Distribution Agreement

In presenting this thesis or dissertation as a partial fulfillment of the requirements for an advanced degree from Emory University, I hereby grant Emory University and its agents the non-exclusive license to archive, make accessible, and display my thesis or dissertation in whole or in part in all forms of media, now or hereafter known, including display on the world wide web. I understand that I may select some access restrictions as part of the online submission of this thesis or dissertation. I retain all ownership rights to the copyright of the thesis or dissertation. I also retain the right to use in future works (such as articles or books) all or part of this thesis or dissertation.

Signature:

Jack Christopher Sharland Date

Overcoming the Limitations of Rhodium-Catalyzed Asymmetric Cyclopropanation and Other Adventures in Strained Ring Synthesis

By

Jack C. Sharland

Doctor of Philosophy

Chemistry

Huw M. L. Davies, Ph.D.
Advisor

Simon B. Blakey, Ph.D.
committee member

Dennis C. Liotta, Ph.D.
committee member

Accepted:

Kimberly Jacob Arriola, Ph.D., M.P.H
Dean of the James T. Laney School of Graduate Studies

Date

Overcoming the Limitations of Rhodium-Catalyzed Asymmetric Cyclopropanation and Other Adventures in Strained Ring Synthesis

By

Jack C. Sharland

B.A., Bowdoin College, 2018

Advisor: Huw M. L. Davies, Ph.D.

An abstract of a dissertation submitted to the faculty of the James T. Laney School of Graduate Studies of Emory University in partial fulfillment of the requirements for the degree of Doctor of Philosophy in Chemistry, 2023.

Abstract

Overcoming the Limitations of Rhodium-Catalyzed Asymmetric Cyclopropanation and Other Adventures in Strained Ring Synthesis

By

Jack C. Sharland

Rhodium-catalyzed carbenoid reactions have been extensively explored over the past 40 years. While much of recent studies in this field of chemistry have been devoted to exploring Csp^3 C–H functionalization reactions and expanding both the synthetic scope and site-selectivity of these transformations, they are rarely used outside of the academic lab. More industrially relevant is the enantioselective cyclopropanation enabled by dirhodium(II) tetracarboxylate catalysts. This reaction is uniquely selective, offering unparalleled diastereoselectivity and enantioselectivity when a donor/acceptor carbene is used, allowing chemists to generate these strained rings in a predictable and controllable manner with excellent yield. While substantial research has already been performed in this arena, there are significant concerns with practicality, scalability, and scope. The work is divided into several chapters devoted to a detailed discussion of three major subjects. Additive enhanced cyclopropanation, computational studies of these additive effects, and a new synthesis of difluorobicyclo[1.1.1]pentanes. A brief summary of the chapter contents follows.

Chapter 1: This chapter will discuss the discovery of $(MeO)_2CO$ as a enantioenhancing reaction media using a medium-throughput condition screen and application towards highly selective asymmetric cyclopropanations at extremely low catalyst loadings.

Chapter 2: This section will discuss the discovery of general cyclopropanation conditions for highly enantioselective transformations of *ortho*-substituted aryldiazoacetates and its application to a broad scope of vinyl aza-heterocycles. This chemistry has also been of significance to an ongoing medicinal chemistry program at AbbVie and this will be discussed briefly.

Chapter 3: This section will explore the role of 1,1,1,3,3,3-hexafluoroisopropanol (HFIP), including its ability to selectively deactivate poisonous and reactive nucleophiles in asymmetric cyclopropanation. This additive has profound effects on catalyst enantioselectivity, reactivity and substrate scope.

Chapter 4: This chapter will explore computational endeavors to rationalize the remarkable effect additives can have on rhodium carbene chemistry. Three additives will be explored in this chapter, *N,N'*-dicyclohexylcarbodiimide (DCC) in C–H functionalization, 2-chloropyridine in asymmetric cyclopropanation, and HFIP's ability to manipulate catalyst selectivity.

Chapter 5: The final chapter will discuss a novel synthetic strategy to access difluorobicyclo[1.1.1]pentanes in one-pot. The generation of unexpected reaction products when difluorocarbene is reacted with 2-aryl bicyclo[1.1.0]butanes will also be explored.

Overcoming the Limitations of Rhodium-Catalyzed Asymmetric Cyclopropanation and Other Adventures in Strained Ring Synthesis

By

Jack C. Sharland

B.A., Bowdoin College, 2018

Advisor: Huw M. L. Davies, Ph.D.

A dissertation submitted to the faculty of the James T. Laney School of Graduate Studies of Emory University in partial fulfillment of the requirements for the degree of Doctor of Philosophy in Chemistry, 2023.

Acknowledgements

Huw Davies: Throughout my years in the group you have been a mentor and a friend. Thank you for guiding my scientific journey with kindness and patience and for all of the opportunities you have given me during my research. Whether it be helping with my scientific writing, playing tennis, or finding me an apartment in Boston on no notice I couldn't have asked for a better mentor. Thank you for all you have done to make me a better scientist.

Simon Blakey, Dennis Liotta, and Nate Jui: Each of you has given invaluable input on my research during our annual committee meetings. You all have given me fantastic advice and encouragement and pushed me to become a better scientist, and I want to thank all of you for guiding me on this journey.

My Family: All of you have been an amazing source of support and encouragement throughout my Ph.D. Even if you don't understand most of what I'm talking about, you have taken the time to listen to me and get excited about my projects. The journey has been long and difficult but no matter what you have been understanding and supportive, thank you for everything.

Maizie Lee: I couldn't think of a better person to share an office with. I know your journey has been tough, but you are a very talented chemist and an amazing person. You continue to be a source of strength and inspiration and I couldn't be more proud that we are finishing this journey together. Good luck on the outside and say in touch, wherever you end up is lucky to have you!

Bo Wei, Yannick Boni, and Zac Garlets: You three have been the biggest lab mentors to me during my Ph.D. Zac, I don't think I would have made it if it wasn't for you. I was terrified when I first got to the Davies lab and knew practically nothing about organic chemistry, but you quickly whipped me into shape and brought me up to speed. Thank you for taking the time to invest in a nervous undergrad from New Jersey and turn me into the scientist I am today. Bo, we've been through it together. I couldn't ask for a better collaborator and you are one of the most talented chemists I know. Thank you for supporting me and guiding me during our projects, without you I don't know what my Ph.D. would look like. Yannick, thank you for being a true friend. Your perseverance and work ethic has been inspirational and there's no one I would rather get lunch with and debate philosophy. I appreciate all of your mentorship and I hope we see each other again soon.

Will Tracy, Josh Sailer, Jasper Luo, and Kristin Shimabukuro: Mentoring you has been a fantastic part of my Ph.D. Each of you are tenacious and talented chemists and it has been an honor to help guide each of you in your research journeys. Will, you are one of the most talented scientists I have ever met. Your

curiosity and skill are impressive and your ability to produce valuable results despite extremely difficult chemistry or compound properties continues to amaze me. We might disagree on some philosophical issues, but your chemical intuition is spot on. I can't wait to see what you do next both in the lab and after you finish your academic career. Josh, we had a major challenge on our hands when you first joined the group, but you were able to make it your own and create a seriously impressive program in the group. It has been a pleasure working with you and I can't wait to see what your group will look like when you become a professor, your future students don't know how lucky they are. Jasper, it has been a blast having you in lab. I don't envy your weekly terrible jokes but I definitely envy your artistic skills. I look forward to watching your continuing growth as a scientist and I couldn't have hoped for a better bay-mate. Kristin, I am so proud of how much you have grown in the Davies lab. We began working on a project with admittedly no direction, but we persevered and together we have created a program that I believe will be the most impactful in the Davies lab for the foreseeable future. Your willingness to dive into new projects and take on huge challenges is commendable and I will leave the group confident that these projects are in good hands. I also want to thank you for your kindness and willingness to help others, I don't know what I would have done outside that Boba shop if you weren't willing to stay and help me. I know you will be extremely successful as you continue your Ph.D. and beyond and I look forward to seeing your journey unfold.

The Davies group and friends outside the lab: There isn't enough space to mention all of you here, but I couldn't have completed this adventure without you. Your support, encouragement, and guidance have been essential sources of inspiration throughout this experience. Thank you for everything.

Table of Contents

List of Abbreviations

BDE: Bond dissociation energy

Kcal/mol: Kilocalories per mole

GSK: Glaxo-Smith Klein

Rt: Room temperature

DMF: *N,N'*-dimethylformamide

MeCN: Acetonitrile

DCM: Dichloromethane

DMSO: Dimethyl sulfoxide

Equiv: equivalents

BOX ligands: *Bis*-oxazoline

DOSP: *N*-(*para*-*n*-dodecylphenyl)sulfonyl prolinate

TBSP: *N*-(*para*-*tert*-butylphenyl)sulfonyl prolinate

ee: Enantiomeric excess

PTAD: phthalimido-adamantyl glycinato

2,2-DMB: 2,2-dimethyl butane

TPCP: triphenylcyclopropane carboxylate.

DiBic: 3,5-di(*p*-$^{t}BuC_6H_4$)TPCP

TriBic: tris(*p*-$^{t}BuC_6H_4$)TPCP

TCPTAD: *tetra*-chlorophthalimido-adamantyl glycinato

r.r: Regioisomeric ratio

d.r: Diastereomeric ratio

TPPTTL: *tetra*-phenylphthalimido-*tert* leucinato

PhCl: Chlorobenzene

TISP: *N*-2,4,6-tris isopropylphenylsulfonyl prolinate

NTTL: Naphthalimido *tert*-leucinato

BMS: Bristol-Meyers Squibb

DCC: *N,N'*-dicyclohexylcarbodiimide

HFIP: 1,1,1,3,3,3-hexafluoroisopropanol

MS: Molecular sieves

Oct: Octanoate

Ar: Aryl

Het: Heteroaryl

DFT: Density functional theory

DPCP: Diarylcyclopropane carboxylate

CFTR: Cystic fibrosis transmembrane conductance regulator

TON: Turnover number

HTE: High-throughput experimentation

HPLC: High-performance liquid chromatography

UHPLC: Ultra high-performance liquid chromatography

THF: Tetrahydrofuran

EtOAc: Ethyl acetate

TFT: Trifluoromethylbenzene

VTNA: Variable time normalization analysis

H-bond: Hydrogen bond

PAPh: Tetramethyl-6-phenyl-2,4,8trioxa-6-phosphaadamantane

dba: Dibenzylacetone diene

TsNIK: Potassium *N*-iodo *p*-toluenesulfonamide

d.e: Diastereomeric excess

2-Clpyridine: 2-Chloropyridine

ppm: parts per-million

wt%: Weight percent

pKa: negative base-10 logarithm of acid dissociation constant

DMAP: *N,N*-dimethylamino pyridine

CCDC: Cambridge crystallography data center

API: Active pharmaceutical ingredient

IR: Infared

PFR: Plug-flow reactor

TPA: Tri-phenyl acetate

OAc: Acetoxy

NTf_2: Bis(trifluoromethane)sulfonimide

TCPTTL: *tetra*-chlorophthalimido-*tert* leucinato

TFPTTL: *tetra*-fluorophthalimido-*tert* leucinato

NMR: Nucleomagnetic resonance

KIE: Kinetic isotope effect

DCE: 1,2-dichloroethane

DBU: 1,8-diazabicyclo (5.4.0)undec-7-ene

DIC: *N,N'*-diisopropyl carbodiimide

HMPA: Hexamethylphosporamide

dppf: 1,1'-Bis(diphenylphosphino)ferrocene

TEMPO: Tetramethylpiperidine N-Oxyl

PSI: (2S,3aS,6R,7aS)-3a-Methyl-2-((perfluorophenyl)thio)-6-(prop-1-en-2-yl)hexahydrobenzo[d][1,3,2]oxathiaphosphole 2-sulfide

Boc: *tert*-Butyloxycarbonyl

TFA: Trifluoroacetic acid

TS: Transition state

ONIOM: Our own n-layered Integrated molecular Orbital and Molecular mechanics

Nu: Nucleophile

HRMS: High resolution mass spectrometry

CPCM: Conductor-like polarizable continuum model

G: Gibbs free energy

H: Enthalpy

HOMO: Highest occupied molecular orbital

LUMO: Lowest unoccupied molecular orbital

NBO: Natural bond orbitals

MD: Molecular dynamics

RDS: Rate determining step

SDS: Selectivity determining step

E: Total energy

PCM: Polarizable continuum model

SAR: Structure-activity relationship

DEL: DNA-encoded library

TMS: Trimethylsilane

DAST: Diethylaminosulfur Trifluoride

DME: 1,2-dimethoxyethane

p-ABSA: *para*-acetamidobenzene-sulfonyl azide

MeO: methoxy

EAS: Electrophilic aromatic substitution

COSY: Homonuclear Correlation Spectroscopy

NOESY: Nuclear Overhauser Effect Spectroscopy

ROESY: Rotating frame Overhauser Effect Spectroscopy

HSQC: Heteronuclear Single Quantum Coherence

HMBC: Heteronuclear Multiple Bond Correlation

FTIR: Fournier transform infared

List of Figures

Introduction

Chapter 1

Chapter 2

Chapter 3

Chapter 4

Chapter 5

Appendix A

Appendix B

Appendix C

Appendix D

List of Schemes

Introduction

Chapter 1

Chapter 2

Chapter 3

Chapter 5

List of Tables

Chapter 1

Chapter 2

Chapter 3

Chapter 5

Appendix D

Introduction:

Strained rings, defined as rings containing >20 kcal/mol BDE in the C-C bonds that comprise them, have been important motifs in all areas of chemistry.[1-6] In total synthesis, strained rings are either part of natural products, often one of the more difficult parts to furnish, or can be used in synthetic intermediates where strain release is the driving force for subsequent reactions.[6-10] In organometallic reactions, strained rings can be leveraged to form more reactive catalysts and the strain release from organometallic intermediates can be used to drive product formation as in the case of Grubbs metathesis.[11] In medicinal chemistry, the use of strained rings is now ubiquitous and they have gained increasing popularity over the past decade as important metabolically stable bioisosteres.[3, 5, 12, 13] Strained rings also impose unusual, but well-defined, relationships between substituents, achieving extreme angles and eclipsed conformations. can also force substituents into unusual angles, allowing them to access new areas of a protein binding pocket.[12, 13] This phenomenon has led to the increasing use of strained rings in medicinal chemistry and collaborations between high profile academic groups like Molander and MacMillan and industrial partners including GSK and Merck.[10, 14-18]

Figure 1: Selected medicinally relevant strained rings.

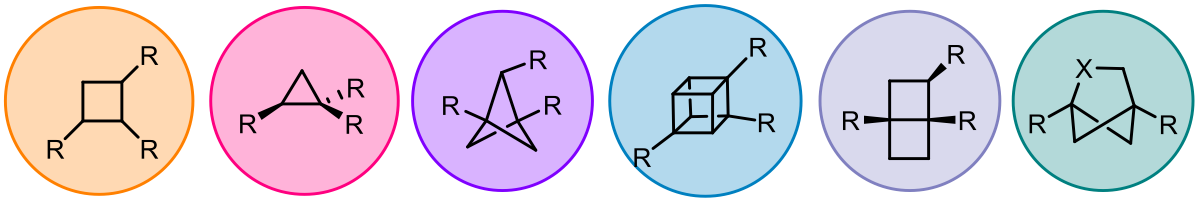

This thesis describes several adventures in strained ring synthesis and includes examples of cyclobutenes, and bicyclo[1.1.1]pentane derivatives, however most of the work (**Chapters 1-4**) will discuss new methods involving cyclopropanation.[19-21] Consequently, a brief introduction to the cyclopropane and established methods for generating this highly strained motif will be given. Cyclopropanes consist of 3 carbon atoms bonded together via σ-bonds to form a highly strained carbocycle.[12] The strain associated with this motif

is exceptionally high and the structure releases around 28 kcal/mol in energy when cleaved depending on the substituents.[1] Due to the narrow angles between the different carbon atoms that comprise the ring (~60°), bonding in cyclopropanes contains far more sigma-character than would be typically expected for a saturated carbocycle (the carbons are sometimes described as sp^5 than sp^3 hybridized).[22, 23] Due to the angle of the carbon-carbon bonds in the system, substituents on the same side of the cyclopropane carbons exist in an eclipsed conformation relative to their neighbors, which can be a useful tool for creating well defined geometries, especially in medicinal chemistry.[6, 9, 12] Despite the high strain, cyclopropanes can be very stable and may be stored at room temperature for years without degrading.[24]

Figure 2: a. Unique physical properties of substituted cyclopropanes make them important motifs in medicinal chemistry. b. Recently approved drugs featuring chiral substituted cyclopropanes.

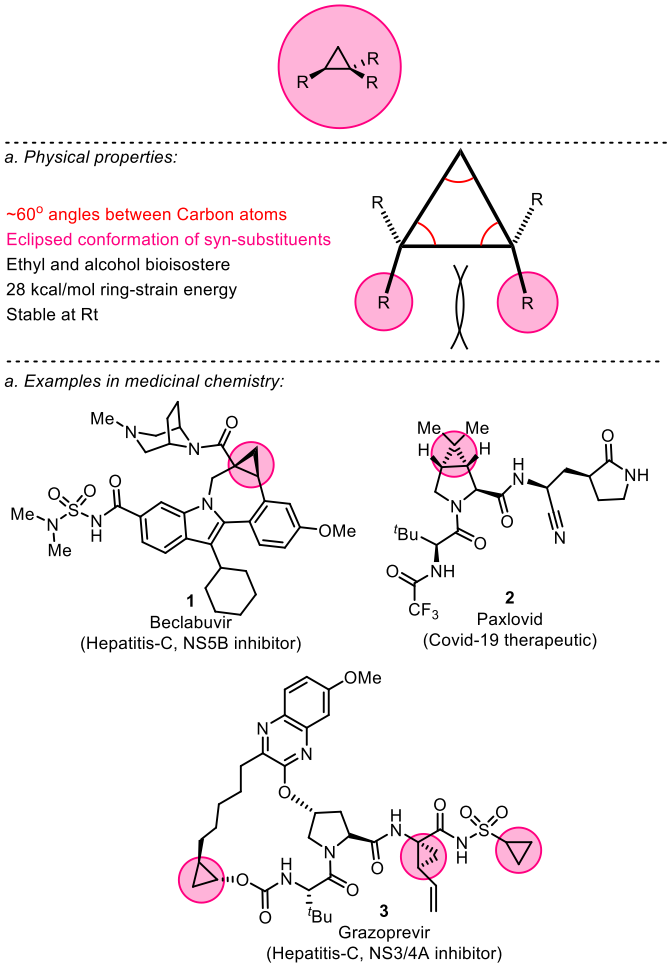

Cyclopropanes have classically been prepared using a variety of methods stretching back to 1958 with the Simmons-smith reaction (Scheme 1).[25, 26] In this reaction, zinc metal is used to generate a zinc carbenoid which can add into an alkene, the resultant negative charge then recaptures the methylene to generate a three membered ring. A few variations of this method have been developed, varying the types of zinc carbenoid that can be generated and the addition of additives that can engender chiral control in the delivery of the carbenoid to the alkene.[27, 28] Directing groups on the substrate like chiral alcohols can also be used to help control stereoselective carbene generation and the reaction has seen uses in a wide variety of applications.[28-30] This chemistry does, however, have some limitations. Organo-zinc species are notoriously pyrophoric and unstable which limits the practical utility of the method as well as the types of zinc carbenoids that can be generated.

Scheme 1: Derivatives and applications of Simmons-Smith cyclopropanation.

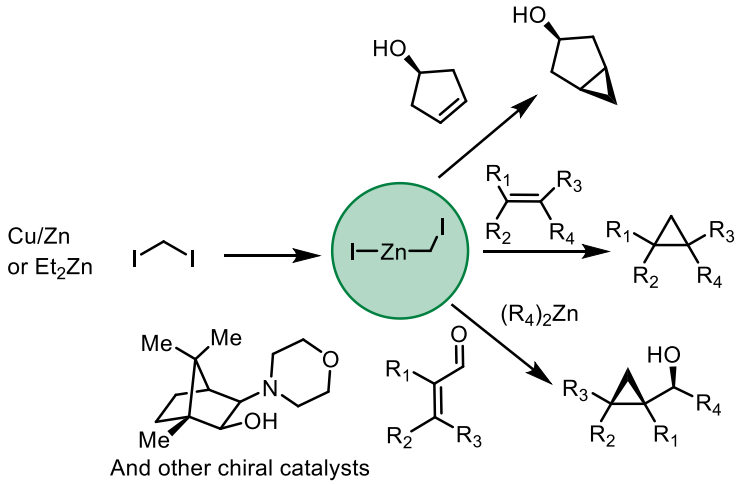

In 1965 a new method was invented by E. J. Corey which employed a sulfur/sulfoxonium ylide to conduct the cyclopropanation (Scheme 2).[31-33] In a similar vein, the negatively charged carbon first attacks an alkene or carbonyl and the new ylide rearranges to generate a 3-membered ring. This method too, while generally useful, suffers from limitations in substrate scope depending on the nature of the sulfur ylide, and can be challenging to render enantioselective.[34-36]

Scheme 2: Derivatives and applications of the Corey-Chaykovsky reaction.

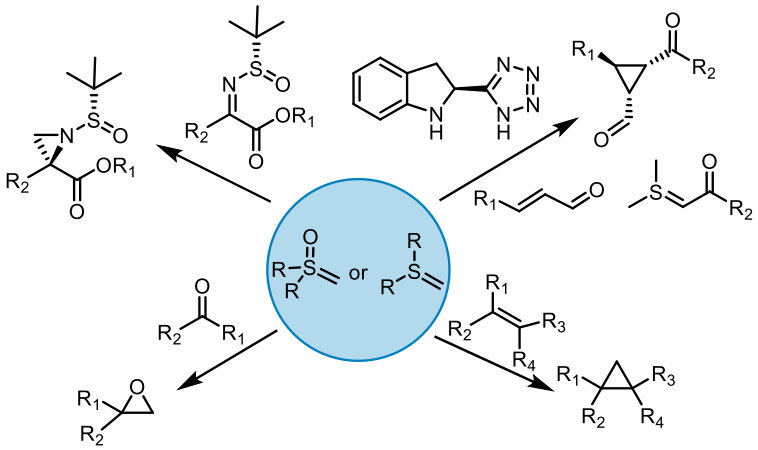

Radical induced cyclopropane formation has garnered significant popularity with the recent resurgence of photocatalysis and a variety of intriguing methods exist, leveraging radical generation to furnish these strained motifs (Scheme 3).[37-40] In general, these reactions rely on the addition of an electrophilic radical to an alkene, followed by SET via reductive quenching of the photocatalyst to generate a carbanion (Scheme 3a.). Finally addition of the carbanion to a carbon featuring a leaving group generates a three membered ring (Scheme 3a).[38, 41] One of the most attractive recent methods developed using this approach is the synthesis of boronated cyclopropanes from carboxylic acid precursors (Scheme 3b).[42] These emerging methods boast a broad substrate scope, mild conditions, and can afford highly substituted products, however the nature of radical reactions often prohibits the formation of these products in an enantioselective fashion. As radical photoredox chemistry gains popularity and research groups like the Yoon group increasingly expand the scope of reactions that can be rendered enantioselective, it is likely that more general chiral versions of this chemistry will become common in the near future.[43-46]

Scheme 3: Radical induced cyclopropanation. a. General mechanism of the reaction. b. Selected examples of photocatalyzed cyclopropanation.

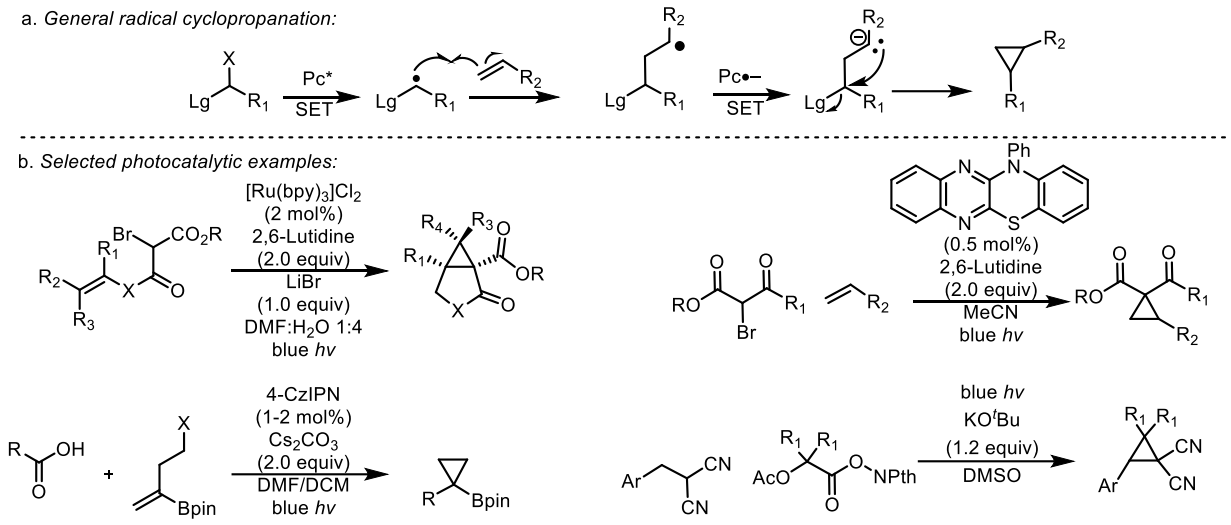

The final, and most relevant to this thesis, method for generating cyclopropanes derives from the use of a metallocarbene generated from the reaction of a precursor compound and a metal catalyst to furnish a highly electrophilic metallocarbene which can do a diverse series of transformations including cyclopropanation.[24, 47] Metals like copper and cobalt have been used in such reactions, however they often have poor catalytic activity (requiring up to 10 mol % catalyst loading) and can also have limited substrate scopes.[48-52] In the case of copper, the best reactivity is often observed with electron deficient acceptor carbenes, reactions of these species can be rendered enantioselective using BOX ligands around the copper core.[48, 53] In the case of cobalt catalysis, the substrate scope is broader, however elaborate ligands like functionalized porphyrins are often required to gain high asymmetric induction.[51, 52, 54] Moving one row down on the periodic table, we arrive at rhodium, and it is here where our story truly begins as dirhodium tetracarboxylate catalysts have been the most broadly successful and industrially utilized catalysts for asymmetric cyclopropanation for the past 30 years.[24, 47, 49, 55, 56] The rhodium carbene is highly electrophilic due to the empty p-orbital centered around the metal-bound carbon, and this electrophilicity is enhanced because rhodium provides very little back-bonding. Though carbenes can be generated from

several species (including ketones, hydrazones, sulfoxonium ylides, alkynes, and iodonium ylides) diazo compounds are typically used to generate the rhodium carbene.[49] These high energy compounds have the distinct advantage of requiring no external base or oxidant for carbene generation and releasing only N_2 as the reaction byproduct.[57]

The field of rhodium carbenoid chemistry encompasses a vast array of reactions, often furnishing structural motifs that would be difficult to furnish in any other way. The unique properties of rhodium generate carbenes that are both reactive enough to conduct difficult transformations like C–H functionalization and cyclopropanation, but also stable enough to achieve high selectivity.[47, 58, 59] Though acceptor and Schrock carbenes have been around for a long time, they often display poor selectivity in combination with a rhodium catalyst (Figure 3).[49, 60] Acceptor carbenes are easily generated from the diazoacetate precursor, however the extremely electron poor carbene that results acts as a super-electrophile and rapidly traps any substrate, including the diazo compound itself. This results in a messy reaction with many side-products most of which are dimers. Though catalysts do exist that can achieve selective transformations with acceptor carbenes (most notably Cu-BOX complexes and engineered enzymes) dirhodium catalysts have yet to achieve similar levels of selectivity with such intermediates.[48, 49, 54, 61] In contrast, Schrock carbenes are far too electron rich to generate effective carbenes for dirhodium catalysis.[62] The lack of a withdrawing group results in an electron rich carbene which is too stable to trap most substrates and so reactions with this group are limited.[63] In the late 1980's, Dr. Huw Davies had the idea to combine these two types of carbenes to generate a balanced carbene complex (Figure 3).[47, 64, 65] This carbene would feature the electron withdrawing group to ensure high reactivity and electrophilicity but would also include an electron donating group.[47] This group would attenuate the selectivity of the metallocarbene by donating electron density into the empty p-orbital, allowing it to achieve longer lifetimes and select between different substrates, providing the potential for chemo, regio and diastereoselectivity.[47, 58] This would be a so-called donor/acceptor carbene (Figure 3).[47, 66]

Figure 3: Historically reported classes of carbene.

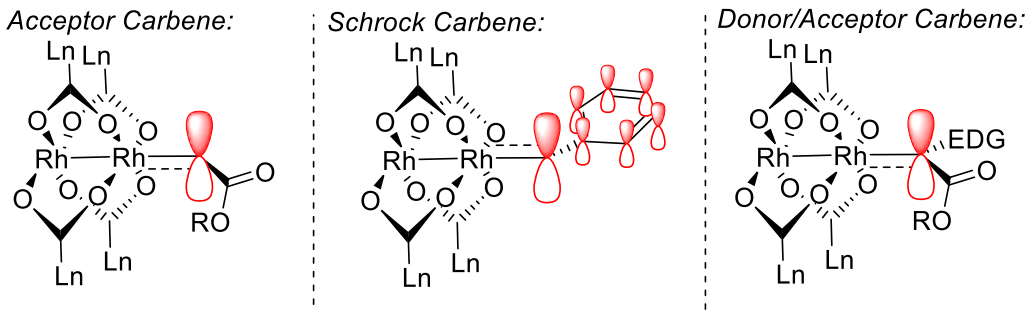

The mechanism of dirhodium catalyzed cyclopropanation with a diazo compound is shown in Figure 4. The reaction begins with the association of the diazo compound with the dirhodium tetracarboxylate (**A**). The donor/acceptor-diazo compound coordinates to **A** via the carbonyl group donating electron density to the rhodium face.[59] To generate the carbene, the rhodium slips to the α-carbon forming a σ-bond to the rhodium atom (**B**).[58, 59, 67] The N_2 group is then extruded resulting in a neutral carbene bound to the rhodium complex (**C**).[59] Once formed, the carbene can react in a multitude of ways, usually through a three-membered transition state.[66-70] In the presence of an alkene the reaction proceeds via a [2+1] cycloaddition to form a substituted cyclopropane (**D**).

Figure 4: Mechanism of dirhodium catalyzed cyclopropanation.

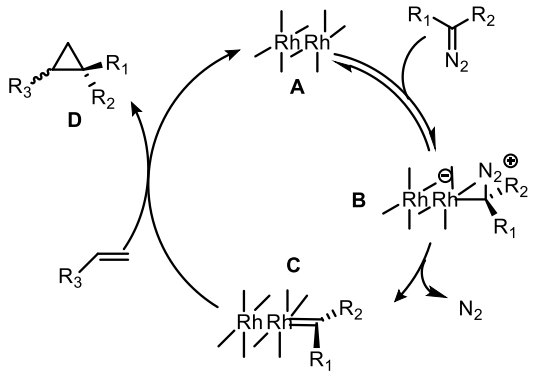

At the outset, the carbene is highly electrophilic as the p-orbital centered on the sp^2 hybridized carbene carbon is empty.[70] Rhodium as a metal provides very little back bonding and the geometry of the carbene

coordination means that it can only bond with the rhodium via the dz^2 orbital rendering the carbene highly electrophilic.[71, 72] In the first step of any rhodium-carbene reaction, the substrate donates electrons into this super electrophilic p-orbital forming a σ-bond and a zwitterionic complex which can then recombine or rearrange to form a new product.[47, 69, 70, 73, 74] The mechanism of product formation can be stepwise or concerted-asynchronous depending on the substrate (Figure 5). In the case of cyclopropanation, for example, the barrier for recombination is so low that it happens almost immediately to efficiently furnish the desired 3-membered ring.[58, 67, 68] In the case of C–H functionalization, however, the mechanism is considered to be stepwise where the initial step (also the rate determining step) is abstraction of the substrate hydride to furnish two zwitterionic species which can then recombine.[19, 69, 75, 76] Sigmatropic rearrangements of the zwitterion in reactions like the stevens rearrangement and the combined C–H functionalization/cope rearrangement are also considered to be stepwise.[76, 77] In the presence of a heteroatom, the first step is instead ylide formation as the heteroatom donates lone-pairs into the empty p-orbital.[78-80] In rare cases these ylides are stable and can be isolated, but more commonly they rearrange to furnish new products as in the case of epoxidation, tertiary alcohol formation, and cascade type transformations.[73, 78, 79]

Figure 5: Mechanisms of interaction between a nucleophilic substrate and a donor/acceptor carbene.

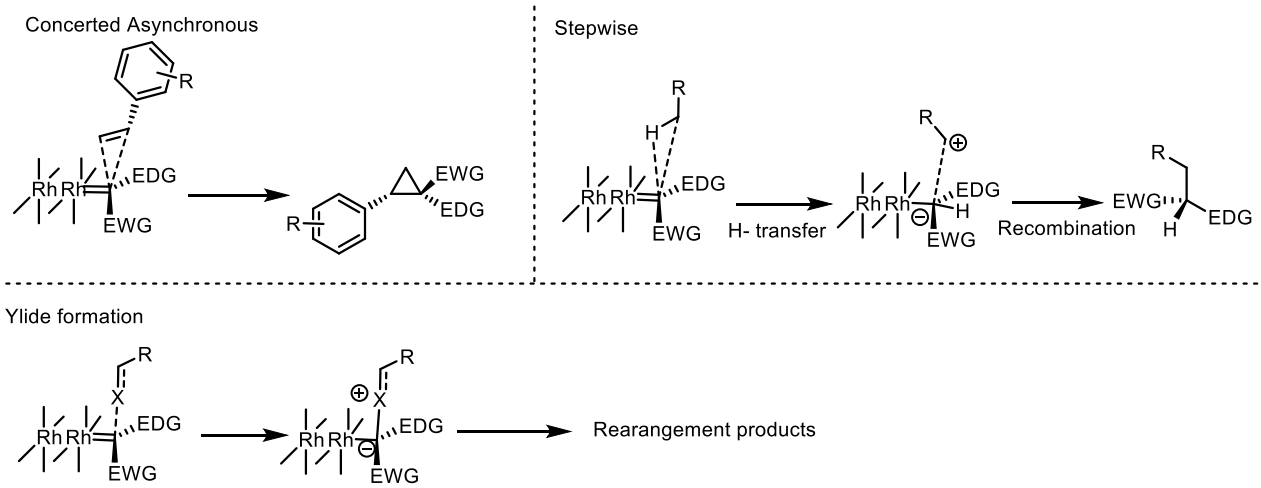

The origins of selectivity in these reactions are more complex, donor/acceptor carbenes are highly diastereoselective and chiral catalysts render them highly enantioselective.[47, 66, 81] Diastereoselectivity and enantioselectivity are both related to the approach of the substrate to the carbene but arise from different controlling elements.[58, 68] Diastereoselectivity is purely derived from substrate control and even reactions catalyzed by achiral complexes like $Rh_2(OAc)_4$ typically exhibit high diastereoselectivity when a donor/acceptor carbene is used.[59, 81] Diastereoselectivity arises from the approach of the substrate to the carbene relative to either the donor or the acceptor side of the carbene (Figure 6). The donor group is generally coplanar with the empty p-orbital as mentioned above and thus has a narrow steric profile, whereas the carbonyl is pointed perpendicular to the p-orbital to minimize orbital overlap (Figure 6).[66, 71, 76] This gives the substrate a clear preference for the approach as the acceptor side is significantly more sterically hindered than the donor-side.[59] This preference is exacerbated by weak non-covalent interactions. Since the donor-group is generally an arene or an alkene, it can π-stack with the substrate or engage in other hydrophobic interactions to help improve the diastereoselectivity of the transformation (Figure 6).[59, 63, 81] As a result, there will always be a *cis*-relationship between the donor group and the substrate if the reaction follows an intermolecular concerted mechanism.[59, 81] Intramolecular mechanisms can obey different trends depending on the substrate, but these will not be discussed at length in this thesis.[82, 83] Stepwise mechanisms can also lose diastereoselectivity as dictated by the rate of zwitterion recombination; if it is slow the diastereomeric ratio will suffer as the molecules may rotate or rearrange prior to recombination.[68]

Figure 6: Model for diastereoselectivity of cyclopropanation of an alkene with a donor/acceptor carbene.

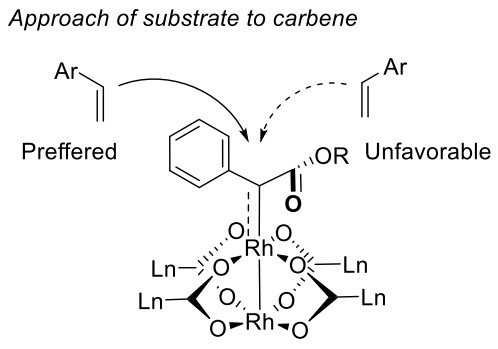

The Davies group achieved success with this new type of carbene early on, achieving levels of diastereoselectivity previously inaccessible to carbenoid transformations.[64, 65] Still unsatisfied, the group wanted to generate enantioselectivity with this new type of carbene and as a result began to invent chiral catalysts based around the dirhodium tetracarboxylate core.[64, 84] At first glance, many assumed that the dirhodium tetracarboxylate lantern structure would be poor platform for chiral catalyst design. Indeed, the carboxylate ligands sit equatorial to the dirhodium core, far away from the axial active site of the catalyst, and so ligands could be expected to have too little influence at the rhodium carbene itself to generate asymmetric induction in such a rapid reaction (Scheme 4a). Despite these doubts, a series of dirhodium catalysts were invented based on an dirhodium *tetra-N*-sulfonyl aryl prolinate scaffold (Scheme 4b, **4** and **5**).[64, 84, 85] Moderate levels of enantioinduction were observed with these early catalysts, however researchers noted that asymmetric induction was highly dependent on the solvent environment, less polar solvents resulted in higher %ee.[47, 64, 85] To capitalize on this observation, the Davies group added an extremely greasy alkyl chain, an *n*-dodecyl group, to the *para*-position of the aryl sulfonyl on the ligand to create a catalyst which would be soluble in pentane, and as a result developed the first highly successful chiral dirhodium tetracarboxylate catalyst, $Rh_2(DOSP)_4$ (**5**).[64] The Davies group exploded the scope of asymmetric transformations that could be achieved with rhodium carbene chemistry using this catalyst including cyclopropanation,[64, 86-88] combined cyclopropanation/cope-rearrangement,[89-91] C–H

functionalization,[85, 92, 93] and the combined C–H functionalization/cope-rearrangement (Scheme 4c/d).[94, 95] This led to a large number of projects within the group, some of which were focused on the synthesis of medicinally relevant compounds including tropanes,[91] others on the total synthesis of complex molecules including colombiasin-A and (+)-elisabethadione.[94-96] Nevertheless the two most prolific programs in the group remained method development and catalyst design.

Scheme 4: a. General dirhodium tetracarboxylate. b. *N*-sulfonyl aryl prolinate derived dirhodium tetracarboxylates. c. Selected examples of $Rh_2(DOSP)_4$ (**5**) catalyzed [2+1] cycloadditions. d. Other $Rh_2(DOSP)_4$ (**5**) catalyzed transformations of donor-acceptor diazo compounds.

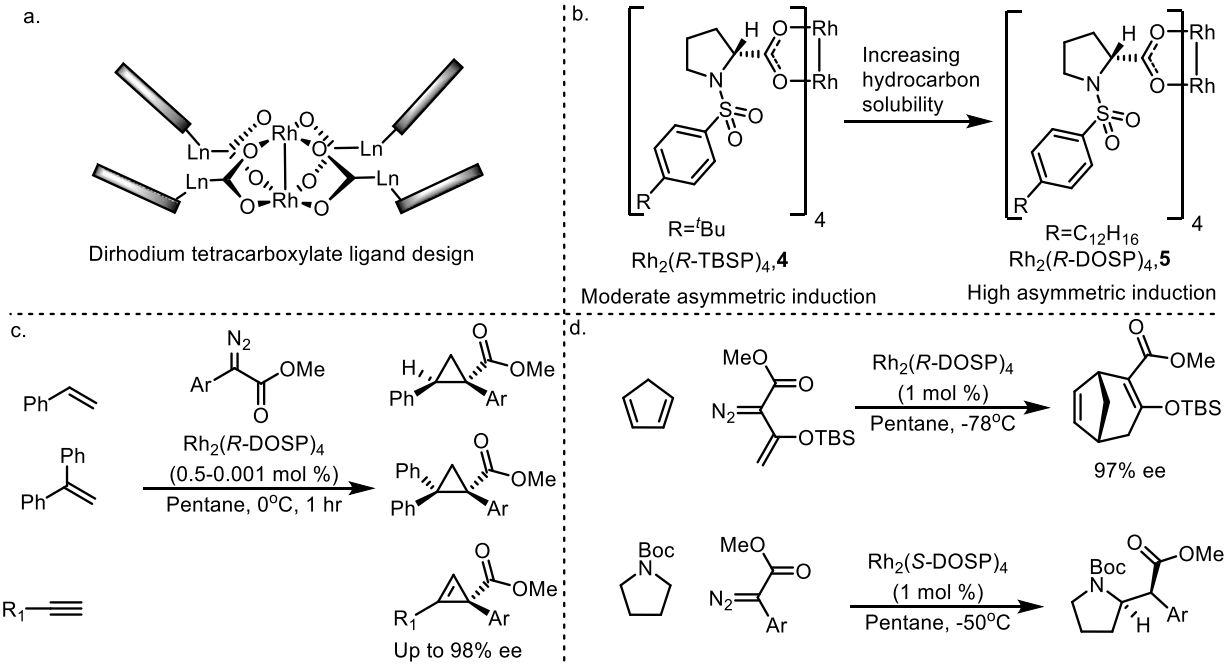

The enantioselectivity of rhodium-carbenoid reactions is controlled purely by the influence of the chiral ligands.[70, 97-99] The carbene essentially has two prochiral faces that can be approached, the *Si* and the *Re*-face, so named due to the isomer they will generate if they react (*Si* produces *S*, *Re* produces *R*). The substrate may approach from the donor side of either the *Si* or the *Re* face of the carbene and the selectivity of one over the other is purely a function of the tetracarboxylate ligand environment (Figure

7).[81, 100] The origins of selectivity imposed by a diverse array of ligands is not fully understood and these effects can be difficult to explore experimentally due to the fleeting nature of the key carbenoid intermediate.[71] Computational investigations are ongoing to determine the origins of selectivity in more detail as will be discussed in **Chapter 4**.

Figure 7: Asymmetric induction determining approach in rhodium catalyzed cyclopropanation.

Enantioselectivity determining approach

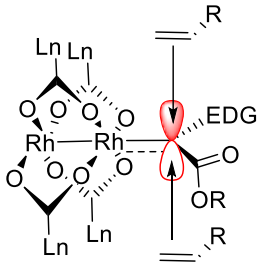

Throughout the Davies group's exploration of the chemistry accessible to the rhodium-carbene system, a diverse series of C–H functionalization reactions were observed.[47, 81, 85, 92, 93] At the same time, other researchers including Fox,[101] Charrette,[102-105] Doyle,[106-108] and Hashimoto[83, 109] were designing their own series of dirhodium tetracarboxylate catalysts for conducting asymmetric transformations. The most broadly successful chiral catalysts in these series were the phthalimido-*tert*-leucinato series pioneered by Hashimoto (**6**) which adopt a C_4-symmetric chiral crown conformation.[109-111] The Davies group swapped the *tert*-leucine group for the bulkier adamantly-glycine group which helped rigidify the catalyst and ensure higher selectivity than the *tert*-leucinato analogues.[69, 99, 112] This first catalyst $Rh_2(PTAD)_4$ (**7**) proved even more selective for transformations involving C–H functionalization than $Rh_2(DOSP)_4$ (**5**) and it too was used for the development of a diverse series of methods (Scheme 5).[113-115]

Scheme 5: Davies expansion on Hashimoto's successful phthalimido-derived catalysts. Selected examples of highly selective transformations with $Rh_2(PTAD)_4$ (**7**).

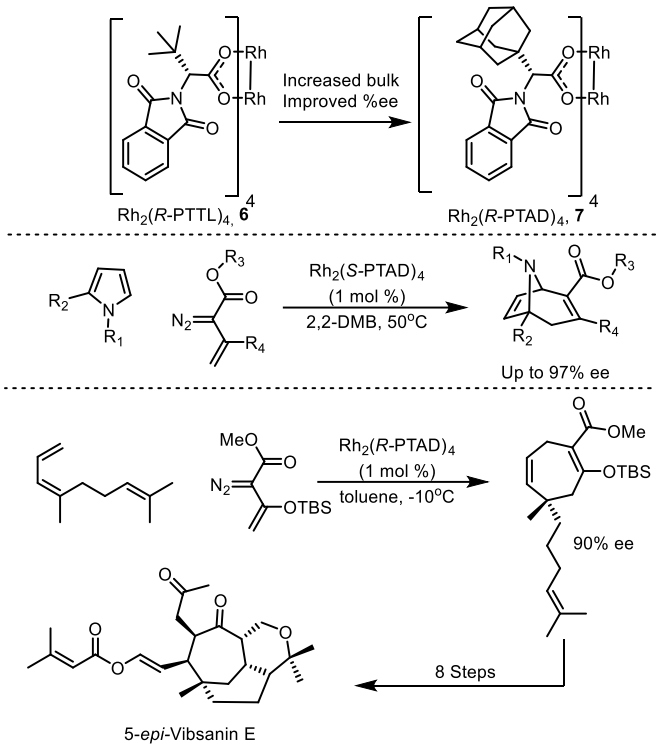

More recently, the Davies group has heavily invested in a new series of catalysts featuring a triaryl-cyclopropane carboxylate (TPCP).[24, 116] These unusual ligand structures were inspired by the highly asymmetric cyclopropanation of 1,1-diphenylethylene by a diverse series of aryldiazoacetates to furnish a new chiral carboxylate that is not naturally derived unlike the prolinate or phthalimido series of catalysts (Figure 8, **8-11**).[88] These catalysts proved to be highly effective for both cyclopropanation and C–H functionalization.[117-119] While previous catalysts were often selective for inserting into the most electronically activated methylene in each system, this series of catalysts created new opportunities for site-selectivity (Figure 8).[119] The high steric demand of the ligands led to catalysts that would react with the most sterically accessible bond instead of the most electronically activated.[55, 119] This effect was taken to the extreme when new catalysts were generated by way of multi-fold Suzuki cross-coupling on the dirhodium complex to furnish catalysts which could distinguish C–H bonds even in unactivated systems

like pentane (**9-10**).[120, 121] More recently, a new catalyst Rh_2(2Cl5Br-TPCP)$_4$ (**10**) was introduced with one of the most sterically demanding pockets so far.[122] This catalyst completely overrides the electronic preference and instead selectively functionalizes only the most accessible methylene site, even in the presence of activated C–H bonds in the molecule (Figure 8).[122, 123] While the TPCP series highlighted the potential for unparalleled site-selectivity in C–H functionalization, they could not access every type of C–H bond and new catalyst structures needed to be developed.

Figure 8: Dirhodium tetrakis(triarylcyclopropane carboxylate) catalysts are capable of unparalleled site selectivity in C–H functionalization of alkanes.

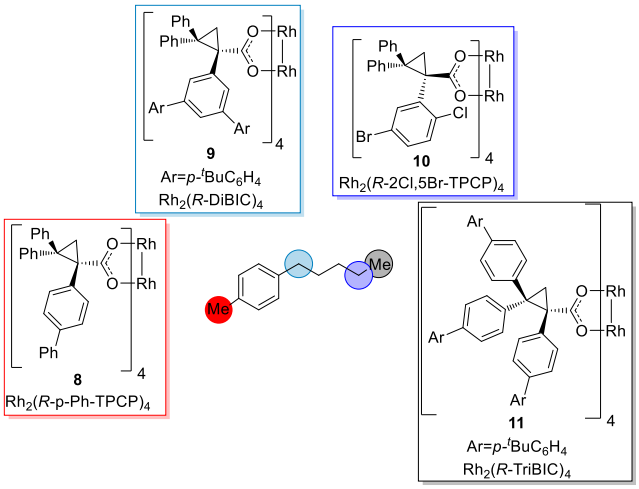

To this end, the group's focus turned from the TPCP series and towards the earlier phthalimido series of catalysts. As previously stated, Rh_2(PTAD)$_4$ (**7**) is selective for activated methylene bonds and it was reasoned that substitution around the phthalimide ring would result in more selective catalysts.[112] The first iteration of this program resulted in the discovery of Rh_2(TCPTAD)$_4$ (**12**), which is a highly selective catalyst for the functionalization of unactivated 3° C–H bonds (Scheme 6).[112, 124] Arguably the most impressive catalyst to come out of this series was Rh_2(TPPTTL)$_4$ (**13**), featuring a per-phenylated phthalimide ligand around the dirhodium core.[19, 20, 98, 125]

Scheme 6: $Rh_2(TCPTAD)_4$ (**12**) is an exceptionally selective catalyst for the C–H functionalization of unactivated tertiary C–H bonds.

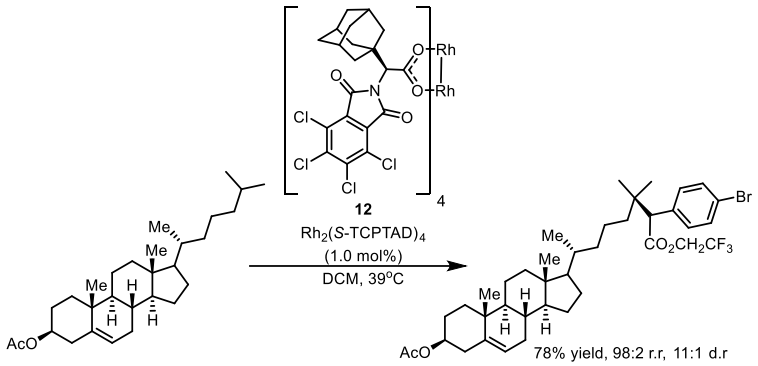

$Rh_2(TPPTTL)_4$ (**15**) is the only Davies catalyst that can be synthesized in two simple high yielding steps. First, *tetra*-phenyl phthalic anhydride (**13**) is condensed with *tert*-leucine to prepare the ligand (Figure 9, **14**). This ligand is then exchanged onto rhodium acetate by refluxing at 160 °C in a Soxhlet extractor with chlorobenzene.[98] The resultant $Rh_2(TPPTTL)_4$ (**15**) complex which features 16 phenyl rings arranged in a C_4-symmetric helical crown conformation around the dirhodium core is then easily purified by column chromatography or recrystallization (Figure 9).[97, 98, 126] In examining crystal structures of this complex, it is clear that the phenyl rings in each ligand tilt in order to favor T-stacking interactions with neighboring ligands creating a type of helical chirality around the bowl of the catalyst.[97, 98] This unique feature of the bowl leads to novel types of site selectivity and reactivity. The original report of this catalyst centered on its ability to selectively functionalize the C-3 equatorial site of substituted cyclohexanes with high site, diastereo, and enantioselectivity (Figure 9).[98] The ability of this catalyst to distinguish between electronically similar C–H bonds with perfect regioselectivity (>20:1) and very high (11:1) diastereoselectivity is unparalleled in the field and a broad scope of substrates was elaborated using this catalyst. The selectivity was rationalized to be a function of the steric environment of the phenyl rings which allowed only one trajectory of the cyclohexane to approach the rhodium carbene (Figure 9).[98] The catalyst was also shown to be surprisingly flexible, and the ligands move to accommodate the carbene

and substrate similar to the way an enzyme binding pocket deforms, highlighting the uniqueness of this catalyst design.[98] Chiral catalysts are often designed to have extremely rigid steric environments in order to ensure predictable and reliable stereoselective reactions but this is not the way nature designs chiral catalysts. Instead, enzyme binding pockets are often highly flexible and can deform either due to substrate binding or even due to allosteric modulation leading to new modes of reactivity.[127] $Rh_2(TPPTTL)_4$ (**15**) is directly analogous to this approach and its promiscuous reactivity has led to a slew of new methodology projects within the Davies group, some of which will be discussed in this thesis (**Chapter 2** and **Chapter 4**). Given the success of this scaffold there have also been attempts to derivatize $Rh_2(TPPTTL)_4$ (**15**) to access new catalysts with related activity, an effort which will briefly be explored in **Chapter 3**.[128] Further elaboration of this intriguing scaffold continues to be part of the catalyst development program as of the writing of this thesis and many of the catalysts related to this scaffold have emerged as the optimal species for ongoing methodological investigations.[21]

Figure 9: a. Synthesis of $Rh_2(TPPTTL)_4$ (**15**) is achieved in two simple high yielding steps, affording a dirhodium tetracarboxylate catalyst with a C_4 symmetric bowl-shaped catalytic pocket. b. The selectivity of this catalyst is rationalized by an analysis of interactions between the bowl and substituted cyclohexane substrates which forces substituted cyclohexanes to adopt a conformation in which the C-3 equitorial site is the most accessible site for functionalization by the carbene. c. Selected transformations in which $Rh_2(TPPTTL)_4$ (**15**) plays a critical role.

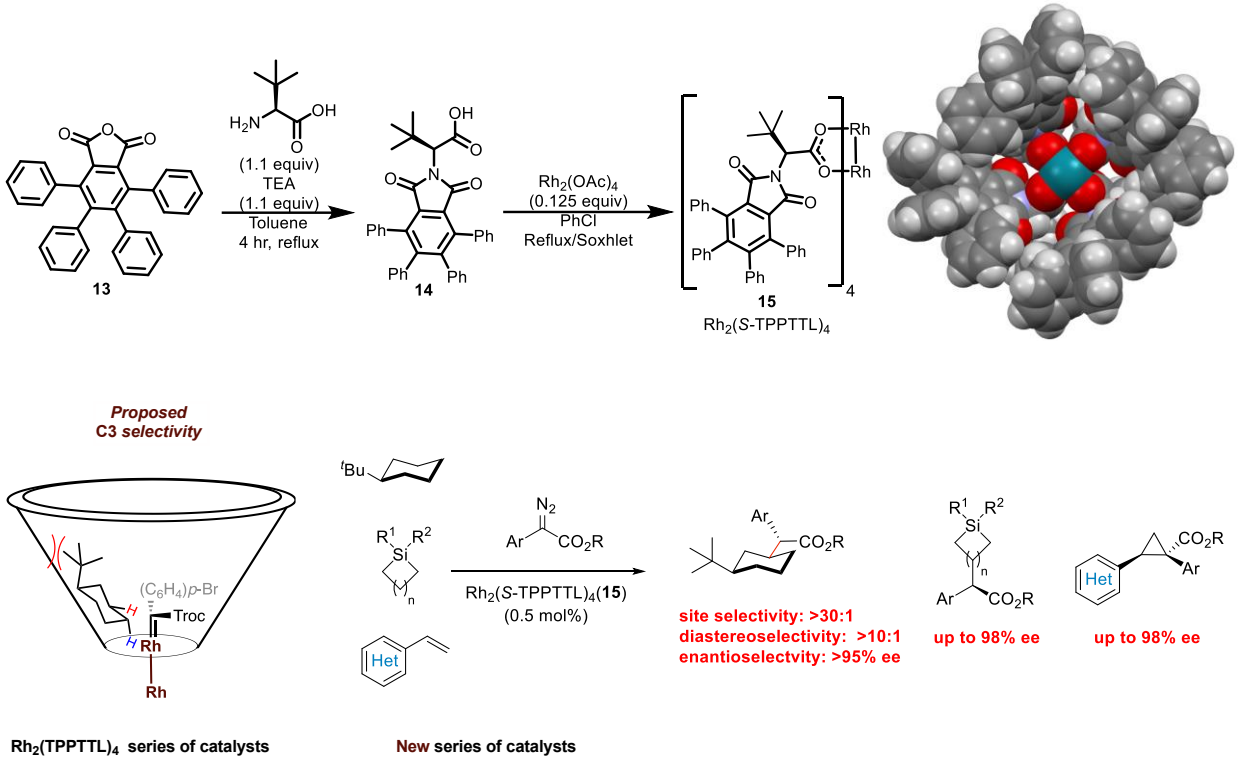

Given the plethora of chiral dirhodium tetracarboxylate catalysts accessible to the Davies group there has been significant interest to apply these catalysts towards the development of new methods, in particular highly selective C–H functionalization and cyclopropanation. This thesis will discuss several of these methods, primarily in the realm of cyclopropanation. Though cyclopropanation has been an important part of Davies group history and highly selective transformations have been performed in the past, the chemistry has three major drawbacks: sustainability, practicality, and substrate scope.

Figure 10: The dirhodium catalyst toolbox in the Davies group.

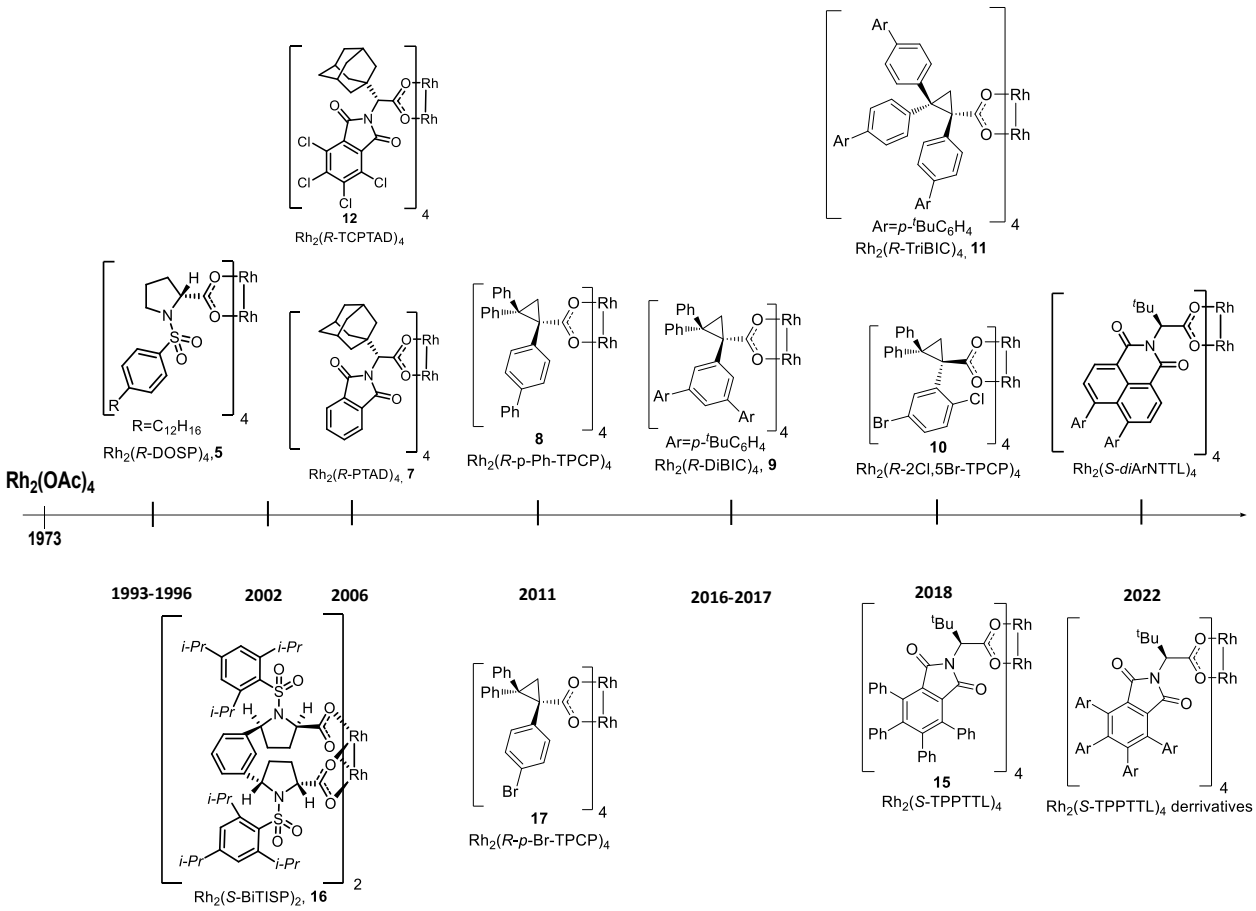

Rhodium is an extremely rare and valuable precious metal and there is considerable interest in developing methods that are operable at extremely low catalyst loadings.[129] Previous approaches to conduct cyclopropanation at low catalyst loadings had required the development of highly complex catalysts like $Rh_2(BiTISP)_2$ (**16**), and conducting the reaction under harsh, impractical conditions.[87, 130, 131] Recent work in the Davies lab has focused around designing methods that can be applied at extremely low catalyst loadings, leveraging the effects of additives to enhance both reactivity and selectivity.[19-21, 129] Another key aspect of sustainability in organic chemistry is the use of green and environmentally solvents.[132] Traditional $Rh_2(DOSP)_4$ (**5**) methodologies required the use of hydrocarbon solvents like 2,2-dimethyl butane and pentanes to ensure high enantioselectivity.[64, 108] Even in the multi-Kg pilot scale synthesis of

the hepatitis-C drug Beclabuvir (**1**), BMS utilized heptanes as solvent to ensure high enantioselectivity for their large scale cyclopropanation.[56] In order to make these methods more attractive to industrial chemists less environmentally damaging solvents need to be utilized as a reaction medium.[132, 133] With the development of new catalysts in the Davies group, catalysts which provided high enantioselectivity in solvents like ethyl acetate and dimethyl carbonate were identified and had the potential to be utilized at extremely low catalyst loadings (Figure 11).[129] A similar campaign was also performed on C–H functionalization where additive effects manifested in a more significant way with the discovery that *N,N*-dicyclohexylcarbodiimide significantly enhanced the competency of catalysts at exceptionally low catalyst loadings (0.00025 mol %) (Figure 11).[19] These efforts are described in **Chapter 1** and **Chapter 4** and go a long way to improving the sustainability of dirhodium catalysis.

Figure 11: Progress on the sustainability of dirhodium carbene catalysis in cyclopropanation and C–H functionalization.

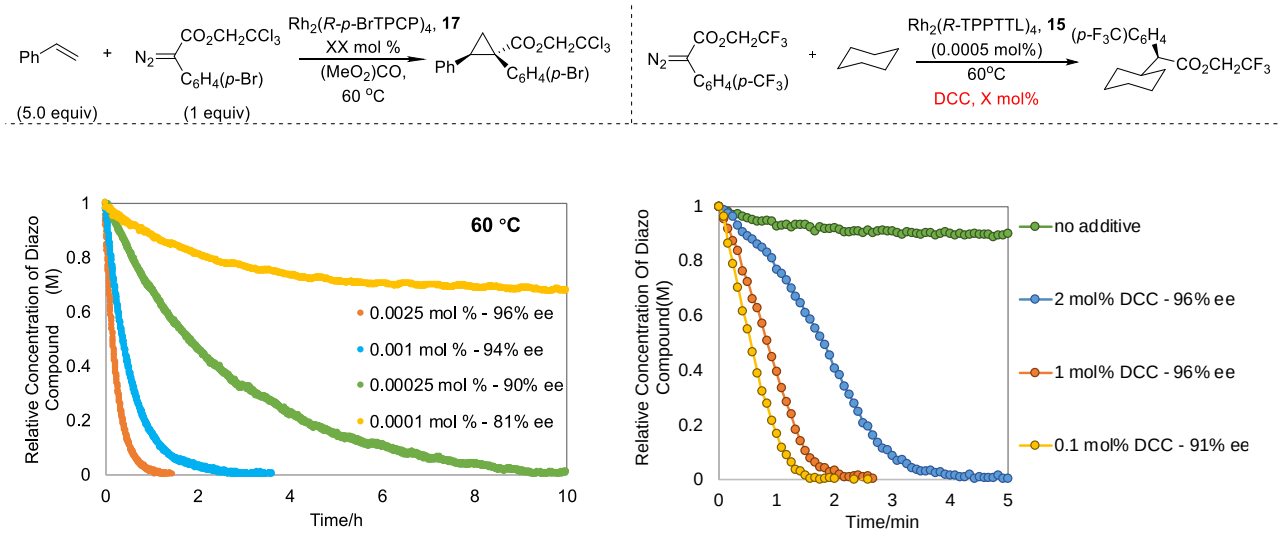

The practicality of rhodium catalyzed reactions is also limited due to the reliance on a transition metal catalyst (Figure 4) to generate the highly reactive carbene intermediate. Nucleophiles like aza-heterocycles are capable of coordinating to the axial sites of the rhodium catalyst, and if the strength of

this interaction is significant, they can do so to the exclusion of the diazo compound.[134-136] This can prevent the generation of the carbene under mild conditions leading to a phenomenon known as catalyst poisoning. While catalyst poisoning is occasionally a useful feature, as in the case of partial hydrogenation of alkynes with Lindlar's catalyst,[137] it is more often a hinderance to scope expansion. Nowhere was this more clear than in the evaluation of heteroaryldiazoacetates in cyclopropanation published in 2001.[86] While several substrates gave a highly selective transformation, many required complex solvent mixtures and high temperatures to ensure a successful transformation.[86] The use of solvent mixtures considerably hurt the selectivity of the transformation as would any deviation from using hydrocarbon media with $Rh_2(DOSP)_4$ (**5**) for the reasons discussed above, however the poor solubility of the heteroaryldiazoacetates made this a challenge.[86] Furthermore, several compounds were poisonous to the rhodium catalyst leading to no reactivity even under forcing conditions.[86] Given the advent of the dirhodium catalyst toolbox these limitations were worth reevaluating especially considering that hydrocarbon solvents are no longer required to generate an enantioselective transformation.[117, 129] The pharmaceutical company, AbbVie, was also interested in methods capable of cyclopropanating vinyl-heterocycles and as a result a collaboration was initiated between the Davies group and AbbVie.[20] The fruits of this partnership are discussed at length in **Chapter 2** including the development of robust methods for the cyclopropanation of vinyl-heterocycles (Scheme 7).[20] Several interesting additive effects emerged from this study including the discovery of 2-chloropyridine as an achiral additive for enhancing the stereoselectivity of cyclopropanation reactions involving *ortho*-substituted aryldiazoacetates and the use of 1,1,1,3,3,3-hexafluoroisopropanol (HFIP) as a dehydrating agent in place of molecular sieves.[20] After the development of this method, the AbbVie process team adapted the synthesis for large scale flow-chemistry and subsequently reported their efforts.[126] Given the unexpected additive effects observed computational studies to understand the origins of the enhancement were performed as will be described in **Chapter 4**.

Scheme 7: Many phases were involved in the development of a generalizable method for the cyclopropanation of vinyl-azaheterocycles with a diverse series of aryldiazoacetates.

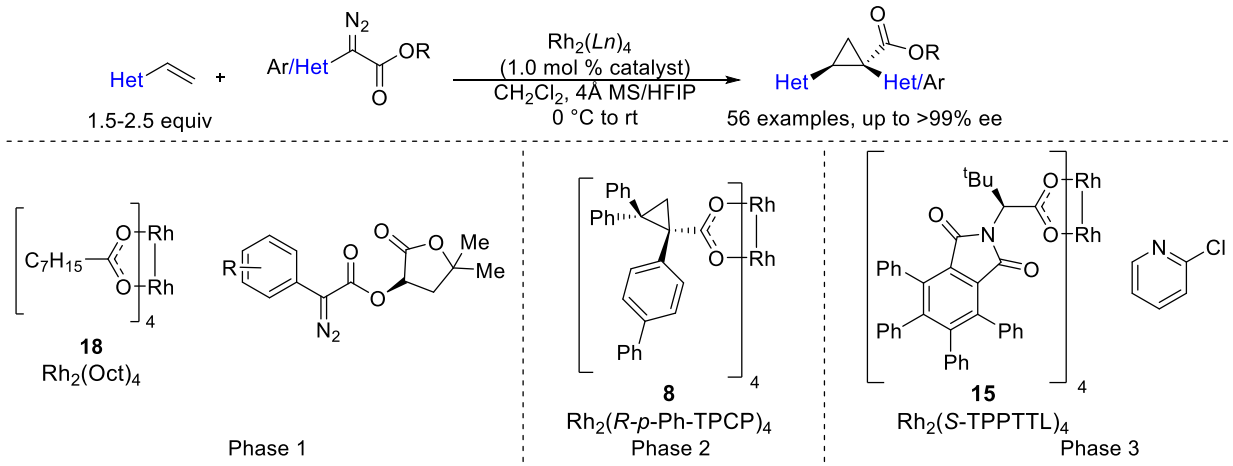

The use of HFIP to prevent water from interfering with catalyst enantioselectivity represented an exciting opportunity to solve the scope limitations of dirhodium catalyzed asymmetric cyclopropanation. In the AbbVie collaboration, the main issue with water was that it caused changes in catalyst enantioselectivity which is highly unconventional.[20] Normally, one would expect that excess water would result in significant O–H insertion as the water competes with the alkene substrate for the highly electrophilic carbene.[74, 138] In this case, however, O–H insertion was not observed. Instead, the water was primarily interfering with catalyst enantioselectivity suggesting that weak coordination to the catalyst or carbene was the main issue.[135, 136, 139] Through hydrogen bonding, HFIP removes this harmful nucleophilic influence and it was hypothesized that it could deal with other nucleophilic poisons (Figure 12).[140, 141] This led to a collaboration with Novartis in which a method was developed leveraging the nucleophile desensitizing power of HFIP to enhance the scope of compounds accessible for derivatization by rhodium catalyzed methods (Figure 12).[142] These efforts are described at length in **Chapter 3**.[21]

Figure 12: The discovery of HFIP for the selective deactivation of poisonous nucleophiles led to the exploration of this method in the presence of 90 different nucleophilic and reactive catalyst poisons and was then leveraged towards the cyclopropanation of complex molecules like (-)-cinchonidine (**19**).

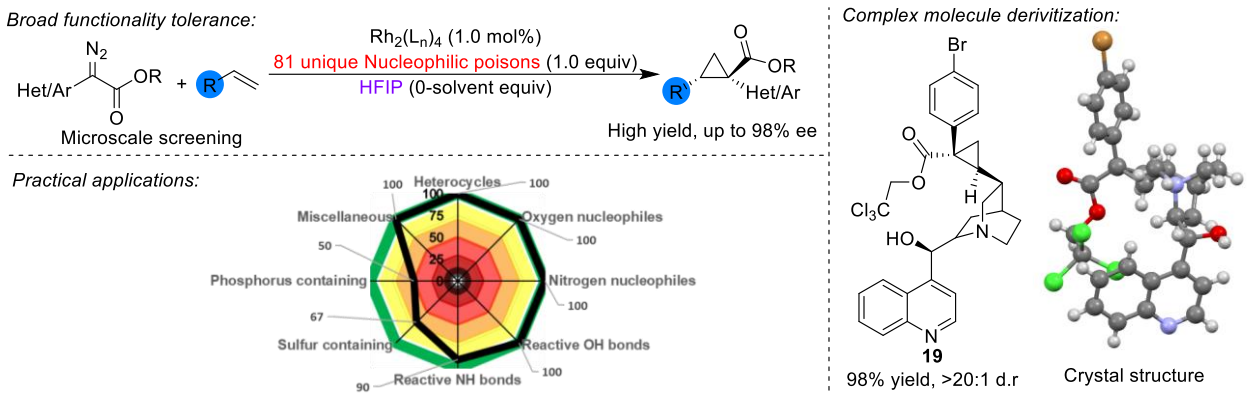

Given the impact of additives on reactivity and selectivity that have observed recently, there was interest in understanding the origins of these effects. Throughout the history of the Davies group, computational analyses have been essential to understanding the selectivity and reactivity of rhodium-carbenoid transformations.[58, 59, 63, 66, 81, 98, 116, 143] To this end, DFT calculations have been performed on a variety of reaction systems explain the unusual additive effects that have been observed (Figure 13). These efforts are described at length in **Chapter 4.**

Figure 13: Computational studies have been imperative in the elucidation of the ability of 2-chloropyridine to enhance the asymmetric induction of cyclopropanation with *ortho*-substituted aryldiazoacetates.

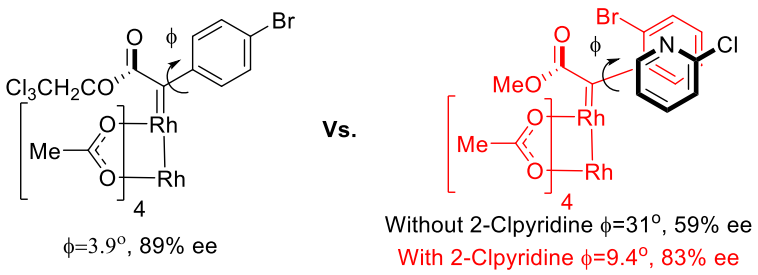

Cyclopropanes are not the only industrially valuable strained rings that are accessible through dirhodium catalysis, many exotic strained motifs including aziridines,[144, 145] tropanes,[91] and bicyclo[1.1.0]butanes[8, 118, 146] are also accessible. In recent years, there has been considerable interest in developing high Csp^3 content phenyl bioisosteres and one of the most successful architectures for this application is the bicyclo[1.1.1]pentane.[4, 5, 147-151] Recently, many groups have collaborated with industrial partners to furnish derivatized versions of these compounds and invent new methods for generating them in a practical and generalizable way.[2, 10, 14, 16-18, 152-155] Slightly lesser-known are 2,2-difluorobicyclo[1.1.1]pentanes which are capable of acting as bioisosteres for *ortho*-fluorinated arenes.[18, 156-158] Initially reported in simultaneous publications from Merck[156] and Enamine,[157] these unusual compounds are derived from the reaction of difluorocarbene with a 3-arylbicyclo[1.1.0]butane and were shown to have improved pharmacological properties compared to an *ortho*-fluoro phenyl.[156] This synthesis represented a significant opportunity for the Davies group to enter the game of bicyclo[1.1.1]pentane synthesis. In 2013, a paper was published describing the ability of a-allyldiazoacetates to undergo intramolecular cyclopropanation to afford 2-arylbicyclo[1.1.0]butanes with high enantioselectivity.[118, 146] These reactions operate at low catalyst loading (0.01 mol %) and can be telescoped to further derivatization.[146] This represented an opportunity to access a novel series of chiral 4-aryl-2,2-difluorobicyclo[1.1.1]pentanes for the first time which could be a valuable new motif for medicinal chemists which will be explored in **Chapter 5** (Figure 14).

Figure 14: A diverse series of complex carbocycles were accessed during the development of a one-pot procedure for the synthesis of highly substituted 2,2,-difluorobicyclo[1.1.1]pentanes.

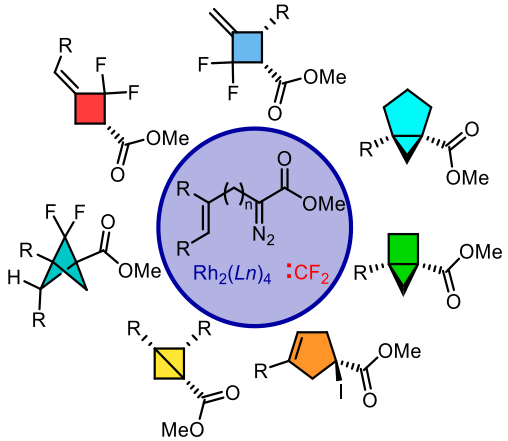

One-pot synthesis. Low catalyst loading. Diverse and modular SM. Accessing novel carbocycles

References:

1. Dudev, T.; Lim, C., Ring strain energies from ab initio calculations. *J. Am. Chem. Soc.* **1998,** *120* (18), 4450-4458.
2. Tyler, J.; Aggarwal, V. K., Synthesis and Applications of Bicyclo [1.1. 0] butyl and Azabicyclo [1.1. 0] butyl Organometallics. *Chem. A Eur. J.* **2023**, e202300008.
3. Bauer, M. R.; Di Fruscia, P.; Lucas, S. C.; Michaelides, I. N.; Nelson, J. E.; Storer, R. I.; Whitehurst, B. C., Put a ring on it: application of small aliphatic rings in medicinal chemistry. *RSC Med. Chem.* **2021,** *12* (4), 448-471.
4. Lovering, F., Escape from Flatland 2: complexity and promiscuity. *MedChemComm* **2013,** *4* (3), 515-519.
5. Lovering, F.; Bikker, J.; Humblet, C., Escape from flatland: increasing saturation as an approach to improving clinical success. *J. Med. Chem.* **2009,** *52* (21), 6752-6756.
6. Gagnon, A.; Duplessis, M.; Fader, L., Arylcyclopropanes: properties, synthesis and use in medicinal chemistry. *Org. Prep. Proced. Int.* **2010,** *42* (1), 1-69.
7. Bennett, S. H.; Fawcett, A.; Denton, E. H.; Biberger, T.; Fasano, V.; Winter, N.; Aggarwal, V. K., Difunctionalization of C–C σ-bonds enabled by the reaction of bicyclo [1.1. 0] butyl boronate complexes with electrophiles: reaction development, scope, and stereochemical origins. *J. Am. Chem. Soc.* **2020,** *142* (39), 16766-16775.
8. Lai, W.; Zhong, K.; Liu, S.; Liu, S.; Chen, H.; Ni, H.; Zeng, Z.; Zhao, Z.; Lan, Y.; Bai, R., How Strain-Release Determines Chemoselectivity: A Mechanistic Study of Rhodium-Catalyzed Bicyclo [1.1. 0] butane Activation. *J. Phys. Chem. Lett.* **2022,** *13* (33), 7694-7701.
9. Salaiin, J.; Bairtr, M., Biologically active cyclopropanes and cyclopropenes. *Curr. Med. Chem* **1995,** *2*, 511-542.
10. McNamee, R. E.; Thompson, A. L.; Anderson, E. A., Synthesis and Applications of Polysubstituted Bicyclo [1.1. 0] butanes. *J. Am. Chem. Soc.* **2021,** *143* (50), 21246-21251.
11. Ogba, O.; Warner, N.; O'leary, D.; Grubbs, R., Recent advances in ruthenium-based olefin metathesis. *Chem. Soc. Rev.* **2018,** *47* (12), 4510-4544.

12. Talele, T. T., The “cyclopropyl fragment” is a versatile player that frequently appears in preclinical/clinical drug molecules. *J. Med. Chem.* **2016,** *59* (19), 8712-8756.
13. Talele, T. T., Opportunities for tapping into three-dimensional chemical space through a quaternary carbon. *J. Med. Chem.* **2020,** *63* (22), 13291-13315.
14. Yen-Pon, E.; Li, L.; Levitre, G.; Majhi, J.; McClain, E. J.; Voight, E. A.; Crane, E. A.; Molander, G. A., On-DNA Hydroalkylation to Introduce Diverse Bicyclo [1.1. 1] pentanes and Abundant Alkyls via Halogen Atom Transfer. *J. Am. Chem. Soc.* **2022,** *144* (27), 12184-12191.
15. Anderson, J. M.; Measom, N. D.; Murphy, J. A.; Poole, D. L., Bridge functionalisation of bicyclo [1.1. 1] pentane derivatives. *Angew. Chem. Int. Ed.* **2021,** *60* (47), 24754-24769.
16. Bychek, R.; Mykhailiuk, P. K., A Practical and Scalable Approach to Fluoro-Substituted Bicyclo [1.1. 1] pentanes. *Angew. Chem. Int. Ed.* **2022,** *61* (29), e202205103.
17. Nugent, J.; Arroniz, C.; Shire, B. R.; Sterling, A. J.; Pickford, H. D.; Wong, M. L.; Mansfield, S. J.; Caputo, D. F.; Owen, B.; Mousseau, J. J., A general route to bicyclo [1.1. 1] pentanes through photoredox catalysis. *ACS. Catal.* **2019,** *9* (10), 9568-9574.
18. Zhao, J.-X.; Chang, Y.-X.; He, C.; Burke, B. J.; Collins, M. R.; Del Bel, M.; Elleraas, J.; Gallego, G. M.; Montgomery, T. P.; Mousseau, J. J., 1, 2-Difunctionalized bicyclo [1.1. 1] pentanes: Long–sought-after mimetics for ortho/meta-substituted arenes. *Proc. Nat. Acad. Sci.* **2021,** *118* (28), e2108881118.
19. Wei, B.; Sharland, J. C.; Blackmond, D. G.; Musaev, D. G.; Davies, H. M. L., In Situ Kinetic Studies of Rh(II)-Catalyzed C–H Functionalization to Achieve High Catalyst Turnover Numbers. *ACS. Catal.* **2022**, 13400-13410.
20. Sharland, J. C.; Wei, B.; Hardee, D. J.; Hodges, T. R.; Gong, W.; Voight, E. A.; Davies, H. M., Asymmetric synthesis of pharmaceutically relevant 1-aryl-2-heteroaryl-and 1, 2-diheteroarylcyclopropane-1-carboxylates. *Chem. Sci.* **2021,** *12* (33), 11181-11190.
21. Sharland, J. C.; Dunstan, D.; Majumdar, D.; Gao, J.; Tan, K.; Malik, H. A.; Davies, H. M., Hexafluoroisopropanol for the Selective Deactivation of Poisonous Nucleophiles Enabling Catalytic Asymmetric Cyclopropanation of Complex Molecules. *ACS. Catal.* **2022,** *12* (20), 12530-12542.
22. Bernett, W. A., A unified theory of bonding for cyclopropanes. *J. Chem. Ed.* **1967,** *44* (1), 17.
23. Veillard, A.; Del Re, G., Hybridization in cyclopropane, cyclobutane and cubane. *Theor. chim. Acta* **1964,** *2* (1), 55-62.
24. Chepiga, K. M.; Qin, C.; Alford, J. S.; Chennamadhavuni, S.; Gregg, T. M.; Olson, J. P.; Davies, H. M., Guide to enantioselective dirhodium (II)-catalyzed cyclopropanation with aryldiazoacetates. *Tetrahedron* **2013,** *69* (27-28), 5765-5771.
25. Simmons, H. E.; Smith, R. D., A new synthesis of cyclopropanes from olefins. *J. Am. Chem. Soc.* **1958,** *80* (19), 5323-5324.
26. Charette, A. B.; Beauchemin, A., Simmons-Smith Cyclopropanation Reaction. *Org. React.* **2004,** *58*, 1-415.
27. Wang, T.; Liang, Y.; Yu, Z.-X., Density Functional Theory Study of the Mechanism and Origins of Stereoselectivity in the Asymmetric Simmons–Smith Cyclopropanation with Charette Chiral Dioxaborolane Ligand. *J. Am. Chem. Soc.* **2011,** *133* (24), 9343-9353.
28. Shitama, H.; Katsuki, T., Asymmetric Simmons–Smith reaction of allylic alcohols with Al Lewis acid/N Lewis base bifunctional Al (salalen) catalyst. *Angew. Chem.* **2008,** *120* (13), 2484-2487.
29. Takahashi, H.; Yoshioka, M.; Ohno, M.; Kobayashi, S., A catalytic enantioselective reaction using a C2-symmetric disulfonamide as a chiral ligand: cyclopropanation of allylic alcohols by the Et2Zn-CH2I2-disulfonamide system. *Tetrahedron Lett.* **1992,** *33* (18), 2575-2578.
30. Grieco, P. A.; Oguri, T.; Wang, C.-L. J.; Williams, E., Stereochemistry and total synthesis of (.+-.)-ivangulin. *J. Org. Chem.* **1977,** *42* (25), 4113-4118.

31. Corey, E.; Chaykovsky, M., Dimethyloxosulfonium methylide ((CH3) 2SOCH2) and dimethylsulfonium methylide ((CH3) 2SCH2). Formation and application to organic synthesis. *J. Am. Chem. Soc.* **1965,** *87* (6), 1353-1364.
32. Corey, E.-J.; Chaykovsky, M., Methylsulfinyl carbanion (CH3-SO-CH2-). Formation and applications to organic synthesis. *J. Am. Chem. Soc.* **1965,** *87* (6), 1345-1353.
33. Chaykovsky, M.; Corey, E., Some New Reactions of Methylsulfinyl and Methylsulfonyl Carbanion1. *J. Org. Chem.* **1963,** *28* (1), 254-255.
34. Zhou, Y.; Li, N.; Cai, W.; Huang, Y., Asymmetric Sequential Corey–Chaykovsky Cyclopropanation/Cloke–Wilson Rearrangement for the Synthesis of 2, 3-Dihydrofurans. *Org. Lett.* **2021,** *23* (22), 8755-8760.
35. Caiuby, C. A.; Furniel, L. G.; Burtoloso, A. C., Asymmetric transformations from sulfoxonium ylides. *Chem. Sci.* **2022,** *13* (5), 1192-1209.
36. Mondal, M.; Connolly, S.; Chen, S.; Mitra, S.; Kerrigan, N. J., Recent Developments in Stereoselective Reactions of Sulfonium Ylides. *Organics* **2022,** *3* (3), 320-363.
37. Chen, Z. L.; Xie, Y.; Xuan, J., Visible Light-Mediated Cyclopropanation: Recent Progress. *Eur. J. Org. Chem.* **2022,** *2022* (44), e202201066.
38. Phelan, J. P.; Lang, S. B.; Compton, J. S.; Kelly, C. B.; Dykstra, R.; Gutierrez, O.; Molander, G. A., Redox-neutral photocatalytic cyclopropanation via radical/polar crossover. *J. Am. Chem. Soc.* **2018,** *140* (25), 8037-8047.
39. Fischer, D. M.; Lindner, H.; Amberg, W. M.; Carreira, E. M., Intermolecular Organophotocatalytic Cyclopropanation of Unactivated Olefins. *J. Am. Chem. Soc.* **2023**.
40. Li, J.; Lear, M. J.; Hayashi, Y., Direct Cyclopropanation of α-Cyano β-Aryl Alkanes by Light-Mediated Single Electron Transfer Between Donor–Acceptor Pairs. *Chem. A Eur. J.* **2021,** *27* (19), 5901-5905.
41. Ide, K.; Furuta, M.; Tokuyama, H., Photoredox-catalyzed intramolecular cyclopropanation of alkenes with α-bromo-β-keto esters. *Org. Biomol. Chem.* **2021,** *19* (42), 9172-9176.
42. Shu, C.; Mega, R. S.; Andreassen, B. J.; Noble, A.; Aggarwal, V. K., Synthesis of Functionalized Cyclopropanes from Carboxylic Acids by a Radical Addition–Polar Cyclization Cascade. *Angew. Chem.* **2018,** *130* (47), 15656-15660.
43. Daub, M. E.; Jung, H.; Lee, B. J.; Won, J.; Baik, M.-H.; Yoon, T. P., Enantioselective [2+ 2] cycloadditions of cinnamate esters: generalizing Lewis acid catalysis of triplet energy transfer. *J. Am. Chem. Soc.* **2019,** *141* (24), 9543-9547.
44. Du, J.; Skubi, K. L.; Schultz, D. M.; Yoon, T. P., A dual-catalysis approach to enantioselective [2+ 2] photocycloadditions using visible light. *Science* **2014,** *344* (6182), 392-396.
45. Girvin, Z. C.; Cotter, L. F.; Yoon, H.; Chapman, S. J.; Mayer, J. M.; Yoon, T. P.; Miller, S. J., Asymmetric Photochemical [2+ 2]-Cycloaddition of Acyclic Vinylpyridines through Ternary Complex Formation and an Uncontrolled Sensitization Mechanism. *J. Am. Chem. Soc.* **2022,** *144* (43), 20109-20117.
46. Chapman, S. J.; Swords, W. B.; Le, C. M.; Guzei, I. A.; Toste, F. D.; Yoon, T. P., Cooperative stereoinduction in asymmetric photocatalysis. *J. Am. Chem. Soc.* **2022,** *144* (9), 4206-4213.
47. Davies, H. M., Finding opportunities from surprises and failures. Development of rhodium-stabilized donor/acceptor carbenes and their application to catalyst-controlled C–H functionalization. *J. Org. Chem.* **2019,** *84* (20), 12722-12745.
48. Zhao, X.; Zhang, Y.; Wang, J., Recent developments in copper-catalyzed reactions of diazo compounds. *Chem. Commun.* **2012,** *48* (82), 10162-10173.
49. Davies, H. M.; Antoulinakis, E. G., Intermolecular metal-catalyzed carbenoid cyclopropanations. *Org. React.* **2004,** *57*, 1-326.
50. Gurmessa, G. T.; Singh, G. S., Recent progress in insertion and cyclopropanation reactions of metal carbenoids from α-diazocarbonyl compounds. *Res.Chem. Intermed.* **2017,** *43*, 6447-6504.

51. Pellissier, H.; Clavier, H., Enantioselective cobalt-catalyzed transformations. *Chem. Rev.* **2014,** *114* (5), 2775-2823.
52. Chawner, S. J.; Cases-Thomas, M. J.; Bull, J. A., Divergent Synthesis of Cyclopropane-Containing Lead-Like Compounds, Fragments and Building Blocks through a Cobalt Catalyzed Cyclopropanation of Phenyl Vinyl Sulfide. *Eur. J. Org. Chem.* **2017,** *2017* (34), 5015-5024.
53. Straub, B. F.; Hofmann, P., Copper (i) Carbenes: The Synthesis of Active Intermediates in Copper-Catalyzed Cyclopropanation. *Angew. Chem.* **2001,** *113* (7), 1328-1330.
54. Zhu, S.; Perman, J. A.; Zhang, X. P., Acceptor/acceptor-substituted diazo reagents for carbene transfers: cobalt-catalyzed asymmetric Z-cyclopropanation of alkenes with α-nitrodiazoacetates. *Angew. Chem. Int. Ed.* **2008,** *47* (44), 8460-8463.
55. Davies, H. M.; Liao, K., Dirhodium tetracarboxylates as catalysts for selective intermolecular C–H functionalization. *Nat. Rev.Chem.* **2019,** *3* (6), 347-360.
56. Bien, J.; Davulcu, A.; DelMonte, A. J.; Fraunhoffer, K. J.; Gao, Z.; Hang, C.; Hsiao, Y.; Hu, W.; Katipally, K.; Littke, A., The first kilogram synthesis of beclabuvir, an HCV NS5B polymerase inhibitor. *Org. Proc. Res. Dev.* **2018,** *22* (10), 1393-1408.
57. Green, S. P.; Wheelhouse, K. M.; Payne, A. D.; Hallett, J. P.; Miller, P. W.; Bull, J. A., Thermal stability and explosive hazard assessment of diazo compounds and diazo transfer reagents. *Org. Proc. Res. Dev.* **2019,** *24* (1), 67-84.
58. Hansen, J.; Autschbach, J.; Davies, H. M., Computational study on the selectivity of donor/acceptor-substituted rhodium carbenoids. *J. Org. Chem.* **2009,** *74* (17), 6555-6563.
59. Ren, Z.; Musaev, D. G.; Davies, H. M., Key Selectivity Controlling Elements in Rhodium-Catalyzed C–H Functionalization with Donor/Acceptor Carbenes. *ACS. Catal.* **2022,** *12* (21), 13446-13456.
60. Doetz, K. H.; Stendel Jr, J., Fischer carbene complexes in organic synthesis: metal-assisted and metal-templated reactions. *Chem. Rev.* **2009,** *109* (8), 3227-3274.
61. Coelho, P. S.; Brustad, E. M.; Kannan, A.; Arnold, F. H., Olefin cyclopropanation via carbene transfer catalyzed by engineered cytochrome P450 enzymes. *Science* **2013,** *339* (6117), 307-310.
62. Schrock, R. R., Recent advances in high oxidation state Mo and W imido alkylidene chemistry. *Chem. Rev.* **2009,** *109* (8), 3211-3226.
63. Lee, M.; Ren, Z.; Musaev, D. G.; Davies, H. M., Rhodium-stabilized diarylcarbenes behaving as donor/acceptor carbenes. *ACS. Catal.* **2020,** *10* (11), 6240-6247.
64. Davies, H. M.; Bruzinski, P. R.; Lake, D. H.; Kong, N.; Fall, M. J., Asymmetric cyclopropanations by rhodium (II) N-(arylsulfonyl) prolinate catalyzed decomposition of vinyldiazomethanes in the presence of alkenes. Practical enantioselective synthesis of the four stereoisomers of 2-phenylcyclopropan-1-amino acid. *J. Am. Chem. Soc.* **1996,** *118* (29), 6897-6907.
65. Davies, H. M.; Oldenburg, C. M.; McAfee, M. J.; Nordahl, J. G.; Henretta, J. P.; Romines, K. R., Novel approach to seven-membered rings by the intramolecular tandem cyclopropanation/cope rearrangement sequence. *Tetrahedron Lett.* **1988,** *29* (9), 975-978.
66. Davies, H. M.; Hodges, L. M.; Matasi, J. J.; Hansen, T.; Stafford, D. G., Effect of carbenoid structure on the reactivity of rhodium-stabilized carbenoids. *Tetrahedron Lett.* **1998,** *39* (25), 4417-4420.
67. Xue, Y.-S.; Cai, Y.-P.; Chen, Z.-X., Mechanism and stereoselectivity of the Rh (II)-catalyzed cyclopropanation of diazooxindole: a density functional theory study. *RSC Adv.* **2015,** *5* (71), 57781-57791.
68. Nowlan, D. T.; Gregg, T. M.; Davies, H. M.; Singleton, D. A., Isotope effects and the nature of selectivity in rhodium-catalyzed cyclopropanations. *J. Am. Chem. Soc.* **2003,** *125* (51), 15902-15911.
69. Davies, H. M.; Manning, J. R., Catalytic C–H functionalization by metal carbenoid and nitrenoid insertion. *Nature* **2008,** *451* (7177), 417-424.
70. Berry, J. F., The role of three-center/four-electron bonds in superelectrophilic dirhodium carbene and nitrene catalytic intermediates. *Dalton Trans.* **2012,** *41* (3), 700-713.

71. Kornecki, K. P.; Briones, J. F.; Boyarskikh, V.; Fullilove, F.; Autschbach, J.; Schrote, K. E.; Lancaster, K. M.; Davies, H. M.; Berry, J. F., Direct spectroscopic characterization of a transitory dirhodium donor-acceptor carbene complex. *Science* **2013,** *342* (6156), 351-354.
72. Berry, J. F.; Lu, C. C., Metal–metal bonds: from fundamentals to applications. *Inorg. Chem.* **2017,** *56* (14), 7577-7581.
73. Fu, L.; Hoang, K.; Tortoreto, C.; Liu, W.; Davies, H. M., Formation of Tertiary Alcohols from the Rhodium-Catalyzed Reactions of Donor/Acceptor Carbenes with Esters. *Organic Lett.* **2018,** *20* (8), 2399-2402.
74. Gillingham, D.; Fei, N., Catalytic X–H insertion reactions based on carbenoids. *Chem. Soc. Rev.* **2013,** *42* (12), 4918-4931.
75. Guo, W.; Hare, S. R.; Chen, S.-S.; Saunders, C. M.; Tantillo, D. J., C–H Insertion in Dirhodium Tetracarboxylate-Catalyzed Reactions despite Dynamical Tendencies toward Fragmentation: Implications for Reaction Efficiency and Catalyst Design. *J. Am. Chem. Soc.* **2022,** *144* (37), 17219-17231.
76. Lian, Y.; Hardcastle, K. I.; Davies, H. M., Computationally Guided Stereocontrol of the Combined C-H Functionalization/Cope Rearrangement. *Angew. Chem. Int. Ed.* **2011,** *50* (40), 9370-9373.
77. Davies, H. M.; Lian, Y., The combined C–H functionalization/cope rearrangement: discovery and applications in organic synthesis. *Acc. Chem. Res.* **2012,** *45* (6), 923-935.
78. Laconsay, C. J.; Tantillo, D. J., Metal Bound or Free Ylides as Reaction Intermediates in Metal-Catalyzed [2, 3]-Sigmatropic Rearrangements? It Depends. *ACS. Catal.* **2021,** *11* (2), 829-839.
79. Li, Z.; Parr, B. T.; Davies, H. M., Highly stereoselective C–C bond formation by rhodium-catalyzed tandem ylide formation/[2, 3]-sigmatropic rearrangement between donor/acceptor carbenoids and chiral allylic alcohols. *J. Am. Chem. Soc.* **2012,** *134* (26), 10942-10946.
80. Li, Z.; Boyarskikh, V.; Hansen, J. H.; Autschbach, J.; Musaev, D. G.; Davies, H. M., Scope and mechanistic analysis of the enantioselective synthesis of allenes by rhodium-catalyzed tandem ylide formation/[2, 3]-sigmatropic rearrangement between donor/acceptor carbenoids and propargylic alcohols. *J. Am. Chem. Soc.* **2012,** *134* (37), 15497-15504.
81. Davies, H. M.; Hansen, T.; Churchill, M. R., Catalytic asymmetric C− H activation of alkanes and tetrahydrofuran. *J. Am. Chem. Soc.* **2000,** *122* (13), 3063-3070.
82. Zhou, Q.; Li, S.; Zhang, Y.; Wang, J., Rhodium (II)-or Copper (I)-Catalyzed Formal Intramolecular Carbene Insertion into Vinylic C (sp2)− H Bonds: Access to Substituted 1H-Indenes. *Angew. Chem.* **2017,** *129* (50), 16229-16233.
83. Hashimoto, S.-i.; Watanabe, N.; Sato, T.; Shiro, M.; Ikegami, S., Enhancement of enantioselectivity in intramolecular CH insertion reactions of α-diazo β-keto esters catalyzed by chiral dirhodium (II) carboxylates. *Tetrahedron Lett.* **1993,** *34* (32), 5109-5112.
84. Davies, H. M.; Panaro, S. A., Novel dirhodium tetraprolinate catalysts containing bridging prolinate ligands for asymmetric carbenoid reactions. *Tetrahedron Lett.* **1999,** *40* (29), 5287-5290.
85. Davies, H. M.; Hansen, T., Asymmetric intermolecular carbenoid C− H insertions catalyzed by rhodium (ii)(S)-N-(p-dodecylphenyl) sulfonylprolinate. *J. Am. Chem. Soc.* **1997,** *119* (38), 9075-9076.
86. Davies, H. M.; Townsend, R. J., Catalytic asymmetric cyclopropanation of heteroaryldiazoacetates. *J. Org. Chem.* **2001,** *66* (20), 6595-6603.
87. Davies, H. M.; Venkataramani, C., Dirhodium tetraprolinate-catalyzed asymmetric cyclopropanations with high turnover numbers. *Org. Lett.* **2003,** *5* (9), 1403-1406.
88. Davies, H. M.; Nagashima, T.; Klino, J. L., Stereoselectivity of methyl aryldiazoacetate cyclopropanations of 1, 1-diarylethylene. Asymmetric synthesis of a cyclopropyl analogue of tamoxifen. *Org. Lett.* **2000,** *2* (6), 823-826.
89. Davies, H. M.; Doan, B. D., Total synthesis of (±)-tremulenolide A and (±)-tremulenediol A via a stereoselective cyclopropanation/Cope rearrangement annulation strategy. *J. Org. Chem.* **1998,** *63* (3), 657-660.

90. Davies, H. M.; Stafford, D. G.; Doan, B. D.; Houser, J. H., Tandem asymmetric cyclopropanation/cope rearrangement. a highly diastereoselective and enantioselective method for the construction of 1, 4-cycloheptadienes. *J. Am. Chem. Soc.* **1998,** *120* (14), 3326-3331.
91. Duanais, J.; Hart, S.; Smith, H.; Letchworth, S.; Davies, H.; Sexton, T.; Bennett, B.; Childers, S.; Porrino, L., Long-acting blockade of biogenic amine transporters in rat brain by administration of the potent novel tropane 2β-propanoyl-3β-(2-naphthyl)-tropane. *J. Pharmacol. Exper. Ther.* **1998**, *287* (2), 814.
92. Davies, H. M.; Hansen, T.; Hopper, D. W.; Panaro, S. A., Highly regio-, diastereo-, and enantioselective CH insertions of methyl aryldiazoacetates into cyclic N-BOC-protected amines. Asymmetric synthesis of novel C-2-symmetric amines and threo-methylphenidate. *J. Am. Chem. Soc.* **1999,** *121* (27), 6509-6510.
93. Davies, H. M.; Antoulinakis, E. G.; Hansen, T., Catalytic asymmetric synthesis of syn-aldol products from intermolecular C− H insertions between allyl silyl ethers and methyl aryldiazoacetates. *Org. Lett.* **1999,** *1* (3), 383-386.
94. Davies, H. M.; Dai, X., Application of the combined C–H activation/Cope rearrangement as a key step in the total syntheses of the assigned structure of (+)-elisabethadione and a (+)-p-benzoquinone natural product. *Tetrahedron* **2006,** *62* (45), 10477-10484.
95. Davies, H. M.; Dai, X.; Long, M. S., Combined C− H activation/cope rearrangement as a strategic reaction in organic synthesis: Total synthesis of (−)-colombiasin A and (−)-elisapterosin B. *J. Am. Chem. Soc.* **2006,** *128* (7), 2485-2490.
96. Davies, H.; Dai, X.; Long, M., Synthesis of (-)-Colombiasin A and (-)-Elisapterosin B. *Synfacts* **2006,** *2006* (07), 0640-0640.
97. DeAngelis, A.; Boruta, D. T.; Lubin, J.-B.; Plampin III, J. N.; Yap, G. P.; Fox, J. M., The chiral crown conformation in paddlewheel complexes. *Chem. Commun.* **2010,** *46* (25), 4541-4543.
98. Fu, J.; Ren, Z.; Bacsa, J.; Musaev, D. G.; Davies, H. M., Desymmetrization of cyclohexanes by site- and stereoselective C–H functionalization. *Nature* **2018,** *564* (7736), 395-399.
99. Hansen, J.; Davies, H. M., High symmetry dirhodium (II) paddlewheel complexes as chiral catalysts. *Coord. Chem. Rev.* **2008,** *252* (5-7), 545-555.
100. Davies, H. M.; Cantrell Jr, W. R., α-Hydroxy esters as inexpensive chiral auxiliaries in rhodium (II)-catalyzed cyclopropanations with vinyldiazomethanes. *Tetrahedron Lett.* **1991,** *32* (45), 6509-6512.
101. Boruta, D. T.; Dmitrenko, O.; Yap, G. P. A.; Fox, J. M., Rh2(S-PTTL)3TPA—a mixed-ligand dirhodium(ii) catalyst for enantioselective reactions of α-alkyl-α-diazoesters. *Chem. Sci.* **2012,** *3* (5), 1589-1593.
102. Lin, W.; Charette, A. B., Rhodium-Catalyzed Asymmetric Intramolecular Cyclopropanation of Substituted Allylic Cyanodiazoacetates. *Advanced Synthesis & Catalysis* **2005,** *347* (11-13), 1547-1552.
103. Lindsay, V. N.; Lin, W.; Charette, A. B., Experimental evidence for the all-up reactive conformation of chiral rhodium (II) carboxylate catalysts: enantioselective synthesis of cis-cyclopropane α-amino acids. *J. Am. Chem. Soc.* **2009,** *131* (45), 16383-16385.
104. Lindsay, V. N.; Charette, A. B., Design and synthesis of chiral heteroleptic rhodium (II) carboxylate catalysts: experimental investigation of halogen bond rigidification effects in asymmetric cyclopropanation. *ACS. Catal.* **2012,** *2* (6), 1221-1225.
105. Lindsay, V.; Lin, W.; Charette, A., Asymmetric Synthesis of cis-Cyclopropane α-Amino Acids by Rhodium (II) Carboxylate. *Synfacts* **2010,** *2010* (02), 0198-0198.
106. Doyle, M. P.; Hu, W.; Phillips, I. M.; Moody, C. J.; Pepper, A. G.; Slawin, A. G., Reactivity enhancement for chiral dirhodium (II) tetrakis (carboxamidates). *Adv. Synth. Catal.* **2001,** *343* (1), 112-117.

107. Doyle, M. P.; Davies, S. B.; Hu, W., Dirhodium (II) tetrakis [methyl 2-oxaazetidine-4-carboxylate]: A chiral dirhodium (II) carboxamidate of exceptional reactivity and selectivity. *Org. Lett.* **2000,** *2* (8), 1145-1147.
108. Doyle, M. P.; Zhou, Q.-L.; Charnsangavej, C.; Longoria, M. A.; McKervey, M. A.; García, C. F., Chiral catalysts for enantioselective intermolecular cyclopropanation reactions with methyl phenyldiazoacetate. Origin of the solvent effect in reactions catalyzed by homochiral dirhodium (II) prolinates. *Tetrahedron Lett.* **1996,** *37* (24), 4129-4132.
109. Tsutsui, H.; Yamaguchi, Y.; Kitagaki, S.; Nakamura, S.; Anada, M.; Hashimoto, S., Dirhodium(II) tetrakis[N-tetrafluorophthaloyl-(S)-tert-leucinate]: an exceptionally effective Rh(II) catalyst for enantiotopically selective aromatic C–H insertions of diazo ketoesters. *Tetrahedron Asymm.* **2003,** *14* (7), 817-821.
110. Adly, F. G.; Maddalena, J.; Ghanem, A., Rh2 (S-1, 2-NTTL) 4: a novel Rh2 (S-PTTL) 4 analog with lower ligand symmetry for asymmetric synthesis of chiral cyclopropylphosphonates. *Chirality* **2014,** *26* (11), 764-774.
111. DeAngelis, A.; Dmitrenko, O.; Yap, G. P.; Fox, J. M., Chiral crown conformation of Rh2 (S-PTTL) 4: Enantioselective cyclopropanation with α-alkyl-α-diazoesters. *J. Am. Chem. Soc.* **2009,** *131* (21), 7230-7231.
112. Reddy, R. P.; Davies, H. M., Dirhodium tetracarboxylates derived from adamantylglycine as chiral catalysts for enantioselective C− H aminations. *Org. Lett.* **2006,** *8* (22), 5013-5016.
113. Nadeau, E.; Li, Z.; Morton, D.; Davies, H. M., Rhodium carbenoid induced intermolecular CH functionalization at tertiary CH bonds. *Synlett* **2009,** *2009* (01), 151-154.
114. Schwartz, B. D.; Denton, J. R.; Davies, H. M.; Williams, C. M., Total Synthesis of (±)-vibsanin E. *Aust. J. Chem.* **2009,** *62* (9), 980-982.
115. Schwartz, B. D.; Denton, J. R.; Lian, Y.; Davies, H. M.; Williams, C. M., Asymmetric [4+ 3] cycloadditions between vinylcarbenoids and dienes: Application to the total synthesis of the natural product (−)-5-epi-vibsanin E. *J. Am. Chem. Soc.* **2009,** *131* (23), 8329-8332.
116. Qin, C.; Boyarskikh, V.; Hansen, J. H.; Hardcastle, K. I.; Musaev, D. G.; Davies, H. M., D 2-symmetric dirhodium catalyst derived from a 1, 2, 2-triarylcyclopropanecarboxylate ligand: design, synthesis and application. *J. Am. Chem. Soc.* **2011,** *133* (47), 19198-19204.
117. Negretti, S.; Cohen, C. M.; Chang, J. J.; Guptill, D. M.; Davies, H. M., Enantioselective dirhodium (II)-catalyzed cyclopropanations with trimethylsilylethyl and trichloroethyl aryldiazoacetates. *Tetrahedron* **2015,** *71* (39), 7415-7420.
118. Qin, C.; Davies, H. M., Enantioselective synthesis of 2-arylbicyclo [1.1. 0] butane carboxylates. *Org. Lett.* **2013,** *15* (2), 310-313.
119. Qin, C.; Davies, H. M., Role of sterically demanding chiral dirhodium catalysts in site-selective C–H functionalization of activated primary C–H bonds. *J. Am. Chem. Soc.* **2014,** *136* (27), 9792-9796.
120. Liao, K.; Negretti, S.; Musaev, D. G.; Bacsa, J.; Davies, H. M., Site-selective and stereoselective functionalization of unactivated C–H bonds. *Nature* **2016,** *533* (7602), 230-234.
121. Liao, K.; Liu, W.; Niemeyer, Z. L.; Ren, Z.; Bacsa, J.; Musaev, D. G.; Sigman, M. S.; Davies, H. M., Site-selective carbene-induced C–H functionalization catalyzed by dirhodium tetrakis (triarylcyclopropanecarboxylate) complexes. *ACS. Catal.* **2018,** *8* (1), 678-682.
122. Liu, W.; Ren, Z.; Bosse, A. T.; Liao, K.; Goldstein, E. L.; Bacsa, J.; Musaev, D. G.; Stoltz, B. M.; Davies, H. M., Catalyst-controlled selective functionalization of unactivated C–H bonds in the presence of electronically activated C–H bonds. *J. Am. Chem. Soc.* **2018,** *140* (38), 12247-12255.
123. Cammarota, R. C.; Liu, W.; Bacsa, J.; Davies, H. M.; Sigman, M. S., Mechanistically Guided Workflow for Relating Complex Reactive Site Topologies to Catalyst Performance in C–H Functionalization Reactions. *J. Am. Chem. Soc.* **2022,** *144* (4), 1881-1898.

124. Liao, K.; Pickel, T. C.; Boyarskikh, V.; Bacsa, J.; Musaev, D. G.; Davies, H. M., Site-selective and stereoselective functionalization of non-activated tertiary C–H bonds. *Nature* **2017,** *551* (7682), 609-613.
125. Fu, J.; Wurzer, N.; Lehner, V.; Reiser, O.; Davies, H. M., Rh (II)-catalyzed monocyclopropanation of pyrroles and its application to the synthesis pharmaceutically relevant compounds. *Org. Lett.* **2019,** *21* (15), 6102-6106.
126. Lathrop, S. P.; Mlinar, L. B.; Manjrekar, O. N.; Zhou, Y.; Harper, K. C.; Sacia, E. R.; Higgins, M.; Bogdan, A. R.; Wang, Z.; Richter, S. M., Continuous Process to Safely Manufacture an Aryldiazoacetate and Its Direct Use in a Dirhodium-Catalyzed Enantioselective Cyclopropanation. *Org. Proc. Res. Dev.* **2022**.
127. Tsou, C. L., Active Site Flexibility in Enzyme Catalysis. *Ann. N. Y. Acad. Sci.* **1998,** *864* (1), 1-8.
128. Garlets, Z. J.; Boni, Y. T.; Sharland, J. C.; Kirby, R. P.; Fu, J.; Bacsa, J.; Davies, H. M., Design, Synthesis, and Evaluation of Extended C4–Symmetric Dirhodium Tetracarboxylate Catalysts. *ACS. Catal.* **2022,** *12*, 10841-10848.
129. Wei, B.; Sharland, J. C.; Lin, P.; Wilkerson-Hill, S. M.; Fullilove, F. A.; McKinnon, S.; Blackmond, D. G.; Davies, H. M., In situ kinetic studies of Rh (II)-catalyzed asymmetric cyclopropanation with low catalyst loadings. *ACS. Catal.* **2019,** *10* (2), 1161-1170.
130. Lian, Y.; Davies, H. M., Rh2 (S-biTISP) 2-catalyzed asymmetric functionalization of indoles and pyrroles with vinylcarbenoids. *Org. Lett.* **2012,** *14* (7), 1934-1937.
131. Pelphrey, P.; Hansen, J.; Davies, H. M., Solvent-free catalytic enantioselective C–C bond forming reactions with very high catalyst turnover numbers. *Chem. Sci.* **2010,** *1* (2), 254-257.
132. Byrne, F. P.; Jin, S.; Paggiola, G.; Petchey, T. H.; Clark, J. H.; Farmer, T. J.; Hunt, A. J.; Robert McElroy, C.; Sherwood, J., Tools and techniques for solvent selection: green solvent selection guides. *Sus. Chem. Proc.* **2016,** *4* (1), 1-24.
133. Tundo, P.; Musolino, M.; Aricò, F., Dialkyl Carbonates in the Green Synthesis of Heterocycles. *Front. Chem.* **2019,** *7*, 300.
134. Ye, Q.-S.; Li, X.-N.; Jin, Y.; Yu, J.; Chang, Q.-W.; Jiang, J.; Yan, C.-X.; Li, J.; Liu, W.-P., Synthesis, crystal structures and catalytic activity of tetrakis (acetato) dirhodium (II) complexes with axial picoline ligands. *Inorg. Chim. Acta* **2015,** *434*, 113-120.
135. Marcoux, D.; Lindsay, V. N.; Charette, A. B., Use of achiral additives to increase the stereoselectivity in Rh (II)-catalyzed cyclopropanations. *Chem. Commun.* **2010,** *46* (6), 910-912.
136. Lebel, H.; Piras, H.; Bartholoméüs, J., Rhodium-Catalyzed Stereoselective Amination of Thioethers with N-Mesyloxycarbamates: DMAP and Bis (DMAP) CH2Cl2 as Key Additives. *Angew. Chem.* **2014,** *126* (28), 7428-7432.
137. Lindlar, H.; Dubuis, R., Palladium catalyst for partial reduction of acetylenes. *Org. Syn.* **2003,** *46*, 89-89.
138. Zhu, S.-F.; Chen, W.-Q.; Zhang, Q.-Q.; Mao, H.-X.; Zhou, Q.-L., Enantioselective Copper-Catalyzed OH Insertion of α-Diazo Phosphonates. *Synlett* **2011,** *2011* (07), 919-922.
139. Nelson, T. D.; Song, Z. J.; Thompson, A. S.; Zhao, M.; DeMarco, A.; Reamer, R. A.; Huntington, M. F.; Grabowski, E. J.; Reider, P. J., Rhodium-carbenoid-mediated intermolecular O–H insertion reactions: a dramatic additive effect. Application in the synthesis of an ascomycin derivative. *Tetrahedron Lett.* **2000,** *41* (12), 1877-1881.
140. Wei, B.; Hatridge, T. A.; Jones, C. W.; Davies, H. M., Copper (II) Acetate-Induced Oxidation of Hydrazones to Diazo Compounds under Flow Conditions Followed by Dirhodium-Catalyzed Enantioselective Cyclopropanation Reactions. *Org. Lett.* **2021,** *23* (14), 5363-5367.
141. Hatridge, T. A.; Wei, B.; Davies, H. M.; Jones, C. W., Copper-Catalyzed, Aerobic Oxidation of Hydrazone in a Three-Phase Packed Bed Reactor. *Org. Proc. Res. Dev.* **2021,** *25* (8), 1911-1922.
142. He, J.; Hamann, L. G.; Davies, H. M.; Beckwith, R. E., Late-stage C–H functionalization of complex alkaloids and drug molecules via intermolecular rhodium-carbenoid insertion. *Nature Commun.* **2015,** *6* (1), 1-9.

143. Wertz, B.; Ren, Z.; Bacsa, J.; Musaev, D. G.; Davies, H. M., Comparison of 1, 2-Diarylcyclopropanecarboxylates with 1, 2, 2-Triarylcyclopropanecarboxylates as Chiral Ligands for Dirhodium-Catalyzed Cyclopropanation and C–H Functionalization. *J. Org. Chem.* **2020,** *85* (19), 12199-12211.
144. Guthikonda, K.; Du Bois, J., A unique and highly efficient method for catalytic olefin aziridination. *J. Am. Chem. Soc.* **2002,** *124* (46), 13672-13673.
145. Boquet, V.; Nasrallah, A.; Dana, A. L.; Brunard, E.; Di Chenna, P. H.; Duran, F. J.; Retailleau, P.; Darses, B.; Sircoglou, M.; Dauban, P., Rhodium (II)-Catalyzed Enantioselective Intermolecular Aziridination of Alkenes. *J. Am. Chem. Soc.* **2022,** *144* (37), 17156-17164.
146. Panish, R.; Chintala, S. R.; Boruta, D. T.; Fang, Y.; Taylor, M. T.; Fox, J. M., Enantioselective synthesis of cyclobutanes via sequential Rh-catalyzed bicyclobutanation/Cu-catalyzed homoconjugate addition. *J. Am. Chem. Soc.* **2013,** *135* (25), 9283-9286.
147. Makarov, I. S.; Brocklehurst, C. E.; Karaghiosoff, K.; Koch, G.; Knochel, P., Synthesis of bicyclo [1.1. 1] pentane bioisosteres of internal alkynes and para-disubstituted benzenes from [1.1. 1] propellane. *Angew. Chem. Int. Ed.* **2017,** *56* (41), 12774-12777.
148. Mykhailiuk, P. K., Saturated bioisosteres of benzene: where to go next? *Org. Biomol. Chem.* **2019,** *17* (11), 2839-2849.
149. Frank, N.; Nugent, J.; Shire, B. R.; Pickford, H. D.; Rabe, P.; Sterling, A. J.; Zarganes-Tzitzikas, T.; Grimes, T.; Thompson, A. L.; Smith, R. C., Synthesis of meta-substituted arene bioisosteres from [3.1. 1] propellane. *Nature* **2022**, 1-6.
150. Herter, L.; Koutsopetras, I.; Turelli, L.; Fessard, T.; Salomé, C., Preparation of new bicyclo [2.1. 1] hexane compact modules: an opening towards novel sp 3-rich chemical space. *Org. Biomol. Chem.* **2022,** *20* (46), 9108-9111.
151. Meanwell, N. A., The influence of bioisosteres in drug design: tactical applications to address developability problems. In *Tactics in Contemporary Drug Design*, Springer: 2013; pp 283-381.
152. Kaleta, J.; Roncevic, I.; Cisarova, I.; Dracinsky, M.; Solinova, V.; Kasicka, V.; Michl, J., Bridge-chlorinated bicyclo [1.1. 1] pentane-1, 3-dicarboxylic acids. *J. Org. Chem.* **2019,** *84* (5), 2448-2461.
153. Garlets, Z. J.; Sanders, J. N.; Malik, H.; Gampe, C.; Houk, K.; Davies, H. M., Enantioselective C–H functionalization of bicyclo [1.1. 1] pentanes. *Nature Catal.* **2020,** *3* (4), 351-357.
154. Yang, Y.; Tsien, J.; Hughes, J. M.; Peters, B. K.; Merchant, R. R.; Qin, T., An intramolecular coupling approach to alkyl bioisosteres for the synthesis of multisubstituted bicycloalkyl boronates. *Nature Chem.* **2021,** *13* (10), 950-955.
155. Rigotti, T.; Bach, T., Bicyclo [2.1. 1] hexanes by Visible Light-Driven Intramolecular Crossed [2+ 2] Photocycloadditions. *Org. Lett.* **2022**.
156. Ma, X.; Sloman, D. L.; Han, Y.; Bennett, D. J., A selective synthesis of 2, 2-difluorobicyclo [1.1. 1] pentane analogues:"BCP-F2". *Org. Lett.* **2019,** *21* (18), 7199-7203.
157. Bychek, R. M.; Hutskalova, V.; Bas, Y. P.; Zaporozhets, O. A.; Zozulya, S.; Levterov, V. V.; Mykhailiuk, P. K., Difluoro-substituted bicyclo [1.1. 1] pentanes for medicinal chemistry: Design, synthesis, and characterization. *J. Org. Chem.* **2019,** *84* (23), 15106-15117.
158. Ma, X.; Nhat Pham, L., Selected topics in the syntheses of bicyclo [1.1. 1] pentane (BCP) analogues. *Asian J. Org. Chem.* **2020,** *9* (1), 8-22.

Chapter 1

Enhancement of asymmetric cyclopropanation with dimethyl carbonate as solvent and applications for low catalyst loading

1.1 Introduction

Dirhodium tetracarboxylates have revolutionized the chemistry of transition-metal-catalyzed reactions of diazo compounds.[1-6] Under mild reaction conditions, they cause the extrusion of nitrogen and generation of transient metal carbene intermediates capable of undergoing a variety of synthetically useful reactions. Since 1996, the Davies group has been particularly interested in developing chiral dirhodium catalysts for enantioselective reactions of donor/acceptor carbenes (Scheme 1.1).[7]

Scheme 1.1: The dirhodium catalyst toolbox in the Davies group.

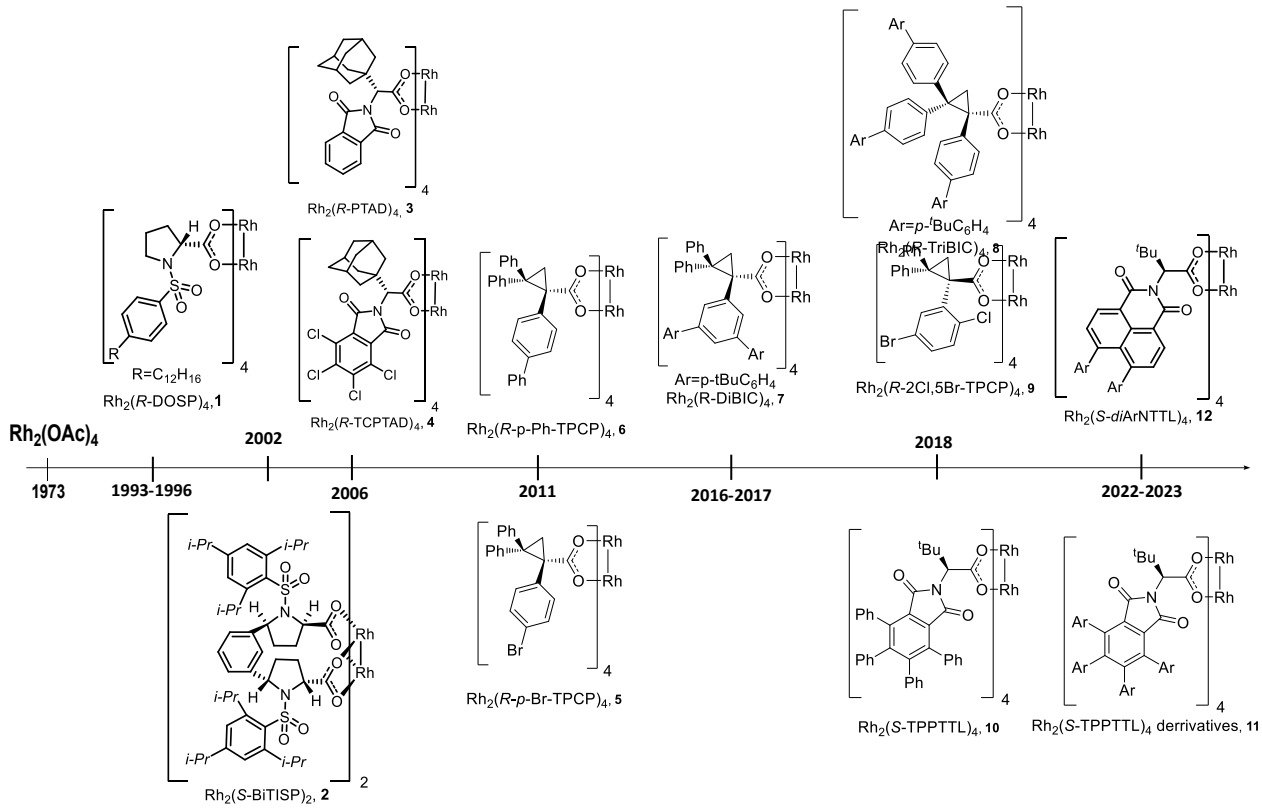

The first generation of catalysts we developed were the chiral *N*-arylsulfonylprolinates, exemplified by $Rh_2(DOSP)_4$ (**1**), which were found to be particularly suited for the reactions of donor/acceptor carbenes

(Figure 1.1).[8, 9] They have been shown to be effective in a wide range of transformations, including cyclopropanation,[5, 10, 11] tandem cyclopropanation /Cope rearrangement,[12, 13] cyclopropenation,[14] various ylide transformations,[15, 16] C–H functionalization[1] and the combined C–H functionalization/Cope rearrangement.[17, 18]$Rh_2(BiTISP)_2$ (**2**), a chiral bridged *N*-arylsulfonylprolinate catalyst, which has also been shown to also be effective in these reactions and is more robust than $Rh_2(DOSP)_4$ (**1**), operating at extremely low catalyst loadings (0.001 mol %).[19, 20] Reactions with these catalysts have classically been performed in hydrocarbon solvents like pentane. Indeed, $Rh_2(DOSP)_4$ (**1**) was specifically designed to have higher solubility in pentane to ensure high enantioselectivity.[21] While reactions with are robust, reliable, and give predictable asymmetric induction, this solvent is not ideal for applications involving complex substrates and diazo-compounds that may not be soluble in hydrocarbon solvents.[22] A paper published by Davies and Townsend in 2001 which evaluates a series of heterocyclic diazoacetates were explored in cyclopropanation, highlights these drawbacks.[23] Though high %ee was observed with several of these substrates, the poor solubility of the heterocycles in pentane and other hydrocarbon solvents led to low enantioselectivity in several examples.[23] In order to address these inadequacies, several advancements in catalyst development needed to be made and a comprehensive protocol for the cyclopropanation of heteroaryldiazoacetates and vinyl-heterocycles will be discussed in detail in **Chapter 2**.

Figure 1.1: While $Rh_2(DOSP)_4$(**1**) found early success as a catalyst for enantioselective cyclopropanation,[21] a more complex bridged-ligand scaffold, $Rh_2(BiTISP)_2$(**2**), was required to improve the competency of the reaction at extremely low catalyst loadings.[20, 24]

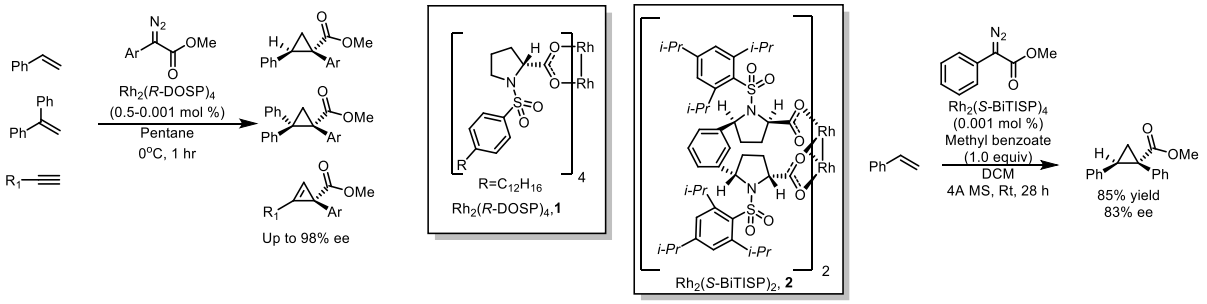

The second and fourth-generation catalysts are related to the phthalimido catalysts developed by Hashimoto.[25] The chiral adamantyl phthalimido catalyst $Rh_2(PTAD)_4$ (**3**) was the first catalyst of this class developed by the Davies group (Figure 1.2).[26] This catalyst tends to give enhanced enantioselectivity compared to the Hashimoto catalysts which contain smaller alkyl groups.[26, 27] Since then, the number of catalysts in this series has exploded to include diverse structures including $Rh_2(TCPTAD)_4$ (**4**),[26] $Rh_2(TPPTTL)_4$ (**10**),[28] and $Rh_2(NTTL)_4$ derivatives (**12**) based on Müller's catalyst.[29] These catalysts feature increasingly larger and deeper bowls and are capable highly site and enantioselective C–H functionalization reactions.[28, 30, 31] Though none of these catalysts are sterically demanding at the carbene, the size of the bowl and the presence of multiple phenyl rings leads to complex interactions with the substrate which results in the unique site-selectivity.[28, 32] Additionally, deeper and wider bowls can lead to novel site-selectivity.[28]

Figure 1.2: Changes in the depth and width of the bowl of C_4 symmetric catalysts as dictated by the ligands has an important influence on the site, diastereo, and enantioselectivity of dirhodium catalyzed transformations.[32]

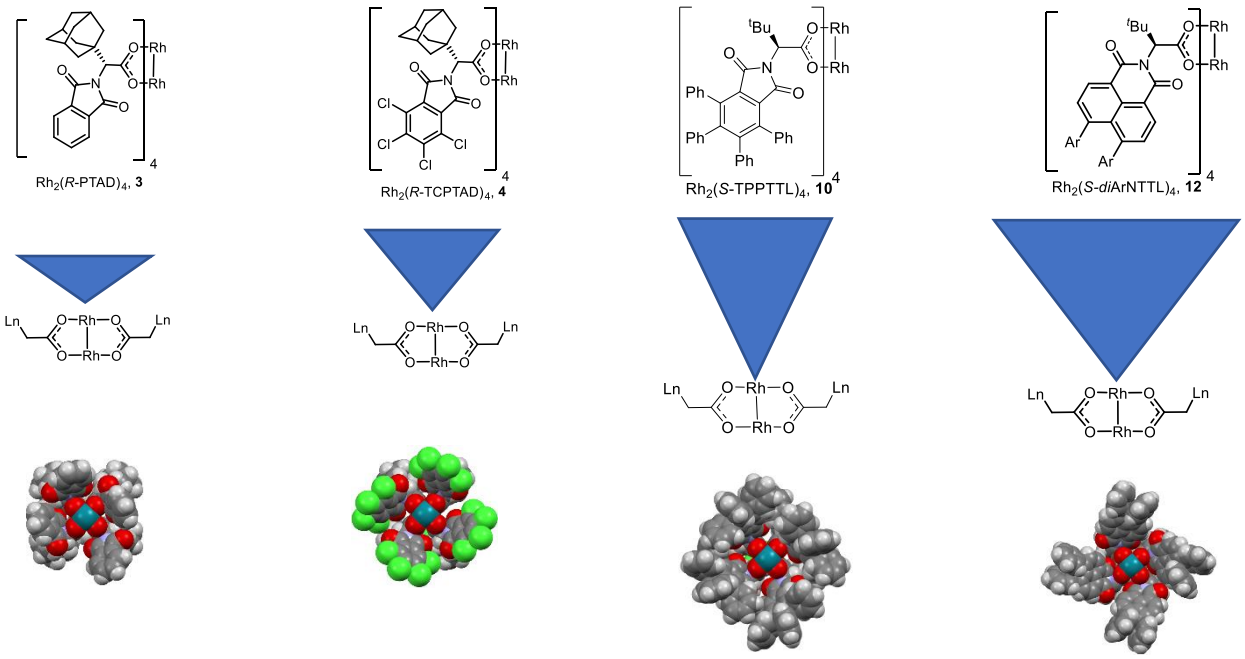

The third-generation catalysts are the triarylcycopropanecarboxylates (TPCP) (Figure 1.3).[33] These catalysts were designed to be more sterically crowded at the carbene than the earlier chiral catalysts. The original catalysts were Rh_2(*p*-Br-TPCP)$_4$ (**5**) and Rh_2(*p*-Ph-TPCP)$_4$ (**6**).[33-35] Since then a variety of even more sterically demanding derivatives have been prepared including Rh_2(*o*-Cl-TPCP)$_4$, Rh_2(2Cl5Br-TPCP)$_4$ (**9**), Rh_2(3,5-di(*p*-^{t}BuC$_6$H$_4$)TPCP)$_4$ (**7**), and Rh_2(tris(*p*-^{t}BuC$_6$H$_4$)TPCP)$_4$ (**8**).[36-39] The high steric demand close to the carbene leads to novel site-selectivity for these catalysts, and the accessibility of the carbene even overrides the electronics of the substrates. In dirhodium-catalyzed C–H functionalization, the reactivity of the C–H bond is proportional to its hydricity, meaning that more electron rich C–H bonds will react preferentially in the presence of less electron rich C–H bonds.[1, 40-42] This leads to a clear C–H bond reactivity series for catalysts with little steric crowding around the carbene: 3°C > 2°C > 1°C. Catalysts like Rh_2(DOSP)$_4$ (**1**), Rh_2(PTAD)$_4$ (**3**), and Rh_2(TCPTAD)$_4$ (**4**) obey this trend and Rh_2(TCPTAD)$_4$ is highly selective for even unactivated 3° C–H bonds over other positions.[30, 43] When the accessibility of the carbene is reduced by constructing a tight chiral pocket around the dirhodium core, this electronic preference can be overridden, and the steric accessibility of the C–H bond takes precedence.[34] For example, in the reaction of *p*-cymene with 2,2,2-trichloroethyl-2-(4-bromophenyl)-2-diazoacetate, Rh_2(*p*-PhTPCP)$_4$ (**6**) is highly selective for the primary C-H bond (>20:1) and affords the product with near perfect enantioselectivity (97% ee).[34] Dr Kuangbiao Liao was able to push this selectivity even further through the use of multi-fold Suzuki cross-coupling to generate an even more sterically demanding catalyst, Rh_2(*tris*(*p*-^{t}BuC$_6$H$_4$)TPCP)$_4$(**8**), which is capable of achieving primary-selective C–H functionalization in unactivated substrates like *n*-pentane.[39] This scaffold has been most extensively applied to achieving novel site selectivity, including reacting with unactivated C–H bonds in the presence of activated ones purely dictated by steric accessibility (Figure 1.3). In 2018, the catalyst Rh_2(2Cl5Br-TPCP)$_4$ (**9**) was shown to react with the most sterically accessible methylene C–H bond in the presence of benzylic C–H bonds which was then applied towards constructing the macrocyclic core of cylindrocyclophane-A.[38] The high rigidity of these catalysts leads to predictable

and high levels of enantioselectivity and is extremely important to their success.[34] Nowhere is this clearer than in studies performed on a series of diarylcyclopropane catalysts ($Rh_2(DPCP)_4$). These catalysts are more flexible than the TPCP catalysts by virtue of the lack of arene adjacent to the carboxylate group in the ligand and as such they are not strictly confined to well defined secondary structures.[44] As a result of this lack of rigidity, the DPCP series cannot achieve the same levels of site and enantioselectivity as the TPCP series. These comparisons highlight the ways in which the rigidity of the TPCP scaffold imparts predictably high asymmetric induction in a wide variety of reactions and under different conditions making them intriguing scaffolds for further investigation.

Figure 1.3: Dirhodium tetrakis(triarylcyclopropane carboxylate) catalysts are capable of unparalleled site selectivity in C–H functionalization.

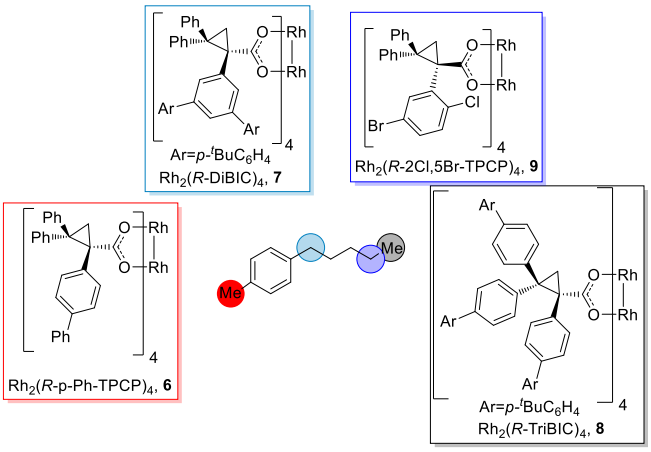

Considering the high cost of rhodium catalysts and the broad utility of donor/acceptor carbenes, we have had a long-standing interest to perform both C–H functionalization and cyclopropanation with very low catalyst loadings.[20, 45, 46] In the Davies lab, cyclopropanation is often viewed as a stepping-stone towards C–H functionalization since it is much more energetically favorable that C–H functionalization.[42, 47] Additionally, when Davies chemistry is applied towards industrial programs, it has historically been applied to generate chiral cyclopropanes as in the example of the multi-Kg scale synthesis of the Hepatitis-

C drug Beclabuvir,[48] and the more recent example of a CFTR program at AbbVie which will be discussed in greater detail in **Chapter 2**.[49] To this, early studies to investigate high catalyst TON were conducted exclusively on cyclopropanation. It was found the bridged catalyst, $Rh_2(BiTISP)_2$ (**2**), enabled the cyclopropanation of styrene to be routinely conducted with 0.001 mol % catalyst loading in 85% ee with a variety of aryldiazoacetates.[20] This catalyst, however, is difficult to synthesize on scale,[24] which has limited its general utility. Even lower catalyst loadings could be achieved for reactions catalyzed by $Rh_2(DOSP)_4$ (**1**) and $Rh_2(PTAD)_4$ (**3**) in the absence of solvent, but the enantioselectivity dropped dramatically under high TON conditions.[46] Additionally, reactions of diazo compounds under neat conditions are impractical for industrial applications due to the high energy associated with the diazo compounds.[50] With several new chiral dirhodium catalysts now available, a systematic study was carried out to determine if the newer catalysts had the potential for practical asymmetric cyclopropanation under extremely low catalyst loadings.[45] Detailed kinetic studies were then performed to determine the relative reactivity of these catalysts and their performance as the reaction progresses. These studies have resulted in the optimization of reaction conditions for highly enantioselective cyclopropanation (86-99% ee) which can be achieved with a range of substrates at a catalyst loading of 0.001 mol %.[45] This chapter will mainly focus on the work performed to optimize the catalyst choice and reaction conditions, only briefly touching on the kinetic studies which were performed by Dr. Bo Wei.[45]

1.2 Results and discussion:

The first stage of the project was to determine the relative enantioselectivity of various catalysts in a standard cyclopropanation of styrene (**13**) with 2,2,2-trichloroethyl-2-(4-bromophenyl)-2-diazoacetate (**14**) to form the cyclopropane (**15**). It has been shown that the trichloroethyl ester offers advantages compared to the traditional methyl ester in terms of site selectivity in C–H functionalization reactions, reaction efficiency and faster reactions.[11, 45, 51] The vast majority of the reported studies on rhodium-

catalyzed reactions of donor/acceptor carbenes have not attempted to conduct the reactions at the lowest catalyst loadings possible.[11, 52, 53] The typical conditions use a catalyst loading of 0.5-1.0 mol % at rt, and under these conditions all the catalysts are very effective. Typically, the reactions are complete in a matter of minutes, although it is very common for the diazo compounds to be added slowly to limit the possibility of carbene dimer formation.[45] The catalysts are so effective that the reactions with reactive trapping substrates can be conducted at temperatures as low as -50 °C.[52] As previously discussed reactions conducted with $Rh_2(DOSP)_4$ (**1**), and $Rh_2(PTAD)_4$ (**3**), give higher levels of asymmetric induction when hydrocarbon solvents are used, but this is far from an optimal solvent for conducting the reaction on large scale with a diverse series of industrially relevant substrates.[22, 54] For newer catalysts dichloromethane is the established optimum solvent, however, there was significant interest in exploring other solvents.[11, 33] While dichloromethane is fairly ubiquitous in organic chemistry it is a concerning solvent for use on large scale in an industrial setting, due to volatility and toxicity issues.[55] We wanted to explore what factors could be used to maintain high enantioselectivity under practical conditions, including low catalyst loadings and environmentally friendly solvents (Figure 1.4). In the original studies with $Rh_2(BiTISP)_2$ (**2**) we had found that high enantioselectivity was maintained only when one equivalent of methyl benzoate was added to the reaction mixture.[20] It was reasoned that the carbonyl of methyl benzoate was weakly interacting with the carbene to form a partial ylide. This weak occupation of the empty p-orbital on the carbene would make it less electrophilic, increasing its stability in the same manner as the donor-aryl group (Figure 1.4).[41] Therefore, we decided to explore whether more practical catalysts could be benefit from a solvent switch, with particular emphasis on solvents containing ester groups. Furthermore, we desired to explore the possibility of using higher boiling solvents, so that we would have the option to conduct low-catalyst-loading reactions with catalysts that had been demonstrated to have slow reaction rates but excellent retention of enantioselectivity, like $Rh_2(p\text{-}BrTPCP)_4$ (**5**), at higher temperatures to expedite the reaction.

Figure 1.4: Weak interactions between coordinating solvents and the rhodium carbene help dictate reaction selectivity.

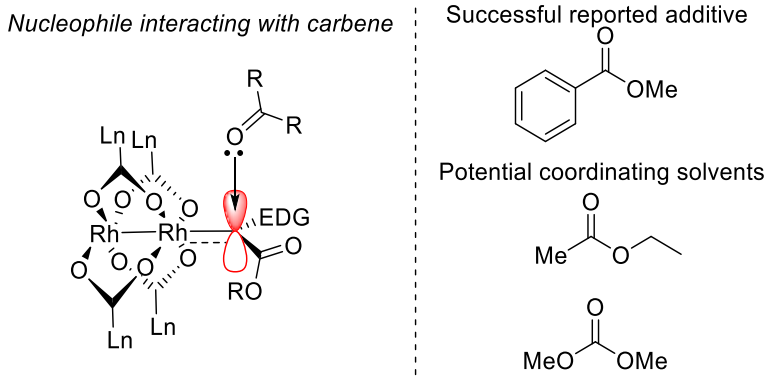

In order to quickly evaluate the effect of solvent on the enantioselectivity of the reaction, it would be most efficient to conduct reactions using a robotic system in a medium-throughput screen (Table 1.1). In recent years, high-throughput experimentation (HTE) has emerged as an essential platform in all major pharmaceutical companies.[56, 57] This workflow enables a single chemist to quickly generate a diverse series of scaffolds or test a variety of different conditions to achieve high yield or novel reactivity.[56] Adapting this system to Davies chemistry proved to be a challenge. Due to the lack of a glove-box and standard HTE amenities including sealable well-plates, flea bars, and powerful magnetic hot chambers for even stirring and heating across the plate, the small-scale reactions had to be conducted open to air and without stirring in PPE microcentrifuge tubes.[45] Dirhodium catalyzed cyclopropanation reactions release N_2 gas over the course of the reaction as the diazo decomposes and it was our hope that this "self-sparging" would both agitate the reaction sufficiently to ensure effective mixing and remove residual O_2 from the solvent which can inhibit the reaction rate.[45] Water can also be a significant catalyst poison and can react with the carbene preferentially to the alkene substrate, leading to unwanted hydroxylated byproducts.[58, 59] Due to the use of plastic reaction vials it would be impossible to dry the reaction vial itself, so the solvent needed to be devoid of water. To address this concern, each solvent in the scope was distilled prior to use

and stored over 4Å molecular sieves. Another problem was that volatile solvents like DCM and pentane would evaporate rapidly under the reaction setup and as a result the reactions would need to be immediately capped after the diazo was dispensed. Lastly, due to all these concerns, it would be inadvisable to run the reaction with low catalyst loading, as the reactions can stall for a variety of reasons and ideally should be run to near completion to get a reasonable estimation of % ee and shorter reaction times reduce the risk of solvent evaporation.[45] Despite these concerns, control experiments showed that the reactions were effective, giving reproducible levels of diastereoselectivity and enantioselectivity, however, under these conditions the isolated yields were low and not truly representative. Each reaction was conducted for 1 h at rt with a catalyst loading on 0.5 mol %, which is sufficient for all catalysts to complete the cyclopropanation in dichloromethane.[45] The automated liquid handling system can dispense solutions in a preprogrammed pattern. To run this reaction, each reaction vial was charged with a 100 µl of 0.125 mM catalyst solution from one of 10 selected catalysts and added to the pipetting palate. Each vial was then filled with 625 µl of 0.243 M styrene solution in the solvent of choice and mixed via pipette. 375 µl of a 52.6 mM solution of the diazo compound **14** was then added to each vial via pipette and the solutions were mixed once more. The vials were capped and allowed to react for 1 h. After this time, HPLC samples of each vial were prepared. Because the robot was programmable to account for time passage, preparation of the HPLC samples was also performed automatically. A 20 µl aliquot of each reaction was added to a vial, suspended in 980 µl HPLC hexanes, and mixed via pipette to generate an HPLC solution. Each crude sample was then subjected to UHPLC analysis to determine the enantioselectivity of the reaction. Despite the sensitivity of both the catalyst and the carbene to atmospheric no diazo dimer or O–H insertion products were observed. The results of the high throughput screening were tabulated and transposed into a heat map to demonstrate the enantioselectivity of the reaction in each solvent for each of the catalyst tested (Table 1.1).[45]

Table 1.1: Medium-throughput screen assessing the selectivity of dirhodium catalyzed cyclopropanation of styrene with 2,2,2-trichloroethyl-2-(4-bromophenyl)-2-diazoacetate as a function of solvent selection and catalyst identity.

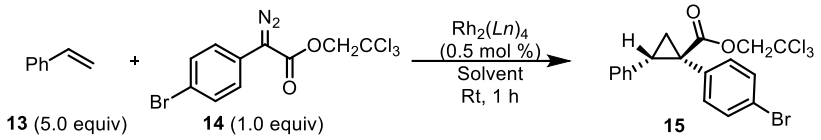

Catalyst	EtOAc	CH_2Cl_2	TFT	*i*-PrOAc	$(MeO)_2CO$	$(EtO)_2CO$	Pentane
$Rh_2(DOSP)_4$	**78.1**	**63.1**	**77.9**	**83.9**	**67.1**	**66.7**	**77**
$Rh_2(PTAD)_4$	**90.9**	**56.6**	**56.9**	**53.5**	**40.5**	**47.1**	**58.9**
$Rh_2(TCPTAD)_4$	**90.7**	**71.5**	**72.9**	**66.7**	**68.1**	**90.7**	
$Rh_2(TPPTTL)_4$	**95.6**	**88.5**	**90.5**	**91.3**	**91.9**	**87.9**	
$Rh_2(o\text{-ClTPCP})_4$	**60.3**	**44.8**	**37.5**	**42.1**	**35.1**	**71.3**	
$Rh_2(2\text{-Cl-5-Br-TPCP})_4$	**39.7**	**72.2**	**70.9**	**77.9**	**63.5**	**70.2**	
$Rh_2(p\text{-Br-TPCP})_4$	**>99**	**92**	**85.1**	**94.7**	**94.7**	**92.5**	**89.6**
$Rh_2(p\text{-Ph-TPCP})_4$	**>99**	**96.7**	**78.5**	**>99**	**>99**	**97.7**	
$Rh_2(\text{tris}(p\text{-}^t\text{BuC}_6\text{H}_4)\text{TPCP})_4$	**98.9**	**95.9**	**89.9**	**96.5**	**93.7**	**>99**	
$Rh_2(3,5\text{-di}(p\text{-}^t\text{BuC}_6\text{H}_4)\text{TPCP})_4$	**87.1**	**73.3**	**91.3**	**82.7**	**61.8**	**89.5**	

>99 % — **% ee** — **0 %**

Color gradient proceeds from red to blue via white middle color which denotes middling % ee. The solvents tested in the screen were ethyl acetate (EtOAc), dichloromethane (CH_2Cl_2), trifluorotoluene (TFT), isopropyl acetate (*i*-PrOAc) dimethyl carbonate ($(MeO)_2CO$), and diethyl carbonate ($(EtO)_2CO$). The majority of the catalysts were insoluble in pentane.

From these data it was clear that later generation, more rigid catalysts were less susceptible to dramatic solvent effects. $Rh_2(p\text{-BrTPCP})_4$ (**5**), $Rh_2(p\text{-PhTPCP})_4$ (**6**), $Rh_2(2Cl5Br\text{-TPCP})_4$ (**9**), and $Rh_2(\text{tris}(p\text{-}^t\text{BuC}_6\text{H}_4)\text{TPCP})_4$ (**8**) maintained similar levels of enantioselectivity regardless of the solvent used. As the catalysts with the least mobility in their ligand structures and the deepest catalyst pockets, this effect was expected and precisely why they were chosen for evaluation in this study. Second generation phthalimido catalysts are significantly more flexible and boast wider catalyst bowls which showed in their susceptibility to solvent effects. The most flexible catalyst of this series $Rh_2(PTAD)_4$ (**3**), displayed up to 43% variability in % ee due to solvent. As the flexibility of the ligand decreases with larger substituents on the phthalimide ring, from

$Rh_2(PTAD)_4$ (**3**) to $Rh_2(TCPTAD)_4$ (**4**) to $Rh_2(TPPTTL)_4$ (**10**), this variability in % ee as a function of solvent decreases highlighting the importance of catalyst rigidity in maintaining high cyclopropane enantioselectivity regardless of the reaction conditions.

Several solvents emerged as promising candidates for further evaluation under high turnover conditions. Particularly interesting were ethyl acetate, isopropyl acetate, and dimethyl carbonate [$(MeO)_2CO$], which provided significant increases in enantioselectivity compared to dichloromethane. Through these studies, ethyl acetate emerged as the optimal solvent for cyclopropanation for several catalysts including $Rh_2(PTAD)_4$ (**3**), $Rh_2(TPPTTL)_4$ (**10**), and Rh_2(*p*-BrTPCP)$_4$ (**5**). This observation is highly advantageous for industrial applications since ethyl acetate and mixtures there-of commonly replace more hazardous solvents.[22] Though previous work has shown that while useful for cyclopropanation, ester solvents would be incompatible with C–H insertion and could also lead to side-reactions at elevated temperatures. Ester solvents like isopropyl acetate can engage the rhodium carbene to form an oxonium ylide and rearrange to install tertiary alcohols (Scheme 1.2),[60] we theorized that carbonates would be compatible with this type of chemistry due to the lack of labile α-hydrogens.[61, 62] Fortunately, dimethyl carbonate ($(MeO)_2CO$) also offered significant enhancement in enantioselectivity compared with classical solvents like dichloromethane for $Rh_2(TPPTTL)_4$(**10**), Rh_2(*p*-BrTPCP)$_4$(**5**), and Rh_2(*p*-PhTPCP)$_4$(**6**). ($(MeO)_2CO$) is a green, environmentally benign solvent that has become widely used as a polar-aprotic solvent instead of potentially hazardous options like dichloromethane, THF, and diethyl ether.[61, 62] Additionally, as later generations of catalysts have become more rigid, polar solvents have become more attractive media and appear to improve the enantioselectivity of C–H insertion reactions.[36, 38] Typically, halogenated solvents like dichloromethane and trifluorotoluene have been used with these catalysts, however this choice of toxic, costly solvent inherently limits the applicability of Davies lab chemistry in an industrial setting. More interestingly we observed an enhancement in enantioselectivity with several catalysts when dimethyl

carbonate was used in comparison to halogenated solvents like dichloromethane and trifluorotoluene.[45] Hence as a safe and industry approved polar solvent, dimethyl carbonate was identified early as a good candidate for halogenated solvent replacement that also offers the potential for C–H insertion compatibility.

Scheme 1.2: Rearrangement of isopropyl acetate in the presence of a rhodium carbene to form chiral tertiary allylic alcohols with high enantioselectivity.[60]

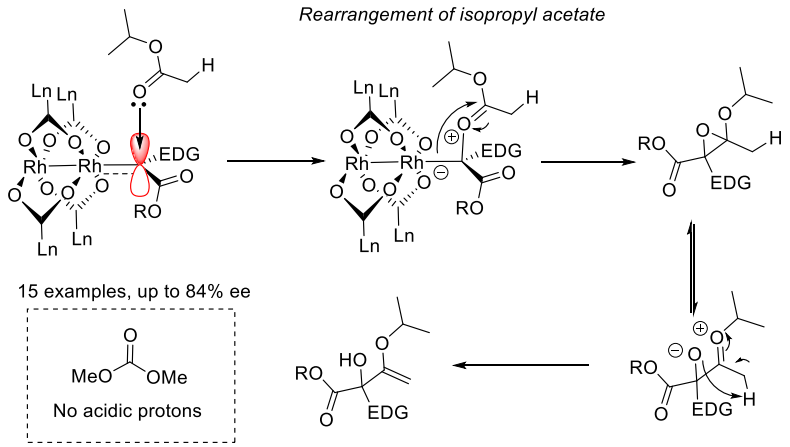

While the flexible dirhodium catalysts, the most significant being $Rh_2(DOSP)_4$ (**1**), exhibited significant deviations in enantioselectivity due to solvent while more rigid third generation catalysts appeared to perform consistently well in a variety of solvents. Rh_2(*p*-BrTPCP)$_4$ (**5**), and Rh_2(*p*-PhTPCP)$_4$ (**6**) displayed an increase in enantioselectivity when the reaction was performed in $(MeO)_2CO$ and ethyl acetate compared with the historically used dichloromethane. This synergistic relationship between the rigidity of the catalyst and the improvement of asymmetric induction in polar solvent was intriguing. In order to rationalize this relationship, one of these catalysts, Rh_2(*R*-*p*-PhTPCP)$_4$ (**6**) was crystallized from a solution of $(MeO)_2CO$. The crystal structure shows dimethyl carbonate coordinated to both the top and bottom rhodium faces of this C_2-symmetric catalyst. Carbene generation occurs within the catalyst bowl however it is conceivable that a molecule of $(MeO)_2CO$ could occupy the bottom rhodium face during carbene

generation and subsequent cyclopropanation. Interactions between the ligands and the axially coordinated dimethyl carbonate molecule may help stabilize the C_2 symmetric bowl conformation and rigidify the entire catalyst which could account for the increased enantioselectivity. Recent computational studies have shown that the enantioselectivity of primary C–H functionalization with Rh_2(*p*-BrTPCP)$_4$, a closely related catalyst, is likely dictated by the conformation of the carbene ester during the rate-determining step.[40] It is conceivable that these results would translate to cyclopropanation in which the enantiodetermining step is similar and it would be interesting to evaluate the ester geometry with and without an axially coordinating $(MeO)_2CO$ molecule *in silico* to see if it can account for these subtle improvements in % ee (Figure 1.5).

Figure 1.5: Interactions between dimethyl carbonate and Rh_2(*p*-PhTPCP)$_4$ (**6**) may help rigidify the catalyst and improve the enantioselectivity of rhodium catalyzed cyclopropanation.

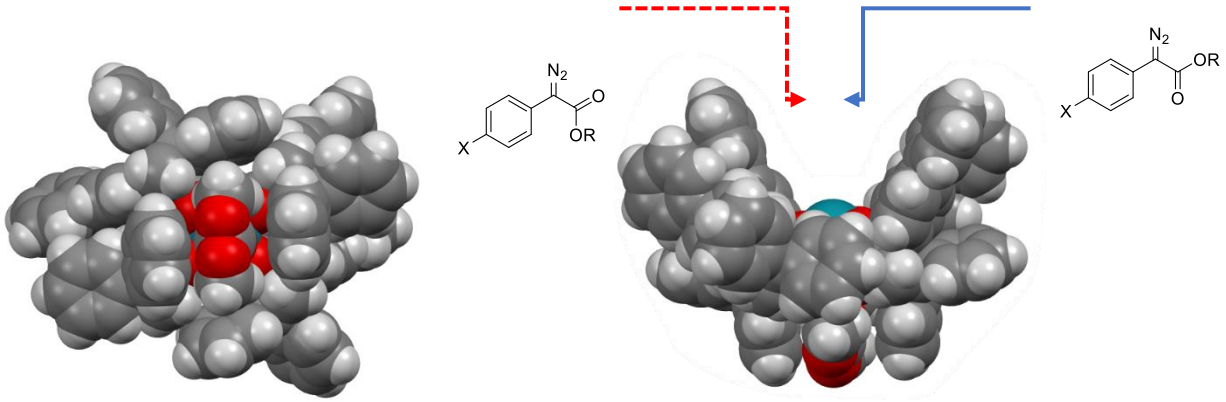

Several solvents were promising candidates for further evaluation under high turnover conditions. Particularly interesting were ethyl acetate, isopropyl acetate, and $(MeO)_2CO$, which provided significant increases in enantioselectivity compared to dichloromethane. Before deciding which solvent would be best suited for low catalyst loading studies, laboratory-scale (100 mg) reactions using 0.5 mol % of catalyst

were performed to both validate results obtained from the high throughput screen and determine the solvent impact on the reaction yield. Rh_2(*p*-Br-TPCP)$_4$ (**5**) was chosen as the catalyst for these reactions because it had been shown to be the optimal catalyst during low-loading kinetic studies in dichloromethane.[45] These lab scale reactions offered some interesting insight into the effect of the solvent on the cyclopropanation. The enantioselectivity enhancements observed in the high throughput screening were confirmed, however, some of the more selective solvents, such as ethyl acetate and isopropyl acetate, had significantly negative impacts on the yield of the reaction (Table 1.2).[60] Additionally ^{t}BuCN, a solvent preferred for Rh-nitrene chemistry in the DuBois lab, was shown to increase enantioselectivity but was significantly detrimental to the yield.[63] Importantly, dimethyl carbonate maintained high yield for the transformation while significantly enhancing the enantioselectivity over dichloromethane. Dimethyl carbonate is a green, high-boiling, environmentally benign solvent that has become widely used as an alternative to potentially hazardous options like dichloromethane and diethyl ether.[22, 61, 62] Hence as a highly enantioselective, high-boiling, green solvent, $(MeO)_2CO$ was identified as a good candidate for optimizing cyclopropanation at low catalyst loading.

Table 1.2: Solvent screening on lab scale for the benchmark cyclopropanation.

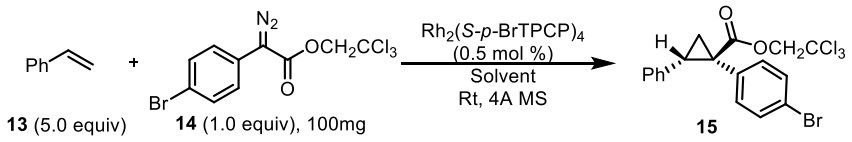

solvent	yield, %	ee, %
CH_2Cl_2	95	91
$(MeO)_2CO$	91	94
EtOAc	66	95
n-hexane	34	87
TFT	88	89
^{t}BuCN	49	97
i-PrOAc	52	91
$(EtO)_2CO$	89	86

Kinetic studies were then performed by Dr. Bo Wei in order to optimize the reaction for low catalyst loadings.[45] Through analysis of the reaction at 0.001 mol % catalyst loading it was identified that even though $Rh_2(DOSP)_4$ (**1**) and $Rh_2(PTAD)_4$ (**3**) boasted impressive overall TON rates, the enantioselectivity of cyclopropanation with these catalysts dropped precipitously between 0.01-0.001 mol % catalyst loading. Conversely, though the more sterically constrained catalysts Rh_2(*p*-Br-TPCP)$_4$ (**5**) and Rh_2(*p*-Ph-TPCP)$_4$ (**6**) were significantly slower, they were better suited to maintain the enantioselectivity under low catalyst loading conditions and are still capable of completing cyclopropanation at 0.0025 mol % catalyst loading in under 2 h at rt.[45]

Figure 1.6: TON of rhodium catalyzed cyclopropanation of styrene with compound **14** as a function of catalyst.

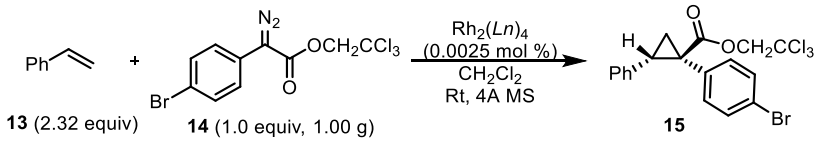

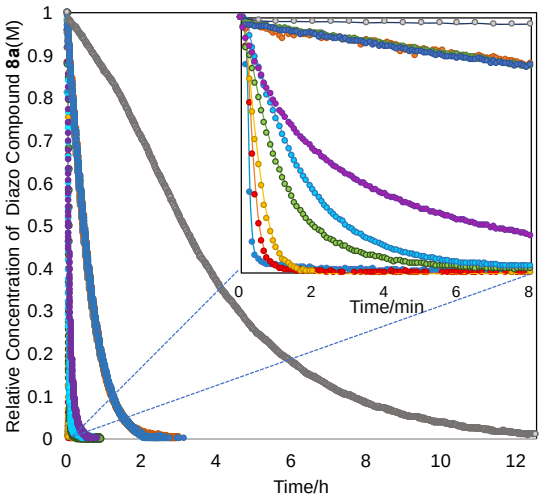

catalyst	ee (**9a**, %)	reaction time	initial TOF/h
$Rh_2(DOSP)_4$	73	2 min	2,880,000
$Rh_2(PTAD)_4$	63	2 min	1,920,000
$Rh_2(TCPTAD)_4$	66	2 min	1,920,000
$Rh_2(TPPTTL)_4$	83	8 min	1,440,000
Rh_2(*o*-ClTPCP)$_4$	37	8 min	1,440,000
Rh_2(2-Cl-5-Br-TPCP)$_4$	43	30 min	1,152,000
Rh_2(*p*-Br-TPCP)$_4$	93	2 h	57,600
Rh_2(*p*-Ph-TPCP)$_4$	90	2 h	58,775
Rh_2(tris(*p*-^{t}BuC$_6$H$_4$)TPCP)$_4$	87	2 h	57,600
Rh_2(3,5-di(*p*-^{t}BuC$_6$H$_4$)TPCP)$_4$	31	12.5 h	5,549

In order to understand better the behavior of these rigid catalysts, Dr. Bo Wei conducted kinetic studies on the cyclopropanation reactions using the Variable Time Normalization Analysis (VTNA) methodology reported by Burés,[43] and determined rate law for the cyclopropanation reaction. The data agreed with earlier computational studies,[46] which showed that the energy barrier for diazo decomposition is much

higher than the cyclopropanation making it the rate-determining step in this reaction. A catalytic cycle that is consistent with the kinetic studies is shown in Scheme 1.4. The rhodium carboxylate **A** coordinates to the aryldiazoacetate in competition with styrene coordination (**B**). This interaction would explain why the rate of the reaction has a reverse relationship to the concentration of styrene. The rate determining step is the extrusion of nitrogen from the rhodium diazo complex **C** to form the rhodium carbene **D**. Reaction of the rhodium carbene **D** with styrene would then generate the final product **E** and recovered catalyst **A**. This mechanism is consistent with computational studies that have been carried out on the cyclopropanation reaction. These studies showed that the formation of the carbene is the rate determining step and the barrier for the cyclopropanation step is very small.[64, 65] Dirhodium tetracarboxylates are very stable complexes. They can be chromatographed and are stable in the open air for years. However, the rhodium carbene intermediate is likely not to be particularly stable and needs to react quickly to prevent catalyst degradation. Hence, an excess of styrene despite its ability to decrease the reaction rate, is better for maintaining the high enantioselectivity under very low catalyst loadings. The X-ray structures of the catalysts always have molecules coordinating to the axial positions (water, ethyl acetate, etc.)[36, 53, 66] These axially coordinating ligands must be displaced for the catalytic reaction to proceed. However, our studies suggest that the kinetic barrier for the loss of the axial ligand must be small since we rarely see a delay before the reaction begins. Nevertheless, dry conditions are required for reproducible reactions at exceedingly low catalyst loading, presumably because excess water would interfere with the small amount of catalyst present.[45]

Figure 1.7: Mechanism of dirhodium catalyzed cyclopropanation.[45]

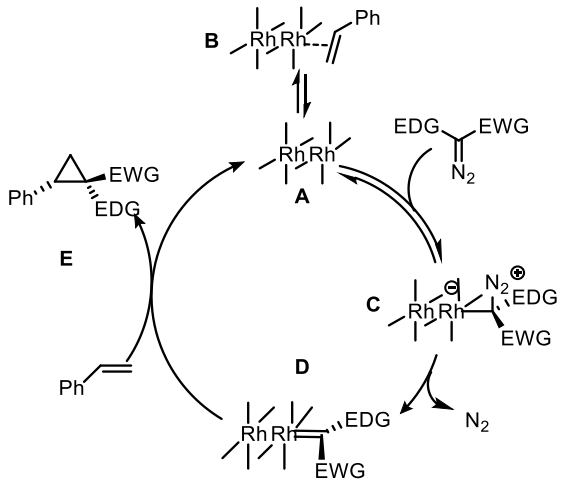

Having established an understanding of the catalytic system at 0.0025 mol % loading, the reaction was then optimized to even lower catalyst loadings by Dr. Bo Wei. Despite some struggles, the use of $(MeO)_2CO$ enabled the reaction to be conducted at catalyst loadings as low as 0.001 mol % without loss of enantioselectivity. The rate of reaction was actually slower in $(MeO)_2CO$ as compared with DCM likely due to the need to displace the solvent from the rhodium catalyst prior to carbene generation which is an energetic sink. In order to achieve these exceptionally low TON's in a reasonable amount of time the reaction temperature was elevated to 60 ^{o}C to speed up the rate of reaction. At this temperature the background decomposition of the diazo compound is negligible and high enantioinduction is therefore retained. This would not have been possible without the use of a high-boiling solvent highlighting the utility of $(MeO)_2CO$ in this study. This reaction was then practically demonstrated in a multiple addition experiment to achieve 750,000 TON on multi-gram scale without loss of enantioselectivity.[45] The scope of the low catalyst loading cyclopropanation was then examined with a range of aryldiazoacetates (Table 1.3). This progressed in tow main steps, first, the substrates were evaluated for yield and %ee on a typical laboratory scale (0.20 mmol and 0.5 mol% catalyst) before being repeated by Dr. Bo Wei under high TON conditions. The initial evaluation was critical, as the high TON conditions required a large amount of diazo compound to be practical (over 1 g) and significantly longer reaction times, making poorly performing

substrates a significant waste of both time and resources.[49] These evaluations also unearthed a problem with the previously optimized catalyst system for high TON. While the Rh_2(*p*-Br-TPCP)$_4$ (**5**)/ dimethyl carbonate system gave high enantioselectivity for some substrates, others delivered enantioselectivities well below 90% ee. During the medium-throughput screen, Rh_2(*p*-Ph-TPCP)$_4$ (**6**) performed extremely well in dimethyl carbonate, giving very high asymmetric induction. Rh_2(*p*-Ph-TPCP)$_4$ (**6**) was briefly examined at low catalyst loading in dimethyl carbonate, its kinetic profile was identical to Rh_2(*p*-Br-TPCP)$_4$ (**5**) but it routinely gave higher levels of enantioselectivity. Based on these results, the published study on the scope of the asymmetric cyclopropanation at low catalyst loading was conducted with Rh_2(*p*-Ph-TPCP)$_4$ (**6**) as the catalyst (Table 1.3). High enantioselectivity and yield was preserved across a broad substrate scope of aryldiazoacetates and styrene derivatives. In some cases, the reactions did not go to completion in 12 h and in those cases, the reactions were repeated using 0.003 mol % catalysts loading. Some of the more intriguing examples are the boronate derivative **21**, the styryl derivative **24** and the heterocyclic derivatives **26** and **27** which all gave excellent enantioselectivity. Compound **24** needed to be synthesized at room temperature due to the thermal degradation of styryldiazoacetate to form the pyrazole which occurs rapidly at relatively low temperature (rapid at 40°C but occurs slowly even if stored at 0°C). Fortunately, under these conditions, the reaction was still competent at low catalyst loading (0.003 mol%), affording the product in 96% ee and 88% yield. Interestingly *ortho*-substituted aryldiazoacetates were not tolerated at all in this method, giving low yield and low enantioselectivity, highlighting the need for the development of a robust method to achieve robust and predicTable 1.high %ee with these substrates as will be discussed in **Chapter 2.**[58]

Table 1.3: Scope of rhodium catalyzed cyclopropanation with extremely low catalyst loadings.

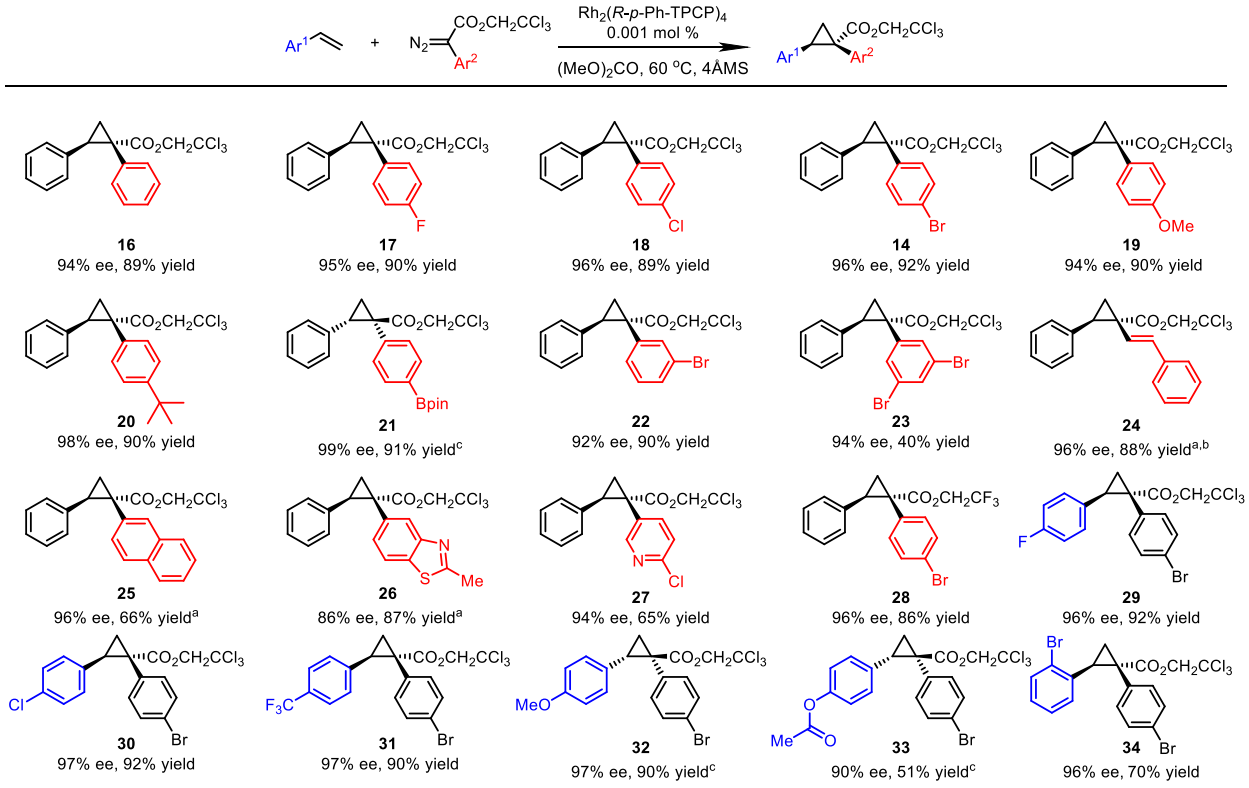

a: Reaction was conducted at 0.003 mol % catalyst loading to ensure reaction proceeds to completion. b: Reaction was conducted at 25 °C to avoid thermal rearrangement of the styryldiazoacetate to a pyrazole. c: Reaction was conducted with Rh_2(*S*-*p*-Ph-TPCP)$_4$ (**6**).

Extension of the Rh_2(*p*-Ph-TPCP)$_4$ -catalyzed cyclopropanation to more sterically bulky substrates was also unsuccessful. 1,1-Diphenylethylene (**35**), a key substrate for the enantioselective synthesis of the third-generation ligands, did not perform very well and cyclopropane **36** was obtained in only 48% ee with Rh_2(*p*-Ph-TPCP)$_4$ (**6**). Therefore, it was necessary to use a less sterically demanding catalyst to achieve high % ee. Rh_2(PTAD)$_4$ (**3**) and $(MeO)_2CO$ were used as the optimal system for this transformation, furnishing the cyclopropane **36** in 94% ee at 0.001 mol % catalyst loading. Additionally, in the cyclopropanation of methyl-2-furate (**37**), the enantioselectivity of the cyclopropane **39** increased from 50% ee with Rh_2(*p*-Ph-TPCP)$_4$ (**6**) to 90% ee with Rh_2(TCPTAD)$_4$ (**4**) in dimethyl carbonate at 0.001 mol % catalyst loading[56] (Scheme 1.5) The necessity of having to use Rh_2(PTAD)$_4$ (**3**) and Rh_2(TCPTAD)$_4$ (**4**) rather than the third-generation catalyst Rh_2(*p*-Ph-TPCP)$_4$ (**6**), is presumably because the less bulky phthalimido series of

catalysts are better suited for reactions of more crowded substrates such as 1,1-diphenylethylene (**35**) and methyl-2-furoate (**37**).

Figure 1.8: Cyclopropanation of bulky substrates with extremely low catalyst loadings requires the use of less sterically encumbered catalysts than Rh_2(*p*-PhTPCP)$_4$ (**6**) like Rh_2(PTAD)$_4$ (**3**) and Rh_2(TCPTAD)$_4$ (**4**).

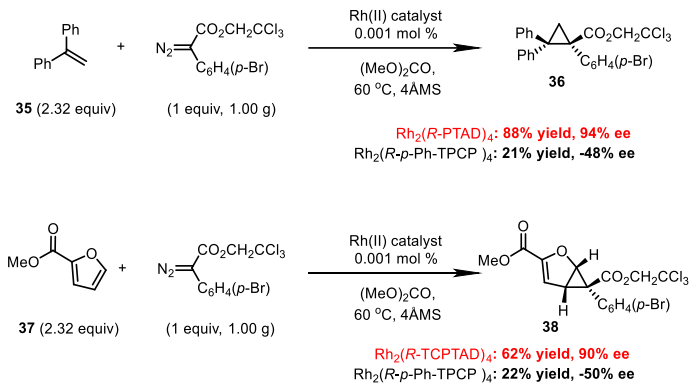

To demonstrate the practicality of the optimized conditions for low catalyst loading cyclopropanation, we decided to re-examine the previously published synthesis of the cyclopropane **41**, a key step in the kilogram scale synthesis of the Hepatitis C drug, Beclabuvir (**42**).[48] (Figure 1.9) The previous synthesis was conducted via a Rh_2(DOSP)$_4$ (**1**)-catalyzed reaction of methyl styryldiazoacetate **39a** with the styrene **40**. Using 0.2 mol % of Rh_2(DOSP)$_4$ (**1**) to afford the desired cyclopropane **41** in 94% yield and 83% ee. The process method was complex, requiring multiple solvent exchanges and drying steps to remove water from the reaction and the use of heptanes as a hydrocarbon solvent to ensure even this moderate level of enantioselectivity. Given our evaluation of catalysts via medium-throughput screening we suspected that this level of enantioselectivity could be improved upon using a more rigid catalyst in combination with $(MeO)_2CO$ as solvent. Under our low catalyst loading conditions using trichloroethyl styryldiazoacetate **39b**, the reaction was carried out with 1/200th the catalyst loading with much higher

asymmetric induction. The Rh_2(*p*-Ph-TPCP)$_4$ (**6**)-catalyzed reaction of **40** using 0.001 mol % catalyst loading at 25 °C with dimethyl carbonate as solvent, generated the cyclopropane **41** in 72% yield and 96% ee.

Figure 1.9: The cyclopropanation of *ortho*-substituted styrene derivative **40** was used as a key reaction in the pilot-scale multi-Kg synthesis of the hepatitis-C drug Beclabuvir (**42**). The same reaction was achieved with higher enantioselectivity and lower catalyst loading with the protocol discovered herein.

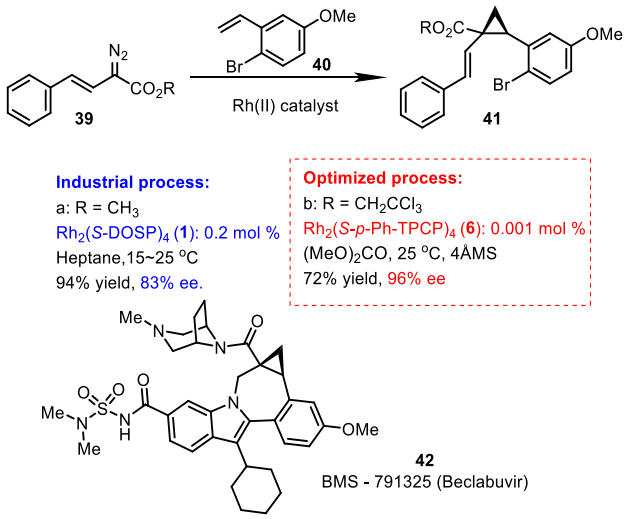

1.3 Conclusion:

Over the course of this comprehensive study, the effect of the ligand on the performance of dirhodium catalysts in combination with solvent choice was investigated. This study highlighted key trends and relationships between catalyst rigidity and enantioselectivity. Polar solvents were also examined which had the ability to improve reaction enantioselectivity of recently developed dirhodium catalysts. The screen also leveraged technology new to the Davies group to synthesize a large volume of useful data in an automated fashion, an approach which has become common in pharma but is still in the early stages of widespread adoption in academia. These evaluations enabled the performance of detailed studies

under the RPKA model to determine the rate law of the cyclopropanation reaction. Further optimization studies identified dimethyl carbonate as a superior solvent in combination with Rh_2(*p*-Ph-TPCP)$_4$ (**6**) for achieving 100,000 catalyst TON's with consistently high enantioselectivity. The optimal catalytic system was then applied to a series of aryldiazoacetates and styrenes and proved to be robust and versatile, achieving high yield and % ee across a broad scope of substrates. The study culminated in the optimization of a key step in the synthesis of the Hepatitis C drug Beclabuvir (**42**) at 200-fold lower catalyst loading than a previously reported procedure developed by the process team at BMS, which highlights the practical utility of this reaction protocol.

1.4 References:

1. Davies, H. M.; Morton, D., Guiding principles for site selective and stereoselective intermolecular C–H functionalization by donor/acceptor rhodium carbenes. *Chem. Soc. Rev.* **2011,** *40* (4), 1857-1869.
2. Ye, T.; McKervey, M. A., Organic synthesis with. alpha.-diazo carbonyl compounds. *Chem. Rev.* **1994,** *94* (4), 1091-1160.
3. Doyle, M. P.; Zhou, Q.-L.; Charnsangavej, C.; Longoria, M. A.; McKervey, M. A.; García, C. F., Chiral catalysts for enantioselective intermolecular cyclopropanation reactions with methyl phenyldiazoacetate. Origin of the solvent effect in reactions catalyzed by homochiral dirhodium (II) prolinates. *Tetrahedron Lett.* **1996,** *37* (24), 4129-4132.
4. Hansen, J.; Davies, H. M., High symmetry dirhodium (II) paddlewheel complexes as chiral catalysts. *Coord. Chem. Rev.* **2008,** *252* (5-7), 545-555.
5. Chepiga, K. M.; Qin, C.; Alford, J. S.; Chennamadhavuni, S.; Gregg, T. M.; Olson, J. P.; Davies, H. M., Guide to enantioselective dirhodium (II)-catalyzed cyclopropanation with aryldiazoacetates. *Tetrahedron* **2013,** *69* (27-28), 5765-5771.
6. Davies, H. M., Finding opportunities from surprises and failures. Development of rhodium-stabilized donor/acceptor carbenes and their application to catalyst-controlled C–H functionalization. *J. Org. Chem.* **2019,** *84* (20), 12722-12745.
7. Davies, H. M.; Liao, K., Dirhodium tetracarboxylates as catalysts for selective intermolecular C–H functionalization. *Nat. Rev. Chem.* **2019,** *3* (6), 347-360.
8. Davies, H. M., Asymmetric synthesis using rhodium-stabilized vinylcarbenoid intermediates. *ALACBI* **1997,** *30* (4), 107-114.
9. Davies, H. M.; Hansen, T., Asymmetric intermolecular carbenoid C− H insertions catalyzed by rhodium (ii)(S)-N-(p-dodecylphenyl) sulfonylprolinate. *J. Am. Chem. Soc.* **1997,** *119* (38), 9075-9076.
10. Davies, H. M.; Nagashima, T.; Klino, J. L., Stereoselectivity of methyl aryldiazoacetate cyclopropanations of 1, 1-diarylethylene. Asymmetric synthesis of a cyclopropyl analogue of tamoxifen. *Org. Lett.* **2000,** *2* (6), 823-826.
11. Negretti, S.; Cohen, C. M.; Chang, J. J.; Guptill, D. M.; Davies, H. M., Enantioselective dirhodium (II)-catalyzed cyclopropanations with trimethylsilylethyl and trichloroethyl aryldiazoacetates. *Tetrahedron* **2015,** *71* (39), 7415-7420.

12. Davies, H. M.; Oldenburg, C. M.; McAfee, M. J.; Nordahl, J. G.; Henretta, J. P.; Romines, K. R., Novel approach to seven-membered rings by the intramolecular tandem cyclopropanation/cope rearrangement sequence. *Tetrahedron Lett.* **1988,** *29* (9), 975-978.
13. Spangler, J. E.; Lian, Y.; Raikar, S. N.; Davies, H. M., Synthesis of complex hexacyclic compounds via a tandem Rh (II)-catalyzed double-cyclopropanation/Cope Rearrangement/Diels–Alder reaction. *Org. Lett.* **2014,** *16* (18), 4794-4797.
14. Briones, J. F.; Hansen, J.; Hardcastle, K. I.; Autschbach, J.; Davies, H. M., Highly enantioselective Rh2 (S-DOSP) 4-catalyzed cyclopropenation of alkynes with styryldiazoacetates. *J. Am. Chem. Soc.* **2010,** *132* (48), 17211-17215.
15. Li, Z.; Parr, B. T.; Davies, H. M., Highly stereoselective C–C bond formation by rhodium-catalyzed tandem ylide formation/[2, 3]-sigmatropic rearrangement between donor/acceptor carbenoids and chiral allylic alcohols. *J. Am. Chem. Soc.* **2012,** *134* (26), 10942-10946.
16. Li, Z.; Boyarskikh, V.; Hansen, J. H.; Autschbach, J.; Musaev, D. G.; Davies, H. M., Scope and mechanistic analysis of the enantioselective synthesis of allenes by rhodium-catalyzed tandem ylide formation/[2, 3]-sigmatropic rearrangement between donor/acceptor carbenoids and propargylic alcohols. *J. Am. Chem. Soc.* **2012,** *134* (37), 15497-15504.
17. Davies, H. M.; Lian, Y., The combined C–H functionalization/cope rearrangement: discovery and applications in organic synthesis. *Acc. Chem. Res.* **2012,** *45* (6), 923-935.
18. Lian, Y.; Hardcastle, K. I.; Davies, H. M., Computationally Guided Stereocontrol of the Combined C-H Functionalization/Cope Rearrangement. *Angew. Chem. Int. Ed.* **2011,** *50* (40), 9370-9373.
19. Nagashima, T.; Davies, H. M., Catalytic asymmetric cyclopropanation using bridged dirhodium tetraprolinates on solid support. *Org. Lett.* **2002,** *4* (12), 1989-1992.
20. Davies, H. M.; Venkataramani, C., Dirhodium tetraprolinate-catalyzed asymmetric cyclopropanations with high turnover numbers. *Org. Lett.* **2003,** *5* (9), 1403-1406.
21. Davies, H. M.; Bruzinski, P. R.; Lake, D. H.; Kong, N.; Fall, M. J., Asymmetric cyclopropanations by rhodium (II) N-(arylsulfonyl) prolinate catalyzed decomposition of vinyldiazomethanes in the presence of alkenes. Practical enantioselective synthesis of the four stereoisomers of 2-phenylcyclopropan-1-amino acid. *J. Am. Chem. Soc.* **1996,** *118* (29), 6897-6907.
22. Byrne, F. P.; Jin, S.; Paggiola, G.; Petchey, T. H.; Clark, J. H.; Farmer, T. J.; Hunt, A. J.; Robert McElroy, C.; Sherwood, J., Tools and techniques for solvent selection: green solvent selection guides. *Sus. Chem. Proc.* **2016,** *4* (1), 1-24.
23. Davies, H. M.; Townsend, R. J., Catalytic asymmetric cyclopropanation of heteroaryldiazoacetates. *J. Org. Chem.* **2001,** *66* (20), 6595-6603.
24. Davies, H. M.; Panaro, S. A., Novel dirhodium tetraprolinate catalysts containing bridging prolinate ligands for asymmetric carbenoid reactions. *Tetrahedron Lett.* **1999,** *40* (29), 5287-5290.
25. Hashimoto, S.-i.; Watanabe, N.; Sato, T.; Shiro, M.; Ikegami, S., Enhancement of enantioselectivity in intramolecular CH insertion reactions of α-diazo β-keto esters catalyzed by chiral dirhodium (II) carboxylates. *Tetrahedron Lett.* **1993,** *34* (32), 5109-5112.
26. Reddy, R. P.; Davies, H. M., Dirhodium tetracarboxylates derived from adamantylglycine as chiral catalysts for enantioselective C− H aminations. *Org. Lett.* **2006,** *8* (22), 5013-5016.
27. Takeda, K.; Oohara, T.; Anada, M.; Nambu, H.; Hashimoto, S., A Polymer-Supported Chiral Dirhodium (II) Complex: Highly Durable and Recyclable Catalyst for Asymmetric Intramolecular C H Insertion Reactions. *Angew. Chem.* **2010,** *122* (39), 7133-7137.
28. Fu, J.; Ren, Z.; Bacsa, J.; Musaev, D. G.; Davies, H. M., Desymmetrization of cyclohexanes by site- and stereoselective C–H functionalization. *Nature* **2018,** *564* (7736), 395-399.
29. Ghanem, A.; Gardiner, M. G.; Williamson, R. M.; Müller, P., First X-ray structure of a N-naphthaloyl-tethered chiral dirhodium (II) complex: structural basis for tether substitution improving asymmetric control in olefin cyclopropanation. *Chem. A Eur. J.* **2010,** *16* (11), 3291-3295.

30. Liao, K.; Pickel, T. C.; Boyarskikh, V.; Bacsa, J.; Musaev, D. G.; Davies, H. M., Site-selective and stereoselective functionalization of non-activated tertiary C–H bonds. *Nature* **2017,** *551* (7682), 609-613.
31. Yamaguchi, A. D.; Chepiga, K. M.; Yamaguchi, J.; Itami, K.; Davies, H. M., Concise syntheses of dictyodendrins A and F by a sequential C–H functionalization strategy. *J. Am. Chem. Soc.* **2015,** *137* (2), 644-647.
32. Garlets, Z. J.; Boni, Y. T.; Sharland, J. C.; Kirby, R. P.; Fu, J.; Bacsa, J.; Davies, H. M., Design, Synthesis, and Evaluation of Extended C4–Symmetric Dirhodium Tetracarboxylate Catalysts. *ACS. Catal.* **2022,** *12*, 10841-10848.
33. Qin, C.; Boyarskikh, V.; Hansen, J. H.; Hardcastle, K. I.; Musaev, D. G.; Davies, H. M., D 2-symmetric dirhodium catalyst derived from a 1, 2, 2-triarylcyclopropanecarboxylate ligand: design, synthesis and application. *J. Am. Chem. Soc.* **2011,** *133* (47), 19198-19204.
34. Qin, C.; Davies, H. M., Role of sterically demanding chiral dirhodium catalysts in site-selective C–H functionalization of activated primary C–H bonds. *J. Am. Chem. Soc.* **2014,** *136* (27), 9792-9796.
35. Fleming, G. S.; Beeler, A. B., Regioselective and Enantioselective Intermolecular Buchner Ring Expansions in Flow. *Org. Lett.* **2017,** *19* (19), 5268-5271.
36. Liao, K.; Liu, W.; Niemeyer, Z. L.; Ren, Z.; Bacsa, J.; Musaev, D. G.; Sigman, M. S.; Davies, H. M., Site-selective carbene-induced C–H functionalization catalyzed by dirhodium tetrakis (triarylcyclopropanecarboxylate) complexes. *ACS. Catal.* **2018,** *8* (1), 678-682.
37. Liao, K.; Negretti, S.; Musaev, D. G.; Bacsa, J.; Davies, H. M., Site-selective and stereoselective functionalization of unactivated C–H bonds. *Nature* **2016,** *533* (7602), 230-234.
38. Liu, W.; Ren, Z.; Bosse, A. T.; Liao, K.; Goldstein, E. L.; Bacsa, J.; Musaev, D. G.; Stoltz, B. M.; Davies, H. M., Catalyst-controlled selective functionalization of unactivated C–H bonds in the presence of electronically activated C–H bonds. *J. Am. Chem. Soc.* **2018,** *140* (38), 12247-12255.
39. Liao, K.; Yang, Y.-F.; Li, Y.; Sanders, J. N.; Houk, K.; Musaev, D. G.; Davies, H. M., Design of catalysts for site-selective and enantioselective functionalization of non-activated primary C–H bonds. *Nat. Chem.* **2018,** *10* (10), 1048-1055.
40. Ren, Z.; Musaev, D. G.; Davies, H. M., Key Selectivity Controlling Elements in Rhodium-Catalyzed C–H Functionalization with Donor/Acceptor Carbenes. *ACS. Catal.* **2022,** *12* (21), 13446-13456.
41. Davies, H. M.; Hodges, L. M.; Matasi, J. J.; Hansen, T.; Stafford, D. G., Effect of carbenoid structure on the reactivity of rhodium-stabilized carbenoids. *Tetrahedron Lett.* **1998,** *39* (25), 4417-4420.
42. Davies, H. M.; Hansen, T.; Churchill, M. R., Catalytic asymmetric C− H activation of alkanes and tetrahydrofuran. *J. Am. Chem. Soc.* **2000,** *122* (13), 3063-3070.
43. Nadeau, E.; Li, Z.; Morton, D.; Davies, H. M., Rhodium carbenoid induced intermolecular CH functionalization at tertiary CH bonds. *Synlett* **2009,** *2009* (01), 151-154.
44. Wertz, B.; Ren, Z.; Bacsa, J.; Musaev, D. G.; Davies, H. M., Comparison of 1, 2-Diarylcyclopropanecarboxylates with 1, 2, 2-Triarylcyclopropanecarboxylates as Chiral Ligands for Dirhodium-Catalyzed Cyclopropanation and C–H Functionalization. *J. Org. Chem.* **2020,** *85* (19), 12199-12211.
45. Wei, B.; Sharland, J. C.; Lin, P.; Wilkerson-Hill, S. M.; Fullilove, F. A.; McKinnon, S.; Blackmond, D. G.; Davies, H. M., In situ kinetic studies of Rh (II)-catalyzed asymmetric cyclopropanation with low catalyst loadings. *ACS. Catal.* **2019,** *10* (2), 1161-1170.
46. Pelphrey, P.; Hansen, J.; Davies, H. M., Solvent-free catalytic enantioselective C–C bond forming reactions with very high catalyst turnover numbers. *Chem. Sci.* **2010,** *1* (2), 254-257.
47. Nowlan, D. T.; Gregg, T. M.; Davies, H. M.; Singleton, D. A., Isotope effects and the nature of selectivity in rhodium-catalyzed cyclopropanations. *J. Am. Chem. Soc.* **2003,** *125* (51), 15902-15911.
48. Bien, J.; Davulcu, A.; DelMonte, A. J.; Fraunhoffer, K. J.; Gao, Z.; Hang, C.; Hsiao, Y.; Hu, W.; Katipally, K.; Littke, A., The first kilogram synthesis of beclabuvir, an HCV NS5B polymerase inhibitor. *Org. Proc. Res. & Dev.* **2018,** *22* (10), 1393-1408.

49. Lathrop, S. P.; Mlinar, L. B.; Manjrekar, O. N.; Zhou, Y.; Harper, K. C.; Sacia, E. R.; Higgins, M.; Bogdan, A. R.; Wang, Z.; Richter, S. M., Continuous Process to Safely Manufacture an Aryldiazoacetate and Its Direct Use in a Dirhodium-Catalyzed Enantioselective Cyclopropanation. *Org. Proc. Res. & Dev.* **2022**.
50. Green, S. P.; Wheelhouse, K. M.; Payne, A. D.; Hallett, J. P.; Miller, P. W.; Bull, J. A., Thermal stability and explosive hazard assessment of diazo compounds and diazo transfer reagents. *Org. Proc. Res. & Dev.* **2019,** *24* (1), 67-84.
51. Guptill, D. M.; Davies, H. M., 2, 2, 2-Trichloroethyl aryldiazoacetates as robust reagents for the enantioselective C–H functionalization of methyl ethers. *J. Am. Chem. Soc.* **2014,** *136* (51), 17718-17721.
52. Davies, H. M.; Antoulinakis, E. G., Intermolecular metal-catalyzed carbenoid cyclopropanations. *Org. React.* **2004,** *57*, 1-326.
53. Davies, H. M.; Pelphrey, P. M., Intermolecular C–H insertions of carbenoids. *Org. React.* **2004,** *75*, 75-212.
54. Pirrung, M. C.; Morehead, A. T., Saturation Kinetics in Dirhodium (II) Carboxylate-Catalyzed Decompositions of Diazo Compounds. *J. Am. Chem. Soc.* **1996,** *118* (34), 8162-8163.
55. Pacheco, C.; Magalhaes, R.; Fonseca, M.; Silveira, P.; Brandão, I., Accidental intoxication by dichloromethane at work place: Clinical case and literature review. *J. Acute Med.* **2016,** *6* (2), 43-45.
56. Friis, S. D.; Weis, E.; Johansson, M. J., HTE as a Tool in C–H Activation Reaction Discovery and Late-Stage Functionalization of Pharmaceuticals. In *The Power of High-Throughput Experimentation: Case Studies from Drug Discovery, Drug Development, and Catalyst Discovery (Volume 2)*, ACS Publications: 2022; pp 161-179.
57. Domostegui, A.; Nieto-Barrado, L.; Perez-Lopez, C.; Mayor-Ruiz, C., Chasing molecular glue degraders: screening approaches. *Chem. Soc. Rev.* **2022**.
58. Sharland, J. C.; Wei, B.; Hardee, D. J.; Hodges, T. R.; Gong, W.; Voight, E. A.; Davies, H. M., Asymmetric synthesis of pharmaceutically relevant 1-aryl-2-heteroaryl-and 1, 2-diheteroarylcyclopropane-1-carboxylates. *Chem. Sci.* **2021,** *12* (33), 11181-11190.
59. Nelson, T. D.; Song, Z. J.; Thompson, A. S.; Zhao, M.; DeMarco, A.; Reamer, R. A.; Huntington, M. F.; Grabowski, E. J.; Reider, P. J., Rhodium-carbenoid-mediated intermolecular O–H insertion reactions: a dramatic additive effect. Application in the synthesis of an ascomycin derivative. *Tetrahedron Lett.* **2000,** *41* (12), 1877-1881.
60. Fu, L.; Hoang, K.; Tortoreto, C.; Liu, W.; Davies, H. M., Formation of Tertiary Alcohols from the Rhodium-Catalyzed Reactions of Donor/Acceptor Carbenes with Esters. *Org. Lett.* **2018,** *20* (8), 2399-2402.
61. Miao, X.; Fischmeister, C.; Bruneau, C.; Dixneuf, P. H., Dimethyl carbonate: An eco-friendly solvent in ruthenium-catalyzed olefin metathesis transformations. *ChemSusChem* **2008,** *1* (10), 813-816.
62. Tundo, P.; Musolino, M.; Aricò, F., Dialkyl Carbonates in the Green Synthesis of Heterocycles. *Front. Chem.* **2019,** *7*, 300.
63. Chiappini, N. D.; Mack, J. B.; Du Bois, J., Intermolecular C (sp3)− H amination of complex molecules. *Angew. Chem. Int. Ed.* **2018,** *57* (18), 4956-4959.
64. Hansen, J.; Autschbach, J.; Davies, H. M., Computational study on the selectivity of donor/acceptor-substituted rhodium carbenoids. *J. Org. Chem.* **2009,** *74* (17), 6555-6563.
65. Xue, Y.-S.; Cai, Y.-P.; Chen, Z.-X., Mechanism and stereoselectivity of the Rh (II)-catalyzed cyclopropanation of diazooxindole: a density functional theory study. *RSC Adv.* **2015,** *5* (71), 57781-57791.
66. Lindsay, V. N.; Lin, W.; Charette, A. B., Experimental evidence for the all-up reactive conformation of chiral rhodium (II) carboxylate catalysts: enantioselective synthesis of cis-cyclopropane α-amino acids. *J. Am. Chem. Soc.* **2009,** *131* (45), 16383-16385.

Chapter 2

Cyclopropanation of Vinyl-azaheterocycles and the 2-Chloropyridine Additive Effect

2.1 Introduction

Heterocycles are ubiquitous in the pharmaceutical industry.[1, 2] The inclusion of heterocyclic functionality can transform molecule potency or biological availability by increasing the polarity of aryl regions or imparting H-bond donors into the molecule of interest.[3-6] It can be difficult for chemical methods developed in academia to break out and gain widespread adoption in the industrial sector, but any method that seeks to break into this market must be able to tolerate a diverse series of heterocycles.[7] In recent years more and more elaborate chiral cyclopropanes have been incorporated into therapeutic scaffolds, such as the trisubstituted cyclopropanes in beclabuvir (**1**),[8] paritaprevir (**2**),[9, 10] grazoprevir (**3**),[11] and paxlovid[12] (**4**, Figure 2.1). In these cases, three substituents are placed in a well-defined orientation. In some cases, the rigid and unique spatial arrangement of substituents around a trisubstituted cyclopropane can allow therapeutic molecules to project functionality into different regions of the protein of interest leading to increased potency.[13] The extreme angles of the bonds in the cyclopropane also makes them difficult to metabolize and as a result, they are often employed as ethyl bioisosteres.[14] In recent years, the incorporation of chiral cyclopropanes has become more important to industrial programs as therapeutic scaffolds have become more elaborate, highlighting the need for robust methodologies that can efficiently prepare these structural motifs.[15] The syntheses of these cyclopropanes, however, are often challenging because they contain two stereogenic centres which need to be generated in a diastereoselective and enantioselective manner.[16] A general method for the stereoselective synthesis of tri- or tetrasubstituted cyclopropanes is the rhodium-catalyzed cyclopropanation of donor/acceptor carbenes.[17] A distinctive characteristic of this cyclopropanation is its high diastereoselectivity, typically >30:1 d.r.[16] Furthermore, effective methods are available to achieve asymmetric induction either with the use of chiral auxiliaries[18] or chiral catalysts.[16, 19-23] In **Chapter 1,** a general method was described to achieve the highly

enantioselective cyclopropanation of a series of vinyl arenes and aryldiazoacetates, however, the method did not include a broad series of heterocycles.[21]

Figure 2.1: Selected examples of drug molecules containing both heterocycles and highly substituted chiral cyclopropanes.

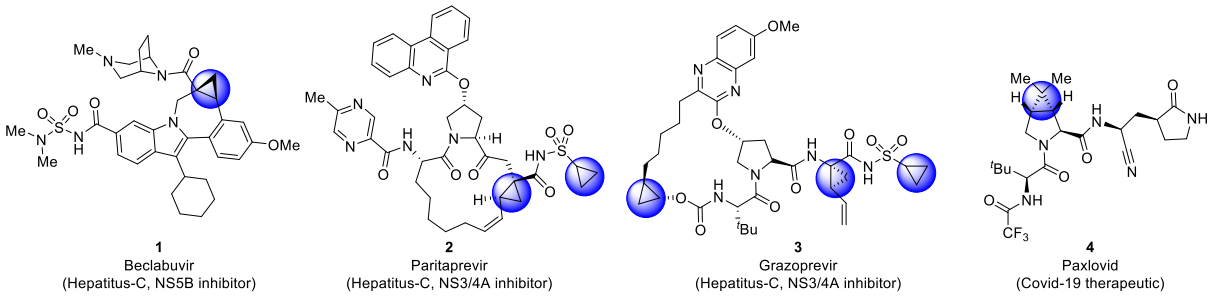

We were motivated to develop a general method to synthesize cyclopropane carboxylates with heterocyclic functionality of potential pharmaceutical interest in collaboration with scientists at AbbVie.[24] Our industrial collaborators were interested in applying this method to an ongoing drug discovery program and as a result had specific molecules of interest that were targeted for the program.[24, 25] Regardless of this target, a general method for cyclopropanation with a broad scope of aza-heterocycles would be valuable to the community at large. The proposed method represents a significant challenge because the dirhodium catalysts and the rhodium-carbene intermediates are susceptible to interactions with nucleophilic sites present in many heterocycles, which could interfere with the desired cyclopropanation unless carefully controlled.[26, 27] Nucleophiles can play two problematic roles in the reaction. The heteroatom can strongly coordinate to the rhodium face and poison the catalyst by preventing carbene formation,[28] or it can donate electrons into the empty p-orbital of the carbene, generating an ylide which leads to undesired side-products (Figure 2.2).[29, 30] **Chapter 3** will delve into ways to overcome these effects,[31] but at this stage, it was more important to tolerate a series of functionalized heterocycles.

Figure 2.2: Interactions between aza-heterocycles and rhodium catalysts/carbenes.

Catalyst poisoning via nucleophillic coordination

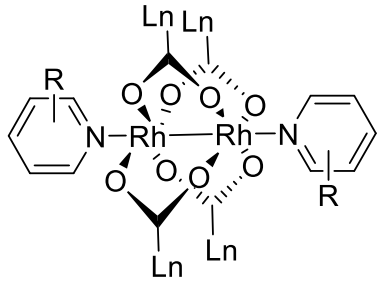

Nucleophile reacting with carbene

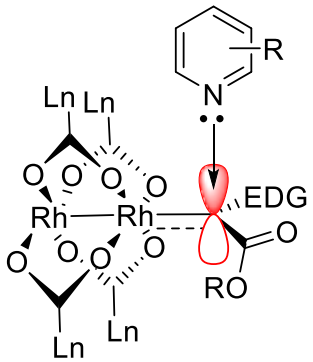

Previous studies on cyclopropanation with heteroaryldiazoacetates as substrates produced mixed results.[21, 32, 33] Rh_2(*S*-DOSP)$_4$ (**5**)-catalyzed cyclopropanation with methyl heteroaryldiazoacetates was generally high yielding and highly diastereoselective, but the levels of enantioselectivity were variable (Table 2.1, 23–89% ee).[33] In particular, heterocycles like indole and pyridine which are extremely important pharmacological motifs suffered in terms of solubility.[34] As stated in **Chapter 1**, Rh_2(*S*-DOSP)$_4$ (**5**) exhibits optimal enantioselectivity in hydrocarbon solvents, and chlorinated solvents or solvent mixtures were required to ensure solubility of many heterocycles, causing the enantioselectivity of the transformation to suffer.[33] It was also evident that nucleophilic heterocycles such as pyridine tended to poison the catalyst and forcing conditions were often required just for the cyclopropanation reaction to proceed.[28, 33] As the reaction temperature increases, so does the reactivity of the carbene which generally decreases the overall enantioselectivity of the cyclopropanation.[35, 36] The enantioselectivity in this reaction derives from the ability of the substrate to preferentially attack from one face of the carbene over the other face as dictated by the chiral environment around the dirhodium core.[37-39] As the reaction temperature increases, this energy gap becomes less relevant since all of the molecules are rotating more rapidly and both modes of attack become accessible to the substrate. As a result, the enantioselectivity decreases as can be seen in this paper.[35]

Table 2.1: Initial report on the cyclopropanation of styrene with heteroaryldiazoacetates in the presence of $Rh_2(DOSP)_4$ (**5**) yielded variable enantioselectivity across a broad substrate scope.[33]

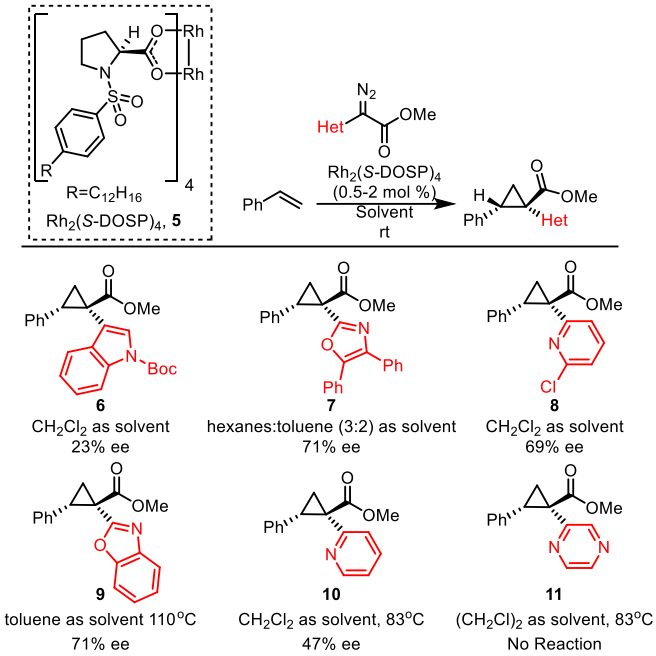

This highlights the need for robust methods to tolerate heterocyclic substrates under ambient conditions. In **Chapter 1**, a few trichloroethyl heteroaryldiazoacetates were shown to be capable of highly enantioselective cyclopropanation of styrene using Rh_2(*R*-*p*-Ph-TPCP)$_4$ (**12**) as catalyst.[21, 32] This catalyst also performs best in polar solvents like dichloromethane (CH_2Cl_2) and dimethyl carbonate ($(MeO)_2CO$) which is encouraging for tolerating heterocycles which would be more soluble in polar solvents compared to hydrocarbon media.[21] Inspired by these promising results, we decided to conduct a systematic study to determine the scope of the heterocycles that can be incorporated in both the diazo compounds and in the trapping alkenes. During early studies on cyclopropanation reactions with donor/acceptor carbenes, the Davies group developed two strategies for asymmetric induction. The first approach used α-hydroxyesters as chiral auxiliaries, and (*R*)-pantolactone was found to be particularly effective.[18] Soon thereafter, chiral dirhodium tetracarboxylate catalysts for asymmetric cyclopropanation were developed as discussed in **Chapter 1**,[16] two which, Rh_2(*R*-*p*-Ph-TPCP)$_4$[21] and Rh_2(*S*-TPPTTL)$_4$[40] (**12** and **13** respectively) play a significant role in this program.

The research program was conducted in three stages (Figure 2.3). In the first stage, a chiral auxiliary approach in combination with $Rh_2(Oct)_4$ as catalyst was used to gain rapid entry to the chiral cyclopropanes and avoid the potential interference of heterocyclic substrates with chiral catalysts.[18] This was the approach used by AbbVie to prepare their lead CFTR therapeutic and so we wanted to elaborate the protocol to highlight its utility to these substrates. The second stage explored the use of chiral catalysts to achieve cyclopropanation of vinyl heterocycles with *para*- and *meta*-substituted aryl- and heteroaryldiazoacetates, which proceeded with high yield and selectivity according to established reaction protocol with Rh_2(*R*-*p*-Ph-TPCP)$_4$ (**12**) as catalyst. The third stage studied *ortho*-substituted diazo compounds, which required considerable optimization, leading to the discovery of coordinating additives with unexpected influence on the enantioselectivity of Rh_2(*S*-TPPTTL)$_4$ (**13**), namely 2-chloropyridine. Finally, studies are described to scale-up the transformation for a multi-gram synthesis and its application to an industrial process which has subsequently been published.[25]

Figure 2.3: The cyclopropanation of aza-heterocycles proceeded in three main phases.

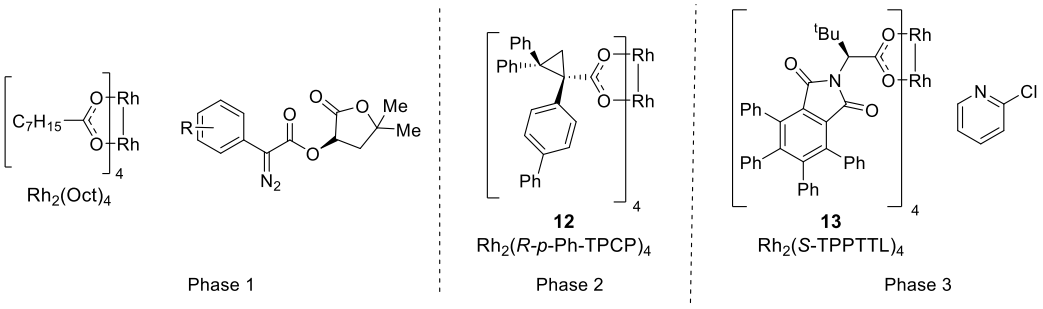

2.2 Results and discussion

At the outset of this project AbbVie required rapid access to chiral 1,2-diaryl(heteroaryl)cyclopropane-1-carboxylates. The first step was to synthesize a diverse series of vinyl heterocycles. Where the starting heteroarylaldehyde was commercially available a simple Wittig reaction was sufficient to furnish the desired substrates (**14-17**).[24] However, these Wittig reactions were often low yielding (~60% yield) and required a lengthy purification (up to 6 separate purification steps depending on the

product). For other substrates it was necessary to conduct a cross-coupling reaction between the heteroaryl bromide and vinyl-pinnacolboronate to furnish the desired substrate (**18-21**). Fortunately, AbbVie was able to provide us with generally effective conditions for these types of cross-coupling reactions leveraging an underutilized phosphine ligand[41] tetramethyl-6-phenyl-2,4,8trioxa-6-phosphaadamantane (PAPh).[42] This ligand, developed by Adjabeng in 2003, combines the qualities of a sterically bulky Buchwald ligand, with the electron donating properties of an alkyl-phosphine ligand to accelerate both the oxidative addition and reductive elimination steps in the cross-coupling.[43] This catalyst was initially developed to conduct cross-couplings with alkyl chlorides while avoiding β-hydride elimination,[42] but it can be even more effective in cross-coupling reactions with heteroaryl halides, including heteroaryl chlorides, and at very low Pd catalyst loadings (0.5 mol % Pd).[24] This reaction was used to furnish the majority of the vinyl heterocycle scope where aldehydes were not commercially available or prohibitively expensive. The remaining substrates were prepared via Chan-Lam coupling (**23-24**) or condensation to form the heterocyclic core (**22**).[24]

Scheme 2.1: Synthesis of a diverse series of vinyl-heterocycles.

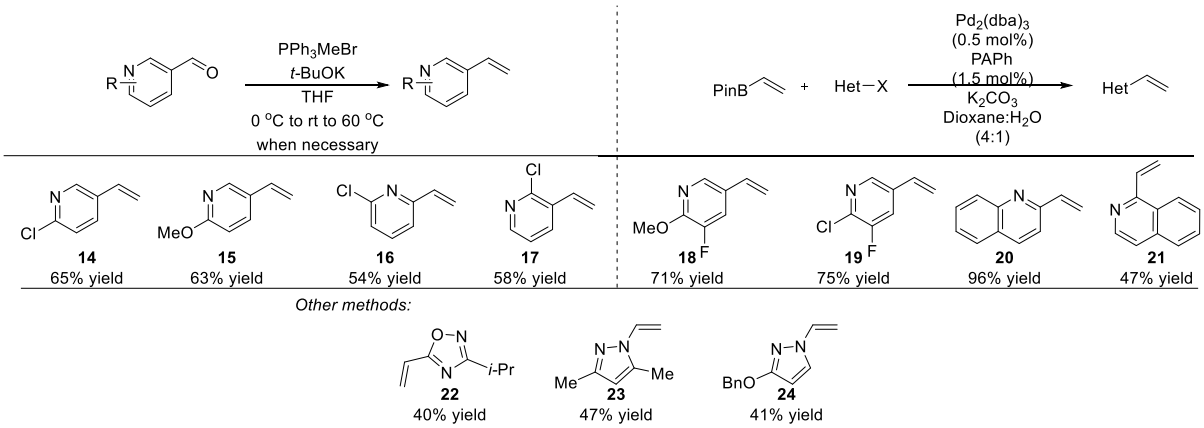

These substrates were then tested for their competency in asymmetric cyclopropanation. Initially, the reaction was performed via the chiral auxiliary approach using (*R*)-pantolactonate diazo compounds.[18] This approach is applicable to a wide range of substrates as summarized in Table 2.2. When applied towards the cyclopropanation of various vinyl heterocycles,[42, 44] the (*R*)-pantolactone-condensed-

aryldiazoacetates gave routinely high asymmetric induction (87-98% d.e.) and the process was suitable for the synthesis of a variety of heterocycle-substituted cyclopropanes. In general, reactions involving a *para*-substituted aryldiazoacetate gave slightly higher asymmetric induction than *ortho*-substituted analogues (**25-28** (97-98% d.e.) vs **29-34** (87-89% d.e.)).

Table 2.2: The cyclopropanation of aza-heterocycles using *R*-Pantolactone as a chiral auxiliary.

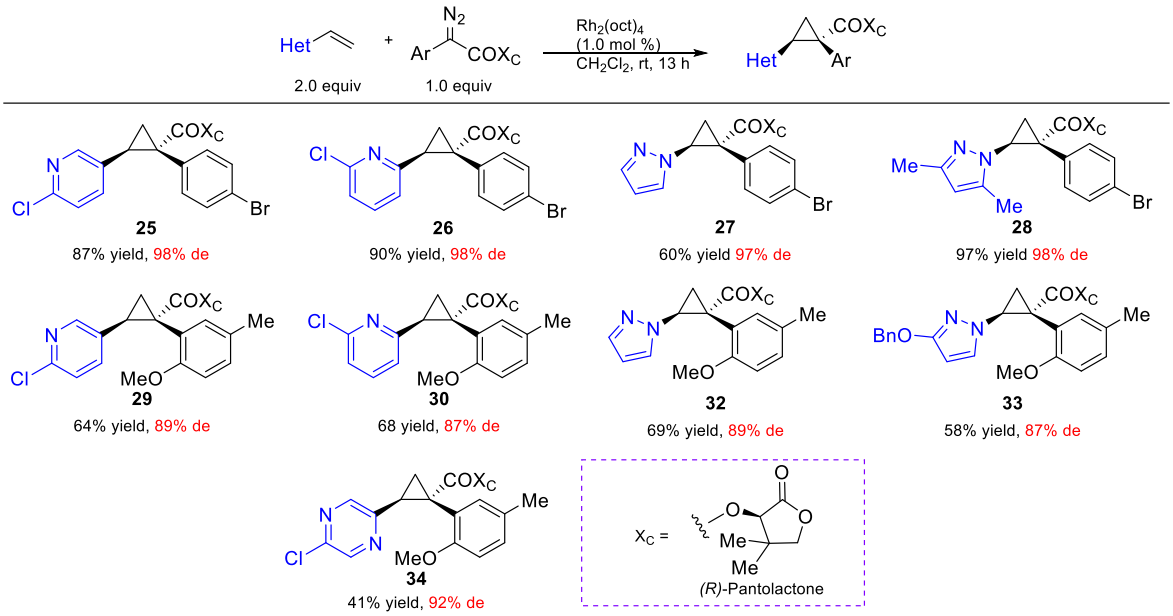

The absolute stereochemistry of **25-34** is assigned by analogy to the previously determined *Si*-face selectivity exhibited by (*R*)-pantolactone in the reactions of donor/acceptor carbenes.[18] The selectivity of this chiral auxiliary has been proposed to derive from weak interactions between the pantolactone ester carbonyl and the empty p-orbital of the carbene.[18] The carbonyl donates electron density into the *Re*-face of the carbene (if *R*-pantolactone is used as the chiral auxiliary), this controls the approach of the substrate to the carbene affording high enantioselectivity. The coordination of the ester carbonyl is a weak interaction and so asymmetric induction can be lost if the substrate displaces the carbonyl. While the chiral auxiliary approach proved generally effective, it does have limitations. The use of a stoichiometric amount of a chiral auxiliary is undesirable on large-scale due the cost and additional synthetic steps incurred for its installation and eventual removal. Additionally, only one of

the enantiomers of pantolactone is relatively inexpensive, limiting the approach to ready accessibility to only one enantiomer of the cyclopropane product.[45] For these reasons, while the (*R*)-pantolactone approach was useful for synthesizing a number of compounds in a short period of time, more contemporary methods using chiral catalysts were desirable.

Scheme 2.2: Rationale for the high enantioinduction achieved with (*R)*-Pantolactonate aryldiazoacetates.

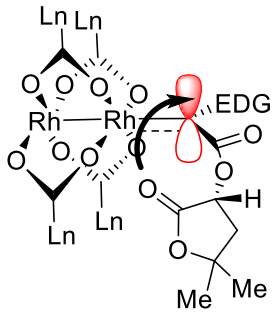

There are few previously reported examples of highly enantioselective dirhodium-catalyzed cyclopropanation involving heteroaryldiazoacetates.[21, 32, 33] Even in the case of successful methodologies, the vast excess of substrate typically used in these reactions raises concerns that vinyl heterocycles, particularly pyridine derivatives, may interfere with the catalyst[26, 46, 47] In order to evaluate the influence of different heterocycles an assortment of vinyl heterocycles (2.32 equiv)[42, 44] were reacted with a broad scope of aryl and heteroaryldiazoacetates (1.0 equiv) (Table 2.3). The catalyst selected for this study was Rh_2(*R*-*p*-Ph-TPCP)$_4$ (**12**, 0.5 mol %), which proved to be the most effective chiral dirhodium tetracarboxylate catalyst for the cyclopropanation of styrene and related vinyl-arenes as demonstrated in **Chapter 1**.[21] Under these conditions, the reaction proved to be robust and highly selective, generating a series of 1-aryl-2-heteroarylcyclopropane-1-carboxylates **35-48** with high enantioselectivity (83->99% ee). Either $(MeO)_2CO$, the optimal solvent identified in **Chapter 1**,[21] or CH_2Cl_2, a generally effective solvent for donor/acceptor carbene transformations, could be used while maintaining high enantioselectivity and the choice merely depends on substrate solubility.[24] The reactions were competent with various pyridine (**35-39**) and quinoline derivatives (**40** and **41**), as well

as five-membered heterocycles (**42** and **43**). The reactions of 2-chloro-5-vinyl pyridine were then conducted with a range of *para*- and *meta*-substituted methyl and trichloroethyl aryldiazoacetates and a styryldiazoacetate to generate the cyclopropanes **44-48**. Again, the reactions proceeded with high enantioselectivity (89-98% ee) except for the case of the 3,4-dimethoxy derivative, which generated the cyclopropane **48** in only 70% ee. The final series of reactions generated cyclopropanes **49-52** (83-95% ee) bearing two heteroaryl rings. These motifs have been completely unexplored in medicinal chemistry possibly due to the lack of available methods to furnish them with high asymmetric induction. It was our hope that this method would open new chemical space to medicinal chemists looking to explore novel motifs like these 1,2-diheteroaryl cyclopropanes.

Table 2.3: Cyclopropanation of vinyl-heterocycles with a diverse series of *para* and *meta*-substituted aryldiazoacetates and heteroaryldiazoacetates using Rh_2(*R*-*p*-Ph-TPCP)$_4$ (**12**) as catalyst.

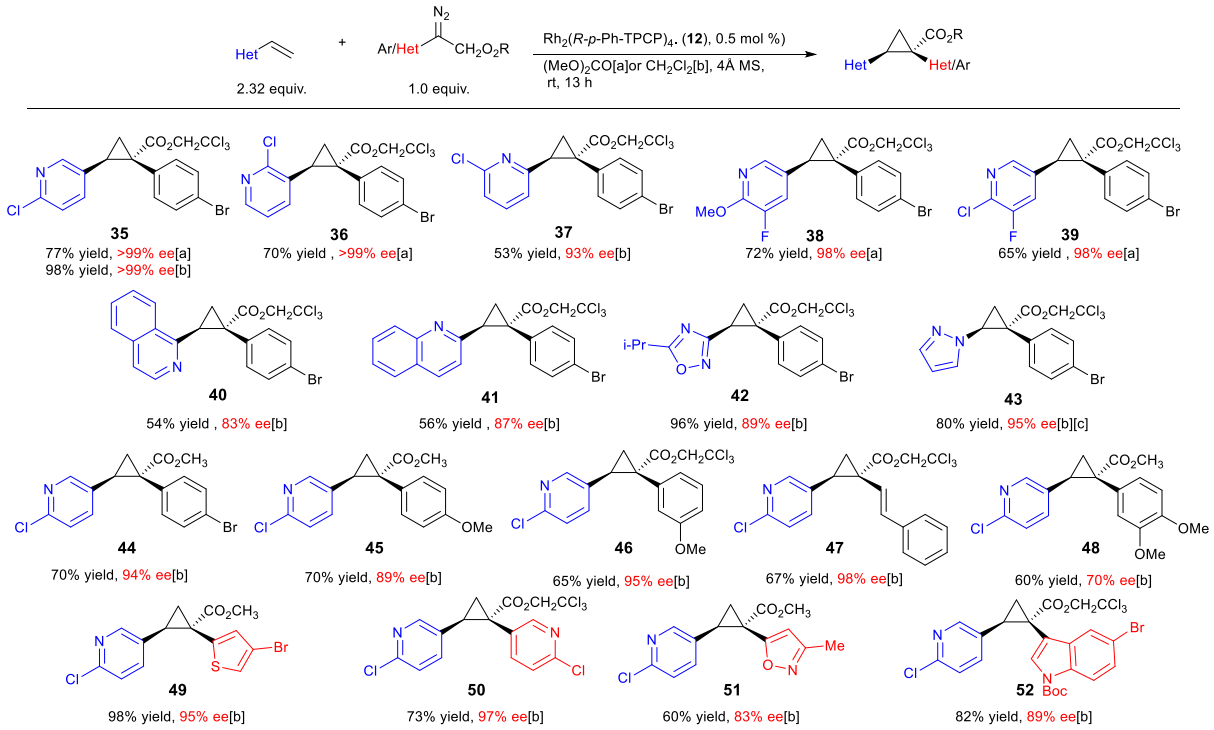

Reactions were conducted on 0.20 mmol scale with 1.0 equiv of diazo-compound, 2.32 equivalents of vinyl-heterocycle, 0.5 mol % catalyst loading (0.1 µmol) and either [a] $(MeO)_2CO$ or [b] CH_2Cl_2 as solvent depending on solubility and optimal enantioselectivity obtained. %Ee was determined by chiral HPLC, absolute configuration of **35** was determined by X-ray crystallography (CCDC 2071127). [c] Reaction was conducted with 1.0 mol % catalyst and run for 48 h at room temperature due to sluggish reactivity.

The *ortho*-substituted aryldiazoacetates were particularly desirable substrates in this study, as these were related to AbbVie's target of interest, specifically methyl 2-diazo-2-(2-methoxy-5-methylphenyl)acetate (**54**). This diazo could not be prepared via conventional diazo transfer methods due to the highly electron-donating *ortho*-methoxy substituent. Instead, this compound was prepared from the anisole via a perfectly regioselective Friedel-Crafts acylation with methyl-oxalyl chloride. The resulting keto-acetate was then converted to the hydrazone via reaction with hydrazine, which required considerable optimization to avoid dimer formation. This product was then oxidized with TsNIK, which efficiently furnished the desired diazo compound in excellent yield.[48] Unfortunately, the Rh_2(*R*-*p*-Ph-TPCP)$_4$ (**12**)-catalyzed process, using the conditions described in Table 2.3, was not successful. The test cyclopropanation of 2-chloro-5-vinylpyridine (**53**) (2.5 equiv), with the *ortho*-substituted aryldiazoacetate **54** under the optimized Rh_2(*R*-*p*-Ph-TPCP)$_4$ (**12**) conditions generated product **55** in only 30% yield and 15% ee (Table 2.4, entry 1). While the stereoselective cyclopropanation of styrene with *ortho*-chlorophenyldiazoacetate has been reported in the presence of a second-generation dirhodium tetracarboxylate catalyst, Rh_2(*S*-PTAD)$_4$ (**56**),[19] this transformation required pentane as solvent to ensure high asymmetric induction, which is incompatible with several of the vinyl heterocycles.[33] The Rh_2(*R*-DOSP)$_4$ (**5**)-catalyzed reaction of **53** with **54** generated the cyclopropane **55** in only 22% ee (Table 2.4, entry 2). Similarly, the Rh_2(*S*-PTAD)$_4$ (**56**)-catalyzed reaction gave low enantioselectivity (26% ee, Table 2.4, entry 3).

Table 2.4: Optimization of the cyclopropanation of 2-chloro-5-vinylpyridine (**54**) with an *ortho*-substituted aryldiazoacetate **55**.

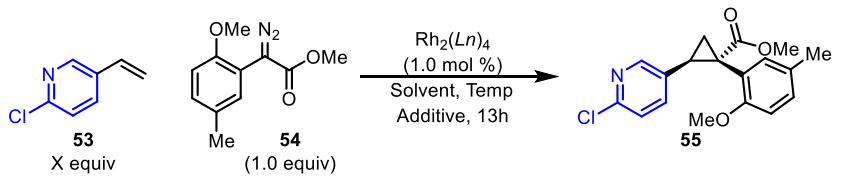

Entry	*Catalyst*	*Temp, ˚C*	*Additive*	*Solvent*	*Equiv **53***	*Ester*	*Yield, %*	*Ee, %*
1	Rh_2(*R-p*-PhTPCP)$_4$ (12)	25˚C	4Å Mol sieves	CH_2Cl_2	2.5	CH_3	30	-15
2	Rh_2(*R*-DOSP)$_4$ (**5**)	25˚C	4Å Mol sieves	CH_2Cl_2	2.5	CH_3	68	-22
3	Rh_2(*S*-PTAD)$_4$ (**56**)	25˚C	4Å Mol sieves	CH_2Cl_2	2.5	CH_3	70	-26
4	Rh_2(*R*-TPPTTL)$_4$ (**13**)	25˚C	4Å Mol sieves	CH_2Cl_2	2.5	CH_3	88	66
5	Rh_2(*R*-TPPTTL)$_4$ (**13**)	25˚C	4Å Mol sieves	$(MeO)_2CO$	2.5	CH_3	78	43
6	Rh_2(*R*-TPPTTL)$_4$ (**13**)	25˚C	4Å Mol sieves	TFT	2.5	CH_3	58	58
7	Rh_2(*R*-TPPTTL)$_4$ (**13**)	25˚C	4Å Mol sieves	CH_2Cl_2	2.5	CH_2CCl_3	47	39
8	Rh_2(*R*-TPPTTL)$_4$ (**13**)	0˚C	4Å Mol sieves	CH_2Cl_2	2.5	CH_3	85	80
9	Rh_2(*R*-TPPTTL)$_4$ (**13**)	0˚C	4Å Mol sieves	CH_2Cl_2	5.0	CH_3	**95**	**98**
10	Rh_2(*R*-TPPTTL)$_4$ (**13**)	0˚C	HFIP	CH_2Cl_2	5.0	CH_3	**93**	**92**

Due to the poor performance of the established catalysts, several of the newer catalysts were evaluated in the reaction. Rh_2(*R*-TPPTTL)$_4$ (**13**)[40, 49] emerged as the optimal catalyst for this system, giving **55** in 88% yield and 66% ee (Table 2.4). Optimization of the Rh_2(*R*-TPPTTL)$_4$ (**13**)-catalyzed reaction by changing solvent (entries 4-6) or changing from the methyl ester to trichloroethyl ester (entry 7), did not improve the reaction. Lowering the reaction temperature to 0 °C increased the level of asymmetric induction to 80% ee (entry 8). The most dramatic effect, however, was to increase the amount of the 2-chloro-5-vinylpyridine (**53**) to 5 equiv, which resulted in the formation of **55** in 95% yield and 98% ee in combination with lower reaction temperature (Table 2.4, entry 9).[27, 50-54] Even though the optimization studies resulted in a considerable improvement in the effectiveness of the reaction, we were concerned that the reaction would not be amenable to scale up. Through Karl-Fischer titrations of the reaction mixture, it was found that as little as 8 ppm water in the reaction harmed the enantioselectivity of the transformation.[24, 25] Interestingly, we never saw appreciable generation of the O–H insertion product which would suggest that coordination of water to the carbene complex during the transformation was responsible for the decrease in enantioselectivity. In

order to control the water content, it was found that 1000 wt % of 4Å molecular sieves was required to ensure a reproducible transformation. Even if the reaction vials were flame dried prior to addition of the reagents, we were unable to avoid the need for molecular sieves. It was later discovered that the vinyl-heterocycles are hygroscopic, and tested samples contain as much as 200 ppm water which could account for the requirement for addition of drying agents to the reaction in addition to rigorous drying of the reaction vessel.[25] Nevertheless, this vast excess of molecular sieves was undesirable for AbbVie's process for a multitude of reasons and so it was important to identify alternative dehydrating strategies for the reaction. We have reported that 1,1,1,3,3,3-hexafluoroisopropanol (HFIP, **57**) has beneficial effects on certain rhodium-catalyzed carbene reactions (Figure 2.4), and it has been shown to subtly alter reactivity and selectivity in various transformations.[49, 55] Therefore, we decided to explore its effect on the optimized cyclopropanation, and we were pleased to observe that 10 equiv of HFIP could be used in place of the 1000 wt % 4Å molecular sieves with retention of high enantioinduction (entry 10). HFIP acts as a powerful hydrogen-bonding agent and it was hypothesized that it sequesters water away from the dirhodium catalyst.[56-58] As a stronger Lewis acid, HFIP can outcompete the weak Lewis acidic rhodium, and it is a privileged secondary alcohol inert to the rhodium carbene.[59] Other fluorinated alcohols were tested but they do not possess the correct balance of nucleophilicity and Lewis acidity to operate effectively as both a water sequestration agent and an inert additive in carbene chemistry. These properties make HFIP an attractive alternative to molecular sieves as a dehydrating agent although it has a much greater potential to influence rhodium carbene chemistry as will be explored in **Chapter 3**.[31]

Figure 2.4: 1,1,1,3,3,3-Hexafluoroisopropanol (**57**) acts as a powerful hydrogen-bonding agent.

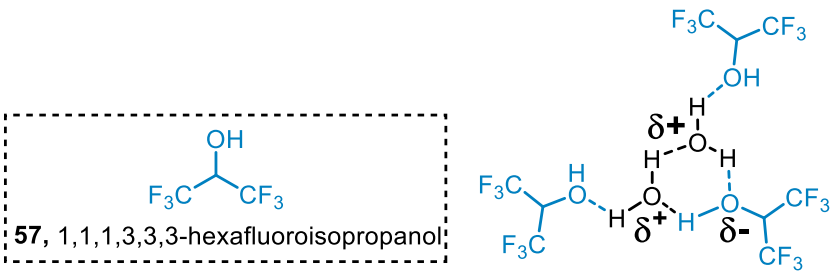

The optimized conditions developed in Table 2.4, were then applied to a range of substrates, but mixed results were obtained (Table 2.5). Interestingly, while the Rh_2(*S*-TPPTTL)$_4$ (**13**)-catalyzed reactions of aryldiazoacetate **54** with various vinyl 2-chloropyridines to form the cyclopropanes **55, 58,** and **59** were highly enantioselective (90-98% ee), the cyclopropanation of styrene with various *ortho*-substituted aryldiazoacetates generated the cyclopropanes **60-62** with low to moderate levels of enantioselectivity (4-64% ee). Improved enantioselectivity was obtained in the formation of cyclopropane **63** (77% ee), derived from a 2-chloropyridyldiazoacetate. The large variation in the levels of enantioselectivity was initially considered to be caused by trace impurities. In their optimization of the cyclopropanation of a styryldiazoacetate with a styrene derivative for their multi-Kg synthesis of the Hepatitis C drug Beclabuvir, BMS identified that trace amounts of triphenyl phosphine (PPh_3) from the Wittig reaction used to furnish the styrene derivative were responsible for crippling the enantioselectivity of the catalyst in question, Rh_2(*R*-DOSP)$_4$ (**5**).[8] Since the vinyl-pyridine substrates were often synthesized via Wittig reaction, the same types of impurities might be at play in this case. But even by repeating the reactions with very carefully purified reagents, rigorously dry conditions, or alkenes not synthesized via Wittig reaction the enantioselectivity remained poor.[60] After a great deal of consideration, we identified that **55, 58, 59,** and **63** all contain a 2-chloropyridyl component and are formed with high levels of enantioselectivity, whereas the substrates that performed poorly all lacked this motif. Therefore, it was proposed that a 2-chloropyridyl group may play a critical role in enhancing the enantioselectivity of the cyclopropanation. Such an effect would be consistent with the observed beneficial effect when using a large excess (5 equiv) of 2-chloro-5-vinylpyridine (**53**) seen in Table 2.2, entry 9.

Table 2.5: The substitution dependant effect of 2-chloropyridine on asymmetric cyclopropanation in the presence of Rh_2(*S*-TPPTTL)$_4$ (**13**).

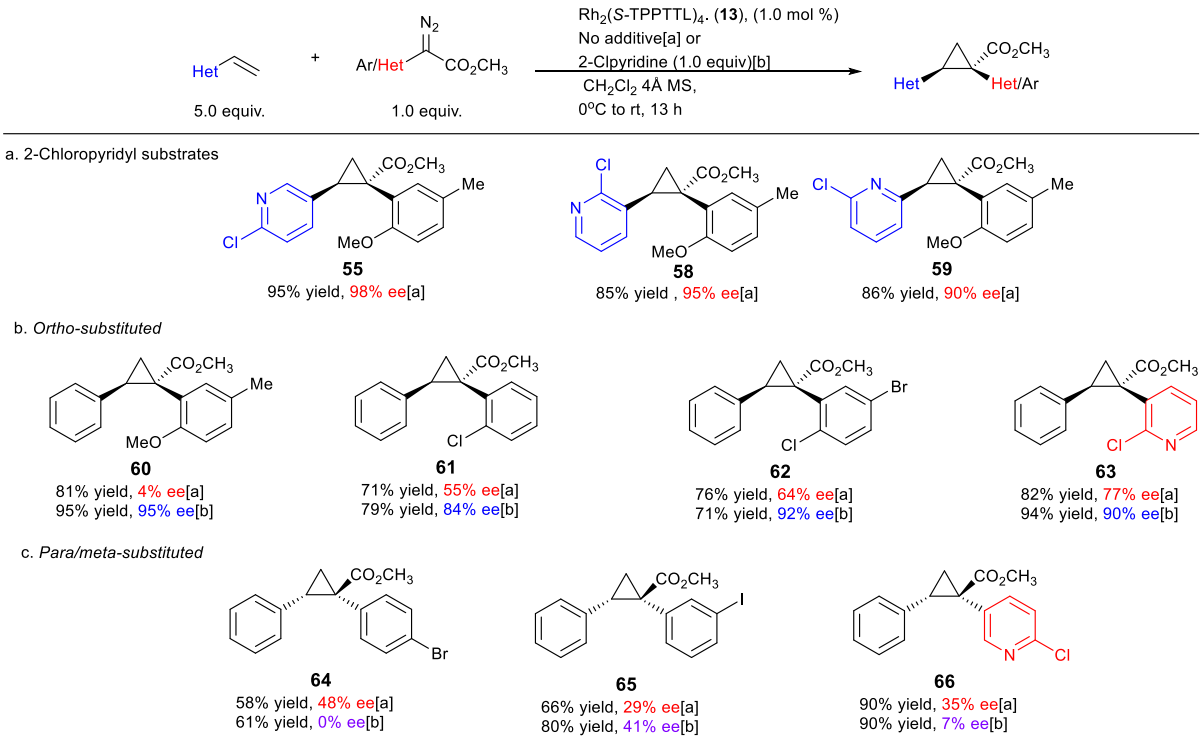

a. Initial scope of vinyl heterocycles compatible with ortho-aryldiazoacetate cyclopropanation. Reactions were conducted on 0.20 mmol scale with 1.0 mol % catalyst loading and DCM as solvent. b. Rh_2(*S*-TPPTTL)$_4$-catalyzed cyclopropanation of styrene with various aryldiazoacetates [a] without additive and [b] with 1.0 equiv of 2-Clpyridine as a coordinating additive. Reactions were conducted on 0.20 mmol scale with 1.0 mol % catalyst loading (0.2 µmol) and DCM as solvent. The absolute configuration of **59** was determined by X-ray crystallography(CCDC 2071154). The absolute configuration of **55, 58-63** is tentatively assigned by analogy to **59**. The absolute configuration of **64-66** is assigned by analogy to the X-ray characterization of the para-substituted product **35**. Rh_2(*S*-TPPTTL)$_4$ affords the opposite configuration in cyclopropanations involving *ortho*-substituted aryldiazoacetates vs. *para*-substituted analogues.

A control reaction was conducted to test this hypothesis. The cyclopropanation to form **60** was repeated in the presence of 1 equiv 2-chloropyridine as an additive. The modified conditions caused a dramatic effect on the enantioselectivity with **60** being formed in 95% ee compared to 4% ee in the absence of the additive. A systematic study was conducted with a range of pyridine and quinoline analogues, which revealed that 2-choropyridine and 2-fluoropyridine were the optimum additives, performing the reaction with similarly high levels of enantio-enhancement (Table 2.6). Pyridines lacking a substituent adjacent to nitrogen tended to poison the catalyst. Quinoline and other 2-substituted pyridines, such as 2-methoxypyridine, also provided considerable enhancement of enantioselectivity (70-92% ee) but none proved superior to 2-chloropyridine in this reaction. The use of additives to enhance the selectivity and reactivity of rhodium catalyzed reactions is not a novel

phenomenon.[27, 51, 61, 62] Several approaches have been used in the past, from the use of axial coordinating tethered ligands[53] to the inclusion of *bis*-DMAP-CH_2Cl_2[50] and *N,N,N'N'*-tetramethyl urea[63] to improve reactivity. This phenomenon has never been observed in the presence of 2-chloropyridine, however. Additionally, though improvement of reactivity is often observed through the addition of axially coordinating ligands additives that enhance enantioselectivity are rare.[50, 64] Solvent effects can change the enantioselectivity of transformations as demonstrated in **Chapter 1** and these effects could be also be related to axial coordination.[21]

Table 2.6: Various heterocyclic and non-heterocyclic additives were assessed for their ability to enhance the enantioselectivity of *ortho*-substituted aryldiazoacetates.

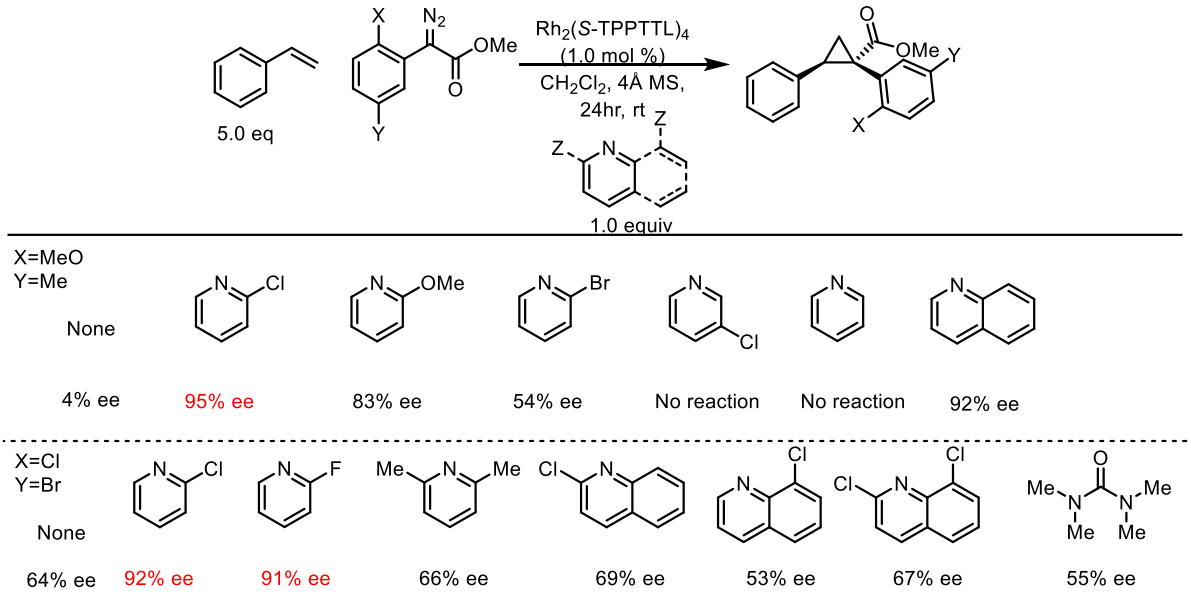

The unexpected positive influence of 2-chloropyridine, prompted us to further evaluate its impact. The Rh_2(*S*-TPPTTL)$_4$ (**13**)-catalyzed cyclopropanation of styrene with representative aryl- and pyridyldiazoacetates were explored under the established system, in the presence or absence of 2-chloropyridine (Table 2.5). In the case of the cyclopropanes **61** and **62** derived from cyclopropanation of styrene with *ortho*-substituted aryldiazoacetates, the presence of 2-chloropyridine in the reaction improved the enantioselectivity from 55-77% ee to 84-92% ee. In contrast to Rh_2(*R*-*p*-Ph-TPCP)$_4$ (**12**), Rh_2(*S*-TPPTTL)$_4$ (**13**) is not a particularly effective chiral catalyst for the formation of the cyclopropanes

64-66, derived from diazo compounds lacking *ortho*-substituents. The enantioselectivity is low in the absence of additive (29-48% ee) and even worse in the presence of 2-chloropyridine (0-41% ee). These studies demonstrated that while 2-chloropyridine as an additive can greatly enhance the enantioselectivity of Rh_2(*S*-TPPTTL)$_4$ (**13**)-catalyzed cyclopropanation, the effect is unique to *ortho*-substituted aryl- and heteroaryldiazoacetates. Other catalysts were evaluated for this effect, but it appeared to be unique to Rh_2(TPPTTL)$_4$ (**13**). The reasons for this enhancement are not well understood but *in silico* investigations into the phenomenon will be discussed in **Chapter 4**. Additionally, *ortho*-substituted aryldiazoacetates gave the opposite enantiomer in combination with Rh_2(*S*-TPPTTL)$_4$ (**13**) which is highly unusual for this chemistry.[19] Most chiral dirhodium tetracarboxylate catalysts give the same enantiomer of the product regardless of the carbene used, and this inversion was extremely puzzling.[16, 19, 20, 65] Furthermore, it was unrelated to the presence of 2-chloropyridine, and the same enantiomer was observed with or without the additive, albeit with different levels of enantioselectivity.[24] To try and solve these mysterious effects, a computational campaign began and the results of these experiments will be summarized in **Chapter 4**. Regardless of our lack of rationale for the effect at this stage, the reaction was extremely reliable and generalizable, hence a scope was investigated to illustrate the applications of this chemistry.

Despite the specificity of these conditions, the effect is generalizable to any *ortho*-substituted aryldiazoacetate across a broad scope. The reactions of *ortho*-substituted aryldiazoacetates was examined with a range of vinyl heterocycles as illustrated in the formation of the cyclopropanes **76-81** (Table 2.7). As many of the vinyl heterocycles are expensive or are not commercially available the reactions were caried out with just 1.5 equiv of the vinyl heterocycle and 3.5 equiv of 2-chloropyridine. The reactions were compatible with a range of heterocycles, including pyridines (**67-69**), quinolines (**72, 73**), a pyrazine (**70**), pyrazoles (**71, 75**), and an oxadiazole (**74**). The reactions proceeded to form the cyclopropanes with generally very high enantioselectivity, ranging from 86% ee to >99% ee. The reaction could also be conducted with methyl 2-(2-chloropyridin-3-yl)-2-diazoacetate and in this case,

1,2-diheteroarylcycloproane carboxylates **82-85** were formed in 72-95% ee. Effective reactions could be caried out using either 4Å molecular sieves or HFIP as dehydrating additive without a dramatic effect on enantioselectivity. Unlike water, 2-chloropyridine is a very poor nucleophile (pKa=0.74) and as a result it is incapable of forming an acid-base pair with HFIP, therefore it's enantioselectivity enhancing effects are preserved regardless of the presence of HFIP.[58, 66] In the case of **55**, **67**-**69** the products were formed with high enantioselectivity using both sets of conditions.

Table 2.7: Scope of cyclopropanation with vinyl-heterocycles under the optimized *ortho*-aryldiazoacetate conditions.

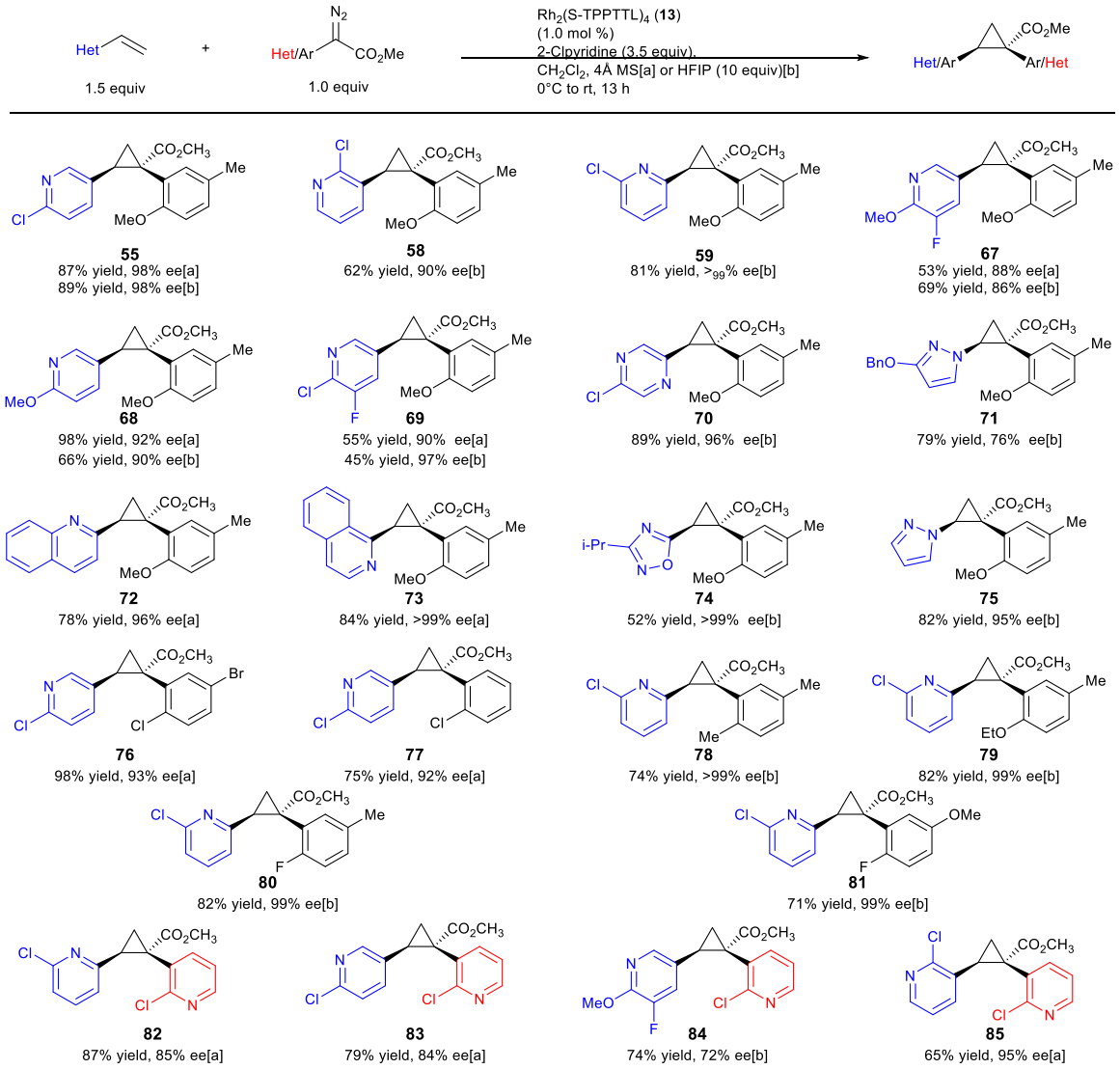

Reactions were conducted on 0.20 mmol scale with 1.0 mol % Rh_2(*S*-TPPTTL)$_4$ (0.2 µmol) CH_2Cl_2 as solvent, and a reduced loading of vinyl-heterocycle (1.5 equiv) balanced out with 2-chloropyridine (3.5 equiv) with [a] 10 weight equiv. 4Å molecular sieves or [b] HFIP (10 equiv.). The absolute configuration of all compounds is assigned by analogy to that of **59,** which was determined by X-ray crystallography (CCDC 2071154).

Exploratory studies were also conducted by AbbVie scientists to determine whether the cyclopropanation reactions were amenable to scale-up.[8, 63, 67-69] The replacement of molecular sieves with HFIP enabled the reaction to be performed on multi-gram scale, providing **59** in 95% yield and 98% ee (Scheme 2.3). Performing the reaction on large scale also enabled the use of considerably lower catalyst loading (0.16 mol % vs. 1.0 mol %). The reaction was conducted at lower temperature to ensure high enantioselectivity regardless of local exotherms, a common trend for dirhodium catalyzed asymmetric cyclopropanation by donor/acceptor carbenes.[18]

Scheme 2.3: Gram scale cyclopropanation of **16**.

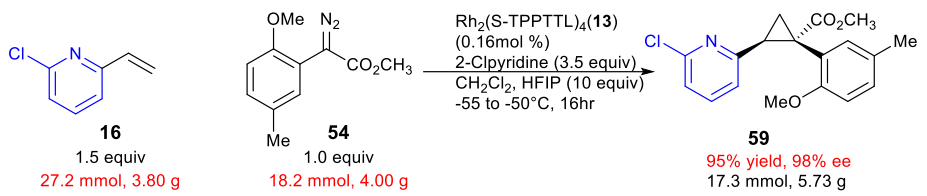

Ultimately, for the reaction to be amenable to very large scale synthesis, the diazo compound would need to be generated in flow to avoid working with large quantities of a high energy intermediate.[70] Fortunately, a copper-catalyzed method for the synthesis of diazo compounds from hydrazones was recently reported, in which the only by-product is water.[71, 72] The copper catalyzed-reaction is greatly accelerated with *N,N*-dimethyl aminopyridine (DMAP), but DMAP, a very nucleophilic pyridine, would be expected to poison the catalyst or react with the carbene under mild conditions.[46, 50] Therefore, we conducted exploratory studies to determine if the unpurified diazo compound from a copper-catalyzed oxidation can be directly used in the rhodium-catalyzed reaction. The copper-catalyzed oxidation of **67** in the presence of DMAP in air generated the desired diazo compound **36** in essentially quantitative yield after stirring for 30 min. This method was later adapted to a flow process by Dr. Bo Wei through collaborations with the Jones group at Georgia Tech.[72] Addition of the resulting solution to another reaction flask containing the reagents for a rhodium-catalyzed cyclopropanation failed to proceed unless HFIP was present.[73] In the presence of HFIP (20 equiv), the cyclopropane was formed

in 83% yield and 98% ee (Scheme 2.5). The HFIP in this case is playing a dual role, both deactivating the undesired effects of DMAP but still allowing the desirable influence of 2-chloropyridine to occur.

Scheme 2.4: Sequential copper-catalyzed diazo formation followed by a rhodium-catalyzed cyclopropanation.[72-74]

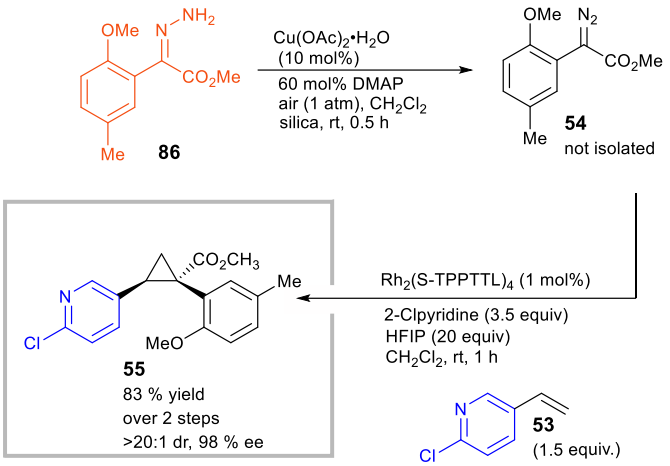

One of the most intriguing features of this study was the dramatic role of additives on reactions involving *ortho*-substituted aryl- and heteroaryldiazoacetates. Typically, the enantioselectivity of rhodium-catalyzed cyclopropanation is not greatly influenced by trace moisture. Certainly, water will tend to cause a decrease in yield because it will competitively react with the carbene. In the case of *ortho*-substituted diazo compounds, trace moisture had a dramatically negative influence and dehydrating agents were essential for reproducibly high enantioselectivity. It was surprising that HFIP could be used in the place of molecular sieves and achieve similar levels of enantioselectivity. HFIP has been demonstrated to have a positive influence on a range of reactions,[56, 59, 75-80] but the role of HFIP in rhodium-catalyzed cyclopropanation was not definitively known at this stage though it was postulated that HFIP engaged in hydrogen-bonding with the water blocking its interference.[76, 81, 82] The most unexpected effect was the role of 2-chloropyridine which was absolutely necessary for high asymmetric induction. In order to understand the influence of 2-chloropyridine, crystals were grown of the 2-chloropyridine complex of Rh_2(*S*-TPPTTL)$_4$ (**13**)(Figure 2.5). The crystal structure contained 2-chloropyridine molecules bound to each rhodium axial site and one additional 2-chloropyridine

situated within the bowl of **13**. An overlay of the previously reported crystal structure of the catalyst[40] and the 2-chloropyridine-coordinated catalyst are shown in Figure 2.5. An intriguing feature of the two overlaid structures is that one of the ligands has been considerably displaced upon coordination to 2-chloropyridine. This led to the hypothesis that appropriate coordinating additives can alter the shape of the catalyst, which was responsible for the change asymmetric induction observed. Certainly, additives that would be expected to coordinate to the axial position of the dirhodium have been shown to influence the general outcome of carbene reactions, but the influence on enantioselectivity has not been extensively explored.[21, 27, 54, 62, 64, 83, 84] While this was our initial theory on how 2-chloropyridine improves catalyst enantioselectivity, the effect is likely to be more intimately related with the carbene intermediate responsible for stereoselectivity. Efforts to identify the rationale behind this phenomenon will be explored in more detail in **Chapter 4**. The cyclopropanation of **53** with **54** generated *in situ* illustrates the additive effects of HFIP and 2-chloropyridine in concert.

Figure 2.5: Structural perturbations in **13** enforced by the coordination of 2-chloropyridine based on X-ray analysis of a single crystal of **13** coordinated to 2-chloropyridine (CCDC 2071667). The top-right ligand is displaced from its original position (green) upon coordination with 2-chloropyridine (blue). The axially coordinated ligands including 2-chlorpyridine ligand located inside of the bowl of the catalysts have been removed in order to give greater clarity of the overlaid structure of the catalysts.

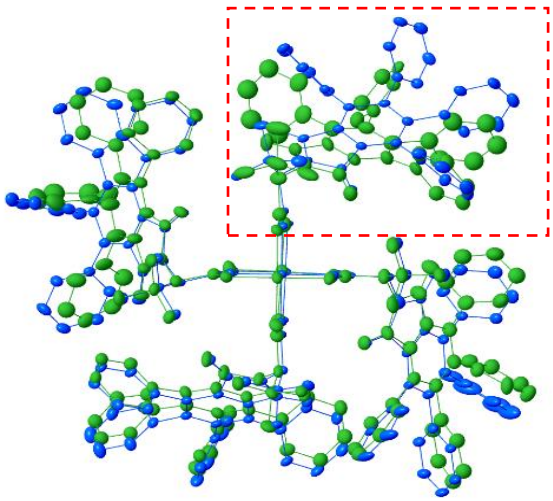

Without the presence of HFIP, the reaction cannot proceed, suggesting that DMAP acts as a poison to the rhodium catalyst, coordinating to the axial position and preventing carbene formation. However, in the presence of HFIP, the DMAP cannot coordinate, suggesting an interaction between DMAP and HFIP, possibly through hydrogen bonding. 2-Chloropyridine, however, is considerably less basic than DMAP,[66] and apparently does not interact with HFIP in the same manner. As a result, the poisonous influence of DMAP is selectively deactivated while the beneficial coordination of 2-chloropyridine proceeds undisturbed. This provides a unique opportunity to expand the scope of dirhodium-catalyzed reactions. If nucleophilic poisons as strong as DMAP can be selectively deactivated without interfering with reaction enantioselectivity, then perhaps other nucleophiles could also be removed from the equation. Efforts to explore this effect will be detailed in **Chapter 3**.[31]

Figure 2.6: Proposed mechanism of selective deactivation of aza-heterocycles by HFIP, with retention of the additive enhancement of 2-chloropyridine for the cyclopropanation of *ortho*-substituted aryldiazoacetates.

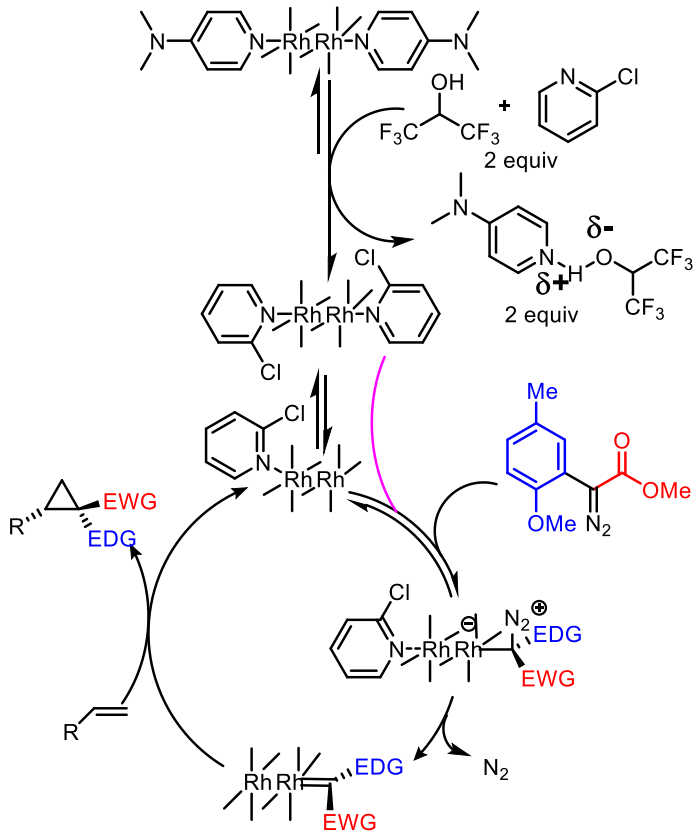

Having designed and optimized a robust and highly enantioselective cyclopropanation of *ortho*-substituted aryldiazoacetates, AbbVie was able to apply this chemistry on 100 g scale to furnish a key intermediate for a CFTR API. While we had demonstrated that in-flow diazo synthesis would be amendable to telescoping with this reaction, process chemists at AbbVie had safety concerns about the copper-catalyzed approach.[72-74] Instead, the scientists at AbbVie developed a different approach to synthesizing the diazo in-flow via a modified Bamford-Stevens elimination from the corresponding sulfonyl hydrazone (Figure 2.7).[25] They then telescoped this transformation with the cyclopropanation reaction and were able to run the reaction at large scale with excellent enantioselectivity (74% yield, 98% ee). AbbVie had concerns about the use of 2-chloropyridine in the reaction as it is a potent toxin and can be difficult to remove from the resultant product.[85] To combat these concerns, the use of 2-fluoropyridine was suggested and preliminary experiments in the Davies lab confirmed that use of this alternative additive would preserve high enantioselectivity for the substrate of interest.

Figure 2.7: Large scale flow-batch synthesis of an API for the treatment of CFTR performed by AbbVie scientists.[25]

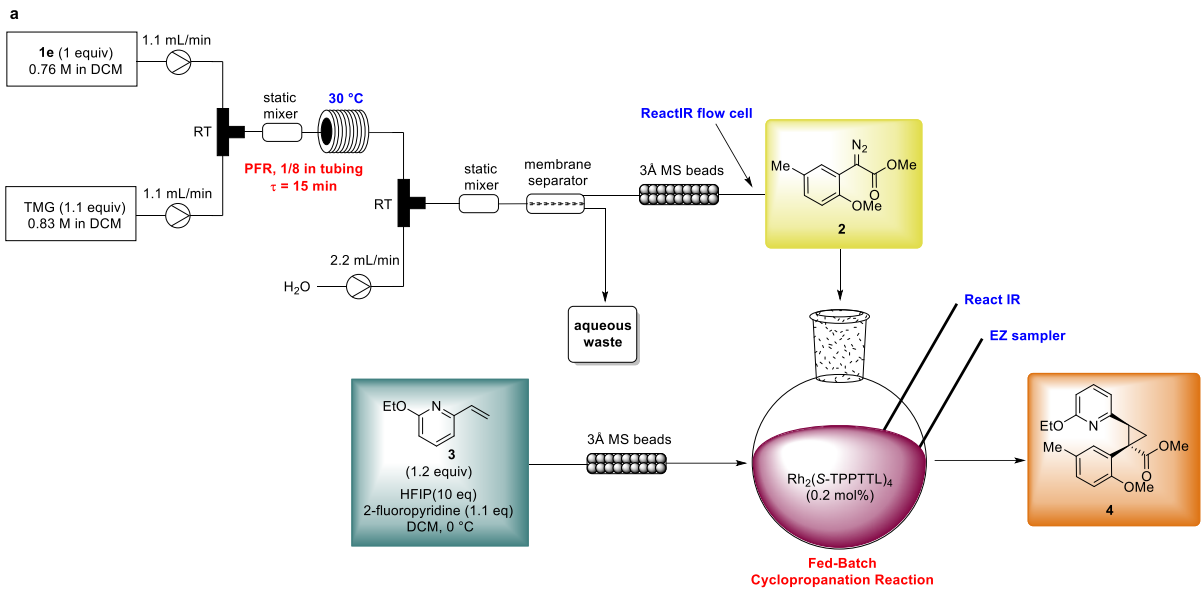

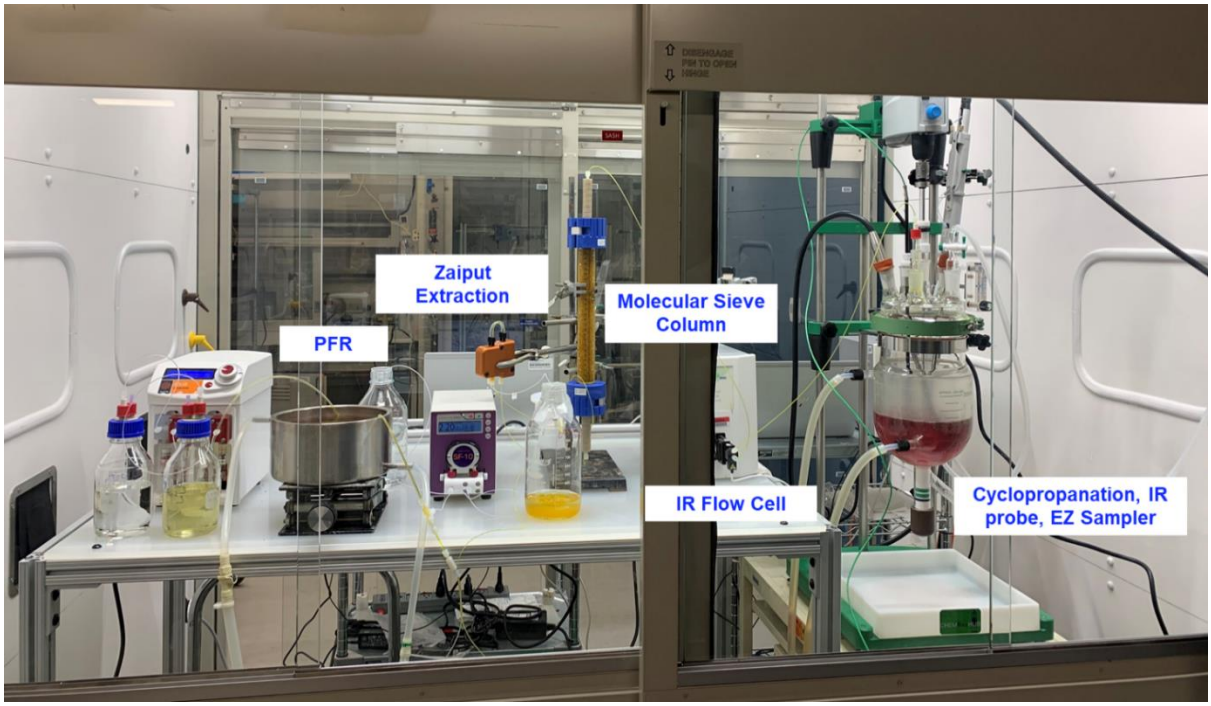

2.3 Conclusion:

Complementary general methodologies for the syntheses of heterocycle-substituted cyclopropanes were developed. Use of (*R*)-pantolactone as a chiral auxiliary was identified as a fast and reliable way

to synthesize 1-aryl-2-heteroaryl- and 1,2-diheteroarylcyclopropane-1-carboxylates with predictably high enantioselectivity, however the limitations of using a chiral auxiliary had to be overcome to convert this reaction into a practical method. Alternatively, 1-aryl-2-heteroaryl- and 1,2-diheteroarylcyclopropane-1-carboxylates could be generated with high enantioselectivity using chiral catalysts after considerable optimization. *Para* or *meta*-substituted aryldiazoacetates performed predictably and with high selectivity Rh_2(*R*-*p*-Ph-TPCP)$_4$ (**12**) as catalyst and the method outlined in **Chapter 1**. The reaction could also be extended to several heteroaryldiazoacetates, enabling access to 1,2-diheteroarylcyclopropane carboxylates, a novel motif which could be useful for medicinal chemists interested in exploring new chemical space. *Ortho*-substituted aryldiazoacetates, however, proved incompatible with these conditions and a different chiral catalyst, Rh_2(*S*-TPPTTL)$_4$ (**13**) was required. During these studies, the role of additives was found to have a major influence. 2-Chloropyridine was discovered as a coordinating additive capable of significantly enhancing the enantioselectivity of cyclopropanation involving *ortho*-substituted aryldiazoacetates. These efforts resulted in a robust and generalizable methodology which was performed on multi-gram scale and made more process-amenable by substituting 4Å molecular sieves for HFIP (**57**) to desensitize the reaction to H_2O. This *in situ* desensitization was further exploited to perform the reaction with aryldiazoacetate generated in situ from the corresponding hydrazone using copper-catalyzed oxidation. Finally, the reaction was conducted on 100g scale by scientists at AbbVie in a flow-batch process for the synthesis of an API for the treatment of CFTR, with the potential to afford 0.5 kg of product per day if run in a continuous process. These unique additive effects have broad implications for other rhodium-catalyzed carbene reactions which will be explored in more detail in subsequent chapters.

2.4 References:

1. Vitaku, E.; Smith, D. T.; Njardarson, J. T., Analysis of the structural diversity, substitution patterns, and frequency of nitrogen heterocycles among US FDA approved pharmaceuticals: miniperspective. *J. Med. Chem.* **2014,** *57* (24), 10257-10274.

2. Mancini, R. S.; Barden, C. J.; Weaver, D. F.; Reed, M. A., Furazans in medicinal chemistry. *J. Med. Chem.* **2021,** *64* (4), 1786-1815.
3. Charifson, P. S.; Walters, W. P., Acidic and basic drugs in medicinal chemistry: a perspective. *J. Med. Chem.* **2014,** *57* (23), 9701-9717.
4. Kumari, S.; Carmona, A. V.; Tiwari, A. K.; Trippier, P. C., Amide bond bioisosteres: strategies, synthesis, and successes. *J. Med. Chem.* **2020,** *63* (21), 12290-12358.
5. Kuhn, B.; Mohr, P.; Stahl, M., Intramolecular hydrogen bonding in medicinal chemistry. *J. Med. Chem.* **2010,** *53* (6), 2601-2611.
6. Caron, G.; Kihlberg, J.; Ermondi, G., Intramolecular hydrogen bonding: An opportunity for improved design in medicinal chemistry. *Med. Res. Rev.* **2019,** *39* (5), 1707-1729.
7. Schultz, D.; Campeau, L.-C., Harder, better, faster. *Nat. Chem.* **2020,** *12* (8), 661-664.
8. Bien, J.; Davulcu, A.; DelMonte, A. J.; Fraunhoffer, K. J.; Gao, Z.; Hang, C.; Hsiao, Y.; Hu, W.; Katipally, K.; Littke, A.; Pedro, A.; Qiu, Y.; Sandoval, M.; Schild, R.; Soltani, M.; Tedesco, A.; Vanyo, D.; Vemishetti, P.; Waltermire, R. E., The First Kilogram Synthesis of Beclabuvir, an HCV NS5B Polymerase Inhibitor. *Org. Process. Res. Dev.* **2018,** *22* (10), 1393-1408.
9. Carrion, A. F.; Gutierrez, J.; Martin, P., New antiviral agents for the treatment of hepatitis C: ABT-450. *Expert Opin. Pharmacother.* **2014,** *15* (5), 711-716.
10. Caspi, D. D.; Cink, R. D.; Clyne, D.; Diwan, M.; Engstrom, K. M.; Grieme, T.; Mei, J.; Miller, R. W.; Mitchell, C.; Napolitano, J. G., Process development of ABT-450–A first generation NS3/4A protease inhibitor for HCV. *Tetrahedron* **2019,** *75* (32), 4271-4286.
11. Xu, F.; McCauley, J. A., Discovery and Chemical Development of Grazoprevir: An HCV NS3/4a Protease Inhibitor for the Treatment of the Hepatitis C Virus Infection. In *Complete Accounts of Integrated Drug Discovery and Development: Recent Examples from the Pharmaceutical Industry Volume 3*, ACS Publications: 2020; pp 285-312.
12. Wen, W.; Chen, C.; Tang, J.; Wang, C.; Zhou, M.; Cheng, Y.; Zhou, X.; Wu, Q.; Zhang, X.; Feng, Z., Efficacy and safety of three new oral antiviral treatment (molnupiravir, fluvoxamine and Paxlovid) for COVID-19 : a meta-analysis. *Ann. Med. Res.* **2022,** *54* (1), 516-523.
13. Talele, T. T., Opportunities for tapping into three-dimensional chemical space through a quaternary carbon. *J. Med. Chem.* **2020,** *63* (22), 13291-13315.
14. Meanwell, N. A., The influence of bioisosteres in drug design: tactical applications to address developability problems. In *Tactics in Contemporary Drug Design*, Springer: 2013; pp 283-381.
15. Talele, T. T., The “cyclopropyl fragment” is a versatile player that frequently appears in preclinical/clinical drug molecules. *J. Med. Chem.* **2016,** *59* (19), 8712-8756.
16. Davies, H. M. L.; Bruzinski, P. R.; Lake, D. H.; Kong, N.; Fall, M. J., Asymmetric Cyclopropanations by Rhodium(II) N-(Arylsulfonyl)prolinate Catalyzed Decomposition of Vinyldiazomethanes in the Presence of Alkenes. Practical Enantioselective Synthesis of the Four Stereoisomers of 2-Phenylcyclopropan-1-amino Acid. *J. Am. Chem. Soc.* **1996,** *118* (29), 6897-6907.
17. Davies, H. M.; Antoulinakis, E. G., Intermolecular Metal-Catalyzed Carbenoid Cyclopropanations. *Org. React.* **2004,** *57*, 1-326.
18. Davies, H. M. L.; Huby, N. J. S.; Cantrell, W. R.; Olive, J. L., .alpha.-Hydroxy esters as chiral auxiliaries in asymmetric cyclopropanations by rhodium(II)-stabilized vinylcarbenoids. *J. Am. Chem. Soc.* **1993,** *115* (21), 9468-9479.
19. Chepiga, K. M.; Qin, C.; Alford, J. S.; Chennamadhavuni, S.; Gregg, T. M.; Olson, J. P.; Davies, H. M. L., Guide to enantioselective dirhodium(II)-catalyzed cyclopropanation with aryldiazoacetates. *Tetrahedron* **2013,** *69* (27), 5765-5771.

20. Negretti, S.; Cohen, C. M.; Chang, J. J.; Guptill, D. M.; Davies, H. M. L., Enantioselective dirhodium(II)-catalyzed cyclopropanations with trimethylsilylethyl and trichloroethyl aryldiazoacetates. *Tetrahedron* **2015,** *71* (39), 7415-7420.
21. Wei, B.; Sharland, J. C.; Lin, P.; Wilkerson-Hill, S. M.; Fullilove, F. A.; McKinnon, S.; Blackmond, D. G.; Davies, H. M. L., In Situ Kinetic Studies of Rh(II)-Catalyzed Asymmetric Cyclopropanation with Low Catalyst Loadings. *ACS Catal.* **2020,** *10* (2), 1161-1170.
22. Yu, Z.; Mendoza, A., Enantioselective Assembly of Congested Cyclopropanes using Redox-Active Aryldiazoacetates. *ACS Catal.* **2019,** *9* (9), 7870-7875.
23. Singha, S.; Buchsteiner, M.; Bistoni, G.; Goddard, R.; Fürstner, A., A New Ligand Design Based on London Dispersion Empowers Chiral Bismuth–Rhodium Paddlewheel Catalysts. *J. Am. Chem. Soc.* **2021**.
24. Sharland, J. C.; Wei, B.; Hardee, D. J.; Hodges, T. R.; Gong, W.; Voight, E. A.; Davies, H. M., Asymmetric synthesis of pharmaceutically relevant 1-aryl-2-heteroaryl-and 1, 2-diheteroarylcyclopropane-1-carboxylates. *Chem. Sci.* **2021,** *12* (33), 11181-11190.
25. Lathrop, S. P.; Mlinar, L. B.; Manjrekar, O. N.; Zhou, Y.; Harper, K. C.; Sacia, E. R.; Higgins, M.; Bogdan, A. R.; Wang, Z.; Richter, S. M., Continuous Process to Safely Manufacture an Aryldiazoacetate and Its Direct Use in a Dirhodium-Catalyzed Enantioselective Cyclopropanation. *Org. Proc. Res. Dev.* **2022**.
26. Ye, Q.-S.; Li, X.-N.; Jin, Y.; Yu, J.; Chang, Q.-W.; Jiang, J.; Yan, C.-X.; Li, J.; Liu, W.-P., Synthesis, crystal structures and catalytic activity of tetrakis(acetato)dirhodium(II) complexes with axial picoline ligands. *Inorg. Chim. Acta.* **2015,** *434*, 113-120.
27. Nelson, T. D.; Song, Z. J.; Thompson, A. S.; Zhao, M.; DeMarco, A.; Reamer, R. A.; Huntington, M. F.; Grabowski, E. J. J.; Reider, P. J., Rhodium-carbenoid-mediated intermolecular O–H insertion reactions: a dramatic additive effect. Application in the synthesis of an ascomycin derivative. *Tetrahedron Lett.* **2000,** *41* (12), 1877-1881.
28. Ye, Q.-S.; Li, X.-N.; Jin, Y.; Yu, J.; Chang, Q.-W.; Jiang, J.; Yan, C.-X.; Li, J.; Liu, W.-P., Synthesis, crystal structures and catalytic activity of tetrakis (acetato) dirhodium (II) complexes with axial picoline ligands. *Inorg. Chim. Acta.* **2015,** *434*, 113-120.
29. Fu, L.; Hoang, K.; Tortoreto, C.; Liu, W.; Davies, H. M., Formation of Tertiary Alcohols from the Rhodium-Catalyzed Reactions of Donor/Acceptor Carbenes with Esters. *Org. Lett.* **2018,** *20* (8), 2399-2402.
30. Laconsay, C. J.; Tantillo, D. J., Metal Bound or Free Ylides as Reaction Intermediates in Metal-Catalyzed [2, 3]-Sigmatropic Rearrangements? It Depends. *ACS. Catal.* **2021,** *11* (2), 829-839.
31. Sharland, J. C.; Dunstan, D.; Majumdar, D.; Gao, J.; Tan, K.; Malik, H. A.; Davies, H. M., Hexafluoroisopropanol for the Selective Deactivation of Poisonous Nucleophiles Enabling Catalytic Asymmetric Cyclopropanation of Complex Molecules. *ACS. Catal.* **2022,** *12* (20), 12530-12542.
32. Fu, L.; Mighion, J. D.; Voight, E. A.; Davies, H. M., Synthesis of 2, 2, 2,-Trichloroethyl Aryl-and Vinyldiazoacetates by Palladium-Catalyzed Cross-Coupling. *Chem. Eur. J.* **2017,** *23* (14), 3272-3275.
33. Davies, H. M. L.; Townsend, R. J., Catalytic Asymmetric Cyclopropanation of Heteroaryldiazoacetates. *J. Org. Chem.* **2001,** *66* (20), 6595-6603.
34. Kumari, A.; Singh, R. K., Medicinal chemistry of indole derivatives: Current to future therapeutic prospectives. *Bioorg. Chem.* **2019,** *89*, 103021.
35. Davies, H. M.; Hodges, L. M.; Matasi, J. J.; Hansen, T.; Stafford, D. G., Effect of carbenoid structure on the reactivity of rhodium-stabilized carbenoids. *Tetrahedron Lett.* **1998,** *39* (25), 4417-4420.
36. Davies, H. M.; Bruzinski, P. R.; Lake, D. H.; Kong, N.; Fall, M. J., Asymmetric cyclopropanations by rhodium (II) N-(arylsulfonyl) prolinate catalyzed decomposition of vinyldiazomethanes in the presence of alkenes. Practical enantioselective synthesis of the four

stereoisomers of 2-phenylcyclopropan-1-amino acid. *J. Am. Chem. Soc.* **1996,** *118* (29), 6897-6907.
37. Lian, Y.; Hardcastle, K. I.; Davies, H. M., Computationally Guided Stereocontrol of the Combined C H Functionalization/Cope Rearrangement. *Angew. Chem. Int. Ed.* **2011,** *50* (40), 9370-9373.
38. Bess, E. N.; Guptill, D. M.; Davies, H. M.; Sigman, M. S., Using IR vibrations to quantitatively describe and predict site-selectivity in multivariate Rh-catalyzed C–H functionalization. *Chem. Sci.* **2015,** *6* (5), 3057-3062.
39. Hansen, J.; Autschbach, J.; Davies, H. M., Computational study on the selectivity of donor/acceptor-substituted rhodium carbenoids. *J. Org. Chem.* **2009,** *74* (17), 6555-6563.
40. Fu, J.; Ren, Z.; Bacsa, J.; Musaev, D. G.; Davies, H. M. L., Desymmetrization of cyclohexanes by site- and stereoselective C–H functionalization. *Nature* **2018,** *564* (7736), 395-399.
41. Hopewell, J.; Jankowski, P.; McMullin, C. L.; Orpen, A. G.; Pringle, P. G., Subtleties in asymmetric catalyst structure: the resolution of a 6-phospha-2, 4, 8-trioxa-adamantane and its applications in asymmetric hydrogenation catalysis. *Chem. Commun.* **2010,** *46* (1), 100-102.
42. Adjabeng, G.; Brenstrum, T.; Wilson, J.; Frampton, C.; Robertson, A.; Hillhouse, J.; McNulty, J.; Capretta, A., Novel Class of Tertiary Phosphine Ligands Based on a Phospha-adamantane Framework and Use in the Suzuki Cross-Coupling Reactions of Aryl Halides under Mild Conditions. *Org. Lett.* **2003,** *5* (6), 953-955.
43. Adjabeng, G. M., Phospha-adamantanes as ligands for palladium-catalyzed cross-coupling reactions. **2003**.
44. Ko, S. Y.; Lerpiniere, J.; Linney, I. D.; Wrigglesworth, R., The total synthesis of epibatidine. *J. Chem. Soc. Chem. Commun.* **1994,** (15), 1775-1776.
45. Calmes, M.; Daunis, J.; Jacquier, R.; Natt, F., Synthesis of (S)-(+) Pantolactone. *Org. Prep. Proced. Int.* **1995,** *27* (1), 107-108.
46. Dennis, A.; Korp, J.; Bernal, I.; Howard, R.; Bear, J., Crystal and molecular structure of the bis (pyridine) adduct of a dinuclear rhodium (II) complex with trifluoroacetamidato bridging ligands. *Inorg. Chem.* **1983,** *22* (10), 1522-1529.
47. Fandzloch, M.; Augustyniak, A.; Dobrzańska, L.; Jędrzejewski, T.; Sitkowski, J.; Wypij, M.; Golińska, P., First dinuclear rhodium (II) complexes with triazolopyrimidines and the prospect of their potential biological use. *J. Inorg. Biochem.* **2020**, 111072.
48. Lee, M.; Ren, Z.; Musaev, D. G.; Davies, H. M., Rhodium-stabilized diarylcarbenes behaving as donor/acceptor carbenes. *ACS. Catal.* **2020,** *10* (11), 6240-6247.
49. Vaitla, J.; Boni, Y. T.; Davies, H. M. L., Distal Allylic/Benzylic C–H Functionalization of Silyl Ethers Using Donor/Acceptor Rhodium(II) Carbenes. *Angew. Chem. Int. Ed.* **2020,** *59* (19), 7397-7402.
50. Lebel, H.; Piras, H.; Bartholoméüs, J., Rhodium-Catalyzed Stereoselective Amination of Thioethers with N-Mesyloxycarbamates: DMAP and Bis(DMAP)CH2Cl2 as Key Additives. *Angew. Chem. Int. Ed.* **2014,** *53* (28), 7300-7304.
51. Kim, M.; Lee, J.; Lee, H.-Y.; Chang, S., Significant Self-Acceleration Effects of Nitrile Additives in the Rhodium-Catalyzed Conversion of Aldoximes to Amides: A New Mechanistic Aspect. *Adv. Synth. Catal.* **2009,** *351* (11-12), 1807-1812.
52. Davies, H. M. L.; Venkataramani, C., Dirhodium Tetraprolinate-Catalyzed Asymmetric Cyclopropanations with High Turnover Numbers. *Org. Lett.* **2003,** *5* (9), 1403-1406.
53. Anderson, B. G.; Cressy, D.; Patel, J. J.; Harris, C. F.; Yap, G. P. A.; Berry, J. F.; Darko, A., Synthesis and Catalytic Properties of Dirhodium Paddlewheel Complexes with Tethered, Axially Coordinating Thioether Ligands. *Inorg. Chem.* **2019,** *58* (3), 1728-1732.
54. Trindade, A. F.; Coelho, J. A. S.; Afonso, C. A. M.; Veiros, L. F.; Gois, P. M. P., Fine Tuning of Dirhodium(II) Complexes: Exploring the Axial Modification. *ACS Catal.* **2012,** *2* (3), 370-383.

55. Boni, Y. T.; Vaitla, J.; Davies, H. M., Catalyst Controlled Site-and Stereoselective Rhodium (II) Carbene C (sp3)–H Functionalization of Allyl Boronates. *Org. Lett.* **2022**.
56. Pozhydaiev, V.; Power, M.; Gandon, V.; Moran, J.; Lebœuf, D., Exploiting hexafluoroisopropanol (HFIP) in Lewis and Brønsted acid-catalyzed reactions. *Chem. Commun.* **2020,** *56* (78), 11548-11564.
57. Colomer, I.; Chamberlain, A. E.; Haughey, M. B.; Donohoe, T. J., Hexafluoroisopropanol as a highly versatile solvent. *Nat. Rev. Chem.* **2017,** *1* (11), 1-12.
58. Milovanović, M. R.; Dherbassy, Q.; Wencel-Delord, J.; Colobert, F.; Zarić, S. D.; Djukic, J. P., The Affinity of Some Lewis Bases for Hexafluoroisopropanol as a Reference Lewis Acid: An ITC/DFT Study. *Chemphyschem* **2020,** *21* (18), 2136-2142.
59. Jana, S.; Yang, Z.; Li, F.; Empel, C.; Ho, J.; Koenigs, R. M., Photoinduced Proton-Transfer Reactions for Mild O-H Functionalization of Unreactive Alcohols. *Angew. Chem. Int. Ed.* **2020,** *59* (14), 5562-5566.
60. Cavani, F.; Trifiro, F., Alternative processes for the production of styrene. *Appl. Catal., A* **1995,** *133* (2), 219-239.
61. Marcoux, D.; Lindsay, V. N.; Charette, A. B., Use of achiral additives to increase the stereoselectivity in Rh (II)-catalyzed cyclopropanations. *Chem. Commun.* **2010,** *46* (6), 910-912.
62. Marcoux, D.; Azzi, S.; Charette, A. B., TfNH2 as achiral hydrogen-bond donor additive to enhance the selectivity of a transition metal catalyzed reaction. Highly enantio-and diastereoselective rhodium-catalyzed cyclopropanation of alkenes using α-cyano diazoacetamide. *J. Am. Chem. Soc.* **2009,** *131* (20), 6970-6972.
63. Gage, J. R.; Chen, F.; Dong, C.; Gonzalez, M. A.; Jiang, Y.; Luo, Y.; McLaws, M. D.; Tao, J.; Development, Semicontinuous Process for GMP Manufacture of a Carbapenem Intermediate via Carbene Insertion Using an Immobilized Rhodium Catalyst. *Org. Process. Res. Dev.* **2020,** *24* (10), 2025-2033.
64. Marcoux, D.; Lindsay, V. N.; Charette, A. B., Use of achiral additives to increase the stereoselectivity in Rh (ii)-catalyzed cyclopropanations. *Chem. Commun.* **2010,** *46* (6), 910-912.
65. Nowlan, D. T.; Gregg, T. M.; Davies, H. M.; Singleton, D. A., Isotope effects and the nature of selectivity in rhodium-catalyzed cyclopropanations. *J. Am. Chem. Soc.* **2003,** *125* (51), 15902-15911.
66. Caballero, N. A.; Melendez, F. J.; Muñoz-Caro, C.; Niño, A., Theoretical prediction of relative and absolute pKa values of aminopyridines. *Biophys. Chem.* **2006,** *124* (2), 155-160.
67. Simpson, J. H.; Godfrey, J.; Fox, R.; Kotnis, A.; Kacsur, D.; Hamm, J.; Totelben, M.; Rosso, V.; Mueller, R.; Delaney, E., A pilot-scale synthesis of (1R)-trans-2-(2, 3-dihydro-4-benzofuranyl) cyclopropanecarboxylic acid: a practical application of asymmetric cyclopropanation using a styrene as a limiting reagent. *Tetrahedron Asymm.* **2003,** *14* (22), 3569-3574.
68. Marcin, L. R.; Denhart, D. J.; Mattson, R. J., Catalytic asymmetric diazoacetate cyclopropanation of 1-tosyl-3-vinylindoles. A route to conformationally restricted homotryptamines. *Org. Lett.* **2005,** *7* (13), 2651-2654.
69. Anthes, R.; Bello, O.; Benoit, S.; Chen, C.-K.; Corbett, E.; Corbett, R. M.; DelMonte, A. J.; Gingras, S.; Livingston, R.; Sausker, J.; Development, Kilogram Synthesis of a Selective Serotonin Reuptake Inhibitor. *Org. Process. Res. Dev.* **2008,** *12* (2), 168-177.
70. Green, S. P.; Wheelhouse, K. M.; Payne, A. D.; Hallett, J. P.; Miller, P. W.; Bull, J. A., Thermal Stability and Explosive Hazard Assessment of Diazo Compounds and Diazo Transfer Reagents. *Org. Process. Res. Dev.* **2020,** *24* (1), 67-84.
71. W, L.; J.Twilton; B. Wei; M. Lee; M. N. Hopkins; J. Bacsa; S. S. Stahl; H. M. L. Davies, *J. Am. Chem. Soc.* **2021,** *11*, 2676-2683.
72. Hatridge, T. A.; Wei, B.; Davies, H. M.; Jones, C. W., Copper-Catalyzed, Aerobic Oxidation of Hydrazone in a Three-Phase Packed Bed Reactor. *Org. Process. Res. Dev.* **2021,** *25* (8), 1911-1922.

73. Wei, B.; Hatridge, T. A.; Jones, C. W.; Davies, H. M., Copper (II) Acetate-Induced Oxidation of Hydrazones to Diazo Compounds under Flow Conditions Followed by Dirhodium-Catalyzed Enantioselective Cyclopropanation Reactions. *Org. Lett.* **2021,** *23* (14), 5363-5367.
74. Liu, W.; Twilton, J.; Wei, B.; Lee, M.; Hopkins, M. N.; Bacsa, J.; Stahl, S. S.; Davies, H. M., Copper-catalyzed oxidation of hydrazones to diazo compounds using oxygen as the terminal oxidant. *ACS. Catal.* **2021,** *11* (5), 2676-2683.
75. Khaksar, S., Fluorinated alcohols: A magic medium for the synthesis of heterocyclic compounds. *J. Fluorine. Chem.* **2015,** *172*, 51-61.
76. Berkessel, A.; Adrio, J. A.; Hüttenhain, D.; Neudörfl, J. M., Unveiling the "booster effect" of fluorinated alcohol solvents: aggregation-induced conformational changes and cooperatively enhanced H-bonding. *J. Am. Chem. Soc.* **2006,** *128* (26), 8421-8426.
77. Colomer, I.; Chamberlain, A. E.; Haughey, M. B.; Donohoe, T. J., Hexafluoroisopropanol as a highly versatile solvent. *Nat. Rev. Chem.* **2017,** *1* (11), 1-12.
78. Sinha, S. K.; Bhattacharya, T.; Maiti, D., Role of hexafluoroisopropanol in C–H activation. *React. Chem. Eng.* **2019,** *4* (2), 244-253.
79. Bhattacharya, T.; Ghosh, A.; Maiti, D., Hexafluoroisopropanol: the magical solvent for Pd-catalyzed C–H activation. *Chem. Sci.* **2021,** *12* (11), 3857-3870.
80. Gray, E. E.; Nielsen, M. K.; Choquette, K. A.; Kalow, J. A.; Graham, T. J.; Doyle, A. G., Nucleophilic (radio) fluorination of α-diazocarbonyl compounds enabled by copper-catalyzed H–F insertion. *J. Am. Chem. Soc* **2016,** *138* (34), 10802-10805.
81. Hollóczki, O.; Berkessel, A.; Mars, J.; Mezger, M.; Wiebe, A.; Waldvogel, S. R.; Kirchner, B., The catalytic effect of fluoroalcohol mixtures depends on domain formation. *ACS Catal.* **2017,** *7* (3), 1846-1852.
82. Borrell, M.; Gil-Caballero, S.; Bietti, M.; Costas, M., Site-selective and product chemoselective aliphatic C–H bond hydroxylation of polyhydroxylated substrates. *ACS. Catal.* **2020,** *10* (8), 4702-4709.
83. Trindade, A. F.; Gois, P. M.; Veiros, L. F.; André, V.; Duarte, M. T.; Afonso, C. A.; Caddick, S.; Cloke, F. G. N., Axial coordination of NHC ligands on dirhodium (II) complexes: Generation of a new family of catalysts. *J. Org. Chem.* **2008,** *73* (11), 4076-4086.
84. Lindsay, V. N.; Nicolas, C.; Charette, A. B., Asymmetric Rh (II)-catalyzed cyclopropanation of alkenes with diacceptor diazo compounds: p-methoxyphenyl ketone as a general stereoselectivity controlling group. *J. Am. Chem. Soc.* **2011,** *133* (23), 8972-8981.
85. Gehring, P.; Torkelson, T.; Oyen, F., A comparison of the lethality of chlorinated pyridines and a study of the acute toxicity of 2-chloropyridine. *Toxicol. Appl. Pharmacol.* **1967,** *11* (2), 361-371.

Chapter 3

1,1,1,3,3,3-Hexafluoroisopropanol for the selective deactivation of poisonous nucleophiles, diversification of complex alkenes, and as a paradigm warping additive for rhodium carbene chemistry.

3.1 Introduction:

Asymmetric rhodium-catalyzed cyclopropanation between diazo compounds and alkenes is an important method for the synthesis of industrially relevant compounds.[1-5] When the carbene bears both a donor and an acceptor group, the cyclopropanation proceeds with high diastereoselectivity (typically >20:1 d.r.) and several chiral dirhodium catalysts have been developed to render the reaction highly enantioselective.[6, 7] While the reaction can be robust and scalable, reliance on the use of a transition metal catalyst and a carbene intermediate means that the substrate scope is inherently limited. Various nucleophiles can coordinate to the rhodium center to the exclusion of the diazo compound, preventing catalytic activity (Scheme 3.1).[8-11] Additionally, reactive bonds (particularly weak and highly polarized heteroatom-H bonds) can outcompete the desired substrate and react with the carbene. Water, alcohols, and protic-amines selectively react with donor/acceptor-carbenes via the heteroatom–H bond to the exclusion of alkene traps like styrene (Scheme 3.1).[12-17] This significantly harms the applicability of rhodium carbene methodology to a commercial setting, where tolerance of trace impurities from earlier synthetic steps, along with the aza-heterocycles and reactive functionality that are common in both therapeutic compounds and natural products, is necessary.[1, 2, 18-20] Additionally, the ability to conduct chemistry without the requirement for pristine, anhydrous reaction conditions is a major benefit for reactions for use in industrial processes.[5]

Scheme 3.1: Cyclopropanation in the presence of nucleophilic poisons fails according to two typical pathways.

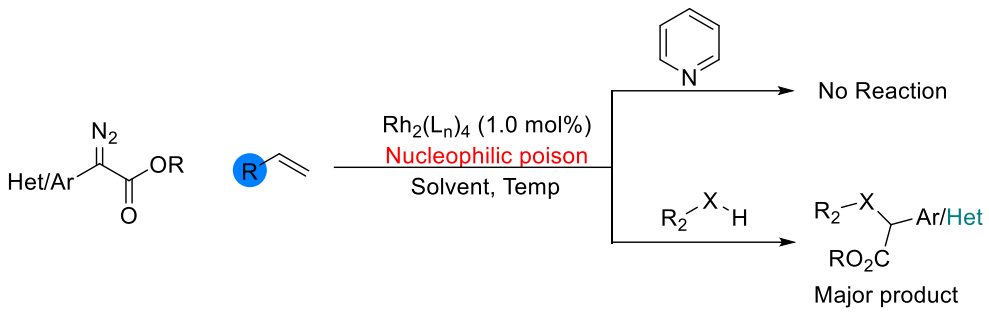

Previous attempts to use Rh-carbene chemistry to functionalize complex molecules containing nucleophilic sites often required the use of high catalyst loading and forcing temperatures to limit catalyst inhibition.[21, 22] In a paper in 2016, the Davies group in collaboration with Novartis scientists attempted to use site-selective C–H functionalization to derivatize a series of natural products and therapeutic compounds.[21] The published manuscript included several examples including brucine (**1**), securinine (**2**), and bicuculine (**3**) however many of the examples were low yielding and had poor diastereoselectivity (Scheme 3.2).[21] It was also impossible to override the electronic activation of sites adjacent to the heteroatom and only α-amino C–H bonds were reactive under the optimized conditions, even when catalysts with different selectivity profiles were used. Even though several of these transformations were successful, the scope was limited to molecules bearing tertiary amines and lacking reactive moieties like alcohols.[21, 22] To avoid interference of the nucleophilic tertiary amines with the rhodium catalyst, the reactions had to be conducted at elevated temperature (83 °C).[21] When conducted at room temperature nitrogen-ylides were observed as the major product, but since ylide formation is reversible, higher temperature encourages C–H functionalization to occur. This limits the choice of solvent to high boiling solvents like trifluorotoluene (CF_3Ph) and lowers the stereoselectivity of the reaction.

Scheme 3.2: Previous work on the late-stage C–H functionalization of complex alkaloids proceeded most successfully with an achiral dirhodium catalyst in terms of site and diastereoselectivity.[21]

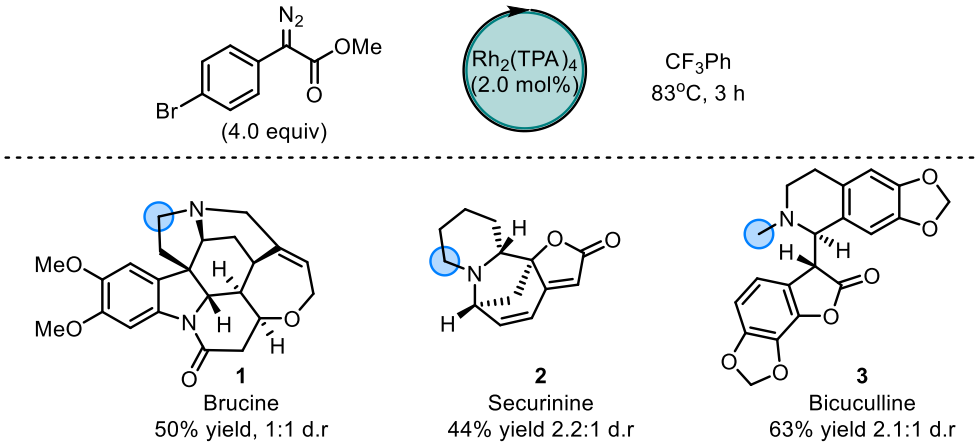

Despite recent interest in the development in C–H functionalization methodologies, we have had a long-standing interest in the cyclopropanation chemistry of donor/acceptor carbenes and in fact this is our most commonly used method in industrial applications.[1, 5] As such, we wished to find a general and procedurally simple approach to conduct cyclopropanation reactions in the presence of the classic nucleophilic poisons or reactive functionality that would be considered to be incompatible with this chemistry.[23] We became intrigued with the possibility that HFIP could be an effective solution to the challenges of functional group intolerance. Reactions conducted in HFIP typically exploit its powerful hydrogen bonding ability to weaken electron rich bonds which can then react under a variety of conditions.[24-28] Other functionality like alcohols and alkenes can be engaged in a similar manner.[29-34] The Laboeuf group has pioneered a diverse series of transformations leveraging the ability of HFIP to enhance reactivity. A few notable transformations include metal free C–H arylation of vinyltrifluoromethanes,[35] calcium catalyzed *ortho*-alkylation of anilines,[36] and application of HFIP promoted aza-Piancatelli reactions for a variety of diverse molecule synthesis (Scheme 3.3).[37]

Scheme 3.3: Examples of methods that leverage the ability of HFIP to potentiate Lewis acid catalysis.[35-37]

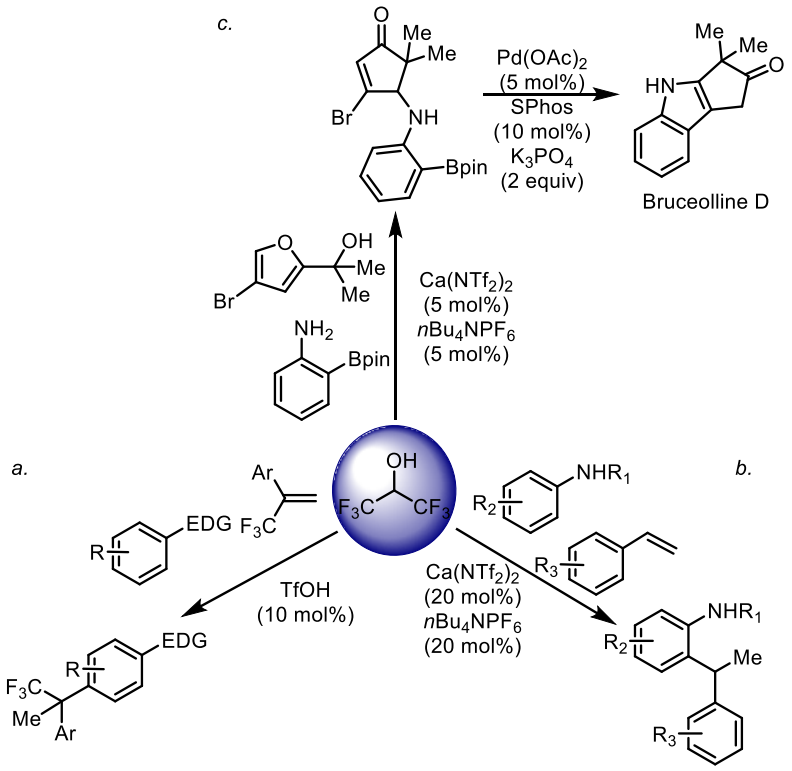

The C–H arylation of vinyltrifluoromethanes (Scheme 3.3a) uses HFIP as solvent to enhance the acidity of triflic acid (TfOH) which enables it to protonate the vinyl trifluoromethane, forming tertiary carbocation.[35] This carbocation can then be engaged by the electron rich arene in an electrophilic aromatic substitution (EAS) mechanism, which forms the observed product. The regioselectivity of the transformation occurs according to typical preferences in EAS reactions, the key role of HFIP in this transformation is to enhance the acidity of TfOH through hydrogen-bond clusters and possibly to reversibly trap the carbocation generated after alkene protonation.[35] The C–H alkylation of anilines, similarly uses a calcium salt ($Ca(NTf_2)_2$) which has been shown to enhance the acidity of HFIP (Scheme 3.3b).[29] This highly acidic HFIP-Ca cluster can protonate tertiary anilines, converting this classically electron donating motif an electron withdrawing group. After this protonation, a vinyl arene can approach this ionic complex and engage the aniline. In a concerted mechanism, the aniline-HFIP-Ca complex donates a proton into the terminal alkene

carbon and the alkene attacks the ortho position of the aniline, which then pushes electrons into the positively charged aniline nitrogen.[36] Rearomatization of this intermediate then occurs to afford the observed *ortho*-alkylated aniline. In this reaction HFIP plays a critical dual role, first generating the charged aniline intermediate and then organizing addition of the vinyl substrate by assisting with protonation of the alkene which accounts for the high regioselectivity of this transformation.[36] Without the addition of a calcium salt, HFIP alone is not acidic enough to promote this transformation, a phenomenon which will become apparent later in this chapter. This cooperative interaction between $Ca(NTf_2)_2$ and HFIP has been exploited for a variety of transformations but has been particularly impactful in the aza-Piancatelli reaction as outlined in Scheme 3.3c. This is a well-studied reaction with a complex mechanism involving the rearrangement of furyl alcohols to cyclopentenones which will not be discussed at length here.[38, 39] In the example shown in Scheme 3.3c, HFIP plays a critical role in the initiation of the rearrangement by dehydrating the tertiary alcohol to generate a carbocation. In previous examples of this transformation, the inclusion of strong lewis acids often led to the oligomerization of the furyl starting material, and the scope was often limited to secondary alcohols.[37, 39] The utility of the HFIP-Ca complex is to act as a moderately strong Lewis acid, generated under mild conditions which allows not only for more efficient conversion in aza-Piancatelli reactions but also a greater substrate scope.[29] Though this reaction has broad applicability to total synthesis, its sensitivity has rarely been leveraged to furnish natural products, however the use of the mild conditions developed by LeBeouf *et. al.* enabled a significantly broader substrate scope and the potential to be applied to natural products like bruceolline as described in Scheme 3.3c.[37]

As discussed above, most of the examples using HFIP rely on enhancing the reactivity of substrates by increasing their electrophilicity.[24] In our case, this strong hydrogen bonding capability would be expected to deactivate nucleophilic sites that would typically poison the reaction (Scheme 3.1). Even though there are a few examples of the deactivating influence of HFIP,[40, 41] it has not been explored extensively,

particularly in the context of rhodium carbene chemistry.[8, 24] One of these examples is the Mn and Fe catalyzed C–H hydroxylation of alkanes.[26] This method uses HFIP to hydrogen bond to existing alcohols in the substrate, converting it from an electronically activating group into a electron withdrawing moiety and hence deactivating proximal bonds towards Mn and Fe catalyzed oxidation (Scheme 3.4).[26]

Scheme 3.4: Manganese and iron catalyzed C–H oxidation of alkyl-alcohols leveraging the deactivating influence of HFIP to achieve site-selectivity.[26]

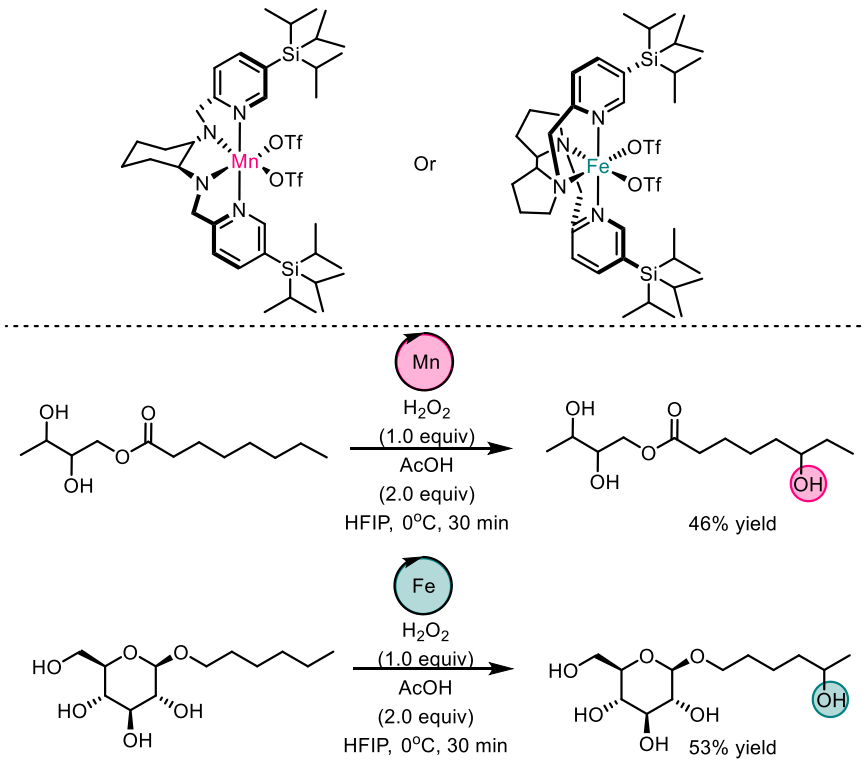

This reaction leverages the ability of metal-oxo species to conduct aliphatic C–H oxidation.[42] This is a common transformation used by metabolic enzymes to degrade biologically active or toxic compounds, but more recently this approach has garnered interest among the medicinal chemistry community as an effective way to install hydroxyl moieties without functional group manipulation.[42-44] The most difficult aspect of this field is engendering site-selectivity in the transformation.[42] Enzymes have complex chiral pockets which allow for high site, chemo, and stereoselectivity however such profiles have been difficult

to replicate with more conventional transition metal catalysts, often leading to poor regioselectivity or over-oxidation to ketones.[42, 44] Given the high reactivity of the metal-oxo intermediate, the site selectivity of these methods is typically related to the reactivity of the C–H bonds in question and under auspicious circumstances, the site of reactivity occurs preferentially at the most reactive (electron rich) C–H bond.[42] To this, heteroatoms often have an inductive effect which can modulate site-selectivity, increasing the electron density of adjacent sites and therefore skewing site selectivity towards them.[21, 42] Noting this trend, the Borrell *et. al.* leveraged the hydrogen bonding capability of HFIP to selectively hydrogen bond with alcohols in complex substrates, converting these inductively activating heteroatoms into inductively deactivating electron poor groups.[26] Then the metal-oxo catalyst (either Mn or Fe depending on the substrate) selected the most activated C–H bond in the system for oxidation, which was distal to this now-deactivating group.[26] The method boasted an impressive substrate scope, including several glyclosides and natural products as shown in Scheme 3.4.[26] Considering this method, it could be analogously applied to the previous example of C–H functionalization of complex molecules (Scheme 3.2).[21] HFIP could coordinate to the amino-functionality and deactivating the adjacent C–H bonds towards insertion of the carbene by inductively reducing the hydricity of these sites.[45] There is also good evidence that this additive would be compatible with rhodium catalyzed carbene reactions.[17, 46] HFIP, unlike other fluorinated alcohols, is essentially inert to rhodium carbenes under mild conditions, and it can be easily removed by rotary evaporation, making it an attractive reaction medium.[17, 47] Indeed, in his exploration of the reactivity of HFIP in the presence of carbenes, Koenigs reported no reaction between HFIP and a rhodium carbene under normal reaction conditions.[17] The carbene had to be generated using blue light in order to achieve a competent reaction with the electron poor alcohol.[17] Generating a carbene in this way forms the triplet state carbene as opposed to the singlet state which is formed upon reaction with a rhodium catalyst.[48, 49] This triplet state includes two unpaired electrons that react in radical-type mechanisms as opposed to the 2-electron chemistry typical of rhodium carbenes (Figure 3.1).[17, 48]

Figure 3.1: Fundamental differences between singlet and triplet state carbenes.

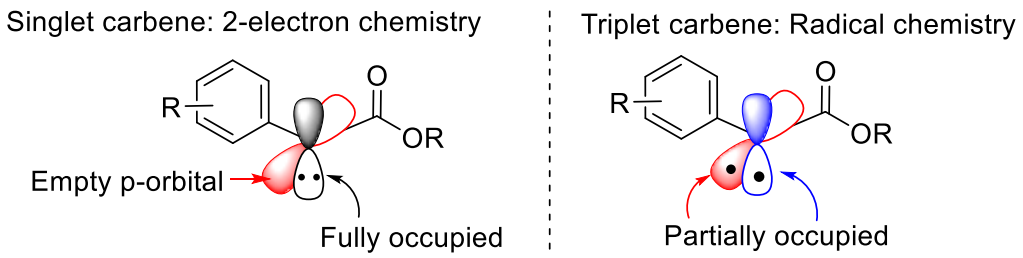

Based on this data and the reactions discussed in **Chapter 2,** which use an excess of HFIP (10 equiv) to control trace water and DMAP in the reaction without effecting yield or % ee,[8] we had good evidence to believe that the rhodium carbene would be inert to HFIP under standard reaction conditions and that chiral catalysis would proceed efficiently.[8, 50, 51] In the first study we developed new catalytic systems with HFIP as an additive to enable high yielding and highly stereoselective cyclopropanation in the presence of a broad scope of poisonous and reactive functionality (Scheme 3.5).[52] The potential of this new approach was then illustrated with the stereoselective derivatization of several elaborate APIs and natural products which bear functionality that would have been previously considered incompatible with the cyclopropanation chemistry.[52] Finally, some new transformations leveraging this deactivating influence are described along with a clear direction for future research in this arena.

Scheme 3.5: Selective deactivation of nucleophilic poisons in rhodium catalyzed cyclopropanation.

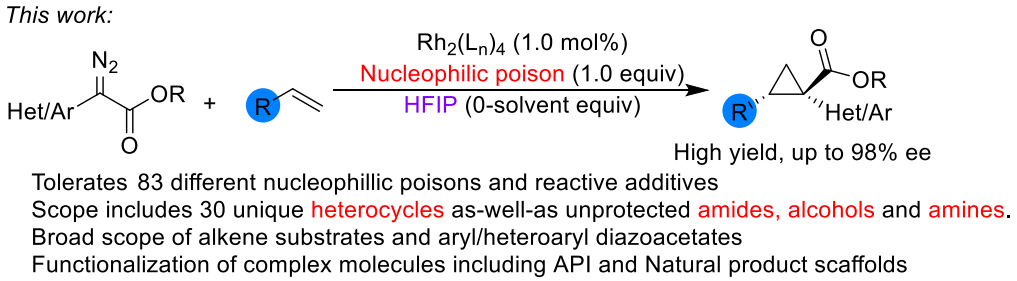

3.2 Results and Discussion:

We have recently become interested in exploring the role of HFIP as an additive in rhodium carbene chemistry. Very small quantities were found to enhance the enantioselectivity in rhodium catalyzed allylic C–H functionalization with 4-aryl-*N*-sulfonyl triazoles.[53] During the development of the chemistry described in **Chapter 2** we discovered that HFIP (10 equiv) desensitizes the reaction to water and *N,N'*-dimethylaminopyridine (**8,** DMAP) (Scheme 3.6).[8, 50] Given this exciting and unexpected result, we suspected that we could leverage this effect to deactivate a wide range of other nucleophilic poisons and reactive functionality that typically interfere with the cyclopropanation reaction.[24, 40, 41] HFIP can hydrogen bond with, or even formally protonate, different nucleophiles due to its relatively high acidity, preventing them from coordinating with the dirhodium catalyst and the rhodium carbene intermediate.[41] We suspected that not only could we prevent poisonous nucleophiles from inhibiting the reaction, but that we may also be able to prevent reactive species like amines and alcohols from preferentially reacting with the carbene through X–H insertion.[16, 41]

Scheme 3.6: Initial observation on the selective deactivation of poisonous heterocycles to rhodium catalyzed cyclopropanation with HFIP.

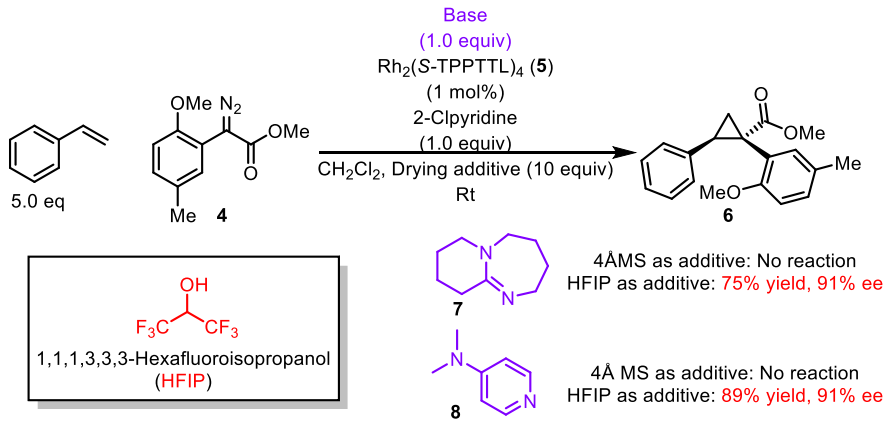

Furthermore, HFIP is inert to the alkene substrate and the rhodium carbene,[8] so the desired cyclopropanation reaction may be able to proceed even in the presence of a vast excess of HFIP.[17] In order to explore this possibility, the reaction of 1-hexene (2.5 equiv) with 2,2,2-trichloroethyl 2-(4-bromophenyl)diazo-2-acetate (**9**) catalyzed by Rh_2(*R*-TPPTTL)$_4$ (**5**, 1.0 mol %) was used as a reference reaction (Table 3.1).[52] The standard reaction in the absence of HFIP resulted in the formation of cyclopropane **10** in 91% yield and 89% ee. Five representative substrates with functionality likely to interfere with the cyclopropanation were examined. These were the tertiary amines, *N*-methyl pyrrolidine (**11**) and pyridine (**13**), and the protic substrates, *tert*-butyl alcohol (**11**) acetoacetamide (**14**) and cyclohexanone oxime (**15**). None of cyclopropane **10** was formed when the standard reaction was conducted in the presence of 1 equiv of these poisons. When HFIP was added, however, the negative influence of these poisons could be blocked.[52] In the presence of 10 equiv of HFIP, cyclopropanation interference no longer occurred with *N*-methyl pyrrolidine (**11**) or *tert*-butyl alcohol (**12**), whereas the use of HFIP as solvent was required to block the interference by pyridine (**13**), acetoacetamide (**14**) and cyclohexanone oxime (**15**). While the reaction displayed promising functionality tolerance in the presence of HFIP, the enantioselectivity of the reaction was negatively affected. Without any HFIP the product was obtained in high selectivity (89% ee). With just 10 equivalents of HFIP, however, the enantioselectivity dropped dramatically (58% ee), and when HFIP was used as the reaction solvent the selectivity dropped further still (15% ee).[52]

Table 3.1: Benchmark reaction of 1-hexene in the presence of reaction poisons and Rh_2(*R*-TPPTTL)$_4$ (**5**).

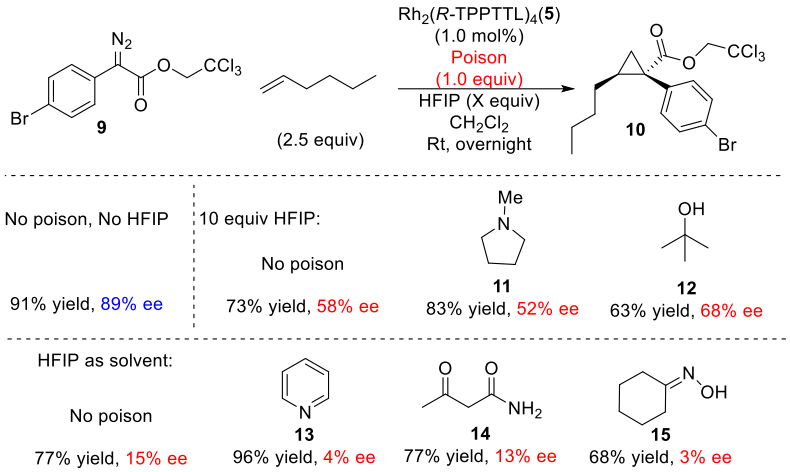

To address this poor enantioselectivity a catalyst screen was performed on the benchmark reaction in the presence of varying quantities of HFIP (10 equiv – solvent) to locate a chiral catalyst which maintained high selectivity even when HFIP is used as solvent (Table 3.2). Many chiral catalysts were examined but they tended to perform poorly in the presence of HFIP.[52] Many catalysts had crippled enantioselectivity including Rh_2(TPPTTL)$_4$ (**5**),[54] Rh_2(DOSP)$_4$,[55] and Rh_2(*p*-PhTPCP)$_4$ (**16**).[56] Interestingly, electron deficient phthalimido-catalysts experienced an inversion in enantioselectivity. Rh_2(TCPTAD)$_4$,[57] Rh_2(TCPTTL)$_4$,[58] and Rh_2(TFPTTL)$_4$[59] gave the opposite major enantiomer when the reaction was performed in HFIP vs DCM. We suspect that HFIP engages in hydrogen bonding with the carboxylate ligand through the various carbonyl moieties present, this could alter the catalyst's C_4 symmetric structure which is key to achieving high asymmetric induction.[54, 60] This hypothesis was explored by crystallizing Rh_2(TCPTTL)$_4$ in the presence of HFIP. The crystal structure indeed showed HFIP hydrogen bonding with both the carboxylate ligands as well as the phthalimide carbonyl oxygens, however that catalyst overall did not show a different geometry to the non-HFIP coordinated catalyst. A few catalysts Rh_2(NTTL)$_4$ (**18**)[61] and Rh_2(PTAD)$_4$[57] actually exhibited higher levels of enantioselectivity when the reaction was conducted in HFIP. The most extreme example being Rh_2(NTTL)$_4$ (**18**) which goes from delivering poor enantioselectivity (35% ee) to a highly selective

catalyst (90% ee).[52] Given the failure of the crystal structure to elucidate the reasons for these alterations in selectivity, the solid-state structure may be irreflexive the catalyst geometry in solution. NMR experiments were performed in deuterated HFIP (D_2-HFIP) with Rh_2(*R*-NTTL)$_4$ (**17**) to see if any of the signals were significantly different in this highly acidic medium.[52] Unfortunately, though some chemical shifts migrated upfield, indicating that the ligand was hydrogen-bonding and thus less electron rich, there was no obvious change in the symmetry of the catalyst.[52] Future work will be needed to determine the true mechanism of enantiomodulation expressed in HFIP, **Chapter 4** will detail some of these efforts.

Table 3.2: Catalyst screen to optimize the enantioselectivity of **10** in the presence of HFIP.[35- 38, 52]

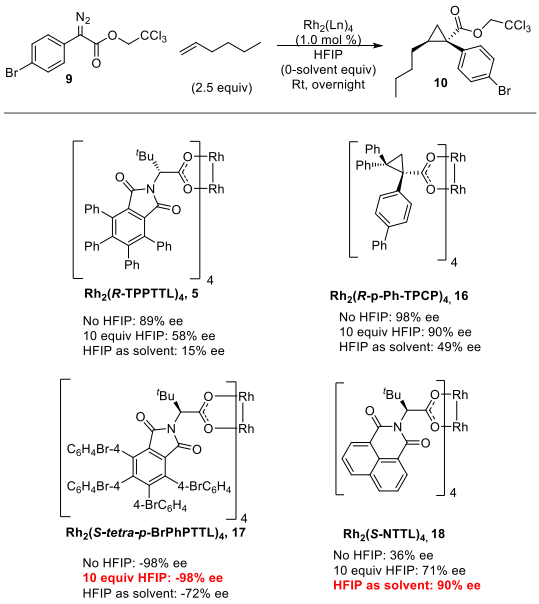

(-) %ee denotes that the opposite enantiomer of **2** from that shown in the scheme was obtained.

Regardless of these unusual effects, the screen identified several promising candidates for a successful transformation, the results of the four most significant are summarized in Table 3.2. The most broadly successful catalyst for asymmetric cyclopropanation with aryldiazoacetates is Rh_2(*S*-*p*-Ph-TPCP)$_4$ (**16**) as explained in **Chapter 1** and **2** but it also suffered from decreasing levels of enantioselectivity on increasing the amount of HFIP.[6, 8, 62] Rh_2(*S*-*tetra*-*p*-BrTPPTTL)$_4$ (**17**), a recently developed catalyst,[60] retained excellent

levels of enantioselectivity (98% ee) when up to 10 equiv of HFIP was used, however, when HFIP was used as solvent the enantioselectivity dropped to 72% ee. Unexpectedly, the best catalyst when HFIP is used as solvent is Rh_2(*S*-NTTL)$_4$ (**18**). Previously, Rh_2(NTTL)$_4$ (**18**), has not shown much promise as a chiral catalyst for the reactions of aryldiazoacetates, and indeed the cyclopropanation in the absence of HFIP afforded only 36% ee.[52] In this case, however, the enantioselectivity improved with increasing amounts of HFIP and when HFIP was used as solvent, the cyclopropane **10** was obtained with 90% ee. As Rh_2(*S-tetra-p*-BrTPPTTL)$_4$ (**17**) will be an important catalyst in this work, its origins and synthesis will be briefly discussed. After the discovery that Rh_2(TPPTTL)$_4$ (**5**) is a catalyst with broad applications,[8, 54, 63, 64] unique site selectivity,[54] and surprising flexibility there was significant interest in derivatizing this scaffold.[60] Dr. Zachary Garlets, a former postdoctoral scholar in the Davies group developed a modular synthesis of tetraphenylated phthalic anhydrides to facilitate these efforts.[60] The synthesis begins with the Claisen-condensation/elimination of two benzyl acetates to generate diaryl propanone **19**. This molecule is condensed with a diarylethanedione to generate tetraarylcyclopentadienone **20**. This intermediate can then be reacted with maleic anhydride/Br_2 in a one-pot Diels-Alder cyclization/aromative oxidation to form the desired phthalic anhydride **21**. The resultant product can then be condensed with *R* or *S-tert*-leucine to generate the chiral *tetra*-phenyl phthalimido *tert*-leucinato ligand **22**. This can then be subjected to ligand exchange with rhodium acetate to afford the desired dirhodium tetracarboxylate catalyst (**17**, **23-28**). These ligand exchanges typically proceed with high yield due to the cooperative self-assembling nature of these ligands.[54, 60] All of the obtained catalysts were crystallized and subjected to X-ray crystallography revealing that they all exhibited the typical C_4 symmetric conformation of the parent catalyst Rh_2(TPPTTL)$_4$ (**5**). The selectivity profiles of these catalysts was then explored and found to be similar to the parent scaffold, though in some cases these expanded catalysts delivered improved selectivity.[60]

Scheme 3.7: Synthesis of extended Rh_2(*S*-TPPTTL)$_4$ derivatives.

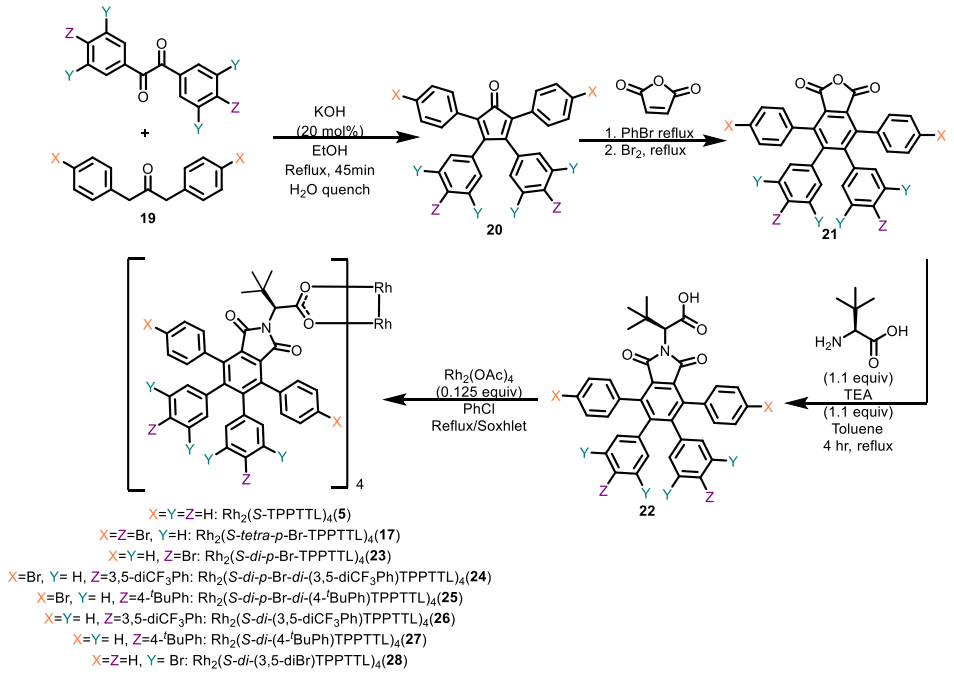

For the cyclopropanation, the two most promising catalysts were then applied towards reactions involving several different additives in a high-throughput screen in collaboration with the Microcycle team at Novartis.[52] Many issues had to be ironed out in the initial stages of the collaboration. We quickly discovered that while % ee values were reproducible between small scale and bench-scale reactions, the % yield was highly variable. This was due to the use of DCM as the reaction medium. The volatility of the solvent posed a problem as the reactions had to be run overnight to ensure high conversion. During this time, the volatile solvent would partially or fully evaporate even within the sealed reaction plate. Control experiments running the same reaction under the same conditions in wells scattered across the plate highlighted these effects as reactions run in the center of the plate tended to display higher yields than reactions towards the edges of the plate. This phenomenon is known as the "edge-effect" and plagues all HTE-type reaction screens as it can make data obtained on microscale unreliable.[65-67] We attempted to use larger reaction vials to combat these effects (2-dram), however the volatility of the solvent remained problematic. To avoid the problematic volatility of CH_2Cl_2 on such small scale, the reactions were

conducted in $(MeO)_2CO$, a high boiling, environmentally benign solvent which retains high enantioselectivity in these types of cyclopropanations as discussed in **Chapter 1**.[8, 62] Other solvents like 1,2-dichloroethane (DCE) were explored but none displayed superior asymmetric induction to $(MeO)_2CO$. Having solved the volatility problem, the reactions were highly reproducible and we were able to proceed to the high-throughput screen.[52] 90 different poisonous and reactive additives were divided into categories based on chemical structure and mode of reactivity. These included aromatic heterocycles (**8**, **13**, **29-46,** Table 3.3), oxygen nucleophiles (**47-55**, Table 3.4), nitrogen nucleophiles (**7, 11**, **56-60**, Table 3.5), reactive O–H bonds (**12, 15, 61-68**, Table 3.6), reactive N–H bonds (**14, 79-87**, Table 3.7), sulfur containing compounds (**88-98,** Table 3.8), phosphorous containing compounds (**99-102**, Table 3.9), and some miscellaneous compounds (**103-111**, Table 3.10). Each additive was assessed according to three reaction protocols. A: Rh_2(*S-tetra-p*-BrTPPTTL)$_4$ as catalyst with no HFIP, B: Rh_2(*S-tetra-p*-BrTPPTTL)$_4$ as catalyst with 10 equiv of HFIP, and C: Rh_2(*R*-NTTL)$_4$ as catalyst with HFIP as solvent. The conditions which yielded optimal results are reported for each compound and can be identified by color coding. Blue color indicates that no HFIP was needed. Green means that 10 equiv of HFIP was required, whereas orange means HFIP had to be used as solvent to avoid interference from the added poison. Molecules in grey regions were not tolerated under any conditions. In general, when HFIP was used as solvent the reaction displayed the broadest functionality tolerance. Reactions that provided ≥30% yield were deemed successful, and several additives were also examined on laboratory scale (0.10 mmol scale) to validate the results.

The development of general procedures to conduct asymmetric cyclopropanation that would be compatible to a wide variety of heterocycles, would greatly increase the pharmaceutical relevance of rhodium-catalyzed cyclopropanation chemistry.[18, 19] While our earlier work on the cyclopropanation of aza-heterocycles sought to address this need, all of the heterocyclic substrates required substitution adjacent to the nitrogen to reduce its nucleophilicity in order to ensure an effective transformation.[8, 9, 68]

Of the 20 aromatic heterocycles examined in this work, only benzothiophene (**29**) was tolerated without the use of HFIP. With 10 equiv of HFIP several heterocycles could be tolerated including strong nucleophiles like oxazole (**31**), DMAP (**8**), and caffeine (**34**). Tolerance to diverse heterocycles was vastly increased when HFIP was used as the reaction solvent. Under these conditions, all 20 of the aromatic heterocycles could be tolerated including pyridine (**13**), several diazines including pyrimidine (**18**) and pyrazine (**36**) and indole (**42**) was also tolerated despite the presence of a reactive N–H bond, along with imidazole (**43**) and triazole (**45**) although the latter caused a reduction in the observed enantioselectivity of the reaction. More complex systems were also compatible with the method including 1,3,5-triazine (**41**), the nucleobase uracil (**46**), isoquinoline (**40**), and several hydroxypyridines (**32**, **37**, and **38**, Table 3.3).[52]

Table 3.3: Tolerance of benchmark reaction to aromatic heterocycles in the presence of various quantities of HFIP.

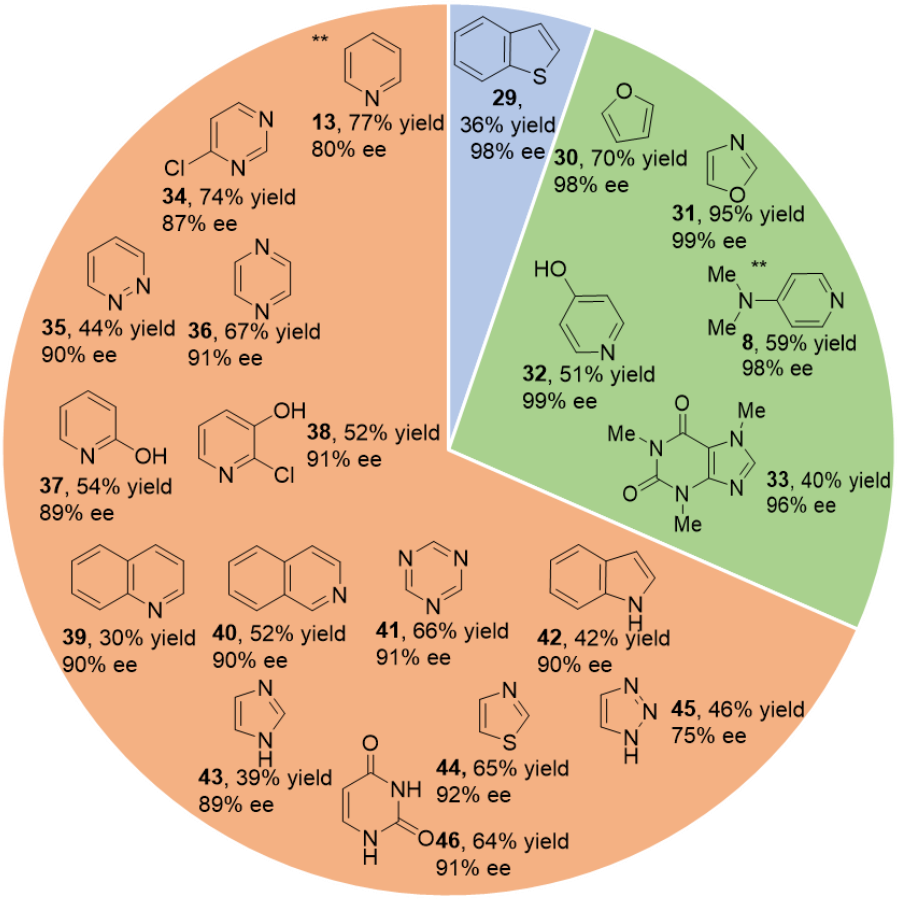

Products are highlighted under the conditions by which best results were obtained in terms of yield and enantioselectivity. Products in blue give optimal results under condition A: Rh_2(*S-tetra-p*-BrPhPTTL)$_4$ (**17**, 1.0 mol%) and dimethyl carbonate as solvent (80ul, 67mM). Products highlighted in green give optimal results under condition B: Rh_2(*S-tetra-p*-BrPhPTTL)$_4$ (**17**, 1.0 mol%) and dimethyl carbonate as solvent (80ul, 67mM) with HFIP (10 equiv). Products highlighted in orange give optimal results under condition C: Rh_2(*R*-NTTL)$_4$ (**18,** 1.0 mol%) and HFIP as solvent (80ul, 67mM). ** This reaction performed on 0.10 mmol scale without molecular sieves and CH_2Cl_2 or HFIP as solvent.

Oxygen nucleophiles are often compatible with dirhodium chemistry.[62, 68] Indeed the solvent used for these transformations, $(MeO)_2CO$, and ethyl acetate can even improve the enantioselectivity of these reactions as described in **Chapter 1**.[62, 69] There is, however, a strong propensity for carbonyls to form ylides with the rhodium carbene, an effect which has been historically exploited in a wide array of important transformations.[45, 70-74] In this study, good reactivity was generally observed with oxygen nucleophiles at low levels of HFIP (Table 3.4). Substrates including acetone (**48**), nitromethane (**49**), and phenylisocyanate

(**50**) were all tolerated without the use of HFIP. However, more nucleophilic compounds, like *N,N'*-dimethylformamide (DMF, **55**) required 10 equiv HFIP to ensure compatibility. Additionally, some substrates like THF (**52**) and aldehydes (**51** and **53**) can undergo competitive reactions with the carbene including C–H insertion[45] and epoxidation,[75, 76] however these side-reactions were shut down in the presence of 10 equiv HFIP (Table 3.4). The identity of reaction side products was not definitively confirmed in any of these cases as the reaction mixture was often complex and the small scale made purification prohibitively difficult.

Table 3.4: Tolerance of benchmark reaction to weak-oxygen nucleophiles in the presence of various quantities of HFIP.

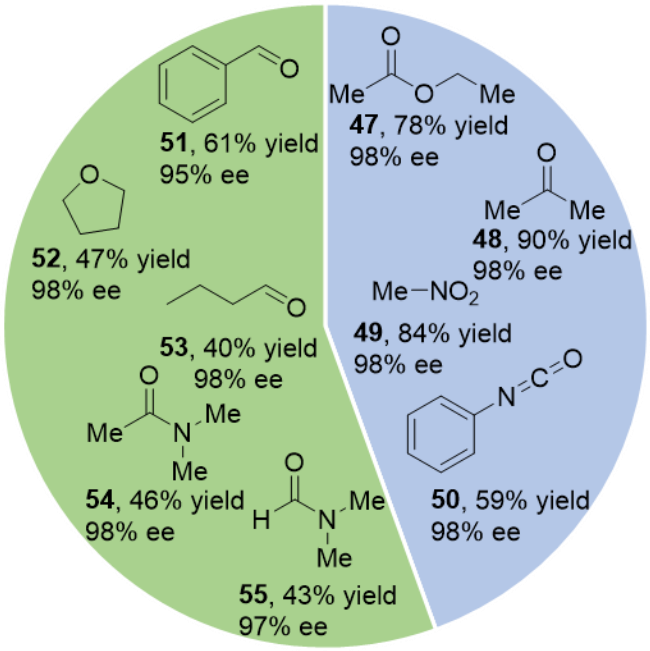

Products are highlighted under the conditions by which best results were obtained in terms of yield and enantioselectivity. Products in blue give optimal results under condition A: Rh_2(*S-tetra-p*-BrPhPTTL)$_4$ (**17**, 1.0 mol%) and dimethyl carbonate as solvent (80ul, 67mM). Products highlighted in green give optimal results under condition B: Rh_2(*S-tetra-p*-BrPhPTTL)$_4$ (**17**, 1.0 mol%) and dimethyl carbonate as solvent (80ul, 67mM) with HFIP (10 equiv).

Basic nitrogen nucleophiles are known to strongly coordinate to many organometallic catalysts. This poses a serious problem for the dirhodium chemistry as not only can nitrogen coordination prevent carbene formation, but the nitrogen can also react strongly with the carbene to generate an ylide which goes on

to do other reactions including the Stevens rearrangement.[13, 71, 77] Indeed, none of the amines tested were tolerated without the use of HFIP with the exception of the bulky tertiary amine triethylamine (**56**). This observation is consistent with the previous study on C–H functionalization of complex molecules in which only bulky tertiary amines were tolerated under standard reaction conditions.[21] Less bulky and more nucleophilic amines including *N*-methyl pyrrolidine (**11**) and quinuclidine (**60**), required 10 equiv HFIP to be deactivated. Imines like 1,8-diazabicyclo (5.4.0)undec-7-ene (DBU, **7**) and *N,N'*-diisopropyl carbodiimide (DIC, **58**) were also well tolerated under these conditions (Table 3.5). While carbodiimides including DIC have been shown to improve the TON of rhodium catalyzed reactions at low concentrations, they act as reaction poisons when in large quantities like those described in this study.[64]

Table 3.5: Tolerance of benchmark reaction to nitrogen nucleophiles in the presence of various quantities of HFIP.

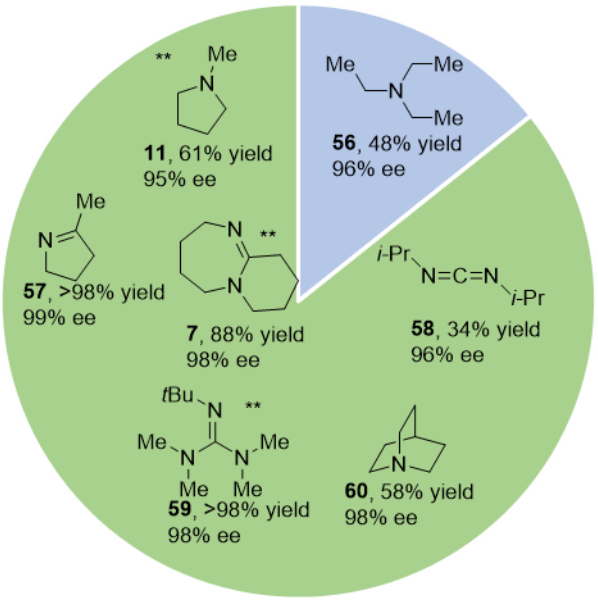

Products are highlighted under the conditions by which best results were obtained in terms of yield and enantioselectivity. Products in blue give optimal results under condition A: Rh_2(*S-tetra-p*-BrPhPTTL)$_4$ (**17**, 1.0 mol%) and dimethyl carbonate as solvent (80ul, 67mM). Products highlighted in green give optimal results under condition B: Rh_2(*S-tetra-p*-BrPhPTTL)$_4$ (**17**, 1.0 mol%) and dimethyl carbonate as solvent (80ul, 67mM) with HFIP (10 equiv). ** This reaction performed on 0.10 mmol scale without molecular sieves and CH_2Cl_2 or HFIP as solvent.

Alcohols and other substrates bearing reactive O–H bonds are well known to insert into metallo-carbenes. This proceeds via initial ylide formation followed by proton transfer in the case of electron rich alcohols,

and by initial protonation of the carbene followed by combination of the resulting charged alkoxide and alkyl-metalated carbon for acidic substrates.[14, 78] Indeed, there is a rich literature around the synthesis of ethers and acetates via this method.[15, 79-86] Unsurprisingly, all of the alcohol substrates reacted with the carbene in the absence of HFIP. Fortunately, several compounds including *tert*-butanol (**12**), salicylic acid (**61**) and acetic acid (**62**) required the use of just 10 equiv HFIP for deactivation (Table 3.6). With larger quantities of HFIP, more reactive nucleophiles including primary and secondary alcohols (**63**-**66**), water (**65**), and phenol (**66**) could also be tolerated. Under these conditions even poly-hydroxylated compounds like ribose (**67**) could be tolerated along with hydroxylamines including cyclohexanone oxime (**15**) and benzohydroxamic acid (**68**, Table 3.6).

Table 3.6: Tolerance of benchmark reaction to reactive O–H bonds in the presence of various quantities of HFIP.

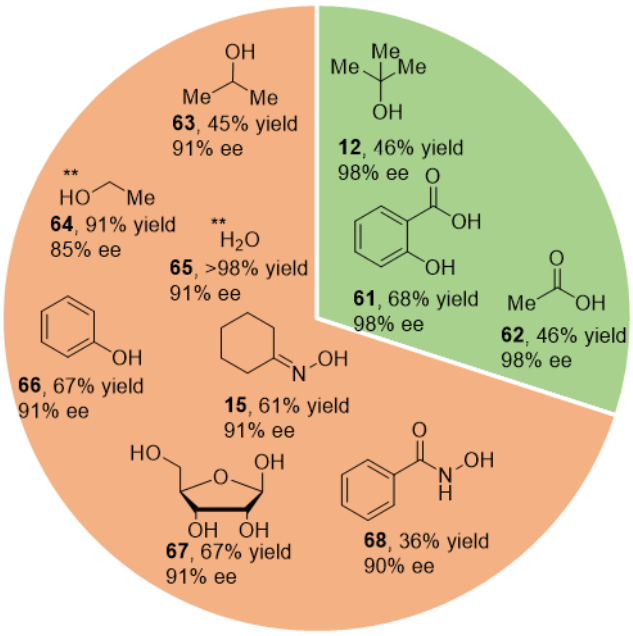

Products are highlighted under the conditions by which best results were obtained in terms of yield and enantioselectivity. Products highlighted in green give optimal results under condition B: Rh_2(*S-tetra-p*-BrPhPTTL)$_4$ (**17**, 1.0 mol%) and dimethyl carbonate as solvent (80ul, 67mM) with HFIP (10 equiv). Products highlighted in orange give optimal results under condition C: Rh_2(*R*-NTTL)$_4$ (**18,** 1.0 mol%) and HFIP as solvent (80ul, 67mM). ** This reaction performed on 0.10 mmol scale without molecular sieves and CH_2Cl_2 or HFIP as solvent.

Reactive N–H bonds are even more challenging to deactivate.[87] Not only can small amines coordinate to the dirhodium catalyst, but the reactive nitrogen can also react with the carbene. The resulting ylide can go on to conduct a multitude of transformations, including 2,3-sigmatropic rearrangements and proton transfer to yield formal N–H insertion products.[4, 16, 88-97] None of the additives tested could be tolerated in the absence of HFIP and led to a multitude of side-products. A few additives like *N*-methyl acetamide (**54**), *N,N'*-di-*p*-tolyl thiourea (**70**), and *D*-proline (**72**) were tolerated with just 10 equiv of HFIP (Table 3.7). Fortunately, most of the compounds tested were tolerated with the use of HFIP as solvent. Under these conditions most reactive species were compatible. Primary amides (**14**, **75** and **76**), ureas (**73**, **77,** and **82**), guanidine (**74**), and even amines (**79** and **80**) were well tolerated. Unfortunately, regardless of the conditions used, pyrrolidine (**85**), aniline (**84**), *N*-methyl aniline (**86**), and diphenyl hydrazone (**87**) exclusively delivered the N–H insertion products (Table 3.7). The reason for this intolerance is as-yet undetermined but could be due to two different reasons. For highly electron-rich nitrogen atoms like pyrrolidine (**85**) and diphenyl hydrazone (**87**) it is possible that even HFIP is unable to fully disrupt ylide formation, leading to the observed side products. In the case of *N*-methyl aniline (**86**) and aniline (**84**) the opposite problem appears to manifest, as these amines are not basic enough to interact with HFIP, but are still capable of forming ylides with the carbene leading to the observed side products.[16]

Table 3.7: Tolerance of benchmark reaction to reactive N–H bonds in the presence of various quantities of HFIP.

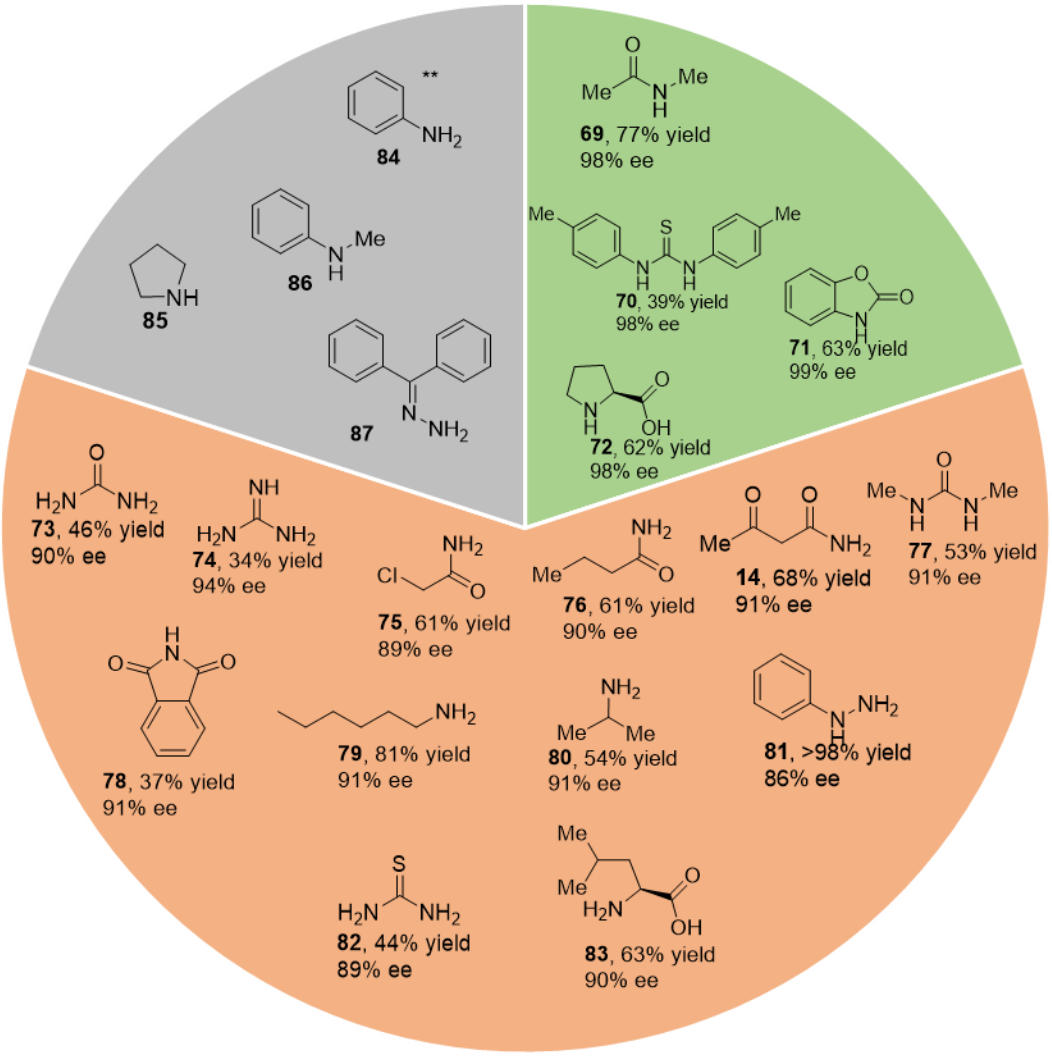

Products are highlighted under the conditions by which best results were obtained in terms of yield and enantioselectivity. Products highlighted in green give optimal results under condition B: Rh_2(*S-tetra-p*-BrPhPTTL)$_4$ (**17**, 1.0 mol%) and dimethyl carbonate as solvent (80ul, 67mM) with HFIP (10 equiv). Products highlighted in orange give optimal results under condition C: Rh_2(*R*-NTTL)$_4$ (**18,** 1.0 mol%) and HFIP as solvent (80ul, 67mM). Products highlighted in grey were not tolerated under any conditions giving 0-29% yield of the desired product on both micro and laboratory scale. ** This reaction performed on 0.10 mmol scale without molecular sieves and CH_2Cl_2 or HFIP as solvent.

The highly polarizable nature of the sulfur atom makes it an excellent ligand for metal catalysts and also makes thiols exceptionally reactive in comparison with the oxygen congeners. As a result, such species can both poison the catalyst through nucleophilic coordination or react with the carbene in a similar manner to nitrogen and oxygen.[16, 93, 98-100] Sulfur also readily forms hypervalent compounds and the atoms directly bound to the sulfur atom can become more reactive as in the case of sulfonic acids and DMSO.

Unsurprisingly, sulfur containing compounds proved difficult to deactivate (Table 3.8). Only diphenyl-disulfide (**88**) was tolerated without any HFIP and, in-fact, when HFIP was included with this additive both reactivity and solubility suffered, possibly due to cleavage of the disulfide bond in this acidic medium. The use of 10 equiv HFIP was enough to deactivate several sulfur-containing additives including carbon disulfide (**74**) and (+)-camphor sulfonic acid (**91**) where atoms other than sulfur are typically reactive in chemical transformations. Solvent equivalents of HFIP effectively deactivate phenyl-isothiocyanate (**93**), dimethyl-sulfoxide (**94**), and *p*-toluene-sulfonamides (**95** and **96**). Unfortunately, thiols like thiophenol (**97**), and benzyl-thiol (**98**) were not tolerated under any conditions (Table 3.8) exclusively affording the corresponding S–H insertion products.

Table 3.8: Tolerance of benchmark reaction to sulfur nucleophiles in the presence of various quantities of HFIP.

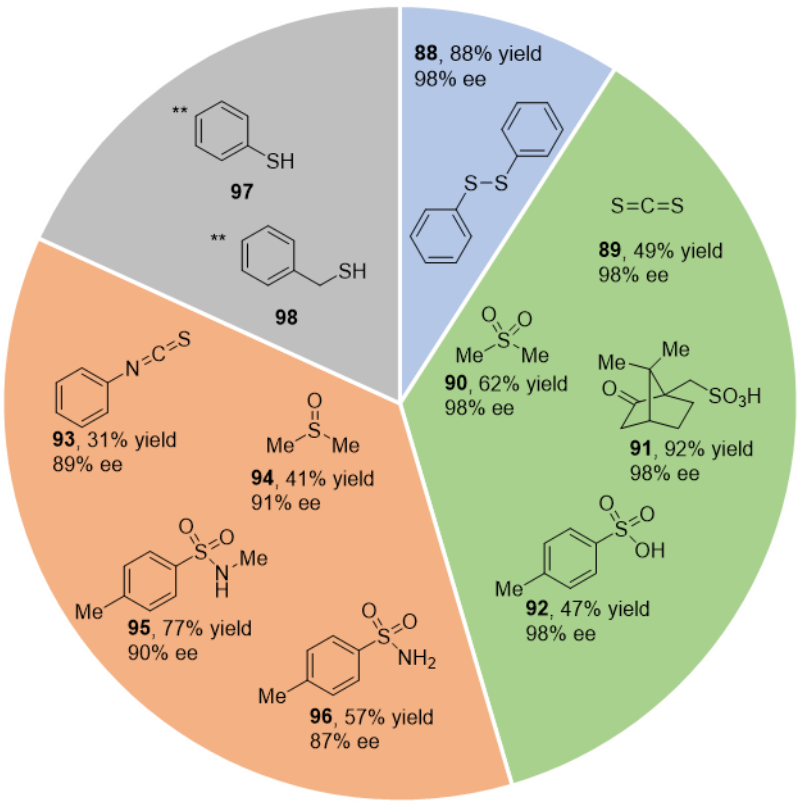

Products are highlighted under the conditions by which best results were obtained in terms of yield and enantioselectivity. Products in blue give optimal results under condition A: Rh_2(*S-tetra-p*-BrPhPTTL)$_4$ (**17**, 1.0 mol%) and dimethyl carbonate as solvent (80ul, 67mM). Products highlighted

in green give optimal results under condition B: Rh_2(*S-tetra-p*-BrPhPTTL)$_4$ (**17**, 1.0 mol%) and dimethyl carbonate as solvent (80ul, 67mM) with HFIP (10 equiv). Products highlighted in orange give optimal results under condition C: Rh_2(*R*-NTTL)$_4$ (**18,** 1.0 mol%) and HFIP as solvent (80ul, 67mM). Products highlighted in grey were not tolerated under any conditions giving 0-29% yield of the desired product on both micro and laboratory scale. ** This reaction performed on 0.10 mmol scale without molecular sieves and CH_2Cl_2 or HFIP as solvent.

Phosphorus is one of the most important elements in inorganic synthesis due to the soft basic nature of phosphorus making it a strongly coordinating ligand for a large variety of metals.[101] Like, sulfur, phosphorus can exist in a multitude of oxidation states and while P(V) ligands are becoming more popular in catalysis,[102, 103] P(III) ligands are still preferred for a majority of catalytic systems, especially Pd catalyzed cross-coupling.[104-106] The compatibility of phosphorus compounds with this method was highly dependent on the phosphorus oxidation state (Table 3.9). P(V) compounds like triphenyl phosphine oxide (**100**) and HMPA (**99**) were well tolerated without the need for any HFIP. The strongly coordinating P(III) species like PPh_3 (**101**) and dppf (**102**), however, were not tolerated under any conditions due to coordination to the dirhodium catalyst, as evidenced by the dark red coloration of the reaction solution upon addition of phosphine, preventing carbene formation.

Table 3.9: Tolerance of benchmark reaction to phosphorus-containing nucleophiles in the presence of various quantities of HFIP.

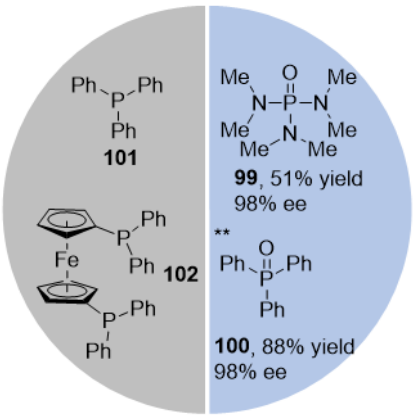

Products are highlighted under the conditions by which best results were obtained in terms of yield and enantioselectivity. Products in blue give optimal results under condition A: Rh_2(*S-tetra-p*-BrPhPTTL)$_4$ (**17**, 1.0 mol%) and dimethyl carbonate as solvent (80ul, 67mM). Products highlighted in grey were not tolerated under any conditions giving 0-29% yield of the desired product on both micro and laboratory scale. ** This reaction performed on 0.10 mmol scale without molecular sieves and CH_2Cl_2 or HFIP as solvent.

Various additives were also examined that did not fit neatly into the other categories (Table 3.10). While acetonitrile (**103**) is a strongly coordinating solvent, it, and related analogues as explored in **Chapter 1,** has been used for a wide array of reactions involving dirhodium nitrenes.[22, 107] While these reactions are generally run at high temperature, the use of acetonitrile suggests that coordination of this ligand is kinetically dynamic. In rhodium carbene chemistry nitriles can cause a drop in yield,[62] but it appears not to react with the carbene when in competition with the cyclopropanation and was tolerated without the need for HFIP. The radical reagent TEMPO (**104**), was also tolerated, it is possible that the singlet nature of the dirhodium carbene prevents modes of radical reactivity and that blue light generation of the carbene would not tolerate TEMPO.[48]

Table 3.10: Tolerance of benchmark reaction to miscellaneous compounds in the presence of various quantities of HFIP.

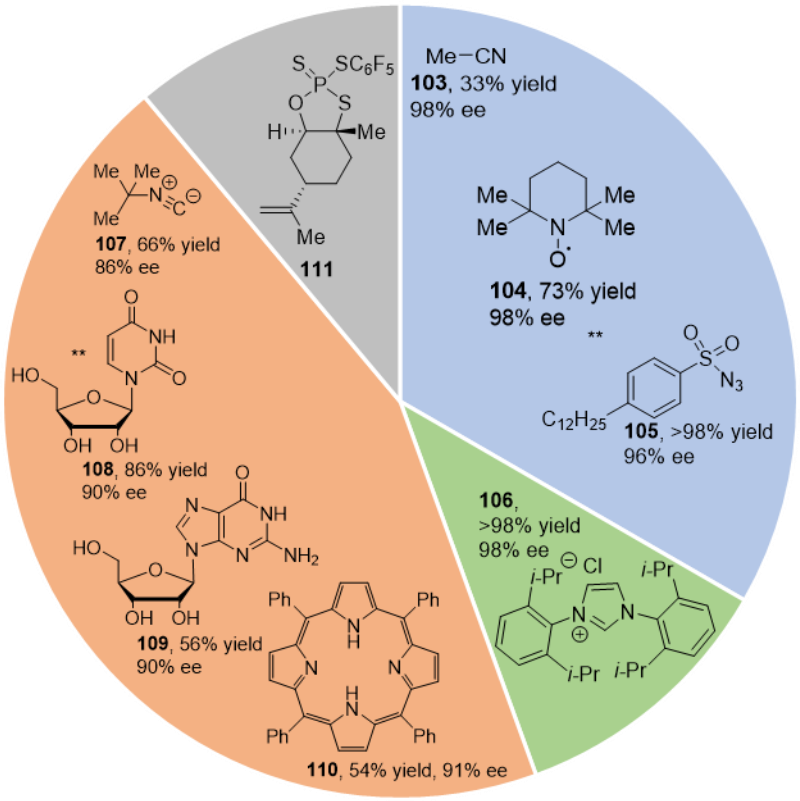

Products are highlighted under the conditions by which best results were obtained in terms of yield and enantioselectivity. Products in blue give optimal results under condition A: Rh_2(*S-tetra-p*-BrPhPTTL)$_4$ (**17**, 1.0 mol%) and dimethyl carbonate as solvent (80ul, 67mM). Products highlighted

in green give optimal results under condition B: Rh_2(*S-tetra-p*-BrPhPTTL)$_4$ (**17**, 1.0 mol%) and dimethyl carbonate as solvent (80ul, 67mM) with HFIP (10 equiv). Products highlighted in orange give optimal results under condition C: Rh_2(*R*-NTTL)$_4$ (**18,** 1.0 mol%) and HFIP as solvent (80ul, 67mM). Products highlighted in grey were not tolerated under any conditions giving 0-29% yield of the desired product on both micro and laboratory scale. ** This reaction performed on 0.10 mmol scale without molecular sieves and CH_2Cl_2 or HFIP as solvent.

Dodecylbenzene sulfonyl azides (**105**) were also tolerated without the use of HFIP although enantioselectivity suffered as a result. An *N*-heterocyclic carbene ligand (**106**) required the use of 10 equiv HFIP to affect deactivation and gratifyingly strongly coordinating *tert*-butyl isocyanide (**107**) was also tolerated with solvent quantities of HFIP.[101, 108] Several complex molecules, including the nucleosides uridine (**108**) and guanosine (**109**) were compatible under this reaction system and even *meso*-tetraphenylporphyrin (**110**) was well tolerated when HFIP was used as the reaction solvent (Table 3.10). Unfortunately, the recently disclosed (+)-PSI-reagent (**111**) from the Baran group[109] was not tolerated under any conditions, instead reacting with the carbene either through the nucleophilic sulfur atom or the terminal alkene on the limonene-derived molecule. Future attempts should be made to identify the byproduct of this reaction as it is entirely possible that derivatives of PSI lacking a terminal alkene would be perfectly compatible with this method. This would increase the applicability of the reaction to include poly-nucleotide processes which may harbor trace amounts of PSI reagent during preparation.

While most of the additives tested had little to no impact on the enantioselectivity of the reaction some additives, like 1,2,3-triazole (**45**) and pyridine (**13**), caused a significant reduction in enantioselectivity. This could be due to incomplete deactivation of the nucleophile or coordination of the nucleophile-HFIP complex to the catalyst. While not strong enough to completely poison the reaction, coordination of the nucleophile to the rhodium-carbene complex or to the carbene itself could cause a change in catalyst structure or carbene accessibility leading to the observed reduction in enantioselectivity.[8, 101] More work is needed both to understand the effect of HFIP and combinations of HFIP and nucleophile on catalyst stereoselectivity. The results of this study may be visualized in a succinct manner through the use radar plots inspired by Glorius (Figure 3.2).[110] In these diagrams, the percentage total additives tested from each category which gave successful reactions under the given condition is plotted as a black line. The radar

plot is color coordinated to visually display the tolerance of each category. Lines within the red/orange regions then the reaction displays poor functionality tolerance (10-50% of additives tested) and if the line lies within the yellow-green region then the reaction tolerates a wide array of different scaffolds with this functionality (75-100% of additives tested). From this visualization the impact of increasing equivalents of HFIP is made clear as the tolerance map expands toward the edges of the diagram, tolerating 90% of all additives tested when HFIP is used as solvent (81 out of 90, Figure 3.2).[52]

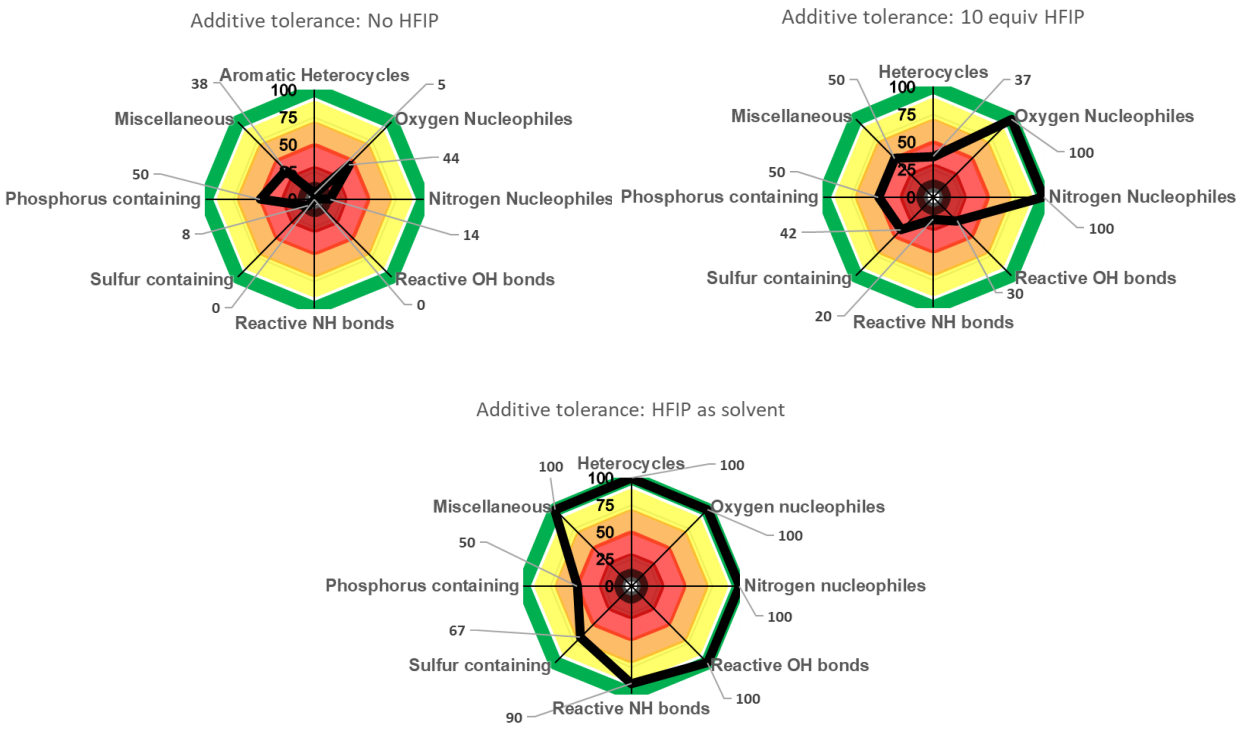

Figure 3.2. Radar plots visualize the tolerance of the described methodologies[110] to the different classes of poisonous and reactive nucleophiles tested. The values listed represent the percentage of substrates tested that were tolerated with each set of conditions.

These results demonstrated a broad array of functionality tolerance. The deactivating effect of HFIP can even be visually observed in real time (Figure 3.3), as in the case of *N*-methyl pyrrolidine (**11**). Without any additive, the dissolved catalyst **17** + 1-hexene appears as a green solution (Figure 3.3a) but upon

addition of **11** a distinct color change is observed, and the solution becomes pink (Figure 3.3b) due to solvatochromism upon coordination of nitrogen to **17**.[111] When HFIP (10 equiv) is added to the solution, another abrupt color change is observed, and the solution becomes a greenish blue coloration (Figure 3.4c). This indicates that the catalyst is no longer coordinated to **11**, and the catalyst **17** is liberated to perform the desired carbene reaction. Upon the addition of diazo compound **9**, the solution briefly becomes yellow and nitrogen gas rapidly evolves (Figure 3.4d). After 30 min, the solution reverts to the bluish green of the catalyst, the diazo compound has been fully consumed and the cyclopropane generated (Figure 3.4d-e).

Figure 3.3: HFIP deactivating a nucleophile in real time. A: The catalyst **17** dissolved in CH_2Cl_2. B: Solution after addition of **11** (1.0 equiv). C: Solution after addition of HFIP (10.0 equiv). D: Solution immediately after addition of **9** (1.0 equiv). E: Solution after stirring at Rt for 30 mins.[52]

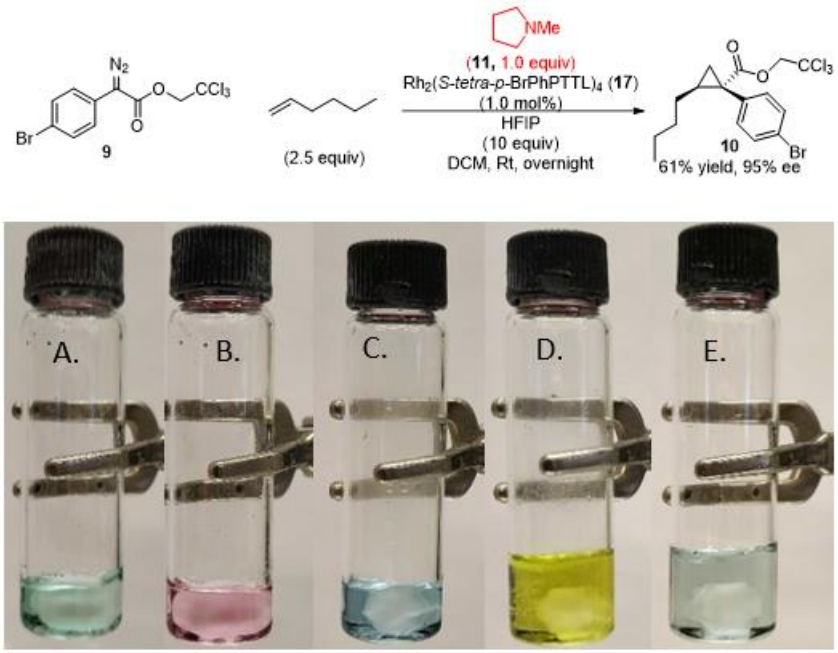

After exploring the tolerance of this methodology, a systematic study was conducted to determine if the optimized reaction conditions were capable of high asymmetric induction in the cyclopropanation with a

range of aryl-and heteroaryldiazoacetates with various alkenes (Table 3.11). The results of the Rh_2(*S-tetra-p*-BrTPPTTL)$_4$ (**17**)-catalyzed reaction and 10 equiv HFIP is indicated in green and the Rh_2(*R*-NTTL)$_4$ (**18**)-catalyzed reaction with HFIP as solvent is indicated in orange. The reactions with Rh_2(*S-tetra-p*-BrTPPTTL)$_4$ (**17**) tended to give high selectivity regardless of substrate, whereas reactions with Rh_2(*R*-NTTL)$_4$ (**18**) exhibited more variable levels of enantioselectivity (71-99% ee). All of the products were obtained with the typically high >20:1 d.r observed with rhodium-catalyzed cyclopropanation with the exception of **125**, which was obtained in 7:1 d.r. The major diastereomer of **125** is identified as the *E*-cyclopropane due to the considerable shielding of the silyl-methylene by the *cis*-phenyl ring (appearing at -0.47 ppm). One particularly interesting example is the reaction of methyl 2-(4-pyridyl)-2-diazoacetate with 1-hexene to form **114**, as the reaction cannot proceed without the use of HFIP as solvent. As discussed in chapter 2, the reactions of *ortho*-substituted aryldiazoacetates is a fundamentally different reaction and requires significant optimization to ensure a successful transformation. It is therefore unsurprising that *ortho*-substituted aryldiazoacetates did not achieve high selectivity under these conditions. Fortunately, in **Chapter 2**, a method for ensuring high enantioselectivity was developed and shown to be compatible with 10 equiv HFIP. When this method was conducted using 1.0 equiv 2-chloropyridine as additive, Rh_2(*S*-TPPTTL)$_4$ (**5**) as the catalyst, and 10 equiv HFIP, the desired cyclopropane **126** was afforded in high yield and enantioselectivity (95% yield, 90% ee). When the reaction was repeated using HFIP as solvent high asymmetric induction was maintained, and the desired cyclopropane was produced in 78% yield and 82% ee. Although this result remains unpublished it is an excellent illustration of the robustness of the additive effect and generality of the method described in **Chapter 2,** as well as the unique status of 2-chloropyridine as an *N*-heterocycle unaffected by the presence of HFIP and thus still able to deliver enantioenhancement regardless of the reaction conditions.[5, 8] Indeed, Rh_2(*S*-TPPTTL)$_4$ (**5**) cannot normally tolerate HFIP as a solvent and when the diazo-compound is *para*-substituted the enantioselectivity drops to practically 0% ee. However, in combination with an *ortho*-substituted aryldiazoacetate and 2-

chloropyridine the enantioenhancemet is preserved and the reaction is rendered highly selective, even with HFIP as solvent.

Table 3.11: Scope of aryl/heteroaryl diazoacetates and olefins tolerated under the complementary methodologies described in this work.

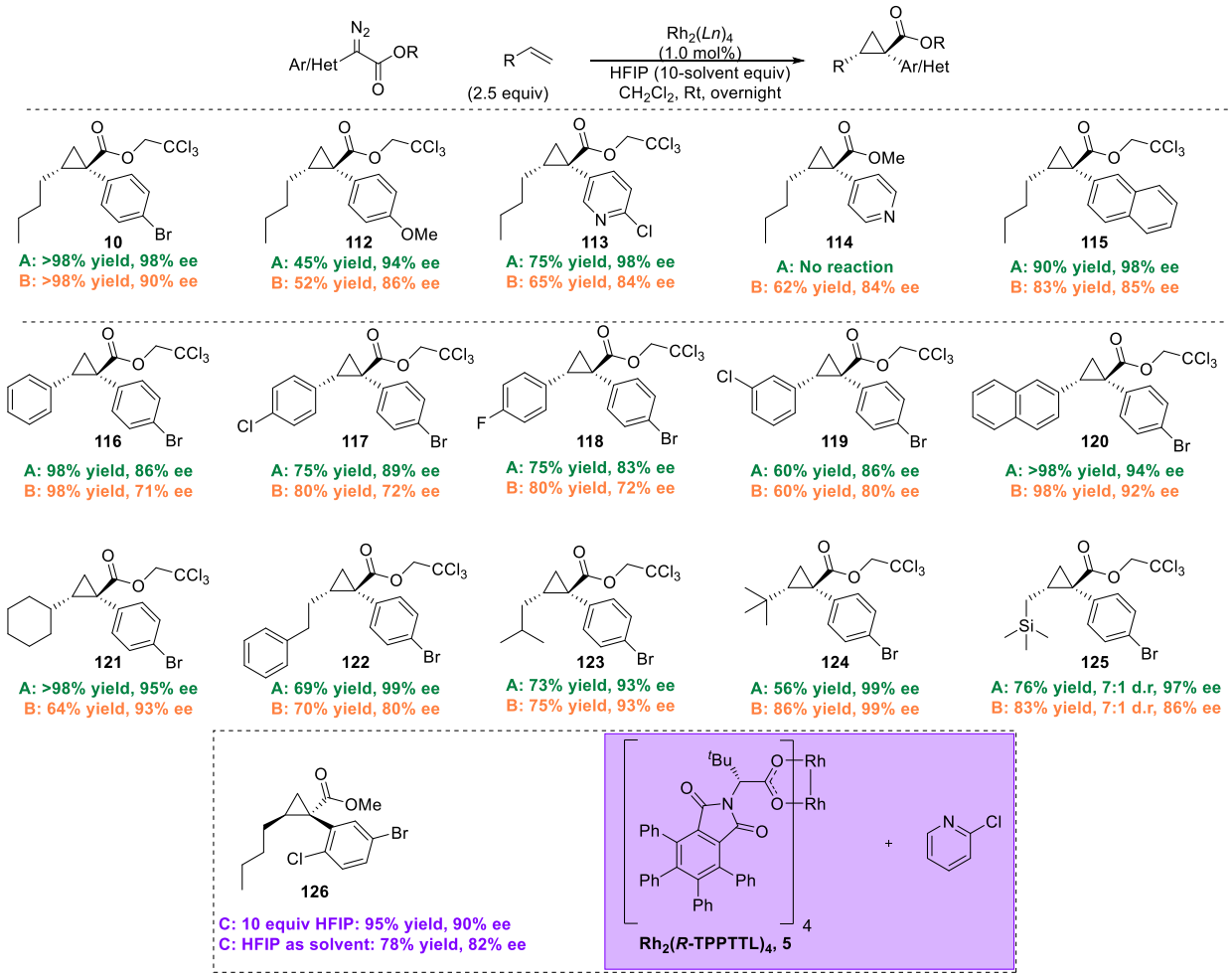

All reactions were conducted at 0.10 mmol scale with 2.5 equivalents of olefin and 1.0 equiv of aryl/heteroaryl diazoacetate in the presence of rhodium catalyst (1.0 mol%) and HFIP. All products were produced in >20:1 d.r. unless indicated. Condition A: Rh_2(*S-tetra-p*-BrPhPTTL)$_4$ (**17**) 10 equiv HFIP. Condition B: Rh_2(*R*-NTTL)$_4$ (**18**) HFIP as solvent. Condition C: Rh_2(*R*-TPPTTL)$_4$ (**5**), 2-chloropyridine (1.0 equiv). Major enantiomer configuration is assigned by analogy to the absolute configuration of **125** determined by X-ray crystallography (CCDC 2182303).

Given the breadth of functionality tolerance the transformation was conducted on several substrates bearing classically poisonous functionality. One of the cleanest transformations occurred with the pharmacologically active progestin Altrenogest (Scheme 3.8).[112, 113] Without HFIP, the reactive alcohol can

selectively react with the carbene and the α-β unsaturated ketone could generate ylides, leading to epoxide and other side-product formation.[75] Fortunately, when HFIP was used as solvent, the compound reacted exclusively at the terminal alkene to afford the desired cyclopropane **127** in 70% yield and with >20:1 d.r. The stereochemical configuration of the cyclopropane is assigned assuming the same preferences for *E*-cyclopropane formation and asymmetric induction seen in Table 3.11.

Scheme 3.8: Cyclopropanation of Altrenogest.

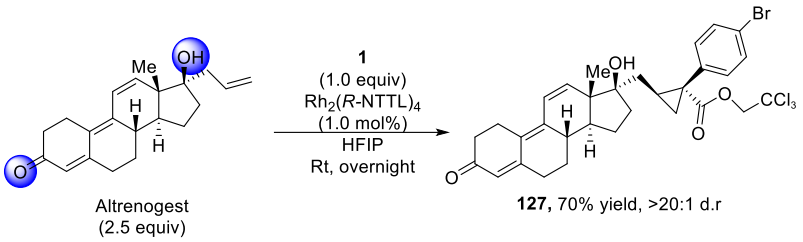

Cinchona alkaloids are an important class of molecules with a wide variety of pharmaceutical and industrial applications.[88, 89] (*S*)-Cinchonidine features several problematic functionalities including a chiral secondary alcohol which could react with the carbene (Scheme 3.9). The molecule also features several poisonous nucleophilic sites including a quinoline, and a quinuclidine ring which coordinates to the catalyst, preventing rhodium carbene generation in the absence of HFIP. Once the reaction was performed in HFIP as solvent with Rh_2(*R*-NTTL)$_4$ (**18**) as catalyst the desired cyclopropane **128** was afforded as in 98% yield and with >20:1 d.r. Although 2.5 equiv of the complex alkene is required for high yield, unreacted starting material was recovered quantitatively during purification. The stereochemical configuration of the cyclopropane was initially assigned assuming the same preferences for *E*-cyclopropane and asymmetric induction seen in the model substrates in Table 3.11, and this was confirmed via X-ray crystallography (CCDC 2182287).

Scheme 3.9: Cyclopropanation of (*S*)-Cinchonidine.

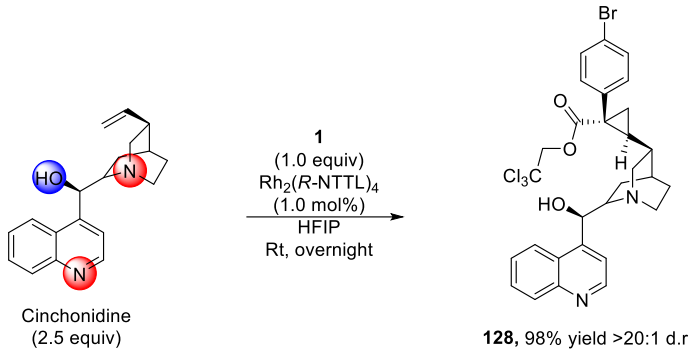

The procaspase-3-activator, PAC-1,[114] was also successful in the reaction and bares a significant amount of problematic functionality including a hydrazide, piperazine, and an unprotected phenol which results in undesired side-reactions in the absence of HFIP (Scheme 3.10). While the transformation occurred at the free alkene as intended using HFIP as solvent, the acidity of the solvent scrambled the *E:Z* ratio of the of the hydrazide. The starting material displayed a 12:1 ratio between these isomers, the product **129** was isolated as a 1:1 mixture that we were unable to separate by HPLC. The stereochemical configuration of the cyclopropane is assigned assuming the same preference for *E*-cyclopropane formation and asymmetric induction seen in the model substrates in Table 3.4. This assignment is further bolstered by the appearance of the minor diastereomer of both the *E* and *Z* isomer methylene at a higher chemical shift (2.75 ppm) than the major product methylene (2.65 ppm). This is due to the shielding experienced by the methylene in the *E*-cyclopropane diastereomer which is absent in the *Z*-cyclopropane. Interestingly, while one of the isomers gives poor diastereoselectivity (6:1 favoring the *E*-cyclopropane), the other isomer gives the typically high diastereoselectivity observed in this work (>20:1 d.r again favoring the *E*-cyclopropane). Due to the complexity of the spectrum, it was not possible to determine whether the *E* or *Z*- configuration of the hydrazide afforded the highest diastereoselectivity.

Scheme 3.10: Cyclopropanation of PAC-1.

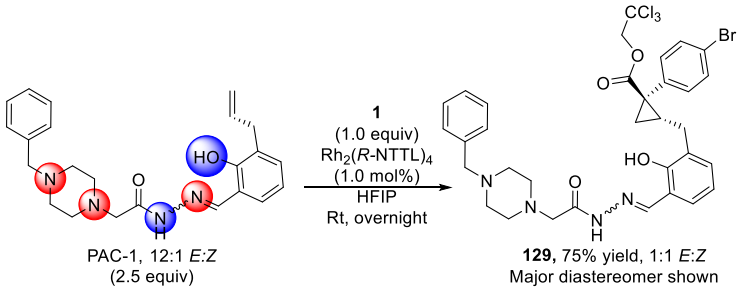

Tacrolimus, or FK-506, is an important calcineurin inhibitor.[115-117] The molecule is a large macrocycle consisting of 21 atoms and bearing a variety of problematic functionality including a three free hydroxyl groups and piperidinyl amide which could react with the carbene (Scheme 3.11). The molecule exists as a dynamic mixture of conformers in solution corresponding to *cis/trans* isomerization around the piperidinyl amide and is used medicinally as this mixture.[118-120] Fortunately, both conformers were reactive under the optimized conditions, and only cyclopropanation of the free alkene was observed. No rearrangement of the macrocyclic core was observed despite the acidic reaction conditions and the identity of the product **130** was confirmed via 2D NMR experiments. The stereochemical configuration of the cyclopropane is assigned assuming the same preference for *E*-cyclopropane formation and asymmetric induction seen in the model substrates in Table 3.11. The diastereoselectivity of this product was not possible to determine due to the complexity of this conformationally dynamic macrocycle. The cyclopropane and methylene signals that are often indicative of the diastereoselectivity are buried underneath the many alkyl signals of the large molecule and further convoluted by the presence of 2 major conformations of the piperidinyl amide in solution, making reliable determination of diastereoselectivity impossible.

Scheme 3.11: Cyclopropanation of FK506(Tacrolimus).

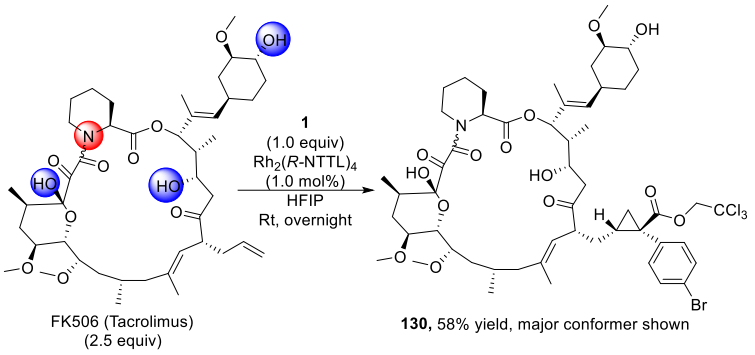

The hepatitis-C drug Asunaprevir[121, 122] was also successfully cyclopropanated to afford **131** (Scheme 3.12). The highly complex scaffold features a diverse array of functionality including a quinoline, a pyrrolidinyl amide, a sulfonamide and a *Boc*-protected *tert*-leucine residue. In the absence of HFIP, the isoquinoline heterocycle could poison the rhodium catalyst or one of the secondary amido nitrogens could preferentially insert into the carbene. Fortunately, when HFIP was used as solvent, only cyclopropanation of the terminal olefin was observed, and the structure was confirmed by 2D NMR, although the resultant product was unstable at elevated temperatures. The use of an acidic reaction medium and TFA as a mobilizing additive in the subsequent HPLC purification led to partial removal of the *Boc*-group. As a result, this compound was not obtained with high purity though it was still possible to confirm the structure of the major product through 2D NMR experimentation. The stereochemical configuration of the cyclopropane is assigned assuming the same preference for *E*-cyclopropane formation and asymmetric induction seen in the model substrates in Table 3.11. This is bolstered by the significant shielding of the diastereotopic cyclopropane methylene adjacent to the site of carbene insertion. In the starting material these signals appear at 1.98 ppm and 1.49 ppm, but in the product, they are no longer close to an alkene and are also significantly shielded by the *p*-bromophenyl ring appearing at 0.66 ppm and 0.45 ppm. This shielding is only present in the *E*-cyclopropane suggesting that the reaction occurs with the high

diastereoselectivity typically observed in this reaction although the minor diastereomer signals could not be confidently assigned due to the complex nature of the NMR.

Scheme 3.12: Cyclopropanation of Asunaprevir.

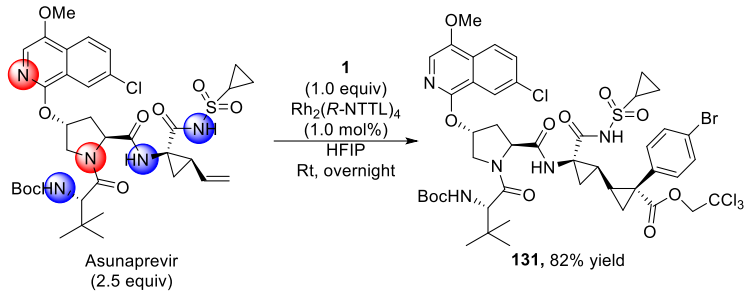

After the publication of these initial experiments, there was interest in investigating other quirks of carbene reactivity in HFIP as solvent. Using HFIP as solvent proved to be the most broadly applicable conditions for the deactivation of poisonous and reactive nucleophiles and so an industrially relevant method for C–H functionalization of complex molecules would need to tolerate HFIP as solvent. There are reasons to doubt the efficacy of C–H functionalization in such a medium despite the success of cyclopropanation under the same conditions. In cyclopropanation, the rate-determining step is dinitrogen extrusion to generate the rhodium carbene as the energetic barrier for cyclopropanation from this unstable intermediate is very low (0-3 kcal/mol).[7, 62, 123, 124] In contrast, the hydride abstraction barrier in C–H functionalization is significantly higher (~5 kcal/mol) and as such this becomes the rate determining step.[45, 64, 125] It is possible that the change in reaction mechanism will cause problems when using HFIP as solvent, additionally, the acidic polar medium could cause different asymmetric induction in C–H insertion, as it did in cyclopropanation. C–H functionalization of cyclohexane proved competent with both Rh_2(*R*-NTTL)$_4$ (**18**) and Rh_2(*S-tetra-p*-BrTPPTTL)$_4$ (**17**) although the phthalimide derived catalyst generated the product in higher %ee (73%). This was encouraging initial data that the reaction could be possible. Even though site-selective catalysts like Rh_2(*p*-PhTPCP)$_4$ (**16**) and Rh_2(TPPTTL)$_4$ (**5**) performed poorly in the

cyclopropanation method, many catalysts have exhibited different levels of enantioinduction in C–H functionalization compared to cyclopropanation. For example, as described in **Chapter 1**, Rh_2(2Cl5Br-TPCP)$_4$ is a highly stereoselective catalyst for C–H functionalization of unactivated C–H bonds in the presence of benzylic C–H bonds, routinely giving >94% ee across a wide substrate scope.[126] However, in cyclopropanation this catalyst is relatively unselective giving at most 63% ee.[62] Future studies will focus on achieving known, highly selective transformations with classically incompatible substrates featuring nucleophilic and reactive sites.

This highly polar medium could also affect selectivity in classical transformations. To this end, *p*-cymene was reacted with **9** in the presence of Rh_2(*R*-TCPTAD)$_4$ (**132**) (Figure 3.4). This catalyst is typically highly selective for tertiary C–H bonds, and the reaction performed in DCM afforded the tertiary insertion product **134** with a >20:1 selectivity over the primary site **133**.[127, 128] Surprisingly, when the reaction was performed in HFIP, **133** was obtained as the major product with 2:1 selectivity over tertiary C–H insertion. The selectivity warping nature of HFIP was indeed surprising, although it can likely be explained through the coordination of HFIP to the carbonyl of the rhodium carbene intermediate. This would make the carbene more electron deficient by enhancing the electron withdrawing nature of the ester, a more electrophilic carbene is also more reactive in C–H functionalization. Site and enantioselectivity in these transformations derive from the ability of the carbene to sample different sites on a substrate and select between them depending on the electronics and sterics of both the catalyst and the substrate.[7, 45, 126, 129, 130] If, however, the carbene is extremely electrophilic then it will instead react with the most kinetically favorable site, and selectivity will be lost or altered, this hypothesis is explored further in **Chapter 4**.

Figure 3.4: Reactions run in HFIP override native catalyst site-selectivity. **132** changes from a tertiary selective catalyst to a primary selective catalyst in HFIP in the reaction of both *p*-cymene and 2-hexene.

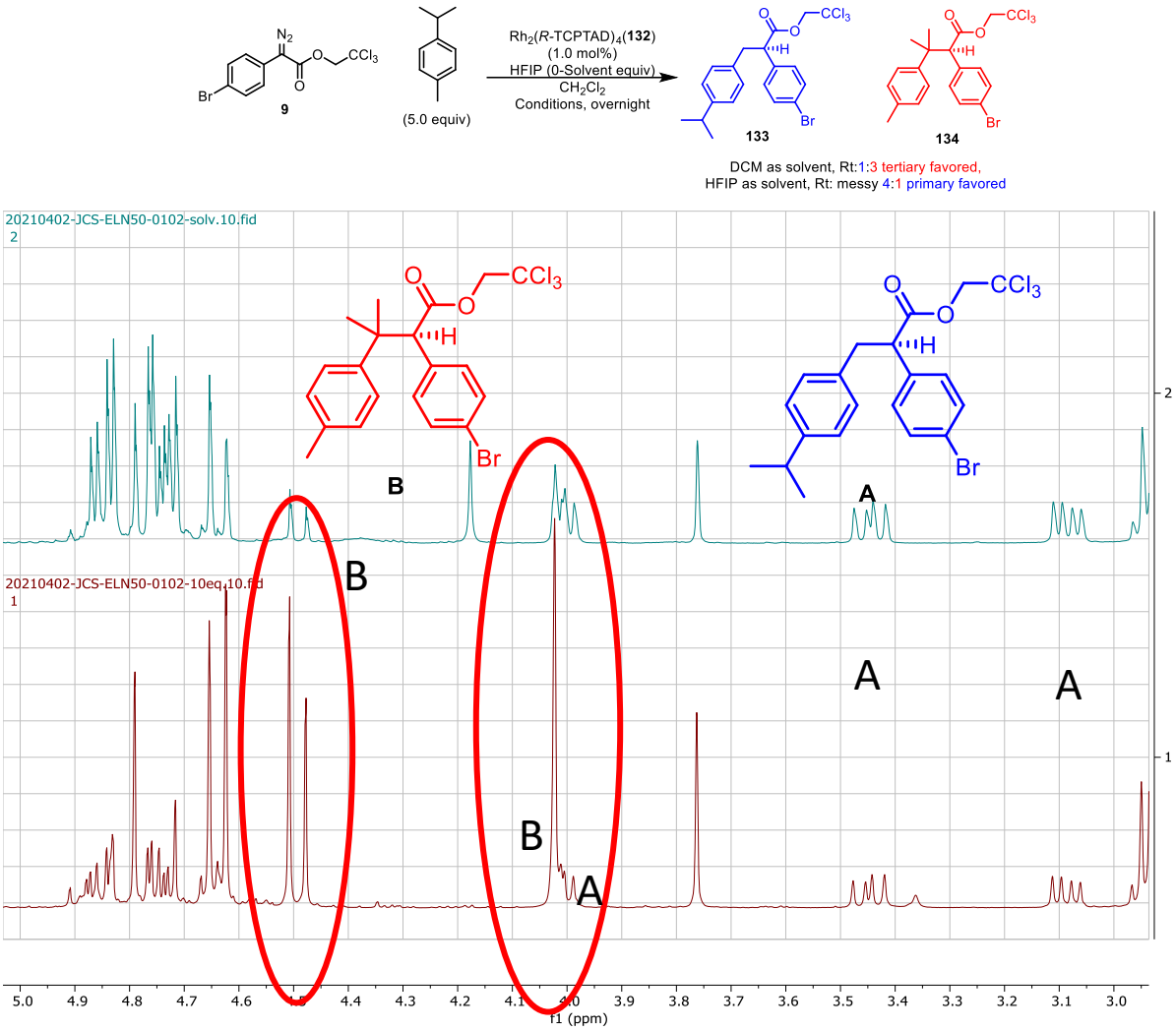

This selectivity also manifests as loss of diastereoselectivity for other substrates (Figure 3.5). For example, the reaction of 2-hexene in the presence of Rh_2(*R*-TCPTAD)$_4$ (**132**) is selective for the C4 allylic methylene (**136**, 8:1 r.r) and gives high diastereoselectivity (8:1 d.r) when the reaction was conducted in DCM. When the reaction was repeated in HFIP, not only was it now selective for the primary allylic C–H bond (**135**), but the diastereoselectivity of the secondary insertion product was also crippled to give just 2:1 d.r. This suggests that the carbene is less selective in the presence of HFIP which causes it to react with the most

sterically accessible activated C–H bond over more electronically activated sites, and it cannot sample different protons at the same site leading to the lack of diastereoselectivity.[45, 125, 131]

Figure 3.5: Changes in carbene reactivity in HFIP translate to changes in site and diastereoselectivity.

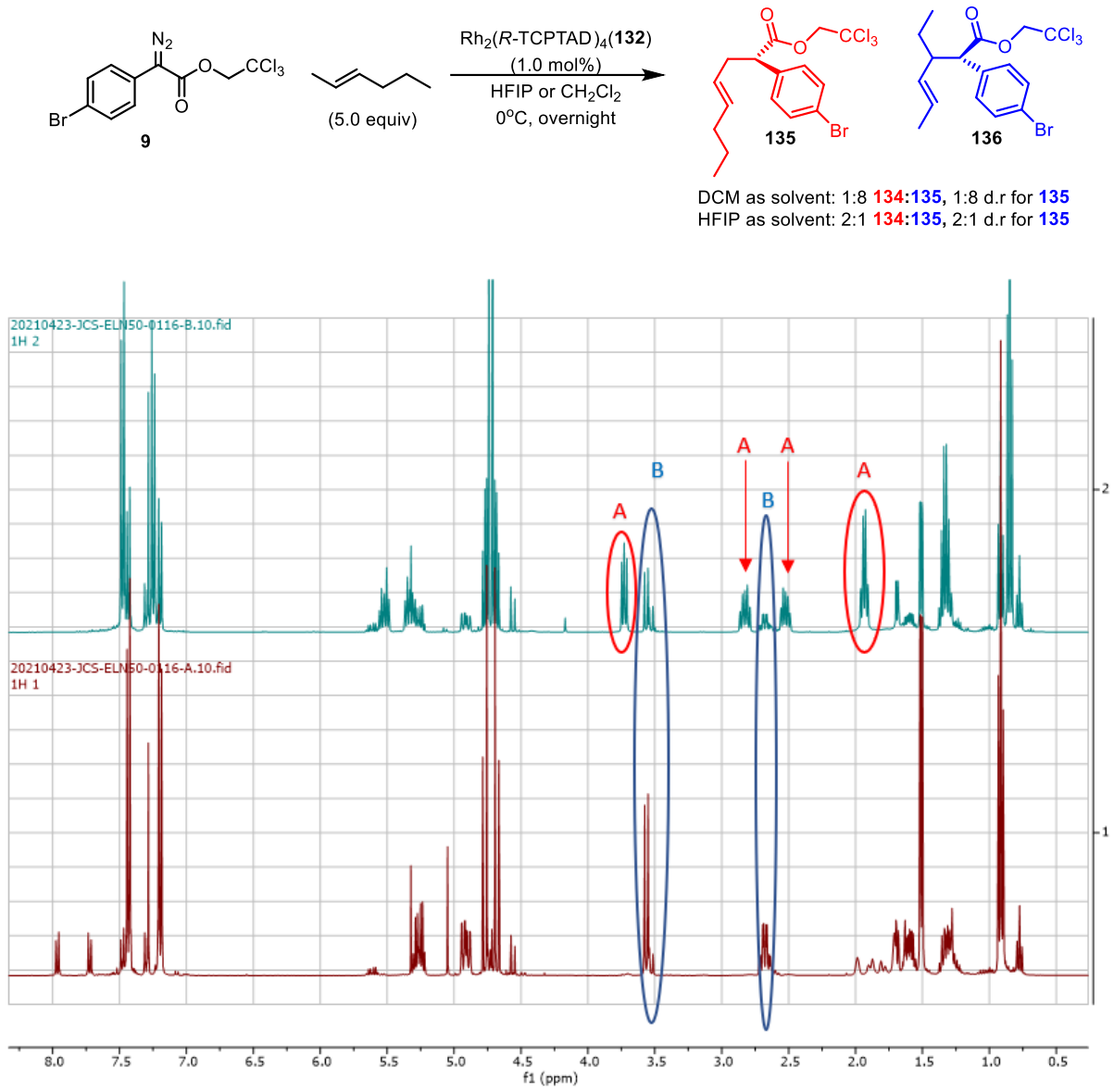

Another interesting feature of reactions with catalyst **132** is that it experiences an inversion in enantioselectivity when HFIP is used as a solvent (Figure 3.6). By varying the amount of HFIP in the reaction, it was discovered that this inversion manifests only in solvent mixtures that include high

concentrations of HFIP (Figure 3.6, minimum 1:1 HFIP:DCM). Through a screen of other solvents it was also determined that the effect is not a function of solvent polarity as solvents with a larger dielectric constant, and hence more polar solvents, did not cause inversion in enantioselectivity (Figure 3.7). We therefore hypothesize that hydrogen bonding interactions between HFIP and the catalyst/**132**-carbene complex are responsible for the enantioinversion.

Figure 3.6: The enantioselectivity of **132** is inverted in the presence of high concentrations of HFIP.

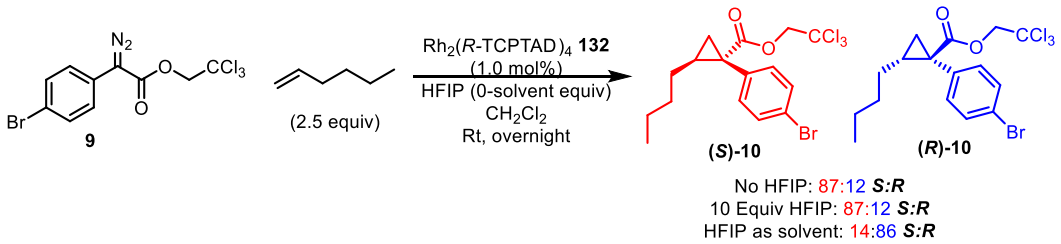

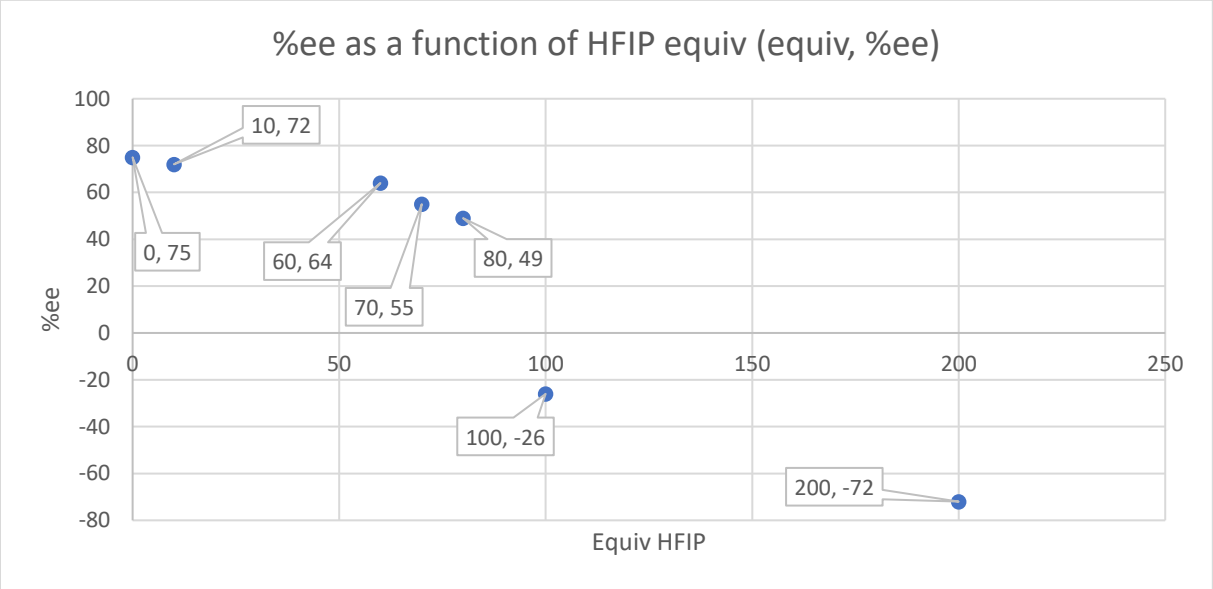

Figure 3.7: Inversion in the enantioselectivity of **132** is not a function of solvent polarity.

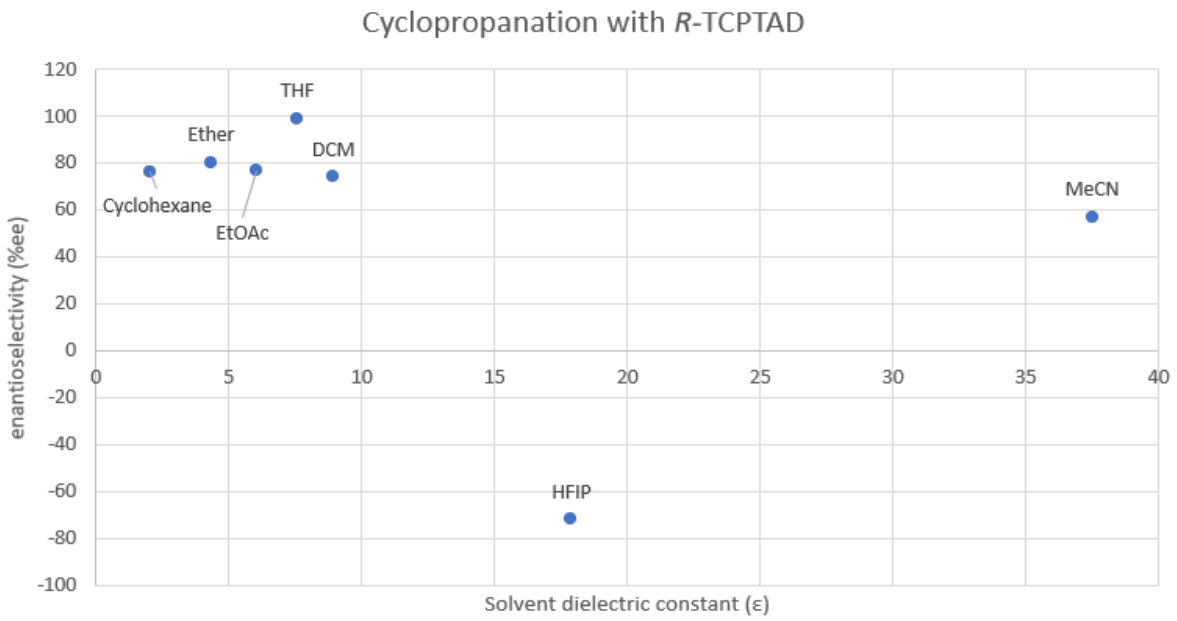

Although cyclohexane and allylic substrates proved competent in C–H functionalization with HFIP as solvent, other substrates proved to be incompatible. Benzylic substrates, for example, often led to a multitude of side products leading to questions about the relative reactivity of different compounds in HFIP. Earlier research in the Davies group has explored the relative reactivity of C–H bonds and other functionality,[45] however the hydrogen bonding capabilities of HFIP appear to warp this trend. Curiously, even when the C–H functionalization substrate is completely inert to the carbene in HFIP (as with *n*-pentane) O–H insertion of the carbene into HFIP is never observed. Instead, an ethereal dimer of **9** is obtained as the exclusive product (**137,** Scheme 3.14). This derives from reaction of the carbene with water to generate the O–H insertion product, this compound then reacts with another equivalent of rhodium carbene to generate **137**. The water in the reaction is likely from the HFIP itself, HFIP is highly hydroscopic as water enables the construction of a hydrogen bonding network in the solvent so molecular sieves can never be fully dehydrate HFIP (Scheme 3.14).[41, 132, 133] HFIP does reduce the nucleophilicity of this water due to hydrogen bonding,[133] this is enough to prevent O–H insertion in cyclopropanation as the

energetic barrier is extremely low, however, if the energetic barrier of C–H functionalization is higher than O–H insertion into HFIP-coordinated water, it will be generated preferentially. The formation of ether instead of simple O–H insertion is likely due to the low concentration of water in the reaction as the HFIP is dried over activated molecular sieves.

Scheme 3.14: The ethereal dimer **137** is observed as the major product when reactions with substrates that are unreactive in HFIP are attempted.

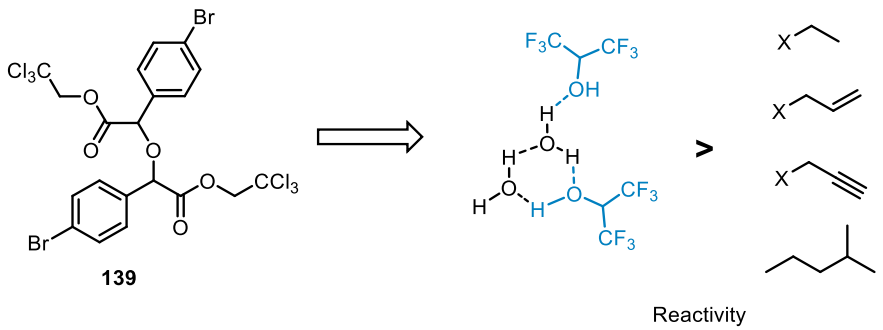

Another quirk or reactions conducted in HFIP is the ability of the solvent to deactivate nucleophile-adjacent sites towards reaction with the carbene. This manifested during exploration of the scope of cyclopropanation of complex molecules. One of the substrates investigated was the terpenoid *S*-(-)-linalool which features a tertiary alcohol adjacent to primary alkene as well as a trisubstituted alkene (Figure 3.8). In DCM, the alcohol forms an ylide with the carbene and rearranges to form homo-allylic alcohol **138**.[78] It was expected that in HFIP, the alcohol would be deactivated towards ylide formation through hydrogen bonding and the terminal alkene would undergo cyclopropanation, however, the exclusive product (**139**) arose from insertion into one of the primary allylic methyl C–H bonds. This observation led to the surprising conclusion that HFIP not only deactivates nucleophilic sites in the molecule, but also adjacent sites by making them less electron rich. As previously stated, the highly electrophilic carbene generated in HFIP as solvent is too reactive to sample multiple sites in the molecule and as a result, it will functionalize the most kinetically active site. In this case, the allylic methyl site was

the most accessible and reactive position, even more reactive than the now electron poor terminal alkene, leading to the observed product in 93% ee.

Figure 3.8: Unexpected selectivity observed in the reaction of a substrate containing an allylic alcohol in the presence of HFIP as a solvent and mechanism of formation.

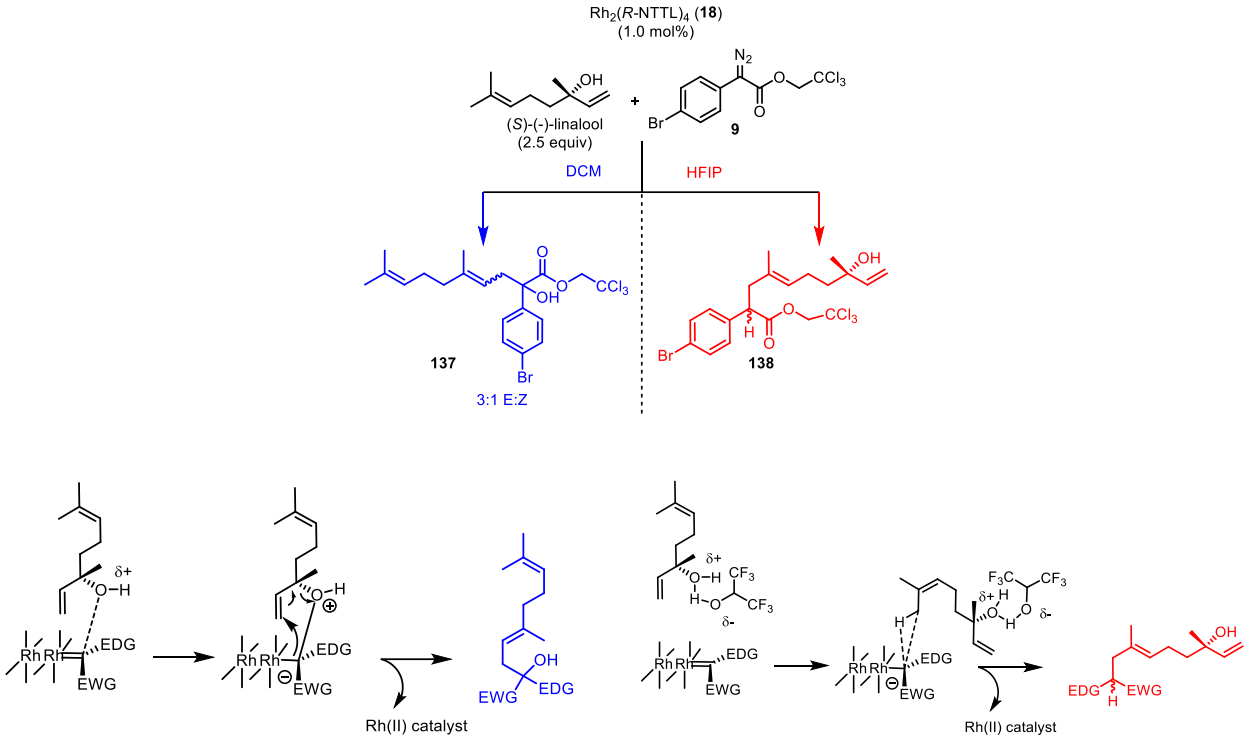

This deactivating influence of HFIP can be used to invert the selectivity of sites that would classically compete with each-other for the carbene. For example, the competitive reaction of 2-methyl-3-buten-2-ol and 3,3-dimethyl-1-butene exclusively gives homo-allylic alcohol product (**140**) when conducted in DCM, and exclusively gives cyclopropanation of 3,3-dimethyl-1-butene (**124**) when conducted in HFIP (Figure 3.10). This effect can be extended to amines as well as alcohols, *N,N*-dimethyl allylamine is unreactive in the presence of HFIP and cyclopropanation occurs preferentially.

Figure 3.9: Competition between nucleophile-containing substrates and other compounds in the presence or absence of HFIP.

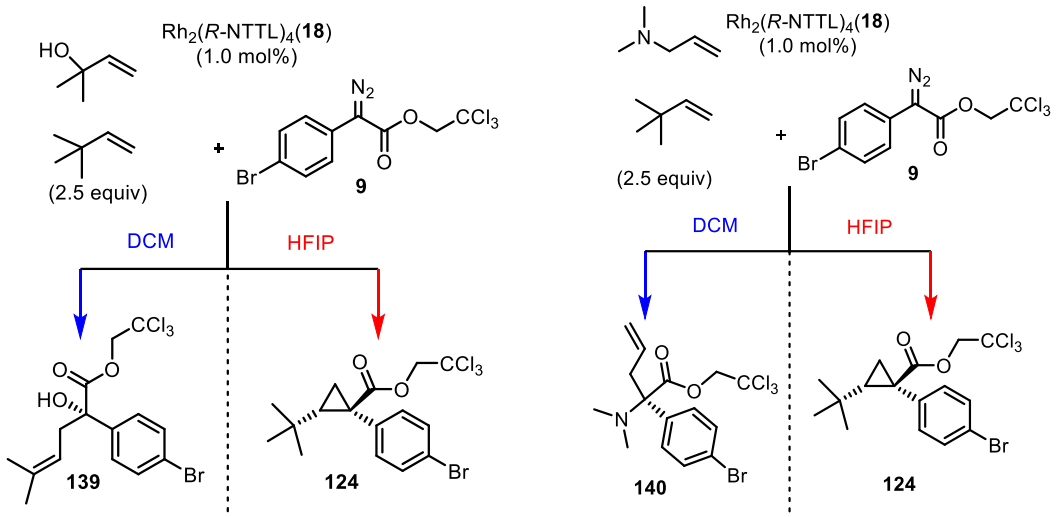

This effect is operative in C–H functionalization substrates as well, examples include THF (Figure 3.10) and the psoralen natural product Trioxsalen (Figure 3.11).[134-136] In competition studies between THF and cyclohexane, the C2 position of THF was determined to be 2000 times more reactive than cyclohexane.[45] This preferential reactivity is confirmed when a competition between THF and cyclohexane is conducted in DCM, as the only observed product in this reaction was **141,** which was obtained in 2:1 d.r and 97% ee when Rh_2(*tetra-p*-BrTPPTTL)$_4$ (**17**) was used as catalyst. However, when the same competition was performed in HFIP as solvent, no C–H insertion into THF was observed and the carbene exclusively reacts with cyclohexane to generate the product **142** in 71% ee. The moderate asymmetric induction was expected as this catalyst often displays diminished enantioselectivity when HFIP is used as solvent (Table 3.2), efforts are ongoing to identify a catalyst which exhibits high selectivity in this reaction in the presence of HFIP as solvent.

Figure 3.10: HFIP allows reaction with unactivated C–H bonds in the presence of C–H bonds adjacent to nucleophiles allowing this chemistry to override native substrate selectivity.

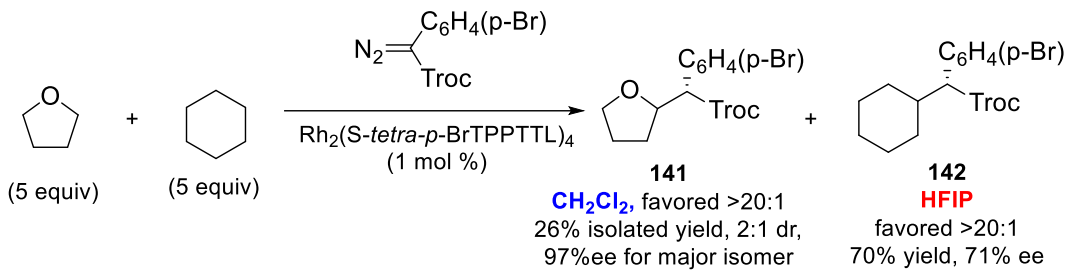

In Trioxsalen, the major product observed in DCM is functionalization of the C3 carbon on the benzofuran ring (**143,** Figure 3.11). This is the most electron rich position in the molecule, hence the reaction progresses in a similar mechanism to electrophilic aromatic insertion. In HFIP, however, hydrogen bonding between the oxygen heteroatoms of Trioxsalen deprives the C3 carbon of electrons, leading reaction with the carbene to occur elsewhere. The next most reactive site in the molecule is the C2 methyl group of the benzofuran. In HFIP, **144** is observed as the exclusive product of the reaction, obtained in 70% ee (Figure 3.11). Further efforts within the group are already underway to expand and explore the scope of substrates and selectivity of rhodium carbene reactions conducted in HFIP.

Figure 3.11: Reaction of Trioxsalen in the presence or absence of HFIP and proposed mechanism for observed selectivity.

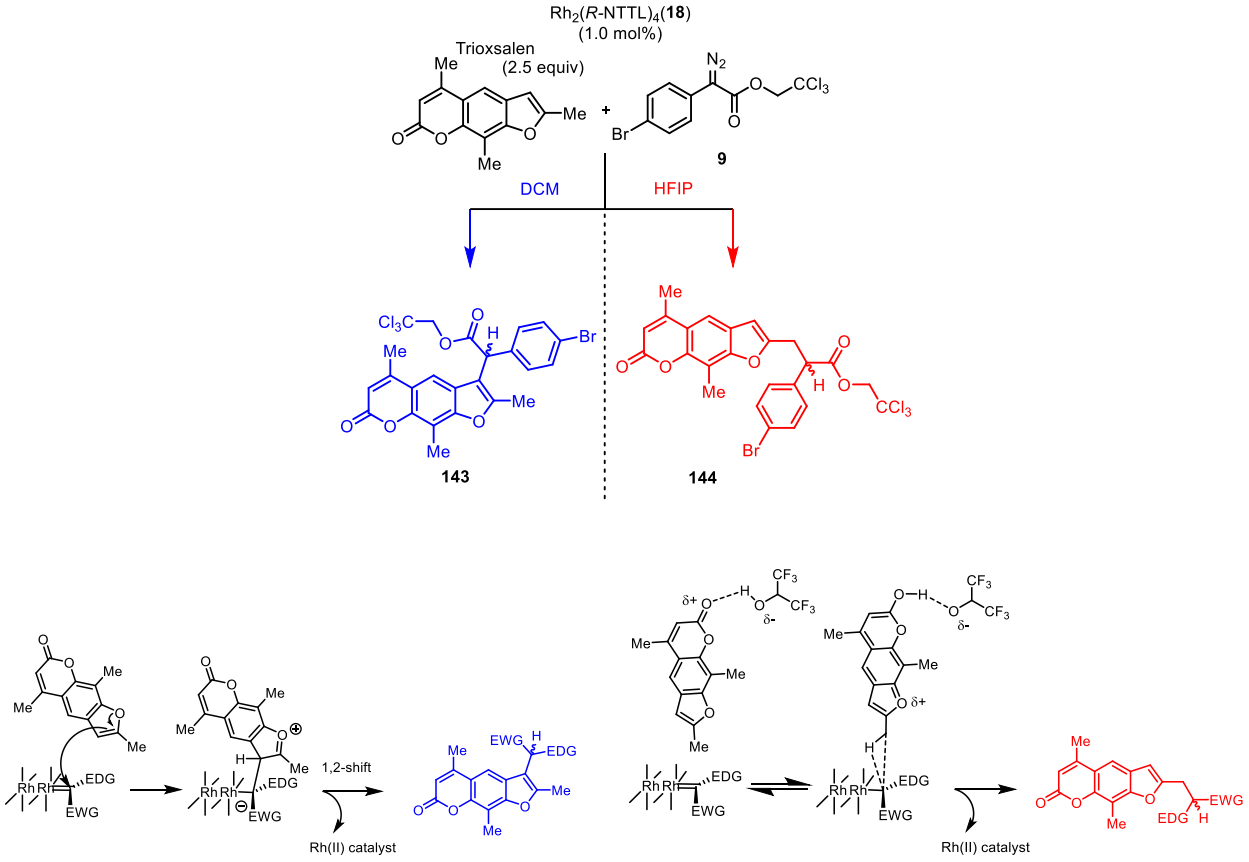

3.3 Conclusion:

The ability of HFIP to selectively deactivate coordinative poisons and desensitize rhodium carbenes to highly reactive substrates has been leveraged to effect highly enantioselective cyclopropanation in the presence of a myriad of poisonous and reactive functionalities. The methodology is applicable to substrates bearing reactive functionality including complex APIs and natural products. This simple additive enables broad functionality tolerance for rhodium carbene transformations making it a more useful tool for accessing chiral molecules and diversifying medicinally relevant scaffolds. This method was then expanded to include other rhodium carbene reactions including functionalization of C–H bonds. HFIP is a privileged additive in this chemistry and warps the existing paradigm of rhodium carbene chemistry

around it. HFIP inverts native catalyst site selectivity by promoting kinetic control over the classical thermodynamically driven selectivity. It deactivates sites adjacent to nucleophiles turning the defined reactivity series on its head and enabling site-selectivity that was considered impossible for a rhodium carbene less than a year ago. Finally, it can stall the progress of polar reaction intermediates through protonation leading to the formation of new products. As future work is done to delve deeper into rhodium carbenoid chemistry involving HFIP it will be interesting to seeing what novel transformations that can be achieved.

3.4 References:

1. Bien, J.; Davulcu, A.; DelMonte, A. J.; Fraunhoffer, K. J.; Gao, Z.; Hang, C.; Hsiao, Y.; Hu, W.; Katipally, K.; Littke, A., The first kilogram synthesis of beclabuvir, an HCV NS5B polymerase inhibitor. *Org. Proc. Res. Dev.* **2018,** *22* (10), 1393-1408.
2. Talele, T. T., The "cyclopropyl fragment" is a versatile player that frequently appears in preclinical/clinical drug molecules. *J. Med. Chem.* **2016,** *59* (19), 8712-8756.
3. Davies, H. M., Finding opportunities from surprises and failures. Development of rhodium-stabilized donor/acceptor carbenes and their application to catalyst-controlled C–H functionalization. *J. Org. Chem.* **2019,** *84* (20), 12722-12745.
4. Gage, J. R.; Chen, F.; Dong, C.; Gonzalez, M. A.; Jiang, Y.; Luo, Y.; McLaws, M. D.; Tao, J., Semicontinuous process for GMP manufacture of a carbapenem intermediate via carbene insertion Using an immobilized rhodium catalyst. *Org. Proc. Res. Dev.* **2020,** *24* (10), 2025-2033.
5. Lathrop, S. P.; Mlinar, L. B.; Manjrekar, O. N.; Zhou, Y.; Harper, K. C.; Sacia, E. R.; Higgins, M.; Bogdan, A. R.; Wang, Z.; Richter, S. M., Continuous Process to Safely Manufacture an Aryldiazoacetate and Its Direct Use in a Dirhodium-Catalyzed Enantioselective Cyclopropanation. *Org. Proc. Res. Dev.* **2022**.
6. Chepiga, K. M.; Qin, C.; Alford, J. S.; Chennamadhavuni, S.; Gregg, T. M.; Olson, J. P.; Davies, H. M., Guide to enantioselective dirhodium (II)-catalyzed cyclopropanation with aryldiazoacetates. *Tetrahedron* **2013,** *69* (27-28), 5765-5771.
7. Hansen, J.; Autschbach, J.; Davies, H. M., Computational study on the selectivity of donor/acceptor-substituted rhodium carbenoids. *J. Org. Chem.* **2009,** *74* (17), 6555-6563.
8. Sharland, J. C.; Wei, B.; Hardee, D. J.; Hodges, T. R.; Gong, W.; Voight, E. A.; Davies, H. M., Asymmetric synthesis of pharmaceutically relevant 1-aryl-2-heteroaryl-and 1, 2-diheteroarylcyclopropane-1-carboxylates. *Chem. Sci.* **2021,** *12* (33), 11181-11190.
9. Ye, Q.-S.; Li, X.-N.; Jin, Y.; Yu, J.; Chang, Q.-W.; Jiang, J.; Yan, C.-X.; Li, J.; Liu, W.-P., Synthesis, crystal structures and catalytic activity of tetrakis (acetato) dirhodium (II) complexes with axial picoline ligands. *Inorg. Chim. Acta* **2015,** *434*, 113-120.
10. Trindade, A. F.; Coelho, J. A.; Afonso, C. A.; Veiros, L. F.; Gois, P. M., Fine tuning of dirhodium (II) complexes: exploring the axial modification. *ACS. Catal.* **2012,** *2* (3), 370-383.
11. Lebel, H.; Piras, H.; Bartholoméüs, J., Rhodium-Catalyzed Stereoselective Amination of Thioethers with N-Mesyloxycarbamates: DMAP and Bis (DMAP) CH2Cl2 as Key Additives. *Angew. Chem.* **2014,** *126* (28), 7428-7432.

12. Doyle, M. P.; Tamblyn, W. H.; Bagheri, V., Highly effective catalytic methods for ylide generation from diazo compounds. Mechanism of the rhodium-and copper-catalyzed reactions with allylic compounds. *J. Org. Chem.* **1981,** *46* (25), 5094-5102.
13. Laconsay, C. J.; Tantillo, D. J., Metal Bound or Free Ylides as Reaction Intermediates in Metal-Catalyzed [2, 3]-Sigmatropic Rearrangements? It Depends. *ACS. Catal.* **2021,** *11* (2), 829-839.
14. Li, Z.; Boyarskikh, V.; Hansen, J. H.; Autschbach, J.; Musaev, D. G.; Davies, H. M., Scope and mechanistic analysis of the enantioselective synthesis of allenes by rhodium-catalyzed tandem ylide formation/[2, 3]-sigmatropic rearrangement between donor/acceptor carbenoids and propargylic alcohols. *J. Am. Chem. Soc.* **2012,** *134* (37), 15497-15504.
15. Nelson, T. D.; Song, Z. J.; Thompson, A. S.; Zhao, M.; DeMarco, A.; Reamer, R. A.; Huntington, M. F.; Grabowski, E. J.; Reider, P. J., Rhodium-carbenoid-mediated intermolecular O–H insertion reactions: a dramatic additive effect. Application in the synthesis of an ascomycin derivative. *Tetrahedron Lett.* **2000,** *41* (12), 1877-1881.
16. Gillingham, D.; Fei, N., Catalytic X–H insertion reactions based on carbenoids. *Chem. Soc. Rev.* **2013,** *42* (12), 4918-4931.
17. Jana, S.; Yang, Z.; Li, F.; Empel, C.; Ho, J.; Koenigs, R. M., Photoinduced Proton-Transfer Reactions for Mild O-H Functionalization of Unreactive Alcohols. *Angew. Chem. Int. Ed.* **2020,** *59* (14), 5562-5566.
18. Gomtsyan, A., Heterocycles in drugs and drug discovery. *Chem. Heterocycl. Compd.* **2012,** *48* (1), 7-10.
19. Soor, H. S.; Appavoo, S. D.; Yudin, A. K., Heterocycles: Versatile control elements in bioactive macrocycles. *Bioorg. Med. Chem.* **2018,** *26* (10), 2774-2779.
20. MacCoss, M.; Lawson, A.; Taylor, R., Rings in Drugs. *J. Med. Chem.* **2014,** *57*, 5845-5859.
21. He, J.; Hamann, L. G.; Davies, H. M.; Beckwith, R. E., Late-stage C–H functionalization of complex alkaloids and drug molecules via intermolecular rhodium-carbenoid insertion. *Nature Commun.* **2015,** *6* (1), 1-9.
22. Chiappini, N. D.; Mack, J. B.; Du Bois, J., Intermolecular C (sp3)− H amination of complex molecules. *Angew. Chem. Int. Ed.* **2018,** *57* (18), 4956-4959.
23. Malik, H. A.; Taylor, B. L.; Kerrigan, J. R.; Grob, J. E.; Houk, K.; Du Bois, J.; Hamann, L. G.; Patterson, A. W., Non-directed allylic C–H acetoxylation in the presence of Lewis basic heterocycles. *Chem. Sci.* **2014,** *5* (6), 2352-2361.
24. Pozhydaiev, V.; Power, M.; Gandon, V.; Moran, J.; Lebœuf, D., Exploiting hexafluoroisopropanol (HFIP) in Lewis and Brønsted acid-catalyzed reactions. *Chem. Commun.* **2020,** *56* (78), 11548-11564.
25. Röckl, J. L.; Dörr, M.; Waldvogel, S. R., Electrosynthesis 2.0 in 1, 1, 1, 3, 3, 3-Hexafluoroisopropanol/Amine Mixtures. *ChemElectroChem* **2020,** *7* (18), 3686-3694.
26. Borrell, M.; Gil-Caballero, S.; Bietti, M.; Costas, M., Site-selective and product chemoselective aliphatic C–H bond hydroxylation of polyhydroxylated substrates. *ACS. Catal.* **2020,** *10* (8), 4702-4709.
27. Sinha, S. K.; Bhattacharya, T.; Maiti, D., Role of hexafluoroisopropanol in C–H activation. *React. Chem. Eng.* **2019,** *4* (2), 244-253.
28. Colomer, I.; Chamberlain, A. E.; Haughey, M. B.; Donohoe, T. J., Hexafluoroisopropanol as a highly versatile solvent. *Nat. Rev. Chem.* **2017,** *1* (11), 1-12.
29. Lebœuf, D.; Marin, L.; Michelet, B.; Perez-Luna, A.; Guillot, R.; Schulz, E.; Gandon, V., Harnessing the Lewis Acidity of HFIP through its Cooperation with a Calcium (II) Salt: Application to the Aza-Piancatelli Reaction. *Chem. A Eur. J.* **2016,** *22* (45), 16165-16171.
30. Qi, C.; Hasenmaile, F.; Gandon, V.; Leboeuf, D., Calcium (II)-catalyzed intra-and intermolecular hydroamidation of unactivated alkenes in hexafluoroisopropanol. *ACS. Catal.* **2018,** *8* (3), 1734-1739.
31. Qi, C.; Yang, S.; Gandon, V.; Lebœuf, D., Calcium (II)-and Triflimide-Catalyzed Intramolecular Hydroacyloxylation of Unactivated Alkenes in Hexafluoroisopropanol. *Org. Lett.* **2019,** *21* (18), 7405-7409.

32. Saito, A.; Kasai, J.; Konishi, T.; Hanzawa, Y., Tandem synthesis of 2, 3-dihydro-4-iminoquinolines via three-component alkyne-imine metathesis. *J. Org. Chem.* **2010,** *75* (20), 6980-6982.
33. Shen, P.-X.; Hu, L.; Shao, Q.; Hong, K.; Yu, J.-Q., Pd (II)-catalyzed enantioselective C (sp3)–H arylation of free carboxylic acids. *J. Am. Chem. Soc.* **2018,** *140* (21), 6545-6549.
34. Okamoto, K.; Chiba, K., Electrochemical total synthesis of pyrrolophenanthridone alkaloids: Controlling the anodically initiated electron transfer process. *Org. Lett.* **2020,** *22* (9), 3613-3617.
35. Vayer, M.; Mayer, R. J.; Moran, J.; Lebœuf, D., Leveraging the Hydroarylation of α-(Trifluoromethyl) styrenes to Access Trifluoromethylated All-Carbon Quaternary Centers. *ACS. Catal.* **2022,** *12* (17), 10995-11001.
36. Wang, S.; Force, G.; Guillot, R.; Carpentier, J.-F.; Sarazin, Y.; Bour, C.; Gandon, V.; Lebœuf, D., Lewis Acid/Hexafluoroisopropanol: A Promoter System for Selective ortho-C-Alkylation of Anilines with Deactivated Styrene Derivatives and Unactivated Alkenes. *ACS. Catal.* **2020,** *10* (18), 10794-10802.
37. Marin, L.; Force, G.; Gandon, V.; Schulz, E.; Lebœuf, D., Aza-Piancatelli Cyclization as a Platform for the Preparation of Scaffolds of Natural Compounds: Application to the Total Synthesis of Bruceolline D. *Eur. J. Org. Chem.* **2020,** *2020* (33), 5323-5328.
38. Faza, O. N.; López, C. S.; Alvarez, R.; De Lera, A. R., Theoretical study of the electrocyclic ring closure of hydroxypentadienyl cations. *Chemistry* **2004,** *10* (17), 4324-4333.
39. Piutti, C.; Quartieri, F., The piancatelli rearrangement: New applications for an intriguing reaction. *Molecules* **2013,** *18* (10), 12290-12312.
40. Berrien, J.-F.; Ourévitch, M.; Morgant, G.; Ghermani, N.; Crousse, B.; Bonnet-Delpon, D., A crystalline H-bond cluster of hexafluoroisopropanol (HFIP) and piperidine: Structure determination by X ray diffraction. *J. Fluorine Chem.* **2007,** *128* (7), 839-843.
41. Milovanović, M. R.; Dherbassy, Q.; Wencel-Delord, J.; Colobert, F.; Zarić, S. D.; Djukic, J. P., The Affinity of Some Lewis Bases for Hexafluoroisopropanol as a Reference Lewis Acid: An ITC/DFT Study. *Chemphyschem* **2020,** *21* (18), 2136-2142.
42. White, M. C.; Zhao, J., Aliphatic C–H oxidations for late-stage functionalization. *J. Am. Chem. Soc.* **2018,** *140* (43), 13988-14009.
43. Freakley, S. J.; Kochius, S.; van Marwijk, J.; Fenner, C.; Lewis, R. J.; Baldenius, K.; Marais, S. S.; Opperman, D. J.; Harrison, S. T.; Alcalde, M., A chemo-enzymatic oxidation cascade to activate C–H bonds with in situ generated H2O2. *Nature Commun.* **2019,** *10* (1), 4178.
44. Li, F.; Zhang, X.; Renata, H., Enzymatic CH functionalizations for natural product synthesis. *Curr. Opin. Chem. Biol.* **2019,** *49*, 25-32.
45. Davies, H. M.; Hansen, T.; Churchill, M. R., Catalytic asymmetric C− H activation of alkanes and tetrahydrofuran. *J. Am. Chem. Soc.* **2000,** *122* (13), 3063-3070.
46. Pei, C.; Koenigs, R. M., A Computational Study on the Photochemical O–H Functionalization of Alcohols with Diazoacetates. *J. Org. Chem.* **2022,** *87* (10), 6832-6837.
47. Gray, E. E.; Nielsen, M. K.; Choquette, K. A.; Kalow, J. A.; Graham, T. J.; Doyle, A. G., Nucleophilic (radio) fluorination of α-diazocarbonyl compounds enabled by copper-catalyzed H–F insertion. *J. Am. Chem. Soc.* **2016,** *138* (34), 10802-10805.
48. Jurberg, I. D.; Davies, H. M., Blue light-promoted photolysis of aryldiazoacetates. *Chem. Sci.* **2018,** *9* (22), 5112-5118.
49. Sakharov, P. A.; Novikov, M. S.; Nguyen, T. K.; Kinzhalov, M. A.; Khlebnikov, A. F.; Rostovskii, N. V., Blue Light-Promoted Cross-Coupling of α-Diazo Esters with Isocyanides: Synthesis of Ester-Functionalized Ketenimines. *ACS Omega* **2022,** *7* (10), 9071-9079.
50. Wei, B.; Hatridge, T. A.; Jones, C. W.; Davies, H. M., Copper (II) Acetate-Induced Oxidation of Hydrazones to Diazo Compounds under Flow Conditions Followed by Dirhodium-Catalyzed Enantioselective Cyclopropanation Reactions. *Org. Lett.* **2021,** *23* (14), 5363-5367.

51. Boni, Y. T.; Vaitla, J.; Davies, H. M., Catalyst Controlled Site-and Stereoselective Rhodium (II) Carbene C (sp3)–H Functionalization of Allyl Boronates. *Org. Lett.* **2022**.
52. Sharland, J. C.; Dunstan, D.; Majumdar, D.; Gao, J.; Tan, K.; Malik, H. A.; Davies, H. M., Hexafluoroisopropanol for the Selective Deactivation of Poisonous Nucleophiles Enabling Catalytic Asymmetric Cyclopropanation of Complex Molecules. *ACS. Catal.* **2022,** *12* (20), 12530-12542.
53. Vaitla, J.; Boni, Y. T.; Davies, H. M., Distal allylic/benzylic C− H functionalization of silyl ethers using donor/acceptor rhodium (II) carbenes. *Angew. Chem.* **2020,** *132* (19), 7467-7472.
54. Fu, J.; Ren, Z.; Bacsa, J.; Musaev, D. G.; Davies, H. M., Desymmetrization of cyclohexanes by site- and stereoselective C–H functionalization. *Nature* **2018,** *564* (7736), 395-399.
55. Davies, H. M.; Bruzinski, P. R.; Lake, D. H.; Kong, N.; Fall, M. J., Asymmetric cyclopropanations by rhodium (II) N-(arylsulfonyl) prolinate catalyzed decomposition of vinyldiazomethanes in the presence of alkenes. Practical enantioselective synthesis of the four stereoisomers of 2-phenylcyclopropan-1-amino acid. *J. Am. Chem. Soc.* **1996,** *118* (29), 6897-6907.
56. Qin, C.; Boyarskikh, V.; Hansen, J. H.; Hardcastle, K. I.; Musaev, D. G.; Davies, H. M., D 2-symmetric dirhodium catalyst derived from a 1, 2, 2-triarylcyclopropanecarboxylate ligand: design, synthesis and application. *J. Am. Chem. Soc.* **2011,** *133* (47), 19198-19204.
57. Reddy, R. P.; Davies, H. M., Dirhodium tetracarboxylates derived from adamantylglycine as chiral catalysts for enantioselective C− H aminations. *Org. Lett.* **2006,** *8* (22), 5013-5016.
58. Lindsay, V. N.; Lin, W.; Charette, A. B., Experimental evidence for the all-up reactive conformation of chiral rhodium (II) carboxylate catalysts: enantioselective synthesis of cis-cyclopropane α-amino acids. *J. Am. Chem. Soc.* **2009,** *131* (45), 16383-16385.
59. Tsutsui, H.; Yamaguchi, Y.; Kitagaki, S.; Nakamura, S.; Anada, M.; Hashimoto, S., Dirhodium(II) tetrakis[N-tetrafluorophthaloyl-(S)-tert-leucinate]: an exceptionally effective Rh(II) catalyst for enantiotopically selective aromatic C–H insertions of diazo ketoesters. *Tetrahedron Asymm.* **2003,** *14* (7), 817-821.
60. Garlets, Z. J.; Boni, Y. T.; Sharland, J. C.; Kirby, R. P.; Fu, J.; Bacsa, J.; Davies, H. M., Design, Synthesis, and Evaluation of Extended C4–Symmetric Dirhodium Tetracarboxylate Catalysts. *ACS. Catal.* **2022,** *12*, 10841-10848.
61. Ghanem, A.; Gardiner, M. G.; Williamson, R. M.; Müller, P., First X-ray structure of a N-naphthaloyl-tethered chiral dirhodium (II) complex: structural basis for tether substitution improving asymmetric control in olefin cyclopropanation. *Chem. A Eur. J.* **2010,** *16* (11), 3291-3295.
62. Wei, B.; Sharland, J. C.; Lin, P.; Wilkerson-Hill, S. M.; Fullilove, F. A.; McKinnon, S.; Blackmond, D. G.; Davies, H. M., In situ kinetic studies of Rh (II)-catalyzed asymmetric cyclopropanation with low catalyst loadings. *ACS. Catal.* **2019,** *10* (2), 1161-1170.
63. Fu, J.; Wurzer, N.; Lehner, V.; Reiser, O.; Davies, H. M., Rh (II)-catalyzed monocyclopropanation of pyrroles and its application to the synthesis pharmaceutically relevant compounds. *Org. Lett.* **2019,** *21* (15), 6102-6106.
64. Wei, B.; Sharland, J. C.; Blackmond, D. G.; Musaev, D. G.; Davies, H. M. L., In Situ Kinetic Studies of Rh(II)-Catalyzed C–H Functionalization to Achieve High Catalyst Turnover Numbers. *ACS. Catal.* **2022**, 13400-13410.
65. Caraus, I.; Alsuwailem, A. A.; Nadon, R.; Makarenkov, V., Detecting and overcoming systematic bias in high-throughput screening technologies: a comprehensive review of practical issues and methodological solutions. *Brief. Bioinformatics* **2015,** *16* (6), 974-986.
66. Malo, N.; Hanley, J. A.; Cerquozzi, S.; Pelletier, J.; Nadon, R., Statistical practice in high-throughput screening data analysis. *Nat. Biotechnol.* **2006,** *24* (2), 167-175.
67. Macarrón, R.; Hertzberg, R. P., Design and implementation of high-throughput screening assays. *High Throughput Screening: Methods and Protocols, Second Edition* **2009**, 1-32.

68. Davies, H. M.; Townsend, R. J., Catalytic asymmetric cyclopropanation of heteroaryldiazoacetates. *J. Org. Chem.* **2001,** *66* (20), 6595-6603.
69. Qin, C.; Davies, H. M., Enantioselective synthesis of 2-arylbicyclo [1.1. 0] butane carboxylates. *Org. Lett.* **2013,** *15* (2), 310-313.
70. Padwa, A., Catalytic Decomposition of Diazo Compounds as a Method for Generating Carbonyl-Ylide Dipoles. *Helv. Chim. Acta* **2005,** *88* (6), 1357-1374.
71. Padwa, A., Domino reactions of rhodium (II) carbenoids for alkaloid synthesis. *Chem. Soc. Rev.* **2009,** *38* (11), 3072-3081.
72. Muthusamy, S.; Babu, S. A.; Gunanathan, C., Novel chemoselective 1, 3-dipolar cycloaddition of rhodium generated carbonyl ylides with arylidenetetralones. *Tetrahedron Lett.* **2000,** *41* (45), 8839-8842.
73. Hodgson, D. M.; Pierard, F. Y.; Stupple, P. A., Catalytic enantioselective rearrangements and cycloadditions involving ylides from diazo compounds. *Chem. Soc. Rev.* **2001,** *30* (1), 50-61.
74. Jia, S.; Dong, G.; Ao, C.; Jiang, X.; Hu, W., Rhodium-catalyzed formal C–O insertion in carbene/alkyne metathesis reactions: Synthesis of 3-substituted 3 H-indol-3-ols. *Org. Lett.* **2019,** *21* (11), 4322-4326.
75. Davies, H. M.; DeMeese, J., Stereoselective synthesis of epoxides by reaction of donor/acceptor-substituted carbenoids with α, β-unsaturated aldehydes. *Tetrahedron Lett.* **2001,** *42* (39), 6803-6805.
76. Doyle, M. P.; Hu, W.; Timmons, D. J., Epoxides and aziridines from diazoacetates via ylide intermediates. *Org. Lett.* **2001,** *3* (6), 933-935.
77. Padwa, A.; Beall, L. S.; Eidell, C. K.; Worsencroft, K. J., An approach toward isoindolobenzazepines using the ammonium ylide/Stevens [1, 2]-rearrangement sequence. *J. Org. Chem.* **2001,** *66* (7), 2414-2421.
78. Li, Z.; Parr, B. T.; Davies, H. M., Highly stereoselective C–C bond formation by rhodium-catalyzed tandem ylide formation/[2, 3]-sigmatropic rearrangement between donor/acceptor carbenoids and chiral allylic alcohols. *J. Am. Chem. Soc.* **2012,** *134* (26), 10942-10946.
79. Zhou, S.; Cai, B.; Hu, C.; Cheng, X.; Li, L.; Xuan, J., Visible light and base promoted OH insertion/cyclization of para-quinone methides with aryl diazoacetates: An approach to 2, 3-dihydrobenzofuran derivatives. *Chin. Chem. Lett.* **2021,** *32* (8), 2577-2581.
80. Noels, A.; Demonceau, A.; Petiniot, N.; Hubert, A. J.; Teyssié, P., Transition-metal-catalyzed reaction of diazocompounds, efficient synthesis of functionalized ethers by carbene insertion into the hydroxylic bond of alcohols. *Tetrahedron* **1982,** *38* (17), 2733-2739.
81. Wu, J.; Li, X.; Qi, X.; Duan, X.; Cracraft, W. L.; Guzei, I. A.; Liu, P.; Tang, W., Site-selective and stereoselective O-alkylation of glycosides by Rh (II)-catalyzed carbenoid insertion. *J. Am. Chem. Soc.* **2019,** *141* (50), 19902-19910.
82. Harada, S.; Tanikawa, K.; Homma, H.; Sakai, C.; Ito, T.; Nemoto, T., Silver-Catalyzed Asymmetric Insertion into Phenolic O− H Bonds using Aryl Diazoacetates and Theoretical Mechanistic Studies. *Chem. A Eur. J.* **2019,** *25* (52), 12058-12062.
83. Shen, H.-Q.; Xie, H.-P.; Sun, L.; Zhou, Y.-G., Enantioselective carbene insertion into O–H of phenols with chiral palladium/2, 2'-biimidazole complexes. *Organometallics* **2019,** *38* (20), 3902-3905.
84. Cenini, S.; Cravotto, G.; Giovenzana, G. B.; Palmisano, G.; Penoni, A.; Tollari, S., Diruthenium (II, II) tetrakis (acetate) as a catalyst of choice for intermolecular insertion of stabilized diazocompounds into O H bonds. *Tetrahedron Lett.* **2002,** *43* (20), 3637-3640.
85. Sacui, I. A.; Zeller, M.; Norris, P., Rhodium (II)-catalyzed decomposition of 3-O-(2-diazo-2-phenylacetyl)-1, 2; 5, 6-di-O-isopropylidene-α-d-allofuranose: diastereoselective ether formation. *Carbohydr. Res.* **2008,** *343* (10-11), 1819-1823.
86. Li, Q.; Cai, B.-G.; Li, L.; Xuan, J., Oxime ether synthesis through O–H Functionalization of oximes with diazo esters under blue LED irradiation. *Org. Lett.* **2021,** *23* (17), 6951-6955.
87. Ramakrishna, K.; Sivasankar, C., Synthesis of aminobenzoic acid derivatives via chemoselective carbene insertion into the− NH bond catalyzed by Cu (I) complex. *J. Org. Chem.* **2016,** *81* (15), 6609-6616.

88. Shi, Y.; Gulevich, A. V.; Gevorgyan, V., Rhodium-Catalyzed NH Insertion of Pyridyl Carbenes Derived from Pyridotriazoles: A General and Efficient Approach to 2-Picolylamines and Imidazo [1, 5-a] pyridines. *Angew. Chem. Int. Ed.* **2014,** *53* (51), 14191-14195.
89. García, C. F.; McKervey, M. A.; Ye, T., Asymmetric catalysis of intramolecular N–H insertion reactions of α-diazocarbonyls. *Chem. Commun.* **1996,** (12), 1465-1466.
90. Davis, F. A.; Yang, B.; Deng, J., Asymmetric synthesis of cis-5-tert-butylproline with metal carbenoid NH insertion. *J. Org. Chem.* **2003,** *68* (13), 5147-5152.
91. Li, M.-L.; Yu, J.-H.; Li, Y.-H.; Zhu, S.-F.; Zhou, Q.-L., Highly enantioselective carbene insertion into N–H bonds of aliphatic amines. *Science* **2019,** *366* (6468), 990-994.
92. Anada, M.; Watanabe, N., Highly enantioselective construction of the key azetidin-2-ones for the synthesis of carbapenem antibiotics via intramolecular C–H insertion reactions of α-methoxycarbonyl-α-diazoacetamides catalysed by chiral dirhodium () carboxylates. *Chem. Commun.* **1998,** (15), 1517-1518.
93. Galardon, E.; Le Maux, P.; Simonneaux, G., Insertion of ethyl diazoacetate into N–H and S–H bonds catalyzed by ruthenium porphyrin complexes. *J. Chem. Soc. Perkin. Trans. 1* **1997,** (17), 2455-2456.
94. Yi, X.; Yu, Y.; Huang, F.; Ding, T.; Zhang, Z.; Feng, J.; Baell, J. B.; Huang, H., Turning waste into valuable catalysts: application of surface-modified sewage sludge in N–H insertion reaction. *Ind. Eng.Chem. Res.* **2020,** *59* (11), 4854-4863.
95. Huang, D.; Jiang, G.-M.; Chen, H.-X.; Gao, W.-D., Preparation of N-Acetyl-2-arylglycin Esters by NH Insertion Reaction of Aryldiazoacetates with Acetamide. *Syn. Commun.* **2009,** *40* (2), 229-234.
96. Deng, Q.-H.; Xu, H.-W.; Yuen, A. W.-H.; Xu, Z.-J.; Che, C.-M., Ruthenium-catalyzed one-pot carbenoid N− H insertion reactions and diastereoselective synthesis of prolines. *Org. Lett.* **2008,** *10* (8), 1529-1532.
97. Kang, J.; Chen, L.; Cui, H.; Zhang, L.; Su, C. Y., N—H Insertion Reactions Catalyzed by a Dirhodium Metal-Organic Cage: A Facile and Recyclable Approach for C—N Bond Formation. *Chin. J. Chem.* **2017,** *35* (6), 964-968.
98. Xu, Y.; Huang, X.; Lv, G.; Lai, R.; Lv, S.; Li, J.; Hai, L.; Wu, Y., Iridium-Catalyzed Carbenoid Insertion of Sulfoxonium Ylides for Synthesis of Quinoxalines and β-Keto Thioethers in Water. *Eur. J. Org. Chem.* **2020,** *2020* (29), 4635-4638.
99. Yang, J.; Wang, G.; Chen, S.; Ma, B.; Zhou, H.; Song, M.; Liu, C.; Huo, C., Catalyst-free, visible-light-promoted S–H insertion reaction between thiols and α-diazoesters. *Org. Biomol. Chem.* **2020,** *18* (46), 9494-9498.
100. Tyagi, V.; Bonn, R. B.; Fasan, R., Intermolecular carbene S–H insertion catalysed by engineered myoglobin-based catalysts. *Chem. Sci.* **2015,** *6* (4), 2488-2494.
101. Hong, B.; Shi, L.; Li, L.; Zhan, S.; Gu, Z., Paddlewheel dirhodium (II) complexes with N-heterocyclic carbene or phosphine ligand: New reactivity and selectivity. *GSC.* **2022**.
102. Tran, V. T.; Nimmagadda, S. K.; Liu, M.; Engle, K. M., Recent applications of chiral phosphoric acids in palladium catalysis. *Org. Biomol. Chem.* **2020,** *18* (4), 618-637.
103. Zhang, D.; Qiu, H.; Jiang, L.; Lv, F.; Ma, C.; Hu, W., Enantioselective Palladium (II) Phosphate Catalyzed Three-Component Reactions of Pyrrole, Diazoesters, and Imines. *Angew. Chem. Int. Ed.* **2013,** *52* (50), 13356-13360.
104. Surry, D. S.; Buchwald, S. L., Biaryl phosphane ligands in palladium-catalyzed amination. *Angew. Chem. Int. Ed.* **2008,** *47* (34), 6338-6361.
105. Martin, R.; Buchwald, S. L., Palladium-catalyzed Suzuki− Miyaura cross-coupling reactions employing dialkylbiaryl phosphine ligands. *Acc. Chem. Res.* **2008,** *41* (11), 1461-1473.
106. Clevenger, A. L.; Stolley, R. M.; Aderibigbe, J.; Louie, J., Trends in the usage of bidentate phosphines as ligands in nickel catalysis. *Chem. Rev.* **2020,** *120* (13), 6124-6196.

107. Kim, M.; Lee, J.; Lee, H. Y.; Chang, S., Significant Self-Acceleration Effects of Nitrile Additives in the Rhodium-Catalyzed Conversion of Aldoximes to Amides: A New Mechanistic Aspect. *Adv. Synth. Catal.* **2009,** *351* (11-12), 1807-1812.
108. Pirrung, M. C.; Morehead Jr, A. T., Electronic effects in dirhodium (II) carboxylates. Linear free energy relationships in catalyzed decompositions of diazo compounds and CO and isonitrile complexation. *J. Am. Chem. Soc.* **1994,** *116* (20), 8991-9000.
109. Knouse, K. W.; deGruyter, J. N.; Schmidt, M. A.; Zheng, B.; Vantourout, J. C.; Kingston, C.; Mercer, S. E.; Mcdonald, I. M.; Olson, R. E.; Zhu, Y., Unlocking P (V): Reagents for chiral phosphorothioate synthesis. *Science* **2018,** *361* (6408), 1234-1238.
110. Pitzer, L.; Schäfers, F.; Glorius, F., Rapid assessment of the reaction-condition-based sensitivity of chemical transformations. *Angew. Chem. Int. Ed.* **2019,** *58* (25), 8572-8576.
111. Warzecha, E.; Berto, T. C.; Wilkinson, C. C.; Berry, J. F., Rhodium rainbow: A colorful laboratory experiment highlighting ligand field effects of dirhodium tetraacetate. *J. Chem. Ed.* **2019,** *96* (3), 571-576.
112. McRobb, L.; Handelsman, D. J.; Kazlauskas, R.; Wilkinson, S.; McLeod, M.; Heather, A. K., Structure–activity relationships of synthetic progestins in a yeast-based in vitro androgen bioassay. *J. Steroid Biochem. Mol. Biol.* **2008,** *110* (1-2), 39-47.
113. Kluber III, E.; Minton, J.; Stevenson, J.; Hunt, M.; Davis, D.; Hoagland, T.; Nelssen, J., Growth, carcass traits, boar odor and testicular and endocrine functions of male pigs fed a progestogen, altrenogest. *J. Anim. Sci.* **1988,** *66* (2), 470-478.
114. Putt, K. S.; Chen, G. W.; Pearson, J. M.; Sandhorst, J. S.; Hoagland, M. S.; Kwon, J.-T.; Hwang, S.-K.; Jin, H.; Churchwell, M. I.; Cho, M.-H., Small-molecule activation of procaspase-3 to caspase-3 as a personalized anticancer strategy. *Nat. Chem. Biol.* **2006,** *2* (10), 543-550.
115. Kino, T.; Hatanaka, H.; Miyata, S.; Inamura, N.; NISHIYAMA, M.; YAJIMA, T.; GOTO, T.; OKUHARA, M.; KOHSAKA, M.; AOKI, H., FK-506, a novel immunosuppressant isolated from a streptomyces II. Immunosuppressive effect of FK-506 in vitro. *J. Antibiot.* **1987,** *40* (9), 1256-1265.
116. Kino, T.; Hatanaka, H.; Hashimoto, M.; Nishiyama, M.; Goto, T.; Okuhara, M.; Kohsaka, M.; Aoki, H.; Imanaka, H., FK-506, a novel immunosuppressant isolated from a Streptomyces I. Fermentation, isolation, and physico-chemical and biological characteristics. *J. Antibiot.* **1987,** *40* (9), 1249-1255.
117. Staatz, C. E.; Tett, S. E., Clinical pharmacokinetics and pharmacodynamics of tacrolimus in solid organ transplantation. *Clin. Pharmacokinet.* **2004,** *43*, 623-653.
118. Yocum, D. E., Cyclosporine, FK-506, rapamycin, and other immunomodulators. *Rheum. Dis. Clin.* **1996,** *22* (1), 133-154.
119. Kawai, M.; Lane, B. C.; Hsieh, G. C.; Mollison, K. W.; Carter, G. W.; Luly, J. R., Structure-activity profiles of macrolactam immunosuppressant FK-506 analogues. *FEBS letters* **1993,** *316* (2), 107-113.
120. Goulet, M. T.; Rupprecht, K. M.; Sinclair, P. J.; Wyvratt, M. J.; Parsons, W. H., The medicinal chemistry of FK-506. *Persp. Drug Discov. Des.* **1994,** *2*, 145-162.
121. Scola, P. M.; Sun, L.-Q.; Wang, A. X.; Chen, J.; Sin, N.; Venables, B. L.; Sit, S.-Y.; Chen, Y.; Cocuzza, A.; Bilder, D. M., The discovery of asunaprevir (BMS-650032), an orally efficacious NS3 protease inhibitor for the treatment of hepatitis C virus infection. *J. Med. Chem.* **2014,** *57* (5), 1730-1752.
122. Mosure, K. W.; Knipe, J. O.; Browning, M.; Arora, V.; Shu, Y.-Z.; Phillip, T.; Mcphee, F.; Scola, P.; Balakrishnan, A.; Soars, M. G., Preclinical pharmacokinetics and in vitro metabolism of asunaprevir (BMS-650032), a potent hepatitis C virus NS3 protease inhibitor. *J. Pharm. Sci.* **2015,** *104* (9), 2813-2823.
123. Xue, Y.-S.; Cai, Y.-P.; Chen, Z.-X., Mechanism and stereoselectivity of the Rh (II)-catalyzed cyclopropanation of diazooxindole: a density functional theory study. *RSC Adv.* **2015,** *5* (71), 57781-57791.
124. Nowlan, D. T.; Gregg, T. M.; Davies, H. M.; Singleton, D. A., Isotope effects and the nature of selectivity in rhodium-catalyzed cyclopropanations. *J. Am. Chem. Soc.* **2003,** *125* (51), 15902-15911.
125. Ren, Z.; Musaev, D. G.; Davies, H. M., Key Selectivity Controlling Elements in Rhodium-Catalyzed C–H Functionalization with Donor/Acceptor Carbenes. *ACS. Catal.* **2022,** *12* (21), 13446-13456.

126. Liu, W.; Ren, Z.; Bosse, A. T.; Liao, K.; Goldstein, E. L.; Bacsa, J.; Musaev, D. G.; Stoltz, B. M.; Davies, H. M., Catalyst-controlled selective functionalization of unactivated C–H bonds in the presence of electronically activated C–H bonds. *J. Am. Chem. Soc.* **2018,** *140* (38), 12247-12255.
127. Nadeau, E.; Li, Z.; Morton, D.; Davies, H. M., Rhodium carbenoid induced intermolecular CH functionalization at tertiary CH bonds. *Synlett* **2009,** *2009* (01), 151-154.
128. Liao, K.; Pickel, T. C.; Boyarskikh, V.; Bacsa, J.; Musaev, D. G.; Davies, H. M., Site-selective and stereoselective functionalization of non-activated tertiary C–H bonds. *Nature* **2017,** *551* (7682), 609-613.
129. Qin, C.; Davies, H. M., Role of sterically demanding chiral dirhodium catalysts in site-selective C–H functionalization of activated primary C–H bonds. *J. Am. Chem. Soc.* **2014,** *136* (27), 9792-9796.
130. Cammarota, R. C.; Liu, W.; Bacsa, J.; Davies, H. M.; Sigman, M. S., Mechanistically Guided Workflow for Relating Complex Reactive Site Topologies to Catalyst Performance in C–H Functionalization Reactions. *J. Am. Chem. Soc.* **2022,** *144* (4), 1881-1898.
131. Davies, H. M.; Hodges, L. M.; Matasi, J. J.; Hansen, T.; Stafford, D. G., Effect of carbenoid structure on the reactivity of rhodium-stabilized carbenoids. *Tetrahedron Lett.* **1998,** *39* (25), 4417-4420.
132. Wu, B.; Hazrah, A. S.; Seifert, N. A.; Oswald, S. n.; Jäger, W.; Xu, Y., Higher-Energy Hexafluoroisopropanol··· Water Isomer and Its Large Amplitude Motions: Rotational Spectra and DFT Calculations. *J. Phys. Chem. A* **2021,** *125* (48), 10401-10409.
133. Ammer, J.; Mayr, H., Solvent nucleophilicities of hexafluoroisopropanol/water mixtures. *J. Phys. Org. Chem.* **2013,** *26* (1), 59-63.
134. Song, P. S.; Tapley, K. J., Photochemistry and photobiology of psoralens. *Photochem. Photobiol.* **1979,** *29* (6), 1177-1197.
135. Kanne, D.; Straub, K.; Rapoport, H.; Hearst, J. E., The psoralen-DNA photoreaction. Characterization of the monoaddition products from 8-methoxypsoralen and 4, 5', 8-trimethylpsoralen. *Biochem.* **1982,** *21* (5), 861-871.
136. Gupta, A. K.; Anderson, T. F., Psoralen photochemotherapy. *JAAD.* **1987,** *17* (5), 703-734.

Chapter 4

Unmasking the additive effect: *in silico* evaluation of rhodium carbene chemistry

4.1 Introduction:

Over the course of the Davies group's investigation of rhodium-carbene chemistry, the use of computation has been invaluable to understanding the unusual reactivity and selectivity observed.[1-11] While kinetic studies can reveal critical pieces of information about the mechanism of a variety of reactions, it is somewhat limited in our case.[7, 12-16] The interaction of rhodium with a diazo-compound results in the generation of a highly electrophilic carbene which is capable of trapping substrates including the classically inert C–H bond.[17, 18] Due to the high reactivity of the carbene it has historically been impossible to trap out and crystallize the carbene in a chiral environment.[19, 20] Furthermore, reactions involving dirhodium tetracarboxylates can be extremely rapid even at extremely low catalyst loadings.[20, 21] While important information about the rate equations of rhodium carbenoid chemistry can be garnered from kinetic studies, the origins of selectivity cannot be investigated through this approach as the transient rhodium carbene cannot be isolated under conventional reaction conditions.[19, 20, 22] The story becomes even more complex when we begin to consider the remarkable additive effects outlined in **Chapters 1-3**.[16, 23, 24] It has been reported that simple organic additives can alter the reaction rate of dirhodium catalyzed cyclopropanation.[25-27] When investigating extremely low catalyst loadings with the bridged-ligand catalyst $Rh_2(BiTISP)_2$, it was reported that methyl-benzoate helped accelerate the reaction rate by eliminating the induction period observed in the kinetic study.[28] While this effect was not observed with later generations of catalysts, other additives have played a critical role in enhancing both reactivity and selectivity in recent years including $(MeO)_2CO$,[16] DCC,[7] 2-chloropyridine,[23] and HFIP.[24]

Figure 4.1: DFT methods are imperative for understanding the role of additives in rhodium carbene chemistry.

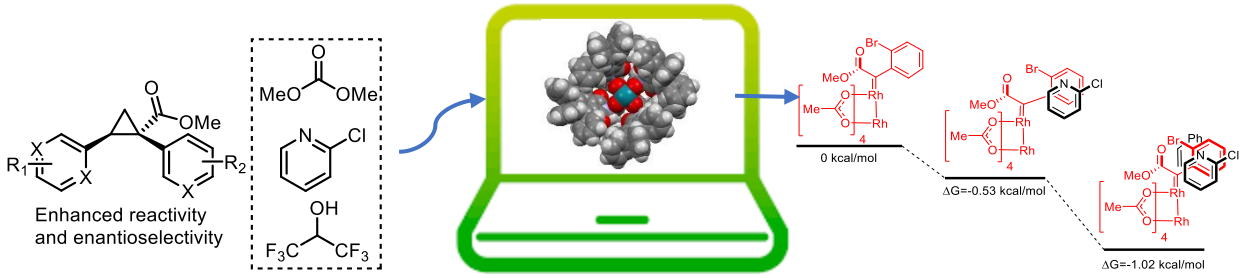

More recently, DFT calculations have been employed to understand site and enantioselectivity in C–H functionalization. While studying the C3 selective C–H functionalization of *tert*-butyl cyclohexane, Dr. Zhi Ren evaluated the selectivity of $Rh_2(TPPTTL)_4$ through analysis of the reaction transition state in the bowl of this catalyst by DFT.[6] This analysis was also critical to obtaining an accurate picture of the structure of $Rh_2(TPPTTL)_4$. In the crystal structure, one of the ligands was tilted in an anti-orientation to the other ligands. However, for dirhodium tetracarboxylates, crystal structures can be irreflexive of the true structure of the catalyst in solution.[6] Indeed, the third-generation catalyst Rh_2(*p*-BrTPCP)$_4$ (**1**) was crystallized as a D_2-symmetric complex,[29] however this structure did not fit the experimentally derived picture of its selectivity which was found to be more similar to Rh_2(*p*-PhTPCP)$_4$ (**3**), known to be a C_2-symmetric catalyst,[30] than $Rh_2(DiBic)_4$ (**2**) (a known D_2-symmetric catalyst).[17, 31]

Figure 4.2: Despite the similarity between the spectroscopically observed crystal structures of TPCP series catalyst the crystal structures cannot explain the reactivity trends of catalysts in this series.

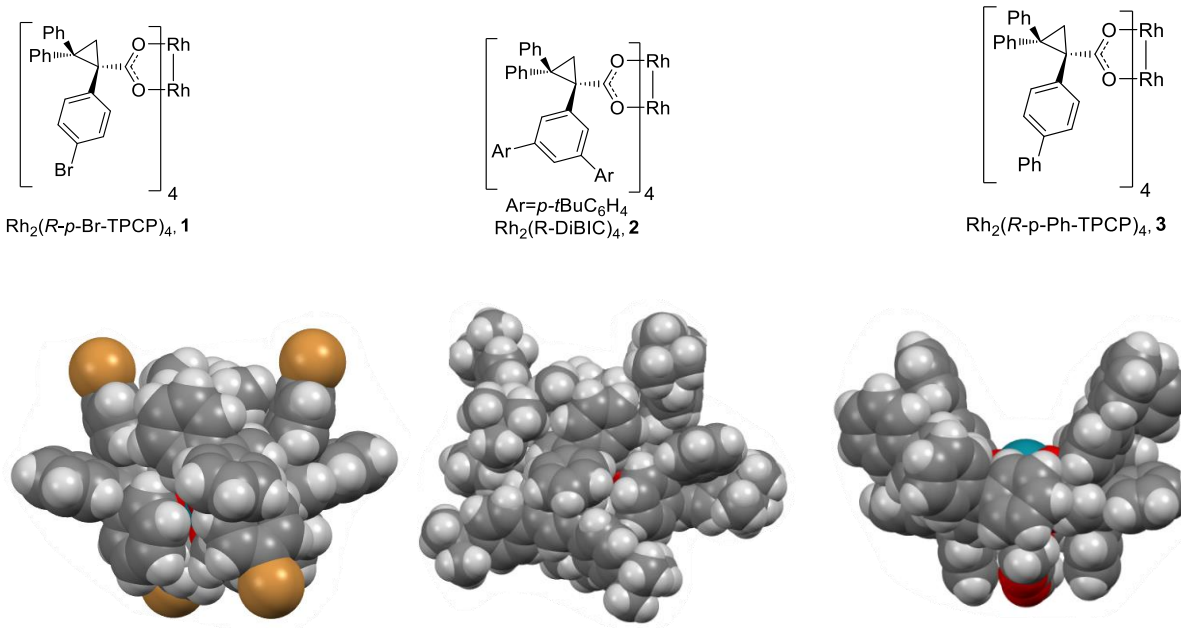

This dynamically derived picture of Rh_2(*p*-BrTPCP)$_4$ (**1**) was then applied towards a comparison of the selectivity of diarylcyclopropanacarboxylate (Rh_2(DPCP)$_4$) complexes in comparison to their triarylated analogues.[32] This analysis was able to show that the high flexibility and similar energy of different symmetry Rh_2(DPCP)$_4$ catalysts led to conformational promiscuity which likely resulted for their poor selectivity profiles.[32] In comparison, the TPCP series of catalysts is highly selective and gives predictable and consistent enantioinduction due to the rigidity of its ligands and the steric demand of the ligands around the open catalyst face.[30] In 2022, the final study of the Rh_2(TPCP)$_4$ system was conducted to rationalize the high enantioselectivity that is observed in these systems.[10] Over the course of these studies, it was discovered that the ester geometry played a critical role in dictating enantioselectivity in primary C–H functionalization. These effects would not have been possible to observe without the use of DFT calculations on the carbene itself, highlighting the importance of *in silico* evaluation of dirhodium carbenoid chemistry in rationalizing selectivity for these highly complex catalysts.

Figure 4.3: Reproduced from Zhi Ren *et. al.* Ester geometries and relevant energetic profiles responsible for the selectivity of C–H functionalization of benzylic substrates with Rh_2(*p*-BrTPCP)$_4$ (**1**).[10]

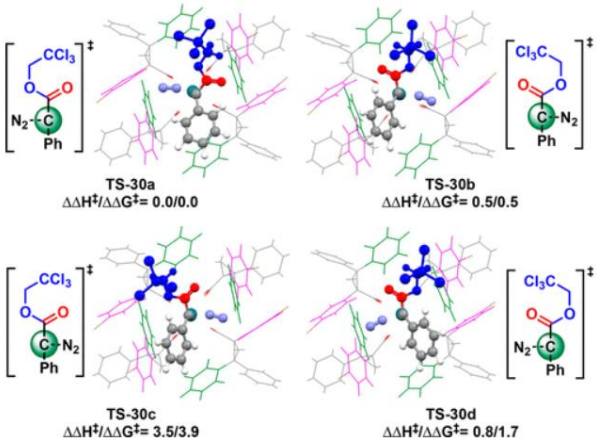

4.2 Results and Discussion:

The role of *N,N'*-dicyclohexylcarbodiimide (DCC) in C–H functionalization of cyclohexane (**4**) at extremely low catalyst loadings (0.0005 mol %) was recently reported.[7] In the optimized system, Rh_2(TPPTTL)$_4$ (**5**) was the catalyst of choice as this catalyst has the highest rate of reactivity as well as asymmetric induction. Curiously, it was observed that while some batches of diazo **6** were competent in C–H functionalization to furnish **7** at catalyst loadings below 0.0025 mol %, others failed.[7] This aberrant reactivity was eventually tracked to the presence of trace amounts of DCC carried over from the esterification step used to furnish the diazo compound.[7] Addition of 1 mol % of DCC back into the reaction resulted in acceleration of the reaction rate, and eventually, this additive proved essential to routinely performing the reaction at 0.0005 mol % with a diverse series of substrates.[7] During the kinetic analysis of the system, Dr. Bo Wei observed that adding DCC to the reaction mixture after the addition of diazo and catalyst had no effect on the reaction rate, however, when a second addition of catalyst was charged into the reaction mixture, the reaction took off and was able to finish in the expected time.[7] This led to the hypothesis that DCC protects the catalyst from degradation, although the degradation of dirhodium tetracarboxylate complexes in

carbene chemistry is not well understood.[7, 16] We hypothesized that DCC coordinates to the carbene complex and prevents this degradation pathway while allowing C–H functionalization to occur however the transient nature of the rhodium carbene prevented experimental interrogation of catalyst degradation. This provided an opportunity to investigate the system computationally.[10, 32]

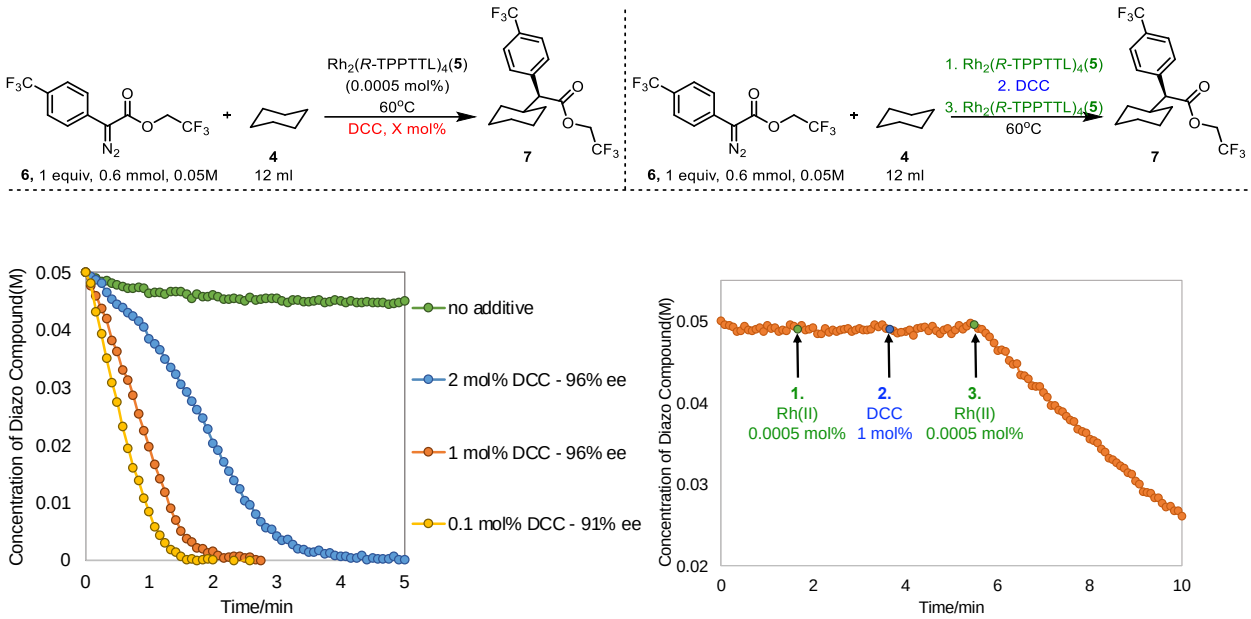

Figure 4.4. Effect of different concentrations of DCC on the reaction kinetic profiles at 60 °C with 0.0005 mol % Rh_2(*R*-TPPTTL)$_4$ (**5**) catalyst loading (left). The reaction with 0.0005 mol % Rh_2(*R*-TPPTTL)$_4$ (**5**) catalyst loading gives no progress until 1 mol % DCC and another 0.0005 mol % Rh_2(*R*-TPPTTL)$_4$ (**5**) catalyst added (right).

To gain greater understanding of the role of DCC in high TON C–H functionalization, the first step was to perform a series of calculations on the simple system of $Rh_2(OAc)_4$-carbene (**8**) with and without a variety of coordinating additives. The actual catalyst, Rh_2(TPPTTL)$_4$ (**5**), is large and complex to calculate due to the presence of 16 phenyl rings on the catalyst periphery which can easily rotate.[6] In combination with the flexibility of the ligand structure, this makes detailed calculations of the system complex and lengthy. Computational systems designed to reduce calculation time like ONIOM would be suboptimal for

interrogating this system due to the importance of the ligand environment to observed reactivity and selectivity.[33] In other words, to get a scientifically accurate picture of the catalyst, the entire structure needs to be calculated at a high level which includes both dispersive interactions and high-level consideration of the ligand environment.[6] Luckily, the enhancement of reaction rate by DCC was not confined to $Rh_2(TPPTTL)_4$ (**5**) and several other catalysts also experienced this effect.[7] As a result, the optimization of the $Rh_2(OAc)_4$-Carbene system was the most practical for conducting calculations. We began by optimizing several structures including $Rh_2(OAc)_4$-Carbene (**8**), $Rh_2(OAc)_4$-Carbene-Nu (Rh coordinated) (**9b**), $Rh_2(OAc)_4$-Carbene-DCC (carbene coordinated) (**10b**). We also wanted to explore additives which were ineffective for enhancing the rate of C–H functionalization, especially a system which is known to poison the reaction, pyridine. The relevant complexes $Rh_2(OAc)_4$-carbene-Nu) (**10**) where Nu stands for nucleophile (DCC or pyridine) and Nu-Rh_2OAc_4-carbene) (**9**) were also calculated. All calculations were performed at the B3LYP-D3(BJ)/6-31G(d,p) level of theory for the main group elements using LANL2DZ for rhodium including effective core potentials. The solvent was accounted for using CPCM and considering dichoromethane as the solvent.

Figure 4.5: General complexes calculated.

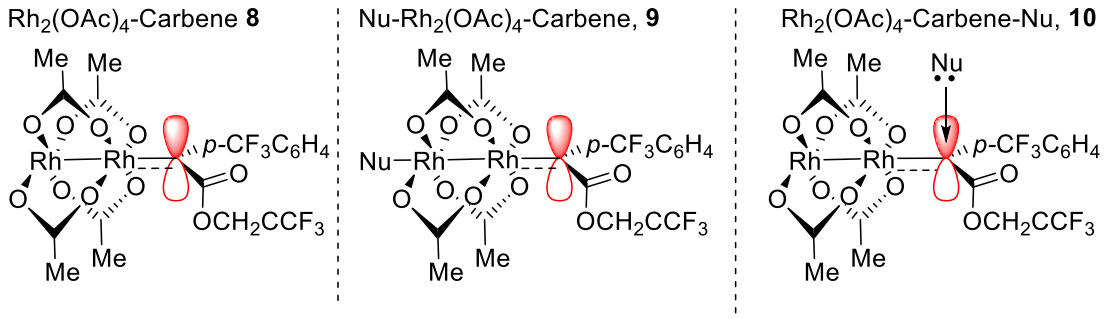

The calculations showed several interesting trends. First, it was clear why pyridine poisons the catalyst as the free energy (ΔG) associated with pyridine binding to $Rh_2(OAc)_4$ is −12.7 kcal/mol, while coordination of the carbonyl of the diazo (the most nucleophilic site) is favorable by just -3.4 kcal/mol.[7] This means that

the diazo compound cannot displace pyridine which is a necessary step for the formation of the catalytically active rhodium carbene intermediate.[16] Even if changes in experimental conditions, such as high temperature, make it possible to generate a rhodium carbene, the presence of pyridine may still prevent the reaction of carbene with alkanes because of the highly energetically favorable formation of a formal ylide (Figure 4.6, **10a**, ΔG = −22.3 kcal/mol). As can be seen in Figure 4.6, the pyridine's axial coordination with the $Rh_2(OAc)_4$-Carbene **8** is only slightly favorable (**9a**, ΔG = −1.9 kcal/mol).

Figure 4.6. *In silico* comparison between pyridine (A) and DCC (B) coordination to rhodium carbene **8**.

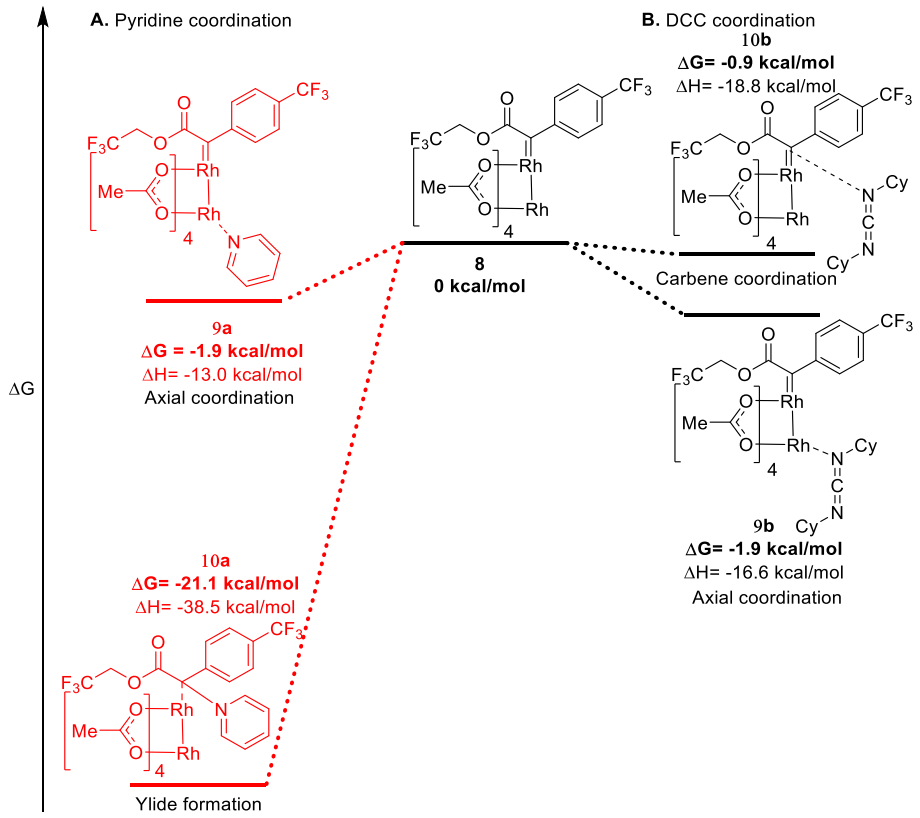

The beneficial influence of DCC was a surprise because we would have expected it to poison the catalyst or react with the carbene to form an ylide.[34, 35] However, calculations revealed that DCC only weakly coordinates with the dirhodium catalyst and the dirhodium carbene intermediate: the calculated (DCC)−$Rh_2(OAc)_4$ and (DCC)− $Rh_2(OAc)_4$ (carbene) bond energies are ΔG = −9.3 kcal/mol and ΔG = −1.9 kcal/mol,

respectively (Figure 4.6). Interestingly, the coordination energy of DCC and pyridine to the open rhodium site of the carbene complex is the same (**9b** and **9a** respectively, ΔG = −1.9 kcal/mol). However, the interaction of DCC with the carbene of the Rh-carbene complex is less energetically favorable (**10b,** ΔG = −0.9 kcal/mol). Therefore, the presence of DCC in proximity to the rhodium carbene is unlikely to initiate ylide formation as pyridine does, likely due to the difference in electronics of the *N*-donor centers of pyridine and DCC in addition to the presence of the sterically bulky cyclohexyl groups in DCC. Instead, the performed calculations enabled us to hypothesize that DCC's weak coordination with the axial site of the dirhodium complex (**10b**) destabilizes the Rh-carbene bond (elongating it by 0.03 Å), modifying the nature of the Rh-carbene bond and changing the energy of the HOMO and LUMO (and other frontier orbitals, Figure 4.7).[7] One should emphasize that similar conclusions have been made by Darko and co-workers in their study of the dirhodium catalysts with tethered axial coordinating groups, thioethers in particular.[36-38] Therefore, we explain the observed rate acceleration upon reaction of the carbene and unactivated traps in our studies through axial coordination with the rhodium carbene. The above presented discussion provides the impression that the presence of any axially coordinating additive in dirhodium tetracarboxylate-catalyzed carbene insertion would accelerate the reaction. However, one should not forget that many such nucleophiles, as exemplified by pyridine, also poison the catalyst, preventing the formation of the catalytically active rhodium-carbene, or react with the carbene through ylide formation, leading to undesired side products.[24, 39] One should emphasize that the unique ability of DCC to enhance the reactivity of the rhodium carbene insertion into the C−H bond derives not only from the unique electronics of the *N*-donor centers but also from the steric bulky nature of its cyclohexyl groups which prohibit ylide formation.

Figure 4.7: Comparative NBO analysis of $Rh_2(OAc)_4$-Carbene **8** (Left) and DCC-$Rh_2(OAc)_4$-Carbene **10a** (right) complexes shows that the LUMO of **10a** is considerably destabilized compared to **8**.

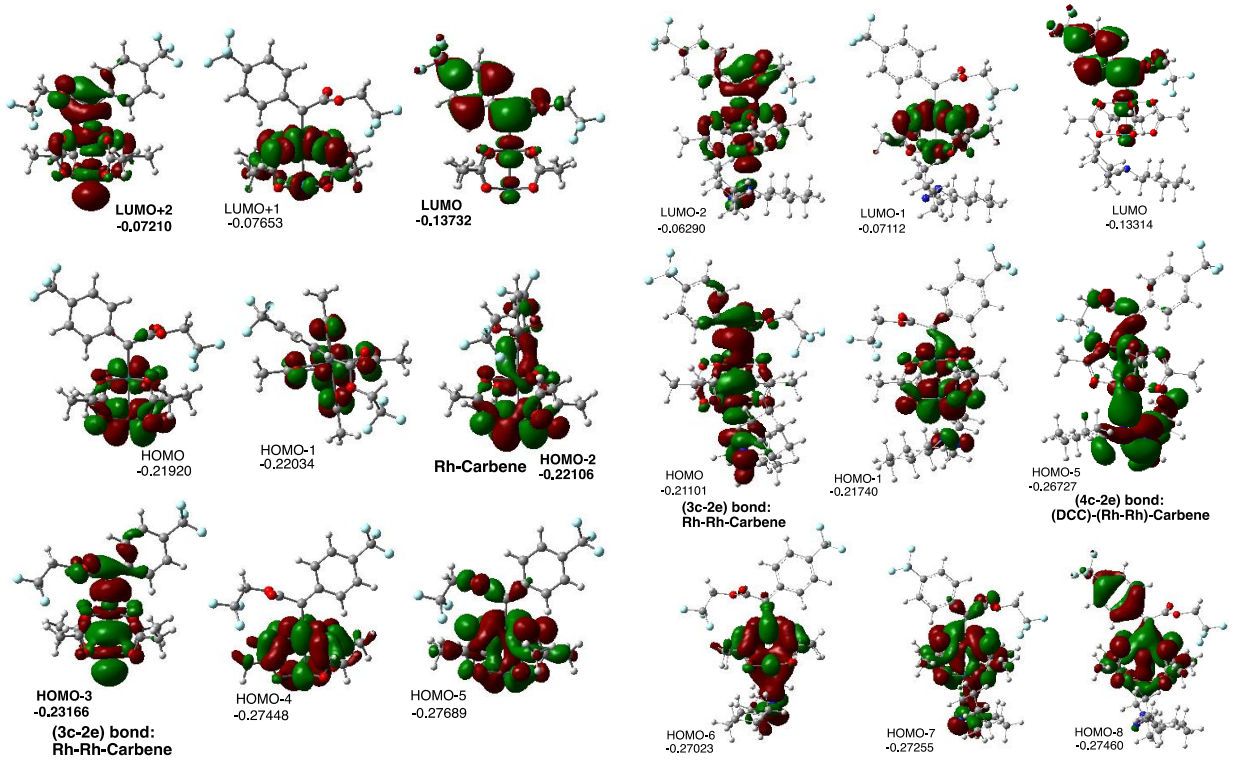

Although this gives us a clear picture of the role of DCC in the simplified achiral system, it may not translate to the actual system of interest which uses $Rh_2(TPPTTL)_4$ (**5**) as catalyst. To mitigate this concern the DCC-$Rh_2(TPPTTL)_4$ complex (**11**), the $Rh_2(TPPTTL)_4$-carbene complex (**12**), and the DCC-$Rh_2(TPPTTL)_4$-carbene complex (**13**) were computed. These calculations showed that indeed DCC can access to sterically bulky axial site of $Rh_2(TPPTTL)_4$ and does so with an even stronger thermodynamic driving force than in the achiral system ((DCC coordination is favorable by -14.4 kcal/mol for **11** and -9.3 kcal/mol for **9b**, $\Delta\Delta G$=-5.1kcal/mol). However, upon coordination, the catalyst bowl deforms (Figure 4.8)

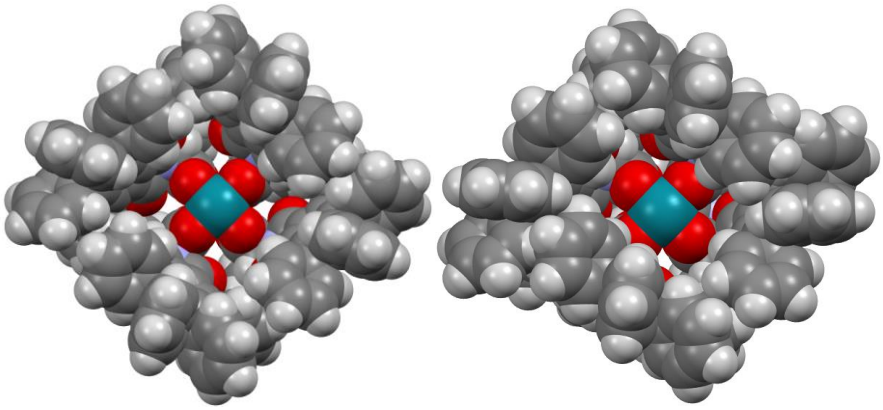

Figure 4.8: Optimized structure of $Rh_2(TPPTTL)_4$ (**5**) (left) and $Rh_2(TPPTTL)_4$-DCC (**11**) (right).

The geometry of the bowl has been reported to be instrumental in controlling the stereoselectivity of C–H functionalization.[6, 40] An interesting feature of the DCC additive effect is that though it enhances reaction rate, the stereoselectivity of the reaction remains unchanged.[7] If DCC deforms the catalyst bowl of the carbene complex, the computational and experimental results could therefore be inconsistent. Fortunately, when DCC- $Rh_2(TPPTTL)_4$-Carbene complex **13** was optimized and compared the geometry with the native $Rh_2(TPPTTL)_4$-Carbene complex **12**, the geometry of the catalyst bowls were almost identical which is consistent with our experimental findings. (Figure 4.9).

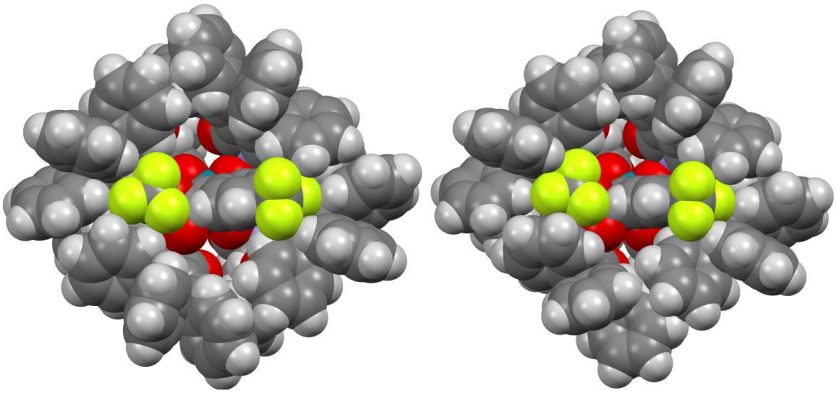

Figure 4.9: Optimized structure of $Rh_2(TPPTTL)_4$-Carbene (**12**) (left), and DCC- $Rh_2(TPPTTL)_4$-Carbene (**13**) (right).

In DCC-$Rh_2(OAc)_4$-Carbene complex **9b** the N-Rh bond length is 2.53Å and the N-Rh bond length in the DCC-$Rh_2(TPPTTL)_4$-Carbene complex **13** was 2.58Å, only 0.05Å longer than in the achiral system. Additionally, while the ligand environment stabilizes the carbene binding significantly through π-stacking ($\Delta\Delta G_{carbene\ generation}$= -18 kcal/mol) the axial coordination of DCC destabilizes the carbene by the same amount of free energy in $Rh_2(TPPTTL)_4$ as it does in $Rh_2(OAc)_4$ (7.0 kcal/mol for **13**, 6.8 kcal/mol for **9b**). As a result, we propose that the achiral model for DCC enhancement (**9b**) is a good fit for the experimental observations.[7] Future work will focus on transition-state DFT calculations and MD simulations to further investigate the key reaction intermediates in this system although ultrafast spectroscopic techniques could also prove invaluable.[20, 22, 41, 42]

The additives described in this thesis have demonstrated the capability to modulate selectivity as well as reactivity, especially in cyclopropanation as discussed in **Chapter 2** and **Chapter 3**.[23, 24] Once again, the easiest way to interrogate these systems was the use of DFT calculations. As described in **Chapter 2**, 2-chloropyridine has a pronounced effect on the selectivity of cyclopropanation involving *ortho*-substituted aryldiazoacetates.[23] In one case, the reaction of methyl 2-diazo-2-(2-methoxy-5-methylphenyl)acetate and styrene, the reaction transforms from 4% ee to 95% ee when 1.0 equiv of 2-chloropyridine is added to the reaction mixture.[23] As stated in **Chapter 2**, the effect has only been observed with *ortho*-substituted aryldiazoacetates in combination with $Rh_2(TPPTTL)_4$ (**5**), a catalyst which could complicate the investigation for the reasons stated above. Furthermore, though the rate determining step (RDS) of the cyclopropanation is N_2-extrusion from the Rh-diazocarbene complex as mentioned in **Chapter 1** this may not be the selectivity determining step (SDS).[2, 10] Instead, the approach and subsequent concerted-asynchronous [2+1] is the selectivity determining step and this is controlled by the chiral ligands (Figure 4.10a).[2, 3, 10] As a result, the reaction is in a Curtin-Hammett situation (meaning that the RDS and SDS are decoupled)[43] where an experimental kinetic investigation of the system would be ineffective for understanding changes in enantioselectivity. Previous work on C–H functionalization with the C_2-

symmetric catalyst Rh_2(*p*-BrTPCP)$_4$ (**1**) has suggested that nitrogen extrusion from the Rh-diazocarbene intermediate dictates the ester geometry of the resultant Rh-carbene complex and this is therefore the selectivity determining step as approach from the ester-side of the carbonyl is always energetically preferred (Figure 4.10b).[10] The argument put forth in this previous study was that the chiral ligands dictate the ester orientation which is allowed to access the catalyst bowl and, hence, that is the true stereoselectivity determining element (Figure 4.10b).[10]

Figure 4.10: Existing paradigms for selectivity in rhodium carbenoid transformations.

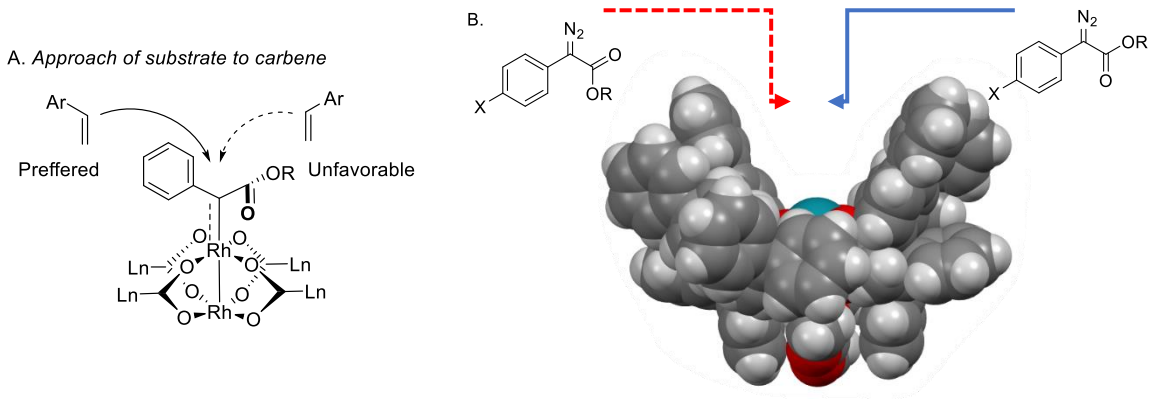

While an interesting hypothesis, previous work may not be analogous to this investigation for several reasons. Firstly, the calculations were performed with C_2 symmetric catalysts and *para*-substituted aryldiazoacetes, the *ortho*-aryldiazoacetate/C_4 symmetric catalyst system could be altogether different.[44-46] Secondly, the reaction investigated was C–H functionalization which has a different rate determining step from cyclopropanation.[7, 16] Cyclopropanation of rhodium carbenes is typically thought to be a barrierless transformation (<0.5 kcal/mol) and has an exceedingly flat potential curve when compared with a reaction like C–H functionalization where the initial hydride abstraction requires overcoming a significant energetic barrier (~16 kcal/mol).[10, 47] Finally, the studied system is experimentally incompatible with *ortho*-substituted aryldiazoacetates. The same catalyst from this study, Rh_2(*p*-BrTPCP)$_4$ (**1**), which has proven to be highly selective with *para*-substituted aryldiazoacetates invariably displays poor selectivity

and reactivity when *ortho*-substituted aryldiazoacetates are used.[16, 23, 48] This suggests that the corresponding carbenes are fundamentally distinct, and analogies between them are likely inappropriate. As a result, a new computational campaign was started to understand the effects at play in the 2-chloropyridine system.

Figure 4.11. Several distinctions in carbene geometry (left), substrate energetics and relative reactivity (middle), and catalyst symmetry (right) prevent analogies between this study and earlier work.

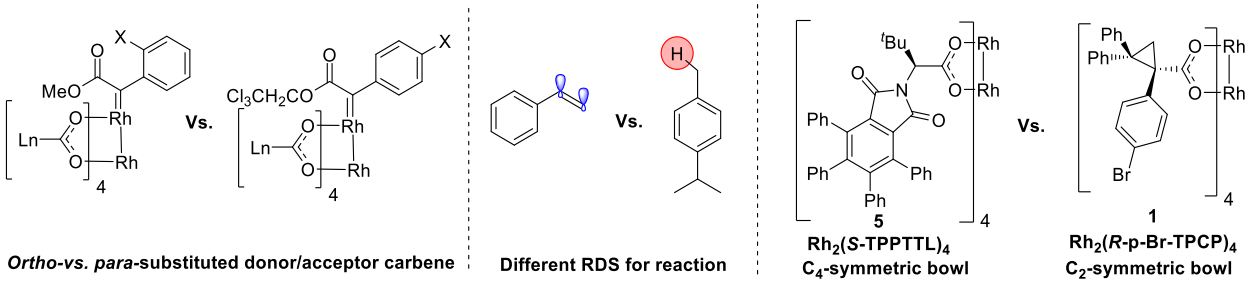

To first analyze the system, calculations were run on the achiral complex and an *ortho*-bromo arylacetato carbene (**14**) was compared with a *para*-bromo arylaceto carbene (**15**) with $Rh_2(OAc)_4$ as the dirhodium complex. All calculations were performed at the B3LYP-D3(BJ)/6-31G(d,p) level of theory for the main group elements using LANL2DZ for rhodium including effective core potentials. The solvent was accounted for using CPCM and considering dichloromethane as the solvent.[10, 32, 47] From a purely geometrical standpoint the carbenes are extremely distinct (Figure 4.12). In a typical donor/acceptor carbene (*para* or *meta*-substituted) the arene is virtually coplanar with the carbene.[3, 49] This occurs due to the π-orbitals of the arene donating electron density into the empty p-orbital of the carbene which serves to stabilize it by reducing electrophilicity.[3, 49, 50] This is a key feature of donor/acceptor carbenes, along with π-stacking between the substrate and the carbene, which allows the carbene to be highly site-selective, enantioselective, and diastereoselective.[2, 3, 10] The computed structure of the *para*-substituted arylacetocarbene **15** shows a shallow dihedral angle between the carbene and the arene of just $\phi=9^{o}$

which is consistent with this established model of carbene selectivity (Figure 4.12). In contrast, the *ortho*-substituted arylacetocarbene **14** experiences a dihedral angle of ϕ=31° between the carbene and the arene which is a significant tilt.[44] This not only creates a different steric environment around the carbene, but also energetically destabilizes the carbene (Figure 4.12). With diminished orbital overlap between the arene and the carbene, the arene cannot as effectively donate electron density into the empty p-orbital of the carbene which raises the total energy (E) of carbene **14** relative to the *para*-congener (**15**) by 3.8 kcal/mol. This higher energy could be responsible for the lack of selectivity observed with the carbene as opposed to the *para*-substituted isomer. Less stable carbenes, in other words more electrophilic carbenes, trap substrates more rapidly.[1] This rapid trapping can override stabilizing weak interactions like π-stacking to simply favor reaction regardless of the substrate trajectory. Similarly, the approach of the substrate to the carbene could be altered by the steric environment of the *ortho*-substitution. The substrate, in this case styrene, π-stacks with the carbene and will approach one face of the carbene as dictated by the ligands.[10] The ester group on the carbene is oriented perpendicular to the p-orbital of the carbene and the substrate also prefers to approach the carbene on the same side as the ester oxygen (not the carbonyl).[2, 45-47] In *ortho*-substituted arylacetocarbene (**14**) the steric bulk of the arene could compromise this approach preference.[44]

Figure 4.12: Energetic and geometrical differences between *ortho* (**14**) and *para* (**15**) substituted carbenes.

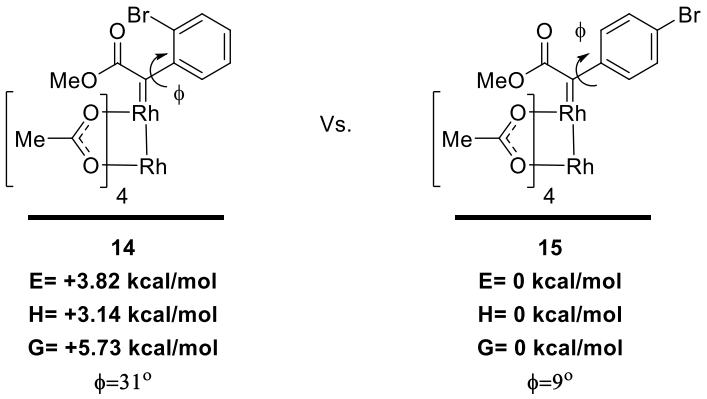

Initially, we wanted to determine the most favorable trajectory for styrene to approach each complex to expedite subsequent transition state calculations (Figure 4.13). This could be difficult, as the cyclopropanation of alkenes with donor/acceptor metallo-carbenes is commonly believed to be virtually barrierless.[45, 47] In the *para*-substituted complex, the approach to the carbene from the carbonyl face (**16**) is energetically unfavorable by 0.3 kcal/mol (Figure 4.13). Interestingly, approach from the ester face of this complex (**17**) cannot be computed as the energetic barrier to [2+1] cycloaddition is so low that attempts to model **17** inevitably resulted in the formation of a cyclopropane during geometry optimization. Based on this data, we propose that the approach of styrene from the ester side in the *para*-substituted donor/acceptor carbene is likely significantly more favorable than the approach from the carbonyl side. Previous studies that calculated this approach did not include diffuse functions or dispersive interactions which could account for the difficulties observed in this study with computing this intermediate as compared to previous work.[2, 3, 45, 46] In the *ortho*-substituted complex, approach of styrene to the carbene occurs favorably from the ester side (**19**, ΔG=-2.2 kcal/mol). The mere fact that approach trajectory of styrene to the ester side of the carbene (**17**) cannot be computed for the *para*-substituted carbene, whereas it can for the *ortho*-substituted carbene (**19**) highlights the major differences between the two complexes despite this superficially subtle structural distinction. As a result, we would expect that the transition states for these two similar substrates will also be energetically distinct.

Figure 4.13: Styrene approach to complexes **14** and **15**. Free energy from left to right: **16**: ΔG=+0.3 kcal/mol, **17**: ΔG cannot be computed. **18**: ΔG=+0.3 kcal/mol. **19**: ΔG=-1.8 kcal/mol.

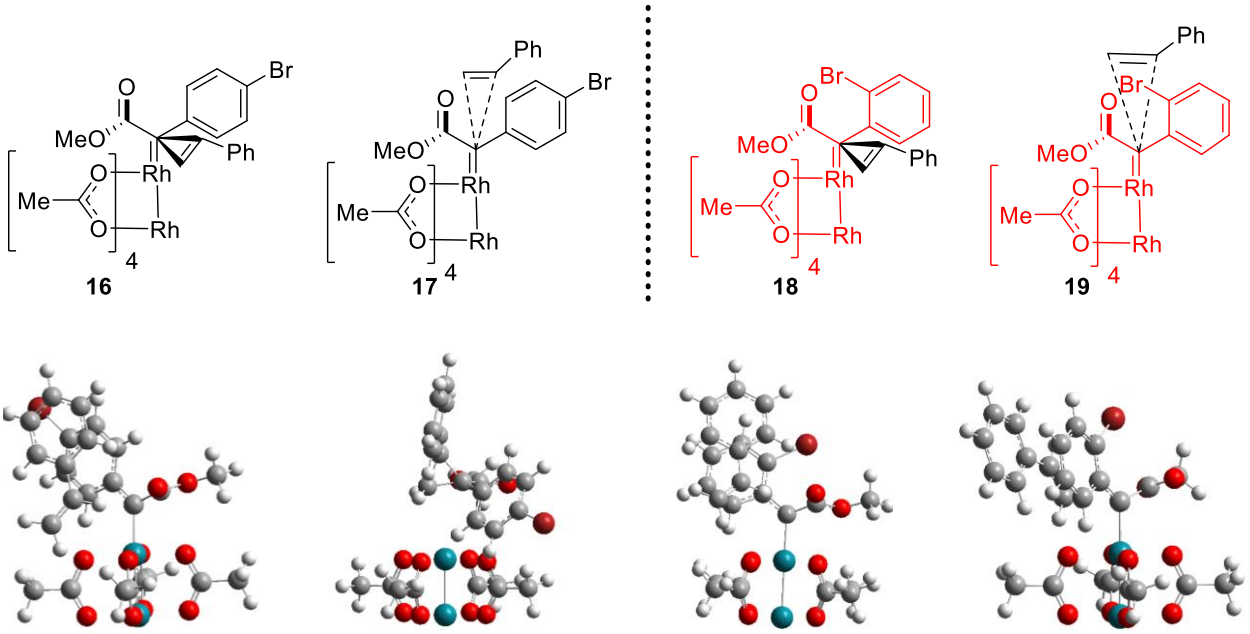

The addition of 2-chloropyridine substantially perturbs the *ortho*-substituted arylacetocarbene complex. As with styrene the trajectory of 2-chloropyridine coordination to the carbene complex needed to be assessed. To this end, the carbonyl-side coordination (**20**) and the ester-side coordination (**21**) complexes were calculated and relative free energies (ΔG) of coordination were compared. Experimentally, we observed that the addition of 2-chloropyridine does not invert the stereoselectivity of the cyclopropanation which suggests it does not occupy the same site as the substrate,[23] of course we need to validate this assumption and so both trajectories were computed. Though the initial geometry of both approach vectors assumed an ylide between the carbene and 2-chloropyridine, this interaction was lost during geometry optimization.[7, 24] This is intuitive as the pKa of 2-chloropyridine is just 0.7, meaning it is non-nucleophilic and unlikely to form a stable ylide with the carbene.[51] By contrast, the known catalyst poison and reactive heterocycle pyridine has a pKa of 5.8.[51] Instead, 2-chloropyridine engages in π-

stacking with the phenyl ring of the carbene. This interaction also occurs favorably on the carbonyl side of the complex (**20**) by ΔG=-1.8 kcal/mol relative to the ester side which offers a rationale as to why enantioinversion was not observed in the system. While this coordination does not significantly lower the overall energy of the complex (ΔG= -0.53 kcal/mol) this could explain why such a significant excess of 2-chloropyridine relative to the carbene is required to observe the effect.[23] While a 1:1 ratio of diazocompound to 2-chloropyridine does not immediately sound like an excess, the catalyst is operating at 1 mol % which means that, at any given time over the course of the reaction, the ratio of rhodium-carbene:2-chloropyridine is actually 1:100.[23] Since the π-stacking of 2-chloropyridine is not very energetically favorable, at least in the achiral model, it is possible that the kinetics of the vast excess of 2-chloropyridine helps to encourage the additive enhancement.

Figure 4.14: Calculated approach of 2-chloropyridine to **14**.

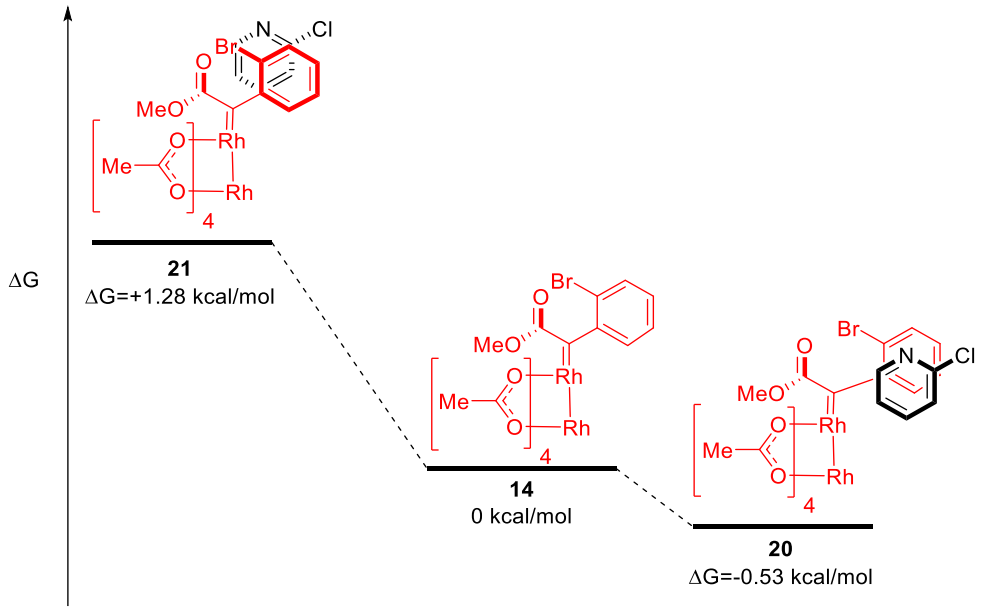

The most interesting feature of the interaction between the carbene and 2-chloropyridine was that it planarizes the *ortho*-substituted arene, reducing the carbene-arene dihedral angle from ϕ=31° (**14**) to ϕ=9.4° (**20**), which is close to *para*-substituted carbene **15** (Figure 4.15, ϕ= 9° for the methyl ester **15**, ϕ=

3.9° for the 2,2,2-trichloroethyl ester **22**).[10] This planarization could explain why 2-chloropyridine helps improve the asymmetric induction of cyclopropanation as a planar arene helps stabilize the empty p-orbital of the carbene and changes the steric profile of the *ortho*-substituted aryl-carbene to be more similar to a *para*-substituted analogue which gives high enantioselectivity without additive enhancement (Figure 4.15).

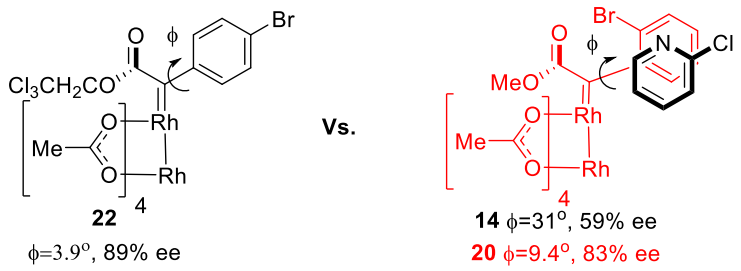

Figure 4.15: Planarization of the arene by 2-chloropyridine, combined with blocking approach from the ester side could be responsible for the increased %ee, as ϕ more closely matches in substrates that are known to give high enantioselectivity.[16, 23]

Once the approach of 2-chloropyridine to the achiral catalyst was assessed the next stage was to compute the transition-state of the cyclopropanation to determine the effect of 2-chloropyridine coordination on this selectivity determining step in the transformation (Figure 4.16). First the TS for the complex both with (**23**) and without 2-chloropyridine (**24**) was computed in the achiral complex (Figure 4.16). This calculation showed that the energetic barrier to cyclopropanation was identical for each complex (ΔG= +2.64 kcal/mol). For the observed experimental difference in selectivity with and without 2-Clpyridine (**26** afforded with 59% ee without 2-chloropyridine and 83% ee in the presence of 2-chloropyridine) we would expect the ΔΔG‡ to be around 0.5 kcal/mol, which these calculations did not show. As a result, more complex calculations will be necessary which include the chiral environment of **5**.

Figure 4.16: Transition-state calculations to assess the activation energy barrier both with and without 2-chloropyridine.

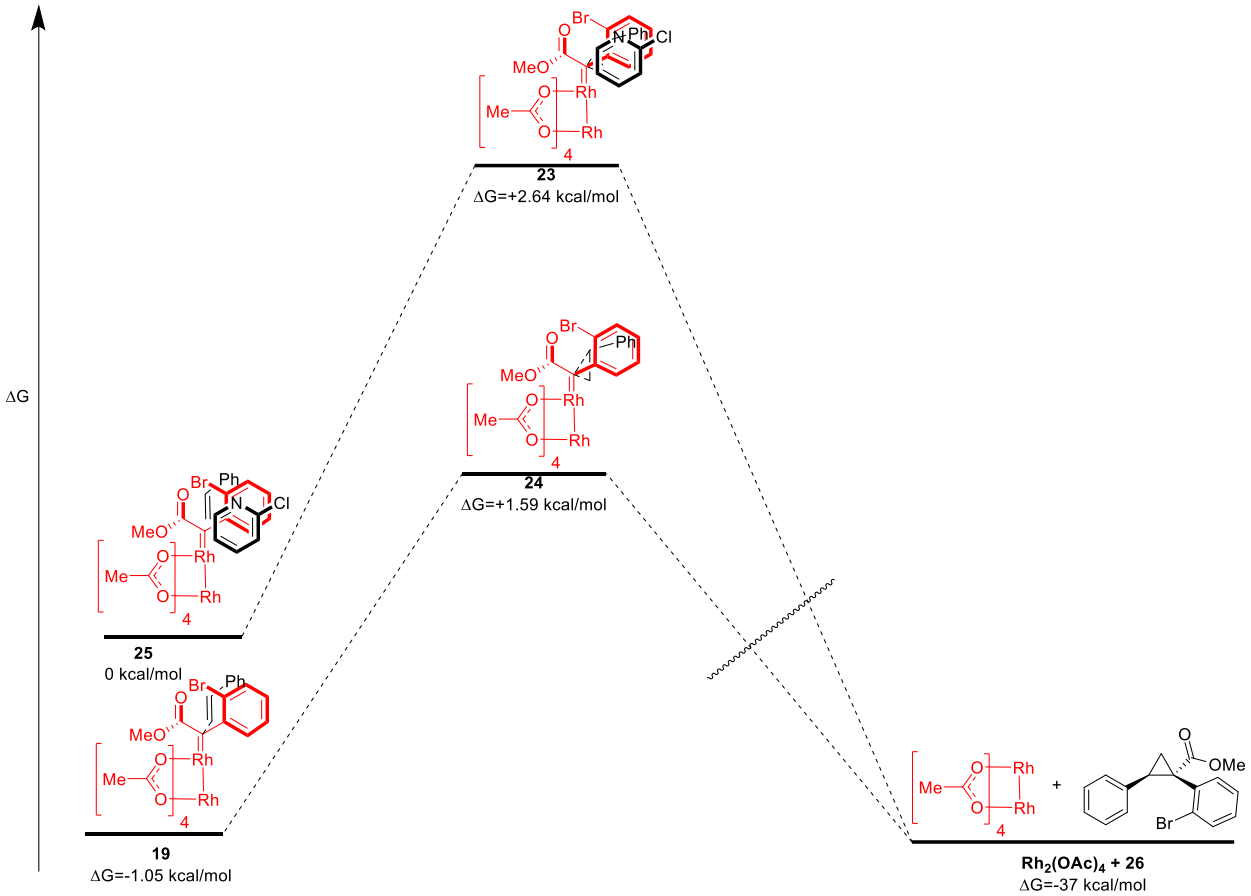

To understand the requirement of the system to use $Rh_2(TPPTTL)_4$ (**5**) as catalyst, these intermediates were calculated in the chiral bowl of this catalyst. The Rh_2(*S*-TPPTTL)$_4$-carbene (**27**), 2clpyr-Rh_2(*S*-TPPTTL)$_4$-carbene (**28**), and 2-clpyr-Rh_2(*S*-TPPTTL)$_4$-carbene-2clpyr (**29**) complexes were optimized. In these complexes, π-stacking between the phenyl rings and the carbene could change the geometry of the carbene and so it was relevant once again to account for these interactions, preventing the use of simplification techniques like ONIOM.[33] The carbene-arene dihedral angle (ϕ) of the *ortho*-substituted aryldiazoacetate was diminished in these complexes but significant tilt was still observed. In complex **27** this angle was 14.8°, in complex **28**, it was 14.1°, and in 2clpyr-Rh_2(*S*-TPPTTL)$_4$-carbene-2clpyr complex **29** it was just 1.1° (Figure 4.17). This shows that the planarizing influence of 2-chloropyridine is preserved in

the chiral catalytic system and is observed only when 2-chloropyridine interacts with the carbene inside the catalyst bowl.

Figure 4.17: Bowl geometries of complexes **27-29**.

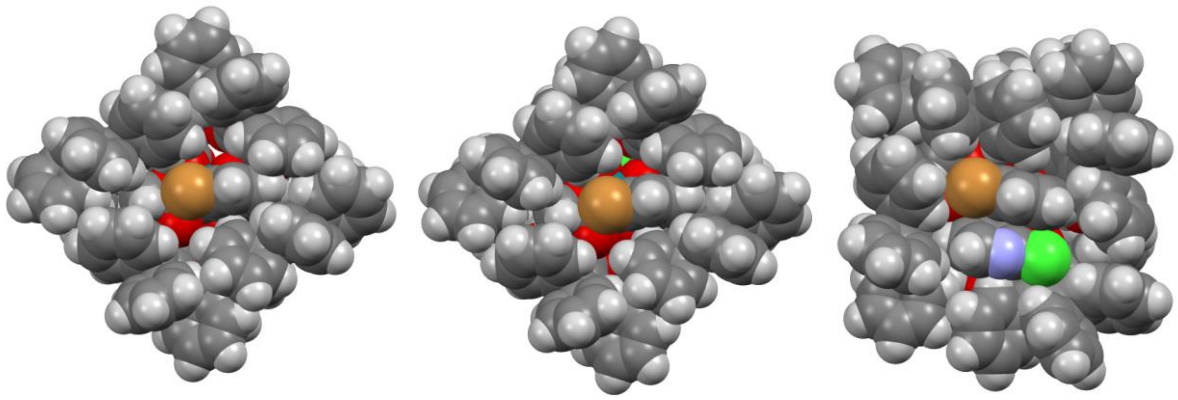

27, ϕ=14.8° **28, ϕ=14.1°** **29, ϕ=1.1°**

Another interesting feature of the system was the disruption in the helical chirality of the bowl.[6, 23, 46, 52] While 4-substituted arylacetocarbenes in the pocket of Rh_2(*S*-TPPTTL)$_4$ (**5**) experience a chiral bowl with a helical chirality in the phenyl rings around the periphery of the catalyst (all rotated clockwise) the 2-substitution of the carbene caused a change in these orientations (Figure 4.18), such that two of the ligands have reversed phenyl ring orientations (**27**, left, right, left, right). In this way the catalyst periphery appears more like a C_2 symmetric structure than a C_4 symmetric structure.[17, 30, 53] This change in catalyst symmetry could also be a critical element governing asymmetric induction with *ortho*-substituted aryldiazoacetates and may explain why the *ortho*-substituted aryldiazoacetates yield the opposite major enantiomer to their *para*-analogues when Rh_2(*S*-TPPTTL)$_4$ (**5**) is used as catalyst.[23] Further calculations are needed to identify the transition states critical for governing cyclopropanation enantioselectivity both with and without the presence of 2-chloropyridine within the bowl of Rh_2(*S*-TPPTTL)$_4$ (**5**).

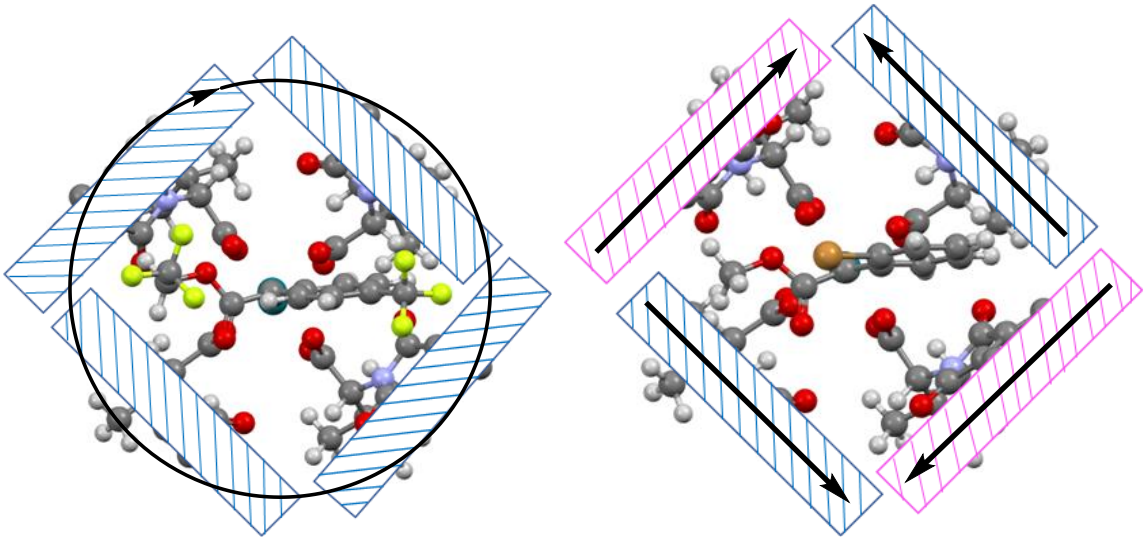

Figure 4.18: Compound **12** highlighting the tilt of the peripheral phenyl rings (left). Rh_2(*S*-TPPTTL)$_4$ with an *ortho*-substituted donor/acceptor carbene (**27**) highlighting the tilt of the peripheral phenyl rings(right).

The final additive to explore was HFIP. As mentioned in **Chapter 3**, this additive has a significant effect on catalyst enantioselectivity as well as reactivity.[24] The reactivity effects of HFIP can be explained through rudimentary analysis of acid-base pairing and hydrogen bonding (Figure 4.19). Questions often arise as to why solvent quantities of HFIP are required for the deactivation of some nucleophiles while others can be deactivated with just 10 equiv HFIP. To answer these questions a cluster of HFIP-H_2O was computed along with the hydrogen bonds between HFIP-DMAP and HFIP-pyridine, compounds which are deactivated with 10 equiv and solvent equiv HFIP respectively (Figure 4.19). These calculations showed that the free energy of HFIP-H_2O cluster formation (ΔG) was -5.4 kcal/mol. This suggests that these clusters will form spontaneously in DCM, and cleavage of the cluster would be required for nucleophilic deactivation to take place as all the alcohol protons of the HFIP molecules are engaged in hydrogen bonding interactions (Figure 4.19). The interaction of DMAP-HFIP had a free energy of -5.99 kcal/mol (Figure 4.19). This suggested that, thermodynamically, DMAP would be able to dissociate an HFIP-H_2O cluster in solution which accounts for the ability of HFIP to deactivate the poisonous influence of DMAP at relatively low

concentrations. In contrast the free energy of formation of the HFIP-pyridine interaction was -4.4 kcal/mol (Figure 4.19). This suggests that the interaction would not be strong enough to dissociate an HFIP-H_2O cluster and hence pyridine requires a full hydrogen bonding network of HFIP to effect deactivation.

Figure 4.19: Interactions between different nucleophiles compared with a known HFIP-H_2O cluster.

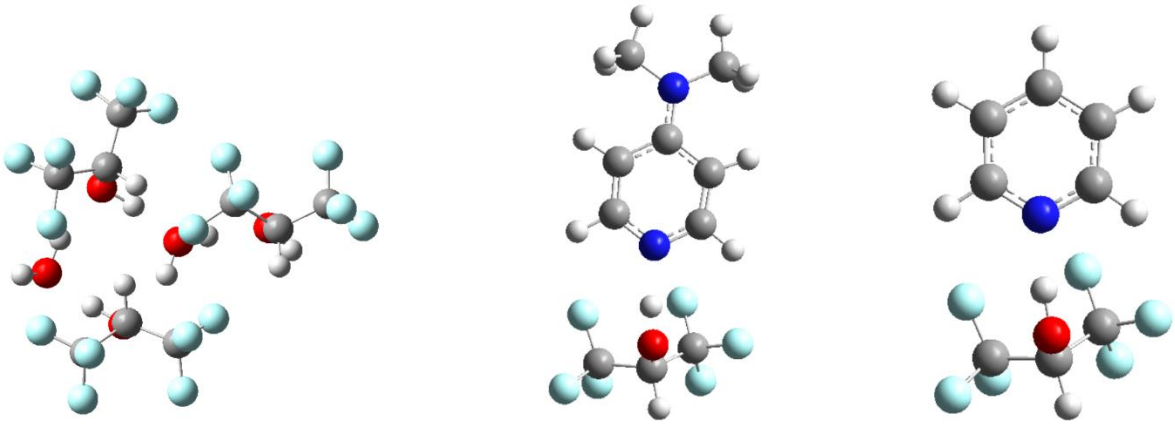

The selectivity effects of HFIP on a variety of rhodium catalysts may be more complex due to the reasons stated above.[54] For this analysis, the most significant system, Rh_2(*S*-TCPTAD)$_4$ (which experiences full enantioinversion as described in **Chapter 3**) will be considered. Once again, the first step is to optimize the achiral system before applying it to a chiral environment. HFIP is a non-nucleophilic alcohol and as a result it will not form a stable ylide to the carbene, nor will it coordinate to the rhodium face itself.[55-58] Instead the most likely interactions are between the ester oxygens and HFIP, although it was unknown which interaction will be the most thermodynamically favorable.[54, 55] As a result, both interactions were computed and initially, the coordination to the ester oxygen was slightly more favorable (ΔG= ~-0.1 kcal/mol). Since the reaction system requires solvent equivalents of HFIP in order to experience these dramatic effects. We also needed to compute the coordination of multiple HFIP molecules to the carbene. All calculations including two HFIP molecules preserved the carbonyl coordination and ejected the ester coordinating HFIP molecule from the carbene. Rather than exiting the complex entirely, this HFIP molecule

instead engaged in hydrogen bonding with the carboxylate of one of the axial ligands. This interaction was also evident in crystal structures obtained of Rh_2(*S*-TCPTTL)$_4$ and Rh_2(*R*-NTTL)$_4$ in HFIP and could be a contributing factor to the changes in asymmetric induction. With these valuable initial structures computed, NBO analysis was then performed on the optimized structure, which showed that the carbene is indeed rendered more electrophilic due to the draining of electron density from the empty p-orbital of the carbene through the hydrogen bonded ester, as evidenced by the lower HOMO ($\Delta E_{\mathbf{22\text{-}33}}$= -1.34 kcal/mol) and LUMO ($\Delta E_{\mathbf{22\text{-}33}}$= -2.04 kcal/mol) energy (Figure 4.20).

Figure 4.20: NBO analysis of HFIP coordinated **22.**

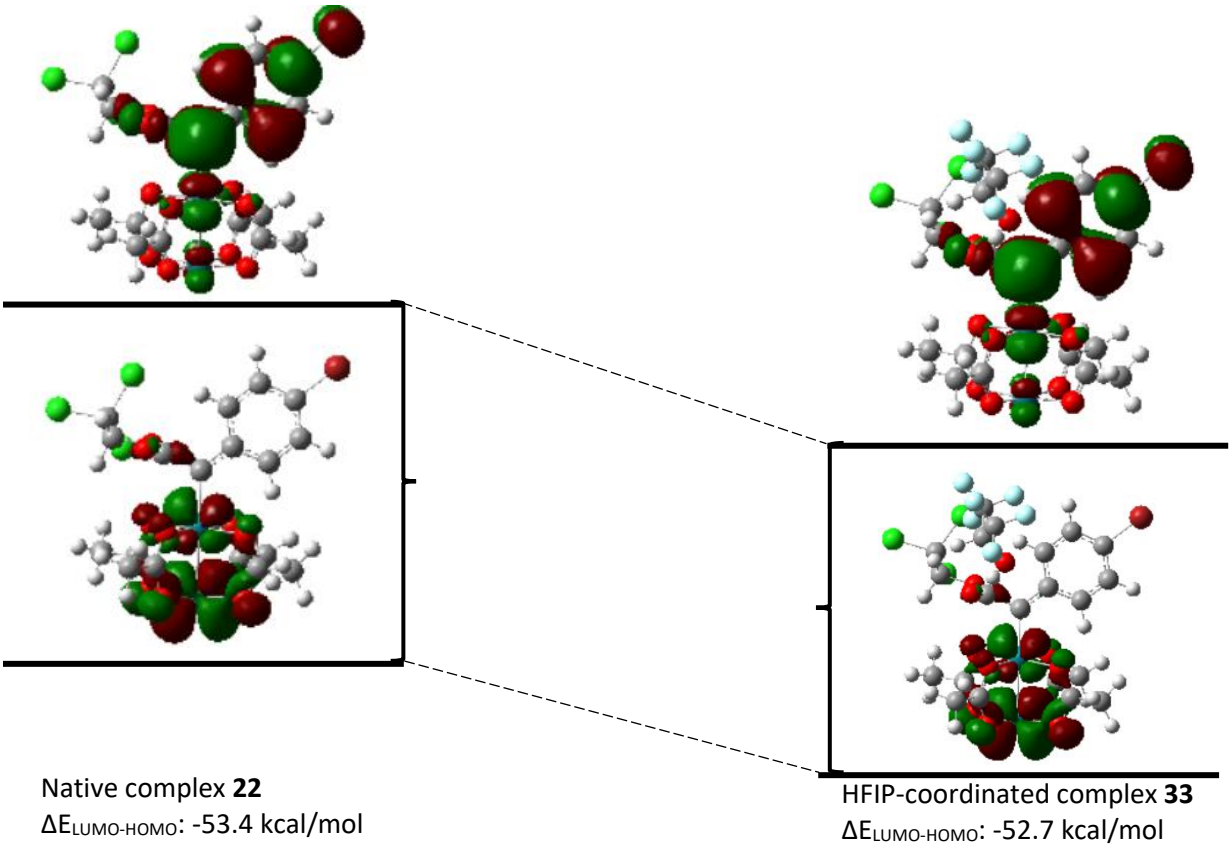

Next, an analysis of the chiral system was performed. It should be noted that while HFIP as solvent is where the most dramatic effects are observed, 1:1 solvent mixtures of DCM:HFIP also exhibit dramatic changes in enantioselectivity. Thus, while there is not a well-established PCM for HFIP modelling,

structures computed considering DCM as solvent under PCM are still highly relevant to the experimental system.[59-61] The first step was to compute the structure of Rh_2(*S*-TCPTAD)$_4$ in the presence HFIP based on the crystal structure of a similar complex, Rh_2(*S*-TCPTTL)$_4$, grown from an HFIP solution, and optimize the geometry. Crystal structures are excellent tools for understanding molecular structure and sometimes reaction intermediates, but they can be poor simulacra for dynamic reaction systems.[10, 29, 32] Crystal structures only display a static image of a molecule in the solid state, and with a highly polar additive like HFIP, gaining an accurate picture of the molecule's lowest energy states by letting it evolve in a solvent field is critical.[60, 61] The optimized structure of [Rh_2(*S*-TCPTAD)$_4$•4HFIP] (**34**) showed several hydrogen bonds between the catalyst and HFIP and water was often assisting to form the network.[54, 61] Although these water molecules were not considered in later computational models, the inclusion of some water could account for differences in experimental observations and the calculations. HFIP is never fully devoid of water, and the water is rendered non-nucleophilic due to hydrogen bonding with HFIP so they could play a role in the reaction selectivity as hydrogen bond intermediaries between HFIP and the catalyst.[62] The optimized structure shows HFIP coordinating to the carboxylates on the bottom face of the catalyst as well as in the chiral bowl. It also shows HFIP molecules coordinating to the phthalimide carbonyls, all of which can affect selectivity.[25, 63] Furthermore, the ligand environment is slightly different to the native catalyst to accommodate these highly favorable hydrogen bonds. The most major perturbation occurs with the ligand marked in pink in Figure 4.21, where the marked dihedral angle changes from 51° in the native catalyst to 53° in the HFIP coordinated structure. This change in ligand tilt, while minor, was not observed in the crystal structure, once more highlighting the importance of DFT calculations to understanding these catalysts.

Figure 4.21: Selected views of [Rh_2(*S*-TCPTAD)$_4$•4HFIP] complex **34**.

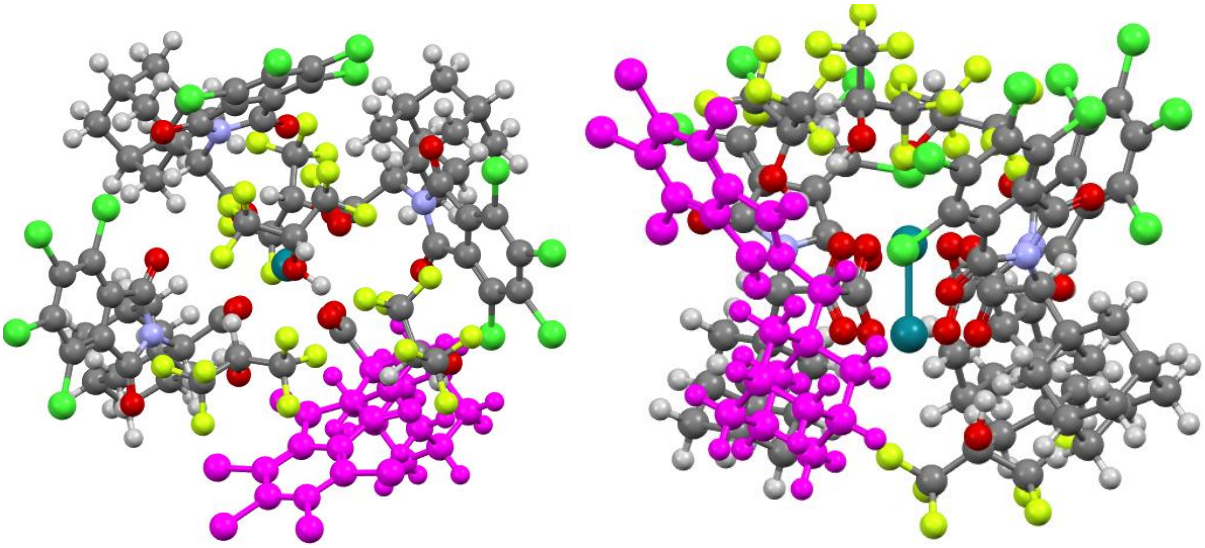

Once these calculations were complete, the carbene complexes were then optimized in the presence of HFIP. These structures showed some startling changes. When the Rh_2(*S*-TCPTAD)$_4$-carbene complex (**35**) is calculated, it displays the typical C_4 symmetric geometry of the phthalimido series of catalysts which is commonly implicated as the key stereoselectivity controlling element.[6, 40, 46, 52, 64] When this optimized structure is populated with the HFIP molecules to afford complex **36** (including the preferred hydrogen bond to the carbene carbonyl) the ligand on the same face of the carbene carbonyl rotates 90° to accommodate the HFIP. The energy associated with this ligand distortion was calculated by single point calculation of **35** without HFIP was measured to be ΔE= +29.1 kcal/mol. This energetic barrier is overcome by the introduction of new hydrogen bonds between HFIP molecules both in the bowl and on the bottom face of the catalyst which are only accessible through this twisted geometry. This new bowl conformation makes the carbonyl face of the carbene significantly more sterically accessible to the typically attacked ester face of the carbene, which may explain why this catalyst experiences enantioinversion with high concentrations of HFIP.[3, 10, 45, 47] Additionally, this ligand distortion only occurs upon introduction of the carbene which likely explains why no substantial changes in ligand geometry were observed in NMR

studies of the catalyst in HFIP. It could also explain how the catalyst enantioselectivity is restored upon removal of HFIP as described in **Chapter 3**. The catalyst naturally prefers to be C_4 symmetric and hence once the carbene is removed, even in the presence of HFIP, the ligand will revert to its natural position.[46, 52, 65] This effect it analogous to heteroleptic dirhodium tetracarboxylate complexes which have been well known in the literature to improve asymmetric induction or reactivity in a variety of reactions.[63, 66-68] These catalysts have not been reported to yield opposite asymmetric induction to the parent homoleptic complexes but the lack of chiral substitution at a given position is a permanent feature of these complexes as opposed to a transient feature of the reaction intermediate as observed in this study.[65-68] This means that the approach of the diazo compound, nitrogen extrusion, and subsequent carbene trapping all occur in the presence of achiral substitution at one of the equatorial sites to the lantern complex for heteroleptic complexes. The fundamentally different nature of this system to previously reported heteroleptic complexes is that achiral substitution only manifests in the presence of the reactive carbene intermediate. This means that the chiral ligand influences dictating diazo approach and carbene reactivity could be decoupled, leading to inversion.

Figure 4.22: Analysis of [**23**-Rh_2(*S*-TCPTAD)$_4$•4HFIP] complex **36**, and comparison with **35**.

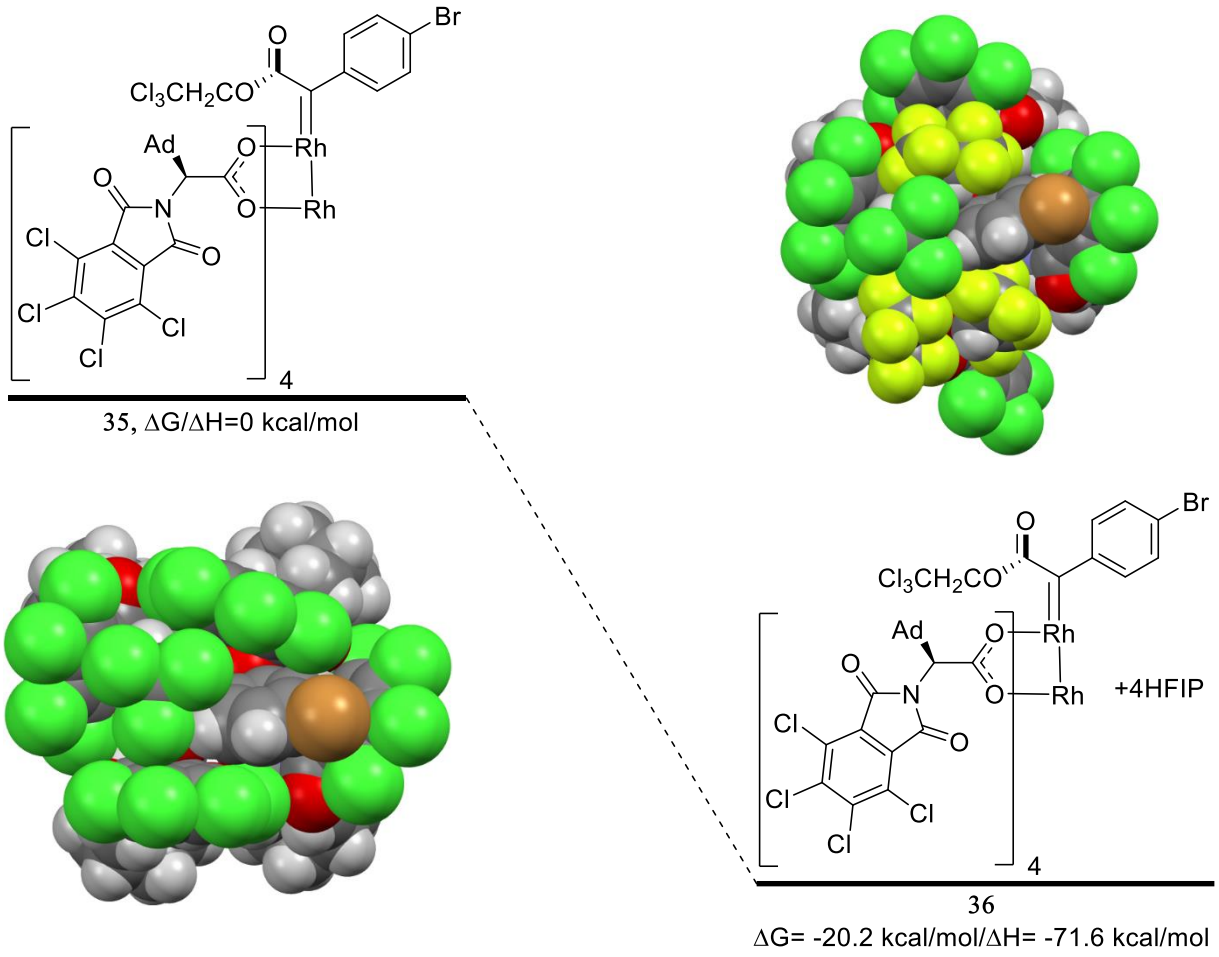

If the bowl remains intact upon initial approach of the diazo compound, the typical ester geometry selection criteria of the catalyst is maintained for initial carbene generation (Figure 4.23).[10, 45, 46] Once the carbene is formed however (or during N_2 extrusion), the ligand tilts and the open face of the carbene is subsequently reversed (Figure 4.23). Other catalysts do not experience as dramatic effects likely due to differences in ligand geometry and electronics. Only electron deficient catalysts experience full enantioinversion (Rh_2(*S*-TCPTAD)$_4$, Rh_2(*S*-TCPTTL)$_4$, Rh_2(*S*-TFPTTL)$_4$) as discussed in **Chapter 3**.[69] Rh_2(*S*-TCPTAD)$_4$ has extremely electron deficient carbonyl groups due to the presence of the per-chlorinated phthalimido ring which makes it a much better hydrogen bond acceptor than non-halogenated phthalimido catalysts. These strong hydrogen bonds may allow the ligand to overcome the high rotation

barrier as opposed to bulky or electron rich catalysts like Rh_2(*tetra-p*-BrTPPTTL)$_4$ which would experience weaker hydrogen bonding interactions and may have larger barriers to ligand rotation due to steric bulk. This could explain why Rh_2(*tetra-p*-BrTPPTTL)$_4$ is able to maintain relatively high enantioselectivity (73% ee when HFIP is solvent vs 98% ee when DCM is used as solvent) when HFIP is used as solvent.[24, 40] While other catalysts do not experience enantioinversion, all experience changes in enantioselectivity in the presence of HFIP which could be due to variable levels of ligand tilting, Rh_2(*S*-TCPTAD)$_4$ is merely the most extreme example.[24] As with 2-chloropyridine coordination, future work will explore these systems and evaluate the key transition states for enantioselectivity.

Figure 4.23: Proposed mechanism of enantioinversion in the presence of HFIP with Rh_2(*S*-TCPTAD)$_4$. Proposed mechanism without HFIP (left) proposed mechanism in HFIP featuring ligand distortion(right).

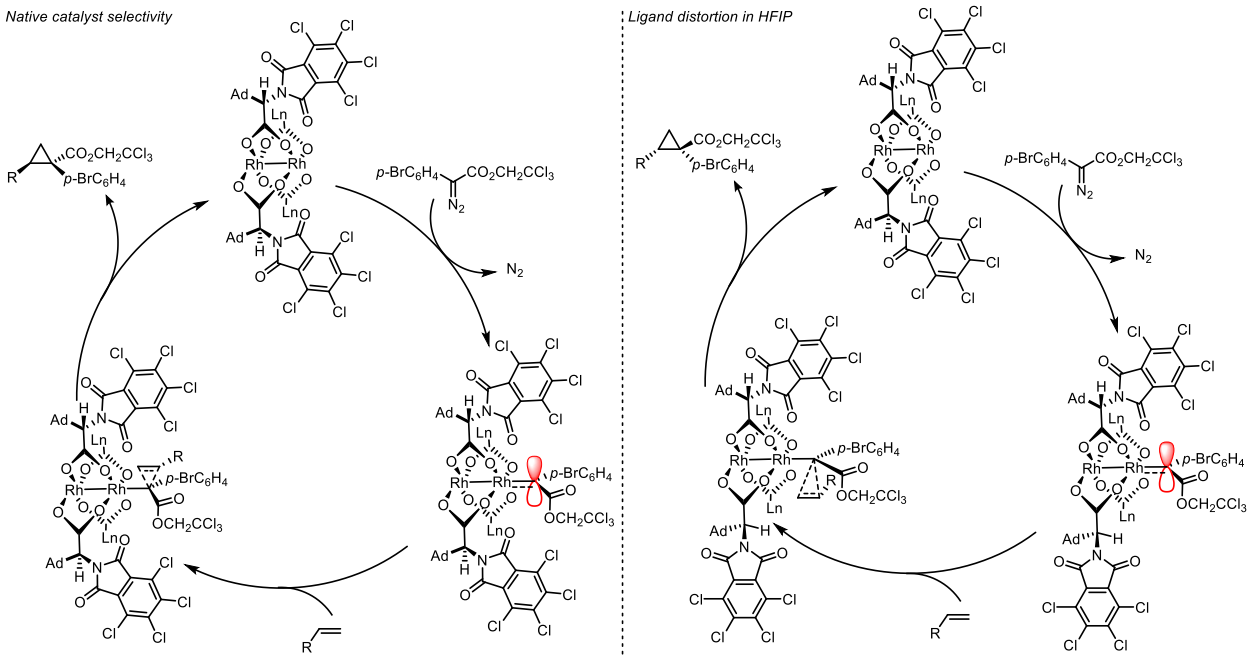

4.3 Conclusion:

DFT calculations have once again shone light on the origins of selectivity and reactivity in rhodium carbenoid transformations, this time in the presence of the coordinating additives discussed in earlier chapters. All calculations were performed at the B3LYP-D3(BJ)/6-31G(d,p) level of theory for the main group elements using LANL2DZ for rhodium including effective core potentials. The solvent was accounted for using CPCM and considering dichloromethane as the solvent, which was determined early on to be the optimum level of theory for analyzing these complexes.[10, 32, 50] These additives can affect both reactivity and selectivity and, in each case, the rationale for these effects was distinct. DCC was shown to enhance catalyst TON at extremely low catalyst loadings, DFT calculations showed that this was likely due to destabilization of the carbene, enhancing the trapping efficiency of unactivated substrates like cyclohexane.[7] Aberrant selectivity observed with *ortho*-substituted aryldiazoacetates could be linked to the steric and electronic influence of the *ortho*-substituent which substantially destabilizes the carbene. 2-Chloropyridine helps planarize this structure and the association of this additive to the carbene complex is favorable in the $Rh_2(TPPTTL)_4$ catalyst pocket which may be responsible for the observed enhancement in enantioselectivity. Finally, the role of HFIP to dramatically change enantioselectivity and reactivity was evaluated through an analysis of several structures on the achiral system. The observed optimized geometries were then translated to $Rh_2(TCPTAD)_4$, revealing interactions which could be responsible for both enantioinversion and enantioenhancement under this unusual additive paradigm.[24]

4.4 References:

1. Davies, H. M.; Hodges, L. M.; Matasi, J. J.; Hansen, T.; Stafford, D. G., Effect of carbenoid structure on the reactivity of rhodium-stabilized carbenoids. *Tetrahedron Lett.* **1998,** *39* (25), 4417-4420.
2. Nowlan, D. T.; Gregg, T. M.; Davies, H. M.; Singleton, D. A., Isotope effects and the nature of selectivity in rhodium-catalyzed cyclopropanations. *J. Am. Chem. Soc.* **2003,** *125* (51), 15902-15911.
3. Hansen, J.; Autschbach, J.; Davies, H. M., Computational study on the selectivity of donor/acceptor-substituted rhodium carbenoids. *J. Org. Chem.* **2009,** *74* (17), 6555-6563.
4. Davies, H. M.; Hansen, T.; Churchill, M. R., Catalytic asymmetric C− H activation of alkanes and tetrahydrofuran. *J. Am. Chem. Soc.* **2000,** *122* (13), 3063-3070.

5. Li, Z.; Boyarskikh, V.; Hansen, J. H.; Autschbach, J.; Musaev, D. G.; Davies, H. M., Scope and mechanistic analysis of the enantioselective synthesis of allenes by rhodium-catalyzed tandem ylide formation/[2, 3]-sigmatropic rearrangement between donor/acceptor carbenoids and propargylic alcohols. *J. Am. Chem. Soc.* **2012,** *134* (37), 15497-15504.
6. Fu, J.; Ren, Z.; Bacsa, J.; Musaev, D. G.; Davies, H. M., Desymmetrization of cyclohexanes by site- and stereoselective C–H functionalization. *Nature* **2018,** *564* (7736), 395-399.
7. Wei, B.; Sharland, J. C.; Blackmond, D. G.; Musaev, D. G.; Davies, H. M. L., In Situ Kinetic Studies of Rh(II)-Catalyzed C–H Functionalization to Achieve High Catalyst Turnover Numbers. *ACS. Catal.* **2022**, 13400-13410.
8. Cammarota, R. C.; Liu, W.; Bacsa, J.; Davies, H. M.; Sigman, M. S., Mechanistically Guided Workflow for Relating Complex Reactive Site Topologies to Catalyst Performance in C–H Functionalization Reactions. *J. Am. Chem. Soc.* **2022,** *144* (4), 1881-1898.
9. Boni, Y. T.; Cammarota, R. C.; Liao, K.; Sigman, M. S.; Davies, H. M., Leveraging Regio-and Stereoselective C (sp3)–H Functionalization of Silyl Ethers to Train a Logistic Regression Classification Model for Predicting Site-Selectivity Bias. *J. Am. Chem. Soc.* **2022,** *144* (34), 15549-15561.
10. Ren, Z.; Musaev, D. G.; Davies, H. M., Key Selectivity Controlling Elements in Rhodium-Catalyzed C–H Functionalization with Donor/Acceptor Carbenes. *ACS. Catal.* **2022,** *12* (21), 13446-13456.
11. Lian, Y.; Hardcastle, K. I.; Davies, H. M., Computationally Guided Stereocontrol of the Combined C H Functionalization/Cope Rearrangement. *Angew. Chem. Int. Ed.* **2011,** *50* (40), 9370-9373.
12. Pirrung, M. C.; Morehead, A. T., Saturation Kinetics in Dirhodium (II) Carboxylate-Catalyzed Decompositions of Diazo Compounds. *J. Am. Chem. Soc.* **1996,** *118* (34), 8162-8163.
13. Blackmond, D. G., Reaction progress kinetic analysis: a powerful methodology for mechanistic studies of complex catalytic reactions. *Angew. Chem. Int. Ed.* **2005,** *44* (28), 4302-4320.
14. Nielsen, C. D.-T.; Burés, J., Visual kinetic analysis. *Chemical science* **2019,** *10* (2), 348-353.
15. Blackmond, D. G., Kinetic profiling of catalytic organic reactions as a mechanistic tool. *J. Am. Chem. Soc.***2015,** *137* (34), 10852-10866.
16. Wei, B.; Sharland, J. C.; Lin, P.; Wilkerson-Hill, S. M.; Fullilove, F. A.; McKinnon, S.; Blackmond, D. G.; Davies, H. M., In situ kinetic studies of Rh (II)-catalyzed asymmetric cyclopropanation with low catalyst loadings. *ACS. Catal.* **2019,** *10* (2), 1161-1170.
17. Liao, K.; Liu, W.; Niemeyer, Z. L.; Ren, Z.; Bacsa, J.; Musaev, D. G.; Sigman, M. S.; Davies, H. M., Site-selective carbene-induced C–H functionalization catalyzed by dirhodium tetrakis (triarylcyclopropanecarboxylate) complexes. *ACS. Catal.* **2018,** *8* (1), 678-682.
18. Davies, H. M., Finding opportunities from surprises and failures. Development of rhodium-stabilized donor/acceptor carbenes and their application to catalyst-controlled C–H functionalization. *J. Org. Chem.* **2019,** *84* (20), 12722-12745.
19. Kornecki, K. P.; Briones, J. F.; Boyarskikh, V.; Fullilove, F.; Autschbach, J.; Schrote, K. E.; Lancaster, K. M.; Davies, H. M.; Berry, J. F., Direct spectroscopic characterization of a transitory dirhodium donor-acceptor carbene complex. *Science* **2013,** *342* (6156), 351-354.
20. Burdzinski, G.; Platz, M. S., Ultrafast kinetics of carbene reactions. *Contemporary Carbene Chemistry* **2013**, 166-192.
21. Buron, C.; Gornitzka, H.; Romanenko, V.; Bertrand, G., Stable versions of transient push-pull carbenes: Extending lifetimes from nanoseconds to weeks. *Science* **2000,** *288* (5467), 834-836.
22. Wang, J.; Burdzinski, G.; Kubicki, J.; Platz, M. S., Ultrafast UV− Vis and IR Studies of p-Biphenylyl Acetyl and Carbomethoxy Carbenes. *J. Am. Chem.Soc.* **2008,** *130* (33), 11195-11209.
23. Sharland, J. C.; Wei, B.; Hardee, D. J.; Hodges, T. R.; Gong, W.; Voight, E. A.; Davies, H. M., Asymmetric synthesis of pharmaceutically relevant 1-aryl-2-heteroaryl-and 1, 2-diheteroarylcyclopropane-1-carboxylates. *Chem. Sci.* **2021,** *12* (33), 11181-11190.

24. Sharland, J. C.; Dunstan, D.; Majumdar, D.; Gao, J.; Tan, K.; Malik, H. A.; Davies, H. M., Hexafluoroisopropanol for the Selective Deactivation of Poisonous Nucleophiles Enabling Catalytic Asymmetric Cyclopropanation of Complex Molecules. *ACS. Catal.* **2022,** *12* (20), 12530-12542.
25. Nelson, T. D.; Song, Z. J.; Thompson, A. S.; Zhao, M.; DeMarco, A.; Reamer, R. A.; Huntington, M. F.; Grabowski, E. J.; Reider, P. J., Rhodium-carbenoid-mediated intermolecular O–H insertion reactions: a dramatic additive effect. Application in the synthesis of an ascomycin derivative. *Tetrahedron Lett.* **2000,** *41* (12), 1877-1881.
26. Lebel, H.; Piras, H.; Bartholoméüs, J., Rhodium-Catalyzed Stereoselective Amination of Thioethers with N-Mesyloxycarbamates: DMAP and Bis (DMAP) CH2Cl2 as Key Additives. *Angew. Chem.* **2014,** *126* (28), 7428-7432.
27. Marcoux, D.; Lindsay, V. N.; Charette, A. B., Use of achiral additives to increase the stereoselectivity in Rh (II)-catalyzed cyclopropanations. *Chem. Commun.* **2010,** *46* (6), 910-912.
28. Davies, H. M.; Venkataramani, C., Dirhodium tetraprolinate-catalyzed asymmetric cyclopropanations with high turnover numbers. *Org. Lett.* **2003,** *5* (9), 1403-1406.
29. Qin, C.; Boyarskikh, V.; Hansen, J. H.; Hardcastle, K. I.; Musaev, D. G.; Davies, H. M., D 2-symmetric dirhodium catalyst derived from a 1, 2, 2-triarylcyclopropanecarboxylate ligand: design, synthesis and application. *J. Am. Chem. Soc.* **2011,** *133* (47), 19198-19204.
30. Qin, C.; Davies, H. M., Role of sterically demanding chiral dirhodium catalysts in site-selective C–H functionalization of activated primary C–H bonds. *J. Am. Chem. Soc.* **2014,** *136* (27), 9792-9796.
31. Liao, K.; Negretti, S.; Musaev, D. G.; Bacsa, J.; Davies, H. M., Site-selective and stereoselective functionalization of unactivated C–H bonds. *Nature* **2016,** *533* (7602), 230-234.
32. Wertz, B.; Ren, Z.; Bacsa, J.; Musaev, D. G.; Davies, H. M., Comparison of 1, 2-Diarylcyclopropanecarboxylates with 1, 2, 2-Triarylcyclopropanecarboxylates as Chiral Ligands for Dirhodium-Catalyzed Cyclopropanation and C–H Functionalization. *J. Org. Chem.* **2020,** *85* (19), 12199-12211.
33. Chung, L. W.; Sameera, W.; Ramozzi, R.; Page, A. J.; Hatanaka, M.; Petrova, G. P.; Harris, T. V.; Li, X.; Ke, Z.; Liu, F., The ONIOM method and its applications. *Chem. Rev.* **2015,** *115* (12), 5678-5796.
34. Wang, H.; Guptill, D. M.; Varela-Alvarez, A.; Musaev, D. G.; Davies, H. M., Rhodium-catalyzed enantioselective cyclopropanation of electron-deficient alkenes. *Chem. Sci.* **2013,** *4* (7), 2844-2850.
35. Doyle, M. P.; Tamblyn, W. H.; Bagheri, V., Highly effective catalytic methods for ylide generation from diazo compounds. Mechanism of the rhodium-and copper-catalyzed reactions with allylic compounds. *J. Org. Chem.* **1981,** *46* (25), 5094-5102.
36. Anderson, B. G.; Cressy, D.; Patel, J. J.; Harris, C. F.; Yap, G. P.; Berry, J. F.; Darko, A., Synthesis and catalytic properties of dirhodium paddlewheel complexes with tethered, axially coordinating thioether ligands. *Inorg. Chem.* **2019,** *58* (3), 1728-1732.
37. Cressy, D.; Zavala, C.; Abshire, A.; Sheffield, W.; Darko, A., Tuning Rh (II)-catalysed cyclopropanation with tethered thioether ligands. *Dalton Trans.* **2020,** *49* (44), 15779-15787.
38. Sheffield, W.; Abshire, A.; Darko, A., Effect of Tethered, Axial Thioether Coordination on Rhodium (II)-Catalyzed Silyl-Hydrogen Insertion. *Eur. J. Org. Chem.* **2019,** *2019* (37), 6347-6351.
39. Ye, Q.-S.; Li, X.-N.; Jin, Y.; Yu, J.; Chang, Q.-W.; Jiang, J.; Yan, C.-X.; Li, J.; Liu, W.-P., Synthesis, crystal structures and catalytic activity of tetrakis (acetato) dirhodium (II) complexes with axial picoline ligands. *Inorg. Chim. Acta* **2015,** *434*, 113-120.
40. Garlets, Z. J.; Boni, Y. T.; Sharland, J. C.; Kirby, R. P.; Fu, J.; Bacsa, J.; Davies, H. M., Design, Synthesis, and Evaluation of Extended C4–Symmetric Dirhodium Tetracarboxylate Catalysts. *ACS. Catal.* **2022,** *12*, 10841-10848.
41. Zhang, Y.; Burdzinski, G.; Kubicki, J.; Platz, M. S., Direct observation of carbene and diazo formation from aryldiazirines by ultrafast infrared spectroscopy. *J. Am. Chem. Soc.* **2008,** *130* (48), 16134-16135.

42. Wang, J.; Burdzinski, G.; Gustafson, T. L.; Platz, M. S., Ultrafast study of p-biphenylyldiazoethane. The chemistry of the diazo excited state and the relaxed carbene. *J. Am. Chem. Soc.* **2007,** *129* (9), 2597-2606.
43. Burés, J.; Armstrong, A.; Blackmond, D. G., Curtin–Hammett paradigm for stereocontrol in organocatalysis by diarylprolinol ether catalysts. *J. Am. Chem. Soc.* **2012,** *134* (15), 6741-6750.
44. Guo, W.; Hare, S. R.; Chen, S.-S.; Saunders, C. M.; Tantillo, D. J., C–H Insertion in Dirhodium Tetracarboxylate-Catalyzed Reactions despite Dynamical Tendencies toward Fragmentation: Implications for Reaction Efficiency and Catalyst Design. *J. Am. Chem. Soc.* **2022,** *144* (37), 17219-17231.
45. Goto, T.; Takeda, K.; Shimada, N.; Nambu, H.; Anada, M.; Shiro, M.; Ando, K.; Hashimoto, S., Highly enantioselective cyclopropenation reaction of 1-alkynes with α-alkyl-α-diazoesters catalyzed by dirhodium (II) carboxylates. *Angew. Chem. Int. Ed.* **2011,** *50* (30), 6803-6808.
46. DeAngelis, A.; Dmitrenko, O.; Yap, G. P.; Fox, J. M., Chiral crown conformation of Rh2 (S-PTTL) 4: Enantioselective cyclopropanation with α-alkyl-α-diazoesters. *J. Am. Chem. Soc.* **2009,** *131* (21), 7230-7231.
47. Xue, Y.-S.; Cai, Y.-P.; Chen, Z.-X., Mechanism and stereoselectivity of the Rh (II)-catalyzed cyclopropanation of diazooxindole: a density functional theory study. *RSC Adv.* **2015,** *5* (71), 57781-57791.
48. Negretti, S.; Cohen, C. M.; Chang, J. J.; Guptill, D. M.; Davies, H. M., Enantioselective dirhodium (II)-catalyzed cyclopropanations with trimethylsilylethyl and trichloroethyl aryldiazoacetates. *Tetrahedron* **2015,** *71* (39), 7415-7420.
49. Werle, C.; Goddard, R.; Philipps, P.; Farès, C.; Fürstner, A., Structures of reactive donor/acceptor and donor/donor rhodium carbenes in the solid state and their implications for catalysis. *J. Am. Chem. Soc.* **2016,** *138* (11), 3797-3805.
50. Lee, M.; Ren, Z.; Musaev, D. G.; Davies, H. M., Rhodium-stabilized diarylcarbenes behaving as donor/acceptor carbenes. *ACS. Catal.* **2020,** *10* (11), 6240-6247.
51. Caballero, N.; Melendez, F.; Muñoz-Caro, C.; Nino, A., Theoretical prediction of relative and absolute pKa values of aminopyridines. *Biophys. Chem.* **2006,** *124* (2), 155-160.
52. DeAngelis, A.; Boruta, D. T.; Lubin, J.-B.; Plampin III, J. N.; Yap, G. P.; Fox, J. M., The chiral crown conformation in paddlewheel complexes. *Chem. Commun.* **2010,** *46* (25), 4541-4543.
53. Davies, H. M.; Liao, K., Dirhodium tetracarboxylates as catalysts for selective intermolecular C–H functionalization. *Nature Rev. Chem.* **2019,** *3* (6), 347-360.
54. Milovanović, M. R.; Dherbassy, Q.; Wencel-Delord, J.; Colobert, F.; Zarić, S. D.; Djukic, J. P., The Affinity of Some Lewis Bases for Hexafluoroisopropanol as a Reference Lewis Acid: An ITC/DFT Study. *Chemphyschem* **2020,** *21* (18), 2136-2142.
55. Colomer, I.; Chamberlain, A. E.; Haughey, M. B.; Donohoe, T. J., Hexafluoroisopropanol as a highly versatile solvent. *Nature Rev. Chem.* **2017,** *1* (11), 1-12.
56. Bhattacharya, T.; Ghosh, A.; Maiti, D., Hexafluoroisopropanol: The magical solvent for Pd-catalyzed C–H activation. *Chem. Sci.* **2021,** *12* (11), 3857-3870.
57. Fu, L.; Hoang, K.; Tortoreto, C.; Liu, W.; Davies, H. M., Formation of Tertiary Alcohols from the Rhodium-Catalyzed Reactions of Donor/Acceptor Carbenes with Esters. *Org. Lett.* **2018,** *20* (8), 2399-2402.
58. Zhu, S.-F.; Chen, W.-Q.; Zhang, Q.-Q.; Mao, H.-X.; Zhou, Q.-L., Enantioselective Copper-Catalyzed OH Insertion of α-Diazo Phosphonates. *Synlett* **2011,** *2011* (07), 919-922.
59. Wang, X.; Li, Z.-Q.; Mai, B. K.; Gurak, J. A.; Xu, J. E.; Tran, V. T.; Ni, H.-Q.; Liu, Z.; Liu, Z.; Yang, K. S., Controlling cyclization pathways in palladium (II)-catalyzed intramolecular alkene hydro-functionalization via substrate directivity. *Chem. Sci.* **2020,** *11* (41), 11307-11314.
60. Miller, E.; Mai, B. K.; Read, J. A.; Bell, W. C.; Derrick, J. S.; Liu, P.; Toste, F. D., A Combined DFT, Energy Decomposition, and Data Analysis Approach to Investigate the Relationship Between Noncovalent Interactions and Selectivity in a Flexible DABCOnium/Chiral Anion Catalyst System. *ACS. Catal.* **2022,** *12* (19), 12369-12385.

61. Wu, B.; Hazrah, A. S.; Seifert, N. A.; Oswald, S. n.; Jäger, W.; Xu, Y., Higher-Energy Hexafluoroisopropanol··· Water Isomer and Its Large Amplitude Motions: Rotational Spectra and DFT Calculations. *J. Phys. Chem. A* **2021,** *125* (48), 10401-10409.
62. Ammer, J.; Mayr, H., Solvent nucleophilicities of hexafluoroisopropanol/water mixtures. *J. Phys. Org. Chem.* **2013,** *26* (1), 59-63.
63. Abshire, A.; Moore, D.; Courtney, J.; Darko, A., Heteroleptic dirhodium (ii, ii) paddlewheel complexes as carbene transfer catalysts. *Org. Biomol. Chem.* **2021,** *19* (41), 8886-8905.
64. Reddy, R. P.; Davies, H. M., Dirhodium tetracarboxylates derived from adamantylglycine as chiral catalysts for enantioselective C− H aminations. *Org. Lett.* **2006,** *8* (22), 5013-5016.
65. Lindsay, V. N.; Lin, W.; Charette, A. B., Experimental evidence for the all-up reactive conformation of chiral rhodium (II) carboxylate catalysts: enantioselective synthesis of cis-cyclopropane α-amino acids. *J. Am. Chem. Soc.* **2009,** *131* (45), 16383-16385.
66. Lindsay, V. N.; Charette, A. B., Design and synthesis of chiral heteroleptic rhodium (II) carboxylate catalysts: experimental investigation of halogen bond rigidification effects in asymmetric cyclopropanation. *ACS. Catal.* **2012,** *2* (6), 1221-1225.
67. DeAngelis, A.; Panish, R.; Fox, J. M., Rh-catalyzed intermolecular reactions of α-alkyl-α-diazo carbonyl compounds with selectivity over β-hydride migration. *Acc. Chem Res.* **2016,** *49* (1), 115-127.
68. Boruta, D. T.; Dmitrenko, O.; Yap, G. P. A.; Fox, J. M., Rh2(S-PTTL)3TPA—a mixed-ligand dirhodium(ii) catalyst for enantioselective reactions of α-alkyl-α-diazoesters. *Chem. Sci.* **2012,** *3* (5), 1589-1593.
69. Tsutsui, H.; Yamaguchi, Y.; Kitagaki, S.; Nakamura, S.; Anada, M.; Hashimoto, S., Dirhodium(II) tetrakis[N-tetrafluorophthaloyl-(S)-tert-leucinate]: an exceptionally effective Rh(II) catalyst for enantiotopically selective aromatic C–H insertions of diazo ketoesters. *Tetrahedron Asymm.* **2003,** *14* (7), 817-821.

Chapter 5

One-pot synthesis of difluorobicyclo[1.1.1]pentanes and related *gem*-difluorinated carbocycles from α-allyl diazoacetates.

5.1 Introduction

For the past two decades, industrial chemists have been attempting to "escape from flatland", trying to avoid the trap of synthesizing relatively planar molecules (high Csp^2 content) in favor of more three-dimensionality (high Csp^3 content).[1, 2] This move has several advantages, the proteins of interest for medicinal chemistry programs have binding pockets that are three dimensional and molecules which can access new areas inside these pockets can often lead to enhanced activity.[1] Furthermore, metabolism of Csp^3 centers is more challenging for enzymes than oxidation of "flat" features like phenyl rings and alkenes, hence molecules with a higher surface-area:volume ratio can offer enhanced metabolic stability.[1, 2] Lastly, alterations to the polar surface area of molecules occur and with higher Csp^3 content, therapeutic scaffolds are more soluble under biological conditions than high Csp^2 content counterparts. These advantages are, however, balanced out by the major drawback of high Csp^3 content molecules: they are hard to synthesize. Indeed, one of the main reasons that biaryls became so common in drug discovery and subsequently in the clinic from 1990 onwards was due to the discovery of Suzuki-cross-coupling and related methods which allowed for facile synthesis of these motifs and boasted an enormous substrate scope (Figure 5.1).[3-7] The ubiquity of the biaryl disconnection has led to a saturated market, however, and whether to avoid patent infringement, solve pharmacokinetic pitfalls, or improve potency, major pharmaceutical companies are now moving away from Suzuki coupling in continuing development of SAR platforms.[1, 2, 8-10]

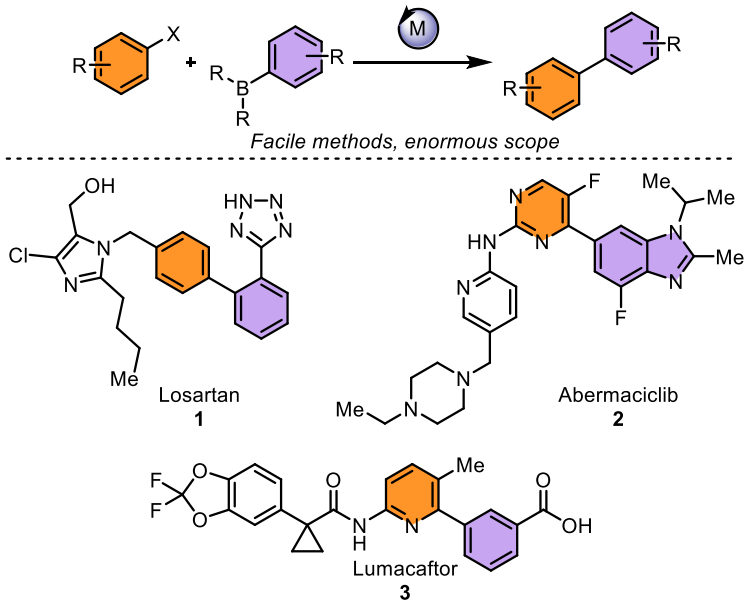

Figure 5.1: Suzuki cross-coupling has enabled drug discovery campaigns for the past 20 years and lead to countless clinical compounds, including these selected examples (**1-3**).[3]

Nevertheless, the phenyl group is an important medicinal motif, and a great deal of emphasis has been placed recently on locating high Csp^3 content bioisosteres to use in place of the phenyl ring.[11] One such motif which has seen a boom recently is the bicyclo[1.1.1]pentane.[12] These molecules feature a caged architecture with 3-methylene carbons and two methine carbons, allowing them to occupy a large 3-D volume, but the arrangement of substituents around the cage can mimic phenyl substitution (Figure 5.2).[13] 1,3-Disubstituted bicyclo[1.1.1]pentanes have seen use as *para*-substituted phenyl bioisosteres[14, 15] (Figure 5.2a) and the recent development of facile methods to synthesize these compounds have seen them adapted to a variety of roles in big pharma, from SAR to DNA-encoded library (DEL) synthesis (Figure 5.2a).[16-22] Even more recently, 2-substituted bicyclo[1.1.1]pentanes have been prepared as analogues for *ortho*-substituted arenes via several methods, however as of the writing of this thesis, no chiral preparations of these compounds has been achieved (Figure 5.2b).[23-27] There is also significant need to

address the challenge of atropoisomerism in drug discovery, a need which could potentially be met through new methods for the asymmetric synthesis of 2-substituted bicyclo[1.1.1]pentanes.[28, 29]

Figure 5.2: Bicyclo[1.1.1]pentanes have been investigated in recent years as high Csp^3 content phenyl bioisosteres by many high-profile groups leading to the discovery of several elegant transformations. The substitution of the motif dictates the properties of the arene that are mimicked.

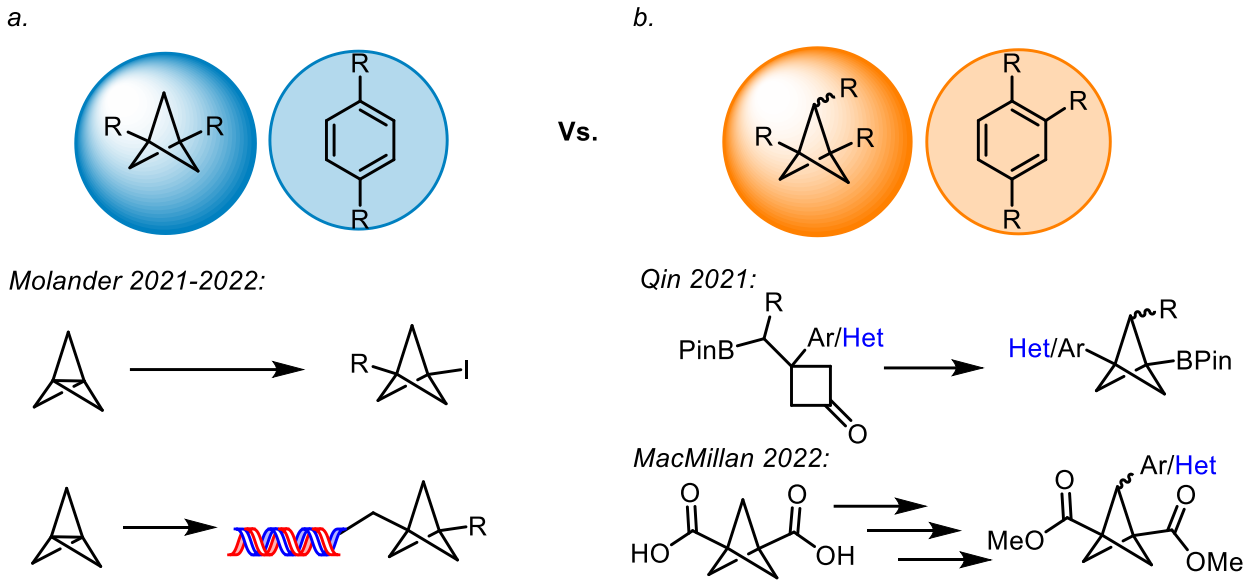

Difluorobicylco[1.1.1]pentanes have become interesting molecules in recent years due to their role as *ortho*-fluorophenyl bioisosteres (Figure 5.3).[30, 31] Inclusion of these groups in the place of phenyl rings can serve to eliminate metabolic liabilities in drug molecules and often provide substances with greater potency than the phenylated analogue.

Figure 5.3: Difluorobicyclo[1.1.1]pentanes have been used as stable bioisosteres for *ortho*-fluoro substituted arenes.

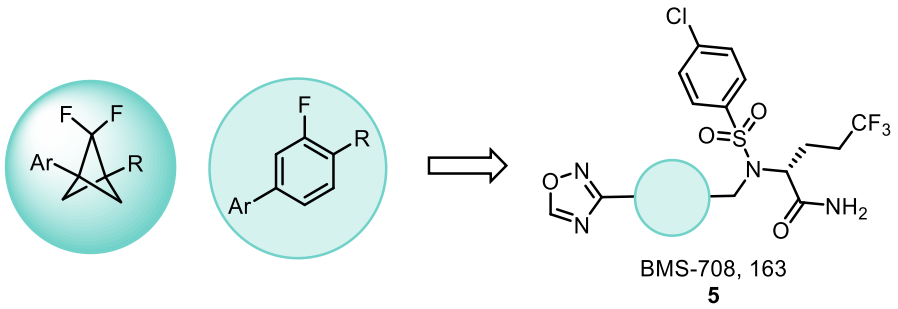

Increased potency and metabolic stability with higher Csp^3 content

Papers published in 2019 by Merck and Enamine disclosed routes to access this new motif through the reaction of 3-arylbicylco[1.1.0]butanes with a difluorocarbene source under mild conditions. While this route was practical for the exploration of several substrates, the scope of the transformation was limited due to the synthetic accessibility of bicyclo[1.1.0]butane precursors. 3-Aryl bicyclo[1.1.0]butanes are classically synthesized according to the procedure outlined in Scheme 5.1.[31] First, an aryl-magnesium chloride is added to cyclobutanone carboxylic acid to generate the resultant tertiary alcohol. The alcohol is then converted to a tertiary alkyl chloride via reaction with HCl. The free acid is then esterified to prevent further reactivity. The resultant product is then reacted with a bulky amine base to generate an enolate which collapses to generate the desired bicyclo[1.1.0]butane. While this is a generally effective method for the synthesis of several 3-arylbicyclo[1.1.0]butane products, it has scope limitations due to the use of a Grignard reagent and harsh ring-closure conditions (Scheme 5.1). Furthermore, the use of 3-aryl bicyclo[1.1.0]butanes precluded the possibility of synthesizing highly substituted difluorobicyclo[1.1.1]pentanes and generating chirality through substitution at the 2-position. While several effective methods have recently emerged for generating 2-substituted bicyclo[1.1.1]pentanes, these methods are achiral and have not yet been applied to fluorinated analogues (Figure 5.2b).[23, 25, 27]

Scheme 5.1: Established synthesis of difluoro[1.1.1]bicyclopentanes.[31]

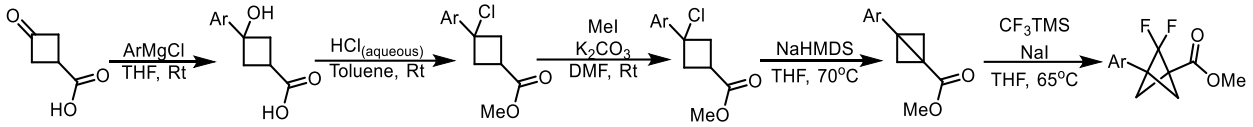

In 2013, the Davies group disclosed a method for the asymmetric synthesis of 2-aryl-bicyclo[1.1.0]butanes through the intramolecular cyclopropanation of α-allyl-diazoacetates in the presence of a chiral dirhodium tetracarboxylate catalyst.[32] This method was able to generate a diverse series of 2-aryl-bicyclo[1.1.0]butanes with high yield and enantioselectivity under the optimized conditions (Scheme 5.2).

Scheme 5.2: Reported asymmetric synthesis of 2-arylbicyclo[1.1.0]butanes.

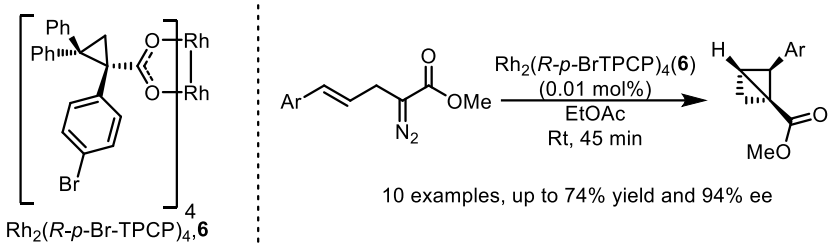

If these compounds could be diversified through reaction with a difluorocarbene(difluorocarbene) source, highly substituted chiral difluorobicyclo[1.1.1]pentanes would be synthesized for the first time. This chapter will describe these efforts and the unusual reactivity observed, followed by the disclosure of an expedient route to 3-aryl-difluorobicyclo[1.1.1]pentanes in a single pot from a diazo precursor along with ring-expanded variants (Figure 5.4).

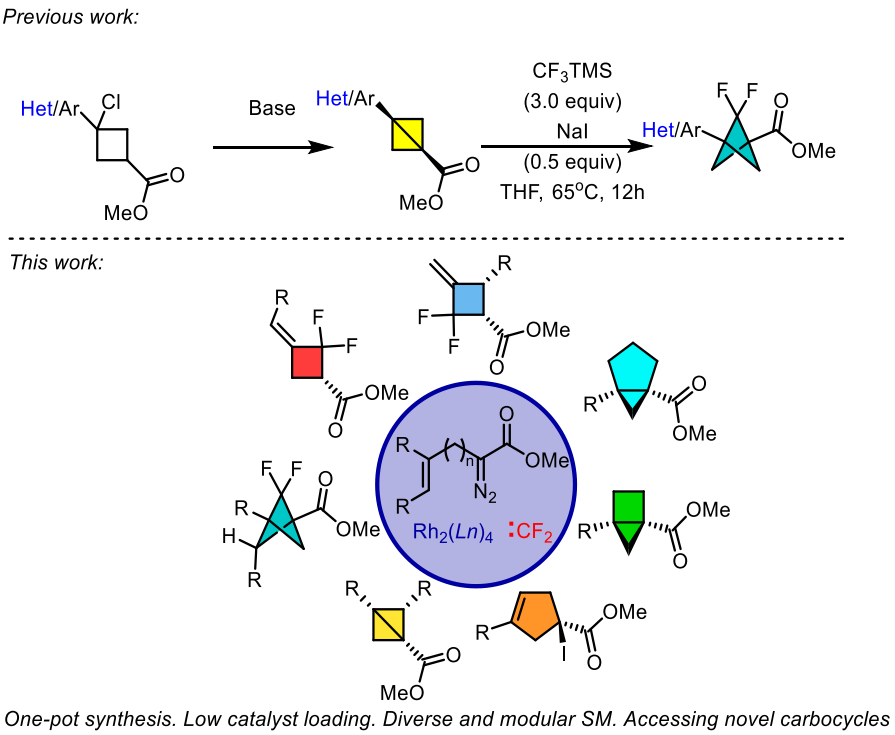

One-pot synthesis. Low catalyst loading. Diverse and modular SM. Accessing novel carbocycles

Figure 5.4: Use of α-allyldiazoacetates for intramolecular cyclopropanation allows access to a diverse series of molecules and *gem*-difluorinated carbocyles when telescoped to include a reaction with difluorocarbene.

5.2 Results and Discussion:

Methyl (*E*)-2-diazo-5-phenylpent-4-enoate (**7**) was prepared according to the published literature procedure.[32] This diazo-compound was then reacted with $Rh_2(Oct)_4$ (0.01 mol %) to generate racemic 2-phenyl bicyclo[1.1.0]butane **8** in 45 min.[32] After confirming the presence of product by ^{1}H NMR of the crude reaction mixture, the solvent was removed *in vacuo* and the product was resuspended in THF. To this mixture, under an inert nitrogen atmosphere, was added NaI (0.5 equiv) and Rupert-Prakash reagent (CF_3TMS, 3.0 equiv) before heating the reaction to 65 °C and allowing it to progress overnight. These were the optimized conditions reported by both Merck and Enamine for generating difluorocarbene (difluorocarbene) and reacting it with 3-arylbicyclo[1.1.0]butanes to generate the desired

difluorobicyclo[1.1.1]pentane products.[30, 31] Upon completion of the reaction, the products were isolated and analyzed by ^{1}H and ^{19}F NMR but no difluorobicyclo[1.1.1]pentane products were observed. Instead, the reaction yielded a 2:1 mixture of methylene-difluorocyclobutene (**9**):methylene-difluorocyclobutene (**10**) products in overall 74% yield (Scheme 5.3).

Scheme 5.3: Intramolecular cyclopropanation of methyl (*E*)-2-diazo-5-phenylpent-4-enoate (**7**) and subsequent reaction with difluorocarbene generates novel and unexpected products.

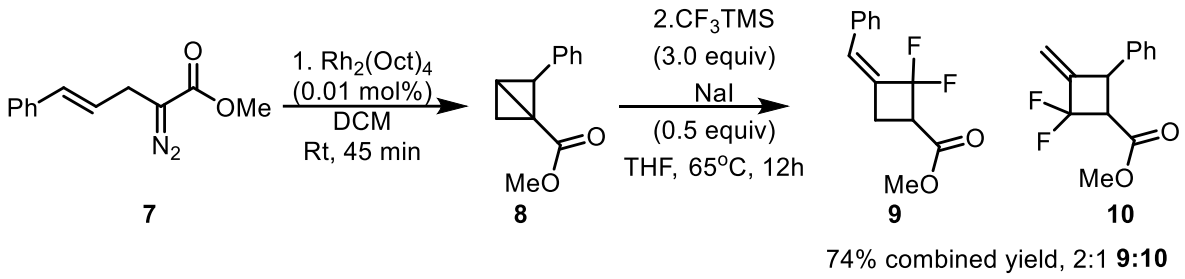

Surprised by the efficient generation of these previously undisclosed exomethylene difluorocyclobutenes, we wanted to understand the mechanism of the reaction and attempt to rationalize the observed selectivity. After careful consideration of the mechanism, we propose that the products arise from the base-catalyzed ring-opening of the desired difluorobicyclo[1.1.1]pentane (Figure 5.5).[33] Previous reports suggest that the insertion of difluorocarbene is a step-wise process beginning with attack by the central C1-C3 bond of the bicyclo[1.1.0]butane on the empty p-orbital of difluorocarbene, followed by recombination of the resultant zwitterion to form a 2,2-difluorobicyclo[1.1.1]pentane.[30, 31, 34, 35] In our system, we propose that the formation of the difluorobicyclo[1.1.1]pentane proceeds as expected, however under the reaction conditions, the compound is unstable. Attempts to trap out the difluorobicyclo[1.1.1]pentane intermediate by skipping workup or running the reaction for short times (1 h) invariably failed, suggesting that the decomposition of this intermediate is almost immediate. The methine C3 proton is highly acidic due to its proximity to the difluoromethylene group and the geometry of the bicyclo[1.1.1]pentane moiety. It is well known that deprotonation and radical reactivity of the

bicyclo[1.1.1]pentane methine proceeds easily under mild conditions, and it appears that the iodide present in the reaction mixture is sufficiently basic to catalyze this process.[16, 22] The bicyclo[1.1.1]pentane then rearranges to form an alkene with either of the adjacent carbons, and the cage and the C1-C2/C1-C4 bond is protonated by the resultant conjugate acid. This opens the caged compound resulting in the formation of isomeric 3-methylene-2,2-difluorocyclobutenes (Figure 5.5). In 2-arylbicyclo[1.1.0]butanes, the weakest C–C bond (C1-C2) is the most easily cleaved during alkene formation which explains the 2:1 product distribution in favor of compound **9**. Interestingly only one alkene isomer of **9** was obtained in the reaction which indicates that the addition of difluorocarbene to the bicyclo[1.1.0]butane intermediate was diastereoselective as has been previously reported.[34]

Figure 5.5: Proposed mechanism of difluorocycle formation.

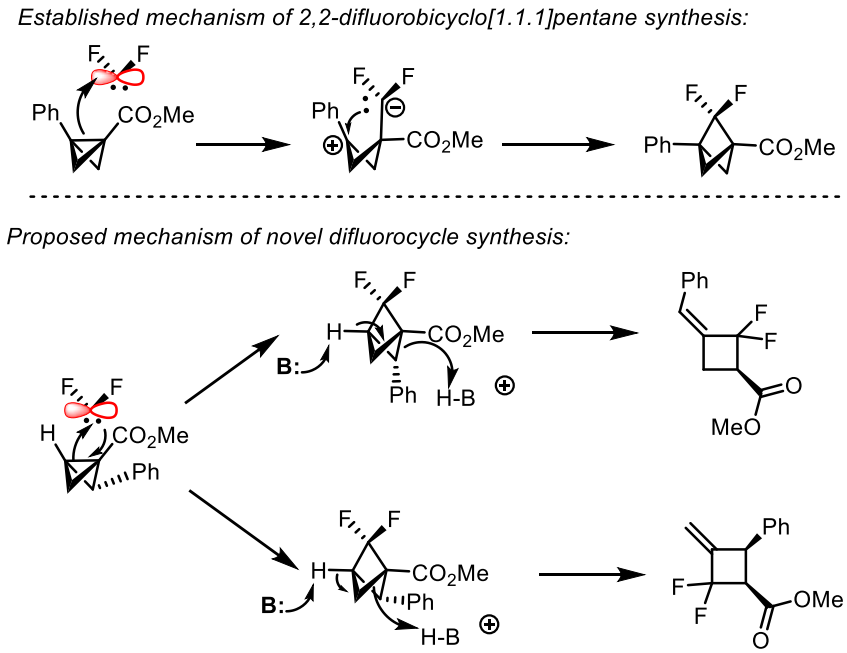

Though unintended, these difluorocarbocycle products are interesting in their own right and have not been reported in the literature previously.[36-38] This creates new opportunities for drug discovery, as such motifs would be otherwise extremely difficult to furnish. In recent years, *gem*-difluorocycloalkanes have become popular in therapeutic compounds but they can be difficult to synthesize, commonly requiring

harsh reactions including deoxyfluorination with DAST or even exposure to F_2 gas, which limits the diversity of these building blocks.[39, 40] As a result, there are few examples of poly-substituted *gem*-difluorocyclobutanes in the literature, and chiral examples are rarer still.[39] In contrast, **9** and **10** contain a high degree of substitution and feature functional handles including an arene, olefin and carboxylate for further diversification. Additionally, thanks to the high asymmetric induction of the cyclopropanation step and the concerted mechanism of difluorocarbene addition, the products should be obtained in high enantioselectivity on the basis of the initial cyclopropanation. This hypothesis was confirmed when the reaction as repeated under the optimal conditions for high asymmetric induction, (Rh_2(*S*-*p*-BrTPCP)$_4$ (**6,** 0.01 mol % and EtOAc as solvent) the products were obtained with high enantioselectivity.[32] Compound **9** was isolated in up to 75% ee and compound **10** was isolated in up to 91% ee. Given the success of this reaction and opportunity to access new chemical space, a short scope of known α-allyl-diazoacetates were synthesized (Table 5.1).[32]

Table 5.1: Preparation of a series of α-allyldiazoacetates according to known literature procedure.[32]

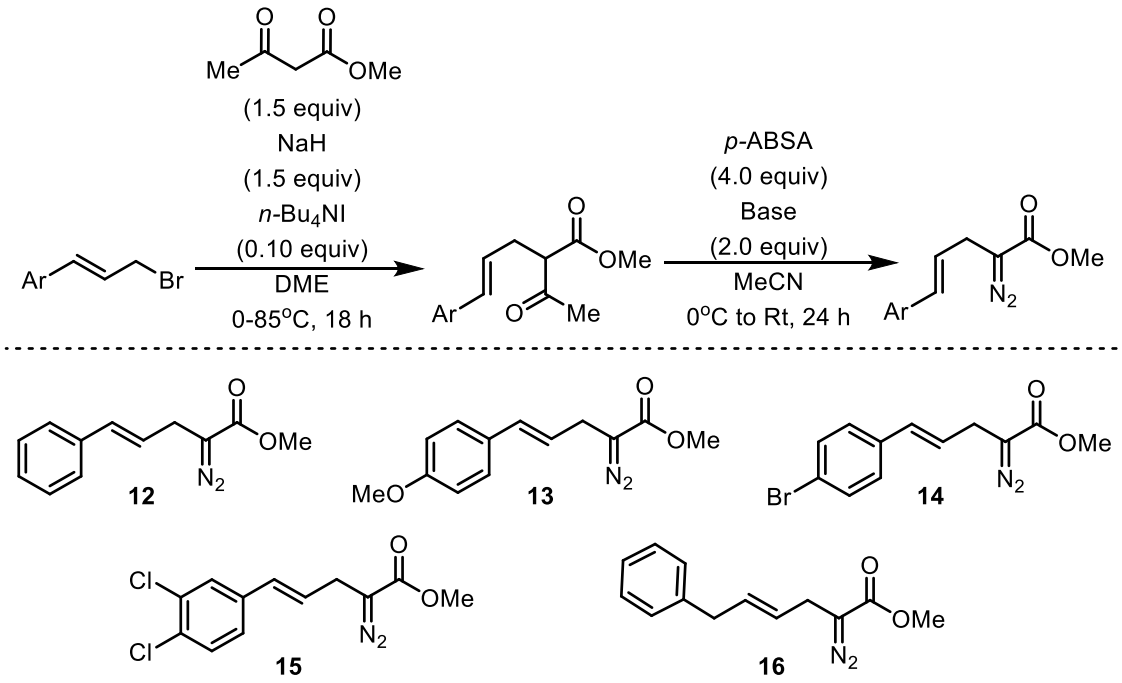

These diazo compounds were then reacted according to the previously described one-pot procedure (Table 5.2). This method well tolerates both electron withdrawing and electron donating substitution on the aryl ring allowing compounds **17** and **18** to be afforded in the same yield as **21** and **22** despite the inclusion of 3,4-dichlorosubstitution in compound **15** and the highly electron donating *p*-MeO substitution of compound **13**. Despite the different electronics of these systems, both afforded the 3-methylene-2,2-difluorocyclobutenes **17** and **18** in the same ratio with similarly high levels of asymmetric induction. We also wanted to examine the reaction of a 2-benzylbicyclo[1.1.0]butane with difluorocarbene since the 2-position of this bicyclo[1.1.0]butane is more sterically accessible and less electronically activated than the aryl derivatives. In this case, compounds **23** and **24** were generated in a 1:1 ratio instead of the typical 2:1 ratio observed in the remainder of the scope, albeit with high asymmetric induction in both cases. Lastly, a 4-bromo substituted arene (**14**) was included to illustrate the potential for diversification of the obtained products **19** and **20**. Purification of these products was extremely challenging and many attempts to isolate the constitutional isomers failed including Ag-impregnated silica, various solvent mixtures, and even reversed-phase preparative HPLC. The only method that was remotely effective for obtaining material for characterization was to run an extremely slow column from 0-1% ether/hexanes and taking an NMR of each fraction to confirm product presence. Once the products were isolated, they degrade in a matter of hours, liberating difluoromethylene and forming a linear diene, the structure of which was confirmed by X-ray crystallography. Even though the products were too unstable to obtain full characterization of purified, the structural assignments were confirmed through extensive NMR analysis, as described in the experimental. Despite this data, the isolated material should not be regarded as pure product, nor the data obtained conclusive of either yield or asymmetric induction. Many of the NMR spectra obtained show byproduct as did the HPLC/SFC traces. FTIR data is also likely inaccurate due to the impurity. At this stage the purpose of reporting these compounds is to illustrate our high degree of confidence that they are

formed over the course of the unusual reaction, but they should not be regarded as either stable or isolable materials and future work will center on the diversification of these products *in situ.*

Table 5.2: Scope of one-pot synthesis of difluorocyclobutenes their rapid degradation to a linear alkene.

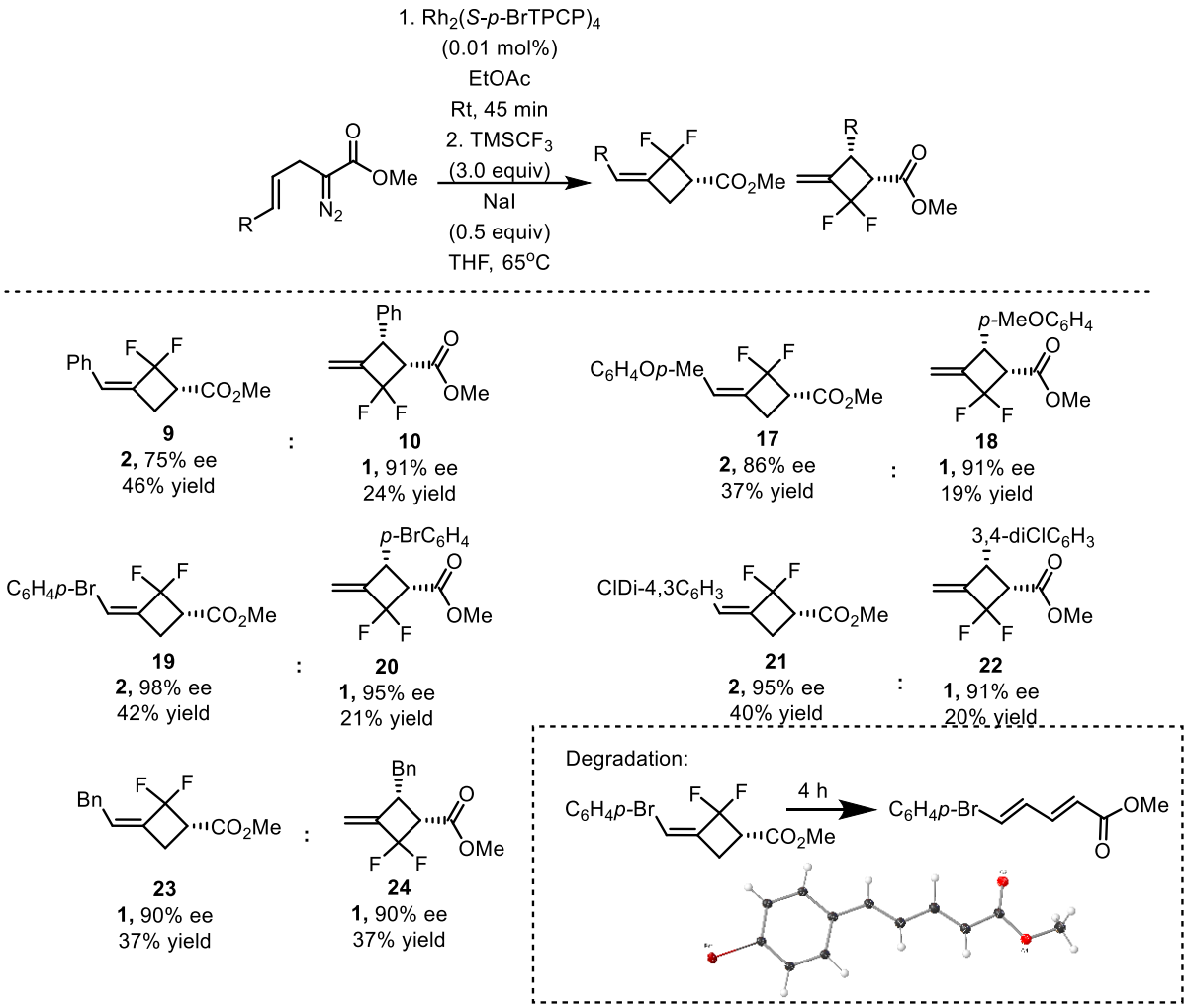

After completion of this scope, it became clear that an alternative approach was required to access difluorobicyclo[1.1.1]pentanes. By applying intramolecular cyclopropanation to a novel class of α-allyl diazoacetates it would be possible to generate 3-aryl-bicyclo[1.1.0]butanes which could react with difluorocarbene according to the established mechanism to generate the desired products. These compounds would, of course, be achiral *meso*-compounds, however if a group could be installed at the 2-position, a chiral highly substituted difluorobicyclo[1.1.1]pentane could be generated. The modular nature

of the diazo synthesis would also allow facile access to expanded ring systems including bicyclo[2.1.0]pentanes and bicyclo[3.1.0]hexanes which have thus far been unexplored as substrates for difluorocarbene reactions. These compounds were expected to react at the most polarized central C–C bond like the 3-aryl bicyclo[1.1.0]butane derivatives, but if new reactivity trends were observed this would still yield interesting products. In order to probe the possibility of performing a one-pot synthesis of difluorobicyclo[1.1.1]pentanes, a series of α-allyl diazoacetates were prepared from the corresponding α-allyl bromides following the established literature procedure and reacted in the presence of a dirhodium catalyst to afford a series of 3-aryl bicyclo[1.1.0]butanes in high yield (Table 5.3).

Table 5.3: Intramolecular cyclopropanation of a novel series of α-allyldiazoacetates to generate 3-aryl/heteroarylbicyclo[1.1.0]butane carboxylates.

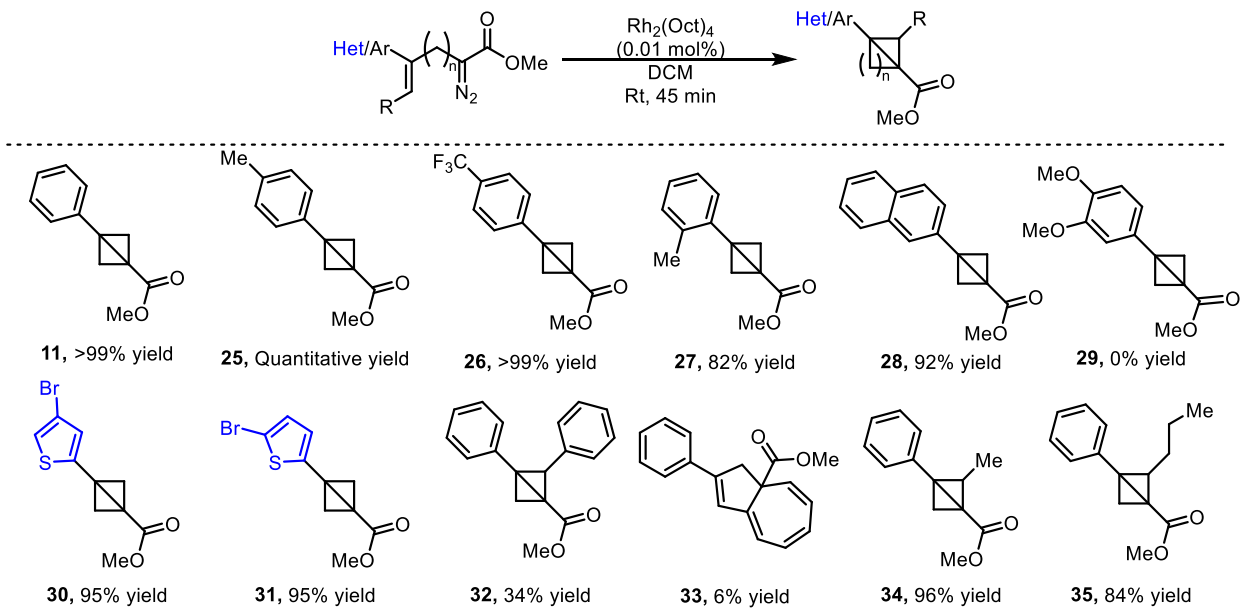

Of note is the formation of compound **27** which includes an *ortho*-substituted arene and compounds **30** and **31** which feature thiophene heterocycles (Table 5.3). Each of these compounds were inaccessible through the previously reported routes to access 3-aryl-bicyclo[1.1.0]butanes.[30] Unfortunately, electron-rich arenes were not compatible with this method as can be seen with compound **29** (Table 5.3), this is likely due to instability of the product which degrades almost immediately upon forming, the diazo

precursor to this product is also unstable and rapidly degrades even if stored at -20 °C.[30] Weak electron donating substitution is tolerated however, and the method efficiently prepares compounds **25**, **27**, and **28**. Several 2-substituted 3-phenyl-bicyclobutanes were also prepared via this method (Table 5.3, **32, 34-35**). Compounds **34** and **35** were generated in excellent yield, however compound **31** was obtained in lower yield.

During the synthesis of the diazo precursor to **32**, the strain associated with the *cis* arrangement of the phenyl rings led to partial isomerization of the alkene to the thermodynamically favorable *trans*-isomer (Scheme 5.5). This isomer was inseparable from the *cis*-isomer but in the presence of a rhodium catalyst, appeared to generate a different product to the *cis*-isomer. Instead, the proximity of the C5-arene to the rhodium carbene caused a rapid cyclopropanation of the arene to occur.[41-43] This highly strained intermediate then underwent a pericyclic rearrangement, resulting in the formation of a phenyl-azulene derivative **33** which was separable from the bicyclo[1.1.0]butane product **32** by column chromatography (Scheme 5.5). The structure of this compound was confirmed through a suite of 2D NMR spectra including COSY, HSQC, and HMBC, and similar analogues are known in the literature.[44, 45]

Scheme 5.4: Proposed strain induced isomerization of diphenyl-trisubstituted α-allyldiazoacetate **36** and **37** leads to two products (**32** and **33**) upon reaction with $Rh_2(Oct)_4$.

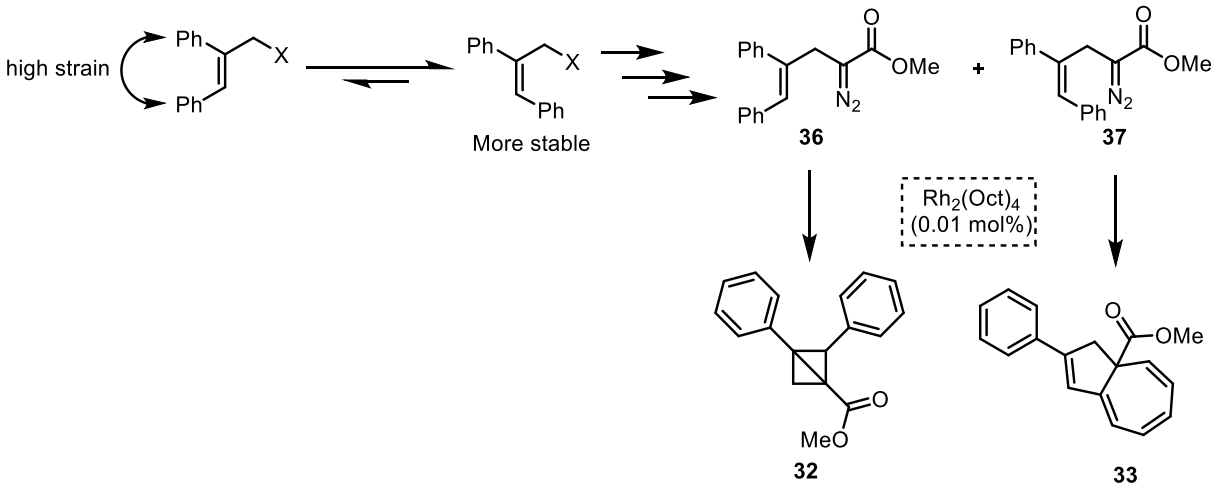

There was interest in determining if chiral information could be generated in the synthesis of products **32-34.** To this end, an exhaustive screen of chiral catalysts was performed (32 chiral catalysts in total). Unfortunately, only one catalyst, Rh_2(*S*-NTTL)$_4$, was able to afford the product with moderate enantioselectivity (50% ee) regardless of the conditions used. Even complex derivatives of Rh_2(*S*-NTTL)$_4$ prepared by Dr. Yannick Boni were unable to improve upon this low level of enantioselectivity and as a result, the scope was elaborated using achiral intramolecular cyclopropanation with Rh_2(Oct)$_4$ as catalyst. To further expand the scope of this transformation larger ring systems were synthesized to see if the strained C2-C3 bond would also be susceptible to insertion of difluorocarbene to generate difluorobicyclo[2.1.1]hexanes and difluorobicyclo[3.1.1]heptanes. Both of these products would provide access to novel highly functionalized *meta*-substituted phenyl bioisosteres.[46] To this effect diazo compounds were synthesized and the intramolecular cyclopropanation was performed to generate the novel bicyclo[2.1.0]pentane **38** and bicyclo[3.1.0]hexane **39** (Scheme 5.6). Both of these products were afforded in excellent yield highlighting the robustness of the intramolecular cyclopropanation despite the modular design of the diazo compound precursors and regardless of the ring size generated. Additionally, unlike the 2,3-disubstituted bicyclo[1.1.0]butanes, these products could be afforded with variable enantioselectivity (11% ee for **38** and 65% ee for **39**, Scheme 5.6) providing hope for achieving an enantioselective difluorocarbene transformation downstream, albeit to generate different products.

Scheme 5.5: Synthesis of bicyclo[2.1.0]pentane and bicyclo[3.1.0]hexane by intramolecular cyclopropanation of β and γ-allyldiazoacetates respectively.

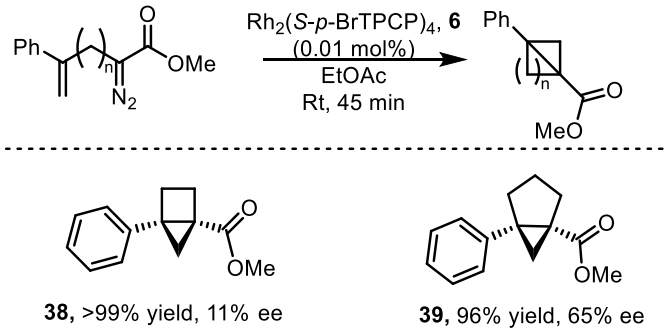

With this novel method for synthesizing 3-arylbicyclo[1.1.0]butanes and larger ring systems in hand, we wanted to evaluate the efficacy of difluorocarbene insertion to generate difluorobicyclo[1.1.1]pentanes. Previous methods have isolated the bicyclo[1.1.0]butane intermediate by column chromatography before conducting this transformation but we reasoned that the small amount of dirhodium catalyst (0.01 mol %) and the lack of un-reacted starting material obviated the need for isolation of the cyclopropanation product.[44] Instead, once the intramolecular cyclopropanation was finished (as determined by FTIR in the disappearance of the $C{=}N_2$ stretch at ~2100 cm^{-1}) the solvent was removed via rotary evaporation and the crude product was suspended in dry THF. NaI (0.5 equiv) and CF_3TMS (3.0 equiv) were added, and the reaction was stirred at 60 °C overnight. After aqueous workup and isolation of the products by column chromatography, the desired difluorobicyclo[1.1.1]pentanes were afforded in comparable yield to previous literature reports (Table 5.4).[30, 31]

Table 5.4: Scope of one-pot synthesis of difluorobicyclo[1.1.1]pentanes.

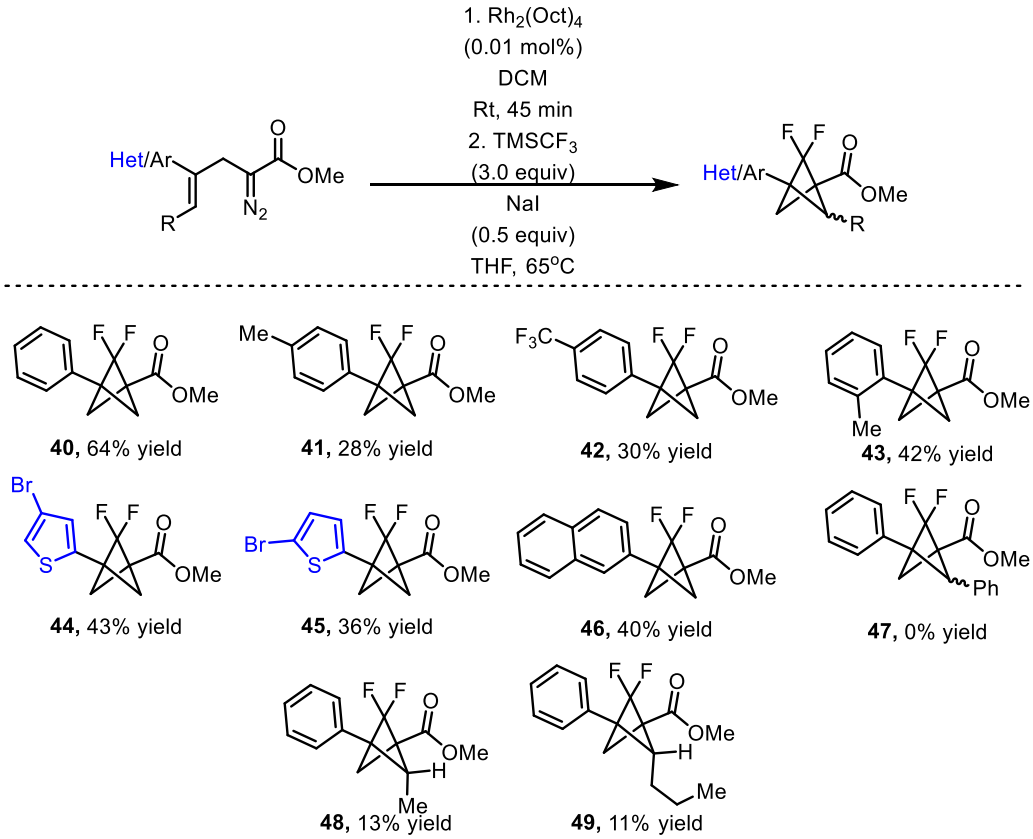

3-Aryl-bicyclo[1.1.0]butanes were generally effective for forming the desired product in moderate yield as has been previously observed and, due to the modular synthesis of the initial diazo compound and the robustness of the subsequent intramolecular cyclopropanation, several novel difluorobicyclo[1.1.1]pentanes could be synthesized by this method (Table 5.4). The previously inaccessible bicyclo[1.1.0]butanes **27, 30,** and **31** proved competent upon reaction with difluorocarbene and afforded the respective novel difluorobicyclo[1.1.1]pentanes in moderate yield.[30] Unfortunately, the 2-substituted derivatives struggled in this reaction (Table 5.4). Compound **36** gave none of the desired product **47**, instead generating *gem*-difluoroalkene as the exclusive difluorocarbene insertion product,[31] product **33** generated from the minor stereoisomer did not react with difluorocarbene. The *gem*-difluoroalkene is the typical byproduct of reactions between bicyclo[1.1.0]butanes and difluorocarbene and is well explored in the literature.[47-49] This compound arises from the same zwitterionic intermediate as the desired diflurobicyclo[1.1.1]pentane product (Scheme 5.7a). However, instead of the two charges recombining to generate the difluorobicyclo[1.1.1]pentane, the electrons on the difluorocarbanion push down into the α-position and the cyclobutane ring opens to reform the alkene present in the starting material (Scheme 5.7a).[31] There are other, well studied methods for generating these *gem*-difluoroalkenes from modified Wittig-type reagents and either carbonyls or diazo-compounds (Scheme 5.7b).[47-49] This was the major product observed in reactions with **34** and **35** also, however these substrates did afford a small amount of the desired 2,2-difluorobicyclo[1.1.1]pentane products albeit in low yield and with no enantioselectivity, even when a chiral catalyst was used in the first step. Interestingly, only a single diastereomer was isolated for both **48** and **49** which indicated that addition of difluorocarbene to the bicyclo[1.1.0]butane is controlled by the substitution around the ring. Only addition to the opposite face from the substituents was observed likely due to steric blocking of the other face which explains this diastereoselectivity (Figure 5.7c). A similar phenomenon has been reported in the literature although the only extant example of this type of reaction has been reported with deuterium as the 2-substituent.[34]

Other difluorocarbene sources were also evaluated including 2,2-difluoro-2-(triphenylphosphonio)acetate ($PPh_3CF_2CO_2$)[49] and the combination of trimethylsilyl 2,2-difluoro-2-(fluorosulfonyl)acetate and NaF (Scheme 5.7b), but the combination of CF_3TMS and NaI proved the most effective as was previously reported.[30, 31]

Scheme 5.6: Mechanism of byproduct formation and alternative difluorocarbene sources.

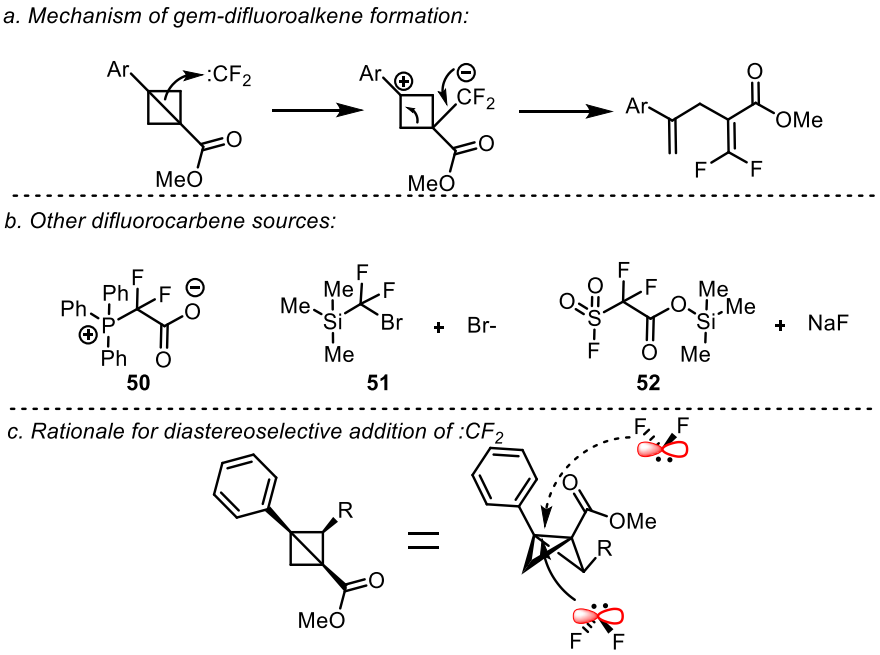

Additionally, neither of the expanded ring systems were able to successfully react with difluorocarbene. It is likely that **39** does not contain sufficient ring strain across the C2–C4 bond to engage with difluorocarbene under these mild conditions. More forcing conditions were used and at higher temperature (trimethylsilyl 2,2-difluoro-2-(fluorosulfonyl)acetate and NaF (**52**) at 90 °C and 2,2-difluoro-2-(triphenylphosphonio)acetate (**50**) at 120 °C) to improve the reaction kinetics. These attempts were also unsuccessful. Compound **38** contains considerably higher ring strain across the C1–C3 bond, and did react under these conditions. However it did not form the desired difluorobicyclo[2.1.1]hexane, instead forming α-iodocyclopentene **53** in 47% yield the structure of which was confirmed by X-ray crystallography (Scheme 5.8a). This product likely arises from the trapping of iodine generated by NaI *in situ.* Given the

promising reactivity of compound other difluorocarbene sources were screened as described in Scheme 5.7b. Reaction involving system **51** was a mess by NMR, however the use of phosphine ylide compound **50** was promising. Unfortunately, upon deeper evaluation, the only products obtained in this reaction were the cyclopentene **54** and an unusual bis(difluoromethyl)triphenyl-λ5-phosphane. It is possible that further evaluation of different difluorocarbene sources could yield the desired compound, however this was not further explored. Nevertheless it remains clear that **38** is a highly reactive compound suitable for further derivatization and future methodological work done by the Davies group to diversify this interesting bicyclo[2.1.0]pentane will be pursued.

Scheme 5.7: Reaction of bicyclo[2.1.0]pentane with various difluorocarbene sources.

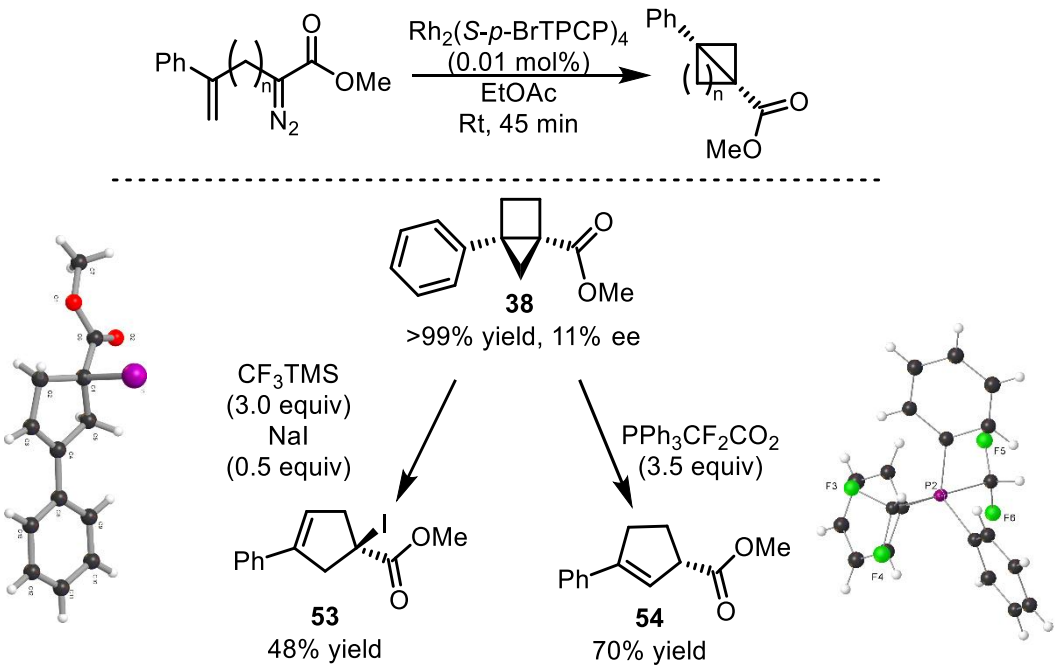

5.3 Conclusion:

A novel approach to synthesizing 3-arylbicyclo[1.1.0]butanes and related structures from an α-allyl diazoacetate precursors was developed. We were also able to explore difluorocarbene insertion of 2-arylbicyclo[1.1.0]butanes and determine the unusual 3-methylene-2,2-difluorocyclobutene products generated as well a propose a mechanism for their formation. The novel method for synthesizing 3-

arylbicyclo[1.1.0]butanes is tolerant of various functionality and generally proceeds with very high yield at low catalyst loading (0.01 mol %), enabling the synthesis of bicyclo[1.1.0]butanes that were inaccessible by previously reported methods. It was also possible to generate a series of 2,2-difluorobicyclo[1.1.1]pentanes from the α-allyl diazoacetate in a one-pot process with comparable yields to previous reports. Several more-highly substituted compounds were also evaluated, and though they were less competent in difluorobicyclo[1.1.1]pentane synthesis, these are interesting compounds in their own right. Ring expanded variants were also compatible with the intramolecular cyclopropanation method, although were ineffective for generating difluorocarbocycles when exposed to various difluorocarbene sources. Future work will be conducted to determine the scope of transformations accessible to these highly substituted bicyclo[1.1.0]butanes and improving the asymmetric synthesis of these novel compounds.

5.4 References:

1. Lovering, F.; Bikker, J.; Humblet, C., Escape from flatland: increasing saturation as an approach to improving clinical success. *J. Med. Chem.* **2009,** *52* (21), 6752-6756.
2. Lovering, F., Escape from Flatland 2: complexity and promiscuity. *MedChemComm* **2013,** *4* (3), 515-519.
3. Buskes, M. J.; Blanco, M.-J., Impact of cross-coupling reactions in drug discovery and development. *Molecules* **2020,** *25* (15), 3493.
4. Maiti, S.; Li, Y.; Sasmal, S.; Guin, S.; Bhattacharya, T.; Lahiri, G. K.; Paton, R. S.; Maiti, D., Expanding chemical space by para-C− H arylation of arenes. *Nat. Commun.* **2022,** *13* (1), 1-10.
5. Yasuda, N., Application of cross-coupling reactions in Merck. *J. Organomet. Chem.* **2002,** *653* (1-2), 279-287.
6. Noël, T.; Buchwald, S. L., Cross-coupling in flow. *Chem. Soc. Rev.* **2011,** *40* (10), 5010-5029.
7. Kadu, B. S., Suzuki–Miyaura cross coupling reaction: recent advancements in catalysis and organic synthesis. *Catal. Sci. Technol.* **2021,** *11* (4), 1186-1221.
8. Erlanson, D. A.; Fesik, S. W.; Hubbard, R. E.; Jahnke, W.; Jhoti, H., Twenty years on: the impact of fragments on drug discovery. *Nat. Rev. Drug Discov.* **2016,** *15* (9), 605-619.
9. Moir, M.; Danon, J. J.; Reekie, T. A.; Kassiou, M., An overview of late-stage functionalization in today's drug discovery. *Expert Opin. Drug Discov.* **2019,** *14* (11), 1137-1149.
10. Guillemard, L.; Kaplaneris, N.; Ackermann, L.; Johansson, M. J., Late-stage C–H functionalization offers new opportunities in drug discovery. *Nat. Rev. Chem.* **2021,** *5* (8), 522-545.
11. Mykhailiuk, P. K., Saturated bioisosteres of benzene: where to go next? *Org. Biomol. Chem.* **2019,** *17* (11), 2839-2849.
12. Ma, X.; Nhat Pham, L., Selected topics in the syntheses of bicyclo [1.1. 1] pentane (BCP) analogues. *Asian J. Org. Chem.* **2020,** *9* (1), 8-22.

13. Bauer, M. R.; Di Fruscia, P.; Lucas, S. C.; Michaelides, I. N.; Nelson, J. E.; Storer, R. I.; Whitehurst, B. C., Put a ring on it: application of small aliphatic rings in medicinal chemistry. *RSC Med. Chem.* **2021,** *12* (4), 448-471.
14. Talele, T. T., Opportunities for tapping into three-dimensional chemical space through a quaternary carbon. *J. Med. Chem.* **2020,** *63* (22), 13291-13315.
15. Makarov, I. S.; Brocklehurst, C. E.; Karaghiosoff, K.; Koch, G.; Knochel, P., Synthesis of bicyclo [1.1. 1] pentane bioisosteres of internal alkynes and para-disubstituted benzenes from [1.1. 1] propellane. *Angew. Chem. Int. Ed.* **2017,** *56* (41), 12774-12777.
16. Yen-Pon, E.; Li, L.; Levitre, G.; Majhi, J.; McClain, E. J.; Voight, E. A.; Crane, E. A.; Molander, G. A., On-DNA Hydroalkylation to Introduce Diverse Bicyclo [1.1. 1] pentanes and Abundant Alkyls via Halogen Atom Transfer. *J. Am. Chem. Soc.* **2022,** *144* (27), 12184-12191.
17. Yu, S.; Jing, C.; Noble, A.; Aggarwal, V. K., 1, 3-Difunctionalizations of [1.1. 1] Propellane via 1, 2-Metallate Rearrangements of Boronate Complexes. *Angew. Chem. Int. Ed.* **2020,** *59* (10), 3917-3921.
18. Measom, N. D.; Down, K. D.; Hirst, D. J.; Jamieson, C.; Manas, E. S.; Patel, V. K.; Somers, D. O., Investigation of a Bicyclo [1.1. 1] pentane as a Phenyl Replacement within an LpPLA2 Inhibitor. *ACS Med. Chem. Lett.* **2017,** *8* (1), 43-48.
19. Wong, M. L.; Sterling, A. J.; Mousseau, J. J.; Duarte, F.; Anderson, E. A., Direct catalytic asymmetric synthesis of α-chiral bicyclo [1.1. 1] pentanes. *Nature Commun.* **2021,** *12* (1), 1-9.
20. Rentería-Gómez, A.; Lee, W.; Yin, S.; Davis, M.; Gogoi, A. R.; Gutierrez, O., General and Practical Route to Diverse 1-(Difluoro) alkyl-3-aryl Bicyclo [1.1. 1] pentanes Enabled by an Fe-Catalyzed Multicomponent Radical Cross-Coupling Reaction. *ACS. Catal.* **2022,** *12*, 11547-11556.
21. Han, H.; Zhu, B.; Du, X.; Zhu, Y.; Yu, C.; Jiang, X., Synthesis of 1-azido-3-heteroaryl bicyclo [1.1. 1] pentanes via azidoheteroarylation of [1.1. 1] propellane. *Green Chem.* **2021,** *23* (24), 10132-10136.
22. Garlets, Z. J.; Sanders, J. N.; Malik, H.; Gampe, C.; Houk, K.; Davies, H. M., Enantioselective C–H functionalization of bicyclo [1.1. 1] pentanes. *Nature Catal.* **2020,** *3* (4), 351-357.
23. Yang, Y.; Tsien, J.; Hughes, J. M.; Peters, B. K.; Merchant, R. R.; Qin, T., An intramolecular coupling approach to alkyl bioisosteres for the synthesis of multisubstituted bicycloalkyl boronates. *Nature Chem.* **2021,** *13* (10), 950-955.
24. Zhao, J.-X.; Chang, Y.-X.; He, C.; Burke, B. J.; Collins, M. R.; Del Bel, M.; Elleraas, J.; Gallego, G. M.; Montgomery, T. P.; Mousseau, J. J., 1, 2-Difunctionalized bicyclo [1.1. 1] pentanes: Long–sought-after mimetics for ortho/meta-substituted arenes. *Proceedings of the National Academy of Sciences* **2021,** *118* (28), e2108881118.
25. Kaleta, J.; Roncevic, I.; Cisarova, I.; Dracinsky, M.; Solinova, V.; Kasicka, V.; Michl, J., Bridge-chlorinated bicyclo [1.1. 1] pentane-1, 3-dicarboxylic acids. *J. Org. Chem.* **2019,** *84* (5), 2448-2461.
26. Ma, X.; Han, Y.; Bennett, D. J., Selective synthesis of 1-dialkylamino-2-alkylbicyclo-[1.1. 1] pentanes. *Org. Lett.* **2020,** *22* (22), 9133-9138.
27. Anderson, J. M.; Measom, N. D.; Murphy, J. A.; Poole, D. L., Bridge functionalisation of bicyclo [1.1. 1] pentane derivatives. *Angew. Chem. Int. Ed.* **2021,** *60* (47), 24754-24769.
28. Clayden, J.; Moran, W. J.; Edwards, P. J.; LaPlante, S. R., The challenge of atropisomerism in drug discovery. *Angew. Chem. Int. Ed.* **2009,** *48* (35), 6398-6401.
29. Joshi, G.; Kaur, M.; Kumar, R., Dynamic axial chirality in drug design and discovery: Introduction to atropisomerism, classification, significance, recent trends and Challenges. *Drug Discov. Dev.* **2021**, 103-124.
30. Ma, X.; Sloman, D. L.; Han, Y.; Bennett, D. J., A selective synthesis of 2, 2-difluorobicyclo [1.1. 1] pentane analogues:"BCP-F2". *Org. Lett.* **2019,** *21* (18), 7199-7203.
31. Bychek, R. M.; Hutskalova, V.; Bas, Y. P.; Zaporozhets, O. A.; Zozulya, S.; Levterov, V. V.; Mykhailiuk, P. K., Difluoro-substituted bicyclo [1.1. 1] pentanes for medicinal chemistry: Design, synthesis, and characterization. *J. Org. Chem.* **2019,** *84* (23), 15106-15117.

32. Qin, C.; Davies, H. M., Enantioselective synthesis of 2-arylbicyclo [1.1. 0] butane carboxylates. *Org. Lett.* **2013,** *15* (2), 310-313.
33. Semeno, V. V.; Vasylchenko, V. O.; Vashchenko, B. V.; Lutsenko, D. O.; Iminov, R. T.; Volovenko, O. B.; Grygorenko, O. O., Building the Housane: Diastereoselective Synthesis and Characterization of Bicyclo [2.1. 0] pentane Carboxylic Acids. *J. Org. Chem* **2019,** *85* (4), 2321-2337.
34. McNamee, R. E.; Thompson, A. L.; Anderson, E. A., Synthesis and Applications of Polysubstituted Bicyclo [1.1. 0] butanes. *J. Am. Chem. Soc.* **2021,** *143* (50), 21246-21251.
35. García-Domínguez, A.; West, T. H.; Primozic, J. J.; Grant, K. M.; Johnston, C. P.; Cumming, G. G.; Leach, A. G.; Lloyd-Jones, G. C., Difluorocarbene Generation from TMSCF3: Kinetics and Mechanism of NaI-Mediated and Si-Induced Anionic Chain Reactions. *J. Am. Chem. Soc.* **2020,** *142* (34), 14649-14663.
36. Shen, Q.; Hammond, G. B., Regiospecific Synthesis of Bicyclo-and Heterobicyclo-g em-difluorocyclobutenes Using Functionalized Fluoroallenes and a Novel Mo-Catalyzed Intramolecular [2+ 2] Cycloaddition Reaction. *J. Am. Chem. Soc.* **2002,** *124* (23), 6534-6535.
37. Chang, J.; Xu, C.; Gao, J.; Gao, F.; Zhu, D.; Wang, M., Me3SiCF2Br-self-assisted Domino reaction: Catalytic synthesis of α, α-difluorocyclopentanones from methylvinylketones. *Org. Lett.* **2017,** *19* (7), 1850-1853.
38. Zhang, M.; Li, H.; Zhao, J.; Li, Y.; Zhang, Q., Copper-catalyzed [3+ 1] cyclization of cyclopropenes/diazo compounds and bromodifluoroacetamides: facile synthesis of α, α-difluoro-β-lactam derivatives. *Chem. Sci.* **2021,** *12* (35), 11805-11809.
39. Grygorenko, O. O.; Melnykov, K. P.; Holovach, S.; Demchuk, O., Fluorinated Cycloalkyl Building Blocks for Drug Discovery. *ChemMedChem* **2022**, e202200365.
40. Chernykh, A. V.; Melnykov, K. P.; Tolmacheva, N. A.; Kondratov, I. S.; Radchenko, D. S.; Daniliuc, C. G.; Volochnyuk, D. M.; Ryabukhin, S. V.; Kuchkovska, Y. O.; Grygorenko, O. O., Last of the gem-difluorocycloalkanes: synthesis and characterization of 2, 2-difluorocyclobutyl-substituted building blocks. *J. Org. Chem.* **2019,** *84* (13), 8487-8496.
41. Zhou, Q.; Li, S.; Zhang, Y.; Wang, J., Rhodium (II)-or Copper (I)-Catalyzed Formal Intramolecular Carbene Insertion into Vinylic C (sp2)− H Bonds: Access to Substituted 1H-Indenes. *Angew. Chem.* **2017,** *129* (50), 16229-16233.
42. Dong, K.; Fan, X.; Pei, C.; Zheng, Y.; Chang, S.; Cai, J.; Qiu, L.; Yu, Z.-X.; Xu, X., Transient-axial-chirality controlled asymmetric rhodium-carbene C (sp2)-H functionalization for the synthesis of chiral fluorenes. *Nature Commun.* **2020,** *11* (1), 1-10.
43. Lian, Y.; Davies, H. M., Rh2 (S-biTISP) 2-catalyzed asymmetric functionalization of indoles and pyrroles with vinylcarbenoids. *Org. Lett.* **2012,** *14* (7), 1934-1937.
44. Panish, R.; Chintala, S. R.; Boruta, D. T.; Fang, Y.; Taylor, M. T.; Fox, J. M., Enantioselective synthesis of cyclobutanes via sequential Rh-catalyzed bicyclobutanation/Cu-catalyzed homoconjugate addition. *J. Am. Chem. Soc.* **2013,** *135* (25), 9283-9286.
45. Hoshi, T.; Ota, E.; Inokuma, Y.; Yamaguchi, J., Asymmetric Synthesis of a 5, 7-Fused Ring System Enabled by an Intramolecular Buchner Reaction with Chiral Rhodium Catalyst. *Org. Lett.* **2019,** *21* (24), 10081-10084.
46. Frank, N.; Nugent, J.; Shire, B. R.; Pickford, H. D.; Rabe, P.; Sterling, A. J.; Zarganes-Tzitzikas, T.; Grimes, T.; Thompson, A. L.; Smith, R. C., Synthesis of meta-substituted arene bioisosteres from [3.1. 1] propellane. *Nature* **2022**, 1-6.
47. Jiang, Q.; Liang, Y.; Zhang, Y.; Zhao, X., Chalcogenide-Catalyzed Intermolecular Electrophilic Thio- and Halofunctionalization of gem-Difluoroalkenes: Construction of Diverse Difluoroalkyl Sulfides and Halides. *Org. Lett.* **2020,** *22* (19), 7581-7587.
48. Zhang, Z.; Yu, W.; Wu, C.; Wang, C.; Zhang, Y.; Wang, J., Reaction of Diazo Compounds with Difluorocarbene: An Efficient Approach towards 1, 1-Difluoroolefins. *Angew. Chem. Int. Ed.* **2016,** *55* (1), 273-277.

49. Zheng, J.; Cai, J.; Lin, J.-H.; Guo, Y.; Xiao, J.-C., Synthesis and decarboxylative Wittig reaction of difluoromethylene phosphobetaine. *Chem. Commun.* **2013,** *49* (68), 7513-7515.

Appendix A: Chapter 1 Supporting information.

CAUTION: Diazo compounds are high energy compounds and need to be treated carefully. Even though we had no problems in own work, care should be taken in handling large quantities of diazo compounds. Large scale reactions should be conducted behind a blast shield. For a more complete analysis of the risks associated with diazo compounds see the recent review by Bull *et. al.*[1]

1. General Considerations

For details on low loading experiments see the published work.[2] All experiments were carried out in oven-dried glassware under argon atmosphere unless otherwise stated. Flash column chromatography was performed on silica gel. 4Å molecular sieves were activated under vacuum at 300 °C for 4 hours. After time elapsed, the flask was cooled to 60 °C under inert nitrogen atmosphere and stored in a 140 °C oven for future use. All solvents were distilled using a short-path distillation system and stored over 4Å molecular sieves under argon atmosphere. Unless otherwise noted, all other reagents were obtained from commercial sources (Sigma Aldrich, Fisher, TCI Chemicals, and AK Scientific) and used as received without purification. ^{1}H, ^{13}C, and ^{19}F NMR spectra were recorded at either 400 MHz (^{13}C at 100 MHz) on VNMR 400 spectrometer or 600 MHz (^{13}C at 150 MHz) on INOVA 600 or Bruker 600 spectrometer. NMR spectra were run in solutions of deuterated chloroform ($CDCl_3$) with residual chloroform taken as an internal standard (7.26 ppm for ^{1}H, and 77.16 ppm for ^{13}C), and were reported in parts per million (ppm). The abbreviations for multiplicity are as follows: s = singlet, d = doublet, t = triplet, q = quartet, p = pentet, m = multiplet, dd = doublet of doublet, etc. Coupling constants (J values) are obtained from the spectra. Thin layer chromatography was performed on aluminum-back silica gel plates with UV light to visualize. *In situ* IR reaction monitoring experiments were carried out with a Mettler Toledo ReactIR 45m instrument equipped with a 9.5 mm x 12'' AgX 1.5 m SiComp probe. Mass spectra were taken on a Thermo Finnigan LTQ-FTMS spectrometer with APCI, ESI or NSI. Melting points (mp) were measured in open capillary tubes with a Mel-Temp Electrothermal melting points apparatus and are uncorrected. IR spectra were collected on a Nicolet iS10 FT-IR spectrometer from Thermo Scientific and reported in unit of cm^{-1}. Optical rotations were measured on Jasco P-2000 polarimeters. Enantiomeric excess (ee) data were obtained on a Varian

Prostar chiral HPLC instrument, eluting the purified products using a mixed solution of HPLC-grade 2-propanol (*i*-PrOH) and *n*-hexane.

2. Preparation of Substrates

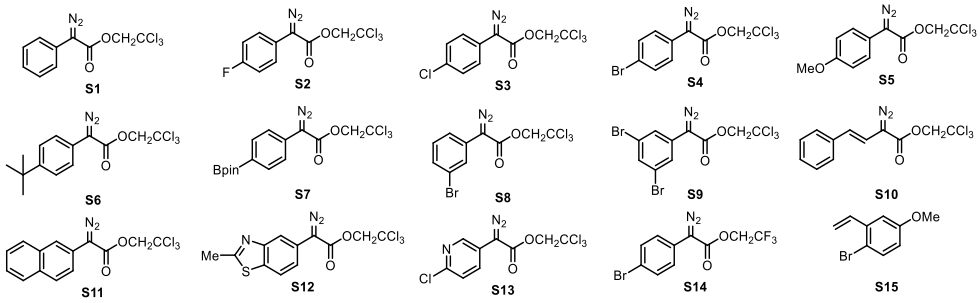

Figure A1: Starting materials.

Diazo compounds **s1**, **s3**, **s5**, **s7**, **s8**, **s10**, **s11**, **s12** were prepared using the procedure reported in the literature.[3]

Diazo compounds **s2**, **s4**, **s6**, were prepared using the procedure reported in the literature.[4]

Diazo compound **s9** was prepared using the procedure reported in literature.[5]

Diazo compound **s14** was prepared using the procedure reported in literature.[6]

Compound **s15** was prepared using the procedure reported in literature.[7]

3. Procedure for high-throughput screen and laboratory scale cyclopropanation reactions

3.1 General procedure for scope preparation:

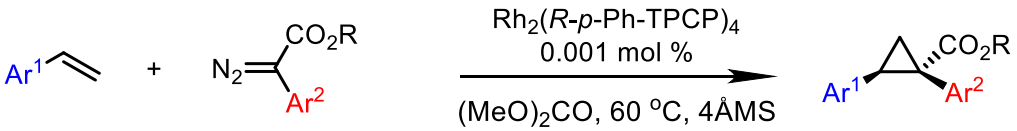

The ReactIR instrument was filled with liquid nitrogen and allowed to equilibrate while the reaction flask was being set-up. An oven-dried 100 mL 3-neck round-bottom flask with 1.5 g 4 Å molecular sieves was fitted with a rubber septum (left neck, 14/20), ReactIR probe (center neck, 24/40 to 19/25 adapter, 19/25 neck), and argon inlet (right neck, 14/20). The flask was cooled to room temperature under vacuum, then backfilled with argon and placed in a water or oil bath, with the temperature of the stir plate set to the desired temperature and stir rate on 700 rpm. Once the reaction flask was at the desired temperature, the background and water vapor spectrum were taken via the ReactIR instrument. The syringe and needle used for the solvent was primed with argon from the flask before adding 27 ml solvent through the rubber septum. The data collection was started on the ReactIR™ software, and the solvent was allowed to stir for 15 min. After a reference spectrum of the solvent was taken, styrene (pre-purified by passing through a pipette column) was added using a plastic syringe. The reaction mixture was allowed to stir while the diazo compound was weighed out. A reference spectrum of alkene substrate was taken after

subtracting out the solvent spectrum, and then the diazo compound (solid) was added by removing and quickly replacing the rubber septum. A reference spectrum of the diazo compound was taken after subtracting out the reference spectrum of alkene, and the reaction mixture was allowed to stir for 15 min. 1 mL of the catalyst stock solution was added to the reaction mixture and allowed to stir until the complete consumption of the diazo compound by tracking the disappearance of the $C{=}N_2$ stretch frequencies (around 2103 cm^{-1}). Upon reaction completion, the solution was passed through a celite filter to remove molecular sieves and the solvent was removed in vacuo. The crude residue was purified by flash column chromatography. Pure product fractions were combined, and solvent was evaporated to afford the desired product. Asymmetric induction of the pure product was determined by chiral-HPLC.

3.2 General procedure for high throughput screen:

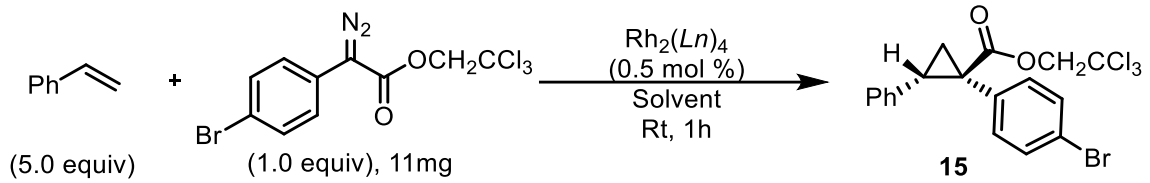

Stock solutions of aryl-diazo acetate **S4** and styrene were prepared for a 11 mg scale reaction. Styrene was freshly columned through a short silica plug and added (158 mg, 143 µl, 1.52 mmol) to a 15 mL conical centrifuge tube and diluted in 6.25 mL of the solvent being examined. 2,2,2-trichloroethyl 2-(4-bromophenyl)-2-diazoacetate (**S4**, 93.1 mg, 0.250 mmol) was added to a separate 15 ml conical vial and dissolved in 4.75 ml of the solvent being examined. Each catalyst being tested (0.00125 mmol) was separately dissolved in 1.000 ml of solvent being tested. Then, 100 µl of each resultant catalyst solution was added to a different 1.7 ml Eppendorf tube. For volatile solvents, these tubes were capped until substrate was dispensed in the reaction vial. A solution of 2 % isopropanol in hexanes was prepared as the HPLC dilution solvent and 10 ml was added to a separate 15 ml conical vial. All reactions were carried out for 1 h under air. All reactions performed for the purpose of the solvent screen were performed in an automated manner according to a specially designed protocol for the robot as listed below.

Protocol steps

1: Dispense 625 µL from 15 mL conical centrifuge tube “Styrene” to 1.5 mL conical µtube “1.5 mL conical µtube #1”: wells A1:A5, B1:B2

- Speed: Slow
- Viscosity: High
- Do not change tip between pipetting
  - Pipetting from Liquid level (Source) / Pipetting on-the-fly (Destination)

2: Dispense 375 µL from 15 mL conical centrifuge tube “Diazo” to 1.5 mL conical µtube “1.5 mL conical µtube #1”: wells A1:A5, B1:B2

- Speed: Slow
  - Viscosity: High
- Do not change tip between pipetting

- Pipetting from Liquid level (Source) / Pipetting on-the-fly (Destination)
3: START timer #1 for 1 h 00 00 4 END of timer #1 after 1 h 00 00 5
Verbalize: “Take the cap off of the HPLC solvent”
6: Dispense 20 µL from 1.5 mL conical µtube “1.5 mL conical µtube #1”: well A1 to 1.5 mL conical µtube “1.5 mL conical µtube #1”: well B4
- Pipette: M100E
- Do not change tip between pipetting
- Pipetting on-the-fly (Destination)
7: Dispense 20 µL from 1.5 mL conical µtube “1.5 mL conical µtube #1”: well A2 to 1.5 mL conical µtube “1.5 mL conical µtube #1”: well B5
- Pipette: M100E
- Do not change tip between pipetting
- Pipetting on-the-fly (Destination)
8: Dispense 20 µL from 1.5 mL conical µtube “1.5 mL conical µtube #1”: well A3 to 1.5 mL conical µtube “1.5 mL conical µtube #1”: well C1
- Pipette: M100E
- Do not change tip between pipetting
- Pipetting on-the-fly (Destination)
9: Dispense 20 µL from 1.5 mL conical µtube “1.5 mL conical µtube #1”: well A4 to 1.5 mL conical µtube “1.5 mL conical µtube #1”: well C2
- Pipette: M100E
- Do not change tip between pipetting
- Pipetting on-the-fly (Destination)
10: Dispense 20 µL from 1.5 mL conical µtube “1.5 mL conical µtube #1”: well A5 to 1.5 mL conical µtube “1.5 mL conical µtube #1”: well C3
- Pipette: M100E
- Do not change tip between pipetting
- Pipetting on-the-fly (Destination)
11: Dispense 20 µL from 1.5 mL conical µtube “1.5 mL conical µtube #1”: well B1 to 1.5 mL conical µtube “1.5 mL conical µtube #1”: well C4
- Pipette: M100E
- Do not change tip between pipetting
- Pipetting on-the-fly (Destination)
12: Dispense 20 µL from 1.5 mL conical µtube “1.5 mL conical µtube #1”: well B2 to 1.5 mL conical µtube “1.5 mL conical µtube #1”: well C5
- Pipette: M100E
- Do not change tip between pipetting
- Pipetting on-the-fly (Destination)
13: Dispense 980 µL from 15 mL conical centrifuge tube “HPLC Hexanes” to 1.5 mL conical µtube “1.5 mL conical µtube #1”: wells B4:B5, C1:C5
- Do not change tip between pipetting

- Pipetting from Liquid level (Source) / Pipetting on-the-fly (Destination)

Resultant diluted reaction samples were directly characterized by Agilent Infinity UHPLC to determine % ee. Method: IAU column, 6 min, 0.500 ml/min, 1% IPA/hexanes. Enantiomers elute: ~2.2 min and ~2.7min

3.3 General procedure for laboratory scale cyclopropanation reactions:

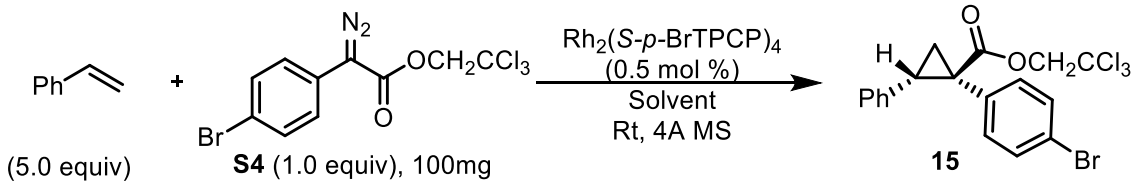

In a flame-dried, 10 mL round-bottomed flask, equipped with a magnetic stir bar and 4Å activated molecular sieves (~0.5 g), Rh_2(*S*-*p*-Br-TPCP)$_4$ (2.32 mg, 1.34 µmol, 0.5 mol%) and styrene (140 mg, 1.34 mmol, 5.0 equiv. columned through a small silica plug immediately prior to reaction) were added. The catalyst and substrate were then dissolved in distilled solvent (5 mL) at room temperature under an inert argon atmosphere. Then 2,2,2-trichloroethyl 2-(4-bromophenyl)-2-diazoacetate (100 mg, 0.269 mmol, 1.0 equiv.) was dissolved in distilled solvent (3 ml) under argon and added dropwise to the reaction mixture. The flask used to dissolve the diazo compound and the needle/syringe were rinsed with 2 mL of distilled solvent, which was added to the reaction. The solution was stirred overnight at room temperature. Upon reaction completion, the solution was passed through a celite filter to remove molecular sieves and the solvent was removed in vacuo. The crude residue was purified based on Rf by flash column chromatography (TLC developed in 5% EtOAc/hexanes, Rf: styrene=0.60 non CAM stain active, cyclopropane product: 0.45 as a CAM stain active dark blue spot). Pure product fractions were combined, and solvent was evaporated to yield a white crystalline solid. Product was characterized by chiral-HPLC. Varian Prostar, OJ-H chiracel column: method: 30min, 1ml/min, 1 % IPA/Hexanes, Major enantiomer: 8.55 min Minor enantiomer: 13.8 min

4. Characterization of the cyclopropanation products

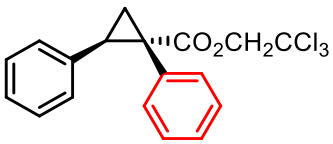

16

2,2-trichloroethyl (1*S*,2*R*)-1,2-diphenylcyclopropane-1-carboxylate

This compound was prepared according to the general procedure 3.1 for cyclopropanation reactions, using styrene (6.24 mmol, 650.0 mg, 2.32 equiv.) as the substrate, 2,2,2-trichloroethyl 2-diazo-2-phenylacetate (2.69 mmol, 789.6 mg, 1.0 equiv.) and Rh_2(*R*-*p*-Ph-TPCP)$_4$ catalyst (0.0000269 mmol, 0.0474 mg, 0.001 mol %). After flash chromatography (0%, then 5% - 15% Et_2O

in hexanes) the product was obtained as a white solid (885.2 mg, 89% yield).

^{1}H NMR (400 MHz, Chloroform-*d*) δ 7.17 – 7.10 (m, 3H), 7.07 (hept, *J* = 3.1 Hz, 5H), 6.80 (dd, *J* = 6.7, 3.0 Hz, 2H), 4.84 (d, *J* = 11.9 Hz, 1H), 4.64 (d, *J* = 11.9 Hz, 1H), 3.22 (dd, *J* = 9.4, 7.4 Hz, 1H), 2.28 (dd, *J* = 9.4, 5.1 Hz, 1H), 2.01 (dd, *J* = 7.4, 5.1 Hz, 1H).

^{13}C NMR (151 MHz, Chloroform-*d*) δ 172.26, 135.88, 133.81, 132.16, 128.26, 127.94, 127.83, 127.43, 126.73, 95.21, 74.51, 37.37, 33.99, 20.43.

Chiral HPLC: (OJ-H, 30 min, 1 mL/min, 1 % iPrOH in hexanes, UV 230 nm) tR: Major: 15.3 min, Minor: 9.0 min, 94% ee.

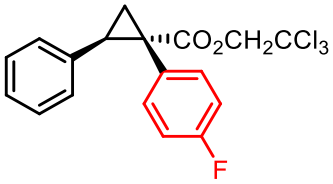

17

2,2,2-trichloroethyl (1*S*,2*R*)-1-(4-fluorophenyl)-2-phenylcyclopropane-1-carboxylate

This compound was prepared according to the general procedure 3.1 for cyclopropanation reactions, using styrene (6.24 mmol, 650.0 mg, 2.32 equiv.) as the substrate, 2,2,2-trichloroethyl 2-diazo-2-(4-fluorophenyl)acetate (2.69 mmol, 838.0 mg, 1.0 equiv.), and Rh_2(*R*-*p*-Ph-TPCP)$_4$ catalyst (0.0000269 mmol, 0.0474 mg, 0.001 mol %). After flash chromatography (0 %, then 5 % - 15 % Et_2O in hexanes) the product was obtained as a white solid (938 .5 mg, 90 % yield).

^{1}H NMR (400 MHz, Chloroform-*d*) δ 7.16 – 7.08 (m, 3H), 7.07 – 6.98 (m, 2H), 6.87 – 6.74 (m, 4H), 4.82 (d, *J* = 11.9 Hz, 1H), 4.65 (d, *J* = 11.9 Hz, 1H), 3.21 (dd, *J* = 9.4, 7.4 Hz, 1H), 2.29 (dd, *J* = 9.4, 5.2 Hz, 1H), 1.98 (dd, *J* = 7.4, 5.2 Hz, 1H).

^{13}C NMR (151 MHz, Chloroform-*d*) δ 172.08, 135.56, 133.77, 133.71, 129.78, 128.24, 128.08, 126.91, 114.91, 114.76, 95.13, 74.56, 36.57, 34.07, 20.55.

^{19}F NMR (376 MHz, Chloroform-*d*) δ -114.59.

Chiral HPLC: (OJ-H, 30 min, 1 mL/min, 1 % iPrOH in hexanes, UV 230 nm) tR: Major: 14.4 min, Minor: 8.8 min, 95% ee.

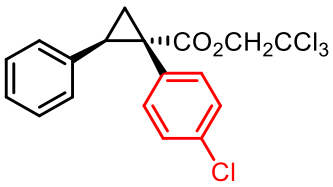

18

2,2,2-trichloroethyl (1*S*,2*R*)-1-(4-chlorophenyl)-2-phenylcyclopropane-1-carboxylate

This compound was prepared according to the general procedure 3.1 for cyclopropanation reactions, using styrene (6.24 mmol, 650.0 mg, 2.32 equiv.) as the substrate, 2,2,2-trichloroethyl 2-(4-chlorophenyl)-2-diazoacetate (2.69 mmol, 882.2 mg, 1.0 equiv.), and Rh_2(*R*-*p*-Ph-TPCP)$_4$ catalyst (0.0000269 mmol, 0.0474 mg, 0.001 mol %). After flash chromatography (0%, then 5% - 15% Et_2O in hexanes) the product was obtained as a white solid (967.5 mg, 89% yield).

^{1}H NMR (400 MHz, Chloroform-*d*) δ 7.17 – 7.06 (m, 5H), 7.04 – 6.95 (m, 2H), 6.80 (dd, *J* = 6.6, 3.0

Hz, 2H), 4.83 (d, *J* = 11.9 Hz, 1H), 4.64 (d, *J* = 11.9 Hz, 1H), 3.22 (dd, *J* = 9.4, 7.5 Hz, 1H), 2.29 (dd, *J* = 9.4, 5.2 Hz, 1H), 1.98 (dd, *J* = 7.5, 5.2 Hz, 1H).

^{13}C NMR (151 MHz, Chloroform-*d*) δ 171.83, 135.39, 133.44, 133.39, 132.55, 128.23, 128.16, 128.11, 127.00, 95.11, 74.55, 36.66, 34.12, 20.37.

Chiral HPLC: (OJ-H, 30 min, 1 mL/min, 1 % iPrOH in hexanes, UV 230 nm) tR: Major: 13.2 min, Minor: 8.3 min, 96% ee.

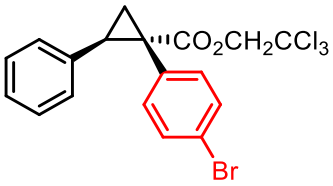

14

2,2,2-trichloroethyl (1*S*,2*R*)-1-(4-bromophenyl)-2-phenylcyclopropane-1-carboxylate

This compound was prepared according to the general procedure 3.1 for cyclopropanation reactions, using styrene (6.24 mmol, 650.0 mg, 2.32 equiv.) as the substrate, 2,2,2-trichloroethyl 2-(4-bromophenyl)-2-diazoacetate (2.69 mmol, 1000.0 mg, 1.0 equiv.) and Rh_2(*R*-*p*-Ph-TPCP)$_4$ catalyst (0.0000269 mmol, 0.0474 mg, 0.001 mol %). After flash chromatography (0%, then 5% - 15% Et_2O in hexanes) the product was obtained as a white solid (1110.0 mg, 90% yield).

^{1}H NMR (400 MHz, Chloroform-*d*) δ 7.28 – 7.24 (m, 3H), 7.16 – 7.05 (m, 2H), 6.98 – 6.86 (m, 2H), 6.86 – 6.75 (m, 2H), 4.83 (d, *J* = 11.9 Hz, 1H), 4.64 (d, *J* = 11.9 Hz, 1H), 3.22 (dd, *J* = 9.4, 7.5 Hz, 1H), 2.28 (dd, *J* = 9.4, 5.2 Hz, 1H), 1.97 (dd, *J* = 7.5, 5.2 Hz, 1H).

^{13}C NMR (151 MHz, Chloroform-*d*) δ 171.74, 135.35, 133.79, 133.07, 131.06, 128.23, 128.18, 127.02, 121.67, 95.10, 74.54, 36.74, 34.09, 20.32.

Chiral HPLC: (OJ-H, 30 min, 1 mL/min, 1 % iPrOH in hexanes, UV 230 nm) tR: Major:13.4 min, Minor: 8.8 min, 96% ee.

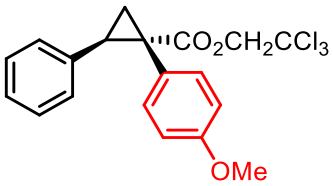

19

2,2,2-trichloroethyl (1*S*,2*R*)-1-(4-methoxyphenyl)-2-phenylcyclopropane-1-carboxylate

This compound was prepared according to the general procedure 3.1 for cyclopropanation reactions, using styrene (6.24 mmol, 650.0 mg, 2.32 equiv.) as the substrate, 2,2,2-trichloroethyl 2-diazo-2-(4-methoxyphenyl)acetate (2.69 mmol, 870.3 mg, 1.0 equiv), and Rh_2(*R*-*p*-Ph-TPCP)$_4$ catalyst (0.0000269 mmol, 0.0474 mg, 0.001 mol %). After flash chromatography (0%, then 5% - 15% Et_2O in hexanes) the product was obtained as a clear oil (967.6 mg, 90% yield).

^{1}H NMR (400 MHz, Chloroform-*d*) δ 7.15 – 7.05 (m, 3H), 7.05 – 6.95 (m, 2H), 6.88 – 6.78 (m, 2H), 6.73 – 6.63 (m, 2H), 4.86 (d, *J* = 11.9 Hz, 1H), 4.66 (d, *J* = 11.9 Hz, 1H), 3.72 (s, 3H), 3.20 (dd, *J* = 9.4, 7.4 Hz, 1H), 2.29 (dd, *J* = 9.4, 5.0 Hz, 1H), 1.97 (dd, *J* = 7.4, 5.0 Hz, 1H).

^{13}C NMR (151 MHz, Chloroform-*d*) δ 172.52, 158.82, 136.03, 133.21, 128.33, 127.99, 126.71,

125.94, 113.33, 95.33, 74.49, 55.25, 36.71, 34.07, 20.66.

Chiral HPLC: (*R,R*-Whelk , 45 min, 1 mL/min, 1 % iPrOH in hexanes, UV 230 nm) tR: Major: 30.3 min, Minor: 19.7 min, 94% ee.

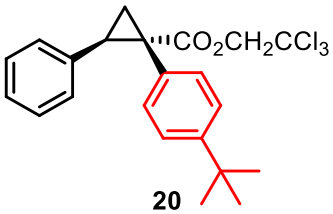

20

2,2,2-trichloroethyl (1*S*,2*R*)-1-(4-(*tert*-butyl)phenyl)-2-phenylcyclopropane-1-carboxylate

This compound was prepared according to the general procedure 3.1 for cyclopropanation reactions, using styrene (6.24 mmol, 650.0 mg, 2.32 equiv.) as the substrate, 2,2,2-trichloroethyl 2-(4-(tert-butyl)phenyl)-2-diazoacetate (2.69 mmol, 940.5 mg, 1.0 equiv.), and Rh_2(*R*-*p*-Ph-TPCP)$_4$ catalyst (0.0000269 mmol, 0.0474 mg, 0.001 mol %). After flash chromatography (0%, then 5% - 15% Et_2O in hexanes) the product was obtained as a white solid (1030.8 mg, 90 % yield).

^{1}H NMR (400 MHz, Chloroform-*d*) δ 7.18 – 7.10 (m, 2H), 7.07(dd, *J* =4.9, 1.8 Hz, 3H), 7.01 – 6.95 (m, 2H), 6.79(dtd, *J* = 4.9, 3.2, 2.7, 1.4 Hz, 2H), 4.84 (d, *J* = 11.9 Hz, 1H), 4.66 (d, *J* = 11.9 Hz, 1H), 3.20 (dd, *J* = 9.4, 7.4 Hz, 1H), 2.29 (dd, *J* = 9.4, 5.0 Hz, 1H), 1.98 (dd, *J* = 7.4, 5.1 Hz, 1H), 1.23 (s, 9H).

^{13}C NMR (151 MHz, Chloroform-*d*) δ 172.35, 150.27, 136.06, 131.70, 130.62, 128.25, 127.80, 126.59, 124.70, 95.29, 74.40, 37.01, 34.52, 33.87, 31.39, 20.49.

Chiral HPLC: (*R,R*-Whelk, 30 min, 1 mL/min, 1 % iPrOH in hexanes, UV 230 nm) tR: Major: 11.2min, Minor: 8.4 min, 98% ee.

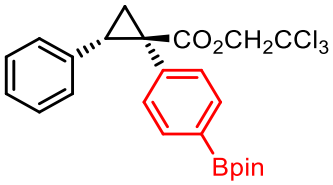

21

2,2,2-trichloroethyl(1*S*,2*R*)-2-phenyl-1-(4-(4,4,5,5-tetramethyl-1,3,2-dioxaborolan-2-yl)phenyl)cyclopropane-1-carboxylate

This compound was prepared according to the general procedure 3.1 for cyclopropanation reactions, using styrene (6.24 mmol, 650.0 mg, 2.32 equiv.) as the substrate, 2,2,2-trichloroethyl 2-diazo-2-(4-(4,4,5,5-tetramethyl-1,3,2-dioxaborolan-2-yl)phenyl)acetate (2.69 mmol, 1128.4 mg, 1.0 equiv), and Rh_2(*S*-p-Ph-TPCP)$_4$ catalyst (0.0000269 mmol, 0.0474 mg, 0.001 mol %). After flash chromatography (0%, then 5% - 15% Et_2O in hexanes) the product was obtained as a clear oil (1213.3 mg, 91 % yield).

^{1}H NMR (400 MHz, Chloroform-*d*) δ 7.64 – 7.52 (m, 2H), 7.14 – 7.03 (m, 5H), 6.88 – 6.74 (m, 2H), 4.86 (d, *J* = 11.9 Hz, 1H), 4.63 (d, *J* = 11.9 Hz, 1H), 3.23 (dd, *J* = 9.4, 7.5 Hz, 1H), 2.28 (dd, *J* = 9.4, 5.1 Hz, 1H), 2.02 (dd, *J* = 7.5, 5.1 Hz, 1H), 1.32 (s, 12H).

^{13}C NMR (151 MHz, Chloroform-*d*) δ 172.02, 136.90, 135.68, 134.29, 131.48, 128.24, 128.04, 126.78, 95.18, 83.85, 74.44, 37.43, 34.12, 25.04, 24.99, 20.32.

Chiral HPLC: (*S,S*-Whelk, 30 min, 1 mL/min, 1 % iPrOH in hexanes, UV 230 nm) tR: Major: 10.5 min, Minor: 12.8 min, 99% ee.

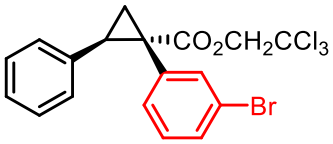

22

2,2,2-trichloroethyl (1*S*,2*R*)-1-(3-bromophenyl)-2-phenylcyclopropane-1-carboxylate

This compound was prepared according to the general procedure 3.1 for cyclopropanation reactions, using styrene (6.24 mmol, 650.0 mg, 2.32 equiv.) as the substrate, 2,2,2-trichloroethyl 2-(3-bromophenyl)-2-diazoacetate (2.69 mmol, 1000.0 mg, 1.0 equiv.) and Rh_2(*R*-*p*-Ph-TPCP)$_4$ catalyst (0.0000269 mmol, 0.0474 mg, 0.001 mol %). After flash chromatography (0%, then 5% - 15% Et_2O in hexanes) the product was obtained as a clear oil (1086.0 mg, 90% yield).

^{1}H NMR (400 MHz, Chloroform-*d*) δ 7.26(dt, *J* = 7.0, 1.7 Hz, 2H), 7.17-7.05 (m, 3H), 7.02 – 6.90 (m, 2H), 6.87– 6.78 (m, 2H), 4.84 (d, *J* = 11.9 Hz, 1H), 4.62 (d, *J* = 11.9 Hz, 1H), 3.22 (dd, *J* = 9.4, 7.5 Hz, 1H), 2.27 (dd, *J* = 9.4, 5.2 Hz, 1H), 2.00 (dd, *J* = 7.5, 5.3 Hz, 1H).

^{13}C NMR (151 MHz, Chloroform-*d*) δ 171.64, 136.25, 135.21, 135.09, 130.92, 130.59, 129.26, 128.23, 128.14, 127.06, 121.69, 95.07, 74.57, 36.83, 34.18, 20.21.

Chiral HPLC: (OJ-H, 30 min, 1 mL/min, 1 % iPrOH in hexanes, UV 230 nm) tR: Major: 14.4 min, Minor: 10.2 min, 92% ee.

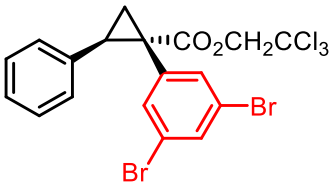

23

2,2,2-trichloroethyl (1*S*,2*R*)-1-(3,5-dibromophenyl)-2-phenylcyclopropane-1-carboxylate

This compound was prepared according to the general procedure 3.1 for cyclopropanation reactions, using styrene (6.24 mmol, 650.0 mg, 2.32 equiv.) as the substrate, 2,2,2-trichloroethyl 2-diazo-2-(3,5-dibromophenyl)acetate (2.69 mmol, 1214.1 mg, 1.0 equiv.), and Rh_2(*R*-*p*-Ph-TPCP)$_4$ catalyst (0.0000807 mmol, 0.1422 mg, 0.003 mol %). After flash chromatography (0%, then 5% - 15% Et_2O in hexanes) the product was obtained as a clear oil (567.5 mg, 40 % yield).

[a]$^{20}_D$ = -5° (c = 0.20, $CHCl_3$)

^{1}H NMR (400 MHz, Chloroform-*d*) δ 7.43 (t, *J* = 1.8 Hz, 1H), 7.21 – 7.05 (m, 5H), 6.85 (dd, *J* = 7.5, 2.1 Hz, 2H), 4.86 (d, *J* = 11.9 Hz, 1H), 4.62 (d, *J* = 11.9 Hz, 1H), 3.23 (dd, *J* = 9.5, 7.6 Hz, 1H), 2.27 (dd, *J* = 9.4, 5.4 Hz, 1H), 2.00 (dd, *J* = 7.5, 5.4 Hz, 1H).

^{13}C NMR (151 MHz, Chloroform-*d*) δ 171.10, 137.96, 134.63, 134.02, 133.20, 128.36, 128.21, 127.43, 122.04, 94.97, 74.66, 36.40, 34.41, 20.00.

IR(neat): 3029, 2970, 1736, 1585, 1552, 1498, 1365, 1235, 1156, 1113, 860, 814, 698 cm^{-1}

HR-MS： (+p APCI) calcd for [C18H13Br2Cl3O2+] 523.8348 found 523.83376

Chiral HPLC: (OD-H, 30 min, 1 mL/min, 1 % iPrOH in hexanes, UV 230 nm) tR: Major: 9.7 min, Minor: 9.0 min, 94% ee.

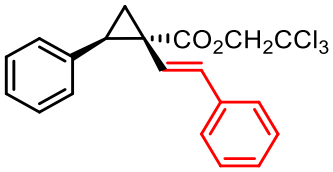

24

2,2,2-trichloroethyl (1*R*,2*R*)-2-phenyl-1-((E)-styryl)cyclopropane-1-carboxylate

This compound was prepared according to the general procedure 3.1 for cyclopropanation reactions, using styrene (6.24 mmol, 650.0 mg, 2.32 equiv.) as the substrate, 2,2,2-trichloroethyl (E)-2-diazo-4-phenylbut-3-enoate (2.69mmol, 859.6 mg, 1.0 equiv.), and Rh_2(*R*-*p*-Ph-TPCP)$_4$ catalyst (0.0000807 mmol, 0.1422 mg, 0.003 mol %) at 25°C. After flash chromatography (0 %, then 5 % - 15 % Et_2O in hexanes) the product was obtained as a white solid (936.7 mg, 88 % yield).

MP: 71 – 72 °C

[a]$^{20}_{D}$ = +73° (c = 0.10, $CHCl_3$)

^{1}H NMR (400 MHz, Chloroform-*d*) δ 7.36 – 7.05 (m, 10H), 6.45 (d, *J* = 16.1 Hz, 1H), 6.19 (d, *J* = 16.2 Hz, 1H), 4.87 (qd, *J* = 12.2, 2.2 Hz, 2H), 3.20 (dd, *J* = 9.2, 7.4 Hz, 1H), 2.22 (dd, *J* = 9.3, 5.2 Hz, 1H), 1.97 (dd, *J* = 7.5, 5.2 Hz, 1H).

^{13}C NMR (151 MHz, Chloroform-*d*) δ 172.03, 137.08, 135.10, 133.73, 129.34, 128.53, 128.26, 127.56, 127.20, 126.39, 123.17, 95.26, 74.47, 35.94, 33.04, 19.19.

IR(neat):3027, 2924, 1732, 1602, 1500, 1455, 1377, 1312, 1243, 1208, 1149, 1128, 1109, 1092, 1053, 975, 953, 897, 857, 813, 773, 747, 710, 694, 576, 477 cm^{-1}

HR-MS： (+p APCI) calcd for [C20H17Cl3O2+H] 395.0367 found 395.03652

Chiral HPLC: (ADH, 30 min, 1 mL/min, 1 % iPrOH in hexanes, UV 230 nm) tR: Major: 10.3 min, Minor: 8.8min, 96% ee.

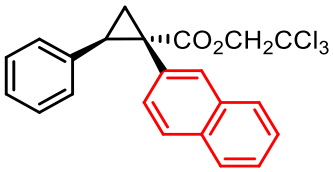

25

2,2,2-trichloroethyl (1*S*,2*R*)-1-(naphthalen-2-yl)-2-phenylcyclopropane-1-carboxylate

This compound was prepared according to the general procedure 3.1 for cyclopropanation reactions, using styrene (6.24 mmol, 650.0 mg, 2.32 equiv.) as the substrate, 2,2,2-trichloroethyl 2-diazo-2-(naphthalen-2-yl)acetate (2.69 mmol, 924.2 mg, 1.0 equiv.), and Rh_2(*R*-*p*-Ph-TPCP)$_4$ catalyst (0.0000807 mmol, 0.1422 mg, 0.003 mol %). After flash chromatography (0 %, then 5 % - 15 % Et_2O in hexanes) the product was obtained as a white solid (745.2 mg, 66 % yield).

MP: 127 – 128 °C

[a]$^{20}_{D}$ = -81.3° (c = 0.10, $CHCl_3$)

^{1}H NMR (400 MHz, Chloroform-*d*) δ 7.77 – 7.68 (m, 2H), 7.66 (d, *J* = 1.7 Hz, 1H), 7.55 (d, *J* = 8.5 Hz, 1H), 7.45 – 7.37 (m, 2H), 7.11 (dd, *J* = 8.5, 1.8 Hz, 1H), 7.06 – 6.96 (m, 3H), 6.88 – 6.80 (m, 2H), 4.89 (d, *J* = 11.9 Hz, 1H), 4.63 (d, *J* = 11.9 Hz, 1H), 3.30 (dd, *J* = 9.4, 7.4 Hz, 1H), 2.38 (dd, *J* = 9.4, 5.1 Hz, 1H), 2.16 (dd, *J* = 7.4, 5.1 Hz, 1H).

^{13}C NMR (151 MHz, Chloroform-*d*) δ 172.26, 135.66, 133.11, 132.72, 131.69, 130.87, 130.21, 128.26, 128.01, 127.91, 127.71, 127.25, 126.78, 126.04, 125.84, 95.20, 74.48, 37.49, 34.19, 20.52.

IR(neat):3057, 2924, 1732, 1602, 1500, 1455, 1377, 1312, 1243, 1208, 1149, 1128, 1109, 1092, 1053, 975, 953, 897, 857, 813, 773, 747, 710, 694, 576, 477 cm^{-1}

HR-MS： (+p APCI) calcd for [C22H17Cl3O2+H] 419.0367 found 419.03622

Chiral HPLC: (ADH, 30min, 1 mL/min, 1 % iPrOH in hexanes, UV 230 nm) tR: Major: 11.6 min, Minor: 10.1 min, 96% ee.

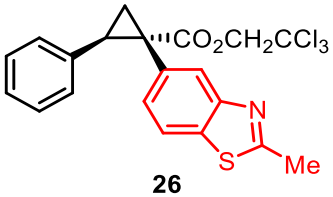

26

2,2,2-trichloroethyl(1*S*,2*R*)-1-(2-methylbenzo[d]thiazol-5-yl)-2-phenylcyclopropane-1-carboxylate

This compound was prepared according to the general 3.1 procedure for cyclopropanation reactions, using styrene (6.24 mmol, 650.0 mg, 2.32 equiv.) as the substrate, 2,2,2-trichloroethyl 2-diazo-2-(naphthalen-2-yl)acetate (2.69 mmol, 980.8 mg, 1.0 equiv.), and Rh_2(*R*-*p*-Ph-TPCP)$_4$ catalyst (0.0000807 mmol, 0.1422 mg, 0.003 mol %). After flash chromatography (0%, then 5% - 15% Et_2O in hexanes) the product was obtained as a clear oil (1031.5 mg, 87 % yield).

^{1}H NMR (400 MHz, Chloroform-*d*) δ 7.77 (d, *J* = 1.7 Hz, 1H), 7.51 (d, *J* = 8.3 Hz, 1H), 7.09 – 6.99 (m, 3H), 6.98 (dd, *J* = 8.3, 1.7 Hz, 1H), 6.86 – 6.77 (m, 2H), 4.85 (d, *J* = 11.9 Hz, 1H), 4.65 (d, *J* = 11.9 Hz, 1H), 3.29 (dd, *J* = 9.4, 7.4 Hz, 1H), 2.78 (s, 3H), 2.35 (dd, *J* = 9.4, 5.2 Hz, 1H), 2.11 (dd, *J* = 7.5, 5.2 Hz, 1H).

^{13}C NMR (151 MHz, Chloroform-*d*) δ 172.04, 167.22, 153.26, 135.48, 134.77, 132.16, 129.23, 128.22, 128.03, 126.80, 125.49, 120.54, 95.12, 74.47, 37.27, 34.19, 20.50, 20.21.

Chiral HPLC: (OJ-H, 30 min, 1 mL/min, 1 % iPrOH in hexanes, UV 230 nm) tR: Major: 21.8min, Minor: 15.8 min, 86% ee.

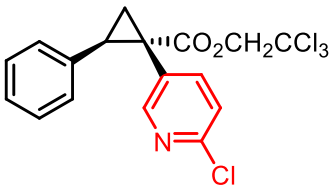

27

2,2,2-trichloroethyl (1*S*,2*R*)-1-(6-chloropyridin-3-yl)-2-phenylcyclopropane-1-carboxylate

This compound was prepared according to the general procedure 3.1 for cyclopropanation reactions, using styrene (6.24 mmol, 650.0 mg, 2.32 equiv.) as the substrate, 2,2,2-trichloroethyl 2-(6-chloropyridin-3-yl)-2-diazoacetate (2.69 mmol, 884.9 mg, 1.0 equiv.), and Rh_2(*R*-*p*-Ph-TPCP)$_4$

catalyst (0.0000269 mmol, 0.0474 mg, 0.001 mol %). After flash chromatography (0%, then 5% - 10% EtOAC in hexanes) the product was obtained as a slight yellow oil (708.3 mg, 65 % yield).

^{1}H NMR (400 MHz, Chloroform-*d*) δ 8.17-8.11 (m, 1H),7.30-7.23 ppm (m, 1H), 7.14 (dd, *J* = 4.9, 1.9 Hz, 3H), 7.06 (d, *J* = 8.3 Hz, 1H), 6.83 (dd, *J* = 6.7, 2.9 Hz, 2H), 4.84 (d, *J* = 11.9 Hz, 1H), 4.65 (d, *J* = 11.9 Hz, 1H), 3.27 (dd, *J* = 9.5, 7.5 Hz, 1H), 2.35 (dd, *J* = 9.4, 5.4 Hz, 1H), 2.05 (dd, *J* = 7.5, 5.4 Hz, 1H).

^{13}C NMR (151 MHz, Chloroform-*d*) δ 171.03, 152.54, 150.53, 142.52, 134.40, 129.25, 128.54, 128.25, 127.53, 123.40, 94.90, 74.68, 34.06, 34.00, 19.65.

Chiral HPLC: (OJ-H, 30 min, 1 mL/min, 1 % iPrOH in hexanes, UV 230 nm) tR: Major: 25.2 min, Minor: 21.9 min, 94% ee.

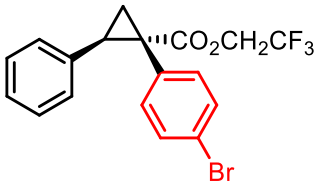

28

2,2,2-trifluoroethyl (1*S*,2*R*)-1-(4-bromophenyl)-2-phenylcyclopropane-1-carboxylate

This compound was prepared according to the general procedure 3.1 for cyclopropanation reactions, using styrene (6.24 mmol, 650.0 mg, 2.32 equiv.) as the substrate and 2,2,2-trifluoroethyl 2-(4-bromophenyl)-2-diazoacetate (2.69 mmol, 869.1 mg, 1.0 equiv.) under the catalysis of Rh_2(*R*-*p*-Ph-TPCP)$_4$ (0.0000269 mmol, 0.0474 mg, 0.001 mol%). After flash chromatography (0%, then 5% - 15% Et_2O in hexanes) the product was obtained as a clear oil (923.5 mg, 86 % yield).

^{1}H NMR (400 MHz, Chloroform-*d*) δ 7.31 – 7.22 (m, 3H), 7.20 – 7.03 (m, 3H), 6.93 – 6.85 (m, 2H), 6.79 (dd, *J* = 6.7, 3.0 Hz, 2H), 4.54 (dq, *J* = 12.7, 8.4 Hz, 1H), 4.40 (dq, *J* = 12.6, 8.3 Hz, 1H), 3.17 (dd, *J* = 9.4, 7.5 Hz, 1H), 2.22 (dd, *J* = 9.4, 5.2 Hz, 1H), 1.96 (dd, *J* = 7.5, 5.2 Hz, 1H).

^{13}C NMR (151 MHz, Chloroform-*d*) δ 171.87, 135.21, 133.61, 132.98, 131.17, 128.22, 128.18, 127.06, 121.75, 61.20, 60.96, 36.52, 34.06, 20.56.

^{19}F NMR (376 MHz, Chloroform-*d*) δ -73.92, -73.94, -73.96.

Chiral HPLC: (OJ-H, 30 min, 1 mL/min, 1 % iPrOH in hexanes, UV 230 nm) tR: Major: 16.7 min, Minor: 9.6 min, 96% ee.

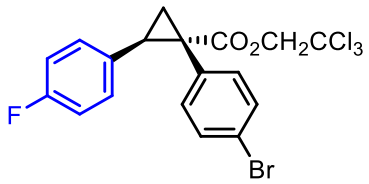

29

2,2,2-trichloroethyl (1*S*,2*R*)-1-(4-bromophenyl)-2-(4-fluorophenyl)cyclopropane-1-carboxylate

This compound was prepared according to the general procedure 3.1 for cyclopropanation reactions, using 1-fluoro-4-vinylbenzene (6.24 mmol, 762.3 mg, 2.32 equiv.) as the substrate, 2,2,2-trichloroethyl 2-(4-bromophenyl)-2-diazoacetate (2.69 mmol, 1000.0 mg, 1.0 equiv.), and

Rh_2(*R*-*p*-Ph-TPCP)$_4$ catalyst (0.0000269 mmol, 0.0474 mg, 0.001 mol %). After flash chromatography (0%, then 5% - 15% Et_2O in hexanes) the product was obtained as a white solid (1154.6 mg, 92 % yield).

[α]$^{20}_D$: -10° (c=0.10, $CHCl_3$).

MP: 106 – 108 °C

^{1}H NMR (400 MHz, Chloroform-*d*) δ 7.33 – 7.22 (m, 3H), 6.98 – 6.89 (m, 2H), 6.85 – 6.72 (m, 4H), 4.83 (d, *J* = 11.9 Hz, 1H), 4.64 (d, *J* = 11.9 Hz, 1H), 3.20 (dd, *J* = 9.4, 7.4 Hz, 1H), 2.28 (dd, *J* = 9.5, 5.3 Hz, 1H), 1.92 (dd, *J* = 7.4, 5.3 Hz, 1H).

^{13}C NMR (151 MHz, Chloroform-*d*) δ 171.59, 133.74, 132.85, 131.18, 131.10, 129.69, 129.63, 121.80, 115.24, 115.09, 95.06, 74.56, 36.60, 33.29, 20.44.

^{19}F NMR (376 MHz, Chloroform-*d*) δ -115.40.

IR(neat): 2954, 1733, 1607, 1513, 1490, 1395, 1375, 1239, 1152, 1011, 838, 716, 575 cm^{-1}

HR-MS： (+p APCI) calcd for [C18H13BrCl3FO2+H] 464.9221 found 464.92158

Chiral HPLC: (OJ-H, 30 min, 1 mL/min, 1 % iPrOH in hexanes, UV 230 nm) tR: Major: 17.8 min, Minor: 10.6 min, 96% ee.

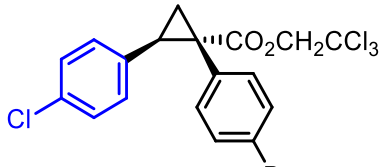

30

2,2,2-trichloroethyl (1*S*,2*R*)-1-(4-bromophenyl)-2-(4-chlorophenyl)cyclopropane-1-carboxylate

This compound was prepared according to the general procedure 3.1 for cyclopropanation reactions, using 1-chloro-4-vinylbenzene (6.24 mmol, 864.9 mg , 2.32 equiv.) as the substrate, 2,2,2-trichloroethyl 2-(4-bromophenyl)-2-diazoacetate (2.69 mmol, 1000 mg, 1.0 equiv.), and Rh_2(*R*-*p*-Ph-TPCP)$_4$ catalyst (0.0000269 mmol, 0.0474 mg, 0.001 mol %). After flash chromatography (0%, then 5% - 15% Et_2O in hexanes) the product was obtained as a white solid. (1195.3 mg, 92 % yield).

^{1}H NMR (400 MHz, Chloroform-*d*) δ 7.31 – 7.26 (m, 2H), 6.96 – 6.90 (m, 2H), 6.85 – 6.77 (m, 2H), 6.77 (dd, *J* = 8.5, 5.6 Hz, 2H), 4.83 (d, *J* = 11.9 Hz, 1H), 4.64 (dd, *J* = 11.9, 0.6 Hz, 1H), 3.20 (dd, *J* = 9.4, 7.4 Hz, 1H), 2.28 (dd, *J* = 9.4, 5.3 Hz, 1H), 1.92 (dd, *J* = 7.4, 5.3 Hz, 1H).

^{13}C NMR (151 MHz, Chloroform-*d*) δ 171.59, 133.73, 132.85, 131.18, 131.10, 129.68, 129.63, 121.80, 115.23, 115.09, 95.06, 74.54, 36.59, 33.28, 20.42.

Chiral HPLC: (OJ-H, 30 min, 1 mL/min, 1 % iPrOH in hexanes, UV 230 nm) tR: Major:25.1 min, Minor: 14.1 min, 96% ee.

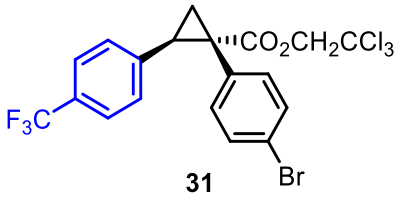

31

2,2,2-trichloroethyl(1*S*,2*R*)-1-(4-bromophenyl)-2-(4-(trifluoromethyl)phenyl)cyclopropane-1-carboxylate

This compound was prepared according to the general procedure 3.1 for cyclopropanation reactions, using 1-(trifluoromethyl)-4-vinylbenzene (6.24 mmol, 1074.4 mg, 2.32 equiv.) as the substrate, 2,2,2-trichloroethyl 2-(4-bromophenyl)-2-diazoacetate (2.69 mmol, 1000 mg, 1.0 equiv.), and Rh_2(*R*-*p*-Ph-TPCP)$_4$ catalyst (0.0000269 mmol, 0.0474 mg, 0.001 mol %). After flash chromatography (0 %, then 5 % - 15 % Et_2O in hexanes) the product was obtained as a white solid (1250.6 mg, 90% yield).

MP: 98 - 100 °C

[a]$^{20}_{D}$ = -13° (c = 0.10, $CHCl_3$)

^{1}H NMR (400 MHz, Chloroform-*d*) δ 7.37 (d, *J* = 8.1 Hz, 2H), 7.33 – 7.28 (m, 2H), 6.98 – 6.84 (m, 4H), 4.83 (d, *J* = 11.9 Hz, 1H), 4.64 (d, *J* = 11.9 Hz, 1H), 3.24 (dd, *J* = 9.4, 7.4 Hz, 1H), 2.33 (dd, *J* = 9.4, 5.3 Hz, 1H), 1.99 (dd, *J* = 7.4, 5.3 Hz, 1H).

^{13}C NMR (151 MHz, Chloroform-*d*) δ 171.36, 139.81, 133.64, 132.40, 131.36, 128.46, 125.14, 125.11, 125.09, 122.09, 94.97, 74.64, 37.23, 33.31, 20.75.

^{19}F NMR (376 MHz, $cdcl_3$) δ -62.51.

IR(neat): 2955, 1735, 1620, 1489, 1323, 1239, 1154, 1115, 1067, 1011, 927, 842, 764, 715, 573, 509 cm^{-1}

HR-MS： (+p APCI) calcd for [C19H13BrCl3F3O2+] 513.9111 found 513.91045

Chiral HPLC: (OJ-H, 30 min, 1 mL/min, 1 % iPrOH in hexanes, UV 230 nm) tR: Major:21.7 min, Minor: 12.0 min, 97% ee.

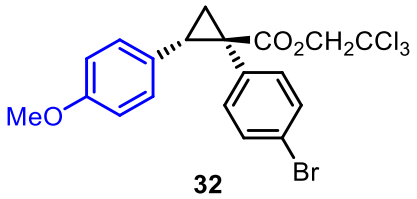

32

2,2,2-trichloroethyl(1*S*,2*R*)-1-(4-bromophenyl)-2-(4-methoxyphenyl)cyclopropane-1-carboxylate

This compound was prepared according to the general procedure for cyclopropanation reactions, using 1-methoxy-4-vinylbenzene (6.24 mmol, 837.4 mg, 2.32 equiv.) as the substrate, 2,2,2-trichloroethyl 2-(4-bromophenyl)-2-diazoacetate (2.69 mmol, 1000 mg, 1.0 equiv), and Rh_2(*S*-p-Ph-TPCP)$_4$ catalyst (0.0000269 mmol, 0.0474 mg, 0.001 mol %). After flash chromatography (0 %, then 5 % - 15 % Et_2O in hexanes) the product was obtained as a clear oil (1158.7 mg, 90 % yield).

^{1}H NMR (400 MHz, Chloroform-*d*) δ 7.29 – 7.22 (m, 2H), 6.97 – 6.87 (m, 2H), 6.70 (d, *J* = 8.7 Hz, 2H) 6.71-6.59 (m, 2H), 4.81 (dd, *J* = 11.9, 0.8 Hz, 1H), 4.61 (dd, *J* = 12.0, 0.8 Hz, 1H), 3.71 (s, 3H), 3.15 (dd, *J* = 9.5, 7.5 Hz, 1H), 2.25 (ddd, *J* = 9.4, 5.2, 0.8 Hz, 1H), 1.88 (dd, *J* = 7.5, 5.2 Hz, 1H).

^{13}C NMR (151 MHz, Chloroform-*d*) δ 171.79, 158.62, 133.84, 133.25, 131.05, 129.24, 127.27, 121.59, 113.64, 95.14, 74.49, 55.29, 36.45, 33.74, 20.40.

Chiral HPLC: (*S,S*-Whelk, 30 min, 1 mL/min, 1 % iPrOH in hexanes, UV 230 nm) tR: Major: 15.0min, Minor: 18.4 min, 97% ee.

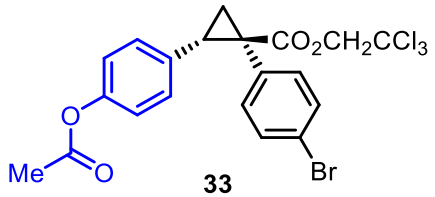

33

2,2,2-trichloroethyl (1*S*,2*R*)-2-(4-acetoxyphenyl)-1-(4-bromophenyl)cyclopropane-1-carboxylate

This compound was prepared according to the general procedure for cyclopropanation reactions, using 4-vinylphenyl acetate (6.24 mmol, 1012.2 mg, 2.32 equiv.) as the substrate, 2,2,2-trichloroethyl 2-(4-bromophenyl)-2-diazoacetate (2.69 mmol, 1000 mg, 1.0 equiv.), and Rh_2(*S*-p-Ph-TPCP)$_4$ catalyst (0.0000269 mmol, 0.0474 mg, 0.001 mol %). After flash chromatography (0 %, then 5 % - 15 % Et_2O in hexanes) the product was obtained as a white solid (695.0 mg, 51 % yield).

MP: 95 - 98 °C

[a]$^{20}_{D}$ = -9.2° (c = 1.00, $CHCl_3$)

^{1}H NMR (400 MHz, Chloroform-*d*) δ 7.32 – 7.23 (m, 2H), 6.98 – 6.90 (m, 2H), 6.89 – 6.82 (m, 2H), 6.82 – 6.76 (m, 2H), 4.83 (d, *J* = 11.9 Hz, 1H), 4.63 (d, *J* = 12.0 Hz, 1H), 3.20 (dd, *J* = 9.5, 7.4 Hz, 1H), 2.29 (dd, *J* = 9.5, 5.2 Hz, 1H), 2.24 (s, 3H), 1.92 (dd, *J* = 7.4, 5.3 Hz, 1H).

^{13}C NMR (151 MHz, Chloroform-*d*) δ 171.60, 169.35, 149.63, 133.77, 133.00, 132.84, 131.17, 129.10, 121.81, 121.27, 95.05, 74.54, 36.71, 33.43, 21.24, 20.64.

IR(neat): 3041, 1757, 1630, 1505, 1367, 1186, 1163, 1108, 1012, 907, 850, 626, 490 cm^{-1}

HR-MS： (+p APCI) calcd for [C20H16BrCl3O4+]503.9298 found 503.92901

Chiral HPLC: (ADH, 40 min, 1 mL/min, 1 % iPrOH in hexanes, UV 230 nm) tR: Major: 24.0 min, Minor: 30.0 min, 90% ee.

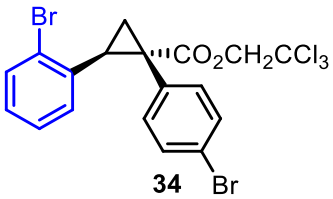

34

2,2,2-trichloroethyl (1*S*,2*S*)-2-(2-bromophenyl)-1-(4-bromophenyl)cyclopropane-1-carboxylate

This compound was prepared according to the general procedure for cyclopropanation reactions, using 1-bromo-2-vinylbenzene (6.24 mmol, 1142.4 mg, 2.32 equiv.) as the substrate, 2,2,2-trichloroethyl 2-(4-bromophenyl)-2-diazoacetate (2.69 mmol, 1000 mg, 1.0 equiv.), and Rh_2(*R*-*p*-Ph-TPCP)$_4$ catalyst (0.0000269 mmol, 0.0474 mg, 0.001 mol %). After flash chromatography (0%, then 5% - 15% Et2O in hexanes) the product was obtained as a clear oil (993.2 mg, 70 % yield).

[a]$^{20}_{D}$ = +4.0° (c = 0.03, $CHCl_3$)

^{1}H NMR (400 MHz, Chloroform-*d*) δ 7.57 – 7.43 (m, 1H), 7.25 – 7.18 (m, 2H), 7.10 – 7.02 (m, 2H), 7.02 – 6.90 (m, 2H), 6.65 – 6.48 (m, 1H), 4.90 (d, *J* = 11.9 Hz, 1H), 4.65 (d, *J* = 11.9 Hz, 1H), 3.47 (dd, *J* = 9.2, 7.7 Hz, 1H), 2.26 (dd, *J* = 9.2, 5.3 Hz, 1H), 2.12 (dd, *J* = 7.7, 5.3 Hz, 1H).

^{13}C NMR (151 MHz, Chloroform-*d*) δ 171.42, 135.01, 133.16, 133.01, 132.72, 131.03, 128.73, 127.85, 127.22, 127.20, 121.69, 95.01, 74.61, 35.90, 35.00, 18.98.

IR(neat):2952, 1735, 1592, 1469, 1439, 1376, 1242, 1206, 1156, 1125, 1090, 1073, 1059, 1045,

1011, 969, 827, 768, 718, 575, 515 cm^{-1}

HR-MS： (+p APCI) calcd for [C18H13Br2Cl3O2+H] 524.8421 found 524.84200

Chiral HPLC: (OD-H, 30 min, 1 mL/min, 1 % iPrOH in hexanes, UV 230 nm) tR: Major: 17.3 min, Minor: 11.9 min, 96% ee.

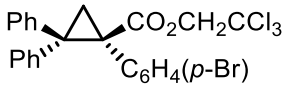

36

2,2,2-trichloroethyl (*R*)-1-(4-bromophenyl)-2,2-diphenylcyclopropane-1-carboxylate

This compound was prepared according to the general procedure for cyclopropanation reactions, using 1,1-diphenylethylene (6.24 mmol, 1124.9 mg, 2.32 equiv.) as the substrate, 2,2,2-trichloroethyl 2-(4-bromophenyl)-2-diazoacetate (2.69 mmol, 1000 mg, 1.0 equiv.), and Rh_2(*R*-PTAD)$_4$ catalyst(0.0000269 mmol, 0.0419 mg, 0.001 mol %). After flash chromatography (0 %, then 5 % - 15 % Et_2O in hexanes) the product was obtained as a clear oil (1242.0 mg, 88 % yield).

^{1}H NMR (400 MHz, Chloroform-*d*) δ 7.58 – 7.52 (m, 2H), 7.37 – 7.23 (m, 7H), 7.11 – 6.95 (m, 5H), 4.54 (d, *J* = 11.8 Hz, 1H), 4.15 (d, *J* = 11.9 Hz, 1H), 2.78 (d, *J* = 5.7 Hz, 1H), 2.52 (d, *J* = 5.7 Hz, 1H).

^{13}C NMR (151 MHz, Chloroform-*d*) δ 169.19, 134.05, 133.70, 130.86, 130.10, 128.80, 128.74, 128.04, 127.49, 126.77, 121.59, 94.42, 75.37, 45.77, 42.28, 23.10.

Chiral UHPLC: (IAU, 6 min, 0.500 mL/min, 1.0 % iPrOH in hexanes, UV 230 nm) tR: Major: 5.1 min, Minor: 3.3 min, 94% ee.

(Rh_2(*R*-*p*-Ph-TPCP)$_4$ as catalyst: AD-H, 30 min, 1 mL/min, 1 % iPrOH in hexanes, UV 230 nm) tR: Major: 10.5 min, Minor: 18.8 min, -48% ee)

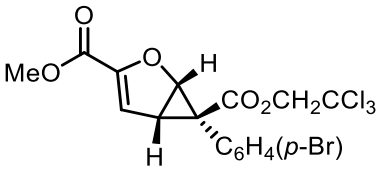

38

3-methyl 6-(2,2,2-trichloroethyl) (1*S*,5*S*,6*R*)-6-(4-bromophenyl)-2-oxabicyclo[3.1.0]hex-3-ene-3,6-dicarboxylate

This compound was prepared according to the general procedure 3.1 for cyclopropanation reactions, using methyl furan-2-carboxylate (6.24 mmol, 787.0 mg, 2.32 equiv.) as the substrate, 2,2,2-trichloroethyl 2-(4-bromophenyl)-2-diazoacetate (2.69 mmol, 1000 mg, 1.0 equiv.), and $Rh_{2(}$*R*-TCPTAD)$_4$ catalyst (0.0000269 mmol, 0.0568 mg, 0.001 mol %). After flash chromatography ((silica gel, hexanes/EtOAc = 50:1, 25:1, 15:1, 3:1) the product was obtained as a yellow oil (784.7 mg, 62 % yield).

[a]$^{20}_D$ = -39.8° (c = 1.5, $CHCl_3$)

^{1}H NMR (600 MHz, Chloroform-*d*) δ 7.39 (d, *J* = 8.0 Hz, 1H), 7.11 (d, *J* = 8.0 Hz, 1H), 6.13 (d, *J* = 3.0 Hz, 1H), 5.33 (d, *J* = 5.2 Hz, 1H), 4.75 – 4.70 (m, 1H), 4.66 – 4.61 (m, 1H), 3.64 (d, *J* = 2.3 Hz, 3H), 3.50 (dd, *J* = 5.4, 2.9 Hz, 1H).

^{13}C NMR (151 MHz, Chloroform-*d*) δ 170.49, 158.61, 149.58, 134.02, 131.49, 127.87, 122.32, 113.45, 94.71, 74.40, 71.22, 52.35, 40.22, 28.08.

IR (neat): 2954, 2257, 1727, 1611, 1490, 1438, 1396, 1338, 1264, 1226, 1208, 1115, 1040, 1012, 952, 906, 793, 725, 576, 524 cm^{-1}

HR-MS: (NSI) *m/z*: calculated for C16H13BrCl3O5H+ 468.9012, observed 468.9015.

Chiral UHPLC: (IAU, 15 min, 0.500 mL/min, 5.0 % iPrOH in hexanes, UV 230 nm) tR: Major: 4.8 min, Minor: 9.1 min, 90% ee.

(Rh_2(*R*-*p*-Ph-TPCP)$_4$ as catalyst: OD-H, 40 min, 1 mL/min, 3 % iPrOH in hexanes, UV 230 nm) tR: Major: 25.7 min, Minor: 14.2 min, -50% ee)

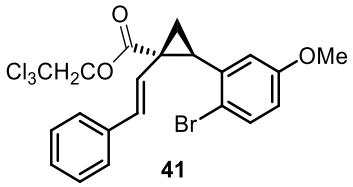

41

2,2,2-trichloroethyl (1*S*,2*R*)-2-(2-bromo-5-methoxyphenyl)-1-styrylcyclopropane-1-carboxylate

This compound was prepared according to the general procedure 3.1 for cyclopropanation reactions, using 1-bromo-4-methoxy-2-vinylbenzene (6.24 mmol, 1329.7 mg, 2.32 equiv.) as the substrate, 2,2,2-trichloroethyl (1S, 2R)-2-diazo-4-phenylbut-3-enoate (2.69 mmol, 859.6 mg, 1.0 equiv.), and Rh_2(*R*-*p*-Ph-TPCP)$_4$ catalyst (0.0000269 mmol, 0.0474 mg, 0.001 mol%) at 25 °C. After flash chromatography (0%, then 5% - 15% Et2O in hexanes) the product was obtained as a white solid (977.4 mg, 72% yield).

MP: 98 - 99 °C

$[a]^{20}_{D}$ = -52.4° (c = 0.10, $CHCl_3$)

^{1}H NMR (400 MHz, Chloroform-*d*) δ 7.40 (d, *J* = 8.7 Hz, 1H), 7.24 – 7.09 (m, 5H), 6.72 – 6.59 (m, 2H), 6.34 (d, *J* = 16.1Hz, 1H), 6.24 (d, *J* = 16.1Hz, 1H), 4.91 (d, *J* = 11.9 Hz, 1H), 4.81 (d, *J* = 11.9 Hz, 1H), 3.72 (s, 3H), 3.22 – 3.08 (m, 1H), 2.28 – 2.11 (m, 1H), 1.94 (dd, *J* = 7.6, 5.3 Hz, 1H).

^{13}C NMR (151 MHz, Chloroform-*d*) δ 171.84, 158.80, 137.05, 136.45, 132.99, 132.43, 128.50, 127.51, 126.42, 122.50, 117.81, 116.91, 113.95, 95.13, 74.60, 55.59, 37.58, 32.42, 19.06.

IR(neat):3024, 2954, 2836, 1734, 1596, 1571, 1472, 1449, 1419, 1375, 1294, 1274, 1228, 1195, 1169, 1137,1097, 1064, 1016, 961, 804, 787, 751, 730, 716, 693, 604, 576 cm^{-1}

HR-MS： (+p APCI) calcd for [C21H18BrCl3O3+H] 502.9578 found 502.95765

Chiral HPLC: (*R,R*-Whelk, 35 min, 1mL/min, 1 % iPrOH in hexanes, UV 230 nm) tR: Major: 24.8 min, Minor: 23.0 min.

4. HPLC Chromatograms

4.1 HPLC Chromatograms of High-throughput experiment

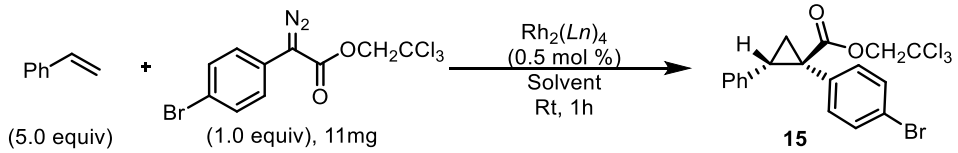

Racemic cyclopropane 15:

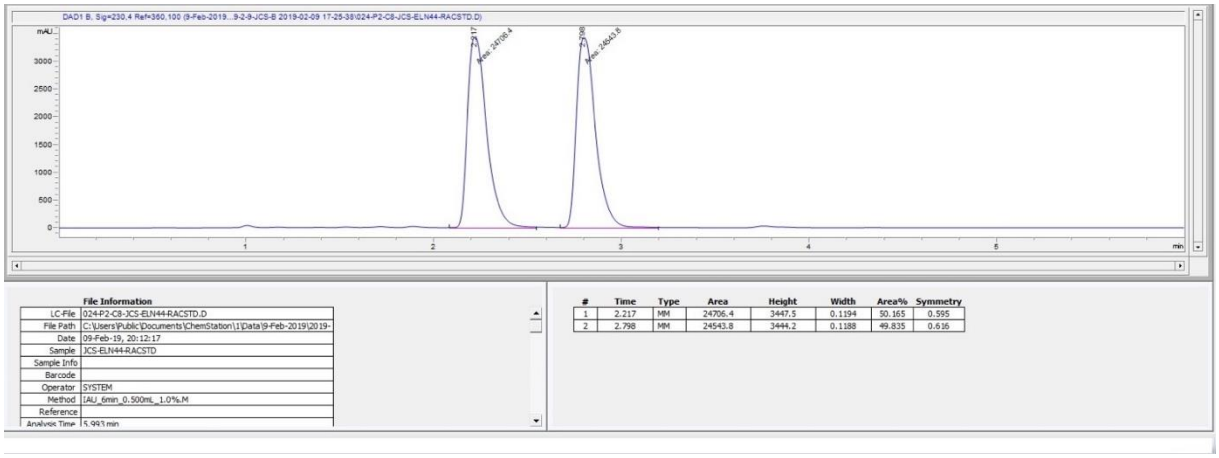

Results for dichloromethane (DCM) solvent:

15 prepared with Rh_2(*S*-DOSP)$_4$

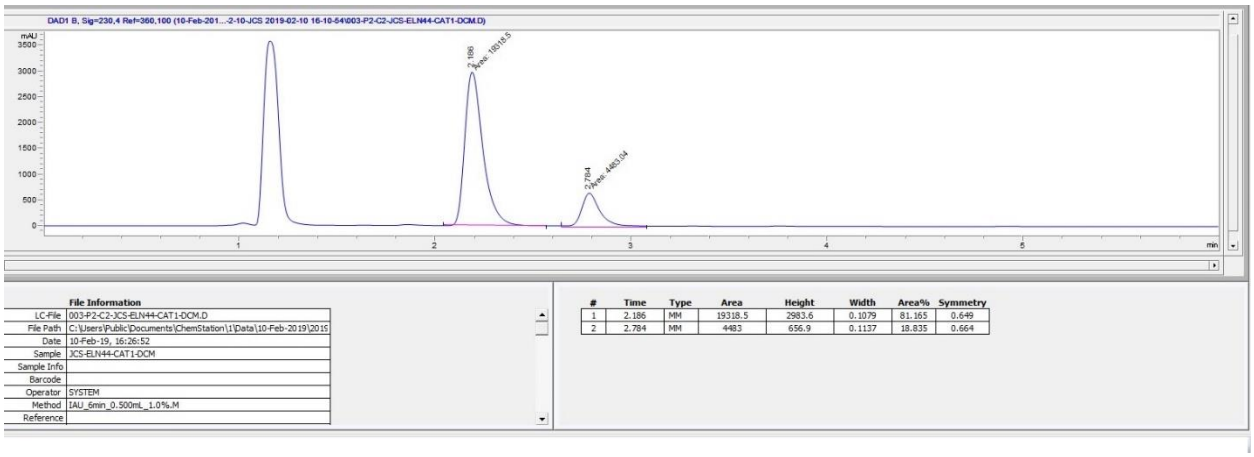

15 prepared with Rh_2(*S*-*p*-Br-TPCP)$_4$

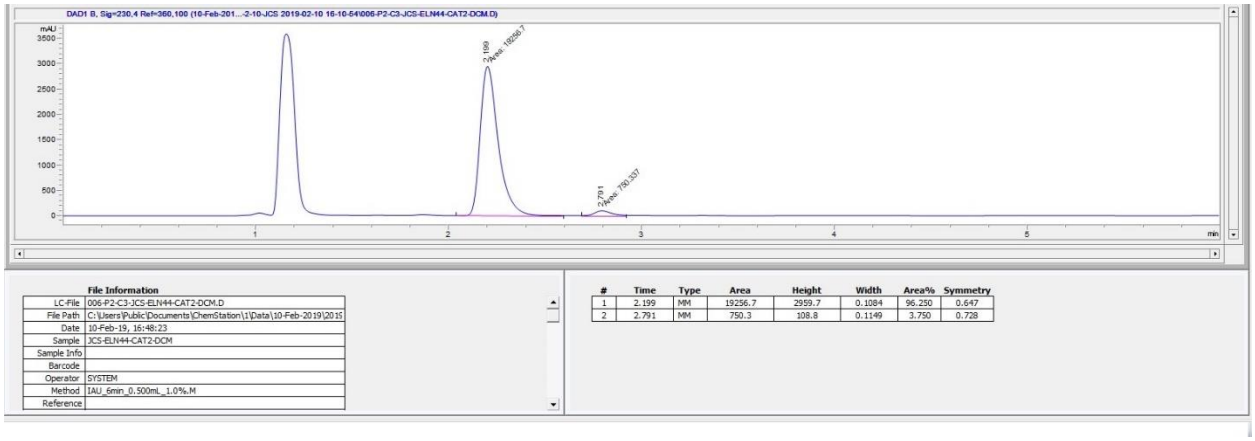

15 prepared with Rh_2(*R*-*p*-Ph-TPCP)$_4$

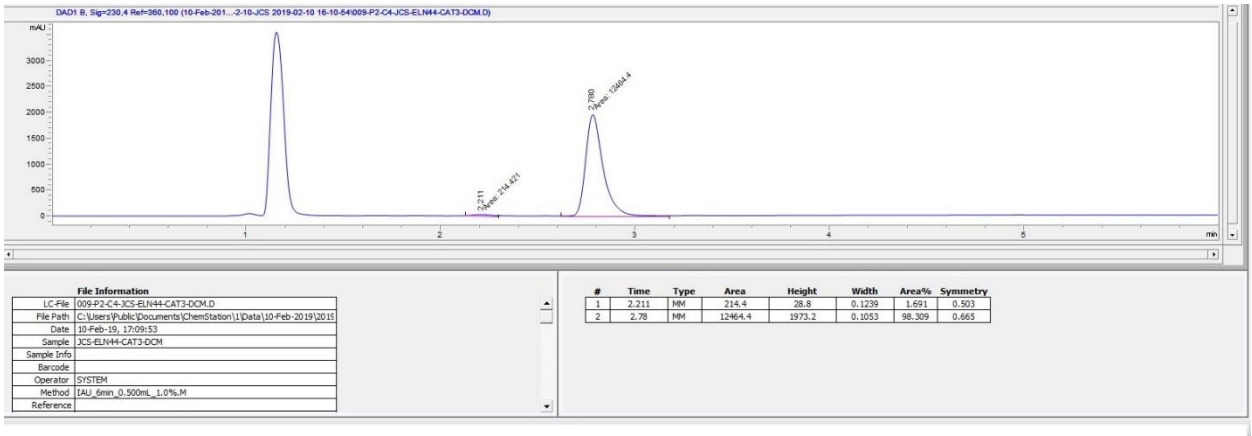

15 prepared with Rh_2(*R*-TPPTTL)$_4$

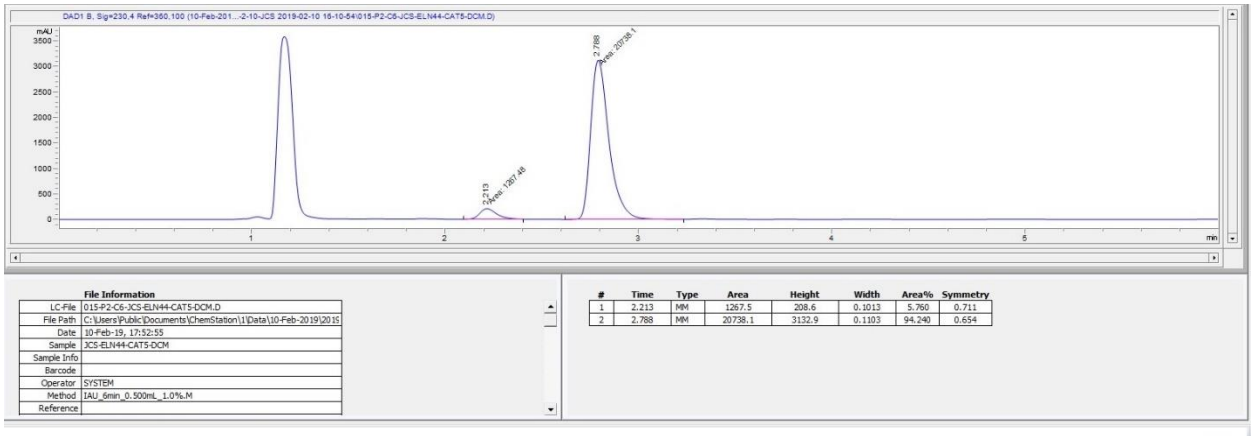

15 prepared with Rh_2(*R*-PTAD)$_4$

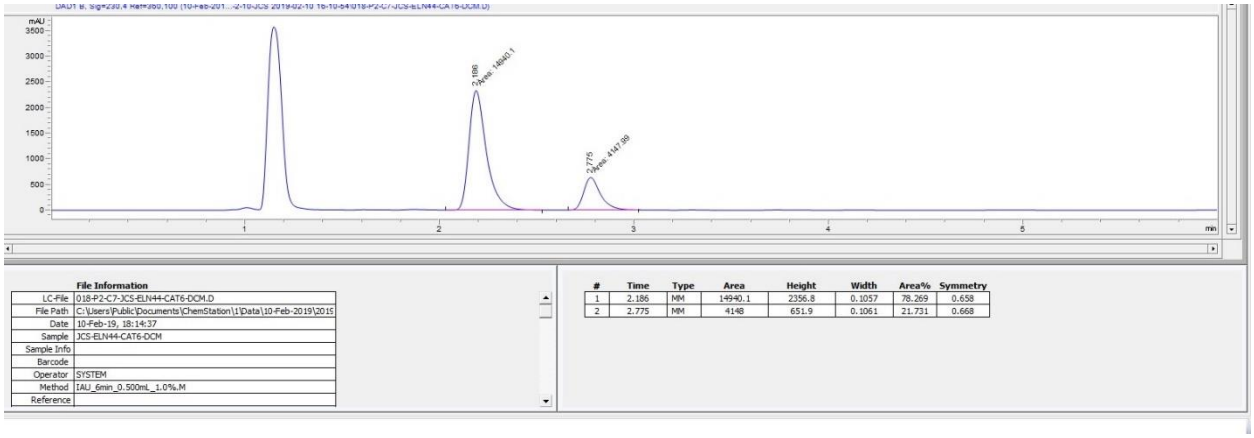

15 prepared with Rh_2(*R*-TCPTAD)$_4$

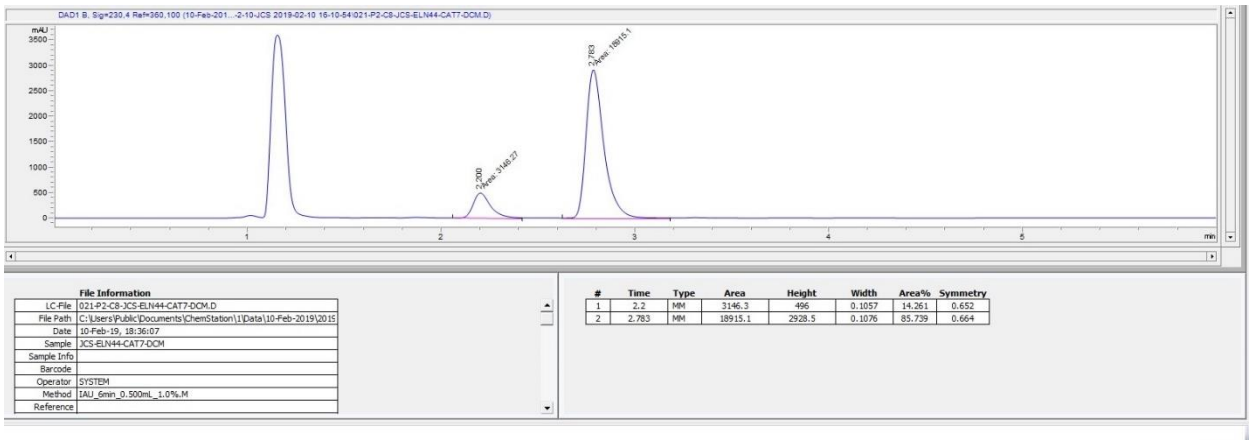

15 prepared with Rh_2(*S*-*o*-Cl-TPCP)$_4$

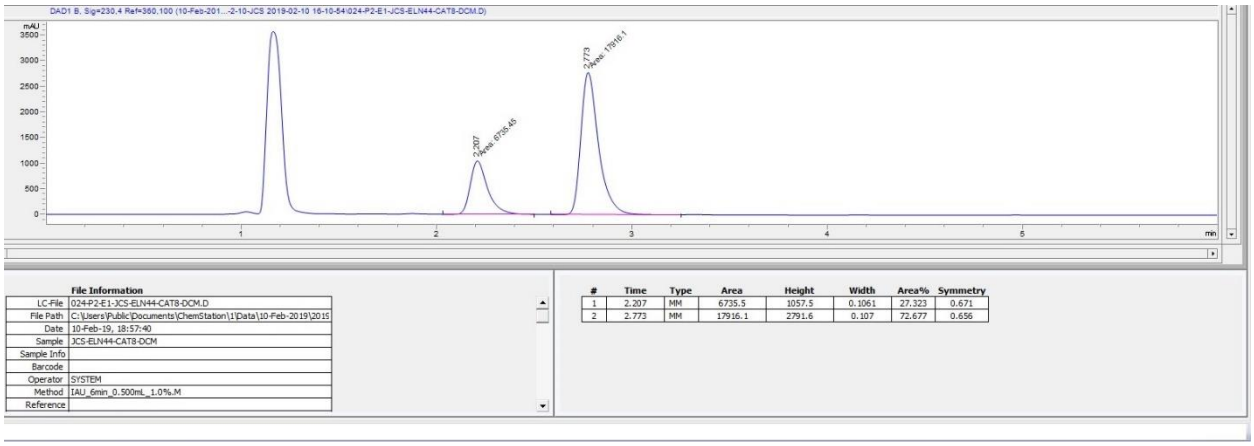

15 prepared with Rh_2(*S*-2-Cl-5-Br-TPCP)$_4$

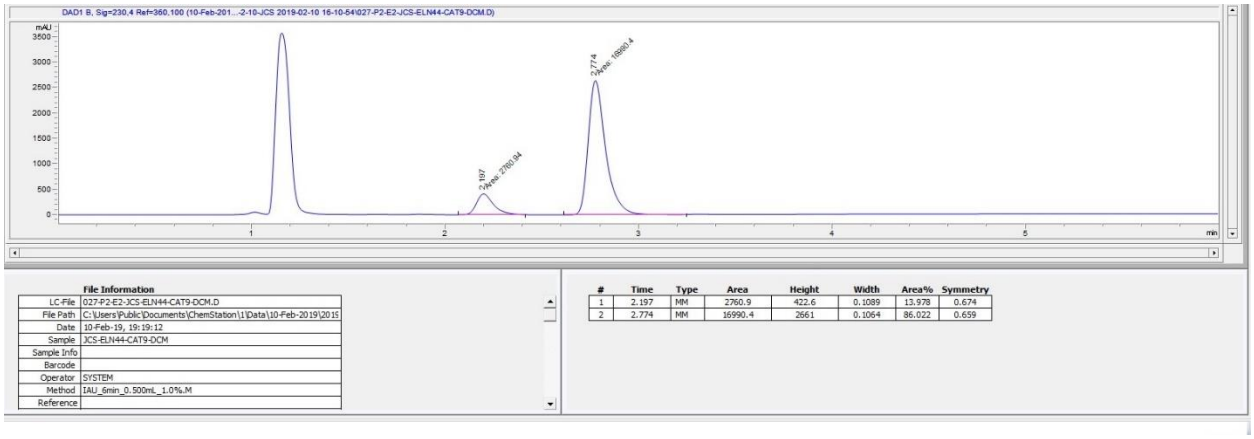

15 prepared with Rh_2(*R*-3,5-di(*p*-^{t}BuC$_6$H$_4$)TPCP)$_4$

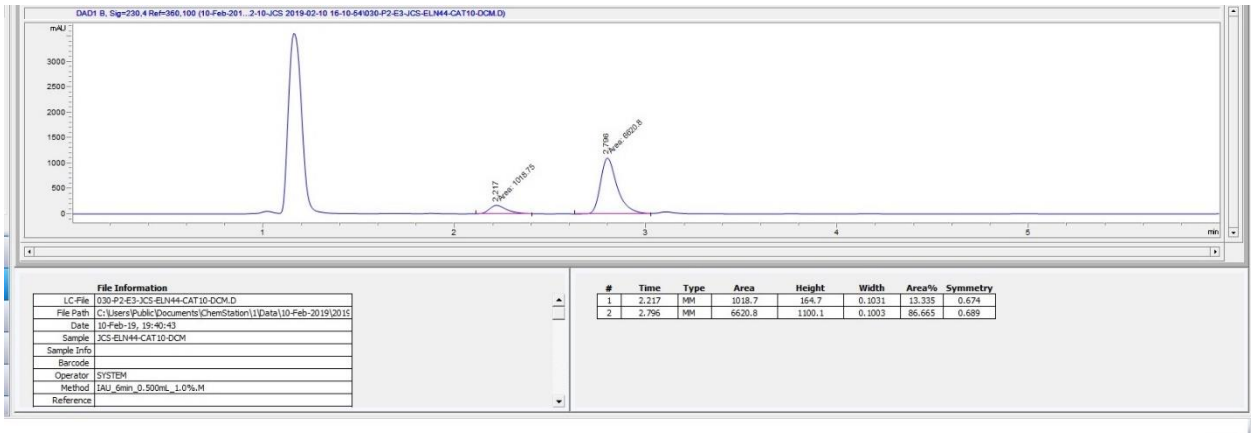

15 prepared with Rh_2(*S*-tris(*p*-^{t}BuC_6H_4)TPCP)$_4$

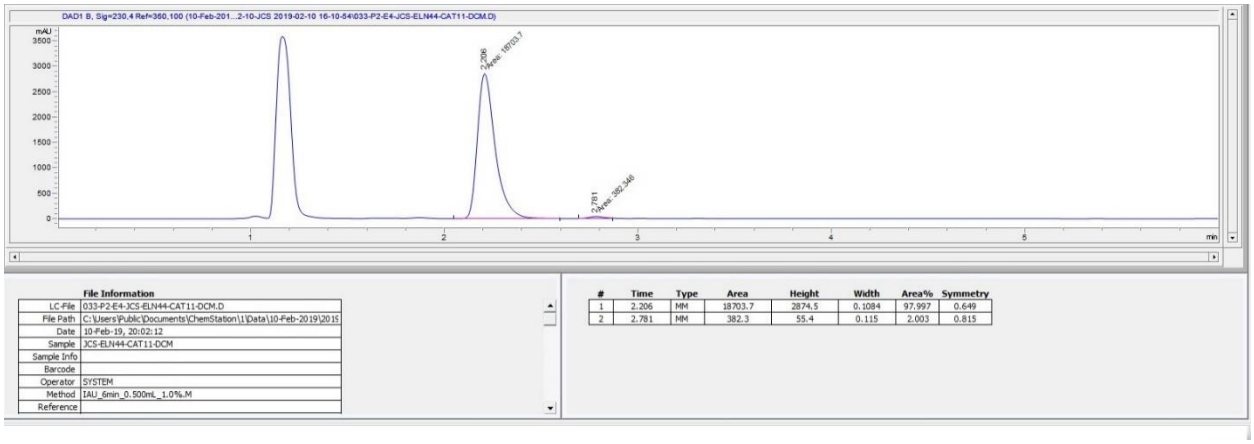

Results for diethyl carbonate ($(EtO)_2CO$) solvent

15 prepared with Rh_2(*S*-DOSP)$_4$

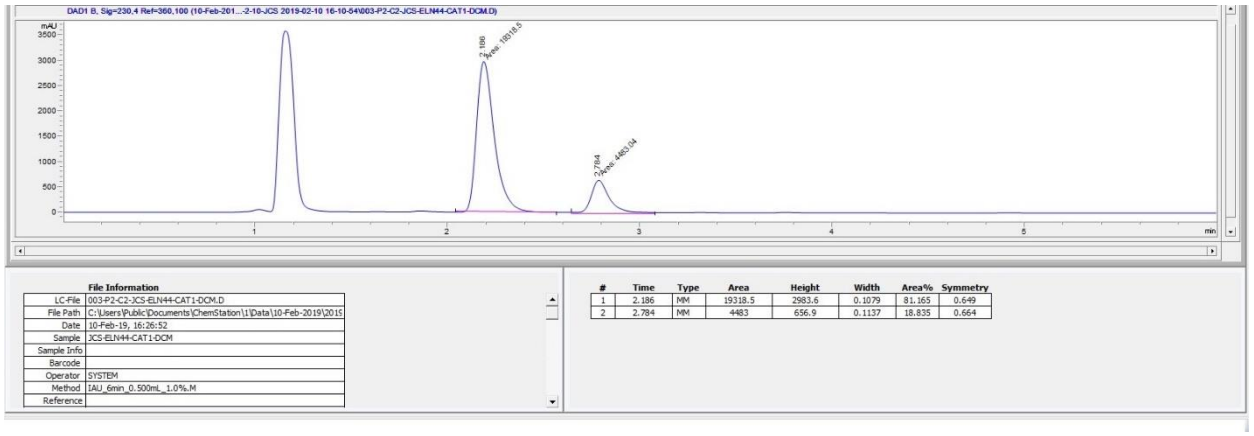

15 prepared with Rh_2(*S*-*p*-Br-TPCP)$_4$

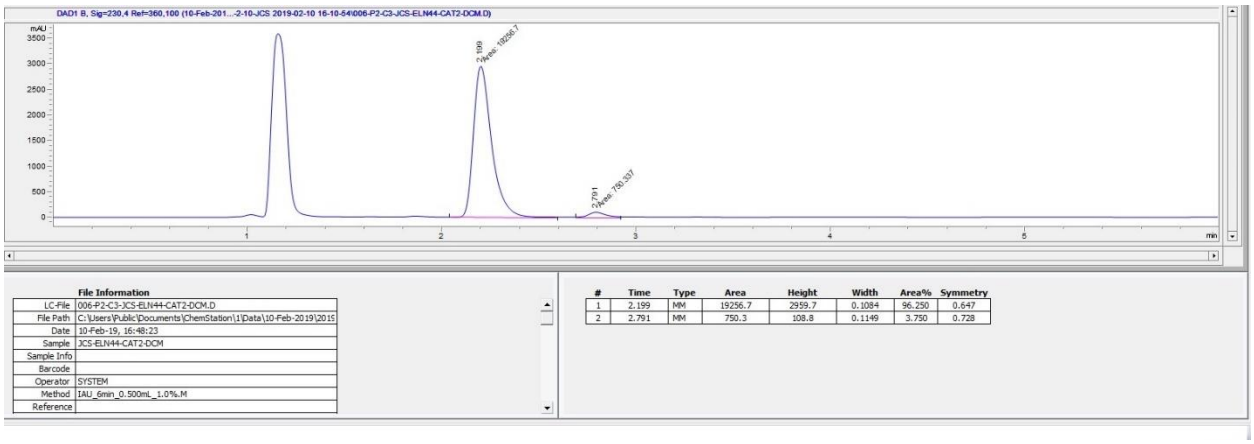

#	Time	Type	Area	Height	Width	Area%	Symmetry
1	2.199	MM	19256.7	2959.7	0.1084	96.250	0.647
2	2.791	MM	750.3	108.8	0.1149	3.750	0.728

15 prepared with Rh_2(*S*-*p*-Ph-TPCP)$_4$

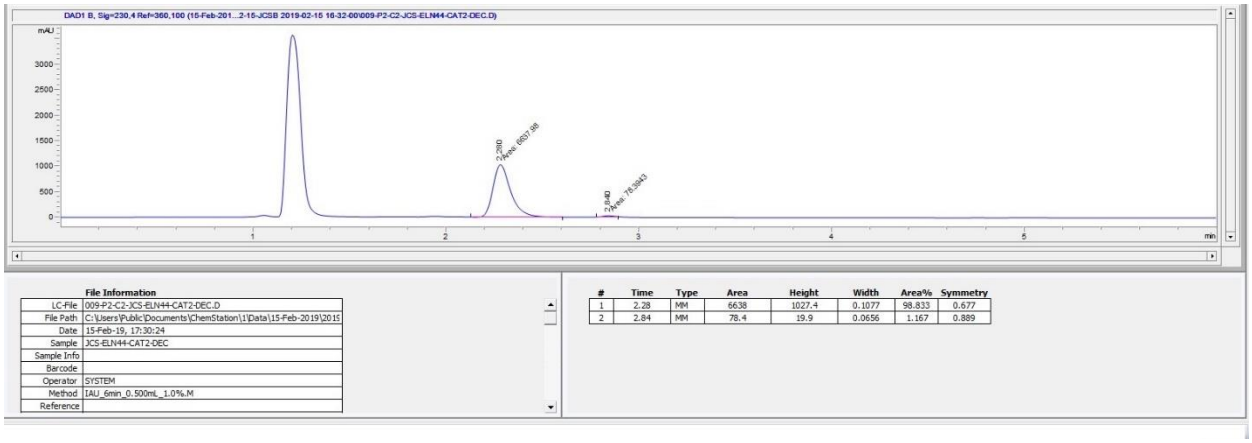

#	Time	Type	Area	Height	Width	Area%	Symmetry
1	2.28	MM	6638	1027.4	0.1077	98.833	0.677
2	2.84	MM	78.4	19.9	0.0656	1.167	0.889

15 prepared with Rh_2(*R*-TPPTTL)$_4$

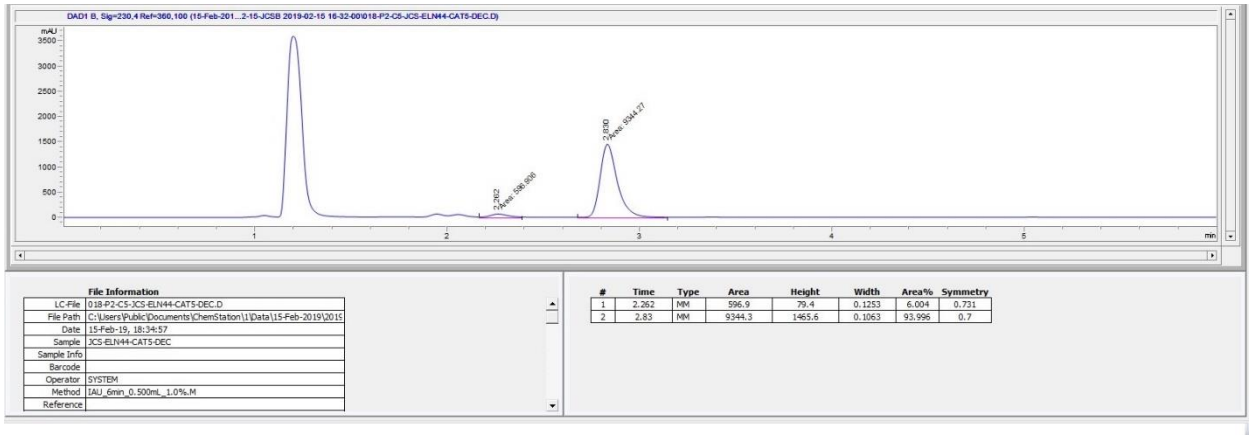

#	Time	Type	Area	Height	Width	Area%	Symmetry
1	2.262	MM	596.9	79.4	0.1253	6.004	0.731
2	2.83	MM	9344.3	1465.6	0.1063	93.996	0.7

15 prepared with Rh_2(*R*-PTAD)$_4$

15 prepared with Rh_2(*S*-TCPTAD)$_4$

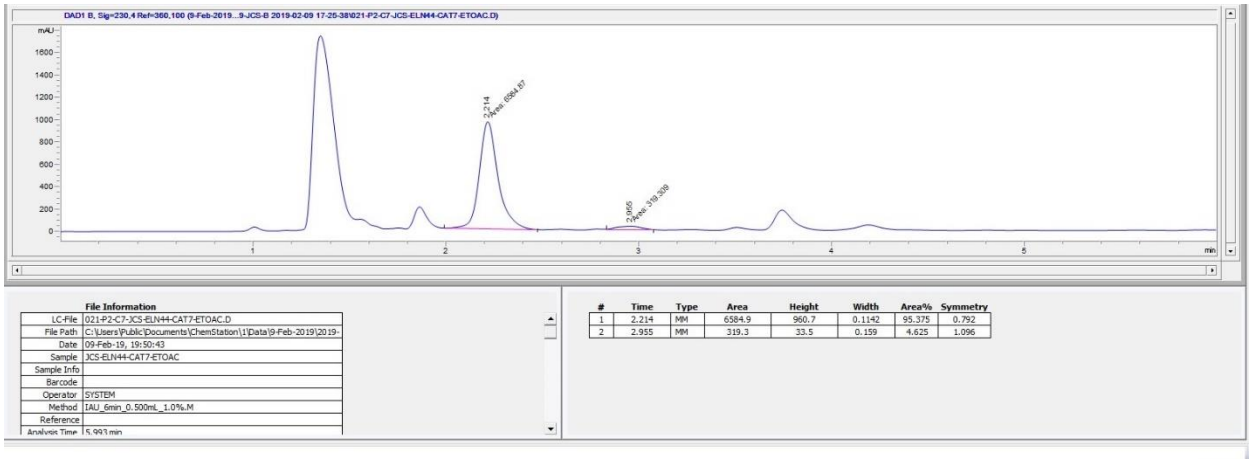

15 prepared with Rh_2(*S*-*o*-Cl-TPCP)$_4$

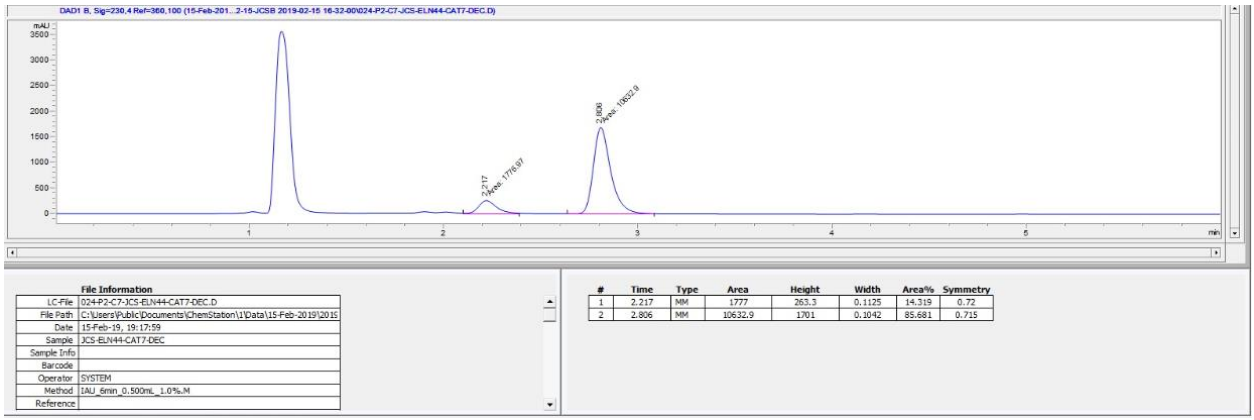

15 prepared with Rh_2(*S*-2-Cl-5-Br-TPCP)$_4$

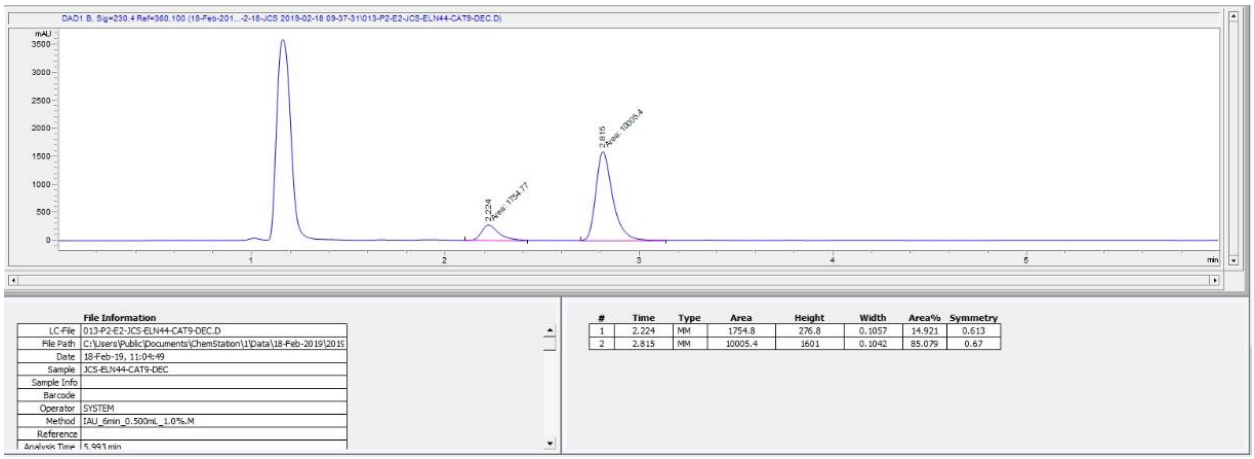

15 prepared with Rh_2(*R*-3,5-di(*p*-^{t}BuC_6H_4)TPCP)$_4$

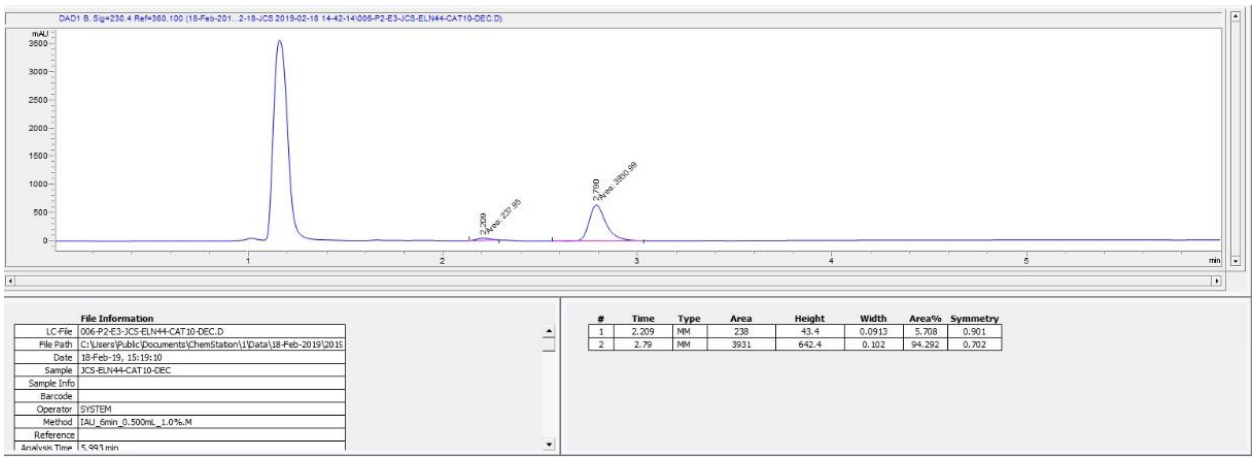

15 prepared with Rh_2(*S*-tris(*p*-^{t}BuC_6H_4)TPCP)$_4$

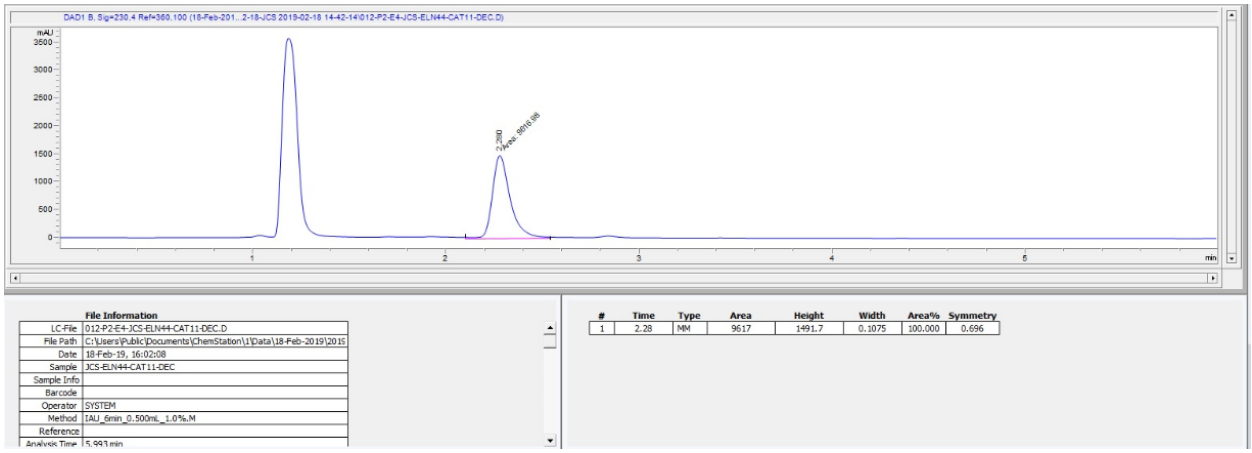

Results for dimethyl carbonate ($(MeO)_2CO$) solvent:

15 prepared with Rh_2(*S*-DOSP)$_4$

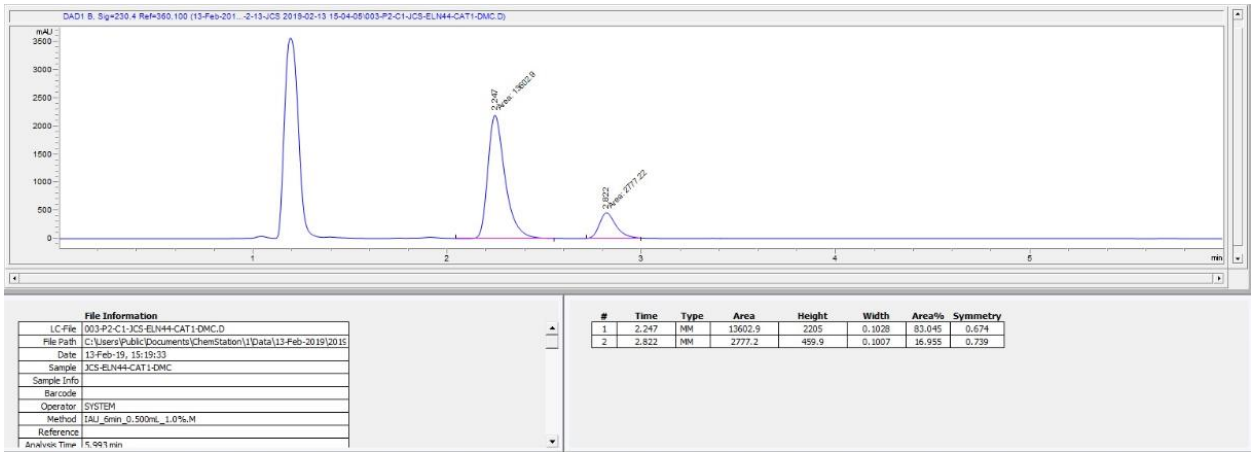

#	Time	Type	Area	Height	Width	Area%	Symmetry
1	2.247	MM	13602.9	2205	0.1028	83.045	0.674
2	2.822	MM	2777.2	459.9	0.1007	16.955	0.739

15 prepared with Rh_2(*S*-*p*-Br-TPCP)$_4$

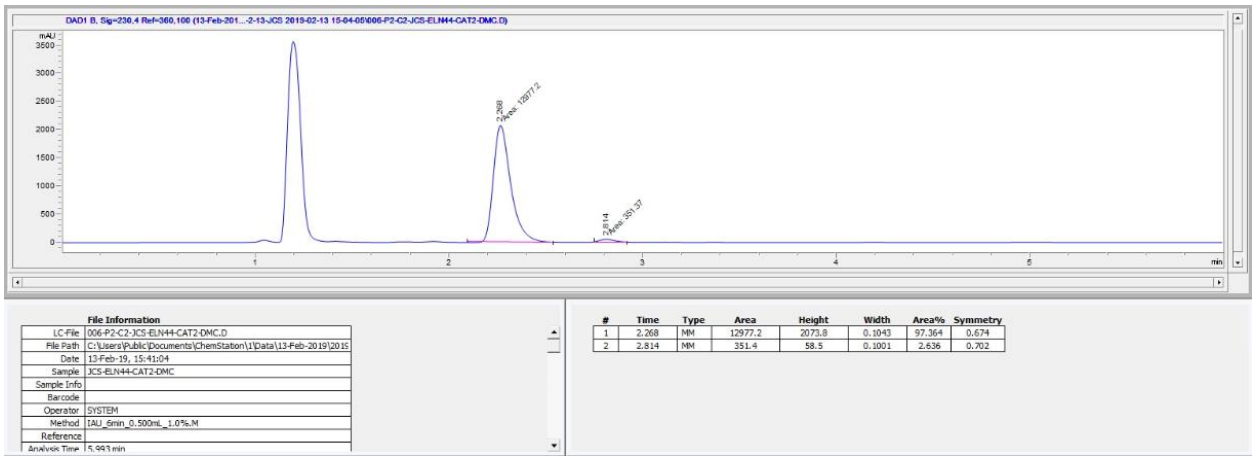

#	Time	Type	Area	Height	Width	Area%	Symmetry
1	2.268	MM	12977.2	2073.8	0.1043	97.364	0.674
2	2.814	MM	351.4	58.5	0.1001	2.636	0.702

15 prepared with Rh_2(*R*-*p*-Ph-TPCP)$_4$

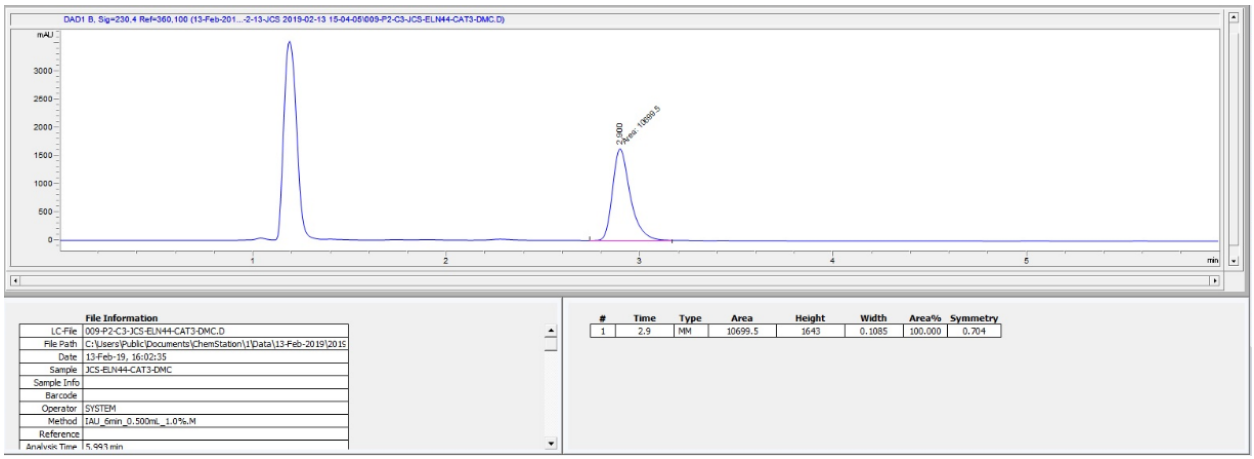

#	Time	Type	Area	Height	Width	Area%	Symmetry
1	2.9	MM	10699.5	1643	0.1085	100.000	0.704

15 prepared with Rh_2(*R*-TPPTTL)$_4$

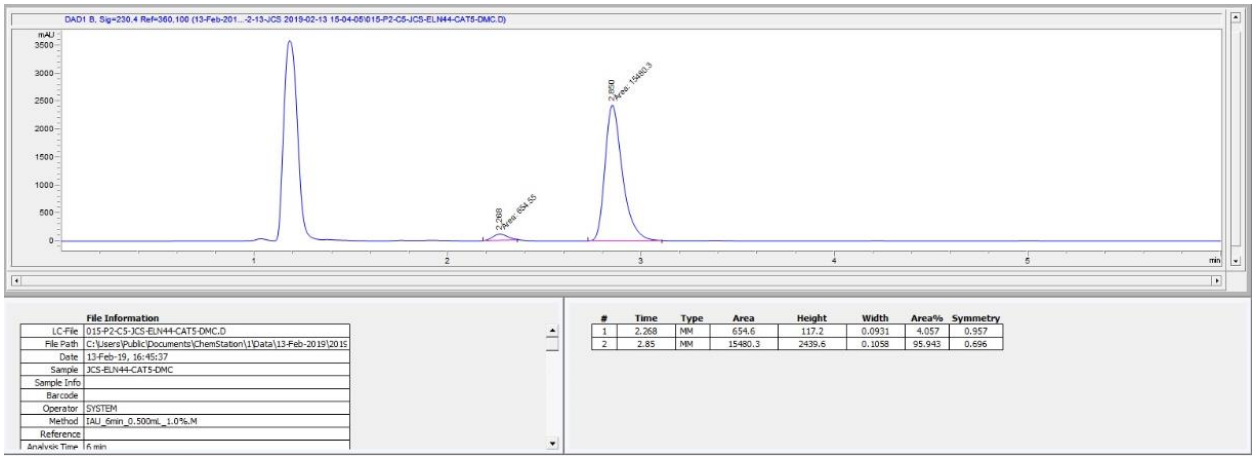

#	Time	Type	Area	Height	Width	Area%	Symmetry
1	2.268	MM	654.6	117.2	0.0931	4.057	0.957
2	2.85	MM	15480.3	2439.6	0.1058	95.943	0.696

15 prepared with Rh_2(*R*-PTAD)$_4$

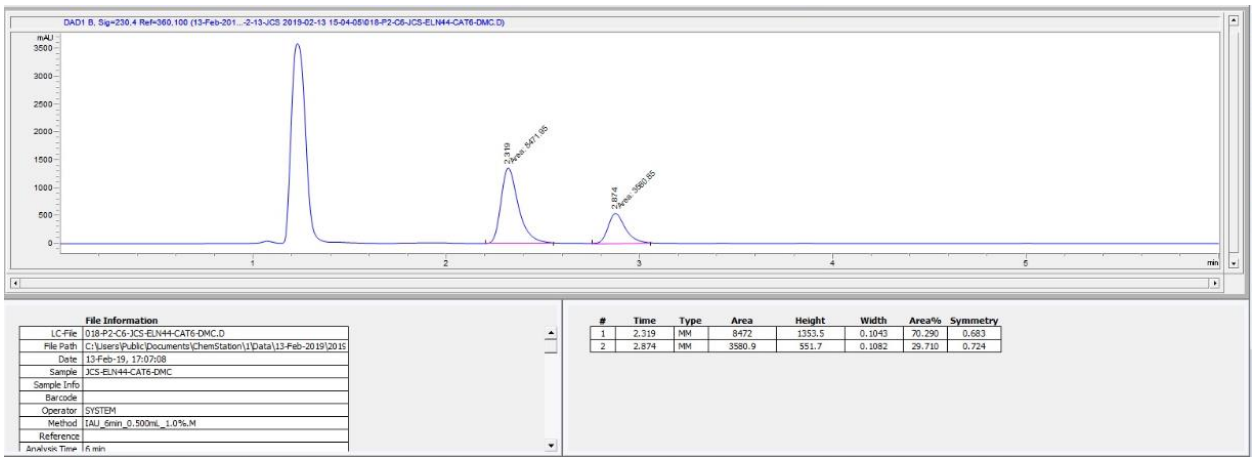

#	Time	Type	Area	Height	Width	Area%	Symmetry
1	2.319	MM	8472	1353.5	0.1043	70.290	0.683
2	2.874	MM	3580.9	551.7	0.1082	29.710	0.724

15 prepared with Rh_2(*R*-TCPTAD)$_4$

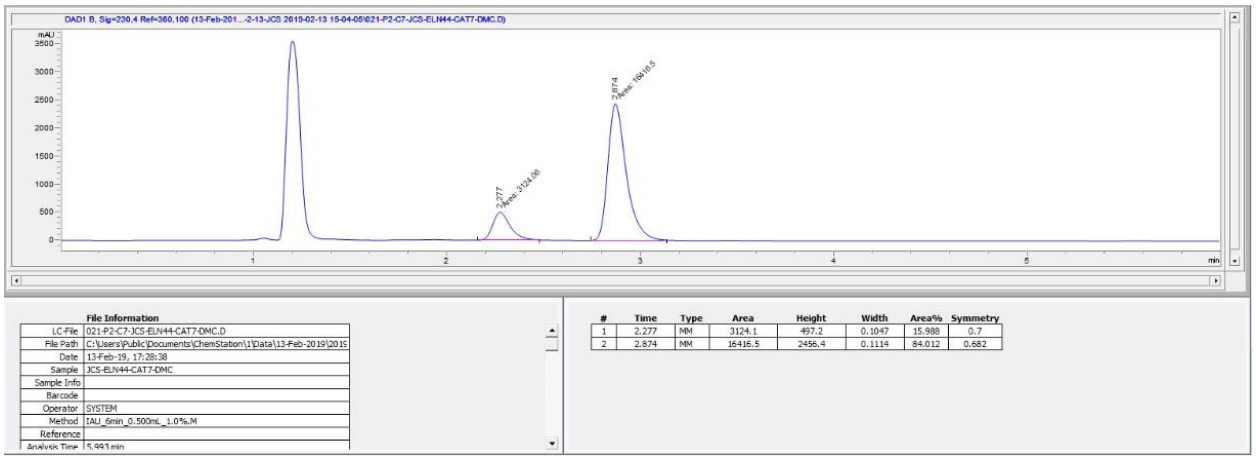

#	Time	Type	Area	Height	Width	Area%	Symmetry
1	2.277	MM	3124.1	497.2	0.1047	15.988	0.7
2	2.874	MM	16416.5	2456.4	0.1114	84.012	0.682

15 prepared with Rh_2(*S*-*o*-Cl-TPCP)$_4$

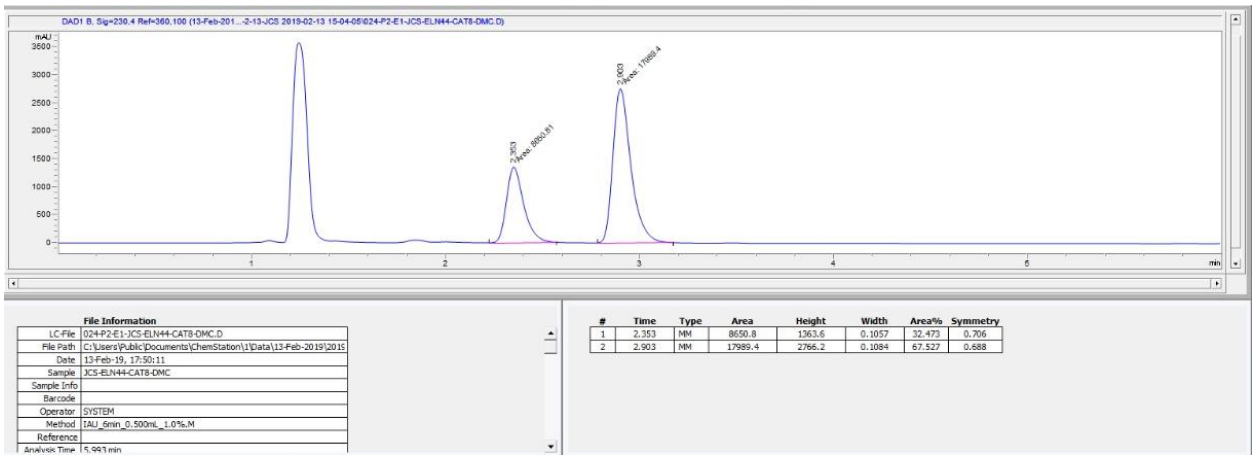

15 prepared with Rh_2(*S*-2-Cl-5-Br-TPCP)$_4$

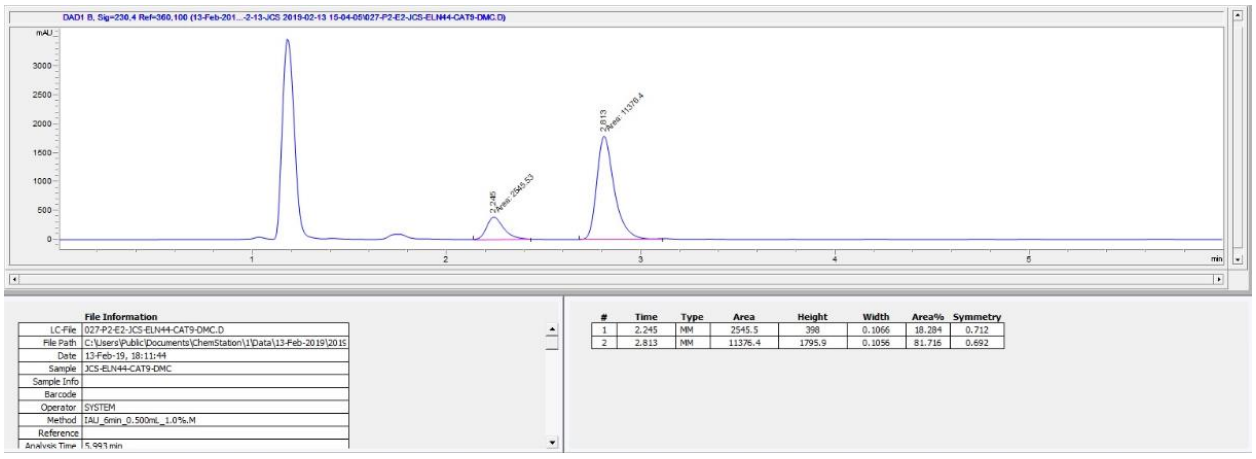

15 prepared with Rh_2(*R*-3,5-di(*p*-^{t}BuC$_6$H$_4$)TPCP)$_4$

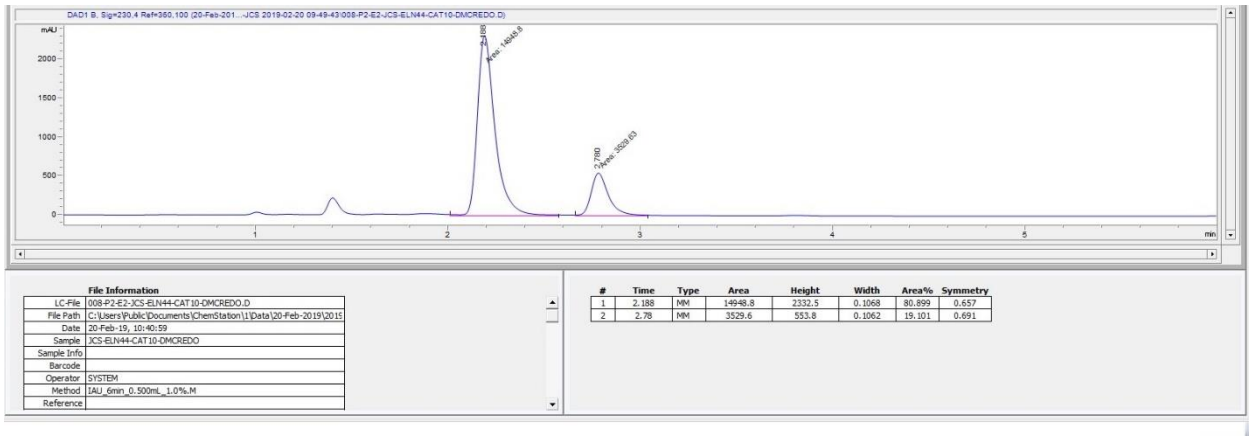

15 prepared with Rh_2(*S*-tris(*p*-^{t}BuC_6H_4)TPCP)$_4$

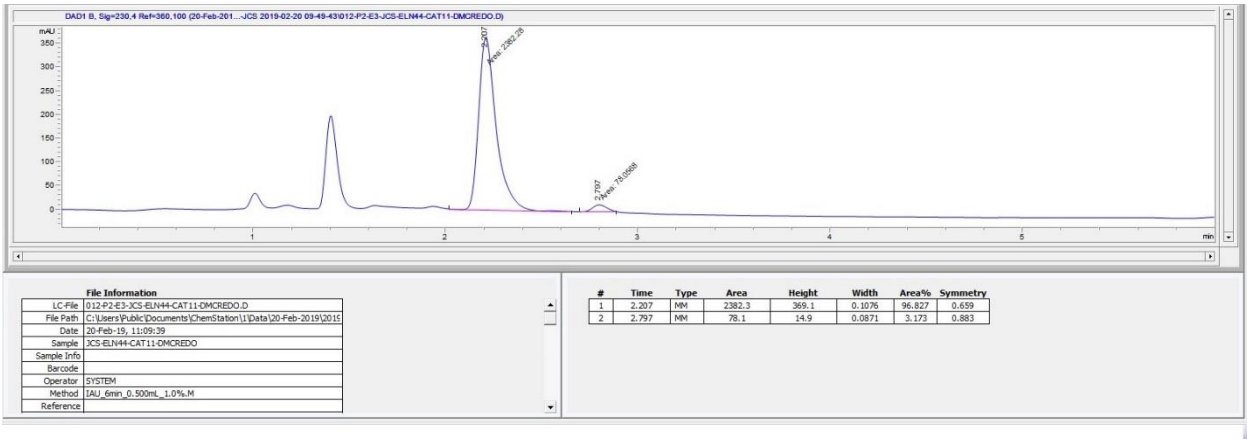

Results for ethyl acetate (EtOAc) solvent:

15 prepared with Rh_2(*S*-DOSP)$_4$

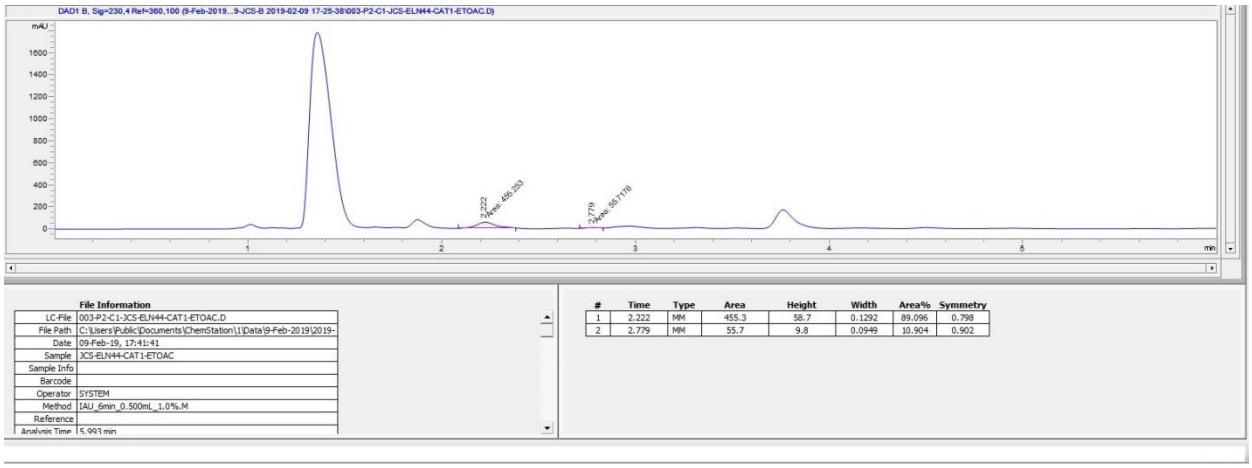

15 prepared with Rh_2(*S*-*p*-Br-TPCP)$_4$

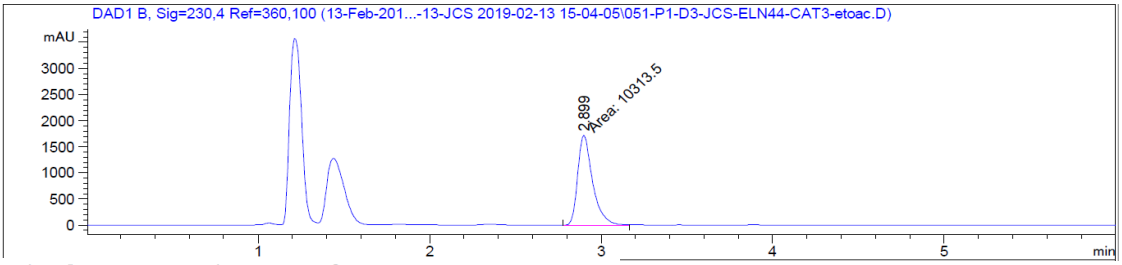

Signal 2: DAD1 B, Sig=230,4 Ref=360,100

Peak #	RetTime [min]	Type	Width [min]	Area [mAU*s]	Height [mAU]	Area %
1	2.899	MM	0.1001	1.03135e4	1717.97571	100.0000

Totals : 1.03135e4 1717.97571

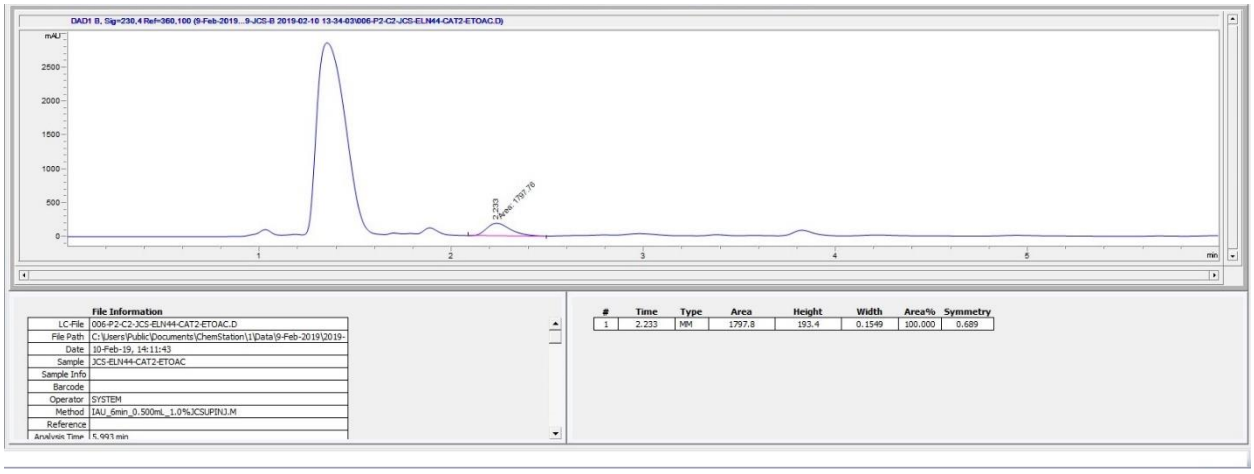

15 prepared with Rh_2(*R*-*p*-Ph-TPCP)$_4$

15 prepared with Rh_2(*R*-TPPTTL)$_4$

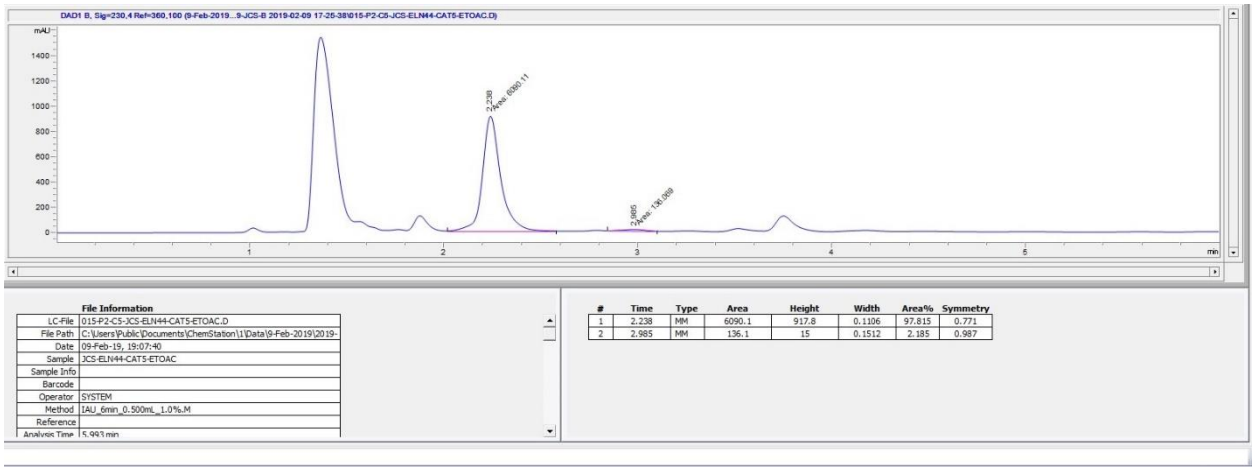

15 prepared with Rh_2(*R*-PTAD)$_4$

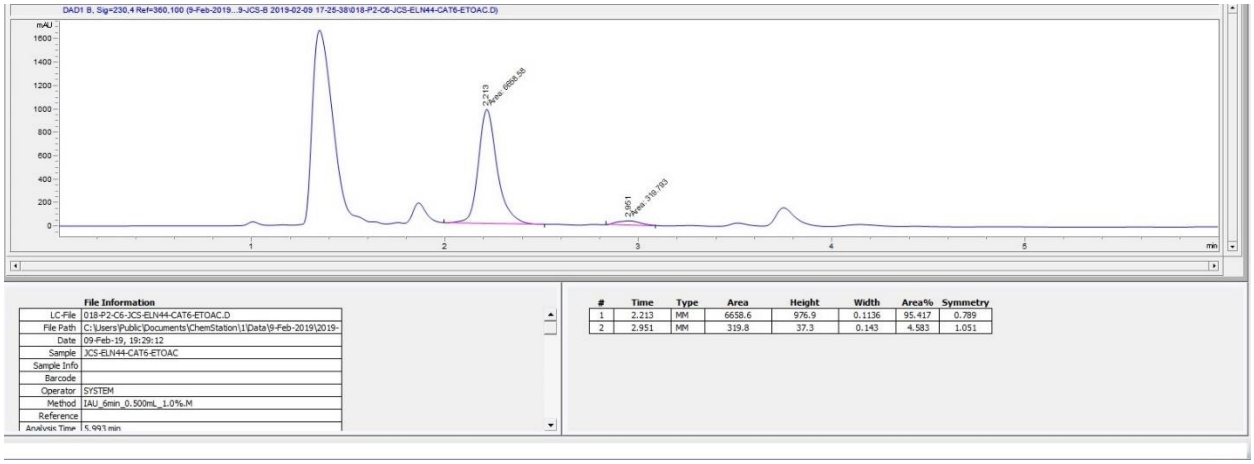

15 prepared with Rh_2(*R*-TCPTAD)$_4$

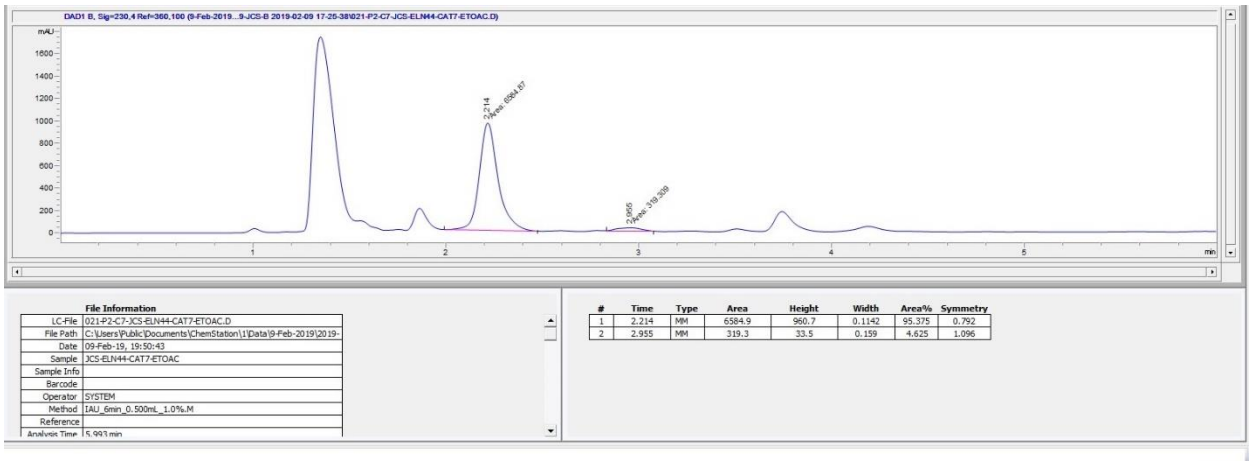

15 prepared with Rh_2(*S*-*o*-Cl-TPCP)$_4$

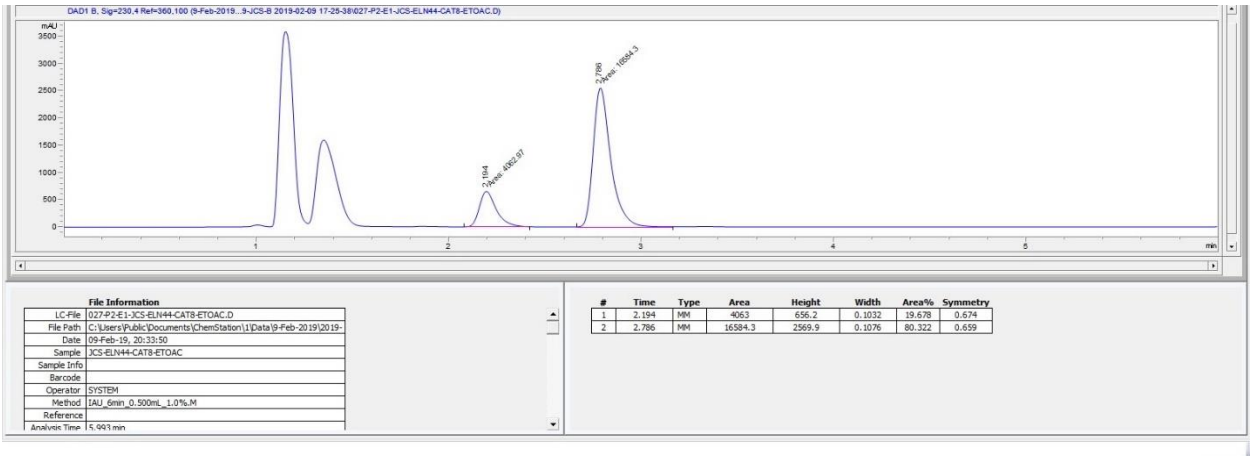

15 prepared with Rh_2(*S*-2-Cl-5-Br-TPCP)$_4$

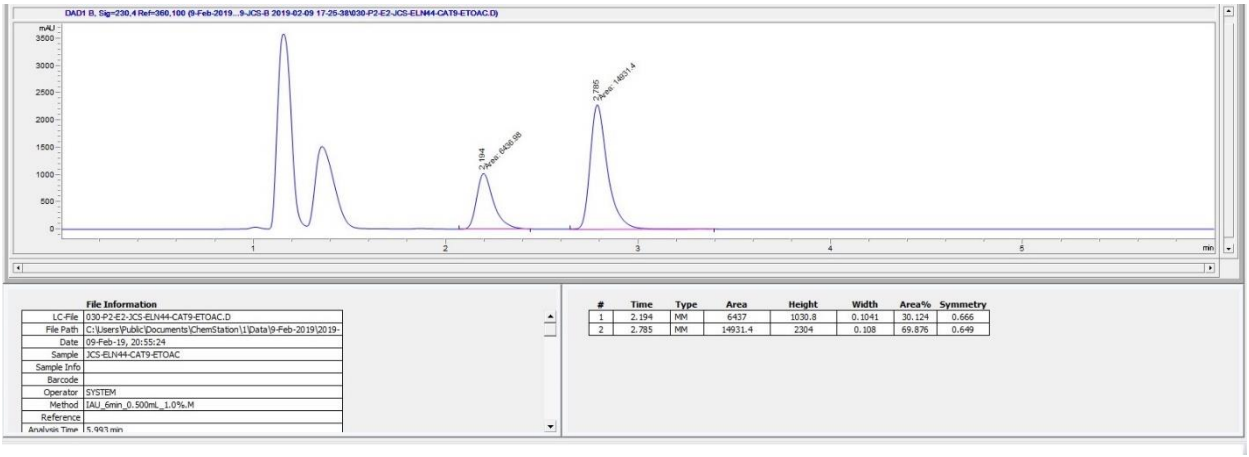

15 prepared with Rh_2(*R*-3,5-di(*p*-^{t}BuC_6H_4)TPCP)$_4$

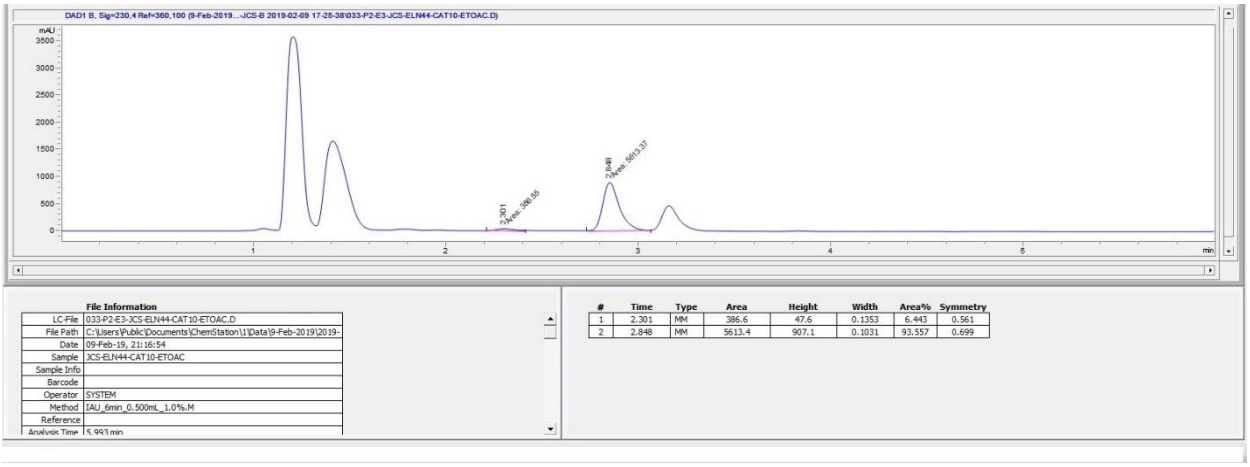

15 prepared with Rh_2(*S*-tris(*p*-^{t}BuC_6H_4)TPCP)$_4$

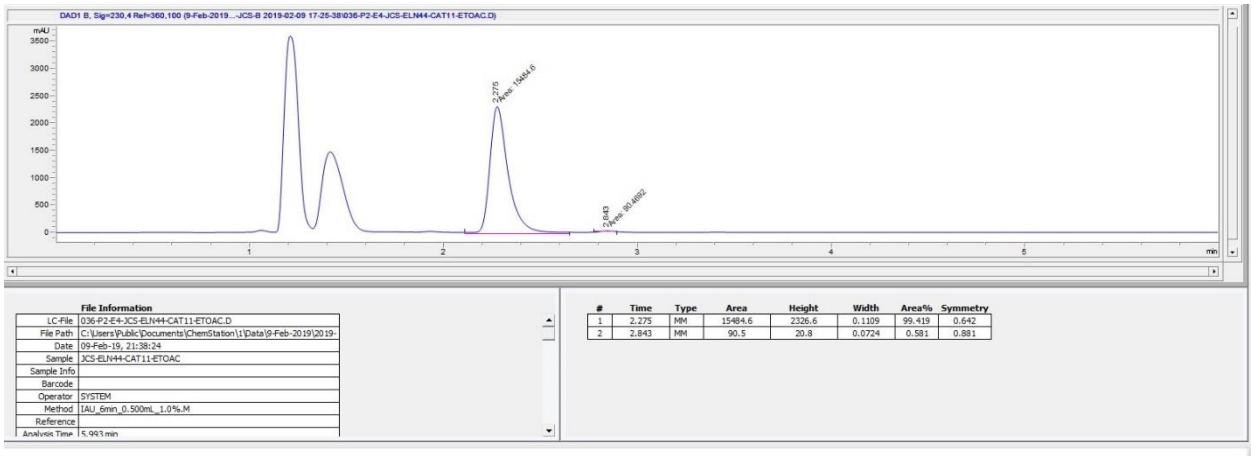

Results for isopropyl acetate (*i*-PrOAc) solvent:

15 prepared with Rh_2(*S*-DOSP)$_4$

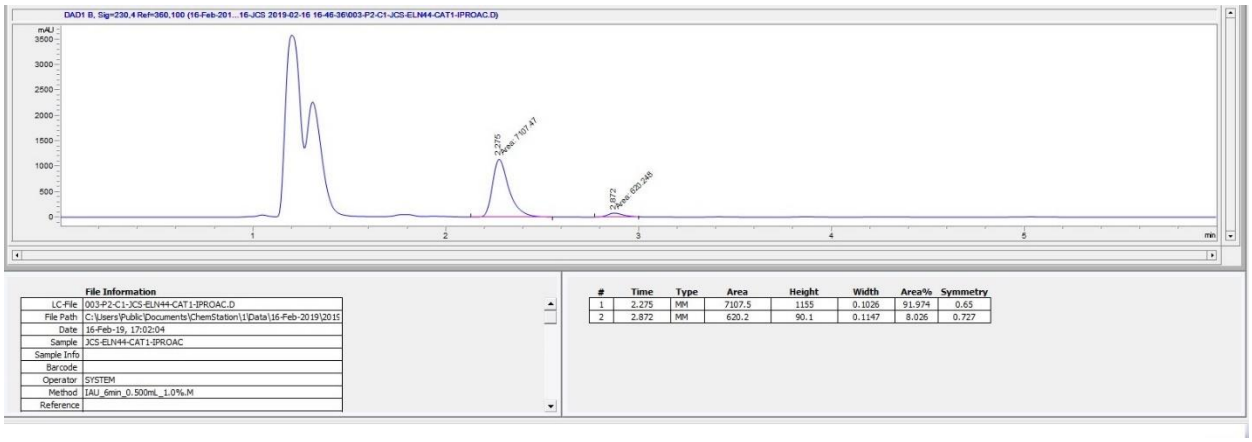

15 prepared with Rh_2(*S*-*p*-Br-TPCP)$_4$

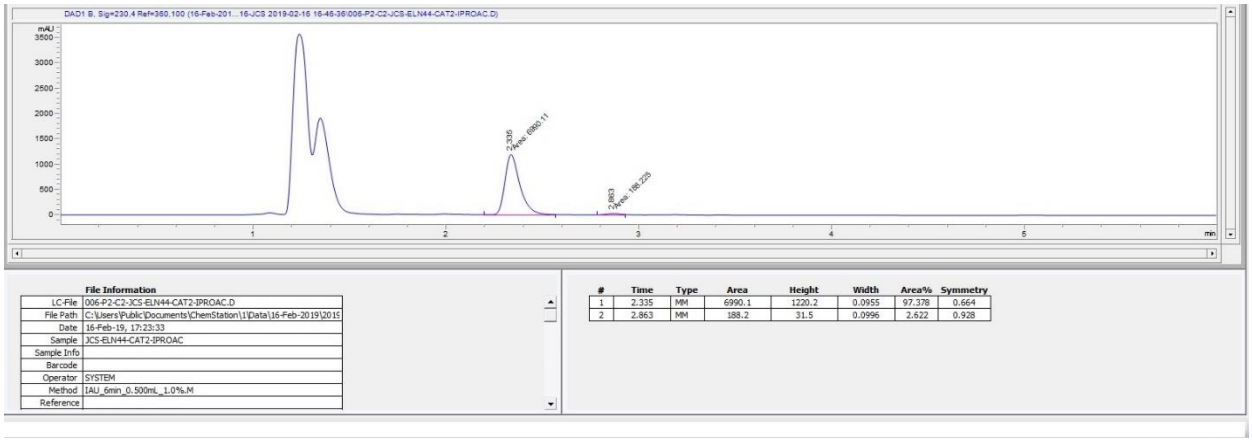

15 prepared with Rh_2(*R*-*p*-Ph-TPCP)$_4$

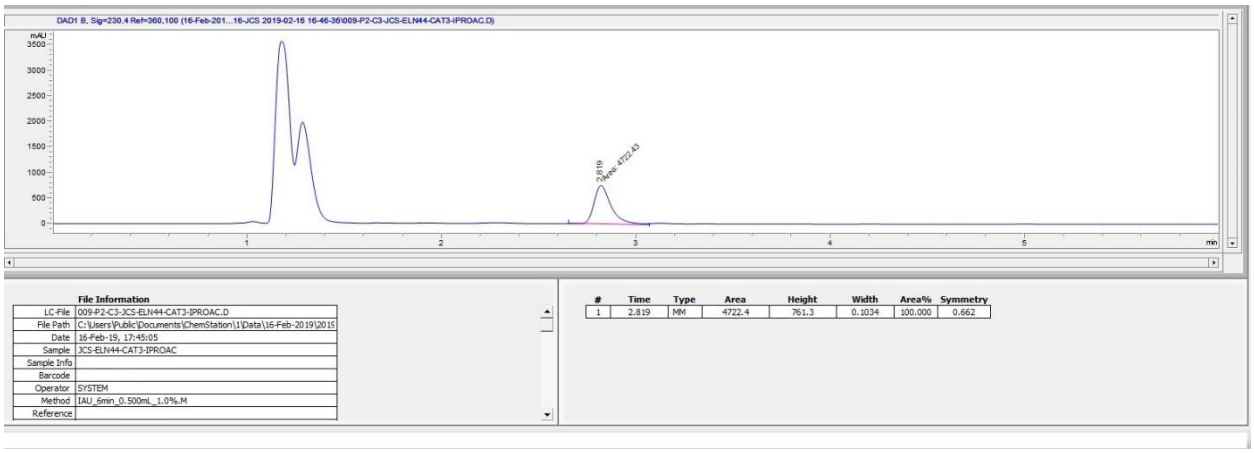

15 prepared with Rh_2(*R*-TPPTTL)$_4$

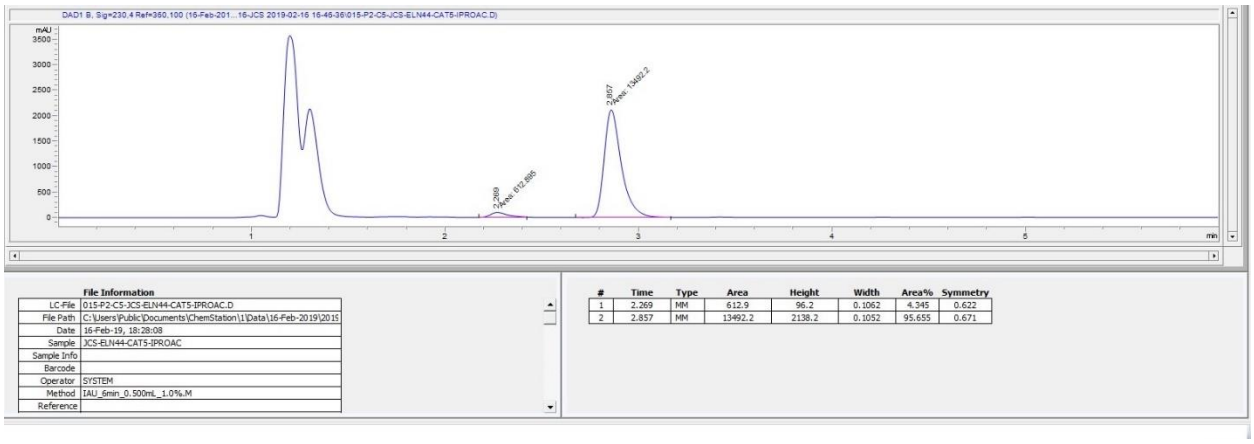

15 prepared with Rh_2(*R*-PTAD)$_4$

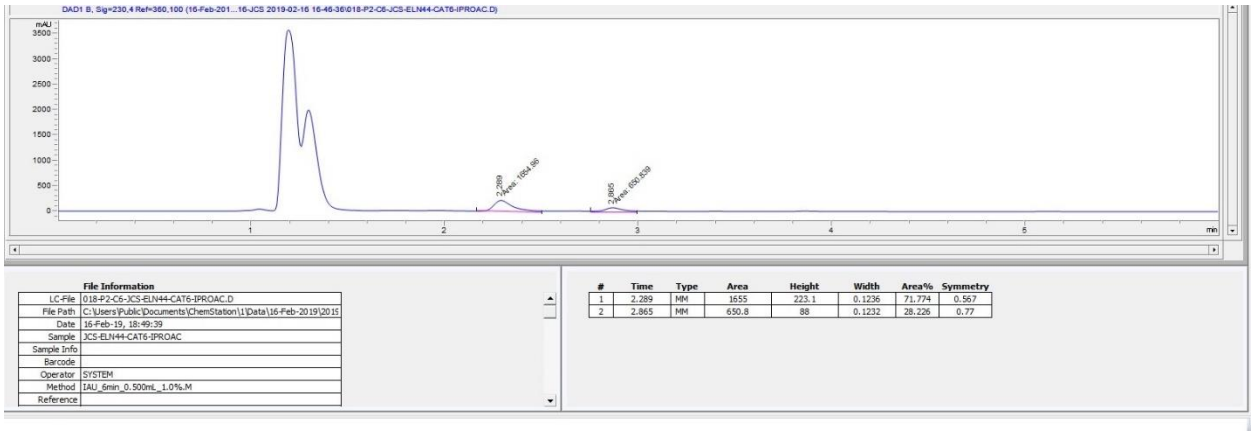

15 prepared with Rh_2(*R*-TCPTAD)$_4$

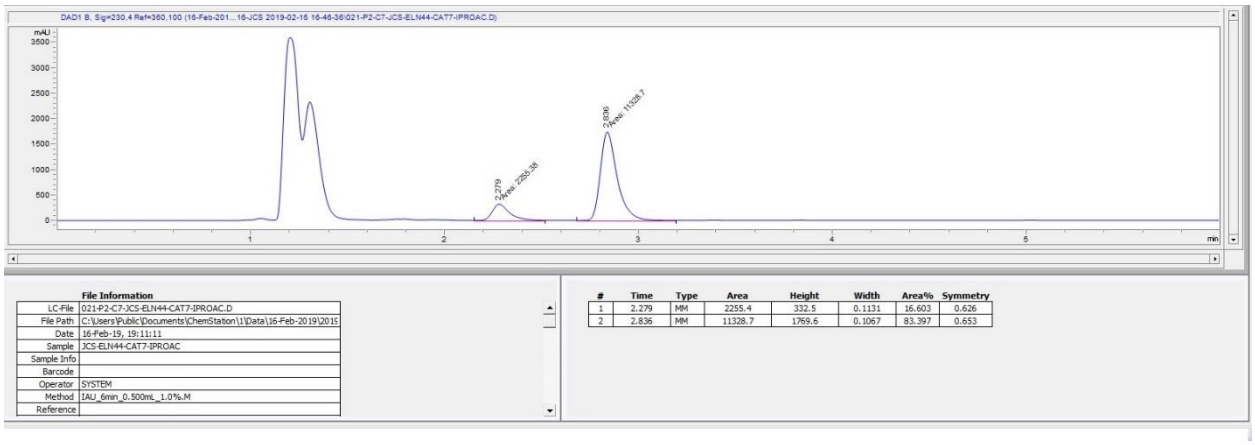

15 prepared with Rh_2(*S*-o-Cl-TPCP)$_4$

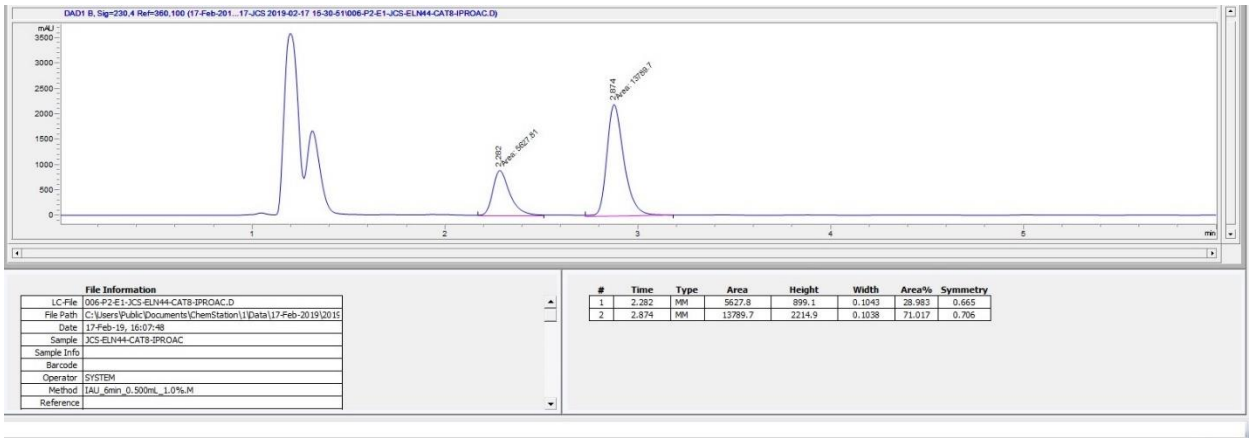

15 prepared with Rh_2(*S*-2-Cl-5-Br-TPCP)$_4$

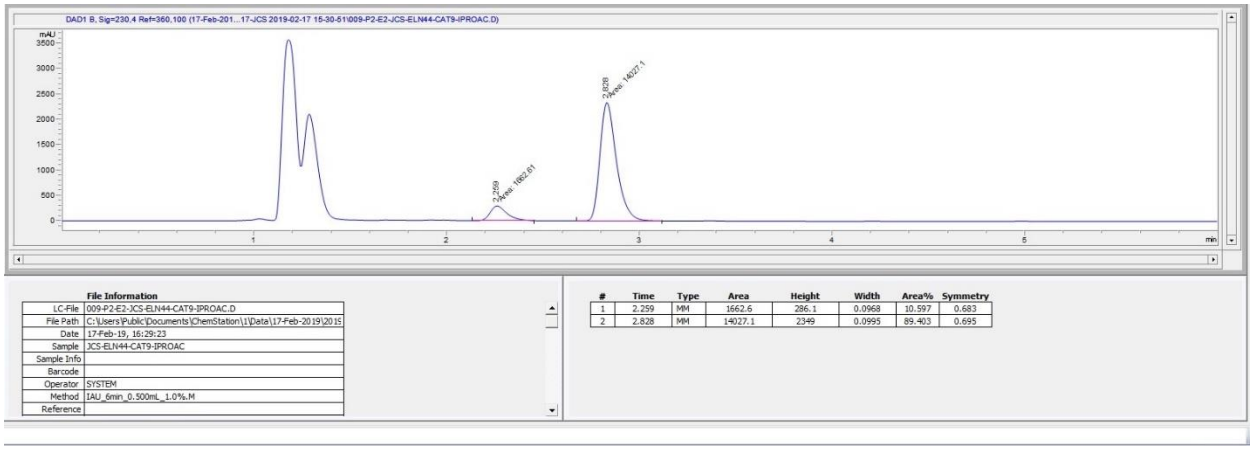

15 prepared with Rh_2(*R*-3,5-di(*p*-^{t}BuC_6H_4)TPCP)$_4$

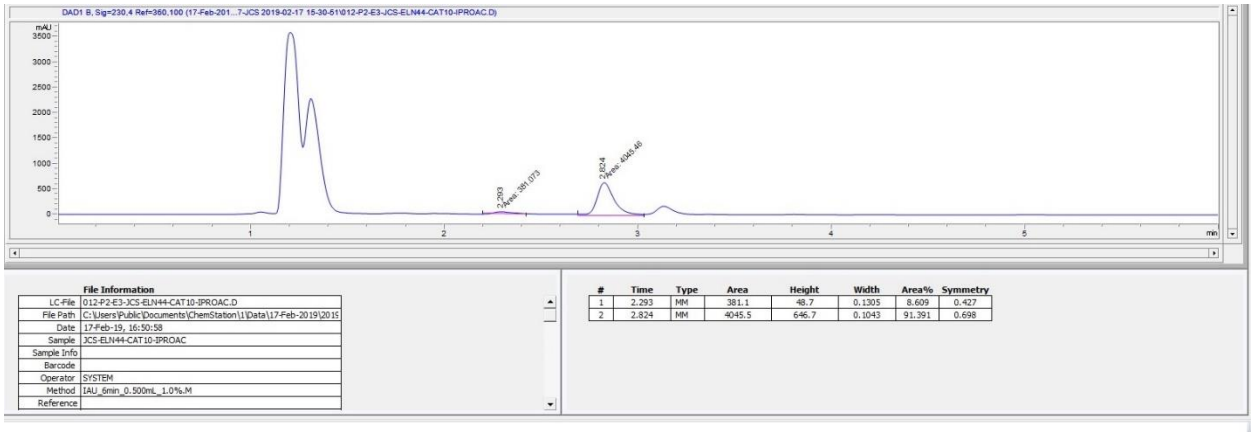

15 prepared with Rh_2(*S*-tris(*p*-^{t}BuC_6H_4)TPCP)$_4$

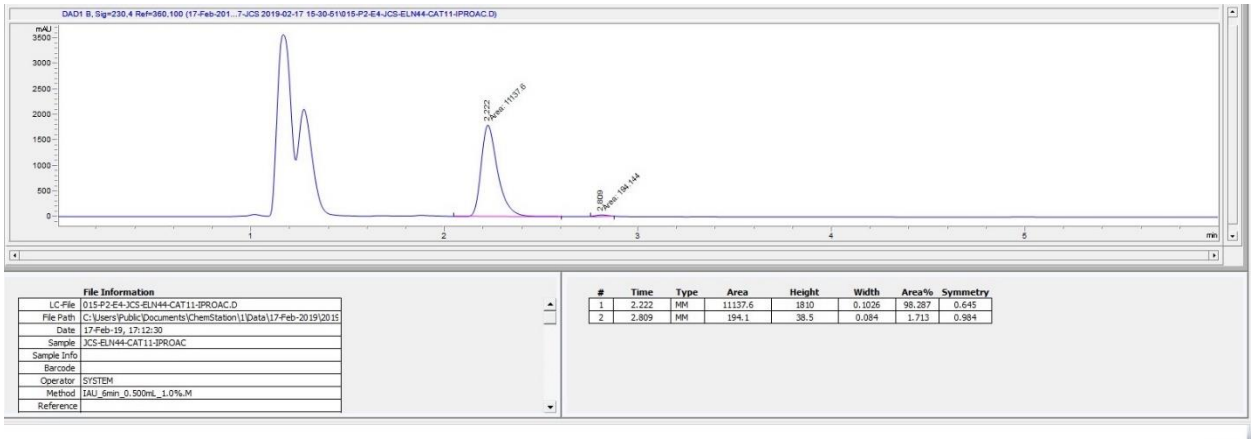

Results for Trifluorotoluene (TFT) solvent:

15 prepared with Rh_2(*S*-DOSP)$_4$

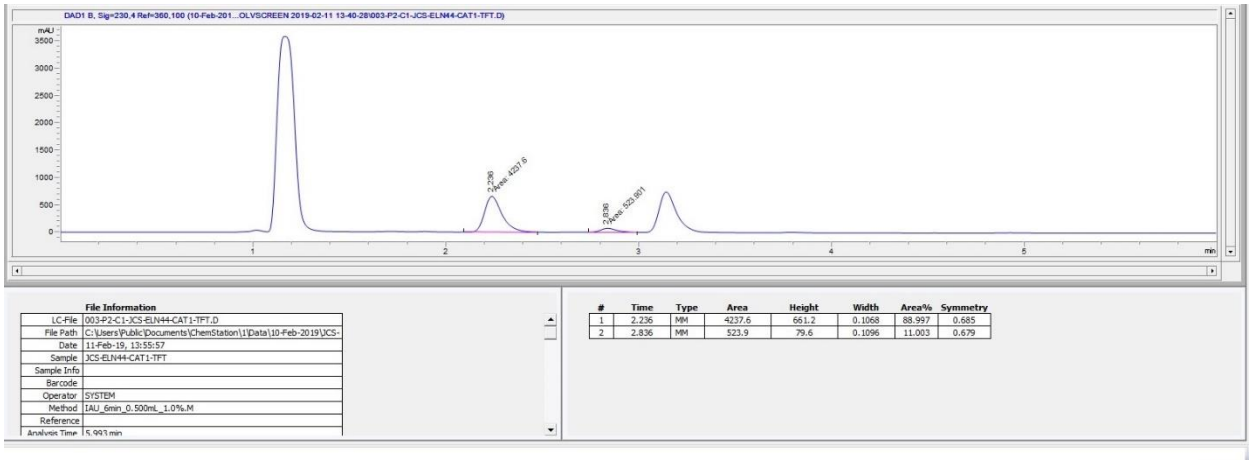

15 prepared with Rh_2(*S*-*p*-Br-TPCP)$_4$

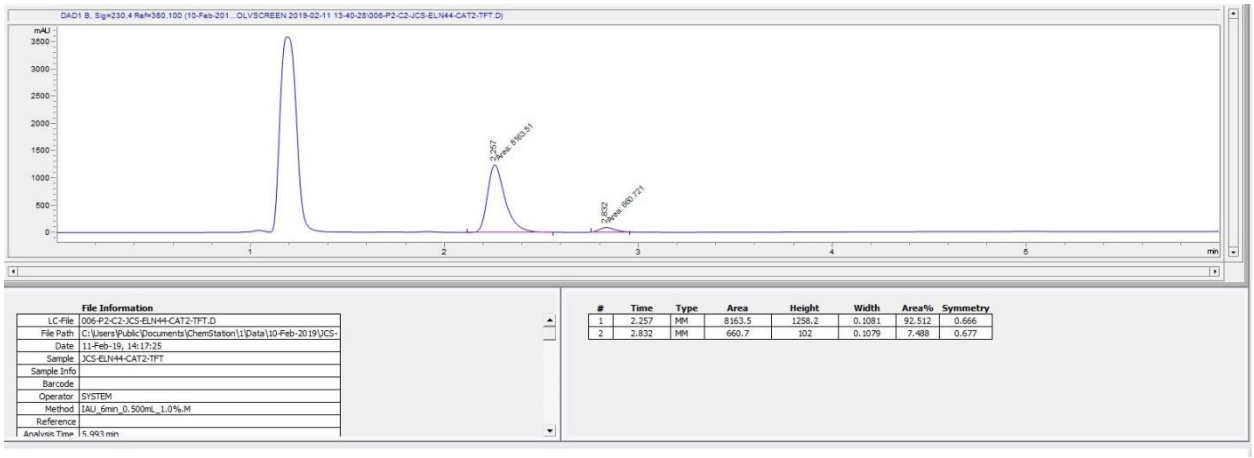

15 prepared with Rh_2(*R*-*p*-Ph-TPCP)$_4$

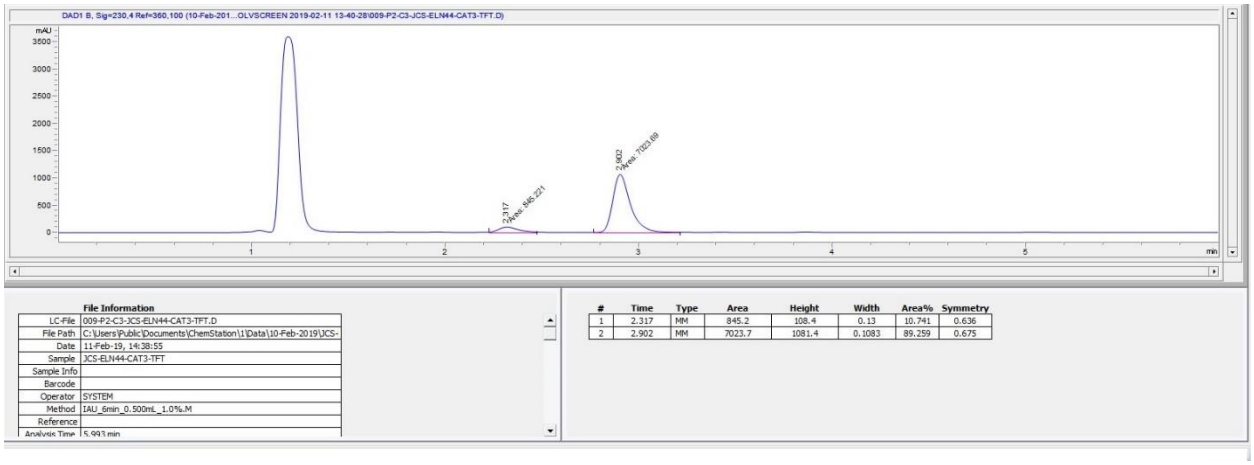

15 prepared with Rh_2(*R*-TPPTTL)$_4$

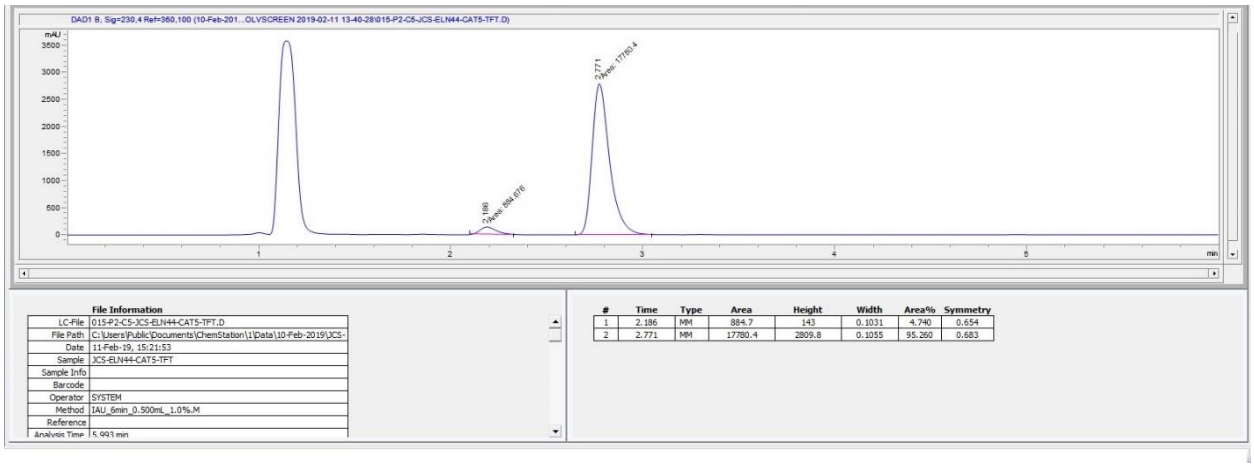

15 prepared with Rh_2(*R*-PTAD)$_4$

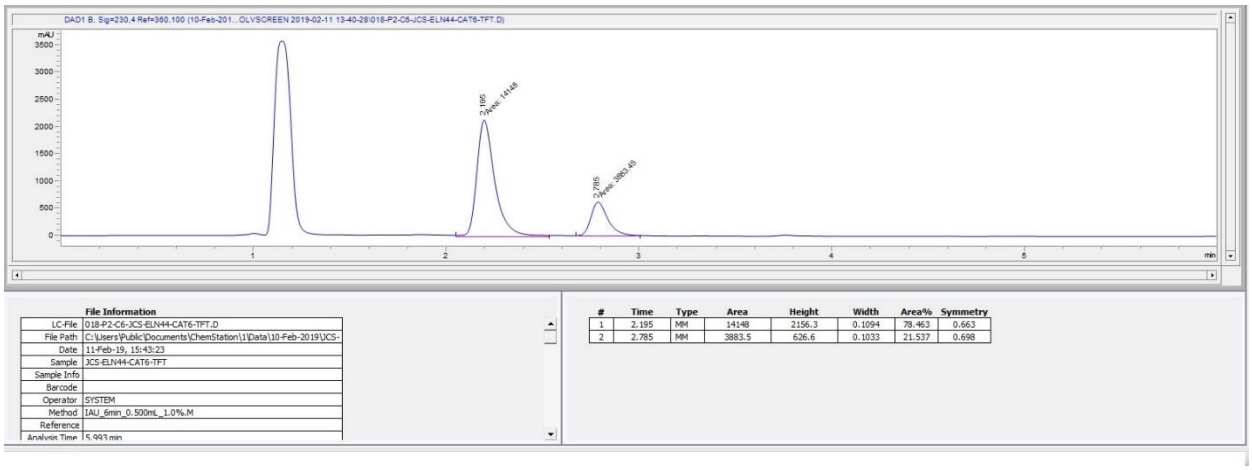

15 prepared with Rh_2(*R*-TCPTAD)$_4$

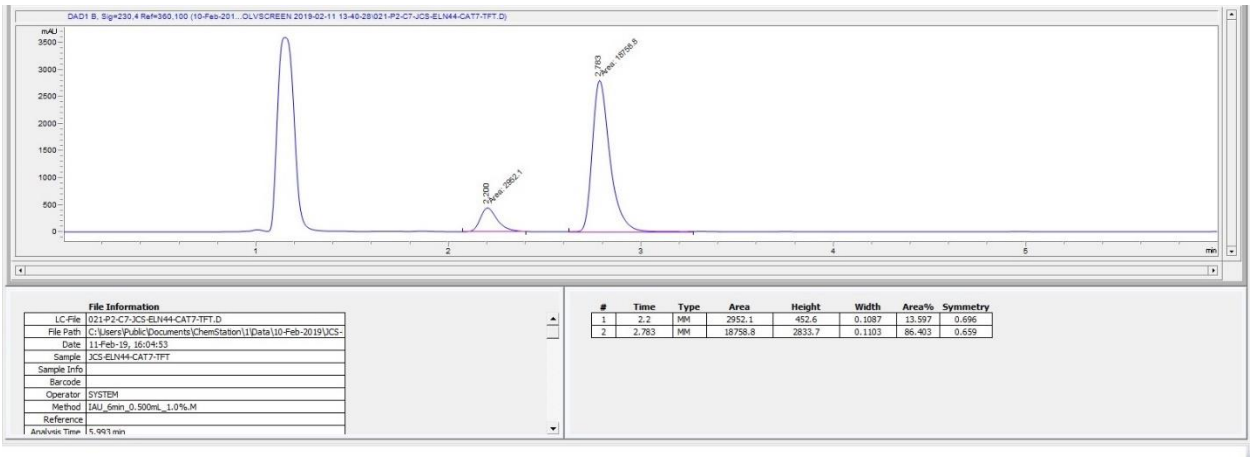

15 prepared with Rh_2(*S*-*o*-Cl-TPCP)$_4$

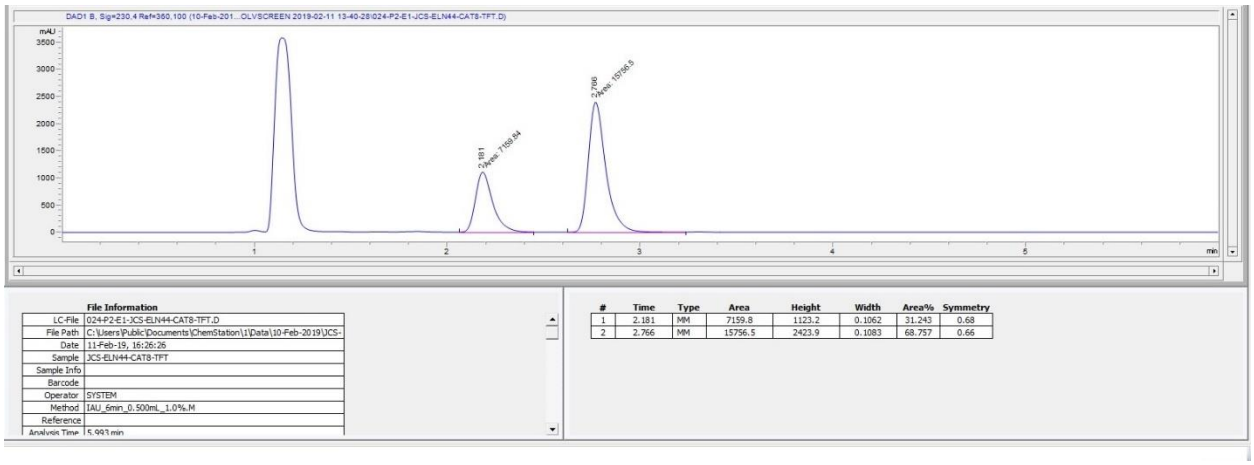

15 prepared with Rh_2(*S*-2-Cl-5-Br-TPCP)$_4$

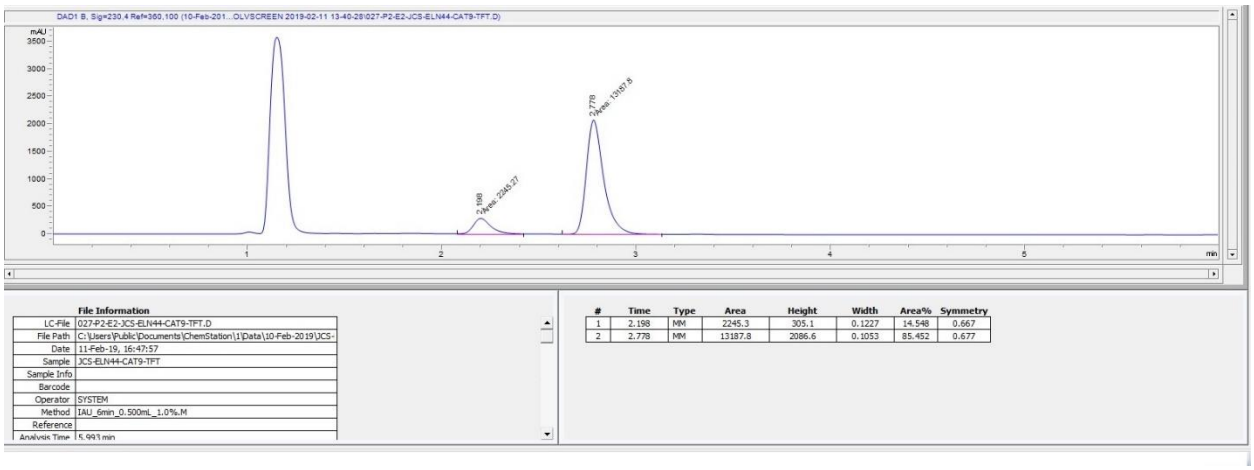

15 prepared with Rh_2(*R*-3,5-di(*p*-^{t}BuC_6H_4)TPCP)$_4$

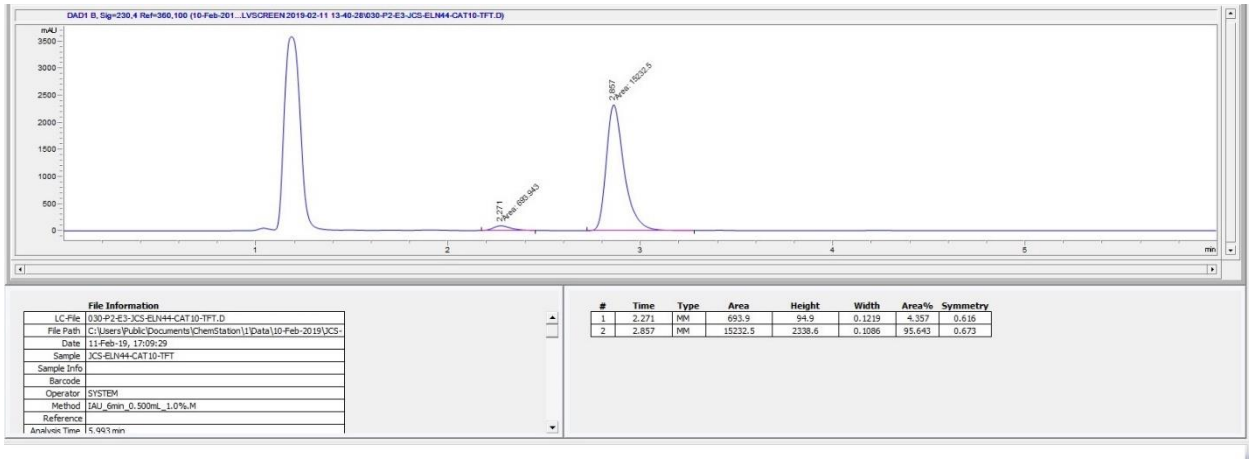

15 prepared with Rh_2(*S*-tris(*p*-^{t}BuC_6H_4)TPCP)$_4$

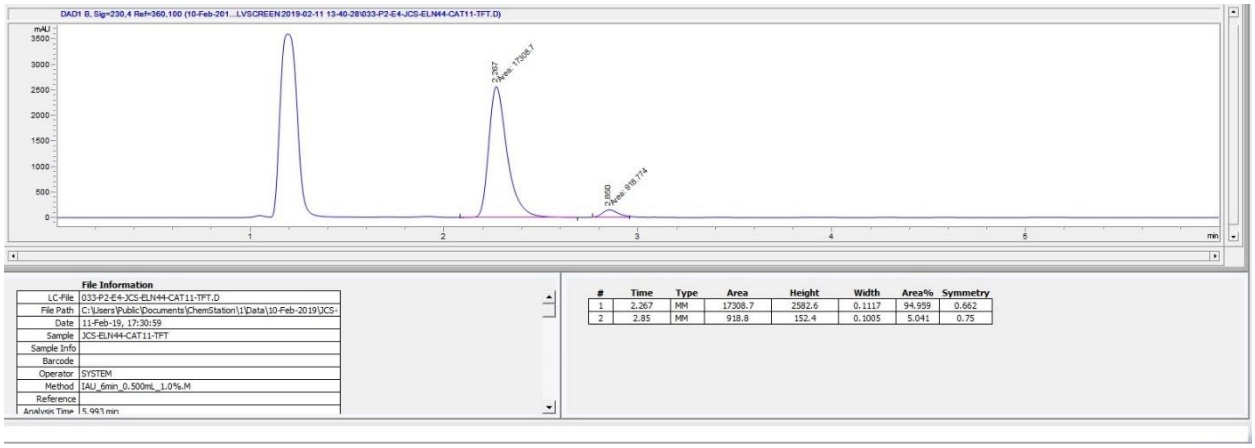

OH insertion: elution at 1.00 min and styrene 7: elution at 1.26 min

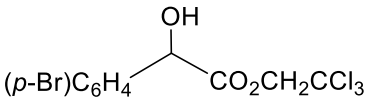

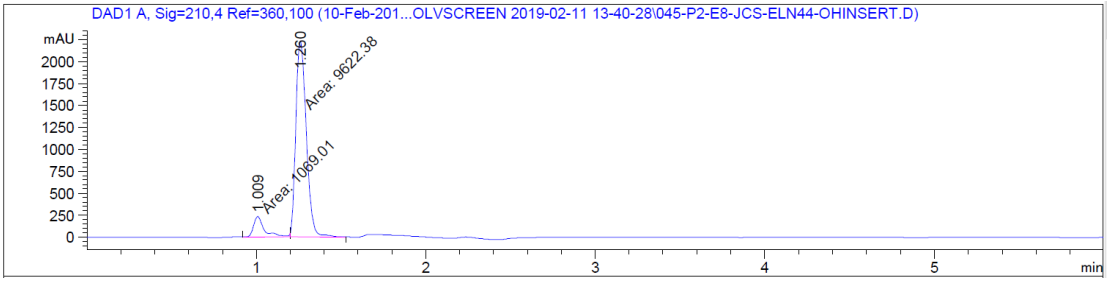

Signal 1: DAD1 A, Sig=210,4 Ref=360,100

Peak #	RetTime [min]	Type	Width [min]	Area [mAU*s]	Height [mAU]	Area %
1	1.009	MM	0.0742	1069.00745	240.26186	9.9988
2	1.260	MM	0.0714	9622.38379	2244.79980	90.0012
Totals :				1.06914e4	2485.06166	

7.4 HPLC Chromatograms of lab scale experiment.

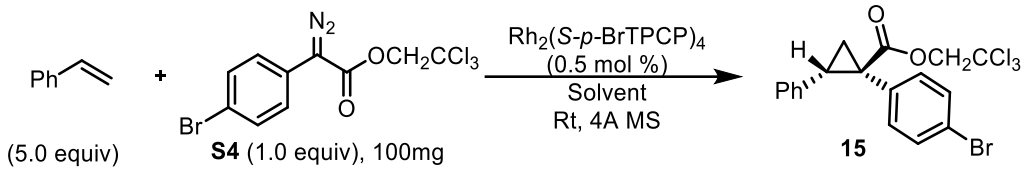

DCM/ Rh_2(*S*-*p*-Br-TPCP)$_4$

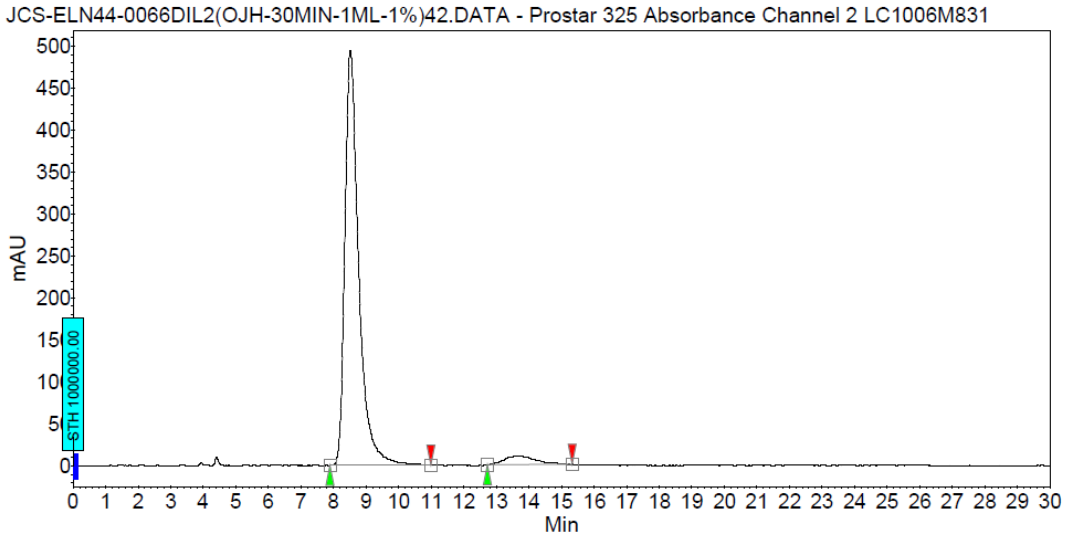

Peak results :

Index	Name	Time [Min]	Quantity [% Area]	Height [mAU]	Area [mAU.Min]	Area % [%]
1	UNKNOWN	8.51	95.35	493.2	243.3	95.353
2	UNKNOWN	13.70	4.65	10.5	11.9	4.647
Total			100.00	503.7	255.1	100.000

DMC/ Rh_2(*S*-*p*-Br-TPCP)$_4$

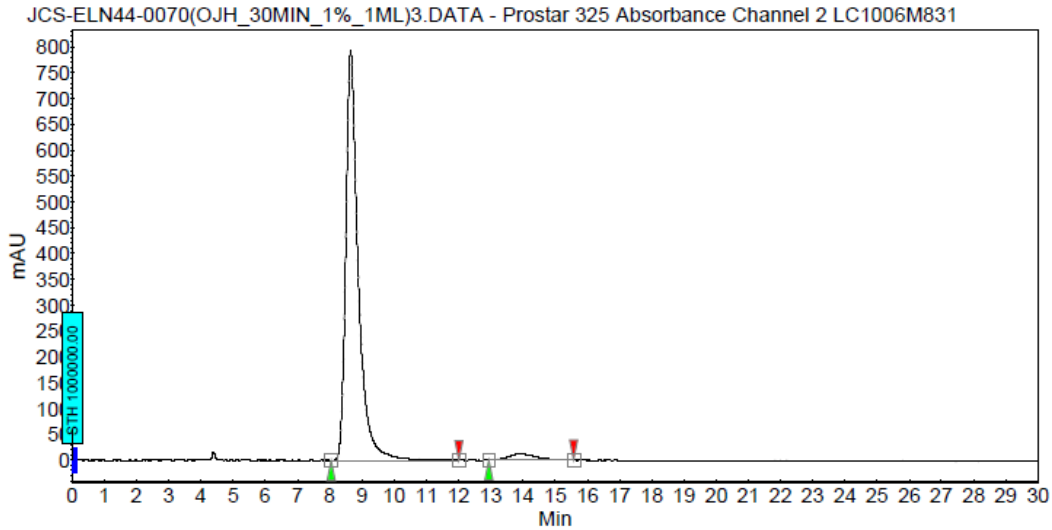

Peak results :

Index	Name	Time [Min]	Quantity [% Area]	Height [mAU]	Area [mAU.Min]	Area % [%]
1	UNKNOWN	8.65	96.72	793.0	356.1	96.725
2	UNKNOWN	13.86	3.28	10.9	12.1	3.275
Total			100.00	803.9	368.1	100.000

DEC/ Rh_2(*S-p*-Br-TPCP)$_4$

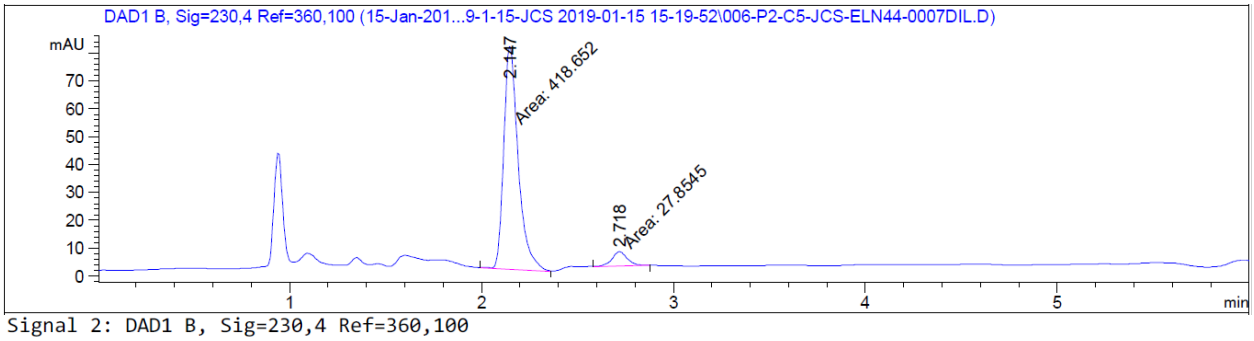

Signal 2: DAD1 B, Sig=230,4 Ref=360,100

Peak #	RetTime [min]	Type	Width [min]	Area [mAU*s]	Height [mAU]	Area %
1	2.147	MM	0.0869	418.65164	80.32243	93.7617
2	2.718	MM	0.0910	27.85451	5.09939	6.2383
Totals :				446.50615	85.42183	

EtOAc/ Rh_2(*S-p*-Br-TPCP)$_4$

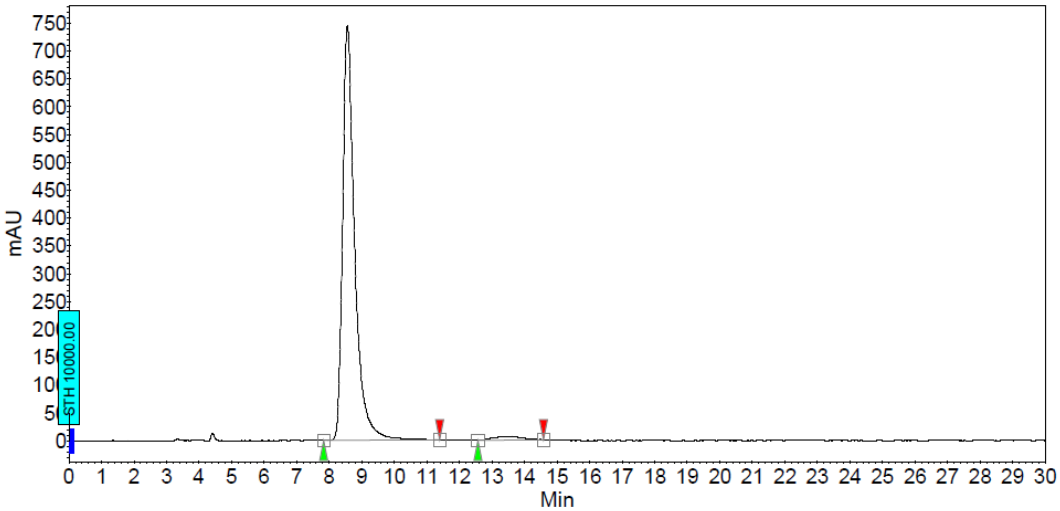

Peak results :

Index	Name	Time [Min]	Quantity [% Area]	Height [mAU]	Area [mAU.Min]	Area % [%]
1	UNKNOWN	8.55	97.82	743.7	319.3	97.825
2	UNKNOWN	13.45	2.18	7.1	7.1	2.175
Total			100.00	750.8	326.4	100.000

iPrOAc/ Rh_2(*S*-*p*-Br-TPCP)$_4$

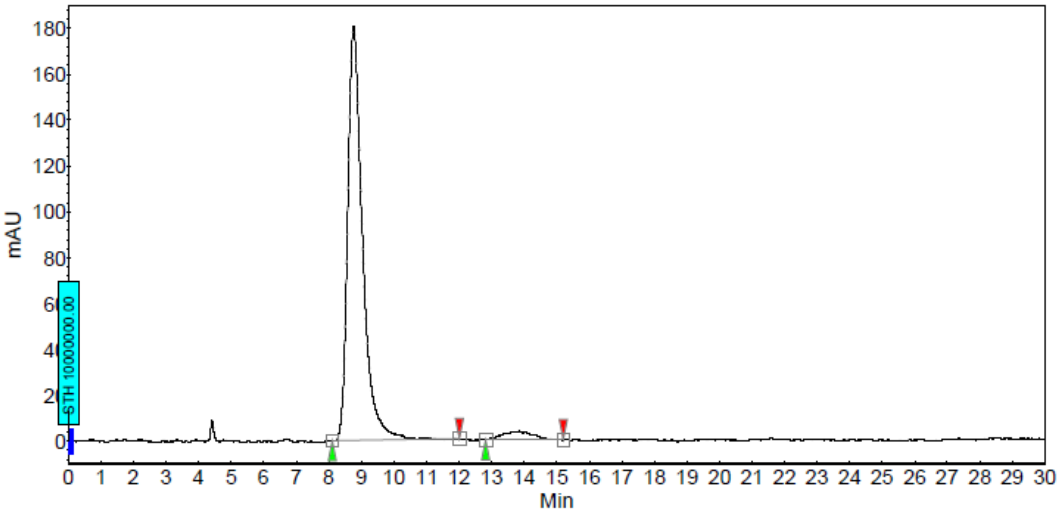

Peak results :

Index	Name	Time [Min]	Quantity [% Area]	Height [mAU]	Area [mAU.Min]	Area % [%]
1	UNKNOWN	8.76	95.95	180.3	95.7	95.955
2	UNKNOWN	13.84	4.05	3.7	4.0	4.045
Total			100.00	184.0	99.7	100.000

PivCN/ Rh_2(*S*-*p*-Br-TPCP)$_4$

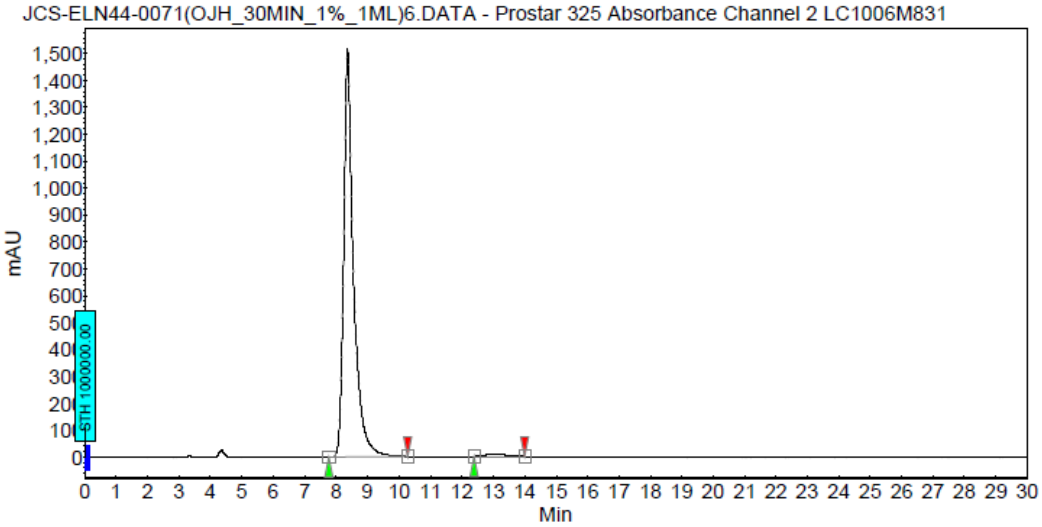

Peak results :

Index	Name	Time [Min]	Quantity [% Area]	Height [mAU]	Area [mAU.Min]	Area % [%]
1	UNKNOWN	8.36	98.65	1514.5	551.6	98.649
2	UNKNOWN	13.01	1.35	9.0	7.6	1.351
Total			100.00	1523.6	559.1	100.000

TFT/ Rh_2(*S*-*p*-Br-TPCP)$_4$

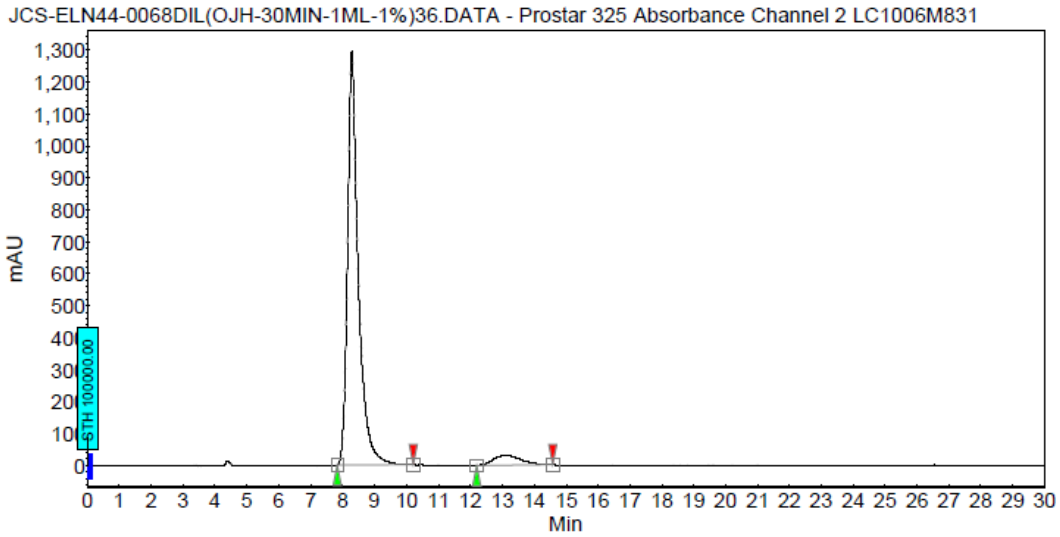

Peak results :

Index	Name	Time [Min]	Quantity [% Area]	Height [mAU]	Area [mAU.Min]	Area % [%]
1	UNKNOWN	8.28	94.28	1293.4	509.3	94.279
2	UNKNOWN	13.05	5.72	30.1	30.9	5.721
Total			100.00	1323.5	540.2	100.000

7.7 HPLC Chromatograms of the scope

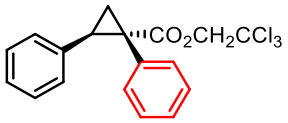

16

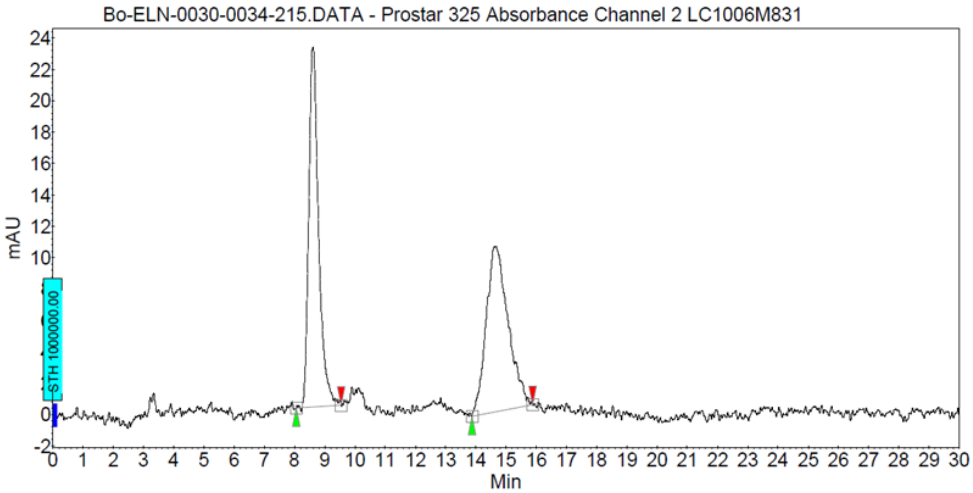

Peak results :

Index	Name	Time [Min]	Quantity [% Area]	Height [mAU]	Area [mAU.Min]	Area % [%]
2	UNKNOWN	8.60	49.42	22.9	8.7	49.421
1	UNKNOWN	14.60	50.58	10.6	8.9	50.579
Total			100.00	33.5	17.6	100.000

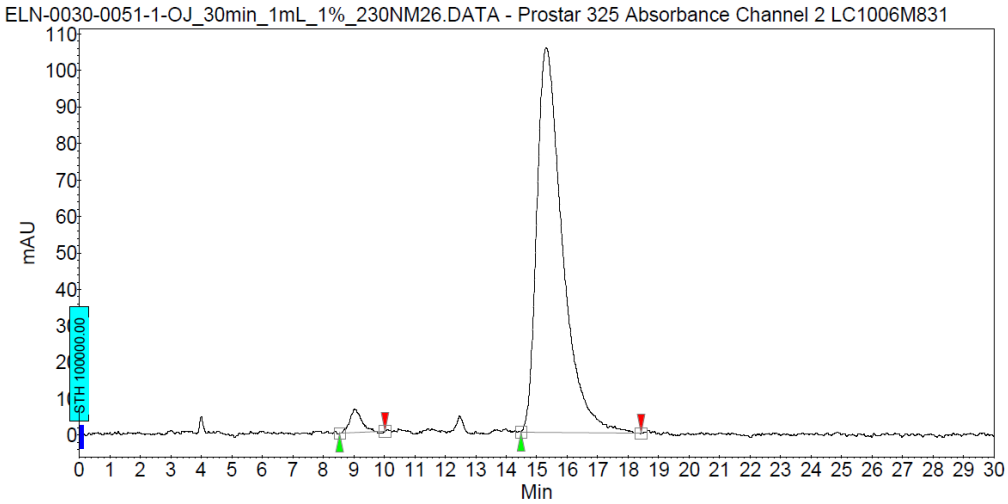

Peak results :

Index	Name	Time [Min]	Quantity [% Area]	Height [mAU]	Area [mAU.Min]	Area % [%]
1	UNKNOWN	9.01	2.71	6.5	2.9	2.713
2	UNKNOWN	15.31	97.29	105.4	102.9	97.287
Total			100.00	111.9	105.7	100.000

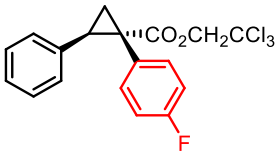

17

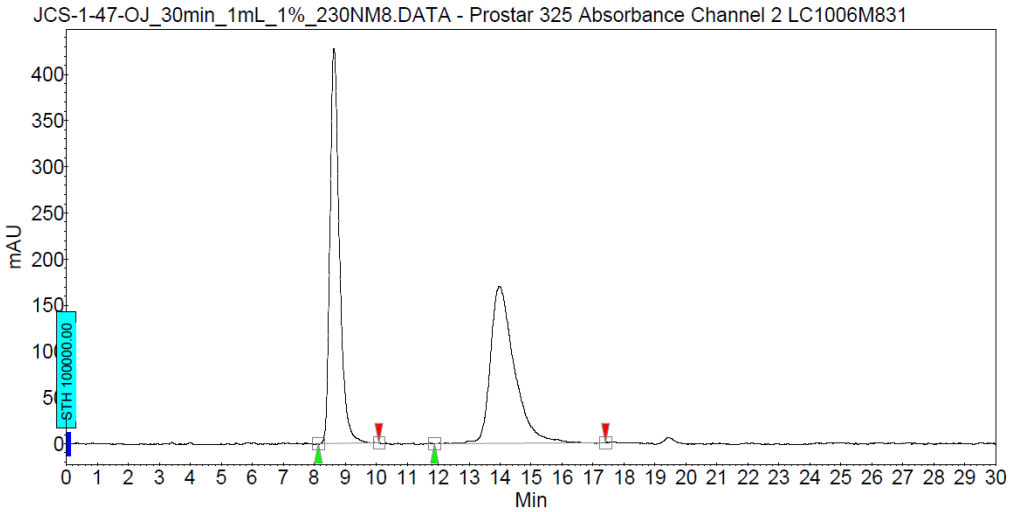

Peak results :

Index	Name	Time [Min]	Quantity [% Area]	Height [mAU]	Area [mAU.Min]	Area % [%]
2	UNKNOWN	8.64	50.17	427.5	151.7	50.174
1	UNKNOWN	13.97	49.83	170.3	150.6	49.826
Total			100.00	597.8	302.3	100.000

ELN-0030-0047-OJ_30min_1mL_1%_230NM8.DATA - Prostar 325 Absorbance Channel 2 LC1006M831

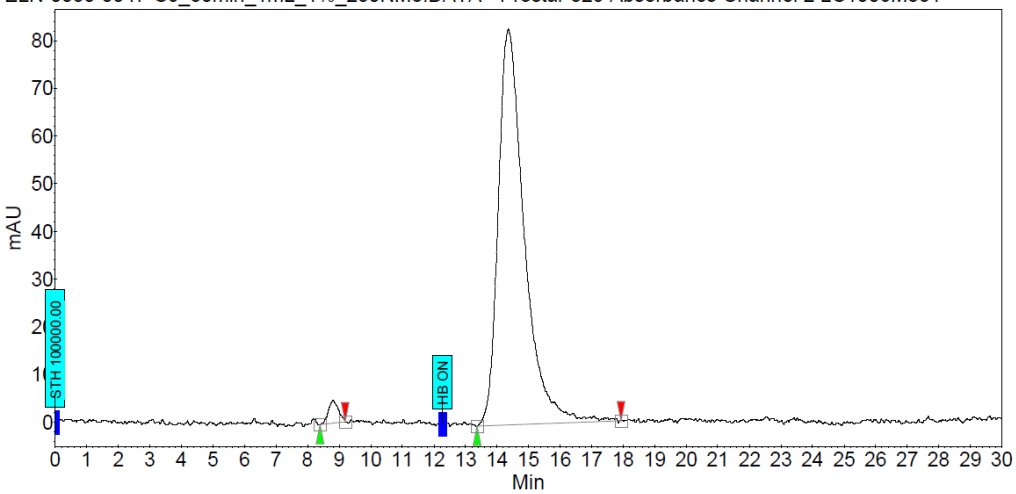

Peak results :

Index	Name	Time [Min]	Quantity [% Area]	Height [mAU]	Area [mAU.Min]	Area % [%]
1	UNKNOWN	8.81	2.16	4.8	1.8	2.162
2	UNKNOWN	14.36	97.84	83.0	79.5	97.838
Total			100.00	87.7	81.2	100.000

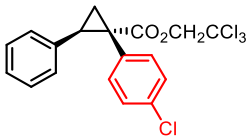

18

pcl-1222.DATA - Prostar 325 Absorbance Channel 2 LC1006M831

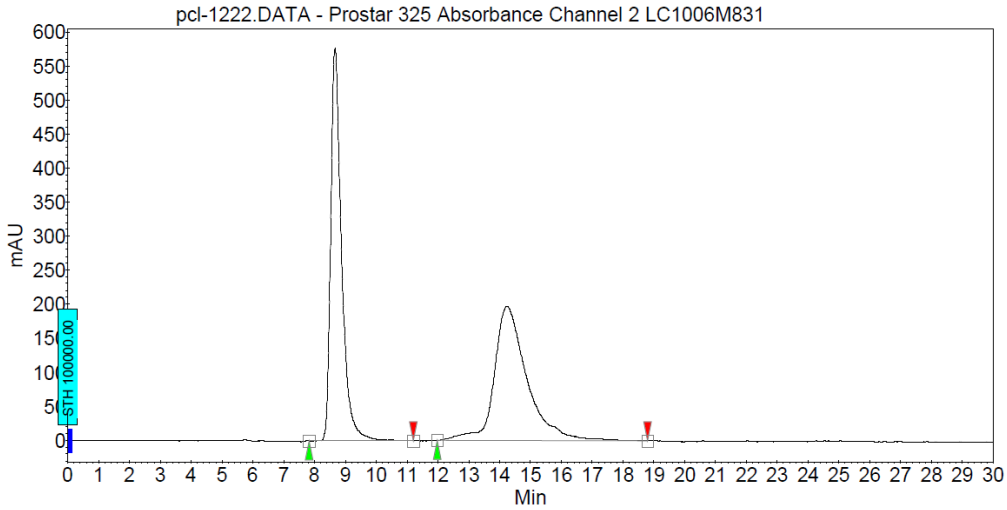

Peak results :

Index	Name	Time [Min]	Quantity [% Area]	Height [mAU]	Area [mAU.Min]	Area % [%]
1	UNKNOWN	8.66	49.03	576.9	234.9	49.032
2	UNKNOWN	14.24	50.97	197.4	244.2	50.968
Total			100.00	774.3	479.2	100.000

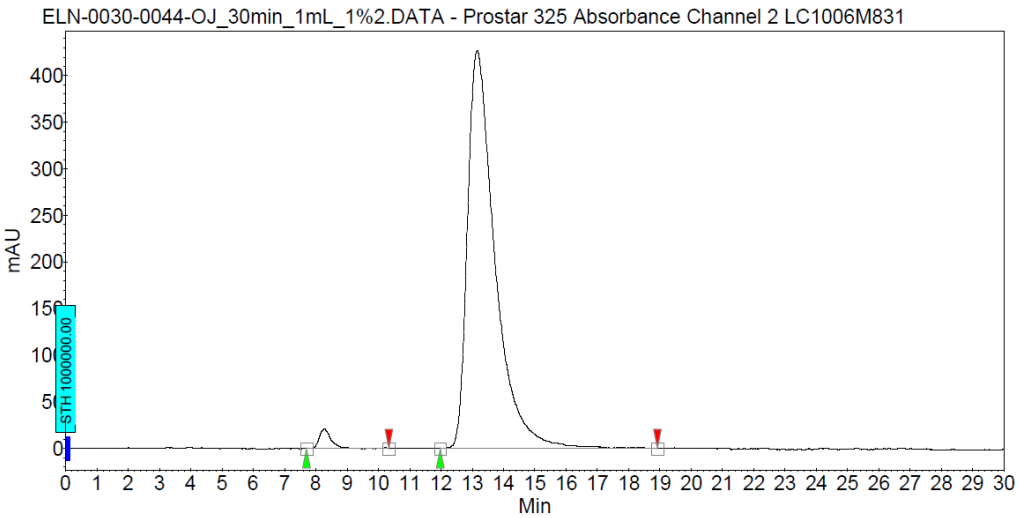

Peak results :

Index	Name	Time [Min]	Quantity [% Area]	Height [mAU]	Area [mAU.Min]	Area % [%]
2	UNKNOWN	8.28	2.08	21.0	9.2	2.082
1	UNKNOWN	13.16	97.92	426.3	434.4	97.918
Total			100.00	447.3	443.7	100.000

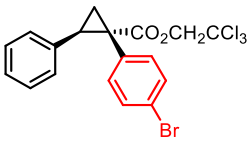

14

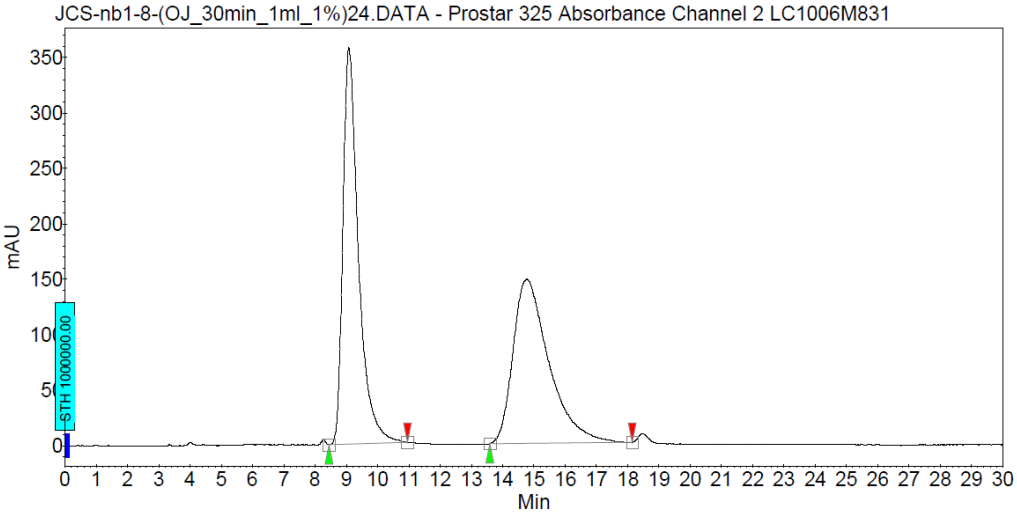

Peak results :

Index	Name	Time [Min]	Quantity [% Area]	Height [mAU]	Area [mAU.Min]	Area % [%]
2	UNKNOWN	9.08	51.18	357.7	206.3	51.180
1	UNKNOWN	14.77	48.82	148.0	196.8	48.820
Total			100.00	505.7	403.1	100.000

ELN-30-0043-re-OJ_30min_1mL_1%_230NM8.DATA - Prostar 325 Absorbance Channel 2 LC1006M831

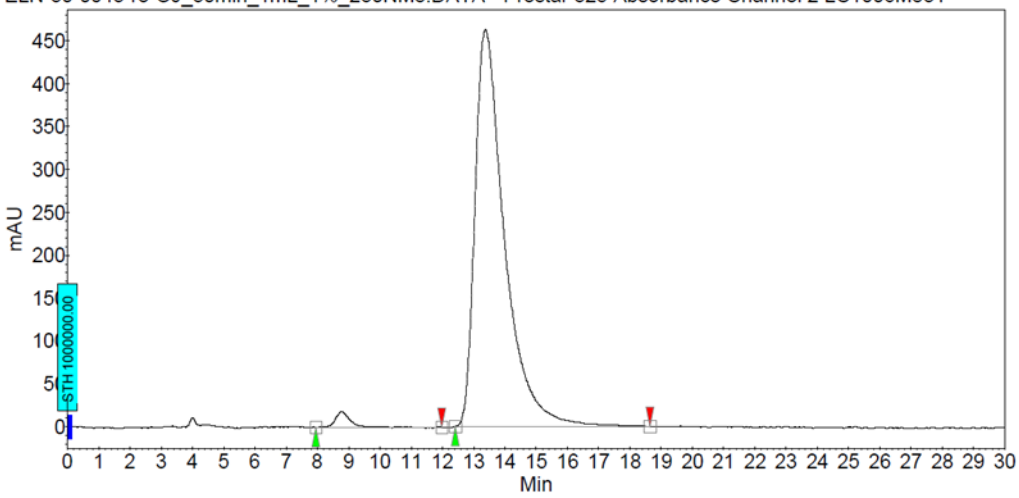

Peak results :

Index	Name	Time [Min]	Quantity [% Area]	Height [mAU]	Area [mAU.Min]	Area % [%]
2	UNKNOWN	8.78	1.97	18.2	10.2	1.970
1	UNKNOWN	13.38	98.03	462.6	507.0	98.030
Total			100.00	480.8	517.2	100.000

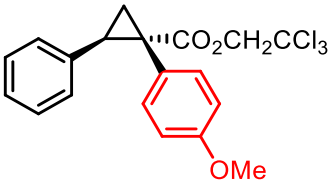

19

ELN-30-0032-RAC-RRW_45min_1mL_1%_230nm23.DATA - Prostar 325 Absorbance Channel 2 LC1006M831

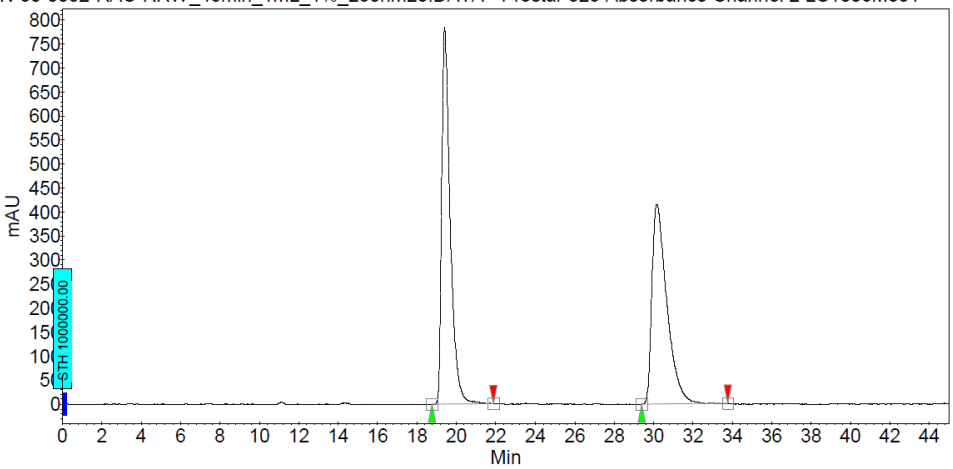

Peak results :

Index	Name	Time [Min]	Quantity [% Area]	Height [mAU]	Area [mAU.Min]	Area % [%]
2	UNKNOWN	19.40	51.62	783.9	390.5	51.625
1	UNKNOWN	30.17	48.38	415.6	365.9	48.375
Total			100.00	1199.6	756.5	100.000

ELN-0030-0050-3-new-RRW-30min_1mL_1%_230nm2.DATA - Prostar 325 Absorbance Channel 2 LC1006M831

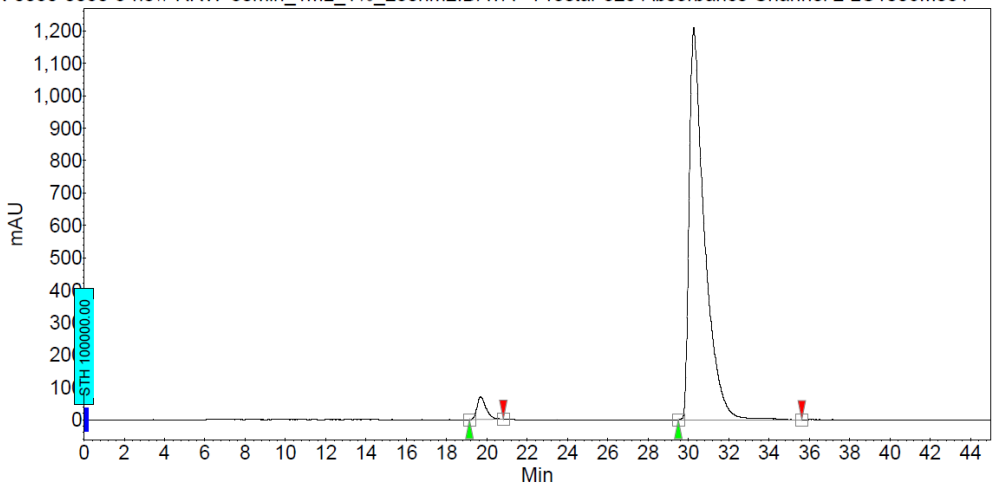

Peak results :

Index	Name	Time [Min]	Quantity [% Area]	Height [mAU]	Area [mAU.Min]	Area % [%]
2	UNKNOWN	19.68	3.29	70.6	36.0	3.294
1	UNKNOWN	30.26	96.71	1208.0	1056.7	96.706
Total			100.00	1278.6	1092.7	100.000

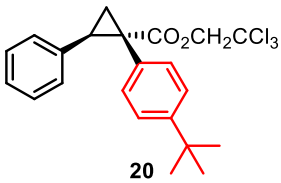

20

ELN-0030-0045-RE-RRW_30min_1mL_1%_230nm47.DATA - Prostar 325 Absorbance Channel 2 LC1006M831

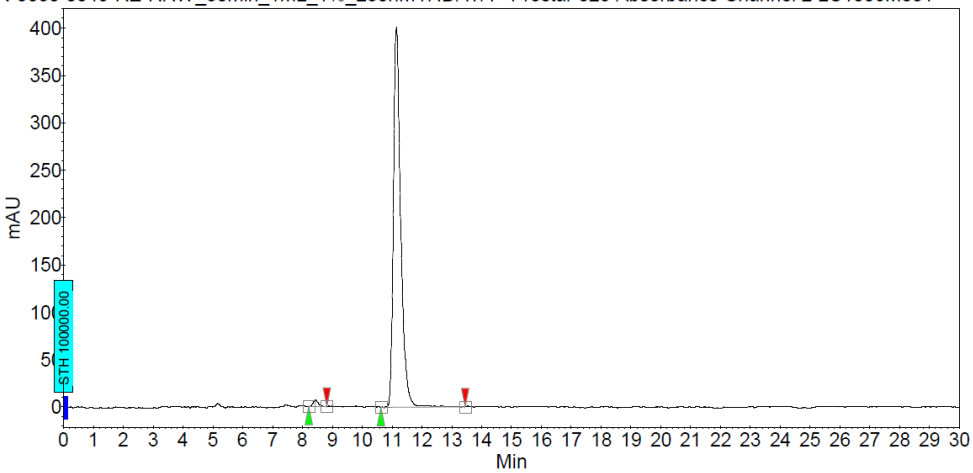

Peak results :

Index	Name	Time [Min]	Quantity [% Area]	Height [mAU]	Area [mAU.Min]	Area % [%]
1	UNKNOWN	8.43	1.15	7.0	1.3	1.152
2	UNKNOWN	11.15	98.85	400.7	113.5	98.848
Total			100.00	407.7	114.8	100.000

ELN-0030-0048-S250_30min_1mL_1%_230nm23.DATA - Prostar 325 Absorbance Channel 2 LC1006M831

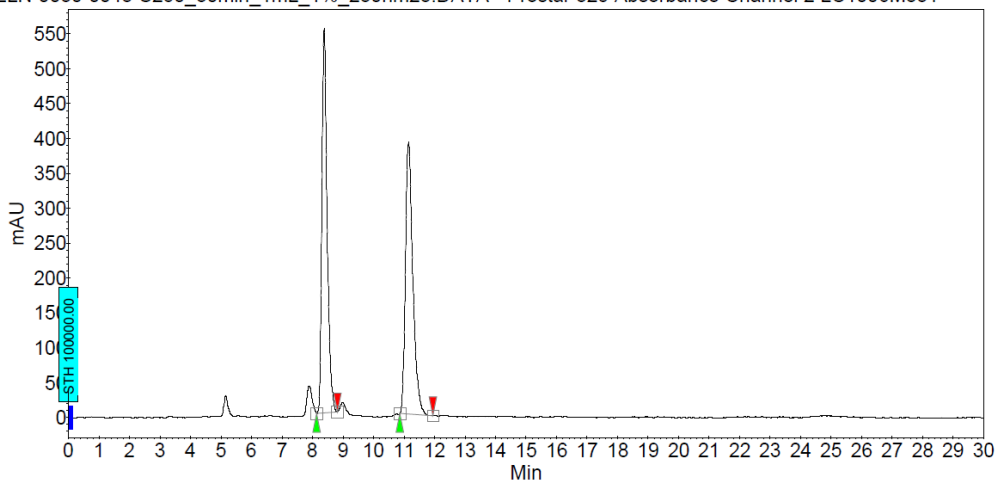

Peak results :

Index	Name	Time [Min]	Quantity [% Area]	Height [mAU]	Area [mAU.Min]	Area % [%]
1	UNKNOWN	8.38	50.06	550.9	109.8	50.056
2	UNKNOWN	11.15	49.94	389.7	109.5	49.944
Total			100.00	940.6	219.3	100.000

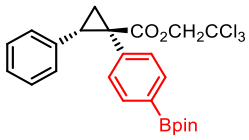

21

ELN-0030-0057-OLD-SSW_30min_1mL_1%_230nm20.DATA - Prostar 325 Absorbance Channel 1 LC1006M831

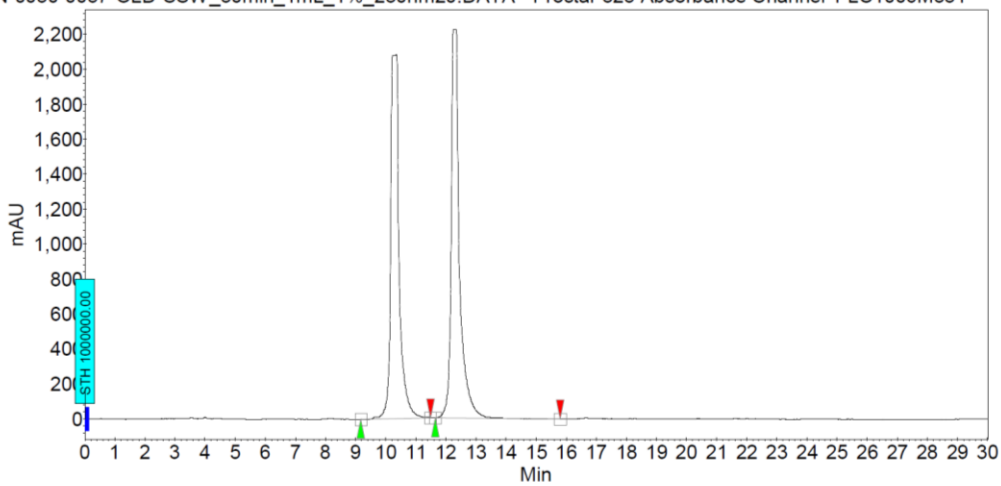

Peak results :

Index	Name	Time [Min]	Quantity [% Area]	Height [mAU]	Area [mAU.Min]	Area % [%]
1	UNKNOWN	10.36	49.27	2082.8	693.4	49.274
2	UNKNOWN	12.32	50.73	2223.5	713.9	50.726
Total			100.00	4306.3	1407.3	100.000

ELN-0030-0061-OLD-SSW_30min_1mL_1%_230nm23.DATA - Prostar 325 Absorbance Channel 2 LC1006M831

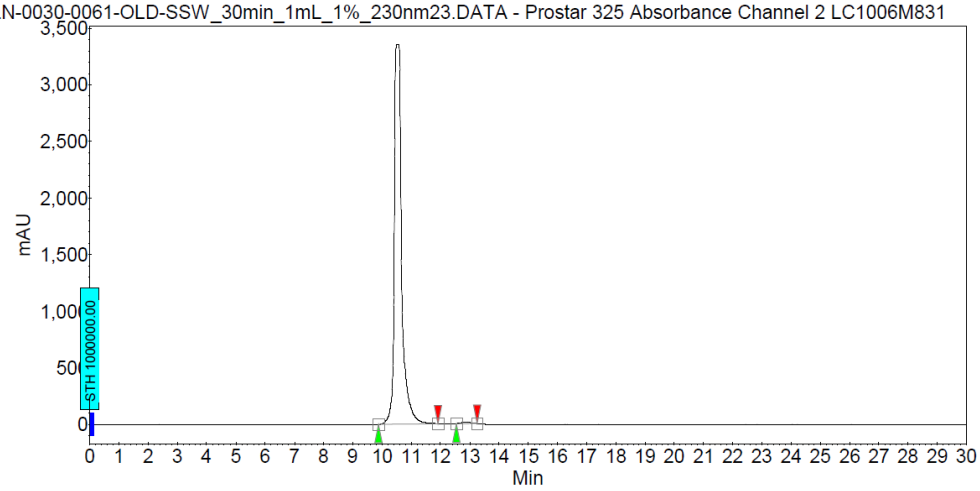

Peak results :

Index	Name	Time [Min]	Quantity [% Area]	Height [mAU]	Area [mAU.Min]	Area % [%]
1	UNKNOWN	10.49	99.47	3348.7	979.5	99.466
2	UNKNOWN	12.84	0.53	14.4	5.3	0.534
Total			100.00	3363.1	984.8	100.000

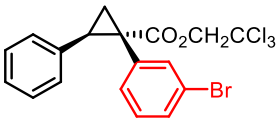

22

Bo-ELN-0030-0073-OJH_30min_1mL_1%2.DATA - Prostar 325 Absorbance Channel 2 LC1006M831

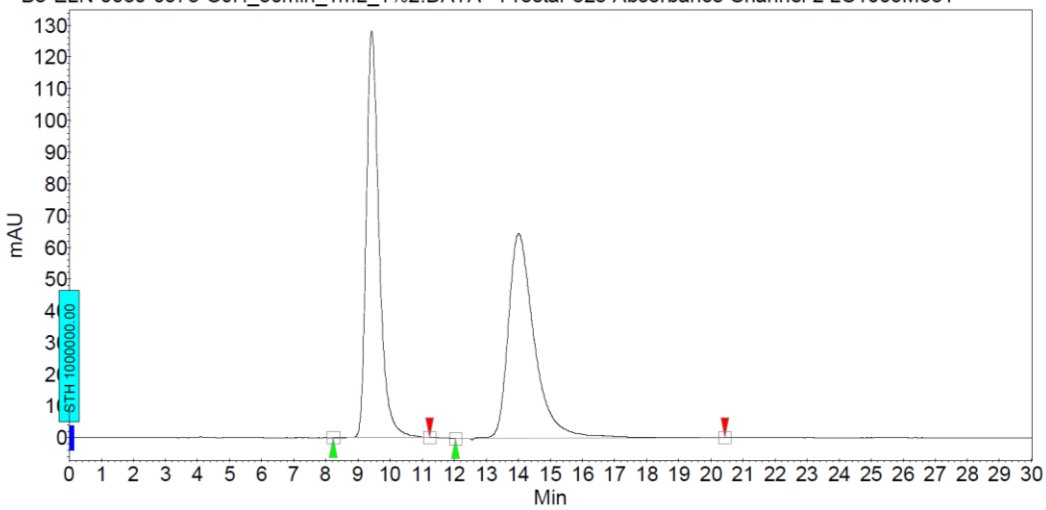

Peak results :

Index	Name	Time [Min]	Quantity [% Area]	Height [mAU]	Area [mAU.Min]	Area % [%]
1	UNKNOWN	9.43	49.33	128.4	59.2	49.330
2	UNKNOWN	14.01	50.67	64.5	60.8	50.670
Total			100.00	192.9	120.1	100.000

Bo-ELN-0030-0068-OJ_30min_1mL_1%_230NM11.DATA - Prostar 325 Absorbance Channel 2 LC1006M831

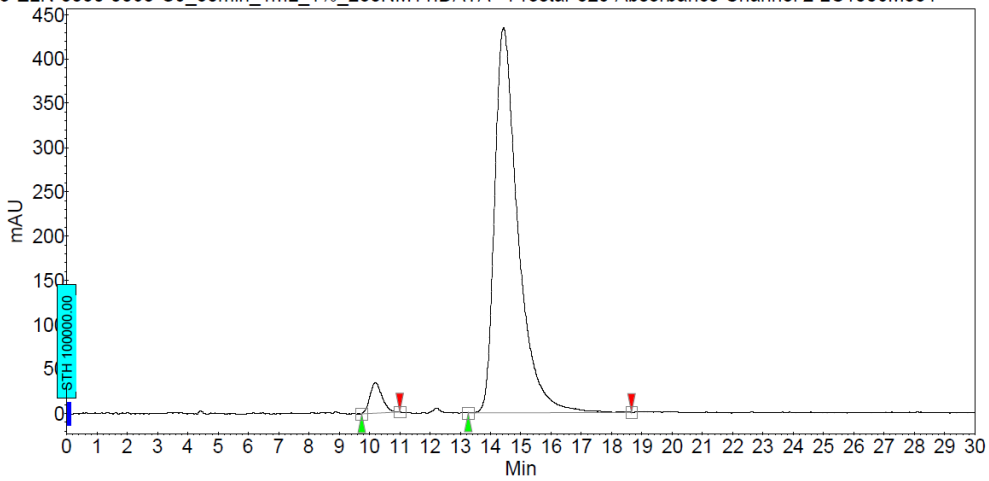

Peak results :

Index	Name	Time [Min]	Quantity [% Area]	Height [mAU]	Area [mAU.Min]	Area % [%]
2	UNKNOWN	10.20	3.94	34.4	15.9	3.942
1	UNKNOWN	14.43	96.06	434.4	388.7	96.058
Total			100.00	468.8	404.6	100.000

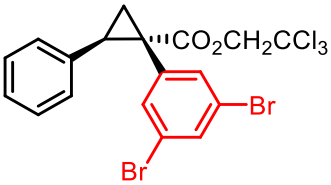

23

Bo-ELN-0030-0075-ODH-30min_1mL_1%_210_2305.DATA - Prostar 325 Absorbance Channel 2 LC1006M831

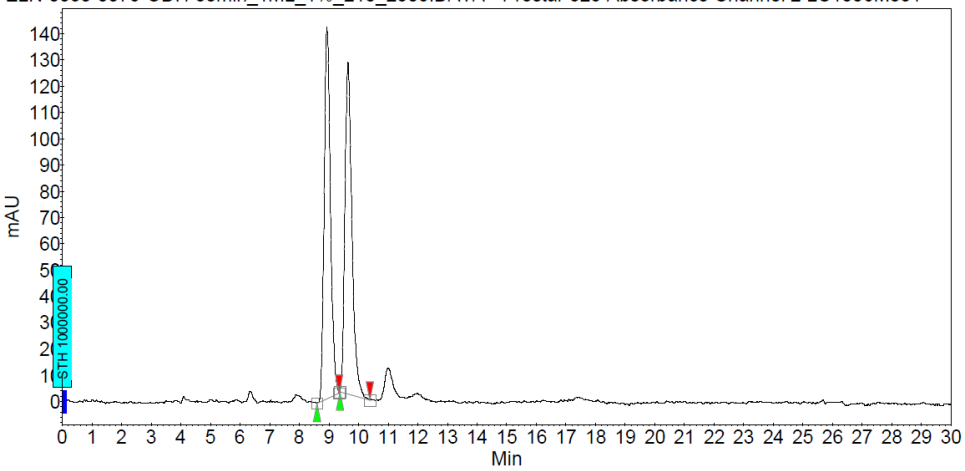

Peak results :

Index	Name	Time [Min]	Quantity [% Area]	Height [mAU]	Area [mAU.Min]	Area % [%]
1	UNKNOWN	8.93	49.87	141.4	34.7	49.871
2	UNKNOWN	9.64	50.13	126.3	34.9	50.129
Total			100.00	267.7	69.6	100.000

Bo-ELN-0030-0074-ODH-30min_1mL_1%_210_23015.DATA - Prostar 325 Absorbance Channel 2 LC1006M831

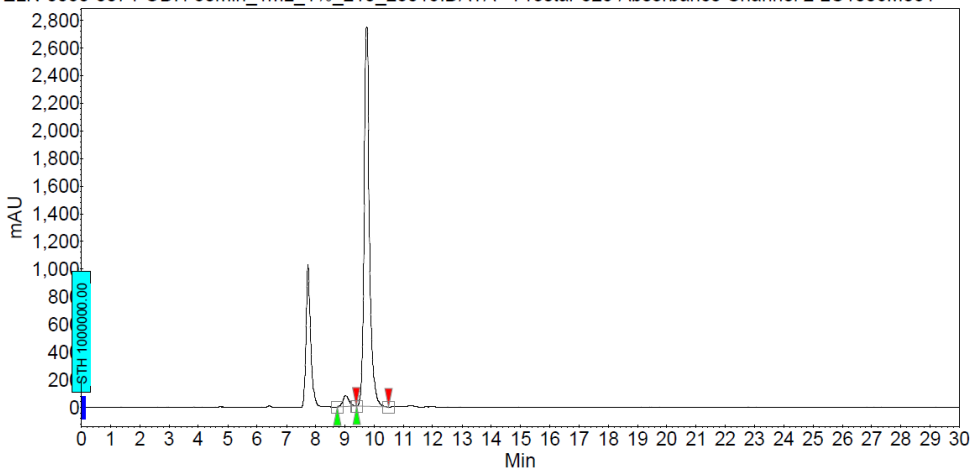

Peak results :

Index	Name	Time [Min]	Quantity [% Area]	Height [mAU]	Area [mAU.Min]	Area % [%]
1	UNKNOWN	9.03	3.17	77.1	18.9	3.165
2	UNKNOWN	9.75	96.83	2741.1	578.7	96.835
Total			100.00	2818.3	597.7	100.000

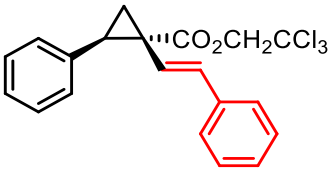

24

rac-JCS-0015-ADH_30min_1mL_1%_230nm37.DATA - Prostar 325 Absorbance Channel 2 LC1006M831

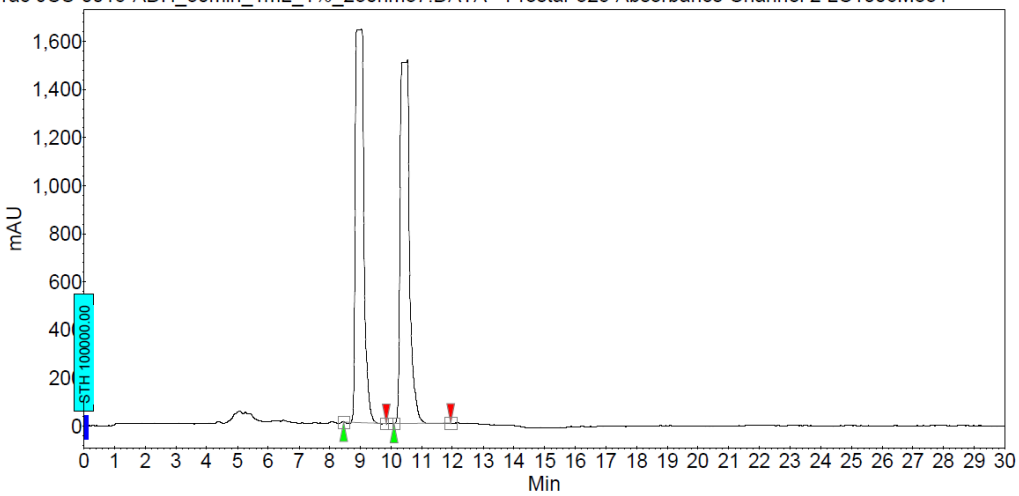

Peak results :

Index	Name	Time [Min]	Quantity [% Area]	Height [mAU]	Area [mAU.Min]	Area % [%]
1	UNKNOWN	9.05	49.63	1637.7	522.8	49.635
2	UNKNOWN	10.54	50.37	1513.5	530.5	50.365
Total			100.00	3151.3	1053.3	100.000

ELN-0030-0067-3RD-ADH_30min_1mL_1%_230NM40.DATA - Prostar 325 Absorbance Channel 2 LC1006M831

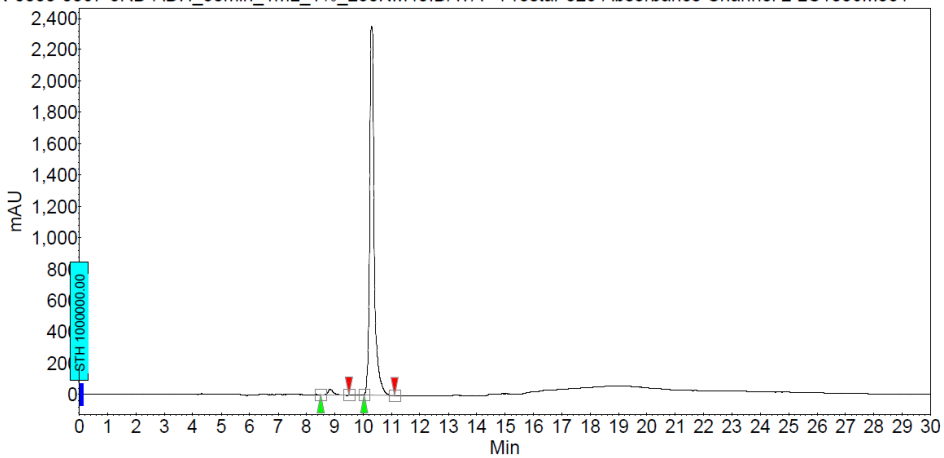

Peak results :

Index	Name	Time [Min]	Quantity [% Area]	Height [mAU]	Area [mAU.Min]	Area % [%]
1	UNKNOWN	8.84	1.63	36.5	7.3	1.630
2	UNKNOWN	10.30	98.37	2349.2	440.5	98.370
Total			100.00	2385.7	447.8	100.000

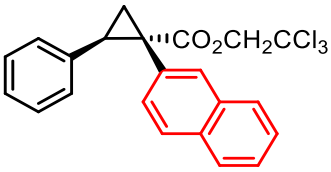

25

Bo-ELN-0030-0072-ADH_30min_1mL_1%_230nm44.DATA - Prostar 325 Absorbance Channel 2 LC1006M831

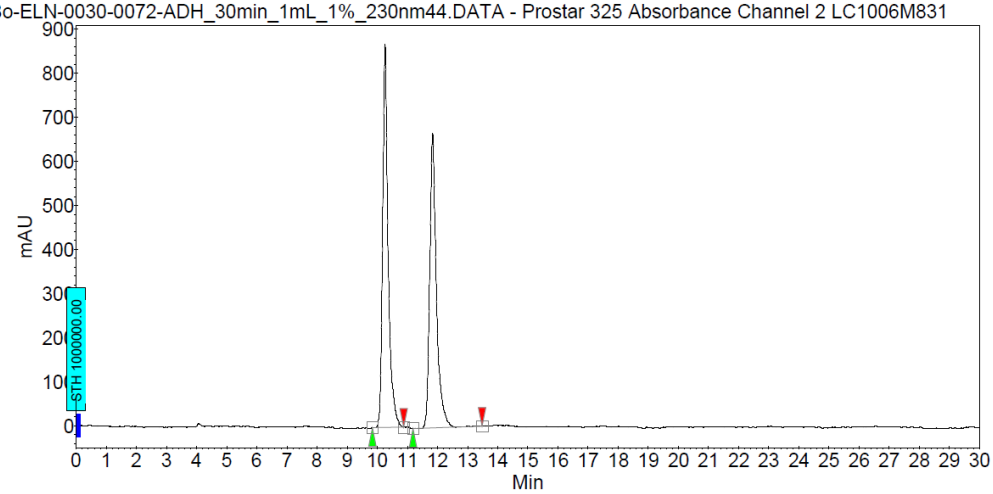

Peak results :

Index	Name	Time [Min]	Quantity [% Area]	Height [mAU]	Area [mAU.Min]	Area % [%]
2	UNKNOWN	10.26	51.77	868.7	183.8	51.767
1	UNKNOWN	11.84	48.23	667.9	171.2	48.233
Total			100.00	1536.6	355.0	100.000

Bo-ELN-0030-0069-ADH-30min_1mL_1%_210_2302.DATA - Prostar 325 Absorbance Channel 2 LC1006M831

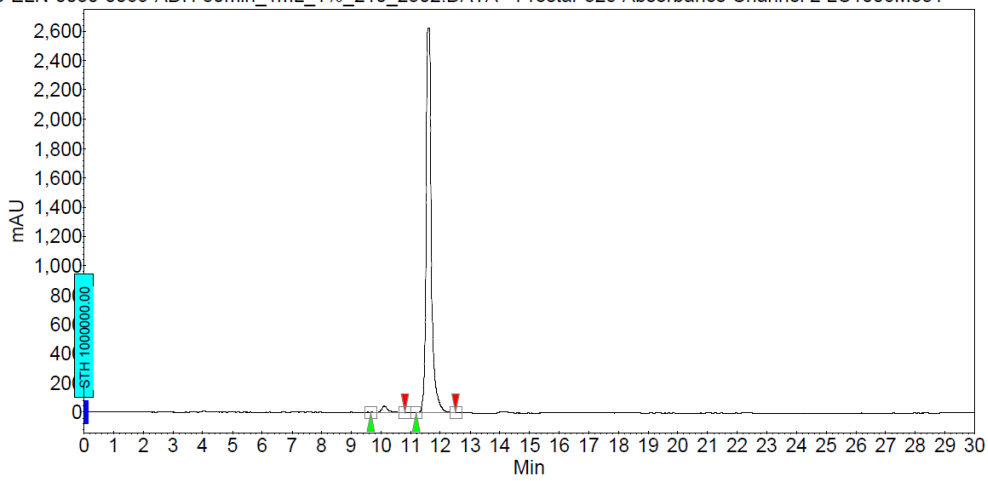

Peak results :

Index	Name	Time [Min]	Quantity [% Area]	Height [mAU]	Area [mAU.Min]	Area % [%]
2	UNKNOWN	10.11	1.81	42.7	9.9	1.811
1	UNKNOWN	11.60	98.19	2622.2	538.0	98.189
Total			100.00	2664.9	547.9	100.000

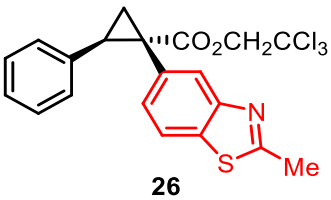

26

ELN-0030-0056-OJ_30min_1mL_3%_230nm2.DATA - Prostar 325 Absorbance Channel 2 LC1006M831

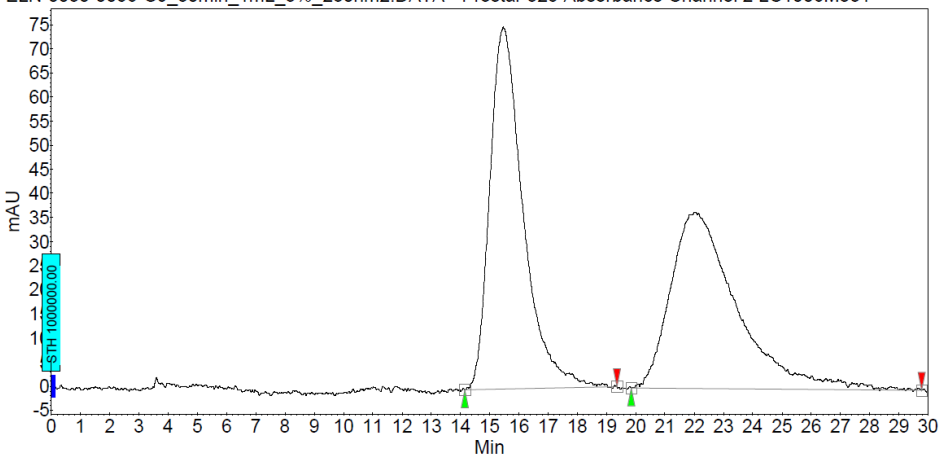

Peak results :

Index	Name	Time [Min]	Quantity [% Area]	Height [mAU]	Area [mAU.Min]	Area % [%]
2	UNKNOWN	15.47	50.79	75.1	99.1	50.790
1	UNKNOWN	22.05	49.21	36.6	96.1	49.210
Total			100.00	111.7	195.2	100.000

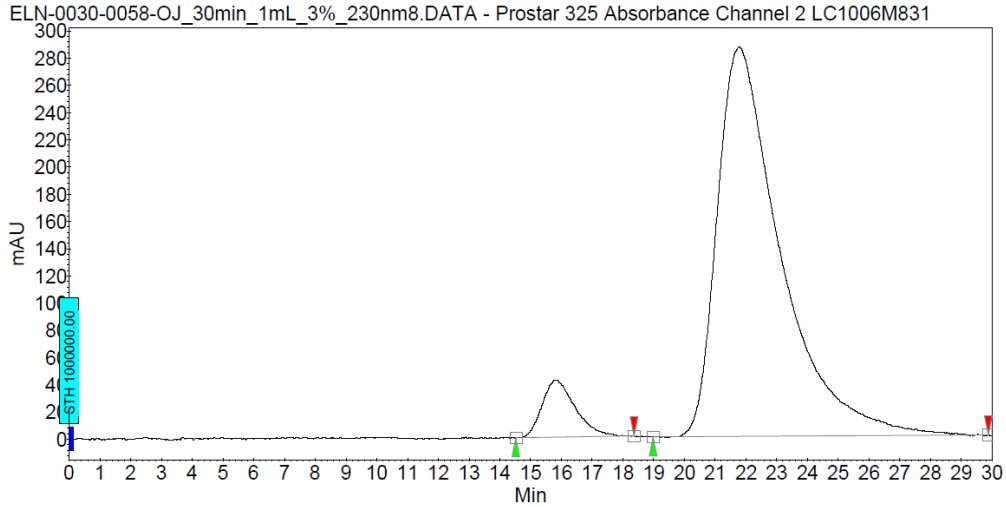

Peak results :

Index	Name	Time [Min]	Quantity [% Area]	Height [mAU]	Area [mAU.Min]	Area % [%]
1	UNKNOWN	15.83	7.07	41.9	51.9	7.067
2	UNKNOWN	21.77	92.93	286.0	681.8	92.933
Total			100.00	327.9	733.7	100.000

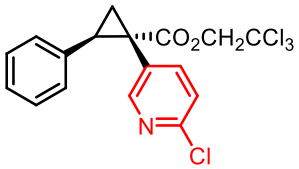

27

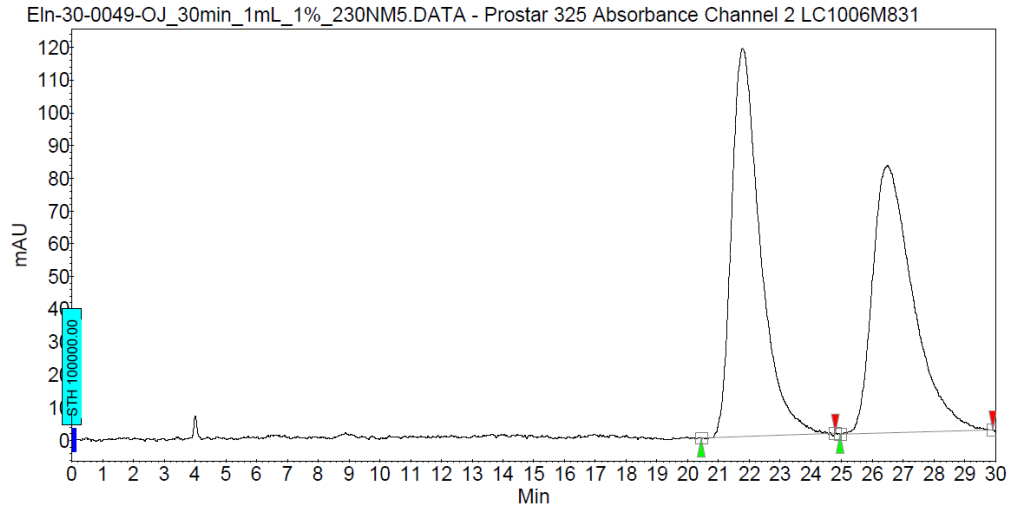

Peak results :

Index	Name	Time [Min]	Quantity [% Area]	Height [mAU]	Area [mAU.Min]	Area % [%]
1	UNKNOWN	21.77	50.77	118.5	127.8	50.771
2	UNKNOWN	26.49	49.23	81.7	123.9	49.229
Total			100.00	200.2	251.7	100.000

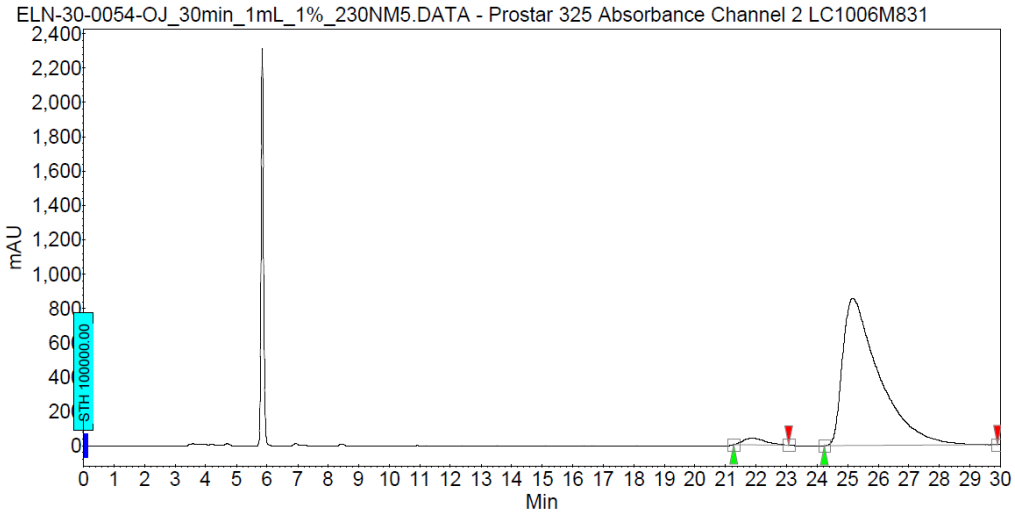

Peak results :

Index	Name	Time [Min]	Quantity [% Area]	Height [mAU]	Area [mAU.Min]	Area % [%]
2	UNKNOWN	21.88	2.69	38.6	32.7	2.690
1	UNKNOWN	25.17	97.31	853.5	1182.5	97.310
Total			100.00	892.1	1215.2	100.000

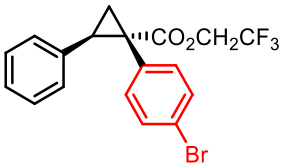

28

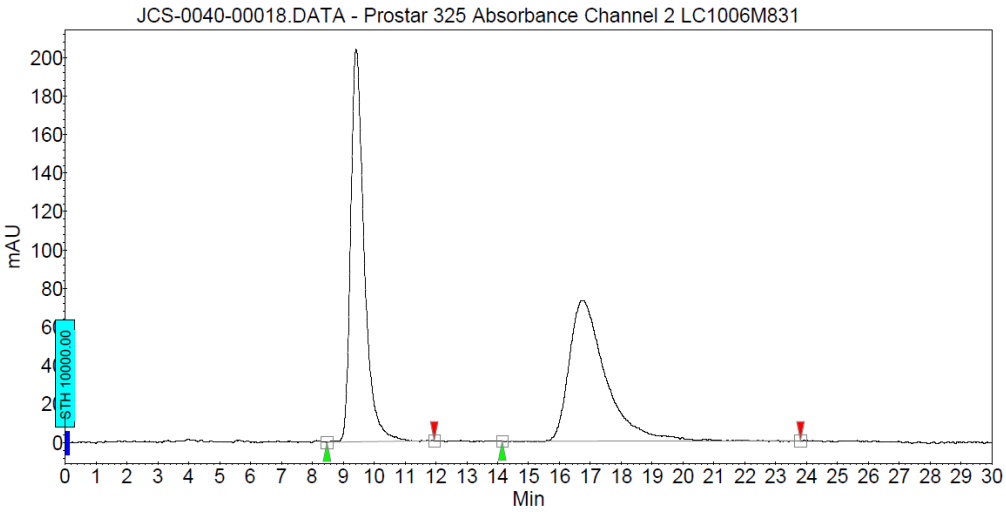

Peak results :

Index	Name	Time [Min]	Quantity [% Area]	Height [mAU]	Area [mAU.Min]	Area % [%]
1	UNKNOWN	9.42	50.84	203.8	103.4	50.836
2	UNKNOWN	16.77	49.16	73.2	100.0	49.164
Total			100.00	277.0	203.5	100.000

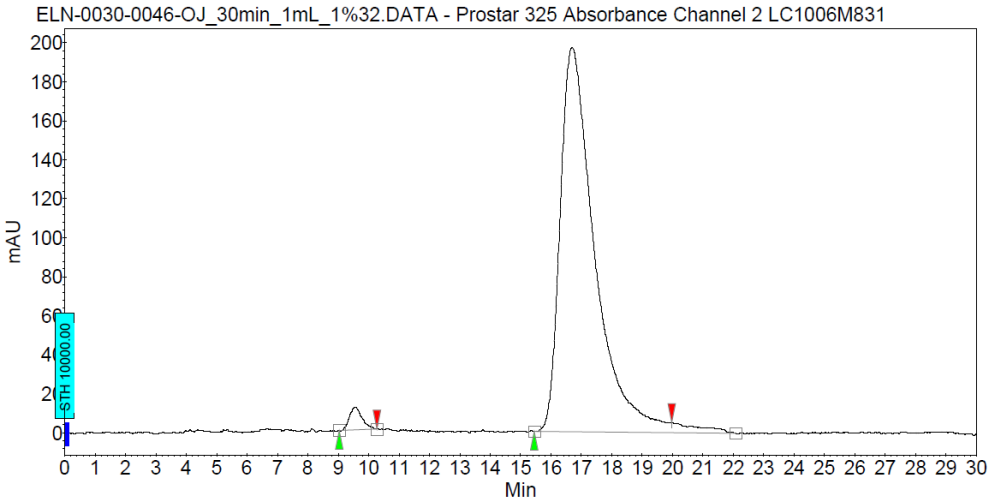

Peak results :

Index	Name	Time [Min]	Quantity [% Area]	Height [mAU]	Area [mAU.Min]	Area % [%]
1	UNKNOWN	9.57	2.09	11.6	5.5	2.094
2	UNKNOWN	16.70	97.91	196.9	258.0	97.906
Total			100.00	208.5	263.6	100.000

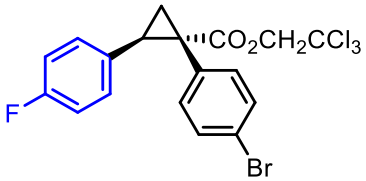

29

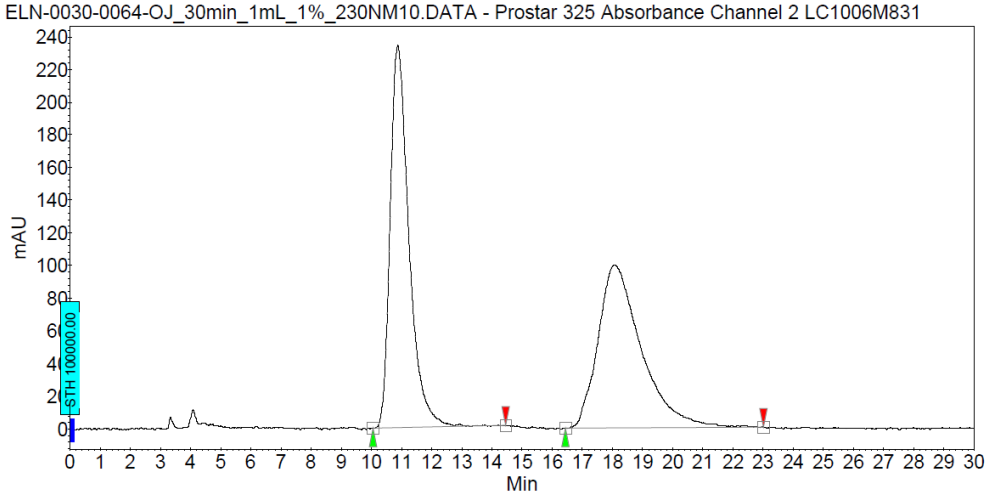

Peak results :

Index	Name	Time [Min]	Quantity [% Area]	Height [mAU]	Area [mAU.Min]	Area % [%]
1	UNKNOWN	10.88	50.46	233.7	168.5	50.457
2	UNKNOWN	18.04	49.54	99.4	165.4	49.543
Total			100.00	333.2	333.9	100.000

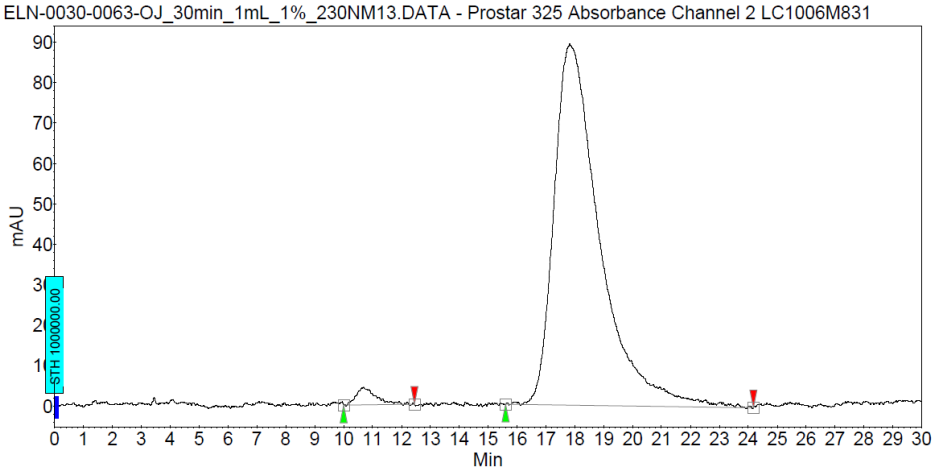

Peak results :

Index	Name	Time [Min]	Quantity [% Area]	Height [mAU]	Area [mAU.Min]	Area % [%]
2	UNKNOWN	10.69	2.03	4.4	3.4	2.033
1	UNKNOWN	17.82	97.97	89.4	163.1	97.967
Total			100.00	93.7	166.4	100.000

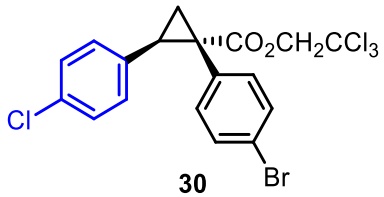

30

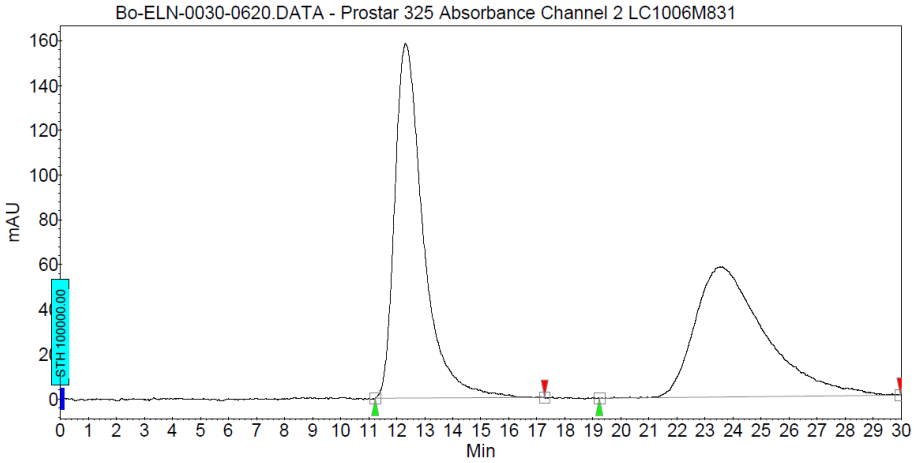

Peak results :

Index	Name	Time [Min]	Quantity [% Area]	Height [mAU]	Area [mAU.Min]	Area % [%]
2	UNKNOWN	12.31	52.61	158.2	185.8	52.607
1	UNKNOWN	23.63	47.39	58.1	167.4	47.393
Total			100.00	216.3	353.2	100.000

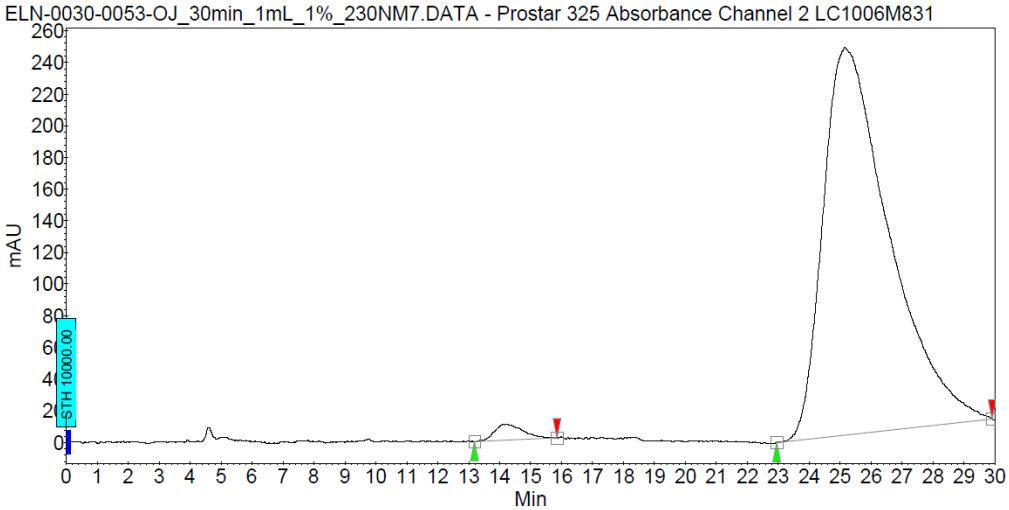

Peak results :

Index	Name	Time [Min]	Quantity [% Area]	Height [mAU]	Area [mAU.Min]	Area % [%]
1	UNKNOWN	14.12	1.76	10.3	10.8	1.756
2	UNKNOWN	25.15	98.24	244.7	606.0	98.244
Total			100.00	255.0	616.8	100.000

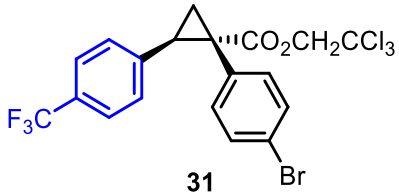

31

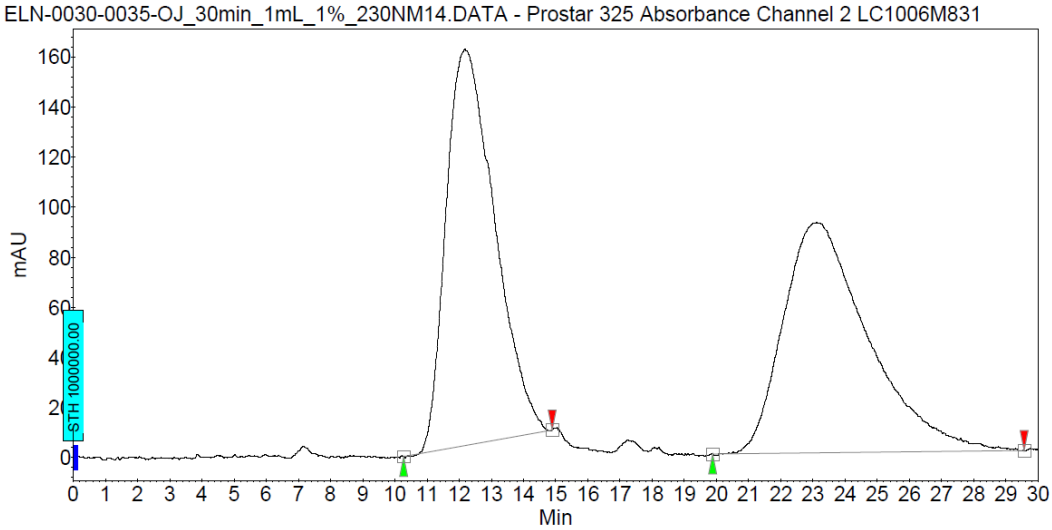

Peak results :

Index	Name	Time [Min]	Quantity [% Area]	Height [mAU]	Area [mAU.Min]	Area % [%]
2	UNKNOWN	12.18	49.67	158.3	277.2	49.675
1	UNKNOWN	23.11	50.33	92.0	280.9	50.325
Total			100.00	250.2	558.1	100.000

ELN-0030-0059-OJ_30min_1mL_1%_230NM3.DATA - Prostar 325 Absorbance Channel 2 LC1006M831

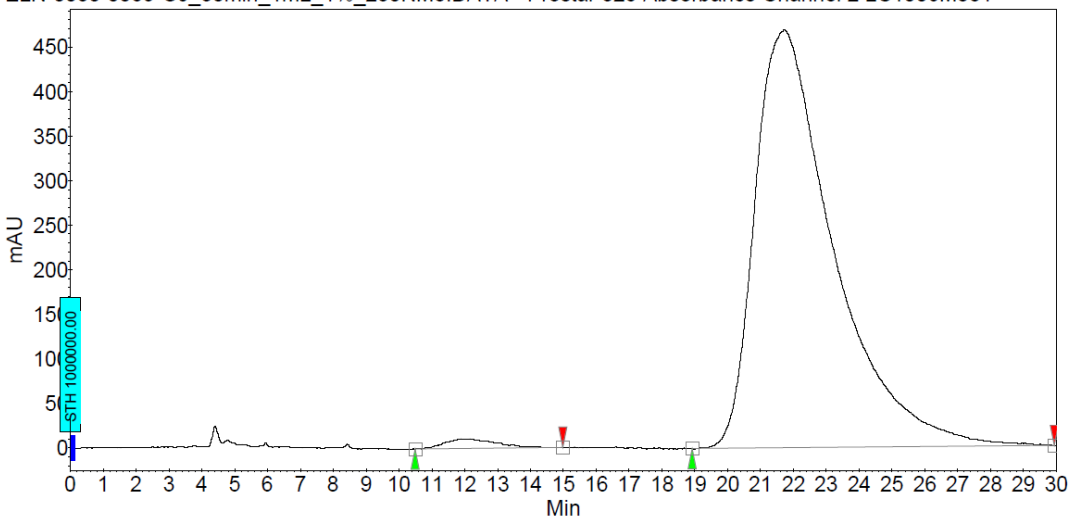

Peak results :

Index	Name	Time [Min]	Quantity [% Area]	Height [mAU]	Area [mAU.Min]	Area % [%]
2	UNKNOWN	12.05	1.49	10.8	19.6	1.486
1	UNKNOWN	21.72	98.51	468.5	1297.4	98.514
Total			100.00	479.3	1316.9	100.000

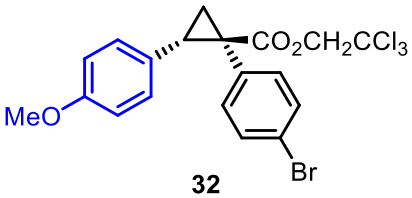

32

ELN-0030-04-OLD-SSW_30min_1mL_1%_230nm26.DATA - Prostar 325 Absorbance Channel 2 LC1006M831

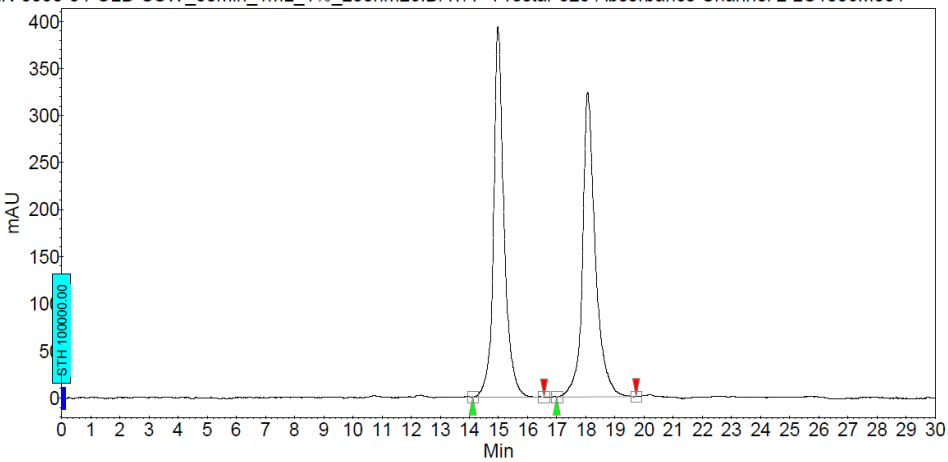

Peak results :

Index	Name	Time [Min]	Quantity [% Area]	Height [mAU]	Area [mAU.Min]	Area % [%]
1	UNKNOWN	14.98	49.73	393.2	163.7	49.734
2	UNKNOWN	18.06	50.27	323.9	165.5	50.266
Total			100.00	717.1	329.2	100.000

ELN-0030-0060-OLD-SSW_30min_1mL_1%_230nm29.DATA - Prostar 325 Absorbance Channel 2 LC1006M831

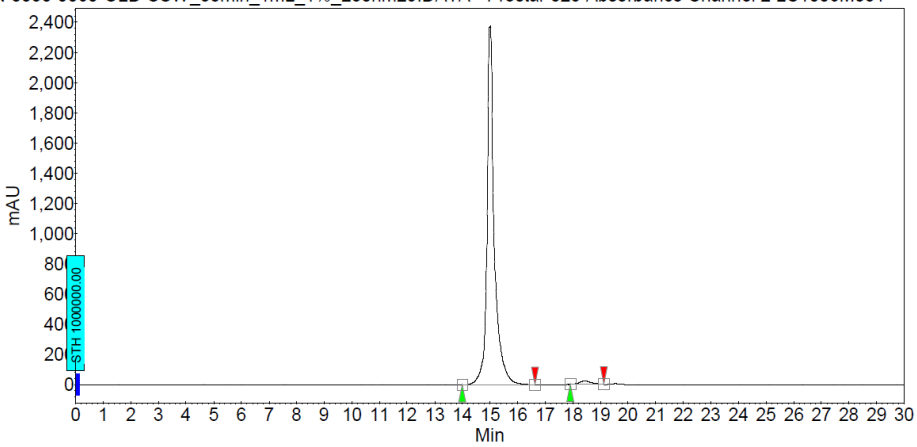

Peak results :

Index	Name	Time [Min]	Quantity [% Area]	Height [mAU]	Area [mAU.Min]	Area % [%]
2	UNKNOWN	15.02	98.60	2374.4	724.5	98.598
1	UNKNOWN	18.43	1.40	22.4	10.3	1.402
Total			100.00	2396.9	734.8	100.000

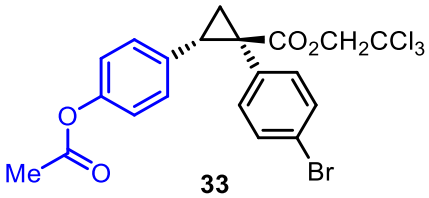

33

ELN-0030-0055-ADH_40min_1mL_1%-230nm2.DATA - Prostar 325 Absorbance Channel 2 LC1006M831

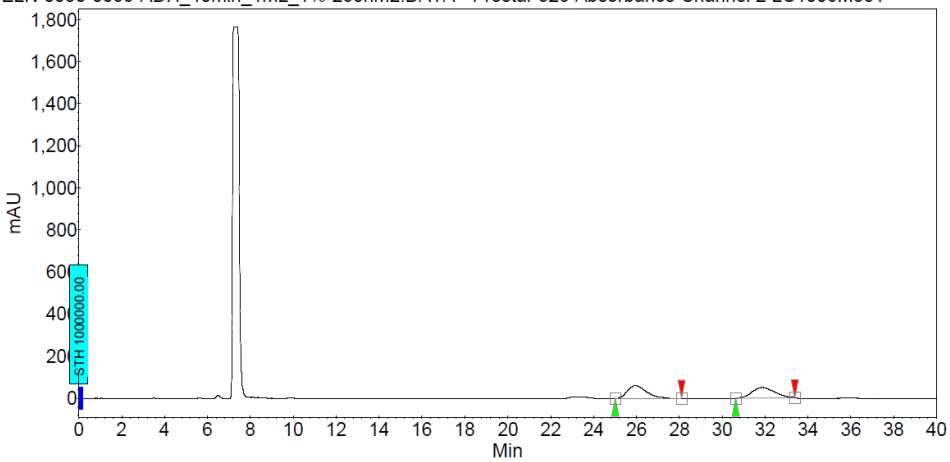

Peak results :

Index	Name	Time [Min]	Quantity [% Area]	Height [mAU]	Area [mAU.Min]	Area % [%]
1	UNKNOWN	25.98	50.83	61.1	62.6	50.830
2	UNKNOWN	31.85	49.17	49.3	60.5	49.170
Total			100.00	110.4	123.1	100.000

ELN-0030-0052-ADH_40min_1mL_1%-230nm5.DATA - Prostar 325 Absorbance Channel 2 LC1006M831

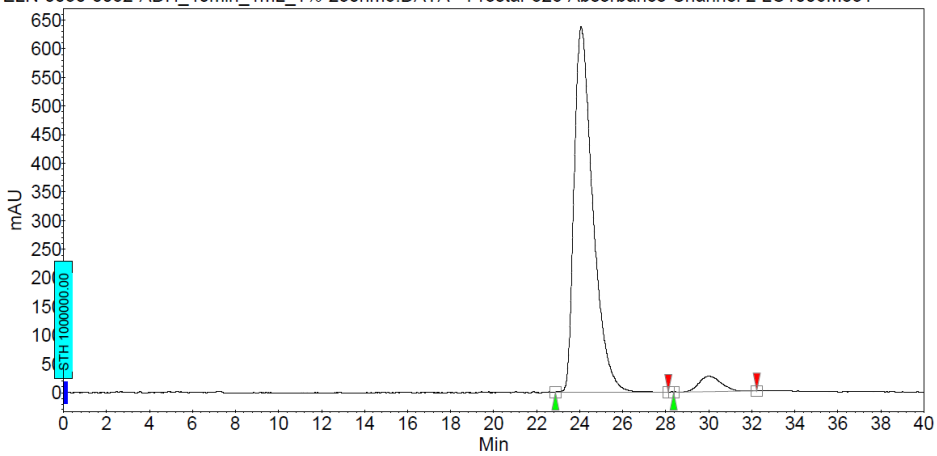

Peak results :

Index	Name	Time [Min]	Quantity [% Area]	Height [mAU]	Area [mAU.Min]	Area % [%]
1	UNKNOWN	24.06	95.22	637.6	642.8	95.220
2	UNKNOWN	30.03	4.78	27.4	32.3	4.780
Total			100.00	665.0	675.1	100.000

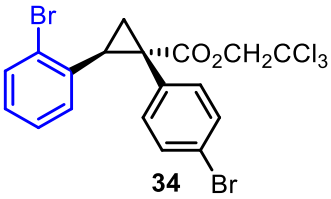

34

ELN-0030-0087-RAC-ADH_30min_1mL_1%-230nm17.DATA - Prostar 325 Absorbance Channel 2 LC1006M831

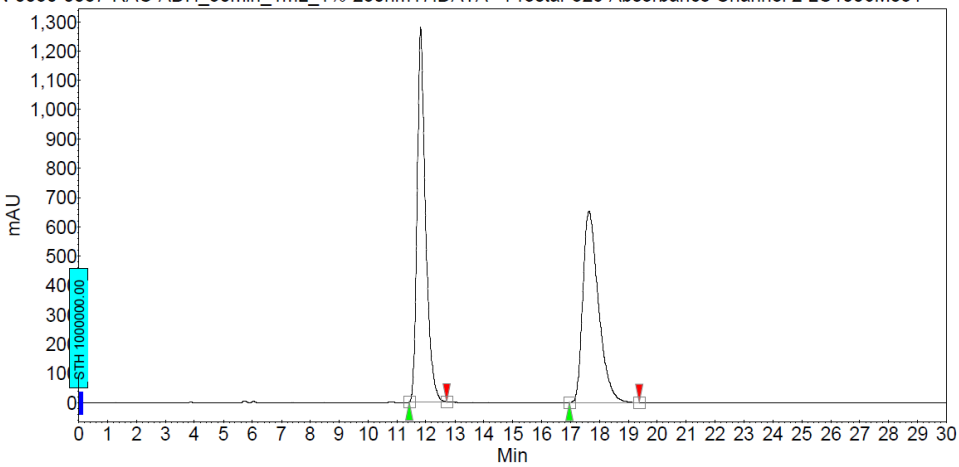

Peak results :

Index	Name	Time [Min]	Quantity [% Area]	Height [mAU]	Area [mAU.Min]	Area % [%]
1	UNKNOWN	11.82	51.51	1278.0	433.4	51.506
2	UNKNOWN	17.64	48.49	653.2	408.0	48.494
Total			100.00	1931.2	841.4	100.000

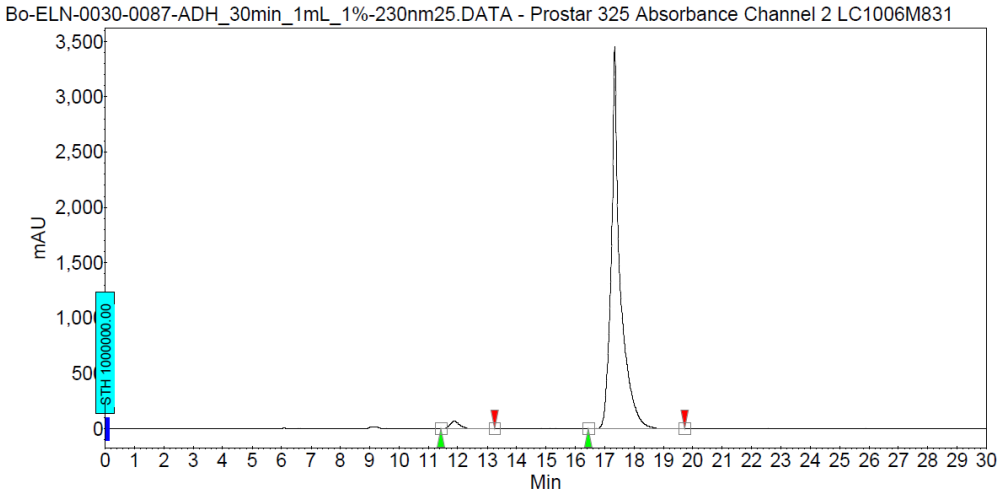

Peak results :

Index	Name	Time [Min]	Quantity [% Area]	Height [mAU]	Area [mAU.Min]	Area % [%]
1	UNKNOWN	11.88	2.04	65.4	25.2	2.038
2	UNKNOWN	17.35	97.96	3448.3	1210.7	97.962
Total			100.00	3513.7	1235.9	100.000

7.8 HPLC Chromatograms of the more crowded substrates

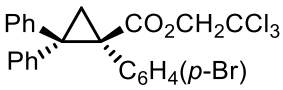

36

racemic of 36:

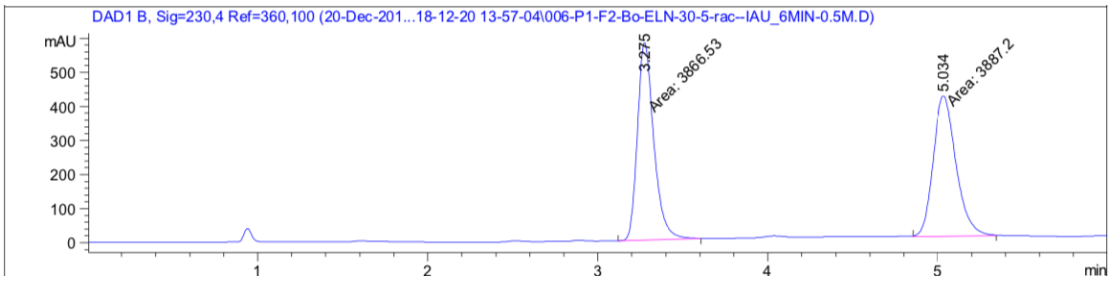

Signal 2: DAD1 B, Sig=230, 4 Ref=360, 100

Peak #	Ret Time [min]	Type	Width [min]	Area [mAU*s]	Height [mAU]	Area %
1	3.275	MM	0.1112	3866.53198	579.74060	49.8667
2	5.034	MM	0.1568	3887.20142	413.27756	50.1333

Totals : 7753.73340 993.01816

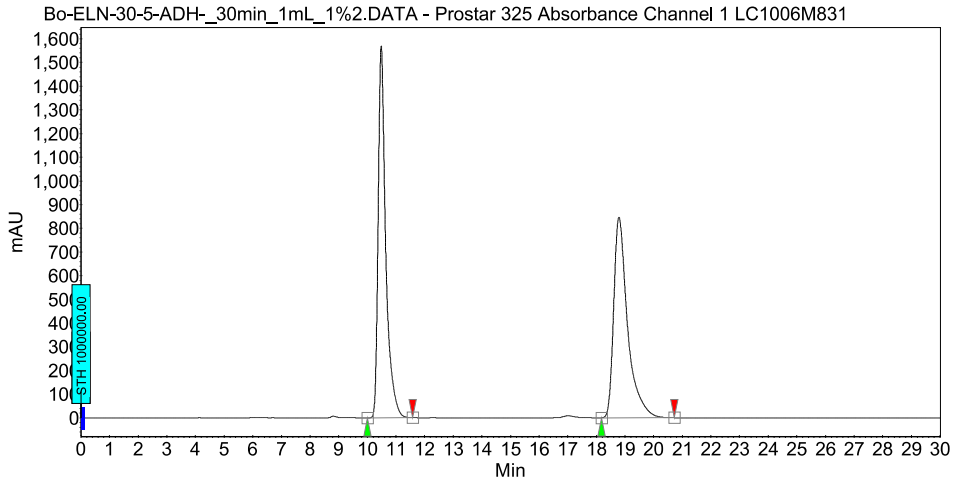

Peak results :

Index	Name	Time [Min]	Quantity [% Area]	Height [mAU]	Area [mAU.Min]	Area % [%]
1	UNKNOWN	10.48	50.35	1568.9	481.0	50.354
2	UNKNOWN	18.79	49.65	846.0	474.3	49.646
Total			100.00	2414.9	955.3	100.000

Rh_2(*S*-*p*-Br-TPCP)$_4$ as catalyst:

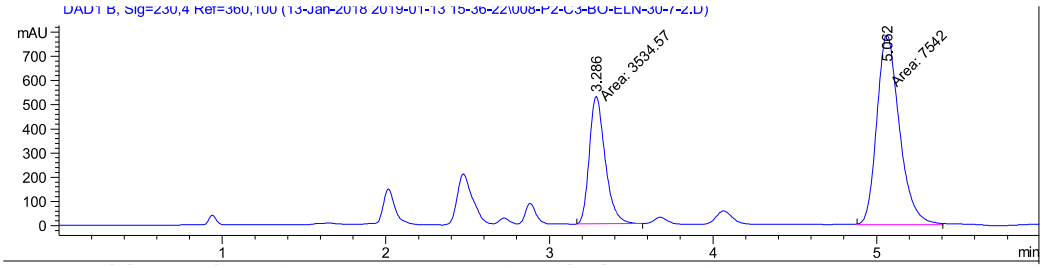

Signal 2: DAD1 B, Sig=230,4 Ref=360,100

Peak #	Ret Time [min]	Type	Width [min]	Area [mAU*s]	Height [mAU]	Area %
1	3.286	MM	0.1116	3534.56616	528.00745	31.9103
2	5.062	MM	0.1599	7542.00146	785.92395	68.0897

Totals : 1.10766e4 1313.93140

Rh_2(*R*-*p*-Ph-TPCP)$_4$ as catalyst:

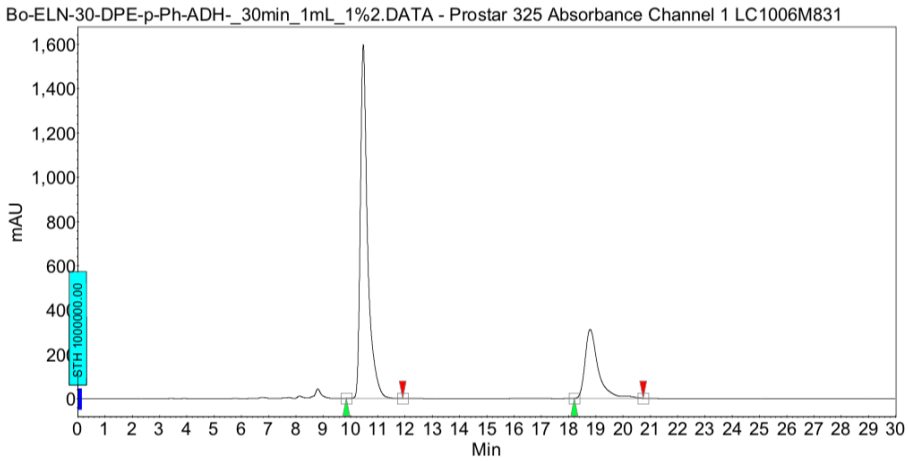

Peak results :

Index	Name	Time [Min]	Quantity [% Area]	Height [mAU]	Area [mAU.Min]	Area % [%]
1	UNKNOWN	10.47	73.87	1597.6	492.5	73.871
2	UNKNOWN	18.79	26.13	311.6	174.2	26.129
Total			100.00	1909.2	666.7	100.000

Rh_2(*R*-PTAD)$_4$ as catalyst:

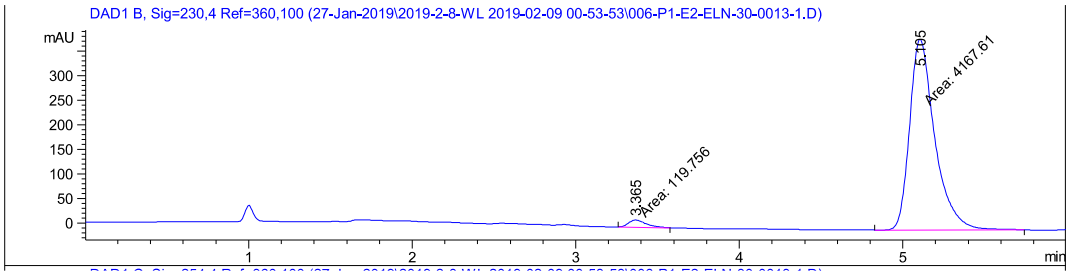

Signal 2: DAD1 B, Sig=230,4 Ref=360,100

Peak #	Ret Time [min]	Type	Width [min]	Area [mAU*s]	Height [mAU]	Area %
1	3.365	MM	0.1323	119.75571	15.08606	2.7932
2	5.105	MM	0.1788	4167.60596	388.56750	97.2068

Totals : 4287.36166 403.65356

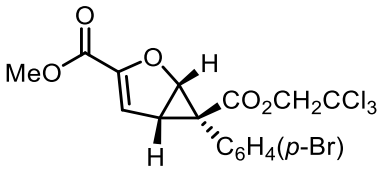

38

racemic of 38:

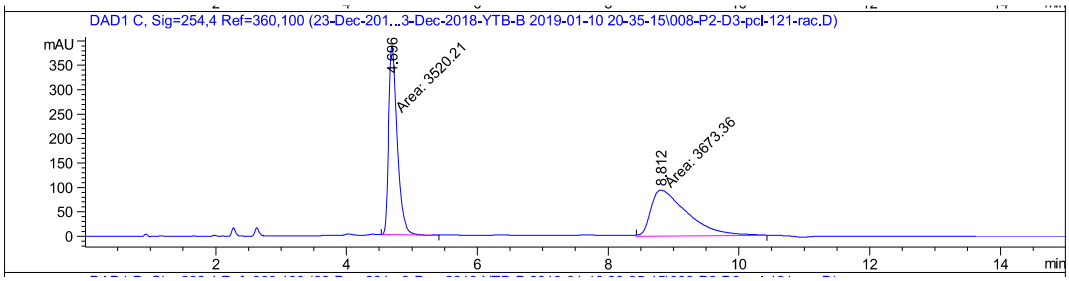

Signal 3: DAD1 C, Sig=254, 4 Ref=360, 100

Peak #	Ret Time [min]	Type	Width [min]	Area [mAU*s]	Height [mAU]	Area %
1	4.696	MM	0.1521	3520.20972	385.77090	48.9355
2	8.812	MM	0.6494	3673.36060	94.27181	51.0645
Totals :				7193.57031	480.04272	

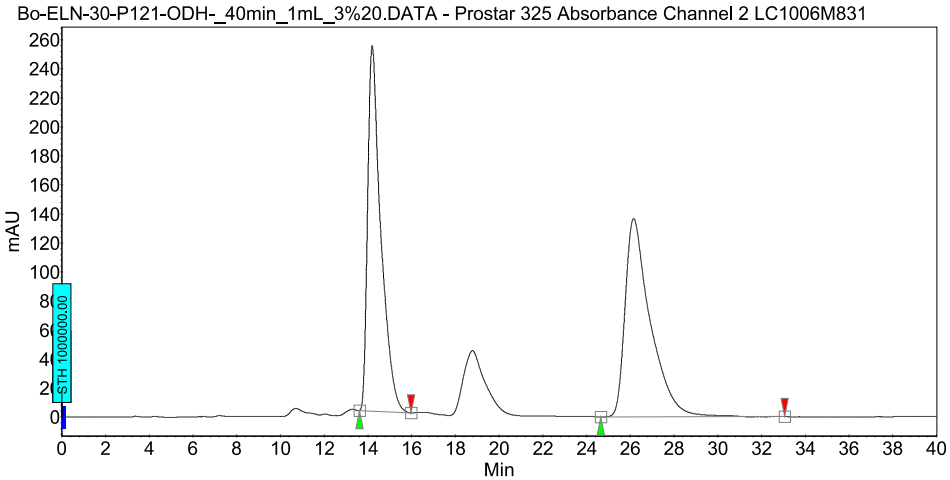

Peak results :

Index	Name	Time [Min]	Quantity [% Area]	Height [mAU]	Area [mAU.Min]	Area % [%]
1	UNKNOWN	14.19	49.08	251.9	175.9	49.084
2	UNKNOWN	26.15	50.92	136.8	182.4	50.916
Total			100.00	388.7	358.3	100.000

Rh_2(*S*-*p*-Br-TPCP)$_4$ as catalyst:

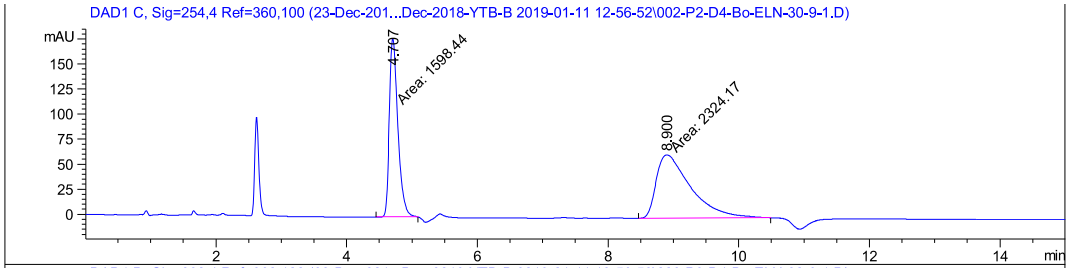

Signal 3: DAD1 C, Sig=254,4 Ref=360,100

Peak #	Ret Time [min]	Type	Width [min]	Area [mAU*s]	Height [mAU]	Area %
1	4.707	MM	0.1495	1598.43738	178.22815	40.7494
2	8.900	MM	0.6106	2324.17017	63.44468	59.2506

Totals : 3922.60754 241.67282

Rh_2(*R*-*p*-Ph-TPCP)$_4$ as catalyst:

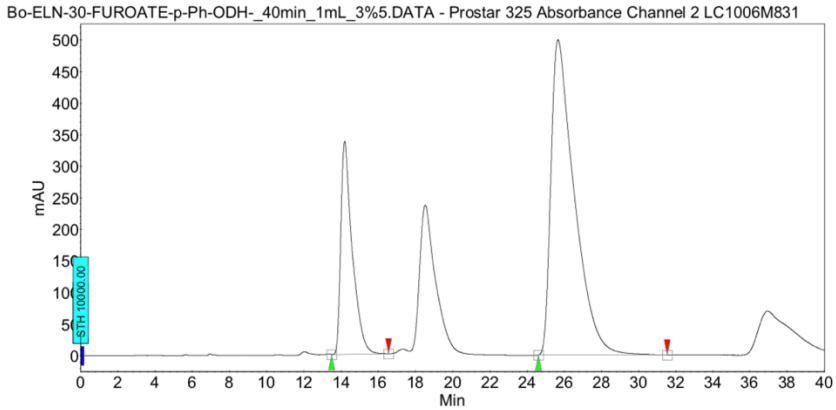

Peak results :

Index	Name	Time [Min]	Quantity [% Area]	Height [mAU]	Area [mAU.Min]	Area % [%]
1	UNKNOWN	14.19	24.76	337.6	239.9	24.762
2	UNKNOWN	25.66	75.24	500.0	728.8	75.238
Total			100.00	837.7	968.7	100.000

Rh_2(*R*-TCPTAD)$_4$ as catalyst:

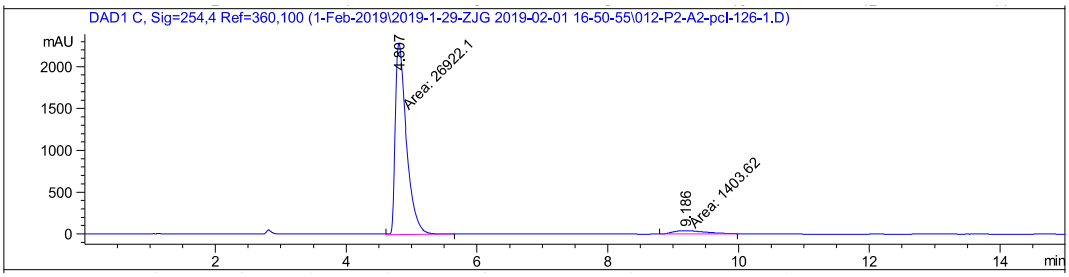

Signal 3: DAD1 C, Sig=254,4 Ref=360,100

Peak #	Ret Time [min]	Type	Width [min]	Area [mAU*s]	Height [mAU]	Area %
1	4.807	MM	0.1963	2.69221e4	2285.21484	95.0447
2	9.186	MM	0.5763	1403.61926	40.59235	4.9553

Totals : 2.83257e4 2325.80720

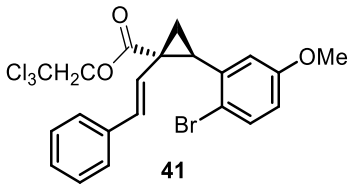

41

Racemate of **41:**

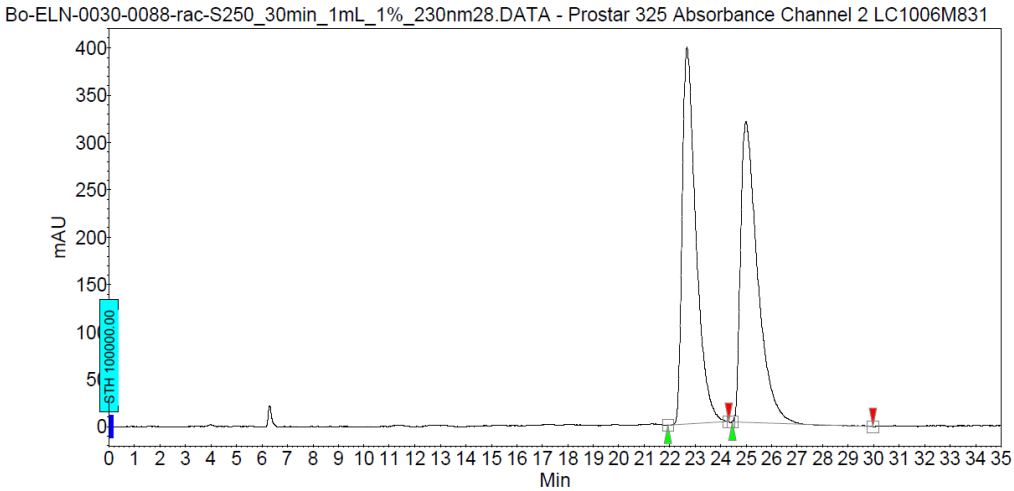

Peak results :

Index	Name	Time [Min]	Quantity [% Area]	Height [mAU]	Area [mAU.Min]	Area % [%]
1	UNKNOWN	22.68	50.40	398.0	248.5	50.403
2	UNKNOWN	24.99	49.60	317.8	244.5	49.597
Total			100.00	715.9	493.0	100.000

Rh_2(*S*-*p*-Ph-TPCP)$_4$ as catalyst:

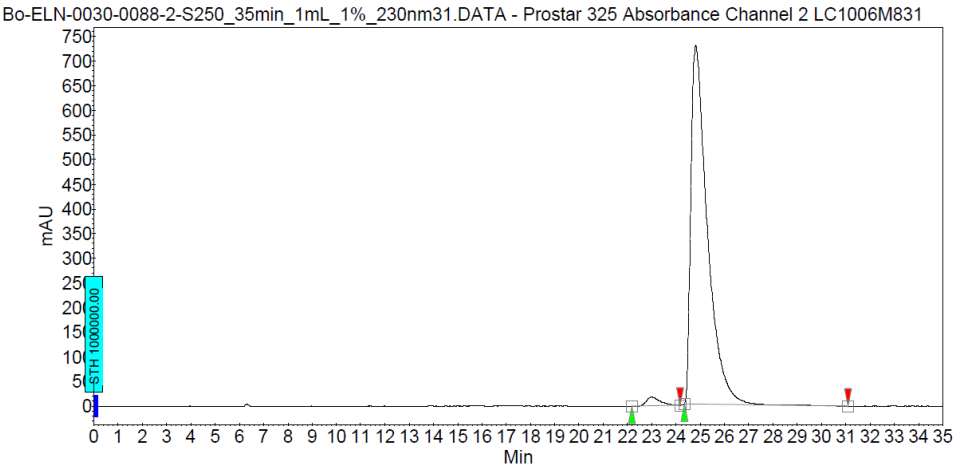

Peak results :

Index	Name	Time [Min]	Quantity [% Area]	Height [mAU]	Area [mAU.Min]	Area % [%]
1	UNKNOWN	23.01	1.99	18.1	11.7	1.988
2	UNKNOWN	24.82	98.01	728.0	575.4	98.012
Total			100.00	746.1	587.1	100.000

8. NMR Spectra

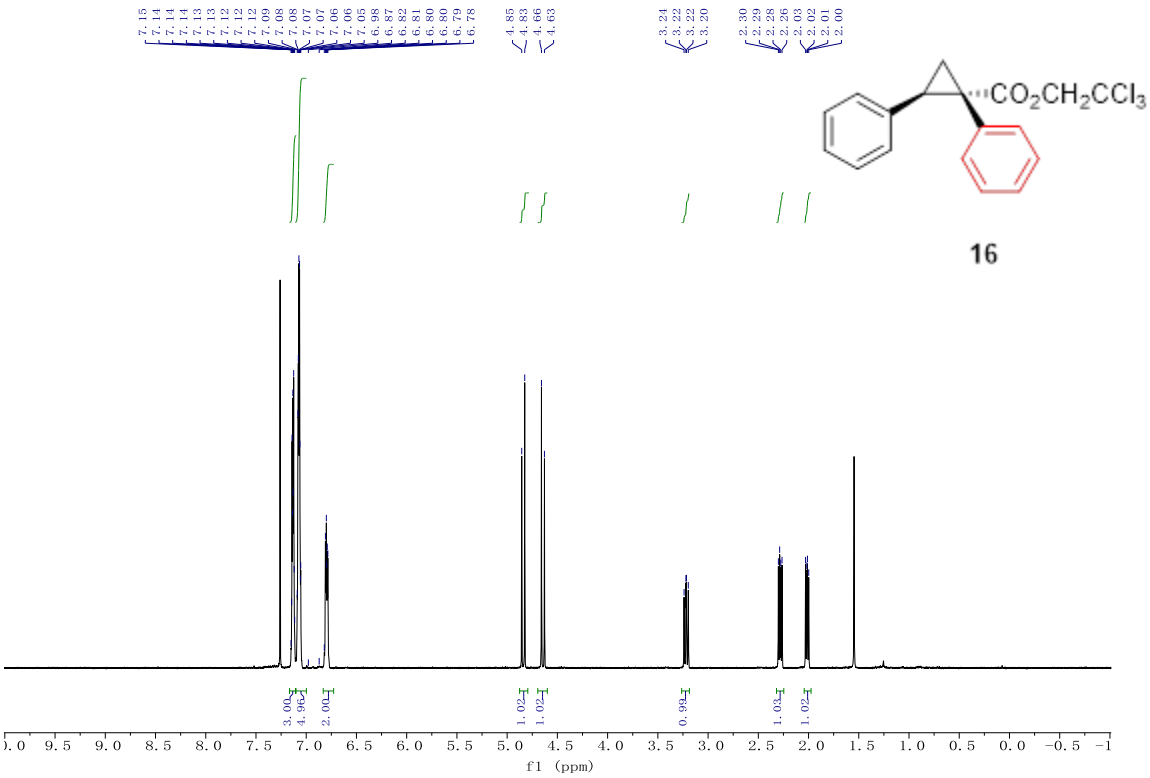

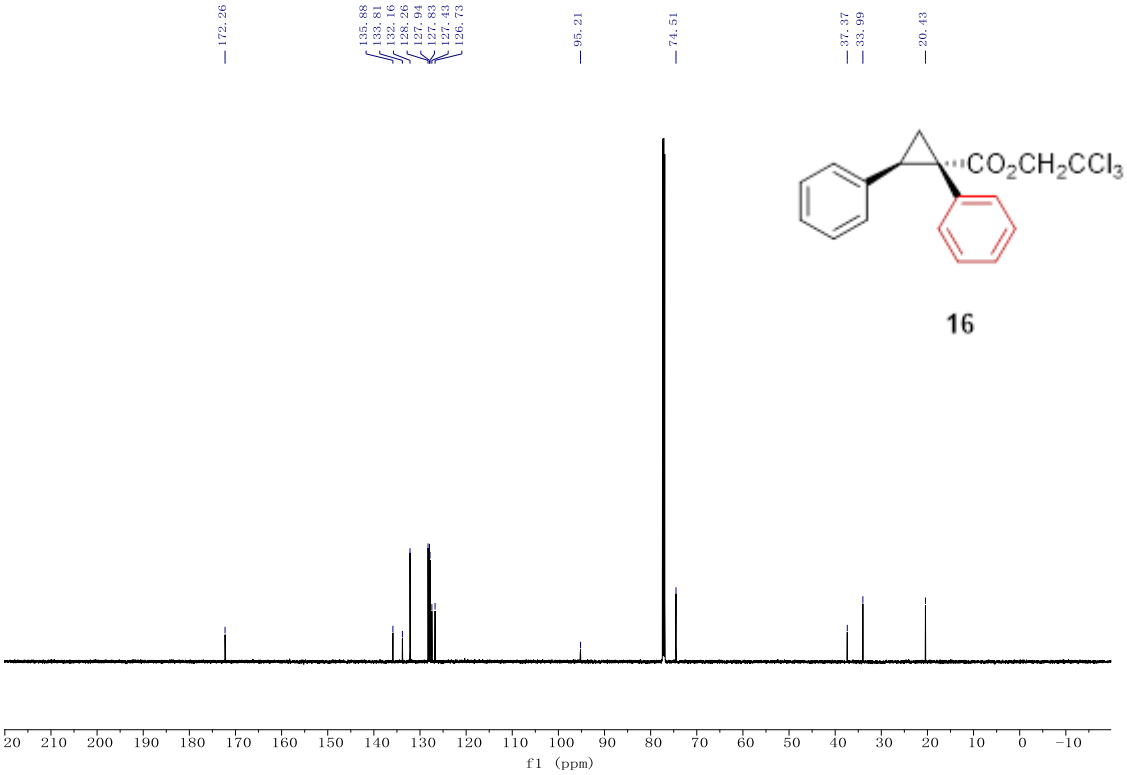

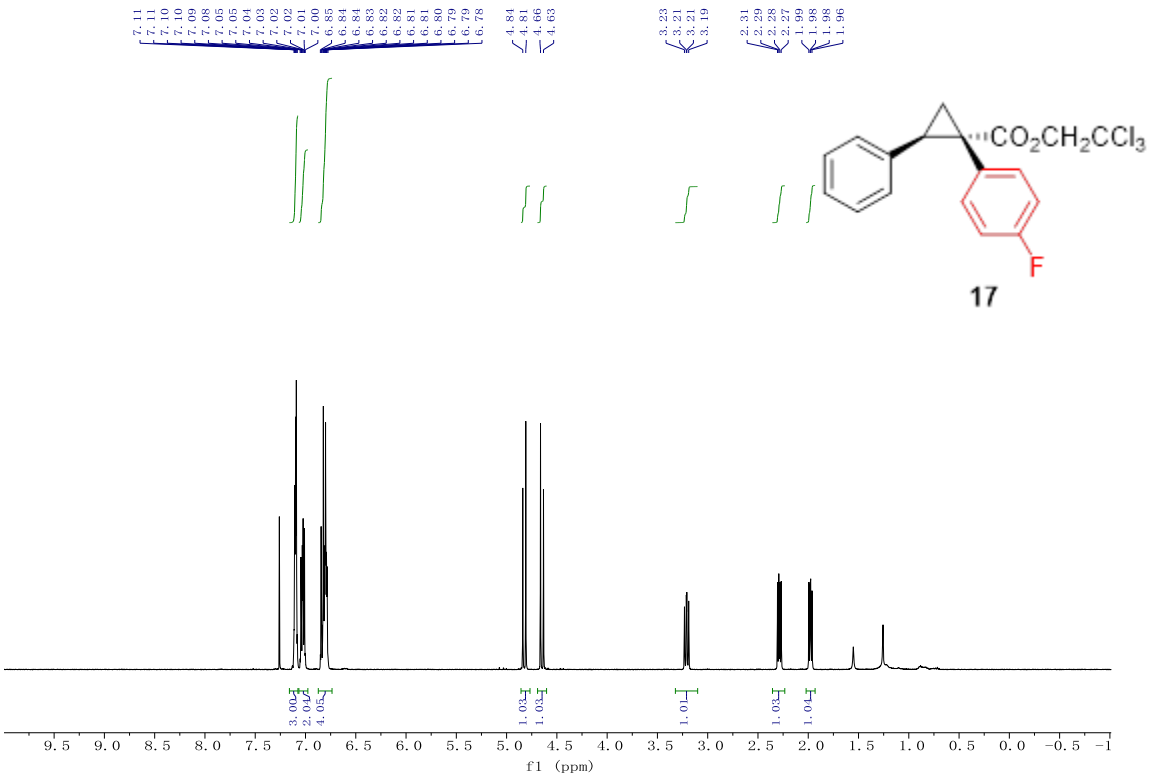
7.11
7.11
7.10
7.10
7.09
7.08
7.05
7.05
7.04
7.03
7.02
7.02
7.01
7.00
6.85
6.84
6.84
6.83
6.82
6.82
6.81
6.81
6.80
6.79
6.79
6.78
4.84
4.81
4.66
4.63
3.23
3.21
3.21
3.19
2.31
2.29
2.28
2.27
1.99
1.98
1.98
1.96
CO2CH2CCl3
F
17
3.00
2.04
4.05
1.03
1.03
1.01
1.03
1.04
9.5 9.0 8.5 8.0 7.5 7.0 6.5 6.0 5.5 5.0 4.5 4.0 3.5 3.0 2.5 2.0 1.5 1.0 0.5 0.0 −0.5 −1
f1 (ppm)

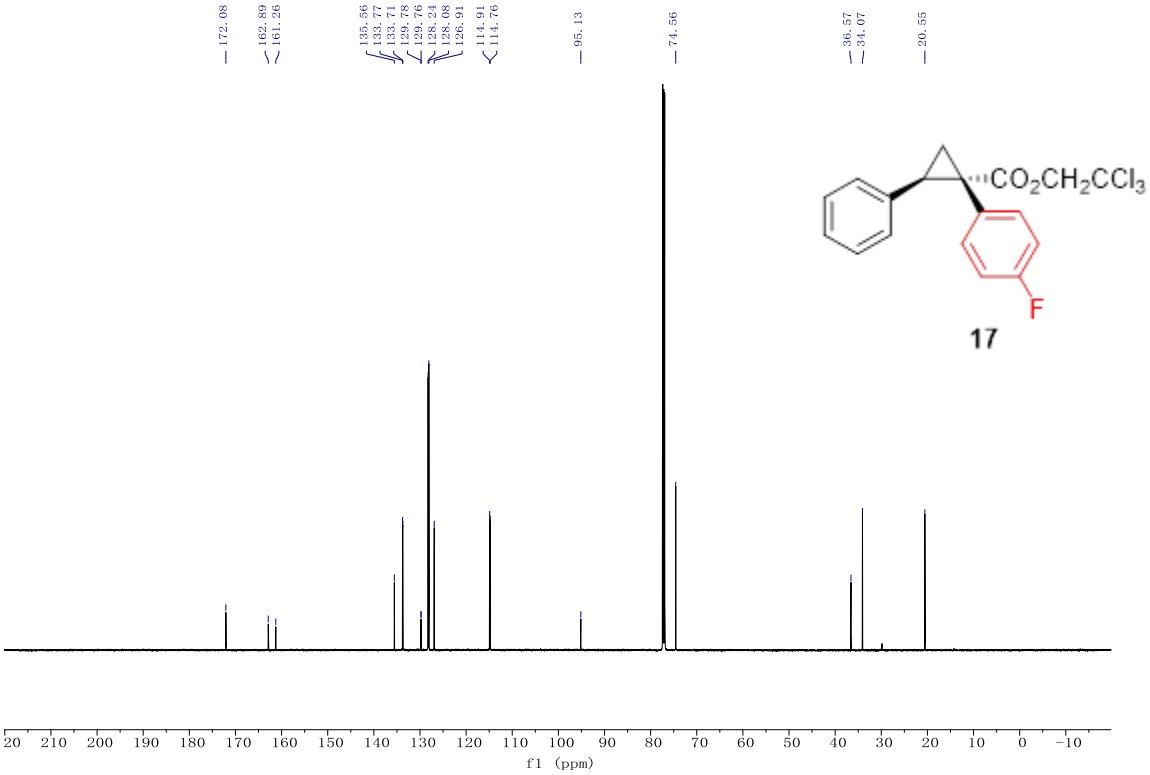
172.08
162.89
161.26
135.56
133.77
133.71
129.78
129.76
128.24
128.08
126.91
114.91
114.76
95.13
74.56
36.57
34.07
20.55
CO2CH2CCl3
F
17
20 210 200 190 180 170 160 150 140 130 120 110 100 90 80 70 60 50 40 30 20 10 0 −10
f1 (ppm)

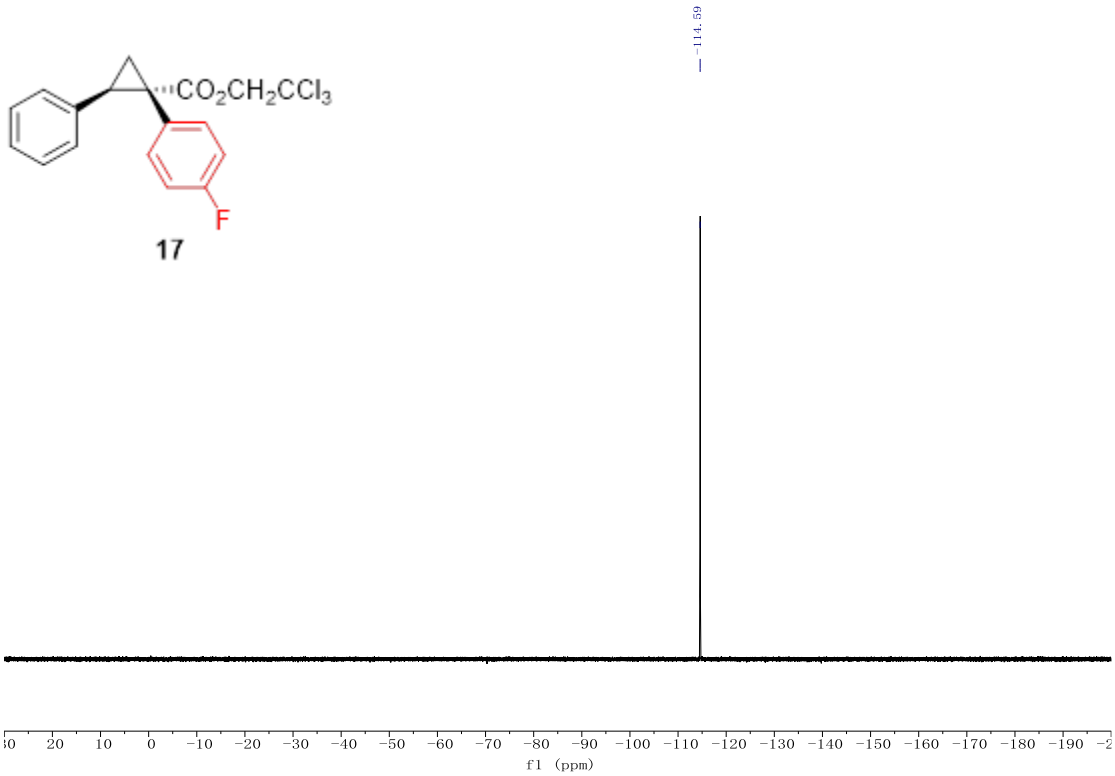
CO2CH2CCl3
F
17
-114.59
f1 (ppm)

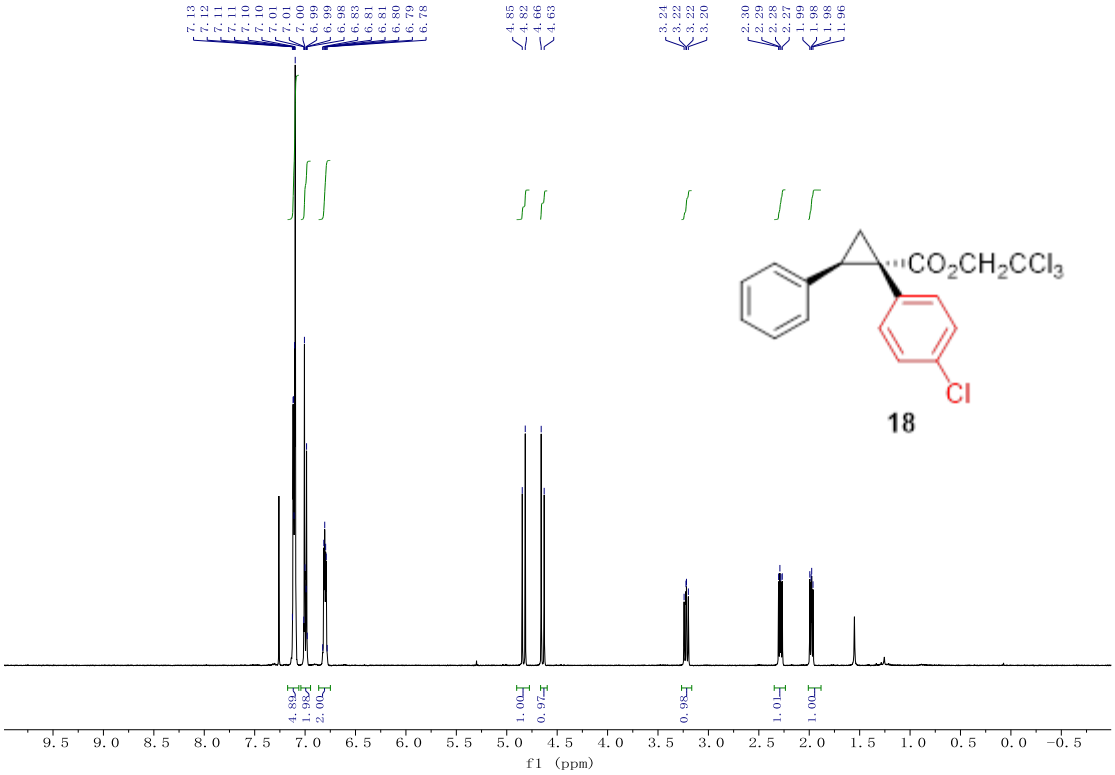
7.13
7.12
7.11
7.11
7.10
7.10
7.01
7.01
7.00
6.99
6.99
6.98
6.83
6.81
6.81
6.80
6.79
6.78
4.85
4.82
4.66
4.63
3.24
3.22
3.22
3.20
2.30
2.29
2.28
2.27
1.99
1.98
1.98
1.96
CO2CH2CCl3
Cl
18
4.89
1.98
2.00
1.00
0.97
0.98
1.01
1.00
f1 (ppm)

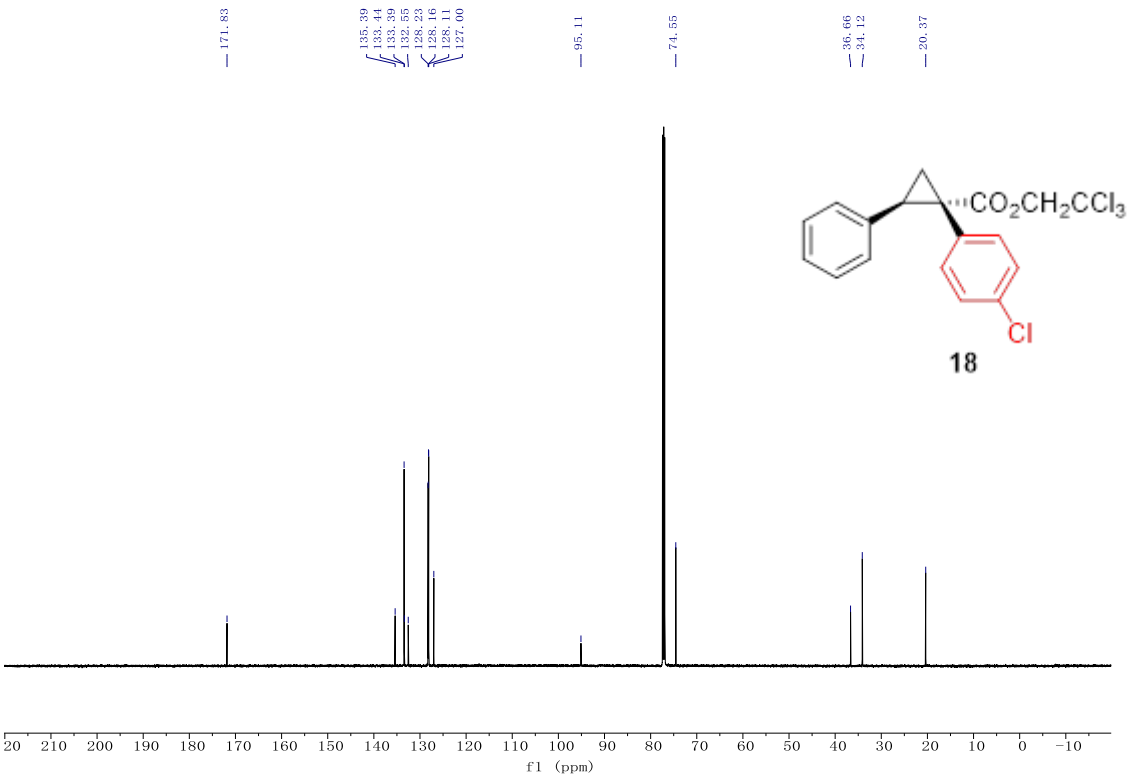
171.83
135.39
133.44
133.39
132.55
128.23
128.16
128.11
127.00
95.11
74.55
36.66
34.12
20.37
CO2CH2CCl3
Cl
18
f1 (ppm)

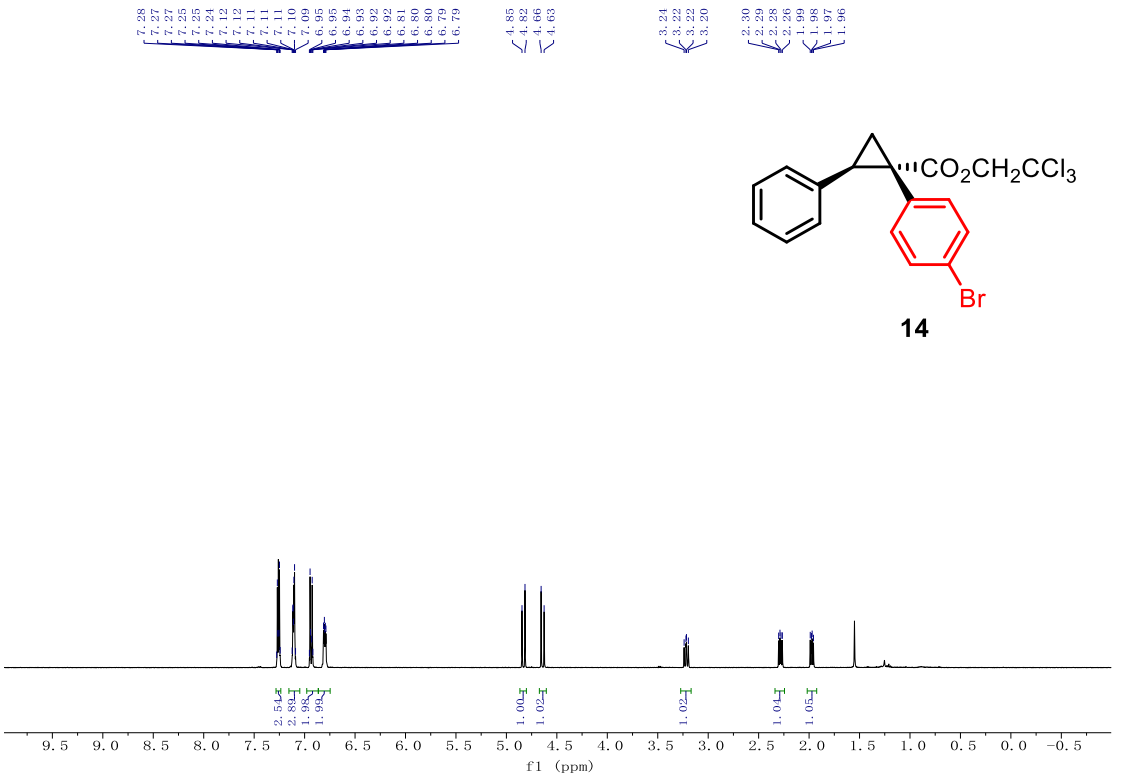
7.28
7.27
7.27
7.25
7.25
7.24
7.12
7.12
7.11
7.11
7.11
7.10
7.09
6.95
6.95
6.94
6.93
6.92
6.92
6.81
6.80
6.80
6.79
6.79
4.85
4.82
4.66
4.63
3.24
3.22
3.22
3.20
2.30
2.29
2.28
2.26
1.99
1.98
1.97
1.96
CO2CH2CCl3
Br
14
2.54
2.89
1.98
1.99
1.00
1.02
1.02
1.04
1.05
f1 (ppm)

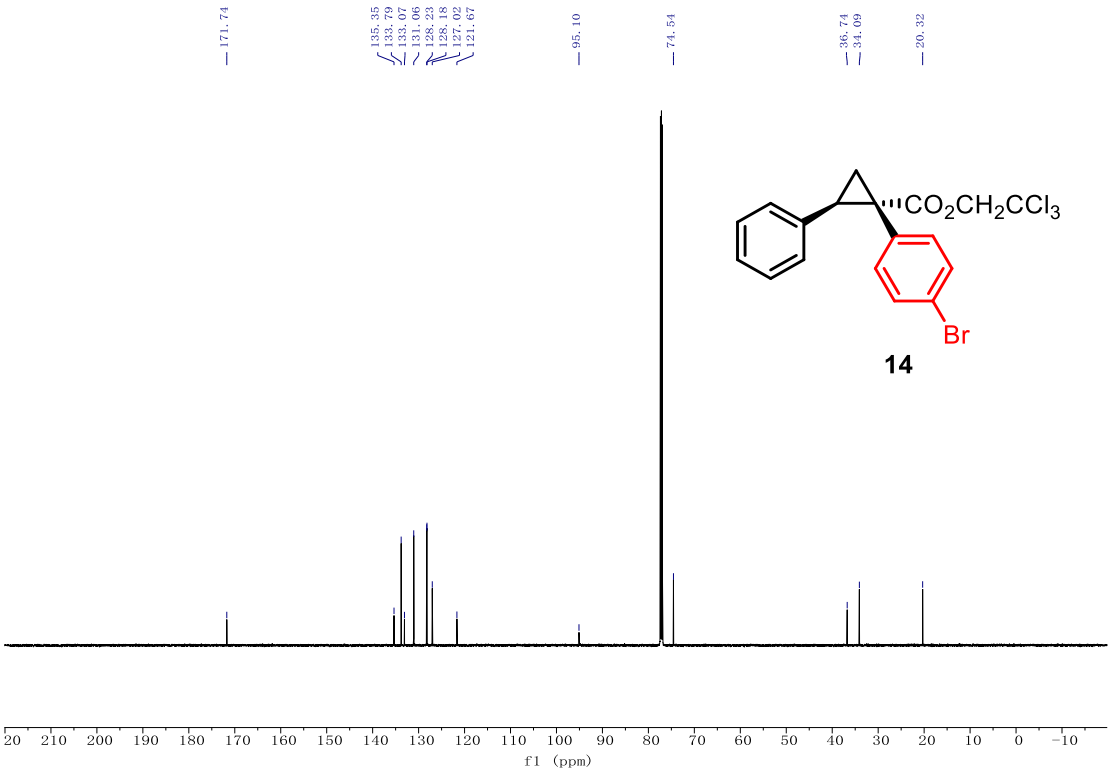
171.74
135.35
133.79
133.07
131.06
128.23
128.18
127.02
121.67
95.10
74.54
36.74
34.09
20.32
CO2CH2CCl3
Br
14
f1 (ppm)

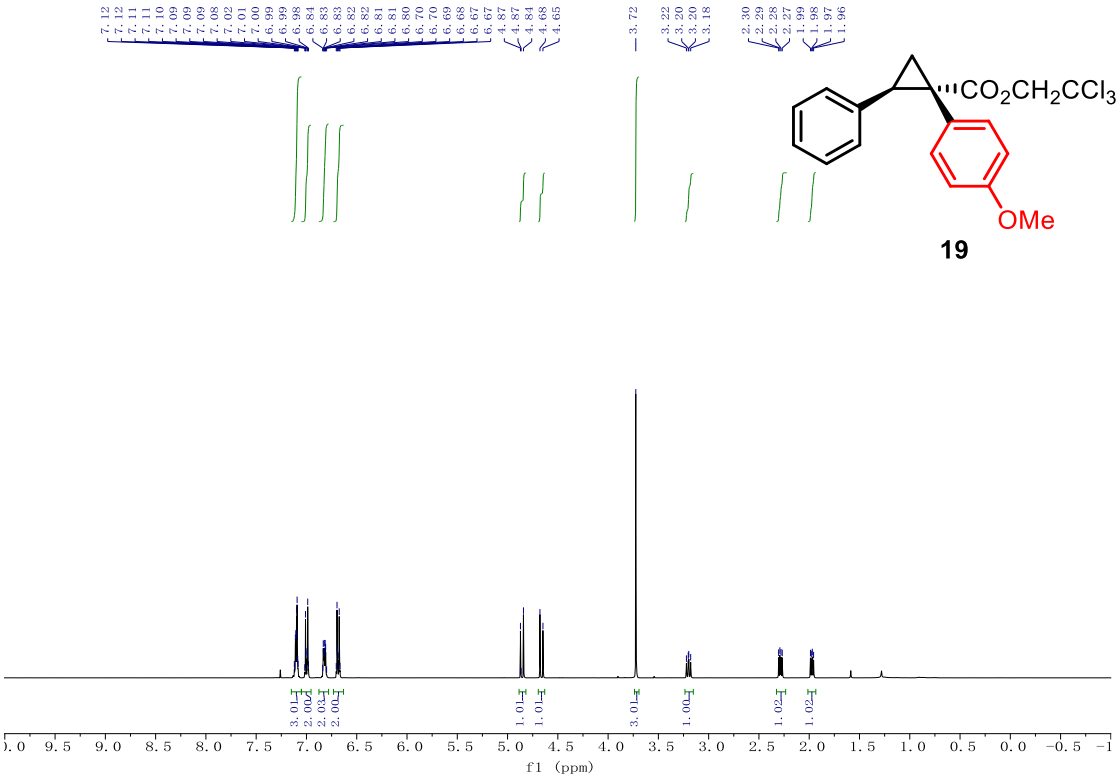
3.72
3.22
3.20
3.20
3.18
2.30
2.29
2.28
2.27
1.99
1.98
1.97
1.96
4.87
4.87
4.84
4.68
4.65
CO2CH2CCl3
OMe
19
f1 (ppm)

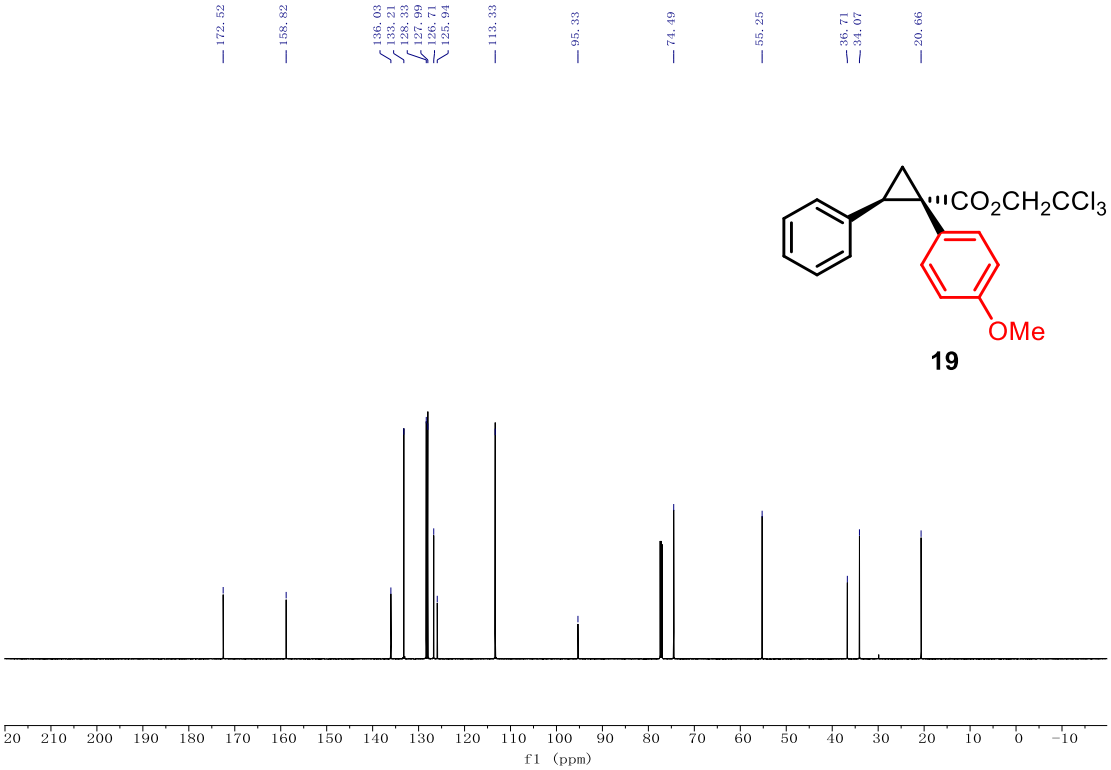
172.52
158.82
136.03
133.21
128.33
127.99
126.71
125.94
113.33
95.33
74.49
55.25
36.71
34.07
20.66
CO2CH2CCl3
OMe
19
f1 (ppm)

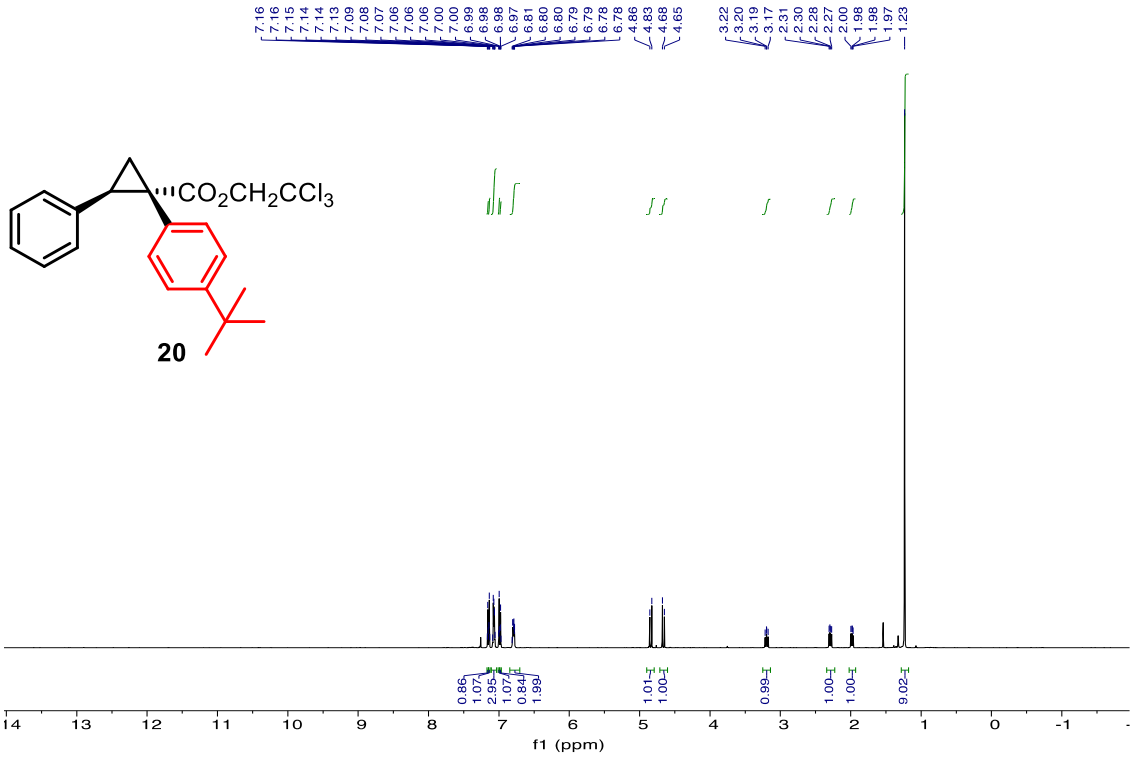
7.16
7.16
7.15
7.14
7.14
7.13
7.09
7.08
7.07
7.06
7.06
7.06
7.00
7.00
6.99
6.98
6.98
6.97
6.81
6.80
6.80
6.79
6.79
6.78
6.78
4.86
4.83
4.68
4.65
3.22
3.20
3.19
3.17
2.31
2.30
2.28
2.27
2.00
1.98
1.98
1.97
1.23
CO2CH2CCl3
20
0.86
1.07
2.95
1.07
0.84
1.99
1.01
1.00
0.99
1.00
1.00
9.02
f1 (ppm)

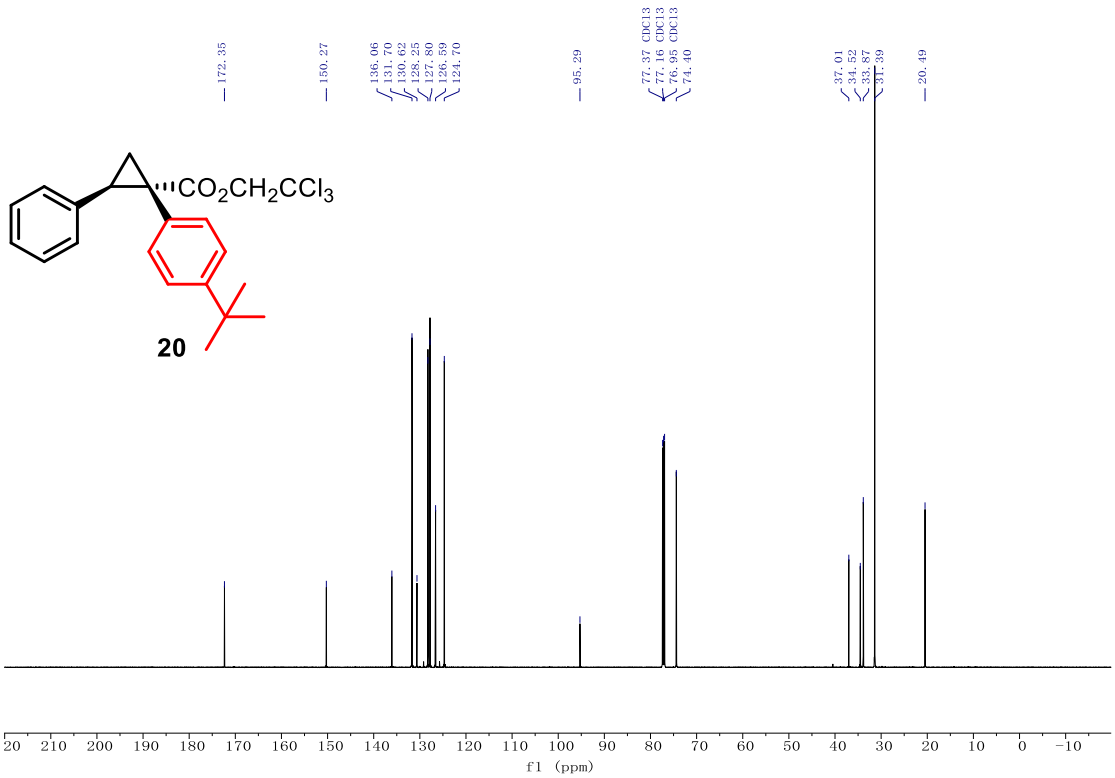
172.35
150.27
136.06
131.70
130.62
128.25
127.80
126.59
124.70
95.29
77.37 CDCl3
77.16 CDCl3
76.95 CDCl3
74.40
37.01
34.52
33.87
31.39
20.49
CO2CH2CCl3
20
f1 (ppm)

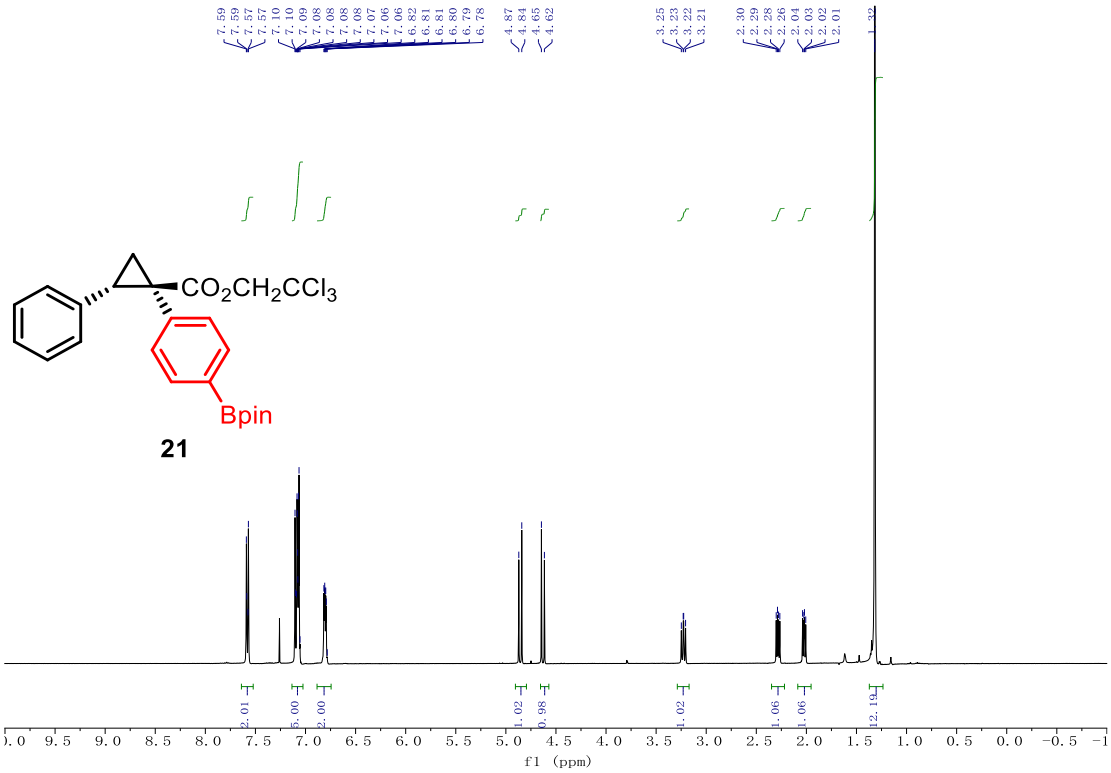
7.59
7.59
7.57
7.57
7.10
7.10
7.09
7.08
7.08
7.08
7.08
7.07
7.06
7.06
6.82
6.81
6.81
6.80
6.79
6.78
4.87
4.84
4.65
4.62
3.25
3.23
3.22
3.21
2.30
2.29
2.28
2.26
2.04
2.03
2.02
2.01
1.32
CO2CH2CCl3
Bpin
21
2.01
5.00
2.00
1.02
0.98
4.02
1.06
1.06
12.19
f1 (ppm)

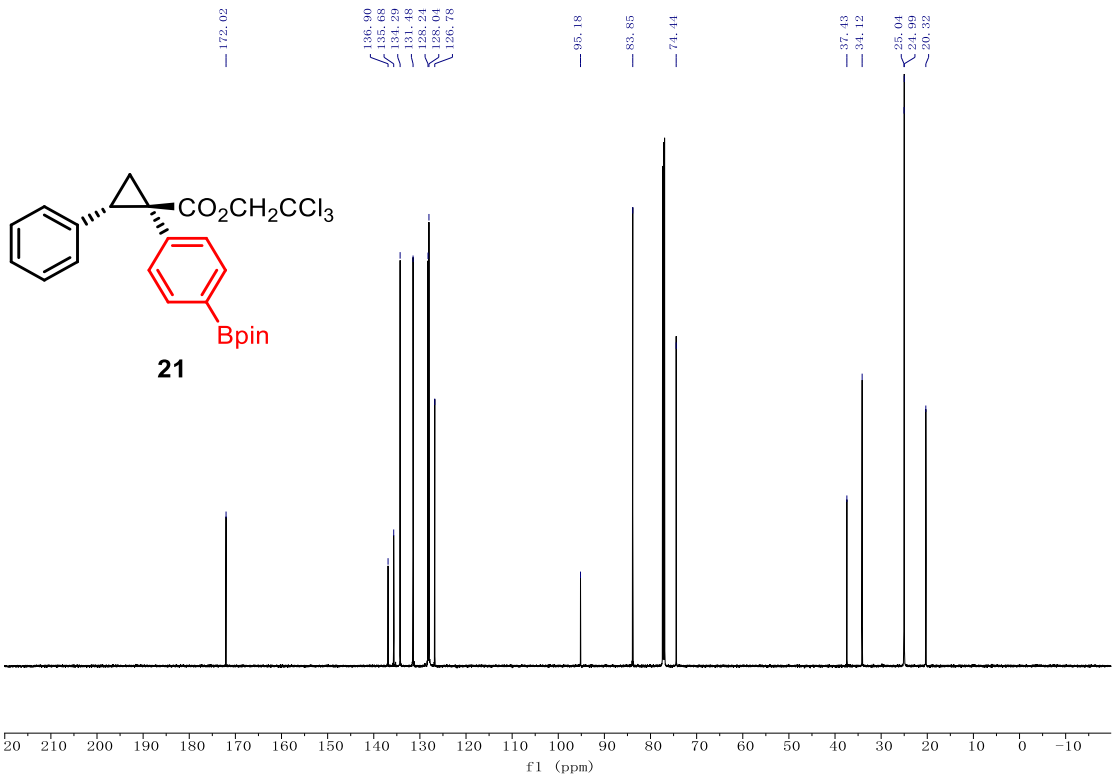
172.02
136.90
135.68
134.29
131.48
128.24
128.04
126.78
95.18
83.85
74.44
37.43
34.12
25.04
24.99
20.32
CO2CH2CCl3
Bpin
21
f1 (ppm)

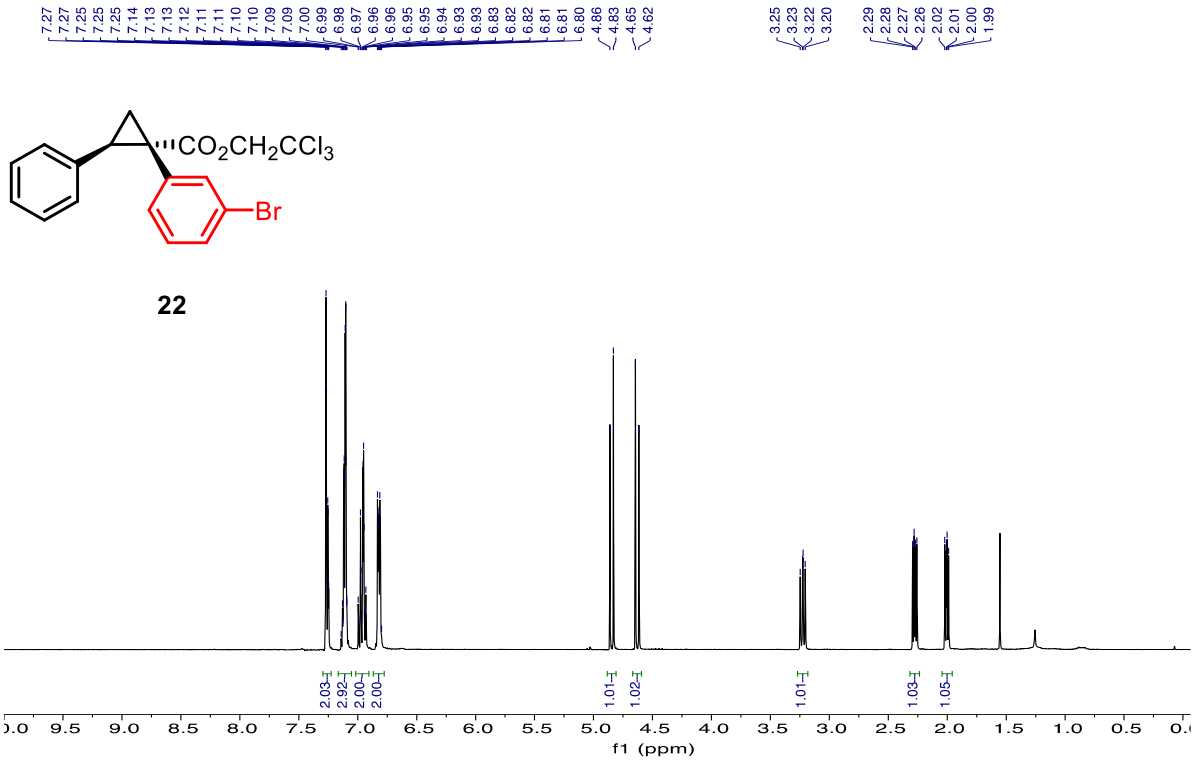
7.27
7.27
7.25
7.25
7.25
7.14
7.13
7.13
7.12
7.11
7.11
7.10
7.10
7.09
7.09
7.00
6.99
6.98
6.97
6.96
6.96
6.95
6.95
6.94
6.93
6.93
6.83
6.82
6.82
6.81
6.81
6.80
4.86
4.83
4.65
4.62
3.25
3.23
3.22
3.20
2.29
2.28
2.27
2.26
2.02
2.01
2.00
1.99
CO2CH2CCl3
Br
22
2.03
2.92
2.00
2.00
1.01
1.02
1.01
1.03
1.05
f1 (ppm)

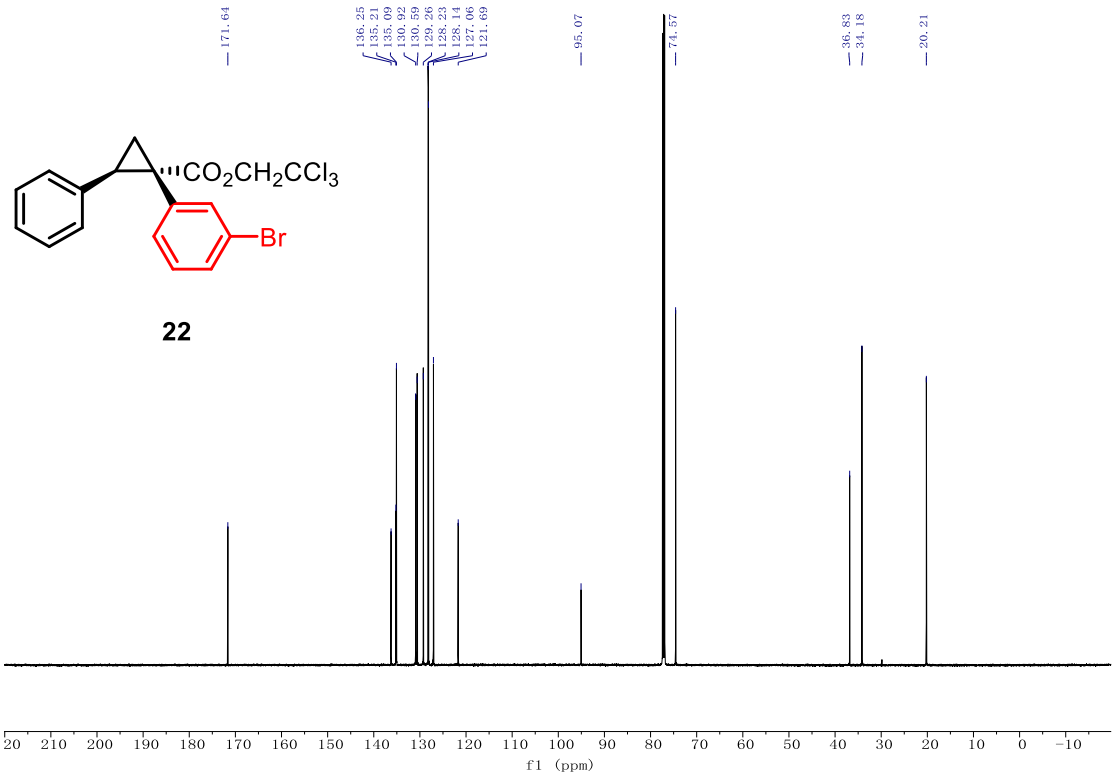
171.64
136.25
135.21
135.09
130.92
130.59
129.26
128.23
128.14
127.06
121.69
95.07
74.57
36.83
34.18
20.21
CO2CH2CCl3
Br
22
f1 (ppm)

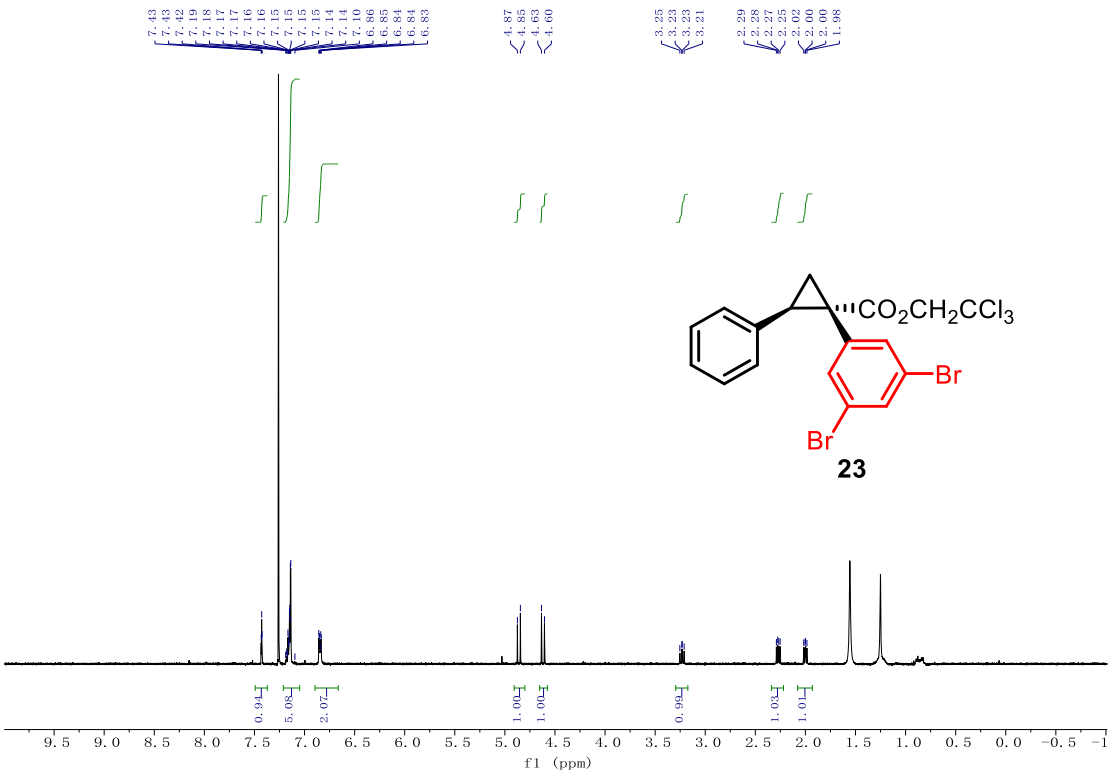
7.43
7.43
7.42
7.19
7.18
7.17
7.17
7.16
7.16
7.15
7.15
7.15
7.15
7.14
7.14
7.10
6.86
6.85
6.84
6.84
6.83
4.87
4.85
4.63
4.60
3.25
3.23
3.23
3.21
2.29
2.28
2.27
2.25
2.02
2.00
2.00
1.98
CO2CH2CCl3
Br
Br
23
0.94
5.08
2.07
1.00
1.00
0.99
1.03
1.01
f1 (ppm)

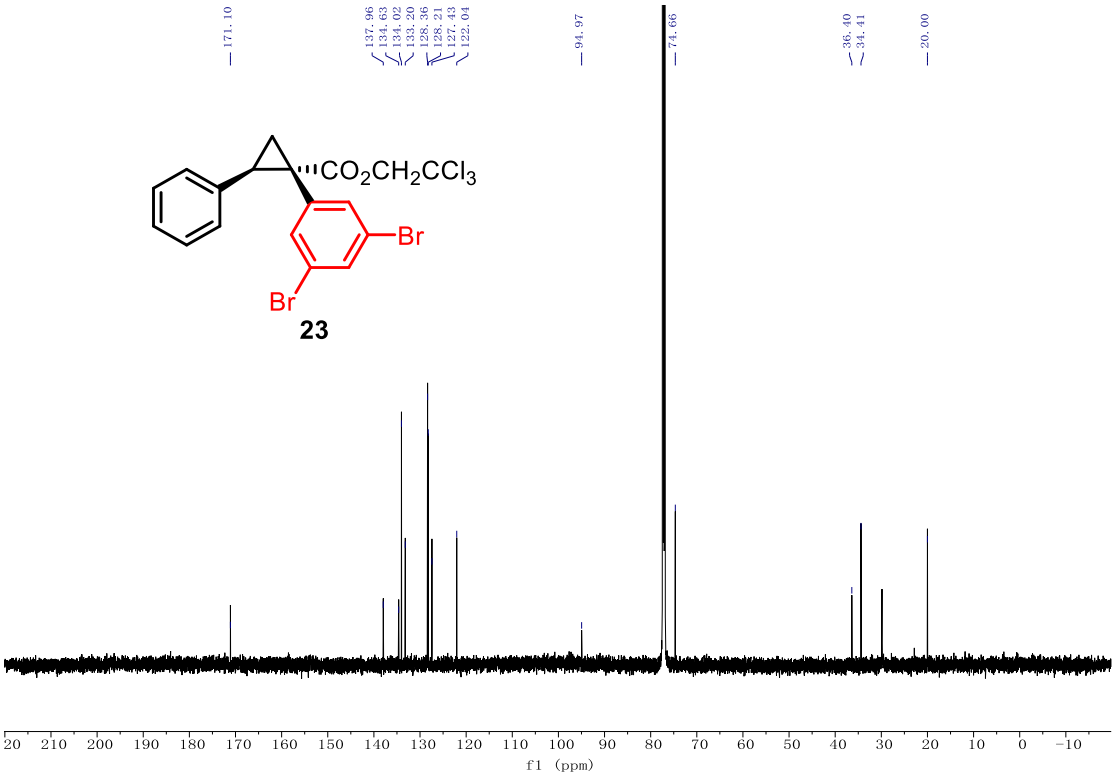
171.10
137.96
134.63
134.02
133.20
128.36
128.21
127.43
122.04
94.97
74.66
36.40
34.41
20.00
CO2CH2CCl3
Br
Br
23
f1 (ppm)

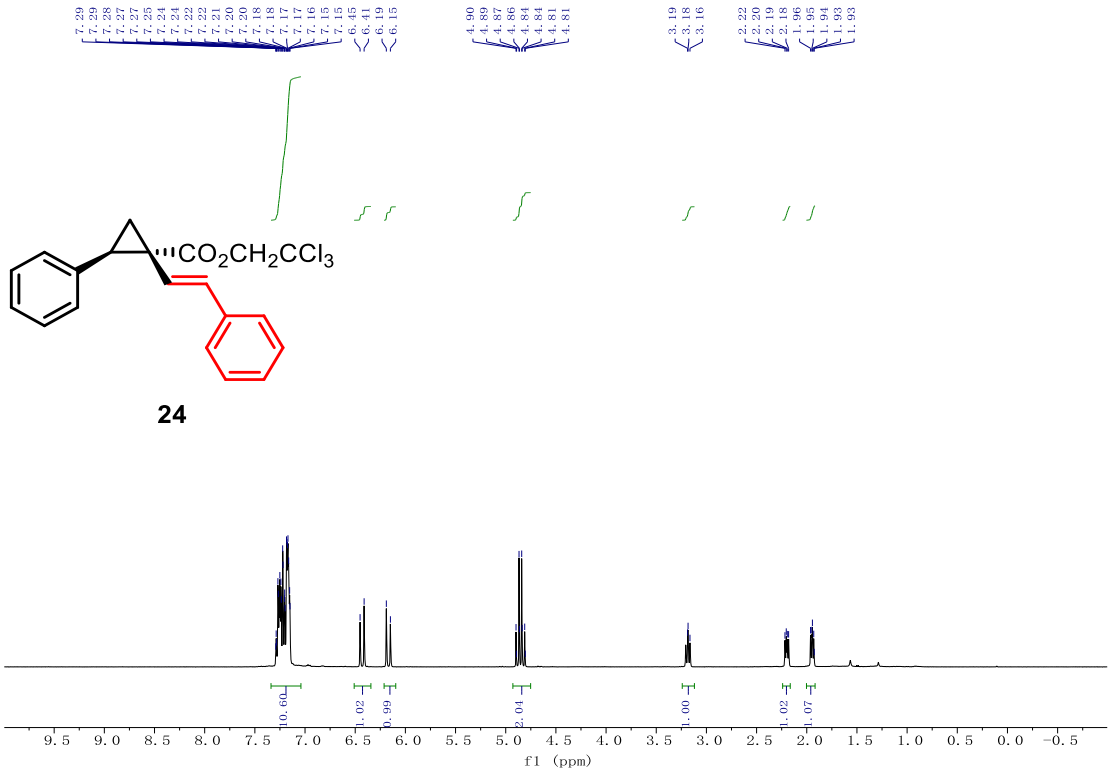
7.29
7.29
7.28
7.27
7.27
7.25
7.24
7.24
7.22
7.22
7.21
7.20
7.20
7.18
7.18
7.17
7.17
7.16
7.15
7.15
6.45
6.41
6.19
6.15
4.90
4.89
4.87
4.86
4.84
4.84
4.81
4.81
3.19
3.18
3.16
2.22
2.20
2.19
2.18
1.96
1.95
1.94
1.93
1.93
CO2CH2CCl3
24
10.60
1.02
0.99
2.04
1.00
1.02
1.07
f1 (ppm)

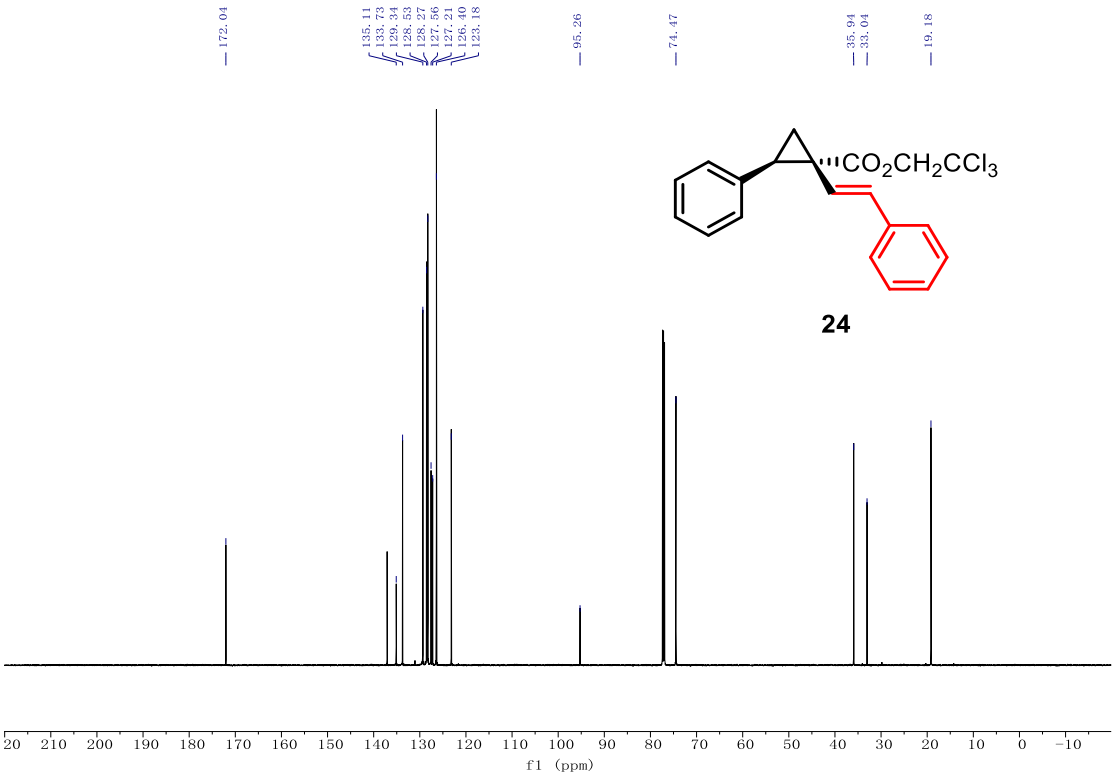
172.04
135.11
133.73
129.34
128.53
128.27
127.56
127.21
126.40
123.18
95.26
74.47
35.94
33.04
19.18
CO2CH2CCl3
24
f1 (ppm)

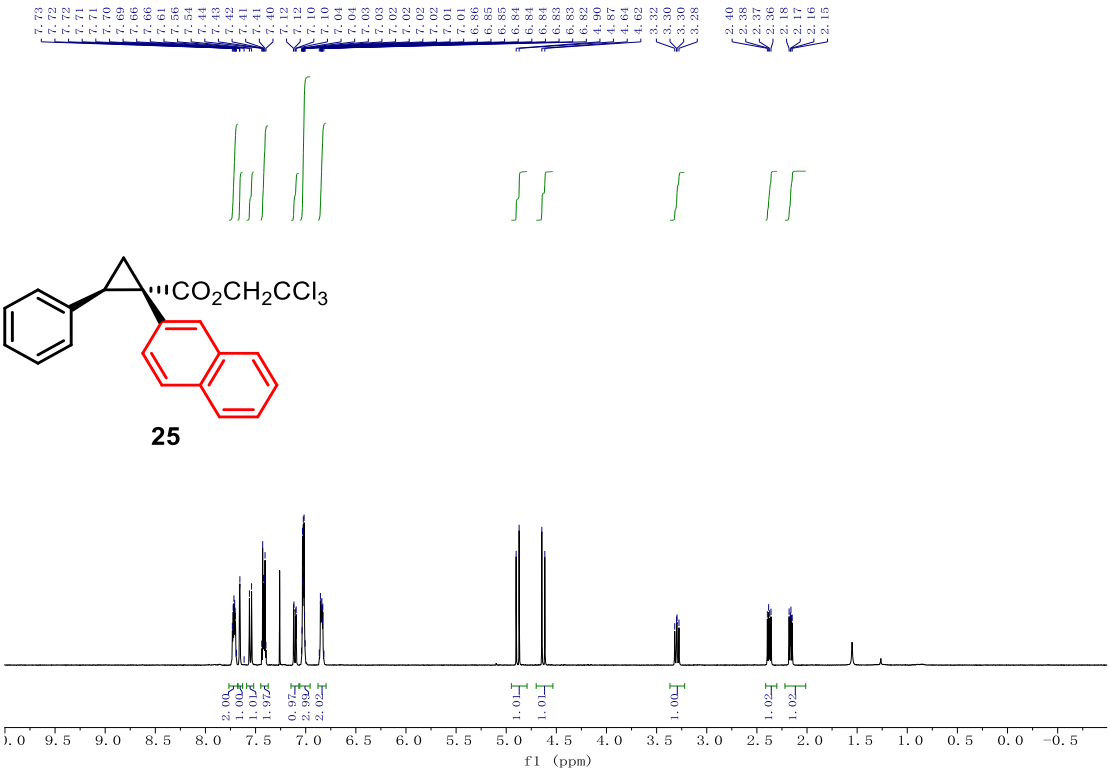
CO2CH2CCl3
25
f1 (ppm)

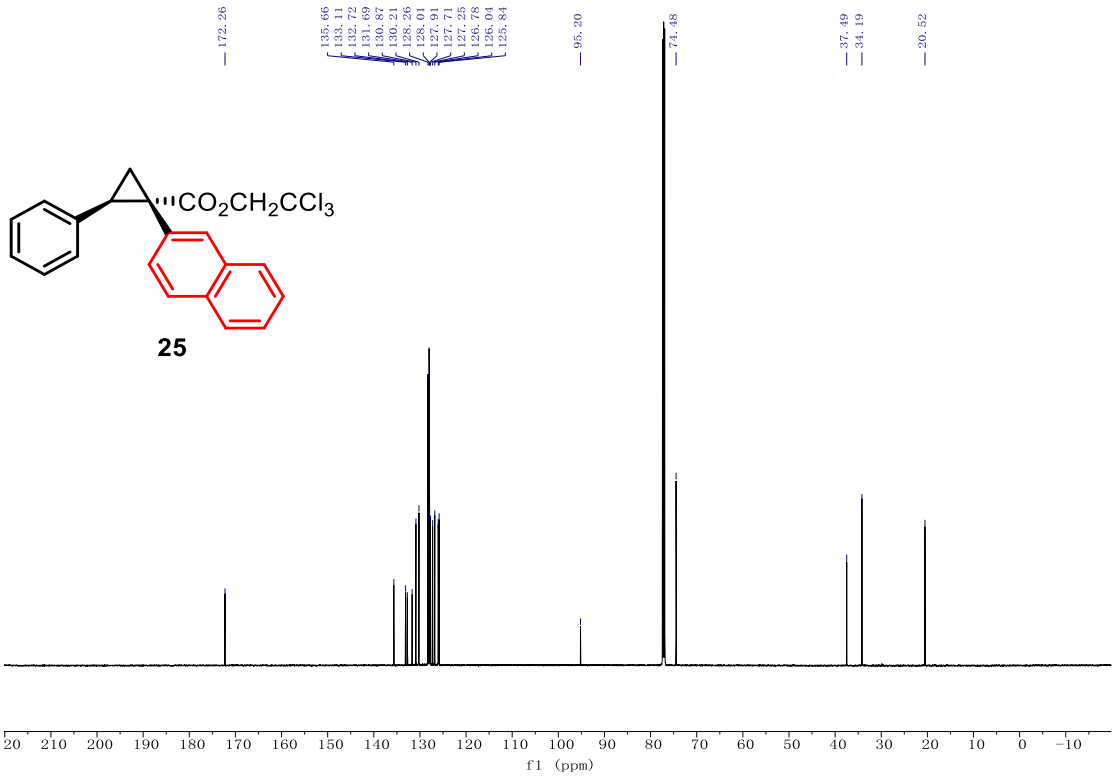
172.26
135.66
133.11
132.72
131.69
130.57
130.21
128.26
128.01
127.91
127.71
127.25
126.78
126.04
125.84
95.20
74.48
37.49
34.19
20.52
CO2CH2CCl3
25
f1 (ppm)

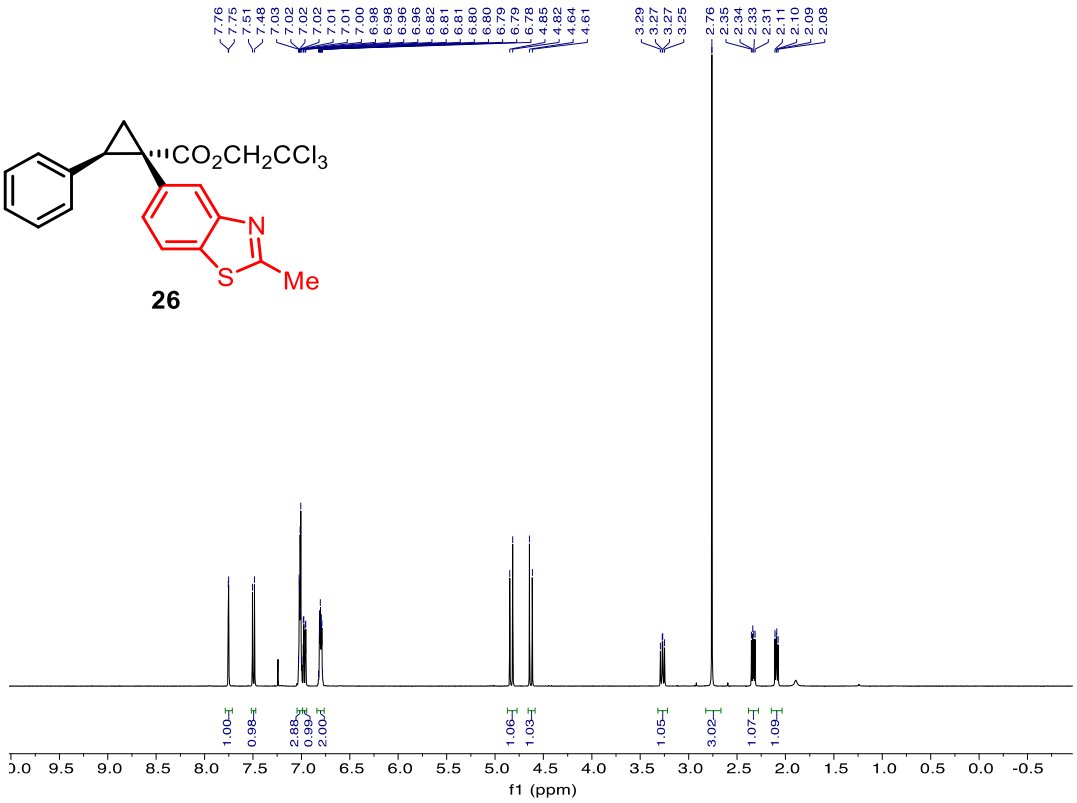
7.76
7.75
7.51
7.48
7.03
7.02
7.02
7.02
7.01
7.01
7.00
6.98
6.98
6.96
6.96
6.82
6.81
6.81
6.80
6.80
6.79
6.79
6.78
4.85
4.82
4.64
4.61
3.29
3.27
3.27
3.25
2.76
2.35
2.34
2.33
2.31
2.11
2.10
2.09
2.08
CO2CH2CCl3
N
S
Me
26
1.00
0.98
2.88
0.99
2.00
1.06
1.03
1.05
3.02
1.07
1.09
f1 (ppm)

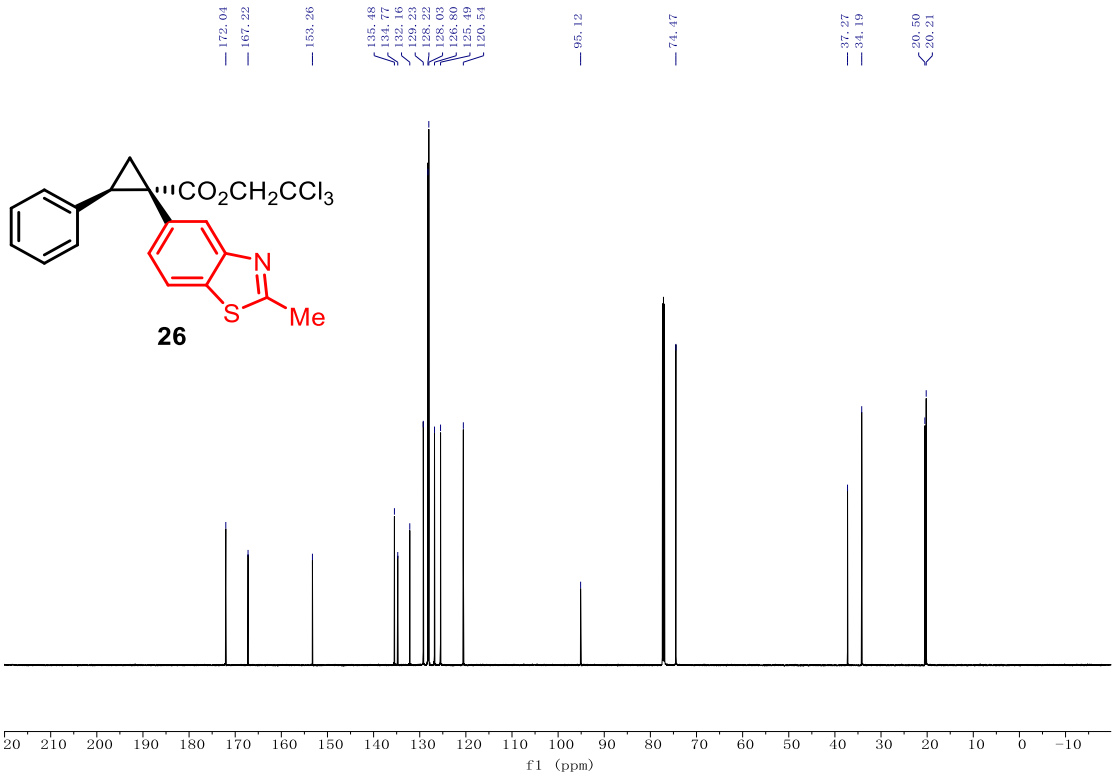
172.04
167.22
153.26
135.48
134.77
132.16
129.23
128.22
128.03
126.80
125.49
120.54
95.12
74.47
37.27
34.19
20.50
20.21
CO2CH2CCl3
N
S
Me
26
f1 (ppm)

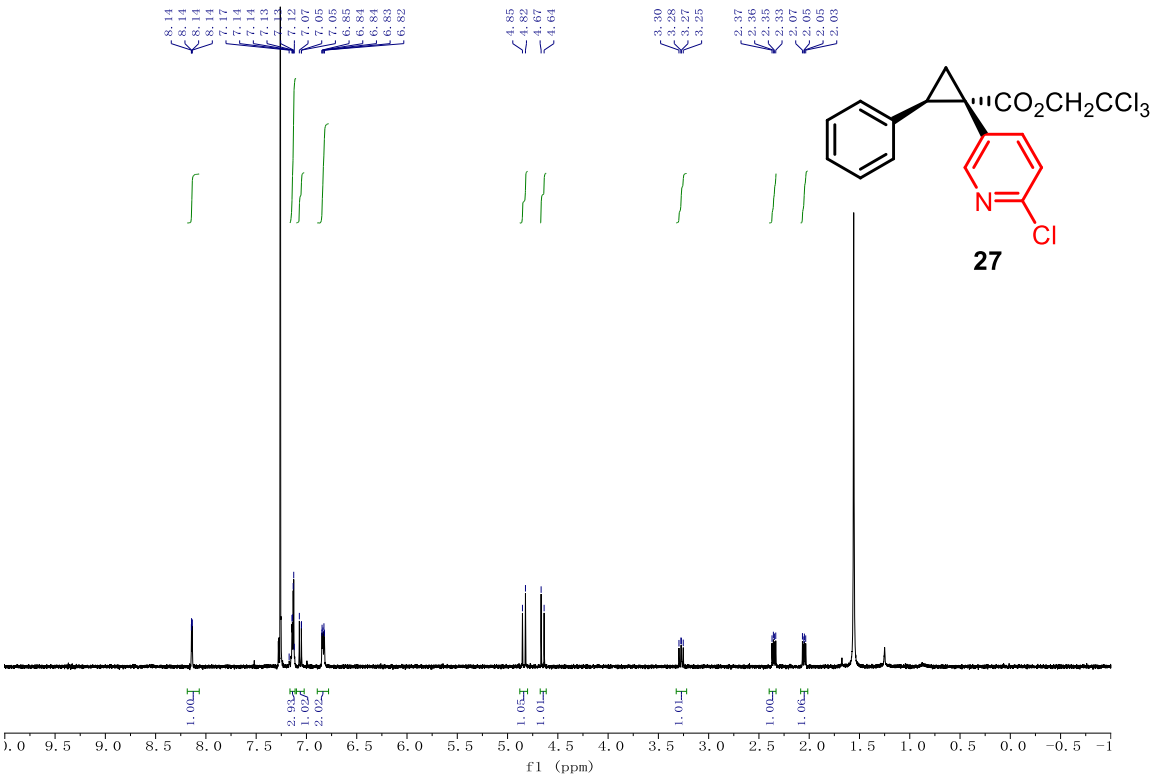
8.14
7.17
7.14
7.13
7.12
7.07
7.05
6.85
6.84
6.83
6.82
4.85
4.82
4.67
4.64
3.30
3.28
3.27
3.25
2.37
2.36
2.35
2.33
2.07
2.05
2.03
CO2CH2CCl3
N
Cl
27
1.00
2.93
1.02
2.02
1.05
1.01
1.01
1.00
1.06
f1 (ppm)

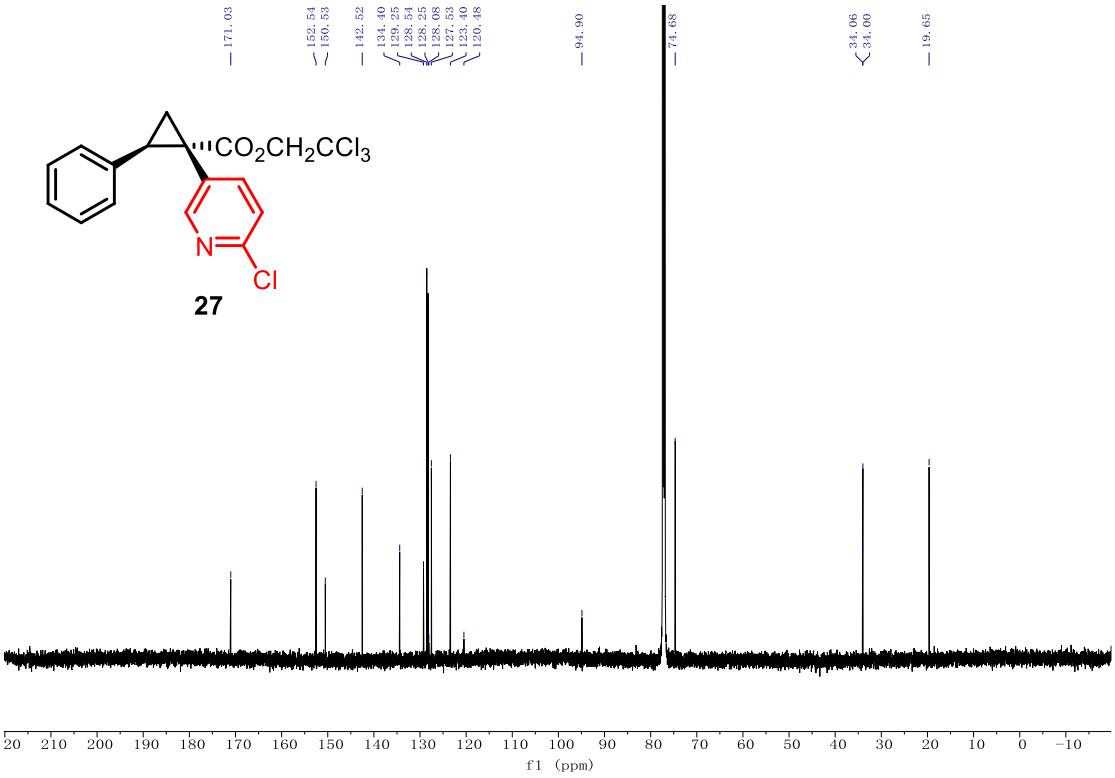
171.03
152.54
150.53
142.52
134.40
129.25
128.54
128.25
126.08
125.53
123.40
120.48
94.90
74.68
34.06
34.00
19.65
CO2CH2CCl3
N
Cl
27
f1 (ppm)

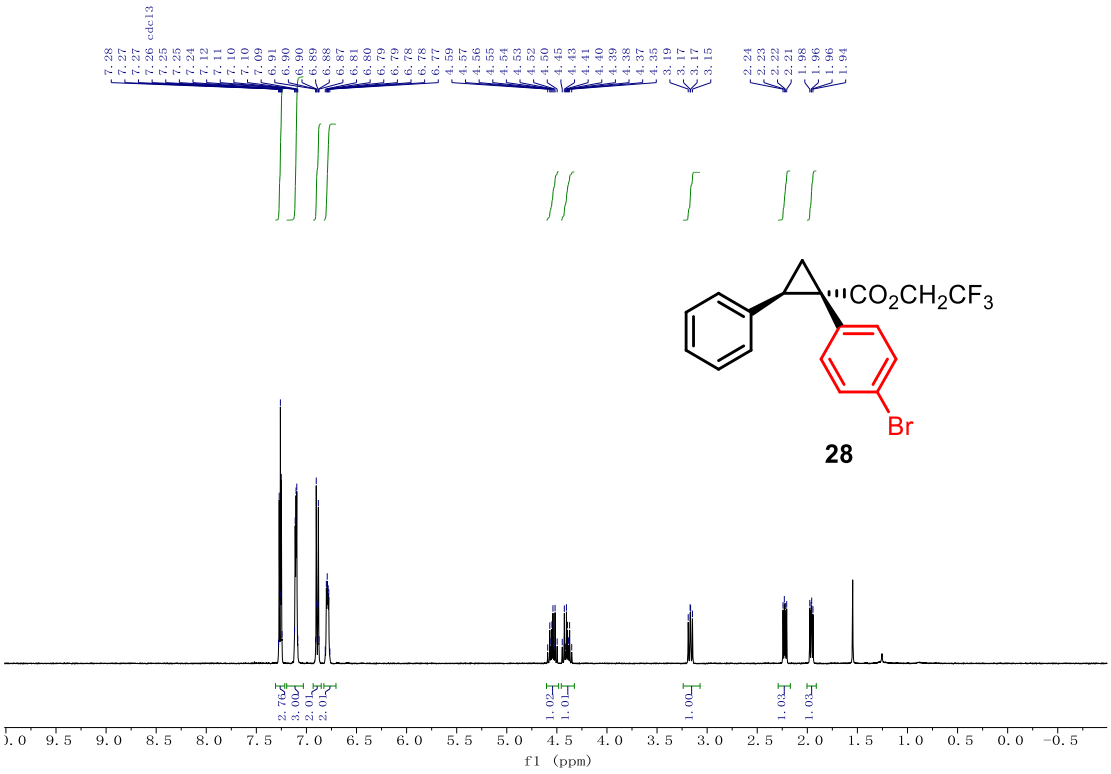
cdcl3
CO2CH2CF3
Br
28
f1 (ppm)

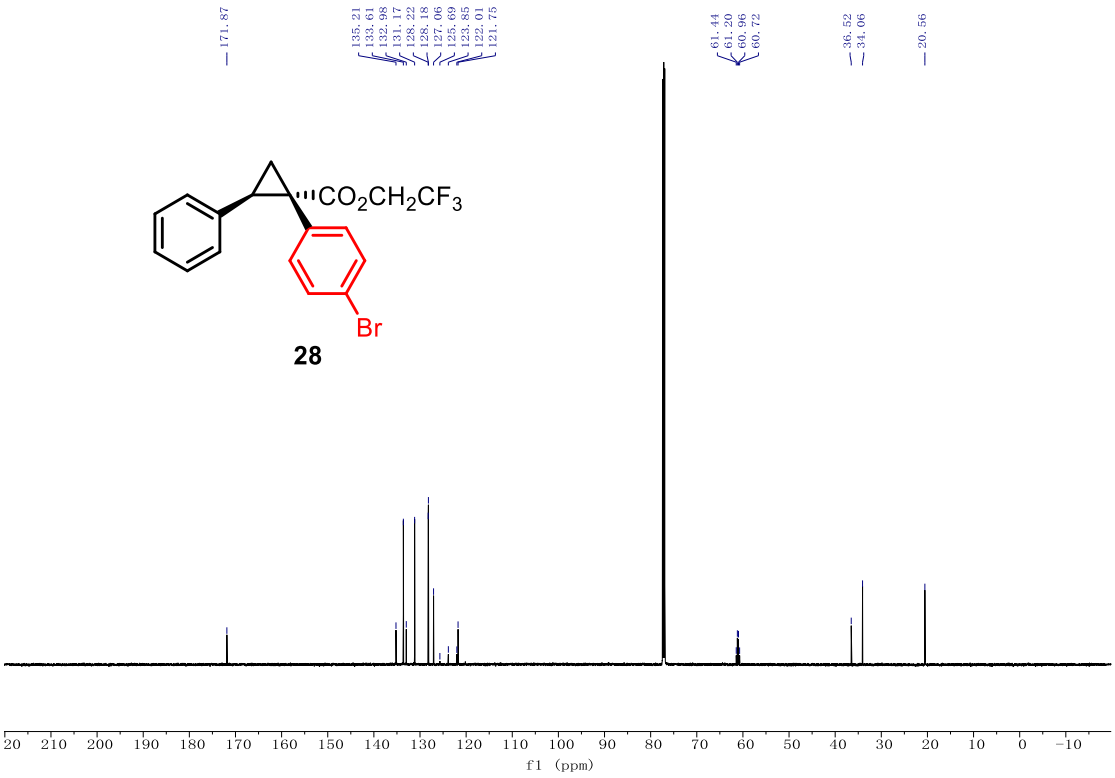
171.87
135.21
133.61
132.98
131.17
128.22
128.18
127.06
125.69
123.85
122.01
121.75
61.44
61.20
60.96
60.72
36.52
34.06
20.56
CO2CH2CF3
Br
28
f1 (ppm)

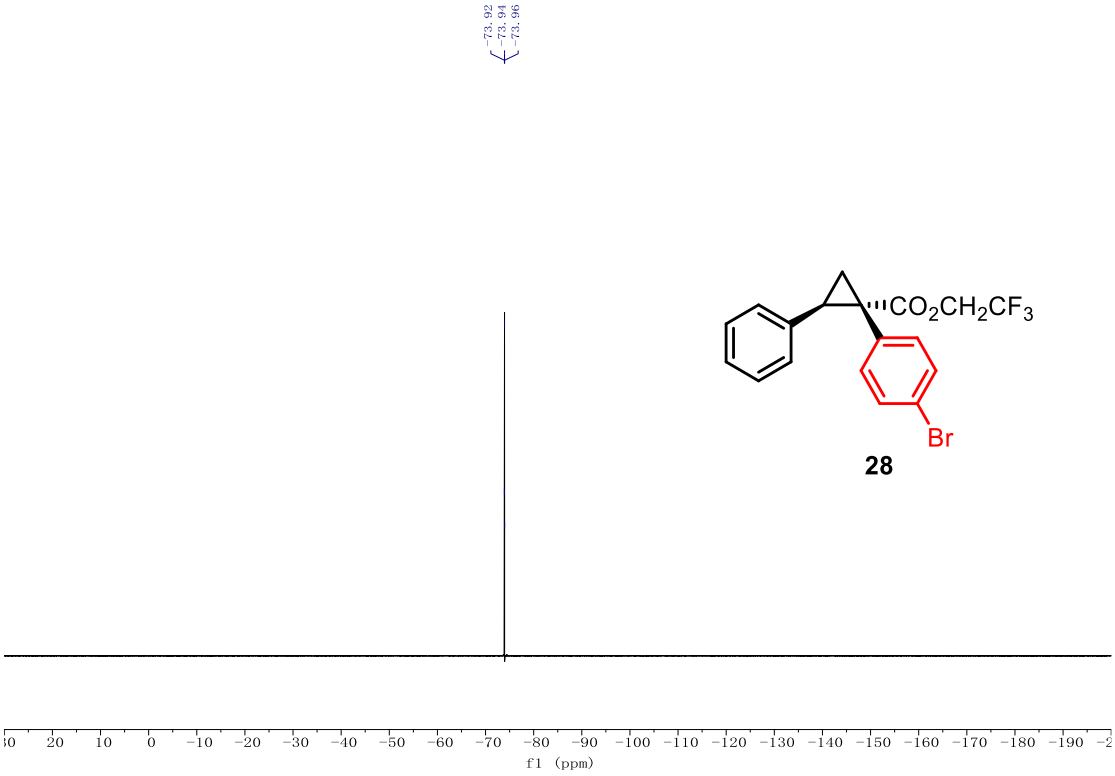
-73.92
-73.94
-73.96
CO2CH2CF3
Br
28
f1 (ppm)

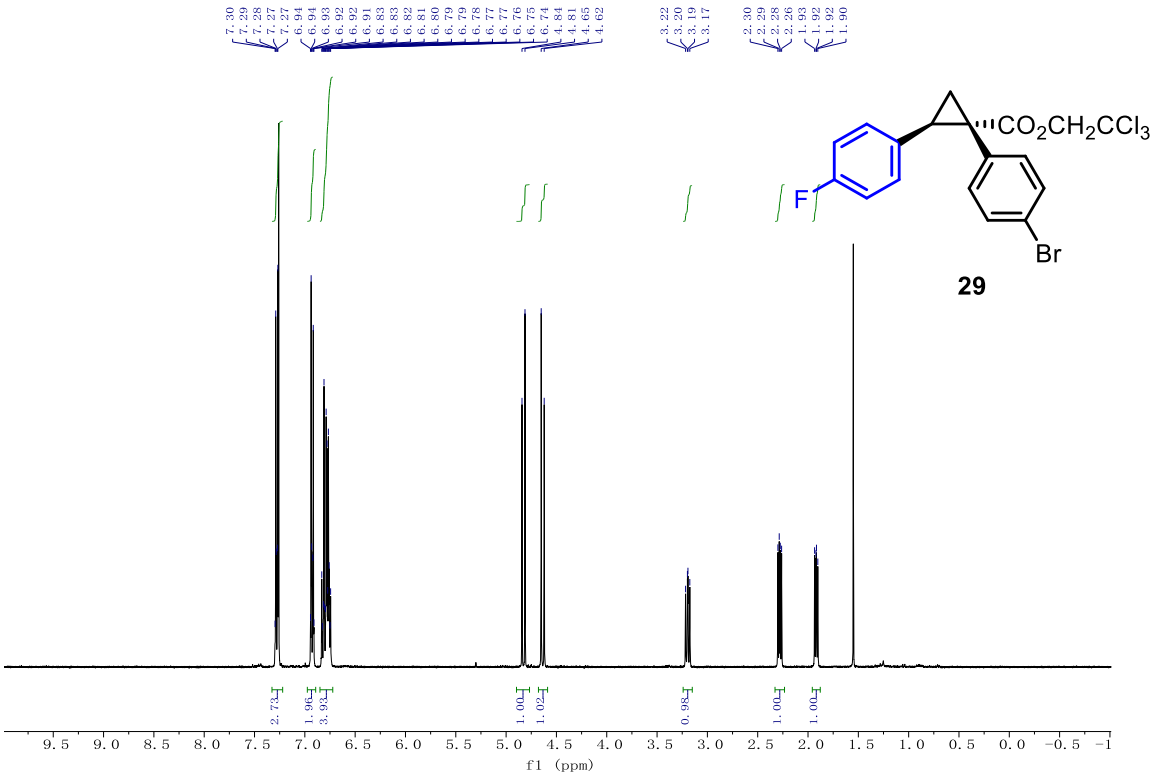
7.30
7.29
7.28
7.27
7.27
6.94
6.94
6.93
6.92
6.92
6.91
6.83
6.83
6.82
6.81
6.80
6.79
6.79
6.78
6.77
6.77
6.76
6.75
6.74
4.84
4.81
4.65
4.62
3.22
3.20
3.19
3.17
2.30
2.29
2.28
2.26
1.93
1.92
1.92
1.90
2.73
1.96
3.93
1.00
1.02
0.98
1.00
1.00
9.5 9.0 8.5 8.0 7.5 7.0 6.5 6.0 5.5 5.0 4.5 4.0 3.5 3.0 2.5 2.0 1.5 1.0 0.5 0.0 −0.5 −1
f1 (ppm)
CO2CH2CCl3
F
Br
29

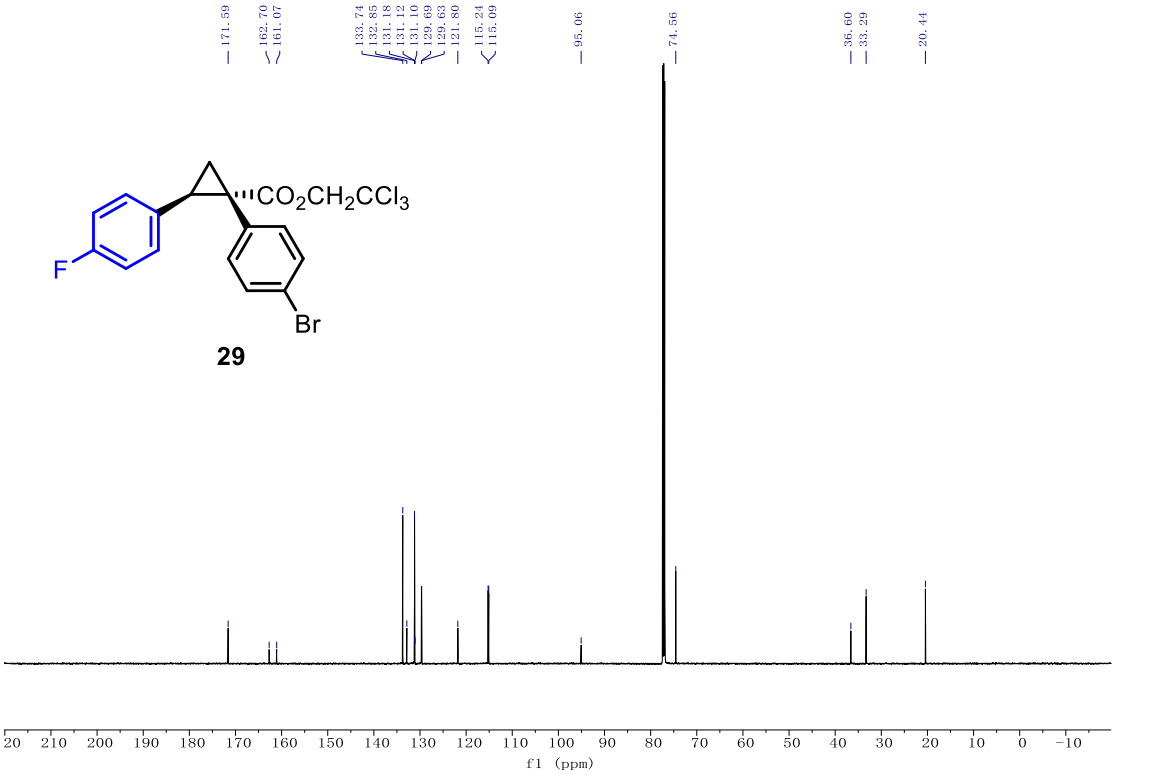
171.59
162.70
161.07
133.74
132.85
131.18
131.12
131.10
129.69
129.63
121.80
115.24
115.09
95.06
74.56
36.60
33.29
20.44
210 200 190 180 170 160 150 140 130 120 110 100 90 80 70 60 50 40 30 20 10 0 −10
f1 (ppm)
CO2CH2CCl3
F
Br
29

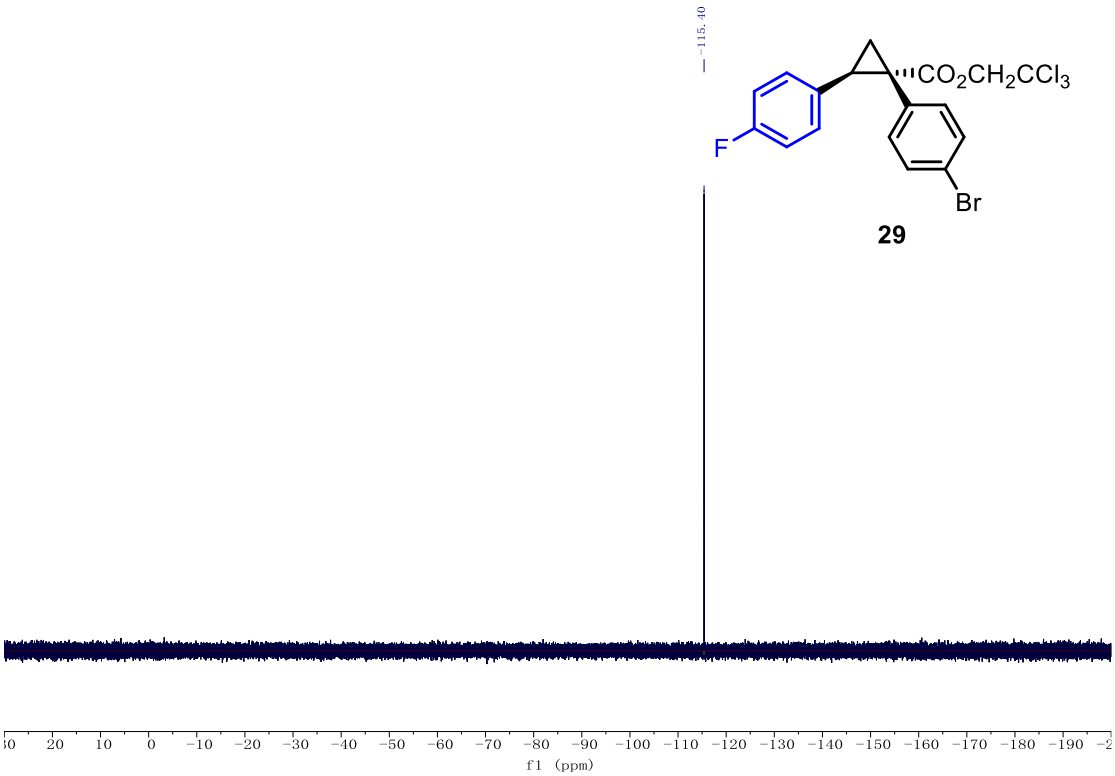
−115.40
CO2CH2CCl3
F
Br
29
f1 (ppm)

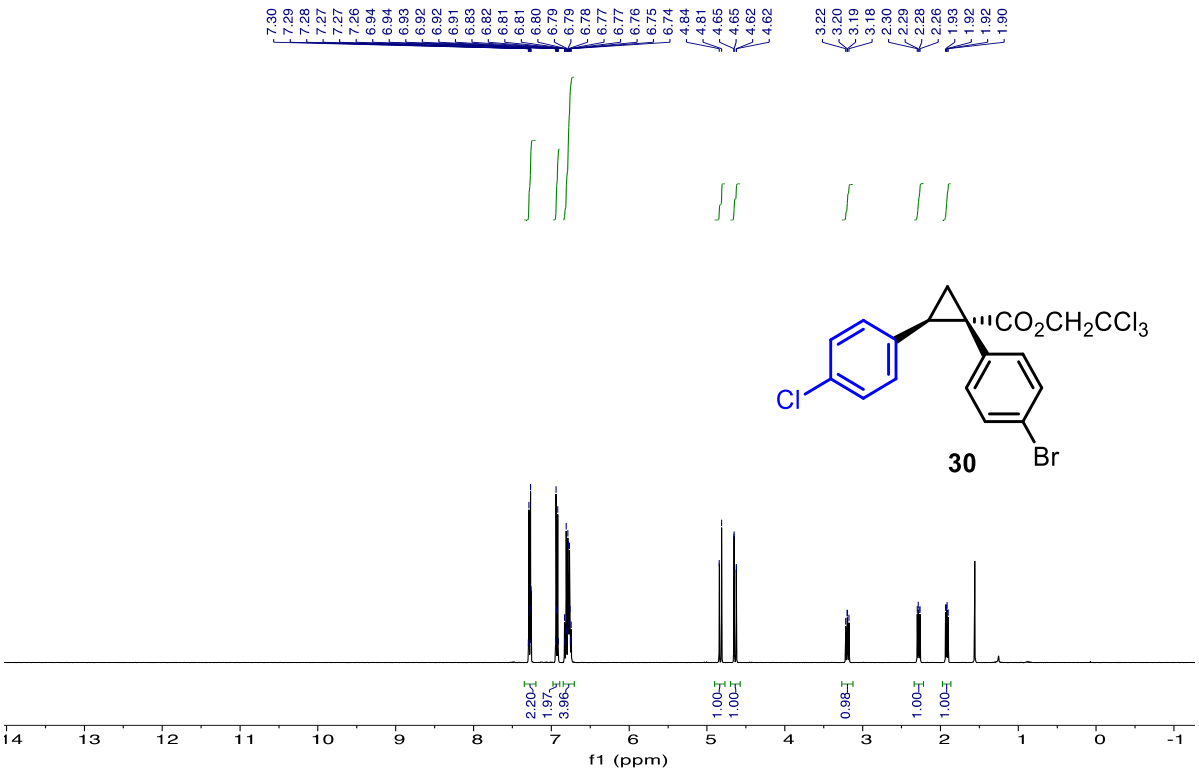
7.30
7.29
7.28
7.27
7.27
7.26
6.94
6.94
6.93
6.92
6.92
6.91
6.83
6.82
6.81
6.81
6.80
6.79
6.79
6.78
6.77
6.77
6.76
6.75
6.74
4.84
4.81
4.65
4.65
4.62
4.62
3.22
3.20
3.19
3.18
2.30
2.29
2.28
2.26
1.93
1.92
1.92
1.90
CO2CH2CCl3
Cl
Br
30
2.20
1.97
3.96
1.00
1.00
0.98
1.00
1.00
f1 (ppm)

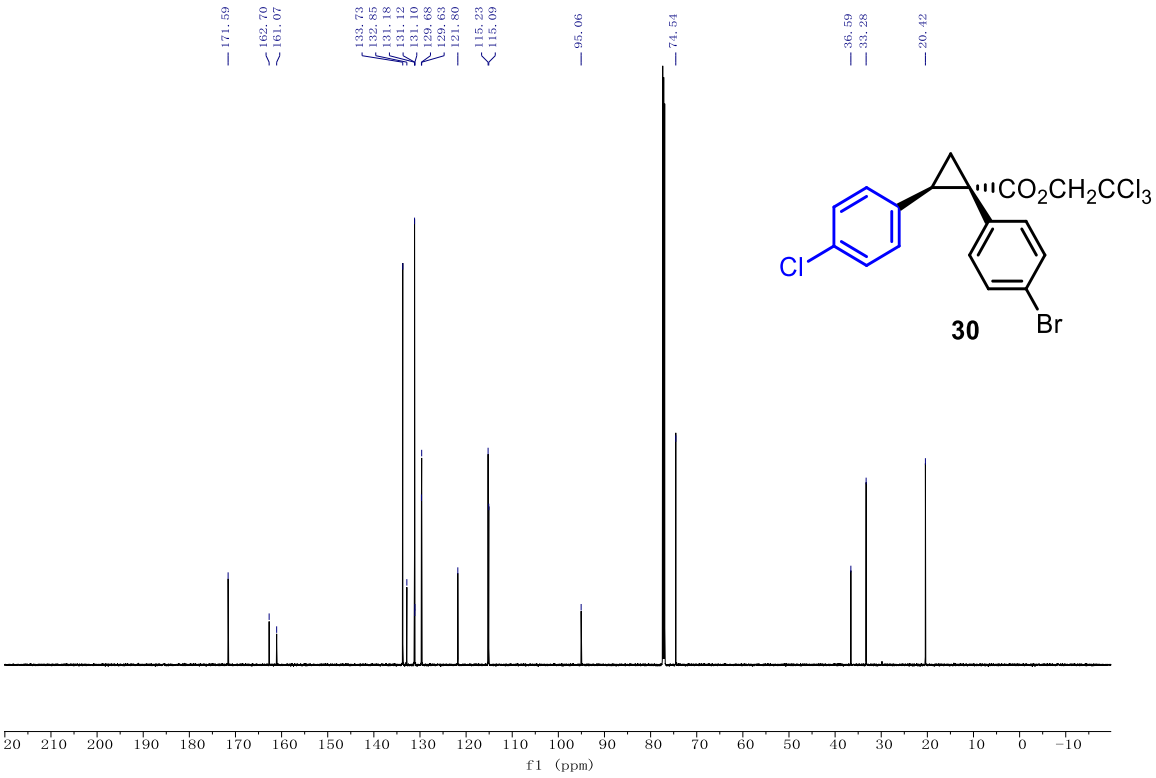
171.59
162.70
161.07
133.73
132.85
131.18
131.12
131.10
129.68
129.63
121.80
115.23
115.09
95.06
74.54
36.59
33.28
20.42
CO2CH2CCl3
Cl
Br
30
f1 (ppm)

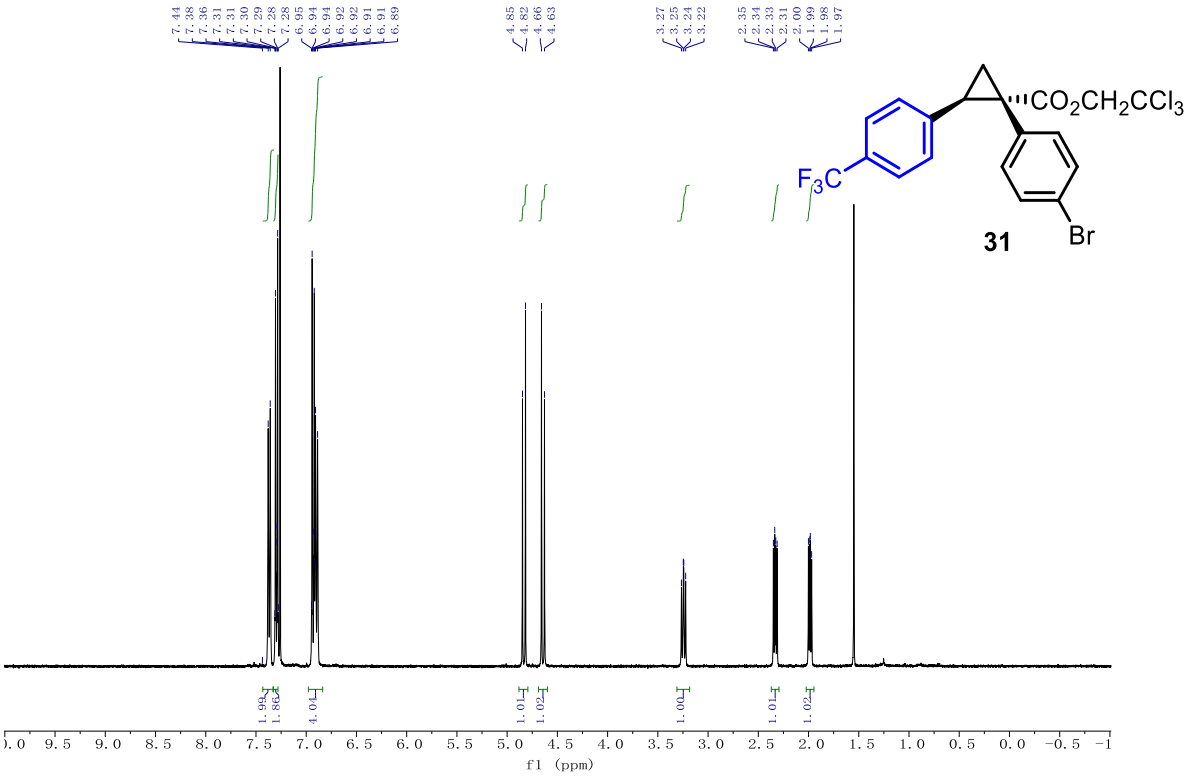
7.44
7.38
7.36
7.31
7.31
7.30
7.29
7.28
7.28
6.95
6.94
6.94
6.92
6.92
6.91
6.91
6.89
4.85
4.82
4.66
4.63
3.27
3.25
3.24
3.22
2.35
2.34
2.33
2.31
2.00
1.99
1.98
1.97
CO2CH2CCl3
F3C
Br
31
1.99
1.86
4.01
1.01
1.02
1.00
1.01
1.02
f1 (ppm)

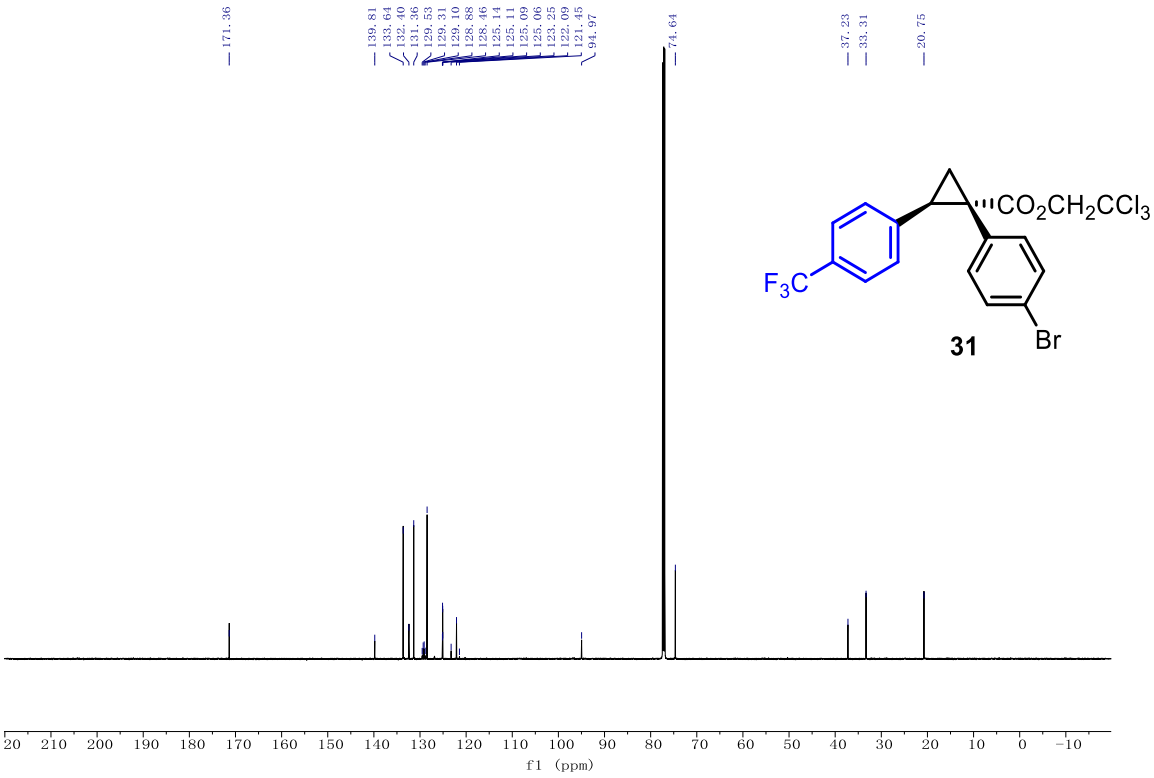
171.36
139.81
133.64
132.40
131.36
129.53
129.31
129.10
128.88
128.46
125.14
125.11
125.09
125.06
123.25
122.09
121.45
94.97
74.64
37.23
33.31
20.75
CO2CH2CCl3
F3C
Br
31
f1 (ppm)

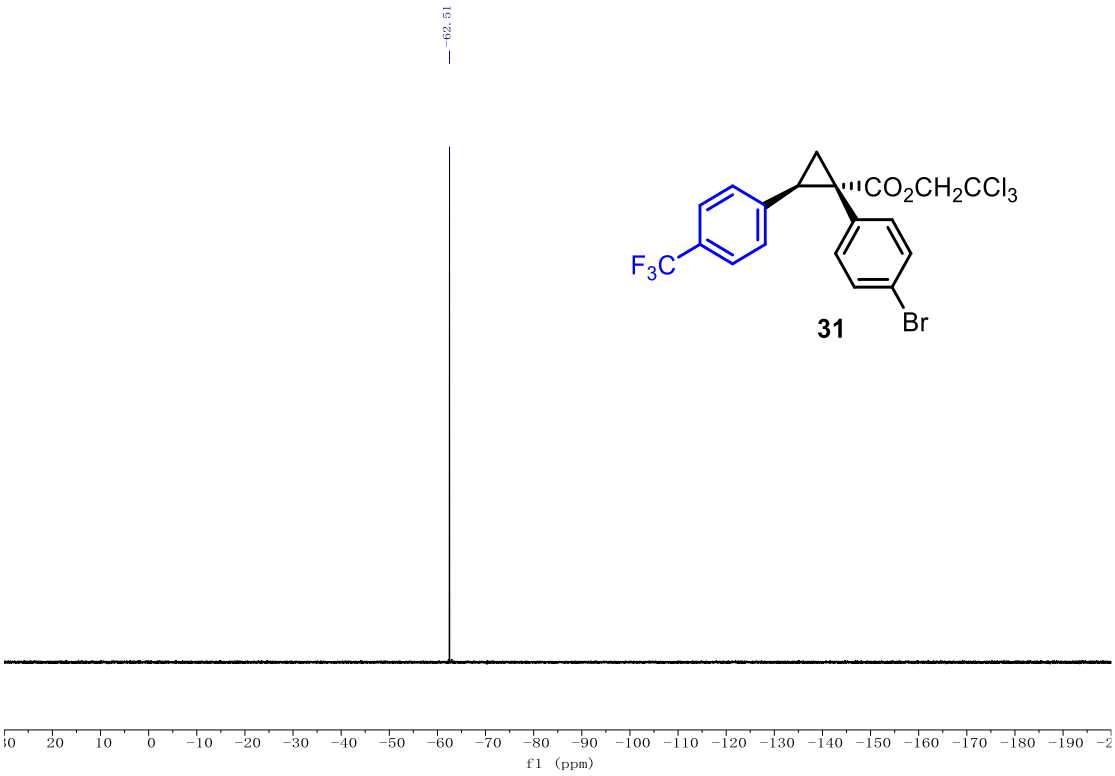
-62.51
CO2CH2CCl3
F3C
Br
31
f1 (ppm)

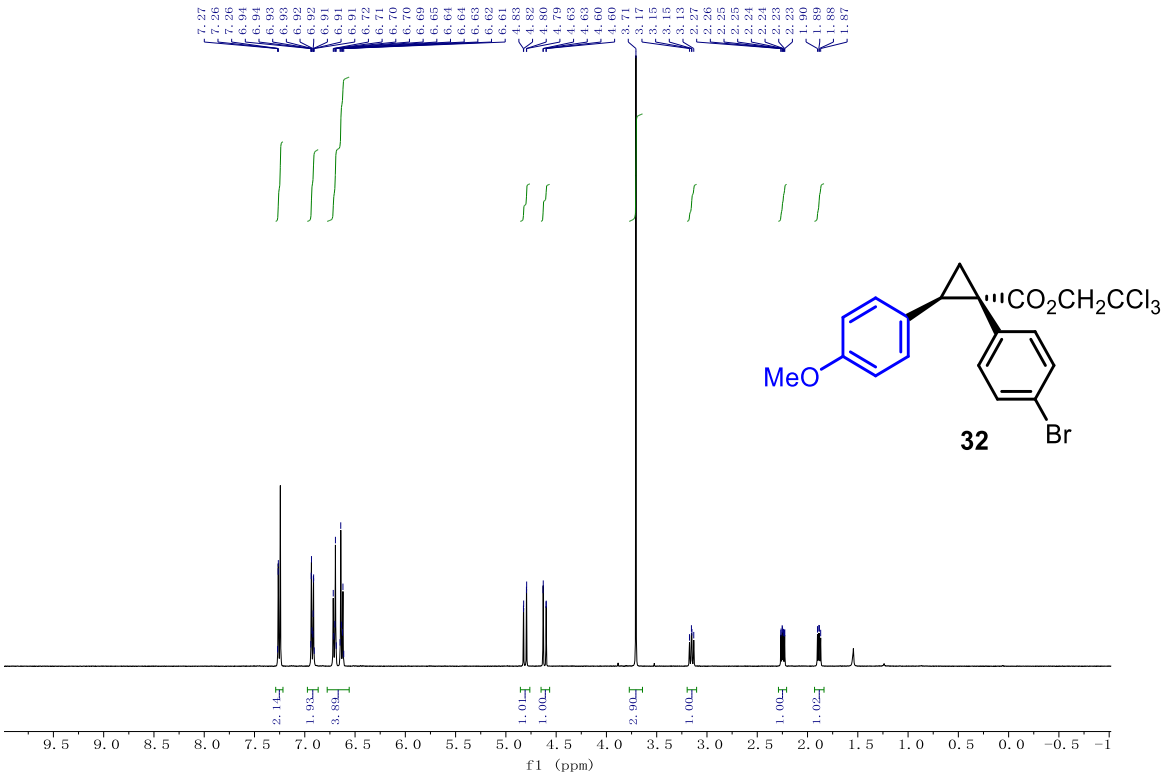
7.27 7.26 7.26 6.94 6.94 6.93 6.93 6.92 6.92 6.91 6.91 6.91 6.91 6.72 6.71 6.70 6.70 6.69 6.65 6.64 6.64 6.63 6.62 6.61
4.83 4.82 4.80 4.79 4.63 4.63 4.60 4.60
3.71 3.17 3.15 3.15 3.13
2.27 2.26 2.25 2.25 2.24 2.24 2.23 2.23
1.90 1.89 1.88 1.87
CO2CH2CCl3
MeO
Br
32
2.14 1.93 3.89 1.01 1.00 2.90 1.00 1.00 1.02
9.5 9.0 8.5 8.0 7.5 7.0 6.5 6.0 5.5 5.0 4.5 4.0 3.5 3.0 2.5 2.0 1.5 1.0 0.5 0.0 −0.5 −1
f1 (ppm)

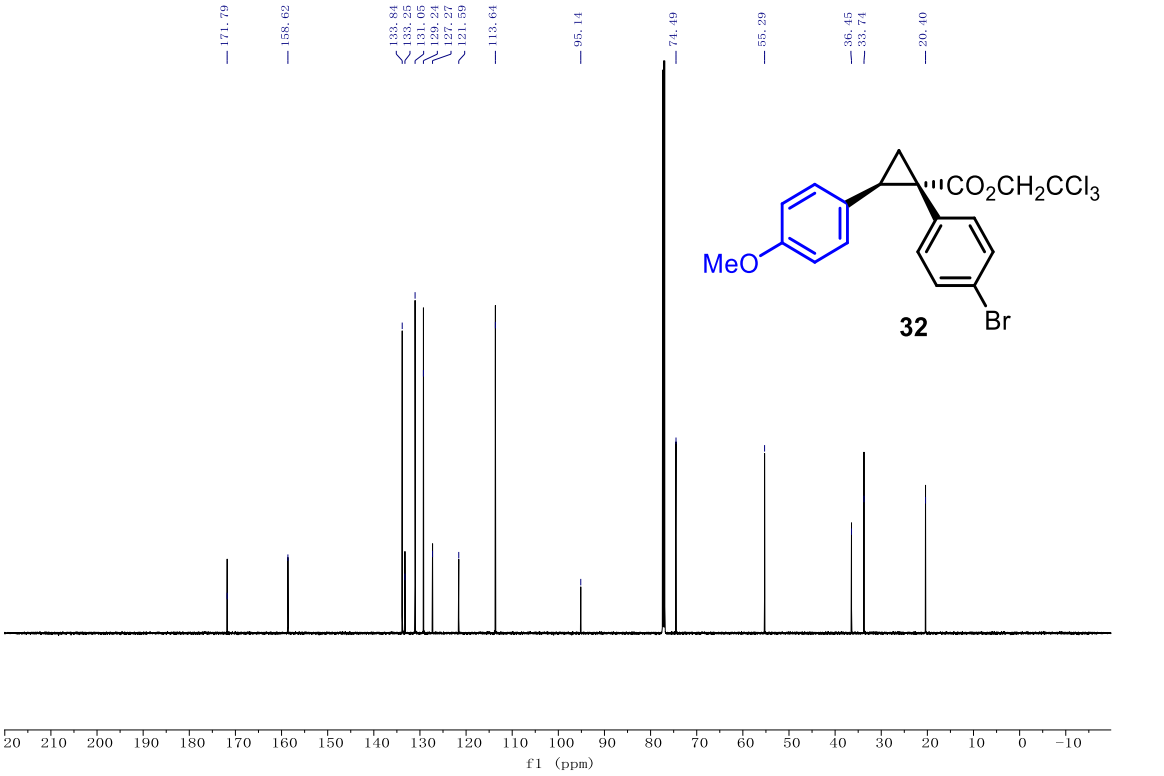
171.79
158.62
133.84 133.25 131.65 129.24 127.27 121.59
113.64
95.14
74.49
55.29
36.45 33.74
20.40
CO2CH2CCl3
MeO
Br
32
220 210 200 190 180 170 160 150 140 130 120 110 100 90 80 70 60 50 40 30 20 10 0 −10
f1 (ppm)

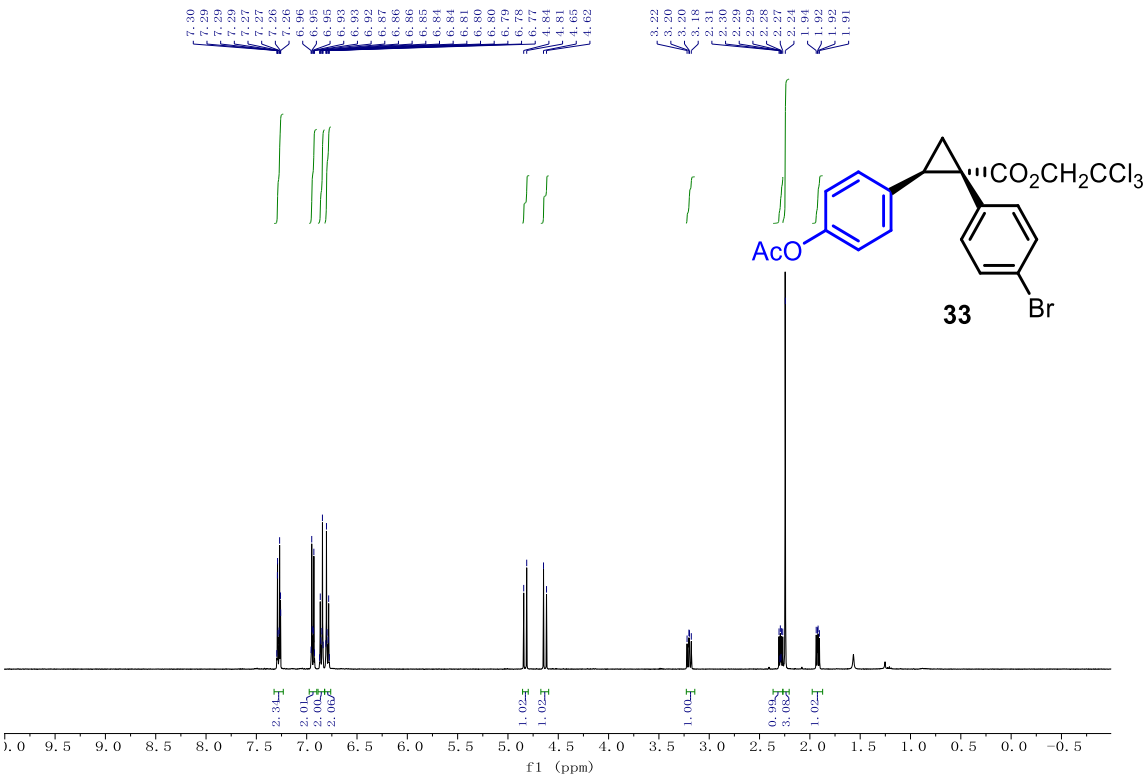
7.30 7.29 7.29 7.29 7.27 7.27 7.26 7.26 6.96 6.95 6.95 6.93 6.93 6.92 6.87 6.86 6.86 6.85 6.84 6.84 6.81 6.80 6.80 6.79 6.78 6.77 4.84 4.81 4.65 4.62
3.22 3.20 3.20 3.18 2.31 2.30 2.29 2.29 2.28 2.27 2.24 1.94 1.92 1.92 1.91
2.34 2.01 2.00 2.06 1.02 1.02 1.00 0.99 3.08 1.02
f1 (ppm)
AcO
CO2CH2CCl3
Br
33

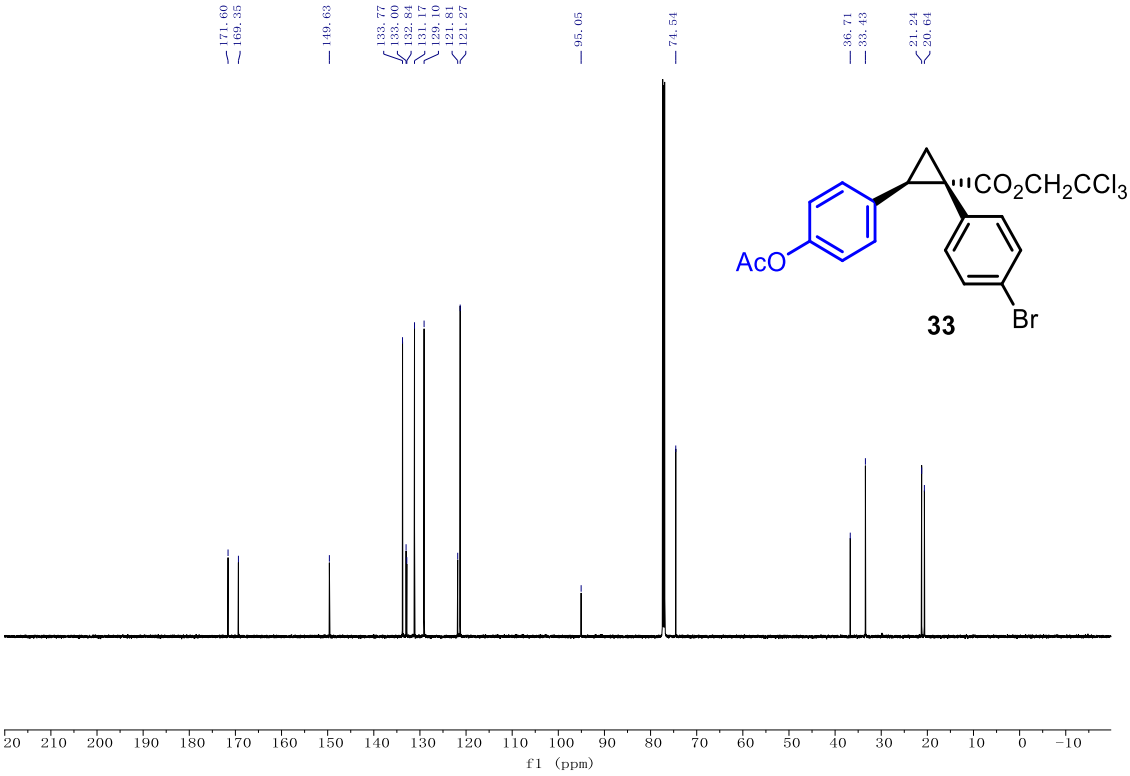
171.60 169.35 149.63 133.77 133.00 132.84 131.17 129.10 121.81 121.27 95.05 74.54 36.71 33.43 21.24 20.64
f1 (ppm)
AcO
CO2CH2CCl3
Br
33

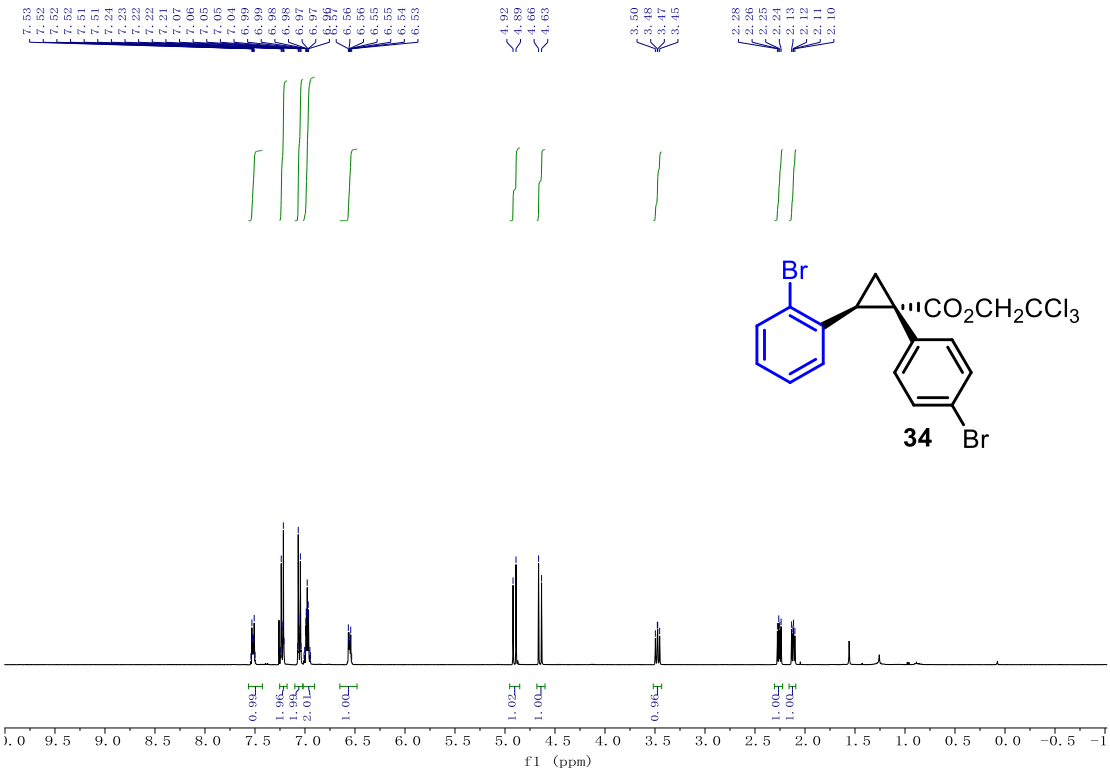
Br
CO2CH2CCl3
34
Br
f1 (ppm)

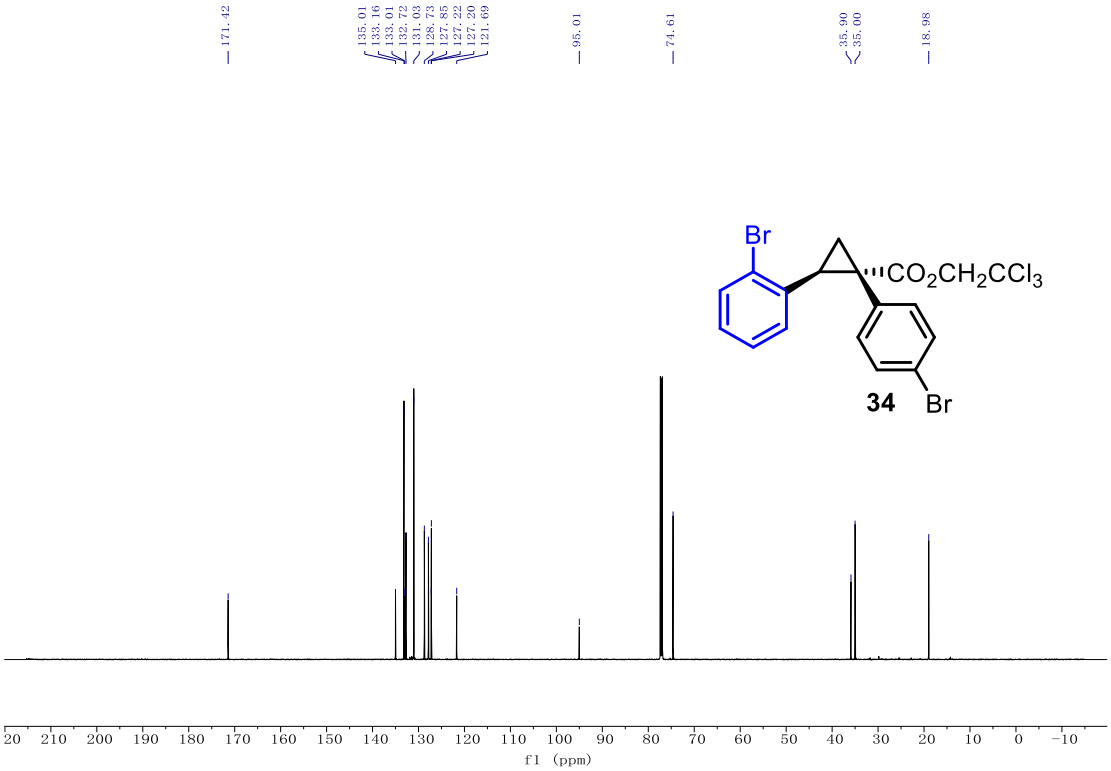
Br
CO2CH2CCl3
34
Br
f1 (ppm)

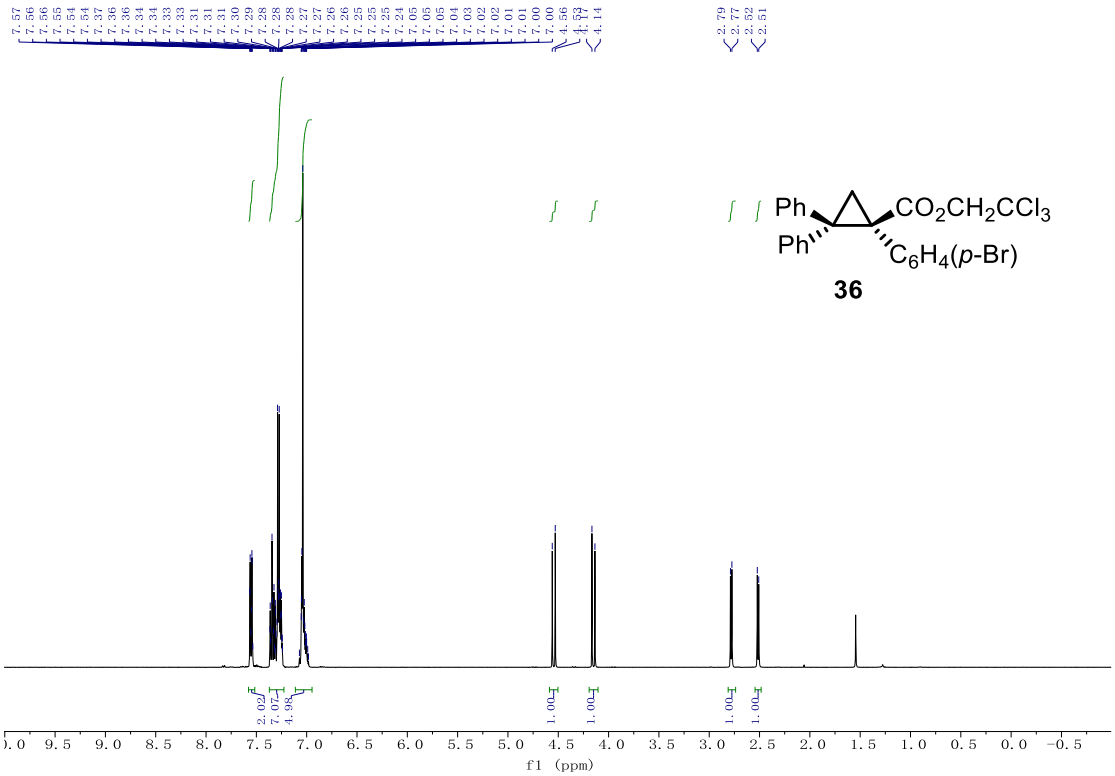
Ph
Ph
CO2CH2CCl3
C6H4(p-Br)
36
f1 (ppm)

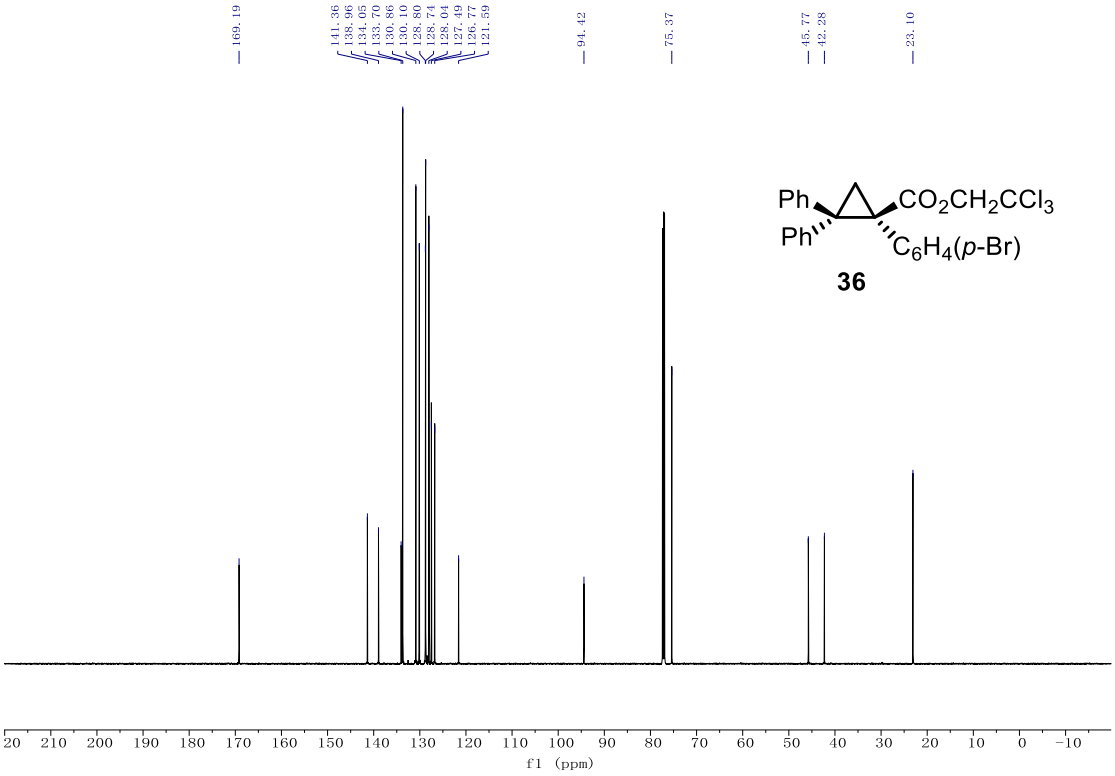
Ph
Ph
CO2CH2CCl3
C6H4(p-Br)
36
f1 (ppm)

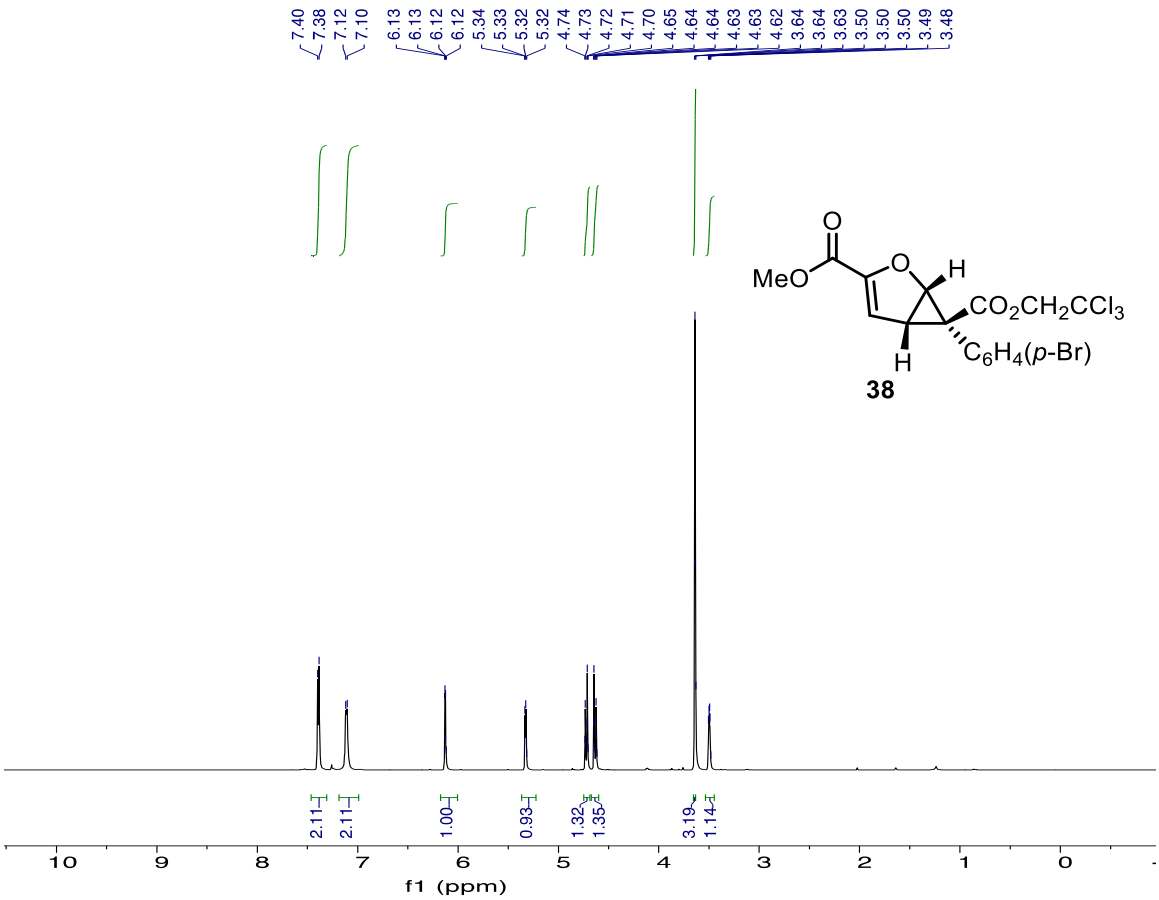
7.40
7.38
7.12
7.10
6.13
6.13
6.12
6.12
5.34
5.33
5.32
5.32
4.74
4.73
4.72
4.71
4.70
4.65
4.64
4.64
4.63
4.63
4.62
3.64
3.64
3.63
3.50
3.50
3.50
3.49
3.48
MeO
O
O
H
H
CO2CH2CCl3
C6H4(p-Br)
38
2.11
2.11
1.00
0.93
1.32
1.35
3.19
1.14
10
9
8
7
6
5
4
3
2
1
0
f1 (ppm)

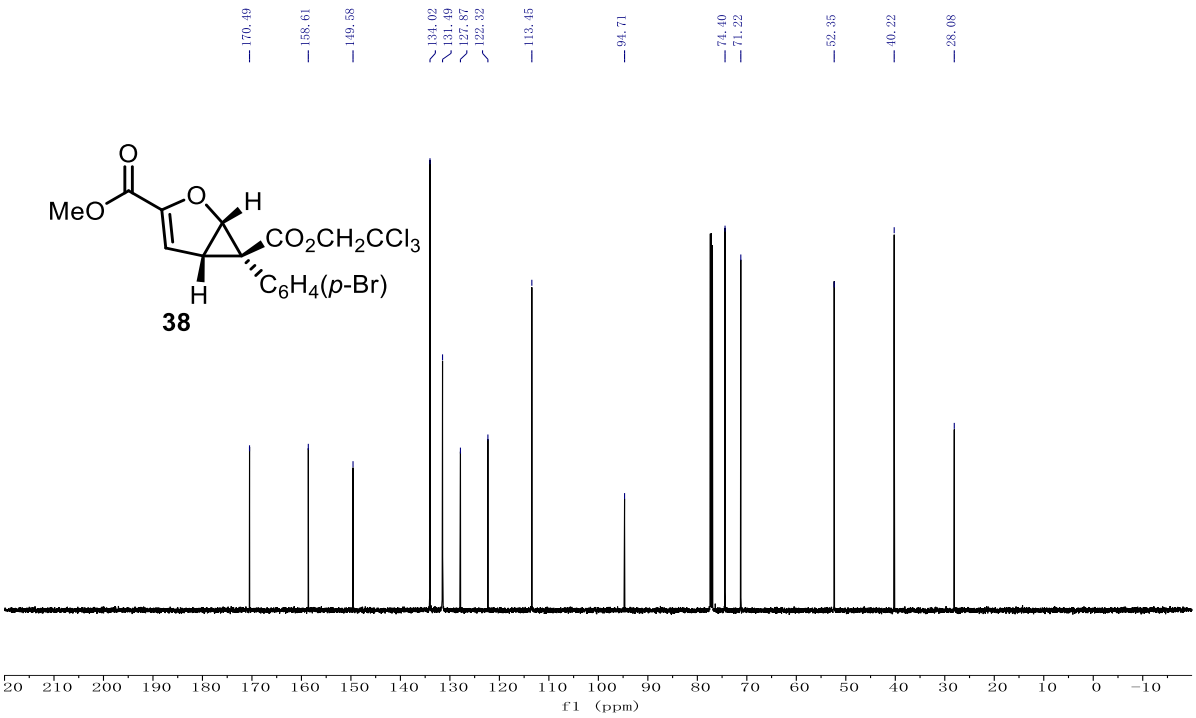
170.49
158.61
149.58
134.02
131.49
127.87
122.32
113.45
94.71
74.40
71.22
52.35
40.22
28.08
MeO
O
O
H
H
CO2CH2CCl3
C6H4(p-Br)
38
f1 (ppm)

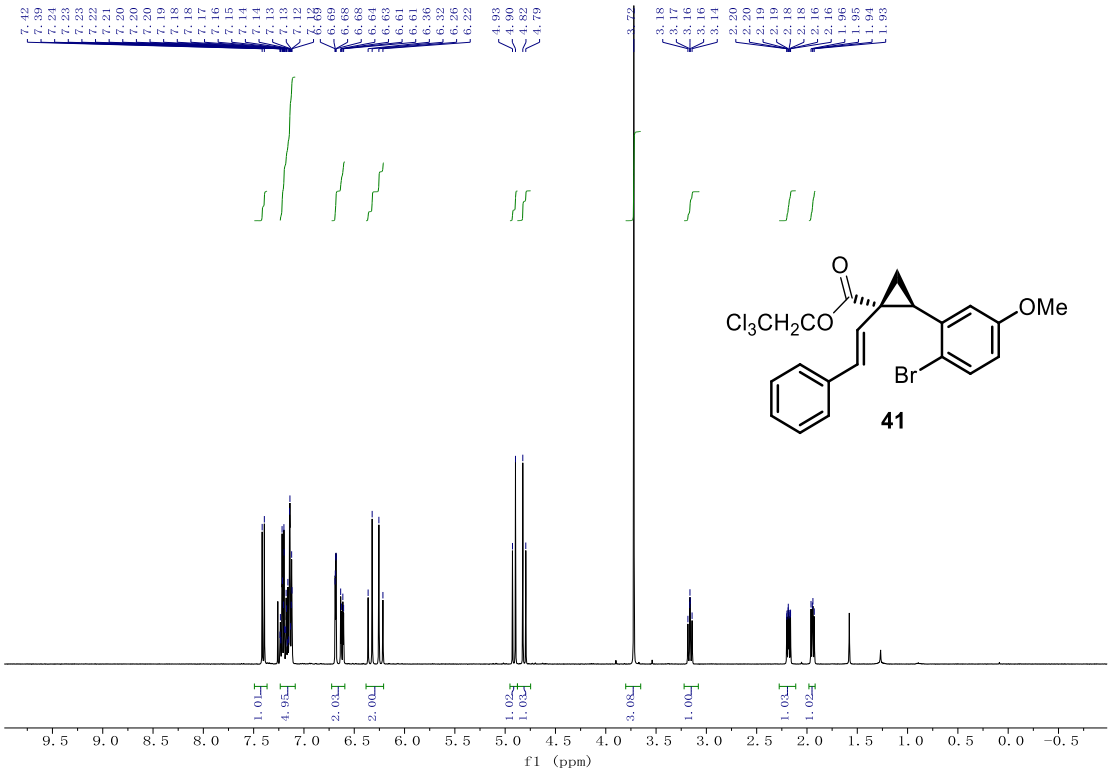
Cl3CH2CO
O
OMe
Br
41
f1 (ppm)

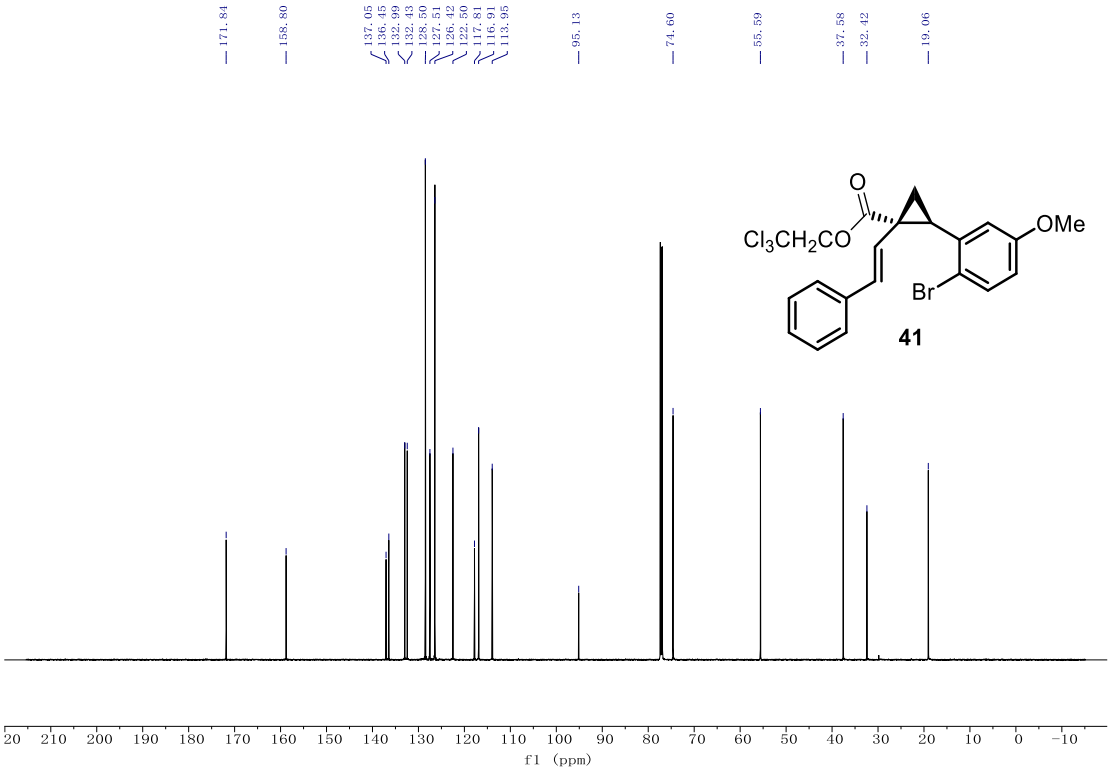
Cl3CH2CO
O
OMe
Br
41
f1 (ppm)

5. References

1. Green, S. P.; Wheelhouse, K. M.; Payne, A. D.; Hallett, J. P.; Miller, P. W.; Bull, J. A., Thermal stability and explosive hazard assessment of diazo compounds and diazo transfer reagents. *Org. Proc. Res. Dev. Dev.* **2019,** *24* (1), 67-84.
2. Wei, B.; Sharland, J. C.; Lin, P.; Wilkerson-Hill, S. M.; Fullilove, F. A.; McKinnon, S.; Blackmond, D. G.; Davies, H. M., In situ kinetic studies of Rh (II)-catalyzed asymmetric cyclopropanation with low catalyst loadings. *ACS. Catal.* **2019,** *10* (2), 1161-1170.
3. Fu, L.; Mighion, J. D.; Voight, E. A.; Davies, H. M., Synthesis of 2, 2, 2,-Trichloroethyl Aryl- and Vinyldiazoacetates by Palladium-Catalyzed Cross-Coupling. *Chem. A Eur. J.* **2017,** *23* (14), 3272-3275.
4. Guptill, D. M.; Davies, H. M., 2, 2, 2-Trichloroethyl aryldiazoacetates as robust reagents for the enantioselective C–H functionalization of methyl ethers. *J. Am. Chem. Soc.* **2014,** *136* (51), 17718-17721.
5. Liao, K.; Negretti, S.; Musaev, D. G.; Bacsa, J.; Davies, H. M., Site-selective and stereoselective functionalization of unactivated C–H bonds. *Nature* **2016,** *533* (7602), 230-234.
6. Liu, W.; Ren, Z.; Bosse, A. T.; Liao, K.; Goldstein, E. L.; Bacsa, J.; Musaev, D. G.; Stoltz, B. M.; Davies, H. M., Catalyst-controlled selective functionalization of unactivated C–H bonds in the presence of electronically activated C–H bonds. *J. Am. Chem. Soc.* **2018,** *140* (38), 12247-12255.
7. Bien, J.; Davulcu, A.; DelMonte, A. J.; Fraunhoffer, K. J.; Gao, Z.; Hang, C.; Hsiao, Y.; Hu, W.; Katipally, K.; Littke, A., The first kilogram synthesis of beclabuvir, an HCV NS5B polymerase inhibitor. *Org. Proc. Res. Dev.* **2018,** *22* (10), 1393-1408.

Appendix B: Chapter 2 Supporting information.

CAUTION: Diazo compounds are high energy compounds and need to be treated with respect. Even though we experienced no energetic decomposition in this work, care should be taken in handling large quantities of diazo compounds. Large scale reactions should be conducted behind a blast shield. For a more complete analysis of the risks associated with diazo compounds see the recent review by Bull *et. al.*[1]

1. General Considerations

All experiments were carried out in oven-dried glassware under argon atmosphere unless otherwise stated. Flash column chromatography was performed on silica gel. 4Å molecular sieves were activated under vacuum at 300 °C for 4 h. After time elapsed, the flask was cooled to 60 °C under inert nitrogen atmosphere and stored in a 140 °C oven for future use. All solvents were distilled using a short-path distillation system and stored over 4Å molecular sieves under argon atmosphere. Unless otherwise noted, all other reagents were obtained from commercial sources (Sigma Aldrich, Fisher, TCI Chemicals, AK Scientific, Combi Blocks, Oakwood Chemicals) and used as received without purification. ^{1}H, ^{13}C, and ^{19}F NMR spectra were recorded at either 400 MHz (^{13}C at 100 MHz) on Bruker 400 spectrometer or 600 MHz (^{13}C at 151 MHz) on INOVA 600 or Bruker 600 spectrometer. NMR spectra were run in solutions of deuterated chloroform ($CDCl_3$) with residual chloroform taken as an internal standard (7.26 ppm for ^{1}H, and 77.16 ppm for ^{13}C), and were reported in parts per million (ppm). The abbreviations for multiplicity are as follows: s = singlet, d = doublet, t = triplet, q = quartet, p = pentet, m = multiplet, dd = doublet of doublet, etc. Coupling constants (J values) are obtained from the spectra. Thin layer chromatography was performed on aluminum-back silica gel plates with UV light and cerium aluminum molybdate (CAM) or permanganate ($KMnO_4$)stain to visualize. Mass spectra were taken on a Thermo Finnigan LTQ-FTMS spectrometer with APCI, ESI or NSI. Melting points (mp) were measured in open capillary tubes with a Mel-Temp Electrothermal melting points apparatus and are uncorrected. IR spectra were collected on a Nicolet iS10 FT-IR spectrometer from Thermo Scientific and reported in unit of cm^{-1}. Enantiomeric excess (% ee) data were obtained on a Varian Prostar chiral HPLC instrument, an Agilent 1100 HPLC, or an Agilent 1290 Infinity UHPLC, eluting the purified products using a mixed solution of HPLC-grade 2-propanol (*i*-PrOH) and *n*-hexane.

Experimental Procedures

2. Preparation of Substrates:

2.1 Preparation of known substrates.

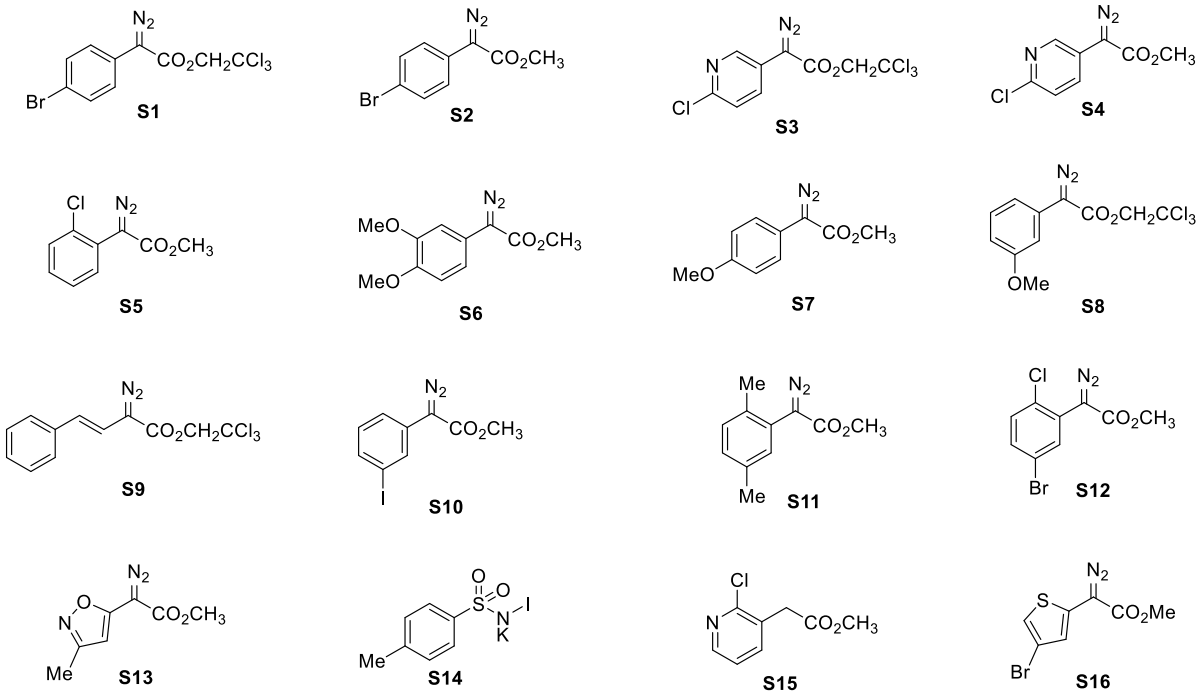

Figure B1: ***Known substrate starting materials***

Diazo compounds **s1-4** were prepared according to the established literature and matched the reported spectra.[2]
Diazo compounds **S5-7,** were prepared according to the established literature and matched the reported spectra.[3]
Diazo compounds **S8-9** were prepared according to the established literature and matched the reported spectra.[4]
Diazo compound **S10** was prepared according to the established literature and matched the reported spectra.[5]
Diazo compound **S11** was prepared according to the established literature and matched the reported spectra.[6]
Diazo compound **S12** was prepared according to the established literature and matched the reported spectra.[7]
Diazo compound **S13** was prepared according to the established literature and matched the reported spectra.[8]
Compound **s14** matched the spectra reported in the literature. [9]
Compound **s15** matched the spectra reported in the literature. [10]
Compound **s16** matched the spectra reported in the literature.[11]

2.2 Preparation of novel substrates:

2.2.1 Preparation of (*R*)-4,4-dimethyl-2-oxotetrahydrofuran-3-yl 2-(4-bromophenyl)-2-diazoacetate (S17).

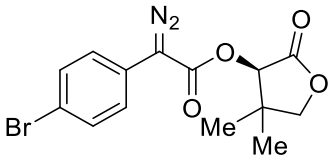

2.2.1.1 Esterification towards (*R*)-4,4-dimethyl-2-oxotetrahydrofuran-3-yl 2-(4-bromophenyl)acetate.

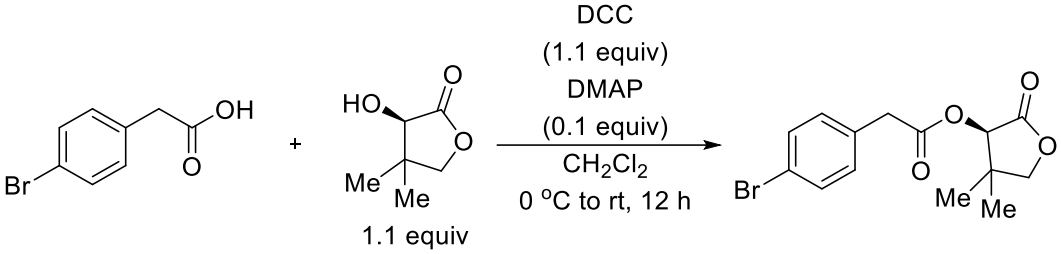

4-Bromophenylacetic acid (5.00 g, 23.3 mmol), *N,N*-dimethyl 4-aminopyridine (DMAP, 0.1 equiv, 284mg, 2.33 mmol), and (*R*)-3-hydroxy-4,4-dimethyldihydrofuran-2(*3H*)-one (*R*-pantolactone, 1.1 equiv, 3.33g, 25.6mmol) were added to a flame-dried round bottom flask. The reagents were dissolved in 100 mL CH_2Cl_2 (DCM) and the solution was cooled to 0 °C. A solution of *N,N'*-dicyclohexylcarbodiimide (DCC, 1.1 equiv, 5.28g, 25.6mmol) in CH_2Cl_2 (30 mL) was added to the reaction mixture via syringe over 5 minutes (min). The reaction mixture was removed from the ice bath allowed to stir overnight at room temperature. The reaction mixture was filtered by vacuum filtration over a pad of celite and washed with diethyl ether (Et_2O, 100 mL). The filtrate was concentrated and purified by flash column chromatography (0-5% EtOAc/hexanes over 30CV on isolera) to give pure (*R*)-4,4-dimethyl-2-oxotetrahydrofuran-3-yl 2-(4-bromophenyl)acetate as off-white needlelike crystals (70% yield, 5.3 g, 16 mmol) after aggregation and evaporation of appropriate fractions.

2.2.1.2 Diazo transfer to form (*R*)-4,4-dimethyl-2-oxotetrahydrofuran-3-yl 2-(4-bromophenyl)-2-diazoacetate.

(*R*)-4,4-dimethyl-2-oxotetrahydrofuran-3-yl 2-(4-bromophenyl)acetate (2.00 g, 6.11 mmol) and 4-acetamidobenzenesulfonyl azide (*p*-ABSA, 1.3 equiv, 1.91 g, 7.95 mmol) were added to a flame-dried round bottom flask and dissolved in acetonitrile (MeCN, 50mL) at 0 ℃ in an ice-bath. 1,8-diazabicyclo[5.4.0]undec-7-ene (DBU, 1.0 equiv, 0.921 mL) was added dropwise to the cooled stirring solution causing it to change from a clear-colorless solution to a deep orange solution. The reaction was left to stir overnight before quenching with saturated ammonium chloride solution (NH_4Cl in H_2O, 50mL). The aqueous and organic layers were separated, and the aqueous layer was extracted with Et_2O (2 X 25 mL). The combined organic layers were dried over anhydrous sodium sulfate (Na_2SO_4) before loading onto silica. The diazo -impregnated silica was then purified by flash column chromatography (100 g silica cartridge, 0% EtOAc/hexanes 3 CV, 0-20% EtOAc/Hexanes for 30 CV, 20% EtOAc/hexanes for 5 CV) to afford (*R*)-4,4-dimethyl-2-oxotetrahydrofuran-3-yl 2-(4-bromophenyl)-2-diazoacetate as a powdery bright orange solid (**S17,** 60% yield, 1.30 g, 3.68 mmol) after aggregation and evaporation of appropriate fractions.

2.2.2 Preparation of (*R*)-4,4-dimethyl-2-oxotetrahydrofuran-3-yl 2-diazo-2-(2-methoxy-5-methylphenyl)acetate (S18)

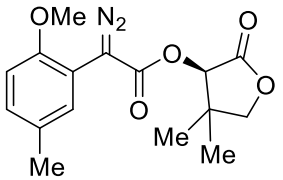

2.2.2.1 Friedel-Crafts acylation towards methyl 2-(2-methoxy-5-methylphenyl)-2-oxoacetate.

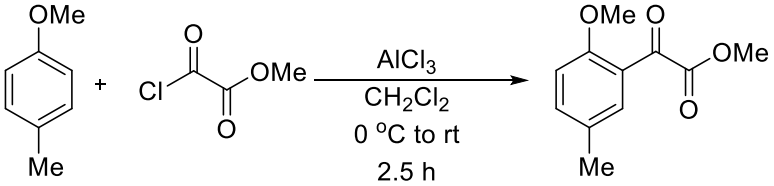

A solution of 1-methoxy-4-methylbenzene (1.0 equiv, 10.0 g, 10.3 mL, 81.9 mmol) and methyl 2-chloro-2-oxoacetate (1.5 equiv, 15.0 g, 11.3 mL, 122.8 mmol) in CH_2Cl_2 (50 mL) was added dropwise to a stirred suspension of aluminium chloride ($AlCl_3$, 1.0 equiv, 10.9 g, 81.85 mmol) in CH_2Cl_2 (150 mL) in a flame-dried round-bottom flask under an inert nitrogen atmosphere. The temperature maintained below 5 °C throughout addition. When the addition was complete, the deep purple mixture was stirred at 25 °C for 2.5 h and then poured onto 100 g of ice. The aqueous layer was washed once with CH_2Cl_2 (100 mL). The combined organic extracts were washed with 3 M HCl (200 mL), 1 M HCl (200 mL), DI water (200 mL), and

saturated NaCl (200 mL). Then the organic layer was filtered over a plug of basic alumina (25 g) and dried over sodium sulfate (Na_2SO_4) then organic solvent was concentrated to yield a yellow liquid. The crude product was then purified by flash chromatography (0-5% Et_2O/hexane over 25 CV) and the major peak containing fractions were aggregated and evaporated to yield the title product as a light yellow oil (93% yield, 15.9 g, 76.4 mmol).

2.2.2.2 Hydrolysis to afford 2-(2-methoxy-5-methylphenyl)-2-oxoacetic acid

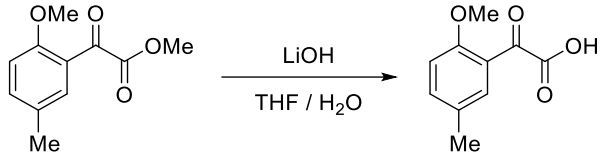

Lithium hydroxide (1.06 g, 44.3 mmol) was added to a solution of methyl 2-(2-methoxy-5-methylphenyl)-2-oxoacetate (4.61 g, 22.1 mmol) in tetrahydrofuran (30 mL) and water (15 mL) at room temperature. After stirring for 2 h the reaction was acidified with 1M HCl and extracted with EtOAc. The organic phase was washed with brine, dried with $MgSO_4$, filtered, and concentrated under reduced pressure to give the title compound (4.03 g, 20.8 mmol, 94% yield) as a gray solid without further purification. 1H NMR (600 MHz, DMSO-d6) δ 7.55 – 7.48 (m, 2H), 7.15 (d, J = 8.5 Hz, 1H), 3.81 (s, 3H), 2.29 (t, J = 0.7 Hz, 3H); MS(APCI+) m/z 195.6 (M+H)+. The material was used in the next step without further characterization.

2.2.2.3 Esterification towards (*R*)-4,4-dimethyl-2-oxotetrahydrofuran-3-yl 2-(2-methoxy-5-methylphenyl)-2-oxoacetate.

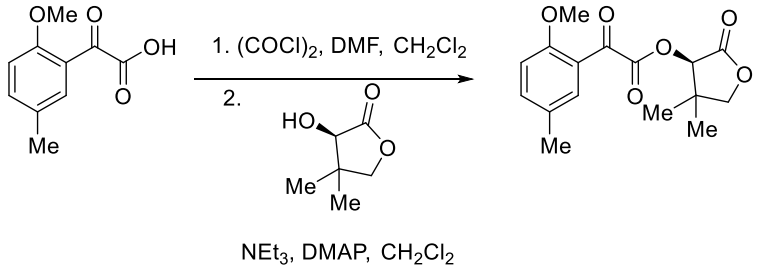

Oxalyl chloride (8.66 mL, 99 mmol) was added dropwise to a mixture of 2-(2-methoxy-5-methylphenyl)-2-oxoacetic acid (9.6 g, 49.4 mmol) and DMF (0.038 mL, 0.494 mmol) in CH_2Cl_2 (100 mL) at 0 °C. The reaction was slowly warmed to room temperature and stirred for 16 h before being concentrated under reduced pressure. The resulting residue was then taken up in CH_2Cl_2 (100 mL) and cooled in an ice bath. Triethylamine (TEA, 17.23 mL, 124 mmol), DMAP (0.060 g, 0.494 mmol), and *R*-pantolactone (9.65 g, 74.2 mmol, CombiBlocks) were then sequentially added before warming the mixture to room temperature. After stirring for 2 h the reaction was washed with 1M HCl, saturated $NaHCO_3$, and brine. The organic phase was then dried with $MgSO_4$, filtered, and concentrated under reduced pressure. The crude residue was purified by flash chromatography (ISCO Combiflash, 0-50% EtOAc/heptanes,120 g Redisep gold silica column) to give the title compound (13.8 g, 45.1 mmol, 91% yield) as a light yellow oil after aggregation and evaporation of appropriate fractions. 1H NMR (500 MHz, DMSO-d6) δ 7.62 – 7.55 (m, 2H), 7.19 (d, J = 8.5 Hz, 1H), 5.82 (s, 1H), 4.22 – 4.17 (m, 1H), 4.12 (d, J = 8.6 Hz, 1H), 3.84 (s, 3H), 2.31 (d, J = 0.8 Hz, 3H), 1.21 (s, 3H), 0.99 (s, 3H); MS(APCI+) m/z 307.3 (M+H)+. The material was used in the next step without further characterization.

2.2.2.4 One-pot diazotization of (*R*)-4,4-dimethyl-2-oxotetrahydrofuran-3-yl 2-(2-methoxy-5 -methylphenyl)-2-oxoacetate.

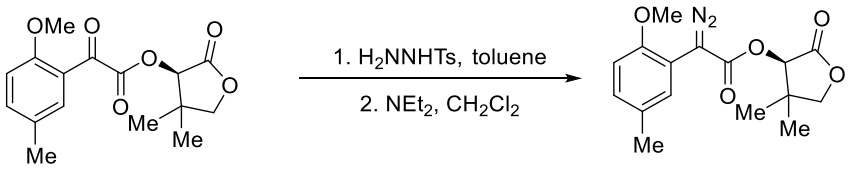

A mixture of (R)-4,4-dimethyl-2-oxotetrahydrofuran-3-yl 2-(2-methoxy-5-methylphenyl)-2-oxoacetate (8.53 g, 27.8 mmol) and 4-methylbenzenesulfonohydrazide (5.19 g, 27.8 mmol, Aldrich) in toluene (56 mL) was heated to reflux with a Dean-Stark trap. After 16 h the reaction was concentrated under reduced pressure and CH_2Cl_2 (56 mL) and TEA (5.82 mL, 41.8 mmol) were added to the resulting residue. After stirring at room temperature for 16 h the reaction was washed with saturated $NaHCO_3$ and brine, dried with $MgSO_4$, filtered, and concentrated under reduced pressure. The crude residue was purified by flash chromatography (ISCO Combiflash, 0-40% EtOAc/heptanes, 120 g Redisep gold silica column) to yield (*R*)-4,4-dimethyl-2-oxotetrahydrofuran-3-yl 2-diazo-2-(2-methoxy-5-methylphenyl)acetate (**S18,** 7.3 g, 23 mmol, 82% yield) as a yellow solid after aggregation and evaporation of appropriate fractions.

2.2.3 Preparation of methyl 2-diazo-2-(2-methoxy-5-methylphenyl)acetate (54).

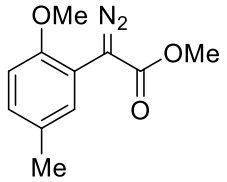

2.2.3.1 Hydrazine condensation towards methyl (*E*/*Z*)-2-hydrazineylidene-2-(2-methoxy-5-methylphenyl) acetate.

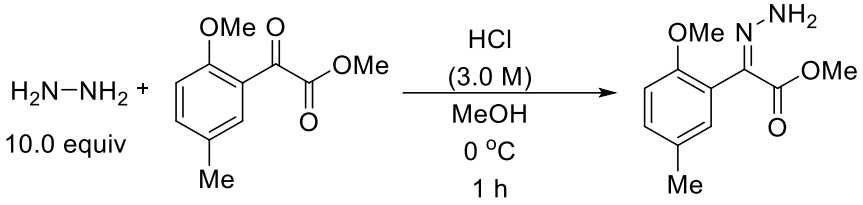

Hydrazine hydrate (50 wt% in H_2O, 10.0 equiv, 24 mL, 384 mmol) was dissolved in methanol (100 mL) in a round-bottom flask and placed into an ice bath. 3M HCl (9.0 equiv, 120 mL, 346 mmol) was added dropwise to the stirring cold solution. After the addition was complete, methyl 2-(2'-methoxy-5'-methylphenyl)-2-oxoacetate (1.0 equiv, 8.00 g, 38.4 mmol) dissolved in methanol (30 mL) was added dropwise to the stirring solution. The solution was left to stir for 1.5 h. Reaction completion was determined by the presence of only two CAM stain active spots on TLC. If the reaction is left to run too long, a yellow precipitate is generated, possibly the azine dimer. This byproduct has the same rf as the starting material by TLC and thus disappearance of the starting material cannot be used to determine reaction completion. The reaction was quenched with a saturated sodium bicarbonate ($NaHCO_3$) solution (150 mL) and left to stir and quench overnight. The reaction mixture was concentrated via rotovap to remove methanol. The solution was then extracted with EtOAc (2 X 100 mL) and the organic layer was washed with DI H_2O (100 mL) and saturated NaCl solution (100 mL) before drying over Na_2SO_4 and concentrating in vacuo. Hydrazone was purified by flash column chromatography (0-25% EtOAc/hec over 8 CV, 25% EtOAc/hex for 6 CV, 25-45% EtOAc/hexanes over 6 CV, 45% EtOAc/hex for 10 CV, then 65% EtOAC/hex- 85% EtOAc/Hex for 10 CV). Both the *E* and *Z* isomers of the hydrazone product were isolated as separate peaks CAM active peaks and combined. The *E* and *Z* isomers may be isolated separately as white powders in their pure form, either isomer or a mixture of the two is suitable for the subsequent diazotization. Product containing fractions were concentrated to afford the title compound as a clear colorless oil (89% yield, 7.56 g, 34 mmol).

2.2.3.2 Iodamine-T (TsNIK) oxidation of methyl (*E*/*Z*)-2-hydrazineylidene-2-(2-methoxy-5-methylphenyl)acetate.

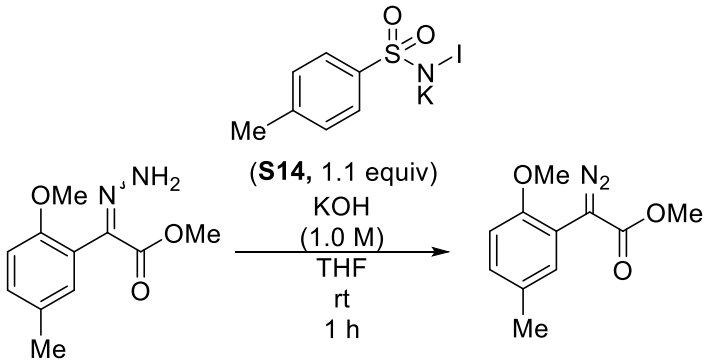

Mixture of E and Z isomers

Iodamine-T (TsNIK, **S14**, 1.1 equiv, 5.19 g, 15.47 mmol) was suspended in a solution of methyl (*E*/*Z*)-2-hydrazineylidene-2-(2-methoxy-5-methylphenyl)acetate (1.0 equiv, 3.13 g, 14.06 mmol) in THF (20 mL). Aqueous 1.0 M KOH (1.1 equiv, 15 mL, 15.47 mmol) was slowly added to the suspension, causing the solution to change in coloration from yellow to deep red. After stirring for 1 h at room temperature, the reaction solution was poured into aqueous KOH (1.0 M, 20 mL) and extracted with Et_2O (2 X 20 mL). The organic layer was washed with KOH (1.0 M, 20 mL), DI H_2O (20 mL) and saturated NaCl solution (40 mL) before being dried over Na_2SO_4. The organic layer was concentrated via rotovap and purified by flash column

chromatography (1% EtOAc/hexanes over 24 CV) to afford methyl 2-diazo-2-(2-methoxy-5-methylphenyl)acetate (**54**) as a bright orange, crystalline powder (80% yield, 2.5 g, 11.3 mmol) after aggregation and evaporation of appropriate fractions..

2.2.4 Synthesis of methyl 2-(2-chloropyridin-3-yl)-2-diazoacetate (S20).

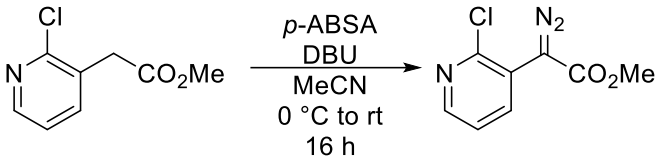

Methyl 2-(2-chloropyridin-3-yl)acetate (**S15,** 1.0 equiv, 5.39 g, 29.1 mmol) and *p*-ABSA (1.2 equiv, 8.38 g, 34.9 mmol) were added to a flame-dried 250 mL round-bottom flask under an inert nitrogen atmosphere. They were dissolved in dry acetonitrile (MeCN, 150 mL) and cooled to 0 ˚C in an ice-bath. Then DBU (1.2 equiv, 5.31 g, 5.20 mL, 10.9 mmol) was added dropwise to the stirring solution which slowly became deep yellow. The reaction was allowed to warm to room temperature over 18 h. Reaction was then quenched with saturated NH_4Cl (100 mL) and the organic layer was separated. The aqueous layer was extracted with CH_2Cl_2 (2 X 50 mL) and organic extracts were combined, dried over Na_2SO_4, and dry-loaded onto silica (5 g). The product was then purified by flash column chromatography (0-50% EtOAc/hexanes). Yellow fractions were combined and evaporated to yield methyl 2-(2-chloropyridin-3-yl)-2-diazoacetate (**S20**) as a bright yellow fluffy solid (96% yield, 5.9 g, 27.9 mmol).

2.2.5 Synthesis of methyl 2-diazo-2-(2-ethoxy-5-methylphenyl)acetate (S21).

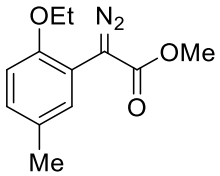

2.2.5.1 Friedel-Crafts acylation towards methyl 2-(2-ethoxy-5-methylphenyl)-2-oxoacetate.

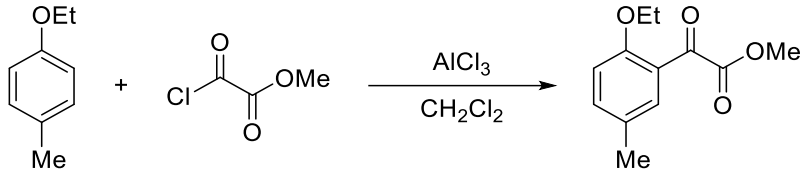

1-Ethoxy-4-methylbenzene (1.35 mL, 9.6 mmol) was added dropwise to a suspension of $AlCl_3$ (1.60 g, 12.0 mmol) in CH_2Cl_2 (38.5 mL) at 0 °C. After 5 min, methyl 2-chloro-2-oxoacetate (1.106 mL, 12.02 mmol, Aldrich) was added dropwise and the reaction was warmed to room temperature. After stirring for 16 h the reaction was poured into 250 mL of 1M HCl and extracted with CH_2Cl_2. The organic phase was washed with 1M HCl and brine, dried with $MgSO_4$ and concentrated under reduced pressure. The crude residue was then purified by flash chromatography (ISCO Combiflash, 0-30% EtOAc/heptanes, 80 g Redisep gold silica column) to yield the title compound (1.42 g, 6.39 mmol, 66.4 % yield) as a light yellow oil after aggregation and evaporation of appropriate fractions. 1H NMR (400 MHz, $CDCl_3$) δ 7.68 (dd, J = 2.4, 1.0 Hz, 1H), 7.40 7.30 (m, 1H), 6.86 (d, J = 8.5 Hz, 1H), 4.07 (q, J = 7.0 Hz, 2H), 3.91 (s, 3H), 2.32 (d, J = 0.7 Hz, 3H), 1.39 (t, J = 7.0 Hz, 3H); MS(APCI+) *m/z* 223.4 $(M+H)^+$. The material was used in the next step without further characterization.

2.2.5.2 One-pot diazotization of (methyl 2-(2-ethoxy-5-methylphenyl)-2-oxoacetate.

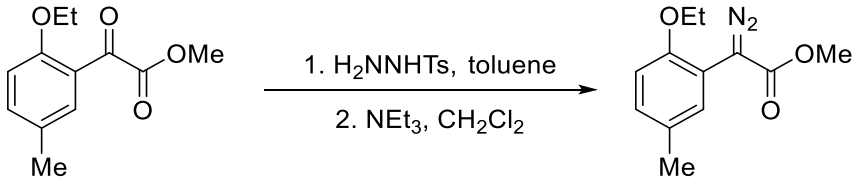

A mixture of methyl 2-(2-ethoxy-5-methylphenyl)-2-oxoacetate (1.29 g, 5.80 mmol) and 4-methylbenzenesulfonohydrazide (1.08 g, 5.80 mmol) in toluene (14.5 mL) was heated at reflux with a Dean-Stark trap for 16 h. The reaction was then concentrated under reduced pressure and the resulting residue was taken up in CH_2Cl_2 (14.5 mL) and cooled in an ice bath. TEA (1.214 mL, 8.71 mmol) was added in one portion and after 5 minthe reaction was warmed to room temperature. After stirring for 16 h the reaction was washed with sat. $NaHCO_3$ dried with $MgSO_4$, and concentrated under reduced pressure. The crude residue was then purified by flash chromatography (ISCO Combiflash, 0-20% EtOAc/heptanes, 40 g Redisep gold silica column) to yield the title compound (**S21,** 1.08 g, 4.61 mmol, 79 % yield) as an orange oil that crystallized upon standing after aggregation and evaporation of appropriate fractions..

2.2.6 Synthesis of methyl 2-diazo-2-(2-fluoro-5-methylphenyl)acetate (S22).

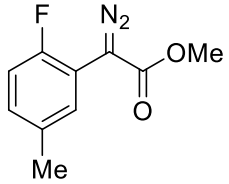

2.2.6.1 Synthesis of methyl 2-(2-fluoro-5-methylphenyl)-2-oxoacetate

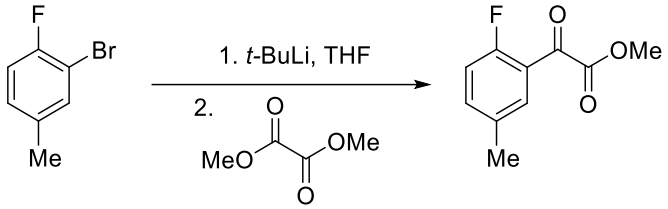

tert-Butyllithium (*t*-BuLi, 13.4 mL, 22.8 mmol, 1.7 M in pentane) was added dropwise to a solution of 2-bromo-1-fluoro-4-methylbenzene (1.43 mL, 11.4 mmol, Aldrich) in THF (57 mL) at -78 °C. After 20 min a solution of dimethyl oxalate (2.69 g, 22.75 mmol, Aldrich) in THF (3 mL) was added in one portion and the reaction was warmed to 0 °C. After stirring for 16 h the reaction was quenched with DI H_2O and extracted with EtOAc. The organic phase was washed with brine, dried with Na_2SO_4, filtered, and concentrated under reduced pressure. The crude material was purified by flash chromatography (ISCO Combiflash, 0-50% EtOAc/heptanes, 40 g Redisep gold silica column) to give the title compound (1.21 g, 6.17 mmol, 54.2 % yield) as a yellow oil after aggregation and evaporation of appropriate fractions.. ^{1}H NMR (600 MHz, $CDCl_3$) δ 7.70 (ddd, J = 6.7, 2.4, 0.9 Hz, 1H), 7.43 (dddd, J = 8.5, 5.0, 2.4, 0.7 Hz, 1H), 7.05 (dd, J = 10.5, 8.5 Hz, 1H), 3.96 (s, 3H), 2.42 – 2.33 (m, 3H); MS(APCI+) *m/z* 197.5 $(M+H)^+$. The material was used in the next step without further characterization.

2.2.6.2 Diazotization of methyl 2-(2-fluoro-5-methylphenyl)-2-oxoacetate.

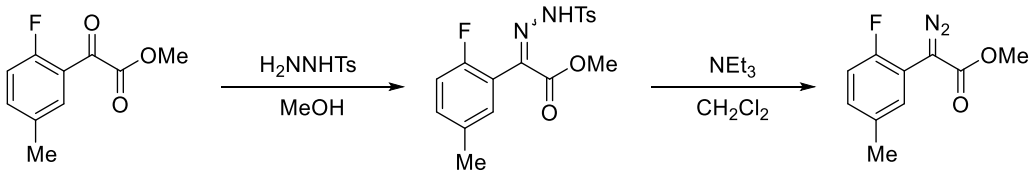

Methyl 2-(2-fluoro-5-methylphenyl)-2-oxoacetate (1.28 g, 6.52 mmol) was added to a slurry of 4-methylbenzenesulfonhydrazide (1.28 g, 6.85 mmol) in methanol (6 mL) at room temperature to give a yellow solution. After stirring for 16 h at room temperature a white precipitate formed that was collected by filtration and washed with methyl-*tert*-butyl ether (MTBE) to give 819 mg of intermediate hydrazone. The mother liquor was concentrated under reduced pressure and the resulting solid was triturated with MTBE to yield an additional 700 mg of hydrazone as a white solid. This material was used directly in the next step without further purification. CH_2Cl_2 (10 mL) and TEA (0.627 mL, 4.50 mmol) were added to the first 819 mg batch of white solid. After stirring at room temperature for 16 h the reaction was concentrated under reduced pressure. The crude material was purified by flash chromatography (ISCO Combiflash, 0-20% EtOAc / heptanes, 24 g Redisep gold silica column) to yield the title compound as a yellow solid (**S22,** 406 mg, 1.950 mmol, 87 % yield) after aggregation and evaporation of appropriate fractions.

2.2.7 Synthesis of methyl 2-diazo-2-(2-fluoro-5-methoxyphenyl)acetate (S23).

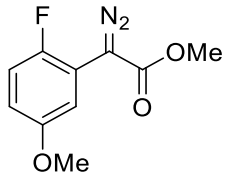

2.2.7.1 Esterification of methyl 2-(2-fluoro-5-methoxyphenyl)acetate

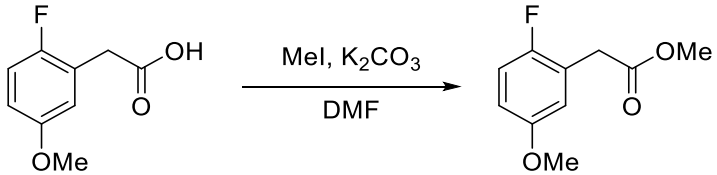

Methyl iodide (0.82 mL, 13.0 mmol) was added to a mixture of 2-(2-fluoro-5-methoxyphenyl)acetic acid (2 g, 10.86 mmol, Astatech) and potassium carbonate (K_2CO_3, 1.95 g, 14.1 mmol) in DMF (11 mL) at room temperature. After stirring for 16 h the reaction was diluted with EtOAc and washed twice with DI H_2O and once with saturated NaCl solution. The organic phase was dried with $MgSO_4$ filtered, and concentrated under reduced pressure to give methyl 2-(2-fluoro-5-methoxyphenyl)acetate (1.66 g, 8.38 mmol, 77 % yield) as a light yellow oil without further purification. ^{1}H NMR (500 MHz, $CDCl_3$) δ 7.01 – 6.95 (m, 1H), 6.80 – 6.74 (m, 2H), 3.77 (s, 3H), 3.71 (s, 3H), 3.64 (d, J = 1.3 Hz, 2H). The material was used in the next step without further characterization.

2.2.7.2 Diazo transfer to form methyl 2-diazo-2-(2-fluoro-5-methoxyphenyl)acetate.

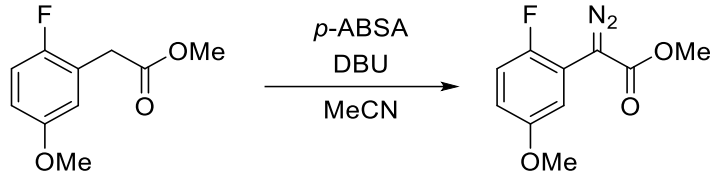

DBU (1.27 mL, 8.40 mmol) was added to a solution of methyl 2-(2-fluoro-5-methoxyphenyl)acetate (1.19 g, 6.00 mmol) and *p*-ABSA (1.73 g, 7.20 mmol, Aldrich) in MeCN (18 mL) at room temperature. After stirring for 16 h the reaction was diluted with EtOAc and washed twice with DI H_2O and once with brine. The organic phase was dried with $MgSO_4$, filtered, and concentrated under reduced pressure. The crude residue was purified by flash column chromatography (ISCO Combiflash, 0-40% EtOAc / heptanes, 40 g Redisep gold silica column) to yield the title compound (**S23,** 977 mg, 4.36 mmol, 72.6 % yield) after evaporation of appropriate fractions as a bright yellow solid.

2.2.9 Synthesis of substituted vinyl-heterocycles

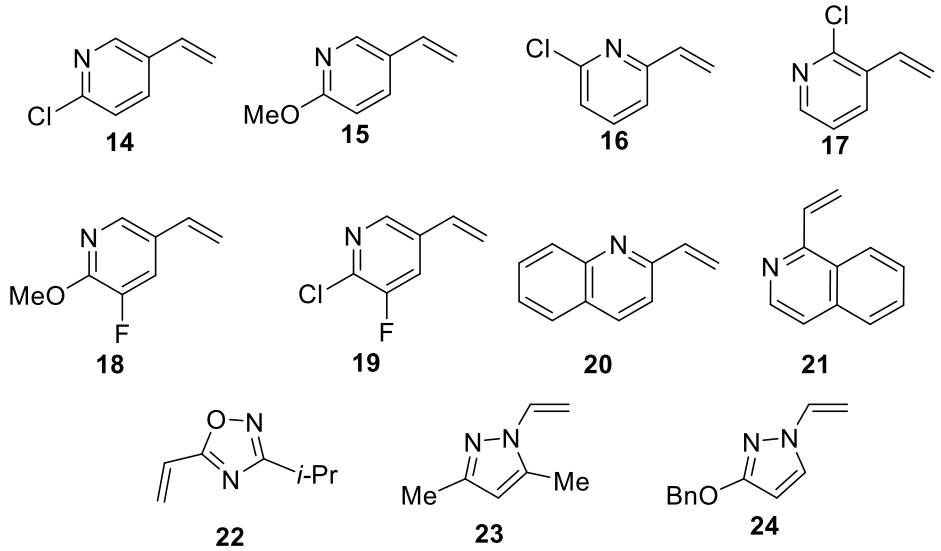

Figure B2: Vinyl-heteroaryl substrates for cyclopropanation of aza-heterocycles. Compounds **14, 16, 15-17** were synthesized using general procedure A. Compounds **18-21** were synthesized using general procedure B. Compounds **22-24** were synthesized according to alternative procedures.

2.2.8.1 General procedure A, Wittig olefination of pyridyl-aldehydes.

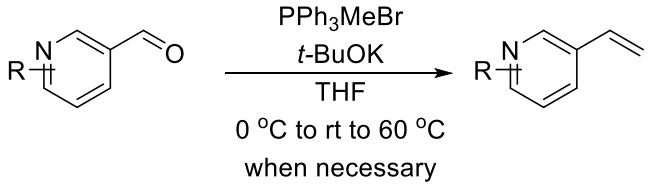

Reaction may be conducted on large scale, up to 140 mmol, although slightly lower yields may be observed. To 0 °C, stirred slurry of methyltriphenylphosphonium bromide (1.2 equiv) under an inert nitrogen atmosphere in tetrahydrofuran (150 mL) was added potassium *tert*-butoxide dissolved in 30 mL THF ((*t*-BuOK, 1.2 equiv) portionwise over a 5 minute period to produce a yellow ylide slurry. After 30 min, pyridyl aldehyde (1.0 equiv) was added slowly to produce a colored slurry (color ranges from brown to blue depending on pyridyl substitution). TLC was conducted every hour to monitor reaction progress (5% EtOAc in hexanes) warming to rt or heating to 60 ˚C if reaction was incomplete after 2 h. After the reaction had stopped the reaction mixture was treated with saturated aqueous ammonium chloride (160 mL) and a majority of the THF was removed in vacuo (concentrated via rotovap). The resulting mixture (often a brown liquid) was washed with ethyl acetate, the

combined organic layers washed with saturated aqueous brine and stirred over activated charcoal for 1hr to remove colored impurities. The mixture was then filtered over Celite, dried over Na_2SO_4 and concentrated in vacuo. The resulting semi-solid/oil was stirred overnight in pentanes (150 mL) to precipitate phosphine byproduct. Then the solution was filtered through a silica plug (~50 g) and the solids washed with an additional portion of 2:1 Et_2O/pentane (500 mL) until olefin spots (as confirmed by TLC (5% EtOAc/hexanes) developed with permanganate stain) no longer eluted from the plug. The combined filtrates were concentrated in vacuo and purified by flash column chromatography (0-5% Et_2O/hexanes over 40 CV) and product containing fractions were combined and evaporated to afford the vinyl-pyridine as a colorless or yellow oil (40-65% yield). Products **14, 16, 15,** and **17** were synthesized via this method.

2.2.8.2 General procedure B, Suzuki-coupling towards vinyl-heterocycles.

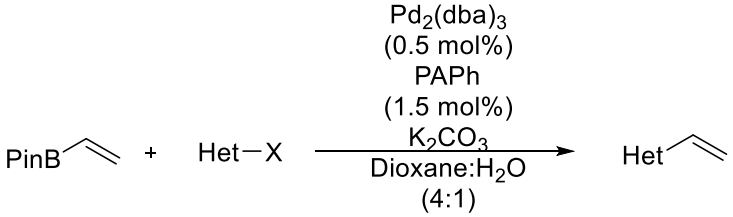

Reaction may be run on a variety of scales and is effective for heteroaryl iodides, bromides, and chlorides although higher catalyst and ligand loading (2 mol % Pd/ 5 mol % PAPh) was most effective for heteroaryl-chlorides. Heteroaryl-halide (1.0 equiv), 1,3,5,7-tetramethyl-6-phenyl-2,4,8-trioxa-6-phosphaadamantane (PAPh, 1.5 mol %), and potassium carbonate (K_3CO_3, 2.5 equiv) were combined in a round-bottom flask containing a stir bar and charged with a dioxane:water (4:1 v:v) solution. The mixture was sparged with nitrogen for 10 minbefore adding tris(dibenzylideneacetone)dipalladium(0) ($Pd_2(dba)_3$, 0.5 mol %). After the solution had turned a deep red color, neat vinylboronic acid pinacol ester (1.5 equiv) was added dropwise. The reaction mixture was then heated overnight at 80 °C. Disappearance of starting heteroaryl-halide was monitored by TLC (1% EtOAc/hexanes) to determine reaction completion. The reaction mixture was decanted into a separatory funnel and DI water (20 mL) was added. The aqueous mixture was extracted with Et_2O (2 X 20 mL). Organic extracts were combined and washed with DI H_2O (1x 50 mL) and saturated NaCl solution (1x 50 mL). The organic layer was then filtered over celite and dried over Na_2SO_4 before concentrating in vacuo. The material was then purified via flash column chromatography (0-2% EtOAc / hexanes, 18 CV) and the pure product fractions (identified by permanganate stain) were combined to afford the desired vinyl-heterocycle (**18-21**, 47-96% yield).

2.2.9 Synthesis of 3-isopropyl-5-vinyl-1,2,4-oxadiazole (22)

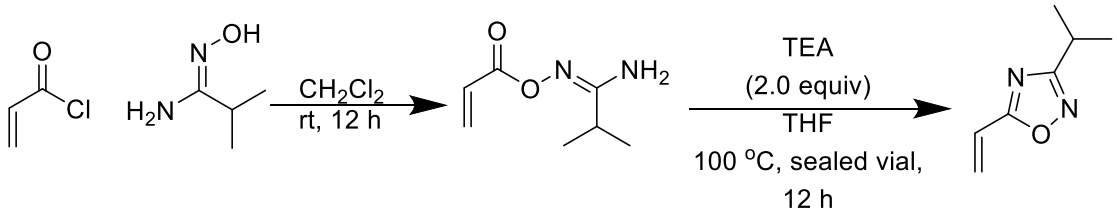

Acryloyl chloride (1.20 equiv, 1.06 g, 11.7 mmol) was added slowly to a solution of (*E*)-*N*'-hydroxyisobutyrimidamide (1.00 g, 9.79 mmol) in CH_2Cl_2 (8 mL) at rt. After 12 hr, the reaction mixture was neutralized using sat. $NaHCO_3$, extracted 3 X using CH_2Cl_2, dried over anhydrous Na_2SO_4, and concentrated to afford crude (*E*)-*N*'-(acryloyloxy)isobutyrimidamide (1.53 g, 9.78 mmol) as a white solid. Crude (*E*)-*N*'-(acryloyloxy)isobutyrimidamide (1.53 g, 9.78 mmol) and TEA (2.76 mL, 19.81 mmol) were then dissolved in THF (20 mL) in a sealed microwave vial. The reaction mixture was heated to 100 °C and stirred for 12 h and then cooled to rt. After the vial had cooled, the mixture was filtered over celite, washed with ether, and concentrated. The crude residue was purified by flash column chromatography (0% ether/hexanes for 3 CV, 0%-5% ether/hexanes over 15 CV, 5% ether/hexanes for 5 CV). The appropriate fractions (identified by permanganate stain) were concentrated via rotovap (with a bath temp of 23 °C) to afford 3-isopropyl-5-vinyl-1,2,4-oxadiazole (**22,** 550mg, 3.98 mmol, 40% yield) as a clear colorless liquid.

2.2.10 Synthesis of 3,5-dimethyl-1-vinyl-*1H*-pyrazole (23)

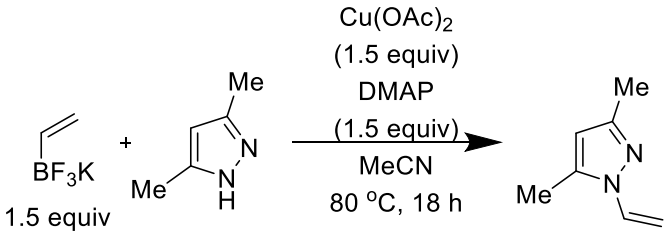

This product was synthesized via Chan-Lam coupling. $Cu(OAc)_2$ (1.5 equiv, 8.5 g, 47 mmol), DMAP (1.5 equiv, 5.7 g, 47 mmol), trifluoro(vinyl)-l4-borane potassium salt (1.5 equiv, 6.3 g, 47mmol), and 3,5-dimethyl-*1H*-pyrazole (1.0 equiv, 3.0 g, 31 mmol) were added to a 250 mL round-bottom flask and dissolved in MeCN (100 mL). The flask was sealed and heated to 80 °C under inert nitrogen atmosphere. After stirring for 18 h, the reaction was cooled to rt, diluted with Et_2O, and filtered off the solids by passing through a short silica plug. The filtrate was concentrated carefully via rotovap in order to not lose the volatile product. The resulting crude residue was purified by flash column chromatography (0-100% Et_2O/hexanes over 40 CV) and product containing fractions (identified by permanganate stain) were carefully concentrated to afford 3,5-dimethyl-1-vinyl-*1H*-pyrazole (**23,** 1.8 g, 15 mmol, 47% yield) as a clear colorless liquid.

2.2.11 Synthesis of 3-(benzyloxy)-1-vinyl-*1H*-pyrazole (24)

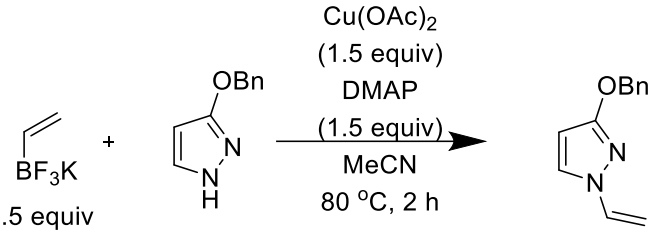

This product was synthesized via Chan-Lam coupling. Mixed DMAP (1.052 g, 8.61 mmol), $Cu(OAc)_2$ (1.564 g, 8.61 mmol), trifluoro(vinyl)-l4-borane potassium salt (1.153 g, 8.61 mmol), and 3-(benzyloxy)-*1H*-pyrazole (1 g, 5.74 mmol) in MeCN (14.4 mL). The mixture was heated at 80 °C for 2 h under ambient atmosphere. The mixture was cooled to rt, diluted with MTBE, mixed with celite, filtered, washed with additional MTBE, and loaded onto additional celite by removing the solvent under vacuum. The material was then purified by flash column chromatography (RediSep Rf Gold® Normal-Phase Silica, 24 g, 0-50% EtOAc/heptanes) and product containing fractions (identified by permanganate stain) were concentrated to afford 3-(benzyloxy)-1-vinyl-*1H*-pyrazole (**24** 475 mg, 2.372 mmol, 41.3 % yield) as a clear colorless oil.

2.3 Catalyst preparation:

All catalysts were synthesized according to known procedures and used directly.

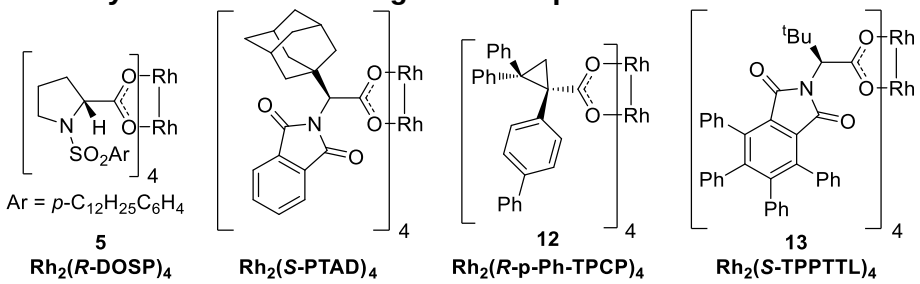

Figure B3: Dirhodium tetracarboxylate catalysts used for cyclopropanation involving aza-heterocycles.
Rh_2(*R*-DOSP)$_4$ **5** was prepared using the procedure reported in the literature.[12]
Rh_2(*S*-PTAD)$_4$ was prepared using the procedure reported in the literature.[13]
Rh_2(*R*-*p*-Ph-TPCP)$_4$ **12** was prepared using the procedure reported in the literature.[14]
Rh_2(*R*-TPPTTL)$_4$ and Rh_2(*S*-TPPTTL)$_4$ **13** were prepared using the procedure reported in the literature.[15]

3. Procedures for cyclopropanation involving aza-heterocycles.

3.1 General procedure for cyclopropanation of vinyl-heterocycles with aryl-diazo-(*R*)-pantolactonates.

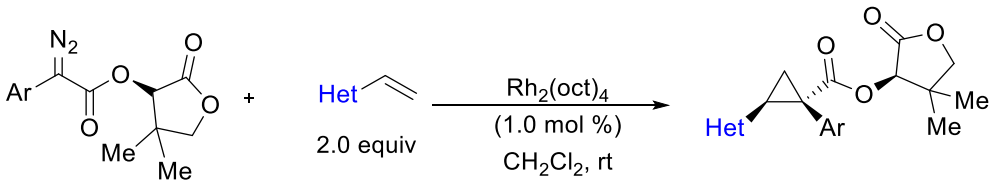

A 10 mL vial containing a stir bar was flame dried under vacuum along with a small round-bottom flask. Vessels were evacuated and purged with nitrogen 2 times to establish an inert atmosphere. Then catalytic rhodium octanoate dimer ($Rh_2(oct)_4$, 1.0 mol %, 1.6 mg, 2.0 µmol) was added to the vial. Solid aryl-diazo-(*R*)-pantolactonate (1.0 equiv, 0.20 mmol) was added to the flame dried round bottom flask. Then vacuum was reestablished on both the vial and the flask to further

remove air from the system. After 5 min, the system was flushed with nitrogen and vinyl-heterocycle (2.0 equiv, 0.40 mmol) was added to the vial via preweighed syringe along with 2 mL dry CH_2Cl_2 was added to the vial. The nitrogen line attached to the vial was then replaced by a balloon filled with argon. Diazo compound was dissolved in 3 mL dry CH_2Cl_2 under an inert atmosphere. The round bottom flask was swirled to ensure all diazo had dissolved before the solution was loaded into a syringe. The syringe was then inserted through the vial septum and the full contents were injected into the vial in one portion. The reaction was stirred at room temperature overnight under argon (at least 13 h). The reaction solution was subjected to TLC to determine reaction completion (30% EtOAc/hexanes). Crude reaction was concentrated via rotovap and asymmetric induction was determined by ^{1}H NMR of the crude reaction mixture. Purified by flash column chromatography (0% Et_2O/hexanes for 3CV, 0-100% Et_2O /hexanes over 30 CV, 100% Et_2O for 3CV). Fractions containing only product by TLC were aggregated and concentrated via rotovap. Products **8-16** were synthesized via this method.

3.2. General procedure for the additive free cyclopropanation of vinyl-heterocycles with non-*ortho*-substituted aryl/heteroaryl-diazoacetates.

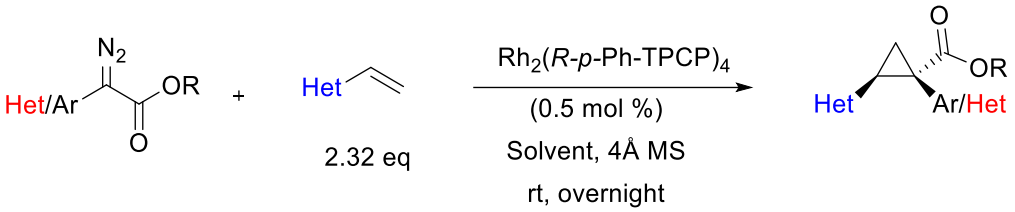

Compounds were prepared according to the established literature procedure for lab-scale cyclopropanation.[16] A 10 mL vial containing 4Å activated molecular sieves (0.5 g) and a stir bar was flame dried under vacuum along with a small round-bottom flask. Vessels were evacuated and purged with nitrogen 2 times to establish an inert atmosphere. Then catalytic Rh_2(*R*-*p*-Ph-TPCP)$_4$ (0.5 mol %, 1.8 mg, 0.0001 mmol) was added to the vial. Solid diazo compound (1.0 equiv, 0.20 mmol) was added to the flame dried round bottom flask. Then vacuum was reestablished on both the vial and the flask to further remove air from the system. After 5 min, the system was flushed with nitrogen and vinyl-heterocycle (2.32 equiv, 1.0 mmol) was added to the vial via preweighed syringe along with 2 mL dry $(MeO)_2CO$ or CH_2Cl_2. The nitrogen line attached to the vial was then replaced by a balloon filled with argon. Diazo compound was dissolved in 3 mL dry $(MeO)_2CO$ or CH_2Cl_2 under an inert atmosphere. The round bottom flask was swirled to ensure all diazo had dissolved before the solution was loaded into a syringe. The syringe was then inserted through the vial septum and the full contents were injected into the vial in one portion. The reaction was stirred overnight under argon (at least 13 h). The reaction solution was subjected to TLC to determine reaction completion (20% EtOAc/hexanes). After completion the solution was filtered through celite to remove molecular sieves before concentrating via rotovap. The crude concentrate was then directly purified by flash column chromatography (5% EtOAc/hexanes 3 CV, 5% EtOAc/hexanes to 30% EtOAc/hexanes 15 CV, 30% EtOAc/hexanes for 3-10 CV). Fractions containing only product by TLC were aggregated and concentrated via rotovap. Enantioselectivity was determined by chiral HPLC. Products **17-33** were synthesized via this method.

3.2.1 Synthesis of *Tert*-butyl 5-bromo-3-(1-diazo-2-oxo-2-(2,2,2-trichloroethoxy)ethyl)-*1H*-indole-1-carboxylate (52).

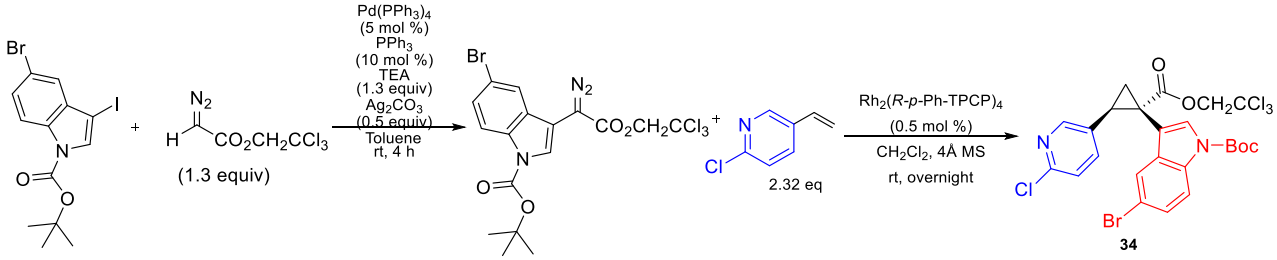

The diazo compound in question proved difficult to work with, but effective cyclopropanation was achieved by using the compound directly after a short column. Tetrakis(triphenylphosphine)palladium(0) (273.8 mg, 0.05 equiv, 236.9 µmol), triphenylphosphine (124.3 mg, 0.1 equiv, 473.9 µmol), *tert*-butyl 5-bromo-3-iodo-*1H*-indole-1-carboxylate (2.000 g, 1.0 equiv, 4.739 mmol), silver carbonate (653.3 mg, 0.5 equiv, 2.369 mmol) were added to a 100 mL flame-dried round bottom flask equipped with a magnetic stir-bar. The reagents were suspended in toluene (20 mL) under nitrogen, followed by addition of triethylamine (623.4 mg, 0.859 mL, 1.3 equiv, 6.160 mmol) and 2,2,2-trichloroethyl 2-diazoacetate (1.133 g, 1.1 equiv, 5.213 mmol). The resulting reaction was stirred at room temperature for 4 h and then filtered through a short path of silica gel, eluting with ethyl acetate. The volatile compounds were removed through reduced pressure and the residue was purified by column chromatography(1% -15% EtOAc in hexane) to give the desired product (2.259 g, 93% yield), ***tert*-butyl 5-bromo-3-(1-diazo-2-oxo-2-(2,2,2-trichloroethoxy)ethyl)-*1H*-indole-1-carboxylate,** as a bright orange solid after aggregation and evaporation of appropriate fractions. **^{1}H NMR** (400 MHz, $CDCl_3$) δ 8.11 (d, *J* = 88 Hz, 1H), 7.87 (s, 1H), 7.63 (d, *J* = 1.9 Hz, 1H), 7.46 (dd, *J* = 8.9, 1.9 Hz, 1H), 4.93 (s, 2H), 1.66 (s, 9H).**HRMS:** (+p APCI) Peak calculated for [$C_{17}H_{15}BrCl_3N_3O_4$+ minus $C_5H_9O_2$ minus N_2 plus 3H] 381.88095, found 381.88001. **IR**(neat): 2954, 2091, 1737, 1713, 1451, 1370, 1306, 1270, 1249, 1243, 1120, 1153, 1113, 1050, 1009, 897, 853, 841, 803, 778, 766, 717, 634, 615, 586, 573 cm^{-1}.

The product was used immediately in the subsequent cyclopropanation without further characterization. A 10 mL vial containing 4Å activated molecular sieves (0.5 g) and a stir bar was flame dried under vacuum along with a small round-bottom flask. Vessels were evacuated and purged with nitrogen 2 times to establish an inert atmosphere. Then catalytic Rh_2(*R*-*p*-Ph-TPCP)$_4$ (0.5 mol %, 1.8 mg, 0.0001 mmol) was added to the vial. Solid diazo compound (1.0 equiv, 100 mg, 0.20 mmol) was added to the flame dried round bottom flask. Then vacuum was reestablished on both the vial and the flask to further remove air from the system. After 5 min, the system was flushed with nitrogen and **14** (2.32 equiv, 0.46 mmol, 65 mg) was added to the vial via preweighed syringe along with 2 mL dry CH_2Cl_2. The nitrogen line attached to the vial was then replaced by a balloon filled with argon. Diazo compound was dissolved in 3 mL dry CH_2Cl_2 under an inert atmosphere. The round bottom flask was swirled to ensure all diazo had dissolved before the solution was loaded into a syringe. The syringe was then inserted through the vial septum and the full contents were injected into the vial in one portion. The reaction was stirred overnight under argon (at least 13 h). The reaction solution was subjected to TLC to determine reaction completion (20% EtOAc/hexanes). After completion the solution was filtered through celite to remove molecular sieves before concentrating via rotovap. The crude concentrate was then directly purified by flash column chromatography (5% EtOAc/hexanes 3 CV, 5% EtOAc/hexanes to 30% EtOAc/hexanes 15 CV, 30% EtOAc/hexanes for 3-10 CV). Fractions containing only product by TLC were aggregated and concentrated via rotovap. Product (**52**) was obtained as a brown oil in 82% yield and 89% ee (0.16 mmol, 102 mg). Enantioselectivity was determined by chiral HPLC.

3.3 General procedure for the additive free cyclopropanation of vinyl-heterocycles with *ortho*-substituted aryl/heteroaryl-diazoacetates

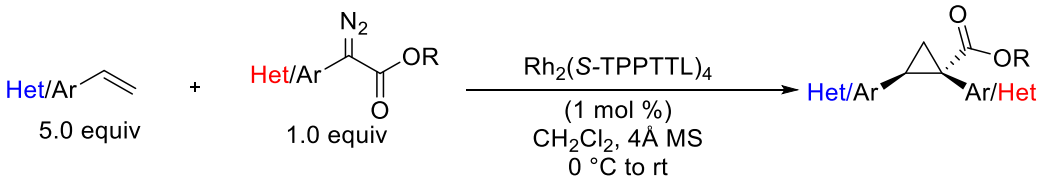

A 10 mL vial containing 4Å activated molecular sieves (0.5 g) and a stir bar was flame dried under vacuum along with a small round-bottom flask. Vessels were evacuated and purged with nitrogen 2 times to establish an inert atmosphere. Then catalyst Rh_2(*S*-TPPTTL)$_4$ (1.0 mol %, 4.9 mg, 0.002 mmol) was added to the vial. Solid diazo compound (1.0 equiv, 0.20 mmol) was added to the flame dried round bottom flask. Then vacuum was reestablished on both the vial and the flask to further remove air from the system. After 5 min, the system was flushed with nitrogen and vinyl pyridine (5.0 equiv, 1.0 mmol) was added to the vial via preweighed syringe and 2 mL distilled CH_2Cl_2 was added to the vial. The nitrogen line attached to the vial was then replaced by a balloon filled with argon and the vial was added to an ice bath to maintain the temperature at 0 ˚C and let stir. Temperature of the ice bath was monitored by thermocouple external to the reaction vessel. While the vial cooled for approximately 10 min, the diazo compound was dissolved in 3 mL distilled CH_2Cl_2 added via syringe. The round bottom flask was swirled to ensure all diazo had dissolved before the solution was loaded into the syringe. The syringe was then inserted through the vial septum and the full contents were injected into the vial in one portion maintaining the bath at 0 ˚C throughout the addition. The reaction was stirred overnight under argon in the ice bath which slowly warmed to room temperature (at least 13 h). The reaction solution was subjected to TLC to determine reaction completion (20% EtOAc/hexanes). After completion the solution was filtered through celite to remove molecular sieves before concentrating via rotovap. The crude concentrate was then directly purified by flash column chromatography (5% EtOAc/hexanes 3 CV, 5% EtOAc/hexanes to 30% EtOAc/hexanes 15 CV, 30% EtOAc/hexanes for 3-10 CV). Fractions containing only product by TLC were aggregated and concentrated via rotovap. Enantioselectivity was determined by chiral HPLC. Products **55-46** were synthesized via this method.

3.4 General procedure for the additive promoted cyclopropanation involving *ortho*-substituted aryl/heteroaryl-diazoacetates.

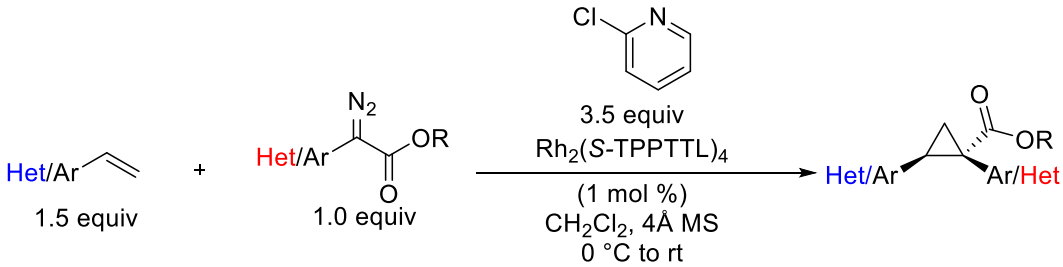

A 10 mL vial containing 4Å activated molecular sieves (0.5 g) and a stir bar was flame dried under vacuum along with a small round-bottom flask. Vessels were evacuated and purged with nitrogen 2 times to establish an inert atmosphere. Then catalytic Rh_2(*S*-TPPTTL)$_4$ (1.0 mol %, 4.9 mg, 0.002 mmol) was added to the vial. Solid diazo compound (1.0 equiv, 0.20 mmol) was added to the flame dried round bottom flask. Then vacuum was reestablished on both the vial and the flask to further remove air from the system. After 5 min, the system was flushed with nitrogen, vinyl-heterocycle (1.5 equiv, 0.30 mmol), and 2-Clpyridine (3.5 equiv, 79 mg, 66 µl, 0.70 mmol) was added to the vial via syringe along with 2 mL dry CH_2Cl_2.

The nitrogen line attached to the vial was then replaced by a balloon filled with argon and the vial was added to an ice bath to maintain the temperature at 0 ˚C and let stir. Temperature of the ice bath was monitored by thermocouple external to the reaction vessel. While the vial cooled for approximately 10 min, the diazo compound was dissolved in 3 mL dry CH_2Cl_2 added via syringe. The round bottom flask was swirled to ensure all diazo had dissolved before the solution was loaded into the syringe. The syringe was then inserted through the vial septum and the full contents were injected into the vial in one portion maintaining the bath at 0 ˚C throughout the addition. The reaction was stirred overnight under argon in the ice bath which slowly warmed to room temperature (at least 13 h). The reaction solution was subjected to TLC to determine reaction completion (20% EtOAc/hexanes). After completion the solution was filtered through celite to remove molecular sieves before concentrating via rotovap. The crude concentrate was then directly purified by flash column chromatography (5% EtOAc/hexanes 3 CV, 5% EtOAc/hexanes to 30% EtOAc/hexanes 15 CV, 30% EtOAc/hexanes for 3-10 CV). Fractions containing only product by TLC were aggregated and concentrated via rotovap. Enantioselectivity was determined by chiral HPLC. Products **55, 47-49, 52-53, 56-57, 62-65** were synthesized via this method.

3.5 General procedure for the additive promoted cyclopropanation involving *ortho*-substituted aryl/heteroaryl-diazoacetates and HFIP.

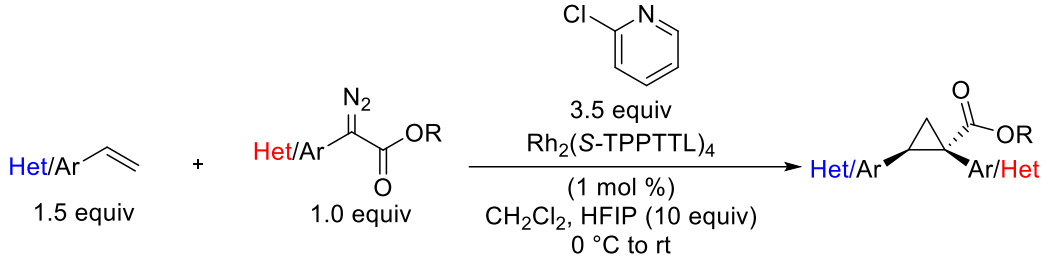

A 10 mL vial containing a stir bar was flame dried under vacuum along with a small round-bottom flask. Vessels were evacuated and purged with nitrogen 2 times to establish an inert atmosphere. Then catalytic Rh_2(*S*-TPPTTL)$_4$ (1.0 mol %, 4.9 mg, 0.002 mmol) was added to the vial. Solid diazo compound (1.0 equiv, 0.20 mmol) was added to the flame dried round bottom flask. Then vacuum was reestablished on both the vial and the flask to further remove air from the system. After 5 min, the system was flushed with nitrogen, vinyl-heterocycle (1.5 equiv, 0.30 mmol), 2-Clpyridine (3.5 equiv, 79 mg, 66 µl, 0.70 mmol), and 1,1,1-3,3,3-hexafluoroisopropanol (HFIP, 10 equiv, 340 mg, 0.21 mL, 2.0 mmol) was added to the vial via syringe along with 2 mL dry CH_2Cl_2. The nitrogen line attached to the vial was then replaced by a balloon filled with argon and the vial was added to an ice bath to maintain the temperature at 0 ˚C and let stir. Temperature of the ice bath was monitored by thermocouple external to the reaction vessel. While the vial cooled for approximately 10 min, the diazo compound was dissolved in 3 mL distilled CH_2Cl_2 added via syringe. The round bottom flask was swirled to ensure all diazo had dissolved before the solution was loaded into the syringe. The syringe was then inserted through the vial septum and the full contents were injected into the vial in one portion maintaining the bath at 0 ˚C throughout the addition. The reaction was stirred overnight under argon and allowed to warm to room temperature (at least 13 h). The reaction solution was subjected to TLC to determine reaction completion (20% EtOAc/hexanes). After completion the solution was filtered through celite to remove molecular sieves before concentrating via rotovap. The crude concentrate was then directly purified by flash column chromatography (5% EtOAc/hexanes 3 CV, 5% EtOAc/hexanes to 30% EtOAc/hexanes 15CV, 30% EtOAc/hexanes for 3-10 CV). Fractions containing product by TLC were aggregated and concentrated via rotovap. Enantioselectivity was determined by chiral HPLC. Products **55-39, 47-51, 54-55, 58-61** were synthesized via this method.

3.6 Procedure for one-Pot hydrazone oxidation/cyclopropanation

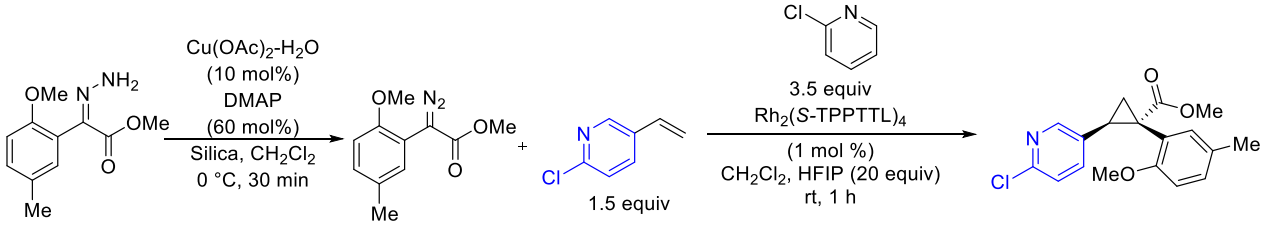

In the first step: A 20 mL scintillation vial was charged with $Cu(OAc)_2$-H_2O (3.9 mg, 0.020 mmol, 10 mol %), silica powder (44.4 mg, 100 wt%, SiliaFlash® P60, 40-63 µm), and 1.0 mL solution of 0.06 mol/L DMAP in CH_2Cl_2 The initial mixture was stirred vigorously with a stir bar (600 rpm) under air for 5 min before hydrazone was added. In a 4 mL scintillation vial, methyl (*Z*)-2-hydrazineylidene-2-(2-methoxy-5-methylphenyl)acetate (44.4 mg, 0.20 mmol, 1.0 equiv) was dissolved in 1.0 mL of the 0.06 mol/L DMAP in CH_2Cl_2 solution. The hydrazone/DMAP CH_2Cl_2 solution was then transferred by syringe in one portion to the initial mixture of $Cu(OAc)_2$-H_2O/silica/DMAP CH_2Cl_2 solution. The reaction was stirred for 0.5 h before next step to afford a crude solution of **54**.

In the second step: a 20 mL scintillation vial equipped with a stir bar was flame dried under vacuum. After cooling down, the vail was charged with Rh_2(*S*-TPPTTL)$_4$ (4.9 mg, 1.0 mol %, 0.0020 mmol), then flushed with nitrogen for 3 times and the nitrogen balloon was left on the septum. Then HFIP (672.2 mg, 0.42 mL, 20 equiv, 4.0 mmol), 2-chloropyridine (79.5 mg, 66 µL, 3.5 equiv, 0.70 mmol), 2-chloro-5-vinylpyridine (**14,** 41.9 mg, 1.5 equiv, 0.30 mmol) and 2.0 mL CH_2Cl_2 were added sequentially via syringe, the mixture was stirred at 600 rpm for 10 min before crude diazo injection. The crude diazo mixture from step **1** (~1.5 mL) was added by syringe to the 2-chloro-5-vinylpyridine/Rh_2(*S*-TPPTTL)$_4$/HFIP/2-chloropyridine solution in one portion. The reaction was then stirred 1 h under nitrogen at r.t. After completion the solution was concentrated under rotovap and purified by flash column chromatography (5 % EtOAc/hexanes 3 CV, 5 % EtOAc/hexanes to 30 % EtOAc/hexanes 15 CV, 30 % EtOAc/hexanes 10 CV). Cyclopropanation product was concentrated to give a clear colorless oil in 83% yield (**55,** 55.2 mg,0.166 mmol) and 98% ee. Repeating the same reaction without addition of the HFIP resulted in recovery of unreacted diazo compound **54**.

Results and Discussion

4. Characterization of synthesized compounds.

4.1 Characterization of novel starting materials

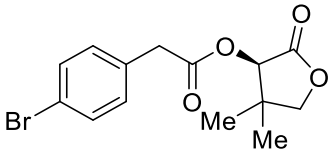

(*R*)-4,4-dimethyl-2-oxotetrahydrofuran-3-yl 2-(4-bromophenyl)acetate. This compound was prepared according to the procedure outlined in **2.2.1.1** on 23.3 mmol scale. After isolation the product was obtained as off-white crystalline solid (70% yield, 5.3 g, 16 mmol).
MP: 62-63℃
^{1}H NMR (400 MHz, $CDCl_3$) δ 7.45(d, *J* = 8.2 Hz, 2H), 7.18 (d, *J* = 8.2 Hz, 2H), 5.34 (s, 1H), 4.05 – 3.95 (m, 2H), 3.72 (s, 2H), 1.12 (s, 3H), 0.99 (s, 3H).
^{13}C NMR (151 MHz, $CDCl_3$) δ 172.1, 169.9, 132.2, 131.8, 131.1, 121.5, 76.2, 75.5, 40.2, 40.2, 22.9, 19.8.
HRMS: (+p APCI) calculated for [$C_{14}H_{16}O_4{}^{79}Br$ +] 327.0227, found 327.0227
IR(neat): 2967, 2931, 1779, 1745, 1592, 1488, 1465, 1400, 1269, 1351, 1297, 1242, 1139, 1072, 1031, 1012, 997, 914, 851, 801, 754, 735, 573, 540, 491 cm^{-1}

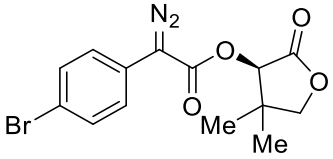

(*R*)-4,4-dimethyl-2-oxotetrahydrofuran-3-yl 2-(4-bromophenyl)-2-diazoacetate S17. This compound was prepared according to the procedure outlined **in 2.2.1.2** on 6.11 mmol scale. After isolation the product was obtained as a powdery orange solid (60% yield, 1.30 g, 3.68 mmol).
MP: 95-99℃ diazo decomposes rapidly after melting
^{1}H NMR(400 MHz, $CDCl_3$) δ 7.59 – 7.42 (m, 2H), 7.42 – 7.31 (m, 2H), 5.52 (s, 1H), 4.08 (m, 2H), 1.25 (s, 3H), 1.13 (s, 3H).
^{13}C NMR (151 MHz, $CDCl_3$) δ 172.1, 163.4, 132.2, 125.5, 123.9, 119.9, 76.2, 75.4, 40.2, 22.9, 19.8.
HRMS: (+p APCI) Compound decomposed in ESI-MS to give OH-insertion product. Peak calculated for [$C_{14}H_{14}O_4{}^{79}Br$ +] 325.007, found 325.0075
IR(neat): 2970, 2089, 1783, 1738, 1490, 1464, 1365, 1275, 1230, 1217, 1141, 1086, 1031, 1009, 996, 970, 920, 821, 781, 731, 647, 575, 543, 528, 515, 493 cm^{-1}

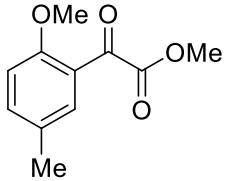

Methyl 2-(2-methoxy-5-methylphenyl)-2-oxoacetate. This compound was prepared according to the procedure outlined in **2.2.2.1** from the reaction between 4-methyl anisole and methyl-oxalyl chloride on 81.9 mmol scale. After isolation the product was obtained as a light yellow liquid (93% yield, 15.9 g, 76.4 mmol).
^{1}H NMR (600 MHz, $CDCl_3$) δ 7.67 (d, *J* = 2.5 Hz, 1H), 7.39 (dd, *J* = 8.5, 2.4 Hz, 1H), 6.88 (d, *J* = 8.5 Hz, 1H), 3.91 (s, 3H), 3.84 (s, 3H).

^{13}C NMR (151 MHz, $CDCl_3$) δ186.4, 165.7, 158.5, 137.1, 130.9, 130.6, 122.4, 112.2, 56.3, 52.3, 20.2.
HRMS: (+p APCI) calculated for [$C_{11}H_{13}O_4$+] 209.0808, found 209.0806
IR(neat): 2951, 1739, 1667, 1608, 1581, 1497, 1412, 1272, 1245, 1224, 1179, 1155, 1133, 1019, 947, 901, 864, 813, 778, 712,669, 588, 537, 489 cm^{-1}

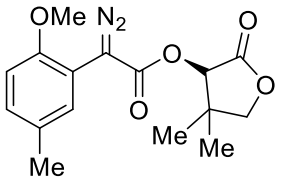

(*R*)-4,4-dimethyl-2-oxotetrahydrofuran-3-yl 2-diazo-2-(2-methoxy-5-methylphenyl)acetate S18.
This compound was prepared according to the procedure outlined in **2.2.2.4** from (*R*)-4,4-dimethyl-2-oxotetrahydrofuran-3-yl 2-(2-methoxy-5-methylphenyl)-2-oxoacetate. After isolation the product was obtained as a yellow solid (7.3 g, 23 mmol, 82% yield).
^{1}H NMR (500 MHz, $CDCl_3$) δ 7.37 (d, J = 2.2 Hz, 1H), 7.09 – 7.04 (m, 1H), 6.80 (d, J = 8.4 Hz, 1H), 5.50 (s, 1H), 4.10 – 4.02 (m, 2H), 3.84 (s, 3H), 2.33 – 2.29 (m, 3H), 1.25 (s, 3H), 1.12 (s, 3H);
^{13}C NMR (101 MHz, CDCL3) δ 172.4, 153.5, 130.6, 130.5, 129.4, 112.5, 110.9, 76.2, 75.2, 55.6, 40.2, 23.0, 20.5, 19.8
HRMS: (ESI) m/z calculated for $C_{16}H_{18}N_2O_5Na$ [M+Na]+, 475.1533; found 475.1545.

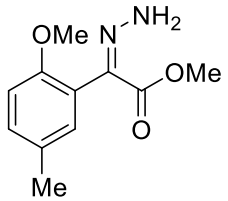

Methyl (*E*/*Z*)-2-hydrazineylidene-2-(2-methoxy-5-methylphenyl)acetate. This compound was prepared according to the procedure outlined in **2.2.3.1** between methyl 2-(2-methoxy-5-methylphenyl)-2-oxoacetate and hydrazine on 38.4 mmol scale. After isolation the product was obtained as a mixture of isomers as a clear, colorless clear colorless oil (89% yield, 7.56 g, 34 mmol). Pure *Z*-isomer appears as an off-white solid, pure *E*-isomer is obtained as a white solid.
MP: 63-65 ˚C – *Z*-isomer, 72-75 ˚C – *E*-isomer,
^{1}H NMR (400 MHz, $CDCl_3$) *Z*-Isomer: δ 8.13 (s, 2H), 7.14 – 7.12 (m, 2H), 7.10 (dt, J = 2.4, 0.8 Hz, 1H), 6.79 (d, J = 8.1 Hz, 1H), 3.76 (s, 3H), 3.73 (s, 3H), 2.30 (d, J = 0.8 Hz, 3H). *E*-isomer: δ 7.21 (ddq, J = 8.6, 2.3, 0.7 Hz, 1H), 6.97 (dt, J = 2.3, 0.6 Hz, 1H), 6.90 (d, J = 8.4 Hz, 1H), 6.11 (s, 2H), 3.83 (s, 3H), 3.77 (s, 3H).
^{13}C NMR (151 MHz, $CDCl_3$) *Z*-Isomer: δ163.7, 155.9, 130.7, 130.3, 130.2, 126.3, 111.1, 56.0, 51.6, 20.6. *E*-isomer: δ 165.3, 155.1, 136.1, 131.9, 130.8, 130.7, 118.3, 111.9, 56.1, 52.6, 20.7.
HRMS: (+p APCI) calculated for [$C_{11}H_{15}O_3N_2$+] 223.1077, found 223.1077 for *Z* isomer, found 223.1079 for *E* isomer.
IR(neat): *Z*-Isomer: 3454, 3293, 2948, 2836, 1695, 1575, 1498, 1463, 1435, 1295, 1266, 1245, 1186, 1150, 1130, 1037, 1025, 993, 887, 808, 730, 670, 496. *E*-Isomer: 3407,3294, 3210, 2948, 2838, 1708, 1608, 1557, 1496, 1435, 1316, 1238, 1185, 1119, 1046, 1025, 950, 872, 810, 781, 729, 468 cm^{-1}

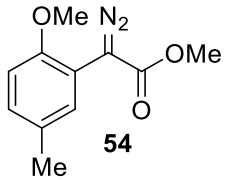

54

Methyl 2-diazo-2-(2-methoxy-5-methylphenyl)acetate (54)
This compound was prepared according to the procedure outlined in **2.2.3.2** between methyl (*E*/*Z*)-2-hydrazineylidene-2-(2-methoxy-5-methylphenyl)acetate and TsNIK on 14.06 mmol scale. After isolation the product was obtained as a mixture of isomers as a bright orange powder (80% yield, 2.5 g, 11.3 mmol).
MP: 55-60 ˚C
^{1}H NMR (600 MHz, $CDCl_3$) δ 7.36 (s, 1H), 7.06 (d, *J* = 8.41 Hz, 1H), 6.79 (d, *J* = 8.42 Hz, 1H), 3.83 (s, 3H), 3.82 (s, 3H), 2.31 (s, 3H).
^{13}C NMR (151 MHz, $CDCl_3$) δ 166.8, 153.5, 130.7, 130.5, 129.2, 113.3, 110.9, 55.7, 51.9, 20.6. Please note that the diazo carbon was not visible by 13C NMR.
HRMS: (+p APCI) calculated for [$C_{11}H_{13}O_3N_2$+] 221.0921, found 221.0922
IR(neat): 2090, 1693, 1503, 1434, 1339, 1291, 1248, 1186, 1138, 1048, 804, 743 cm^{-1}

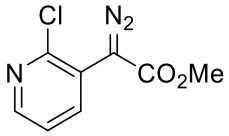

Methyl 2-(2-chloropyridin-3-yl)-2-diazoacetate (S20). This compound was prepared according to the procedure outlined in **2.2.4** between methyl 2-(2-chloropyridin-3-yl)acetate and *p*-ABSA on 29.1 mmol scale. After isolation the product was obtained as a bright yellow solid (96% yield, 5.9 g, 27.9 mmol).
MP: 71-73℃
^{1}H NMR (400 MHz, $CDCl_3$) δ 8.35 (dd, *J* = 4.7, 1.9 Hz, 1H), 7.95 (dd, *J* = 7.8, 1.9 Hz, 1H), 7.32 (dd, *J* = 7.8, 4.7 Hz, 1H), 3.86 (s, 3H).
^{13}C NMR (151 MHz, $CDCl_3$) δ 165.4, 149.2, 148.9, 140.5, 122.7, 121.6, 52.5. Please note that the diazo carbon was not visible by 13C NMR.
HRMS: (+p APCI) calculated for [$C_8H_7O_2N_3{}^{35}Cl$ +] 212.0221, found 212.0222
IR(neat): 2097, 1694, 1555, 1455, 1435, 1402, 1344, 1272, 1211, 1193, 1162, 1128, 1099, 1060, 1023, 1006, 798, 737, 727 cm^{-1}

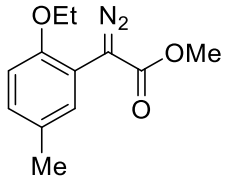

Methyl 2-diazo-2-(2-ethoxy-5-methylphenyl)acetate (S21)
This compound was prepared according to the procedure outlined in **2.2.5.2** from methyl 2-(2-ethoxy-5-methylphenyl)-2-oxoacetate on 9.6 mmol scale. After isolation the product was obtained as an orange oil which crystallized upon standing (1.08 g, 4.61 mmol, 52% yield over 2 steps)
^{1}H NMR (400 MHz, $CDCl_3$) d 7.36 (d, J = 2.3 Hz, 1H), 7.02 (ddd, J = 8.4, 2.3, 0.8 Hz, 1H), 6.77 (d, J = 8.4 Hz, 1H), 4.02 (q, J = 7.0 Hz, 2H), 3.83 (s, 3H), 2.29 (d, J = 0.7 Hz, 3H), 1.41 (t, J = 6.9 Hz, 3H);
^{13}C NMR (101 MHz, CDCL3) δ 166.9, 152.8, 130.6, 130.4, 129.0, 113.3, 111.7, 64.2, 52.0, 20.7, 14.8;
HRMS (ESI) m/z calculated for $C_{12}H_{14}N_2O_3Na$ [M+Na]+, 257.0897; found 257.0899.

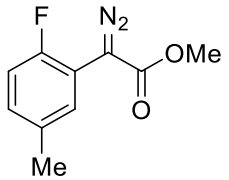

Methyl 2-diazo-2-(2-fluoro-5-methylphenyl)acetate (S22)
This compound was prepared according to the procedure outlined in **2.2.6** from 2-bromo-1-fluoro-4-methylbenzene. After isolation the product was obtained as a yellow solid (406 mg, 1.950 mmol, 47% yield over 2 steps)
^{1}H NMR (500 MHz, $CDCl_3$) δ 7.49 – 7.43 (m, 1H), 7.05 – 6.99 (m, 1H), 6.96 (dd, J = 10.8, 8.4 Hz, 1H), 3.86 (s, 3H), 2.33 (q, J = 0.8 Hz, 3H);
^{13}C NMR (101 MHz, $CDCl_3$) δ 157.9, 155.5, 134.2, 134.2, 129.7 (d, *J* = 2.0 Hz), 129.2 (d, *J* = 8.0 Hz), 115.4, 115.2, 52.1 20.8.
^{19}F NMR (376 MHz, DMSO) δ -118.92 (q, *J* = 7.9 Hz).
HRMS (ESI) m/z calculated for $C_{10}H_9FN_2O_2Na$ [M+Na]+, 231.054; found 231.0543.

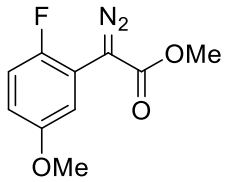

Methyl 2-diazo-2-(2-fluoro-5-methoxyphenyl)acetate (S23)
This compound was prepared according to the procedure outlined in **2.2.7** from 2-(2-fluoro-5-methoxyphenyl)acetic acid. After isolation the product was obtained as a bright yellow solid (977 mg, 4.36 mmol, 56% yield over 2 steps)
^{1}H NMR (600 MHz, $CDCl_3$) δ 7.29 – 7.22 (m, 1H), 6.98 (dd, J = 10.6, 9.0 Hz, 1H), 6.74 (ddd, J = 9.0, 3.9, 3.1 Hz, 1H), 3.86 (s, 3H), 3.79 (s, 3H);
^{13}C NMR (101 MHz, $CDCl_3$) δ 165.6, 156.0, 155.9, 153.9, 151.5, 116.2, 116.0, 113.9 (d, *J* = 8.1 Hz), 113.4 (d, *J* = 2.2 Hz), 55.8, 52.2.
^{19}F NMR (376 MHz, $CDCl_3$) δ -124.99.
HRMS (ESI) m/z calculated for $C_{10}H_9FN_2O_3Na$ [M+Na]+, 247.0489; found 247.0490

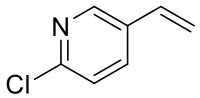

14

2-Chloro-5-vinylpyridine (14). This compound was prepared according the procedure outlined in **2.2.8.1** from the Wittig reaction between methyltriphenylphosphinium bromide (1.2 equiv, 85 mmol, 30.3 g), 6-chloronicotinaldehyde (71 mmol, 10 g), and potassium *tert*-butoxide (1.2 equiv, 85 mmol, 9.5 g). After isolation, the product was obtained as a clear colorless oil (65% yield, 6.4g, 46 mmol).
^{1}H NMR (600 MHz, $CDCl_3$) δ 8.31 (d, *J* = 2.36, 1H), 7.65 (dd, *J* = 2.64, 8.42 Hz, 1H), 7.23 (d, *J* = 8.33 Hz, 1H), 6.61 (dd, *J*= 10.97, 17.58 Hz, 1H), 5.76 (d, *J*= 17.61 Hz, 1H), 5.36 (d, *J*= 10.93 Hz, 1H).
^{13}C NMR (151 MHz, $CDCl_3$) δ 150.3, 147.9, 135.3, 132.0, 124.0, 124.0, 116.9
HRMS: (+p APCI) calculated for [$C_7H_7N^{35}Cl$ +] 140.0262, found 140.0261
IR(neat): 1633, 1592, 1558, 1458, 1422, 1360, 1142, 1099, 1019, 999, 919, 834, 804, 748, 639, 631, 622, 502, 489 cm^{-1}

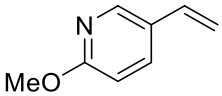

2-Methoxy-5-vinylpyridine (15). This compound was prepared according the procedure outlined in **2.2.8.1** from the Wittig reaction between methyltriphenylphosphinium bromide (1.2 equiv, 85 mmol, 30.3 g), 6-methoxynicotinaldehyde (71 mmol, 10 g), and potassium *tert*-butoxide (1.2 equiv, 85 mmol, 9.5 g). After isolation, the product was obtained as a clear colorless oil (63% yield).
^{1}H NMR (600 MHz, $CDCl_3$) δ 8.11 (d, *J* = 2.28, 1H), 7.68 (dd, *J* = 2.53, 8.85 Hz, 1H), 6.70 (d, *J* = 8.57 Hz, 1H), 6.63 (dd, *J*= 10.81, 17.32 Hz, 1H), 5.62 (d, *J*= 17.50 Hz, 1H), 5.20 (d, *J*= 10.92 Hz, 1H), 3.92 (s, 3H).
^{13}C NMR (151 MHz, $CDCl_3$) δ 163.8, 145.5, 135.2, 133.0, 126.7, 112.9, 110.8, 53.4
HRMS: (+p APCI) calculated for [$C_8H_{10}ON$ +] 136.0757, found 136.0757
IR(neat): 1632, 1598, 1566, 1491, 1461, 1368, 1303, 1282, 1255, 1126, 1019, 987, 901, 830, 764, 729, 587, 554, 509 cm^{-1}

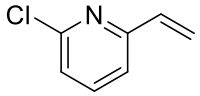

16

2-Chloro-6-vinylpyridine (16). This compound was prepared according to the procedure outlined in **2.2.8.1** from the Wittig reaction between methyltriphenylphosphinium bromide (1.2 equiv, 42.4 mmol, 15.1 g), 2-chloronicotinaldehyde (35.3 mmol, 5.0 g), and potassium *tert*-butoxide (1.2 equiv, 42.4 mmol, 4.76 g). 6-chloropicolinaldehyde. After isolation, the product was obtained as a clear yellow oil (54% yield, 19 mmol, 2.65 g).
^{1}H NMR (400 MHz, $CDCl_3$) δ 7.58 (t, *J* = 7.7 Hz, 1H), 7.21 (d, *J* = 7.6 Hz, 1H), 7.16 (d, *J* = 7.9 Hz, 1H), 6.72 (dd, *J* = 17.4, 10.8 Hz, 1H), 6.24 (d, *J* = 17.4 Hz, 1H), 5.50 (d, *J* = 10.8 Hz, 1H).
^{13}C NMR (151 MHz, $CDCl_3$) δ 156.4, 151.2, 139.0, 135.4, 122.9, 119.9, 119.6.
HRMS: (+p APCI) calculated for [$C_7H_7N^{35}Cl$ +] 140.0262, found 140.0263
IR(neat): 1580, 1551, 1441, 1411, 1396, 1161, 1135, 983, 931, 846, 803, 744, 676 cm^{-1}

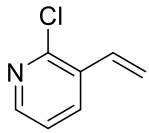

2-Chloro-3-vinylpyridine (17). This compound was prepared according to the procedure outlined in **2.2.8.1** from the Wittig reaction between methyltriphenylphosphinium bromide (1.2 equiv, 42.4 mmol, 15.1g), 2-chloronicotinaldehyde (35.3 mmol, 5.0 g), and potassium *tert*-butoxide (1.2 equiv, 42.4 mmol, 4.76 g). After isolation, the product was obtained as a clear colorless oil (58% yield, 20.6 mmol, 2.88 g).
^{1}H NMR (400 MHz, $CDCl_3$) δ 8.18 (t, *J*=2.35 Hz, 1H), 7.76 (dd, *J*=1.96, 7.75 Hz, 1H), 7.13 (dd, *J*=4.71, 7.75 Hz, 1H), 6.91 (dd, *J*=11.01, 17.54 Hz, 1H), 5.68 (d, *J*= 17.49 Hz, 1H), 5.38 (d, *J*=10.99 Hz, 1H)
^{13}C NMR (151 MHz, $CDCl_3$) δ 149.8, 148.5, 134.9, 132.2, 131.9, 122.7, 118.6
HRMS: (+p APCI) calculated for [$C_7H_7N^{35}Cl$ +] 140.0262, found 140.0262
IR(neat): 1627, 1577, 1558, 1450, 1426, 1410, 1380, 1186, 1128, 1062, 1028, 985, 921, 804, 752, 683, 658 cm^{-1}

2-Methoxy-3-fluoro-5-vinylpyridine (18). This compound was prepared according to the procedure outlined in **2.2.8.2** from the Suzuki coupling between 2-methoxy-3-fluoro-5-bromopyridine (6.65 mmol, 1.37 g) and vinylboronic acid pinacol ester (1.5 equiv, 1.54 g, 9.98 mmol) in the presence of PAPh (1.5 mol %, 0.1mmol, 29 mg), and K_2CO_3 (2.5 equiv, 16.6 mmol, 2.3

g) and $Pd_2(dba)_3$ (0.5 mol %, 0.03 mmol, 30.4 mg). After isolation, the product was obtained as a clear colorless oil (71% yield, 4.73 mmol, 725 mg).
^{1}H NMR (600 MHz, $CDCl_3$) δ 7.86 (s, 1H), 7.43 (d, *J* = 11.00 Hz, 1H), 6.62 (dd, *J* = 11.26, 17.59 Hz, 1H), 5.61 (d, *J*= 17.58 Hz, 1H), 5.26 (d, *J*= 10.96 Hz, 1H), 4.02 (s, 3H).
^{13}C NMR (151 MHz, $CDCl_3$) δ 152.9 d, *J* = 11.5 Hz), 148.6, 139.8, 132.1, 127.9, 119.1 (d, *J* = 15.5 Hz), 114.3, 53.8
^{19}F NMR (151 MHz, $CDCl_3$) δ -140.15 (d, *J* = 11.2 Hz).
HRMS: (+p APCI) calculated for [C_8H_9ONF +] 154.0663, found 154.0662
IR(neat): 1633, 1611, 1571, 1493, 1460, 1440, 1420, 1400, 1318, 1255, 1211, 1196, 1173, 1146, 1133, 1042, 1013, 986, 959, 896, 778, 750, 700, 627, 555, 525, 500, 440, 423 cm^{-1}

2-Chloro-3-fluoro-5-vinylpyridine (19). This compound was prepared according to the procedure outlined in **2.2.8.2** from the Suzuki coupling between 2-methoxy-3-chloro-5-bromopyridine (12 mmol, 2.5 g) and vinylboronic acid pinacol ester (1.5 equiv, 2.7 g, 18 mmol) in the presence of PAPh (1.5 mol %, 0.18 mmol, 52 mg), and K_2CO_3 (2.5 equiv, 30 mmol, 4.1 g) and $Pd_2(dba)_3$ (0.5 mol %, 0.06 mmol, 54 mg). After isolation, the product was obtained as a clear colorless oil which crystallizes in the freezer as needlelike crystals that melt at room temperature (75% yield, 8.57 mmol, 1.35 g).
MP: 25 ℃
^{1}H NMR (400 MHz, $CDCl_3$) δ 8.18 (d, *J* = 2.0 Hz, 1H), 7.51 (dd, *J* = 9.0, 2.0 Hz, 1H), 6.67 (dd, *J* = 17.5, 11.0 Hz, 1H), 5.83 (d, *J* = 17.6 Hz, 1H), 5.48 (d, *J* = 11.0 Hz, 1H).
^{13}C NMR (151 MHz, $CDCl_3$) δ 155.7, 153.9, 142.9 (d, *J* = 5.0 Hz), 137.8 (d, *J* = 19.8 Hz), 134.5 (d, *J* = 2.9 Hz), 131.3, 120.6 (d, *J* = 19.0 Hz), 118.4.
^{19}F NMR (376 MHz, $CDCl_3$) δ -119.60 (d, *J*=9.0 Hz).
HRMS: (+p APCI) calculated for [$C_7H_6N^{35}ClF$ +]158.0167, found 158.0168
IR(neat): 3057, 1633, 1593, 1560, 1453, 1420, 1394, 1293, 1208, 1168, 1087, 985, 919, 896, 731, 710 690, 649, 635, 545, 471 cm^{-1}

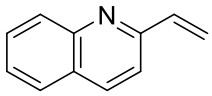

2-Vinylquinoline (20). This compound was prepared according the procedure outlined in **2.2.8.2** from the Suzuki coupling between 2-chloroquinoline (5.0 mmol, 818 mg) and vinylboronic acid pinacol ester (1.2 equiv, 924 mg, 6.0 mmol) in the presence of PAPh (5.0 mol %, 0.25 mmol, 73.1 mg), and K_2CO_3 (2.5 equiv, 12.5 mmol, 1.73 g) and $Pd_2(dba)_3$ (2.0 mol %, 0.10 mmol, 91.6 mg). After isolation, the product was obtained as a light yellow oil (96% yield, 4.81 mmol, 746 mg). Over time product polymerizes to a dark green liquid even if stored at -20 ℃ in the dark. The polymer may be separated from the title compound by short silica-plug through a pipette, eluting with CH_2Cl_2 as a yellow solution while the dark colored polymer remains adhered to silica gel. Batches of the title compound either freshly columned or those that contained a high degree of polymer were equally suitable for highly enantioselective cyclopropanation.
^{1}H NMR (600 MHz, $CDCl_3$) δ 8.04 (d, *J* = 8.5 Hz, 1H), 7.97 (d, *J* = 8.6 Hz, 1H), 7.70 (d, *J* = 8.4 Hz, 1H), 7.68-7.62 (m, 1H) 7.52 (d, *J* = 8.6 Hz, 1H), 7.44 (m, 1H), 7.02 (dd, *J* = 17.6, 10.9 Hz, 1H), 6.25 (d, *J* = 17.6 Hz, 1H), 5.63 (d, *J* = 10.9 Hz, 1H).
^{13}C NMR (126 MHz, $CDCl_3$) δ 156.0, 148.0, 137.9, 136.3, 129.6, 129.4, 127.5, 127.5, 126.3, 119.8, 118.4.
HRMS: (+p APCI) calculated for [$C_{11}H_{10}N$ +] 156.0808, found 156.0808
IR(neat): 3016, 1738, 1616, 1597, 1504, 1427, 1373, 1339, 1231, 1217, 1097, 991, 926, 834, 764, 715, 699, 616, 472 cm^{-1}

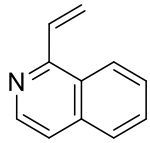

1-Vinylisoquinoline (21). This compound was prepared according to the procedure outlined in **2.2.8.2** from the Suzuki coupling between 1-chloroisoquinoline (5.0 mmol, 818 mg) and vinylboronic acid pinacol ester (1.2 equiv, 924 mg, 6.0 mmol) in the presence of PAPh (5.0 mol %, 0.25 mmol, 73.1 mg), and K_3CO_3 (2.5 equiv, 12.5 mmol, 1.73 g) and $Pd_2(dba)_3$ (2.0 mol %, 0.10 mmol, 91.6 mg). After isolation, the product was obtained as a light yellow oil which rapidly polymerizes, changing appearance to a dark brown liquid (47% yield, 2.29 mmol, 356 mg). The polymer may be separated from the title compound by short silica-plug through a pipette, eluting with CH_2Cl_2 as a yellow solution while the dark colored polymer remains adhered to silica gel. Batches of the title compound either freshly columned or those that contained a high degree of polymer were equally suitable for highly enantioselective cyclopropanation.
^{1}H NMR (400 MHz, $CDCl_3$) δ 8.52 (d, *J* = 5.6 Hz, 1H), 8.22 (dt, *J* = 8.5, 1.1 Hz, 1H), 7.83 – 7.73 (m, 1H), 7.69 – 7.60 (m, 2H), 7.57 (ddd, *J* = 13.0, 6.1, 4.2 Hz, 3H), 6.53 (dd, *J* = 16.9, 2.0 Hz, 1H), 5.71 (dd, *J* = 10.8, 2.0 Hz, 1H).
^{13}C NMR (151 MHz, $CDCl_3$ δ 154.8, 142.4, 136.6, 132.2, 129.9, 127.2, 127.2, 126.4, 124.6, 121.7, 120.3.
HRMS: (+p APCI) calculated for [$C_{11}H_{10}N$ +] 156.0808, found 156.0809
IR(neat): 3048, 1738, 1617, 1579, 1553, 1500, 1414, 1320, 1244, 1217, 1140, 1013, 979, 936, 869, 822, 745, 710, 536 cm^{-1}

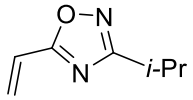

3-Isopropyl-5-vinyl-1,2,4-oxadiazole (22). This compound was prepared according to the procedure outlined in **2.2.9** on 9.8 mmol scale. After isolation, the product was obtained as a clear colorless oil (550 mg, 3.98 mmol, 40% yield over 2 steps)
^{1}H NMR (400 MHz, $CDCl_3$) δ 6.66 (dd, *J* = 17.7, 11.1 Hz, 1H), 6.46 (d, *J* = 17.7 Hz, 1H), 5.91 (d, *J* = 11.1 Hz, 1H), 3.08 (hept, *J* = 6.9 Hz, 1H), 1.33 (d, *J* = 7.0 Hz, 6H).
^{13}C NMR (151 MHz, $CDCl_3$) δ 175.5, 174.2, 128.2, 120.7, 26.7, 20.5.
HRMS: (+p APCI) calculated for [$C_7H_{11}ON_2$ +] 139.0866, found 139.0867
IR(neat): 2973, 2934, 1651, 1571, 1547, 1505, 1465, 1415, 1387, 1353, 1310, 1261, 1215, 1164, 1096, 1066, 1024, 1015, 981, 953, 900, 878, 793, 728, 729, 710, 693 cm^{-1}

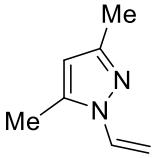

3,5-Dimethyl-1-vinyl-*1H*-pyrazole (23). This compound was prepared according to the procedure outlined in **2.2.10** on 31 mmol scale. After isolation, the product was obtained as a clear colorless oil (1.8 g, 15 mmol, 47% yield)
^{1}H NMR (400 MHz, $CDCl_3$) δ 6.83 (dd, *J* = 15.4, 8.9 Hz, 1H), 5.82 (s, 1H), 5.55 (d, *J* = 15.4 Hz, 1H), 4.72 (d, *J* = 8.9 Hz, 1H), 2.22 (d, *J* = 1.0 Hz, 6H).
^{13}C NMR (151 MHz, $CDCl_3$) δ 149.8, 139.1, 129.2, 106.8, 99.5, 13.6, 10.9.
HRMS: (+p APCI) calculated for [$C_7H_{11}N_2$+] 123.0917, found 123.0918
IR(neat): 2924, 1720, 1645, 1561, 1446, 1427, 1372, 1344, 1283, 1240, 1119, 1044, 1014, 957, 912, 874, 793, 732, 699, 626 543 cm^{-1}

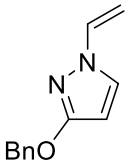

3-(benzyloxy)-1-vinyl-*1H*-pyrazole (24)
This compound was prepared according to the procedure outlined in **2.2.11** on 5.74 mmol scale. After isolation, the product was obtained as a clear colorless oil (475 mg, 2.372 mmol, 41.3 % yield).
^{1}H NMR (400 MHz, $CDCl_3$) δ 7.49 – 7.42 (m, 2H), 7.42 – 7.27 (m, 4H), 6.81 (dd, J = 15.5, 8.8 Hz, 1H), 5.81 (d, J = 2.6 Hz, 1H), 5.39 (d, J = 15.5 Hz, 1H), 5.25 (s, 2H), 4.67 (d, J = 8.8 Hz, 1H);
^{13}C NMR (101 MHz, $CDCl_3$) δ 164.3, 136.9, 132.7, 129.5, 128.5, 128.1, 128.0, 98.1, 93.2, 71.3;
HRMS (ESI) m/z calculated for [$C_{12}H_{13}N_2O$+H+], 201.1022; found 201.1019.

4.1 Characterization of known cyclopropanation products

All products shown with absolute stereo-configuration generated with Rh_2(S-TPPTTL)$_4$* **(7)

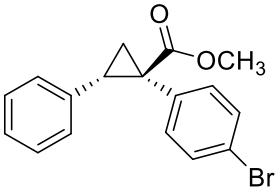

Methyl (1*R*,2*S*)-1-(4-bromophenyl)-2-phenylcyclopropane-1-carboxylate (44)
This compound was prepared according to **General procedure 3.3** and **General procedure 3.4** from the reaction between **S2** (0.20 mmol, 50 mg) and freshly columned styrene (5.0 equiv, 1.00 mmol, 100 mg). Compound prepared according to **General procedure 3.3** was isolated in 58% yield and 48% ee (0.11 mmol, 38 mg). Compound prepared according to **General procedure 3.4** was isolated in 61% yield and 0% ee (0.12 mmol, 40 mg). After isolation, product was obtained as a white solid.
^{1}H NMR (400 MHz, $CDCl_3$) δ 7.28 – 7.24 (m, 3H), 7.16 – 7.05 (m, 2H), 6.98 – 6.86 (m, 2H), 6.86 – 6.75 (m, 2H), 4.83 (d, *J* = 11.9 Hz, 1H), 4.64 (d, *J* = 11.9 Hz, 1H), 3.22 (dd, *J* = 9.4, 7.5 Hz, 1H), 2.28 (dd, *J* = 9.4, 5.2 Hz, 1H), 1.97 (dd, *J* = 7.5, 5.2 Hz, 1H).
^{13}C NMR (151 MHz, $CDCl_3$) δ 171.7, 135.4, 133.8, 133.1, 131.1, 128.2, 128.2, 127.0, 121.7, 95.1, 74.6, 36.7, 34.1, 20.3.
Chiral HPLC: (OJ-H, 30 min, 1 mL/min, 1% *i*-PrOH in *n*-hexane, UV 230 nm) RT: 10.03 min, 14.97 min.

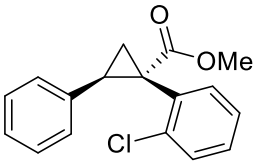

Methyl (1*S*,2*R*)-1-(2-chlorophenyl)-2-phenylcyclopropane-1-carboxylate (61)
This compound was prepared according to **General procedure 3.3** and **General procedure 3.4** from the reaction between **S5** (0.20 mmol, 42 mg) and freshly columned styrene (5.0 equiv, 1.00 mmol, 100 mg). Compound prepared according to **General procedure 3.3** was isolated in 71% yield and 55% ee (0.14 mmol, 40 mg). Compound prepared according to **General procedure 3.4** was isolated in 79% yield and 84% ee (0.16 mmol, 45 mg). After isolation, enantio-enriched product was obtained as a clear colorless oil.
^{1}H NMR (400 MHz, $CDCl_3$) δ 7.15 (broad m, 4H), 7.08 (m, 3H), 6.87 – 6.76 (dd, *J* = 6.9, 2.0 Hz 2H), 3.70 (s, 3H), 3.34 (t, *J* = 8.4 Hz, 1H), 2.13 (s, 1H), 1.94 (dd, *J* = 7.5, 5.2 Hz, 1H).
^{13}C NMR (151 MHz, $CDCl_3$) δ 173.4, 137.3, 133.3, 129.3, 128.6, 127.9, 129.4, 126.4, 126.1, 64.4, 52.7, 33.3, 25.4, 21.5
Chiral HPLC: (OJ-H, 30 min, 1 mL/min, 1% *i*-PrOH in *n*-hexane, UV 230 nm) RT: 12.80 min, 20.73 min

4.3 Characterization of novel cyclopropanation products

All products shown with absolute stereo-configuration generated with Rh_2(S-TPPTTL)$_4$* **(13) *or Rh_2(R-p-Ph-TPCP)$_4$* **(12)**

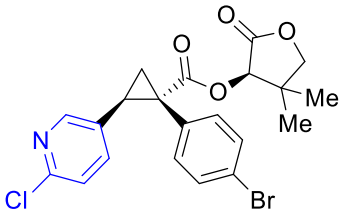

(*R*)-4,4-Dimethyl-2-oxotetrahydrofuran-3-yl-(1*S*,2*R*)-1-(4-bromophenyl)-2-(6-chloropyridin-3-yl) cyclopropane-1-carboxylate (25)
This compound was prepared according to **General procedure 3.1** from the reaction between **S17** (0.20 mmol, 71 mg) and **14** (2.0 equiv, 0.40 mmol, 56 mg). After isolation, product was obtained as a light yellow oil in 87% yield and 98% d.e as determined from the crude NMR (0.17 mmol, 81 mg).
^{1}H NMR (400 MHz, $CDCl_3$) δ 8.08 (d, *J* = 2.6 Hz, 1H), 7.40 – 7.31 (m, 2H), 7.05 (d, *J* = 8.3 Hz, 1H), 7.00 – 6.94 (m, 2H), 6.87 (dd, *J* = 8.3, 2.5 Hz, 1H), 5.33 (d, *J* = 6.9 Hz, 1H), 4.01 (s, 2H), 3.28 (dd, *J* = 9.4, 7.3 Hz, 1H), 2.31 (dd, *J* = 9.4, 5.4 Hz, 1H), 1.94 (dd, *J* = 7.3, 5.5 Hz, 1H), 1.19 (s, 3H), 0.89 (s, 3H).
^{13}C NMR (151 MHz, $CDCl_3$) δ 171.8, 171.4, 149.9, 149.7, 137.3, 133.3, 132.1, 131.6, 130.7, 123.5, 122.2, 40.1, 36.9, 29.7, 22.9, 20.8, 19.6.
HRMS: (+p APCI) calculated for [$C_{21}H_{20}O_4N^{79}Br^{35}Cl$+] 464.0259, found 464.0258
IR(neat): 2970, 1786, 1728, 1587, 1560, 1490, 1464, 1397, 1370, 1352, 1296, 1237, 1216, 1152, 1091, 1071, 1012, 997, 976, 943, 910, 837, 730, 648, 580, 548, 525 cm^{-1}

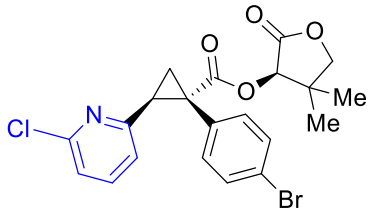

(*R*)-4,4-dimethyl-2-oxotetrahydrofuran-3-yl (1*S*,2*S*)-1-(4-bromophenyl)-2-(6-chloropyridin-2-yl)cyclopropane -1-carboxylate (26)
This compound was prepared according to **General procedure 3.1** from the reaction between **S17** (0.20 mmol, 71 mg) and **16** (2.0 equiv, 0.40 mmol, 56 mg). After isolation, product was obtained as a clear colorless oil in 90% yield and 98% d.e as determined from the crude NMR (0.18 mmol, 84 mg)
^{1}H NMR (400 MHz, $CDCl_3$) δ 7.40 (t, *J* = 7.8 Hz, 1H), 7.32 – 7.22 (m, 2H), 7.01 (dd, *J* = 7.9, 0.8 Hz, 1H), 6.99 – 6.93 (m, 2H), 6.88 (dd, *J* = 7.7, 0.8 Hz, 1H), 5.32 (d, *J* = 5.3 Hz, 1H), 3.99 (d, *J* = 1.4 Hz, 2H), 3.44 (dd, *J* = 9.0, 7.1 Hz, 1H), 2.37 (dd, *J* = 7.1, 4.9 Hz, 1H), 2.26 – 2.16 (m, 1H), 1.17 (s, 3H), 0.88 (s, 3H).
^{13}C NMR (151 MHz, $CDCl_3$) δ 171.9, 171.5, 156.3, 150.4, 138.4, 133.2, 132.8, 130.9, 122.1, 121.7, 121.5, 76.1, 75.9, 40.1, 37.4, 33.9, 22.9, 20.3, 19.6.
HRMS: (+p APCI) calculated for [$C_{21}H_{20}O_4N^{79}Br^{35}Cl$ +] 464.0259, found 464.0262
IR(neat): 2967, 1788, 1729, 1584, 1559, 1490, 1464, 1435, 1399, 1377, 1298, 1244, 1152, 1095, 1072, 1031, 1011, 996, 910, 827, 827, 798, 762, 732, 649, 532 cm^{-1}

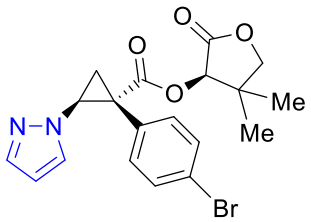

(*R*)-4,4-dimethyl-2-oxotetrahydrofuran-3-yl (1*R*,2*S*)-1-(4-bromophenyl)-2-(*1H*-pyrazol-1-yl)cyclopropane-1-carboxylate (27)

This compound was prepared according to **General procedure 3.1** from the reaction between **S17** (0.20 mmol, 71 mg) and ***N*-vinyl-pyrazole** (2.0 equiv, 0.40 mmol, 56 mg, Enamine). After isolation, product was obtained as a white waxy solid in 66% yield and 97% d.e as determined from the crude NMR (0.13 mmol, 55 mg).

MP: 142-144℃

^{1}H NMR (400 MHz, $CDCl_3$) δ 7.34 (t, *J* = 1.1 Hz, 1H), 7.29 – 7.19 (m, 3H), 7.17 (d, *J* = 2.4 Hz, 1H), 7.11 – 6.94 (m, 2H), 6.06 (t, *J* = 2.1 Hz, 1H), 5.31 (s, 1H), 4.79 – 4.65 (m, 1H), 3.98 (d, *J* = 1.1 Hz, 2H), 2.48 (d, *J* = 6.1 Hz, 1H), 2.41 – 2.31 (m, 1H), 1.17 (s, 3H), 0.85 (s, 3H).

^{13}C NMR (151 MHz, $CDCl_3$) δ 171.6, 170.4, 140.1, 132.5, 131.4, 131.0, 128.9, 122.1, 106.2, 76.0, 45.9, 40.0, 35.4, 22.9, 19.6, 19.4.

HRMS: (+p APCI) calculated for [$C_{19}H_{20}O_4N_2{}^{79}Br$ +] 419.0601, found 419.0600

IR(neat): 2967, 2930, 1789, 1731, 1518, 1491, 1465, 1398, 1378, 1347, 1251, 1199, 1153, 1098, 1071, 1032, 1012, 996, 859, 762, 733, 721, 647, 614, 543 cm^{-1}

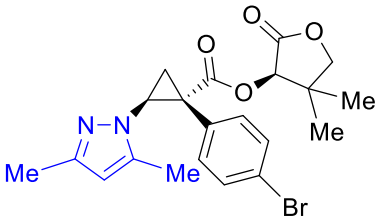

(*R*)-4,4-Dimethyl-2-oxotetrahydrofuran-3-yl (1*R*,2*S*)-1-(4-bromophenyl)-2-(3,5-dimethyl-*1H*-pyrazol-1-yl)cyclopropane-1-carboxylate (28)

This compound was prepared according to **General procedure 3.1** from the reaction between **S17** (0.20 mmol, 71 mg) and **23** (2.0 equiv, 0.40 mmol, 49 mg). After isolation, product was obtained as a crystalline white solid in 97% yield and 98% d.e as determined from the crude NMR (0.19 mmol, 87 mg).

MP: 132-138℃

^{1}H NMR (400 MHz, $CDCl_3$) δ 7.31 – 7.19 (d, *J* = 8.5 Hz, 2H), 6.99 (d, *J* = 8.5 Hz, 2H), 5.68 (s, 1H), 5.37 (s, 1H), 4.43 (dd, *J* = 8.9, 5.6 Hz, 1H), 4.02 (s, 2H), 2.97 (t, *J* = 5.7 Hz, 1H), 2.41 – 2.31 (m, 3H), 2.29 (dd, *J* = 8.9, 5.9 Hz, 1H), 1.92 (s, 3H), 1.20 (s, 3H), 0.99 (s, 3H).

^{13}C NMR (151 MHz, $CDCl_3$) δ 171.9, 170.5, 147.1, 132.3, 131.3, 130.9, 121.8, 106.6, 76.1, 75.7, 44.0, 40.0, 35.2, 22.9, 19.8, 18.4, 13.1, 11.1.

HRMS: (+p APCI) calculated for [$C_{21}H_{24}O_4N_2{}^{79}Br$ +] 447.0914, found 447.0916

IR(neat): 2970, 1788, 1736, 1560, 1491, 1464, 1370, 1299, 1229, 1217, 1204, 1148, 1127, 1092, 1072, 1011, 997, 913, 851, 790, 763, 731, 719, 647, 578, 541, 528 cm^{-1}

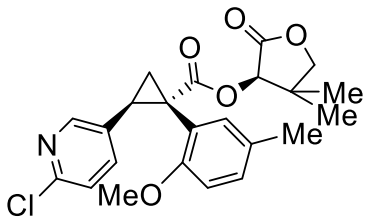

(*R*)-4,4-dimethyl-2-oxotetrahydrofuran-3-yl (*1S,2R*)-2-(6-chloropyridin-3-yl)-1-(2-methoxy-5-methylphenyl) cyclopropane-1-carboxylate (29)

This compound was prepared according to **General procedure 3.1** from the reaction between **S18** (0.20 mmol, 64 mg) and **14** (2.0 equiv, 0.40 mmol, 56 mg). After isolation the product was obtained as a white solid in 64% yield and 89% d.e as determined from the crude NMR (0.13 mmol, 86 mg)

^{1}H NMR (400 MHz, $CDCl_3$) δ 8.07 (d, J = 2.5 Hz, 1H), 7.06 (d, J = 2.3 Hz, 1H), 6.98 – 6.89 (m, 2H), 6.86 (dd, J = 8.3, 2.5 Hz, 1H), 6.41 (d, J = 8.3 Hz, 1H), 5.34 (s, 1H), 3.99 – 3.89 (m, 2H), 3.38 (s, 3H), 3.27 (dd, J = 9.3, 7.3 Hz, 1H), 2.25 (s, 3H), 2.09 (dd, J = 9.2, 5.4 Hz, 1H), 1.93 (dd, J = 7.3, 5.4 Hz, 1H), 1.13 (s, 3H), 0.74 (s, 3H);

^{13}C NMR (101 MHz, DMSO-d6) δ 172.9, 172.4, 156.1, 149.8, 148.3, 138.6, 132.4, 132.0, 129.9, 128.8, 122.8, 122.0, 110.0, 75.7, 75.6, 55.2, 40.2, 34.0, 29.0, 21.8, 20.5, 19.6, 19.1;

HRMS: (ESI) m/z calculated for $C_{23}H_{25}ClNO_5$ [M+H]+, 430.1427; found 430.1426.

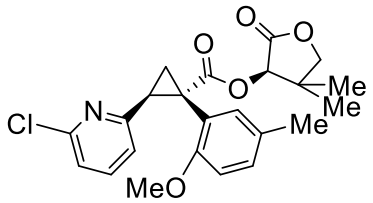

(*R*)-4,4-dimethyl-2-oxotetrahydrofuran-3-yl (1*S*,2*S*)-2-(6-chloropyridin-2-yl)-1-(2-methoxy-5-methylphenyl) cyclopropane-1-carboxylate (30)

This compound was prepared according to **General procedure 3.1** from the reaction between **S18** (0.20 mmol, 64 mg) and **16** (2.0 equiv, 0.40 mmol, 56 mg). After isolation the product was obtained as a white solid in 68% yield and 87% d.e as determined from the crude NMR (0.13 mmol, 92 mg)

^{1}H NMR (400 MHz, $CDCl_3$) δ 7.29 (d, J = 7.8 Hz, 1H), 7.10 (d, J = 2.3 Hz, 1H), 6.94 – 6.84 (m, 2H), 6.76 (dd, J = 7.8, 0.9 Hz, 1H), 6.35 (d, J = 8.3 Hz, 1H), 5.33 (s, 1H), 3.97 – 3.89 (m, 2H), 3.45 (dd, J = 9.0, 7.0 Hz, 1H), 3.37 (s, 3H), 2.34 (dd, J = 7.1, 4.9 Hz, 1H), 2.25 (s, 3H), 2.04 (dd, J = 9.0, 4.8 Hz, 1H), 1.13 (s, 3H), 0.76 (s, 3H);

^{13}C NMR (101 MHz, DMSO-d6) δ 172.8, 172.2, 157.1, 156.2, 148.8, 138.8, 132.7, 129.4, 128.4, 122.5, 122.2, 121.8, 109.8, 75.7, 75.6, 55.2, 40.3, 34.6, 33.0, 21.9, 20.5, 19.9, 19.2;

HRMS (ESI) m/z calculated for $C_{23}H_{25}ClNO_5$ [M+H]+, 430.1427; found 430.1430.

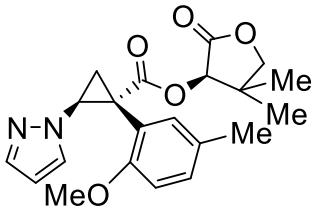

(*R*)-4,4-dimethyl-2-oxotetrahydrofuran-3-yl (1*R*,2*S*)-1-(2-methoxy-5-methylphenyl)-2-(*1H*-pyrazol-1-yl) cyclopropane-1-carboxylate (32)

This compound was prepared according to **General procedure 3.1** from the reaction between **S18** (0.20 mmol, 64 mg) and ***N*-vinyl pyrazole** (2.0 equiv, 0.40 mmol, 38 mg, Enamine). After isolation the product was obtained as a white foam in 69% yield and 89% d.e as determined from the crude NMR (0.14 mmol, 83 mg)

^{1}H NMR (400 MHz, $CDCl_3$) δ 7.24 (dd, J = 2.4, 0.7 Hz, 1H), 7.20 (dd, J = 1.8, 0.7 Hz, 1H), 6.94 – 6.90 (m, 2H), 6.54 – 6.49 (m, 1H), 6.00 (dd, J = 2.4, 1.8 Hz, 1H), 5.34 (s, 1H), 4.74 (dd, J = 8.7, 5.7 Hz, 1H), 4.01 – 3.88 (m, 2H), 3.67 (s, 3H), 2.64 (t, J = 6.0 Hz, 1H), 2.19 – 2.12 (m, 4H), 1.15 (s, 3H), 0.79 (s, 3H);

^{13}C NMR (101 MHz, $CDCl_3$) δ 172.0, 171.4, 156.3, 138.4, 132.1, 129.8, 129.6, 129.4, 120.7, 109.3, 105.5, 76.0, 75.4, 54.9, 45.2, 40.1, 32.6, 22.7, 20.4, 19.24, 19.21;

HRMS (ESI) m/z calculated for $C_{21}H_{25}N_2O_5$ [M+H]+, 385.1758; found 385.1767.

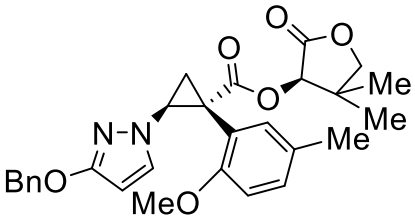

(*R*)-4,4-dimethyl-2-oxotetrahydrofuran-3-yl (1*R*,2*S*)-2-(3-(benzyloxy)-*1H*-pyrazol-1-yl)-1-(2-methoxy-5-methylphenyl)cyclopropane-1-carboxylate (33)

This compound was prepared according to **General procedure 3.1** from the reaction between **S18** (0.20 mmol, 64 mg) and **24** (2.0 equiv, 0.40 mmol, 80 mg). After isolation the product was obtained as a clear oil in 58% yield and 87% d.e as determined from the crude NMR (0.12 mmol, 89 mg)

^{1}H NMR (400 MHz, $CDCl_3$) δ 7.38 – 7.26 (m, 5H), 7.02 (d, J = 2.5 Hz, 1H), 6.99 – 6.91 (m, 2H), 6.54 (d, J = 8.1 Hz, 1H), 5.43 (d, J = 2.5 Hz, 1H), 5.33 (s, 1H), 5.00 (d, J = 11.9 Hz, 1H), 4.89 (d, J = 12.0 Hz, 1H), 4.58 (dd, J = 8.7, 5.7 Hz, 1H), 3.94 (d, J = 2.2 Hz, 2H), 3.66 (s, 3H), 2.54 (t, J = 5.9 Hz, 1H), 2.18 (s, 3H), 2.10 (dd, J = 8.7, 6.1 Hz, 1H), 1.15 (s, 3H), 0.79 (s, 3H);

^{13}C NMR (101 MHz, $CDCl_3$) δ 172.0, 171.4, 162.0, 156.5, 137.2, 132.2, 131.2, 129.5, 129.2, 128.3, 127.8, 127.7, 121.0, 109.4, 91.4, 76.0, 75.3, 70.7, 54.9, 45.5, 40.1, 32.5, 22.7, 20.4, 19.2, 19.1;

HRMS (ESI) m/z calculated for $C_{28}H_{31}N_2O_6$ [M+H]+, 491.2177; found 491.2184.

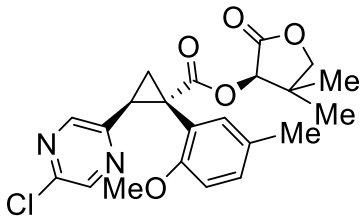

(*R*)-4,4-dimethyl-2-oxotetrahydrofuran-3-yl (1*S*,2*S*)-2-(5-chloropyrazin-2-yl)-1-(2-methoxy-5-methylphenyl) cyclopropane-1-carboxylate (34)

This compound was prepared according to **General procedure 3.1** from the reaction between **S18** (0.20 mmol, 64 mg) and **2-chloro-5-ethenyl-pyrimidine** (2.0 equiv, 0.40 mmol, 56 mg, Enamine). After isolation the product was obtained as a white foam in 41% yield and 92% d.e as determined from the crude NMR (0.08 mmol, 56 mg)

^{1}H NMR (400 MHz, $CDCl_3$) δ 8.24 (d, J = 1.4 Hz, 1H), 8.04 (d, J = 1.3 Hz, 1H), 7.10 (d, J = 2.2 Hz, 1H), 6.91 (ddd, J = 8.2, 2.3, 0.9 Hz, 1H), 6.35 (d, J = 8.3 Hz, 1H), 5.33 (s, 1H), 4.01 – 3.89 (m, 2H), 3.47 (dd, J = 8.9, 7.0 Hz, 1H), 3.41 (s, 3H), 2.43 (dd, J = 7.0, 4.7 Hz, 1H), 2.25 (s, 3H), 2.07 (dd, J = 8.9, 4.7 Hz, 1H), 1.13 (s, 3H), 0.74 (s, 3H);

^{13}C NMR (101 MHz, $CDCl_3$) δ 172.1, 172.0, 155.4, 150.7, 146.4, 144.7, 142.0, 133.0, 129.6, 129.5, 121.5, 108.9, 76.1, 75.5, 53.6, 40.2, 34.9, 30.4, 22.7, 20.5, 20.0, 19.2;

HRMS (ESI) m/z calculated for $C_{22}H_{24}ClN_2O_5$ [M+H]+, 431.1368; found 431.1377.

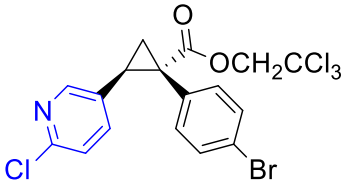

2,2,2-trichloroethyl (1*S*,2*R*)-1-(4-bromophenyl)-2-(6-chloropyridin-3-yl)cyclopropane-1-carboxylate (35)

This compound was prepared according to **General procedure 3.2** from the reaction between **s1** (0.20 mmol, 74 mg) and **14** (2.32 equiv, 0.46 mmol, 65 mg) with $(MeO)_2CO$ as solvent in 77% yield and >99% ee (0.15 mmol, 75 mg). After isolation, enantio-enriched product was obtained as an off-white greasy crystalline solid.

MP: 136-137℃

^{1}H NMR (600 MHz, $CDCl_3$) δ 8.05 (d, *J* = 2.5 Hz, 1H), 7.36 – 7.30 (m, 2H), 7.03 (d, *J* = 8.3 Hz, 1H), 6.96 – 6.90 (m, 2H), 6.83 (dd, *J* = 8.4, 2.5 Hz, 1H), 4.84 (d, *J* = 11.9 Hz, 1H), 4.64 (d, *J* = 11.9 Hz, 1H), 3.18 (dd, *J* = 9.4, 7.3 Hz, 1H), 2.34 (dd, *J* = 9.4, 5.5 Hz, 1H), 1.93 (dd, *J* = 7.3, 5.5 Hz, 1H).

^{13}C NMR (151 MHz, $CDCl_3$) δ 171.1, 150.2, 149.9, 137.4, 133.7, 131.9, 131.7, 130.7, 123.7, 122.5, 94.9, 74.8, 37.0, 30.3, 20.5.

HRMS: (+p APCI) calculated for $[C_{17}H_{13}O_2N^{79}Br^{35}Cl_4+]$ 481.8878, found 481.8878

IR(neat): 2954, 1737, 1587, 1561, 1490, 1464, 1396, 1367, 1349, 1237, 1210, 1156, 1111, 1071, 1057, 1024, 1011, 973, 909, 836, 801, 767, 740, 717, 646, 575, 521 cm^{-1}

Chiral HPLC: (OD-H, 60 min, 1 mL/min, 1% *i*-PrOH in *n*-hexane, UV 230 nm) RT: 30.65 min, 38.71 min.

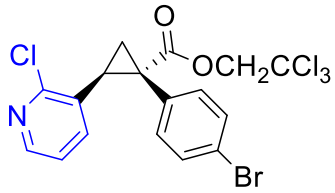

2,2,2-trichloroethyl (1*R*,2*R*)-1-(4-bromophenyl)-2-(2-chloropyridin-3-yl)cyclopropane-1-carboxylate (36)

This compound was prepared according to **General procedure 3.2** from the reaction between **s1** (0.20 mmol, 74 mg) and **17** (2.32 equiv, 0.46 mmol, 65 mg) with $(MeO)_2CO$ as solvent in 70% yield and >99% ee (0.14 mmol, 68 mg)**.** After isolation, enantio-enriched product was obtained as a clear colorless oil.

^{1}H NMR (400 MHz, $CDCl_3$) δ 8.15 (s, 1H), 7.32 – 7.19 (m, 3H), 7.15 – 7.01 (m, 2H), 6.92 (s, 1H), 6.86 (dd, *J* = 7.7, 1.7 Hz, 1H), 4.90 (d, *J* = 11.9 Hz, 1H), 4.67 (d, *J* = 11.9 Hz, 1H), 3.47 (dd, *J* = 9.1, 7.6 Hz, 1H), 2.31 (dd, *J* = 9.2, 5.5 Hz, 1H), 2.07 (dd, *J* = 7.6, 5.5 Hz, 1H).

^{13}C NMR (151 MHz, $CDCl_3$) δ 170.9, 153.2, 147.9, 135.9, 132.8, 132.2, 131.2, 130.5, 122.0, 121.9, 94.7, 74.4, 36.0, 31.2, 18.2.

HRMS: (+p APCI) calculated for $[C_{17}H_{13}O_2N^{79}Br^{35}Cl_4+]$ 481.8878, found 481.8884

IR(neat): 3016, 2770, 1737, 1564, 1490, 1440, 1409, 1367, 1234, 1193, 1156, 1131, 1091, 1071, 1011, 909, 818, 809, 767, 751, 716, 677, 575, 521 cm^{-1}

Chiral HPLC: (OD-H, 30 min, 1 mL/min, 1% *i*-PrOH in *n*-hexane, UV 230 nm) RT: 33.41 min, 39.16 min.

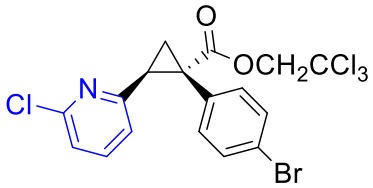

2,2,2-trichloroethyl (1*S*,2*S*)-1-(4-bromophenyl)-2-(6-chloropyridin-2-yl)cyclopropane-1-carboxylate (37)
This compound was prepared according **General procedure 3.2** from the reaction between **s1** (0.20 mmol, 74 mg) and **16** (2.32 equiv, 0.46 mmol, 65 mg) with CH_2Cl_2 as solvent in 53% yield and 93% ee (0.11 mmol, 51 mg)**.** After isolation, enantio-enriched product was obtained as a yellow oil.
^{1}H NMR (400 MHz, $CDCl_3$) δ 7.40 (t, *J* = 7.8 Hz, 1H), 7.33 – 7.23 (m, 2H), 7.03 (d, *J* = 7.9 Hz, 1H), 6.98 (d, *J* = 6.5 Hz, 1H), 6.83 (d, *J* = 7.6 Hz, 1H), 4.85 (d, *J* = 11.9 Hz, 1H), 4.64 (d, *J* = 11.9 Hz, 1H), 3.40 (dd, *J* = 9.0, 7.1 Hz, 1H), 2.38 (dd, *J* = 7.1, 4.9 Hz, 1H), 2.28 (dd, *J* = 9.0, 4.9 Hz, 1H).
^{13}C NMR (151 MHz, $CDCl_3$) δ 170.9, 156.1, 150.5, 138.3, 133.3, 132.4, 132.0, 130.8, 129.2, 122.1, 121.6, 121.4, 94.7, 74.5, 37.3, 34.2, 19.7.
HRMS: (+p APCI) calculated for [$C_{17}H_{13}O_2N^{79}Br^{35}Cl_4$+] 481.8878, found 481.8881
IR(neat): 2953, 1736, 1584, 1559, 1490, 1434, 1408, 1396, 1378, 1238, 1155, 1096, 1071, 1012, 990, 909, 831, 798, 766, 738, 717, 672, 574, 539 cm^{-1}
Chiral HPLC: (AD-H, 30 min, 1 mL/min, 1% *i*-PrOH in *n*-hexane, UV 230 nm) RT: 10.71 min, 14.49 min.

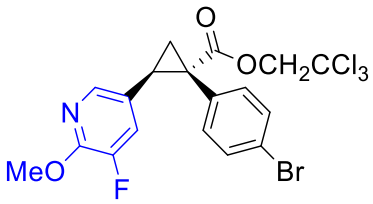

2,2,2-trichloroethyl (1*S*,2*R*)-1-(4-bromophenyl)-2-(5-fluoro-6-methoxypyridin-3-yl)cyclopropane-1-carboxylate (38)
This compound was prepared according **General procedure 3.2** from the reaction between **s1** (0.20 mmol, 74 mg) and **18** (2.32 equiv, 0.46 mmol, 71 mg) with CH_2Cl_2 as solvent in 72% yield and 98% ee (0.14 mmol, 72 mg). After isolation, enantio-enriched product was obtained as a clear colorless oil.
^{1}H NMR (400 MHz, $CDCl_3$) δ 7.59 (d, *J* = 2.0 Hz, 1H), 7.39 – 7.28 (m, 2H), 7.04 – 6.88 (m, 2H), 6.58 (dd, *J* = 11.0, 2.1 Hz, 1H), 4.96 – 4.75 (m, 1H), 4.63 (dd, *J* = 11.9, 0.7 Hz, 1H), 3.94 (d, *J* = 0.9 Hz, 3H), 3.14 (dd, *J* = 9.5, 7.3 Hz, 1H), 2.35 – 2.22 (m, 1H), 1.87 (dd, *J* = 7.3, 5.4 Hz, 1H).
^{13}C NMR (151 MHz, $CDCl_3$) δ 171.1, 152.3 (d, *J* = 11.4 Hz), 147.6, 145.9, 140.9 (d, *J* = 5.7 Hz), 133.4, 132.1, 131.3, 125.2, 122.1, 122.0, 122.0, 94.8, 74.4, 53.7, 36.3, 30.2, 20.0.
^{19}F NMR (376 MHz, $CDCl_3$) δ -139.93 (d, *J* = 10.9 Hz).
HRMS: (+p APCI) calculated for [$C_{18}H_{15}O_3N^{79}Br^{35}Cl_3F$ +] 495.9279, found 495.9284
IR(neat): 1732, 1617, 1577, 1495, 1443, 1412, 1382, 1315, 1198, 1140, 1197, 1162, 1140, 1091, 1071, 1057, 1011, 970, 907, 850, 827, 806, 779, 766, 718, 649, 622, 573, 546, 526, 500 cm^{-1}
Chiral HPLC: (OD-H, 30 min, 1 mL/min, 1% *i*-PrOH in *n*-hexane, UV 230 nm) RT: 14.14 min, 23.37 min.

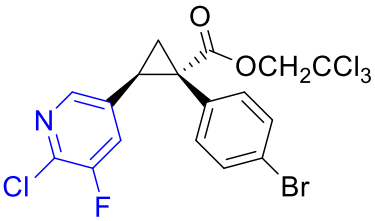

2,2,2-trichloroethyl (1*S*,2*R*)-1-(4-bromophenyl)-2-(6-chloro-5-fluoropyridin-3-yl)cyclopropane-1-carboxylate (39)
This compound was prepared according to **General procedure 3.2** from the reaction between **s1** (0.20 mmol, 74 mg) and **19** (2.32 equiv, 0.46 mmol, 73 mg) with CH_2Cl_2 as solvent in 65% yield and 98% ee (0.13 mmol, 65 mg). After isolation, enantio-enriched product was obtained as a white solid.
MP: 109-116℃
^{1}H NMR (400 MHz, $CDCl_3$) δ 7.87 (d, *J* = 2.1 Hz, 1H), 7.44 – 7.30 (m, 2H), 7.04 – 6.91 (m, 2H), 6.69 (dd, *J* = 9.0, 2.1 Hz, 1H), 4.84 (d, *J* = 11.9 Hz, 1H), 4.64 (d, *J* = 11.8 Hz, 1H), 3.20 (dd, *J* = 9.4, 7.2 Hz, 1H), 2.36 (dd, *J* = 9.4, 5.5 Hz, 1H), 1.92 (dd, *J* = 7.3, 5.5 Hz, 1H).
^{13}C NMR (151 MHz, $CDCl_3$) δ 170.6, 155.0, 153.2, 144.5 (d, *J* = 5.1 Hz), 137.5, 137.4, 133.3, 131.6, 131.3, 123.1, 123.0, 122.5, 94.6, 74.6, 37.0, 29.6, 20.5.
^{19}F NMR (376 MHz, $CDCl_3$) δ -119.18 (d, *J* = 8.9 Hz).
HRMS: (+p APCI) calculated for [$C_{17}H_{12}O_2N^{79}Br^{35}Cl_4F$ +] 499.8784, found 499.8786
IR(neat): 2955, 1736, 1594, 1568, 1490, 1414, 1381, 1241, 1187, 1152, 1071, 1059, 1012, 970, 904, 828, 807, 767, 728, 717, 573, 542 cm^{-1}

Chiral HPLC: (OD-H, 60 min, 1 mL/min, 1% *i*-PrOH in *n*-hexane, UV 230 nm) RT: 25.63 min, 39.39 min.

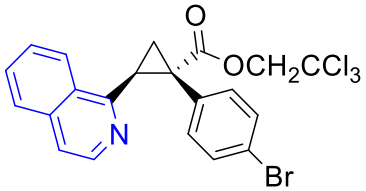

2,2,2-trichloroethyl (1*S*,2*S*)-1-(4-bromophenyl)-2-(isoquinolin-1-yl)cyclopropane-1-carboxylate (40)
This compound was prepared according to **General procedure 3.2** from the reaction between **s1** (0.20 mmol, 74 mg) and **21** (2.32 equiv, 0.46 mmol, 72 mg) with CH_2Cl_2 as solvent in 54% yield and 83% ee (0.11 mmol, 54 mg). After isolation, enantio-enriched product was obtained as a yellow solid.
MP: 124-127℃
^{1}H NMR (400 MHz, $CDCl_3$) δ 8.39 (d, *J* = 8.0 Hz, 1H), 8.11 (d, *J* = 5.7 Hz, 1H), 7.79 (d, *J* = 7.5 Hz, 1H), 7.70 (dd, *J* = 8.7, 6.8 Hz, 2H), 7.47 – 7.30 (m, 1H), 7.15 – 6.96 (m, 2H), 6.88 – 6.68 (m, 2H), 4.96 (d, *J* = 11.9 Hz, 1H), 4.74 (d, *J* = 11.9 Hz, 1H), 4.03 (dd, *J* = 8.9, 7.0 Hz, 1H), 2.98 (s, 1H), 2.31 (dd, *J* = 8.9, 4.4 Hz, 1H).
^{13}C NMR (151 MHz, $CDCl_3$) δ 171.4, 153.8, 141.3, 135.9, 132.6(2 C), 132.6, 130.5(2 C), 130.1, 128.8, 127.7, 127.5, 124.4, 121.3, 119.9, 95.0, 74.3, 37.3, 31.9, 18.4.
HRMS: (+p APCI) calculated for [$C_{21}H_{16}O_2N^{79}Br^{35}Cl_3$+] 497.9424, found 497.9415
IR(neat): 1733, 1623, 1585, 1563, 1491, 1407, 1396, 1367, 1311, 1272, 1237, 1197, 1170, 1150, 1095, 1059, 1011, 972, 906, 825, 799, 767, 730, 649, 573, 532 cm^{-1}
Chiral HPLC: (AD-H, 30 min, 1 mL/min, 1% *i*-PrOH in *n*-hexane, UV 230 nm) RT: 15.62 min, 19.25 min.

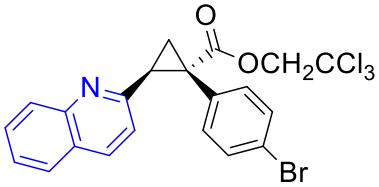

2,2,2-trichloroethyl (1*S*,2*S*)-1-(4-bromophenyl)-2-(quinolin-2-yl)cyclopropane-1-carboxylate (41)
This compound was prepared according to **General procedure 3.2** from the reaction between **s1** (0.20 mmol, 74 mg) and **20** (2.32 equiv, 0.46 mmol, 72 mg) with CH_2Cl_2 as solvent in 56% yield and 87% ee (0.11 mmol, 56 mg). After isolation, enantio-enriched product was obtained as a light yellow oil.
^{1}H NMR (400 MHz, $CDCl_3$) δ 7.88 (dd, *J* = 8.5, 0.8 Hz, 1H), 7.83 – 7.77 (m, 1H), 7.68 (dd, *J* = 8.2, 1.4 Hz, 1H), 7.61 (ddd, *J* = 8.5, 6.9, 1.5 Hz, 1H), 7.44 (ddd, *J* = 8.1, 6.9, 1.2 Hz, 1H), 7.20 – 7.08 (m, 2H), 7.02 – 6.97 (m, 2H), 6.95 (d, *J* = 8.5 Hz, 1H), 4.85 (d, *J* = 11.9 Hz, 1H), 4.66 (d, *J* = 11.9 Hz, 1H), 3.59 (dd, *J* = 9.1, 7.2 Hz, 1H), 2.56 (dd, *J* = 7.2, 4.8 Hz, 1H), 2.35 (dd, *J* = 9.1, 4.8 Hz, 1H).
^{13}C NMR (151 MHz, $CDCl_3$) δ 171.2, 155.3, 147.5, 135.7, 133.3, 132.8, 130.8, 129.5, 128.9, 127.4, 126.6, 126.1, 121.4, 120.8, 94.8, 74.5, 37.5, 35.4, 20.1.
HRMS: (+p APCI) calculated for [$C_{21}H_{16}O_2N^{79}Br^{35}Cl_3$+] 497.9425, found 497.9428
IR(neat): 2952, 1736, 1618, 1598, 1505, 1489, 1426, 1366, 1237, 1192, 1155, 1094, 1071, 1012, 988, 909, 834, 758, 732, 719, 575, 527 cm^{-1}
Chiral HPLC: (AD-H, 90 min, 1 mL/min, 1% *i*-PrOH in *n*-hexane, UV 230 nm) RT: 17.42 min, 54.21 min.

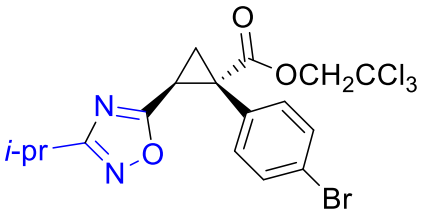

2,2,2-trichloroethyl (1*S*,2*R*)-1-(4-bromophenyl)-2-(3-Isopropyl-5-vinyl-1,2,4-oxadiazole)cyclopropane-1-carboxylate (42)
This compound was prepared according to **General procedure 3.2** from the reaction between **s1** (0.20 mmol, 74 mg) and **22** (2.32 equiv, 0.46 mmol, 64 mg) with CH_2Cl_2 as solvent in 96% yield and 89% ee (0.19 mmol, 93 mg). After isolation, enantio-enriched product was obtained as a clear colorless oil.
^{1}H NMR (400 MHz, $CDCl_3$) δ 7.34 (d, *J* = 8.4 Hz, 2H), 7.04 (d, *J* = 8.5 Hz, 2H), 4.83 (d, *J* = 11.9 Hz, 1H), 4.64 (d, *J* = 11.9 Hz, 1H), 3.40 (dd, *J* = 9.0, 6.8 Hz, 1H), 2.87 (hept, *J* = 6.9 Hz, 1H), 2.42 – 2.30 (two overlapped signals, m, 2H), 1.10 (dd, *J* = 6.9, 2.0 Hz, 6H).
^{13}C NMR (151 MHz, $CDCl_3$) δ 174.9, 174.5, 169.8, 132.4, 131.7, 131.3, 122.4, 94.4, 74.7, 36.9, 26.4, 23.6, 20.4, 20.1, 19.9.
HRMS: (+p APCI) calculated for [$C_{17}H_{17}O_3N_2^{79}Br^{35}Cl_3$ +] 480.9482, found 480.9484
IR(neat): 2970, 1739, 1588, 1489, 1435, 1366, 1230, 1217, 1158, 1094, 1070, 1012, 969, 909, 830, 809, 785, 767, 717, 574, 543, 528 cm^{-1}
Chiral HPLC: (OJ-H, 30 min, 1 mL/min, 1% *i*-PrOH in *n*-hexane, UV 230 nm) RT: 12.63 min, 15.08 min.

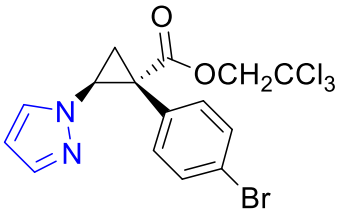

2,2,2-trichloroethyl (1*R*,2*S*)-1-(4-bromophenyl)-2-(*1H*-pyrazol-1-yl)cyclopropane-1-carboxylate (43)
This compound was prepared according to **General procedure 3.2** from the reaction between **s1** (0.20 mmol, 74 mg) and ***N*-vinyl pyrazole** (2.32 equiv, 0.46 mmol, 44 mg) purchased from Enamine with CH_2Cl_2 as solvent. The reaction had to be conducted with elevated catalyst loading (1.0 mol % Rh_2(*R*-*p*-Ph-TPCP)$_4$, 2.0 μmol, 2.6 mg) and longer reaction time (48 h) to achieve high yield and selectivity, 80% yield and 95% ee (0.16 mmol, 70 mg). After isolation, product was obtained as a white solid.
MP: 90-93℃
^{1}H NMR (400 MHz, $CDCl_3$) δ 7.36 (d, *J* = 1.8 Hz, 1H), 7.33 – 7.26 (m, 2H), 7.17 (s, 1H), 7.11 – 6.99 (m, 2H), 6.09 (t, *J* = 2.1 Hz, 1H), 4.89 – 4.78 (m, 1H), 4.72 (dd, *J* = 8.8, 5.8 Hz, 1H), 4.66 (d, *J* = 11.9 Hz, 1H), 2.53 (t, *J* = 6.0 Hz, 1H), 2.42 (dd, *J* = 8.8, 6.3 Hz, 1H).
^{13}C NMR (151 MHz, $CDCl_3$) δ 169.8, 140.1, 132.6, 131.7, 131.0, 128.8, 128.3, 122.2, 106.3, 94.6, 74.7, 74.5, 46.0, 35.5, 18.8.
HRMS: (+p APCI) calculated for [$C_{15}H_{13}O_2N_2{}^{79}Br^{35}Cl_3$+] 436.9220, found 436.9220
IR(neat): 1735, 1593, 1517, 1489, 1448, 1395, 1330, 1242, 1156, 1097, 1071, 1011, 986, 911, 858, 827, 808, 767, 718, 667, 641, 612, 574, 491 cm^{-1}
Chiral HPLC: (OJ-H, 45 min, 1 mL/min, 1% *i*-PrOH in *n*-hexane, UV 230 nm) RT: 22.60 min, 18.87 min.

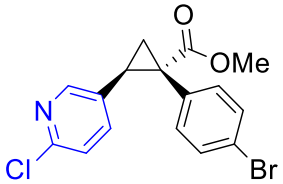

Methyl (1*S*,2*R*)-1-(4-bromophenyl)-2-(6-chloropyridin-3-yl)cyclopropane-1-carboxylate (44)
This compound was prepared according to **General procedure 3.2** from the reaction between **s2** (0.20 mmol, 51 mg) and **14** (2.32 equiv, 0.46 mmol, 65 mg) with CH_2Cl_2 as solvent in 70% yield and 94% ee (0.14 mmol, 51 mg). After isolation, enantio-enriched product was obtained as a white waxy solid.
MP: 152-156℃
^{1}H NMR (400 MHz, $CDCl_3$) δ 8.06 (d, *J* = 2.6 Hz, 1H), 7.37 – 7.31 (m, 2H), 7.03 (d, *J* = 8.4 Hz, 1H), 6.96 – 6.84 (m, 2H), 6.80 (dd, *J* = 8.3, 2.6 Hz, 1H), 3.70 (s, 3H), 3.11 (dd, *J* = 9.3, 7.2 Hz, 1H), 2.23 (dd, *J* = 9.4, 5.2 Hz, 1H), 1.82 (dd, *J* = 7.2, 5.2 Hz, 1H).
^{13}C NMR (151 MHz, $CDCl_3$) δ 173.0, 149.7, 149.6, 137.1, 133.4, 132.7, 131.4, 131.1, 123.3, 121.9, 52.9, 37.0, 29.4, 20.3.
HRMS: (+p APCI) calculated for [$C_{16}H_{14}O_2N^{79}Br^{35}Cl$+] 365.9891, found 365.9894
IR(neat): 2951, 1716, 1587, 1560, 1489, 1464, 1434, 1395, 1349, 1258, 1211, 1193, 1163, 1142, 1111, 1080, 1025, 1011, 967, 910, 863, 834, 801, 766, 739, 647, 629, 573, 522 cm^{-1}
Chiral HPLC: (AD-H, 60 min, 1 mL/min, 1% *i*-PrOH in *n*-hexane, UV 230 nm) RT: 37.89 min, 46.52 min.

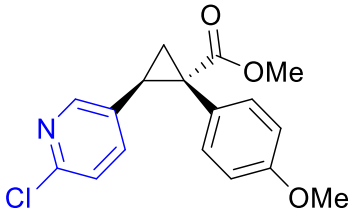

Methyl (1*S*,2*R*)-2-(6-chloropyridin-3-yl)-1-(4-methoxyphenyl)cyclopropane-1-carboxylate (45)
This compound was prepared according to **General procedure 3.2** from the reaction between **S7** (0.20 mmol, 41 mg) and **14** (2.32 equiv, 0.46 mmol, 65 mg) with CH_2Cl_2 as solvent in 70% yield and 89% ee (0.14 mmol, 45 mg). After isolation, enantio-enriched product was obtained as a clear colorless oil.
^{1}H NMR (400 MHz, $CDCl_3$) δ 8.01 (d, *J* = 2.5 Hz, 1H), 6.97 (d, *J* = 8.3 Hz, 1H), 6.95 – 6.90 (m, 2H), 6.75 (dd, *J* = 8.4, 2.6 Hz, 1H), 6.73 – 6.66 (m, 2H), 3.75 (s, 3H), 3.67 (s, 3H), 3.04 (dd, *J* = 9.3, 7.1 Hz, 1H), 2.18 (dd, *J* = 9.3, 5.1 Hz, 1H), 1.78 (dd, *J* = 7.1, 5.1 Hz, 1H), 1.57 (s, 3H).
^{13}C NMR (151 MHz, $CDCl_3$) δ 174.1, 159.0, 149.9, 149.5, 137.4, 133.0, 132.0, 125.7, 123.3, 113.9, 55.3, 53.0, 37.1, 29.7, 21.0.
HRMS: (+p APCI) calculated for [$C_{17}H_{17}O_3N^{35}Cl$ +] 318.0891, found 318.0885
IR(neat): 2952, 1717, 1612, 1584, 1560, 1516, 1463, 1435, 1349, 1264, 1247, 1211, 1176, 1163, 1109, 1031, 967, 835, 803, 756, 745, 653, 632, 604, 537, cm^{-1}

Chiral HPLC: (AD-H, 30 min, 1 mL/min, 3% *i*-PrOH in *n*-hexane, UV 230 nm) RT: 19.34 min, 21.92 min.

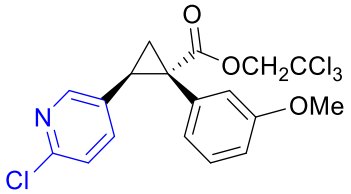

2,2,2-trichloroethyl (1*S*,2*R*)-2-(6-chloropyridin-3-yl)-1-(3-methoxyphenyl)cyclopropane-1-carboxylate (46)
This compound was prepared according to **General procedure 3.2** from the reaction between **S8** (0.20 mmol, 65 mg) and **14** (2.32 equiv, 0.46 mmol, 65 mg) with CH_2Cl_2 as solvent in 65% yield and 95% ee (0.13 mmol, 55 mg). After isolation, enantio-enriched product was obtained as a clear colorless oil.
^{1}H NMR (400 MHz, $CDCl_3$) δ 8.05 (d, *J* = 2.6 Hz, 1H), 7.10 (t, *J* = 7.9 Hz, 1H), 6.99 (d, *J* = 8.3 Hz, 1H), 6.83 (dd, *J* = 8.3, 2.6 Hz, 1H), 6.73 (ddt, *J* = 8.3, 2.6, 0.8 Hz, 1H), 6.65 (ddt, *J* = 7.7, 1.6, 0.7 Hz, 1H), 6.63 – 6.56 (m, 1H), 4.86 (dd, *J* = 12.0, 0.6 Hz, 1H), 4.63 (dd, *J* = 11.9, 0.6 Hz, 1H), 3.67 (d, *J* = 0.5 Hz, 3H), 3.16 (dd, *J* = 9.4, 7.2 Hz, 1H), 2.47 – 2.16 (m, 1H), 1.95 (dd, *J* = 7.2, 5.3 Hz, 1H).
^{13}C NMR (151 MHz, $CDCl_3$) δ 171.5, 159.5, 149.9, 149.8, 137.4, 134.1, 131.2, 129.4, 124.5, 123.4, 117.8, 113.7, 95.0, 74.6, 55.3, 37.6, 30.2, 20.7.
HRMS: (+p APCI) calculated for [$C_{18}H_{16}O_3N^{35}Cl_4$+] 433.9878, found 433.9881
IR(neat): 2954, 1733, 1601, 1585, 1561, 1494, 1463, 1435, 1367, 1347, 1288, 1238, 1208, 1153, 1110, 1046, 978, 910, 803, 753, 736, 713, 700, 573 cm^{-1}
Chiral HPLC: (AD-H, 30 min, 1 mL/min, 5% *i*-PrOH in *n*-hexane, UV 230 nm) RT: 12.15 min, 14.45 min.

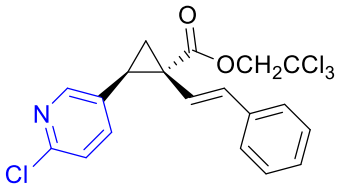

2,2,2-trichloroethyl (1*R*,2*R*)-2-(6-chloropyridin-3-yl)-1-((E)-styryl)cyclopropane-1-carboxylate (47)
This compound was prepared according to **General procedure 3.2** from the reaction between **S9** (0.20 mmol, 64 mg) and **14** (2.32 equiv, 0.46 mmol, 65 mg) with CH_2Cl_2 as solvent in 67% yield and 98% ee (0.13 mmol, 57 mg). After isolation, enantio-enriched product was obtained as a yellow oil.
^{1}H NMR (400 MHz, $CDCl_3$) δ 8.28 (s, 1H), 7.38 (dd, *J* = 8.3, 2.2 Hz, 1H), 7.33 – 7.25 (m, 3H), 7.25 – 7.11 (m, 3H), 6.45 (d, *J* = 16.0 Hz, 1H), 6.19 (d, *J* = 16.0 Hz, 1H), 4.95 – 4.77 (m, 2H), 3.09 (dd, *J* = 9.3, 7.3 Hz, 1H), 2.25 (ddd, *J* = 9.3, 5.5, 0.8 Hz, 1H), 1.94 (dd, *J* = 7.3, 5.5 Hz, 1H).
^{13}C NMR (151 MHz, $CDCl_3$) δ 171.2, 150.4, 150.1, 138.9, 136.1, 134.9, 130.1, 128.6 (2 C), 128.0, 126.3 (2 C), 123.6, 121.5, 94.9, 74.5, 33.2, 31.7, 18.4.
HRMS: (+p APCI) calculated for [$C_{19}H_{16}O_2N^{35}Cl_4$+] 429.9929, found 429.9934
IR(neat): 3026, 2970, 1736, 2586, 1560, 1493, 1463, 1448, 1365, 1230, 1217, 1131, 1109, 1059, 966, 910, 835, 806, 783, 746, 718, 694, 646, 633, 572, 528 cm^{-1}
Chiral HPLC: (AD-H, 30 min, 1 mL/min, 3% *i*-PrOH in *n*-hexane, UV 230 nm) RT: 16.04 min, 20.66 min.

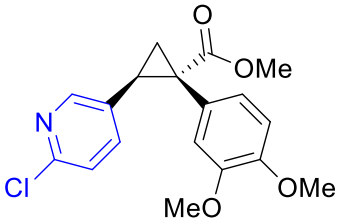

Methyl (1*S*,2*R*)-2-(6-chloropyridin-3-yl)-1-(3,4-dimethoxyphenyl)cyclopropane-1-carboxylate (48)
This compound was prepared according to **General procedure 3.2** from the reaction between **S6** (0.20 mmol, 47 mg) and **14** (2.32 equiv, 0.46 mmol, 65 mg) with CH_2Cl_2 as solvent in 60% yield and 71% ee (0.12 mmol, 41 mg). After isolation, enantio-enriched product was obtained as a clear colorless oil.
^{1}H NMR (400 MHz, $CDCl_3$) δ 8.08 (s, 1H), 6.97 (d, *J* = 8.3 Hz, 1H), 6.73 (dd, *J* = 8.1, 2.6 Hz, 1H), 6.70 (d, *J* = 8.2 Hz, 1H), 6.63 (dd, *J* = 8.3, 2.0 Hz, 1H), 6.43 (s, 1H), 3.83 (s, 3H), 3.69 (s, 3H), 3.66 (s, 3H), 3.05 (dd, *J* = 9.2, 7.1 Hz, 1H), 2.19 (dd, *J* = 9.4, 5.0 Hz, 1H), 1.79 (dd, *J* = 7.1, 5.1 Hz, 1H).
^{13}C NMR (151 MHz, $CDCl_3$) δ 173.8, 149.7, 149.4, 148.4, 148.4, 136.9, 131.8, 125.9, 124.1, 123.1, 115.0, 110.6, 55.8, 55.7, 52.8, 37.3, 29.4, 20.9.
HRMS: (+p APCI) calculated for [$C_{18}H_{19}O_4N^{35}Cl$ +] 348.0997, found 348.0996
IR(neat): 3003, 2969, 2950, 1737, 1721, 1587, 1551, 1517, 1462, 1435, 1414, 1365, 1352, 1252, 1227, 1217, 1157, 1140, 1108, 1026, 908, 742, 658, 528 cm^{-1}
Chiral HPLC: (AD-H, 60 min, 1 mL/min, 3% *i*-PrOH in *n*-hexane, UV 230 nm) RT: 32.96 min, 45.12 min.

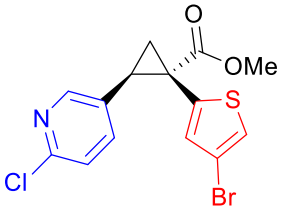

Methyl (1*R*,2*R*)-1-(4-bromothiophen-2-yl)-2-(6-chloropyridin-3-yl)cyclopropane-1-carboxylate (49)
This compound was prepared according **General procedure 3.2** from the reaction between **S16** (0.20 mmol, 52 mg) and **14** (2.32 equiv, 0.46 mmol, 65 mg) with CH_2Cl_2 as solvent in 98% yield and 95% ee (0.20 mmol, 73 mg). After isolation, enantio-enriched product was obtained as a light brown solid.
MP: 126-127℃
^{1}H NMR (400 MHz, $CDCl_3$) δ 8.11 (dt, *J* = 2.5, 0.7 Hz, 1H), 7.10 (dd, *J* = 8.3, 0.8 Hz, 1H), 7.06 (dd, *J* = 2.5, 0.5 Hz, 1H), 7.03 (d, *J* = 1.5 Hz, 1H), 6.69 (d, *J* = 1.5 Hz, 1H), 3.74 (s, 3H), 3.13 (dd, *J* = 9.3, 7.4 Hz, 1H), 2.28 (dd, *J* = 9.3, 5.3 Hz, 1H), 1.95 (dd, *J* = 7.4, 5.3 Hz, 1H).
^{13}C NMR (151 MHz, $CDCl_3$) δ 172.2, 150.4, 149.9, 138.8, 137.6, 132.3, 130.5, 124.2, 123.7, 108.9, 53.4, 32.1, 31.3, 22.0.
HRMS: (+p APCI) calculated for [$C_{14}H_{12}O_2N^{79}Br^{35}Cl^{32}S$+] 371.9455, found 371.9458
IR(neat): 3105, 2951, 1720, 1586, 1561, 1528, 1464, 1434, 1348, 1265, 1208, 1155, 1108, 1023, 963, 915, 881, 836, 799, 733, 678, 633, 604, 563 cm^{-1}
Chiral HPLC: (OD-H, 60 min, 1 mL/min, 1% *i*-PrOH in *n*-hexane, UV 230 nm) RT: 43.1 min, 50.5 min.

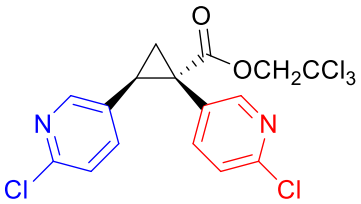

2,2,2-trichloroethyl (1*S*,2*R*)-1,2-bis(6-chloropyridin-3-yl)cyclopropane-1-carboxylate (50)
This compound was prepared according to **General procedure 3.2** from the reaction between **S3** (0.20 mmol, 66 mg) and **14** (2.32 equiv, 0.46 mmol, 65 mg) with CH_2Cl_2 as solvent in 73% yield and 97% ee (0.15 mmol, 64 mg). After isolation, enantio-enriched product was obtained as a crystalline yellow solid.
MP: 88-89℃
^{1}H NMR (400 MHz, $CDCl_3$) δ 8.19 (d, *J* = 2.5 Hz, 1H), 8.09 (d, *J* = 2.6 Hz, 1H), 7.34 (dd, *J* = 8.3, 2.5 Hz, 1H), 7.23 – 7.15 (m, 1H), 7.11 (d, *J* = 8.3 Hz, 1H), 6.94 (dd, *J* = 8.3, 2.6 Hz, 1H), 4.87 (d, *J* = 11.9 Hz, 1H), 4.67 (d, *J* = 11.9 Hz, 1H), 3.26 (dd, *J* = 9.5, 7.4 Hz, 1H), 2.44 (dd, *J* = 9.4, 5.7 Hz, 1H), 2.03 (dd, *J* = 7.4, 5.7 Hz, 1H).
^{13}C NMR (151 MHz, $CDCl_3$) δ 170.1, 152.2, 151.0, 150.4, 149.6, 142.3, 137.5, 129.6, 128.0, 123.9, 94.5, 74.6, 34.1, 30.0, 19.4.
HRMS: (+p APCI) calculated for [$C_{16}H_{12}O_2N_2{}^{35}Cl_5$+] 438.9335, found 438.9337
IR(neat): 3016, 2970, 1738, 1587, 1560, 1463, 1366, 1230, 1217, 1162, 1113, 1060, 1022, 912, 839, 812, 779, 749, 528 cm^{-1}
Chiral HPLC: (AD-H, 60 min, 1 mL/min, 7% *i*-PrOH in *n*-hexane, UV 230 nm) RT: 36.61 min, 44.71 min.

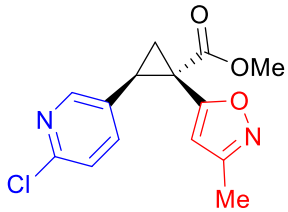

Methyl (1*S*,2*R*)-2-(6-chloropyridin-3-yl)-1-(3-methylisoxazol-5-yl)cyclopropane-1-carboxylate (51)
This compound was prepared according **General procedure 3.2** from the reaction between **S13** (0.20 mmol, 36 mg) and **14** (2.32 equiv, 0.46 mmol, 65 mg) with CH_2Cl_2 as solvent in 60% yield and 83% ee (0.12 mmol, 35 mg). After isolation, enantio-enriched product was obtained as a clear colorless oil.
^{1}H NMR (600 MHz, $CDCl_3$) δ 8.13 (dt, *J* = 2.6, 0.7 Hz, 1H), 7.24 (ddd, *J* = 8.3, 2.5, 0.6 Hz, 1H), 7.12 (dd, *J* = 8.4, 0.8 Hz, 1H), 5.91 (s, 1H), 3.76 (s, 3H), 3.18 (dd, *J* = 9.2, 7.8 Hz, 1H), 2.24 – 2.20 (m, 1H), 2.20 – 2.16 (m, 1H), 2.15 (s, 3H).
^{13}C NMR (151 MHz, $CDCl_3$) δ 170.6, 165.3, 160.1, 150.6, 150.0, 138.2, 129.9, 123.9, 106.8, 53.3, 31.2, 29.3, 19.9, 11.6
HRMS: (+p APCI) calculated for [$C_{14}H_{14}O_3N_2{}^{35}Cl$ +] 293.0687, found 293.0687
IR(neat): 2954, 1725, 1612, 1588, 1561, 1463, 1435, 1414, 1351, 1319, 1265, 1219, 1200, 1157, 1108, 1077, 1024, 1008, 986, 964, 914, 835, 799, 761, 736, 696, 645, 633, 561, 458 cm^{-1}
Chiral HPLC: (OD-H, 60 min, 1 mL/min, 3% *i*-PrOH in *n*-hexane, UV 230 nm) RT: 39.76 min, 51.41 min.

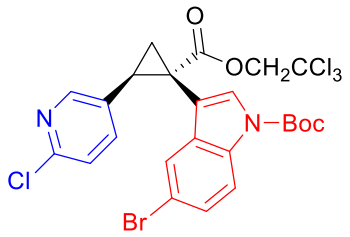

***Tert*-butyl 5-bromo-3-((1*S*,2*R*)-)-2-(6-chloropyridin-3-yl)-1-((2,2,2-trichloroethoxy)carbonyl)cyclopropyl)-1H-indole-1-carboxylate (52)**

This compound was prepared according to the procedure outlined in **3.2.1.** After isolation, enantio-enriched product was obtained as a brown oil in 82% yield and 89% ee (0.16 mmol, 102 mg).

^{1}H NMR (400 MHz, $CDCl_3$) δ 8.04 (s, 1H), 7.87 (d, *J* = 8.8 Hz, 1H), 7.44 (s, 1H), 7.30 (dd, *J* = 8.8, 2.0 Hz, 1H), 7.25 – 7.14 (m, 1H), 7.02 (d, *J* = 8.3 Hz, 1H), 4.87 (d, *J* = 11.9 Hz, 1H), 4.65 (d, *J* = 11.9 Hz, 1H), 3.28 (dd, *J* = 9.4, 7.3 Hz, 1H), 2.36 (dd, *J* = 9.4, 5.2 Hz, 1H), 2.00 (dd, *J* = 7.4, 5.2 Hz, 1H), 1.63 (s, 9H).

^{13}C NMR (151 MHz, $CDCl_3$) δ 170.8, 150.0, 148.9, 138.2, 133.8, 131.5, 130.3, 128.1, 127.5, 123.2, 122.5, 116.6, 116.0, 113.0, 94.6, 84.6, 74.5, 29.7, 28.1 (3 C), 20.0.

HRMS: (+p APCI) calculated for [$C_{24}H_{22}O_4N_2{}^{79}Br^{35}Cl_4$+] 620.9511, found 620.9509

IR(neat): 2980, 1732, 1587, 1561, 1451, 1371, 1304, 1274, 1240, 1215, 1197, 1152, 1121, 1055, 1026, 961, 908, 839, 801, 789, 765, 731, 648, 636, 572 cm^{-1}

Chiral HPLC: (OD-H, 30 min, 1 mL/min, 3% *i*-PrOH in *n*-hexane, UV 230 nm) RT: 15.17 min, 21.87 min.

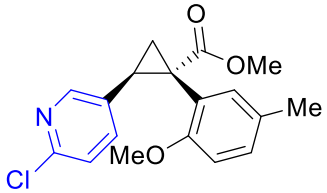

Methyl (1*S*,2*R*)-2-(6-chloropyridin-3-yl)-1-(2-methoxy-5-methylphenyl)cyclopropane-1-carboxylate (55)

This compound was prepared according to **General procedure 3.2, General procedure 3.3, General procedure 3.4, General procedure 3.5,** and **General procedure 3.6** from the reaction between **14** and **54** with varying levels of enantioselectivity depending on the method and conditions used. **General procedure 3.2: 54** (0.20 mmol, 44 mg) and **14** (2.32 equiv, 0.46 mmol, 65 mg) with CH_2Cl_2 as solvent in 22% yield and 22% ee (0.04 mmol, 15 mg). **General procedure 3.3: 54** (0.20 mmol, 44 mg) and **14** (5.0 equiv, 1.00 mmol, 160 mg) in 95% yield and 98% ee (0.19 mmol, 63 mg)**. General procedure 3.4: 54** (0.20 mmol, 44 mg) and **14** (1.5 equiv, 0.30 mmol, 42 mg) with CH_2Cl_2 as solvent in 87% yield and 98% ee (0.17 mmol, 58 mg). **General procedure 3.5: 54** (0.20 mmol, 44 mg) and **14** (1.5 equiv, 0.30 mmol, 42 mg) with CH_2Cl_2 as solvent in 89% yield and 98% ee (0.18 mmol, 59 mg). Only optimized results for each procedure are reported here, enantioselectivity data corresponding to other variants in Table 1 and Table 2 may be found in section **5.3**. **General procedure 3.6:** Reaction was performed according to the described procedure and **55** was obtained in 83% yield over two steps and 98% ee. After isolation, enantio-enriched product was obtained as a clear colorless oil, racemate is obtained as colorless orthorhombic crystals.

MP: 126-127℃

^{1}H NMR (600 MHz, $CDCl_3$) δ 8.00 (d, *J*= 2.53 Hz, 1H), 6.98 (s, 1H), 6.94 (d, *J*= 8.19 Hz, 1H), 6.89 (d, *J* = 8.23 Hz, 1H), 6.81 (dd, *J*= 2.51, 8.33 Hz, 1H), 6.44 (d, *J*= 8.24 Hz, 1H), 3.63 (s, 3H), 3.37 (s, 3H), 3.17 (m, 1H), 2.23 (s, 3H), 1.98 (m, 1H), 1.78 (m, 1H).

^{13}C NMR (151 MHz, $CDCl_3$) δ 173.8, 156.2, 149.6, 148.8, 136.6, 131.9, 129.7, 129.3, 122.3, 110.2, 55.0, 52.6, 34.1, 28.7, 25.3, 20.4, 20.0

HRMS: (+p APCI) calculated for [$C_{18}H_{19}O_3N^{35}Cl$ +] 332.1048, found 332.1046

IR(neat): 1716, 1562, 1501, 1461, 1434, 1348, 1262, 1241, 1158, 1140, 1107, 1029, 972, 905, 808, 732, 671, 548 cm^{-1}

Chiral HPLC: (OD-H, 30 min, 1 mL/min, 1% *i*-PrOH in *n*-hexane, UV 230 nm) RT: 19.46 min, 22.97 min.

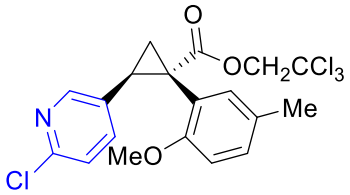

2,2,2-Trichloroethyl (1*S*,2*R*)-2-(6-chloropyridin-3-yl)-1-(2-methoxy-5-methylphenyl)cyclopropane-1-carboxylate (Table 2, **entry 7)**

This compound was prepared according to **General procedure 3.3** from the reaction between **2,2,2-Trichloroethy-1-(2-methoxy-5-methylphenyl)-1-carboxylate** (0.20 mmol, 70 mg) and **14** (5.0 equiv, 1.00 mmol, 140 mg) in in 47% yield and 39% ee (0.09 mmol, 44 mg). After isolation, enantio-enriched product was obtained as a clear colorless oil.

^{1}H NMR (400 MHz, $CDCl_3$) δ 8.04 (d, *J* = 2.5 Hz, 1H), 7.08 – 6.82 (m, 4H), 6.44 (d, *J* = 8.3 Hz, 1H), 4.88 (d, *J* = 11.9 Hz, 1H), 4.57 (d, *J* = 11.9 Hz, 1H), 3.40 (s, 3H), 3.26 (dd, *J* = 9.3, 7.3 Hz, 1H), 2.25 (s, 3H), 2.13 (dd, *J* = 9.3, 5.4 Hz, 1H), 1.92 (dd, *J* = 7.3, 5.4 Hz, 1H).
^{13}C NMR (151 MHz, $CDCl_3$) δ 171.5, 156.1, 149.6, 149.0, 136.8, 131.9, 131.4, 130.0, 129.2, 122.4, 121.2, 109.9, 94.9, 74.4, 54.8, 34.0, 29.2, 20.5, 20.1.
HRMS: (+p APCI) calculated for [$C_{19}H_{18}O_3N^{35}Cl_4$+] 448.0035, found 448.0033
IR(neat): 2925, 1736, 1613, 1587, 1562, 1503, 1462, 1367, 1239, 1138, 1108, 1058, 1034, 978, 911, 805, 767, 726, 572 cm^{-1}
Chiral HPLC: (AD-H, 60 min, 1 mL/min, 0.5 % *i*-PrOH in *n*-hexane, UV 230 nm) RT: 37.07 min, 40.77 min.

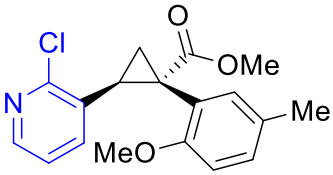

Methyl (1*S*,2*S*)-2-(2-chloropyridin-3-yl)-1-(2-methoxy-5-methylphenyl)cyclopropane-1-carboxylate (58)
This compound was prepared according to **General procedure 3.3, General procedure 3.4,** and **General procedure 3.5** from the reaction between **17** and **54. General procedure 3.3: 54** (0.20 mmol, 44 mg) and **17** (5.0 equiv, 1.00 mmol, 160 mg) in 85% yield and 95% ee (0.17 mmol, 56 mg) **General procedure 3.5: 54** (0.20 mmol, 44 mg) and **17** (1.5 equiv, 0.30 mmol, 42 mg) in 62% yield and 90% ee (0.12 mmol, 41 mg). After isolation, enantio-enriched product was obtained as a white solid.
MP: 143-152℃
^{1}H NMR (600 MHz, $CDCl_3$) δ 8.03 (dd, *J*=1.94, 4.73, 1H), 7.01 (t, *J*=3.70, 1H), 6.93 (d, *J*=8.460, 1H), 6.72 (dd, *J*=4.67, 7.66), 6.47 (d, *J*=1.94, 1H), 6.40 (d, *J*=8.15, 1H), 3.67 (s, 3H), 3.63 (m, 1H), 3.38 (s, 3H), 2.25 (s, 3H), 2.05 (m, 1H), 1.84 (m, 1H)
^{13}C NMR (151 MHz, $CDCl_3$) δ 173.5, 156.4, 153.2, 146.3, 133.8, 132.5, 131.7, 129.5, 128.9, 122.4, 120.8, 109.8, 54.8, 52.6, 34.4, 28.5, 20.4, 19.9.
HRMS: (+p APCI) calculated for [$C_{18}H_{19}O_3N^{35}Cl$ +] 332.1048, found 332.1048
IR(neat): 2919, 1720, 1585, 1557, 1433, 1264, 1244, 1158, 1140, 1034, 910, 800, 733 cm^{-1}
Chiral HPLC: (OD-H, 30 min, 1 mL/min, 1% *i*-PrOH in *n*-hexane, UV 230 nm) RT: 12.44 min, 22.31 min.

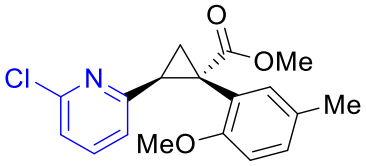

Methyl (1*S*,2*S*)-2-(6-chloropyridin-2-yl)-1-(2-methoxy-5-methylphenyl)cyclopropane-1-carboxylate (59)
This compound was prepared according to **General procedure 3.3, General procedure 3.4,** and **General procedure 3.5** from the reaction between **16** and **54. General procedure 3.3: 54** (0.20 mmol, 44 mg) and **16** (5.0 equiv, 1.00 mmol, 160 mg) in 86% yield and 90% ee (0.17 mmol, 57 mg), **General procedure 3.5: 54** (0.20 mmol, 44 mg) and **16** (1.5 equiv, 0.30 mmol, 42 mg) in 81% yield and >99% ee (0.16 mmol, 54 mg). After isolation, enantio-enriched product was obtained as a white solid.
MP: 114-116℃
^{1}H NMR (400 MHz, $CDCl_3$) δ 7.31 – 7.16 (m, 2H), 7.02 (d, *J* = 2.3 Hz, 1H), 6.91 (ddd, *J* = 7.7, 5.6, 1.3 Hz, 2H), 6.74 (dd, *J* = 7.6, 0.8 Hz, 1H), 6.41 (d, *J* = 8.3 Hz, 1H), 3.64 (s, 3H), 3.44 – 3.31 (buried m under main s, 4H), 2.28 – 2.17 (buried m under main s, 4H), 1.96 (dd, *J* = 8.9, 4.7 Hz, 1H).
^{13}C NMR (151 MHz, $CDCl_3$) δ 173.8, 157.9, 156.3, 149.5, 137.2, 132.6, 129.0, 128.9, 122.7, 121.0, 121.0, 109.6, 55.0, 52.5, 34.8, 32.9 29.7, 20.4
HRMS: (+p APCI) calculated for [$C_{18}H_{19}O_3N^{35}Cl$ +] 332.1048, found 332.1044
IR(neat): 2916, 2849, 1721, 1585, 1557, 1502, 1433, 1376, 1263, 1242, 1158, 1141, 1033, 910, 800, 720 cm^{-1}
Chiral HPLC: (OD-H, 60 min, 1 mL/min, 1% *i*-PrOH in *n*-hexane, UV 230 nm) RT: 22.93 min, 36.26 min.

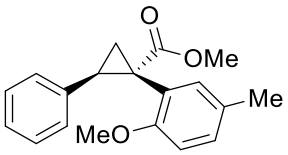

Methyl (1*S*,2*R*)-1-(2-methoxy-5-methylphenyl)-2-phenylcyclopropane-1-carboxylate (60)
This compound was prepared according to **General procedure 3.3** and **General procedure 3.4** from the reaction between **54** and freshly columned styrene. **General procedure 3.3: 54** (0.20 mmol, 44 mg) and styrene (5.0 equiv, 1.00 mmol, 100 mg) in 81% yield and 4% ee (0.16 mmol, 48 mg) **General procedure 3.4: 54** (0.20 mmol, 44 mg) and styrene (5.0 equiv, 0.30 mmol, 100 mg) in the presence of 2-chloropyridine (1.0 equiv, 0.20 mmol, 23 mg) in 95% yield and 95% ee (0.19 mmol, 56 mg). After isolation, enantio-enriched product was obtained as a clear colorless oil. Other coordinating additives gave different levels of enantioselectivity as reported in **section 5.3**.

^{1}H NMR (400 MHz, $CDCl_3$) δ 7.02 (dd, *J* = 5.1, 1.9 Hz, 3H), 6.96 (d, *J* = 2.3 Hz, 1H), 6.94 – 6.86 (m, 1H), 6.83 – 6.71 (m, 2H), 6.43 (d, *J* = 8.2 Hz, 1H), 3.65 (s, 3H), 3.31 (s, 3H), 3.21 (dd, *J* = 9.3, 7.4 Hz, 1H), 2.23 (s, 3H), 1.97 (dd, *J* = 9.3, 4.9 Hz, 1H), 1.82 (dd, *J* = 7.3, 5.0 Hz, 1H).
^{13}C NMR (151 MHz, $CDCl_3$) δ 174.5, 156.9, 136.9, 132.3, 129.0, 128.8, 127.7, 127.7, 127.0, 125.8, 123.5, 110.1, 55.0, 55.0, 52.4, 34.0, 32.4, 20.6, 20.5.
HRMS: (+p APCI) calculated for [$C_{19}H_{20}O_3$+] 296.1407, found 296.1409
IR(neat): 1716, 1502, 1460, 1436, 1410, 1354, 1263, 1244, 1186, 1159, 1144, 1067, 1031, 907, 806, 729, 683, 646, 503 cm^{-1}
Chiral HPLC: (OD-H, 30 min, 1 mL/min, 1% *i*-PrOH in *n*-hexane, UV 230 nm) RT: 10.89 min, 12.80 min. or (AD-H, 30 min, 1 mL/min, 1% *i*-PrOH in *n*-hexane, UV 230 nm) RT: 9.61 min, 11.17 min.

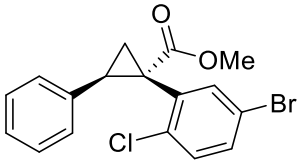

Methyl (1*S*,2*R*)-1-(5-bromo-2-chlorophenyl)-2-phenylcyclopropane-1-carboxylate (62)
This compound was prepared according to **General procedure 3.3** and **General procedure 3.4** from the reaction between **S12** and freshly columned styrene. **General procedure 3.3: S12** (0.20 mmol, 58 mg) and styrene (5.0 equiv, 1.00 mmol, 100 mg) in 76% yield and 64% ee (0.15 mmol, 56 mg) **General procedure 3.4: S12** (0.20 mmol, 58 mg) and styrene (5.0 equiv, 0.30 mmol, 100 mg) in the presence of 2-chloropyridine (1.0 equiv, 0.20 mmol, 23 mg) in 71% yield and 92% ee (0.14 mmol, 52 mg). After isolation, enantio-enriched product was obtained as a clear colorless oil. Other coordinating additives gave different levels of enantioselectivity as reported in the following section.
^{1}H NMR (600 MHz, $CDCl_3$) δ 7.23 (dd, *J*=2.23, 8.46 Hz, 1H), 7.10 (s, 4H), 7.02 (broad s, 1H), 6.86 (m, 2H), 3.68 (s, 3H) 3.32 (m, 1H), 2.10 (broad s, 1H), 1.90 (m, 1H)
^{13}C NMR (151 MHz, $CDCl_3$) δ 172.6, 136.8, 135.5, 134.0, 131.5, 130.6, 127.9, 127.6, 127.6, 119.5, 52.7, 33.3, 33.3, 21.4
HRMS: (+p APCI) calculated for [$C_{17}H_{15}O_2{}^{79}Br^{35}Cl$+] 364.9938, found 364.9932
IR(neat): 3027, 2970, 2949, 1720, 1458, 1433, 1266, 1246, 1208, 1192, 116, 1115, 1085, 1045, 969, 814, 770, 731, 695, 526 cm^{-1}
Chiral HPLC: (OJ-H, 30 min, 1 mL/min, 1% *i*-PrOH in *n*-hexane, UV 230 nm) RT: 9.07 min, 11.82 min

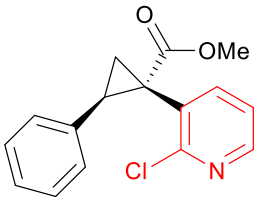

Methyl (1*S*,2*R*)-1-(2-chloropyridin-3-yl)-2-phenylcyclopropane-1-carboxylate (63)
This compound was prepared according to **General procedure 3.3** and **General procedure 3.4** from the reaction between **S20** and freshly columned styrene. **General procedure 3.3: S20** (0.20 mmol, 42 mg) and styrene (5.0 equiv, 1.00 mmol, 100 mg) in 82% yield and 77% ee (0.16 mmol, 47 mg) **General procedure 3.4: S20** (0.20 mmol, 42 mg) and styrene (5.0 equiv, 0.30 mmol, 100 mg) in the presence of 2-chloropyridine (1.0 equiv, 0.20 mmol, 23 mg) in 94% yield and 90% ee (0.19 mmol, 54 mg). After isolation, enantio-enriched product was obtained as a clear crystalline solid.
MP: 115-119℃
^{1}H NMR (600 MHz, $CDCl_3$) δ 8.19 (m, 1H), 7.09 (broad s, 5H), 6.85 (m, 2H), 3.68 (s, 3H), 3.34 (m, 1H), 2.18 (broad s, 1H), 1.92 (dd, *J*= 5.46, 7.59 Hz, 1H)
^{13}C NMR (151 MHz, $CDCl_3$) δ 172,5, 154.3, 148.1, 141.3, 134.9, 130.4, 129.3 128.0, 127.8, 126.9, 121.6, 52.7, 34.1, 33.5, 25.3, 20.0
HRMS: (+p APCI) calculated for [$C_{16}H_{15}O_2N^{35}Cl$ +] 288.0785, found 288.0786
IR(neat): 1720, 1452, 1433, 1397, 1262, 1221, 1163, 1132, 1059, 966, 908, 776, 750, 728, 697, 646, 562 cm^{-1}
Chiral HPLC: (AD-H, 30 min, 1 mL/min, 1% *i*-PrOH in *n*-hexane, UV 230 nm) RT: 20.19 min, 23.41 min.

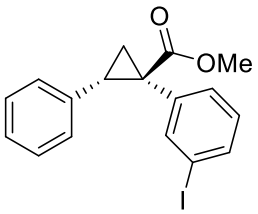

Methyl (1*R*,2*S*)-1-(3-iodophenyl)-2-phenylcyclopropane-1-carboxylate (65)
This compound was prepared according to **General procedure 3.3** and **General procedure 3.4** from the reaction between **S10** and freshly columned styrene. **General procedure 3.3: S10** (0.20 mmol, 60 mg) and styrene (5.0 equiv, 1.00 mmol, 100 mg) in 66% yield and 29% ee (0.13 mmol, 50 mg) **General procedure 3.4: S10** (0.20 mmol, 60 mg) and styrene (5.0

equiv, 0.30 mmol, 100 mg) in the presence of 2-chloropyridine (1.0 equiv, 0.20 mmol, 23 mg) in 80% yield and 41% ee (0.16 mmol, 61 mg). After isolation, product was obtained as a colorless oil.
^{1}H NMR (400 MHz, $CDCl_3$) δ 7.52 – 7.38 (m, 2H), 7.10 (dd, *J* = 5.2, 2.0 Hz, 3H), 6.98 – 6.85 (m, 1H), 6.84 (d, *J* = 7.7 Hz, 1H), 6.82 – 6.72 (m, 2H), 3.67 (s, 3H), 3.11 (dd, *J* = 9.3, 7.3 Hz, 1H), 2.13 (dd, *J* = 9.3, 5.0 Hz, 1H), 1.85 (dd, *J* = 7.4, 5.0 Hz, 1H).
^{13}C NMR (151 MHz, $CDCl_3$) δ 173.6, 140.7, 137.2, 136.1, 135.7, 131.4, 129.2, 128.0, 127.8, 126.6, 93.3, 52.7, 36.7, 33.1, 20.2.
HRMS: (+p APCI) calculated for [$C_{17}H_{16}O_2{}^{127}I$ +] 379.0189, found 379.0184
IR(neat): 1713, 1590, 1559, 1474, 1455, 1431, 1250, 1209, 1190, 1095, 1054, 995, 965, 936, 908, 884, 789, 763, 729, 696, 678, 645, 592, 565 cm^{-1}
Chiral HPLC: (OD-H, 30 min, 1 mL/min, 1% *i*-PrOH in *n*-hexane, UV 230 nm) RT: 8.23 min, 9.27 min.

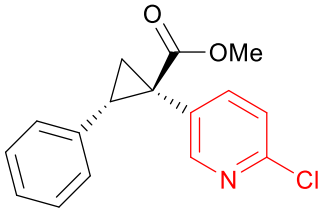

Methyl (1*R*,2*S*)-1-(6-chloropyridin-3-yl)-2-phenylcyclopropane-1-carboxylate (66)
This compound was prepared according to **General procedure 3.3** and **General procedure 3.4** from the reaction between **S4** and freshly columned styrene. **General procedure 3.3: S4** (0.20 mmol, 42 mg) and styrene (5.0 equiv, 1.00 mmol, 100 mg) in 90% yield and 35% ee (0.18 mmol, 52 mg) **General procedure 3.4: S4** (0.20 mmol, 42 mg) and styrene (5.0 equiv, 0.30 mmol, 100 mg) in the presence of 2-chloropyridine (1.0 equiv, 0.20 mmol, 23 mg) in 90% yield and 7% ee (0.18 mmol, 52 mg). After isolation, enantio-enriched product was obtained as a clear colorless oil.
^{1}H NMR (600 MHz, $CDCl_3$) δ 8.08 (dd, J = 2.6, 0.8 Hz, 1H), 7.21 (dd, J = 8.2, 2.5 Hz, 1H), 7.11 (dq, J = 4.5, 2.3 Hz, 3H), 7.05 (dd, J = 8.2, 0.7 Hz, 1H), 6.87 – 6.71 (m, 2H), 3.67 (d, J = 3.5 Hz, 3H), 3.16 (dd, J = 9.3, 7.3 Hz, 1H), 2.21 (dd, J = 9.4, 5.2 Hz, 1H), 1.96 – 1.86 (m, 1H).
^{13}C NMR (151 MHz, $CDCl_3$) δ 173.2, 152.7, 150.2, 142.4, 135.1, 130.3, 128.5, 128.2, 127.3, 123.5, 53.0, 34.3, 33.1, 19.7.
HRMS: (+p APCI) calculated for [$C_{16}H_{15}O_2N^{35}Cl$+] 288.0785, found 288.0786
IR(neat): 2952, 1720, 1588, 1560, 1499, 1463, 1433, 1366, 1261, 1164, 1112, 1022, 965, 779, 742, 719, 696, 559, 485 cm^{-1}
Chiral HPLC: (OD-H, 30 min, 1 mL/min, 1% *i*-PrOH in *n*-hexane, UV 230 nm) RT: 22.14 min, 25.67 min.

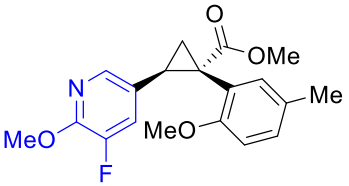

Methyl-(1*S*,2*R*)-2-(5-fluoro-6-methoxypyridin-3-yl)-1-(2-methoxy-5-methylphenyl)cyclopropane-1-carboxylate (67)
This compound was prepared according to **General procedure 3.4,** and **General procedure 3.5** from the reaction between **54** and **18. General procedure 3.4: 54** (0.20 mmol, 44 mg) and **18** (1.5 equiv, 0.30 mmol, 46 mg) in 53% yield and 88% ee (0.16 mmol, 37 mg)**., General procedure 3.5: 54** (0.20 mmol, 44 mg) and **18** (1.5 equiv, 0.30 mmol, 46 mg) in 69% yield and 86% ee (0.16 mmol, 48 mg). After isolation, enantio-enriched product was obtained as a white solid.
MP: 114-116℃
^{1}H NMR (400 MHz, $CDCl_3$) δ 7.57 (s, 1H), 6.98 – 6.91 (m, 2H), 6.65 (dd, *J* = 11.6, 1.9 Hz, 1H), 6.53 – 6.46 (m, 1H), 3.91 (s, 3H), 3.65 (s, 3H), 3.48 (s, 3H), 3.15 (dd, *J* = 9.3, 7.2 Hz, 1H), 2.24 (s, 3H), 1.93 (dd, *J* = 9.3, 5.1 Hz, 1H), 1.74 (dd, *J* = 7.2, 5.2 Hz, 2H).
^{13}C NMR (151 MHz, $CDCl_3$) δ 174.1, 151.5 (d, *J* = 11.3 Hz), 140.6, 140.6, 131.7, 129.5, 129.3, 126.9, 122.2, 122.1, 110.2, 55.0, 53.6, 52.5, 33.5, 29.7, 28.5, 20.5, 19.8.
^{19}F NMR (151 MHz, $CDCl_3$) δ -142.02 (d, *J* = 11.6 Hz)
HRMS: (+p APCI) calculated for [$C_{19}H_{21}O_4NF$ +] 346.1449, found 346.1448
IR(neat): 2948, 2850, 1720, 1616, 1577, 1495, 1440, 1411, 1378, 1296, 1240, 1194, 1161, 1136, 1085, 1016, 965, 906, 808, 778, 726, 647, 631, 560, 513 cm^{-1}
Chiral HPLC: (OD-H, 30 min, 1 mL/min, 1% *i*-PrOH in *n*-hexane, UV 230 nm) RT: 10.90 min, 16.19 min.
.

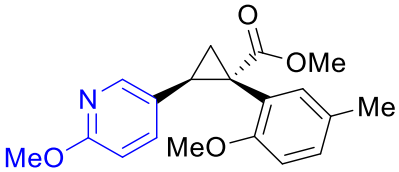

Methyl-(1*S*,2*R*)-1-(2-methoxy-5-methylphenyl)-2-(6-methoxypyridin-3-yl)cyclopropane-1-carboxylate (68)

This compound was prepared according to **General procedure 3.4** and **General procedure 3.5** from the reaction between **15** and **54. General procedure 3.4: 54** (0.20 mmol, 44 mg) and **15** (1.5 equiv, 30 mmol, 46 mg) in 98% yield and 92% ee (0.20 mmol, 64 mg) **General procedure 3.5: 54** (0.20 mmol, 44 mg) and **15** (1.5 equiv, 0.30 mmol, 46 mg) in 66% yield and 90% ee (0.13 mmol, 43 mg). After isolation, enantio-enriched product was obtained as a clear colorless oil.
^{1}H NMR (400 MHz, $CDCl_3$) δ 7.78 (d, *J* = 2.5 Hz, 1H), 6.97 – 6.89 (m, 2H), 6.83 (dd, *J* = 8.6, 2.5 Hz, 1H), 6.46 (d, *J* = 8.1 Hz, 1H), 6.35 (d, *J* = 8.6 Hz, 1H), 3.81 (s, 3H), 3.64 (s, 3H), 3.42 (s, 3H), 3.14 (dd, *J* = 9.3, 7.3 Hz, 1H), 2.23 (s, 3H), 1.92 (dd, *J* = 9.3, 5.1 Hz, 1H), 1.76 (dd, *J* = 7.3, 5.1 Hz, 1H).
^{13}C NMR (151 MHz, $CDCl_3$) δ 174.3, 162.6, 156.5, 146.4, 137.3, 131.9, 129.3, 129.1, 125.3, 123.1, 110.1, 108.9, 55.0, 53.2, 52.5, 33.5, 29.1, 20.5, 19.8.
HRMS: (+p APCI) calculated for [$C_{19}H_{22}O_4N$ +] 328.1543, found 328.1537
IR(neat): 2948, 1716, 1607, 1571, 1496, 1463, 1435, 1399, 1352, 1259, 1242, 1191, 1157, 1143, 1130, 1084, 1029, 971, 907, 827, 808, 769, 726, 608, 588, 550 cm^{-1}
Chiral HPLC: (OD-H, 30 min, 1 mL/min, 1% *i*-PrOH in *n*-hexane, UV 230 nm) RT: 10.74 min, 18.24 min.

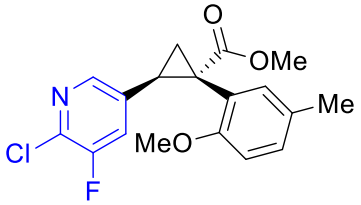

Methyl-(1*S*,2*R*)-2-(6-chloro-5-fluoropyridin-3-yl)-1-(2-methoxy-5-methylphenyl)cyclopropane-1-carboxylate (69)
This compound was prepared according to **General procedure 3.4** and **General procedure 3.5** from the reaction between **19** and **54. General procedure 3.4: 54** (0.20 mmol, 44 mg) and **19** (1.5 equiv, 30 mmol, 47 mg) in 55% yield and 90% ee (0.11 mmol, 38mg) **General procedure 3.5: 54** (0.20 mmol, 44 mg) and **19** (1.5 equiv, 0.30 mmol, 47 mg) in 45% yield and 97% ee (0.09 mmol, 31 mg). After isolation, enantio-enriched product was obtained as a white solid.
MP: 124-127℃
^{1}H NMR (400 MHz, $CDCl_3$) δ 7.87 (d, *J* = 2.0 Hz, 1H), 7.06 – 6.94 (m, 2H), 6.68 (dd, *J* = 9.4, 2.1 Hz, 1H), 6.48 (d, *J* = 8.9 Hz, 1H), 3.65 (s, 3H), 3.43 (s, 3H), 3.21 (dd, *J* = 9.2, 7.1 Hz, 1H), 2.25 (s, 3H), 2.00 (dd, *J* = 9.2, 5.3 Hz, 1H), 1.78 (dd, *J* = 7.1, 5.3 Hz, 1H).
^{13}C NMR (151 MHz, $CDCl_3$) δ 173.6, 156.1, 154.4, 152.7, 144.6 (d, *J* = 5.0 Hz), 135.0 (d, *J* = 3.1 Hz), 131.7, 130.0, 129.5, 122.6 (d, *J* = 19.4 Hz), 122.0, 110.3, 55.0, 52.7, 34.3, 28.2, 20.5, 20.3.
^{19}F NMR (376 MHz, $CDCl_3$) δ -121.30 (d, *J* = 9.4 Hz).
HRMS: (+p APCI) calculated for [$C_{18}H_{18}O_3N^{35}ClF$ +] 350.0953, found 350.0951
IR(neat): 2950 1716, 1501, 1433, 1411, 1379, 1263, 1241, 1210, 1181, 1155, 1142, 1074, 1031, 964, 907, 808, 728, 703, 678, 647, 619, 559, 488 cm^{-1}
Chiral HPLC: (*R*,*R*-Whelk, 60 min, 1 mL/min, 1% *i*-PrOH in *n*-hexane, UV 230 nm) RT: 43.60 min, 52.05 min.

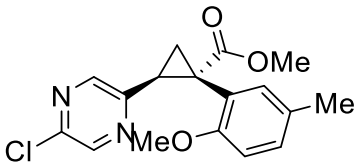

Methyl (1S,2S)-2-(5-chloropyrazin-2-yl)-1-(2-methoxy-5-methylphenyl)cyclopropane-1-carboxylate (70)
This compound was prepared according to **General procedure 3.5** from the reaction between **54** (0.20 mmol, 44 mg) and **2-chloro-5-ethenyl-pyrimidine** (1.5 equiv, 0.30 mmol, 84 mg, Enamine) in 89% yield and 96% ee (0.16 mmol, 59 mg). After isolation, enantio-enriched product was obtained as a viscous colorless oil.
^{1}H NMR (400 MHz, $CDCl_3$) δ 8.20 (d, J = 1.4 Hz, 1H), 8.03 (d, J = 1.4 Hz, 1H), 7.03 (d, J = 2.3 Hz, 1H), 6.96 – 6.91 (m, 1H), 6.39 (d, J = 8.3 Hz, 1H), 3.65 (s, 3H), 3.41 (s, 3H), 3.40 – 3.36 (m, 1H), 2.30 (dd, J = 6.9, 4.5 Hz, 1H), 2.25 (s, 3H), 1.98 (dd, J = 8.8, 4.5 Hz, 1H);
^{13}C NMR (101 MHz, $CDCl_3$) δ 173.6, 155.9, 151.1, 146.2, 144.6, 142.0, 132.7, 129.5, 129.2, 122.3, 109.5, 54.9, 52.7, 35.1, 30.1, 20.5, 19.5;
HRMS (ESI) m/z calculated for [$C_{17}H_{18}ClN_2O_3$+H]+, 333.1000; found 333.1006.
Chiral SFC: (ChiralCel-OD 3 µm column, 3 mL / minute, 5-50% MeOH / CO_2 over 5 min, RT: 0.99 min, 1.13 min.

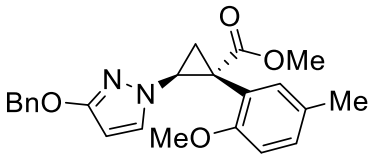

Methyl (1*R*,2*S*)-2-(3-(benzyloxy)-*1H*-pyrazol-1-yl)-1-(2-methoxy-5-methylphenyl)cyclopropane-1-carboxylate (71)
This compound was prepared according to **General procedure 3.5** from the reaction between **54** (0.20 mmol, 44 mg) and **24** (1.5 equiv, 0.30 mmol, 60 mg) in 79% yield and 96% ee (0.16 mmol, 62mg). After isolation, enantio-enriched product was obtained as a viscous colorless oil.

^{1}H NMR (400 MHz, $CDCl_3$) δ 7.39 – 7.25 (m, 5H), 7.03 – 6.93 (m, 2H), 6.88 (d, J = 2.3 Hz, 1H), 6.60 (d, J = 8.3 Hz, 1H), 5.42 (d, J = 2.4 Hz, 1H), 5.06 – 4.88 (m, 2H), 4.49 (dd, J = 8.7, 5.6 Hz, 1H), 3.69 (s, 3H), 3.64 (s, 3H), 2.37 (t, J = 5.8 Hz, 1H), 2.17 (s, 3H), 2.04 (dd, J = 8.7, 6.0 Hz, 1H);
^{13}C NMR (101 MHz, $CDCl_3$) δ 173.0, 162.2, 156.9, 137.3, 131.9, 131.1, 129.4, 129.1, 128.4, 127.8, 127.7, 121.8, 110.0, 91.3, 70.7, 55.3, 52.5, 45.4, 32.5, 20.5, 18.7;
HRMS (ESI) m/z calculated for $[C_{23}H_{25}N_2O_4+H]+$, 393.1809; found 393.1818.
Chiral SFC: (ChiralPak-AD 3 µm column, 3 mL / minute, 5-50% MeOH / CO_2 over 5 min, RT: 1.18 min,1.39 min.

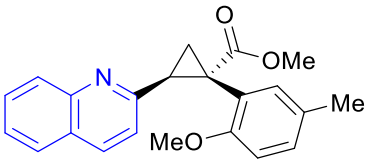

Methyl (1*S*,2*S*)-1-(2-methoxy-5-methylphenyl)-2-(quinolin-2-yl)cyclopropane-1-carboxylate (72)
This compound was prepared according to **General procedure 3.4** from the reaction between **54** (0.20 mmol, 44 mg) and **20** (1.5 equiv, 0.30 mmol, 47 mg) in 78% yield and 96% ee (0.16 mmol, 54mg). After isolation, enantio-enriched product was obtained as a brown solid.
MP: 158-159℃
^{1}H NMR (400 MHz, $CDCl_3$) δ 7.77 (dd, *J* = 8.8, 6.4 Hz, 2H), 7.63 (dd, *J* = 8.1, 1.5 Hz, 1H), 7.54 (ddd, *J* = 8.5, 6.8, 1.5 Hz, 1H), 7.37 (ddd, *J* = 8.1, 6.8, 1.2 Hz, 1H), 7.07 (d, *J* = 2.3 Hz, 1H), 6.94 (d, *J* = 8.5 Hz, 1H), 6.86 – 6.76 (m, 1H), 6.28 (d, *J* = 8.2 Hz, 1H), 3.67 (s, 3H), 3.58 (dd, *J* = 8.9, 7.1 Hz, 1H), 3.25 (s, 3H), 2.42 (dd, *J* = 7.0, 4.5 Hz, 1H), 2.20 (s, 3H), 2.06 (dd, *J* = 8.9, 4.5 Hz, 1H).
^{13}C NMR (151 MHz, $CDCl_3$) δ 174.0, 157.1, 156.5, 134.3, 132.6, 128.9, 128.8, 128.8, 127.1, 126.5, 125.4, 123.2, 121.1, 109.6, 54.9, 52.5, 34.8, 34.2, 20.4, 20.4.
HRMS: (+p APCI) calculated for $[C_{22}H_{22}O_3N +]$ 348.1594, found 348.1594
IR(neat): 2949. 1716, 1600, 1561, 1502, 1463, 1433, 1372, 1297, 1263, 1243, 1213, 1190, 1159, 1142, 1090, 1033, 961, 911, 827, 808, 770, 732, 700, 647, 586, 503 cm^{-1}
Chiral HPLC: (AD-H, 60 min, 1 mL/min, 1% *i*-PrOH in *n*-hexane, UV 230 nm) RT: 20.15 min, 33.06 min.

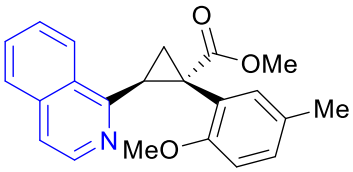

Methyl (1*S*,2*S*)-2-(isoquinolin-1-yl)-1-(2-methoxy-5-methylphenyl)cyclopropane-1-carboxylate (73)
This compound was prepared according to **General procedure 3.4** from the reaction between **54** (0.20 mmol, 44 mg) and **21** (1.5 equiv, 30 mmol, 47 mg) in 84% yield and >99% ee (0.17 mmol, 59 mg). After isolation, enantio-enriched product was obtained as a white solid. In order to resolve enantiomers by chiral UHPLC, the product had to be reduced to the corresponding alcohol. The product (0.16 mmol 57mg) was dissolved in dry THF (1 mL) and LAH (1.5 equiv, 0.25 mmol, 0.25 mL 1.0 M solution in THF) was added dropwise to the stirring solution. The reaction was allowed to stir for 2 h before quenching with excess Na_2SO_4 • 10 H_2O. Quench ran for 30 min. Then the solids were filtered off and the crude residue was evaporated to dryness. The crude residue was dissolved in isopropanol, diluted with hexanes and used directly for UHPLC characterization.
MP: 118-120℃
^{1}H NMR (400 MHz, $CDCl_3$) δ 8.63 – 8.47 (m, 1H), 8.01 (d, *J* = 5.7 Hz, 1H), 7.77 – 7.69 (m, 1H), 7.65 (dq, *J* = 6.8, 4.3 Hz, 2H), 7.27 (s, 2H), 7.07 (d, *J* = 2.2 Hz, 1H), 6.78 (ddd, *J* = 8.2, 2.3, 0.8 Hz, 1H), 6.13 (d, *J* = 8.2 Hz, 1H), 4.18 (dd, *J* = 8.7, 6.9 Hz, 1H), 3.73 (s, 3H), 2.88 (broad s, 1H), 2.81 (s, 3H), 2.21 (s, 3H), 1.97 (dd, *J* = 8.7, 4.2 Hz, 1H).
^{13}C NMR (151 MHz, $CDCl_3$) δ 174.5, 156.0, 155.5, 140.6, 135.5, 132.5, 129.4, 128.8, 128.5 (2 C), 126.7, 126.4, 126.3, 122.8, 118.8, 108.7, 53.9, 52.6, 35.4, 29.9, 20.4, 18.6.
HRMS: (+p APCI) calculated for $[C_{22}H_{22}O_3N +]$ 348.1594, found 348.1593
IR(neat): 3005, 2949, 2833, 1717, 1621, 1585, 1561, 1501, 1461,1435, 1404, 1365, 1271, 1240, 1216, 1171, 1141, 1092, 1032, 992, 971, 908, 871, 822, 807, 727, 683, 647, 618, 582, 529, 505 cm^{-1}
Chiral HPLC: (AD-H, 30 min, 3 mL/min, 3% *i*-PrOH in *n*-hexane, UV 230 nm) RT: 7.98 min, 11.62 min.

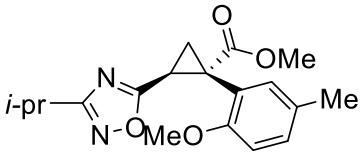

Methyl (1*S*,2*S*)-2-(3-isopropyl-1,2,4-oxadiazol-5-yl)-1-(2-methoxy-5-methylphenyl)cyclopropane-1-carboxylate (74)
This compound was prepared according to **General procedure 3.5** from the reaction between **54** (0.20 mmol, 44 mg) and **22** (1.5 equiv, 0.30 mmol, 42 mg) in 52% yield and >99% ee (0.10 mmol, 34 mg). After isolation, enantio-enriched product was obtained as a viscous colorless oil.

^{1}H NMR (400 MHz, $CDCl_3$) δ 7.01 – 6.97 (m, 2H), 6.54 (d, J = 8.8 Hz, 1H), 3.66 (s, 3H), 3.54 (s, 3H), 3.40 (dd, J = 9.0, 6.9 Hz, 1H), 2.84 (hept, J = 6.9 Hz, 1H), 2.24 (d, J = 0.7 Hz, 3H), 2.17 (dd, J = 6.8, 4.8 Hz, 1H), 2.11 (dd, J = 9.0, 4.8 Hz, 1H), 1.07 (dd, J = 11.2, 6.9 Hz, 6H);
^{13}C NMR (101 MHz, $CDCl_3$) δ 176.4, 174.4, 172.6, 156.5, 132.2, 129.7, 129.2, 122.1, 109.8, 55.2, 52.9, 34.5, 26.4, 23.0, 21.1, 20.6, 20.4, 20.0;
HRMS (ESI) m/z calculated for $[C_{18}H_{23}N_2O_4+H]+$, 331.1652; found 331.1659.
Chiral SFC: (ChiralPak-IB N-3 3µm column, 3 mL / minute, 5-30% *i*PrOH / CO_2 with DEA additive over 5 min, RT: 1.39 min, 1.75 min.

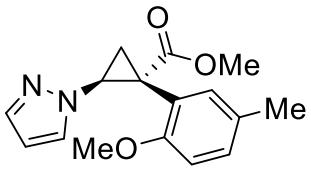

Methyl (1*R*,2*S*)-1-(2-methoxy-5-methylphenyl)-2-(*1H*-pyrazol-1-yl)cyclopropane-1-carboxylate (75)
This compound was prepared according to **General procedure 3.5** from the reaction between **54** (0.20 mmol, 44 mg) and ***N*-vinylpyrazole** (1.5 equiv, 0.30 mmol, 28 mg, Enamine) in 82% yield and 96% ee (0.16 mmol, 47 mg). After isolation, enantio-enriched product was obtained as a viscous colorless oil.
^{1}H NMR (400 MHz, $CDCl_3$) δ 7.22 (ddd, J = 3.9, 2.1, 0.7 Hz, 2H), 6.94 (dtd, J = 8.3, 1.4, 0.7 Hz, 1H), 6.85 – 6.80 (m, 1H), 6.57 (d, J = 8.3 Hz, 1H), 5.99 (dd, J = 2.4, 1.8 Hz, 1H), 4.65 (dd, J = 8.7, 5.6 Hz, 1H), 3.69 (s, 3H), 3.65 (d, J = 0.5 Hz, 3H), 2.50 (t, J = 5.8 Hz, 1H), 2.16 (t, J = 0.7 Hz, 3H), 2.08 (dd, J = 8.7, 6.0 Hz, 1H);
^{13}C NMR (101 MHz, $CDCl_3$) δ 172.9, 156.7, 138.4, 131.7, 129.9, 129.5, 129.3, 121.5, 109.9, 105.5, 55.2, 52.5, 45.1, 32.6, 20.4, 18.7;
HRMS (ESI) m/z calculated for $[C_{16}H_{19}N_2O_3 +H]+$, 287.1390; found 287.1395.
Chiral SFC: (Lux i-Cellulose-5 (IC) column, 3 mL / minute, 5-50% MeOH / CO_2 over 5 min, RT: 1.40 min, 1.56 min.

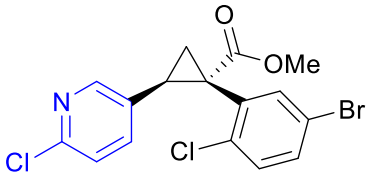

Methyl (1*S*,2*R*)-1-(5-bromo-2-chlorophenyl)-2-(6-chloropyridin-3-yl)cyclopropane-1-carboxylate (76)
This compound was prepared according to **General procedure 3.4** from the reaction between **S12** (0.20 mmol, 58 mg) and **14** (1.5 equiv, 0.30 mmol, 42 mg) in 98% yield and 93% ee (0.20 mmol, 78 mg). After isolation, enantio-enriched product was obtained as a white solid.
MP: 96-99℃
^{1}H NMR (400 MHz, $CDCl_3$) δ 8.07 – 7.91 (s, 1H), 7.52 (s, 1H), 7.32 (dd, *J* = 8.5, 2.4 Hz, 1H), 7.11 – 7.00 (m, 2H), 6.96 (dd, *J* = 8.3, 2.2 Hz, 1H), 3.71 (s, 3H), 3.33 (t, *J* = 7.9 Hz, 1H), 2.14 (s, 1H), 1.90 (dd, *J* = 7.3, 5.5 Hz, 1H).
^{13}C NMR (151 MHz, $CDCl_3$) δ 171.9, 149.7, 149.3, 137.0, 135.8, 135.0, 134.6, 132.4, 131.0, 130.2, 122.9, 120.2, 53.0, 36.7, 29.6, 20.8.
HRMS: (+p APCI) calculated for $[C_{16}H_{13}O_2N^{79}Br^{35}Cl_2 +]$ 399.9501 found 399.9501
IR(neat): 3016, 2951, 1722, 1586, 1560, 1465, 1434, 1365, 1350, 1270, 1248, 1208, 1166, 1141, 1114, 1045, 1024, 970, 909, 892, 815, 741, 730, 647, 634, 533 cm^{-1}
Chiral HPLC: (OD-H, 60 min, 1 mL/min, 1% *i*-PrOH in *n*-hexane, UV 230 nm) RT: 26.38 min, 29.94 min.

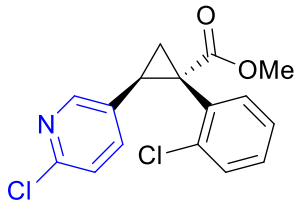

Methyl (1*S*,2*R*)-1-(2-chlorophenyl)-2-(6-chloropyridin-3-yl)cyclopropane-1-carboxylate (77)
This compound was prepared according to **General procedure 3.4** from the reaction between **S5** (0.20 mmol, 42 mg) and **14** (1.5 equiv, 0.30 mmol, 42 mg) in 75% yield and 92% ee (0.15 mmol, 49 mg). After isolation, enantio-enriched product was obtained as a clear colorless oil.
^{1}H NMR (400 MHz, $CDCl_3$) δ 7.98 (d, *J* = 2.5 Hz, 1H), 7.49 – 7.27 (m, 1H), 7.25 – 7.12 (m, 3H), 6.94 (d, *J* = 8.3 Hz, 1H), 6.87 (dd, *J* = 8.3, 2.6 Hz, 1H), 3.68 (s, 3H), 3.30 (t, *J* = 8.4 Hz, 1H), 2.11 (t, *J* = 8.2 Hz, 1H), 1.89 (dd, *J* = 7.3, 5.4 Hz, 1H).
^{13}C NMR (151 MHz, $CDCl_3$) δ 172.8, 149.6, 149.7, 137.2, 137.1, 132.5, 130.9, 129.9, 129.6, 126.9, 123.0, 53.1, 37.0, 29.7
HRMS: (+p APCI) calculated for $[C_{16}H_{14}O_2N^{35}Cl_2+]$ 322.0396, found 322.0399
IR(neat): 2923, 2852, 1720, 1586, 1561, 1464, 1434, 1397, 1348, 1269, 1250, 1208, 1165, 1143, 1110, 1034, 1023, 992, 968, 909, 885, 833, 802, 780, 741, 699, 660, 647, 586, 518, 470, 434 cm^{-1}
Chiral HPLC: (OD-H, 60 min, 1 mL/min, 1% *i*-PrOH in *n*-hexane, UV 230 nm) RT: 28.71 min, 32.79 min

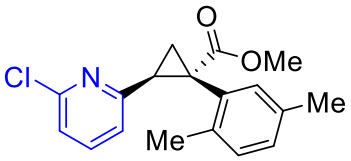

Methyl (1*S*,2*S*)-2-(6-chloropyridin-2-yl)-1-(2,5-dimethylphenyl)cyclopropane-1-carboxylate (78)
This compound was prepared according to **General procedure 3.5: S11** (0.20 mmol, 41 mg) and **16** (1.5 equiv, 0.30 mmol, 42 mg) in 74% yield and >99% ee (0.15 mmol, 47 mg). After isolation, enantio-enriched product was obtained as a clear colorless oil.
^{1}H NMR (500 MHz, $CDCl_3$) δ 7.29 – 7.05 (m, 2H), 6.97 (d, J = 7.8 Hz, 1H), 6.93 – 6.86 (m, 1H), 6.80 (s, 1H), 6.50 (d, J = 7.1 Hz, 1H), 3.66 (s, 3H), 3.46 – 3.32 (m, 1H), 2.48 – 1.82 (m, 8H);
^{13}C NMR (101 MHz, $CDCl_3$) δ 173.5, 157.6, 149.8, 137.7, 136.0, 134.6, 132.2, 129.6, 128.3, 121.4, 120.2, 52.6, 33.8, 21.7, 20.9, 18.8;
HRMS (ESI) m/z calculated for $C_{18}H_{19}ClNO_2$ [M+H]+, 316.1104; found 316.1097.
Chiral SFC: (ChiralPakIC column, 3 mL / minute, 5-30% MeOH / CO_2 over 10 min, RT: 2.15 min, 2.57 min.

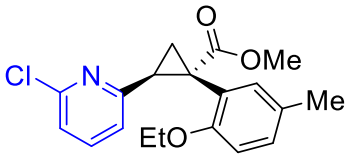

Methyl (1*S*,2*S*)-2-(6-chloropyridin-2-yl)-1-(2-ethoxy-5-methylphenyl)cyclopropane-1-carboxylate (79)
This compound was prepared according to **General procedure 3.5: S21** (0.20 mmol, 47 mg) and **16** (1.5 equiv, 0.30 mmol, 42 mg) in 82% yield and 99% ee (0.16 mmol, 56 mg). After isolation, enantio-enriched product was obtained as a clear colorless oil.
^{1}H NMR (500 MHz, $CDCl_3$) δ 7.25 (t, J = 7.8 Hz, 1H), 7.01 (d, J = 2.4 Hz, 1H), 6.92 – 6.87 (m, 2H), 6.70 (dd, J = 7.8, 0.8 Hz, 1H), 6.40 (d, J = 8.2 Hz, 1H), 3.79 (dq, J = 8.7, 7.0 Hz, 1H), 3.64 (s, 3H), 3.41 (ddd, J = 15.9, 9.1, 7.0 Hz, 2H), 2.27 – 2.20 (m, 4H), 1.94 (dd, J = 8.9, 4.8 Hz, 1H), 1.24 (t, J = 7.0 Hz, 3H);
^{13}C NMR (101 MHz, $CDCl_3$) δ 173.9, 158.0, 155.7, 149.4, 137.3, 132.5, 129.0, 128.7, 122.6, 121.0, 120.9, 110.1, 62.9, 52.4, 34.9, 32.8, 20.4, 20.1, 14.7;
HRMS (ESI) m/z calculated for $C_{19}H_{21}ClNO_3$ [M+H]+, 346.1215; found 346.1208.
Chiral SFC: (ChiralPakIC column, 3 mL / minute, 5-30% MeOH / CO_2 over 10 min, RT: 2.63 min, 2.96 min.

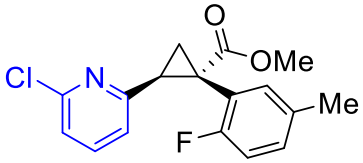

Methyl (1*S*,2*S*)-2-(6-chloropyridin-2-yl)-1-(2-fluoro-5-methylphenyl)cyclopropane-1-carboxylate (80)
This compound was prepared according to **General procedure 3.5: S22** (0.20 mmol, 42 mg) and **16** (1.5 equiv, 0.30 mmol, 42 mg) in 81% yield and >99% ee (0.16 mmol, 52 mg). After isolation, enantio-enriched product was obtained as a clear colorless oil.
^{1}H NMR (500 MHz, $CDCl_3$) δ 7.37 (t, J = 7.8 Hz, 1H), 7.02 – 6.93 (m, 3H), 6.93 – 6.88 (m, 1H), 6.62 (dd, J = 9.9, 8.3 Hz, 1H), 3.68 (s, 3H), 3.34 (dd, J = 8.9, 7.0 Hz, 1H), 2.35 (dd, J = 7.0, 4.7 Hz, 1H), 2.24 (d, J = 1.0 Hz, 3H), 2.06 (dd, J = 8.9, 4.7 Hz, 1H); **^{13}C NMR** (101 MHz, $CDCl_3$) δ 173.0, 161.5, 159.1, 156.8, 149.9, 138.0, 133.1 (d, *J* = 3.7 Hz), 129.6 (d, *J* = 8.1 Hz),121.9, 121.6, 114.3, 114.1, 52.8, 33.6, 33.1, 20.5, 19.5.
^{19}F NMR (376 MHz, $CDCl_3$) δ -119.37 (dt, *J* = 10.9, 6.0 Hz).
HRMS (ESI) m/z calculated for $C_{17}H_{16}ClFNO_2$ [M+H]+, 320.0859; found 320.0857.
Chiral SFC: ChiralPak-IB column, 3 mL / minute, 5-50% MeOH / CO_2 over 10 min, RT: 0.96 min, 1.07 min.

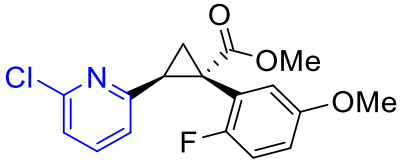

Methyl (1*S*,2*S*)-2-(6-chloropyridin-2-yl)-1-(2-fluoro-5-methoxyphenyl)cyclopropane-1-carboxylate (81)
This compound was prepared according to **General procedure 3.5: S23** (0.20 mmol, 45 mg) and **16**(1.5 equiv, 0.30 mmol, 42 mg) in 71% yield and >99% ee (0.14 mmol, 48 mg). After isolation, enantio-enriched product was obtained as a white solid.
^{1}H NMR (400 MHz, $CDCl_3$) δ 7.38 (t, J = 7.7 Hz, 1H), 7.02 6.93 (m, 2H), 6.72 – 6.59 (m, 3H), 3.70 (s, 3H), 3.69 (s, 3H), 3.34 (dd, J = 9.0, 7.0 Hz, 1H), 2.34 (dd, J = 7.0, 4.7 Hz, 1H), 2.07 (dd, J = 8.9, 4.7 Hz, 1H);
^{13}C NMR (101 MHz, $CDCl_3$) δ 172.7, 157.8, 156.7, 155.5, 155.0 (d, *J* = 2.0 Hz), 150.0, 138.0, 121.9, 121.6, 117.6 (d, *J* = 3.7 Hz), 115.2, 114.9, 114.5 (d, *J* = 8.2 Hz), 55.8, 52.7, 33.3, 19.7.

^{19}F NMR (376 MHz, $CDCl_3$) δ -124.68 (dt, *J* = 8.6, 5.5 Hz).
HRMS (ESI) m/z calculated for [$C_{17}H_{16}ClFNO_3$ +H]+, 336.0808; found 336.0808.
Chiral SFC: Lux i-Cellulose column, 3 mL / minute, 5-25% IPA / CO_2 over 10 min, RT: 2.08 min, 2.40 min.

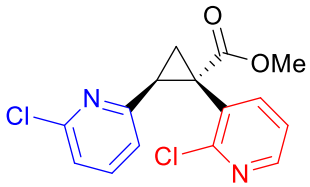

Methyl (1*S*,2*S*)-2-(6-chloropyridin-2-yl)-1-(2-chloropyridin-3-yl)cyclopropane-1-carboxylate (82)
This compound was prepared according to **General procedure 3.4** from the reaction between **S20** (0.20 mmol, 42 mg) and **16** (1.5 equiv, 30 mmol, 42 mg) in 87% yield and 85% ee (0.17 mmol, 56 mg). After isolation, enantio-enriched product was obtained as a clear colorless oil.
^{1}H NMR (400 MHz, $CDCl_3$) δ 8.21 (ddd, *J* = 10.3, 4.9, 1.9 Hz, 2H), 7.32 (broad s, 1H), 7.03 (broad s, 1H), 6.88 (broad s, 1H), 6.65 (broad s, 1H), 3.72 (s, 3H), 3.65 (broad s, 1H), 2.33 (broad s, 1H), 1.90 (dd, *J* = 7.8, 5.7 Hz, 1H).
^{13}C NMR (151 MHz, $CDCl_3$) δ 171.7, 154.1, 153.4, 148.6 (2 C), 147.8, 141.6, 129.6, 121.9 (2 C), 121.7, 53.1, 29.6, 25.3, 20.9.
HRMS: (+p APCI) calculated for [$C_{15}H_{13}O_2N_2{}^{35}Cl_2$+] 323.0348, found 323.0340
IR(neat): 1724, 1563, 1436, 1411, 1398, 1357, 1268, 1220, 1196, 1166, 1132, 1063, 756, 732, 682cm^{-1}
Chiral HPLC: (AD-H, 30 min, 1 mL/min, 1% *i*-PrOH in *n*-hexane, UV 230 nm) RT: 10.65 min, 11.71 min.

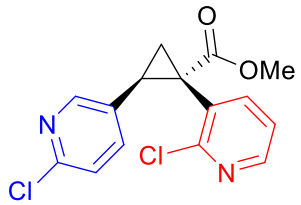

Methyl (1*S*,2*R*)-1-(2-chloropyridin-3-yl)-2-(6-chloropyridin-3-yl)cyclopropane-1-carboxylate (83)
This compound was prepared according to **General procedure 3.4** from the reaction between **S20** (0.20 mmol, 42 mg) and **14** (1.5 equiv, 30 mmol, 42 mg) in 79% yield and 84% ee (0.16 mmol, 51 mg). After isolation, enantio-enriched product was obtained as a clear colorless oil.
^{1}H NMR (600 MHz, $CDCl_3$) δ 8.27 (s, 1H), 7.98 (s, 1H), 7.19 (s, 1H), 7.03 (s, 3 H), 3.70 (s, 3H), 3.36 (m, 1 H), 2.18 (broad S, 1H), 1.69 (broad s, 1H)
^{13}C NMR (151 MHz, $CDCl_3$) δ 171.7, 153.9, 149.9, 149.1, 148.8, 137.5, 129.4, 123.1, 122.1, 53.0, 36.0, 29.6, 29.6, 25.3
HRMS: (+p APCI) calculated for [$C_{15}H_{13}O_2N_2{}^{35}Cl_2$+] 323.0348, found 323.0349
IR(neat): 3016, 2970, 2950, 1721, 1562, 1464, 1434, 1397, 1348, 1265, 1221, 1165, 1132, 1108, 1058, 1023, 967, 911, 835, 801, 779, 754, 728, 659, 647, 633, 437 cm^{-1}
Chiral HPLC: (AD-H, 60 min, 1 mL/min, 1% *i*-PrOH in *n*-hexane, UV 230 nm) RT: 29.56 min, 34.74 min.

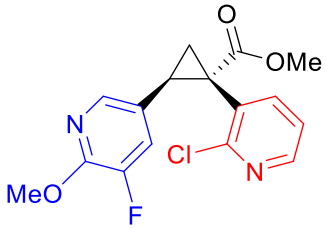

Methyl (1*S*,2*R*)-1-(2-chloropyridin-3-yl)-2-(5-fluoro-6-methoxypyridin-3-yl)cyclopropane-1-carboxylate (84)
This compound was prepared according to **General procedure 3.4** from the reaction between **S20** (0.20 mmol, 42 mg) and **18** (1.5 equiv, 30 mmol, 46 mg) in 74% yield and 72% ee (0.15 mmol, 50 mg). After isolation, enantio-enriched product was obtained as clear colorless oil.
^{1}H NMR (400 MHz, $CDCl_3$) δ 8.25 (dd, *J* = 4.8, 1.9 Hz, 1H), 7.58 (d, *J* = 2.1 Hz, 1H), 7.48 (d, *J* = 48.6 Hz, 1H), 7.17 (s, 1H), 6.67 (dd, *J* = 11.2, 2.1 Hz, 1H), 3.92 (s, 3H), 3.69 (s, 3H), 3.31 (t, *J* = 8.4 Hz, 1H), 2.14 (s, 1H), 1.81 (dd, *J* = 7.4, 5.6 Hz, 1H).
^{13}C NMR (151 MHz, $CDCl_3$) δ 172.0, 154.0, 152.3 (d, *J* = 11.5 Hz), 148.6, 147.4, 145.7, 140.8 (d, *J* = 5.7 Hz), 129.8, 124.5, 122.1, 122.0, 121.9, 53.7, 52.9, 35.6, 29.7.
^{19}F NMR (376 MHz, $CDCl_3$) δ -140.38 (d, *J* = 11.2 Hz).
HRMS: (+p APCI) calculated for [$C_{16}H_{15}O_3N_2{}^{35}ClF$ +] 337.0749, found 337.0747
IR(neat): 2952, 1720, 1617, 1579, 1564, 1496, 1437, 1413, 1398, 1264, 1219, 1196, 1169, 1140, 1059, 959, 909, 776, 751, 731, 654, 564, 503 cm^{-1}
Chiral HPLC: (AD-H, 80 min, 1 mL/min, 1% *i*-PrOH in *n*-hexane, UV 230 nm) RT: 40.39 min, 66.59 min

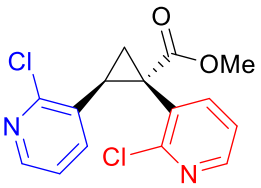

Methyl (1*S*,2*S*)-1,2-bis(2-chloropyridin-3-yl)cyclopropane-1-carboxylate (85)
This compound was prepared according to **General procedure 3.4** from the reaction between **S20** (0.20 mmol, 42 mg) and **17** (1.5 equiv, 30 mmol, 42 mg) in 65% yield and 95% ee (0.13 mmol, 42 mg). After isolation, enantio-enriched product was obtained as a clear colorless oil.
^{1}H NMR (400 MHz, $CDCl_3$) δ 8.20 (dd, *J* = 4.8, 1.9 Hz, 1H), 7.77 (s, 1H), 7.43 (t, *J* = 7.7 Hz, 1H), 7.20 (broad s, 1H), 6.94 (d, *J* = 7.9 Hz, 1H), 3.69 (s, 3H), 3.49 – 3.40 (m, 1H), 2.44 (broad s, 1H), 2.05 (broad s, 1H).
^{13}C NMR (151 MHz, $CDCl_3$) δ 172.1, 155.7, 153.3, 149.9, 148.1, 141.8, 138.1, 130.1, 123.6, 121.8, 52.9, 37.0, 33.0, 29.7, 22.7, 20.9.
HRMS: (+p APCI) calculated for $[C_{15}H_{13}O_2N_2{}^{35}Cl_2+]$ 323.0348, found 323.0346
IR(neat): 1722, 1583, 1558, 1434, 1398, 1377, 1265, 1220, 1162, 1132, 1096, 1058, 991, 941, 910, 810, 796, 770, 752, 730, 714, 654 cm^{-1}
Chiral HPLC: (AD-H, 30 min, 1 mL/min, 1% *i*-PrOH in *n*-hexane, UV 230 nm) RT: 22.81 min, 24.16 min.

5. Determination of enantioselectivity

5.1: Diastereoselectivity of *R*-pantolactonate cyclopropanes.

Diastereoselectivity of these products was determined through analysis of the crude cyclopropanation products via ^{1}H NMR. The reaction has the potential to form 4 stereoisomers. 2 arise from the enantiocontrol of the pantolactonate, and 2 arise from the cis/trans diastereoselectivity inherent to donor-acceptor rhodium carbenes. In-order to resolve the identity of these stereoisomers, a control experiment may be performed in the presence of a chiral catalyst. One of the isomers of the chiral catalyst will oppose the enantioselectivity imparted by the pantolactonate, leading to increased production of the minor-stereoisomer that would arise from imperfect enantiocontrol by the pantolactonate. However, due to the inherent cis/trans diastereoselectivity of donor/acceptor carbenes, the ratio of cis/trans stereoisomers is not affected. By comparing distinctive peaks in the stereo-scrambled product to the crude reaction mixture of the chiral reaction the asymmetric induction of the chiral-auxiliary reaction may be determined unambiguously (**Figure B4**).

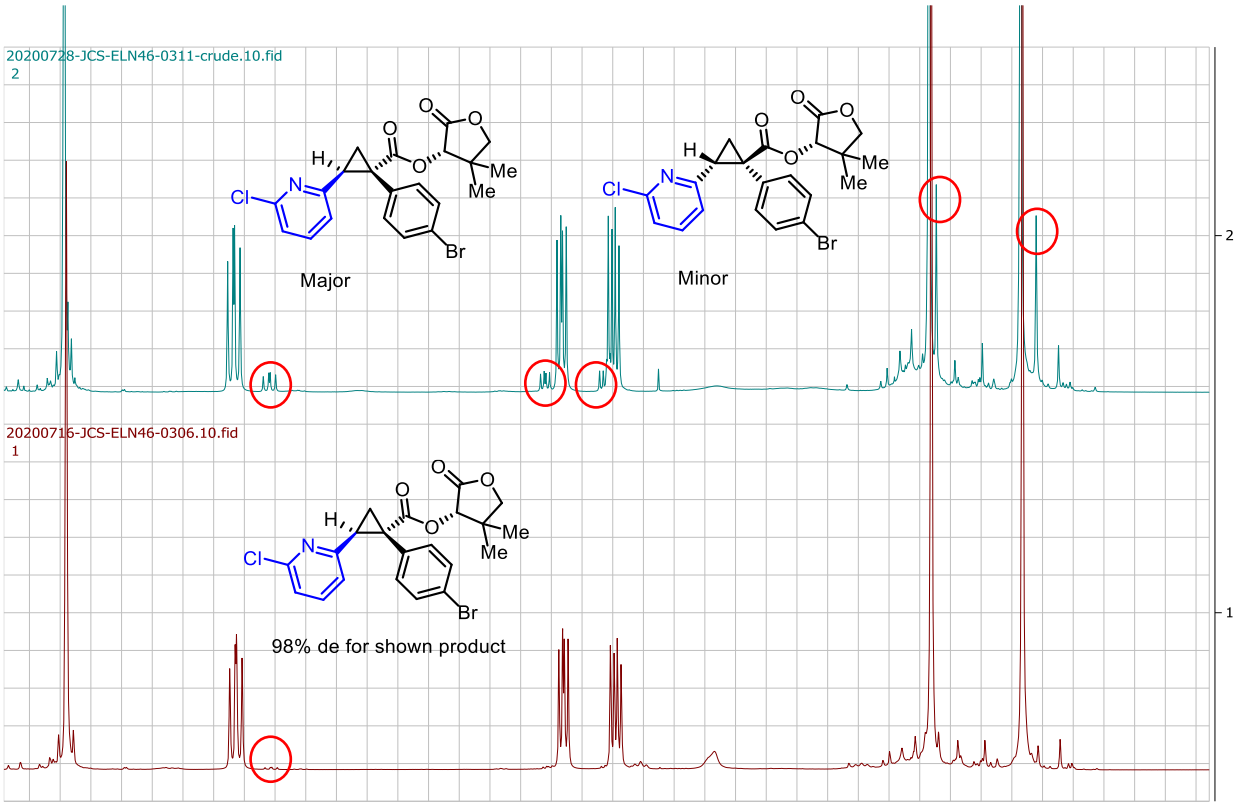

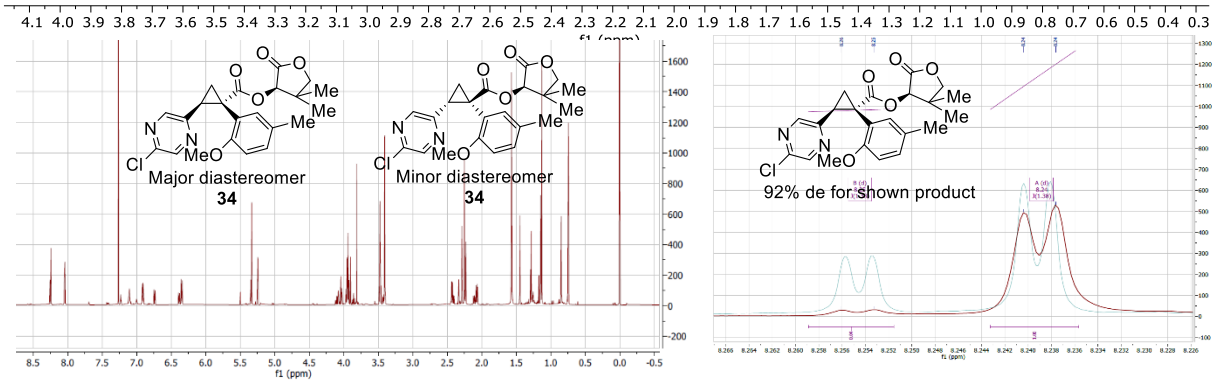

Figure B4a. Determination of diastereomeric excess of compound **26** based on identification of peaks in the reaction crude (Red) corresponding to the minor stereo-isomer due to imperfect enantiocontrol. The benzylic cyclopropyl proton gives the clearest determination of %de due to its separation from the major stereoisomer in the crude spectrum. Regardless several characteristic peaks of the minor stereoisomer are observed in the stereo-scrambled product (Blue) as circled in red. The scrambled product was obtained from the reaction between **S17** and **16** in the presence of a 1:1 mixture of Rh_2(*S*-DOSP)$_4$ and Rh_2(*R*-DOSP)$_4$ (1.0 mol % total catalyst loading), in CH_2Cl_2 at rt for 24hr. Diastereomeric excess is determined by subtracting the integration of the minor stereoisomer from the normalized integration of the major stereoisomer. **B4b.** For compounds bearing an *ortho*-substituent, comparison of protons in the aryl region corresponding to the azaheterocycle may be used for determination of diastereomeric excess due to the lack of surrounding clutter. Diastereo-scrambled products were prepared using blue-light to generate the carbene in absence of a chiral environment, the example shown is **34** from the reaction between **S18** and **2-chloro-5-ethenyl-pyrimidine** (Enamine) in CH_2Cl_2 under blue light irradiation at rt for 24hr.

5.1.1: Crude ^{1}H NMRs of *R*-pantolactonate cyclopropanes for %d.e determination:

Compound 25

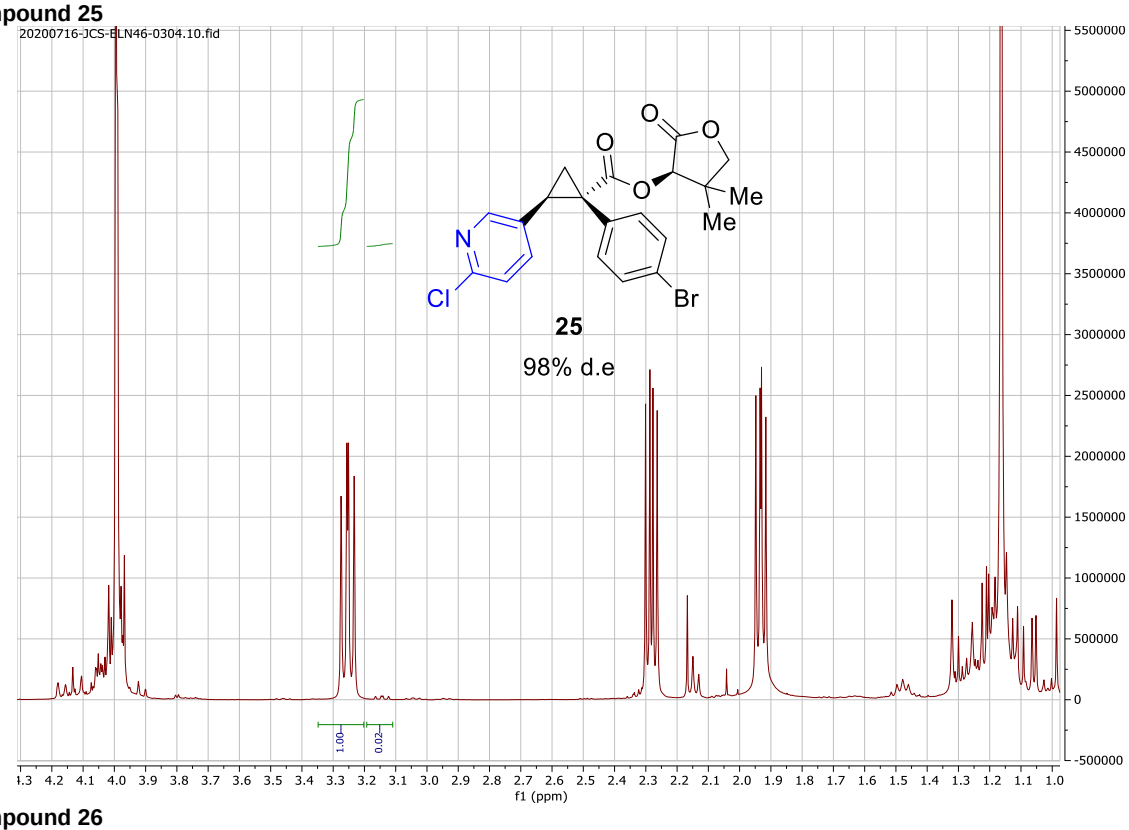

Compound 26

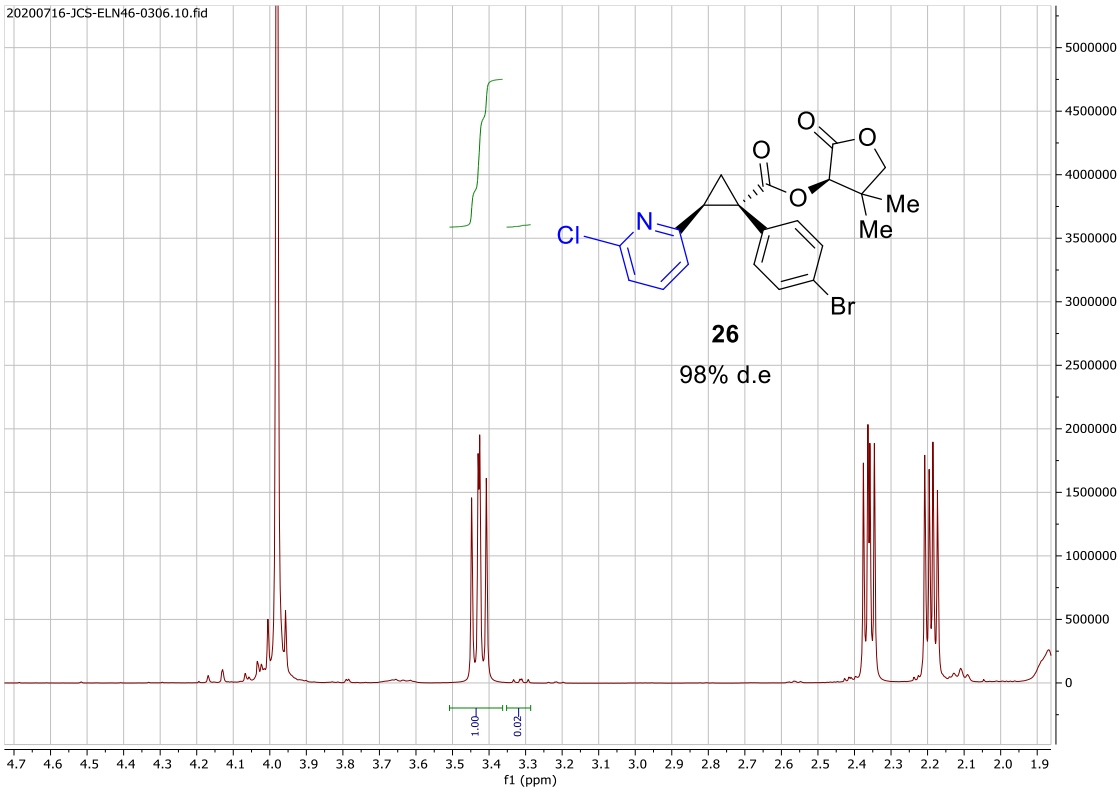

Compound 27

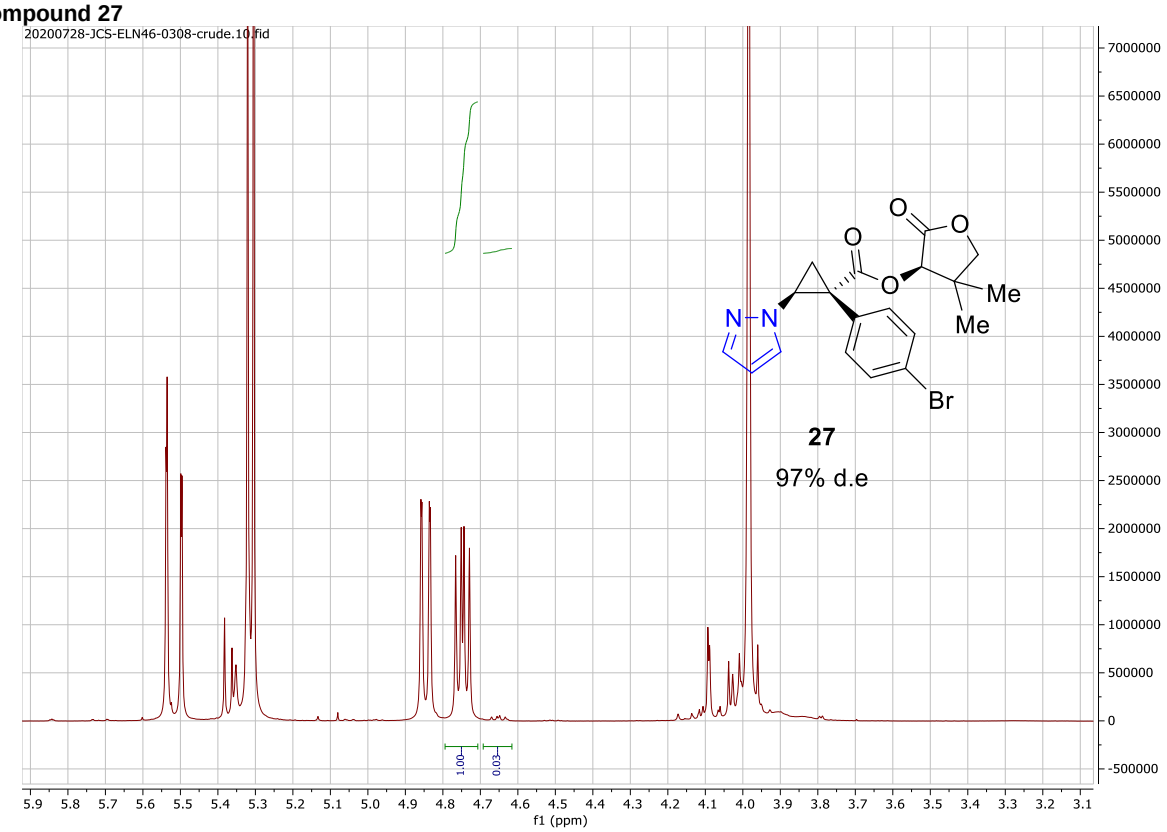

Compound 28

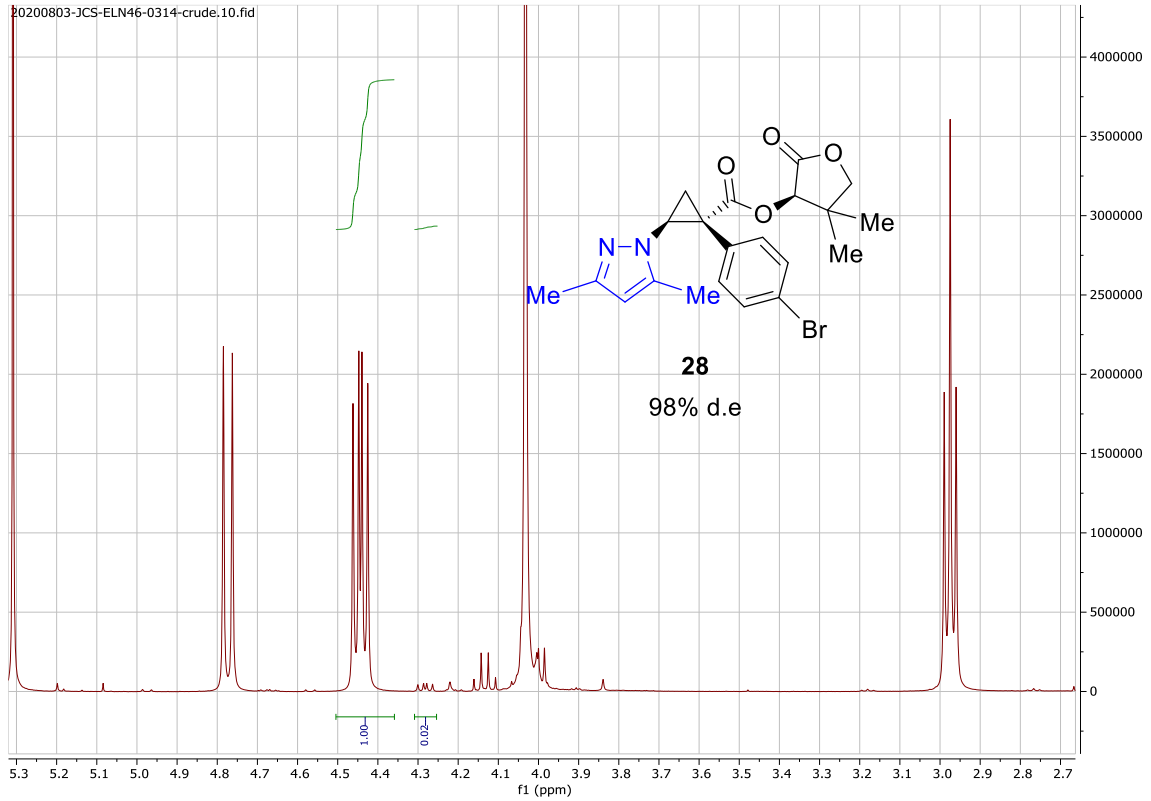

Compound 29:

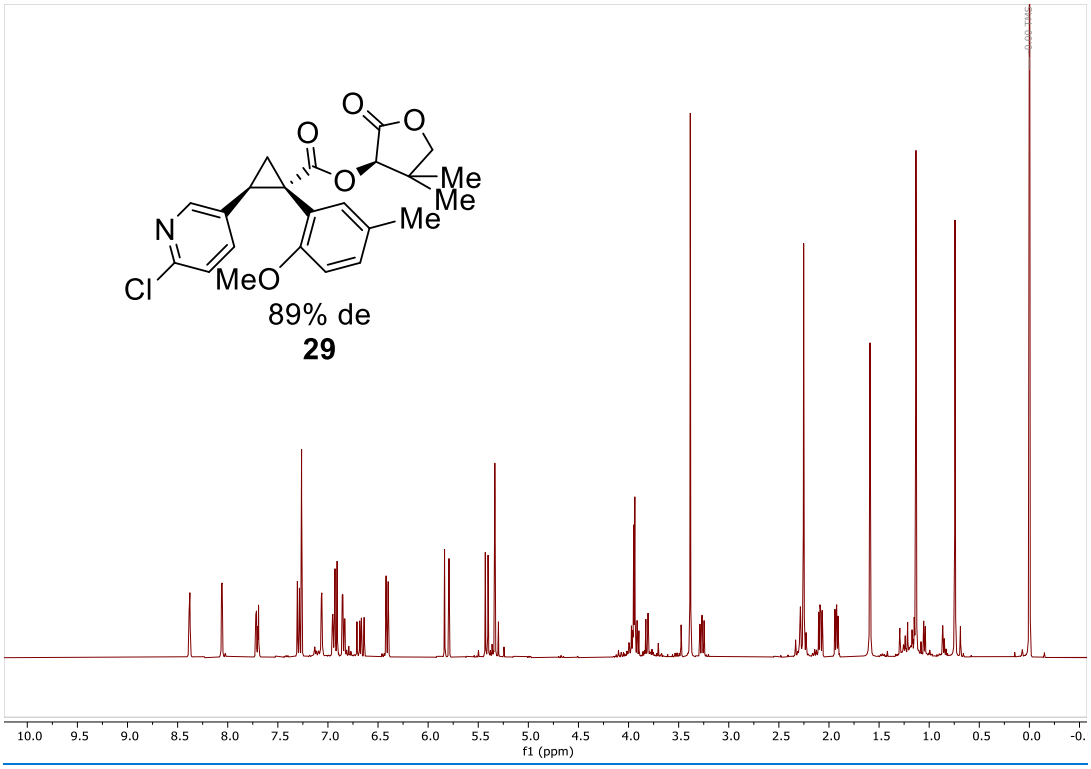

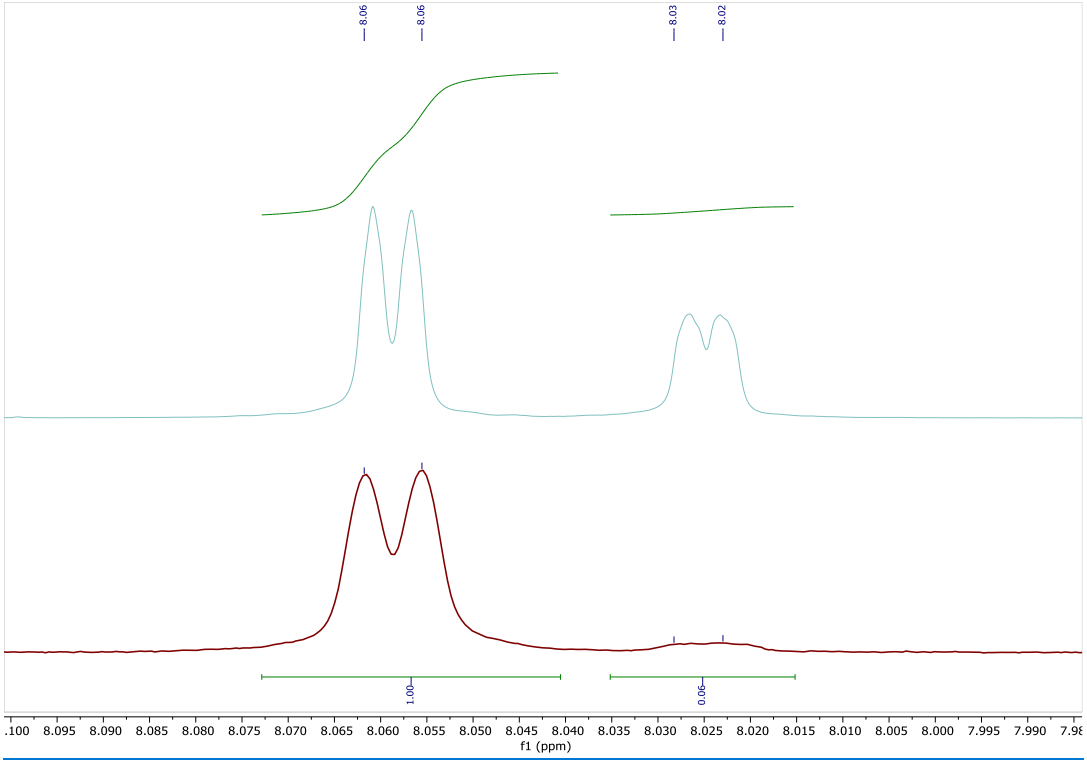

Compound 30:

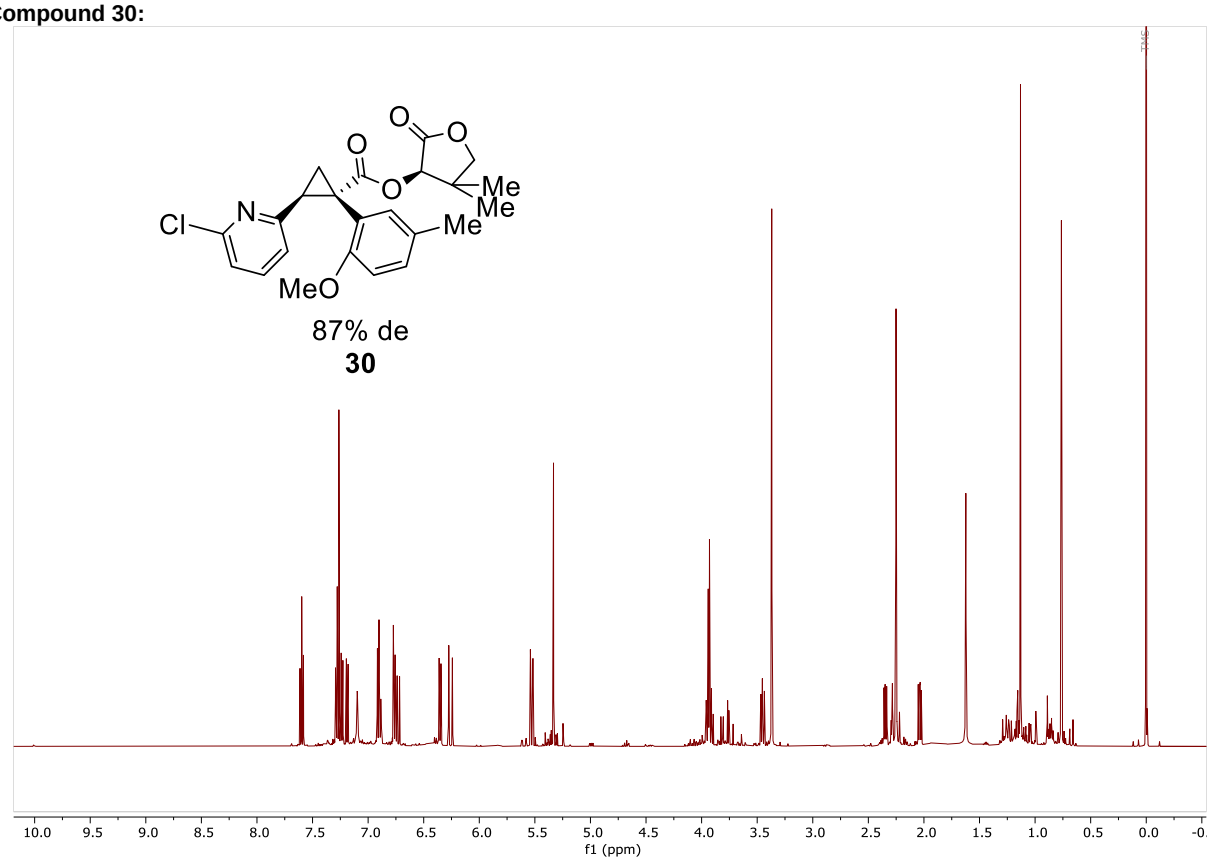

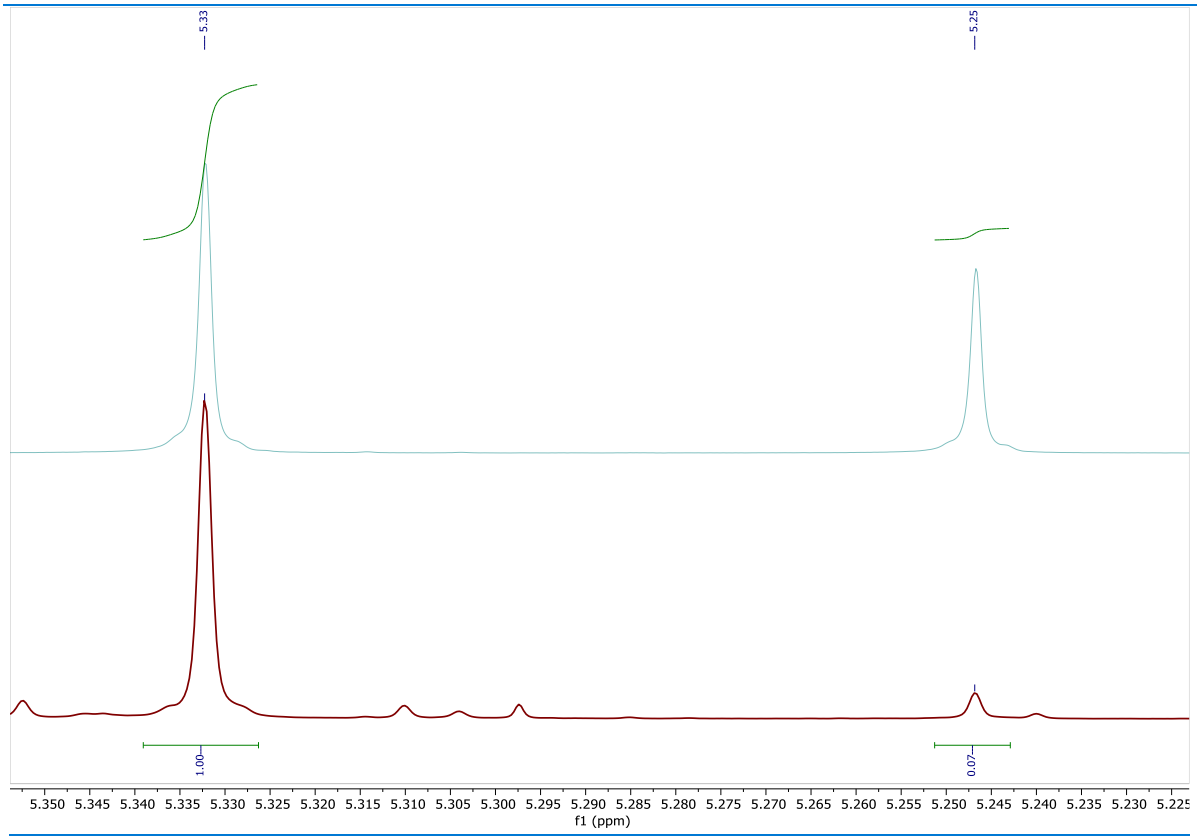

Compound 32:

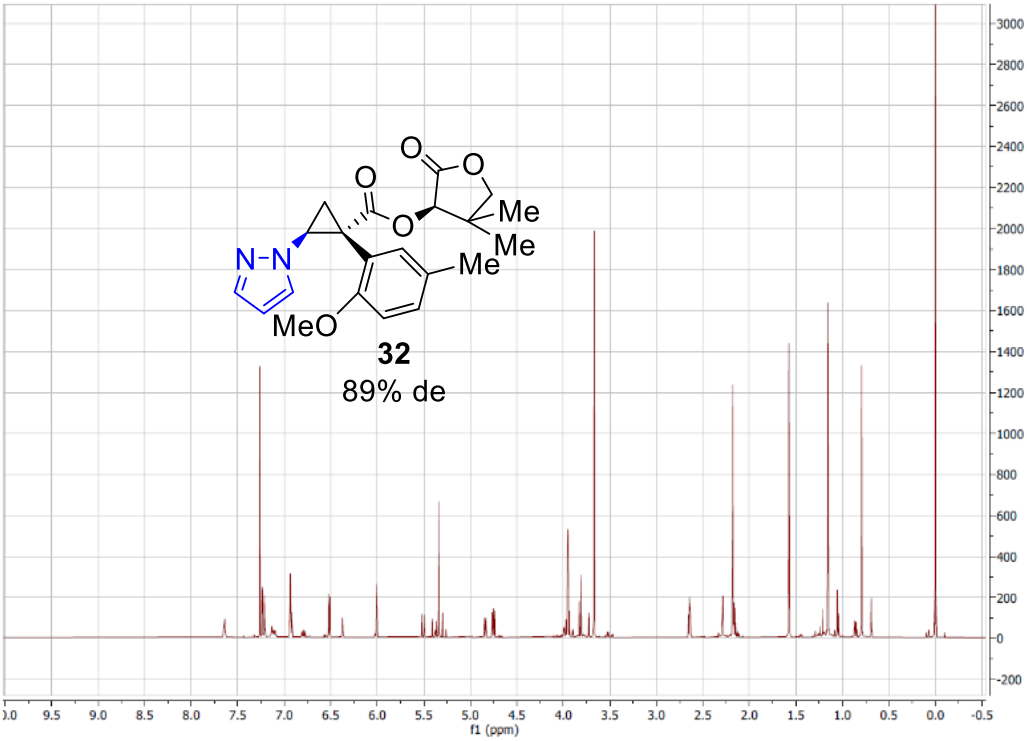

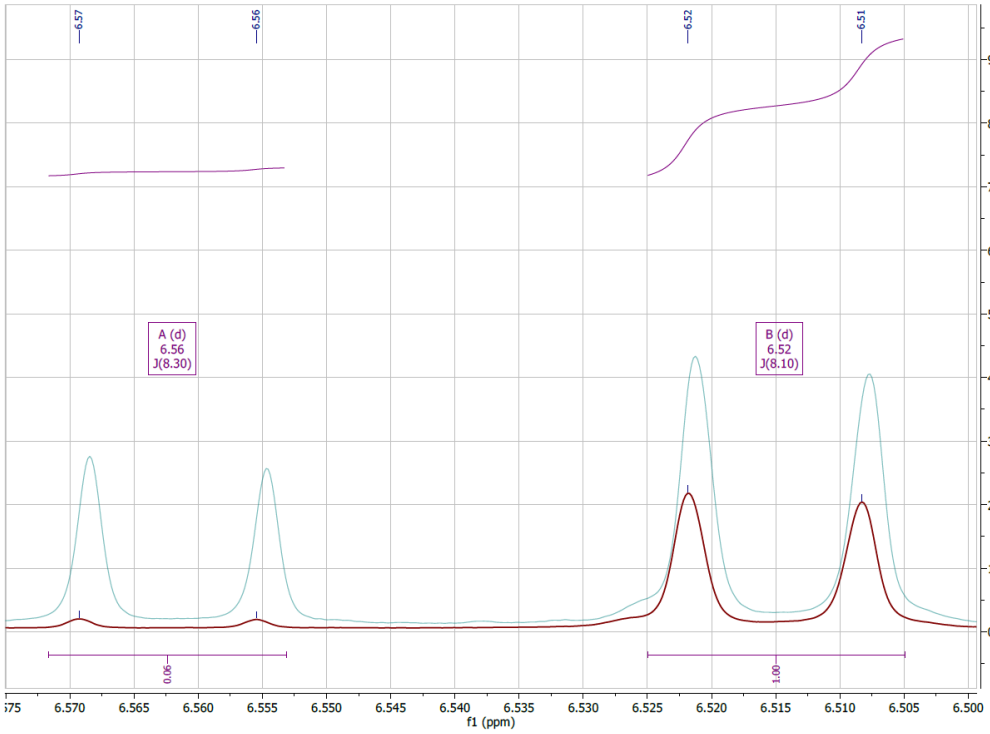

Compound 33:

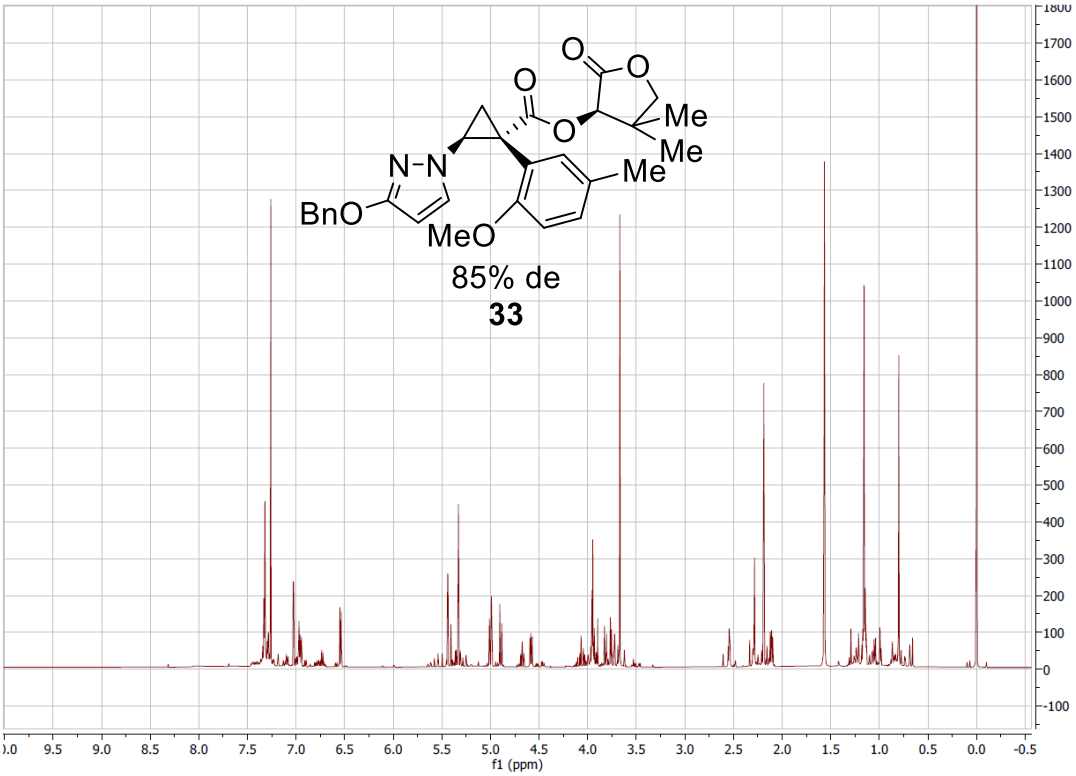

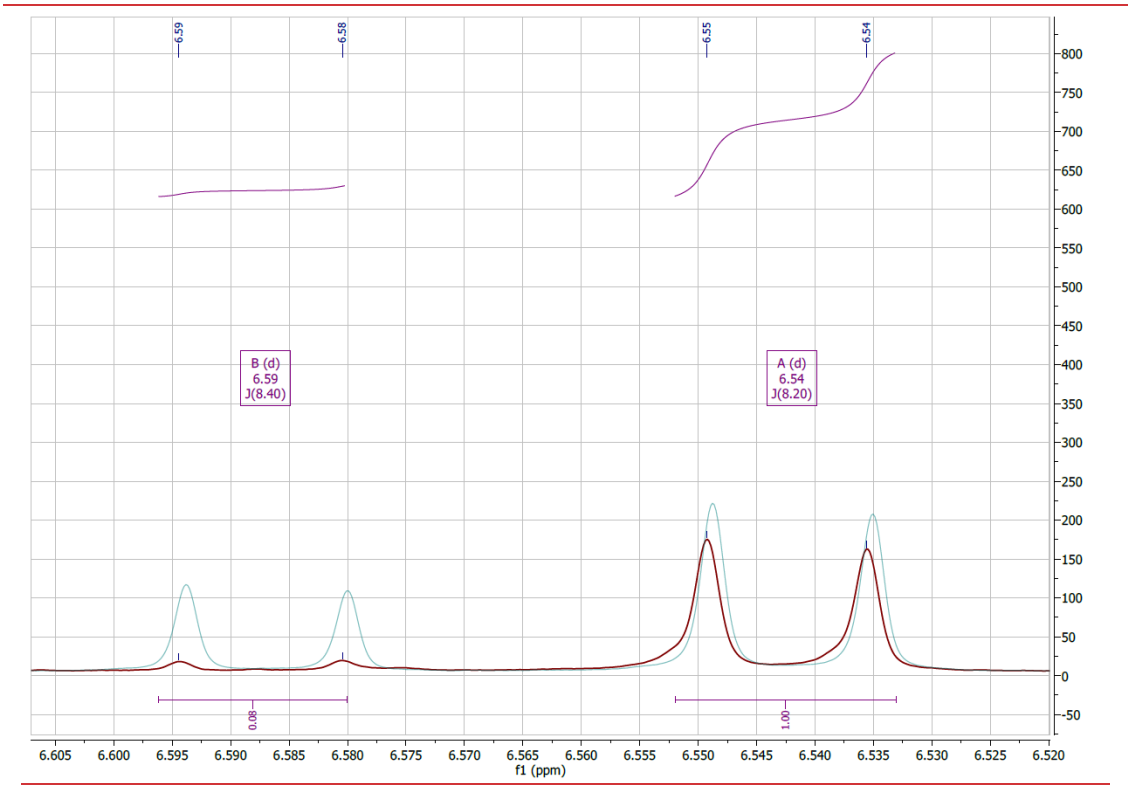

Compound 34:

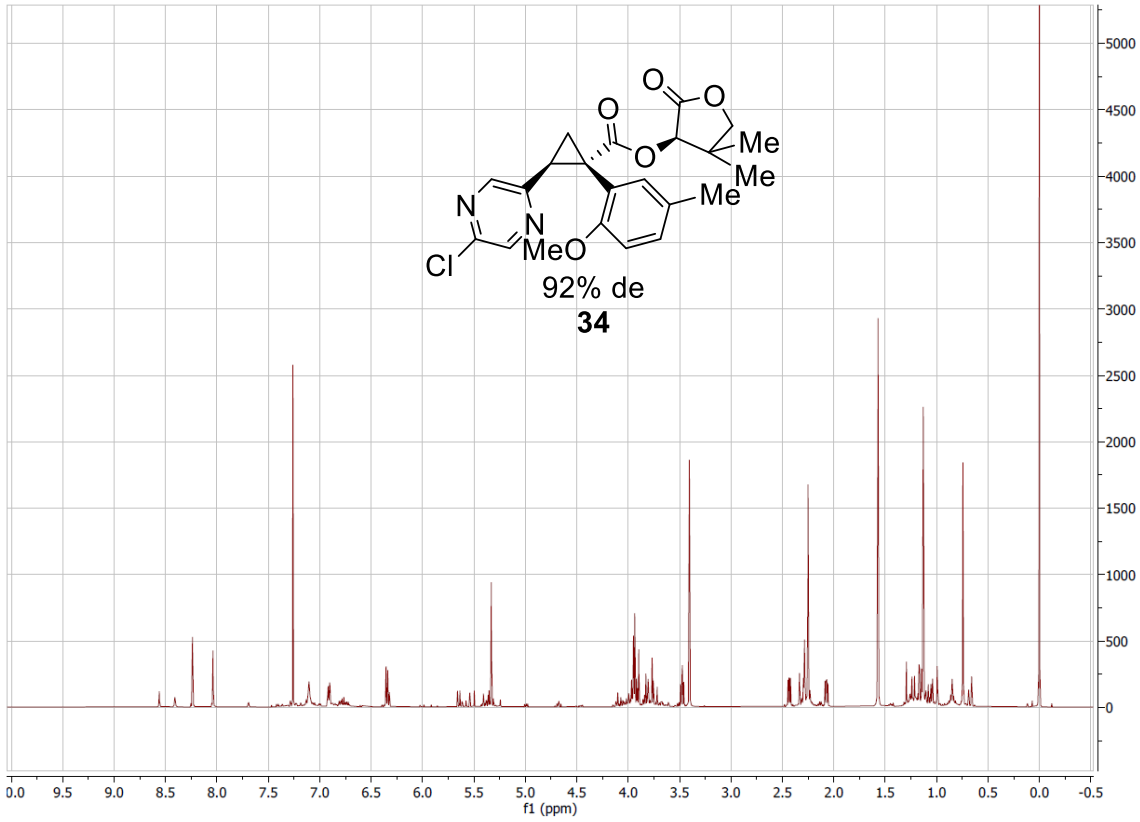
92% de
34
f1 (ppm)

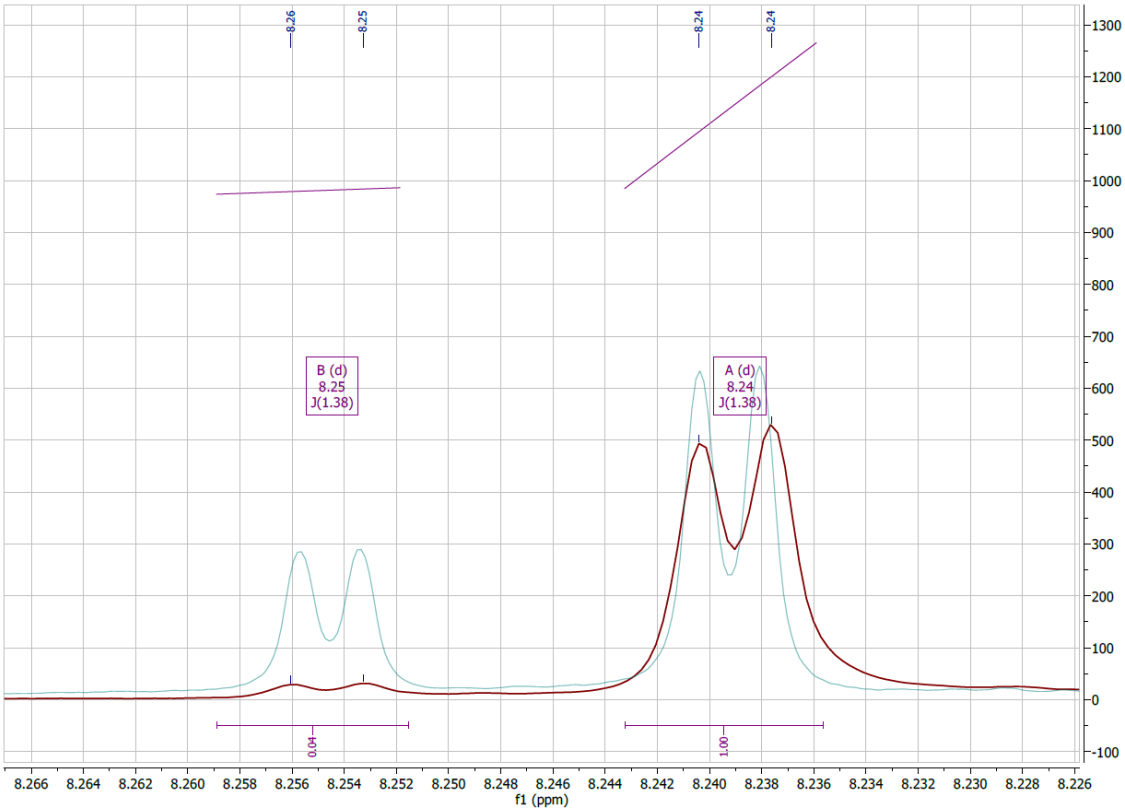
8.26
8.25
8.24
8.24
B (d)
8.25
J(1.38)
A (d)
8.24
J(1.38)
0.04
1.00
f1 (ppm)

5.2: Enantioselectivity of cyclopropanes synthesized with chiral catalysts was determined by chiral HPLC, UHPLC, of SFC.

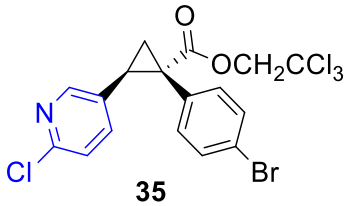

35

Racemic trace:

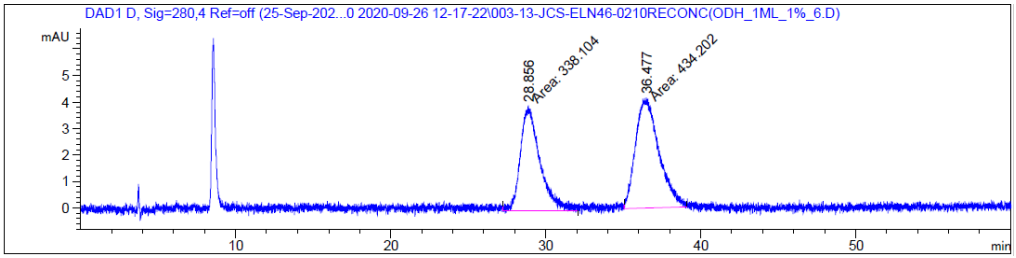


```
Signal 4: DAD1 D, Sig=280,4 Ref=off

Peak RetTime Type  Width     Area      Height     Area
  #   [min]        [min]   [mAU*s]     [mAU]       %
----|-------|----|-------|----------|----------|--------|
   1  28.856 MM    1.4272  338.10449    3.94839  43.7785
   2  36.477 MM    1.7347  434.20224    4.17165  56.2215

Totals :                   772.30673    8.12004
```

25℃, 0.5 mol % Rh_2(*R*-*p*-Ph-TPCP)$_4$, reaction performed according to procedure 3.2 with $(MeO)_2CO$ as solvent

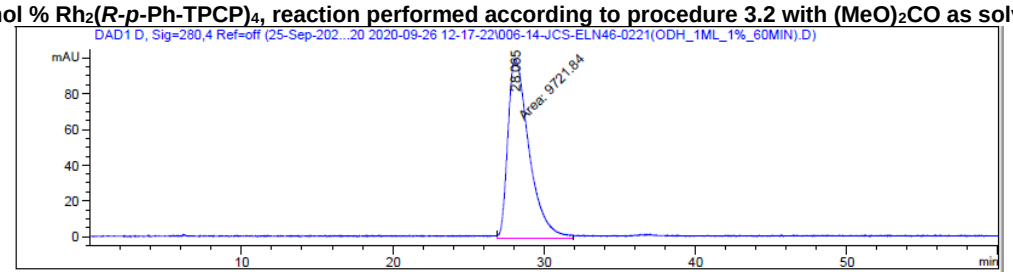


```
Signal 4: DAD1 D, Sig=280,4 Ref=off

Peak RetTime Type  Width     Area      Height     Area
  #   [min]        [min]   [mAU*s]     [mAU]       %
----|-------|----|-------|----------|----------|--------|
   1  28.065 MM    1.6141 9721.84082  100.38266 100.0000

Totals :                  9721.84082  100.38266
```

25 ℃, 0.5 mol % Rh_2(*R-p*-Ph-TPCP)$_4$, reaction performed according to procedure 3.2 with CH_2Cl_2 as solvent

Chromatogram :
JCS-ELN46-0211(ODH_1ML_1%_60MIN)11_channel2

System : Prostar LC System
Method : ADH_30min_1mL_1%-230nm
User : User1

Acquired : 2/3/2020 5:14:08 PM
Processed : 2/4/2020 12:14:28 PM
Printed : 9/12/2020 12:01:47 PM

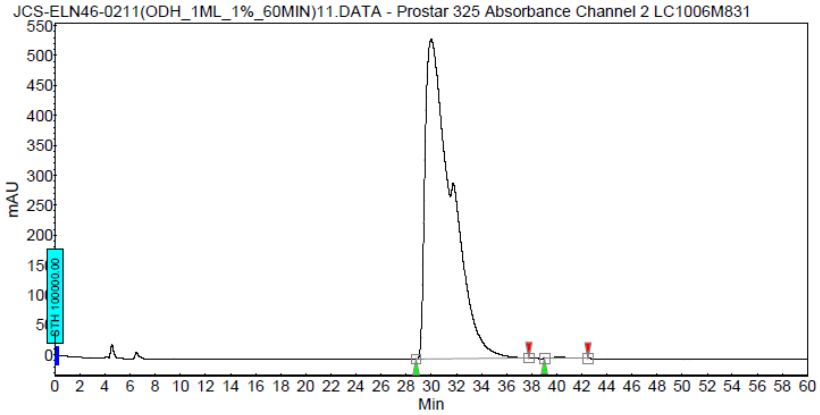

Peak results :

Index	Name	Time [Min]	Quantity [% Area]	Height [mAU]	Area [mAU.Min]	Area % [%]
1	UNKNOWN	29.99	99.72	533.4	1307.9	99.723
2	UNKNOWN	40.16	0.28	2.2	3.6	0.277
Total			100.00	535.6	1311.5	100.000

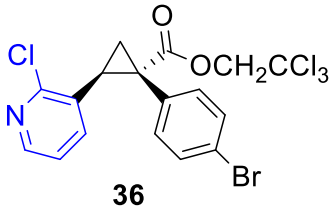

36

Racemic trace:

Chromatogram :
JCS-ELN46-0224(ADH_1ML_1%_60MIN)31_channel1

System : Prostar LC System
Method : DACHDNB_30min_1mL_1%-230nm
User : User1

Acquired : 2/7/2020 6:12:59 AM
Processed : 2/8/2020 11:36:01 AM
Printed : 9/12/2020 11:57:24 AM

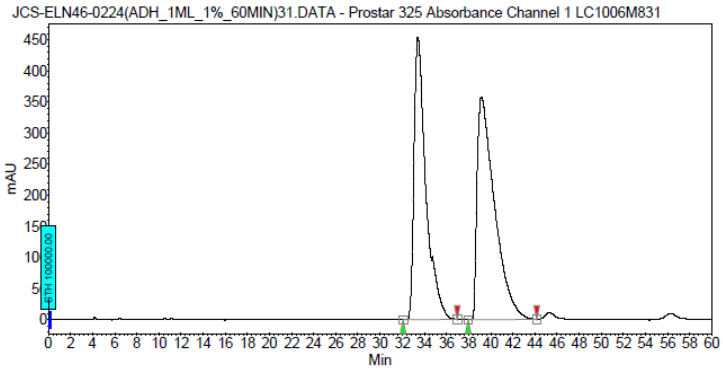

Peak results :

Index	Name	Time [Min]	Quantity [% Area]	Height [mAU]	Area [mAU.Min]	Area % [%]
1	UNKNOWN	33.41	46.30	453.4	566.0	46.298
2	UNKNOWN	39.16	53.70	358.0	656.4	53.702
Total			100.00	811.5	1222.4	100.000

25 ˚C, 0.5 mol % Rh_2(*R-p*-Ph-TPCP)$_4$, reaction performed according to procedure 3.2

Chromatogram :
JCS-ELN46-0225(ADH_1ML_1%_60min)76_channel1

System : Prostar LC System
Method : DACHDNB_30min_1mL_1%-230nm
User : User1

Acquired : 2/8/2020 7:25:39 AM
Processed : 2/8/2020 11:36:31 AM
Printed : 9/12/2020 11:57:09 AM

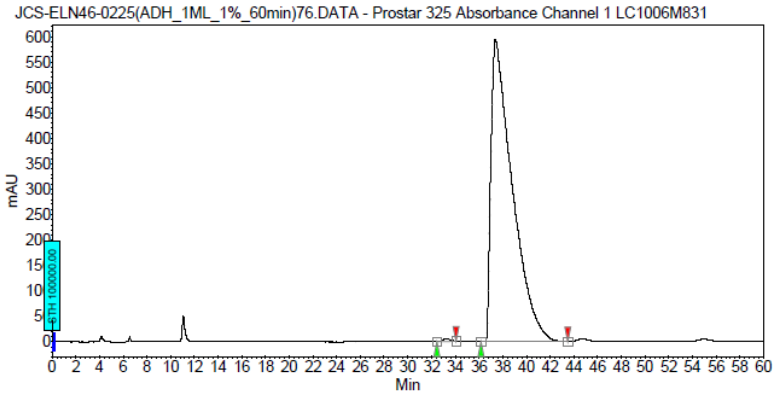

Peak results :

Index	Name	Time [Min]	Quantity [% Area]	Height [mAU]	Area [mAU.Min]	Area % [%]
1	UNKNOWN	33.25	0.31	5.4	3.9	0.314
2	UNKNOWN	37.38	99.69	594.2	1238.7	99.686
Total			100.00	599.6	1242.6	100.000

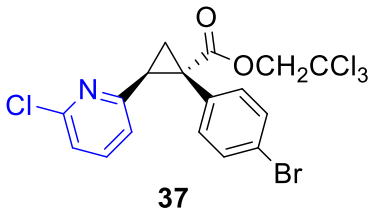

37

Racemic trace:

Chromatogram :
JCS-ELN46-0226(ADH_1ML_1%_60MIN)34_channel1

System : Prostar LC System
Method : DACHDNB_30min_1mL_1%-230nm
User : User1

Acquired : 2/7/2020 8:01:53 AM
Processed : 9/12/2020 11:56:08 AM
Printed : 9/12/2020 11:56:13 AM

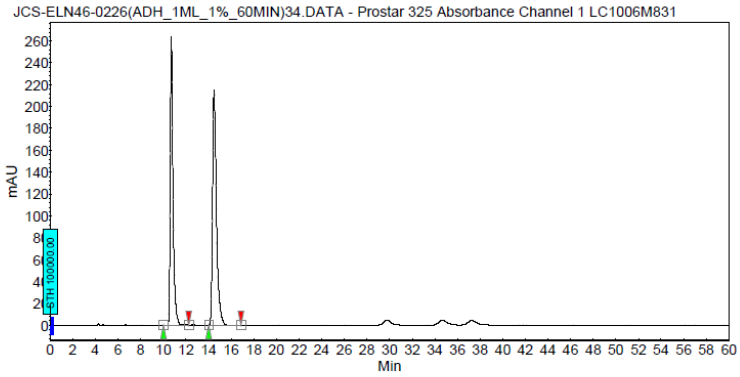

Peak results :

Index	Name	Time [Min]	Quantity [% Area]	Height [mAU]	Area [mAU.Min]	Area % [%]
1	UNKNOWN	10.71	47.51	263.2	75.0	47.514
2	UNKNOWN	14.49	52.49	214.9	82.9	52.486
Total			100.00	478.1	157.9	100.000

25 ℃, 0.5 mol % Rh_2(*R-p*-Ph-TPCP)$_4$, reaction performed according to procedure 3.2

Chromatogram :
JCS-ELN46-0227(ADH_1ML_1%_30min)79_channel1

System : Prostar LC System
Method : DACHDNB_30min_1mL_1%-230nm
User : User1

Acquired : 2/8/2020 9:14:11 AM
Processed : 9/12/2020 11:56:41 AM
Printed : 9/12/2020 11:56:45 AM

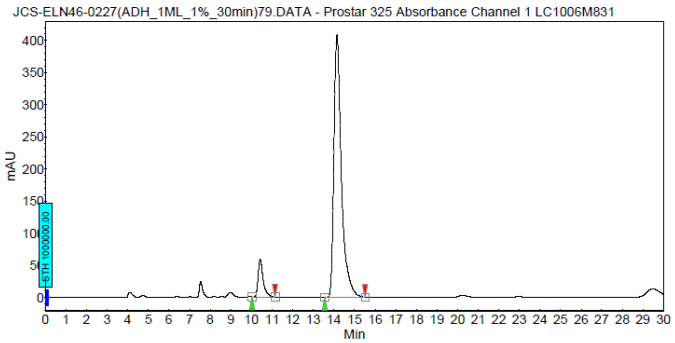

Peak results :

Index	Name	Time [Min]	Quantity [% Area]	Height [mAU]	Area [mAU.Min]	Area % [%]
2	UNKNOWN	10.42	8.92	58.8	16.7	8.916
1	UNKNOWN	14.14	91.08	408.1	170.8	91.084
Total			100.00	467.0	187.5	100.000

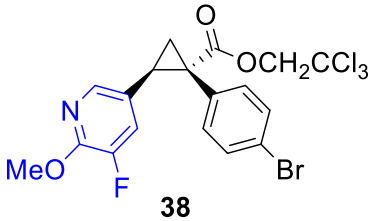

38

Racemic trace:

Chromatogram :
JCS-ELN46-0228(ODH_1ML_1%_60MIN)9_channel1

System : Prostar LC System
Method : ADH_30min_1mL_1%-230nm
User : User1

Acquired : 2/6/2020 6:25:51 PM
Processed : 2/8/2020 11:39:19 AM
Printed : 9/12/2020 11:54:43 AM

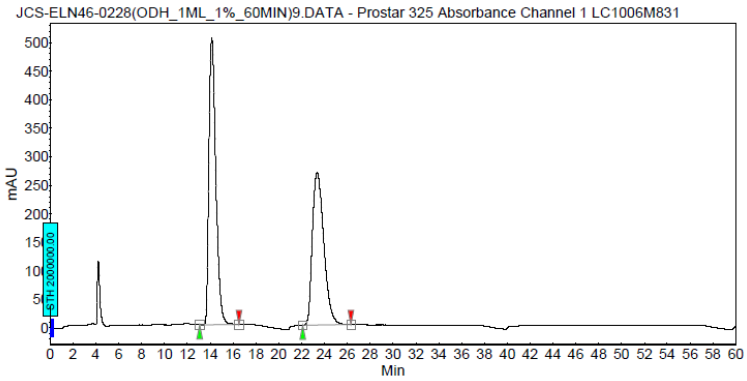

Peak results :

Index	Name	Time [Min]	Quantity [% Area]	Height [mAU]	Area [mAU.Min]	Area % [%]
1	UNKNOWN	14.14	53.42	502.8	357.7	53.415
2	UNKNOWN	23.37	46.58	268.3	312.0	46.585
Total			100.00	771.1	669.7	100.000

25 ℃, 0.5 mol % Rh_2(*R-p*-Ph-TPCP)$_4$, reaction performed according to procedure 3.2

Chromatogram :
JCS-ELN46-0229(ODH_1ML_30MIN_1%)54_chann el2

System : Prostar LC System
Method : ADH_30min_1mL_1%-230nm
User : User1

Acquired : 2/7/2020 5:29:57 PM
Processed : 2/8/2020 11:40:03 AM
Printed : 9/12/2020 11:54:21 AM

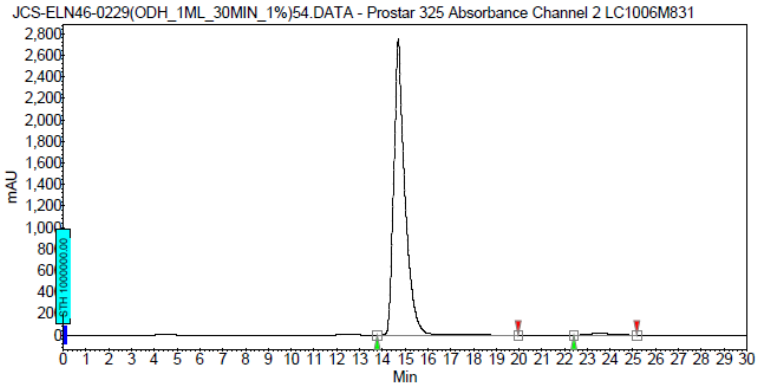

Peak results :

Index	Name	Time [Min]	Quantity [% Area]	Height [mAU]	Area [mAU.Min]	Area % [%]
2	UNKNOWN	14.70	99.01	2751.0	1541.2	99.011
1	UNKNOWN	23.54	0.99	15.0	15.4	0.989
Total			100.00	2765.9	1556.6	100.000

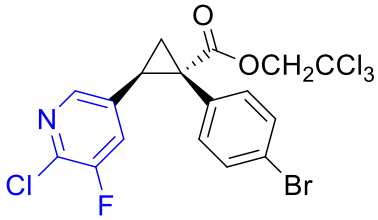

39

Racemic trace:

Chromatogram :
JCS-ELN46-0230(ODH_1ML_1%_60MIN)12_chann el1

System : Prostar LC System
Method : ADH_30min_1mL_1%-230nm
User : User1

Acquired : 2/6/2020 8:14:14 PM
Processed : 2/8/2020 11:38:02 AM
Printed : 9/12/2020 11:54:07 AM

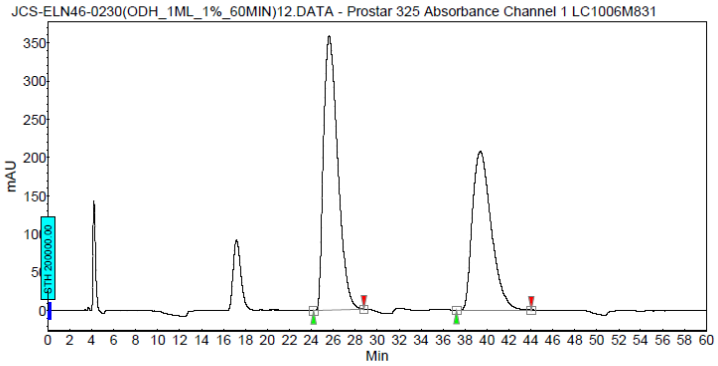

Peak results :

Index	Name	Time [Min]	Quantity [% Area]	Height [mAU]	Area [mAU.Min]	Area % [%]
1	UNKNOWN	25.63	56.49	357.9	537.0	56.492
2	UNKNOWN	39.39	43.51	207.4	413.6	43.508
Total			100.00	565.3	950.6	100.000

25 ℃, 0.5 mol % Rh_2(*R-p*-Ph-TPCP)$_4$, reaction performed according to procedure 3.2

Chromatogram :
JCS-ELN46-0231(ODH_1ML_60MIN_1%)57_channel2

System : Prostar LC System
Method : ADH_30min_1mL_1%-230nm
User : User1

Acquired : 2/7/2020 6:47:17 PM
Processed : 2/8/2020 11:38:42 AM
Printed : 9/12/2020 11:53:49 AM

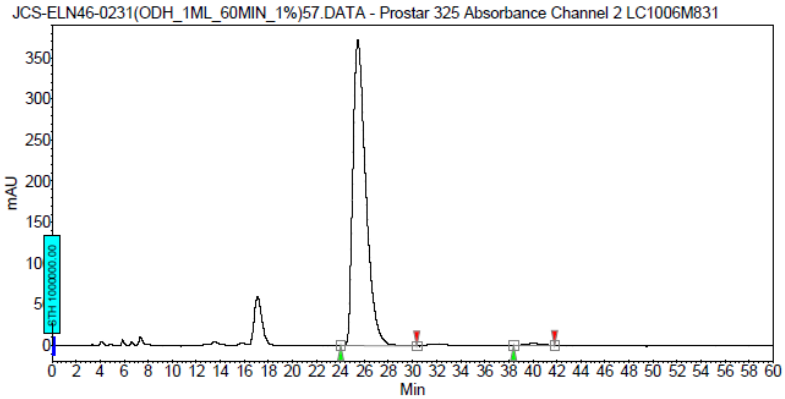

Peak results :

Index	Name	Time [Min]	Quantity [% Area]	Height [mAU]	Area [mAU.Min]	Area % [%]
2	UNKNOWN	25.44	99.08	371.7	464.2	99.076
1	UNKNOWN	40.06	0.92	2.8	4.3	0.924
Total			100.00	374.5	468.5	100.000

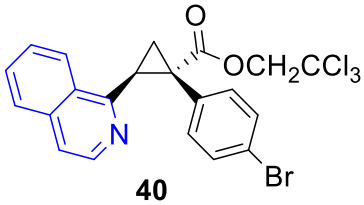

40

Racemic trace:

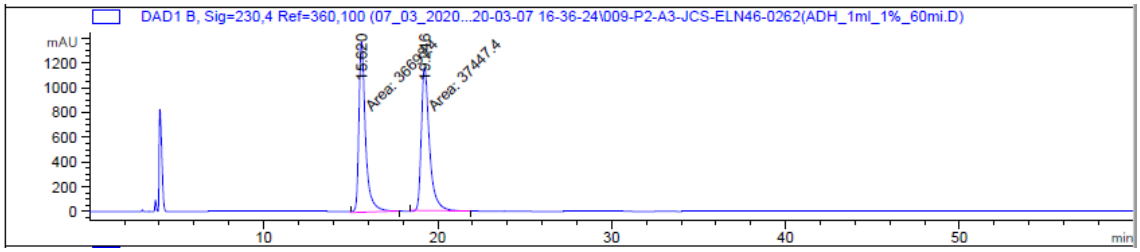


```
Signal 2: DAD1 B, Sig=230,4 Ref=360,100

Peak RetTime Type  Width     Area      Height     Area
  #   [min]        [min]   [mAU*s]     [mAU]       %
----|-------|----|-------|----------|----------|--------|
   1  15.620 MM    0.4448 3.66934e4  1375.04175  49.4915
   2  19.246 MM    0.5396 3.74474e4  1156.70520  50.5085

Totals :                  7.41407e4  2531.74695
```

25 ℃, 0.5 mol % Rh_2(*R-p*-Ph-TPCP)$_4$, reaction performed according to procedure 3.2

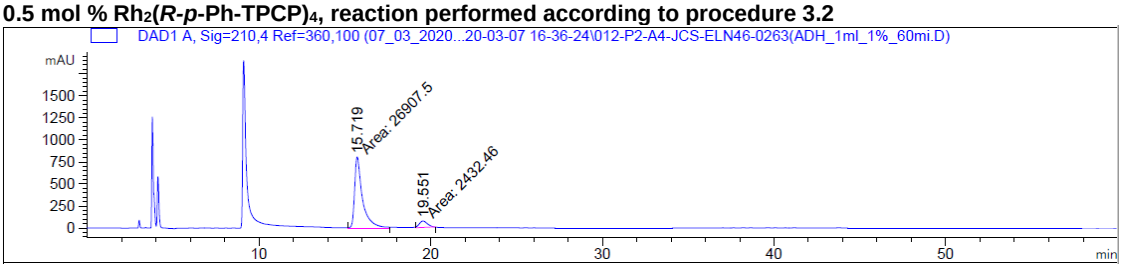

```
Signal 1: DAD1 A, Sig=210,4 Ref=360,100

Peak RetTime Type  Width     Area      Height     Area
  #   [min]        [min]   [mAU*s]     [mAU]       %
----|-------|----|-------|----------|----------|--------|
   1  15.719 MM    0.5516 2.69075e4   812.98846  91.7094
   2  19.551 MM    0.5503 2432.45801   73.66758   8.2906

Totals :                 2.93400e4   886.65604
```

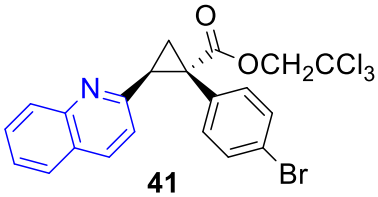

Racemic trace:

Chromatogram :
JCS-ELN46-0258(ADH_1ML_1%_90MIN)36_channel2

Prostar LC System
Method : OJ_30min_1mL_1%_230NM
User : User1

Acquired : 3/5/2020 4:42:38 PM
Processed : 9/12/2020 9:53:46 AM
Printed : 9/12/2020 9:54:03 AM

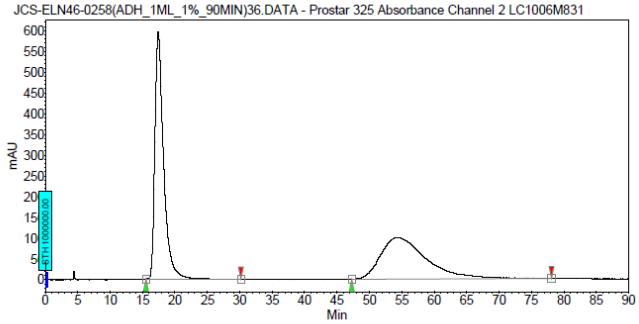

Peak results :

Index	Name	Time [Min]	Quantity [% Area]	Height [mAU]	Area [mAU.Min]	Area % [%]
1	UNKNOWN	17.42	52.95	595.3	927.8	52.950
2	UNKNOWN	54.21	47.05	99.8	824.4	47.050
Total			100.00	695.1	1752.3	100.000

25 ℃, 0.5 mol % Rh_2(*R-p*-Ph-TPCP)$_4$, reaction performed according to procedure 3.2

Chromatogram :
JCS-ELN46-0259RE(ADH_1ML_1%_90MIN)19_channel2

Prostar LC System
Method : OJ_30min_1mL_1%_230NM
User : User1

Acquired : 3/10/2020 6:10:24 PM
Processed : 3/11/2020 10:29:05 AM
Printed : 9/12/2020 9:50:41 AM

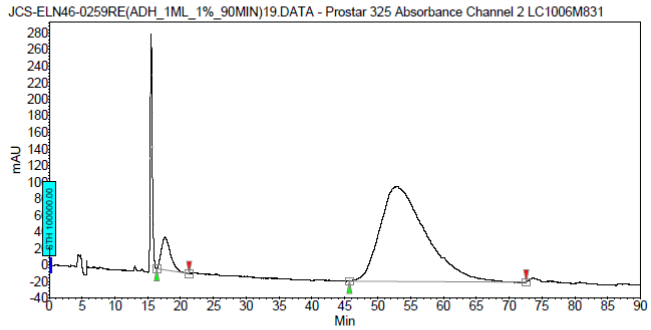

Peak results :

Index	Name	Time [Min]	Quantity [% Area]	Height [mAU]	Area [mAU.Min]	Area % [%]
2	UNKNOWN	17.62	6.50	40.0	64.3	6.502
1	UNKNOWN	52.99	93.50	114.5	925.0	93.498
Total			100.00	154.5	989.3	100.000

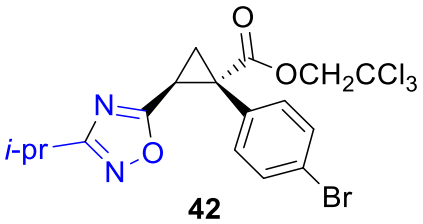

42

Racemic trace:

Chromatogram :
JCS-ELN46-0303(OJH_1ML_1%_30MIN)3_channel1

System : Prostar LC System
Method : DACHDNB_30min_1mL_1%-230nm
User : User1

Acquired : 7/16/2020 8:42:40 PM
Processed : 9/12/2020 9:34:44 AM
Printed : 9/12/2020 9:37:17 AM

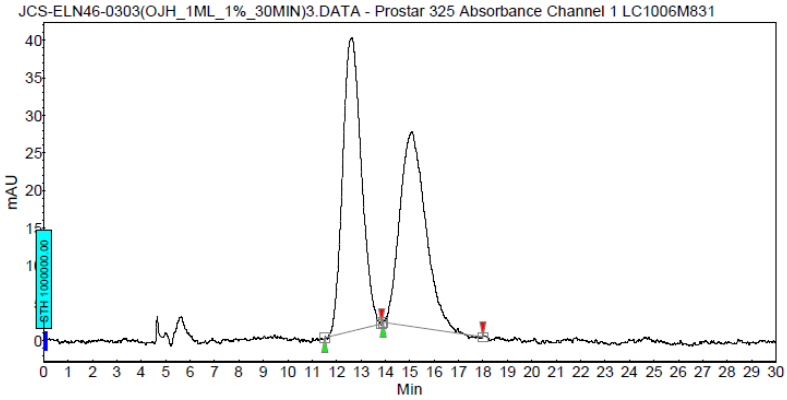

Peak results :

Index	Name	Time [Min]	Quantity [% Area]	Height [mAU]	Area [mAU.Min]	Area % [%]
1	UNKNOWN	12.63	52.26	38.9	34.5	52.261
2	UNKNOWN	15.08	47.74	25.9	31.6	47.739
Total			100.00	64.9	66.1	100.000

25 ℃, 0.5 mol % Rh_2(*R*-*p*-Ph-TPCP)$_4$, reaction performed according to procedure 3.2

Chromatogram :
JCS-ELN46-0302A(OJH_1ML_1%_30MIN)6_channel1

System : Prostar LC System
Method : DACHDNB_30min_1mL_1%-230nm
User : User1

Acquired : 7/16/2020 10:00:24 PM
Processed : 7/18/2020 12:09:01 PM
Printed : 9/12/2020 9:37:22 AM

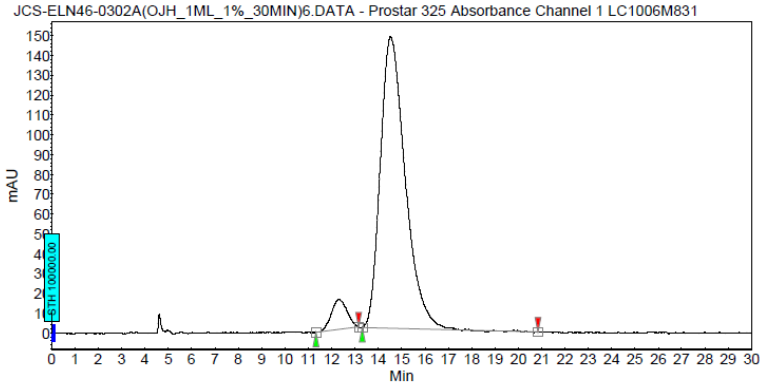

Peak results :

Index	Name	Time [Min]	Quantity [% Area]	Height [mAU]	Area [mAU.Min]	Area % [%]
1	UNKNOWN	12.33	5.99	15.0	11.6	5.990
2	UNKNOWN	14.52	94.01	146.9	182.2	94.010
Total			100.00	161.9	193.9	100.000

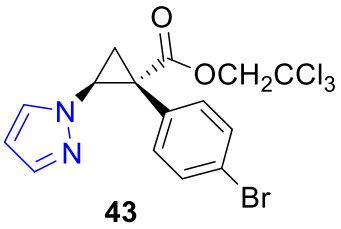

43

Racemic trace:

Chromatogram :
JCS-ELN46-0309(OJH_45min_1ml_1%)3_channel1

System : Prostar LC System
Method : DACHDNB_30min_1mL_1%-230nm
User : User1

Acquired : 7/30/2020 1:57:01 PM
Processed : 7/30/2020 5:45:01 PM
Printed : 9/12/2020 9:31:34 AM

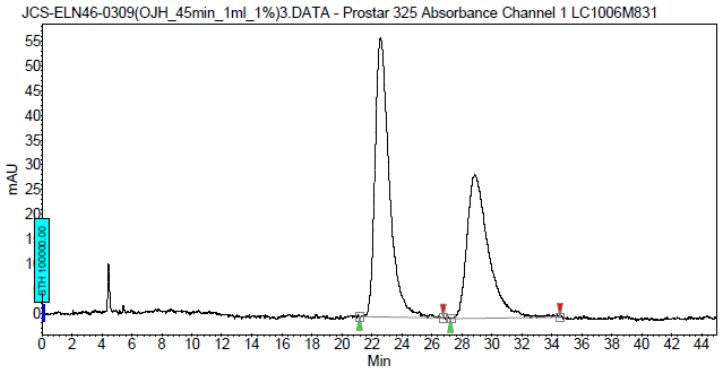

Peak results :

Index	Name	Time [Min]	Quantity [% Area]	Height [mAU]	Area [mAU.Min]	Area % [%]
1	UNKNOWN	22.60	56.44	56.5	62.2	56.439
2	UNKNOWN	28.87	43.56	29.1	48.0	43.561
Total			100.00	85.5	110.1	100.000

25 ℃, 1 mol % Rh_2(*R*-*p*-Ph-TPCP)$_4$, reaction performed according to procedure 3.2

Chromatogram :
JCS-ELN46-0310BRE(OJH_45min_1ml_1%)6_channel1

System : Prostar LC System
Method : DACHDNB_30min_1mL_1%-230nm
User : User1

Acquired : 8/1/2020 2:55:50 PM
Processed : 8/3/2020 1:18:21 PM
Printed : 9/12/2020 9:31:01 AM

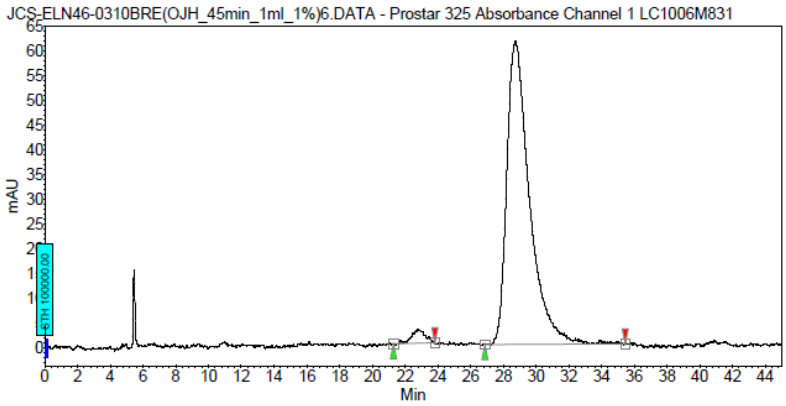

Peak results :

Index	Name	Time [Min]	Quantity [% Area]	Height [mAU]	Area [mAU.Min]	Area % [%]
1	UNKNOWN	22.84	2.62	2.8	2.7	2.622
2	UNKNOWN	28.74	97.38	61.3	98.5	97.378
Total			100.00	64.1	101.1	100.000

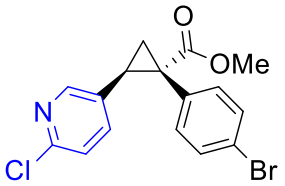

44

Racemic trace:

Chromatogram :
Bo-ELN36-0104(ADH_1ML_1%_60MIN)8_channel1

System : Prostar LC System
Method : DACHDNB_30min_1mL_1%-230nm
User : User1

Acquired : 2/4/2020 1:08:05 PM
Processed : 9/21/2020 6:17:22 PM
Printed : 9/21/2020 6:17:25 PM

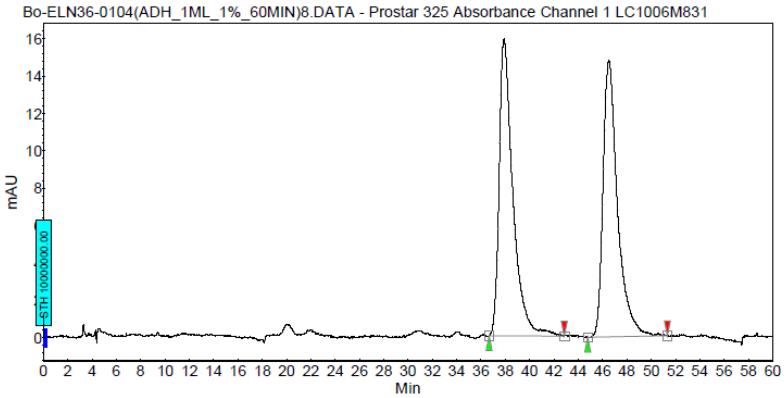

Peak results :

Index	Name	Time [Min]	Quantity [% Area]	Height [mAU]	Area [mAU.Min]	Area % [%]
1	UNKNOWN	37.89	50.44	15.9	20.8	50.437
2	UNKNOWN	46.52	49.56	14.8	20.5	49.563
Total			100.00	30.7	41.3	100.000

25 ℃, 0.5 mol % Rh_2(*R*-*p*-Ph-TPCP)$_4$, reaction performed according to procedure 3.2

Chromatogram :
JCS-ELN46-0215(ADH_1ML_1%_60MIN)10_chann
el1

System : Prostar LC System
Method : DACHDNB_30min_1mL_1%-230nm
User : User1

Acquired : 2/4/2020 2:56:34 PM
Processed : 2/5/2020 9:28:29 AM
Printed : 9/12/2020 11:59:59 AM

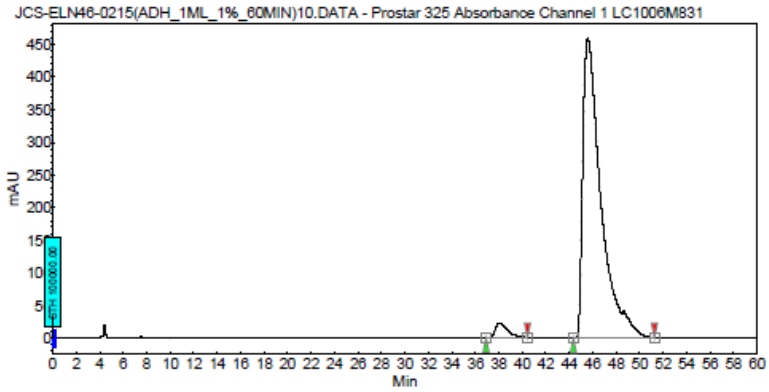

Peak results :

Index	Name	Time [Min]	Quantity [% Area]	Height [mAU]	Area [mAU.Min]	Area % [%]
1	UNKNOWN	38.05	3.20	22.9	27.0	3.197
2	UNKNOWN	45.59	96.80	458.6	818.0	96.803
Total			100.00	481.5	845.0	100.000

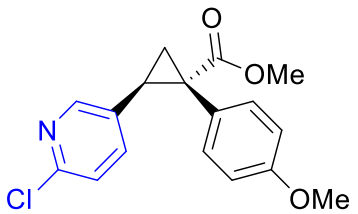

45

Racemic trace:

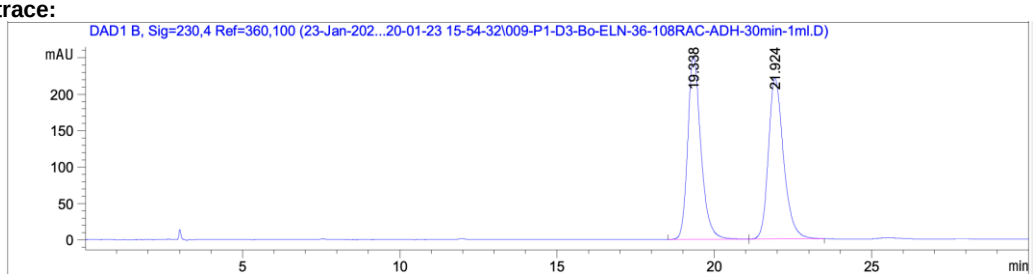


```
Signal 2: DAD1 B, Sig=230,4 Ref=360,100

Peak RetTime Type  Width     Area      Height     Area
  #   [min]        [min]   [mAU*s]     [mAU]       %
----|-------|----|-------|----------|----------|--------|
   1  19.338 BB    0.4391 7316.83301  251.73724  49.7532
   2  21.924 BB    0.5079 7389.43115  221.10867  50.2468
```

25 ℃, 0.5 mol % Rh_2(*R*-*p*-Ph-TPCP)$_4$, reaction performed according to procedure 3.2

Chromatogram :
JCS-ELN46-0232(ADH_1ML_3%_30MIN)109_channel2

System : Prostar LC System
Method : DACHDNB_30min_1mL_3%-230nm
User : User1

Acquired : 2/8/2020 6:44:06 PM
Processed : 2/10/2020 8:45:18 AM
Printed : 9/12/2020 11:53:36 AM

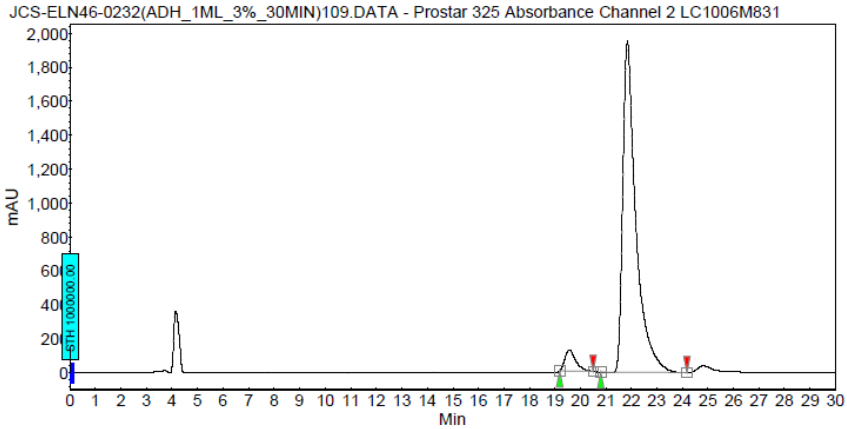

Peak results :

Index	Name	Time [Min]	Quantity [% Area]	Height [mAU]	Area [mAU.Min]	Area % [%]
1	UNKNOWN	19.57	5.01	123.8	61.0	5.010
2	UNKNOWN	21.84	94.99	1953.7	1156.0	94.990
Total			100.00	2077.5	1216.9	100.000

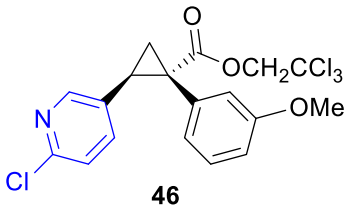

46

Racemic trace:

Chromatogram :
BO-ELN36-0102(ADH_1ML_5%_45min)89_channel1

System : Prostar LC System
Method : DACHDNB_30min_1mL_5%_230nm
User : User1

Acquired : 2/8/2020 2:20:55 PM
Processed : 9/25/2020 4:50:39 PM
Printed : 9/25/2020 4:50:46 PM

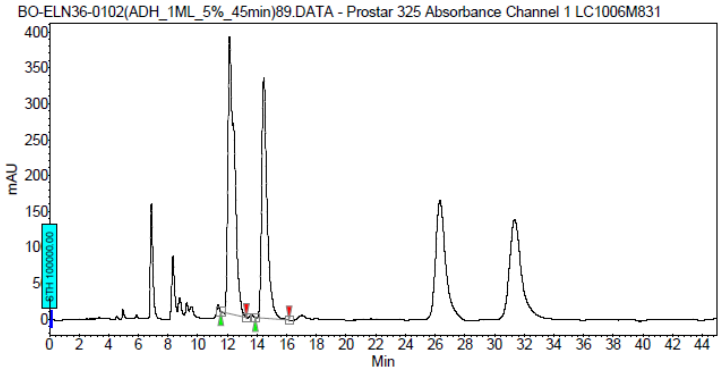

Peak results :

Index	Name	Time [Min]	Quantity [% Area]	Height [mAU]	Area [mAU.Min]	Area % [%]
1	UNKNOWN	12.15	57.51	385.2	192.0	57.512
2	UNKNOWN	14.45	42.49	334.2	141.9	42.488
Total			100.00	719.4	333.9	100.000

25 ℃, 0.5 mol % Rh_2(*R*-*p*-Ph-TPCP)$_4$, reaction performed according to procedure 3.2

Chromatogram :
JCS-ELN46-0233(ADH_1ML_5%_45min)92_channel2

System : Prostar LC System
Method : DACHDNB_30min_1mL_5%_230nm
User : User1

Acquired : 2/8/2020 3:53:38 PM
Processed : 2/10/2020 8:43:26 AM
Printed : 9/12/2020 11:53:20 AM

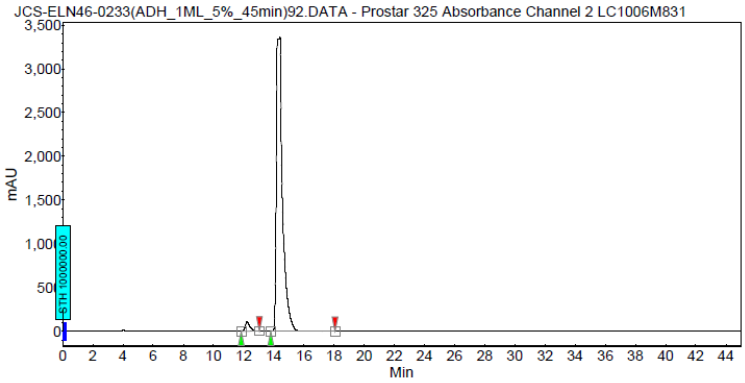

Peak results :

Index	Name	Time [Min]	Quantity [% Area]	Height [mAU]	Area [mAU.Min]	Area % [%]
1	UNKNOWN	12.23	2.40	105.1	39.8	2.404
2	UNKNOWN	14.43	97.60	3358.7	1616.3	97.596
Total			100.00	3463.9	1656.1	100.000

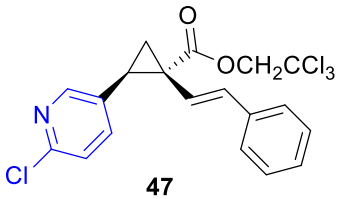

47

Racemic trace:

Chromatogram :
JCS-ELN46-0242A(ADH_1ML_3%_60MIN)15_channel2

System : Prostar LC System
Method : ADH_30min_1mL_3%-230nm
User : User1

Acquired : 2/13/2020 12:04:37 AM
Processed : 9/12/2020 11:49:31 AM
Printed : 9/12/2020 11:49:36 AM

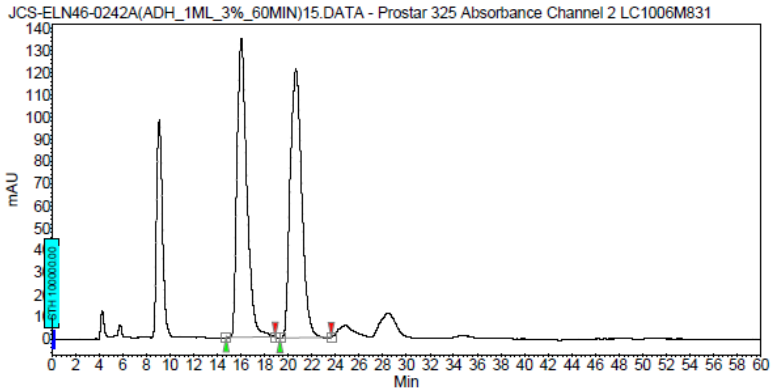

Peak results :

Index	Name	Time [Min]	Quantity [% Area]	Height [mAU]	Area [mAU.Min]	Area % [%]
1	UNKNOWN	16.04	48.67	134.3	129.6	48.668
2	UNKNOWN	20.66	51.33	120.9	136.7	51.332
Total			100.00	255.2	266.4	100.000

25 ℃, 0.5 mol % Rh_2(*R-p*-Ph-TPCP)$_4$, reaction performed according to procedure 3.2

Chromatogram :
JCS-ELN46-0243(ODH_1ML_3%_30MIN)18_channel1

System : Prostar LC System
Method : ADH_30min_1mL_3%-230nm
User : User1

Acquired : 2/13/2020 9:21:41 PM
Processed : 2/14/2020 12:33:29 PM
Printed : 9/12/2020 11:47:01 AM

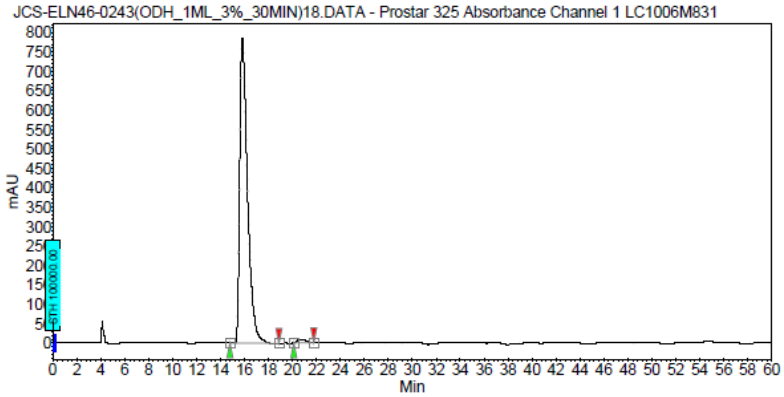

Peak results :

Index	Name	Time [Min]	Quantity [% Area]	Height [mAU]	Area [mAU.Min]	Area % [%]
1	UNKNOWN	15.83	98.96	784.2	595.5	98.955
2	UNKNOWN	20.74	1.04	8.3	6.3	1.045
Total			100.00	792.5	601.8	100.000

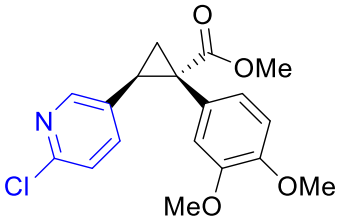

48

Racemic trace:

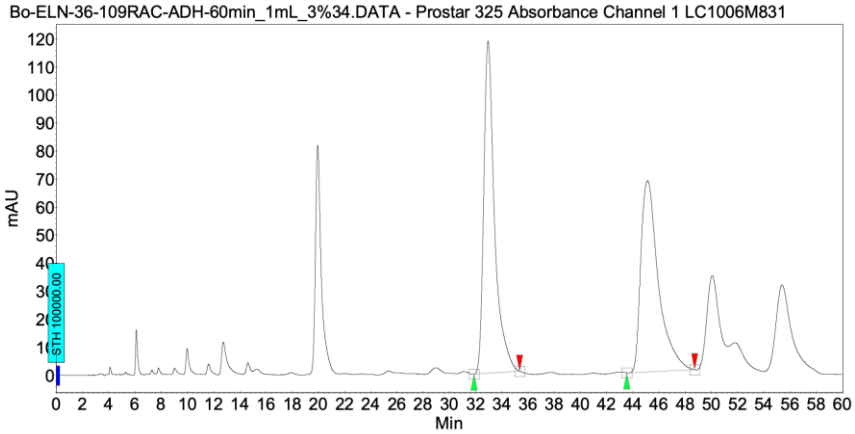

Peak results :

Index	Name	Time [Min]	Quantity [% Area]	Height [mAU]	Area [mAU.Min]	Area % [%]
1	UNKNOWN	32.96	51.67	118.6	113.3	51.674
2	UNKNOWN	45.12	48.33	68.2	106.0	48.326
Total			100.00	186.8	219.3	100.000

25 ℃, 0.5 mol % Rh_2(*R*-*p*-Ph-TPCP)$_4$, reaction performed according to procedure 3.2

Chromatogram :

JCS-ELN46-0245RE(ADH_1ML_3%_60MIN)3_channel1

Instrument : Prostar LC System
Method : DACHDNB_30min_1mL_3%-230nm
User : User1

Acquired : 2/19/2020 11:11:37 AM
Processed : 2/19/2020 12:19:49 PM
Printed : 9/12/2020 11:43:05 AM

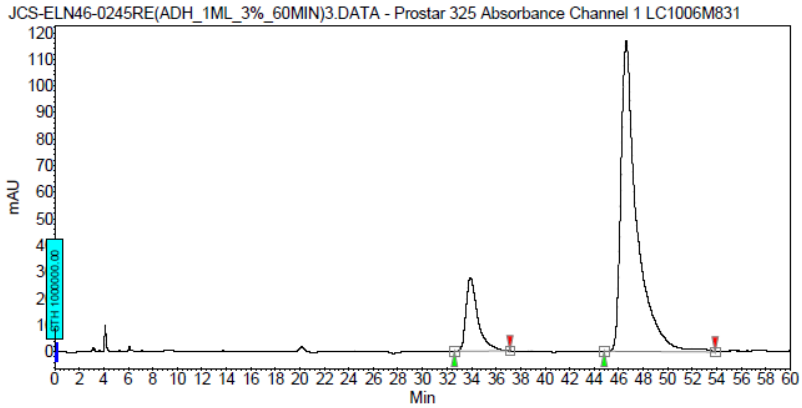

Peak results :

Index	Name	Time [Min]	Quantity [% Area]	Height [mAU]	Area [mAU.Min]	Area % [%]
1	UNKNOWN	33.90	14.93	27.4	30.8	14.930
2	UNKNOWN	46.61	85.07	116.9	175.5	85.070
Total			100.00	144.3	206.3	100.000

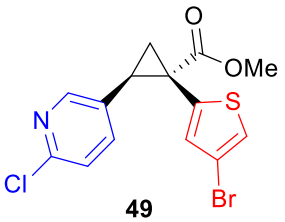

49

Racemic trace:

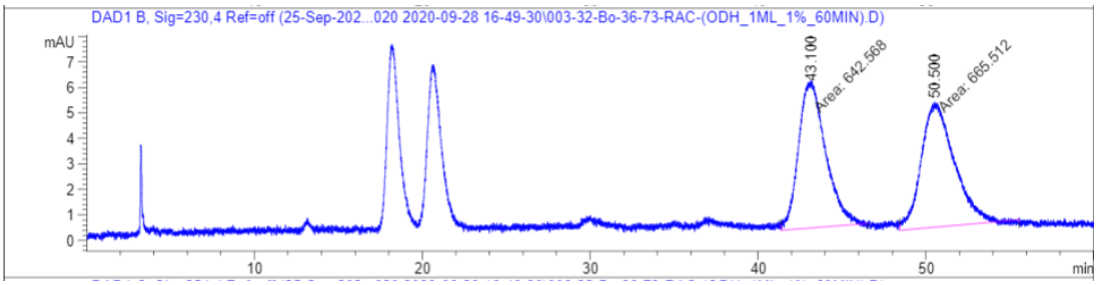

Signal 2: DAD1 B, Sig=230,4 Ref=off

Peak #	RetTime [min]	Type	Width [min]	Area [mAU*s]	Height [mAU]	Area %
1	43.100	MM	1.8564	642.56848	5.76899	49.1230
2	50.500	MM	2.2602	665.51190	4.90745	50.8770
Totals :				1308.08038	10.67644	

25 ℃, 0.5 mol % Rh_2(*R-p*-Ph-TPCP)$_4$, reaction performed according to procedure 3.2

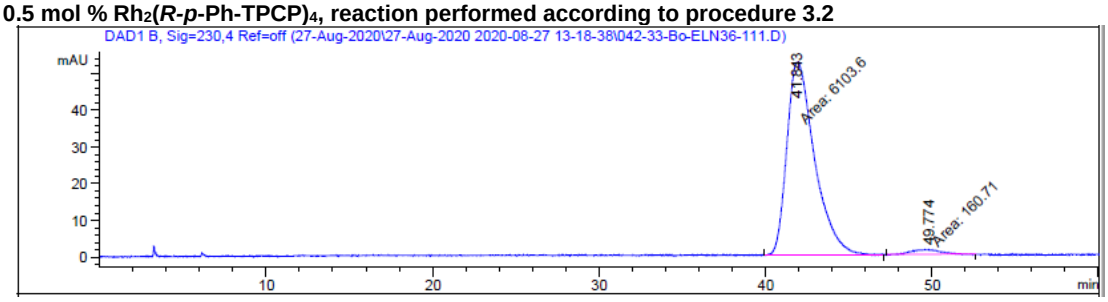

Signal 2: DAD1 B, Sig=230,4 Ref=off

Peak #	RetTime [min]	Type	Width [min]	Area [mAU*s]	Height [mAU]	Area %
1	41.843	MM	1.9352	6103.60498	52.56713	97.4345
2	49.774	MM	1.9571	160.70956	1.36859	2.5655
Totals :				6264.31454	53.93572	

Signal 3: DAD1 C, Sig=254,4 Ref=off

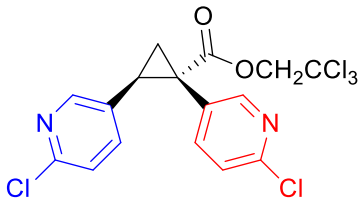

50

Racemic trace:

Chromatogram :
JCS-ELN46-0234RACFINAL(ADH_1ML_7%_60MIN)6.channel1

System : Prostar 325 Absorbance System
Method : DACHDNB_30min_1mL_7%
User : User1

Acquired : 2/19/2020 6:16:26 PM
Processed : 9/12/2020 11:43:33 AM
Printed : 9/12/2020 11:43:42 AM

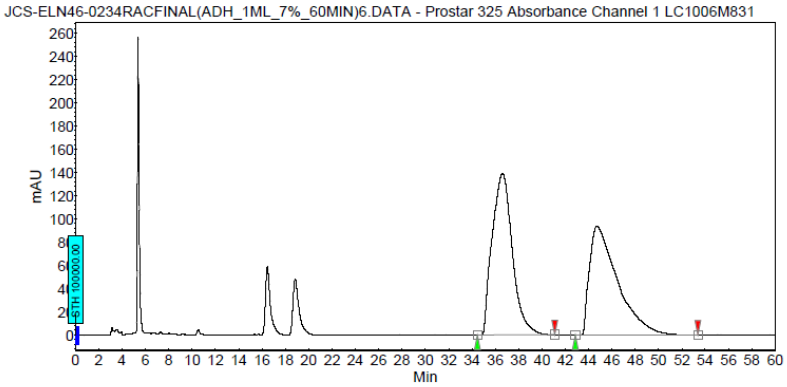

Peak results :

Index	Name	Time [Min]	Quantity [% Area]	Height [mAU]	Area [mAU.Min]	Area % [%]
1	UNKNOWN	36.61	51.67	138.8	278.8	51.672
2	UNKNOWN	44.71	48.33	93.6	260.8	48.328
Total			100.00	232.4	539.6	100.000

25 ˚C, 0.5 mol % Rh_2(*R-p*-Ph-TPCP)$_4$, reaction performed according to procedure 3.2

Chromatogram :
JCS-ELN46-0234RE(ADH_1ML_7%_60MIN)3_channel1

Prostar LC System
Method : DACHDNB_30min_1mL_7%
User : User1

Acquired : 2/20/2020 9:32:24 AM
Processed : 2/20/2020 11:01:57 AM
Printed : 9/12/2020 12:08:20 PM

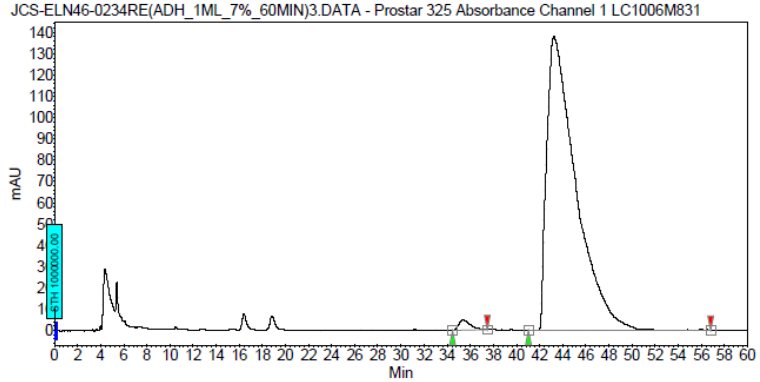

Peak results :

Index	Name	Time [Min]	Quantity [% Area]	Height [mAU]	Area [mAU.Min]	Area % [%]
1	UNKNOWN	35.37	1.42	4.8	5.8	1.415
2	UNKNOWN	43.25	98.58	138.1	402.4	98.585
Total			100.00	142.9	408.1	100.000

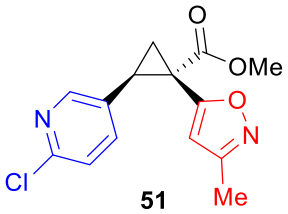

51

Racemic trace:

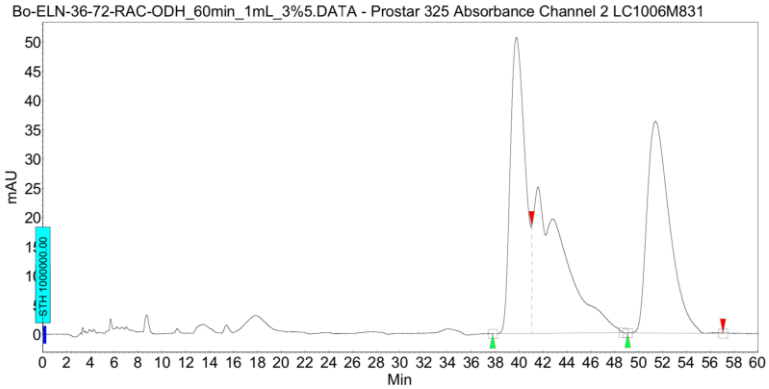

Peak results :

Index	Name	Time [Min]	Quantity [% Area]	Height [mAU]	Area [mAU.Min]	Area % [%]
2	UNKNOWN	39.76	47.92	50.7	73.0	47.918
1	UNKNOWN	51.41	52.08	36.2	79.4	52.082
Total			100.00	86.9	152.4	100.000

25 ℃, 0.5 mol % Rh_2(*R*-*p*-Ph-TPCP)$_4$, reaction performed according to procedure 3.2

Chromatogram :
JCS-ELN46-0235RE(ODH_1ML_3%_60MIN)30_channel2

Prostar LC System
Method : ADH_30min_1mL_3%-230nm
User : User1

Acquired : 2/14/2020 4:35:50 AM
Processed : 2/14/2020 12:36:05 PM
Printed : 9/12/2020 11:46:24 AM

JCS-ELN46-0235RE(ODH_1ML_3%_60MIN)30.DATA - Prostar 325 Absorbance Channel 2 LC1006M831

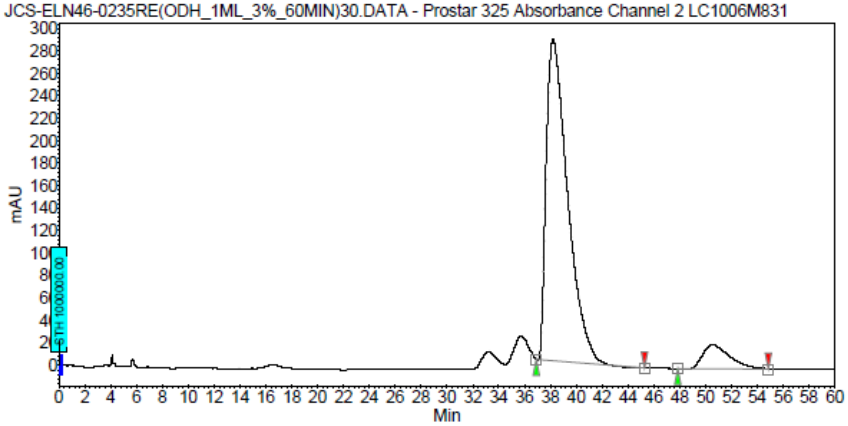

Peak results :

Index	Name	Time [Min]	Quantity [% Area]	Height [mAU]	Area [mAU.Min]	Area % [%]
1	UNKNOWN	38.21	91.41	285.8	547.1	91.409
2	UNKNOWN	50.56	8.59	21.1	51.4	8.591
Total			100.00	306.9	598.6	100.000

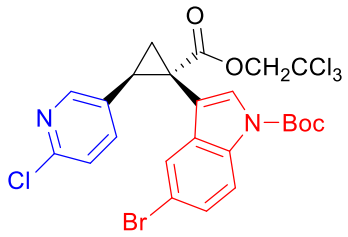

52

Racemic trace:

Chromatogram :
JCS-ELN46-0238A(ADH_1ML_3%_60MIN)3_channel1

System : Prostar LC System
Method : ADH_30min_1mL_3%-230nm
User : User1

Acquired : 2/12/2020 4:50:11 PM
Processed : 9/12/2020 11:51:40 AM
Printed : 9/12/2020 11:51:45 AM

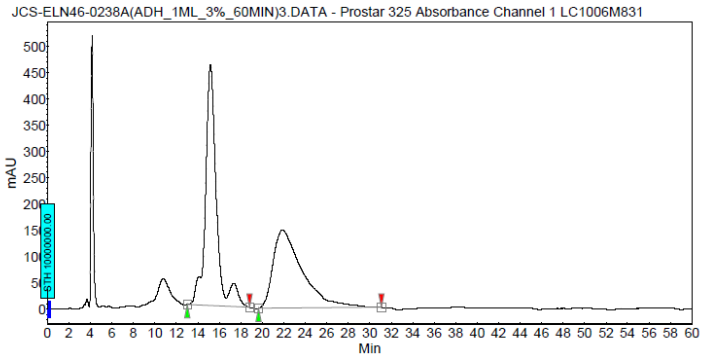

Peak results :

Index	Name	Time [Min]	Quantity [% Area]	Height [mAU]	Area [mAU.Min]	Area % [%]
1	UNKNOWN	15.17	53.91	457.7	547.2	53.912
2	UNKNOWN	21.87	46.09	147.8	467.8	46.088
Total			100.00	605.5	1015.0	100.000

25 ℃, 0.5 mol % Rh_2(*R-p*-Ph-TPCP)$_4$, reaction performed according to procedure 3.2

Chromatogram :
JCS-ELN46-0239(ODH_1ML_3%_30MIN)9_channel2

System : Prostar LC System
Method : ADH_30min_1mL_3%-230nm
User : User1

Acquired : 2/13/2020 4:27:23 PM
Processed : 2/13/2020 5:37:57 PM
Printed : 9/12/2020 11:47:49 AM

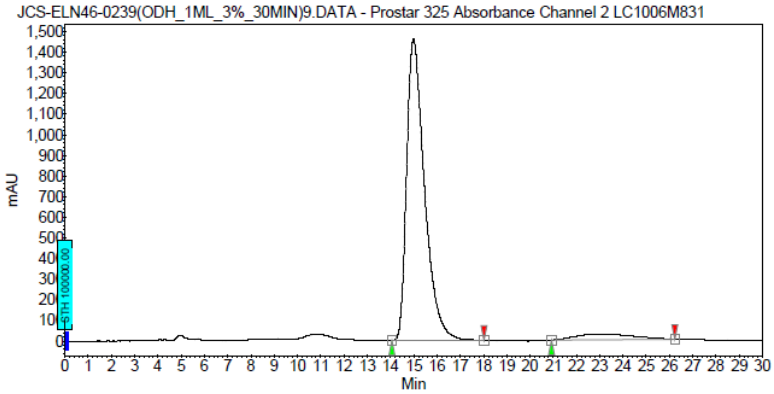

Peak results :

Index	Name	Time [Min]	Quantity [% Area]	Height [mAU]	Area [mAU.Min]	Area % [%]
1	UNKNOWN	14.99	94.21	1460.7	1300.2	94.213
2	UNKNOWN	23.00	5.79	27.2	79.9	5.787
Total			100.00	1487.9	1380.0	100.000

Racemic trace:

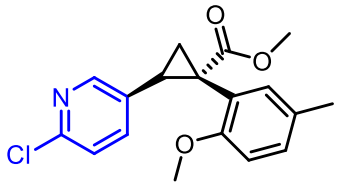

55

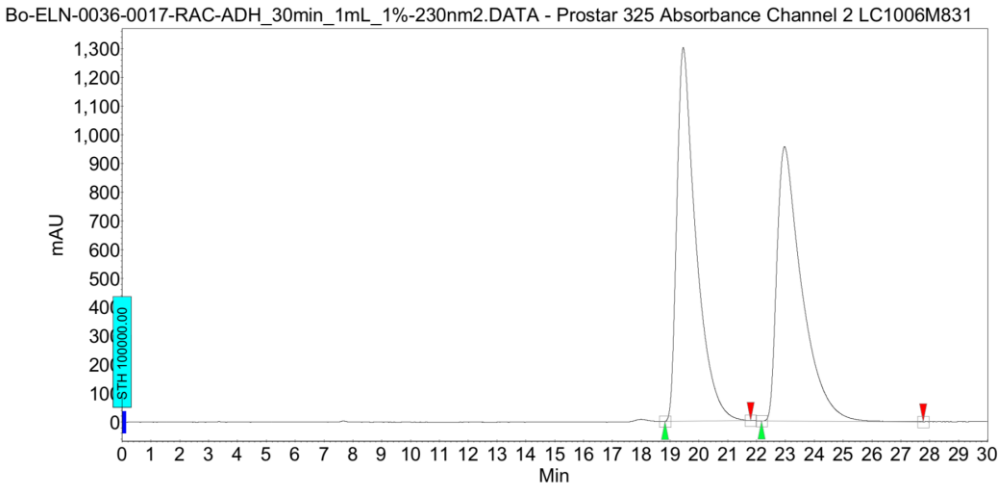

Peak results :

Index	Name	Time [Min]	Quantity [% Area]	Height [mAU]	Area [mAU.Min]	Area % [%]
2	UNKNOWN	19.46	51.18	1301.1	997.7	51.179
1	UNKNOWN	22.97	48.82	954.5	951.7	48.821
Total			100.00	2255.5	1949.4	100.000

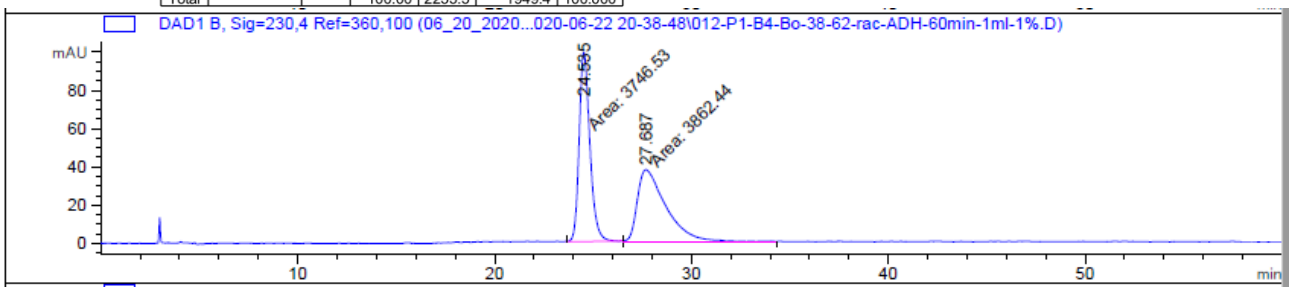


```
Signal 2: DAD1 B, Sig=230,4 Ref=360,100

Peak RetTime Type  Width     Area      Height     Area
  #   [min]        [min]   [mAU*s]     [mAU]       %
----|-------|----|-------|----------|----------|--------|
   1  24.535 MM    0.6308 3746.52588   98.99397  49.2383
   2  27.687 MM    1.7056 3862.44385   37.74244  50.7617

Totals :                 7608.96973  136.73640
```

25 ̊C, 1 mol % Rh_2(*S*-Tris(*p*-^{t}BuPh)-TPCP)$_4$, 2.5 equiv of vinyl pyridine, reaction performed according to procedure 3.3

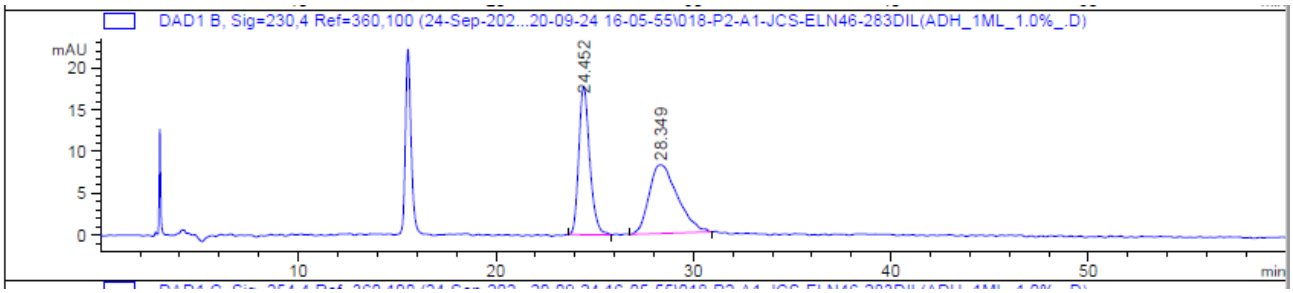

Signal 2: DAD1 B, Sig=230,4 Ref=360,100

Peak #	RetTime [min]	Type	Width [min]	Area [mAU*s]	Height [mAU]	Area %
1	24.452	BB	0.5913	682.12305	17.71050	45.3337
2	28.349	BB	1.1946	822.54871	8.19809	54.6663
Totals :				1504.67175		25.90858

25℃, 1 mol % Rh_2(*R*-*p*-Ph-TPCP)$_4$, 2.5 equiv of vinyl pyridine, reaction performed according to procedure 3.3

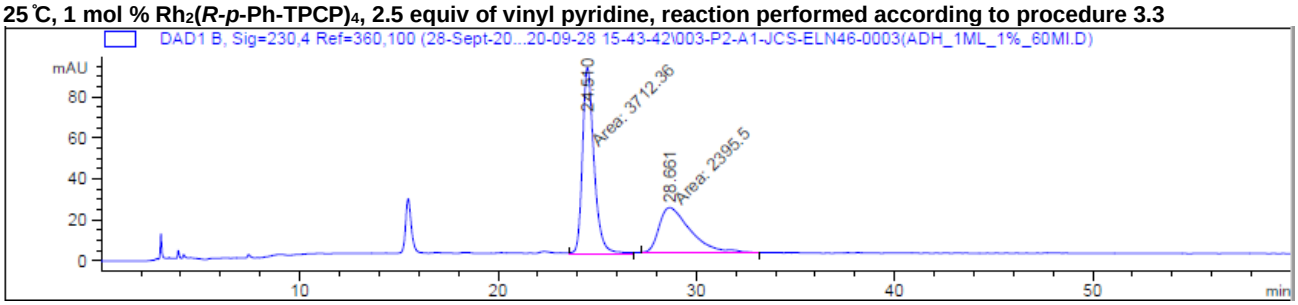

Signal 2: DAD1 B, Sig=230,4 Ref=360,100

Peak #	RetTime [min]	Type	Width [min]	Area [mAU*s]	Height [mAU]	Area %
1	24.510	MM	0.6798	3712.36304	91.01790	60.7801
2	28.661	MM	1.8180	2395.49829	21.96103	39.2199
Totals :				6107.86133		112.97893

25℃, 1 mol % Rh_2(*S*-PTAD)$_4$, 2.5 equiv of vinyl pyridine, reaction performed according to procedure 3.3

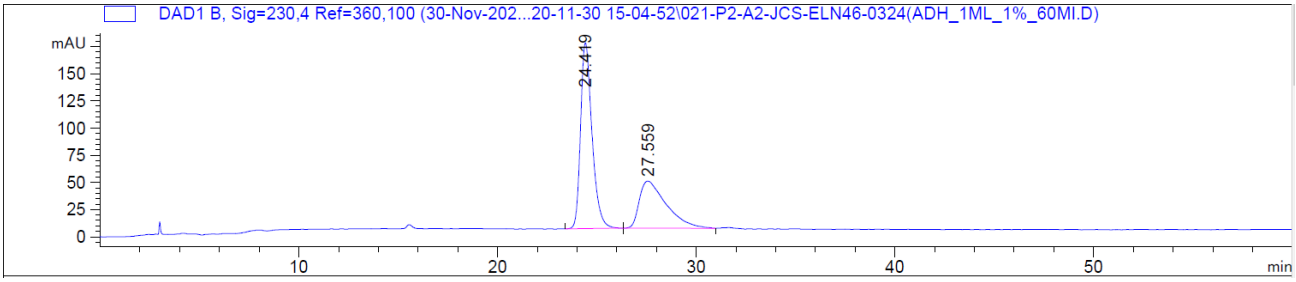

Signal 2: DAD1 B, Sig=230,4 Ref=360,100

Peak #	RetTime [min]	Type	Width [min]	Area [mAU*s]	Height [mAU]	Area %
1	24.419	BB	0.6104	6852.22852	170.68393	62.7498
2	27.559	BB	1.3235	4067.68384	43.24023	37.2502
Totals :				1.09199e4	213.92416	

25℃, 1 mol % Rh_2(*R*-DOSP)$_4$, 2.5 equiv of vinyl pyridine, reaction performed according to procedure 3.3

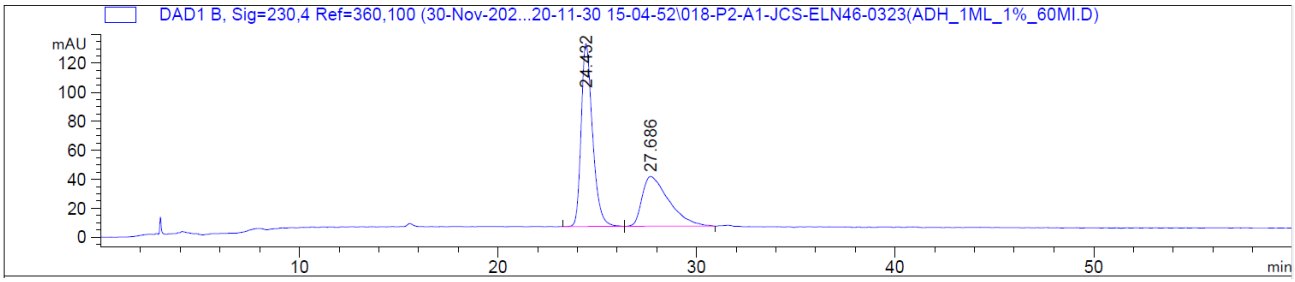

Signal 2: DAD1 B, Sig=230,4 Ref=360,100

Peak #	RetTime [min]	Type	Width [min]	Area [mAU*s]	Height [mAU]	Area %
1	24.432	BB	0.6066	5040.94482	126.03858	60.9987
2	27.686	BB	1.2961	3223.07275	34.36885	39.0013
Totals :				8264.01758	160.40743	

25 ̊C, 1 mol % Rh_2(*S*-TPPTTL)$_4$, 2.5 equiv of vinyl pyridine, reaction performed according to procedure 5.3

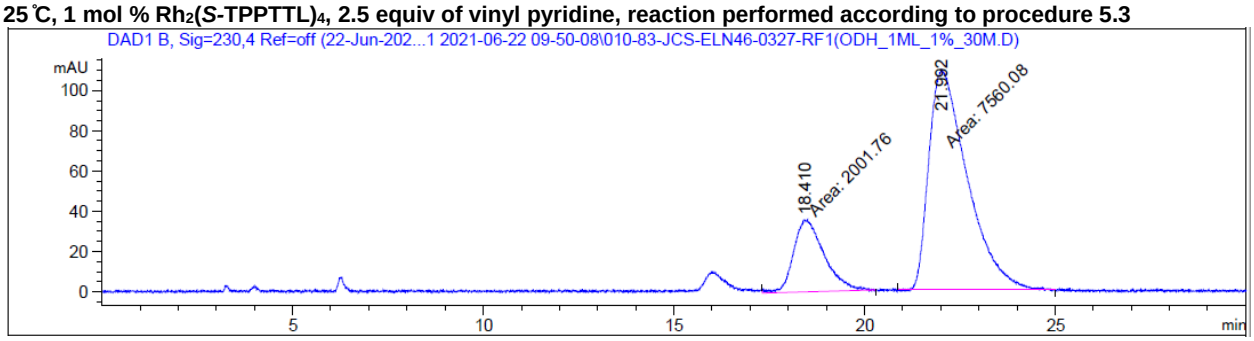

Signal 2: DAD1 B, Sig=230,4 Ref=off

Peak #	RetTime [min]	Type	Width [min]	Area [mAU*s]	Height [mAU]	Area %
1	18.410	MM	0.9206	2001.76111	36.24048	20.9349
2	21.992	MM	1.1563	7560.07959	108.97326	79.0651
Totals :				9561.84070	145.21374	

25 ̊C, 1 mol % Rh_2(*S*-TPPTTL)$_4$, 2.5 equiv of vinyl pyridine, trifluorotoluene as solvent, reaction performed according to procedure 3.3

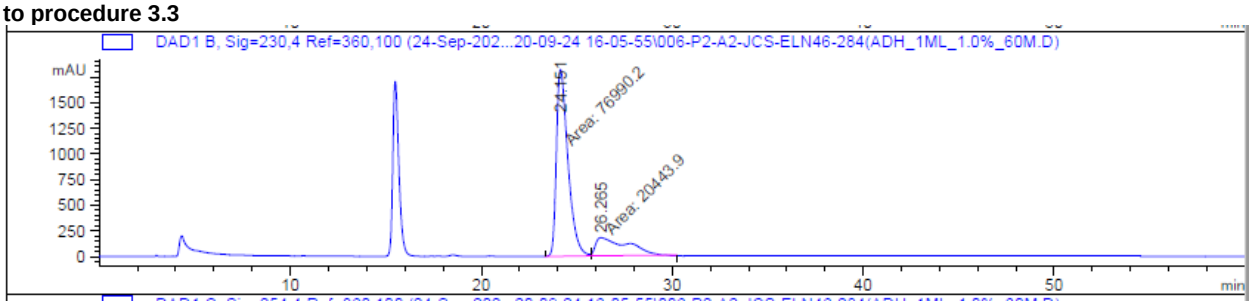

Signal 2: DAD1 B, Sig=230,4 Ref=360,100

Peak #	RetTime [min]	Type	Width [min]	Area [mAU*s]	Height [mAU]	Area %
1	24.151	MM	0.7051	7.69902e4	1819.95508	79.0177
2	26.265	MM	1.9219	2.04439e4	177.29097	20.9823
Totals :				9.74341e4	1997.24605	

25 ℃, 1.0 mol % Rh_2(*S*-TPPTTL)$_4$, 2.5 equiv vinyl heterocycle, $(MeO)_2CO$ as solvent, reaction performed according to procedure 3.3

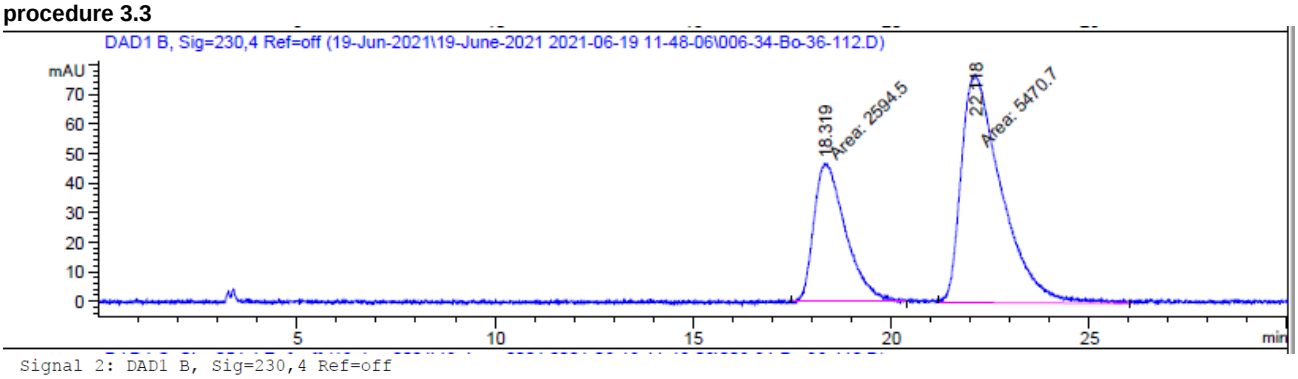


```
Signal 2: DAD1 B, Sig=230,4 Ref=off

Peak RetTime Type  Width     Area      Height     Area
  #   [min]        [min]   [mAU*s]     [mAU]       %
----|-------|----|-------|----------|----------|--------|
   1  18.319 MM    0.9232 2594.49976   46.84001  32.1691
   2  22.118 MM    1.1747 5470.69922   77.62168  67.8309

Totals :                 8065.19897  124.46169
```

0 ℃, 1.0 mol % Rh_2(*S*-TPPTTL)$_4$, 2.5 equiv vinyl heterocycle, CH_2Cl_2 as solvent, reaction performed according to procedure 3.3

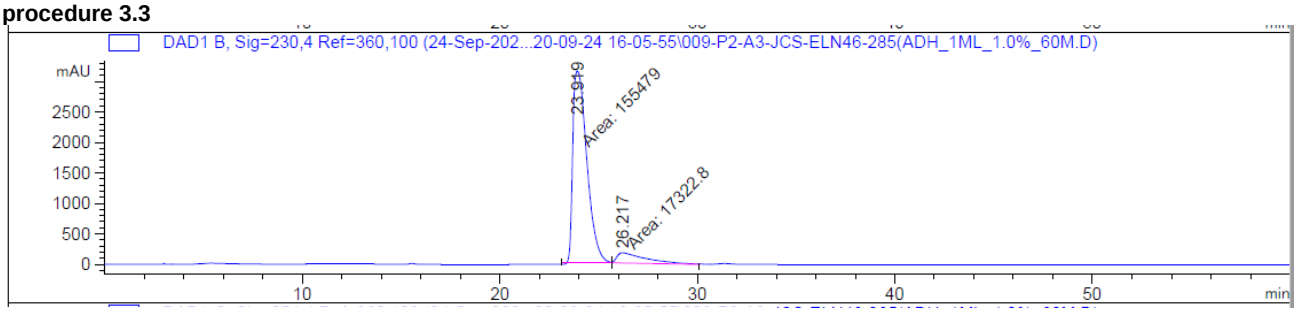


```
Signal 2: DAD1 B, Sig=230,4 Ref=360,100

Peak RetTime Type  Width     Area      Height     Area
  #   [min]        [min]   [mAU*s]     [mAU]       %
----|-------|----|-------|----------|----------|--------|
   1  23.919 MM    0.8237 1.55479e5  3145.96094  89.9753
   2  26.217 MM    1.7319 1.73228e4   166.70610  10.0247

Totals :                 1.72802e5  3312.66704
```

–50 ℃, 1.0 mol % Rh_2(*R*-TPPTTL)$_4$, 2.5 equiv vinyl heterocycle, CH_2Cl_2 as solvent, reaction performed according to procedure 3.3

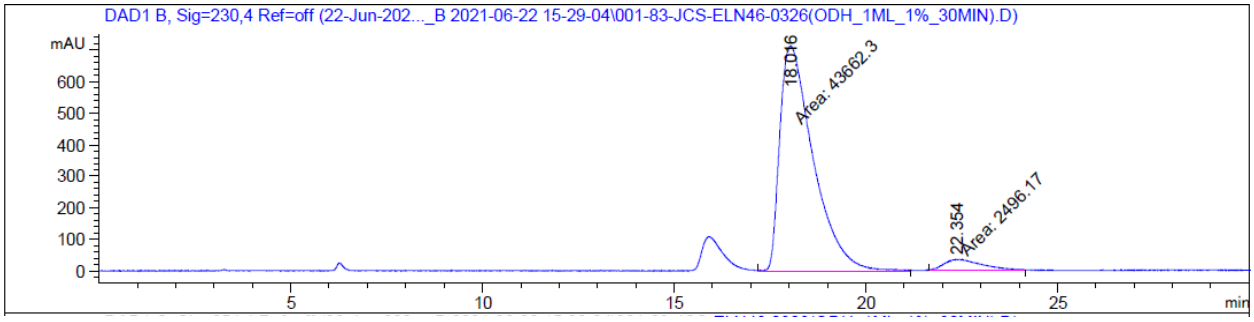


```
Signal 2: DAD1 B, Sig=230,4 Ref=off

Peak RetTime Type  Width     Area      Height     Area
  #   [min]        [min]   [mAU*s]     [mAU]       %
----|-------|----|-------|----------|----------|--------|
   1  18.016 MM    1.0163 4.36623e4   716.00336  94.5922
   2  22.354 MM    1.1754 2496.16895   35.39403   5.4078

Totals :                 4.61585e4   751.39739
```

0 ℃, 1.0 mol % Rh_2(*S*-TPPTTL)$_4$, 5.0 equiv vinyl heterocycle, CH_2Cl_2 as solvent, reaction performed according to procedure 3.3

Chromatogram :
JCS-ELN46-0088(OD-H_30min_1ml_1%)23_channel2

System : Prostar LC System
Method : ADH_30min_1mL_1%-230nm
User : User1

Acquired : 10/10/2019 4:30:32 PM
Processed : 10/10/2019 5:01:43 PM
Printed : 9/30/2020 3:25:52 PM

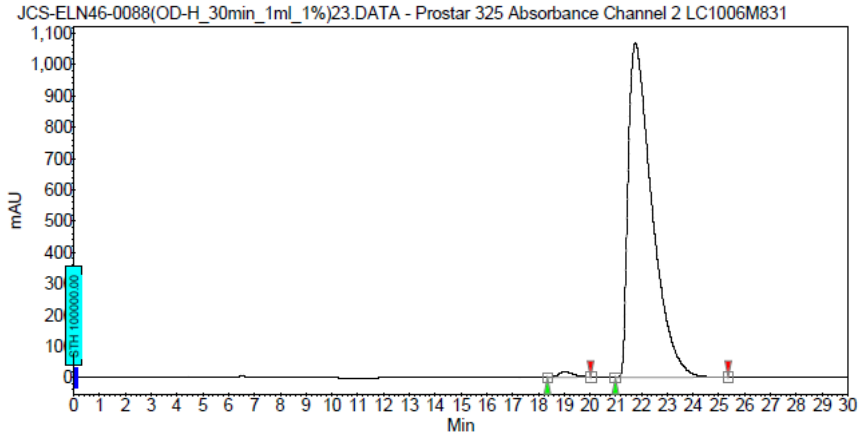

Peak results :

Index	Name	Time [Min]	Quantity [% Area]	Height [mAU]	Area [mAU.Min]	Area % [%]
1	UNKNOWN	19.04	1.08	17.1	12.5	1.084
2	UNKNOWN	21.76	98.92	1068.8	1142.0	98.916
Total			100.00	1085.9	1154.6	100.000

0 ℃, 1.0 mol % Rh_2(*S*-TPPTTL)$_4$, 10.0 equiv vinyl heterocycle, CH_2Cl_2 as solvent, reaction performed according to procedure 3.3

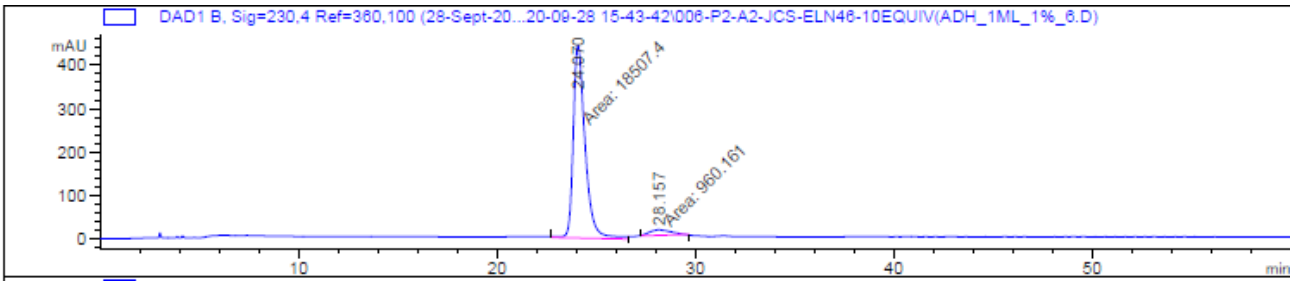


```
Signal 2: DAD1 B, Sig=230,4 Ref=360,100

Peak RetTime Type  Width     Area      Height     Area
  #   [min]        [min]   [mAU*s]     [mAU]       %
----|-------|----|-------|----------|----------|--------|
   1  24.070 MM    0.6933 1.85074e4   444.89807  95.0679
   2  28.157 MM    1.2559  960.16119   12.74203   4.9321

Totals :                 1.94676e4   457.64010
```

0 ˚C, 1.0 mol % Rh_2(*S*-TPPTTL)$_4$, 1.5 equiv vinyl heterocycle, 3.5 equiv 2-chloropyridine, CH_2Cl_2 as solvent, reaction performed according to procedure 3.4

Chromatogram :
JCS-ELN46-0085(OD-H_30min_1ml_1%)20_channel2

System : Prostar LC System
Method : ADH_30min_1mL_1%-230nm
User : User1

Acquired : 10/10/2019 3:13:03 PM
Processed : 10/10/2019 3:52:13 PM
Printed : 9/30/2020 3:25:44 PM

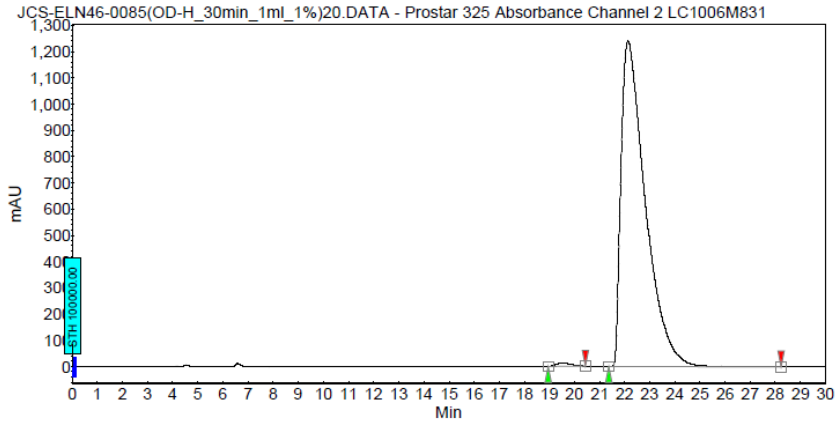

Peak results :

Index	Name	Time [Min]	Quantity [% Area]	Height [mAU]	Area [mAU.Min]	Area % [%]
1	UNKNOWN	19.54	0.67	13.0	9.4	0.670
2	UNKNOWN	22.14	99.33	1239.6	1387.0	99.330
Total			100.00	1252.6	1396.4	100.000

0 ˚C, 1.0 mol % Rh_2(*S*-TPPTTL)$_4$, 1.5 equiv vinyl heterocycle, 2.5 equiv 2-chloropyridine, CH_2Cl_2 as solvent, reaction performed according to procedure 3.4

Chromatogram :
JCS-ELN46-2.5P(ODH_30MIN_1ML_1%)9_channe l2

System : Prostar LC System
Method : ADH_30min_1mL_1%-230nm
User : User1

Acquired : 12/10/2019 4:34:30 PM
Processed : 12/11/2019 11:15:42 AM
Printed : 12/31/2019 12:04:53 PM

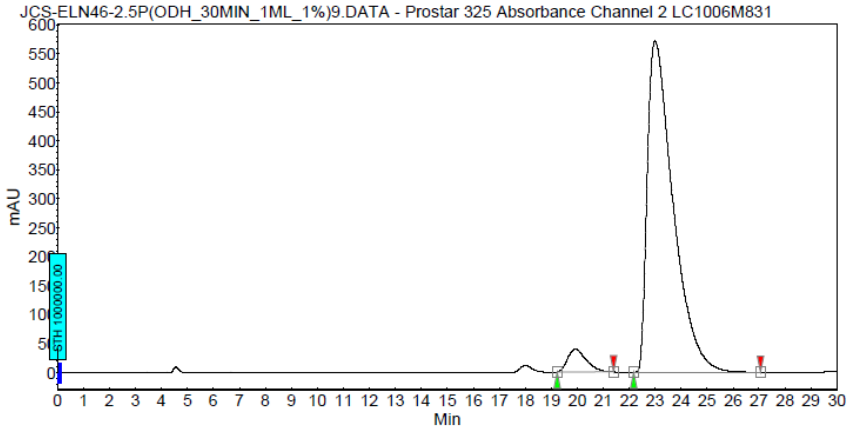

Peak results :

Index	Name	Time [Min]	Quantity [% Area]	Height [mAU]	Area [mAU.Min]	Area % [%]
1	UNKNOWN	19.92	4.75	39.3	32.8	4.753
2	UNKNOWN	23.00	95.25	571.8	657.6	95.247
Total			100.00	611.1	690.4	100.000

0 ℃, 1.0 mol % Rh_2(*S*-TPPTTL)$_4$, 1.5 equiv vinyl heterocycle, 1.5 equiv 2-chloropyridine, CH_2Cl_2 as solvent, reaction performed according to procedure 3.4

Chromatogram :
JCS-ELN46-1.5P(ODH_30MIN_1ML_1%)6_channe l2

System : Prostar LC System
Method : ADH_30min_1mL_1%-230nm
User : User1

Acquired : 12/10/2019 3:17:21 PM
Processed : 12/11/2019 11:15:02 AM
Printed : 12/31/2019 12:04:31 PM

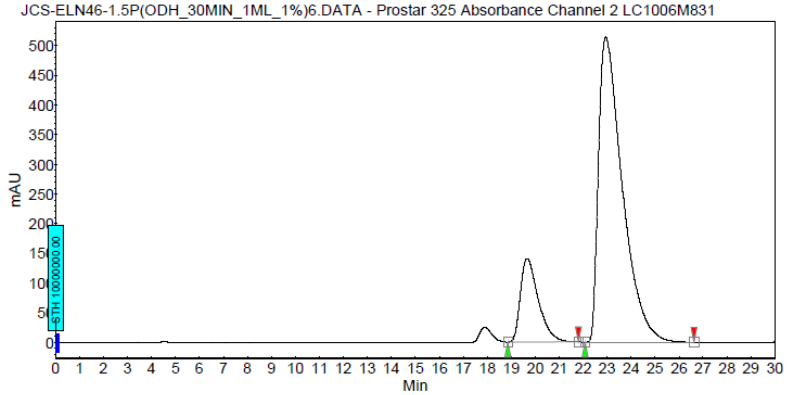

Peak results :

Index	Name	Time [Min]	Quantity [% Area]	Height [mAU]	Area [mAU.Min]	Area % [%]
1	UNKNOWN	19.66	17.07	140.3	121.7	17.068
2	UNKNOWN	22.94	82.93	513.6	591.4	82.932
Total			100.00	653.9	713.1	100.000

0 ℃, 1.0 mol % Rh_2(*S*-TPPTTL)$_4$, 1.5 equiv vinyl heterocycle, 3.5 equiv 2-chloropyridine, CH_2Cl_2 as solvent, no drying additive present, reaction performed according to procedure 3.4

Chromatogram :
JCS-ELN46-0046re(ADH_1ml_1%_60min)2_channel1

System : Prostar LC System
Method : DACHDNB_30min_1mL_1%-230nm
User : User1

Acquired : 8/28/2019 5:38:18 PM
Processed : 8/29/2019 11:36:36 AM
Printed : 9/30/2020 3:29:25 PM

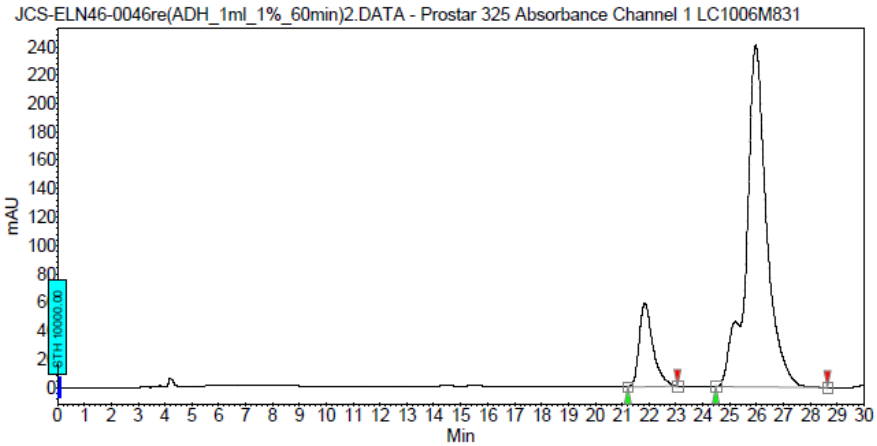

Peak results :

Index	Name	Time [Min]	Quantity [% Area]	Height [mAU]	Area [mAU.Min]	Area % [%]
1	UNKNOWN	21.84	14.11	59.4	34.9	14.110
2	UNKNOWN	25.97	85.89	241.1	212.6	85.890
Total			100.00	300.5	247.5	100.000

0 ℃, 1.0 mol % Rh_2(*S*-TPPTTL)$_4$, 1.5 equiv vinyl heterocycle, 3.5 equiv 2-chloropyridine, CH_2Cl_2 as solvent, 10 equiv HFIP, reaction performed according to procedure 3.5

Chromatogram :
JCS-ELN46-0185(ODH_1ML_1%_30MIN)67_channel2

System : Prostar LC System
Method : ADH_30min_1mL_1%-230nm
User : User1

Acquired : 12/11/2019 10:42:37 PM
Processed : 12/12/2019 9:45:36 AM
Printed : 9/12/2020 12:15:49 PM

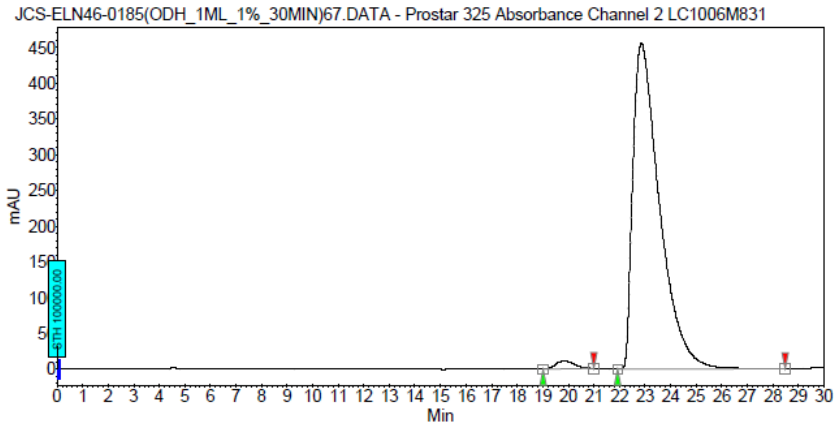

Peak results :

Index	Name	Time [Min]	Quantity [% Area]	Height [mAU]	Area [mAU.Min]	Area % [%]
1	UNKNOWN	19.82	1.71	11.3	9.6	1.714
2	UNKNOWN	22.86	98.29	455.9	550.6	98.286
Total			100.00	467.2	560.2	100.000

0 ℃, 1.0 mol % Rh_2(*S*-TPPTTL)$_4$, 1.5 equiv vinyl heterocycle, 3.5 equiv 2-chloropyridine, CH_2Cl_2 as solvent, 5 equiv HFIP, reaction performed according to procedure 3.5

Chromatogram :
JCS-ELN46-0144(ODSH_1ml_1%_30min)3_channel2

System : Prostar LC System
Method : ADH_30min_1mL_1%-230nm
User : User1

Acquired : 11/21/2019 11:16:20 AM
Processed : 11/21/2019 11:57:48 AM
Printed : 12/31/2019 12:18:07 PM

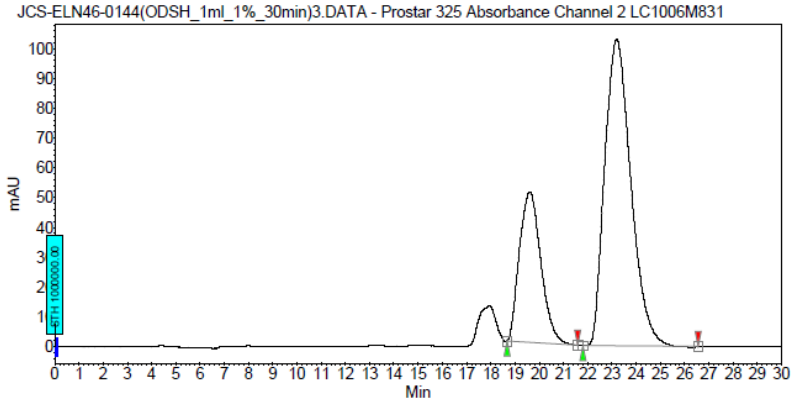

Peak results :

Index	Name	Time [Min]	Quantity [% Area]	Height [mAU]	Area [mAU.Min]	Area % [%]
1	UNKNOWN	19.61	28.83	50.4	51.9	28.830
2	UNKNOWN	23.20	71.17	102.7	128.0	71.170
Total			100.00	153.1	179.9	100.000

0 ℃, 1.0 mol % Rh_2(*S*-TPPTTL)$_4$, 1.5 equiv vinyl heterocycle, 3.5 equiv 2-chloropyridine, CH_2Cl_2 as solvent, 1.0 equiv HFIP, reaction performed according to procedure 3.5

Chromatogram :
JCS-ELN46-0146(ODSH_1ml_1%_30min)9_channel2

System : Prostar LC System
Method : ADH_30min_1mL_1%-230nm
User : User1

Acquired : 11/21/2019 1:54:03 PM
Processed : 11/25/2019 3:27:35 PM
Printed : 12/31/2019 12:18:17 PM

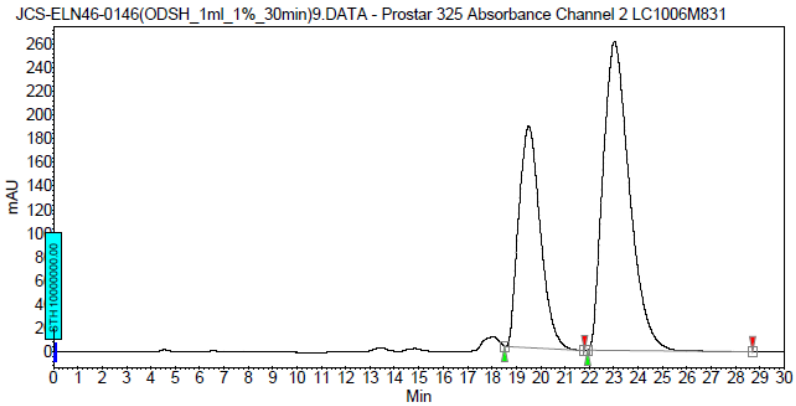

Peak results :

Index	Name	Time [Min]	Quantity [% Area]	Height [mAU]	Area [mAU.Min]	Area % [%]
1	UNKNOWN	19.51	37.00	187.6	192.8	36.999
2	UNKNOWN	23.03	63.00	260.8	328.3	63.001
Total			100.00	448.4	521.1	100.000

25℃, 1.0 mol % Rh_2(*S*-TPPTTL)$_4$, 1.5 equiv vinyl heterocycle, 3.5 equiv 2-chloropyridine, CH_2Cl_2 as solvent 20 equiv HFIP, reaction performed according to procedure 3.6

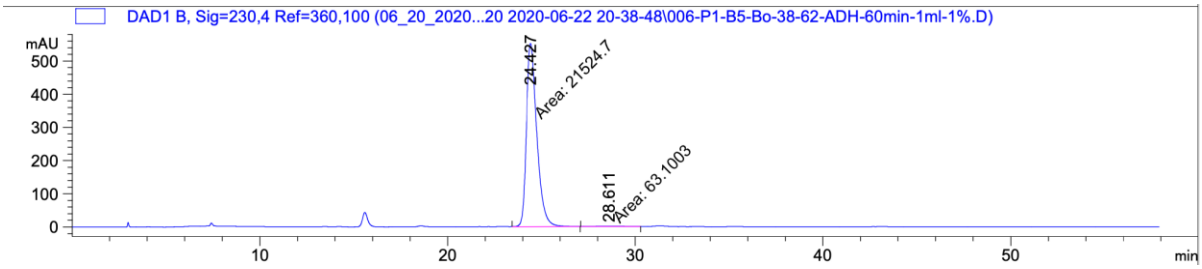

Signal 2: DAD1 B, Sig=230,4 Ref=360,100

Peak #	RetTime [min]	Type	Width [min]	Area [mAU*s]	Height [mAU]	Area %
1	24.427	MM	0.6497	2.15247e4	552.13348	99.7077
2	28.611	MM	1.2945	63.10027	8.12402e-1	0.2923

Totals : 2.15878e4 552.94589

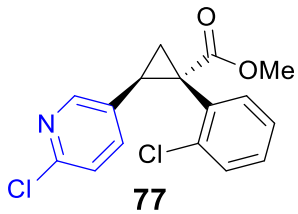

77

Racemic Trace:

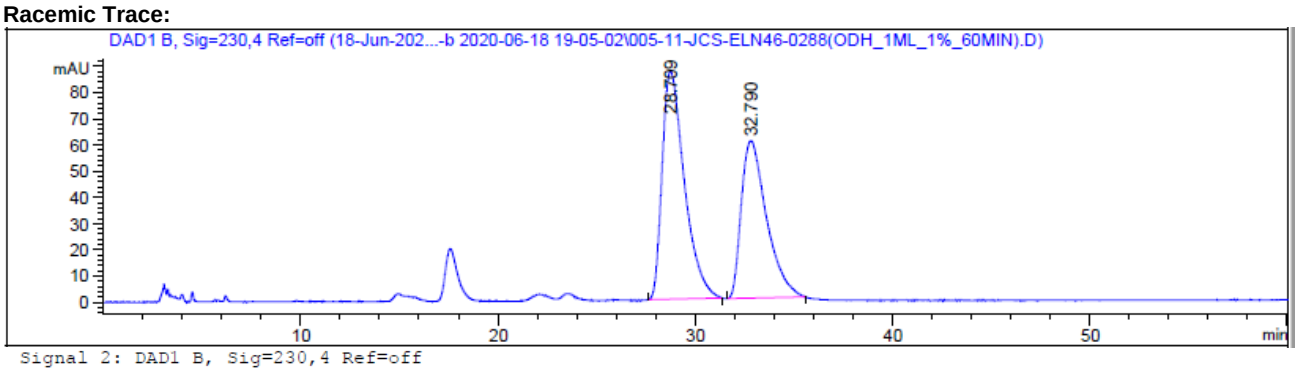

Signal 2: DAD1 B, Sig=230,4 Ref=off

Peak #	RetTime [min]	Type	Width [min]	Area [mAU*s]	Height [mAU]	Area %
1	28.709	VV R	0.9181	6819.27051	86.98462	56.0344
2	32.790	VV R	1.0426	5350.51172	60.01482	43.9656

Totals : 1.21698e4 146.99944

0 ℃, 1.0 mol % Rh_2(*S*-TPPTTL)$_4$, 1.5 equiv vinyl heterocycle, 3.5 equiv 2-chloropyridine, CH_2Cl_2 as solvent, reaction performed according to procedure 3.4

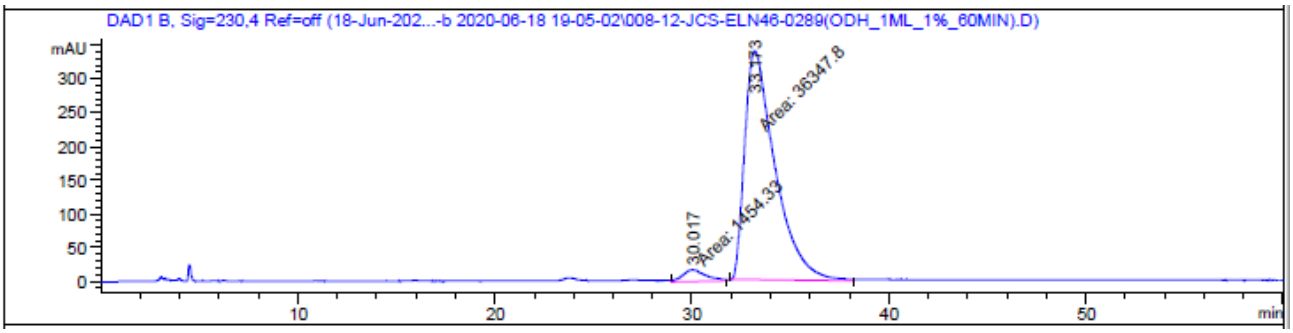

Signal 2: DAD1 B, Sig=230,4 Ref=off

Peak #	RetTime [min]	Type	Width [min]	Area [mAU*s]	Height [mAU]	Area %
1	30.017	MM	1.3712	1454.32605	17.67680	3.8472
2	33.173	MM	1.7882	3.63478e4	338.76584	96.1528

Totals : 3.78022e4 356.44263

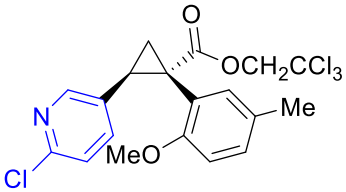

Table 2, Entry 7

Racemic Trace:

Chromatogram :
JCS-ELN-46-0018conc(ADH_30min_1mL_0.5%-230nm6.channel2

Method : ADH_30min_1mL_0.5%-230nm
User : User1

Acquired : 7/17/2019 9:11:27 AM
Processed : 9/21/2020 5:15:00 PM
Printed : 9/21/2020 5:15:08 PM

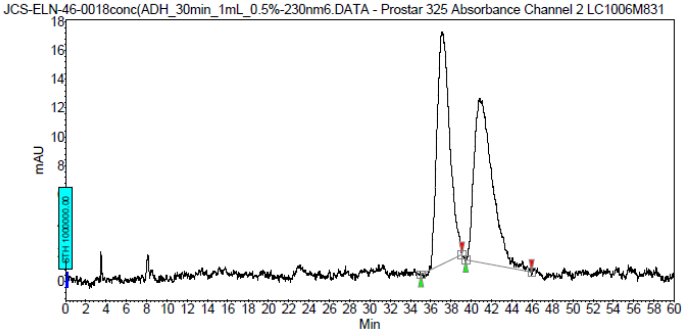

Peak results :

Index	Name	Time [Min]	Quantity [% Area]	Height [mAU]	Area [mAU.Min]	Area % [%]
1	UNKNOWN	37.07	49.19	16.1	23.1	49.195
2	UNKNOWN	40.77	50.81	11.4	23.9	50.805
Total			100.00	27.4	47.0	100.000

25 ℃, 1.0 mol % Rh_2(*R*-TPPTTL)$_4$, 2.5 equiv vinyl heterocycle, CH_2Cl_2 as solvent, reaction performed according to procedure 3.3

Chromatogram :
JCS-ELN-46-0019conc(ADH_30min_1mL_0.5%-2
30nm16_channel2

Method : ADH_30min_1mL_0.5%-230nm
User : User1

Acquired : 7/17/2019 10:59:49 AM
Processed : 12/31/2019 12:36:29 PM
Printed : 9/21/2020 5:14:37 PM

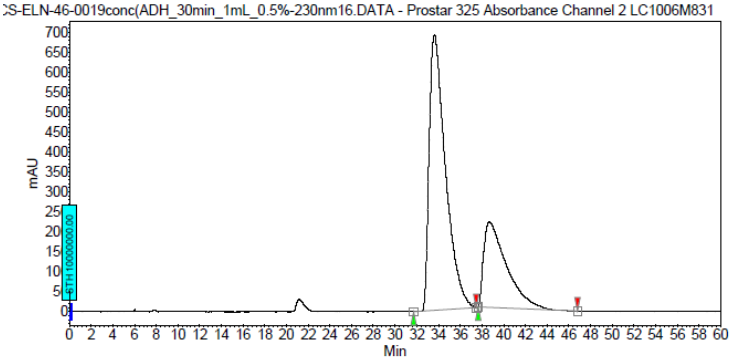

Peak results :

Index	Name	Time [Min]	Quantity [% Area]	Height [mAU]	Area [mAU.Min]	Area % [%]
1	UNKNOWN	33.63	69.60	690.8	1200.9	69.601
2	UNKNOWN	38.71	30.40	215.1	524.5	30.399
Total			100.00	905.9	1725.4	100.000

Racemic Trace:

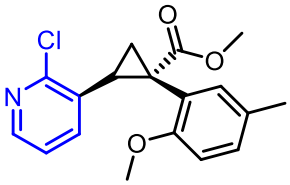

58

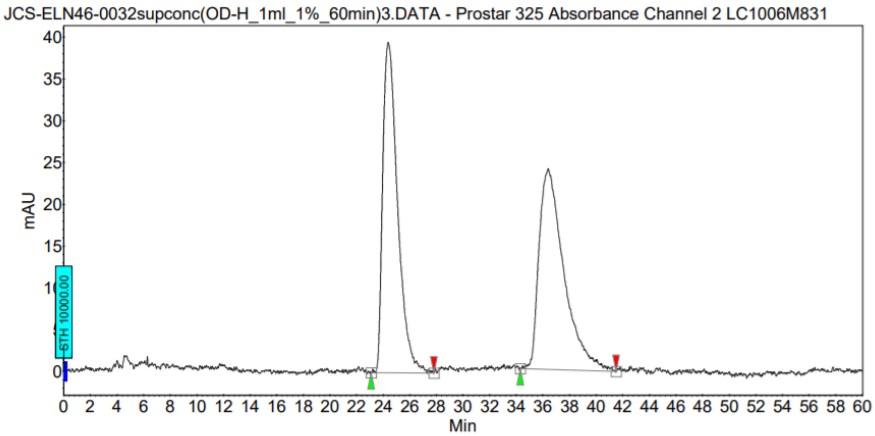

Peak results :

Index	Name	Time [Min]	Quantity [% Area]	Height [mAU]	Area [mAU.Min]	Area % [%]
1	UNKNOWN	24.36	49.68	39.5	51.3	49.675
2	UNKNOWN	36.40	50.32	24.0	52.0	50.325
Total			100.00	63.6	103.2	100.000

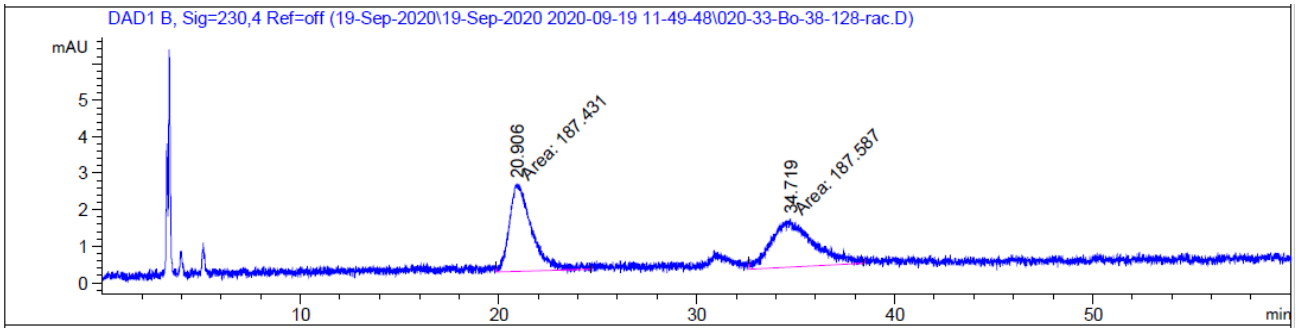


```
Signal 2: DAD1 B, Sig=230,4 Ref=off

Peak RetTime Type  Width     Area      Height     Area
  #   [min]        [min]   [mAU*s]     [mAU]       %
----|-------|----|-------|----------|----------|--------|
   1  20.906 MM    1.2927  187.43066    2.41649  49.9792
   2  34.719 MM    2.3695  187.58693    1.31948  50.0208

Totals :                  375.01759    3.73597
```

0 ℃, 1.0 mol % Rh_2(*R*-TPPTTL)$_4$ 5.0 equiv vinyl heterocycle, CH_2Cl_2 as solvent, reaction performed according to procedure 3.3

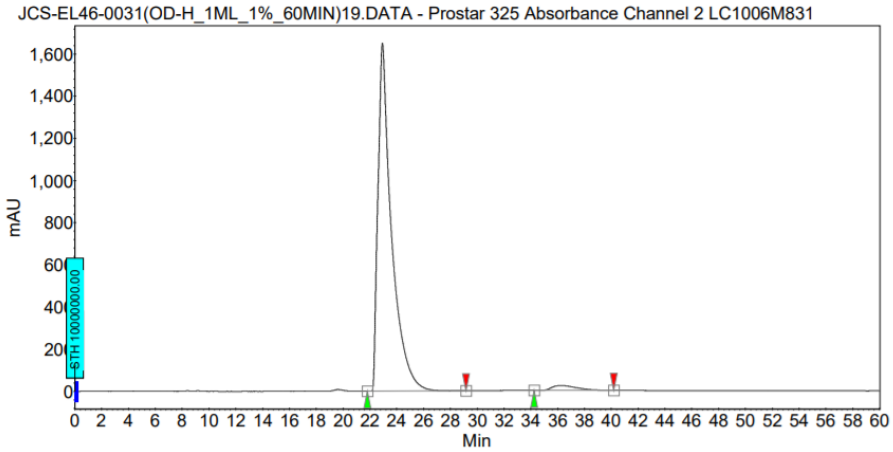

Peak results :

Index	Name	Time [Min]	Quantity [% Area]	Height [mAU]	Area [mAU.Min]	Area % [%]
1	UNKNOWN	22.93	97.43	1649.8	1929.1	97.427
2	UNKNOWN	36.26	2.57	23.4	50.9	2.573
Total			100.00	1673.3	1980.0	100.000

0 ℃, 1.0 mol % Rh_2(*S*-TPPTTL)$_4$, 1.5 equiv vinyl heterocycle, 3.5 equiv 2-chloropyridine, CH_2Cl_2 as solvent, 10 equiv HFIP, reaction performed according to procedure 3.5

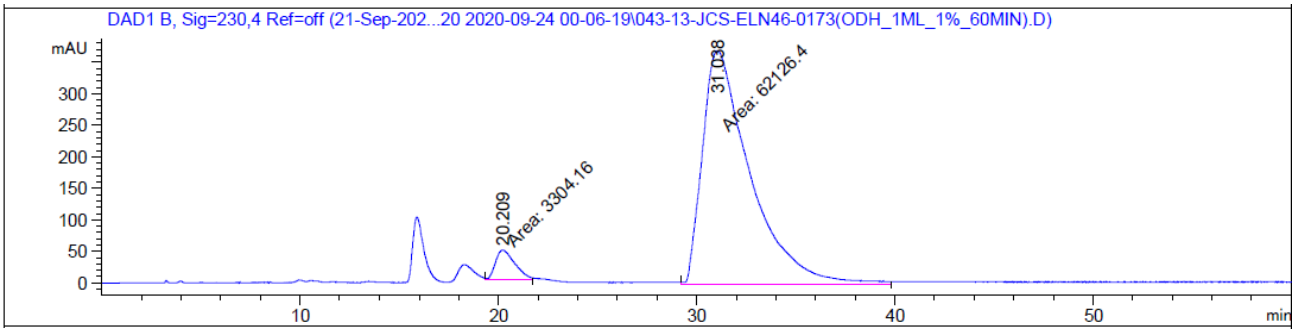


```
Signal 2: DAD1 B, Sig=230,4 Ref=off

Peak RetTime Type  Width     Area      Height     Area
  #   [min]        [min]   [mAU*s]     [mAU]       %
----|-------|----|-------|----------|----------|--------|
   1  20.209 MM    1.1572 3304.15601   47.58920   5.0499
   2  31.038 MM    2.7909 6.21264e4   371.00339  94.9501

Totals :                 6.54305e4   418.59259
```

Racemic Trace:

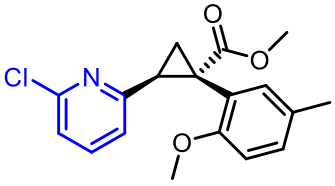

59

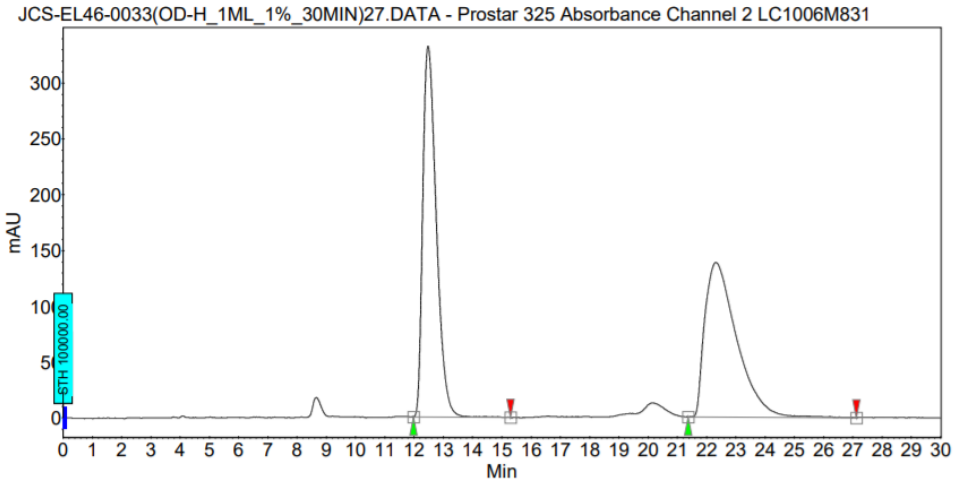

Peak results :

Index	Name	Time [Min]	Quantity [% Area]	Height [mAU]	Area [mAU.Min]	Area % [%]
1	UNKNOWN	12.48	50.48	332.2	178.2	50.479
2	UNKNOWN	22.31	49.52	138.6	174.9	49.521
Total			100.00	470.8	353.1	100.000

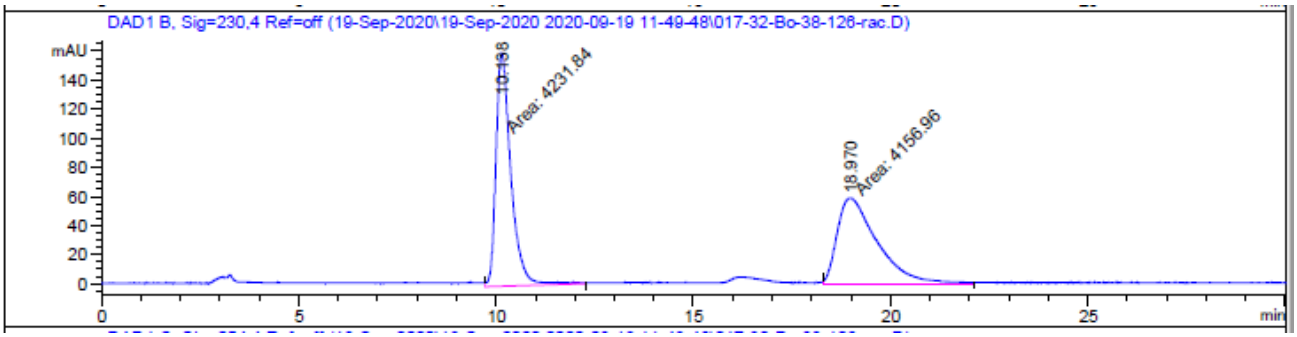

Signal 2: DAD1 B, Sig=230,4 Ref=off

Peak #	RetTime [min]	Type	Width [min]	Area [mAU*s]	Height [mAU]	Area %
1	10.138	MM	0.4400	4231.83789	160.27992	50.4463
2	18.970	MM	1.1751	4156.95947	58.95683	49.5537
Totals :				8388.79736	219.23675	

0 ℃, 1.0 mol % Rh_2(*R*-TPPTTL)$_4$ 5.0 equiv vinyl heterocycle, CH_2Cl_2 as solvent, reaction performed according to procedure 3.3

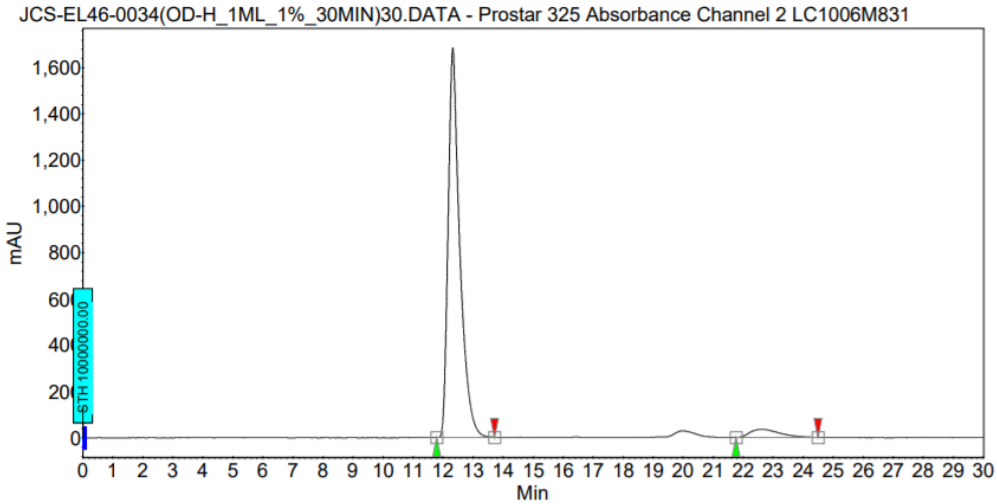

Peak results :

Index	Name	Time [Min]	Quantity [% Area]	Height [mAU]	Area [mAU.Min]	Area % [%]
1	UNKNOWN	12.32	94.97	1683.9	756.0	94.972
2	UNKNOWN	22.59	5.03	35.0	40.0	5.028
Total			100.00	1718.9	796.0	100.000

0 ˚C, 1.0 mol % Rh_2(*S*-TPPTTL)$_4$, 1.5 equiv vinyl heterocycle, 3.5 equiv 2-chloropyridine, CH_2Cl_2 as solvent, 10 equiv HFIP, reaction performed according to procedure 3.5

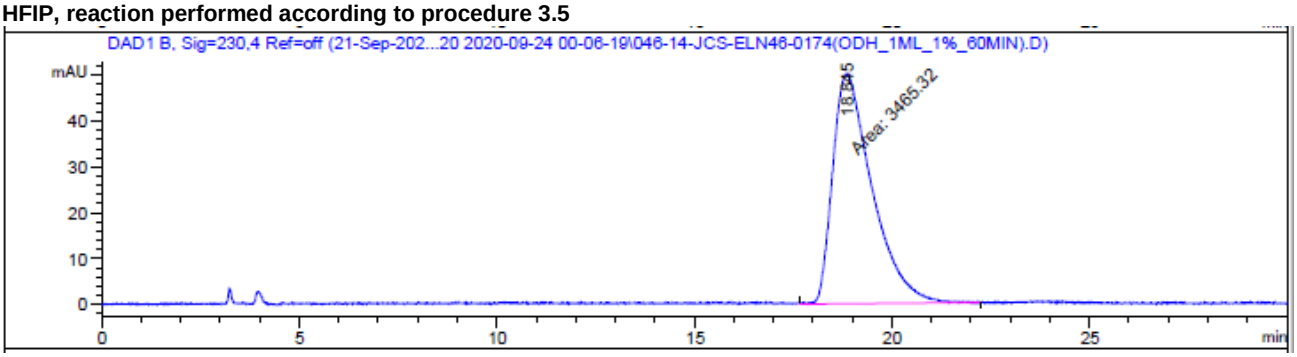


```
Signal 2: DAD1 B, Sig=230,4 Ref=off

Peak RetTime Type  Width     Area      Height     Area
  #   [min]        [min]   [mAU*s]     [mAU]       %
----|-------|----|-------|----------|----------|--------|
   1  18.845 MM    1.1559 3465.31787   49.96665 100.0000

Totals :                  3465.31787   49.96665
```

Racemic trace:

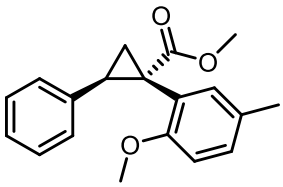

60

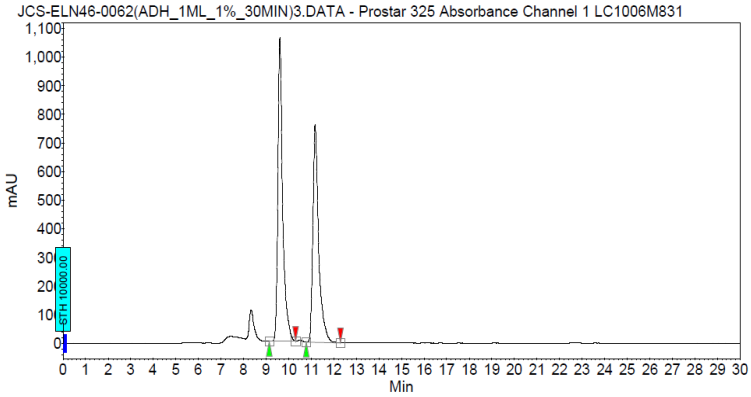

Peak results :

Index	Name	Time [Min]	Quantity [% Area]	Height [mAU]	Area [mAU.Min]	Area % [%]
1	UNKNOWN	9.61	53.67	1060.1	260.5	53.666
2	UNKNOWN	11.17	46.33	760.0	224.9	46.334
Total			100.00	1820.2	485.3	100.000

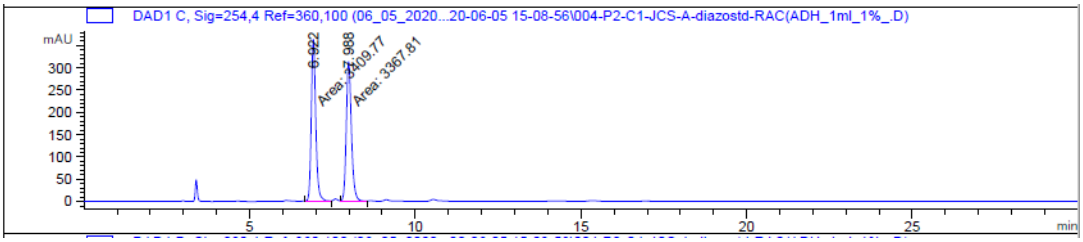

```
Signal 3: DAD1 C, Sig=254,4 Ref=360,100

Peak RetTime Type  Width     Area      Height     Area
  #   [min]        [min]   [mAU*s]     [mAU]       %
----|-------|----|-------|----------|----------|--------|
   1   6.922 MM    0.1564 3409.76978  363.26288  50.3095
   2   7.988 MM    0.1792 3367.81470  313.22736  49.6905

Totals :                  6777.58447  676.49023
```

0 ℃, 1.0 mol % Rh_2(*S*-TPPTTL)$_4$ 5.0 equiv styrene, CH_2Cl_2 as solvent, reaction performed according to procedure 3.3

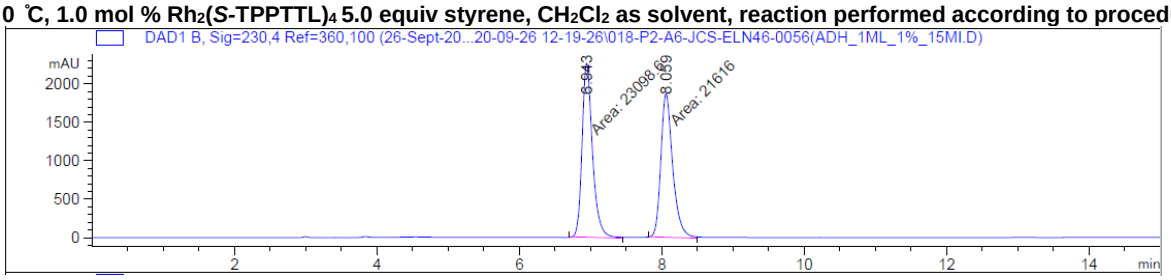


```
Signal 2: DAD1 B, Sig=230,4 Ref=360,100

Peak RetTime Type  Width     Area      Height     Area
  #   [min]        [min]   [mAU*s]     [mAU]       %
----|-------|----|-------|----------|----------|--------|
   1   6.943 MM    0.1701 2.30986e4  2263.13354  51.6578
   2   8.059 MM    0.1933 2.16160e4  1863.70142  48.3422

Totals :                  4.47146e4  4126.83496
```

0 ℃, 1.0 mol % Rh_2(*S*-TPPTTL)$_4$ 5.0 equiv styrene, 1.0 equiv 2-chloropyridine, CH_2Cl_2 as solvent, reaction performed according to procedure 3.4

Chromatogram :
JCS-ELN46-0095DIL(ADH_30MIN_1ml_1%)3_channel 1

Prostar LC System
Method : DACHDNB_30min_1mL_1%-230nm
User : User1

Acquired : 10/17/2019 9:55:29 AM
Processed : 10/17/2019 10:44:45 AM
Printed : 12/31/2019 12:32:50 PM

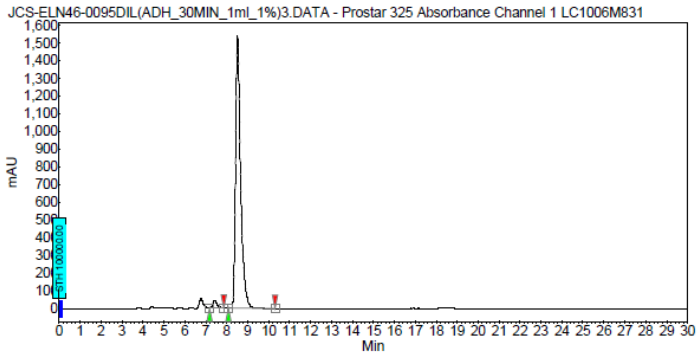

Peak results :

Index	Name	Time [Min]	Quantity [% Area]	Height [mAU]	Area [mAU.Min]	Area % [%]
2	UNKNOWN	7.41	2.41	44.3	10.6	2.413
1	UNKNOWN	8.52	97.59	1536.4	429.5	97.587
Total			100.00	1580.6	440.1	100.000

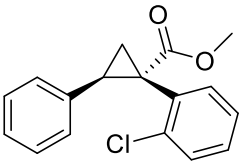

61

Racemic trace:

Chromatogram :
JCS-ELN46-0070(OJH_1ml_1%_30min)6_channe
l2

System : Prostar LC System
Method : OD_30min_1mL_1%_230nm
User : User1

Acquired : 10/2/2019 2:34:15 PM
Processed : 12/31/2019 12:46:22 PM
Printed : 12/31/2019 12:46:27 PM

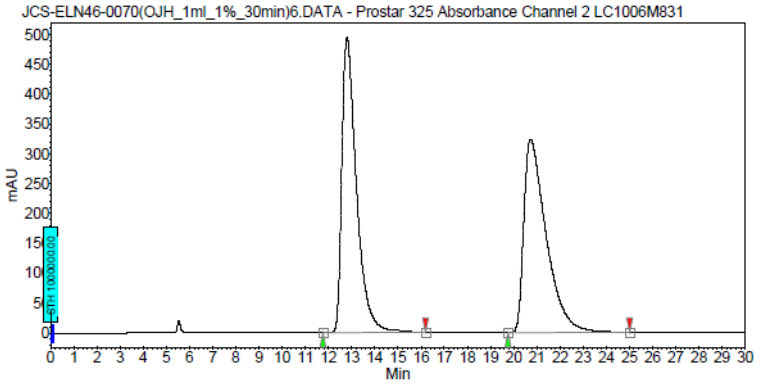

Peak results :

Index	Name	Time [Min]	Quantity [% Area]	Height [mAU]	Area [mAU.Min]	Area % [%]
1	UNKNOWN	12.80	49.85	493.8	360.6	49.854
2	UNKNOWN	20.73	50.15	323.5	362.7	50.146
Total			100.00	817.3	723.4	100.000

0 ℃, 1.0 mol % Rh_2(*S*-TPPTTL)$_4$ 5.0 equiv styrene, CH_2Cl_2 as solvent, reaction performed according to procedure 3.3

Chromatogram :
JCS-ELN46-0071(OJH_1ml_1%_30min)9_channe
l2

System : Prostar LC System
Method : OD_30min_1mL_1%_230nm
User : User1

Acquired : 10/2/2019 3:51:39 PM
Processed : 12/31/2019 12:46:44 PM
Printed : 12/31/2019 12:46:49 PM

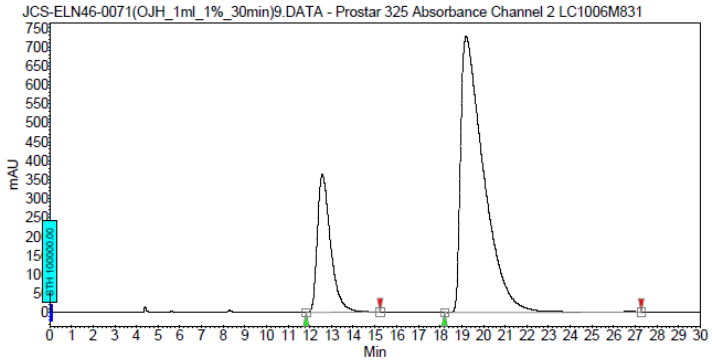

Peak results :

Index	Name	Time [Min]	Quantity [% Area]	Height [mAU]	Area [mAU.Min]	Area % [%]
1	UNKNOWN	12.57	22.27	363.9	257.5	22.266
2	UNKNOWN	19.20	77.73	728.1	898.8	77.734
Total			100.00	1092.0	1156.2	100.000

0 ℃, 1.0 mol % Rh_2(*S*-TPPTTL)$_4$ 5.0 equiv styrene, 1.0 equiv 2-chloropyridine, CH_2Cl_2 as solvent, reaction performed according to procedure 3.4

Chromatogram :
JCS-ELN46-0072F7-8RERUNOJH_1ML_1%_30MIN)58_channel2

System : Prostar LC System
Method : OD_30min_1mL_1%_230nm
User : User1

Acquired : 10/4/2019 5:19:31 PM
Processed : 12/31/2019 12:45:42 PM
Printed : 12/31/2019 12:45:46 PM

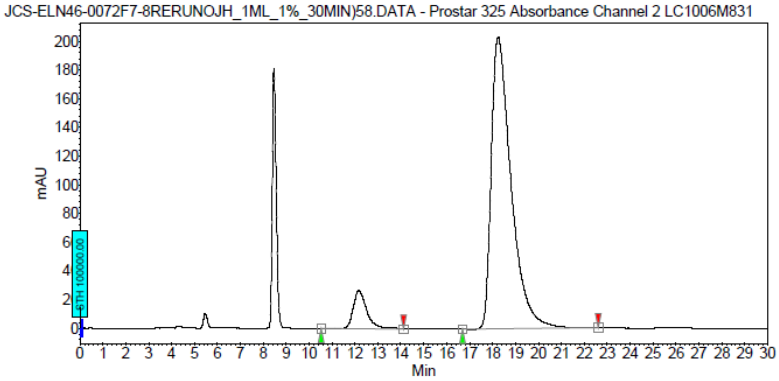

Peak results :

Index	Name	Time [Min]	Quantity [% Area]	Height [mAU]	Area [mAU.Min]	Area % [%]
1	UNKNOWN	12.17	8.19	26.5	18.2	8.194
2	UNKNOWN	18.24	91.81	203.3	204.2	91.806
Total			100.00	229.9	222.4	100.000

Racemic trace:

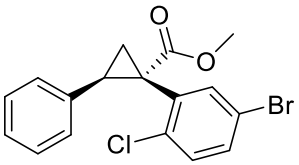

62

Chromatogram :
JCS-ELN46-0080(OJH_1ML_1%_30MIN)11_channel2

System : Prostar LC System
Method : OD_30min_1mL_1%_210_230nm
User : User1

Acquired : 10/8/2019 4:32:30 PM
Processed : 10/8/2019 5:19:04 PM
Printed : 12/31/2019 12:44:41 PM

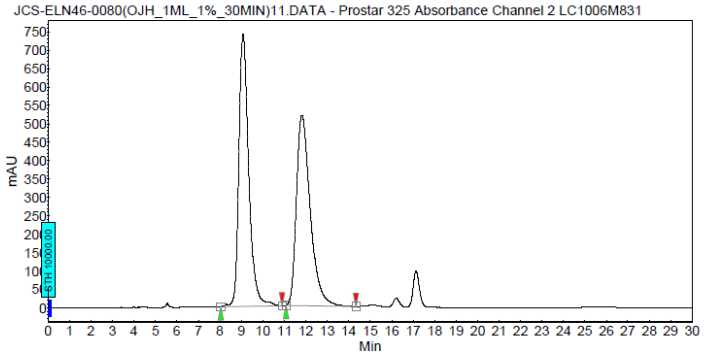

Peak results :

Index	Name	Time [Min]	Quantity [% Area]	Height [mAU]	Area [mAU.Min]	Area % [%]
1	UNKNOWN	9.07	50.51	739.1	394.0	50.510
2	UNKNOWN	11.82	49.49	516.8	386.0	49.490
Total			100.00	1255.9	780.0	100.000

0 ℃, 1.0 mol % Rh_2(*S*-TPPTTL)$_4$ 5.0 equiv styrene, CH_2Cl_2 as solvent, reaction performed according to procedure 3.3

Chromatogram :
JCS-ELN46-0078(OJH_1ML_1%_30MIN)14_channel2

System : Prostar LC System
Method : OD_30min_1mL_1%_210_230nm
User : User1

Acquired : 10/8/2019 5:49:55 PM
Processed : 10/9/2019 8:51:34 AM
Printed : 12/31/2019 12:44:37 PM

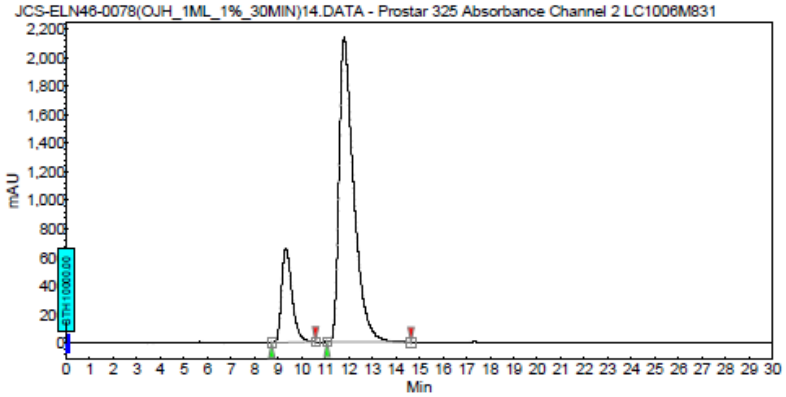

Peak results :

Index	Name	Time [Min]	Quantity [% Area]	Height [mAU]	Area [mAU.Min]	Area % [%]
1	UNKNOWN	9.33	18.01	664.7	338.8	18.006
2	UNKNOWN	11.81	81.99	2130.8	1542.8	81.994
Total			100.00	2795.5	1881.6	100.000

0 ℃, 1.0 mol % Rh_2(*S*-TPPTTL)$_4$ 5.0 equiv styrene, 1.0 equiv 2-chloropyridine, CH_2Cl_2 as solvent, reaction performed according to procedure 3.4

Chromatogram :
JCS-ELN46-0079DIL(OJH_30MIN_1ML_1%)3_channel2

System : Prostar LC System
Method : OD_30min_1mL_1%_230nm
User : User1

Acquired : 10/9/2019 9:44:19 AM
Processed : 12/31/2019 12:43:26 PM
Printed : 12/31/2019 12:43:28 PM

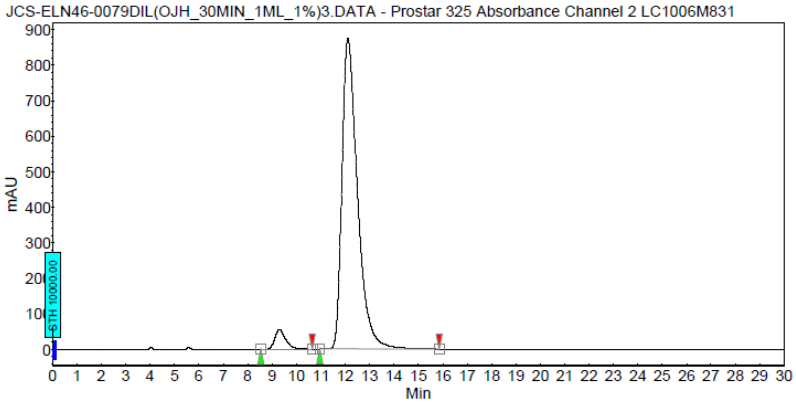

Peak results :

Index	Name	Time [Min]	Quantity [% Area]	Height [mAU]	Area [mAU.Min]	Area % [%]
1	UNKNOWN	9.30	4.30	55.7	29.0	4.303
2	UNKNOWN	12.11	95.70	872.6	643.9	95.697
Total			100.00	928.3	672.8	100.000

Racemic trace:

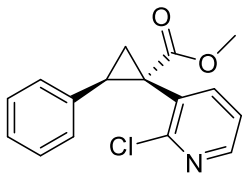

63

Chromatogram :
JCS-ELN46-0040(ADH_1ml_1%_60min)2_channel2

System : Prostar LC System
Method : DACHDNB_30min_1mL_1%-230nm
User : User1

Acquired : 8/23/2019 10:20:38 AM
Processed : 8/26/2019 10:23:30 AM
Printed : 9/30/2020 3:27:58 PM

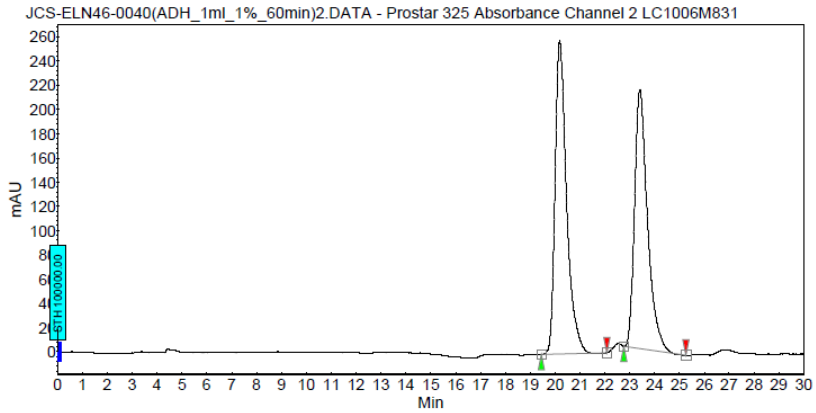

Peak results :

Index	Name	Time [Min]	Quantity [% Area]	Height [mAU]	Area [mAU.Min]	Area % [%]
1	UNKNOWN	20.19	51.66	258.3	138.2	51.657
2	UNKNOWN	23.41	48.34	214.0	129.4	48.343
Total			100.00	472.3	267.6	100.000

0 ℃, 1.0 mol % Rh_2(*R*-TPPTTL)$_4$ 5.0 equiv styrene, CH_2Cl_2 as solvent, reaction performed according to procedure 3.3

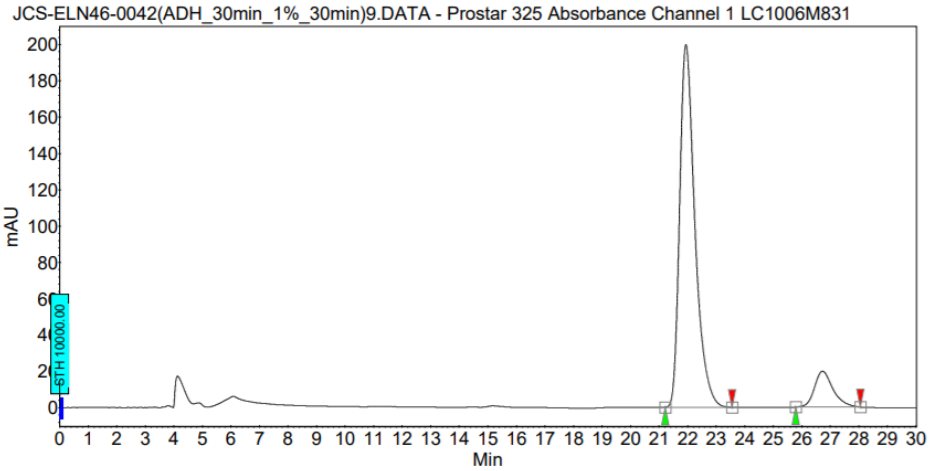

Peak results :

Index	Name	Time [Min]	Quantity [% Area]	Height [mAU]	Area [mAU.Min]	Area % [%]
1	UNKNOWN	21.94	89.24	199.8	123.6	89.238
2	UNKNOWN	26.72	10.76	19.8	14.9	10.762
Total			100.00	219.6	138.5	100.000

0 ℃, 1.0 mol % Rh_2(*S*-TPPTTL)$_4$ 5.0 equiv styrene, 1.0 equiv 2-chloropyridine, CH_2Cl_2 as solvent, reaction performed according to procedure 3.4

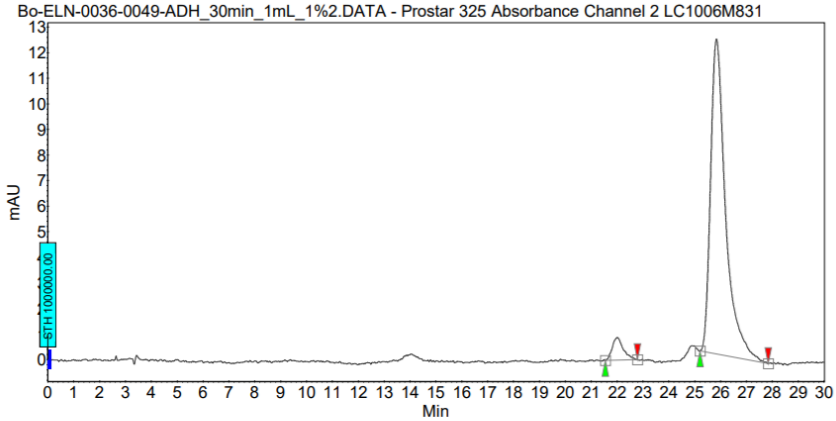

Peak results :

Index	Name	Time [Min]	Quantity [% Area]	Height [mAU]	Area [mAU.Min]	Area % [%]
2	UNKNOWN	22.01	5.01	0.9	0.4	5.010
1	UNKNOWN	25.84	94.99	12.3	8.3	94.990
Total			100.00	13.2	8.7	100.000

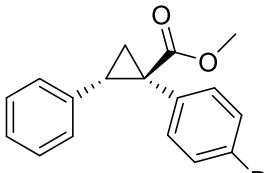

64

Racemic trace:

Chromatogram :
JCS-ELN46-0109(OJH_1ml_1%_30min)3_channe
11

System : Prostar LC System
Method : S4900_30min_1mL_1%_230nm
User : User1

Acquired : 10/29/2019 5:28:42 PM
Processed : 10/30/2019 9:10:55 AM
Printed : 12/31/2019 12:29:24 PM

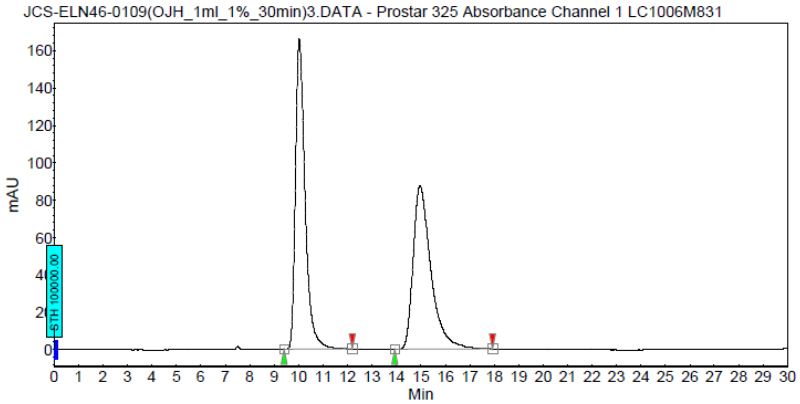

Peak results :

Index	Name	Time [Min]	Quantity [% Area]	Height [mAU]	Area [mAU.Min]	Area % [%]
1	UNKNOWN	10.03	50.57	165.9	75.6	50.571
2	UNKNOWN	14.97	49.43	87.5	73.9	49.429
Total			100.00	253.4	149.5	100.000

0 ℃ , 1.0 mol % Rh_2(*S*-TPPTTL)$_4$ 5.0 equiv styrene, CH_2Cl_2 as solvent, reaction performed according to procedure 3.3

Chromatogram :
JCS-ELN46-0110(OJH_1ml_1%_30min)6_channe
11

System : Prostar LC System
Method : S4900_30min_1mL_1%_230nm
User : User1

Acquired : 10/29/2019 6:46:05 PM
Processed : 10/30/2019 9:11:19 AM
Printed : 12/31/2019 12:29:32 PM

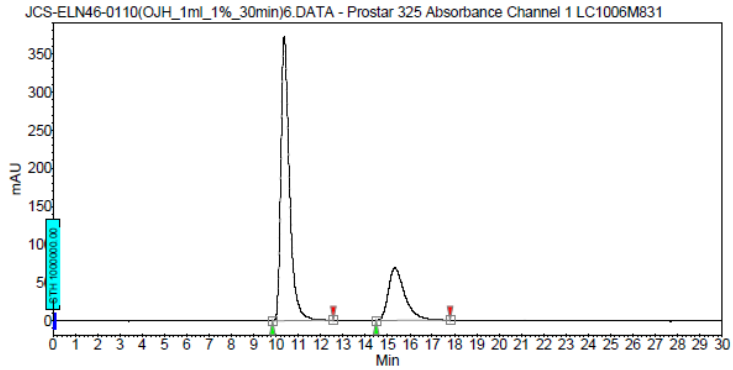

Peak results :

Index	Name	Time [Min]	Quantity [% Area]	Height [mAU]	Area [mAU.Min]	Area % [%]
1	UNKNOWN	10.37	73.78	371.9	166.1	73.781
2	UNKNOWN	15.33	26.22	68.7	59.0	26.219
Total			100.00	440.6	225.1	100.000

0 ℃, 1.0 mol % Rh_2(*S*-TPPTTL)$_4$ 5.0 equiv styrene, 1.0 equiv 2-chloropyridine, CH_2Cl_2 as solvent, reaction performed according to procedure 3.4

Chromatogram :
JCS-ELN46-0111(OJH_1ml_1%_30min)9_channe
11

System : Prostar LC System
Method : S4900_30min_1mL_1%_230nm
User : User1

Acquired : 10/29/2019 8:03:22 PM
Processed : 10/30/2019 9:11:45 AM
Printed : 12/31/2019 12:29:28 PM

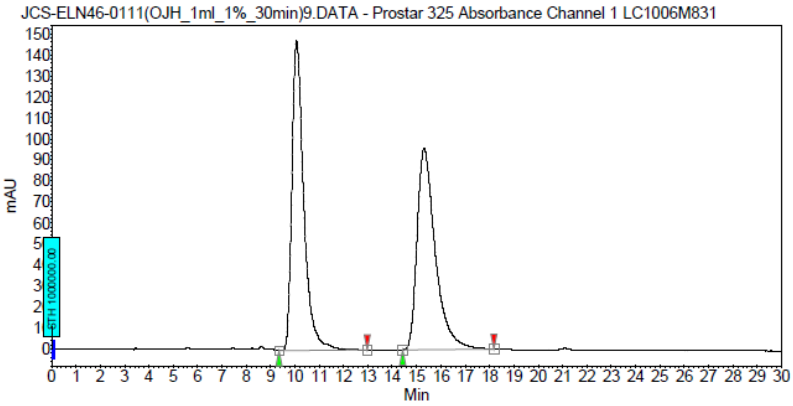

Peak results :

Index	Name	Time [Min]	Quantity [% Area]	Height [mAU]	Area [mAU.Min]	Area % [%]
1	UNKNOWN	10.07	50.07	147.5	83.6	50.070
2	UNKNOWN	15.31	49.93	95.7	83.4	49.930
Total			100.00	243.3	167.0	100.000

Racemic trace:

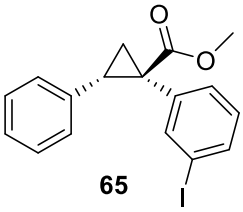

65

Chromatogram :
JCS-ELN46-0181(ODH_30MIN_1ML_1%)48_channel2

System : Prostar LC System
Method : ADH_30min_1mL_1%-230nm
User : User1

Acquired : 12/11/2019 4:01:46 PM
Processed : 12/12/2019 9:38:09 AM
Printed : 12/31/2019 12:05:13 PM

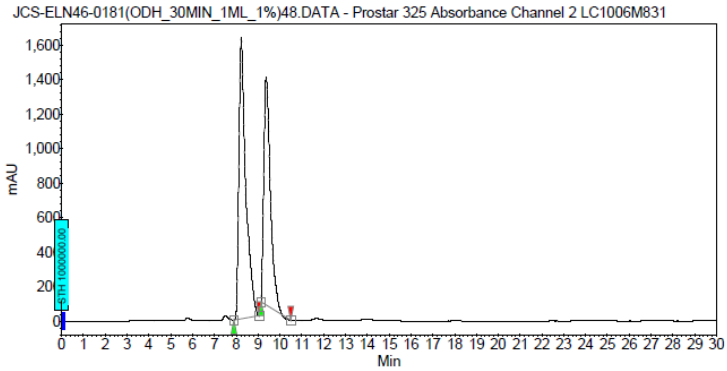

Peak results :

Index	Name	Time [Min]	Quantity [% Area]	Height [mAU]	Area [mAU.Min]	Area % [%]
1	UNKNOWN	8.23	56.24	1631.2	592.4	56.236
2	UNKNOWN	9.37	43.76	1320.4	461.0	43.764
Total			100.00	2951.6	1053.3	100.000

0 ℃, 1.0 mol % Rh_2(*S*-TPPTTL)$_4$ 5.0 equiv styrene, CH_2Cl_2 as solvent, reaction performed according to procedure 3.3

Chromatogram :
JCS-ELN46-0182(ODH_30MIN_1ML_1%)51_channel2

System : Prostar LC System
Method : ADH_30min_1mL_1%-230nm
User : User1

Acquired : 12/11/2019 5:19:44 PM
Processed : 12/12/2019 9:38:35 AM
Printed : 12/31/2019 12:05:08 PM

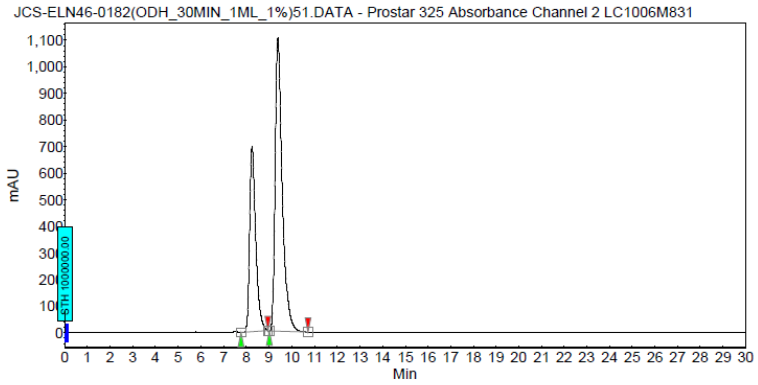

Peak results :

Index	Name	Time [Min]	Quantity [% Area]	Height [mAU]	Area [mAU.Min]	Area % [%]
1	UNKNOWN	8.25	35.34	699.4	221.1	35.336
2	UNKNOWN	9.39	64.66	1102.8	404.6	64.664
Total			100.00	1802.3	625.7	100.000

0 ℃, 1.0 mol % Rh_2(*S*-TPPTTL)$_4$ 5.0 equiv styrene, 1.0 equiv 2-chloropyridine, CH_2Cl_2 as solvent, reaction performed according to procedure 3.4

Chromatogram :
JCS-ELN46-0183P1(ODH_30MIN_1ML_1%)54_channel2

Prostar LC System
Method : ADH_30min_1mL_1%-230nm
User : User1

Acquired : 12/11/2019 6:37:10 PM
Processed : 12/12/2019 9:39:14 AM
Printed : 12/31/2019 12:04:57 PM

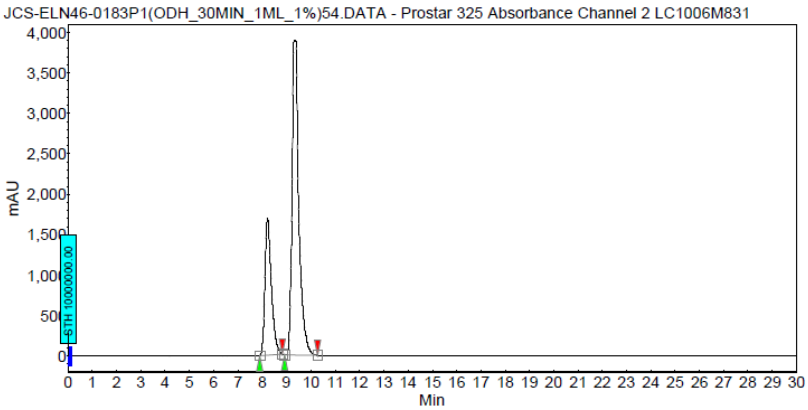

Peak results :

Index	Name	Time [Min]	Quantity [% Area]	Height [mAU]	Area [mAU.Min]	Area % [%]
1	UNKNOWN	8.21	29.17	1691.5	523.5	29.169
2	UNKNOWN	9.36	70.83	3884.5	1271.2	70.831
Total			100.00	5576.1	1794.8	100.000

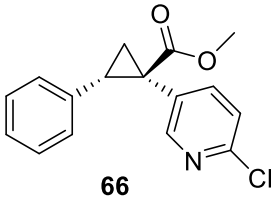

66

Racemic trace:

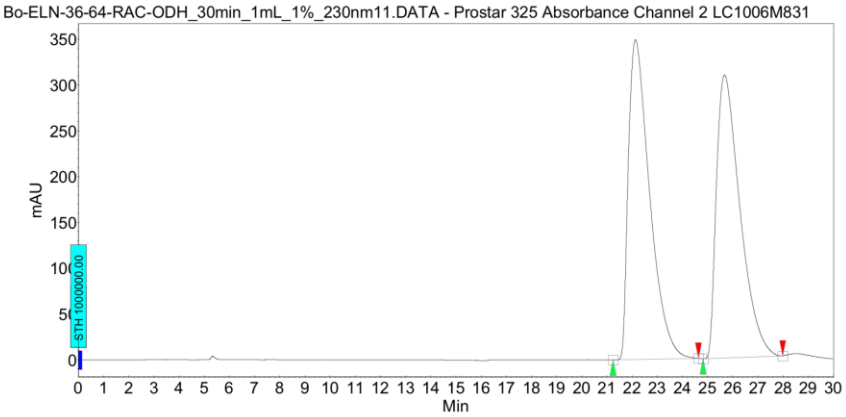

Peak results :

Index	Name	Time [Min]	Quantity [% Area]	Height [mAU]	Area [mAU.Min]	Area % [%]
1	UNKNOWN	22.14	50.51	349.2	341.9	50.507
2	UNKNOWN	25.67	49.49	309.1	335.0	49.493
Total			100.00	658.2	676.9	100.000

0 ℃, 1.0 mol % Rh_2(*S*-TPPTTL)$_4$ 5.0 equiv styrene, CH_2Cl_2 as solvent, reaction performed according to procedure 3.3

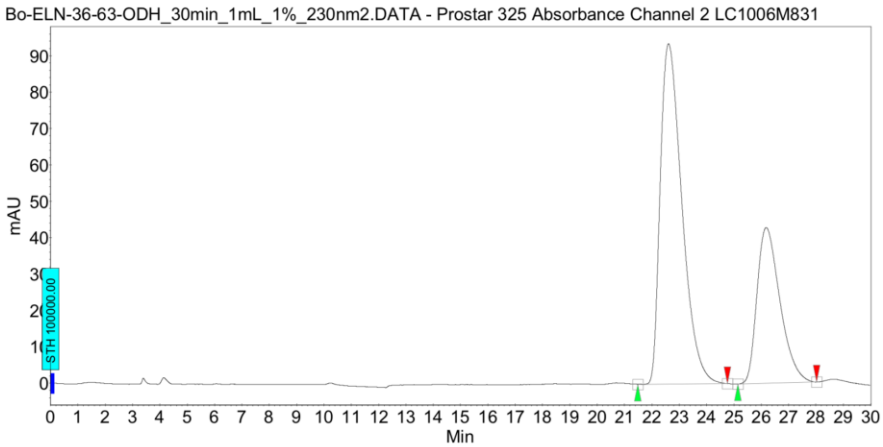

Peak results :

Index	Name	Time [Min]	Quantity [% Area]	Height [mAU]	Area [mAU.Min]	Area % [%]
1	UNKNOWN	22.61	67.37	93.5	86.0	67.366
2	UNKNOWN	26.18	32.63	42.8	41.6	32.634
Total			100.00	136.3	127.6	100.000

0 ℃, 1.0 mol % Rh_2(*S*-TPPTTL)$_4$ 5.0 equiv styrene, 1.0 equiv 2-chloropyridine, CH_2Cl_2 as solvent, reaction performed according to procedure 3.4

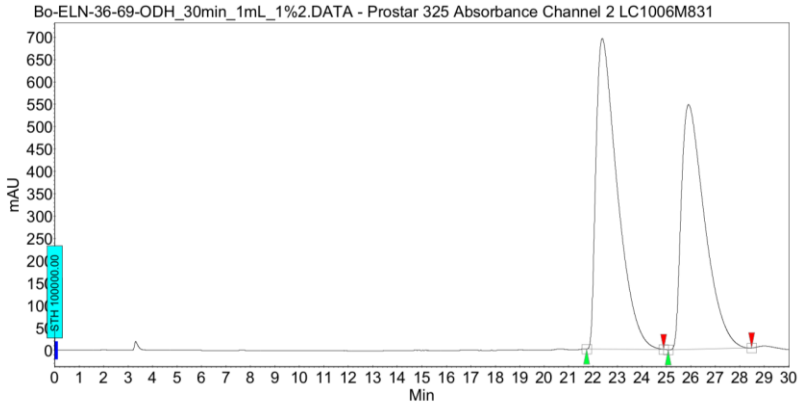

Peak results :

Index	Name	Time [Min]	Quantity [% Area]	Height [mAU]	Area [mAU.Min]	Area % [%]
1	UNKNOWN	22.38	53.63	694.8	701.8	53.635
2	UNKNOWN	25.91	46.37	547.3	606.6	46.365
Total			100.00	1242.1	1308.4	100.000

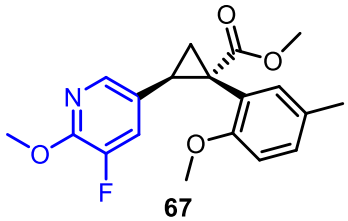

67

Racemic trace:

Chromatogram :
JCS-ELN46-0160(ODH_30min_1ml_1%)6_channel2

System : Prostar LC System
Method : ADH_30min_1mL_1%-230nm
User : User1

Acquired : 11/26/2019 12:28:10 PM
Processed : 11/30/2019 1:57:41 PM
Printed : 12/31/2019 12:16:50 PM

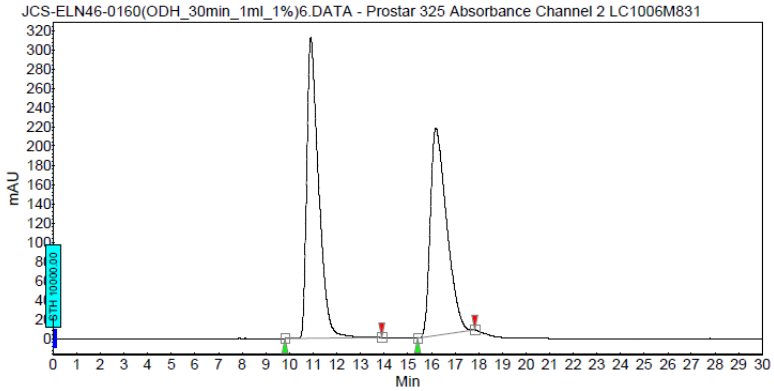

Peak results :

Index	Name	Time [Min]	Quantity [% Area]	Height [mAU]	Area [mAU.Min]	Area % [%]
1	UNKNOWN	10.90	51.23	312.1	182.2	51.230
2	UNKNOWN	16.19	48.77	215.7	173.4	48.770
Total			100.00	527.8	355.6	100.000

0 ℃, 1.0 mol % Rh_2(*S*-TPPTTL)$_4$ 5.0 equiv vinyl heterocycle, CH_2Cl_2 as solvent, reaction performed according to procedure 3.3

Chromatogram :
JCS-ELN46-0161(ODH_30min_1ml_1%)18_channel2

System : Prostar LC System
Method : ADH_30min_1mL_1%-230nm
User : User1

Acquired : 11/26/2019 5:37:29 PM
Processed : 11/27/2019 9:48:33 AM
Printed : 11/30/2019 1:58:04 PM

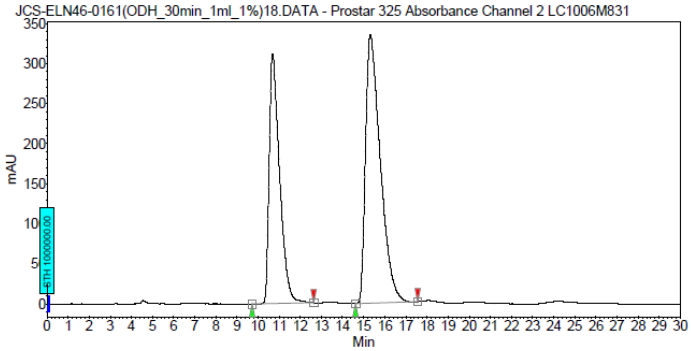

Peak results :

Index	Name	Time [Min]	Quantity [% Area]	Height [mAU]	Area [mAU.Min]	Area % [%]
2	UNKNOWN	10.69	39.64	312.2	178.6	39.641
1	UNKNOWN	15.32	60.36	335.3	272.0	60.359
Total			100.00	647.6	450.6	100.000

0 ℃, 1.0 mol % Rh_2(*S*-TPPTTL)$_4$ 1.5 equiv vinyl heterocycle, 3.5 equiv 2-chloropyridine, CH_2Cl_2 as solvent, reaction performed according to procedure 3.4

Chromatogram :
JCS-ELN46-0162(ODH_30min_1ml_1%)21_channel2

System : Prostar LC System
Method : ADH_30min_1mL_1%-230nm
User : User1

Acquired : 11/26/2019 6:54:56 PM
Processed : 11/30/2019 1:58:24 PM
Printed : 12/31/2019 12:16:37 PM

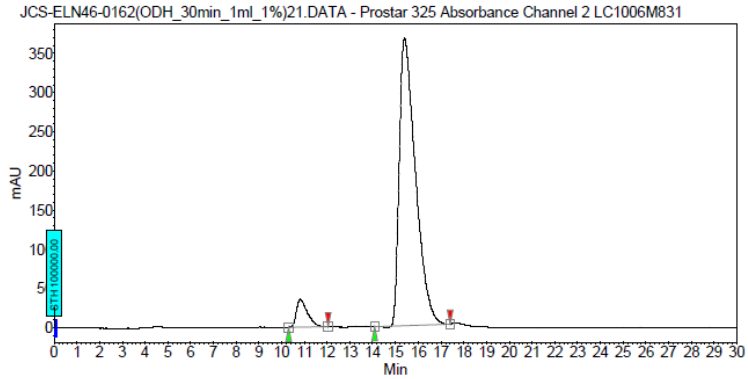

Peak results :

Index	Name	Time [Min]	Quantity [% Area]	Height [mAU]	Area [mAU.Min]	Area % [%]
1	UNKNOWN	10.82	6.24	35.7	20.1	6.239
2	UNKNOWN	15.40	93.76	367.4	301.3	93.761
Total			100.00	403.1	321.4	100.000

0 ℃, 1.0 mol % Rh_2(*S*-TPPTTL)$_4$ 1.5 equiv vinyl heterocycle, 3.5 equiv 2-chloropyridine, CH_2Cl_2 as solvent, 10 equiv HFIP, reaction performed according to procedure 3.5

Chromatogram :
JCS-ELN46-0186(ODH_1ML_1%_30MIN)70_channel2

System : Prostar LC System
Method : ADH_30min_1mL_1%-230nm
User : User1

Acquired : 12/11/2019 11:59:57 PM
Processed : 12/12/2019 9:45:57 AM
Printed : 12/31/2019 12:04:34 PM

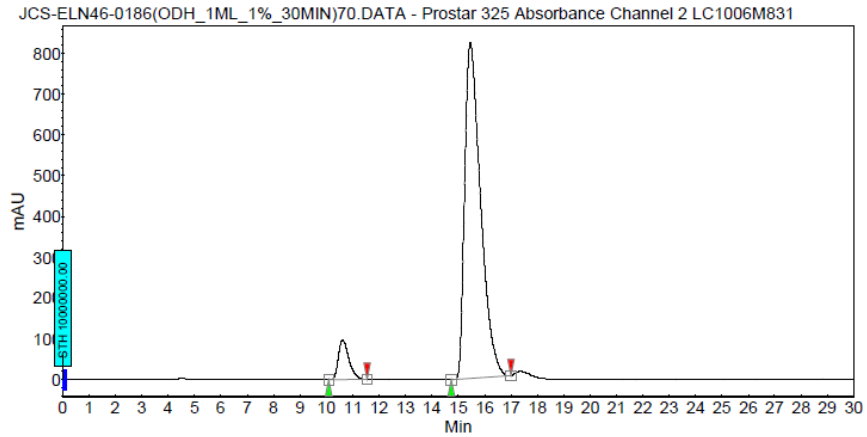

Peak results :

Index	Name	Time [Min]	Quantity [% Area]	Height [mAU]	Area [mAU.Min]	Area % [%]
1	UNKNOWN	10.61	7.21	97.1	44.4	7.209
2	UNKNOWN	15.46	92.79	821.4	571.9	92.791
Total			100.00	918.5	616.3	100.000

Racemic Trace:

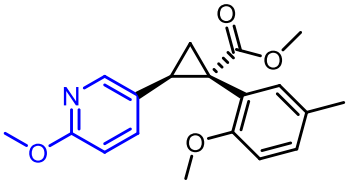

68

Chromatogram :
JCS-ELN46-0103(ODH_30MIN_1ML_1%)16_channel2

System : Prostar LC System
Method : ADH_30min_1mL_1%-230nm
User : User1

Acquired : 10/17/2019 6:04:06 PM
Processed : 10/18/2019 8:04:05 AM
Printed : 10/23/2019 4:33:17 PM

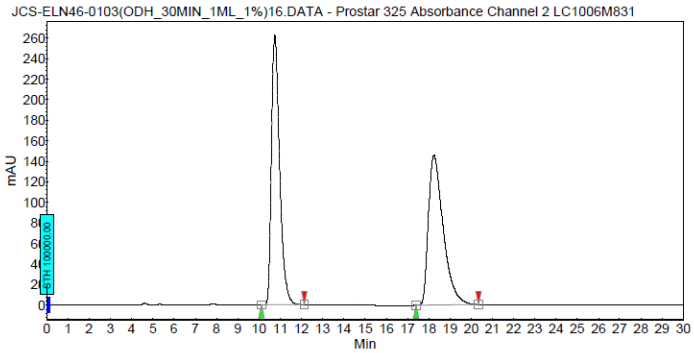

Peak results :

Index	Name	Time [Min]	Quantity [% Area]	Height [mAU]	Area [mAU.Min]	Area % [%]
1	UNKNOWN	10.74	49.79	262.2	117.0	49.792
2	UNKNOWN	18.24	50.21	145.9	118.0	50.208
Total			100.00	408.0	234.9	100.000

0 ℃, 1.0 mol % Rh_2(*S*-TPPTTL)$_4$, 1.5 equiv vinyl heterocycle, 3.5 equiv 2-chloropyridine, CH_2Cl_2 as solvent, reaction performed according to procedure 3.4

Chromatogram :
JCS-ELN46-0106(ODH_30MIN_1ML_1%)25_channel2

System : Prostar LC System
Method : ADH_30min_1mL_1%-230nm
User : User1

Acquired : 10/17/2019 9:56:08 PM
Processed : 10/18/2019 8:05:47 AM
Printed : 12/31/2019 12:32:45 PM

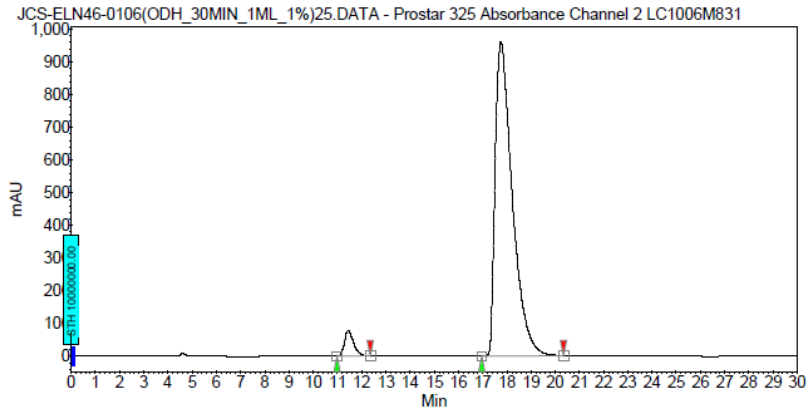

Peak results :

Index	Name	Time [Min]	Quantity [% Area]	Height [mAU]	Area [mAU.Min]	Area % [%]
1	UNKNOWN	11.45	4.11	77.2	33.7	4.106
2	UNKNOWN	17.75	95.89	961.0	787.3	95.894
Total			100.00	1038.2	821.0	100.000

0 ℃, 1.0 mol % Rh_2(*S*-TPPTTL)$_4$, 1.5 equiv vinyl heterocycle, 3.5 equiv 2-chloropyridine, CH_2Cl_2 as solvent, 10 equiv HFIP, reaction performed according to procedure 3.5

Chromatogram :
JCS-ELN46-0172(ODH_30MIN_1ML_1%)12_channel2

System : Prostar LC System
Method : ADH_30min_1mL_1%-230nm
User : User1

Acquired : 11/30/2019 6:11:24 PM
Processed : 12/2/2019 8:41:54 AM
Printed : 12/31/2019 12:15:28 PM

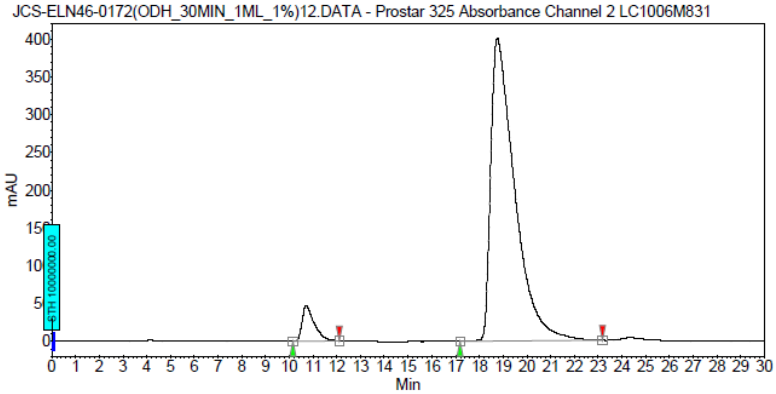

Peak results :

Index	Name	Time [Min]	Quantity [% Area]	Height [mAU]	Area [mAU.Min]	Area % [%]
1	UNKNOWN	10.71	5.61	47.2	27.8	5.609
2	UNKNOWN	18.76	94.39	400.5	468.1	94.391
Total			100.00	447.7	495.9	100.000

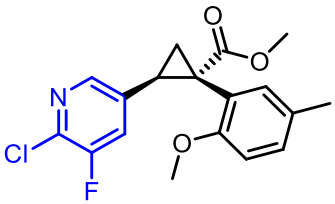

69

Racemic trace:

Chromatogram :
JCS-ELN46-0189RE(R,R-WHELK_60MIN_1ML_1%)3_channel2

System : Prostar LC System
Method : OD_30min_1mL_1%_230nm
User : User1

Acquired : 12/16/2019 9:41:58 AM
Processed : 12/16/2019 3:26:28 PM
Printed : 12/31/2019 12:59:07 PM

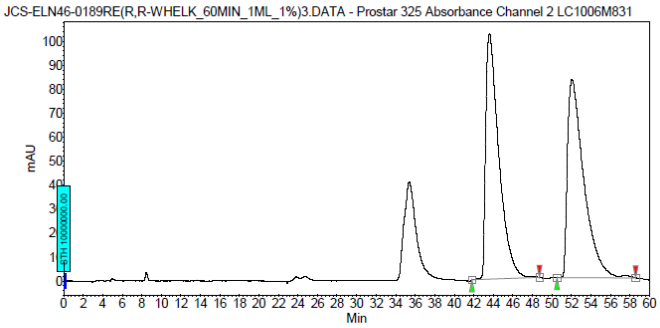

Peak results :

Index	Name	Time [Min]	Quantity [% Area]	Height [mAU]	Area [mAU.Min]	Area % [%]
1	UNKNOWN	43.60	49.93	102.4	160.2	49.933
2	UNKNOWN	52.05	50.07	82.8	160.7	50.067
Total			100.00	185.1	320.9	100.000

0 ℃, 1.0 mol % Rh_2(*S*-TPPTTL)$_4$ 1.5 equiv vinyl heterocycle, 3.5 equiv 2-chloropyridine, CH_2Cl_2 as solvent, reaction performed according to procedure 3.4

Chromatogram :
JCS-ELN46-0192(WHELK_60MIN_1ML_1%)16_channel2

Prostar LC System
Method : OD_30min_1mL_1%_230nm
User : User1

Acquired : 12/16/2019 5:09:25 PM
Processed : 12/16/2019 8:55:34 PM
Printed : 12/31/2019 12:59:13 PM

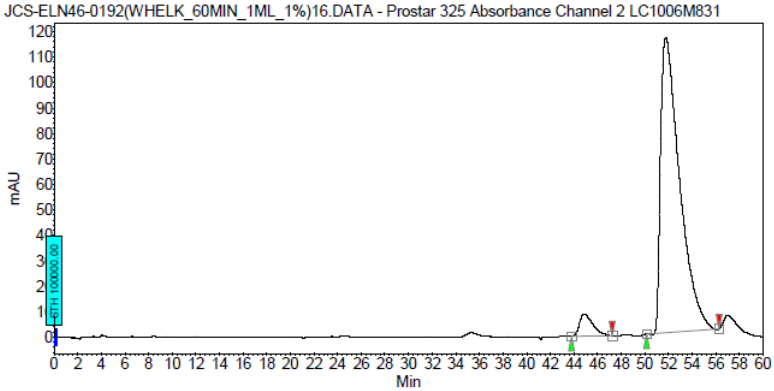

Peak results :

Index	Name	Time [Min]	Quantity [% Area]	Height [mAU]	Area [mAU.Min]	Area % [%]
1	UNKNOWN	44.88	5.04	8.7	11.5	5.037
2	UNKNOWN	51.77	94.96	115.9	216.7	94.963
Total			100.00	124.6	228.2	100.000

0 ℃, 1.0 mol % Rh_2(*S*-TPPTTL)$_4$ 1.5 equiv vinyl heterocycle, 3.5 equiv 2-chloropyridine, CH_2Cl_2 as solvent, 10 equiv HFIP, reaction performed according to procedure 3.5

Chromatogram :
JCS-ELN46-0198(WHELK_60MIN_1ML_1%)3_channel2

Prostar LC System
Method : OD_30min_1mL_1%_230nm
User : User1

Acquired : 12/20/2019 11:37:43 AM
Processed : 9/23/2020 5:58:12 PM
Printed : 9/23/2020 5:58:19 PM

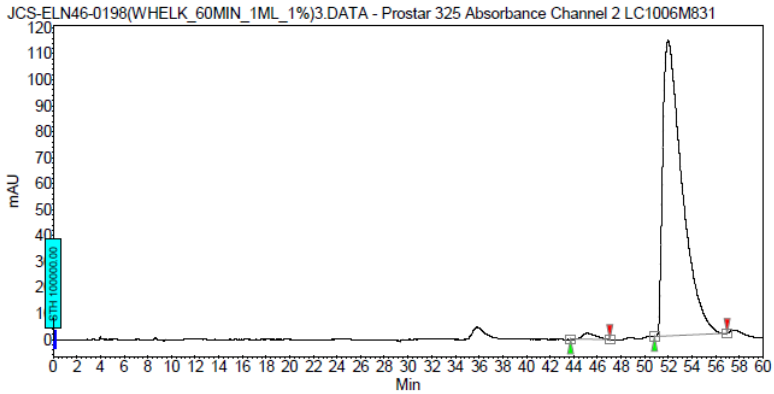

Peak results :

Index	Name	Time [Min]	Quantity [% Area]	Height [mAU]	Area [mAU.Min]	Area % [%]
1	UNKNOWN	45.17	1.43	2.4	3.1	1.434
2	UNKNOWN	51.97	98.57	114.0	216.4	98.566
Total			100.00	116.3	219.6	100.000

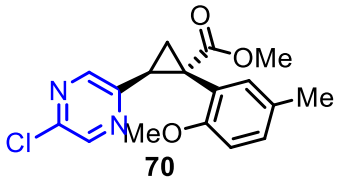

70

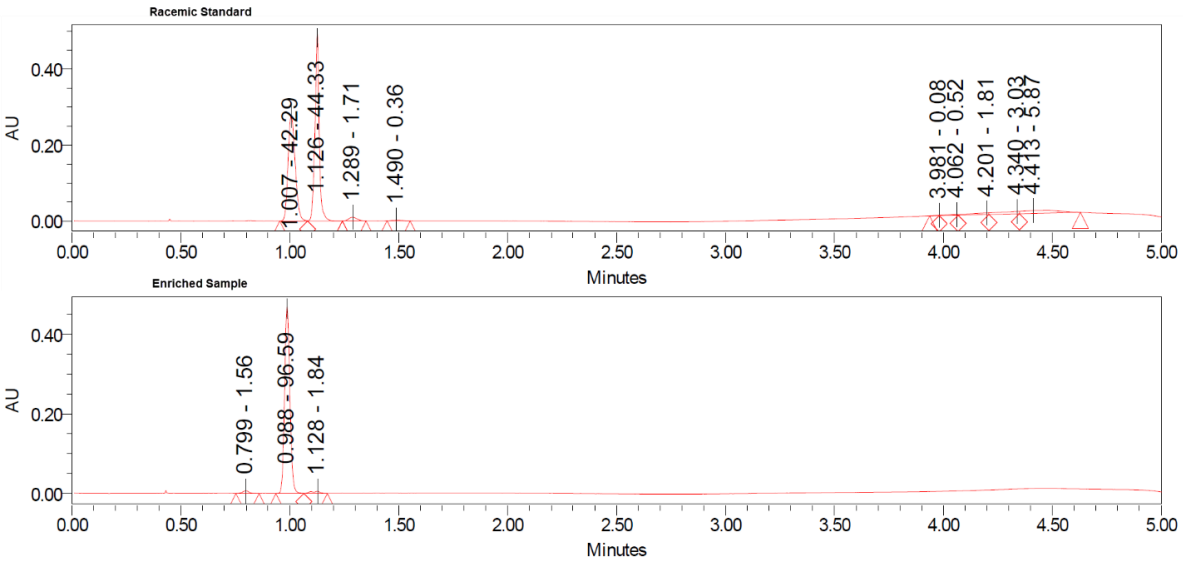

Racemic Standard	Enriched Sample
RT = 1.007 min Area = 42.29	RT_{major} = 0.988 min Area = 96.59
RT = 1.126 min Area = 44.33	RT_{minor} = 1.128 min Area = 1.84

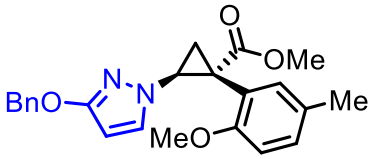

71

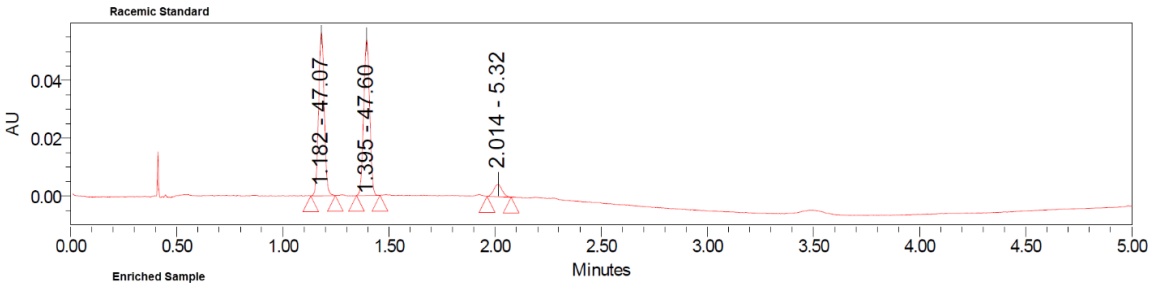

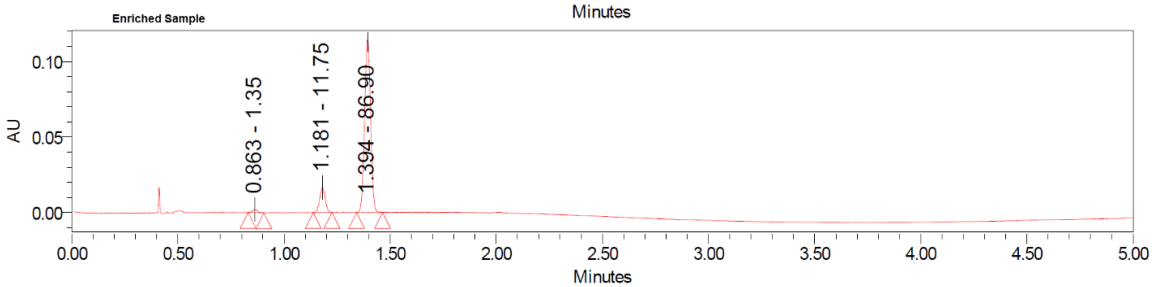

Racemic Standard	Enriched Sample
RT = 1.182 min Area = 47.07	RT_{minor} = 1.181 min Area = 11.75
RT = 1.395 min Area = 47.60	RT_{major} = 1.394 min Area = 86.90

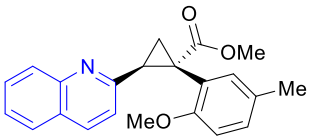

72

Racemic trace:

Chromatogram :
JCS-ELN46-0277conc(ADH_1ML_1%_60MIN)44_channel2

Instrument : Prostar LC System
Method : OJ_30min_1mL_1%_230NM
User : User1

Acquired : 6/7/2020 4:59:26 AM
Processed : 9/12/2020 9:43:51 AM
Printed : 9/12/2020 9:43:58 AM

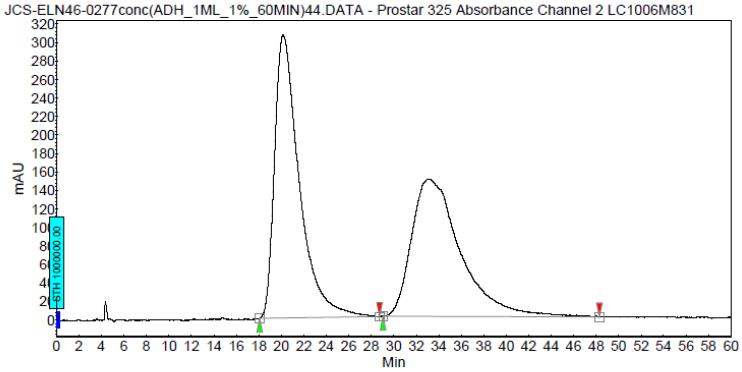

Peak results :

Index	Name	Time [Min]	Quantity [% Area]	Height [mAU]	Area [mAU.Min]	Area % [%]
1	UNKNOWN	20.15	51.09	306.0	780.3	51.090
2	UNKNOWN	33.06	48.91	148.7	747.0	48.910
Total			100.00	454.7	1527.2	100.000

0 ˚C, 1.0 mol % Rh_2(*S*-TPPTTL)$_4$ 1.5 equiv vinyl heterocycle, 3.5 equiv 2-chloropyridine, CH_2Cl_2 as solvent, reaction performed according to procedure 3.4

Chromatogram :
JCS-ELN46-0278conc(ADH_1ml_1%_60min)5_channel2

Prostar LC System
Method : OJ_30min_1mL_1%_230NM
User : User1

Acquired : 6/9/2020 6:17:52 PM
Processed : 6/10/2020 4:48:38 PM
Printed : 9/12/2020 9:40:49 AM

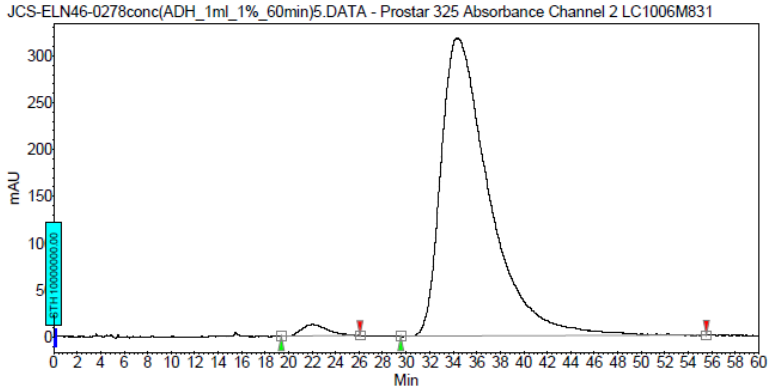

Peak results :

Index	Name	Time [Min]	Quantity [% Area]	Height [mAU]	Area [mAU.Min]	Area % [%]
1	UNKNOWN	22.04	2.03	12.5	31.3	2.034
2	UNKNOWN	34.36	97.97	317.8	1508.3	97.966
Total			100.00	330.3	1539.6	100.000

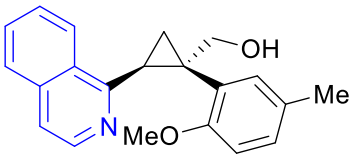

(73-reduced)

LAH reduction of **73** was required to achieve separation of the enantiomers by chiral UHPLC. See section 4.3 for experimental details.

Racemic trace of reduced product:

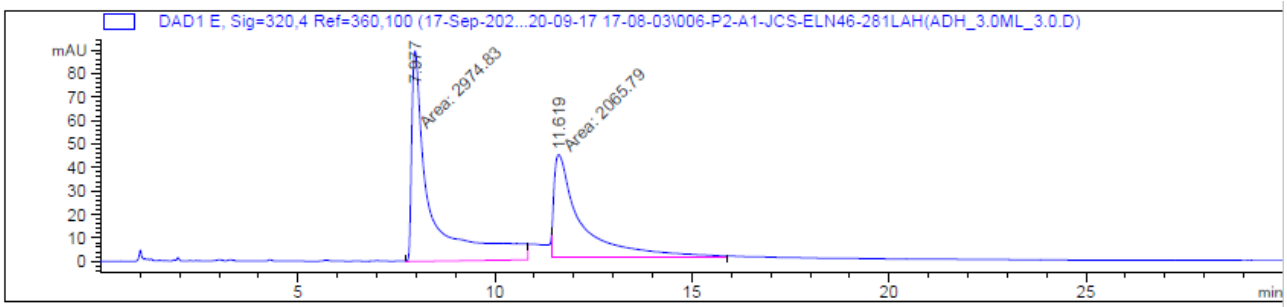

Signal 5: DAD1 E, Sig=320,4 Ref=360,100

Peak #	RetTime [min]	Type	Width [min]	Area [mAU*s]	Height [mAU]	Area %
1	7.977	MM	0.5532	2974.82690	89.62110	59.0172
2	11.619	MM	0.7913	2065.78540	43.50774	40.9828
Totals :				5040.61230	133.12885	

0 ℃, 1.0 mol % Rh_2(*S*-TPPTTL)$_4$ 1.5 equiv vinyl heterocycle, 3.5 equiv 2-chloropyridine, CH_2Cl_2 as solvent, reaction performed according to procedure 3.4 prior to LAH reduction.

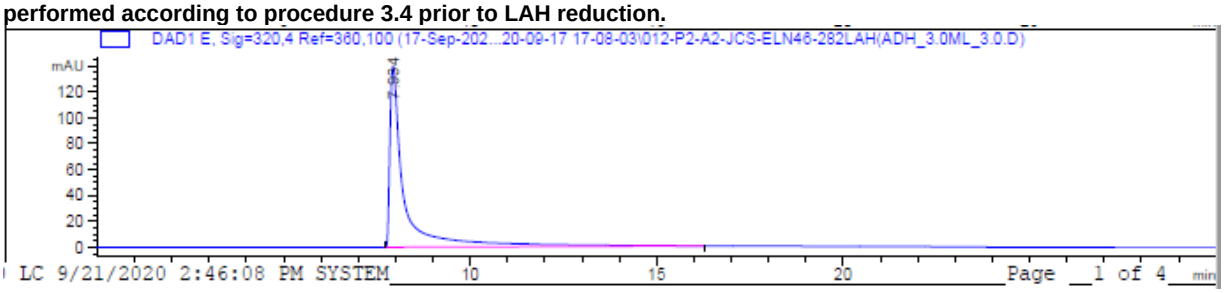

Signal 5: DAD1 E, Sig=320,4 Ref=360,100

Peak #	RetTime [min]	Type	Width [min]	Area [mAU*s]	Height [mAU]	Area %
1	7.934	BB	0.3805	3865.99292	139.85376	100.0000
Totals :				3865.99292	139.85376	

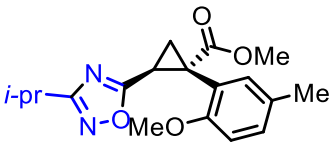

74

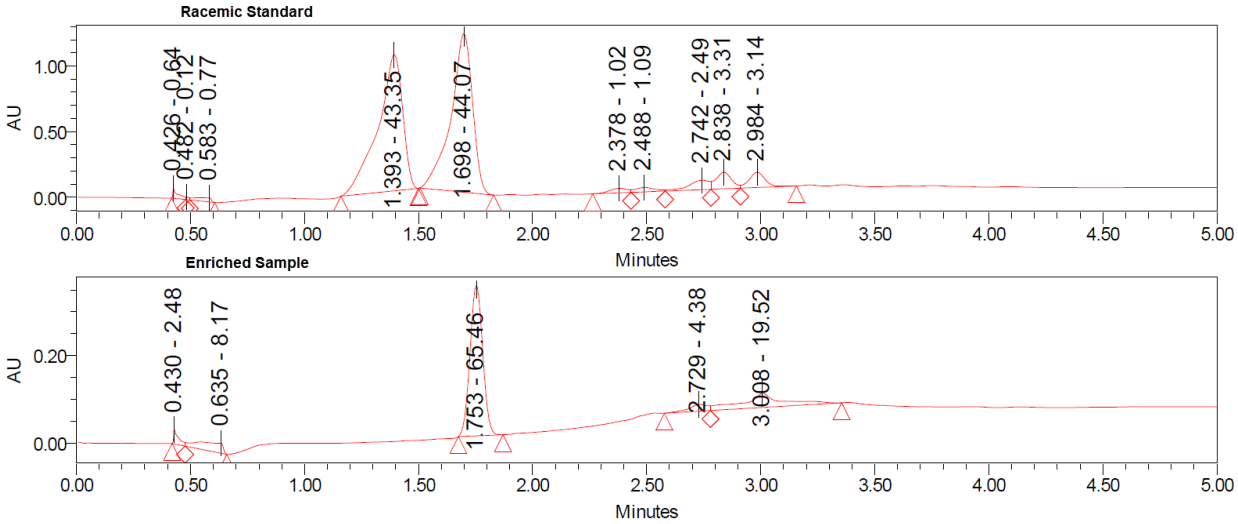

Racemic Standard	Enriched Sample
RT = 1.393 min Area = 43.35	RT_{minor} = n.d. Area = n.d.
RT = 1.698 min Area = 44.07	RT_{major} = 1.753 min Area = 65.46

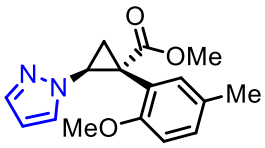

75

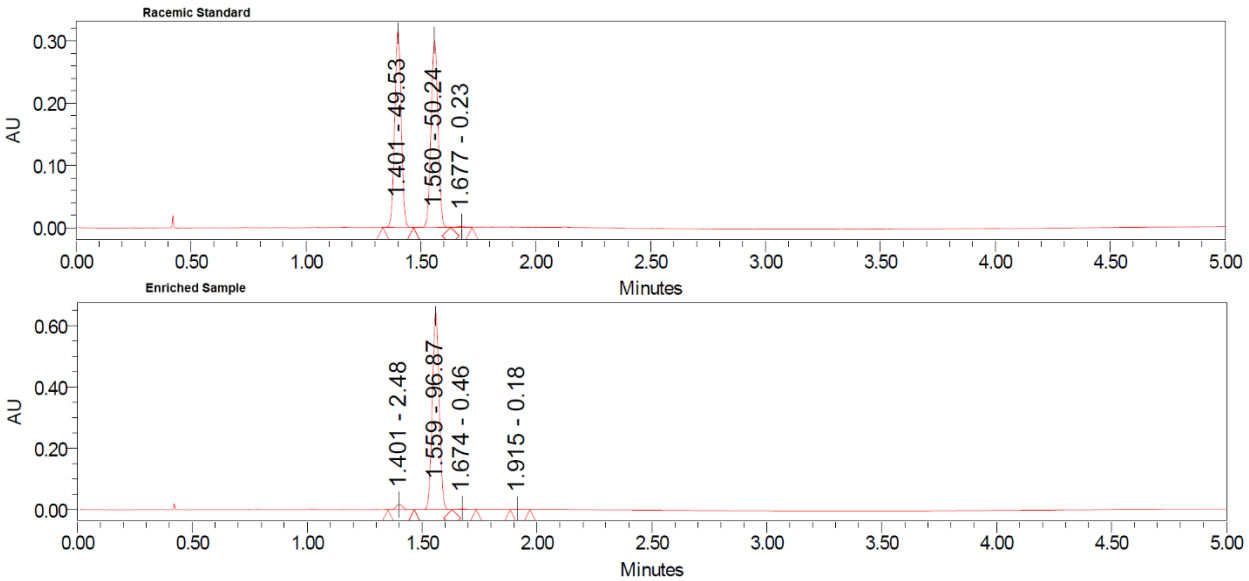

Racemic Standard	Enriched Sample
RT = 1.401 min Area = 49.53	RT_{minor} = 1.401 min Area = 2.48
RT = 1.560 min Area = 50.24	RT_{major} = 1.559 min Area = 96.87

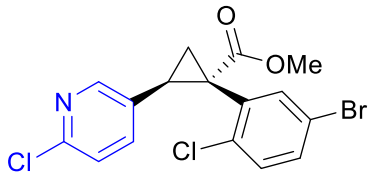

76

Racemic trace:

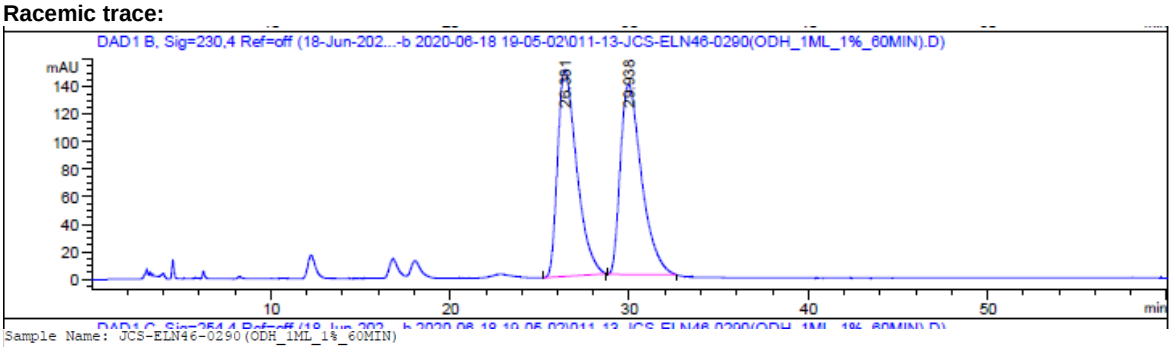

Sample Name: JCS-ELN46-0290(ODH_1ML_1%_60MIN)

Peak #	RetTime [min]	Type	Width [min]	Area [mAU*s]	Height [mAU]	Area %
1	26.381	VV R	0.8758	1.12299e4	150.62157	49.6462
2	29.938	VV R	0.9626	1.13900e4	138.47125	50.3538
Totals :				2.26198e4	289.09282	

0 ˚C, 1.0 mol % Rh_2(*S*-TPPTTL)$_4$ 1.5 equiv vinyl heterocycle, 3.5 equiv 2-chloropyridine, CH_2Cl_2 as solvent, reaction performed according to procedure 3.4

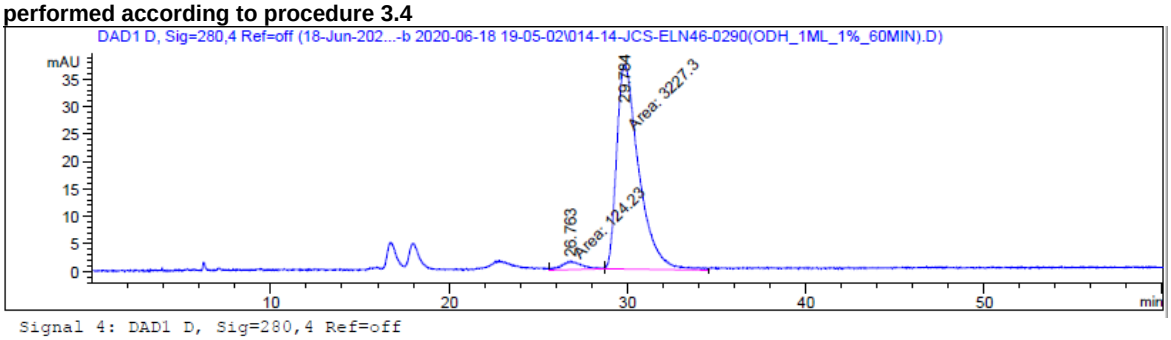

Signal 4: DAD1 D, Sig=280,4 Ref=off

Peak #	RetTime [min]	Type	Width [min]	Area [mAU*s]	Height [mAU]	Area %
1	26.763	MM	1.3216	124.23034	1.56664	3.7067
2	29.784	MM	1.4409	3227.30420	37.33059	96.2933

Totals : 3351.53454 38.89723

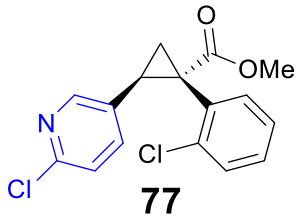

77

Racemic Trace:

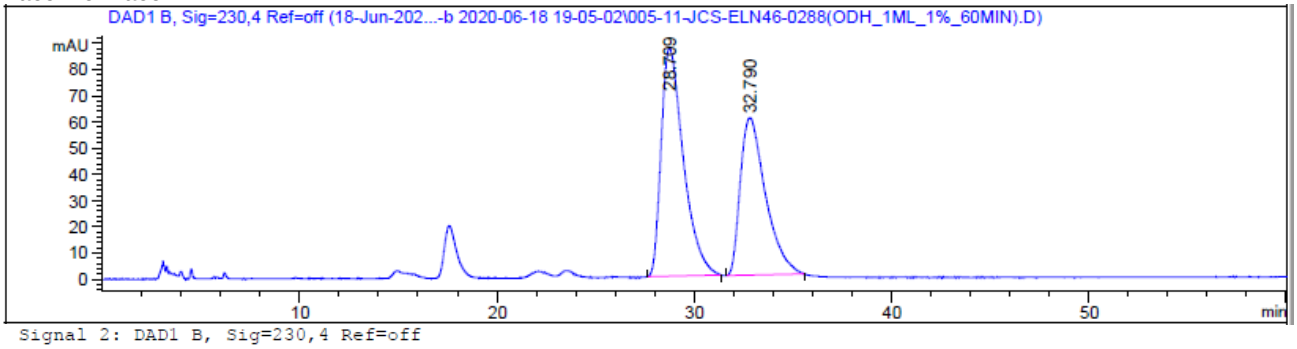

Signal 2: DAD1 B, Sig=230,4 Ref=off

Peak #	RetTime [min]	Type	Width [min]	Area [mAU*s]	Height [mAU]	Area %
1	28.709	VV R	0.9181	6819.27051	86.98462	56.0344
2	32.790	VV R	1.0426	5350.51172	60.01482	43.9656

Totals : 1.21698e4 146.99944

0 ˚C, 1.0 mol % Rh_2(*S*-TPPTTL)$_4$, 1.5 equiv vinyl heterocycle, 3.5 equiv 2-chloropyridine, CH_2Cl_2 as solvent, reaction performed according to procedure 3.4

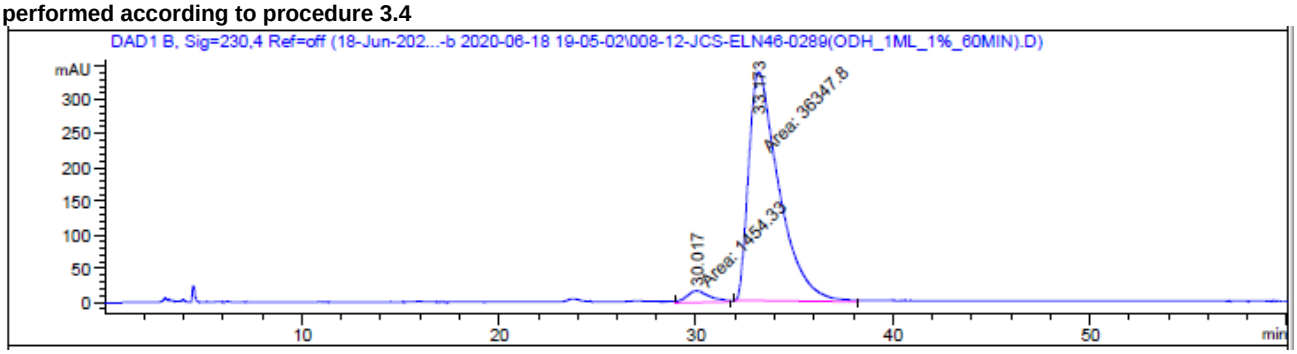


```
Signal 2: DAD1 B, Sig=230,4 Ref=off

Peak RetTime Type  Width     Area      Height     Area
  #   [min]        [min]   [mAU*s]     [mAU]       %
----|-------|----|-------|----------|----------|--------|
   1  30.017 MM    1.3712 1454.32605   17.67680   3.8472
   2  33.173 MM    1.7882 3.63478e4   338.76584  96.1528

Totals :                 3.78022e4   356.44263
```

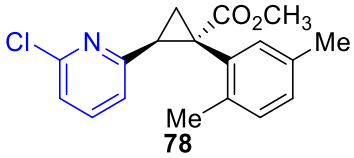

78

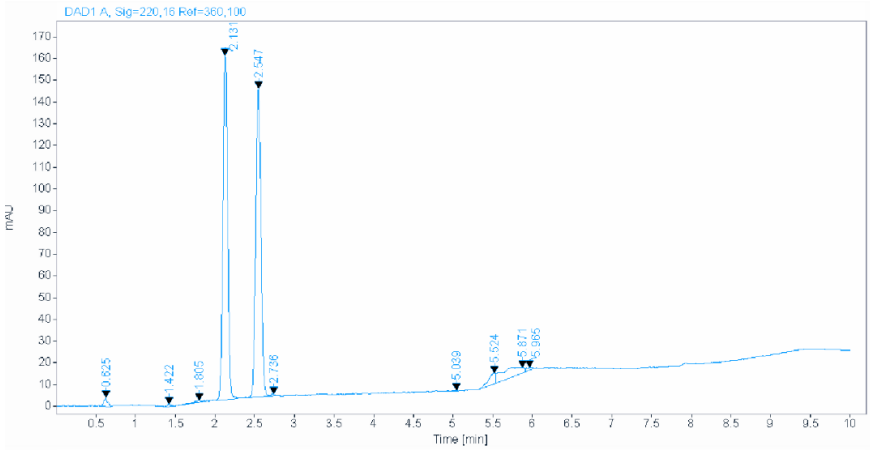

Racemic Standard
RT = 2.13 min Area = 647.6
RT = 2.55 min Area = 646.9

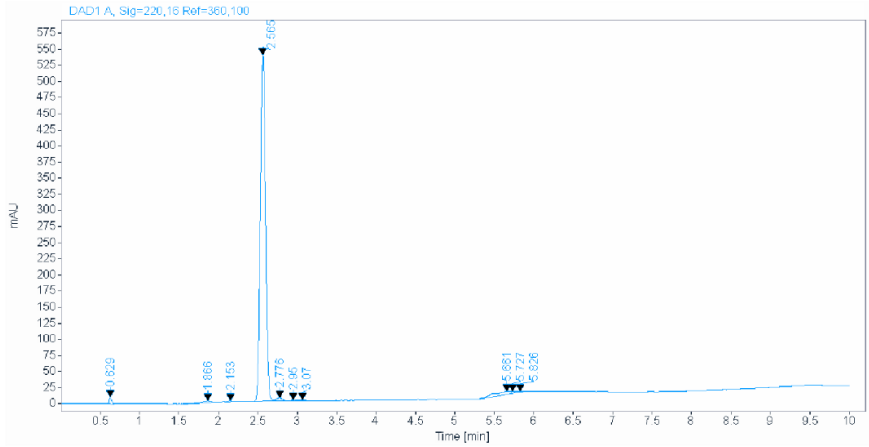

Enriched Sample
RT_{minor} = 2.15 min Area = 5.4
RT_{major} = 2.57 min Area = 2451.9

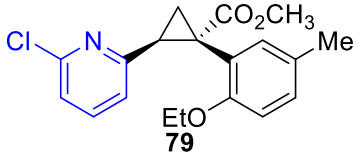

79

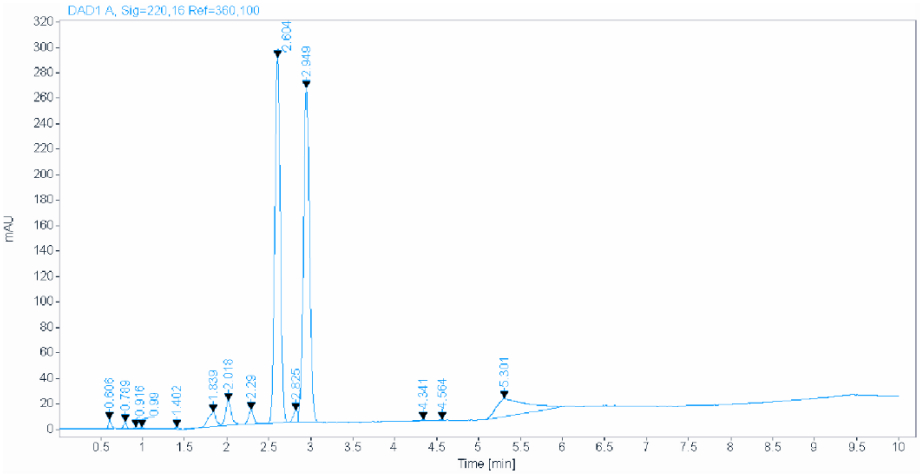

Racemic Standard
RT = 2.60 min Area = 1318.7
RT = 2.95 min Area = 1334.2

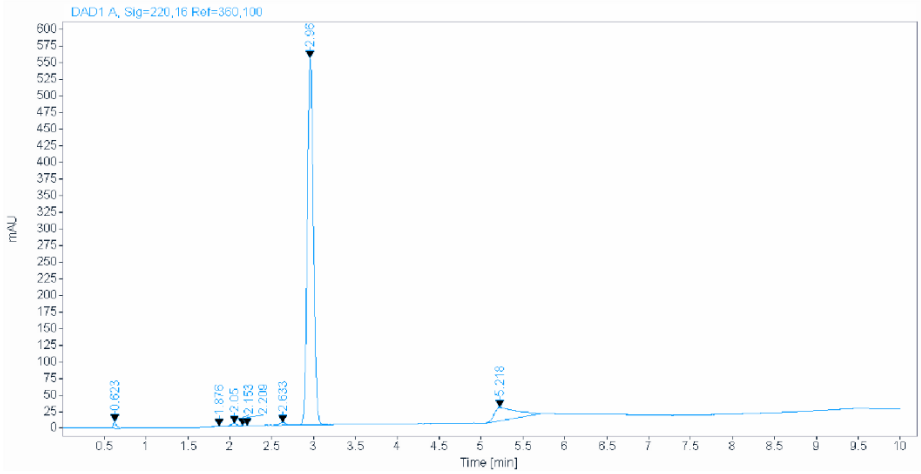

Enriched Sample
RT_{minor} = 2.63 min Area = 19.7
RT_{major} = 2.96 min Area = 2782.0

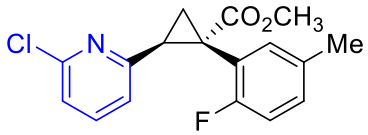

80

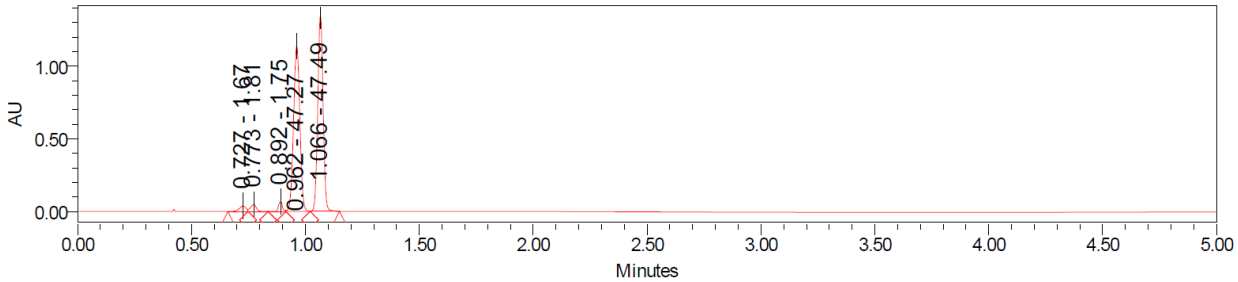

Racemic Standard
RT = 0.96 min Area = 47.27
RT = 1.07 min Area = 47.49

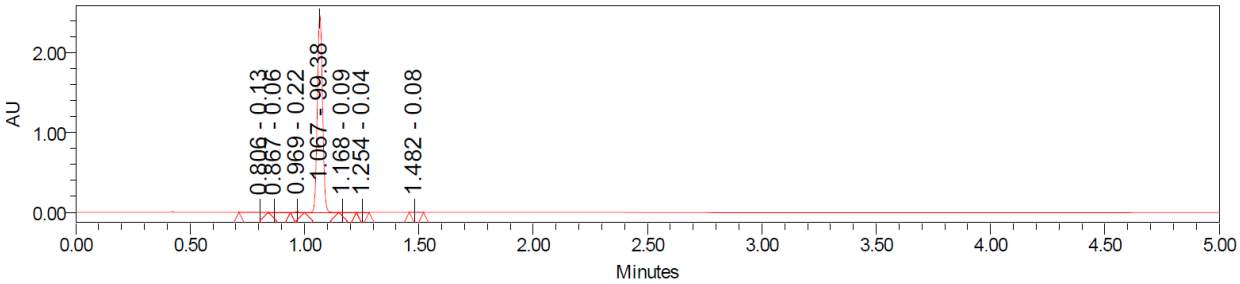

Enriched Sample
RT_{minor} = 0.97 min Area = 0.22
RT_{major} = 1.07 min Area = 99.38

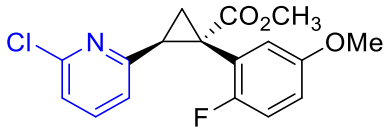

81

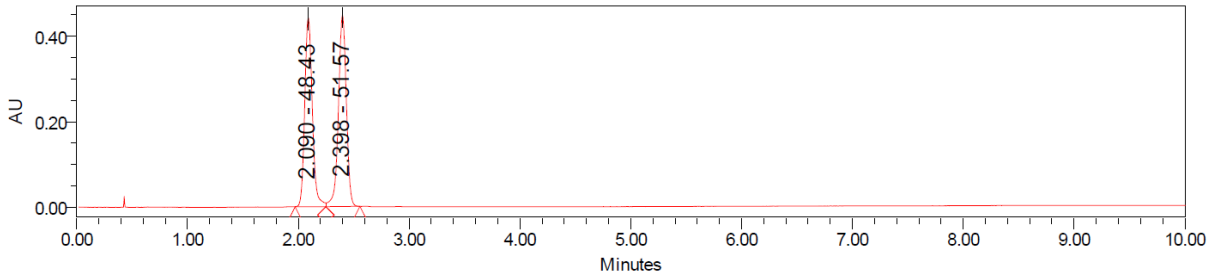

Racemic Standard
RT = 2.09 min Area = 48.43
RT = 2.40 min Area = 51.57

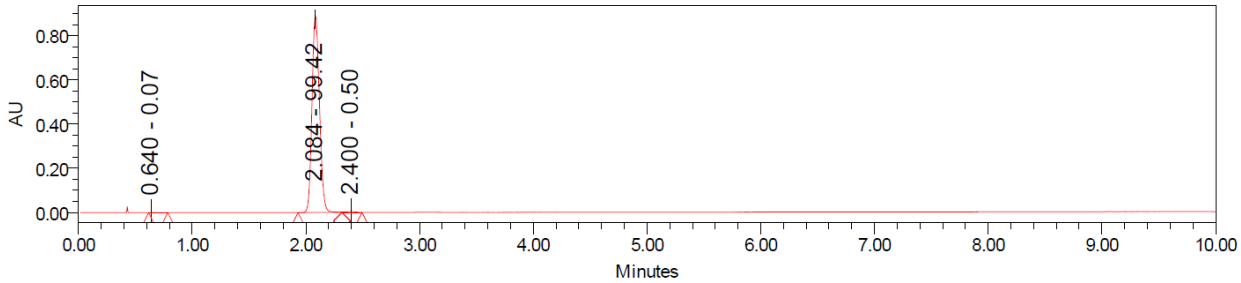

Enriched Sample
RT_{major} = 2.08 min Area = 99.42
RT_{minor} = 2.40 min Area = 0.50

Racemic trace:

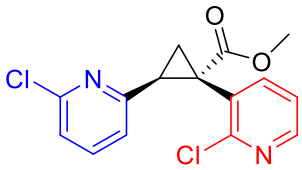

82

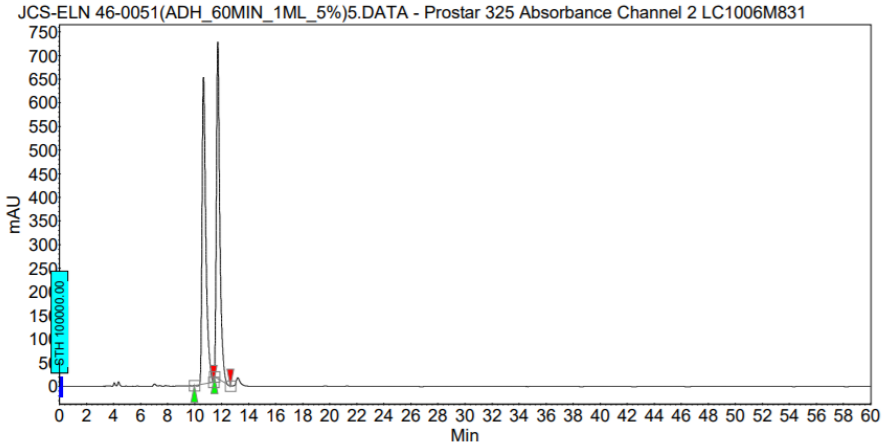

Peak results :

Index	Name	Time [Min]	Quantity [% Area]	Height [mAU]	Area [mAU.Min]	Area % [%]
1	UNKNOWN	10.65	50.25	649.3	210.6	50.254
2	UNKNOWN	11.71	49.75	712.3	208.5	49.746
Total			100.00	1361.7	419.1	100.000

0 ℃, 1.0 mol % Rh_2(*S*-TPPTTL)$_4$ 1.5 equiv vinyl heterocycle, 3.5 equiv 2-chloropyridine, CH_2Cl_2 as solvent, reaction performed according to procedure 3.4

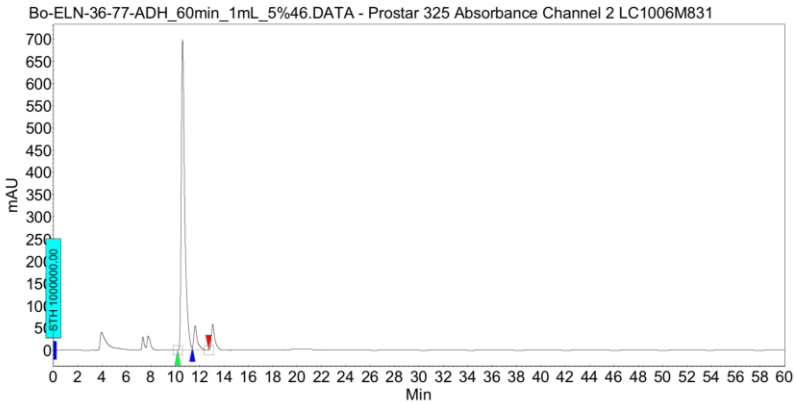

Peak results :

Index	Name	Time [Min]	Quantity [% Area]	Height [mAU]	Area [mAU.Min]	Area % [%]
1	UNKNOWN	10.60	92.62	698.2	230.9	92.622
2	UNKNOWN	11.63	7.38	54.6	18.4	7.378
Total			100.00	752.7	249.3	100.000

Racemic trace:

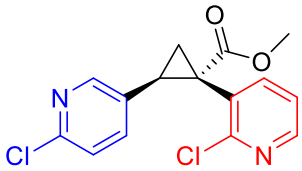

83

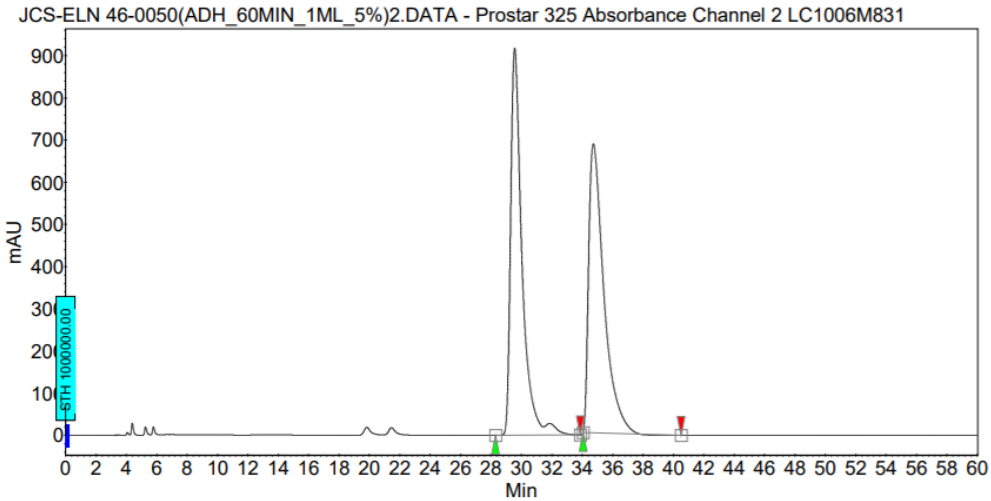

Peak results :

Index	Name	Time [Min]	Quantity [% Area]	Height [mAU]	Area [mAU.Min]	Area % [%]
1	UNKNOWN	29.56	50.43	917.3	801.0	50.427
2	UNKNOWN	34.74	49.57	684.2	787.4	49.573
Total			100.00	1601.4	1588.4	100.000

0 ℃, 1.0 mol % Rh_2(*S*-TPPTTL)$_4$1.5 equiv vinyl heterocycle, 3.5 equiv 2-chloropyridine, CH_2Cl_2 as solvent, reaction performed according to procedure 3.4

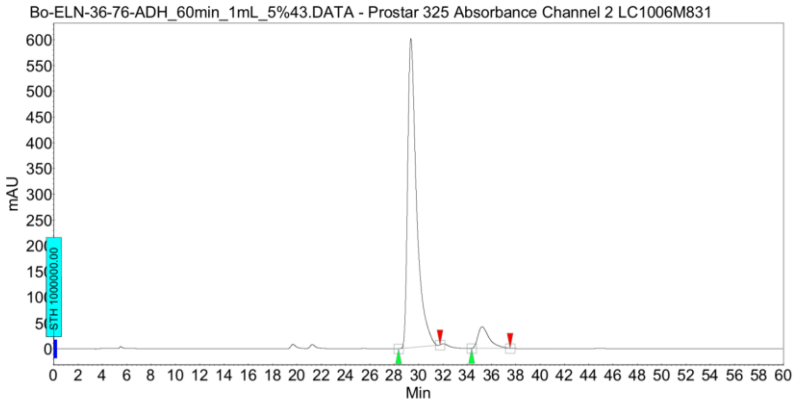

Peak results :

Index	Name	Time [Min]	Quantity [% Area]	Height [mAU]	Area [mAU.Min]	Area % [%]
2	UNKNOWN	29.37	91.81	599.4	508.8	91.813
1	UNKNOWN	35.23	8.19	41.9	45.4	8.187
Total			100.00	641.3	554.2	100.000

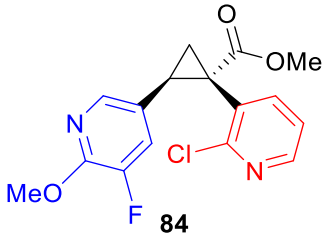

84

Racemic trace:

Chromatogram :
JCS-ELN46-202(ADH_80MIN_1ML_1%)3_channel1

System : Prostar LC System
Method : DACHDNB_30min_1mL_1%-230nm
User : User1

Acquired : 1/27/2020 9:42:16 AM
Processed : 1/30/2020 9:32:53 AM
Printed : 9/12/2020 12:07:06 PM

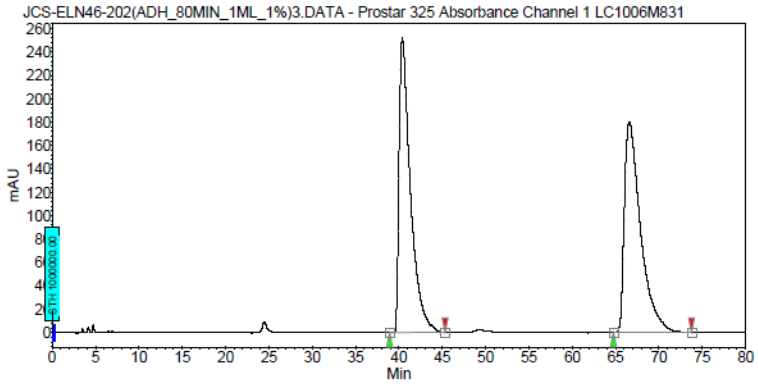

Peak results :

Index	Name	Time [Min]	Quantity [% Area]	Height [mAU]	Area [mAU.Min]	Area % [%]
1	UNKNOWN	40.39	49.63	252.0	384.1	49.626
2	UNKNOWN	66.59	50.37	180.0	389.9	50.374
Total			100.00	432.0	774.0	100.000

0 ℃, 1.0 mol % Rh_2(*S*-TPPTTL)$_4$ 1.5 equiv vinyl heterocycle, 3.5 equiv 2-chloropyridine, CH_2Cl_2 as solvent, reaction performed according to procedure 3.4

Chromatogram :
JCS-ELN46-203(ADH_80MIN_1ML_1%)6_channel1

System : Prostar LC System
Method : DACHDNB_30min_1mL_1%-230nm
User : User1

Acquired : 1/27/2020 11:52:55 AM
Processed : 1/27/2020 1:22:55 PM
Printed : 9/12/2020 12:08:16 PM

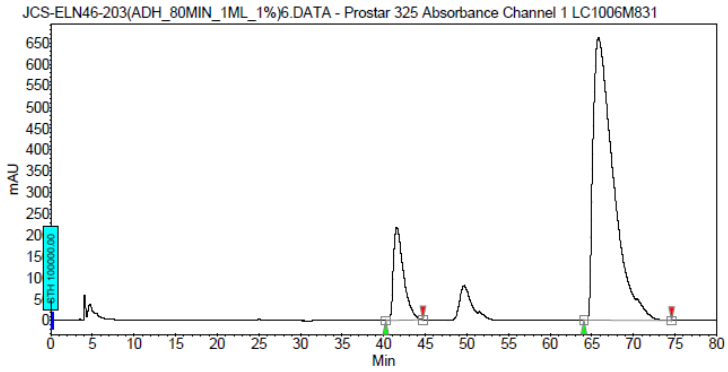

Peak results :

Index	Name	Time [Min]	Quantity [% Area]	Height [mAU]	Area [mAU.Min]	Area % [%]
1	UNKNOWN	41.57	14.09	218.8	306.3	14.092
2	UNKNOWN	65.80	85.91	661.4	1867.1	85.908
Total			100.00	880.2	2173.4	100.000

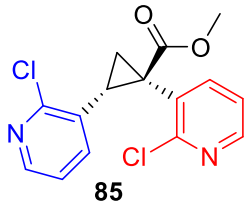

85

Racemic trace:

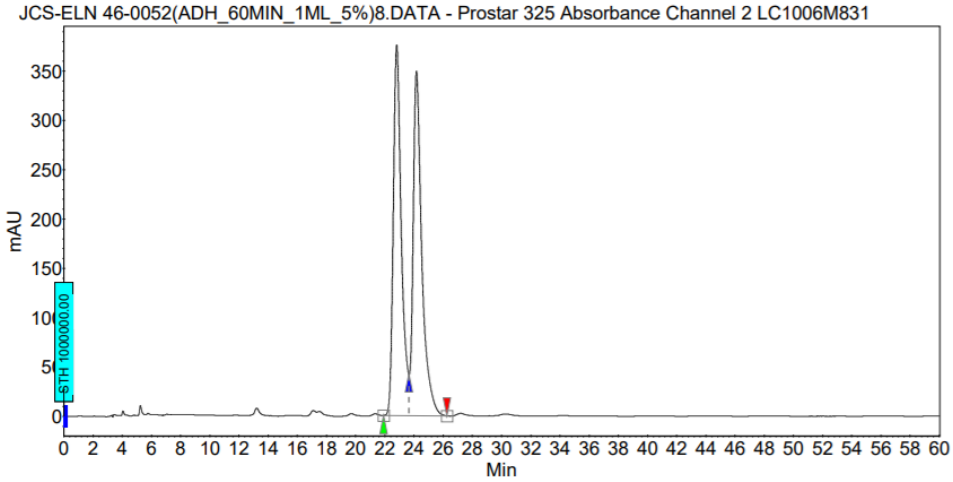

Peak results :

Index	Name	Time [Min]	Quantity [% Area]	Height [mAU]	Area [mAU.Min]	Area % [%]
1	UNKNOWN	22.81	49.64	375.9	239.1	49.641
2	UNKNOWN	24.16	50.36	349.3	242.6	50.359
Total			100.00	725.2	481.8	100.000

0 ℃, 1.0 mol % Rh_2(*S*-TPPTTL)$_4$ 1.5 equiv vinyl heterocycle, 3.5 equiv 2-chloropyridine, CH_2Cl_2 as solvent, reaction performed according to procedure 3.4

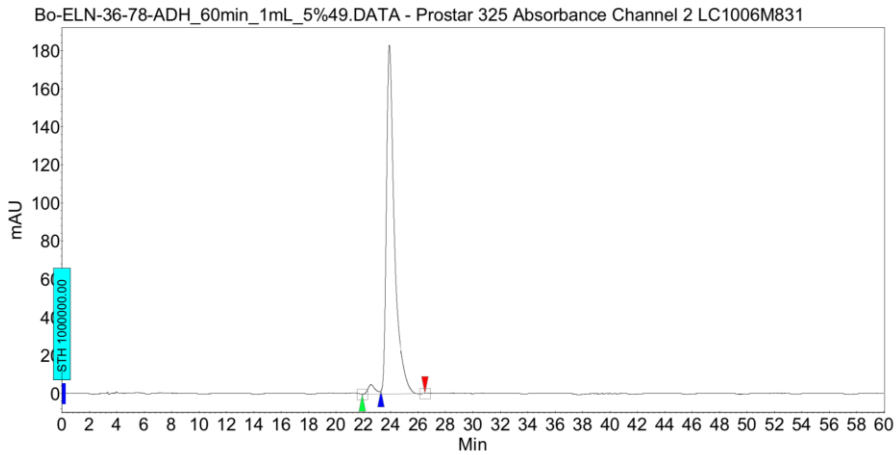

Peak results :

Index	Name	Time [Min]	Quantity [% Area]	Height [mAU]	Area [mAU.Min]	Area % [%]
1	UNKNOWN	22.54	2.40	4.9	3.1	2.396
2	UNKNOWN	23.89	97.60	183.1	124.9	97.604
Total			100.00	188.0	127.9	100.000

5.3: Screening of different coordinating additives for optimal %ee enhancement in cyclopropanation with *ortho*-substituted aryl/heteroaryl diazoacetates.

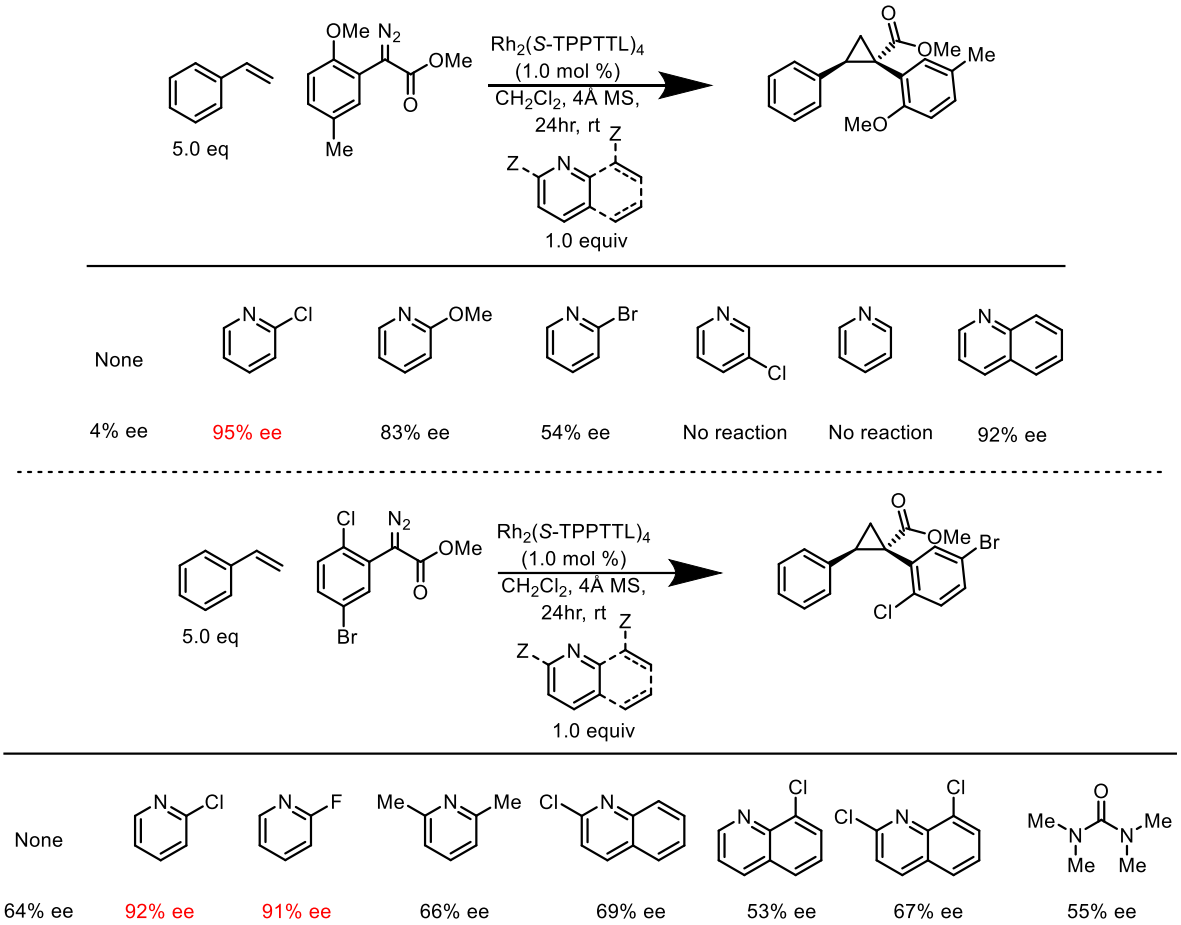

Figure B5. Examination of various coordinating additives to determine the optimal compound to enhance the enantioselectivity of cyclopropanation involving *ortho*-substituted aryl diazo acetates. Two aryldiazoacetates were examined to ensure generalizability. Reactions were conducted on 0.20 mmol scale with 5.0 equiv styrene, 1.0 equiv coordinating additive, 1.0 mol % catalyst loading, and CH_2Cl_2 as solvent. The reaction was conducted at room temperature and run for at least 13 hr. Of the additives tested, 2-chloropyridine and 2-fluoropyridine (red) gave the best levels of enantio-enhancement. Other additives seemed to hamper the enantioselectivity of the reaction, in particular substituted quinolines and tetra-methyl urea. 3-Chloropyridine and pyridine served to poison the reaction, no rhodium-carbene was generated and the diazo-starting material was recovered.

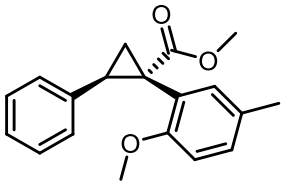

60

Racemic trace, AD-H column:

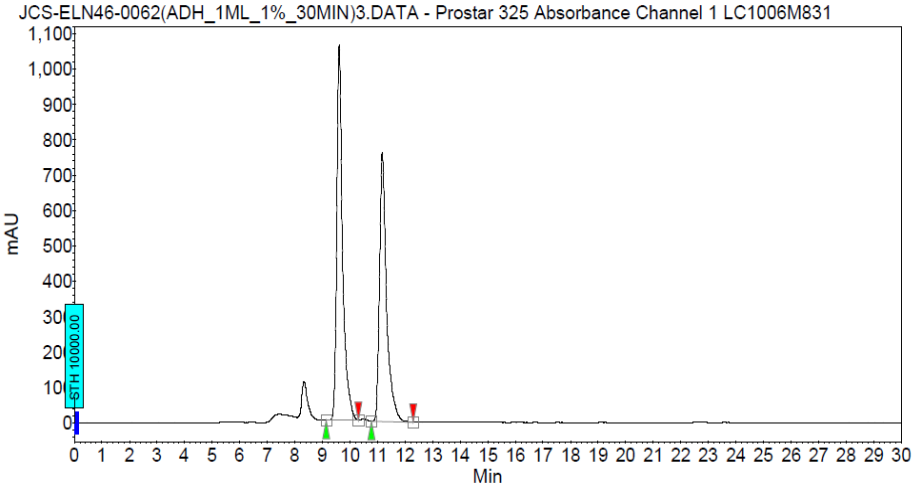

Peak results :

Index	Name	Time [Min]	Quantity [% Area]	Height [mAU]	Area [mAU.Min]	Area % [%]
1	UNKNOWN	9.61	53.67	1060.1	260.5	53.666
2	UNKNOWN	11.17	46.33	760.0	224.9	46.334
Total			100.00	1820.2	485.3	100.000

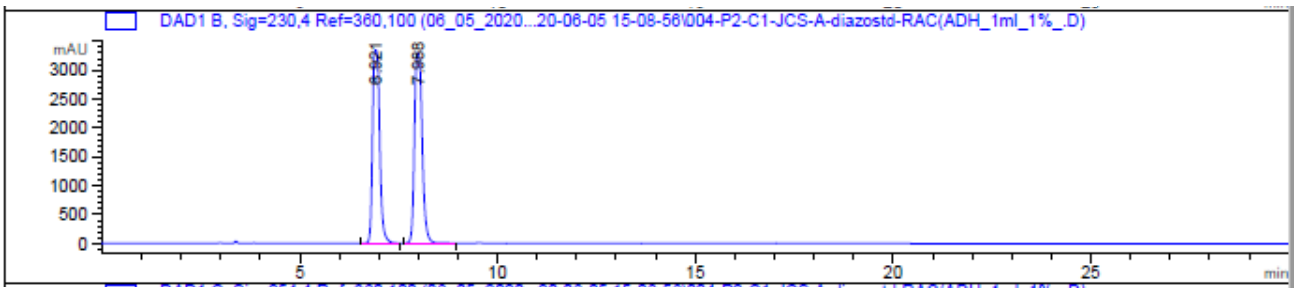

Signal 2: DAD1 B, Sig=230,4 Ref=360,100

Peak #	RetTime [min]	Type	Width [min]	Area [mAU*s]	Height [mAU]	Area %
1	6.921	BB	0.1986	4.20731e4	3348.93286	48.2033
2	7.988	BV R	0.2130	4.52095e4	3305.63135	51.7967
Totals :				8.72826e4	6654.56421	

0 ℃, 1.0 mol % Rh_2(*S*-TPPTTL)$_4$, 5.0 equiv styrene, 1.0 equiv 2-chloropyridine, CH_2Cl_2 as solvent, reaction performed according to procedure 3.4

Chromatogram :
JCS-ELN46-0095DIL(ADH_30MIN_1ml_1%)3_channel 1

Instrument : Prostar LC System
Method : DACHDNB_30min_1mL_1%-230nm
User : User1

Acquired : 10/17/2019 9:55:29 AM
Processed : 10/17/2019 10:44:45 AM
Printed : 12/31/2019 12:32:50 PM

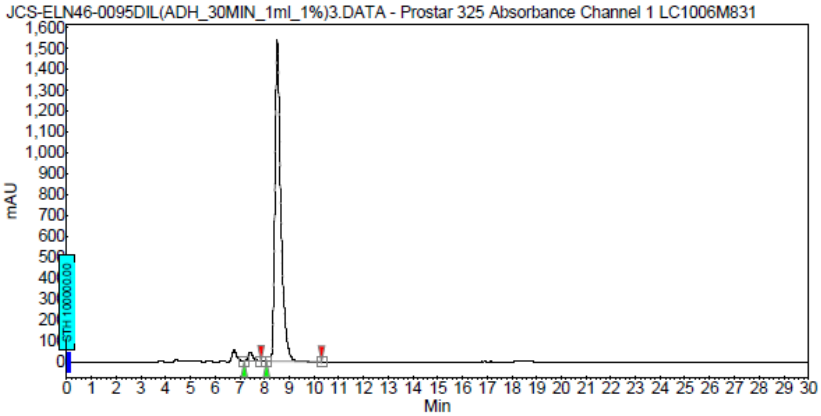

Peak results :

Index	Name	Time [Min]	Quantity [% Area]	Height [mAU]	Area [mAU.Min]	Area % [%]
2	UNKNOWN	7.41	2.41	44.3	10.6	2.413
1	UNKNOWN	8.52	97.59	1536.4	429.5	97.587
Total			100.00	1580.6	440.1	100.000

0 ℃, 1.0 mol % Rh_2(*S*-TPPTTL)$_4$, 5.0 equiv styrene, 1.0 equiv 2-MeOpyridine, CH_2Cl_2 as solvent, reaction performed according to procedure 3.4

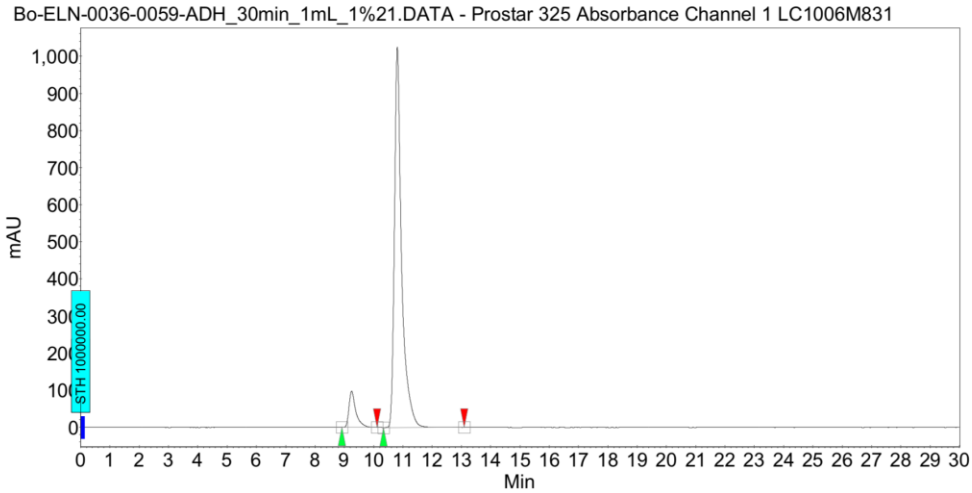

Peak results :

Index	Name	Time [Min]	Quantity [% Area]	Height [mAU]	Area [mAU.Min]	Area % [%]
2	UNKNOWN	9.25	8.27	97.7	26.3	8.274
1	UNKNOWN	10.81	91.73	1025.7	291.2	91.726
Total			100.00	1123.4	317.5	100.000

0 ℃, 1.0 mol % Rh_2(*S*-TPPTTL)$_4$, 5.0 equiv styrene, 1.0 equiv 2-Brpyridine, CH_2Cl_2 as solvent, reaction performed according to procedure 3.4

Chromatogram :
JCS-ELN46-0100(ADH_30MIN_1ml_1%)8_channel1

System : Prostar LC System
Method : DACHDNB_30min_1mL_1%-230nm
User : User1

Acquired : 10/16/2019 7:22:07 PM
Processed : 10/17/2019 8:59:27 AM
Printed : 12/31/2019 12:34:44 PM

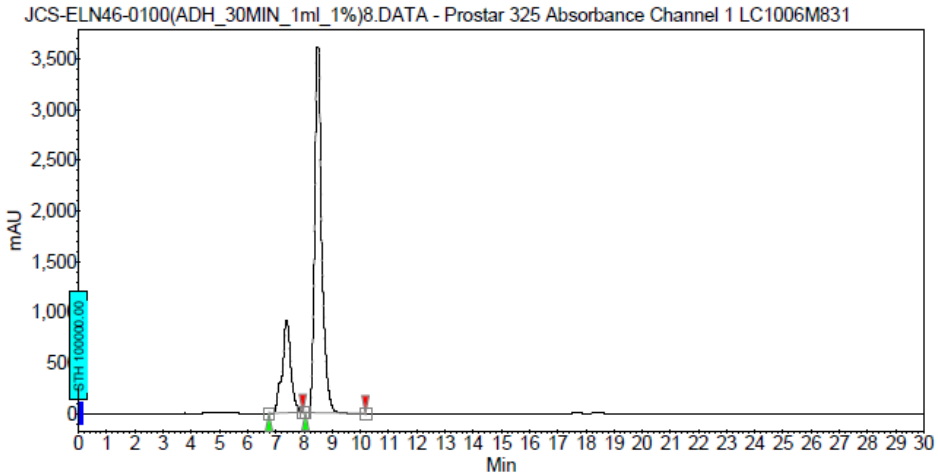

Peak results :

Index	Name	Time [Min]	Quantity [% Area]	Height [mAU]	Area [mAU.Min]	Area % [%]
2	UNKNOWN	7.38	23.23	916.7	323.5	23.230
1	UNKNOWN	8.50	76.77	3610.0	1069.1	76.770
Total			100.00	4526.7	1392.6	100.000

0 ℃, 1.0 mol % Rh_2(*S*-TPPTTL)$_4$, 5.0 equiv styrene, 1.0 equiv quinoline, CH_2Cl_2 as solvent, reaction performed according to procedure 3.4

Chromatogram :
JCS-ELN46-0102(ADH_30MIN_1ml_1%)11_channel1

System : Prostar LC System
Method : DACHDNB_30min_1mL_1%-230nm
User : User1

Acquired : 10/16/2019 8:39:23 PM
Processed : 10/17/2019 8:58:20 AM
Printed : 1/3/2020 11:11:40 AM

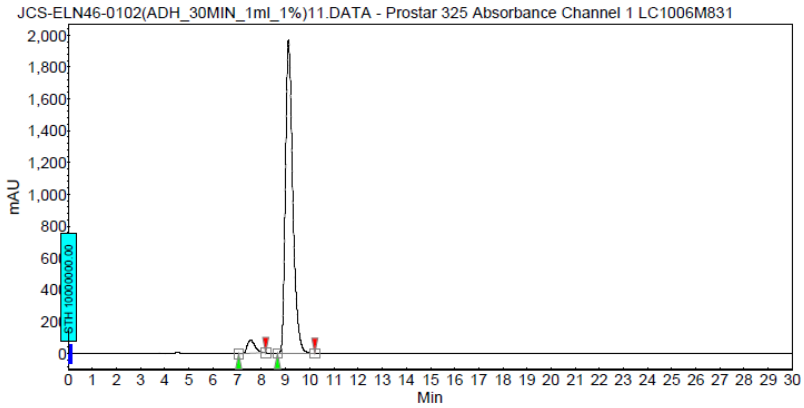

Peak results :

Index	Name	Time [Min]	Quantity [% Area]	Height [mAU]	Area [mAU.Min]	Area % [%]
1	UNKNOWN	7.54	4.24	81.7	30.5	4.245
2	UNKNOWN	9.12	95.76	1966.1	687.8	95.755
Total			100.00	2047.8	718.3	100.000

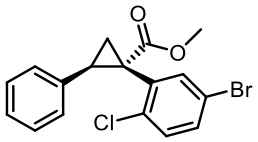

62

Racemic trace:

Chromatogram :
JCS-ELN46-0080(OJH_1ML_1%_30MIN)11_channel2

System : Prostar LC System
Method : OD_30min_1mL_1%_210_230nm
User : User1

Acquired : 10/8/2019 4:32:30 PM
Processed : 10/8/2019 5:19:04 PM
Printed : 12/31/2019 12:44:41 PM

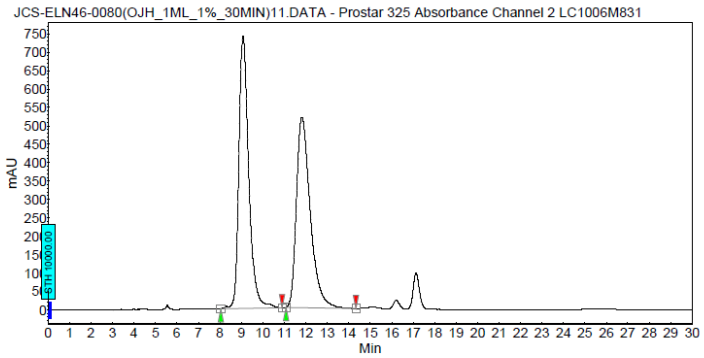

Peak results :

Index	Name	Time [Min]	Quantity [% Area]	Height [mAU]	Area [mAU.Min]	Area % [%]
1	UNKNOWN	9.07	50.51	739.1	394.0	50.510
2	UNKNOWN	11.82	49.49	516.8	386.0	49.490
Total			100.00	1255.9	780.0	100.000

0 ℃, 1.0 mol % Rh_2(*S*-TPPTTL)$_4$, 5.0 equiv styrene, 1.0 equiv 2-Clpyridine, CH_2Cl_2 as solvent, reaction performed according to procedure 3.4

Chromatogram :
JCS-ELN46-0079DIL(OJH_30MIN_1ML_1%)3_channel2

System : Prostar LC System
Method : OD_30min_1mL_1%_230nm
User : User1

Acquired : 10/9/2019 9:44:19 AM
Processed : 12/31/2019 12:43:26 PM
Printed : 12/31/2019 12:43:28 PM

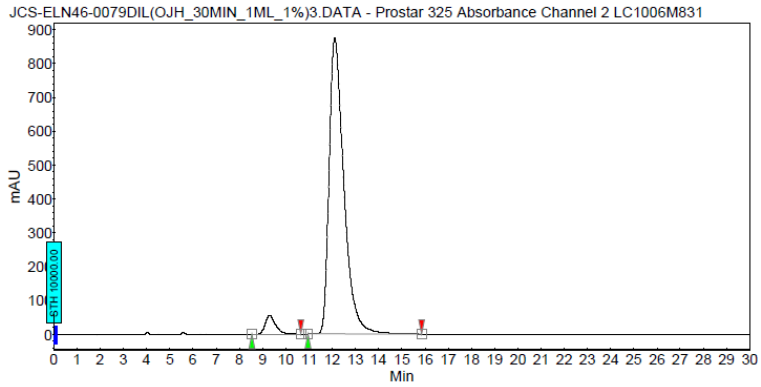

Peak results :

Index	Name	Time [Min]	Quantity [% Area]	Height [mAU]	Area [mAU.Min]	Area % [%]
1	UNKNOWN	9.30	4.30	55.7	29.0	4.303
2	UNKNOWN	12.11	95.70	872.6	643.9	95.697
Total			100.00	928.3	672.8	100.000

0 ℃, 1.0 mol % Rh_2(*S*-TPPTTL)$_4$, 5.0 equiv styrene, 1.0 equiv 2-Clquinoline, CH_2Cl_2 as solvent, reaction performed according to procedure 3.4

Chromatogram :
JCS-ELN46-0115RE(OJH_30MIN_1ML_1%)23_channel2

Prostar LC System
Method : S4900_30min_1mL_1%_230nm
User : User1

Acquired : 11/10/2019 12:14:54 AM
Processed : 9/29/2020 4:40:17 PM
Printed : 9/29/2020 4:40:29 PM

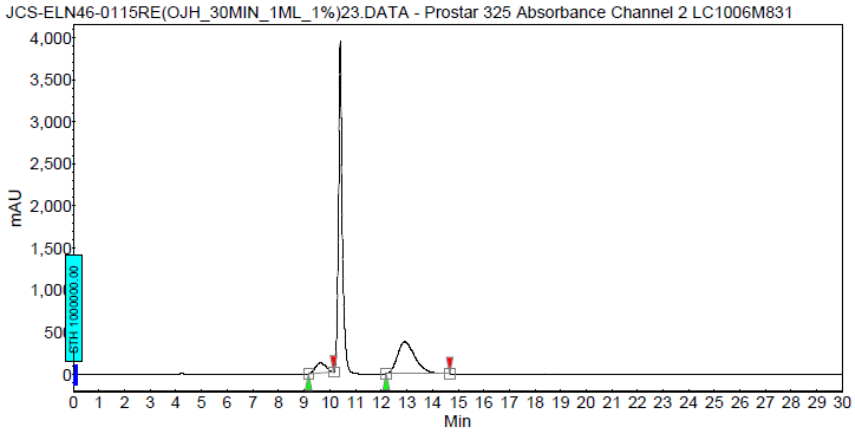

Peak results :

Index	Name	Time [Min]	Quantity [% Area]	Height [mAU]	Area [mAU.Min]	Area % [%]
1	UNKNOWN	9.62	15.41	120.3	55.1	15.411
2	UNKNOWN	12.92	84.59	379.7	302.3	84.589
Total			100.00	500.0	357.4	100.000

0 ℃, 1.0 mol % Rh_2(*S*-TPPTTL)$_4$, 5.0 equiv styrene, 1.0 equiv 2,8-dichloroquinoline, CH_2Cl_2 as solvent, reaction performed according to procedure 3.4

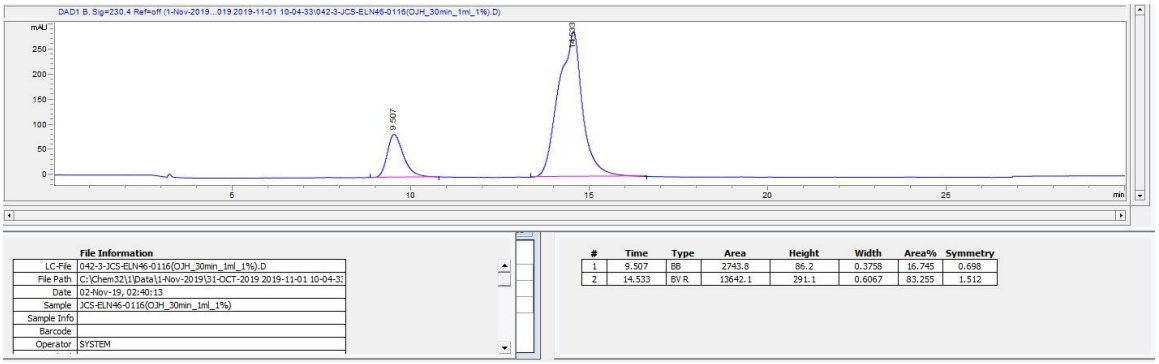

0 ℃, 1.0 mol % Rh_2(*S*-TPPTTL)$_4$, 5.0 equiv styrene, 1.0 equiv 8-chloroquinoline, CH_2Cl_2 as solvent, reaction performed according to procedure 3.4

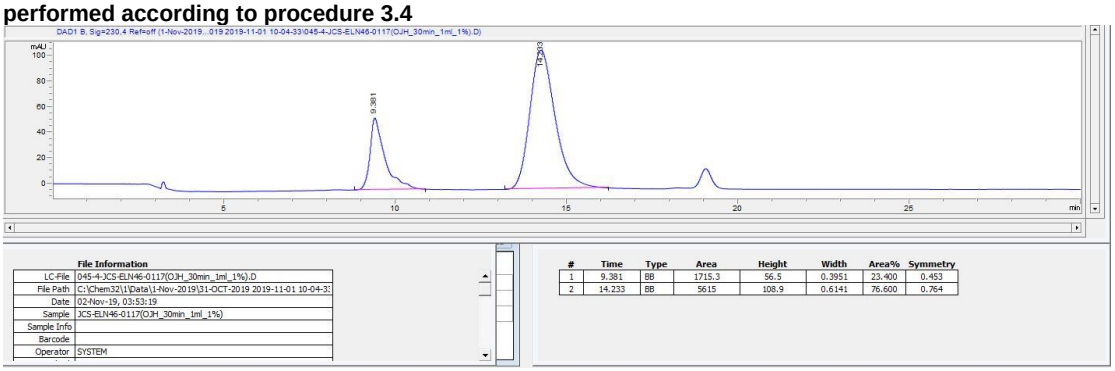

0 ℃, 1.0 mol % Rh_2(*S*-TPPTTL)$_4$, 5.0 equiv styrene, 1.0 equiv 2-Fpyridine, CH_2Cl_2 as solvent, reaction performed according to procedure 3.4

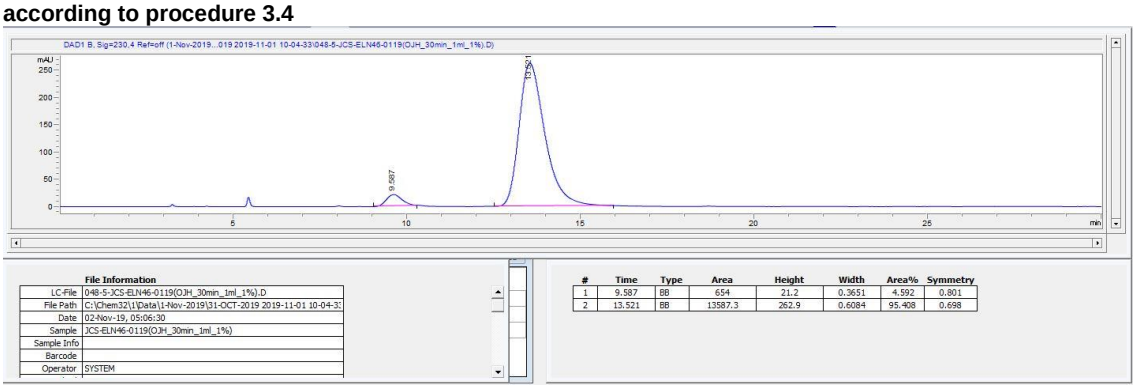

0 ℃, 1.0 mol % Rh_2(*S*-TPPTTL)$_4$, 5.0 equiv styrene, 1.0 equiv 2,6-lutidine, CH_2Cl_2 as solvent, reaction performed according to procedure 3.4

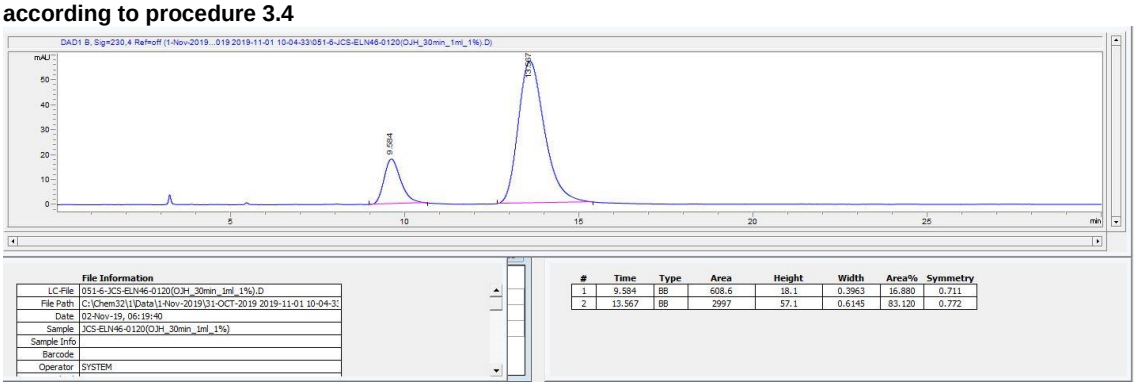

0 ℃, 1.0 mol % Rh_2(*S*-TPPTTL)$_4$, 5.0 equiv styrene, 1.0 equiv *N,N,N'N'*- tetramethyl urea, CH_2Cl_2 as solvent, reaction performed according to procedure 3.4

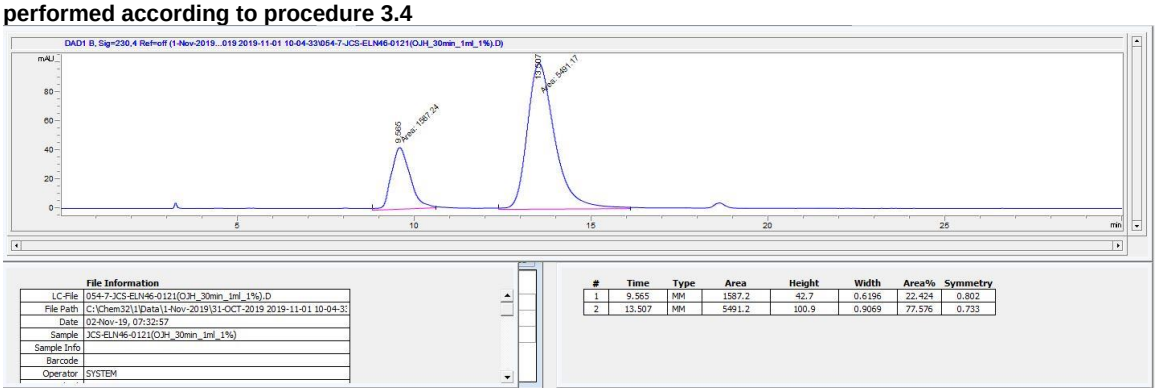

6. NMR Spectra:

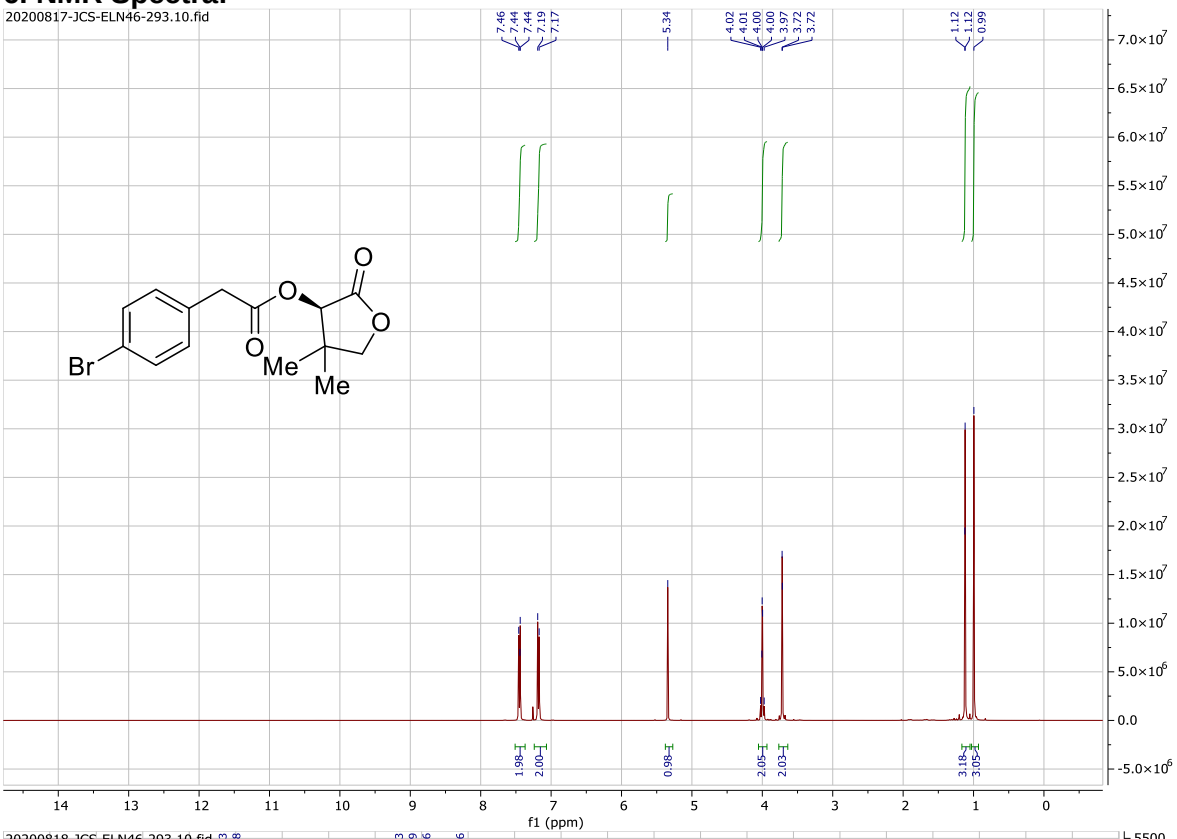

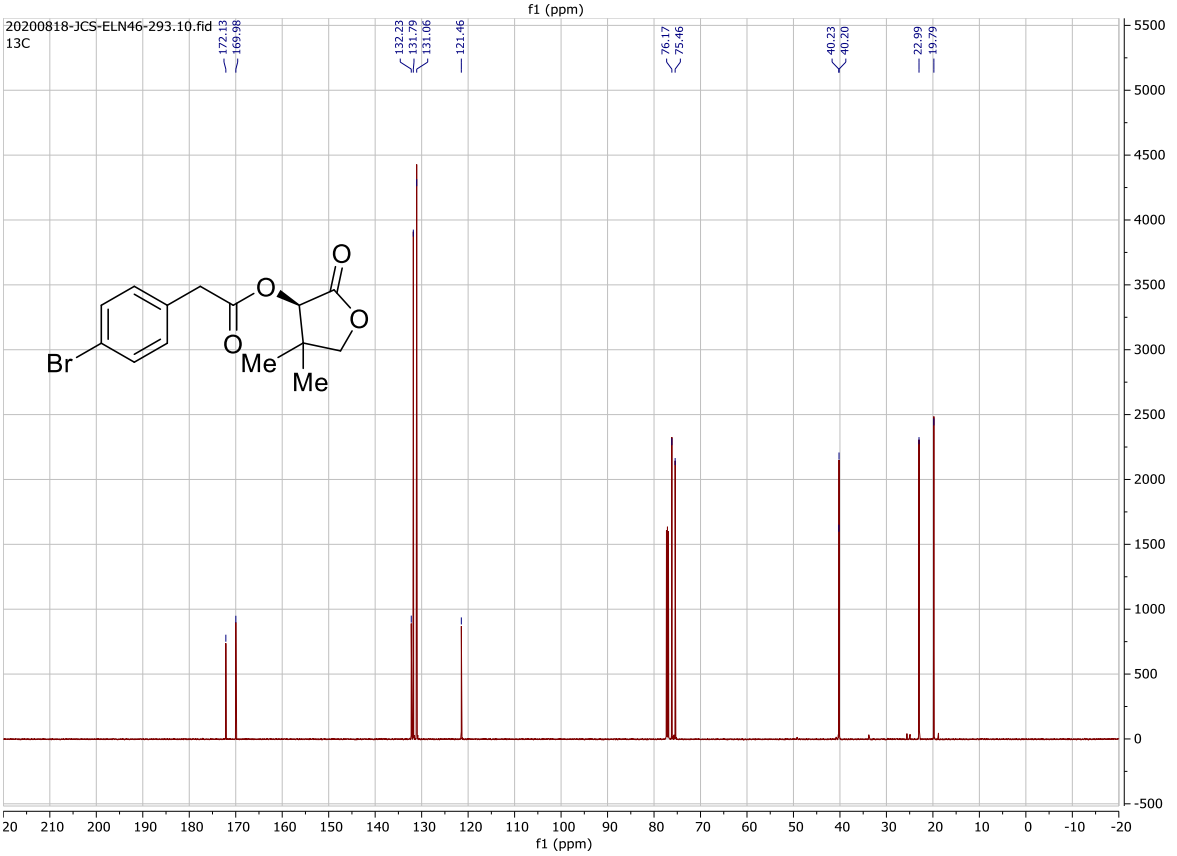

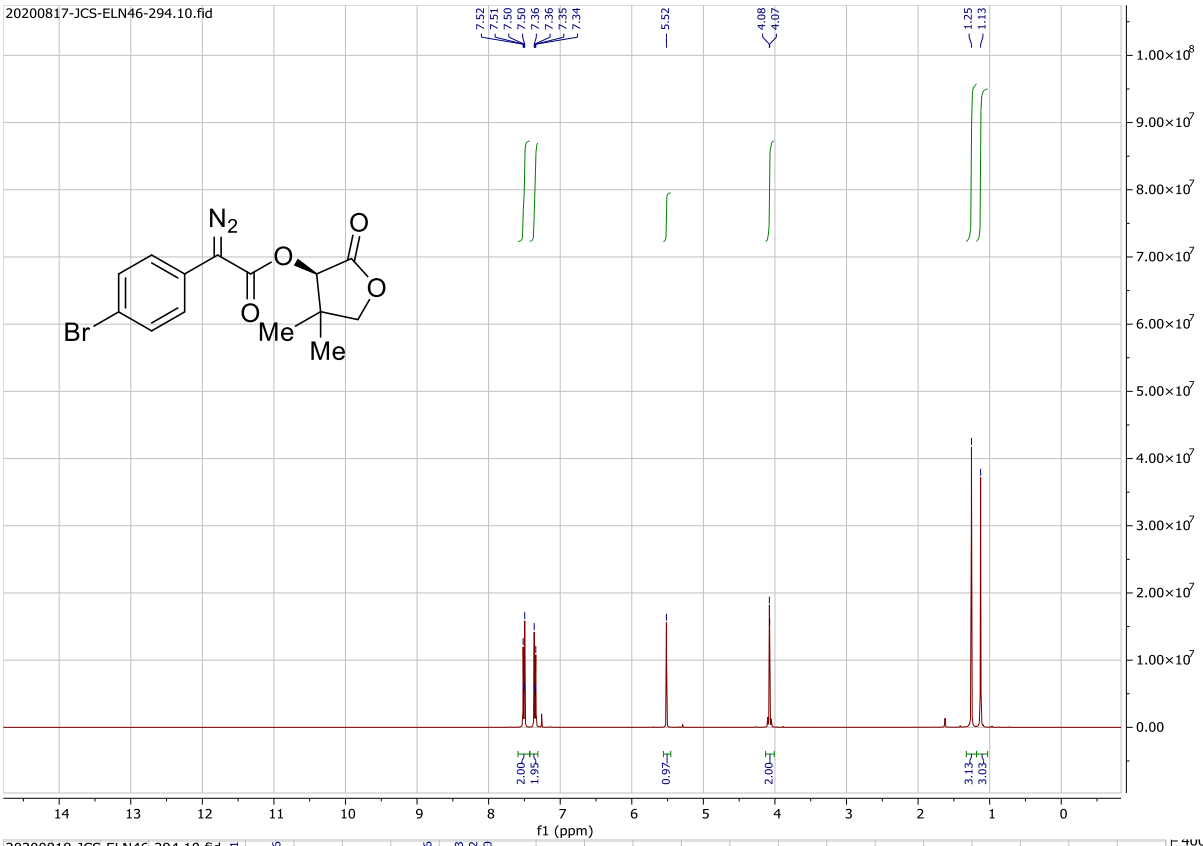
20200817-JCS-ELN46-294.10.fid
7.52
7.51
7.50
7.50
7.36
7.36
7.35
7.34
5.52
4.08
4.07
1.25
1.13
2.00
1.95
0.97
2.00
3.13
3.03
f1 (ppm)

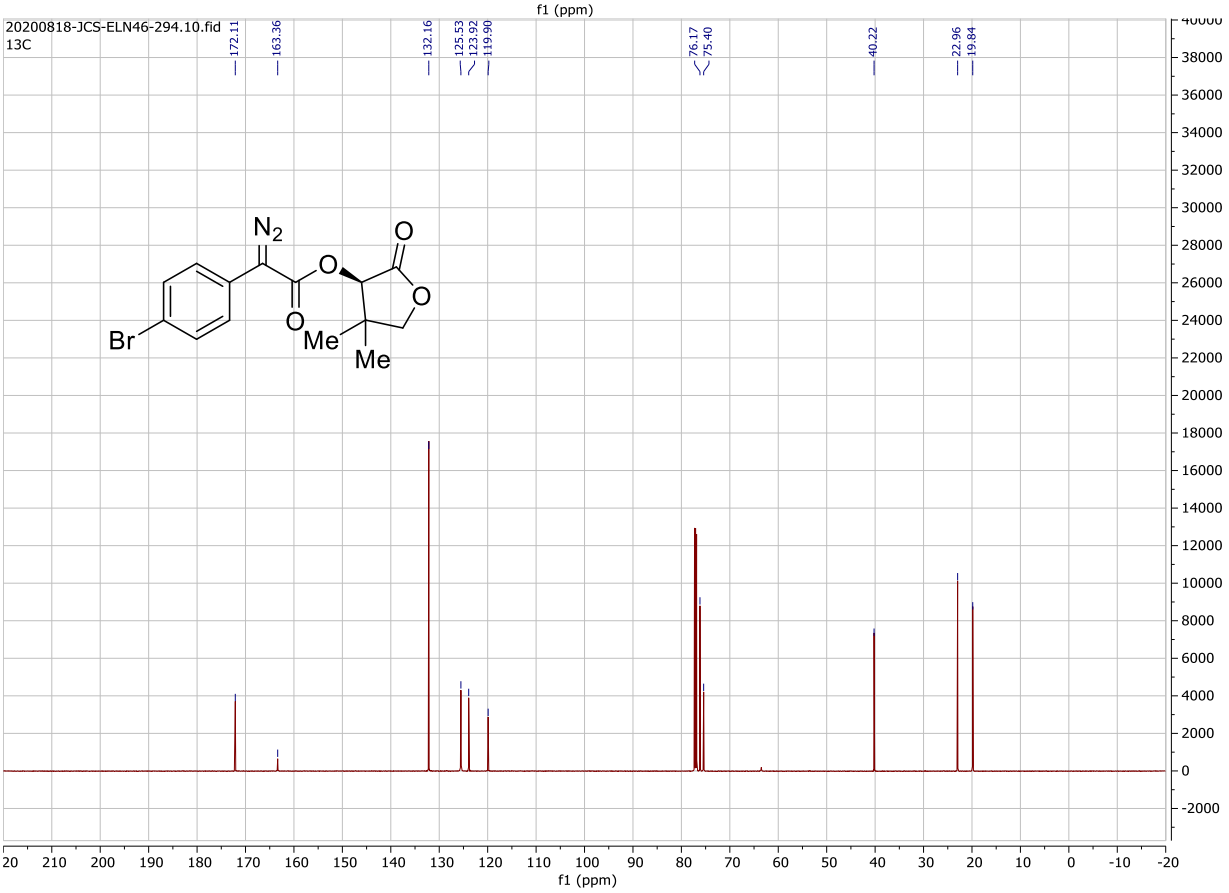
20200818-JCS-ELN46-294.10.fid
13C
172.11
163.36
132.16
125.53
123.92
119.90
76.17
75.40
40.22
22.96
19.84
f1 (ppm)

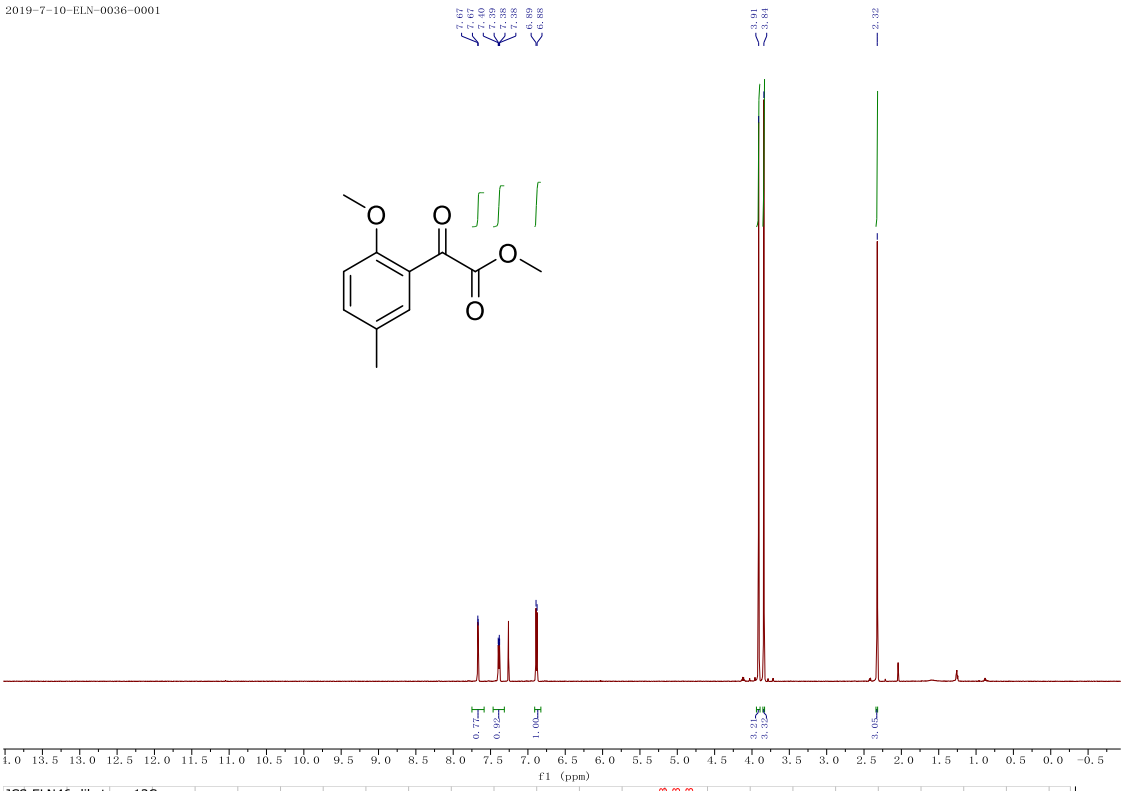
2019-7-10-ELN-0036-0001
7.67
7.67
7.40
7.39
7.38
7.38
6.89
6.88
3.91
3.84
2.32
0.77
0.99
1.00
3.21
3.32
3.05
f1 (ppm)

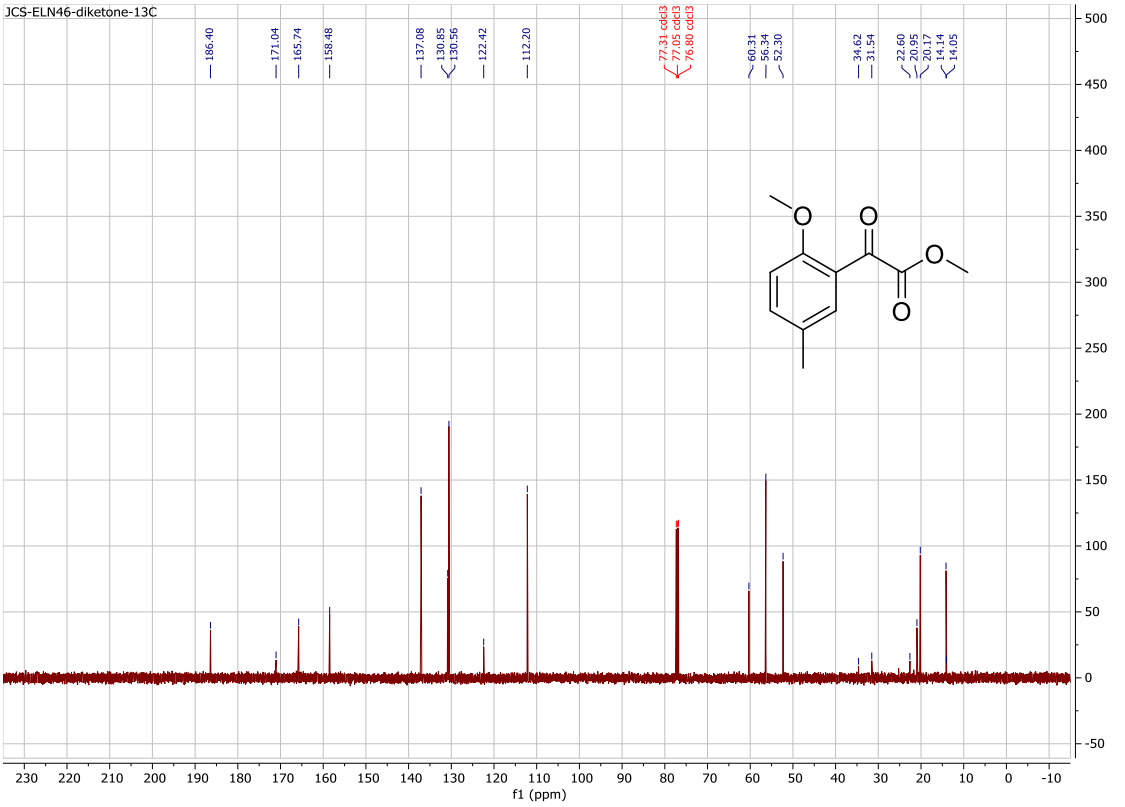
JCS-ELN46-diketone-13C
186.40
171.04
165.74
158.48
137.08
130.85
130.56
122.42
112.20
77.31 cdcl3
77.05 cdcl3
76.80 cdcl3
60.31
56.34
52.30
34.62
31.54
22.60
20.95
20.17
14.14
14.05
f1 (ppm)

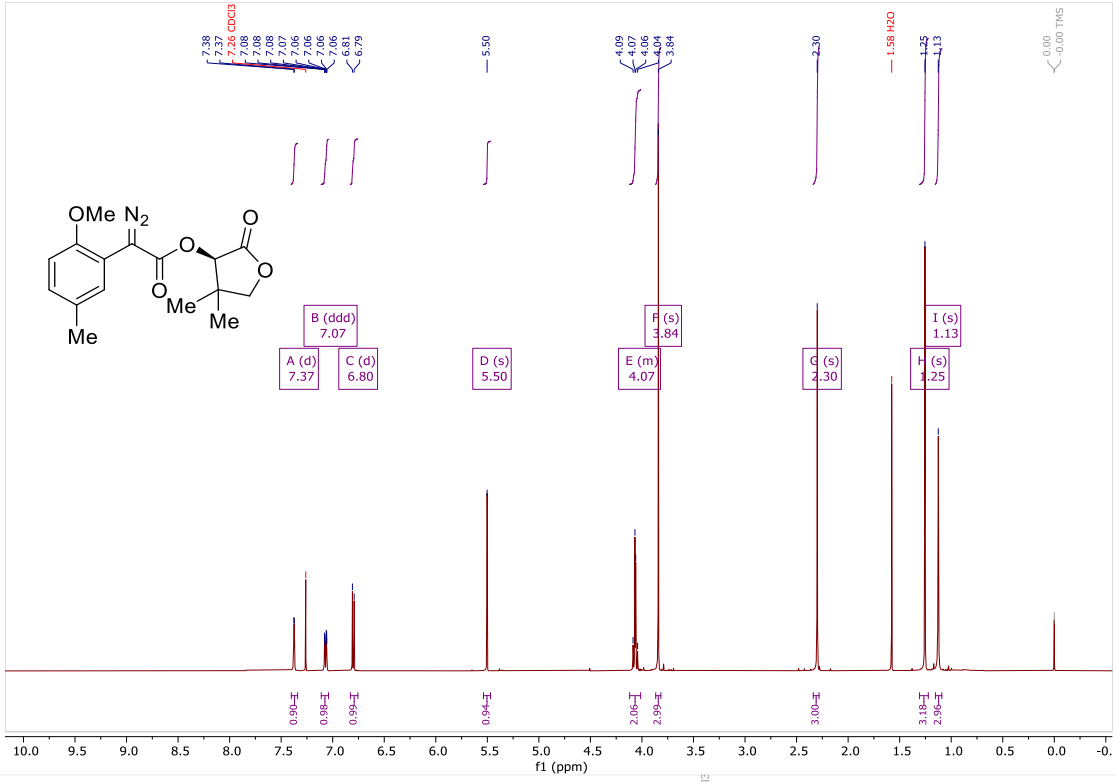
OMe N2
O
O
O
O
Me
Me
Me
A (d) 7.37
B (ddd) 7.07
C (d) 6.80
D (s) 5.50
E (m) 4.07
F (s) 3.84
G (s) 2.30
H (s) 1.25
I (s) 1.13
1.58 H2O
7.26 CDCl3
f1 (ppm)

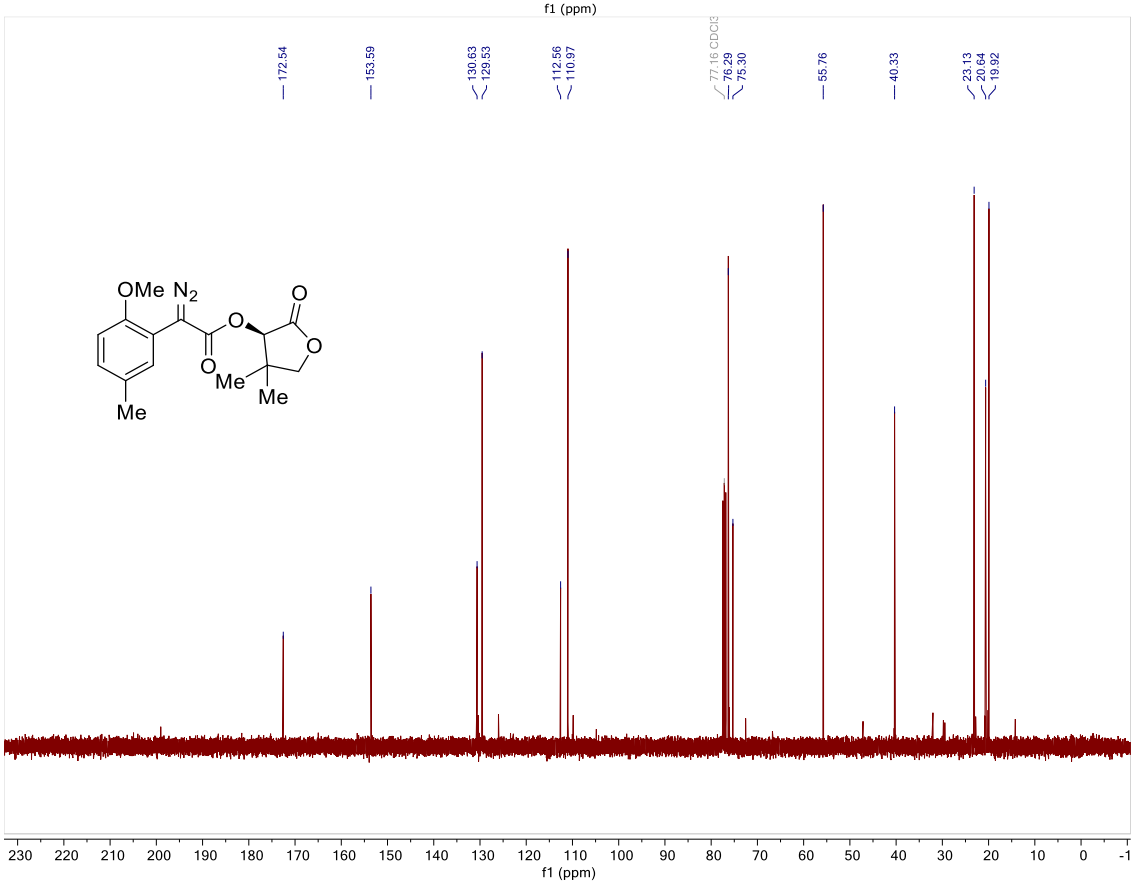
OMe N2
O
O
O
O
Me
Me
Me
172.54
153.59
130.63
129.53
112.56
110.97
77.16 CDCl3
76.29
75.30
55.76
40.33
23.13
20.64
19.92
f1 (ppm)

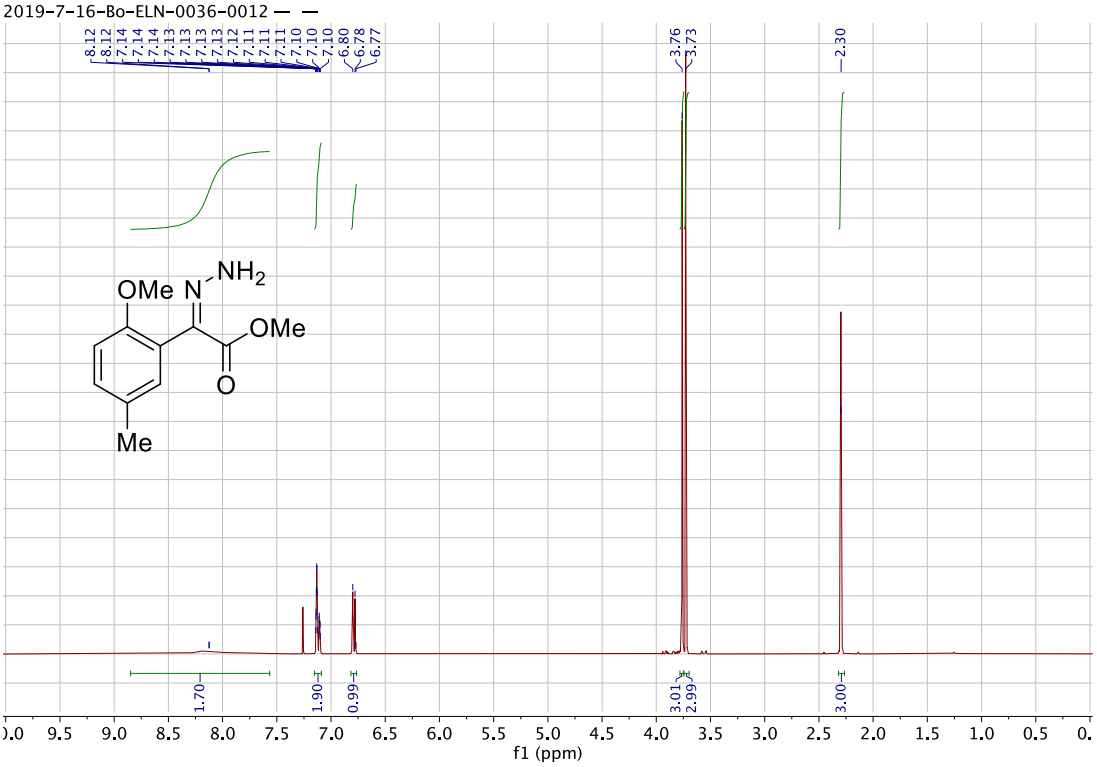
2019-7-16-Bo-ELN-0036-0012
8.12
8.12
7.14
7.14
7.14
7.13
7.13
7.13
7.13
7.12
7.11
7.11
7.11
7.10
7.10
7.10
6.80
6.78
6.77
3.76
3.73
2.30
OMe
N
NH2
OMe
O
Me
1.70
1.90
0.99
3.01
2.99
3.00
f1 (ppm)

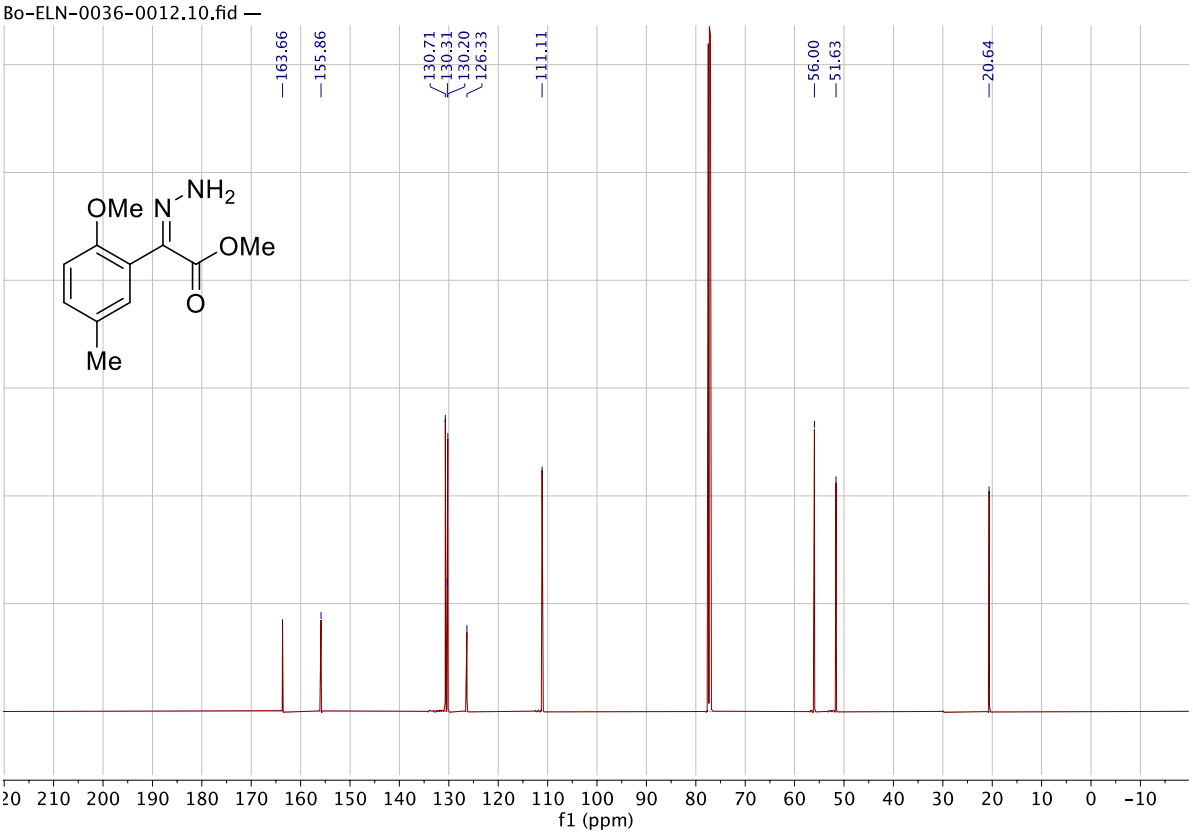
Bo-ELN-0036-0012.10.fid
163.66
155.86
130.71
130.31
130.20
126.33
111.11
56.00
51.63
20.64
OMe
N
NH2
OMe
O
Me
f1 (ppm)

20200729-Bo-38-E.10.fid —

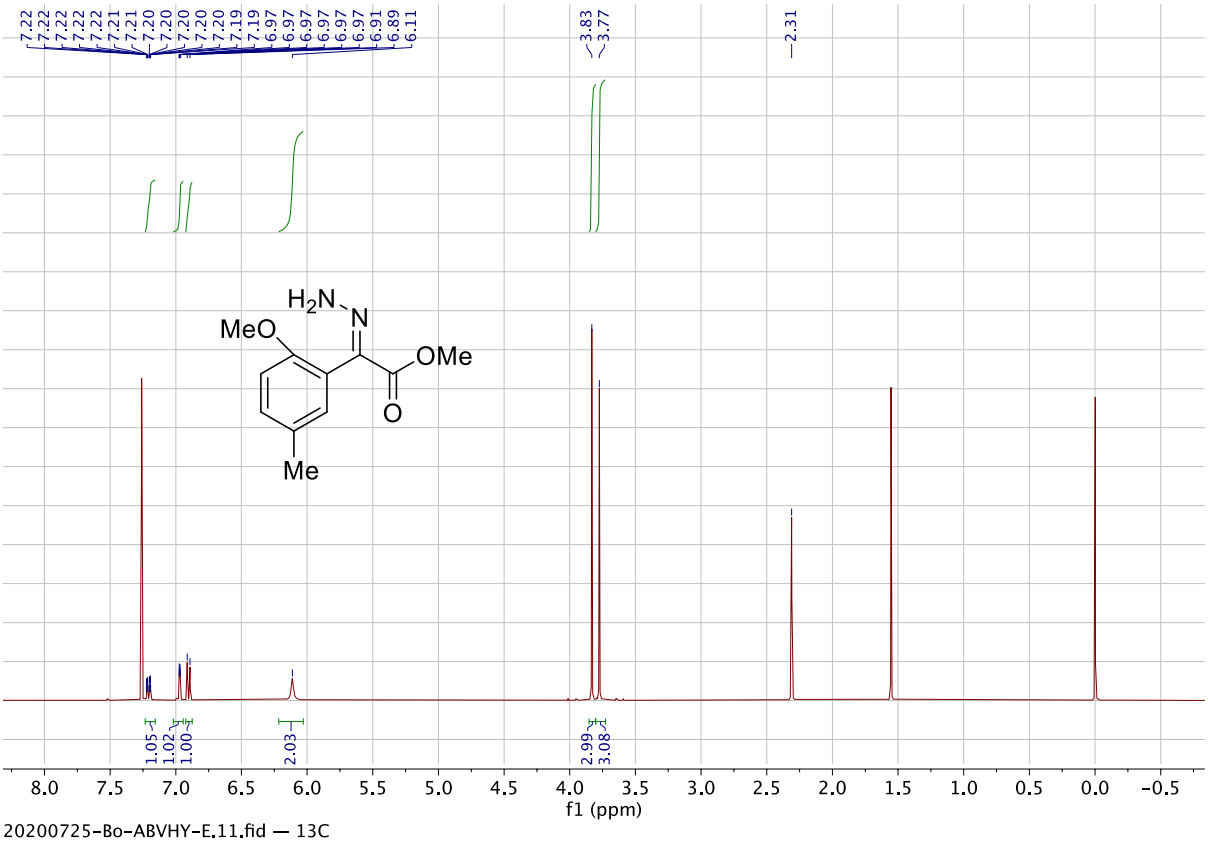

20200725-Bo-ABVHY-E.11.fid — 13C

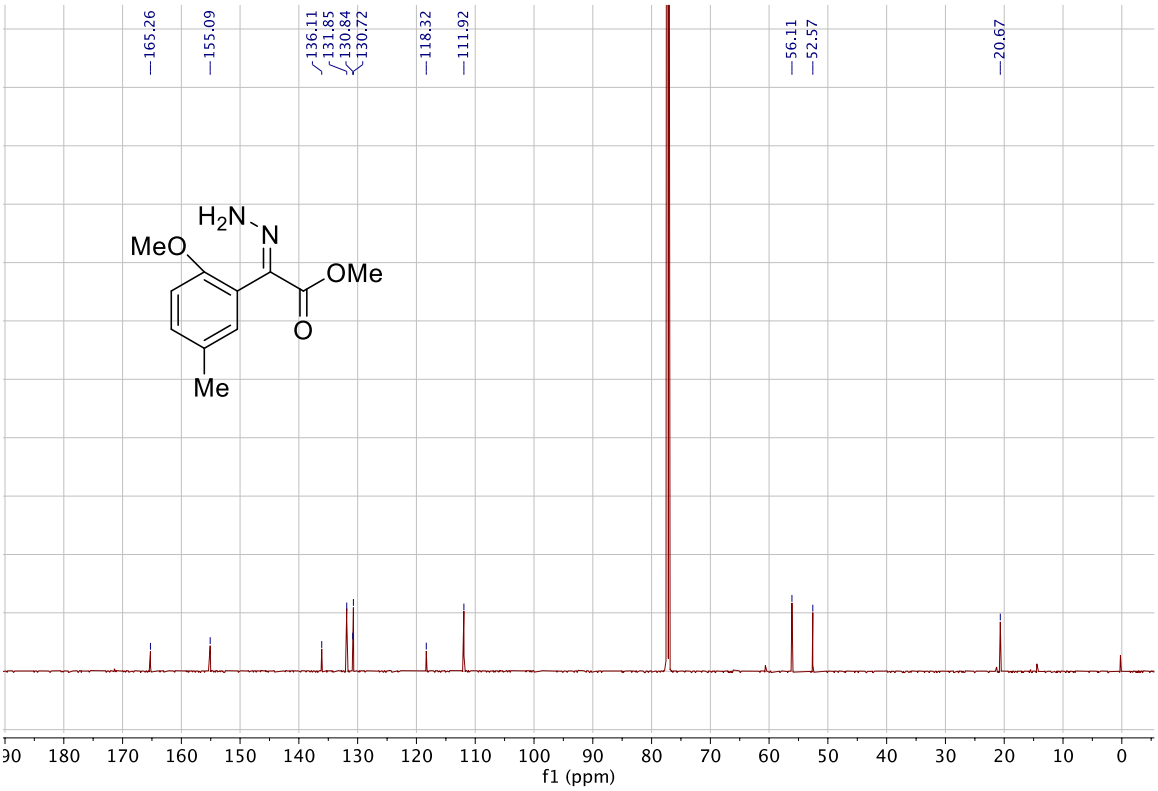

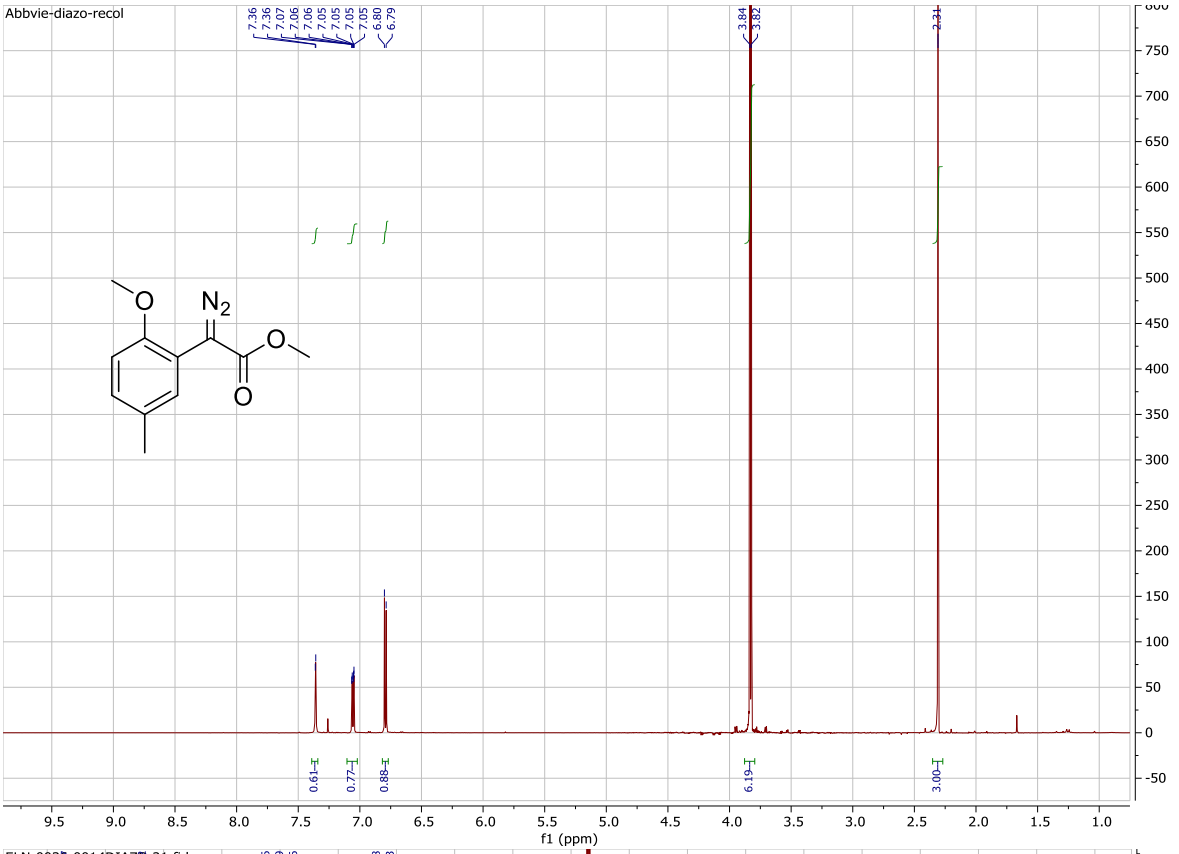
Abbvie-diazo-recol
7.36
7.36
7.07
7.06
7.06
7.05
7.05
7.05
6.80
6.79
3.84
3.82
2.31
0.61
0.77
0.88
6.19
3.00
f1 (ppm)

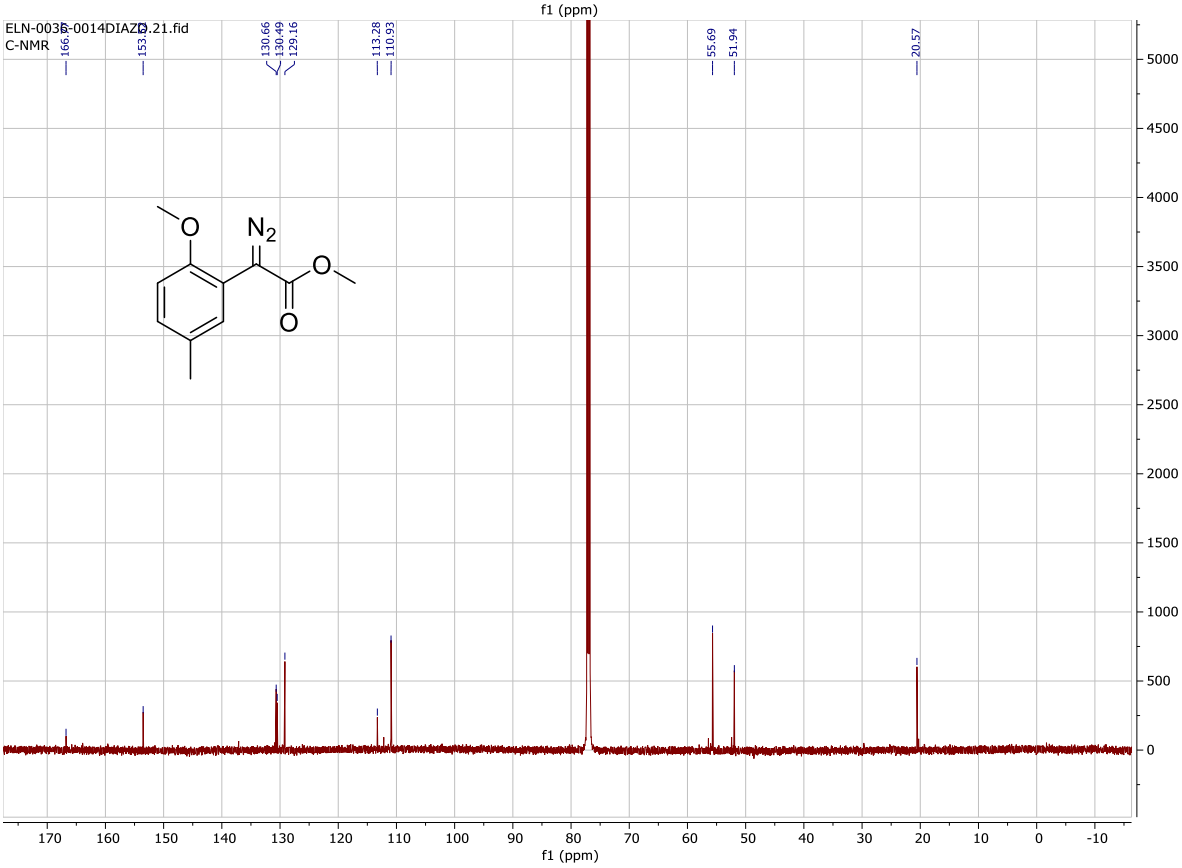
ELN-0035-0014DIAZO.21.fid
C-NMR
166.6
153.0
130.66
130.49
129.16
113.28
110.93
55.69
51.94
20.57
f1 (ppm)

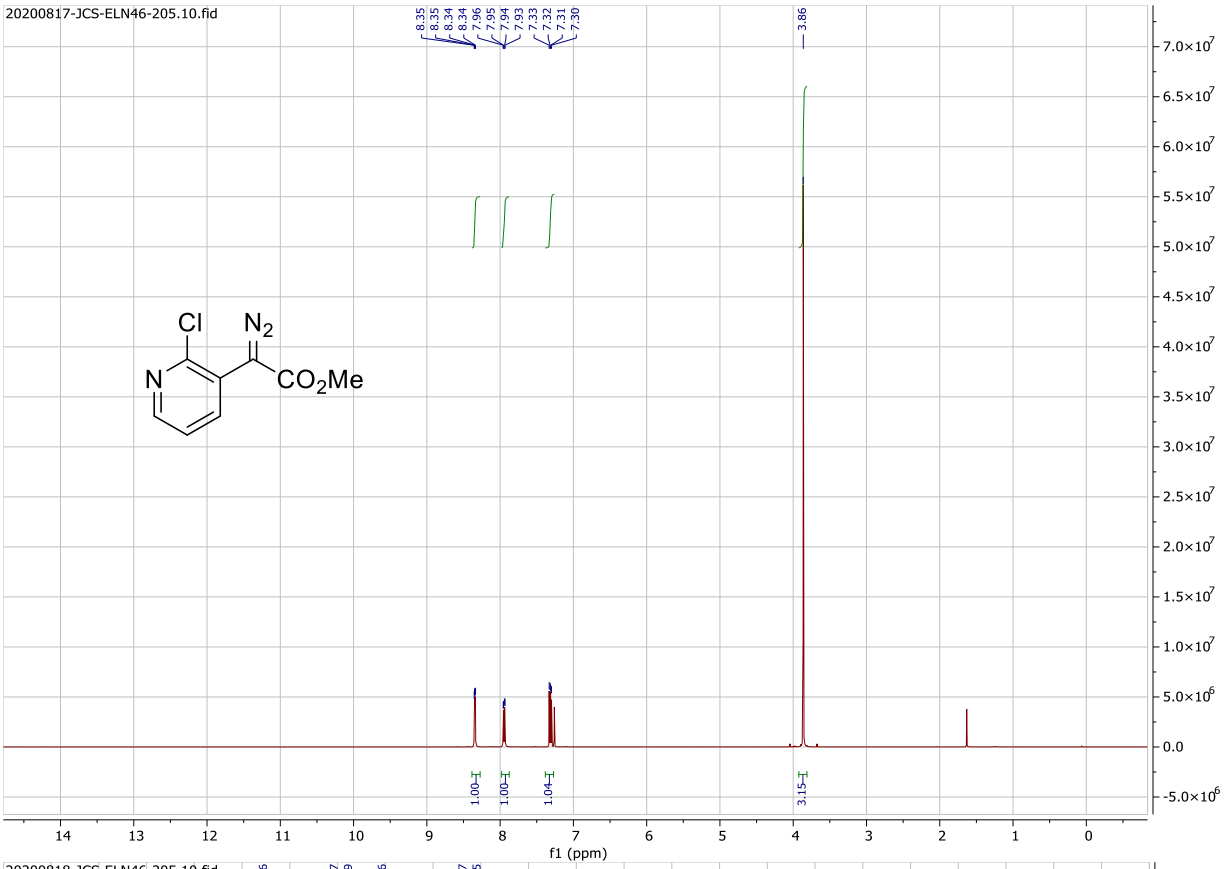
20200817-JCS-ELN46-205.10.fid
8.35
8.35
8.34
8.34
7.96
7.95
7.94
7.93
7.33
7.32
7.31
7.30
3.86
Cl
N2
N
CO2Me
1.00
1.00
1.04
3.15
f1 (ppm)

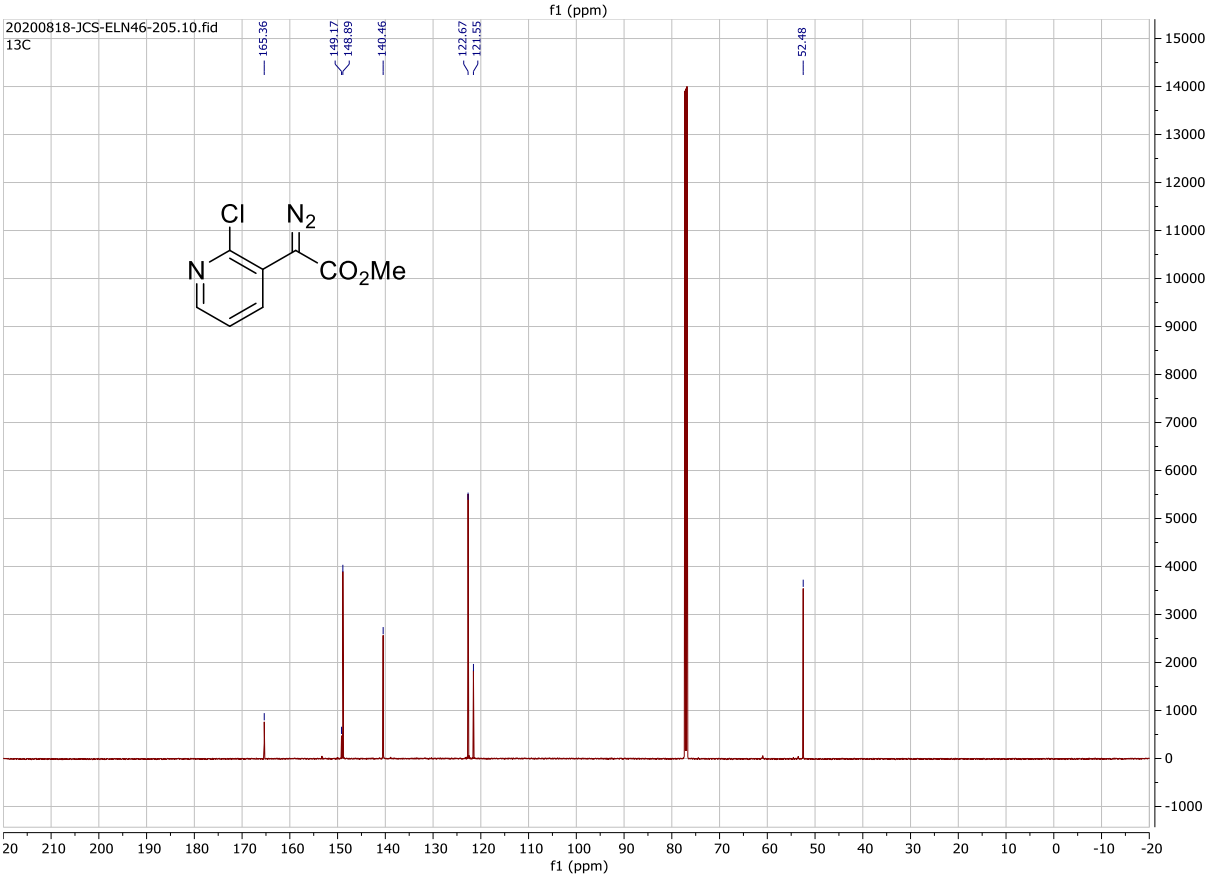
20200818-JCS-ELN46-205.10.fid
13C
165.36
149.17
148.89
140.46
122.67
121.55
52.48
Cl
N2
N
CO2Me
f1 (ppm)

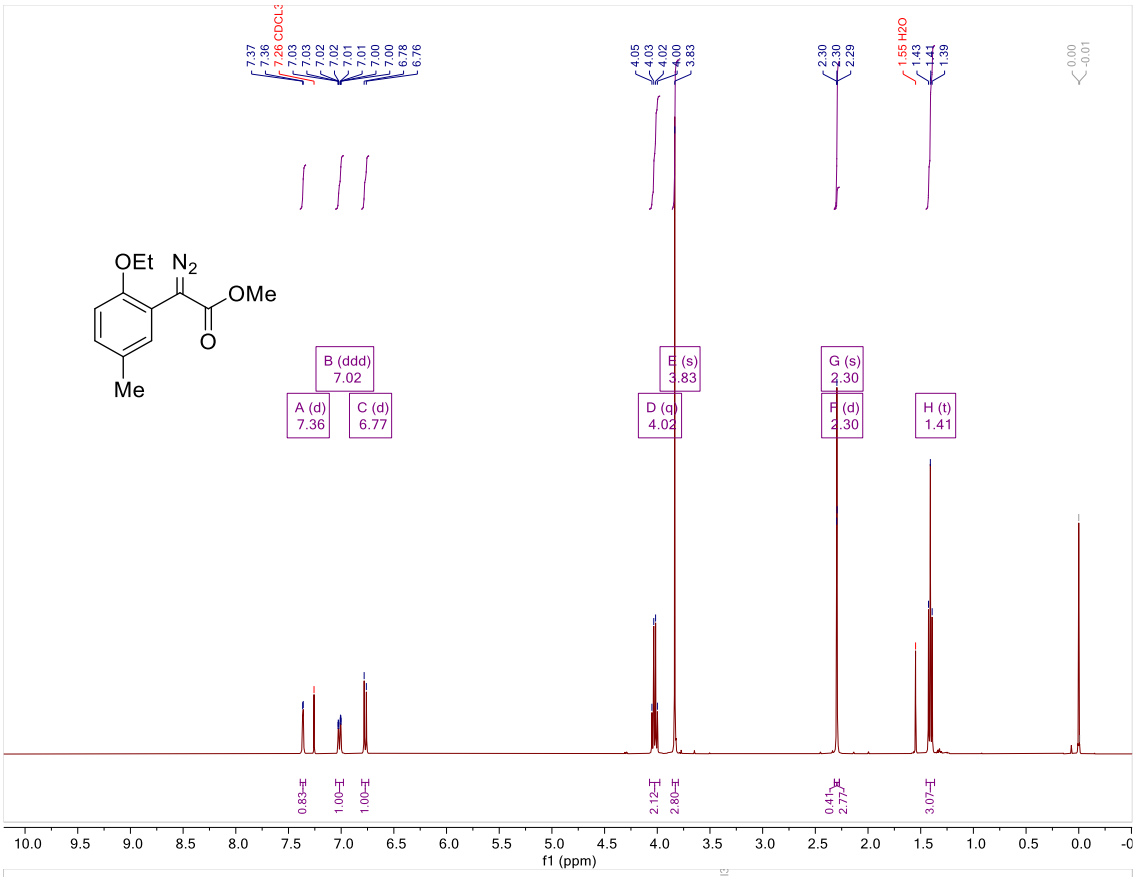
7.37
7.36
7.26 CDCl3
7.03
7.03
7.02
7.02
7.01
7.01
7.00
7.00
6.78
6.76
4.05
4.03
4.02
4.00
3.83
2.30
2.30
2.29
1.55 H2O
1.43
1.41
1.39
0.00
-0.01
OEt
N2
OMe
O
Me
B (ddd)
7.02
A (d)
7.36
C (d)
6.77
E (s)
3.83
D (q)
4.02
G (s)
2.30
F (d)
2.30
H (t)
1.41
0.83
1.00
1.00
2.12
2.80
0.41
2.77
3.07
f1 (ppm)

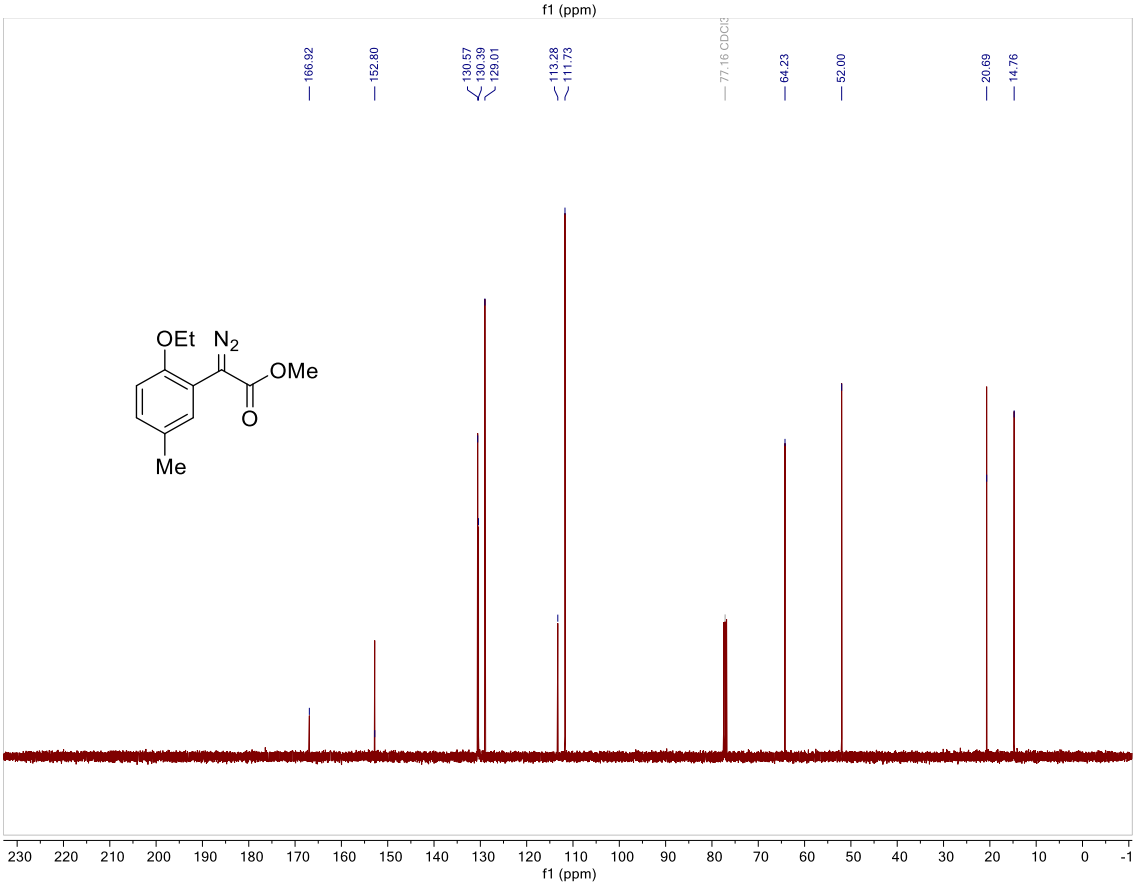
166.92
152.80
130.57
130.39
129.01
113.28
111.73
77.16 CDCl3
64.23
52.00
20.69
14.76
OEt
N2
OMe
O
Me
f1 (ppm)

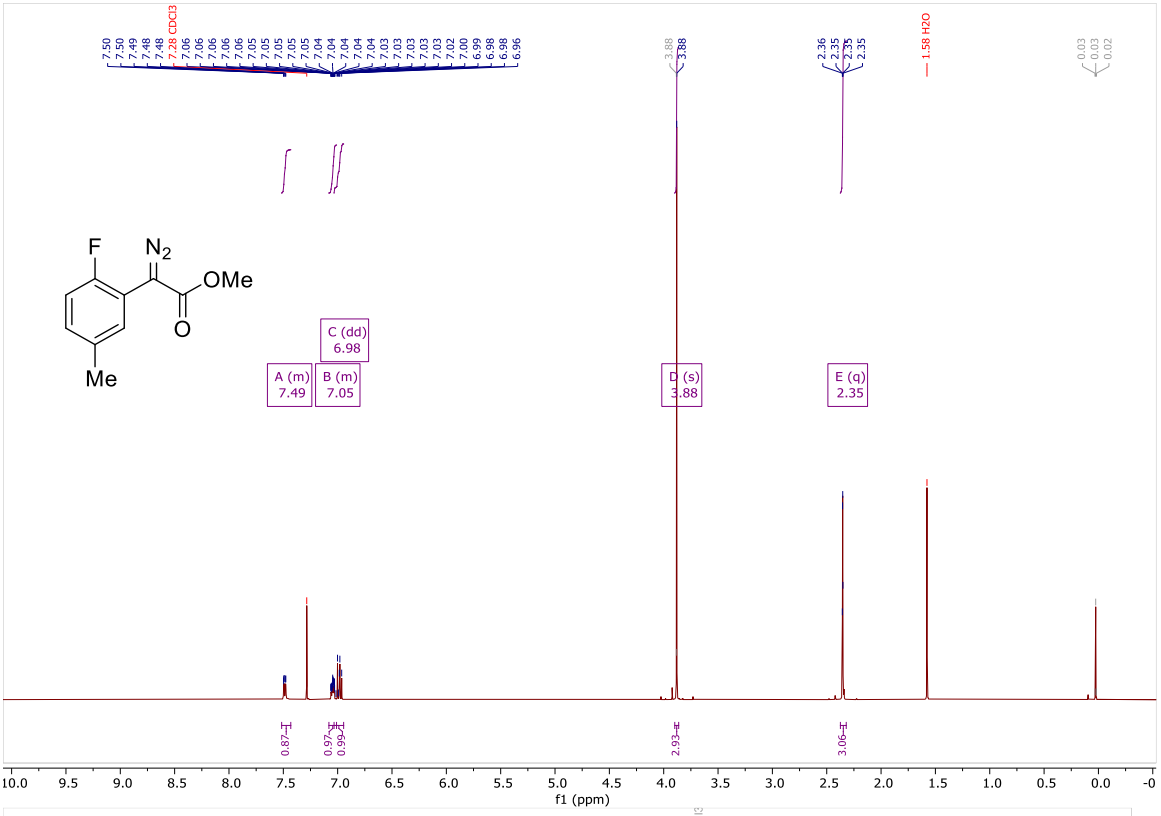
F
N2
OMe
O
Me
A (m) 7.49
B (m) 7.05
C (dd) 6.98
D (s) 3.88
E (q) 2.35
1.58 H2O
f1 (ppm)

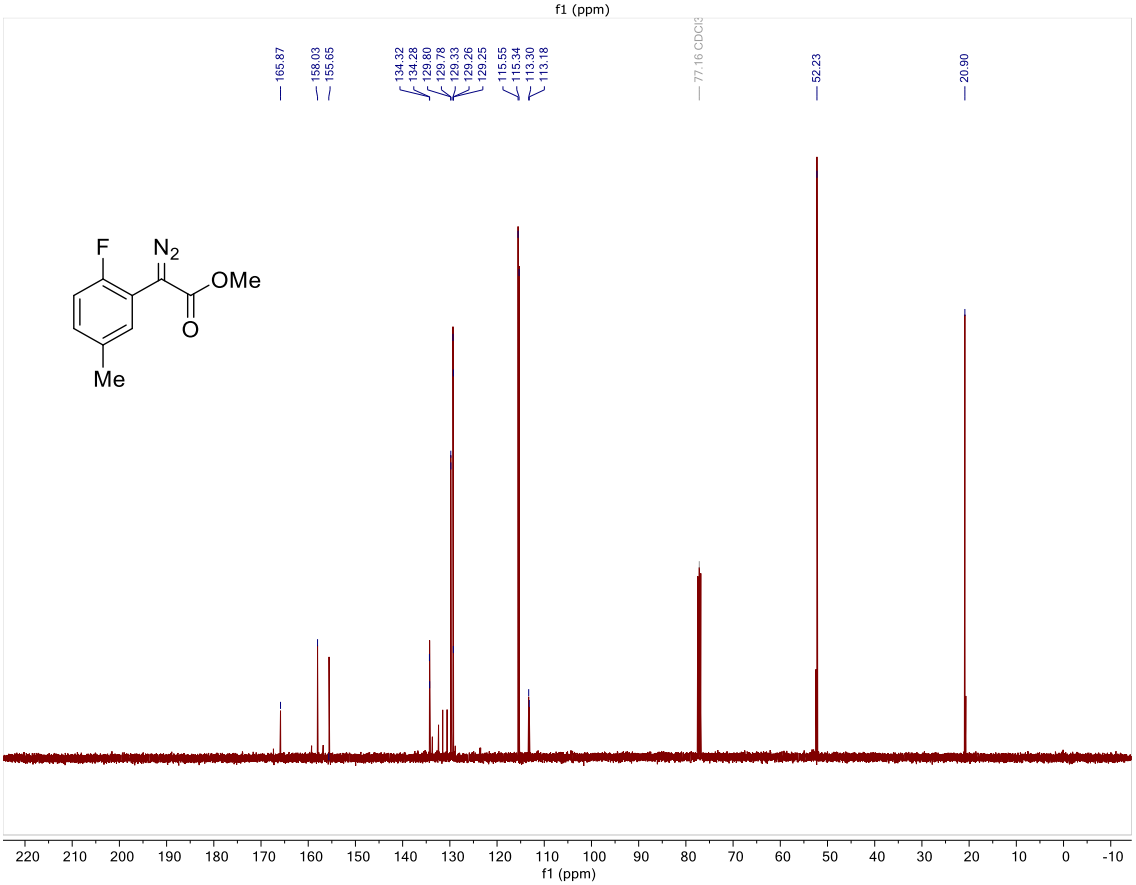
F
N2
OMe
O
Me
165.87
158.03
155.65
134.32
134.28
129.90
129.78
129.73
129.26
129.25
115.55
115.34
113.30
113.18
77.16 CDCl3
52.23
20.90
f1 (ppm)

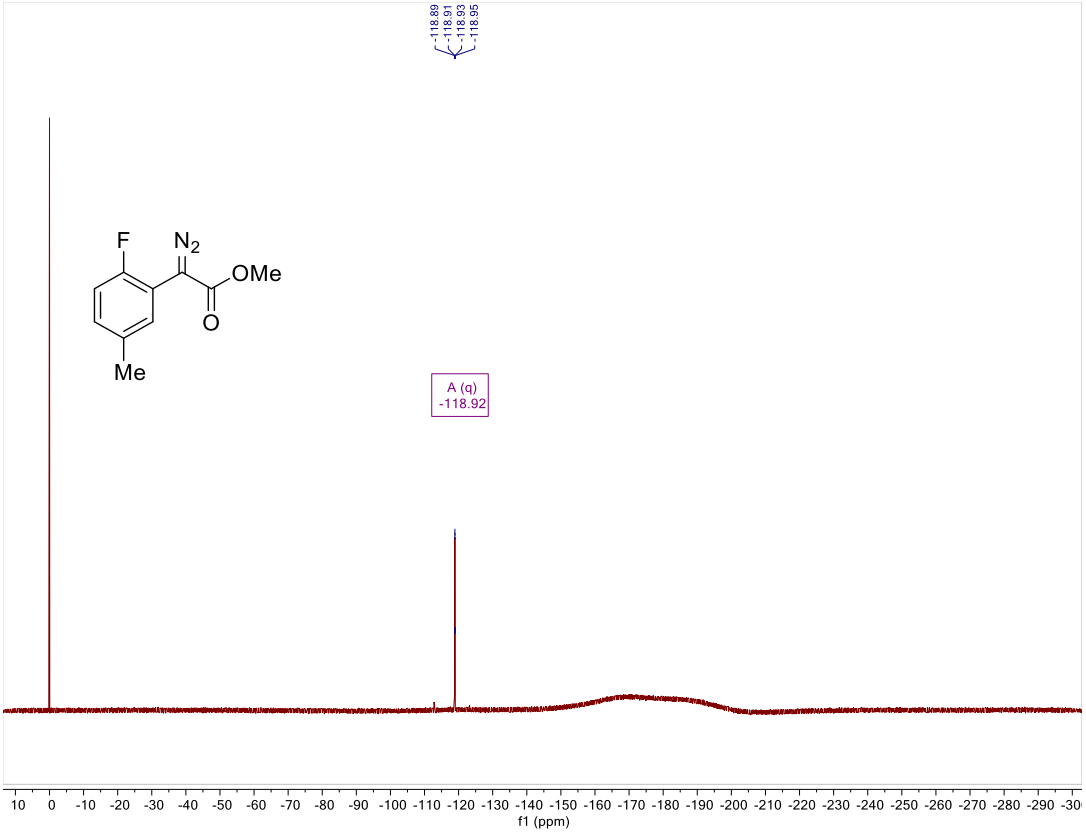
-118.89
-118.91
-118.93
-118.95
F
N2
OMe
O
Me
A (q)
-118.92
f1 (ppm)

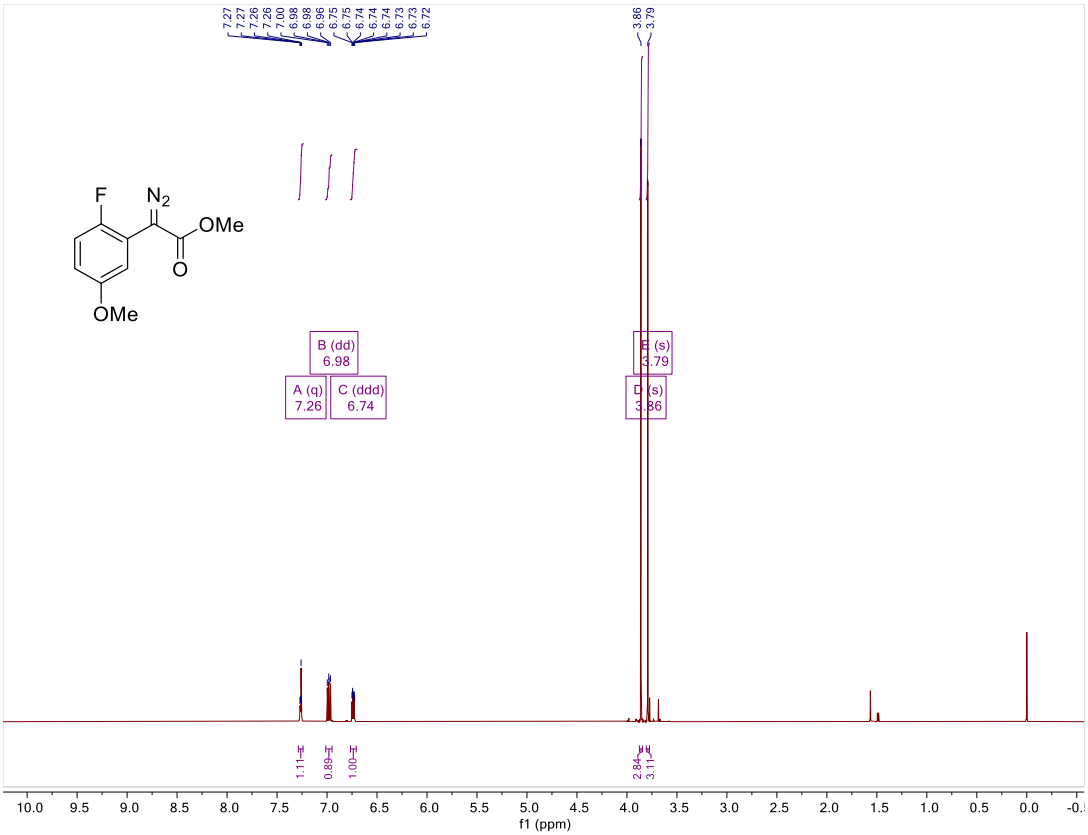
7.27
7.27
7.26
7.26
7.00
6.98
6.98
6.96
6.75
6.74
6.74
6.74
6.73
6.73
6.72
3.86
3.79
F
N2
OMe
O
OMe
B (dd)
6.98
A (q)
7.26
C (ddd)
6.74
E (s)
3.79
D (s)
3.86
1.11
0.89
1.00
2.84
3.11
f1 (ppm)

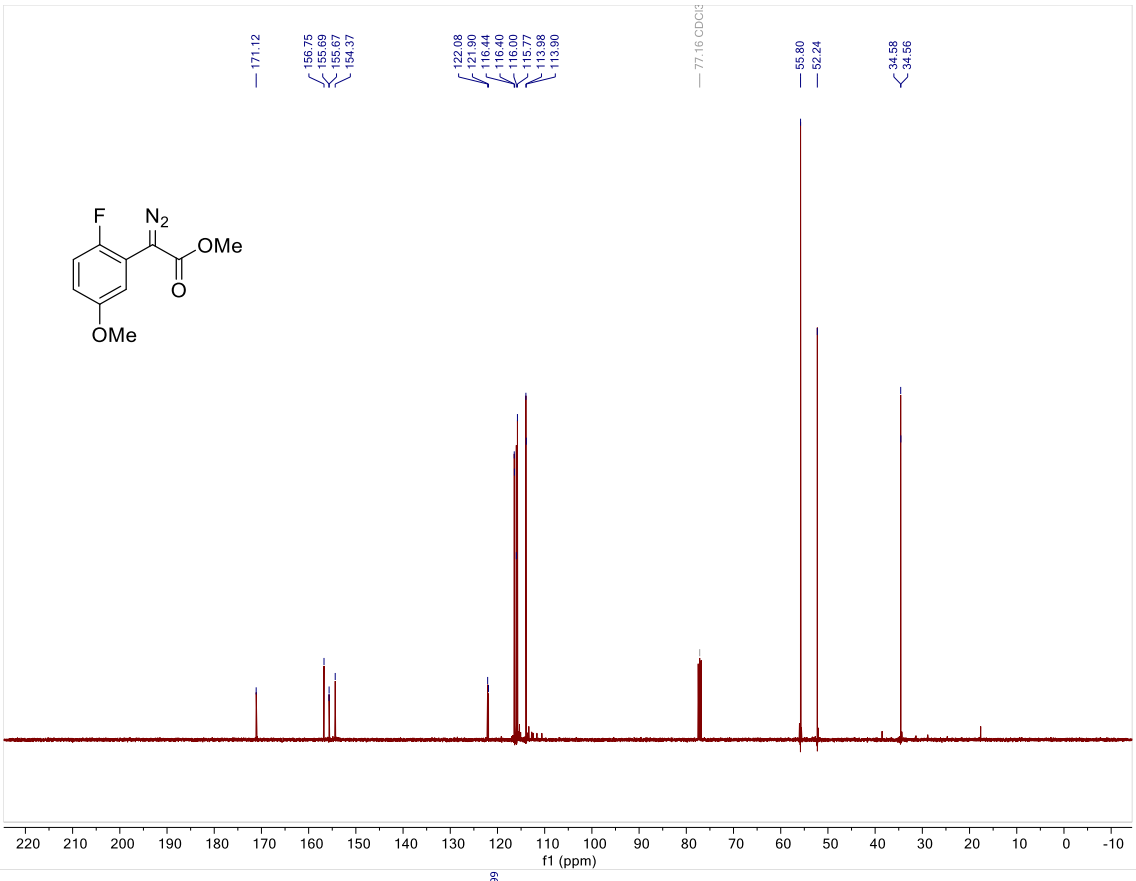
171.12
156.75
155.69
155.67
154.37
122.08
121.90
116.44
116.40
116.00
115.77
113.98
113.90
77.16 CDCl3
55.80
52.24
34.58
34.56
F
N2
OMe
O
OMe
f1 (ppm)

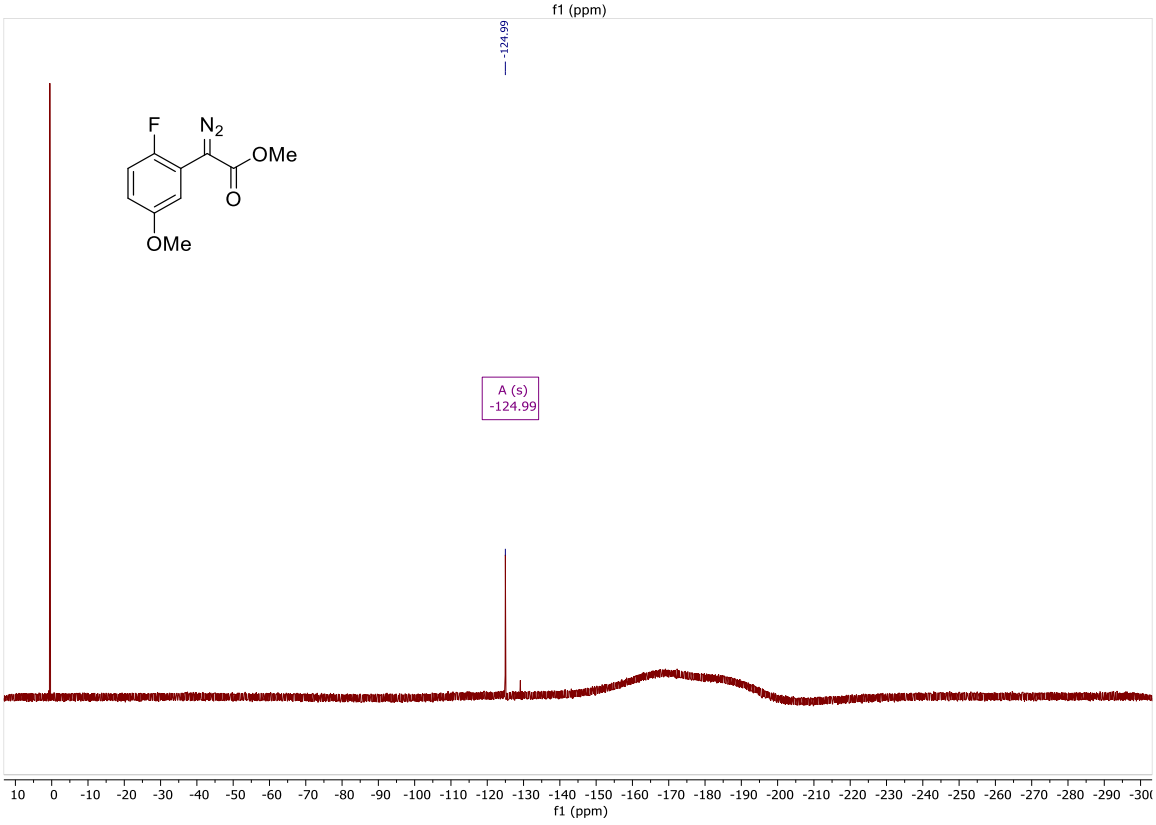
-124.99
F
N2
OMe
O
OMe
A (s)
-124.99
f1 (ppm)

2020-1-24-Bo-ELN-36-py-recycle — —

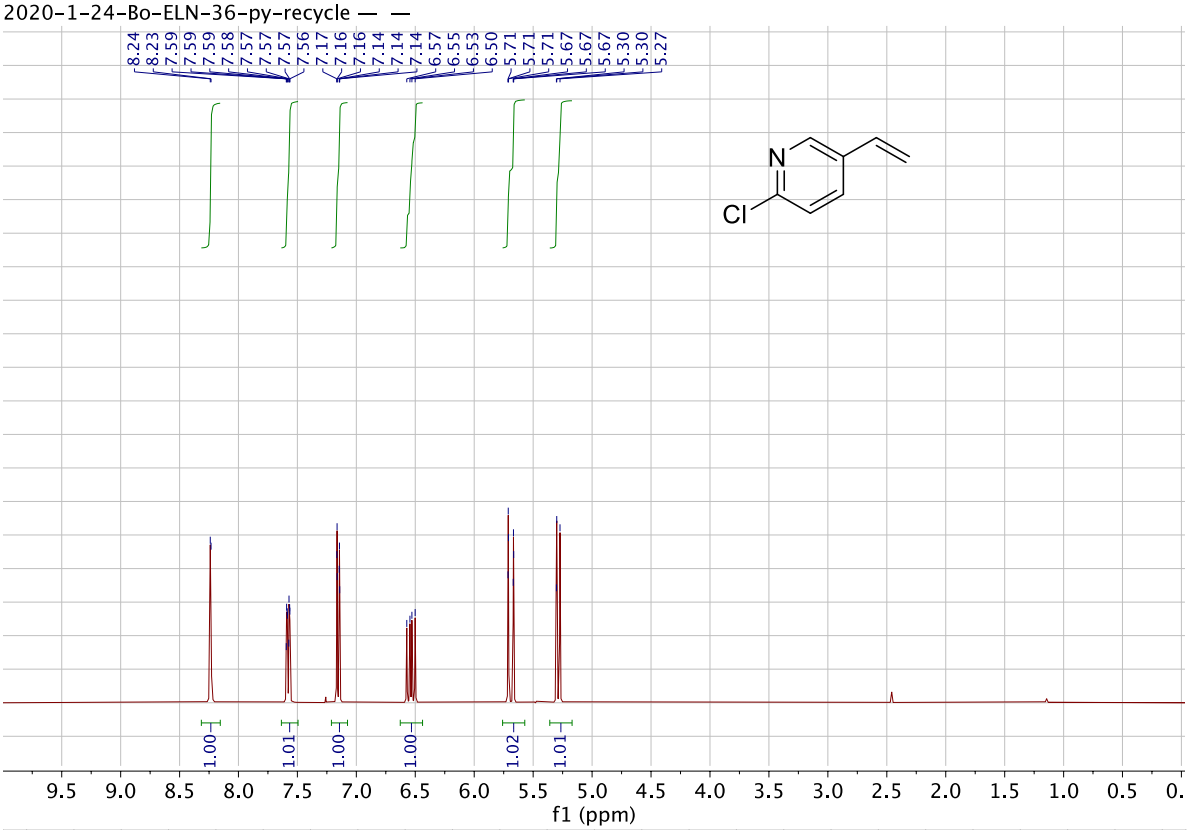

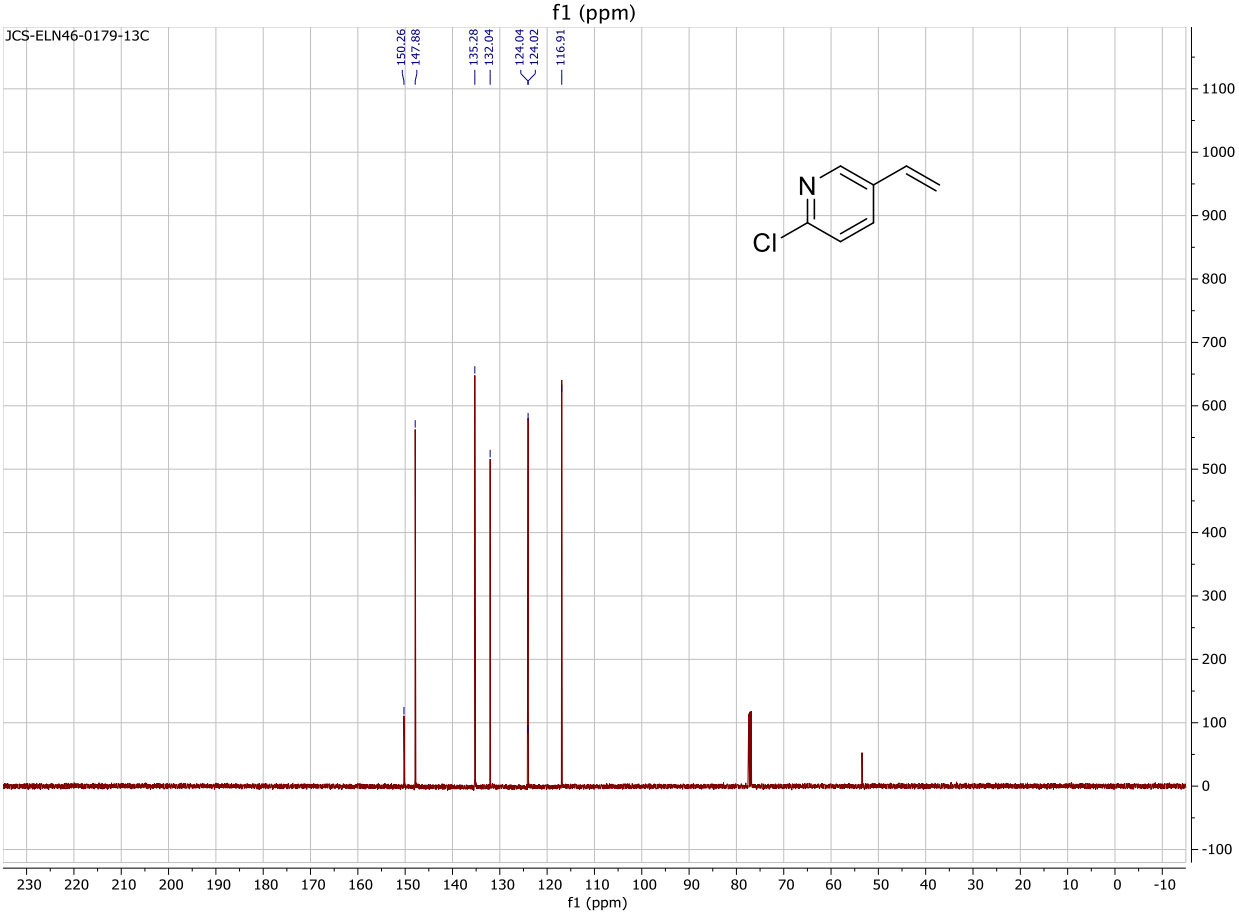

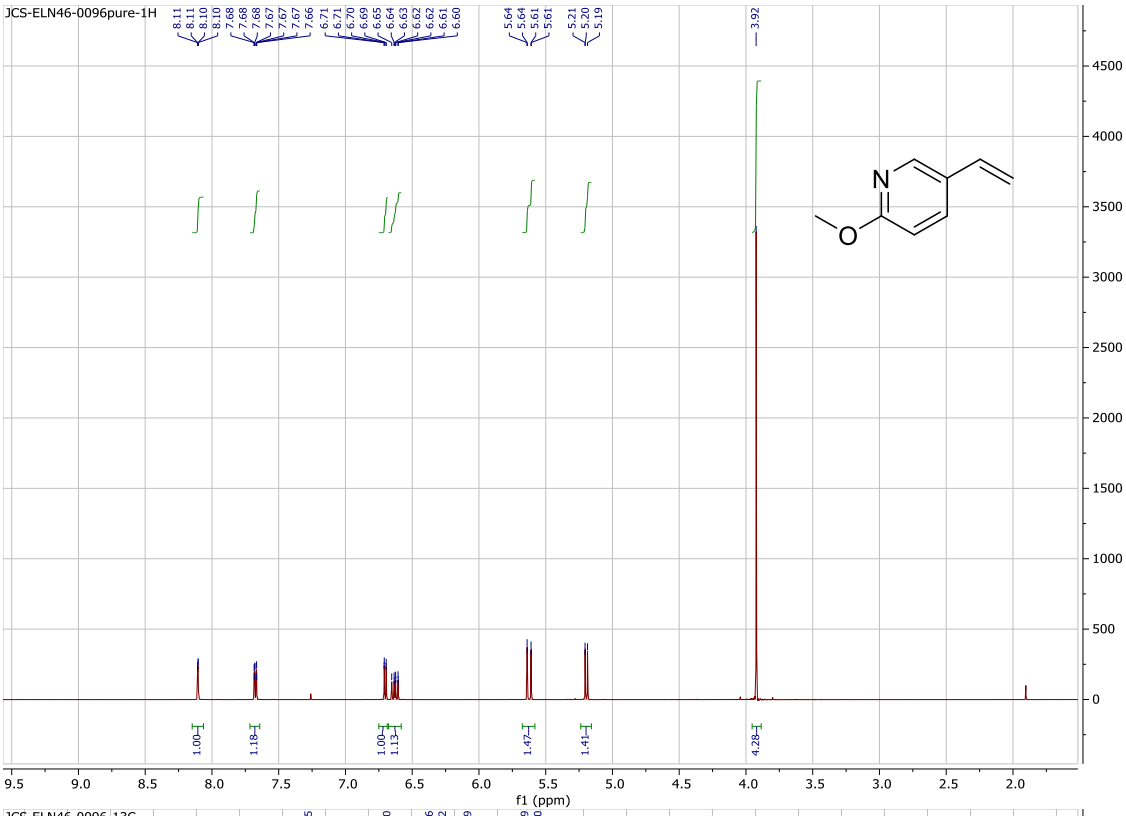
JCS-ELN46-0096pure-1H
8.11
8.11
8.10
8.10
7.68
7.68
7.68
7.67
7.67
7.67
7.66
6.71
6.71
6.70
6.69
6.65
6.64
6.63
6.62
6.62
6.61
6.60
5.64
5.64
5.61
5.61
5.21
5.20
5.19
3.92
1.00
1.18
1.00
1.13
1.47
1.41
4.28
N
O
f1 (ppm)

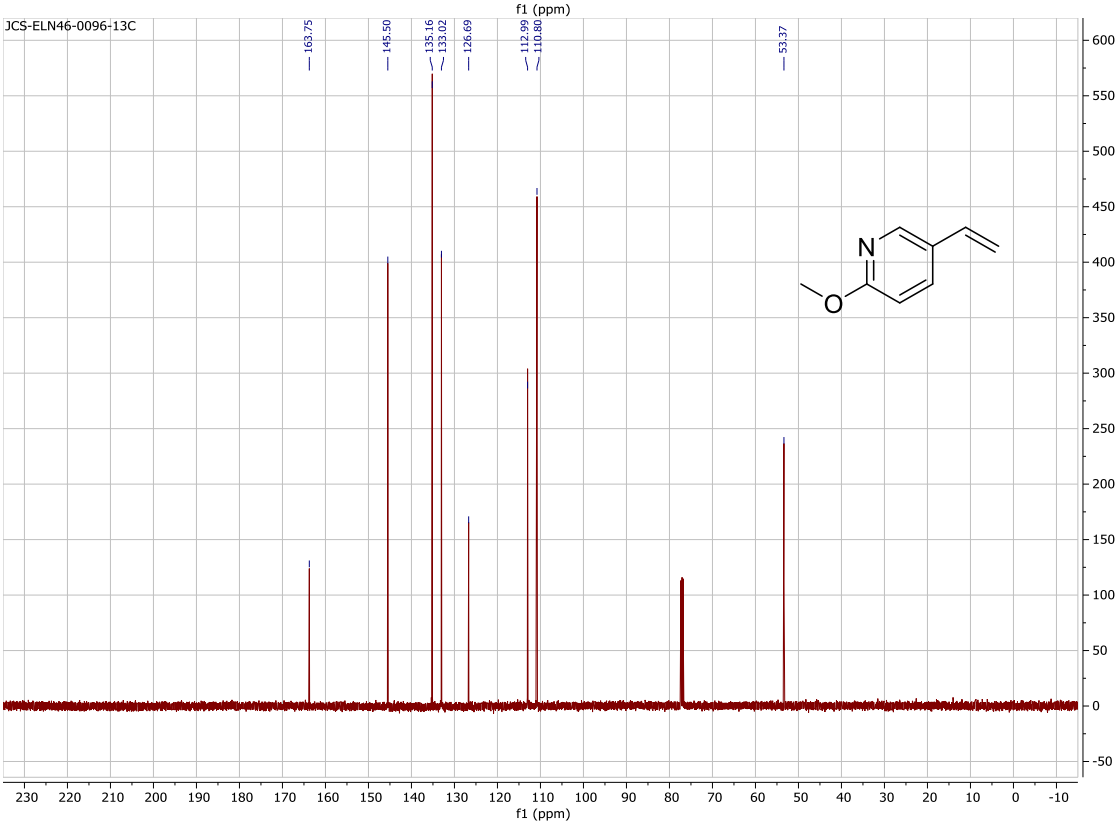
JCS-ELN46-0096-13C
163.75
145.50
135.16
133.02
126.69
112.99
110.80
53.37
N
O
f1 (ppm)

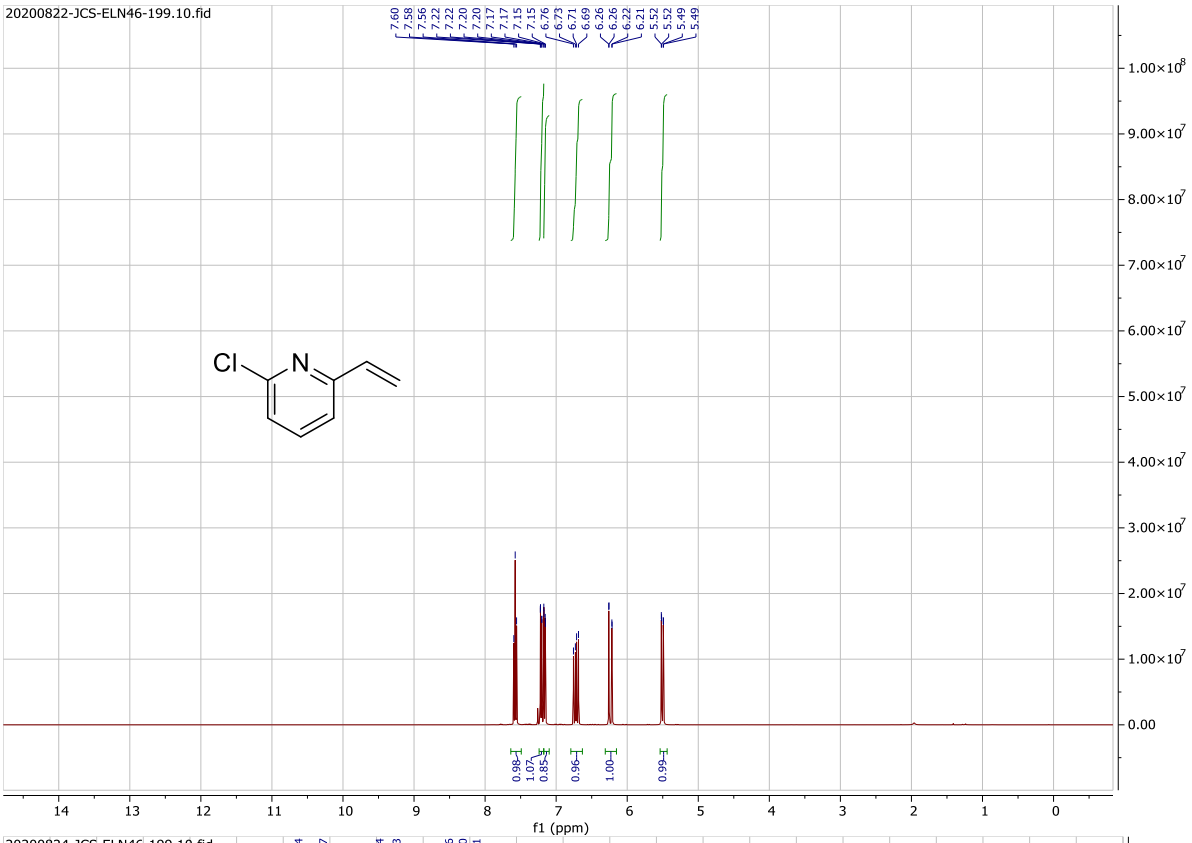
20200822-JCS-ELN46-199.10.fid
7.60 7.58 7.56 7.22 7.22 7.20 7.20 7.17 7.17 7.15 7.15 6.76 6.73 6.71 6.69 6.26 6.26 6.22 6.21 5.52 5.52 5.49 5.49
Cl
N
0.98 1.07 0.85 0.96 1.00 0.99
f1 (ppm)

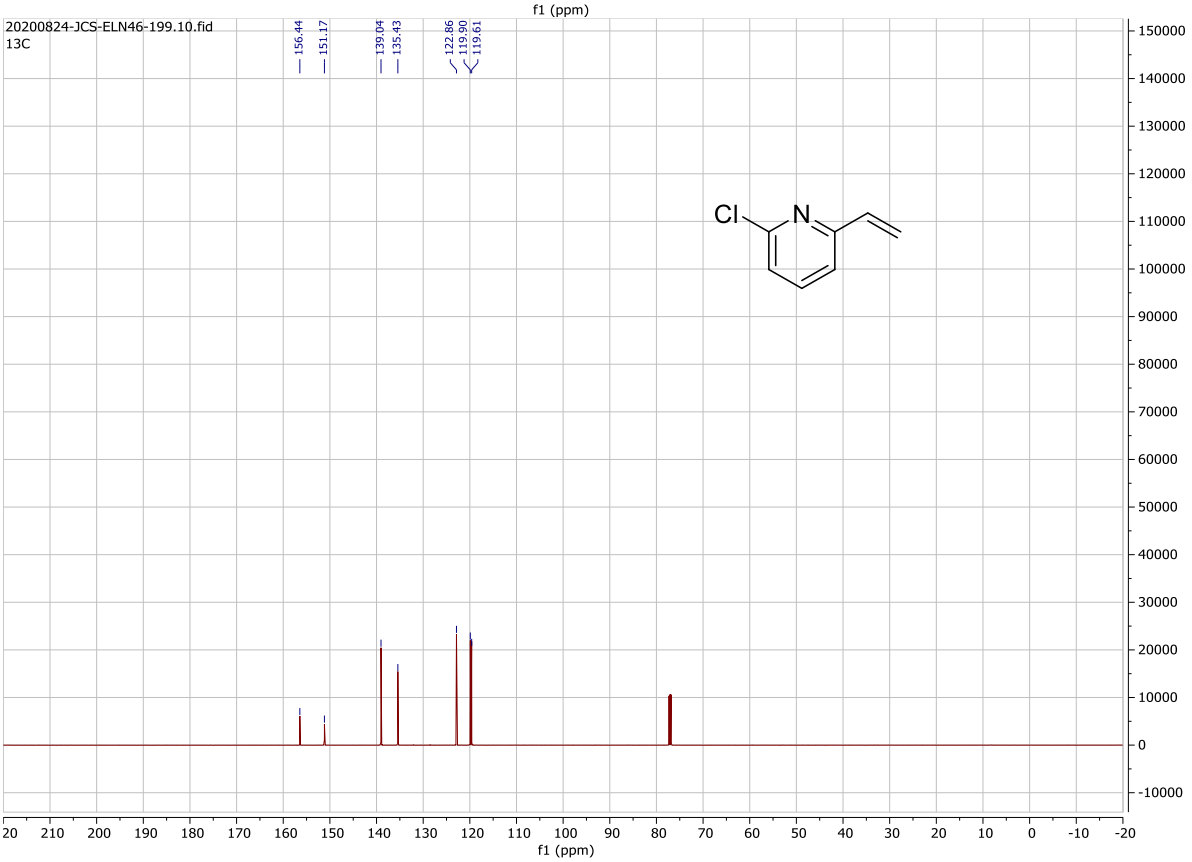
20200824-JCS-ELN46-199.10.fid
13C
156.44 151.17 139.04 135.43 122.86 119.90 119.61
Cl
N
f1 (ppm)

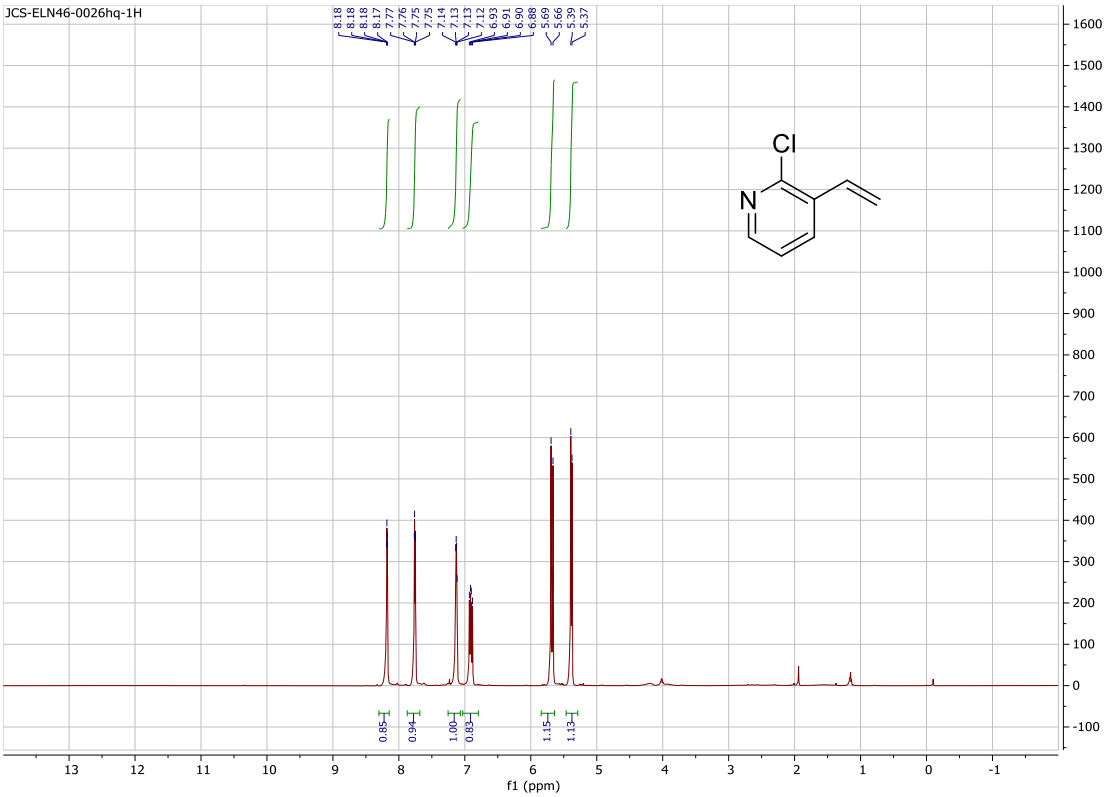
JCS-ELN46-0026hq-1H
8.18
8.18
8.18
8.17
7.77
7.76
7.75
7.75
7.75
7.14
7.13
7.13
7.12
6.93
6.91
6.90
6.88
5.69
5.66
5.39
5.37
Cl
N
0.85
0.94
1.00
0.83
1.15
1.13
f1 (ppm)

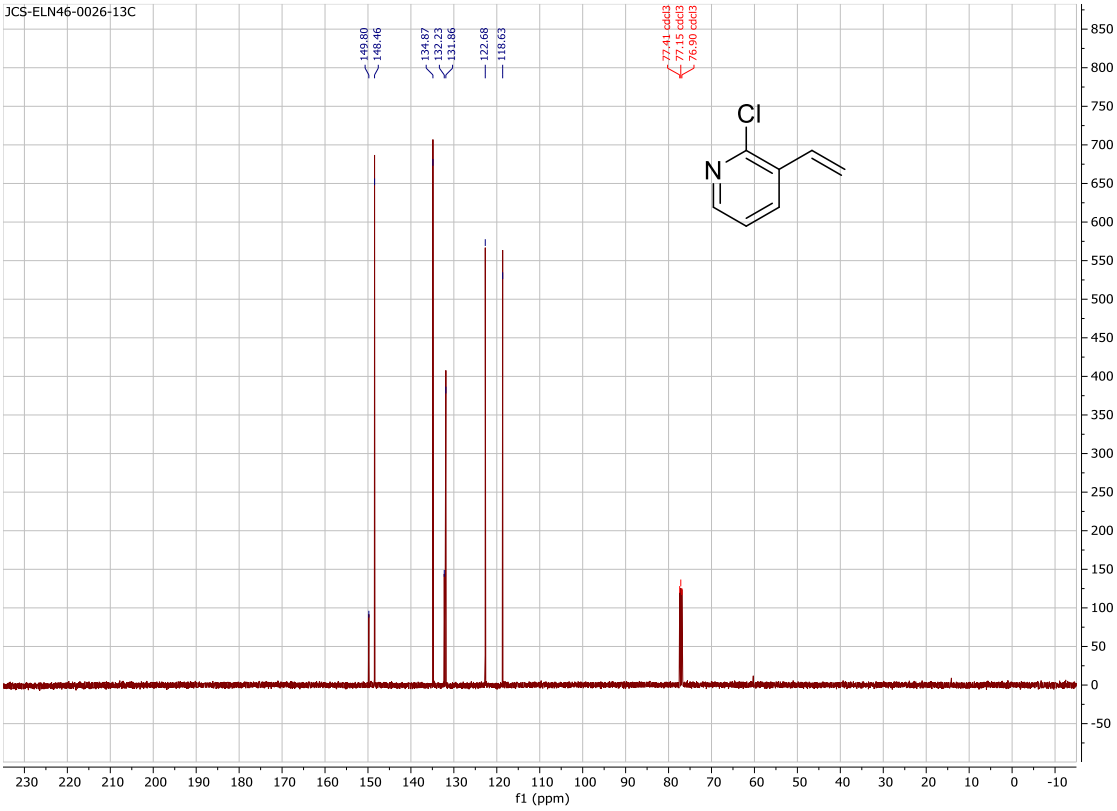
JCS-ELN46-0026-13C
149.80
148.46
134.87
132.23
131.86
122.68
118.63
77.41 cdcl3
77.15 cdcl3
76.90 cdcl3
Cl
N
f1 (ppm)

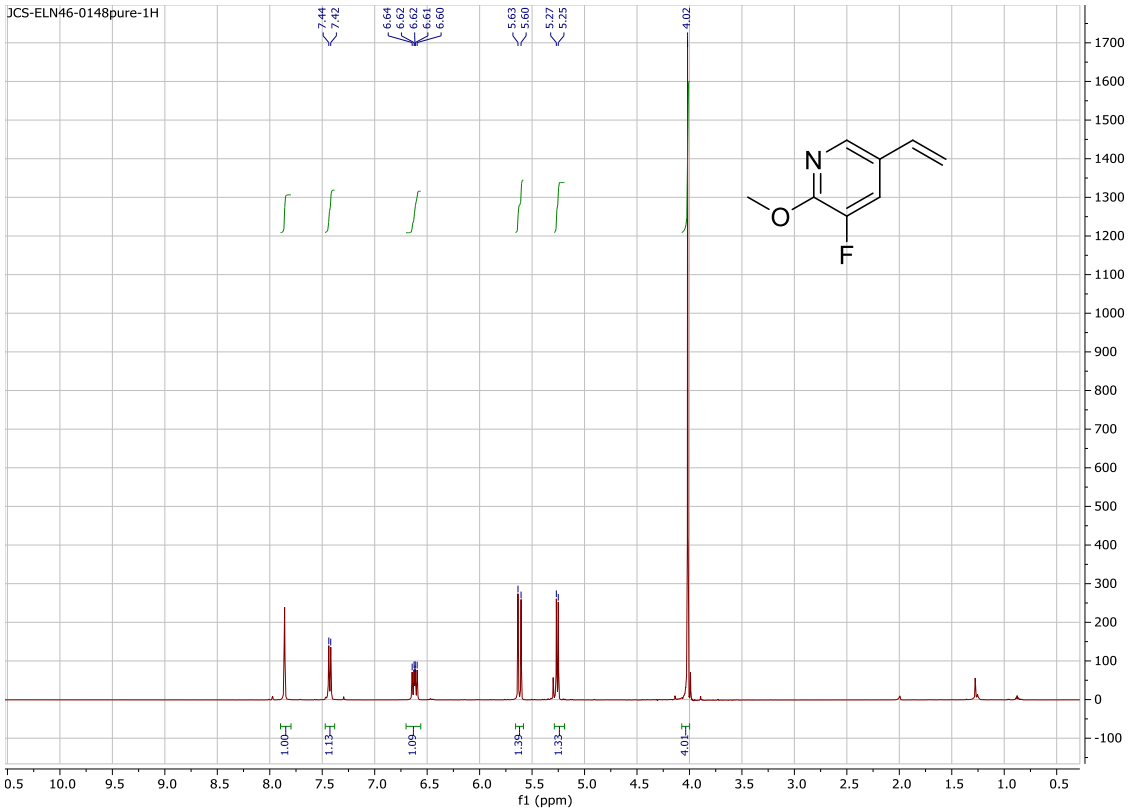
JCS-ELN46-0148pure-1H
7.44
7.42
6.64
6.62
6.62
6.61
6.60
5.63
5.60
5.27
5.25
4.02
1.00
1.13
1.09
1.39
1.33
4.01
N
O
F
f1 (ppm)

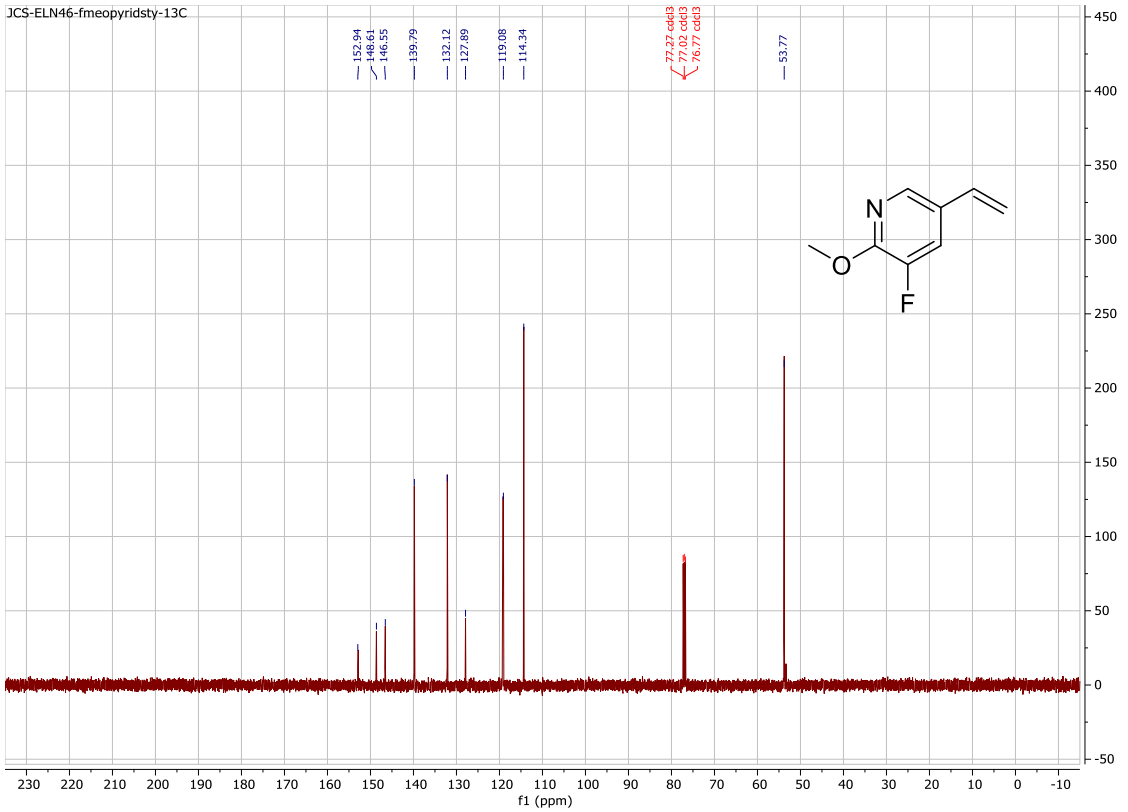
JCS-ELN46-fmeopyridsty-13C
152.94
148.61
146.55
139.79
132.12
127.89
119.08
114.34
77.27 cdcl3
77.02 cdcl3
76.77 cdcl3
53.77
N
O
F
f1 (ppm)

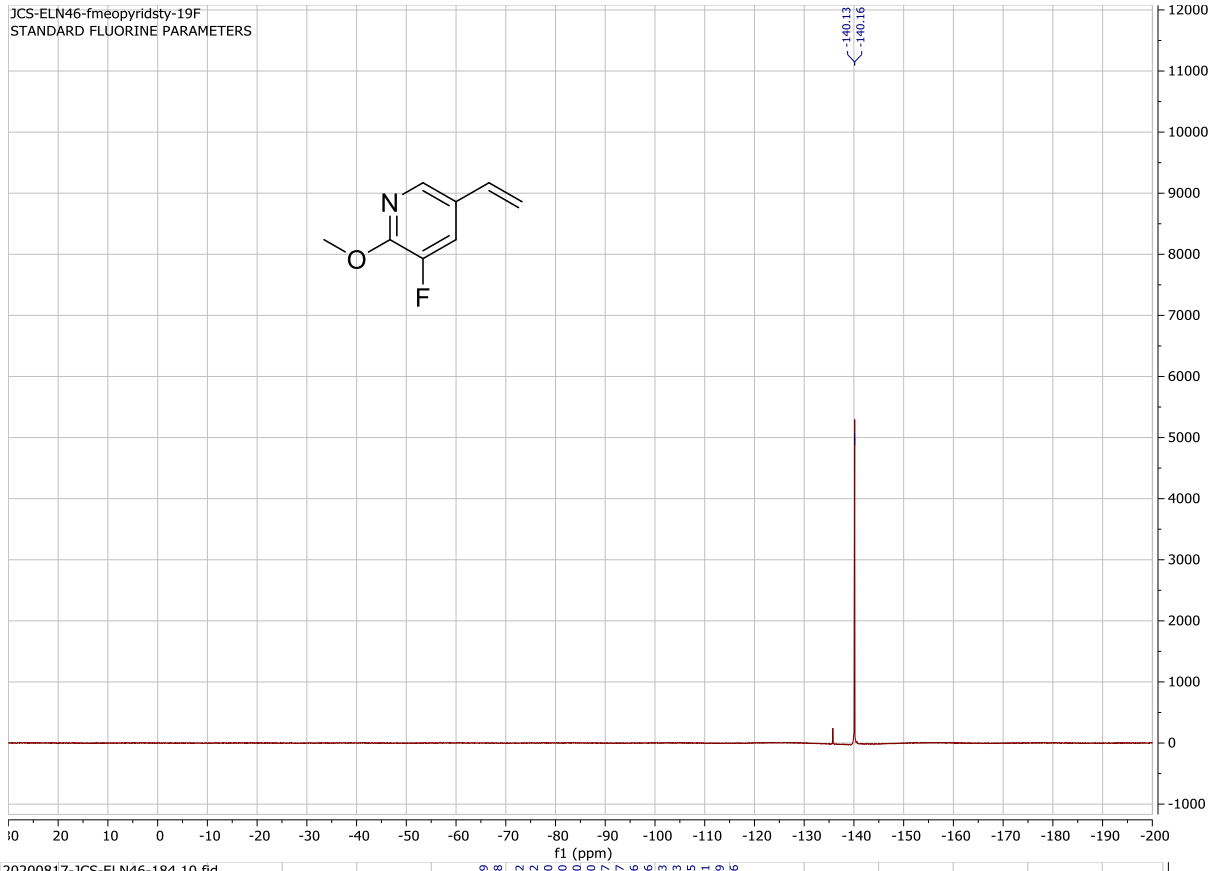
JCS-ELN46-fmeopyridsty-19F
STANDARD FLUORINE PARAMETERS
-140.13
-140.16
N
O
F
f1 (ppm)

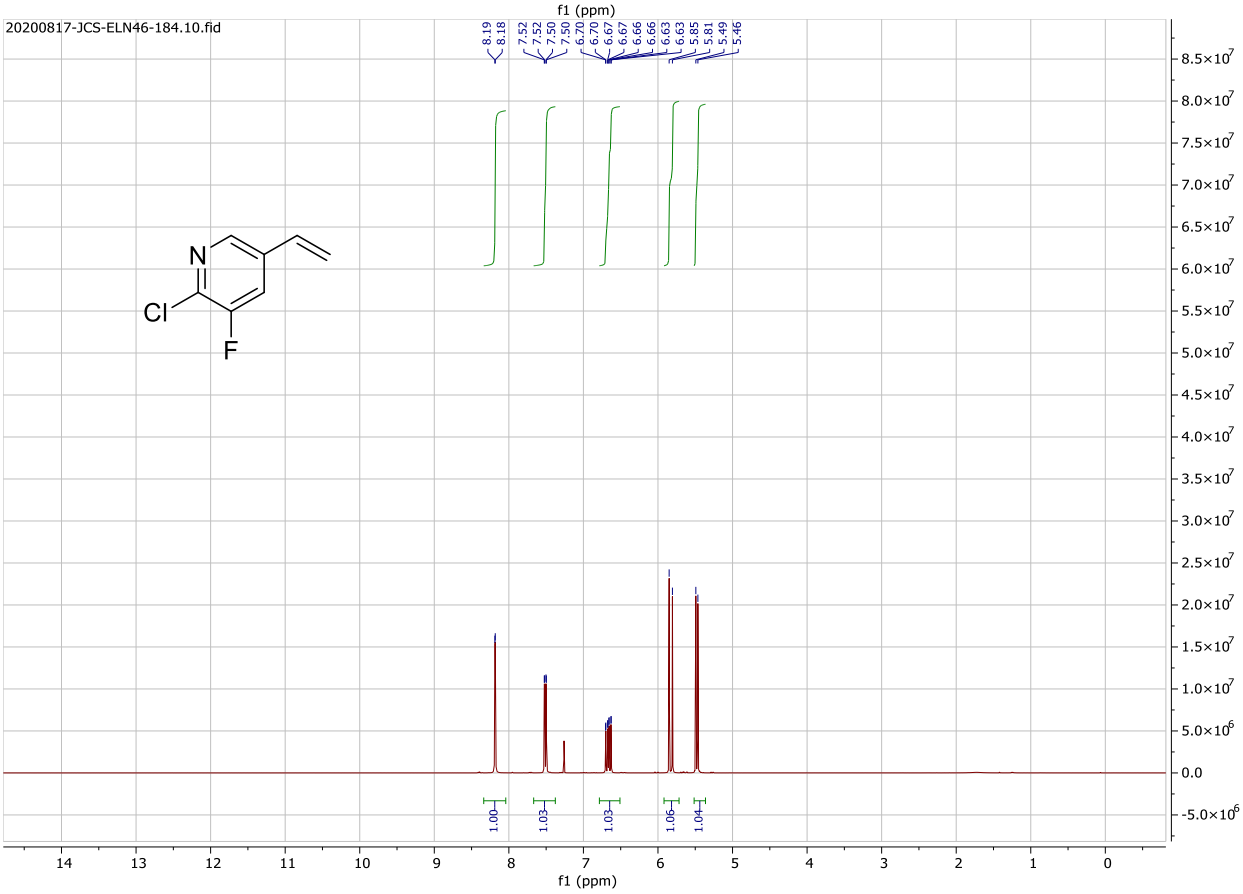
20200817-JCS-ELN46-184.10.fid
8.19
8.18
7.52
7.52
7.50
7.50
6.70
6.67
6.67
6.66
6.66
6.63
5.85
5.81
5.49
5.46
N
Cl
F
1.00
1.03
1.03
1.06
1.04
f1 (ppm)

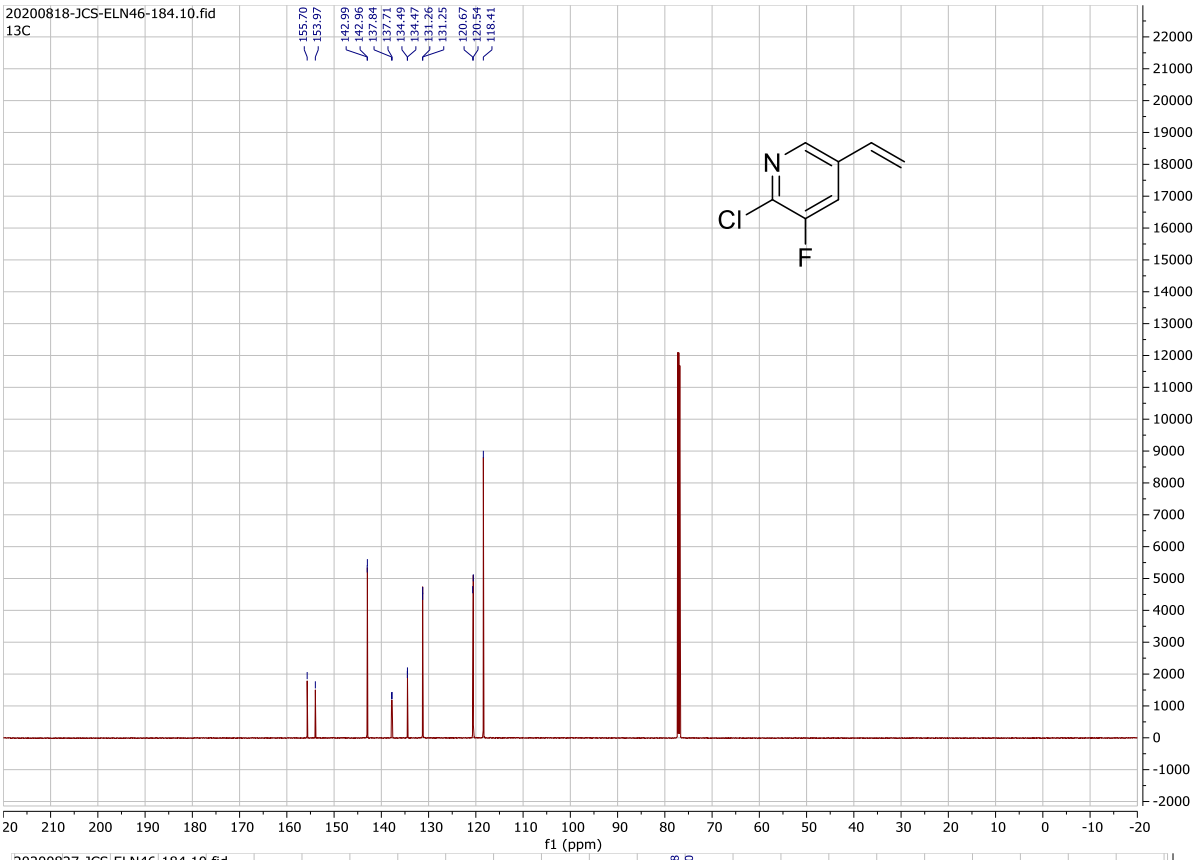
20200818-JCS-ELN46-184.10.fid
13C
155.70
153.97
142.99
142.96
137.84
137.71
134.49
134.47
131.26
131.25
120.67
120.54
118.41
N
Cl
F
f1 (ppm)

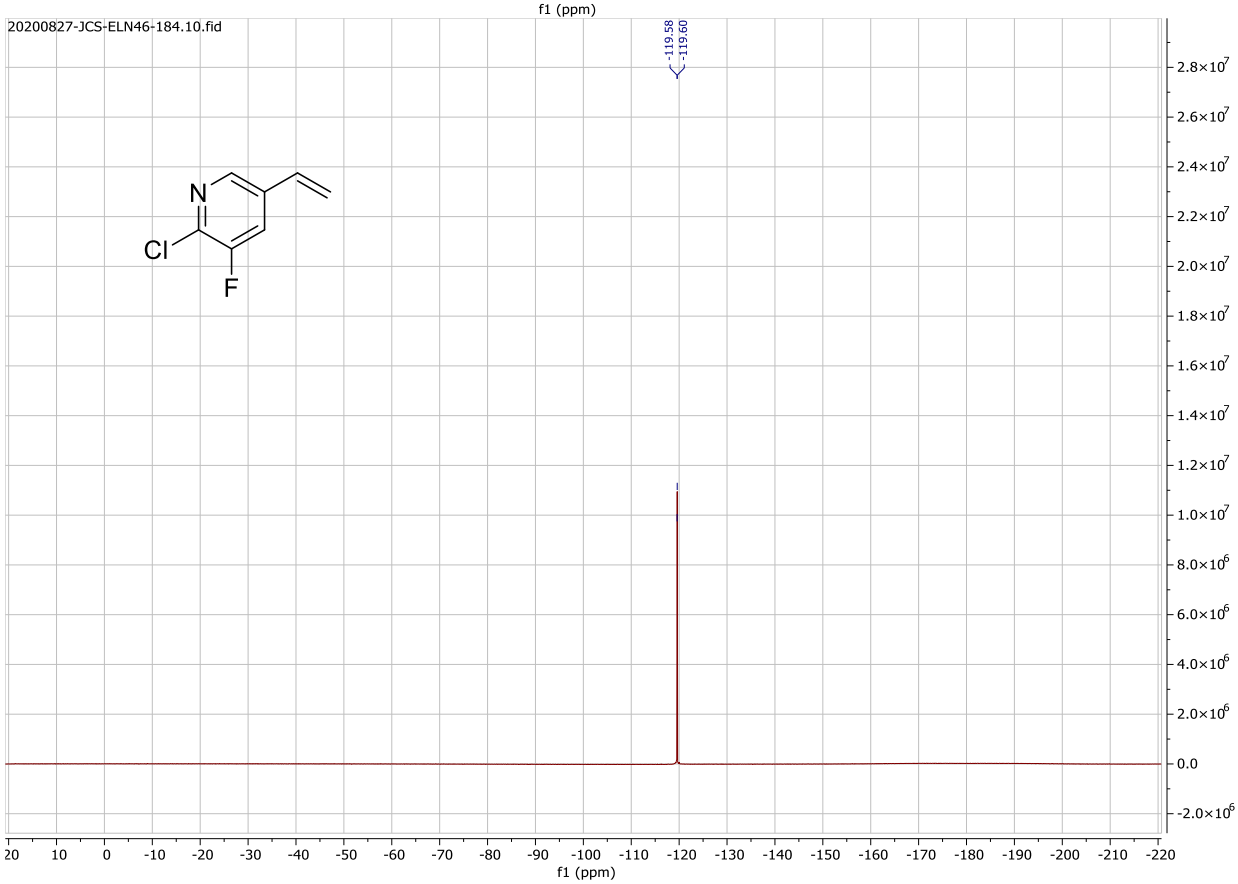
20200827-JCS-ELN46-184.10.fid
-119.58
-119.60
N
Cl
F
f1 (ppm)

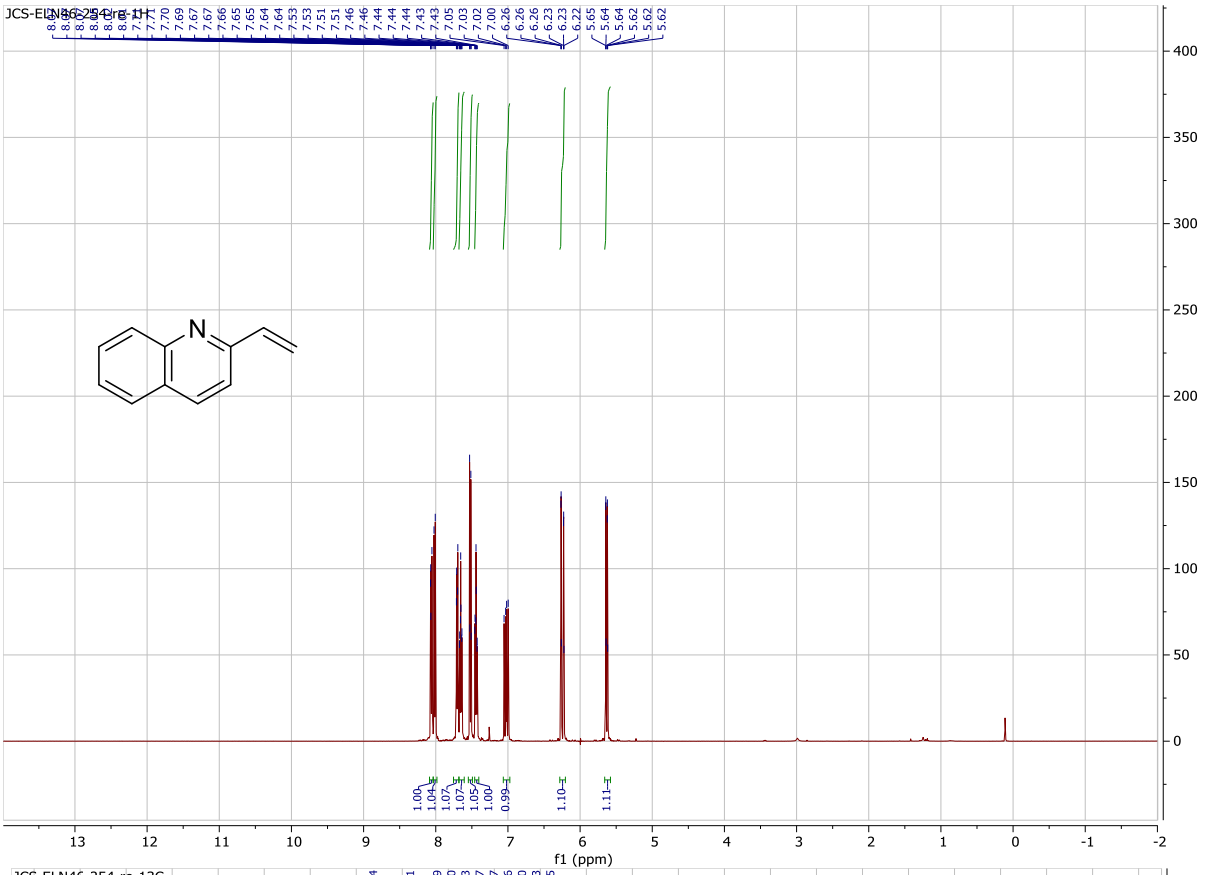
JCS-ELN46-254-re-1H
8.86 8.86 8.85 8.85 8.84 8.84 8.83 8.83 8.82 8.82 8.81 8.81 7.71 7.70 7.69 7.67 7.67 7.66 7.65 7.65 7.64 7.64 7.53 7.53 7.51 7.51 7.46 7.46 7.44 7.44 7.44 7.43 7.43 7.05 7.03 7.02 7.00 6.26 6.26 6.26 6.23 6.23 6.22 5.65 5.64 5.64 5.62 5.62 5.62
N
1.00 1.04 1.07 1.07 1.05 1.00 0.99 1.10 1.11
f1 (ppm)

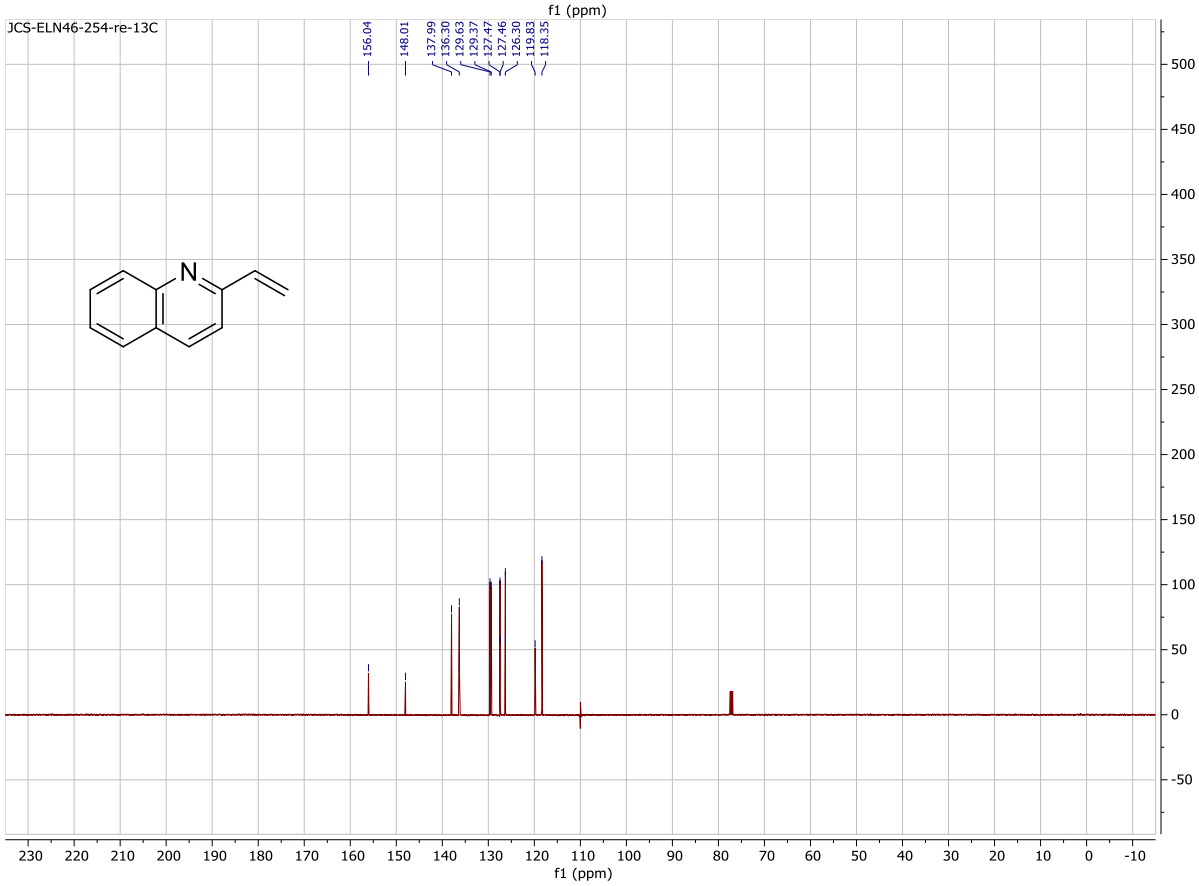
JCS-ELN46-254-re-13C
156.04 148.01 137.99 136.30 129.63 129.37 127.47 127.46 126.30 119.83 118.35
N
f1 (ppm)

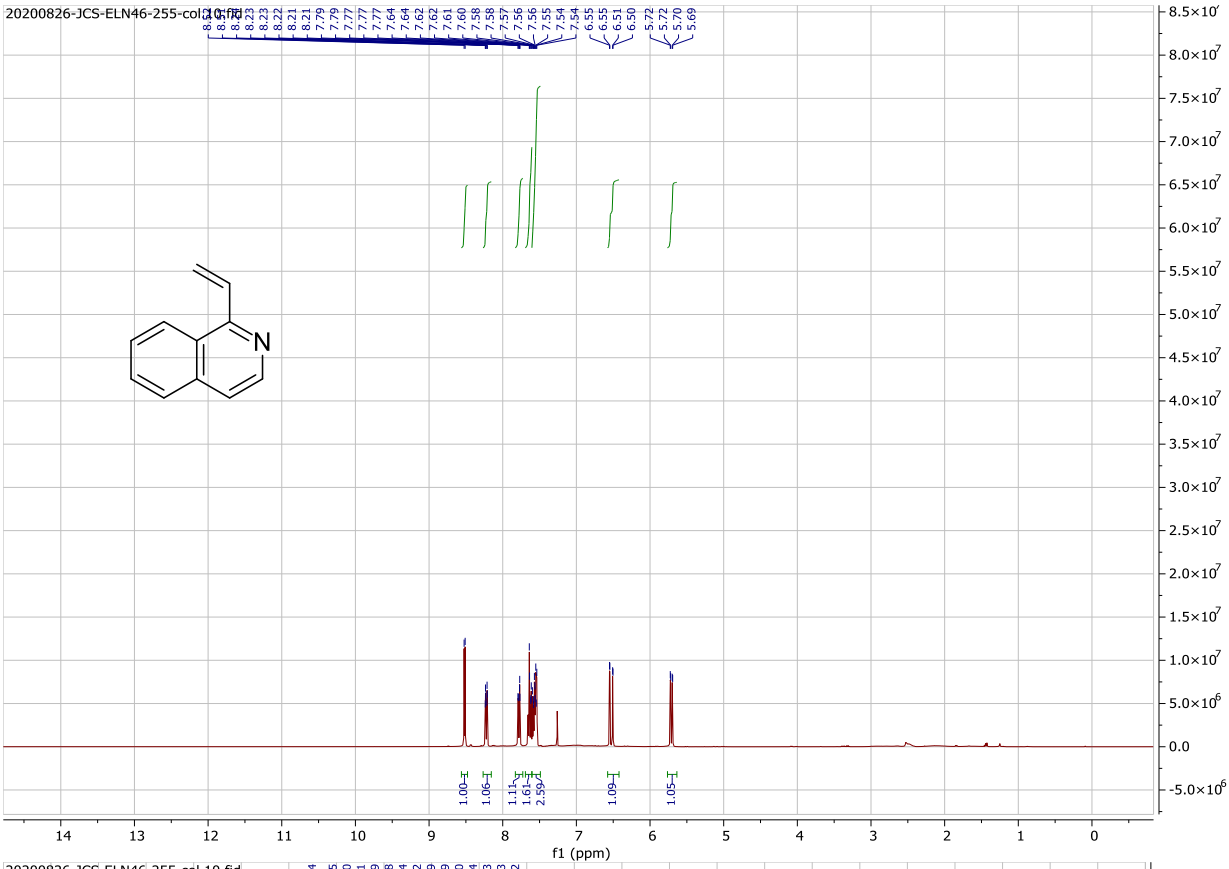
20200826-JCS-ELN46-255-col.10.fid
N
f1 (ppm)

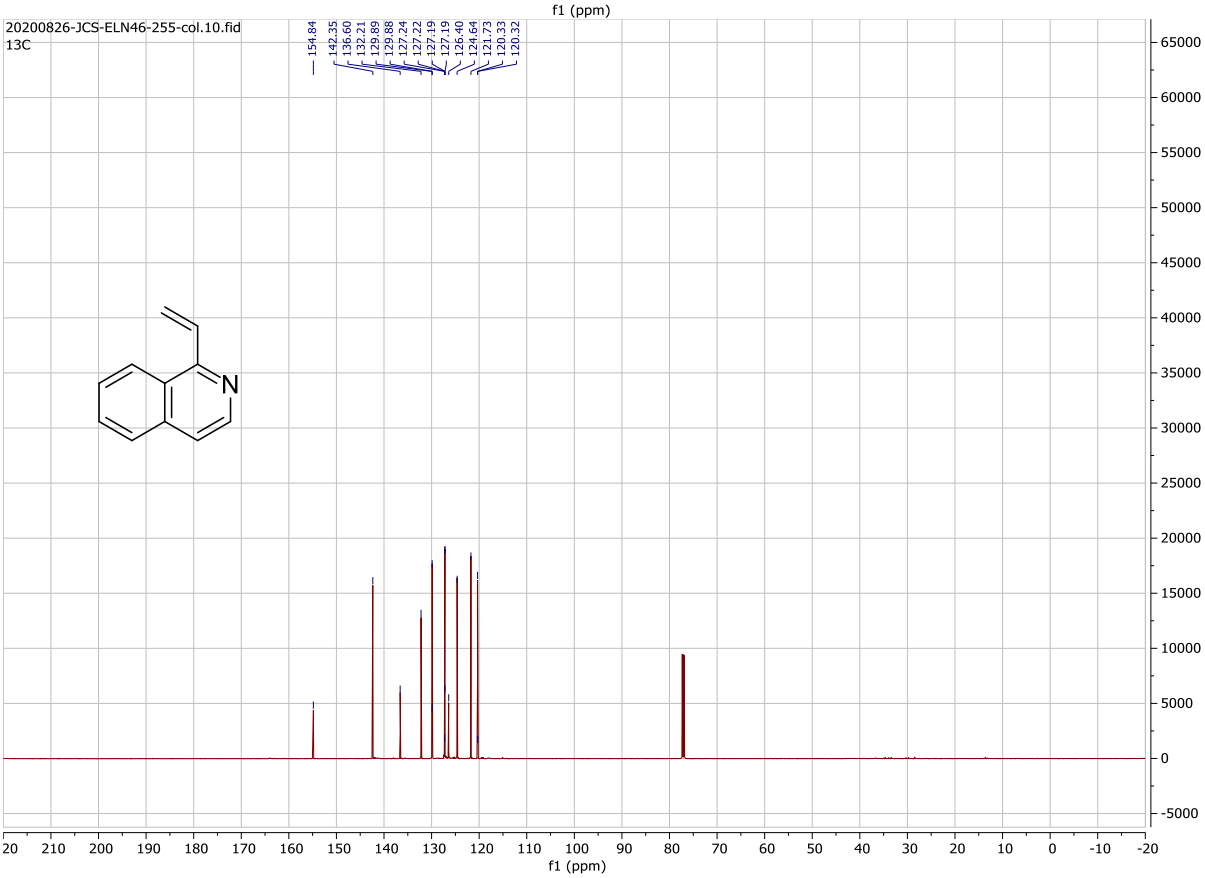
20200826-JCS-ELN46-255-col.10.fid
13C
154.84
142.35
136.60
132.21
129.89
129.88
127.24
127.22
127.19
127.19
126.40
124.64
121.73
120.33
120.32
N
f1 (ppm)

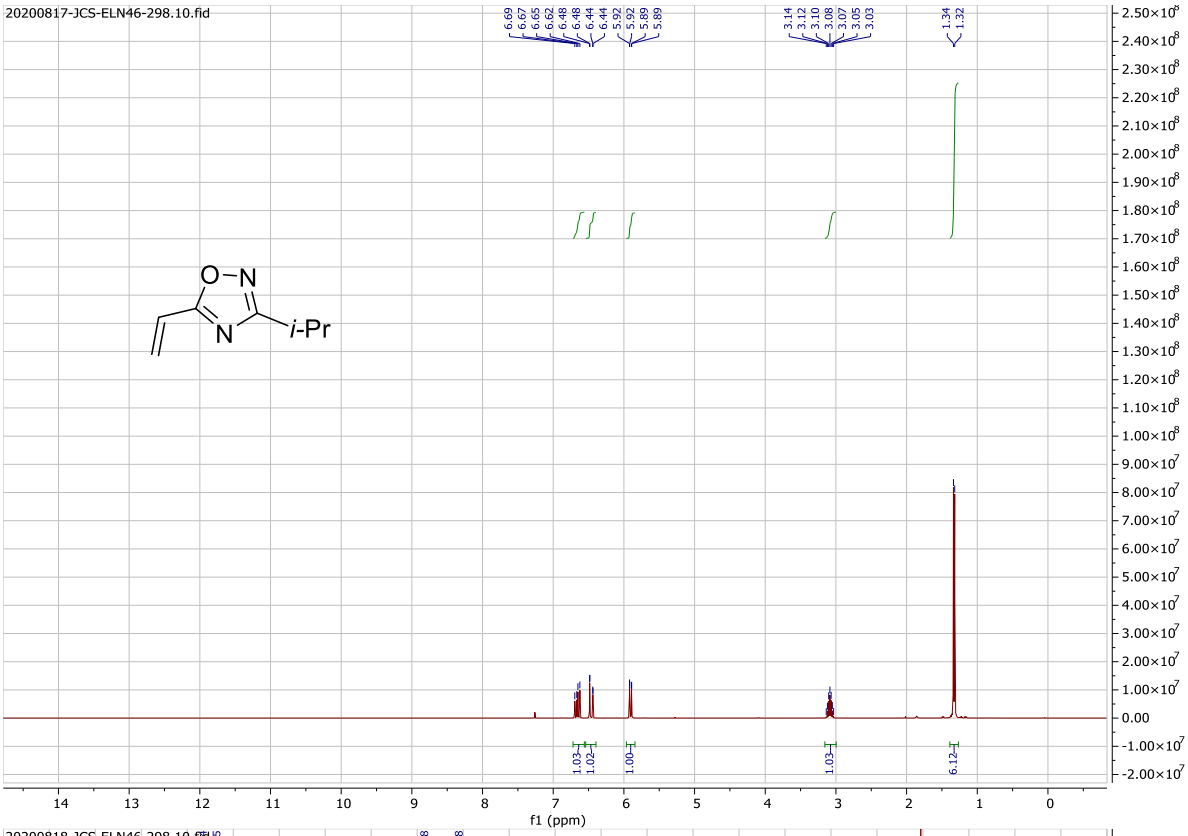
20200817-JCS-ELN46-298.10.fid
6.69
6.67
6.65
6.62
6.48
6.44
6.44
5.92
5.92
5.89
5.89
3.14
3.12
3.10
3.08
3.07
3.05
3.03
1.34
1.32
O
N
N
i-Pr
1.03
1.02
1.00
1.03
6.12
f1 (ppm)

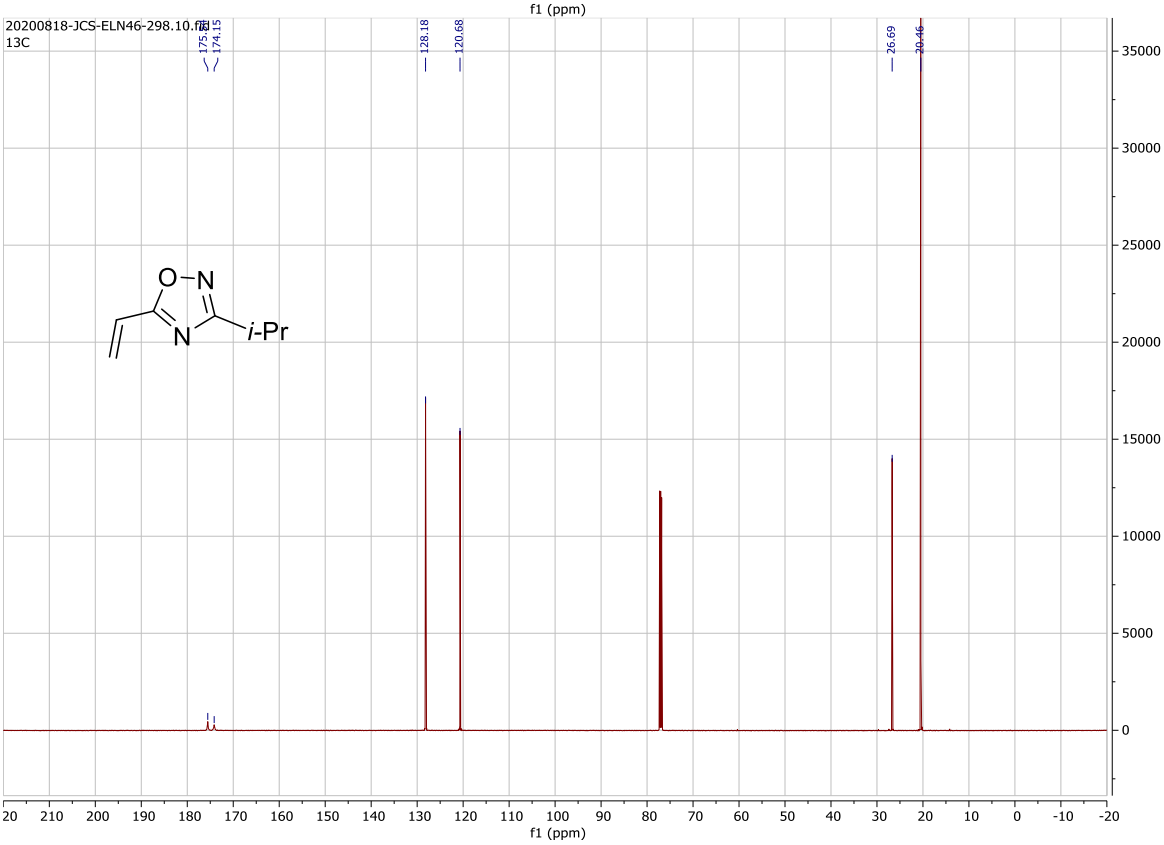
20200818-JCS-ELN46-298.10.fid
13C
175.41
174.15
128.18
120.68
26.69
20.46
O
N
N
i-Pr
f1 (ppm)

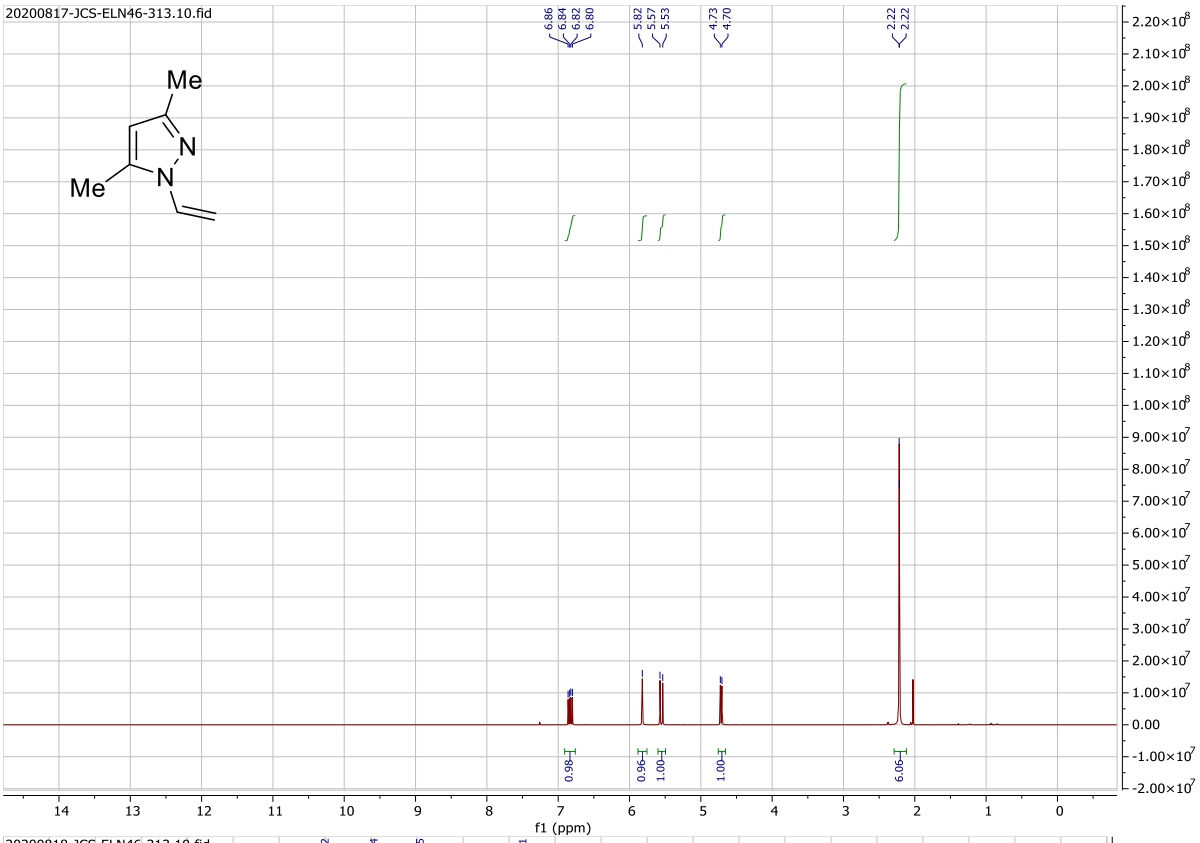
20200817-JCS-ELN46-313.10.fid
6.86
6.84
6.82
6.80
5.82
5.57
5.53
4.73
4.70
2.22
2.22
Me
N
N
Me
0.98
0.96
1.00
1.00
6.06
f1 (ppm)

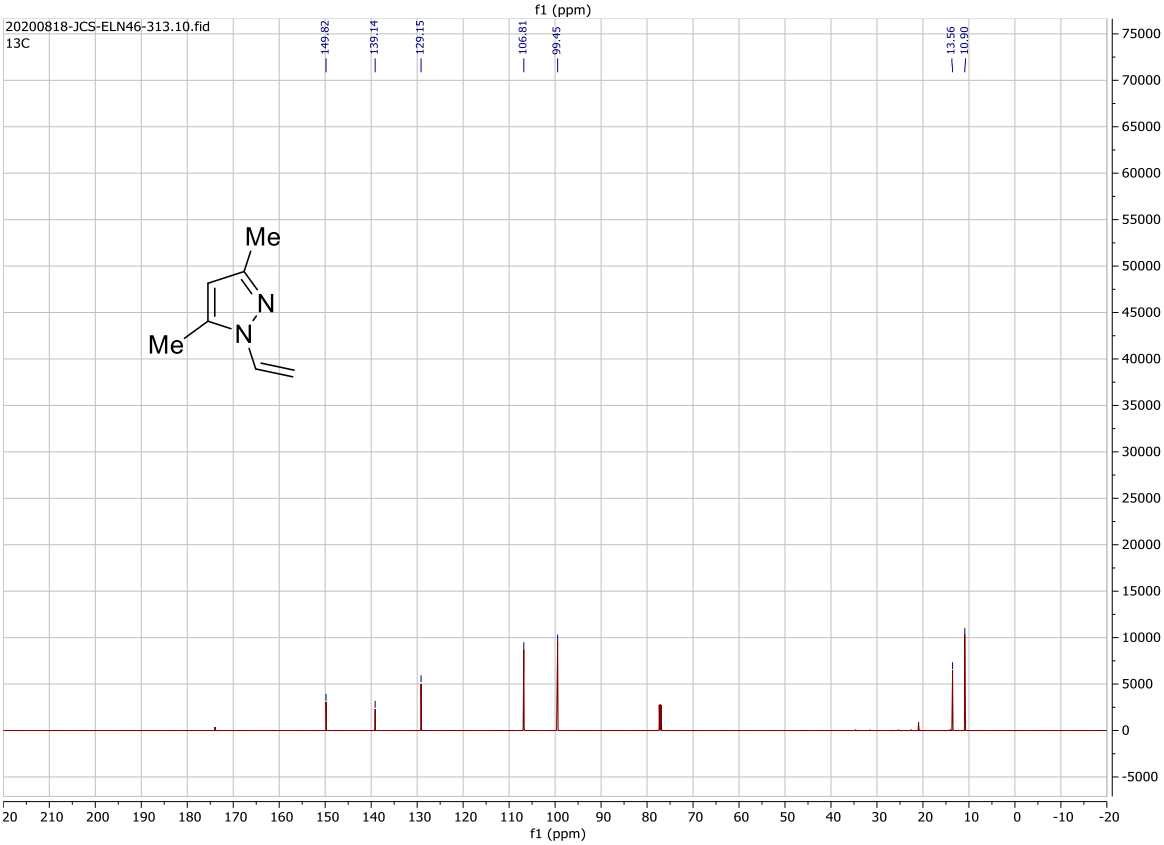
20200818-JCS-ELN46-313.10.fid
13C
149.82
139.14
129.15
106.81
99.45
13.56
10.90
Me
N
N
Me
f1 (ppm)

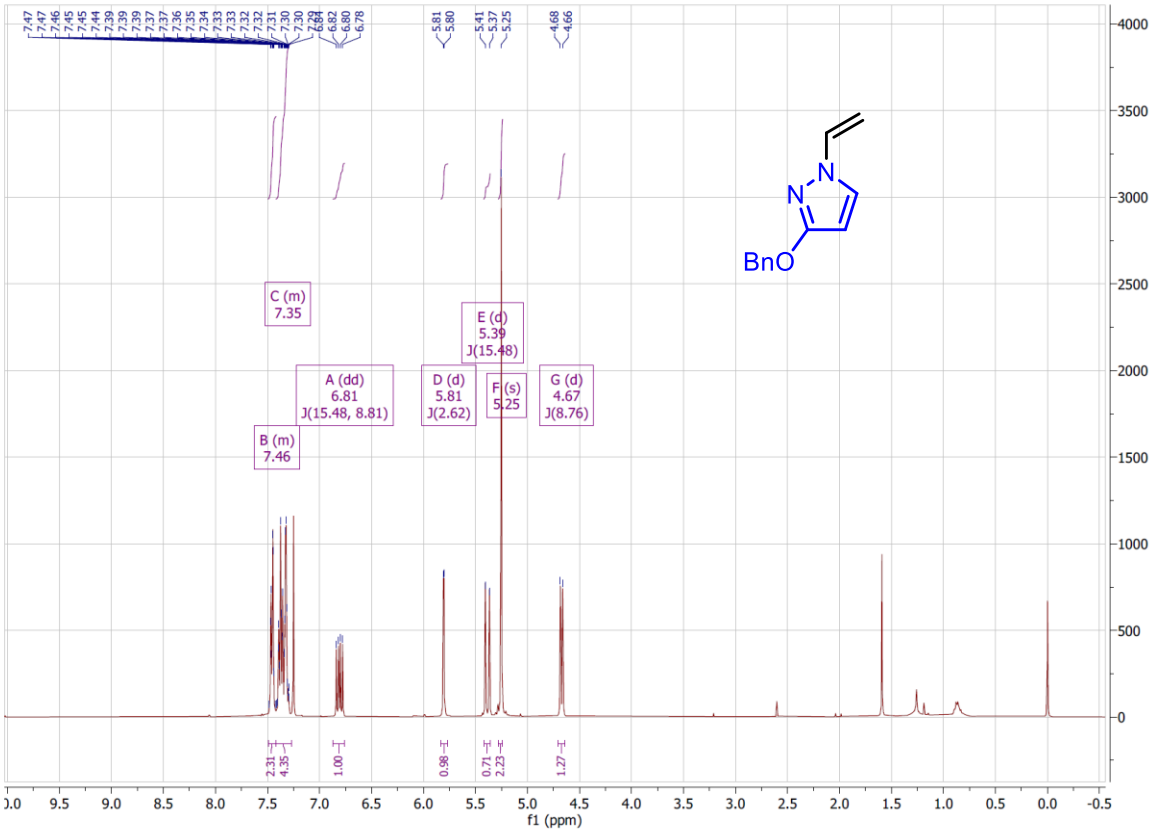
C (m)
7.35
B (m)
7.46
A (dd)
6.81
J(15.48, 8.81)
D (d)
5.81
J(2.62)
E (d)
5.39
J(15.48)
F (s)
5.25
G (d)
4.67
J(8.76)
BnO
f1 (ppm)

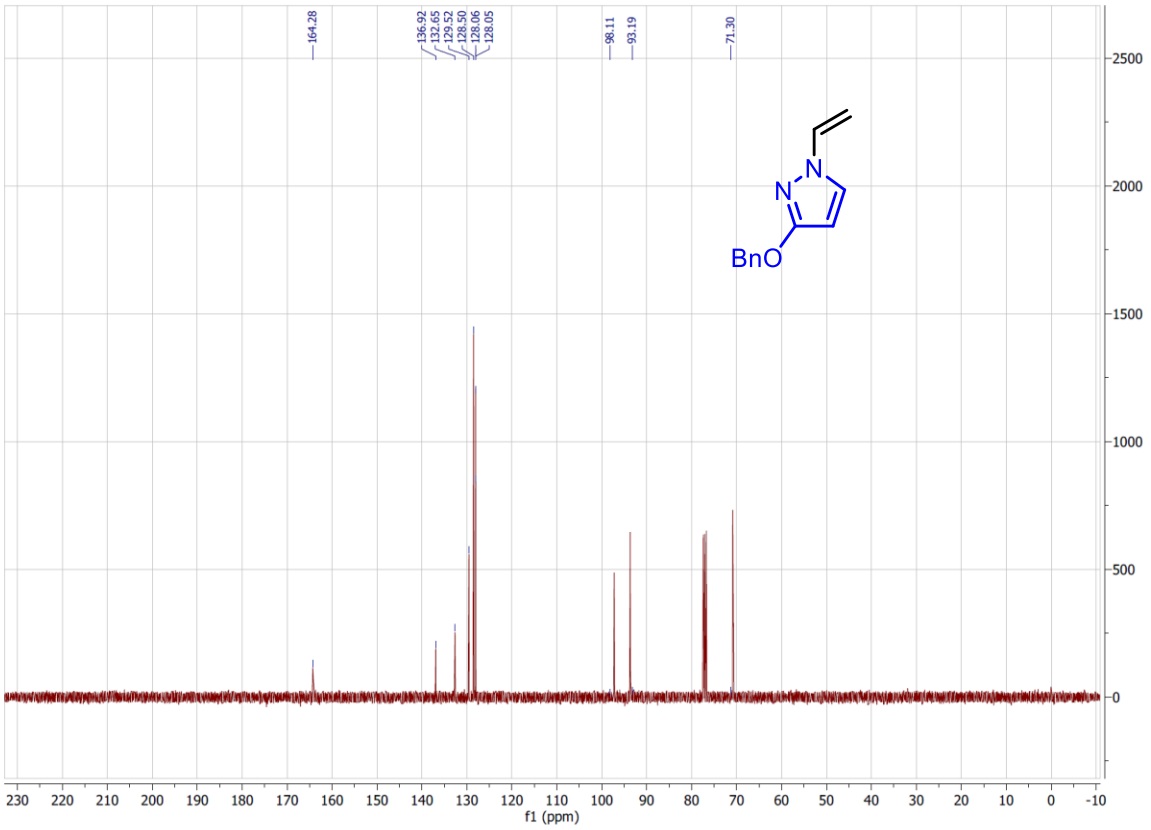
164.28
136.92
132.65
129.52
128.50
128.06
128.05
98.11
93.19
71.30
BnO
f1 (ppm)

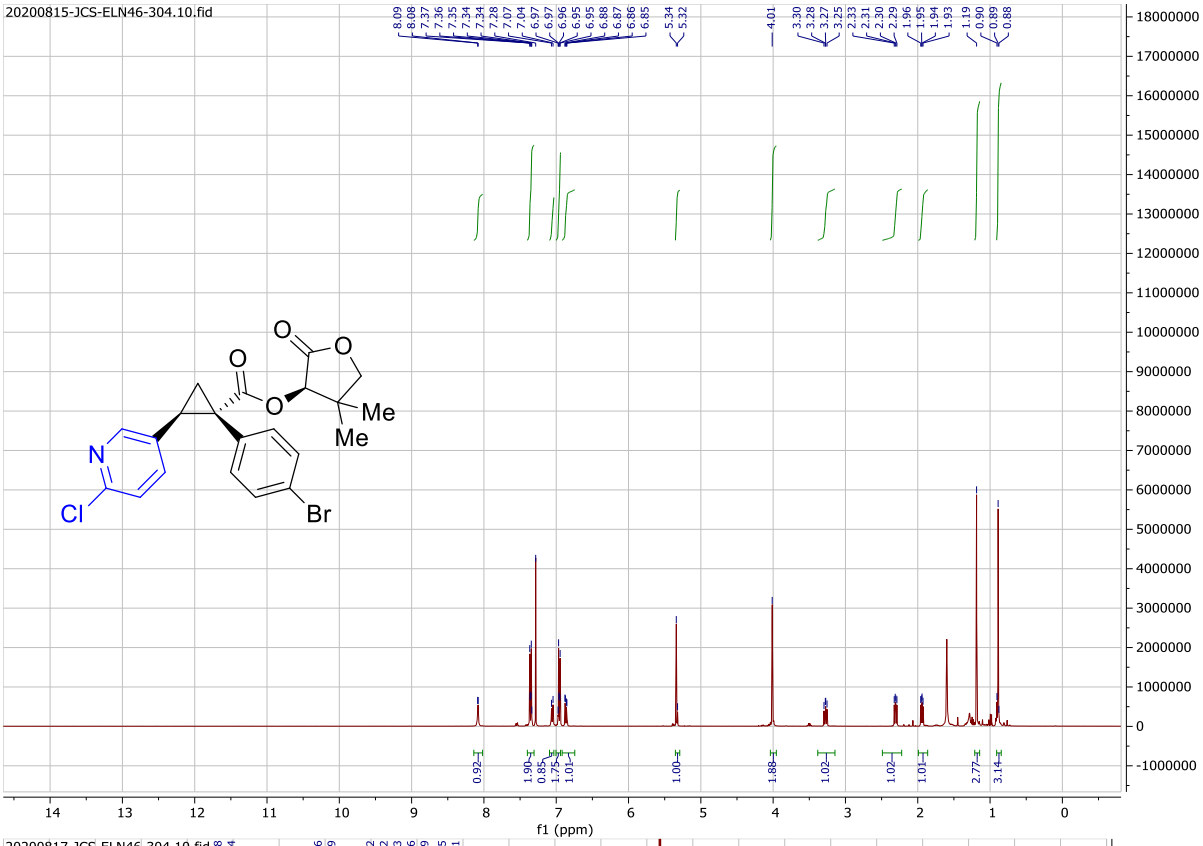
20200815-JCS-ELN46-304.10.fid
8.09
8.08
7.37
7.36
7.35
7.34
7.34
7.28
7.07
7.04
6.97
6.97
6.96
6.95
6.95
6.88
6.87
6.86
6.85
5.34
5.32
4.01
3.30
3.28
3.27
3.25
2.33
2.31
2.30
2.29
1.96
1.95
1.94
1.93
1.19
0.90
0.89
0.88
O
O
O
O
Me
Me
N
Cl
Br
0.92
1.90
0.85
1.75
1.01
1.00
1.88
1.02
1.02
1.01
2.77
3.14
f1 (ppm)

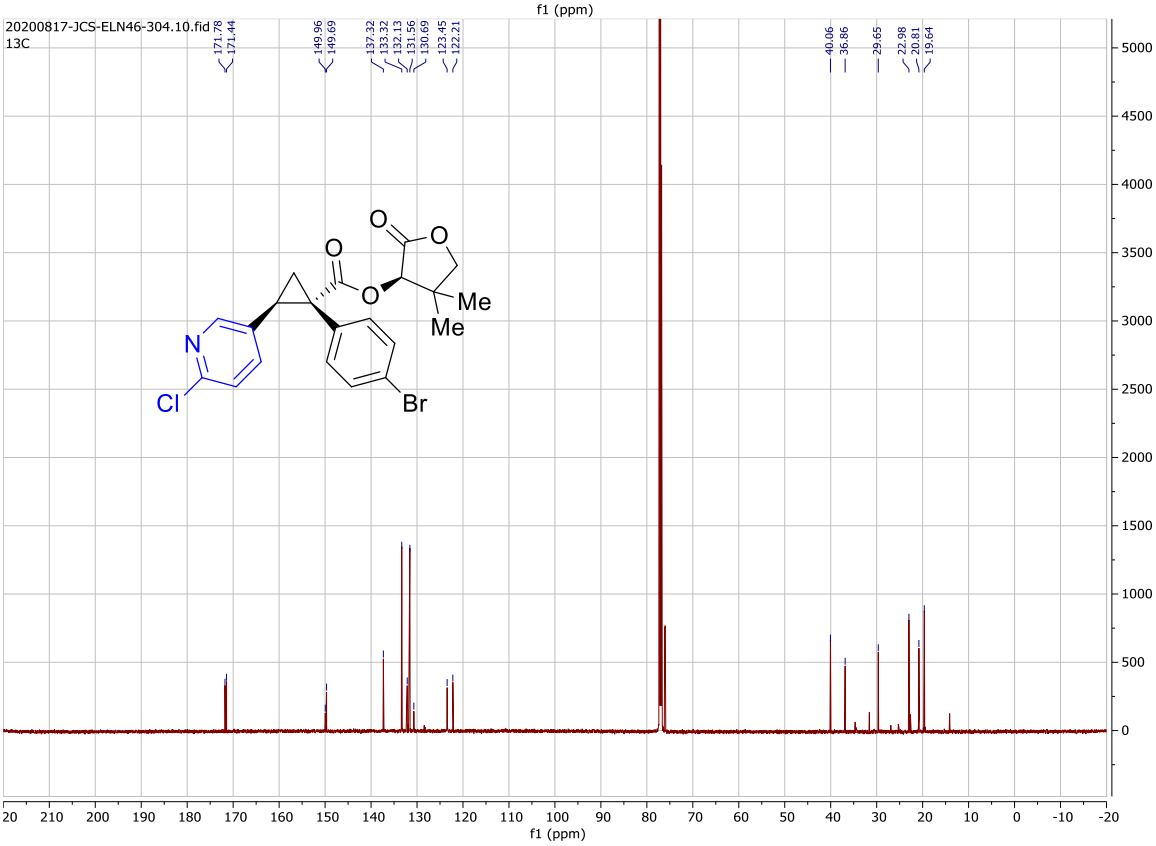
20200817-JCS-ELN46-304.10.fid
13C
171.78
171.44
149.96
149.69
137.32
133.32
132.13
131.56
130.69
123.45
122.21
40.06
36.86
29.65
22.98
20.81
19.64
O
O
O
O
Me
Me
N
Cl
Br
f1 (ppm)

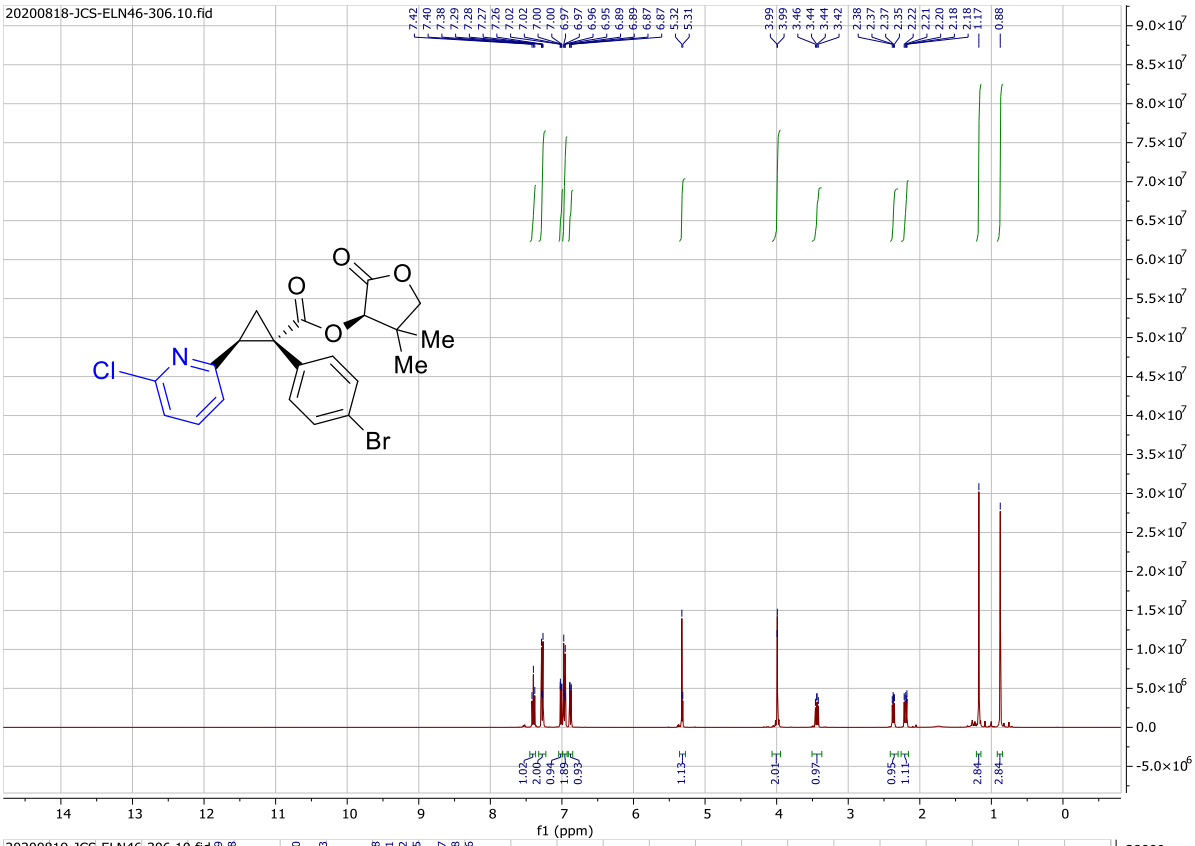
20200818-JCS-ELN46-306.10.fid
7.42 7.40 7.38 7.29 7.28 7.27 7.26 7.02 7.02 7.00 7.00 6.97 6.97 6.96 6.95 6.89 6.89 6.87 6.87 5.32 5.31
3.99 3.99 3.46 3.44 3.44 3.42
2.38 2.37 2.37 2.35 2.22 2.21 2.20 2.18 2.18 1.17
0.88
1.02 2.00 0.94 1.89 0.93
1.13
2.01
0.97
0.95 1.11
2.84 2.84
Cl
N
O
O
O
O
Me
Me
Br
f1 (ppm)

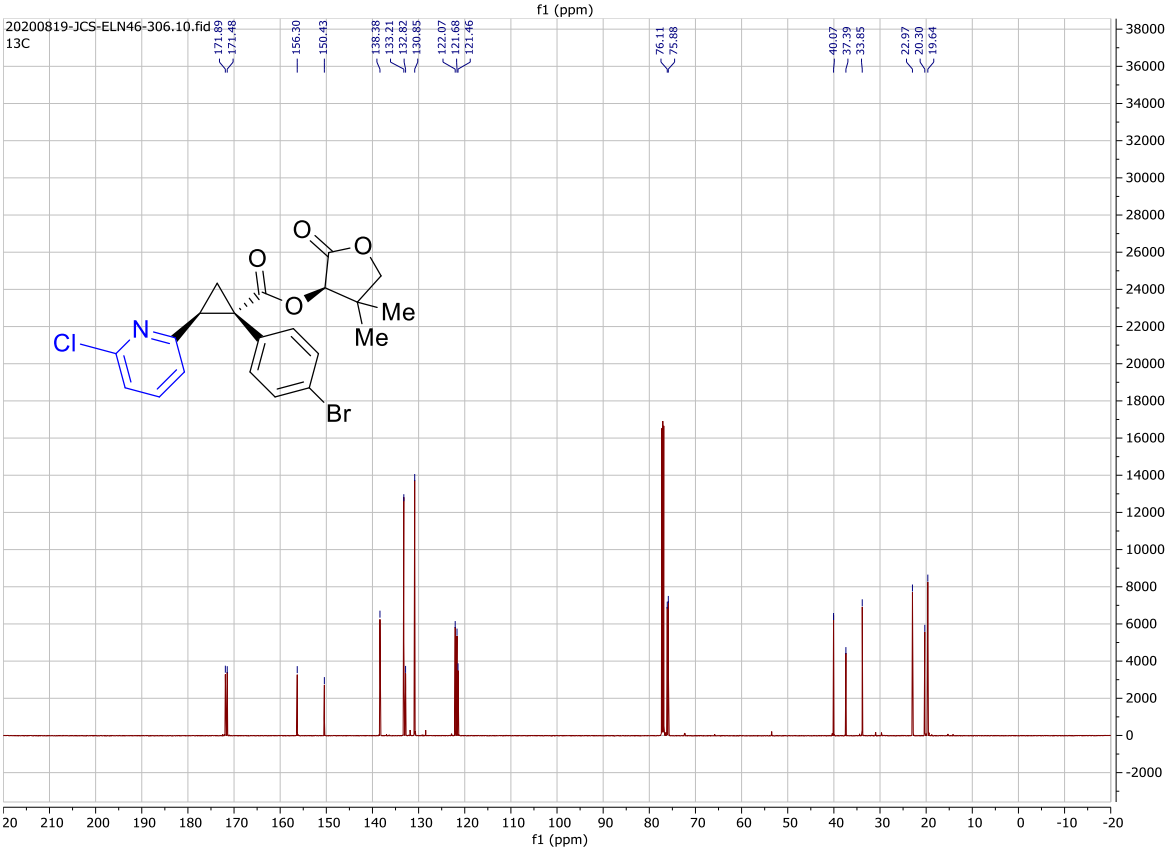
20200819-JCS-ELN46-306.10.fid
13C
171.89 171.48
156.30
150.43
138.38 133.21 132.82 130.85
122.07 121.68 121.46
76.11 75.88
40.07 37.39 33.85
22.97 20.30 19.64
Cl
N
O
O
O
O
Me
Me
Br
f1 (ppm)

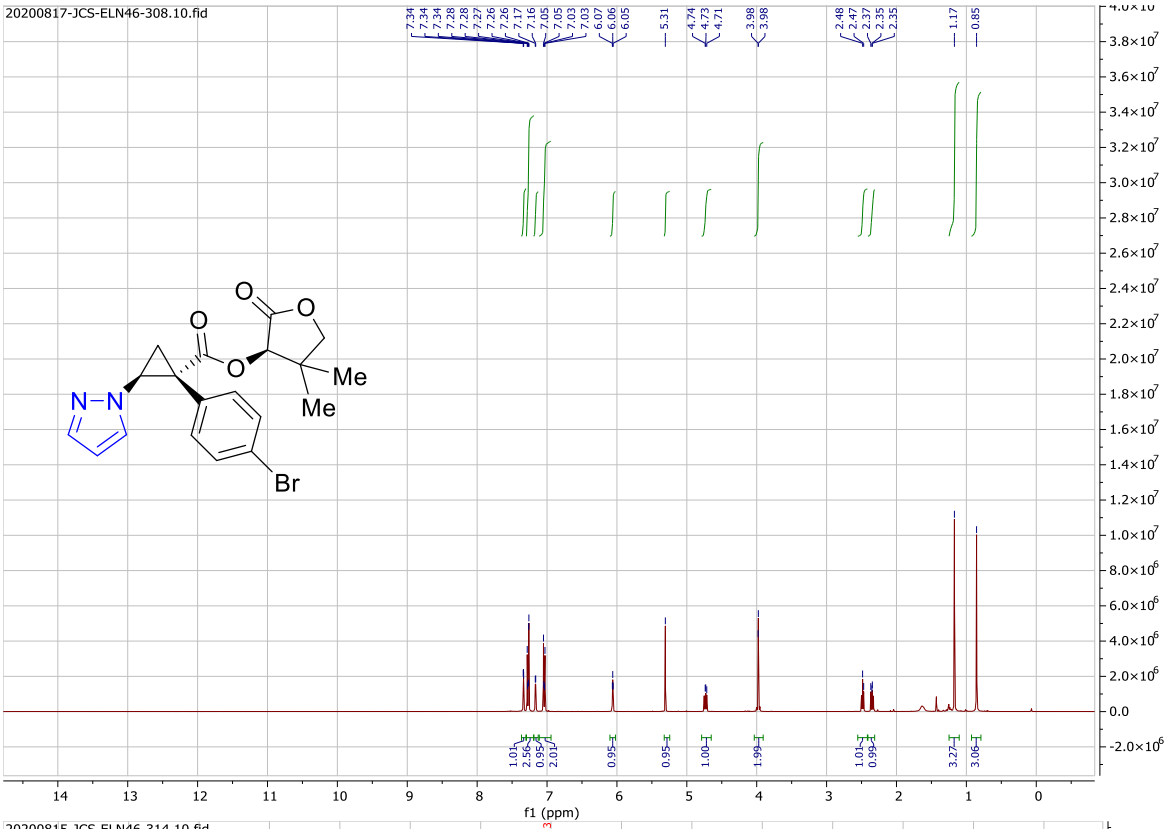
20200817-JCS-ELN46-308.10.fid
f1 (ppm)

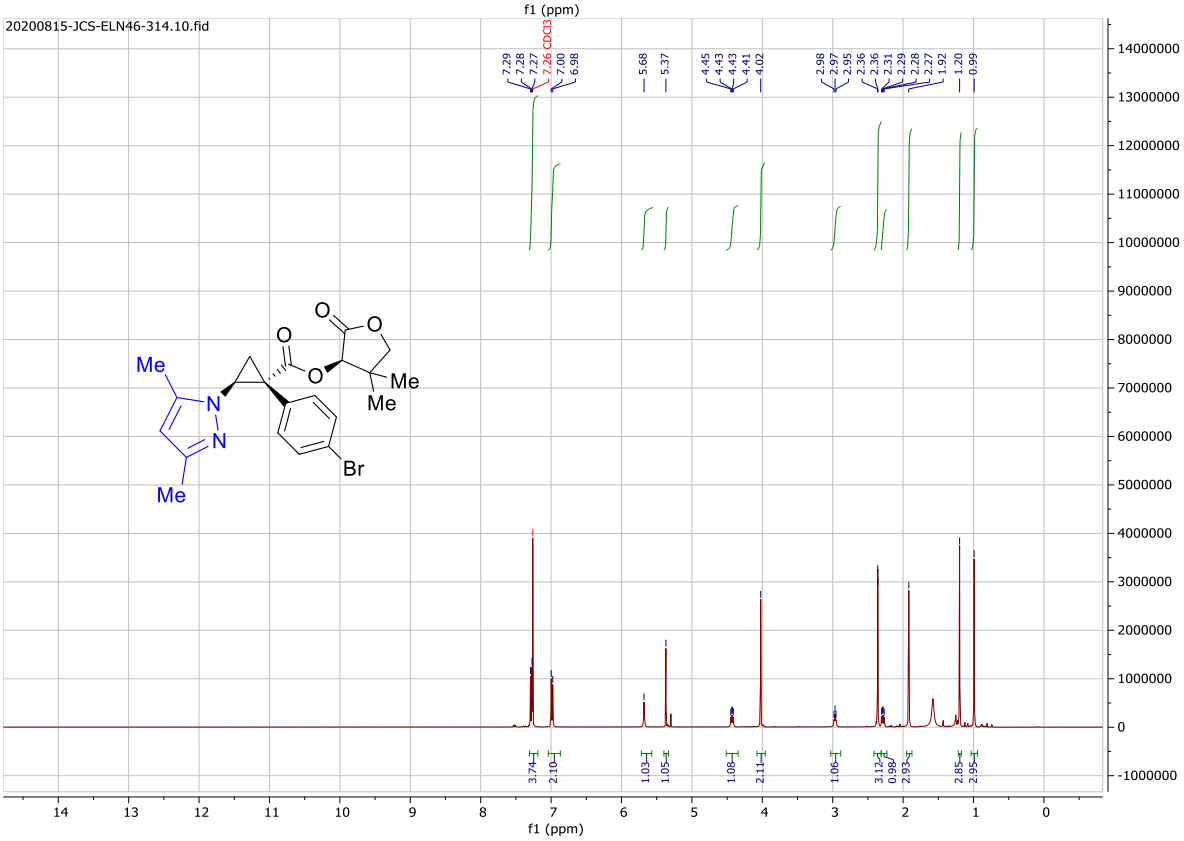
20200815-JCS-ELN46-314.10.fid
CDCl3
f1 (ppm)

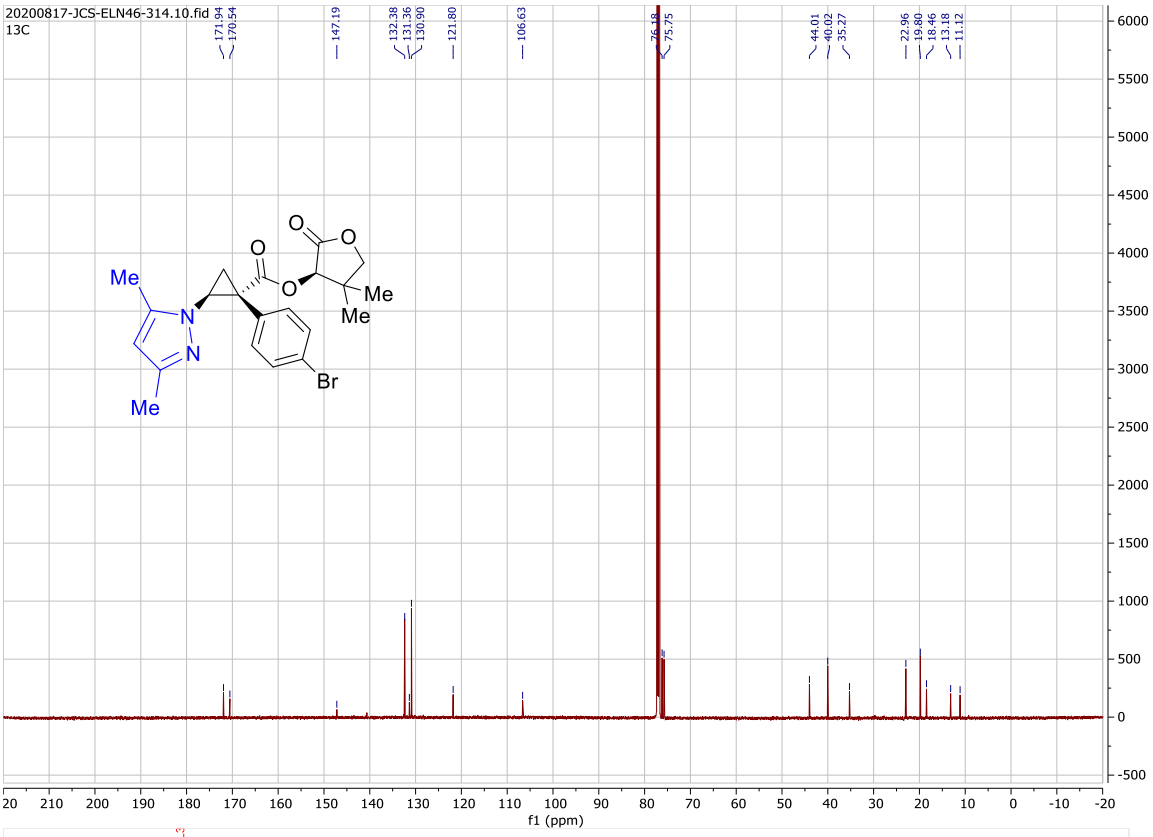
20200817-JCS-ELN46-314.10.fid
13C
171.94
170.54
147.19
132.38
131.36
130.90
121.80
106.63
76.18
75.75
44.01
40.02
35.27
22.96
19.80
18.46
13.18
11.12
Me
N
N
Me
O
O
O
O
Me
Me
Br
f1 (ppm)

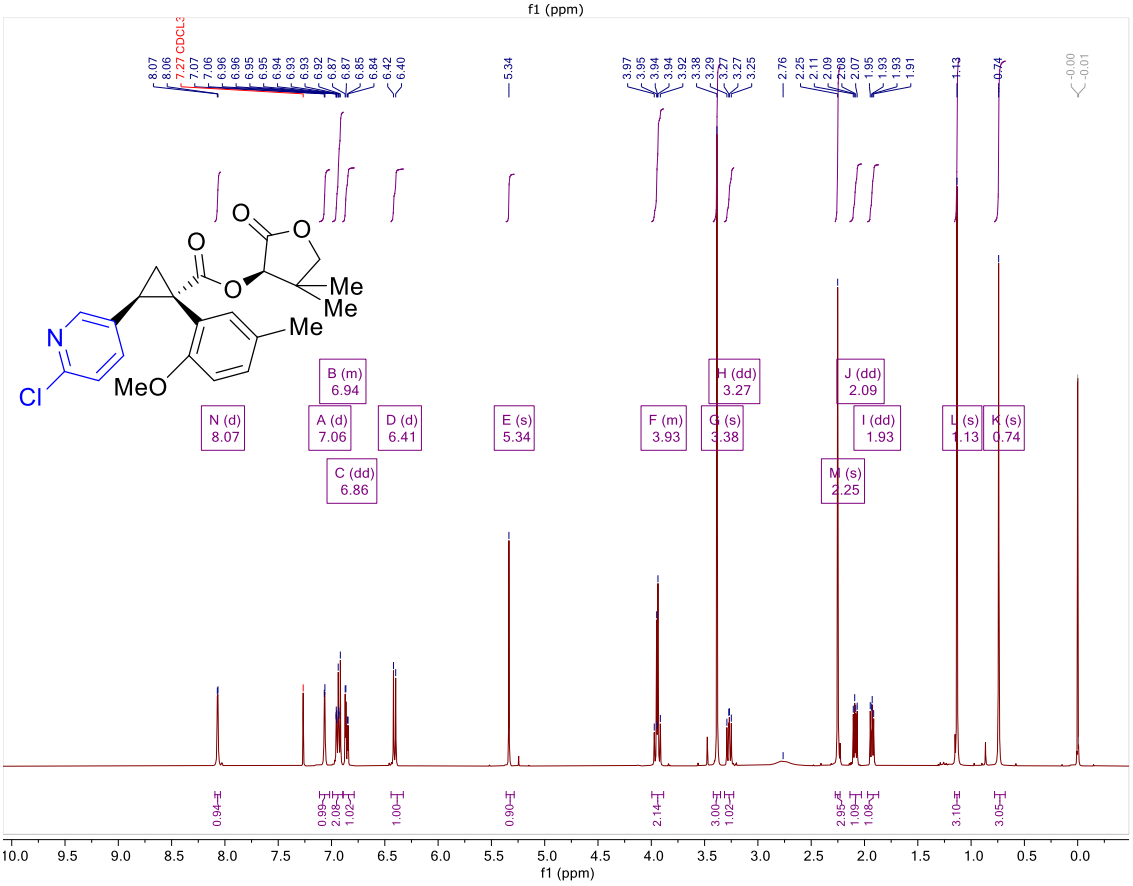
CDCl3
N
Cl
MeO
Me
Me
Me
O
O
O
O
N (d) 8.07
A (d) 7.06
B (m) 6.94
C (dd) 6.86
D (d) 6.41
E (s) 5.34
F (m) 3.93
G (s) 3.38
H (dd) 3.27
I (dd) 1.93
J (dd) 2.09
M (s) 2.25
L (s) 1.13
K (s) 0.74
f1 (ppm)

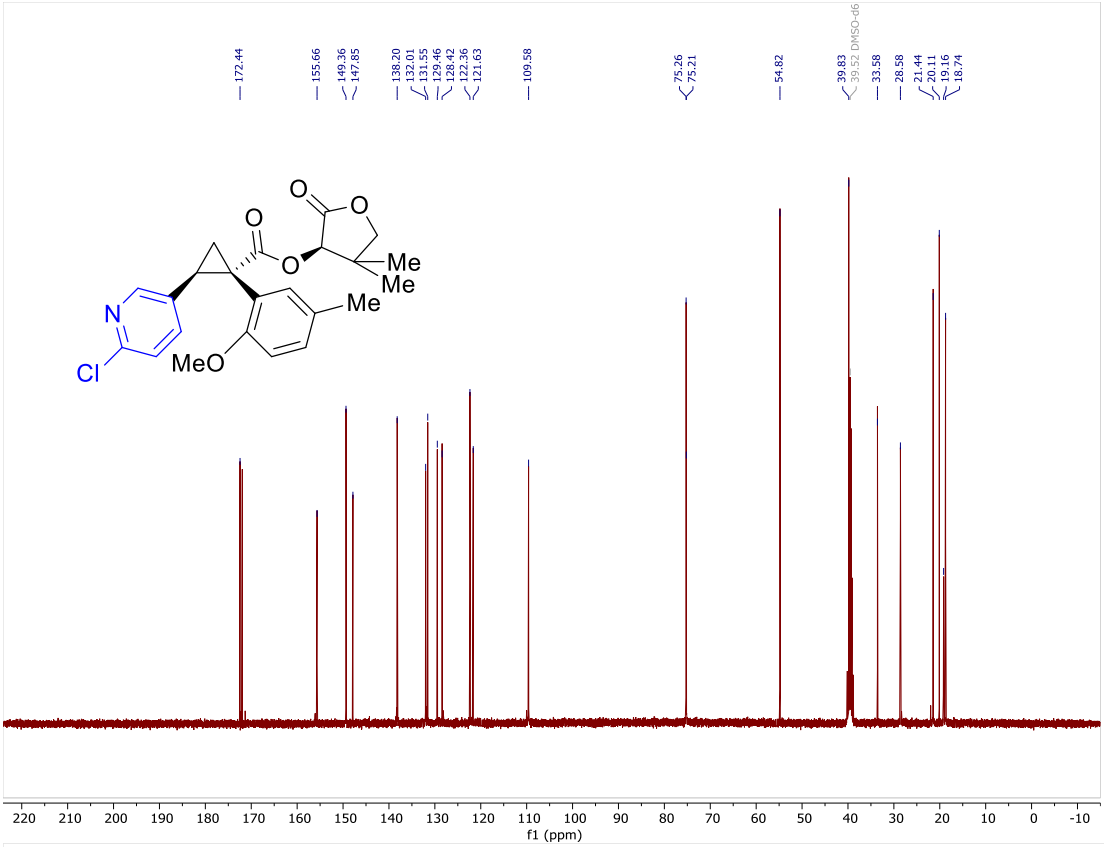
172.44
155.66
149.36
147.85
138.20
132.01
131.55
129.46
128.42
122.36
121.63
109.58
75.26
75.21
54.82
39.83
39.52 DMSO-d6
33.58
28.58
21.44
20.11
19.16
18.74
f1 (ppm)

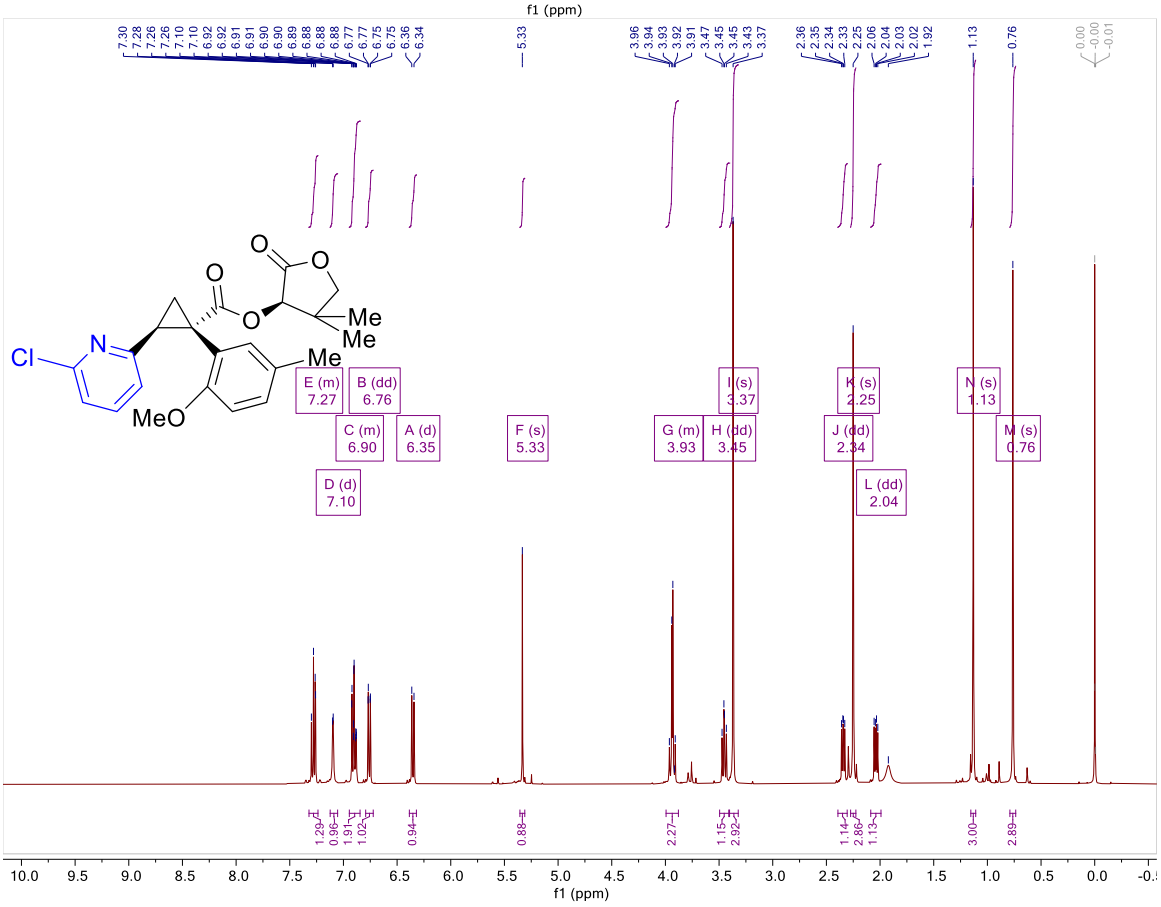
E (m) 7.27
B (dd) 6.76
C (m) 6.90
A (d) 6.35
D (d) 7.10
F (s) 5.33
G (m) 3.93
H (dd) 3.45
I (s) 3.37
K (s) 2.25
J (dd) 2.34
L (dd) 2.04
N (s) 1.13
M (s) 0.76
f1 (ppm)

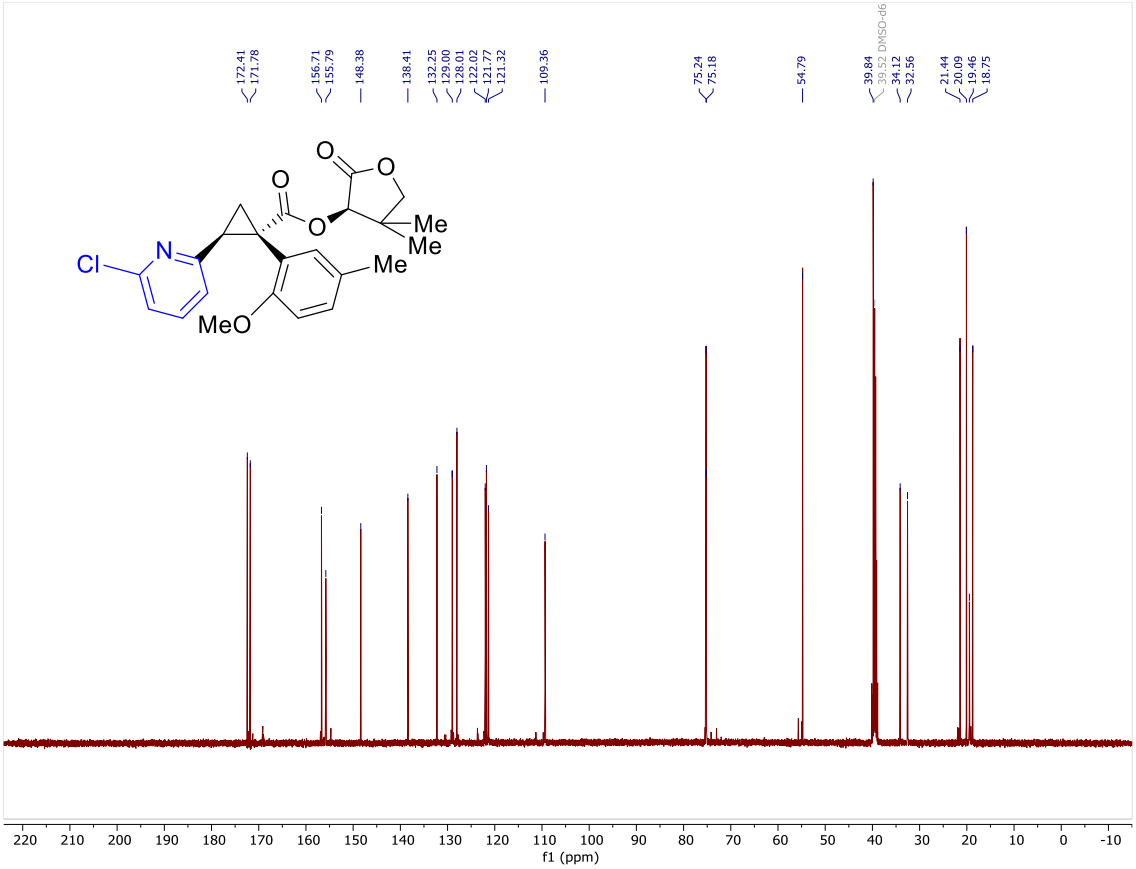
172.41
171.78
156.71
155.79
148.38
138.41
132.25
129.00
128.01
122.02
121.77
121.32
109.36
75.24
75.18
54.79
39.84
39.52 DMSO-d6
34.12
32.56
21.44
20.09
19.46
18.75
Cl
N
O
O
O
O
Me
Me
Me
MeO
f1 (ppm)

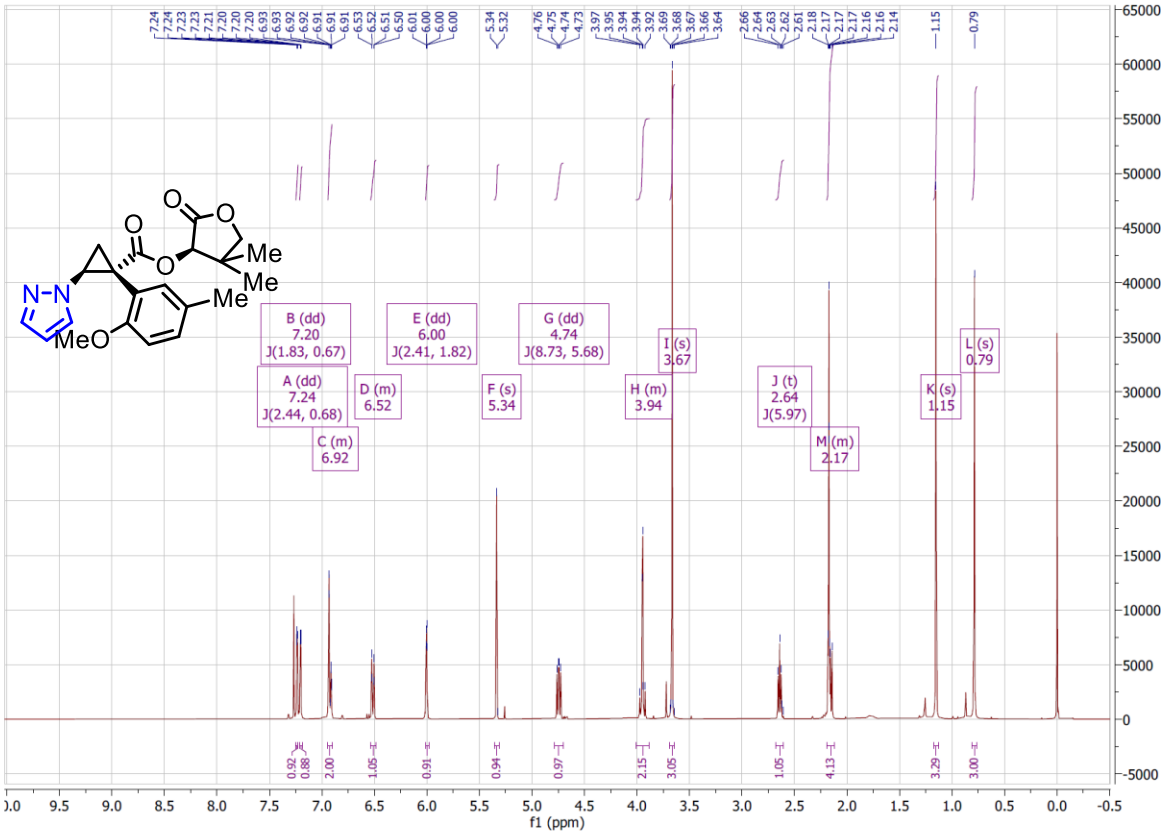
N-N
O
O
O
O
Me
Me
Me
MeO
B (dd)
7.20
J(1.83, 0.67)
A (dd)
7.24
J(2.44, 0.68)
C (m)
6.92
D (m)
6.52
E (dd)
6.00
J(2.41, 1.82)
F (s)
5.34
G (dd)
4.74
J(8.73, 5.68)
H (m)
3.94
I (s)
3.67
J (t)
2.64
J(5.97)
M (m)
2.17
K (s)
1.15
L (s)
0.79
f1 (ppm)

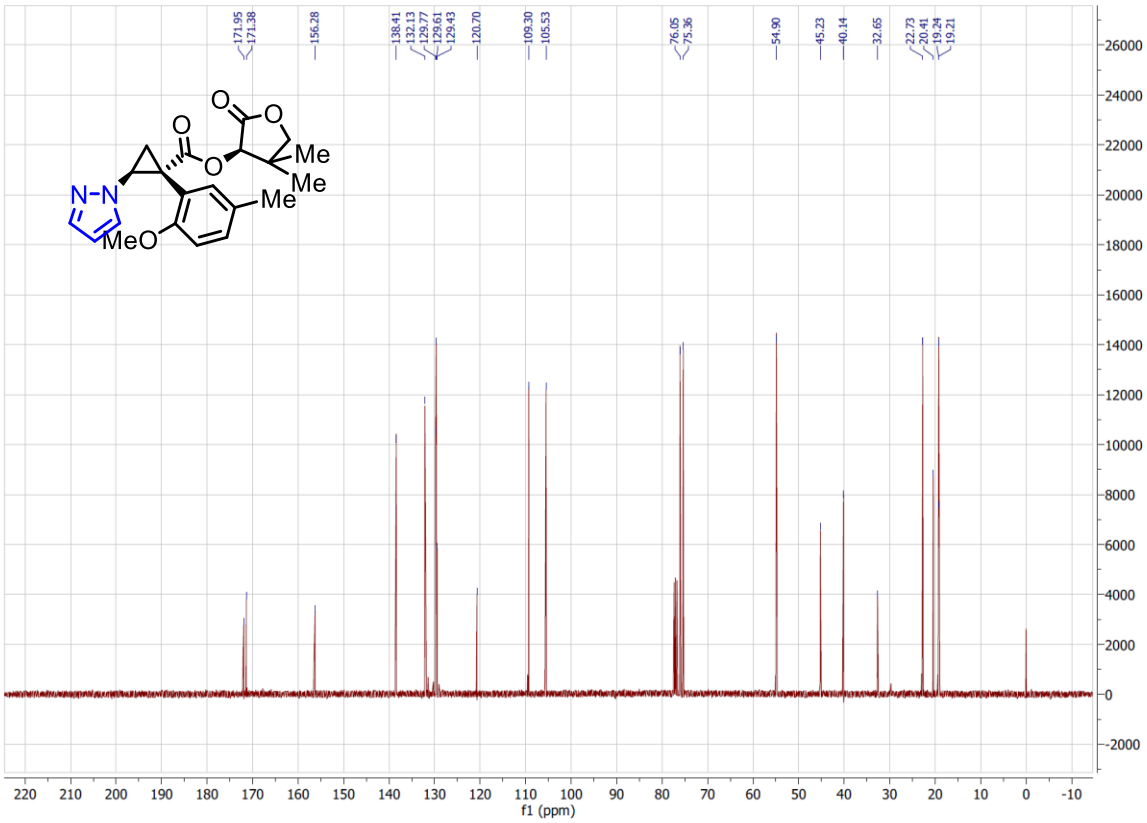
171.95
171.38
156.28
138.41
132.13
129.77
129.61
129.43
120.70
109.30
105.53
76.05
75.36
54.90
45.23
40.14
32.65
22.73
20.41
19.24
19.21
f1 (ppm)

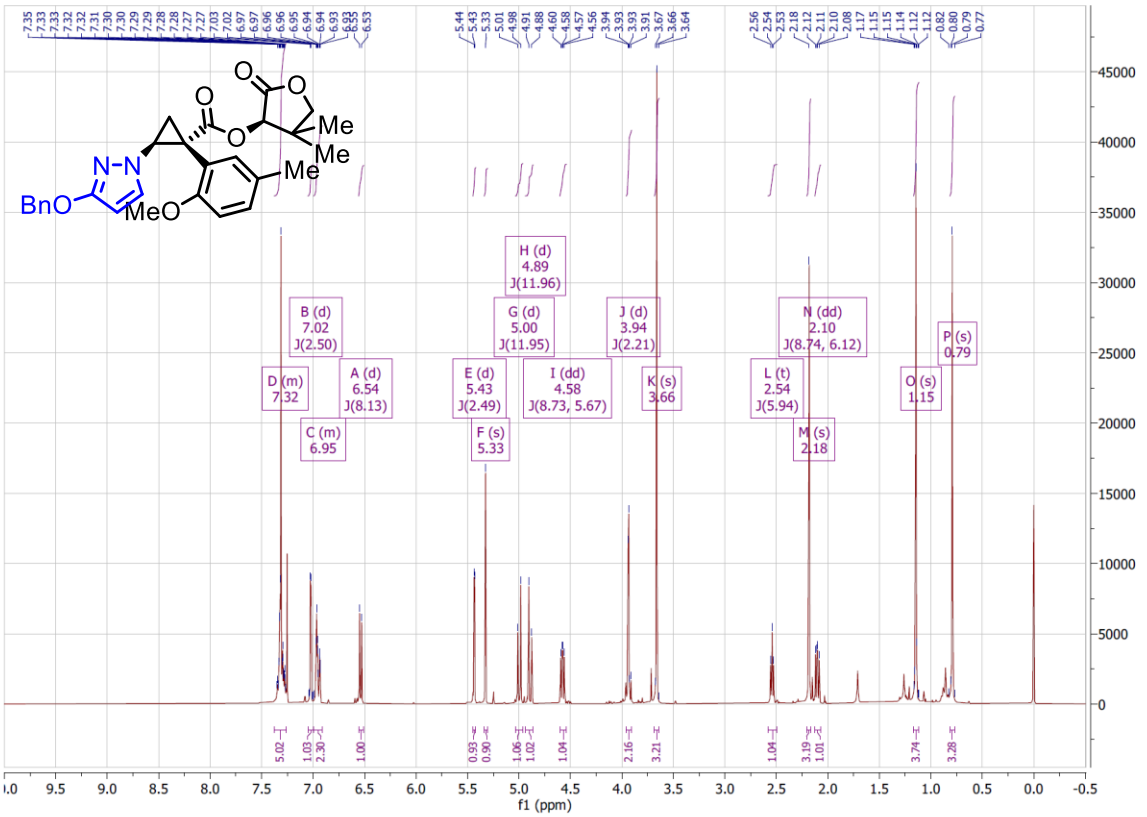
H (d)
4.89
J(11.96)
B (d)
7.02
J(2.50)
G (d)
5.00
J(11.95)
J (d)
3.94
J(2.21)
N (dd)
2.10
J(8.74, 6.12)
P (s)
0.79
D (m)
7.32
A (d)
6.54
J(8.13)
E (d)
5.43
J(2.49)
I (dd)
4.58
J(8.73, 5.67)
K (s)
3.66
L (t)
2.54
J(5.94)
O (s)
1.15
C (m)
6.95
F (s)
5.33
M (s)
2.18
f1 (ppm)

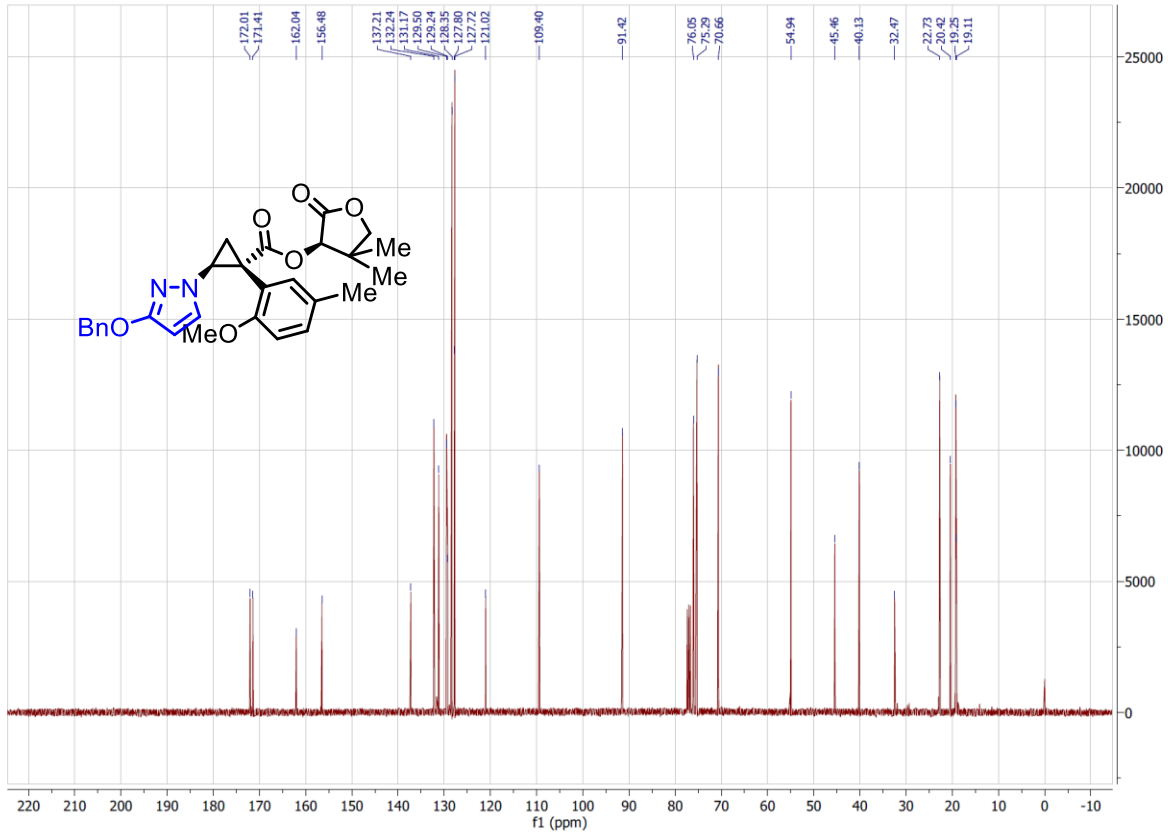
172.01
171.41
162.04
156.48
137.21
132.24
131.17
129.50
129.24
128.35
127.80
127.72
121.02
109.40
91.42
76.05
75.29
70.66
54.94
45.46
40.13
32.47
22.73
20.42
19.25
19.11
f1 (ppm)

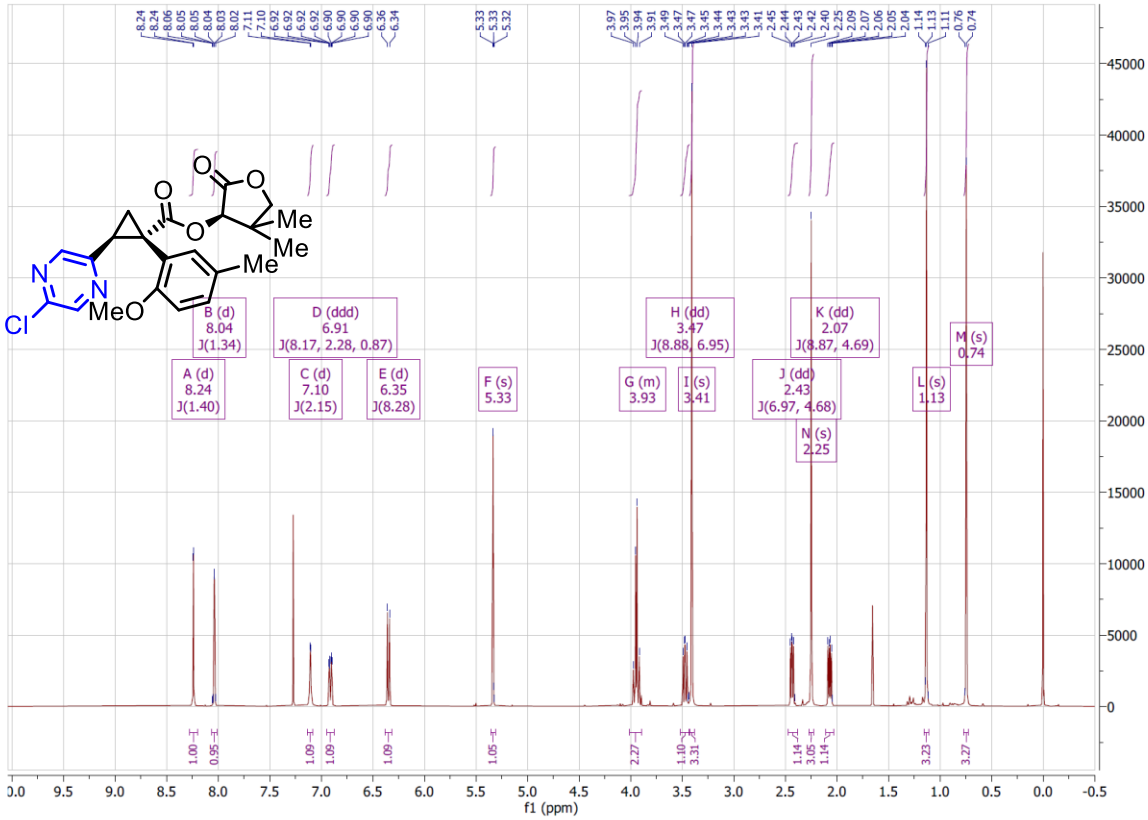
A (d)
8.24
J(1.40)
B (d)
8.04
J(1.34)
C (d)
7.10
J(2.15)
D (ddd)
6.91
J(8.17, 2.28, 0.87)
E (d)
6.35
J(8.28)
F (s)
5.33
G (m)
3.93
H (dd)
3.47
J(8.88, 6.95)
I (s)
3.41
J (dd)
2.43
J(6.97, 4.68)
K (dd)
2.07
J(8.87, 4.69)
N (s)
2.25
L (s)
1.13
M (s)
0.74
f1 (ppm)

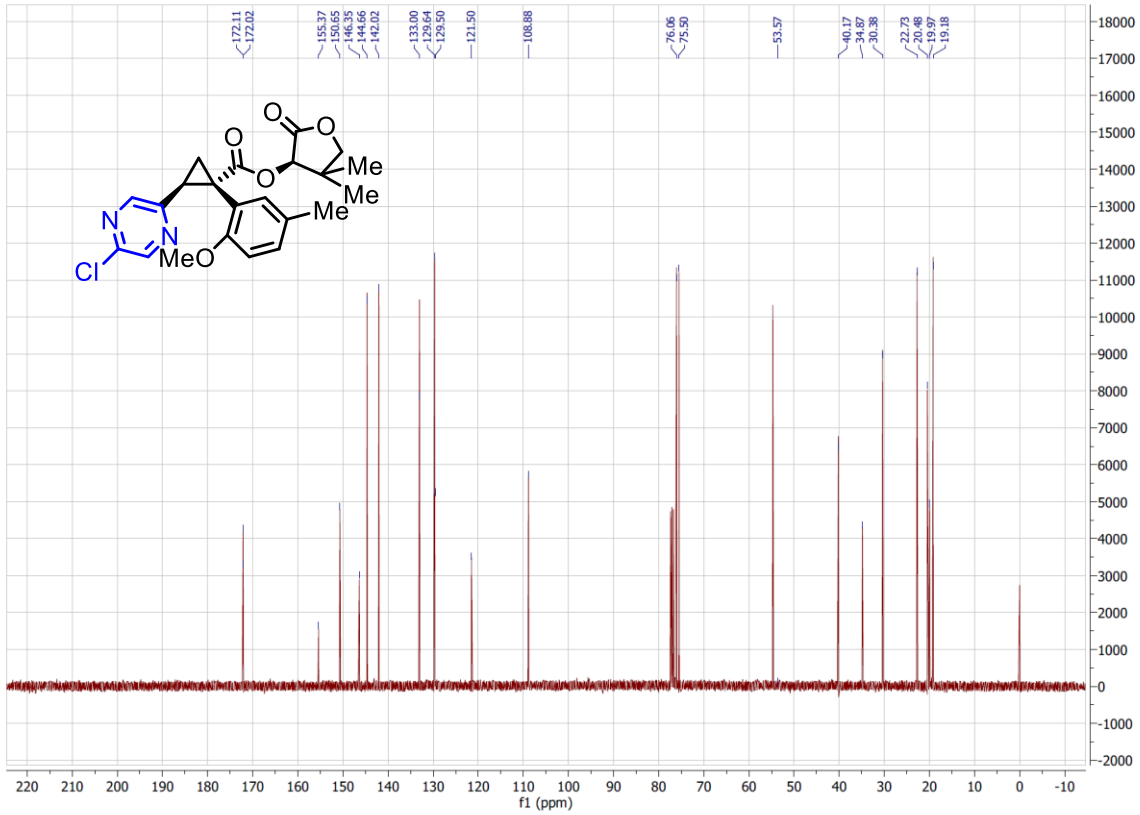
172.11
172.02
155.37
150.65
146.35
144.66
142.02
133.00
129.64
129.50
121.50
108.88
76.06
75.50
53.57
40.17
34.67
30.38
22.73
20.48
19.97
19.18
Me
Me
Me
MeO
Cl
f1 (ppm)

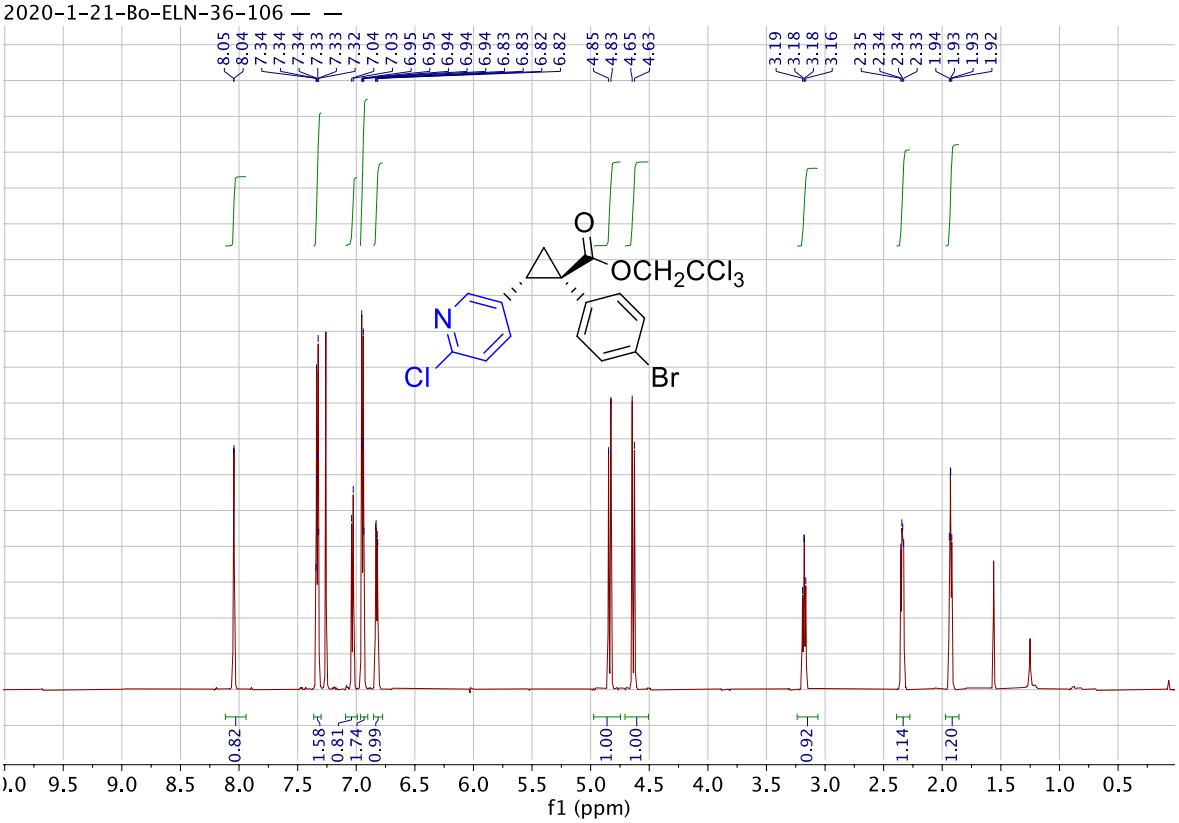
2020-1-21-Bo-ELN-36-106 — —
8.05
8.04
7.34
7.34
7.34
7.33
7.33
7.32
7.04
7.03
6.95
6.95
6.94
6.94
6.94
6.83
6.83
6.82
6.82
4.85
4.83
4.65
4.63
3.19
3.18
3.18
3.16
2.35
2.34
2.34
2.33
1.94
1.93
1.93
1.92
OCH2CCl3
Cl
Br
0.82
1.58
0.81
1.74
0.99
1.00
1.00
0.92
1.14
1.20
f1 (ppm)

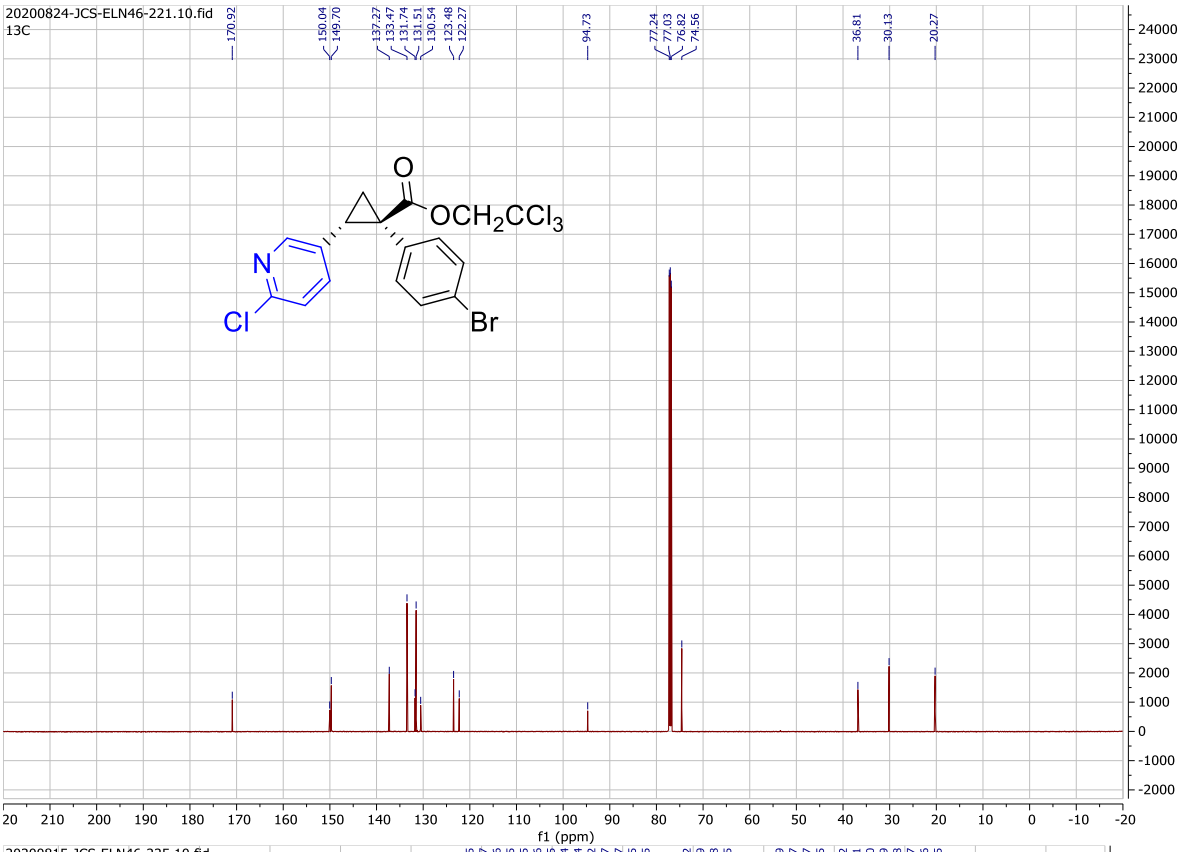
20200824-JCS-ELN46-221.10.fid
13C
170.92
150.04
149.70
137.27
133.47
131.74
131.51
130.54
123.48
122.27
94.73
77.24
77.03
76.82
74.56
36.81
30.13
20.27
O
OCH2CCl3
N
Cl
Br
f1 (ppm)

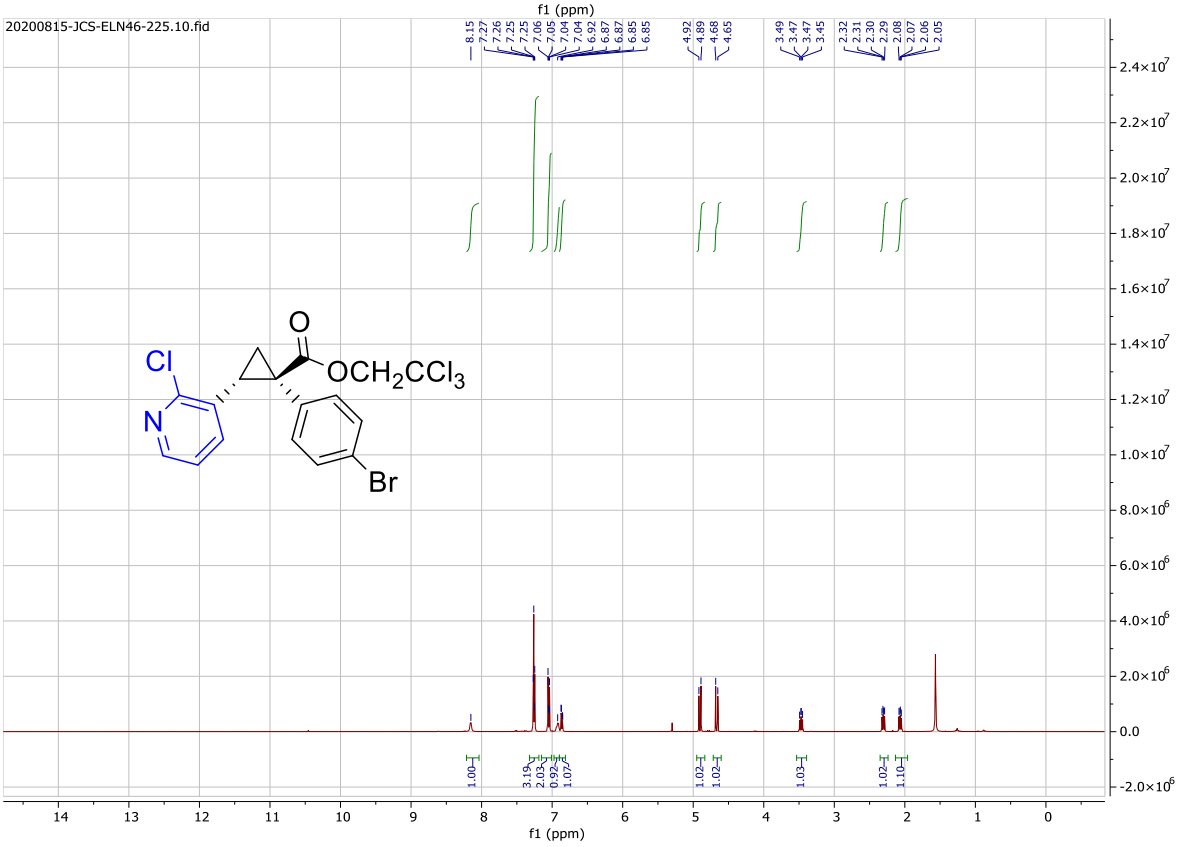
20200815-JCS-ELN46-225.10.fid
8.15
7.27
7.26
7.25
7.06
7.05
7.04
6.92
6.87
6.85
4.92
4.89
4.68
4.65
3.49
3.47
3.45
2.32
2.31
2.30
2.29
2.08
2.07
2.06
2.05
1.00
3.19
2.03
0.92
1.07
1.02
1.02
1.03
1.02
1.10
Cl
N
O
OCH2CCl3
Br
f1 (ppm)

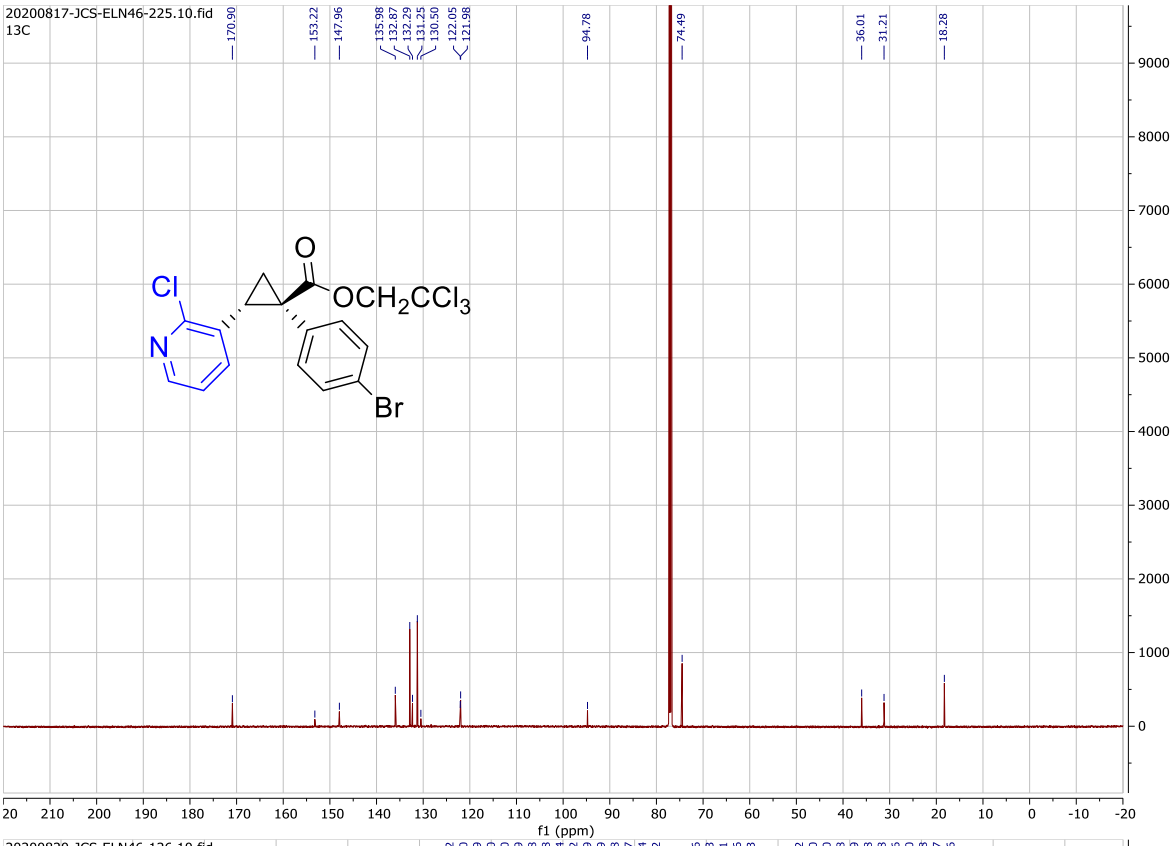
20200817-JCS-ELN46-225.10.fid
13C
170.90
153.22
147.96
135.98
132.87
132.29
131.25
130.50
122.05
121.98
94.78
74.49
36.01
31.21
18.28
O
Cl
N
OCH2CCl3
Br
f1 (ppm)

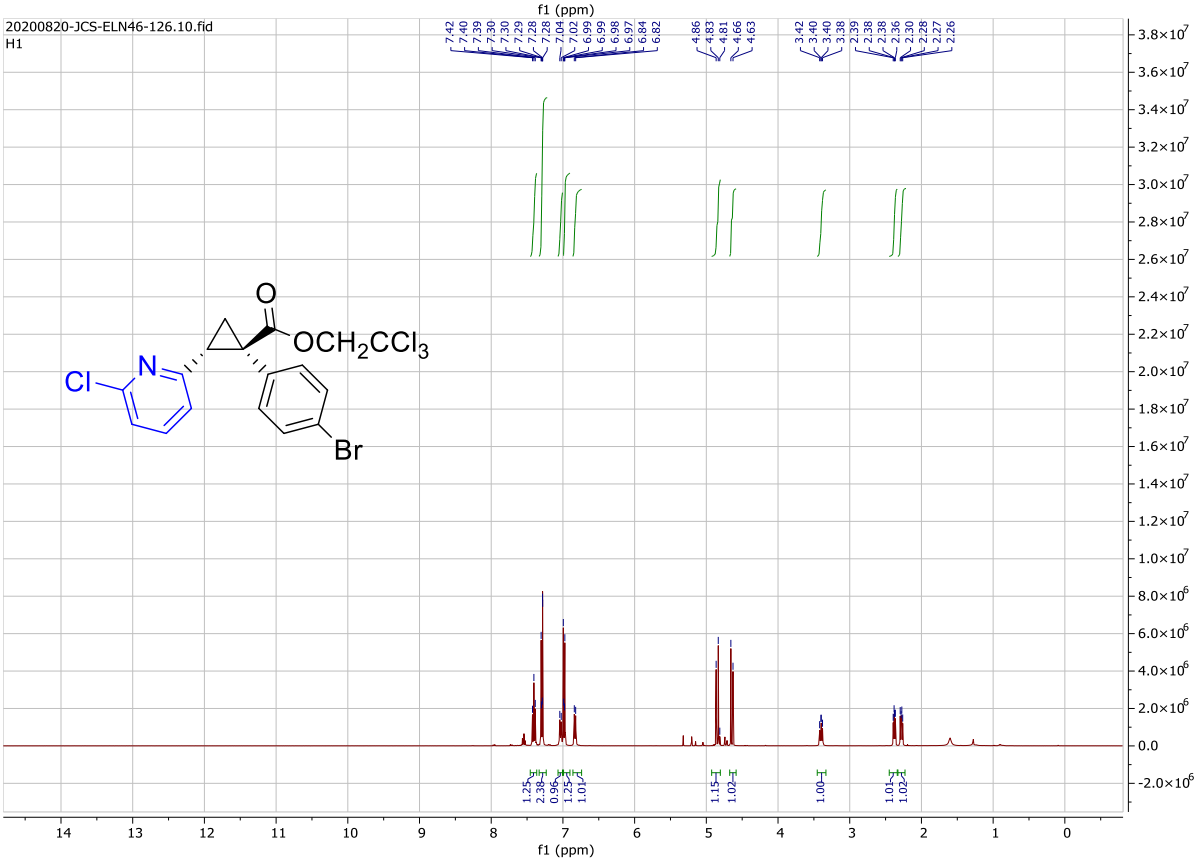
20200820-JCS-ELN46-126.10.fid
H1
7.42
7.40
7.39
7.30
7.30
7.29
7.28
7.28
7.04
7.02
6.99
6.99
6.98
6.97
6.84
6.82
4.86
4.83
4.81
4.66
4.63
3.42
3.40
3.40
3.38
2.39
2.38
2.38
2.36
2.30
2.28
2.27
2.26
1.25
2.36
0.96
1.25
1.07
1.15
1.02
1.00
1.01
1.02
O
Cl
N
OCH2CCl3
Br
f1 (ppm)

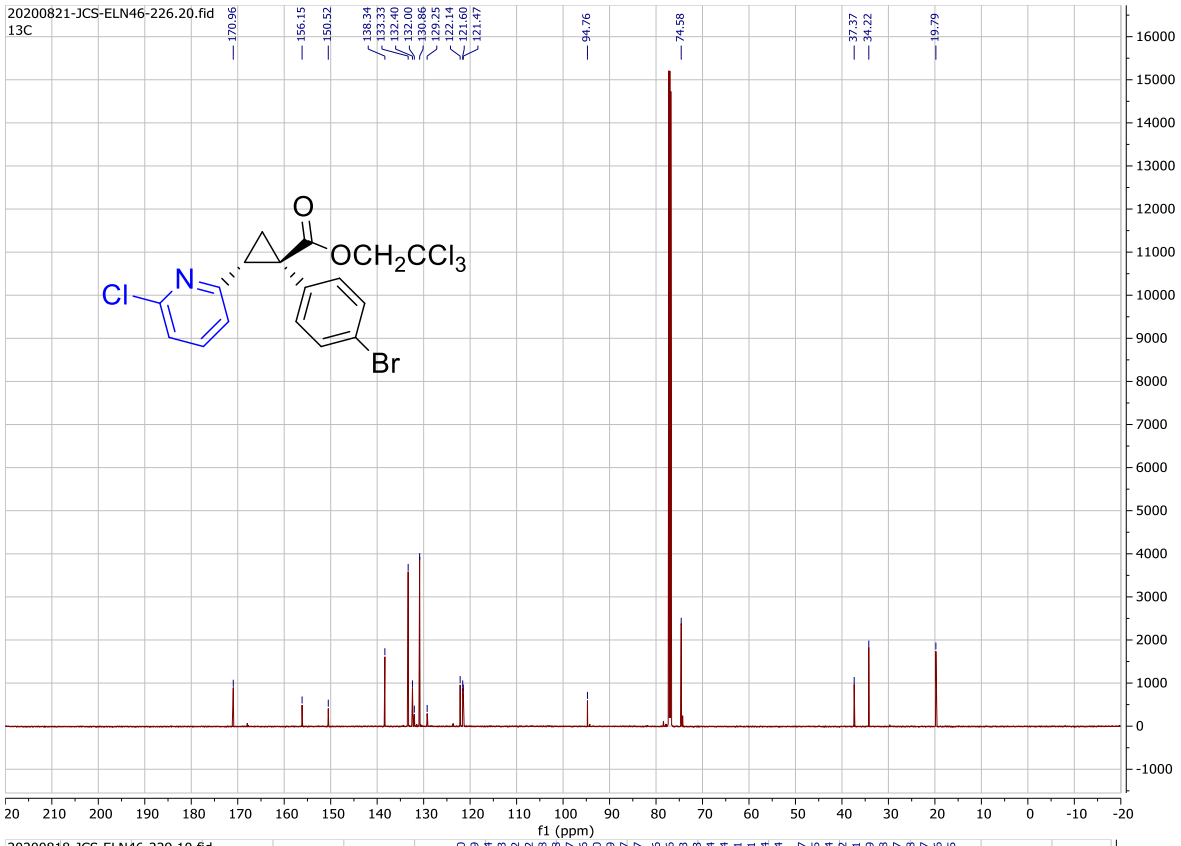
20200821-JCS-ELN46-226.20.fid
13C
170.96
156.15
150.52
138.34
133.33
132.40
132.00
130.86
129.25
122.14
121.60
121.47
94.76
74.58
37.37
34.22
19.79
O
OCH2CCl3
Cl
N
Br
f1 (ppm)

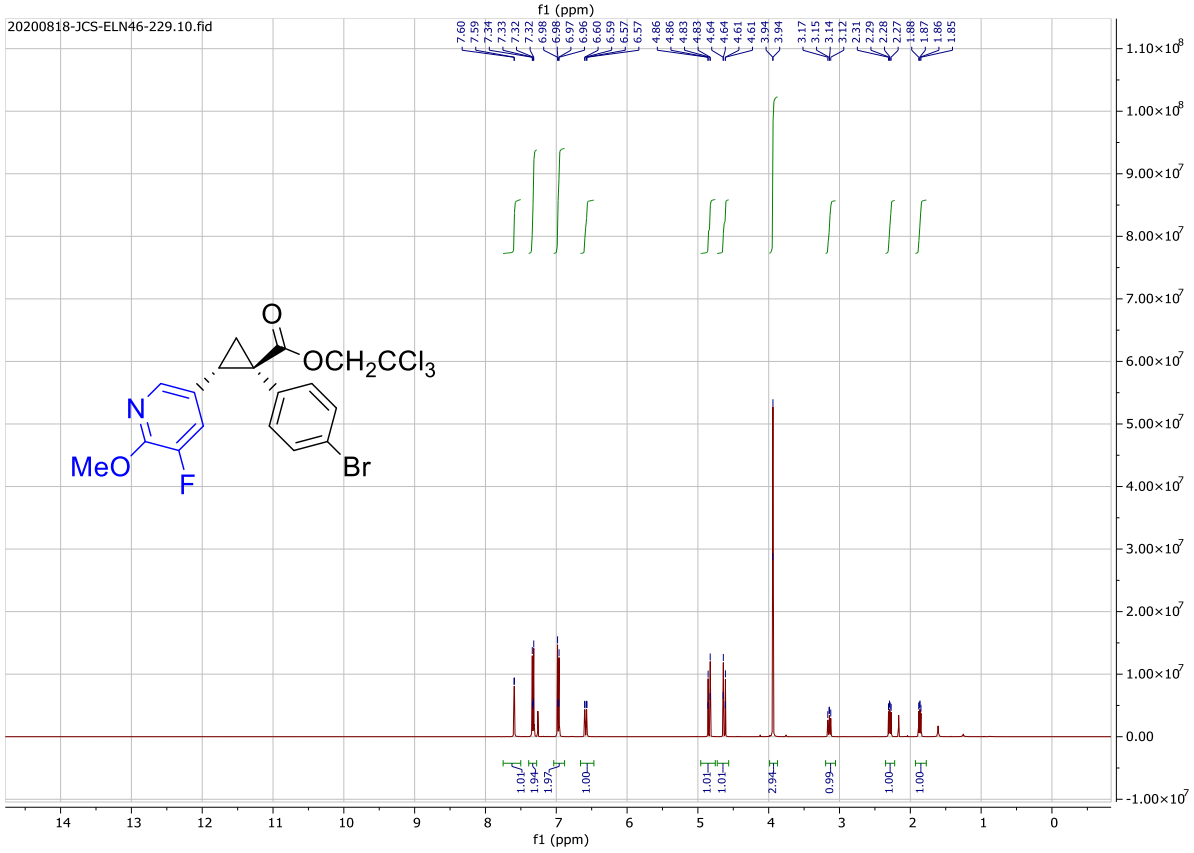
20200818-JCS-ELN46-229.10.fid
7.60
7.59
7.34
7.33
7.32
7.32
6.98
6.97
6.96
6.60
6.59
6.57
4.86
4.86
4.83
4.83
4.64
4.64
4.61
4.61
3.94
3.94
3.17
3.15
3.14
3.12
2.31
2.29
2.28
2.27
1.88
1.87
1.86
1.85
1.01
1.94
1.97
1.00
1.01
1.01
2.94
0.99
1.00
1.00
O
OCH2CCl3
N
MeO
F
Br
f1 (ppm)

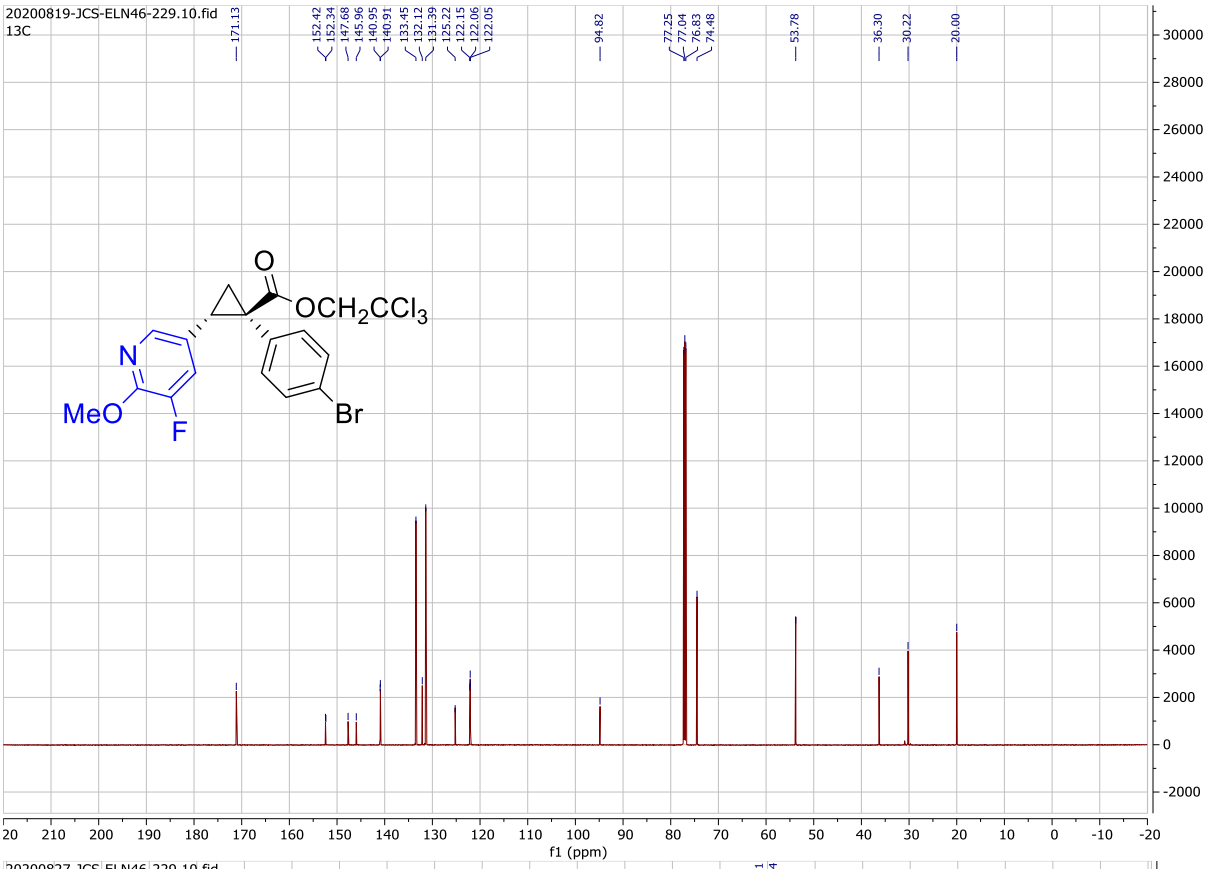
20200819-JCS-ELN46-229.10.fid
13C
171.13
152.42
152.34
147.68
145.96
140.95
140.91
133.45
132.12
131.39
125.22
122.15
122.06
122.05
94.82
77.25
77.04
76.83
74.48
53.78
36.30
30.22
20.00
O
OCH2CCl3
N
MeO
F
Br
f1 (ppm)

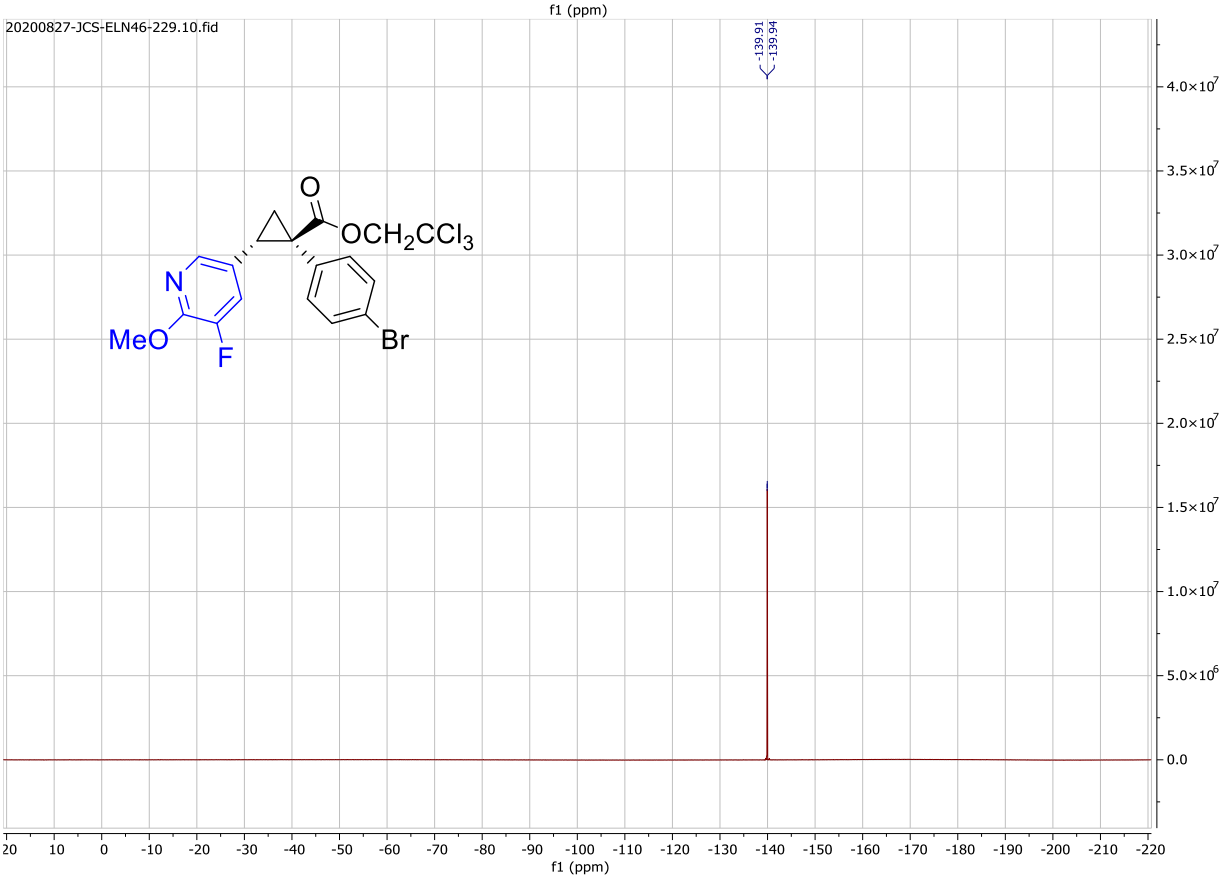
20200827-JCS-ELN46-229.10.fid
-139.91
-139.94
O
OCH2CCl3
N
MeO
F
Br
f1 (ppm)

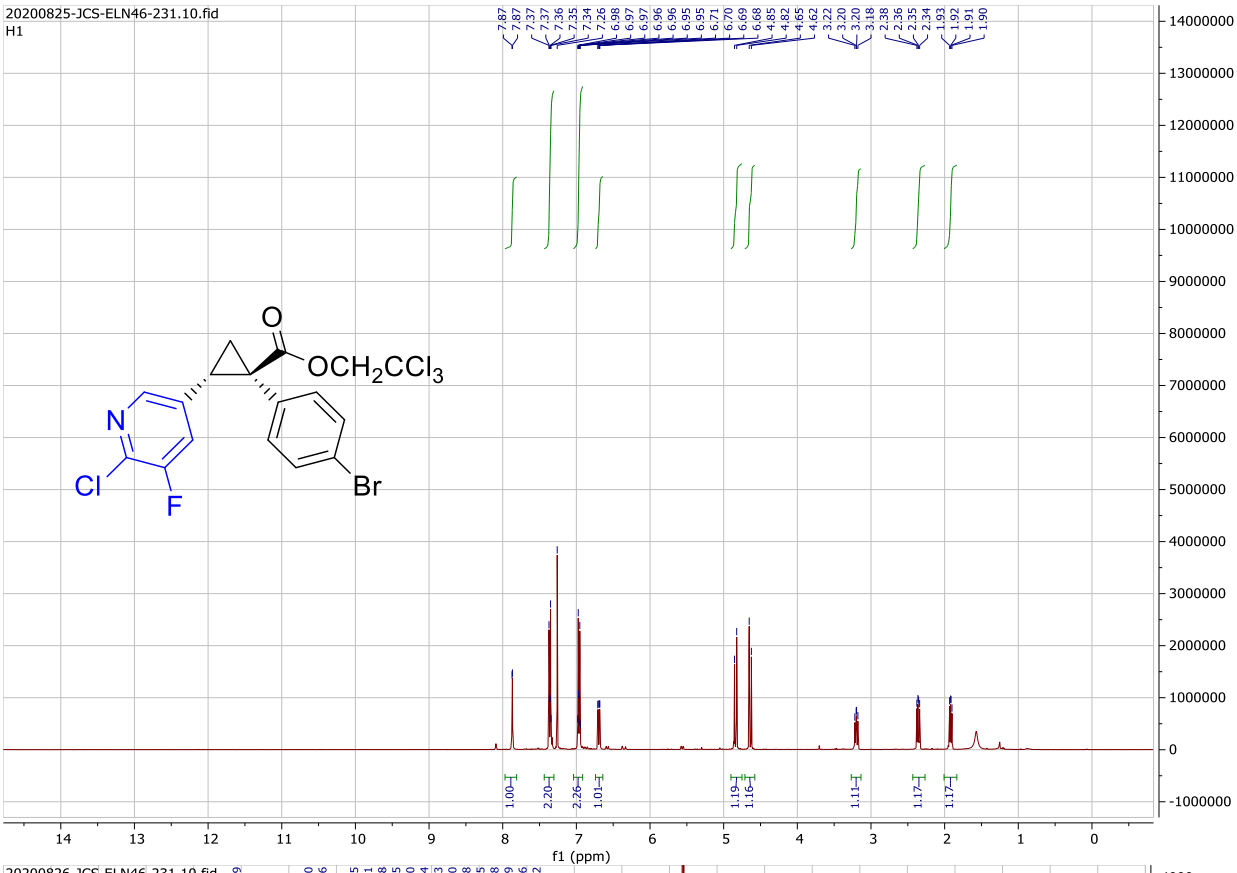
20200825-JCS-ELN46-231.10.fid
H1
7.87 7.87 7.37 7.37 7.36 7.35 7.34 7.26 6.98 6.97 6.97 6.96 6.96 6.95 6.95 6.71 6.70 6.69 6.68 4.85 4.82 4.65 4.62 3.22 3.20 3.20 3.18 2.38 2.36 2.35 2.34 1.93 1.92 1.91 1.90
O
OCH2CCl3
N
Cl
F
Br
1.00 2.20 2.26 1.01 1.19 1.16 1.11 1.17 1.17
f1 (ppm)

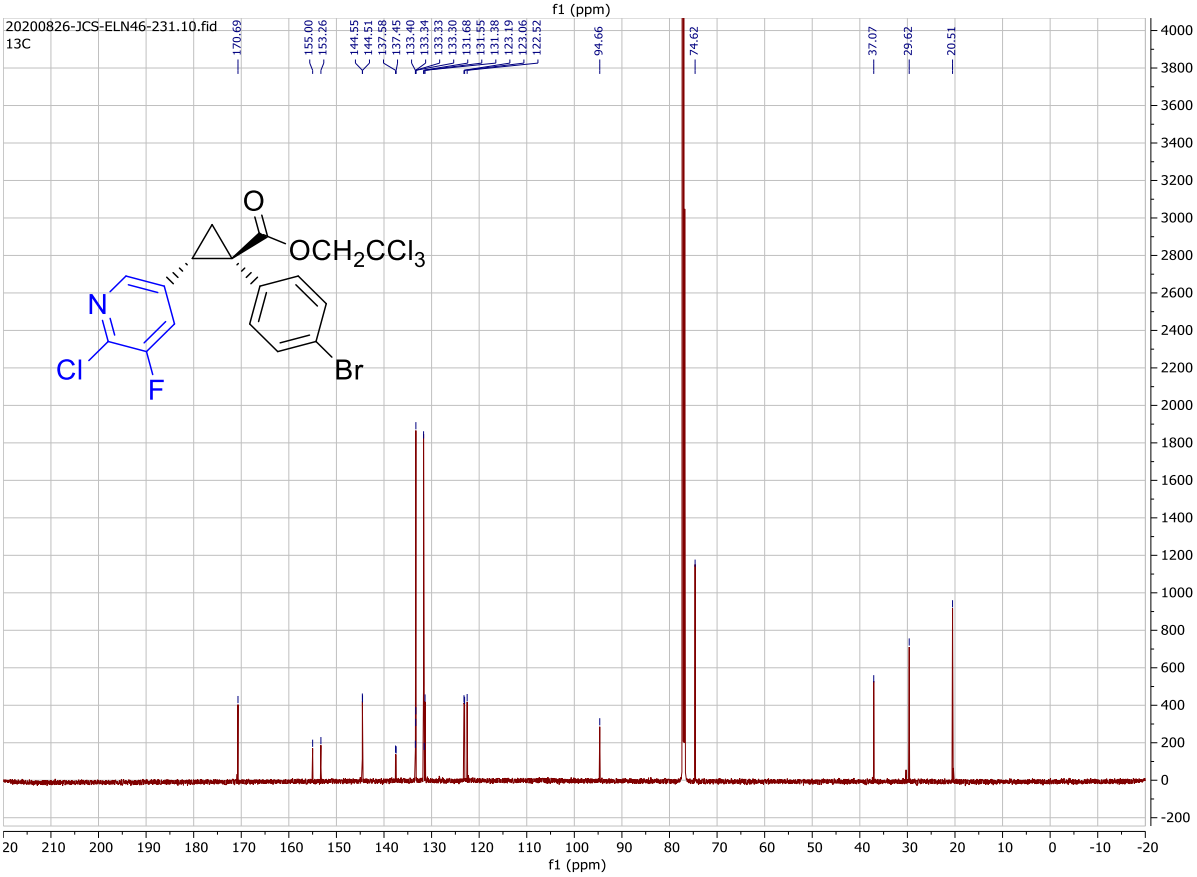
20200826-JCS-ELN46-231.10.fid
13C
170.69 155.00 153.26 144.55 144.51 137.58 137.45 133.40 133.34 133.33 133.30 131.68 131.55 131.38 123.19 123.06 122.52 94.66 74.62 37.07 29.62 20.51
O
OCH2CCl3
N
Cl
F
Br
f1 (ppm)

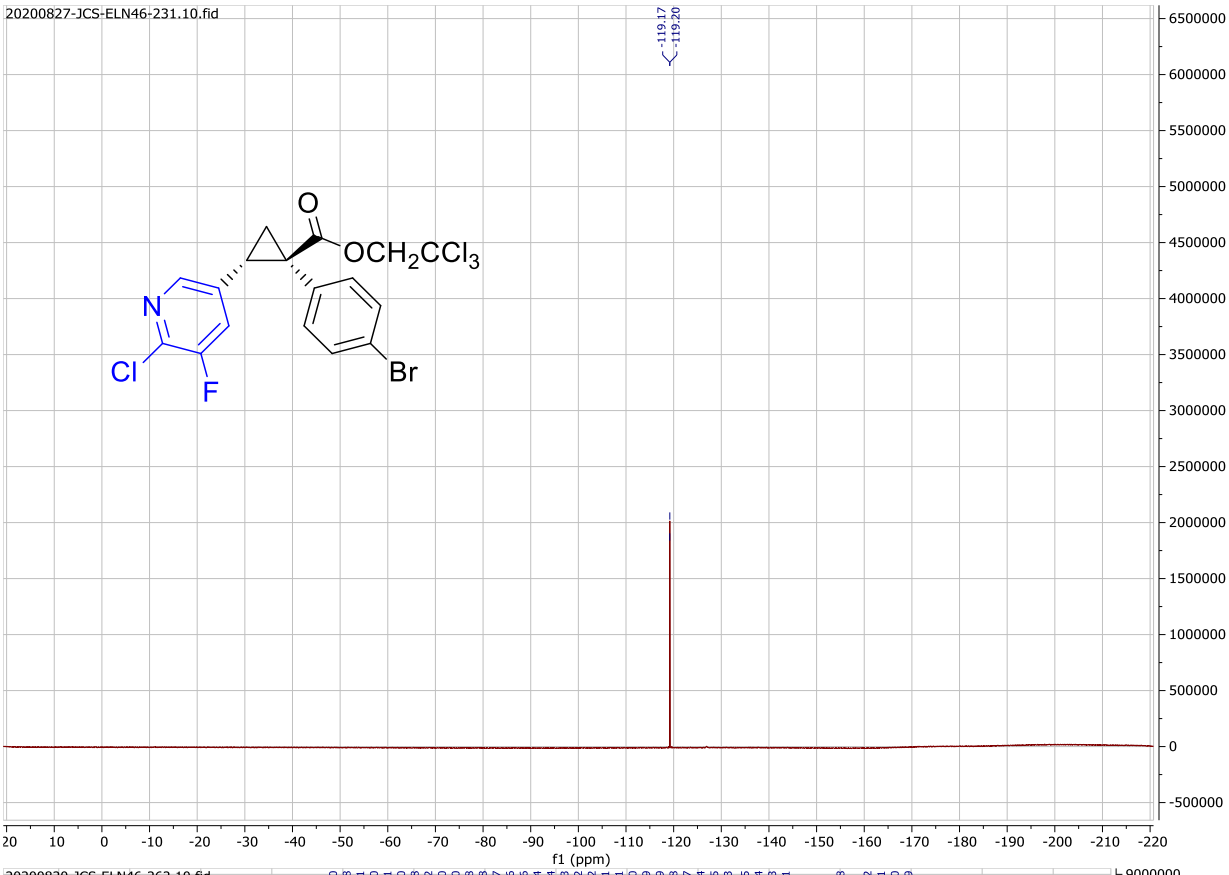
20200827-JCS-ELN46-231.10.fid
-119.17
-119.20
O
OCH2CCl3
N
Cl
F
Br
f1 (ppm)

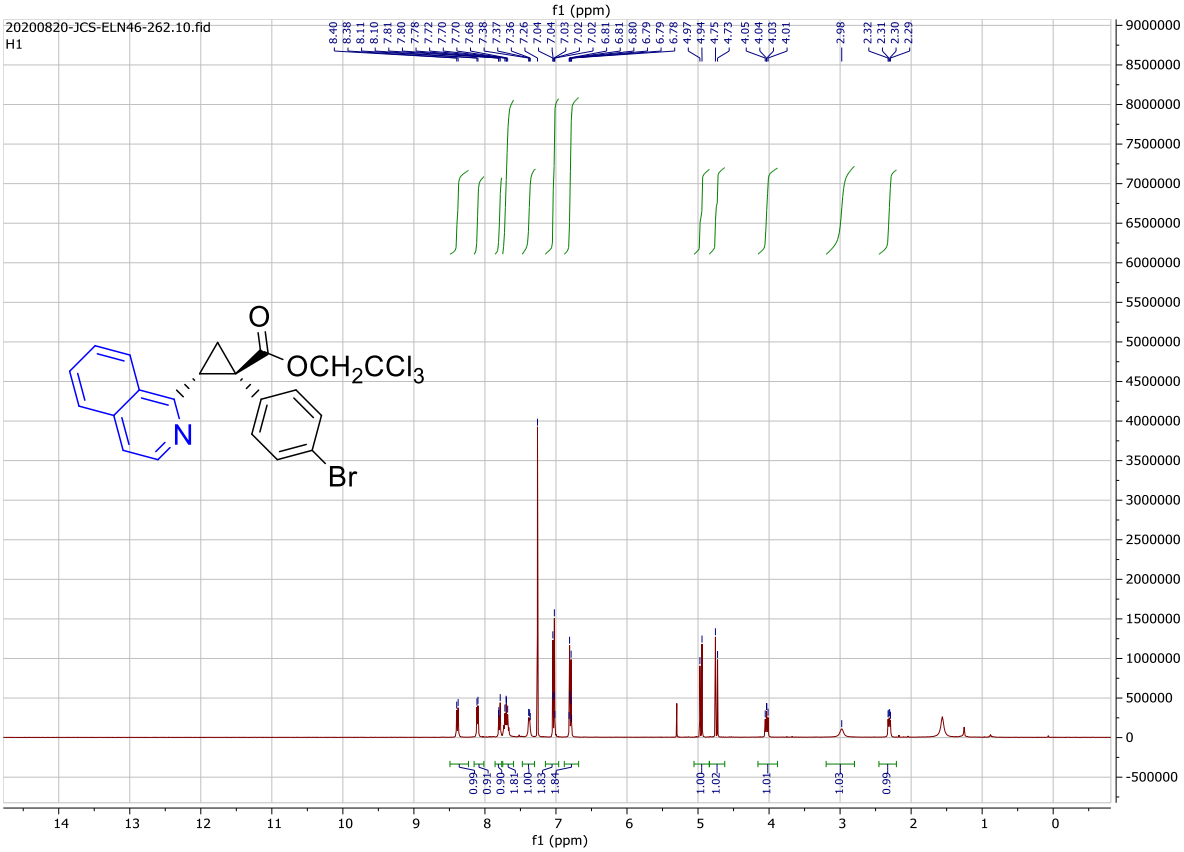
20200820-JCS-ELN46-262.10.fid
H1
8.40
8.38
8.11
8.10
7.81
7.80
7.78
7.72
7.70
7.70
7.70
7.68
7.38
7.37
7.37
7.36
7.04
7.04
7.03
7.02
7.02
6.81
6.81
6.80
6.79
6.79
6.78
4.97
4.94
4.75
4.73
4.05
4.04
4.03
4.01
2.98
2.32
2.31
2.30
2.29
O
OCH2CCl3
N
Br
0.99
0.91
0.90
1.81
1.00
1.83
1.86
1.00
1.02
1.01
1.03
0.99
f1 (ppm)

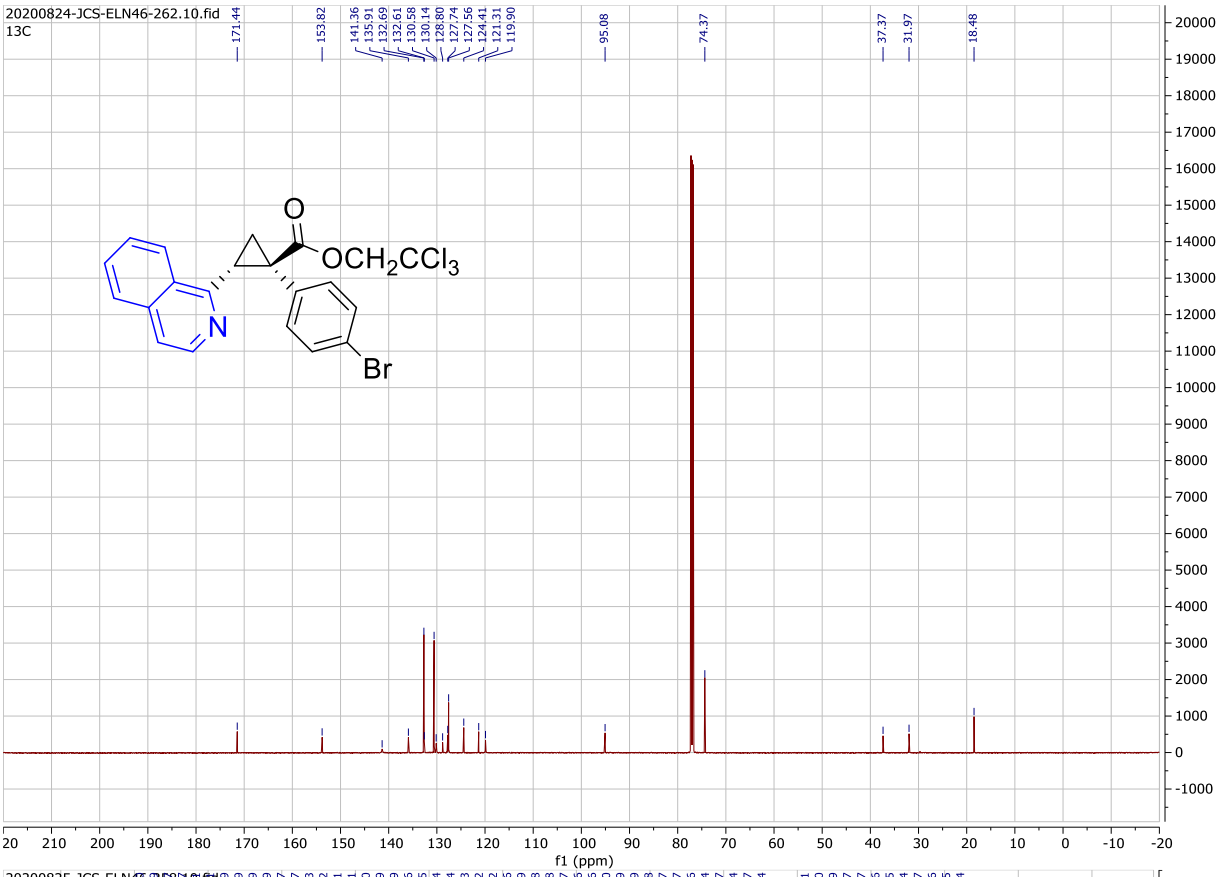
20200824-JCS-ELN46-262.10.fid
13C
171.44
153.82
141.36
135.91
132.69
132.61
130.58
130.14
128.80
127.74
127.56
124.41
121.31
119.90
95.08
74.37
37.37
31.97
18.48
O
OCH2CCl3
N
Br
f1 (ppm)

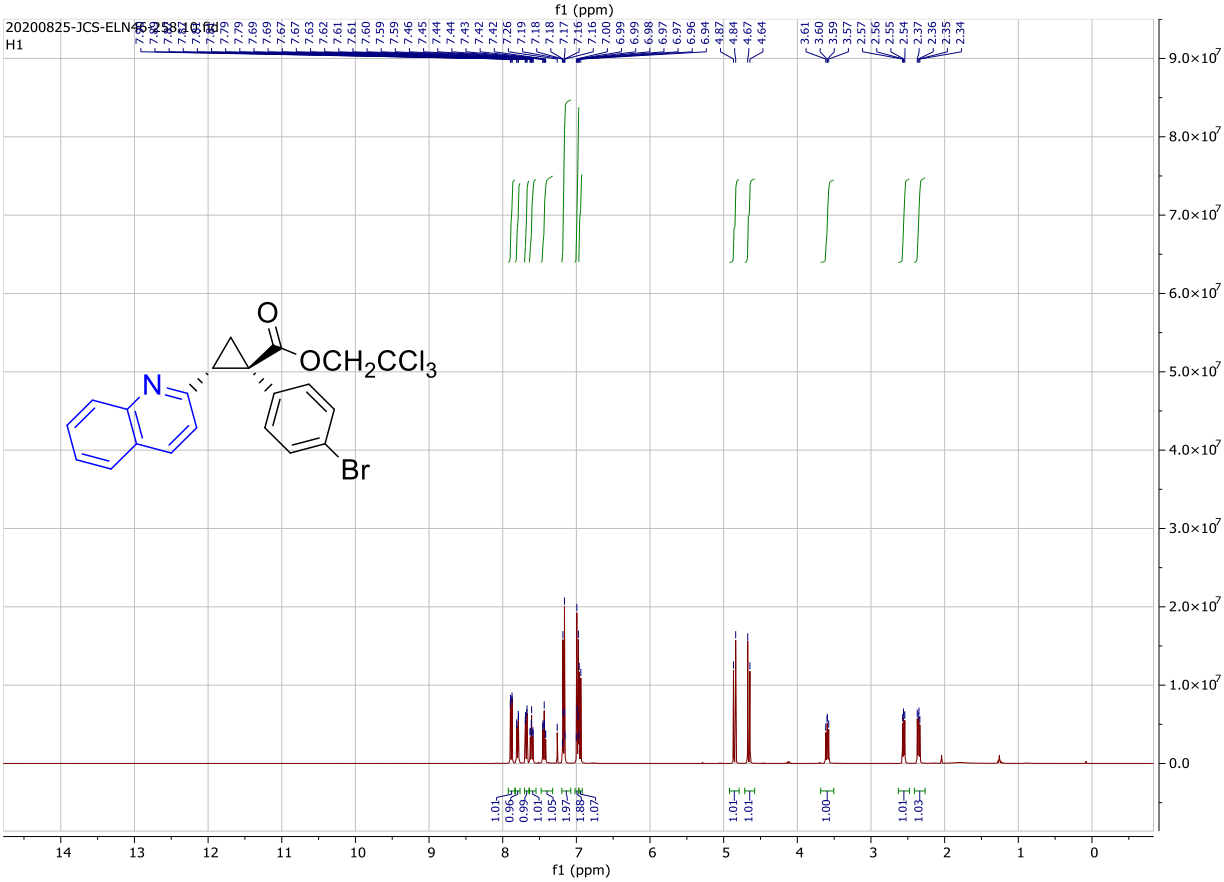
20200825-JCS-ELN46-258.10.fid
H1
O
OCH2CCl3
N
Br
f1 (ppm)

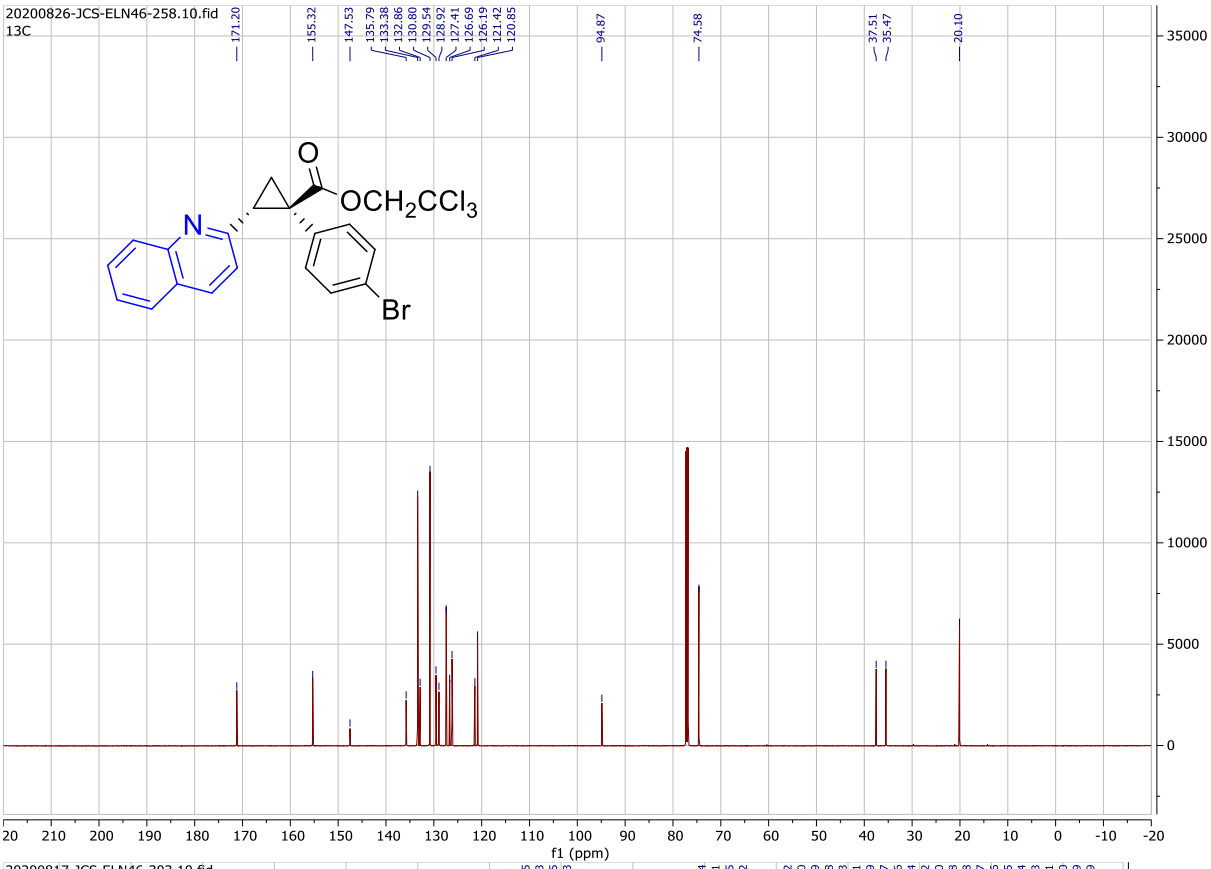
20200826-JCS-ELN46-258.10.fid
13C
171.20
155.32
147.53
135.79
133.38
132.86
130.80
129.54
128.92
127.41
126.69
126.19
121.42
120.85
94.87
74.58
37.51
35.47
20.10
O
OCH2CCl3
N
Br
f1 (ppm)

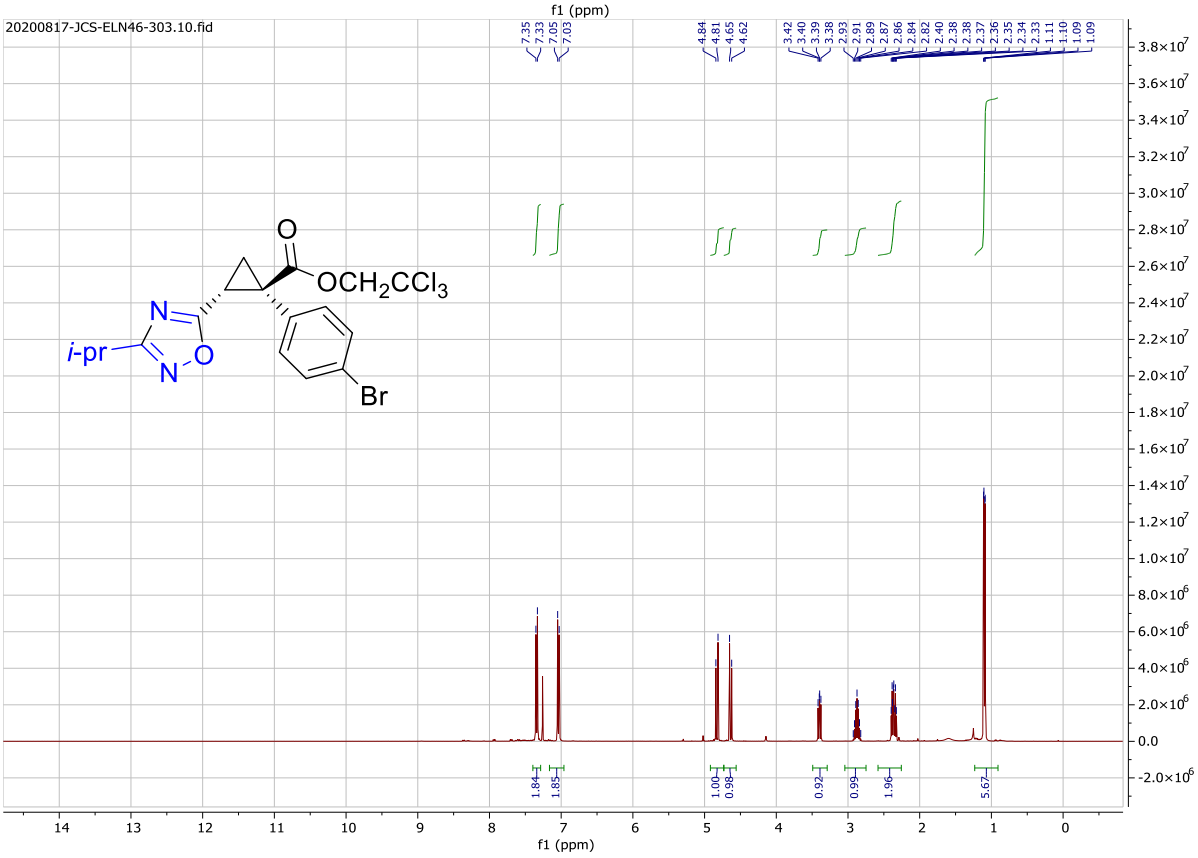
20200817-JCS-ELN46-303.10.fid
7.35
7.33
7.05
7.03
4.84
4.81
4.65
4.62
3.42
3.40
3.39
3.38
2.93
2.91
2.89
2.87
2.86
2.84
2.82
2.40
2.38
2.38
2.37
2.36
2.35
2.34
2.33
1.11
1.10
1.09
1.09
O
OCH2CCl3
N
i-pr
N
O
Br
1.84
1.85
1.00
0.98
0.92
0.99
1.96
5.67
f1 (ppm)

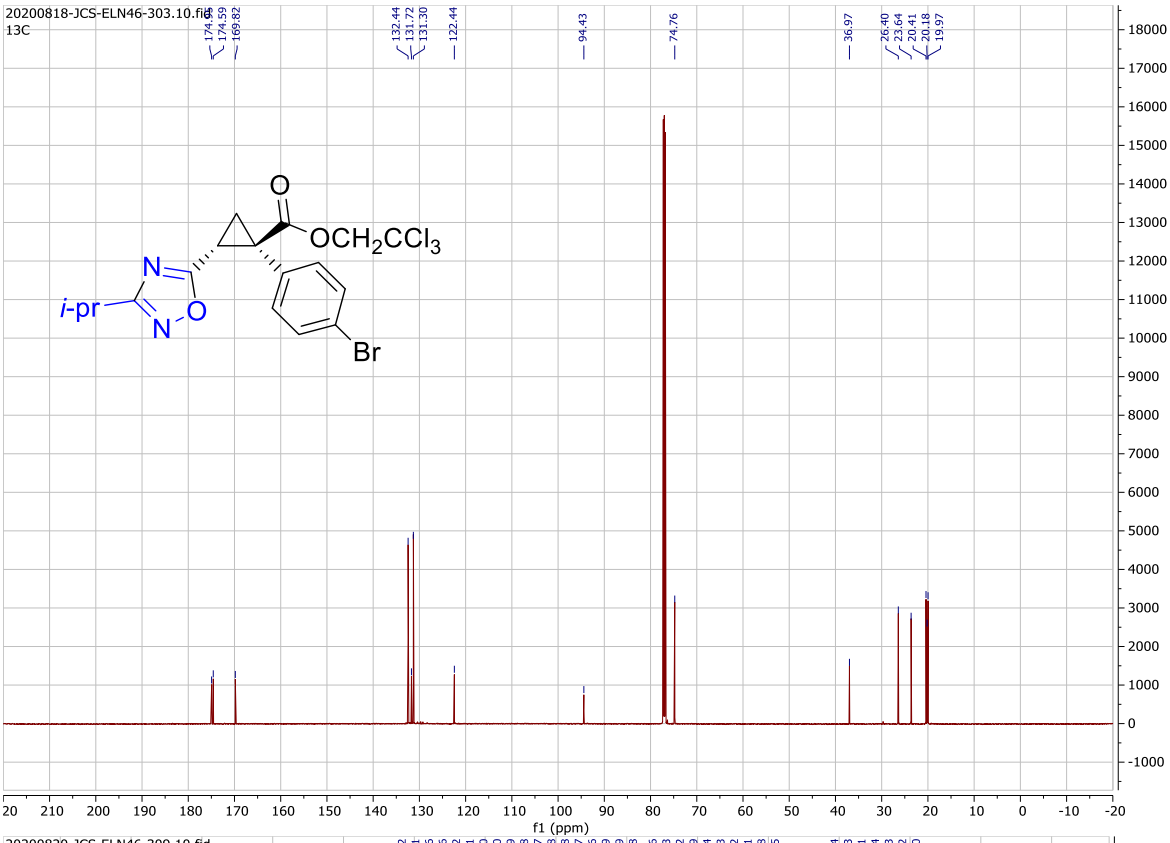
20200818-JCS-ELN46-303.10.fid
13C
174.48
174.59
169.82
132.44
131.72
131.30
122.44
94.43
74.76
36.97
26.40
23.64
20.41
20.18
19.97
O
OCH2CCl3
N
N
O
i-pr
Br
f1 (ppm)

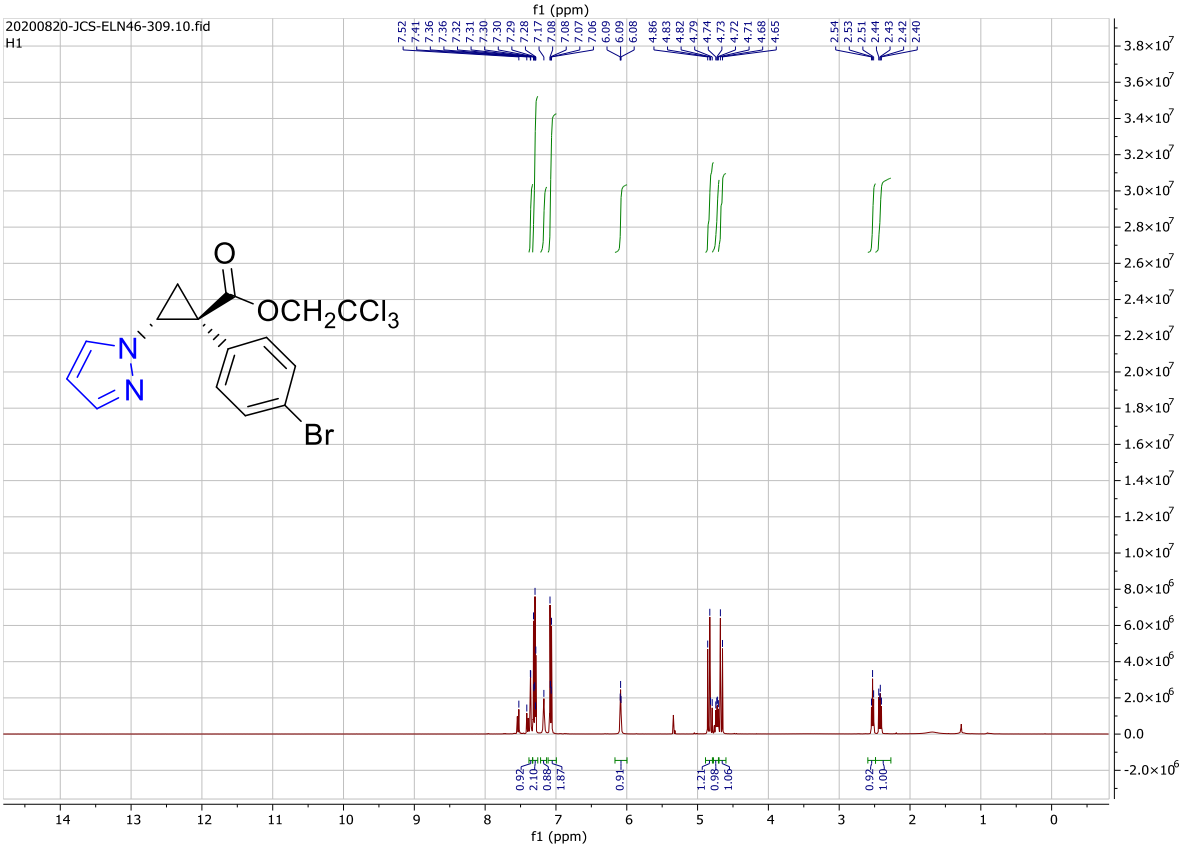
20200820-JCS-ELN46-309.10.fid
H1
7.52
7.41
7.36
7.36
7.32
7.31
7.30
7.30
7.29
7.28
7.17
7.08
7.08
7.07
7.06
6.09
6.09
6.08
4.86
4.83
4.82
4.79
4.74
4.74
4.73
4.72
4.71
4.68
4.65
2.54
2.53
2.51
2.44
2.43
2.42
2.40
0.92
2.10
0.88
1.87
0.91
1.21
0.98
1.06
0.92
1.00
O
OCH2CCl3
N
N
Br
f1 (ppm)

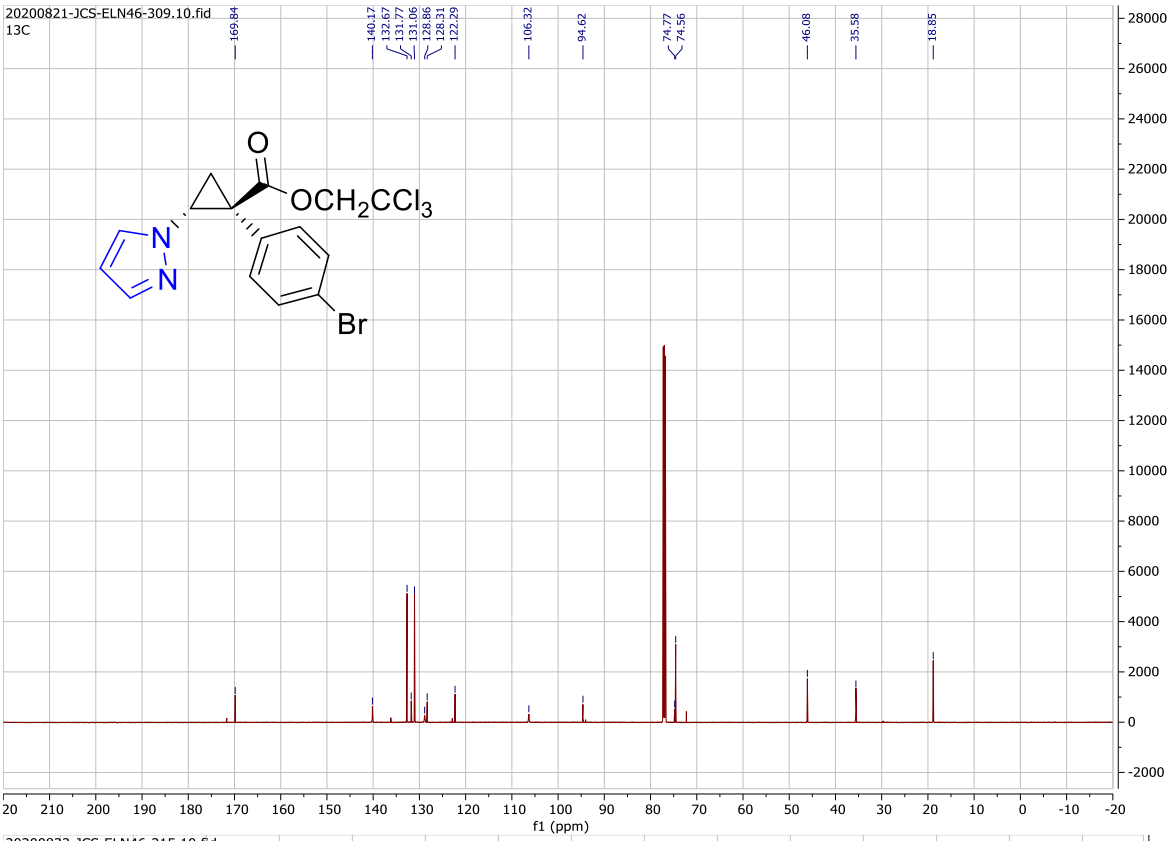
20200821-JCS-ELN46-309.10.fid
13C
169.84
140.17
132.67
131.77
131.06
128.86
128.31
122.29
106.32
94.62
74.77
74.56
46.08
35.58
18.85
O
OCH2CCl3
N
N
Br
f1 (ppm)

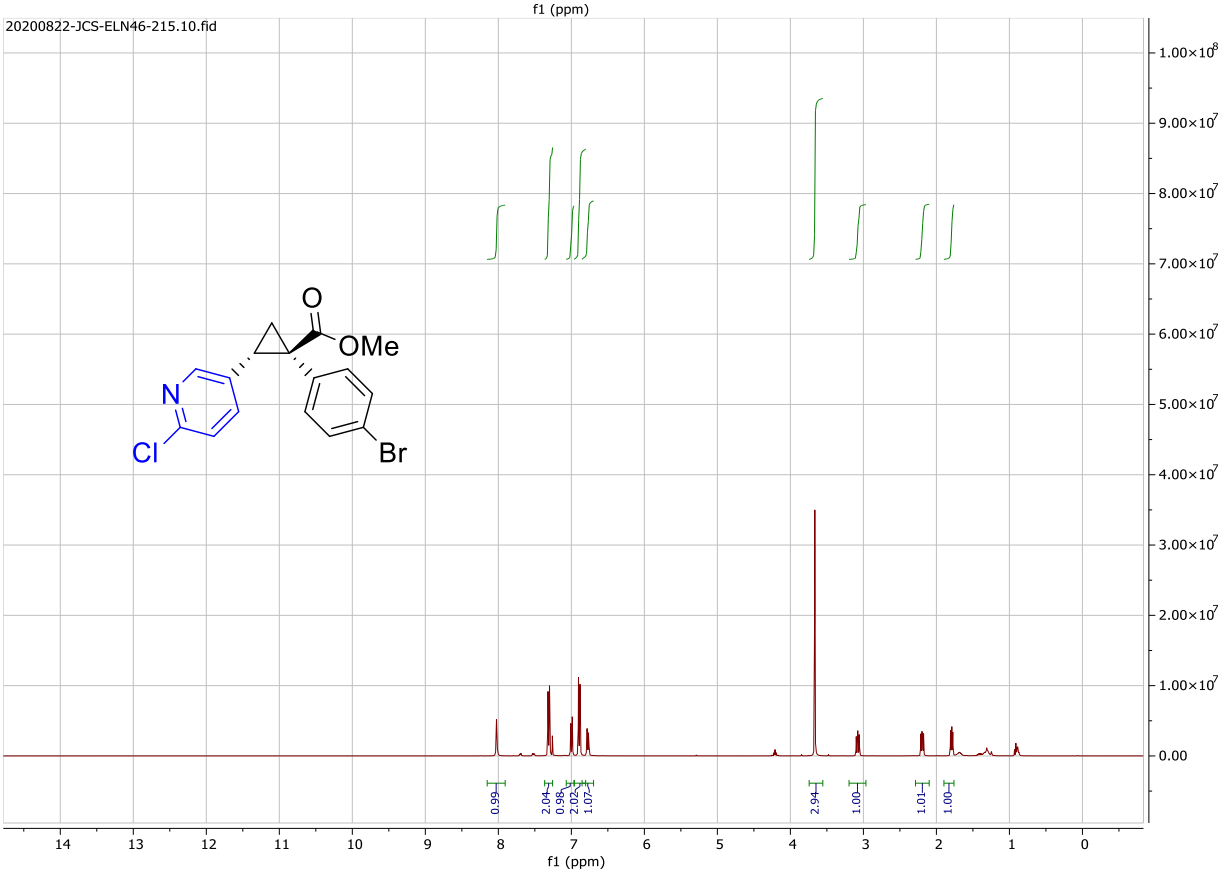
20200822-JCS-ELN46-215.10.fid
O
OMe
N
Cl
Br
0.99
2.04
0.98
2.02
1.07
2.94
1.00
1.01
1.00
f1 (ppm)

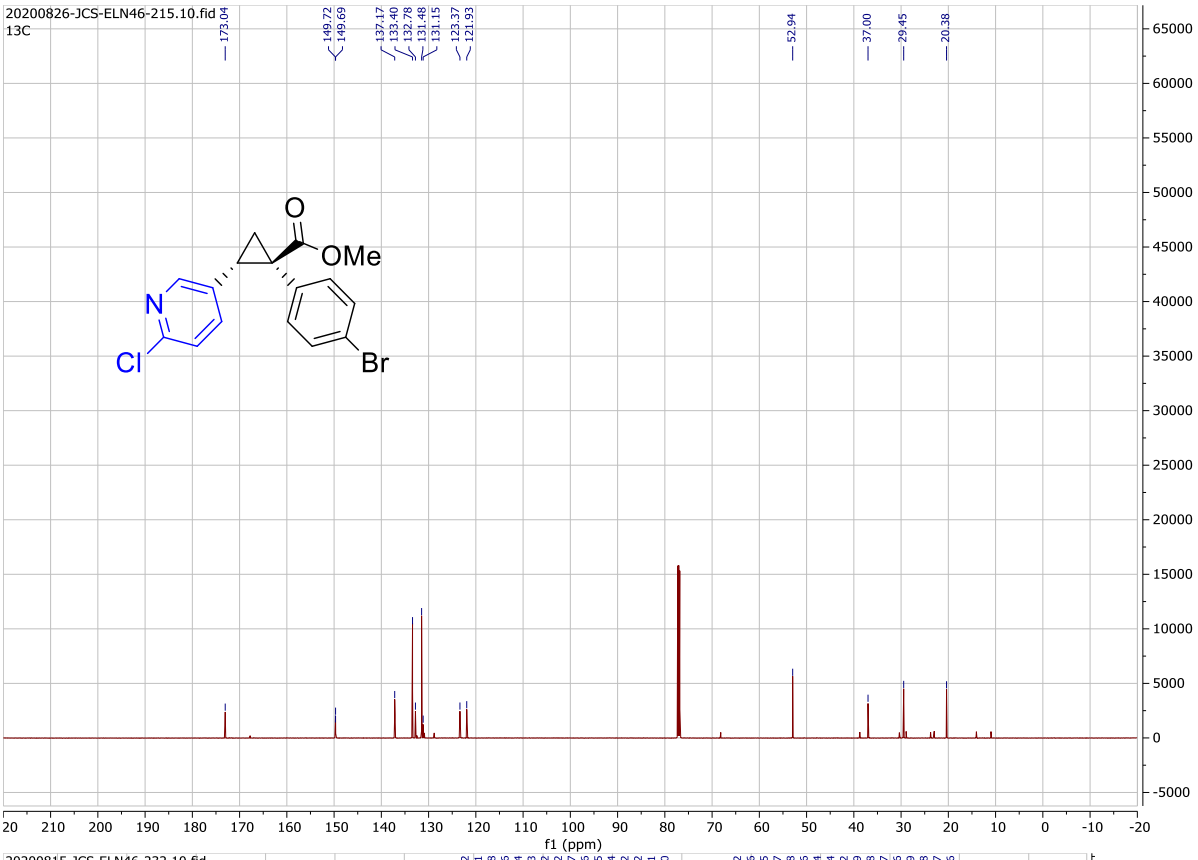
20200826-JCS-ELN46-215.10.fid
13C
173.04
149.72
149.69
137.17
133.40
132.78
131.48
131.15
123.37
121.93
52.94
37.00
29.45
20.38
O
OMe
N
Cl
Br
f1 (ppm)

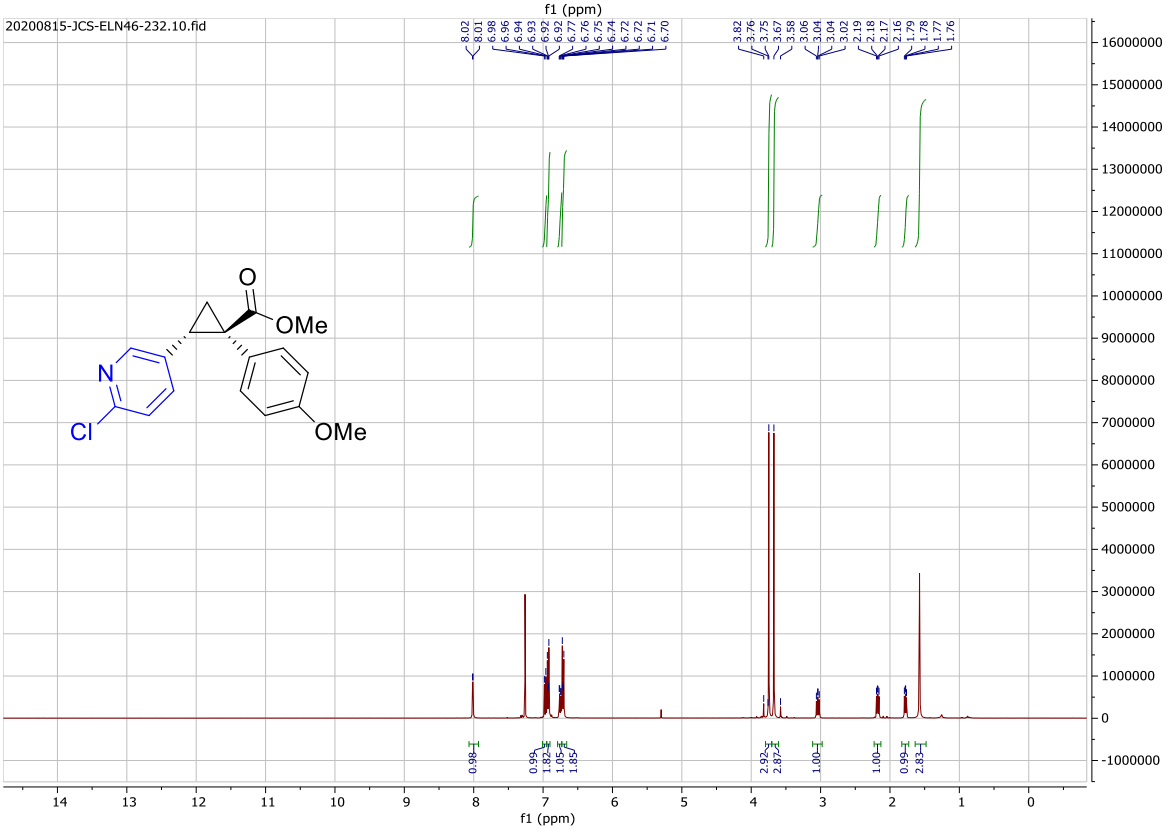
20200815-JCS-ELN46-232.10.fid
8.02
8.01
6.98
6.96
6.94
6.93
6.92
6.92
6.77
6.76
6.75
6.74
6.72
6.72
6.71
6.70
3.82
3.76
3.75
3.67
3.58
3.06
3.04
3.02
2.19
2.18
2.17
2.16
1.79
1.78
1.77
1.76
O
OMe
N
Cl
OMe
0.98
0.99
1.82
1.05
1.85
2.92
2.87
1.00
1.00
0.99
2.83
f1 (ppm)

20200123-Bo-ELN-36-108-C.10.fid —

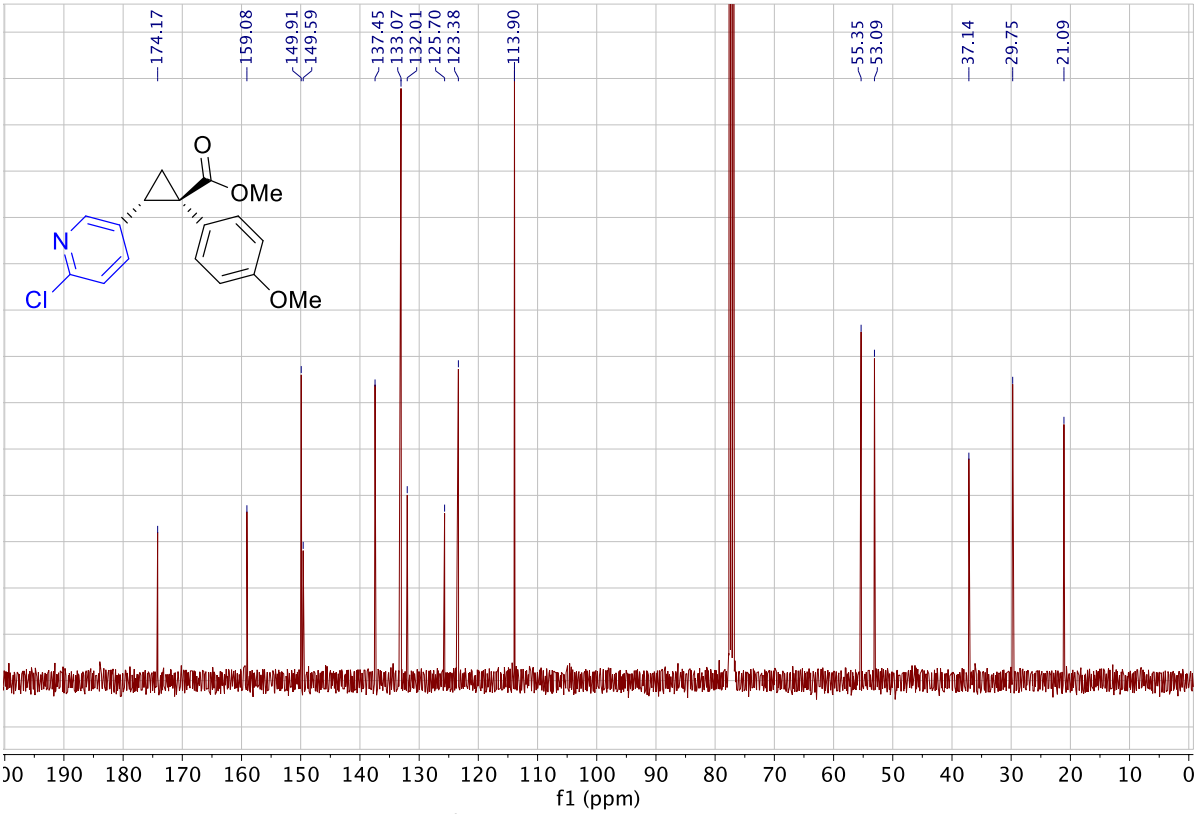

2020-1-15-Bo-ELN-36-102 — Xun-3-156-crude-INOVA600 —

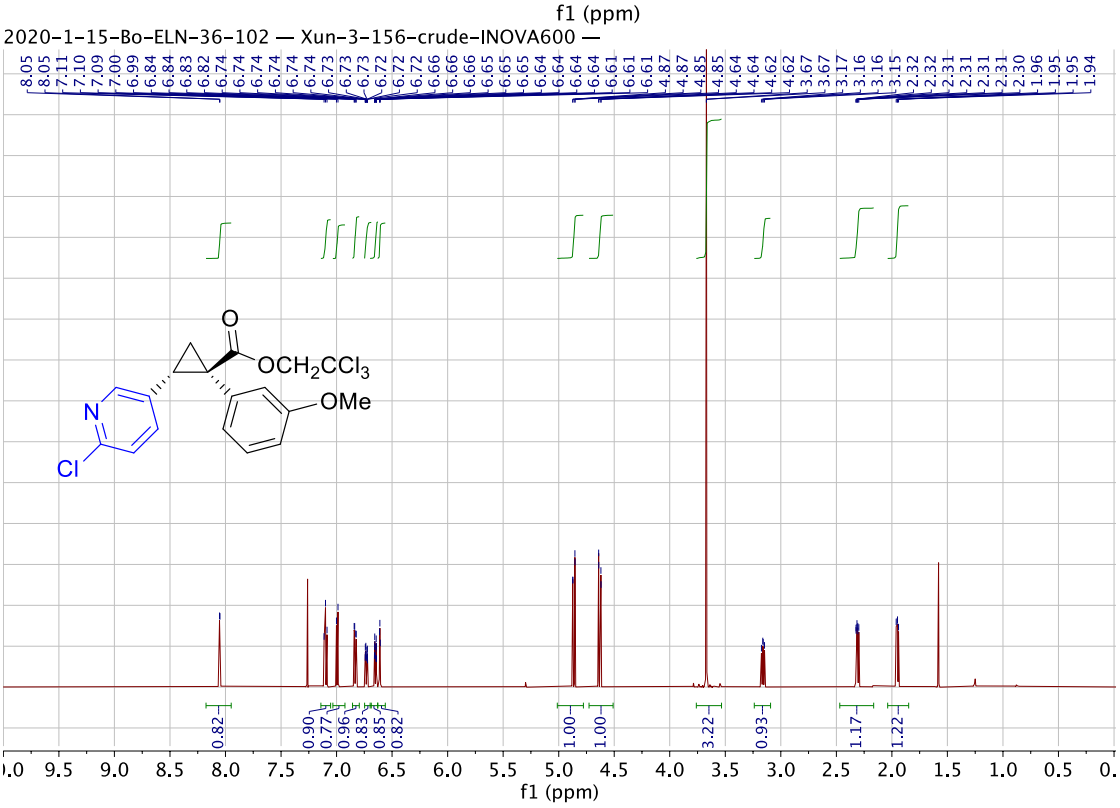

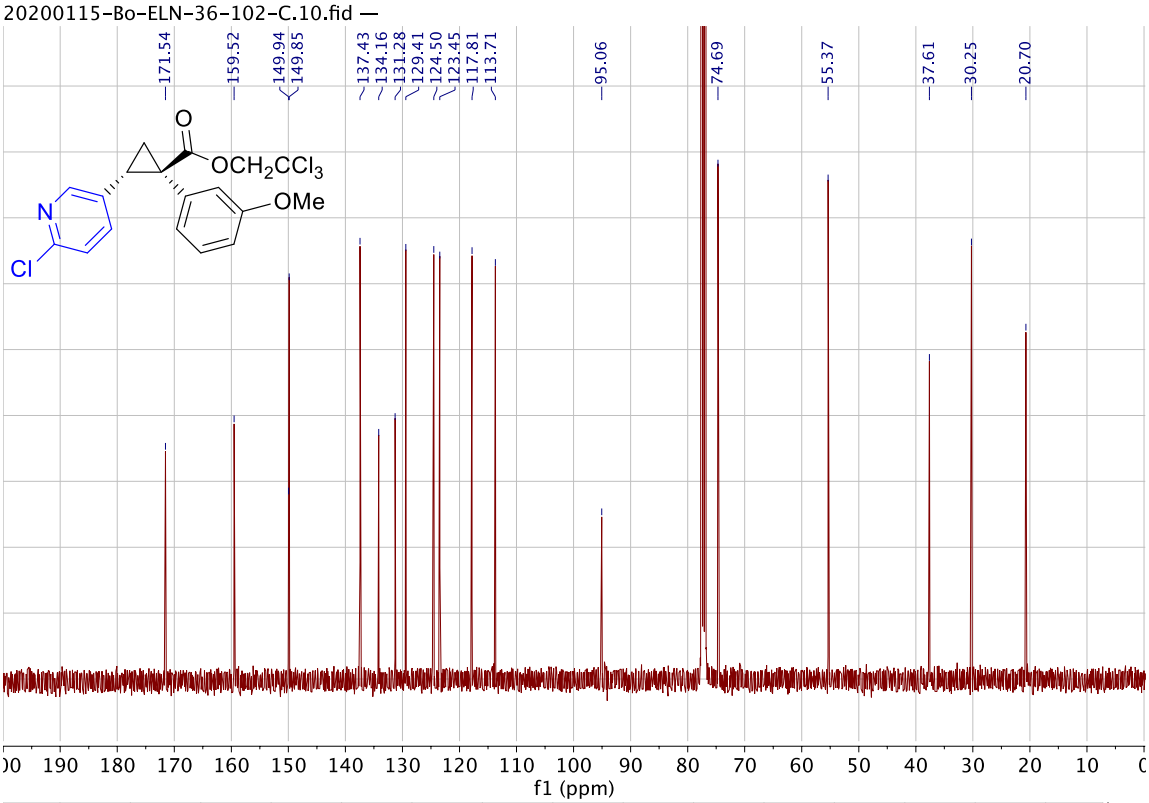
20200115-Bo-ELN-36-102-C.10.fid
171.54
159.52
149.94
149.85
137.43
134.16
131.28
129.41
124.50
123.45
117.81
113.71
95.06
74.69
55.37
37.61
30.25
20.70
O
OCH2CCl3
OMe
N
Cl
f1 (ppm)

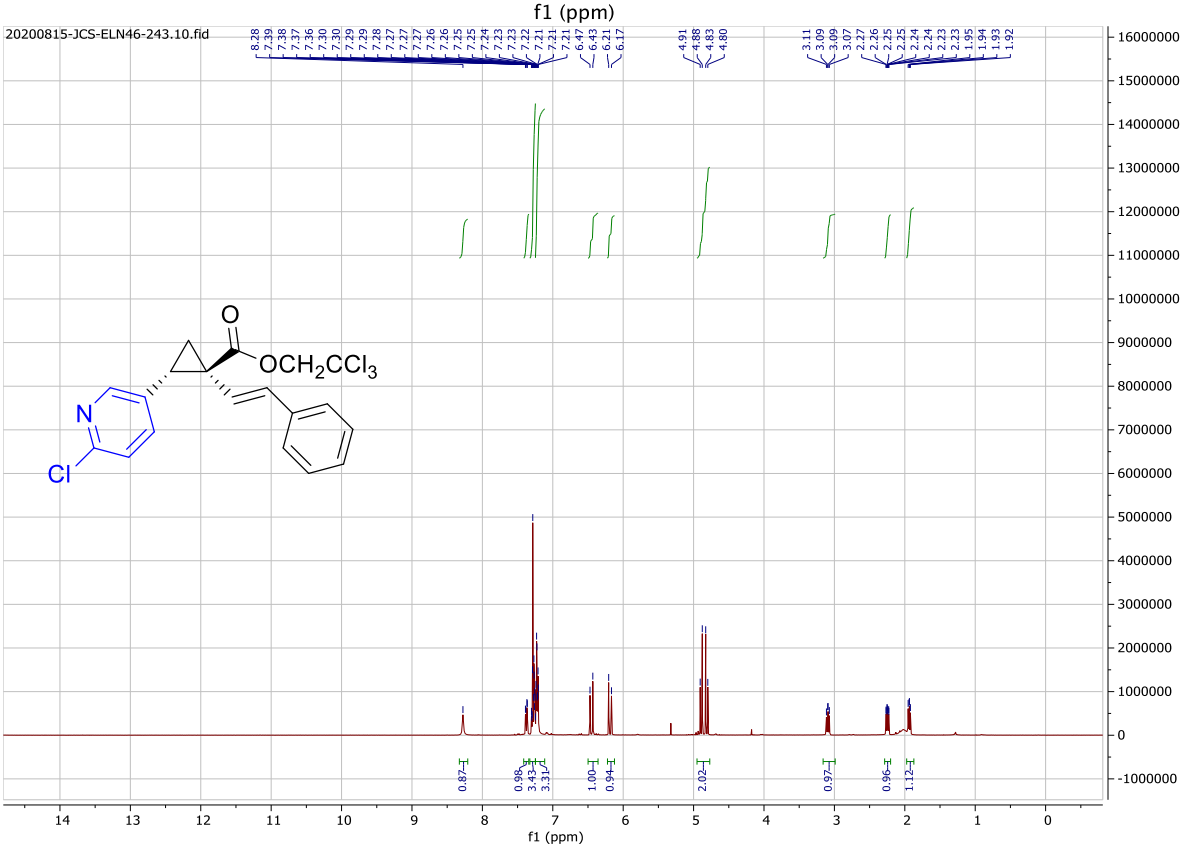
20200815-JCS-ELN46-243.10.fid
O
OCH2CCl3
N
Cl
f1 (ppm)

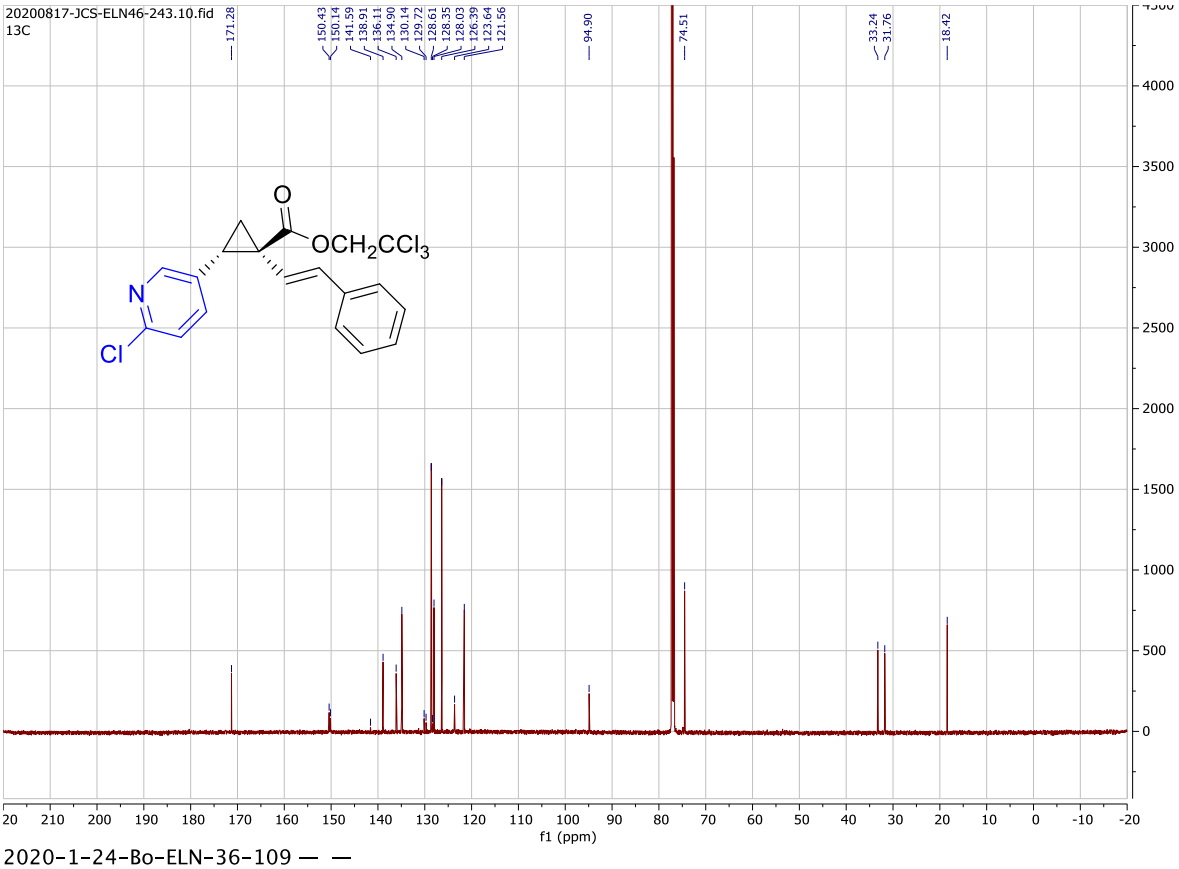
20200817-JCS-ELN46-243.10.fid
13C
171.28
150.43
150.14
141.59
138.91
136.11
134.90
130.14
129.72
128.61
128.35
128.03
126.39
123.64
121.56
94.90
74.51
33.24
31.76
18.42
O
OCH2CCl3
N
Cl
f1 (ppm)

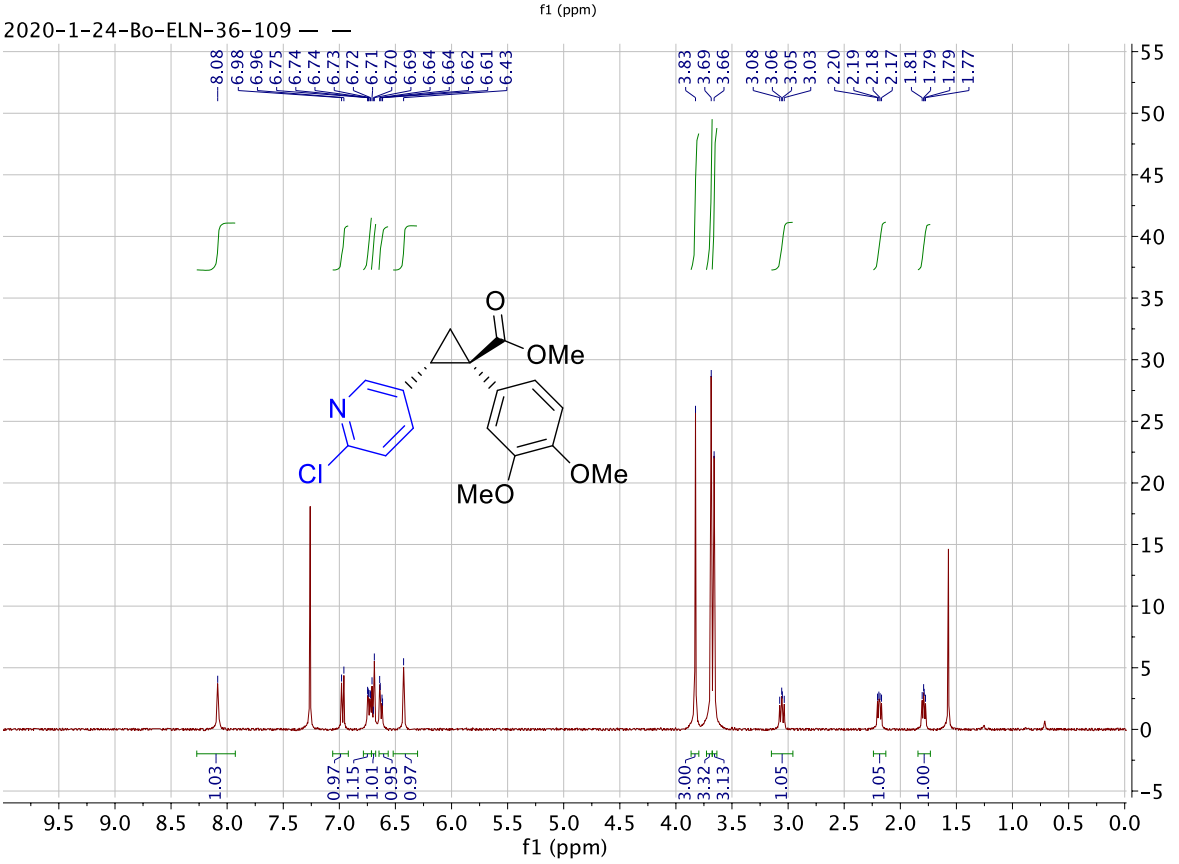
2020-1-24-Bo-ELN-36-109
8.08
6.98
6.96
6.75
6.74
6.74
6.73
6.72
6.71
6.70
6.69
6.64
6.64
6.62
6.61
6.43
3.83
3.69
3.66
3.08
3.06
3.05
3.03
2.20
2.19
2.18
2.17
1.81
1.79
1.79
1.77
1.03
0.97
1.15
1.01
0.95
0.97
3.00
3.32
3.13
1.05
1.05
1.00
O
OMe
N
Cl
MeO
OMe
f1 (ppm)

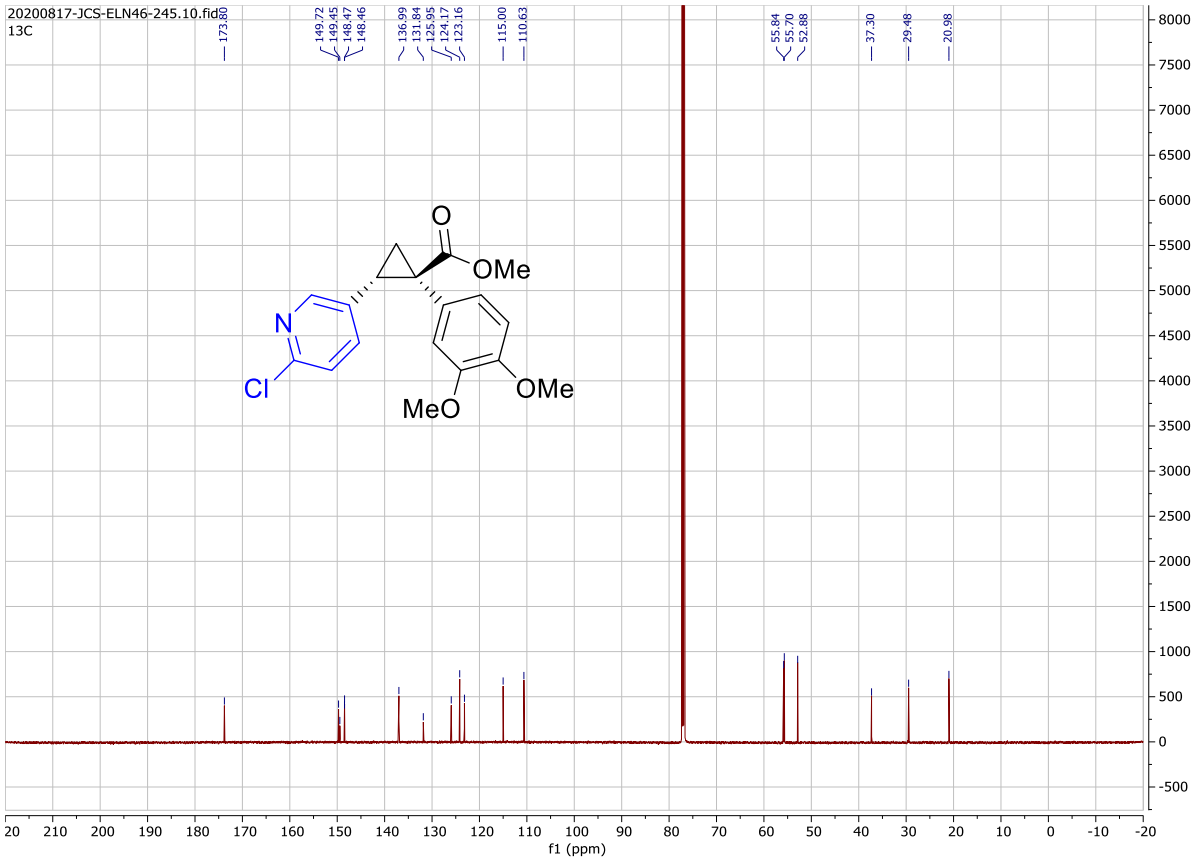

2019-7-11-ELN-0036-0014 — Silica plugged —

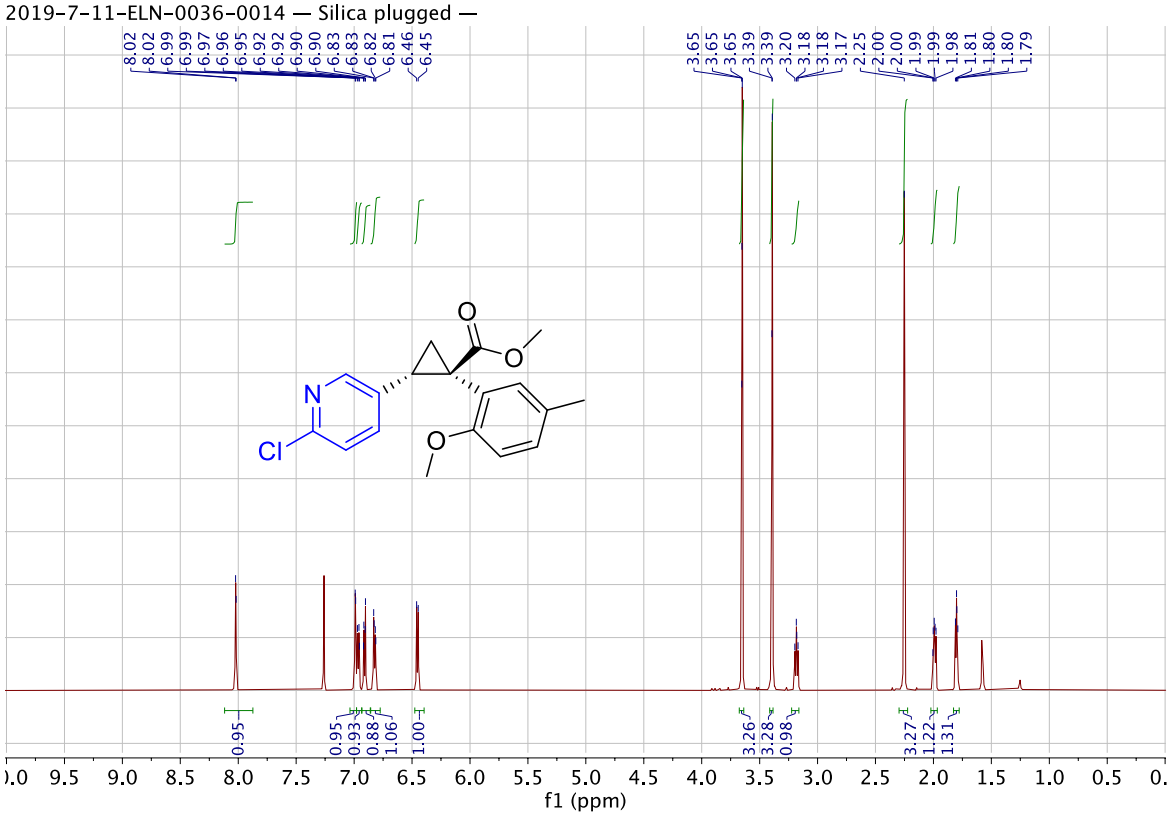

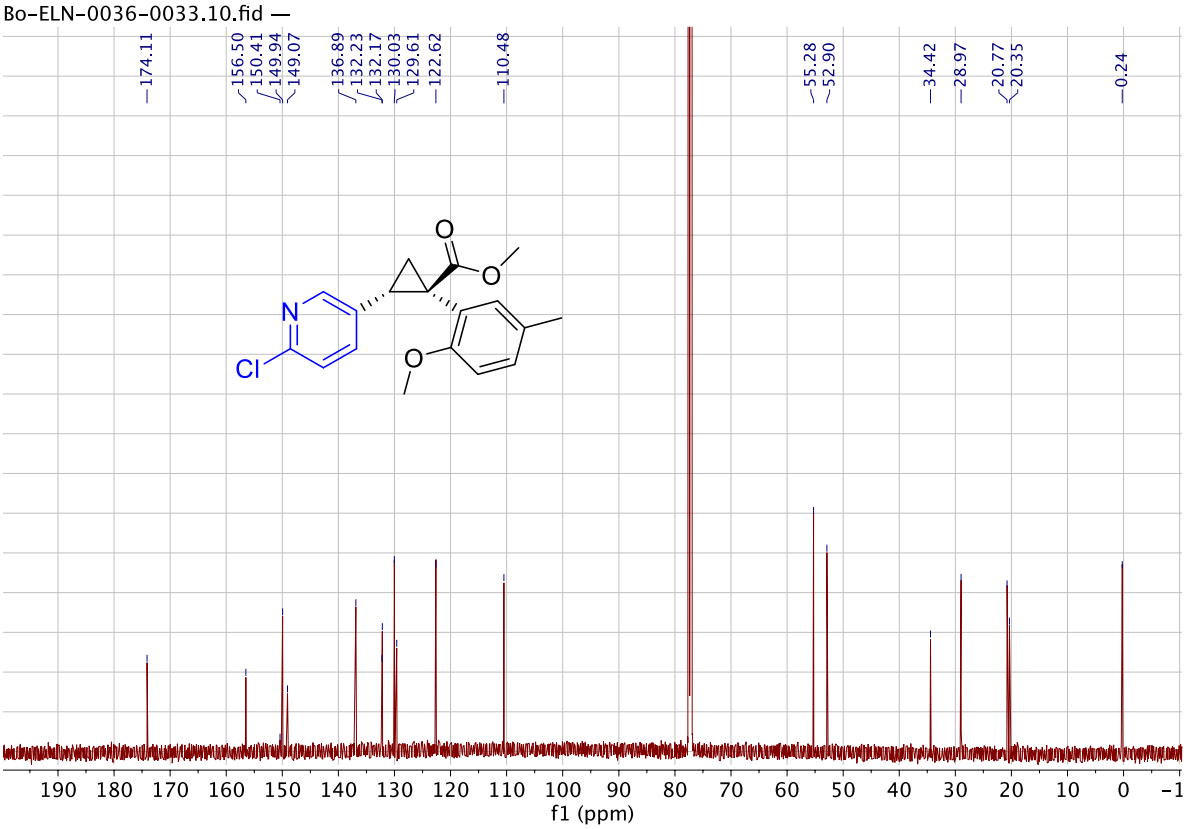
Bo-ELN-0036-0033.10.fid
174.11
156.50
150.41
149.94
149.07
136.89
132.23
132.17
130.03
129.61
122.62
110.48
55.28
52.90
34.42
28.97
20.77
20.35
0.24
f1 (ppm)

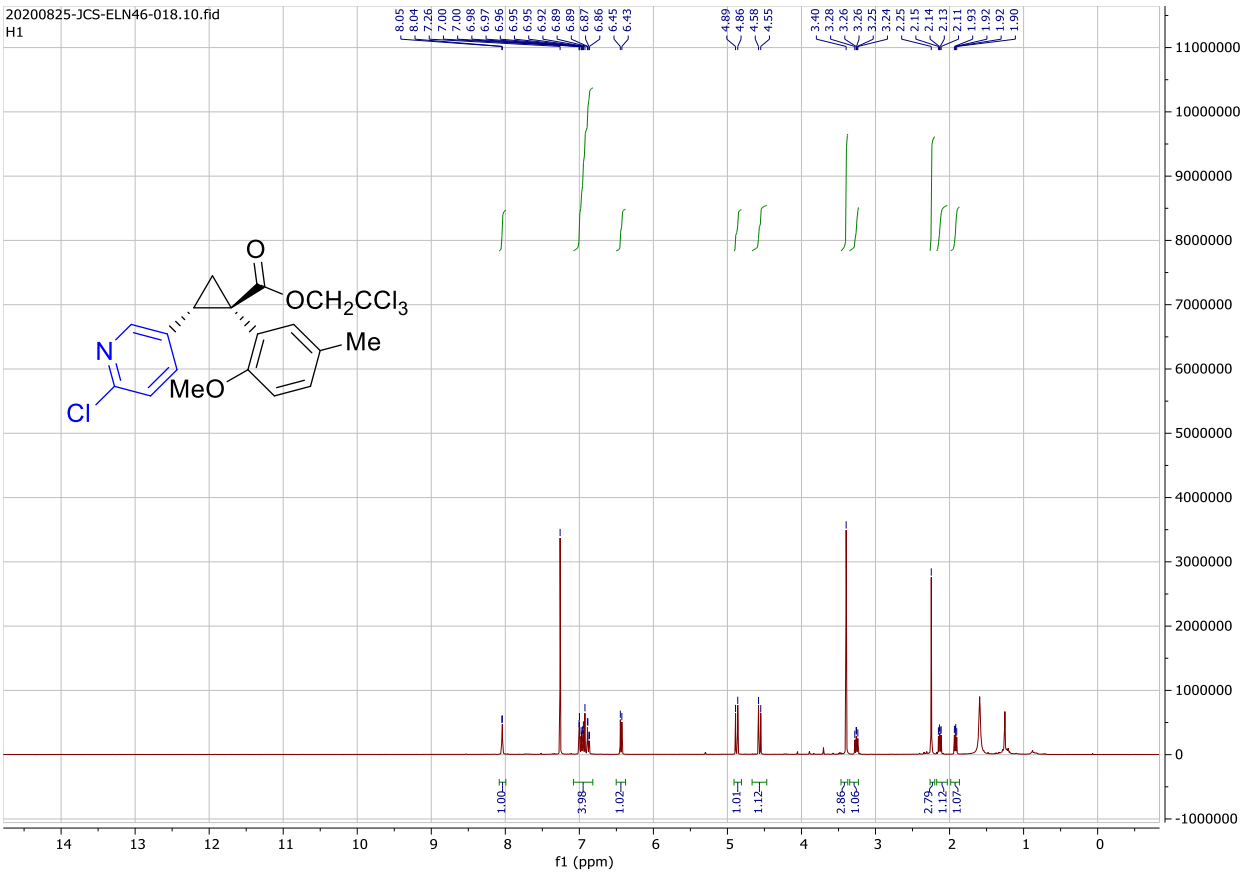
20200825-JCS-ELN46-018.10.fid
H1
f1 (ppm)

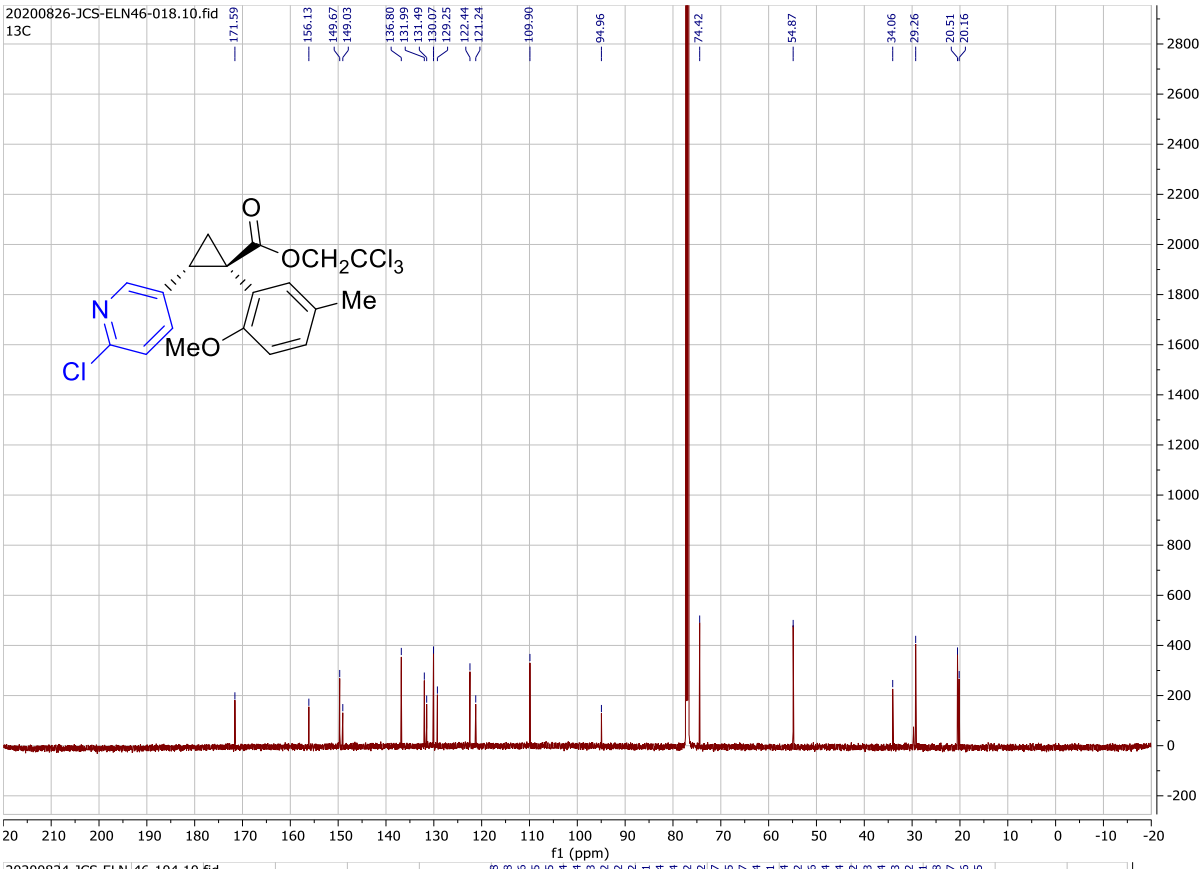
20200826-JCS-ELN46-018.10.fid
13C
171.59
156.13
149.67
149.03
136.80
131.99
131.49
130.07
129.25
122.44
121.24
109.90
94.96
74.42
54.87
34.06
29.26
20.51
20.16
O
OCH2CCl3
Me
N
MeO
Cl
f1 (ppm)

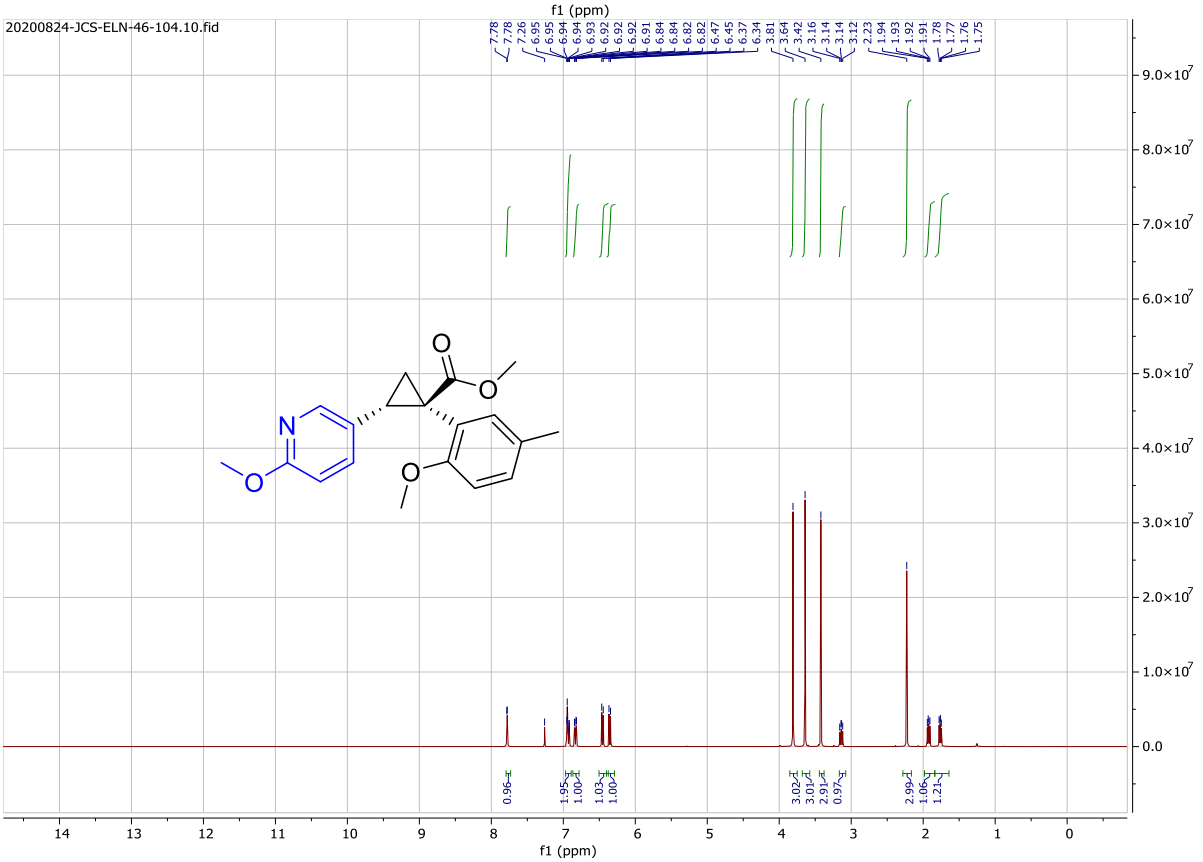
20200824-JCS-ELN-46-104.10.fid
7.78
7.26
6.95
6.94
6.93
6.92
6.91
6.84
6.82
6.47
6.45
6.37
6.34
3.81
3.64
3.42
3.16
3.14
3.12
2.23
1.94
1.93
1.92
1.91
1.78
1.77
1.76
1.75
O
O
N
O
O
0.96
1.95
1.00
1.03
1.00
3.02
3.01
2.91
0.97
2.99
1.06
1.21
f1 (ppm)

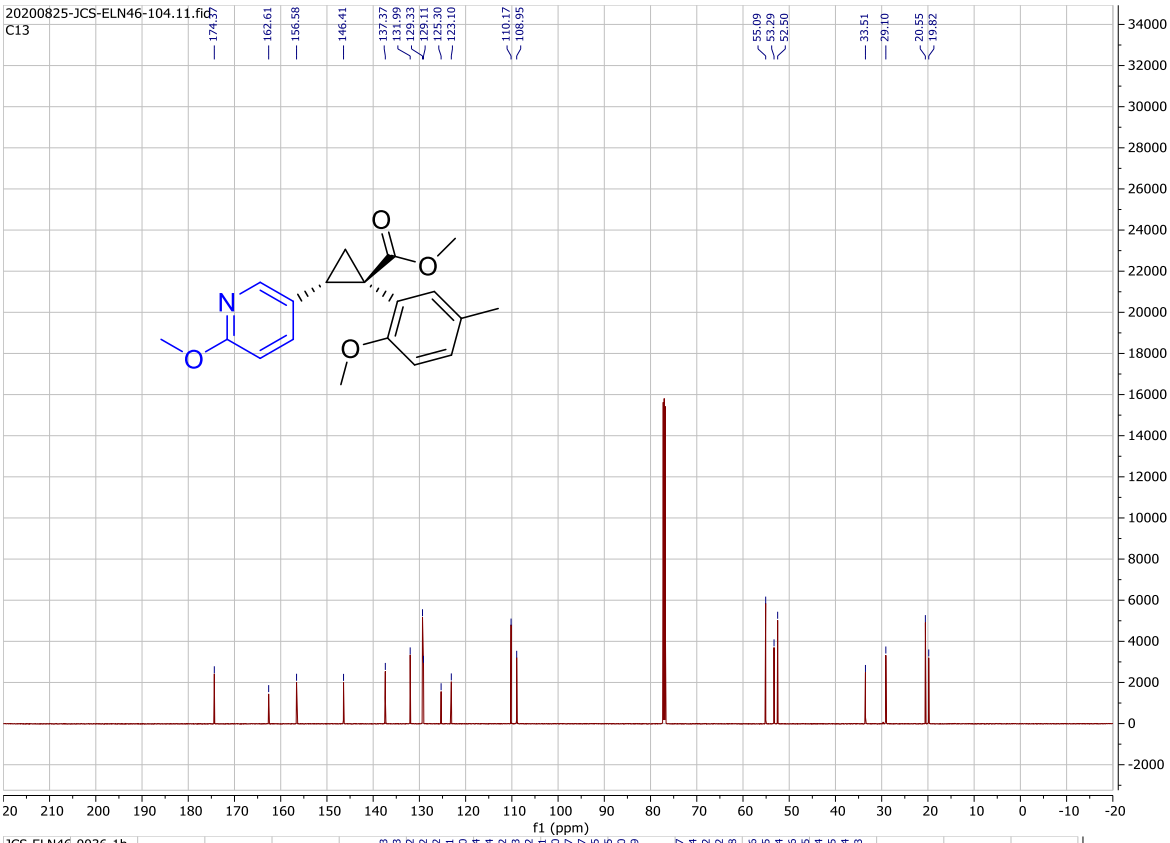
20200825-JCS-ELN46-104.11.fid
C13
174.37
162.61
156.58
146.41
137.37
131.99
129.33
129.11
125.30
123.10
110.17
108.95
55.09
53.29
52.50
33.51
29.10
20.55
19.82
f1 (ppm)

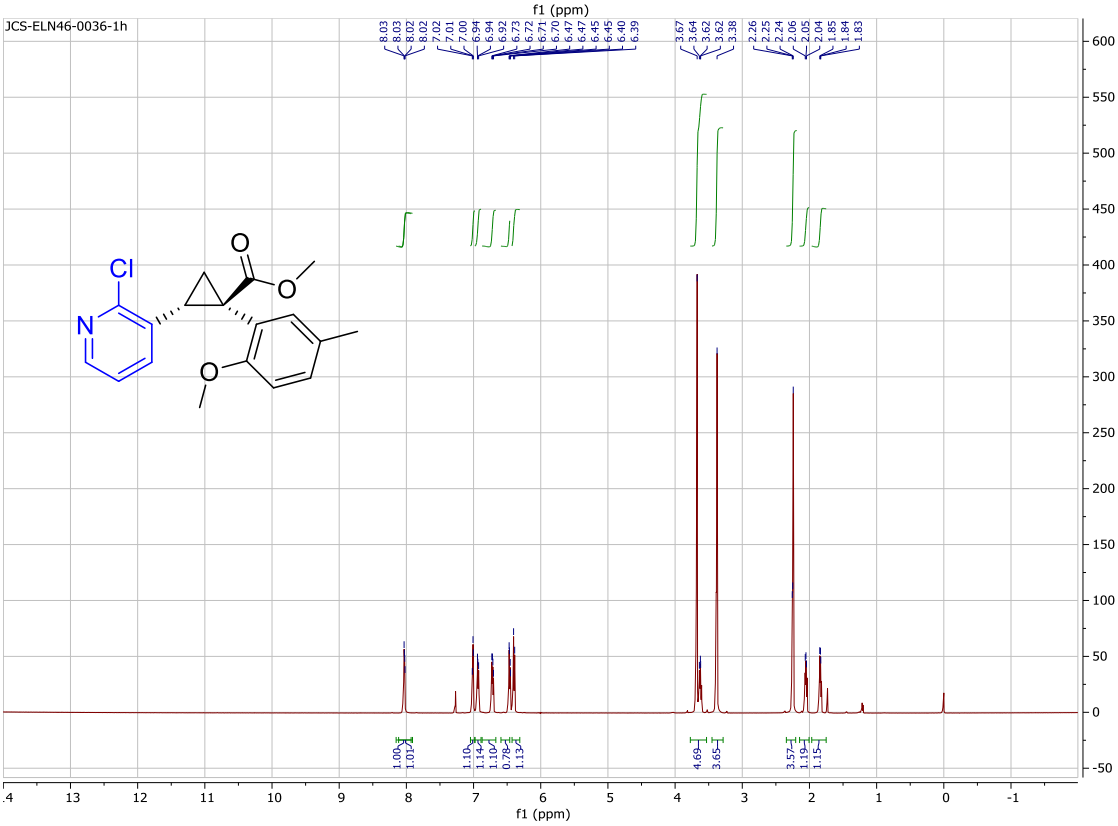
JCS-ELN46-0036-1h
8.03
8.03
8.02
8.02
7.02
7.01
7.00
6.94
6.94
6.92
6.73
6.72
6.71
6.70
6.47
6.47
6.45
6.45
6.40
6.39
3.67
3.64
3.62
3.62
3.38
2.26
2.25
2.24
2.06
2.05
2.04
1.85
1.84
1.83
1.00
1.01
1.10
1.14
1.10
0.78
1.13
4.69
3.65
3.57
1.19
1.15
f1 (ppm)

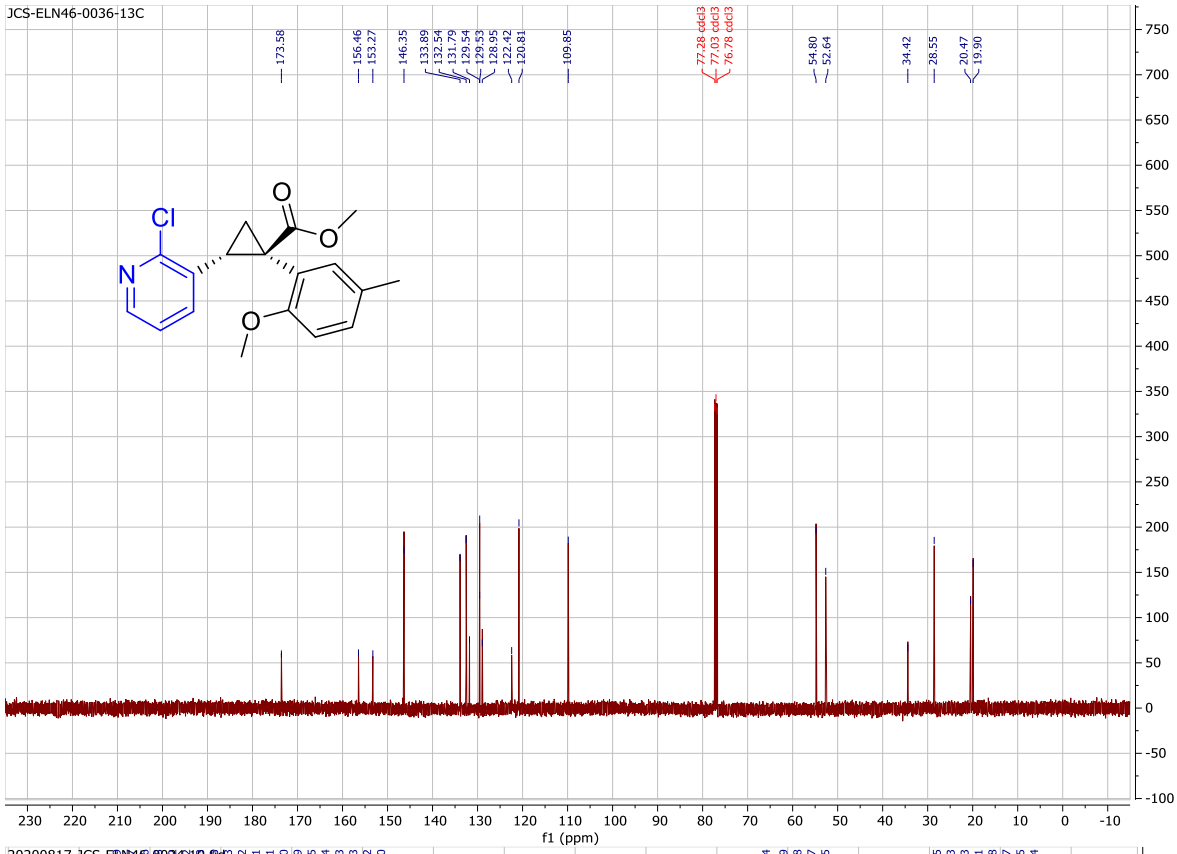
JCS-ELN46-0036-13C
173.58
156.46
153.27
146.35
133.89
132.54
131.79
129.54
129.53
128.95
122.42
120.81
109.85
77.28 cdcl3
77.03 cdcl3
76.78 cdcl3
54.80
52.64
34.42
28.55
20.47
19.90
Cl
N
O
O
O
f1 (ppm)

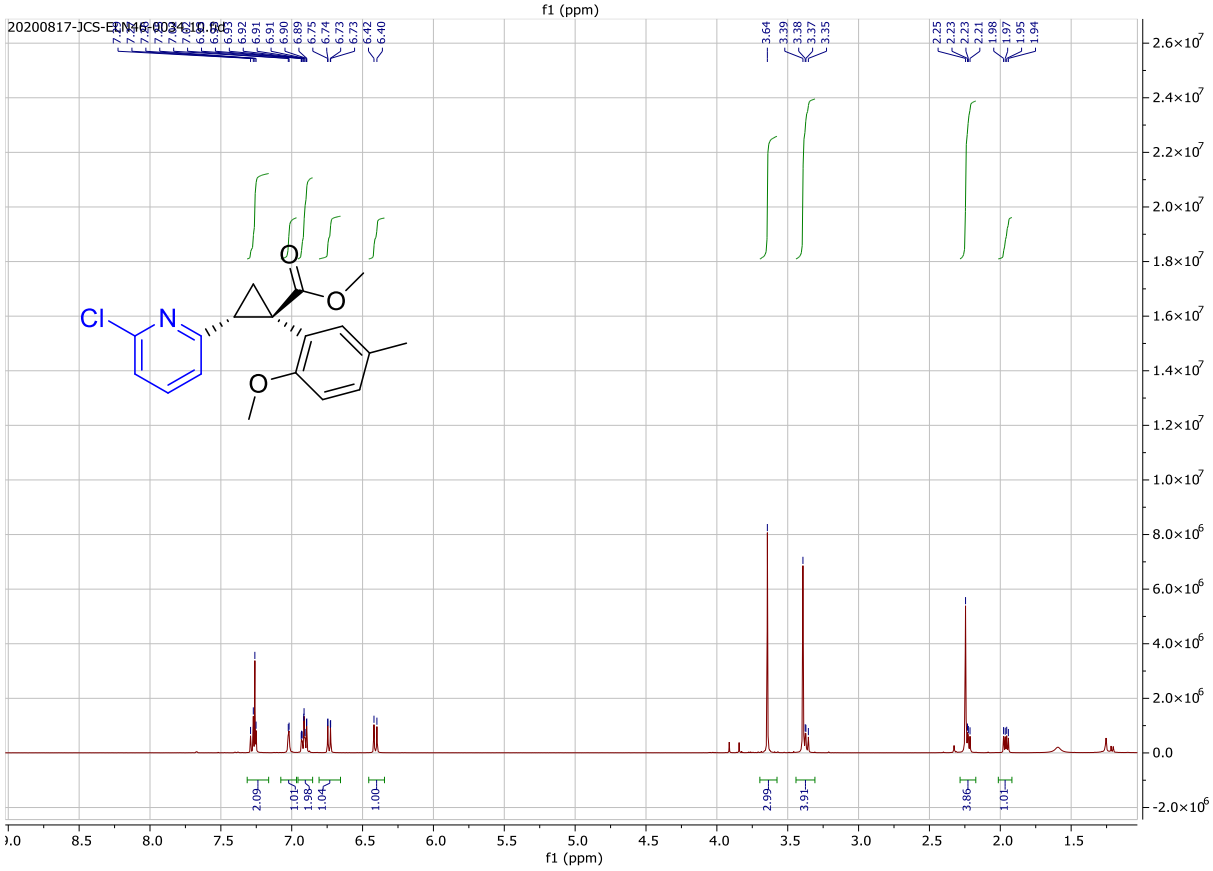
20200817-JCS-ELN46-0036-1H-01
3.64
3.39
3.38
3.37
3.35
2.25
2.23
2.23
2.21
1.98
1.97
1.95
1.94
6.75
6.74
6.73
6.73
6.42
6.40
2.09
1.01
1.98
1.04
1.00
2.99
3.91
3.86
1.01
Cl
N
O
O
O
f1 (ppm)

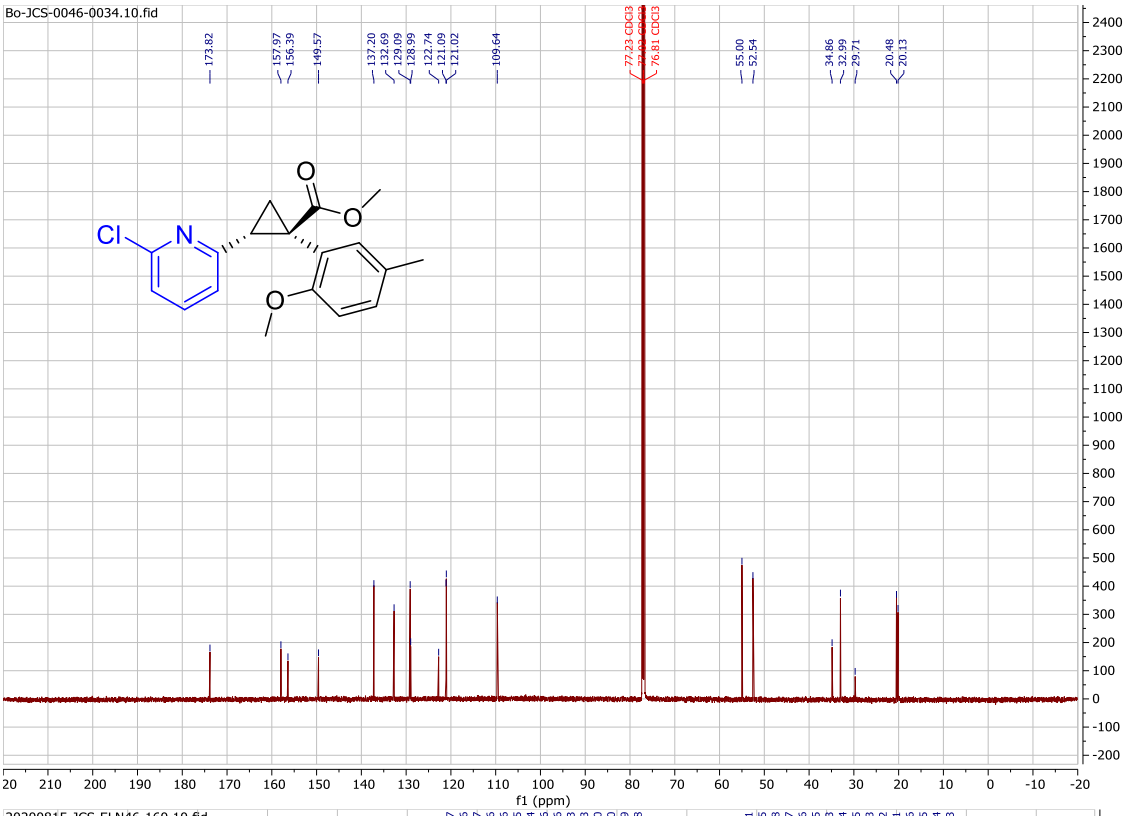
Bo-JCS-0046-0034.10.fid
173.82
157.97
156.39
149.57
137.20
132.69
129.09
128.99
122.74
121.09
121.02
109.64
77.23 CDCl3
76.81 CDCl3
55.00
52.54
34.86
32.99
29.71
20.48
20.13
Cl
N
O
O
O
f1 (ppm)

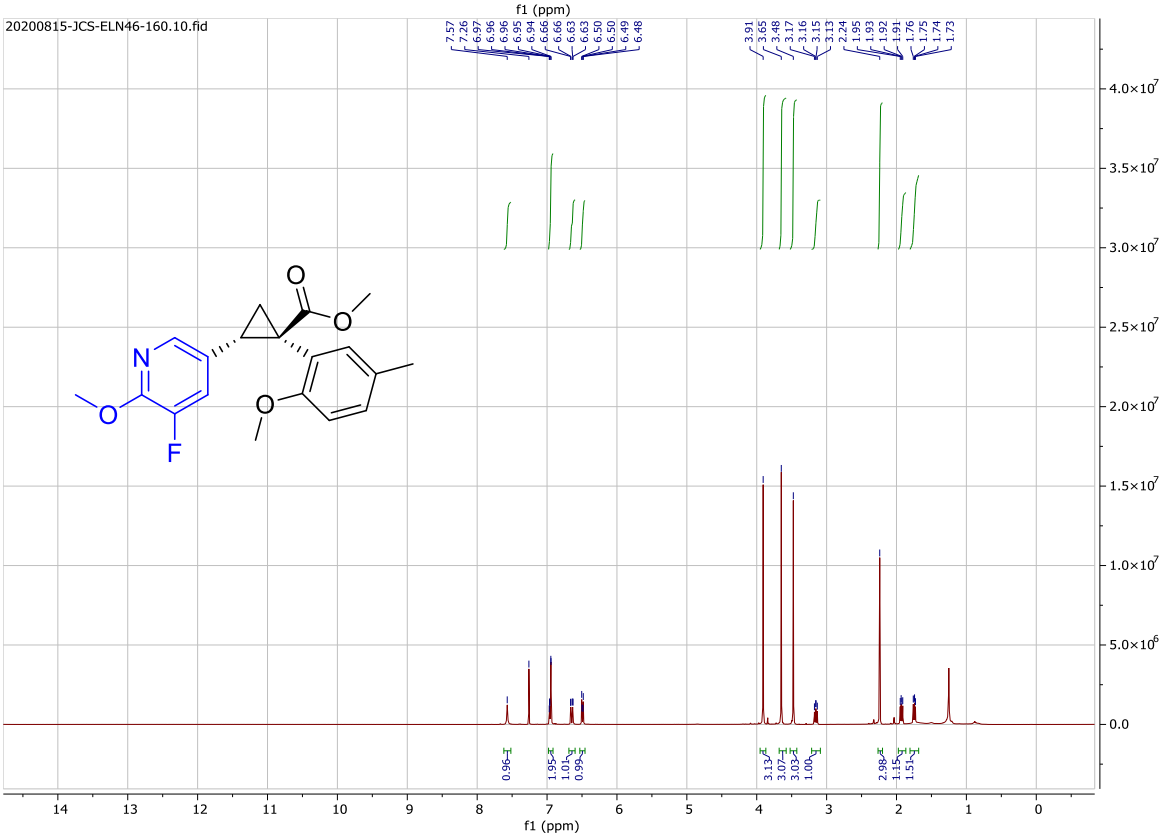
20200815-JCS-ELN46-160.10.fid
7.57
7.26
6.97
6.96
6.96
6.95
6.94
6.66
6.66
6.63
6.63
6.50
6.50
6.49
6.48
3.91
3.65
3.48
3.17
3.16
3.15
3.13
2.24
1.95
1.93
1.92
1.91
1.76
1.75
1.74
1.73
0.96
1.95
1.01
0.99
3.13
3.07
3.03
1.00
2.98
1.15
1.51
N
O
F
O
O
O
f1 (ppm)

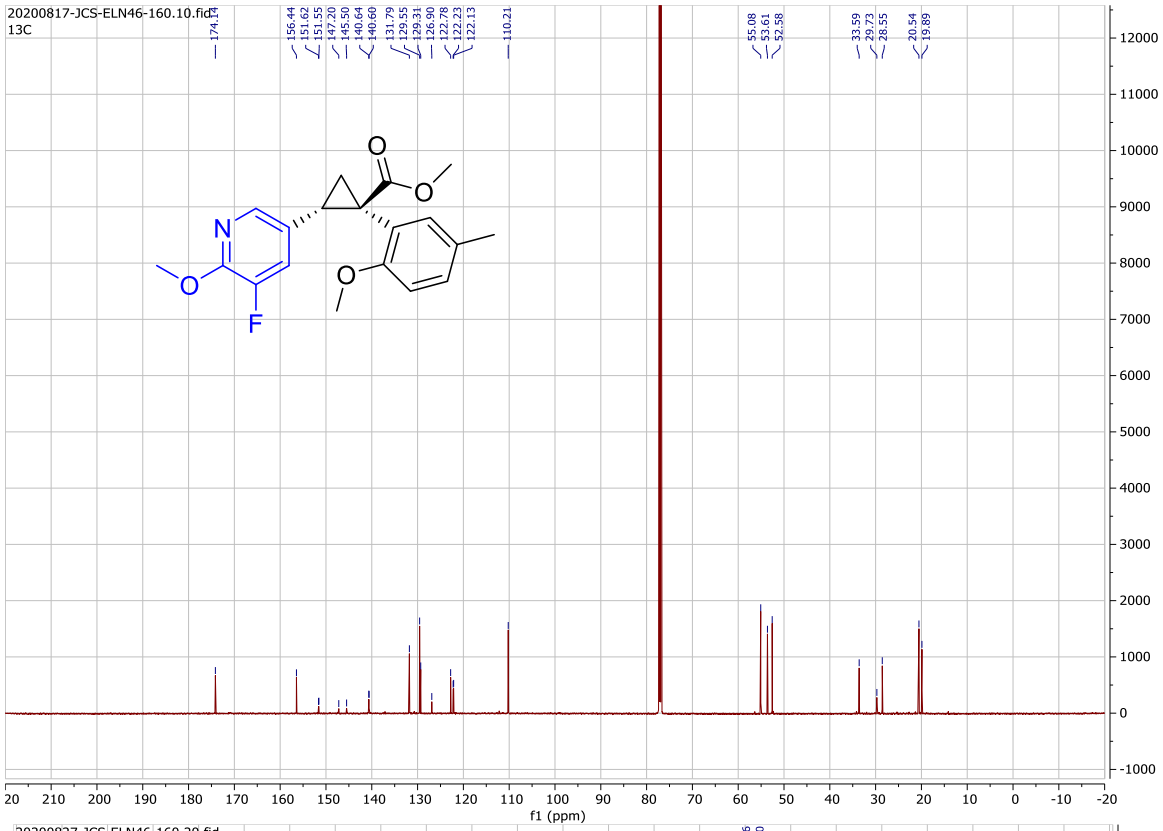
20200817-JCS-ELN46-160.10.fid
13C
174.11
156.44
151.62
151.55
147.20
145.50
140.64
140.60
131.79
129.55
129.31
126.90
122.78
122.23
122.13
110.21
55.08
53.61
52.58
33.59
29.73
28.55
20.54
19.89
f1 (ppm)

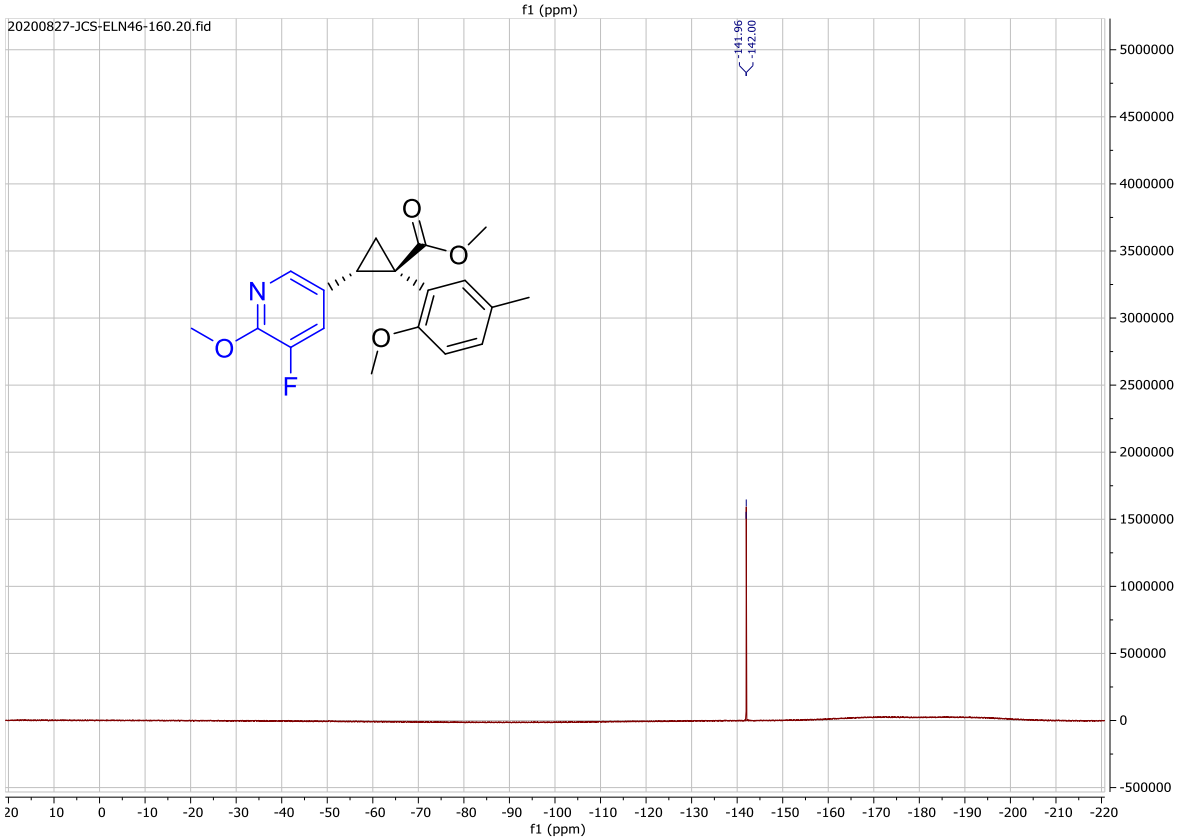
20200827-JCS-ELN46-160.20.fid
-141.96
-142.00
f1 (ppm)

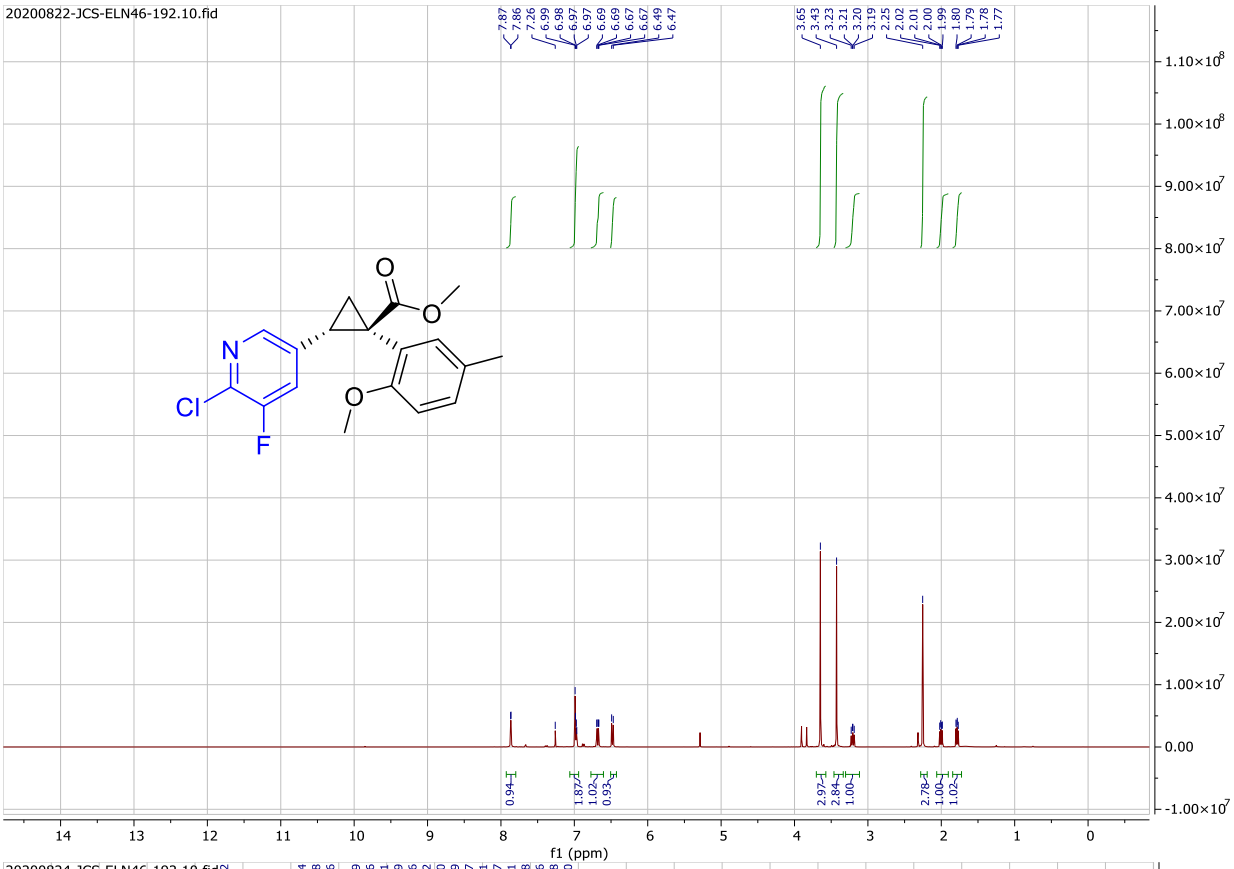
20200822-JCS-ELN46-192.10.fid
7.87
7.86
7.26
6.99
6.98
6.97
6.97
6.69
6.69
6.67
6.67
6.49
6.47
3.65
3.43
3.23
3.21
3.20
3.19
2.25
2.02
2.01
2.00
1.99
1.80
1.79
1.78
1.77
0.94
1.87
1.02
0.93
2.97
2.84
1.00
2.78
1.00
1.02
f1 (ppm)

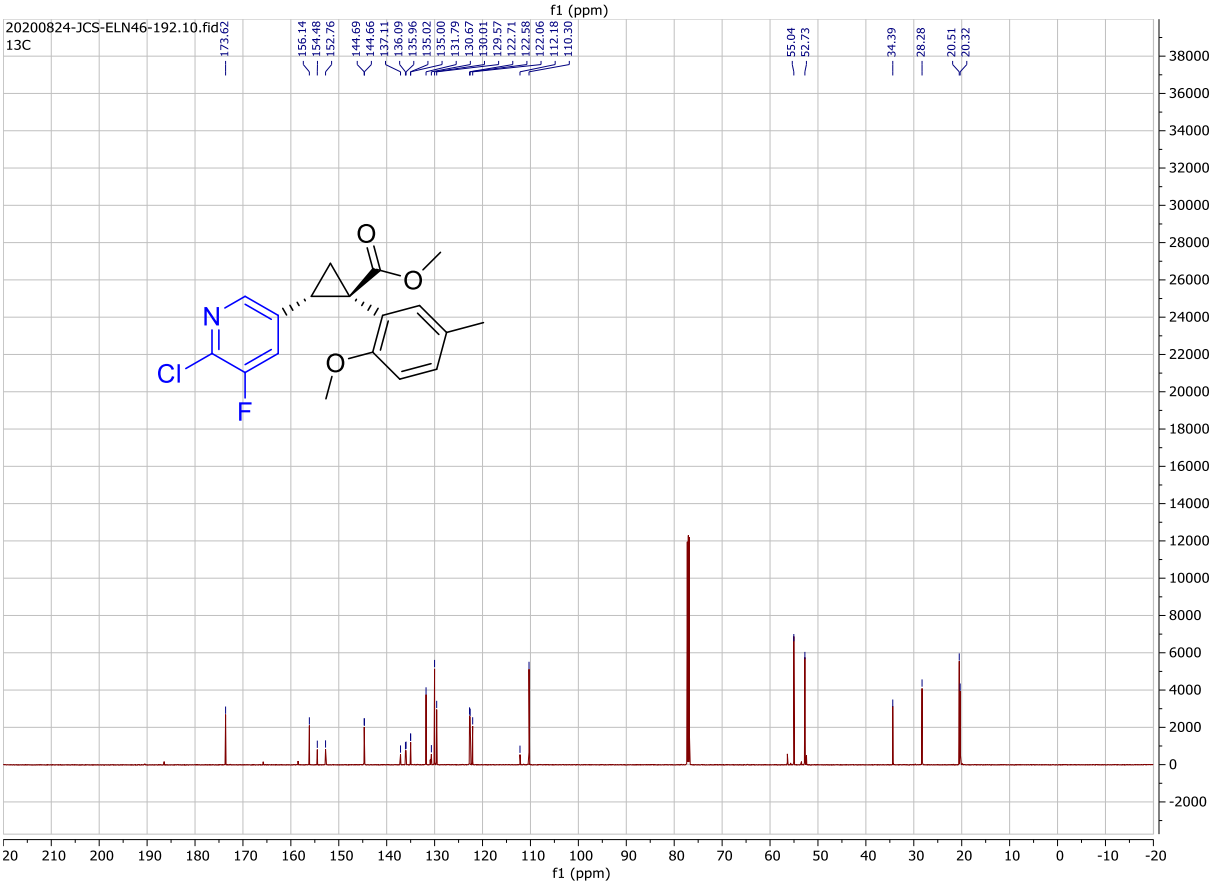
20200824-JCS-ELN46-192.10.fid
13C
173.62
156.14
154.48
152.76
144.69
144.66
137.11
136.09
135.96
135.02
135.00
131.79
130.67
130.61
129.57
122.71
122.58
122.06
112.18
110.30
55.04
52.73
34.39
28.28
20.51
20.32
f1 (ppm)

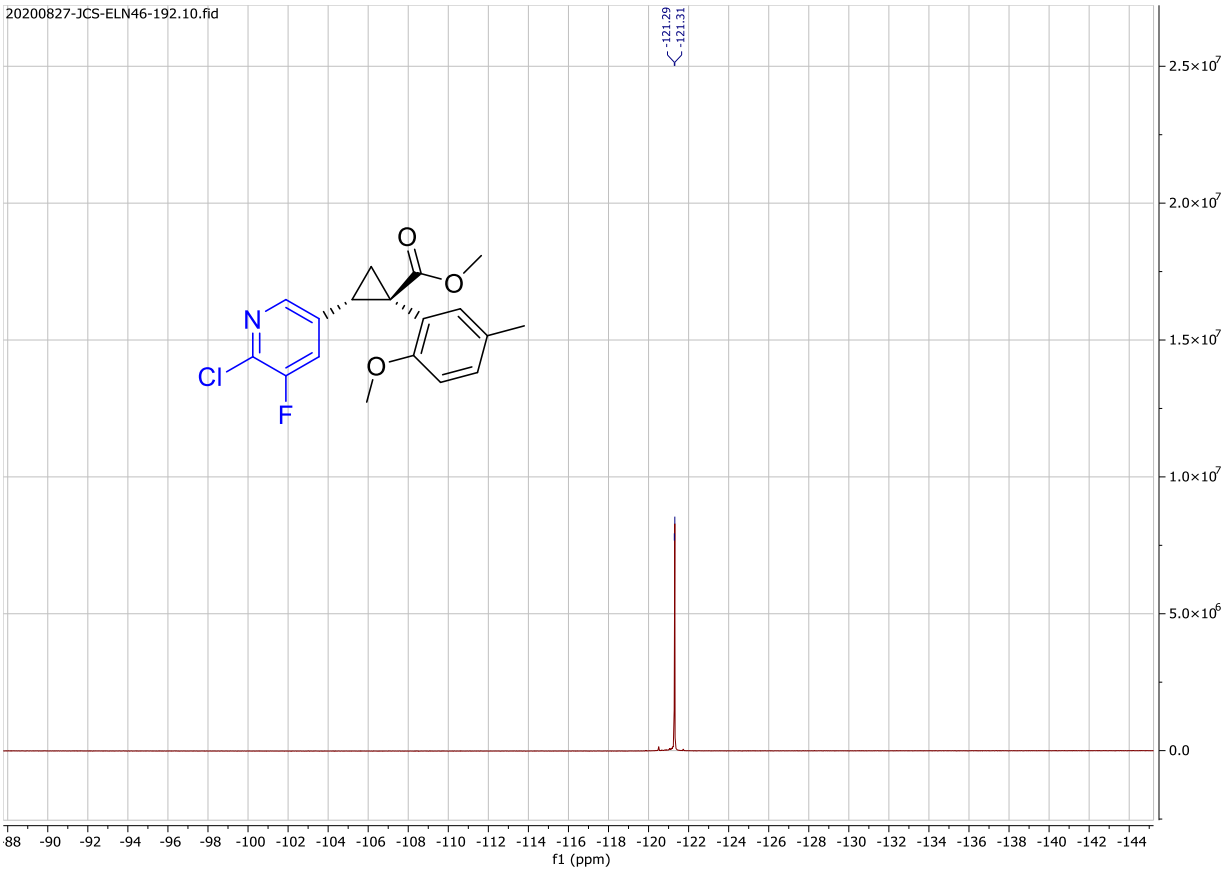
20200827-JCS-ELN46-192.10.fid
-121.29
-121.31
f1 (ppm)

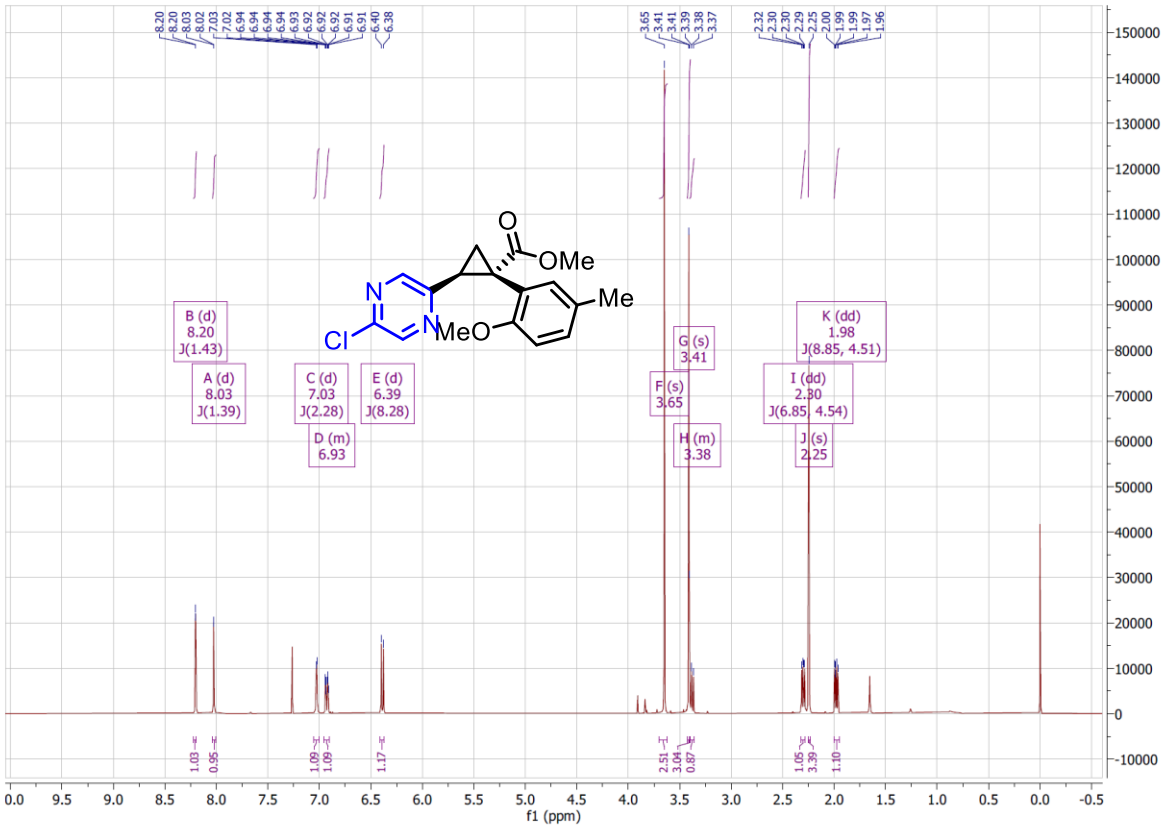
B (d)
8.20
J(1.43)
A (d)
8.03
J(1.39)
C (d)
7.03
J(2.28)
D (m)
6.93
E (d)
6.39
J(8.28)
F (s)
3.65
G (s)
3.41
H (m)
3.38
I (dd)
2.30
J(6.85, 4.54)
J (s)
2.25
K (dd)
1.98
J(8.85, 4.51)
f1 (ppm)

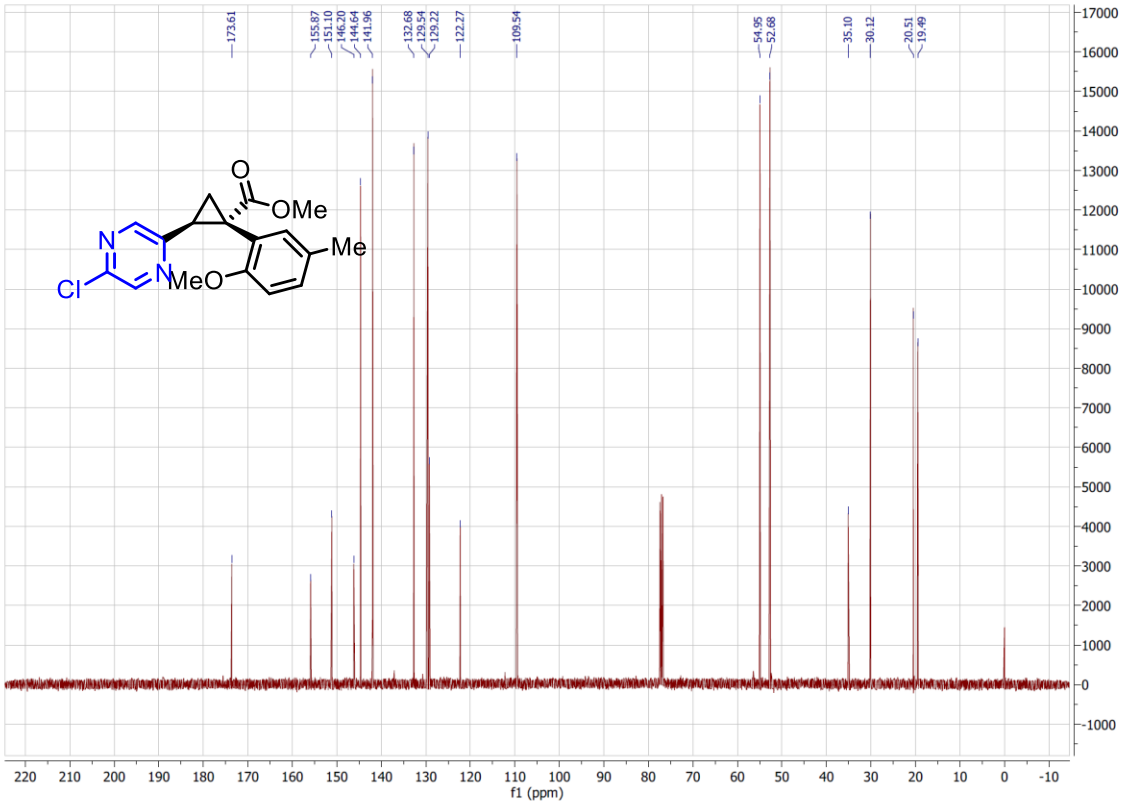
173.61
155.87
151.10
146.20
144.64
141.96
132.68
129.54
129.22
122.27
109.54
54.95
52.68
35.10
30.12
20.51
19.49
O
OMe
N
N
Cl
MeO
Me
f1 (ppm)

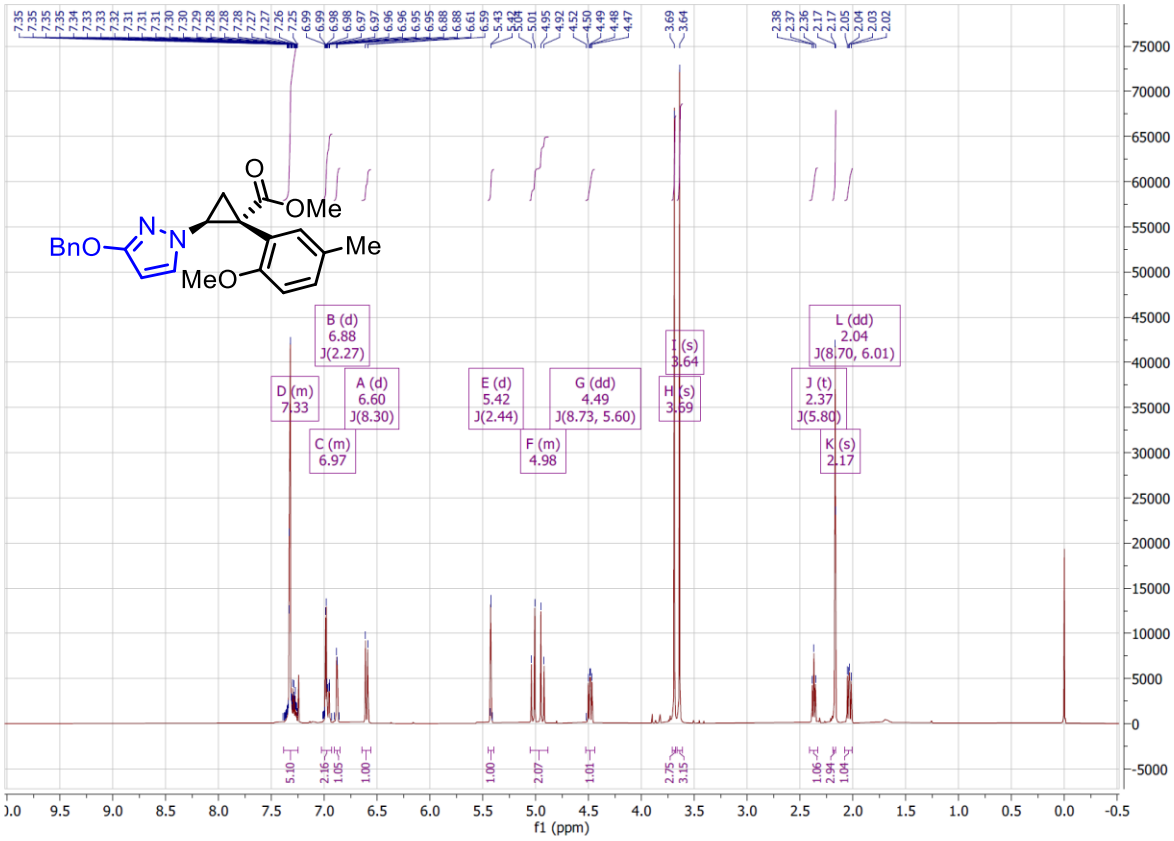
O
OMe
N
N
BnO
MeO
Me
B (d)
6.88
J(2.27)
D (m)
7.33
A (d)
6.60
J(8.30)
C (m)
6.97
E (d)
5.42
J(2.44)
F (m)
4.98
G (dd)
4.49
J(8.73, 5.60)
I (s)
3.64
H (s)
3.69
L (dd)
2.04
J(8.70, 6.01)
J (t)
2.37
J(5.80)
K (s)
2.17
f1 (ppm)

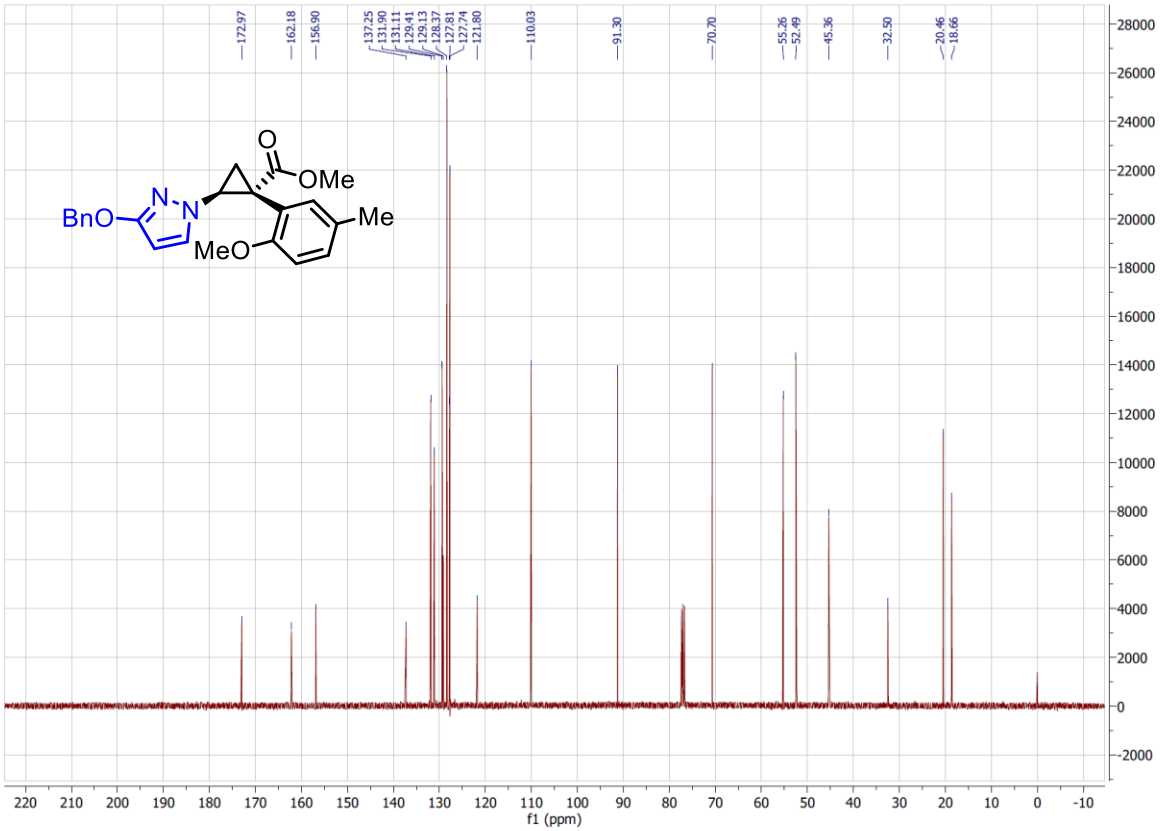
172.97
162.18
156.90
137.25
131.90
131.11
129.41
129.13
128.37
127.31
127.14
121.80
110.03
91.30
70.70
55.26
52.49
45.36
32.50
20.46
18.66
O
OMe
BnO
N
N
Me
MeO
f1 (ppm)

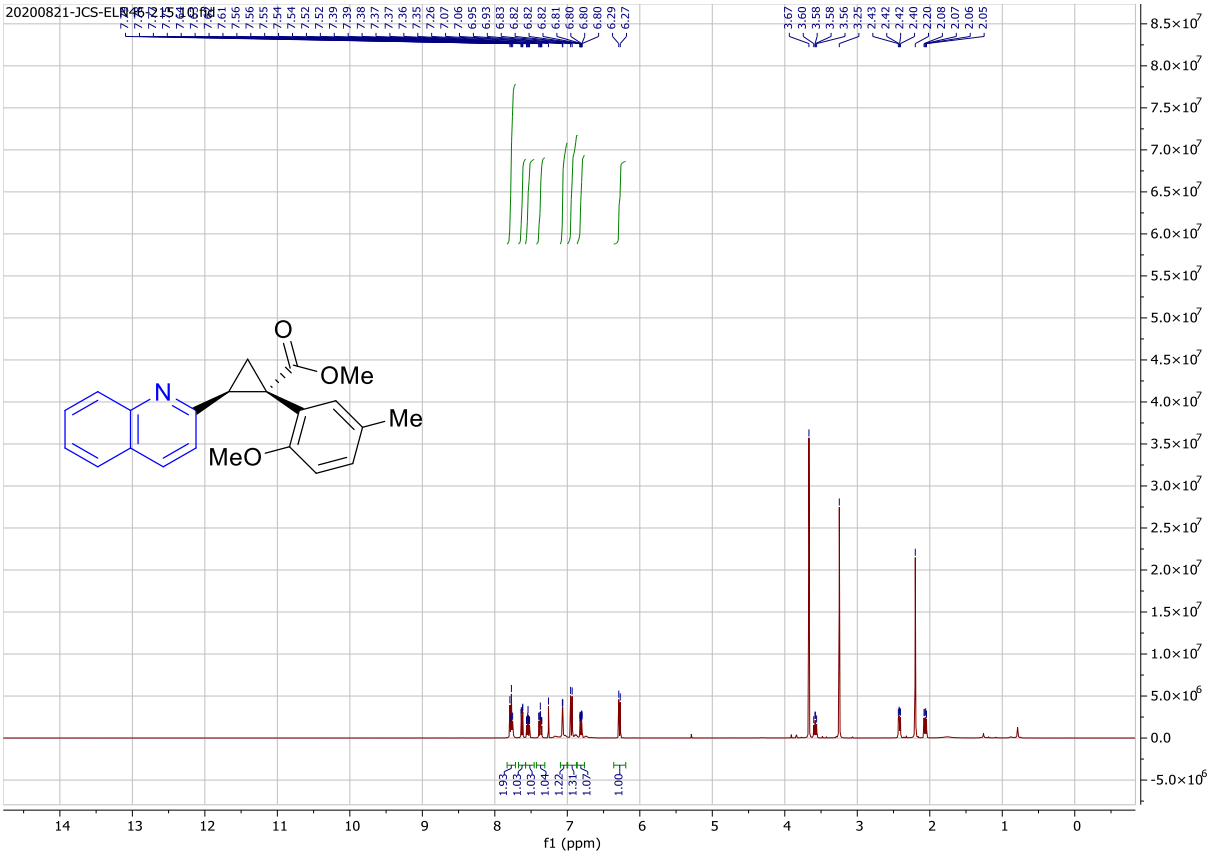
20200821-JCS-ELM-215-10-52
3.67
3.60
3.58
3.58
3.56
3.25
2.43
2.42
2.42
2.40
2.20
2.08
2.07
2.06
2.05
1.93
1.03
1.03
1.04
1.22
1.31
1.07
1.00
O
OMe
N
Me
MeO
f1 (ppm)

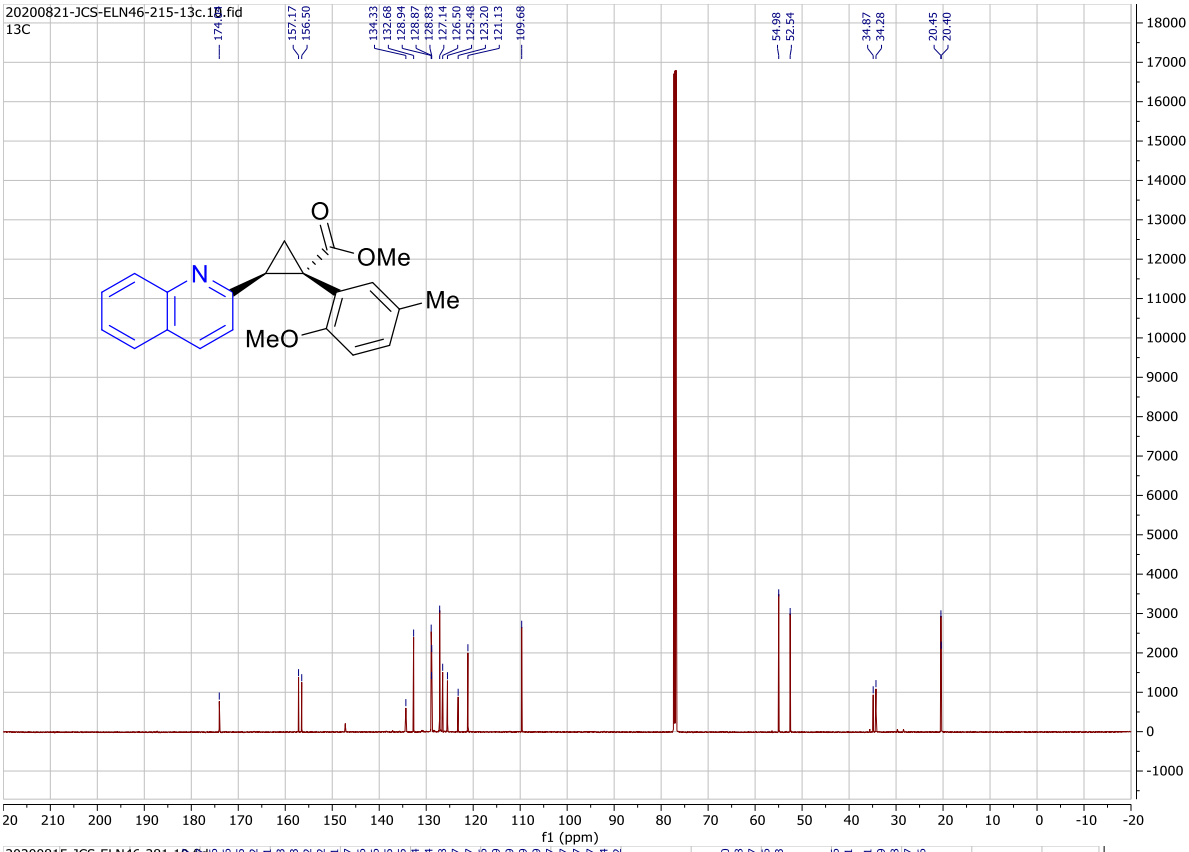
20200821-JCS-ELN46-215-13c.1.fid
13C
174.
157.17
156.50
134.33
132.68
128.94
128.87
128.83
127.14
126.50
125.48
123.20
121.13
109.68
54.98
52.54
34.87
34.28
20.45
20.40
O
OMe
N
Me
MeO
f1 (ppm)

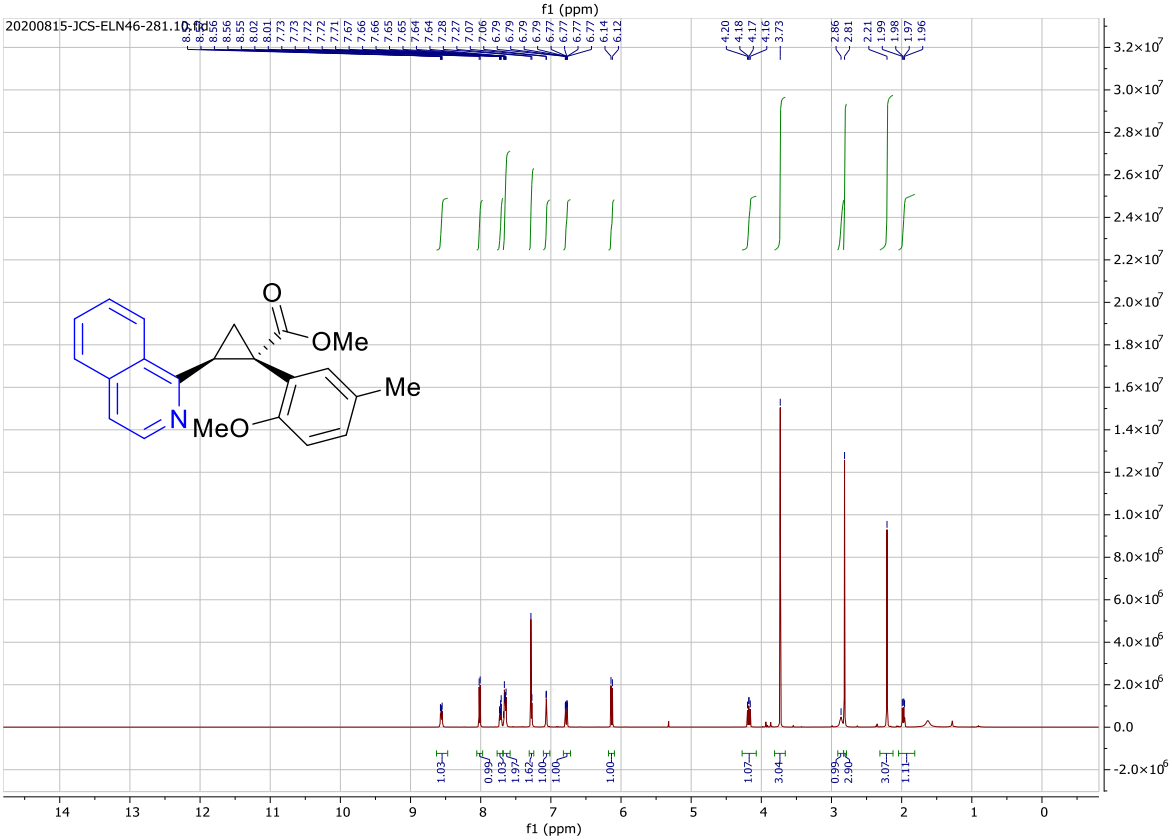
20200815-JCS-ELN46-281.10.fid
8.57
8.56
8.56
8.55
8.02
8.01
7.73
7.73
7.72
7.72
7.71
7.67
7.66
7.66
7.65
7.65
7.64
7.64
7.28
7.27
7.07
7.06
6.79
6.79
6.79
6.79
6.77
6.77
6.77
6.77
6.14
6.12
4.20
4.18
4.17
4.16
3.73
2.86
2.81
2.21
1.99
1.98
1.97
1.96
1.03
0.99
1.03
1.97
1.62
1.06
1.00
1.00
1.07
3.04
0.99
2.90
3.07
1.11
O
OMe
N
Me
MeO
f1 (ppm)

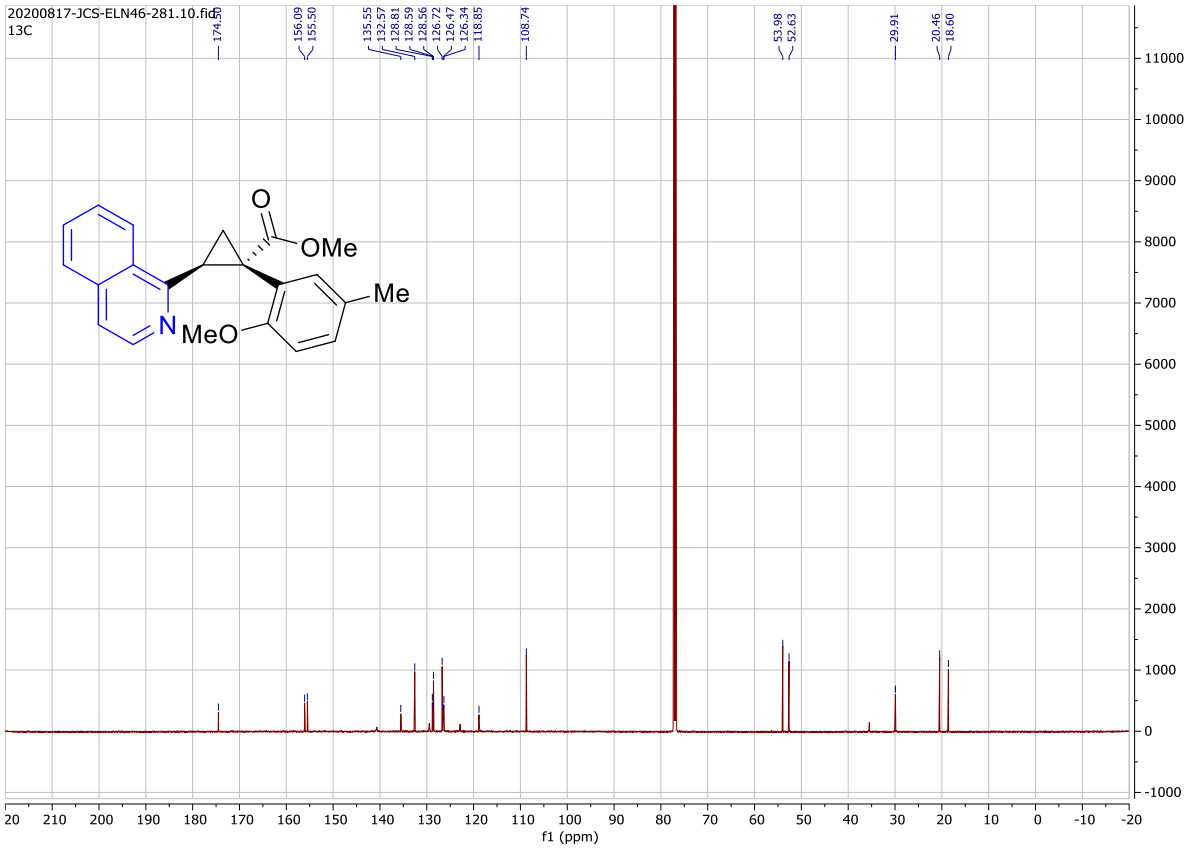
20200817-JCS-ELN46-281.10.fid
13C
174.50
156.09
155.50
135.55
132.57
128.81
128.59
128.56
126.72
126.47
126.34
118.85
108.74
53.98
52.63
29.91
20.46
18.60
O
OMe
Me
N
MeO
f1 (ppm)

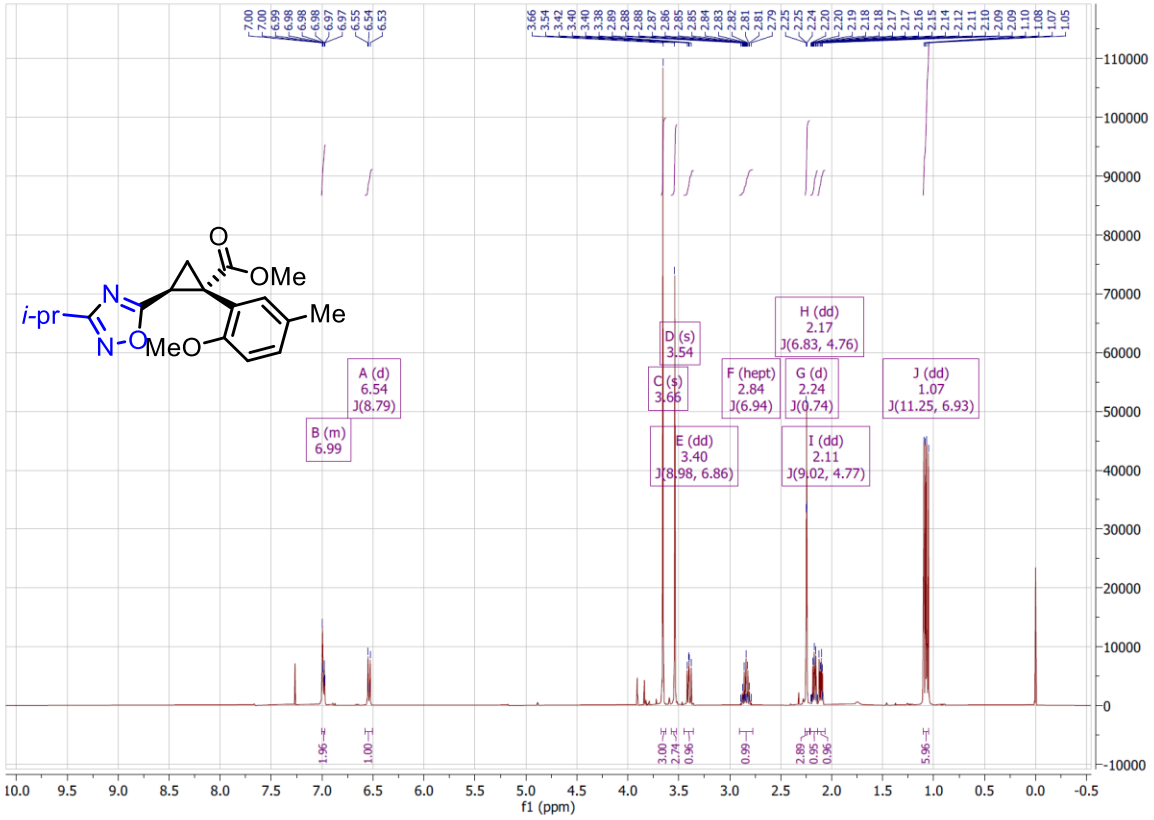
O
OMe
Me
N
i-pr
N-O
MeO
A (d)
6.54
J(8.79)
B (m)
6.99
C (s)
3.66
D (s)
3.54
E (dd)
3.40
J(8.98, 6.86)
F (hept)
2.84
J(6.94)
G (d)
2.24
J(0.74)
H (dd)
2.17
J(6.83, 4.76)
I (dd)
2.11
J(9.02, 4.77)
J (dd)
1.07
J(11.25, 6.93)
f1 (ppm)

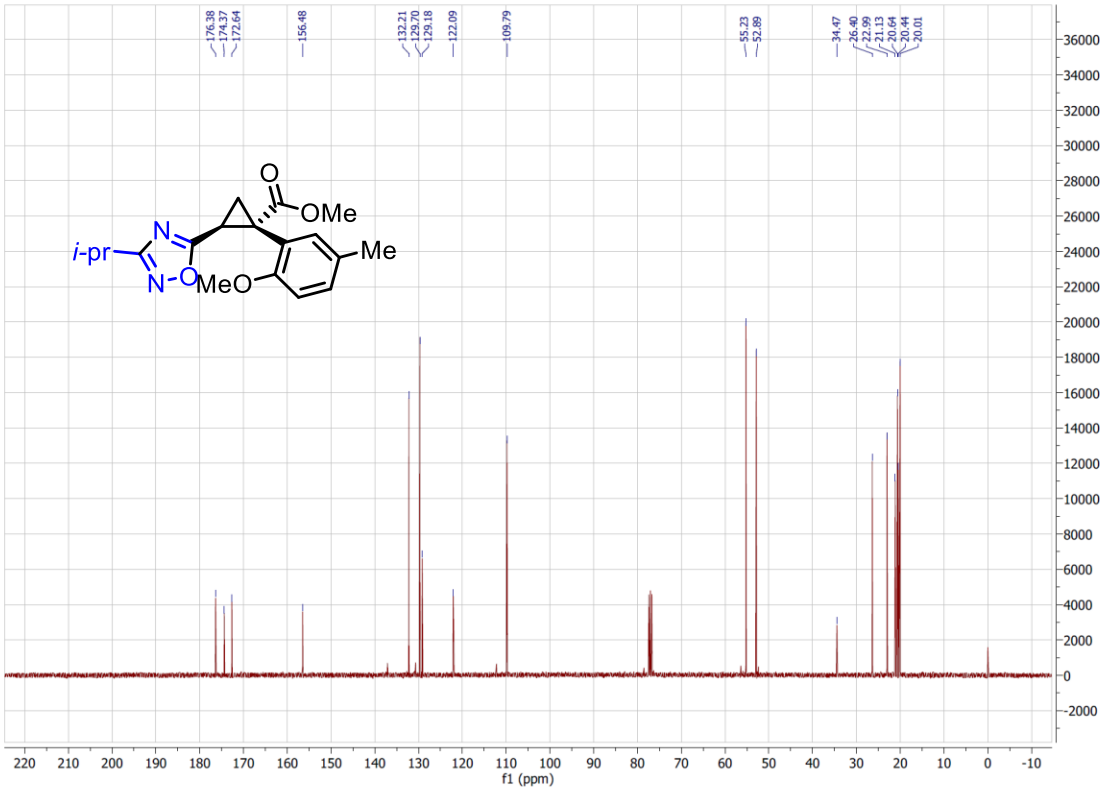
176.38
174.37
172.64
156.48
132.21
129.70
129.18
122.09
109.79
55.23
52.89
34.47
26.40
22.99
21.13
20.64
20.44
20.01
O
OMe
Me
i-pr
N
N-O
MeO
f1 (ppm)

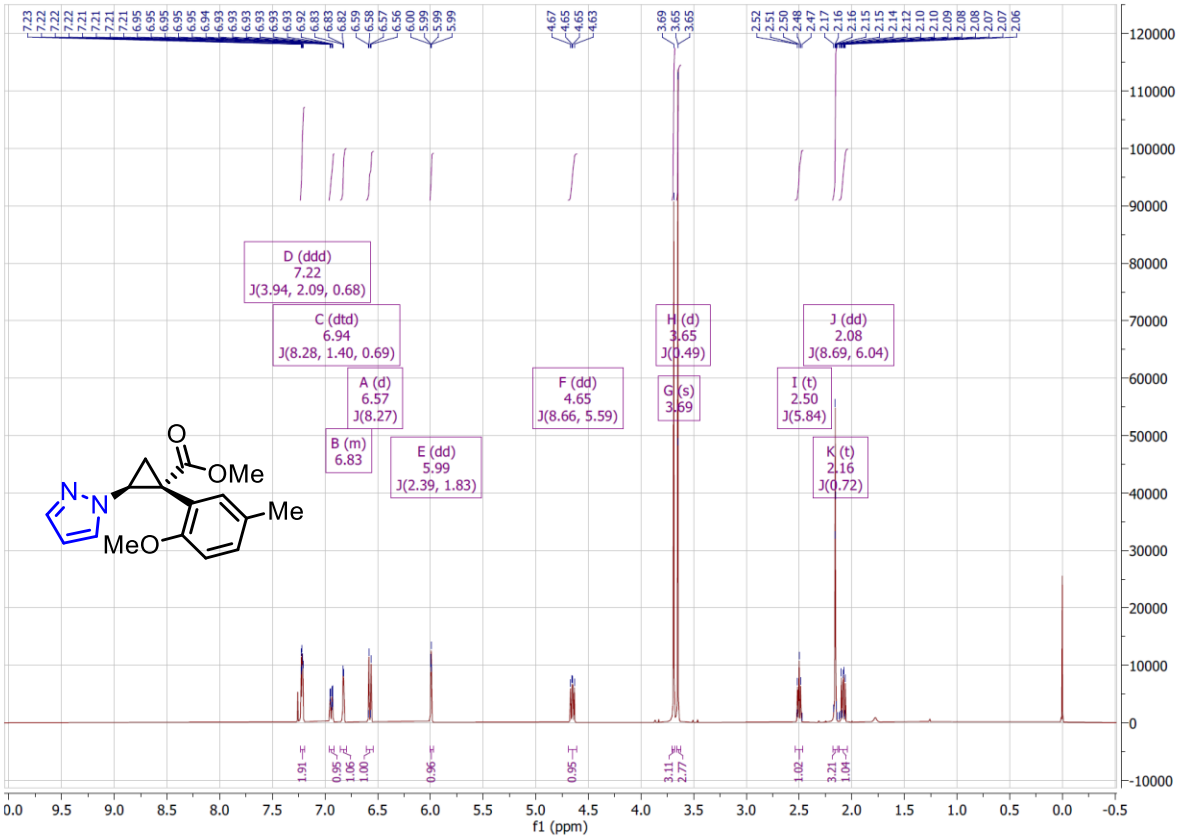
D (ddd)
7.22
J(3.94, 2.09, 0.68)
C (dtd)
6.94
J(8.28, 1.40, 0.69)
A (d)
6.57
J(8.27)
B (m)
6.83
E (dd)
5.99
J(2.39, 1.83)
F (dd)
4.65
J(8.66, 5.59)
H (d)
3.65
J(0.49)
G (s)
3.59
J (dd)
2.08
J(8.69, 6.04)
I (t)
2.50
J(5.84)
K (t)
2.16
J(0.72)
O
OMe
Me
MeO
N
N
f1 (ppm)

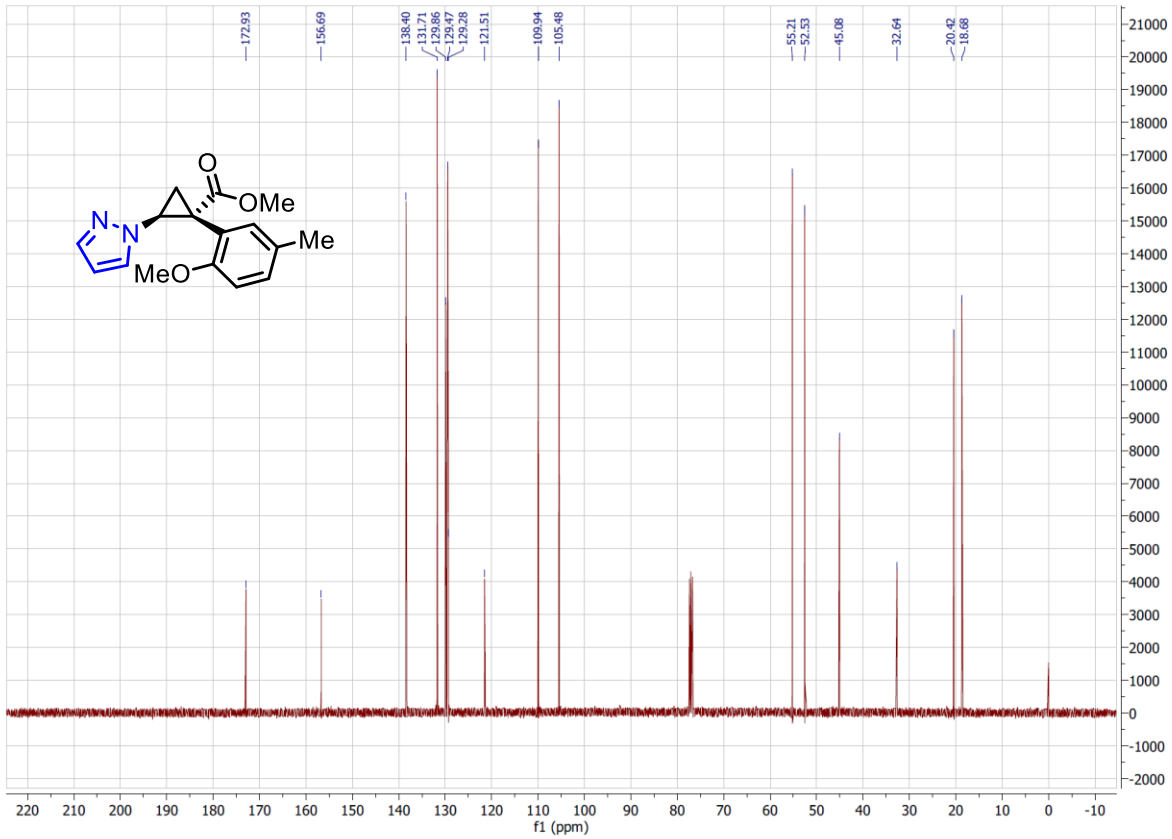
172.93
156.69
138.40
131.71
129.86
129.47
129.28
121.51
109.94
105.48
55.21
52.53
45.08
32.64
20.42
18.68
O
OMe
N
N
Me
MeO
f1 (ppm)

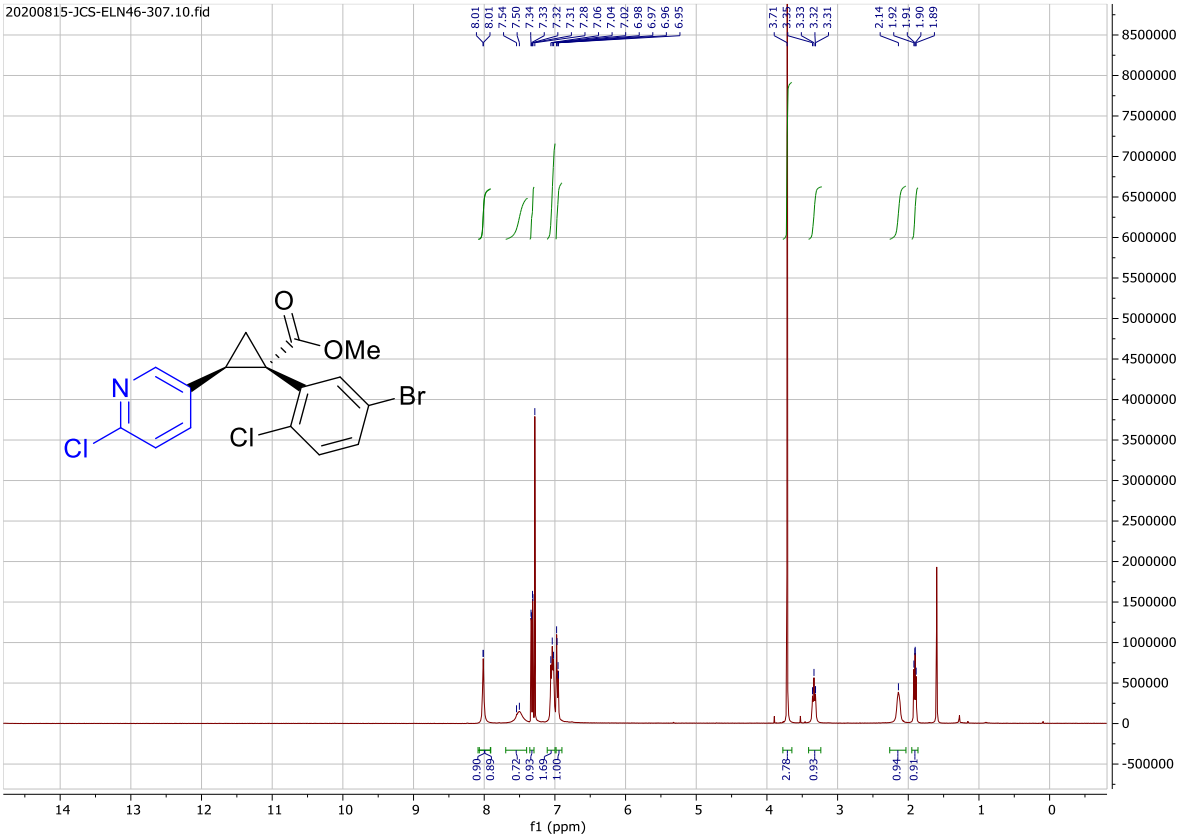
20200815-JCS-ELN46-307.10.fid
8.01
8.01
7.54
7.50
7.34
7.33
7.32
7.31
7.28
7.06
7.04
7.02
6.98
6.97
6.96
6.95
3.71
3.35
3.33
3.32
3.31
2.14
1.92
1.91
1.90
1.89
O
OMe
N
Br
Cl
Cl
0.90
0.89
0.72
0.93
1.69
1.00
2.78
0.93
0.94
0.91
f1 (ppm)

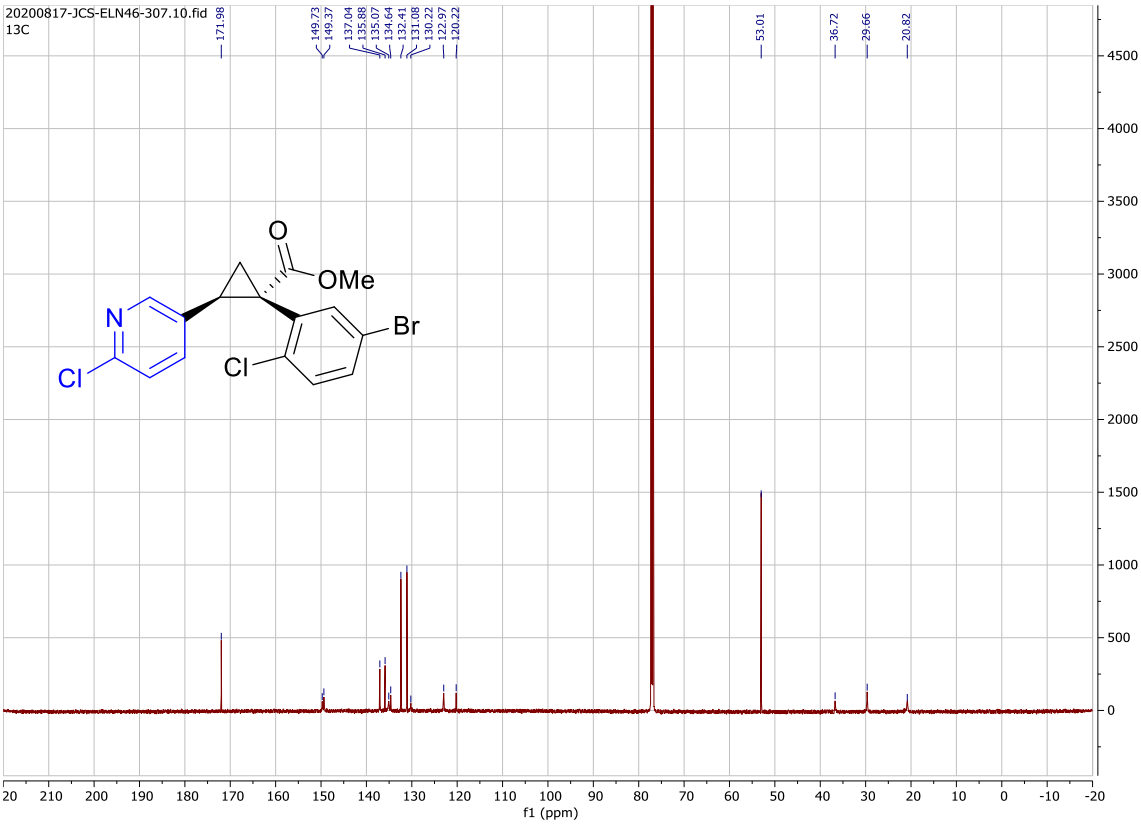
20200817-JCS-ELN46-307.10.fid
13C
171.98
149.73
149.37
137.04
135.88
135.07
134.64
132.41
131.08
130.22
122.97
120.22
53.01
36.72
29.66
20.82
O
OMe
N
Cl
Cl
Br
f1 (ppm)

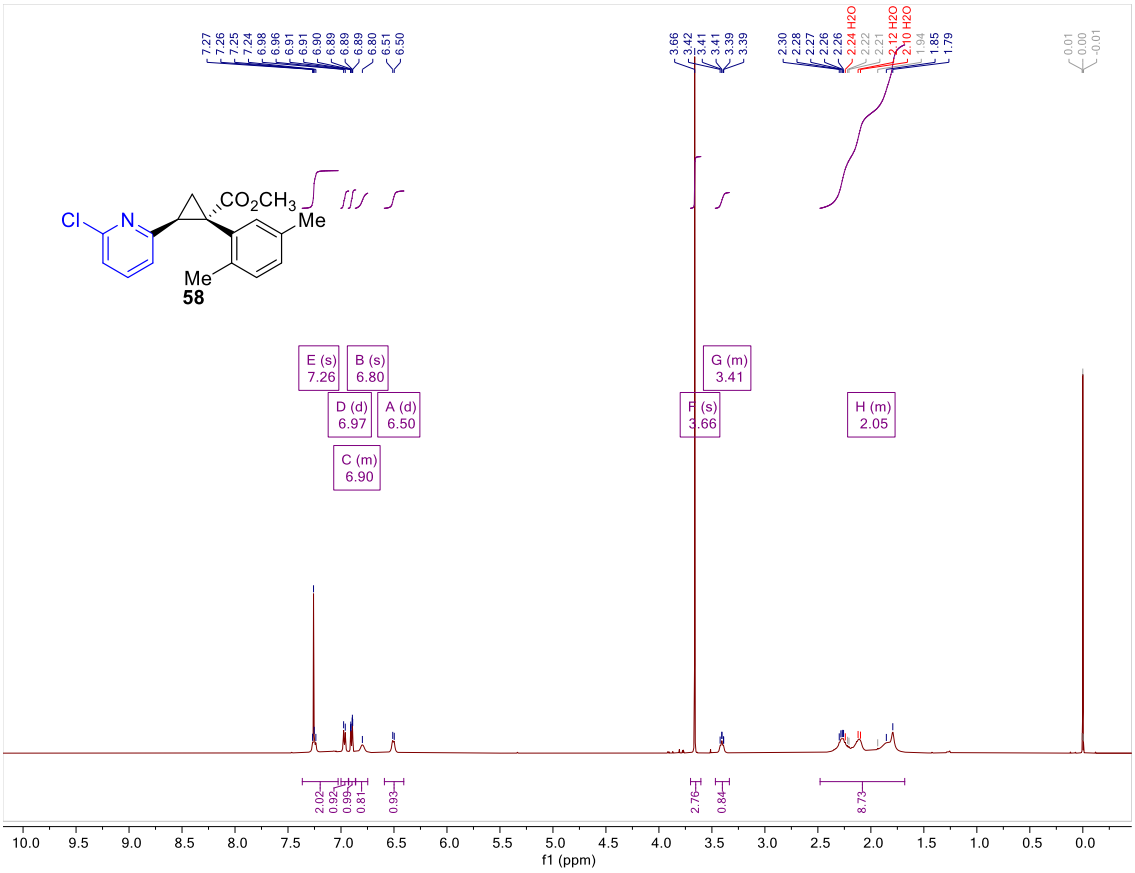
7.27
7.26
7.25
7.24
6.98
6.96
6.91
6.91
6.91
6.90
6.89
6.89
6.89
6.80
6.51
6.50
3.66
3.42
3.41
3.41
3.39
3.39
2.30
2.28
2.27
2.26
2.26
2.24 H2O
2.22
2.21
2.12 H2O
2.10 H2O
1.94
1.85
1.79
0.01
0.00
-0.01
Cl
N
CO2CH3
Me
Me
58
E (s) 7.26
B (s) 6.80
D (d) 6.97
A (d) 6.50
C (m) 6.90
G (m) 3.41
F (s) 3.66
H (m) 2.05
2.02
0.92
0.99
0.81
0.93
2.76
0.84
8.73
f1 (ppm)

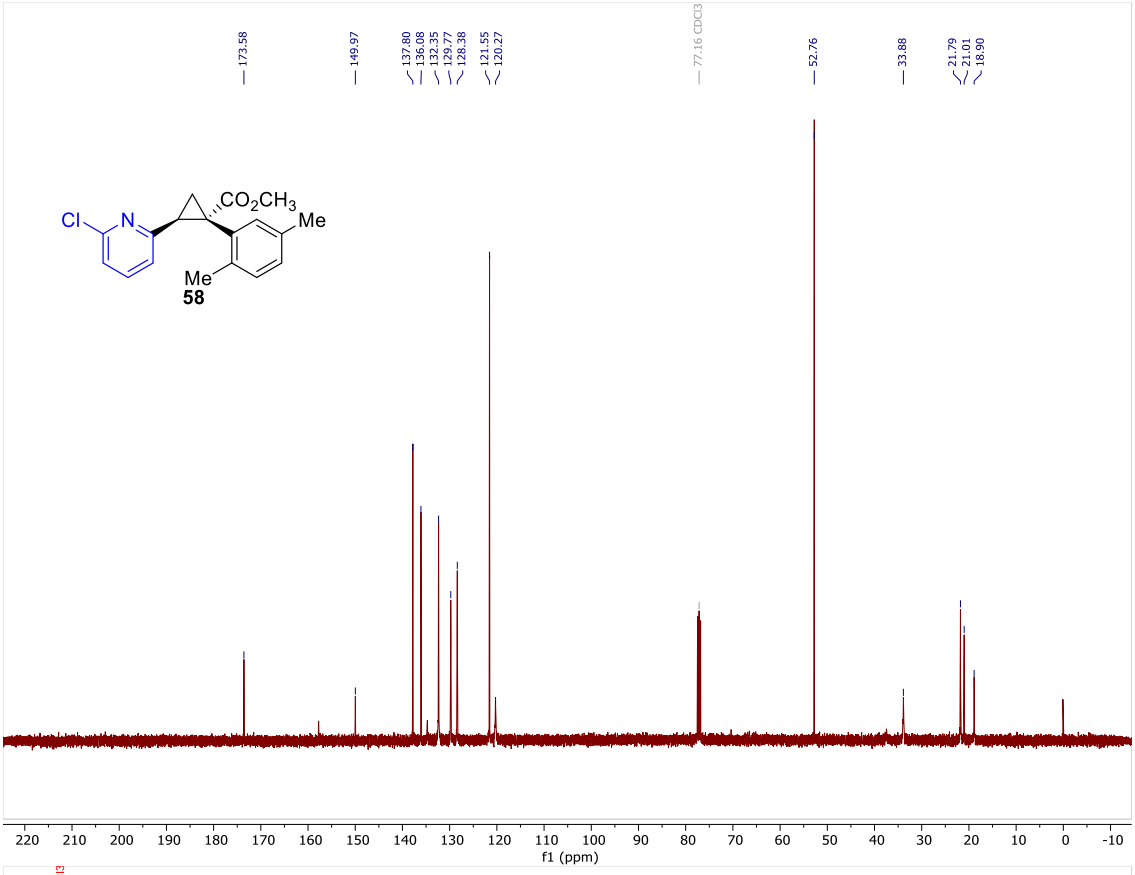
173.58
149.97
137.80
136.08
132.35
129.77
128.38
121.55
120.27
77.16 CDCl3
52.76
33.88
21.79
21.01
18.90
Cl
N
CO2CH3
Me
Me
58
f1 (ppm)

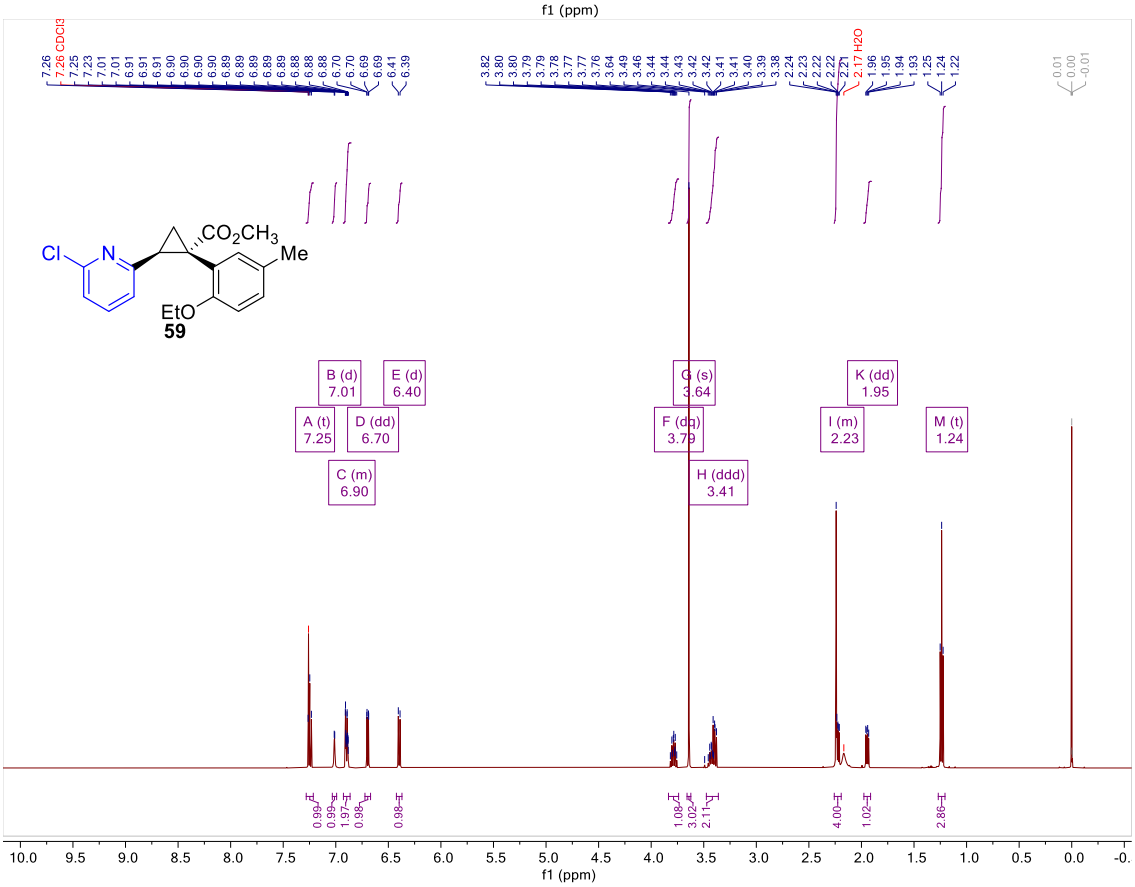
7.26 CDCl3
2.17 H2O
Cl
N
CO2CH3
Me
EtO
59
B (d) 7.01
E (d) 6.40
A (t) 7.25
D (dd) 6.70
C (m) 6.90
G (s) 3.64
F (dq) 3.79
H (ddd) 3.41
K (dd) 1.95
I (m) 2.23
M (t) 1.24
f1 (ppm)

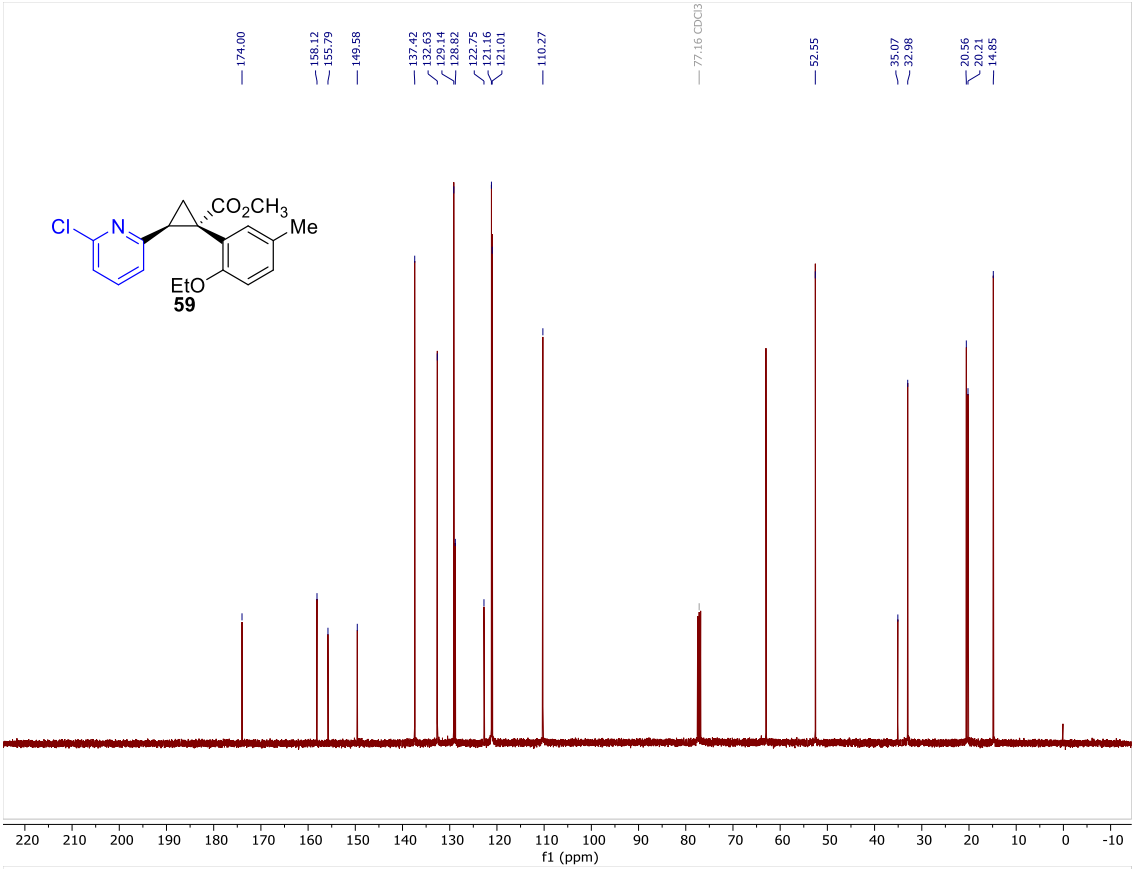
174.00
158.12
155.79
149.58
137.42
132.63
129.14
128.82
122.75
121.16
121.01
110.27
77.16 CDCl3
52.55
35.07
32.98
20.56
20.21
14.85
CO2CH3
Me
Cl
N
EtO
59
f1 (ppm)

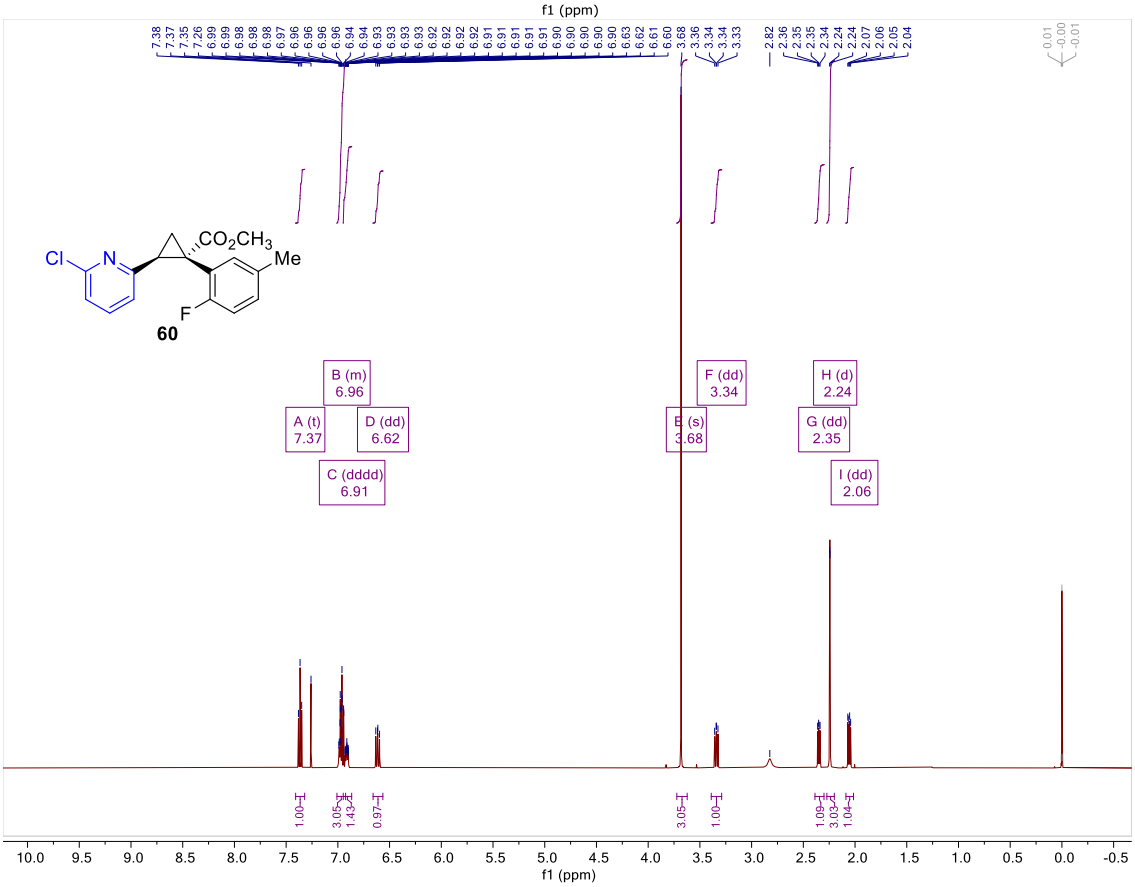
CO2CH3
Me
Cl
N
F
60
A (t) 7.37
B (m) 6.96
C (dddd) 6.91
D (dd) 6.62
E (s) 3.68
F (dd) 3.34
G (dd) 2.35
H (d) 2.24
I (dd) 2.06
f1 (ppm)

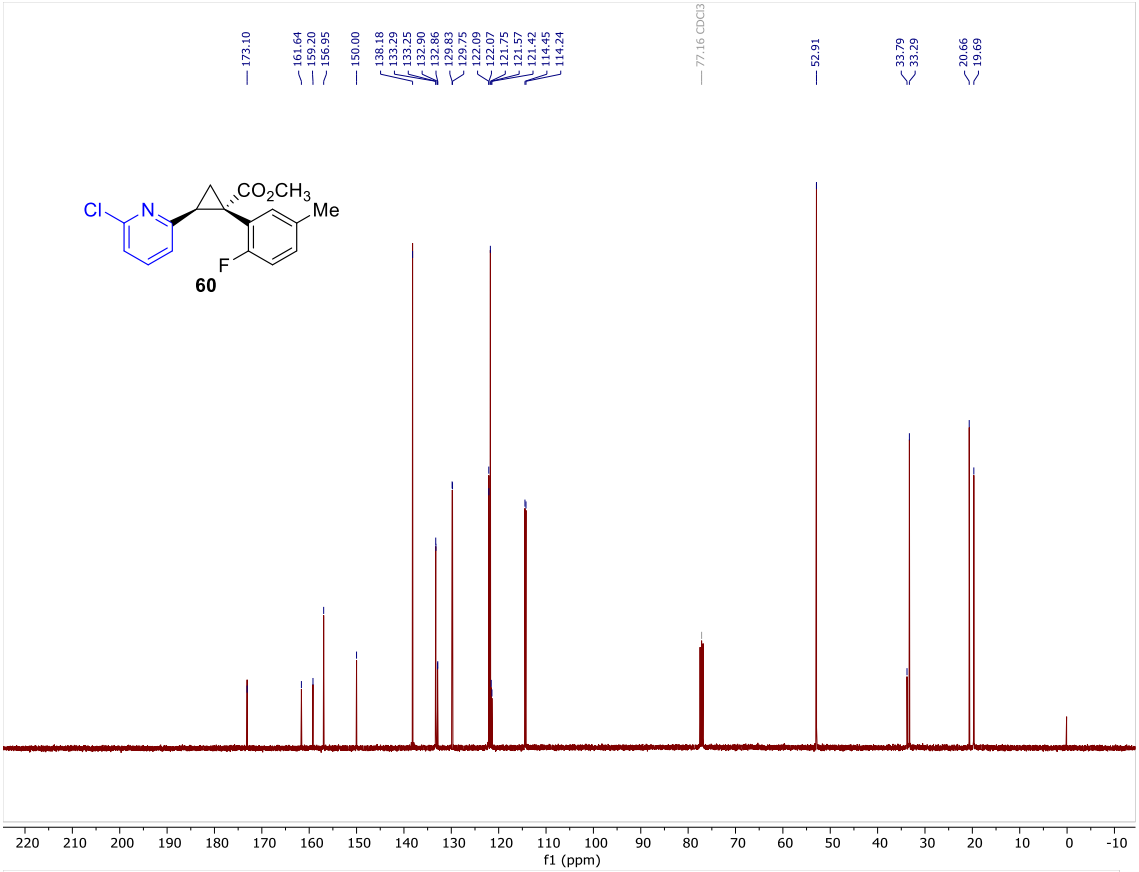
173.10
161.64
159.20
156.95
150.00
138.18
133.29
133.25
132.90
132.86
129.83
129.75
122.09
122.07
121.75
121.57
121.42
114.45
114.24
77.16 CDCl3
52.91
33.79
33.29
20.66
19.69
Cl
N
CO2CH3
Me
F
60
f1 (ppm)

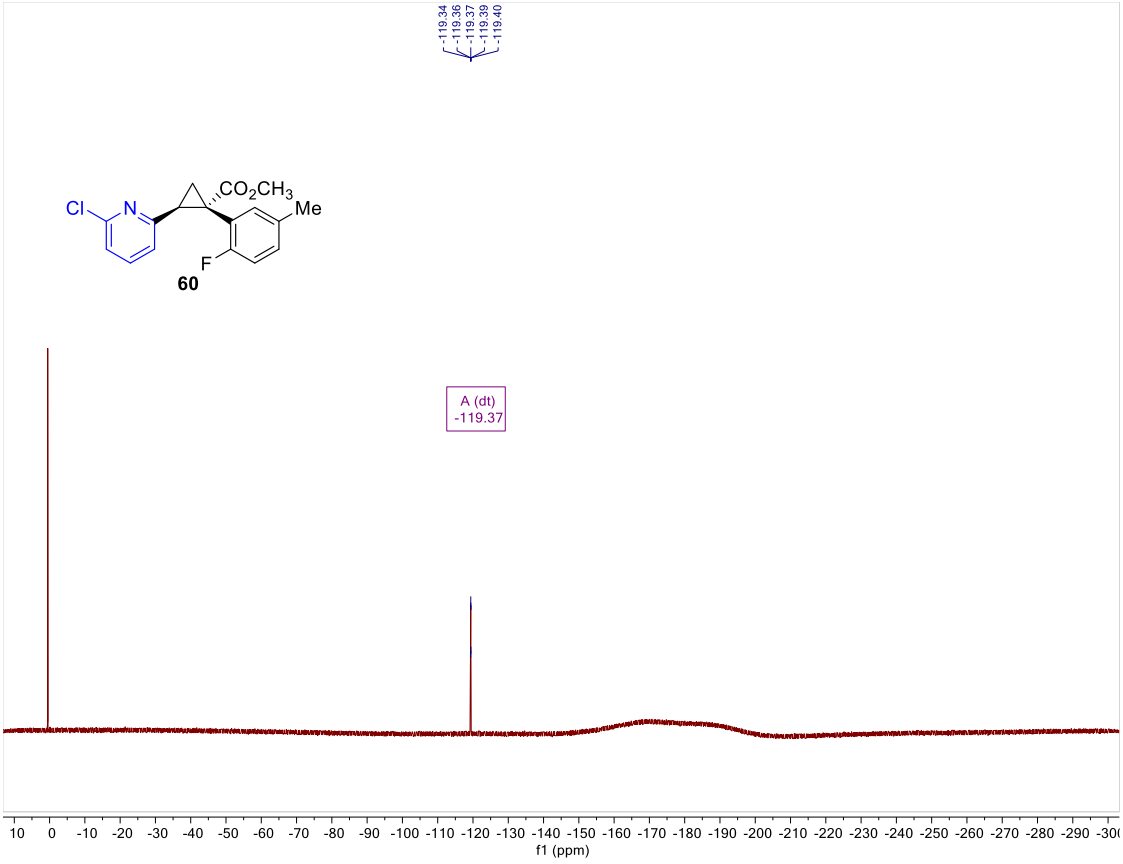
-119.34
-119.36
-119.37
-119.39
-119.40
Cl
N
CO2CH3
Me
F
60
A (dt)
-119.37
f1 (ppm)

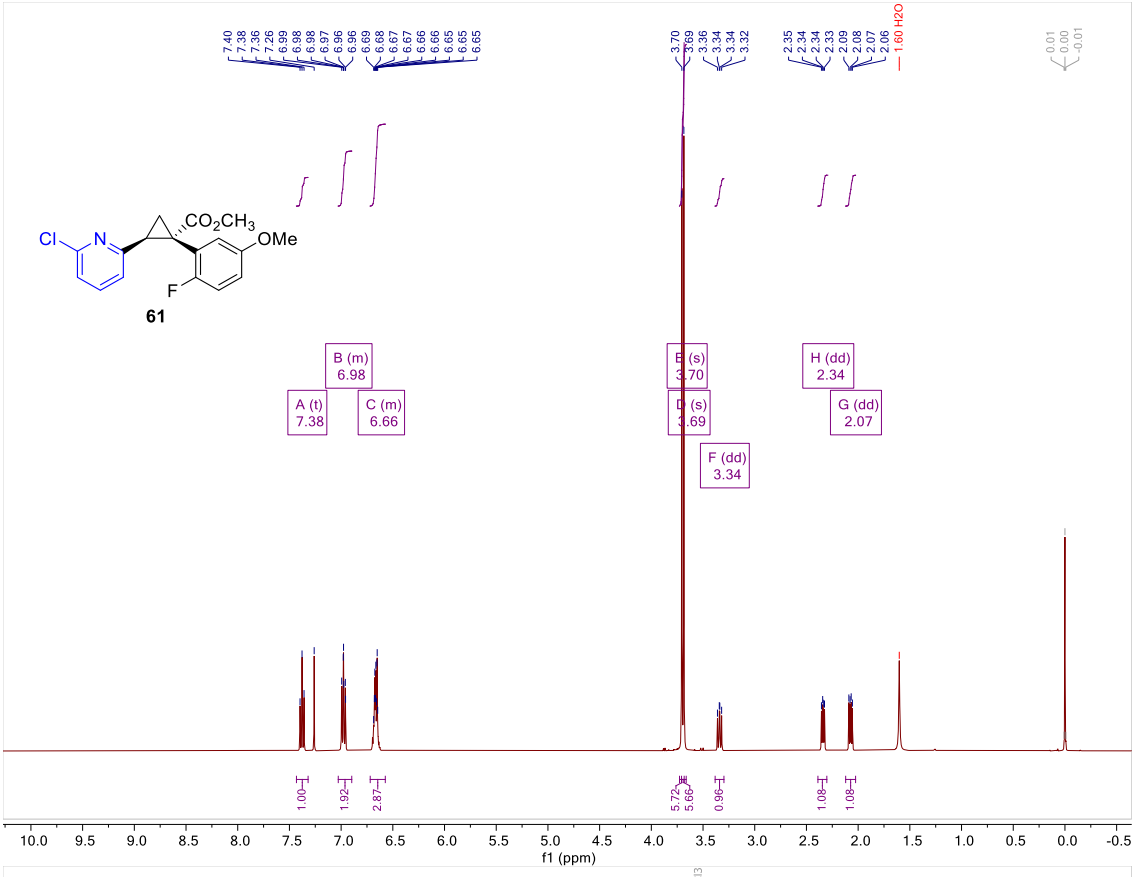
61
A (t) 7.38
B (m) 6.98
C (m) 6.66
D (s) 3.69
E (s) 3.70
F (dd) 3.34
G (dd) 2.07
H (dd) 2.34
1.60 H2O
f1 (ppm)

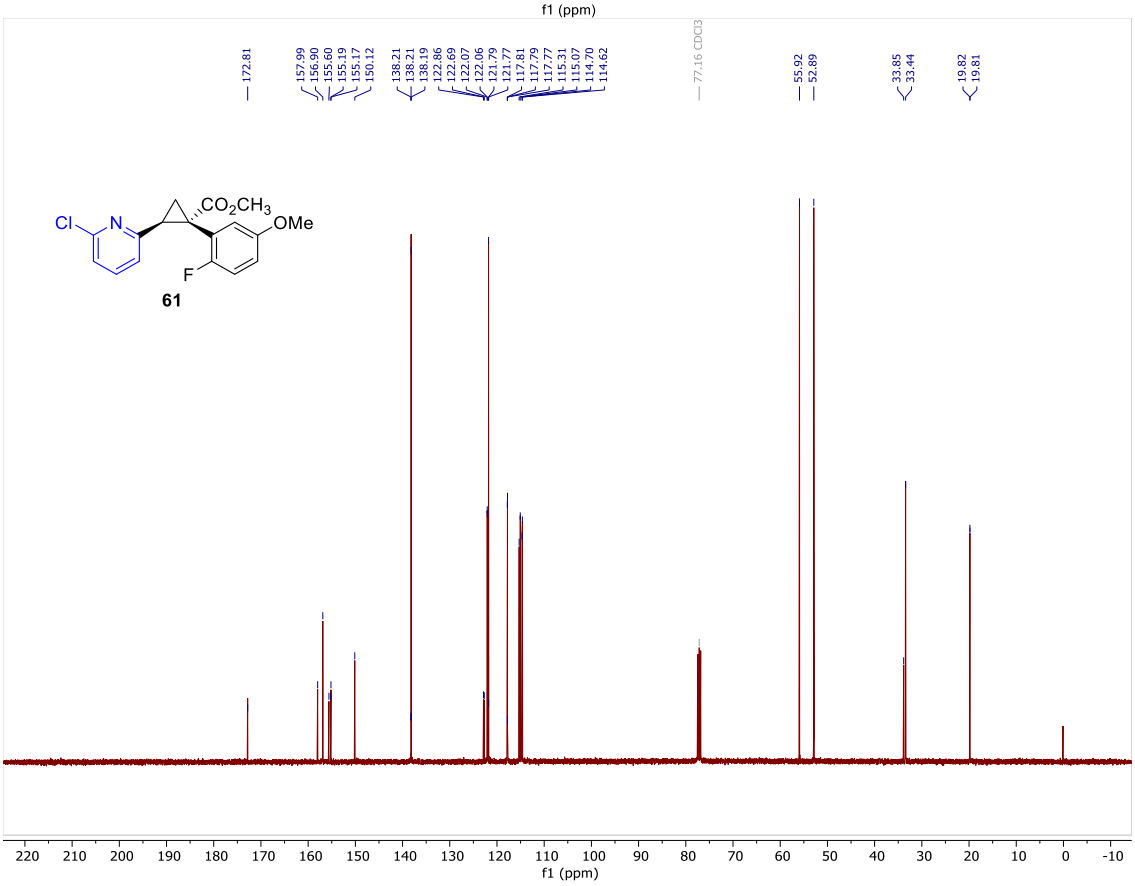
61
77.16 CDCl3
f1 (ppm)

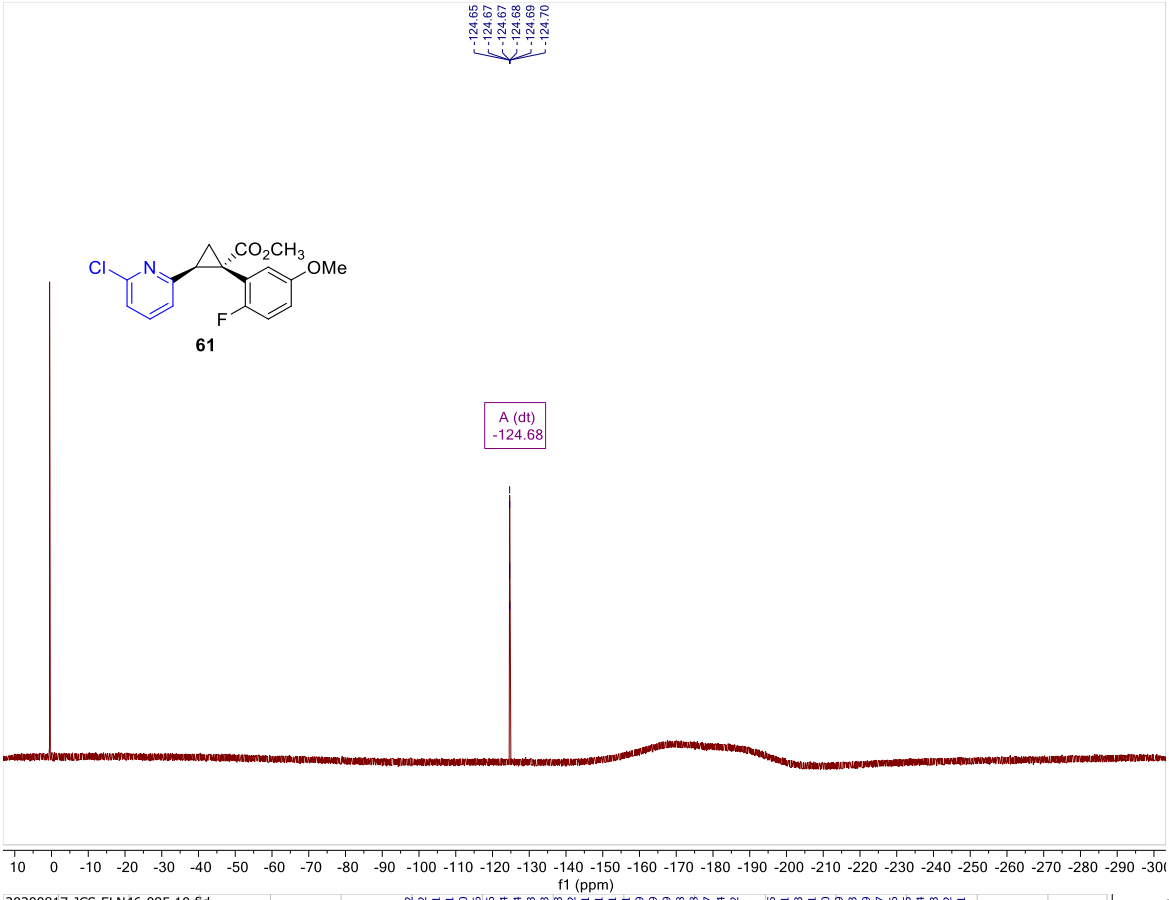
-124.65
-124.67
-124.67
-124.67
-124.68
-124.69
-124.70
Cl
N
CO2CH3
OMe
F
61
A (dt)
-124.68
f1 (ppm)

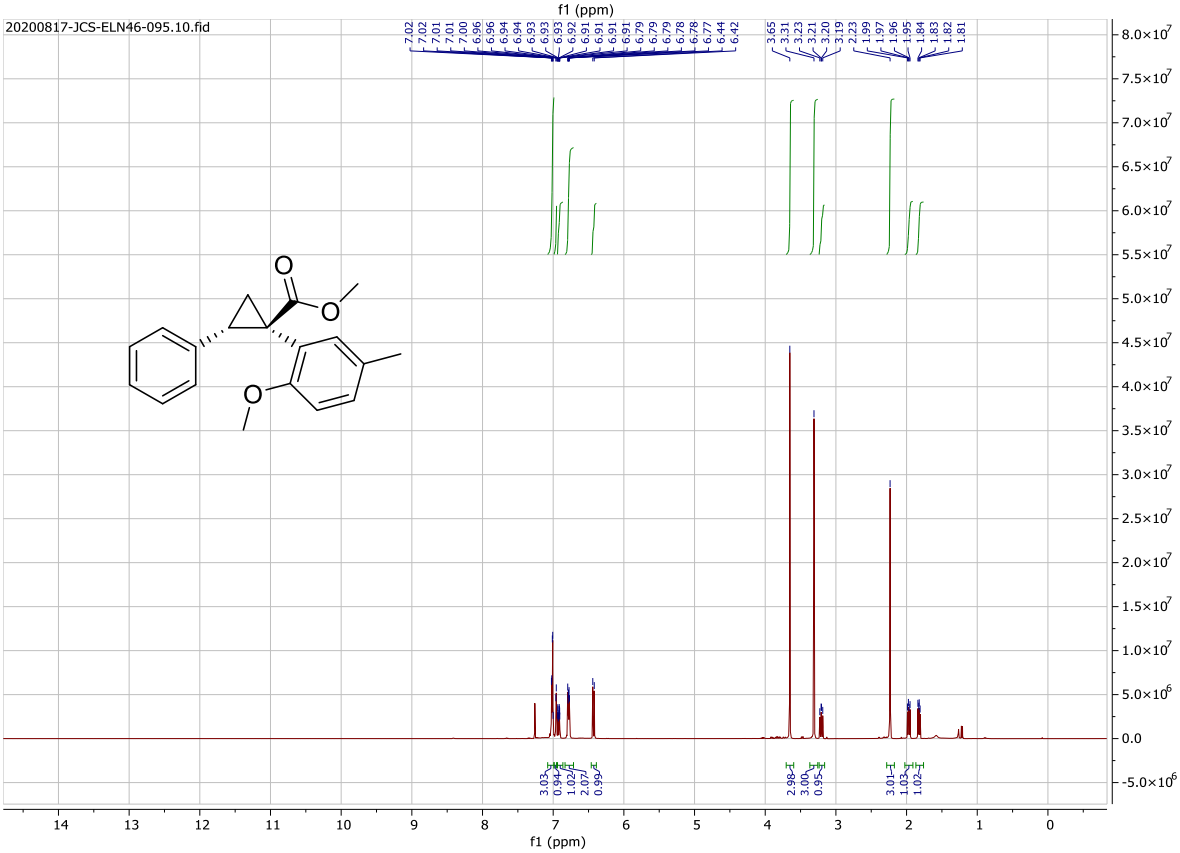
20200817-JCS-ELN46-095.10.fid
O
O
O
f1 (ppm)

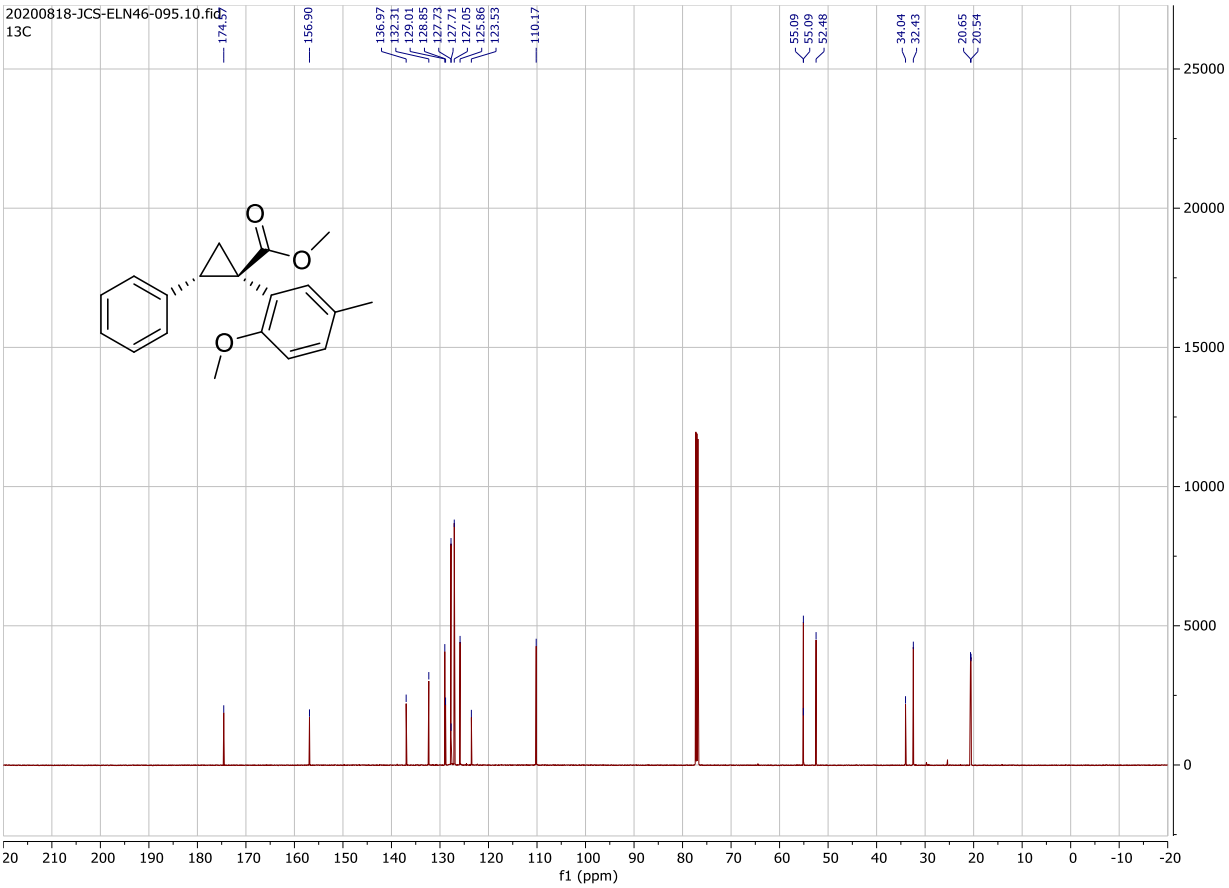
20200818-JCS-ELN46-095.10.fid
13C
174.57
156.90
136.97
132.31
129.01
128.85
127.73
127.71
127.05
125.86
123.53
110.17
55.09
55.09
52.48
34.04
32.43
20.65
20.54
f1 (ppm)

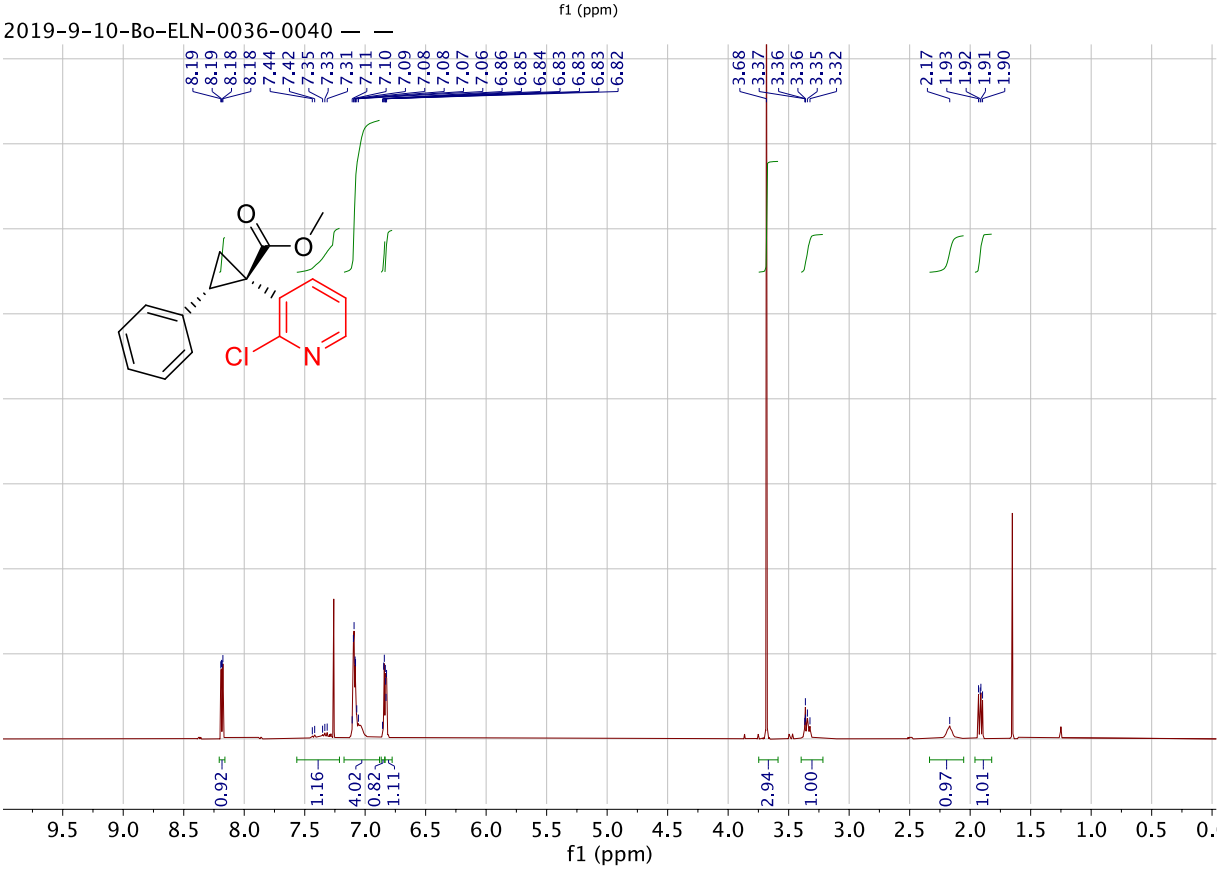
2019-9-10-Bo-ELN-0036-0040 — —
8.19
8.19
8.18
8.18
7.44
7.42
7.35
7.33
7.31
7.11
7.10
7.09
7.08
7.08
7.07
7.06
6.86
6.85
6.84
6.83
6.83
6.83
6.82
3.68
3.37
3.36
3.36
3.35
3.32
2.17
1.93
1.92
1.91
1.90
0.92
1.16
4.02
0.82
1.11
2.94
1.00
0.97
1.01
f1 (ppm)

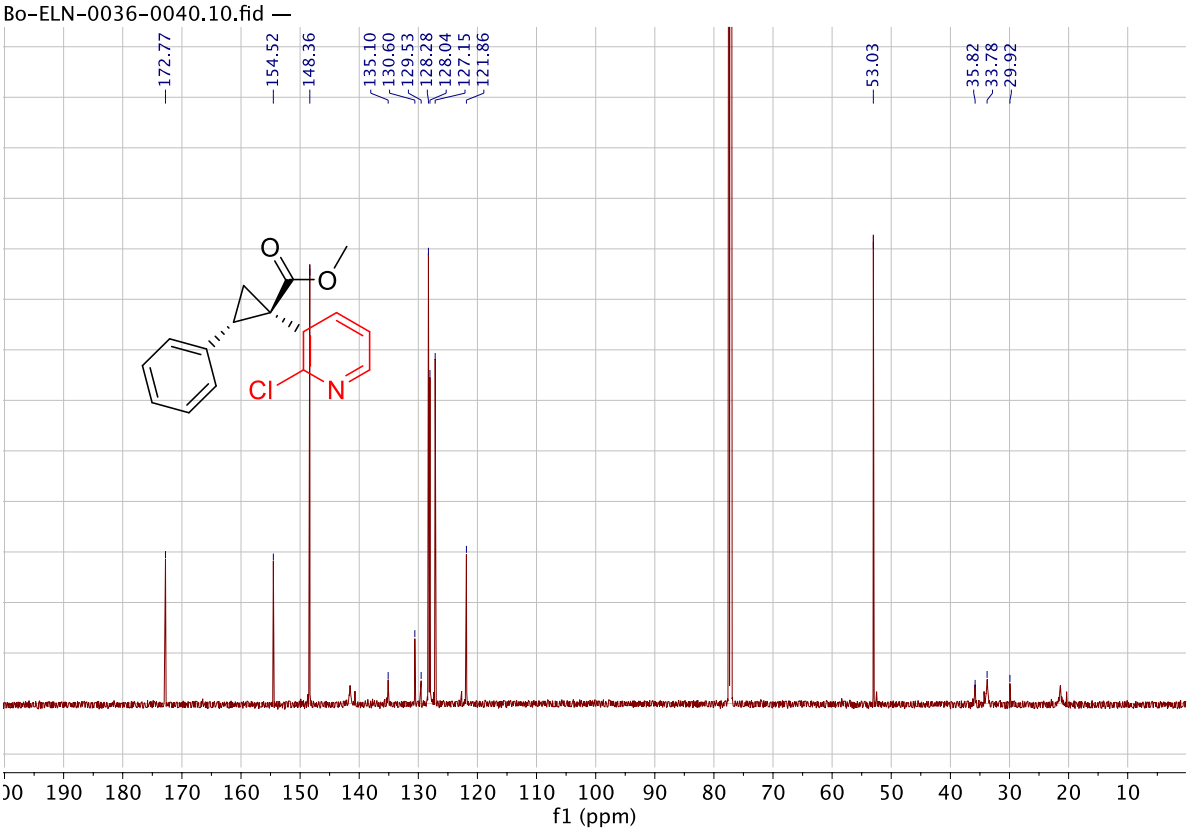
Bo-ELN-0036-0040.10.fid —
172.77
154.52
148.36
135.10
130.60
129.53
128.28
128.04
127.15
121.86
53.03
35.82
33.78
29.92
O
O
Cl
N
f1 (ppm)

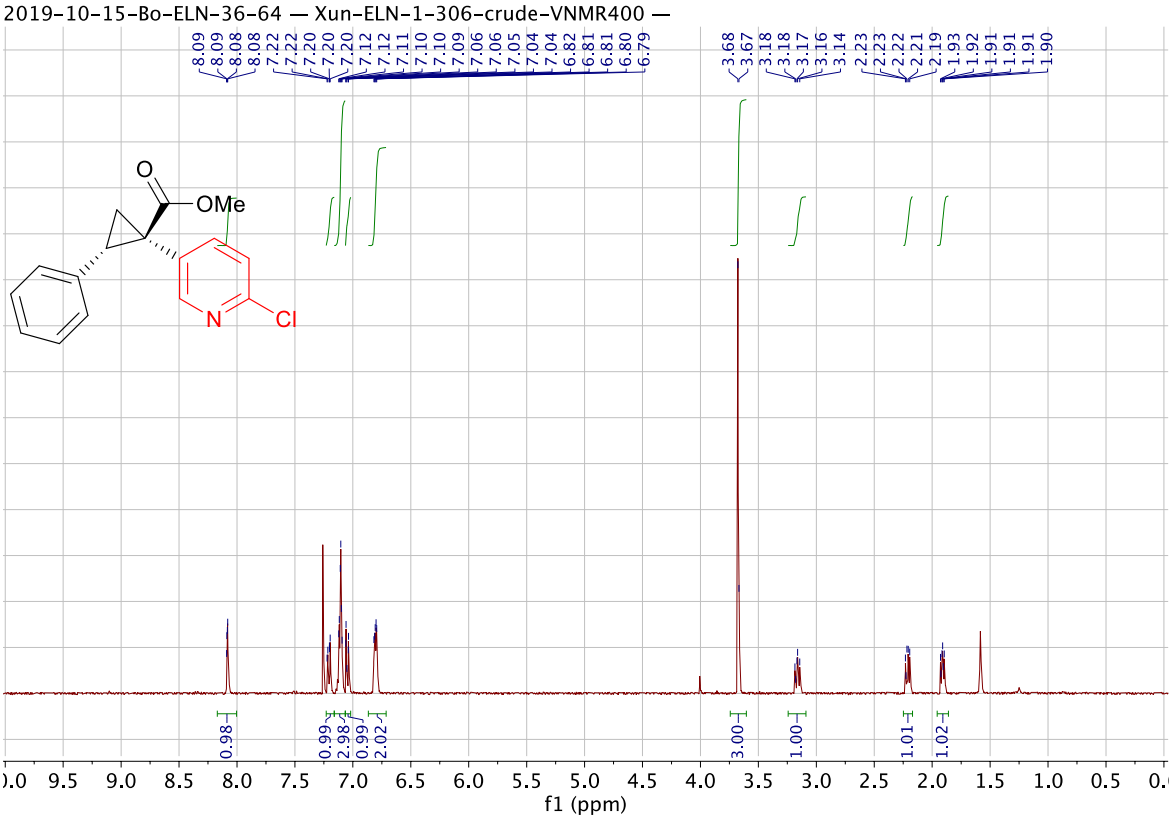
2019-10-15-Bo-ELN-36-64 — Xun-ELN-1-306-crude-VNMR400 —
8.09
8.09
8.08
8.08
7.22
7.22
7.20
7.20
7.20
7.12
7.12
7.11
7.10
7.10
7.09
7.06
7.06
7.05
7.04
7.04
6.82
6.81
6.81
6.80
6.79
3.68
3.67
3.18
3.18
3.17
3.16
3.14
2.23
2.23
2.22
2.21
2.19
1.93
1.92
1.91
1.91
1.91
1.90
O
OMe
N
Cl
0.98
0.99
2.98
0.99
2.02
3.00
1.00
1.01
1.02
f1 (ppm)

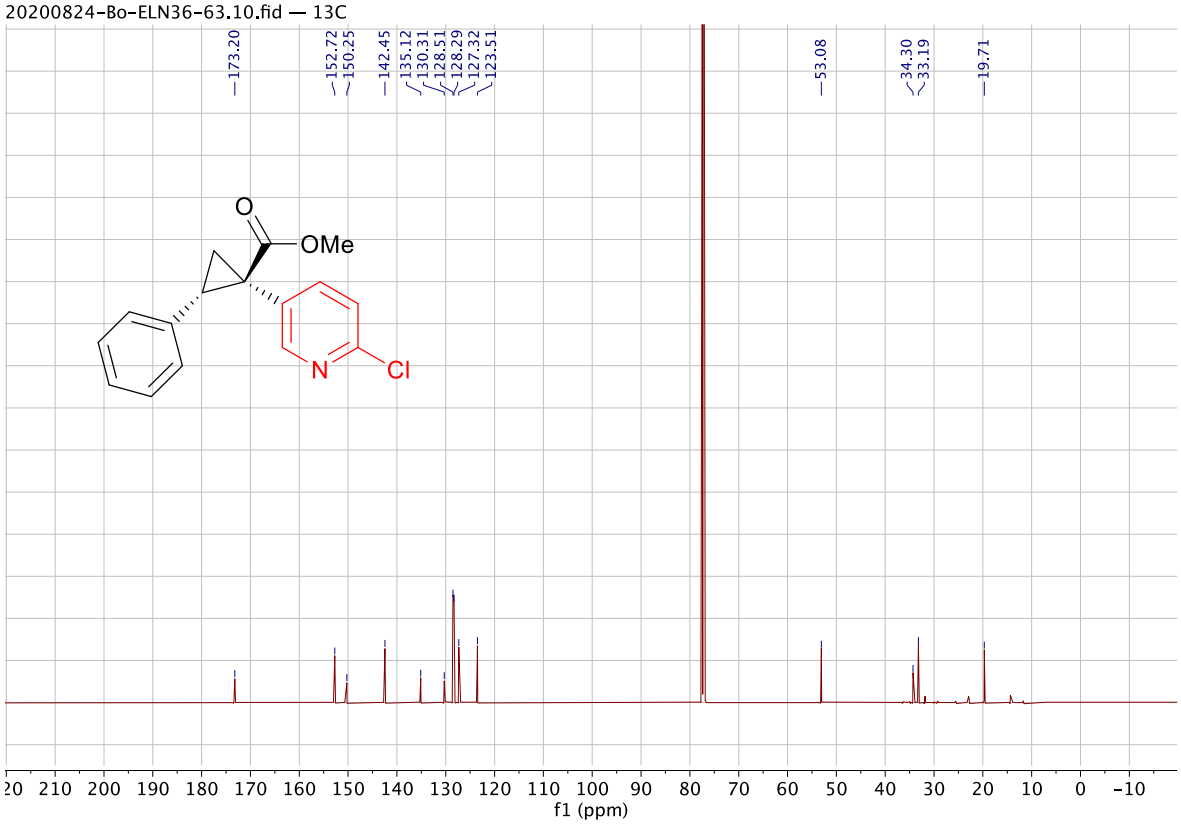
20200824-Bo-ELN36-63.10.fid — 13C
173.20
152.72
150.25
142.45
135.12
130.31
128.51
128.29
127.32
123.51
53.08
34.30
33.19
19.71
O
OMe
N
Cl
f1 (ppm)

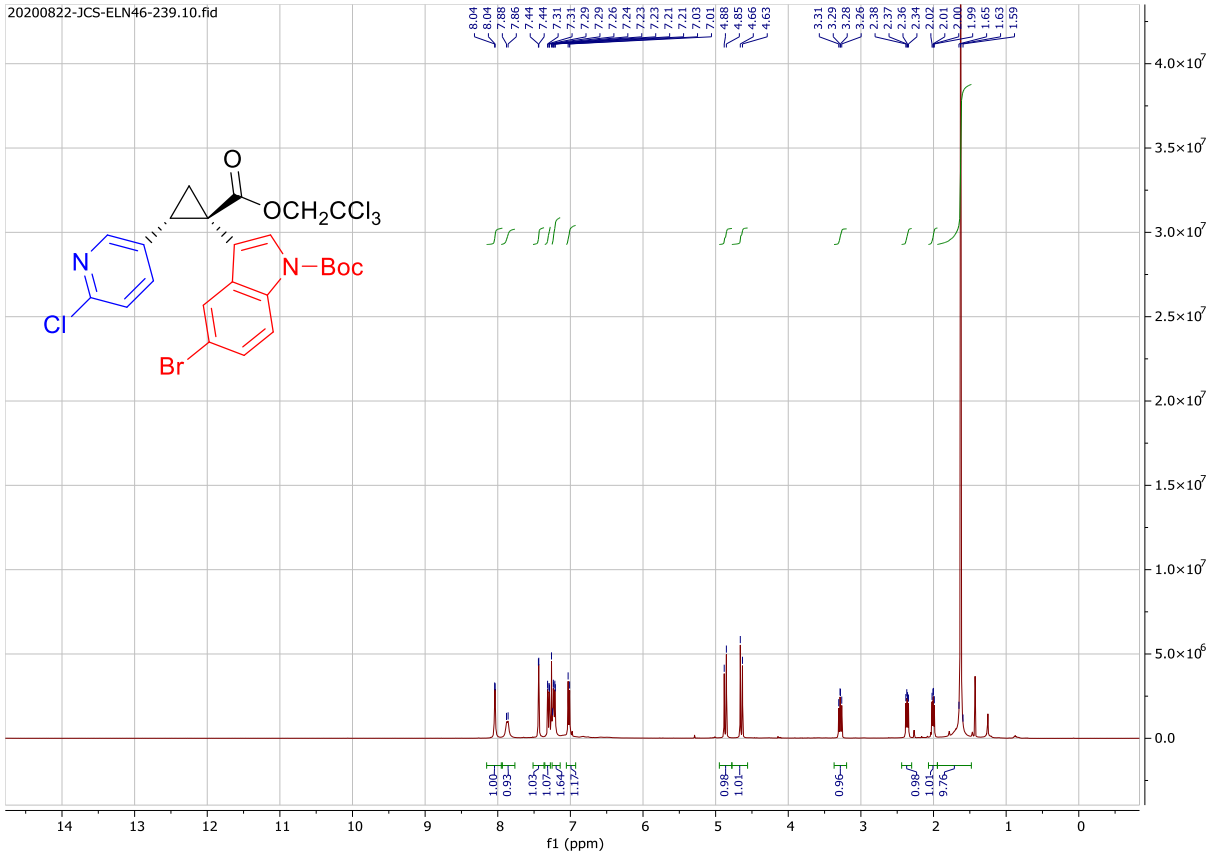
20200822-JCS-ELN46-239.10.fid
O
OCH2CCl3
N
Cl
N−Boc
Br
f1 (ppm)

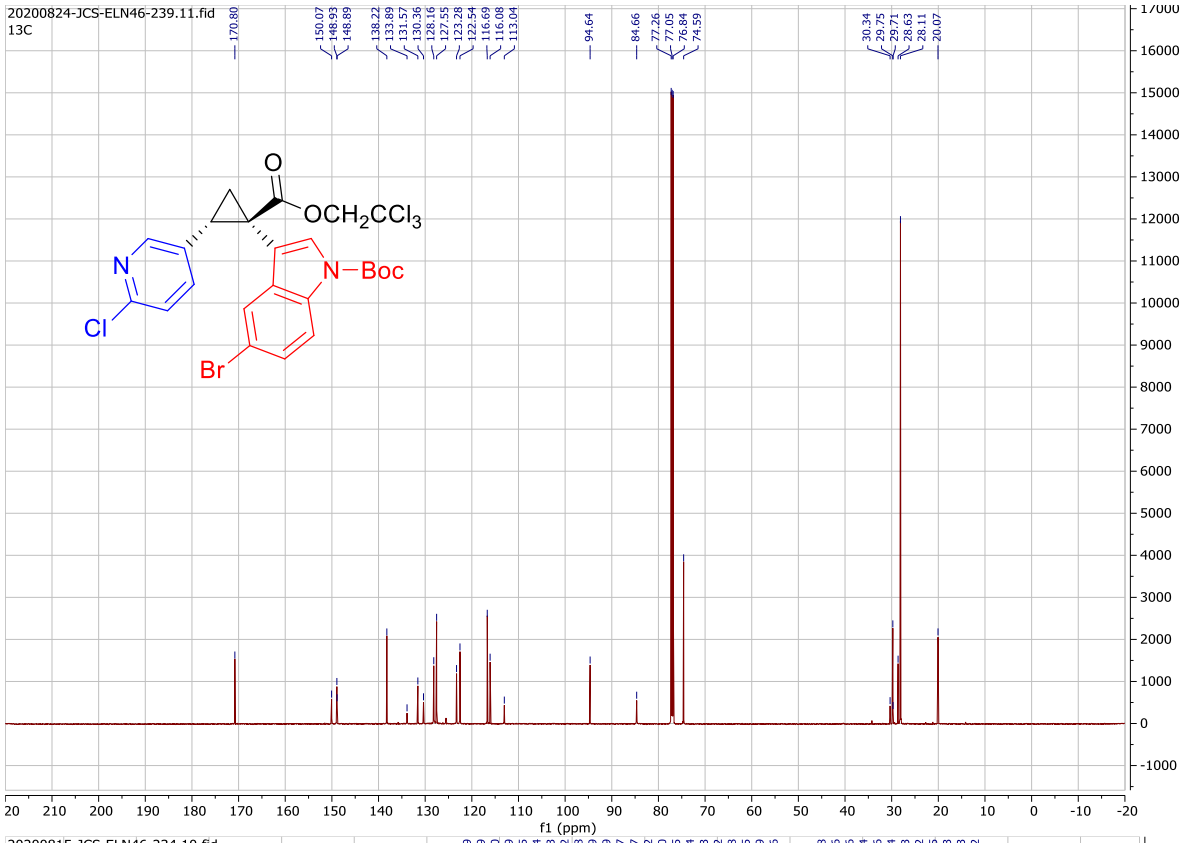
20200824-JCS-ELN46-239.11.fid
13C
170.80
150.07
146.93
146.89
138.22
133.89
131.57
130.36
128.16
127.55
123.28
122.54
116.69
116.08
113.04
94.64
84.66
77.26
77.05
76.84
74.59
30.34
29.75
29.71
28.63
28.11
20.07
O
OCH2CCl3
N
Cl
N−Boc
Br
f1 (ppm)

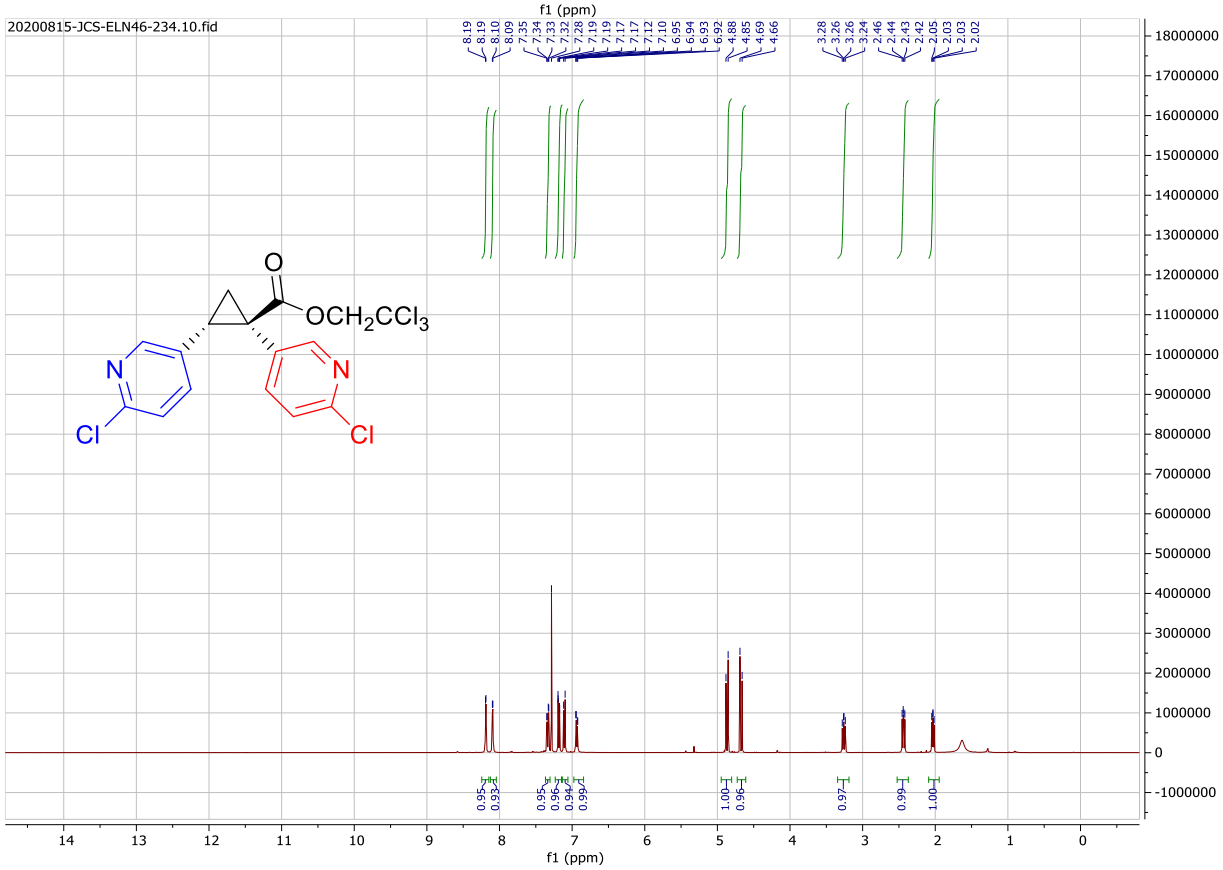
20200815-JCS-ELN46-234.10.fid
8.19
8.19
8.10
8.09
7.35
7.34
7.33
7.32
7.28
7.19
7.19
7.17
7.17
7.12
7.10
6.95
6.94
6.93
6.92
4.88
4.85
4.69
4.66
3.28
3.26
3.26
3.24
2.46
2.44
2.43
2.42
2.05
2.03
2.03
2.02
O
OCH2CCl3
N
Cl
N
Cl
0.95
0.93
0.95
0.96
0.94
0.99
1.00
0.96
0.97
0.99
1.00
f1 (ppm)

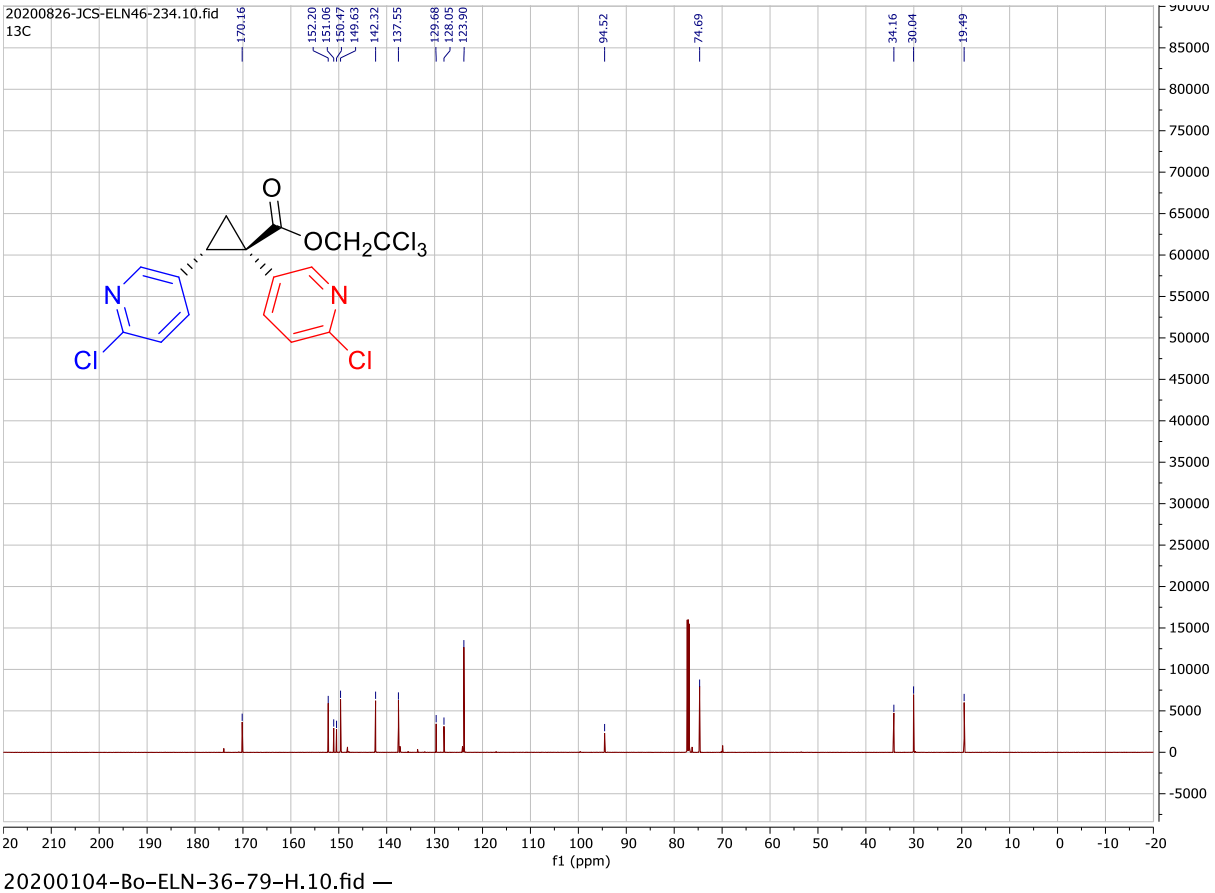
20200826-JCS-ELN46-234.10.fid
13C
170.16
152.20
151.06
150.47
149.63
142.32
137.55
129.68
128.05
123.90
94.52
74.69
34.16
30.04
19.49
O
OCH2CCl3
N
Cl
N
Cl
f1 (ppm)

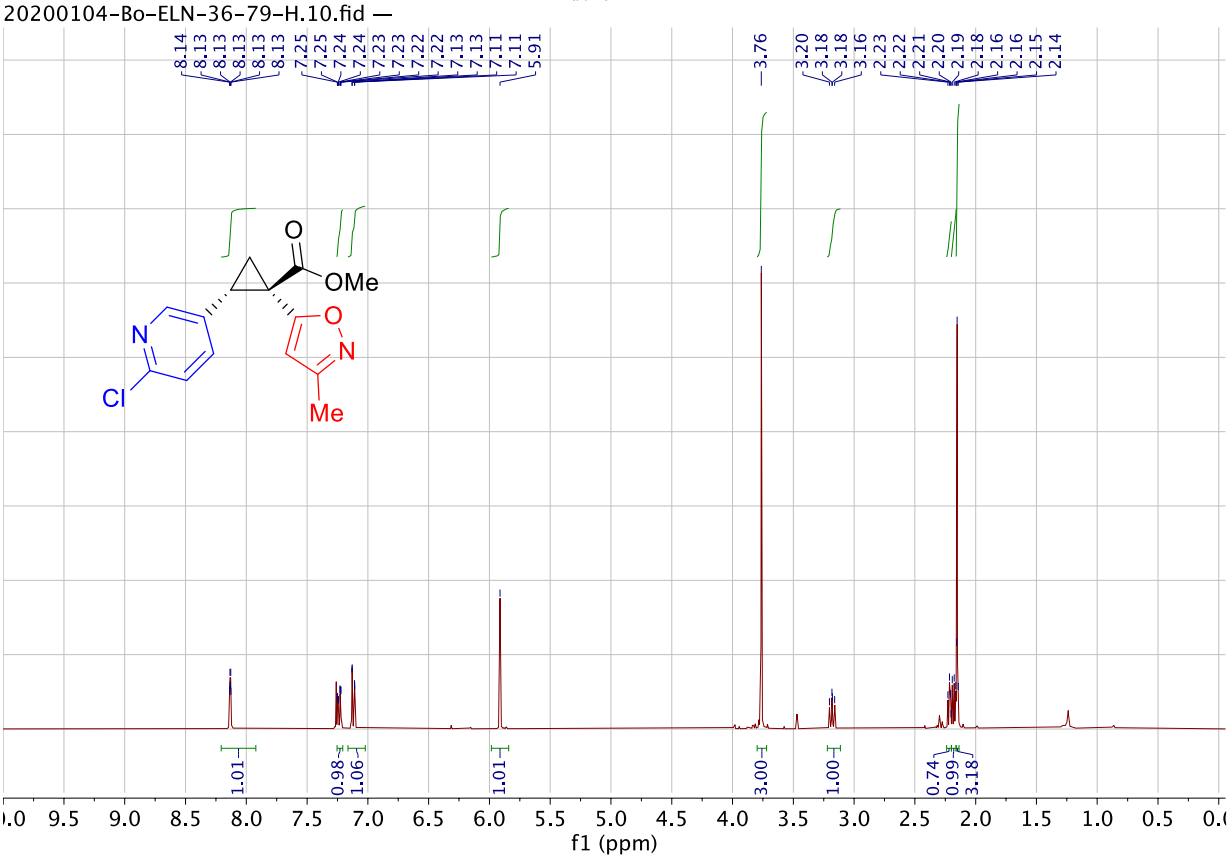
20200104-Bo-ELN-36-79-H.10.fid —
8.14
8.13
8.13
8.13
8.13
7.25
7.25
7.24
7.24
7.24
7.23
7.23
7.22
7.22
7.22
7.13
7.13
7.11
7.11
5.91
3.76
3.20
3.18
3.18
3.16
2.23
2.22
2.21
2.20
2.19
2.18
2.16
2.15
2.14
O
OMe
N
Cl
O
N
Me
1.01
0.98
1.06
1.01
3.00
1.00
0.74
0.99
3.18
f1 (ppm)

20200104-Bo-ELN-36-79-C.10.fid —

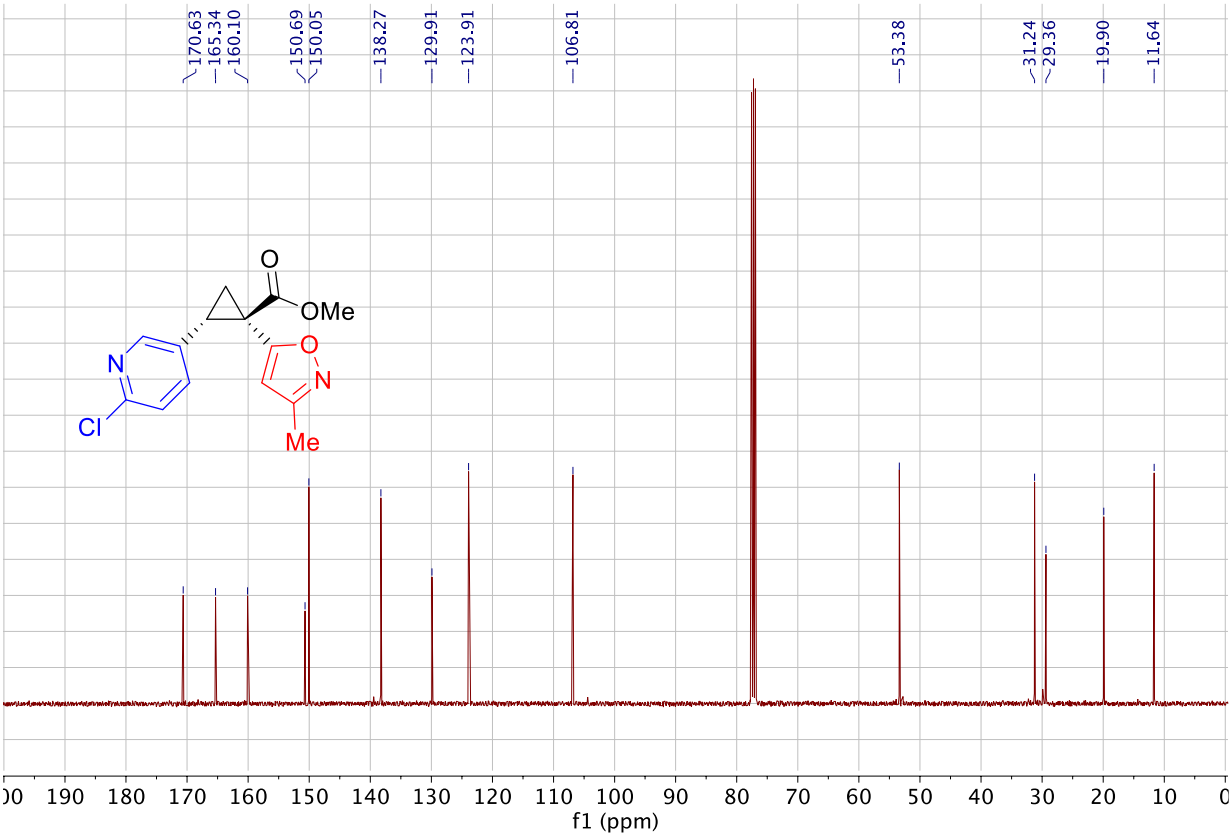

2019-9-14-Bo-ELN-0036-0051 — —

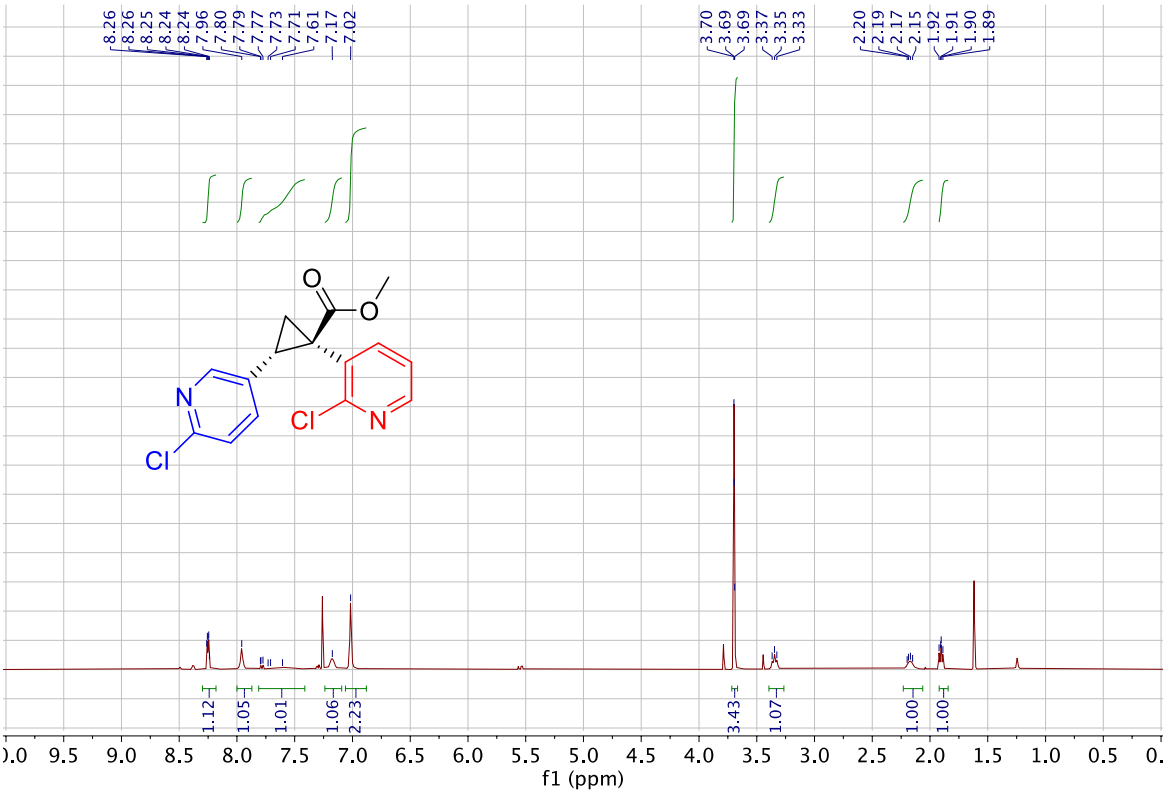

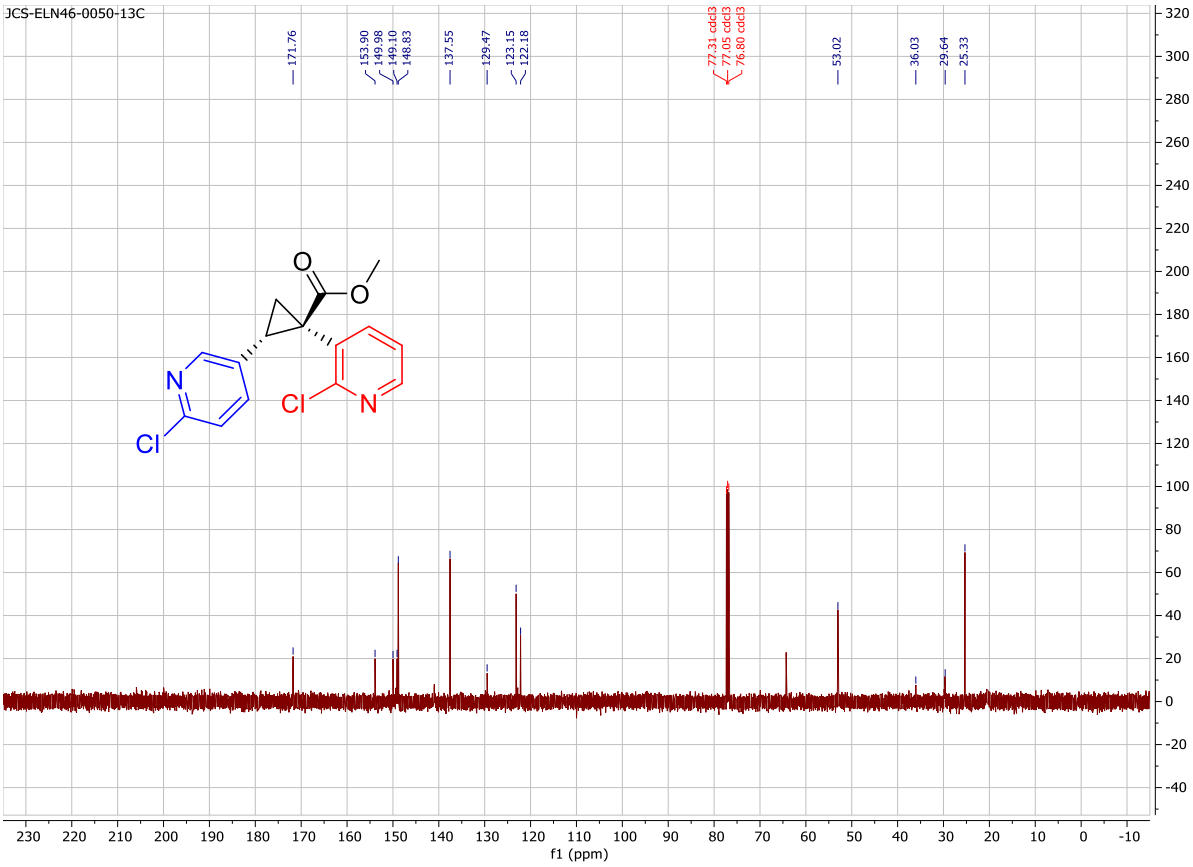
JCS-ELN46-0050-13C
171.76
153.90
149.98
149.10
148.83
137.55
129.47
123.15
122.18
77.31 cdcl3
77.05 cdcl3
76.80 cdcl3
53.02
36.03
29.64
25.33
f1 (ppm)

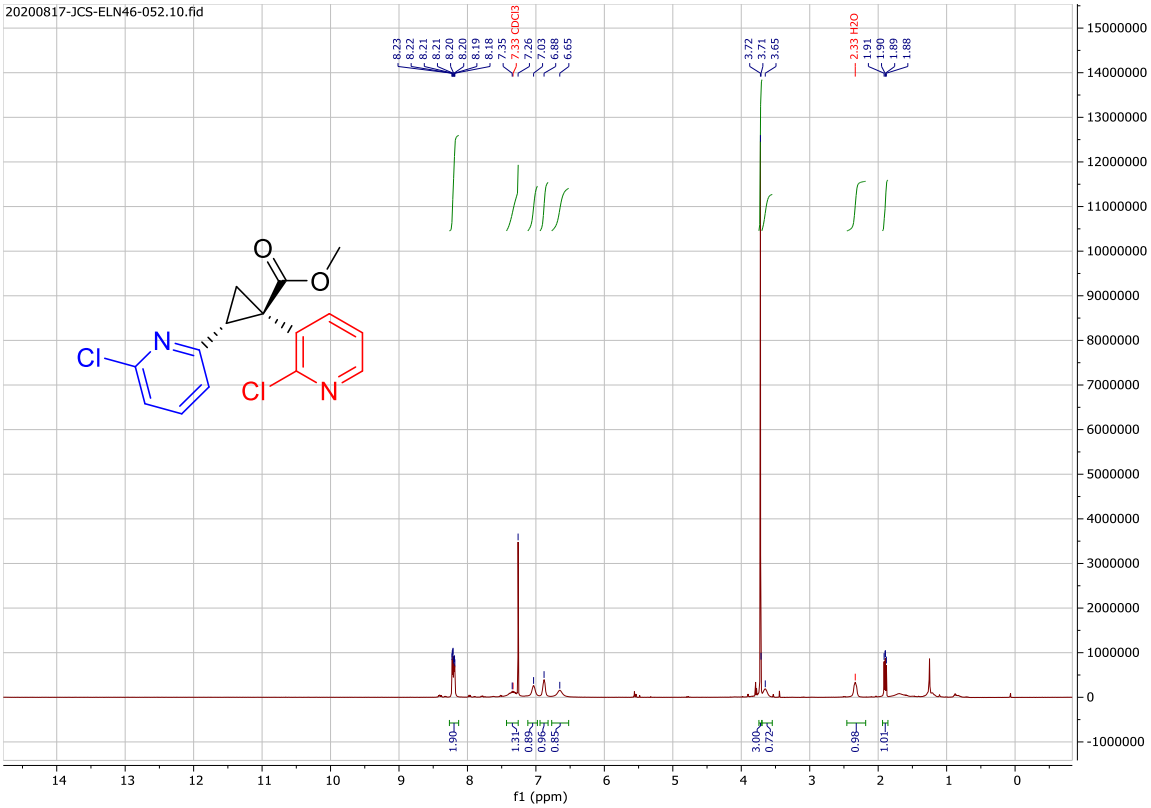
20200817-JCS-ELN46-052.10.fid
8.23
8.22
8.21
8.21
8.20
8.20
8.19
8.18
7.35
7.33 CDCl3
7.26
7.03
6.88
6.65
3.72
3.71
3.65
2.33 H2O
1.91
1.90
1.89
1.88
1.90
1.31
0.89
0.96
0.85
3.00
0.72
0.98
1.01
f1 (ppm)

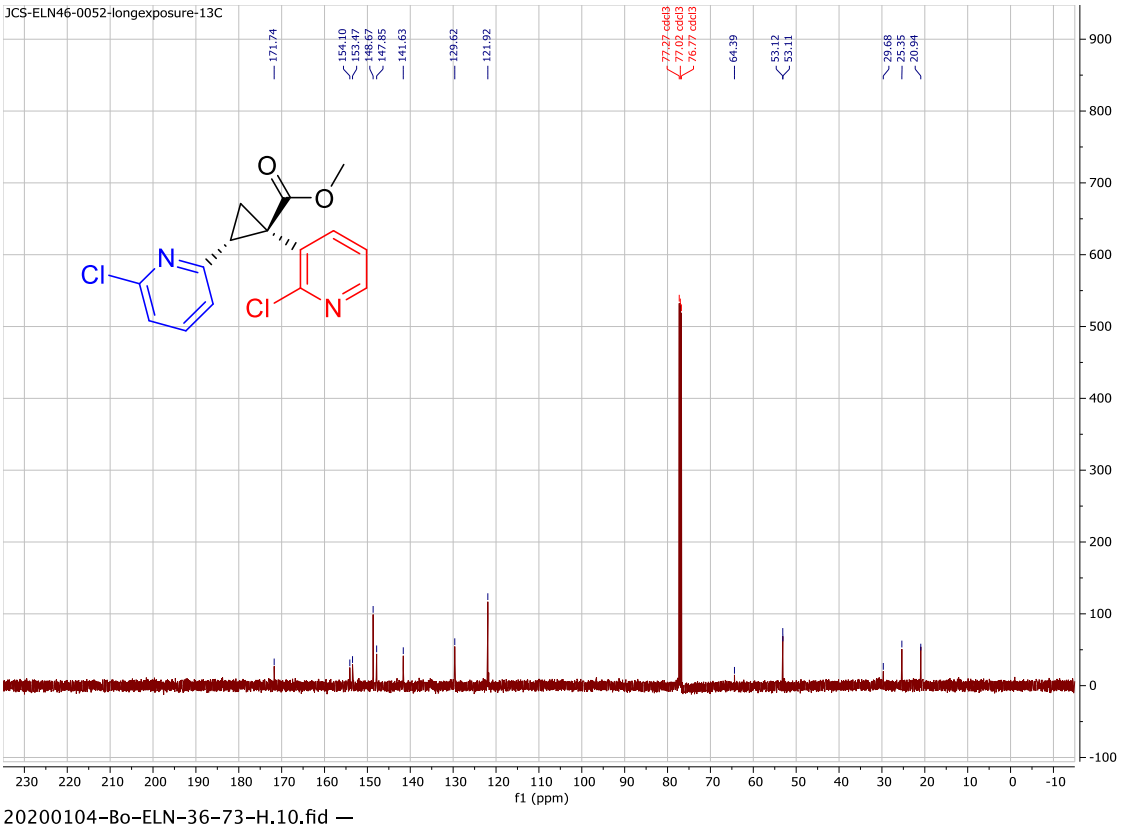
JCS-ELN46-0052-longexposure-13C
171.74
154.10
153.47
148.67
147.85
141.63
129.62
121.92
77.27 cdcl3
77.02 cdcl3
76.77 cdcl3
64.39
53.12
53.11
29.68
25.35
20.94
f1 (ppm)

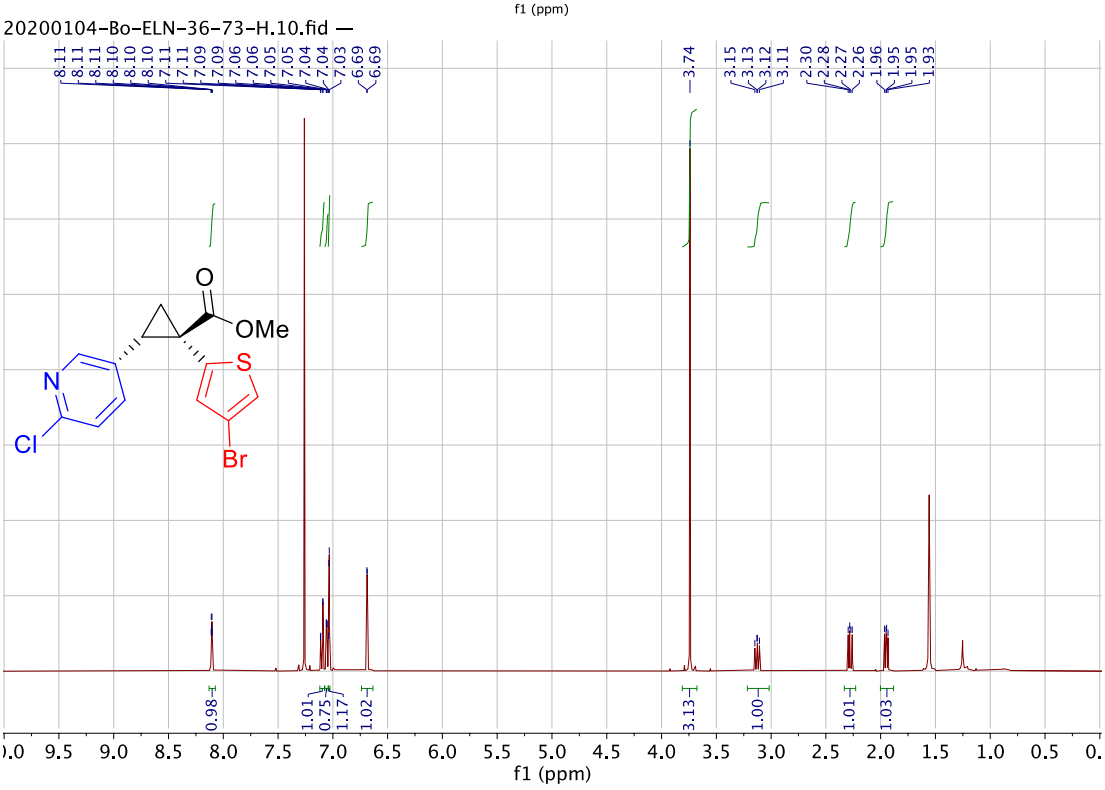
20200104-Bo-ELN-36-73-H.10.fid
8.11
8.11
8.11
8.10
8.10
8.10
7.11
7.11
7.09
7.09
7.06
7.06
7.05
7.05
7.04
7.04
7.03
6.69
6.69
3.74
3.15
3.13
3.12
3.11
2.30
2.28
2.27
2.26
1.96
1.95
1.95
1.93
0.98
1.01
0.75
1.17
1.02
3.13
1.00
1.01
1.03
f1 (ppm)

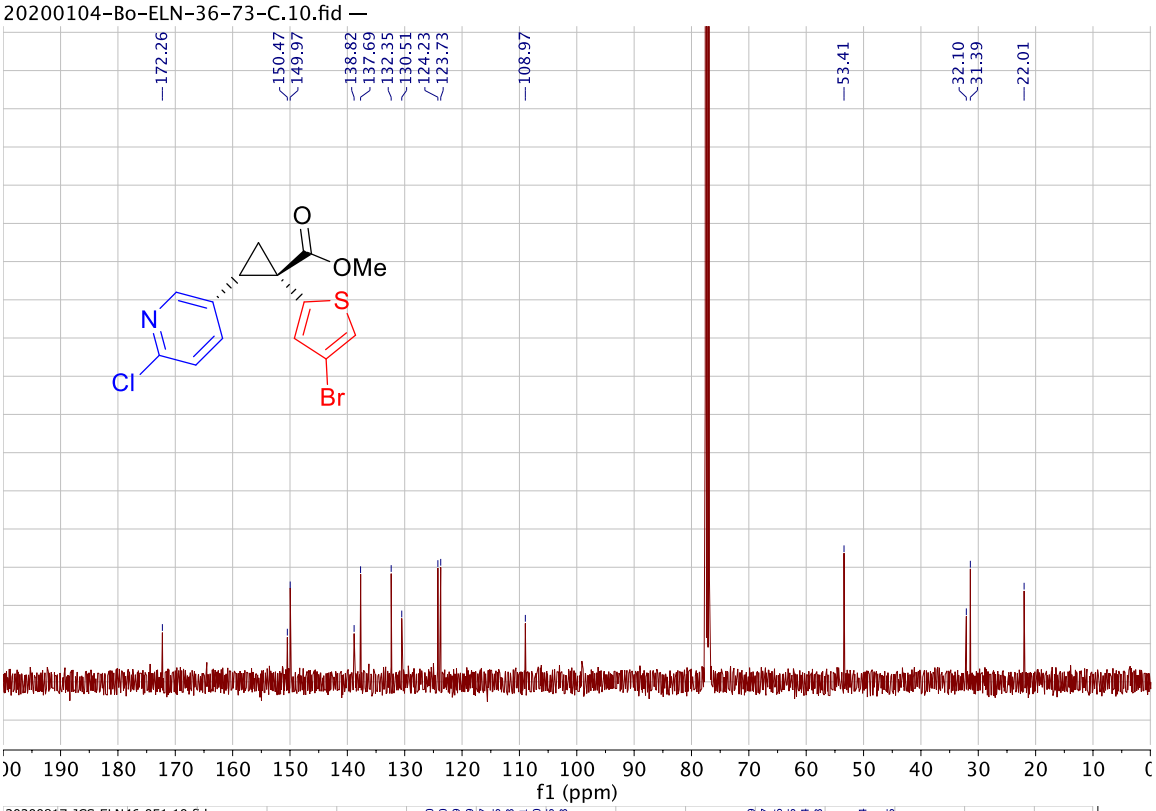
20200104-Bo-ELN-36-73-C.10.fid
172.26
150.47
149.97
138.82
137.69
132.35
130.51
124.23
123.73
108.97
53.41
32.10
31.39
22.01
O
OMe
N
S
Cl
Br
f1 (ppm)

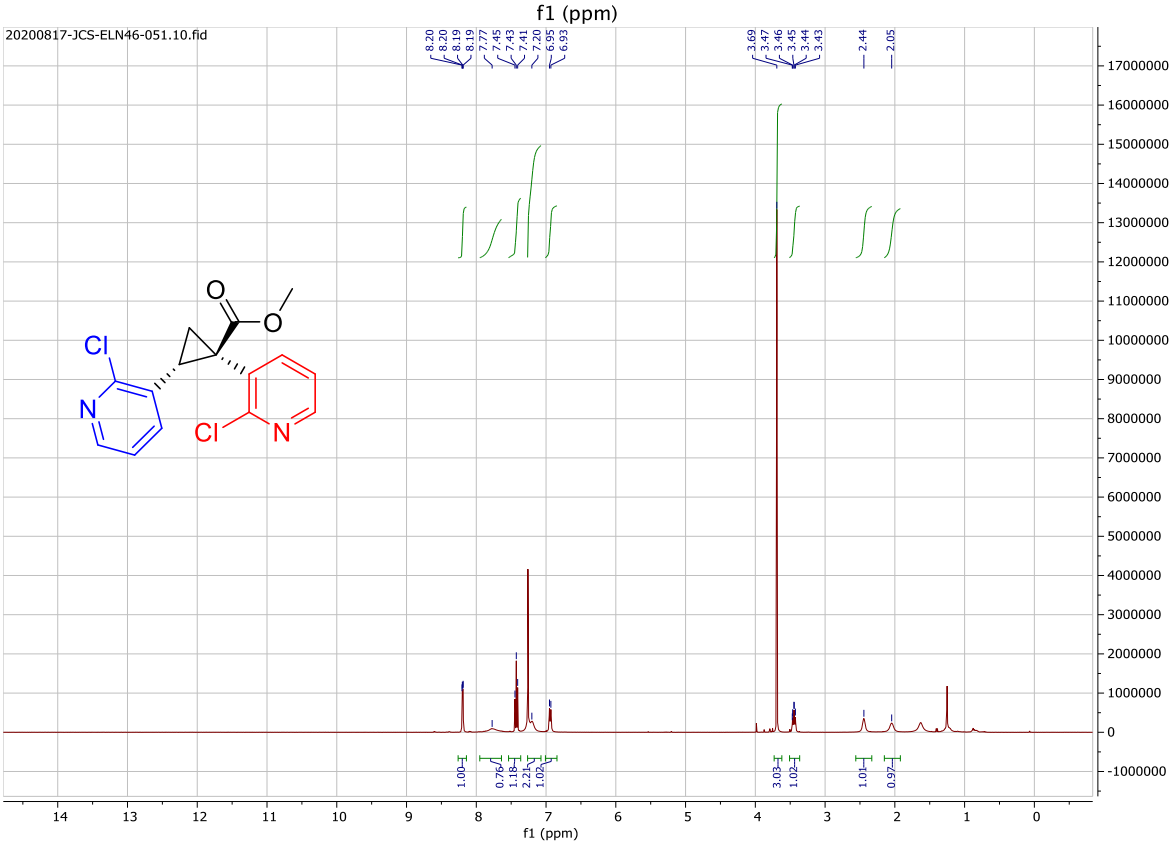
20200817-JCS-ELN46-051.10.fid
8.20
8.20
8.19
8.19
7.77
7.77
7.45
7.43
7.41
7.20
6.95
6.93
3.69
3.47
3.46
3.45
3.44
3.43
2.44
2.05
1.00
0.76
1.18
2.22
1.02
3.03
1.02
1.01
0.97
O
O
Cl
N
Cl
N
f1 (ppm)

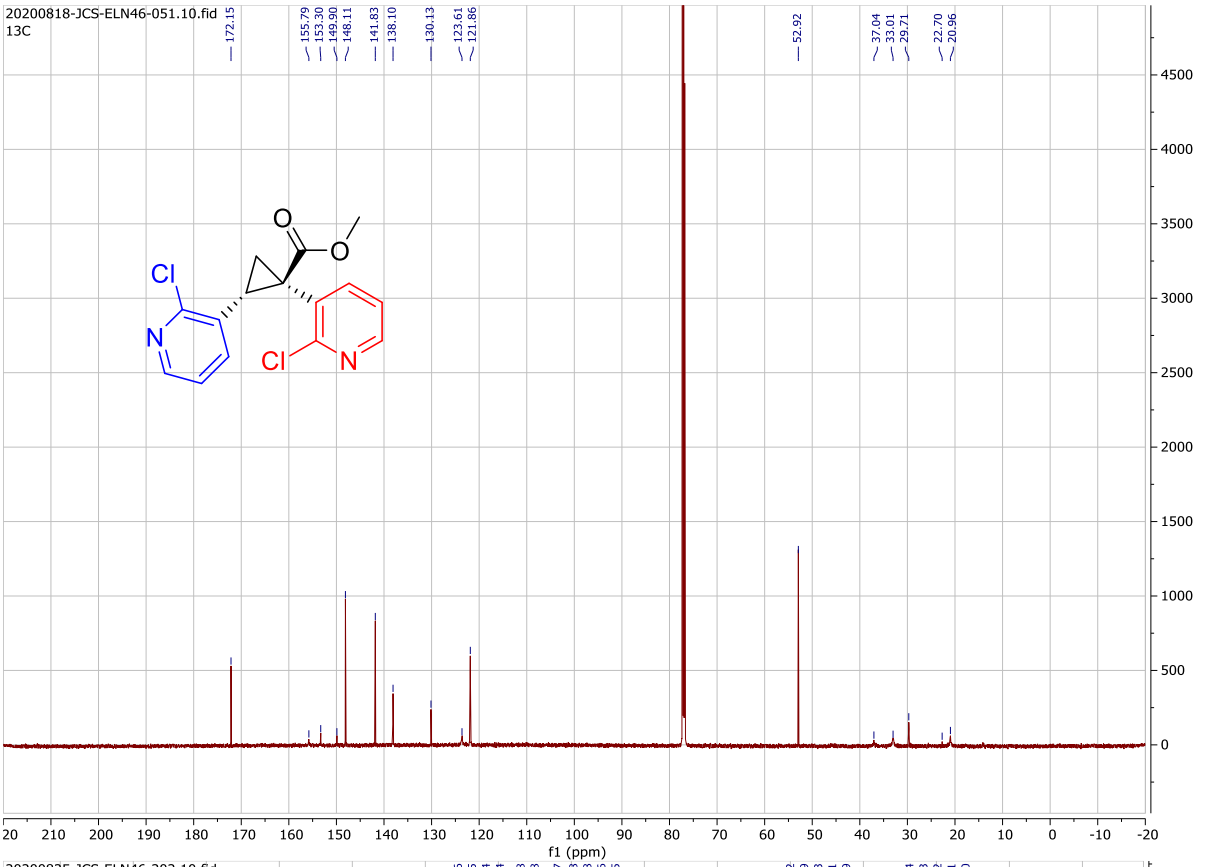
20200818-JCS-ELN46-051.10.fid
13C
172.15
155.79
153.30
149.90
148.11
141.83
138.10
130.13
123.61
121.86
52.92
37.04
33.01
29.71
22.70
20.96
f1 (ppm)

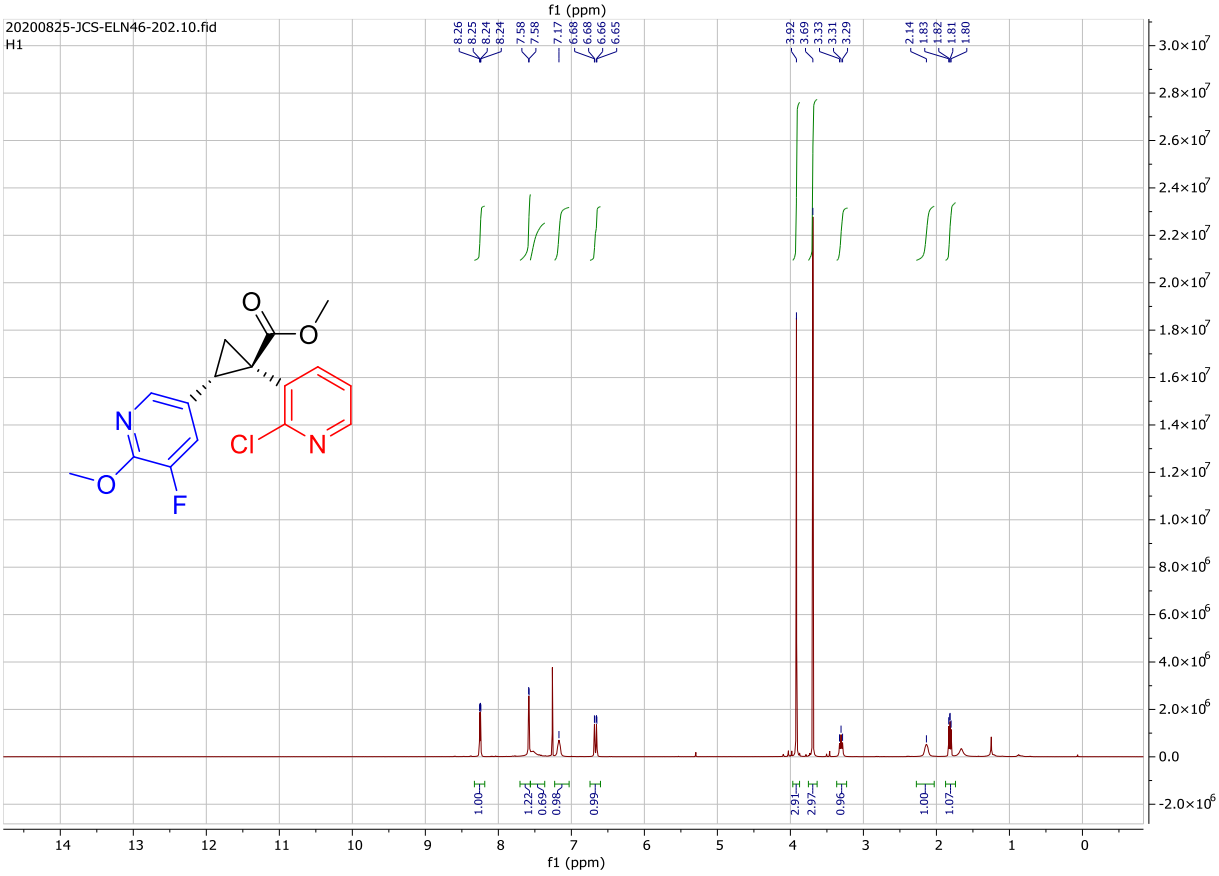
20200825-JCS-ELN46-202.10.fid
H1
8.26
8.25
8.24
8.24
7.58
7.58
7.17
6.68
6.68
6.66
6.65
3.92
3.69
3.33
3.31
3.29
2.14
1.83
1.82
1.81
1.80
1.00
1.22
0.69
0.98
0.99
2.91
2.97
0.96
1.00
1.07
f1 (ppm)

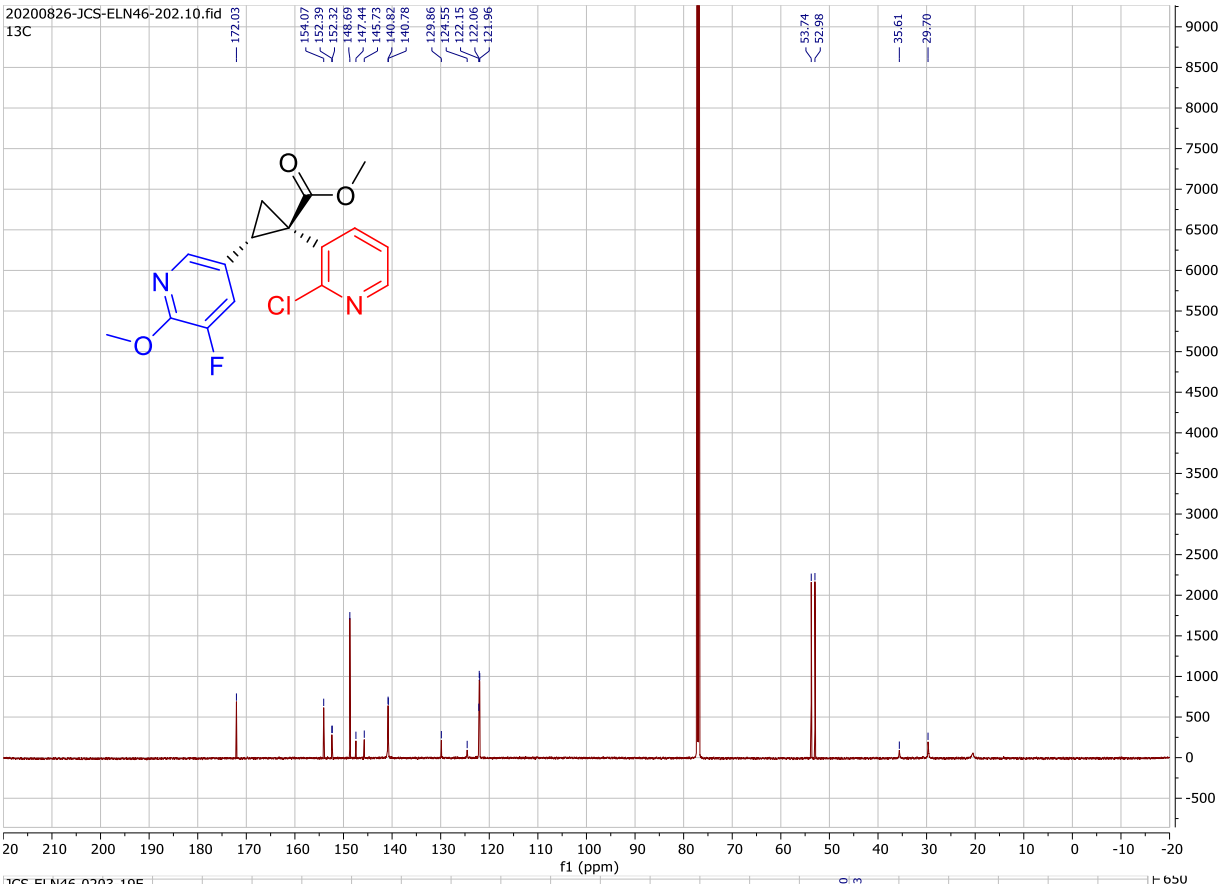
20200826-JCS-ELN46-202.10.fid
13C
172.03
154.07
152.39
152.32
148.69
147.44
145.73
140.82
140.78
129.86
124.55
122.15
122.06
121.96
53.74
52.98
35.61
29.70
f1 (ppm)

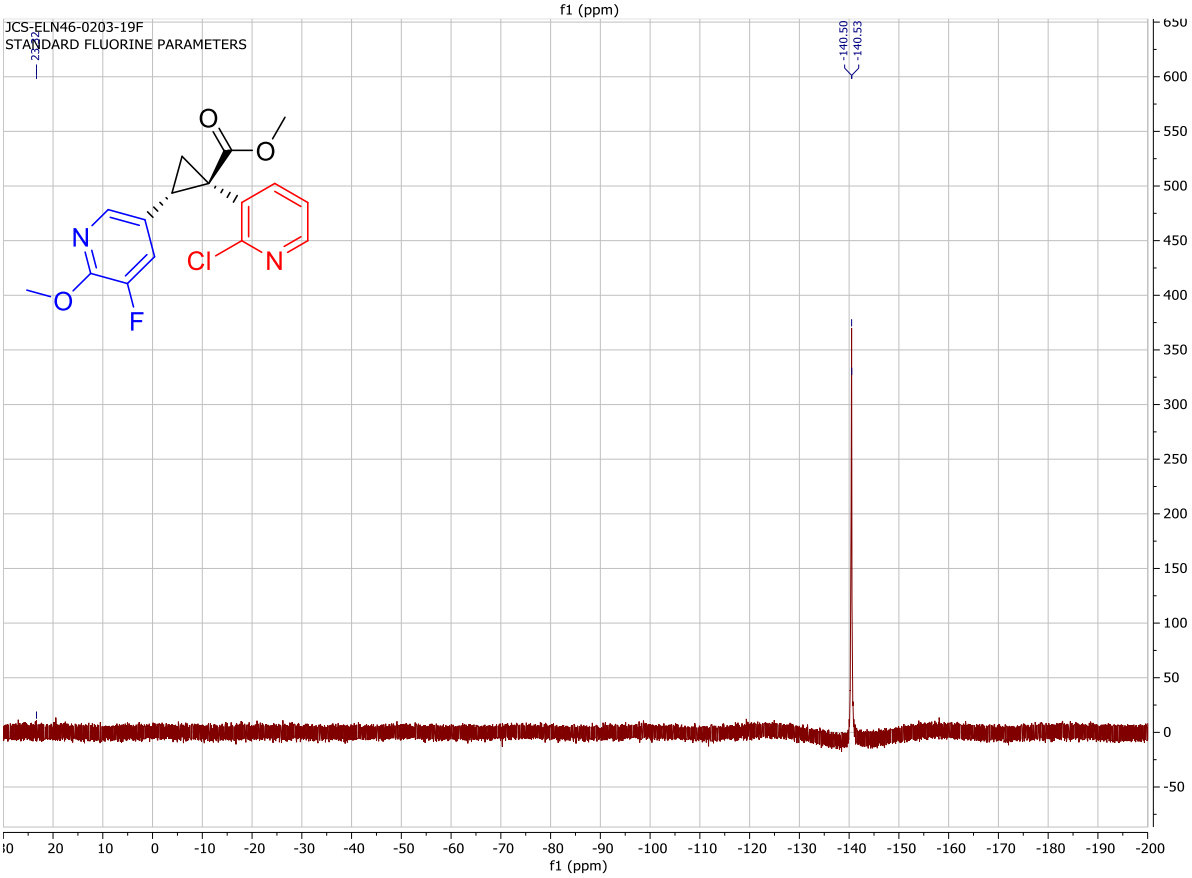
JCS-ELN46-0203-19F
STANDARD FLUORINE PARAMETERS
-140.50
-140.53
f1 (ppm)

20200104-Bo-ELN-36-55-H.10.fid —

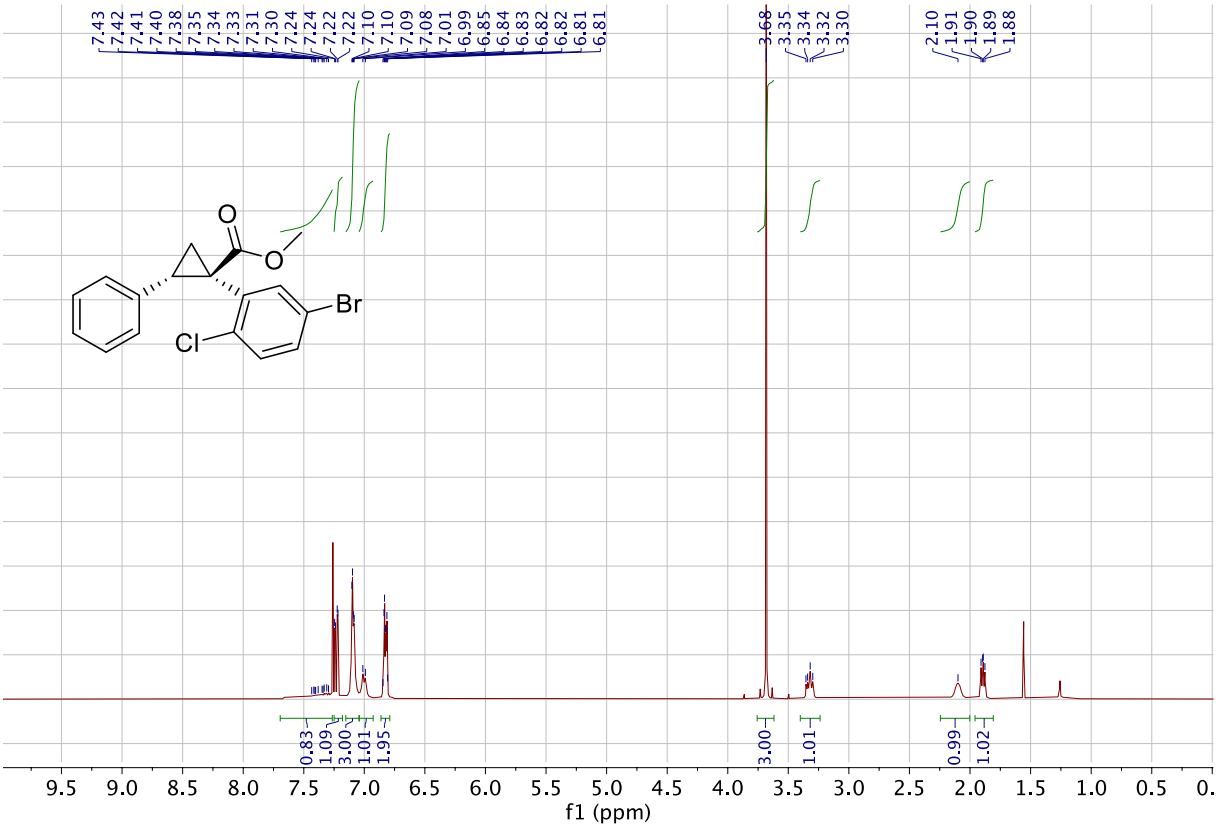

20200104-Bo-ELN-36-55-C.10.fid —

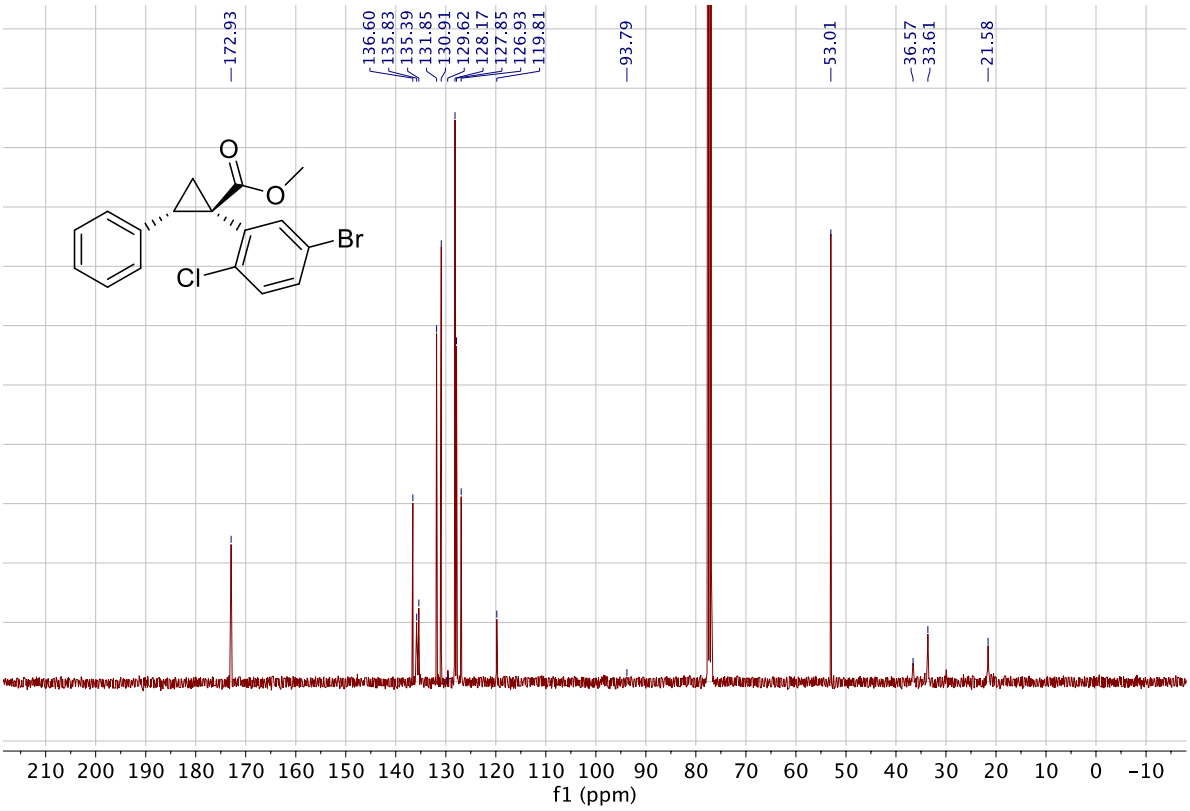

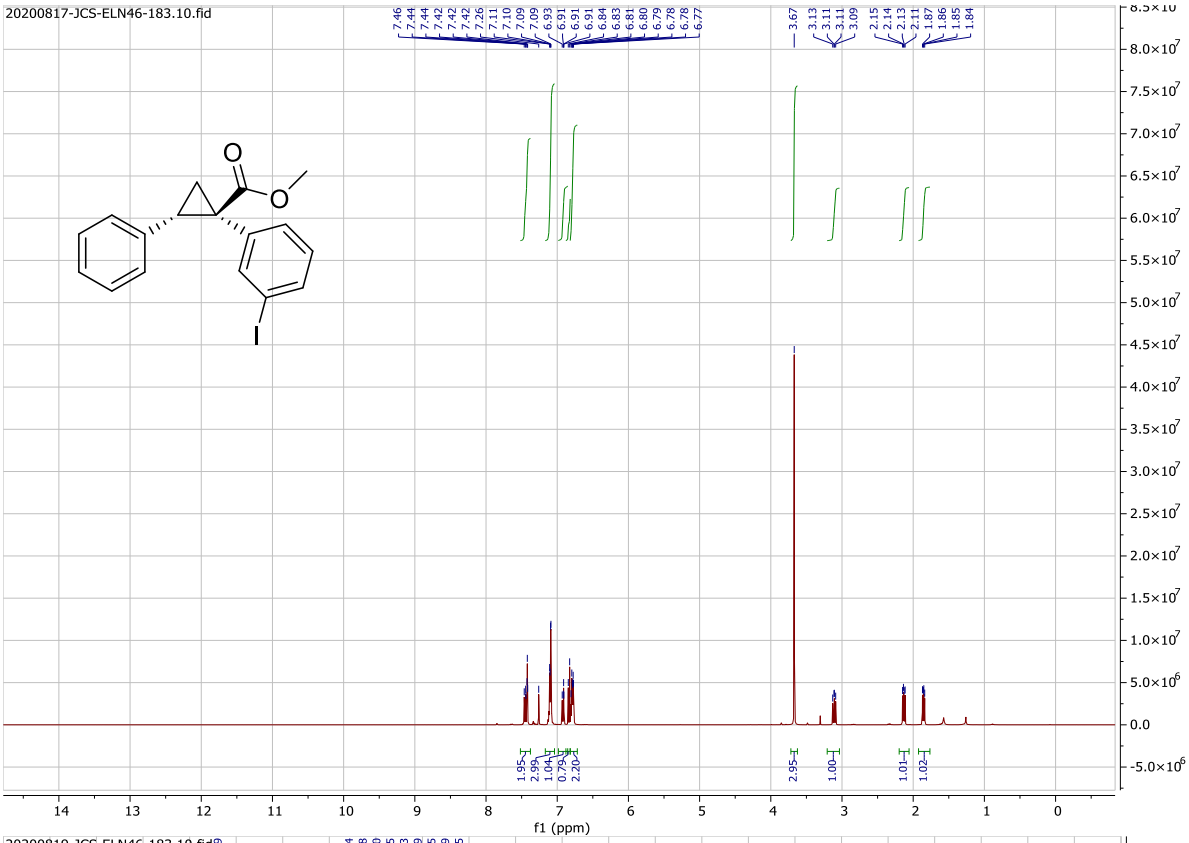
20200817-JCS-ELN46-183.10.fid
7.46 7.44 7.44 7.42 7.42 7.42 7.26 7.11 7.10 7.09 7.09 6.93 6.91 6.91 6.91 6.84 6.83 6.81 6.80 6.79 6.78 6.78 6.77
3.67 3.13 3.11 3.11 3.09 2.15 2.14 2.13 2.11 1.87 1.86 1.85 1.84
1.95 2.99 1.04 0.79 2.20 2.95 1.00 1.01 1.02
f1 (ppm)

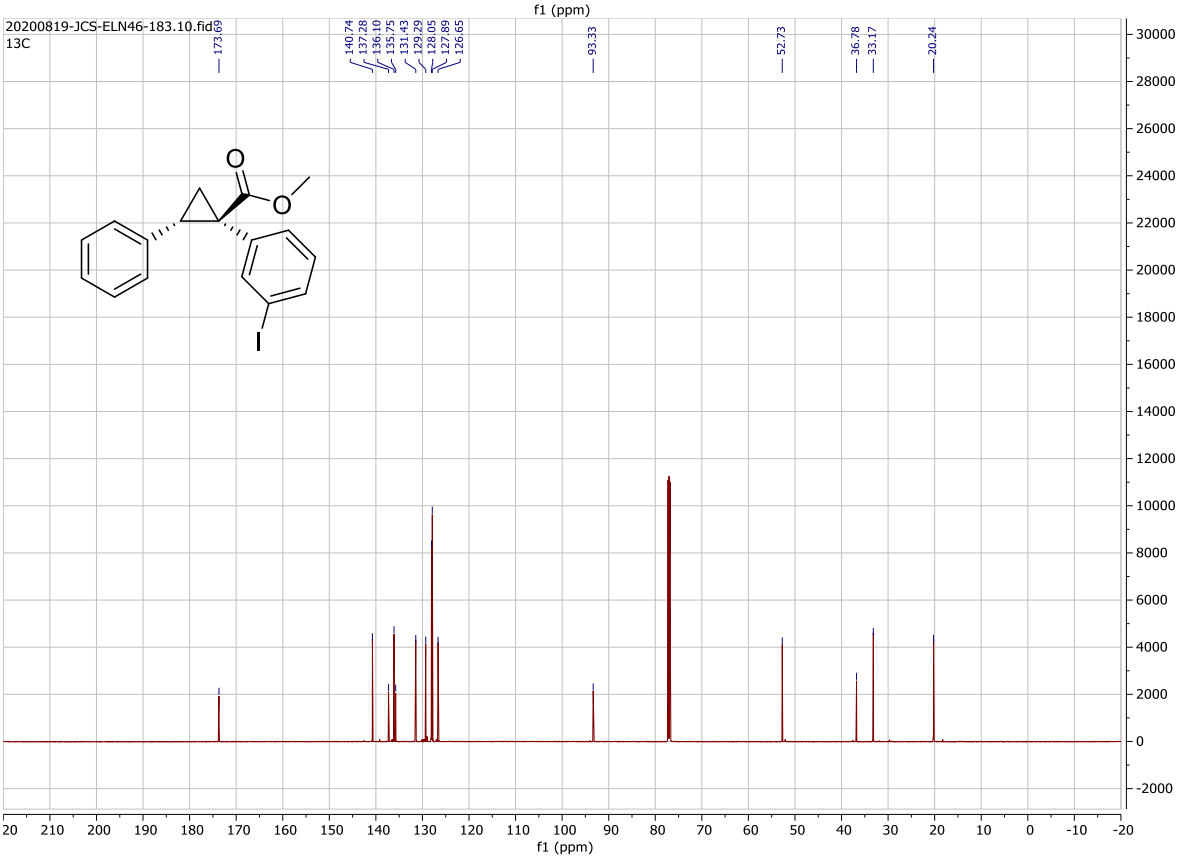
20200819-JCS-ELN46-183.10.fid
13C
173.69
140.74 137.28 136.10 135.75 131.43 129.29 128.05 127.89 126.65
93.33
52.73
36.78 33.17
20.24
f1 (ppm)

7. References

1. S. P. Green, K. M. Wheelhouse, A. D. Payne, J. P. Hallett, P. W. Miller and J. A. Bull, *Org. Process. Res. Dev.*, 2020, **24**, 67-84.
2. D. M. Guptill and H. M. L. Davies, *J. Am. Chem. Soc.*, 2014, **154**, 17718-17721.
3. K. M. Chepiga, C. Qin, J. S. Alford, S. Chennamadhavuni, T. M. Gregg, J. P. Olson and H. M. L. Davies, *Tetrahedron*, 2013, **69**, 5765-5771.
4. L. Fu, J. D. Mighion, E. A. Voight and H. M. L. Davies, *Chem. Eur. J.*, 2017, **23**, 3272-3275.
5. S. Harada, K. Tanikawa, H. Homma, C. Sakai, T. Ito and T. Nemoto, *Chem. Eur. J.*, 2019, **25**, 12058-12062.
6. X. B. Wang, Z. J. Zheng, J. L. Xie, X. W. Gu, Q. C. Mu, G. W. Yin, F. Ye, Z. Xu and L. W. Xu, *Angew. Chem. Int. Ed.*, 2020, **59**, 790-797.
7. L. Fu, K. Hoang, C. Tortoreto, W. Liu and H. M. L. Davies, *Org. Lett.*, 2018, **20**, 2399-2402.
8. H. M. L. Davies and R. J. Townsend, *J. Org. Chem.*, 2001, **16**, 6595-6603.
9. S. M. Nicolle and C. J. Moody, *Chem. Eur. J.*, 2014, **20**, 4420-4425.
10. P.-C. Lv, A.-Q. Jiang, W.-M. Zhang and H.-L. Zhu, *Expert. Opin. Ther. Pat.*, 2018, **28**, 139-145.
11. J. Fu, N. Wurzer, V. Lehner, O. Reiser and H. M. L. Davies, *Org. Lett.*, 2019, **21**, 6102-6106.
12. H. M. L. Davies, P. R. Bruzinski, D. H. Lake, N. Kong and M. J. Fall, *J. Am. Chem. Soc.*, 1996, **118**, 6897-6907.
13. R. P. Reddy, G. H. Lee and H. M. L. Davies, *Org. Lett.*, 2006, **8**, 3437-3440.
14. C. Qin and H. M. L. Davies, *J. Am. Chem. Soc.*, 2014, **154**, 9792-9796.
15. J. Fu, Z. Ren, J. Bacsa, D. G. Musaev and H. M. L. Davies, *Nature*, 2018, **564**, 395-399.
16. B. Wei, J. C. Sharland, P. Lin, S. M. Wilkerson-Hill, F. A. Fullilove, S. McKinnon, D. G. Blackmond and H. M. L. Davies, *ACS Catal.*, 2020, **10**, 1161-1170.

Appendix C: Chapter 3 Supporting Information

CAUTION: Diazo compounds are high energy compounds and need to be treated with respect. Even though we experienced no energetic decomposition in this work, care should be taken in handling large quantities of diazo compounds. Large scale reactions should be conducted behind a blast shield. For a more complete analysis of the risks associated with diazo compounds see the recent review by Bull *et. al.*[1]

1. General Considerations

All experiments on large (≥0.10mmol) scale were carried out in flame-dried glassware under nitrogen atmosphere unless otherwise stated. Reactions on microscale (5.0µmol) were performed in 300µl vials in a 96 well-plate in the presence of 4Å molecular sieves under an inert nitrogen atmosphere in a Braun glovebox. Flash column chromatography was performed on silica gel. 4Å molecular sieves were activated under vacuum at 300 °C for 4 h. After time elapsed, the flask was cooled under inert nitrogen atmosphere and stored in a 140 °C oven for future use. All solvents were stored over 4Å molecular sieves under nitrogen atmosphere. Unless otherwise noted, all other reagents were obtained from commercial sources (Sigma Aldrich, Fisher, TCI Chemicals, AK Scientific, Combi Blocks, Ambeed, Oakwood Chemicals) and used as received without purification. ^{1}H, ^{13}C, and ^{19}F NMR spectra were recorded at either 400 MHz (^{13}C at 100 MHz) on Bruker 400 spectrometer or 600 MHz (^{13}C at 151 MHz) on INOVA 600 or Bruker 600 spectrometer. NMR spectra were run in solutions of deuterated chloroform ($CDCl_3$) with residual chloroform taken as an internal standard (7.26 ppm for ^{1}H, and 77.16 ppm for ^{13}C), deuterated dimethyl sulfoxide (d6-DMSO) with residual DMSO taken as an internal standard (2.50 ppm for ^{1}H, and 39.51 ppm for ^{13}C), or deuterated methanol (MeOD) with residual MeOH taken as an internal standard (3.31 ppm for ^{1}H, and 49.00 ppm for ^{13}C) and were reported in parts per million (ppm). The abbreviations for multiplicity are as follows: s = singlet, d = doublet, t = triplet, q = quartet, p = pentet, m = multiplet, dd = doublet of doublet, etc. Coupling constants (J values) are obtained from the spectra. Thin layer chromatography was performed on aluminum-back silica gel plates with UV light and cerium aluminum molybdate (CAM) or permanganate ($KMnO_4$) stain to visualize. Mass spectra at Emory were taken on a Thermo Finnigan LTQ-FTMS spectrometer with APCI, ESI or NSI. Melting points (mp) were measured in open capillary tubes with a Mel-Temp Electrothermal melting point apparatus and are uncorrected. IR spectra were collected on a Nicolet iS10 FT-IR spectrometer from Thermo Scientific and reported in units of wavenumbers (cm^{-1}). Enantiomeric excess (% ee) data were obtained on an Agilent 1100 HPLC, an Agilent 1290 Infinity UHPLC, or a Waters SFC, eluting the purified products using a mixed solution of HPLC-grade 2-propanol (*i*-PrOH) and *n*-hexane for HPLC and a mixed solution of *i*-PrOH or MeOH and supercritical CO_2 for SFC.

Experimental Procedures

2. Preparation of Substrates:

2.1 Preparation of known substrates.

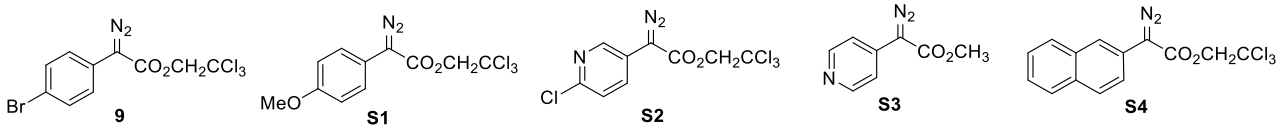

Figure C1: ***Known diazo starting materials***

Diazo compounds **1, S1** and **S2** were prepared according to the established literature and matched the reported spectra.[2]
Diazo compound **S3,** was prepared according to the established literature and matched the reported spectra.[3]
Diazo compound **S4** was prepared according to the established literature and matched the reported spectra.[4]

2.2 Catalyst preparation:

All catalysts were synthesized according to known procedures and used directly.

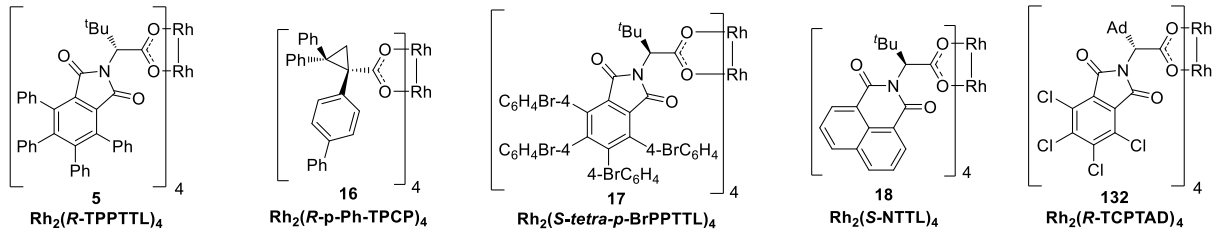

Figure C2: Dirhodium tetracarboxylate catalysts relevant to the scope of this work

Rh_2(*R*-TPPTTL)$_4$ and Rh_2(*S*-TPPTTL)$_4$ **5** were prepared using the procedure reported in the literature.[5]
Rh_2(*R*-*p*-Ph-TPCP)$_4$ **16** was prepared using the procedure reported in the literature.[6]
Rh_2(*S*-*tetra*-*p*-Br-PhPTTL)$_4$ **17** were prepared using the procedure reported in the literature.[7]
Rh_2(*R*-NTTL)$_4$ and Rh_2(*S*-NTTL)$_4$ **18** were prepared using the procedure reported in the literature.[8]
Rh_2(*R*-TCPTAD)$_4$ **132** was prepared using the procedure reported in the literature.[9]

3. Procedures for cyclopropanation.

3.1. General procedure for the cyclopropanation of olefins with aryl/heteroaryl diazoacetates on 0.10 mmol scale.

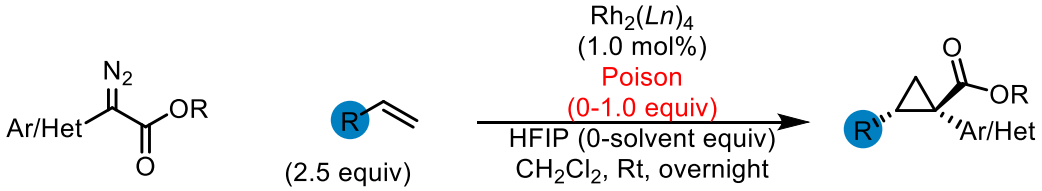

A 8 mL vial containing a stir bar was flame dried under vacuum. The vial was then evacuated and purged with nitrogen 2 times to establish an inert atmosphere. Then catalyst (1.0 mol%, 0.0001 mmol) was added to the vial. The reaction vial bearing catalyst was flushed with nitrogen and olefin (2.5 equiv, 0.25 mmol) was added to the vial via syringe along with 1 mL dry CH_2Cl_2 or HFIP. If poisonous additive is to be included in the reaction it is added neat at this stage (1.0 equiv, 0.10mmol) to the reaction vial. If 10 equiv HFIP is to be used in the reaction, it is added at this stage to the reaction vial (10 equiv, 0.10ml, 1.0 mmol) via syringe. The nitrogen line attached to the vial was then replaced by a balloon filled with argon and the reaction mixture was stirred for 5 mins. Solid diazo compound (1.0 equiv, 0.10 mmol) was weighed out and added to a separate vial (not dried in any way). Diazo compound was dissolved in 1 mL dry CH_2Cl_2 or HFIP and sonicated to ensure all diazo had dissolved before the solution was loaded into a syringe. The syringe was then inserted through the vial septum

and the full contents were injected into the vial in one portion. The reaction was stirred overnight under argon (at least 13 h). The reaction solution was subjected to TLC to determine reaction completion (5% EtOAc/hexanes). After completion the solution was concentrated via rotovap and resuspended in $CDCl_3$ for analysis by crude ^1H NMR to determine product distribution. The crude concentrate was then directly purified by flash column chromatography (0% Et_2O/hexanes 3 CV, 0% Et_2O/hexanes to 10% Et_2O/hexanes 15 CV, 10% Et_2O/hexanes for 3-10 CV) if it contained product based on ^1H NMR analysis. Fractions containing only product by TLC were aggregated and concentrated via rotovap. Enantioselectivity was determined by chiral HPLC. Products **2, 97-125** were synthesized via this method.

3.2 General procedure for the cyclopropanation of complex molecules with 2,2,2-trichloroethyl-2-(4-bromophenyl)diazo-2-acetate.

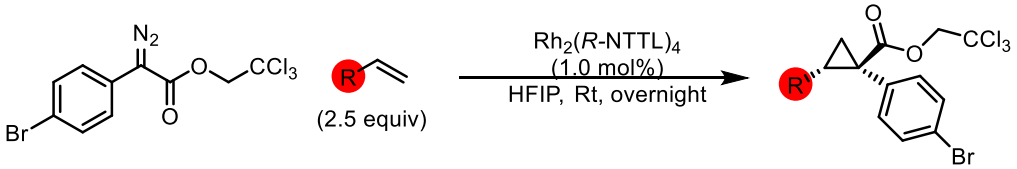

A 8 mL vial containing a stir bar and 4Å molecular sieves (0.2g) was flame dried under vacuum. The vial was then evacuated and purged with nitrogen 2 times to establish an inert atmosphere. Then Rh_2(*R*-NTTL)$_4$ (1.0 mol%) was added to the vial. 2,2,2-Trichloroethyl-2-(4-bromophenyl)diazo-2-acetate (**1,** 1.0 equiv) was weighed out and added to a separate vial (not dried in any way). The system was flushed with nitrogen and complex olefin (2.5 equiv) was added to the vial along with 1 mL HFIP. The nitrogen line attached to the vial was then replaced by a balloon filled with argon and the solution was stirred for 5 mins. Diazo compound was dissolved in 1 mL HFIP and sonicated to ensure all diazo had dissolved before the solution was loaded into a syringe. The syringe was then inserted through the vial septum and the full contents were injected into the vial in one portion. The reaction was stirred overnight under argon (at least 13 h). After completion the solution was concentrated via rotovap and resuspended in MeCN. The crude concentrate was then directly purified by preperative HPLC (95-0% H_2O/MeCN, 25ml/min, 45min). Fractions containing product were aggregated and concentrated via rotovap and further dried under high vacuum for several days. Products **127-125** were synthesized via this method.

4. Characterization of synthesized compounds.

4.1 Characterization of cyclopropanation products

All products shown with absolute stereo-configuration generated with Rh_2(S-tetra-p-BrPhPTTL)$_4$* **(17) *and Rh_2(R-NTTL)$_4$* **(18),** *relative stereochemistry of the cyclopropane product is assigned by analogy to the major enantiomer of compound* ***125*** *and* ***127*** *as confirmed by X-Ray crystallography.*

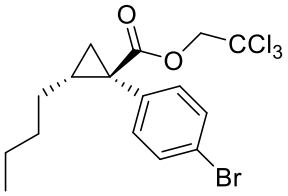

2,2,2-trichloroethyl (1R,2R)-1-(4-bromophenyl)-2-butylcyclopropane-1-carboxylate (10)

This compound was prepared according to **General procedure 3.1 and 3.2** from the reaction between **1** (0.10 mmol/0.00537mmol, 37 mg/20ul stock solution) and 1-hexene (2.5 equiv, 0.25 mmol/xmmol, 31 ul/40ul stock solution). After isolation of 0.10 mmol scale reaction, product was obtained as a clear colorless oil in up to 99% yield and >98% ee (0.10 mmol, 43 mg).

^{1}H NMR: (600 MHz, CDCl3) δ 7.46 (d, J= hz) , 7.45(d, *J* = 8.5 Hz, 1H), 7.19 (d, *J* = 8.6 Hz, 1H), 4.67 (a,b quartet 2H), 1.93 (m, 1H), 1.86 (dd, *J* = 9.1, 4.2 Hz, 1H), 1.35(m, 4H), 1.26(m, 5H), 1.18 (dd, *J* = 6.9, 4.3 Hz, 1H), 0.83 (t, *J*= 7.45 Hz, 3H), 0.57 (m, 1H).

^{13}C NMR (151 MHz, $CDCl_3$) δ 172.52, 134.42, 133.13, 131.16, 121.43, 95.01, 74.27, 33.05, 31.18, 29.96, 29.63, 22.39, 21.94, 13.98.

IR(neat): 3015, 2970, 2951, 2858, 1735, 1489, 1435, 1365, 1229, 1216, 1161, 1100, 1072, 1045, 1010, 974, 888, 828, 805, 763, 715, 573, 527, 515 cm^{-1}

Chiral HPLC: (Column R,R-Welk, 60 min, 1ml/min, 0% IPA/Hexanes) RT: 16.0 min, 28.1 min

Chiral SFC: (Column SS-Welk-O, 5 min, 3ml/min, 5% IPA/CO_2) RT: 2.18 min, 3.35 min

HRMS: (+p APCI) calculated for $C_{16}H_{19}O_2{}^{79}Br^{35}Cl_3$ [426.96285] found [426.96292]

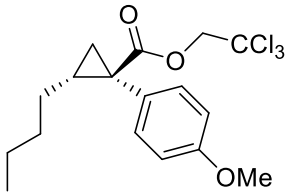

2,2,2-trichloroethyl (1R,2R)-2-butyl-1-(4-methoxyphenyl)cyclopropane-1-carboxylate (112)
This compound was prepared according to **General procedure 3.1** from the reaction between **S1** (0.10 mmol, 32 mg) and 1-hexene (2.5 equiv, 0.25 mmol, 31 ul). After isolation, product was obtained as a clear colorless oil in up to 52% yield and 94% ee (52 µmol, 20 mg).
^{1}H NMR (400 MHz, $CDCl_3$) δ 7.25 (d, *J* = 8.8 Hz, 2H), 6.88 (d, *J* = 8.8 Hz, 2H), 4.70 (dd, *J* = 96.9, 11.9 Hz, 2H), 3.83 (s, 4H), 1.91 (ddd, *J* = 8.8, 6.6, 5.0 Hz, 1H), 1.85 (dd, *J* = 9.3, 3.9 Hz, 1H), 1.50 – 1.33 (m, 4H), 1.28 (dtd, *J* = 15.3, 7.4, 1.9 Hz, 2H), 1.20 (dd, *J* = 6.6, 4.0 Hz, 1H), 0.85 (t, *J* = 7.2 Hz, 3H), 0.74 – 0.53 (m, 1H).
^{13}C NMR (101 MHz, $CDCl_3$) δ 173.38, 158.70, 132.46, 127.37, 113.37, 95.18, 74.19, 55.23, 32.80, 31.28, 29.94, 29.64, 22.45, 21.99, 14.05.
IR(neat): 3004, 2955, 2930, 2858, 1736, 1612, 1581, 1515, 1441, 1366, 1292, 1244, 1217, 1158, 1101, 1034, 974, 889, 832, 813, 796, 753, 724, 640, 605, 574, 528 cm^{-1}
Chiral HPLC: (Column AD-H, 15 min, 1ml/min, 1% IPA/Hexanes) RT: 5.8 min, 6.3 min.
HRMS: (+p APCI) calculated for $C_{17}H_{22}O_3{}^{35}Cl_3$ [379.0629] found [379.06258]

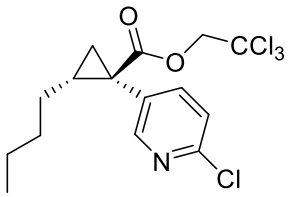

2,2,2-trichloroethyl (1R,2R)-2-butyl-1-(6-chloropyridin-3-yl)cyclopropane-1-carboxylatecarboxylate (113)
This compound was prepared according to **General procedure 3.1** from the reaction between **S2** (0.10 mmol, 33 mg) and 1-hexene (2.5 equiv, 0.25 mmol 31 ul). After isolation, product was obtained as a clear colorless oil in up to 75% yield and 98% ee (75 µmol, 29 mg).
^{1}H NMR: (600 MHz, CDCl3) δ 8.35 (d, *J* = 2.5 Hz, 1H), 7.64 (dd, *J* = 8.2, 2.5 Hz, 1H), 7.33 (d, *J* = 8.2 Hz, 1H), 4.70 (dd, *J* = 128.6, 11.9 Hz, 2H), 2.15 – 1.85 (m, 2H), 1.46 – 1.35 (m, 3H), 1.27 (dtd, *J* = 17.2, 6.6, 3.2 Hz, 3H), 0.86 (t, *J* = 7.3 Hz, 3H), 0.68 – 0.46 (m, 1H).
^{13}C NMR: (151 MHz, $CDCl_3$) δ 171.74, 152.13, 150.46, 141.89, 130.34, 123.58, 94.78, 74.42, 31.05, 30.55, 30.05, 29.63, 22.35, 21.74, 13.93.
IR(neat): 3015, 2970, 2950, 2859, 1735, 1588, 1560, 1461, 1366, 1260, 1228, 1216, 1166, 1138, 1107, 1048, 1019, 895, 836, 811, 777, 743, 722, 573, 538, 527, 515 cm^{-1}
Chiral HPLC: (Column OD-H, 60 min, 1ml/min, 0% IPA/Hexanes) RT: 7.50 min, 20.1 min.
HRMS: (+p APCI) calculated for $C_{15}H_{18}O_2N^{35}Cl_4$ [384.00862] found [384.00849]

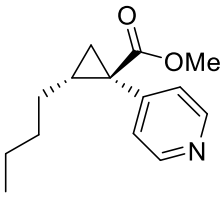

Methyl (1R,2R)-2-butyl-1-(pyridin-4-yl)cyclopropane-1-carboxylate (114)
This compound was prepared according to **General procedure 3.1** from the reaction between **S3** (0.10 mmol, 18 mg) and 1-hexene (2.5 equiv, 0.25 mmol, 31 ul). After isolation, product was obtained as a clear colorless oil in up to 62% yield and 84% ee (62 µmol, 15 mg).
^{1}H NMR (400 MHz, $CDCl_3$) δ 8.57 – 8.46 (m, 2H), 7.61 (ddd, *J* = 7.8, 2.3, 1.7 Hz, 1H), 7.35 – 7.23 (ddd, J = 7.5, 4.8, 0.9 Hz, 1H), 3.63 (s, 3H), 1.91 – 1.84 (m, 1H), 1.86 – 1.75 (m, 1H), 1.47 – 1.31 (m, 3H), 1.29 – 1.19 (m, 3H), 1.14 (dd, *J* = 6.7, 4.2 Hz, 1H), 0.83 (t, *J* = 7.2 Hz, 3H), 0.51 (m, 1H).
^{13}C NMR (101 MHz, $CDCl_3$) δ 174.32, 152.47, 148.19, 138.94, 132.33, 122.93, 52.48, 31.30, 31.16, 30.07, 28.70, 22.37, 21.34, 13.97.
IR(neat): 2954, 2929, 2858, 1717, 1573, 1480, 1432, 1415, 1387, 1329, 1266, 1245, 1196, 1173, 1106, 1052, 1023, 990, 961, 870, 812, 764, 715, 680, 620 cm^{-1}
Chiral HPLC: (Column OD-H, 60 min, 1ml/min, 2% IPA/Hexanes) RT: 11.3 min, 14.8 min.
HRMS: (+p APCI) calculated for $C_{14}H_{20}O_2N$ [234.14886] found [234.14873]

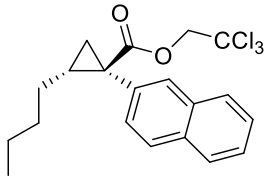

2,2,2-Trichloroethyl (1R,2R)-2-butyl-1-(naphthalen-2-yl)cyclopropane-1-carboxylate (115)
This compound was prepared according to **General procedure 3.1** from the reaction between **S4** (0.10 mmol, 34 mg) and 1-hexene (2.5 equiv, 0.25 mmol, 31 ul). After isolation, product was obtained as a clear light yellow oil in up to 90% yield and 98% ee (0.09 mmol, 36 mg).
^{1}H NMR: (500 MHz, $CDCl_3$) δ 7.88 – 7.83 (m, 1H), 7.81 (d, *J* = 8.8 Hz, 2H), 7.74 (d, *J* = 1.8 Hz, 1H), 7.51 – 7.43 (m, 3H), 4.70 (ab-quartet, 2H), 2.02 (tdd, *J* = 9.1, 6.8, 4.7 Hz, 1H), 1.94 (dd, *J* = 9.0, 4.2 Hz, 1H), 1.47 – 1.30 (m, 3H), 1.28 – 1.14 (m, 2H), 0.80 (t, *J* = 7.3 Hz, 3H), 0.65 – 0.54 (m, 1H).
^{13}C NMR: (151 MHz, $CDCl_3$) δ 173.08, 133.18, 133.06, 132.70, 129.90, 129.86, 127.83, 127.64, 127.38, 125.94, 95.12, 74.22, 33.74, 31.32, 29.86, 29.85, 22.39, 21.90, 14.01.
IR(neat): 2956, 2930, 2858, 1735, 1620, 1506, 1435, 1367, 1260, 1236, 1217, 1160, 1128, 1099, 1047, 905, 858, 815, 753, 711, 657, 573, 478 cm^{-1}
Chiral HPLC: (Column AD-H, 15 min, 1ml/min, 1% IPA/Hexanes) RT: 4.9 min, 5.4 min.
HRMS: (+p APCI) calculated for $C_{20}H_{21}O_2{}^{35}Cl_3$ [398.06016] found [398.06017]

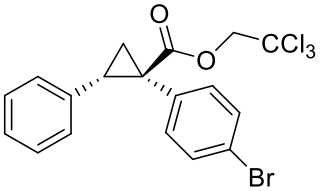

2,2,2-Trichloroethyl (1R,2S)-1-(4-bromophenyl)-2-phenylcyclopropane-1-carboxylate(116)
This compound was prepared according to **General procedure 3.1** from the reaction between **1** (0.10 mmol, 37 mg) and styrene (2.5 equiv, 0.25 mmol, 29 ul). After isolation, product was obtained as a clear crystalline solid in up to 98% yield and 86% ee (98 µmol, 44 mg). Spectra and characterization matched literature reported values.[10]
Chiral HPLC: (Column AD-H, 1ml/ml, 1% IPA/hexane, 15min) RT: 6.7 min, 8.4 min.

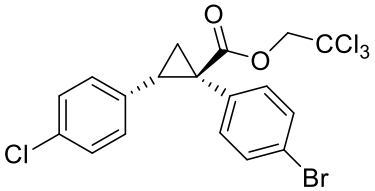

2,2,2-trichloroethyl (1R,2S)-1-(4-bromophenyl)-2-(4-chlorophenyl)cyclopropane-1-carboxylate (117)
This compound was prepared according to **General procedure 3.1** from the reaction between **1** (0.10 mmol, 37 mg) and 4-chlorostyrene (2.5 equiv, 0.25 mmol, 35 mg). After isolation, product was obtained as a white solid in up to 80% yield and 89% ee (0.08 mmol, 39 mg). Spectra and characterization matched literature reported values.[10]
Chiral HPLC: (Column AD-H, 1ml/ml, 1% IPA/hexane, 15min) RT: 8.8 min, 11.5 min.

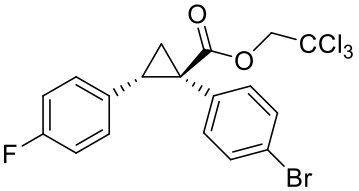

2,2,2-trichloroethyl (1R,2S)-1-(4-bromophenyl)-2-(4-fluorophenyl)cyclopropane-1-carboxylate (118)
This compound was prepared according to **General procedure 3.1** from the reaction between **1** (0.10 mmol, 37 mg) and 4-fluorostyrene (2.5 equiv, 0.25 mmol 31 mg). After isolation, product was obtained as a white solid in up to 80% yield and 83% ee (0.08 mmol, 37 mg). Spectra and characterization matched literature reported values.[10]
Chiral HPLC: (Column AD-H, 1ml/ml, 1% IPA/hexane, 15min) RT: 8.0 min, 10.7 min.

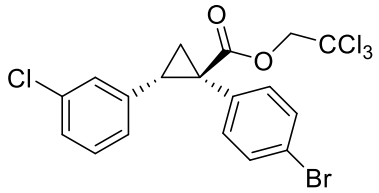

2,2,2-trichloroethyl (1R,2S)-1-(4-bromophenyl)-2-(3-chlorophenyl)cyclopropane-1-carboxylate (119)
This compound was prepared according to **General procedure 3.1** from the reaction between **1** (0.10 mmol, 37 mg) and 1-chloro-3-vinylbenzene (2.5 equiv, 0.25 mmol, 35mg). After isolation, product was obtained as a white solid in up to 60% yield and 86% ee (60 µmol, 29 mg).
MP:102-104ºC
^{1}H NMR : (600 MHz, CDCl3) δ 7.29 (d, *J* = 8.5 Hz, 1H), 7.11 – 7.06 (m, 1H), 7.02 (t, *J* = 7.9 Hz, 1H), 6.94 (d, *J* = 8.4 Hz, 1H), 6.60 (d, *J* = 7.7 Hz, 1H), 4.73 (dd, *J* = 105.9, 11.9 Hz, 2H), 3.18 (dd, *J* = 9.3, 7.4 Hz, 1H), 2.28 (dd, *J* = 9.3, 5.4 Hz, 1H), 1.95 (dd, *J* = 7.4, 5.4 Hz, 1H).
^{13}C NMR : (151 MHz, $CDCl_3$) δ 171.29, 137.51, 133.97, 133.51, 132.44, 131.10, 129.21, 128.52, 127.09, 125.95, 121.79, 94.86, 74.47, 36.75, 33.19, 20.20.
IR(neat): 3015, 2970, 2947, 1735, 1597, 1571, 1440, 1366, 1229, 1216, 1151, 1091, 1071, 1051, 1011, 971, 906, 828, 785, 764, 715, 700, 679, 574, 527, 515 cm^{-1}
Chiral HPLC: (Column AD-H, 30 min, 1ml/min, 1% IPA/Hexanes) RT: 7.5 min, 9.5 min.
HRMS: (+p APCI) calculated for $C_{18}H_{14}O_2{}^{79}Br^{35}Cl_4$ [480.89258] found [480.89274]

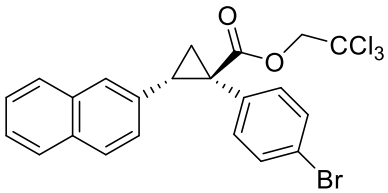

2,2,2-trichloroethyl (1R,2S)-1-(4-bromophenyl)-2-(naphthalen-2-yl)cyclopropane-1-carboxylate (120)
This compound was prepared according to **General procedure 3.1** from the reaction between **1** (0.10 mmol, 37 mg) and 2-vinylnaphthalene (2.5 equiv, 0.25 mmol, 39 mg). After isolation, product was obtained as a white crystalline solid in up to >98% yield and 94% ee (0.10 mmol, 50 mg).
MP: 100-104ºC
^{1}H NMR: (600 MHz, CDCl3) δ 7.77 – 7.72 (m, 1H), 7.69 – 7.63 (m, 1H), 7.60 (d, *J* = 8.5 Hz, 1H), 7.44 (qd, *J* = 7.0, 3.4 Hz, 2H), 7.39 (d, *J* = 1.8 Hz, 1H), 7.24 (d, *J* = 8.4 Hz, 2H), 7.00 (d, *J* = 8.4 Hz, 2H), 6.87 (dd, *J* = 8.5, 1.8 Hz, 1H), 4.78 (dd, *J* = 103.2, 11.9 Hz, 2H), 3.41 (dd, *J* = 9.3, 7.4 Hz, 1H), 2.39 (dd, *J* = 9.4, 5.2 Hz, 1H), 2.13 (dd, *J* = 7.5, 5.2 Hz, 1H).
^{13}C NMR: (151 MHz, $CDCl_3$) δ 171.59, 133.60, 133.02, 132.91, 132.89, 132.32, 131.00, 127.60, 127.58, 127.54, 127.27, 126.15, 125.87, 125.79, 121.59, 94.97, 74.46, 36.78, 34.16, 20.49.
IR(neat): 3015, 2970, 2947, 1739, 1435, 1365, 1228, 1216, 1149, 1092, 895, 766, 749, 716, 538, 527, 515 cm^{-1}
Chiral HPLC: (Column OD-H, 30 min, 1ml/min, 1% IPA/Hexanes) RT: 13.9 min, 16.2 min.
HRMS: (+p APCI) calculated for $C_{22}H_{16}O_2{}^{79}Br^{35}Cl_3$ [495.93938] found [495.93943]

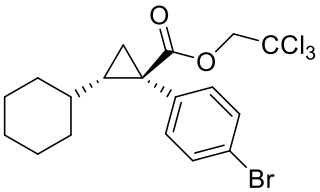

2,2,2-trichloroethyl (1R,2S)-1-(4-bromophenyl)-2-cyclohexylcyclopropane-1-carboxylate (121)
This compound was prepared according to **General procedure 3.1** from the reaction between **1** (0.10 mmol, 37 mg) and vinyl cyclohexane (2.5 equiv, 0.25 mmol, 28mg). After isolation, product was obtained as a clear colorless oil in up to >98% yield and 95% ee (0.10 mmol, 45 mg).
^{1}H NMR: (600 MHz, $CDCl_3$) δ 7.30 (dd, *J* = 8.6, 2.2 Hz, 2H), 7.08 (dd, *J* = 8.6, 2.2 Hz, 2H), 4.53 (ab-quartet, 2H), 1.68 – 1.58 (m, 4H), 1.51 – 1.46 (m, 1H), 1.45 – 1.37 (m, 3H), 1.11 (q, *J* = 3.5 Hz, 1H), 1.05 – 0.94 (m, 3H), 0.92 – 0.82 (m, 1H), 0.82 – 0.68 (m, 1H), 0.16 (qt, *J* = 10.7, 3.5 Hz, 1H).
^{13}C NMR: (151 MHz, $CDCl_3$) δ 172.50, 134.14, 133.15, 131.04, 121.42, 95.08, 74.24, 37.29, 36.62, 33.77, 32.85, 32.75, 26.17, 25.94, 25.59, 19.52.
IR(neat): 3015, 2970, 2925, 2850, 1735, 1489, 1447, 1366, 1270, 1216, 1172, 1158, 1120, 1091, 1073, 1046, 1010, 967, 904, 825, 806, 764, 745, 717, 574, 539, 527, 515 cm^{-1}
Chiral HPLC: (Column AD-H, 60 min, 1ml/min, 0% IPA/Hexanes) RT: 13.1 min, 28.8 min.
HRMS: (+p APCI) calculated for $C_{18}H_{21}O_2{}^{79}Br^{35}Cl_3$ [452.9785] found [452.97838]

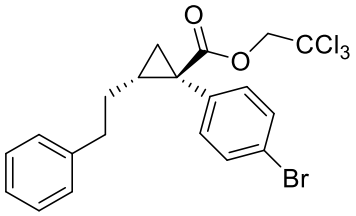

2,2,2-trichloroethyl (1R,2R)-1-(4-bromophenyl)-2-phenethylcyclopropane-1-carboxylate (122)
This compound was prepared according to **General procedure 3.1** from the reaction between **1** (0.10 mmol, 37 mg) and but-3-en-1-ylbenzene (2.5 equiv, 0.25 mmol, 33mg). After isolation, product was obtained as a clear colorless oil in up to 70% yield and 99% ee (70 µmol, 33 mg).
^{1}H NMR: (600 MHz, CDCl3) δ 7.47 (d, *J* = 8.3 Hz, 2H), 7.35 – 7.24 (m, 2H), 7.20 (d, *J* = 8.2 Hz, 2H), 7.10 (d, *J* = 7.6 Hz, 2H), 4.69 (dd, *J* = 129.0, 11.9, Hz, 2H), 2.71 (qdd, *J* = 14.0, 8.9, 6.4 Hz, 2H), 2.07 – 1.97 (m, 1H), 1.88 (dd, *J* = 9.1, 4.5 Hz, 1H), 1.70 (ddt, *J* = 14.3, 9.0, 5.9 Hz, 1H), 1.20 (dd, *J* = 7.0, 4.5 Hz, 1H), 0.96 (dtd, *J* = 15.0, 8.9, 6.3 Hz, 1H).
^{13}C NMR: (151 MHz, $CDCl_3$) δ 172.31, 141.35, 134.13, 133.08, 131.26, 128.41, 126.01, 121.58, 94.95, 74.31, 35.24, 33.16, 32.29, 29.05, 21.73.
IR(neat): 3015, 2970, 2946, 1735, 1435, 1366, 1216, 1158, 1105, 1092, 1044, 909, 730, 539, 527, 515 cm^{-1}
Chiral HPLC: (Column AD-H, 30 min, 1ml/min, 1% IPA/Hexanes) RT: 6.9 min, 8.8 min.
HRMS: (+p APCI) calculated for $C_{20}H_{19}O_2{}^{79}Br^{35}Cl_3$ [474.96285] found [474.96312]

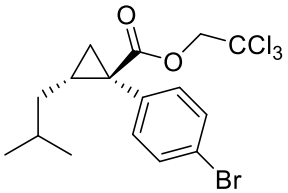

2,2,2-trichloroethyl (1R,2R)-1-(4-bromophenyl)-2-isobutylcyclopropane-1-carboxylate (123)
This compound was prepared according to **General procedure 3.1** from the reaction between **1** (0.10 mmol, 37 mg) and 4-methylpent-1-ene (2.5 equiv, 0.25 mmol, 21mg). After isolation, product was obtained as a clear colorless oil in up to 73% yield and 93% ee (73 µmol, 31 mg).
^{1}H NMR: (600 MHz, CDCl3) δ 7.48 (d, *J* = 8.4 Hz, 2H), 7.20 (d, *J* = 8.4 Hz, 2H), 4.70 (dd, *J* = 133.4, 11.9 Hz, 2H), 1.99 (tdd, *J* = 9.6, 6.8, 4.2 Hz, 1H), 1.92 (dd, *J* = 9.0, 4.2 Hz, 1H), 1.70 (dp, *J* = 13.4, 6.7 Hz, 1H), 1.40 (ddd, *J* = 13.9, 6.5, 4.2 Hz, 1H), 1.22 (dd, *J* = 6.9, 4.2 Hz, 1H), 0.90 (dd, *J* = 6.7, 2.7 Hz, 5H), 0.36 (ddd, *J* = 13.9, 9.7, 7.2 Hz, 1H).
^{13}C NMR: (151 MHz, $CDCl_3$) δ 172.60, 134.41, 133.14, 131.16, 121.43, 95.01, 74.28, 39.33, 32.42, 28.28, 28.13, 22.64, 22.52, 22.47.
IR(neat): 3015, 2970, 2949, 1735, 1435, 1366, 1229, 1216, 1162, 1112, 1092, 1073, 1044, 1011, 909, 831, 807, 764, 731, 718, 574, 539, 527, 515 cm^{-1}
Chiral HPLC: (Column R,R-Welk, 30 min, 1ml/min, 0% IPA/Hexanes) RT: 12.3 min, 25.4 min.
HRMS: (+p APCI) calculated for $C_{16}H_{18}O_2{}^{79}Br^{35}Cl_3$ [425.95503] found [425.95481]

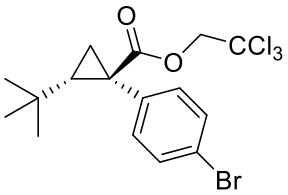

2,2,2-trichloroethyl (1R,2S)-1-(4-bromophenyl)-2-(tert-butyl)cyclopropane-1-carboxylate (124)
This compound was prepared according to **General procedure 3.1** from the reaction between **1** (0.10 mmol, 37 mg) and 3,3-dimethylbut-1-ene (2.5 equiv, 0.25 mmol ,21mg). After isolation, product was obtained as a clear colorless oil in up to 86% yield and 99% ee (86 µmol, 37 mg).
^{1}H NMR: (600 MHz, CDCl3) δ 7.45 (d, *J* = 8.7 Hz, 2H), 7.32 (d, *J* = 8.0 Hz, 2H), 4.70 (dd, *J* = 183.1, 11.9 Hz, 2H), 1.95 (dd, *J* = 10.0, 8.2 Hz, 1H), 1.72 (dd, *J* = 10.0, 4.6 Hz, 1H), 1.62 – 1.44 (m, 1H), 0.74 (s, 9H)
^{13}C NMR: (151 MHz, $CDCl_3$) δ 172.66, 134.12, 130.90, 121.38, 95.05, 74.37, 41.47, 33.59, 31.31, 28.81, 16.51.
IR(neat): 3015, 2970, 2950, 1735, 1438, 1435, 1365, 1228, 1216, 1161, 1092, 1070, 1010, 897, 828, 805, 761, 719, 573, 538, 527, 515 cm^{-1}
Chiral HPLC: (Column R,R-Welk, 30 min, 1ml/min, 0% IPA/Hexanes) RT: 9.7 min, 20.7 min.
HRMS: (+p APCI) calculated for $C_{16}H_{18}O_2{}^{79}Br^{35}Cl_3$ [425.95503] found [425.95483]

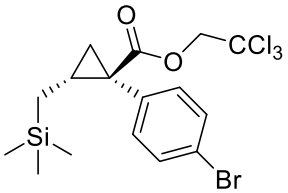

2,2,2-trichloroethyl (1R,2R)-1-(4-bromophenyl)-2-((trimethylsilyl)methyl)cyclopropane-1-carboxylate (125)
This compound was prepared according to **General procedure 3.1** from the reaction between **1** (0.10 mmol, 37 mg) and allyltrimethylsilane (2.5 equiv, 0.25 mmol, 29mg). After isolation, product was obtained as a colorless crystalline solid in up to 83% yield, 7:1 d.r, and 99% ee (83 µmol, 38 mg). Absolute configuration was confirmed by X-Ray crytallography, d.r was determined by 1H NMR.
MP: 58-59ºC
^{1}H NMR (major diastereomer): (600 MHz, CDCl3) δ 7.47 (d, *J* = 8.2 Hz, 2H), 7.17 (d, *J* = 8.3 Hz, 2H), 4.66 (dd, *J* = 132.7, 11.9 Hz, 2H), 1.97 – 1.81 (m, 2H), 1.09 (d, *J* = 3.0 Hz, 1H), 0.87 (dd, *J* = 6.7, 2.3 Hz, 1H), 0.83 (dd, *J* = 14.0, 2.5 Hz, 1H), 0.01 (s, 8H), -0.47 (dd, *J* = 14.3, 11.5 Hz, 1H).
^{13}C NMR (major diastereomer): (151 MHz, $CDCl_3$) δ 172.52, 134.47, 133.49, 133.14, 131.17, 121.38, 95.04, 74.26, 33.02, 26.85, 23.52, 18.28, -1.52, -1.55.
IR(neat): 3015, 2970, 2949, 1735, 1488, 1435, 1366, 1228, 1216, 1125, 1092, 1073, 1044, 1010, 895, 836, 805, 761, 717, 573, 539, 527, 515 cm^{-1}
Chiral HPLC: (Column R,R-Welk, 30 min, 1ml/min, 0% IPA/Hexanes) RT: 11.9 min, 25.1 min.
HRMS: (+p APCI) calculated for $C_{16}H_{21}O_2{}^{79}Br^{35}Cl_3{}^{28}Si$ [456.95543] found [456.95544]
CCDC#: 2182302

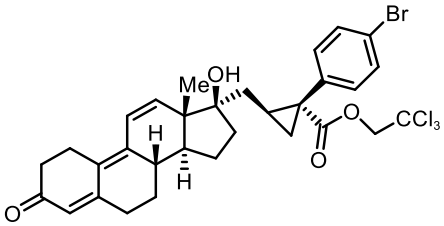

2,2,2-trichloroethyl (1R,2S)-1-(4-bromophenyl)-2-(((8S,13S,14S,17R)-17-hydroxy-13-methyl-3-oxo-2,3,6,7,8,13,14,15,16,17-decahydro-1H-cyclopenta[a]phenanthren-17-yl)methyl)cyclopropane-1-carboxylate (127)
This compound was prepared according to **General procedure 3.4** from the reaction between **1** (54 µmol, 20 mg) and Altrenogest (2.5 equiv, 0.13 mmol, 42 mg). The reaction mixture was purified by preperative HPLC. After isolation, product was obtained as a brown oil in 70% yield, and >20:1 d.r (25 mg, 37 mmol). Structural assignment of compound by 2D NMR can be found on **S349-S355.** D.r was determined by 1H NMR and SFC.
^{1}H NMR: (600 MHz, CDCl3) δ 7.47 (d, *J* = 8.5 Hz, 1H), 7.18 (d, *J* = 8.5 Hz, 1H), 6.37 (d, *J* = 10.0 Hz, 1H), 6.09 (d, *J* = 10.0 Hz, 1H), 5.83 (s, 1H), 4.71 (dd, *J* = 95.8, 12.0 Hz, 2H), 3.71 (Broad s, 1H), 2.92 – 2.72 (m, 2H), 2.71 – 2.54 (m, 2H), 2.50 (td, *J* = 7.2, 2.7 Hz, 2H), 2.40 (t, *J* = 11.5 Hz, 1H), 2.28 – 2.06 (m, 2H), 1.98 (dd, *J* = 9.1, 4.5 Hz, 1H), 1.90 (dq, *J* = 11.6, 3.9 Hz, 1H), 1.77 (dd, *J* = 15.2, 10.6 Hz, 1H), 1.71 – 1.61 (m, 1H), 1.53 (dd, *J* = 14.3, 4.4 Hz, 1H), 1.49 – 1.44 (m, 1H), 1.40 (dd, *J* = 7.0, 4.5 Hz, 1H), 1.34 – 1.17 (m, 1H), 0.98 (s, 3H), 0.87 (ddd, *J* = 14.6, 8.6, 1.5 Hz, 1H).
^{13}C NMR: (101 MHz, $CDCl_3$) δ 172.50, 157.50, 142.17, 141.10, 133.86, 133.14, 131.43, 127.32, 124.24, 123.58, 121.79, 95.05, 82.60, 74.45, 49.13, 47.79, 38.42, 38.15, 36.56, 35.93, 32.36, 31.63, 27.08, 25.38, 24.34, 23.31, 22.64, 16.59.
IR(neat): 3456, 3015, 2970, 1739, 1568, 1435, 1365, 1229, 1217, 1092, 1010, 900, 766, 718, 539, 527, 516 cm^{-1}
Chiral SFC: (Column CEL-1, 10 min, 2.5ml/min, 20% MeOH/CO_2) RT: 3.7 min, 4.5 min.
HRMS: (+p APCI) calculated for $C_{31}H_{33}O_4{}^{79}Br^{35}Cl_3$ [653.06223] found [653.06224]

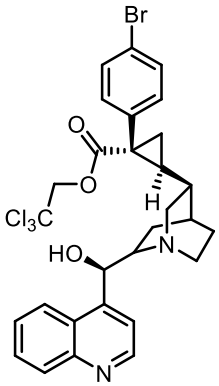

2,2,2-trichloroethyl (1R,2S)-1-(4-bromophenyl)-2-((1S,3S,4S)-6-((R)-hydroxy(quinolin-4-yl)methyl)quinuclidin-3-yl)cyclopropane-1-carboxylate (128)

This compound was prepared according to **General procedure 3.4** from the reaction between **S1** (0.10 mmol, 37 mg) and (*S*)-Cinchonidine (2.5 equiv, 0.25 mmol, 74mg). After isolation of large scale reaction, product was obtained as an powdery off-white solid in >98% yield, >20:1 d.r, (0.10 mmol, 64 mg). Identity of the product was confirmed via X-ray crystallography.

^{1}H NMR: (400 MHz, $CDCl_3$) δ 12.34 (s, 1H), 8.87 (d, *J* = 4.7 Hz, 1H), 7.99 (d, *J* = 8.5 Hz, 1H), 7.83 (d, *J* = 8.5 Hz, 1H), 7.73 (d, *J* = 4.6 Hz, 1H), 7.57 (t, *J* = 7.6 Hz, 1H), 7.51 (d, *J* = 8.3 Hz, 2H), 7.32 (t, *J* = 7.7 Hz, 1H), 7.09 (d, *J* = 8.2 Hz, 2H), 6.36 (s, 1H), 4.71 – 4.45 (ab-quartet, 2H), 4.36 (d, *J* = 13.4 Hz, 1H), 3.43 (t, *J* = 9.0 Hz, 1H), 3.23 (dd, *J* = 13.3, 10.4 Hz, 1H), 3.17 – 3.07 (m, 1H), 2.91 (td, *J* = 12.1, 5.2 Hz, 1H), 2.26 (dd, *J* = 13.6, 7.7 Hz, 1H), 2.15 (d, *J* = 12.0 Hz, 1H), 2.03 (t, *J* = 3.1 Hz, 1H), 1.78 – 1.63 (m, 2H), 1.59 – 1.40 (m, 1H), 1.24 – 1.13 (m, 1H), 0.92 (d, *J* = 14.5 Hz, 1H).

^{13}C NMR: (101 MHz, $CDCl_3$) δ 171.01, 148.70, 147.32, 145.98, 133.03, 132.65, 131.94, 130.08, 128.94, 127.94, 124.21, 122.48, 121.87, 118.62, 94.51, 74.30, 66.20, 60.78, 56.10, 43.67, 34.62, 33.86, 33.14, 26.16, 24.28, 19.31, 18.58.

IR(neat): 3213, 2922, 2851, 1743, 1591, 1509, 1489, 1462, 1395, 1370, 1258, 1238, 1157, 1104, 1048, 1010, 958, 908, 806, 783, 765, 730, 646, 573, 459 cm^{-1}

HRMS: (+p APCI) calculated for $C_{29}H_{29}O_3N_2{}^{79}Br^{35}Cl_3$ [637.04216] found [637.04255]

CCDC#: 2182287

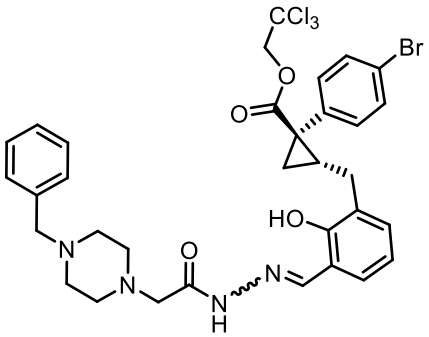

2,2,2-trichloroethyl (1R,2R)-2-(3-((E/Z)-(2-(2-(4-benzylpiperazin-1-yl)acetyl)hydrazineylidene)methyl)-2-hydroxybenzyl)-1-(4-bromophenyl)cyclopropane-1-carboxylate (129)

This compound was prepared according to **General procedure 3.4** from the reaction between **1** (27 µmol, 10 mg) and PAC-1 (2.5 equiv, 67 µmol, 26 mg). After isolation product was obtained as a yellow oil in up to 88% yield, 1:1 E:Z ratio, 13:1 overall d.r (24 umol, 18 mg). The *E* and *Z* isomers of the hydrazide were inseperable by prep-HPLC, however the products were resolvable by NMR and are reported seperately herein. Structural assignment of both compounds by 2D NMR can be found on **S357-S368.**

^{1}H NMR: **E-isomer** (600 MHz, $CDCl_3$) δ 11.00 (s, 1H), 8.05 (s, 1H), 7.51 – 7.34 (m, 15H), 7.25 – 7.08 (m, 5H), 7.04 (dd, *J* = 14.3, 7.5 Hz, 3H), 6.80 (dt, *J* = 32.1, 7.5 Hz, 2H), 4.83 – 4.77 (m, 2H), 4.59 – 4.50 (m, 2H), 4.28 – 4.18 (m, 6H), 3.74 (s, 4H), 3.58 (d, *J* = 11.9 Hz, 7H), 2.65 (ddd, *J* = 29.0, 15.1, 5.5 Hz, 2H), 2.36 – 2.26 (m, 2H), 1.94 – 1.85 (m, 3H), 1.38 (dd, *J* = 6.9, 4.6 Hz, 1H).

^{1}H NMR: **Z-isomer** (600 MHz, $CDCl_3$) δ 8.24 (s, 1H), 7.53 – 7.37 (m, 16H), 7.27 – 7.11 (m, 6H), 7.06 (dd, *J* = 14.3, 7.5 Hz, 3H), 6.82 (dt, *J* = 32.1, 7.5 Hz, 2H), 4.86 – 4.79 (m, 2H), 4.62 – 4.53 (m, 2H), 4.30 – 4.20 (m, 6H), 4.03 (s, 2H), 3.68 (s, 5H), 3.60 (d, *J* = 11.9 Hz, 8H), 2.39 – 2.28 (m, 2H), 1.97 – 1.87 (m, 3H), 1.84 (dd, *J* = 9.0, 4.4 Hz, 1H), 1.38 – 1.34 (m, 1H).

^{13}C NMR: E-isomer (151 MHz, $CDCl_3$) δ 152.01, 152.01, 133.34, 133.34, 133.34, 131.25, 120.14, 119.66, 74.42, 74.42, 74.42, 74.42, 61.22, 60.90, 49.96, 30.16, 30.00, 30.00, 30.00, 28.06

^{13}C NMR: Z-isomer (151 MHz, $CDCl_3$) δ 153.23, 133.27, 133.27, 133.27, 131.18, 120.07, 119.59, 74.36, 74.36, 74.36, 74.36, 61.16, 60.83, 56.81, 30.09, 29.93, 29.93, 29.93, 28.00

IR(neat): Both isomers 3455, 3015, 2970, 2948, 1738, 1670, 1609, 1489, 1447, 1365, 1228, 1216, 1203, 1136, 1092, 1075, 1011, 956, 897, 833, 799, 766, 752, 721, 702, 574, 538, 528, 517 cm^{-1}
HRMS: (+p APCI) calculated for $C_{33}H_{35}O_4N_4{}^{79}Br^{35}Cl_3$ [735.09018] found [735.08967]

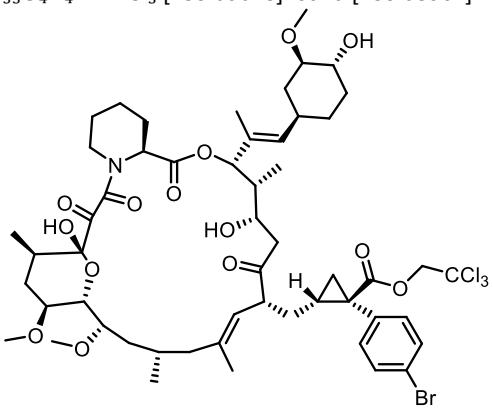

2,2,2-trichloroethyl (1R,2R)-1-(4-bromophenyl)-2-(((3S,4R,5S,8R,12S,14S,15R,16S,18R,19R,26aS,E)-5,19-dihydroxy-3-((E)-1-((1R,3R,4R)-4-hydroxy-3-methoxycyclohexyl)prop-1-en-2-yl)-14,16-dimethoxy-4,10,12,18-tetramethyl-1,7,20,21-tetraoxo-1,4,5,6,7,8,11,12,13,14,15,16,17,18,19,20,21,23,24,25,26,26a-docosahydro-3H-15,19-epoxypyrido[2,1-c][1]oxa[4]azacyclotricosin-8-yl)methyl)cyclopropane-1-carboxylate (130)
This compound was prepared according to **General procedure 3.4** from the reaction between **1** (0.10 mmol, 37 mg) and FK506 (Tacrolimus, 2.0 equiv, 74 mmol, 160mg). After isolation product was obtained as a powdery white solid in up to 58% yield (58 µmol, 66 mg). The starting material is sold as a conformer mixture, and both the starting material conformers and product conformers are not resolved by preperative HPLC or NMR, as they readily interconvert in solution. Structural assignment of the major confromer of the compound by 2D NMR can be found on **S369-S374.**
^{1}H NMR (Major diastereomer reported): (600 MHz, MeOD) δ 7.51 – 7.48 (d, *J* = 8.5 Hz, 2H), 7.27 (d, *J* = 8.5 Hz, 2H), 4.74 (ab-quartet, 2H), 4.35 (d, *J* = 14.0 Hz, 2H), 3.91 (ddd, *J* = 7.3, 5.9, 3.4 Hz, 1H), 3.74 (ddd, *J* = 9.6, 5.8, 2.1 Hz, 2H), 3.70 – 3.55 (m, 3H), 3.45 (dd, *J* = 4.4, 1.6 Hz, 1H), 3.41 (s, 2H), 3.40 (s, 3H), 3.33 (multiple nucleides, d, *J* = 2.3 Hz, 5H), 3.02 (dddd, *J* = 11.0, 8.8, 4.4, 1.9 Hz, 1H), 2.99 – 2.94 (m, 1H), 2.77 (dd, *J* = 14.3, 5.9 Hz, 1H), 2.36 – 2.27 (m, 1H), 2.21 – 2.15 (m, 2H), 2.14 – 2.07 (m, 1H), 2.01 (s, 5H), 1.97 – 1.90 (m, 4H), 1.83 – 1.71 (m, 15H), 1.70 – 1.64 (m, 4H), 1.60 (dd, *J* = 10.0, 1.3 Hz, 3H), 1.55 – 1.48 (m, 1H), 1.48 – 1.40 (m, 1H), 1.41 – 1.31 (m, 3H), 1.24 (t, *J* = 7.1 Hz, 6H), 1.13 – 1.04 (m, 1H), 0.95 (d, *J* = 6.4 Hz, 3H), 0.90 (ddd, *J* = 7.0, 4.4, 2.5 Hz, 12H).
^{13}C NMR (Major diastereomer reported): (151 MHz, MeOD) δ 212.63, 198.39, 173.50, 170.65, 167.48, 140.59, 135.83, 134.55, 133.13, 132.23, 132.21, 124.08, 122.40, 99.01, 96.46, 85.21, 81.60, 76.86, 75.32, 75.11, 74.66, 74.62, 73.86, 70.63, 57.95, 57.86, 57.65, 57.36, 56.66, 56.20, 54.00, 50.11, 47.41, 41.83, 40.27, 36.79, 36.30, 36.16, 35.14, 34.38, 33.53, 33.15, 33.04, 31.83, 28.44, 28.19, 27.20, 25.35, 22.11, 20.85, 20.24, 16.49, 16.37, 13.51, 10.78.
IR(neat): 3460, 2970, 2941, 1738, 1650, 1447, 1365, 1229, 1217, 1092, 909, 765, 719, 528 cm^{-1}
HRMS: (+p APCI) calculated for $C_{54}H_{75}O_{14}N^{79}Br^{35}Cl_3{}^{23}Na$ [1168.33287] found [1168.3347]

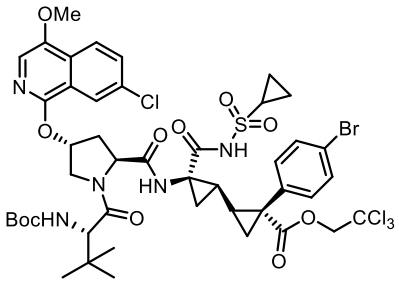

2,2,2-trichloroethyl (1R,1'R,2R,2'R)-2-(4-bromophenyl)-2'-((2S,4R)-1-((S)-2-((tert-butoxycarbonyl)amino)-3,3-dimethylbutanoyl)-4-((7-chloro-4-methoxyisoquinolin-1-yl)oxy)pyrrolidine-2-carboxamido)-2'-((cyclopropylsulfonyl)carbamoyl)-[1,1'-bi(cyclopropane)]-2-carboxylate (131)
This compound was prepared according to **General procedure 3.4** from the reaction between **1** (26.9 µmol, 10.0 mg) and Asunaprevir (2.5 equiv, 67 µmol, 50mg). After isolation product was obtained as a off white solid in about 82% yield (22 µmol, 24 mg). Upon heating above 40°C the compound is prone to decomposition to give an unidentified orange oil. Furthermore, the acidic nature of the reaction and subsequent purification led to partial removal of the Boc protecting group and **115** was therefore not obtained as a pure compound. Structural assignment of compound by 2D NMR can be found on **S375-S381.**
^{1}H NMR: (600 MHz, DMSO) δ 10.60 (s, 1H), 8.44 (s, 0H), 8.06 (d, J = 8.9 Hz, 1H), 7.99 (d, J = 2.3 Hz, 1H), 7.82 – 7.75 (m, 1H), 7.72 – 7.64 (m, 2H), 7.57 – 7.51 (m, 2H), 7.32 – 7.27 (m, 2H), 6.60 (d, J = 8.3 Hz, 1H), 5.68 (s, 1H), 4.82 (dd, J = 80.9, 12.2 Hz, 2H), 4.40 (dd, J = 10.5, 7.1 Hz, 1H), 4.33 (d, J = 11.6 Hz, 1H), 3.96 (s, 4H), 3.88 (d, J = 11.3 Hz, 1H), 3.00 – 2.94

+(m, 1H), 2.43 (dd, J = 13.7, 7.0 Hz, 1H), 2.12 (d, J = 9.9 Hz, 2H), 1.71 (dd, J = 9.2, 5.1 Hz, 1H), 1.55 (t, J = 6.1 Hz, 1H), 1.35 – 1.29 (m, 2H), 1.23 (s, 17H), 1.13 (d, J = 4.2 Hz, 3H), 1.04 (d, J = 11.8 Hz, 3H), 0.92 (s, 12H), 0.66 (d, J = 7.0 Hz, 1H), 0.47 – 0.42 (m, 1H).

^{13}C NMR: (151 MHz, DMSO) δ 173, 171.2, 170.9, 168.5, 155.4, 151.8, 145.6, 133.9, 133.2, 133.2, 132.1, 130.8, 130.8, 130.8, 128.7, 123.3, 121.9, 120.6, 120, 119, 95.2, 78, 74.2, 73.2, 58.8, 58.8, 56.1, 53.3, 53.3, 40.1, 34.2, 33.9, 32.1, 30.3, 30.3, 27.5, 26.2, 25.5, 20.5, 19.8, 5.3, 5.3

IR(neat): 3403, 2957, 2928, 2858, 1725, 1463, 1380, 1271, 1201, 1123, 1072, 1039, 743, 705, 571 cm^{-1}

HRMS: (+p APCI) calculated for $C_{45}H_{53}O_{11}N_5{}^{79}Br^{35}Cl_4{}^{32}S$ [1090.13943] found [1090.13899]

5. High-throughput screening for synthesis of compound 2 in the presence of poisonous and reactive nucleophiles.

5.1 General procedure for the cyclopropanation of 9-hexene with 2,2,2-trichloroethyl-2-(4-bromophenyl)diazo-2-acetate in the presence of poisonous additives on microscale.

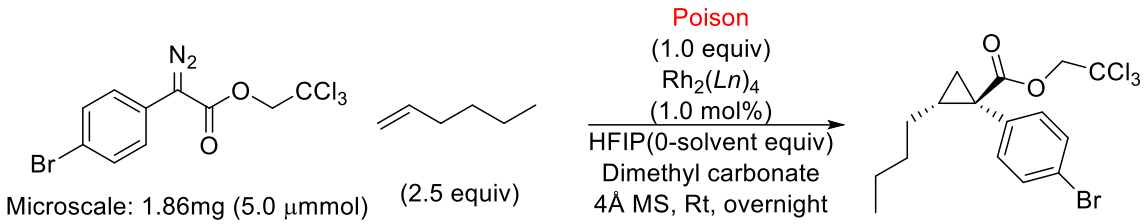

A 96 aluminum wellplate with a rubber seal was prepared bearing 96 300µl vials. This wellplate was then brought into a glovebox under an inert nitrogen atmosphere and dry stirbars and 4Å molecular sieves were added to each vial (1 sieve per vial). Stock solution of catalyst and 1-hexene was prepared according to the conditions being explored (0.00125M catalyst and 0.31M 1-hexene in DMC or HFIP). For reactions run in with 10 equiv HFIP the catalyst stock solution was prepared from a 1.25M solution of HFIP in DMC (50µmol of HFIP per 40µl). Then stock solutions of each additive were prepared according to the conditions being explored (0.25M in DMC or HFIP). Then stock solution of 2,2,2-trichloroethyl-2-(4-bromophenyl)diazo-2-acetate **1** was prepared according to the conditions being explored (0.25M in DMC or HFIP). Then catalyst solution (40µl, 0.05 µmol catalyst, 12.5 µmol 1-hexene) was added to each vial by multichannel automatic pipette. Next additive stock solution (20µl, 5.0 µmol) was added to each vial individually by automatic pipette. Every vial contains a different additive and identity is assigned according to wellplate position. The wellplate was briefly swirled to encourage mixing between the additive and catalyst solutions before adding the diazo solution to each vial via multichannel automatic pipette (20µl, 5.0 µmol). The wellplate was then sealed with the rubber septum via use of a screwdriver and removed from the glovebox. The reactions were stirred at 400rpm for 24 hours via stirrer. The reaction solutions were then dried under a stream of N_2 and resuspended in a solution of 1.0M Glyburide (glibenclamide) in MeOH (350µl). The resultant solutions were then vortex mixed for 10mins and centrifuged at 1200 rpm for 8 mins to settle the molecular sieve dust. 50 µl of the solution from each vial was then transferred to a 96 wellplate and the crude reaction mixture was analyzed by LC/MS and UV spectroscopy to determine reaction yield as function of the ratio between the area of the Glyburide peak and the product peak. Glyburide RT: 1.41 min, product RT: 2.17 min.

Seperation conditions: Waters Acquity Classic UPLC, (Column: Waters Acquity BEH C18 1.7um, 2.1x50mm)

Solvents: Water with 0.1% formic acid (A), acetonitrile with 0.1% formic acid (B)

Injection volume: 2uL

Flow rate: 1mL/min, Gradient run:

Time (min)	%A	%B
Initial	98	2
0.1	98	2
2.1	2	98
2.6	2	98
2.7	98	2
3	98	2

Reactions that exhibited >30% yield were regarded as successful. 150 µl of analyte from successful reactions was then transferred to an HPLC vial fitted with a low volume insert and subjected to chiral SFC to determine enantioselectivity of the reaction. Column conditions: SS-Welk-O, 5 min, 3ml/min, 5% IPA/CO_2) RT: 2.18 min, 3.35 min

5.2 Calibration curve for yield determination

The yield of products obtained by **general procedure 5.1** was determined by LC/UV-Vis spectroscopy. Since significant variation can be observed in high throughput screens as a function of sample preperation, yield was determined as a function of the ratio of UV/Vis absorbance between the product and an internal standard. Glibenclamide (glyburide) was selected as the internal standard since significant seperation was observed between this compound and the product 2,2,2-trichloroethyl (*1R,2R*)-1-(4-bromophenyl)-2-butylcyclopropane-1-carboxylate by LC/MS (column conditions). A calibration curve was generated plotting the %yield of the reaction as a function of the ratio between product UV absorbance at 220nm: glyburide UV absorbance at 220 nm. Projected yield was determined by serial dilution of a known sample of pure 2,2,2-trichloroethyl (1R,2R)-1-(4-bromophenyl)-2-butylcyclopropane-1-carboxylate with 1.0M glyburide solution in MeOH with a dilution factor of 1.25. This technique generated the below calibration curve which was used to determine the yield of high-throughput reactions (**Figure C**3). The equation derived from this calibration curve (Equation 1) was used to determine the yield of reactions performed and analyzed according to **general procedure 5.1**. Reactions that afforded >30% yield are considered to be successful and the data from these reactions are reported herein. The results of the analysis as a function of condition used and the corresponding UV spectra for successful reactions are listed below.

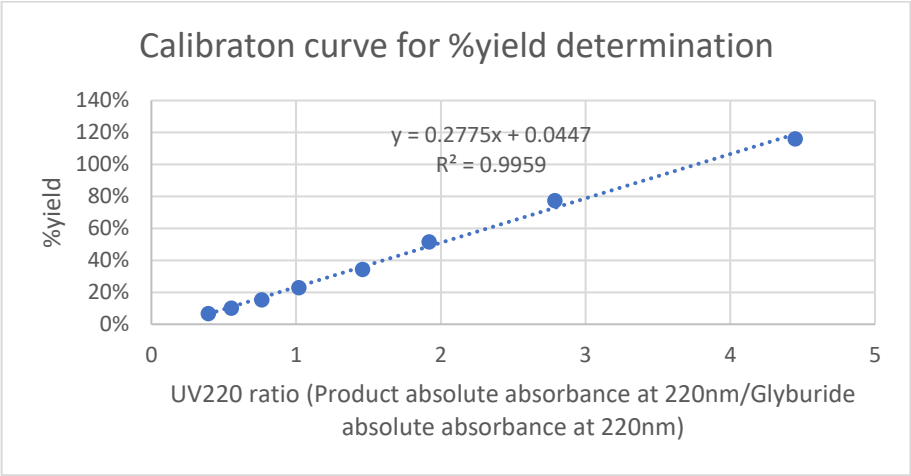

Figure C3: Calibration curve for %yield determination in high throughput reaction screen.

$$\boldsymbol{Equation\ 1}: \%\ Yield = \left(0.2775 \times \frac{Absolute\ integration\ of\ product\ (\mathbf{2})peak}{Absolute\ integration\ of\ glyburide\ peak} + 0.0447\right) \times 100$$

As an example of how this equation was used to derive yield consider the following result for poison A2 (Furan, **13**) in the absence of HFIP. In the yield chromatogram the absolute integration of the product peak was: 10173.68 and the absolute integration of the glyburide peak was: 8561.55. Therefore, the ratio between the two peaks ($\frac{Absolute\ integration\ of\ product\ (\mathbf{2})peak}{Absolute\ integration\ of\ glyburide\ peak}$) is 1.19. Plugging this into equation 1 we can calculate the %yield as 37%.

5.3 Successful reactions performed with Rh_2(*S-tetra-p*-Br-PhPTTL)$_4$ as catalyst in the absence of HFIP.

The following dataset represents reactions that were successful when performed according to **general procedure 5.1** in the absence of HFIP using Rh_2(*S-tetra-p*-Br-PhPTTL)$_4$ as catalyst and dimethyl carbonate as solvent. Each additive is described according to the well plate designation in the study as well as the compound number it was assigned in the main text. The yield of the reaction in the presence of each additive is reported in **Figure C**4 and what follows is the HPLC data from which the yield was calculated according to equation 1.

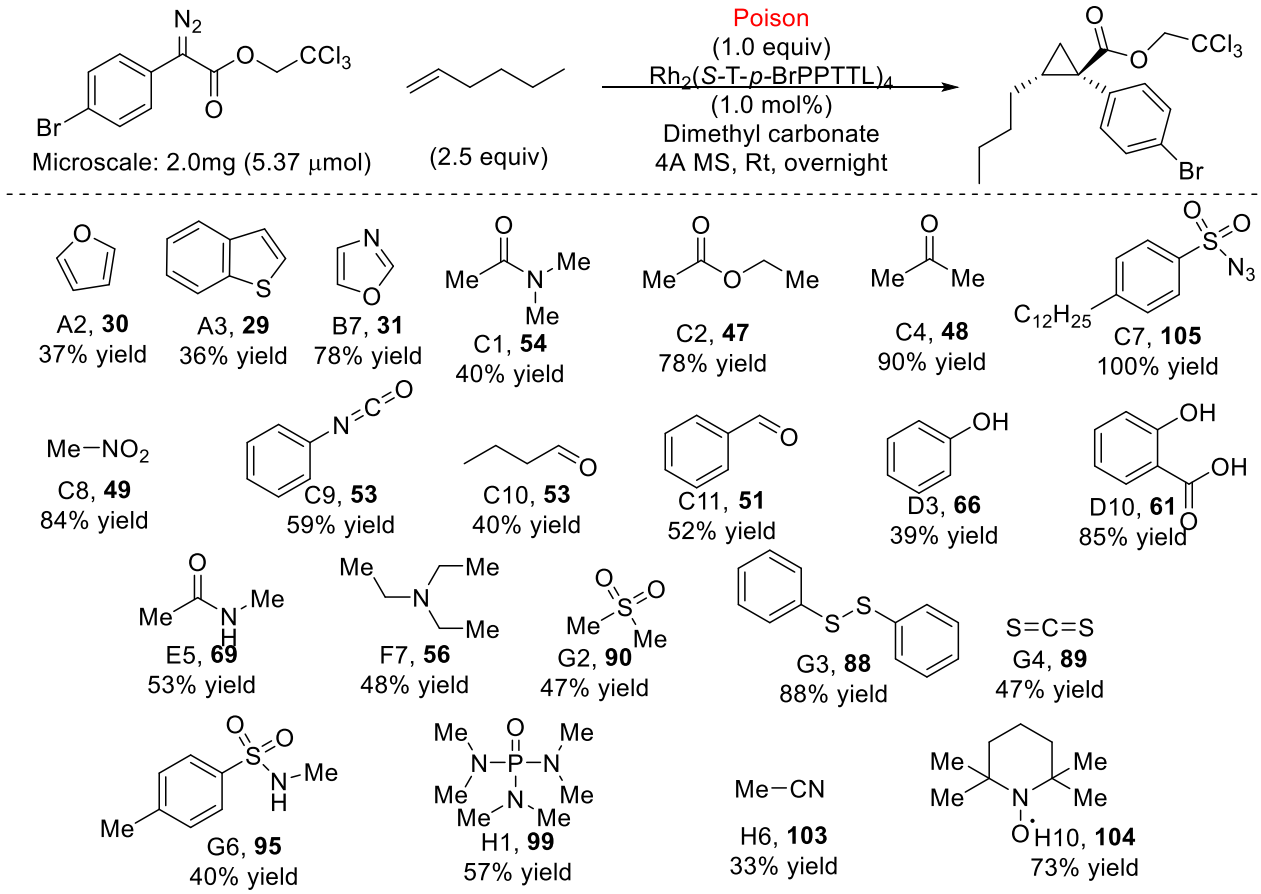

Figure C4: Reactions giving >30% yield (successful reactions) without the use of HFIP in the presence of Rh_2(*S-tetra-p*-Br-PhPTTL)$_4$ and dimethyl carbonate as solvent.

Single Sample Report
Sample Name: SHARLJA1-exp100-0025_11_29_2021_A2
Filename: sharlja1-exp100-0025_11_29_2021_a2.raw
Submitter:

A2,
37% yield

Peak #	Formula	Target …	Target …	Time	Found	Area %	Area Abs
10	C23H28C…	493.1	Glyburi…	1.411	Yes	30.4	8561.55
19	C16H18B…	426.0	Product	2.071	Yes	36.1	10173.68

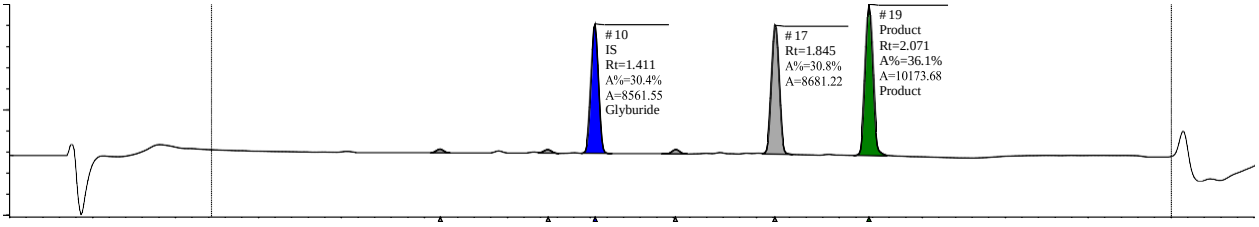

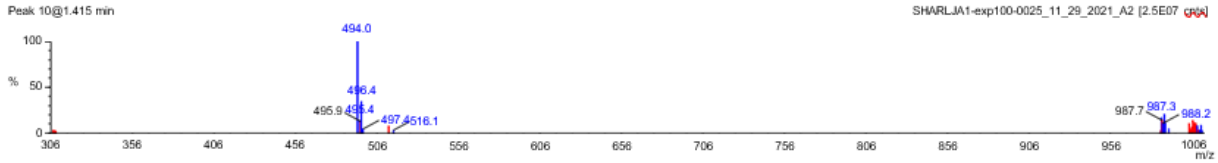

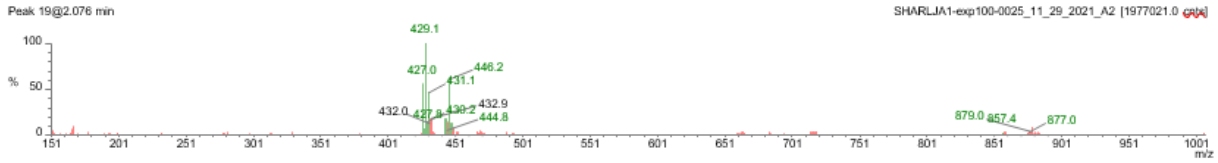

Name	Y/N	Type	Formula	Mass
Glyburide	Y	IS	C23H28ClN3O5S	493.1
Product	Y	Product	C16H18BrCl3O2	426.0

Single Sample Report
Sample Name: SHARLJA1-exp100-0025_11_29_2021_A3
Filename: sharlja1-exp100-0025_11_29_2021_a3.raw
Submitter:

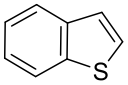

A3,
36% yield

Peak #	Formula	Target …	Target …	Time	Found	Area %	Area Abs
8	C23H28C…	493.1	Glyburi…	1.411	Yes	14.4	7255.35
18	C16H18B…	426.0	Product	2.071	Yes	16.9	8492.35

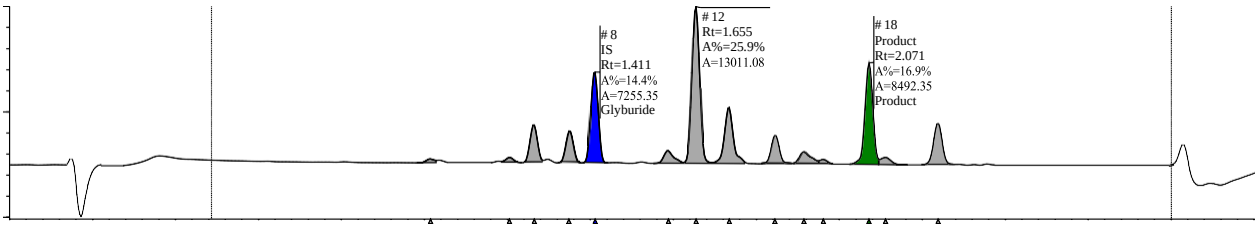

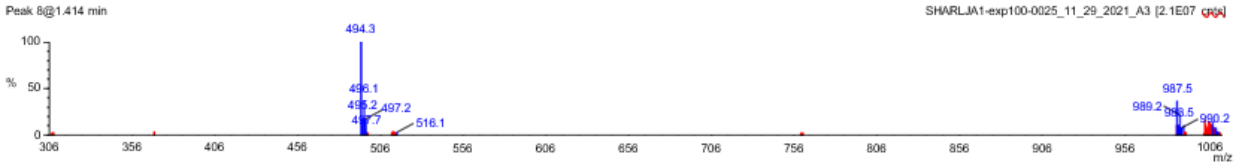

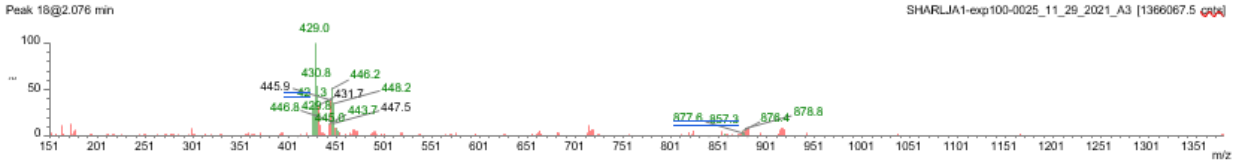

Name	Y/N	Type	Formula	Mass
Glyburide	Y	IS	C23H28ClN3O5S	493.1
Product	Y	Product	C16H18BrCl3O2	426.0

Single Sample Report
Sample Name: SHARLJA1-exp100-0025_11_29_2021_B7
Filename: sharlja1-exp100-0025_11_29_2021_b7.raw
Submitter:

B7,
78% yield

Peak #	Formula	Target …	Target …	Time	Found	Area %	Area Abs
12	C23H28C…	493.1	Glyburi…	1.408	Yes	23.4	5724.13
23	C16H18B…	426.0	Product	2.071	Yes	55.6	13597.32

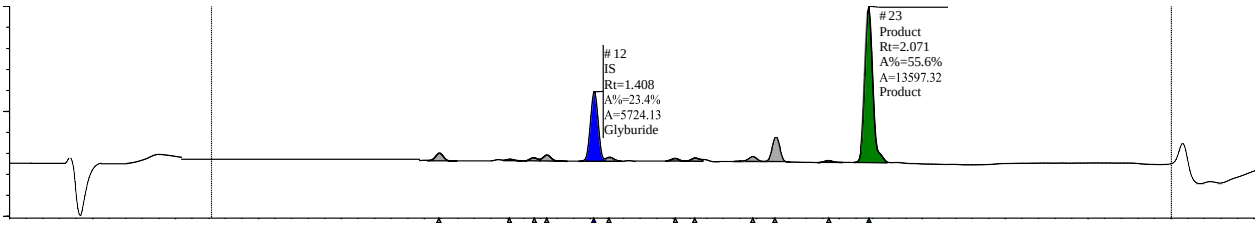

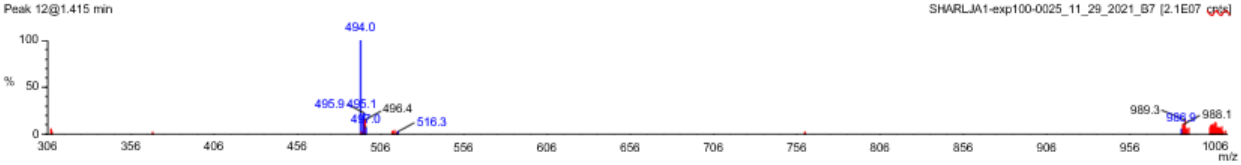

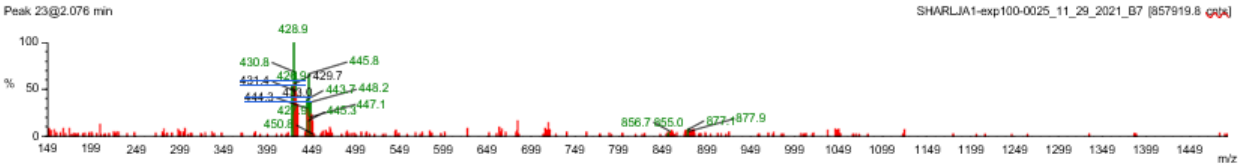

Name	Y/N	Type	Formula	Mass
Glyburide	Y	IS	C23H28ClN3O5S	493.1
Product	Y	Product	C16H18BrCl3O2	426.0

Sample Name: SHARLJA1-exp100-0025_11_29_2021_C1
Filename: sharlja1-exp100-0025_11_29_2021_c1.raw
Submitter:

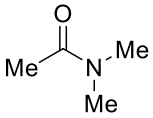

C1,
40% yield

Peak #	Formula	Target …	Target …	Time	Found	Area %	Area Abs
11	C23H28C…	493.1	Glyburi…	1.411	Yes	18.4	7659.20
22	C16H18B…	426.0	Product	2.075	Yes	23.6	9858.73

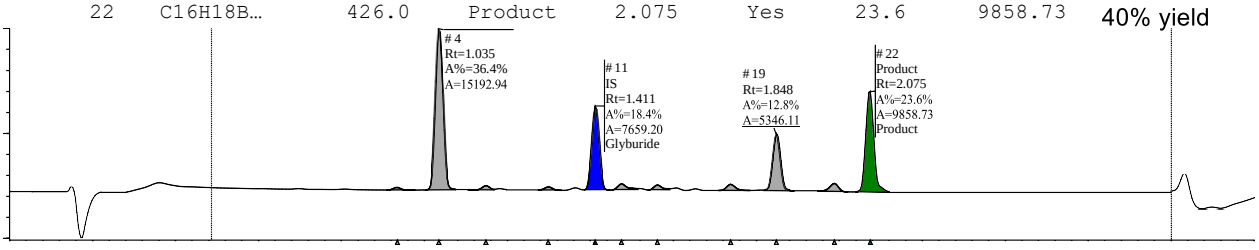

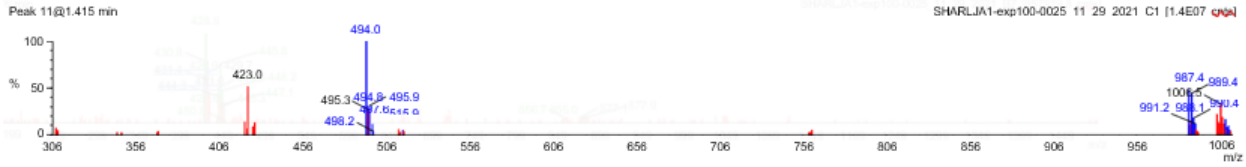

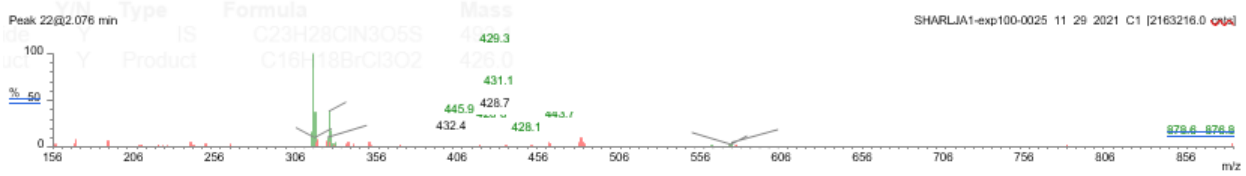

Name	Y/N	Type	Formula	Mass
Glyburide	Y	IS	C23H28ClN3O5S	493.1
Product	Y	Product	C16H18BrCl3O2	426.0

Single Sample Report
Sample Name: SHARLJA1-exp100-0025_11_29_2021_C2
Filename: sharlja1-exp100-0025_11_29_2021_c2.raw**Submitter:**

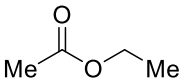

Peak #	Formula	Target …	Target …	Time	Found	Area %	Area Abs
7	C23H28C…	493.1	Glyburi…	1.411	Yes	25.8	8669.68
16	C16H18B…	426.0	Product	2.071	Yes	44.2	14871.45

C2,
78% yield

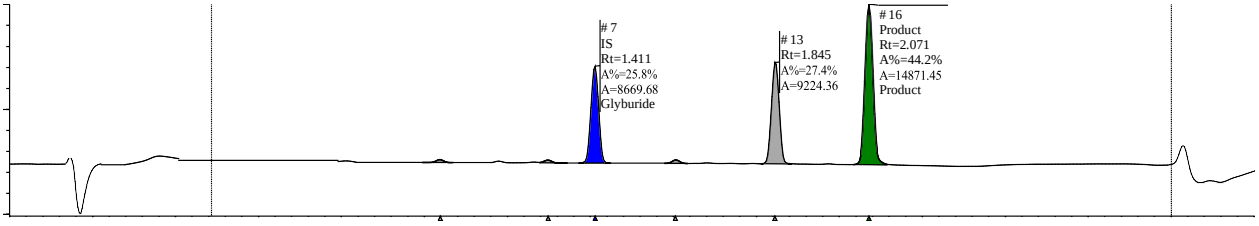

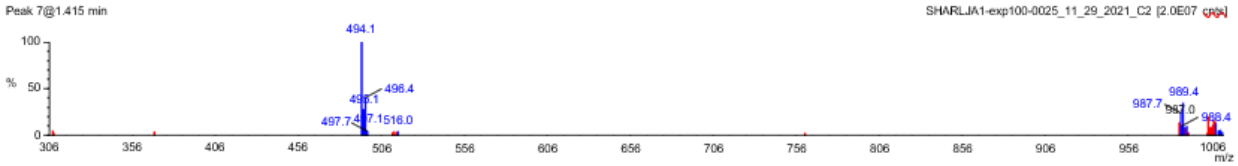

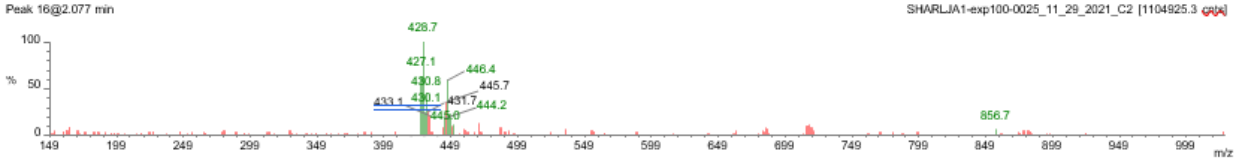

Name	Y/N	Type	Formula	Mass
Glyburide	Y	IS	C23H28ClN3O5S	493.1
Product	Y	Product	C16H18BrCl3O2	426.0

Single Sample Report
Sample Name: SHARLJA1-exp100-0025_11_29_2021_C4
Filename: sharlja1-exp100-0025_11_29_2021_c4.raw
Submitter:

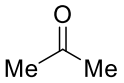

C4,
90% yield

Peak #	Formula	Target …	Target …	Time	Found	Area %	Area Abs
7	C23H28C…	493.1	Glyburi…	1.408	Yes	23.4	4104.33
17	C16H18B…	426.0	Product	2.071	Yes	63.5	11128.40

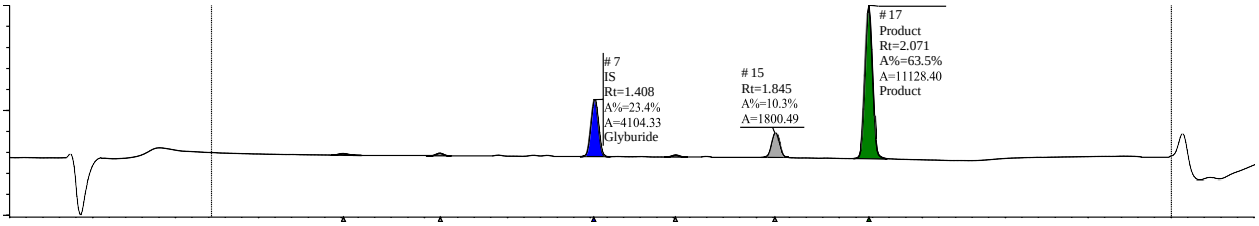

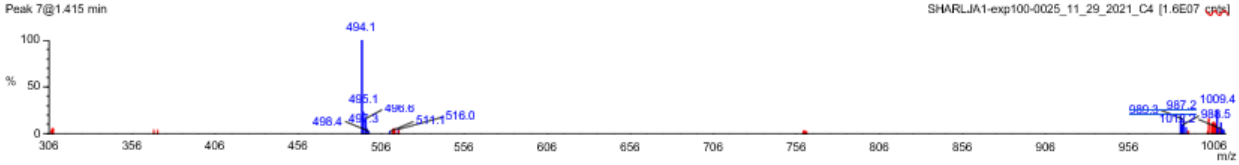

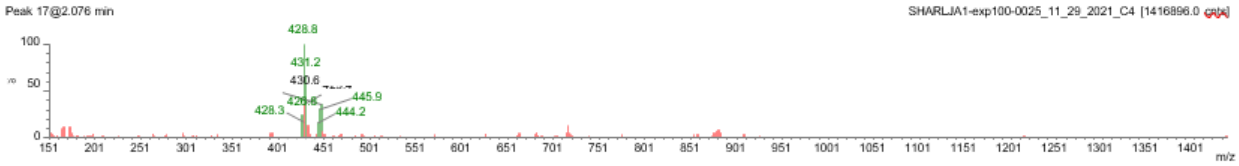

Name	Y/N	Type	Formula	Mass
Glyburide	Y	IS	C23H28ClN3O5S	493.1
Product	Y	Product	C16H18BrCl3O2	426.0

Single Sample Report
Sample Name: SHARLJA1-exp100-0025_11_29_2021_C7
Filename: sharlja1-exp100-0025_11_29_2021_c7.raw
Submitter:

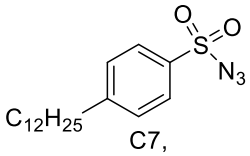

C7,
100% yield

Peak #	Formula	Target …	Target …	Time	Found	Area %	Area Abs
6	C23H28C…	493.1	Glyburi…	1.411	Yes	14.7	3843.77
14	C16H18B…	426.0	Product	2.075	Yes	44.1	11527.89

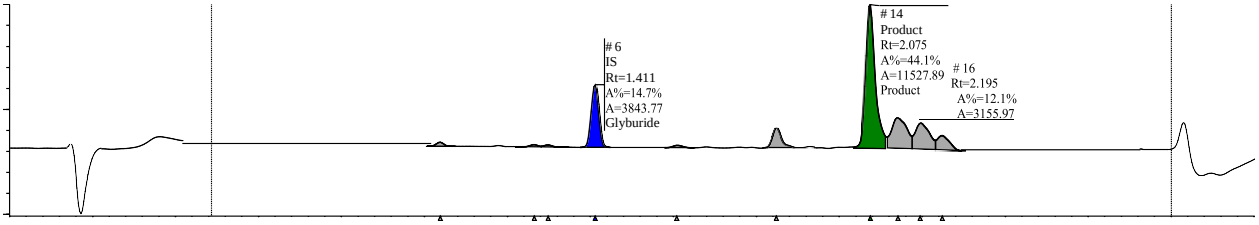

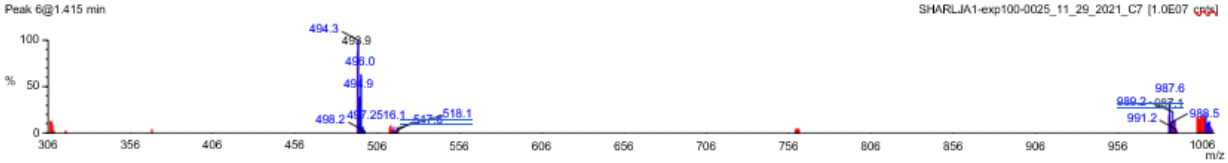

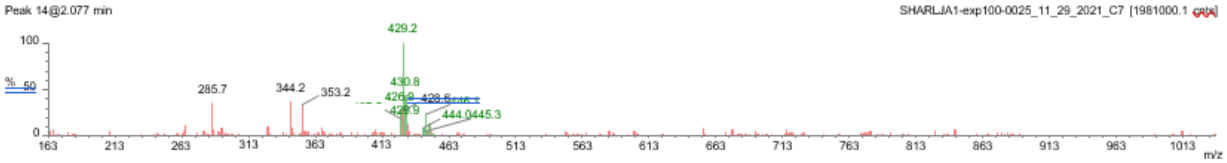

Name	Y/N	Type	Formula	Mass
Glyburide	Y	IS	C23H28ClN3O5S	493.1
Product	Y	Product	C16H18BrCl3O2	426.0

Me—NO_2

C8,
84% yield

Single Sample Report
Sample Name: SHARLJA1-exp100-0025_11_29_2021_C8
Filename: sharlja1-exp100-0025_11_29_2021_c8.raw
Submitter:

Peak #	Formula	Target …	Target …	Time	Found	Area %	Area Abs
7	C23H28C…	493.1	Glyburi…	1.411	Yes	20.1	5721.63
15	C16H18B…	426.0	Product	2.071	Yes	51.2	14581.75

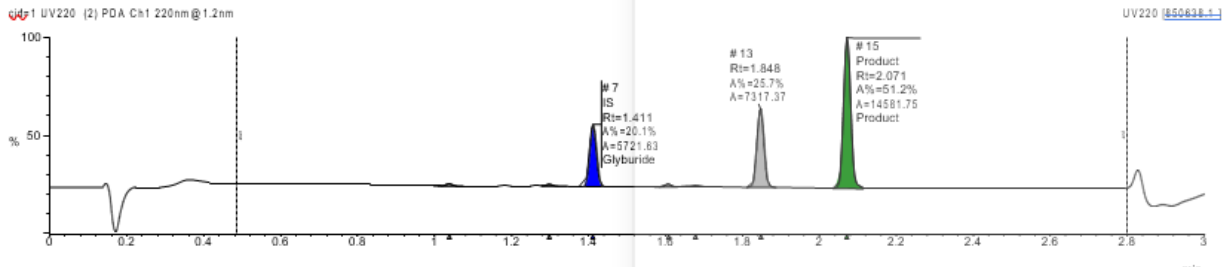

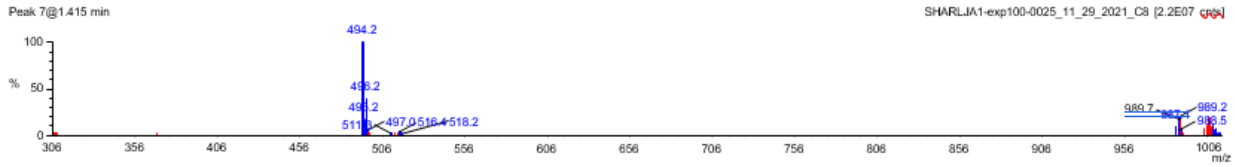

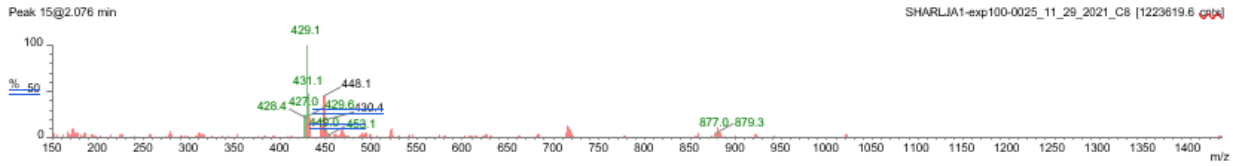

Name	Y/N	Type	Formula	Mass
Glyburide	Y	IS	C23H28ClN3O5S	493.1
Product	Y	Product	C16H18BrCl3O2	426.0

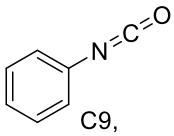

C9,
59% yield

Single Sample Report
Sample Name: SHARLJA1-exp100-0025_11_29_2021_C9
Filename: sharlja1-exp100-0025_11_29_2021_c9.raw
Submitter:

Peak #	Formula	Target …	Target …	Time	Found	Area %	Area Abs
9	C23H28C…	493.1	Glyburi…	1.408	Yes	20.2	3877.05
20	C16H18B…	426.0	Product	2.071	Yes	37.2	7144.62

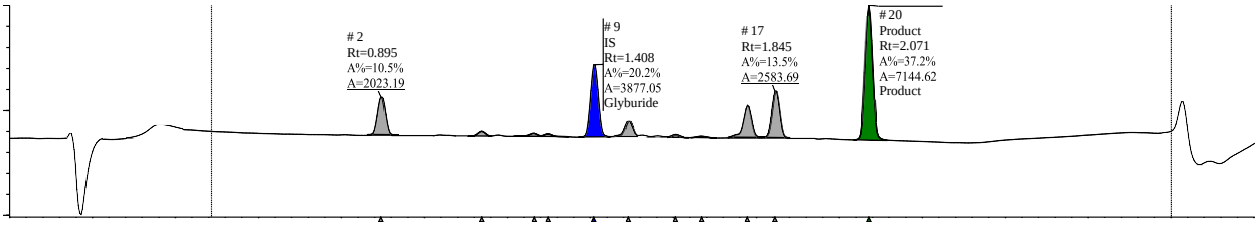

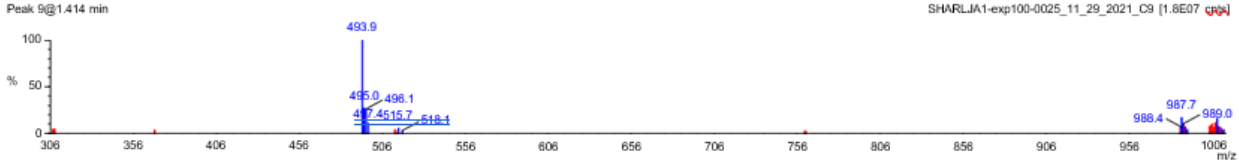

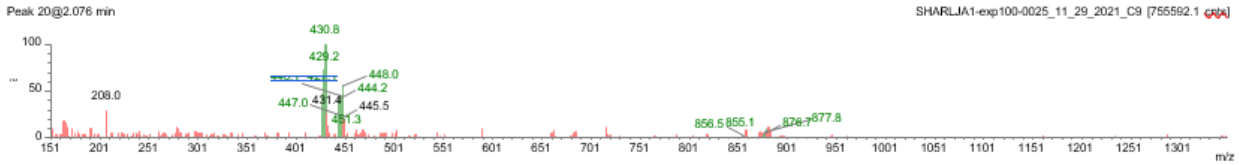

Name	Y/N	Type	Formula	Mass
Glyburide	Y	IS	C23H28ClN3O5S	493.1
Product	Y	Product	C16H18BrCl3O2	426.0

Single Sample Report
Sample Name: SHARLJA1-exp100-0025_11_29_2021_C10
Filename: sharlja1-exp100-0025_11_29_2021_c10.raw
Submitter:

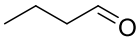

C10,
40% yield

Peak #	Formula	Target …	Target …	Time	Found	Area %	Area Abs
9	C23H28C…	493.1	Glyburi…	1.411	Yes	25.0	4054.35
20	C16H18B…	426.0	Product	2.075	Yes	32.5	5273.84

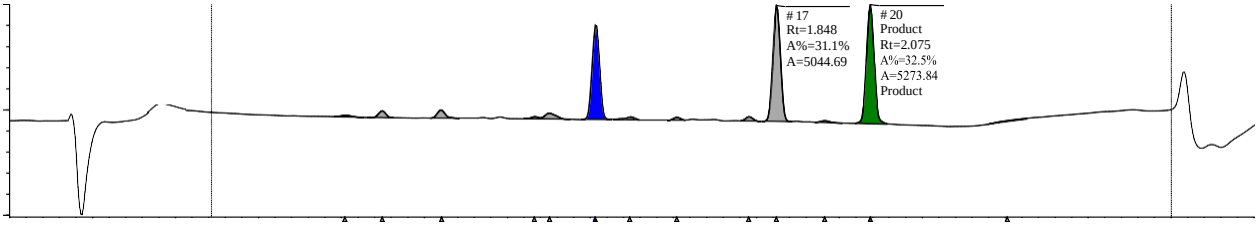

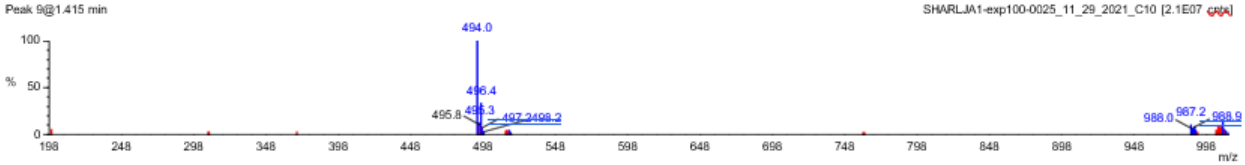

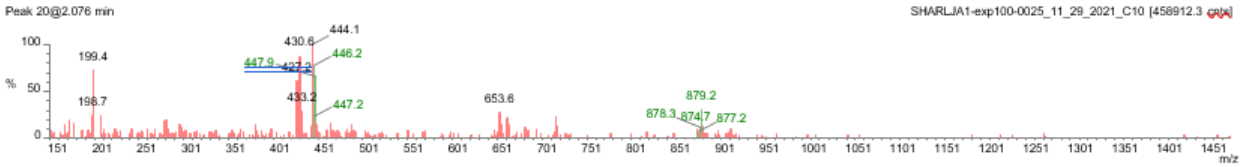

Name	Y/N	Type	Formula	Mass
Glyburide	Y	IS	C23H28ClN3O5S	493.1
Product	Y	Product	C16H18BrCl3O2	426.0

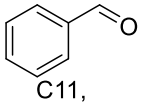

C11,
52% yield

Sample Name: SHARLJA1-exp100-0025_11_29_2021_C11
Filename: sharlja1-exp100-0025_11_29_2021_c11.raw
Submitter:

Peak #	Formula	Target …	Target …	Time	Found	Area %	Area Abs
7	C23H28C…	493.1	Glyburi…	1.411	Yes	19.9	4169.94
13	C16H18B…	426.0	Product	2.075	Yes	32.4	6775.54

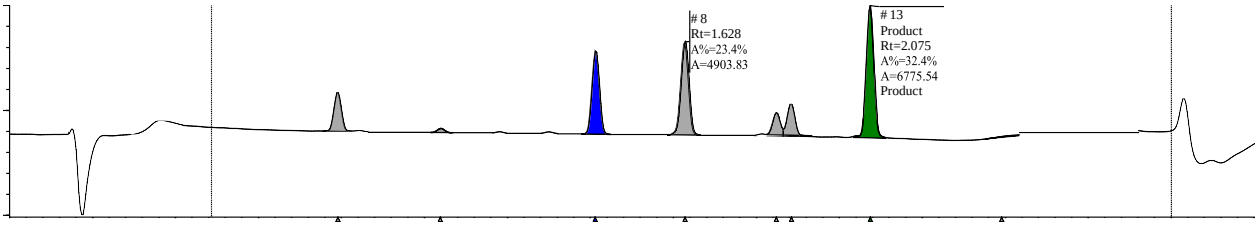

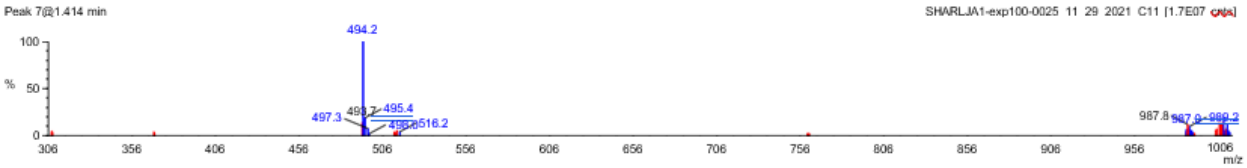

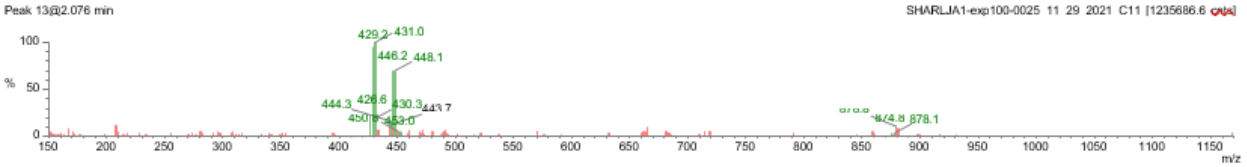

Name	Y/N	Type	Formula	Mass
Glyburide	Y	IS	C23H28ClN3O5S	493.1
Product	Y	Product	C16H18BrCl3O2	426.0

Single Sample Report
Sample Name: SHARLJA1-exp100-0025_11_29_2021_D3
Filename: sharlja1-exp100-0025_11_29_2021_d3.raw
Submitter:

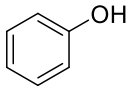

D3,
39% yield

Peak #	Formula	Target …	Target …	Time	Found	Area %	Area Abs
9	C23H28C…	493.1	Glyburi…	1.411	Yes	19.3	1498.38
16	C16H18B…	426.0	Product	2.071	Yes	24.4	1902.26

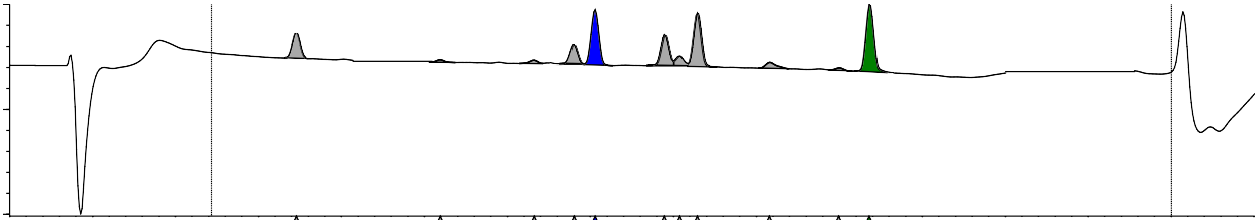

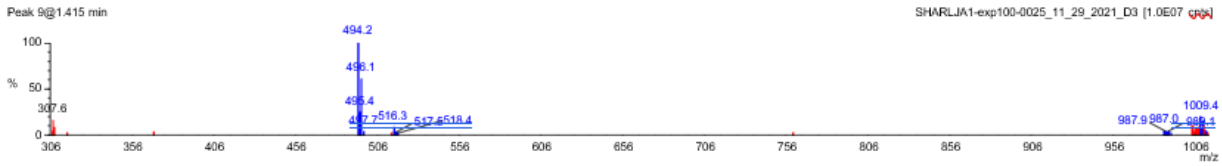

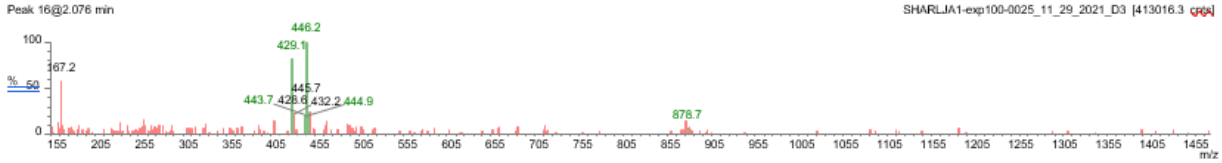

Name	Y/N	Type	Formula	Mass
Glyburide	Y	IS	C23H28ClN3O5S	493.1
Product	Y	Product	C16H18BrCl3O2	426.0

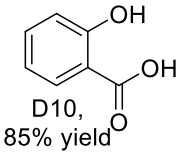

Single Sample Report
Sample Name: SHARLJA1-exp100-0025_11_29_2021_D10
Filename: sharlja1-exp100-0025_11_29_2021_d10.raw
Submitter:

Peak #	Formula	Target …	Target …	Time	Found	Area %	Area Abs
7	C23H28C…	493.1	Glyburi…	1.411	Yes	7.9	2671.93
17	C16H18B…	426.0	Product	2.071	Yes	20.2	6889.44

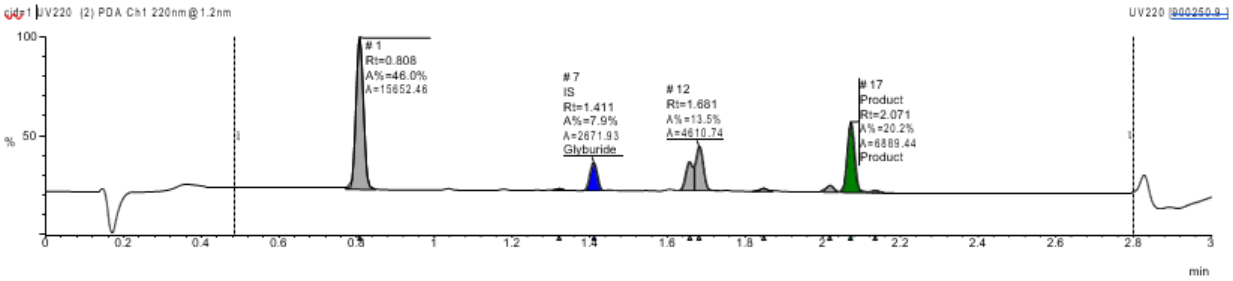

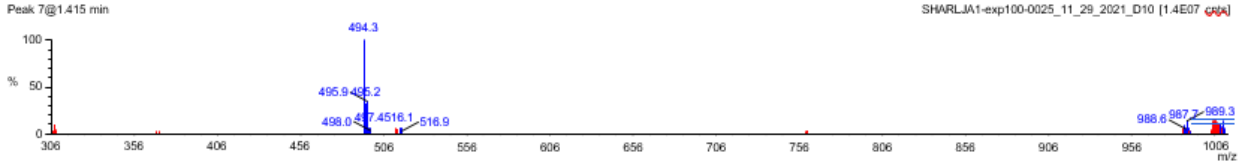

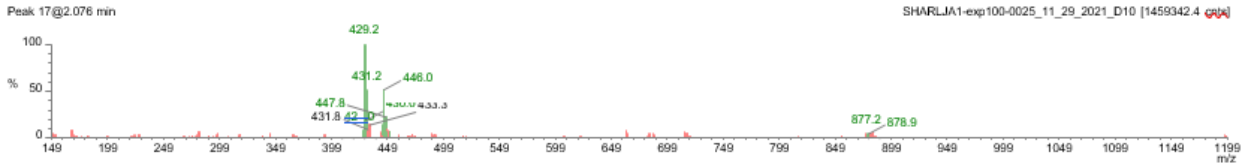

Name	Y/N	Type	Formula	Mass
Glyburide	Y	IS	C23H28ClN3O5S	493.1
Product	Y	Product	C16H18BrCl3O2	426.0

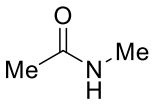

E5,
53% yield

Single Sample Report
Sample Name: SHARLJA1-exp100-0025_11_29_2021_E5
Filename: sharlja1-exp100-0025_11_29_2021_e5.raw
Submitter:

Peak #	Formula	Target …	Target …	Time	Found	Area %	Area Abs
11	C23H28C…	493.1	Glyburi…	1.411	Yes	17.2	3965.46
20	C16H18B…	426.0	Product	2.075	Yes	28.8	6631.44

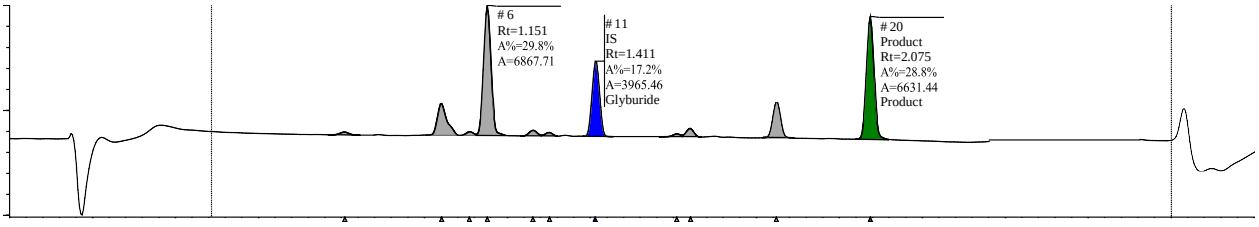

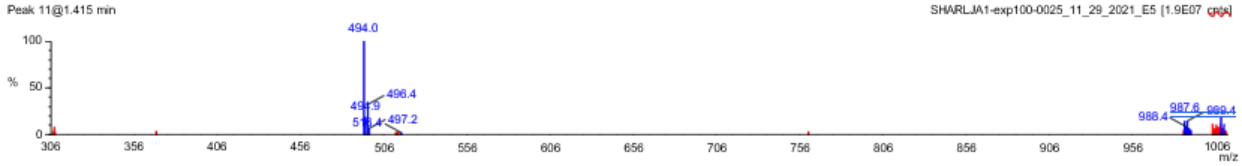

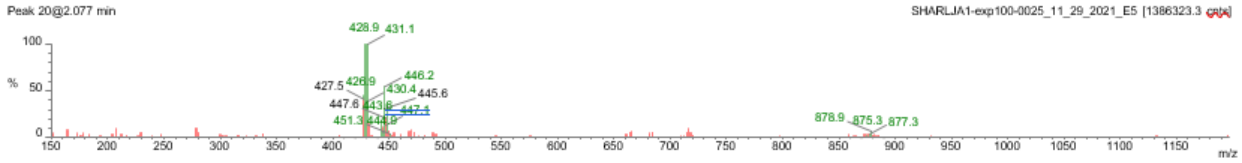

Name	Y/N	Type	Formula	Mass
Glyburide	Y	IS	C23H28ClN3O5S	493.1
Product	Y	Product	C16H18BrCl3O2	426.0

Single Sample Report
Sample Name: SHARLJA1-exp100-0025_11_29_2021_F7
Filename: sharlja1-exp100-0025_11_29_2021_f7.raw
Submitter:

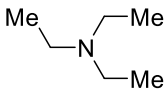

F7,
48% yield

Peak #	Formula	Target …	Target …	Time	Found	Area %	Area Abs
9	C23H28C…	493.1	Glyburi…	1.408	Yes	24.2	7606.53
16	C16H18B…	426.0	Product	2.071	Yes	37.2	11673.87

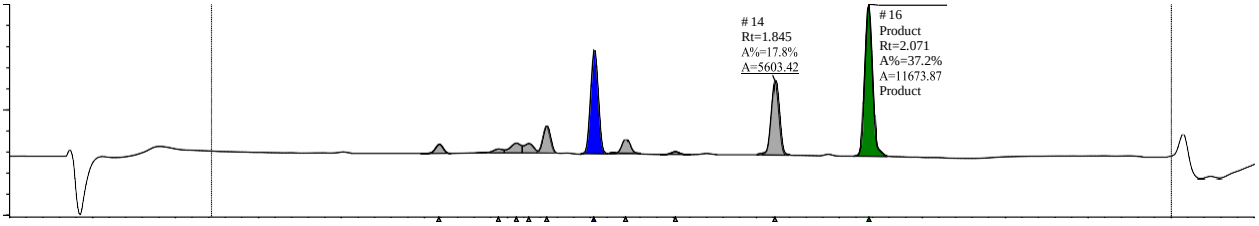

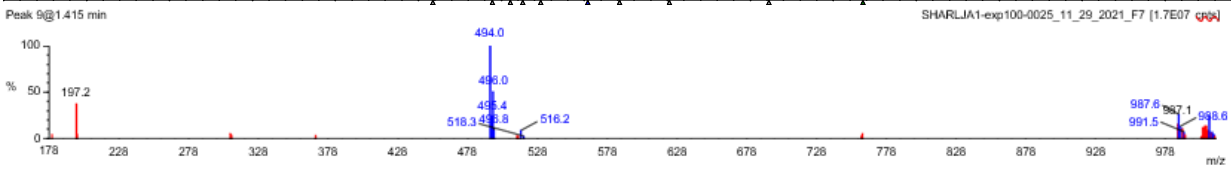

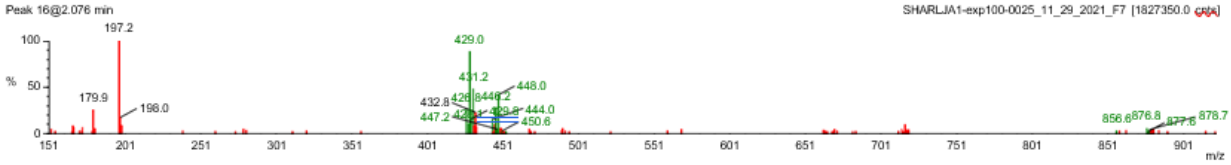

Name	Y/N	Type	Formula	Mass
Glyburide	Y	IS	C23H28ClN3O5S	493.1
Product	Y	Product	C16H18BrCl3O2	426.0

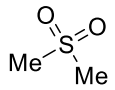

G2,
47% yield

Single Sample Report
Sample Name: SHARLJA1-exp100-0025_11_29_2021_G2
Filename: sharlja1-exp100-0025_11_29_2021_g2.raw
Submitter:

Peak #	Formula	Target …	Target …	Time	Found	Area %	Area Abs
9	C23H28C…	493.1	Glyburi…	1.411	Yes	27.1	3226.02
15	C16H18B…	426.0	Product	2.075	Yes	40.5	4809.65

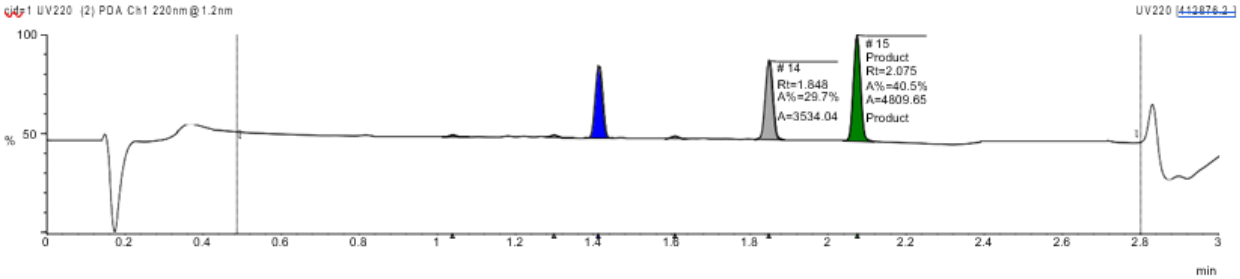

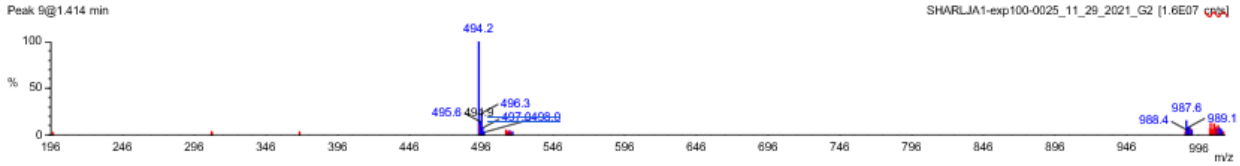

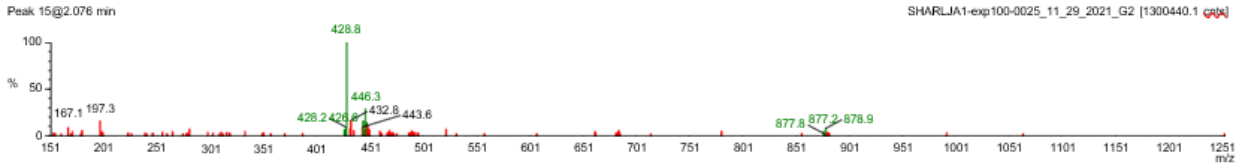

Name	Y/N	Type	Formula	Mass
Glyburide	Y	IS	C23H28ClN3O5S	493.1
Product	Y	Product	C16H18BrCl3O2	426.0

Single Sample Report
Sample Name: SHARLJA1-exp100-0025_11_29_2021_G3
Filename: sharlja1-exp100-0025_11_29_2021_g3.raw
Submitter:

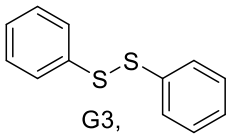

G3,
88% yield

Peak #	Formula	Target …	Target …	Time	Found	Area %	Area Abs
9	C23H28C…	493.1	Glyburi…	1.411	Yes	12.8	3843.11
20	C16H18B…	426.0	Product	2.071	Yes	34.1	10233.64

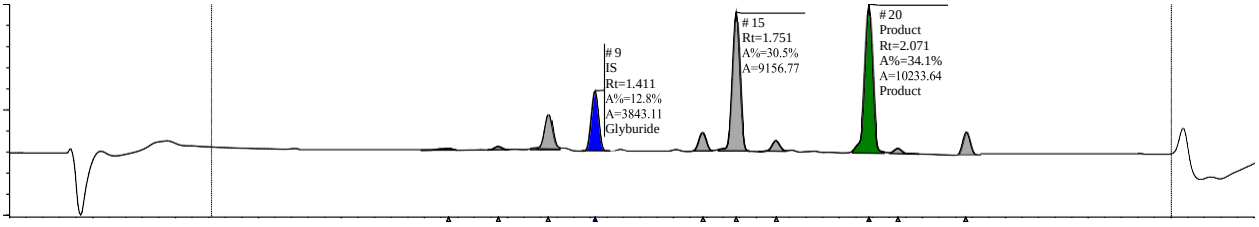

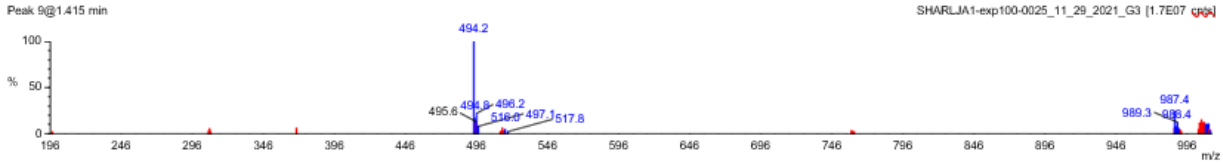

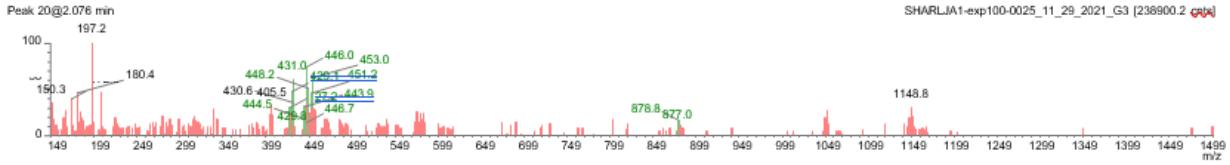

Name	Y/N	Type	Formula	Mass
Glyburide	Y	IS	C23H28ClN3O5S	493.1
Product	Y	Product	C16H18BrCl3O2	426.0

S=C=S
G4,
47% yield

Single Sample Report
Sample Name: SHARLJA1-exp100-0025_11_29_2021_G4
Filename: sharlja1-exp100-0025_11_29_2021_g4.raw
Submitter:

Peak #	Formula	Target …	Target …	Time	Found	Area %	Area Abs
9	C23H28C…	493.1	Glyburi…	1.411	Yes	25.6	4166.68
17	C16H18B…	426.0	Product	2.075	Yes	38.6	6280.02

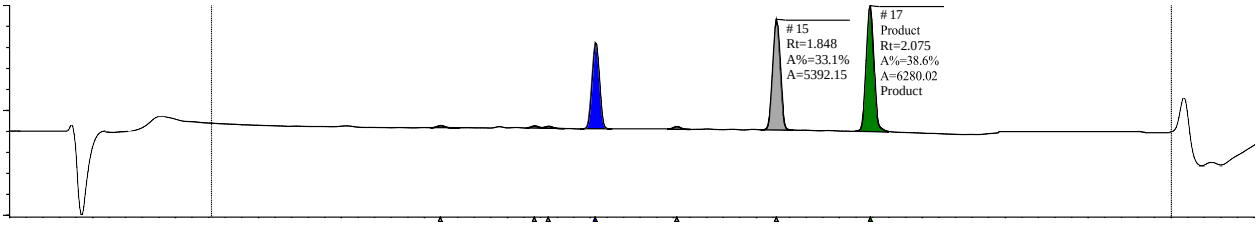

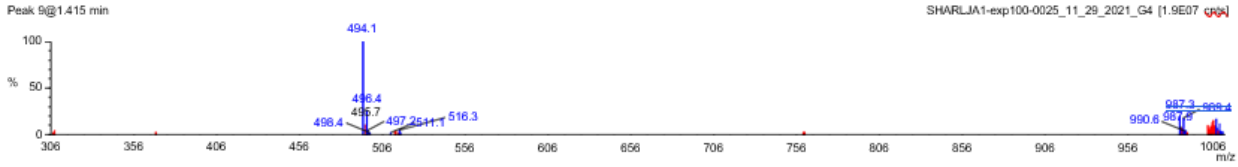

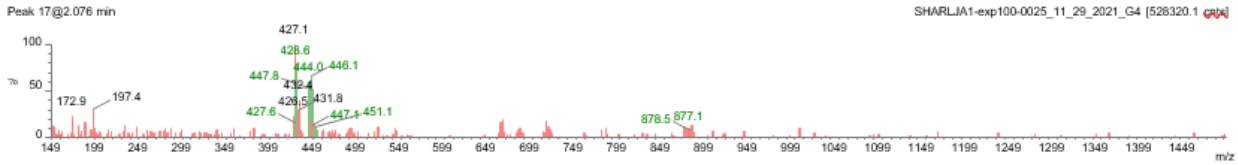

Name	Y/N	Type	Formula	Mass
Glyburide	Y	IS	C23H28ClN3O5S	493.1
Product	Y	Product	C16H18BrCl3O2	426.0

Single Sample Report
Sample Name: SHARLJA1-exp100-0025_11_29_2021_G6
Filename: sharlja1-exp100-0025_11_29_2021_g6.raw
Submitter:

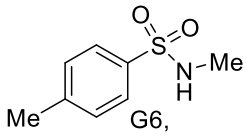

G6,
40% yield

Peak #	Formula	Target …	Target …	Time	Found	Area %	Area Abs
12	C23H28C…	493.1	Glyburi…	1.411	Yes	12.9	4117.15
22	C16H18B…	426.0	Product	2.071	Yes	16.8	5333.95

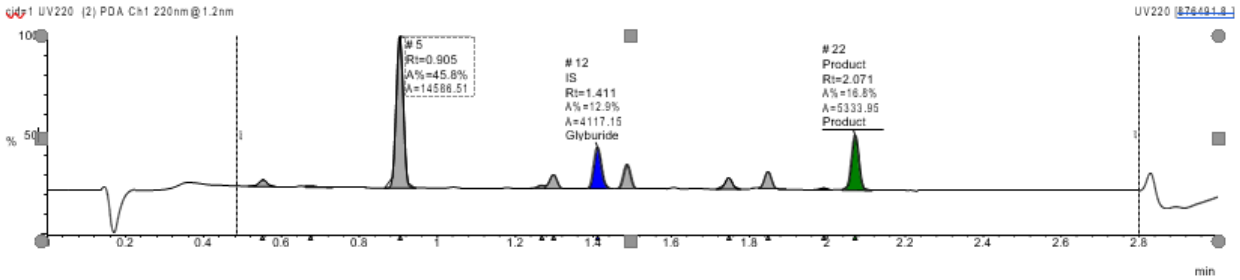

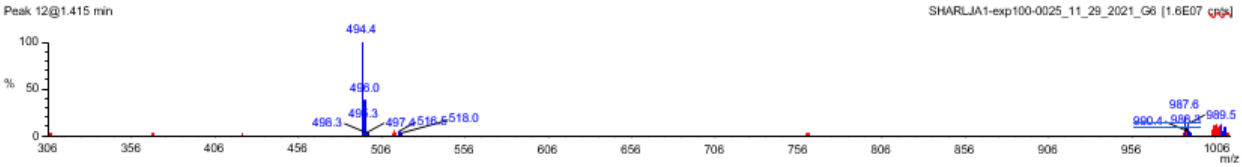

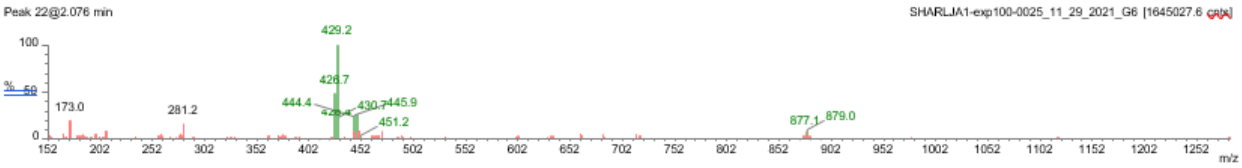

Name	Y/N	Type	Formula	Mass
Glyburide	Y	IS	C23H28ClN3O5S	493.1
Product	Y	Product	C16H18BrCl3O2	426.0

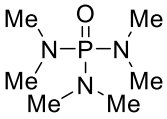

H1,
57% yield

Sample Name: SHARLJA1-exp100-0025_11_29_2021_H1
Filename: sharlja1-exp100-0025_11_29_2021_h1.raw

Peak #	Formula	Target …	Target …	Time	Found	Area %	Area Abs
8	C23H28C…	493.1	Glyburi…	1.411	Yes	17.7	3899.23
15	C16H18B…	426.0	Product	2.075	Yes	31.3	6896.73

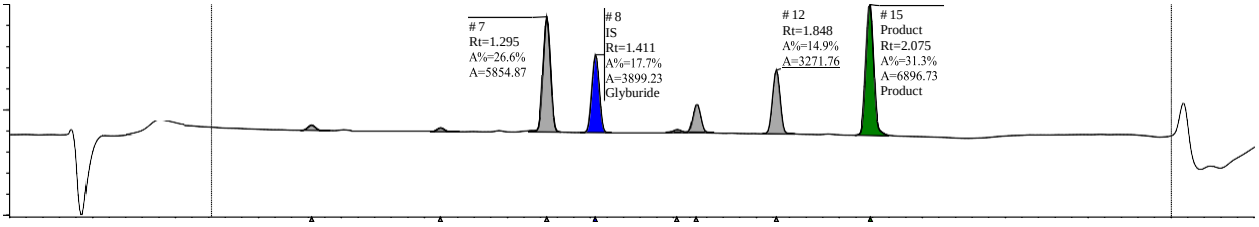

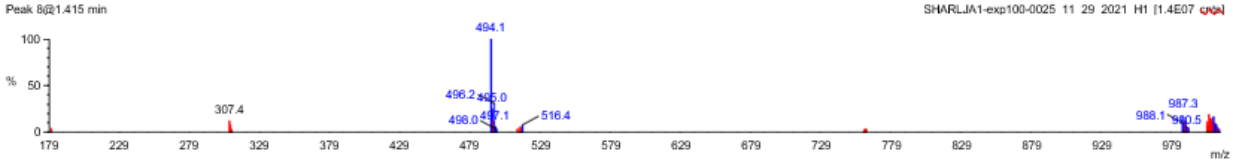

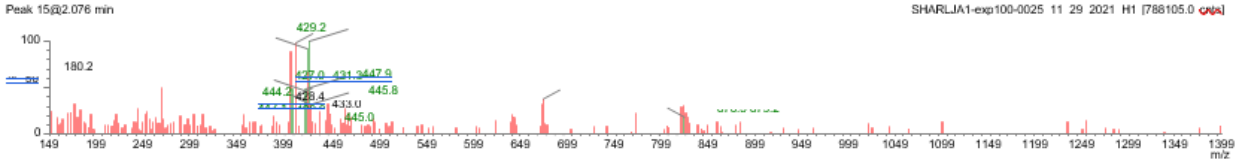

Name	Y/N	Type	Formula	Mass
Glyburide	Y	IS	C23H28ClN3O5S	493.1
Product	Y	Product	C16H18BrCl3O2	426.0

Me−CN

H6,
33% yield

Single Sample Report
Sample Name: SHARLJA1-exp100-0025_11_29_2021_H6
Filename: sharlja1-exp100-0025_11_29_2021_h6.raw
Submitter:

Peak #	Formula	Target …	Target …	Time	Found	Area %	Area Abs
9	C23H28C…	493.1	Glyburi…	1.415	Yes	30.3	8042.17
17	C16H18B…	426.0	Product	2.075	Yes	33.2	8800.80

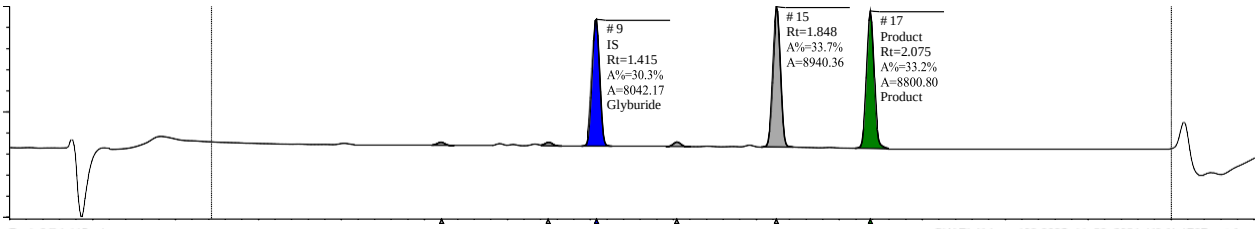

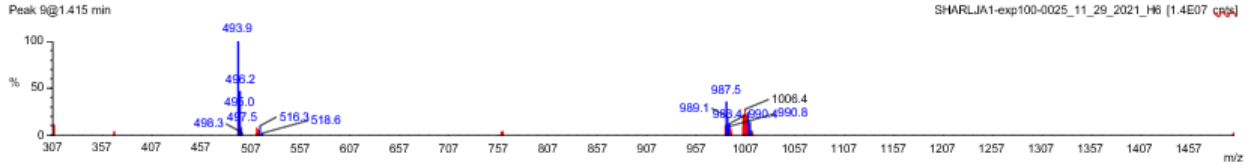

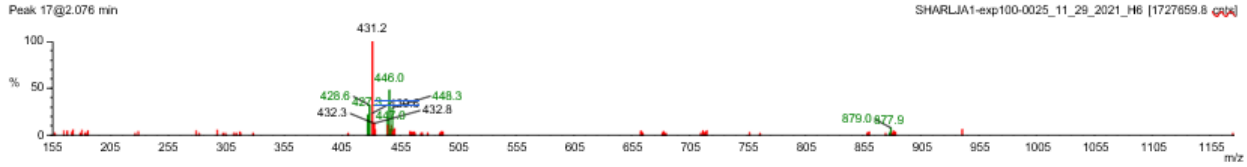

Name	Y/N	Type	Formula	Mass
Glyburide	Y	IS	C23H28ClN3O5S	493.1
Product	Y	Product	C16H18BrCl3O2	426.0

Single Sample Report
Sample Name: SHARLJA1-exp100-0025_11_29_2021_H10
Filename: sharlja1-exp100-0025_11_29_2021_h10.raw
Submitter:

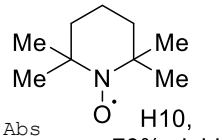

H10,
73% yield

Peak #	Formula	Target …	Target …	Time	Found	Area %	Area Abs
8	C23H28C…	493.1	Glyburi…	1.411	Yes	21.7	7339.01
17	C16H18B…	426.0	Product	2.071	Yes	48.3	16320.76

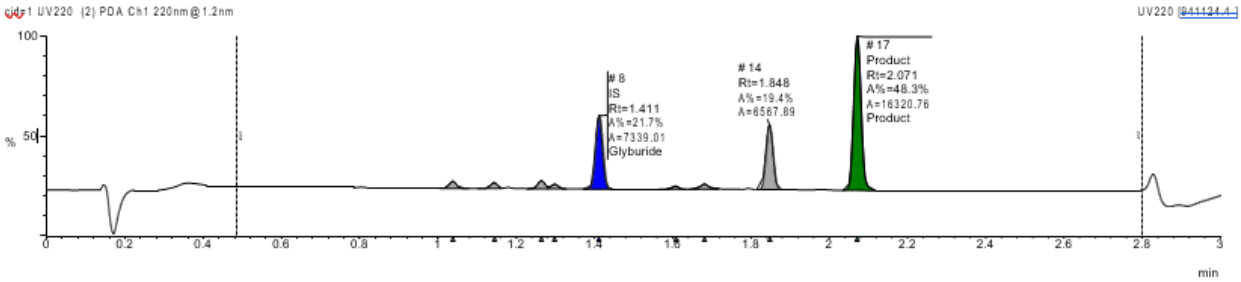

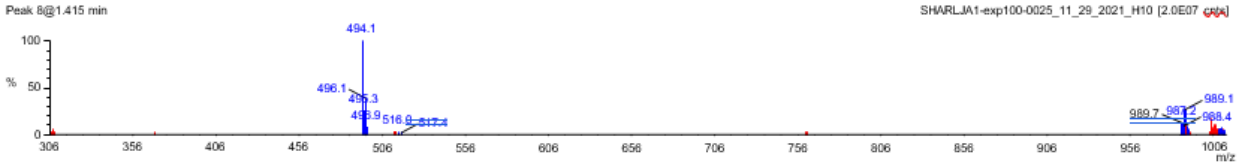

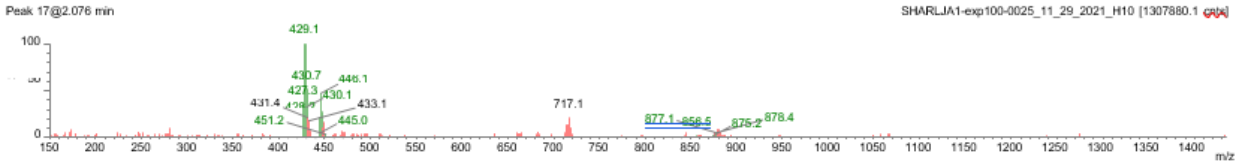

Name	Y/N	Type	Formula	Mass
Glyburide	Y	IS	C23H28ClN3O5S	493.1
Product	Y	Product	C16H18BrCl3O2	426.0

5.3: Enantioselectivity of successful reactions with Rh_2(*S-tetra-p*-Br-PhPTTL)$_4$ and $(CH_3O)_2CO$ as solvent:

The following dataset represents reactions that were successful when performed according to **general procedure 5.1** using Rh_2(*S-tetra-p*-Br-PhPTTL)$_4$ as catalyst and dimethyl carbonate as solvent. Each additive is described according to the well plate designation in the study as well as the compound number it was assigned in the main text. The enantioselectivity of the reaction in the presence of each additive is reported in **Figure C**5 and what follows is the SFC data from which the asymmetric induction was determined.

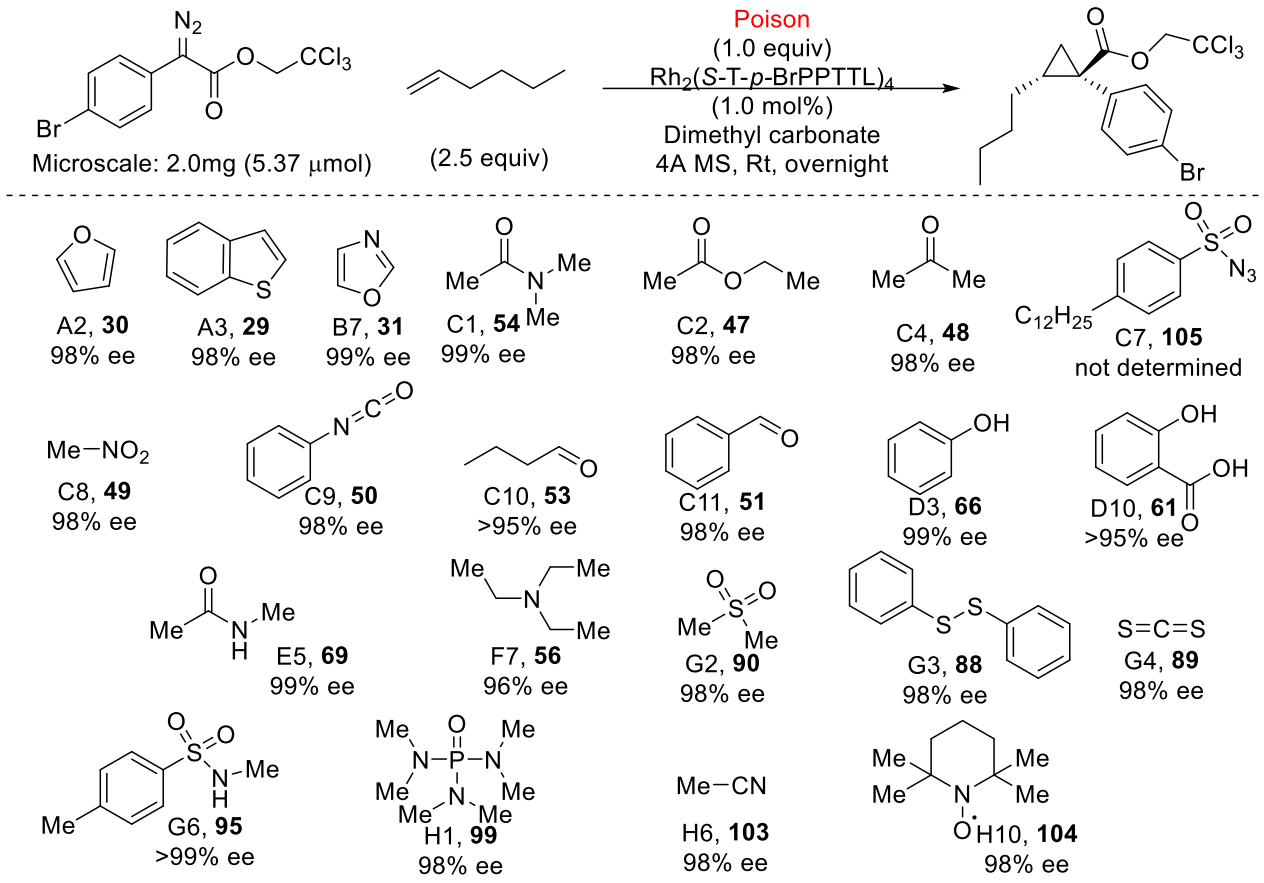

Figure C5: Successful additives using Rh_2(S-*tetra-p*-BrPhPTTL)$_4$ as catalyst (1.0 mol%) and dimethyl carbonate as solvent on microscale according to **general procedure 5.1**. This figure is followed by the SFC data.

Racemate:

Openlynx Report - DUSTADA1 Page 1

Sample: 135 Vial:2:1 ID:Racemate
File:DUSTADA1_20211008_139 Date:20-Oct-2021 Time:10:47:55
Description:(S,S)WO1 4.6x100mm 5µ Conditions:5% IPA over 5min 3mL/min

Printed: Thu Dec 16 11:33:15 2021

Sample Report:

Sample 135 Vial 2:1 ID Racemate File DUSTADA1_20211008_139 Date 20-Oct-2021 Time 10:47:55 Description (S,S)WO1 4.6x100mm 5µ

2: UV Detector: 230 Nm 2.0000-2.3500: Smooth (Mn, 2x3), 3.1000-3.5500: Smooth (Mn, 2x3) 9.103e-2
Range: 1.048e-1

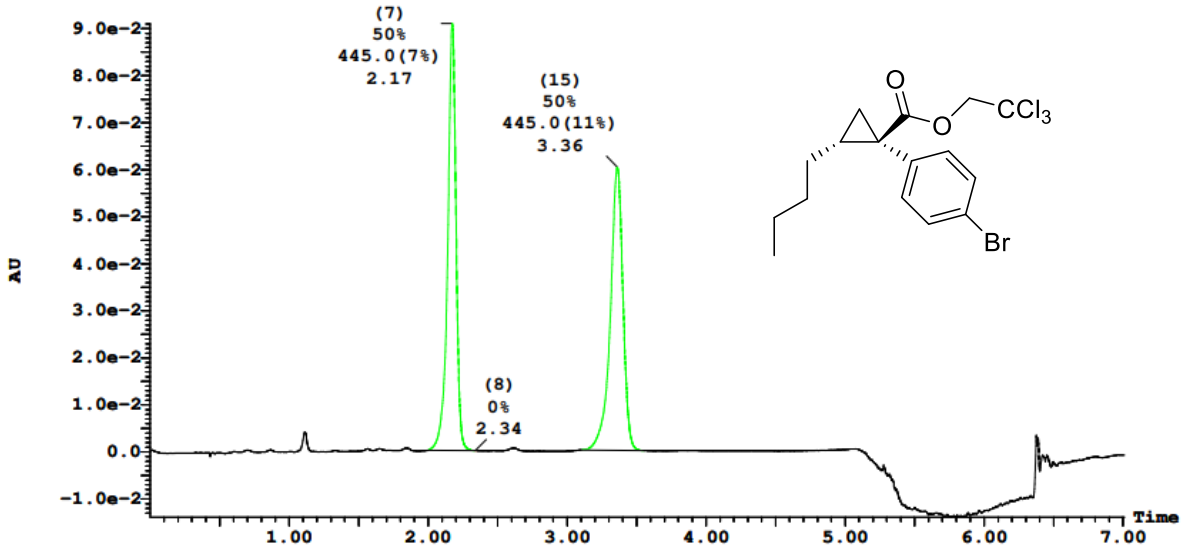

Peak Number	Compound	Time	AreaAbs	Area %Total	Width	Height	Mass Found
7	Found	2.17	6e+003	49.93	0	9e+004	445.0000
8		2.34	2e-001	0.00	0	3e+001	Not Found
15	Found	3.36	6e+003	50.07	0	6e+004	445.0000

A2: 98% ee

Openlynx Report - SHARLJA1

Sample: 1
File:SHARLJA1_20211118_1
Description:(S,S)WO1 4.6x100mm 5µ

Vial:1:1
Date:18-Nov-2021
Conditions:5% IPA over 5min 3mL/min

ID:26-A1
Time:11:31:22

A2,
98% ee

Page 1

Printed: Thu Dec 16 11:07:53 2021

Sample Report:

Sample 1 Vial 1:1 ID 26-A1 File SHARLJA1_20211118_1 Date 18-Nov-2021 Time 11:31:22 Description (S,S)WO1 4.6x100mm 5µ

2: UV Detector: 230 Nm 2.0000-2.3500: Smooth (Mn, 2x3), 3.1000-3.5500: Smooth (Mn, 2x3) 6.147e-1
Range: 6.376e-1

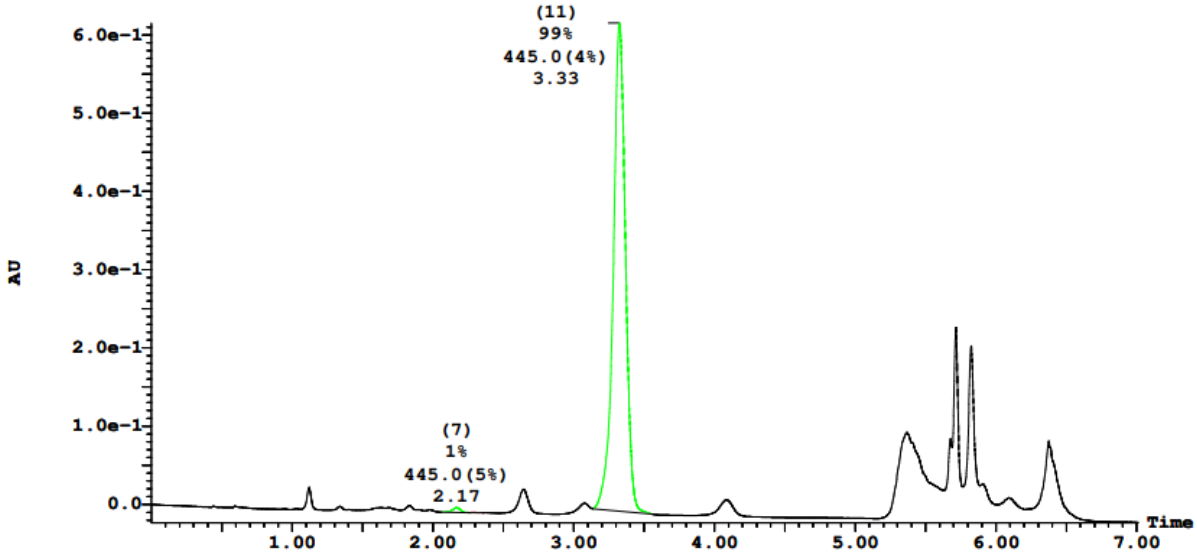

Peak Number	Compound	Time	AreaAbs	Area %Total	Width	Height	Mass Found
7	Found	2.17	4e+002	0.64	0	6e+003	445.0000
8		2.30	1e+001	0.02	0	2e+002	Not Found
11	Tentative	3.33	6e+004	99.35	0	6e+005	445.0000

A3: 98% ee

Openlynx Report - SHARLJA1

Sample: 2
File:SHARLJA1_20211118_2
Description:(S,S)WO1 4.6x100mm 5µ

Vial:1:2
Date:18-Nov-2021
Conditions:5% IPA over 5min 3mL/min

ID:26-A2
Time:11:40:53

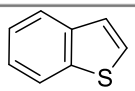

A3,
98% ee

Printed: Thu Dec 16 11:07:53 2021

Sample Report (continued):

Sample 2 Vial 1:2 ID 26-A2 File SHARLJA1_20211118_2 Date 18-Nov-2021 Time 11:40:53 Description (S,S)WO1 4.6x100mm 5µ

2: UV Detector: 230 Nm 2.0000-2.3500: Smooth (Mn, 2x3), 3.1000-3.5500: Smooth (Mn, 2x3) 8.464e-1
Range: 8.477e-1

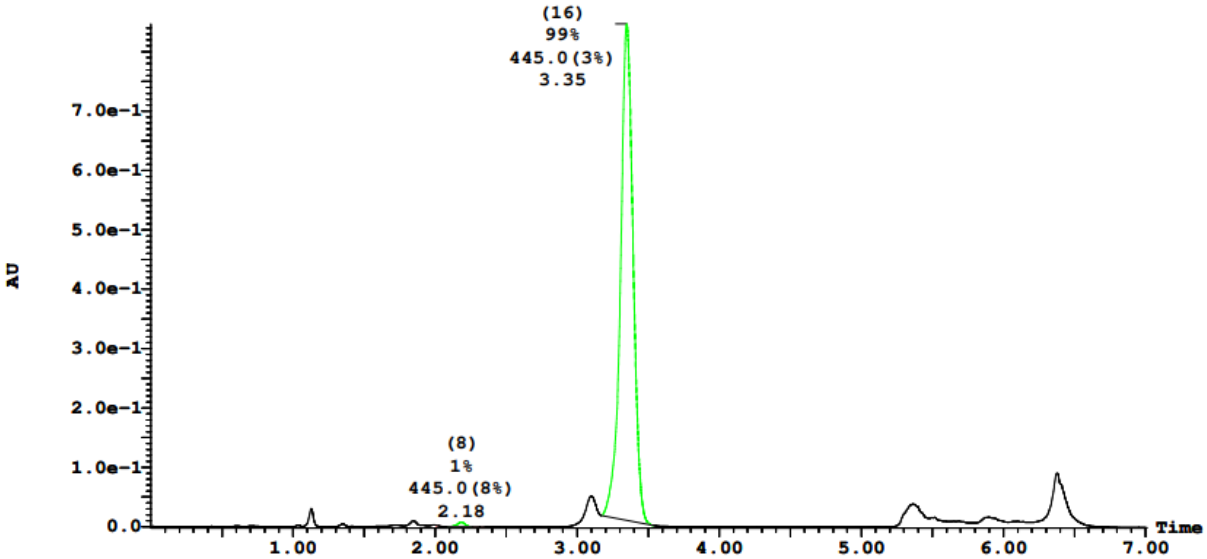

Peak Number	Compound	Time	AreaAbs	Area %Total	Width	Height	Mass Found
7		2.00	9e-001	0.00	0	1e-002	Not Found
8	Found	2.18	5e+002	0.57	0	8e+003	445.0000
9		2.30	1e+001	0.01	0	4e+002	Not Found
10		2.31	7e+000	0.01	0	3e+002	Not Found
16	Tentative	3.35	9e+004	99.41	0	8e+005	445.0000

B7: 99% ee

Openlynx Report - SHARLJA1

Sample: 6
File:SHARLJA1_20211118_6
Description:(S,S)WO1 4.6x100mm 5µ

Vial:1:6
Date:18-Nov-2021
Conditions:5% IPA over 5min 3mL/min

ID:26-B7
Time:12:13:24

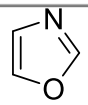

B7,
99% ee

Page 11

Printed: Thu Dec 16 11:07:53 2021

Sample Report (continued):

Sample 6 Vial 1:6 ID 26-B7 File SHARLJA1_20211118_6 Date 18-Nov-2021 Time 12:13:24 Description (S,S)WO1 4.6x100mm 5µ

2: UV Detector: 230 Nm 2.0000-2.3500: Smooth (Mn, 2x3), 3.1000-3.5500: Smooth (Mn, 2x3) 7.072e-1
Range: 7.077e-1

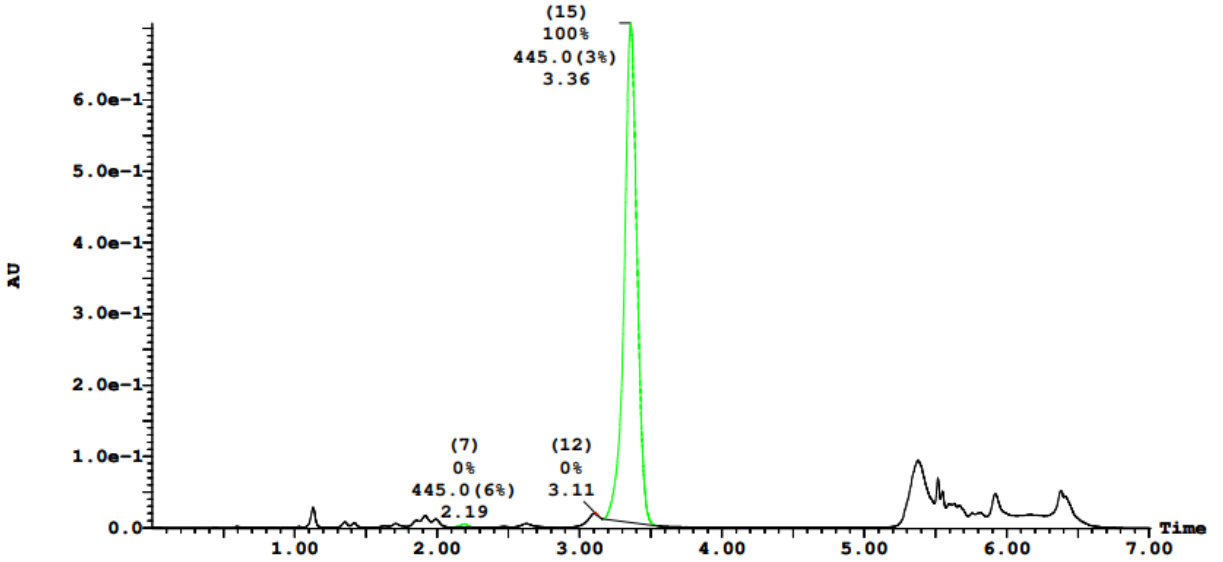

Peak Number	Compound	Time	AreaAbs	Area %Total	Width	Height	Mass Found
7	Found	2.19	3e+002	0.36	0	4e+003	445.0000
8		2.31	1e+001	0.02	0	3e+002	Not Found
12		3.11	6e+001	0.09	0	1e+003	Not Found
15	Tentative	3.36	7e+004	99.54	0	7e+005	445.0000

C1: 99% ee

Openlynx Report - SHARLJA1

Sample: 8
File:SHARLJA1_20211118_8
Description:(S,S)WO1 4.6x100mm 5µ

Vial:1:8
Date:18-Nov-2021
Conditions:5% IPA over 5min 3mL/min

ID:26-C1
Time:12:29:40

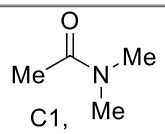

C1,
99% ee

Page 15

Printed: Thu Dec 16 11:07:53 2021

Sample Report (continued):

Sample 8 Vial 1:8 ID 26-C1 File SHARLJA1_20211118_8 Date 18-Nov-2021 Time 12:29:40 Description (S,S)WO1 4.6x100mm 5µ

2: UV Detector: 230 Nm 2.0000-2.3500: Smooth (Mn, 2x3), 3.1000-3.5500: Smooth (Mn, 2x3) 4.209e-1
Range: 4.214e-1

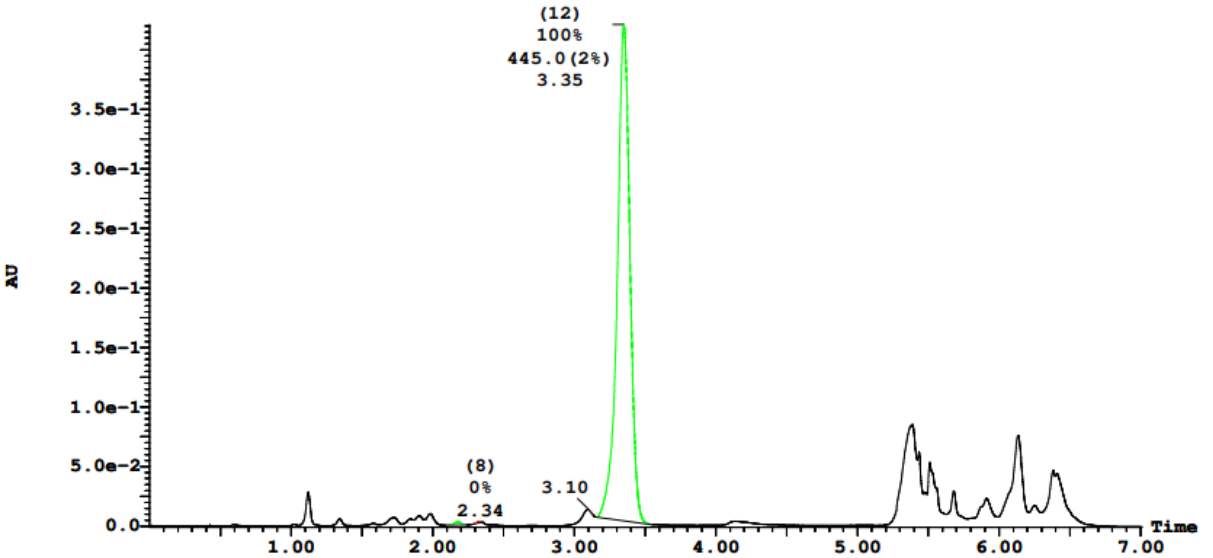

Peak Number	Compound	Time	AreaAbs	Area %Total	Width	Height	Mass Found
7	Tentative	2.18	2e+002	0.36	0	3e+003	445.0000
8		2.34	4e+001	0.09	0	8e+002	Not Found
10		3.10	1e+001	0.02	0		Not Found
12	Tentative	3.35	4e+004	99.53	0	4e+005	445.0000

C2: 98% ee

Openlynx Report - SHARLJA1

Sample: 9
File:SHARLJA1_20211118_9
Description:(S,S)WO1 4.6x100mm 5µ

Vial:1:9
Date:18-Nov-2021
Conditions:5% IPA over 5min 3mL/min

ID:26-C2
Time:12:37:47

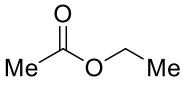

C2,
98% ee

Page 17

Printed: Thu Dec 16 11:07:53 2021

Sample Report (continued):

Sample 9 Vial 1:9 ID 26-C2 File SHARLJA1_20211118_9 Date 18-Nov-2021 Time 12:37:47 Description (S,S)WO1 4.6x100mm 5µ

2: UV Detector: 230 Nm 2.0000-2.3500: Smooth (Mn, 2x3), 3.1000-3.5500: Smooth (Mn, 2x3) 8.496e-1
Range: 8.497e-1

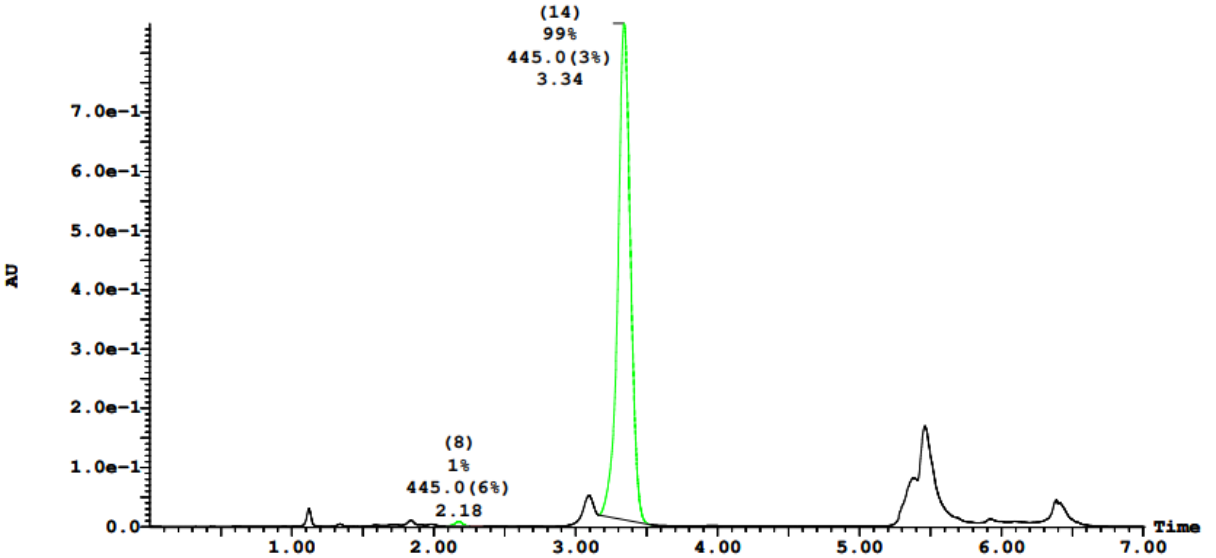

Peak Number	Compound	Time	AreaAbs	Area %Total	Width	Height	Mass Found
8	Found	2.18	5e+002	0.57	0	8e+003	445.0000
9		2.30	2e+001	0.02	0	4e+002	Not Found
14	Tentative	3.34	9e+004	99.41	0	8e+005	445.0000

C4: 98% ee

Openlynx Report - SHARLJA1

Sample: 11
File:SHARLJA1_20211118_11
Description:(S,S)WO1 4.6x100mm 5µ

Vial:1:11
Date:18-Nov-2021
Conditions:5% IPA over 5min 3mL/min

ID:26-C4
Time:12:54:03

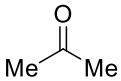

C4,
98% ee

Page 21

Printed: Thu Dec 16 11:07:53 2021

Sample Report (continued):

Sample 11 Vial 1:11 ID 26-C4 File SHARLJA1_20211118_11 Date 18-Nov-2021 Time 12:54:03 Description (S,S)WO1 4.6x100mm 5µ

2: UV Detector: 230 Nm 2.0000-2.3500: Smooth (Mn, 2x3), 3.1000-3.5500: Smooth (Mn, 2x3) 8.656e-1
Range: 8.66e-1

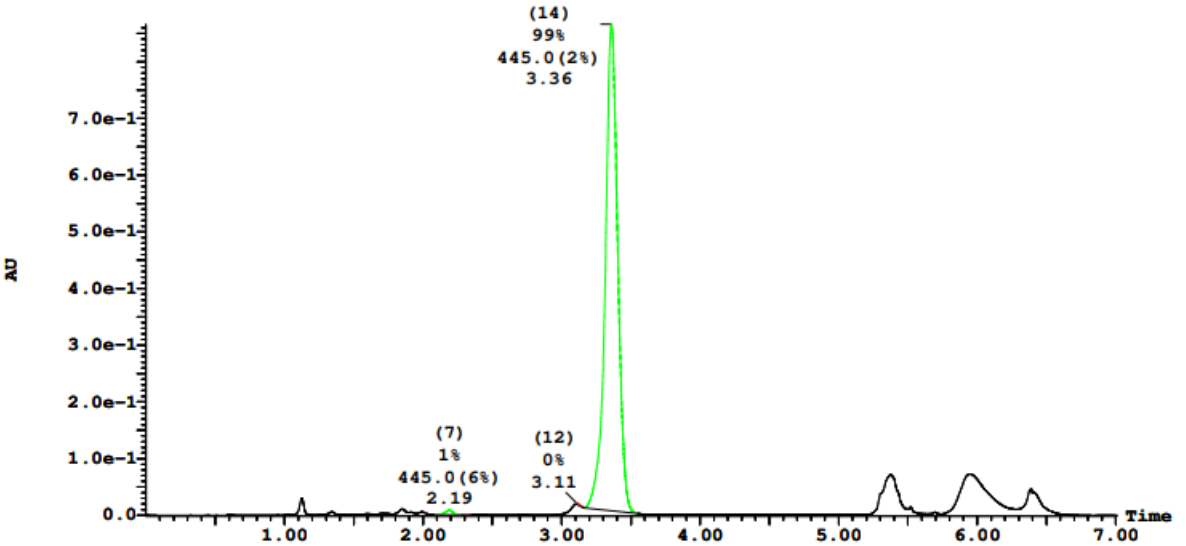

Peak Number	Compound	Time	AreaAbs	Area %Total	Width	Height	Mass Found
6		2.00	2e+000	0.00	0	1e-002	Not Found
7	Found	2.19	5e+002	0.59	0	8e+003	445.0000
8		2.32	4e+000	0.00	0	1e+002	Not Found
8		2.34	4e-001	0.00	0	6e+001	Not Found
12		3.11	7e+001	0.08	0	2e+003	Not Found
14	Tentative	3.36	9e+004	99.32	0	9e+005	445.0000

C7: %ee could not be determined due to overlap with minor enantiomer**.**

Openlynx Report - SHARLJA1
Sample: 13
File:SHARLJA1_20211118_13
Description:(S,S)WO1 4.6x100mm 5µ

Printed: Thu Dec 16 11:07:53 2021

Vial:1:13
Date:18-Nov-2021
Conditions:5% IPA over 5min 3mL/min

ID:26-C7
Time:13:10:18

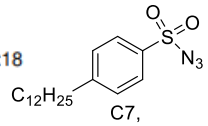

C7,
not determined

Sample Report (continued):

Sample 13 Vial 1:13 ID 26-C7 File SHARLJA1_20211118_13 Date 18-Nov-2021 Time 13:10:18 Description (S,S)WO1 4.6x100mm 5µ

2: UV Detector: 230 Nm 2.0000-2.3500: Smooth (Mn, 2x3), 3.1000-3.5500: Smooth (Mn, 2x3) 8.28e-1
Range: 8.285e-1

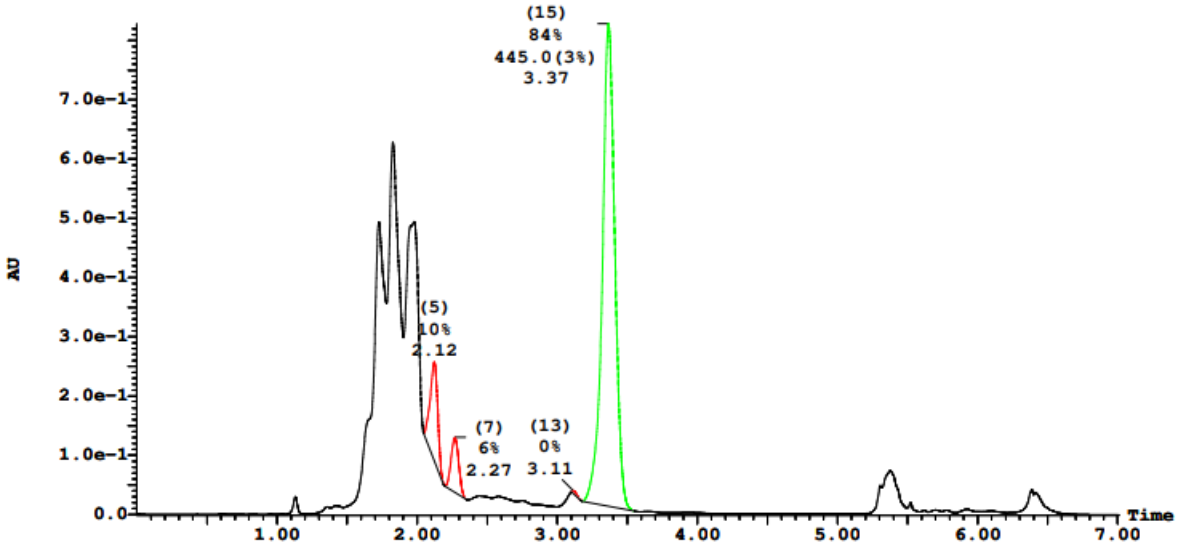

Peak Number	Compound	Time	AreaAbs	Area %Total	Width	Height	Mass Found
5		2.12	1e+004	10.35	0	2e+005	Not Found
7		2.27	6e+003	5.79	0	9e+004	Not Found
13		3.11	2e+002	0.18	0	4e+003	Not Found
15	Tentative	3.37	8e+004	83.68	0	8e+005	445.0000

C8: 98% ee

Openlynx Report - SHARLJA1 Page 27

Sample: 14 Vial:1:14 ID:26-C8
File:SHARLJA1_20211118_14 Date:18-Nov-2021 Time:13:18:27
Description:(S,S)WO1 4.6x100mm 5µ Conditions:5% IPA over 5min 3mL/min

Printed: Thu Dec 16 11:07:53 2021

Me—NO_2

C8,
98% ee

Sample Report (continued):

Sample 14 Vial 1:14 ID 26-C8 File SHARLJA1_20211118_14 Date 18-Nov-2021 Time 13:18:27 Description (S,S)WO1 4.6x100mm 5µ

2: UV Detector: 230 Nm 2.0000-2.3500: Smooth (Mn, 2x3), 3.1000-3.5500: Smooth (Mn, 2x3) 7.668e-1
Range: 7.693e-1

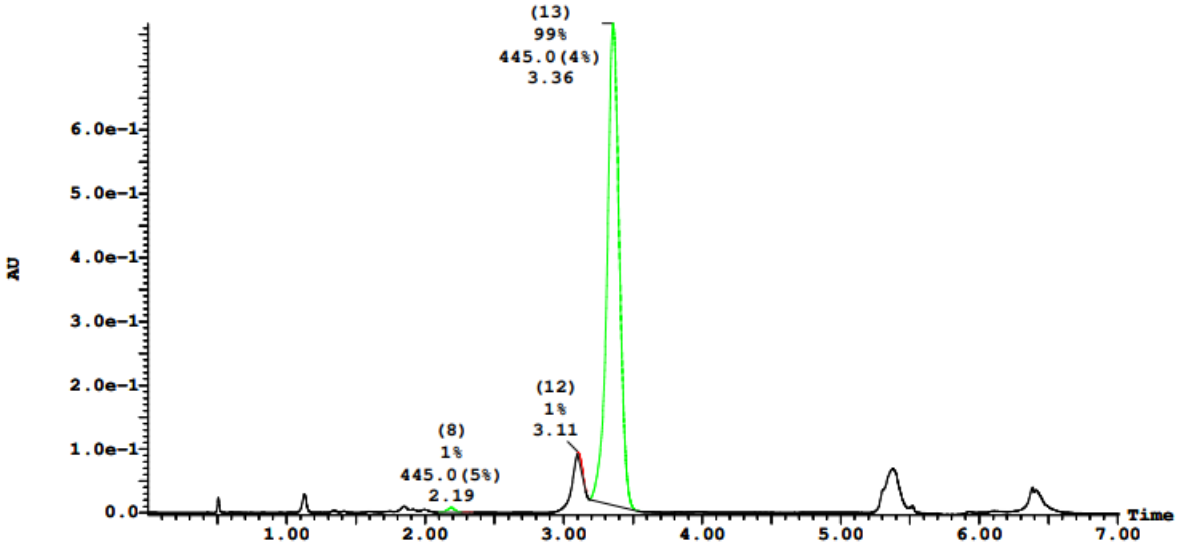

Peak Number	Compound	Time	AreaAbs	Area %Total	Width	Height	Mass Found
8	Found	2.19	5e+002	0.64	0	8e+003	445.0000
9		2.31	2e+001	0.03	0	6e+002	Not Found
9		2.32	8e+000	0.01	0	4e+002	Not Found
12		3.11	4e+002	0.56	0	7e+003	Not Found
13	Tentative	3.36	8e+004	98.77	0	8e+005	445.0000

C9: 98% ee

Openlynx Report - SHARLJA1

Sample: 15
File:SHARLJA1_20211118_15
Description:(S,S)WO1 4.6x100mm 5µ

Vial:1:15
Date:18-Nov-2021
Conditions:5% IPA over 5min 3mL/min

ID:26-C9
Time:13:26:34

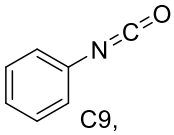

C9,
98% ee

Printed: Thu Dec 16 11:07:53 2021

Sample Report (continued):

Sample 15 Vial 1:15 ID 26-C9 File SHARLJA1_20211118_15 Date 18-Nov-2021 Time 13:26:34 Description (S,S)WO1 4.6x100mm 5µ

2: UV Detector: 230 Nm 2.0000-2.3500: Smooth (Mn, 2x3), 3.1000-3.5500: Smooth (Mn, 2x3) 6.433e-1
Range: 6.442e-1

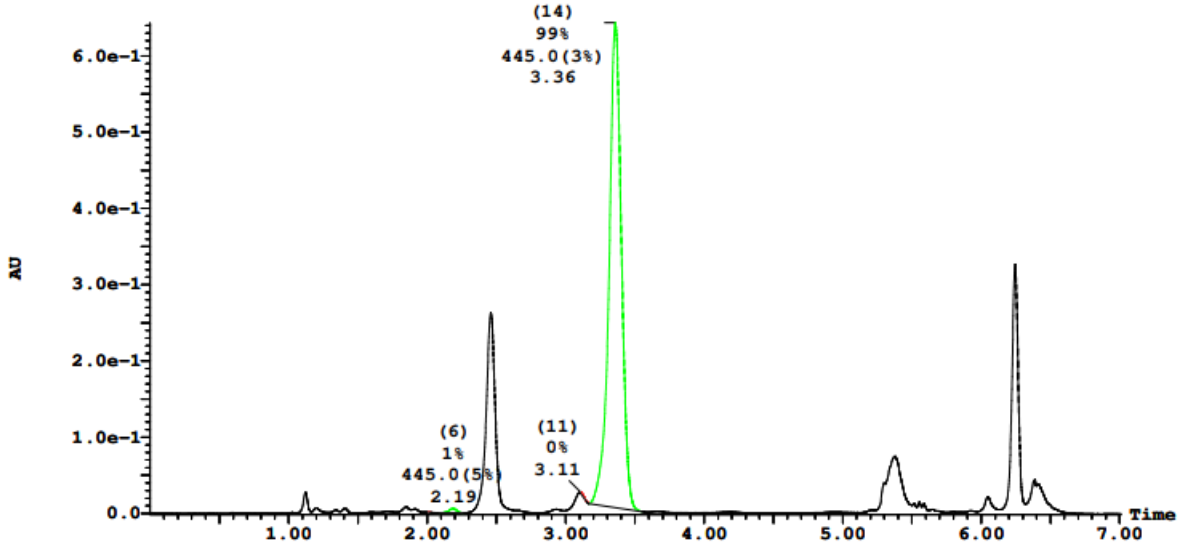

Peak Number	Compound	Time	AreaAbs	Area %Total	Width	Height	Mass Found
4		2.00	1e+000	0.00	0		Not Found
6	Found	2.19	4e+002	0.59	0	6e+003	445.0000
11		3.11	9e+001	0.13	0	1e+003	Not Found
14	Tentative	3.36	7e+004	99.28	0	6e+005	445.0000

C10: >95% ee

Openlynx Report - SHARLJA1

Sample: 16
File:SHARLJA1_20211118_16
Description:(S,S)WO1 4.6x100mm 5µ

Vial:1:16
Date:18-Nov-2021
Conditions:5% IPA over 5min 3mL/min

ID:26-C10
Time:13:34:42

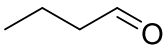

C10,
>95% ee

Page 31

Printed: Thu Dec 16 11:07:53 2021

Sample Report (continued):

Sample 16 Vial 1:16 ID 26-C10 File SHARLJA1_20211118_16 Date 18-Nov-2021 Time 13:34:42 Description (S,S)WO1 4.6x100mm 5µ

2: UV Detector: 230 Nm 2.0000-2.3500: Smooth (Mn, 2x3), 3.1000-3.5500: Smooth (Mn, 2x3) 5.205e-1
Range: 5.214e-1

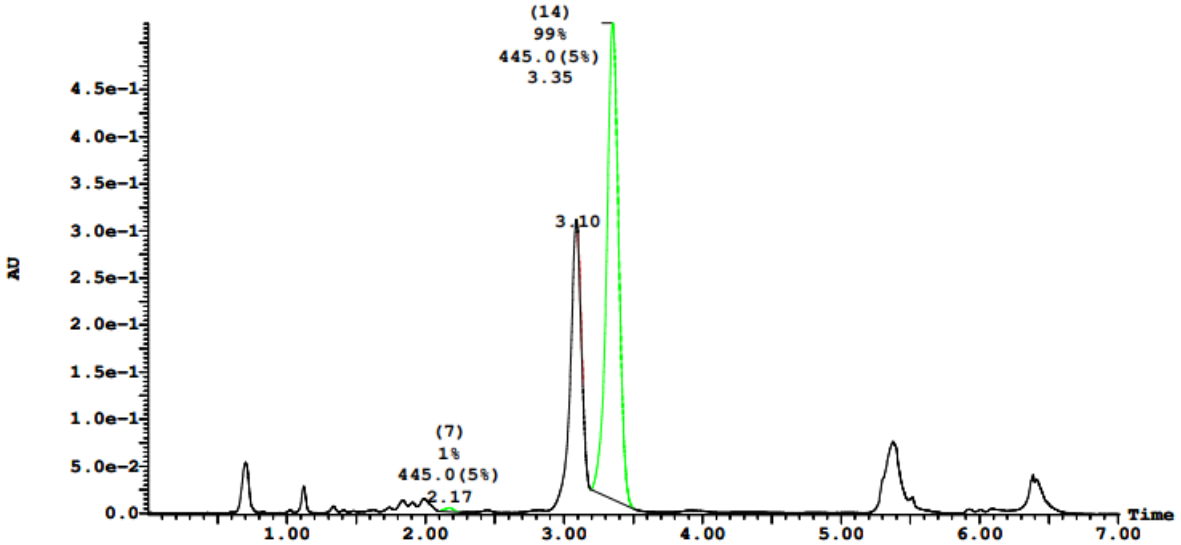

Peak Number	Compound	Time	AreaAbs	Area %Total	Width	Height	Mass Found
7	Found	2.17	3e+002	0.60	0	4e+003	445.0000
12		3.10	2e+002	0.42	0	4e-001	Not Found
14	Tentative	3.35	5e+004	98.99	0	5e+005	445.0000

C11: 99% ee

Openlynx Report - SHARLJA1

Sample: 17
File:SHARLJA1_20211118_17
Description:(S,S)WO1 4.6x100mm 5µ

Vial:1:17
Date:18-Nov-2021
Conditions:5% IPA over 5min 3mL/min

ID:26-C11
Time:13:42:49

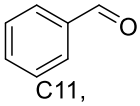

C11,
98% ee

Printed: Thu Dec 16 11:07:53 2021

Sample Report (continued):

Sample 17 Vial 1:17 ID 26-C11 File SHARLJA1_20211118_17 Date 18-Nov-2021 Time 13:42:49 Description (S,S)WO1 4.6x100mm 5µ

2: UV Detector: 230 Nm 2.0000-2.3500: Smooth (Mn, 2x3), 3.1000-3.5500: Smooth (Mn, 2x3) 7.217e-1
Range: 7.226e-1

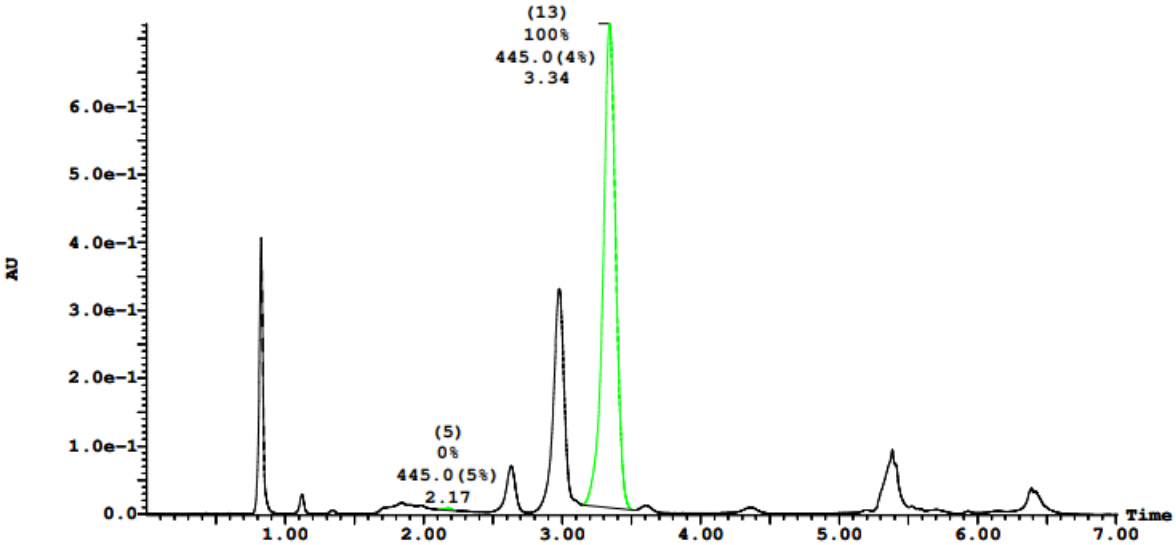

Peak Number	Compound	Time	AreaAbs	Area %Total	Width	Height	Mass Found
5	Found	2.17	2e+002	0.25	0	3e+003	445.0000
13	Tentative	3.34	8e+004	99.75	0	7e+005	445.0000

D3: 99% ee

Openlynx Report - SHARLJA1

Sample: 21
File:SHARLJA1_20211118_21
Description:(S,S)WO1 4.6x100mm 5µ

Vial:1:21
Date:18-Nov-2021
Conditions:5% IPA over 5min 3mL/min

ID:26-D3
Time:14:15:20

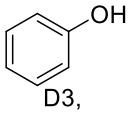

D3,
99% ee

Printed: Thu Dec 16 11:07:53 2021

Sample Report (continued):

Sample 21 Vial 1:21 ID 26-D3 File SHARLJA1_20211118_21 Date 18-Nov-2021 Time 14:15:20 Description (S,S)WO1 4.6x100mm 5µ

2: UV Detector: 230 Nm 2.0000-2.3500: Smooth (Mn, 2x3), 3.1000-3.5500: Smooth (Mn, 2x3) 2.372
Range: 2.372

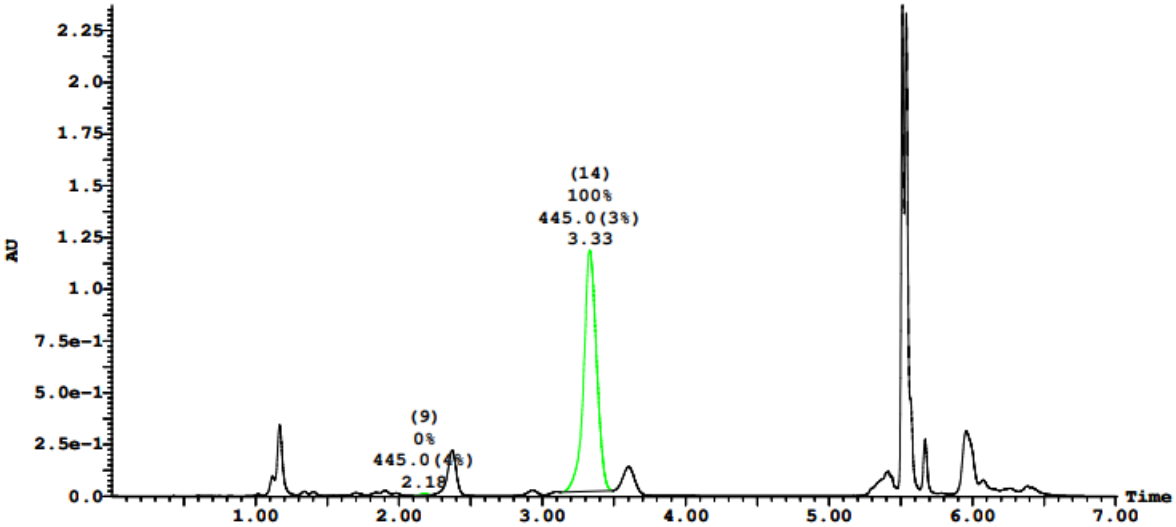

Peak Number	Compound	Time	AreaAbs	Area %Total	Width	Height	Mass Found
9	Found	2.18	4e+002	0.34	0	8e+003	445.0000
14	Tentative	3.33	1e+005	99.66	0	1e+006	445.0000

D10: >95% ee

Openlynx Report - SHARLJA1

Sample: 24
File:SHARLJA1_20211118_24
Description:(S,S)WO1 4.6x100mm 5µ

Vial:1:24
Date:18-Nov-2021
Conditions:5% IPA over 5min 3mL/min

ID:26-D10
Time:14:39:43

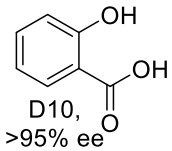

Printed: Thu Dec 16 11:07:53 2021

Sample Report (continued):

Sample 24 Vial 1:24 ID 26-D10 File SHARLJA1_20211118_24 Date 18-Nov-2021 Time 14:39:43 Description (S,S)WO1 4.6x100mm 5µ

2: UV Detector: 230 Nm 2.0000-2.3500: Smooth (Mn, 2x3), 3.1000-3.5500: Smooth (Mn, 2x3) 4.785e-1
Range: 4.788e-1

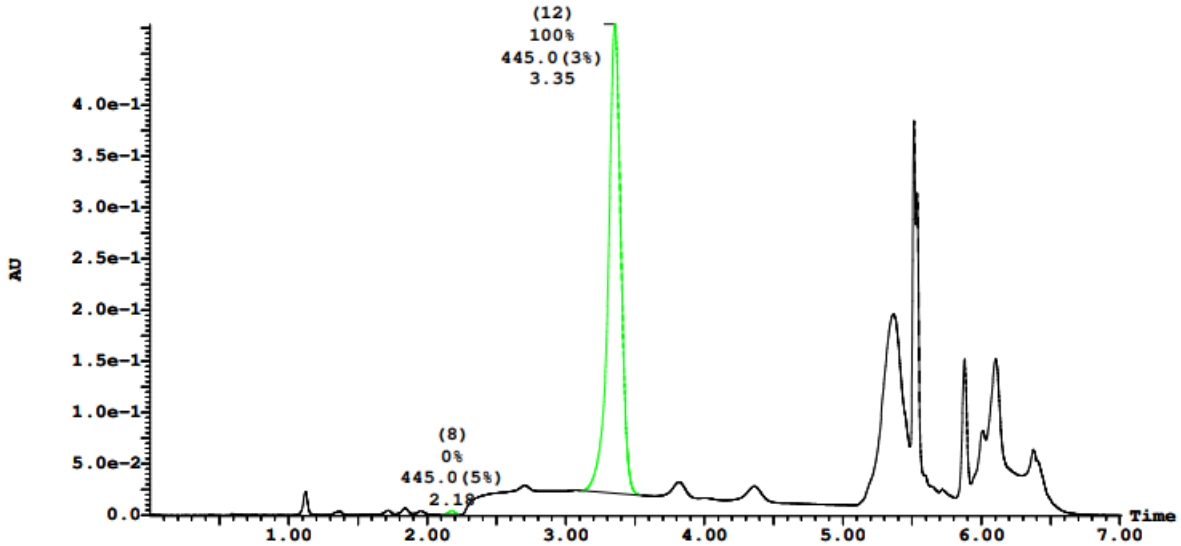

Peak Number	Compound	Time	AreaAbs	Area %Total	Width	Height	Mass Found
8	Tentative	2.18	2e+002	0.46	0	4e+003	445.0000
12	Tentative	3.35	5e+004	99.54	0	5e+005	445.0000

E5: 99% ee

Openlynx Report - SHARLJA1

Sample: 27
File:SHARLJA1_20211118_27
Description:(S,S)WO1 4.6x100mm 5µ

Vial:1:27
Date:18-Nov-2021
Conditions:5% IPA over 5min 3mL/min

ID:26-E5
Time:15:04:06

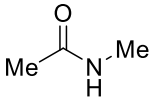

E5,
99% ee

Page 53

Printed: Thu Dec 16 11:07:53 2021

Sample Report (continued):

Sample 27 Vial 1:27 ID 26-E5 File SHARLJA1_20211118_27 Date 18-Nov-2021 Time 15:04:06 Description (S,S)WO1 4.6x100mm 5µ

2: UV Detector: 230 Nm 2.0000-2.3500: Smooth (Mn, 2x3), 3.1000-3.5500: Smooth (Mn, 2x3) 6.996e-1
Range: 6.999e-1

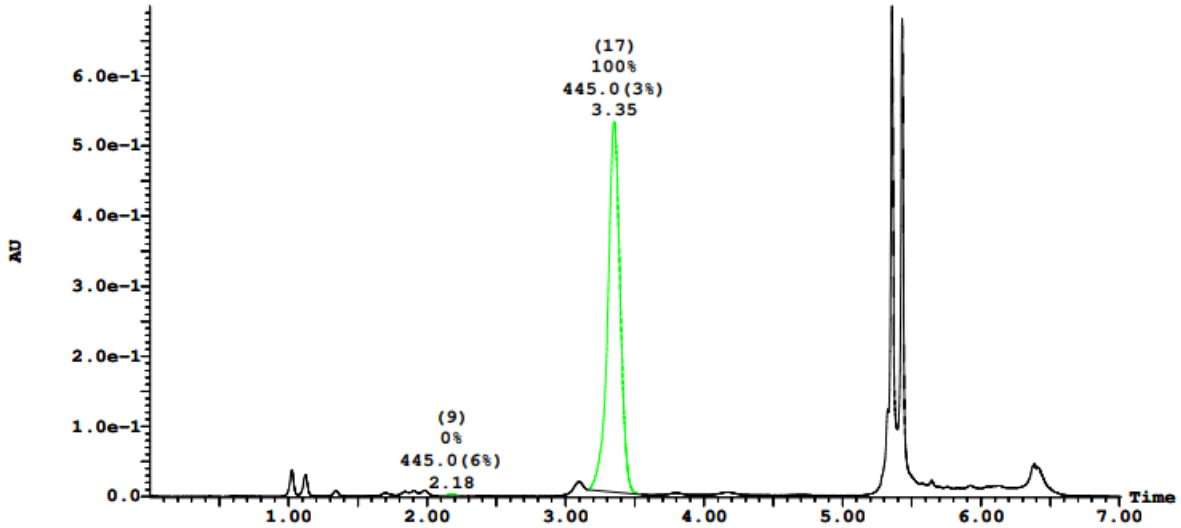

Peak Number	Compound	Time	AreaAbs	Area %Total	Width	Height	Mass Found
9	Found	2.18	2e+002	0.39	0	4e+003	445.0000
10		2.29	1e+001	0.02	0	4e+002	Not Found
11		2.31	1e+001	0.02	0	5e+002	Not Found
12		2.34	3e+000	0.01	0	2e+002	Not Found
17	Tentative	3.35	5e+004	99.56	0	5e+005	445.0000

F7: 96% ee

Openlynx Report - SHARLJA1

Sample: 32
File:SHARLJA1_20211118_32
Description:(S,S)WO1 4.6x100mm 5µ

Vial:1:32
Date:18-Nov-2021
Conditions:5% IPA over 5min 3mL/min

ID:26-F7
Time:15:44:45

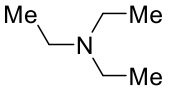

F7,
96% ee

Printed: Thu Dec 16 11:07:53 2021

Sample Report (continued):

Sample 32 Vial 1:32 ID 26-F7 File SHARLJA1_20211118_32 Date 18-Nov-2021 Time 15:44:45 Description (S,S)WO1 4.6x100mm 5µ

2: UV Detector: 230 Nm 2.0000-2.3500: Smooth (Mn, 2x3), 3.1000-3.5500: Smooth (Mn, 2x3) 6.822e-1
Range: 6.826e-1

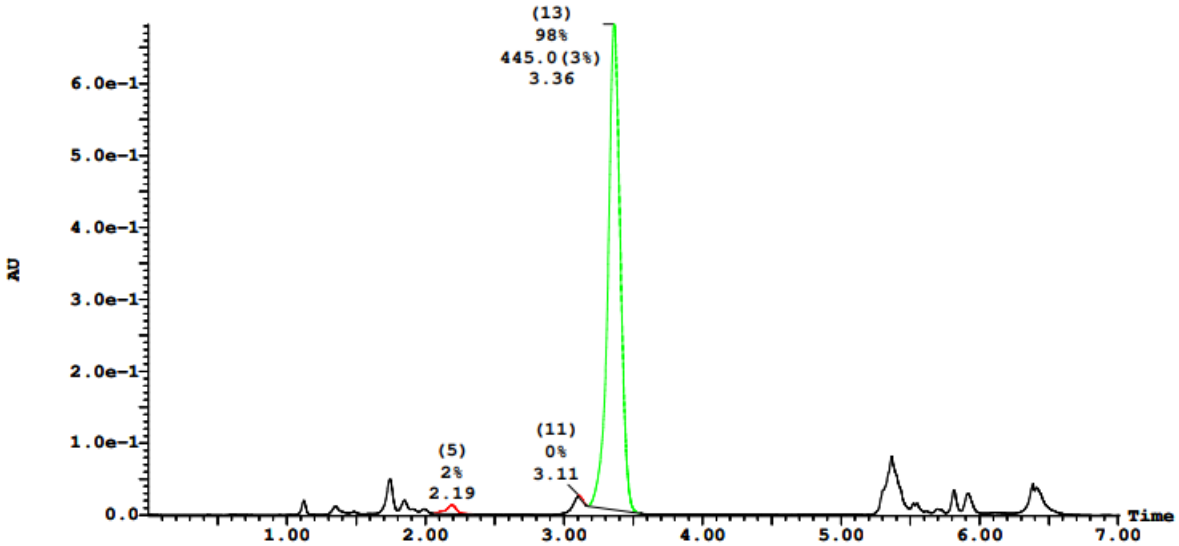

Peak Number	Compound	Time	AreaAbs	Area %Total	Width	Height	Mass Found
5		2.19	1e+003	1.56	0	1e+004	Not Found
11		3.11	1e+002	0.17	0	3e+003	Not Found
13	Tentative	3.36	7e+004	98.28	0	7e+005	445.0000

G2: 98% ee

Openlynx Report - SHARLJA1

Sample: 35
File:SHARLJA1_20211118_35
Description:(S,S)WO1 4.6x100mm 5µ

Vial:1:35
Date:18-Nov-2021
Conditions:5% IPA over 5min 3mL/min

ID:26-G2
Time:16:09:09

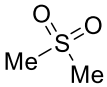

G2,
98% ee

Printed: Thu Dec 16 11:07:53 2021

Sample Report (continued):

Sample 35 Vial 1:35 ID 26-G2 File SHARLJA1_20211118_35 Date 18-Nov-2021 Time 16:09:09 Description (S,S)WO1 4.6x100mm 5µ

2: UV Detector: 230 Nm 2.0000-2.3500: Smooth (Mn, 2x3), 3.1000-3.5500: Smooth (Mn, 2x3) 8.207e-1
Range: 8.235e-1

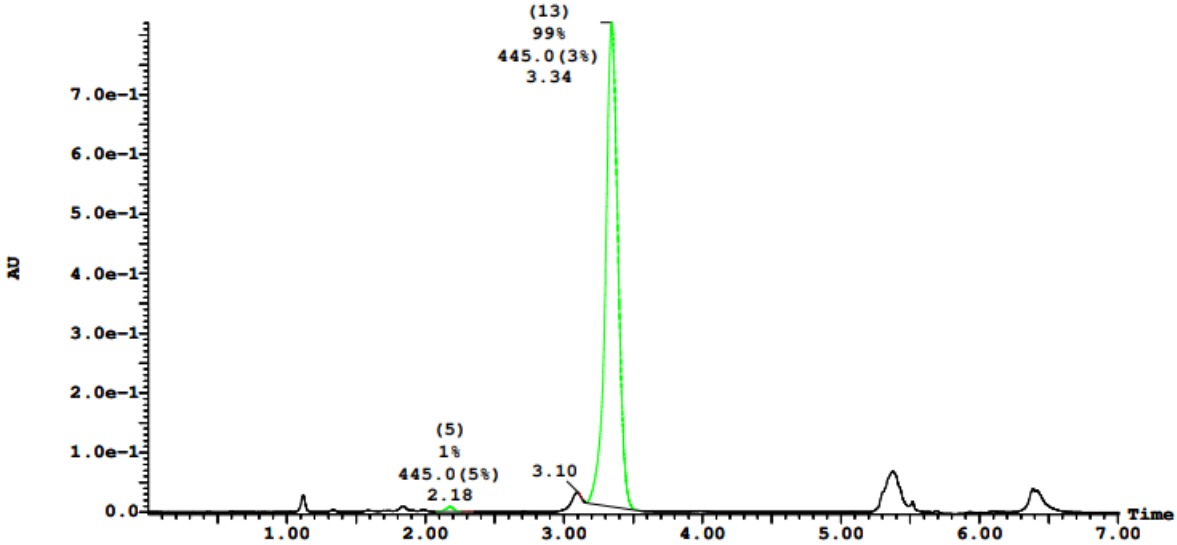

Peak Number	Compound	Time	AreaAbs	Area %Total	Width	Height	Mass Found
5	Found	2.18	6e+002	0.66	0	8e+003	445.0000
6		2.31	8e+000	0.01	0	3e+002	Not Found
7		2.33	5e+000	0.01	0	2e+002	Not Found
11		3.10	4e+001	0.04	0	2e-002	Not Found
13	Tentative	3.34	8e+004	99.29	0	8e+005	445.0000

G3: 98% ee

Openlynx Report - SHARLJA1

Sample: 36
File:SHARLJA1_20211118_36
Description:(S,S)WO1 4.6x100mm 5µ

Vial:1:36
Date:18-Nov-2021
Conditions:5% IPA over 5min 3mL/min

ID:26-G3
Time:16:17:18

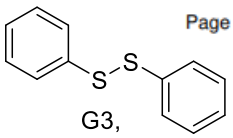

G3,
98% ee

Printed: Thu Dec 16 11:07:53 2021

Sample Report (continued):

Sample 36 Vial 1:36 ID 26-G3 File SHARLJA1_20211118_36 Date 18-Nov-2021 Time 16:17:18 Description (S,S)WO1 4.6x100mm 5µ

2: UV Detector: 230 Nm 2.0000-2.3500: Smooth (Mn, 2x3), 3.1000-3.5500: Smooth (Mn, 2x3) 2.789
Range: 2.79

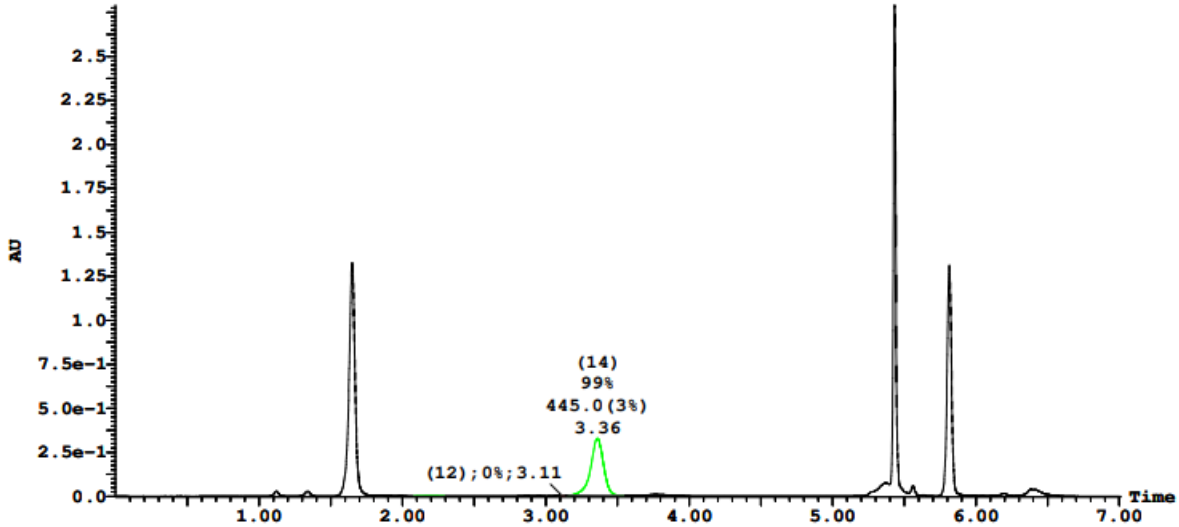

Peak Number	Compound	Time	AreaAbs	Area %Total	Width	Height	Mass Found
6	Tentative	2.18	3e+002	0.86	0	3e+003	445.0000
12		3.11	3e+000	0.01	0	2e+002	Not Found
14	Tentative	3.36	3e+004	99.13	0	3e+005	445.0000

G4: 98% ee

Openlynx Report - SHARLJA1

Page 73

Sample: 37
File:SHARLJA1_20211118_37
Description:(S,S)WO1 4.6x100mm 5µ

Vial:1:37
Date:18-Nov-2021
Conditions:5% IPA over 5min 3mL/min

ID:26-G4
Time:16:25:25

S=C=S
G4,
98% ee

Printed: Thu Dec 16 11:07:53 2021

Sample Report (continued):

Sample 37 Vial 1:37 ID 26-G4 File SHARLJA1_20211118_37 Date 18-Nov-2021 Time 16:25:25 Description (S,S)WO1 4.6x100mm 5µ

2: UV Detector: 230 Nm 2.0000-2.3500: Smooth (Mn, 2x3), 3.1000-3.5500: Smooth (Mn, 2x3) 6.93e-1
Range: 6.942e-1

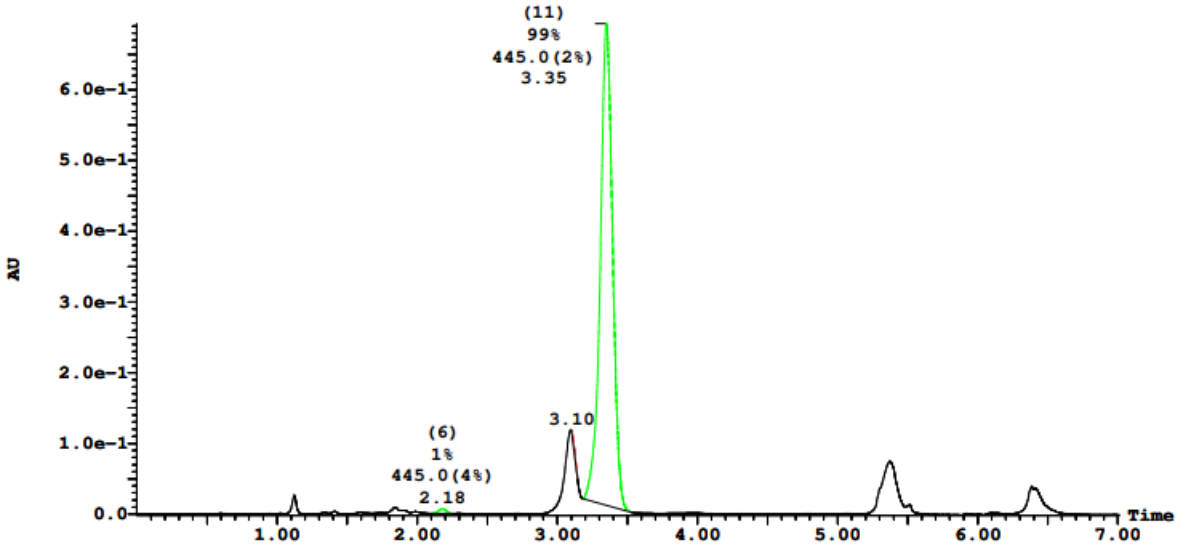

Peak Number	Compound	Time	AreaAbs	Area %Total	Width	Height	Mass Found
6	Found	2.18	4e+002	0.62	0	7e+003	445.0000
9		3.10	2e+002	0.25	0	2e-002	Not Found
11	Tentative	3.35	7e+004	99.12	0	7e+005	445.0000

G6: >99% ee

Openlynx Report - SHARLJA1

Sample: 38
File:SHARLJA1_20211118_38
Description:(S,S)WO1 4.6x100mm 5µ

Vial:1:38
Date:18-Nov-2021
Conditions:5% IPA over 5min 3mL/min

ID:26-G6
Time:16:33:33

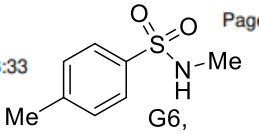

G6,
>99% ee

Printed: Thu Dec 16 11:07:53 2021

Sample Report (continued):

Sample 38 Vial 1:38 ID 26-G6 File SHARLJA1_20211118_38 Date 18-Nov-2021 Time 16:33:33 Description (S,S)WO1 4.6x100mm 5µ

2: UV Detector: 230 Nm 2.0000-2.3500: Smooth (Mn, 2x3), 3.1000-3.5500: Smooth (Mn, 2x3) 2.811
Range: 2.813

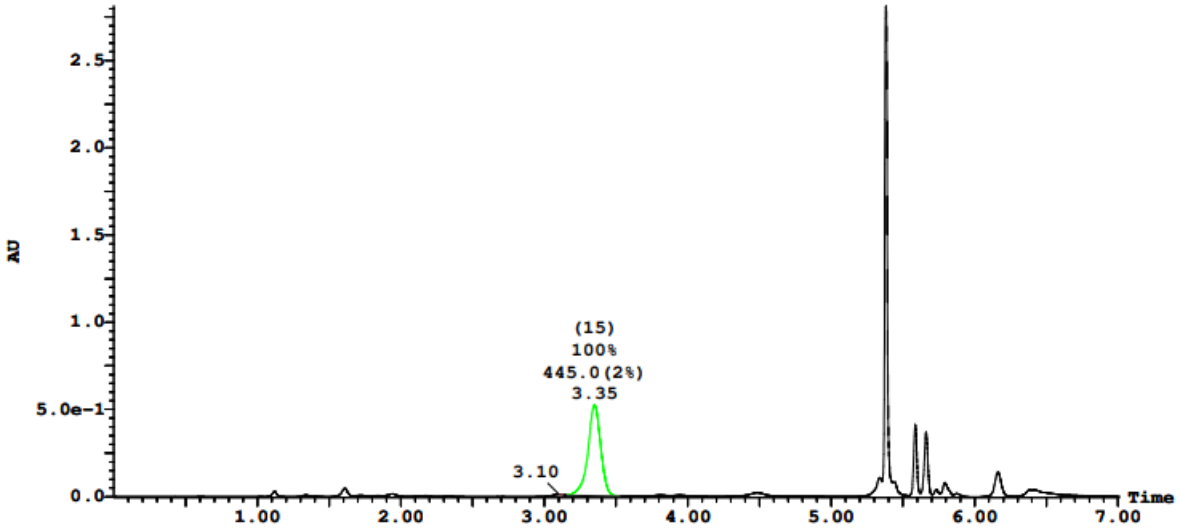

Peak Number	Compound	Time	AreaAbs	Area %Total	Width	Height	Mass Found
13		3.10	1e+001	0.02	0	1e-002	Not Found
15	Tentative	3.35	5e+004	99.98	0	5e+005	445.0000

H1: 98% ee

Openlynx Report - SHARLJA1

Sample: 41
File:SHARLJA1_20211118_41
Description:(S,S)WO1 4.6x100mm 5µ

Printed: Thu Dec 16 11:07:53 2021

Vial:1:41
Date:18-Nov-2021
Conditions:5% IPA over 5min 3mL/min

ID:26-H1
Time:16:57:57

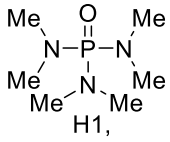

H1,
98% ee

Sample Report (continued):

Sample 41 Vial 1:41 ID 26-H1 File SHARLJA1_20211118_41 Date 18-Nov-2021 Time 16:57:57 Description (S,S)WO1 4.6x100mm 5µ

2: UV Detector: 230 Nm 2.0000-2.3500: Smooth (Mn, 2x3), 3.1000-3.5500: Smooth (Mn, 2x3) 5.948e-1
Range: 5.954e-1

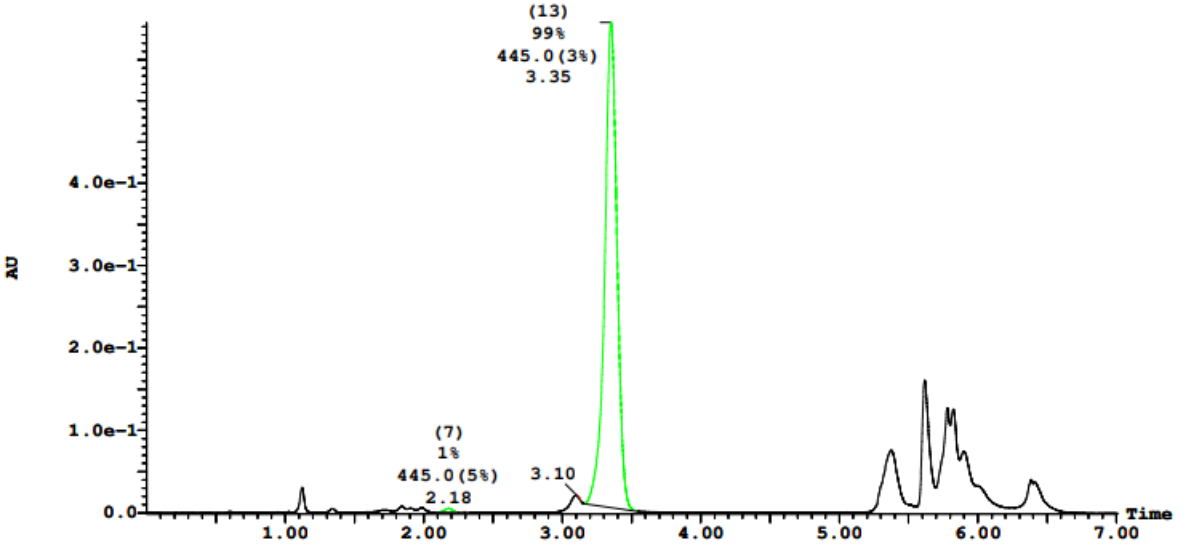

Peak Number	Compound	Time	AreaAbs	Area %Total	Width	Height	Mass Found
7	Found	2.18	3e+002	0.50	0	5e+003	445.0000
8		2.28	1e+001	0.02	0	4e+002	Not Found
9		2.30	8e+000	0.01	0	4e+002	Not Found
11		3.10	3e+001	0.05	0		Not Found
13	Tentative	3.35	6e+004	99.42	0	6e+005	445.0000

H6: 98% ee

Openlynx Report - SHARLJA1 Page 87

Sample: 44 Vial:1:44 ID:26-H6 Me−CN
File:SHARLJA1_20211118_44 Date:18-Nov-2021 Time:17:22:21
Description:(S,S)WO1 4.6x100mm 5µ Conditions:5% IPA over 5min 3mL/min

H6,
98% ee

Printed: Thu Dec 16 11:07:53 2021

Sample Report (continued):

Sample 44 Vial 1:44 ID 26-H6 File SHARLJA1_20211118_44 Date 18-Nov-2021 Time 17:22:21 Description (S,S)WO1 4.6x100mm 5µ

2: UV Detector: 230 Nm 2.0000-2.3500: Smooth (Mn, 2x3), 3.1000-3.5500: Smooth (Mn, 2x3) 8.615e-1
Range: 8.631e-1

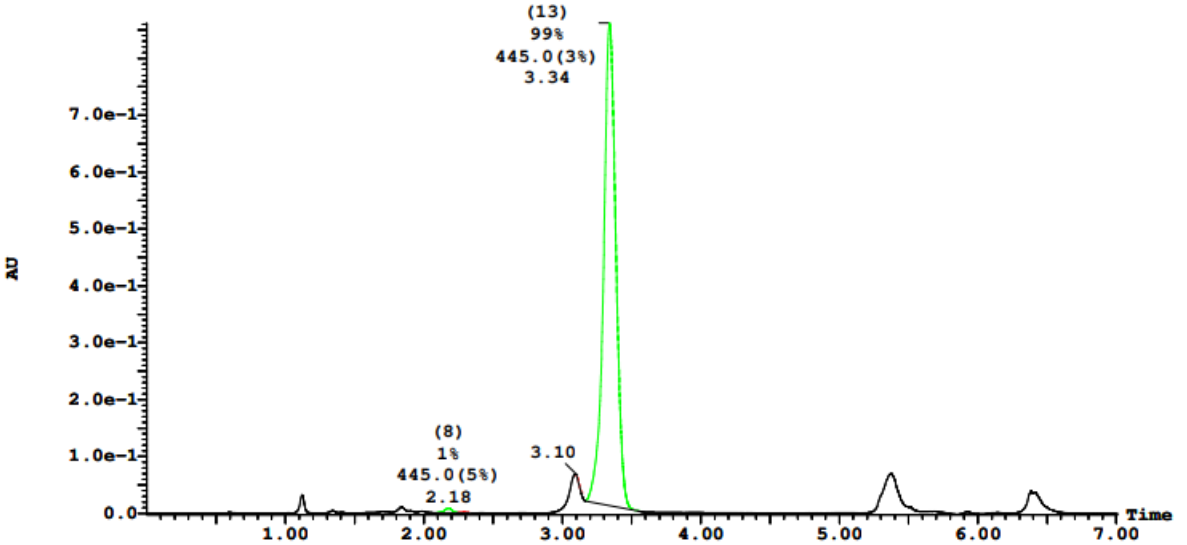

Peak Number	Compound	Time	AreaAbs	Area %Total	Width	Height	Mass Found
8	Found	2.18	5e+002	0.62	0	8e+003	445.0000
9		2.29	5e+001	0.05	0	9e+002	Not Found
9		2.32	8e+000	0.01	0	5e+002	Not Found
11		3.10	6e+001	0.06	0	1e-002	Not Found
13	Tentative	3.34	9e+004	99.26	0	8e+005	445.0000

H10: 98% ee

Openlynx Report - SHARLJA1
Sample: 46
File:SHARLJA1_20211118_46
Description:(S,S)WO1 4.6x100mm 5µ

Vial:1:46
Date:18-Nov-2021
Conditions:5% IPA over 5min 3mL/min

ID:26-H10
Time:17:38:37

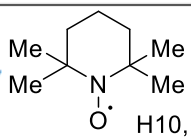

Printed: Thu Dec 16 11:07:53 2021

Sample Report (continued):

Sample 46 Vial 1:46 ID 26-H10 File SHARLJA1_20211118_46 Date 18-Nov-2021 Time 17:38:37 Description (S,S)WO1 4.6x100mm 5µ

2: UV Detector: 230 Nm 2.0000-2.3500: Smooth (Mn, 2x3), 3.1000-3.5500: Smooth (Mn, 2x3) 8.172e-1
Range: 8.205e-1

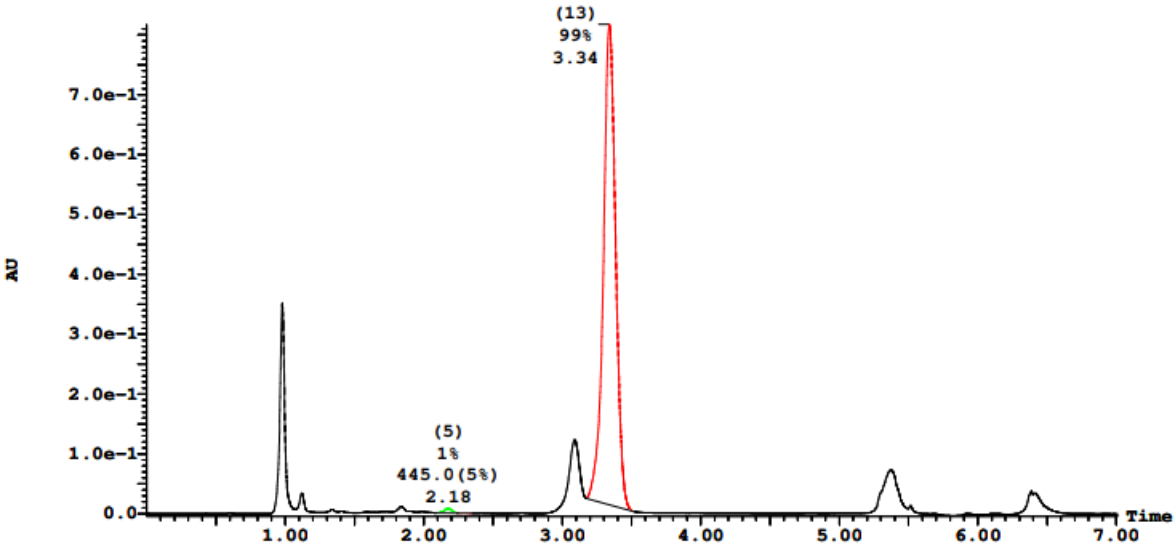

Peak Number	Compound	Time	AreaAbs	Area %Total	Width	Height	Mass Found
5	Found	2.18	5e+002	0.59	0	8e+003	445.0000
6		2.29	4e+001	0.05	0	7e+002	Not Found
13		3.34	8e+004	99.37	0	8e+005	Not Found

5.3 Successful reactions performed with Rh_2(*S-tetra-p*-Br-PhPTTL)$_4$ as catalyst in the presence of 90 equiv of HFIP.

The following dataset represents reactions that were successful when performed according to **general procedure 5.1** in the presence of 10 equiv HFIP using Rh_2(*S-tetra-p*-Br-PhPTTL)$_4$ as catalyst and dimethyl carbonate as solvent. Each additive is described according to the well plate designation in the study as well as the compound number it was assigned in the main text. The yield of the reaction in the presence of each additive is reported in **Figure C**6 and what follows is the HPLC data from which the yield was calculated according to equation 1.

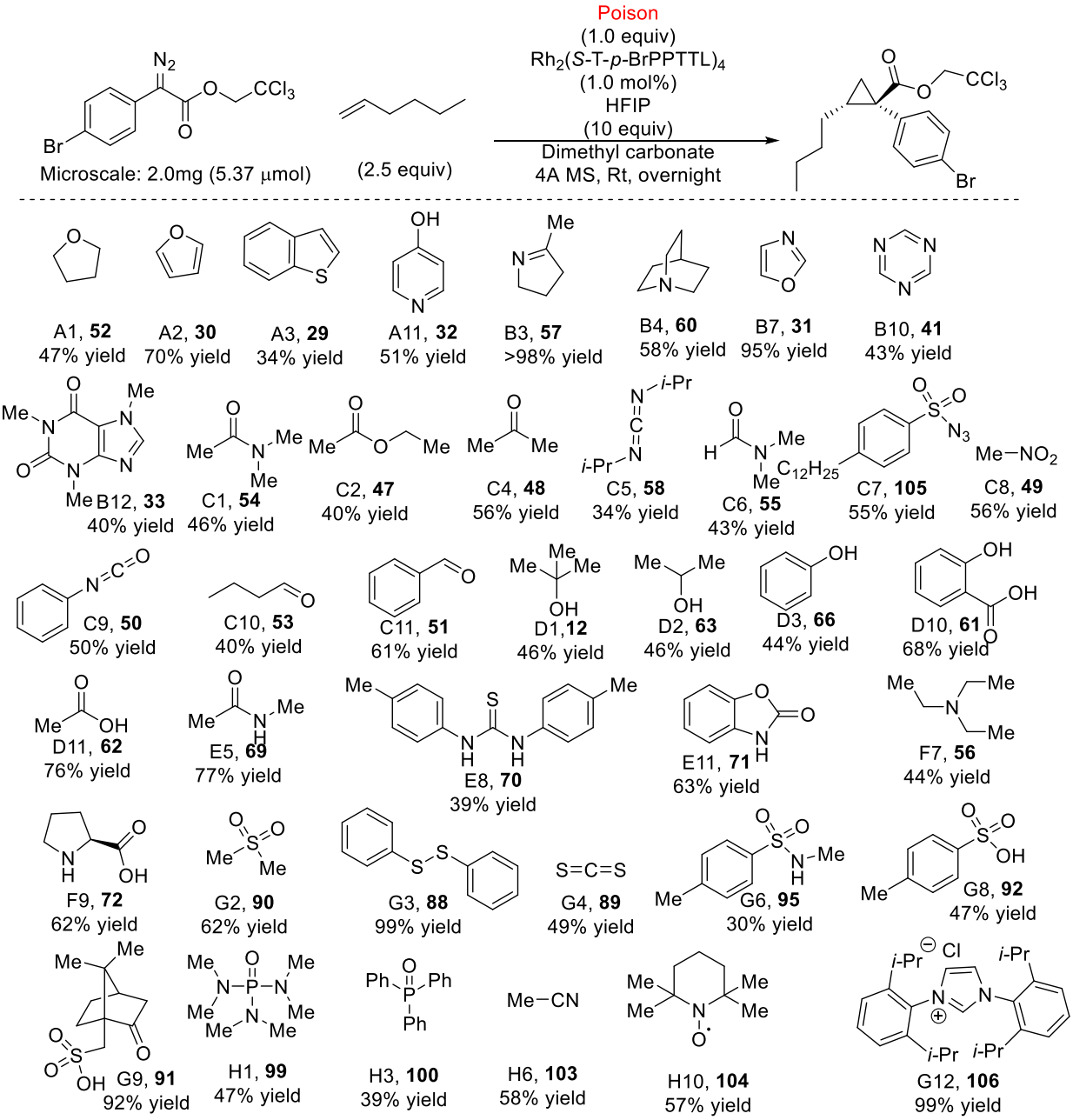

Figure C6: Reactions giving >30% yield (successful reactions) with the use of 10 equiv. HFIP in the presence of Rh_2(*S-tetra-p*-Br-PhPTTL)$_4$ and dimethyl carbonate as solvent.

A1,
47% yield

Single Sample Report
Sample Name: SHARLJA1-exp100-0026_11_30_2021_A1-re
Filename: sharlja1-exp100-0026_11_30_2021_a1-re.raw
Submitter:

Peak #	Formula	Target …	Target …	Time	Found	Area %	Area Abs
9	C23H28C…	493.1	Glyburi…	1.411	Yes	27.2	2484.26
19	C16H18B…	426.0	Product	2.071	Yes	48.0	4379.48

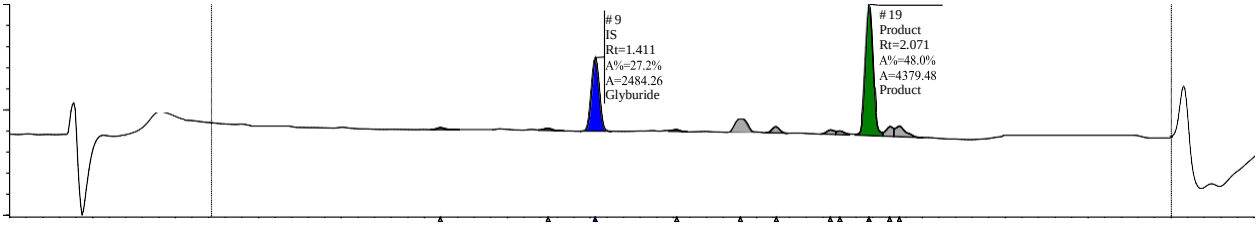

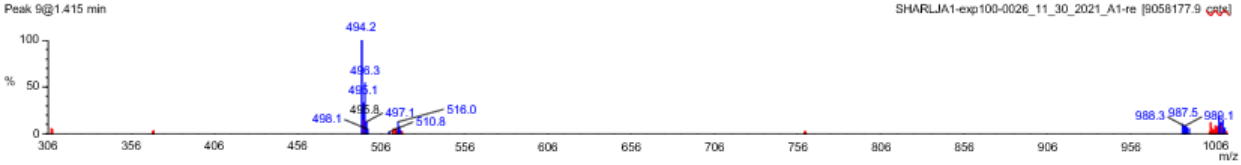

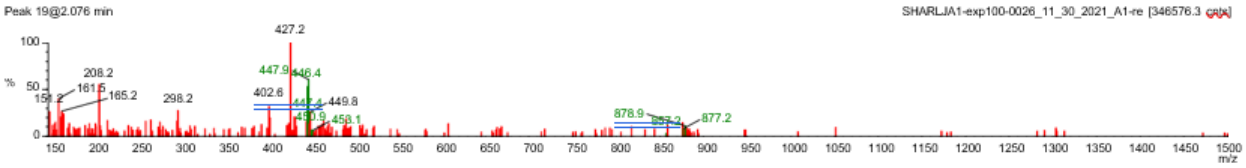

Name	Y/N	Type	Formula	Mass
Glyburide	Y	IS	C23H28ClN3O5S	493.1
Product	Y	Product	C16H18BrCl3O2	426.0

Single Sample Report
Sample Name: SHARLJA1-exp100-0026_11_30_2021_A2-re
Filename: sharlja1-exp100-0026_11_30_2021_a2-re.raw
Submitter

A2,
70% yield

Peak #	Formula	Target …	Target …	Time	Found	Area %	Area Abs
8	C23H28C…	493.1	Glyburi…	1.411	Yes	22.4	2732.56
13	C16H18B…	426.0	Product	2.071	Yes	56.5	6885.37

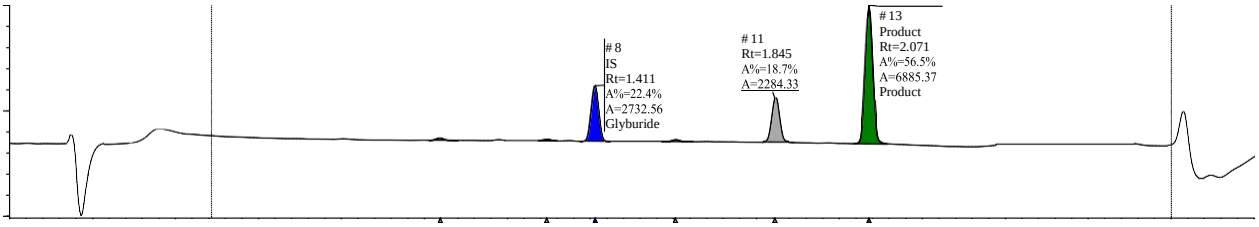

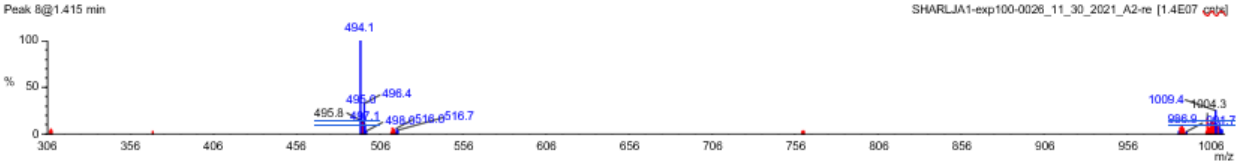

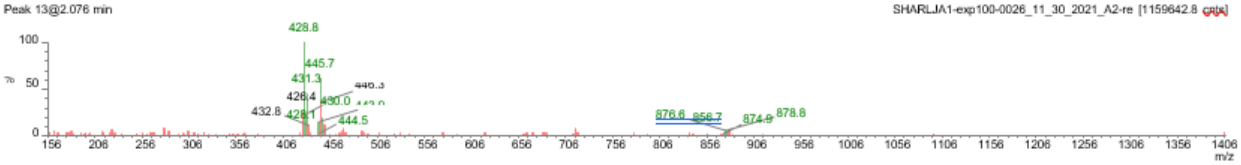

Name	Y/N	Type	Formula	Mass
Glyburide	Y	IS	C23H28ClN3O5S	493.1
Product	Y	Product	C16H18BrCl3O2	426.0

Single Sample Report
Sample Name: SHARLJA1-exp100-0026_11_30_2021_A3
Filename: sharlja1-exp100-0026_11_30_2021_a3.raw
Submitter:

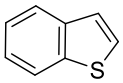

A3,
34% yield

Peak #	Formula	Target …	Target …	Time	Found	Area %	Area Abs
8	C23H28C…	493.1	Glyburi…	1.411	Yes	16.3	2594.57
15	C16H18B…	426.0	Product	2.071	Yes	21.2	3389.34

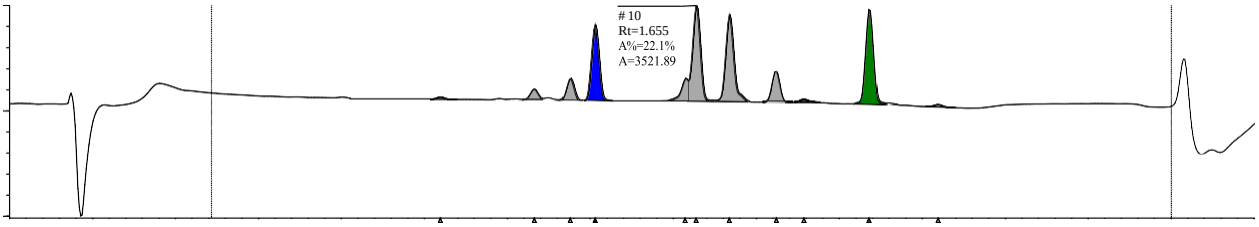

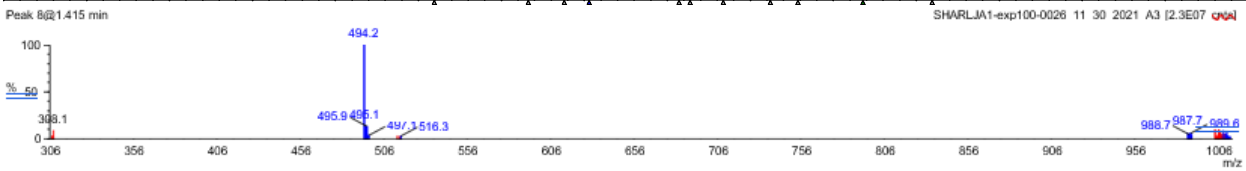

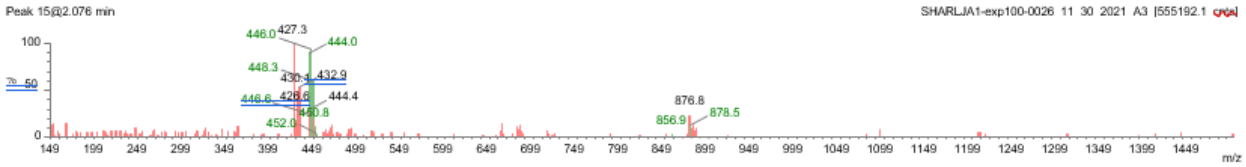

Name	Y/N	Type	Formula	Mass
Glyburide	Y	IS	C23H28ClN3O5S	493.1
Product	Y	Product	C16H18BrCl3O2	426.0

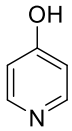

A11,
51% yield

Single Sample Report
Sample Name: SHARLJA1-exp100-0026_11_30_2021_A11
Filename: sharlja1-exp100-0026_11_30_2021_a11.raw
Submitter

Peak #	Formula	Target …	Target …	Time	Found	Area %	Area Abs
11	C23H28C…	493.1	Glyburi…	1.411	Yes	16.6	5981.01
14	C16H18B…	426.0	Product	2.075	Yes	31.3	11301.23

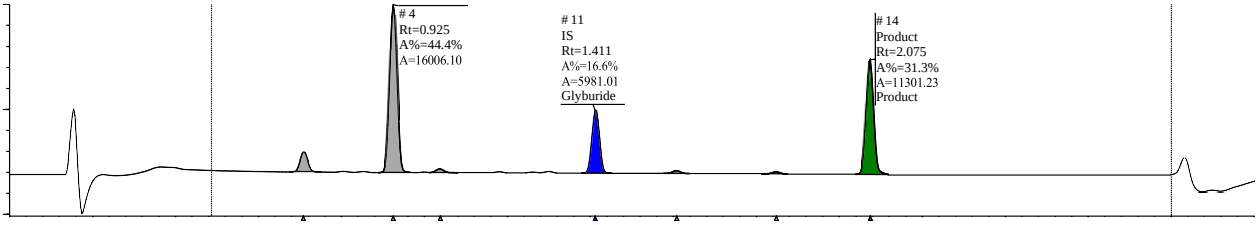

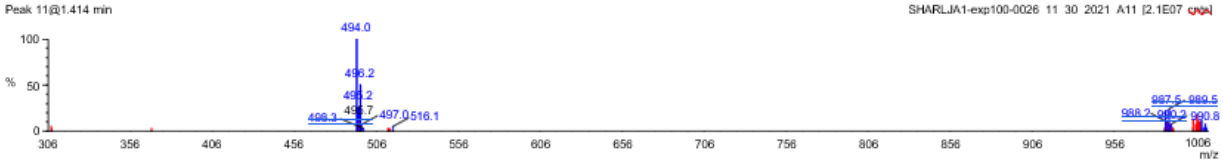

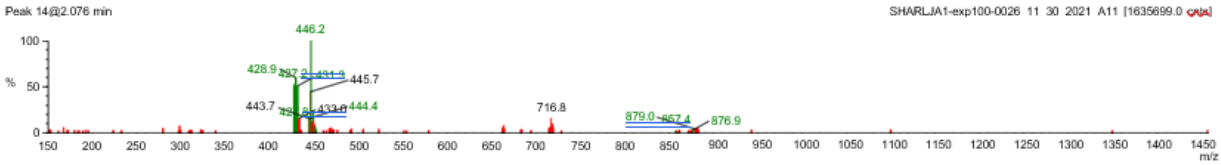

Name	Y/N	Type	Formula	Mass
Glyburide	Y	IS	C23H28ClN3O5S	493.1
Product	Y	Product	C16H18BrCl3O2	426.0

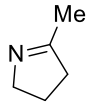

B3,
>98% yield

Single Sample Report

Sample Name: SHARLJA1-exp100-0026_11_30_2021_B3-re **Location:** 18
Filename: sharlja1-exp100-0026_11_30_2021_b3-re.raw **Instrument:**
Submitter: **Job Code:** SHARLJA1_EXP100_0026_resuspended_11_30_2021

Peak #	Formula	Target …	Target …	Time	Found	Area %	Area Abs
15	C23H28C…	493.1	Glyburi…	1.408	Yes	18.1	2834.76
24	C16H18B…	426.0	Product	2.071	Yes	64.0	10019.61

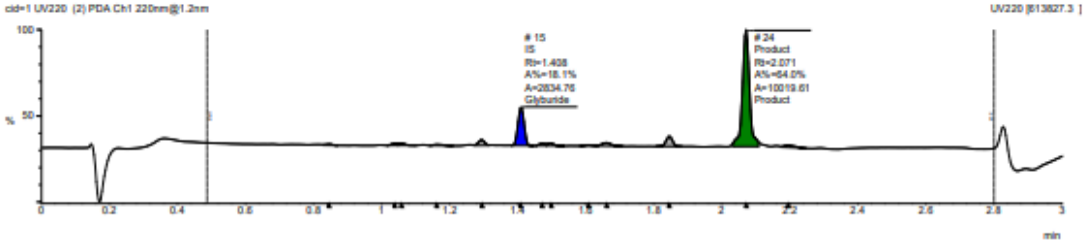

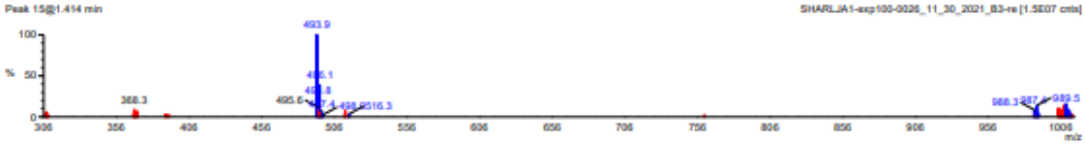

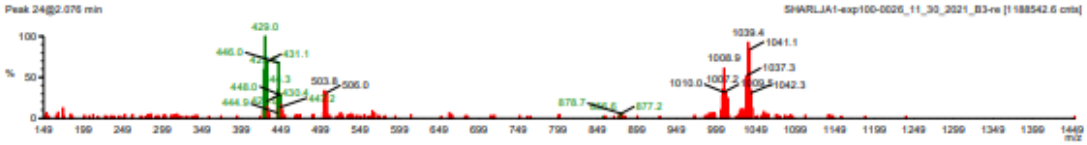

Name	Y/N	Type	Formula	Mass
Glyburide	Y	IS	C23H28ClN3O5S	493.1
Product	Y	Product	C16H18BrCl3O2	426.0

Single Sample Report

Sample Name: SHARLJA1-exp100-0026_11_30_2021_B4
Filename: sharlja1-exp100-0026_11_30_2021_b4.raw
Submitter:

Location: 26
Instrument:
Job Code:
SHARLJA1_EXP100_0026_resuspended_11_30_2021

B4,
58% yield

Peak #	Formula	Target …	Target …	Time	Found	Area %	Area Abs
9	C23H28C…	493.1	Glyburi…	1.411	Yes	18.2	1645.80
13	C16H18B…	426.0	Product	2.071	Yes	9.5	858.86

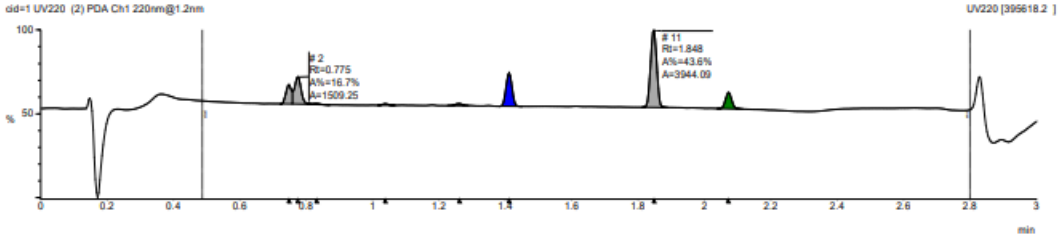

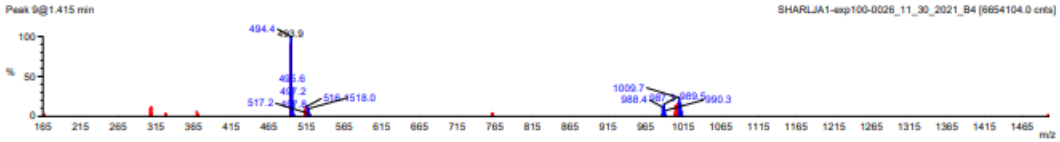

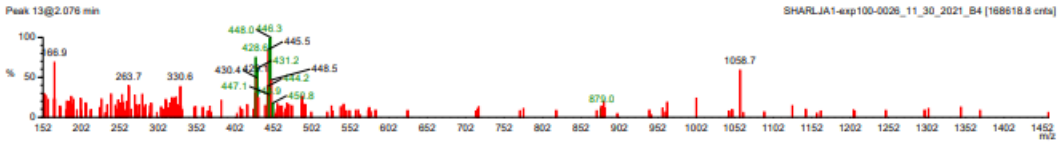

Name	Y/N	Type	Formula	Mass
Glyburide	Y	IS	C23H28ClN3O5S	493.1
Product	Y	Product	C16H18BrCl3O2	426.0

Single Sample Report

Sample Name: SHARLJA1-exp100-0026_11_30_2021_B7

Filename: sharlja1-exp100-0026_11_30_2021_b7.raw

B7, 95% yield

Peak #	Formula	Target …	Target …	Time	Found	Area %	Area Abs
11	C23H28C…	493.1	Glyburi…	1.411	Yes	19.0	4305.82
24	C16H18B…	426.0	Product	2.071	Yes	64.1	14500.93

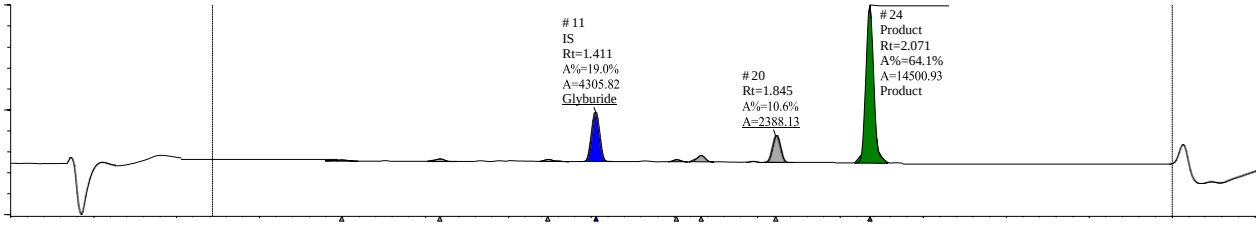

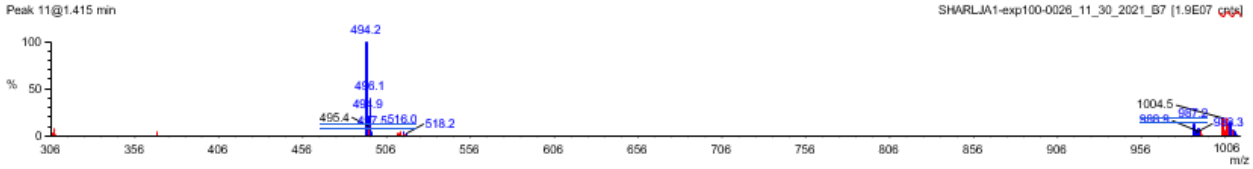

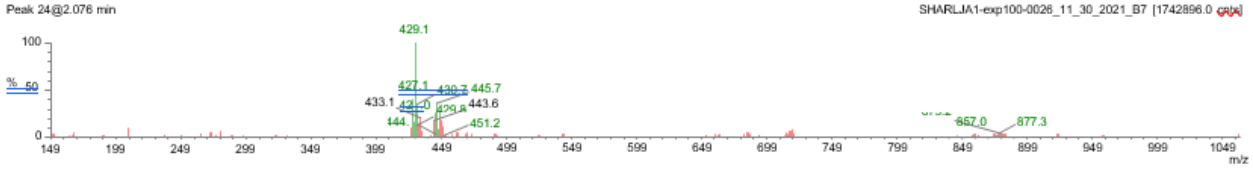

Name	Y/N	Type	Formula	Mass
Glyburide	Y	IS	C23H28ClN3O5S	493.1
Product	Y	Product	C16H18BrCl3O2	426.0

Single Sample Report
Sample Name: SHARLJA1-exp100-0026_11_30_2021_B10
Filename: sharlja1-exp100-0026_11_30_2021_b10.raw
Submitter:

B10,
43% yield

Peak #	Formula	Target …	Target …	Time	Found	Area %	Area Abs
17	C23H28C…	493.1	Glyburi…	1.411	Yes	22.1	5911.46
28	C16H18B…	426.0	Product	2.075	Yes	35.9	9592.75

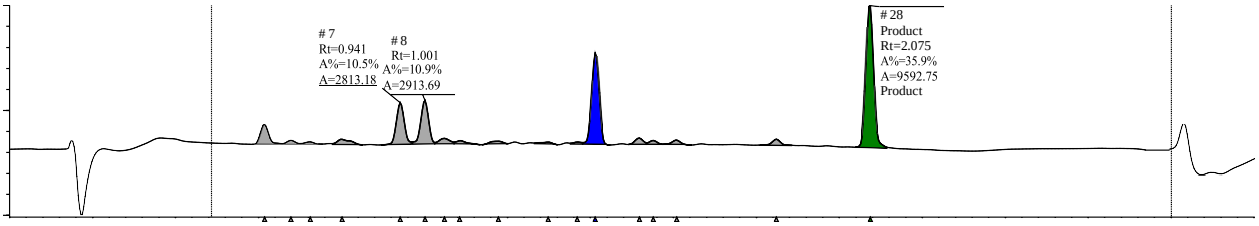

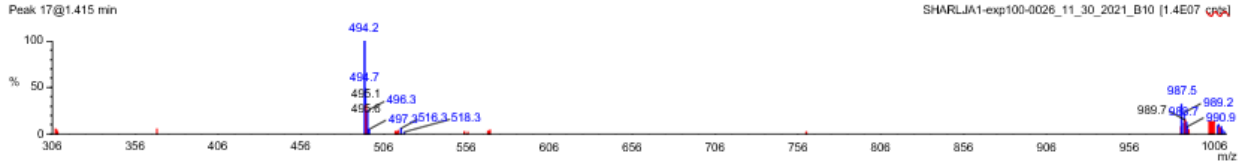

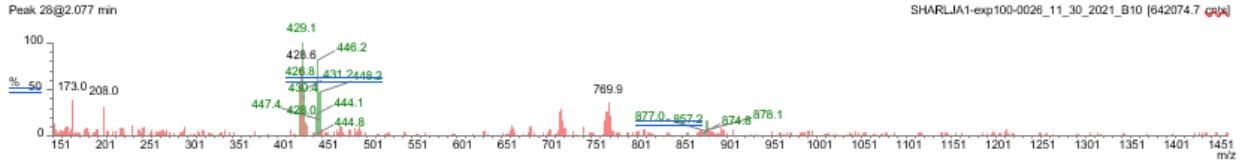

Name	Y/N	Type	Formula	Mass
Glyburide	Y	IS	C23H28ClN3O5S	493.1
Product	Y	Product	C16H18BrCl3O2	426.0

Single Sample Report
Sample Name: SHARLJA1-exp100-0026_11_30_2021_B12
Filename: sharlja1-exp100-0026_11_30_2021_b12.raw
Submitter:

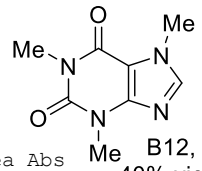

B12,
40% yield

Peak #	Formula	Target …	Target …	Time	Found	Area %	Area Abs
12	C23H28C…	493.1	Glyburi…	1.411	Yes	16.9	9551.70
15	C16H18B…	426.0	Product	2.071	Yes	25.5	14444.52

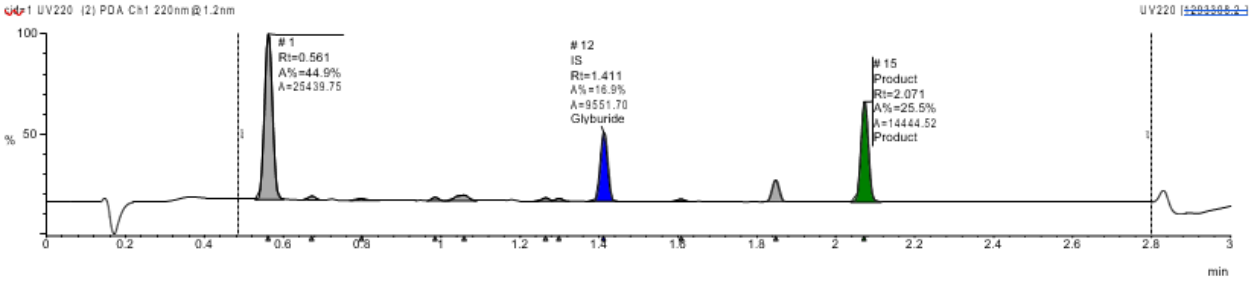

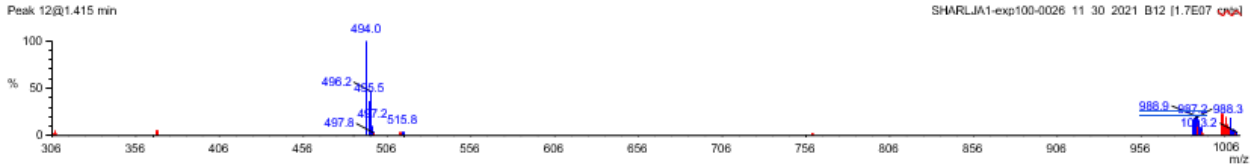

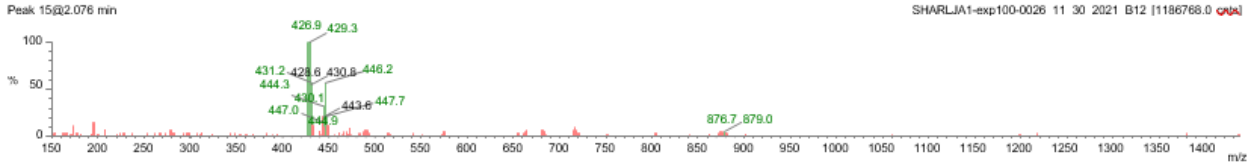

Name	Y/N	Type	Formula	Mass
Glyburide	Y	IS	C23H28ClN3O5S	493.1
Product	Y	Product	C16H18BrCl3O2	426.0

Single Sample Report
Sample Name: SHARLJA1-exp100-0026_11_30_2021_C1
Filename: sharlja1-exp100-0026_11_30_2021_c1.raw
Submitter:

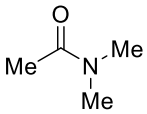

C1,
46% yield

Peak #	Formula	Target …	Target …	Time	Found	Area %	Area Abs
10	C23H28C…	493.1	Glyburi…	1.411	Yes	27.1	3559.79
19	C16H18B…	426.0	Product	2.071	Yes	46.5	6117.62

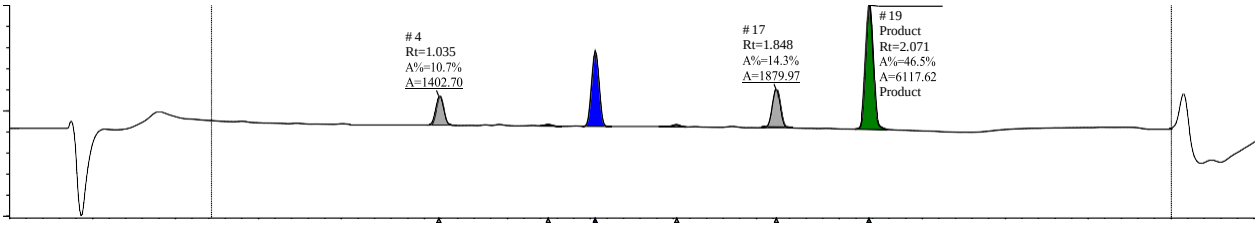

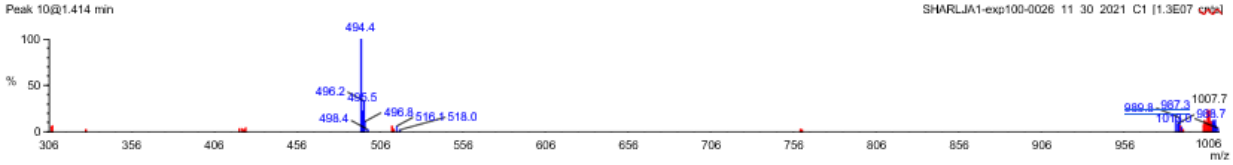

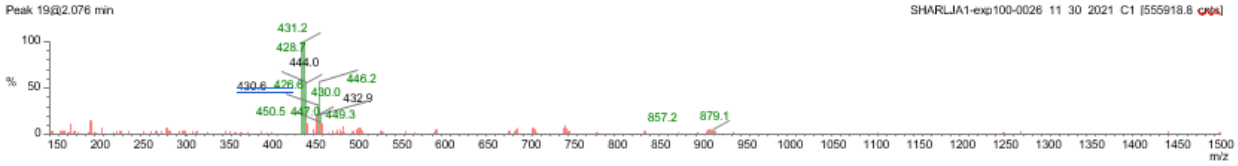

Name	Y/N	Type	Formula	Mass
Glyburide	Y	IS	C23H28ClN3O5S	493.1
Product	Y	Product	C16H18BrCl3O2	426.0

Single Sample Report
Sample Name: SHARLJA1-exp100-0026_11_30_2021_C2
Filename: sharlja1-exp100-0026_11_30_2021_c2.raw
Submitter:

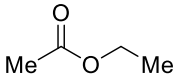

C2,
40% yield

Peak #	Formula	Target …	Target …	Time	Found	Area %	Area Abs
10	C23H28C…	493.1	Glyburi…	1.411	Yes	25.9	5766.04
18	C16H18B…	426.0	Product	2.071	Yes	38.9	8655.46

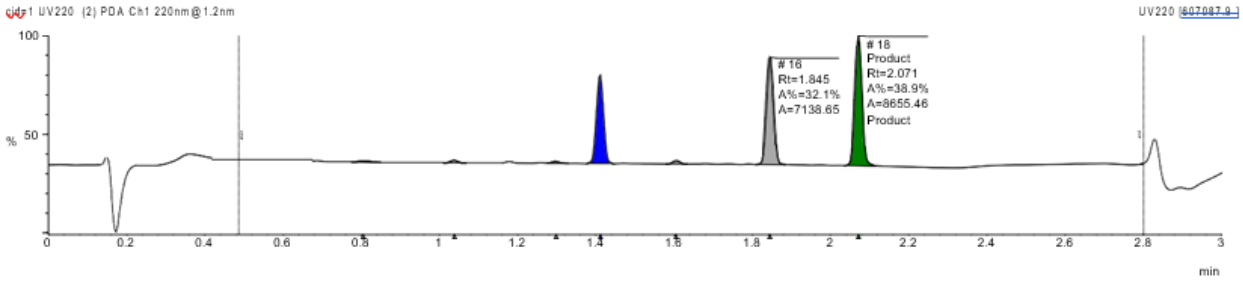

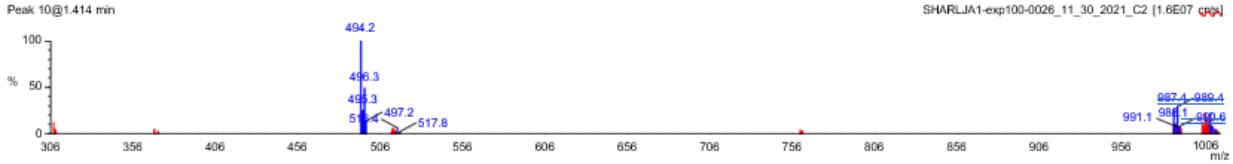

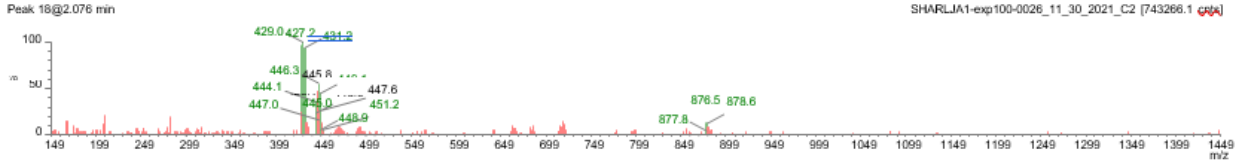

Name	Y/N	Type	Formula	Mass
Glyburide	Y	IS	C23H28ClN3O5S	493.1
Product	Y	Product	C16H18BrCl3O2	426.0

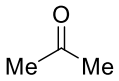

C4,
56% yield

Single Sample Report
Sample Name: SHARLJA1-exp100-0026_11_30_2021_C4-re
Filename: sharlja1-exp100-0026_11_30_2021_c4-re.raw
Submitter:

Peak #	Formula	Target …	Target …	Time	Found	Area %	Area Abs
6	C23H28C…	493.1	Glyburi…	1.411	Yes	25.4	3208.08
10	C16H18B…	426.0	Product	2.071	Yes	51.9	6546.86

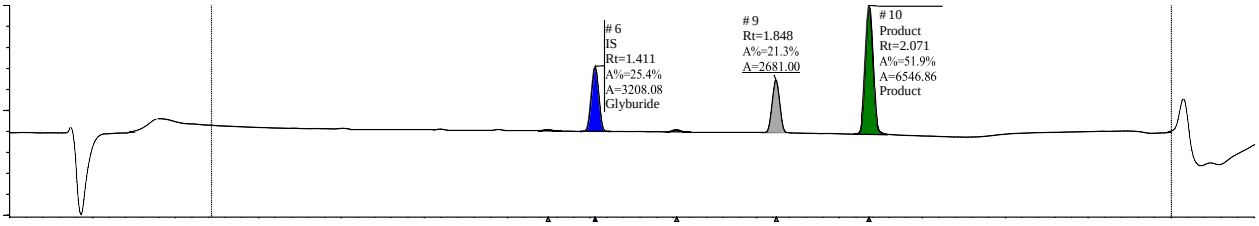

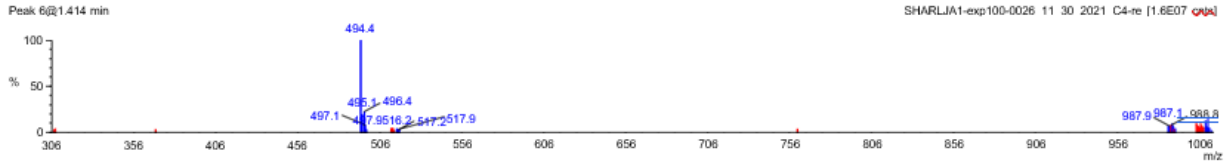

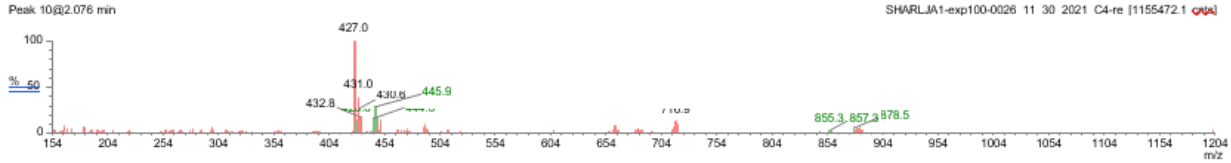

Name	Y/N	Type	Formula	Mass
Glyburide	Y	IS	C23H28ClN3O5S	493.1
Product	Y	Product	C16H18BrCl3O2	426.0

Single Sample Report

Sample Name: SHARLJA1-exp100-0026_11_30_2021_C5
Filename: sharlja1-exp100-0026_11_30_2021_c5.raw
Submitter:

Location: 35
Instrument:
Job Code:
SHARLJA1_EXP100_0026_resuspended_11_30_2021

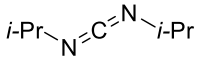

C5,
34% yield

Peak #	Formula	Target …	Target …	Time	Found	Area %	Area Abs
12	C23H28C…	493.1	Glyburi…	1.411	Yes	34.1	4017.06
25	C16H18B…	426.0	Product	2.071	Yes	36.6	4312.69

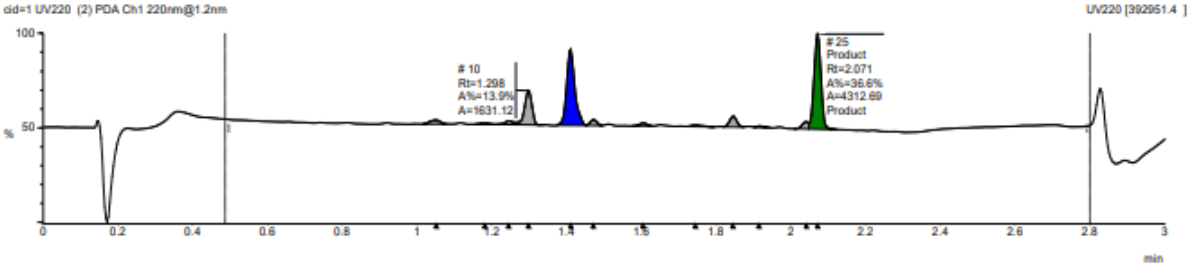

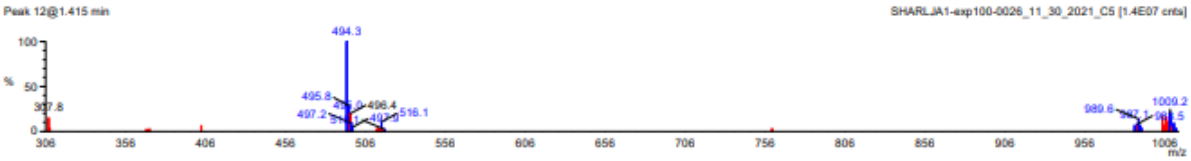

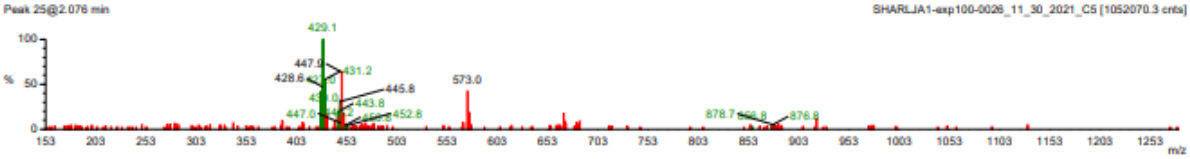

Name	Y/N	Type	Formula	Mass
Glyburide	Y	IS	C23H28ClN3O5S	493.1
Product	Y	Product	C16H18BrCl3O2	426.0

Single Sample Report
Sample Name: SHARLJA1-exp100-0026_11_30_2021_C6-re
Filename: sharlja1-exp100-0026_11_30_2021_c6-re.raw

Peak #	Formula	Target …	Target …	Time	Found	Area %	Area Abs
12	C23H28C…	493.1	Glyburi…	1.408	Yes	17.9	3218.39
18	C16H18B…	426.0	Product	2.071	Yes	29.0	5216.17

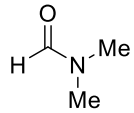

C6,
43% yield

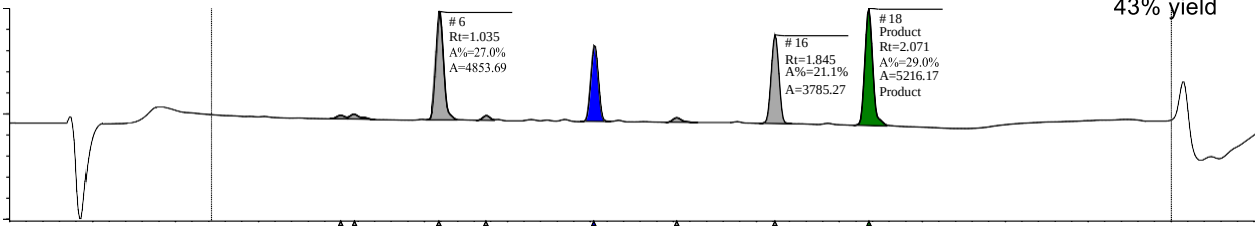

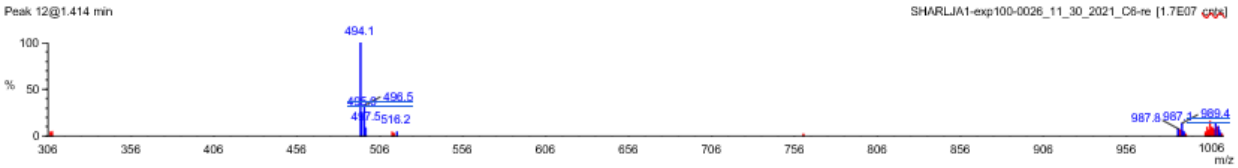

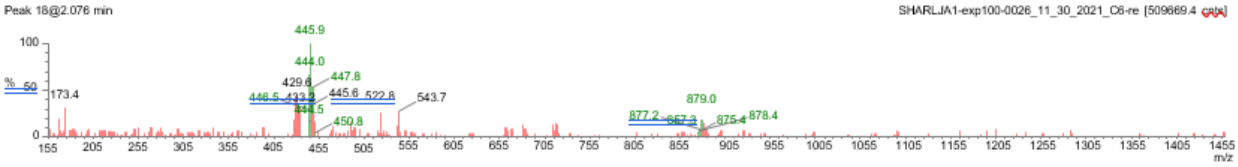

Name	Y/N	Type	Formula	Mass
Glyburide	Y	IS	C23H28ClN3O5S	493.1
Product	Y	Product	C16H18BrCl3O2	426.0

Single Sample Report
Sample Name: SHARLJA1-exp100-0026_11_30_2021_C7-re
Filename: sharlja1-exp100-0026_11_30_2021_c7-re

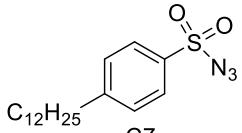

C7,
55% yield

Peak #	Formula	Target …	Target …	Time	Found	Area %	Area Abs
8	C23H28C…	493.1	Glyburi…	1.411	Yes	22.2	2768.93
16	C16H18B…	426.0	Product	2.071	Yes	45.0	5608.19

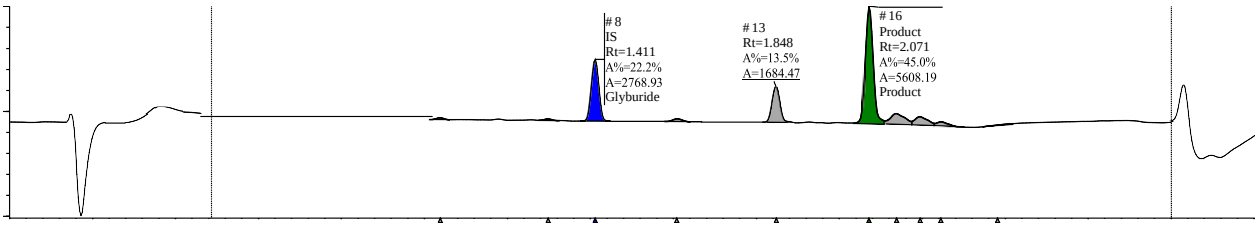

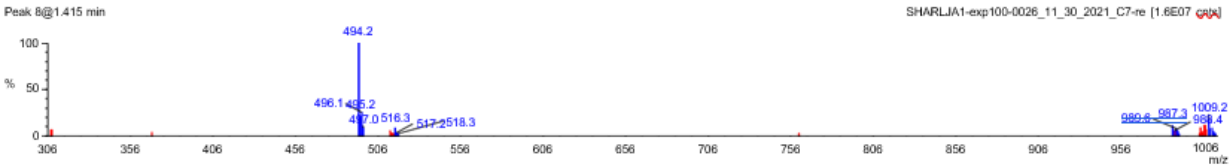

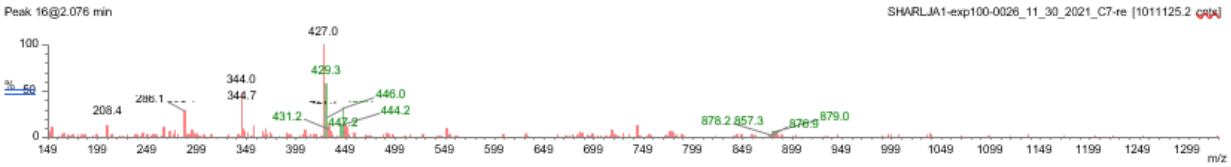

Name	Y/N	Type	Formula	Mass
Glyburide	Y	IS	C23H28ClN3O5S	493.1
Product	Y	Product	C16H18BrCl3O2	426.0

Me−NO_2

C8,
56% yield

Single Sample Report
Sample Name: SHARLJA1-exp100-0026_11_30_2021_C8
Filename: sharlja1-exp100-0026_11_30_2021_c8.raw

Peak #	Formula	Target …	Target …	Time	Found	Area %	Area Abs
7	C23H28C…	493.1	Glyburi…	1.411	Yes	25.7	5755.46
12	C16H18B…	426.0	Product	2.075	Yes	52.7	11808.85

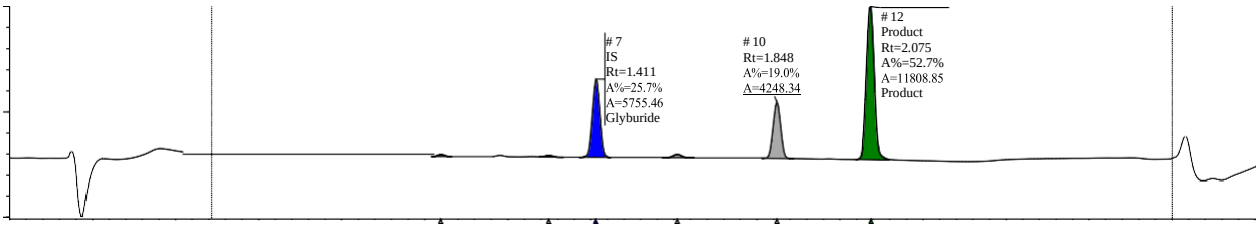

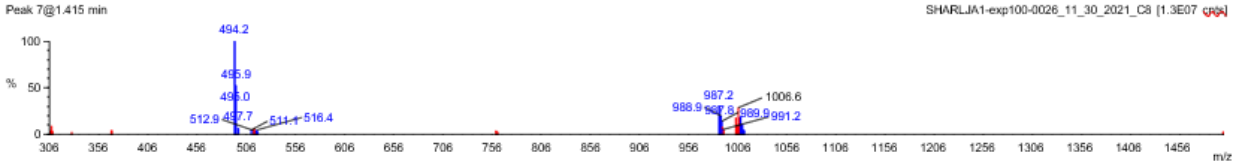

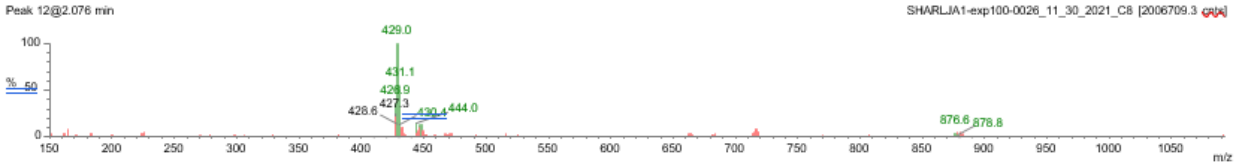

Name	Y/N	Type	Formula	Mass
Glyburide	Y	IS	C23H28ClN3O5S	493.1
Product	Y	Product	C16H18BrCl3O2	426.0

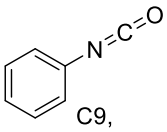

C9,
50% yield

Single Sample Report
Sample Name: SHARLJA1-exp100-0026_11_30_2021_C9
Filename: sharlja1-exp100-0026_11_30_2021_c9.raw
Submitter:

Peak #	Formula	Target …	Target …	Time	Found	Area %	Area Abs
8	C23H28C…	493.1	Glyburi…	1.411	Yes	16.5	3199.07
12	C16H18B…	426.0	Product	2.075	Yes	30.4	5888.22

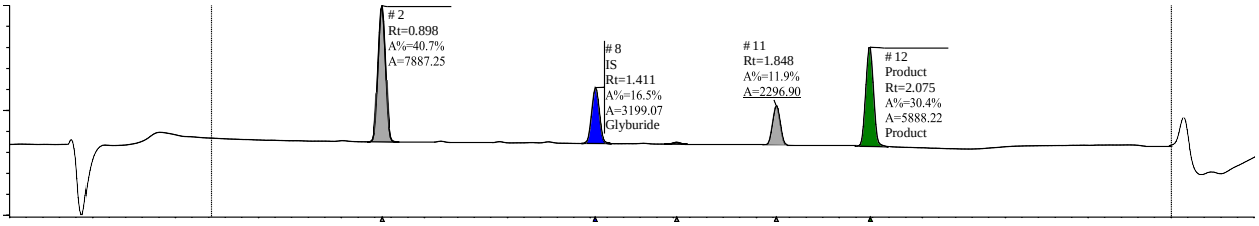

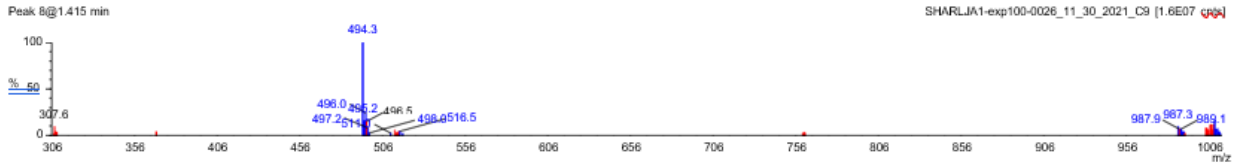

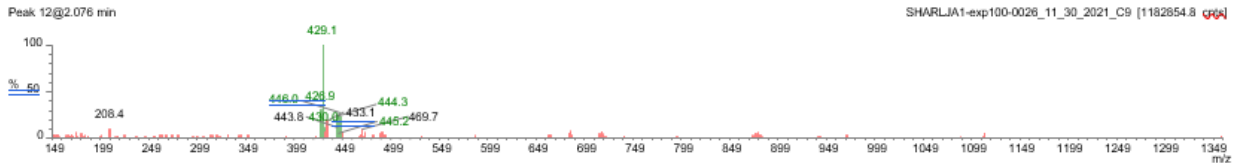

Name	Y/N	Type	Formula	Mass
Glyburide	Y	IS	C23H28ClN3O5S	493.1
Product	Y	Product	C16H18BrCl3O2	426.0

Single Sample Report
Sample Name: SHARLJA1-exp100-0026_11_30_2021_C10
Filename: sharlja1-exp100-0026_11_30_2021_c10.raw
Submitter:

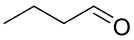

C10,
40% yield

Peak #	Formula	Target …	Target …	Time	Found	Area %	Area Abs
7	C23H28C…	493.1	Glyburi…	1.411	Yes	30.5	3553.13
12	C16H18B…	426.0	Product	2.071	Yes	45.8	5343.80

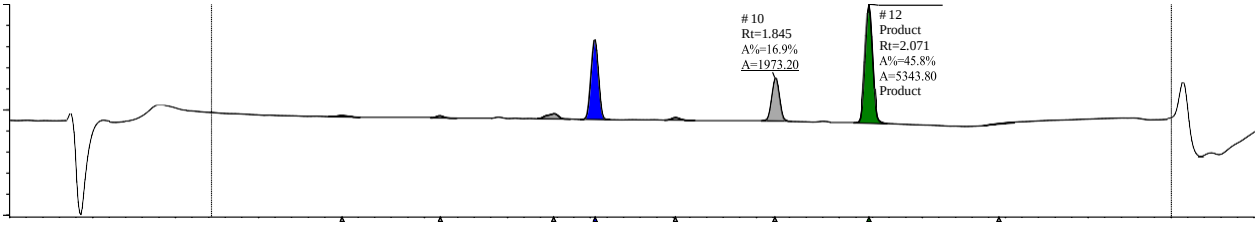

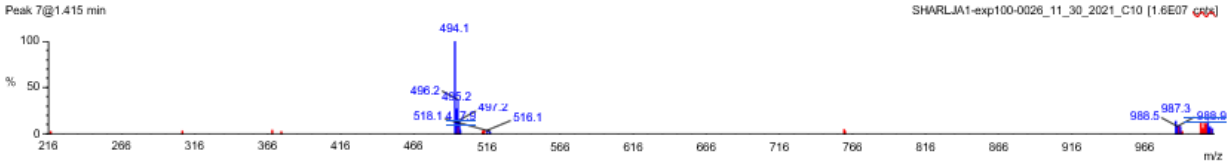

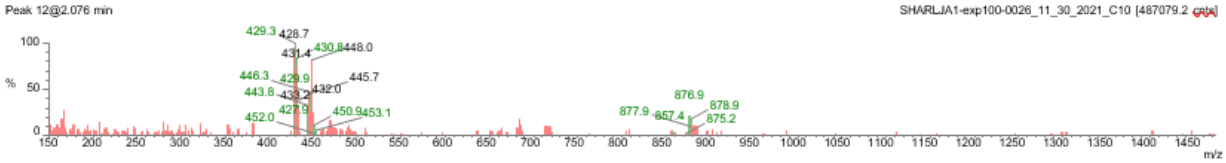

Name	Y/N	Type	Formula	Mass
Glyburide	Y	IS	C23H28ClN3O5S	493.1
Product	Y	Product	C16H18BrCl3O2	426.0

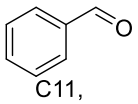

C11,
61% yield

Single Sample Report
Sample Name: SHARLJA1-exp100-0026_11_30_2021_C11
Filename: sharlja1-exp100-0026_11_30_2021_c11.raw
Submitter:

Peak #	Formula	Target …	Target …	Time	Found	Area %	Area Abs
7	C23H28C…	493.1	Glyburi…	1.411	Yes	19.7	4567.02
13	C16H18B…	426.0	Product	2.071	Yes	43.7	10139.35

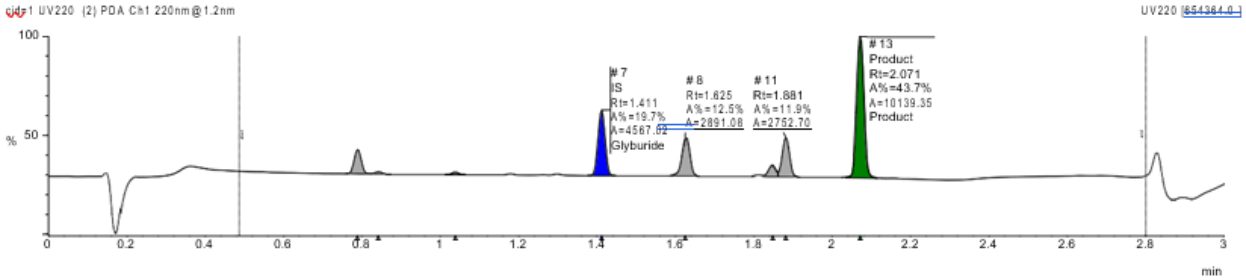

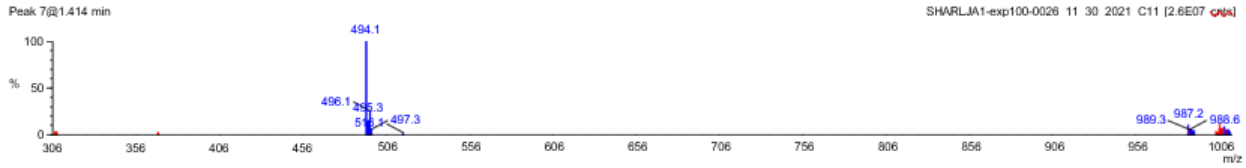

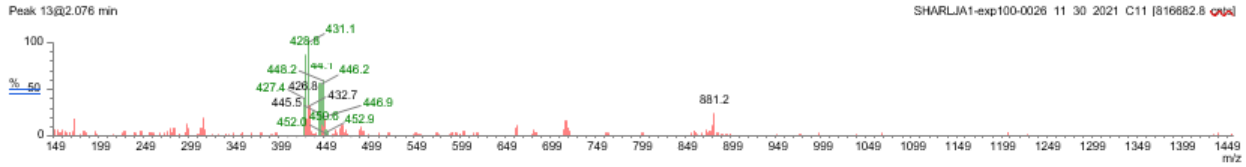

Name	Y/N	Type	Formula	Mass
Glyburide	Y	IS	C23H28ClN3O5S	493.1
Product	Y	Product	C16H18BrCl3O2	426.0

Single Sample Report
Sample Name: SHARLJA1-exp100-0026_11_30_2021_D1-re
Filename: sharlja1-exp100-0026_11_30_2021_d1- re.raw
Submitter:

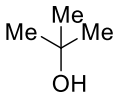

D1,
46% yield

Peak #	Formula	Target …	Target …	Time	Found	Area %	Area Abs
6	C23H28C…	493.1	Glyburi…	1.411	Yes	27.8	2448.15
12	C16H18B…	426.0	Product	2.071	Yes	47.9	4223.10

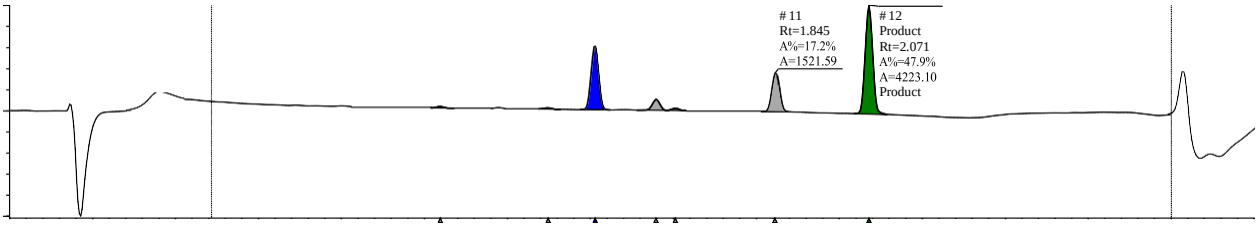

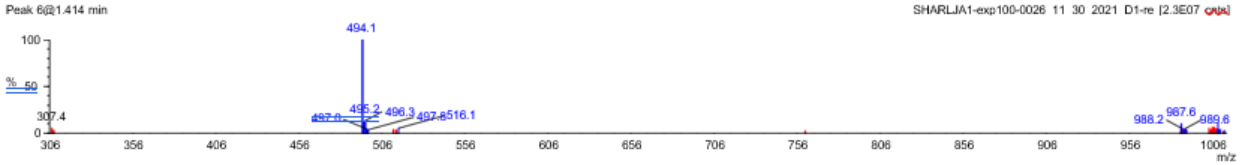

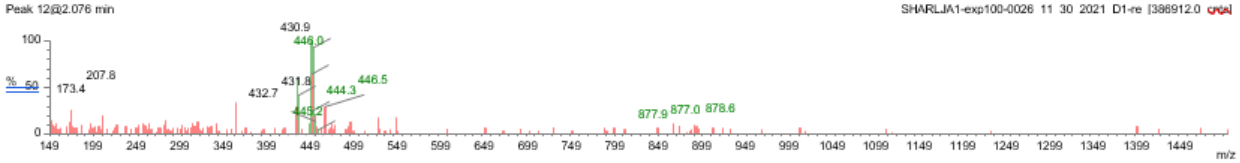

Name	Y/N	Type	Formula	Mass
Glyburide	Y	IS	C23H28ClN3O5S	493.1
Product	Y	Product	C16H18BrCl3O2	426.0

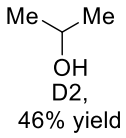

Single Sample Report
Sample Name: SHARLJA1-exp100-0026_11_30_2021_D2-re
Filename: sharlja1-exp100-0026_11_30_2021_d2-re

Peak #	Formula	Target …	Target …	Time	Found	Area %	Area Abs
8	C23H28C…	493.1	Glyburi…	1.411	Yes	21.8	3164.69
13	C16H18B…	426.0	Product	2.071	Yes	37.6	5457.73

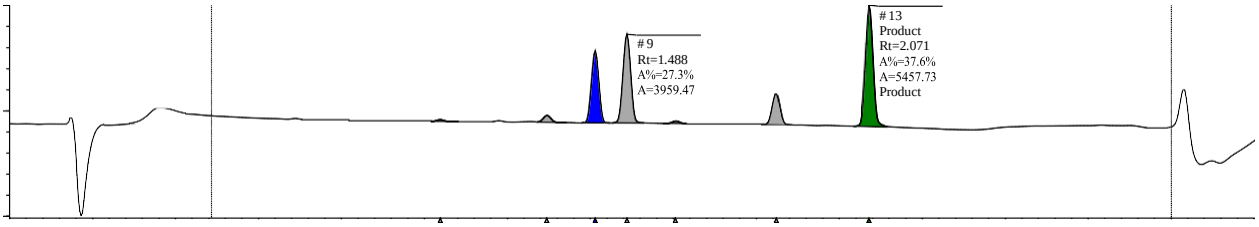

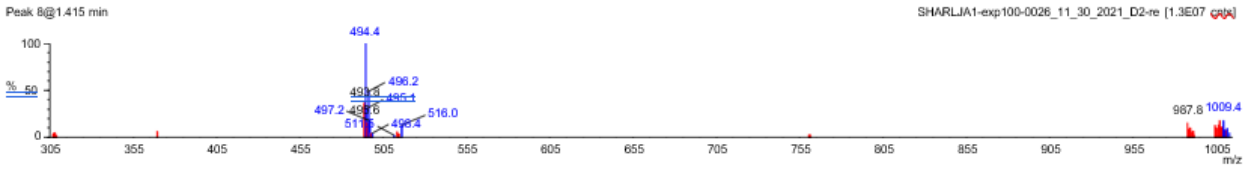

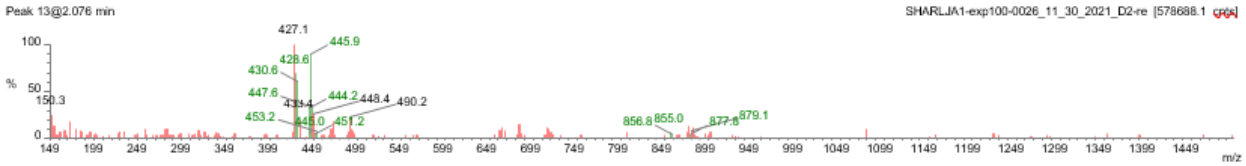

Name	Y/N	Type	Formula	Mass
Glyburide	Y	IS	C23H28ClN3O5S	493.1
Product	Y	Product	C16H18BrCl3O2	426.0

Single Sample Report

Sample Name: SHARLJA1-exp100-0026_11_30_2021_D3

Filename: sharlja1-exp100-0026_11_30_2021_d3.raw

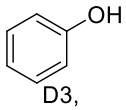

D3,
44% yield

Peak #	Formula	Target …	Target …	Time	Found	Area %	Area Abs
8	C23H28C…	493.1	Glyburi…	1.408	Yes	17.4	2797.98
16	C16H18B…	426.0	Product	2.071	Yes	28.4	4576.34

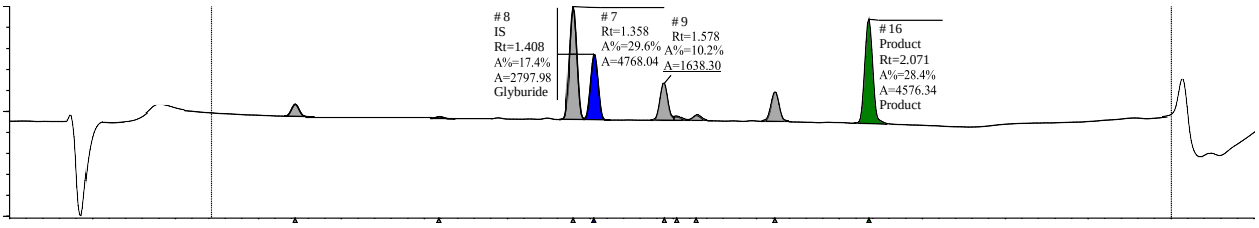

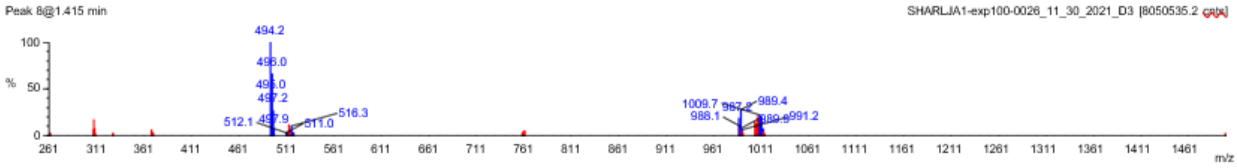

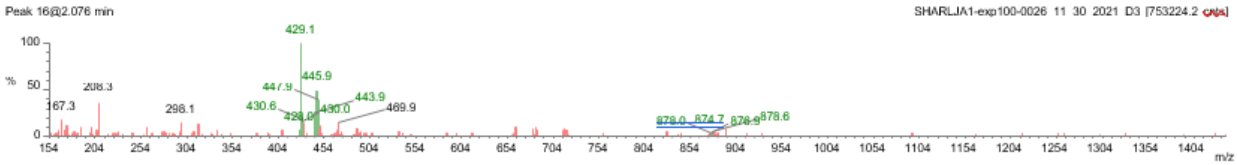

Name	Y/N	Type	Formula	Mass
Glyburide	Y	IS	C23H28ClN3O5S	493.1
Product	Y	Product	C16H18BrCl3O2	426.0

Single Sample Report

Sample Name: SHARLJA1-exp100-0026_11_30_2021_D10

Filename: sharlja1-exp100-0026_11_30_2021_d10.raw

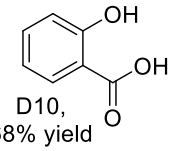

Peak #	Formula	Target …	Target …	Time	Found	Area %	Area Abs
6	C23H28C…	493.1	Glyburi…	1.408	Yes	6.8	1433.91
15	C16H18B…	426.0	Product	2.071	Yes	16.7	3520.23

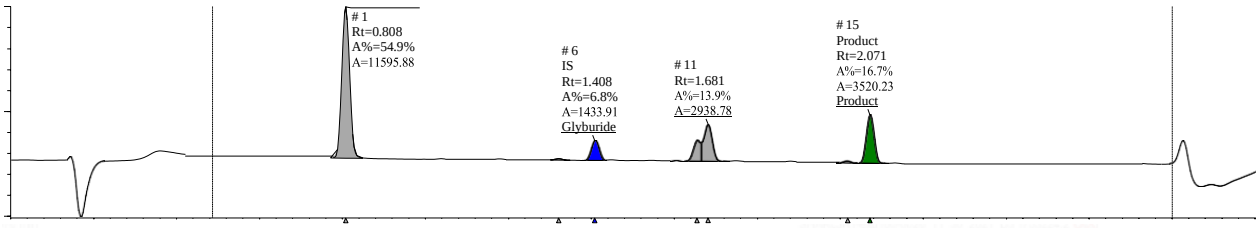

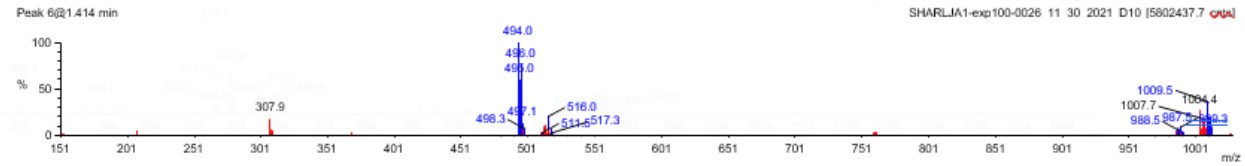

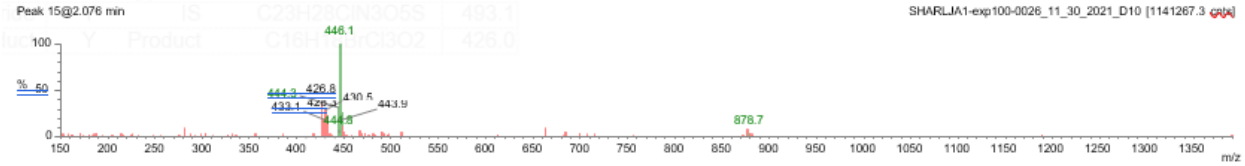

Name	Y/N	Type	Formula	Mass
Glyburide	Y	IS	C23H28ClN3O5S	493.1
Product	Y	Product	C16H18BrCl3O2	426.0

Single Sample Report

Sample Name: SHARLJA1-exp100-0026_11_30_2021_D11-re

Filename: sharlja1-exp100-0026_11_30_2021_d11-re.raw

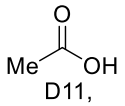

D11,
76% yield

Peak #	Formula	Target …	Target …	Time	Found	Area %	Area Abs
7	C23H28C…	493.1	Glyburi…	1.408	Yes	23.5	4552.62
12	C16H18B…	426.0	Product	2.071	Yes	64.4	12459.17

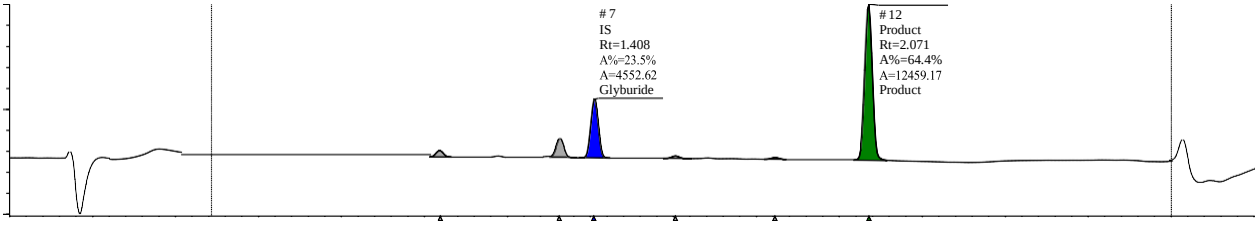

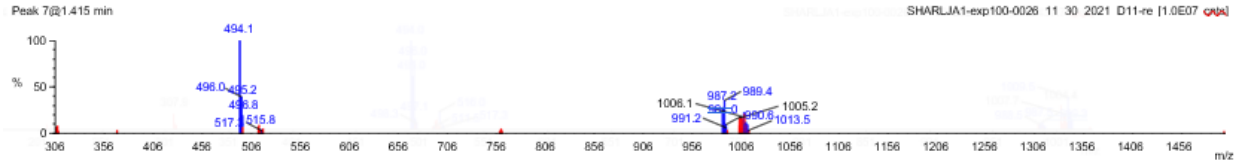

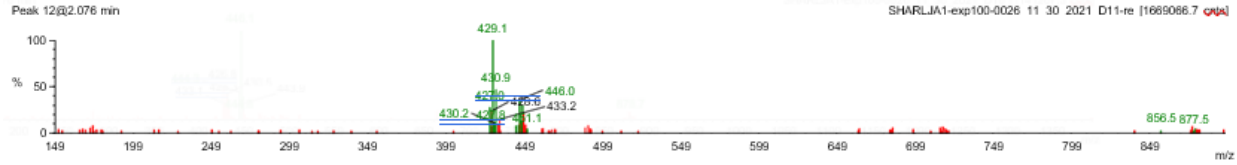

Name	Y/N	Type	Formula	Mass
Glyburide	Y	IS	C23H28ClN3O5S	493.1
Product	Y	Product	C16H18BrCl3O2	426.0

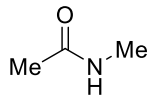

E5,
77% yield

Single Sample Report
Sample Name: SHARLJA1-exp100-0026_11_30_2021_E5-re
Filename: sharlja1-exp100-0026_11_30_2021_e5-re.raw
Submitter:

Peak #	Formula	Target …	Target …	Time	Found	Area %	Area Abs
7	C23H28C…	493.1	Glyburi…	1.411	Yes	18.1	5918.57
15	C16H18B…	426.0	Product	2.075	Yes	50.1	16385.39

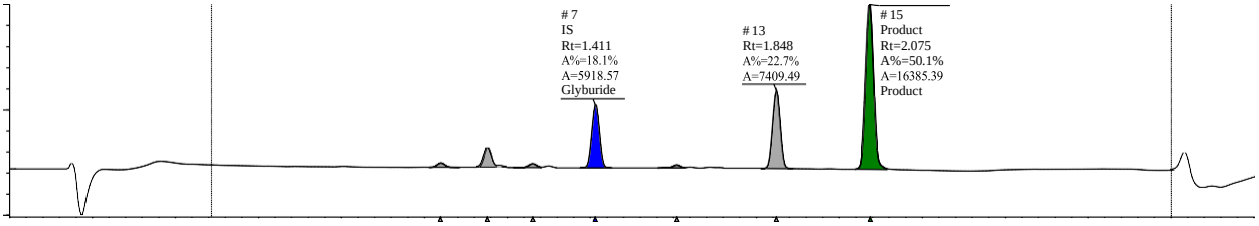

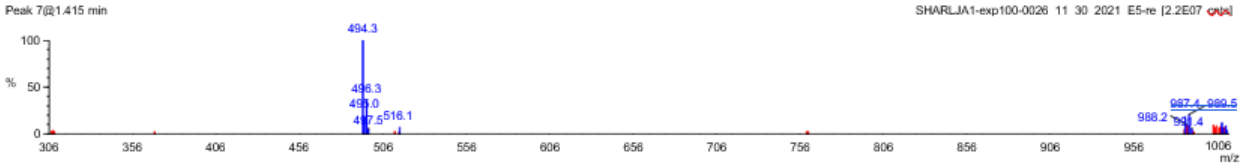

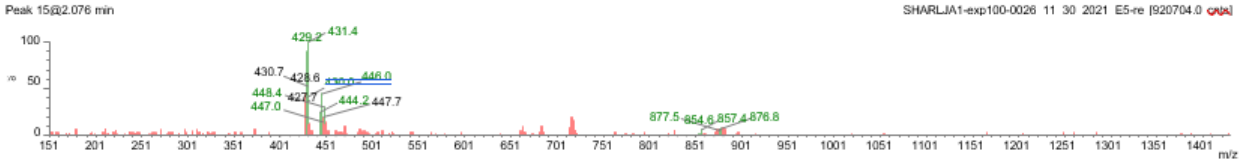

Name	Y/N	Type	Formula	Mass
Glyburide	Y	IS	C23H28ClN3O5S	493.1
Product	Y	Product	C16H18BrCl3O2	426.0

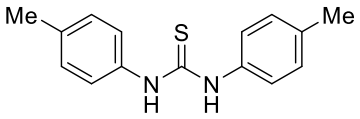

E8,
39% yield

Single Sample Report
Sample Name: SHARLJA1-exp100-0026_11_30_2021_E8
Filename: sharlja1-exp100-0026_11_30_2021_e8.raw
Submitter:

Peak #	Formula	Target …	Target …	Time	Found	Area %	Area Abs
8	C23H28C…	493.1	Glyburi…	1.411	Yes	29.7	3066.21
14	C16H18B…	426.0	Product	2.071	Yes	44.1	4559.51

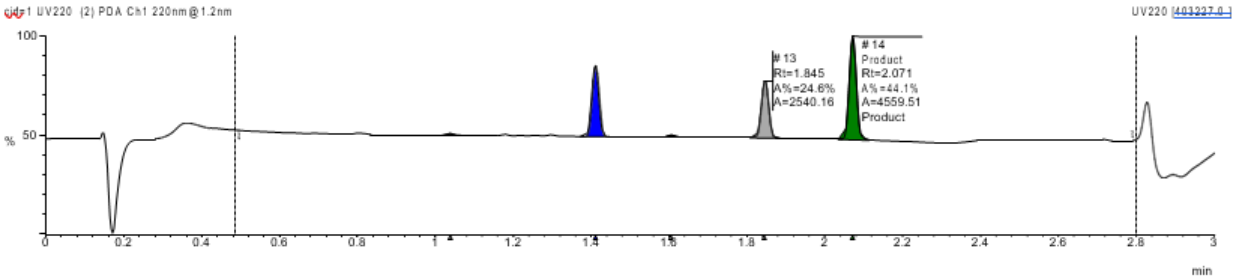

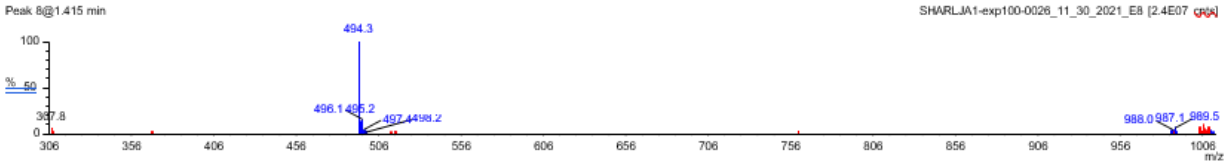

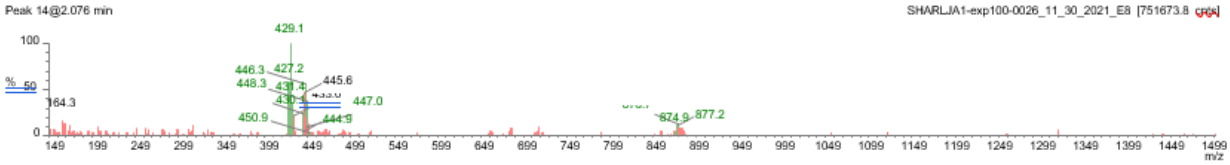

Name	Y/N	Type	Formula	Mass
Glyburide	Y	IS	C23H28ClN3O5S	493.1
Product	Y	Product	C16H18BrCl3O2	426.0

Single Sample Report

Sample Name: SHARLJA1-exp100-0026_11_30_2021_E11

Filename: sharlja1-exp100-0026_11_30_2021_e11.raw

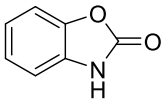

E11,
63% yield

Peak #	Formula	Target …	Target …	Time	Found	Area %	Area Abs
8	C23H28C…	493.1	Glyburi…	1.411	Yes	12.7	3265.51
13	C16H18B…	426.0	Product	2.071	Yes	29.0	7466.04

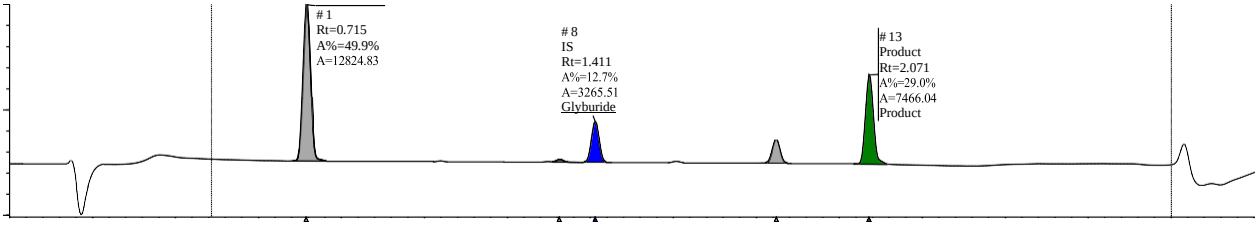

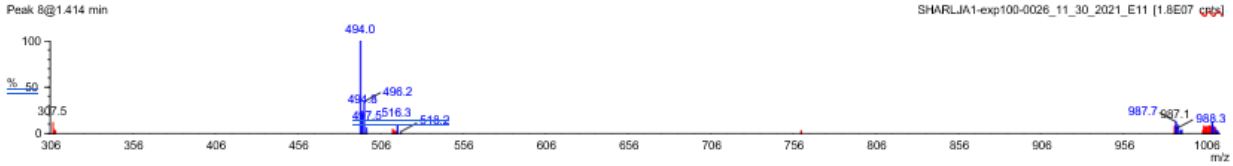

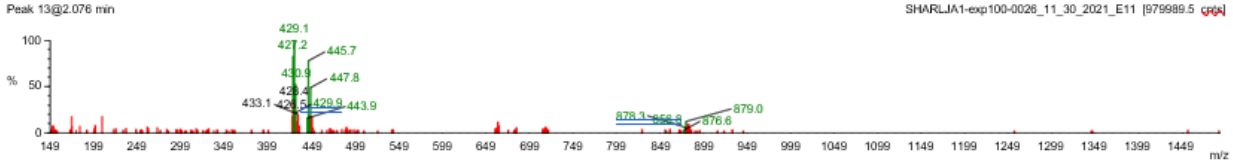

Name	Y/N	Type	Formula	Mass
Glyburide	Y	IS	C23H28ClN3O5S	493.1
Product	Y	Product	C16H18BrCl3O2	426.0

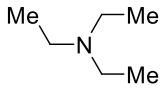

F7,
44% yield

Single Sample Report
Sample Name: SHARLJA1-exp100-0026_11_30_2021_F7
Filename: sharlja1-exp100-0026_11_30_2021_f7.raw
Submitter:

Peak #	Formula	Target …	Target …	Time	Found	Area %	Area Abs
8	C23H28C…	493.1	Glyburi…	1.411	Yes	27.5	3135.17
14	C16H18B…	426.0	Product	2.071	Yes	45.2	5144.09

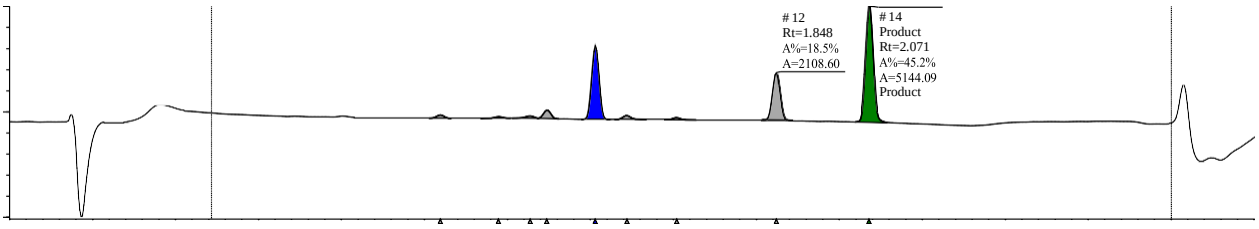

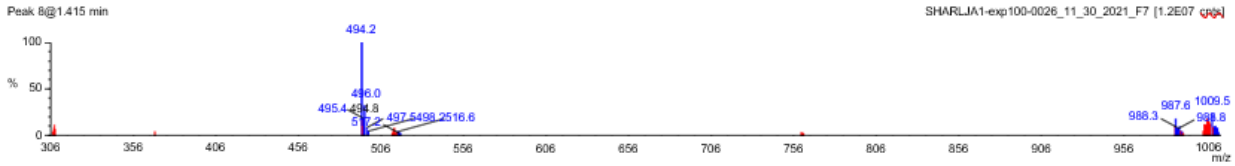

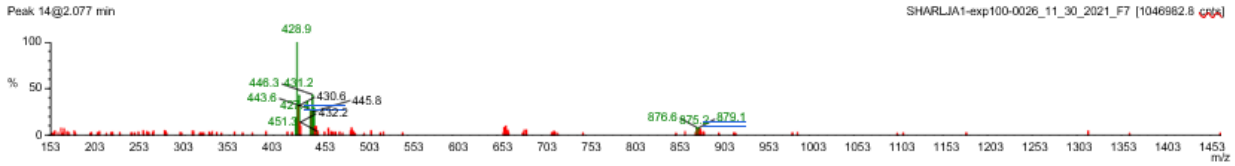

Name	Y/N	Type	Formula	Mass
Glyburide	Y	IS	C23H28ClN3O5S	493.1
Product	Y	Product	C16H18BrCl3O2	426.0

Single Sample Report
Sample Name: SHARLJA1-exp100-0026_11_30_2021_F9-re
Filename: sharlja1-exp100-0026_11_30_2021_f9-re.raw

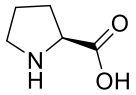

F9,
62% yield

Peak #	Formula	Target …	Target …	Time	Found	Area %	Area Abs
11	C23H28C…	493.1	Glyburi…	1.411	Yes	26.5	3258.88
17	C16H18B…	426.0	Product	2.071	Yes	60.0	7395.65

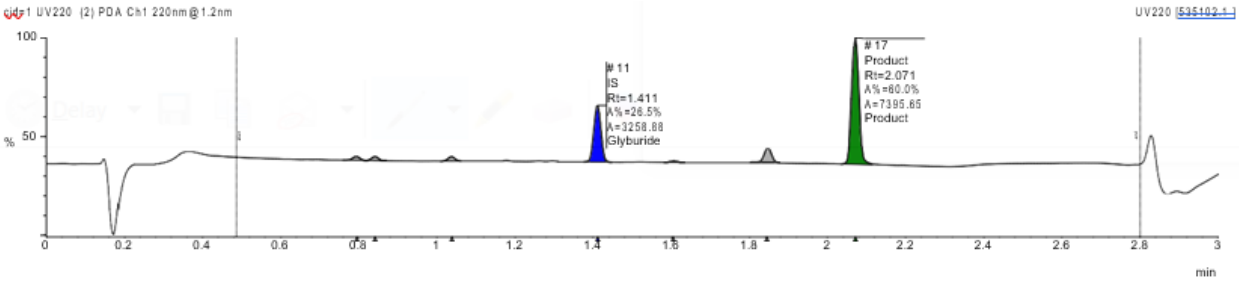

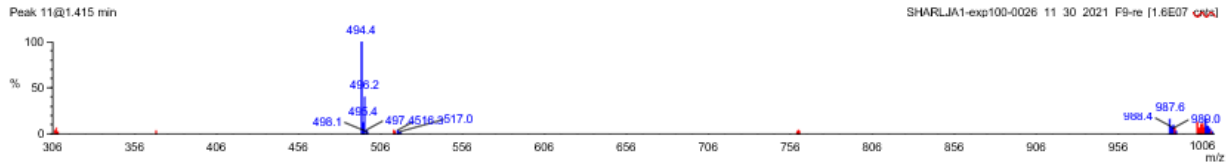

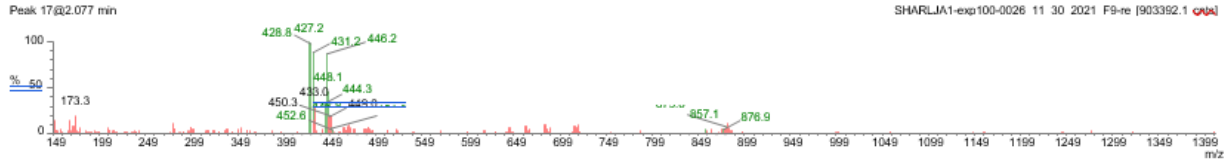

Name	Y/N	Type	Formula	Mass
Glyburide	Y	IS	C23H28ClN3O5S	493.1
Product	Y	Product	C16H18BrCl3O2	426.0

Single Sample Report
Sample Name: SHARLJA1-exp100-0026_11_30_2021_G3
Filename: sharlja1-exp100-0026_11_30_2021_g3.raw
Submitter:

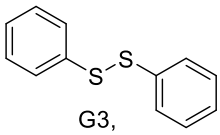

G3,
99% yield

Peak #	Formula	Target …	Target …	Time	Found	Area %	Area Abs
7	C23H28C…	493.1	Glyburi…	1.415	Yes	10.1	4258.00
17	C16H18B…	426.0	Product	2.075	Yes	35.8	15005.23

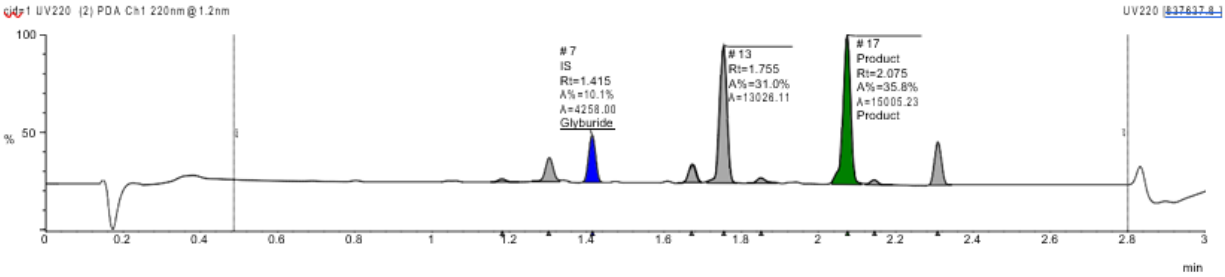

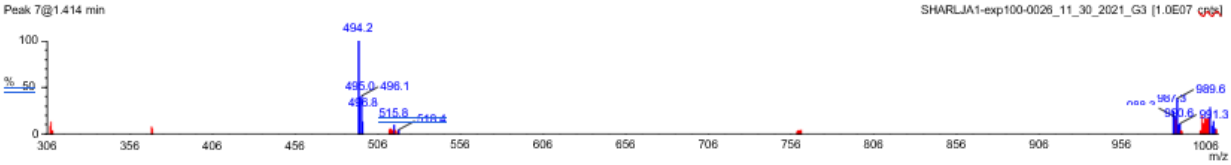

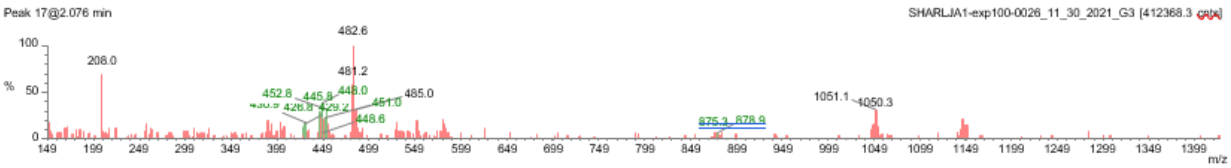

Name	Y/N	Type	Formula	Mass
Glyburide	Y	IS	C23H28ClN3O5S	493.1
Product	Y	Product	C16H18BrCl3O2	426.0

S=C=S

G4,
49% yield

Single Sample Report
Sample Name: SHARLJA1-exp100-0026_11_30_2021_G4
Filename: sharlja1-exp100-0026_11_30_2021_g4.raw
Submitter:

Peak #	Formula	Target …	Target …	Time	Found	Area %	Area Abs
6	C23H28C…	493.1	Glyburi…	1.411	Yes	25.1	3393.58
10	C16H18B…	426.0	Product	2.071	Yes	45.7	6175.07

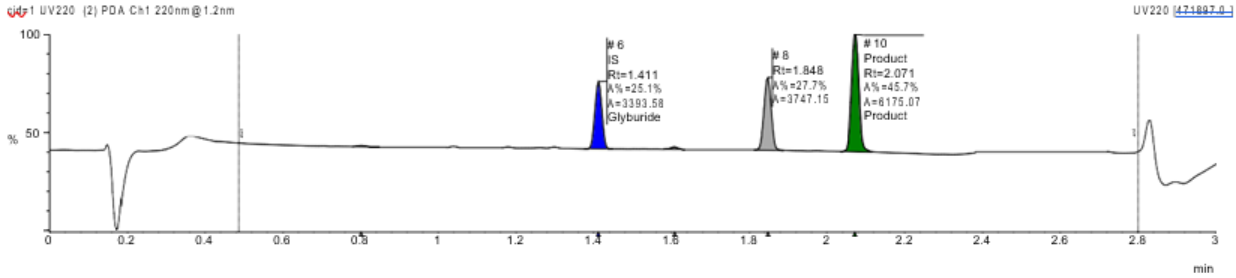

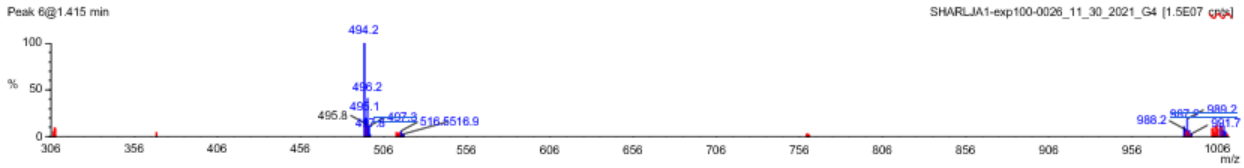

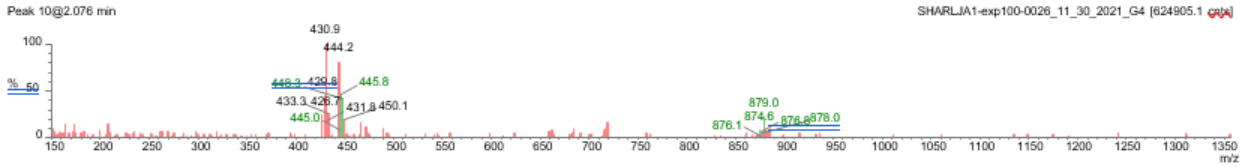

Name	Y/N	Type	Formula	Mass
Glyburide	Y	IS	C23H28ClN3O5S	493.1
Product	Y	Product	C16H18BrCl3O2	426.0

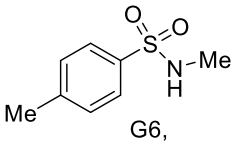

G6,
30% yield

Single Sample Report
Sample Name: SHARLJA1-exp100-0026_11_30_2021_G6
Filename: sharlja1-exp100-0026_11_30_2021_g6.raw
Submitter:

Peak #	Formula	Target …	Target …	Time	Found	Area %	Area Abs
11	C23H28C…	493.1	Glyburi…	1.411	Yes	16.7	2723.54
18	C16H18B…	426.0	Product	2.071	Yes	19.3	3138.12

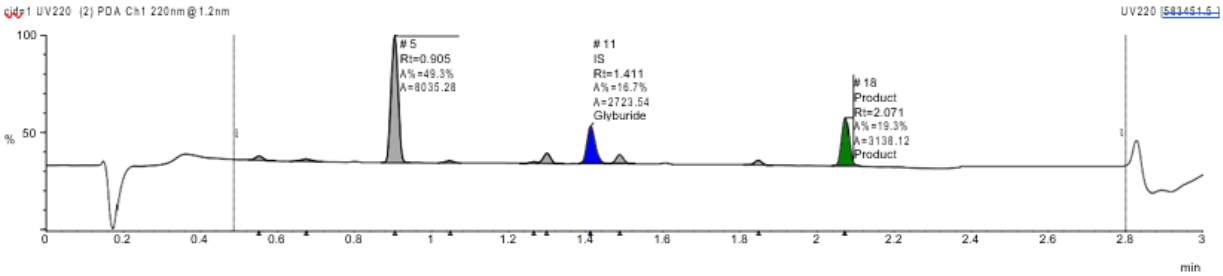

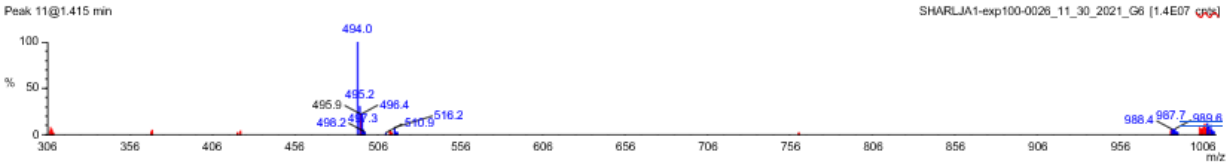

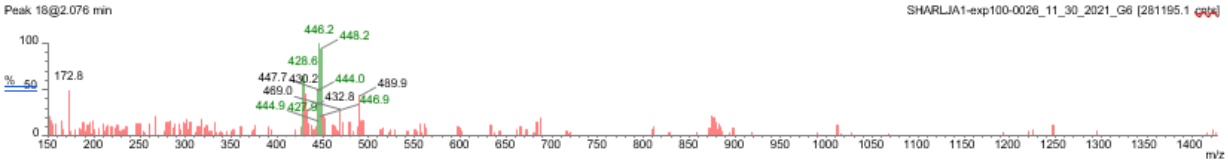

Name	Y/N	Type	Formula	Mass
Glyburide	Y	IS	C23H28ClN3O5S	493.1
Product	Y	Product	C16H18BrCl3O2	426.0

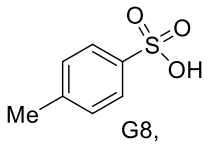

G8,
47% yield

Single Sample Report
Sample Name: SHARLJA1-exp100-0026_11_30_2021_G8-re
Filename: sharlja1-exp100-0026_11_30_2021_g8-re

Peak #	Formula	Target …	Target …	Time	Found	Area %	Area Abs
9	C23H28C…	493.1	Glyburi…	1.411	Yes	24.8	3423.89
17	C16H18B…	426.0	Product	2.071	Yes	43.5	6002.26

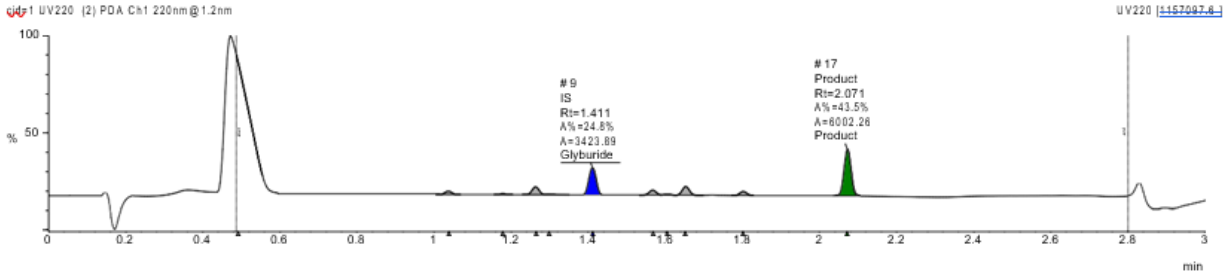

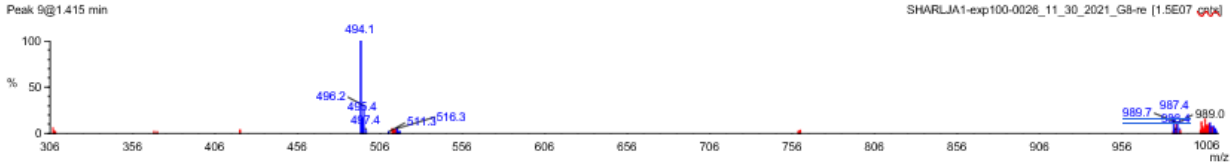

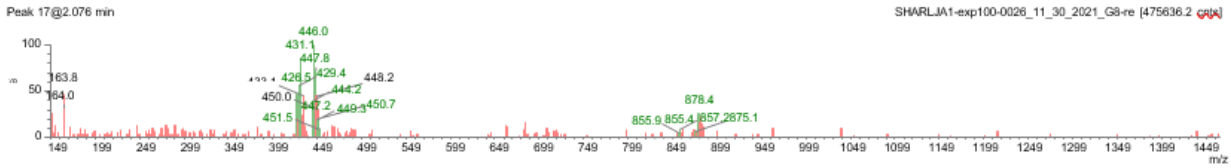

Name	Y/N	Type	Formula	Mass
Glyburide	Y	IS	C23H28ClN3O5S	493.1
Product	Y	Product	C16H18BrCl3O2	426.0

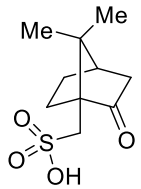

G9,
92% yield

Single Sample Report
Sample Name: SHARLJA1-exp100-0026_11_30_2021_G9-re
Filename: sharlja1-exp100-0026_11_30_2021_g9-re

Peak #	Formula	Target …	Target …	Time	Found	Area %	Area Abs
8	C23H28C…	493.1	Glyburi…	1.411	Yes	21.7	2992.39
13	C16H18B…	426.0	Product	2.071	Yes	70.6	9727.45

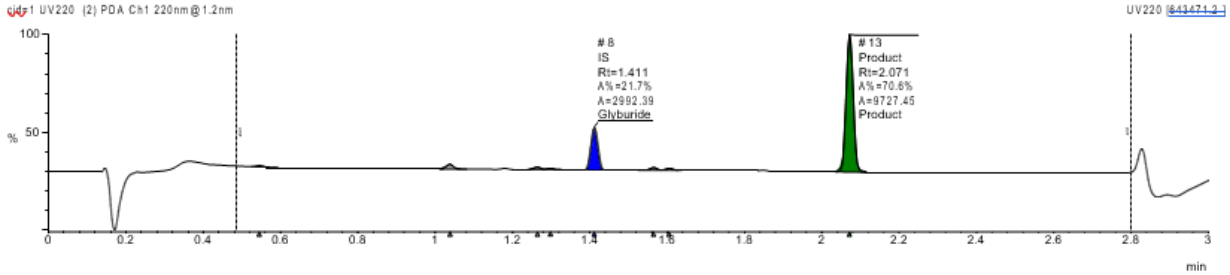

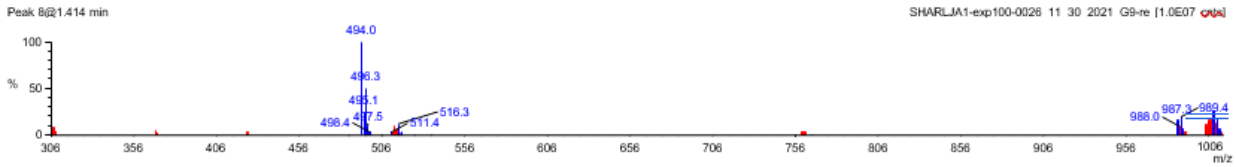

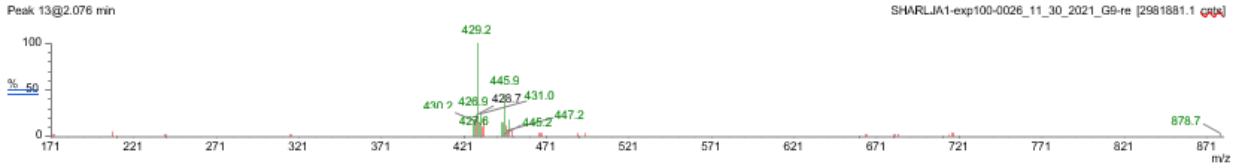

Name	Y/N	Type	Formula	Mass
Glyburide	Y	IS	C23H28ClN3O5S	493.1
Product	Y	Product	C16H18BrCl3O2	426.0

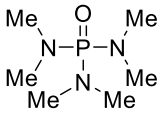

Sample Name: SHARLJA1-exp100-0026_11_30_2021_H1
Filename: sharlja1-exp100-0026_11_30_2021_h1.raw
Submitter:

Peak #	Formula	Target …	Target …	Time	Found	Area %	Area Abs
10	C23H28C…	493.1	Glyburi…	1.411	Yes	26.9	5627.03
16	C16H18B…	426.0	Product	2.071	Yes	46.6	9764.30

H1,
47% yield

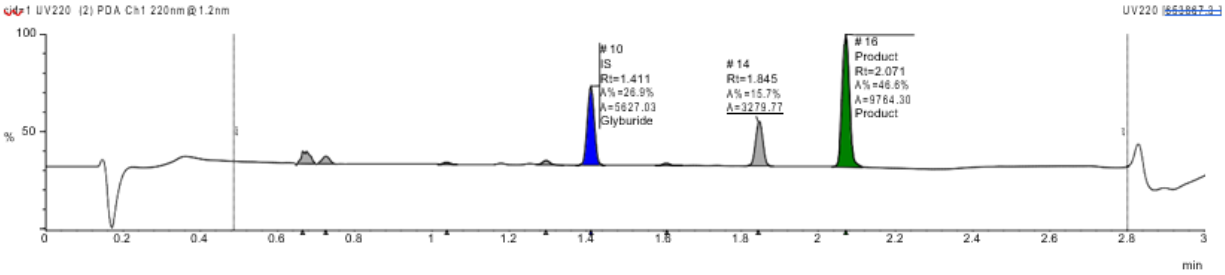

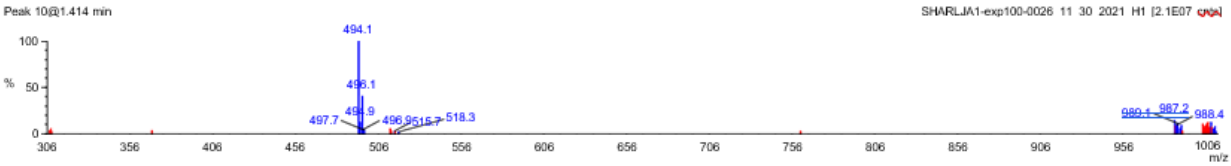

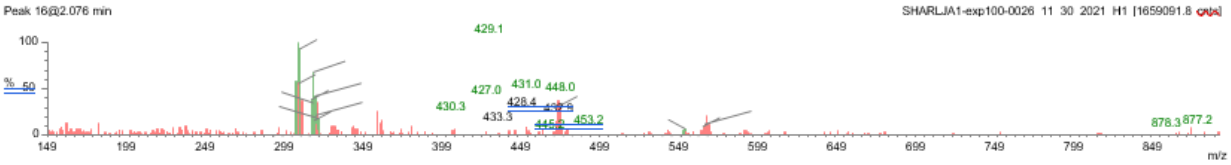

Name	Y/N	Type	Formula	Mass
Glyburide	Y	IS	C23H28ClN3O5S	493.1
Product	Y	Product	C16H18BrCl3O2	426.0

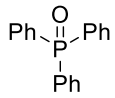

H3,
39% yield

Single Sample Report
Sample Name: SHARLJA1-exp100-0026_11_30_2021_H3
Filename: sharlja1-exp100-0026_11_30_2021_h3.raw
Submitter:

Peak #	Formula	Target …	Target …	Time	Found	Area %	Area Abs
7	C23H28C…	493.1	Glyburi…	1.411	Yes	9.6	2712.41
10	C16H18B…	426.0	Product	2.071	Yes	14.0	3962.81

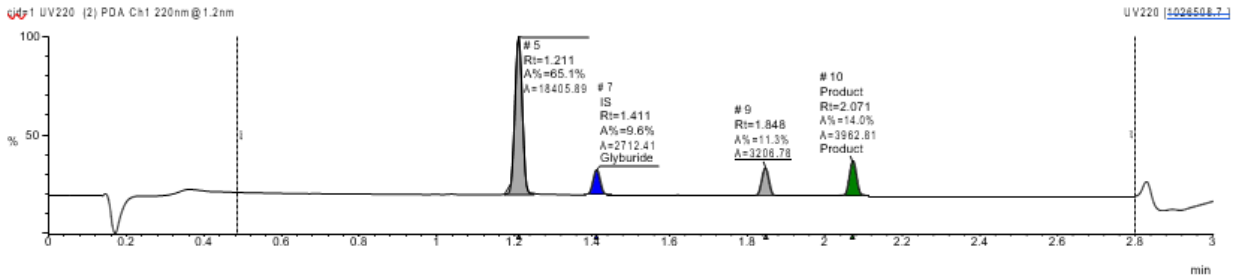

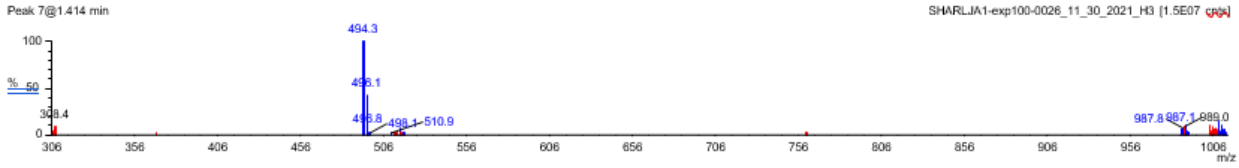

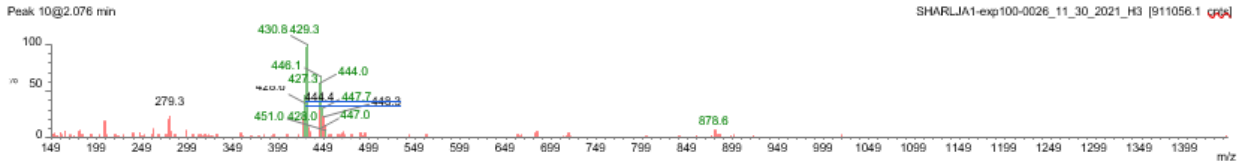

Name	Y/N	Type	Formula	Mass
Glyburide	Y	IS	C23H28ClN3O5S	493.1
Product	Y	Product	C16H18BrCl3O2	426.0

Single Sample Report

Sample Name: SHARLJA1-exp100-0026_11_30_2021_H6

Filename: sharlja1-exp100-0026_11_30_2021_h6.raw

Submitter:

Me−CN

H6,
58% yield

Peak #	Formula	Target …	Target …	Time	Found	Area %	Area Abs
8	C23H28C…	493.1	Glyburi…	1.411	Yes	28.3	5655.77
16	C16H18B…	426.0	Product	2.071	Yes	60.0	11987.56

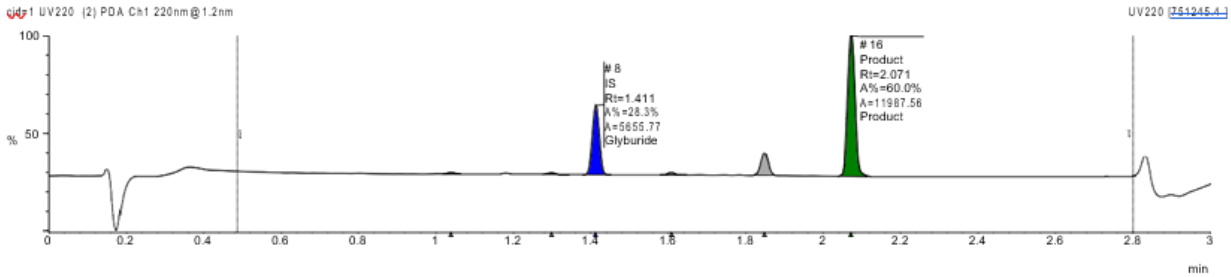

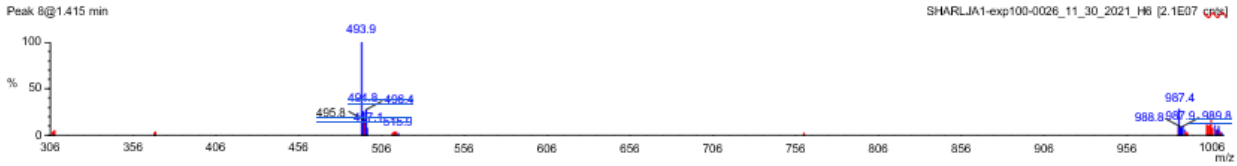

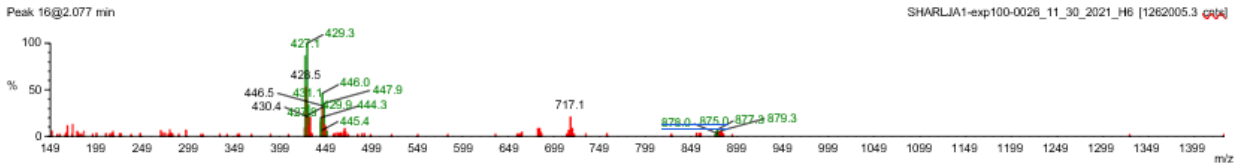

Name	Y/N	Type	Formula	Mass
Glyburide	Y	IS	C23H28ClN3O5S	493.1
Product	Y	Product	C16H18BrCl3O2	426.0

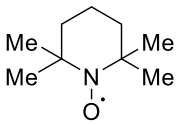

H10,
57% yield

Single Sample Report
Sample Name: SHARLJA1-exp100-0026_11_30_2021_H10
Filename: sharlja1-exp100-0026_11_30_2021_h10.raw
Submitter:

Peak #	Formula	Target …	Target …	Time	Found	Area %	Area Abs
8	C23H28C…	493.1	Glyburi…	1.408	Yes	27.4	3671.84
11	C16H18B…	426.0	Product	2.071	Yes	57.5	7702.63

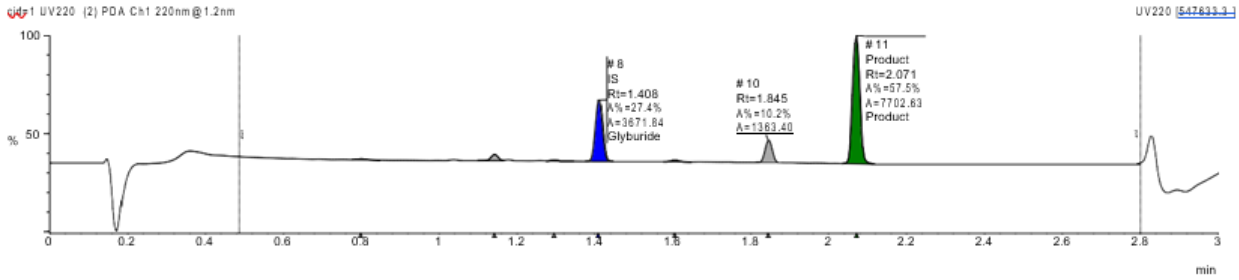

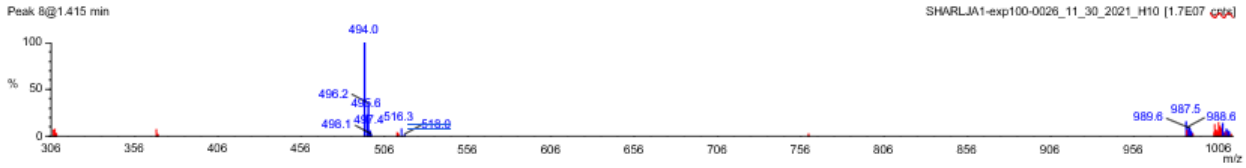

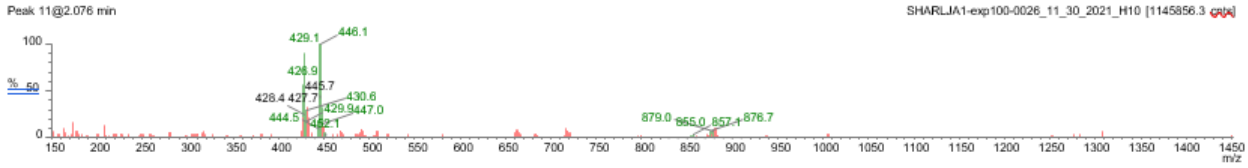

Name	Y/N	Type	Formula	Mass
Glyburide	Y	IS	C23H28ClN3O5S	493.1
Product	Y	Product	C16H18BrCl3O2	426.0

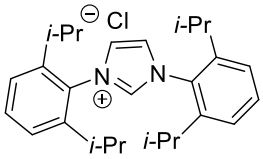

G12,
99% yield

Single Sample Report
Sample Name: SHARLJA1-exp100-0026_11_30_2021_H12-re
Filename: sharlja1-exp100-0026_11_30_2021_h12-re.raw

Peak #	Formula	Target …	Target …	Time	Found	Area %	Area Abs
8	C23H28C…	493.1	Glyburi…	1.411	Yes	5.3	2545.03
12	C16H18B…	426.0	Product	2.075	Yes	18.5	8933.13

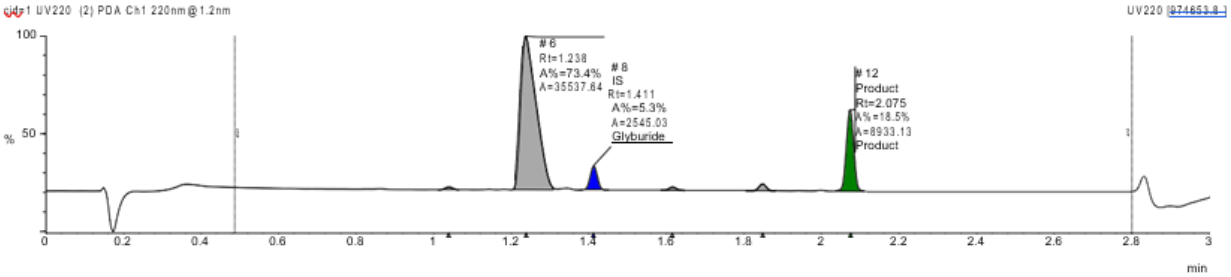

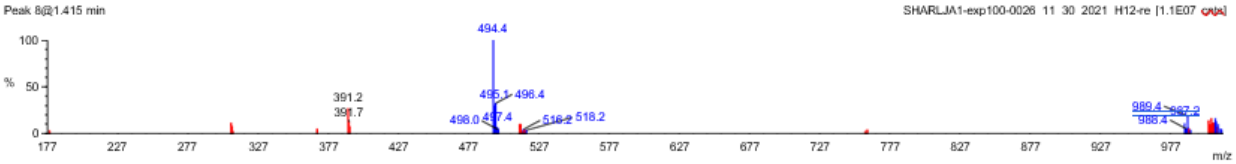

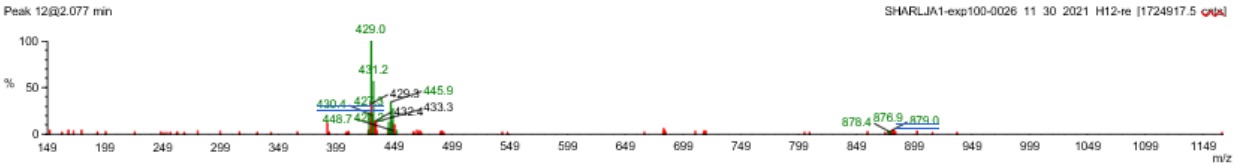

Name	Y/N	Type	Formula	Mass
Glyburide	Y	IS	C23H28ClN3O5S	493.1
Product	Y	Product	C16H18BrCl3O2	426.0

5.4: Enantioselectivity of additive screen with Rh_2(*S-tetra-p*-Br-PhPTTL)$_4$, 10 equiv HFIP, and $(CH_3O)_2CO$ as solvent:

The following dataset represents reactions that were successful when performed according to **general procedure 5.1** in the presence of 10 equiv HFIP using Rh_2(*S-tetra-p*-Br-PhPTTL)$_4$ as catalyst and dimethyl carbonate as solvent. Each additive is described according to the well plate designation in the study as well as the compound number it was assigned in the main text. The enantioselectivity of the reaction in the presence of each additive is reported in **Figure C**7 and what follows is the SFC data from which the asymmetric induction was determined.

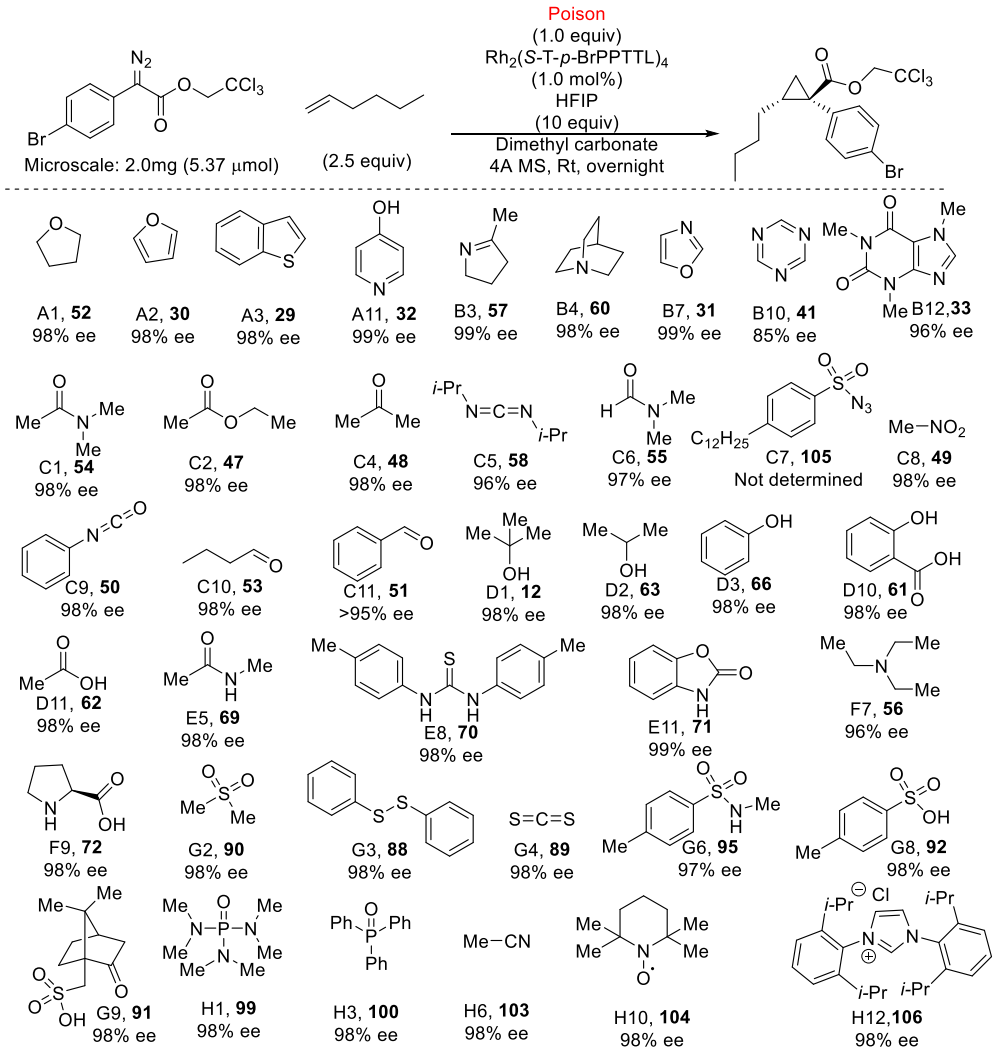

Figure C7: Successful additives using Rh_2(*S-tetra-p*-BrPhPTTL)$_4$ as catalyst (1.0 mol%), 10 equivalents of HFIP, and dimethyl carbonate as solvent on microscale. The observed %ee for each compound is reported and what follows are the SFC traces.

Racemate:

Openlynx Report - DUSTADA1 Page 1

Sample: 135 Vial:2:1 ID:Racemate
File:DUSTADA1_20211008_139 Date:20-Oct-2021 Time:10:47:55
Description:(S,S)WO1 4.6x100mm 5µ Conditions:5% IPA over 5min 3mL/min

Printed: Thu Dec 16 11:33:15 2021

Sample Report:

Sample 135 Vial 2:1 ID Racemate File DUSTADA1_20211008_139 Date 20-Oct-2021 Time 10:47:55 Description (S,S)WO1 4.6x100mm 5µ

2: UV Detector: 230 Nm 2.0000-2.3500: Smooth (Mn, 2x3), 3.1000-3.5500: Smooth (Mn, 2x3) 9.103e-2
Range: 1.048e-1

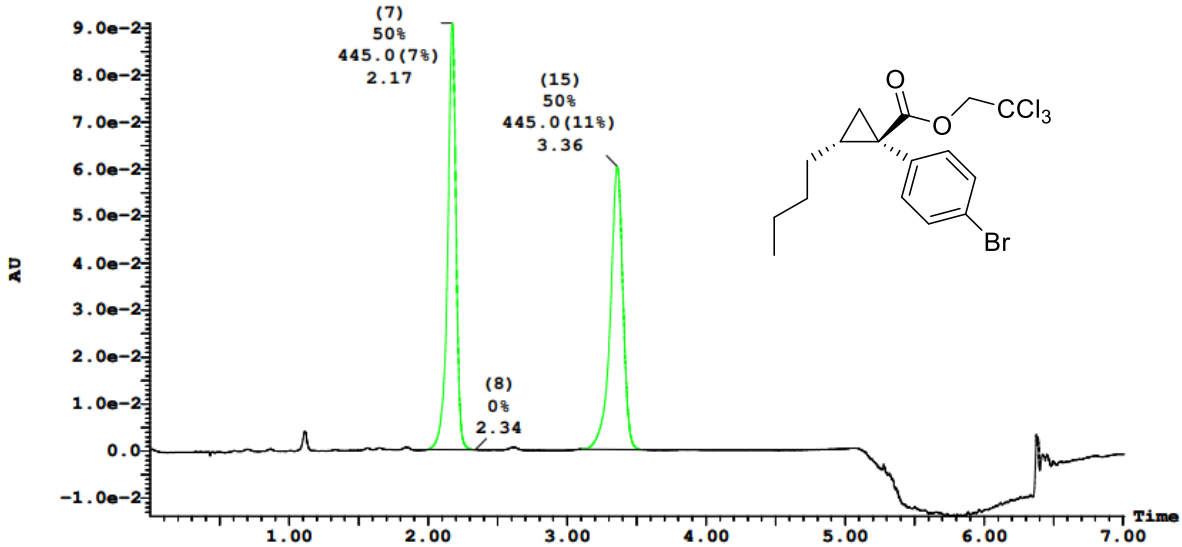

Peak Number	Compound	Time	AreaAbs	Area %Total	Width	Height	Mass Found
7	Found	2.17	6e+003	49.93	0	9e+004	445.0000
8		2.34	2e-001	0.00	0	3e+001	Not Found
15	Found	3.36	6e+003	50.07	0	6e+004	445.0000

A1: 98% ee

Openlynx Report - SHARLJA1

Sample: 1
File:SHARLJA1_20211119_CAROL_1
Description:(S,S)WO1 4.6x100mm 5µ

Vial:1:1
Date:19-Nov-2021
Conditions:5% IPA over 5min 3mL/min

ID:26-A1
Time:17:14:31

A1,
98% ee

Printed: Thu Dec 09 16:26:30 2021

Sample Report:

Sample 1 Vial 1:1 ID 26-A1 File SHARLJA1_20211119_CAROL_1 Date 19-Nov-2021 Time 17:14:31 Description (S,S)WO1 4.6x100mm 5µ

2: UV Detector: 230 Nm 2.0000-2.3500: Smooth (Mn, 2x3), 3.1000-3.5500: Smooth (Mn, 2x3) 7.373e-1
Range: 7.497e-1

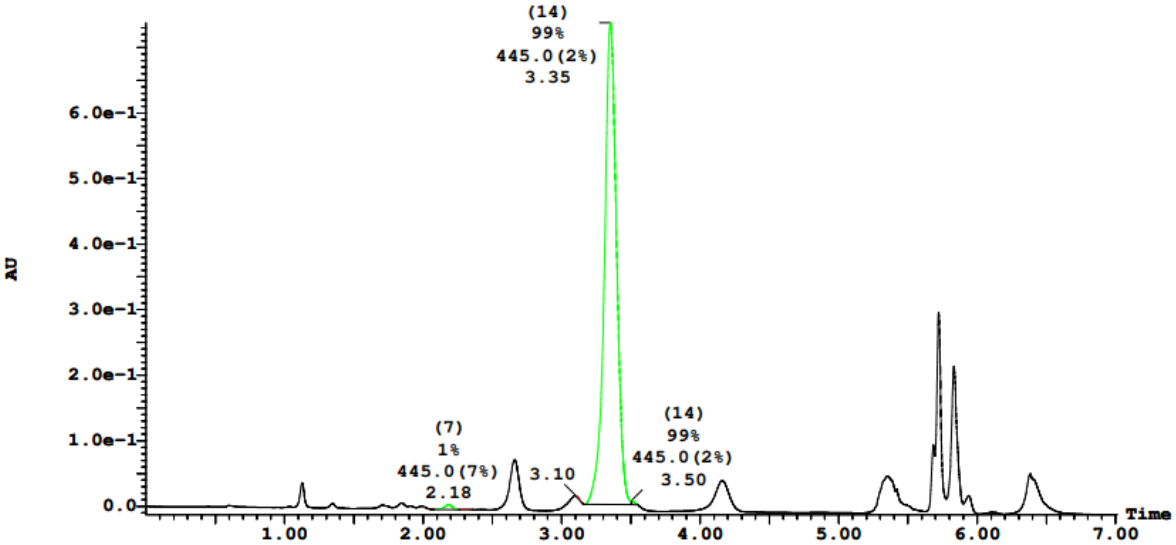

Peak Number	Compound	Time	AreaAbs	Area %Total	Width	Height	Mass Found
6		2.00	1e+000	0.00	0		Not Found
7	Found	2.18	5e+002	0.64	0	8e+003	445.0000
8		2.30	2e+001	0.03	0	5e+002	Not Found
8		2.33	2e+000	0.00	0	1e+002	Not Found
11		3.10	4e+001	0.06	0	2e-002	Not Found
14	Tentative	3.35	7e+004	99.07	0	7e+005	445.0000
16	Tentative	3.50	1e+002	0.19	0	5e+003	445.0000

A2: 98% ee

Openlynx Report - SHARLJA1

Sample: 2
File:SHARLJA1_20211119_CAROL_2
Description:(S,S)WO1 4.6x100mm 5µ

Vial:1:2
Date:19-Nov-2021
Conditions:5% IPA over 5min 3mL/min

ID:26-A2
Time:17:23:12

A2,
98% ee

Printed: Thu Dec 09 16:26:30 2021

Sample Report (continued):

Sample 2 Vial 1:2 ID 26-A2 File SHARLJA1_20211119_CAROL_2 Date 19-Nov-2021 Time 17:23:12 Description (S,S)WO1 4.6x100mm 5µ

2: UV Detector: 230 Nm 2.0000-2.3500: Smooth (Mn, 2x3), 3.1000-3.5500: Smooth (Mn, 2x3) 8.059e-1
Range: 8.113e-1

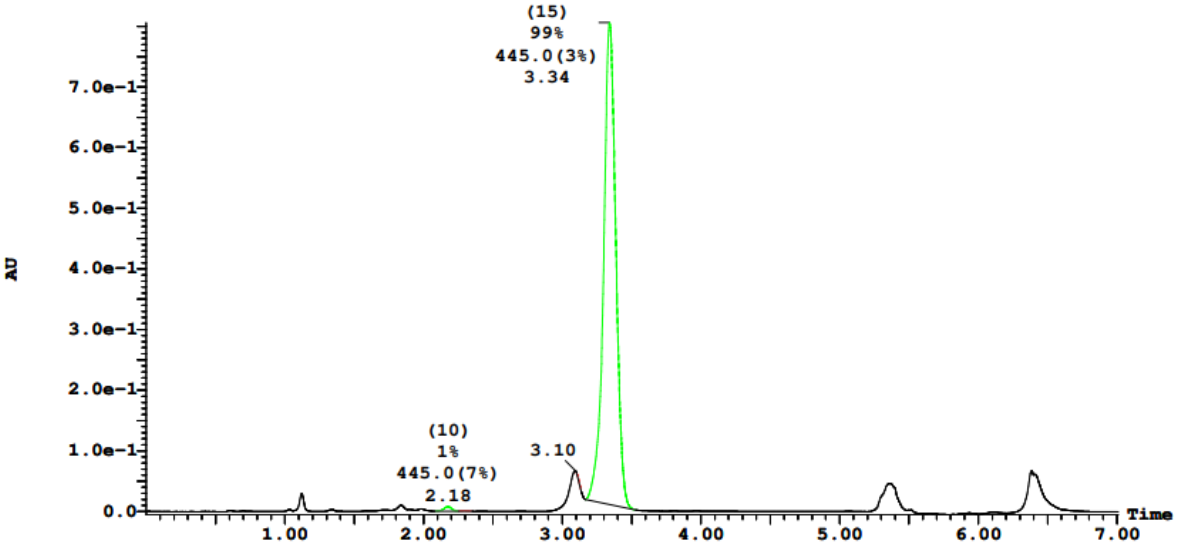

Peak Number	Compound	Time	AreaAbs	Area %Total	Width	Height	Mass Found
10	Found	2.18	5e+002	0.60	0	8e+003	445.0000
11		2.29	4e+001	0.05	0	7e+002	Not Found
13		3.10	6e+001	0.07	0	1e-001	Not Found
15	Tentative	3.34	8e+004	99.28	0	8e+005	445.0000

A3: 98% ee

Openlynx Report - SHARLJA1

Sample: 3
File:SHARLJA1_20211119_CAROL_3
Description:(S,S)WO1 4.6x100mm 5µ

Vial:1:3
Date:19-Nov-2021
Conditions:5% IPA over 5min 3mL/min

ID:26-A3
Time:17:31:19

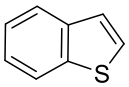

A3,
98% ee

Page 5

Printed: Thu Dec 09 16:26:30 2021

Sample Report (continued):

Sample 3 Vial 1:3 ID 26-A3 File SHARLJA1_20211119_CAROL_3 Date 19-Nov-2021 Time 17:31:19 Description (S,S)WO1 4.6x100mm 5µ

2: UV Detector: 230 Nm 2.0000-2.3500: Smooth (Mn, 2x3), 3.1000-3.5500: Smooth (Mn, 2x3) 1.661
Range: 1.662

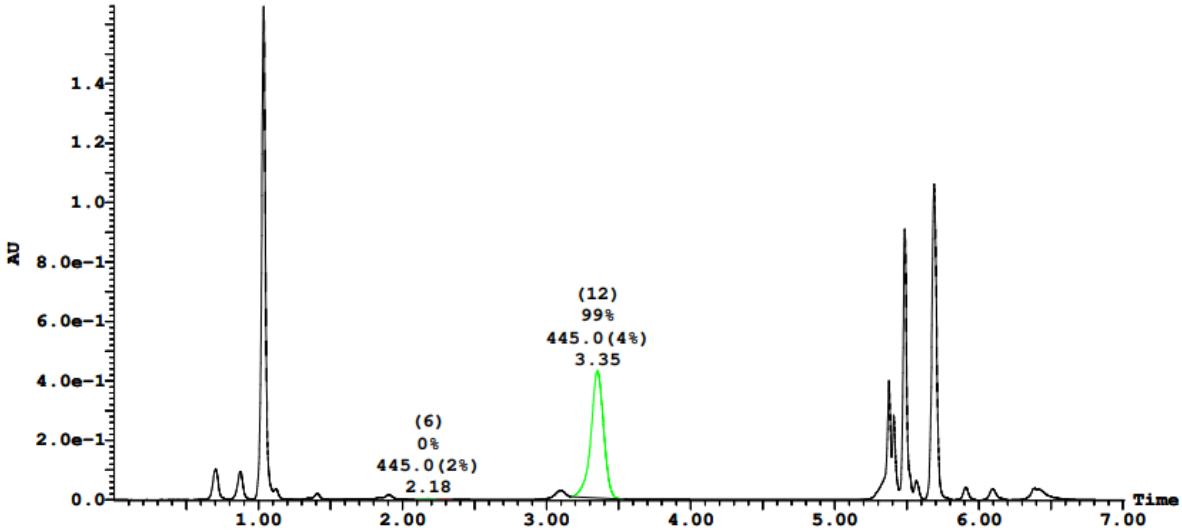

Peak Number	Compound	Time	AreaAbs	Area %Total	Width	Height	Mass Found
6	Tentative	2.18	2e+002	0.45	0	3e+003	445.0000
7		2.30	7e+001	0.15	0	1e+003	Not Found
12	Tentative	3.35	4e+004	99.39	0	4e+005	445.0000

A11: 99% ee

Openlynx Report - SHARLJA1

Sample: 6
File:SHARLJA1_20211119_CAROL_6
Description:(S,S)WO1 4.6x100mm 5µ

Vial:1:6
Date:19-Nov-2021
Conditions:5% IPA over 5min 3mL/min

ID:26-A11
Time:17:55:42

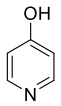

A11,
99% ee

Printed: Thu Dec 09 16:26:30 2021

Sample Report (continued):

Sample 6 Vial 1:6 ID 26-A11 File SHARLJA1_20211119_CAROL_6 Date 19-Nov-2021 Time 17:55:42 Description (S,S)WO1 4.6x100mm 5µ

2: UV Detector: 230 Nm 2.0000-2.3500: Smooth (Mn, 2x3), 3.1000-3.5500: Smooth (Mn, 2x3) 4.505e-1
Range: 4.54e-1

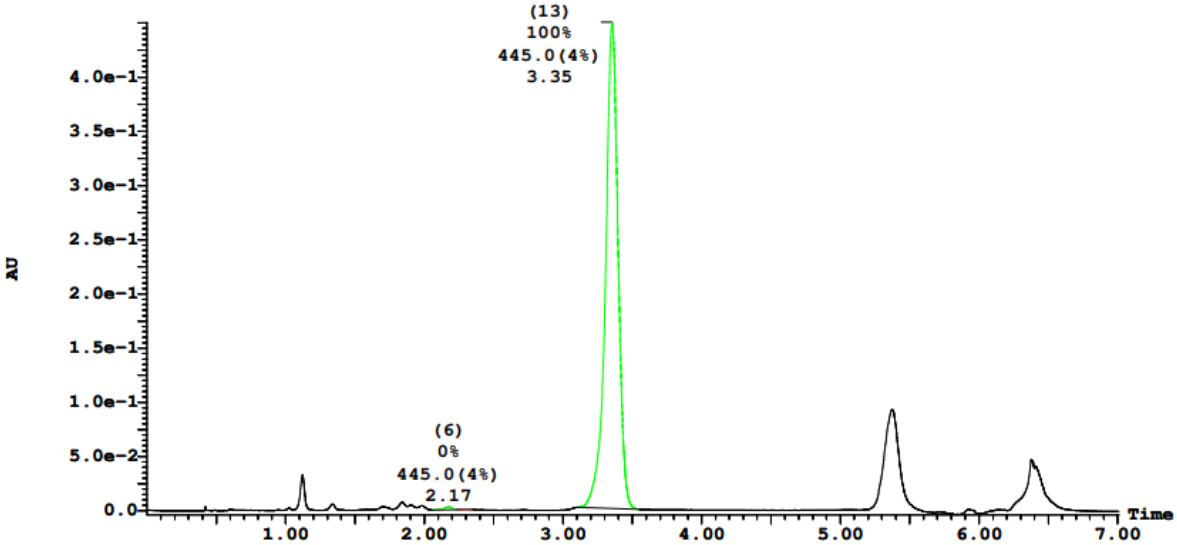

Peak Number	Compound	Time	AreaAbs	Area %Total	Width	Height	Mass Found
6	Tentative	2.17	2e+002	0.39	0	3e+003	445.0000
7		2.30	5e+001	0.10	0	7e+002	Not Found
13	Tentative	3.35	5e+004	99.51	0	4e+005	445.0000

B3: 99% ee

Openlynx Report - SHARLJA1

Sample: 7
File:SHARLJA1_20211119_CAROL_7
Description:(S,S)WO1 4.6x100mm 5µ

Vial:1:7
Date:19-Nov-2021
Conditions:5% IPA over 5min 3mL/min

ID:26-B3
Time:18:03:49

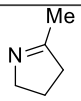

B3,
99% ee

Printed: Thu Dec 09 16:26:30 2021

Sample Report (continued):

Sample 7 Vial 1:7 ID 26-B3 File SHARLJA1_20211119_CAROL_7 Date 19-Nov-2021 Time 18:03:49 Description (S,S)WO1 4.6x100mm

2: UV Detector: 230 Nm 2.0000-2.3500: Smooth (Mn, 2x3), 3.1000-3.5500: Smooth (Mn, 2x3) 5.153e-1
Range: 5.156e-1

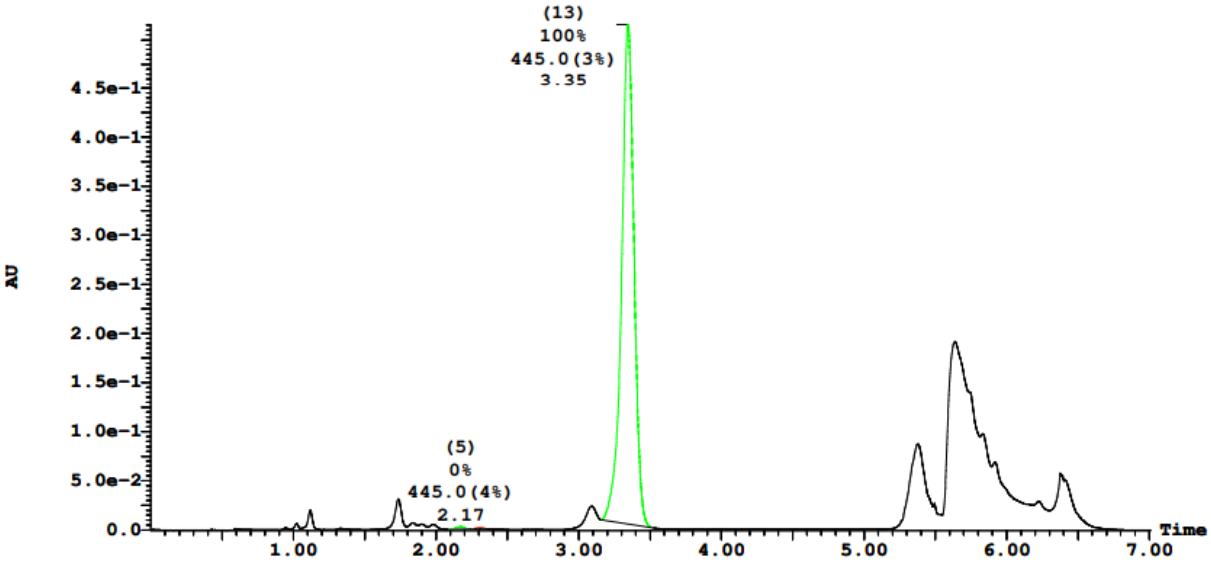

Peak Number	Compound	Time	AreaAbs	Area %Total	Width	Height	Mass Found
5	Tentative	2.17	2e+002	0.32	0	3e+003	445.0000
6		2.28	7e+000	0.01	0	4e+002	Not Found
7		2.31	2e+001	0.03	0	6e+002	Not Found
8		2.31	2e+001	0.03	0	6e+002	Not Found
13	Tentative	3.35	5e+004	99.60	0	5e+005	445.0000

B4: 98% ee

Openlynx Report - SHARLJA1

Page 15

Sample: 8
File:SHARLJA1_20211119_CAROL_8
Description:(S,S)WO1 4.6x100mm 5µ

Vial:1:8
Date:19-Nov-2021
Conditions:5% IPA over 5min 3mL/min

ID:26-B4
Time:18:11:57

B4,
98% ee

Printed: Thu Dec 09 16:26:30 2021

Sample Report (continued):

Sample 8 Vial 1:8 ID 26-B4 File SHARLJA1_20211119_CAROL_8 Date 19-Nov-2021 Time 18:11:57 Description (S,S)WO1 4.6x100mm

2: UV Detector: 230 Nm 2.0000-2.3500: Smooth (Mn, 2x3), 3.1000-3.5500: Smooth (Mn, 2x3) 4.554e-1
Range: 4.555e-1

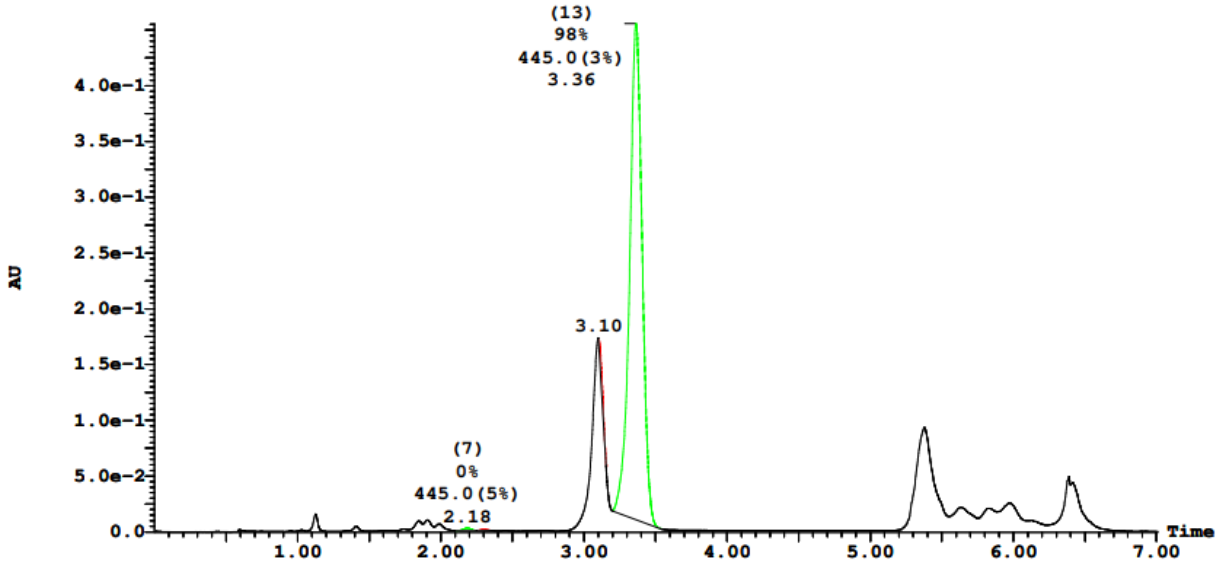

Peak Number	Compound	Time	AreaAbs	Area %Total	Width	Height	Mass Found
7	Found	2.18	1e+002	0.31	0	2e+003	445.0000
8		2.30	4e+001	0.10	0	8e+002	Not Found
11		3.10	6e+002	1.21	0	2e+003	Not Found
13	Tentative	3.36	5e+004	98.38	0	4e+005	445.0000

B7: 99% ee

Openlynx Report - SHARLJA1

Sample: 10
File:SHARLJA1_20211119_CAROL_10
Description:(S,S)WO1 4.6x100mm 5µ

Vial:1:10
Date:19-Nov-2021
Conditions:5% IPA over 5min 3mL/min

ID:26-B7
Time:18:28:13

B7,
99% ee

Printed: Thu Dec 09 16:26:30 2021

Sample Report (continued):

Sample 10 Vial 1:10 ID 26-B7 File SHARLJA1_20211119_CAROL_10 Date 19-Nov-2021 Time 18:28:13 Description (S,S)WO1 4.6x100mm

2: UV Detector: 230 Nm 2.0000-2.3500: Smooth (Mn, 2x3), 3.1000-3.5500: Smooth (Mn, 2x3) 6.957e-1
Range: 6.96e-1

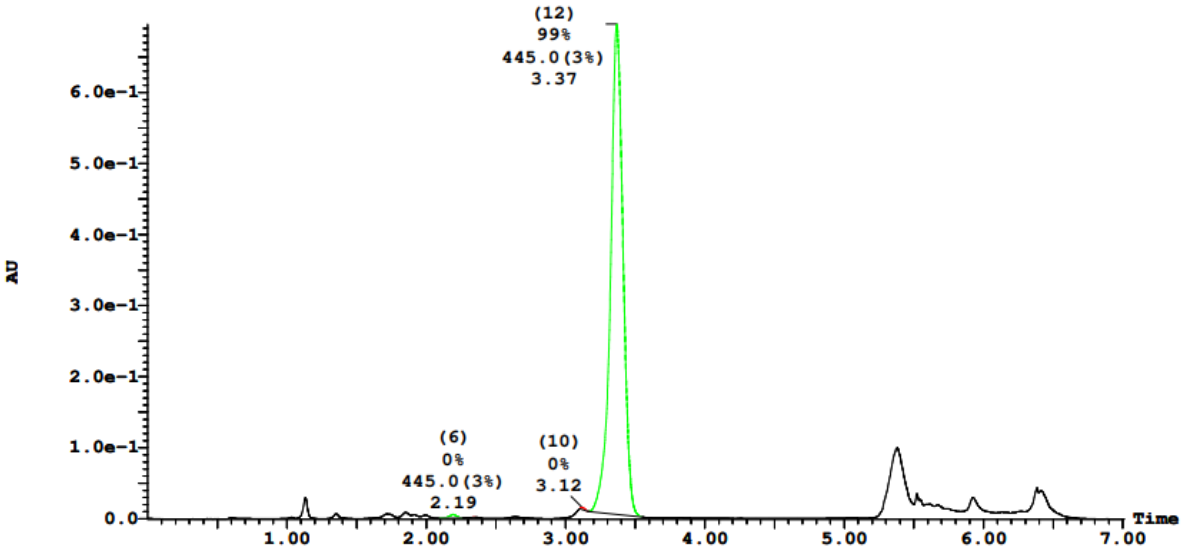

Peak Number	Compound	Time	AreaAbs	Area %Total	Width	Height	Mass Found
6	Found	2.19	3e+002	0.43	0	5e+003	445.0000
7		2.35	1e+000	0.00	0		Not Found
10		3.12	9e+001	0.13	0	3e+003	Not Found
12	Tentative	3.37	7e+004	99.44	0	7e+005	445.0000

B10: 85% ee

Openlynx Report - SHARLJA1

Sample: 11
File:SHARLJA1_20211119_CAROL_11
Description:(S,S)WO1 4.6x100mm 5µ

Vial:1:11
Date:19-Nov-2021
Conditions:5% IPA over 5min 3mL/min

ID:26-B10
Time:18:36:21

B10,
85% ee

Printed: Thu Dec 09 16:26:30 2021

Sample Report (continued):

Sample 11 Vial 1:11 ID 26-B10 File SHARLJA1_20211119_CAROL_11 Date 19-Nov-2021 Time 18:36:21 Description (S,S)WO1 4.6x100

2: UV Detector: 230 Nm 2.0000-2.3500: Smooth (Mn, 2x3), 3.1000-3.5500: Smooth (Mn, 2x3) 3.778e-1
Range: 3.783e-1

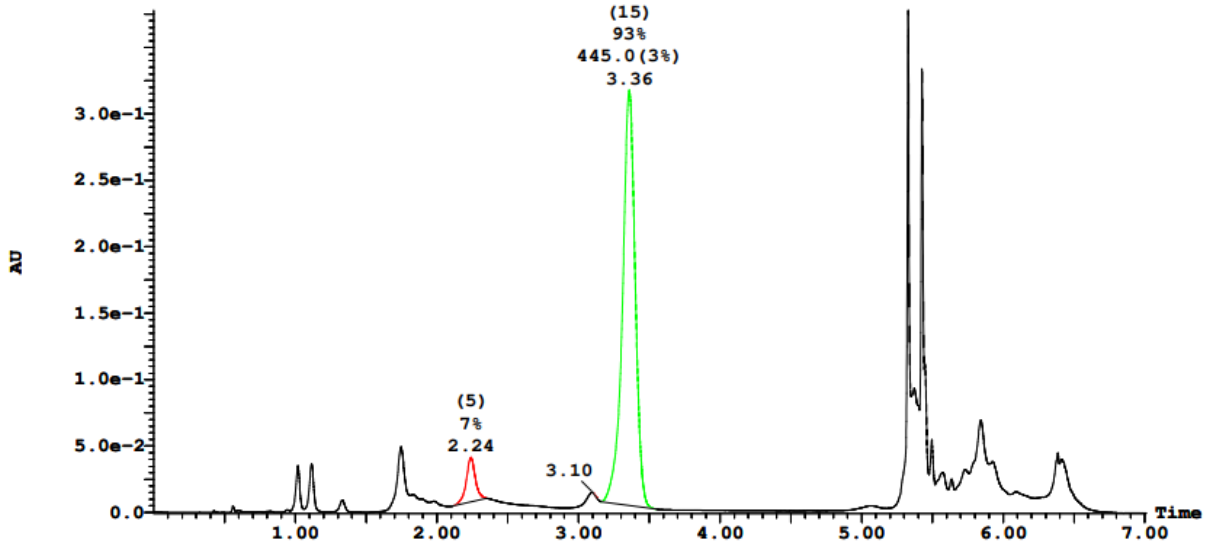

Peak Number	Compound	Time	AreaAbs	Area %Total	Width	Height	Mass Found
5		2.24	3e+003	7.13	0	3e+004	Not Found
12		3.10	1e+001	0.04	0		Not Found
15	Tentative	3.36	3e+004	92.83	0	3e+005	445.0000

B12: 96% ee

Openlynx Report - DUSTADA1

Sample: 208
File:DUSTADA1-12_20_2021_005
Description:(S,S)WO1 4.6x100mm 5µ

Printed: Mon Dec 20 15:37:27 2021

Vial:2:3
Date:20-Dec-2021
Conditions:5% IPA over 5min 3mL/min

ID:EXP026 B12
Time:12:14:51

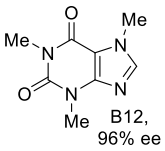

Sample Report (continued):

Sample 208 Vial 2:3 ID EXP026 B12 File DUSTADA1-12_20_2021_005 Date 20-Dec-2021 Time 12:14:51 Description (S,S)WO1 4.6x1

2: UV Detector: 230 Nm 2.0000-2.3500: Smooth (Mn, 2x3), 3.1000-3.5500: Smooth (Mn, 2x3) 8.826e-1
Range: 8.838e-1

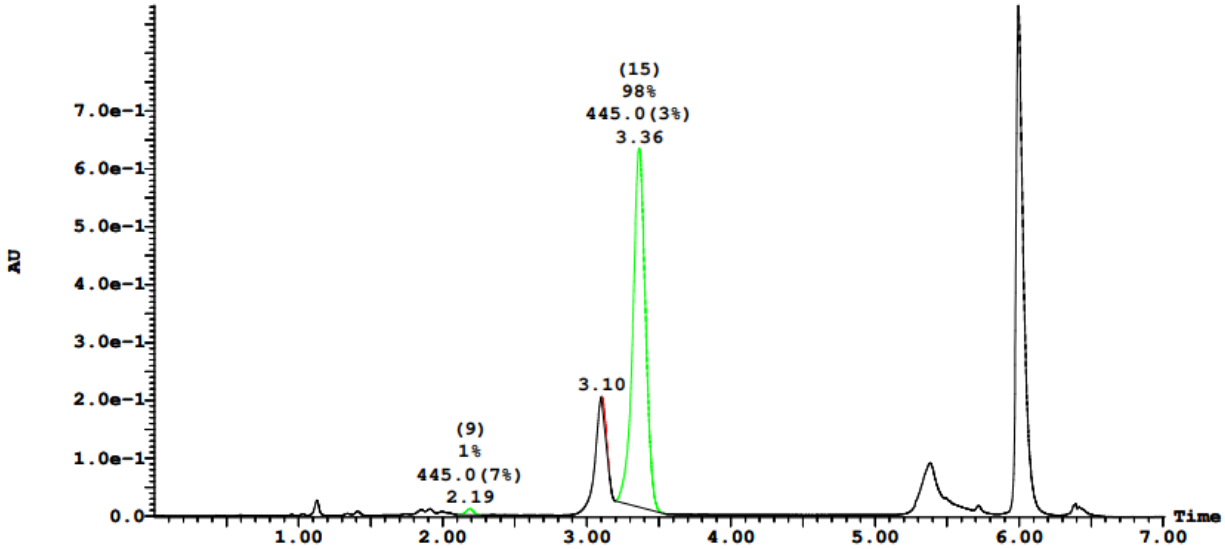

Peak Number	Compound	Time	AreaAbs	Area %Total	Width	Height	Mass Found
9	Found	2.19	7e+002	1.03	0	1e+004	445.0000
12		3.10	8e+002	1.27	0	9e+003	Not Found
15	Tentative	3.36	6e+004	97.70	0	6e+005	445.0000

C1: 98% ee

Openlynx Report - SHARLJA1

Sample: 12
File:SHARLJA1_20211119_CAROL_12
Description:(S,S)WO1 4.6x100mm 5µ

Vial:1:12
Date:19-Nov-2021
Conditions:5% IPA over 5min 3mL/min

ID:26-C1
Time:18:44:28

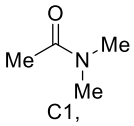

C1,
98% ee

Printed: Thu Dec 09 16:26:30 2021

Sample Report (continued):

Sample 12 Vial 1:12 ID 26-C1 File SHARLJA1_20211119_CAROL_12 Date 19-Nov-2021 Time 18:44:28 Description (S,S)WO1 4.6x100mm

2: UV Detector: 230 Nm 2.0000-2.3500: Smooth (Mn, 2x3), 3.1000-3.5500: Smooth (Mn, 2x3) 7.149e-1
Range: 7.155e-1

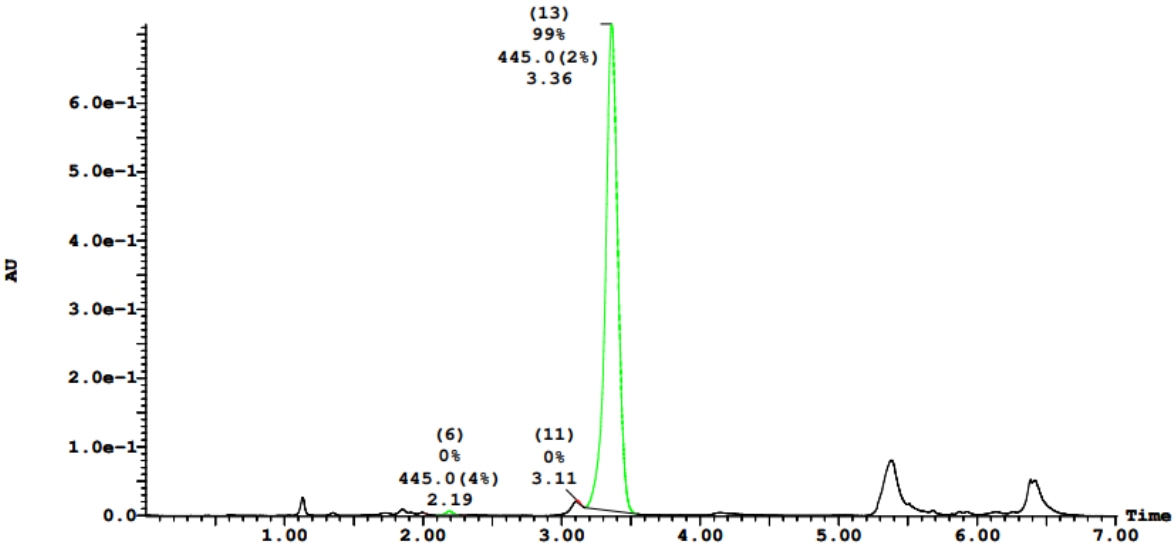

Peak Number	Compound	Time	AreaAbs	Area %Total	Width	Height	Mass Found
5		2.00	3e+000	0.00	0		Not Found
6	Found	2.19	4e+002	0.48	0	6e+003	445.0000
7		2.32	1e+001	0.02	0	3e+002	Not Found
8		2.33	4e+000	0.01	0	3e+002	Not Found
11		3.11	1e+002	0.13	0	2e+003	Not Found
13	Tentative	3.36	7e+004	99.36	0	7e+005	445.0000

C2: 98% ee

Openlynx Report - SHARLJA1

Sample: 13
File:SHARLJA1_20211119_CAROL_13
Description:(S,S)WO1 4.6x100mm 5µ

Vial:1:13
Date:19-Nov-2021
Conditions:5% IPA over 5min 3mL/min

ID:26-C2
Time:18:52:36

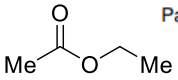

C2,
98% ee

Printed: Thu Dec 09 16:26:30 2021

Sample Report (continued):

Sample 13 Vial 1:13 ID 26-C2 File SHARLJA1_20211119_CAROL_13 Date 19-Nov-2021 Time 18:52:36 Description (S,S)WO1 4.6x100mm

2: UV Detector: 230 Nm 2.0000-2.3500: Smooth (Mn, 2x3), 3.1000-3.5500: Smooth (Mn, 2x3) 7.453e-1
Range: 7.482e-1

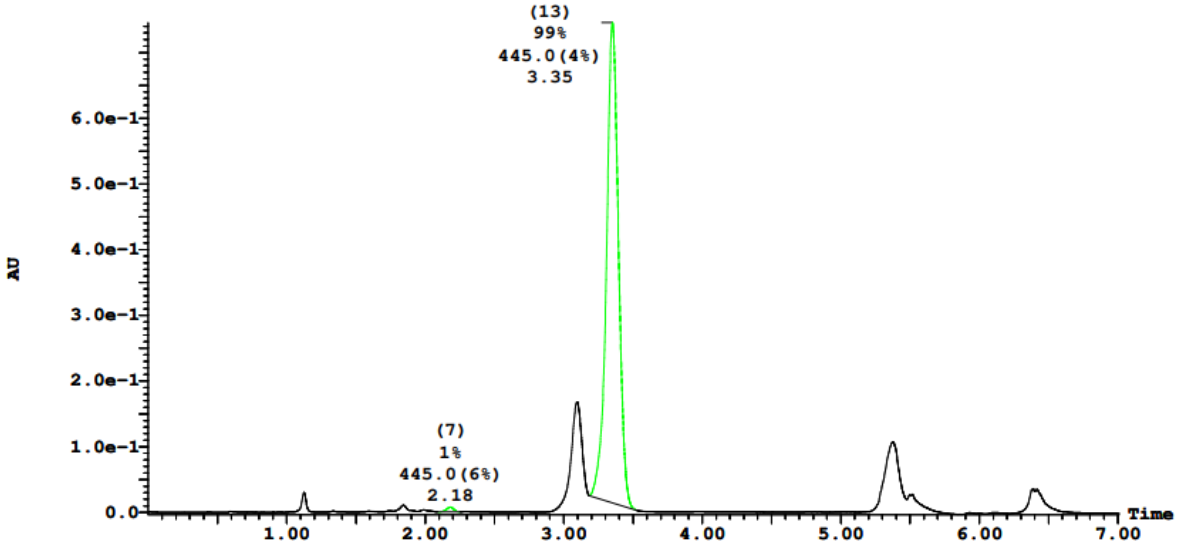

Peak Number	Compound	Time	AreaAbs	Area %Total	Width	Height	Mass Found
7	Found	2.18	4e+002	0.58	0	7e+003	445.0000
13	Tentative	3.35	7e+004	99.42	0	7e+005	445.0000

C4: 98% ee

Openlynx Report - SHARLJA1

Sample: 15
File:SHARLJA1_20211119_CAROL_15
Description:(S,S)WO1 4.6x100mm 5µ

Vial:1:15
Date:19-Nov-2021
Conditions:5% IPA over 5min 3mL/min

ID:26-C4
Time:19:08:53

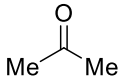

C4,
98% ee

Printed: Thu Dec 09 16:26:30 2021

Sample Report (continued):

Sample 15 Vial 1:15 ID 26-C4 File SHARLJA1_20211119_CAROL_15 Date 19-Nov-2021 Time 19:08:53 Description (S,S)WO1 4.6x10

2: UV Detector: 230 Nm 2.0000-2.3500: Smooth (Mn, 2x3), 3.1000-3.5500: Smooth (Mn, 2x3) 7.438e-1
Range: 7.5e-1

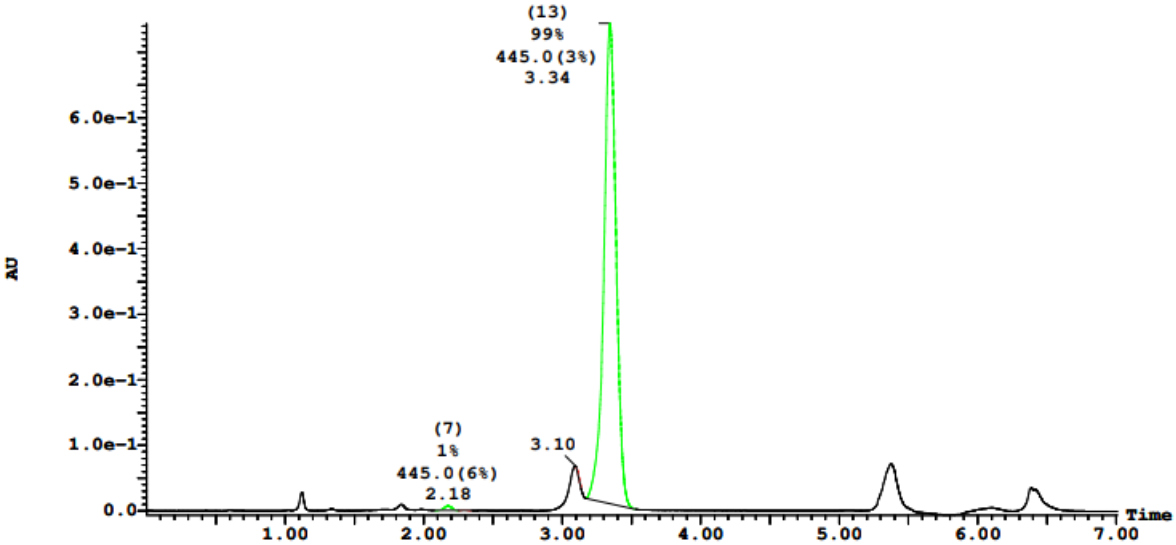

Peak Number	Compound	Time	AreaAbs	Area %Total	Width	Height	Mass Found
7	Found	2.18	5e+002	0.61	0	7e+003	445.0000
8		2.30	5e+001	0.07	0	9e+002	Not Found
12		3.10	6e+001	0.08	0	1e-002	Not Found
13	Tentative	3.34	7e+004	99.25	0	7e+005	445.0000

C5: 96% ee

Openlynx Report - SHARLJA1 Page 31

Sample: 16 Vial:1:16 ID:26-C5
File:SHARLJA1_20211119_CAROL_16 Date:19-Nov-2021 Time:19:17:01
Description:(S,S)WO1 4.6x100mm 5µ Conditions:5% IPA over 5min 3mL/min

Printed: Thu Dec 09 16:26:30 2021

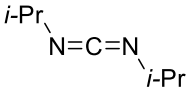

C5,
96% ee

Sample Report (continued):

Sample 16 Vial 1:16 ID 26-C5 File SHARLJA1_20211119_CAROL_16 Date 19-Nov-2021 Time 19:17:01 Description (S,S)WO1 4.6x1(

2: UV Detector: 230 Nm 2.0000-2.3500: Smooth (Mn, 2x3), 3.1000-3.5500: Smooth (Mn, 2x3) 4.424e-1
Range: 4.463e-1

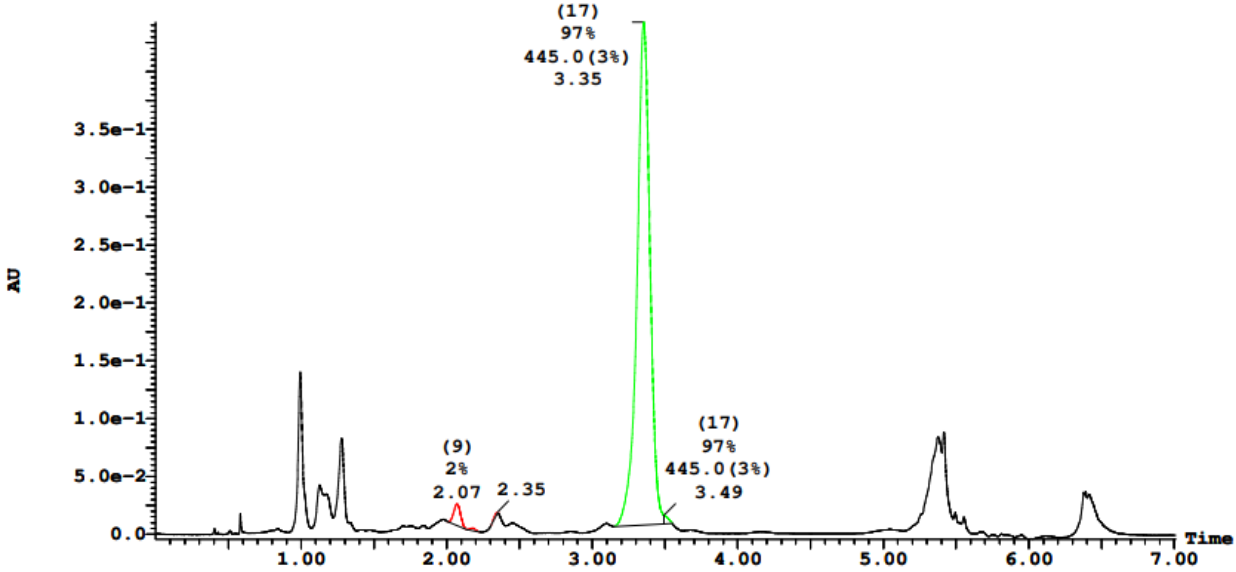

Peak Number	Compound	Time	AreaAbs	Area %Total	Width	Height	Mass Found
9		2.07	1e+003	2.23	0	2e+004	Not Found
10		2.18	9e+001	0.19	0	2e+003	Not Found
12		2.35	6e+001	0.13	0	9e+002	Not Found
17	Tentative	3.35	4e+004	96.93	0	4e+005	445.0000
18	Tentative	3.49	2e+002	0.51	0	7e+003	445.0000

C6: 97% ee

Openlynx Report - SHARLJA1

Sample: 17
File:SHARLJA1_20211119_CAROL_17
Description:(S,S)WO1 4.6x100mm 5µ

Vial:1:17
Date:19-Nov-2021
Conditions:5% IPA over 5min 3mL/min

ID:26-C6
Time:19:25:08

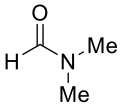

C6,
97% ee

Printed: Thu Dec 09 16:26:30 2021

Sample Report (continued):

Sample 17 Vial 1:17 ID 26-C6 File SHARLJA1_20211119_CAROL_17 Date 19-Nov-2021 Time 19:25:08 Description (S,S)WO1 4.6x100n

2: UV Detector: 230 Nm 2.0000-2.3500: Smooth (Mn, 2x3), 3.1000-3.5500: Smooth (Mn, 2x3) 4.194e-1
Range: 4.231e-1

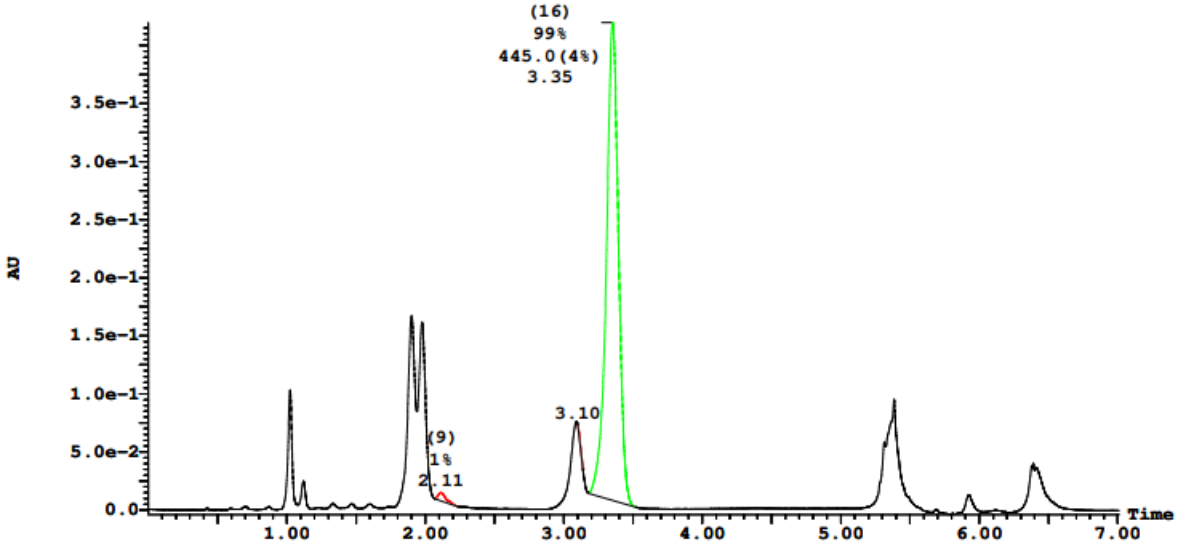

Peak Number	Compound	Time	AreaAbs	Area %Total	Width	Height	Mass Found
9		2.11	4e+002	1.06	0	7e+003	Not Found
14		3.10	6e+001	0.15	0	1e-001	Not Found
16	Tentative	3.35	4e+004	98.78	0	4e+005	445.0000

C7: %ee could not be determined due to overlap with minor enantiomer.

Openlynx Report - SHARLJA1

Sample: 18
File:SHARLJA1_20211119_CAROL_18
Description:(S,S)WO1 4.6x100mm 5µ

Printed: Thu Dec 09 16:26:30 2021

Vial:1:18
Date:19-Nov-2021
Conditions:5% IPA over 5min 3mL/min

ID:26-C7
Time:19:33:17

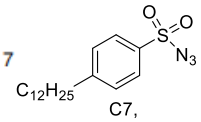

C7,
Not determined

Sample Report (continued):

Sample 18 Vial 1:18 ID 26-C7 File SHARLJA1_20211119_CAROL_18 Date 19-Nov-2021 Time 19:33:17 Description (S,S)WO1 4.6x10(

2: UV Detector: 230 Nm 2.0000-2.3500: Smooth (Mn, 2x3), 3.1000-3.5500: Smooth (Mn, 2x3) 7.502e-1
Range: 7.538e-1

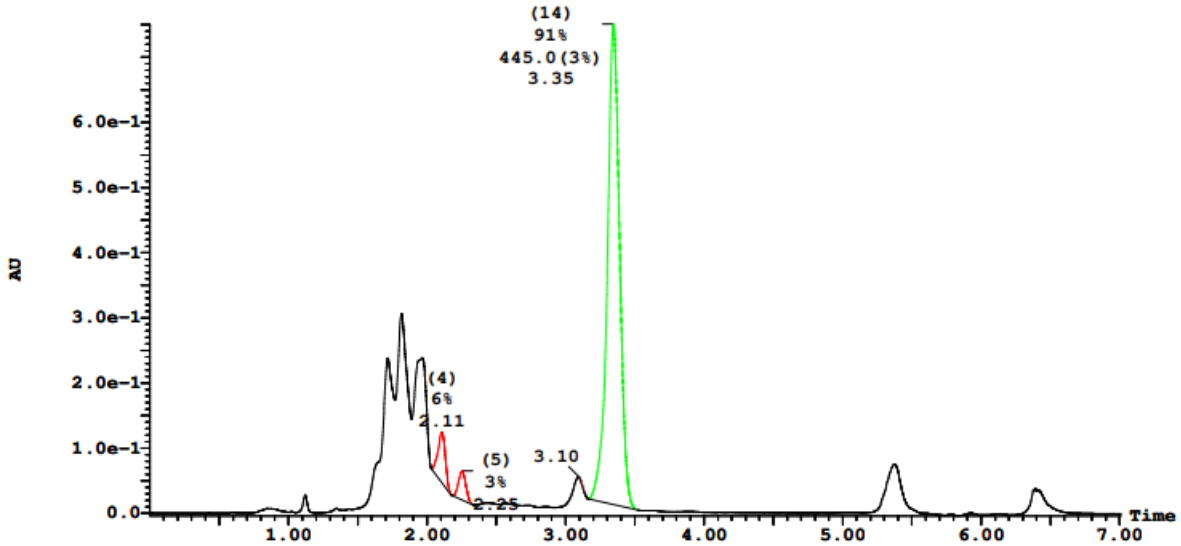

Peak Number	Compound	Time	AreaAbs	Area %Total	Width	Height	Mass Found
4		2.11	5e+003	5.79	0	8e+004	Not Found
5		2.25	3e+003	3.25	0	4e+004	Not Found
12		3.10	4e+001	0.05	0	5e-002	Not Found
14	Tentative	3.35	8e+004	90.91	0	7e+005	445.0000

C8: 98% ee

Openlynx Report - SHARLJA1

Page 37

Sample: 19
File:SHARLJA1_20211119_CAROL_19
Description:(S,S)WO1 4.6x100mm 5µ

Vial:1:19
Date:19-Nov-2021
Conditions:5% IPA over 5min 3mL/min

ID:26-C8
Time:19:41:25

Printed: Thu Dec 09 16:26:30 2021

C8,
98% ee

Sample Report (continued):

Sample 19 Vial 1:19 ID 26-C8 File SHARLJA1_20211119_CAROL_19 Date 19-Nov-2021 Time 19:41:25 Description (S,S)WO1 4.6x100

2: UV Detector: 230 Nm 2.0000-2.3500: Smooth (Mn, 2x3), 3.1000-3.5500: Smooth (Mn, 2x3) 7.689e-1
Range: 7.742e-1

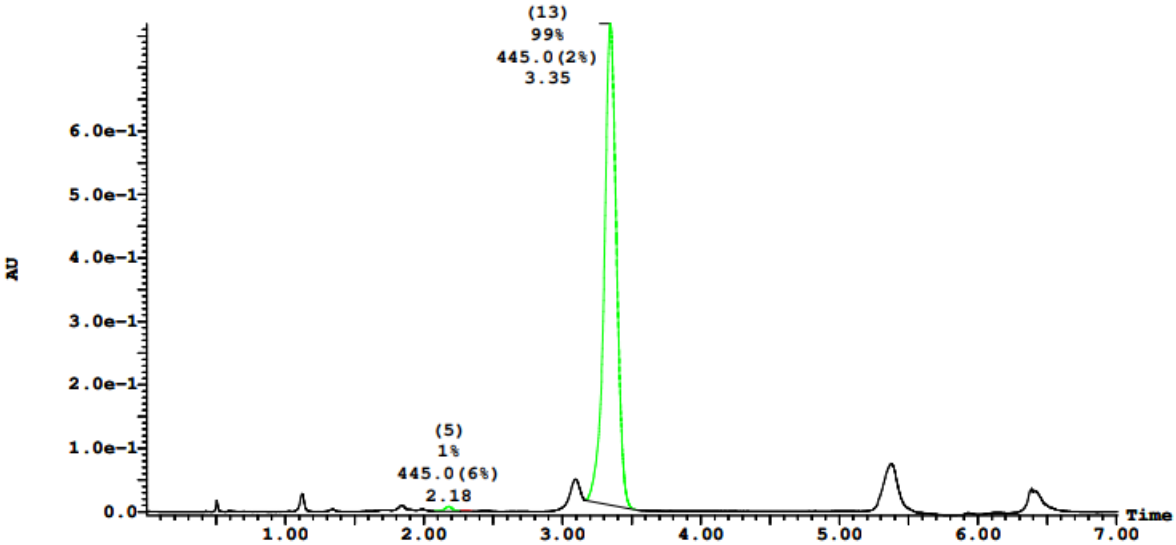

Peak Number	Compound	Time	AreaAbs	Area %Total	Width	Height	Mass Found
5	Found	2.18	5e+002	0.62	0	7e+003	445.0000
6		2.29	5e+001	0.06	0	9e+002	Not Found
13	Tentative	3.35	8e+004	99.32	0	8e+005	445.0000

C9: 98% ee

Openlynx Report - SHARLJA1

Sample: 20
File:SHARLJA1_20211119_CAROL_20
Description:(S,S)WO1 4.6x100mm 5µ

Vial:1:20
Date:19-Nov-2021
Conditions:5% IPA over 5min 3mL/min

ID:26-C9
Time:19:49:33

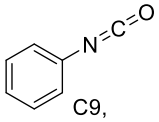

C9,
98% ee

Printed: Thu Dec 09 16:26:30 2021

Sample Report (continued):

Sample 20 Vial 1:20 ID 26-C9 File SHARLJA1_20211119_CAROL_20 Date 19-Nov-2021 Time 19:49:33 Description (S,S)WO1 4.6x100m

2: UV Detector: 230 Nm 2.0000-2.3500: Smooth (Mn, 2x3), 3.1000-3.5500: Smooth (Mn, 2x3) 1.056
Range: 1.06

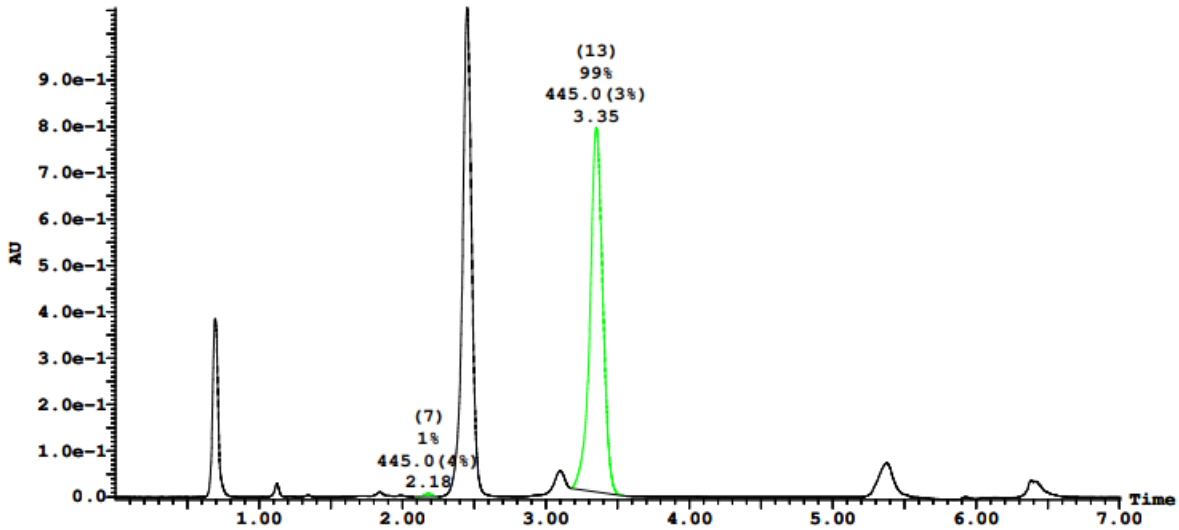

Peak Number	Compound	Time	AreaAbs	Area %Total	Width	Height	Mass Found
7	Tentative	2.18	5e+002	0.56	0	7e+003	445.0000
13	Tentative	3.35	8e+004	99.44	0	8e+005	445.0000

C10: 98% ee

Openlynx Report - SHARLJA1 Page 41

Sample: 21
File:SHARLJA1_20211119_CAROL_21
Description:(S,S)WO1 4.6x100mm 5µ

Vial:1:21
Date:19-Nov-2021
Conditions:5% IPA over 5min 3mL/min

ID:26-C10
Time:19:57:40

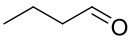

C10,
98% ee

Printed: Thu Dec 09 16:26:30 2021

Sample Report (continued):

Sample 21 Vial 1:21 ID 26-C10 File SHARLJA1_20211119_CAROL_21 Date 19-Nov-2021 Time 19:57:40 Description (S,S)WO1 4.6x10

2: UV Detector: 230 Nm 2.0000-2.3500: Smooth (Mn, 2x3), 3.1000-3.5500: Smooth (Mn, 2x3) 7.243e-1
Range: 7.288e-1

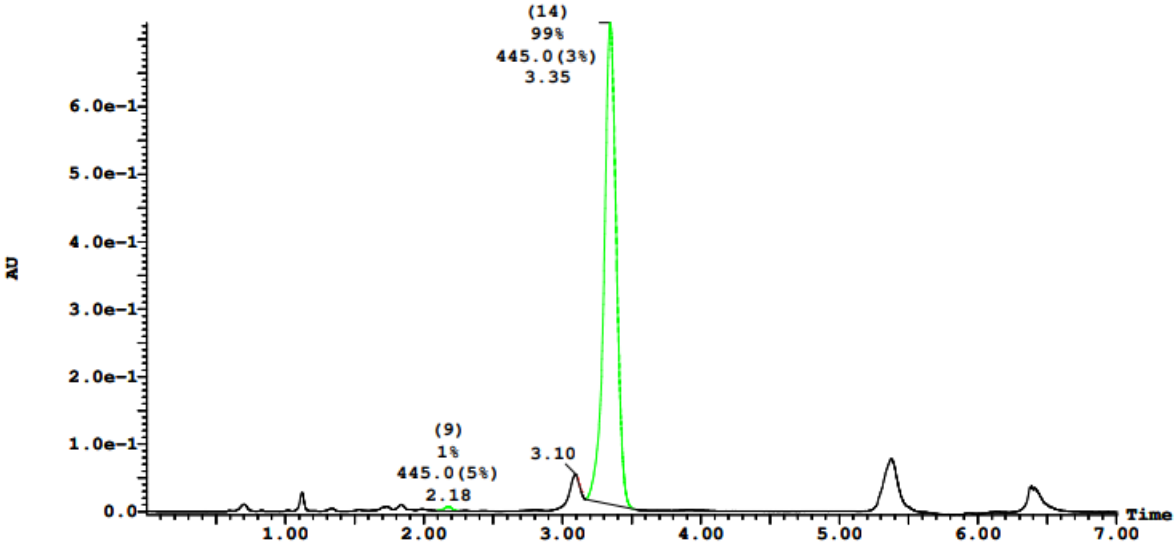

Peak Number	Compound	Time	AreaAbs	Area %Total	Width	Height	Mass Found
9	Found	2.18	4e+002	0.56	0	6e+003	445.0000
12		3.10	5e+001	0.07	0	8e-002	Not Found
14	Tentative	3.35	7e+004	99.37	0	7e+005	445.0000

C11: >95% ee

Openlynx Report - DUSTADA1

Sample: 209
File:DUSTADA1-12_20_2021_006
Description:(S,S)WO1 4.6x100mm 5µ

Vial:2:4
Date:20-Dec-2021
Conditions:5% IPA over 5min 3mL/min

ID:EXP026 C11
Time:12:22:59

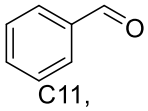

C11,
>95% ee

Printed: Mon Dec 20 15:37:27 2021

Sample Report (continued):

Sample 209 Vial 2:4 ID EXP026 C11 File DUSTADA1-12_20_2021_006 Date 20-Dec-2021 Time 12:22:59 Description (S,S)WO1 4.6x1

2: UV Detector: 230 Nm 2.0000-2.3500: Smooth (Mn, 2x3), 3.1000-3.5500: Smooth (Mn, 2x3) 4.616e-1
Range: 4.622e-1

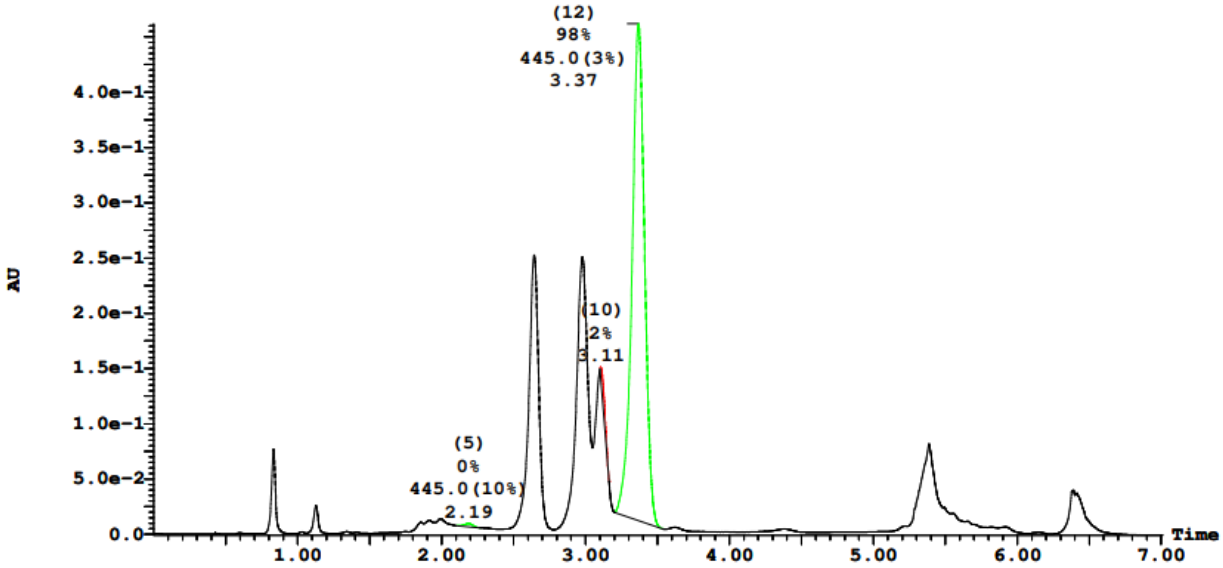

Peak Number	Compound	Time	AreaAbs	Area %Total	Width	Height	Mass Found
5	Found	2.19	2e+002	0.43	0	3e+003	445.0000
10		3.11	7e+002	1.55	0	9e+003	Not Found
12	Tentative	3.37	5e+004	98.02	0	4e+005	445.0000

D1: 98% ee

Openlynx Report - SHARLJA1

Sample: 23
File:SHARLJA1_20211119_CAROL_23
Description:(S,S)WO1 4.6x100mm 5µ

Vial:1:23
Date:19-Nov-2021
Conditions:5% IPA over 5min 3mL/min

ID:26-D1
Time:20:13:56

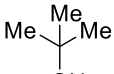

D1,
98% ee

Printed: Thu Dec 09 16:26:30 2021

Sample Report (continued):

Sample 23 Vial 1:23 ID 26-D1 File SHARLJA1_20211119_CAROL_23 Date 19-Nov-2021 Time 20:13:56 Description (S,S)WO1 4.6x10(

2: UV Detector: 230 Nm 2.0000-2.3500: Smooth (Mn, 2x3), 3.1000-3.5500: Smooth (Mn, 2x3) 7.433e-1
Range: 7.474e-1

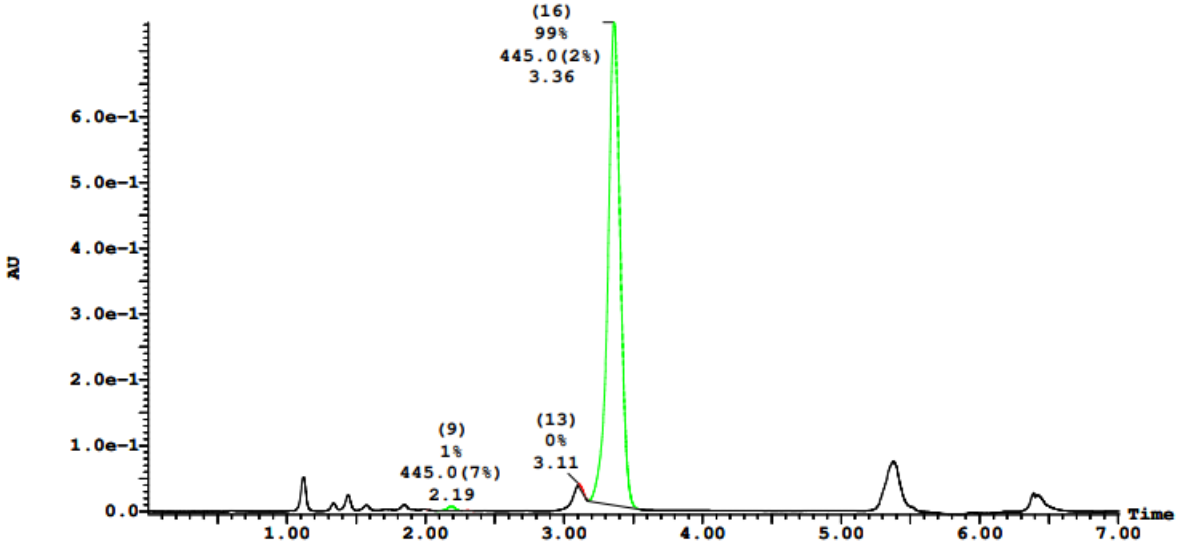

Peak Number	Compound	Time	AreaAbs	Area %Total	Width	Height	Mass Found
8		2.00	8e-001	0.00	0		Not Found
9	Found	2.19	5e+002	0.60	0	7e+003	445.0000
10		2.30	3e+001	0.04	0	5e+002	Not Found
13		3.11	2e+002	0.27	0	4e+003	Not Found
16	Tentative	3.36	8e+004	99.10	0	7e+005	445.0000

D2: 98% ee

Openlynx Report - SHARLJA1

Sample: 24
File:SHARLJA1_20211119_CAROL_24
Description:(S,S)WO1 4.6x100mm 5µ

Vial:1:24
Date:19-Nov-2021
Conditions:5% IPA over 5min 3mL/min

ID:26-D2
Time:20:22:04

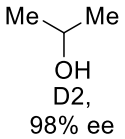

Printed: Thu Dec 09 16:26:30 2021

Sample Report (continued):

Sample 24 Vial 1:24 ID 26-D2 File SHARLJA1_20211119_CAROL_24 Date 19-Nov-2021 Time 20:22:04 Description (S,S)WO1 4.6x10

2: UV Detector: 230 Nm 2.0000-2.3500: Smooth (Mn, 2x3), 3.1000-3.5500: Smooth (Mn, 2x3) 5.98e-1
Range: 6.044e-1

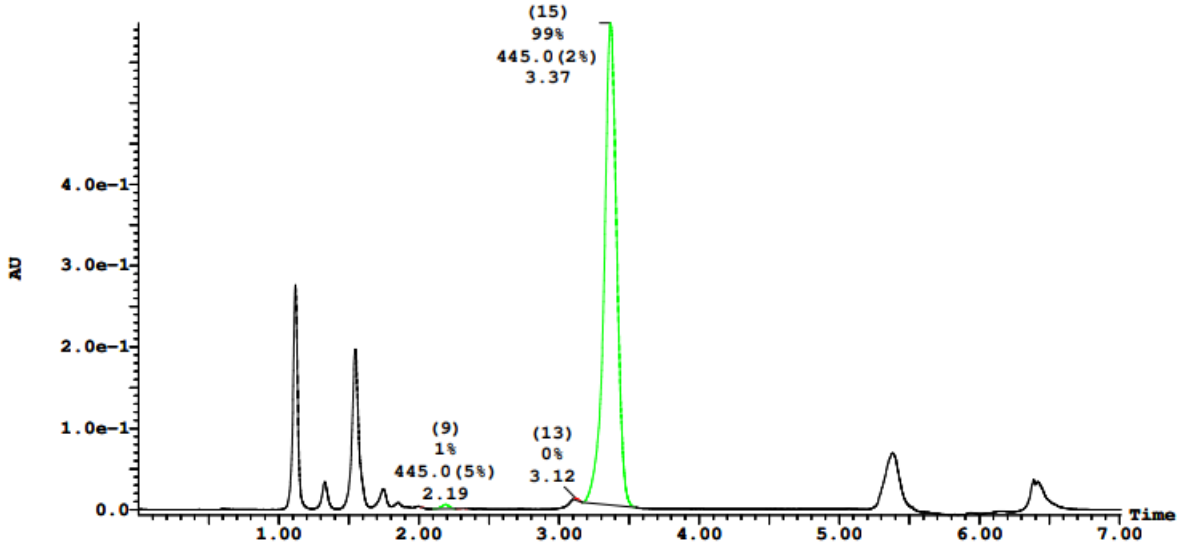

Peak Number	Compound	Time	AreaAbs	Area %Total	Width	Height	Mass Found
8		2.00	2e+000	0.00	0		Not Found
9	Found	2.19	3e+002	0.51	0	5e+003	445.0000
10		2.31	1e+001	0.02	0	3e+002	Not Found
10		2.33	3e+000	0.00	0	2e+002	Not Found
13		3.12	7e+001	0.11	0	2e+003	Not Found
15	Tentative	3.37	6e+004	99.34	0	6e+005	445.0000

D3: 98% ee

Openlynx Report - SHARLJA1

Sample: 25
File:SHARLJA1_20211119_CAROL_25
Description:(S,S)WO1 4.6x100mm 5µ

Vial:1:25
Date:19-Nov-2021
Conditions:5% IPA over 5min 3mL/min

ID:26-D3
Time:20:30:11

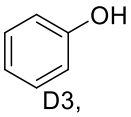

D3,
98% ee

Printed: Thu Dec 09 16:26:30 2021

Sample Report (continued):

Sample 25 Vial 1:25 ID 26-D3 File SHARLJA1_20211119_CAROL_25 Date 19-Nov-2021 Time 20:30:11 Description (S,S)WO1 4.6x100

2: UV Detector: 230 Nm 2.0000-2.3500: Smooth (Mn, 2x3), 3.1000-3.5500: Smooth (Mn, 2x3) 6.043e-1
Range: 6.112e-1

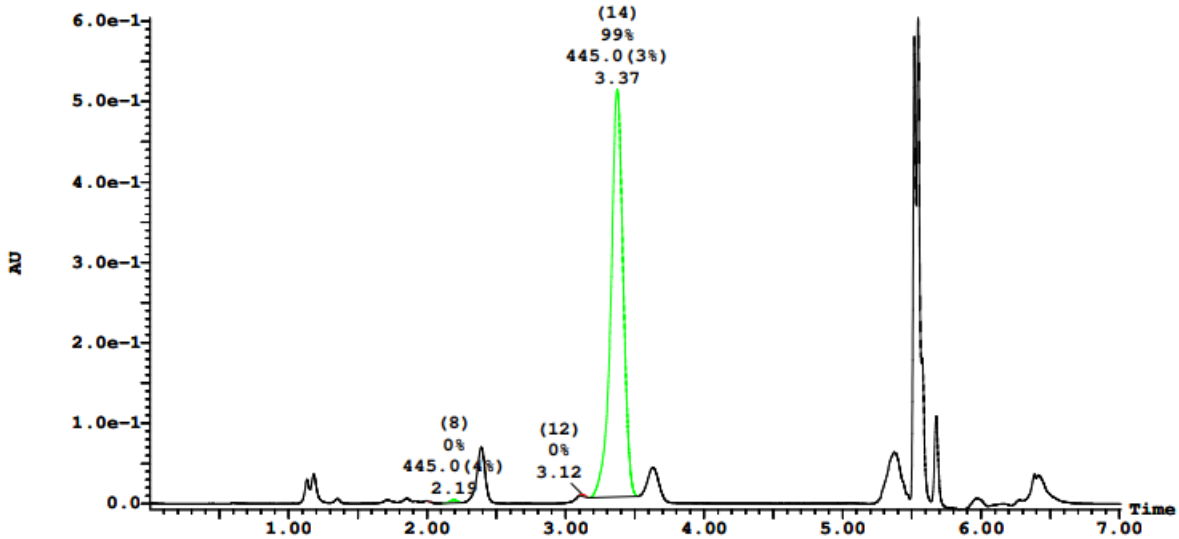

Peak Number	Compound	Time	AreaAbs	Area %Total	Width	Height	Mass Found
7		2.00	5e+000	0.01	0		Not Found
8	Found	2.19	2e+002	0.45	0	4e+003	445.0000
12		3.12	7e+001	0.14	0	2e+003	Not Found
14	Tentative	3.37	5e+004	99.41	0	5e+005	445.0000

D10: 98% ee

Openlynx Report - SHARLJA1

Sample: 29
File:SHARLJA1_20211119_CAROL_29
Description:(S,S)WO1 4.6x100mm 5µ

Vial:1:29
Date:19-Nov-2021
Conditions:5% IPA over 5min 3mL/min

ID:26-D10
Time:21:02:45

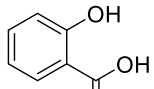

D10,
98% ee

Printed: Thu Dec 09 16:26:30 2021

Sample Report (continued):

Sample 29 Vial 1:29 ID 26-D10 File SHARLJA1_20211119_CAROL_29 Date 19-Nov-2021 Time 21:02:45 Description (S,S)WO1 4.6x1

2: UV Detector: 230 Nm 2.0000-2.3500: Smooth (Mn, 2x3), 3.1000-3.5500: Smooth (Mn, 2x3) 5.754e-1
Range: 5.758e-1

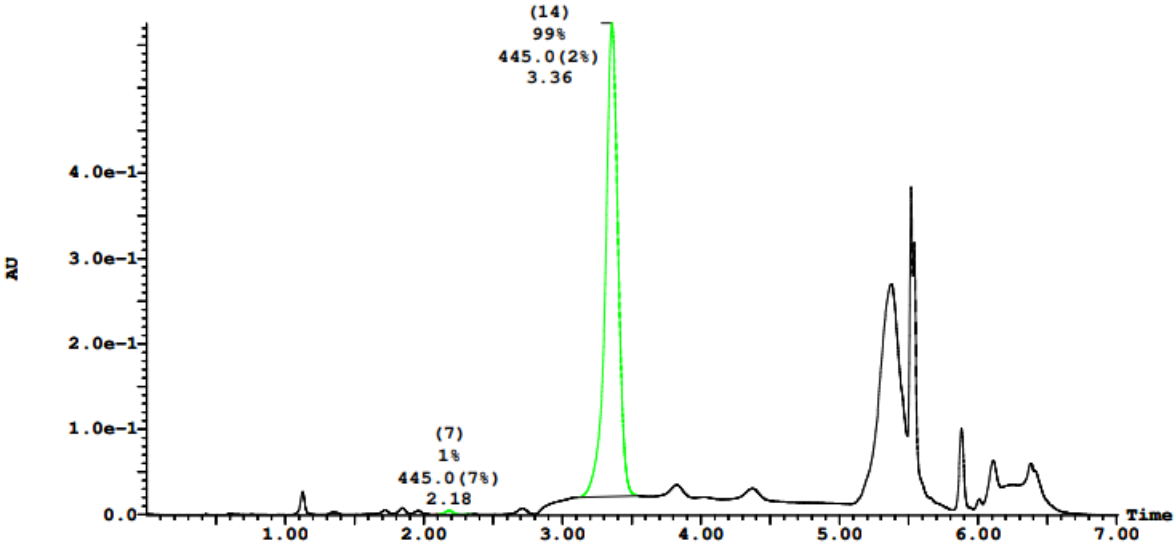

Peak Number	Compound	Time	AreaAbs	Area %Total	Width	Height	Mass Found
6		2.09	4e+000	0.01	0	3e+002	Not Found
7	Found	2.18	3e+002	0.52	0	5e+003	445.0000
8	Tentative	2.32	3e+000	0.00	0	1e+002	445.0000
9	Tentative	2.34	5e+000	0.01	0	2e+002	445.0000
14	Tentative	3.36	6e+004	99.46	0	6e+005	445.0000

D11: 98% ee

Openlynx Report - SHARLJA1

Sample: 30
File:SHARLJA1_20211119_CAROL_30
Description:(S,S)WO1 4.6x100mm 5µ

Vial:1:30
Date:19-Nov-2021
Conditions:5% IPA over 5min 3mL/min

ID:26-D11
Time:21:10:52

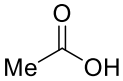

D11,
98% ee

Printed: Thu Dec 09 16:26:30 2021

Sample Report (continued):

Sample 30 Vial 1:30 ID 26-D11 File SHARLJA1_20211119_CAROL_30 Date 19-Nov-2021 Time 21:10:52 Description (S,S)WO1 4.6x1(

2: UV Detector: 230 Nm 2.0000-2.3500: Smooth (Mn, 2x3), 3.1000-3.5500: Smooth (Mn, 2x3) 7.51e-1
Range: 7.521e-1

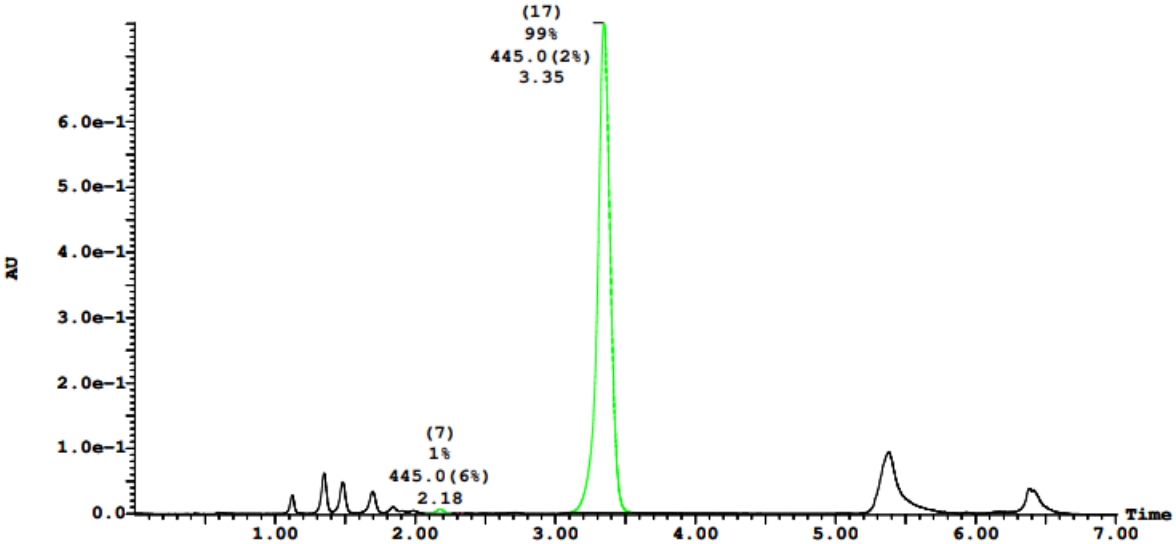

Peak Number	Compound	Time	AreaAbs	Area %Total	Width	Height	Mass Found
7	Tentative	2.18	4e+002	0.56	0	7e+003	445.0000
8		2.32	4e+000	0.00	0	2e+002	Not Found
9		2.33	5e+000	0.01	0	2e+002	Not Found
17	Tentative	3.35	8e+004	99.43	0	7e+005	445.0000

E5: 98% ee

Openlynx Report - SHARLJA1

Sample: 34
File:SHARLJA1_20211119_CAROL_34
Description:(S,S)WO1 4.6x100mm 5µ

Vial:1:34
Date:19-Nov-2021
Conditions:5% IPA over 5min 3mL/min

ID:26-E5
Time:21:43:23

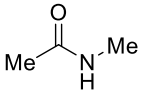

E5,
98% ee

Printed: Thu Dec 09 16:26:30 2021

Sample Report (continued):

Sample 34 Vial 1:34 ID 26-E5 File SHARLJA1_20211119_CAROL_34 Date 19-Nov-2021 Time 21:43:23 Description (S,S)WO1 4.6x10

2: UV Detector: 230 Nm 2.0000-2.3500: Smooth (Mn, 2x3), 3.1000-3.5500: Smooth (Mn, 2x3) 7.927e-1
Range: 7.935e-1

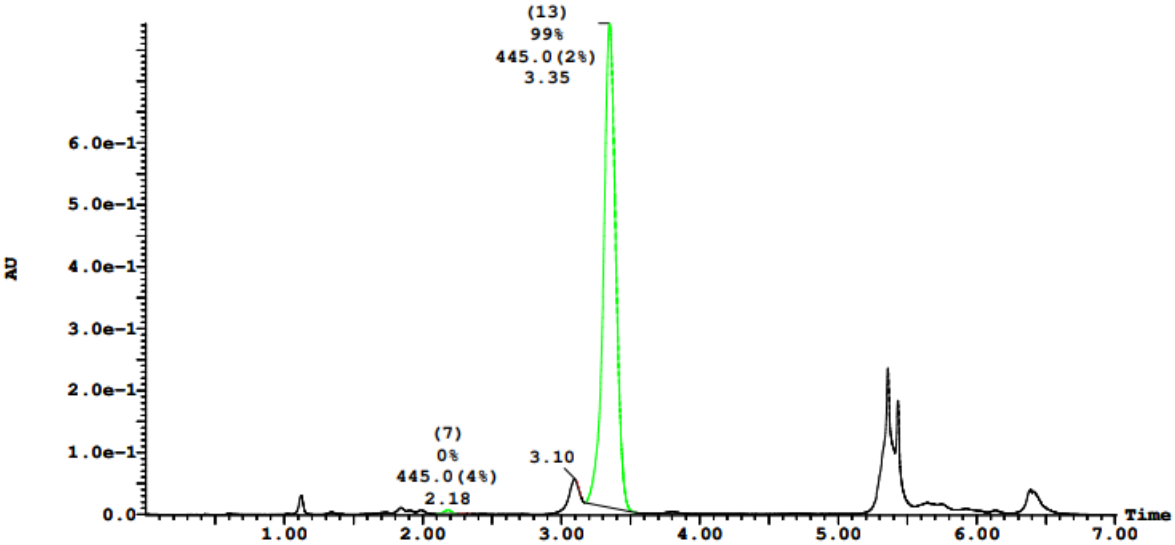

Peak Number	Compound	Time	AreaAbs	Area %Total	Width	Height	Mass Found
7	Found	2.18	4e+002	0.49	0	6e+003	445.0000
8		2.30	3e+001	0.04	0	9e+002	Not Found
8		2.32	1e+001	0.02	0	7e+002	Not Found
12		3.10	9e+001	0.11	0	5e-002	Not Found
13	Tentative	3.35	8e+004	99.35	0	8e+005	445.0000

E8: 98% ee

Openlynx Report - SHARLJA1

Sample: 37
File:SHARLJA1_20211119_CAROL_37
Description:(S,S)WO1 4.6x100mm 5µ

Vial:1:37
Date:19-Nov-2021
Conditions:5% IPA over 5min 3mL/min

ID:26-E8
Time:22:07:46

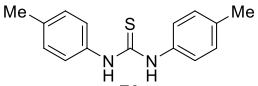

E8,
98% ee

Printed: Thu Dec 09 16:26:30 2021

Sample Report (continued):

Sample 37 Vial 1:37 ID 26-E8 File SHARLJA1_20211119_CAROL_37 Date 19-Nov-2021 Time 22:07:46 Description (S,S)WO1 4.6x100r

2: UV Detector: 230 Nm 2.0000-2.3500: Smooth (Mn, 2x3), 3.1000-3.5500: Smooth (Mn, 2x3) 7.535e-1
Range: 7.588e-1

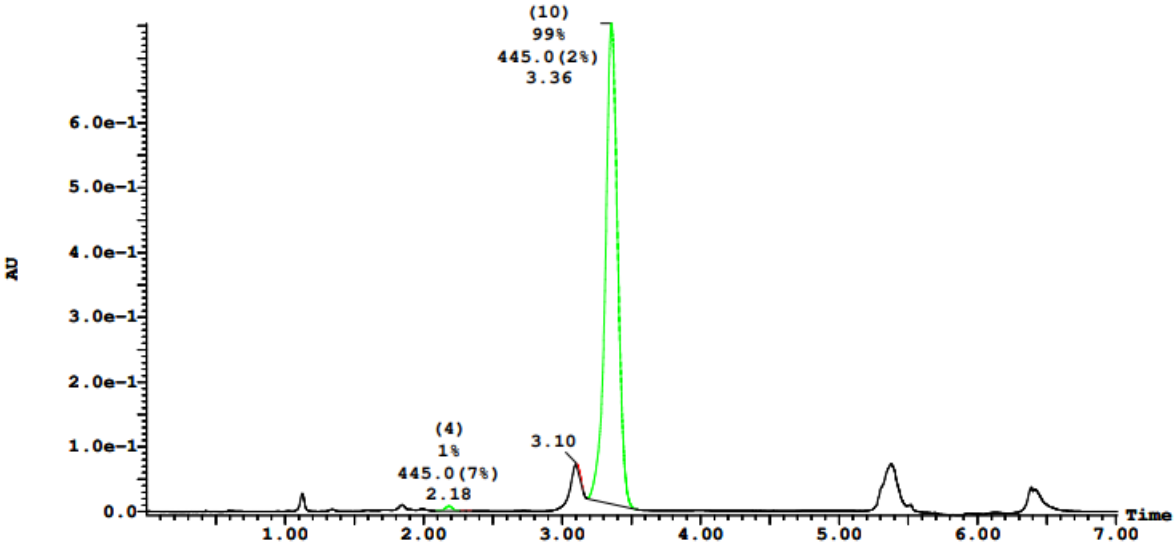

Peak Number	Compound	Time	AreaAbs	Area %Total	Width	Height	Mass Found
4	Found	2.18	5e+002	0.61	0	7e+003	445.0000
5		2.30	7e+000	0.01	0	3e+002	Not Found
6		2.32	1e+001	0.01	0	4e+002	Not Found
9		3.10	3e+002	0.34	0	3e+003	Not Found
10	Tentative	3.36	8e+004	99.03	0	7e+005	445.0000

E11: 99% ee

Openlynx Report - SHARLJA1

Sample: 39
File:SHARLJA1_20211119_CAROL_39
Description:(S,S)WO1 4.6x100mm 5µ

Vial:1:39
Date:19-Nov-2021
Conditions:5% IPA over 5min 3mL/min

ID:26-E11
Time:22:24:02

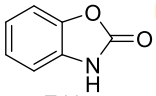

E11,
99% ee

Printed: Thu Dec 09 16:26:30 2021

Sample Report (continued):

Sample 39 Vial 1:39 ID 26-E11 File SHARLJA1_20211119_CAROL_39 Date 19-Nov-2021 Time 22:24:02 Description (S,S)WO1 4.6x100

2: UV Detector: 230 Nm 2.0000-2.3500: Smooth (Mn, 2x3), 3.1000-3.5500: Smooth (Mn, 2x3) 1.168
Range: 1.176

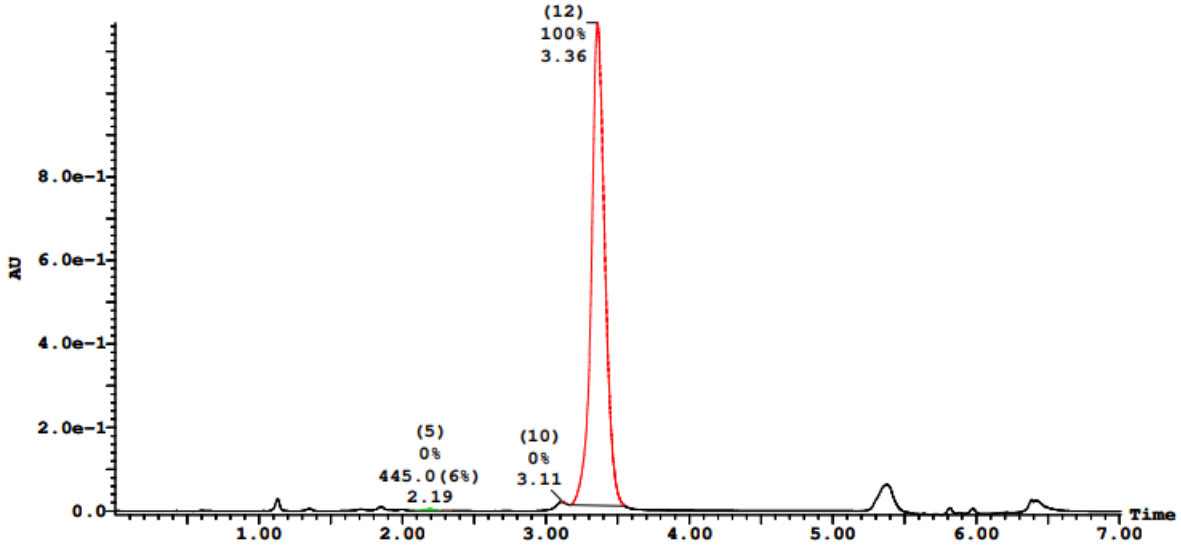

Peak Number	Compound	Time	AreaAbs	Area %Total	Width	Height	Mass Found
5	Found	2.19	4e+002	0.28	0	5e+003	445.0000
6		2.31	1e+001	0.01	0	3e+002	Not Found
10		3.11	1e+002	0.08	0	3e+003	Not Found
12		3.36	1e+005	99.63	0	1e+006	Not Found

F7: 96% ee

Openlynx Report - SHARLJA1

Sample: 44
File:SHARLJA1_20211119_CAROL_44
Description:(S,S)WO1 4.6x100mm 5µ

Vial:1:44
Date:19-Nov-2021
Conditions:5% IPA over 5min 3mL/min

ID:26-F7
Time:23:04:42

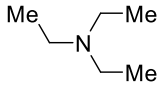

F7,
96% ee

Printed: Thu Dec 09 16:26:30 2021

Sample Report (continued):

Sample 44 Vial 1:44 ID 26-F7 File SHARLJA1_20211119_CAROL_44 Date 19-Nov-2021 Time 23:04:42 Description (S,S)WO1 4.6x100

2: UV Detector: 230 Nm 2.0000-2.3500: Smooth (Mn, 2x3), 3.1000-3.5500: Smooth (Mn, 2x3) 7.09e-1
Range: 7.156e-1

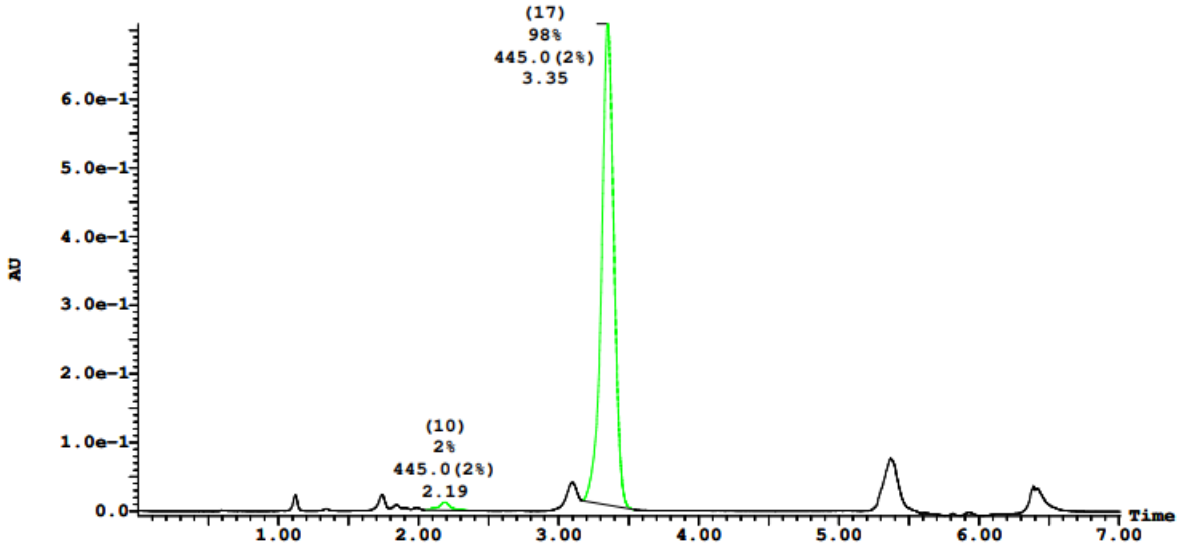

Peak Number	Compound	Time	AreaAbs	Area %Total	Width	Height	Mass Found
10	Tentative	2.19	1e+003	1.58	0	1e+004	445.0000
17	Tentative	3.35	7e+004	98.42	0	7e+005	445.0000

F9: 98% ee

Openlynx Report - SHARLJA1

Sample: 45
File:SHARLJA1_20211119_CAROL_45
Description:(S,S)WO1 4.6x100mm 5µ

Vial:1:45
Date:19-Nov-2021
Conditions:5% IPA over 5min 3mL/min

ID:26-F9
Time:23:12:51

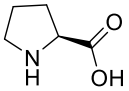

F9,
98% ee

Printed: Thu Dec 09 16:26:30 2021

Sample Report (continued):

Sample 45 Vial 1:45 ID 26-F9 File SHARLJA1_20211119_CAROL_45 Date 19-Nov-2021 Time 23:12:51 Description (S,S)WO1 4.6x1(

2: UV Detector: 230 Nm 2.0000-2.3500: Smooth (Mn, 2x3), 3.1000-3.5500: Smooth (Mn, 2x3) 7.679e-1
Range: 7.748e-1

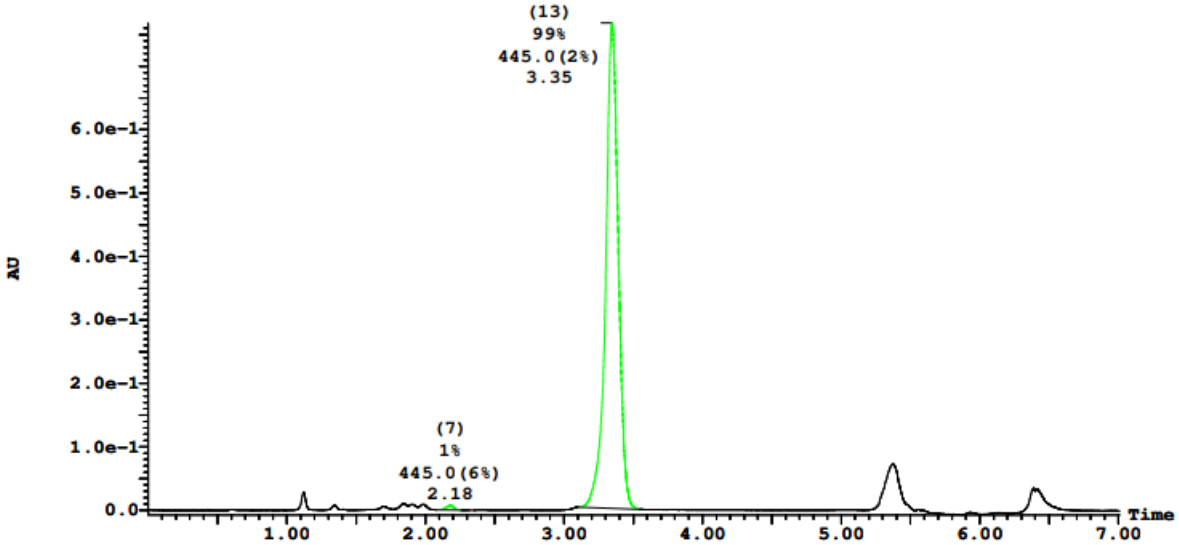

Peak Number	Compound	Time	AreaAbs	Area %Total	Width	Height	Mass Found
7	Found	2.18	5e+002	0.59	0	7e+003	445.0000
8		2.33	3e+000	0.00	0	2e+002	Not Found
13	Tentative	3.35	8e+004	99.41	0	8e+005	445.0000

G2: 98% ee

Openlynx Report - SHARLJA1

Sample: 46
File:SHARLJA1_20211119_CAROL_46
Description:(S,S)WO1 4.6x100mm 5µ

Vial:1:46
Date:19-Nov-2021
Conditions:5% IPA over 5min 3mL/min

ID:26-G2
Time:23:20:58

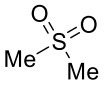

G2,
98% ee

Printed: Thu Dec 09 16:26:30 2021

Sample Report (continued):

Sample 46 Vial 1:46 ID 26-G2 File SHARLJA1_20211119_CAROL_46 Date 19-Nov-2021 Time 23:20:58 Description (S,S)WO1 4.6x10

2: UV Detector: 230 Nm 2.0000-2.3500: Smooth (Mn, 2x3), 3.1000-3.5500: Smooth (Mn, 2x3) 8.037e-1
Range: 8.118e-1

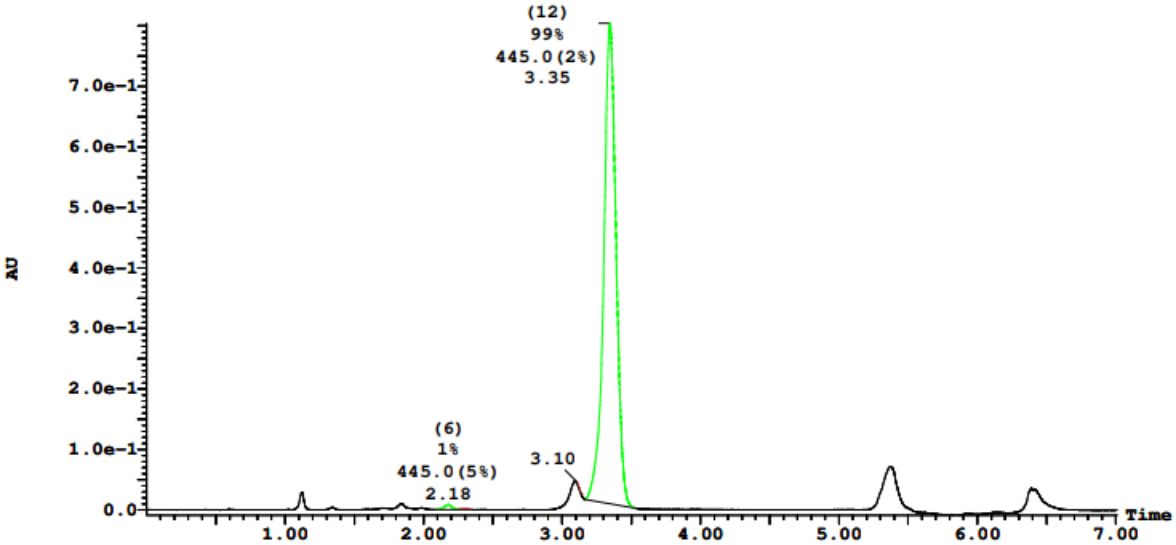

Peak Number	Compound	Time	AreaAbs	Area %Total	Width	Height	Mass Found
6	Found	2.18	5e+002	0.61	0	8e+003	445.0000
7		2.30	4e+001	0.05	0	8e+002	Not Found
9		3.10	5e+001	0.07	0	3e-002	Not Found
12	Tentative	3.35	8e+004	99.28	0	8e+005	445.0000

G3: 98% ee

Openlynx Report - SHARLJA1

Sample: 47
File:SHARLJA1_20211119_CAROL_47
Description:(S,S)WO1 4.6x100mm 5µ

Vial:1:47
Date:19-Nov-2021
Conditions:5% IPA over 5min 3mL/min

ID:26-G3
Time:23:29:06

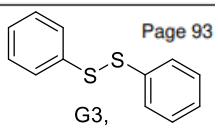

G3,
98% ee

Printed: Thu Dec 09 16:26:30 2021

Sample Report (continued):

Sample 47 Vial 1:47 ID 26-G3 File SHARLJA1_20211119_CAROL_47 Date 19-Nov-2021 Time 23:29:06 Description (S,S)WO1 4.6x1(

2: UV Detector: 230 Nm 2.0000-2.3500: Smooth (Mn, 2x3), 3.1000-3.5500: Smooth (Mn, 2x3) 2.946
Range: 2.951

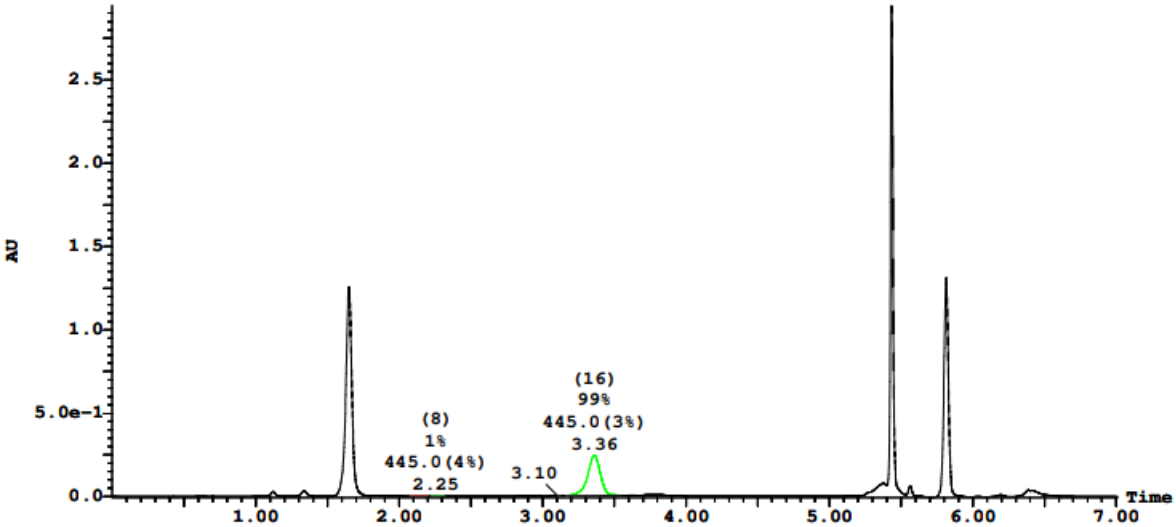

Peak Number	Compound	Time	AreaAbs	Area %Total	Width	Height	Mass Found
7		2.17	2e+002	0.65	0	2e+003	Not Found
8	Found	2.25	1e+002	0.55	0	2e+003	445.0000
14		3.10	4e+000	0.02	0		Not Found
16	Tentative	3.36	3e+004	98.78	0	2e+005	445.0000

G4: 98% ee

Openlynx Report - SHARLJA1

S=C=S

G4,
98% ee

Sample: 48
File:SHARLJA1_20211119_CAROL_48
Description:(S,S)WO1 4.6x100mm 5µ

Vial:1:48
Date:19-Nov-2021
Conditions:5% IPA over 5min 3mL/min

ID:26-G4
Time:23:37:14

Printed: Thu Dec 09 16:26:30 2021

Sample Report (continued):

Sample 48 Vial 1:48 ID 26-G4 File SHARLJA1_20211119_CAROL_48 Date 19-Nov-2021 Time 23:37:14 Description (S,S)WO1 4.6x10

2: UV Detector: 230 Nm 2.0000-2.3500: Smooth (Mn, 2x3), 3.1000-3.5500: Smooth (Mn, 2x3) 7.29e-1
Range: 7.358e-1

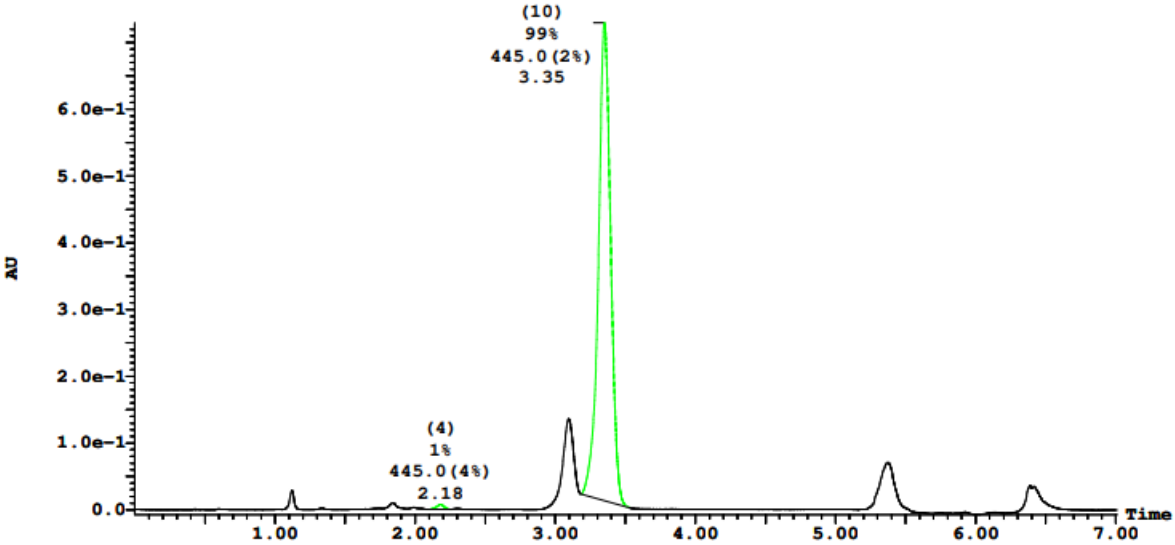

Peak Number	Compound	Time	AreaAbs	Area %Total	Width	Height	Mass Found
4	Found	2.18	4e+002	0.58	0	7e+003	445.0000
10	Tentative	3.35	7e+004	99.42	0	7e+005	445.0000

G6: 97% ee

Openlynx Report - SHARLJA1

Sample: 49
File:SHARLJA1_20211119_CAROL_49
Description:(S,S)WO1 4.6x100mm 5µ

Vial:2:1
Date:19-Nov-2021
Conditions:5% IPA over 5min 3mL/min

ID:26-G6
Time:23:45:21

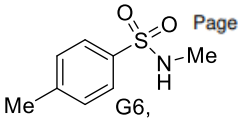

G6,
97% ee

Printed: Thu Dec 09 16:26:30 2021

Sample Report (continued):

Sample 49 Vial 2:1 ID 26-G6 File SHARLJA1_20211119_CAROL_49 Date 19-Nov-2021 Time 23:45:21 Description (S,S)WO1 4.6x100

2: UV Detector: 230 Nm 2.0000-2.3500: Smooth (Mn, 2x3), 3.1000-3.5500: Smooth (Mn, 2x3) 2.7
Range: 2.706

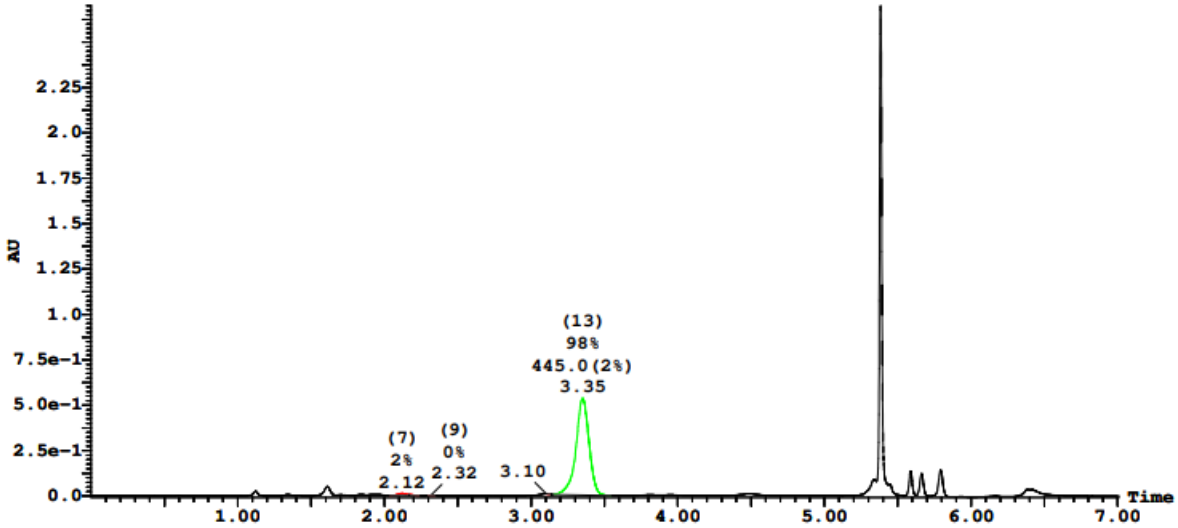

Peak Number	Compound	Time	AreaAbs	Area %Total	Width	Height	Mass Found
7		2.12	8e+002	1.50	0	1e+004	Not Found
7		2.17	2e+002	0.32	0	5e+003	Not Found
9		2.32	9e+000	0.02	0	3e+002	Not Found
11		3.10	1e+001	0.02	0		Not Found
13	Tentative	3.35	6e+004	98.14	0	5e+005	445.0000

G8: 98% ee

Openlynx Report - SHARLJA1

Sample: 50
File:SHARLJA1_20211119_CAROL_50
Description:(S,S)WO1 4.6x100mm 5µ

Vial:2:2
Date:19-Nov-2021
Conditions:5% IPA over 5min 3mL/min

ID:26-G8
Time:23:53:29

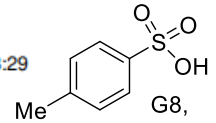

G8,
98% ee

Printed: Thu Dec 09 16:26:30 2021

Sample Report (continued):

Sample 50 Vial 2:2 ID 26-G8 File SHARLJA1_20211119_CAROL_50 Date 19-Nov-2021 Time 23:53:29 Description (S,S)WO1 4.6x100

2: UV Detector: 230 Nm 2.0000-2.3500: Smooth (Mn, 2x3), 3.1000-3.5500: Smooth (Mn, 2x3) 6.36e-1
Range: 6.368e-1

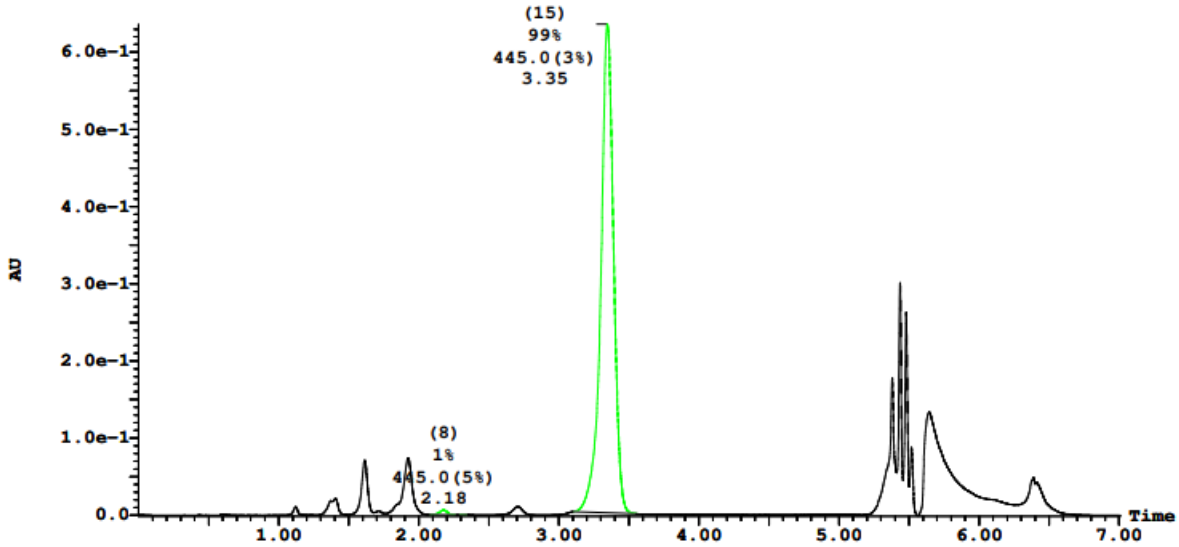

Peak Number	Compound	Time	AreaAbs	Area %Total	Width	Height	Mass Found
8	Found	2.18	4e+002	0.61	0	6e+003	445.0000
9	Tentative	2.32	1e+001	0.02	0	3e+002	445.0000
15	Tentative	3.35	7e+004	99.37	0	6e+005	445.0000

G9: 98% ee

Openlynx Report - SHARLJA1

Sample: 51
File:SHARLJA1_20211119_CAROL_51
Description:(S,S)WO1 4.6x100mm 5µ

Vial:2:3
Date:20-Nov-2021
Conditions:5% IPA over 5min 3mL/min

ID:26-G9
Time:00:01:37

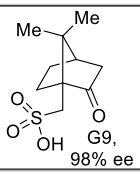

Printed: Thu Dec 09 16:26:30 2021

Sample Report (continued):

Sample 51 Vial 2:3 ID 26-G9 File SHARLJA1_20211119_CAROL_51 Date 20-Nov-2021 Time 00:01:37 Description (S,S)WO1 4.6x100

2: UV Detector: 230 Nm 2.0000-2.3500: Smooth (Mn, 2x3), 3.1000-3.5500: Smooth (Mn, 2x3) 8.743e-1
Range: 8.747e-1

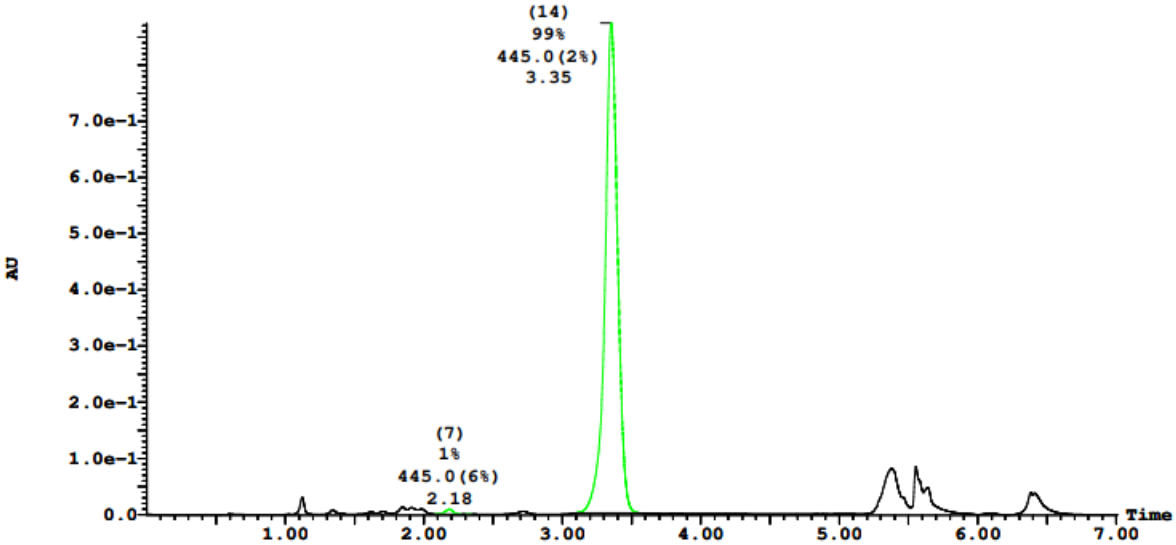

Peak Number	Compound	Time	AreaAbs	Area %Total	Width	Height	Mass Found
7	Found	2.18	6e+002	0.61	0	9e+003	445.0000
8	Tentative	2.33	5e+000	0.01	0	2e+002	445.0000
14	Tentative	3.35	9e+004	99.38	0	9e+005	445.0000

H1: 98% ee

Openlynx Report - SHARLJA1

Sample: 52
File:SHARLJA1_20211119_CAROL_52
Description:(S,S)WO1 4.6x100mm 5µ

Vial:2:4
Date:20-Nov-2021
Conditions:5% IPA over 5min 3mL/min

ID:26-H1
Time:00:09:46

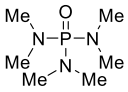

H1,
98% ee

Printed: Thu Dec 09 16:26:30 2021

Sample Report (continued):

Sample 52 Vial 2:4 ID 26-H1 File SHARLJA1_20211119_CAROL_52 Date 20-Nov-2021 Time 00:09:46 Description (S,S)WO1 4.6x100

2: UV Detector: 230 Nm 2.0000-2.3500: Smooth (Mn, 2x3), 3.1000-3.5500: Smooth (Mn, 2x3) 7.602e-1
Range: 7.647e-1

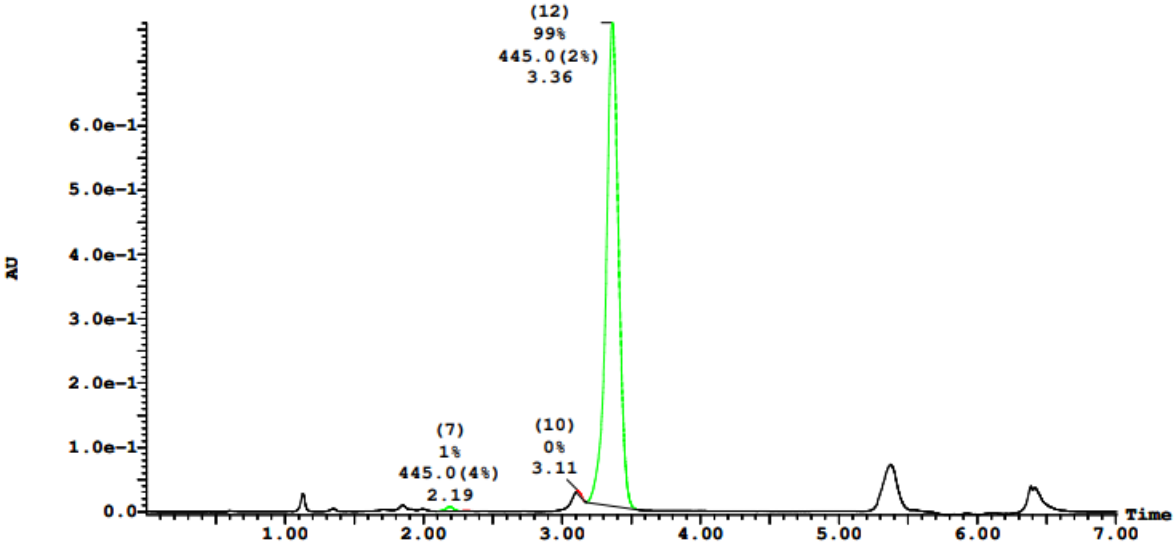

Peak Number	Compound	Time	AreaAbs	Area %Total	Width	Height	Mass Found
7	Found	2.19	5e+002	0.58	0	7e+003	445.0000
8		2.31	3e+001	0.04	0	6e+002	Not Found
10		3.11	2e+002	0.25	0	5e+003	Not Found
12	Tentative	3.36	8e+004	99.14	0	8e+005	445.0000

H3: 98% ee

Openlynx Report - SHARLJA1

Sample: 53
File:SHARLJA1_20211119_CAROL_53
Description:(S,S)WO1 4.6x100mm 5µ

Vial:2:5
Date:20-Nov-2021
Conditions:5% IPA over 5min 3mL/min

ID:26-H3
Time:00:17:53

H3,
98% ee

Printed: Thu Dec 09 16:26:30 2021

Sample Report (continued):

Sample 53 Vial 2:5 ID 26-H3 File SHARLJA1_20211119_CAROL_53 Date 20-Nov-2021 Time 00:17:53 Description (S,S)WO1 4.6x100r

2: UV Detector: 230 Nm 2.0000-2.3500: Smooth (Mn, 2x3), 3.1000-3.5500: Smooth (Mn, 2x3) 1.66
Range: 1.669

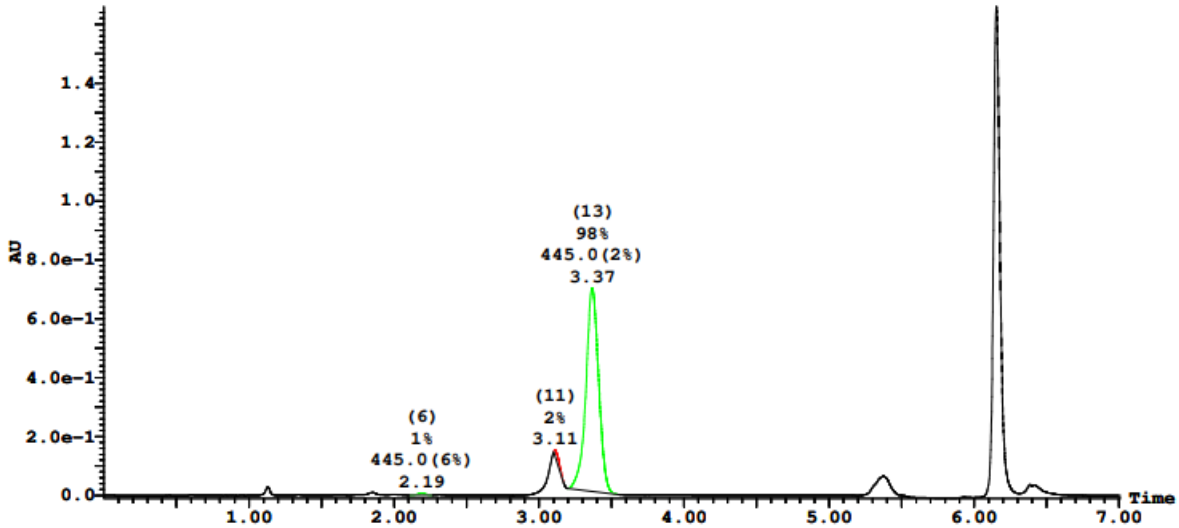

Peak Number	Compound	Time	AreaAbs	Area %Total	Width	Height	Mass Found
6	Found	2.19	4e+002	0.51	0	6e+003	445.0000
11		3.11	1e+003	1.55	0	2e+004	Not Found
13	Tentative	3.37	7e+004	97.94	0	7e+005	445.0000

H6: 98% ee

Openlynx Report - SHARLJA1

Sample: 55
File:SHARLJA1_20211119_CAROL_55
Description:(S,S)WO1 4.6x100mm 5µ

Vial:2:7
Date:20-Nov-2021
Conditions:5% IPA over 5min 3mL/min

ID:26-H6
Time:00:34:08

Me−CN
H6,
98% ee

Printed: Thu Dec 09 16:26:30 2021

Sample Report (continued):

Sample 55 Vial 2:7 ID 26-H6 File SHARLJA1_20211119_CAROL_55 Date 20-Nov-2021 Time 00:34:08 Description (S,S)WO1 4.6x100

2: UV Detector: 230 Nm 2.0000-2.3500: Smooth (Mn, 2x3), 3.1000-3.5500: Smooth (Mn, 2x3) 6.66e-1
Range: 6.735e-1

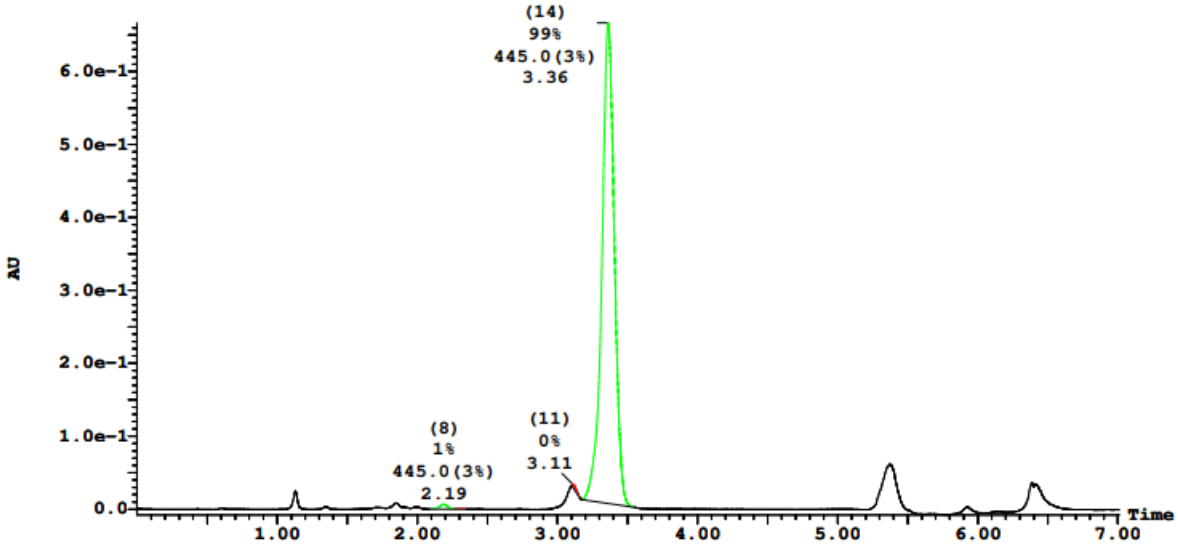

Peak Number	Compound	Time	AreaAbs	Area %Total	Width	Height	Mass Found
8	Found	2.19	4e+002	0.60	0	6e+003	445.0000
9		2.31	3e+001	0.04	0	7e+002	Not Found
11		3.11	2e+002	0.26	0	4e+003	Not Found
14	Tentative	3.36	7e+004	99.10	0	7e+005	445.0000

H10: 98% ee

Openlynx Report - SHARLJA1

Sample: 56
File:SHARLJA1_20211119_CAROL_56
Description:(S,S)WO1 4.6x100mm 5µ

Vial:2:8
Date:20-Nov-2021
Conditions:5% IPA over 5min 3mL/min

ID:26-H10
Time:00:42:15

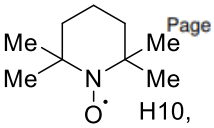

Printed: Thu Dec 09 16:26:30 2021

Sample Report (continued):

Sample 56 Vial 2:8 ID 26-H10 File SHARLJA1_20211119_CAROL_56 Date 20-Nov-2021 Time 00:42:15 Description (S,S)WO1 4.6x10

2: UV Detector: 230 Nm 2.0000-2.3500: Smooth (Mn, 2x3), 3.1000-3.5500: Smooth (Mn, 2x3) 6.844e-1
Range: 6.927e-1

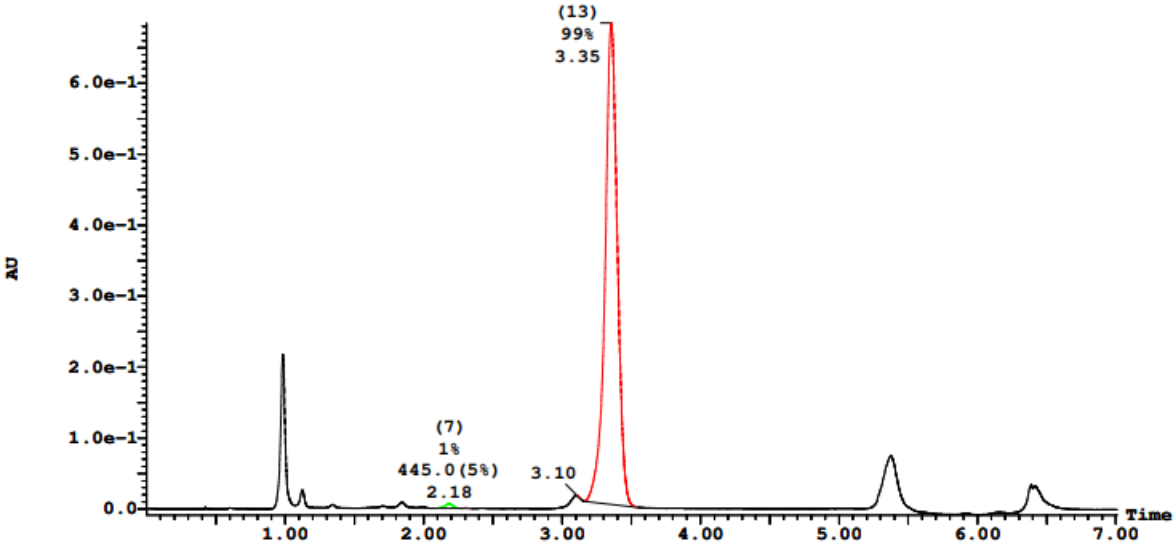

Peak Number	Compound	Time	AreaAbs	Area %Total	Width	Height	Mass Found
7	Found	2.18	4e+002	0.61	0	7e+003	445.0000
8		2.31	2e+001	0.03	0	5e+002	Not Found
11		3.10	4e+001	0.05	0	4e+002	Not Found
13		3.35	7e+004	99.31	0	7e+005	Not Found

H12: 98% ee

Openlynx Report - SHARLJA1

Sample: 57
File:SHARLJA1_20211119_CAROL_57
Description:(S,S)WO1 4.6x100mm 5µ

Vial:2:9
Date:20-Nov-2021
Conditions:5% IPA over 5min 3mL/min

ID:26-H12
Time:00:50:23

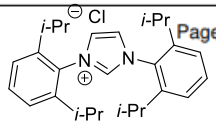

H12,
98% ee

Printed: Thu Dec 09 16:26:30 2021

Sample Report (continued):

Sample 57 Vial 2:9 ID 26-H12 File SHARLJA1_20211119_CAROL_57 Date 20-Nov-2021 Time 00:50:23 Description (S,S)WO1 4.6x100

2: UV Detector: 230 Nm 2.0000-2.3500: Smooth (Mn, 2x3), 3.1000-3.5500: Smooth (Mn, 2x3) 6.923e-1
Range: 7.011e-1

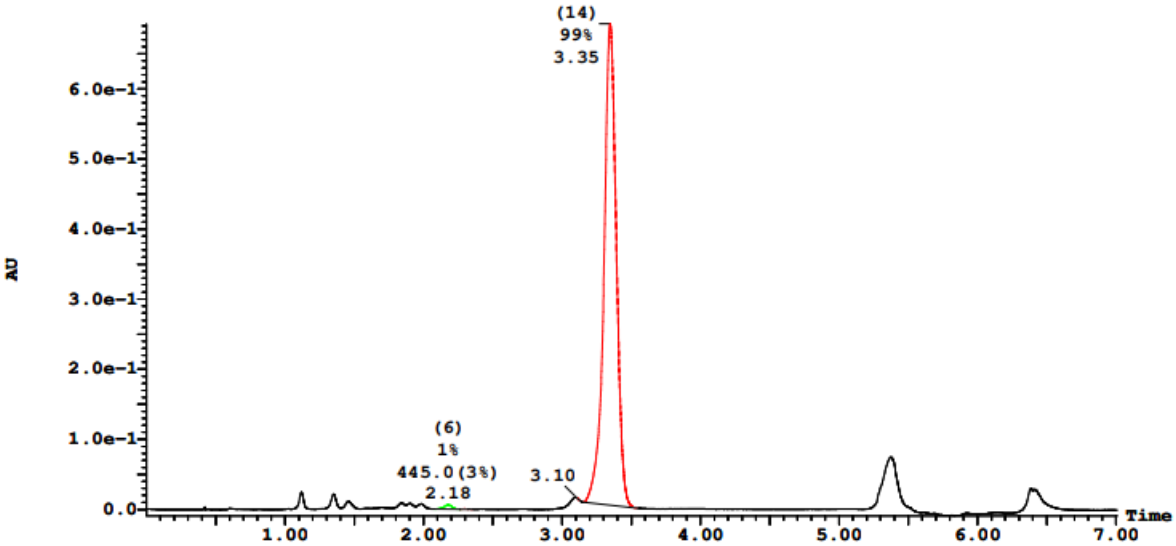

Peak Number	Compound	Time	AreaAbs	Area %Total	Width	Height	Mass Found
6	Tentative	2.18	4e+002	0.55	0	6e+003	445.0000
7		2.30	2e+001	0.02	0	4e+002	Not Found
8		2.33	5e+000	0.01	0	3e+002	Not Found
11		3.10	1e+001	0.02	0	1e-002	Not Found
14		3.35	7e+004	99.40	0	7e+005	Not Found

5.3 Successful reactions performed with Rh_2(*R*-NTTL)$_4$ and HFIP as solvent.

The following dataset represents reactions that were successful when performed according to **general procedure 5.1** using Rh_2(*R*-NTTL)$_4$ as catalyst and HFIP as solvent. Each additive is described according to the well plate designation in the study as well as the compound number it was assigned in the main text. The yield of the reaction in the presence of each additive is reported in **Figure C**8 and what follows is the HPLC data from which the yield was calculated according to equation 1.

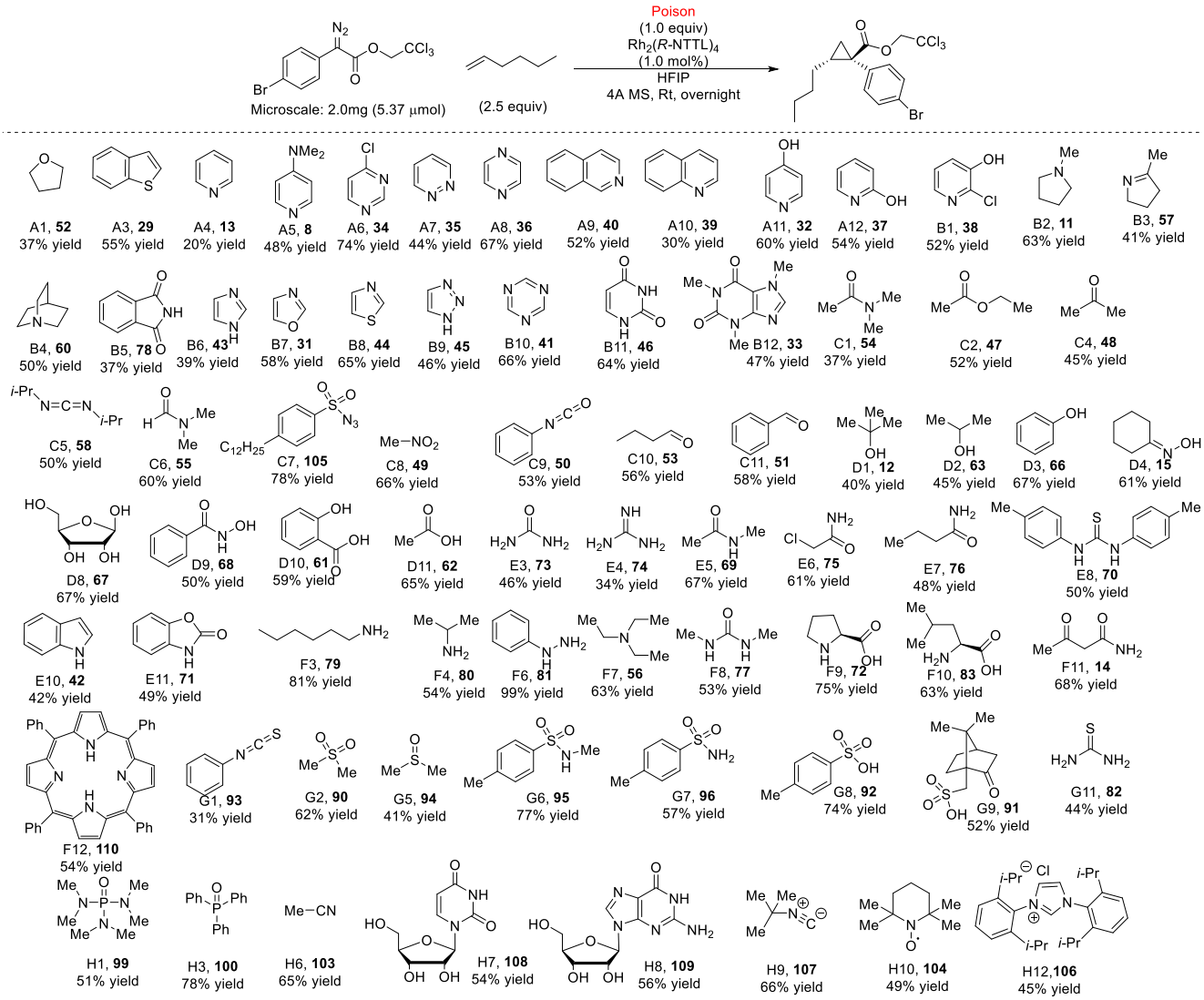

Figure C8: Reactions giving >30% yield (successful reactions) in the presence of Rh_2(*R*-NTTL)$_4$ and HFIP as solvent.

Single Sample Report
Sample Name: SHARLJA1-exp100-0027_12_01_2021_A1
Filename: sharlja1-exp100-0027_12_01_2021_a1.raw
Submitter:

Peak #	Formula	Target …	Target …	Time	Found	Area %	Area Abs
7	C23H28C…	493.1	Glyburi…	1.408	Yes	30.9	7591.85
16	C16H18B…	426.0	Product	2.071	Yes	45.7	11219.74

A1,
37% yield

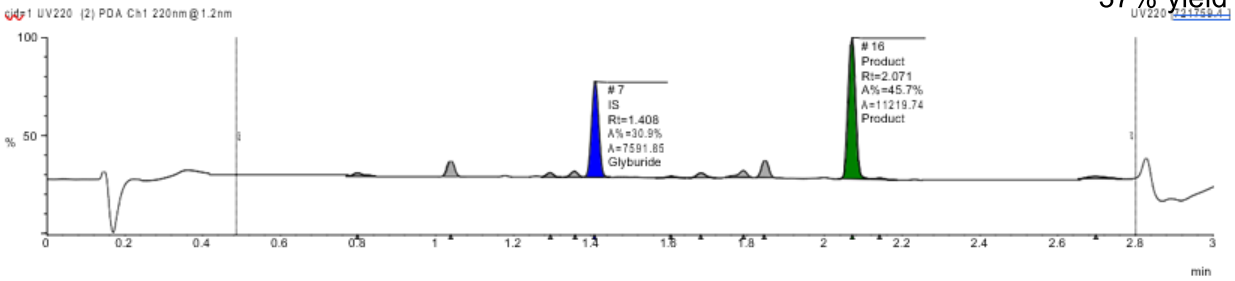

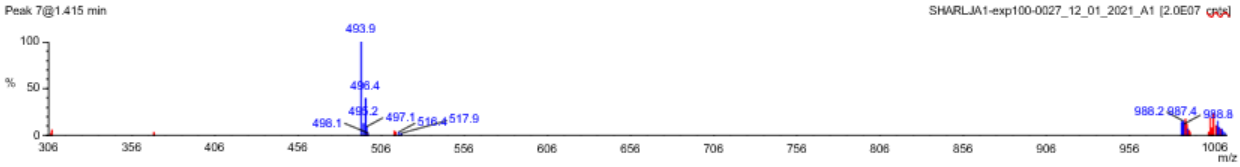

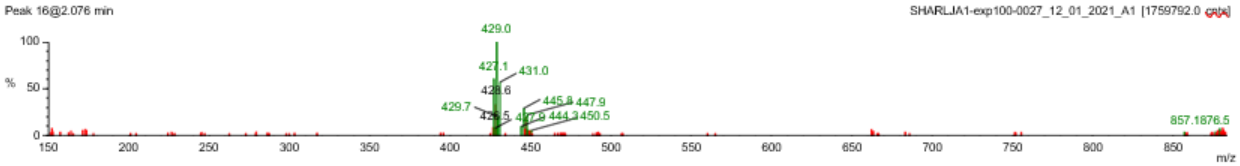

Name	Y/N	Type	Formula	Mass
Glyburide	Y	IS	C23H28ClN3O5S	493.1
Product	Y	Product	C16H18BrCl3O2	426.0

Single Sample Report
Sample Name: SHARLJA1-exp100-0027_12_01_2021_A3
Filename: sharlja1-exp100-0027_12_01_2021_a3.raw
Submitter:

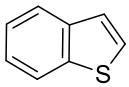

A3,
55% yield

Peak #	Formula	Target …	Target …	Time	Found	Area %	Area Abs
8	C23H28C…	493.1	Glyburi…	1.411	Yes	17.5	3013.31
20	C16H18B…	426.0	Product	2.071	Yes	37.6	6483.95

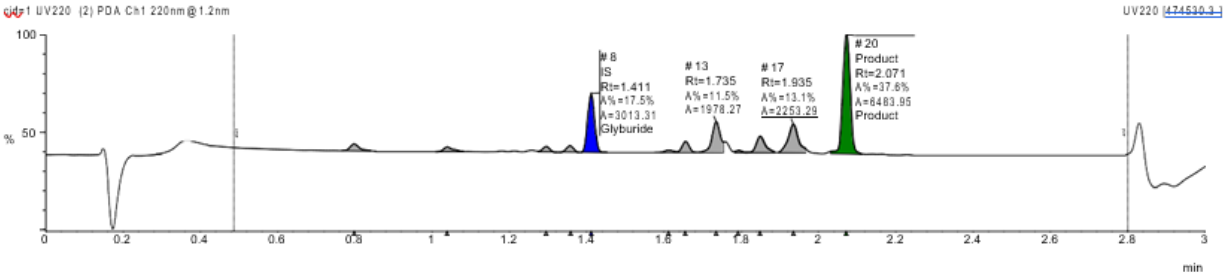

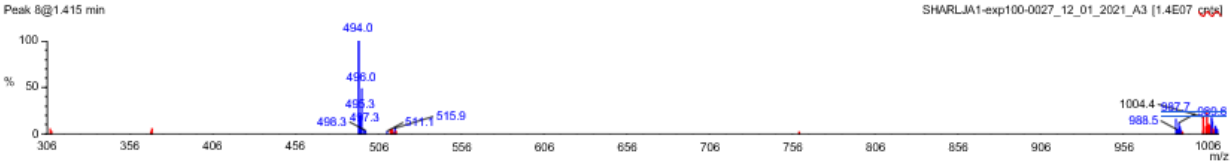

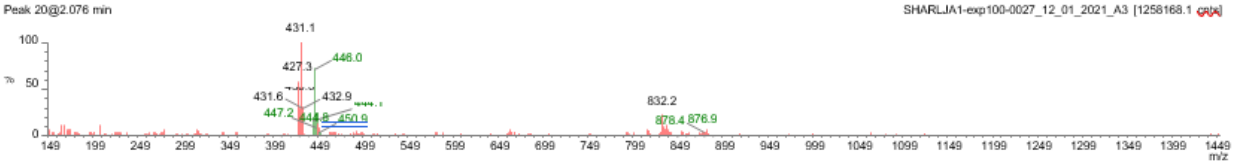

Name	Y/N	Type	Formula	Mass
Glyburide	Y	IS	C23H28ClN3O5S	493.1
Product	Y	Product	C16H18BrCl3O2	426.0

Single Sample Report
Sample Name: SHARLJA1-exp100-0027_12_01_2021_A4
Filename: sharlja1-exp100-0027_12_01_2021_a4.raw
Submitter:

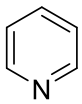

Peak #	Formula	Target …	Target …	Time	Found	Area %	Area Abs
10	C23H28C…	493.1	Glyburi…	1.411	Yes	43.4	10619.91
16	C16H18B…	426.0	Product	2.071	Yes	37.4	9158.44

A4,
20% yield

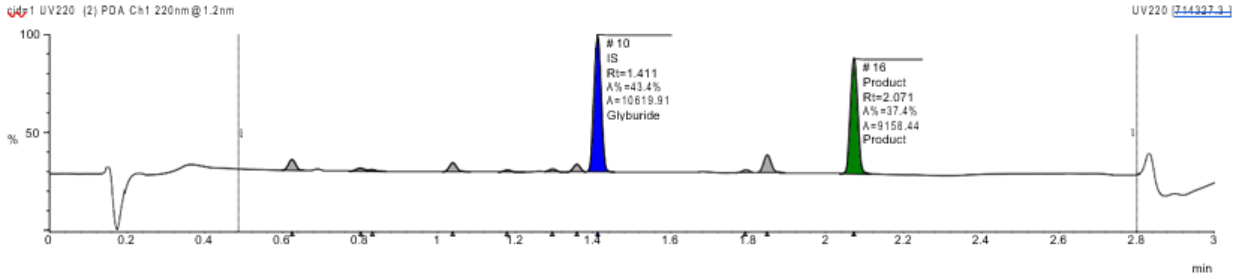

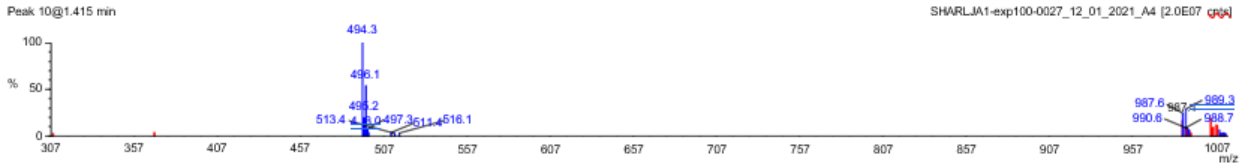

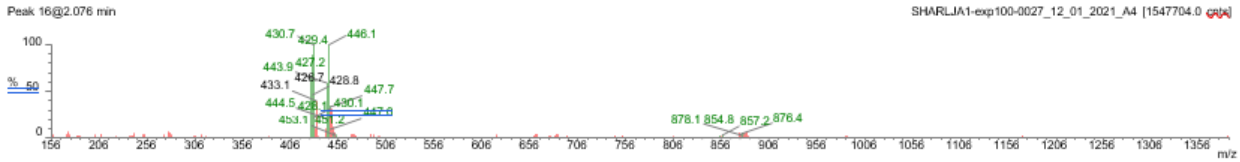

Name	Y/N	Type	Formula	Mass
Glyburide	Y	IS	C23H28ClN3O5S	493.1
Product	Y	Product	C16H18BrCl3O2	426.0

Single Sample Report
Sample Name: SHARLJA1-exp100-0027_12_01_2021_A5
Filename: sharlja1-exp100-0027_12_01_2021_a5.raw
Submitter:

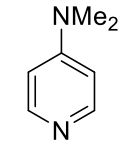

A5,
48% yield

Peak #	Formula	Target …	Target …	Time	Found	Area %	Area Abs
9	C23H28C…	493.1	Glyburi…	1.411	Yes	22.5	7714.25
18	C16H18B…	426.0	Product	2.071	Yes	42.4	14535.41

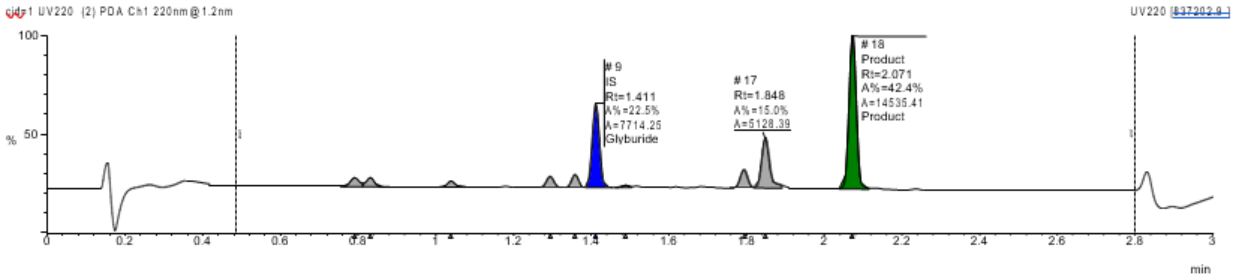

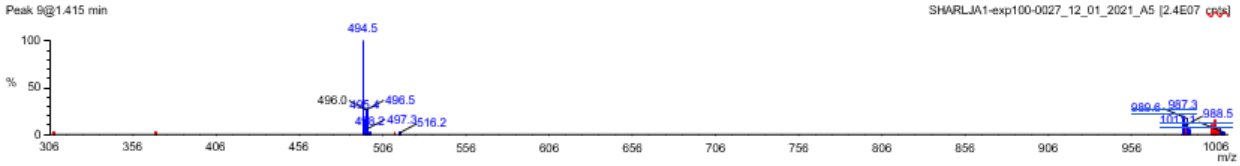

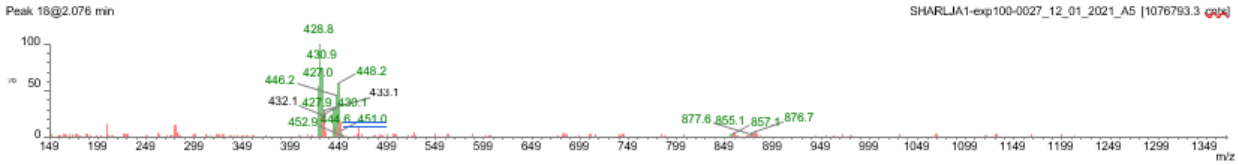

Name	Y/N	Type	Formula	Mass
Glyburide	Y	IS	C23H28ClN3O5S	493.1
Product	Y	Product	C16H18BrCl3O2	426.0

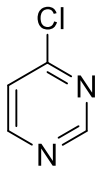

A6,
74% yield

Single Sample Report
Sample Name: SHARLJA1-exp100-0027_12_01_2021_A6
Filename: sharlja1-exp100-0027_12_01_2021_a6.raw
Submitter:

Peak #	Formula	Target …	Target …	Time	Found	Area %	Area Abs
10	C23H28C…	493.1	Glyburi…	1.411	Yes	20.5	6783.78
19	C16H18B…	426.0	Product	2.071	Yes	57.9	19175.76

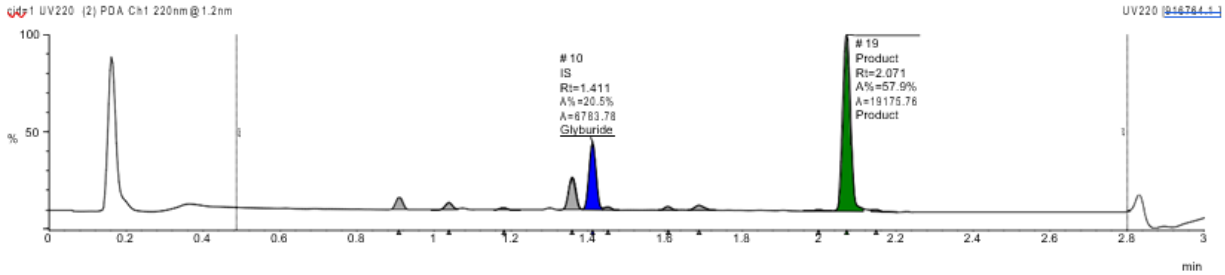

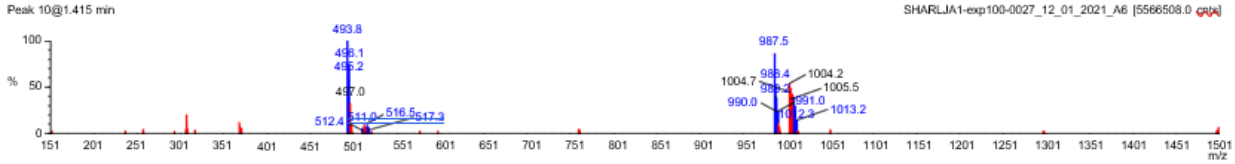

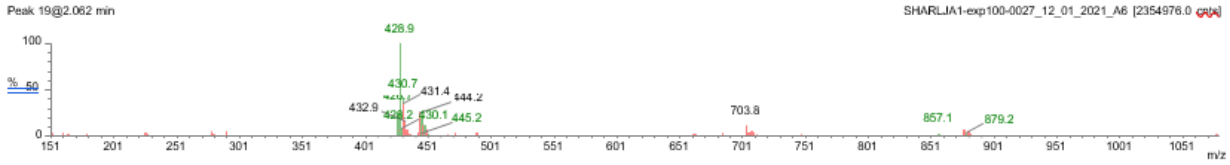

Name	Y/N	Type	Formula	Mass
Glyburide	Y	IS	C23H28ClN3O5S	493.1
Product	Y	Product	C16H18BrCl3O2	426.0

Single Sample Report
Sample Name: SHARLJA1-exp100-0027_12_01_2021_A7
Filename: sharlja1-exp100-0027_12_01_2021_a7.raw
Submitter:

A7,
44% yield

Peak #	Formula	Target …	Target …	Time	Found	Area %	Area Abs
12	C23H28C…	493.1	Glyburi…	1.411	Yes	23.8	7143.93
25	C16H18B…	426.0	Product	2.071	Yes	41.1	12356.90

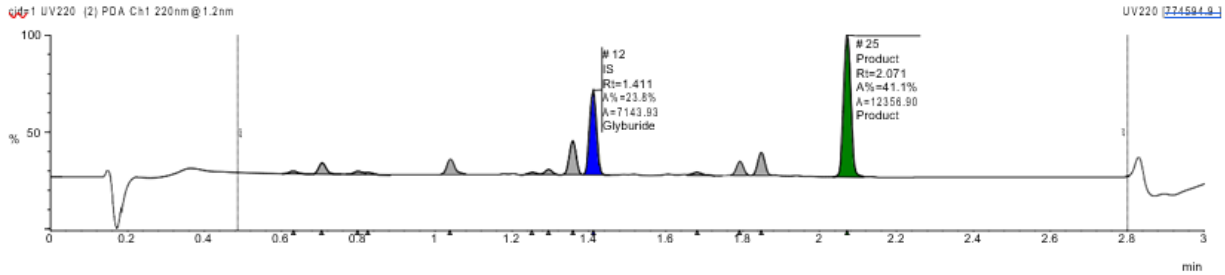

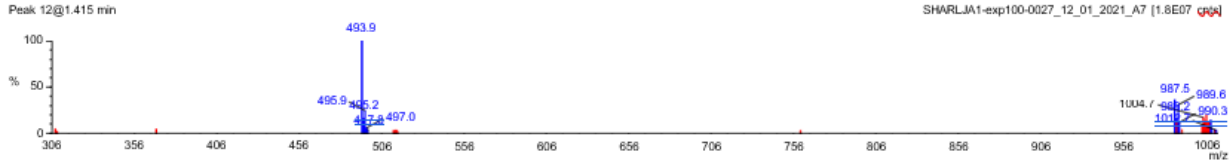

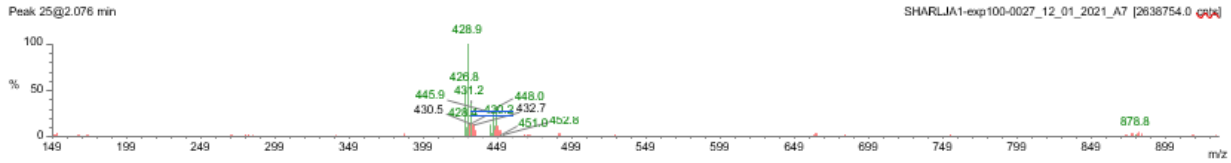

Name	Y/N	Type	Formula	Mass
Glyburide	Y	IS	C23H28ClN3O5S	493.1
Product	Y	Product	C16H18BrCl3O2	426.0

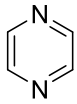

A8,
67% yield

Single Sample Report
Sample Name: SHARLJA1-exp100-0027_12_01_2021_A8
Filename: sharlja1-exp100-0027_12_01_2021_a8.raw
Submitter:

Peak #	Formula	Target …	Target …	Time	Found	Area %	Area Abs
12	C23H28C…	493.1	Glyburi…	1.411	Yes	19.5	6494.20
19	C16H18B…	426.0	Product	2.071	Yes	50.4	16790.71

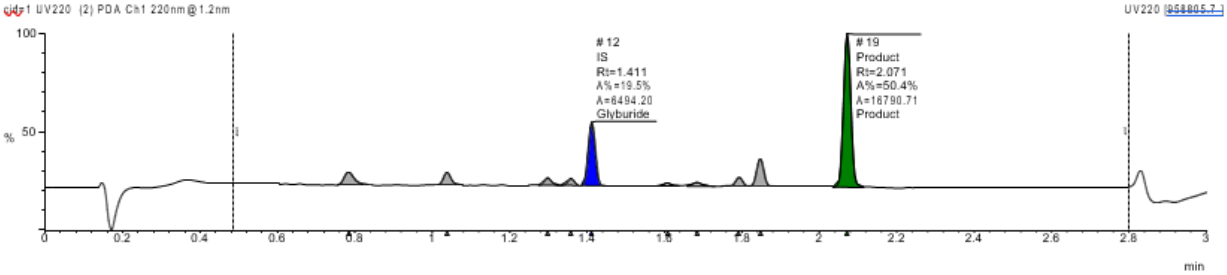

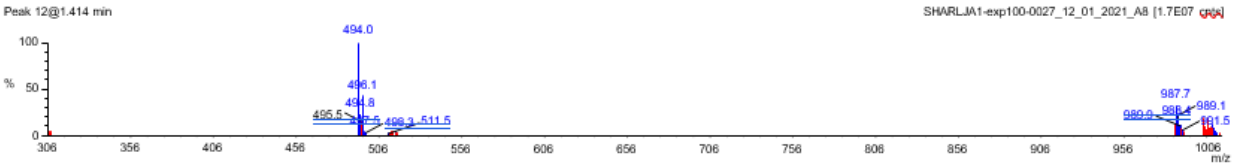

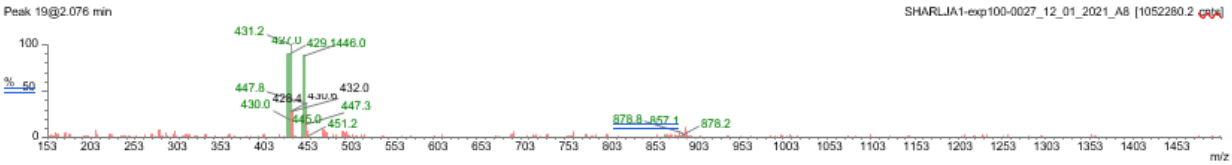

Name	Y/N	Type	Formula	Mass
Glyburide	Y	IS	C23H28ClN3O5S	493.1
Product	Y	Product	C16H18BrCl3O2	426.0

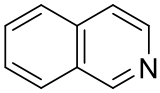

A9,
52% yield

Single Sample Report
Sample Name: SHARLJA1-exp100-0027_12_01_2021_A9
Filename: sharlja1-exp100-0027_12_01_2021_a9.raw
Submitter:

Peak #	Formula	Target …	Target …	Time	Found	Area %	Area Abs
14	C23H28C…	493.1	Glyburi…	1.408	Yes	22.9	6467.37
24	C16H18B…	426.0	Product	2.071	Yes	46.3	13043.57

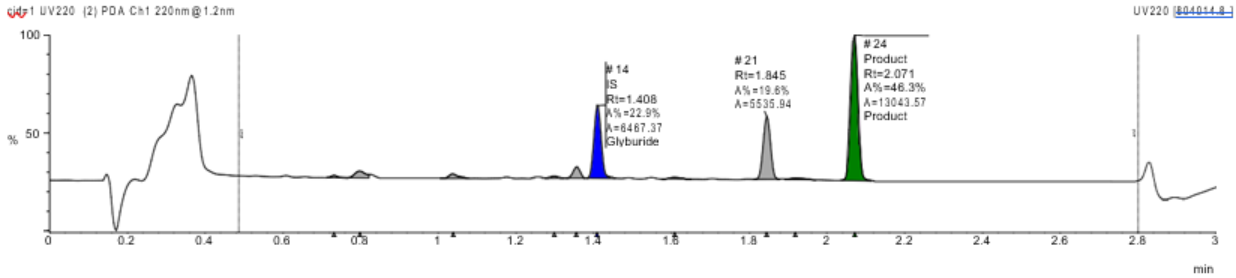

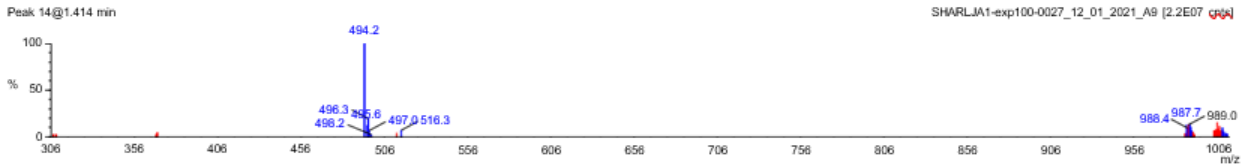

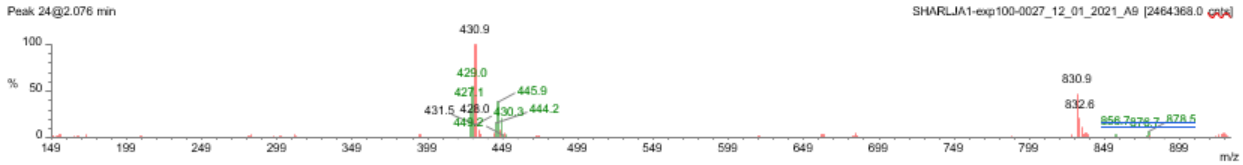

Name	Y/N	Type	Formula	Mass
Glyburide	Y	IS	C23H28ClN3O5S	493.1
Product	Y	Product	C16H18BrCl3O2	426.0

Single Sample Report
Sample Name: SHARLJA1-exp100-0027_12_01_2021_A10
Filename: sharlja1-exp100-0027_12_01_2021_a10.raw
Submitter:

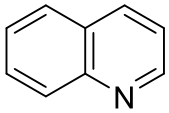

A10,
30% yield

Peak #	Formula	Target …	Target …	Time	Found	Area %	Area Abs
11	C23H28C…	493.1	Glyburi…	1.411	Yes	32.3	7019.56
22	C16H18B…	426.0	Product	2.075	Yes	37.7	8200.84

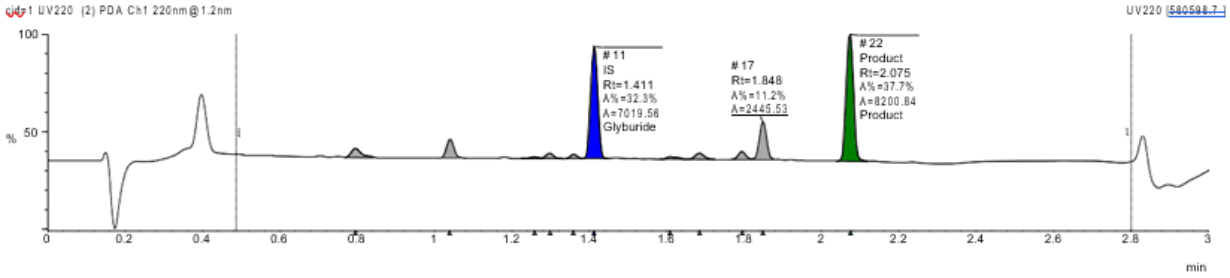

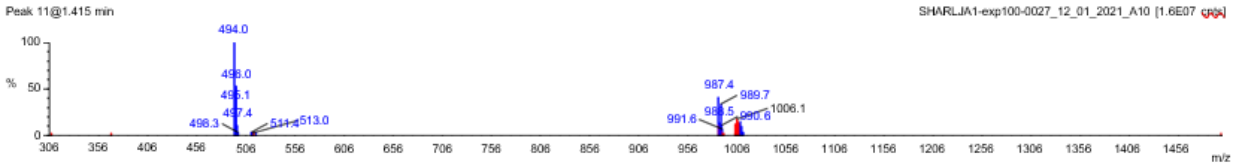

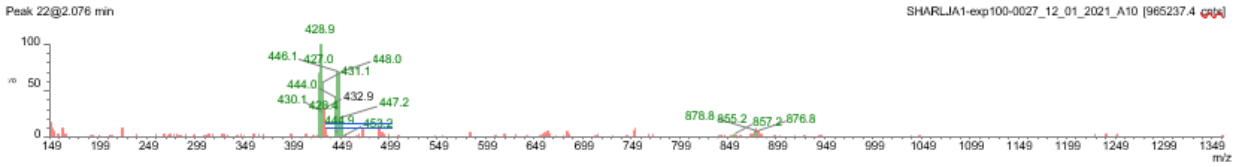

Name	Y/N	Type	Formula	Mass
Glyburide	Y	IS	C23H28ClN3O5S	493.1
Product	Y	Product	C16H18BrCl3O2	426.0

Single Sample Report
Sample Name: SHARLJA1-exp100-0027_12_01_2021_A11
Filename: sharlja1-exp100-0027_12_01_2021_a11.raw
Submitter:

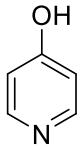

A11,
60% yield

Peak #	Formula	Target …	Target …	Time	Found	Area %	Area Abs
16	C23H28C…	493.1	Glyburi…	1.411	Yes	20.7	6830.00
25	C16H18B…	426.0	Product	2.071	Yes	47.8	15788.45

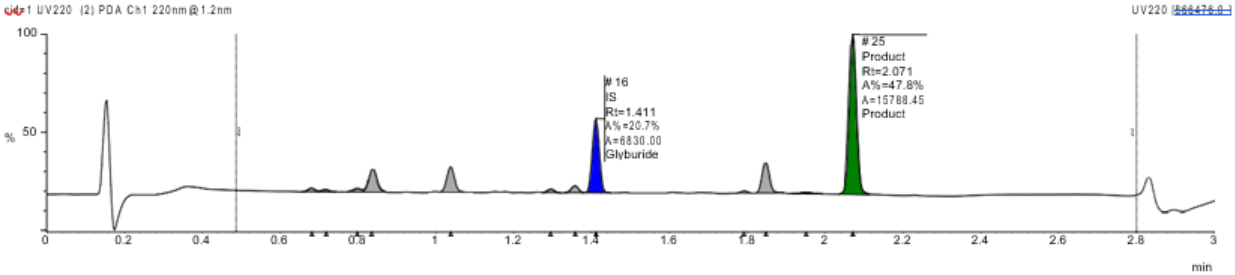

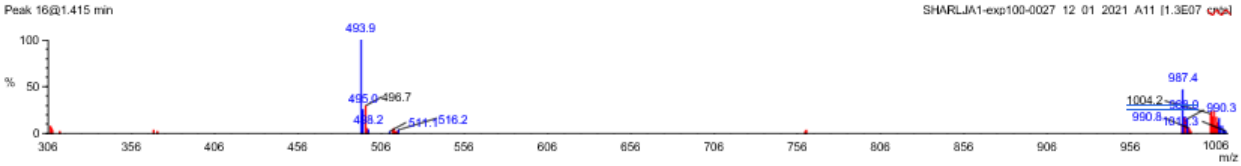

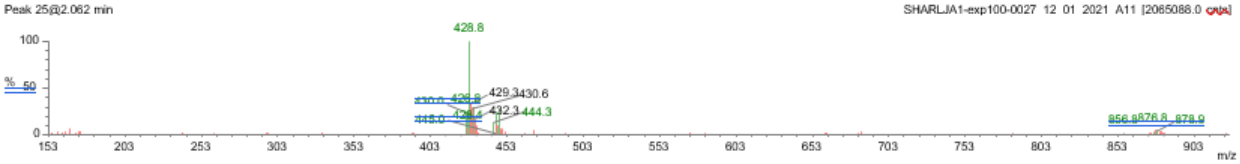

Name	Y/N	Type	Formula	Mass
Glyburide	Y	IS	C23H28ClN3O5S	493.1
Product	Y	Product	C16H18BrCl3O2	426.0

Sample Name: SHARLJA1-exp100-0027_12_01_2021_A12
Filename: sharlja1-exp100-0027_12_01_2021_a12.raw
Submitter:

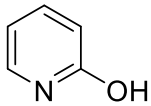

A12,
54% yield

Peak #	Formula	Target …	Target …	Time	Found	Area %	Area Abs
12	C23H28C…	493.1	Glyburi…	1.411	Yes	17.2	6393.56
21	C16H18B…	426.0	Product	2.071	Yes	36.3	13529.62

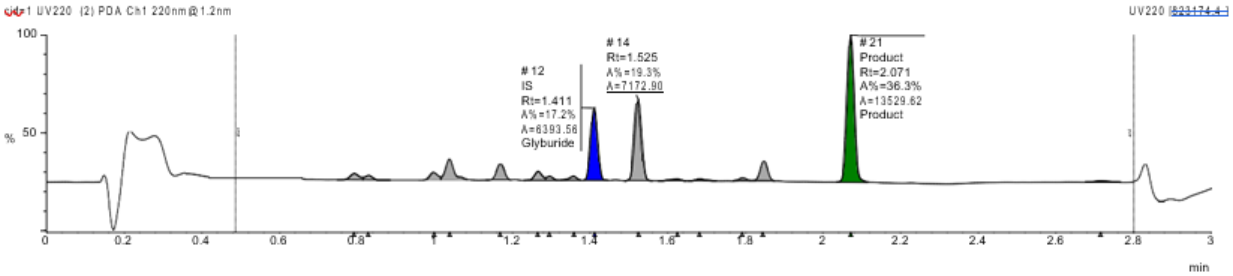

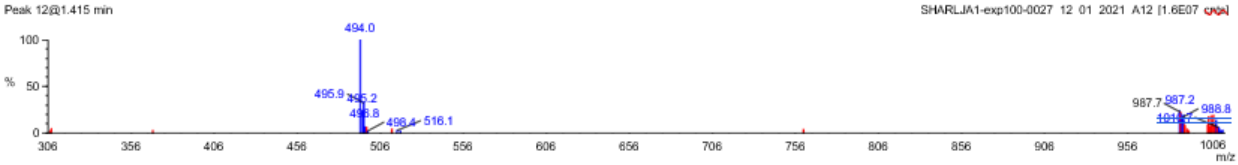

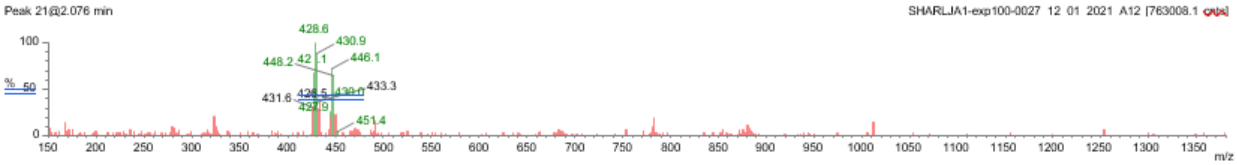

Name	Y/N	Type	Formula	Mass
Glyburide	Y	IS	C23H28ClN3O5S	493.1
Product	Y	Product	C16H18BrCl3O2	426.0

Sample Name: SHARLJA1-exp100-0027_12_01_2021_B1
Filename: sharlja1-exp100-0027_12_01_2021_b1.raw
Submitter:

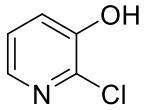

B1,
52% yield

Peak #	Formula	Target …	Target …	Time	Found	Area %	Area Abs
9	C23H28C…	493.1	Glyburi…	1.415	Yes	18.4	6660.32
18	C16H18B…	426.0	Product	2.075	Yes	37.2	13463.23

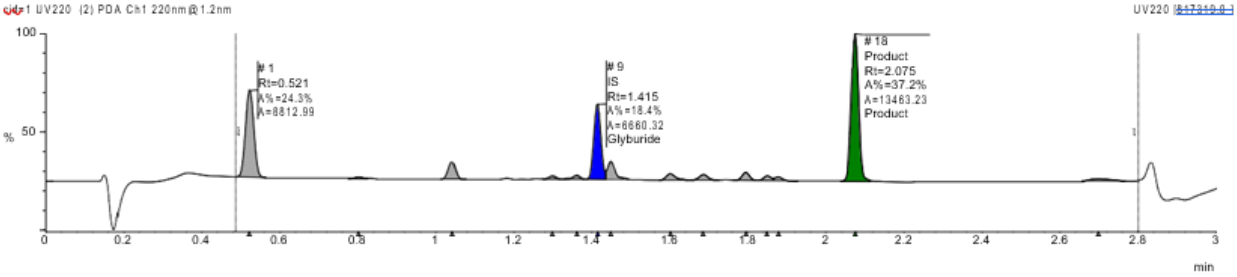

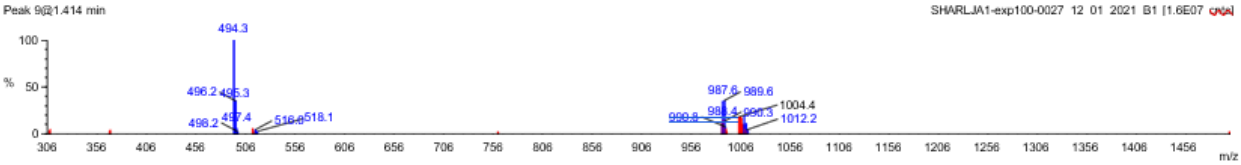

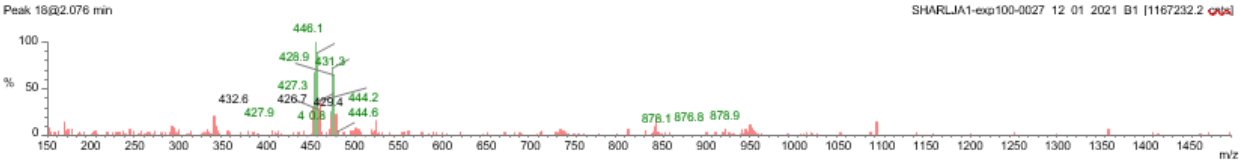

Name	Y/N	Type	Formula	Mass
Glyburide	Y	IS	C23H28ClN3O5S	493.1
Product	Y	Product	C16H18BrCl3O2	426.0

Single Sample Report
Sample Name: SHARLJA1-exp100-0027_12_01_2021_B2
Filename: sharlja1-exp100-0027_12_01_2021_b2.raw
Submitter:

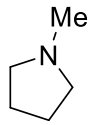

B2,
63% yield

Peak #	Formula	Target …	Target …	Time	Found	Area %	Area Abs
10	C23H28C…	493.1	Glyburi…	1.411	Yes	19.3	5700.96
20	C16H18B…	426.0	Product	2.071	Yes	46.7	13834.50

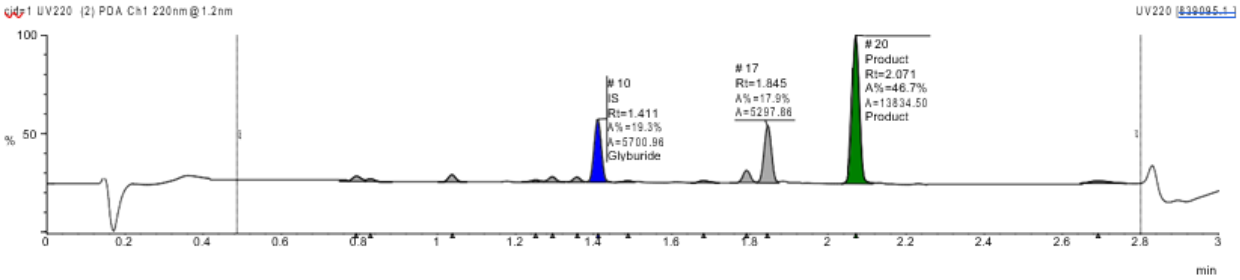

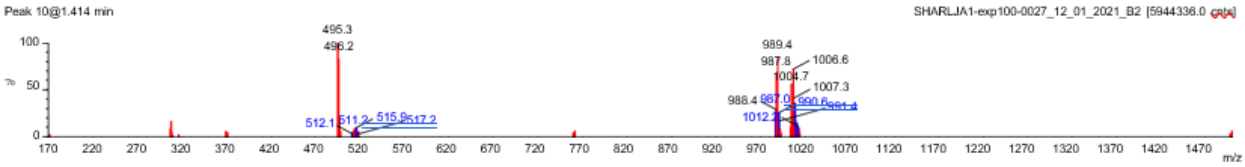

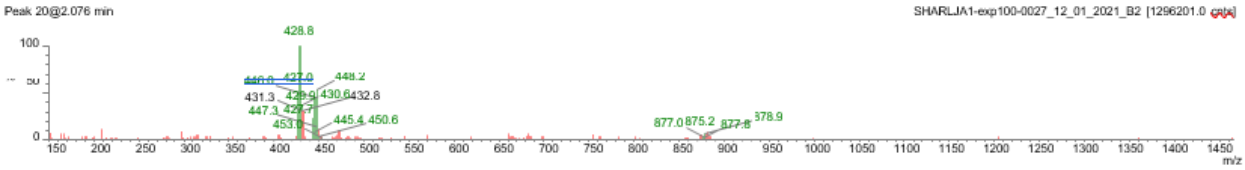

Name	Y/N	Type	Formula	Mass
Glyburide	Y	IS	C23H28ClN3O5S	493.1
Product	Y	Product	C16H18BrCl3O2	426.0

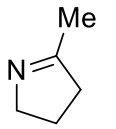

B3,
41% yield

Single Sample Report
Sample Name: SHARLJA1-exp100-0027_12_01_2021_B3
Filename: sharlja1-exp100-0027_12_01_2021_b3.raw
Submitter:

Peak #	Formula	Target …	Target …	Time	Found	Area %	Area Abs
11	C23H28C…	493.1	Glyburi…	1.411	Yes	27.8	3519.77
20	C16H18B…	426.0	Product	2.071	Yes	45.6	5765.17

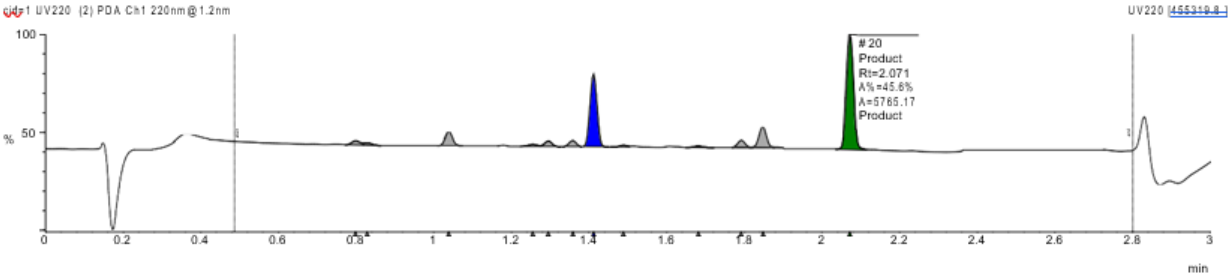

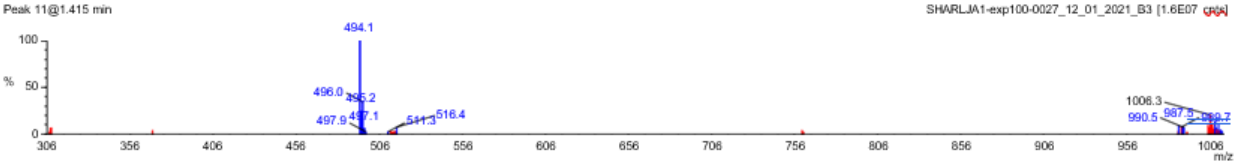

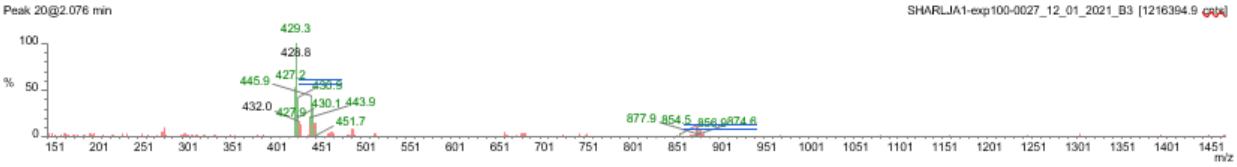

Name	Y/N	Type	Formula	Mass
Glyburide	Y	IS	C23H28ClN3O5S	493.1
Product	Y	Product	C16H18BrCl3O2	426.0

Single Sample Report
Sample Name: SHARLJA1-exp100-0027_12_01_2021_B4
Filename: sharlja1-exp100-0027_12_01_2021_b4.raw
Submitter:

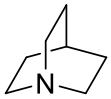

B4,
50% yield

Peak #	Formula	Target …	Target …	Time	Found	Area %	Area Abs
8	C23H28C…	493.1	Glyburi…	1.415	Yes	24.6	3371.49
16	C16H18B…	426.0	Product	2.075	Yes	48.1	6579.16

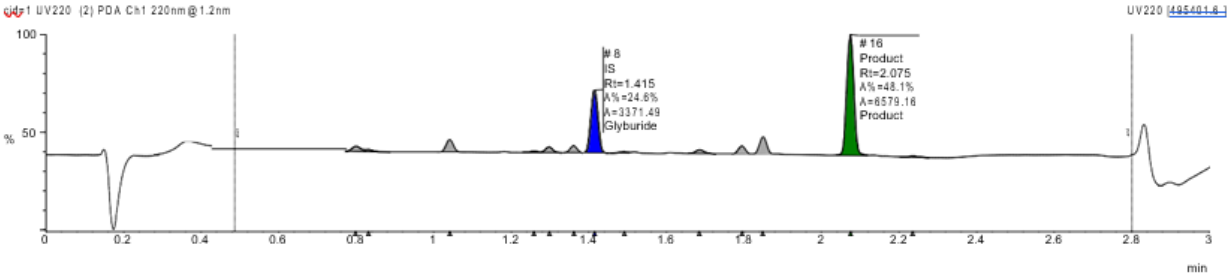

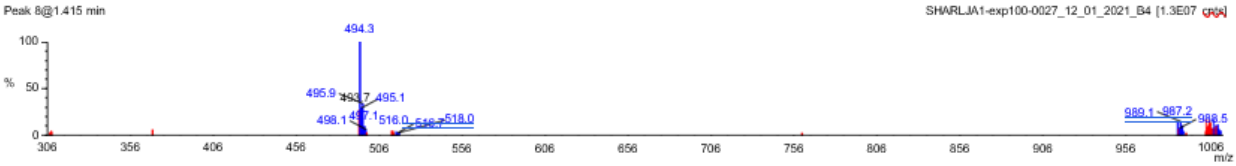

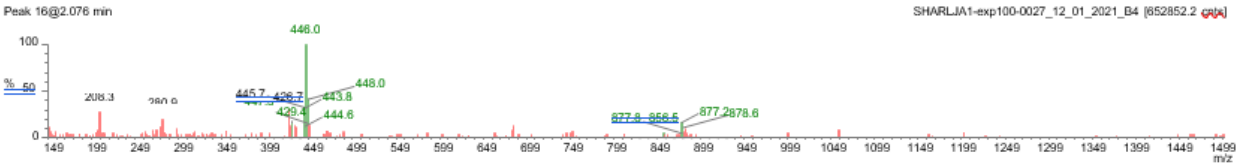

Name	Y/N	Type	Formula	Mass
Glyburide	Y	IS	C23H28ClN3O5S	493.1
Product	Y	Product	C16H18BrCl3O2	426.0

Single Sample Report
Sample Name: SHARLJA1-exp100-0027_12_01_2021_B5
Filename: sharlja1-exp100-0027_12_01_2021_b5.raw
Submitter

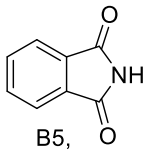

B5,
37% yield

Peak #	Formula	Target …	Target …	Time	Found	Area %	Area Abs
9	C23H28C…	493.1	Glyburi…	1.411	Yes	12.2	6672.64
16	C16H18B…	426.0	Product	2.075	Yes	18.3	10004.96

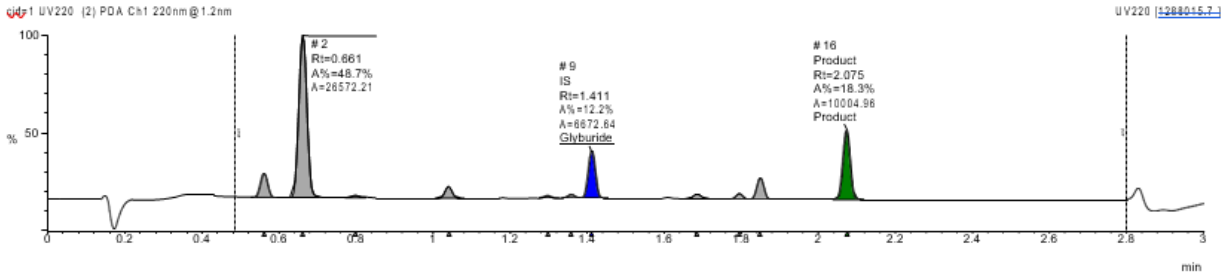

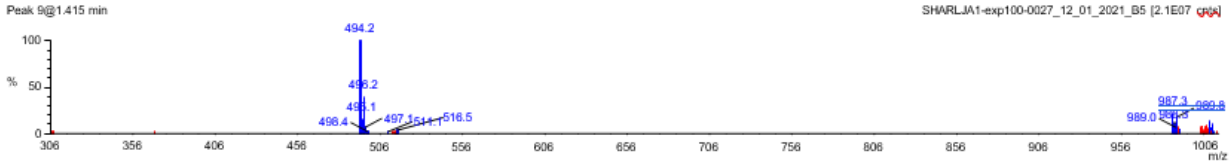

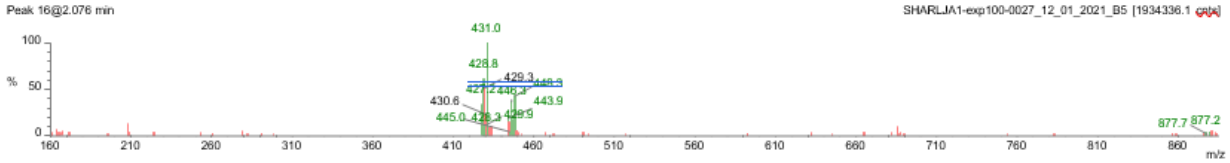

Name	Y/N	Type	Formula	Mass
Glyburide	Y	IS	C23H28ClN3O5S	493.1
Product	Y	Product	C16H18BrCl3O2	426.0

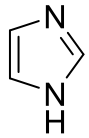

B6,
39% yield

Single Sample Report
Sample Name: SHARLJA1-exp100-0027_12_01_2021_B6
Filename: sharlja1-exp100-0027_12_01_2021_b6.raw
Submitter:

Peak #	Formula	Target …	Target …	Time	Found	Area %	Area Abs
15	C23H28C…	493.1	Glyburi…	1.411	Yes	28.9	4606.10
22	C16H18B…	426.0	Product	2.071	Yes	44.9	7151.44

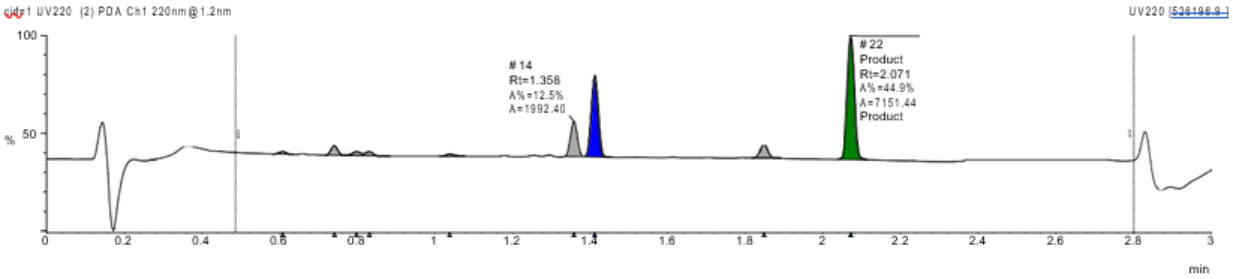

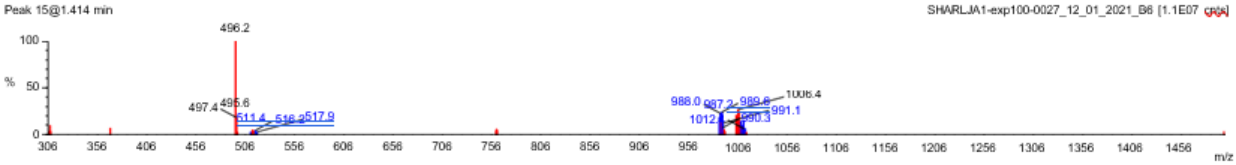

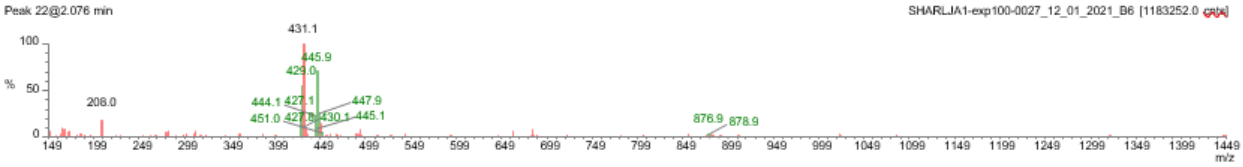

Name	Y/N	Type	Formula	Mass
Glyburide	Y	IS	C23H28ClN3O5S	493.1
Product	Y	Product	C16H18BrCl3O2	426.0

Single Sample Report
Sample Name: SHARLJA1-exp100-0027_12_01_2021_B7
Filename: sharlja1-exp100-0027_12_01_2021_b7.raw
Submitter:

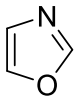

B7,
58% yield

Peak #	Formula	Target …	Target …	Time	Found	Area %	Area Abs
10	C23H28C…	493.1	Glyburi…	1.415	Yes	21.3	6639.31
17	C16H18B…	426.0	Product	2.075	Yes	48.1	15006.77

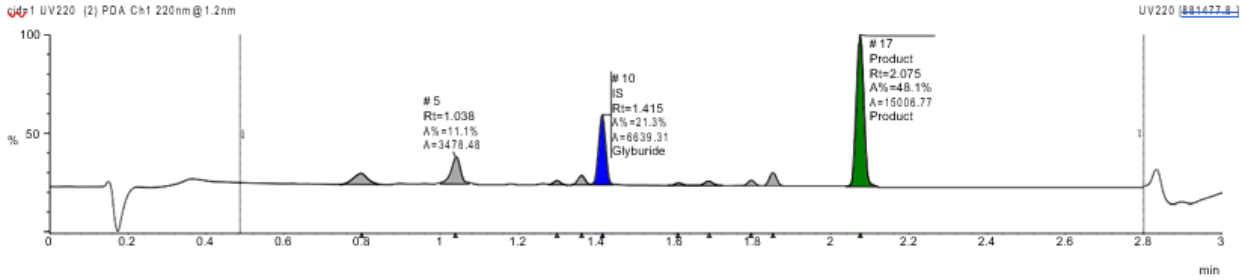

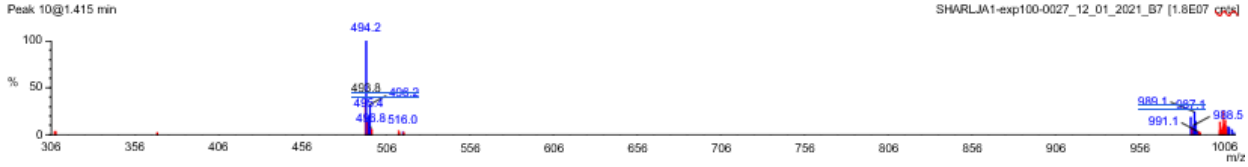

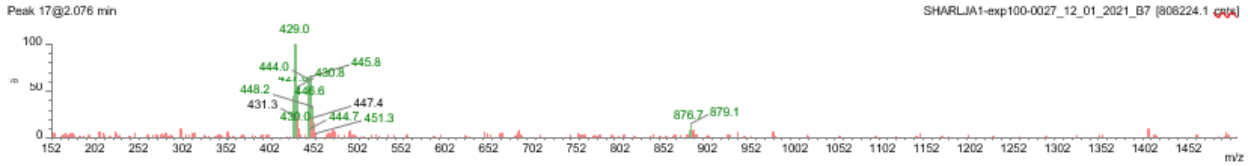

Name	Y/N	Type	Formula	Mass
Glyburide	Y	IS	C23H28ClN3O5S	493.1
Product	Y	Product	C16H18BrCl3O2	426.0

Single Sample Report
Sample Name: SHARLJA1-exp100-0027_12_01_2021_B8
Filename: sharlja1-exp100-0027_12_01_2021_b8.raw
Submitter:

B8,
65% yield

Peak #	Formula	Target …	Target …	Time	Found	Area %	Area Abs
12	C23H28C…	493.1	Glyburi…	1.411	Yes	19.8	7338.80
25	C16H18B…	426.0	Product	2.071	Yes	49.2	18264.42

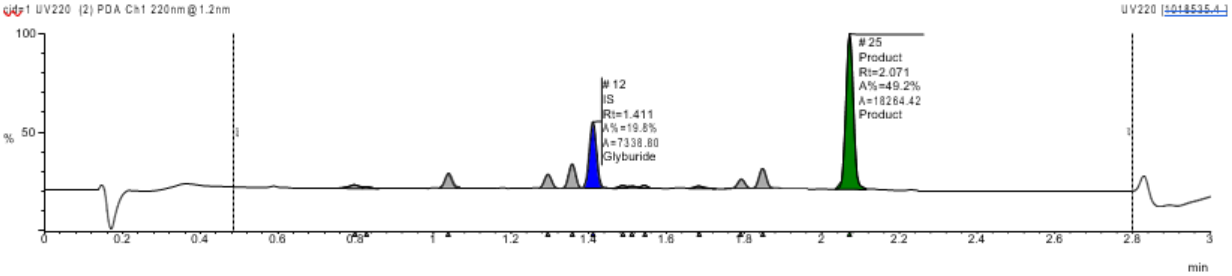

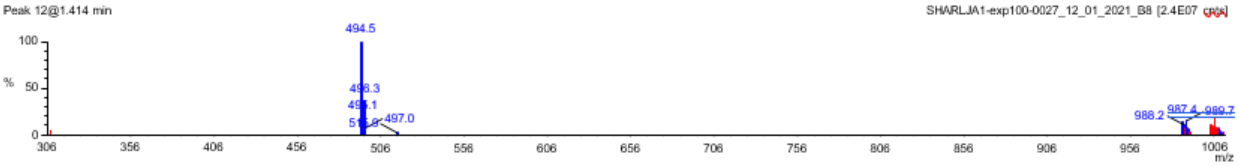

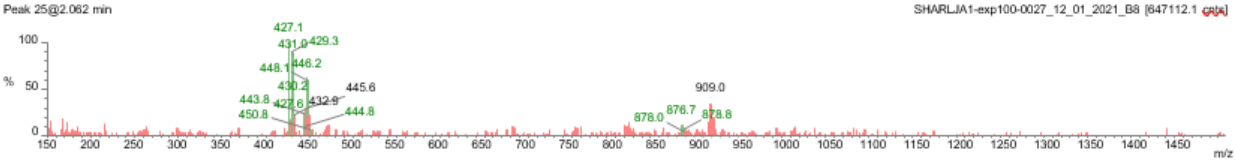

Name	Y/N	Type	Formula	Mass
Glyburide	Y	IS	C23H28ClN3O5S	493.1
Product	Y	Product	C16H18BrCl3O2	426.0

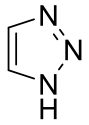

B9,
46% yield

Single Sample Report
Sample Name: SHARLJA1-exp100-0027_12_01_2021_B9
Filename: sharlja1-exp100-0027_12_01_2021_b9.raw
Submitter:

Peak #	Formula	Target …	Target …	Time	Found	Area %	Area Abs
11	C23H28C…	493.1	Glyburi…	1.411	Yes	18.8	6506.90
20	C16H18B…	426.0	Product	2.071	Yes	33.8	11728.29

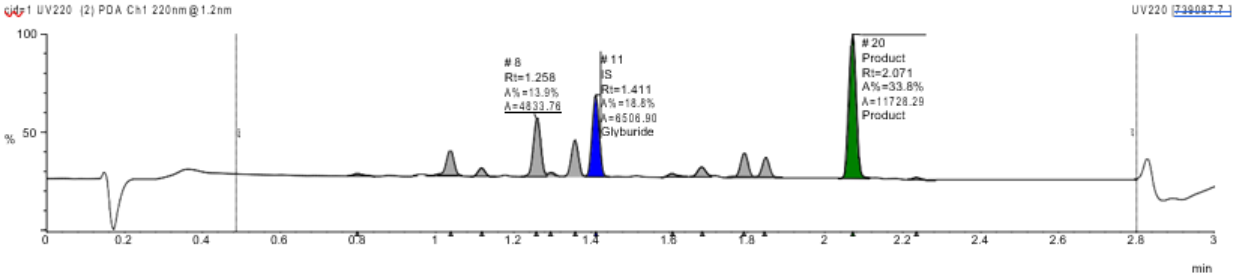

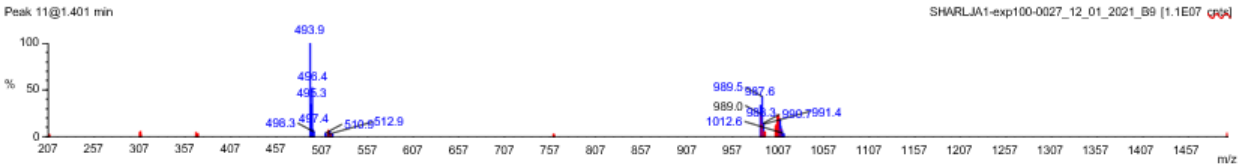

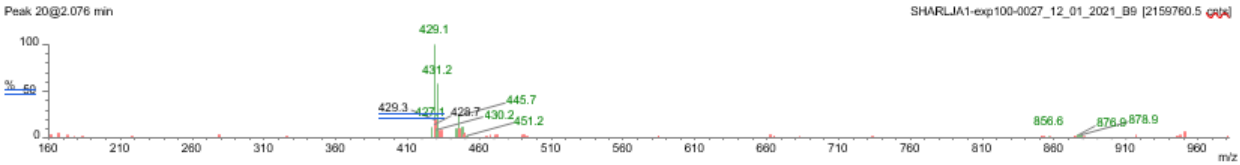

Name	Y/N	Type	Formula	Mass
Glyburide	Y	IS	C23H28ClN3O5S	493.1
Product	Y	Product	C16H18BrCl3O2	426.0

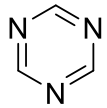

B10,
66% yield

Single Sample Report
Sample Name: SHARLJA1-exp100-0027_12_01_2021_B10
Filename: sharlja1-exp100-0027_12_01_2021_b10.raw
Submitter:

Peak #	Formula	Target …	Target …	Time	Found	Area %	Area Abs
11	C23H28C…	493.1	Glyburi…	1.411	Yes	18.2	6718.44
21	C16H18B…	426.0	Product	2.071	Yes	46.6	17163.61

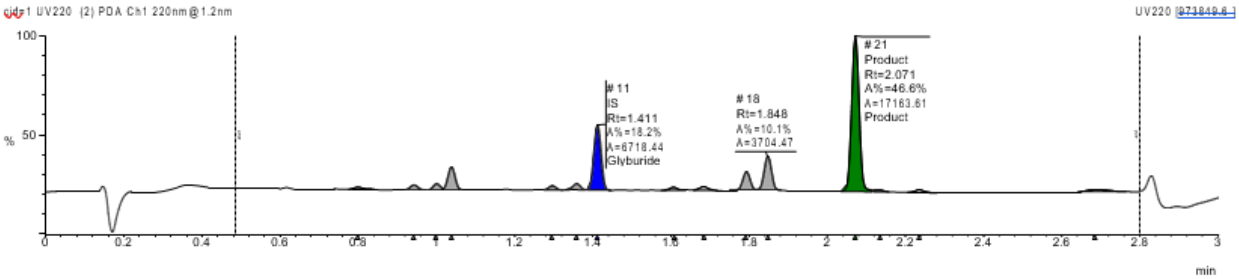

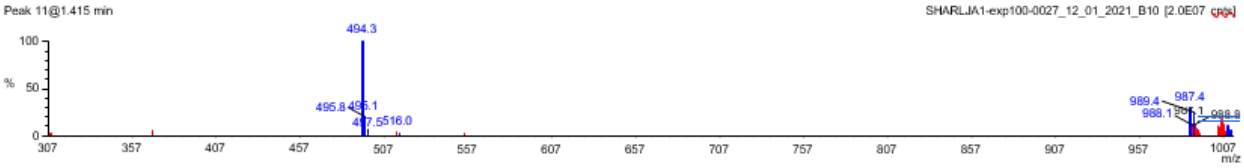

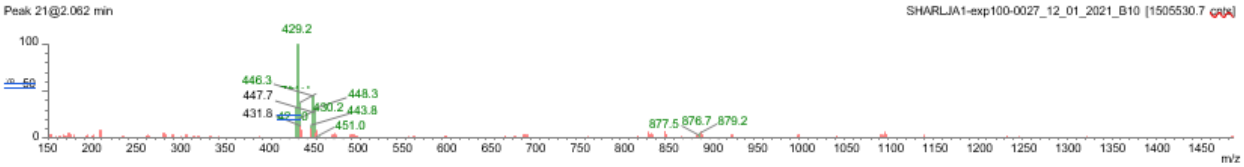

Name	Y/N	Type	Formula	Mass
Glyburide	Y	IS	C23H28ClN3O5S	493.1
Product	Y	Product	C16H18BrCl3O2	426.0

Sample Name: SHARLJA1-exp100-0027_12_01_2021_B11
Filename: sharlja1-exp100-0027_12_01_2021_b11.raw
Submitter:

Peak #	Formula	Target …	Target …	Time	Found	Area %	Area Abs
9	C23H28C…	493.1	Glyburi…	1.411	Yes	19.8	4301.02
17	C16H18B…	426.0	Product	2.075	Yes	48.6	10576.93

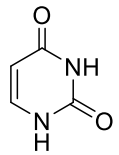

B11,
64% yield

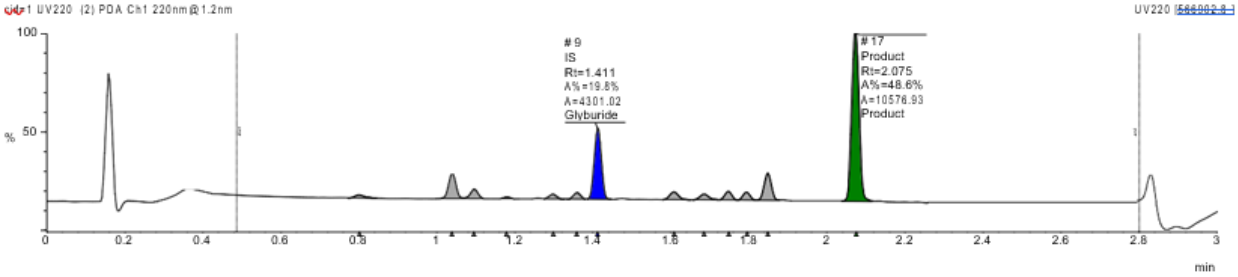

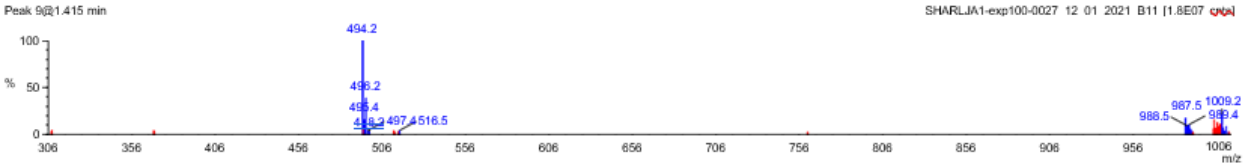

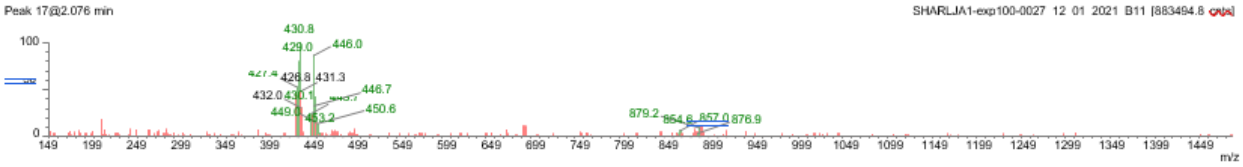

Name	Y/N	Type	Formula	Mass
Glyburide	Y	IS	C23H28ClN3O5S	493.1
Product	Y	Product	C16H18BrCl3O2	426.0

Sample Name: SHARLJA1-exp100-0027_12_01_2021_B12
Filename: sharlja1-exp100-0027_12_01_2021_b12.raw
Submitter:

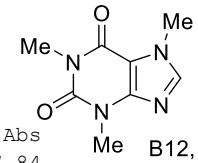

B12, 47% yield

Peak #	Formula	Target …	Target …	Time	Found	Area %	Area Abs
9	C23H28C…	493.1	Glyburi…	1.415	Yes	14.1	6707.84
16	C16H18B…	426.0	Product	2.075	Yes	26.3	12509.34

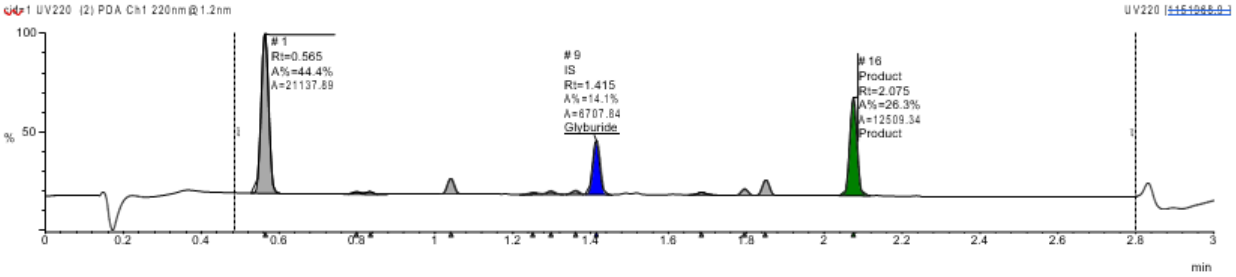

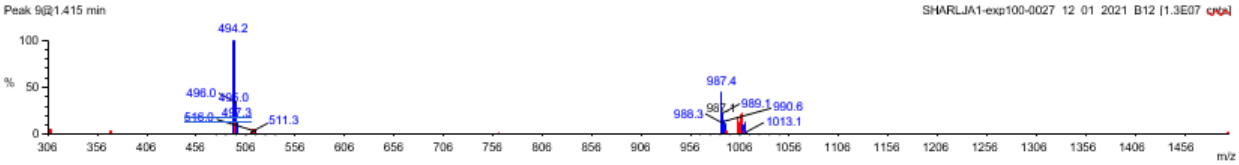

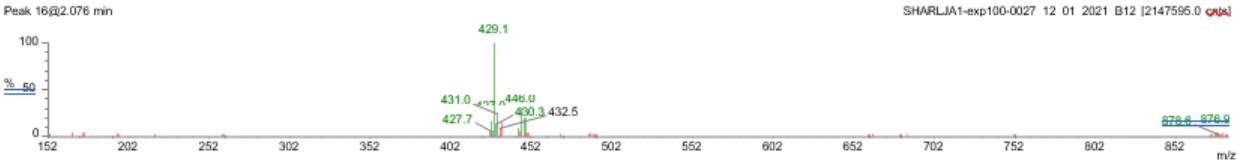

Name	Y/N	Type	Formula	Mass
Glyburide	Y	IS	C23H28ClN3O5S	493.1
Product	Y	Product	C16H18BrCl3O2	426.0

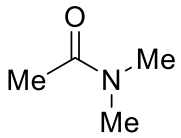

C1,
37% yield

Sample Name: SHARLJA1-exp100-0027_12_01_2021_C1
Filename: sharlja1-exp100-0027_12_01_2021_c1.raw
Submitter:

Peak #	Formula	Target …	Target …	Time	Found	Area %	Area Abs
10	C23H28C…	493.1	Glyburi…	1.411	Yes	29.9	4144.27
18	C16H18B…	426.0	Product	2.075	Yes	44.1	6122.97

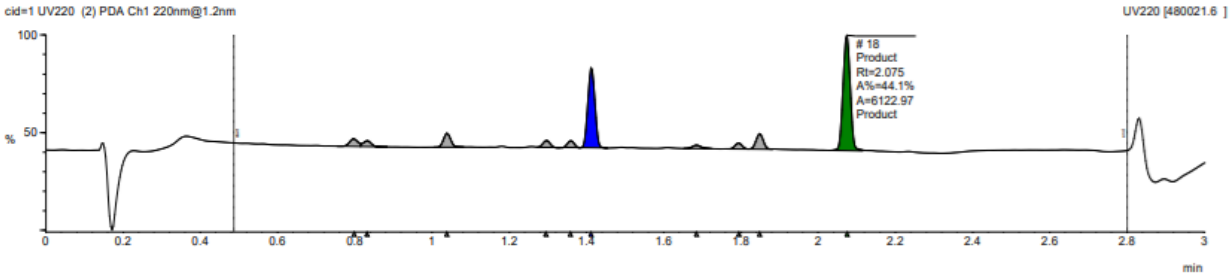

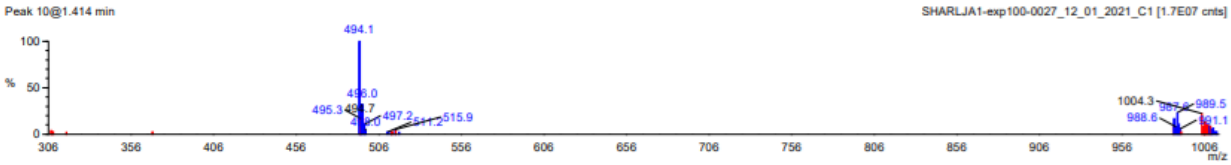

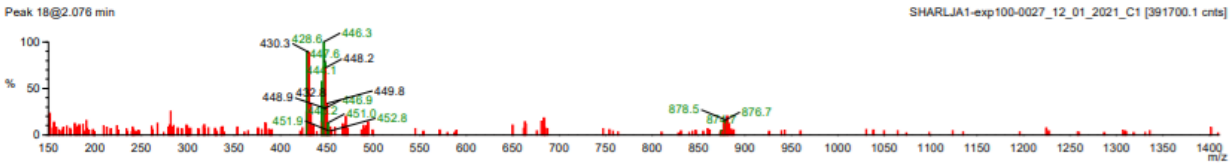

Name	Y/N	Type	Formula	Mass
Glyburide	Y	IS	C23H28ClN3O5S	493.1
Product	Y	Product	C16H18BrCl3O2	426.0

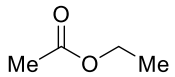

C2,
52% yield

Single Sample Report
Sample Name: SHARLJA1-exp100-0027_12_01_2021_C2
Filename: sharlja1-exp100-0027_12_01_2021_c2.raw
Submitter:

Peak #	Formula	Target …	Target …	Time	Found	Area %	Area Abs
8	C23H28C…	493.1	Glyburi…	1.411	Yes	25.1	6267.86
17	C16H18B…	426.0	Product	2.071	Yes	51.1	12771.66

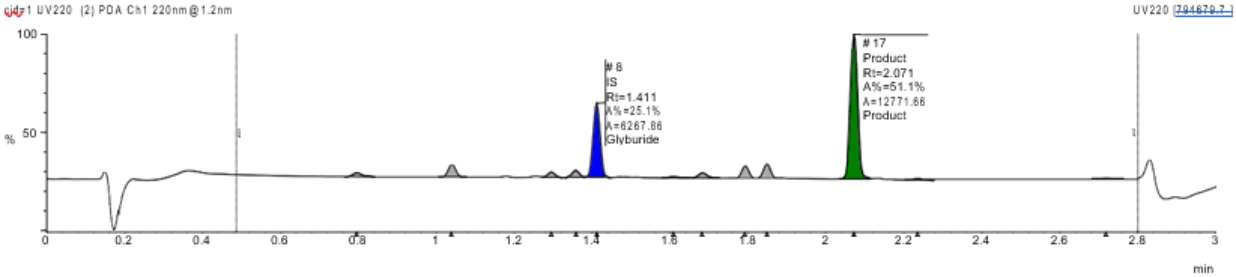

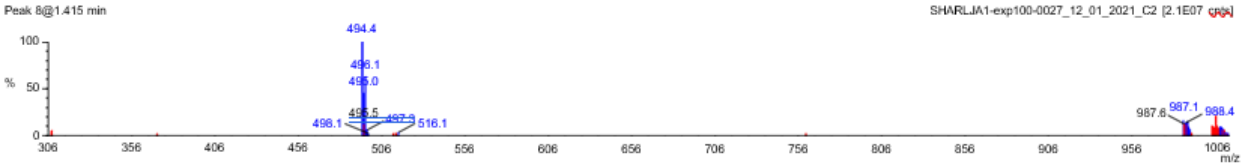

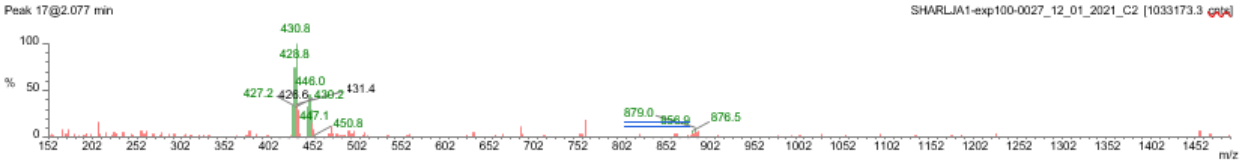

Name	Y/N	Type	Formula	Mass
Glyburide	Y	IS	C23H28ClN3O5S	493.1
Product	Y	Product	C16H18BrCl3O2	426.0

Single Sample Report
Sample Name: SHARLJA1-exp100-0027_12_01_2021_C4
Filename: sharlja1-exp100-0027_12_01_2021_c4.raw
Submitter:

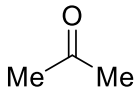

C4,
45% yield

Peak #	Formula	Target …	Target …	Time	Found	Area %	Area Abs
9	C23H28C…	493.1	Glyburi…	1.411	Yes	23.5	6053.42
20	C16H18B…	426.0	Product	2.075	Yes	41.8	10759.47

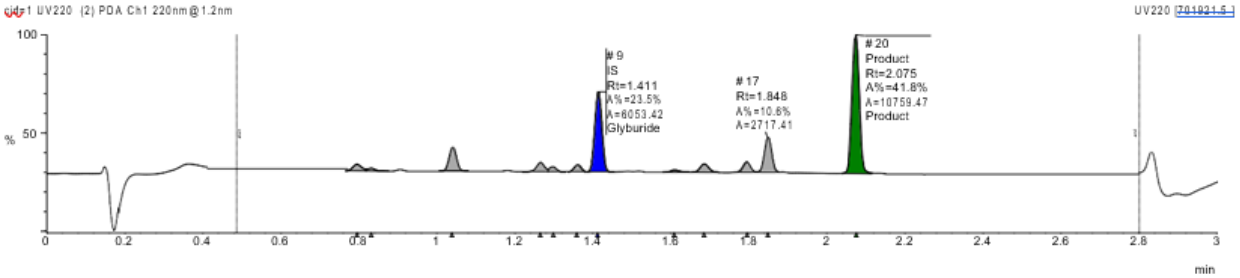

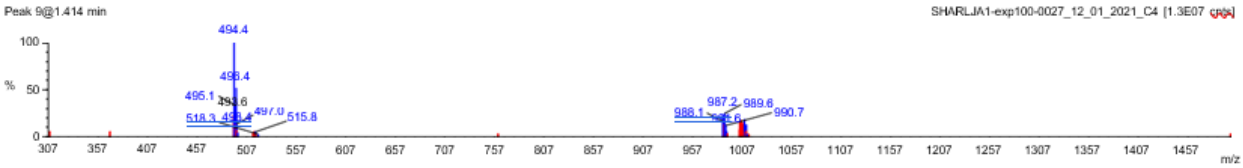

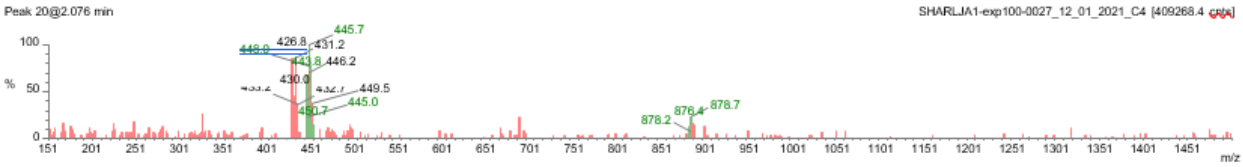

Name	Y/N	Type	Formula	Mass
Glyburide	Y	IS	C23H28ClN3O5S	493.1
Product	Y	Product	C16H18BrCl3O2	426.0

Single Sample Report

Sample Name: SHARLJA1-exp100-0027_12_01_2021_C5
Filename: sharlja1-exp100-0027_12_01_2021_c5.raw
Submitter:

Location: 35
Instrument:
Job Code:
SHARLJA1_EXP100_0027_resuspended_12_01_2021

Acquired: 12/1/2021 11:32 AM
User:

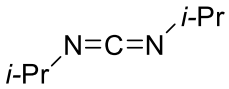

C5,
50% yield

Peak #	Formula	Target …	Target …	Time	Found	Area %	Area Abs
9	C23H28C…	493.1	Glyburi…	1.411	Yes	26.7	4274.02
17	C16H18B…	426.0	Product	2.071	Yes	51.9	8320.01

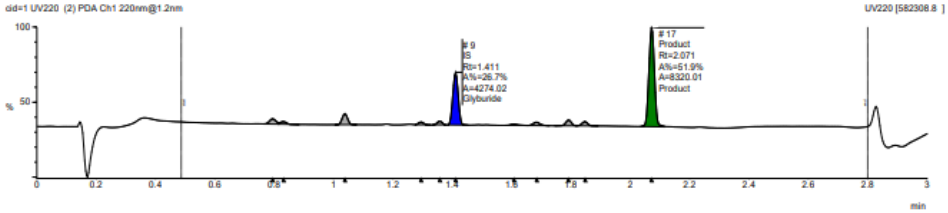

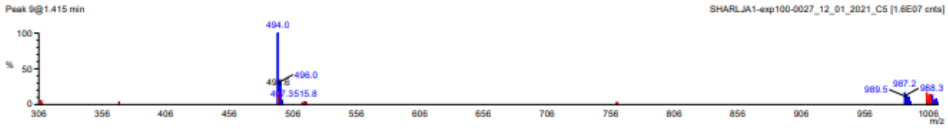

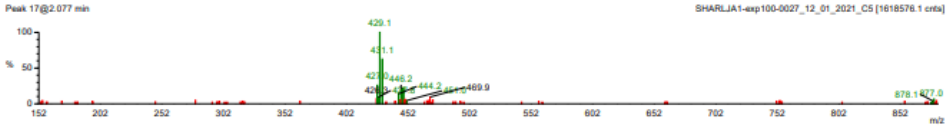

Name	Y/N	Type	Formula	Mass
Glyburide	Y	IS	C23H28ClN3O5S	493.1
Product	Y	Product	C16H18BrCl3O2	426.0

Single Sample Report
Sample Name: SHARLJA1-exp100-0027_12_01_2021_C6
Filename: sharlja1-exp100-0027_12_01_2021_c6.raw
Submitter:

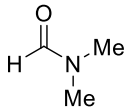

C6,
60% yield

Peak #	Formula	Target …	Target …	Time	Found	Area %	Area Abs
8	C23H28C…	493.1	Glyburi…	1.411	Yes	23.5	3369.37
15	C16H18B…	426.0	Product	2.071	Yes	54.6	7830.04

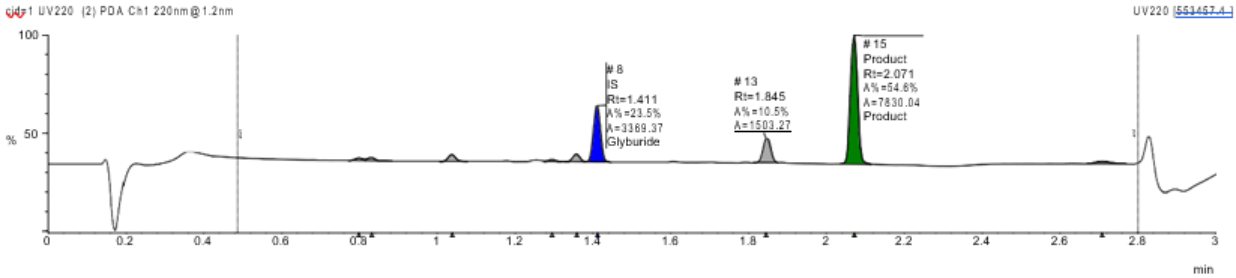

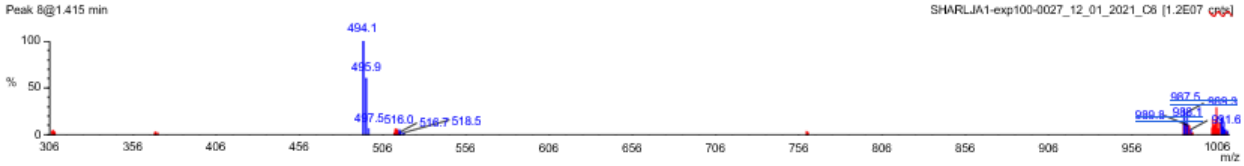

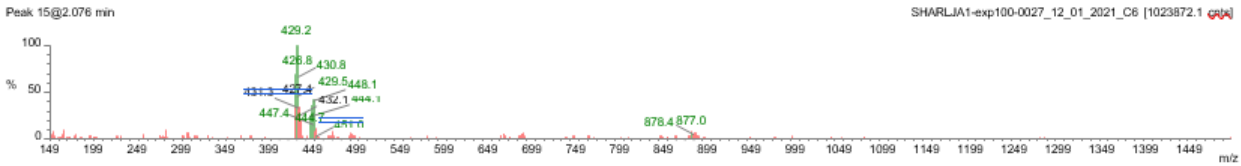

Name	Y/N	Type	Formula	Mass
Glyburide	Y	IS	C23H28ClN3O5S	493.1
Product	Y	Product	C16H18BrCl3O2	426.0

Single Sample Report
Sample Name: SHARLJA1-exp100-0027_12_01_2021_C7
Filename: sharlja1-exp100-0027_12_01_2021_c7.raw
Submitter:

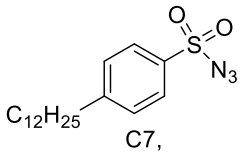

C7,
78% yield

Peak #	Formula	Target …	Target …	Time	Found	Area %	Area Abs
7	C23H28C…	493.1	Glyburi…	1.411	Yes	13.4	6637.53
16	C16H18B…	426.0	Product	2.075	Yes	39.8	19762.38

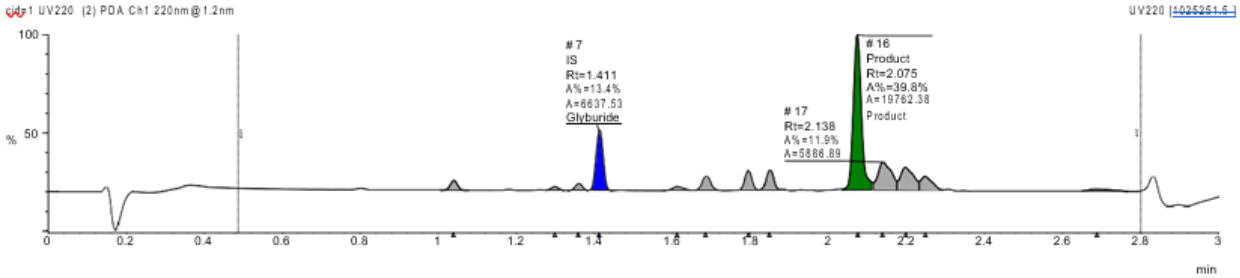

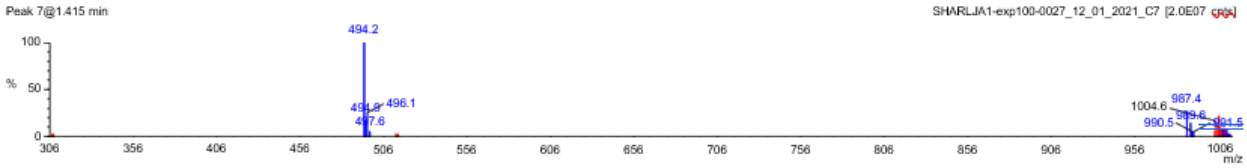

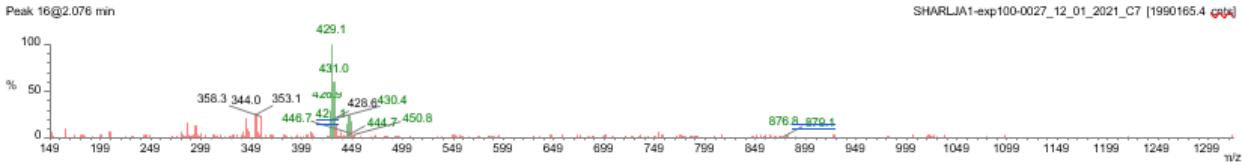

Name	Y/N	Type	Formula	Mass
Glyburide	Y	IS	C23H28ClN3O5S	493.1
Product	Y	Product	C16H18BrCl3O2	426.0

Single Sample Report
Sample Name: SHARLJA1-exp100-0027_12_01_2021_C8
Filename: sharlja1-exp100-0027_12_01_2021_c8.raw
Submitter:

Me—NO_2

C8,
66% yield

Peak #	Formula	Target …	Target …	Time	Found	Area %	Area Abs
8	C23H28C…	493.1	Glyburi…	1.411	Yes	21.0	7118.08
15	C16H18B…	426.0	Product	2.071	Yes	53.4	18118.10

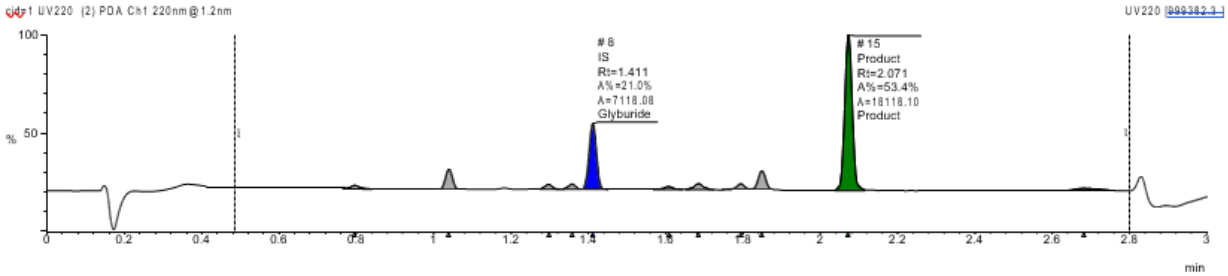

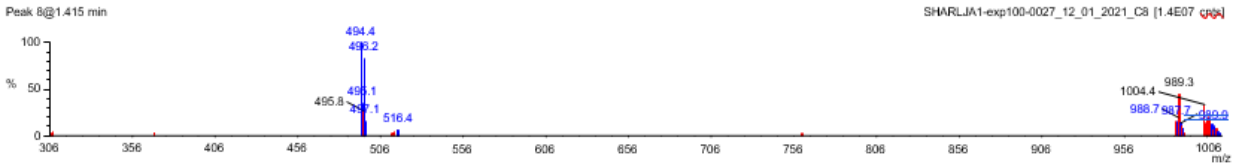

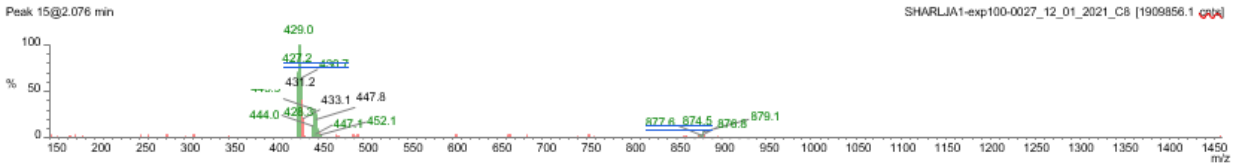

Name	Y/N	Type	Formula	Mass
Glyburide	Y	IS	C23H28ClN3O5S	493.1
Product	Y	Product	C16H18BrCl3O2	426.0

Single Sample Report
Sample Name: SHARLJA1-exp100-0027_12_01_2021_C9
Filename: sharlja1-exp100-0027_12_01_2021_c9.raw
Submitter

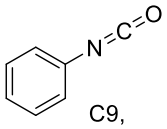

C9,
53% yield

Peak #	Formula	Target …	Target …	Time	Found	Area %	Area Abs
10	C23H28C…	493.1	Glyburi…	1.411	Yes	17.1	3940.45
20	C16H18B…	426.0	Product	2.075	Yes	35.4	8155.19

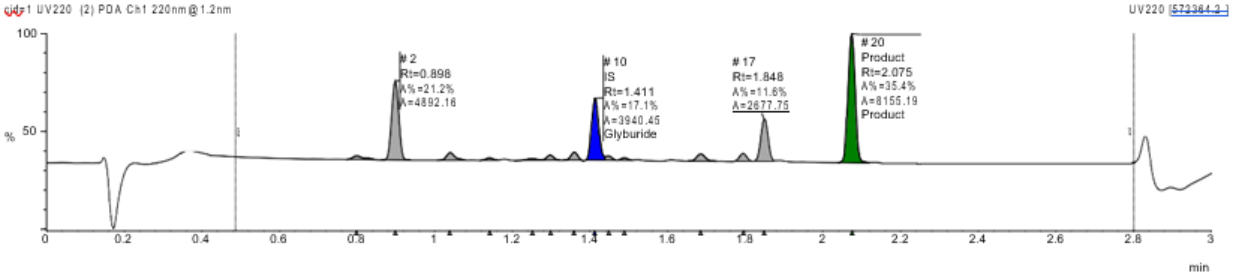

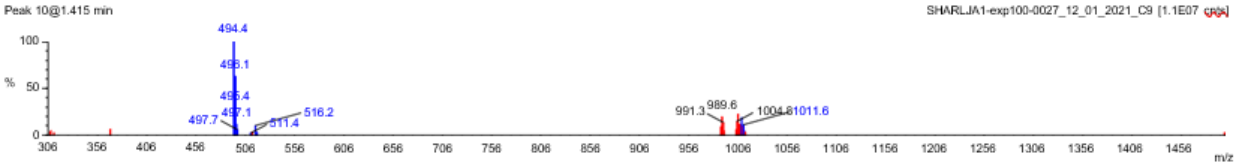

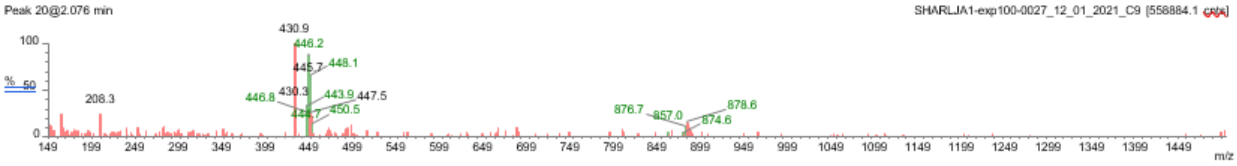

Name	Y/N	Type	Formula	Mass
Glyburide	Y	IS	C23H28ClN3O5S	493.1
Product	Y	Product	C16H18BrCl3O2	426.0

Single Sample Report
Sample Name: SHARLJA1-exp100-0027_12_01_2021_C10
Filename: sharlja1-exp100-0027_12_01_2021_c10.raw
Submitter:

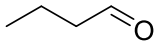

C10,
56% yield

Peak #	Formula	Target …	Target …	Time	Found	Area %	Area Abs
10	C23H28C…	493.1	Glyburi…	1.411	Yes	22.0	6472.67
20	C16H18B…	426.0	Product	2.071	Yes	47.8	14037.76

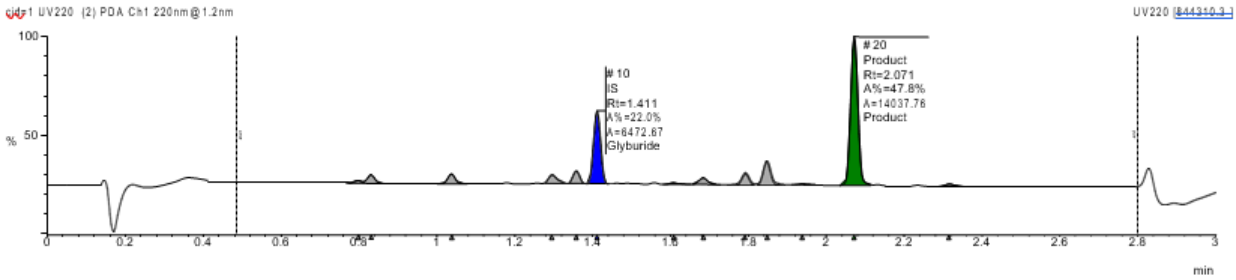

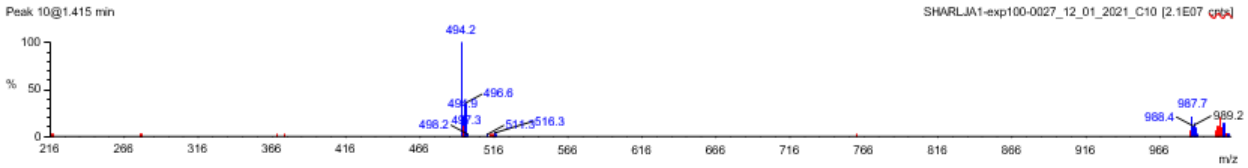

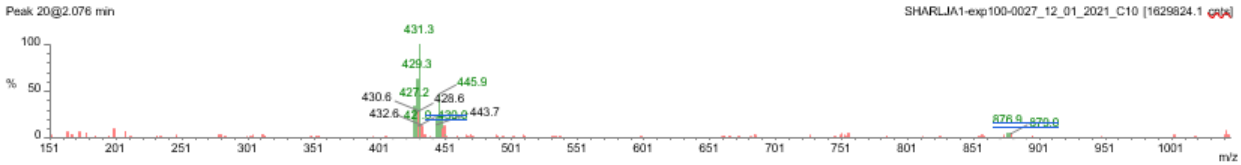

Name	Y/N	Type	Formula	Mass
Glyburide	Y	IS	C23H28ClN3O5S	493.1
Product	Y	Product	C16H18BrCl3O2	426.0

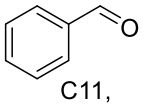

C11,
58% yield

Sample Name: SHARLJA1-exp100-0027_12_01_2021_C11
Filename: sharlja1-exp100-0027_12_01_2021_c11.raw
Submitter:

Peak #	Formula	Target …	Target …	Time	Found	Area %	Area Abs
7	C23H28C…	493.1	Glyburi…	1.411	Yes	19.4	3923.90
15	C16H18B…	426.0	Product	2.075	Yes	43.4	8777.36

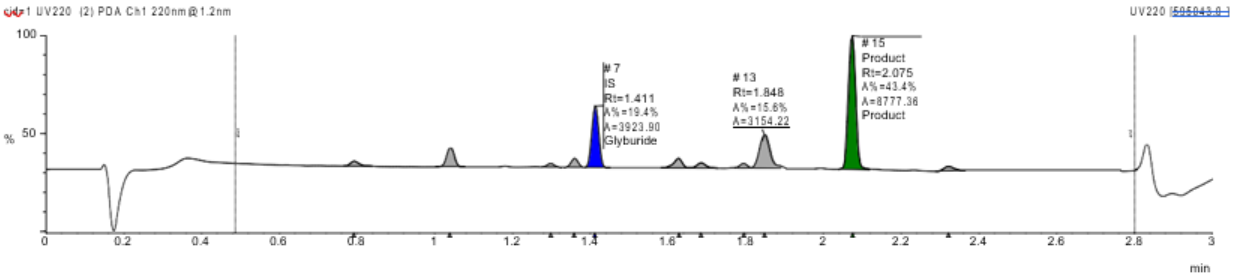

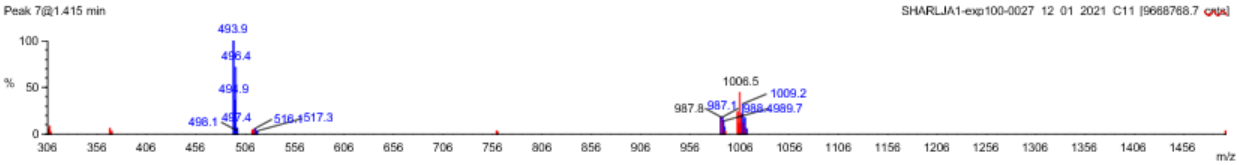

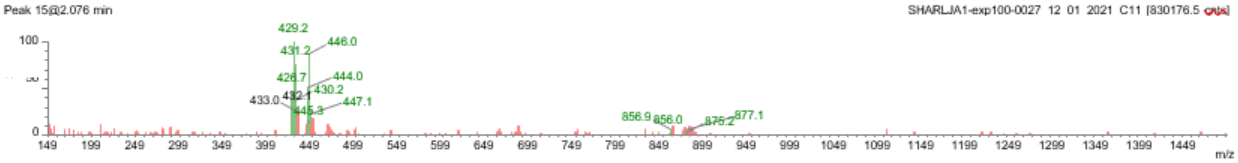

Name	Y/N	Type	Formula	Mass
Glyburide	Y	IS	C23H28ClN3O5S	493.1
Product	Y	Product	C16H18BrCl3O2	426.0

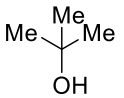

D1,
40% yield

Sample Name: SHARLJA1-exp100-0027_12_01_2021_D1
Filename: sharlja1-exp100-0027_12_01_2021_d1.raw
Submitter:

Peak #	Formula	Target …	Target …	Time	Found	Area %	Area Abs
10	C23H28C…	493.1	Glyburi…	1.411	Yes	31.2	6071.59
19	C16H18B…	426.0	Product	2.071	Yes	50.1	9764.28

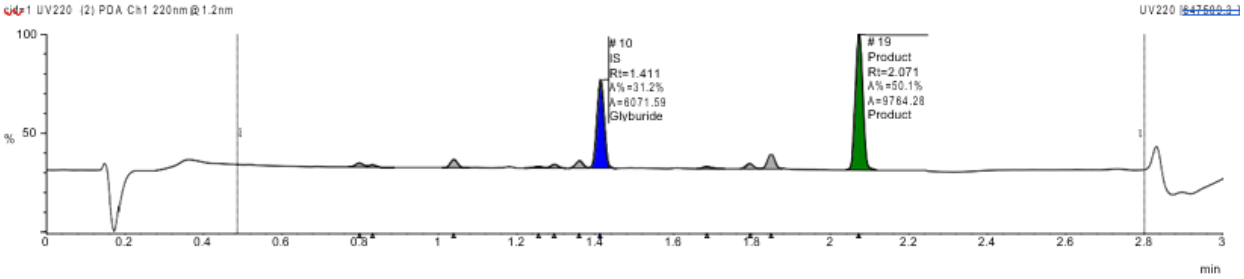

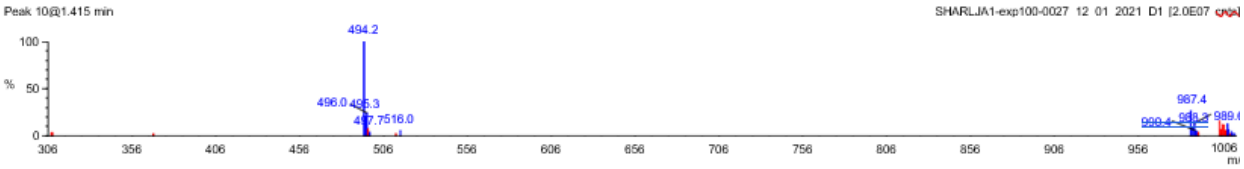

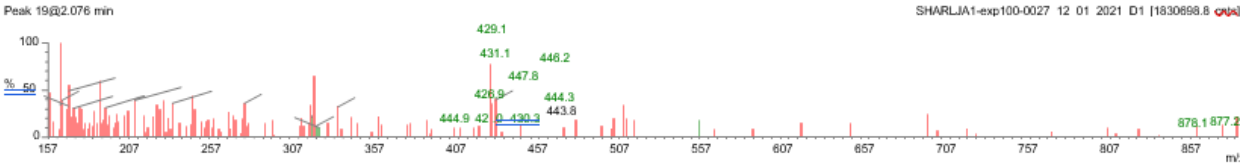

Name	Y/N	Type	Formula	Mass
Glyburide	Y	IS	C23H28ClN3O5S	493.1
Product	Y	Product	C16H18BrCl3O2	426.0

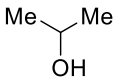

D2,
45% yield

Single Sample Report
Sample Name: SHARLJA1-exp100-0027_12_01_2021_D2
Filename: sharlja1-exp100-0027_12_01_2021_d2.raw
Submitter:

Peak #	Formula	Target …	Target …	Time	Found	Area %	Area Abs
7	C23H28C…	493.1	Glyburi…	1.411	Yes	24.9	6692.16
14	C16H18B…	426.0	Product	2.071	Yes	44.9	12036.12

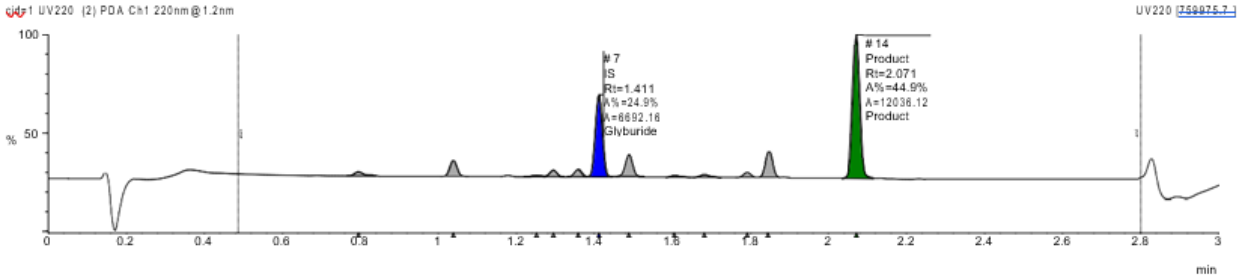

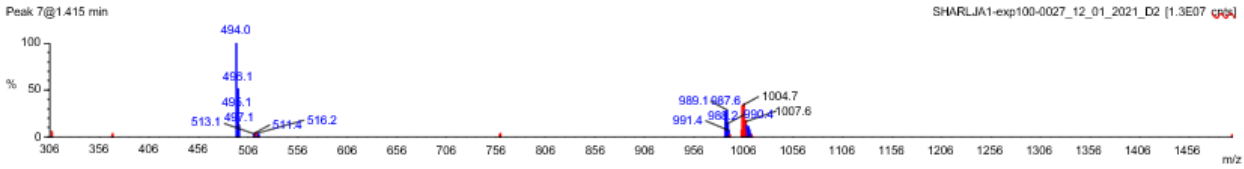

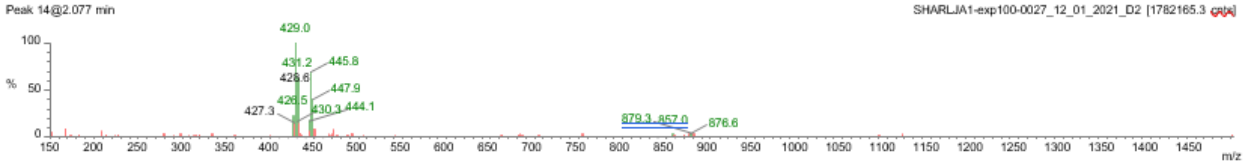

Name	Y/N	Type	Formula	Mass
Glyburide	Y	IS	C23H28ClN3O5S	493.1
Product	Y	Product	C16H18BrCl3O2	426.0

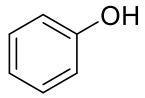

D3,
67% yield

Single Sample Report
Sample Name: SHARLJA1-exp100-0027_12_01_2021_D3
Filename: sharlja1-exp100-0027_12_01_2021_d3.raw
Submitter:

Peak #	Formula	Target …	Target …	Time	Found	Area %	Area Abs
9	C23H28C…	493.1	Glyburi…	1.411	Yes	17.4	5552.02
19	C16H18B…	426.0	Product	2.071	Yes	45.1	14393.81

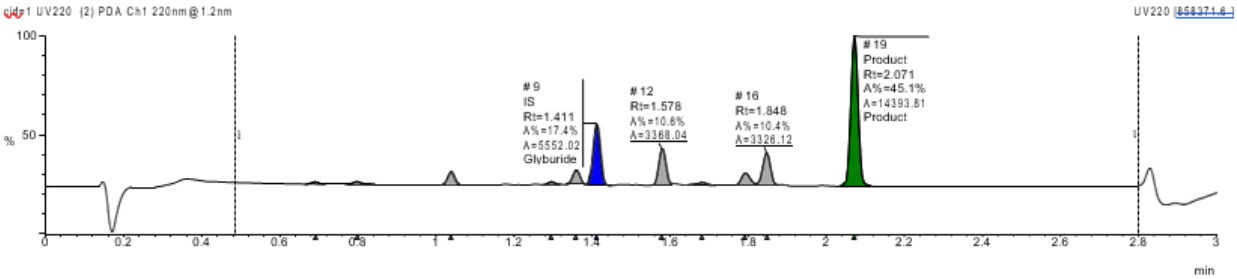

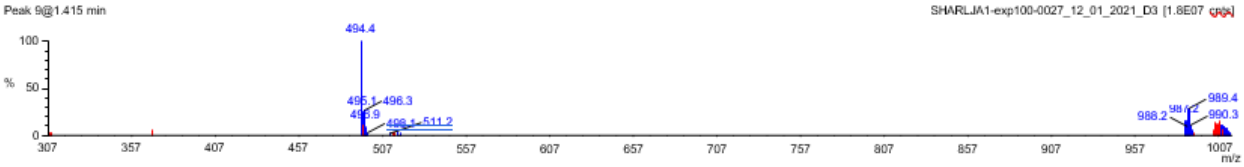

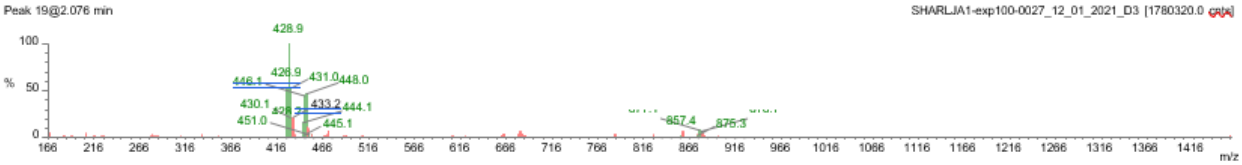

Name	Y/N	Type	Formula	Mass
Glyburide	Y	IS	C23H28ClN3O5S	493.1
Product	Y	Product	C16H18BrCl3O2	426.0

Single Sample Report
Sample Name: SHARLJA1-exp100-0027_12_01_2021_D4
Filename: sharlja1-exp100-0027_12_01_2021_d4.raw
Submitter:

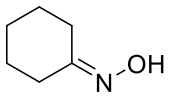

D4,
61% yield

Peak #	Formula	Target …	Target …	Time	Found	Area %	Area Abs
13	C23H28C…	493.1	Glyburi…	1.411	Yes	19.5	5441.17
26	C16H18B…	426.0	Product	2.071	Yes	46.1	12881.51

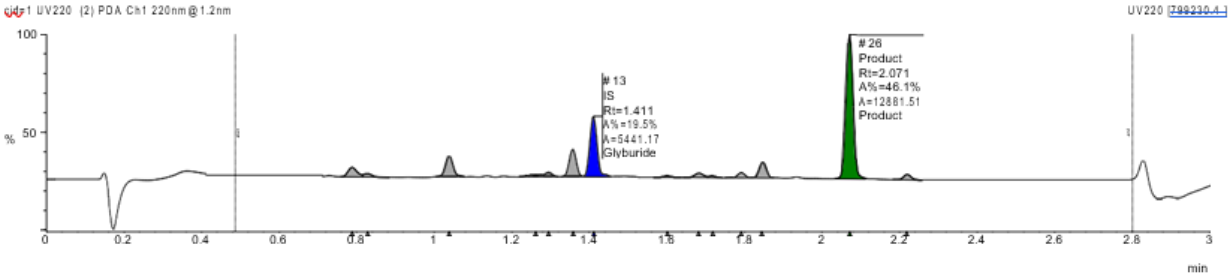

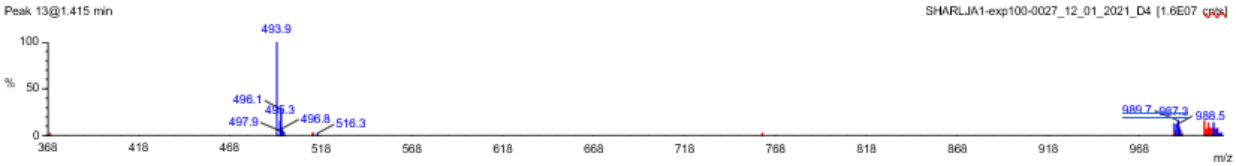

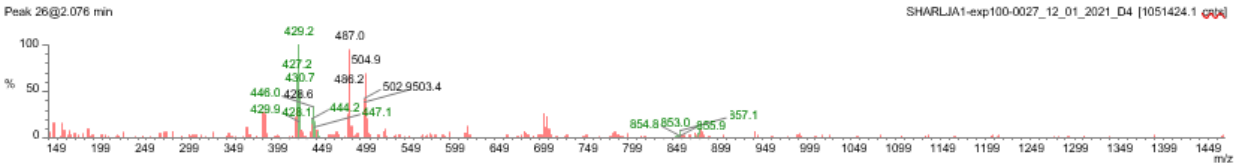

Name	Y/N	Type	Formula	Mass
Glyburide	Y	IS	C23H28ClN3O5S	493.1
Product	Y	Product	C16H18BrCl3O2	426.0

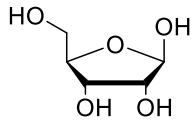

D8,
67% yield

Single Sample Report
Sample Name: SHARLJA1-exp100-0027_12_01_2021_D8
Filename: sharlja1-exp100-0027_12_01_2021_d8.raw
Submitter:

Peak #	Formula	Target …	Target …	Time	Found	Area %	Area Abs
13	C23H28C…	493.1	Glyburi…	1.411	Yes	24.5	866.94
20	C16H18B…	426.0	Product	2.075	Yes	63.1	2230.87

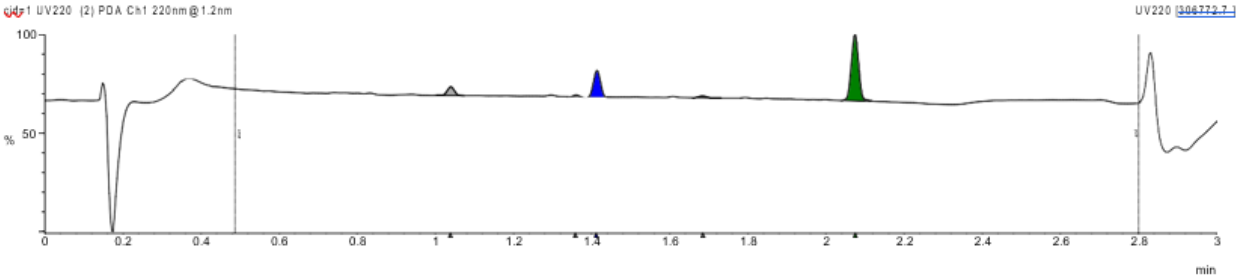

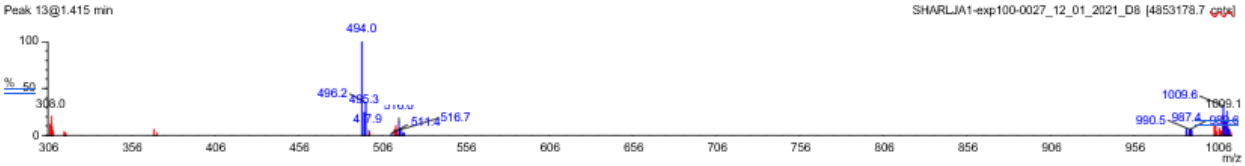

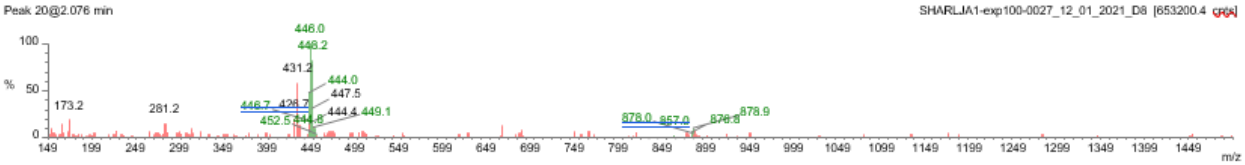

Name	Y/N	Type	Formula	Mass
Glyburide	Y	IS	C23H28ClN3O5S	493.1
Product	Y	Product	C16H18BrCl3O2	426.0

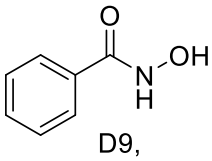

D9,
50% yield

Single Sample Report
Sample Name: SHARLJA1-exp100-0027_12_01_2021_D9
Filename: sharlja1-exp100-0027_12_01_2021_d9.raw
Submitter:

Peak #	Formula	Target …	Target …	Time	Found	Area %	Area Abs
15	C23H28C…	493.1	Glyburi…	1.411	Yes	14.1	3486.87
26	C16H18B…	426.0	Product	2.071	Yes	27.8	6859.95

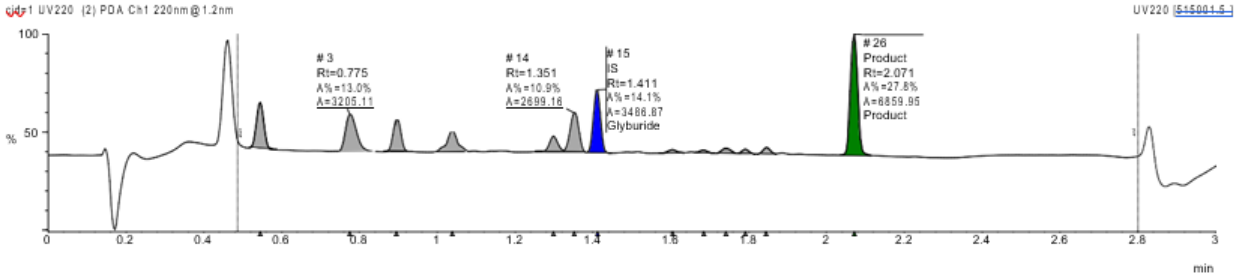

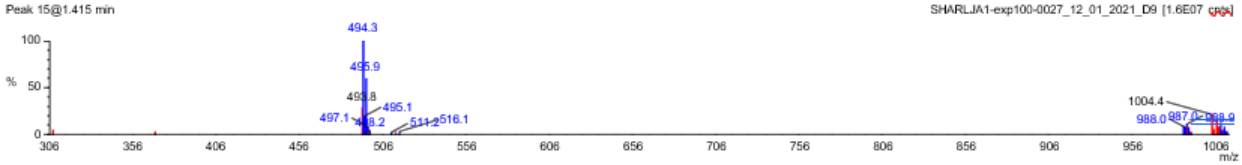

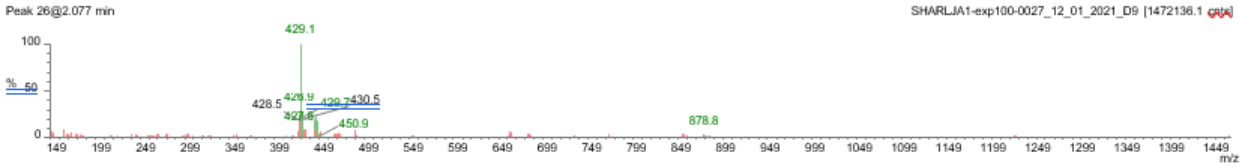

Name	Y/N	Type	Formula	Mass
Glyburide	Y	IS	C23H28ClN3O5S	493.1
Product	Y	Product	C16H18BrCl3O2	426.0

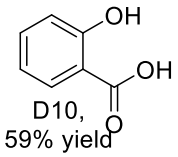

Single Sample Report
Sample Name: SHARLJA1-exp100-0027_12_01_2021_D10
Filename: sharlja1-exp100-0027_12_01_2021_d10.raw
Submitter:

Peak #	Formula	Target …	Target …	Time	Found	Area %	Area Abs
6	C23H28C…	493.1	Glyburi…	1.411	Yes	13.4	6106.16
15	C16H18B…	426.0	Product	2.071	Yes	30.6	13967.41

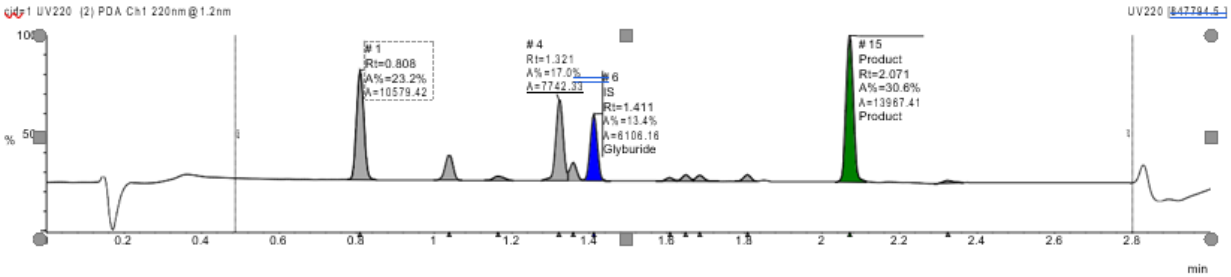

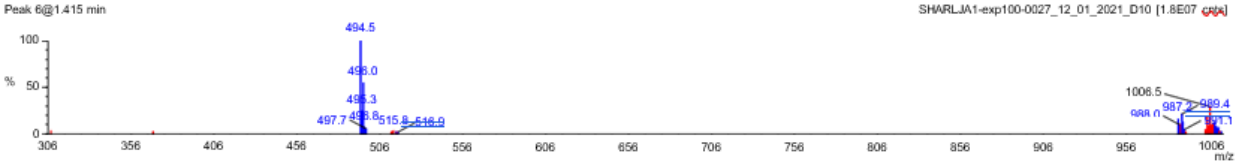

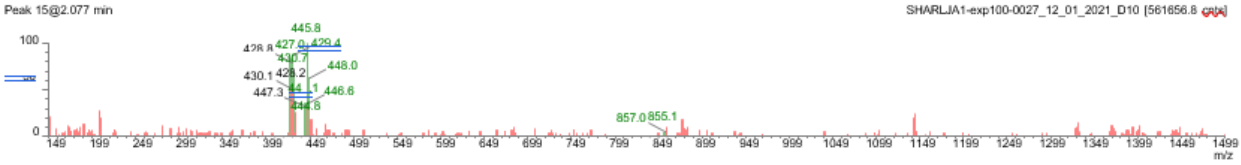

Name	Y/N	Type	Formula	Mass
Glyburide	Y	IS	C23H28ClN3O5S	493.1
Product	Y	Product	C16H18BrCl3O2	426.0

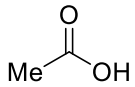

D11,
65% yield

Sample Name: SHARLJA1-exp100-0027_12_01_2021_D11
Filename: sharlja1-exp100-0027_12_01_2021_d11.raw
Submitter:

Peak #	Formula	Target …	Target …	Time	Found	Area %	Area Abs
8	C23H28C…	493.1	Glyburi…	1.411	Yes	18.9	6978.88
16	C16H18B…	426.0	Product	2.075	Yes	47.0	17389.58

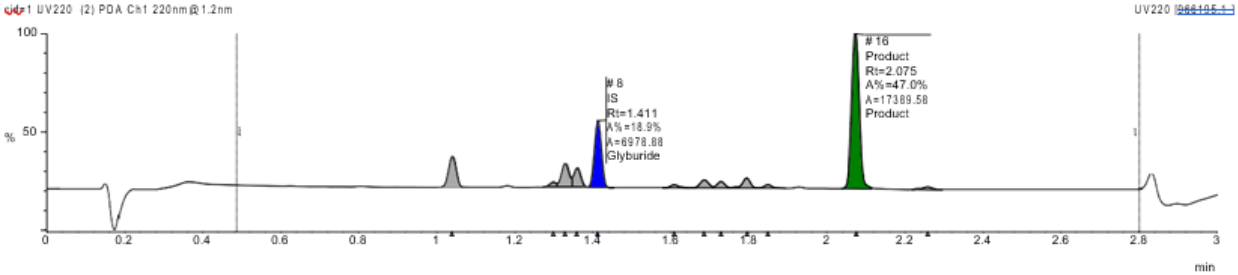

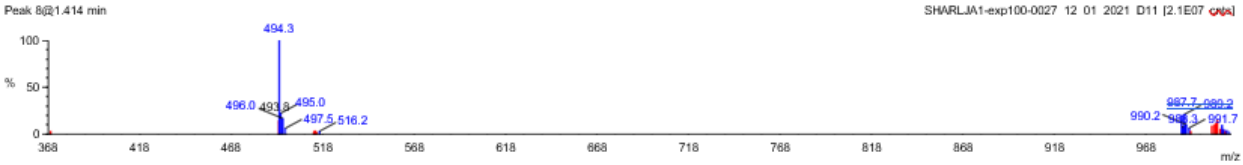

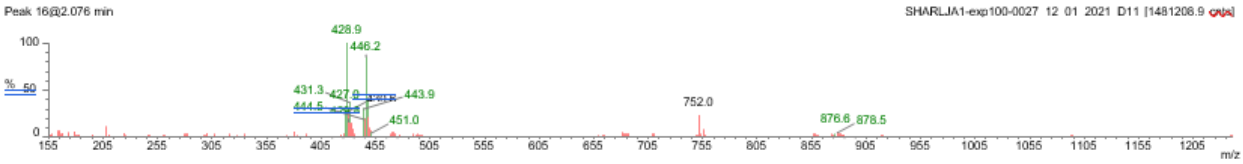

Name	Y/N	Type	Formula	Mass
Glyburide	Y	IS	C23H28ClN3O5S	493.1
Product	Y	Product	C16H18BrCl3O2	426.0

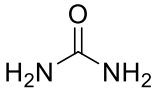

E3,
46% yield

Single Sample Report
Sample Name: SHARLJA1-exp100-0027_12_01_2021_E3
Filename: sharlja1-exp100-0027_12_01_2021_e3.raw
Submitter:

Peak #	Formula	Target …	Target …	Time	Found	Area %	Area Abs
10	C23H28C…	493.1	Glyburi…	1.411	Yes	20.4	6459.11
18	C16H18B…	426.0	Product	2.071	Yes	36.8	11673.92

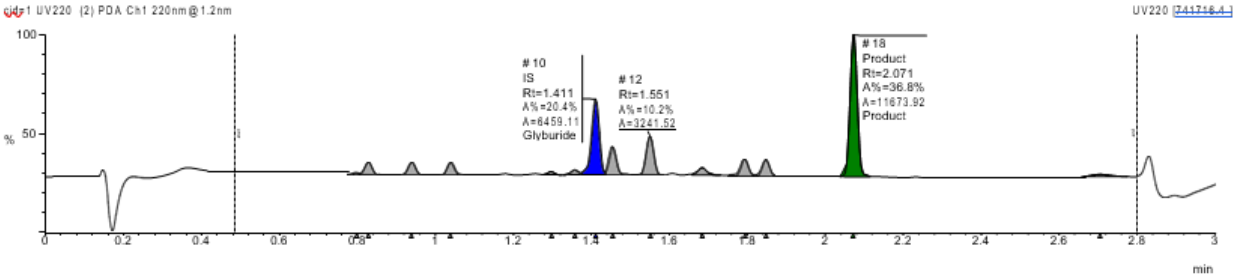

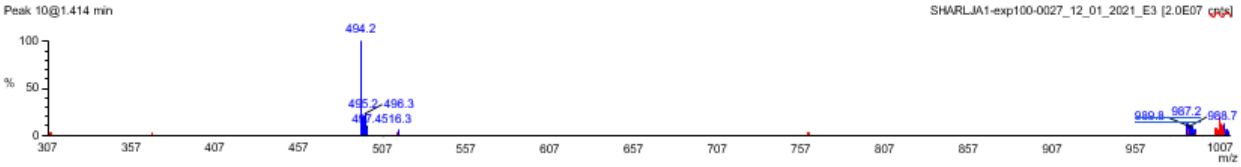

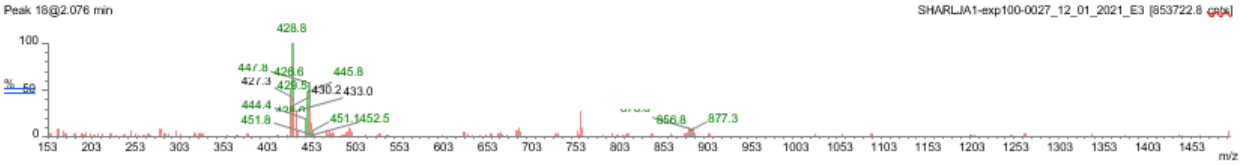

Name	Y/N	Type	Formula	Mass
Glyburide	Y	IS	C23H28ClN3O5S	493.1
Product	Y	Product	C16H18BrCl3O2	426.0

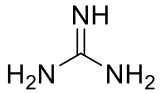

E4,
34% yield

Single Sample Report
Sample Name: SHARLJA1-exp100-0027_12_01_2021_E4
Filename: sharlja1-exp100-0027_12_01_2021_e4.raw
Submitter:

Peak #	Formula	Target …	Target …	Time	Found	Area %	Area Abs
18	C23H28C…	493.1	Glyburi…	1.411	Yes	19.7	5211.14
26	C16H18B…	426.0	Product	2.071	Yes	27.1	7178.63

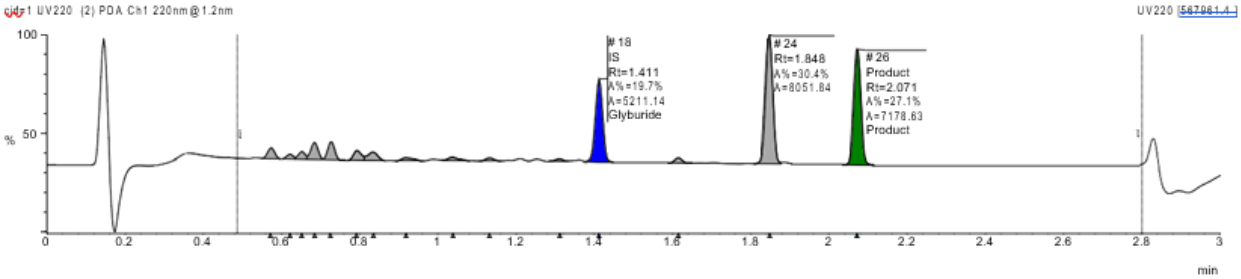

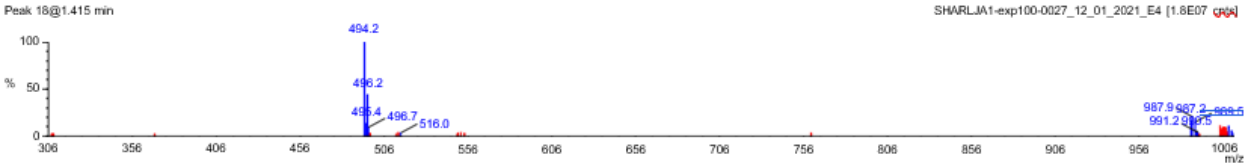

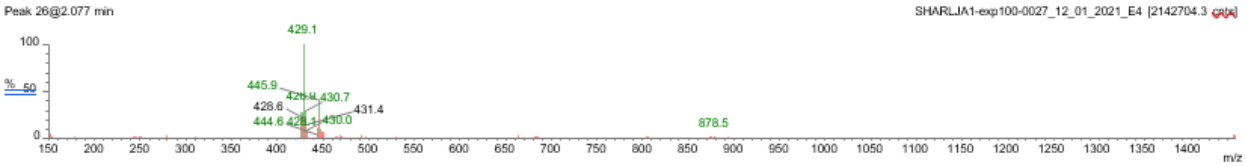

Name	Y/N	Type	Formula	Mass
Glyburide	Y	IS	C23H28ClN3O5S	493.1
Product	Y	Product	C16H18BrCl3O2	426.0

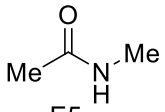

E5,
67% yield

Single Sample Report
Sample Name: SHARLJA1-exp100-0027_12_01_2021_E5
Filename: sharlja1-exp100-0027_12_01_2021_e5.raw
Submitter:

Peak #	Formula	Target …	Target …	Time	Found	Area %	Area Abs
8	C23H28C…	493.1	Glyburi…	1.411	Yes	19.1	6648.10
17	C16H18B…	426.0	Product	2.071	Yes	49.3	17107.87

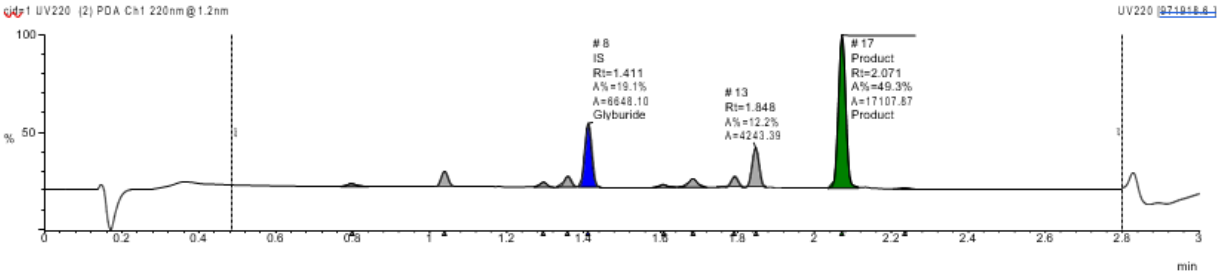

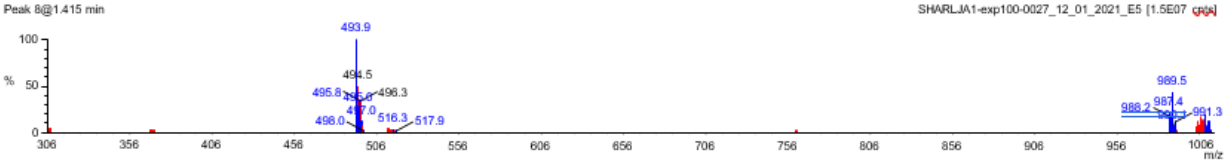

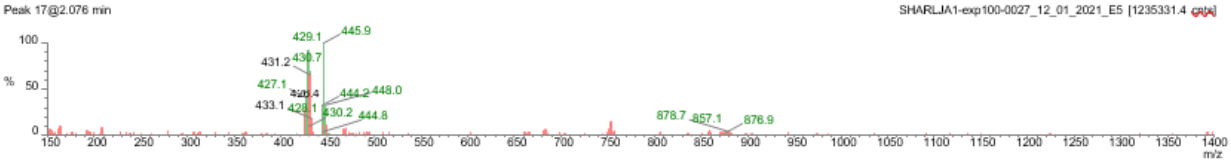

Name	Y/N	Type	Formula	Mass
Glyburide	Y	IS	C23H28ClN3O5S	493.1
Product	Y	Product	C16H18BrCl3O2	426.0

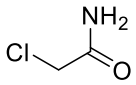

E6,
61% yield

Single Sample Report
Sample Name: SHARLJA1-exp100-0027_12_01_2021_E6
Filename: sharlja1-exp100-0027_12_01_2021_e6.raw
Submitter:

Peak #	Formula	Target …	Target …	Time	Found	Area %	Area Abs
11	C23H28C…	493.1	Glyburi…	1.411	Yes	21.3	3361.98
19	C16H18B…	426.0	Product	2.071	Yes	50.6	7986.03

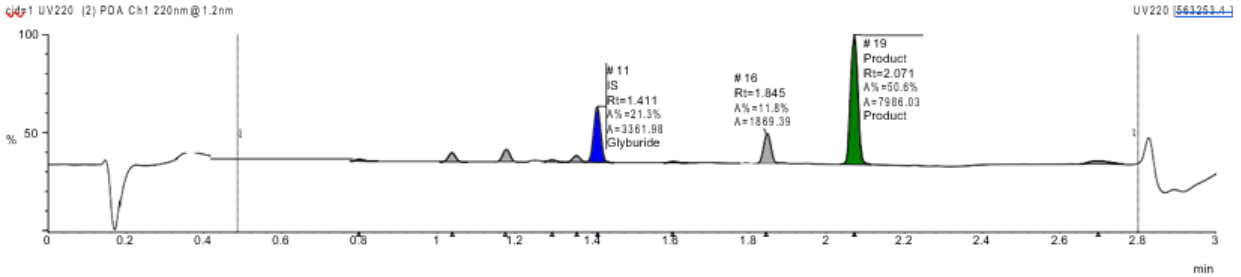

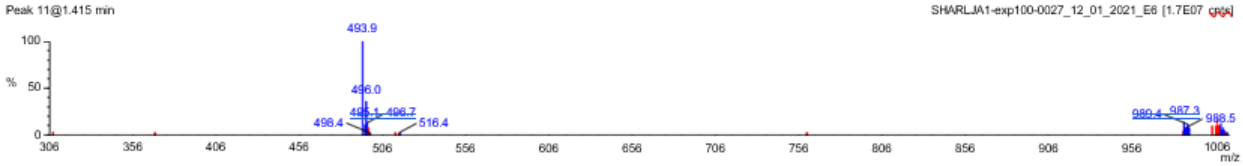

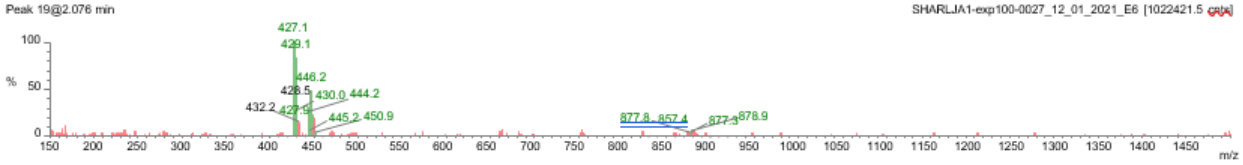

Name	Y/N	Type	Formula	Mass
Glyburide	Y	IS	C23H28ClN3O5S	493.1
Product	Y	Product	C16H18BrCl3O2	426.0

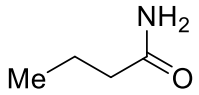

E7,
48% yield

Single Sample Report
Sample Name: SHARLJA1-exp100-0027_12_01_2021_E7
Filename: sharlja1-exp100-0027_12_01_2021_e7.raw
Submitter:

Peak #	Formula	Target …	Target …	Time	Found	Area %	Area Abs
11	C23H28C…	493.1	Glyburi…	1.411	Yes	21.8	6441.59
17	C16H18B…	426.0	Product	2.071	Yes	41.5	12249.73

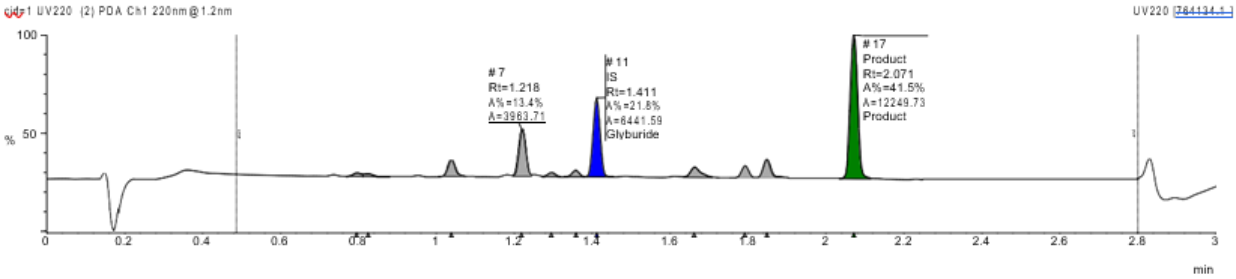

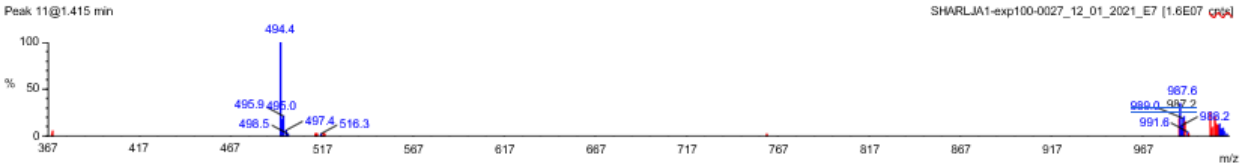

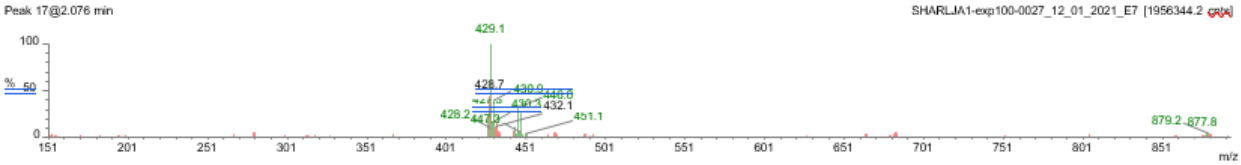

Name	Y/N	Type	Formula	Mass
Glyburide	Y	IS	C23H28ClN3O5S	493.1
Product	Y	Product	C16H18BrCl3O2	426.0

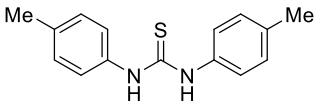

E8,
50% yield

Single Sample Report
Sample Name: SHARLJA1-exp100-0027_12_01_2021_E8
Filename: sharlja1-exp100-0027_12_01_2021_e8.raw
Submitter:

Peak #	Formula	Target …	Target …	Time	Found	Area %	Area Abs
11	C23H28C…	493.1	Glyburi…	1.411	Yes	12.1	6634.37
20	C16H18B…	426.0	Product	2.075	Yes	23.7	13002.61

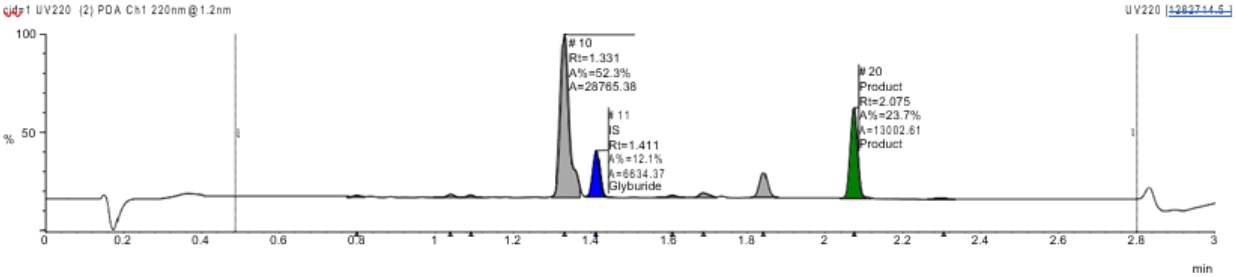

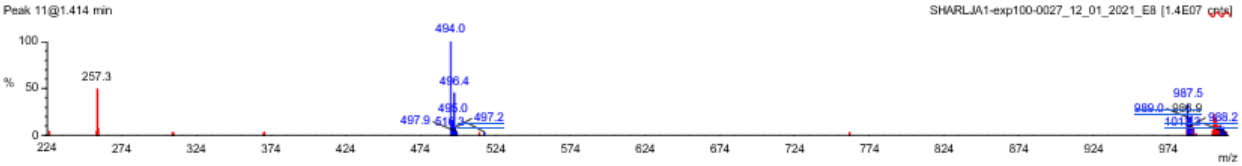

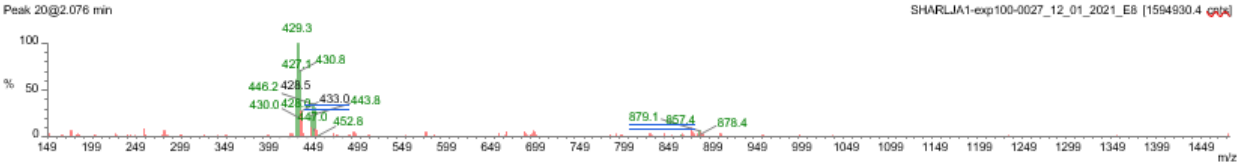

Name	Y/N	Type	Formula	Mass
Glyburide	Y	IS	C23H28ClN3O5S	493.1
Product	Y	Product	C16H18BrCl3O2	426.0

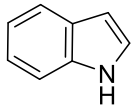

E10,
42% yield

Single Sample Report
Sample Name: SHARLJA1-exp100-0027_12_01_2021_E10
Filename: sharlja1-exp100-0027_12_01_2021_e10.raw
Submitter:

Peak #	Formula	Target …	Target …	Time	Found	Area %	Area Abs
12	C23H28C…	493.1	Glyburi…	1.411	Yes	11.0	6129.18
25	C16H18B…	426.0	Product	2.071	Yes	18.5	10262.16

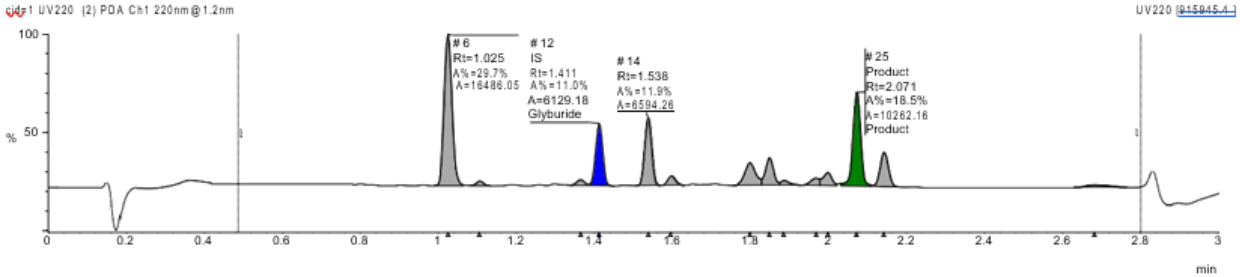

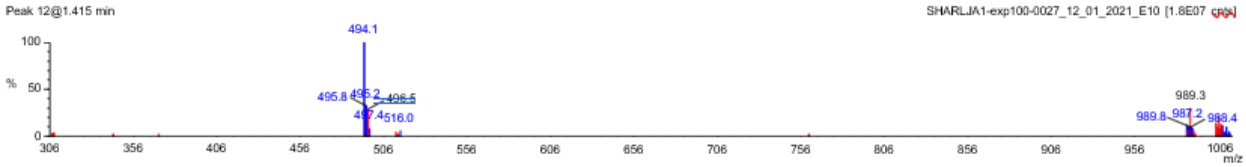

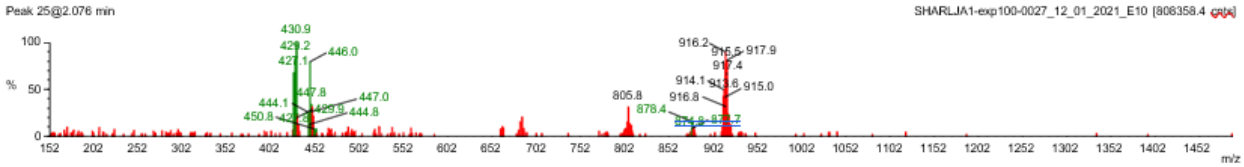

Name	Y/N	Type	Formula	Mass
Glyburide	Y	IS	C23H28ClN3O5S	493.1
Product	Y	Product	C16H18BrCl3O2	426.0

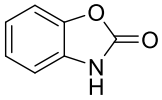

E11,
49% yield

Sample Name: SHARLJA1-exp100-0027_12_01_2021_E11
Filename: sharlja1-exp100-0027_12_01_2021_e11.raw
Submitter:

Peak #	Formula	Target …	Target …	Time	Found	Area %	Area Abs
10	C23H28C…	493.1	Glyburi…	1.411	Yes	15.4	8109.18
18	C16H18B…	426.0	Product	2.071	Yes	29.5	15516.47

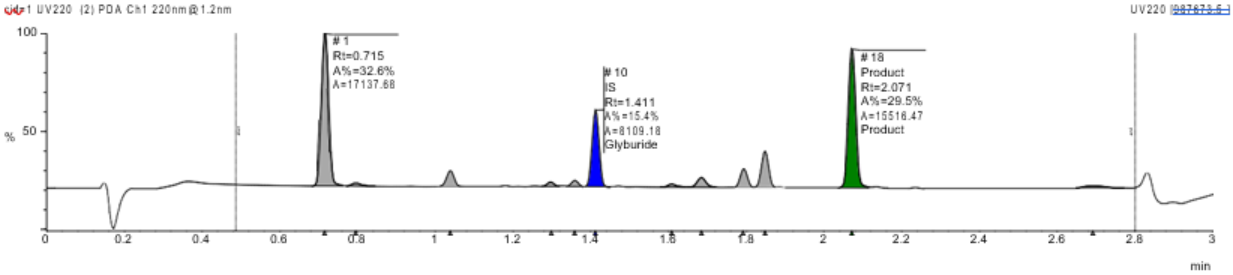

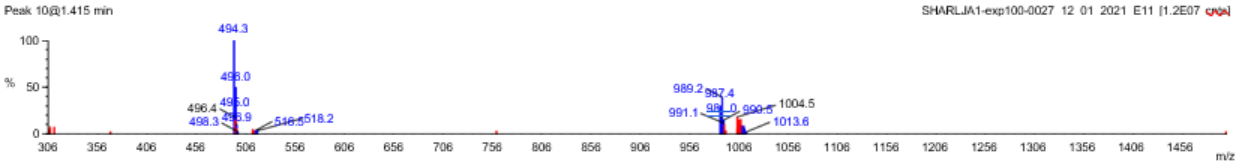

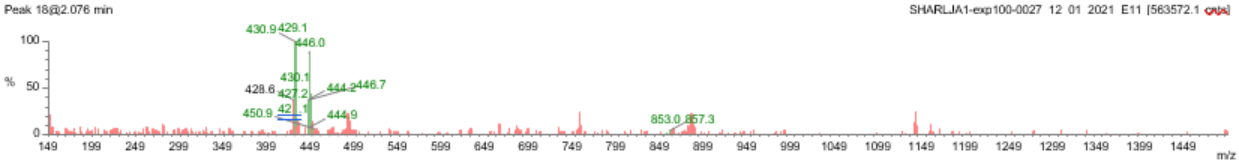

Name	Y/N	Type	Formula	Mass
Glyburide	Y	IS	C23H28ClN3O5S	493.1
Product	Y	Product	C16H18BrCl3O2	426.0

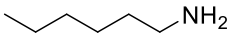

F3,
81% yield

Single Sample Report
Sample Name: SHARLJA1-exp100-0027_12_01_2021_F3
Filename: sharlja1-exp100-0027_12_01_2021_f3.raw
Submitter:

Peak #	Formula	Target …	Target …	Time	Found	Area %	Area Abs
9	C23H28C…	493.1	Glyburi…	1.411	Yes	18.9	4071.01
19	C16H18B…	426.0	Product	2.075	Yes	58.2	12550.66

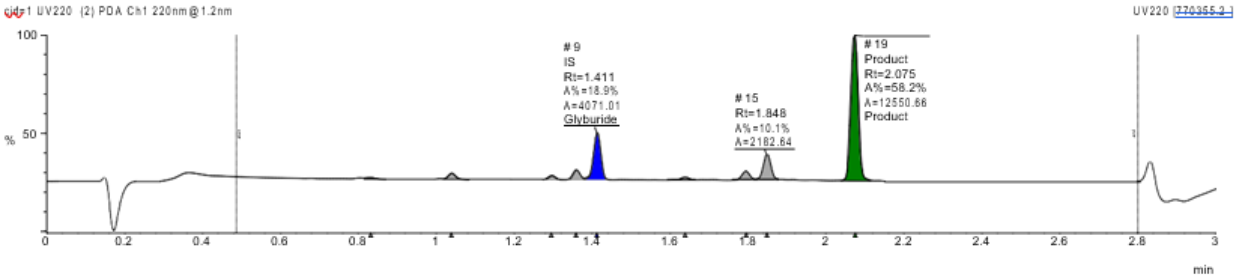

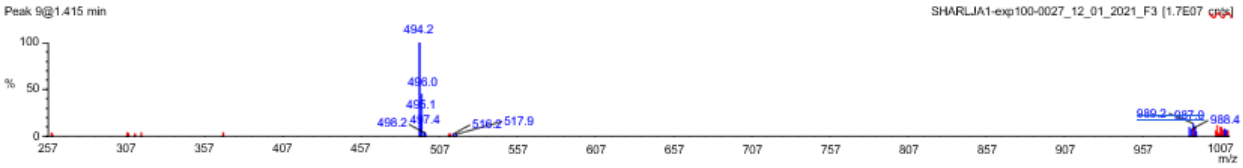

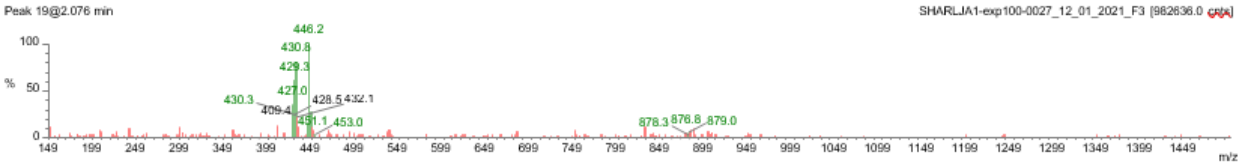

Name	Y/N	Type	Formula	Mass
Glyburide	Y	IS	C23H28ClN3O5S	493.1
Product	Y	Product	C16H18BrCl3O2	426.0

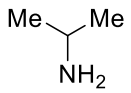

F4,
54% yield

Single Sample Report
Sample Name: SHARLJA1-exp100-0027_12_01_2021_F4
Filename: sharlja1-exp100-0027_12_01_2021_f4.raw
Submitter:

Peak #	Formula	Target …	Target …	Time	Found	Area %	Area Abs
11	C23H28C…	493.1	Glyburi…	1.411	Yes	21.0	5312.57
20	C16H18B…	426.0	Product	2.071	Yes	44.1	11121.94

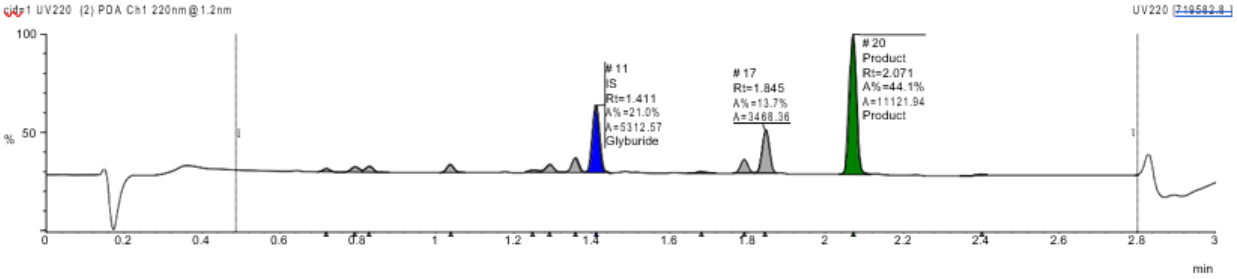

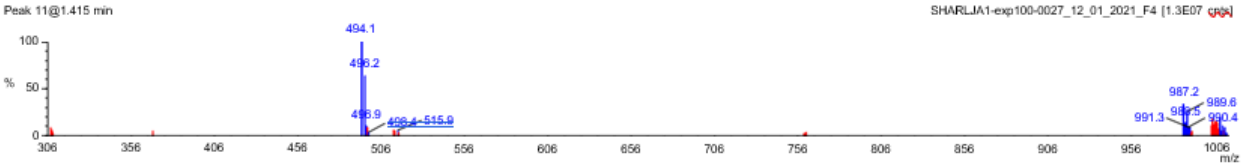

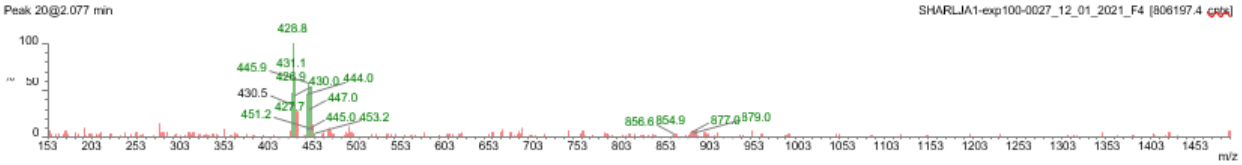

Name	Y/N	Type	Formula	Mass
Glyburide	Y	IS	C23H28ClN3O5S	493.1
Product	Y	Product	C16H18BrCl3O2	426.0

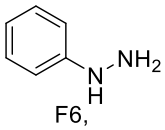

F6,
99% yield

Single Sample Report
Sample Name: SHARLJA1-exp100-0027_12_01_2021_F6
Filename: sharlja1-exp100-0027_12_01_2021_f6.raw
Submitter:

Peak #	Formula	Target …	Target …	Time	Found	Area %	Area Abs
10	C23H28C…	493.1	Glyburi…	1.411	Yes	15.0	3156.31
23	C16H18B…	426.0	Product	2.071	Yes	56.2	11821.88

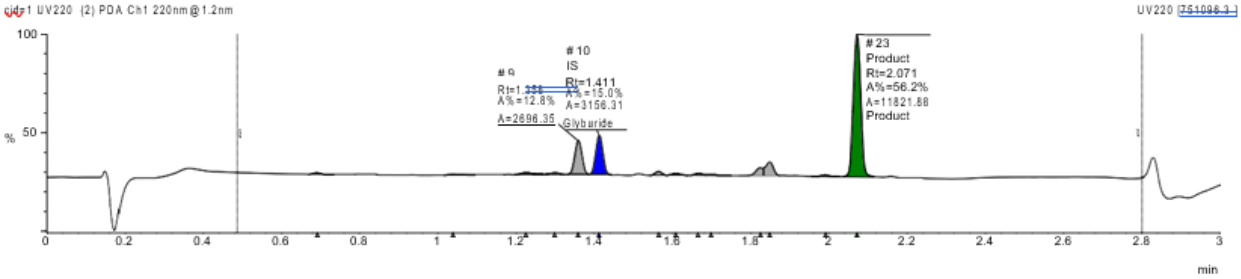

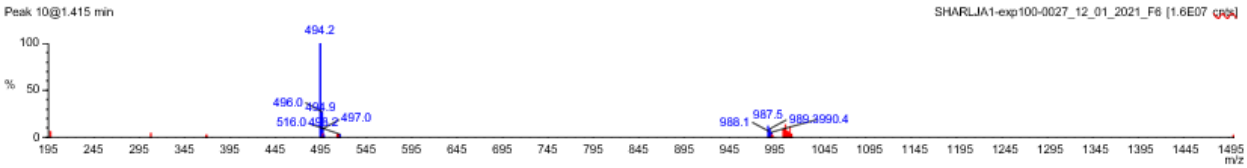

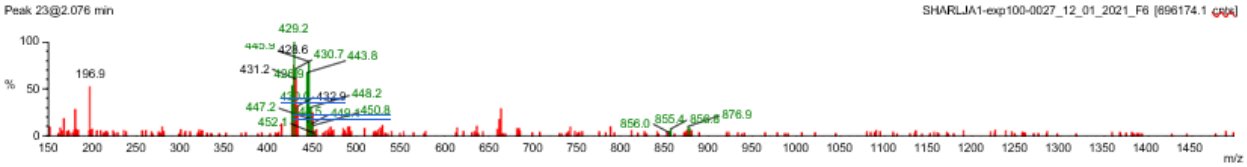

Name	Y/N	Type	Formula	Mass
Glyburide	Y	IS	C23H28ClN3O5S	493.1
Product	Y	Product	C16H18BrCl3O2	426.0

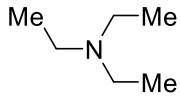

F7,
63% yield

Single Sample Report
Sample Name: SHARLJA1-exp100-0027_12_01_2021_F7
Filename: sharlja1-exp100-0027_12_01_2021_f7.raw
Submitter:

Peak #	Formula	Target …	Target …	Time	Found	Area %	Area Abs
11	C23H28C…	493.1	Glyburi…	1.408	Yes	21.1	6324.44
20	C16H18B…	426.0	Product	2.071	Yes	51.3	15373.18

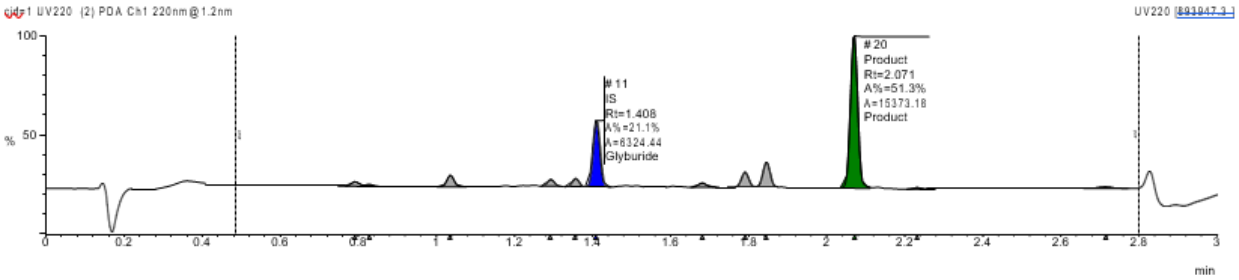

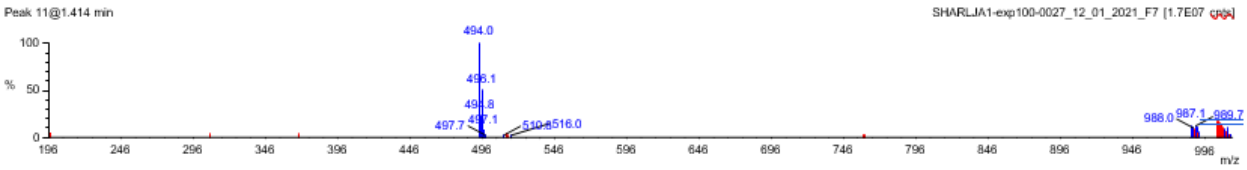

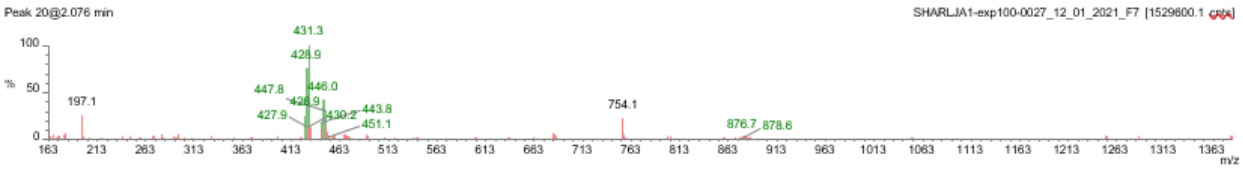

Name	Y/N	Type	Formula	Mass
Glyburide	Y	IS	C23H28ClN3O5S	493.1
Product	Y	Product	C16H18BrCl3O2	426.0

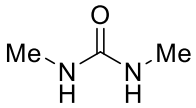

F8,
53% yield

Single Sample Report
Sample Name: SHARLJA1-exp100-0027_12_01_2021_F8
Filename: sharlja1-exp100-0027_12_01_2021_f8.raw
Submitter:

Peak #	Formula	Target …	Target …	Time	Found	Area %	Area Abs
11	C23H28C…	493.1	Glyburi…	1.411	Yes	19.6	6307.51
20	C16H18B…	426.0	Product	2.071	Yes	40.8	13106.44

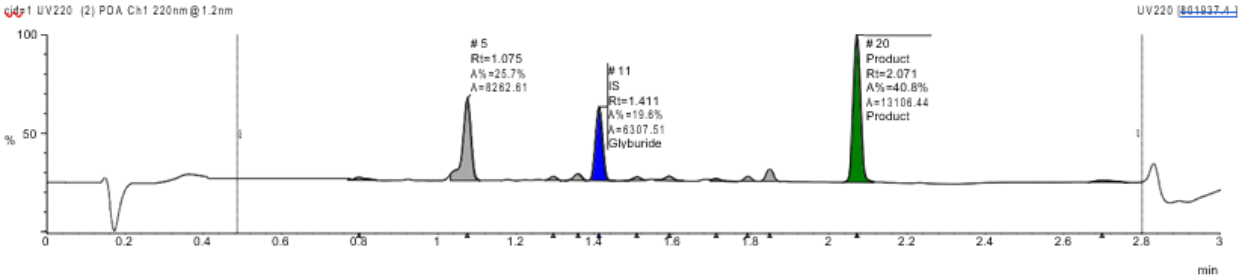

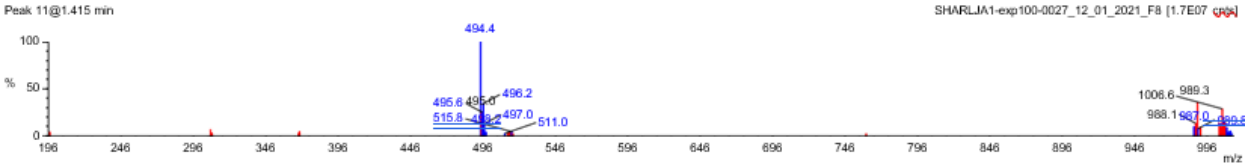

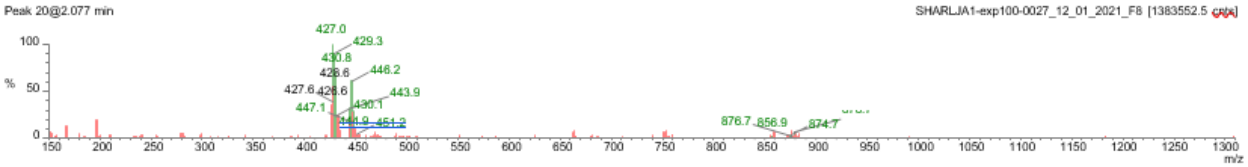

Name	Y/N	Type	Formula	Mass
Glyburide	Y	IS	C23H28ClN3O5S	493.1
Product	Y	Product	C16H18BrCl3O2	426.0

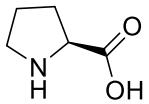

F9,
75% yield

Single Sample Report
Sample Name: SHARLJA1-exp100-0027_12_01_2021_F9
Filename: sharlja1-exp100-0027_12_01_2021_f9.raw
Submitter:

Peak #	Formula	Target …	Target …	Time	Found	Area %	Area Abs
15	C23H28C…	493.1	Glyburi…	1.411	Yes	18.9	6241.42
25	C16H18B…	426.0	Product	2.071	Yes	53.7	17781.45

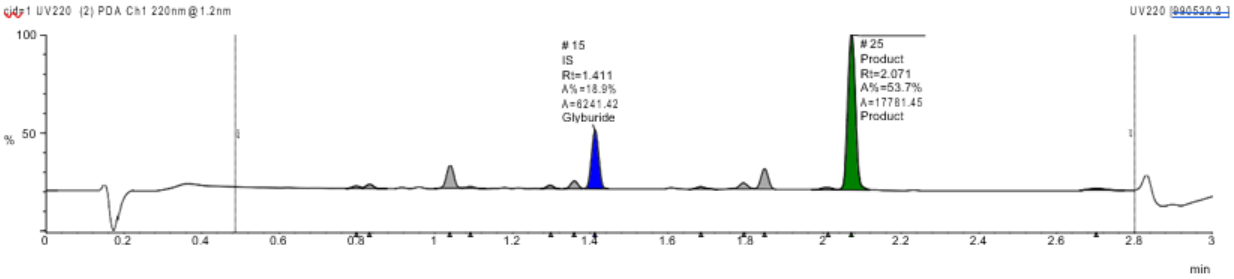

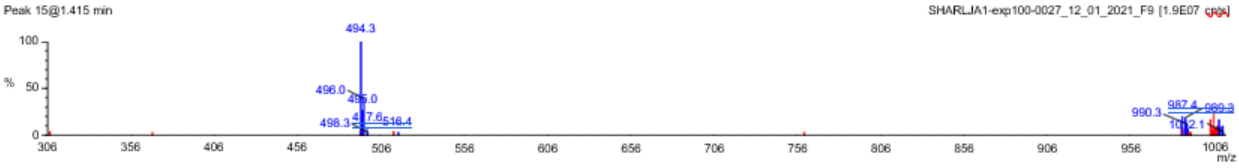

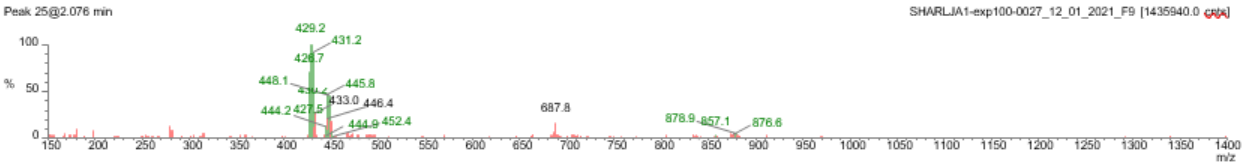

Name	Y/N	Type	Formula	Mass
Glyburide	Y	IS	C23H28ClN3O5S	493.1
Product	Y	Product	C16H18BrCl3O2	426.0

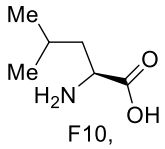

F10,
63% yield

Single Sample Report
Sample Name: SHARLJA1-exp100-0027_12_01_2021_F10
Filename: sharlja1-exp100-0027_12_01_2021_f10.raw
Submitter:

Peak #	Formula	Target …	Target …	Time	Found	Area %	Area Abs
14	C23H28C…	493.1	Glyburi…	1.411	Yes	19.0	6549.58
24	C16H18B…	426.0	Product	2.075	Yes	45.8	15817.55

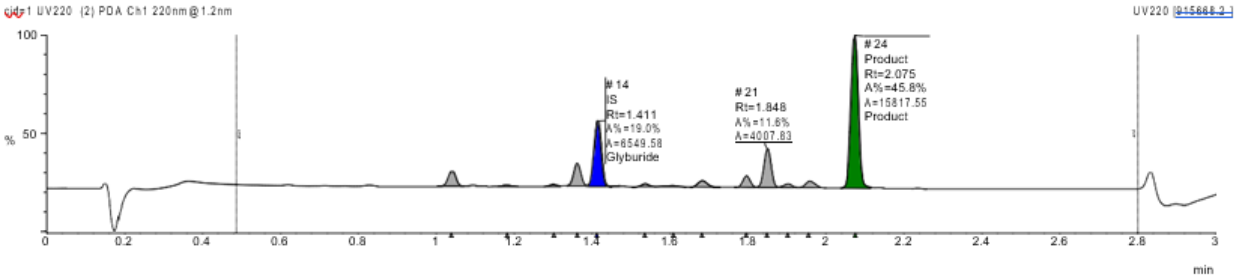

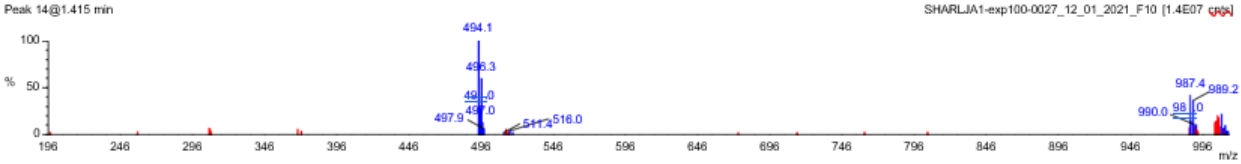

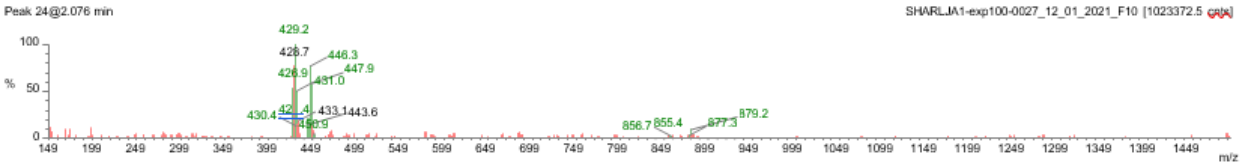

Name	Y/N	Type	Formula	Mass
Glyburide	Y	IS	C23H28ClN3O5S	493.1
Product	Y	Product	C16H18BrCl3O2	426.0

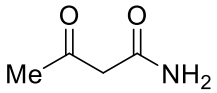

F11,
68% yield

Sample Name: SHARLJA1-exp100-0027_12_01_2021_F11
Filename: sharlja1-exp100-0027_12_01_2021_f11.raw
Submitter:

Peak #	Formula	Target …	Target …	Time	Found	Area %	Area Abs
13	C23H28C…	493.1	Glyburi…	1.411	Yes	18.5	6750.71
24	C16H18B…	426.0	Product	2.071	Yes	48.7	17722.71

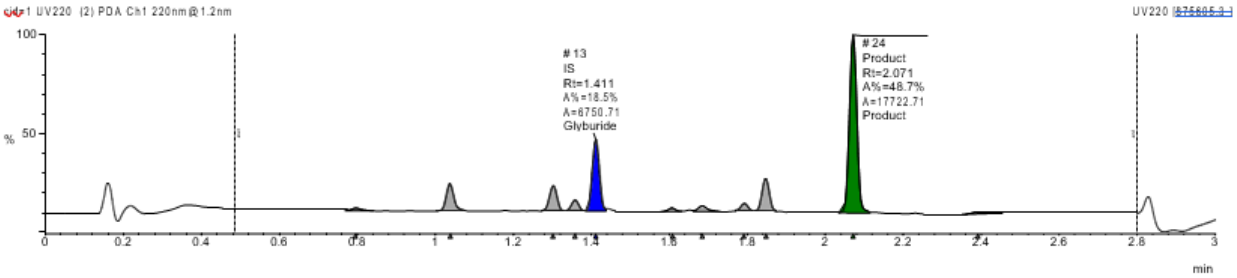

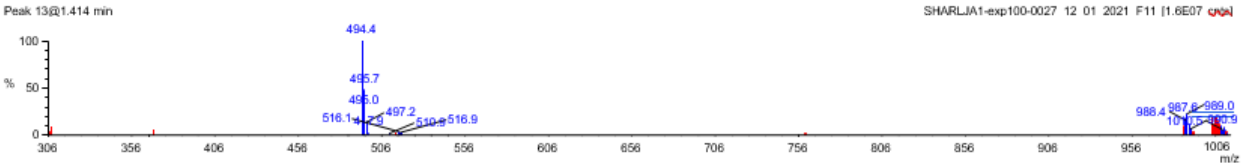

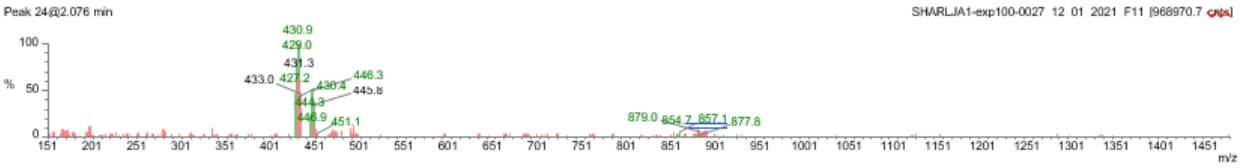

Name	Y/N	Type	Formula	Mass
Glyburide	Y	IS	C23H28ClN3O5S	493.1
Product	Y	Product	C16H18BrCl3O2	426.0

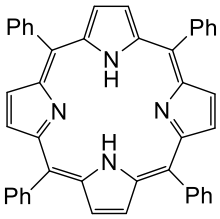

F12,
54% yield

Sample Name: SHARLJA1-exp100-0027_12_01_2021_F12
Filename: sharlja1-exp100-0027_12_01_2021_f12.raw
Submitter:

Peak #	Formula	Target …	Target …	Time	Found	Area %	Area Abs
9	C23H28C…	493.1	Glyburi…	1.411	Yes	24.6	3336.64
17	C16H18B…	426.0	Product	2.075	Yes	51.3	6974.52

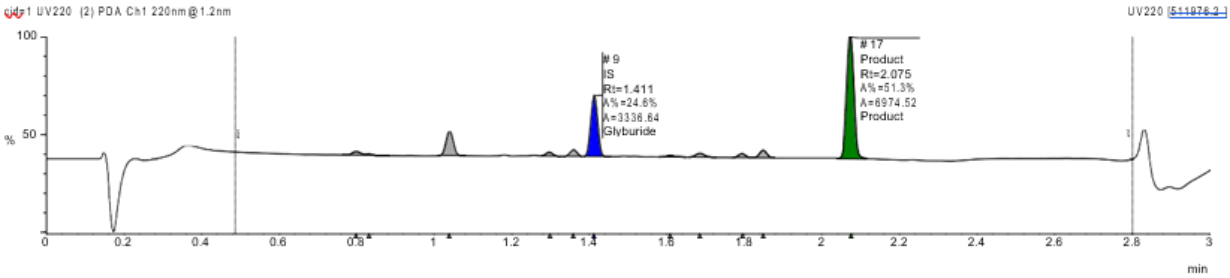

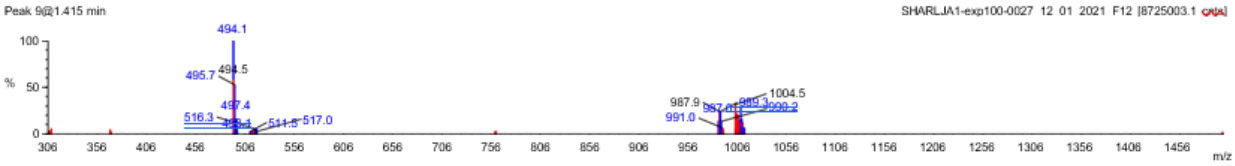

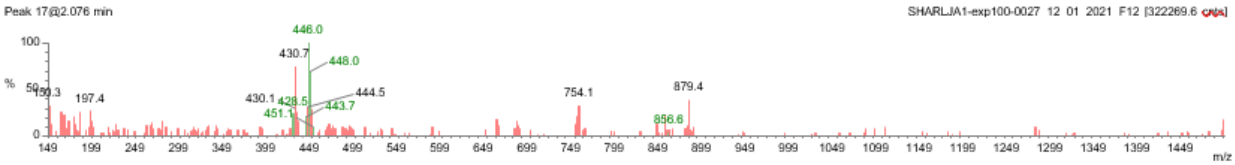

Name	Y/N	Type	Formula	Mass
Glyburide	Y	IS	C23H28ClN3O5S	493.1
Product	Y	Product	C16H18BrCl3O2	426.0

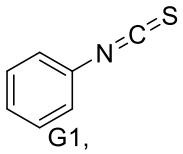

G1,
31% yield

Sample Name: SHARLJA1-exp100-0027_12_01_2021_G1
Filename: sharlja1-exp100-0027_12_01_2021_g1.raw
Submitter:

Peak #	Formula	Target …	Target …	Time	Found	Area %	Area Abs
13	C23H28C…	493.1	Glyburi…	1.415	Yes	28.3	3051.72
25	C16H18B…	426.0	Product	2.075	Yes	36.2	3905.17

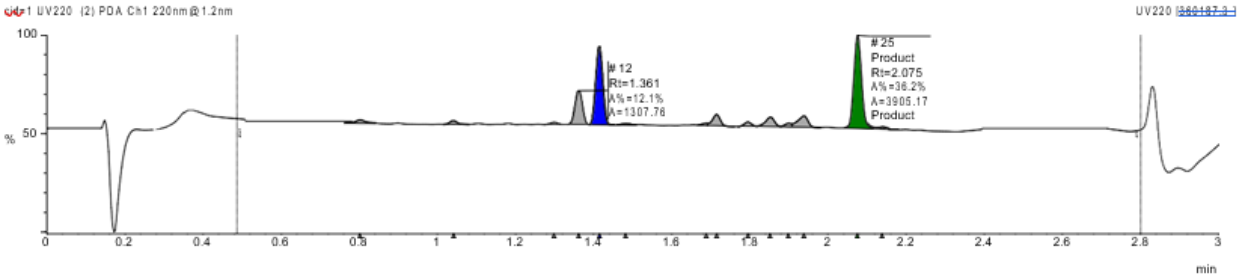

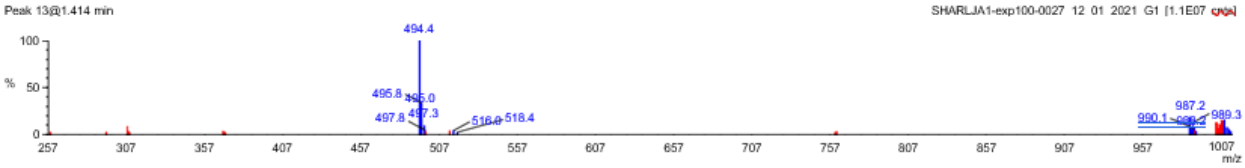

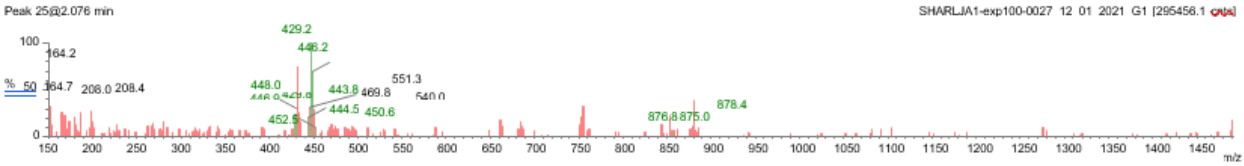

Name	Y/N	Type	Formula	Mass
Glyburide	Y	IS	C23H28ClN3O5S	493.1
Product	Y	Product	C16H18BrCl3O2	426.0

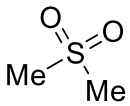

G2,
62% yield

Single Sample Report
Sample Name: SHARLJA1-exp100-0027_12_01_2021_G2
Filename: sharlja1-exp100-0027_12_01_2021_g2.raw
Submitter:

Peak #	Formula	Target …	Target …	Time	Found	Area %	Area Abs
9	C23H28C…	493.1	Glyburi…	1.411	Yes	24.1	5880.80
17	C16H18B…	426.0	Product	2.071	Yes	58.0	14149.06

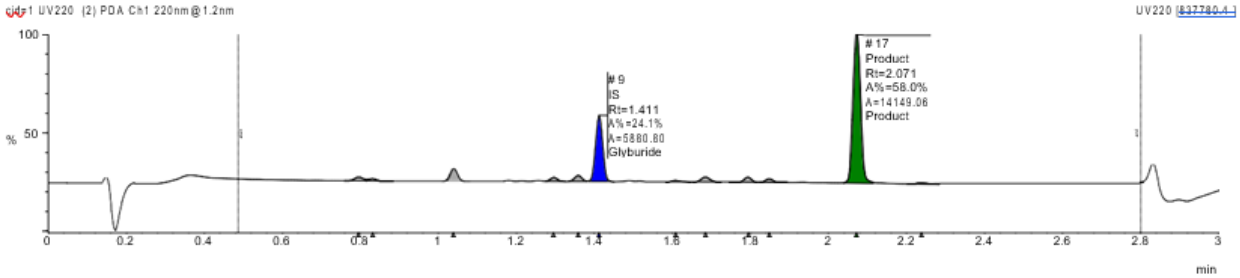

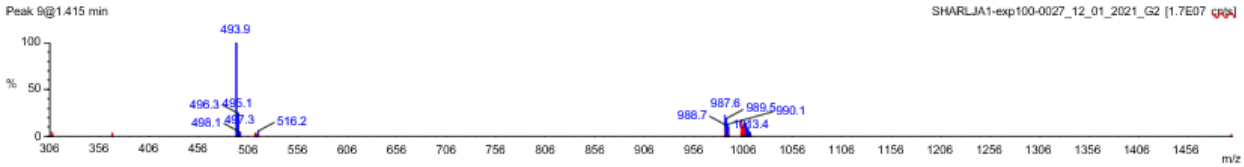

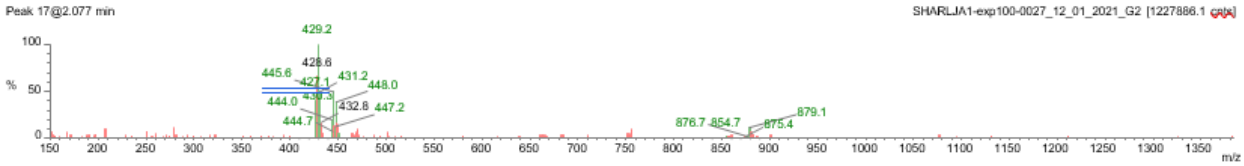

Name	Y/N	Type	Formula	Mass
Glyburide	Y	IS	C23H28ClN3O5S	493.1
Product	Y	Product	C16H18BrCl3O2	426.0

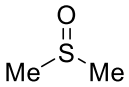

G5,
41% yield

Single Sample Report
Sample Name: SHARLJA1-exp100-0027_12_01_2021_G5
Filename: sharlja1-exp100-0027_12_01_2021_g5.raw
Submitter:

Peak #	Formula	Target …	Target …	Time	Found	Area %	Area Abs
8	C23H28C…	493.1	Glyburi…	1.411	Yes	25.9	2838.99
19	C16H18B…	426.0	Product	2.075	Yes	42.9	4690.97

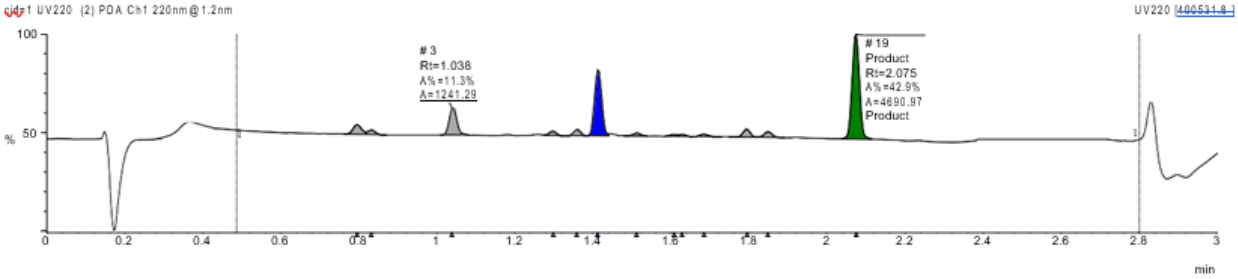

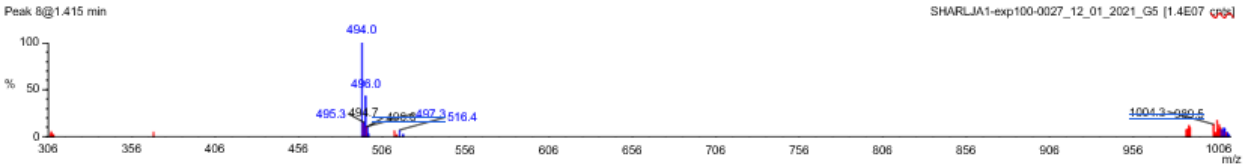

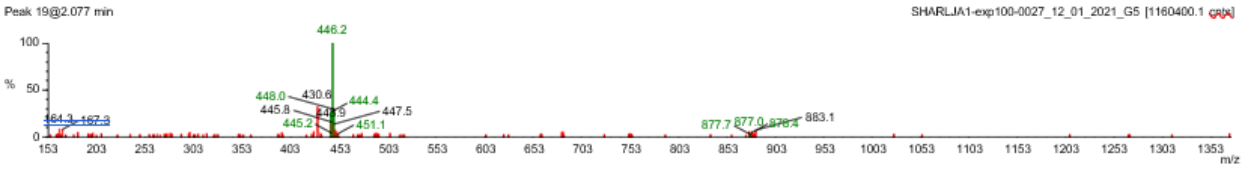

Name	Y/N	Type	Formula	Mass
Glyburide	Y	IS	C23H28ClN3O5S	493.1
Product	Y	Product	C16H18BrCl3O2	426.0

Single Sample Report
Sample Name: SHARLJA1-exp100-0027_12_01_2021_G6
Filename: sharlja1-exp100-0027_12_01_2021_g6.raw
Submitter:

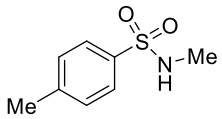

G6,
77% yield

Peak #	Formula	Target …	Target …	Time	Found	Area %	Area Abs
9	C23H28C…	493.1	Glyburi…	1.415	Yes	12.7	4609.64
16	C16H18B…	426.0	Product	2.075	Yes	37.3	13484.31

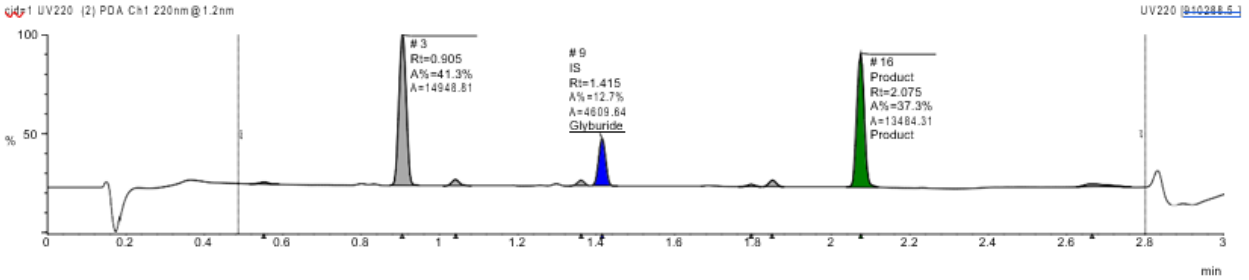

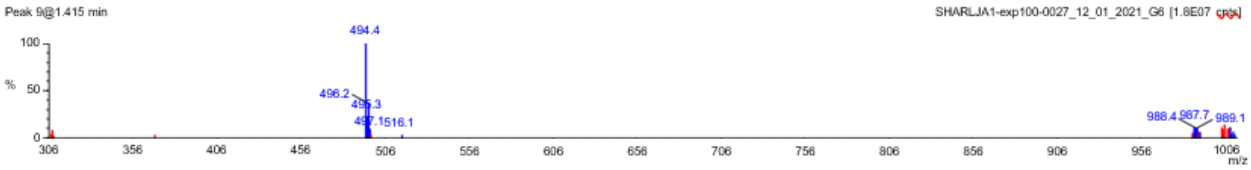

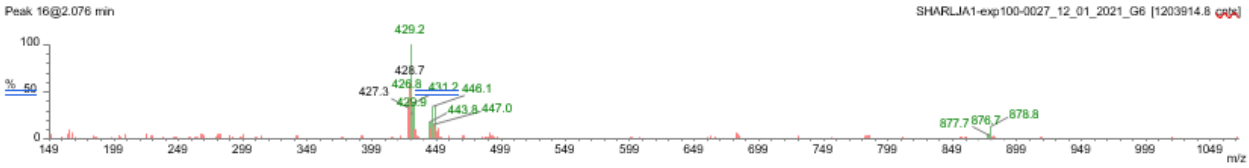

Name	Y/N	Type	Formula	Mass
Glyburide	Y	IS	C23H28ClN3O5S	493.1
Product	Y	Product	C16H18BrCl3O2	426.0

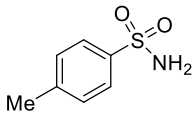

G7,
57% yield

Single Sample Report
Sample Name: SHARLJA1-exp100-0027_12_01_2021_G7
Filename: sharlja1-exp100-0027_12_01_2021_g7.raw
Submitter:

Peak #	Formula	Target …	Target …	Time	Found	Area %	Area Abs
13	C23H28C…	493.1	Glyburi…	1.411	Yes	14.0	8022.52
25	C16H18B…	426.0	Product	2.071	Yes	31.3	17907.99

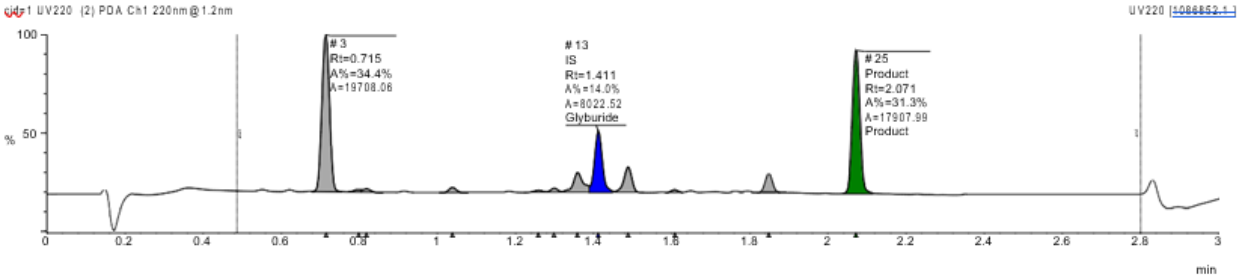

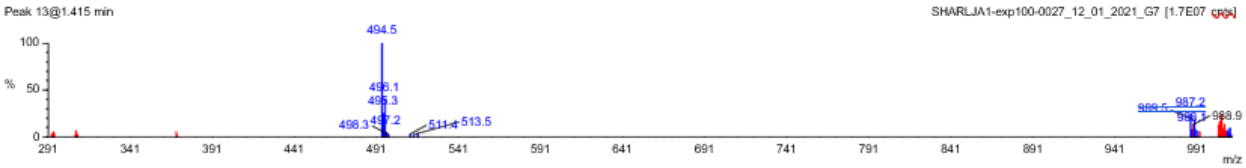

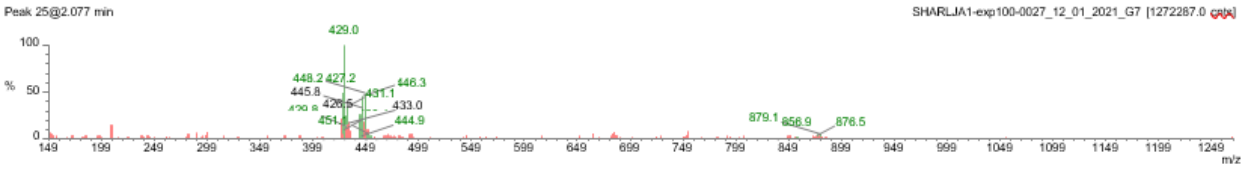

Name	Y/N	Type	Formula	Mass
Glyburide	Y	IS	C23H28ClN3O5S	493.1
Product	Y	Product	C16H18BrCl3O2	426.0

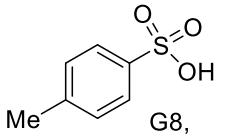

G8,
74% yield

Single Sample Report
Sample Name: SHARLJA1-exp100-0027_12_01_2021_G8
Filename: sharlja1-exp100-0027_12_01_2021_g8.raw
Submitter:

Peak #	Formula	Target …	Target …	Time	Found	Area %	Area Abs
11	C23H28C…	493.1	Glyburi…	1.415	Yes	7.9	1892.31
21	C16H18B…	426.0	Product	2.075	Yes	22.3	5334.93

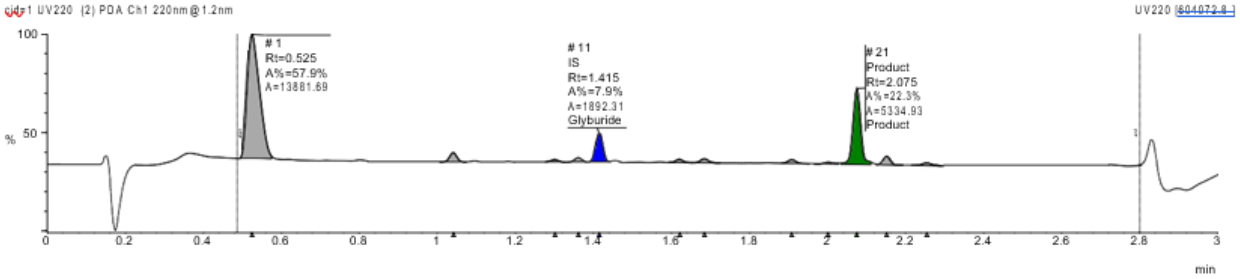

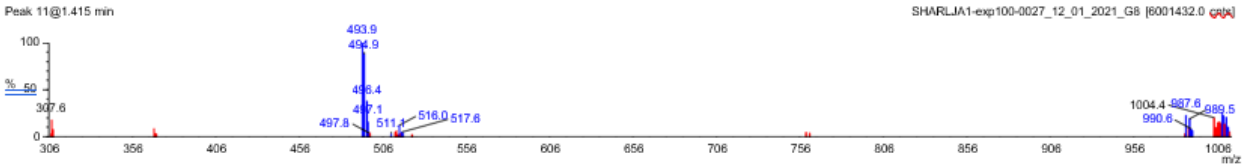

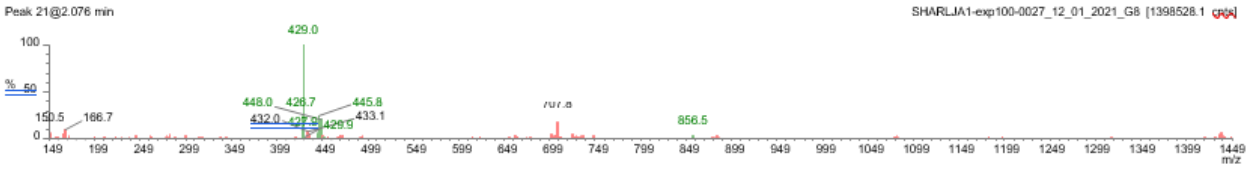

Name	Y/N	Type	Formula	Mass
Glyburide	Y	IS	C23H28ClN3O5S	493.1
Product	Y	Product	C16H18BrCl3O2	426.0

Single Sample Report
Sample Name: SHARLJA1-exp100-0027_12_01_2021_G9
Filename: sharlja1-exp100-0027_12_01_2021_g9.raw
Submitter:

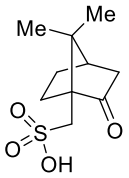

G9,
52% yield

Peak #	Formula	Target …	Target …	Time	Found	Area %	Area Abs
9	C23H28C…	493.1	Glyburi…	1.411	Yes	23.0	2257.18
19	C16H18B…	426.0	Product	2.071	Yes	47.0	4616.06

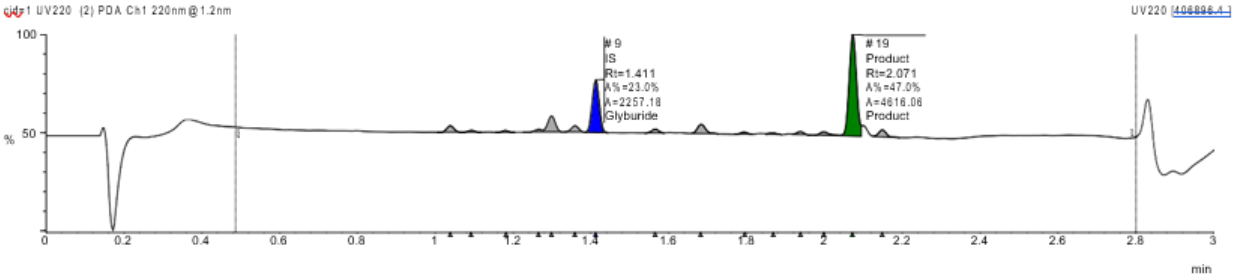

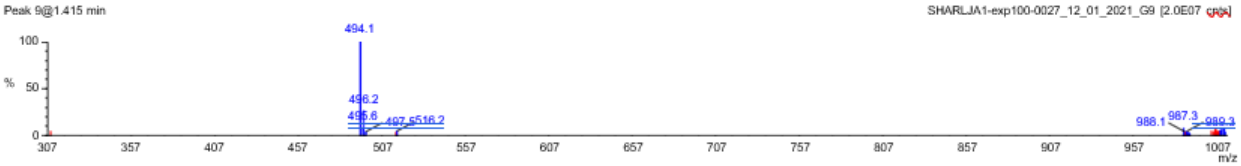

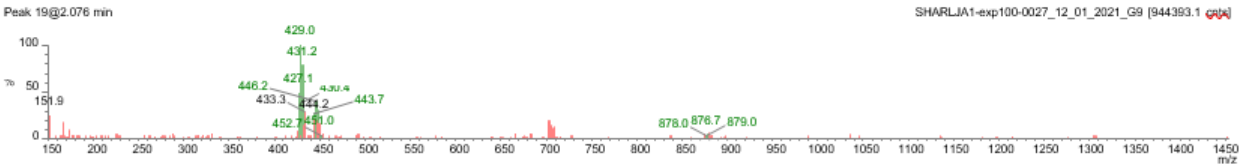

Name	Y/N	Type	Formula	Mass
Glyburide	Y	IS	C23H28ClN3O5S	493.1
Product	Y	Product	C16H18BrCl3O2	426.0

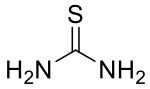

G11,
44% yield

Sample Name: SHARLJA1-exp100-0027_12_01_2021_G11
Filename: sharlja1-exp100-0027_12_01_2021_g11.raw
Submitter:

Peak #	Formula	Target …	Target …	Time	Found	Area %	Area Abs
13	C23H28C…	493.1	Glyburi…	1.411	Yes	15.9	7771.31
26	C16H18B…	426.0	Product	2.071	Yes	27.8	13632.12

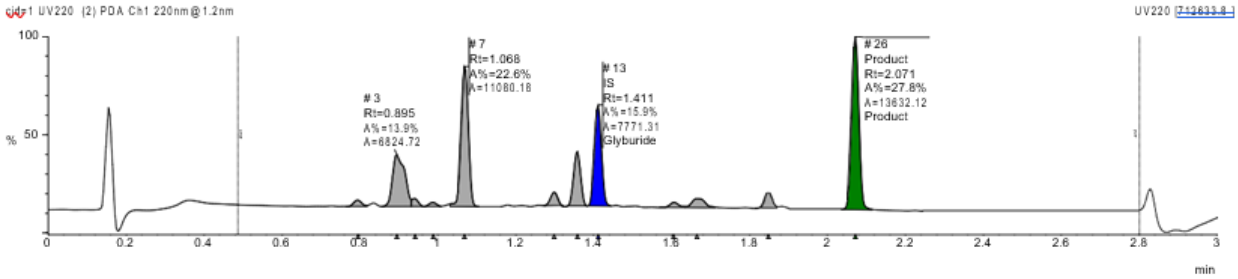

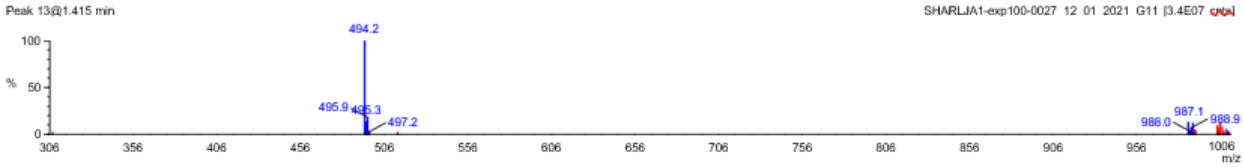

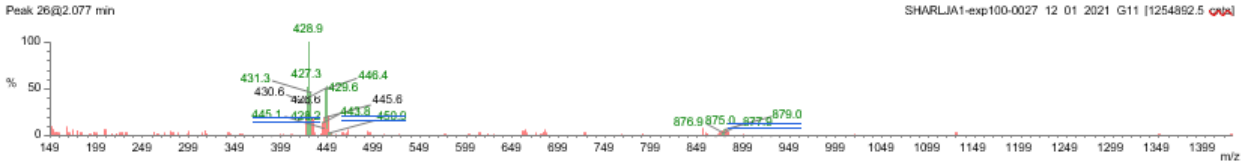

Name	Y/N	Type	Formula	Mass
Glyburide	Y	IS	C23H28ClN3O5S	493.1
Product	Y	Product	C16H18BrCl3O2	426.0

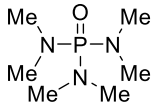

H1,
51% yield

Sample Name: SHARLJA1-exp100-0027_12_01_2021_H1
Filename: sharlja1-exp100-0027_12_01_2021_h1.raw
Submitter:

Peak #	Formula	Target …	Target …	Time	Found	Area %	Area Abs
10	C23H28C…	493.1	Glyburi…	1.415	Yes	28.5	2539.93
18	C16H18B…	426.0	Product	2.075	Yes	56.7	5048.30

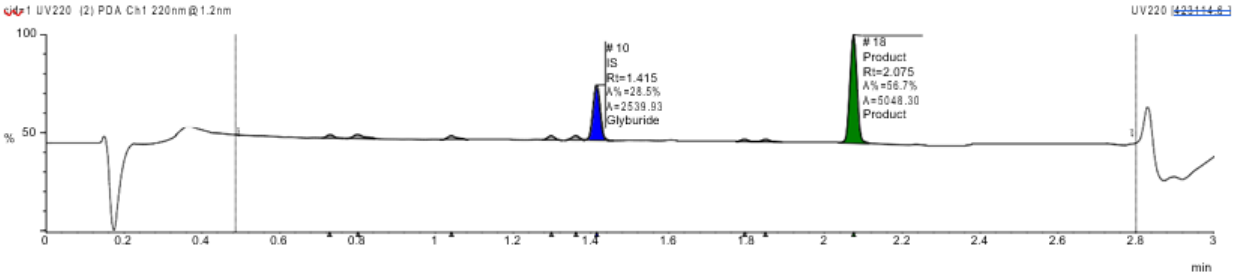

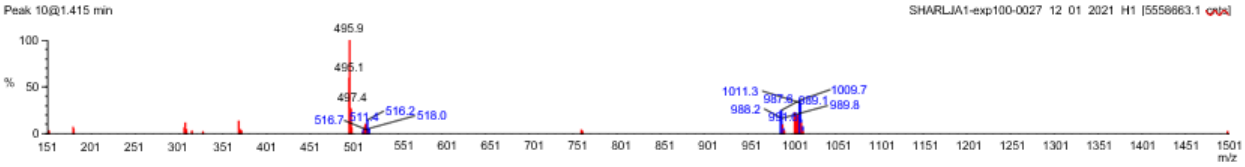

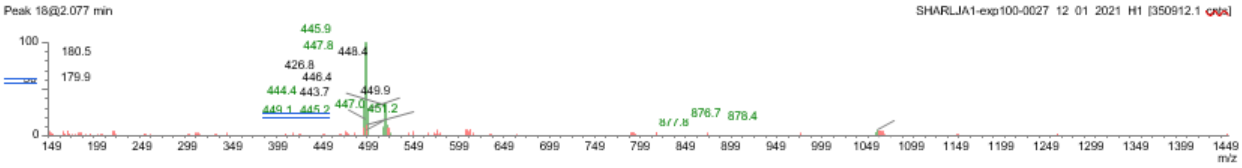

Name	Y/N	Type	Formula	Mass
Glyburide	Y	IS	C23H28ClN3O5S	493.1
Product	Y	Product	C16H18BrCl3O2	426.0

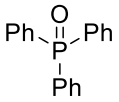

H3,
78% yield

Single Sample Report
Sample Name: SHARLJA1-exp100-0027_12_01_2021_H3
Filename: sharlja1-exp100-0027_12_01_2021_h3.raw
Submitter:

Peak #	Formula	Target …	Target …	Time	Found	Area %	Area Abs
7	C23H28C…	493.1	Glyburi…	1.411	Yes	11.7	5692.15
15	C16H18B…	426.0	Product	2.071	Yes	34.6	16832.59

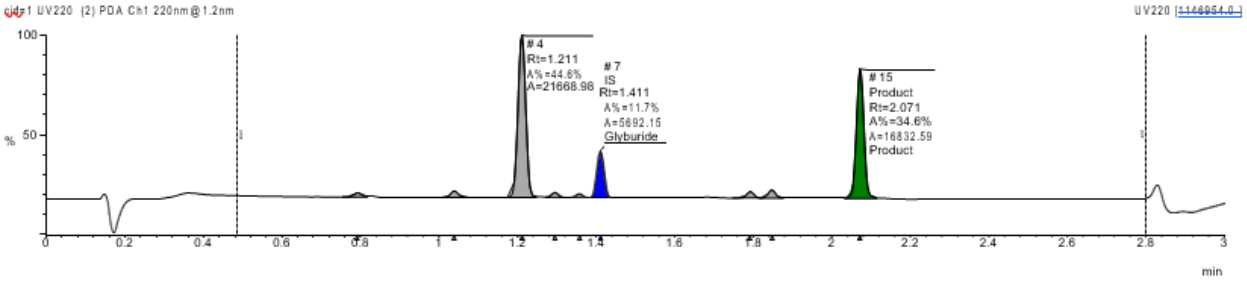

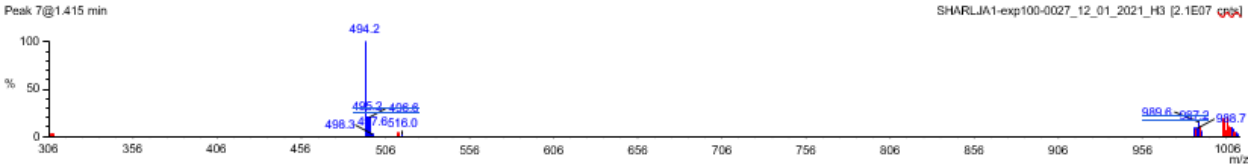

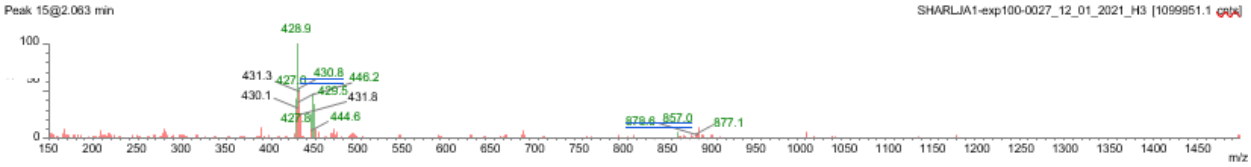

Name	Y/N	Type	Formula	Mass
Glyburide	Y	IS	C23H28ClN3O5S	493.1
Product	Y	Product	C16H18BrCl3O2	426.0

Me−CN
H6,
65% yield

Single Sample Report
Sample Name: SHARLJA1-exp100-0027_12_01_2021_H6
Filename: sharlja1-exp100-0027_12_01_2021_h6.raw
Submitter:

Peak #	Formula	Target …	Target …	Time	Found	Area %	Area Abs
9	C23H28C…	493.1	Glyburi…	1.415	Yes	22.7	6692.34
16	C16H18B…	426.0	Product	2.075	Yes	56.3	16632.29

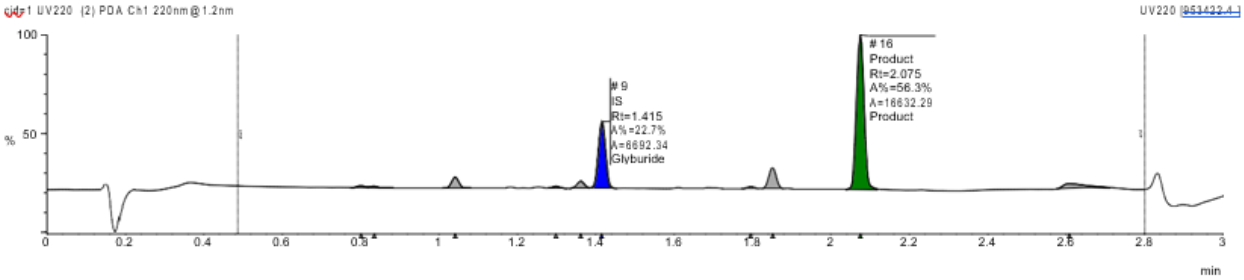

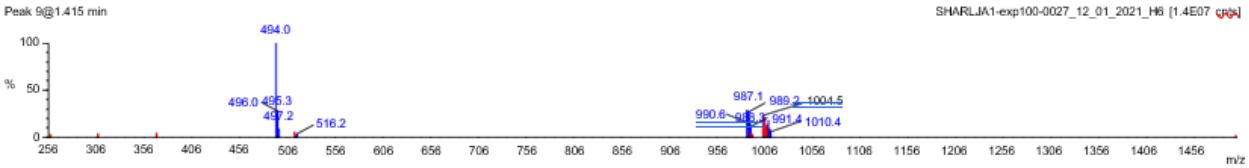

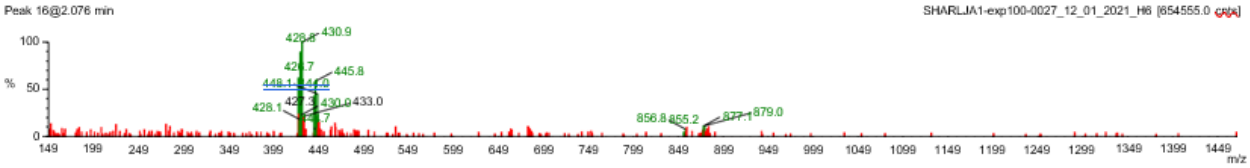

Name	Y/N	Type	Formula	Mass
Glyburide	Y	IS	C23H28ClN3O5S	493.1
Product	Y	Product	C16H18BrCl3O2	426.0

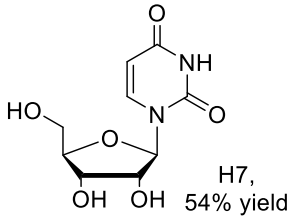

Single Sample Report
Sample Name: SHARLJA1-exp100-0027_12_01_2021_H7
Filename: sharlja1-exp100-0027_12_01_2021_h7.raw
Submitter:

Peak #	Formula	Target …	Target …	Time	Found	Area %	Area Abs
15	C23H28C…	493.1	Glyburi…	1.411	Yes	18.5	7095.79
25	C16H18B…	426.0	Product	2.071	Yes	38.9	14942.70

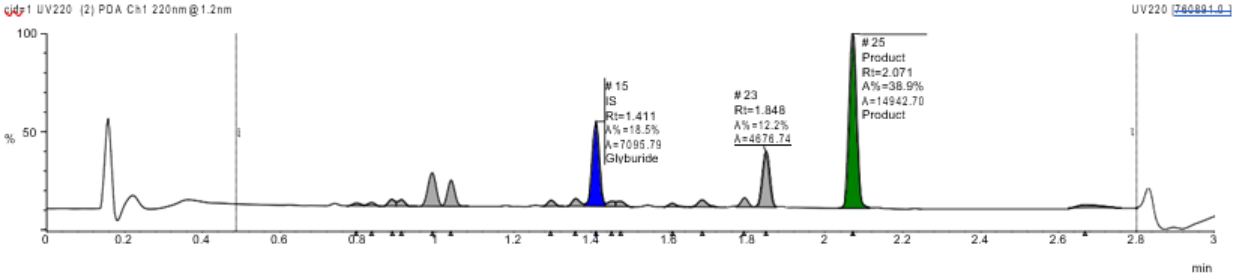

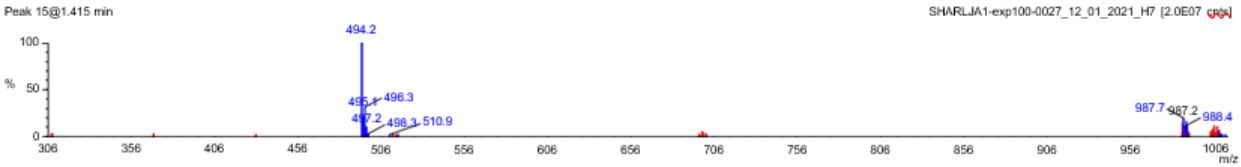

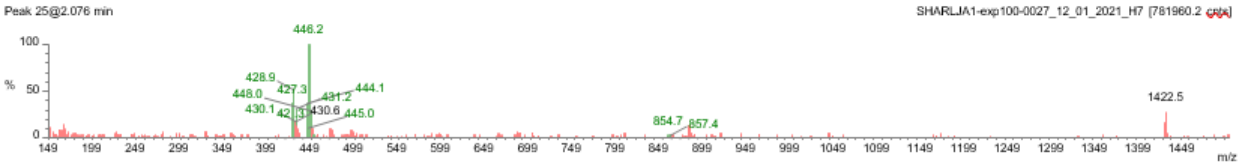

Name	Y/N	Type	Formula	Mass
Glyburide	Y	IS	C23H28ClN3O5S	493.1
Product	Y	Product	C16H18BrCl3O2	426.0

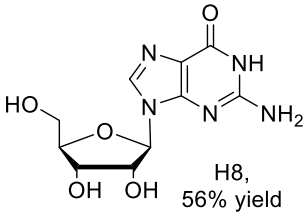

Single Sample Report
Sample Name: SHARLJA1-exp100-0027_12_01_2021_H8
Filename: sharlja1-exp100-0027_12_01_2021_h8.raw
Submitter:

Peak #	Formula	Target …	Target …	Time	Found	Area %	Area Abs
18	C23H28C…	493.1	Glyburi…	1.408	Yes	19.8	4006.79
25	C16H18B…	426.0	Product	2.071	Yes	43.1	8724.87

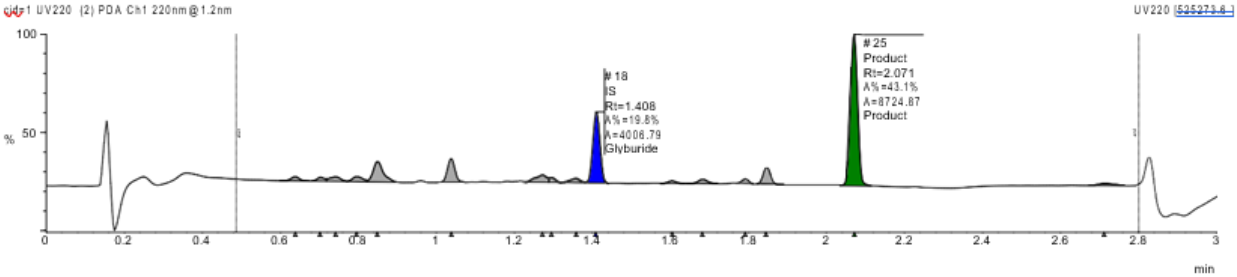

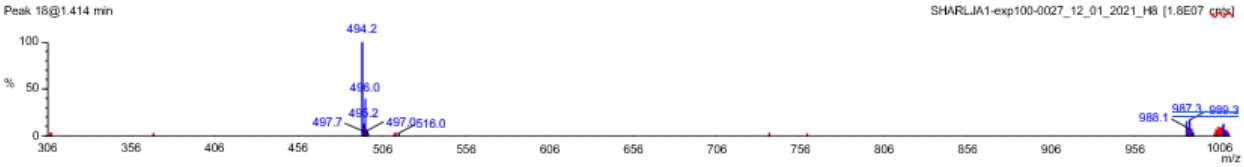

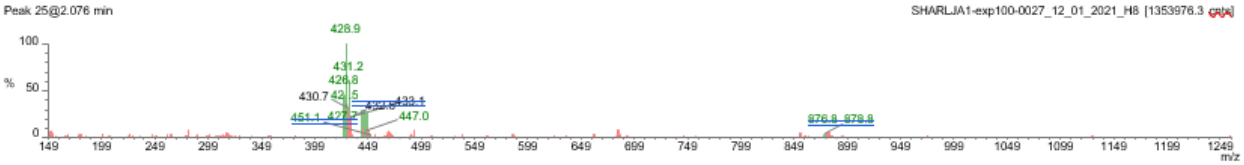

Name	Y/N	Type	Formula	Mass
Glyburide	Y	IS	C23H28ClN3O5S	493.1
Product	Y	Product	C16H18BrCl3O2	426.0

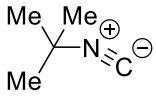

H9,
66% yield

Single Sample Report
Sample Name: SHARLJA1-exp100-0027_12_01_2021_H9
Filename: sharlja1-exp100-0027_12_01_2021_h9.raw
Submitter:

Peak #	Formula	Target …	Target …	Time	Found	Area %	Area Abs
8	C23H28C…	493.1	Glyburi…	1.411	Yes	22.6	3340.87
16	C16H18B…	426.0	Product	2.071	Yes	57.2	8459.05

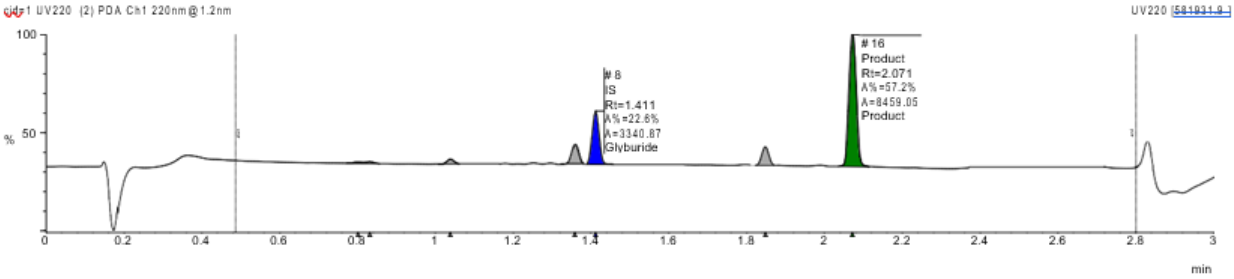

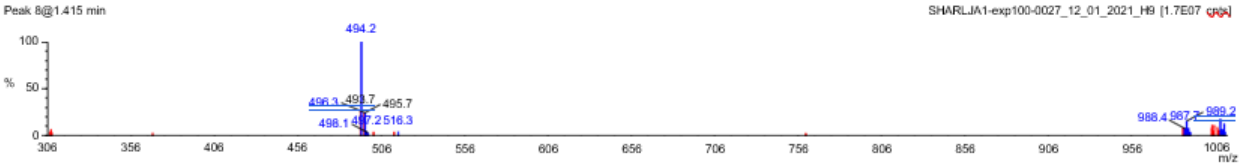

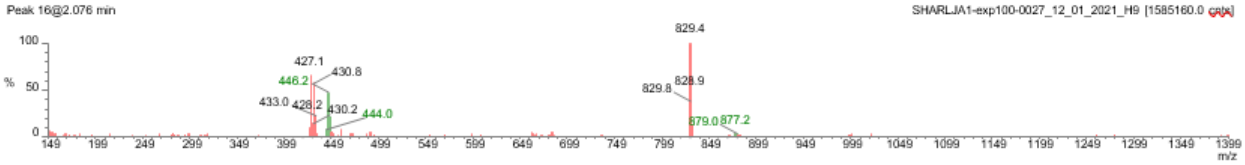

Name	Y/N	Type	Formula	Mass
Glyburide	Y	IS	C23H28ClN3O5S	493.1
Product	Y	Product	C16H18BrCl3O2	426.0

Single Sample Report
Sample Name: SHARLJA1-exp100-0027_12_01_2021_H10
Filename: sharlja1-exp100-0027_12_01_2021_h10.raw
Submitter:

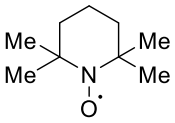

H10,
49% yield

Peak #	Formula	Target …	Target …	Time	Found	Area %	Area Abs
10	C23H28C…	493.1	Glyburi…	1.415	Yes	25.7	5212.08
20	C16H18B…	426.0	Product	2.075	Yes	49.5	10024.08

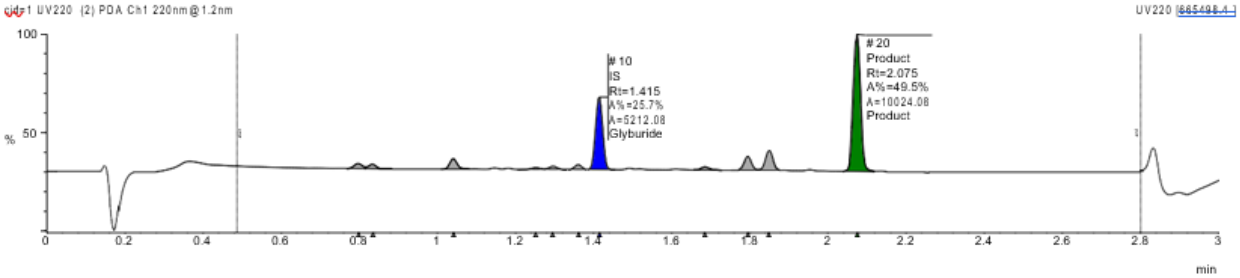

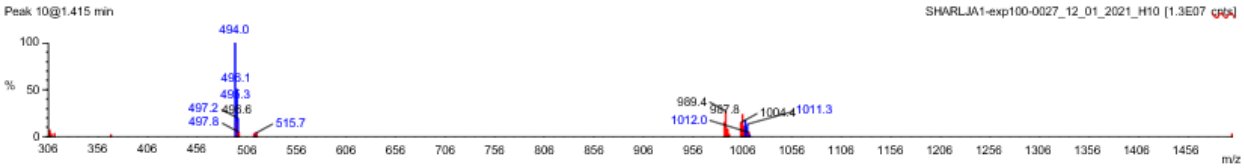

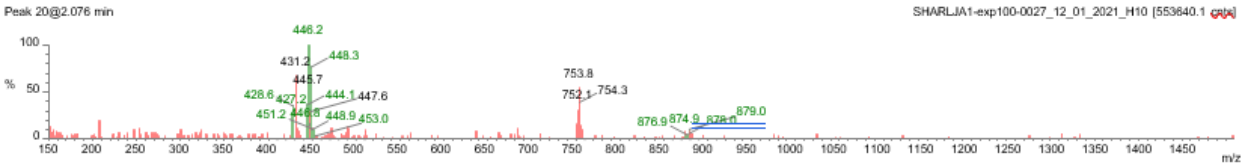

Name	Y/N	Type	Formula	Mass
Glyburide	Y	IS	C23H28ClN3O5S	493.1
Product	Y	Product	C16H18BrCl3O2	426.0

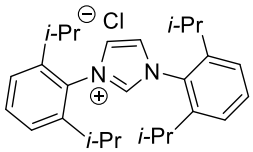

H12,
45% yield

Single Sample Report
Sample Name: SHARLJA1-exp100-0027_12_01_2021_H12
Filename: sharlja1-exp100-0027_12_01_2021_h12.raw
Submitter:

Peak #	Formula	Target …	Target …	Time	Found	Area %	Area Abs
8	C23H28C…	493.1	Glyburi…	1.411	Yes	9.8	4526.59
15	C16H18B…	426.0	Product	2.075	Yes	17.5	8076.70

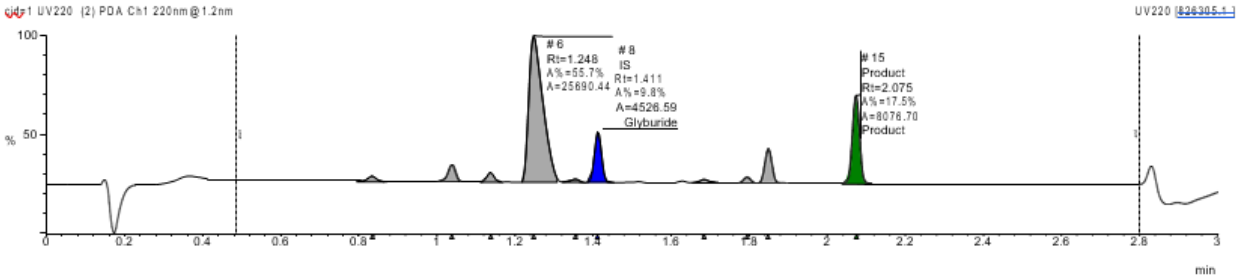

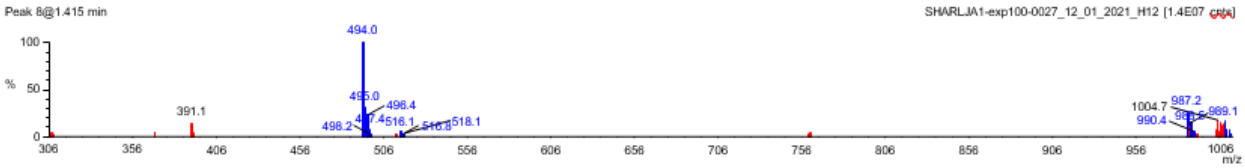

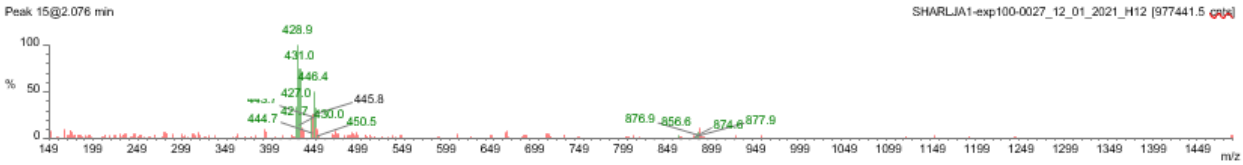

Name	Y/N	Type	Formula	Mass
Glyburide	Y	IS	C23H28ClN3O5S	493.1
Product	Y	Product	C16H18BrCl3O2	426.0

5.5: Enantioselectivity of successful reactions with Rh_2(*R*-NTTL)$_4$ and HFIP as solvent:

The following dataset represents reactions that were successful when performed according to **general procedure 5.1** using Rh_2(*R*-NTTL)$_4$ as catalyst and HFIP as solvent. Each additive is described according to the well plate designation in the study as well as the compound number it was assigned in the main text. The enantioselectivity of the reaction in the presence of each additive is reported in **Figure C**9 and what follows is the SFC data from which the asymmetric induction was determined.

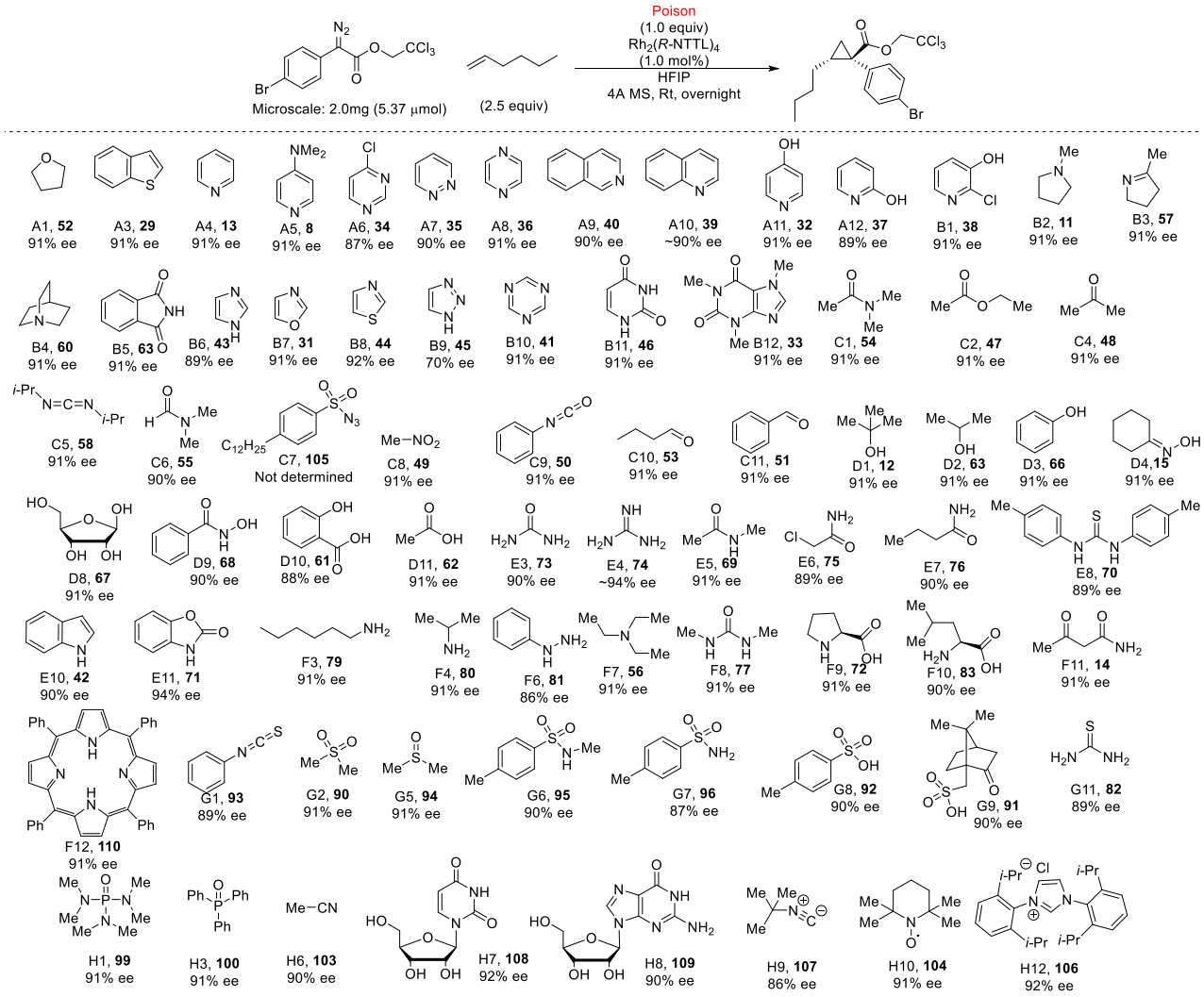

Figure C9: Successful additives using Rh_2(*R*-NTTL)$_4$ as catalyst (1.0 mol%) and HFIP as solvent on microscale. Wellplate designation is listed below additive structure along with the assigned number in the main text. The observed %ee by SFC is reported below the structure and what follows is the SFC data.

A1: 91% ee

Openlynx Report - SHARLJA1

Sample: 1
File:SHARLJA1_20211115_1
Description:(S,S)WO1 4.6x100mm 5µ

Vial:1:1
Date:15-Nov-2021
Conditions:5% IPA over 5min 3mL/min

ID:27-A1
Time:16:10:57

A1,
91% ee

Page 1

Printed: Thu Dec 09 16:42:06 2021

Sample Report:

Sample 1 Vial 1:1 ID 27-A1 File SHARLJA1_20211115_1 Date 15-Nov-2021 Time 16:10:57 Description (S,S)WO1 4.6x100mm 5µ

2: UV Detector: 230 Nm 2.0000-2.3500: Smooth (Mn, 2x3), 3.1000-3.5500: Smooth (Mn, 2x3) 4.084e-1
Range: 4.183e-1

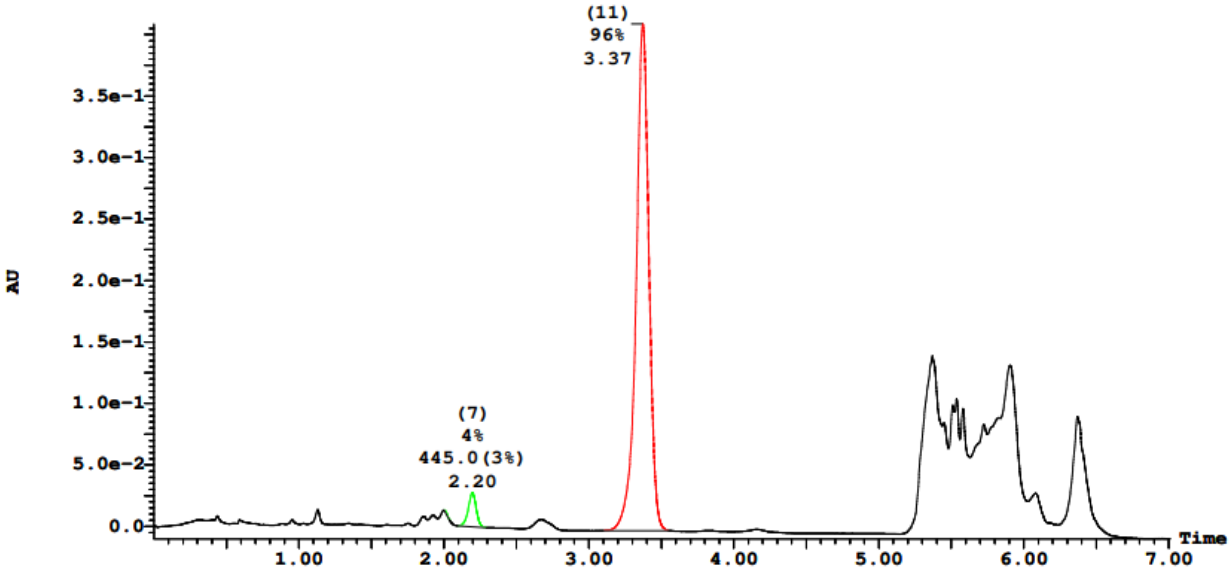

Peak Number	Compound	Time	AreaAbs	Area %Total	Width	Height	Mass Found
6	Tentative	2.00	3e+001	0.07	0	2e+002	445.0000
7	Tentative	2.20	2e+003	4.03	0	3e+004	445.0000
11		3.37	4e+004	95.90	0	4e+005	Not Found

A3: 91% ee

Openlynx Report - SHARLJA1

Sample: 3
File:SHARLJA1_20211115_3
Description:(S,S)WO1 4.6x100mm 5µ

Vial:1:3
Date:15-Nov-2021
Conditions:5% IPA over 5min 3mL/min

ID:27-A3
Time:16:28:08

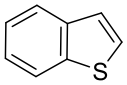

A3,
91% ee

Printed: Thu Dec 09 16:42:06 2021

Sample Report (continued):

Sample 3 Vial 1:3 ID 27-A3 File SHARLJA1_20211115_3 Date 15-Nov-2021 Time 16:28:08 Description (S,S)WO1 4.6x100mm 5µ

2: UV Detector: 230 Nm 2.0000-2.3500: Smooth (Mn, 2x3), 3.1000-3.5500: Smooth (Mn, 2x3) 4.326e-1
Range: 4.329e-1

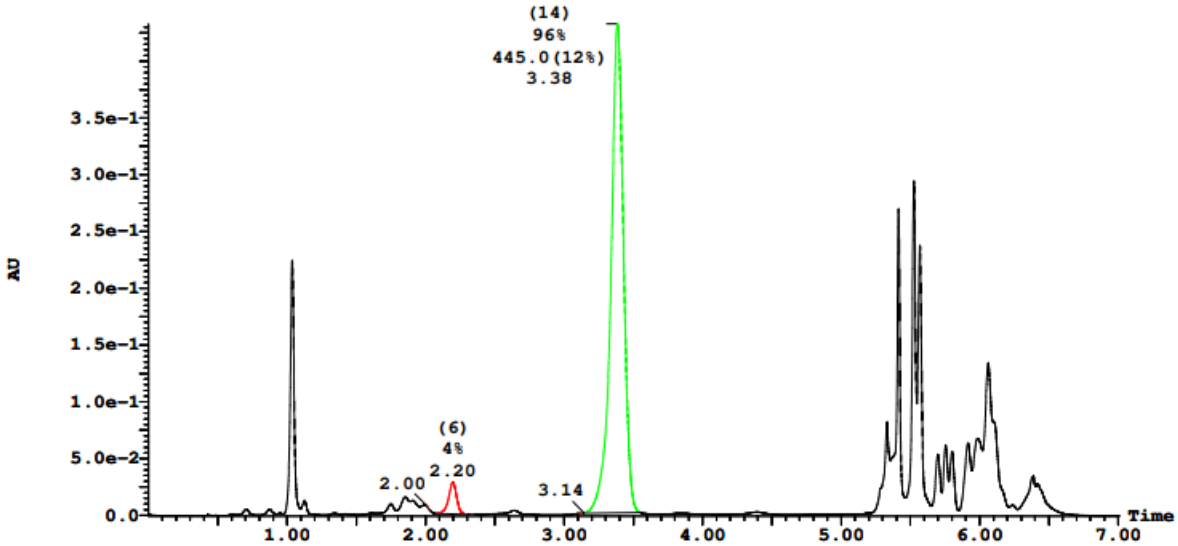

Peak Number	Compound	Time	AreaAbs	Area %Total	Width	Height	Mass Found
5		2.00	8e+000	0.02	0		Not Found
6		2.20	2e+003	3.96	0	3e+004	Not Found
7		2.31	1e+000	0.00	0	5e+001	Not Found
11		3.14	1e+001	0.03	0	7e+002	Not Found
14	Found	3.38	5e+004	95.99	0	4e+005	445.0000

A4: 91% ee

Openlynx Report - SHARLJA1

Sample: 4
File:SHARLJA1_20211115_4
Description:(S,S)WO1 4.6x100mm 5µ

Vial:1:4
Date:15-Nov-2021
Conditions:5% IPA over 5min 3mL/min

ID:27-A4
Time:16:36:16

A4,
91% ee

Page 7

Printed: Thu Dec 09 16:42:06 2021

Sample Report (continued):

Sample 4 Vial 1:4 ID 27-A4 File SHARLJA1_20211115_4 Date 15-Nov-2021 Time 16:36:16 Description (S,S)WO1 4.6x100mm 5µ

2: UV Detector: 230 Nm 2.0000-2.3500: Smooth (Mn, 2x3), 3.1000-3.5500: Smooth (Mn, 2x3) 2.119e-1
Range: 2.13e-1

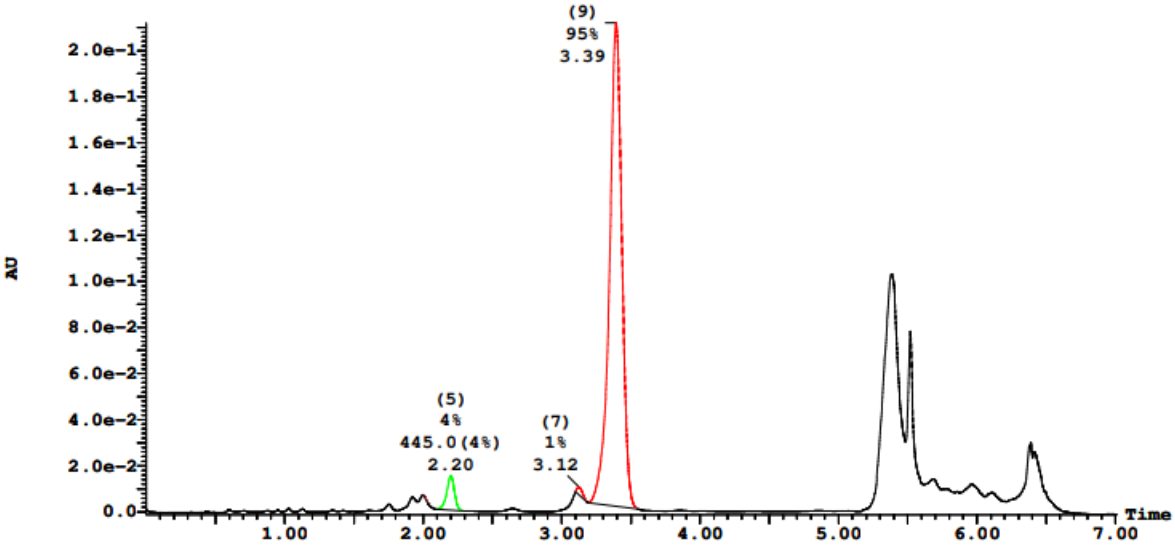

Peak Number	Compound	Time	AreaAbs	Area %Total	Width	Height	Mass Found
4		2.00	1e+001	0.05	0		Not Found
5	Tentative	2.20	1e+003	4.24	0	1e+004	445.0000
7		3.12	2e+002	0.69	0	3e+003	Not Found
9		3.39	2e+004	95.02	0	2e+005	Not Found

A5: 91% ee

Openlynx Report - SHARLJA1

Sample: 5
File:SHARLJA1_20211115_5
Description:(S,S)WO1 4.6x100mm 5µ

Vial:1:5
Date:15-Nov-2021
Conditions:5% IPA over 5min 3mL/min

ID:27-A5
Time:16:44:23

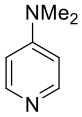

A5,
91% ee

Printed: Thu Dec 09 16:42:06 2021

Sample Report (continued):

Sample 5 Vial 1:5 ID 27-A5 File SHARLJA1_20211115_5 Date 15-Nov-2021 Time 16:44:23 Description (S,S)WO1 4.6x100mm 5µ

2: UV Detector: 230 Nm 2.0000-2.3500: Smooth (Mn, 2x3), 3.1000-3.5500: Smooth (Mn, 2x3) 5.66e-1
Range: 5.669e-1

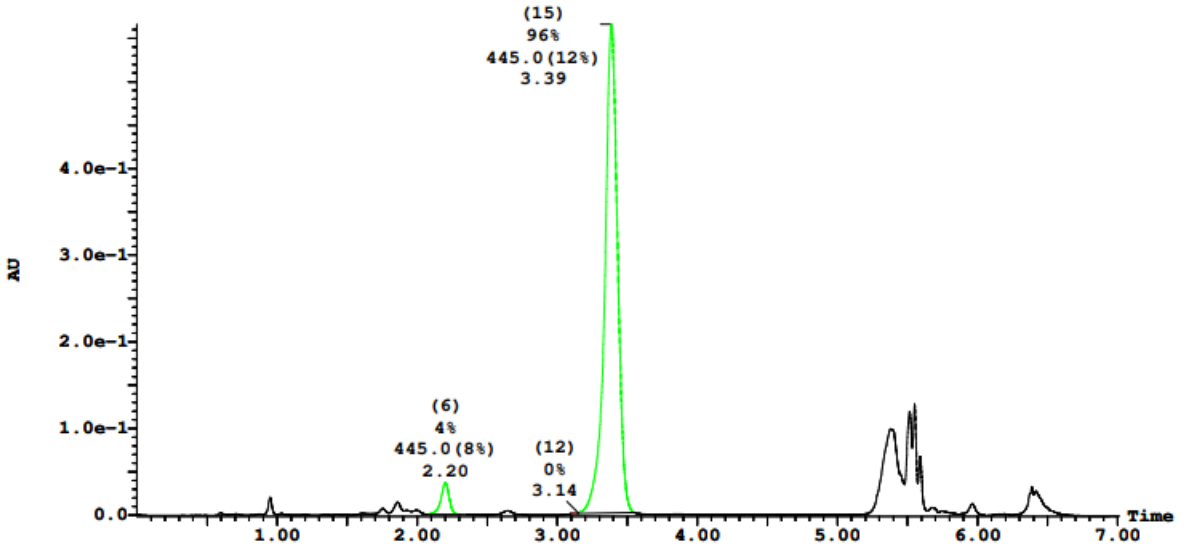

Peak Number	Compound	Time	AreaAbs	Area %Total	Width	Height	Mass Found
6	Found	2.20	2e+003	3.99	0	4e+004	445.0000
7		2.32	2e+000	0.00	0	7e+001	Not Found
12		3.14	3e+001	0.04	0	1e+003	Not Found
15	Found	3.39	6e+004	95.97	0	6e+005	445.0000

A6: 87% ee

Openlynx Report - SHARLJA1

Sample: 6
File:SHARLJA1_20211115_6
Description:(S,S)WO1 4.6x100mm 5µ

Vial:1:6
Date:15-Nov-2021
Conditions:5% IPA over 5min 3mL/min

ID:27-A6
Time:16:52:31

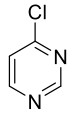

A6,
87% ee

Printed: Thu Dec 09 16:42:06 2021

Sample Report (continued):

Sample 6 Vial 1:6 ID 27-A6 File SHARLJA1_20211115_6 Date 15-Nov-2021 Time 16:52:31 Description (S,S)WO1 4.6x100mm 5µ

2: UV Detector: 230 Nm 2.0000-2.3500: Smooth (Mn, 2x3), 3.1000-3.5500: Smooth (Mn, 2x3) 6.604e-1
Range: 6.617e-1

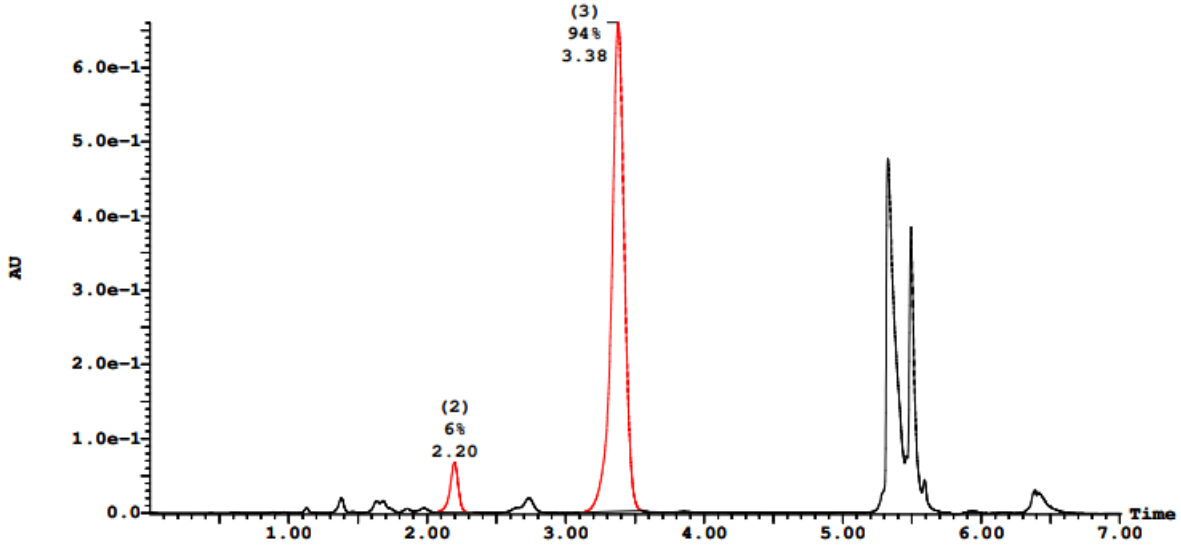

Peak Number	Compound	Time	AreaAbs	Area %Total	Width	Height	Mass Found
2		2.20	5e+003	6.23	0	7e+004	Not Found
3		3.38	7e+004	93.77	0	7e+005	Not Found

A7: 90% ee

Openlynx Report - SHARLJA1

Sample: 7
File:SHARLJA1_20211115_7
Description:(S,S)WO1 4.6x100mm 5µ

Vial:1:7
Date:15-Nov-2021
Conditions:5% IPA over 5min 3mL/min

ID:27-A7
Time:17:00:39

A7,
90% ee

Page 13

Printed: Thu Dec 09 16:42:06 2021

Sample Report (continued):

Sample 7 Vial 1:7 ID 27-A7 File SHARLJA1_20211115_7 Date 15-Nov-2021 Time 17:00:39 Description (S,S)WO1 4.6x100mm 5µ

2: UV Detector: 230 Nm 2.0000-2.3500: Smooth (Mn, 2x3), 3.1000-3.5500: Smooth (Mn, 2x3) 5.77e-1
Range: 5.778e-1

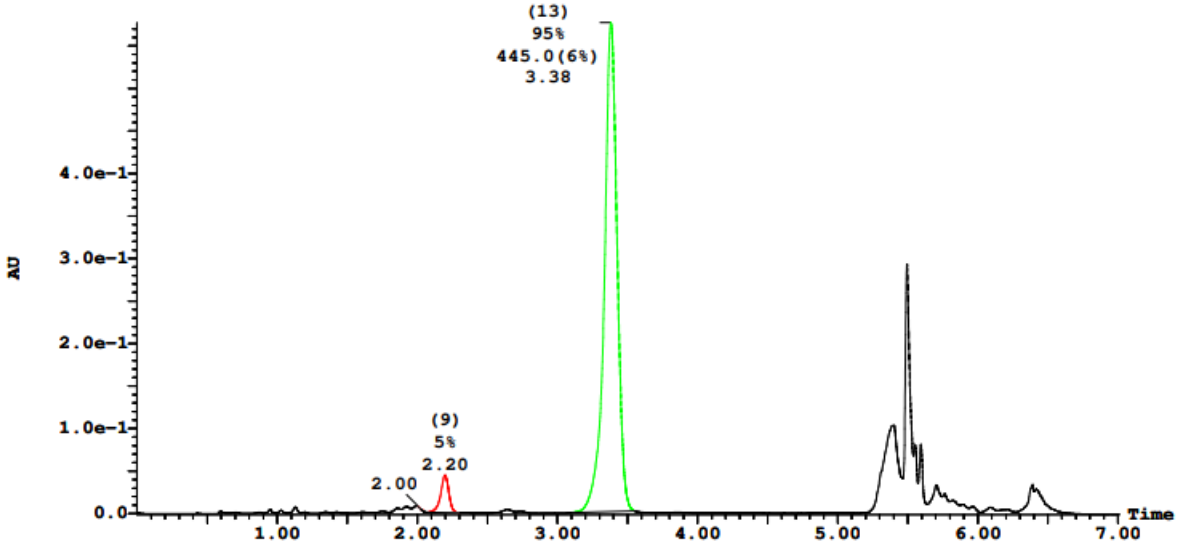

Peak Number	Compound	Time	AreaAbs	Area %Total	Width	Height	Mass Found
8		2.00	8e+000	0.01	0	1e-002	Not Found
9		2.20	3e+003	4.65	0	4e+004	Not Found
13	Found	3.38	6e+004	95.33	0	6e+005	445.0000

A8: 91% ee

Openlynx Report - SHARLJA1

Sample: 8
File:SHARLJA1_20211115_8
Description:(S,S)WO1 4.6x100mm 5µ

Vial:1:8
Date:15-Nov-2021
Conditions:5% IPA over 5min 3mL/min

ID:27-A8
Time:17:08:47

A8,
91% ee

Printed: Thu Dec 09 16:42:06 2021

Sample Report (continued):

Sample 8 Vial 1:8 ID 27-A8 File SHARLJA1_20211115_8 Date 15-Nov-2021 Time 17:08:47 Description (S,S)WO1 4.6x100mm 5µ

2: UV Detector: 230 Nm 2.0000-2.3500: Smooth (Mn, 2x3), 3.1000-3.5500: Smooth (Mn, 2x3) 6.156e-1
Range: 6.163e-1

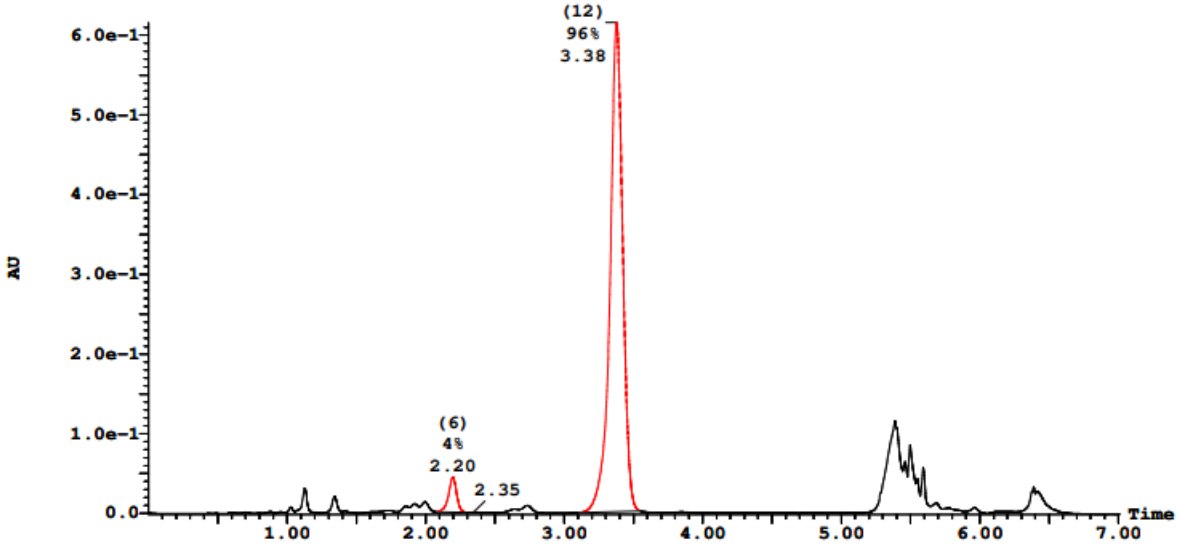

Peak Number	Compound	Time	AreaAbs	Area %Total	Width	Height	Mass Found
6		2.20	3e+003	4.35	0	4e+004	Not Found
7		2.35	6e-001	0.00	0		Not Found
12		3.38	7e+004	95.65	0	6e+005	Not Found

A9: 90% ee

Openlynx Report - SHARLJA1

Sample: 9
File:SHARLJA1_20211115_9
Description:(S,S)WO1 4.6x100mm 5µ

Vial:1:9
Date:15-Nov-2021
Conditions:5% IPA over 5min 3mL/min

ID:27-A9
Time:17:16:56

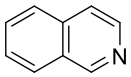

A9,
90% ee

Printed: Thu Dec 09 16:42:06 2021

Sample Report (continued):

Sample 9 Vial 1:9 ID 27-A9 File SHARLJA1_20211115_9 Date 15-Nov-2021 Time 17:16:56 Description (S,S)WO1 4.6x100mm 5µ

2: UV Detector: 230 Nm 2.0000-2.3500: Smooth (Mn, 2x3), 3.1000-3.5500: Smooth (Mn, 2x3) 7.073e-1
Range: 7.081e-1

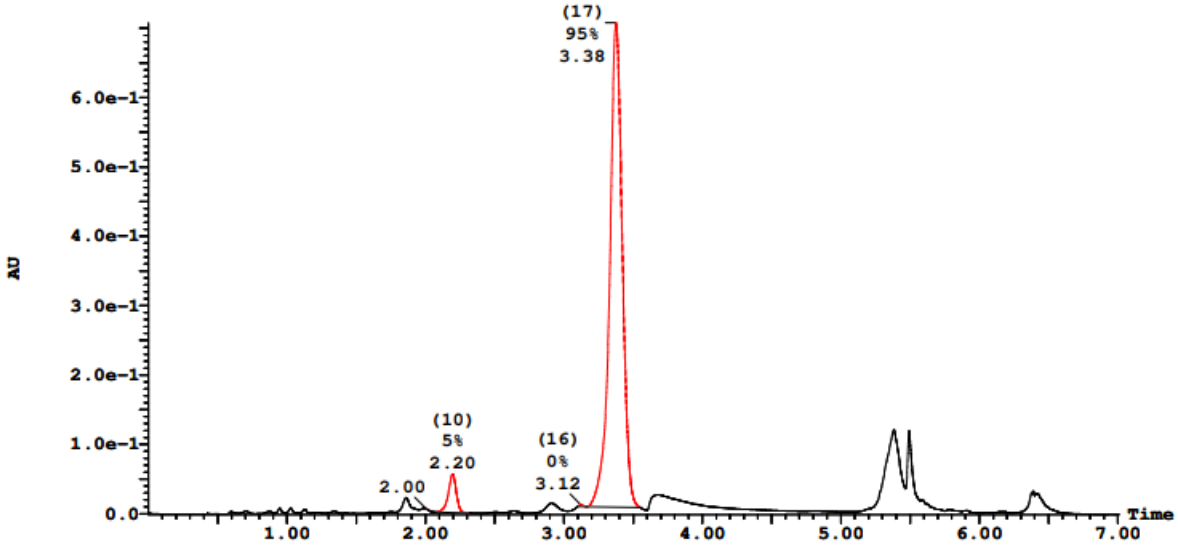

Peak Number	Compound	Time	AreaAbs	Area %Total	Width	Height	Mass Found
8		2.00	2e+000	0.00	0		Not Found
10		2.20	4e+003	4.82	0	6e+004	Not Found
16		3.12	7e+001	0.09	0	2e+003	Not Found
17		3.38	7e+004	95.09	0	7e+005	Not Found

A10: >85% ee

Openlynx Report - SHARLJA1

Sample: 10
File:SHARLJA1_20211115_10
Description:(S,S)WO1 4.6x100mm 5µ

Vial:1:10
Date:15-Nov-2021
Conditions:5% IPA over 5min 3mL/min

ID:27-A10
Time:17:25:03

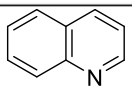

A10,
~90% ee

Printed: Thu Dec 09 16:42:06 2021

Sample Report (continued):

Sample 10 Vial 1:10 ID 27-A10 File SHARLJA1_20211115_10 Date 15-Nov-2021 Time 17:25:03 Description (S,S)WO1 4.6x100mm 5µ

2: UV Detector: 230 Nm 2.0000-2.3500: Smooth (Mn, 2x3), 3.1000-3.5500: Smooth (Mn, 2x3) 6.132e-1
Range: 6.142e-1

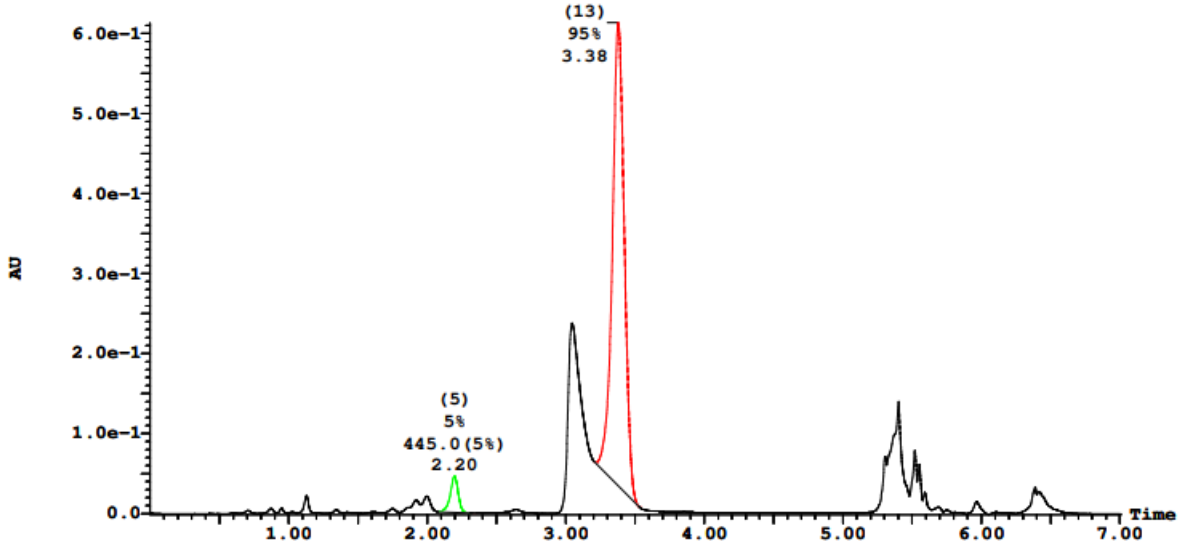

Peak Number	Compound	Time	AreaAbs	Area %Total	Width	Height	Mass Found
5	Found	2.20	3e+003	4.92	0	4e+004	445.0000
6		2.34	6e-001	0.00	0	7e+001	Not Found
13		3.38	6e+004	95.08	0	6e+005	Not Found

A11: 91% ee

Openlynx Report - SHARLJA1

Sample: 11
File:SHARLJA1_20211115_11
Description:(S,S)WO1 4.6x100mm 5µ

Vial:1:11
Date:15-Nov-2021
Conditions:5% IPA over 5min 3mL/min

ID:27-A11
Time:17:33:11

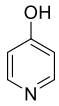

A11,
91% ee

Printed: Thu Dec 09 16:42:06 2021

Sample Report (continued):

Sample 11 Vial 1:11 ID 27-A11 File SHARLJA1_20211115_11 Date 15-Nov-2021 Time 17:33:11 Description (S,S)WO1 4.6x100mm 5µ

2: UV Detector: 230 Nm 2.0000-2.3500: Smooth (Mn, 2x3), 3.1000-3.5500: Smooth (Mn, 2x3) 6.205e-1
Range: 6.21e-1

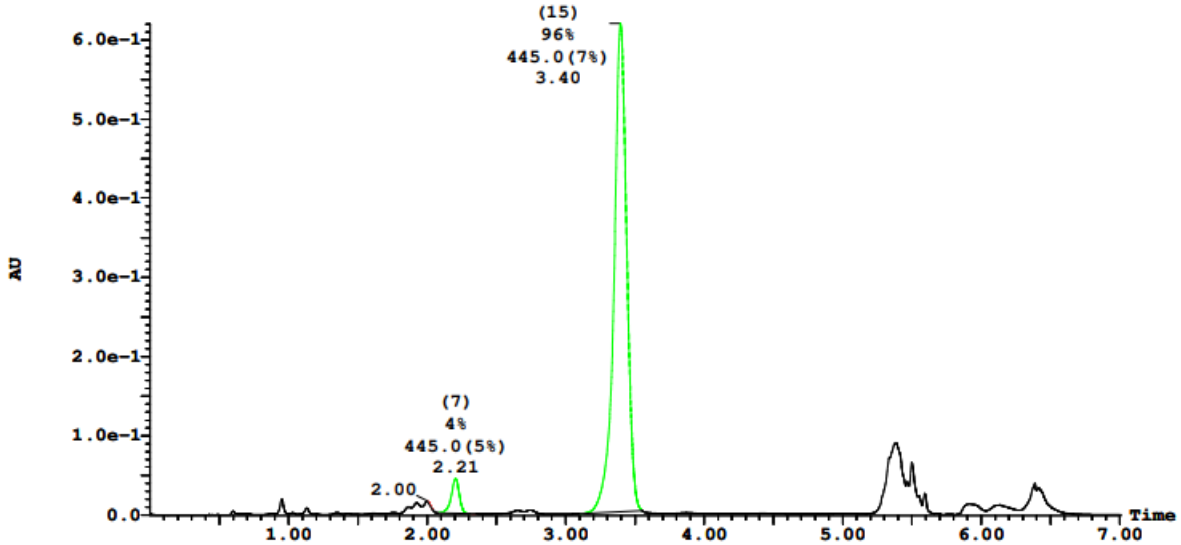

Peak Number	Compound	Time	AreaAbs	Area %Total	Width	Height	Mass Found
6		2.00	3e+001	0.05	0	2e+002	Not Found
7	Tentative	2.21	3e+003	4.33	0	4e+004	445.0000
9		2.31	2e+000	0.00	0	9e+001	Not Found
9		2.34	3e-001	0.00	0	5e+001	Not Found
15	Tentative	3.40	7e+004	95.62	0	6e+005	445.0000

A12: 89% ee

Openlynx Report - SHARLJA1

Sample: 12
File:SHARLJA1_20211115_12
Description:(S,S)WO1 4.6x100mm 5µ

Vial:1:12
Date:15-Nov-2021
Conditions:5% IPA over 5min 3mL/min

ID:27-A12
Time:17:41:18

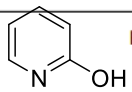

A12,
89% ee

Printed: Thu Dec 09 16:42:06 2021

Sample Report (continued):

Sample 12 Vial 1:12 ID 27-A12 File SHARLJA1_20211115_12 Date 15-Nov-2021 Time 17:41:18 Description (S,S)WO1 4.6x100mm 5µ

2: UV Detector: 230 Nm 2.0000-2.3500: Smooth (Mn, 2x3), 3.1000-3.5500: Smooth (Mn, 2x3) 6.647e-1
Range: 6.652e-1

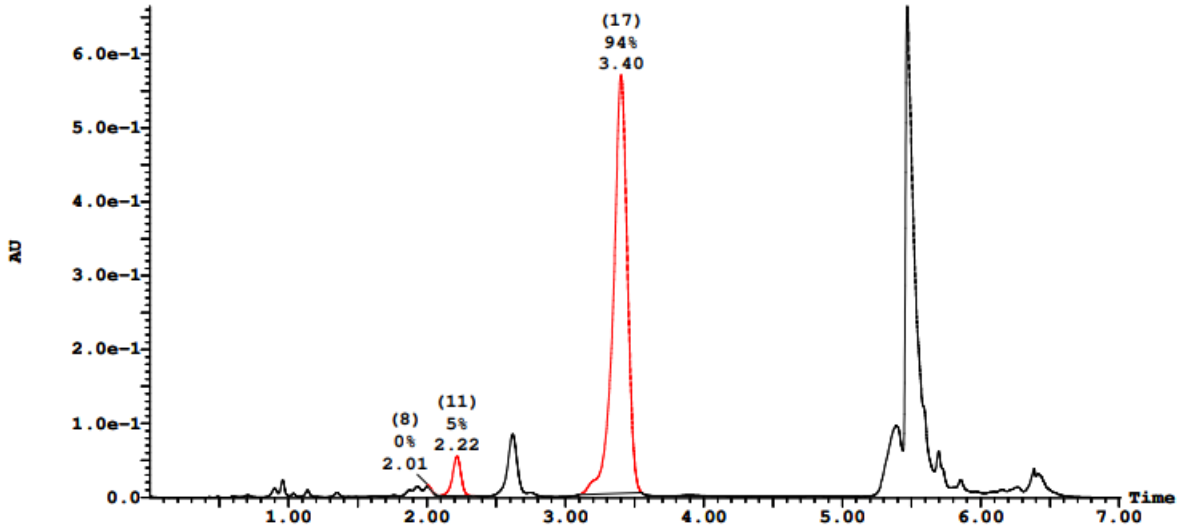

Peak Number	Compound	Time	AreaAbs	Area %Total	Width	Height	Mass Found
8		2.01	9e+001	0.12	0	2e+003	Not Found
11		2.22	4e+003	5.39	0	5e+004	Not Found
12		2.32	6e+000	0.01	0	3e+002	Not Found
17		3.40	7e+004	94.48	0	6e+005	Not Found

B1: 91% ee

Openlynx Report - SHARLJA1

Sample: 13
File:SHARLJA1_20211115_13
Description:(S,S)WO1 4.6x100mm 5µ

Vial:1:13
Date:15-Nov-2021
Conditions:5% IPA over 5min 3mL/min

ID:27-B1
Time:17:49:26

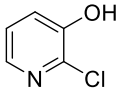

B1,
91% ee

Printed: Thu Dec 09 16:42:06 2021

Sample Report (continued):

Sample 13 Vial 1:13 ID 27-B1 File SHARLJA1_20211115_13 Date 15-Nov-2021 Time 17:49:26 Description (S,S)WO1 4.6x100mm 5µ

2: UV Detector: 230 Nm 2.0000-2.3500: Smooth (Mn, 2x3), 3.1000-3.5500: Smooth (Mn, 2x3) 4.428e-1
Range: 4.446e-1

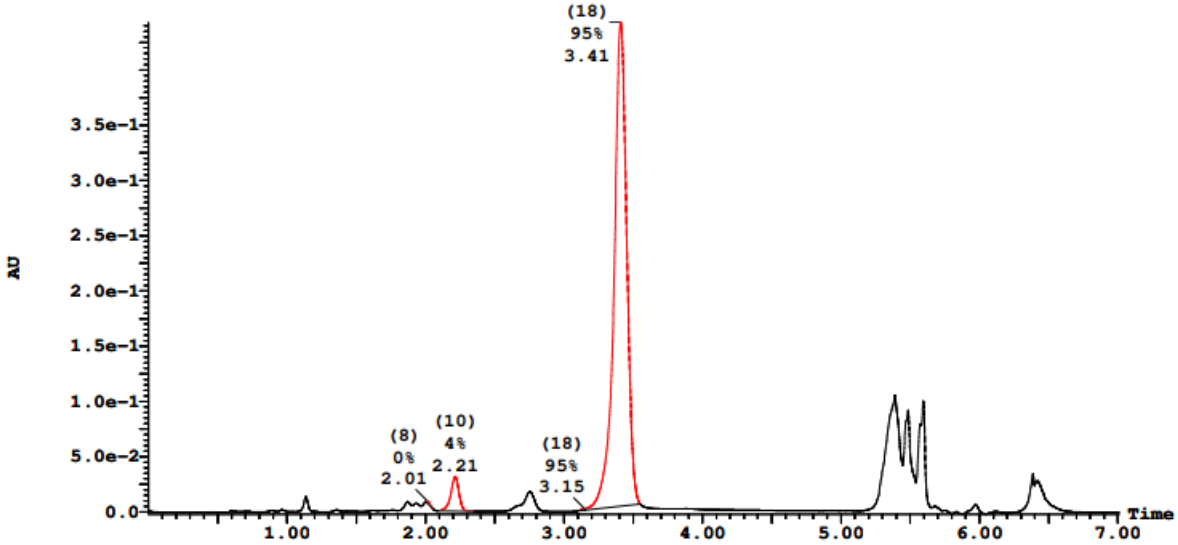

Peak Number	Compound	Time	AreaAbs	Area %Total	Width	Height	Mass Found
8		2.01	7e+001	0.14	0	2e+003	Not Found
10		2.21	2e+003	4.33	0	3e+004	Not Found
12		2.33	8e-001	0.00	0	5e+001	Not Found
16		3.15	3e+001	0.06	0	1e+003	Not Found
18		3.41	5e+004	95.47	0	4e+005	Not Found

B2: 91% ee

Openlynx Report - SHARLJA1

Page 27

Sample: 14
File:SHARLJA1_20211115_14
Description:(S,S)WO1 4.6x100mm 5µ

Vial:1:14
Date:15-Nov-2021
Conditions:5% IPA over 5min 3mL/min

ID:27-B2
Time:17:57:35

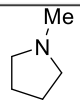

B2,
91% ee

Printed: Thu Dec 09 16:42:06 2021

Sample Report (continued):

Sample 14 Vial 1:14 ID 27-B2 File SHARLJA1_20211115_14 Date 15-Nov-2021 Time 17:57:35 Description (S,S)WO1 4.6x100mm 5µ

2: UV Detector: 230 Nm 2.0000-2.3500: Smooth (Mn, 2x3), 3.1000-3.5500: Smooth (Mn, 2x3) 6.281e-1
Range: 6.313e-1

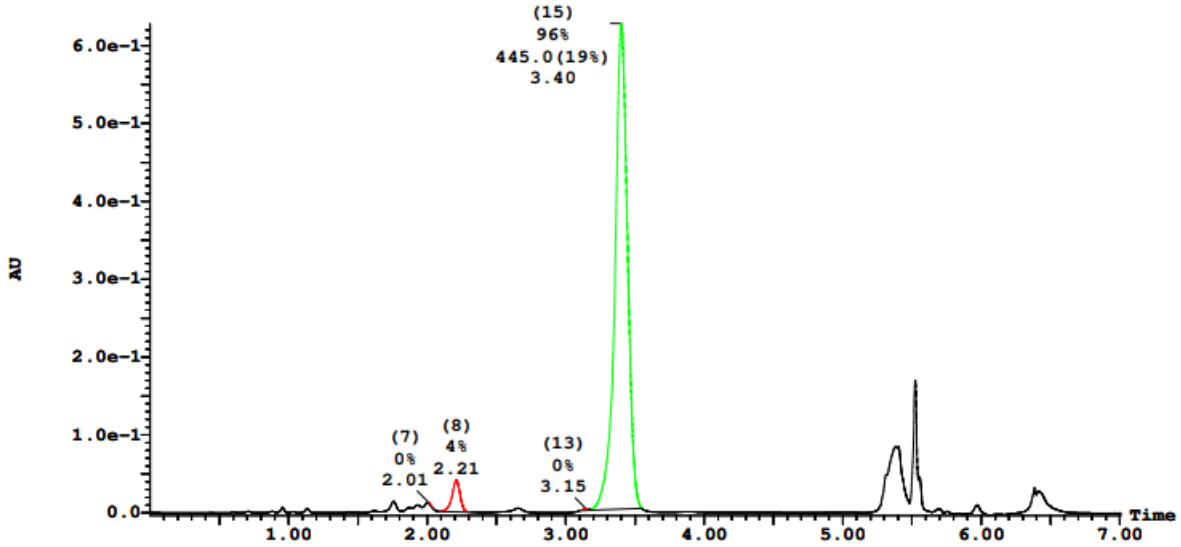

Peak Number	Compound	Time	AreaAbs	Area %Total	Width	Height	Mass Found
7		2.01	6e+001	0.09	0	2e+003	Not Found
8		2.21	3e+003	4.01	0	4e+004	Not Found
13		3.15	1e+002	0.16	0	2e+003	Not Found
15	Found	3.40	7e+004	95.74	0	6e+005	445.0000

B3: 91% ee

Openlynx Report - SHARLJA1

Sample: 15
File:SHARLJA1_20211115_15
Description:(S,S)WO1 4.6x100mm 5µ

Vial:1:15
Date:15-Nov-2021
Conditions:5% IPA over 5min 3mL/min

ID:27-B3
Time:18:05:42

B3,
91% ee

Printed: Thu Dec 09 16:42:06 2021

Sample Report (continued):

Sample 15 Vial 1:15 ID 27-B3 File SHARLJA1_20211115_15 Date 15-Nov-2021 Time 18:05:42 Description (S,S)WO1 4.6x100mm 5µ

2: UV Detector: 230 Nm 2.0000-2.3500: Smooth (Mn, 2x3), 3.1000-3.5500: Smooth (Mn, 2x3) 5.981e-1
Range: 6.028e-1

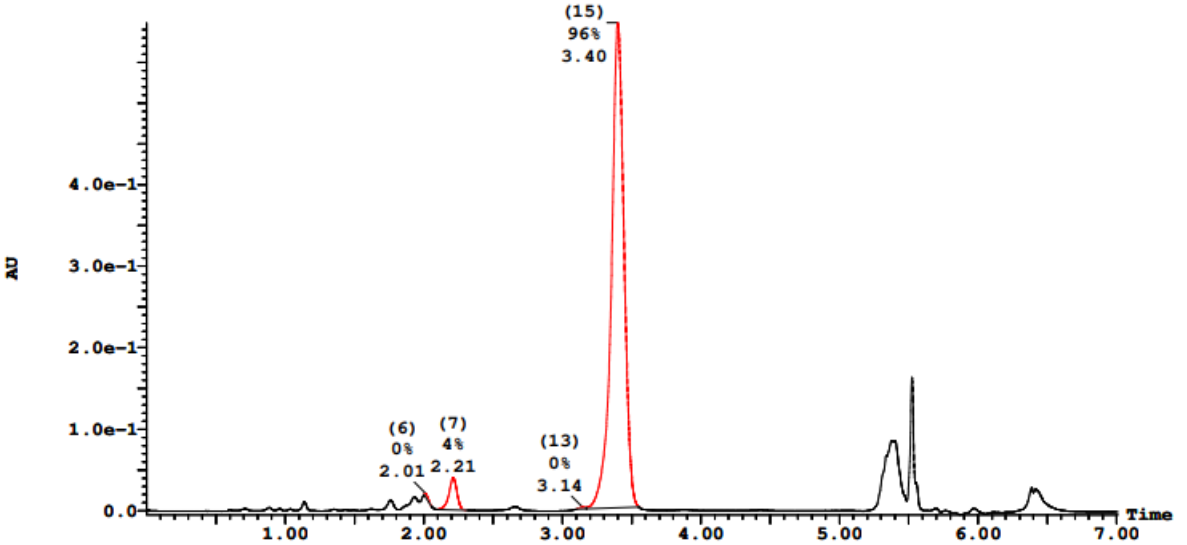

Peak Number	Compound	Time	AreaAbs	Area %Total	Width	Height	Mass Found
6		2.01	1e+002	0.21	0	4e+003	Not Found
7		2.21	3e+003	4.05	0	4e+004	Not Found
13		3.14	1e+002	0.15	0	2e+003	Not Found
15		3.40	6e+004	95.59	0	6e+005	Not Found

B4: 91% ee

Openlynx Report - SHARLJA1

Sample: 16
File:SHARLJA1_20211115_16
Description:(S,S)WO1 4.6x100mm 5µ

Vial:1:16
Date:15-Nov-2021
Conditions:5% IPA over 5min 3mL/min

ID:27-B4
Time:18:13:51

B4,
91% ee

Page 31

Printed: Thu Dec 09 16:42:06 2021

Sample Report (continued):

Sample 16 Vial 1:16 ID 27-B4 File SHARLJA1_20211115_16 Date 15-Nov-2021 Time 18:13:51 Description (S,S)WO1 4.6x100mm 5µ

2: UV Detector: 230 Nm 2.0000-2.3500: Smooth (Mn, 2x3), 3.1000-3.5500: Smooth (Mn, 2x3) 5.725e-1
Range: 5.748e-1

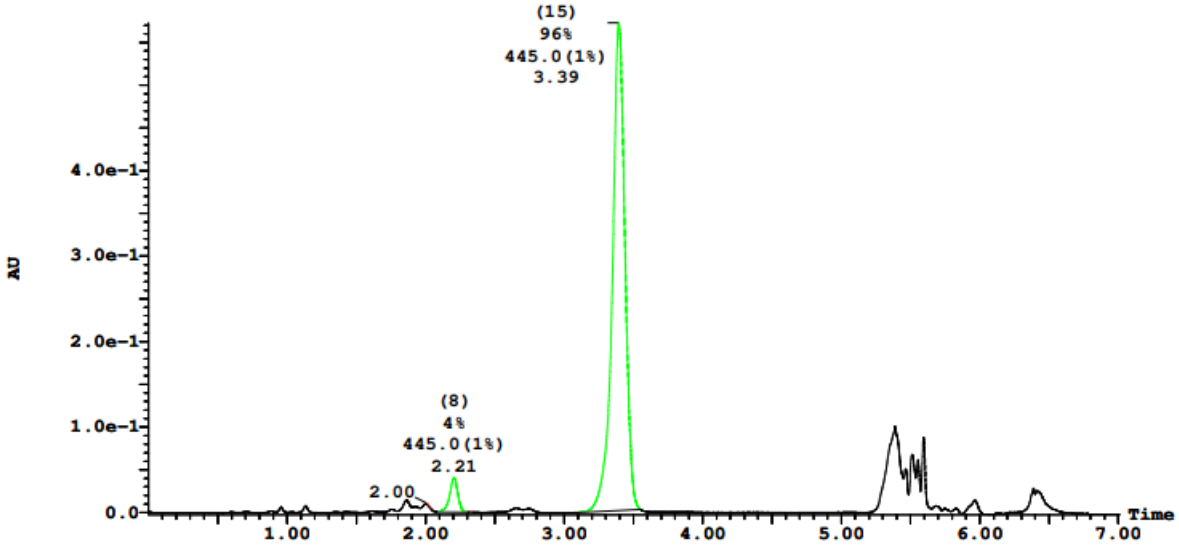

Peak Number	Compound	Time	AreaAbs	Area %Total	Width	Height	Mass Found
7		2.00	3e+001	0.05	0	7e+002	Not Found
8	Tentative	2.21	3e+003	4.33	0	4e+004	445.0000
10		2.31	2e+000	0.00	0	1e+002	Not Found
15	Tentative	3.39	6e+004	95.61	0	6e+005	445.0000

B5: 91% ee

Openlynx Report - SHARLJA1

Sample: 17
File:SHARLJA1_20211115_17
Description:(S,S)WO1 4.6x100mm 5µ

Vial:1:17
Date:15-Nov-2021
Conditions:5% IPA over 5min 3mL/min

ID:27-B5
Time:18:21:58

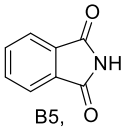

B5,
91% ee

Printed: Thu Dec 09 16:42:06 2021

Sample Report (continued):

Sample 17 Vial 1:17 ID 27-B5 File SHARLJA1_20211115_17 Date 15-Nov-2021 Time 18:21:58 Description (S,S)WO1 4.6x100mm 5µ

2: UV Detector: 230 Nm 2.0000-2.3500: Smooth (Mn, 2x3), 3.1000-3.5500: Smooth (Mn, 2x3) 5.509e-1
Range: 5.545e-1

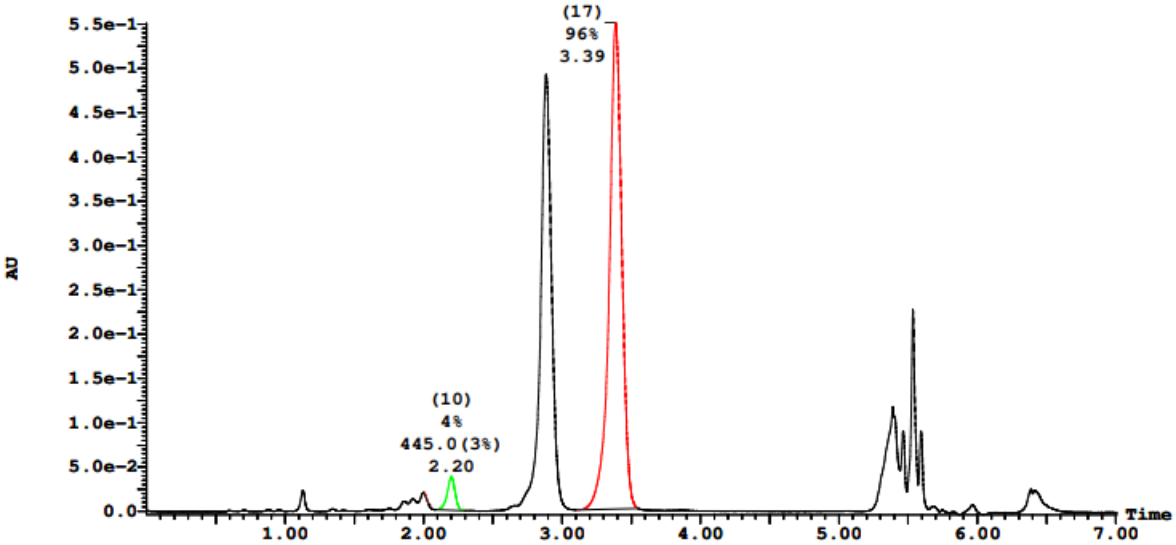

Peak Number	Compound	Time	AreaAbs	Area %Total	Width	Height	Mass Found
9		2.00	4e+001	0.07	0	3e+002	Not Found
10	Found	2.20	3e+003	4.16	0	4e+004	445.0000
11		2.32	8e-001	0.00	0	1e+002	Not Found
17		3.39	6e+004	95.77	0	5e+005	Not Found

B6: 89% ee

Openlynx Report - SHARLJA1

Sample: 18
File:SHARLJA1_20211115_18
Description:(S,S)WO1 4.6x100mm 5µ

Vial:1:18
Date:15-Nov-2021
Conditions:5% IPA over 5min 3mL/min

ID:27-B6
Time:18:30:06

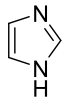

B6,
89% ee

Page 35

Printed: Thu Dec 09 16:42:06 2021

Sample Report (continued):

Sample 18 Vial 1:18 ID 27-B6 File SHARLJA1_20211115_18 Date 15-Nov-2021 Time 18:30:06 Description (S,S)WO1 4.6x100mm 5µ

2: UV Detector: 230 Nm 2.0000-2.3500: Smooth (Mn, 2x3), 3.1000-3.5500: Smooth (Mn, 2x3) 5.749e-1
Range: 5.786e-1

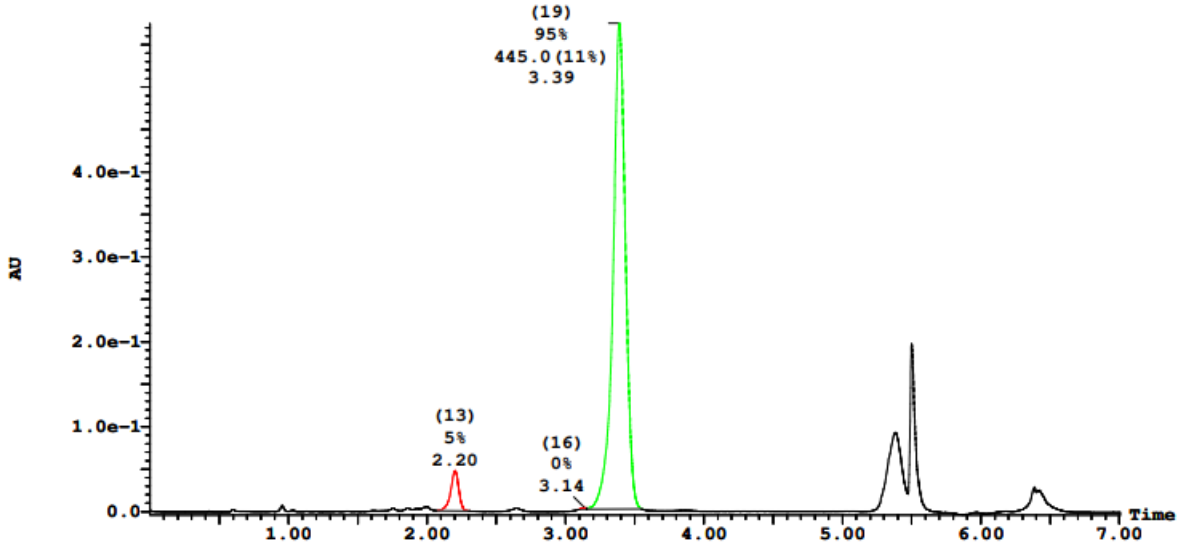

Peak Number	Compound	Time	AreaAbs	Area %Total	Width	Height	Mass Found
13		2.20	3e+003	5.14	0	5e+004	Not Found
16		3.14	5e+001	0.09	0	1e+003	Not Found
19	Found	3.39	6e+004	94.78	0	6e+005	445.0000

B7: 91% ee

Openlynx Report - SHARLJA1

Sample: 19
File:SHARLJA1_20211115_19
Description:(S,S)WO1 4.6x100mm 5µ

Vial:1:19
Date:15-Nov-2021
Conditions:5% IPA over 5min 3mL/min

ID:27-B7
Time:18:38:14

B7,
91% ee

Page 37

Printed: Thu Dec 09 16:42:06 2021

Sample Report (continued):

Sample 19 Vial 1:19 ID 27-B7 File SHARLJA1_20211115_19 Date 15-Nov-2021 Time 18:38:14 Description (S,S)WO1 4.6x100mm 5µ

2: UV Detector: 230 Nm 2.0000-2.3500: Smooth (Mn, 2x3), 3.1000-3.5500: Smooth (Mn, 2x3) 5.846e-1
Range: 5.86e-1

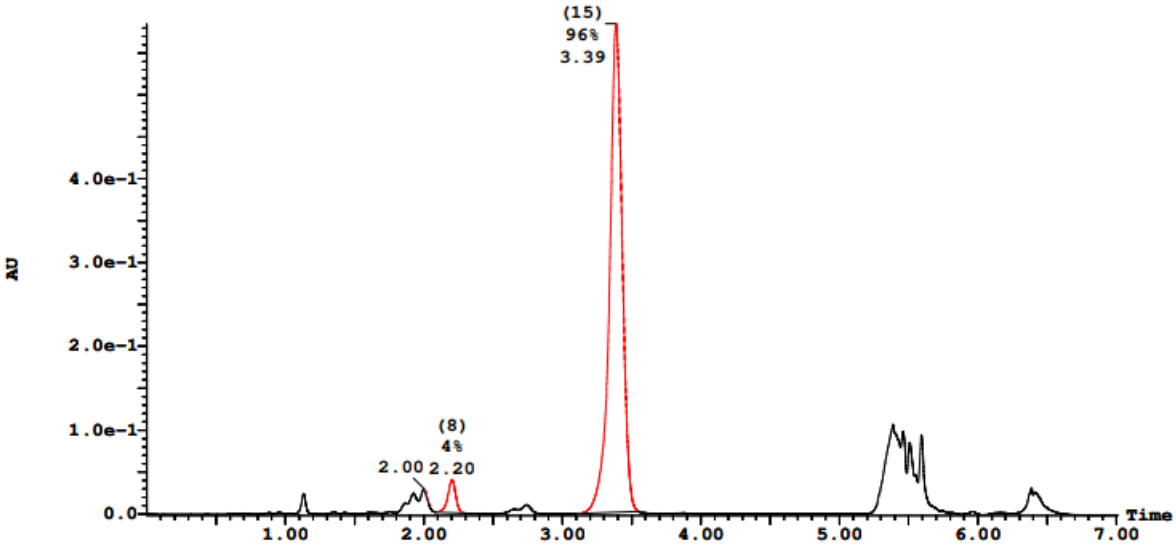

Peak Number	Compound	Time	AreaAbs	Area %Total	Width	Height	Mass Found
6		2.00	6e+001	0.10	0	4e+002	Not Found
8		2.20	3e+003	4.01	0	4e+004	Not Found
15		3.39	6e+004	95.89	0	6e+005	Not Found

B8: 92% ee

Openlynx Report - SHARLJA1

Sample: 20
File:SHARLJA1_20211115_20
Description:(S,S)WO1 4.6x100mm 5µ

Vial:1:20
Date:15-Nov-2021
Conditions:5% IPA over 5min 3mL/min

ID:27-B8
Time:18:46:21

B8,
92% ee

Printed: Thu Dec 09 16:42:06 2021

Sample Report (continued):

Sample 20 Vial 1:20 ID 27-B8 File SHARLJA1_20211115_20 Date 15-Nov-2021 Time 18:46:21 Description (S,S)WO1 4.6x100mm 5µ

2: UV Detector: 230 Nm 2.0000-2.3500: Smooth (Mn, 2x3), 3.1000-3.5500: Smooth (Mn, 2x3) 5.165e-1
Range: 5.176e-1

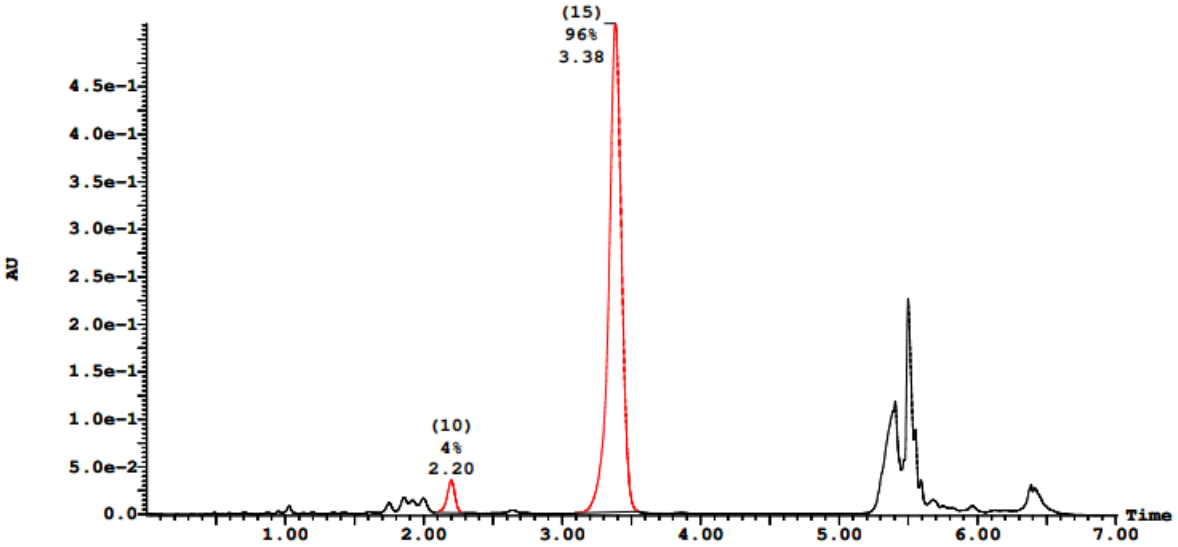

Peak Number	Compound	Time	AreaAbs	Area %Total	Width	Height	Mass Found
10		2.20	2e+003	3.99	0	3e+004	Not Found
15		3.38	5e+004	96.01	0	5e+005	Not Found

B9: 70% ee

Openlynx Report - SHARLJA1

Sample: 21
File:SHARLJA1_20211115_21
Description:(S,S)WO1 4.6x100mm 5µ

Vial:1:21
Date:15-Nov-2021
Conditions:5% IPA over 5min 3mL/min

ID:27-B9
Time:18:54:29

B9,
70% ee

Printed: Thu Dec 09 16:42:06 2021

Sample Report (continued):

Sample 21 Vial 1:21 ID 27-B9 File SHARLJA1_20211115_21 Date 15-Nov-2021 Time 18:54:29 Description (S,S)WO1 4.6x100mm 5µ

2: UV Detector: 230 Nm 2.0000-2.3500: Smooth (Mn, 2x3), 3.1000-3.5500: Smooth (Mn, 2x3) 4.673e-1
Range: 4.683e-1

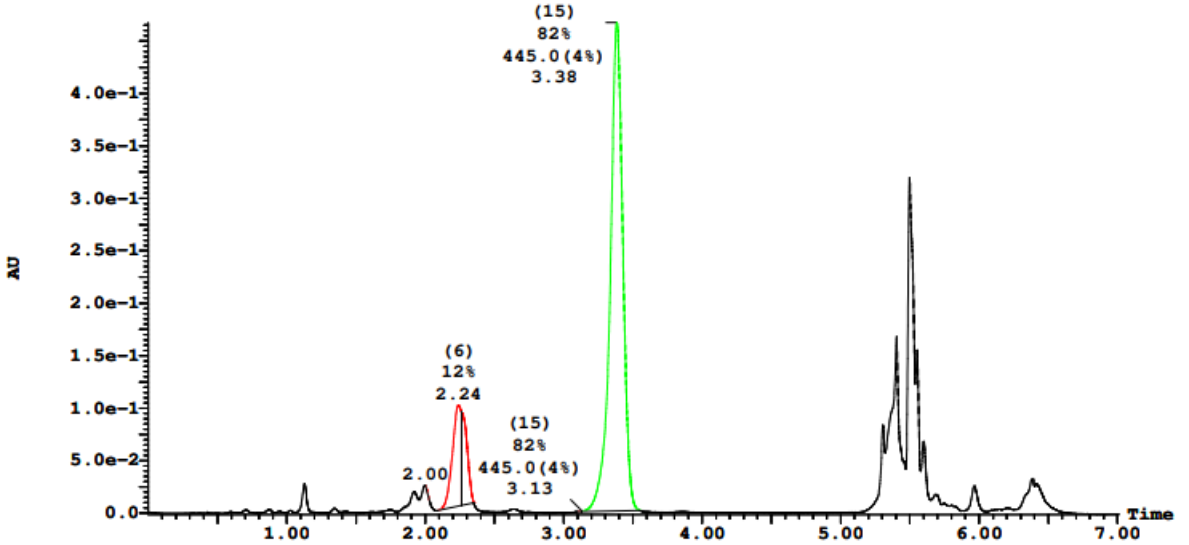

Peak Number	Compound	Time	AreaAbs	Area %Total	Width	Height	Mass Found
5		2.00	3e+001	0.05	0	2e-002	Not Found
6		2.24	7e+003	11.57	0	1e+005	Not Found
6		2.26	4e+003	6.73	0	9e+004	Not Found
12		3.13	8e+000	0.01	0	5e+002	Not Found
15	Tentative	3.38	5e+004	81.63	0	5e+005	445.0000

B10: 91% ee

Openlynx Report - SHARLJA1

Sample: 22
File:SHARLJA1_20211115_22
Description:(S,S)WO1 4.6x100mm 5µ

Vial:1:22
Date:15-Nov-2021
Conditions:5% IPA over 5min 3mL/min

ID:27-B10
Time:19:02:37

B10,
91% ee

Printed: Thu Dec 09 16:42:06 2021

Sample Report (continued):

Sample 22 Vial 1:22 ID 27-B10 File SHARLJA1_20211115_22 Date 15-Nov-2021 Time 19:02:37 Description (S,S)WO1 4.6x100mm 5µ

2: UV Detector: 230 Nm 2.0000-2.3500: Smooth (Mn, 2x3), 3.1000-3.5500: Smooth (Mn, 2x3) 5.311e-1
Range: 5.322e-1

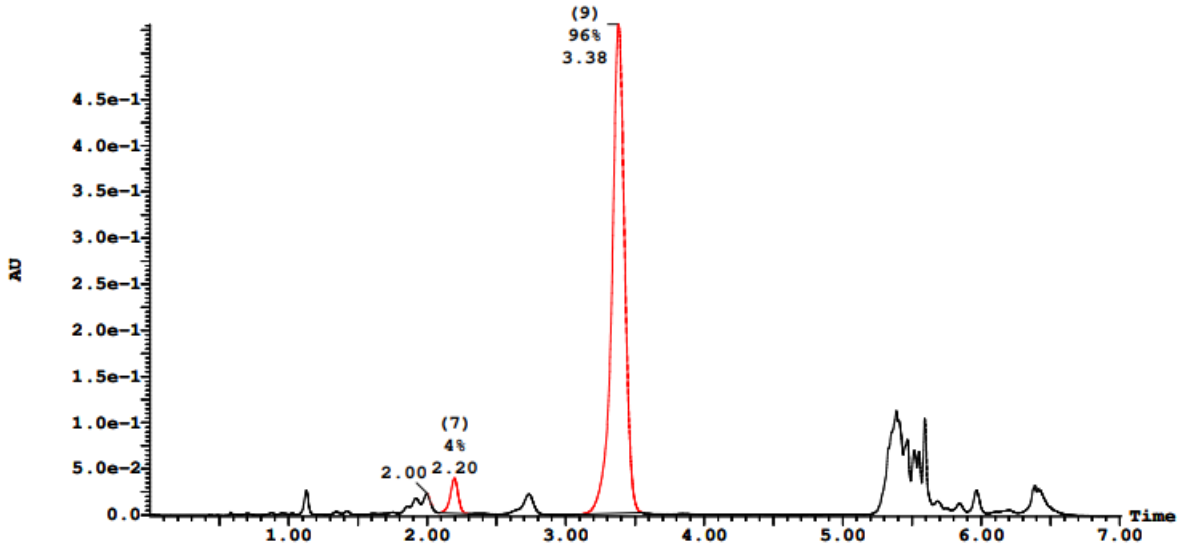

Peak Number	Compound	Time	AreaAbs	Area %Total	Width	Height	Mass Found
5		2.00	2e+001	0.04	0	2e-002	Not Found
7		2.20	3e+003	4.28	0	4e+004	Not Found
9		3.38	6e+004	95.68	0	5e+005	Not Found

B11: 91% ee

Openlynx Report - SHARLJA1

Sample: 23
File:SHARLJA1_20211115_23
Description:(S,S)WO1 4.6x100mm 5µ

Vial:1:23
Date:15-Nov-2021
Conditions:5% IPA over 5min 3mL/min

ID:27-B11
Time:19:10:44

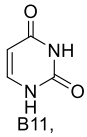

B11,
91% ee

Printed: Thu Dec 09 16:42:06 2021

Sample Report (continued):

Sample 23 Vial 1:23 ID 27-B11 File SHARLJA1_20211115_23 Date 15-Nov-2021 Time 19:10:44 Description (S,S)WO1 4.6x100mm 5µ

2: UV Detector: 230 Nm 2.0000-2.3500: Smooth (Mn, 2x3), 3.1000-3.5500: Smooth (Mn, 2x3) 7.197e-1
Range: 7.208e-1

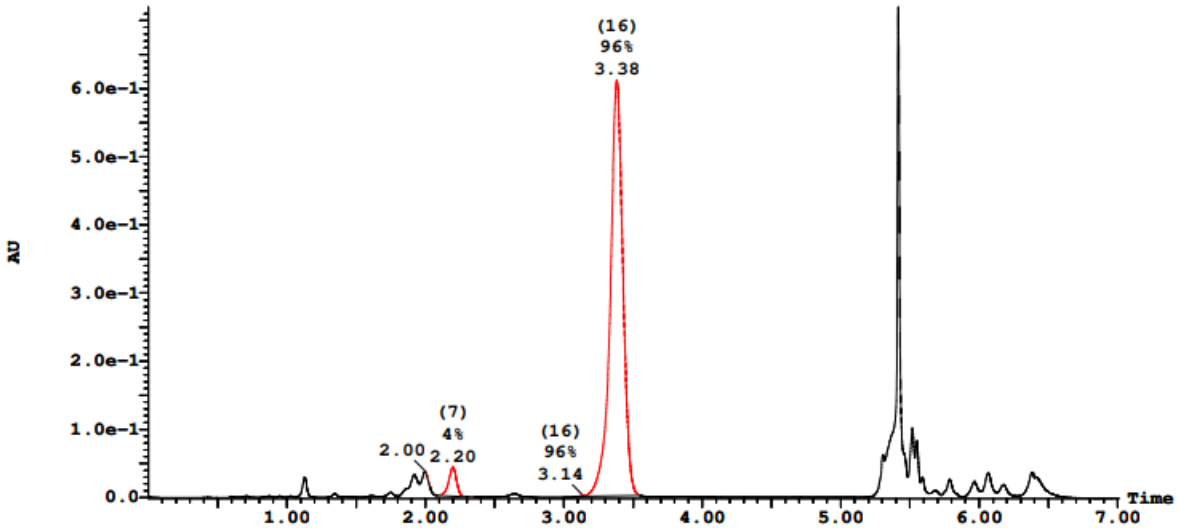

Peak Number	Compound	Time	AreaAbs	Area %Total	Width	Height	Mass Found
6		2.00	5e+001	0.07	0	4e-002	Not Found
7		2.20	3e+003	4.15	0	4e+004	Not Found
8		2.32	3e+000	0.00	0	1e+002	Not Found
13		3.14	2e+001	0.03	0	8e+002	Not Found
16		3.38	7e+004	95.75	0	6e+005	Not Found

B12: 91% ee

Openlynx Report - SHARLJA1

Sample: 24
File:SHARLJA1_20211115_24
Description:(S,S)WO1 4.6x100mm 5µ

Printed: Thu Dec 09 16:42:06 2021

Vial:1:24
Date:15-Nov-2021
Conditions:5% IPA over 5min 3mL/min

ID:27-B12
Time:19:18:51

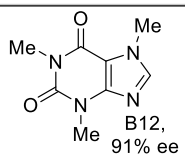

Sample Report (continued):

Sample 24 Vial 1:24 ID 27-B12 File SHARLJA1_20211115_24 Date 15-Nov-2021 Time 19:18:51 Description (S,S)WO1 4.6x100mm 5µ

2: UV Detector: 230 Nm 2.0000-2.3500: Smooth (Mn, 2x3), 3.1000-3.5500: Smooth (Mn, 2x3) 6.775e-1
Range: 6.78e-1

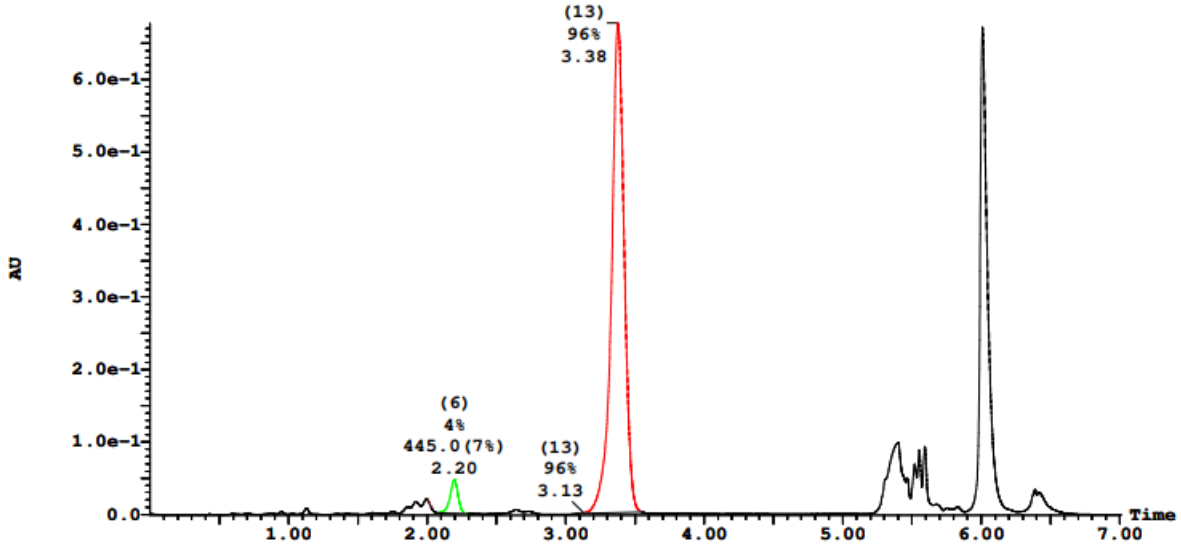

Peak Number	Compound	Time	AreaAbs	Area %Total	Width	Height	Mass Found
5		2.00	2e+001	0.02	0		Not Found
6	Found	2.20	3e+003	4.12	0	5e+004	445.0000
10		3.13	9e+000	0.01	0	6e+002	Not Found
13		3.38	7e+004	95.84	0	7e+005	Not Found

C1: 91% ee

Openlynx Report - SHARLJA1

Sample: 25
File:SHARLJA1_20211115_25
Description:(S,S)WO1 4.6x100mm 5µ

Vial:1:25
Date:15-Nov-2021
Conditions:5% IPA over 5min 3mL/min

ID:27-C1
Time:19:26:59

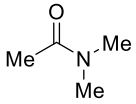

C1,
91% ee

Printed: Thu Dec 09 16:42:06 2021

Sample Report (continued):

Sample 25 Vial 1:25 ID 27-C1 File SHARLJA1_20211115_25 Date 15-Nov-2021 Time 19:26:59 Description (S,S)WO1 4.6x100mm 5µ

2: UV Detector: 230 Nm 2.0000-2.3500: Smooth (Mn, 2x3), 3.1000-3.5500: Smooth (Mn, 2x3) 4.729e-1
Range: 4.735e-1

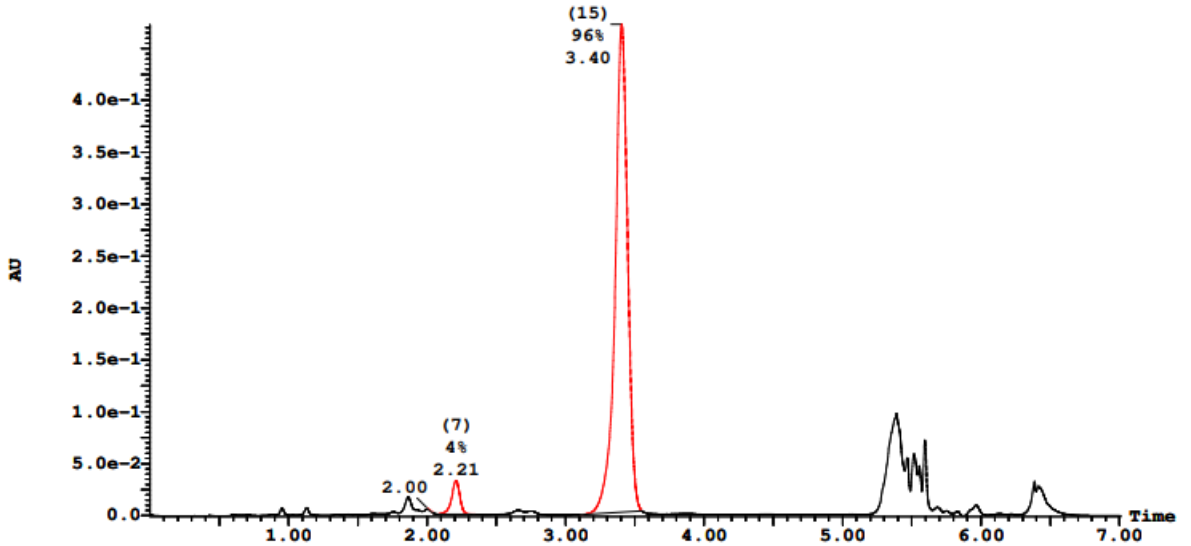

Peak Number	Compound	Time	AreaAbs	Area %Total	Width	Height	Mass Found
5		2.00	2e+001	0.04	0	4e+002	Not Found
7		2.21	2e+003	4.35	0	3e+004	Not Found
9		2.31	5e+000	0.01	0	2e+002	Not Found
15		3.40	5e+004	95.61	0	5e+005	Not Found

C2: 91% ee

Openlynx Report - SHARLJA1

Sample: 26
File:SHARLJA1_20211115_26
Description:(S,S)WO1 4.6x100mm 5µ

Vial:1:26
Date:15-Nov-2021
Conditions:5% IPA over 5min 3mL/min

ID:27-C2
Time:19:35:07

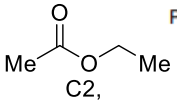

C2,
91% ee

Printed: Thu Dec 09 16:42:06 2021

Sample Report (continued):

Sample 26 Vial 1:26 ID 27-C2 File SHARLJA1_20211115_26 Date 15-Nov-2021 Time 19:35:07 Description (S,S)WO1 4.6x100mm 5µ

2: UV Detector: 230 Nm 2.0000-2.3500: Smooth (Mn, 2x3), 3.1000-3.5500: Smooth (Mn, 2x3) 5.948e-1
Range: 5.984e-1

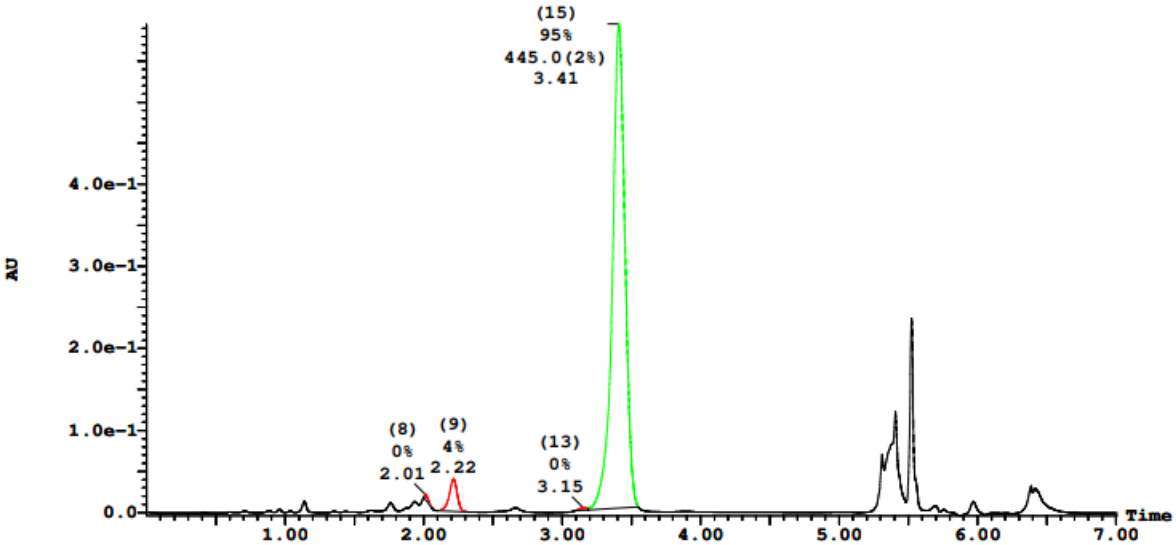

Peak Number	Compound	Time	AreaAbs	Area %Total	Width	Height	Mass Found
8		2.01	2e+002	0.30	0	5e+003	Not Found
9		2.22	3e+003	4.06	0	4e+004	Not Found
13		3.15	1e+002	0.23	0	2e+003	Not Found
15	Found	3.41	6e+004	95.42	0	6e+005	445.0000

C4: 91% ee

Openlynx Report - SHARLJA1

Sample: 28
File:SHARLJA1_20211115_28
Description:(S,S)WO1 4.6x100mm 5µ

Vial:1:28
Date:15-Nov-2021
Conditions:5% IPA over 5min 3mL/min

ID:27-C4
Time:19:51:23

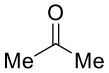

C4,
91% ee

Printed: Thu Dec 09 16:42:06 2021

Sample Report (continued):

Sample 28 Vial 1:28 ID 27-C4 File SHARLJA1_20211115_28 Date 15-Nov-2021 Time 19:51:23 Description (S,S)WO1 4.6x100mm 5µ

2: UV Detector: 230 Nm 2.0000-2.3500: Smooth (Mn, 2x3), 3.1000-3.5500: Smooth (Mn, 2x3) 7.022e-1
Range: 7.056e-1

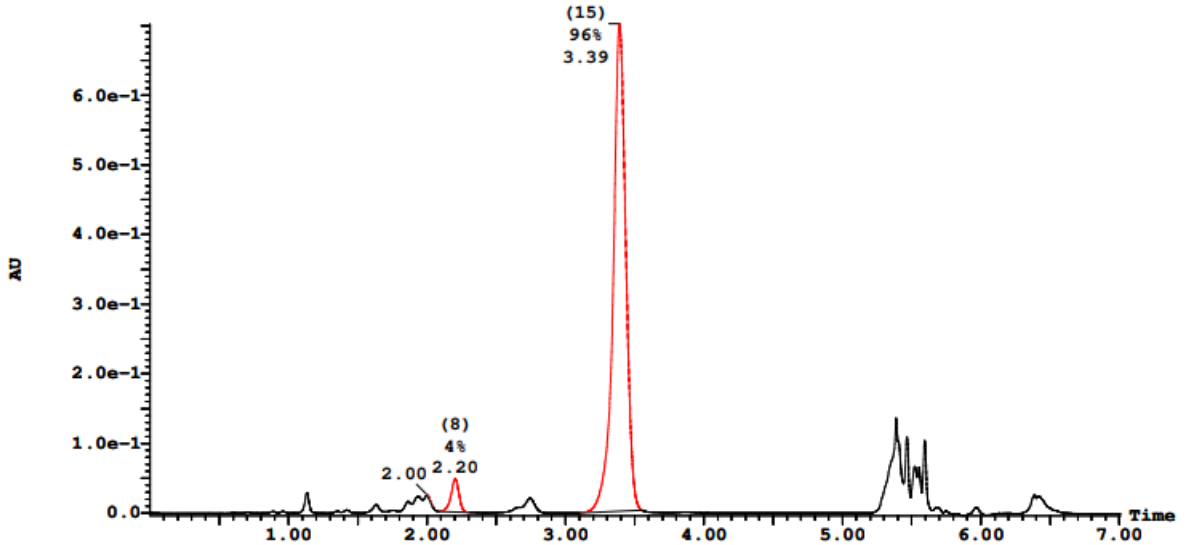

Peak Number	Compound	Time	AreaAbs	Area %Total	Width	Height	Mass Found
7		2.00	7e+001	0.09	0	7e+002	Not Found
8		2.20	3e+003	4.14	0	5e+004	Not Found
15		3.39	7e+004	95.77	0	7e+005	Not Found

C5: 91% ee

Openlynx Report - SHARLJA1 Page 57

Sample: 29
File:SHARLJA1_20211115_29
Description:(S,S)WO1 4.6x100mm 5µ

Vial:1:29
Date:15-Nov-2021
Conditions:5% IPA over 5min 3mL/min

ID:27-C5
Time:19:59:30

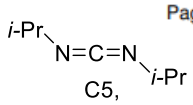

C5,
91% ee

Printed: Thu Dec 09 16:42:06 2021

Sample Report (continued):

Sample 29 Vial 1:29 ID 27-C5 File SHARLJA1_20211115_29 Date 15-Nov-2021 Time 19:59:30 Description (S,S)WO1 4.6x100mm 5µ

2: UV Detector: 230 Nm 2.0000-2.3500: Smooth (Mn, 2x3), 3.1000-3.5500: Smooth (Mn, 2x3) 5.755e-1
Range: 5.776e-1

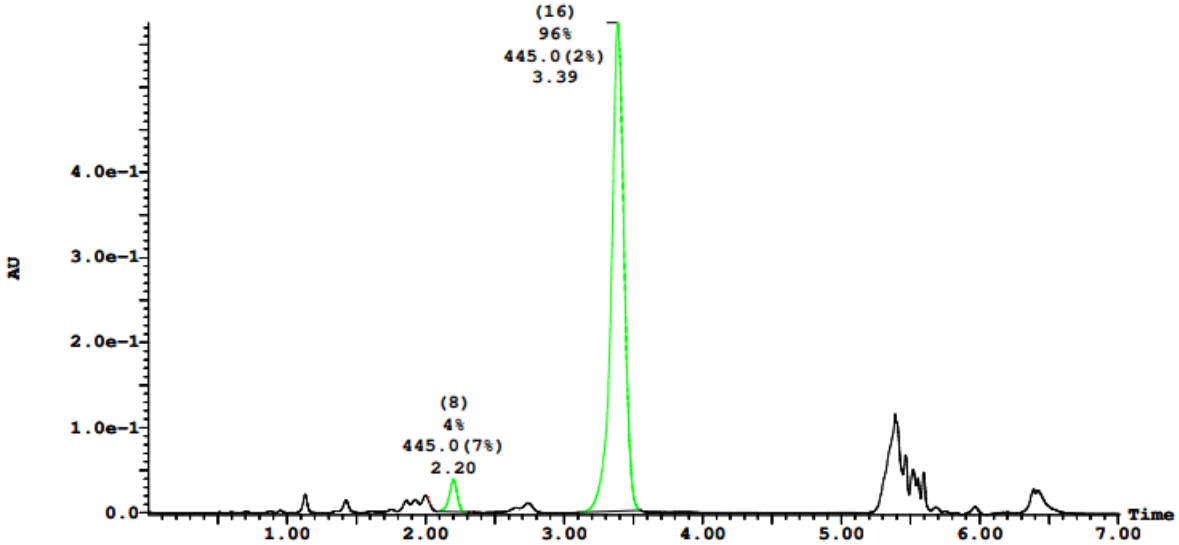

Peak Number	Compound	Time	AreaAbs	Area %Total	Width	Height	Mass Found
7		2.00	5e+001	0.07	0	3e+002	Not Found
8	Found	2.20	3e+003	3.97	0	4e+004	445.0000
9		2.33	7e-001	0.00	0	9e+001	Not Found
16	Found	3.39	6e+004	95.95	0	6e+005	445.0000

C6: 90% ee

Openlynx Report - SHARLJA1

Sample: 30
File:SHARLJA1_20211115_30
Description:(S,S)WO1 4.6x100mm 5µ

Vial:1:30
Date:15-Nov-2021
Conditions:5% IPA over 5min 3mL/min

ID:27-C6
Time:20:07:38

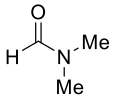

C6,
90% ee

Printed: Thu Dec 09 16:42:06 2021

Sample Report (continued):

Sample 30 Vial 1:30 ID 27-C6 File SHARLJA1_20211115_30 Date 15-Nov-2021 Time 20:07:38 Description (S,S)WO1 4.6x100mm 5µ

2: UV Detector: 230 Nm 2.0000-2.3500: Smooth (Mn, 2x3), 3.1000-3.5500: Smooth (Mn, 2x3) 6.825e-1
Range: 6.856e-1

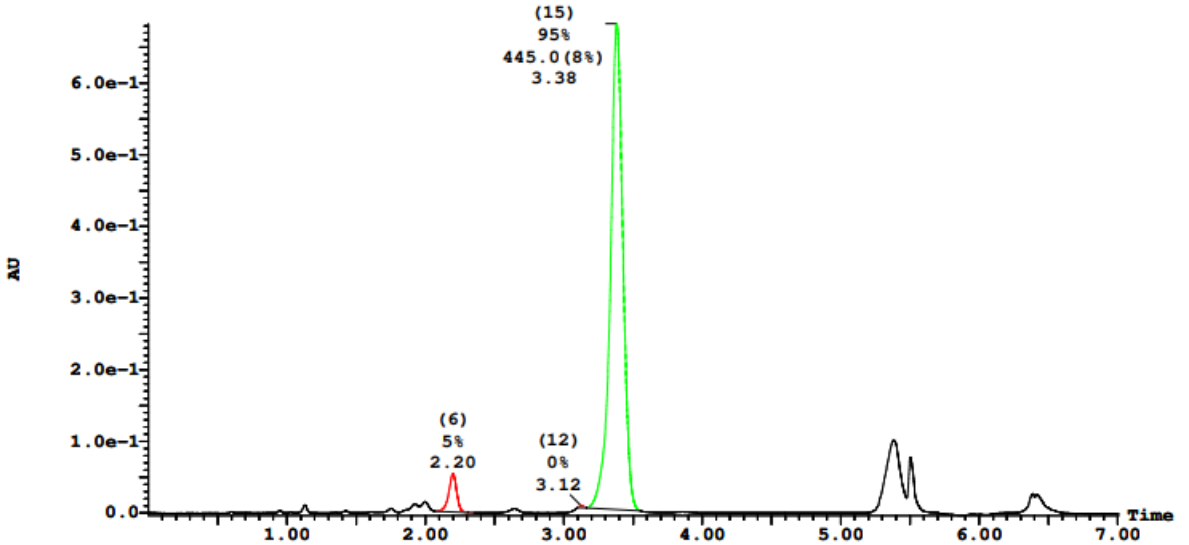

Peak Number	Compound	Time	AreaAbs	Area %Total	Width	Height	Mass Found
6		2.20	4e+003	4.72	0	5e+004	Not Found
7		2.30	3e+000	0.00	0	7e+001	Not Found
12		3.12	1e+002	0.13	0	2e+003	Not Found
15	Found	3.38	7e+004	95.15	0	7e+005	445.0000

C7: %ee could not be determined due to overlap with minor enantiomer**.**

Openlynx Report - SHARLJA1

Sample: 31
File:SHARLJA1_20211115_31
Description:(S,S)WO1 4.6x100mm 5µ

Vial:1:31
Date:15-Nov-2021
Conditions:5% IPA over 5min 3mL/min

ID:27-C7
Time:20:15:46

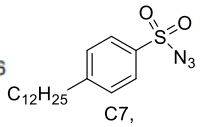

C7,
Not determined

Printed: Thu Dec 09 16:42:06 2021

Sample Report (continued):

Sample 31 Vial 1:31 ID 27-C7 File SHARLJA1_20211115_31 Date 15-Nov-2021 Time 20:15:46 Description (S,S)WO1 4.6x100mm 5µ

2: UV Detector: 230 Nm 2.0000-2.3500: Smooth (Mn, 2x3), 3.1000-3.5500: Smooth (Mn, 2x3) 5.757e-1
Range: 5.771e-1

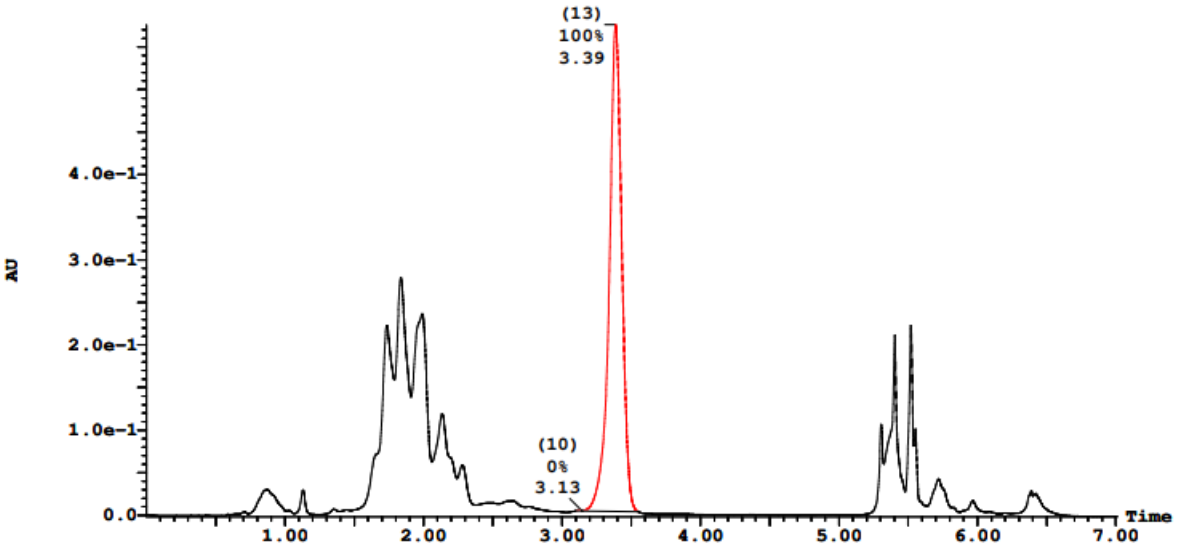

Peak Number	Compound	Time	AreaAbs	Area %Total	Width	Height	Mass Found
10		3.13	3e+001	0.05	0	9e+002	Not Found
13		3.39	6e+004	99.95	0	6e+005	Not Found

C8: 91% ee

Openlynx Report - SHARLJA1 Page 63

Sample: 32
File:SHARLJA1_20211115_32
Description:(S,S)WO1 4.6x100mm 5µ

Vial:1:32
Date:15-Nov-2021
Conditions:5% IPA over 5min 3mL/min

ID:27-C8
Time:20:23:53

Me−NO_2

C8,
91% ee

Printed: Thu Dec 09 16:42:06 2021

Sample Report (continued):

Sample 32 Vial 1:32 ID 27-C8 File SHARLJA1_20211115_32 Date 15-Nov-2021 Time 20:23:53 Description (S,S)WO1 4.6x100mm 5µ

2: UV Detector: 230 Nm 2.0000-2.3500: Smooth (Mn, 2x3), 3.1000-3.5500: Smooth (Mn, 2x3) 6.292e-1
Range: 6.307e-1

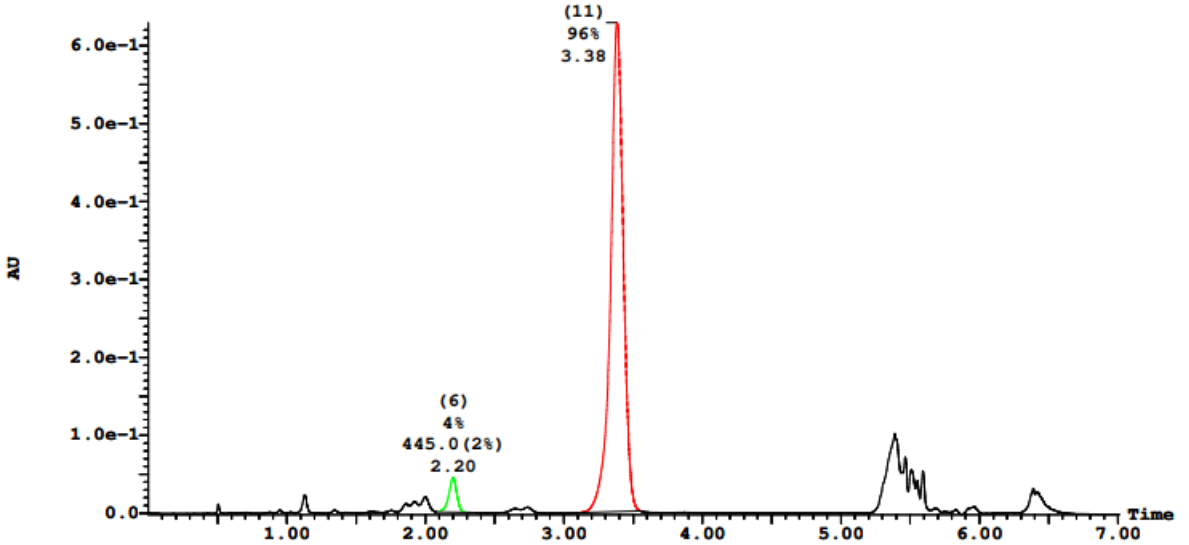

Peak Number	Compound	Time	AreaAbs	Area %Total	Width	Height	Mass Found
6	Tentative	2.20	3e+003	4.27	0	4e+004	445.0000
7		2.32	1e+000	0.00	0	1e+002	Not Found
8		2.34	6e-001	0.00	0	7e+001	Not Found
11		3.38	7e+004	95.72	0	6e+005	Not Found

C9: 91% ee

Openlynx Report - SHARLJA1

Sample: 33
File:SHARLJA1_20211115_33
Description:(S,S)WO1 4.6x100mm 5µ

Vial:1:33
Date:15-Nov-2021
Conditions:5% IPA over 5min 3mL/min

ID:27-C9
Time:20:32:02

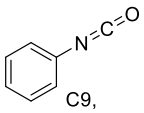

C9,
91% ee

Printed: Thu Dec 09 16:42:06 2021

Sample Report (continued):

Sample 33 Vial 1:33 ID 27-C9 File SHARLJA1_20211115_33 Date 15-Nov-2021 Time 20:32:02 Description (S,S)WO1 4.6x100mm 5µ

2: UV Detector: 230 Nm 2.0000-2.3500: Smooth (Mn, 2x3), 3.1000-3.5500: Smooth (Mn, 2x3) 1.032
Range: 1.033

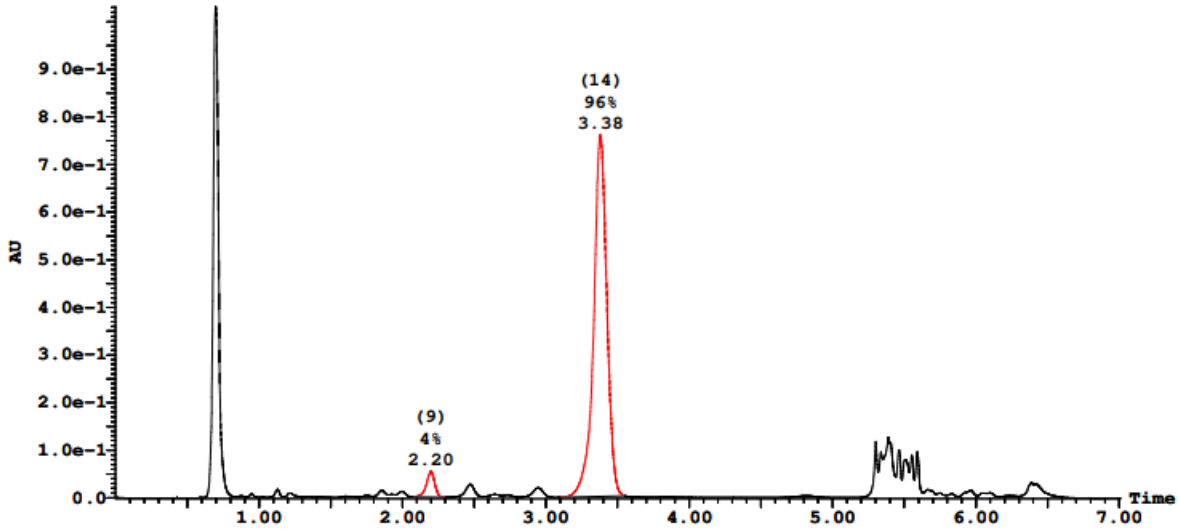

Peak Number	Compound	Time	AreaAbs	Area %Total	Width	Height	Mass Found
9		2.20	4e+003	4.30	0	5e+004	Not Found
14		3.38	8e+004	95.70	0	8e+005	Not Found

C10: 91% ee

Openlynx Report - SHARLJA1

Sample: 34
File:SHARLJA1_20211115_34
Description:(S,S)WO1 4.6x100mm 5µ

Vial:1:34
Date:15-Nov-2021
Conditions:5% IPA over 5min 3mL/min

ID:27-C10
Time:20:40:10

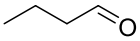

C10,
91% ee

Printed: Thu Dec 09 16:42:06 2021

Sample Report (continued):

Sample 34 Vial 1:34 ID 27-C10 File SHARLJA1_20211115_34 Date 15-Nov-2021 Time 20:40:10 Description (S,S)WO1 4.6x100mm 5µ

2: UV Detector: 230 Nm 2.0000-2.3500: Smooth (Mn, 2x3), 3.1000-3.5500: Smooth (Mn, 2x3) 6.224e-1
Range: 6.237e-1

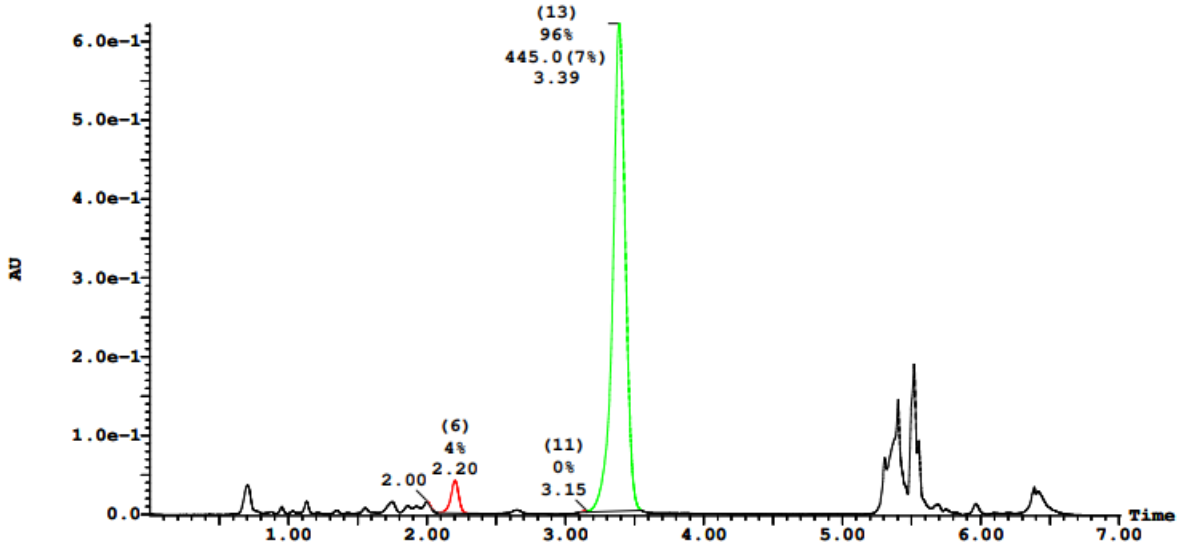

Peak Number	Compound	Time	AreaAbs	Area %Total	Width	Height	Mass Found
5		2.00	4e+001	0.06	0	5e+002	Not Found
6		2.20	3e+003	4.04	0	4e+004	Not Found
11		3.15	5e+001	0.07	0	1e+003	Not Found
13	Found	3.39	7e+004	95.84	0	6e+005	445.0000

C11: 91% ee

Openlynx Report - SHARLJA1

Sample: 35
File:SHARLJA1_20211115_35
Description:(S,S)WO1 4.6x100mm 5µ

Vial:1:35
Date:15-Nov-2021
Conditions:5% IPA over 5min 3mL/min

ID:27-C11
Time:20:48:19

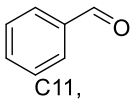

C11,
91% ee

Printed: Thu Dec 09 16:42:06 2021

Sample Report (continued):

Sample 35 Vial 1:35 ID 27-C11 File SHARLJA1_20211115_35 Date 15-Nov-2021 Time 20:48:19 Description (S,S)WO1 4.6x100mm 5µ

2: UV Detector: 230 Nm 2.0000-2.3500: Smooth (Mn, 2x3), 3.1000-3.5500: Smooth (Mn, 2x3) 6.079e-1
Range: 6.09e-1

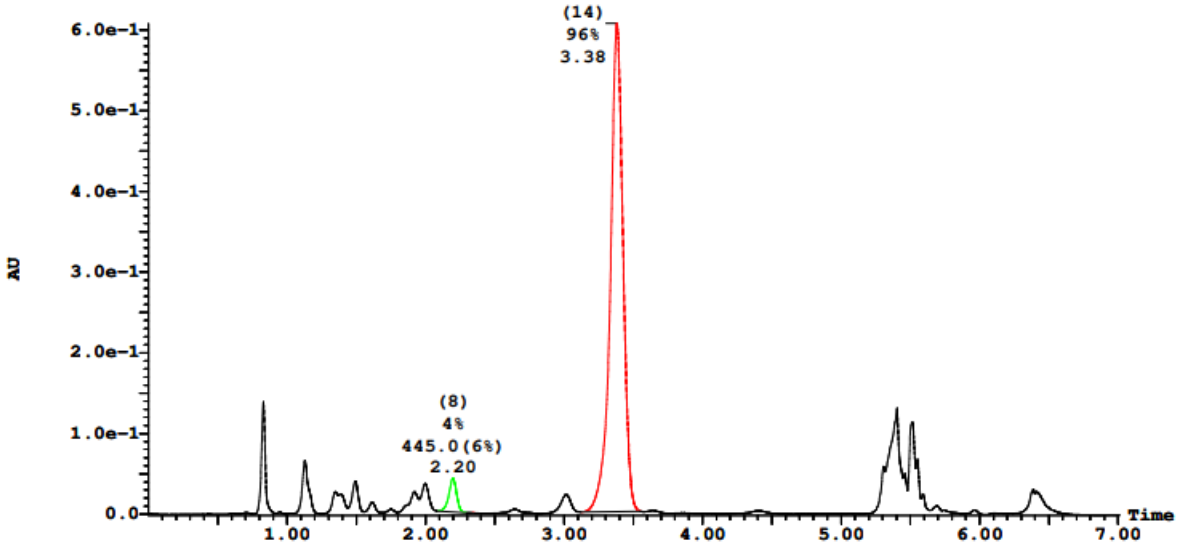

Peak Number	Compound	Time	AreaAbs	Area %Total	Width	Height	Mass Found
8	Found	2.20	3e+003	4.09	0	4e+004	445.0000
9		2.34	2e-001	0.00	0	3e+001	Not Found
14		3.38	6e+004	95.91	0	6e+005	Not Found

D1: 91% ee

Openlynx Report - SHARLJA1

Sample: 37
File:SHARLJA1_20211115_37
Description:(S,S)WO1 4.6x100mm 5µ

Vial:1:37
Date:15-Nov-2021
Conditions:5% IPA over 5min 3mL/min

ID:27-D1
Time:21:04:37

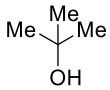

D1,
91% ee

Printed: Thu Dec 09 16:42:06 2021

Sample Report (continued):

Sample 37 Vial 1:37 ID 27-D1 File SHARLJA1_20211115_37 Date 15-Nov-2021 Time 21:04:37 Description (S,S)WO1 4.6x100mm 5µ

2: UV Detector: 230 Nm 2.0000-2.3500: Smooth (Mn, 2x3), 3.1000-3.5500: Smooth (Mn, 2x3) 4.144e-1
Range: 4.15e-1

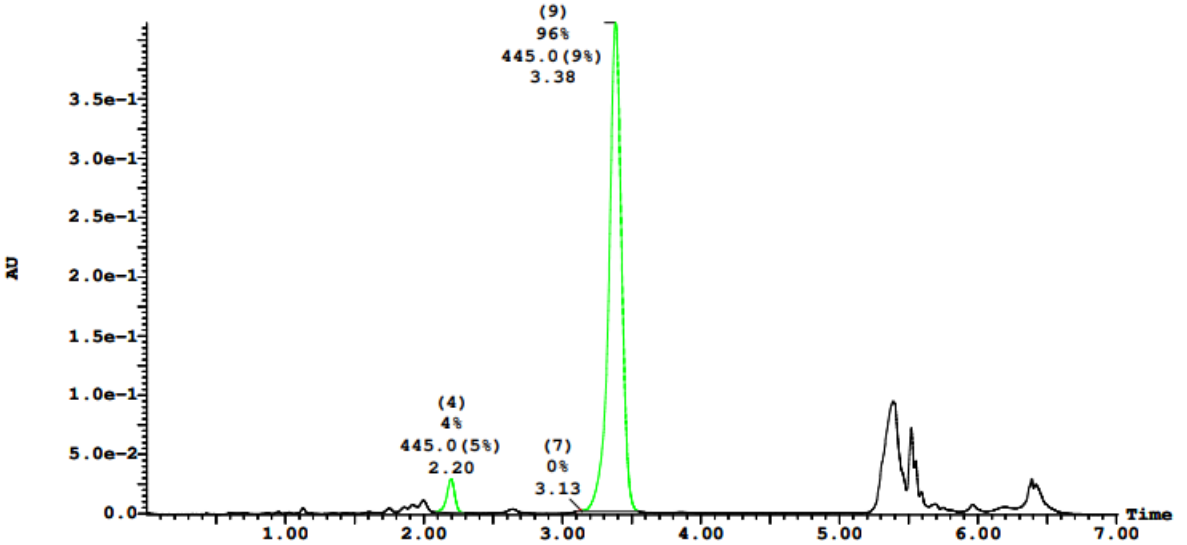

Peak Number	Compound	Time	AreaAbs	Area %Total	Width	Height	Mass Found
4	Found	2.20	2e+003	4.22	0	3e+004	445.0000
7		3.13	2e+001	0.04	0	8e+002	Not Found
9	Found	3.38	4e+004	95.74	0	4e+005	445.0000

D2: 91% ee

Openlynx Report - SHARLJA1

Sample: 38
File:SHARLJA1_20211115_38
Description:(S,S)WO1 4.6x100mm 5µ

Vial:1:38
Date:15-Nov-2021
Conditions:5% IPA over 5min 3mL/min

ID:27-D2
Time:21:12:42

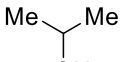

D2,
91% ee

Printed: Thu Dec 09 16:42:06 2021

Sample Report (continued):

Sample 38 Vial 1:38 ID 27-D2 File SHARLJA1_20211115_38 Date 15-Nov-2021 Time 21:12:42 Description (S,S)WO1 4.6x100mm 5µ

2: UV Detector: 230 Nm 2.0000-2.3500: Smooth (Mn, 2x3), 3.1000-3.5500: Smooth (Mn, 2x3) 5.796e-1
Range: 5.801e-1

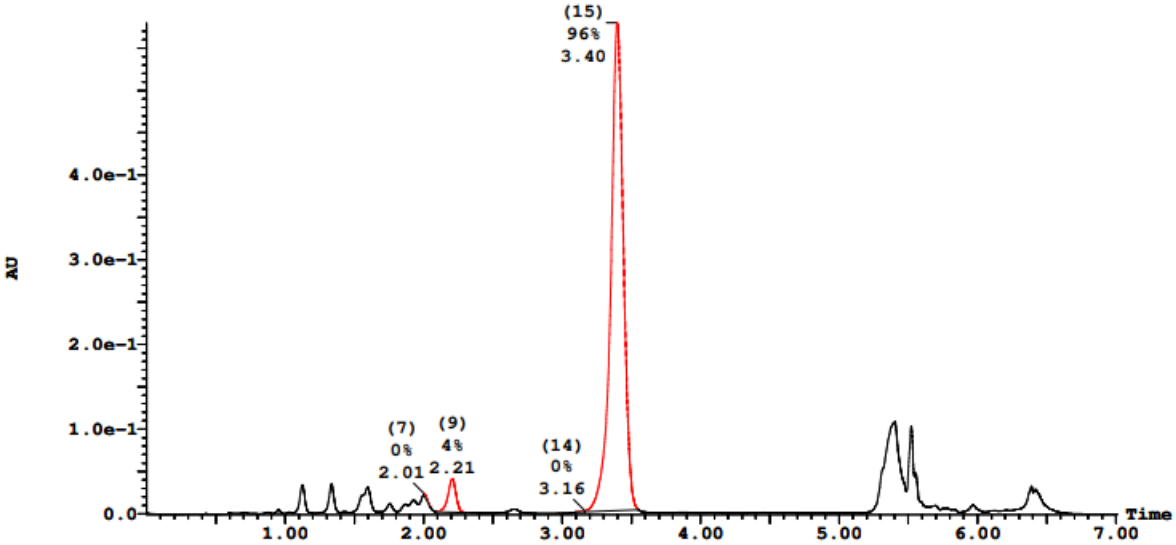

Peak Number	Compound	Time	AreaAbs	Area %Total	Width	Height	Mass Found
7		2.01	9e+001	0.14	0	2e+003	Not Found
9		2.21	3e+003	4.15	0	4e+004	Not Found
10		2.33	7e-001	0.00	0	6e+001	Not Found
14		3.16	5e+001	0.08	0	1e+003	Not Found
15		3.40	6e+004	95.63	0	6e+005	Not Found

D3: 91% ee

Openlynx Report - SHARLJA1

Sample: 39
File:SHARLJA1_20211115_39
Description:(S,S)WO1 4.6x100mm 5µ

Vial:1:39
Date:15-Nov-2021
Conditions:5% IPA over 5min 3mL/min

ID:27-D3
Time:21:20:50

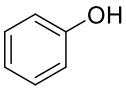

D3,
91% ee

Printed: Thu Dec 09 16:42:06 2021

Sample Report (continued):

Sample 39 Vial 1:39 ID 27-D3 File SHARLJA1_20211115_39 Date 15-Nov-2021 Time 21:20:50 Description (S,S)WO1 4.6x100mm 5µ

2: UV Detector: 230 Nm 2.0000-2.3500: Smooth (Mn, 2x3), 3.1000-3.5500: Smooth (Mn, 2x3) 5.778e-1
Range: 5.785e-1

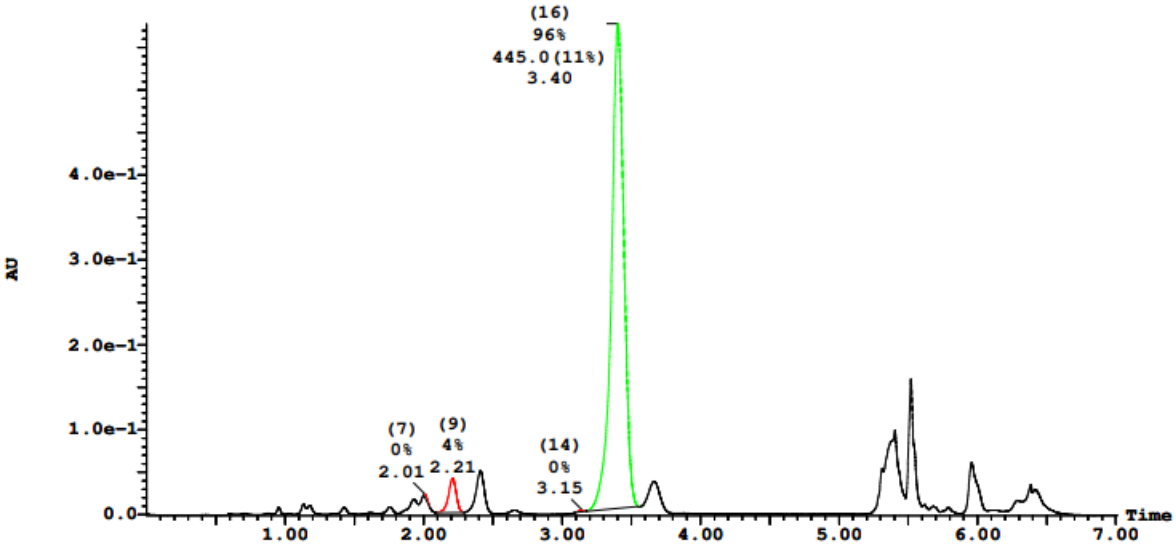

Peak Number	Compound	Time	AreaAbs	Area %Total	Width	Height	Mass Found
7		2.01	1e+002	0.18	0	3e+003	Not Found
9		2.21	3e+003	4.18	0	4e+004	Not Found
14		3.15	8e+001	0.12	0	1e+003	Not Found
16	Found	3.40	6e+004	95.51	0	6e+005	445.0000

D4: 91% ee

Openlynx Report - SHARLJA1

Sample: 40
File:SHARLJA1_20211115_40
Description:(S,S)WO1 4.6x100mm 5µ

Vial:1:40
Date:15-Nov-2021
Conditions:5% IPA over 5min 3mL/min

ID:27-D4
Time:21:28:57

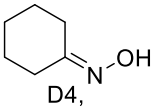

D4,
91% ee

Printed: Thu Dec 09 16:42:06 2021

Sample Report (continued):

Sample 40 Vial 1:40 ID 27-D4 File SHARLJA1_20211115_40 Date 15-Nov-2021 Time 21:28:57 Description (S,S)WO1 4.6x100mm 5µ

2: UV Detector: 230 Nm 2.0000-2.3500: Smooth (Mn, 2x3), 3.1000-3.5500: Smooth (Mn, 2x3) 5.059e-1
Range: 5.066e-1

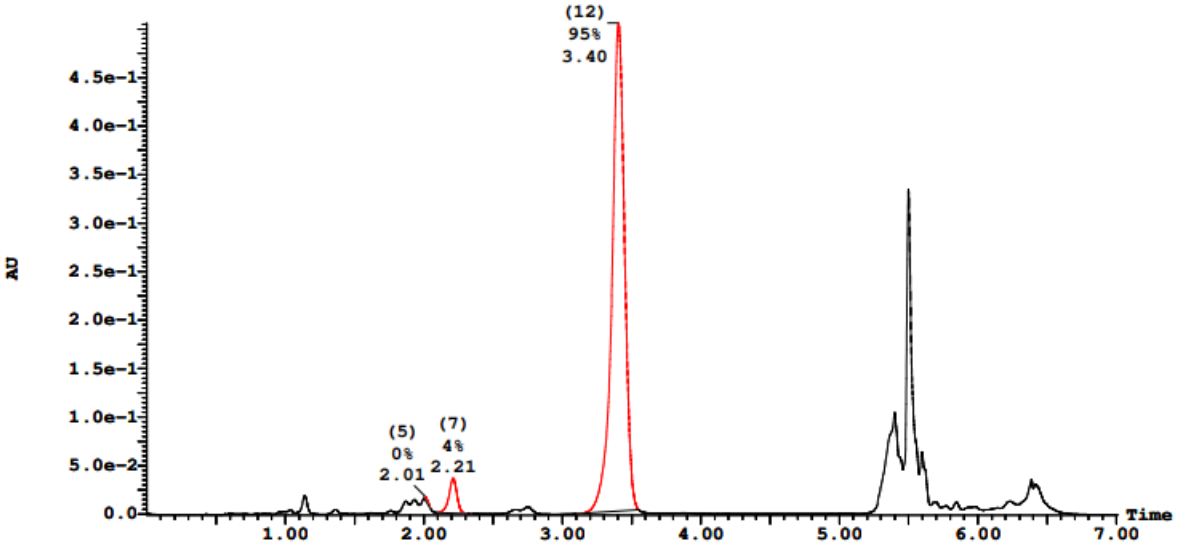

Peak Number	Compound	Time	AreaAbs	Area %Total	Width	Height	Mass Found
5		2.01	1e+002	0.21	0	3e+003	Not Found
7		2.21	2e+003	4.31	0	4e+004	Not Found
9		2.34	3e-001	0.00	0	2e+001	Not Found
12		3.40	5e+004	95.48	0	5e+005	Not Found

D8: 91% ee

Openlynx Report - SHARLJA1

Sample: 44
File:SHARLJA1_20211115_44
Description:(S,S)WO1 4.6x100mm 5µ

Vial:1:44
Date:15-Nov-2021
Conditions:5% IPA over 5min 3mL/min

ID:27-D8
Time:22:01:30

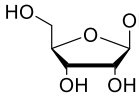

D8,
91% ee

Printed: Thu Dec 09 16:42:06 2021

Sample Report (continued):

Sample 44 Vial 1:44 ID 27-D8 File SHARLJA1_20211115_44 Date 15-Nov-2021 Time 22:01:30 Description (S,S)WO1 4.6x100mm 5µ

2: UV Detector: 230 Nm 2.0000-2.3500: Smooth (Mn, 2x3), 3.1000-3.5500: Smooth (Mn, 2x3) 6.366e-1
Range: 6.383e-1

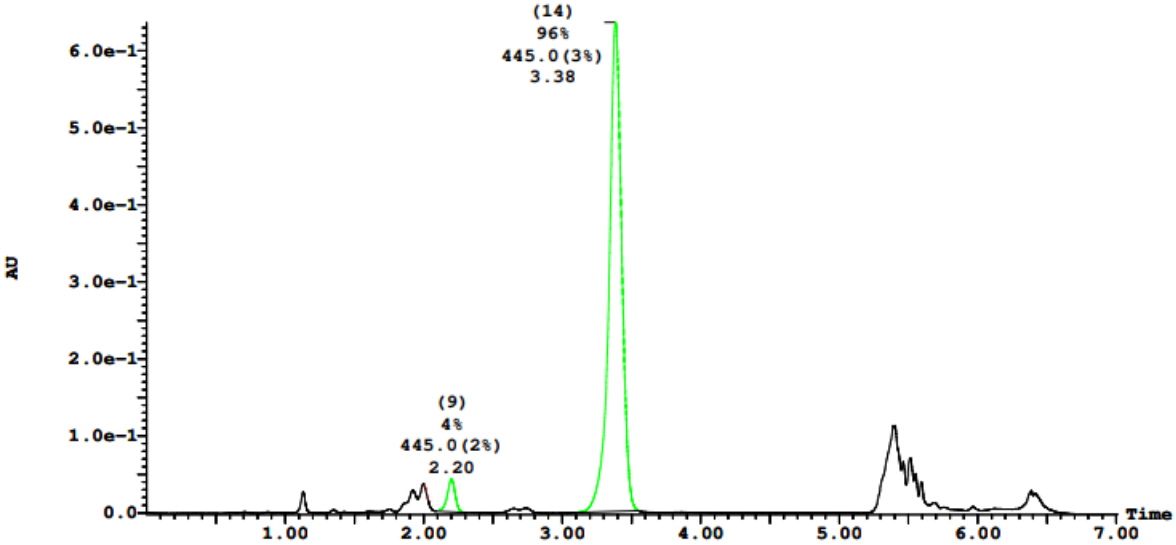

Peak Number	Compound	Time	AreaAbs	Area %Total	Width	Height	Mass Found
7		2.00	6e+001	0.08	0	3e-002	Not Found
9	Tentative	2.20	3e+003	4.01	0	4e+004	445.0000
10		2.33	1e+000	0.00	0	1e+002	Not Found
14	Found	3.38	7e+004	95.91	0	6e+005	445.0000

D9: 90% ee

Openlynx Report - SHARLJA1

Sample: 45
File:SHARLJA1_20211115_45
Description:(S,S)WO1 4.6x100mm 5µ

Vial:1:45
Date:15-Nov-2021
Conditions:5% IPA over 5min 3mL/min

ID:27-D9
Time:22:09:38

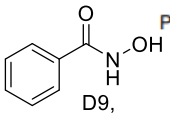

D9,
90% ee

Printed: Thu Dec 09 16:42:06 2021

Sample Report (continued):

Sample 45 Vial 1:45 ID 27-D9 File SHARLJA1_20211115_45 Date 15-Nov-2021 Time 22:09:38 Description (S,S)WO1 4.6x100mm 5µ

2: UV Detector: 230 Nm 2.0000-2.3500: Smooth (Mn, 2x3), 3.1000-3.5500: Smooth (Mn, 2x3) 7.939e-1
Range: 7.95e-1

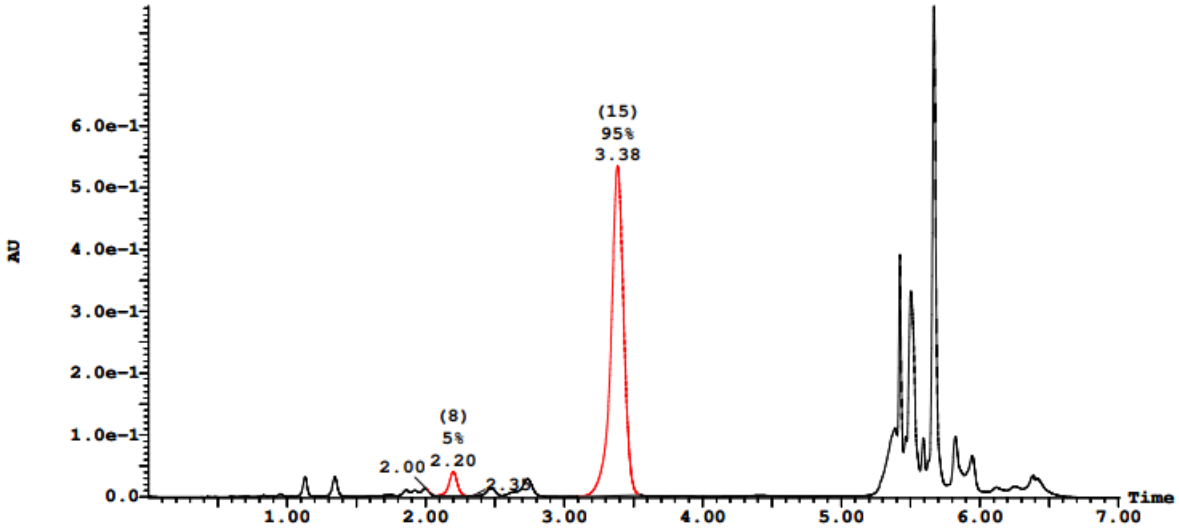

Peak Number	Compound	Time	AreaAbs	Area %Total	Width	Height	Mass Found
6		2.00	2e+001	0.03	0	1e-002	Not Found
8		2.20	3e+003	4.67	0	4e+004	Not Found
10		2.35	6e-001	0.00	0		Not Found
15		3.38	6e+004	95.30	0	5e+005	Not Found

D10: 88% ee

Openlynx Report - SHARLJA1

Sample: 46
File:SHARLJA1_20211115_46
Description:(S,S)WO1 4.6x100mm 5µ

Vial:1:46
Date:15-Nov-2021
Conditions:5% IPA over 5min 3mL/min

ID:27-D10
Time:22:17:45

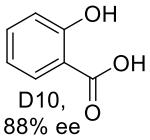

Printed: Thu Dec 09 16:42:06 2021

Sample Report (continued):

Sample 46 Vial 1:46 ID 27-D10 File SHARLJA1_20211115_46 Date 15-Nov-2021 Time 22:17:45 Description (S,S)WO1 4.6x100mm 5µ

2: UV Detector: 230 Nm 2.0000-2.3500: Smooth (Mn, 2x3), 3.1000-3.5500: Smooth (Mn, 2x3) 5.692e-1
Range: 5.7e-1

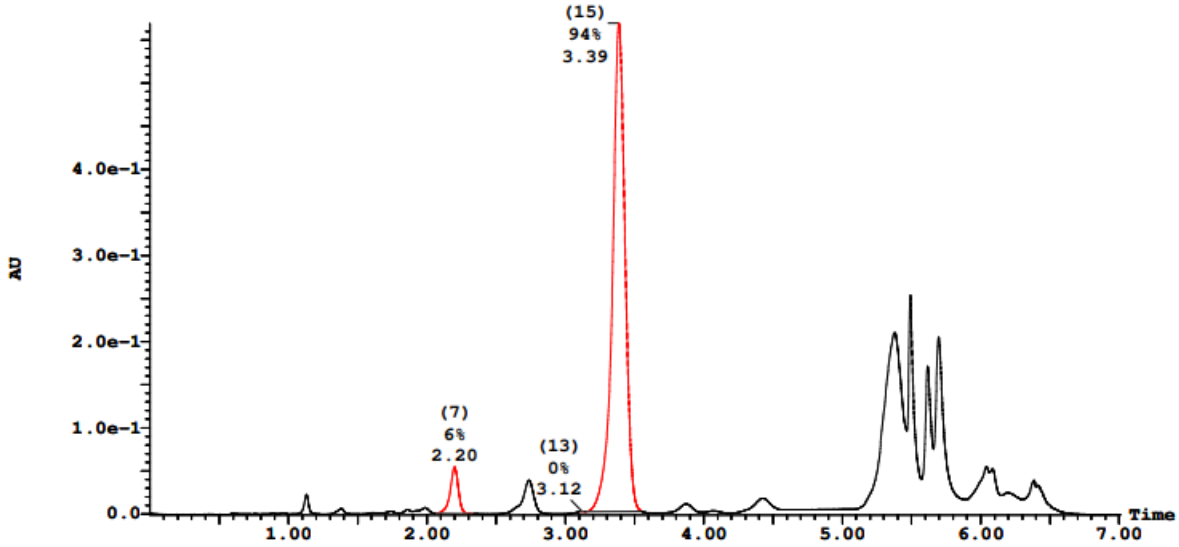

Peak Number	Compound	Time	AreaAbs	Area %Total	Width	Height	Mass Found
7		2.20	4e+003	5.84	0	5e+004	Not Found
8		2.32	3e+000	0.00	0	2e+002	Not Found
13		3.12	9e+000	0.01	0	3e+002	Not Found
15		3.39	6e+004	94.14	0	6e+005	Not Found

D11: 91% ee

Openlynx Report - SHARLJA1

Sample: 47
File:SHARLJA1_20211115_47
Description:(S,S)WO1 4.6x100mm 5µ

Vial:1:47
Date:15-Nov-2021
Conditions:5% IPA over 5min 3mL/min

ID:27-D11
Time:22:25:52

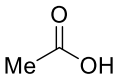

D11,
91% ee

Printed: Thu Dec 09 16:42:06 2021

Sample Report (continued):

Sample 47 Vial 1:47 ID 27-D11 File SHARLJA1_20211115_47 Date 15-Nov-2021 Time 22:25:52 Description (S,S)WO1 4.6x100mm 5µ

2: UV Detector: 230 Nm 2.0000-2.3500: Smooth (Mn, 2x3), 3.1000-3.5500: Smooth (Mn, 2x3) 5.959e-1
Range: 5.974e-1

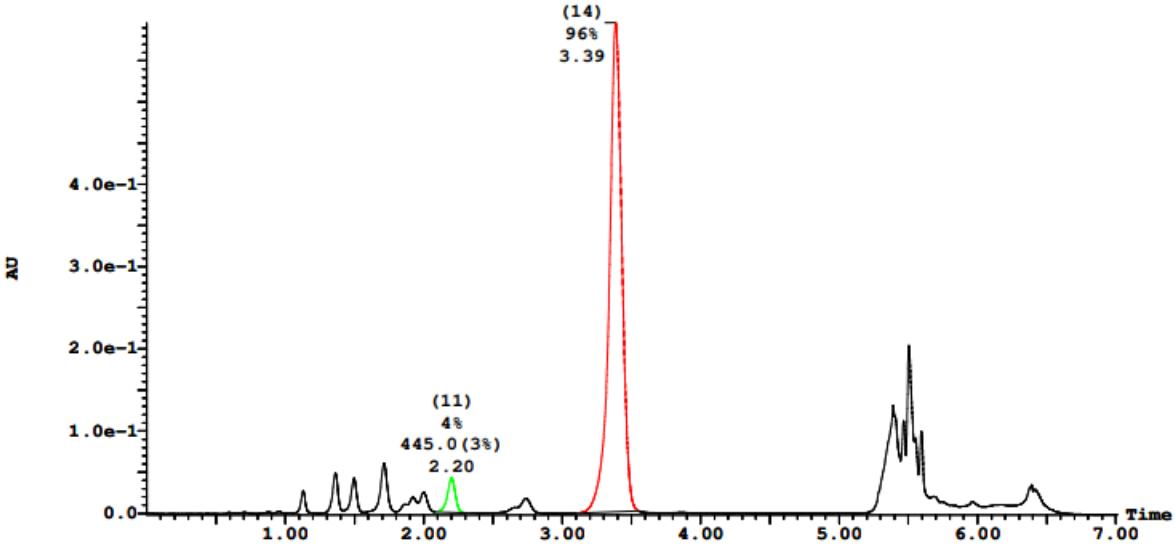

Peak Number	Compound	Time	AreaAbs	Area %Total	Width	Height	Mass Found
11	Tentative	2.20	3e+003	4.25	0	4e+004	445.0000
12		2.33	2e+000	0.00	0	1e+002	Not Found
14		3.39	6e+004	95.75	0	6e+005	Not Found

E3: 90% ee

Openlynx Report - SHARLJA1

Sample: 51
File:SHARLJA1_20211115_51
Description:(S,S)WO1 4.6x100mm 5µ

Vial:2:3
Date:16-Nov-2021
Conditions:5% IPA over 5min 3mL/min

ID:27-E3
Time:09:02:46

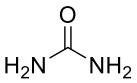

E3,
90% ee

Page 101

Printed: Thu Dec 09 16:42:06 2021

Sample Report (continued):

Sample 51 Vial 2:3 ID 27-E3 File SHARLJA1_20211115_51 Date 16-Nov-2021 Time 09:02:46 Description (S,S)WO1 4.6x100mm 5µ

2: UV Detector: 230 Nm 2.0000-2.3500: Smooth (Mn, 2x3), 3.1000-3.5500: Smooth (Mn, 2x3) 4.739e-1
Range: 4.743e-1

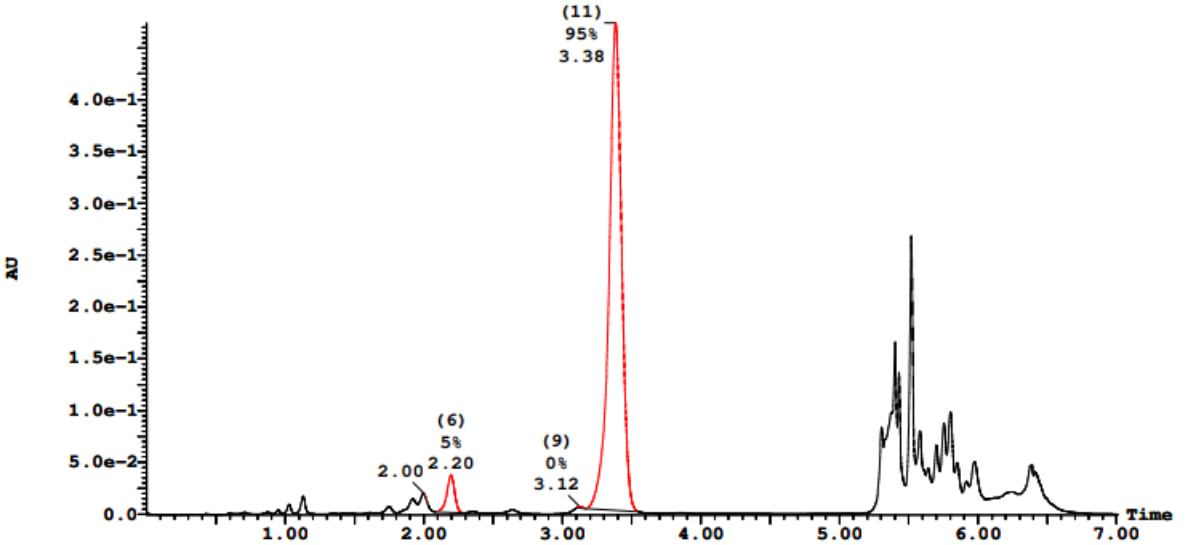

Peak Number	Compound	Time	AreaAbs	Area %Total	Width	Height	Mass Found
5		2.00	2e+001	0.05	0	1e-002	Not Found
6		2.20	2e+003	4.55	0	4e+004	Not Found
9		3.12	6e+001	0.11	0	1e+003	Not Found
11		3.38	5e+004	95.30	0	5e+005	Not Found

E4: >83% ee

Openlynx Report - SHARLJA1

Sample: 52
File:SHARLJA1_20211115_52
Description:(S,S)WO1 4.6x100mm 5µ

Vial:2:4
Date:16-Nov-2021
Conditions:5% IPA over 5min 3mL/min

ID:27-E4
Time:09:10:53

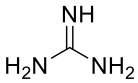

E4,
~94% ee

Printed: Thu Dec 09 16:42:06 2021

Sample Report (continued):

Sample 52 Vial 2:4 ID 27-E4 File SHARLJA1_20211115_52 Date 16-Nov-2021 Time 09:10:53 Description (S,S)WO1 4.6x100mm 5µ

2: UV Detector: 230 Nm 2.0000-2.3500: Smooth (Mn, 2x3), 3.1000-3.5500: Smooth (Mn, 2x3) 4.981e-1
Range: 4.984e-1

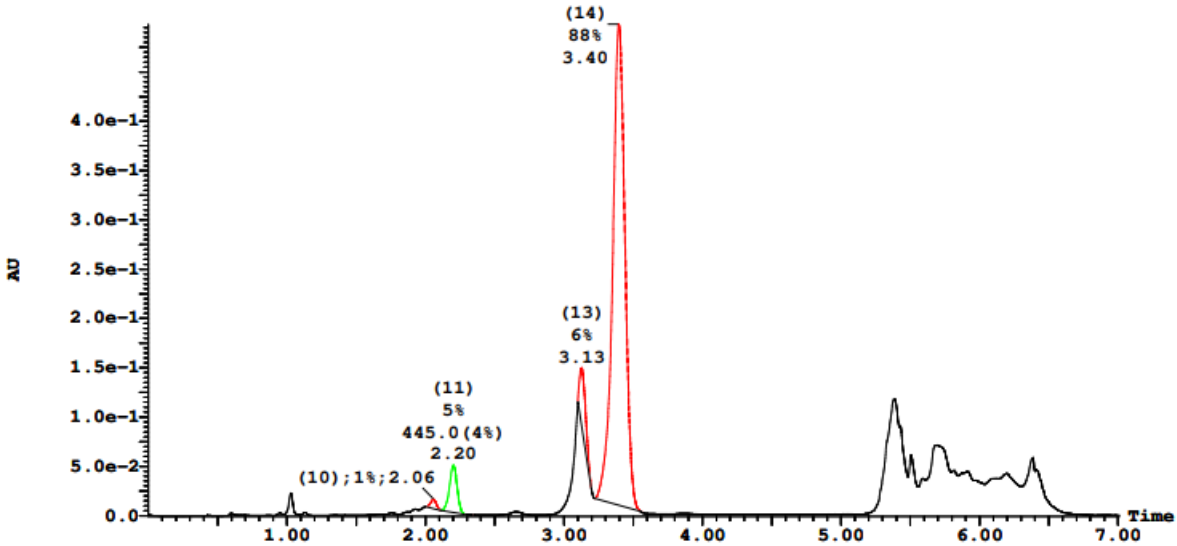

Peak Number	Compound	Time	AreaAbs	Area %Total	Width	Height	Mass Found
10		2.06	5e+002	0.79	0	9e+003	Not Found
11	Tentative	2.20	3e+003	5.37	0	5e+004	445.0000
12		2.34	4e-001	0.00	0	5e+001	Not Found
13		3.13	3e+003	5.53	0	6e+004	Not Found
14		3.40	5e+004	88.31	0	5e+005	Not Found

E5: 91% ee

Openlynx Report - SHARLJA1

Sample: 53
File:SHARLJA1_20211115_53
Description:(S,S)WO1 4.6x100mm 5µ

Vial:2:5
Date:16-Nov-2021
Conditions:5% IPA over 5min 3mL/min

ID:27-E5
Time:09:19:01

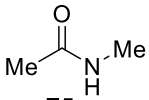

E5,
91% ee

Printed: Thu Dec 09 16:42:06 2021

Sample Report (continued):

Sample 53 Vial 2:5 ID 27-E5 File SHARLJA1_20211115_53 Date 16-Nov-2021 Time 09:19:01 Description (S,S)WO1 4.6x100mm 5µ

2: UV Detector: 230 Nm 2.0000-2.3500: Smooth (Mn, 2x3), 3.1000-3.5500: Smooth (Mn, 2x3) 6.756e-1
Range: 6.76e-1

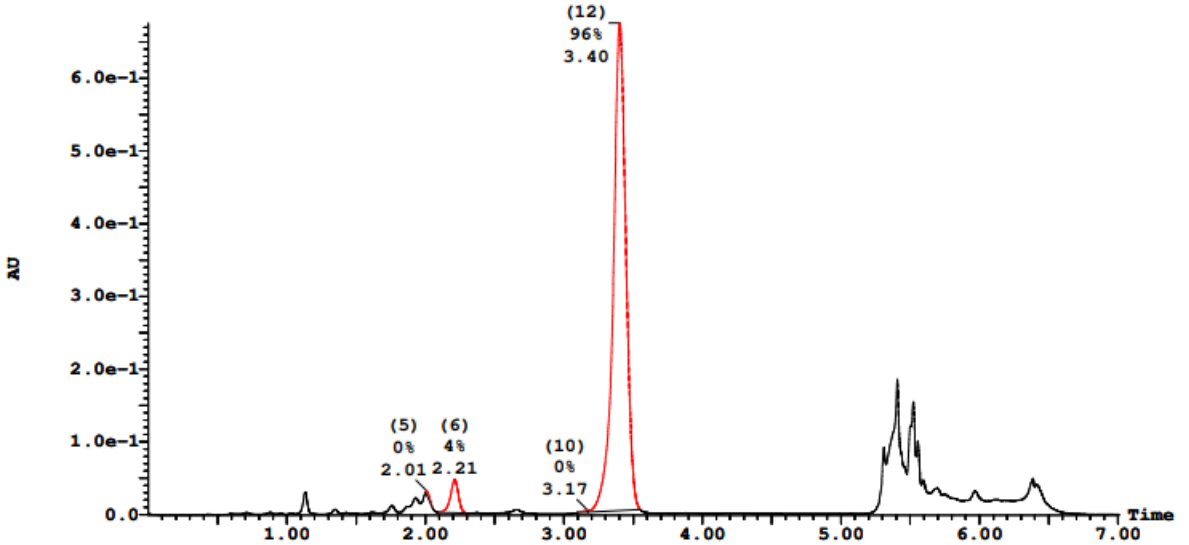

Peak Number	Compound	Time	AreaAbs	Area %Total	Width	Height	Mass Found
5		2.01	2e+002	0.26	0	6e+003	Not Found
6		2.21	3e+003	4.12	0	5e+004	Not Found
10		3.17	9e+001	0.12	0	2e+003	Not Found
12		3.40	7e+004	95.51	0	7e+005	Not Found

E6: 89% ee

Openlynx Report - SHARLJA1

Sample: 54
File:SHARLJA1_20211115_54
Description:(S,S)WO1 4.6x100mm 5µ

Vial:2:6
Date:16-Nov-2021
Conditions:5% IPA over 5min 3mL/min

ID:27-E6
Time:09:27:10

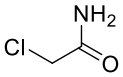

E6,
89% ee

Printed: Thu Dec 09 16:42:06 2021

Sample Report (continued):

Sample 54 Vial 2:6 ID 27-E6 File SHARLJA1_20211115_54 Date 16-Nov-2021 Time 09:27:10 Description (S,S)WO1 4.6x100mm 5µ

2: UV Detector: 230 Nm 2.0000-2.3500: Smooth (Mn, 2x3), 3.1000-3.5500: Smooth (Mn, 2x3) 6.883e-1
Range: 6.89e-1

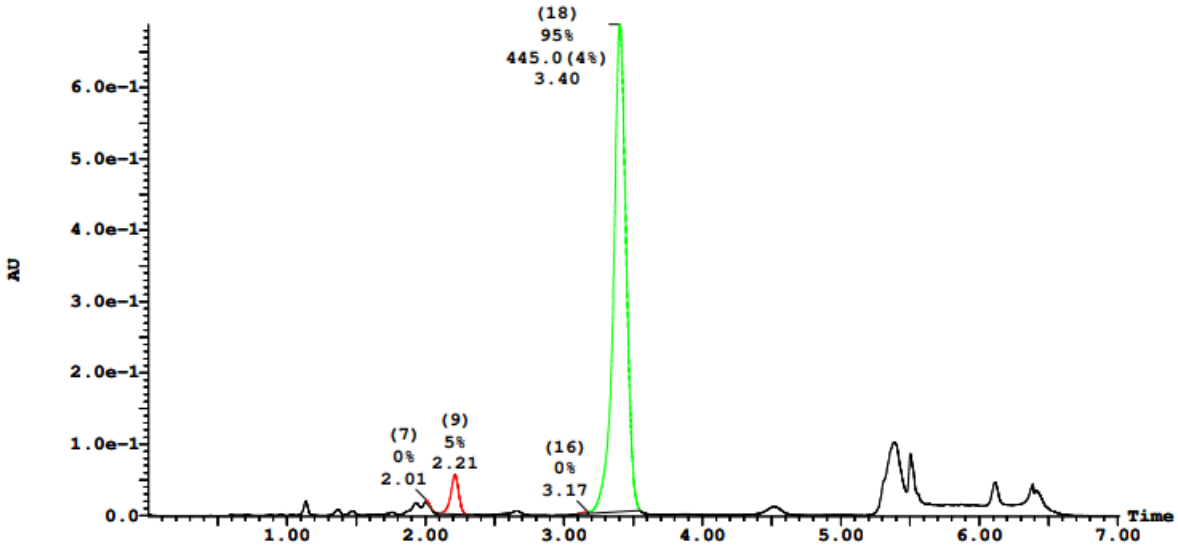

Peak Number	Compound	Time	AreaAbs	Area %Total	Width	Height	Mass Found
7		2.01	1e+002	0.17	0	4e+003	Not Found
9		2.21	4e+003	4.90	0	6e+004	Not Found
10		2.33	1e+000	0.00	0	6e+001	Not Found
16		3.17	1e+002	0.13	0	2e+003	Not Found
18	Found	3.40	7e+004	94.80	0	7e+005	445.0000

E7: 90% ee

Openlynx Report - SHARLJA1

Sample: 55
File:SHARLJA1_20211115_55
Description:(S,S)WO1 4.6x100mm 5µ

Vial:2:7
Date:16-Nov-2021
Conditions:5% IPA over 5min 3mL/min

ID:27-E7
Time:09:35:18

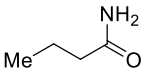

E7,
90% ee

Printed: Thu Dec 09 16:42:06 2021

Sample Report (continued):

Sample 55 Vial 2:7 ID 27-E7 File SHARLJA1_20211115_55 Date 16-Nov-2021 Time 09:35:18 Description (S,S)WO1 4.6x100mm 5µ

2: UV Detector: 230 Nm 2.0000-2.3500: Smooth (Mn, 2x3), 3.1000-3.5500: Smooth (Mn, 2x3) 5.148e-1
Range: 5.155e-1

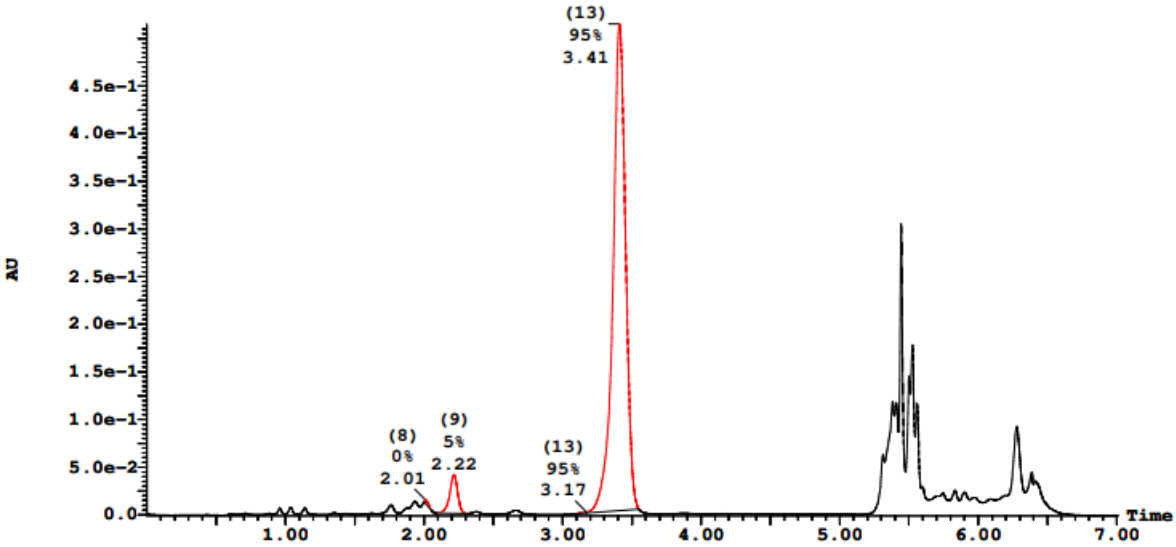

Peak Number	Compound	Time	AreaAbs	Area %Total	Width	Height	Mass Found
8		2.01	1e+002	0.22	0	3e+003	Not Found
9		2.22	3e+003	4.79	0	4e+004	Not Found
11		3.17	4e+001	0.08	0	9e+002	Not Found
13		3.41	5e+004	94.91	0	5e+005	Not Found

E8: 89% ee

Openlynx Report - SHARLJA1 Page 111

Sample: 56
File:SHARLJA1_20211115_56
Description:(S,S)WO1 4.6x100mm 5µ

Vial:2:8
Date:16-Nov-2021
Conditions:5% IPA over 5min 3mL/min

ID:27-E8
Time:09:43:27

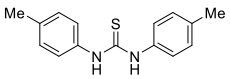

E8,
89% ee

Printed: Thu Dec 09 16:42:06 2021

Sample Report (continued):

Sample 56 Vial 2:8 ID 27-E8 File SHARLJA1_20211115_56 Date 16-Nov-2021 Time 09:43:27 Description (S,S)WO1 4.6x100mm 5µ

2: UV Detector: 230 Nm 2.0000-2.3500: Smooth (Mn, 2x3), 3.1000-3.5500: Smooth (Mn, 2x3) 1.538
Range: 1.539

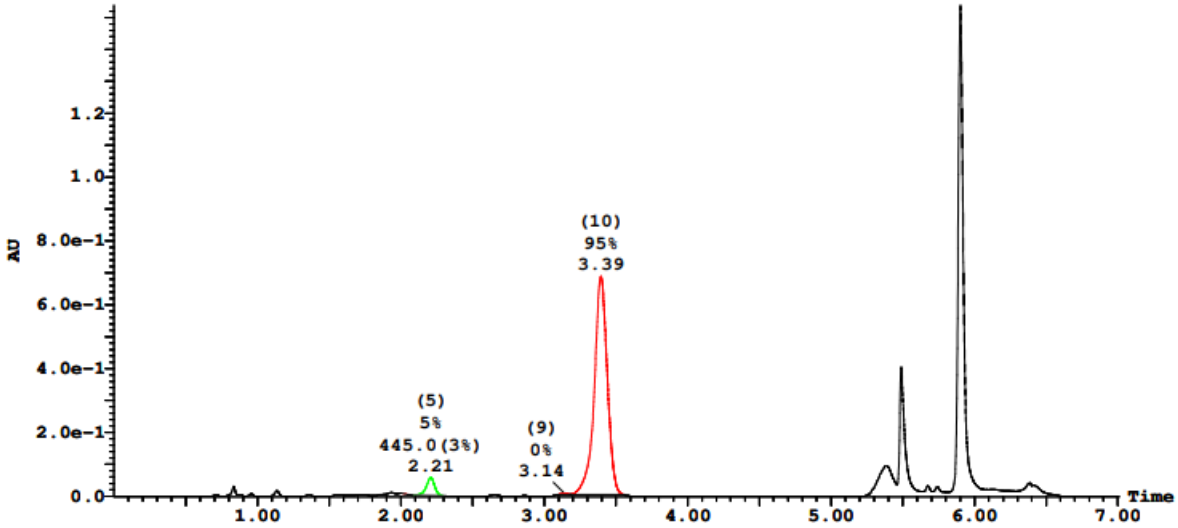

Peak Number	Compound	Time	AreaAbs	Area %Total	Width	Height	Mass Found
4		2.01	3e+001	0.04	0	7e+002	Not Found
5	Found	2.21	4e+003	4.99	0	6e+004	445.0000
6	Tentative	2.32	3e-001	0.00	0		445.0000
9		3.14	2e+002	0.24	0	3e+003	Not Found
10		3.39	7e+004	94.73	0	7e+005	Not Found

E10: 90% ee

Openlynx Report - SHARLJA1

Sample: 58
File:SHARLJA1_20211115_58
Description:(S,S)WO1 4.6x100mm 5µ

Vial:2:10
Date:16-Nov-2021
Conditions:5% IPA over 5min 3mL/min

ID:27-E10
Time:09:59:42

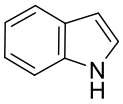

E10,
90% ee

Printed: Thu Dec 09 16:42:06 2021

Sample Report (continued):

Sample 58 Vial 2:10 ID 27-E10 File SHARLJA1_20211115_58 Date 16-Nov-2021 Time 09:59:42 Description (S,S)WO1 4.6x100mm 5µ

2: UV Detector: 230 Nm 2.0000-2.3500: Smooth (Mn, 2x3), 3.1000-3.5500: Smooth (Mn, 2x3) 3.245e-1
Range: 3.255e-1

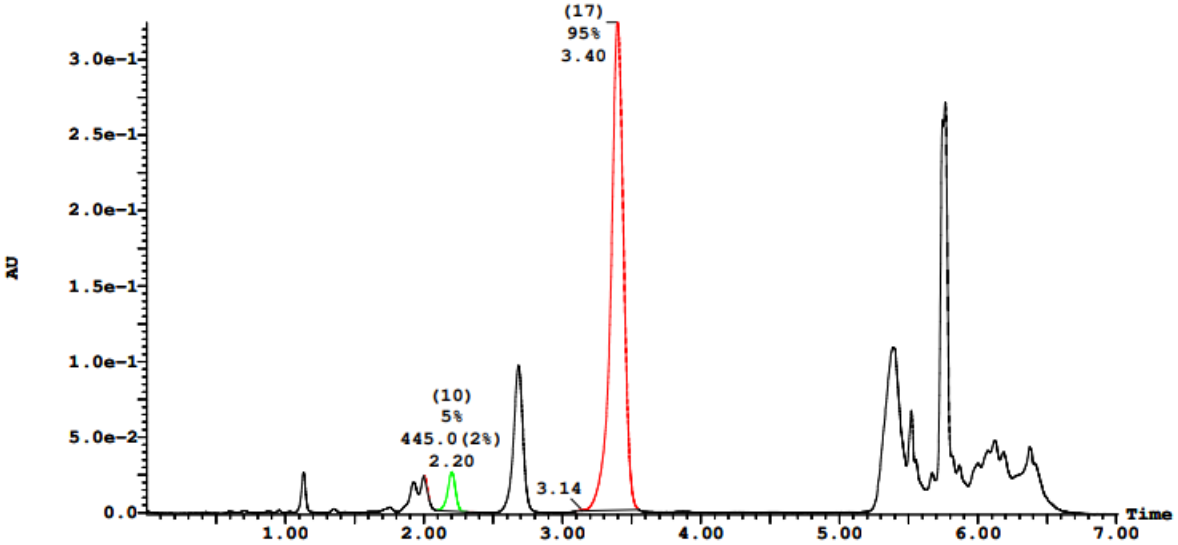

Peak Number	Compound	Time	AreaAbs	Area %Total	Width	Height	Mass Found
9		2.00	7e+001	0.19	0	1e+003	Not Found
10	Tentative	2.20	2e+003	4.75	0	3e+004	445.0000
11		2.33	4e-001	0.00	0	3e+001	Not Found
15		3.14	2e+001	0.04	0	6e+002	Not Found
17		3.40	3e+004	95.02	0	3e+005	Not Found

E11: 94% ee

Openlynx Report - SHARLJA1

Sample: 59
File:SHARLJA1_20211115_59
Description:(S,S)WO1 4.6x100mm 5µ

Vial:2:11
Date:16-Nov-2021
Conditions:5% IPA over 5min 3mL/min

ID:27-E11
Time:10:07:49

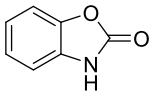

E11,
94% ee

Printed: Thu Dec 09 16:42:06 2021

Sample Report (continued):

Sample 59 Vial 2:11 ID 27-E11 File SHARLJA1_20211115_59 Date 16-Nov-2021 Time 10:07:49 Description (S,S)WO1 4.6x100mm 5µ

2: UV Detector: 230 Nm 2.0000-2.3500: Smooth (Mn, 2x3), 3.1000-3.5500: Smooth (Mn, 2x3) 9.015e-1
Range: 9.027e-1

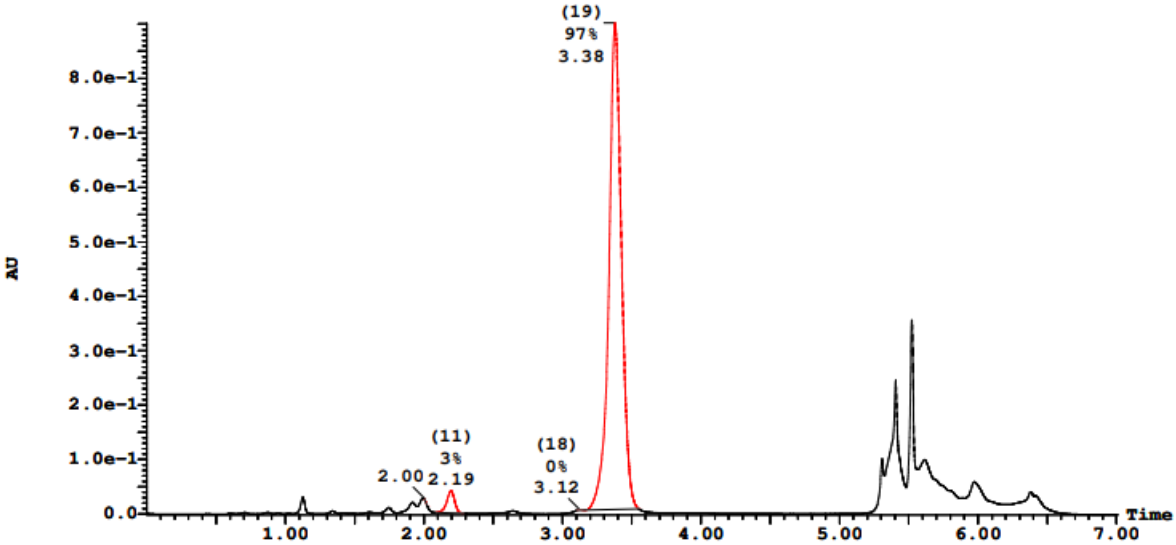

Peak Number	Compound	Time	AreaAbs	Area %Total	Width	Height	Mass Found
9		2.00	1e+001	0.01	0	3e-002	Not Found
11		2.19	3e+003	2.81	0	4e+004	Not Found
18		3.12	4e+001	0.04	0	1e+003	Not Found
19		3.38	9e+004	97.13	0	9e+005	Not Found

F3: 91% ee

Openlynx Report - SHARLJA1 Page 125

Sample: 63
File:SHARLJA1_20211115_63
Description:(S,S)WO1 4.6x100mm 5µ

Vial:2:15
Date:16-Nov-2021
Conditions:5% IPA over 5min 3mL/min

ID:27-F3
Time:10:40:21

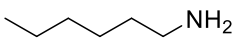

F3,
91% ee

Printed: Thu Dec 09 16:42:06 2021

Sample Report (continued):

Sample 63 Vial 2:15 ID 27-F3 File SHARLJA1_20211115_63 Date 16-Nov-2021 Time 10:40:21 Description (S,S)WO1 4.6x100mm 5µ

2: UV Detector: 230 Nm 2.0000-2.3500: Smooth (Mn, 2x3), 3.1000-3.5500: Smooth (Mn, 2x3) 6.873e-1
Range: 6.883e-1

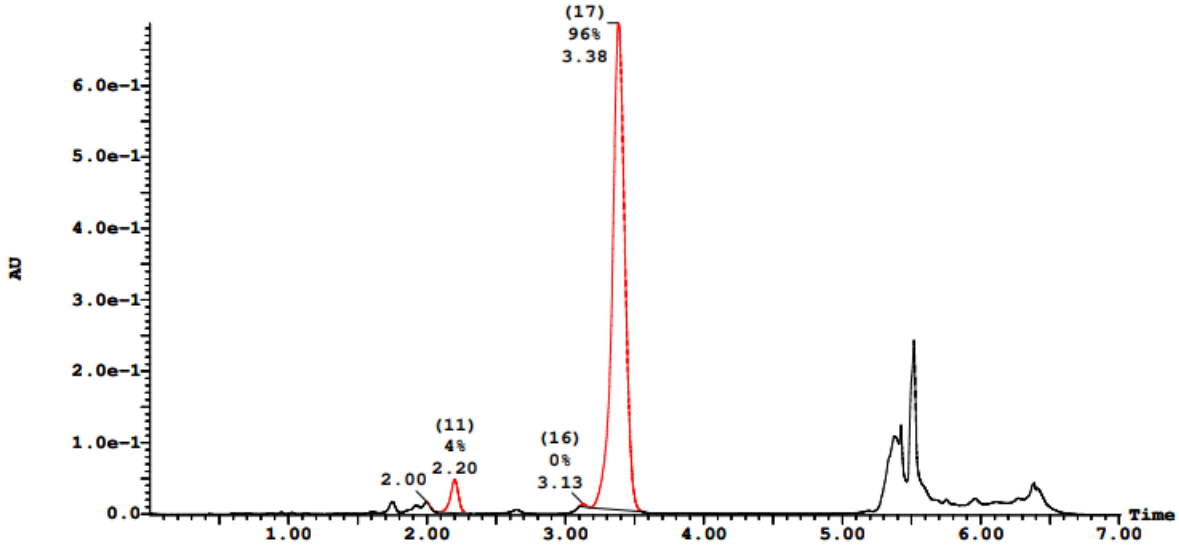

Peak Number	Compound	Time	AreaAbs	Area %Total	Width	Height	Mass Found
9		2.00	2e+001	0.03	0		Not Found
11		2.20	3e+003	4.23	0	5e+004	Not Found
12	Tentative	2.33	6e-001	0.00	0	4e+001	445.0000
16		3.13	2e+002	0.23	0	4e+003	Not Found
17		3.38	7e+004	95.51	0	7e+005	Not Found

F4: 91% ee

Openlynx Report - SHARLJA1

Sample: 64
File:SHARLJA1_20211115_64
Description:(S,S)WO1 4.6x100mm 5µ

Vial:2:16
Date:16-Nov-2021
Conditions:5% IPA over 5min 3mL/min

ID:27-F4
Time:10:48:29

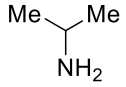

F4,
91% ee

Printed: Thu Dec 09 16:42:06 2021

Sample Report (continued):

Sample 64 Vial 2:16 ID 27-F4 File SHARLJA1_20211115_64 Date 16-Nov-2021 Time 10:48:29 Description (S,S)WO1 4.6x100mm 5µ

2: UV Detector: 230 Nm 2.0000-2.3500: Smooth (Mn, 2x3), 3.1000-3.5500: Smooth (Mn, 2x3) 5.974e-1
Range: 5.983e-1

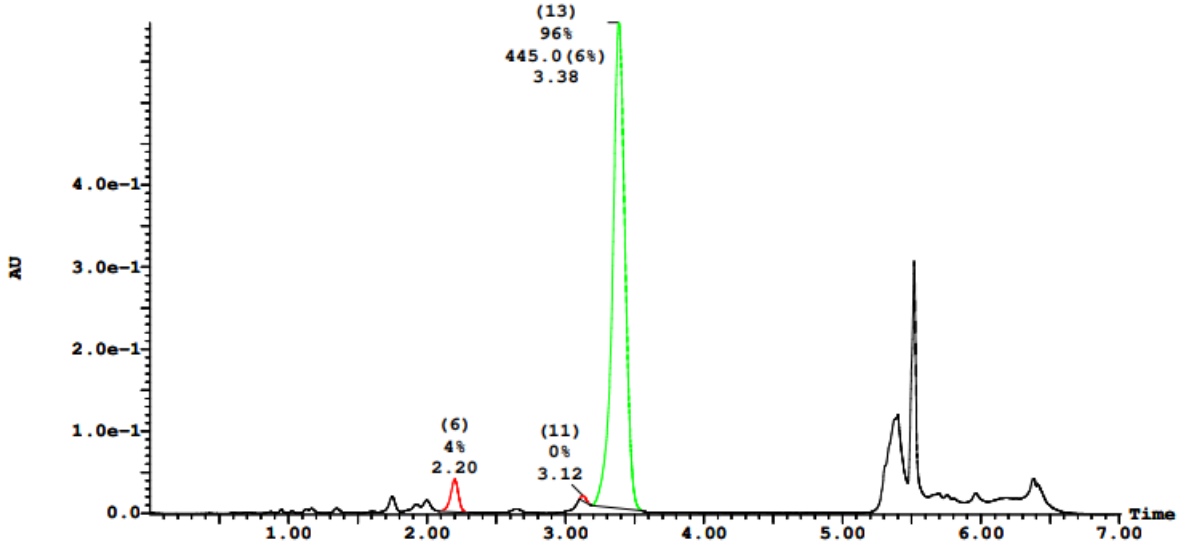

Peak Number	Compound	Time	AreaAbs	Area %Total	Width	Height	Mass Found
6		2.20	3e+003	4.05	0	4e+004	Not Found
11		3.12	3e+002	0.44	0	6e+003	Not Found
13	Found	3.38	6e+004	95.51	0	6e+005	445.0000

F6: 86% ee

Openlynx Report - SHARLJA1

Sample: 66
File:SHARLJA1_20211115_66
Description:(S,S)WO1 4.6x100mm 5µ

Vial:2:18
Date:16-Nov-2021
Conditions:5% IPA over 5min 3mL/min

ID:27-F6
Time:11:04:45

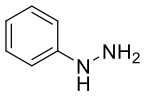

F6,
86% ee

Printed: Thu Dec 09 16:42:06 2021

Sample Report (continued):

Sample 66 Vial 2:18 ID 27-F6 File SHARLJA1_20211115_66 Date 16-Nov-2021 Time 11:04:45 Description (S,S)WO1 4.6x100mm 5µ

2: UV Detector: 230 Nm 2.0000-2.3500: Smooth (Mn, 2x3), 3.1000-3.5500: Smooth (Mn, 2x3) 7.388e-1
Range: 7.394e-1

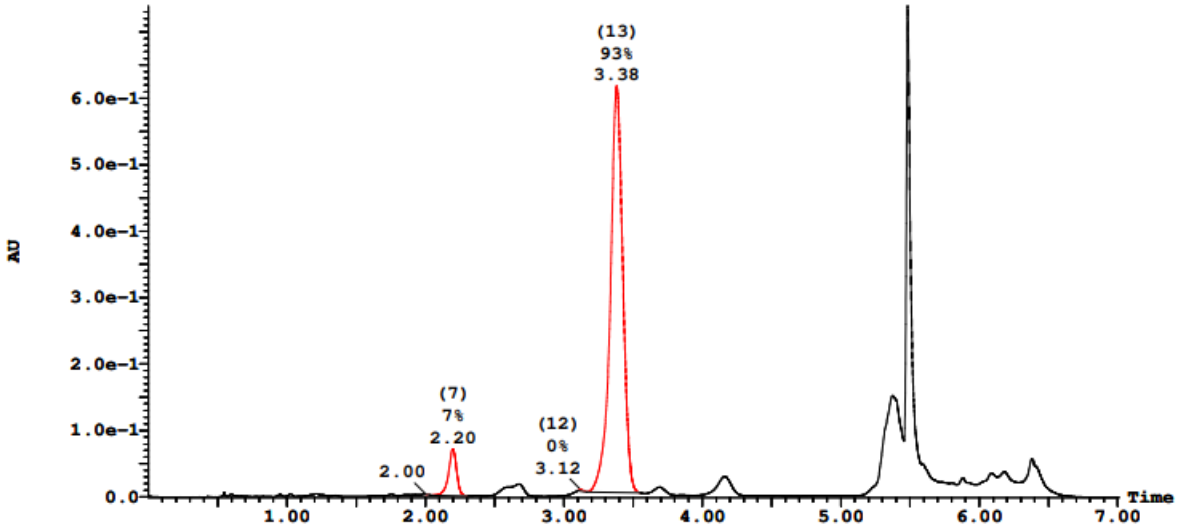

Peak Number	Compound	Time	AreaAbs	Area %Total	Width	Height	Mass Found
4		2.00	3e+000	0.00	0		Not Found
7		2.20	5e+003	6.94	0	7e+004	Not Found
12		3.12	6e+001	0.08	0	2e+003	Not Found
13		3.38	6e+004	92.97	0	6e+005	Not Found

F7: 91% ee

Openlynx Report - SHARLJA1

Sample: 67
File:SHARLJA1_20211115_67
Description:(S,S)WO1 4.6x100mm 5µ

Vial:2:19
Date:16-Nov-2021
Conditions:5% IPA over 5min 3mL/min

ID:27-F7
Time:11:12:53

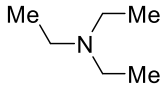

F7,
91% ee

Printed: Thu Dec 09 16:42:06 2021

Sample Report (continued):

Sample 67 Vial 2:19 ID 27-F7 File SHARLJA1_20211115_67 Date 16-Nov-2021 Time 11:12:53 Description (S,S)WO1 4.6x100mm 5µ

2: UV Detector: 230 Nm 2.0000-2.3500: Smooth (Mn, 2x3), 3.1000-3.5500: Smooth (Mn, 2x3) 6.458e-1
Range: 6.468e-1

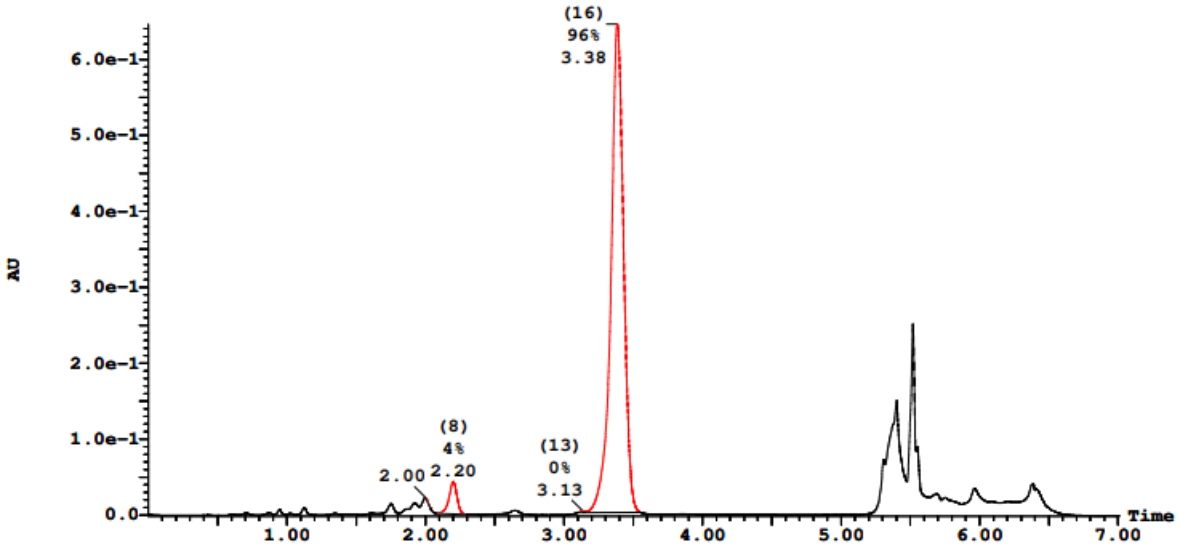

Peak Number	Compound	Time	AreaAbs	Area %Total	Width	Height	Mass Found
7		2.00	4e+001	0.05	0		Not Found
8		2.20	3e+003	3.97	0	4e+004	Not Found
13		3.13	5e+001	0.06	0	1e+003	Not Found
16		3.38	7e+004	95.92	0	6e+005	Not Found

F8: 91% ee

Openlynx Report - SHARLJA1

Sample: 68
File:SHARLJA1_20211115_68
Description:(S,S)WO1 4.6x100mm 5µ

Vial:2:20
Date:16-Nov-2021
Conditions:5% IPA over 5min 3mL/min

ID:27-F8
Time:11:21:00

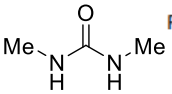

F8,
91% ee

Printed: Thu Dec 09 16:42:06 2021

Sample Report (continued):

Sample 68 Vial 2:20 ID 27-F8 File SHARLJA1_20211115_68 Date 16-Nov-2021 Time 11:21:00 Description (S,S)WO1 4.6x100mm 5µ

2: UV Detector: 230 Nm 2.0000-2.3500: Smooth (Mn, 2x3), 3.1000-3.5500: Smooth (Mn, 2x3) 5.511e-1
Range: 5.519e-1

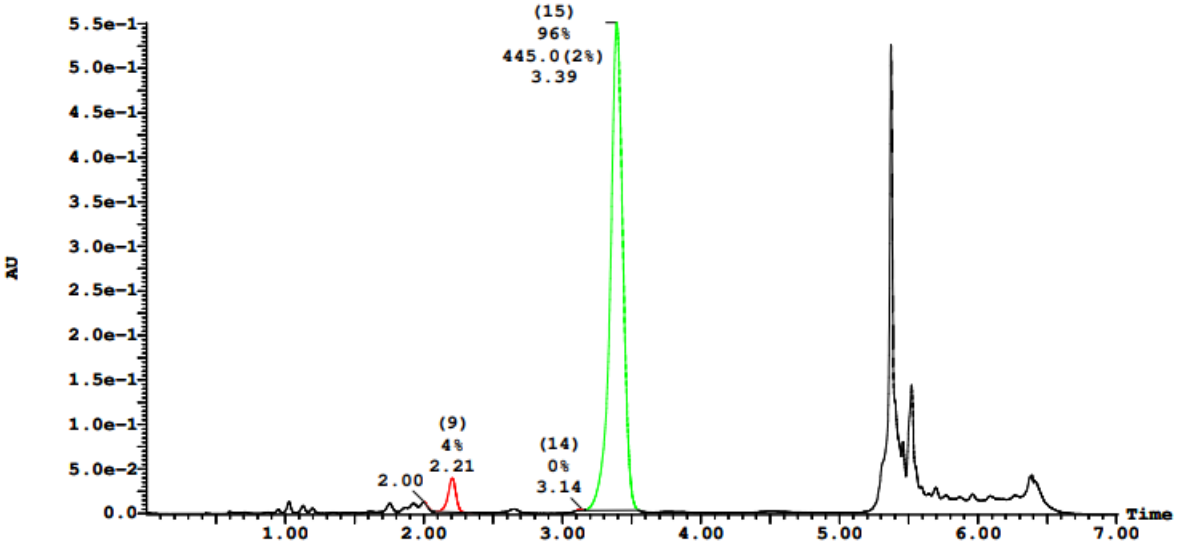

Peak Number	Compound	Time	AreaAbs	Area %Total	Width	Height	Mass Found
7		2.00	3e+001	0.05	0	1e-002	Not Found
9		2.21	3e+003	4.24	0	4e+004	Not Found
11		2.34	1e+000	0.00	0	8e+001	Not Found
14		3.14	7e+001	0.11	0	1e+003	Not Found
15	Found	3.39	6e+004	95.59	0	5e+005	445.0000

F9: 91% ee

Openlynx Report - SHARLJA1

Sample: 69
File:SHARLJA1_20211115_69
Description:(S,S)WO1 4.6x100mm 5µ

Vial:2:21
Date:16-Nov-2021
Conditions:5% IPA over 5min 3mL/min

ID:27-F9
Time:11:29:09

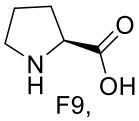

F9,
91% ee

Printed: Thu Dec 09 16:42:06 2021

Sample Report (continued):

Sample 69 Vial 2:21 ID 27-F9 File SHARLJA1_20211115_69 Date 16-Nov-2021 Time 11:29:09 Description (S,S)WO1 4.6x100mm 5µ

2: UV Detector: 230 Nm 2.0000-2.3500: Smooth (Mn, 2x3), 3.1000-3.5500: Smooth (Mn, 2x3) 7.608e-1
Range: 7.615e-1

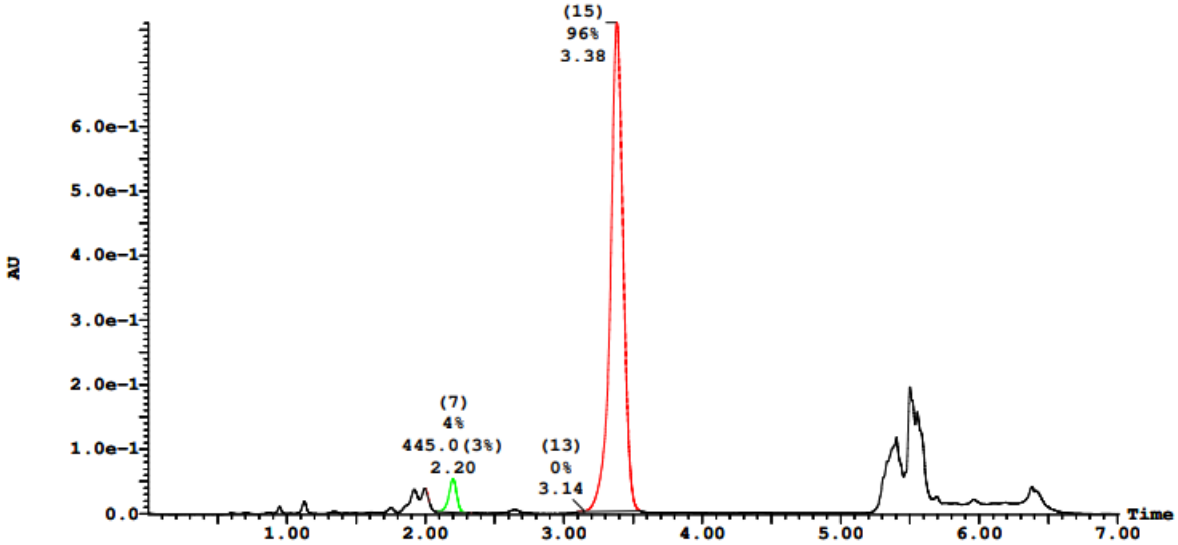

Peak Number	Compound	Time	AreaAbs	Area %Total	Width	Height	Mass Found
6		2.00	5e+001	0.05	0	5e-002	Not Found
7	Tentative	2.20	3e+003	4.13	0	5e+004	445.0000
8		2.33	5e-001	0.00	0	5e+001	Not Found
13		3.14	4e+001	0.04	0	1e+003	Not Found
15		3.38	8e+004	95.77	0	8e+005	Not Found

F10: 90% ee

Openlynx Report - SHARLJA1

Sample: 70
File:SHARLJA1_20211115_70
Description:(S,S)WO1 4.6x100mm 5µ

Vial:2:22
Date:16-Nov-2021
Conditions:5% IPA over 5min 3mL/min

ID:27-F10
Time:11:37:16

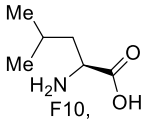

F10,
90% ee

Printed: Thu Dec 09 16:42:06 2021

Sample Report (continued):

Sample 70 Vial 2:22 ID 27-F10 File SHARLJA1_20211115_70 Date 16-Nov-2021 Time 11:37:16 Description (S,S)WO1 4.6x100mm 5µ

2: UV Detector: 230 Nm 2.0000-2.3500: Smooth (Mn, 2x3), 3.1000-3.5500: Smooth (Mn, 2x3) 7.096e-1
Range: 7.102e-1

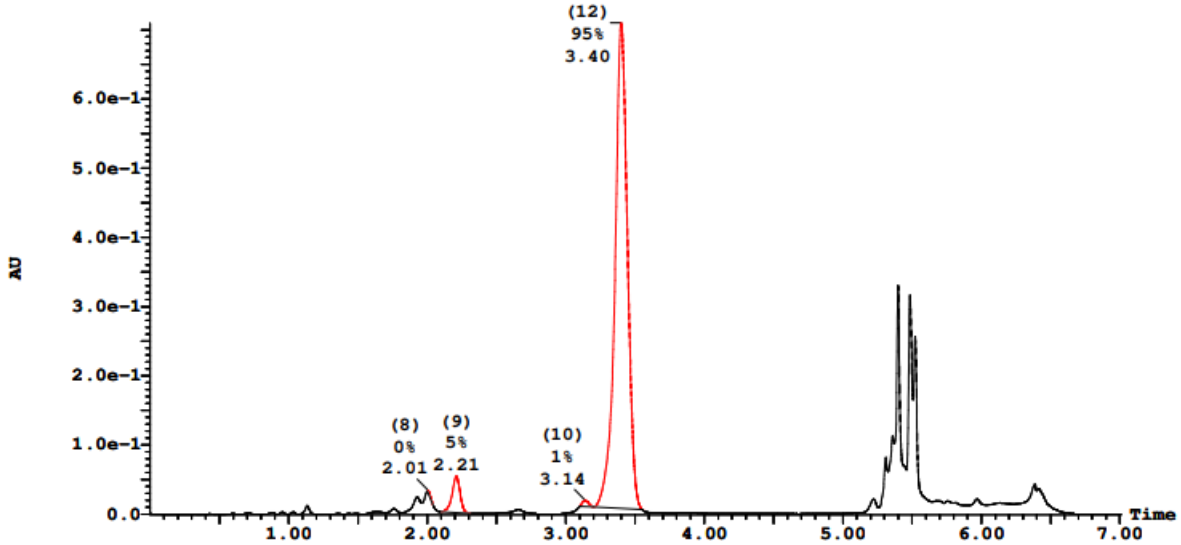

Peak Number	Compound	Time	AreaAbs	Area %Total	Width	Height	Mass Found
8		2.01	1e+002	0.16	0	3e+003	Not Found
9		2.21	4e+003	4.55	0	5e+004	Not Found
10		3.14	5e+002	0.59	0	8e+003	Not Found
12		3.40	7e+004	94.70	0	7e+005	Not Found

F11: 91% ee

Openlynx Report - SHARLJA1

Sample: 71
File:SHARLJA1_20211115_71
Description:(S,S)WO1 4.6x100mm 5µ

Vial:2:23
Date:16-Nov-2021
Conditions:5% IPA over 5min 3mL/min

ID:27-F11
Time:11:45:24

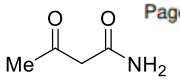

F11,
91% ee

Printed: Thu Dec 09 16:42:06 2021

Sample Report (continued):

Sample 71 Vial 2:23 ID 27-F11 File SHARLJA1_20211115_71 Date 16-Nov-2021 Time 11:45:24 Description (S,S)WO1 4.6x100mm 5µ

2: UV Detector: 230 Nm 2.0000-2.3500: Smooth (Mn, 2x3), 3.1000-3.5500: Smooth (Mn, 2x3) 6.15e-1
Range: 6.155e-1

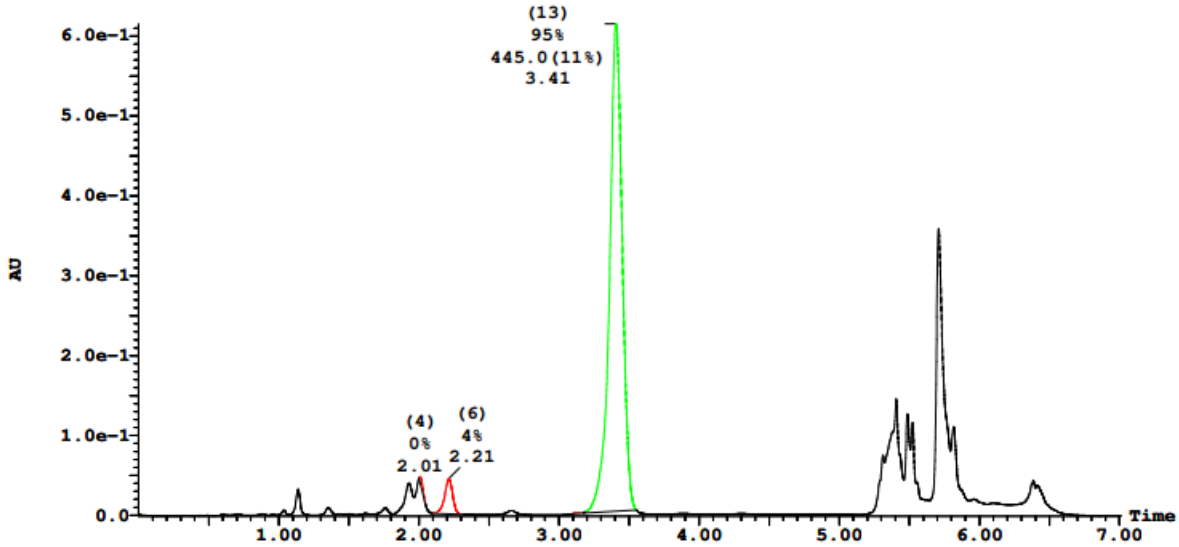

Peak Number	Compound	Time	AreaAbs	Area %Total	Width	Height	Mass Found
4		2.01	2e+002	0.36	0	7e+003	Not Found
6		2.21	3e+003	4.30	0	4e+004	Not Found
11		3.18	9e+001	0.14	0	1e+003	Not Found
13	Found	3.41	6e+004	95.20	0	6e+005	445.0000

F12: 91% ee

Openlynx Report - SHARLJA1

Sample: 72
File:SHARLJA1_20211115_72
Description:(S,S)WO1 4.6x100mm 5µ

Vial:2:24
Date:16-Nov-2021
Conditions:5% IPA over 5min 3mL/min

ID:27-F12
Time:11:53:32

Printed: Thu Dec 09 16:42:06 2021

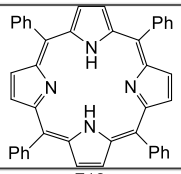

F12,
91% ee

Sample Report (continued):

Sample 72 Vial 2:24 ID 27-F12 File SHARLJA1_20211115_72 Date 16-Nov-2021 Time 11:53:32 Description (S,S)WO1 4.6x100mm 5µ

2: UV Detector: 230 Nm 2.0000-2.3500: Smooth (Mn, 2x3), 3.1000-3.5500: Smooth (Mn, 2x3) 7.204e-1
Range: 7.21e-1

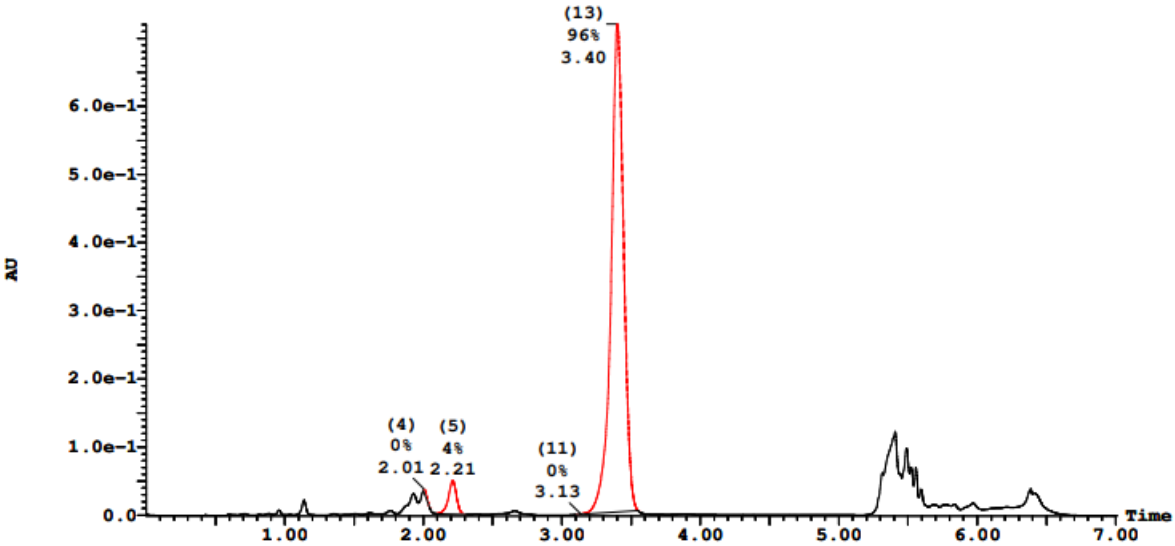

Peak Number	Compound	Time	AreaAbs	Area %Total	Width	Height	Mass Found
4		2.01	2e+002	0.21	0	4e+003	Not Found
5		2.21	3e+003	4.19	0	5e+004	Not Found
11		3.13	9e+000	0.01	0	5e+002	Not Found
13		3.40	8e+004	95.58	0	7e+005	Not Found

G1: 89% ee

Openlynx Report - SHARLJA1

Sample: 73
File:SHARLJA1_20211115_73
Description:(S,S)WO1 4.6x100mm 5µ

Vial:2:25
Date:16-Nov-2021
Conditions:5% IPA over 5min 3mL/min

ID:27-G1
Time:12:01:41

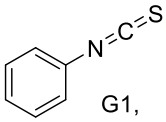

G1,
89% ee

Printed: Thu Dec 09 16:42:06 2021

Sample Report (continued):

Sample 73 Vial 2:25 ID 27-G1 File SHARLJA1_20211115_73 Date 16-Nov-2021 Time 12:01:41 Description (S,S)WO1 4.6x100mm 5µ

2: UV Detector: 230 Nm 2.0000-2.3500: Smooth (Mn, 2x3), 3.1000-3.5500: Smooth (Mn, 2x3) 4.499e-1
Range: 4.509e-1

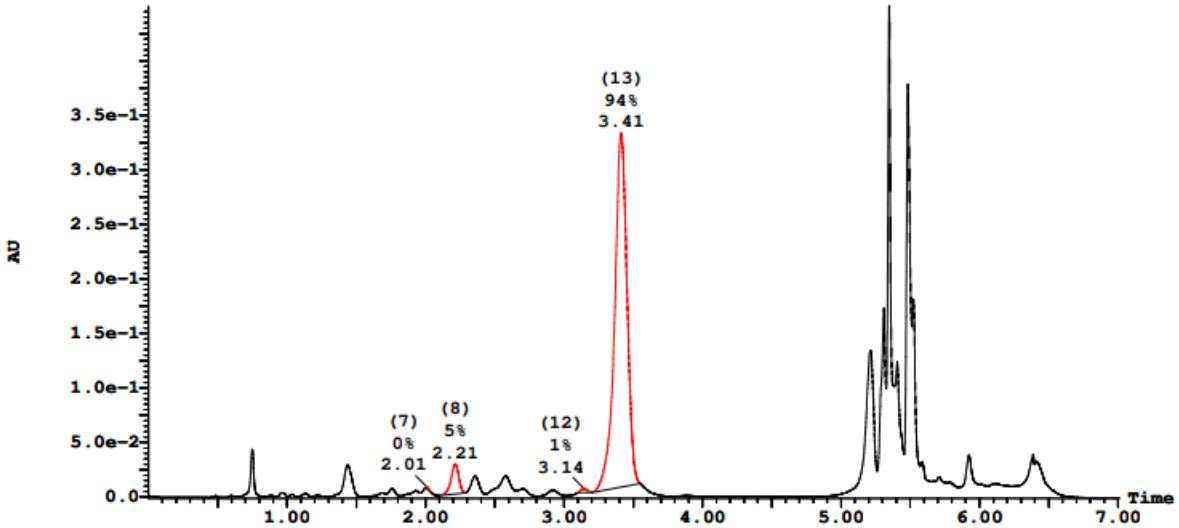

Peak Number	Compound	Time	AreaAbs	Area %Total	Width	Height	Mass Found
7		2.01	5e+001	0.13	0	1e+003	Not Found
8		2.21	2e+003	4.93	0	3e+004	Not Found
12		3.14	2e+002	0.52	0	3e+003	Not Found
13		3.41	3e+004	94.42	0	3e+005	Not Found

G2: 91% ee

Openlynx Report - SHARLJA1

Sample: 74
File:SHARLJA1_20211115_74
Description:(S,S)WO1 4.6x100mm 5µ

Vial:2:26
Date:16-Nov-2021
Conditions:5% IPA over 5min 3mL/min

ID:27-G2
Time:12:09:48

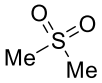

G2,
91% ee

Printed: Thu Dec 09 16:42:06 2021

Sample Report (continued):

Sample 74 Vial 2:26 ID 27-G2 File SHARLJA1_20211115_74 Date 16-Nov-2021 Time 12:09:48 Description (S,S)WO1 4.6x100mm 5µ

2: UV Detector: 230 Nm 2.0000-2.3500: Smooth (Mn, 2x3), 3.1000-3.5500: Smooth (Mn, 2x3) 6.691e-1
Range: 6.705e-1

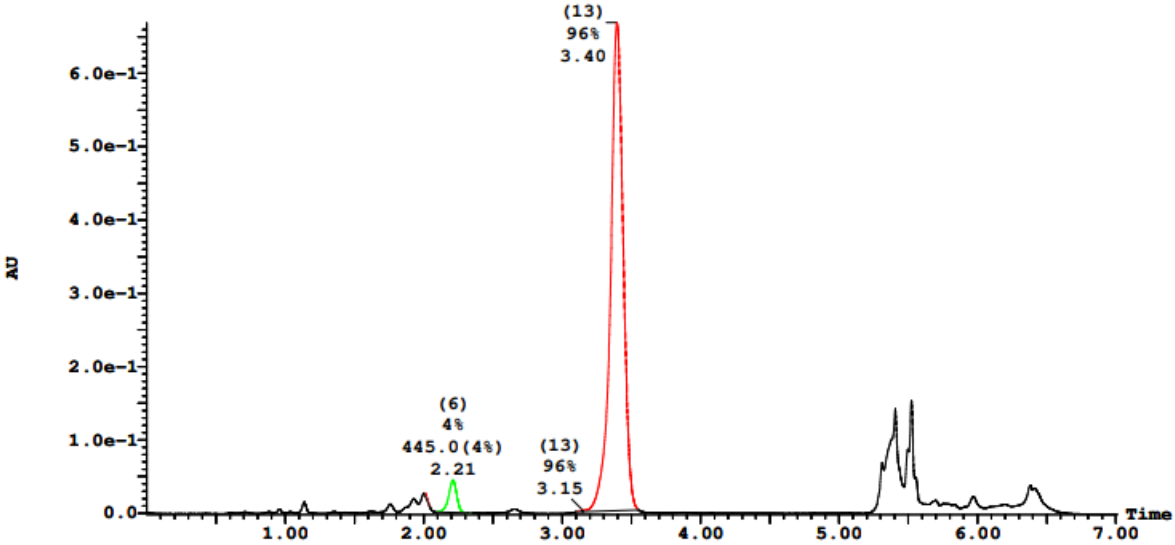

Peak Number	Compound	Time	AreaAbs	Area %Total	Width	Height	Mass Found
5		2.01	1e+002	0.15	0	3e+003	Not Found
6	Found	2.21	3e+003	4.06	0	4e+004	445.0000
7	Tentative	2.33	8e-001	0.00	0	5e+001	445.0000
11		3.15	5e+001	0.07	0	2e+003	Not Found
13		3.40	7e+004	95.72	0	7e+005	Not Found

G5: 91% ee

Openlynx Report - SHARLJA1

Sample: 77
File:SHARLJA1_20211115_77
Description:(S,S)WO1 4.6x100mm 5µ

Vial:2:29
Date:16-Nov-2021
Conditions:5% IPA over 5min 3mL/min

ID:27-G5
Time:12:34:13

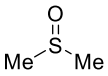

G5,
91% ee

Printed: Thu Dec 09 16:42:06 2021

Sample Report (continued):

Sample 77 Vial 2:29 ID 27-G5 File SHARLJA1_20211115_77 Date 16-Nov-2021 Time 12:34:13 Description (S,S)WO1 4.6x100mm 5µ

2: UV Detector: 230 Nm 2.0000-2.3500: Smooth (Mn, 2x3), 3.1000-3.5500: Smooth (Mn, 2x3) 4.89e-1
Range: 4.899e-1

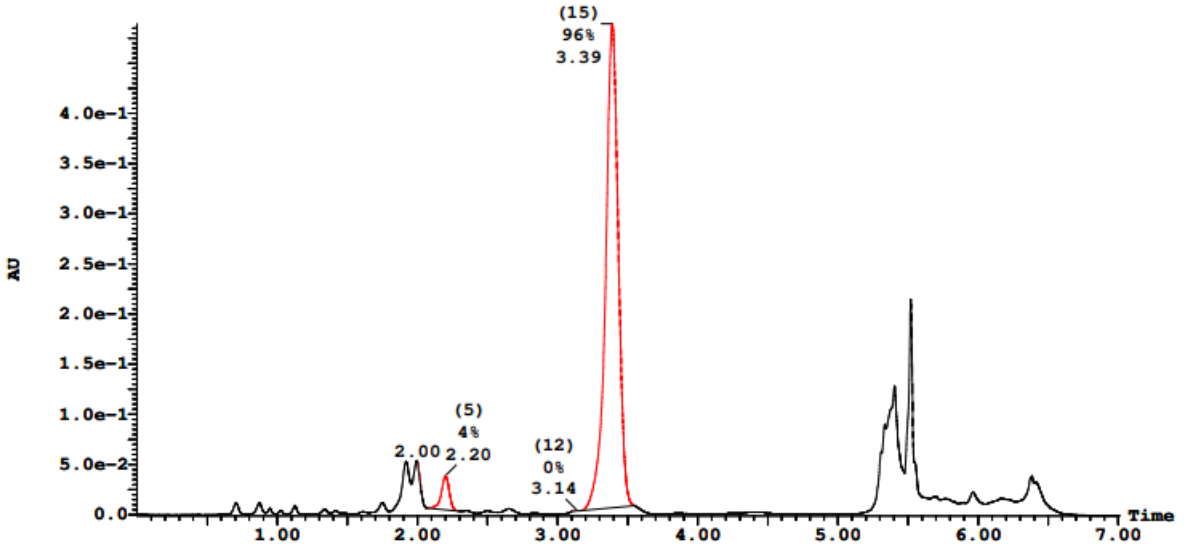

Peak Number	Compound	Time	AreaAbs	Area %Total	Width	Height	Mass Found
4		2.00	4e+001	0.07	0	7e-002	Not Found
5		2.20	2e+003	4.27	0	3e+004	Not Found
12		3.14	3e+001	0.05	0	7e+002	Not Found
15		3.39	5e+004	95.61	0	5e+005	Not Found

G6: 90% ee

Openlynx Report - SHARLJA1

Sample: 78
File:SHARLJA1_20211115_78
Description:(S,S)WO1 4.6x100mm 5µ

Vial:2:30
Date:16-Nov-2021
Conditions:5% IPA over 5min 3mL/min

ID:27-G6
Time:12:42:20

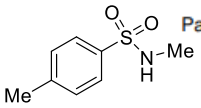

G6,
90% ee

Printed: Thu Dec 09 16:42:06 2021

Sample Report (continued):

Sample 78 Vial 2:30 ID 27-G6 File SHARLJA1_20211115_78 Date 16-Nov-2021 Time 12:42:20 Description (S,S)WO1 4.6x100mm 5µ

2: UV Detector: 230 Nm 2.0000-2.3500: Smooth (Mn, 2x3), 3.1000-3.5500: Smooth (Mn, 2x3) 2.812
Range: 2.813

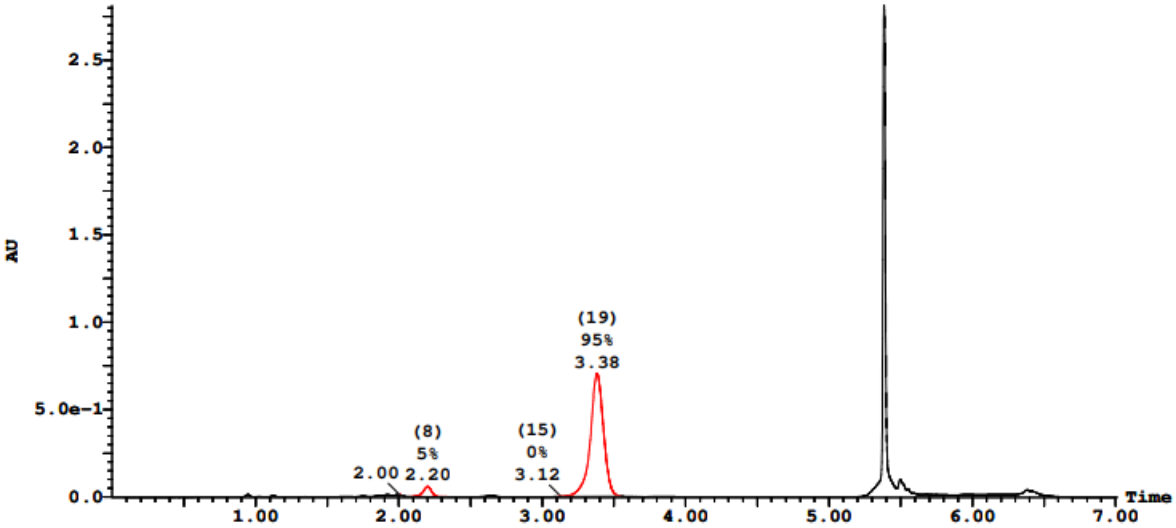

Peak Number	Compound	Time	AreaAbs	Area %Total	Width	Height	Mass Found
7		2.00	9e+000	0.01	0	2e-002	Not Found
8		2.20	4e+003	5.00	0	6e+004	Not Found
10		2.33	1e+001	0.01	0	3e+002	Not Found
15		3.12	1e+001	0.01	0	7e+002	Not Found
19		3.38	8e+004	94.96	0	7e+005	Not Found

G7: 87% ee

Openlynx Report - SHARLJA1

Sample: 79
File:SHARLJA1_20211115_79
Description:(S,S)WO1 4.6x100mm 5µ

Vial:2:31
Date:16-Nov-2021
Conditions:5% IPA over 5min 3mL/min

ID:27-G7
Time:12:50:27

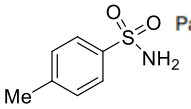

G7,
87% ee

Printed: Thu Dec 09 16:42:06 2021

Sample Report (continued):

Sample 79 Vial 2:31 ID 27-G7 File SHARLJA1_20211115_79 Date 16-Nov-2021 Time 12:50:27 Description (S,S)WO1 4.6x100mm 5µ

2: UV Detector: 230 Nm 2.0000-2.3500: Smooth (Mn, 2x3), 3.1000-3.5500: Smooth (Mn, 2x3) 2.687
Range: 2.688

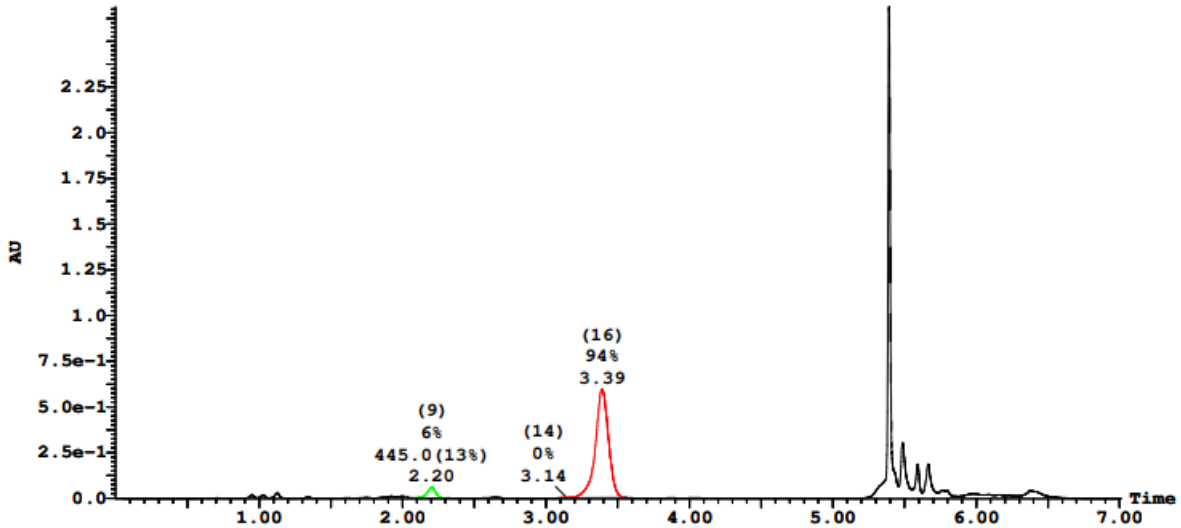

Peak Number	Compound	Time	AreaAbs	Area %Total	Width	Height	Mass Found
7		2.00	1e+001	0.02	0	1e-002	Not Found
9	Found	2.20	4e+003	5.98	0	6e+004	445.0000
10		2.31	1e+001	0.02	0	6e+002	Not Found
10		2.33	2e+000	0.00	0	3e+002	Not Found
14		3.14	3e+001	0.04	0	1e+003	Not Found
16		3.39	6e+004	93.93	0	6e+005	Not Found

G8: 90% ee

Openlynx Report - SHARLJA1

Sample: 80
File:SHARLJA1_20211115_80
Description:(S,S)WO1 4.6x100mm 5µ

Vial:2:32
Date:16-Nov-2021
Conditions:5% IPA over 5min 3mL/min

ID:27-G8
Time:12:58:35

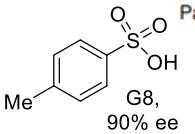

G8,
90% ee

Printed: Thu Dec 09 16:42:06 2021

Sample Report (continued):

Sample 80 Vial 2:32 ID 27-G8 File SHARLJA1_20211115_80 Date 16-Nov-2021 Time 12:58:35 Description (S,S)WO1 4.6x100mm 5µ

2: UV Detector: 230 Nm 2.0000-2.3500: Smooth (Mn, 2x3), 3.1000-3.5500: Smooth (Mn, 2x3) 4.723e-1
Range: 4.737e-1

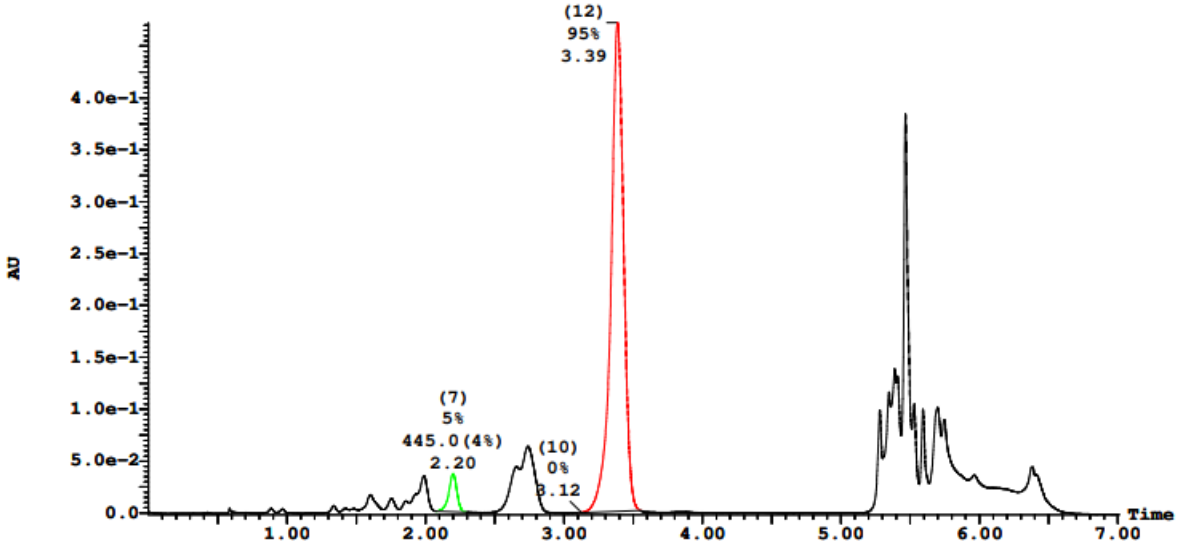

Peak Number	Compound	Time	AreaAbs	Area %Total	Width	Height	Mass Found
7	Found	2.20	3e+003	4.76	0	4e+004	445.0000
10		3.12	4e+000	0.01	0	3e+002	Not Found
12		3.39	5e+004	95.23	0	5e+005	Not Found

G9: 90% ee

Openlynx Report - SHARLJA1

Sample: 81
File:SHARLJA1_20211115_81
Description:(S,S)WO1 4.6x100mm 5µ

Vial:2:33
Date:16-Nov-2021
Conditions:5% IPA over 5min 3mL/min

ID:27-G9
Time:13:06:44

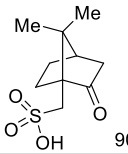

G9,
90% ee

Printed: Thu Dec 09 16:42:06 2021

Sample Report (continued):

Sample 81 Vial 2:33 ID 27-G9 File SHARLJA1_20211115_81 Date 16-Nov-2021 Time 13:06:44 Description (S,S)WO1 4.6x100mm 5µ

2: UV Detector: 230 Nm 2.0000-2.3500: Smooth (Mn, 2x3), 3.1000-3.5500: Smooth (Mn, 2x3) 5.443e-1
Range: 5.455e-1

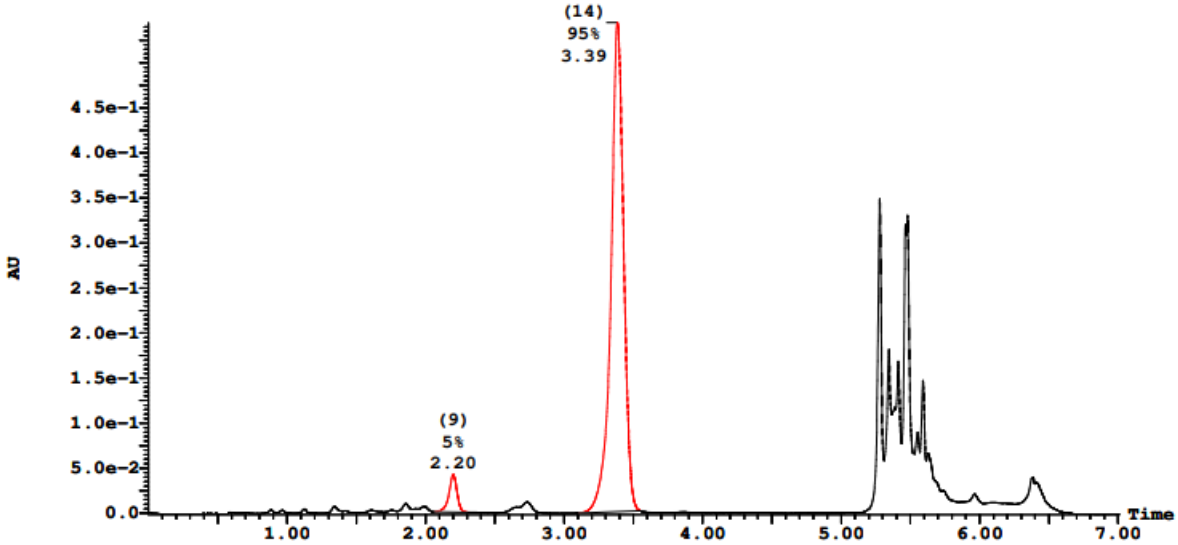

Peak Number	Compound	Time	AreaAbs	Area %Total	Width	Height	Mass Found
9		2.20	3e+003	4.71	0	4e+004	Not Found
14		3.39	6e+004	95.29	0	5e+005	Not Found

G11: 89% ee

Openlynx Report - SHARLJA1

Sample: 83
File:SHARLJA1_20211115_83
Description:(S,S)WO1 4.6x100mm 5µ

Vial:2:35
Date:16-Nov-2021
Conditions:5% IPA over 5min 3mL/min

ID:27-G11
Time:13:22:59

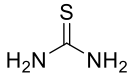

G11,
89% ee

Printed: Thu Dec 09 16:42:06 2021

Sample Report (continued):

Sample 83 Vial 2:35 ID 27-G11 File SHARLJA1_20211115_83 Date 16-Nov-2021 Time 13:22:59 Description (S,S)WO1 4.6x100mm 5µ

2: UV Detector: 230 Nm 2.0000-2.3500: Smooth (Mn, 2x3), 3.1000-3.5500: Smooth (Mn, 2x3) 8.394e-1
Range: 8.402e-1

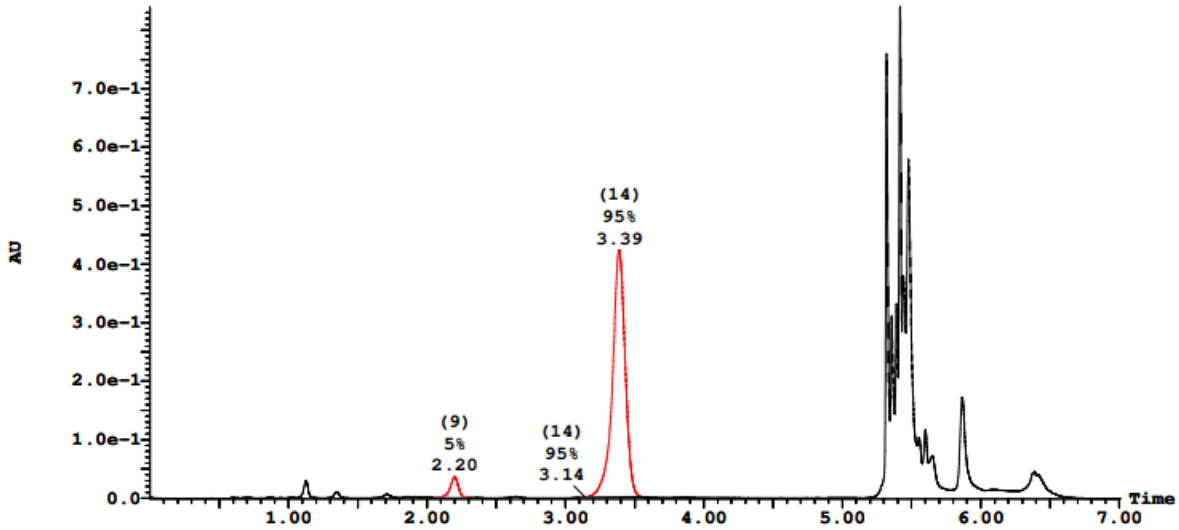

Peak Number	Compound	Time	AreaAbs	Area %Total	Width	Height	Mass Found
9		2.20	2e+003	5.18	0	4e+004	Not Found
10		2.34	1e+000	0.00	0	1e+002	Not Found
12		3.14	2e+001	0.03	0	6e+002	Not Found
14		3.39	4e+004	94.78	0	4e+005	Not Found

H1: 91% ee

Openlynx Report - SHARLJA1

Sample: 85
File:SHARLJA1_20211115_85
Description:(S,S)WO1 4.6x100mm 5µ

Vial:2:37
Date:16-Nov-2021
Conditions:5% IPA over 5min 3mL/min

ID:27-H1
Time:13:39:15

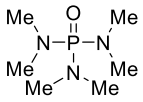

H1,
91% ee

Printed: Thu Dec 09 16:42:06 2021

Sample Report (continued):

Sample 85 Vial 2:37 ID 27-H1 File SHARLJA1_20211115_85 Date 16-Nov-2021 Time 13:39:15 Description (S,S)WO1 4.6x100mm 5µ

2: UV Detector: 230 Nm 2.0000-2.3500: Smooth (Mn, 2x3), 3.1000-3.5500: Smooth (Mn, 2x3) 6.761e-1
Range: 6.767e-1

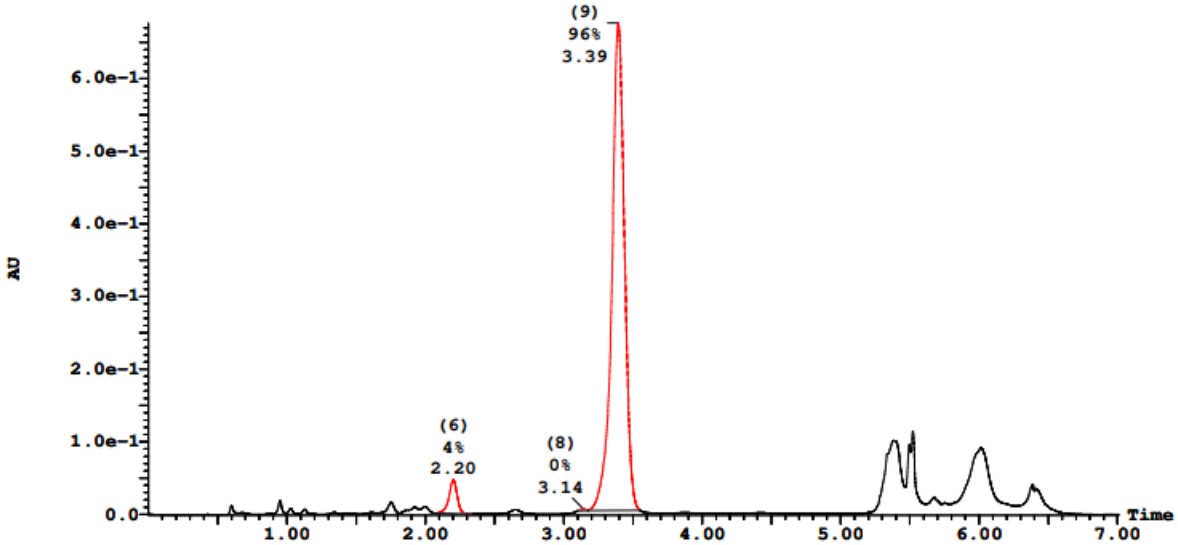

Peak Number	Compound	Time	AreaAbs	Area %Total	Width	Height	Mass Found
6		2.20	3e+003	4.29	0	5e+004	Not Found
8		3.14	1e+002	0.16	0	2e+003	Not Found
9		3.39	7e+004	95.55	0	7e+005	Not Found

H3: 91% ee

Openlynx Report - SHARLJA1

Sample: 87
File:SHARLJA1_20211115_87
Description:(S,S)WO1 4.6x100mm 5µ

Vial:2:39
Date:16-Nov-2021
Conditions:5% IPA over 5min 3mL/min

ID:27-H3
Time:13:55:31

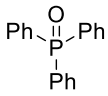

H3,
91% ee

Printed: Thu Dec 09 16:42:06 2021

Sample Report (continued):

Sample 87 Vial 2:39 ID 27-H3 File SHARLJA1_20211115_87 Date 16-Nov-2021 Time 13:55:31 Description (S,S)WO1 4.6x100mm 5µ

2: UV Detector: 230 Nm 2.0000-2.3500: Smooth (Mn, 2x3), 3.1000-3.5500: Smooth (Mn, 2x3) 1.32
Range: 1.321

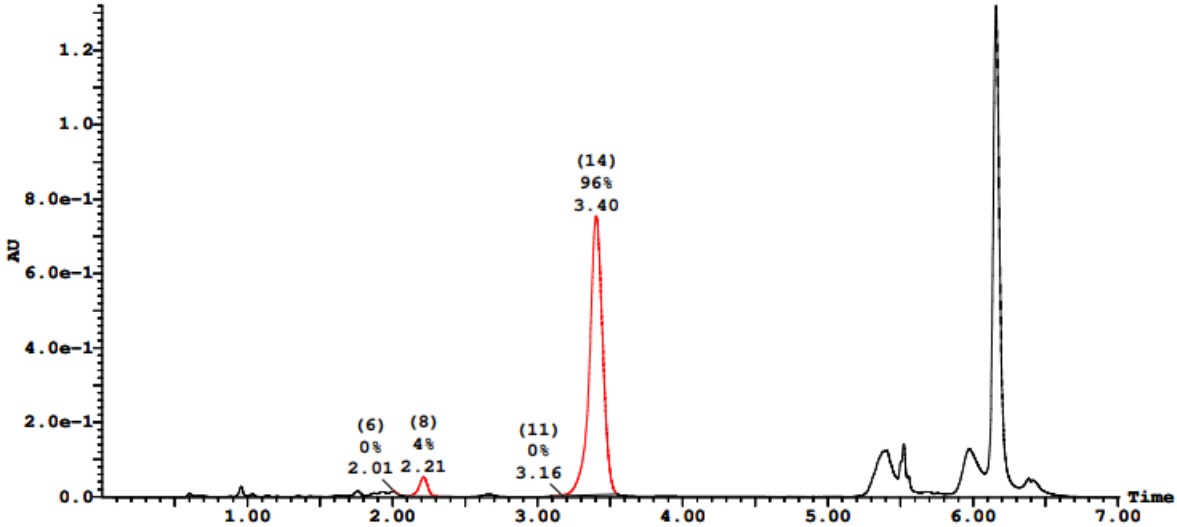

Peak Number	Compound	Time	AreaAbs	Area %Total	Width	Height	Mass Found
6		2.01	8e+001	0.09	0	2e+003	Not Found
8		2.21	4e+003	4.28	0	5e+004	Not Found
11		3.16	9e+001	0.11	0	2e+003	Not Found
14		3.40	8e+004	95.52	0	7e+005	Not Found

H6: 90% ee

Openlynx Report - SHARLJA1

Sample: 90
File:SHARLJA1_20211115_90
Description:(S,S)WO1 4.6x100mm 5µ

Vial:2:42
Date:16-Nov-2021
Conditions:5% IPA over 5min 3mL/min

ID:27-H6
Time:16:55:29

Me−CN
H6,
90% ee

Printed: Thu Dec 09 16:42:06 2021

Sample Report (continued):

Sample 90 Vial 2:42 ID 27-H6 File SHARLJA1_20211115_90 Date 16-Nov-2021 Time 16:55:29 Description (S,S)WO1 4.6x100mm 5µ

2: UV Detector: 230 Nm 2.0000-2.3500: Smooth (Mn, 2x3), 3.1000-3.5500: Smooth (Mn, 2x3) 7.273e-1
Range: 7.278e-1

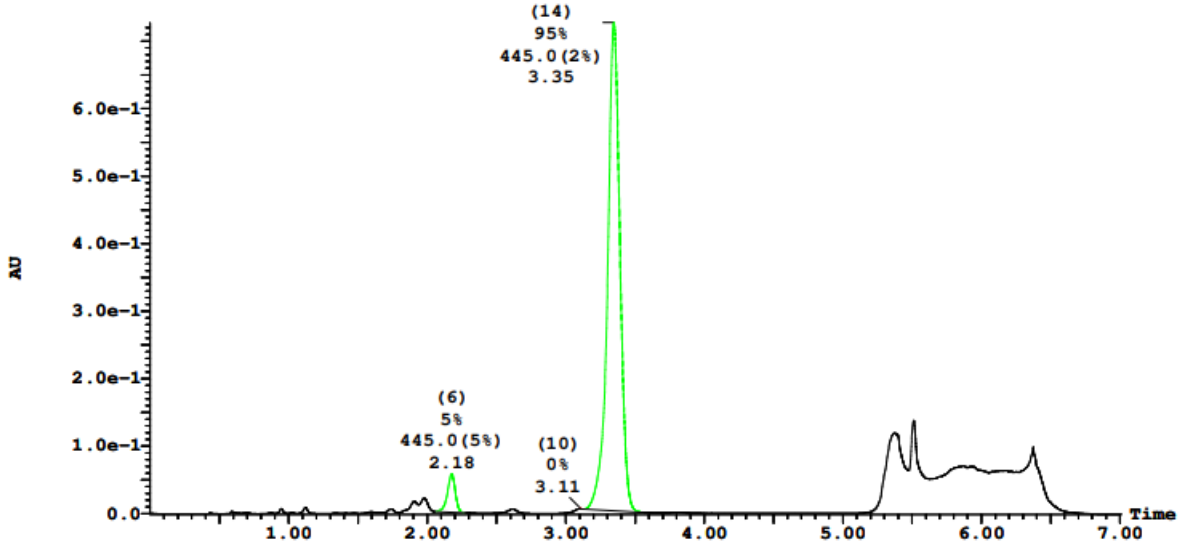

Peak Number	Compound	Time	AreaAbs	Area %Total	Width	Height	Mass Found
6	Found	2.18	4e+003	4.73	0	6e+004	445.0000
10		3.11	3e+000	0.00	0	1e+002	Not Found
14	Tentative	3.35	7e+004	95.26	0	7e+005	445.0000

H7: 92% ee

Openlynx Report - SHARLJA1

Sample: 91
File:SHARLJA1_20211115_91
Description:(S,S)WO1 4.6x100mm 5µ

Vial:2:43
Date:16-Nov-2021
Conditions:5% IPA over 5min 3mL/min

ID:27-H7
Time:17:03:38

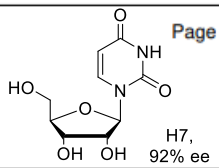

Printed: Thu Dec 09 16:42:06 2021

Sample Report (continued):

Sample 91 Vial 2:43 ID 27-H7 File SHARLJA1_20211115_91 Date 16-Nov-2021 Time 17:03:38 Description (S,S)WO1 4.6x100mm 5µ

2: UV Detector: 230 Nm 2.0000-2.3500: Smooth (Mn, 2x3), 3.1000-3.5500: Smooth (Mn, 2x3) 6.649e-1
Range: 6.65e-1

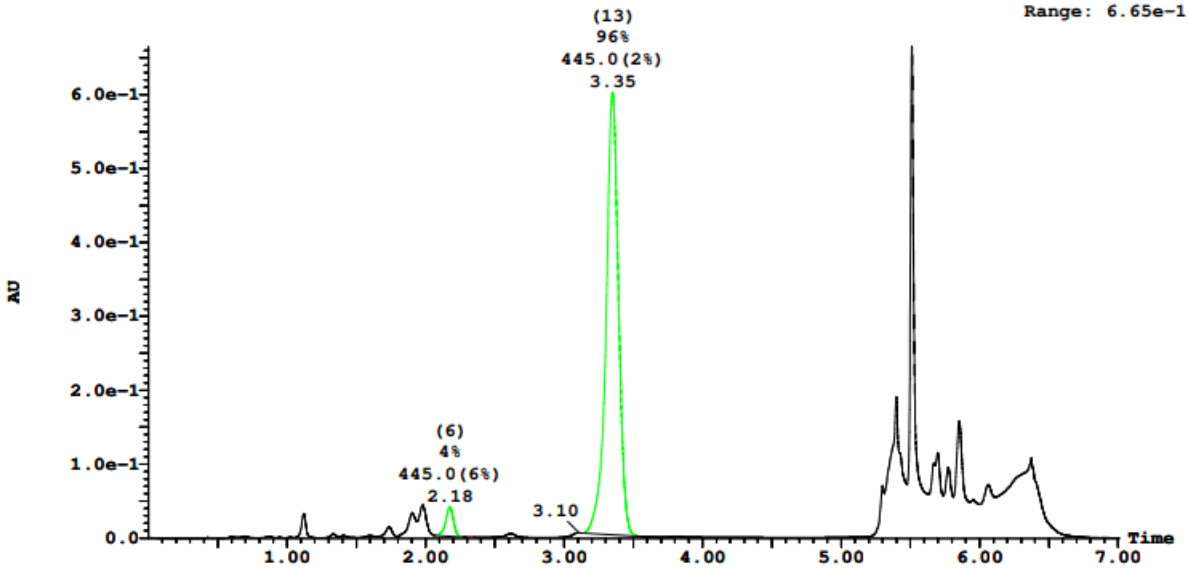

Peak Number	Compound	Time	AreaAbs	Area %Total	Width	Height	Mass Found
6	Found	2.18	3e+003	3.96	0	4e+004	445.0000
7		2.30	1e+000	0.00	0	1e+001	Not Found
10		3.10	2e+000	0.00	0	9e+001	Not Found
13	Tentative	3.35	6e+004	96.03	0	6e+005	445.0000

H8: 90% ee

Openlynx Report - SHARLJA1

Sample: 92
File:SHARLJA1_20211115_92
Description:(S,S)WO1 4.6x100mm 5µ

Vial:2:44
Date:16-Nov-2021
Conditions:5% IPA over 5min 3mL/min

ID:27-H8
Time:17:11:46

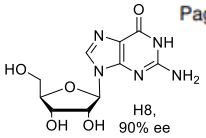

Printed: Thu Dec 09 16:42:06 2021

Sample Report (continued):

Sample 92 Vial 2:44 ID 27-H8 File SHARLJA1_20211115_92 Date 16-Nov-2021 Time 17:11:46 Description (S,S)WO1 4.6x100mm 5µ

2: UV Detector: 230 Nm 2.0000-2.3500: Smooth (Mn, 2x3), 3.1000-3.5500: Smooth (Mn, 2x3) 5.041e-1
Range: 5.046e-1

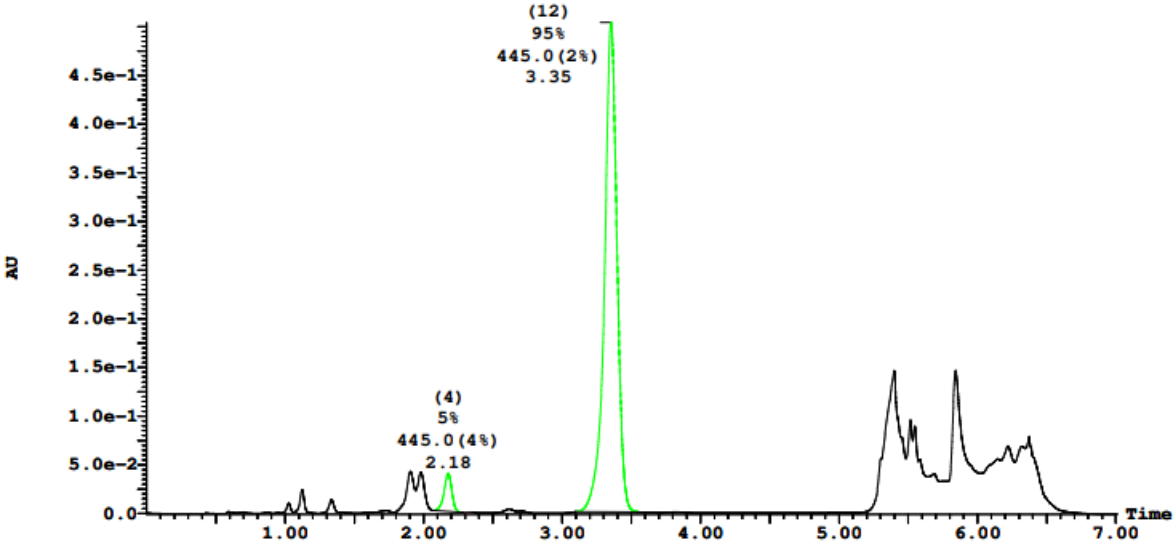

Peak Number	Compound	Time	AreaAbs	Area %Total	Width	Height	Mass Found
4	Tentative	2.18	3e+003	4.61	0	4e+004	445.0000
5		2.34	5e+000	0.01	0	2e+002	Not Found
12	Tentative	3.35	5e+004	95.38	0	5e+005	445.0000

H9: 86% ee

Openlynx Report - SHARLJA1

Sample: 93
File:SHARLJA1_20211115_93
Description:(S,S)WO1 4.6x100mm 5µ

Vial:2:45
Date:16-Nov-2021
Conditions:5% IPA over 5min 3mL/min

ID:27-H9
Time:17:19:54

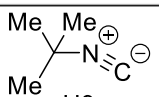

H9,
86% ee

Printed: Thu Dec 09 16:42:06 2021

Sample Report (continued):

Sample 93 Vial 2:45 ID 27-H9 File SHARLJA1_20211115_93 Date 16-Nov-2021 Time 17:19:54 Description (S,S)WO1 4.6x100mm 5µ

2: UV Detector: 230 Nm 2.0000-2.3500: Smooth (Mn, 2x3), 3.1000-3.5500: Smooth (Mn, 2x3) 8.249e-1
Range: 8.253e-1

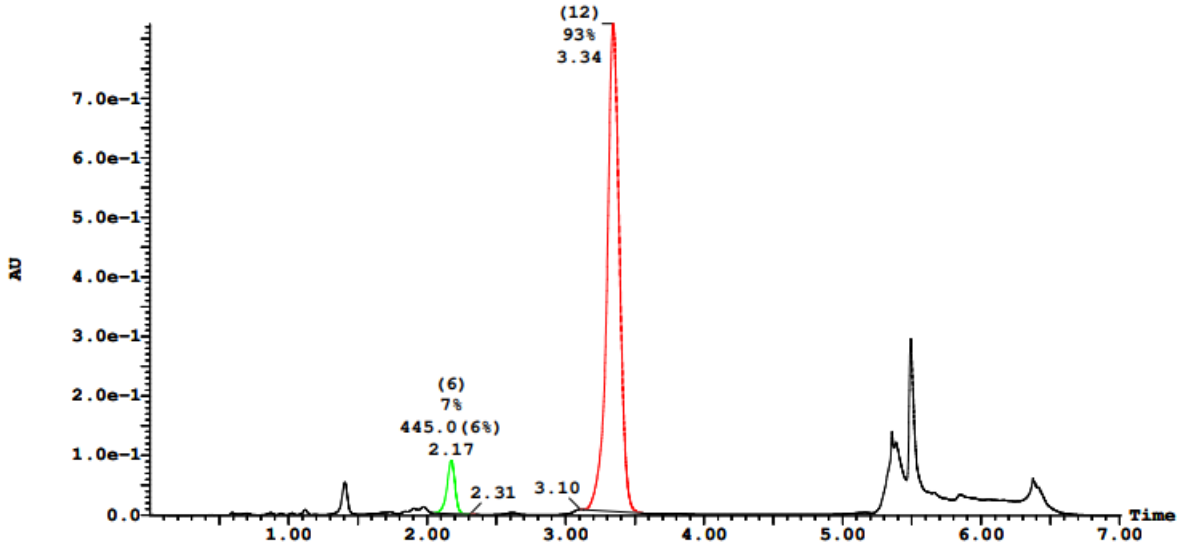

Peak Number	Compound	Time	AreaAbs	Area %Total	Width	Height	Mass Found
6	Found	2.17	6e+003	6.61	0	9e+004	445.0000
8		2.31	4e-001	0.00	0		Not Found
8		2.34	1e-001	0.00	0	4e+000	Not Found
10		3.10	2e+000	0.00	0	1e+002	Not Found
12		3.34	9e+004	93.38	0	8e+005	Not Found

H10: 91% ee

Openlynx Report - SHARLJA1
Sample: 94
File:SHARLJA1_20211115_94
Description:(S,S)WO1 4.6x100mm 5µ

Vial:2:46
Date:16-Nov-2021
Conditions:5% IPA over 5min 3mL/min

ID:27-H10
Time:17:28:01

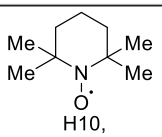

Printed: Thu Dec 09 16:42:06 2021

Sample Report (continued):

Sample 94 Vial 2:46 ID 27-H10 File SHARLJA1_20211115_94 Date 16-Nov-2021 Time 17:28:01 Description (S,S)WO1 4.6x100mm 5µ

2: UV Detector: 230 Nm 2.0000-2.3500: Smooth (Mn, 2x3), 3.1000-3.5500: Smooth (Mn, 2x3) 6.224e-1
Range: 6.226e-1

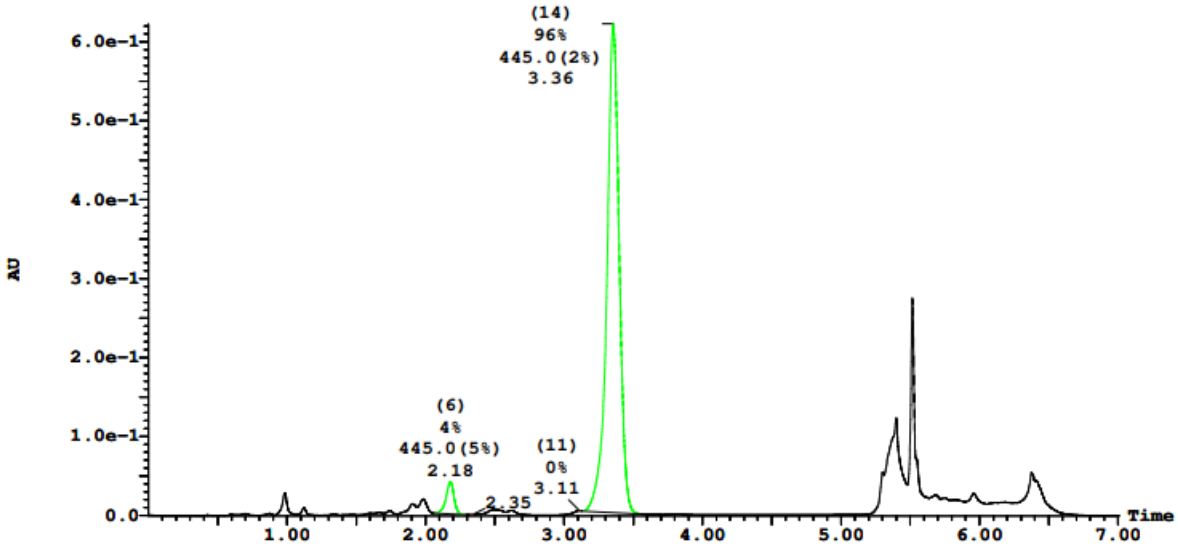

Peak Number	Compound	Time	AreaAbs	Area %Total	Width	Height	Mass Found
6	Found	2.18	3e+003	4.11	0	4e+004	445.0000
7		2.35	6e-001	0.00	0		Not Found
11		3.11	6e+000	0.01	0	3e+002	Not Found
14	Tentative	3.36	6e+004	95.88	0	6e+005	445.0000

H12: 92% ee

Openlynx Report - SHARLJA1

Sample: 96
File:SHARLJA1_20211115_96
Description:(S,S)WO1 4.6x100mm 5µ

Vial:2:48
Date:16-Nov-2021
Conditions:5% IPA over 5min 3mL/min

ID:27-H12
Time:17:44:17

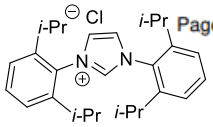

H12,
92% ee

Printed: Thu Dec 09 16:42:06 2021

Sample Report (continued):

Sample 96 Vial 2:48 ID 27-H12 File SHARLJA1_20211115_96 Date 16-Nov-2021 Time 17:44:17 Description (S,S)WO1 4.6x100mm 5µ

2: UV Detector: 230 Nm 2.0000-2.3500: Smooth (Mn, 2x3), 3.1000-3.5500: Smooth (Mn, 2x3) 5.685e-1
Range: 5.688e-1

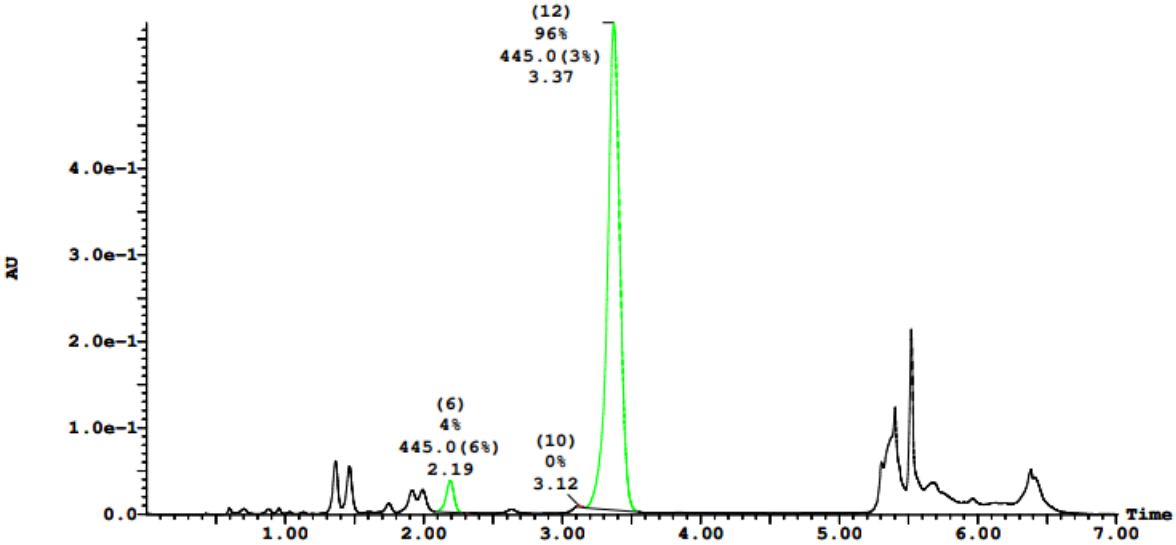

Peak Number	Compound	Time	AreaAbs	Area %Total	Width	Height	Mass Found
6	Found	2.19	2e+003	3.95	0	4e+004	445.0000
7		2.30	7e-001	0.00	0	1e+001	Not Found
10		3.12	5e+001	0.08	0	1e+003	Not Found
12	Tentative	3.37	6e+004	95.97	0	6e+005	445.0000

6. Reactions run at lab (0.10mmol) scale

6.1: Enantioselectivity of cyclopropanes synthesized with chiral catalysts was determined by chiral HPLC, UHPLC, of SFC (summarized in Table 9 in main text).

Table C1: Catalyst screen for benchmark cyclopropanation:

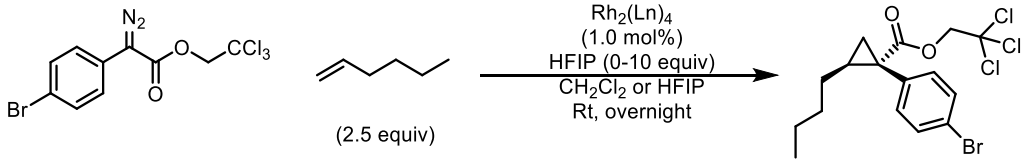

(-) % ee denotes opposite enantiomer was obtained

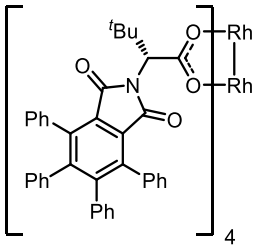

Rh_2(*R*-TPPTTL)$_4$, 5

No HFIP: 89% ee
10 equiv HFIP: 58% ee
HFIP as solvent: 15% ee

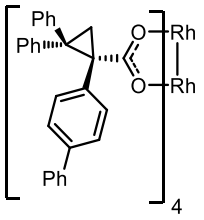

Rh_2(*R*-p-Ph-TPCP)$_4$, 16

No HFIP: 98% ee
10 equiv HFIP: 90% ee
HFIP as solvent: 49% ee

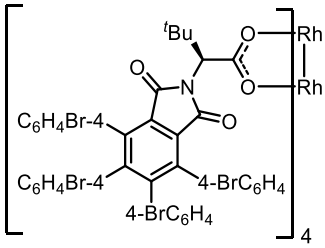

Rh_2(*S-tetra-p*-BrPhPTTL)$_4$, 17

No HFIP: -98% ee
10 equiv HFIP: -98% ee
HFIP as solvent: -72% ee

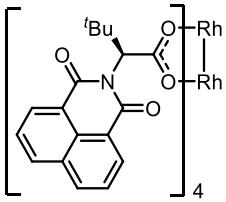

Rh_2(*S*-NTTL)$_4$, 18

No HFIP: 36% ee
10 equiv HFIP: 71% ee
HFIP as solvent: 90% ee

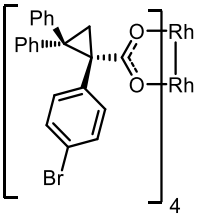

Rh_2(*R*-p-Br-TPCP)$_4$

No HFIP: 94% ee
10 equiv HFIP: 92% ee
HFIP as solvent: 54% ee

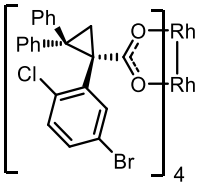

Rh_2(*S*-2Cl5Br-TPCP)$_4$

No HFIP: 64% ee
10 equiv HFIP: 45% ee

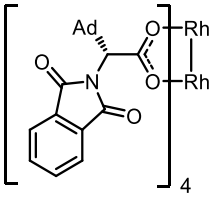

Rh_2(*R*-PTAD)$_4$

No HFIP: -64% ee
10 equiv HFIP: -68% ee
HFIP as solvent: -82% ee

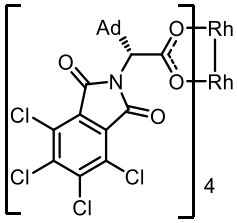

Rh_2(*R*-TCPTAD)$_4$

No HFIP: 75% ee
HFIP as solvent: -72% ee

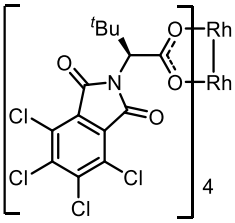

Rh_2(*S*-TCPTTL)$_4$

10 equiv HFIP: -76% ee
HFIP as solvent: 67% ee

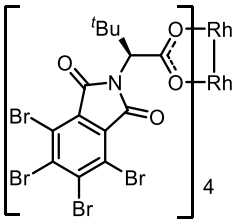

Rh_2(*S*-TBPTTL)$_4$

No HFIP: -87% ee
10 equiv HFIP: -84% ee
HFIP as solvent: -51% ee

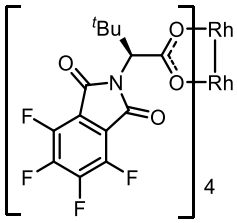

Rh_2(*S*-TFPTTL)$_4$

No HFIP: -38% ee
10 equiv HFIP: -31% ee
HFIP as solvent: 29% ee

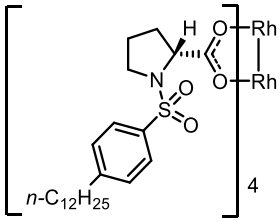

Rh_2(*R*-DOSP)$_4$

10 equiv HFIP: 41% ee
HFIP as solvent: 45% ee

Catalyst screen for cyclopropanation of 1-hexene in the presence of HFIP. All reactions were run at 0.10mmol scale according to **general procedure 3.1**. HPLC data for all entries in this table follow.

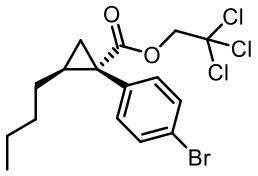
O
O
Cl
Cl
Cl
Br

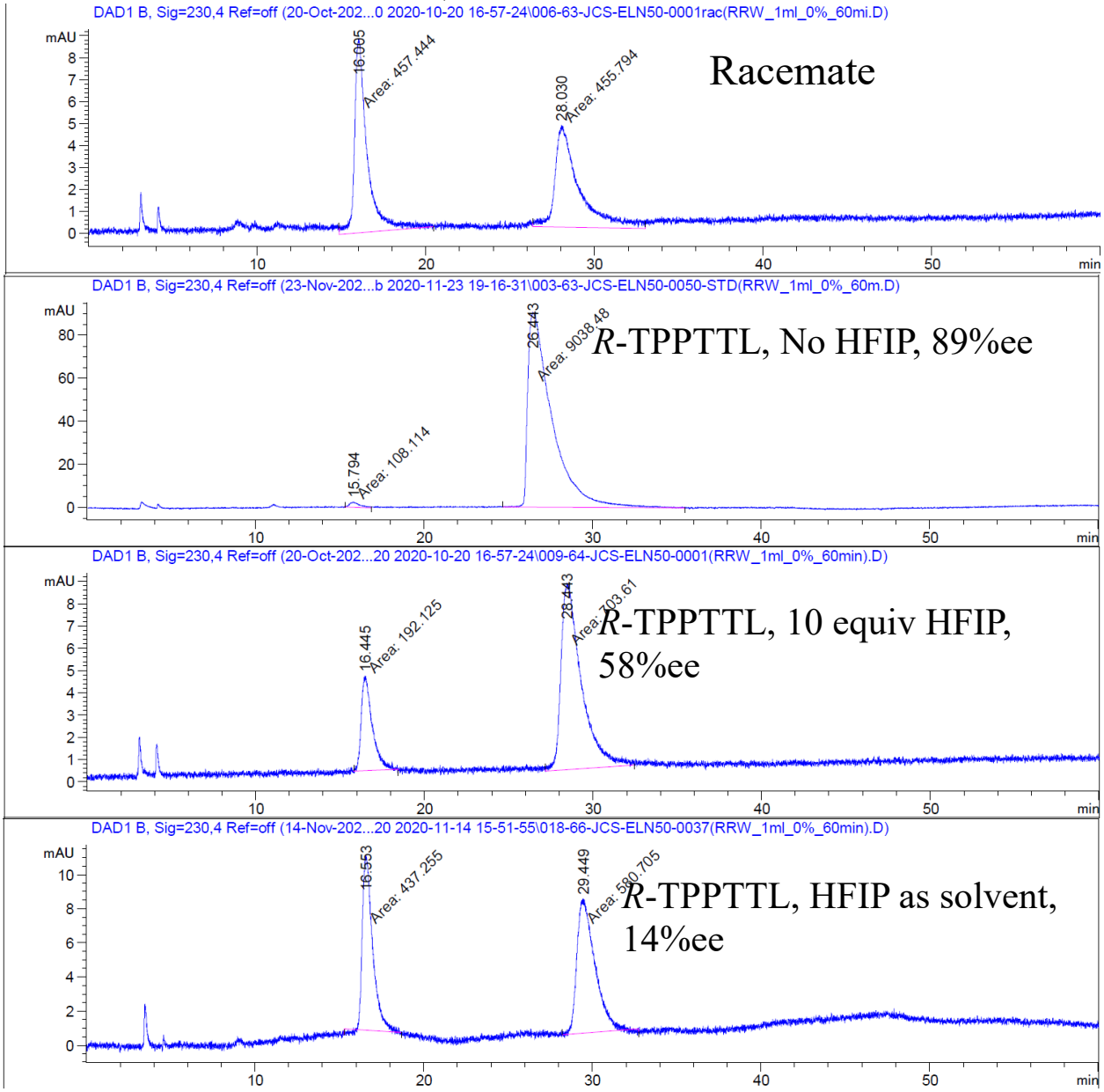
DAD1 B, Sig=230,4 Ref=off (20-Oct-202...0 2020-10-20 16-57-24\006-63-JCS-ELN50-0001rac(RRW_1ml_0%_60mi.D)
Racemate
16.065
Area: 457.444
28.030
Area: 455.794
DAD1 B, Sig=230,4 Ref=off (23-Nov-202...b 2020-11-23 19-16-31\003-63-JCS-ELN50-0050-STD(RRW_1ml_0%_60m.D)
R-TPPTTL, No HFIP, 89%ee
15.794
Area: 108.114
26.443
Area: 9038.48
DAD1 B, Sig=230,4 Ref=off (20-Oct-202...20 2020-10-20 16-57-24\009-64-JCS-ELN50-0001(RRW_1ml_0%_60min).D)
R-TPPTTL, 10 equiv HFIP, 58%ee
16.445
Area: 192.125
28.443
Area: 703.61
DAD1 B, Sig=230,4 Ref=off (14-Nov-202...20 2020-11-14 15-51-55\018-66-JCS-ELN50-0037(RRW_1ml_0%_60min).D)
R-TPPTTL, HFIP as solvent, 14%ee
16.553
Area: 437.255
29.449
Area: 580.705
mAU
min

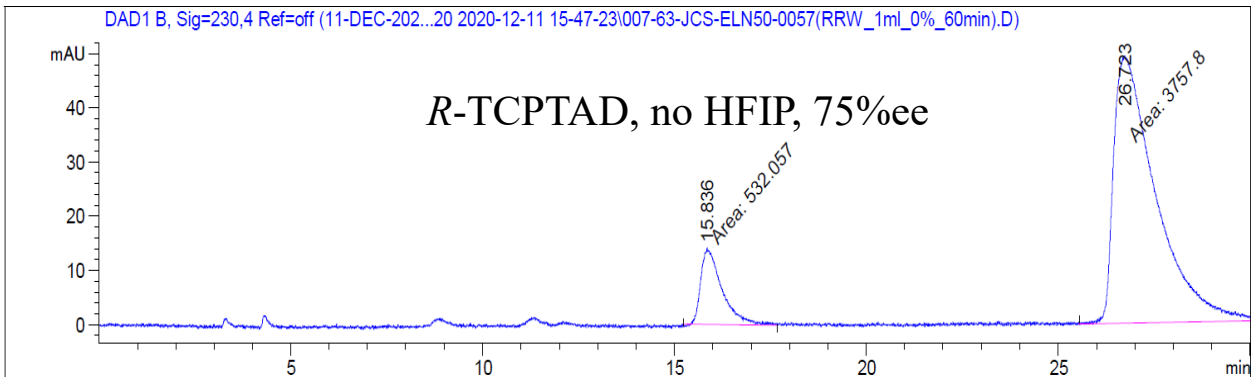
DAD1 B, Sig=230,4 Ref=off (11-DEC-202...20 2020-12-11 15-47-23\007-63-JCS-ELN50-0057(RRW_1ml_0%_60min).D)
mAU
R-TCPTAD, no HFIP, 75%ee
15.836
Area: 532.057
26.723
Area: 3757.8
min

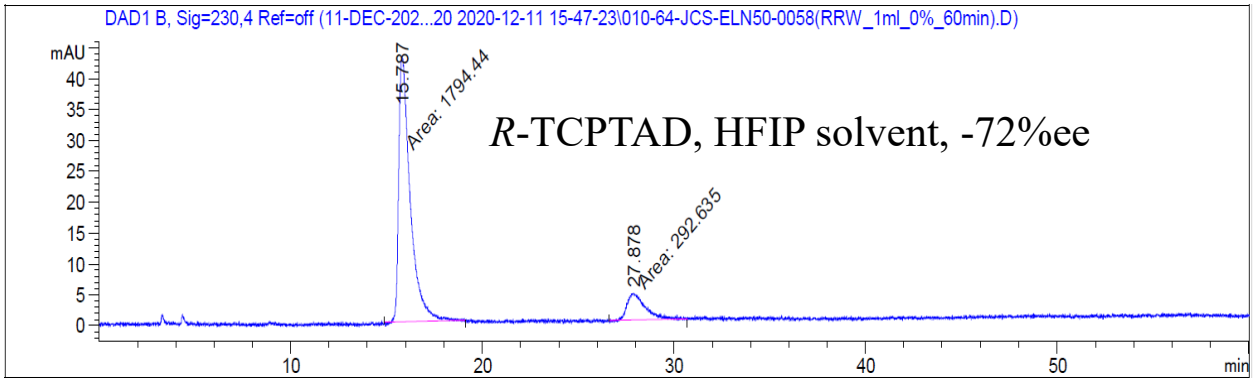
DAD1 B, Sig=230,4 Ref=off (11-DEC-202...20 2020-12-11 15-47-23\010-64-JCS-ELN50-0058(RRW_1ml_0%_60min).D)
mAU
15.787
Area: 1794.44
R-TCPTAD, HFIP solvent, -72%ee
27.878
Area: 292.635
min

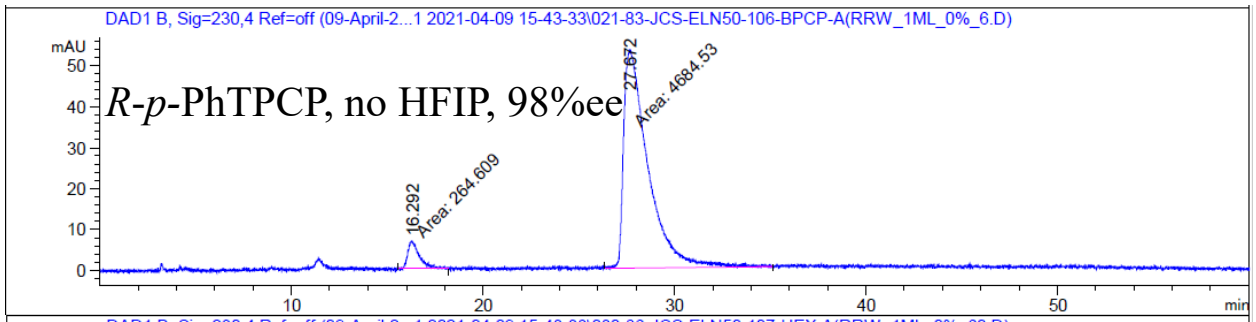
DAD1 B, Sig=230,4 Ref=off (09-April-2...1 2021-04-09 15-43-33\021-83-JCS-ELN50-106-BPCP-A(RRW_1ML_0%_6.D)
mAU
R-*p*-PhTPCP, no HFIP, 98%ee
16.292
Area: 264.609
27.672
Area: 4684.53
min

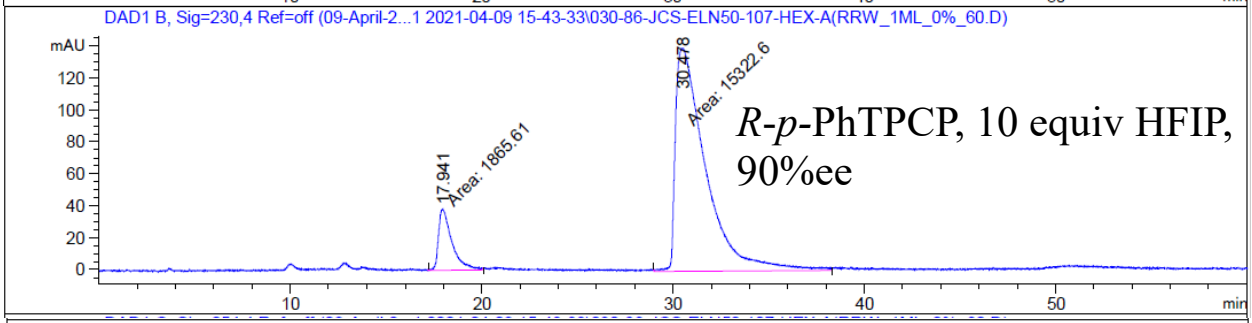
DAD1 B, Sig=230,4 Ref=off (09-April-2...1 2021-04-09 15-43-33\030-86-JCS-ELN50-107-HEX-A(RRW_1ML_0%_60.D)
mAU
17.941
Area: 1865.61
30.478
Area: 15322.6
R-*p*-PhTPCP, 10 equiv HFIP, 90%ee
min

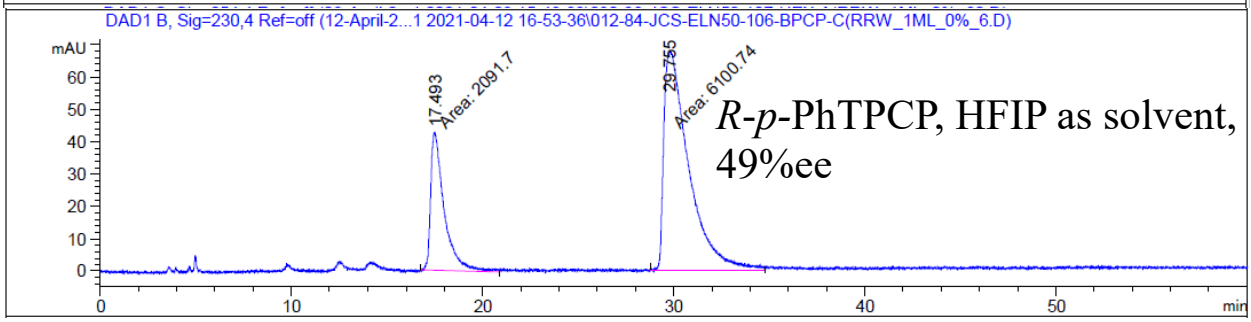
DAD1 B, Sig=230,4 Ref=off (12-April-2...1 2021-04-12 16-53-36\012-84-JCS-ELN50-106-BPCP-C(RRW_1ML_0%_6.D)
mAU
17.493
Area: 2091.7
29.755
Area: 6100.74
R-*p*-PhTPCP, HFIP as solvent, 49%ee
min

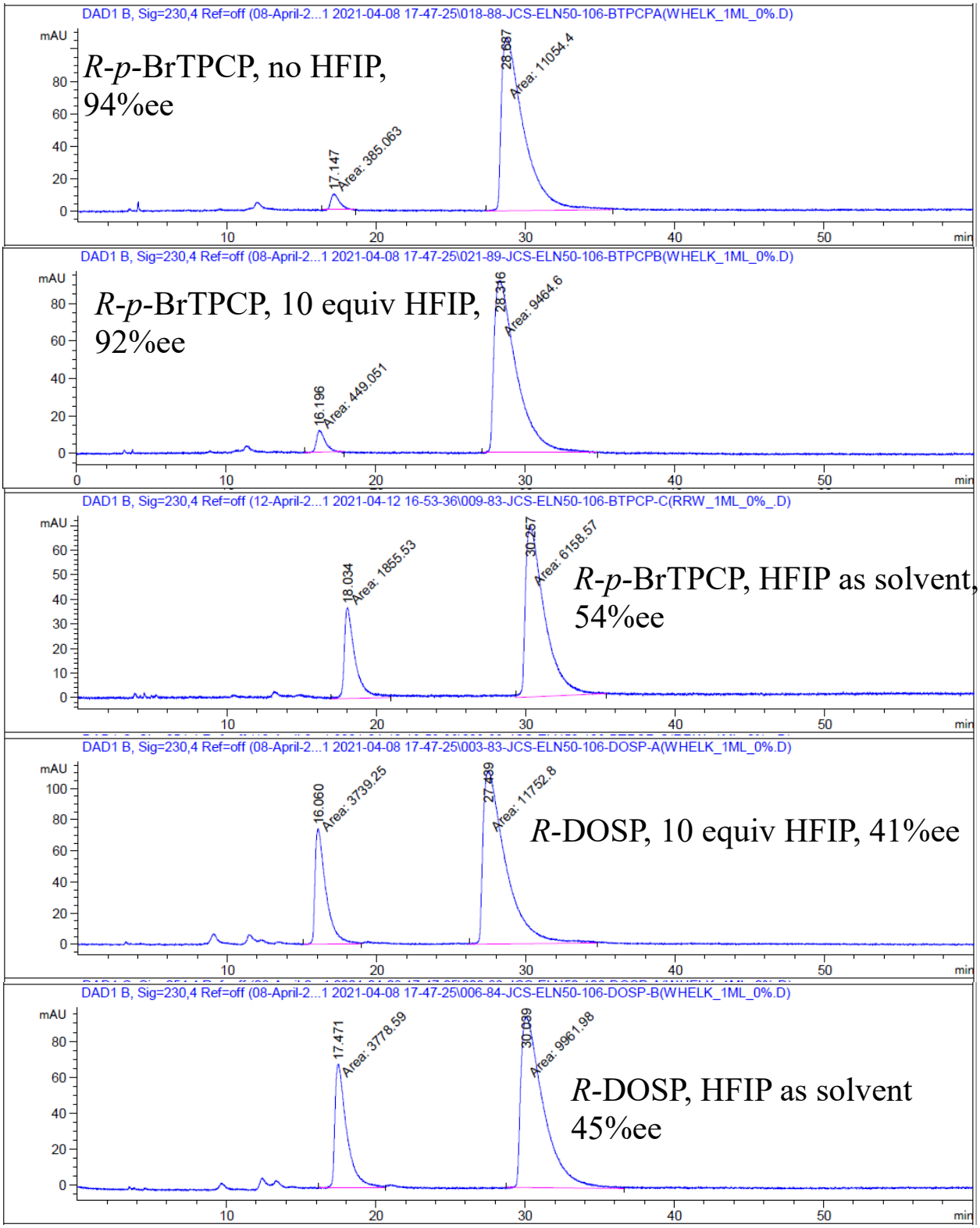
DAD1 B, Sig=230,4 Ref=off (08-April-2...1 2021-04-08 17-47-25\018-88-JCS-ELN50-106-BTPCPA(WHELK_1ML_0%.D)
R-p-BrTPCP, no HFIP, 94%ee
17.147
Area: 385.063
28.687
Area: 11054.4
DAD1 B, Sig=230,4 Ref=off (08-April-2...1 2021-04-08 17-47-25\021-89-JCS-ELN50-106-BTPCPB(WHELK_1ML_0%.D)
R-p-BrTPCP, 10 equiv HFIP, 92%ee
16.196
Area: 449.051
28.316
Area: 9464.6
DAD1 B, Sig=230,4 Ref=off (12-April-2...1 2021-04-12 16-53-36\009-83-JCS-ELN50-106-BTPCP-C(RRW_1ML_0%_.D)
18.034
Area: 1855.53
30.257
Area: 6158.57
R-p-BrTPCP, HFIP as solvent, 54%ee
DAD1 B, Sig=230,4 Ref=off (08-April-2...1 2021-04-08 17-47-25\003-83-JCS-ELN50-106-DOSP-A(WHELK_1ML_0%.D)
16.060
Area: 3739.25
27.439
Area: 11752.8
R-DOSP, 10 equiv HFIP, 41%ee
DAD1 B, Sig=230,4 Ref=off (08-April-2...1 2021-04-08 17-47-25\006-84-JCS-ELN50-106-DOSP-B(WHELK_1ML_0%.D)
17.471
Area: 3778.59
30.039
Area: 9961.98
R-DOSP, HFIP as solvent 45%ee
mAU
min

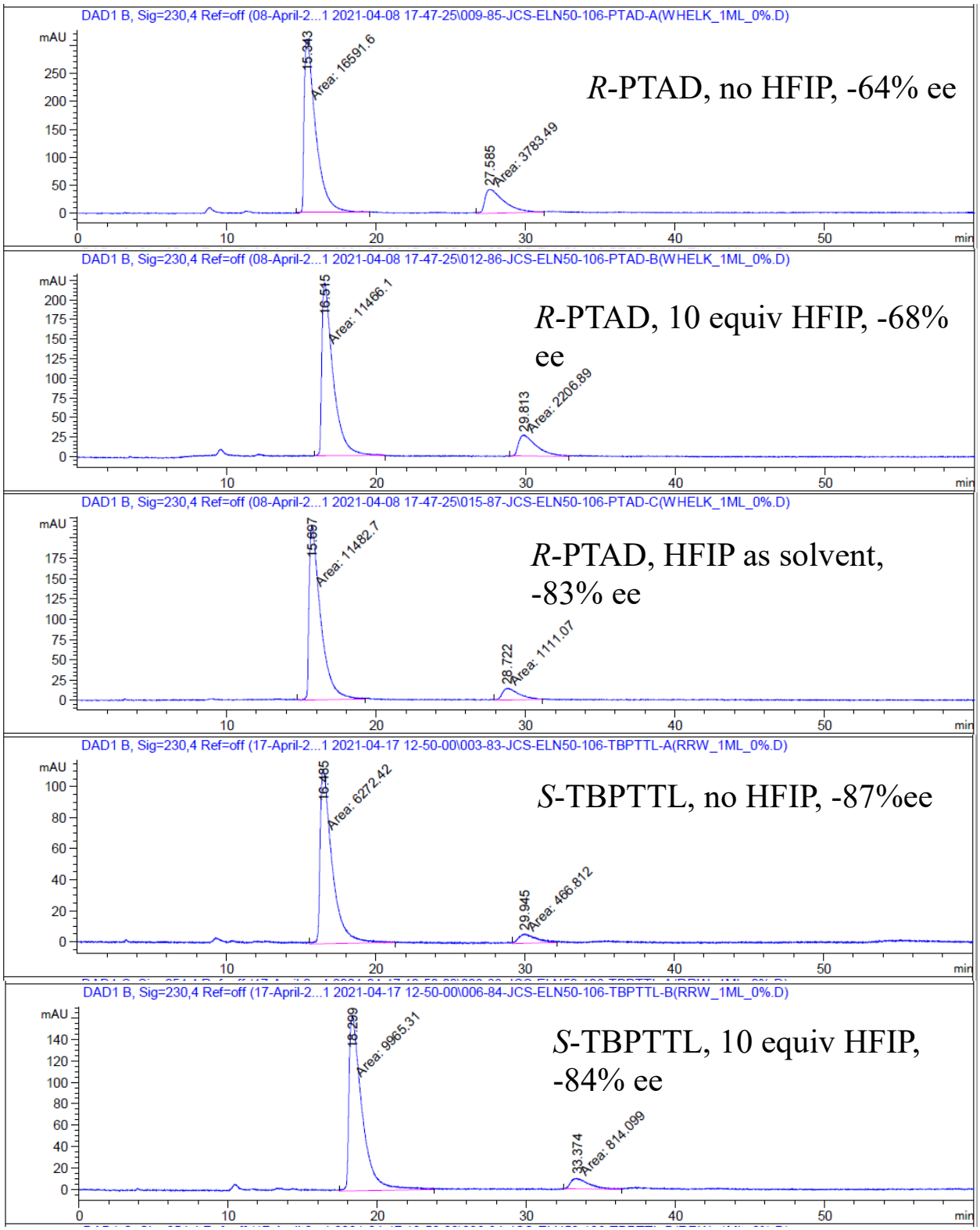
DAD1 B, Sig=230,4 Ref=off (08-April-2...1 2021-04-08 17-47-25\009-85-JCS-ELN50-106-PTAD-A(WHELK_1ML_0%.D)
15.343
Area: 16591.6
27.585
Area: 3783.49
R-PTAD, no HFIP, -64% ee
DAD1 B, Sig=230,4 Ref=off (08-April-2...1 2021-04-08 17-47-25\012-86-JCS-ELN50-106-PTAD-B(WHELK_1ML_0%.D)
16.515
Area: 11466.1
29.813
Area: 2206.89
R-PTAD, 10 equiv HFIP, -68% ee
DAD1 B, Sig=230,4 Ref=off (08-April-2...1 2021-04-08 17-47-25\015-87-JCS-ELN50-106-PTAD-C(WHELK_1ML_0%.D)
15.697
Area: 11482.7
28.722
Area: 1111.07
R-PTAD, HFIP as solvent, -83% ee
DAD1 B, Sig=230,4 Ref=off (17-April-2...1 2021-04-17 12-50-00\003-83-JCS-ELN50-106-TBPTTL-A(RRW_1ML_0%.D)
16.485
Area: 6272.42
29.945
Area: 466.812
S-TBPTTL, no HFIP, -87%ee
DAD1 B, Sig=230,4 Ref=off (17-April-2...1 2021-04-17 12-50-00\006-84-JCS-ELN50-106-TBPTTL-B(RRW_1ML_0%.D)
18.299
Area: 9965.31
33.374
Area: 814.099
S-TBPTTL, 10 equiv HFIP, -84% ee
mAU
min

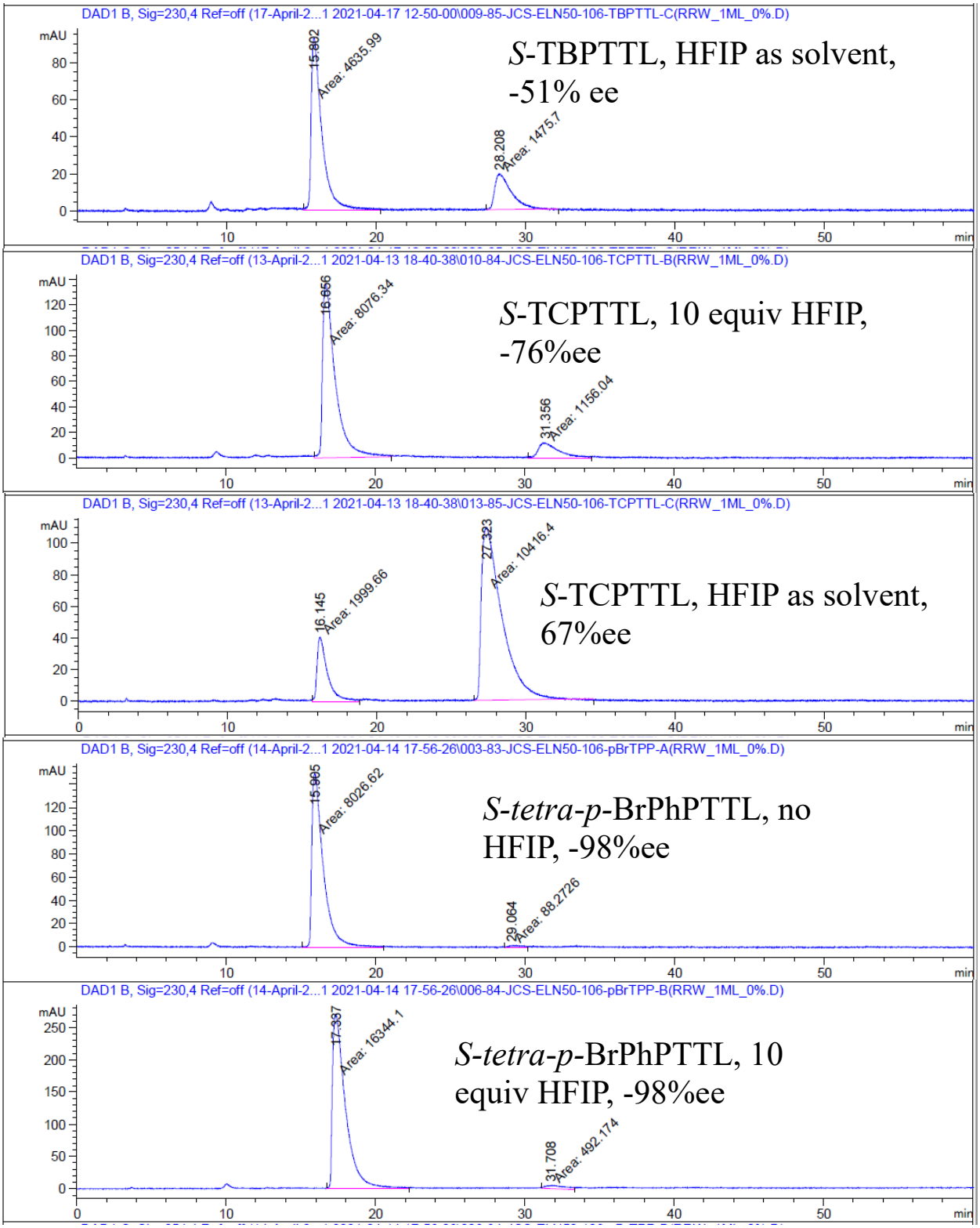
DAD1 B, Sig=230,4 Ref=off (17-April-2...1 2021-04-17 12-50-00\009-85-JCS-ELN50-106-TBPTTL-C(RRW_1ML_0%.D)
mAU
15.982
Area: 4635.99
28.208
Area: 1475.7
S-TBPTTL, HFIP as solvent, -51% ee
min
DAD1 B, Sig=230,4 Ref=off (13-April-2...1 2021-04-13 18-40-38\010-84-JCS-ELN50-106-TCPTTL-B(RRW_1ML_0%.D)
mAU
16.656
Area: 8076.34
31.356
Area: 1156.04
S-TCPTTL, 10 equiv HFIP, -76%ee
min
DAD1 B, Sig=230,4 Ref=off (13-April-2...1 2021-04-13 18-40-38\013-85-JCS-ELN50-106-TCPTTL-C(RRW_1ML_0%.D)
mAU
16.145
Area: 1999.66
27.323
Area: 10416.4
S-TCPTTL, HFIP as solvent, 67%ee
min
DAD1 B, Sig=230,4 Ref=off (14-April-2...1 2021-04-14 17-56-26\003-83-JCS-ELN50-106-pBrTPP-A(RRW_1ML_0%.D)
mAU
15.965
Area: 8026.62
29.064
Area: 88.2726
S-tetra-p-BrPhPTTL, no HFIP, -98%ee
min
DAD1 B, Sig=230,4 Ref=off (14-April-2...1 2021-04-14 17-56-26\006-84-JCS-ELN50-106-pBrTPP-B(RRW_1ML_0%.D)
mAU
17.337
Area: 16344.1
31.708
Area: 492.174
S-tetra-p-BrPhPTTL, 10 equiv HFIP, -98%ee
min

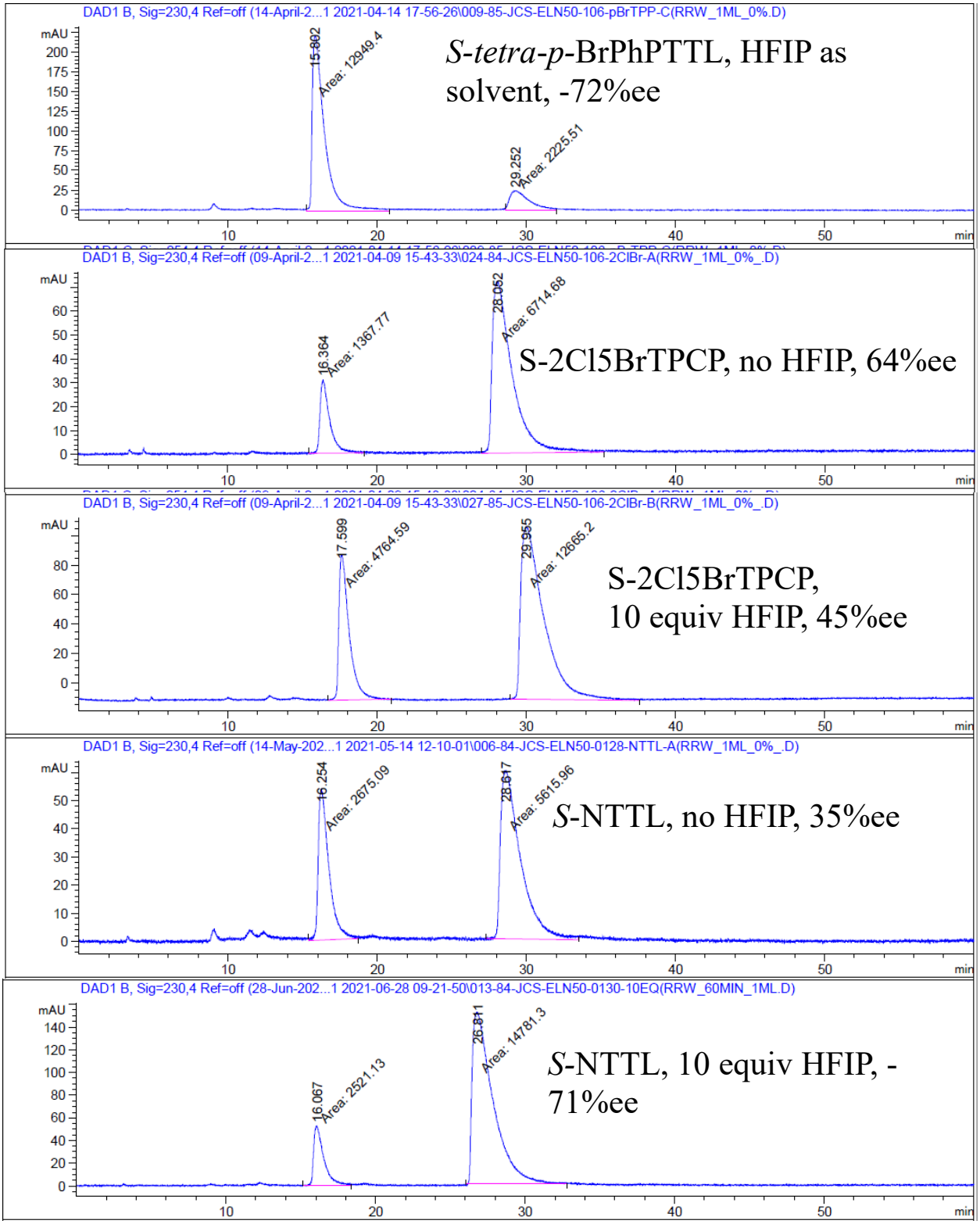
DAD1 B, Sig=230,4 Ref=off (14-April-2...1 2021-04-14 17-56-26\009-85-JCS-ELN50-106-pBrTPP-C(RRW_1ML_0%.D)
mAU
15.882
Area: 12949.4
29.252
Area: 2225.51
S-tetra-p-BrPhPTTL, HFIP as solvent, -72%ee
min
DAD1 B, Sig=230,4 Ref=off (09-April-2...1 2021-04-09 15-43-33\024-84-JCS-ELN50-106-2ClBr-A(RRW_1ML_0%_.D)
mAU
16.364
Area: 1367.77
28.052
Area: 6714.68
S-2Cl5BrTPCP, no HFIP, 64%ee
min
DAD1 B, Sig=230,4 Ref=off (09-April-2...1 2021-04-09 15-43-33\027-85-JCS-ELN50-106-2ClBr-B(RRW_1ML_0%_.D)
mAU
17.599
Area: 4764.59
29.955
Area: 12665.2
S-2Cl5BrTPCP,
10 equiv HFIP, 45%ee
min
DAD1 B, Sig=230,4 Ref=off (14-May-202...1 2021-05-14 12-10-01\006-84-JCS-ELN50-0128-NTTL-A(RRW_1ML_0%_.D)
mAU
16.254
Area: 2675.09
28.617
Area: 5615.96
S-NTTL, no HFIP, 35%ee
min
DAD1 B, Sig=230,4 Ref=off (28-Jun-202...1 2021-06-28 09-21-50\013-84-JCS-ELN50-0130-10EQ(RRW_60MIN_1ML.D)
mAU
16.067
Area: 2521.13
26.811
Area: 14781.3
S-NTTL, 10 equiv HFIP, -71%ee
min

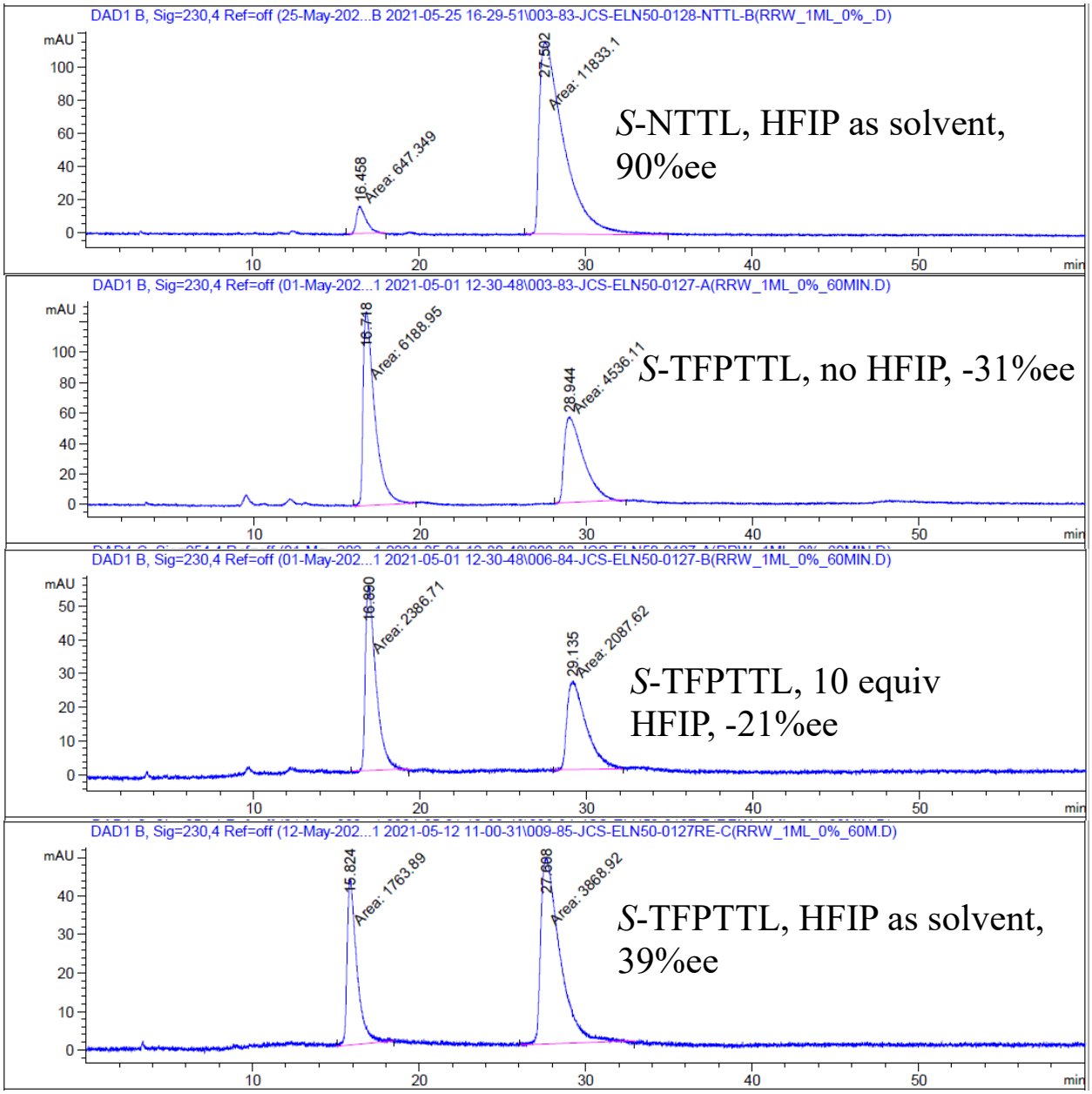
DAD1 B, Sig=230,4 Ref=off (25-May-202...B 2021-05-25 16-29-51\003-83-JCS-ELN50-0128-NTTL-B(RRW_1ML_0%_.D)
mAU
16.458
Area: 647.349
27.582
Area: 11833.1
S-NTTL, HFIP as solvent, 90%ee
min
DAD1 B, Sig=230,4 Ref=off (01-May-202...1 2021-05-01 12-30-48\003-83-JCS-ELN50-0127-A(RRW_1ML_0%_60MIN.D)
mAU
16.718
Area: 6188.95
28.944
Area: 4536.11
S-TFPTTL, no HFIP, -31%ee
min
DAD1 B, Sig=230,4 Ref=off (01-May-202...1 2021-05-01 12-30-48\006-84-JCS-ELN50-0127-B(RRW_1ML_0%_60MIN.D)
mAU
16.890
Area: 2386.71
29.135
Area: 2087.62
S-TFPTTL, 10 equiv HFIP, -21%ee
min
DAD1 B, Sig=230,4 Ref=off (12-May-202...1 2021-05-12 11-00-31\009-85-JCS-ELN50-0127RE-C(RRW_1ML_0%_60M.D)
mAU
15.824
Area: 1763.89
27.688
Area: 3868.92
S-TFPTTL, HFIP as solvent, 39%ee
min

6.2: Initial additive screen with Rh_2(*R*-TPPTTL)$_4$:

Table C2: Table 3 initial additive screen reproduced from main text

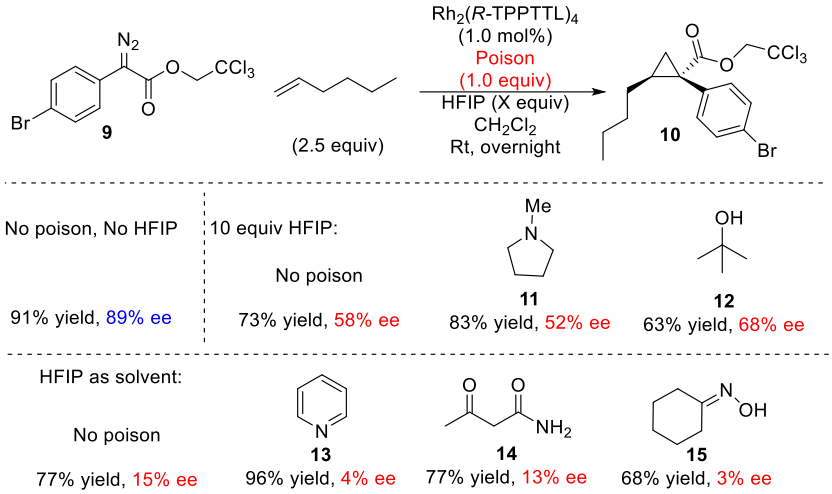

The initial additive screen was performed according to general procedure 3.1 using Rh_2(*R*-TPPTTL)$_4$ as catalyst and varying equivalents of HFIP. Reactions that were successful and the corresponding enantioselectivity are reported in **Table C2** according to the conditions that afforded the best combination of yield and enantioselectivity. The HPLC data for successful reactions are reported below along with the conditions that gave a successful reaction.

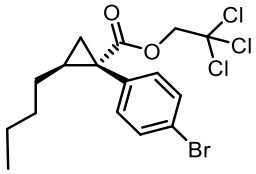

Racemate:

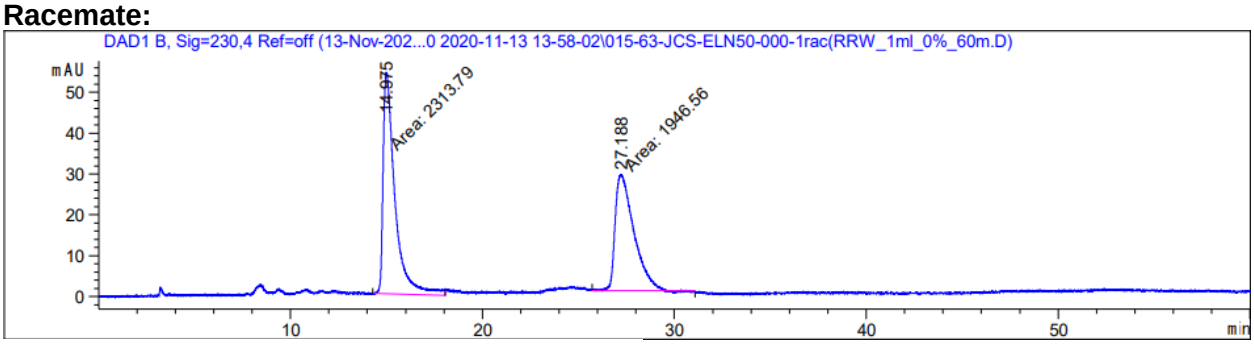

Signal 2: DAD1 B, Sig=230,4 Ref=off

Peak #	RetTime [min]	Type	Width [min]	Area [mAU*s]	Height [mAU]	Area %
1	14.975	MM	0.7108	2313.79248	54.25547	54.3099
2	27.188	MM	1.1311	1946.55518	28.68206	45.6901

Totals : 4260.34766 82.93754

***N*-Methyl pyrrolidine (11):**

10 equiv HFIP:

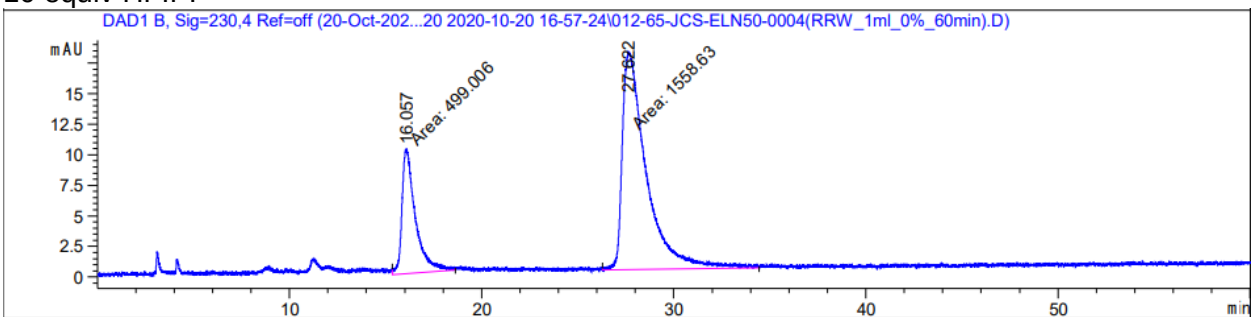

Signal 2: DAD1 B, Sig=230,4 Ref=off

Peak #	RetTime [min]	Type	Width [min]	Area [mAU*s]	Height [mAU]	Area %
1	16.057	MM	0.8141	499.00598	10.21556	24.2515
2	27.622	MM	1.4538	1558.62708	17.86886	75.7485
Totals :				2057.63306	28.08442	

***Tert*-butanol (12):**

10 equiv HFIP:

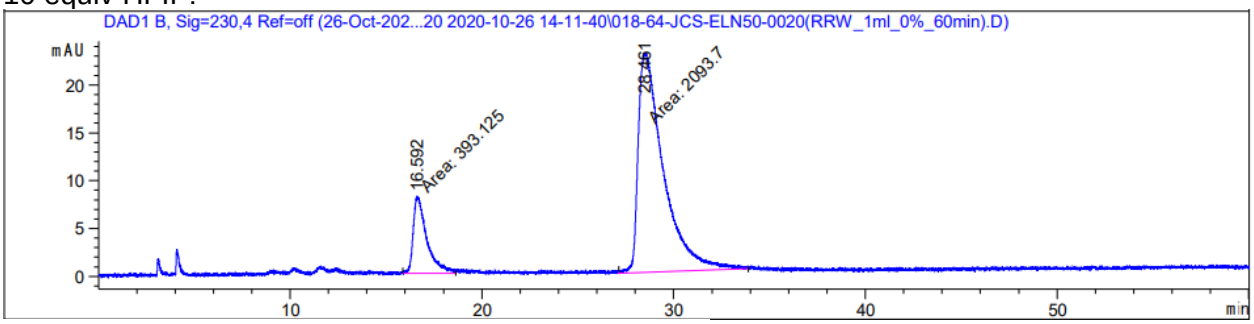

Signal 2: DAD1 B, Sig=230,4 Ref=off

Peak #	RetTime [min]	Type	Width [min]	Area [mAU*s]	Height [mAU]	Area %
1	16.592	MM	0.8128	393.12540	8.06149	15.8083
2	28.461	MM	1.5181	2093.70313	22.98582	84.1917
Totals :				2486.82852	31.04731	

Pyridine (13):

HFIP as solvent:

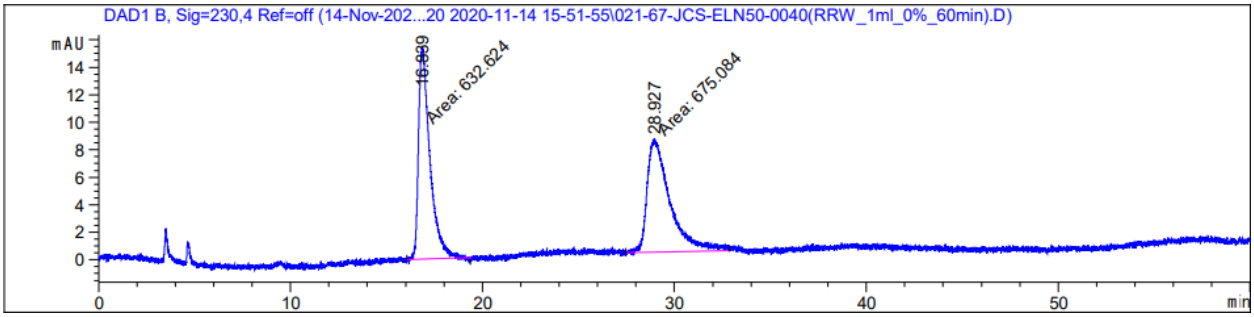

```
Signal 2: DAD1 B, Sig=230,4 Ref=off

Peak RetTime Type  Width     Area      Height     Area
  #   [min]        [min]   [mAU*s]     [mAU]       %
----|-------|----|-------|----------|----------|--------|
   1  16.839 MM    0.6802  632.62427   15.50106  48.3766
   2  28.927 MM    1.3632  675.08411    8.25363  51.6234

Totals :                  1307.70837   23.75469
```

Acetoacetamide (14):

HFIP as solvent:

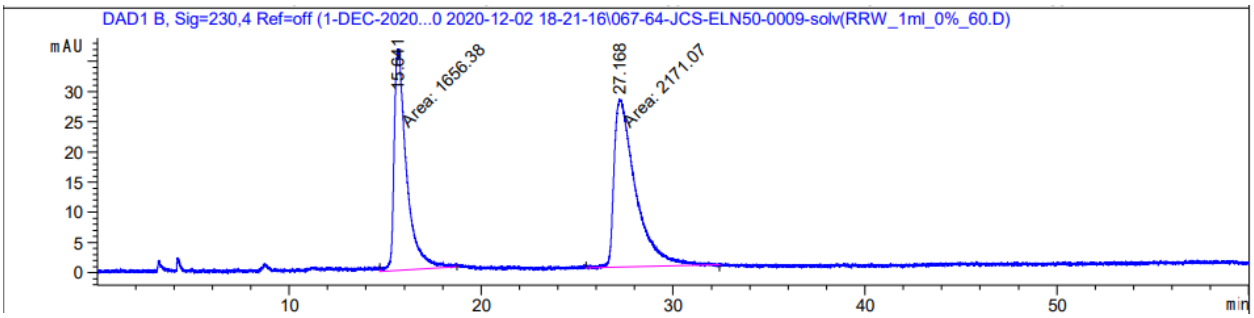


```
Signal 2: DAD1 B, Sig=230,4 Ref=off

Peak RetTime Type  Width     Area      Height     Area
  #   [min]        [min]   [mAU*s]     [mAU]       %
----|-------|----|-------|----------|----------|--------|
   1  15.641 MM    0.7525 1656.38184   36.68562  43.2763
   2  27.168 MM    1.2996 2171.07104   27.84187  56.7237

Totals :                  3827.45288   64.52749
```

Cyclohexanone oxime(14):

HFIP as solvent:

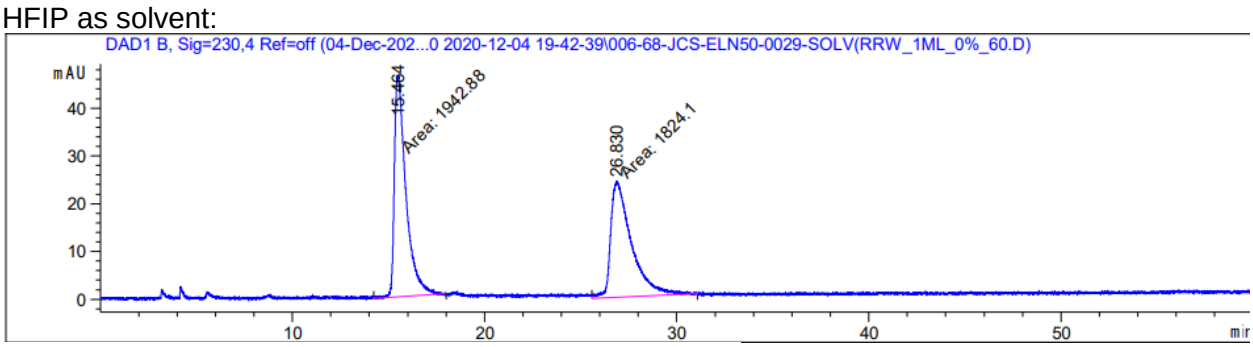


```
Signal 2: DAD1 B, Sig=230,4 Ref=off

Peak RetTime Type  Width     Area      Height     Area
  #   [min]        [min]   [mAU*s]     [mAU]       %
----|-------|----|-------|----------|----------|--------|
   1  15.464 MM    0.6974 1942.87500   46.43016  51.5766
   2  26.830 MM    1.2587 1824.09827   24.15403  48.4234

Totals :                  3766.97327   70.58418
```

5.6 Large scale additive reactions:

All reactions were performed at room temperature according to **general procedure 3.1** and allowed to run for 24 hours. Afterwards, the reactions were filtered over celite to remove mol sieve dust and the solvent was removed *in vacuo.* The reactions were then analyzed by 1H NMR to determine which conditions were successful for each additive. The crude 1H NMR for each attempt is shown according to the addive used, and product generation was determined by compariosn with the pure product 1H NMR which follows this figure. Successful reactions showing significant product formation were purified according to **general procedure 3.1** and isolated yield is reported in each case (**Figure C**10). The pure product was analyzed by HPLC to determine % ee which is reported below (**Figure C**10).

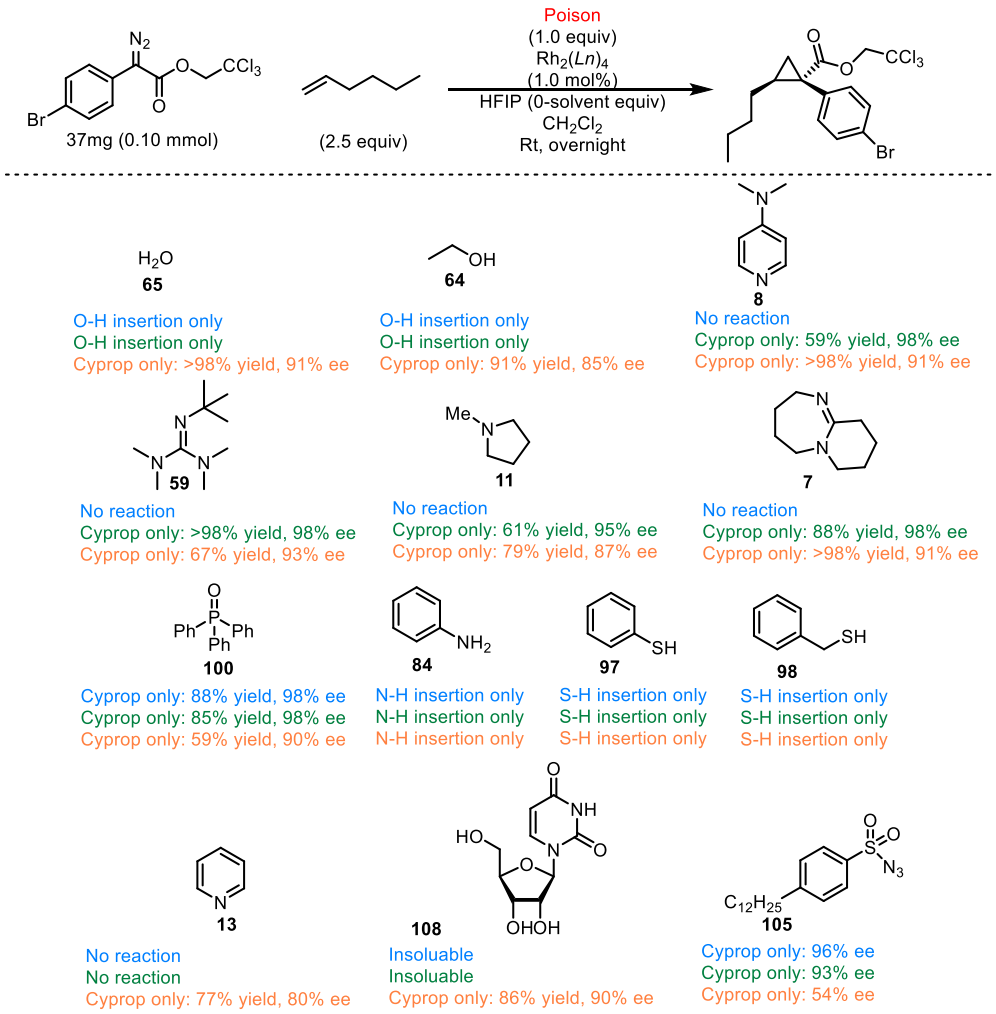

Figure C10**:** Reactions performed with a series of additives on lab-scale according to **general procedure 3.1.** Rh_2(*S-tetra-p*-BrPPTTL)$_4$ without HFIP (0163), Rh_2(*S-tetra-p*-BrPPTTL)$_4$ with 10 equivHFIP(0164), Rh_2(*R*-NTTL)$_4$ with HFIP as solvent (0165).

Pure product (10): See **S4** for peak summary of both spectra

1H NMR:

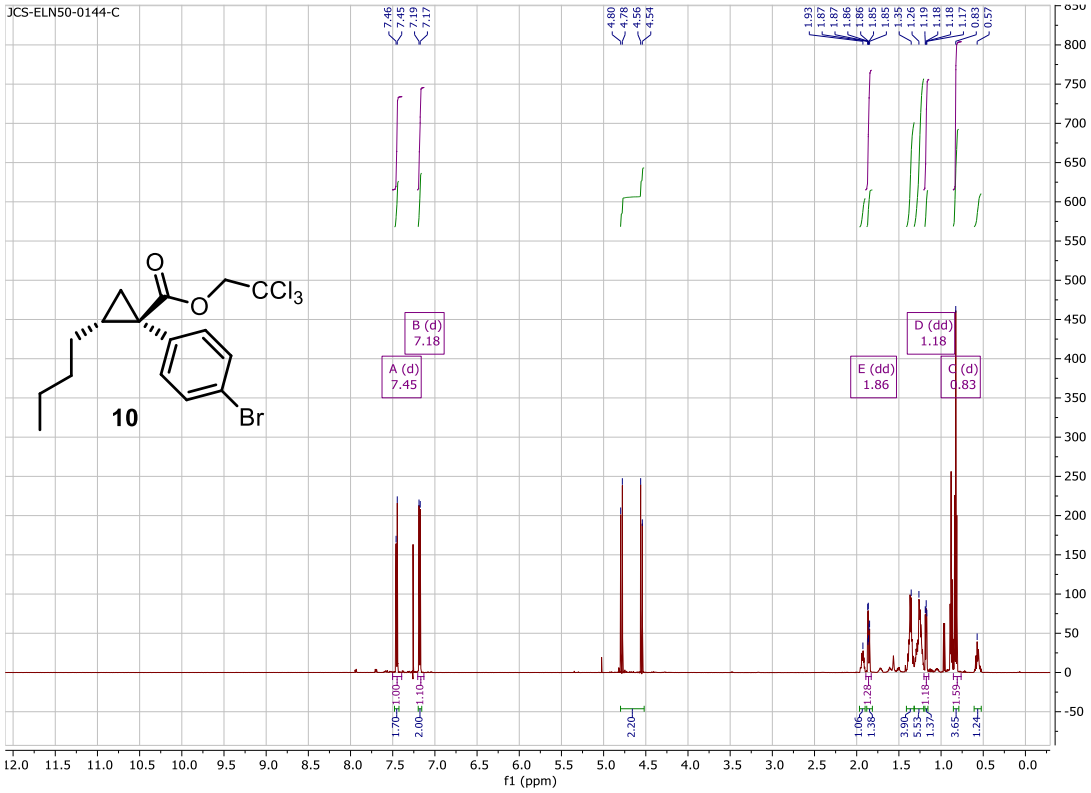

13C NMR:

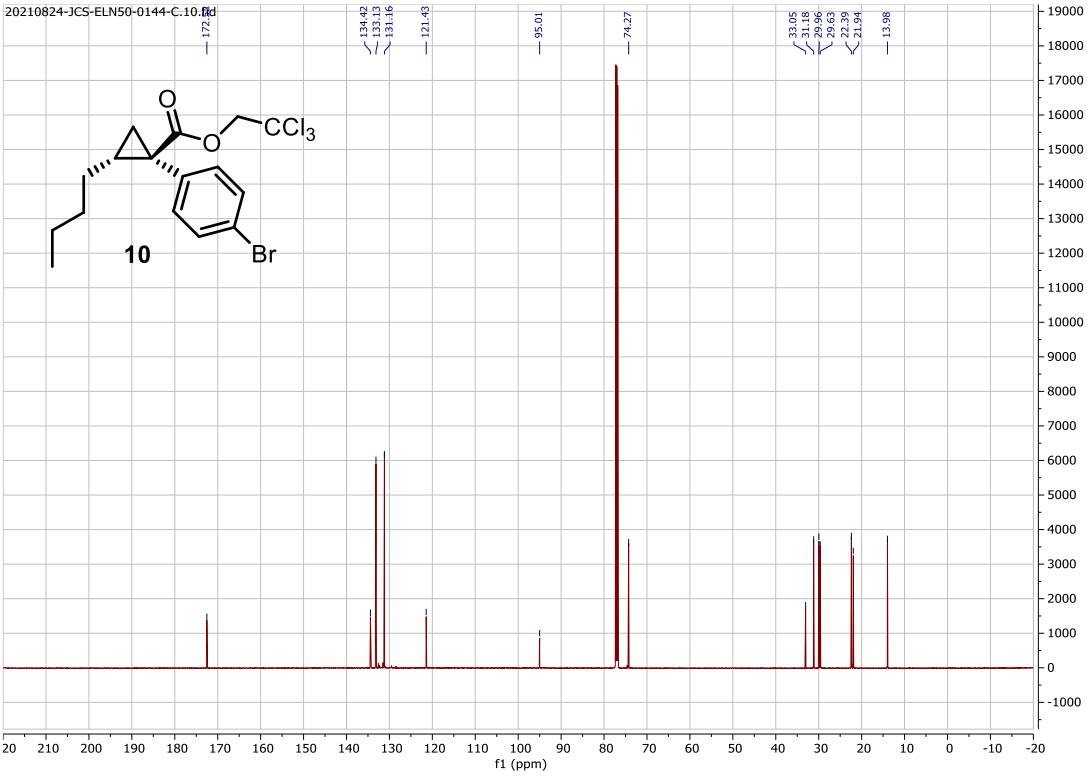

Water (65): Rh_2(*S-tetra-p*-BrPPTTL)$_4$ without HFIP (A), Rh_2(*S-tetra-p*-BrPPTTL)$_4$ with 10 equivHFIP(B), Rh_2(*R*-NTTL)$_4$ with HFIP as solvent (C).

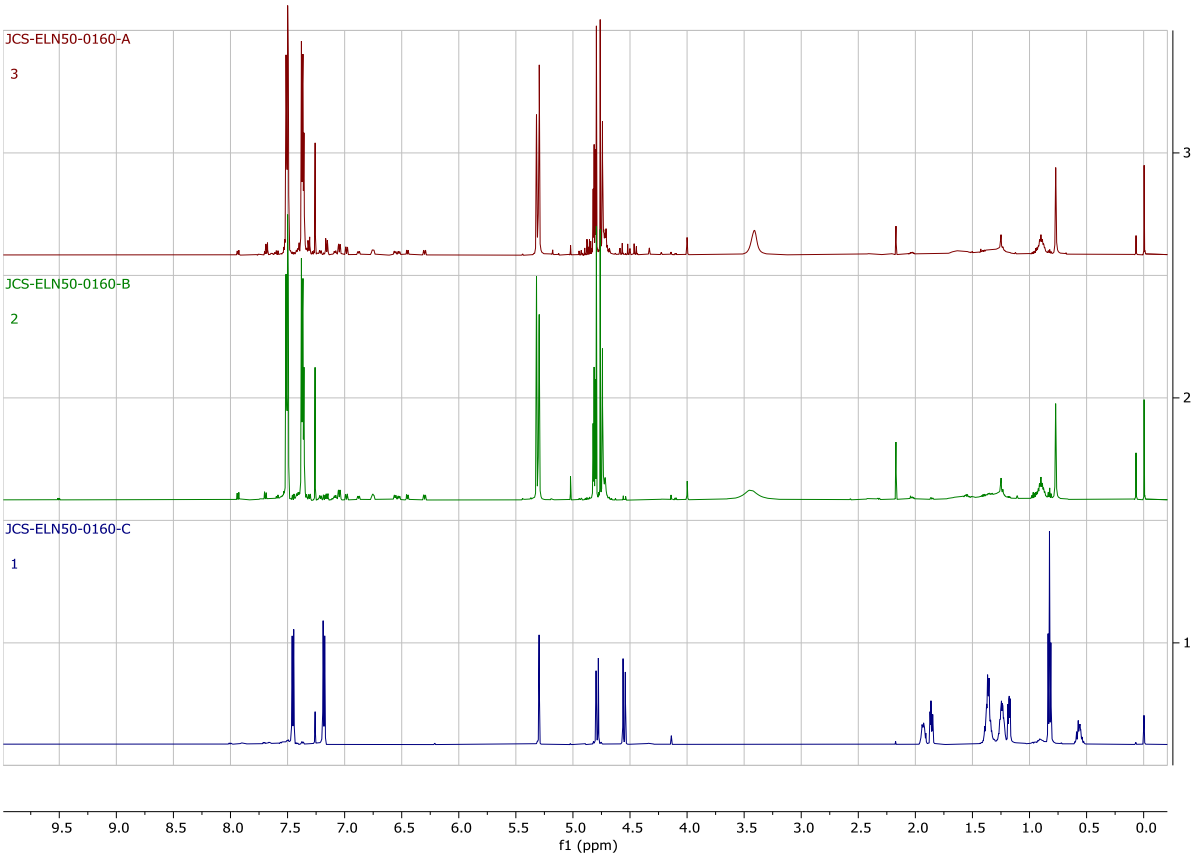

Only Rh_2(*R*-NTTL)$_4$ with HFIP as solvent(165) gave a successful reaction.

Water (HFIP as solvent)

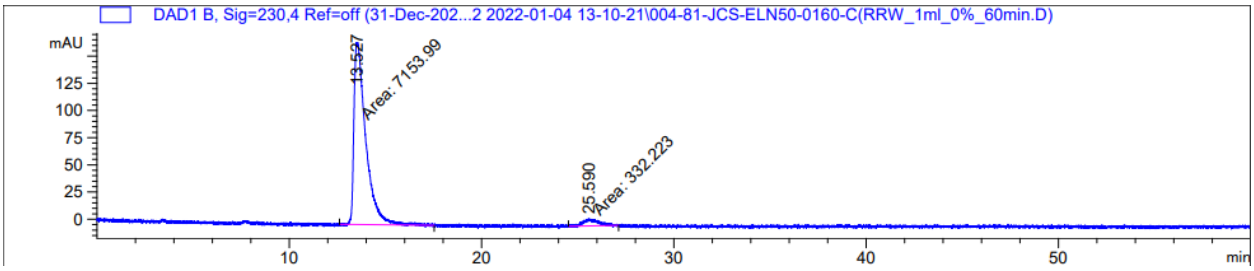


```
Signal 2: DAD1 B, Sig=230,4 Ref=off

Peak RetTime Type  Width     Area      Height     Area
  #   [min]        [min]   [mAU*s]     [mAU]       %
----|-------|----|-------|----------|----------|--------|
   1  13.527 MM    0.7124 7153.99170  167.35742  95.5622
   2  25.590 MM    0.8439  332.22299    6.56139   4.4378

Totals :                  7486.21469  173.91881
```

Ethanol (64): Rh_2(*S-tetra-p*-BrPPTTL)$_4$ without HFIP (163), Rh_2(*S-tetra-p*-BrPPTTL)$_4$ with 10 equiv HFIP (164), Rh_2(*R*-NTTL)$_4$ with HFIP as solvent (165).

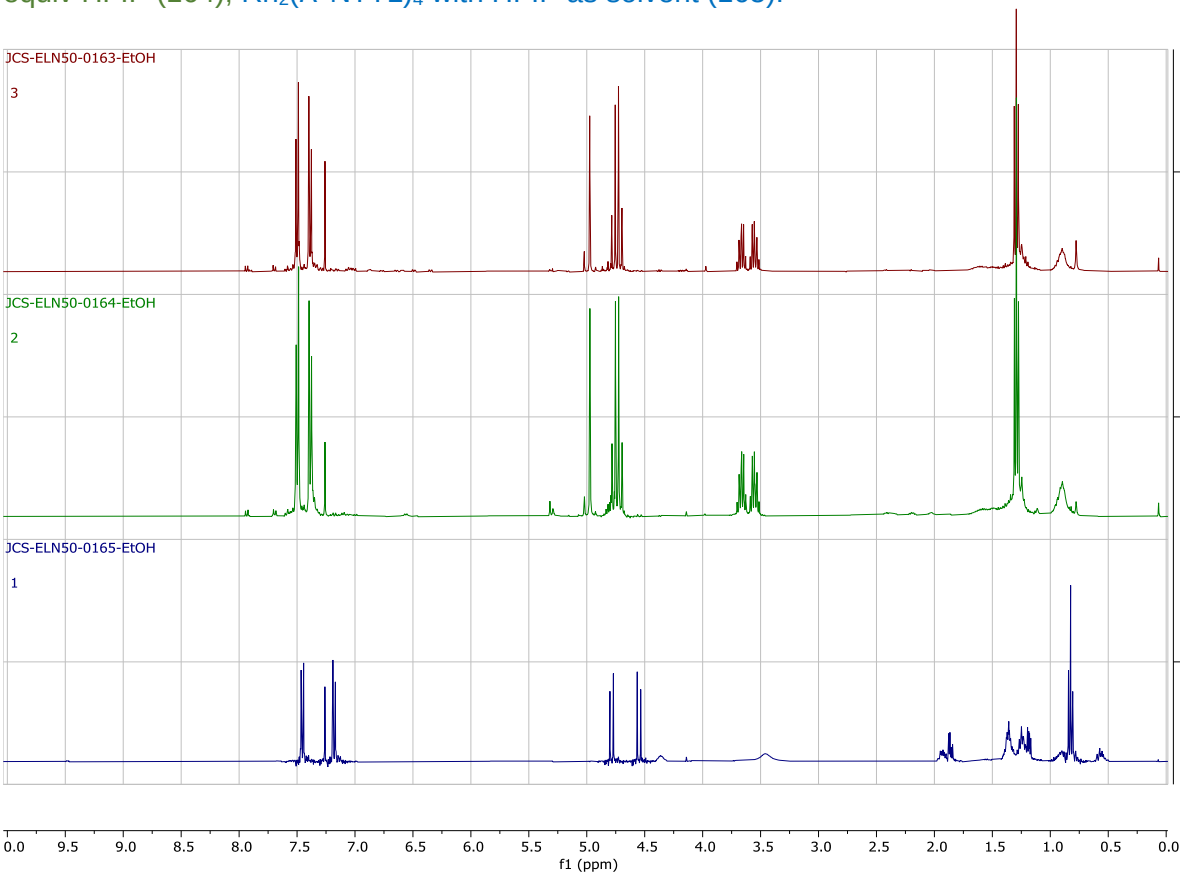

Only Rh_2(*R*-NTTL)$_4$ with HFIP as solvent(165) gave a successful reaction.

Ethanol (HFIP as solvent)

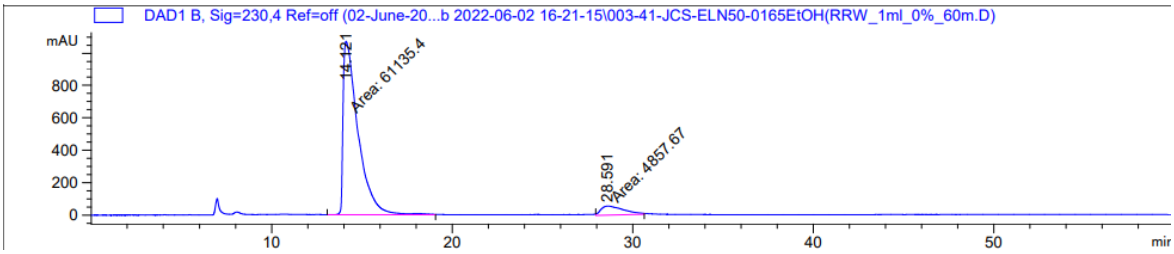

Signal 2: DAD1 B, Sig=230,4 Ref=off

Peak #	RetTime [min]	Type	Width [min]	Area [mAU*s]	Height [mAU]	Area %
1	14.121	MM	0.9510	6.11354e4	1071.37146	92.6391
2	28.591	MM	1.4639	4857.66748	55.30483	7.3609
Totals :				6.59930e4	1126.67629	

DMAP (8): Rh_2(*S-tetra-p*-BrPPTTL)$_4$ without HFIP (163), Rh_2(*S-tetra-p*-BrPPTTL)$_4$ with 10 equivHFIP(164), Rh_2(*R*-NTTL)$_4$ with HFIP as solvent (165).

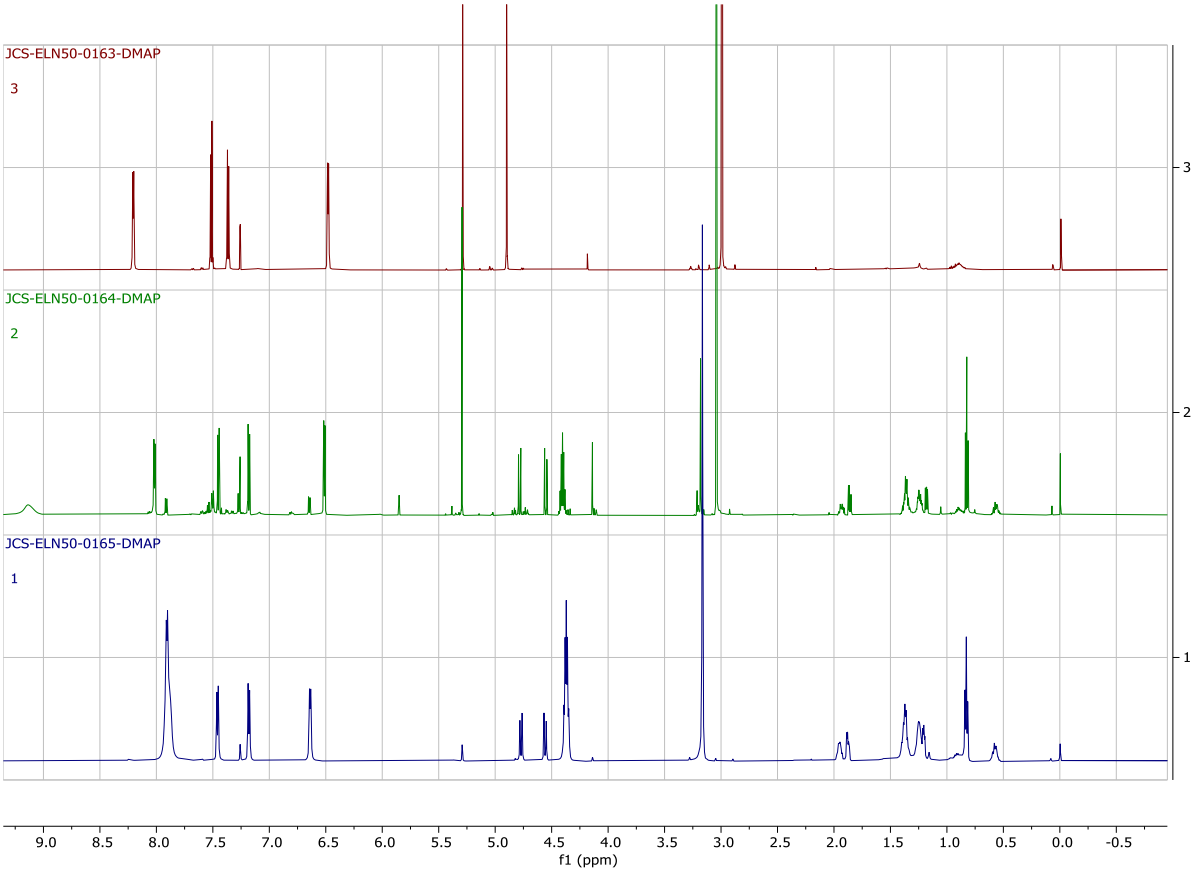

Rh_2(*S-tetra-p*-BrPPTTL)$_4$ with 10 equivHFIP(164) and Rh_2(*R*-NTTL)$_4$ with HFIP as solvent(165) gave successful reactions.

DMAP (10 equiv HFIP)

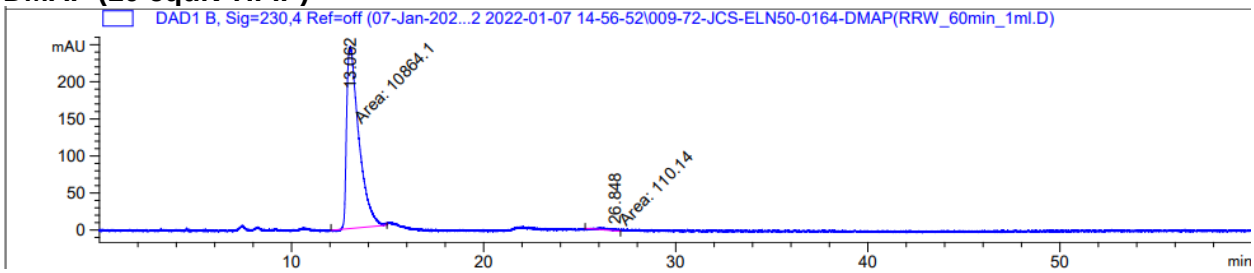

Signal 2: DAD1 B, Sig=230,4 Ref=off

Peak #	RetTime [min]	Type	Width [min]	Area [mAU*s]	Height [mAU]	Area %
1	13.062	MM	0.7359	1.08641e4	246.04532	98.9964
2	26.848	MM	0.5661	110.13956	3.24273	1.0036
Totals :				1.09743e4	249.28805	

DMAP (HFIP as solvent)

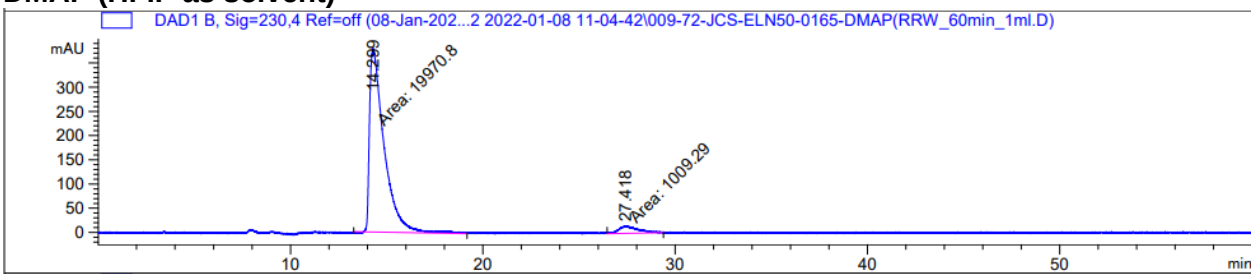

Signal 2: DAD1 B, Sig=230,4 Ref=off

Peak #	RetTime [min]	Type	Width [min]	Area [mAU*s]	Height [mAU]	Area %
1	14.299	MM	0.8778	1.99708e4	379.20023	95.1893
2	27.418	MM	1.1220	1009.29163	14.99290	4.8107
Totals :				2.09801e4	394.19313	

N-*tert*-butyl, N',N',N'',N''-tetramethylguanidine (59): Rh_2(*S-tetra-p*-BrPPTTL)$_4$ without HFIP (163), Rh_2(*S-tetra-p*-BrPPTTL)$_4$ with 10 equivHFIP(164), Rh_2(*R*-NTTL)$_4$ with HFIP as solvent (165).

Rh_2(*S-tetra-p*-BrPPTTL)$_4$ with 10 equivHFIP(164) and Rh_2(*R*-NTTL)$_4$ with HFIP as solvent(165) gave successful reactions.

TMG (10 equiv HFIP)

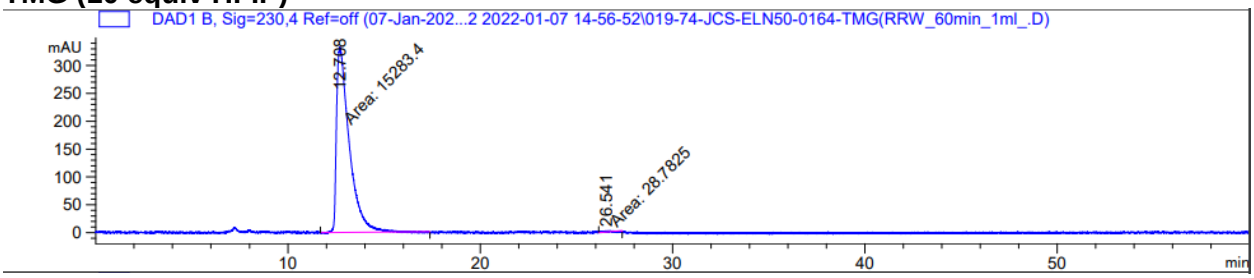

Signal 2: DAD1 B, Sig=230,4 Ref=off

Peak #	RetTime [min]	Type	Width [min]	Area [mAU*s]	Height [mAU]	Area %
1	12.708	MM	0.7656	1.52834e4	332.72964	99.8120
2	26.541	MM	0.1861	28.78253	2.57719	0.1880

Totals : 1.53122e4 335.30684

TMG (HFIP as solvent)

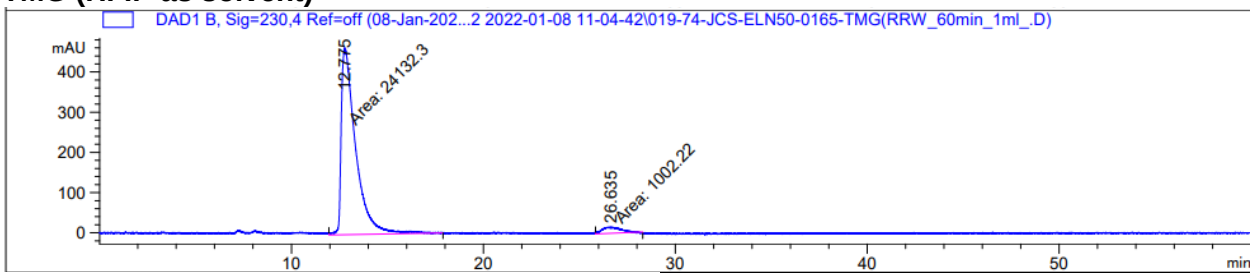

Signal 2: DAD1 B, Sig=230,4 Ref=off

Peak #	RetTime [min]	Type	Width [min]	Area [mAU*s]	Height [mAU]	Area %
1	12.775	MM	0.8643	2.41323e4	465.35959	96.0126
2	26.635	MM	1.0711	1002.21509	15.59518	3.9874

Totals : 2.51345e4 480.95477

***N*-Methyl pyrrolidine (11):** Rh_2(*S-tetra-p*-BrPPTTL)$_4$ without HFIP (163), Rh_2(*S-tetra-p*-BrPPTTL)$_4$ with 10 equivHFIP(164), Rh_2(*R*-NTTL)$_4$ with HFIP as solvent (165).

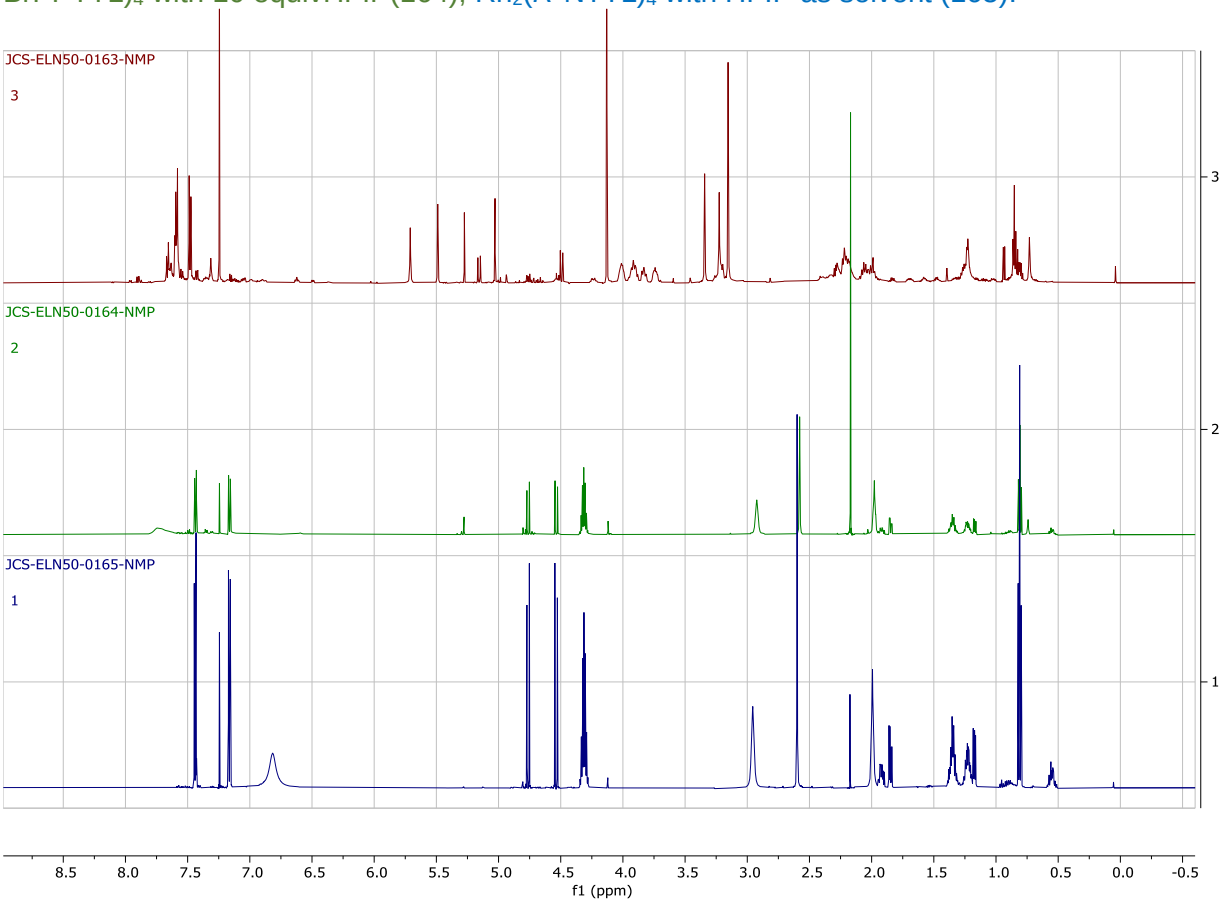

Rh_2(*S-tetra-p*-BrPPTTL)$_4$ with 10 equivHFIP(164) and Rh_2(*R*-NTTL)$_4$ with HFIP as solvent(165) gave successful reactions.

***N*-Methyl pyrrolidine (10 equiv HFIP)**

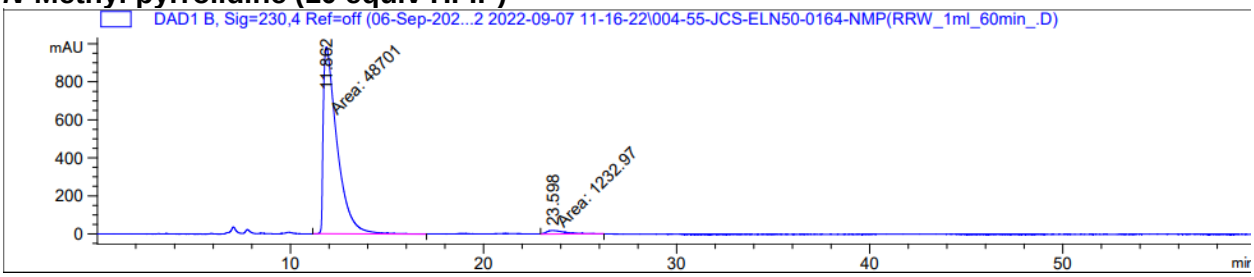


```
Signal 2: DAD1 B, Sig=230,4 Ref=off

Peak RetTime Type  Width     Area      Height     Area
  #   [min]        [min]   [mAU*s]     [mAU]       %
----|-------|----|-------|----------|----------|--------|
   1  11.862 MM    0.8265 4.87010e4   982.09784  97.5308
   2  23.598 MM    1.1103 1232.96826   18.50796   2.4692

Totals :                 4.99339e4  1000.60580
```

***N*-Methyl pyrrolidine (HFIP as solvent)**

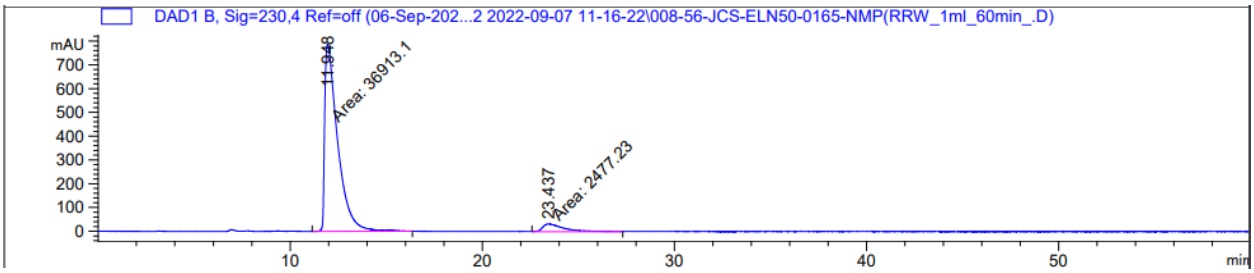

Signal 2: DAD1 B, Sig=230,4 Ref=off

Peak #	RetTime [min]	Type	Width [min]	Area [mAU*s]	Height [mAU]	Area %
1	11.948	MM	0.7820	3.69131e4	786.70319	93.7111
2	23.437	MM	1.2823	2477.23120	32.19671	6.2889
Totals :				3.93903e4	818.89989	

DBU (7): Rh_2(*S-tetra-p*-BrPPTTL)$_4$ without HFIP (163), Rh_2(*S-tetra-p*-BrPPTTL)$_4$ with 10 equivHFIP(164), Rh_2(*R*-NTTL)$_4$ with HFIP as solvent (165).

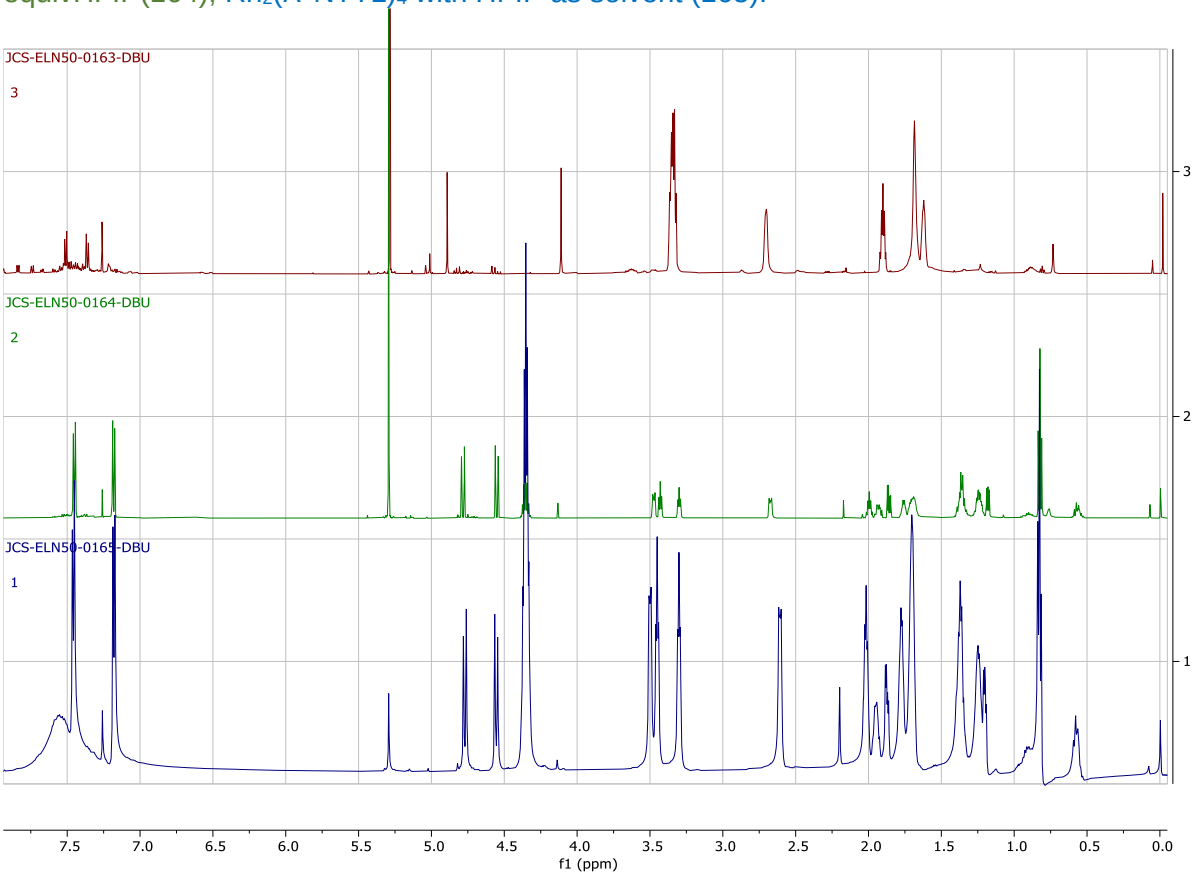

Rh_2(*S-tetra-p*-BrPPTTL)$_4$ with 10 equivHFIP(164) and Rh_2(*R*-NTTL)$_4$ with HFIP as solvent(165) gave successful reactions.

DBU (10 equiv HFIP)

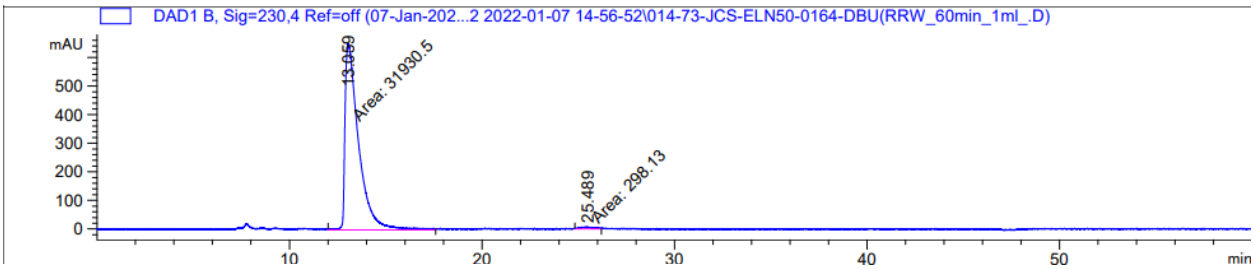

Signal 2: DAD1 B, Sig=230,4 Ref=off

Peak #	RetTime [min]	Type	Width [min]	Area [mAU*s]	Height [mAU]	Area %
1	13.059	MM	0.8183	3.19305e4	650.38055	99.0750
2	25.489	MM	0.7240	298.13007	6.86287	0.9250
Totals :				3.22287e4	657.24342	

DBU (HFIP as solvent)

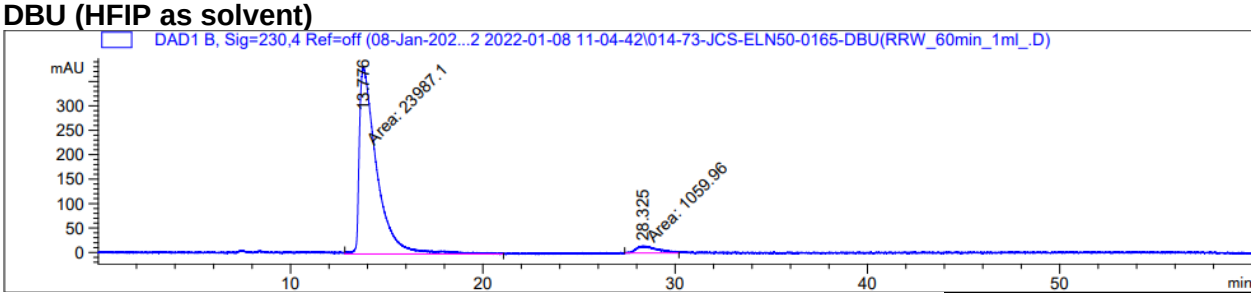

Signal 2: DAD1 B, Sig=230,4 Ref=off

Peak #	RetTime [min]	Type	Width [min]	Area [mAU*s]	Height [mAU]	Area %
1	13.776	MM	1.0492	2.39871e4	381.04593	95.7681
2	28.325	MM	1.1743	1059.95605	15.04420	4.2319
Totals :				2.50471e4	396.09013	

Aniline (84): Rh_2(*S-tetra-p*-BrPPTTL)$_4$ without HFIP (163), Rh_2(*S-tetra-p*-BrPPTTL)$_4$ with 10 equivHFIP(164), Rh_2(*R*-NTTL)$_4$ with HFIP as solvent (165).

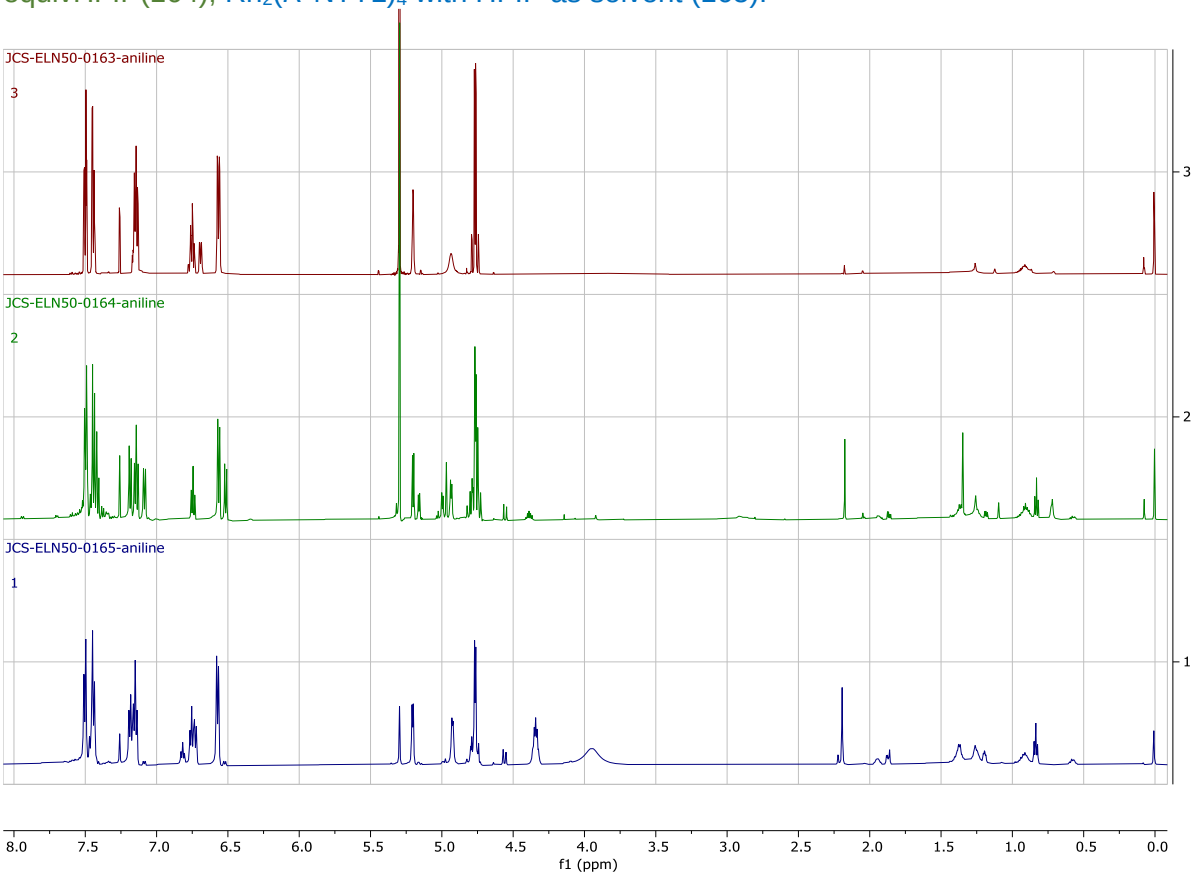

No conditions afforded a successful reaction.

Triphenylphosphine oxide (100): Rh_2(*S-tetra-p*-BrPPTTL)$_4$ without HFIP (163), Rh_2(*S-tetra-p*-BrPPTTL)$_4$ with 10 equivHFIP(164), Rh_2(*R*-NTTL)$_4$ with HFIP as solvent (165).

All conditions afforded a successful reaction

Triphenylphosphine oxide (No HFIP)

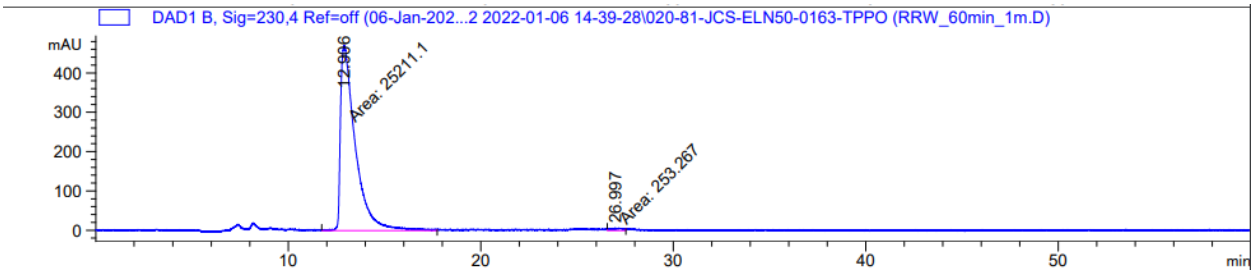


```
Signal 2: DAD1 B, Sig=230,4 Ref=off

Peak RetTime Type  Width     Area      Height     Area
  #   [min]        [min]   [mAU*s]     [mAU]       %
----|-------|----|-------|----------|----------|--------|
   1  12.906 MM    0.8911 2.52111e4   471.51523  99.0054
   2  26.997 MM    0.6310  253.26686    6.68937   0.9946

Totals :                  2.54644e4   478.20460
```

Triphenylphosphine oxide (10 equiv HFIP)

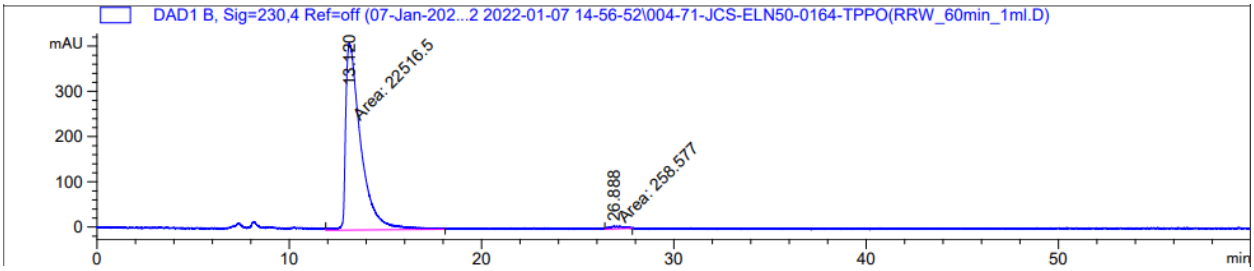

Signal 2: DAD1 B, Sig=230,4 Ref=off

Peak #	RetTime [min]	Type	Width [min]	Area [mAU*s]	Height [mAU]	Area %
1	13.120	MM	0.9078	2.25165e4	413.39267	98.8646
2	26.888	MM	0.6463	258.57736	6.66786	1.1354
Totals :				2.27751e4	420.06053	

Triphenylphosphine oxide (HFIP as solvent)

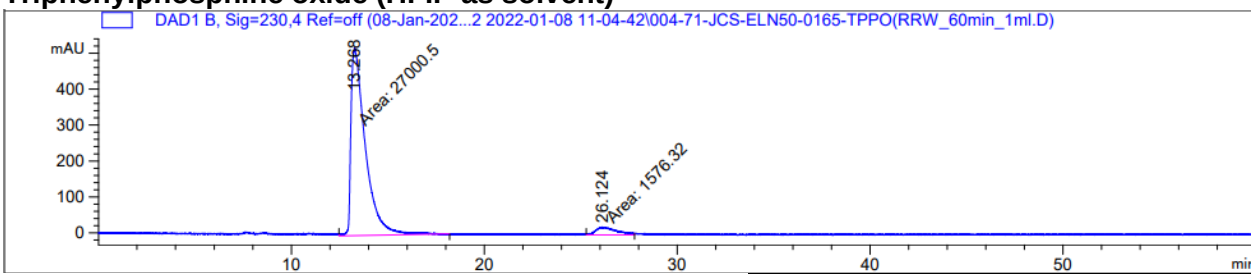

Signal 2: DAD1 B, Sig=230,4 Ref=off

Peak #	RetTime [min]	Type	Width [min]	Area [mAU*s]	Height [mAU]	Area %
1	13.268	MM	0.8626	2.70005e4	521.68585	94.4839
2	26.124	MM	1.2136	1576.31592	21.64865	5.5161
Totals :				2.85768e4	543.33450	

Thiophenol (97): Rh_2(*S-tetra-p*-BrPPTTL)$_4$ without HFIP (163), Rh_2(*S-tetra-p*-BrPPTTL)$_4$ with 10 equivHFIP(164), Rh_2(*R*-NTTL)$_4$ with HFIP as solvent (165).

No conditions afforded a successful reaction.

Benzylthiol (98): Rh_2(*S-tetra-p*-BrPPTTL)$_4$ without HFIP (163), Rh_2(*S-tetra-p*-BrPPTTL)$_4$ with 10 equivHFIP(164), Rh_2(*R*-NTTL)$_4$ with HFIP as solvent (165).

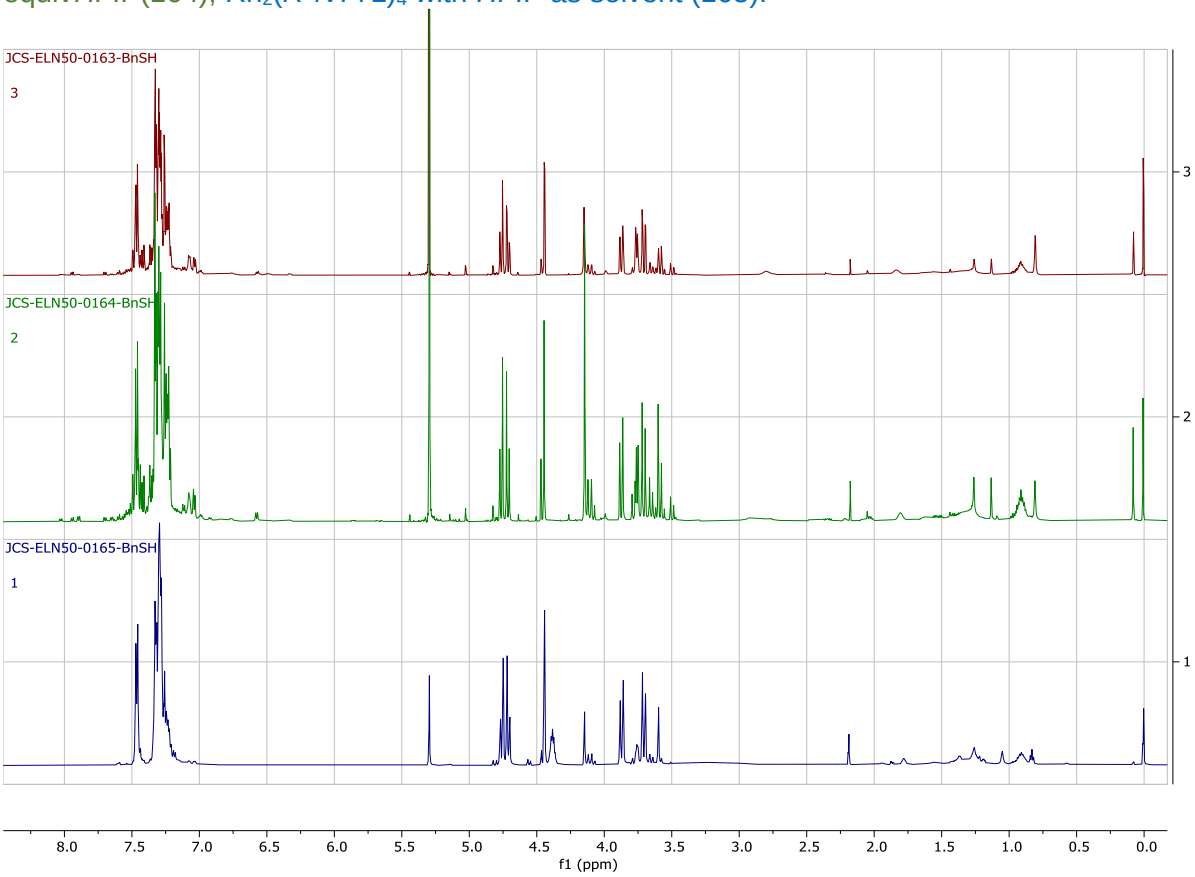

No conditions afforded a successful reaction.

Pyridine (13): Rh_2(*S-tetra-p*-BrPPTTL)$_4$ without HFIP (A), Rh_2(*S-tetra-p*-BrPPTTL)$_4$ with 10 equiv HFIP(B), Rh_2(*R*-NTTL)$_4$ with HFIP as solvent (C).

Only Rh_2(*R*-NTTL)$_4$ with HFIP as solvent(165) gave a successful reaction.

Pyridine (HFIP as solvent)

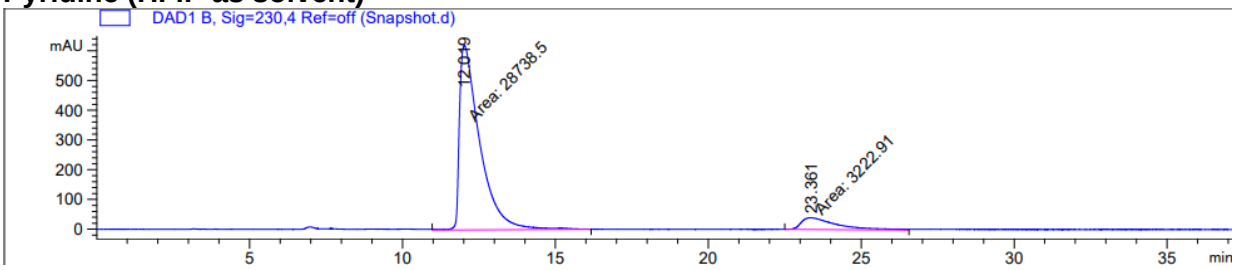

Signal 2: DAD1 B, Sig=230,4 Ref=off

Peak #	RetTime [min]	Type	Width [min]	Area [mAU*s]	Height [mAU]	Area %
1	12.019	MM	0.7720	2.87385e4	620.45660	89.9162
2	23.361	MM	1.3512	3222.91113	39.75453	10.0838

Totals : 3.19614e4 660.21113

Uridine (108): Compound was only soluable when Rh_2(*R*-NTTL)$_4$ was used with HFIP as solvent (165).

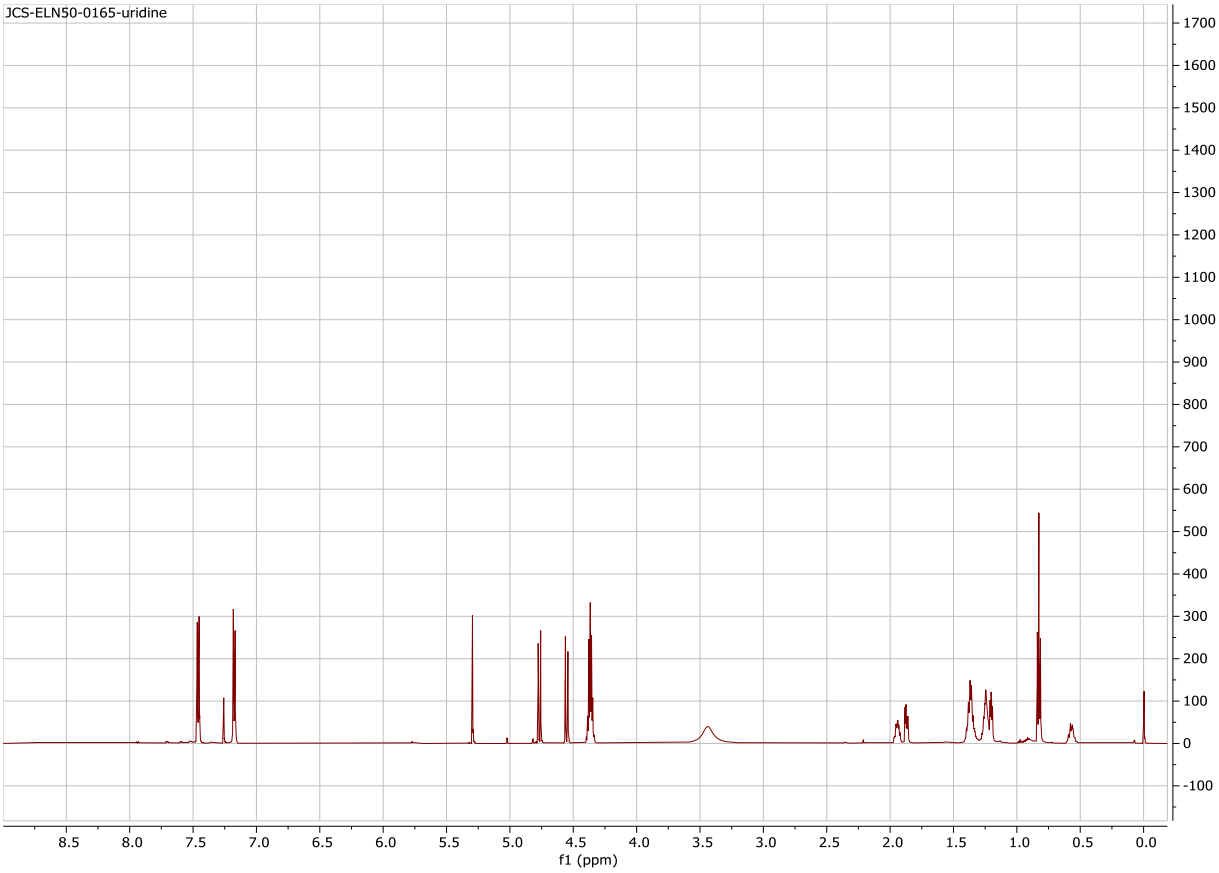

This condition afforded a successful reaction.

Uridine (HFIP as solvent)

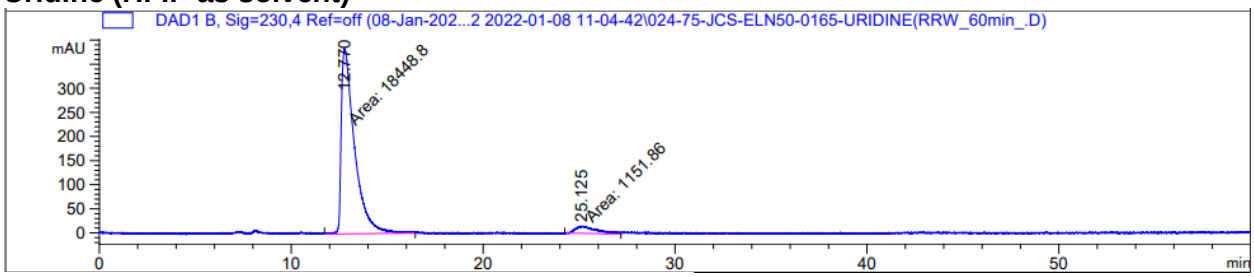

Signal 2: DAD1 B, Sig=230,4 Ref=off

Peak #	RetTime [min]	Type	Width [min]	Area [mAU*s]	Height [mAU]	Area %
1	12.770	MM	0.7986	1.84488e4	385.01071	94.1234
2	25.125	MM	1.2341	1151.85925	15.55553	5.8766

Totals : 1.96007e4 400.56624

Dodecyl sulfonyl azides (105): Rh_2(*S-tetra-p*-BrPPTTL)$_4$ without HFIP (163), Rh_2(*S-tetra-p*-BrPPTTL)$_4$ with 10 equivHFIP(164), Rh_2(*R*-NTTL)$_4$ with HFIP as solvent (165).

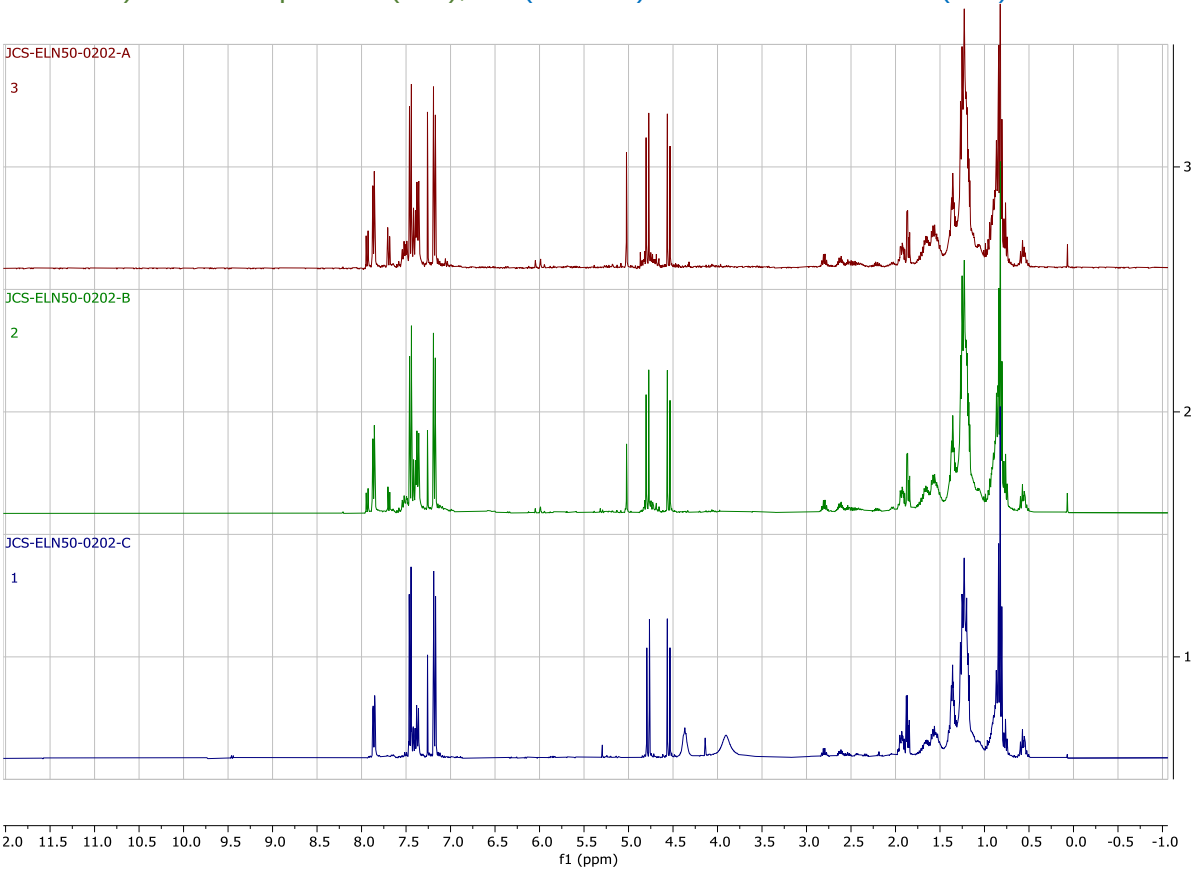

All conditions afforded a successful reaction, however the product was inseperable from the additive by flash chromatography. Therefore yields are not reported for these experiments and should be taken from the additive study performed on microscale featuring this compound.

Dodecyl sulfonyl azides (No HFIP)

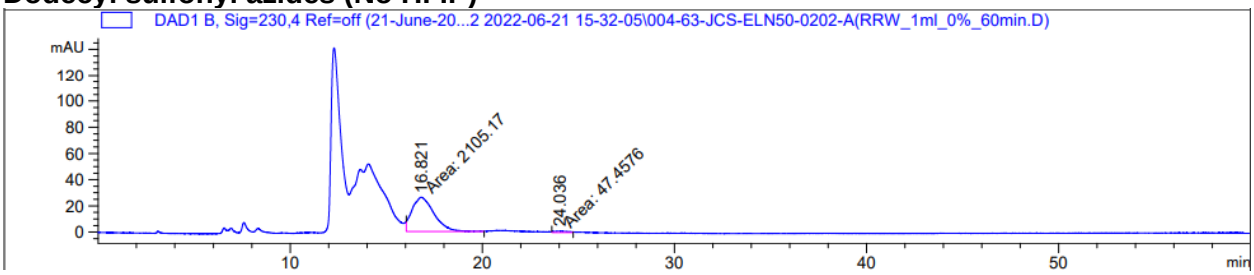

Signal 2: DAD1 B, Sig=230,4 Ref=off

Peak #	RetTime [min]	Type	Width [min]	Area [mAU*s]	Height [mAU]	Area %
1	16.821	MM	1.3355	2105.16943	26.27132	97.7954
2	24.036	MM	0.7670	47.45763	1.03126	2.2046
Totals :				2152.62706	27.30258	

Dodecyl sulfonyl azides (10 equiv HFIP)

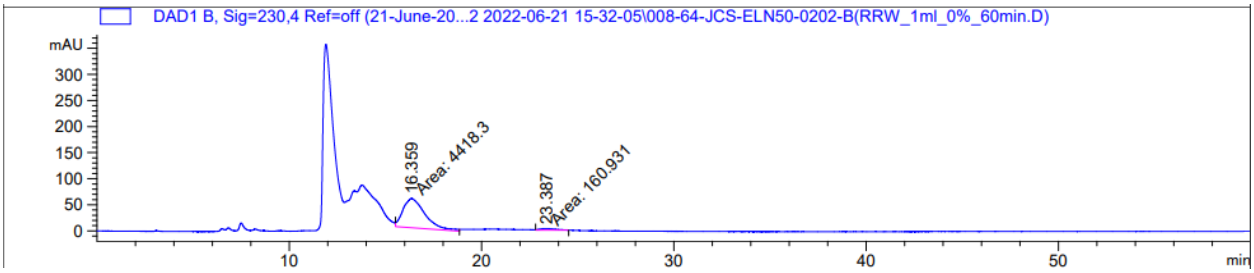

Signal 2: DAD1 B, Sig=230,4 Ref=off

Peak #	RetTime [min]	Type	Width [min]	Area [mAU*s]	Height [mAU]	Area %
1	16.359	MM	1.3128	4418.29834	56.09409	96.4856
2	23.387	MM	0.8950	160.93123	2.99683	3.5144
Totals :				4579.22957	59.09091	

Dodecyl sulfonyl azides (HFIP as solvent)

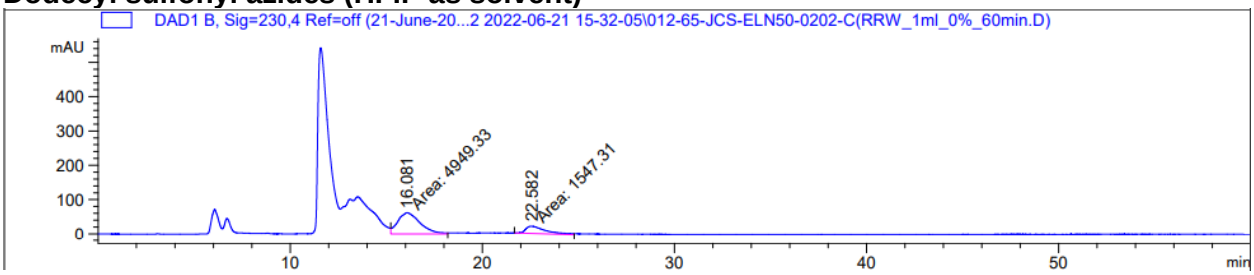

Signal 2: DAD1 B, Sig=230,4 Ref=off

Peak #	RetTime [min]	Type	Width [min]	Area [mAU*s]	Height [mAU]	Area %
1	16.081	MM	1.3382	4949.33008	61.64021	76.1829
2	22.582	MM	1.2172	1547.31116	21.18666	23.8171
Totals :				6496.64124	82.82687	

7. Substrate scope:

What follows are the substrates prepared according to **general procedure 3.1** either in the presence of Rh_2(*S-tetra-p*-Br-PhPTTL)$_4$ and 10 equiv HFIP or Rh_2(*R*-NTTL)$_4$ and HFIP as solvent. The yield of each product is the isolated yield and the pure product NMR is reported below. This spectral data is followed by the HPLC traces used to determine the enantioselectivity of the reaction. The conditions by which the product was prepared are reported on each trace along with the observed %ee. For known compounds only the HPLC traces reporting enantioselectivity under the designated conditions are reported. Refer to the initial reports of these compounds for details on their characterization. For individual HPLC conditions or a summary of the NMR spectra of each novel compound refer to the characterization report **S4-S8.**

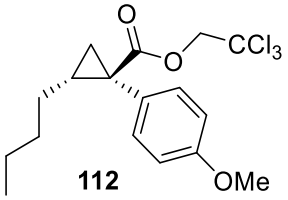

112

1H NMR:

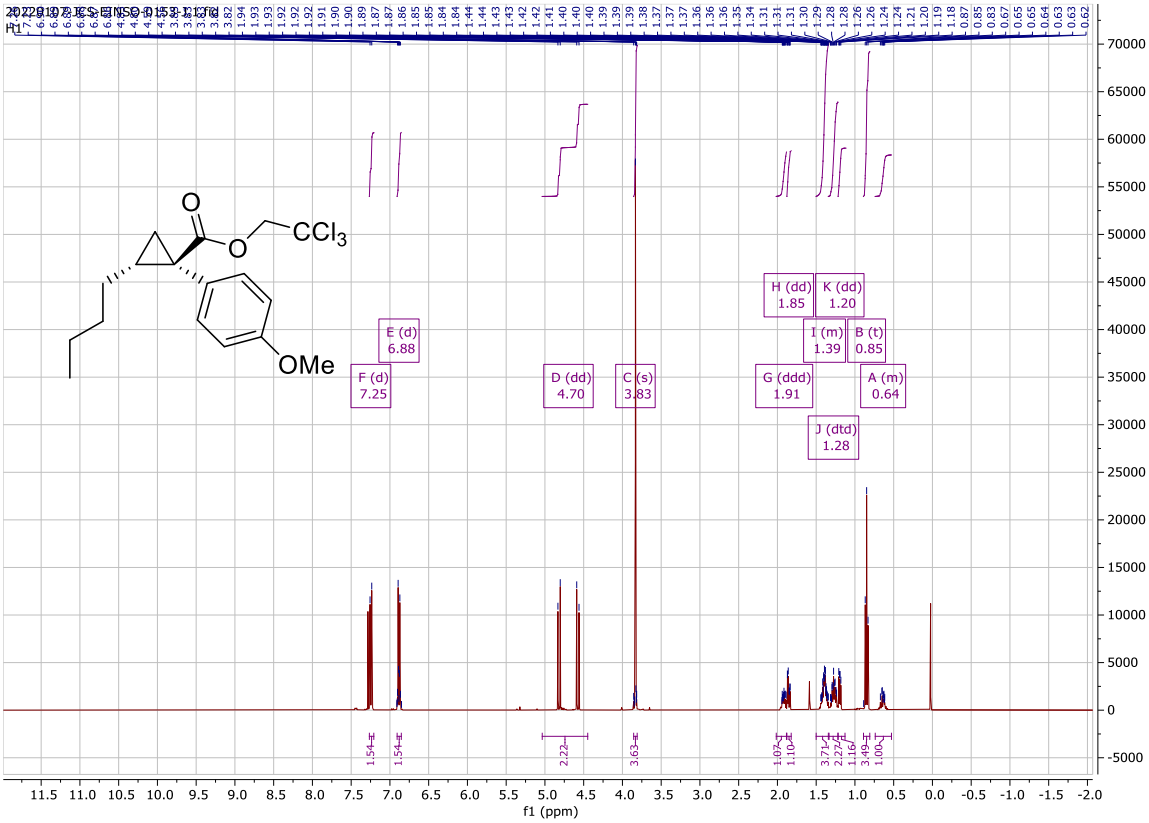

13C NMR:

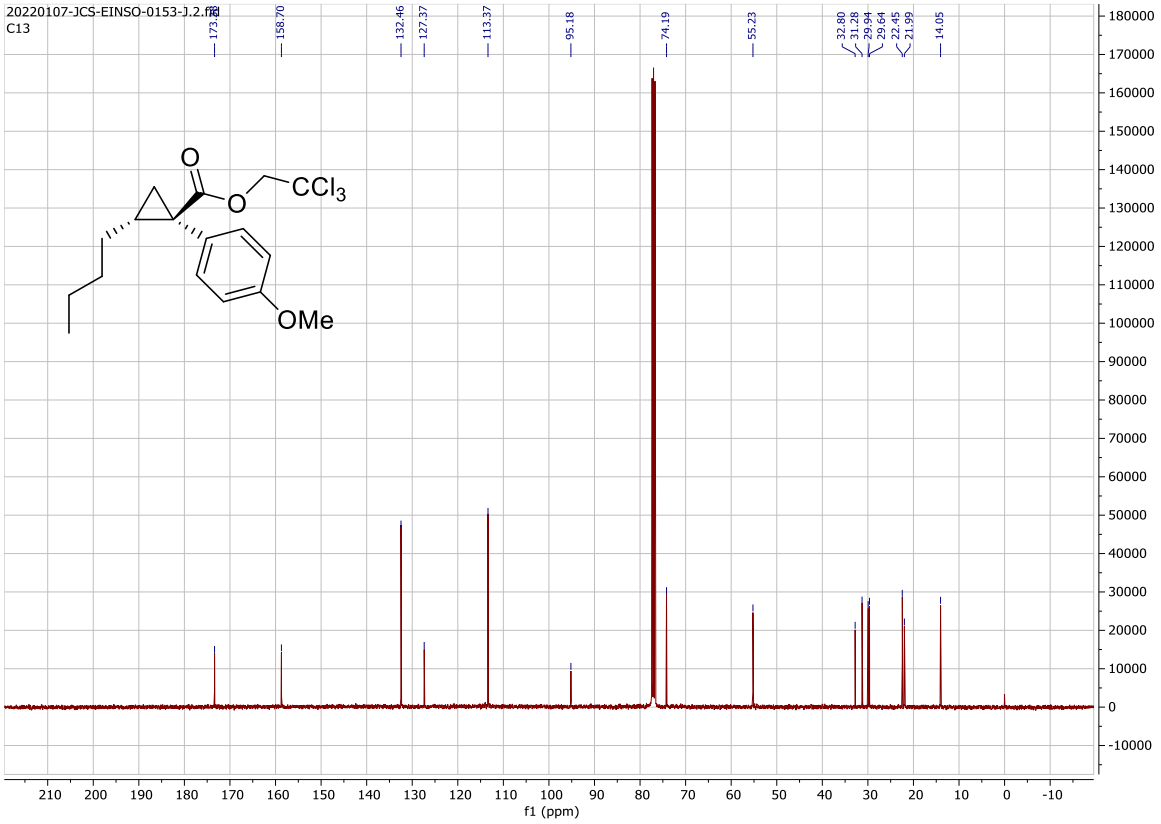

Racemate:

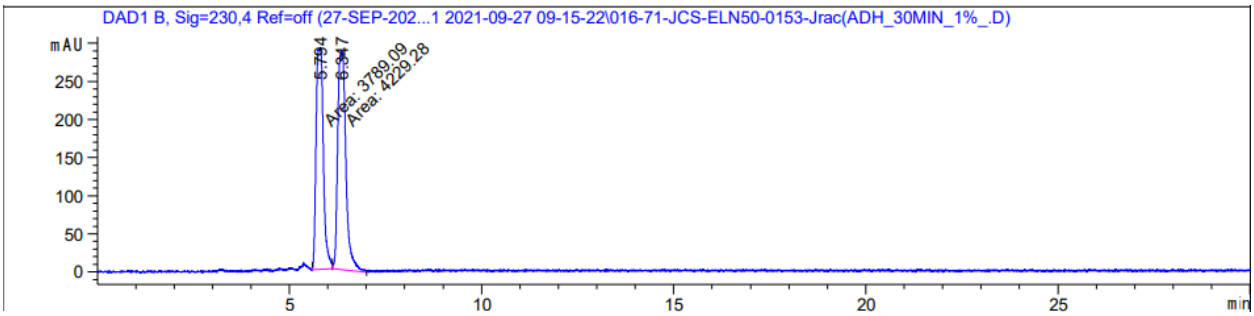

Signal 2: DAD1 B, Sig=230,4 Ref=off

Peak #	RetTime [min]	Type	Width [min]	Area [mAU*s]	Height [mAU]	Area %
1	5.794	MM	0.2172	3789.08813	290.80249	47.2551
2	6.347	MM	0.2460	4229.27930	286.57526	52.7449
Totals :				8018.36743	577.37775	

Chiral reactions:

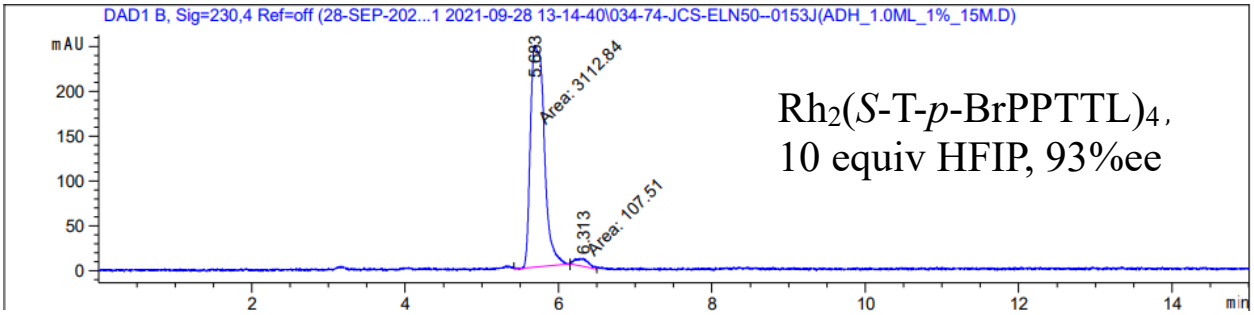

Rh_2(*S*-T-*p*-BrPPTTL)$_4$, 10 equiv HFIP, 93%ee

Signal 2: DAD1 B, Sig=230,4 Ref=off

Peak #	RetTime [min]	Type	Width [min]	Area [mAU*s]	Height [mAU]	Area %
1	5.683	MM	0.2101	3112.84497	246.98019	96.6616
2	6.313	MM	0.2088	107.50985	8.57996	3.3384

Totals : 3220.35482 255.56015

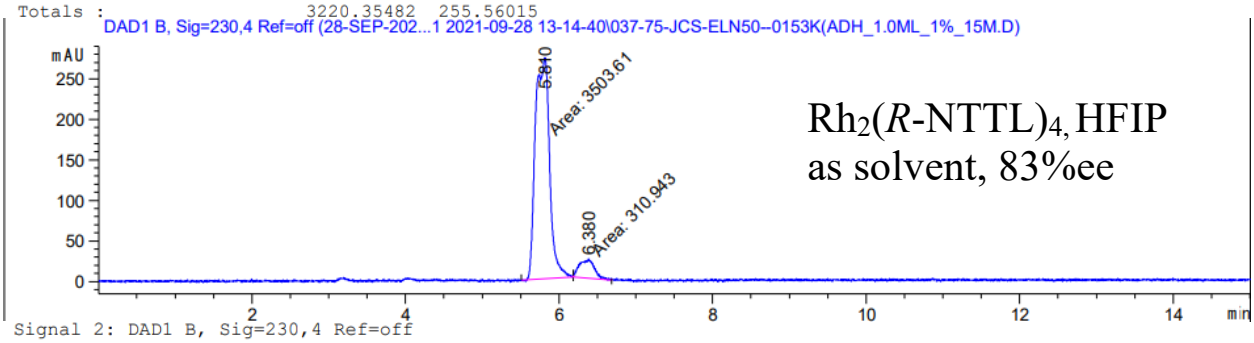

Rh_2(*R*-NTTL)$_4$, HFIP as solvent, 83%ee

Signal 2: DAD1 B, Sig=230,4 Ref=off

Peak #	RetTime [min]	Type	Width [min]	Area [mAU*s]	Height [mAU]	Area %
1	5.810	MM	0.2140	3503.61377	272.86456	91.8485
2	6.380	MM	0.2228	310.94336	23.26229	8.1515

Totals : 3814.55713 296.12686

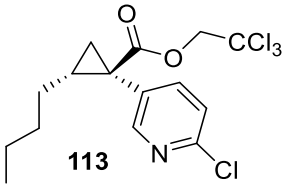

113

1H NMR:

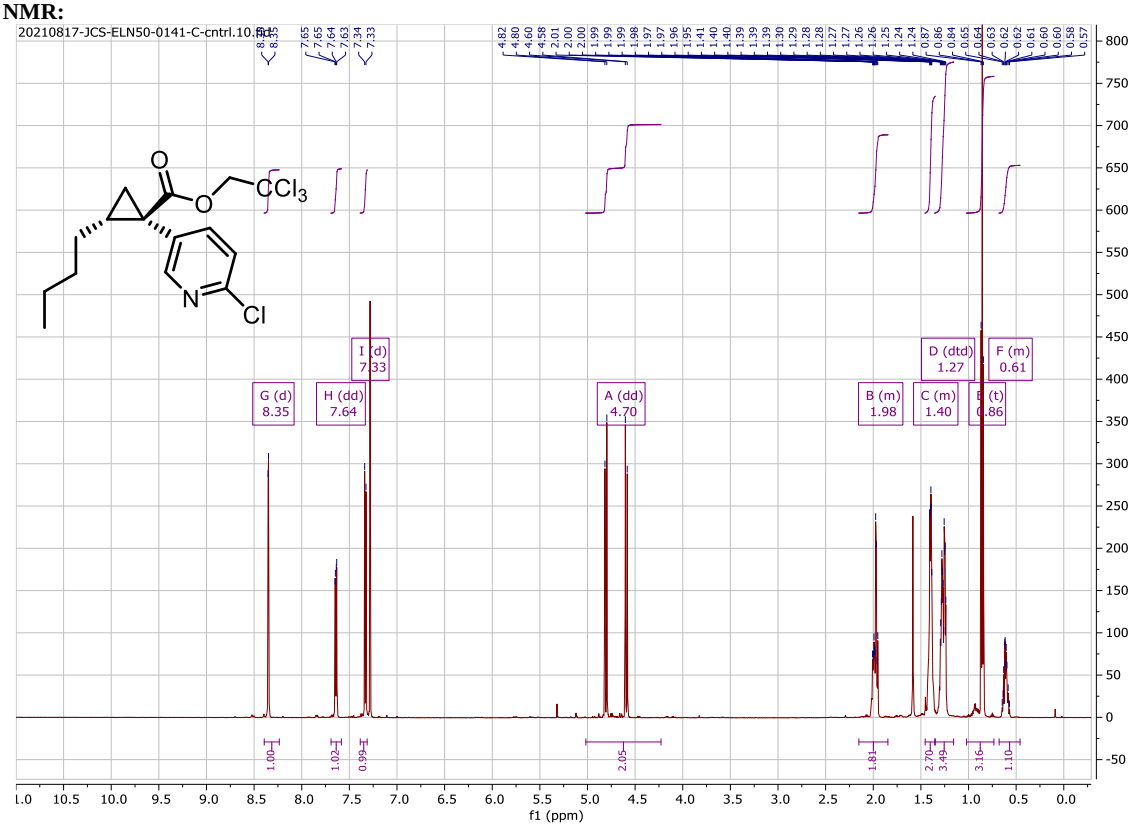

13C NMR:

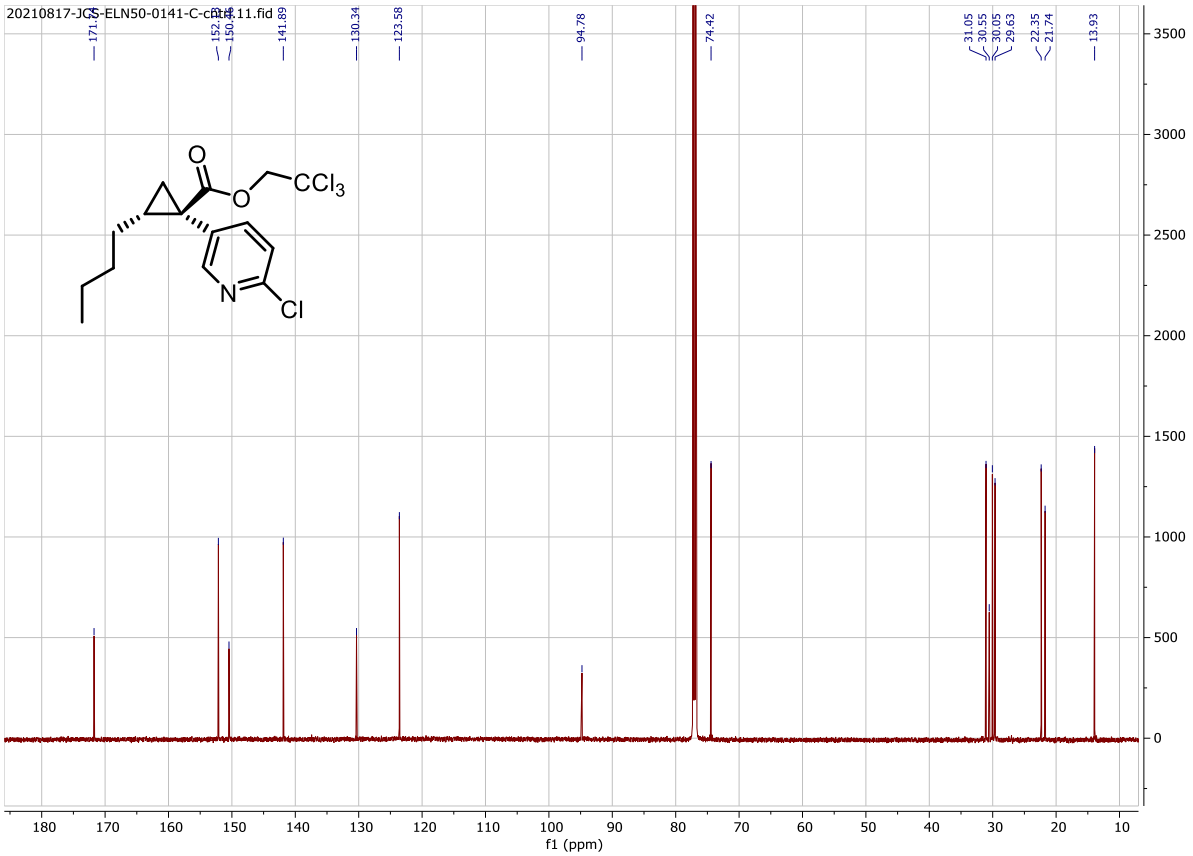

Racemate:

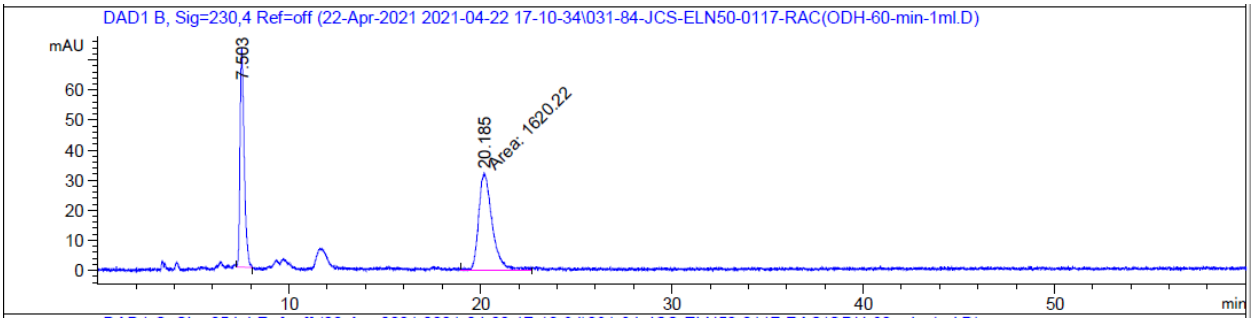

Chiral reactions:

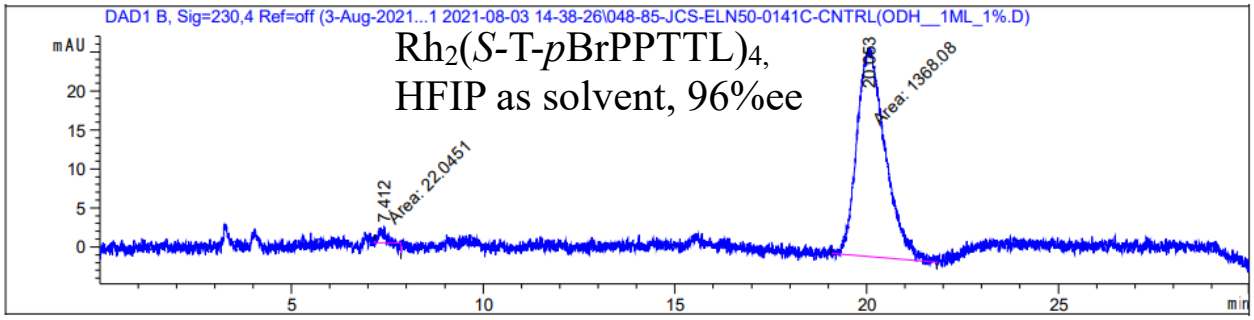

Signal 2: DAD1 B, Sig=230,4 Ref=off

Peak #	RetTime [min]	Type	Width [min]	Area [mAU*s]	Height [mAU]	Area %
1	7.412	MM	0.1798	22.04512	2.04351	1.5858
2	20.053	MM	0.8496	1368.08252	26.83847	98.4142

Totals : 1390.12764 28.88198

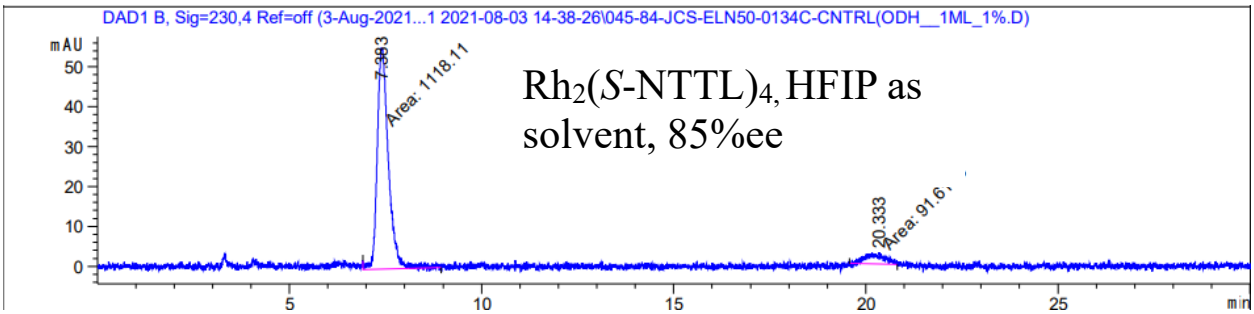

Peak #	RetTime [min]	Type	Width [min]	Area [mAU*s]	Height [mAU]	Area %
1	7.383	MM	0.3362	1118.11096	55.43184	92.4270
2	20.333	MM	0.5414	91.61176	2.82029	7.5730

Totals : 1209.72272 58.25212

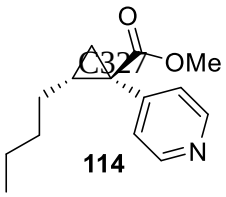

C327

1H NMR:

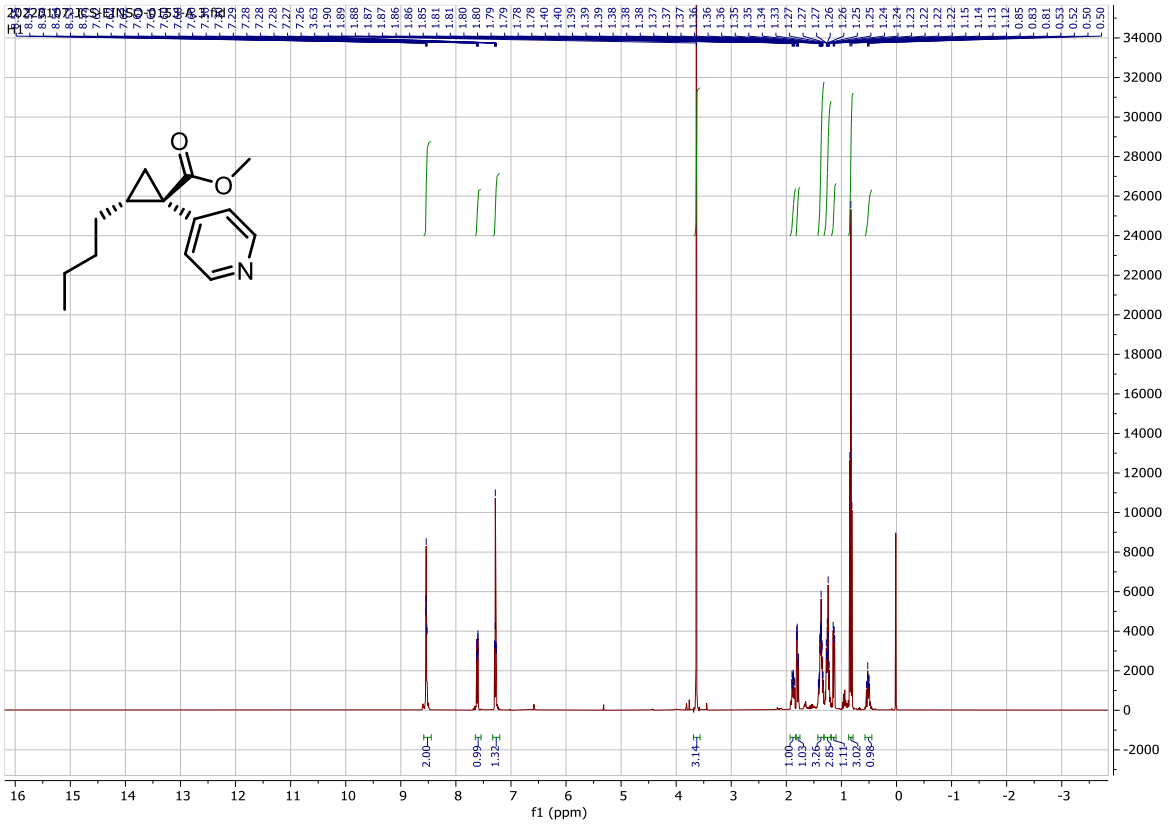

13C NMR:

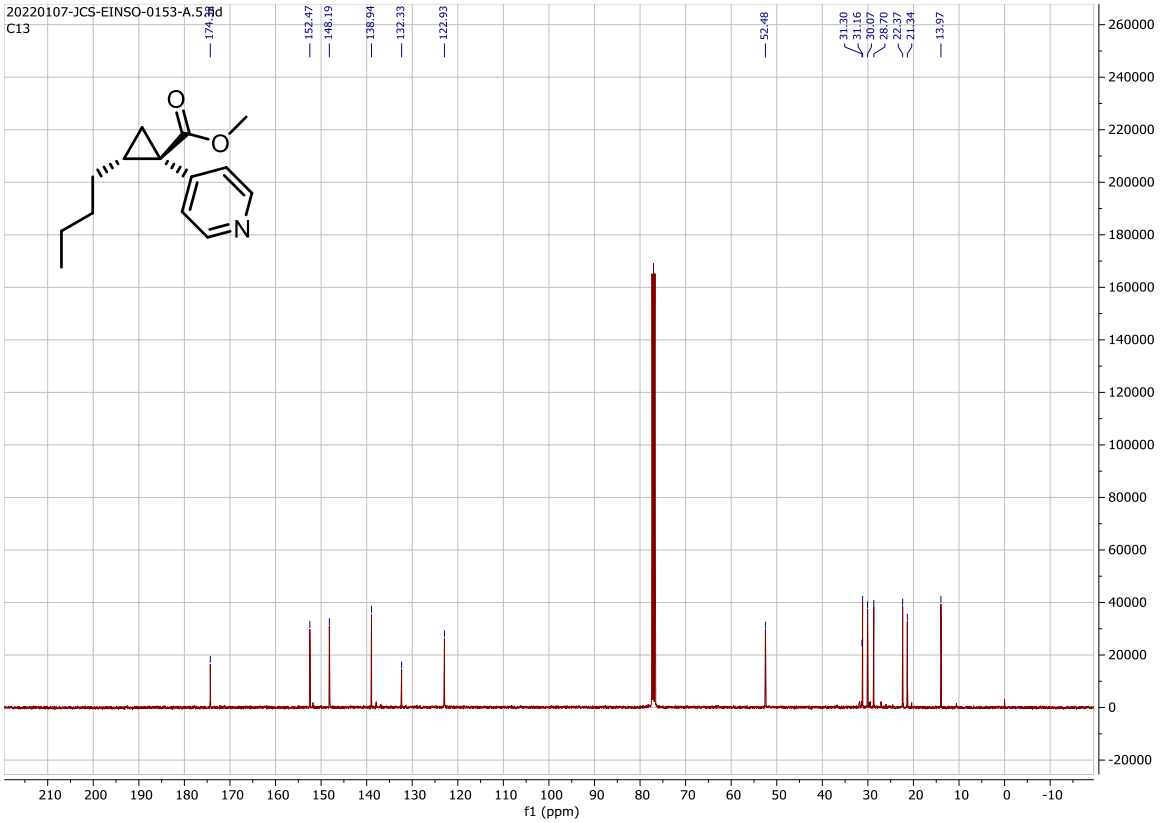

Racemate:

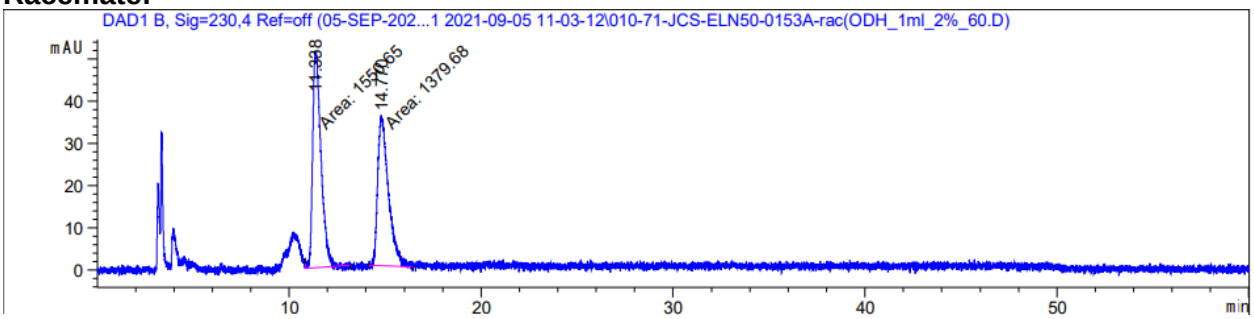

Signal 2: DAD1 B, Sig=230,4 Ref=off

Peak #	RetTime [min]	Type	Width [min]	Area [mAU*s]	Height [mAU]	Area %
1	11.338	MM	0.5022	1550.64990	51.45989	52.9173
2	14.770	MM	0.6466	1379.67664	35.56256	47.0827
Totals :				2930.32654	87.02245	

Chiral reactions:

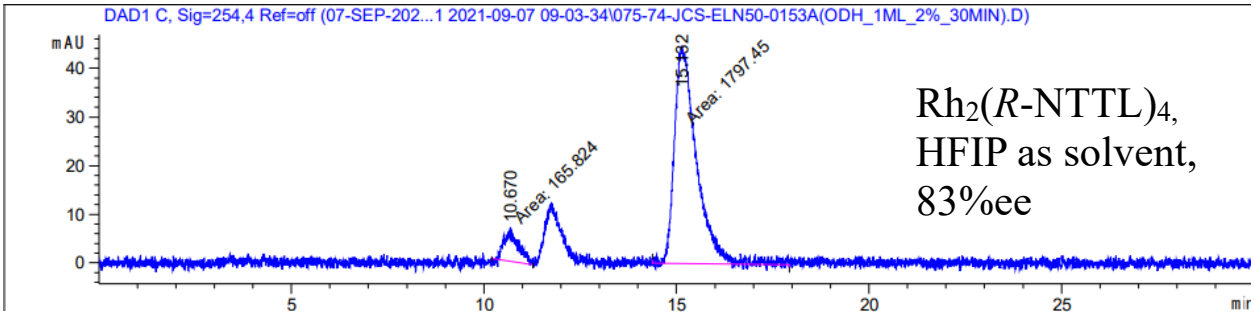

Signal 3: DAD1 C, Sig=254,4 Ref=off

Peak #	RetTime [min]	Type	Width [min]	Area [mAU*s]	Height [mAU]	Area %
1	10.670	MM	0.3946	165.82394	7.00427	8.4463
2	15.132	MM	0.6689	1797.45129	44.78339	91.5537

Totals : 1963.27524 51.78766

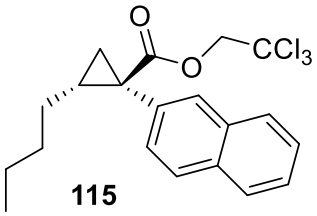

1H NMR:

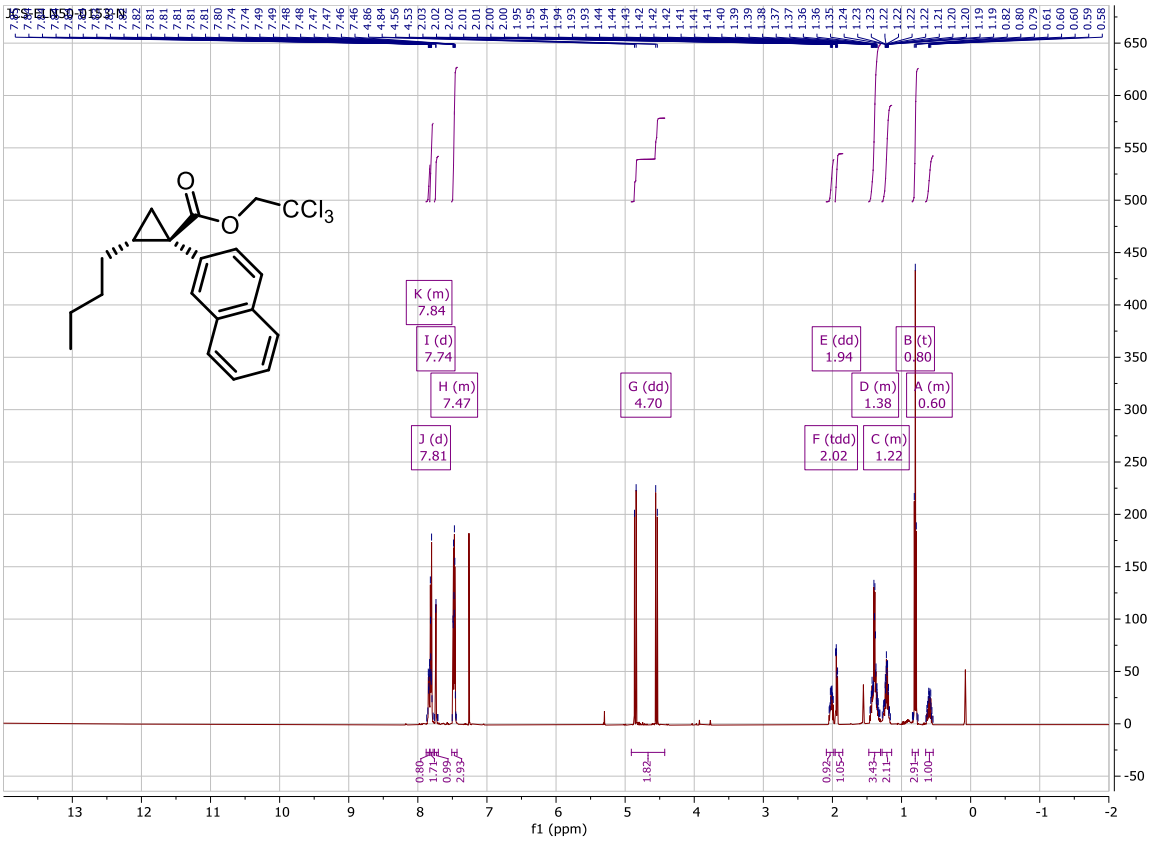

13C NMR:

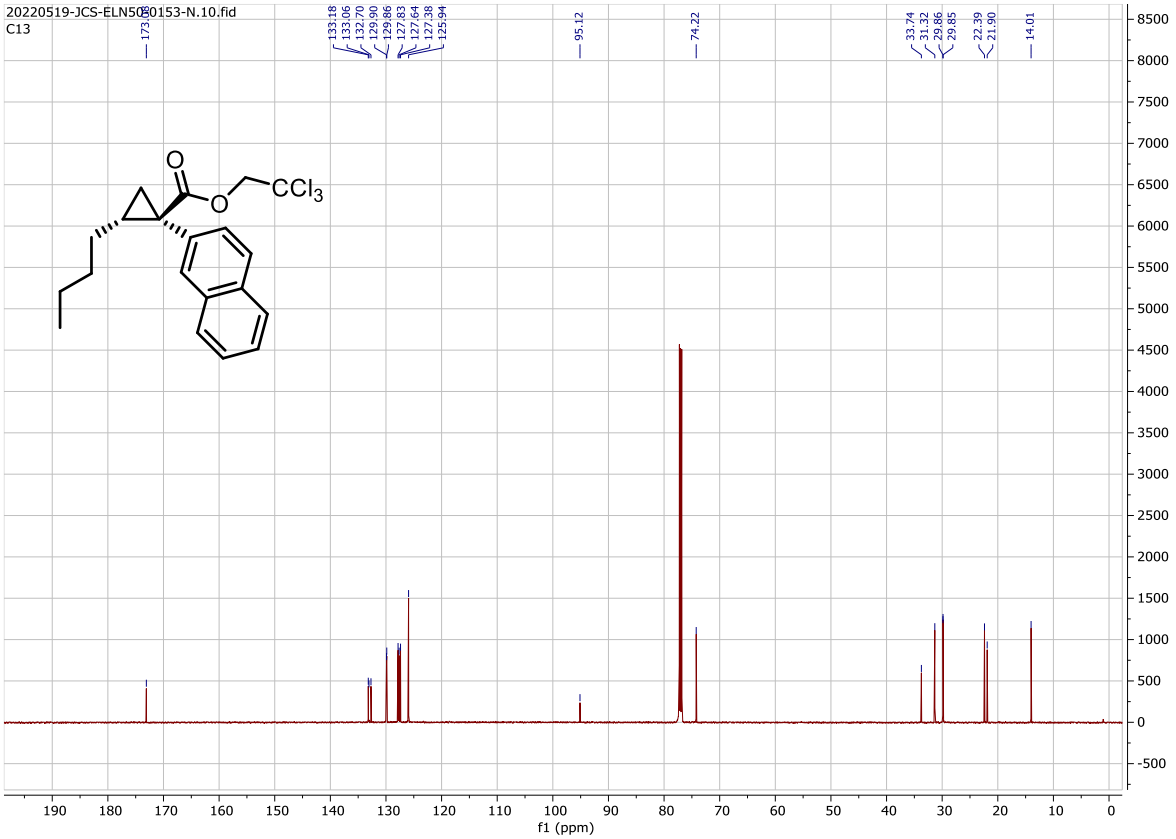

Racemate:

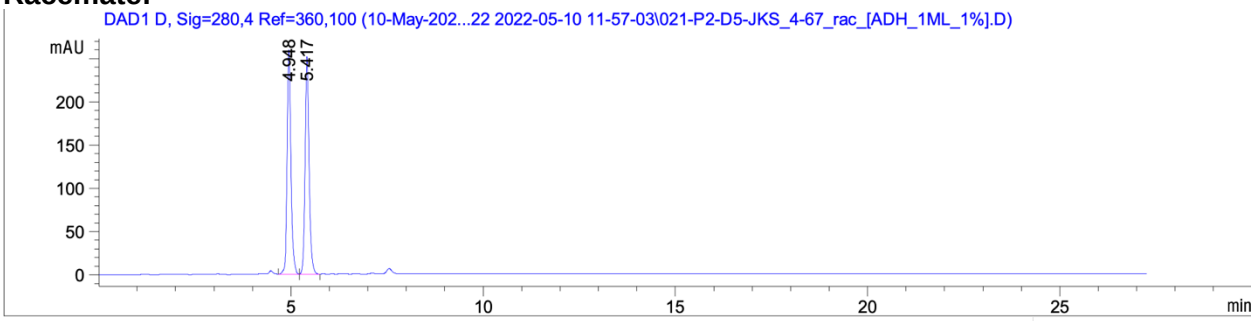

Signal 4: DAD1 D, Sig=280,4 Ref=360,100

Peak #	RetTime [min]	Type	Width [min]	Area [mAU*s]	Height [mAU]	Area %
1	4.948	BB	0.1040	1782.91492	260.08020	48.9374
2	5.417	BB	0.1123	1860.34387	251.58144	51.0626
Totals :				3643.25879	511.66164	

Chiral reactions:

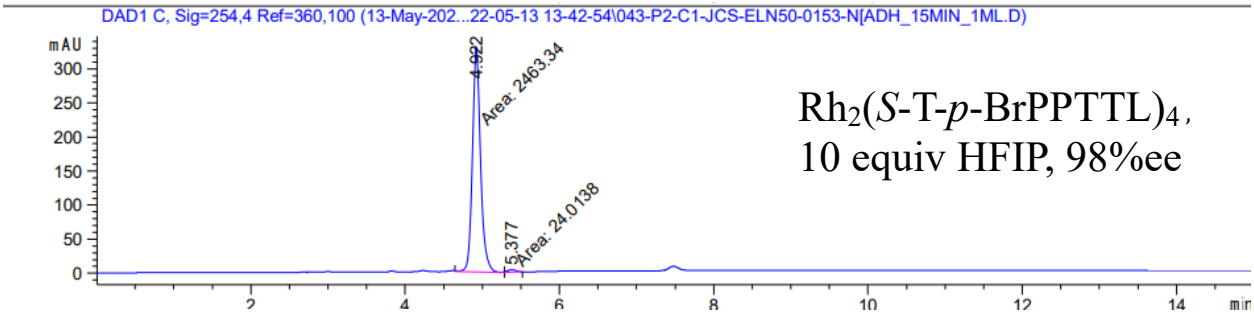

Rh_2(*S*-T-*p*-BrPPTTL)$_4$, 10 equiv HFIP, 98%ee

Signal 3: DAD1 C, Sig=254,4 Ref=360,100

Peak #	RetTime [min]	Type	Width [min]	Area [mAU*s]	Height [mAU]	Area %
1	4.922	MM	0.1245	2463.33618	329.87711	99.0346
2	5.377	MM	0.1106	24.01382	3.61916	0.9654

Totals : 2487.35001 333.49627

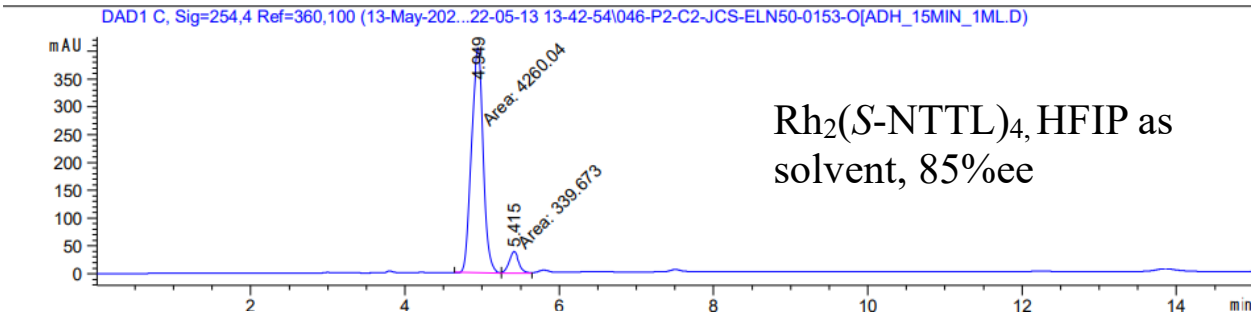

Rh_2(*S*-NTTL)$_4$, HFIP as solvent, 85%ee

Signal 3: DAD1 C, Sig=254,4 Ref=360,100

Peak #	RetTime [min]	Type	Width [min]	Area [mAU*s]	Height [mAU]	Area %
1	4.949	MM	0.1756	4260.04248	404.36258	92.6154
2	5.415	MM	0.1452	339.67264	38.97867	7.3846

Totals : 4599.71512 443.34125

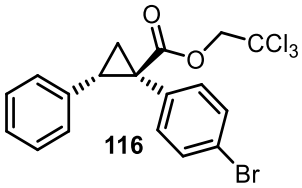

116

Chiral reactions:

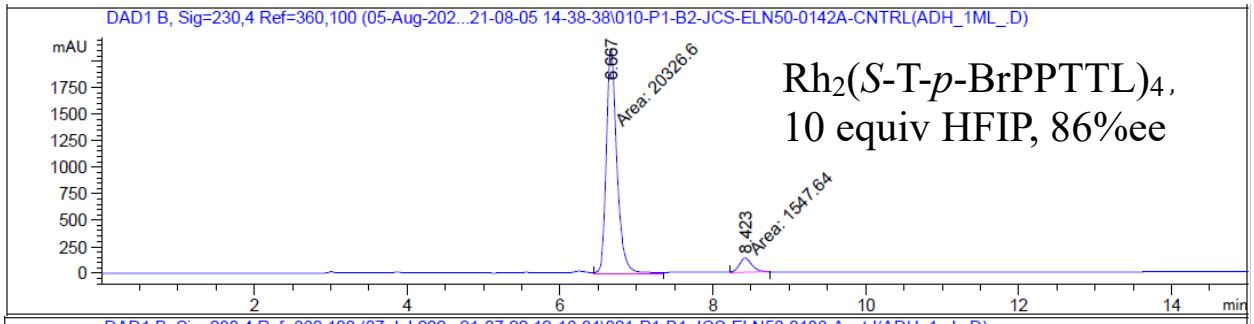

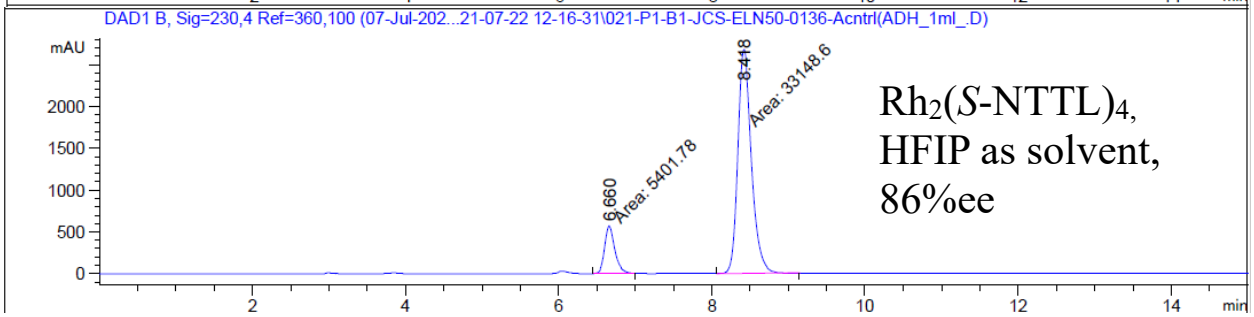

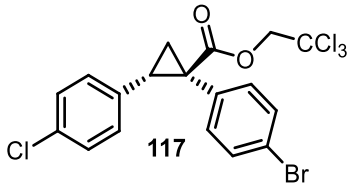

117

Chiral reactions:

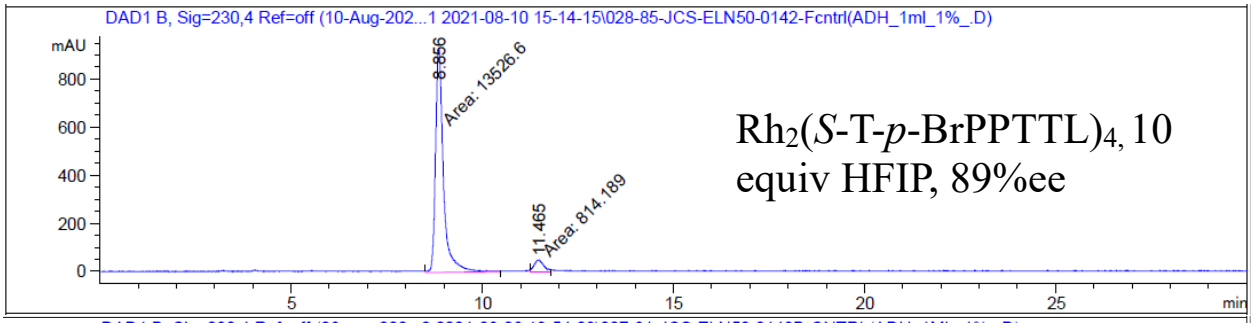

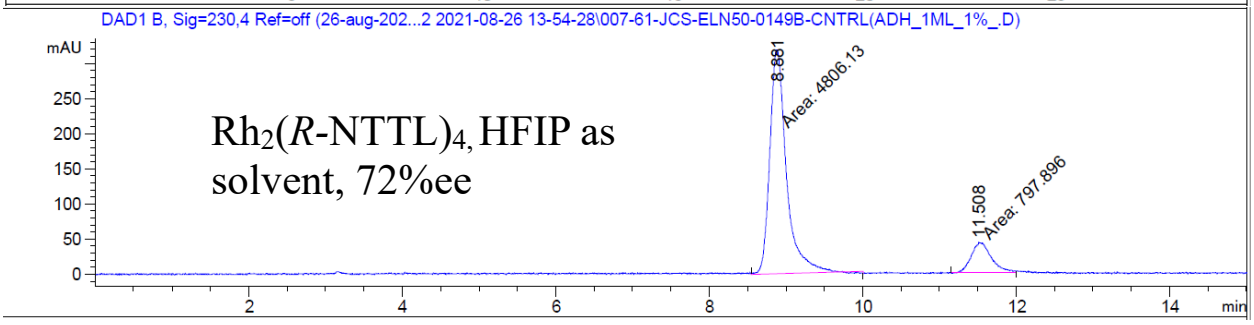

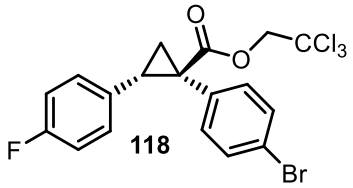

Chiral reactions:

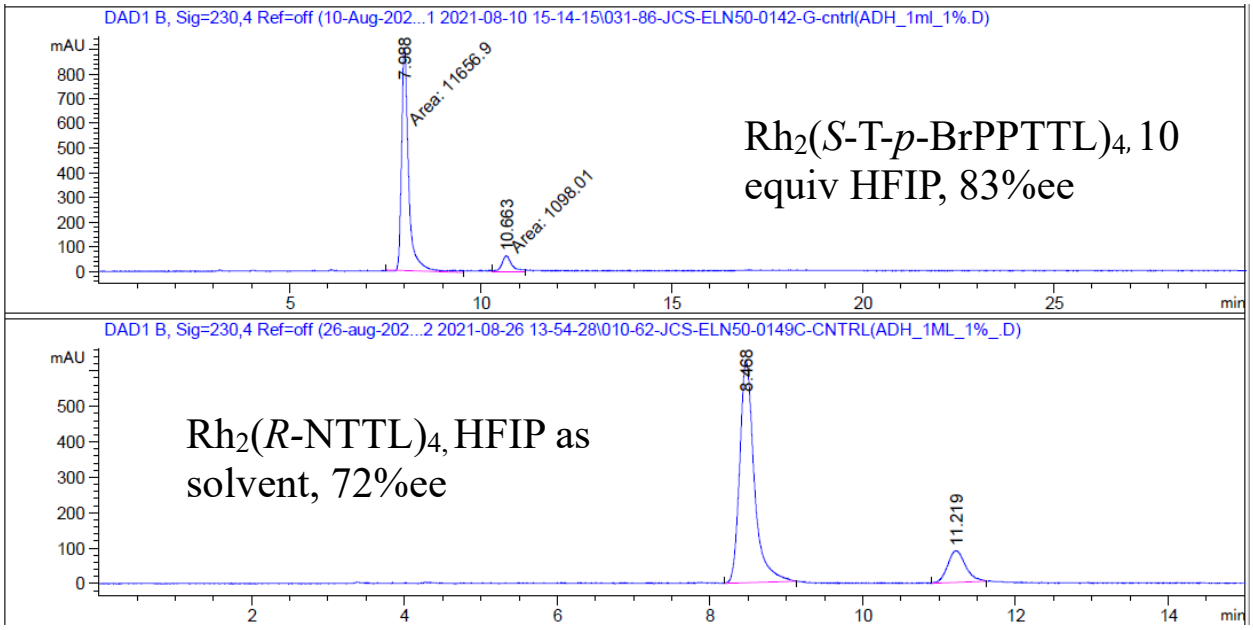

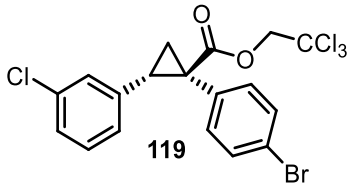

119

1H NMR:

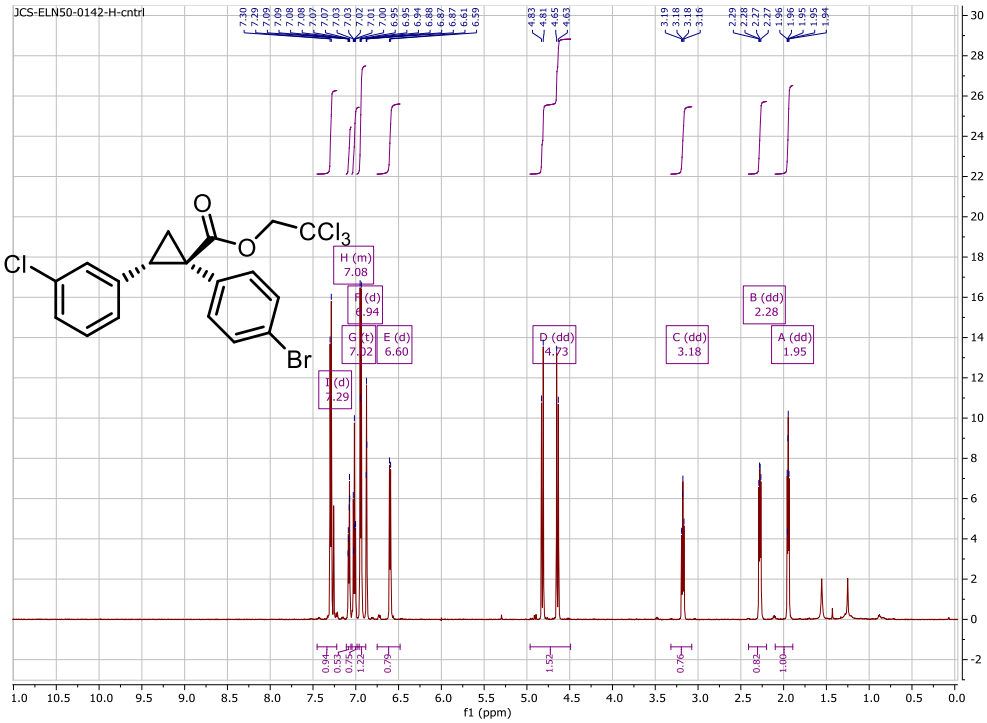

13C NMR:

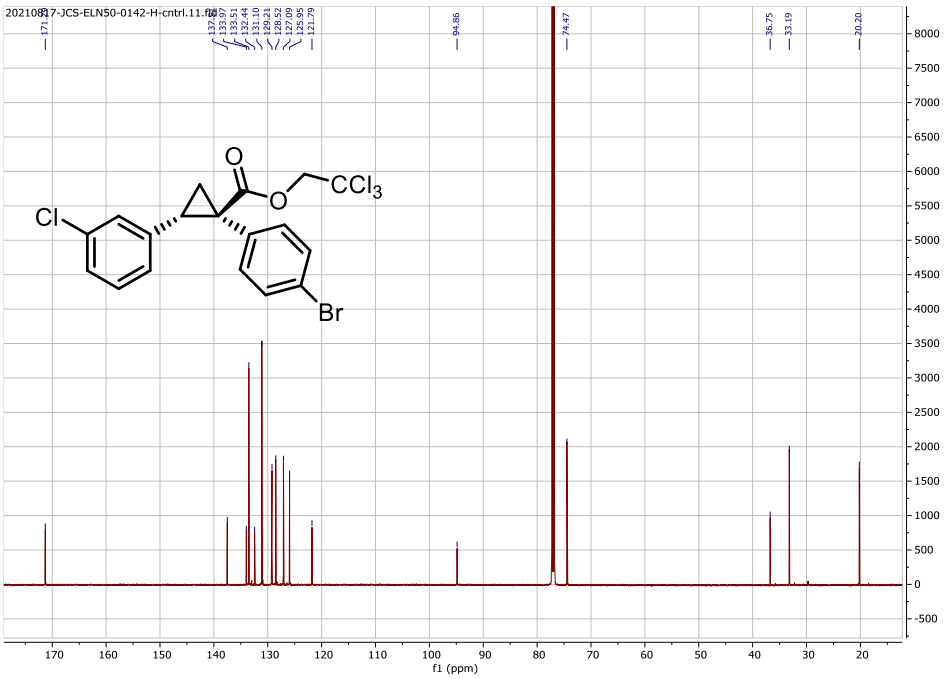

Racemate:

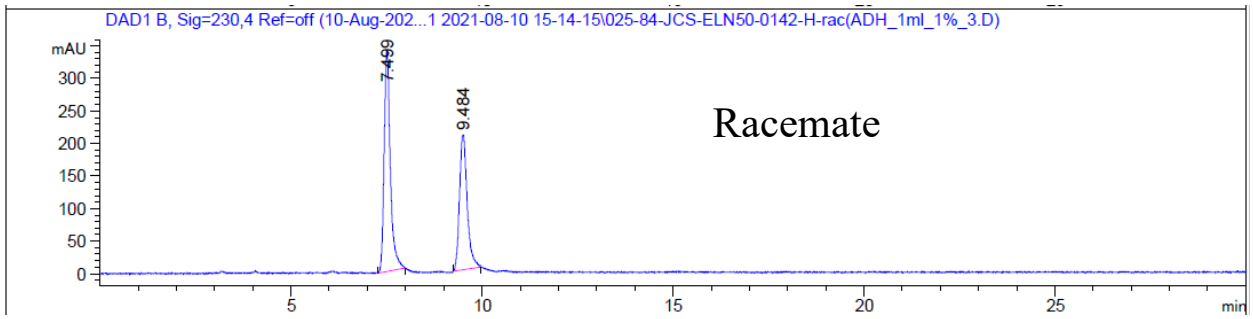

Chiral reactions:

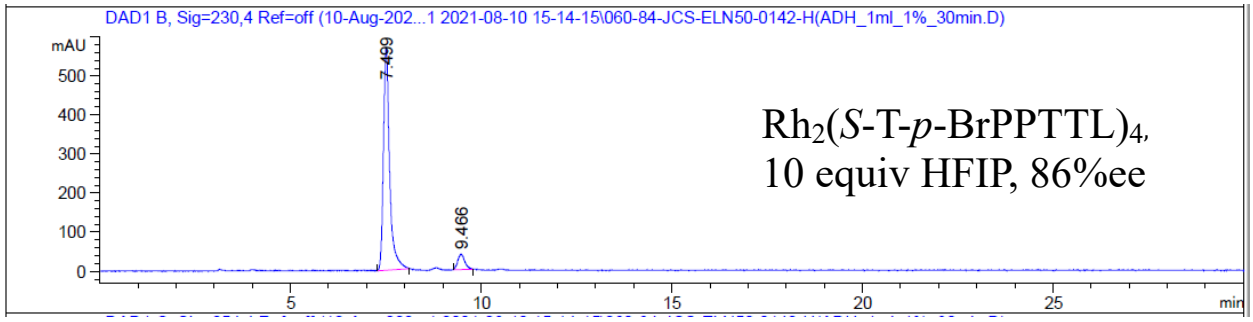

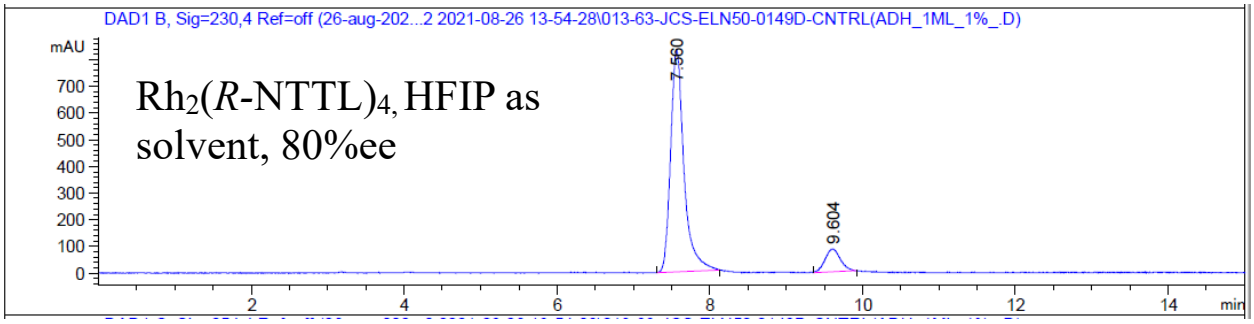

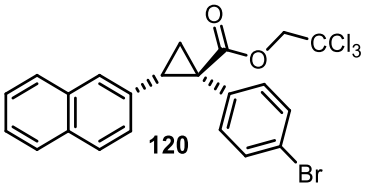
O
O
CCl3
Br

120

1H NMR:

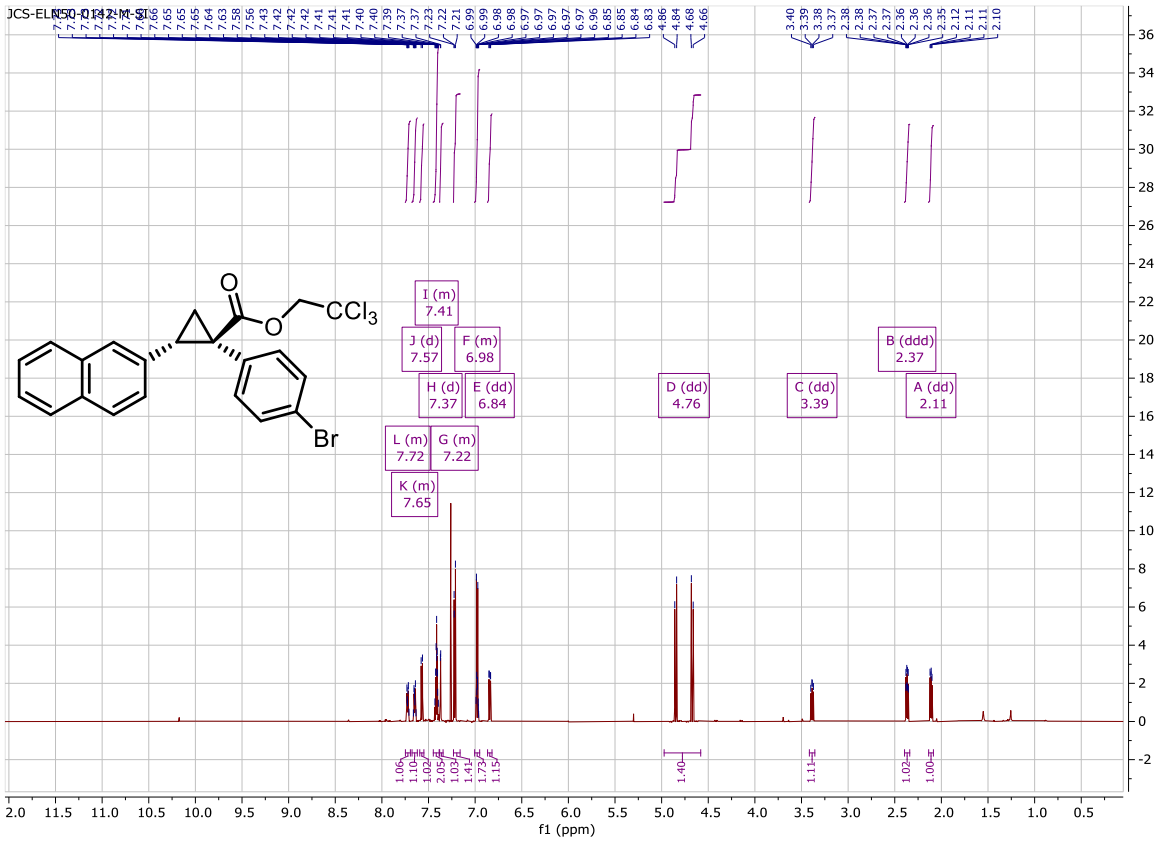
JCS-ELN50-0142-M-S1
I (m) 7.41
J (d) 7.57
F (m) 6.98
H (d) 7.37
E (dd) 6.84
L (m) 7.72
G (m) 7.22
K (m) 7.65
D (dd) 4.76
C (dd) 3.39
B (ddd) 2.37
A (dd) 2.11
f1 (ppm)

13C NMR:

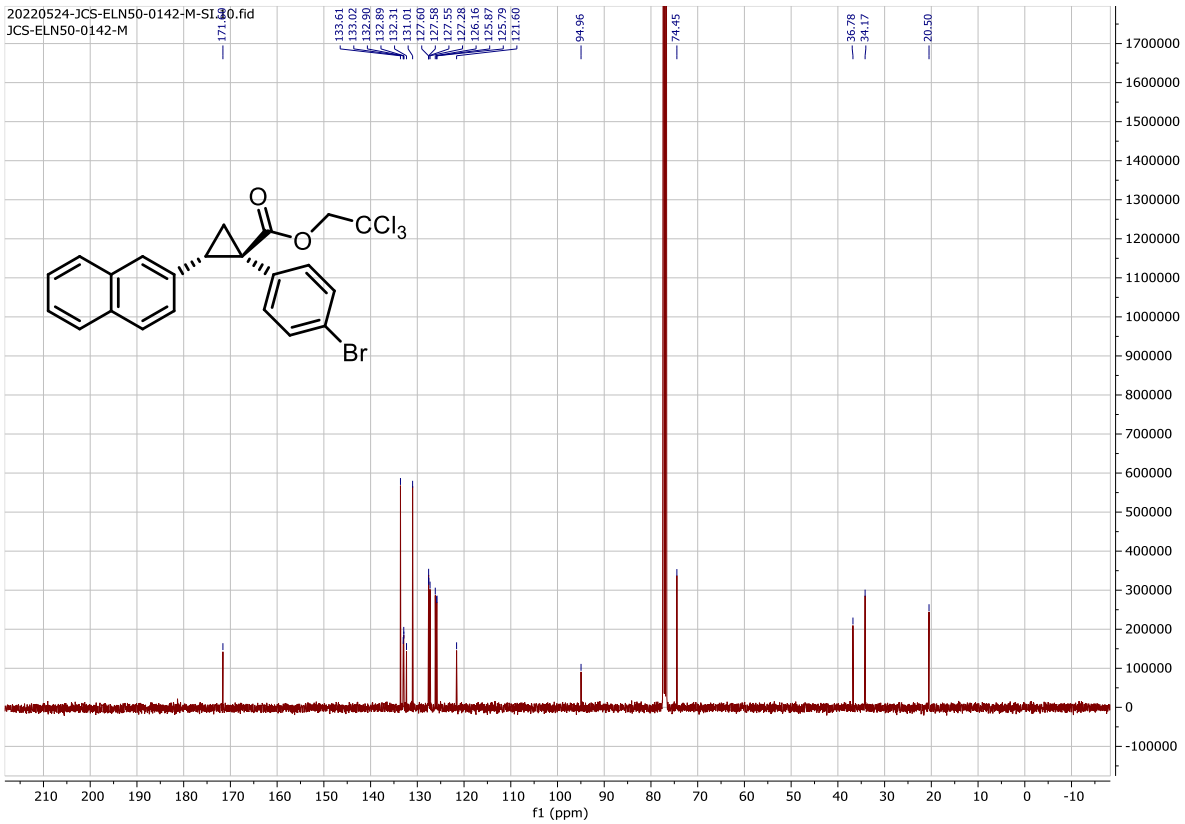
20220524-JCS-ELN50-0142-M-SI.10.fid
JCS-ELN50-0142-M
171.43
133.61
133.02
132.90
132.89
132.31
131.01
127.60
127.58
127.55
127.28
126.16
125.87
125.79
121.60
94.96
74.45
36.78
34.17
20.50
O
O
CCl3
Br
f1 (ppm)

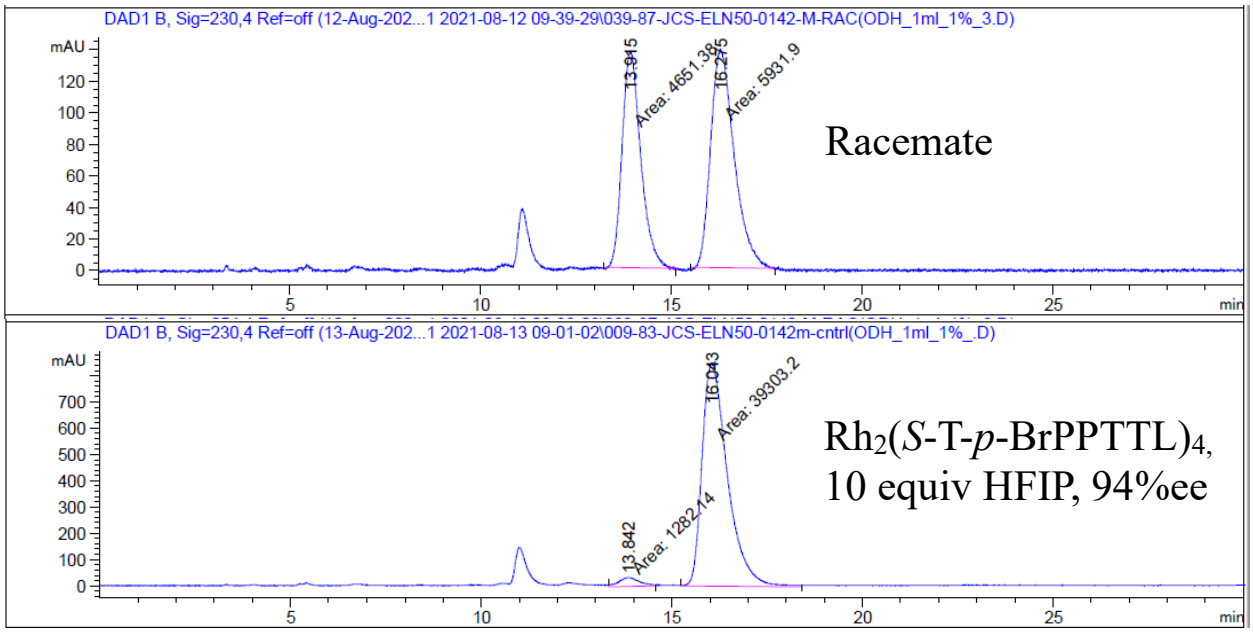
DAD1 B, Sig=230,4 Ref=off (12-Aug-202...1 2021-08-12 09-39-29\039-87-JCS-ELN50-0142-M-RAC(ODH_1ml_1%_3.D)
mAU
13.915
Area: 4651.38
16.275
Area: 5931.9
Racemate
min
DAD1 B, Sig=230,4 Ref=off (13-Aug-202...1 2021-08-13 09-01-02\009-83-JCS-ELN50-0142m-cntrl(ODH_1ml_1%_.D)
mAU
16.043
Area: 39303.2
13.842
Area: 1282.14
Rh2(S-T-p-BrPPTTL)4,
10 equiv HFIP, 94%ee
min

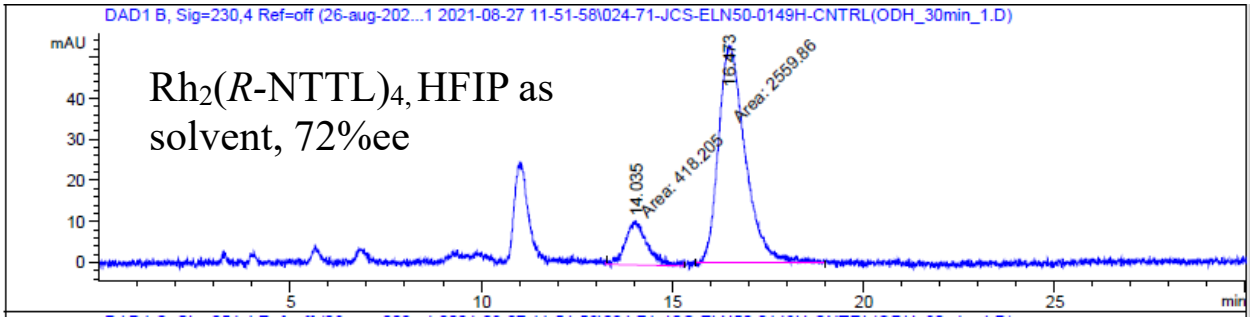
DAD1 B, Sig=230,4 Ref=off (26-aug-202...1 2021-08-27 11-51-58\024-71-JCS-ELN50-0149H-CNTRL(ODH_30min_1.D)
mAU
Rh2(R-NTTL)4, HFIP as solvent, 72%ee
14.035
Area: 418.205
16.473
Area: 2559.86
min

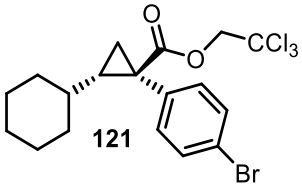
O
O
CCl3
Br

121

1H NMR:

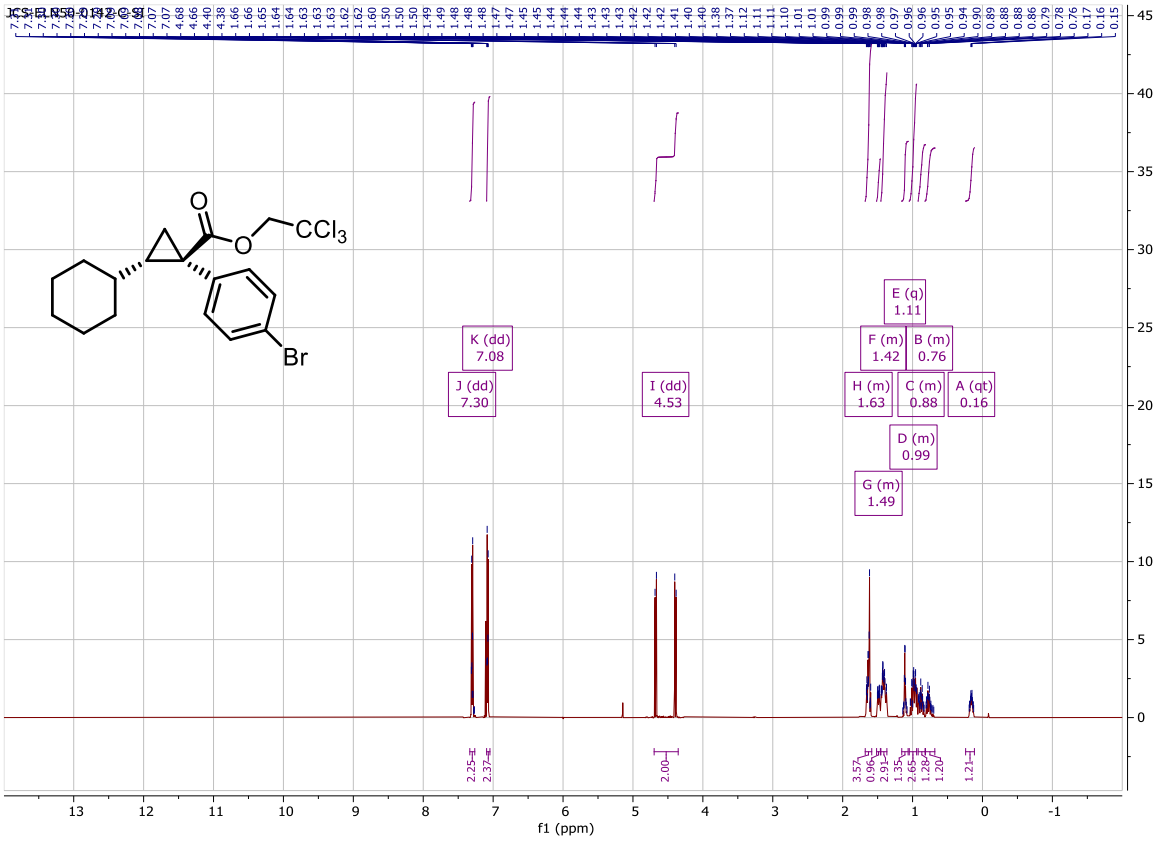
JCS-ELN50-0142
K (dd) 7.08
J (dd) 7.30
I (dd) 4.53
E (q) 1.11
F (m) 1.42
B (m) 0.76
H (m) 1.63
C (m) 0.88
A (qt) 0.16
D (m) 0.99
G (m) 1.49
f1 (ppm)

13C NMR:

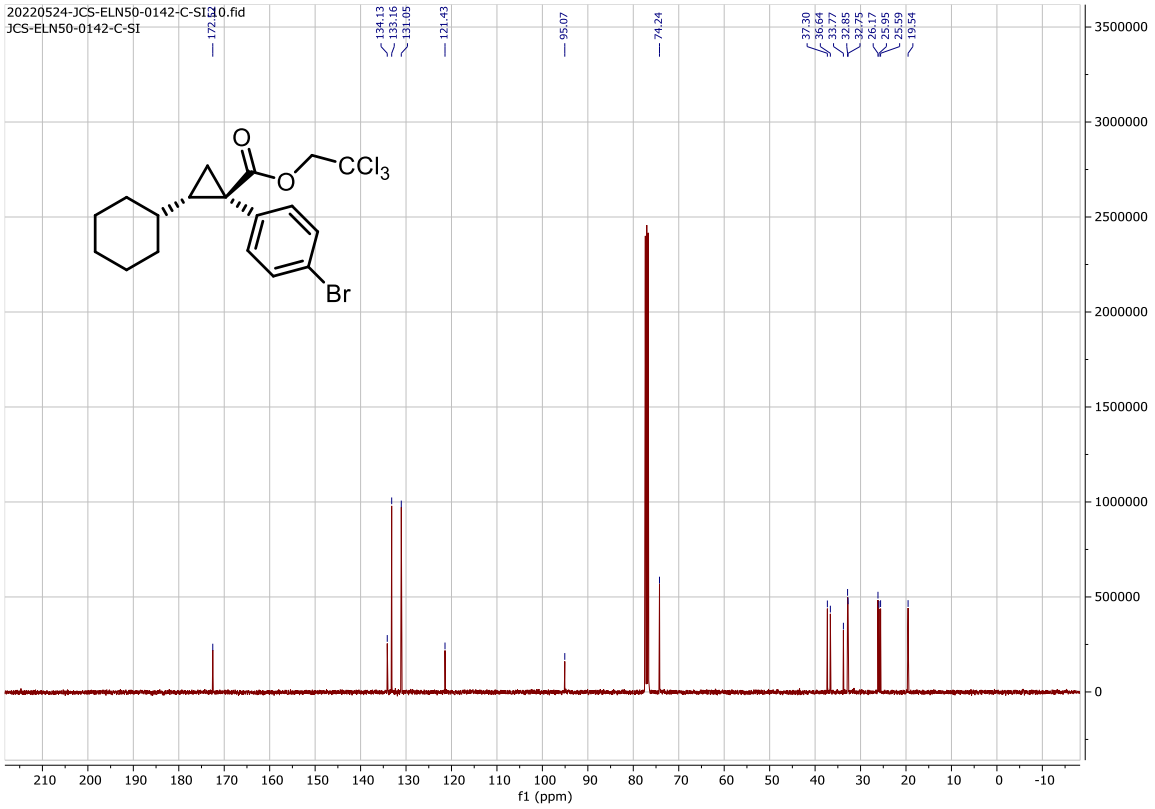

Racemate:

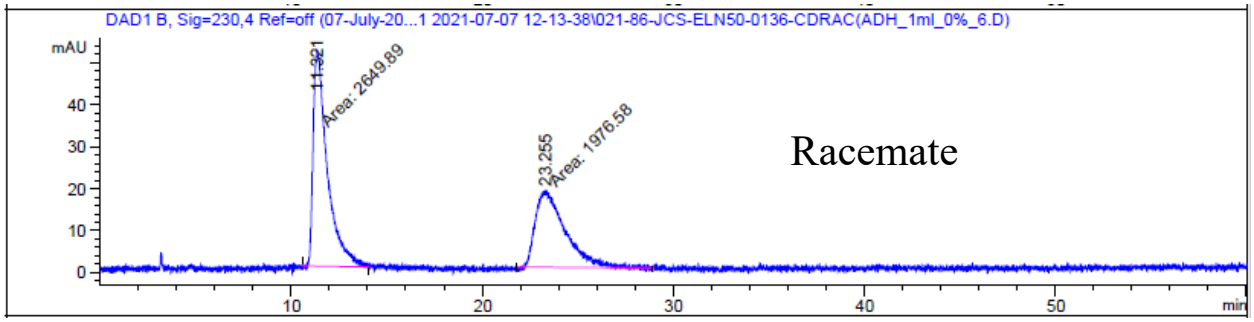

Chiral reactions:

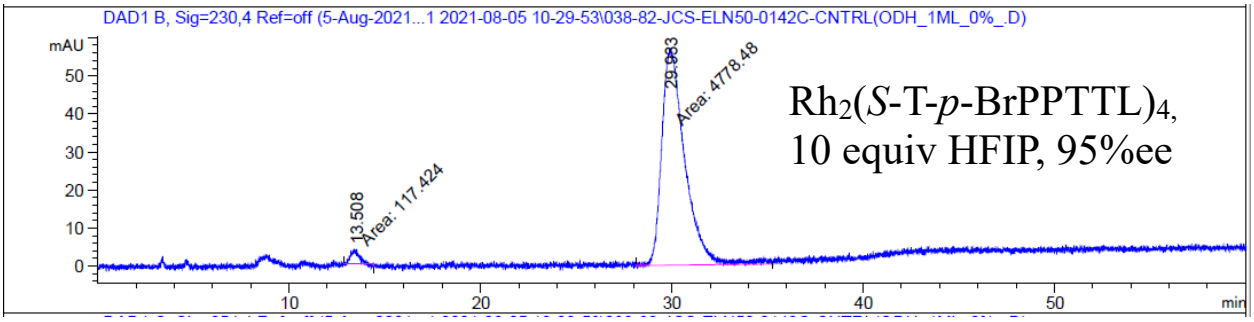

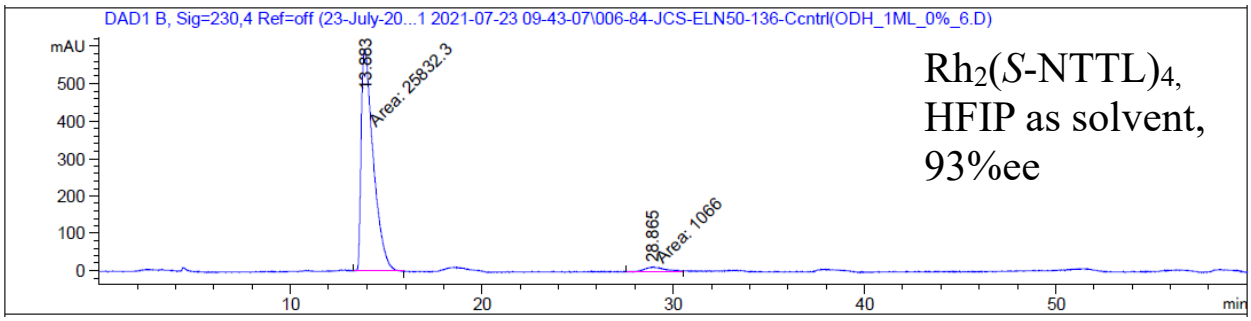
DAD1 B, Sig=230,4 Ref=off (23-July-20...1 2021-07-23 09-43-07\006-84-JCS-ELN50-136-Ccntrl(ODH_1ML_0%_6.D)
mAU
13.883
Area: 25832.3
28.865
Area: 1066
Rh2(S-NTTL)4,
HFIP as solvent,
93%ee
min

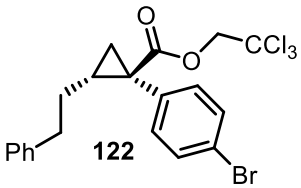
O
O
CCl3
Ph
122
Br

1H NMR:

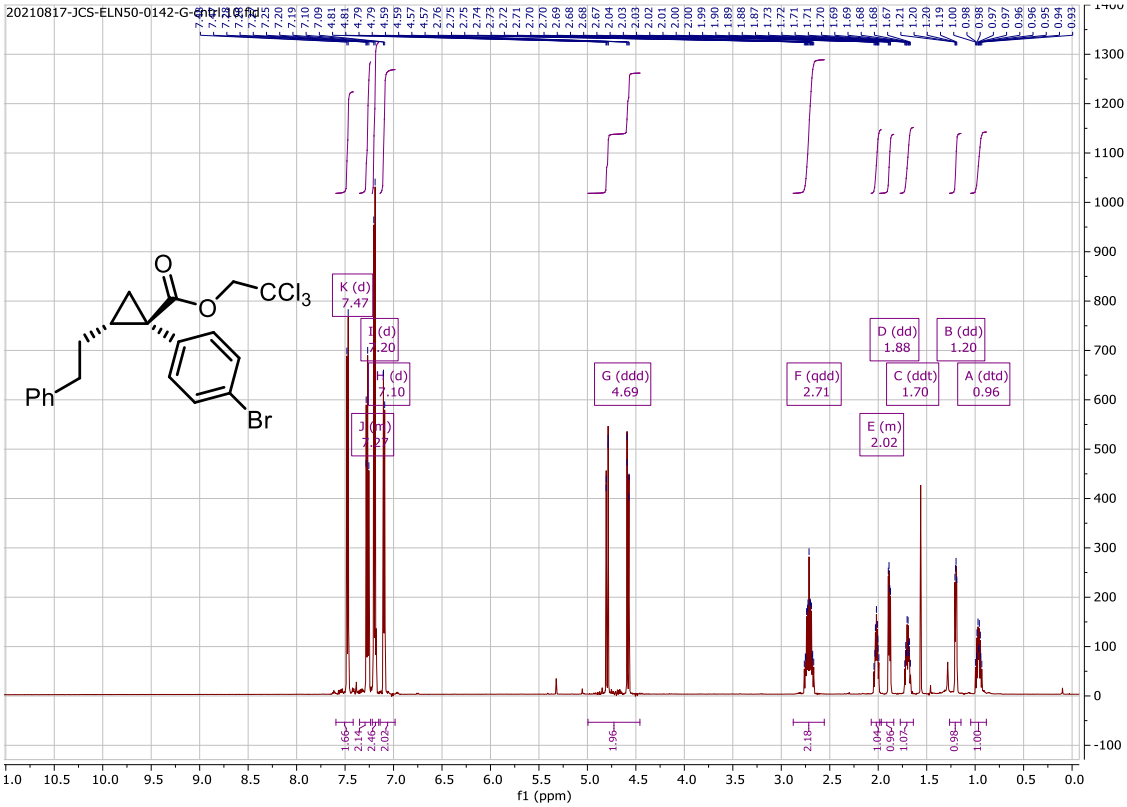
20210817-JCS-ELN50-0142-G-ch
K (d)
7.47
I (d)
7.20
H (d)
7.10
J (m)
7.07
G (ddd)
4.69
F (qdd)
2.71
D (dd)
1.88
B (dd)
1.20
C (ddt)
1.70
A (dtd)
0.96
E (m)
2.02
f1 (ppm)

13C NMR:

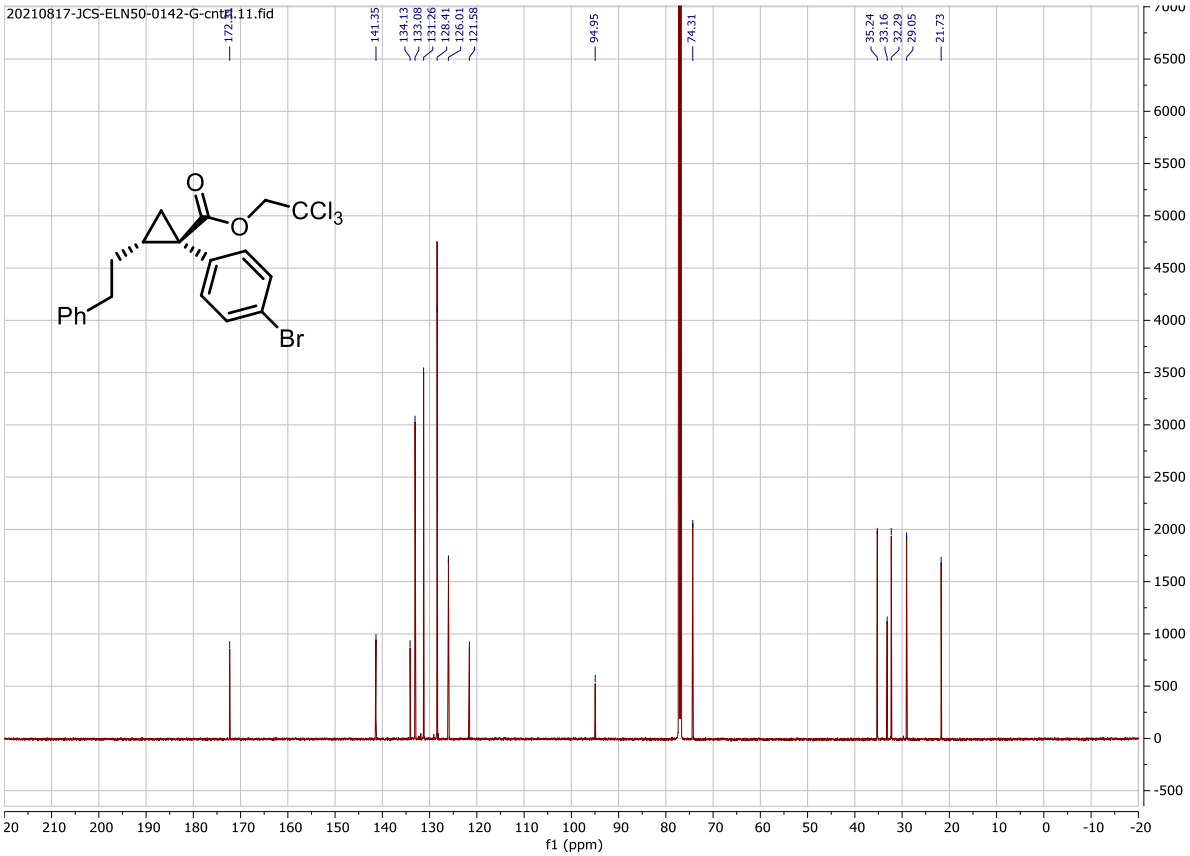

Racemate:

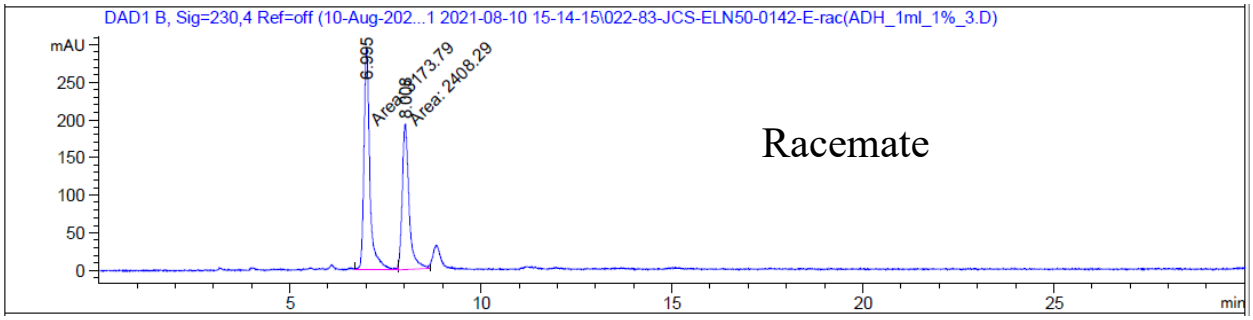

Chiral reactions:

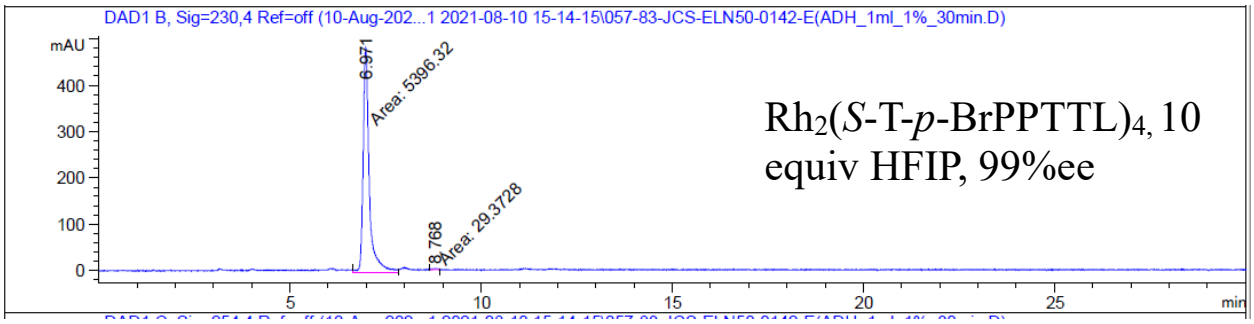

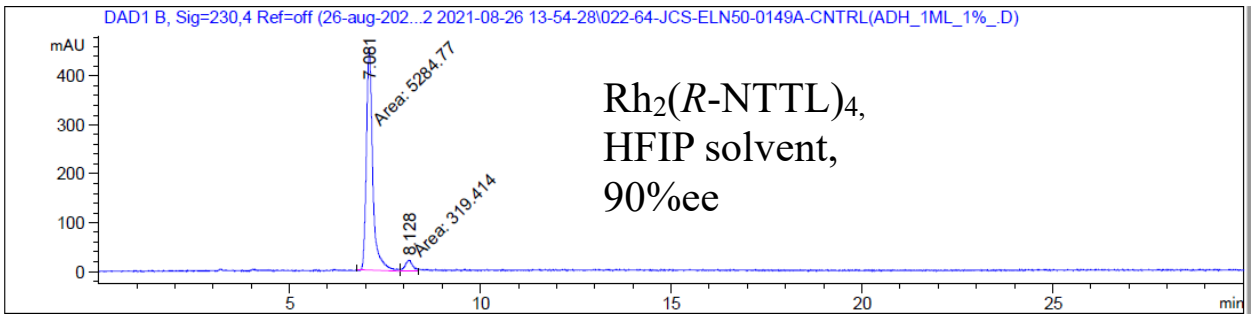
DAD1 B, Sig=230,4 Ref=off (26-aug-202...2 2021-08-26 13-54-28\022-64-JCS-ELN50-0149A-CNTRL(ADH_1ML_1%_.D)
mAU
7.081
Area: 5284.77
8.128
Area: 319.414
Rh2(R-NTTL)4,
HFIP solvent,
90%ee
min

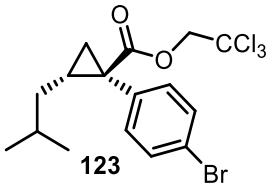
O
O
CCl3
Br

123

1H NMR:

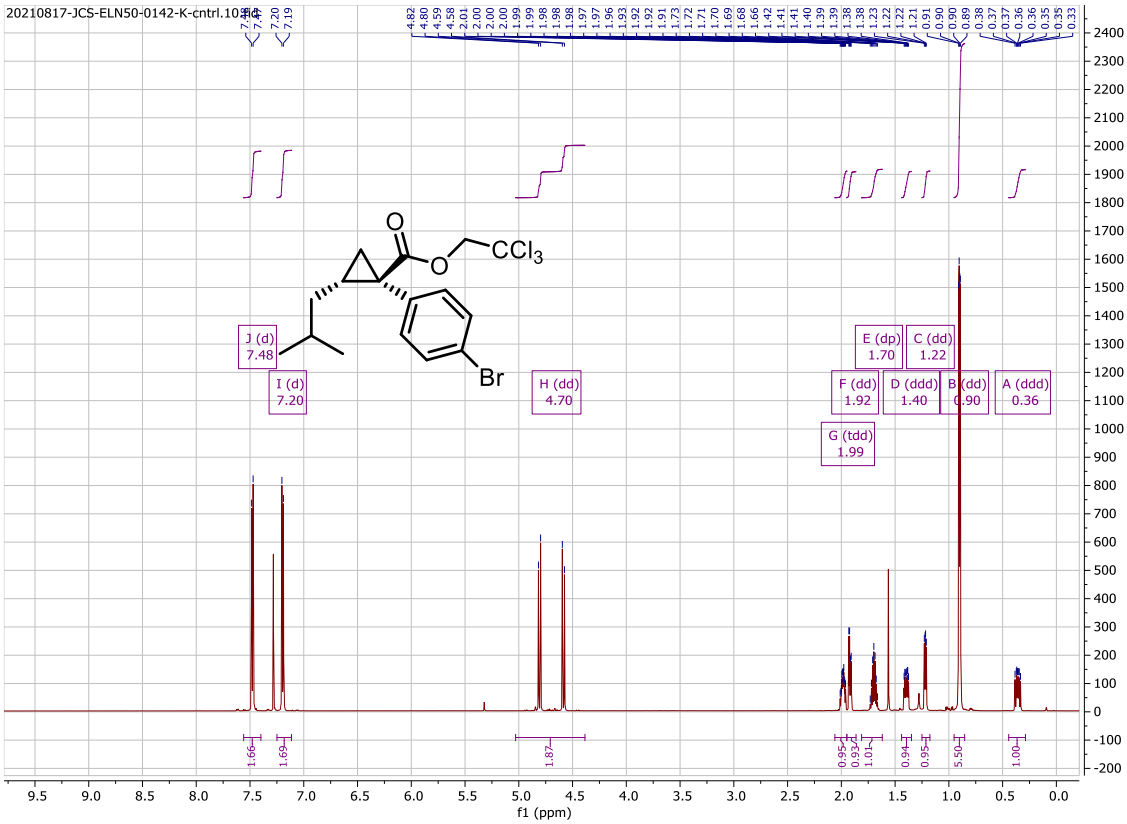
20210817-JCS-ELN50-0142-K-cntrl.1014
J (d)
7.48
I (d)
7.20
H (dd)
4.70
E (dp)
1.70
C (dd)
1.22
F (dd)
1.92
D (ddd)
1.40
B (dd)
0.90
A (ddd)
0.36
G (tdd)
1.99
f1 (ppm)

13C NMR:

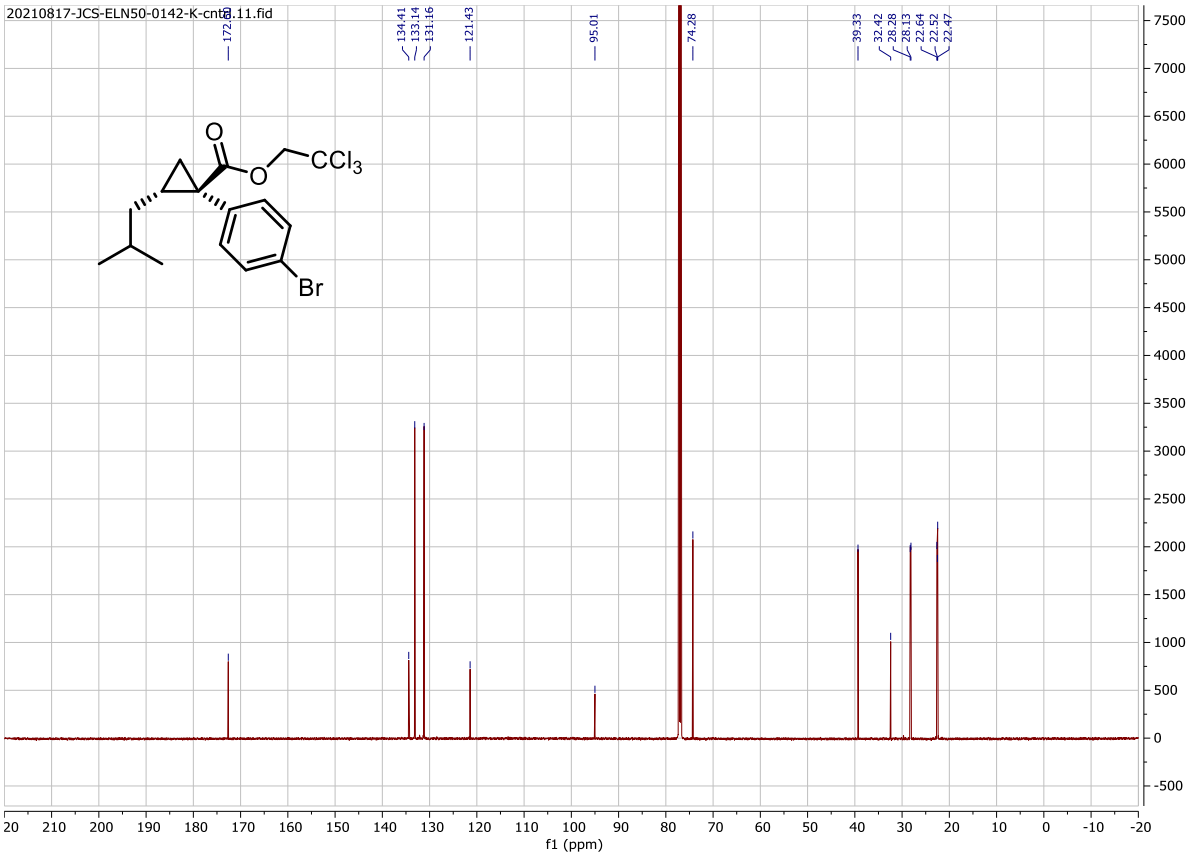

Racemate:

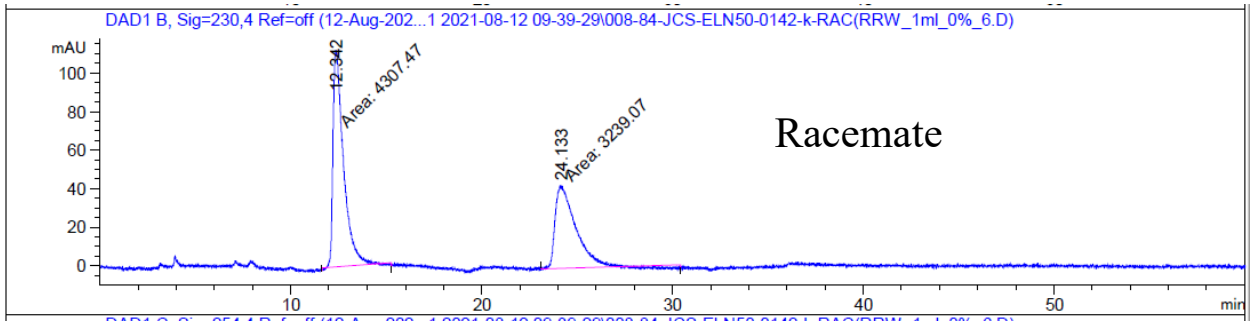

Chiral reactions:

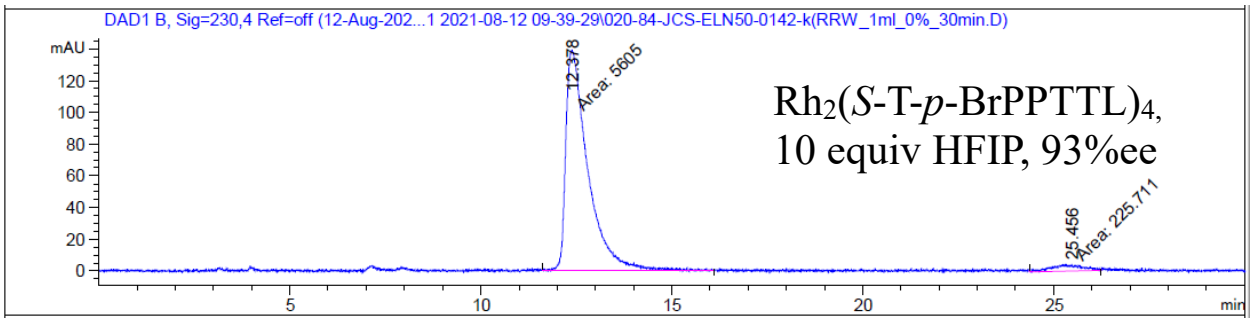

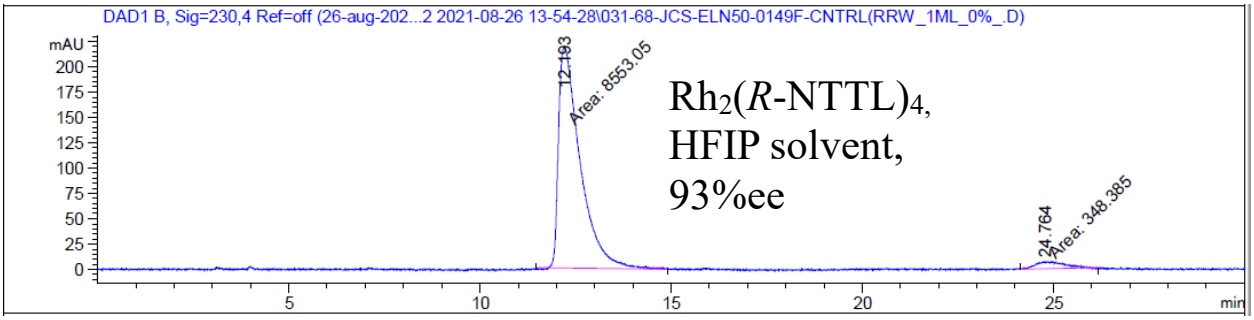
DAD1 B, Sig=230,4 Ref=off (26-aug-202...2 2021-08-26 13-54-28\031-68-JCS-ELN50-0149F-CNTRL(RRW_1ML_0%_.D)
mAU
12.183
Area: 8553.05
Rh2(R-NTTL)4,
HFIP solvent,
93%ee
24.764
Area: 348.385
min

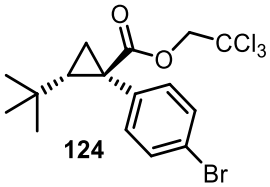
O
O
CCl3
Br

124

1H NMR:

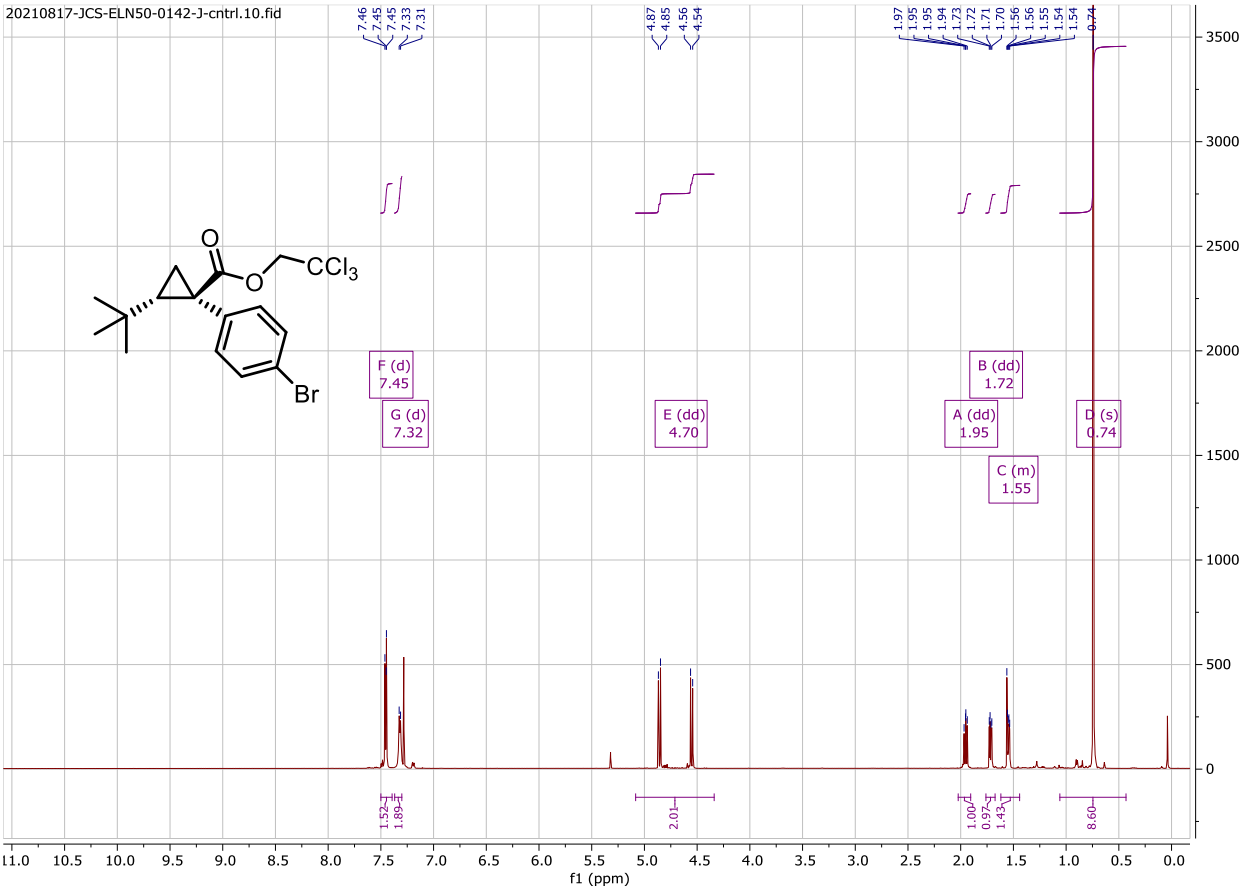
20210817-JCS-ELN50-0142-J-cntrl.10.fid
F (d)
7.45
G (d)
7.32
E (dd)
4.70
B (dd)
1.72
A (dd)
1.95
C (m)
1.55
D (s)
0.74
f1 (ppm)

13C NMR:

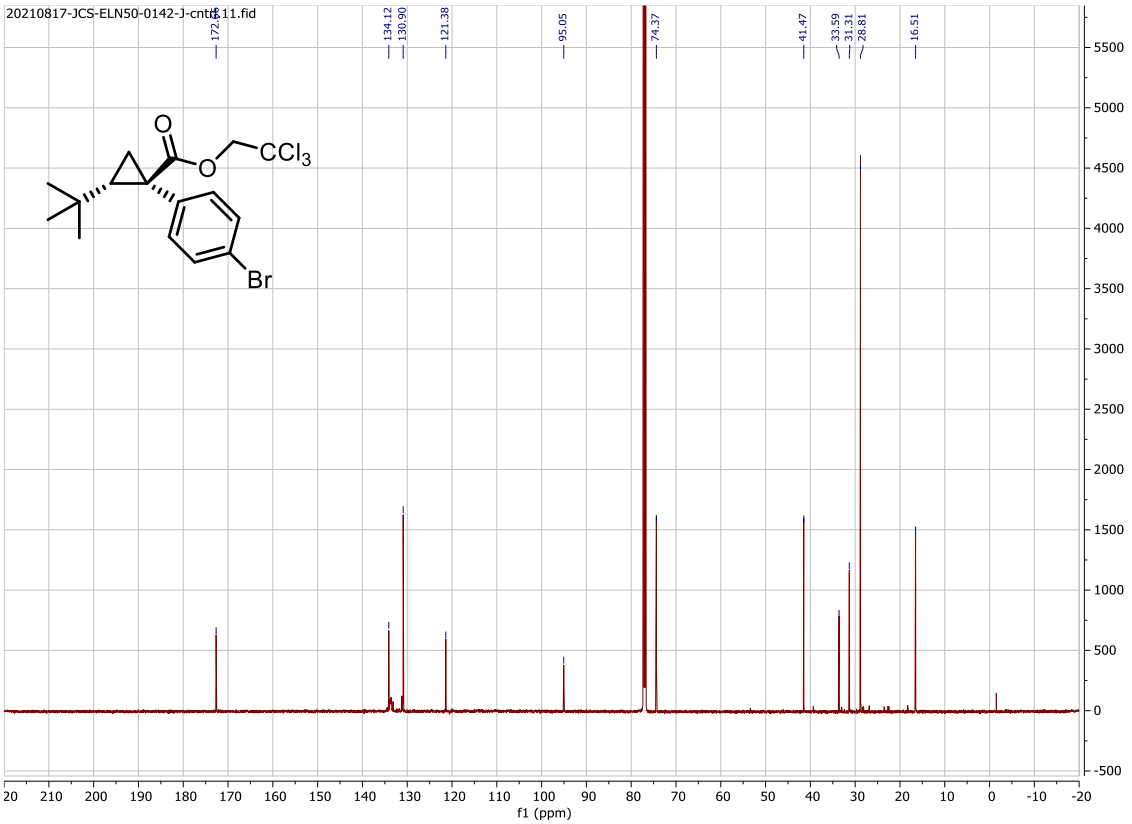

Racemate:

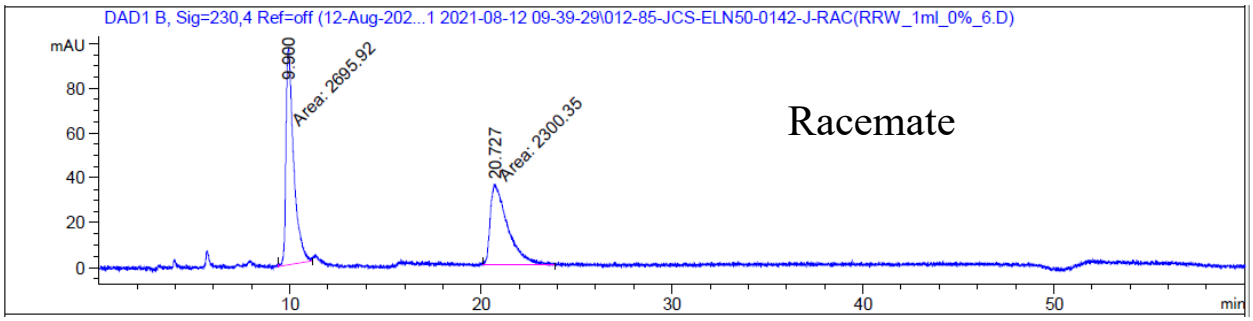

Chiral reactions:

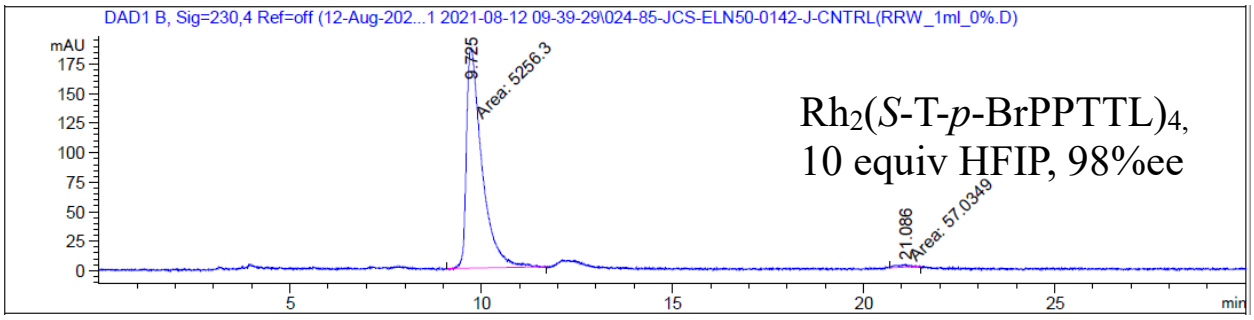

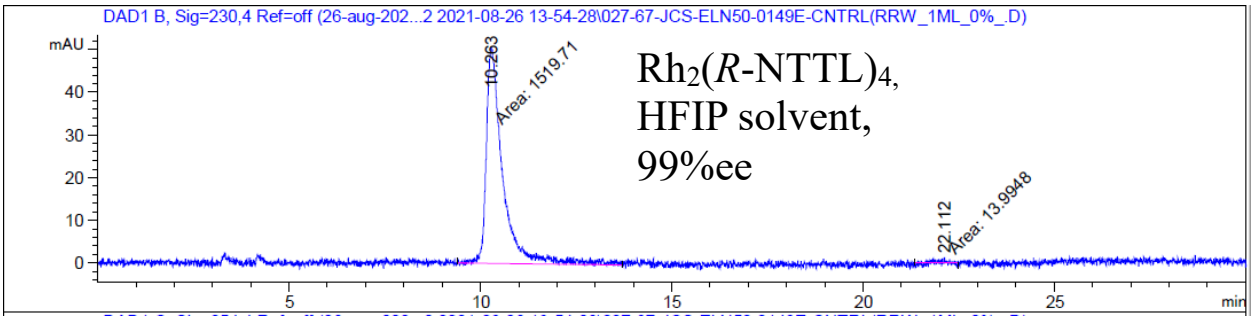

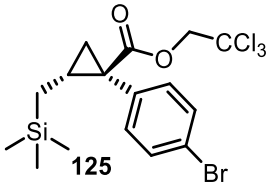

125

1H NMR: D.r was determined to be 7:1 due to the relative integrations of peaks appearing at 0.32 and -0.47 ppm corresponding to the silyl methylene which is significantly shielded by the adjacent phenyl in the major *E*-cyclopropane isomer. Absolute stereoconfiguration of this compound was confirmed by X-Ray crystallography.

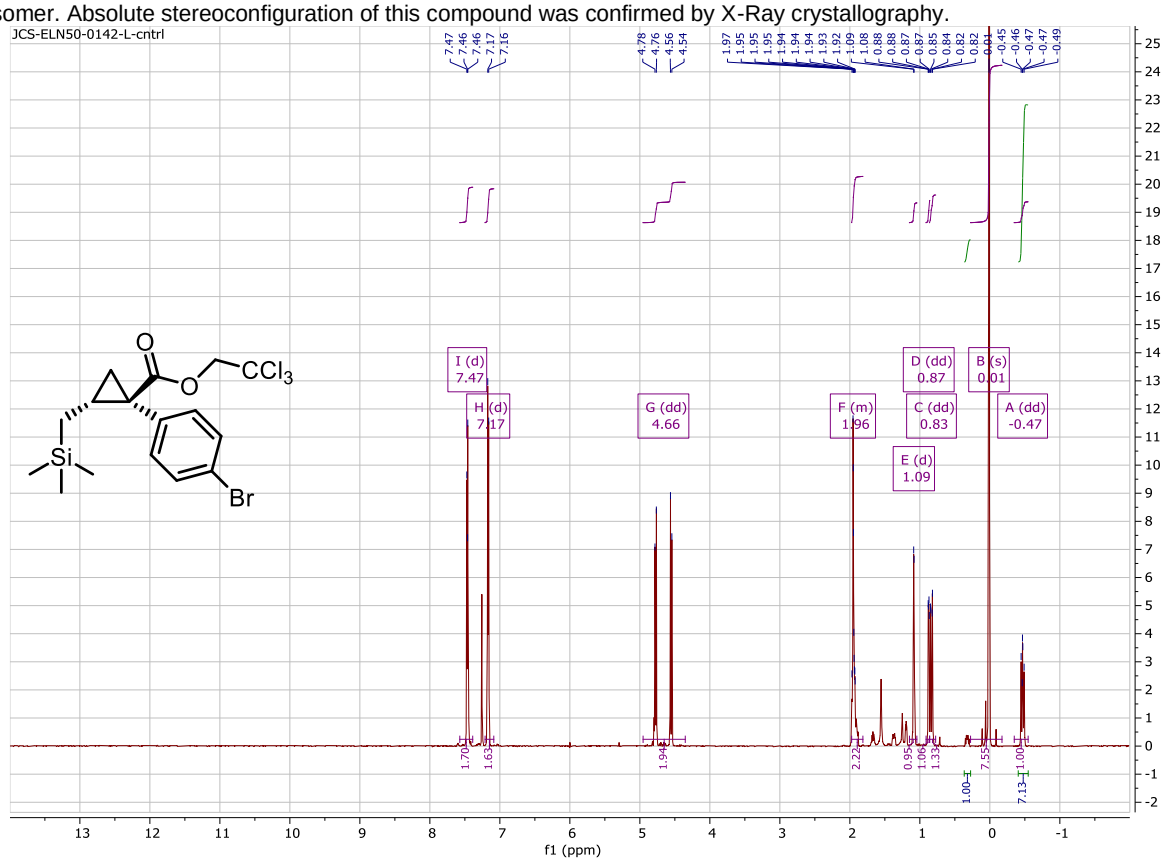

13C NMR:

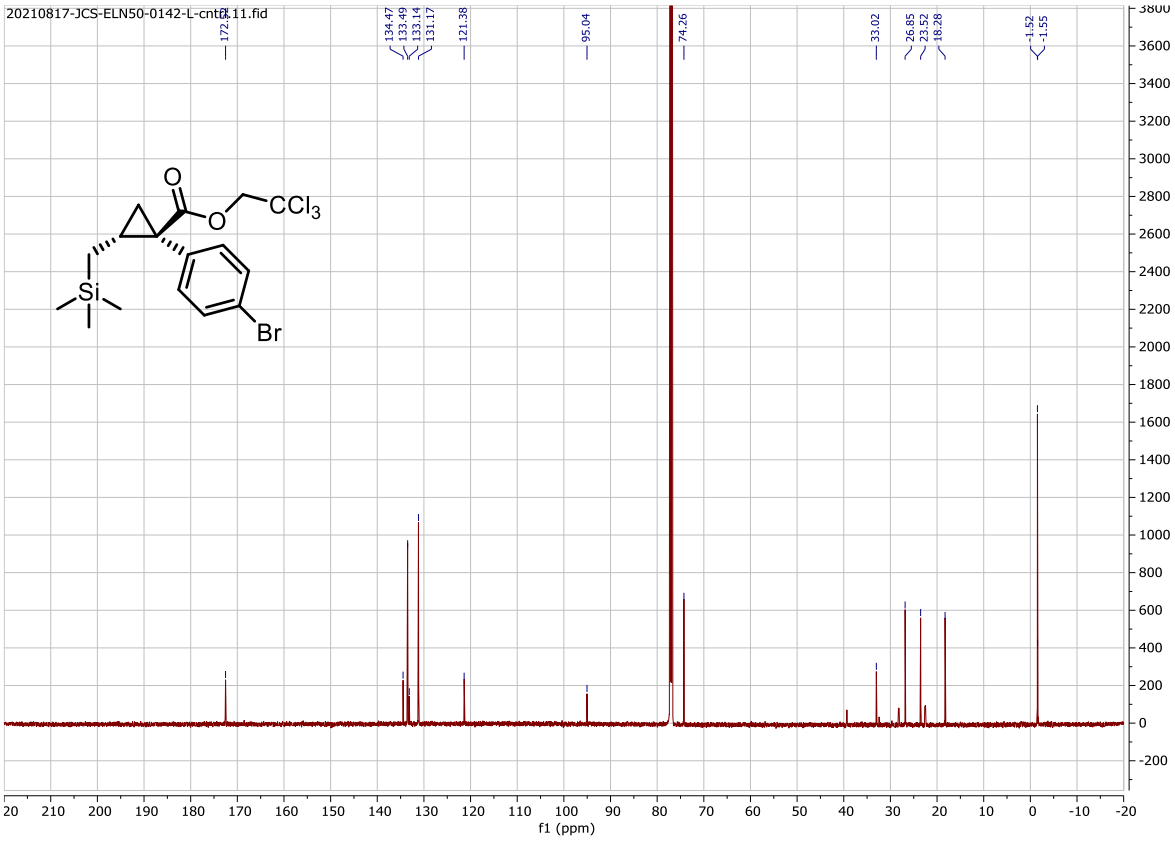

Racemate:

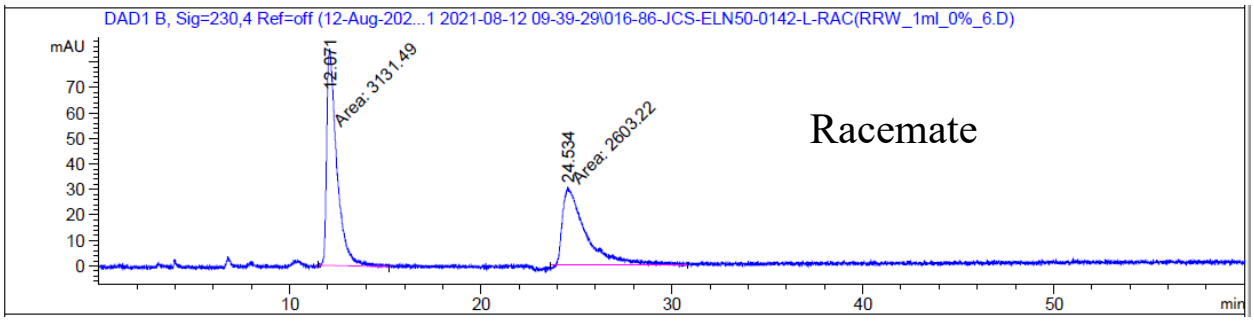

Chiral reactions:

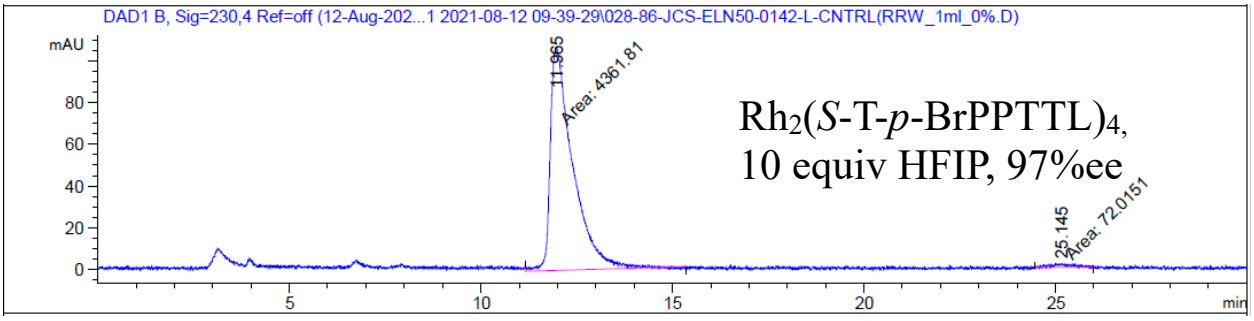

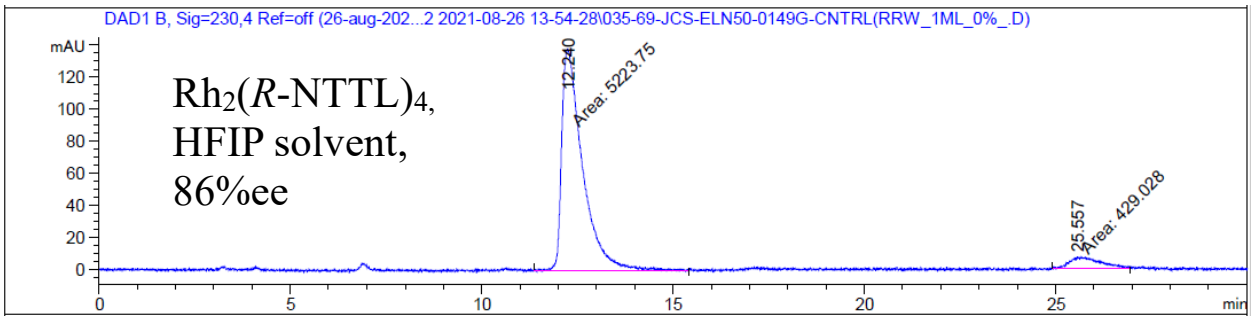

8. Complex API/Natural product substrate scope:

What follows are the substrates prepared according to **general procedure 3.2** in the presence of Rh_2(*R*-NTTL)$_4$ and HFIP as solvent. The yield of each product is the isolated yield and the product NMR is reported below. This data is followed by the 2D spectral suite, where nessecary, that was used to characterize the product. Cross peaks in the 2D spectrum indicate a correlation between the atoms labelled upon the axis and raw data for more detailed examination of the products can be made available upon request. This spectral data is followed by the SFC trace, in the case of compound **111,** used to determine the enantioselectivity of the reaction. For the summary of the 1H and 13C NMR spectra of each novel refer to the characterization report **S8-S11.**

Compound 127:

A 2D NMR suite was used to confirm the structure of **127** including COSY, NOESY, HSQC, and HMBC. Atom assignments are given on the labelled structures adjacent to the spectra. Diastereoselectivity of the **127** was assessed through SFC and analysis of the 1H NMR. D.r was found to be >20:1 due to the relative integrations of peaks appearing at 0.63 ppm and 0.84 ppm corresponiding to methylene 19 and its minor diastereomer. Selectivity of the carbene transformation itself was assessed by SFC which follows this NMR data and was determined to be 32:1 d.r. (95% excess of shown cyclopropane). Relative stereochemistry of the cyclopropane product is assigned by analogy to the major enantiomer of compound **125** and **128** as confirmed by X-Ray crystallography.

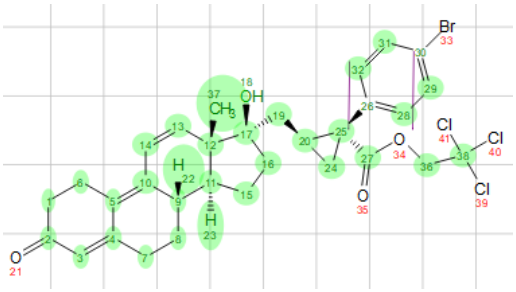

1H NMR:

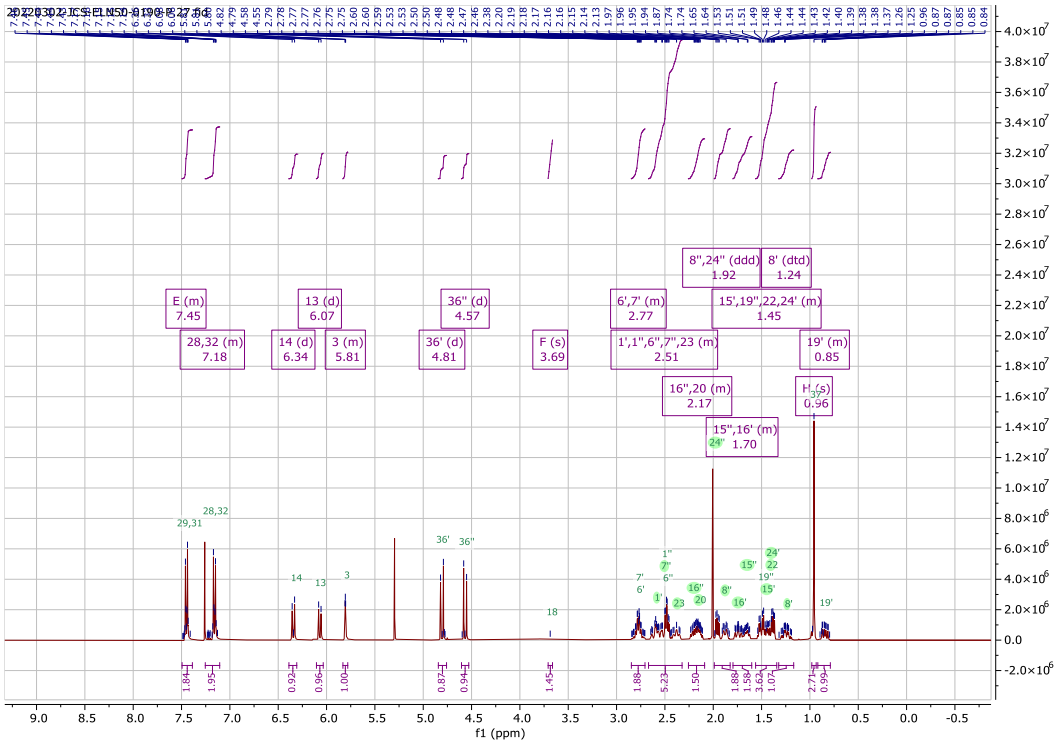

13C NMR:

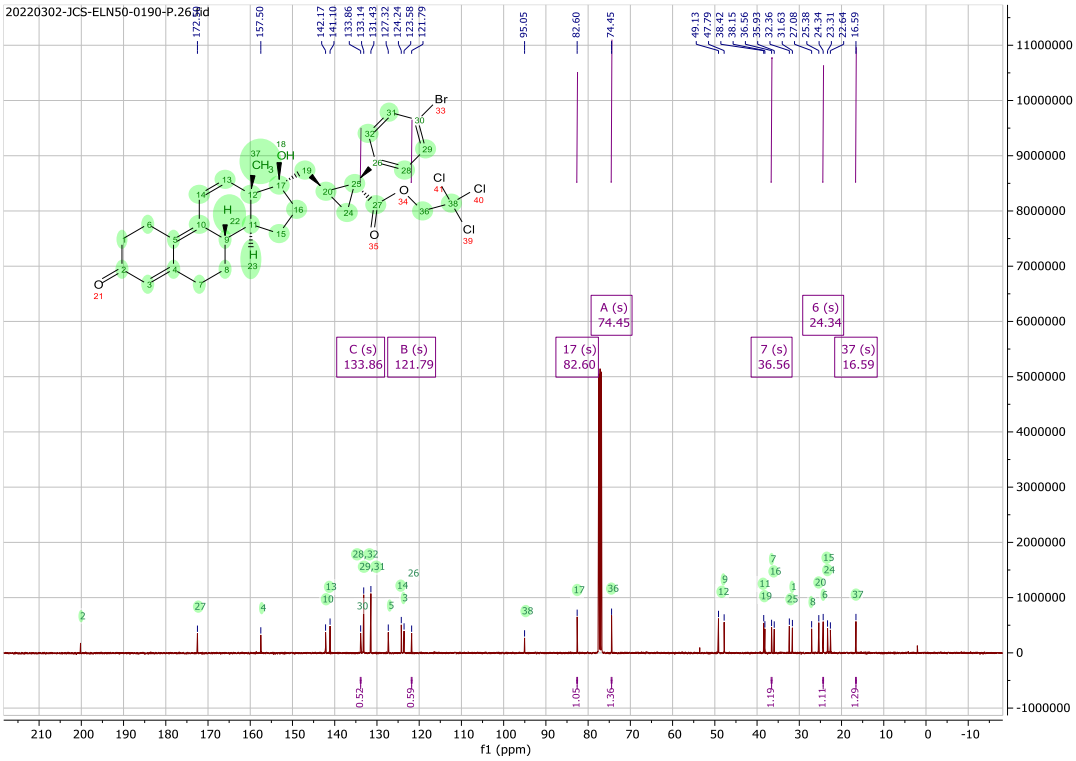

COSY:

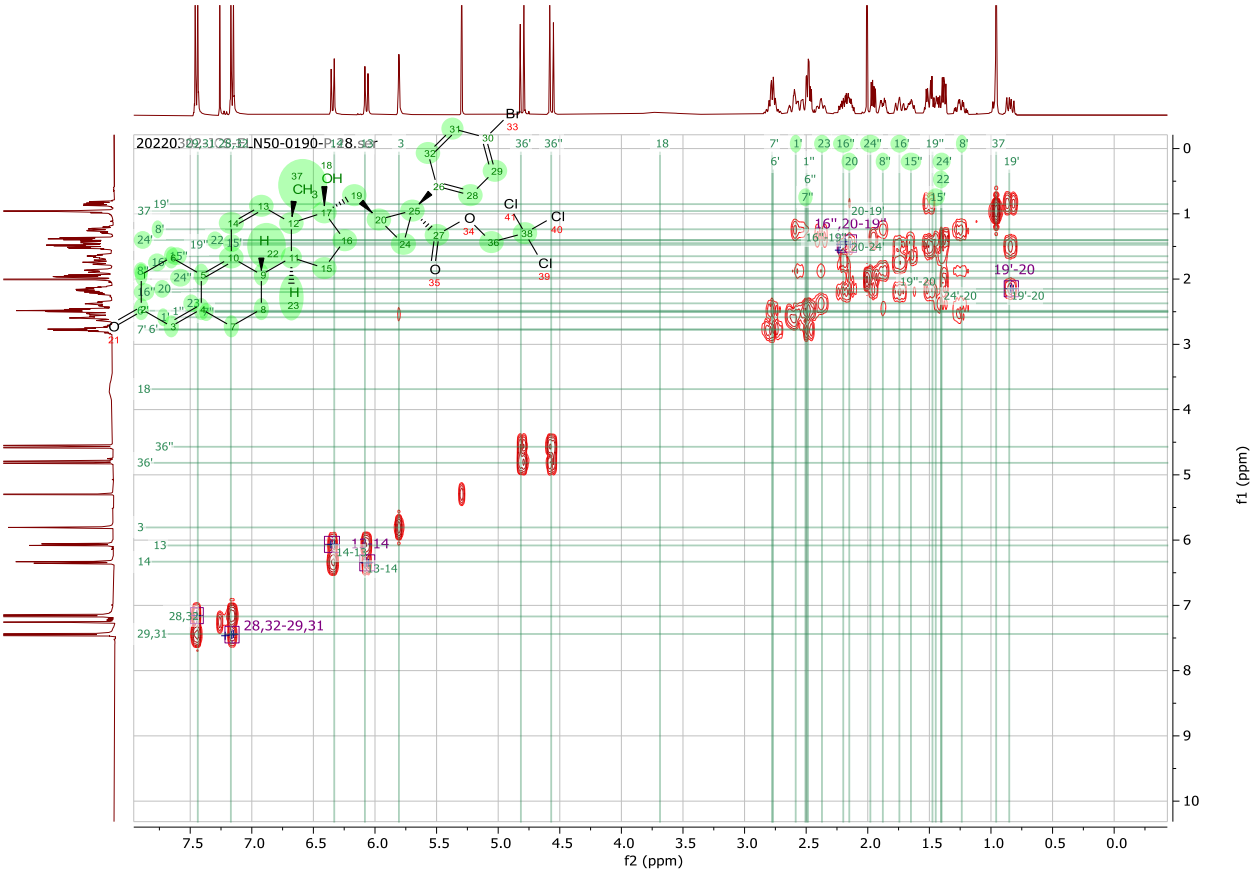

NOESY:

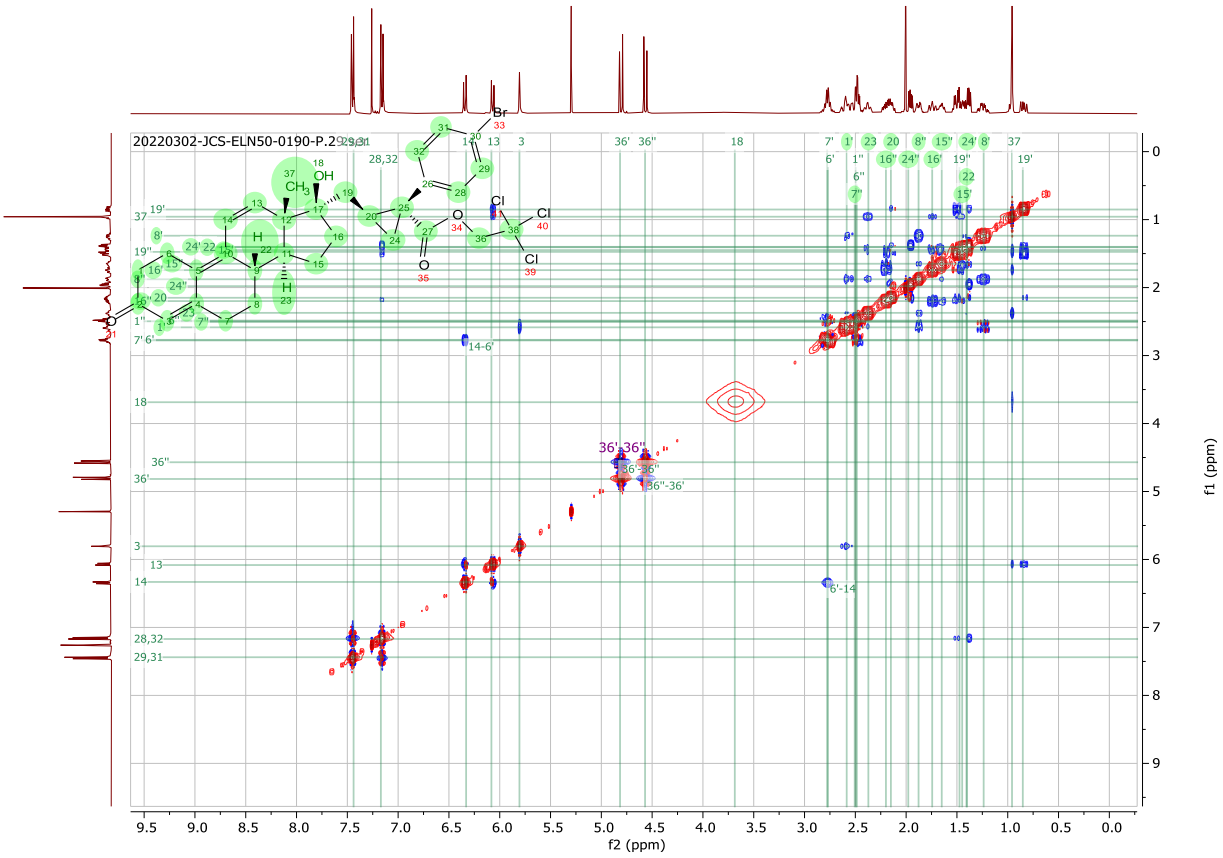

HSQC:

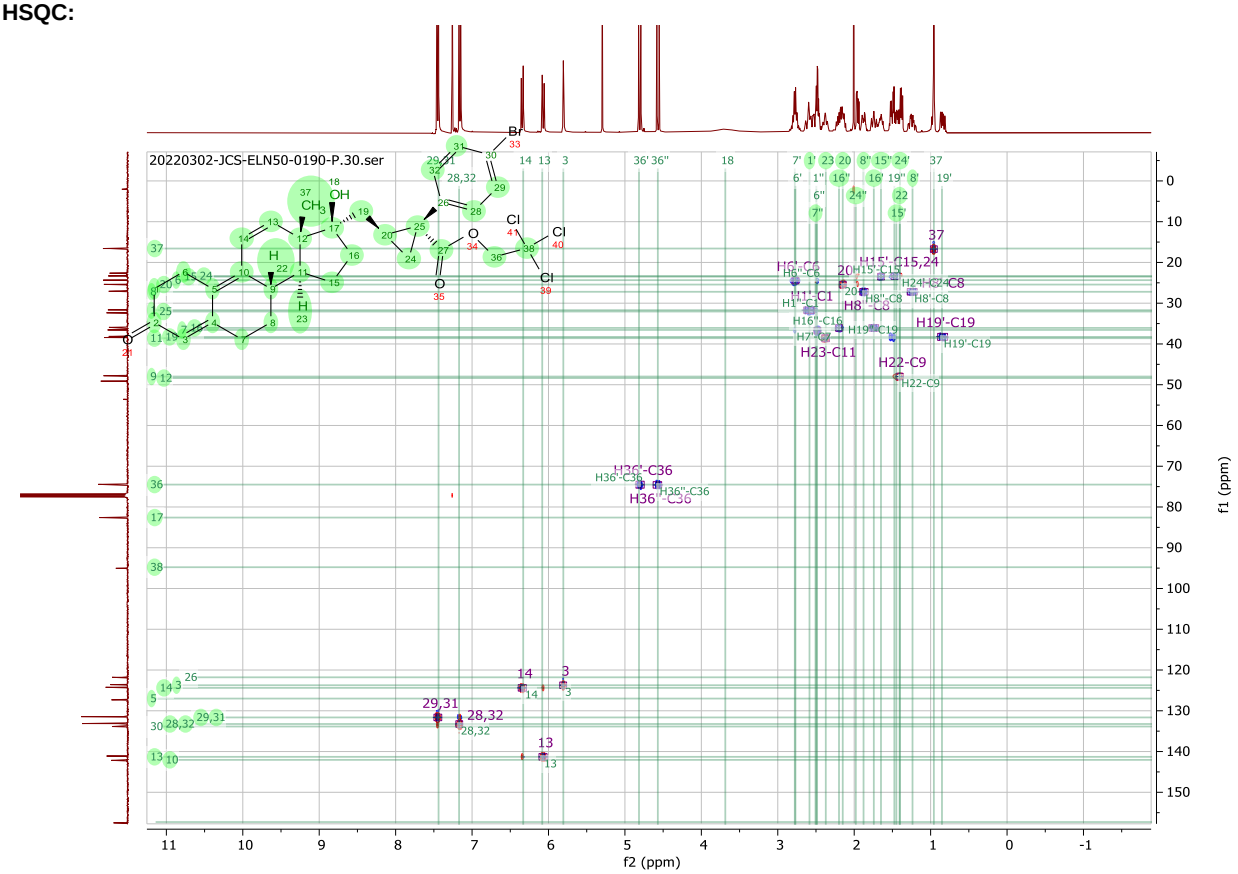

HMBC:

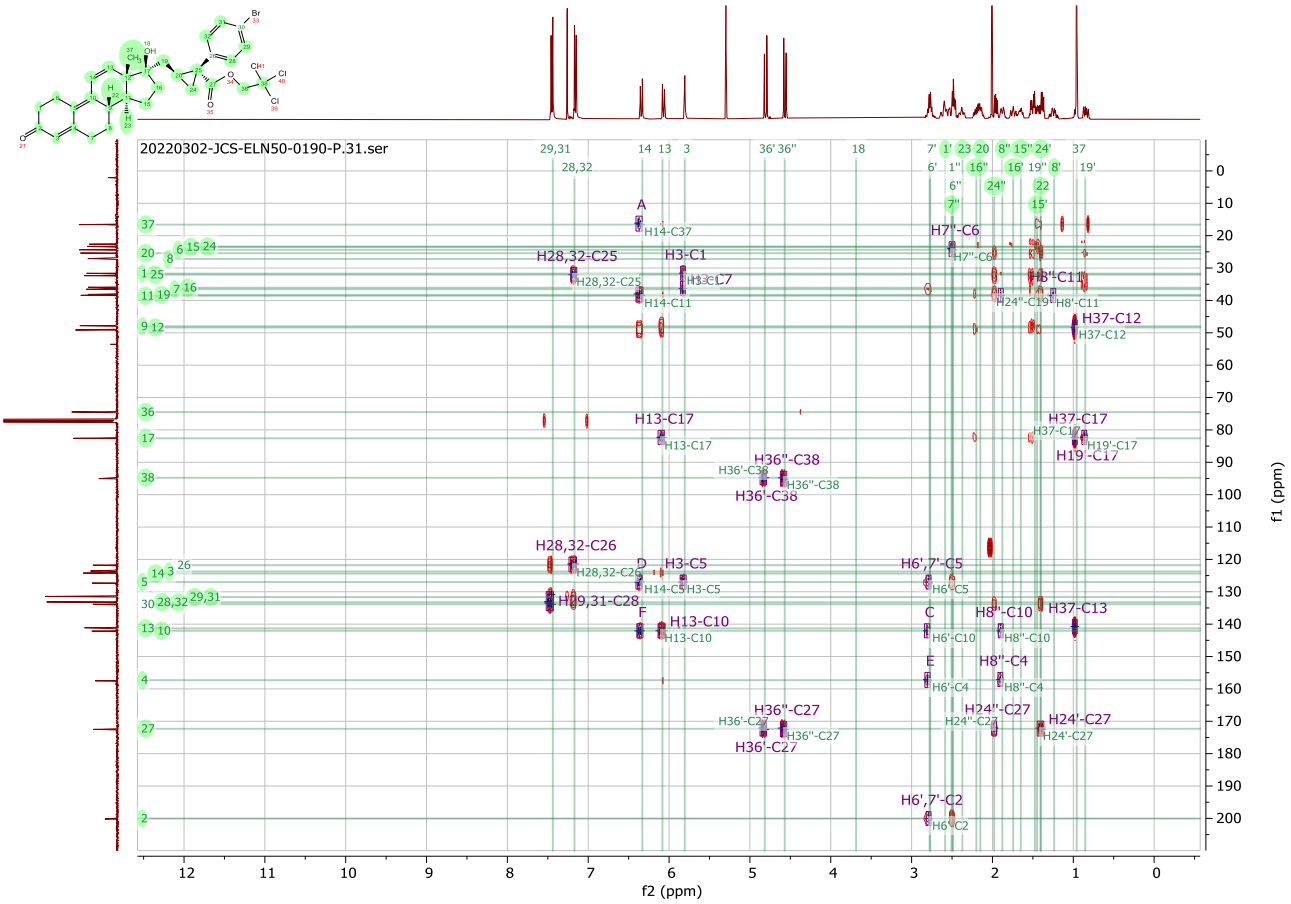
20220302-JCS-ELN50-0190-P.31.ser
f2 (ppm)
f1 (ppm)
H28,32-C25
H3-C1
H13-C17
H36''-C38
H36'-C38
H28,32-C26
H3-C5
H6',7'-C5
H29,31-C28
H13-C10
H8''-C10
H37-C13
H8''-C4
H36''-C27
H36'-C27
H24''-C27
H24'-C27
H6',7'-C2
H37-C12
H37-C17
H19'-C17
H7''-C6
H8'-C11
H14-C37
H14-C11
H14-C5
H6'-C5
H6'-C10
H6'-C4
H6'-C2

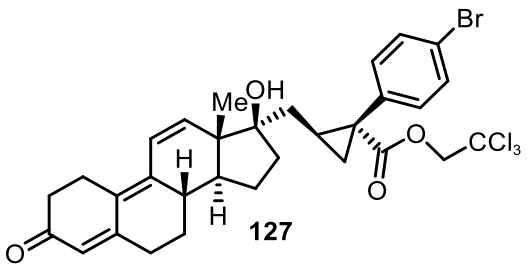

127

Racemate:

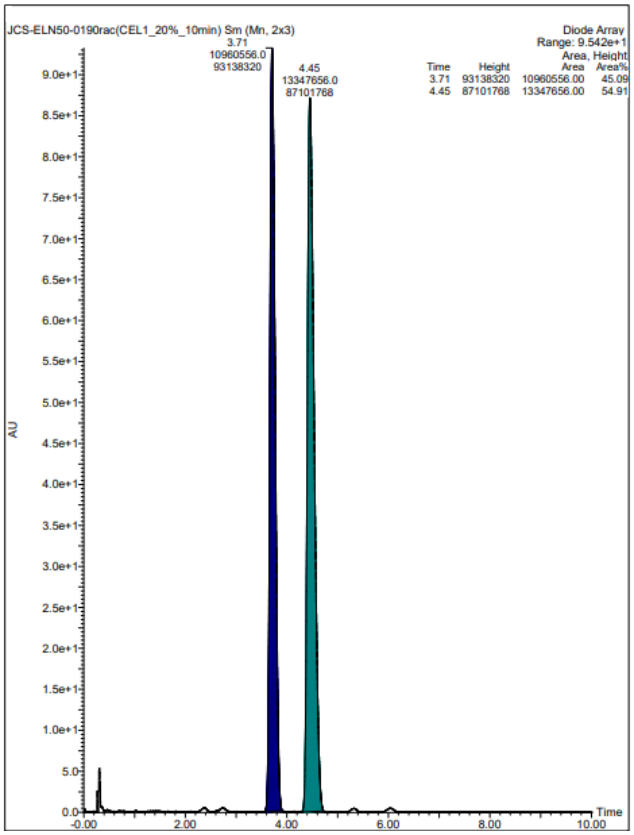

Rh_2(*R*-NTTL)$_4$ HFIP as solvent, 95% d.e

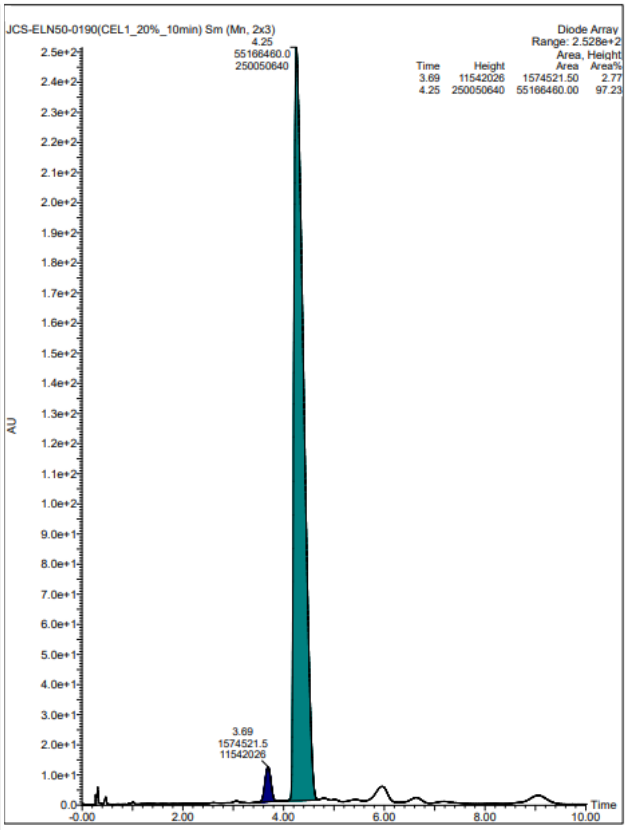

Compound 128: Full structure was charactrized by X-Ray crystallography (CCDC: 2182287).

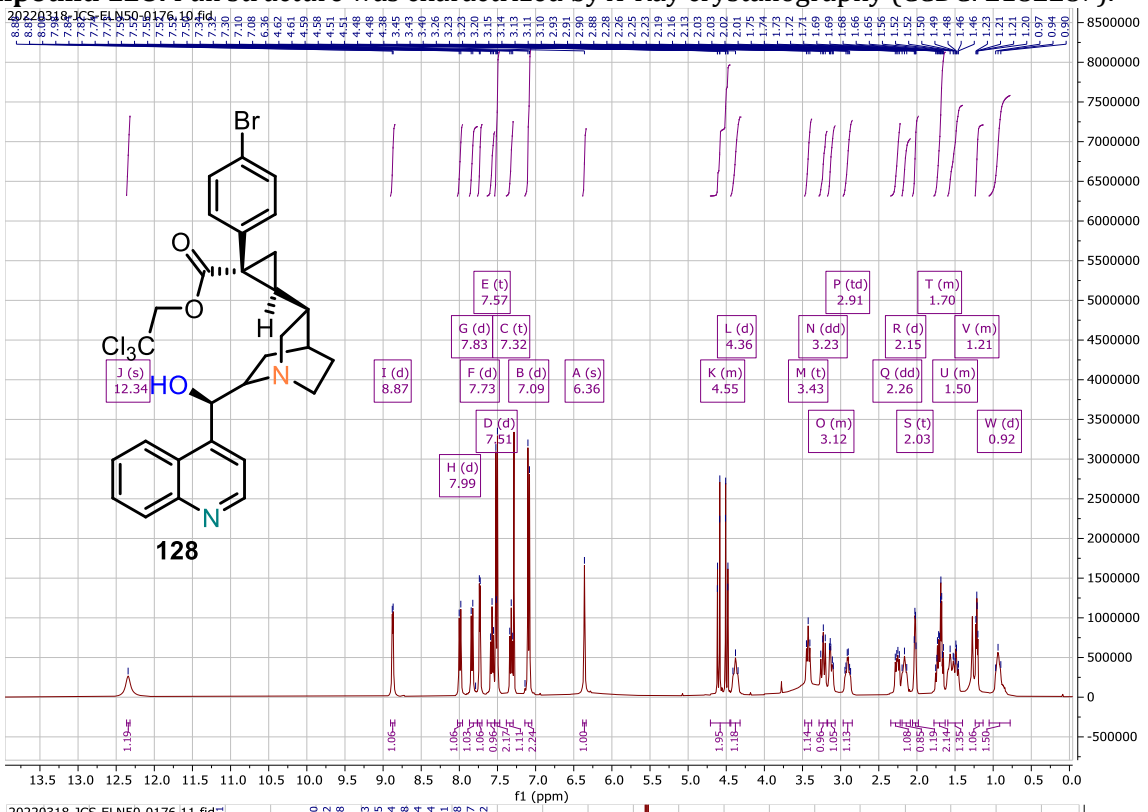

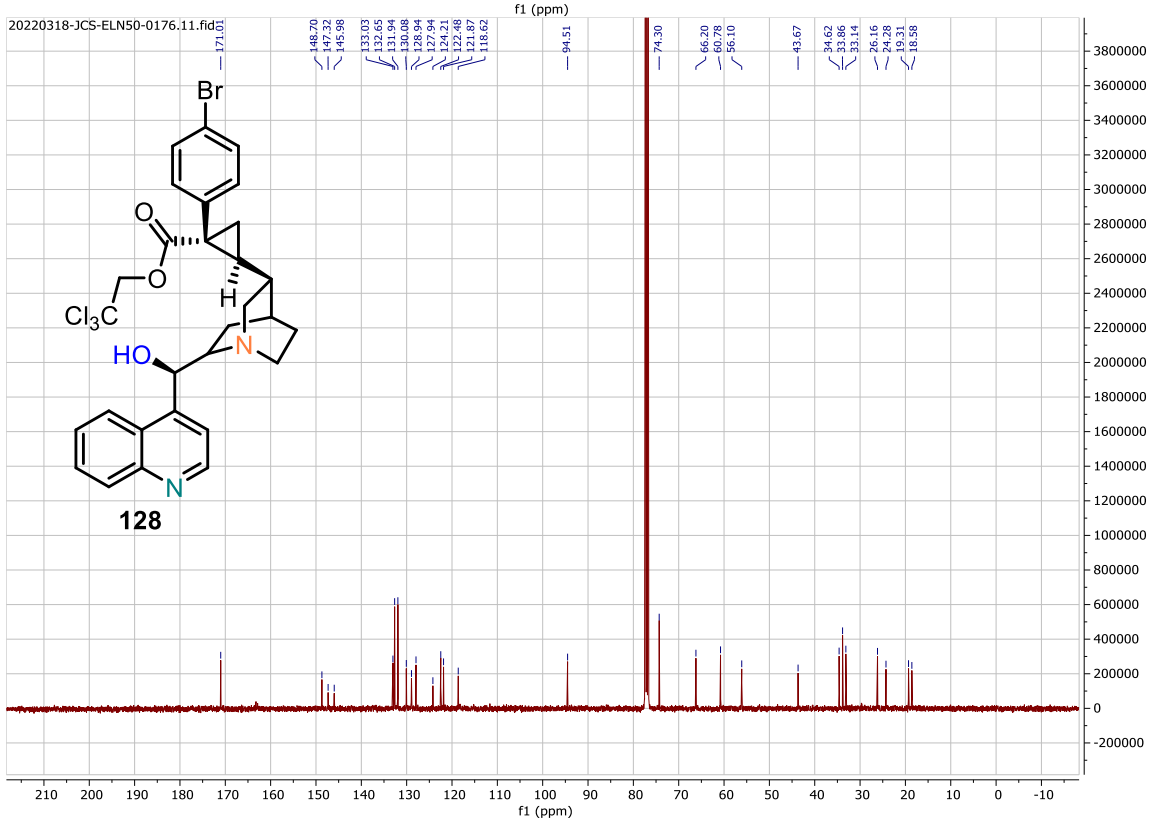

Compound 129:

A 2D NMR suite was used to confirm the structure of **129** including COSY, NOESY, HSQC, and HMBC, and made it possible to resolve the *Z* and *E* isomers. Atom assignments are given on the labelled structures adjacent to the spectra. Diastereoselectivity of the **129** was assessed through analysis of the 1H NMR. D.r was found to be >20:1 for one of the isomers and 6:1 for the other isomer. These values were determined by the relative integrations of peaks appearing at 1.49 and either 1.40 or 1.37 ppm for the >20:1 d.r.,and the relative integrations of the peaks at 1.46 ppm and either 1.40 or 1.37 ppm for the 6:1 d.r. This signal corresponids to methylene 31 and its minor diastereomer. Signals corresponding to the major diastereomers of **129** are shielded relative to the minor diastereomers which suggests that the major diastereomers experience shielding from both the phenyl and benzyl groups of the *E*-cyclopropane which is expected based on the analysis of absolute configuration of other substrates in this work. Due to the complexity of this product mixture the identity of the product obtained with high d.r could not be determined. Relative stereochemistry of the cyclopropane product is assigned by analogy to the major enantiomer of compound **125** and **128** as confirmed by X-Ray crystallography.

Z-isomer:

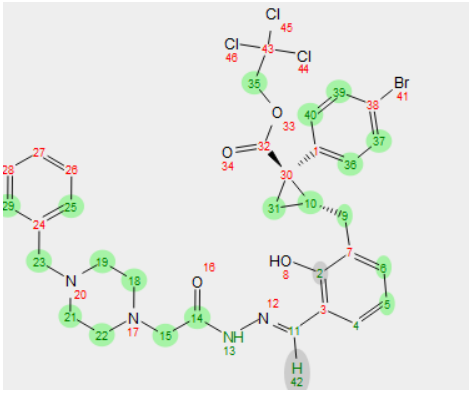

1H NMR:

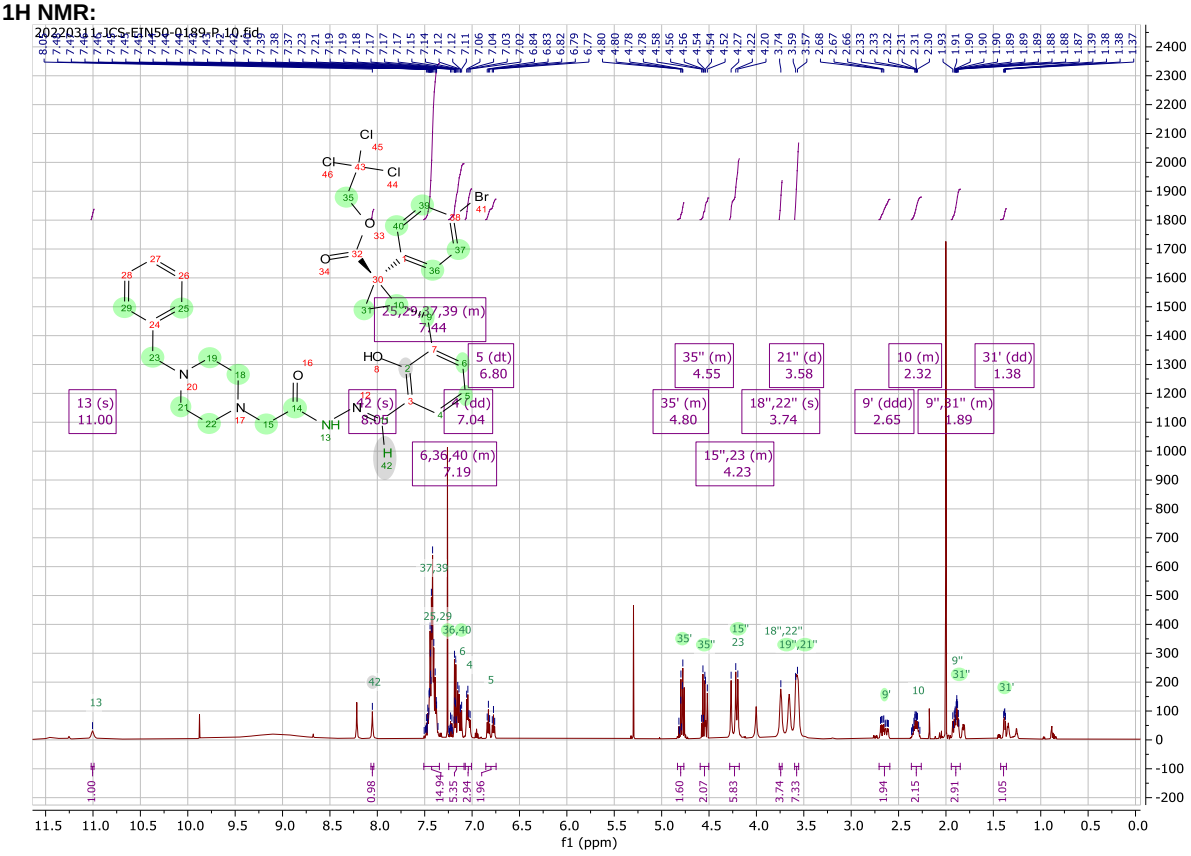

13C NMR:

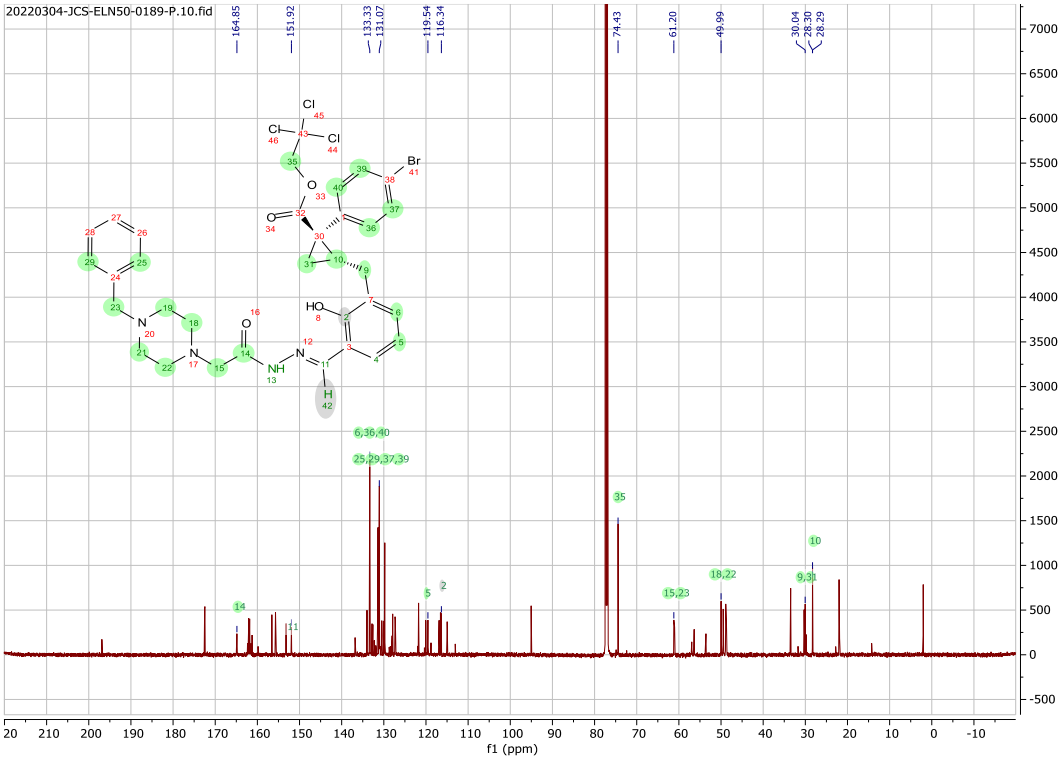
20220304-JCS-ELN50-0189-P.10.fid
164.85
151.92
133.33
131.07
119.54
116.34
74.43
61.20
49.99
30.04
28.70
28.29
6,36,40
25,29,37,39
35
10
18,22
9,31
15,23
5
2
14
11
f1 (ppm)

COSY:

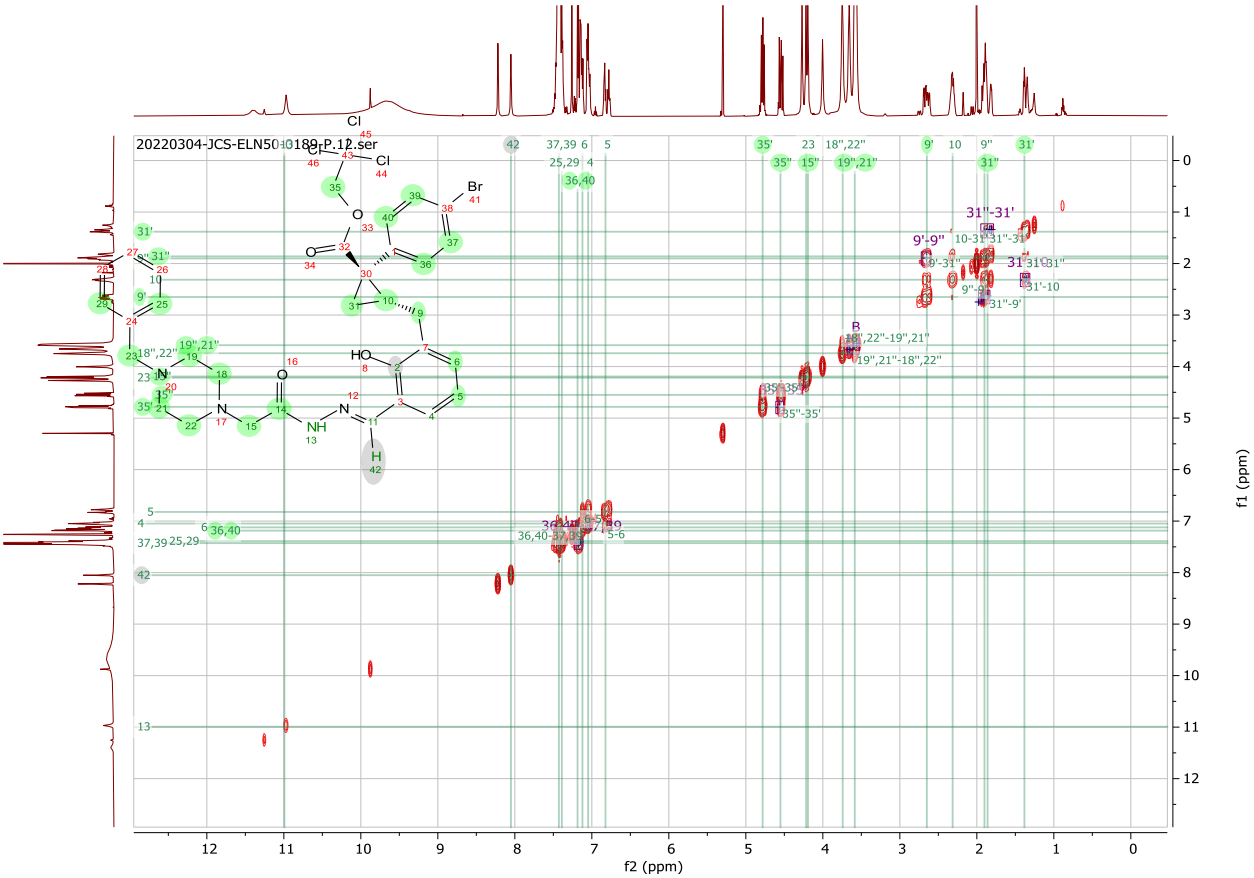

2D-NOESY:

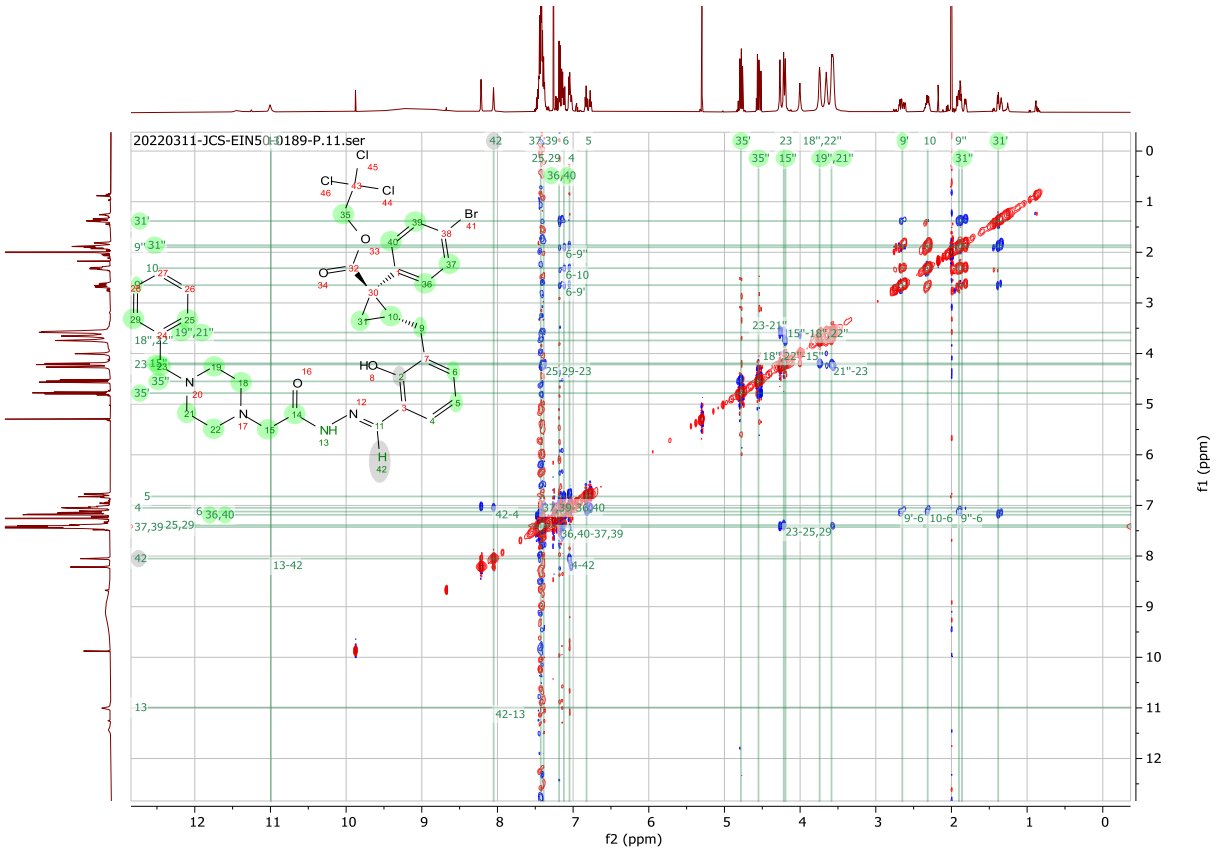
20220311-JCS-EIN50189-P.11.ser
f2 (ppm)
f1 (ppm)

HSQC:

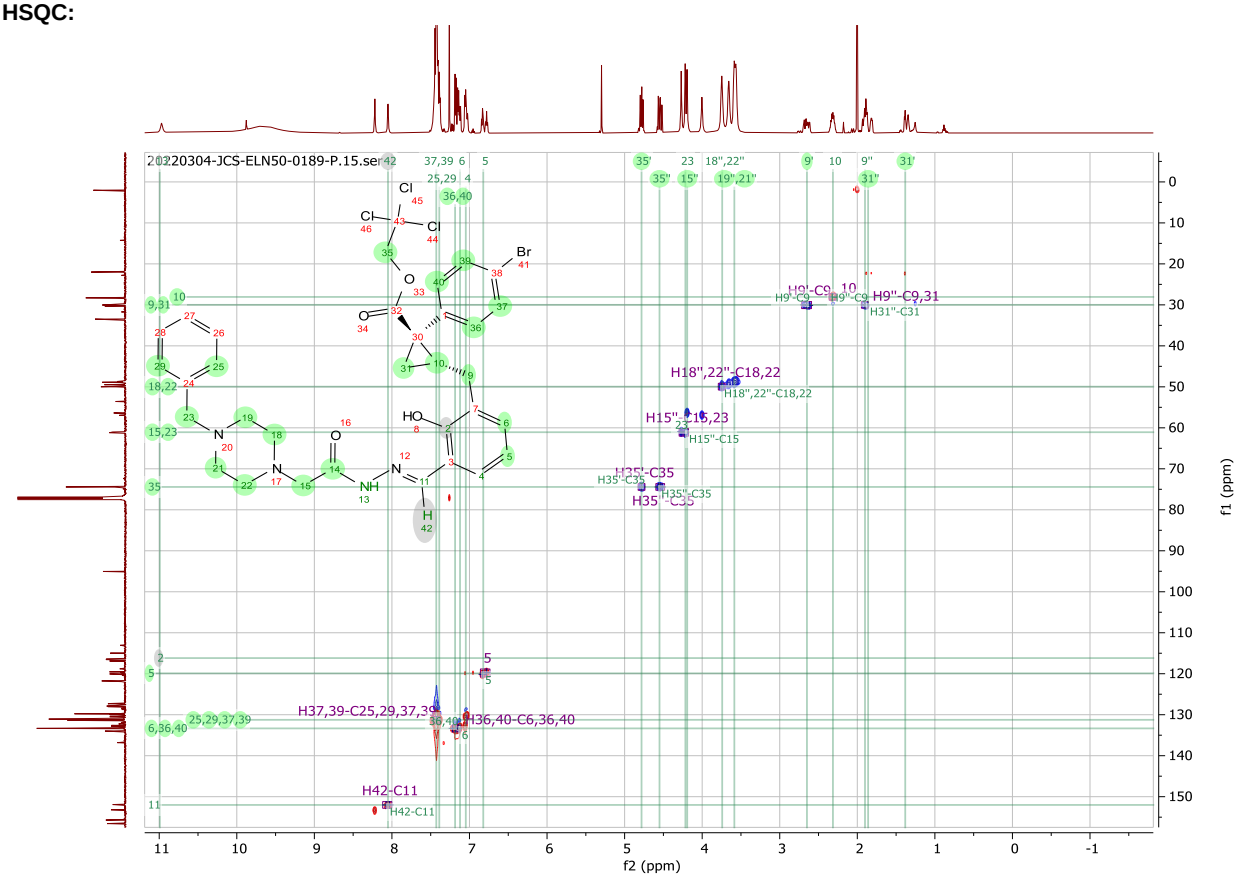
20220304-JCS-ELN50-0189-P.15.ser
f2 (ppm)
f1 (ppm)
H9'-C9,10
H9''-C9,31
H31''-C31
H18'',22''-C18,22
H15''-C15,23
H35'-C35
H35''-C35
H37,39-C25,29,37,39
H36,40-C6,36,40
H42-C11

HMBC:

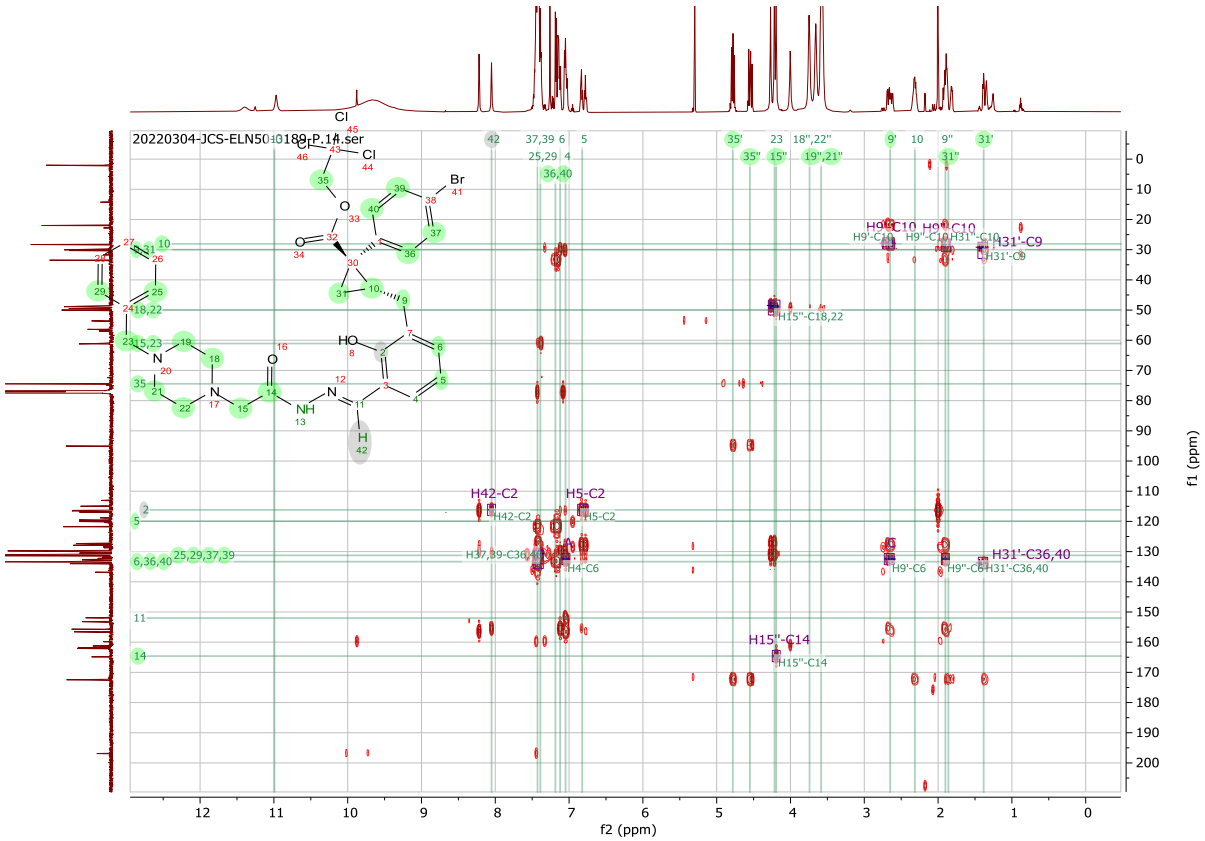

Compound 129, *E*-Isomer:

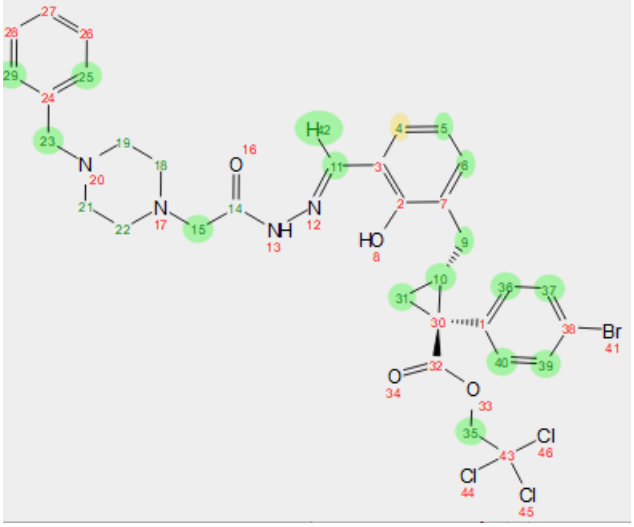

1H NMR:

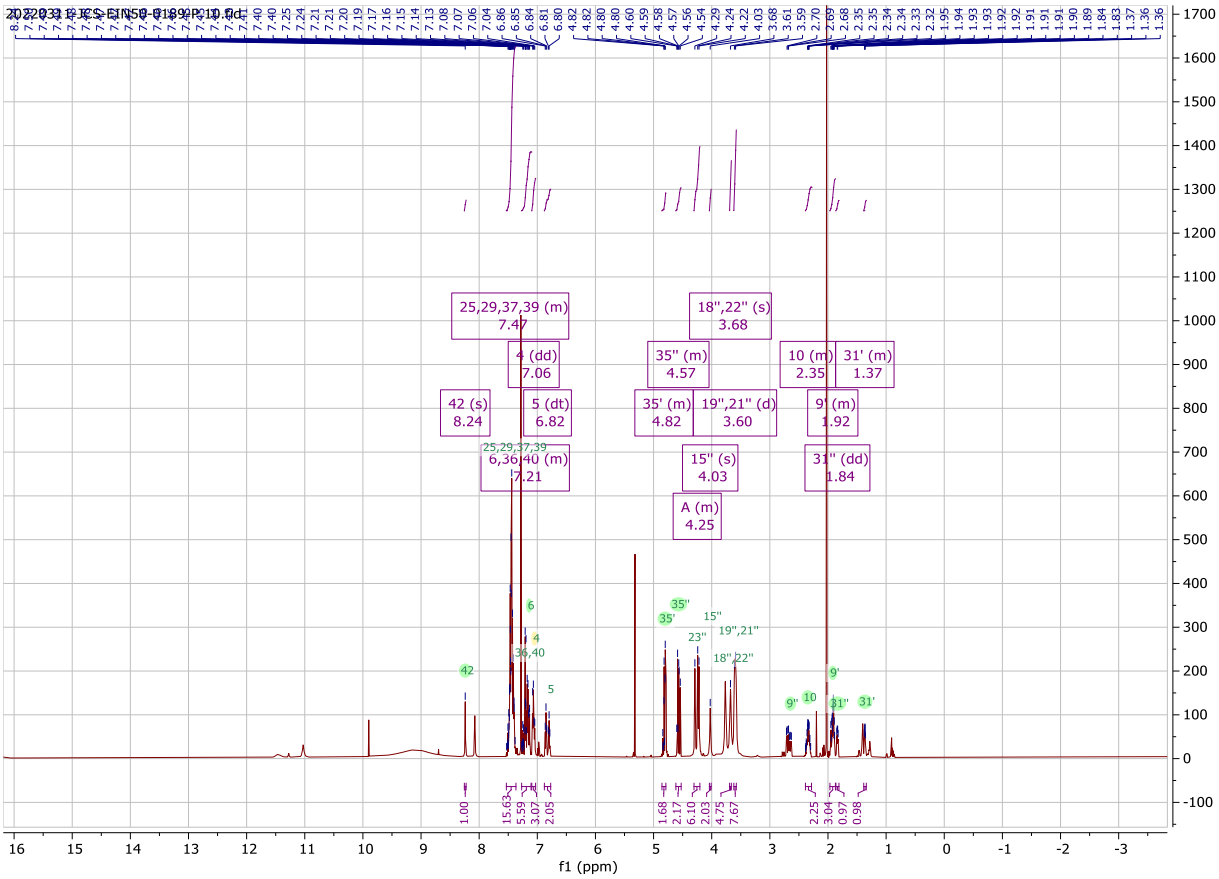

13C NMR:

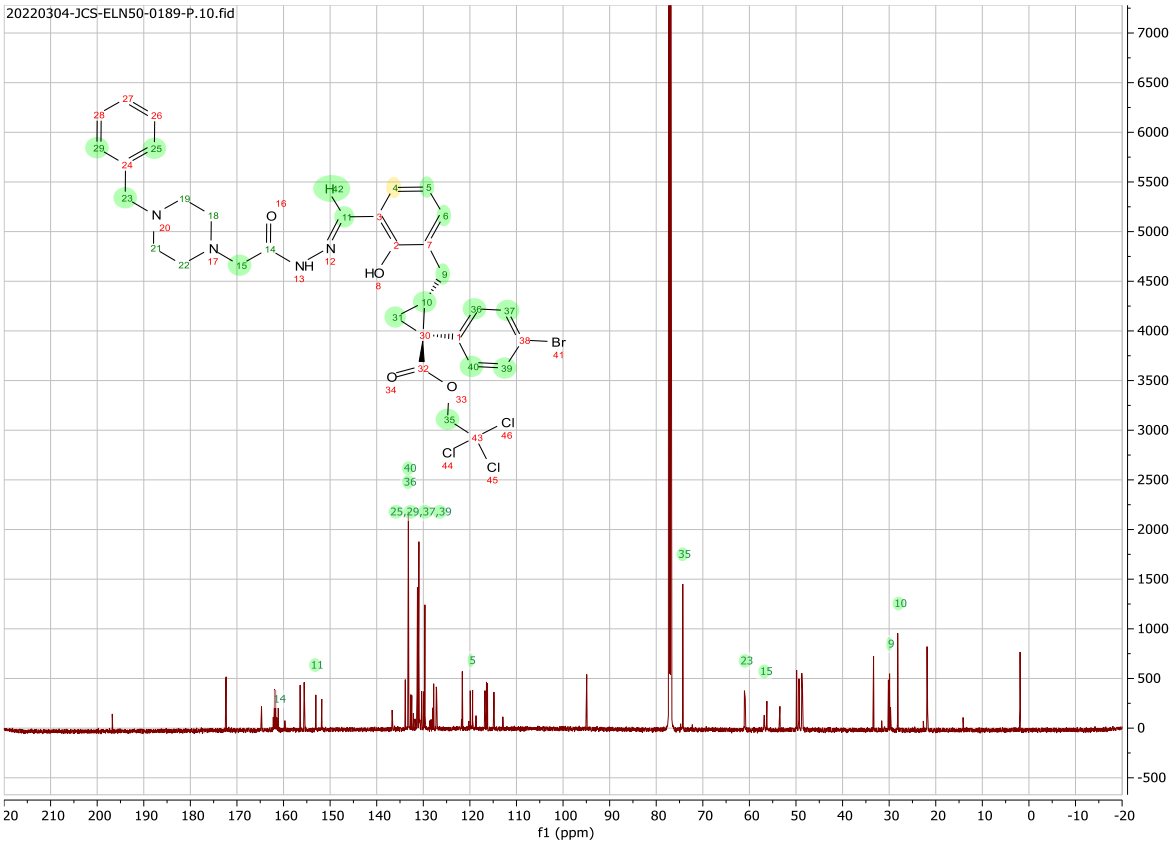

COSY:

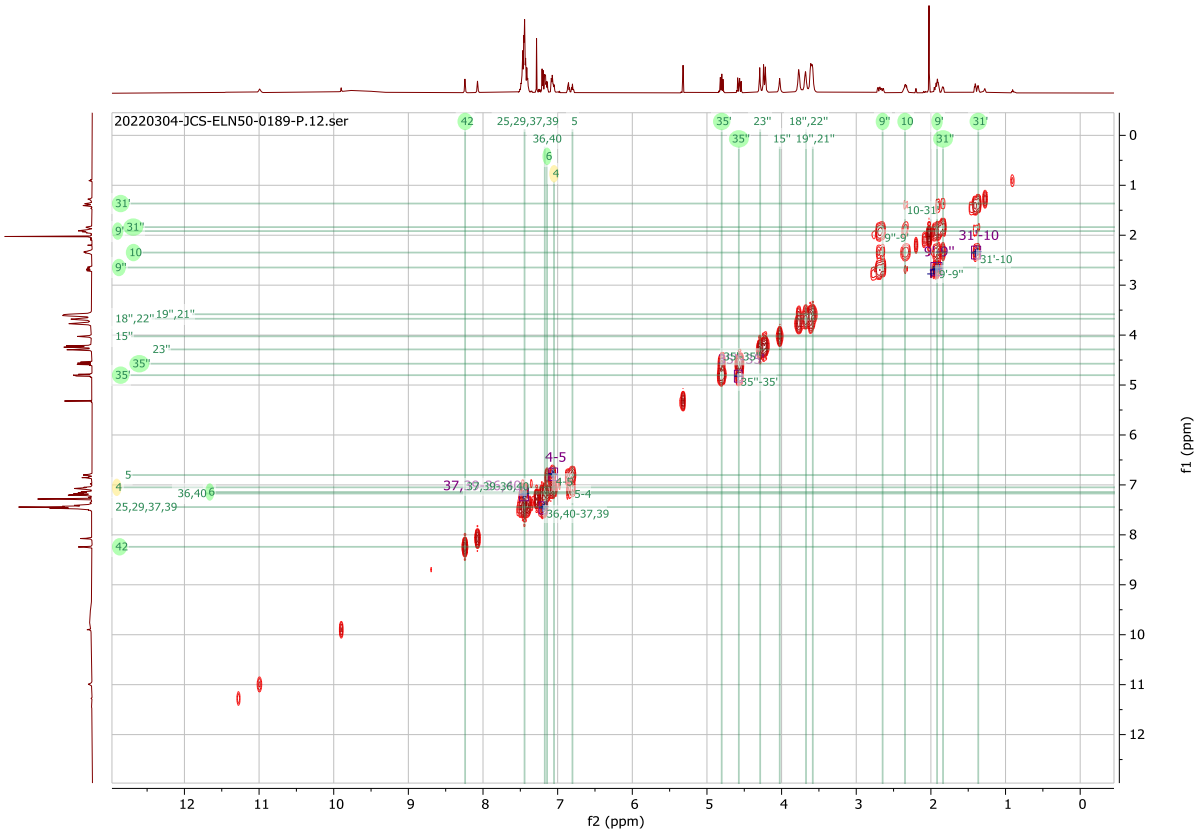
20220304-JCS-ELN50-0189-P.12.ser
f2 (ppm)
f1 (ppm)

NOESY:

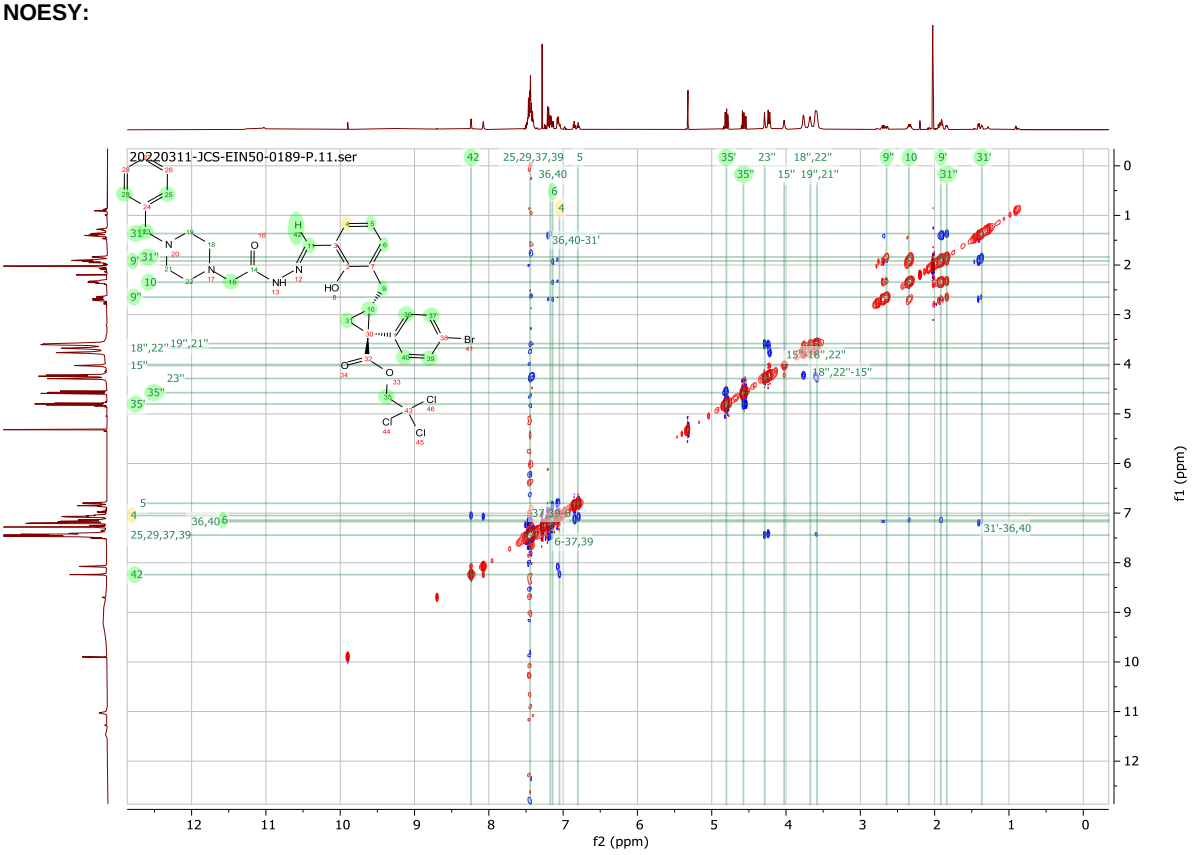

HSQC:

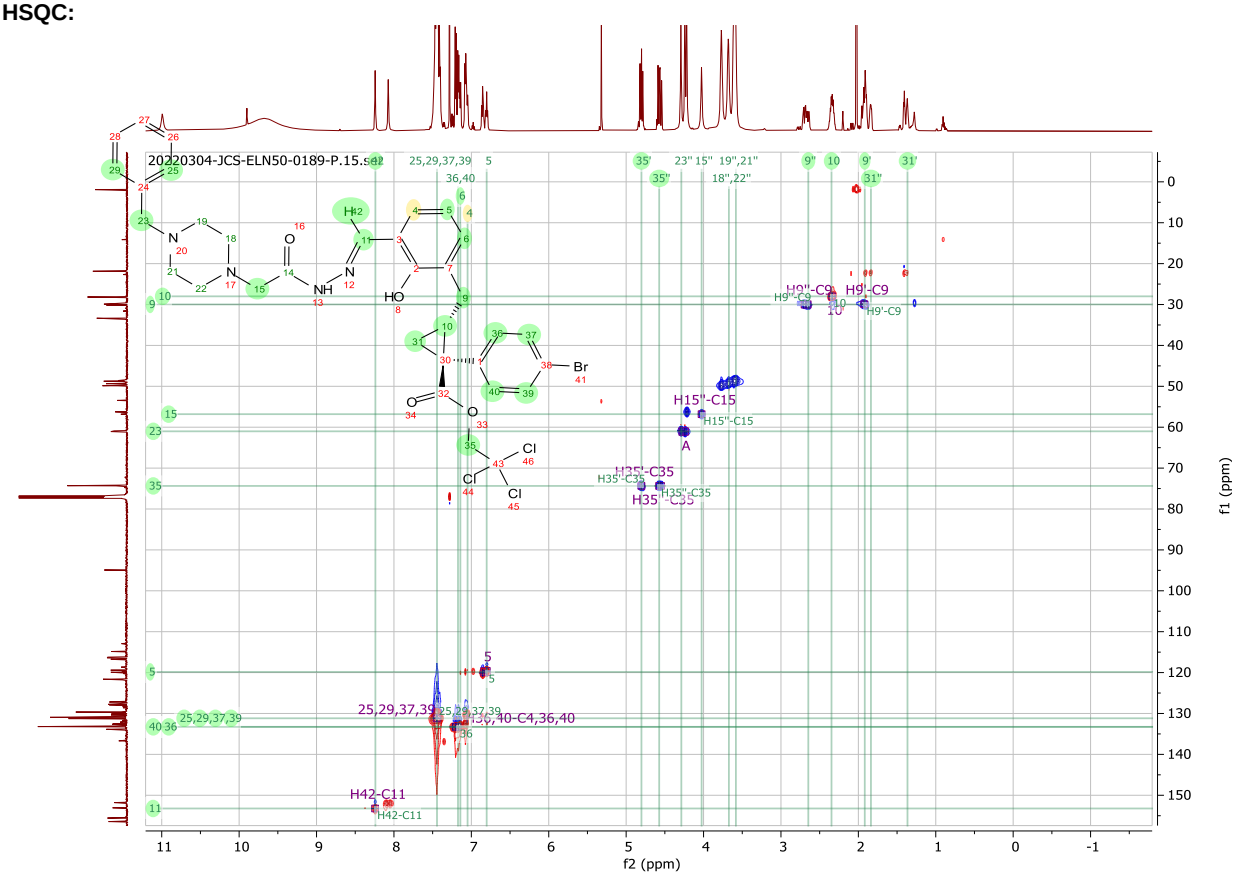
20220304-JCS-ELN50-0189-P.15.se2
f2 (ppm)
f1 (ppm)
H15''-C15
H9''-C9
H9'-C9
H35''-C35
H35'-C35
H42-C11
25,29,37,39-C4,36,40
A

HMBC:

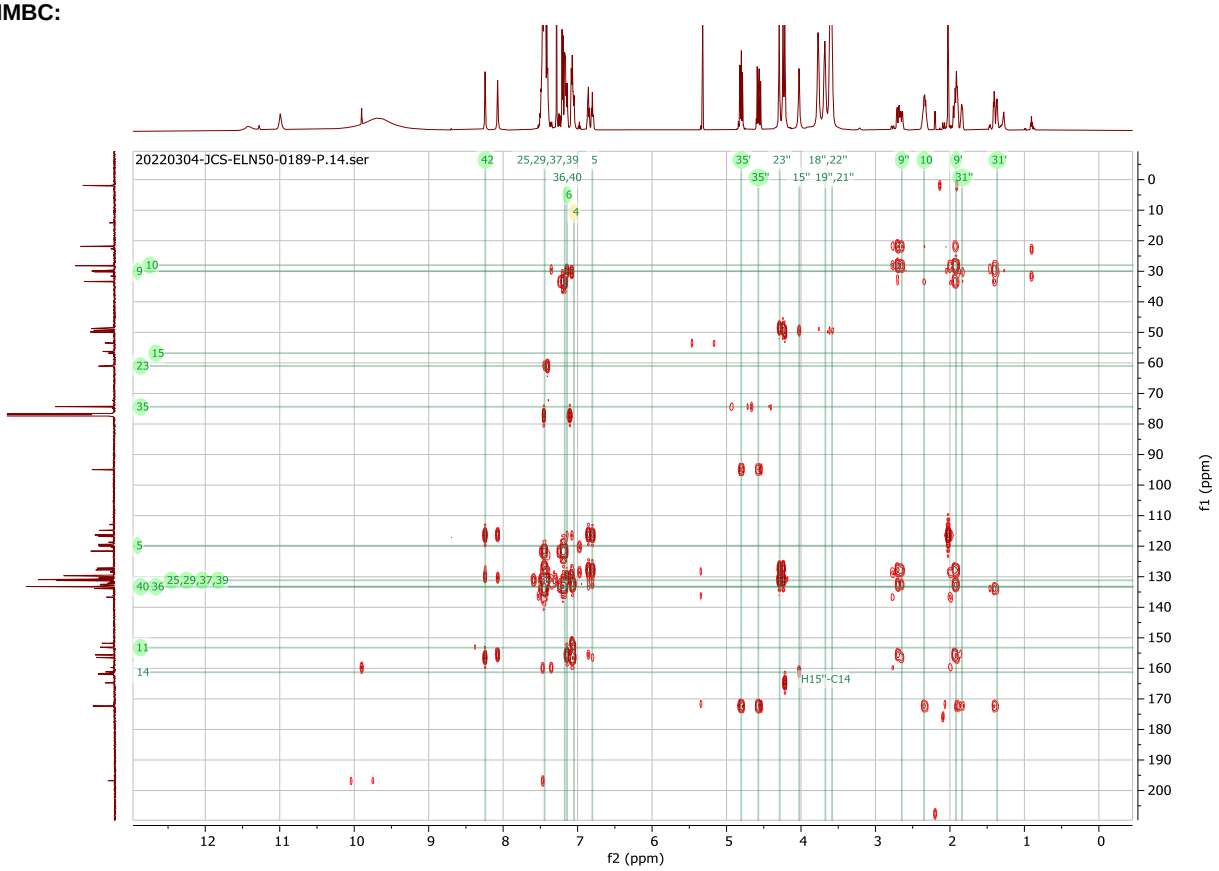

Compound 130:

A 2D NMR suite was used to confirm the structure of **130** including COSY, ROESY, HSQC, and HMBC. Atom assignments are given on the labelled structures adjacent to the spectra. Diastereoselectivity of **130** was not possible to determine due to

the conformational dynamism of the macrocycle. The geometry of the piperidinyl amide can readily interconvert between *cis* and *trans* isomers changing most signals in the NMR. For simplicity, only the major isomer visible by NMR was assigned in this work. Additionally, D.r of the carbene insertion cannot be determined due to the burial of all cyclopropane peaks beneath the many alkyl signals of the macrocycle. Additionally the presence of 2 major conformers of **130** would make confident assignment of the cyclopropane diastereomers impossible. Relative stereochemistry of the cyclopropane product is assigned by analogy to the major enantiomer of compound **125** and **128** as confirmed by X-Ray crystallography.

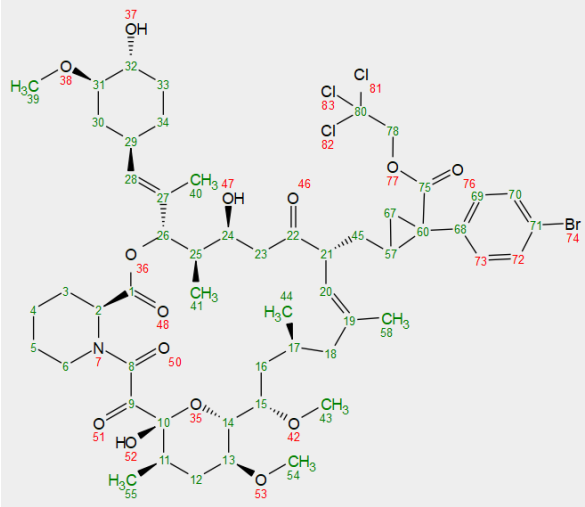

1H NMR:

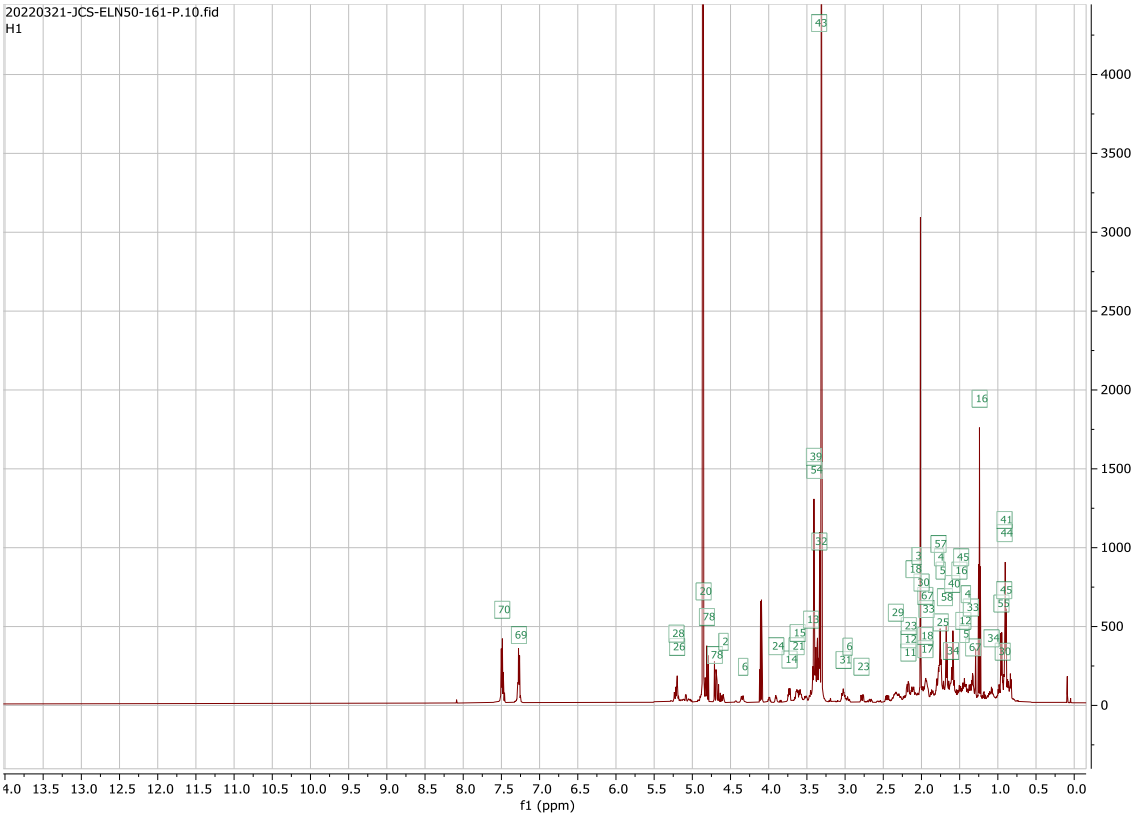

13C NMR:

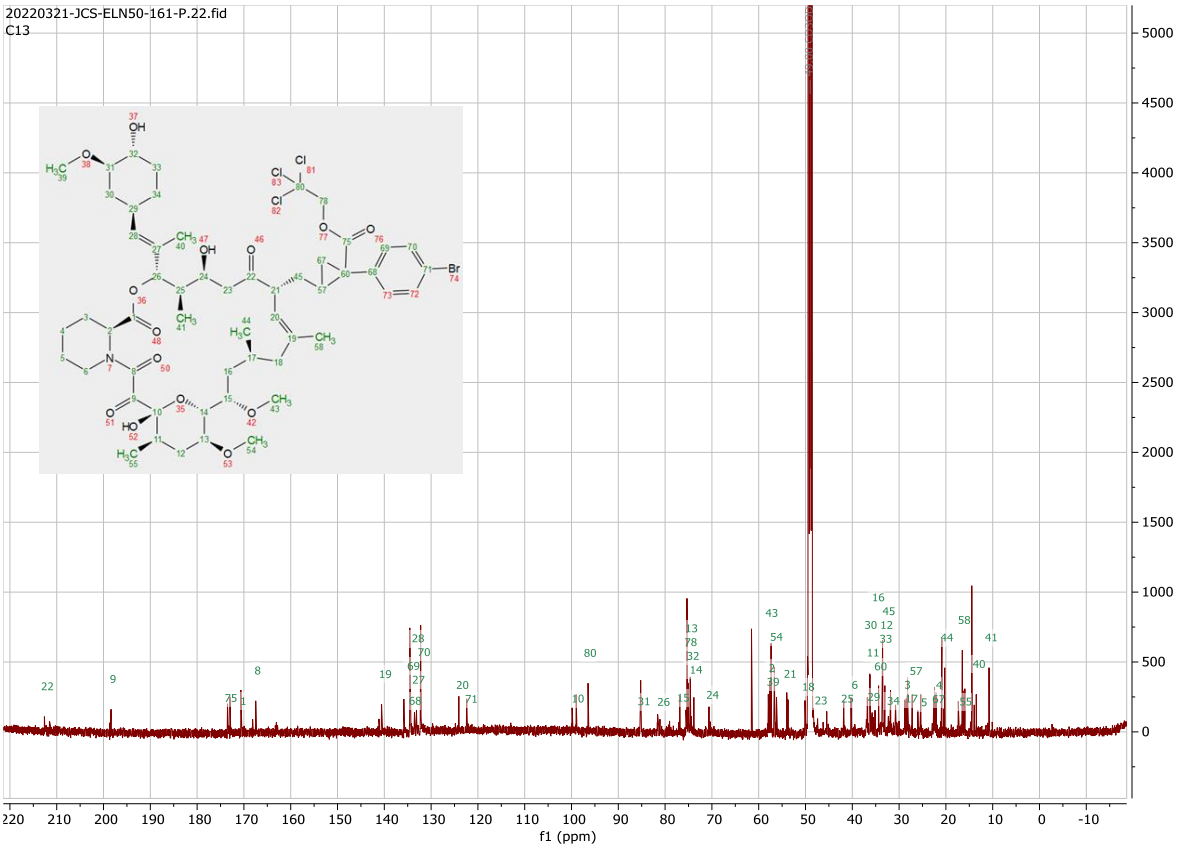

COSY:

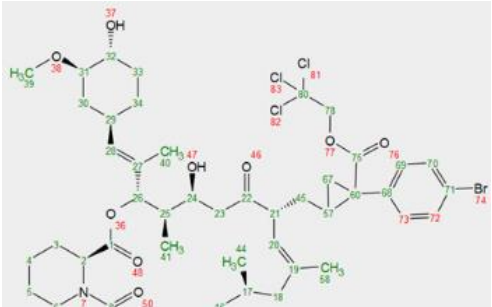

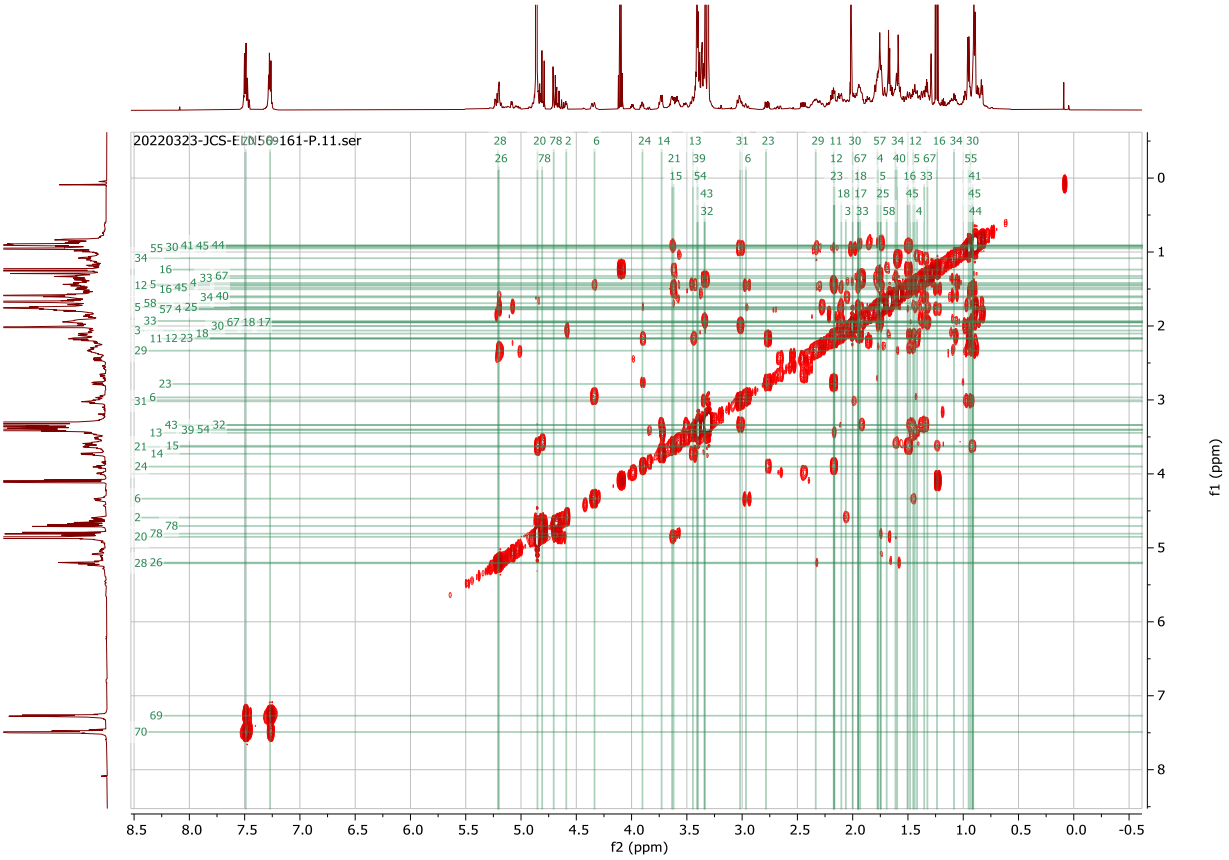

ROESY:

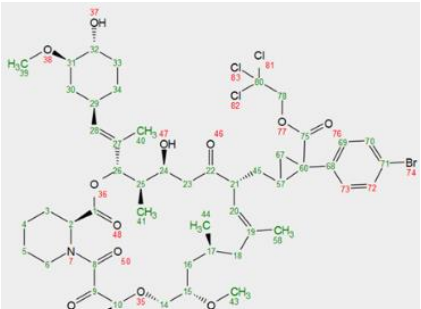

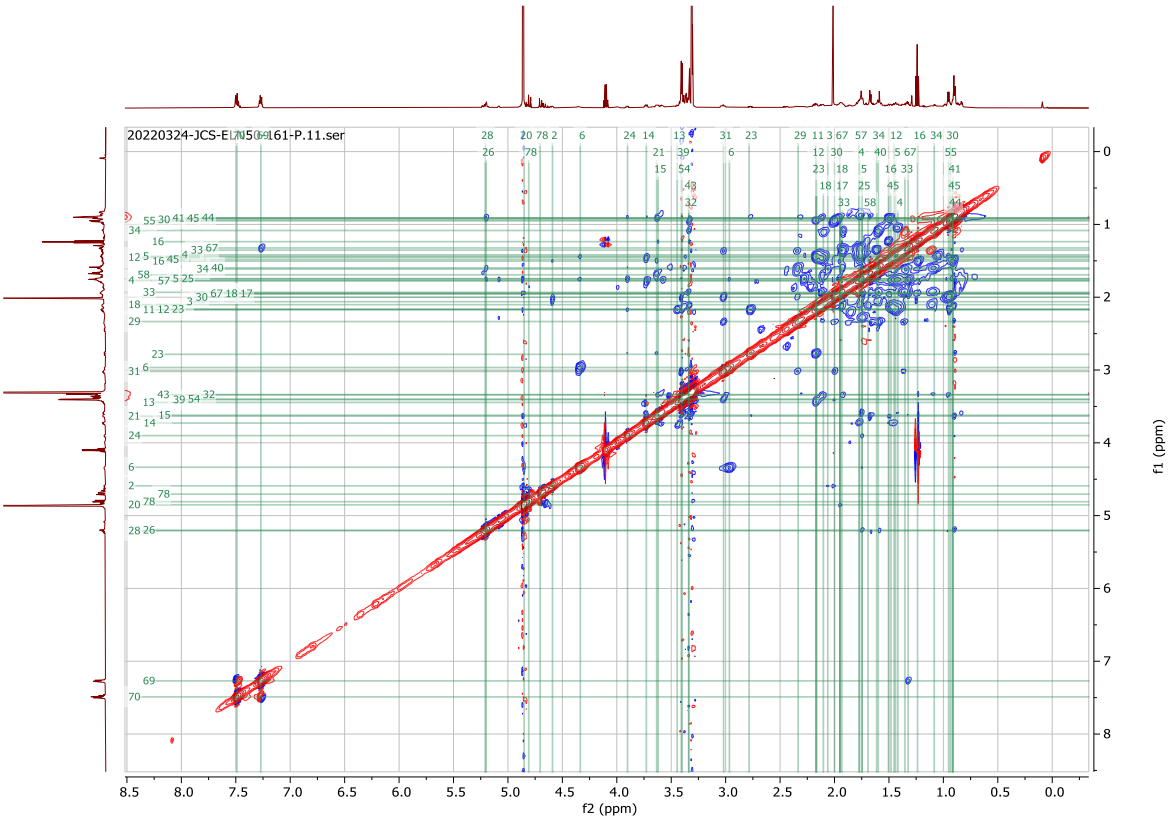

HSQC:

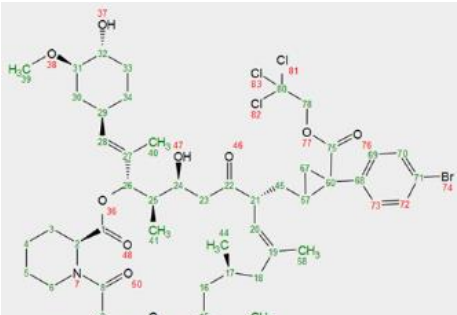

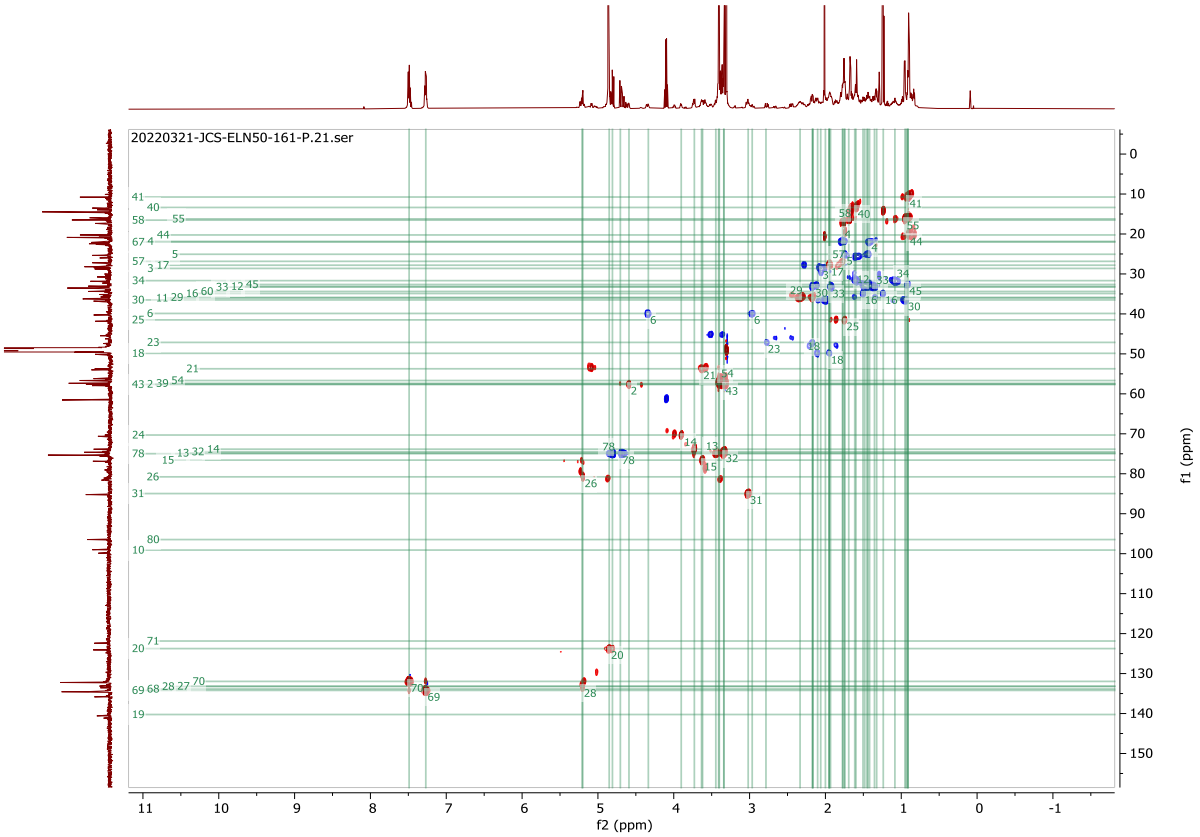

HMBC:

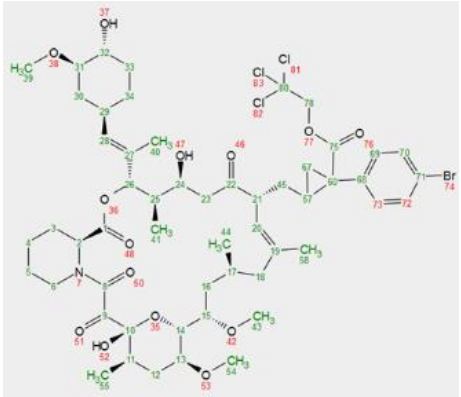

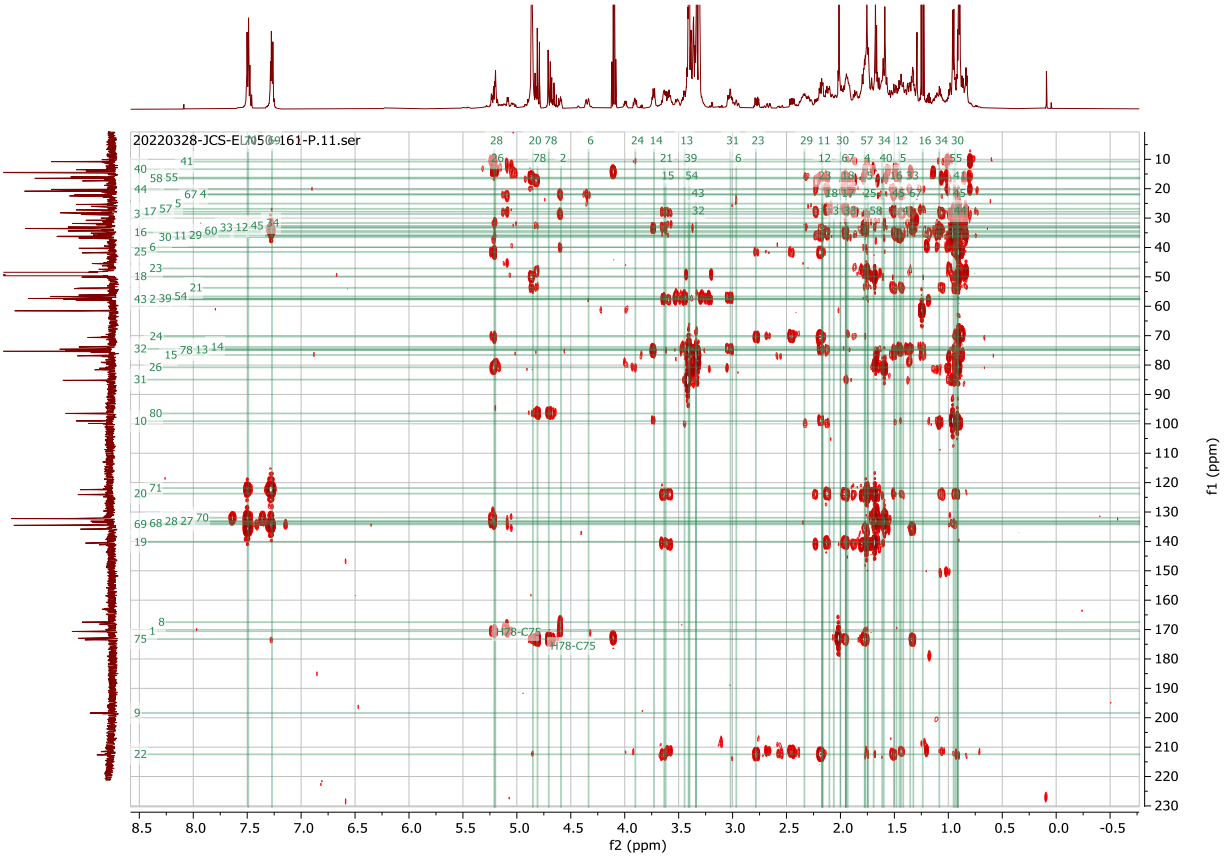

Compound 131:

A 2D NMR suite was used to confirm the structure of **131** including COSY, ROESY, TOCSY, HSQC, and HMBC. Atom assignments are given on the labelled structures adjacent to the spectra. Due to the acidic reaction medium and use of TFA as a mobilizing additive during preperative HPLC purification of the product, partial removal of the Boc-protecting group was observed and the product obtained was not pure. Nevertheless, the structure of the compound can be assigned with the aid of the 2D spectral suite. Diastereoselectivity of **131** was not possible to confidently assigned due to the presence of these impurities however the signals at 0.44 and 0.66 corresponding to the diastereotopic cyclopropane protons of 29 are significantly shielded. This suggests that the major diastereomer experience shielding from the phenyl group of the *E*-cyclopropane which is expected based on the analysis of absolute configuration of other substrates in this work. Relative stereochemistry of the cyclopropane product is assigned by analogy to the major enantiomer of compound **125** and **128** as confirmed by X-Ray crystallography.

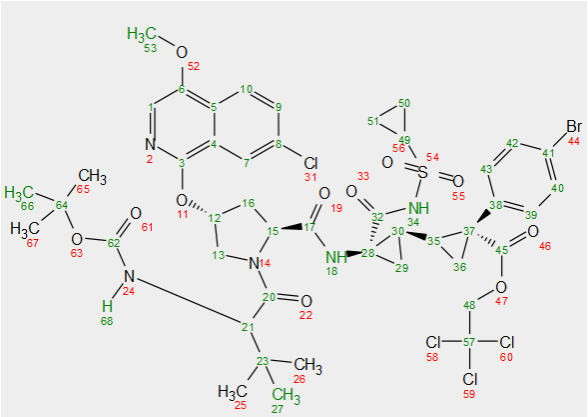

1H NMR:

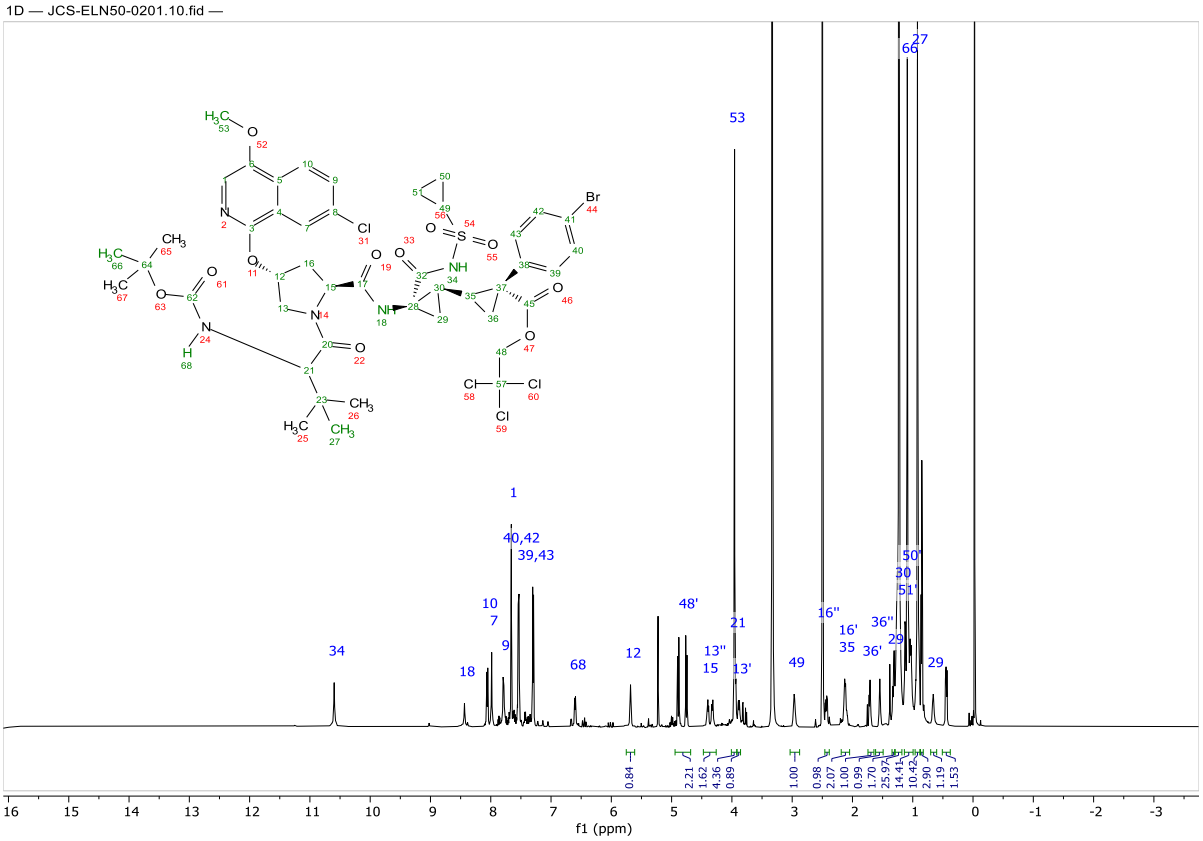

13C NMR:

1D — JCS-ELN50-0201.17.fid —

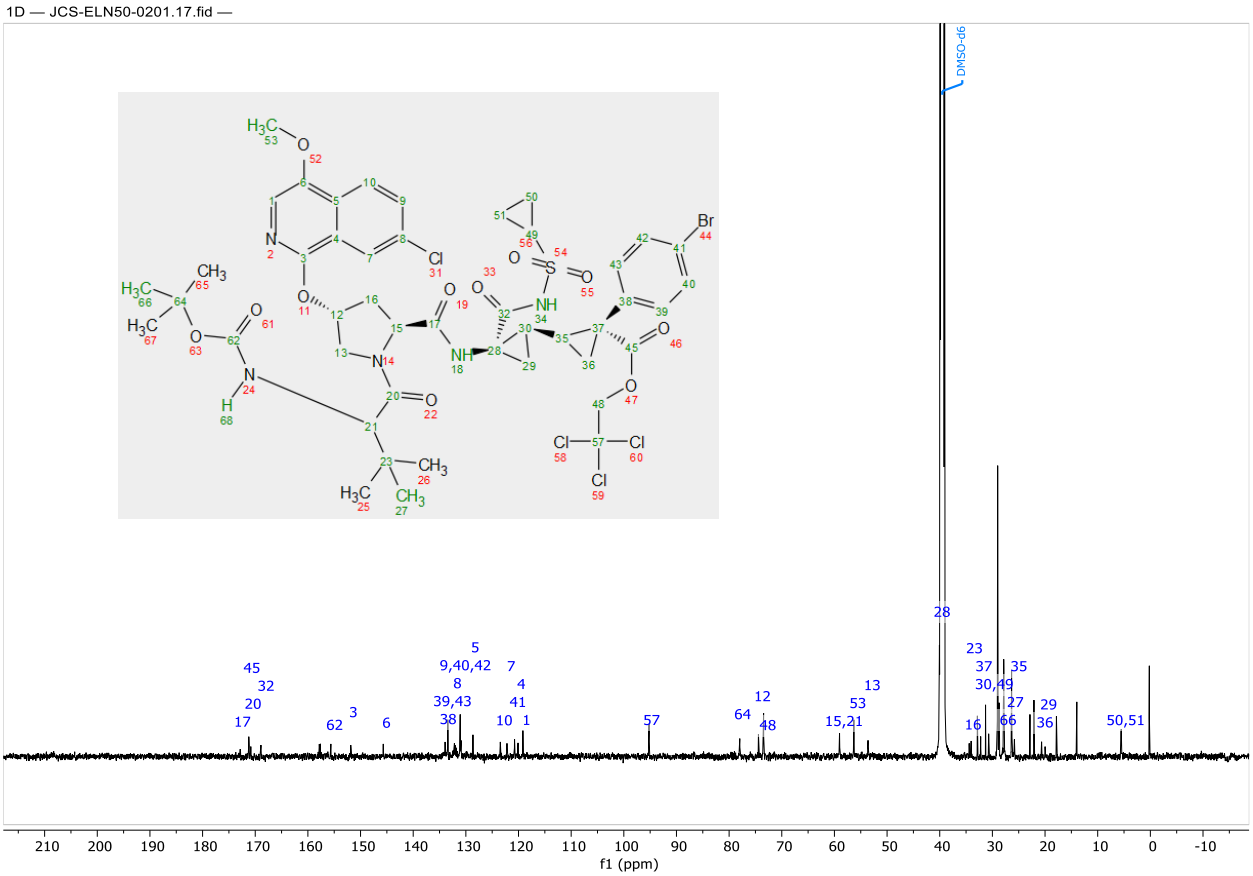

COSY:

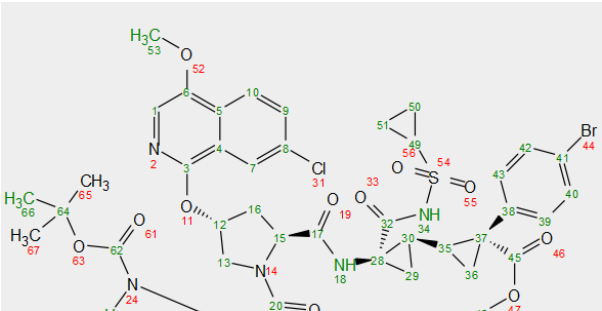

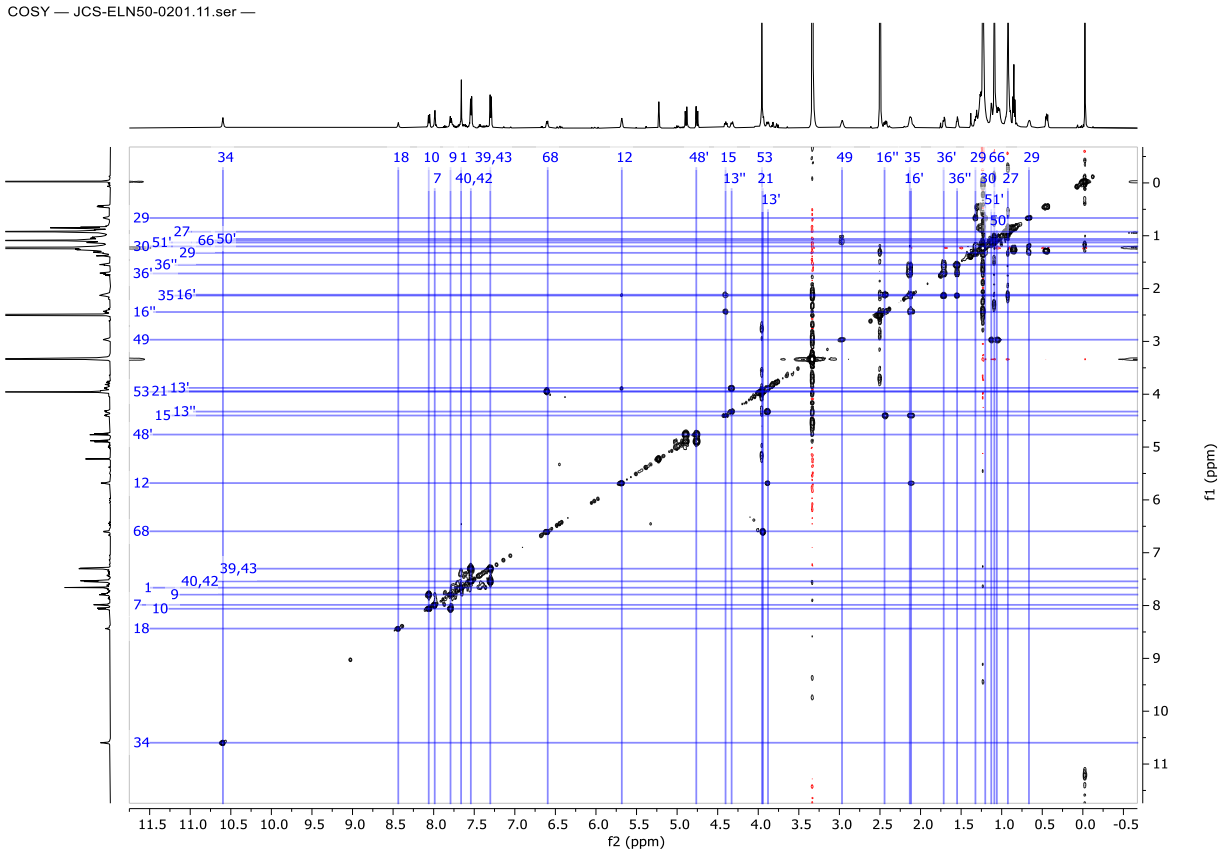

TOCSY:

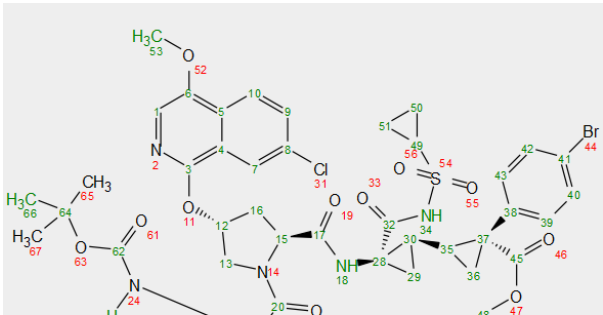

TOCSY — JCS-ELN50-0201.12.ser —

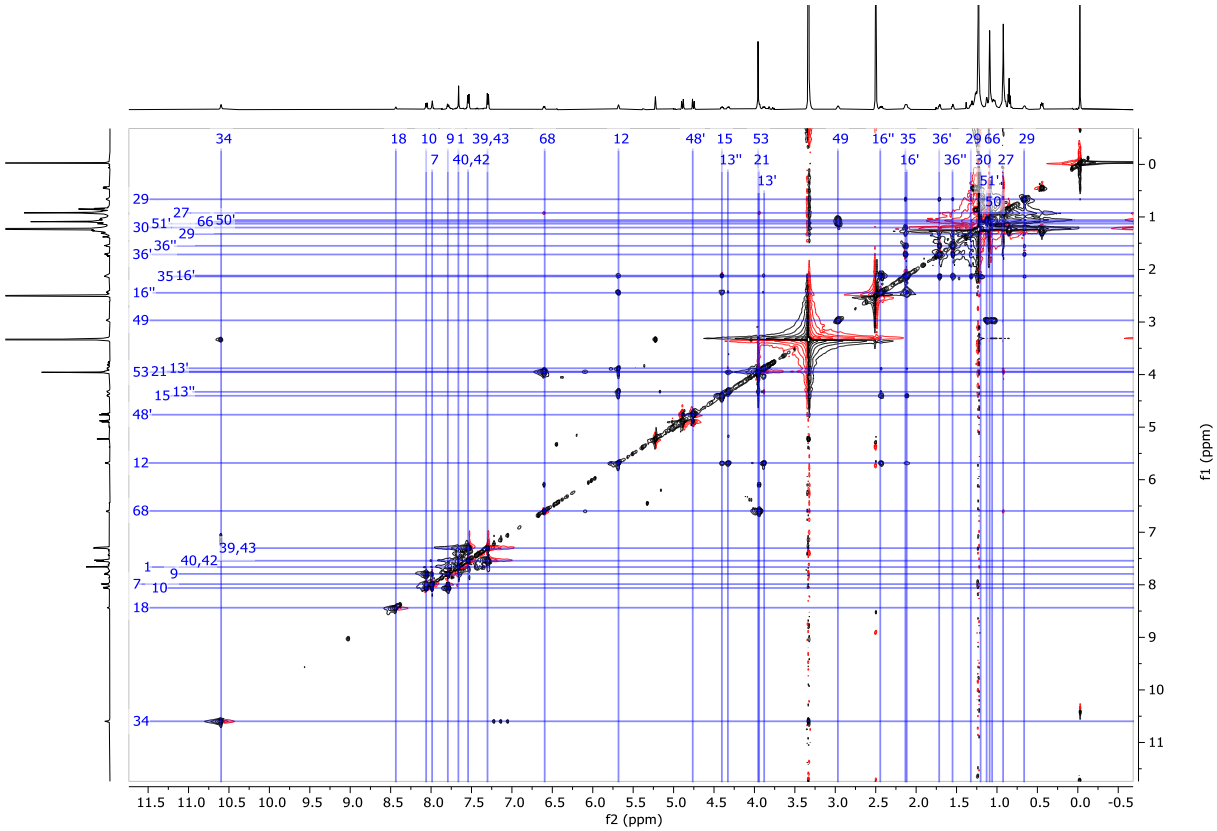

HSQC:

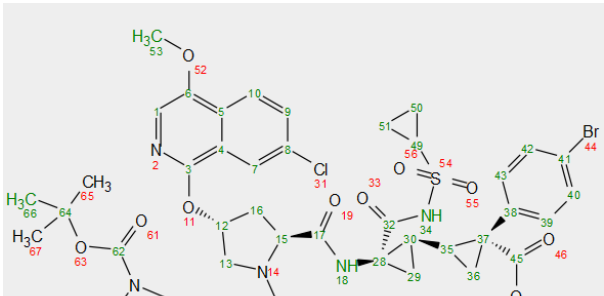

HSQC-EDITED — JCS-ELN50-0201.13.ser —

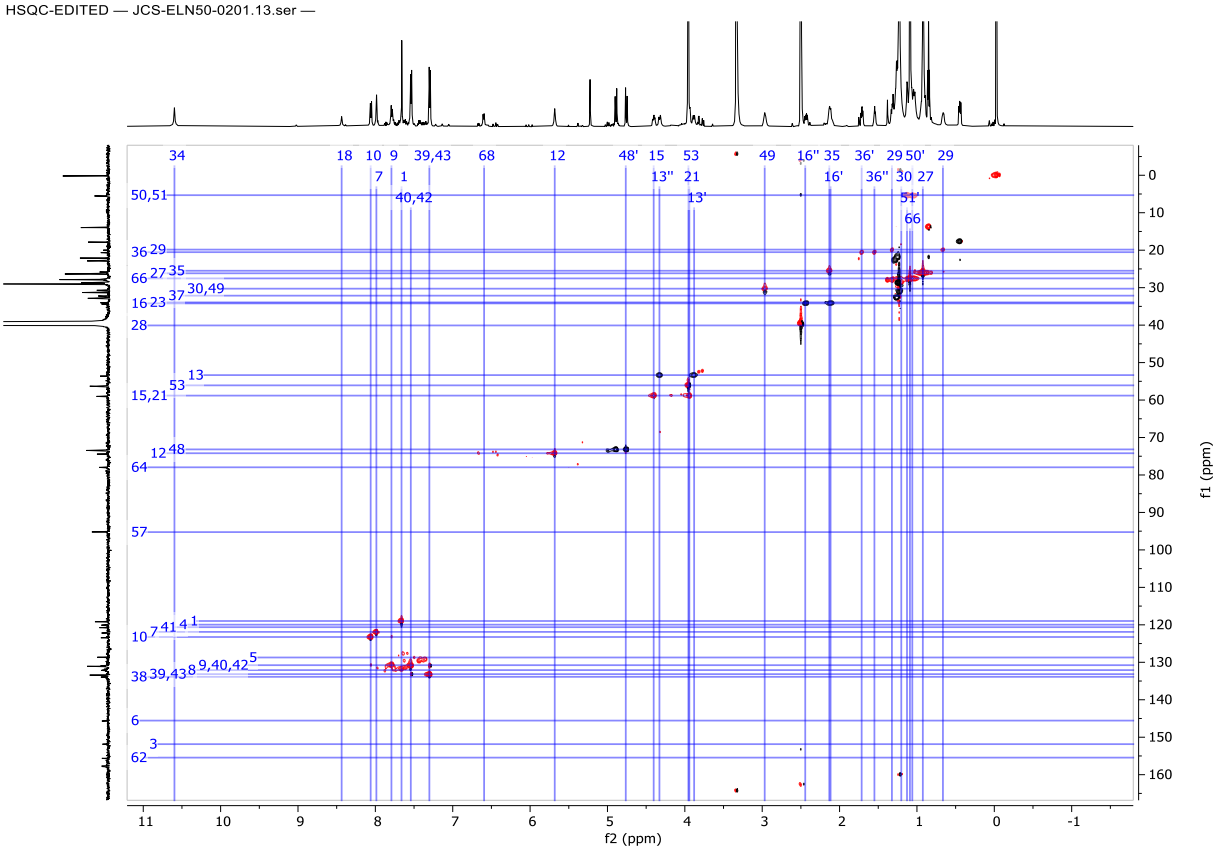

HMBC:

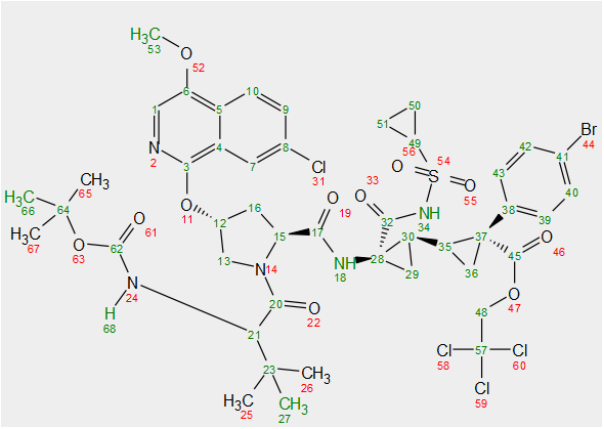

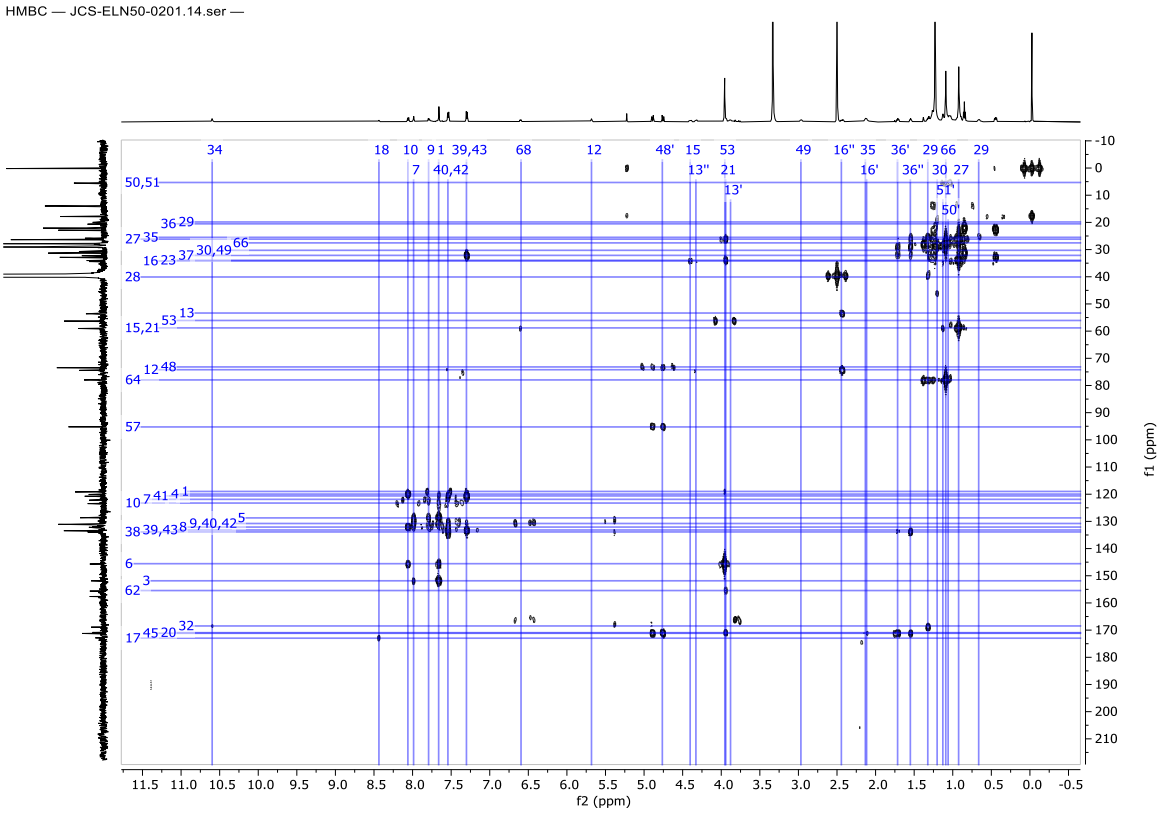
HMBC — JCS-ELN50-0201.14.ser —
f2 (ppm)
f1 (ppm)

ROESY:

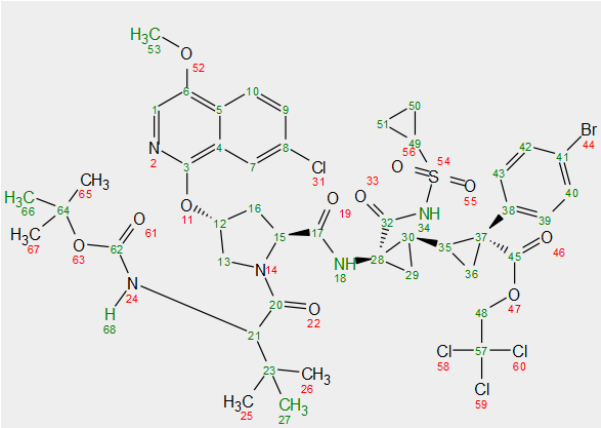

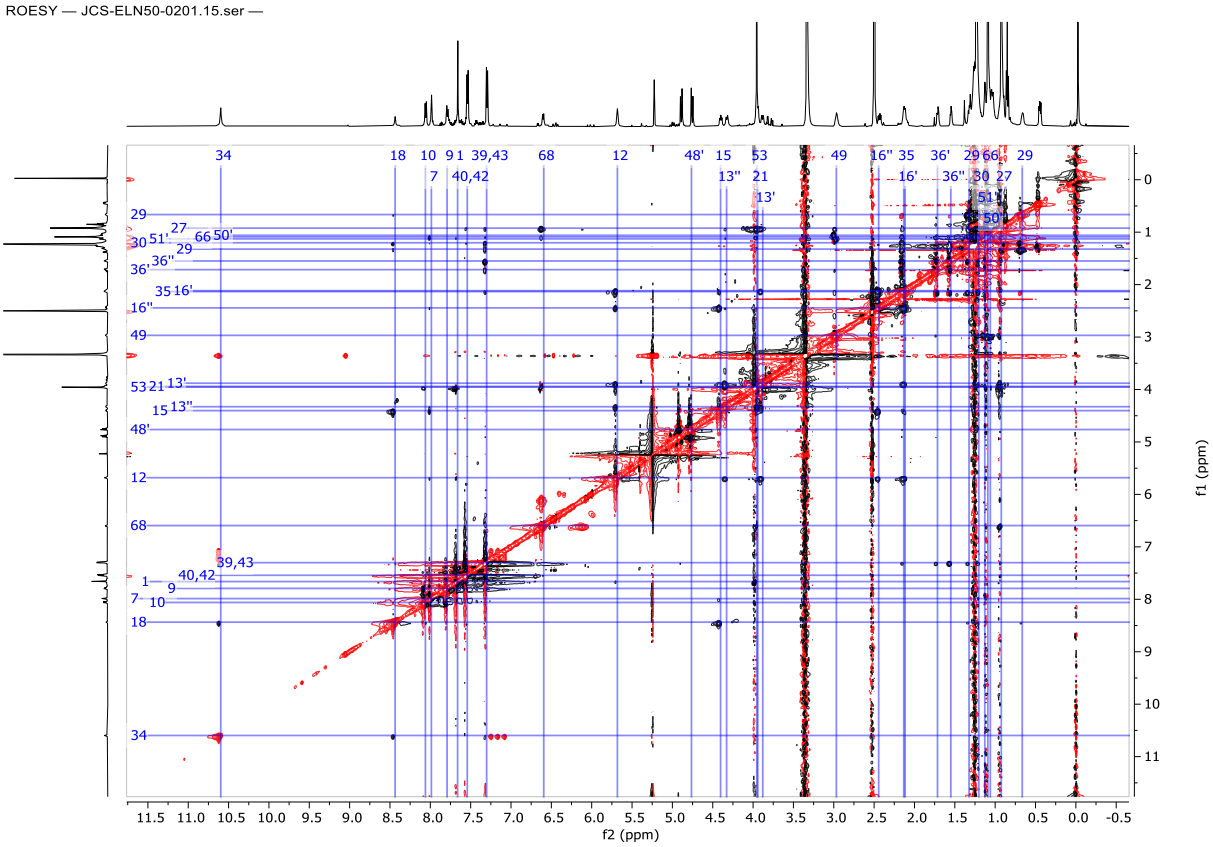

9. Analysis of Rh_2(*R*-NTTL)$_4$(18)in different solvents:

In order to understand the origin of enhanced enantioselectivity of Rh_2(*R*-NTTL)$_4$ when using HFIP as solvent compared with CH_2Cl_2 1H NMR was taken of the catalyst in both CDCl3 (top) and D2-HFIP (bottom). What follows is a blowup of the aryl region of both experiments. While the protons have different chemical shifts in the two solvents the number of peaks remains the same. This suggests that the symmetry of the catalyst is the same in both solvents, and that the catalyst is C4 symmetric as there are only 6 aryl signals. While the protons in the naphthalimide are all unique due to the secondary structure of the catalyst, all of the ligands are identical. Hence this experiment does not suggest that catalyst geometry is significantly altered in HFIP to account for the observed differences in enantioselectivity.

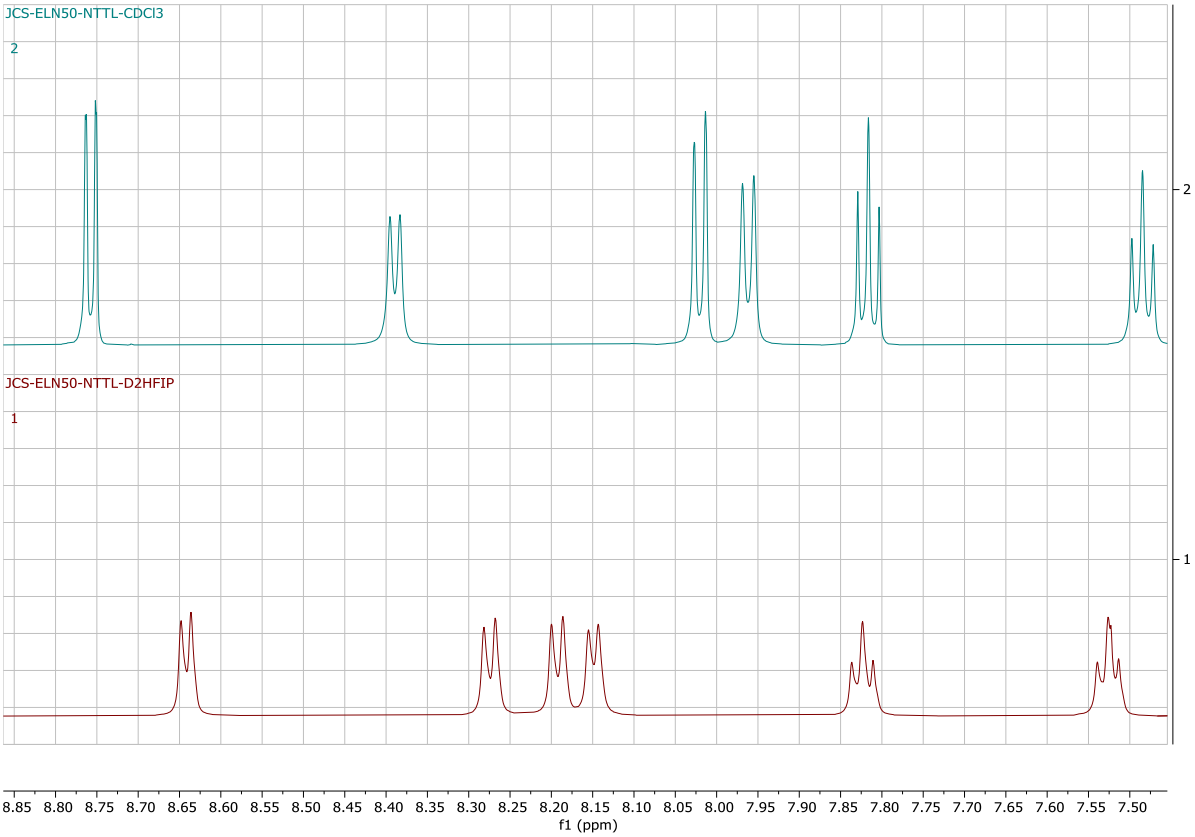

Figure C11. 1H NMR of Rh_2(*R*-NTTL)$_4$ in both $CDCl_3$ (top) and D2-HFIP (bottom).

10. Unpublished results with HFIP

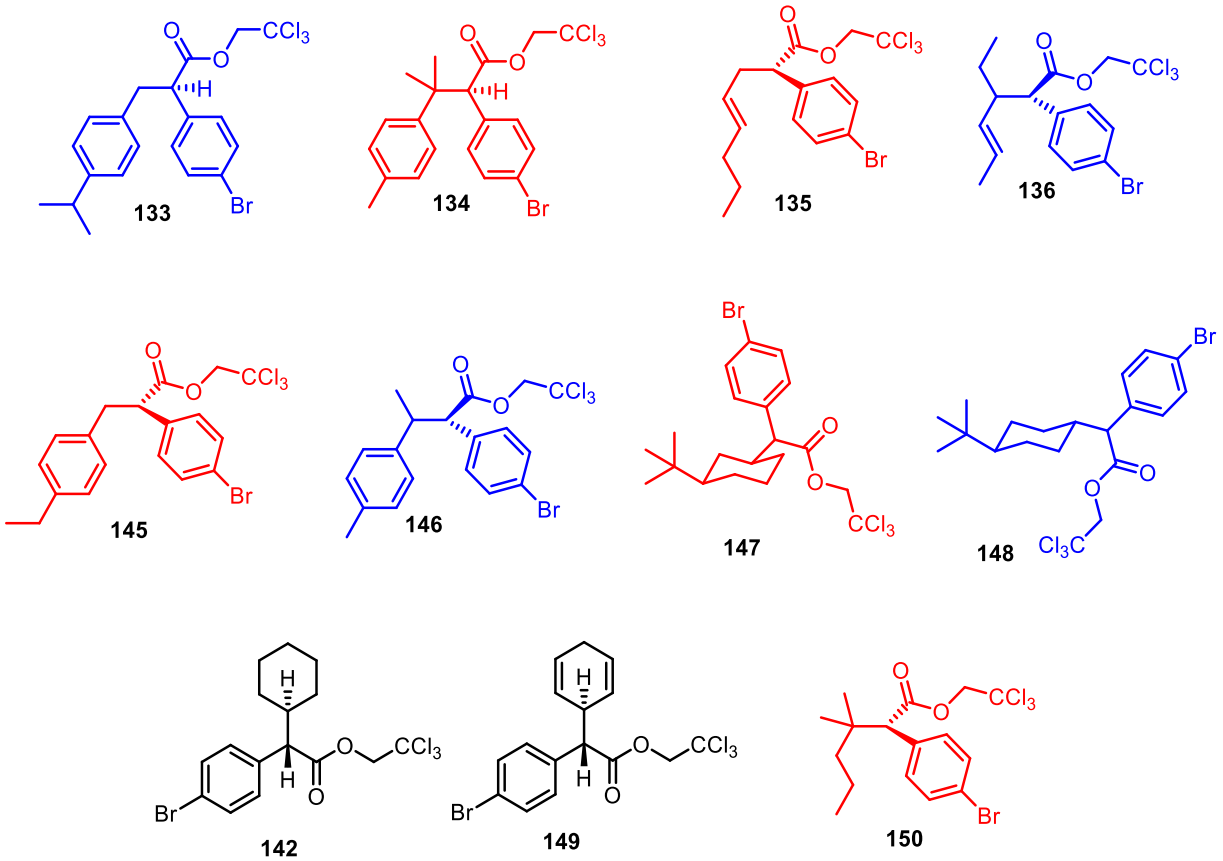

Figure C12: Known supplemental substrates.
Compounds **133, 134, 145, and 146** matched the reported literature spectra.[11]
Compounds **135** and **136** matched the reported literature spectra.[12]
Compounds **142, 147** and **148** matched the reported literature spectra.[13]
Compound **149** matched the reported literature spectra.[14]
Compound **150** matched the reported literature spectra.[15]

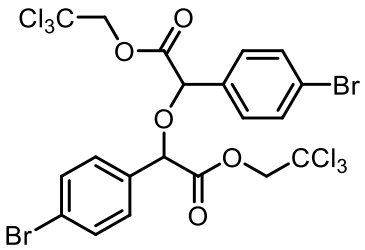

Bis(2,2,2-trichloroethyl) 2,2'-oxybis(2-(4-bromophenyl)acetate) (139): Product is obtained as the major product obtained when reactions are performed without an adequate trap for rhodium carbene generated from the diazo compound 2,2,2-trichloroethyl 2-(4-bromophenyl)-2-diazoacetate in the presence of HFIP as solvent. The product appears as a clear colorless oil.
1H NMR: (600 MHz, CDCl3) δ 7.55 (dd, *J* = 8.5, 6.7 Hz, 3H), 7.42 (d, *J* = 8.5 Hz, 1H), 7.39 (d, *J* = 8.5 Hz, 1H), 5.21 (s, 1H), 5.15 (s, 1H), 4.83 (dd, *J* = 11.9, 4.6 Hz, 2H), 4.73 (dd, *J* = 11.9, 3.1 Hz, 2H).

^{13}C NMR (151 MHz, $CDCl_3$) δ 167.96, 167.72, 133.38, 133.29, 132.09, 132.01, 129.24, 129.14, 123.72, 123.67, 94.29, 94.24, 78.40, 77.85, 74.27.
IR(neat): 3015, 2970, 2947, 173572,5, 1487, 1435, 1366, 1216, 1158, 1120, 1093, 1071, 1011, 907, 826, 762, 718, 539, 527, 515, 493 cm^{-1}
HRMS(+pESI, [M-H]): Expected: 684.73063 Found: 684.73164

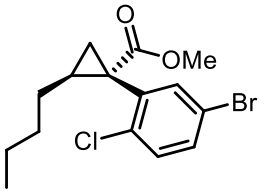

Methyl (1S,2S)-1-(5-bromo-2-chlorophenyl)-2-butylcyclopropane-1-carboxylate (126): Product was prepared according to **general method B** from the reaction between methyl 2-(5-bromo-2-chlorophenyl)-2-diazoacetate (29 mg, 0.10 mmol) and 1-hexene (21 mg, 31µl, 0.25 mmol) in the presence of Rh_2(*R*-TPPTTL)$_4$ (1.0 mol%, 2.5 mg) and 2-chloropyridine (1.0 equiv, 11mg, 10µl, 0.10mmol) at various equivalents of HFIP (10equiv-solvent). The product was obtained as a clear colorless oil in up to 90% ee and 95% yield (33mg, 95µmol).
1H NMR: (600 MHz, CDCl3) δ7.52 – 7.32 (m, 2H), 7.29 – 7.13 (m, 2H), 3.64 (s, 3H), 2.12 (s, 1H), 1.81 – 1.60 (m, 2H), 1.42 – 1.24 (m, 3H), 1.11 (s, 1H), 0.86 (t, *J* = 7.2 Hz, 3H), 0.29 (s, 1H). Note: Hindered rotation of the arene leads to very broad spectral features by NMR.
^{13}C NMR (151 MHz, $CDCl_3$) δ 173.51, 136.21, 134.77, 131.47, 130.86, 120.06, 52.47, 33.07, 31.74, 31.34, 28.49, 28.31, 26.84, 22.35, 14.08.
IR(neat): 3015, 2970, 2951, 2859, 1736, 1434, 1365, 1269, 1228, 1216, 1174, 1111, 1086, 1034, 963, 900, 811, 538, 527, 515, 481 cm^{-1}
HRMS: (+p-APCI, M+H), Expected: 345.02515 Found: 345.02579
Chiral HPLC: (Column OD-H, 60 min, 1ml/min, 0% IPA/Hexanes) RT: 14.5 min, 20.0 min.

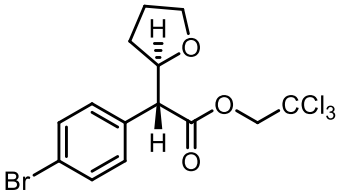

2,2,2-Trichloroethyl (R)-2-(4-bromophenyl)-2-((R)-tetrahydrofuran-2-yl)acetate (141): Product was prepared according to from the reaction between 2,2,2-trichloroethyl 2-(4-bromophenyl)-2-diazoacetate (37 mg, 0.10 mmol) and tetrahydrofuran (5.0 equiv, 40µl, 36mg, 0.50 mmol) in the presence of Rh_2(*tetra-p*-BrTPPTTL)$_4$ as catalyst (1.0 mol%, 3.7mg, 0.10 µmol) and DCM as solvent. The product was obtained as a clear colorless oil as a 2:1 mixture of diastereomers in up to 97% ee and 27% yield (11mg, 26µmol).
1H NMR(600 MHz, CDCl3): 7.54 – 7.44 (m, 5H), 7.32 (d, J = 8.5 Hz, 2H), 7.29 (d, J = 6.8 Hz, 2H), 4.90 – 4.66 (m, 5H), 4.56 (ddt, J = 22.4, 8.4, 6.9 Hz, 3H), 4.00 – 3.76 (m, 4H), 3.74 (d, J = 8.4 Hz, 2H), 3.68 (d, J = 9.7 Hz, 1H), 2.33 – 2.08 (m, 1H), 2.01 – 1.84 (m, 4H), 1.84 – 1.75 (m, 1H), 1.75 – 1.63 (m, 1H), 1.58 – 1.41 (m, 1H).
^{13}C NMR (151 MHz, $CDCl_3$) δ 170.36, 169.93, 134.62, 133.95, 132.00, 131.94, 131.80, 131.73, 130.59, 130.31, 122.15, 121.99, 94.73, 94.66, 80.12, 79.43, 74.18, 74.09, 68.60, 68.48, 56.81, 56.24, 30.27, 29.48, 25.66, 25.42.

IR(neat): 2953, 2873, 1751, 1706, 1665, 1609, 1589, 1489, 1445, 1408, 1374, 1339, 1297, 1274, 1182, 1141, 1072, 1011, 907, 826, 762, 718, 571, 509 cm^{-1}
HRMS: (-p-APCI, M-H), Expected: 412.91191 Found: 412.91169
Chiral SFC: (Column CEL2, 5min, 2.5ml/min, 5% 1:1 MeOH:IPA(+0.2%FA)/CO_2) RT: 1.36 min, 1.69 min.

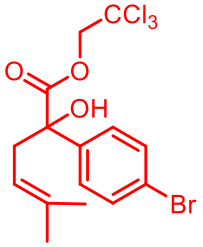

2,2,2-Trichloroethyl 2-(4-bromophenyl)-2-hydroxy-5-methylhex-4-enoate (139): Product was prepared during competition studies from the reaction between 2,2,2-trichloroethyl 2-(4-bromophenyl)-2-diazoacetate (37 mg, 0.10 mmol) and 2-methylbut-3-en-2-ol (2.5 equiv, 22mg, 26µl, 0.25mmol) in the presence of Rh_2(*R*-NTTL)$_4$ as catalyst (1.0 mol%, 1.4mg, 0.10µmol) and DCM as solvent. The product was obtained as a clear colorless oil.
1H NMR: (600 MHz, cdcl3) δ 7.59 (d, J = 8.7 Hz, 2H), 7.51 (d, J = 8.6 Hz, 2H), 5.15 (dddd, J = 7.2, 5.8, 2.9, 1.5 Hz, 1H), 4.84 – 4.69 (a,b-quartet, 2H), 3.52 (s, 1H), 3.04 (dd, J = 14.7, 7.2 Hz, 1H), 2.77 (dd, J = 14.5, 7.1 Hz, 1H), 1.73 (d, J = 1.5 Hz, 3H), 1.67 (s, 3H)
^{13}C NMR (151 MHz, $CDCl_3$) δ 172.96, 139.52, 137.66, 131.76, 131.37, 127.77, 122.30, 116.59, 94.14, 78.18, 75.11, 38.66, 26.04, 18.30.
IR(neat): 3459, 3016, 2970, 1739, 14861435, 1365, 1228, 1216, 1092, 1010, 900, 830, 789, 719, 539, 527, 515 cm^{-1}
HRMS: (+p ESI, M+H), Expected: 428.94212 Found: 428.94281

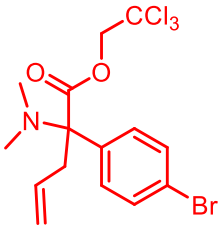

2,2,2-Trichloroethyl 2-(4-bromophenyl)-2-(dimethylamino)pent-4-enoate (140): Product was prepared during competition studies from the reaction between 2,2,2-trichloroethyl 2-(4-bromophenyl)-2-diazoacetate (37 mg, 0.10 mmol) and *N,N*-dimethylallylamine (2.5 equiv, 21mg, 30µl, 0.25mmol) in the presence of Rh_2(*R*-NTTL)$_4$ as catalyst (1.0 mol%, 1.4mg, 0.10µmol) and DCM as solvent. The product was obtained as a clear colorless oil.
1H NMR: (600 MHz, cdcl3) δ 7.46 (d, J = 8.7 Hz, 2H), 7.30 (d, J = 8.7 Hz, 2H), 5.52 (ddt, J = 17.2, 10.3, 7.0 Hz, 1H), 5.00 – 4.95 (m, 1H), 4.93 (d, J = 1.8 Hz, 1H), 4.92 – 4.79 (a,b-quartet, 2H), 2.91 – 2.77 (m, 2H), 2.40 (s, 6H).
^{13}C NMR (151 MHz, $CDCl_3$) δ 168.92, 138.65, 138.62, 132.56, 130.71, 129.93, 121.18, 118.79, 118.75, 94.57, 74.46, 73.98, 42.48, 40.24.
IR(neat): 2950, 2792, 1734, 1639, 1589, 1486, 1449, 1396, 1366, 1284, 1192, 1166, 1112, 1073, 1046, 1009, 967, 918, 808, 779, 718, 629, 574, 520 cm^{-1}
HRMS: (+p APCI, M+H), Expected: 427.9581 Found: 427.95881

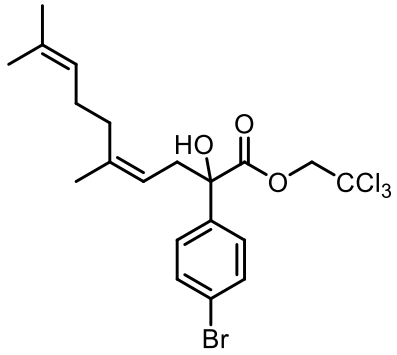

3:1 E:Z

2,2,2-Trichloroethyl (E/Z)-2-(4-bromophenyl)-2-hydroxy-5,9-dimethyldeca-4,8-dienoate (137): Product was prepared according to from the reaction between 2,2,2-trichloroethyl 2-(4-bromophenyl)-2-diazoacetate (37 mg, 0.10 mmol) and (-)-linalool (2.5 equiv, 39mg, 45µl, 0.25mmol) in the presence of Rh_2(*R*-NTTL)$_4$ as catalyst (1.0 mol%, 1.4mg, 0.10µmol) and DCM as solvent. The product was obtained as a white crystalline solid up to 3:1 E:Z ratio and 20% yield (10mg, 20µmol).
1H NMR(600 MHz, cdcl3): δ 7.56 (d, J = 8.8 Hz, 1H), 7.49 (d, J = 8.6 Hz, 1H), 5.13 (tdd, J = 8.5, 4.3, 3.0 Hz, 1H), 5.01 (tt, J = 6.9, 1.6 Hz, 1H), 4.81 – 4.62 (m, 2H), 3.49 (s, 1H), 3.04 (dd, J = 14.6, 7.1 Hz, 1H), 2.75 (dd, J = 14.3, 7.5 Hz, 1H), 2.03 (dtd, J = 15.5, 10.2, 4.4 Hz, 4H), 1.68 (d, J = 1.4 Hz, 3H), 1.64 (d, J = 1.4 Hz, 2H), 1.58 (d, J = 1.3 Hz, 2H).
^{13}C NMR (151 MHz, $CDCl_3$) δ 171.72, 136.14, 133.37, 131.78, 130.63, 129.87, 128.30, 122.90, 94.01, 82.73, 75.67, 74.80, 72.24, 29.72, 22.67.
IR(neat): 3456, 3016, 2970, 1739, 1487, 1435, 1365, 1228, 1216, 1091, 1072, 1011, 909, 827, 765, 720, 572, 527, 516 cm^{-1}
HRMS: (-p-APCI, M-H), Expected: 494.99016 Found: 494.98943

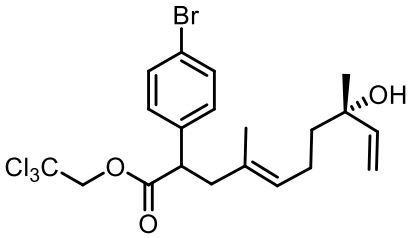

2,2,2-Trichloroethyl (8S,E)-2-(4-bromophenyl)-8-hydroxy-4,8-dimethyldeca-4,9-dienoate (138): Product was prepared according to from the reaction between 2,2,2-trichloroethyl 2-(4-bromophenyl)-2-diazoacetate (37 mg, 0.10 mmol) and (-)-linalool (2.5 equiv, 39mg, 45µl, 0.25mmol) in the presence of Rh_2(*R*-NTTL)$_4$ as catalyst (1.0 mol%, 1.4mg, 0.10µmol) and HFIP as solvent. The product was obtained as a white crystalline solid in up to 93% ee and 42% yield (21mg, 42µmol).
1H NMR: (600 MHz, cdcl3) δ 7.44 (d, J = 8.5 Hz, 2H), 7.22 (d, J = 8.5 Hz, 2H), 5.86 (dd, J = 17.3, 10.8 Hz, 1H), 5.21 – 5.12 (m, 3H), 5.05 (dd, J = 10.8, 1.2 Hz, 1H), 4.75 – 4.54 (m, 3H), 3.86 (dd, J = 8.9, 6.8 Hz, 1H), 2.81 (dd, J = 13.9, 8.6 Hz, 1H), 2.43 (dd, J = 14.2, 6.7 Hz, 2H), 2.07 (s, 4H), 2.00 – 1.86 (m, 2H), 1.60 (d, J = 1.4 Hz, 4H), 1.50 – 1.37 (m, 3H), 1.25 (s, 3H).
^{13}C NMR (151 MHz, $CDCl_3$) δ 171.71, 144.85, 136.14, 131.78, 131.71, 131.19, 129.90, 128.30, 122.90, 111.82, 94.01, 74.80, 74.23, 73.25, 72.24, 49.54, 43.07, 41.73, 29.72, 27.91, 22.67, 15.99.
IR(neat): 3456, 3015, 2970, 1739, 1487, 1435, 1365, 1228, 1216, 1091, 1072, 1011, 910, 827, 764, 720, 573, 527, 515 cm^{-1}
HRMS: (-p-APCI, M-H), Expected: 494.99016 Found: 494.98865

Chiral SFC: (Column OZ-3, 5.00min, 2.5ml/min, 5% 1:1 MeOH:IPA(+0.2%FA)/CO_2) RT: 2.26 min, 2.52 min.

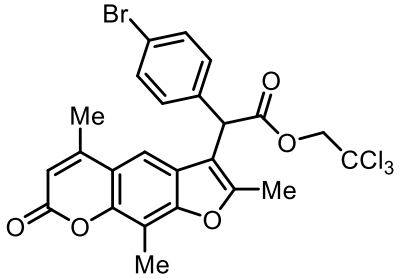

2,2,2-Trichloroethyl 2-(4-bromophenyl)-2-(2,5,9-trimethyl-7-oxo-7H-furo[3,2-g]chromen-3-yl)acetate (143): Product was prepared according to from the reaction between 2,2,2-trichloroethyl 2-(4-bromophenyl)-2-diazoacetate (37 mg, 0.10 mmol) and trioxsalen (2.5 equiv, 57mg, 0.25 mmol) in the presence of Rh_2(*R*-NTTL)$_4$ as catalyst (1.0 mol%, 1.4mg, 0.10µmol) and DCM as solvent . The product was obtained as a white powdery solid.

1H NMR: (600 MHz, cdcl3) δ 7.55 (s, 1H), 7.53 (d, J = 6.5 Hz, 3H), 7.40 (d, J = 8.4 Hz, 2H), 6.44 (q, J = 1.1 Hz, 1H), 6.26 (t, J = 1.3 Hz, 1H), 5.35 (d, J = 2.6 Hz, 1H), 4.91 – 4.66 (m, 3H), 3.35 (s, 1H), 2.61 (d, J = 0.6 Hz, 3H), 2.52 (d, J = 1.1 Hz, 3H), 2.51 (d, J = 1.2 Hz, 3H).

^{13}C NMR (151 MHz, $CDCl_3$) δ 171.71, 161.66, 157.39, 155.48, 153.29, 148.91, 136.15, 131.78, 128.30, 125.39, 122.89, 116.09, 112.78, 112.18, 109.16, 102.63, 94.02, 74.80, 72.24, 19.31, 14.24, 8.59.

IR(neat): 3016, 2970, 2948, 1739, 1608, 1591, 1486, 1435, 1365, 1276, 1228, 1216, 1166, 1104, 1071, 1010, 928, 868, 826, 758, 719, 652, 600, 564, 527, 489 cm^{-1}

HRMS: (+p-APCI, M+H), Expected: 570.9476 Found: 570.94722

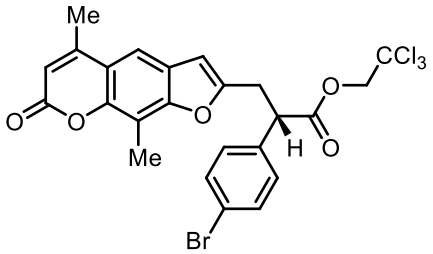

2,2,2-Trichloroethyl (S)-2-(4-bromophenyl)-3-(5,9-dimethyl-7-oxo-7H-furo[3,2-g]chromen-2-yl)propanoate (144): Product was prepared according to from the reaction between 2,2,2-trichloroethyl 2-(4-bromophenyl)-2-diazoacetate (37 mg, 0.10 mmol) and Trioxsalen (2.5 equiv, 57mg, 0.25 mmol) in the presence of Rh_2(*R*-NTTL)$_4$ as catalyst (1.0 mol%, 1.4mg, 0.10µmol) and HFIP as solvent. The product was obtained as a white powdery solid in up to 70% ee and 37% yield (21mg, 37µmol).

1H NMR: (600 MHz, cdcl3) δ 7.52 (s, 1H), 7.47 (d, J = 8.4 Hz, 2H), 7.29 – 7.21 (m, 2H), 6.42 (s, 1H), 6.27 (d, J = 1.5 Hz, 1H), 4.85 – 4.54 (2H), 4.26 (dd, J = 8.4, 7.2 Hz, 1H), 3.66 (ddd, J = 15.4, 8.5, 0.9 Hz, 1H), 3.31 (ddd, J = 15.4, 7.2, 1.0 Hz, 1H), 2.56 (s, 3H), 2.48 (s, 2H).

^{13}C NMR (151 MHz, $CDCl_3$) δ 170.67, 161.41, 156.55, 155.38, 153.09, 149.24, 135.60, 132.07, 129.68, 124.53, 122.21, 116.41, 113.06, 112.85, 109.40, 104.23, 94.50, 74.31, 49.21, 32.00, 19.28, 8.64.

IR(neat): 3016, 2970, 2946, 1738, 1435, 1365, 1228, 1216, 1105, 900, 538, 527, 515 cm^{-1}

HRMS: (+p-APCI, M+H), Expected: 570.9476 Found: 570.94765

Chiral SFC: (Column AS-3, 5 min, 2.5ml/min, 25% 1:1 MeOH:IPA(+0.2%FA)/CO_2) RT: 2.09min, 2.79 min.

Competition Studies:

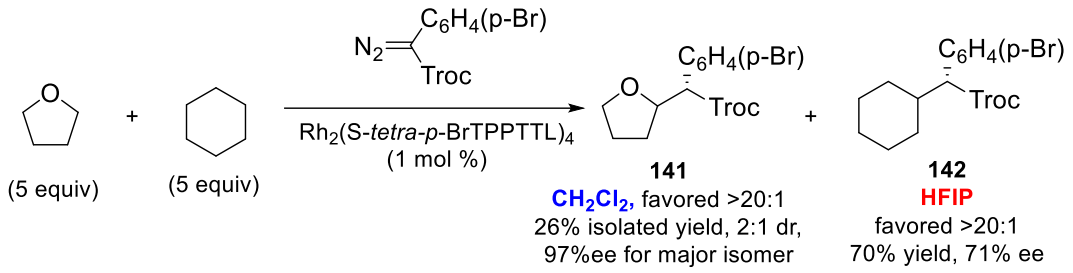

141
CH_2Cl_2, favored >20:1
26% isolated yield, 2:1 dr,
97%ee for major isomer

142
HFIP
favored >20:1
70% yield, 71% ee

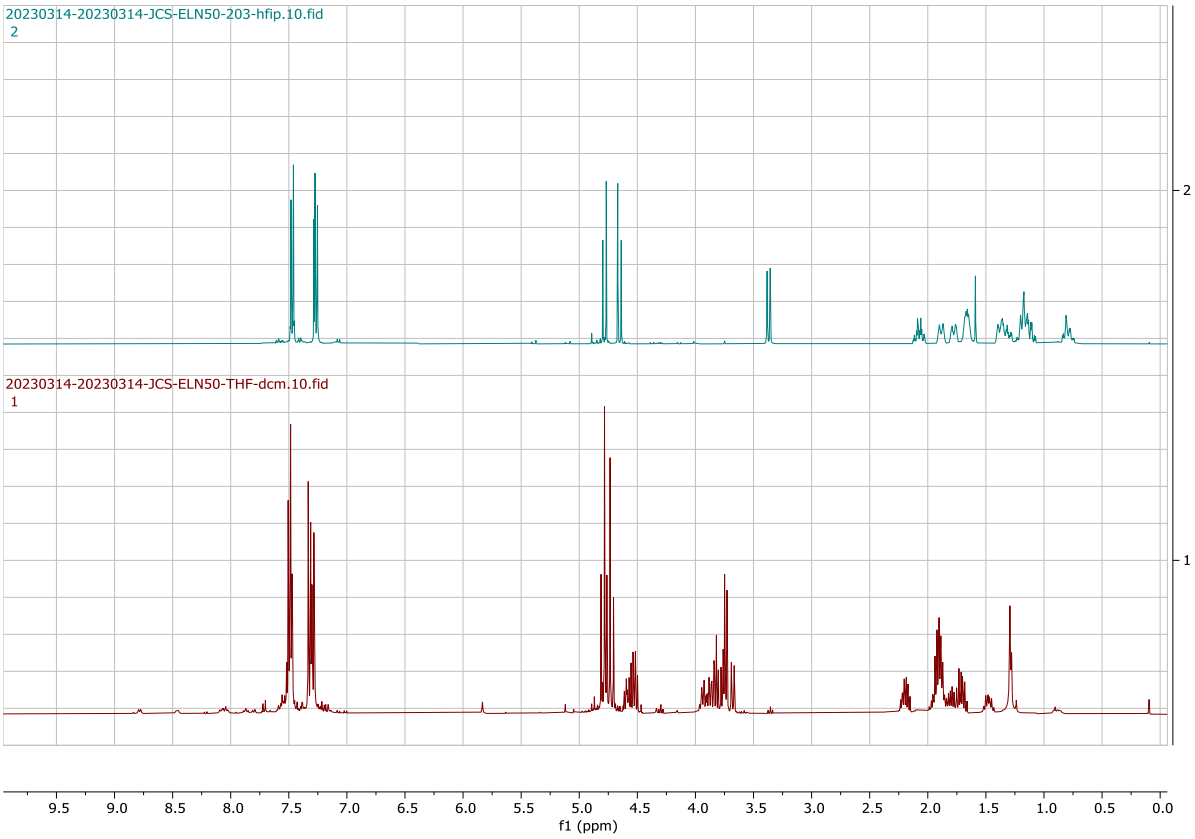

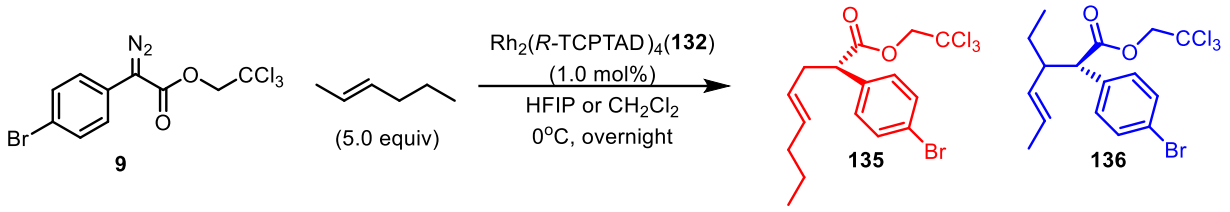

DCM as solvent: 1:8 **134**:**135**, 1:8 d.r for **135**
HFIP as solvent: 2:1 **134**:**135**, 2:1 d.r for **135**

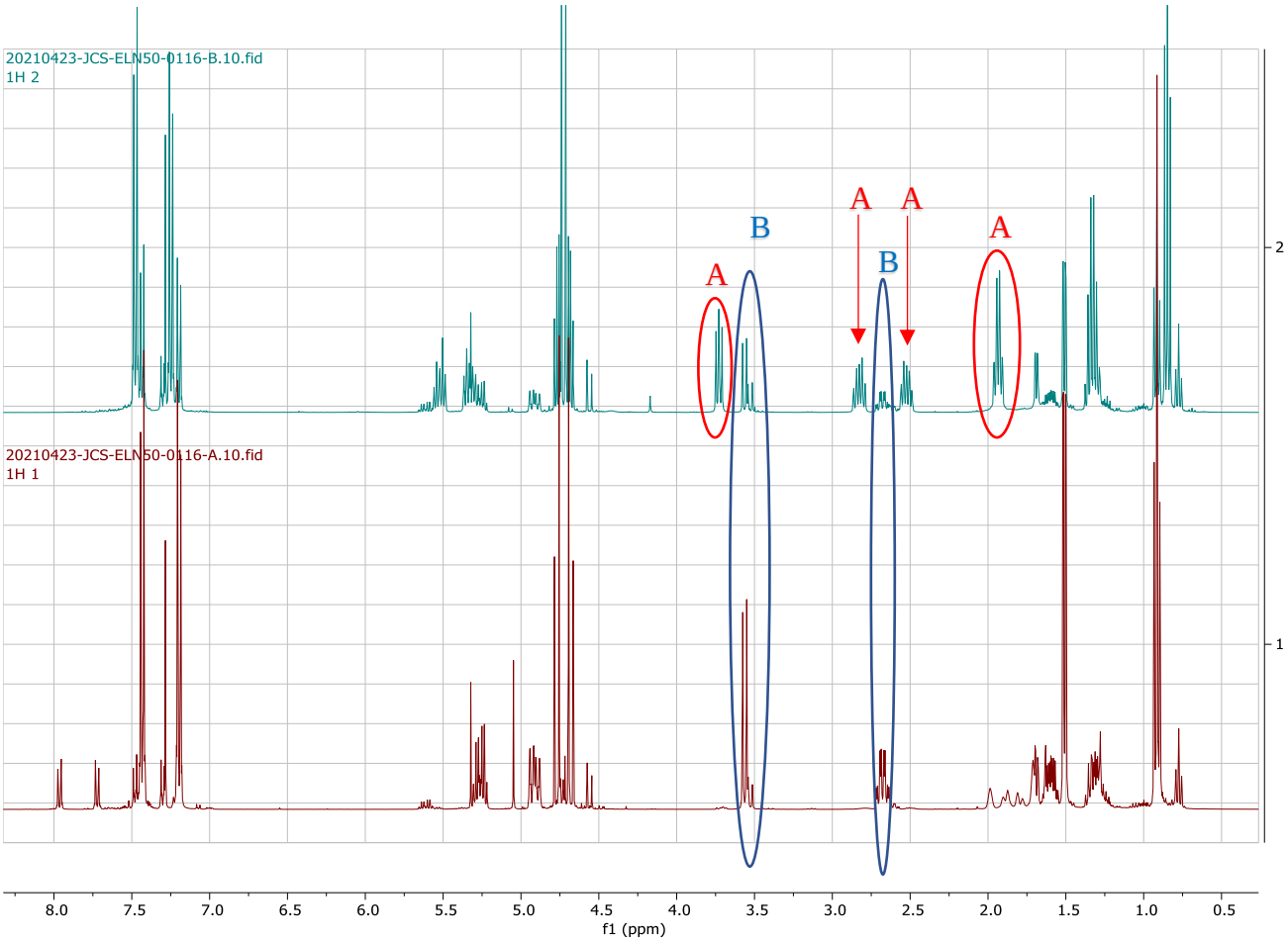

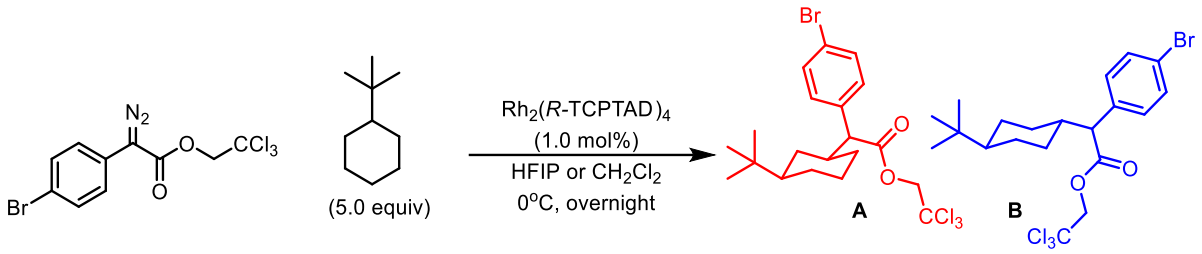

A: DCM as solvent: 1:1 **A:B**
B: HFIP as solvent: 1:1 **A:B+minor ether formation**

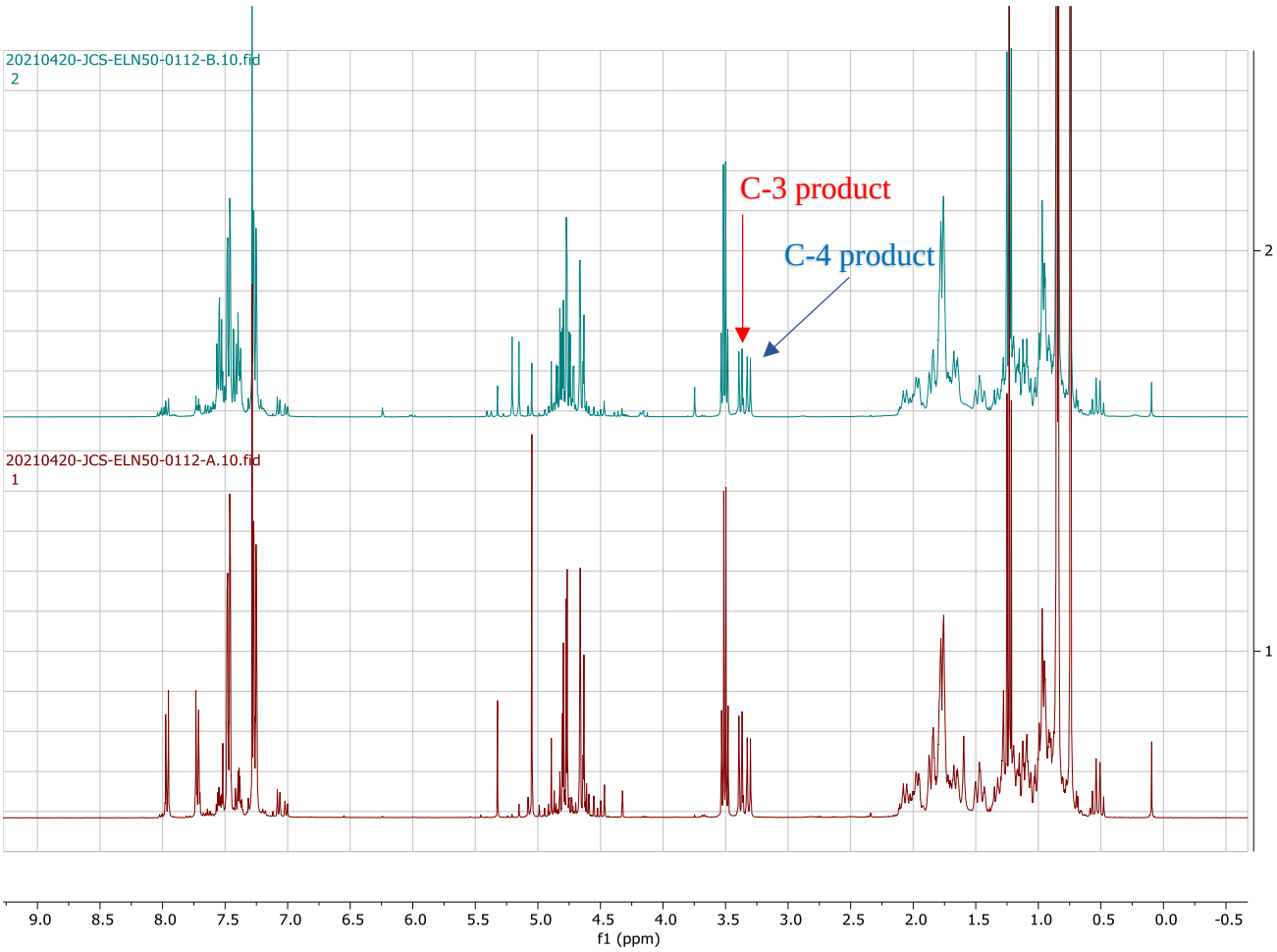

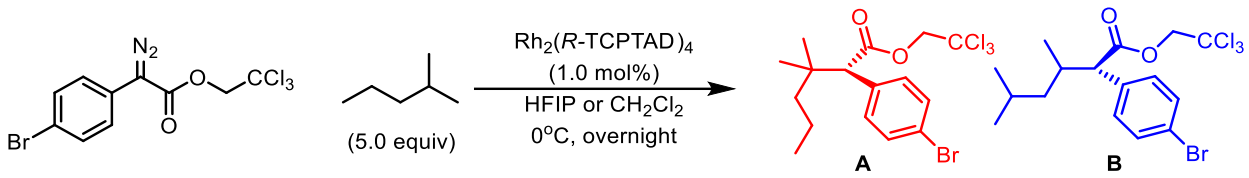

A: DCM as solvent: 10:1 **A:B**
B: HFIP as solvent: Ether=major product

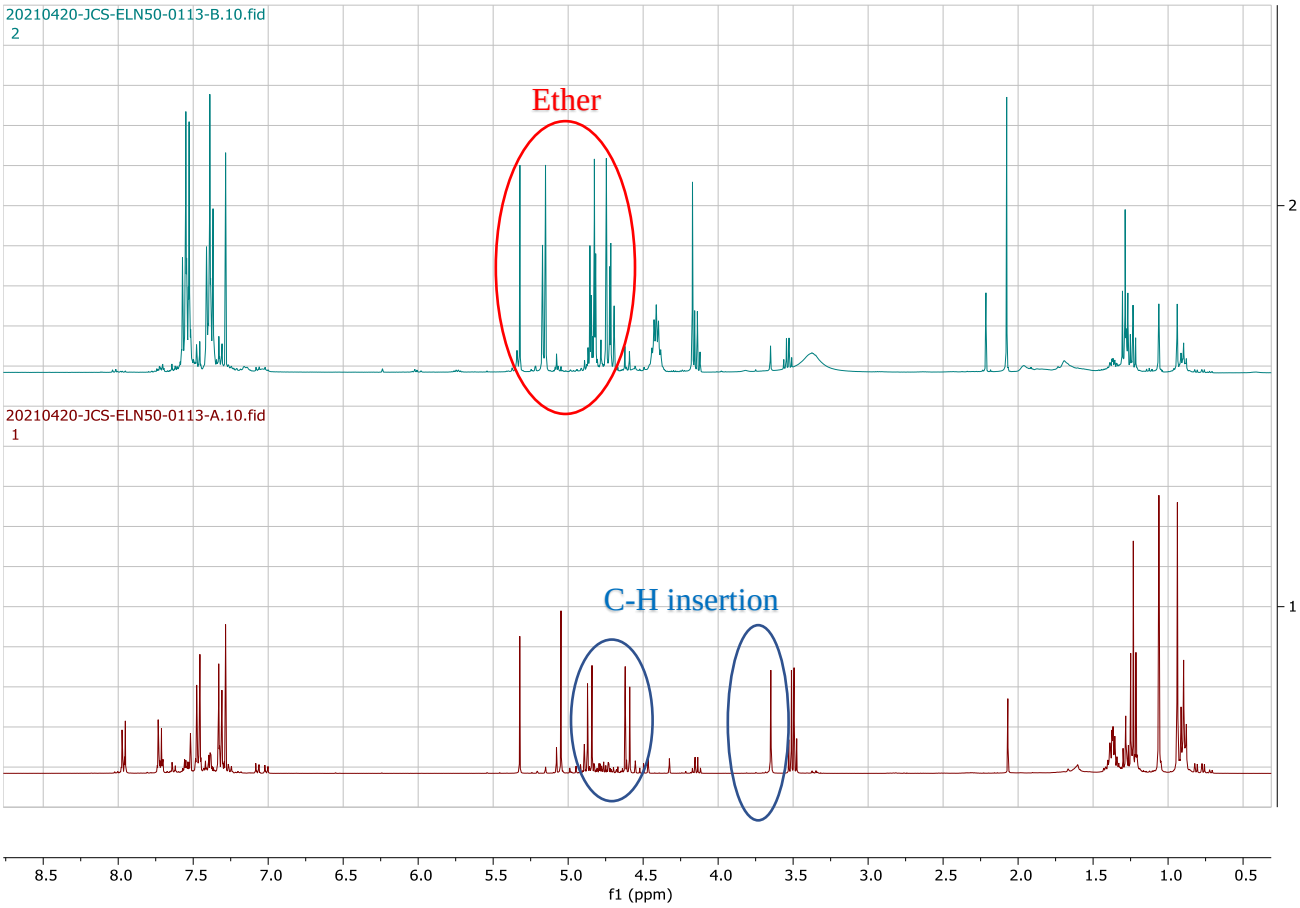

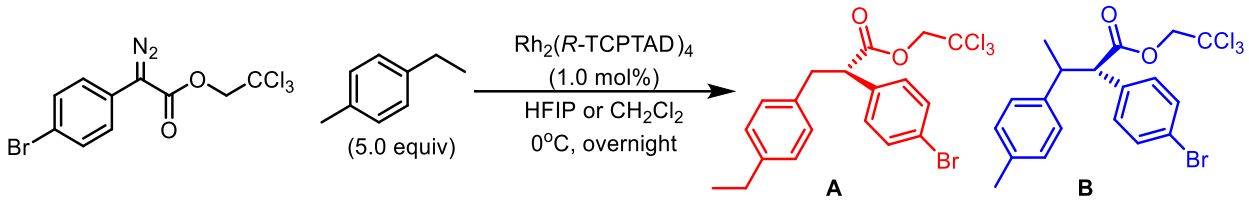

A: DCM as solvent: 1:22 **A:B**, 6:1 d.r. for **B**
B: HFIP as solvent: 1:8 **A:B**, 3:1 d.r. for **B**

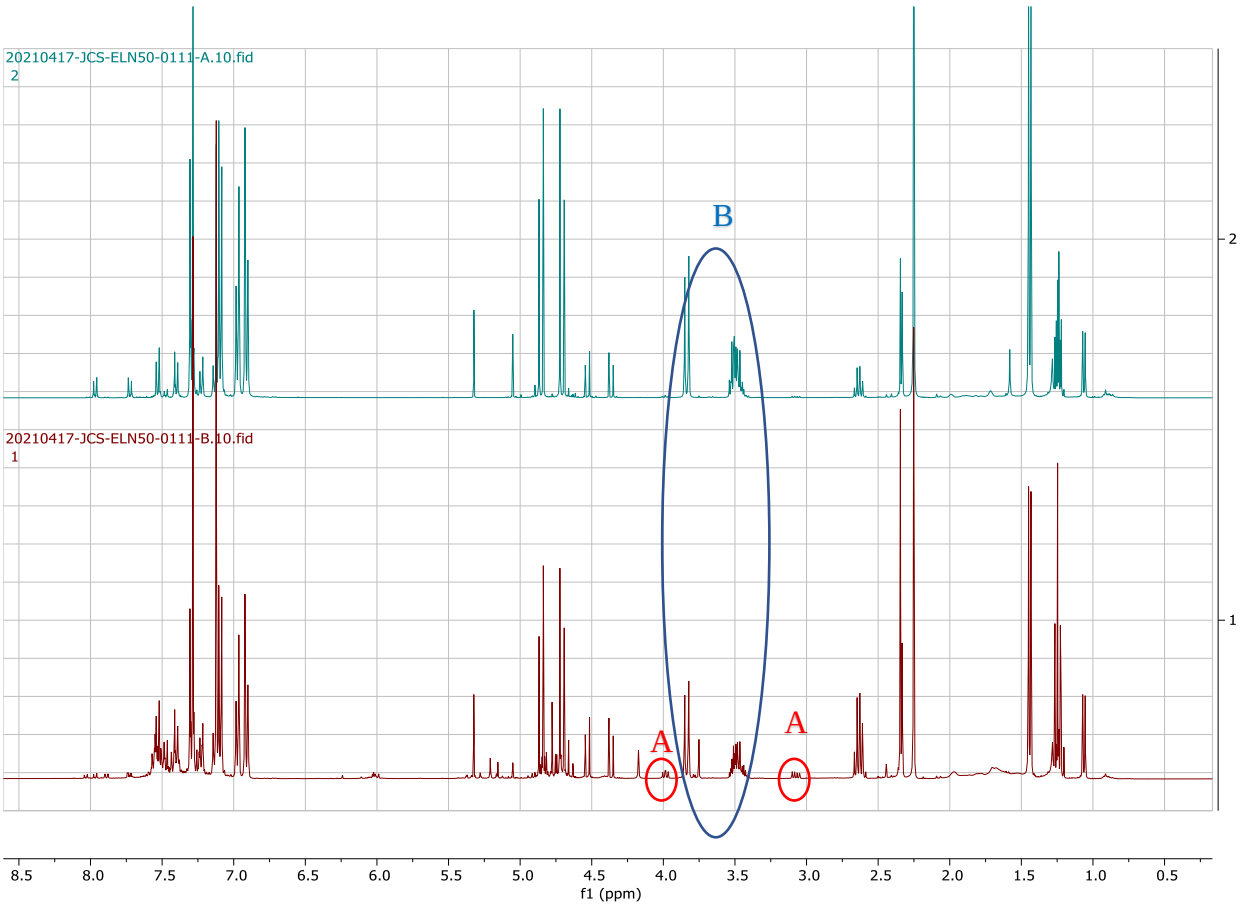

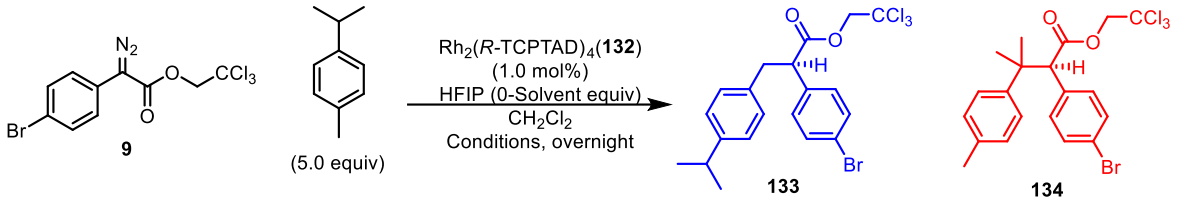

DCM as solvent, Rt:1:3 tertiary favored,
HFIP as solvent, Rt: messy 4:1 primary favored

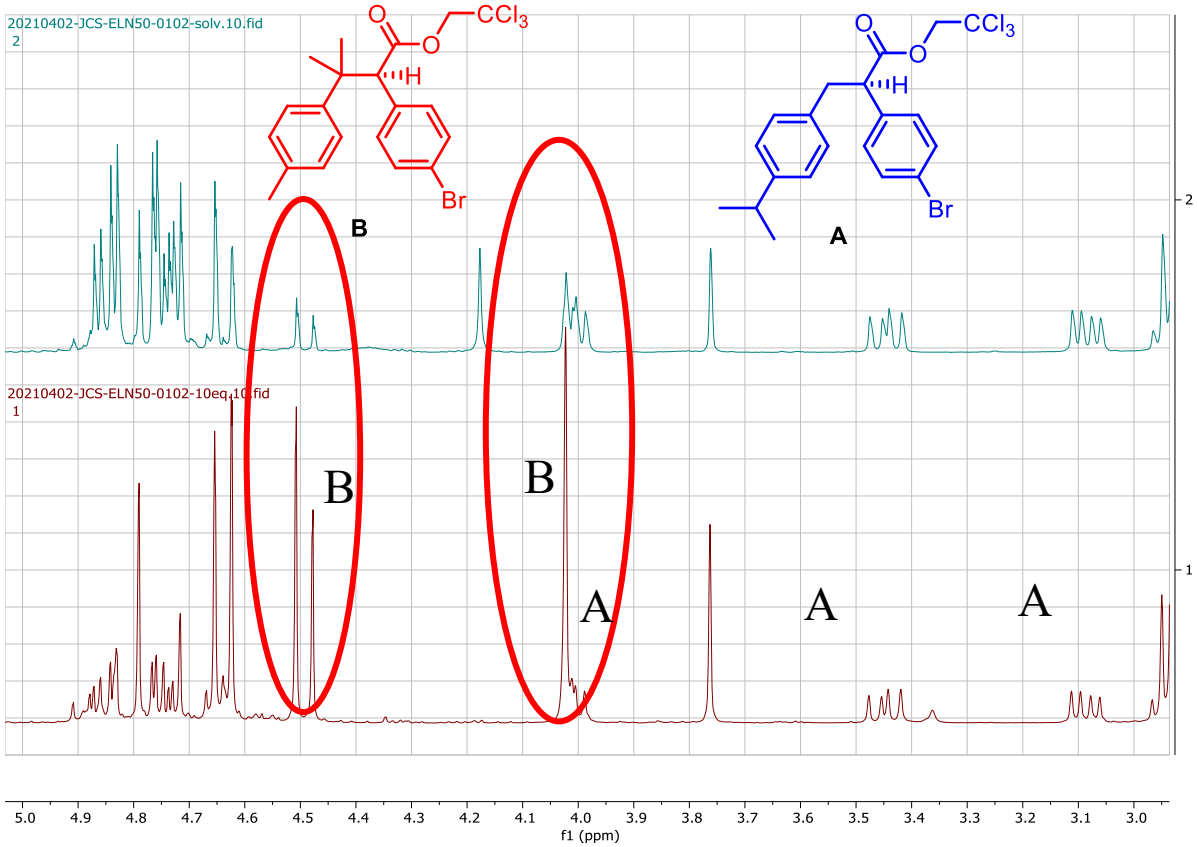

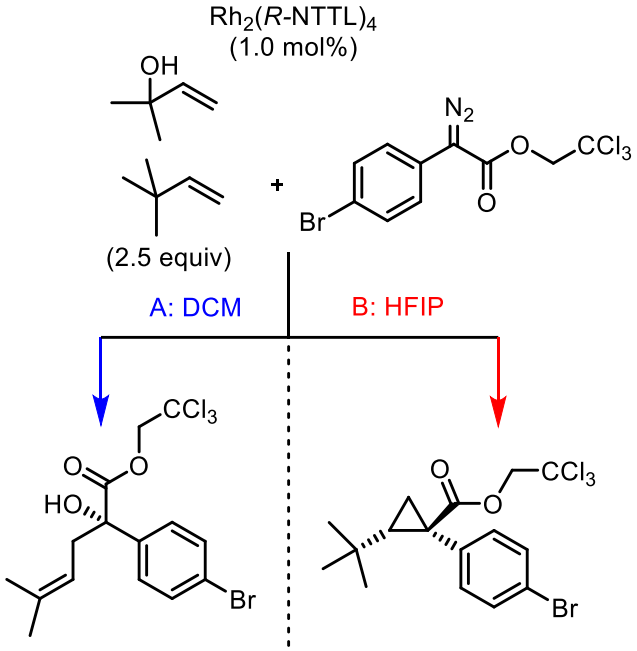
Rh2(R-NTTL)4
(1.0 mol%)
OH
N2
CCl3
O
Br
(2.5 equiv)
A: DCM
B: HFIP
HO
Br

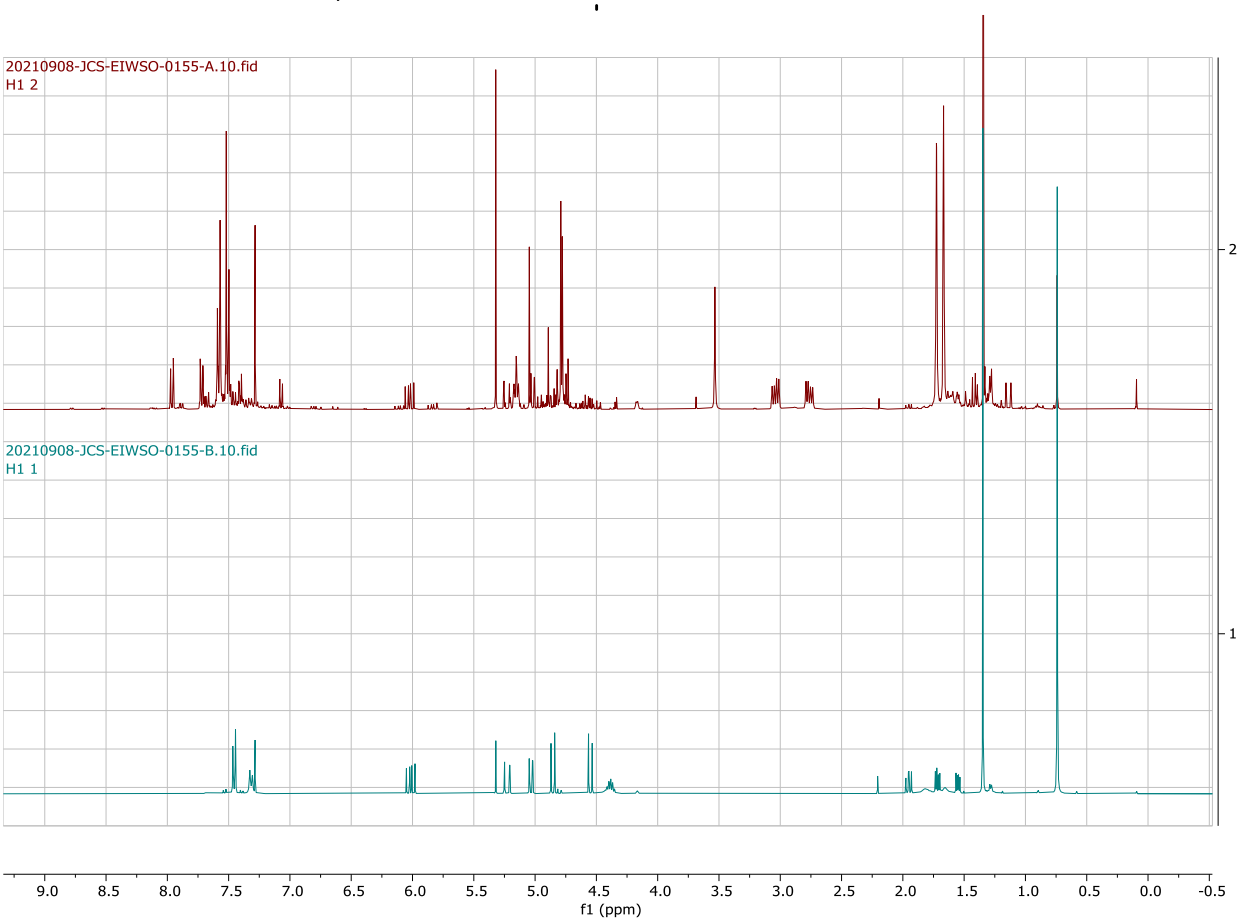
20210908-JCS-EIWSO-0155-A.10.fid
H1 2
20210908-JCS-EIWSO-0155-B.10.fid
H1 1
2
1
9.0 8.5 8.0 7.5 7.0 6.5 6.0 5.5 5.0 4.5 4.0 3.5 3.0 2.5 2.0 1.5 1.0 0.5 0.0 -0.5
f1 (ppm)

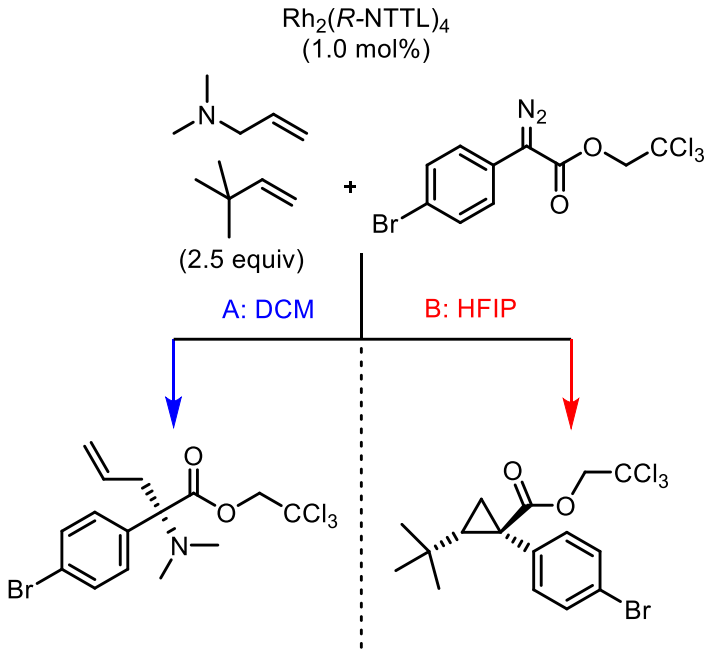
Rh2(R-NTTL)4
(1.0 mol%)
(2.5 equiv)
A: DCM
B: HFIP

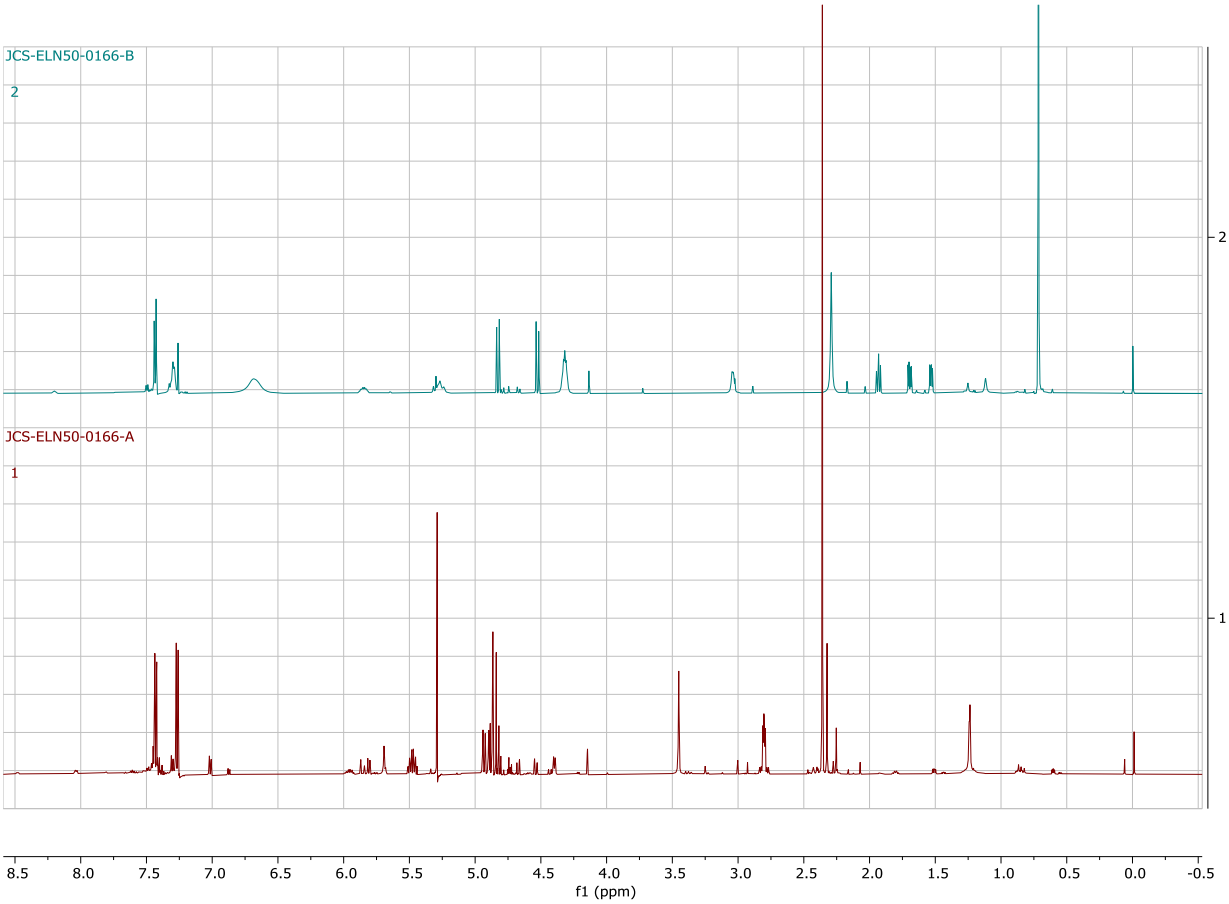
JCS-ELN50-0166-B
JCS-ELN50-0166-A
f1 (ppm)

NMR spectra:

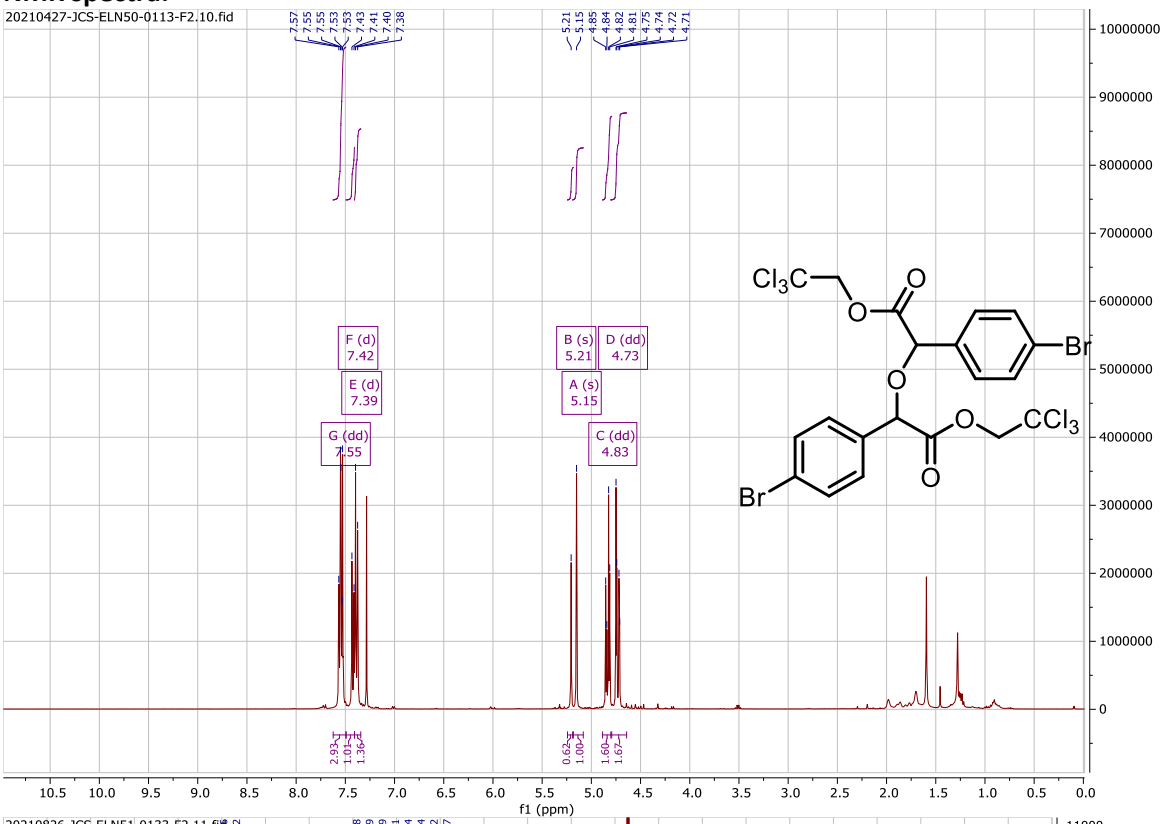
20210427-JCS-ELN50-0113-F2.10.fid
F (d) 7.42
E (d) 7.39
G (dd) 7.55
B (s) 5.21
D (dd) 4.73
A (s) 5.15
C (dd) 4.83
f1 (ppm)

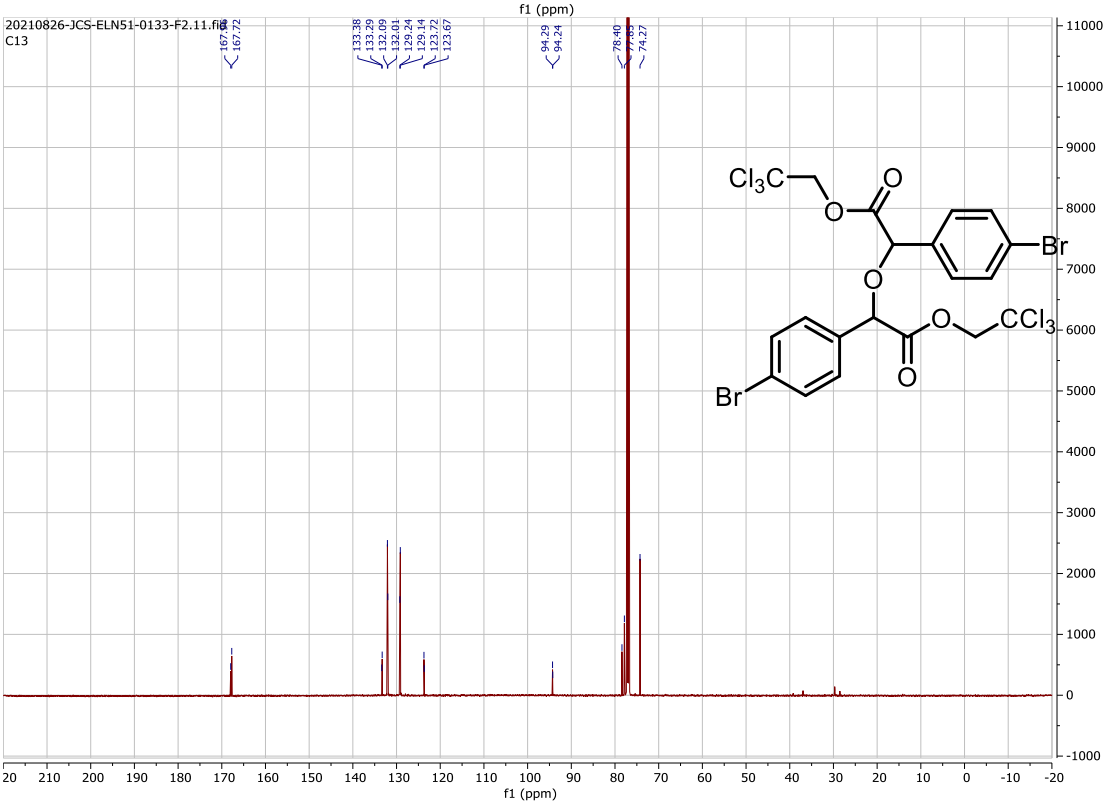
20210826-JCS-ELN51-0133-F2.11.fid
C13
f1 (ppm)

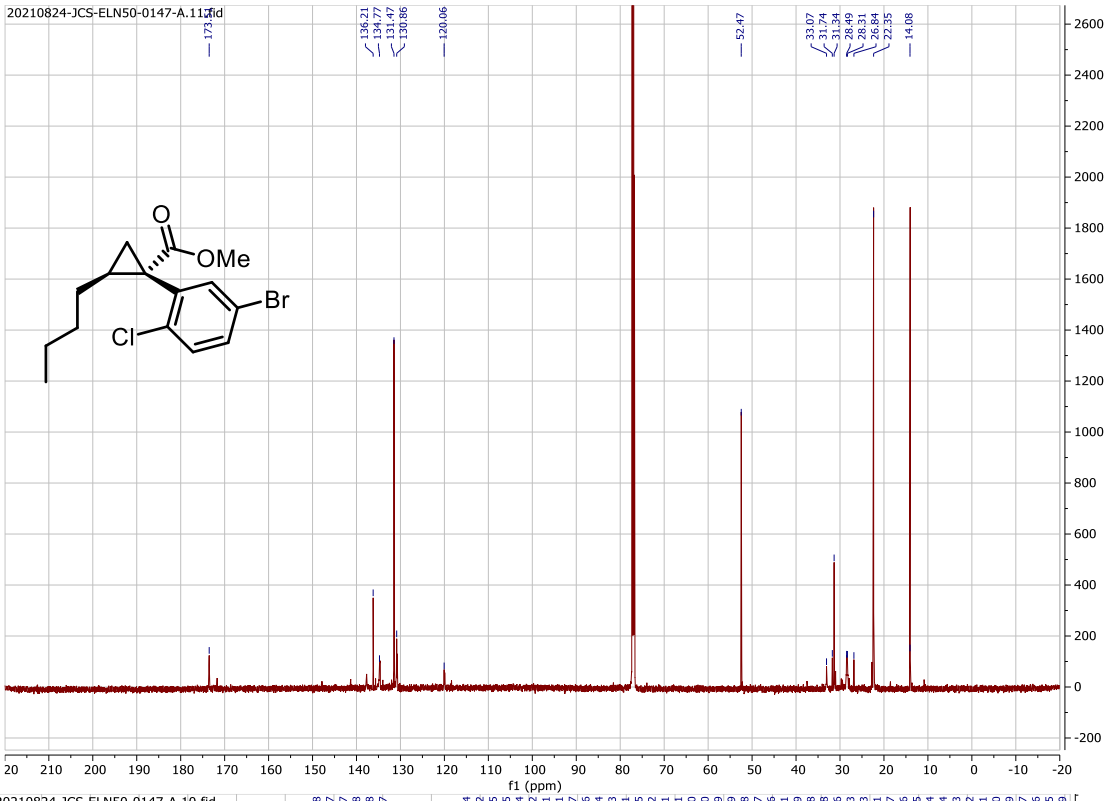
20210824-JCS-ELN50-0147-A.11.fid
173.54
136.21
134.77
131.47
130.86
120.06
52.47
33.07
31.74
31.34
28.49
28.31
26.84
22.35
14.08
O
OMe
Br
Cl
f1 (ppm)

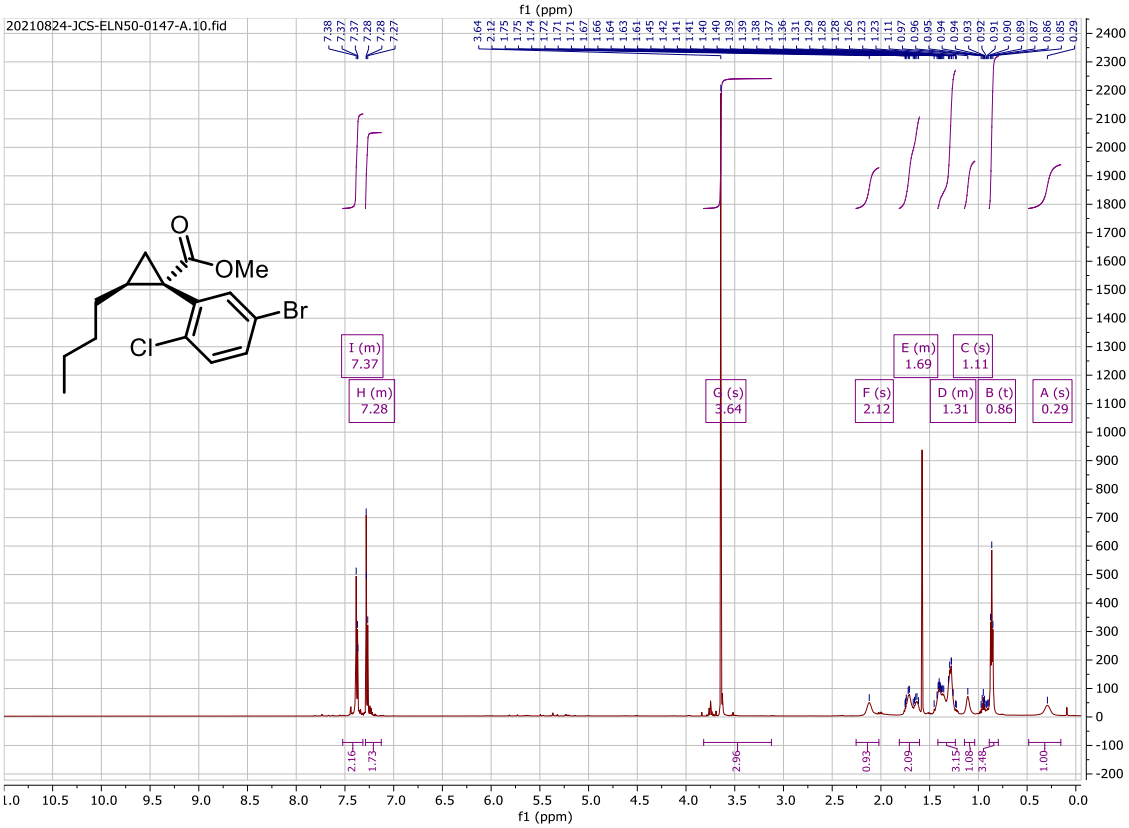
20210824-JCS-ELN50-0147-A.10.fid
I (m) 7.37
H (m) 7.28
G (s) 3.64
F (s) 2.12
E (m) 1.69
D (m) 1.31
C (s) 1.11
B (t) 0.86
A (s) 0.29
O
OMe
Br
Cl
f1 (ppm)

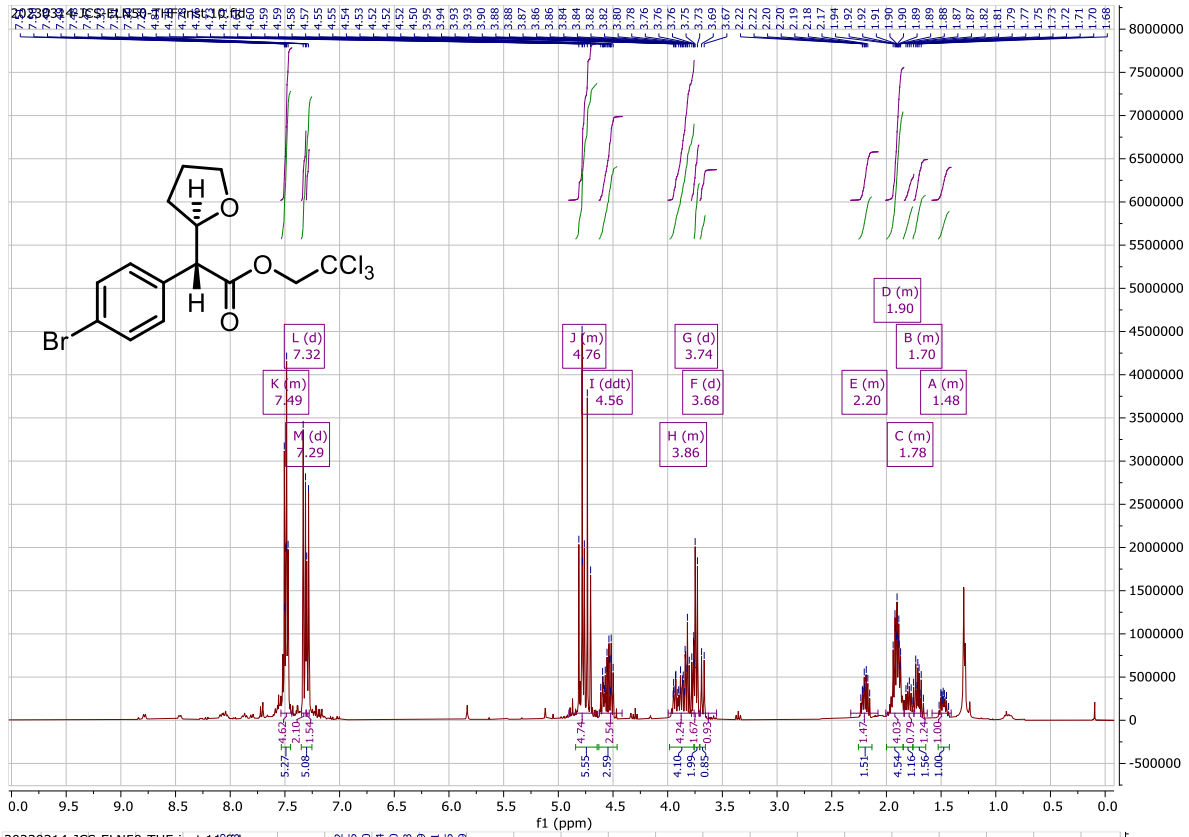
20230314-JCS-ELN50-THF-inst.10.fid
L (d) 7.32
K (m) 7.49
M (d) 7.29
J (m) 4.76
I (ddt) 4.56
G (d) 3.74
F (d) 3.68
H (m) 3.86
D (m) 1.90
B (m) 1.70
E (m) 2.20
A (m) 1.48
C (m) 1.78
f1 (ppm)

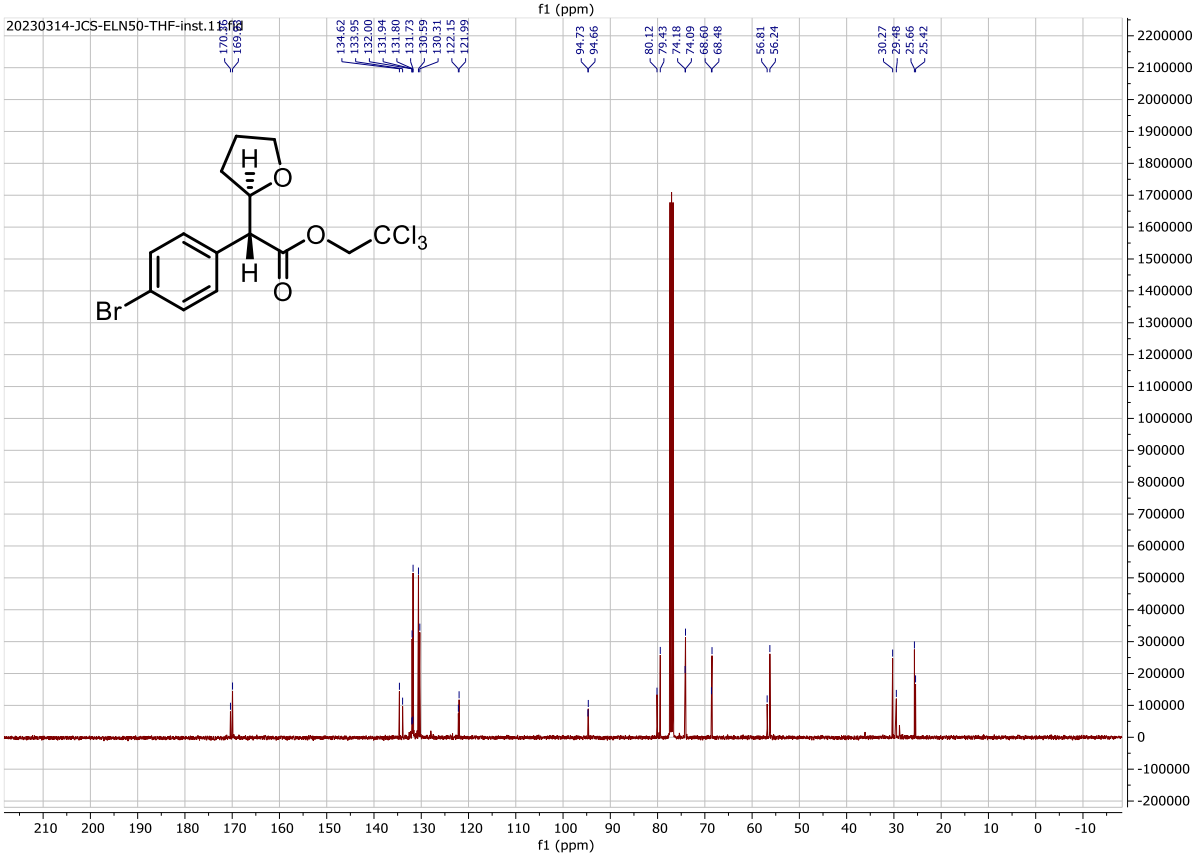
20230314-JCS-ELN50-THF-inst.11.fid
170.03
169.63
134.62
133.95
132.00
131.94
131.80
131.73
130.59
130.31
122.15
121.99
94.73
94.66
80.12
79.43
74.18
74.09
68.60
68.48
56.81
56.24
30.27
29.48
25.66
25.42
f1 (ppm)

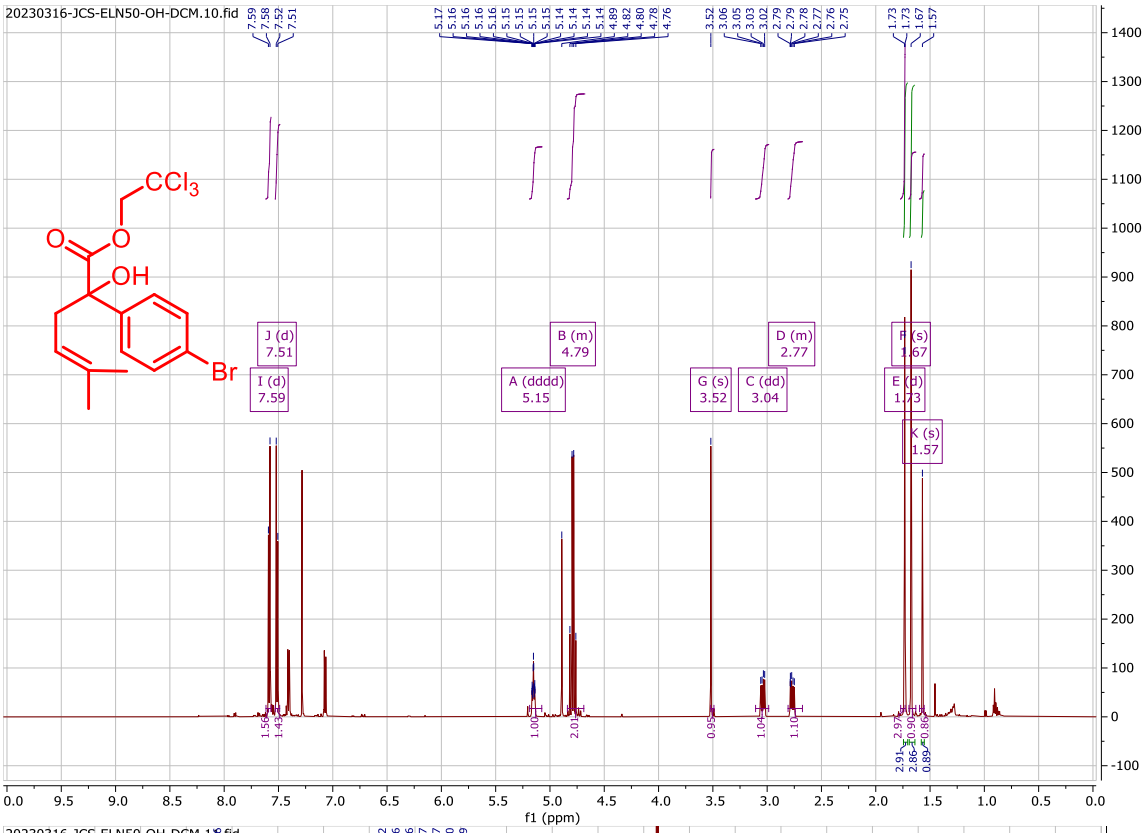
20230316-JCS-ELN50-OH-DCM.10.fid
J (d) 7.51
I (d) 7.59
A (dddd) 5.15
B (m) 4.79
G (s) 3.52
C (dd) 3.04
D (m) 2.77
F (s) 1.67
E (d) 1.73
K (s) 1.57
f1 (ppm)

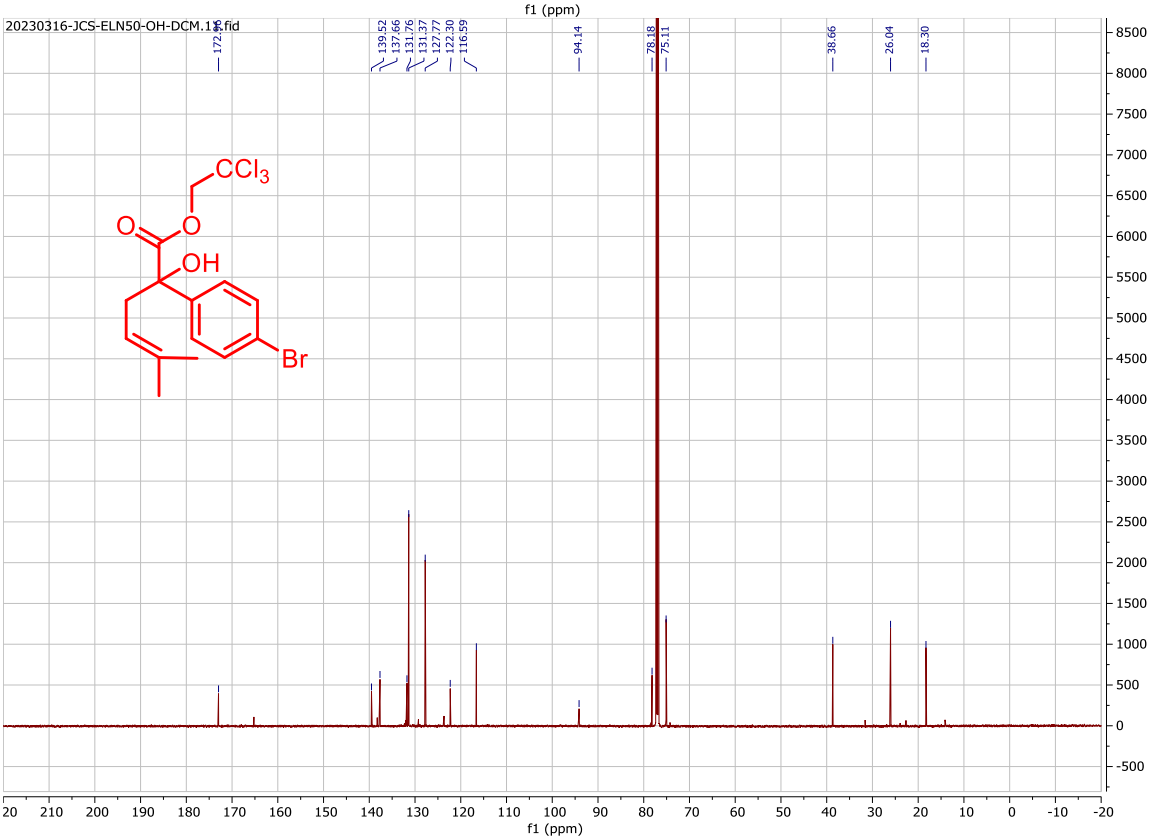
20230316-JCS-ELN50-OH-DCM.11.fid
172.90
139.52
137.66
131.76
131.37
127.77
122.30
116.59
94.14
78.18
75.11
38.66
26.04
18.30
f1 (ppm)

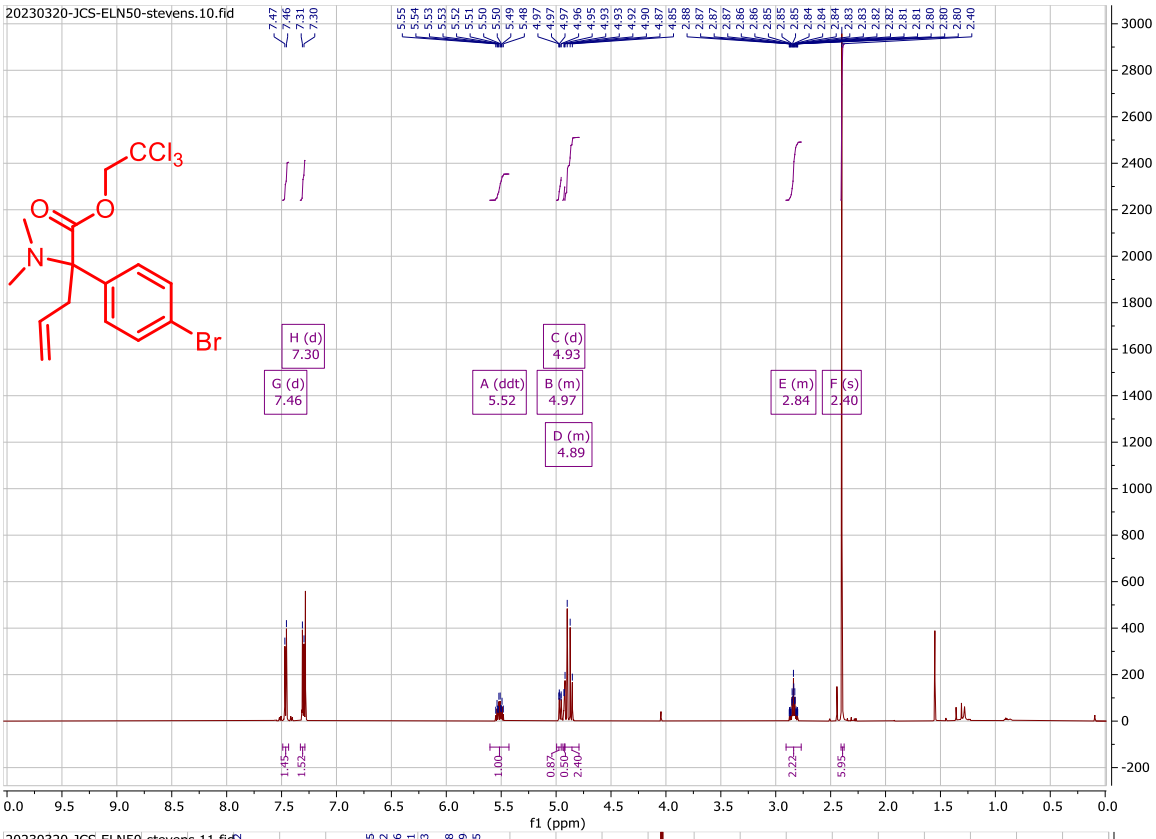
20230320-JCS-ELN50-stevens.10.fid
CCl3
O
O
N
Br
H (d)
7.30
G (d)
7.46
A (ddt)
5.52
C (d)
4.93
B (m)
4.97
D (m)
4.89
E (m)
2.84
F (s)
2.40
f1 (ppm)

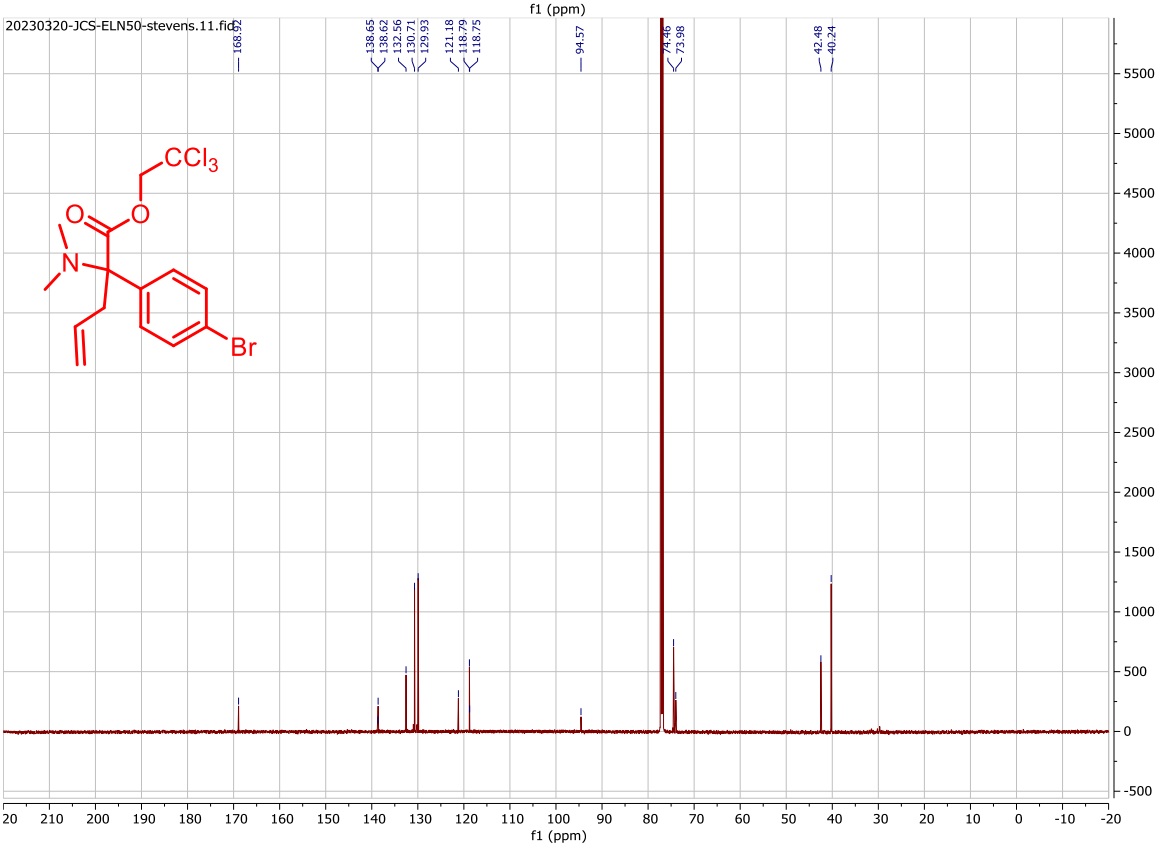
20230320-JCS-ELN50-stevens.11.fid
168.92
138.65
138.62
132.56
130.71
129.93
121.18
118.79
118.75
94.57
74.46
73.98
42.48
40.24
CCl3
O
O
N
Br
f1 (ppm)

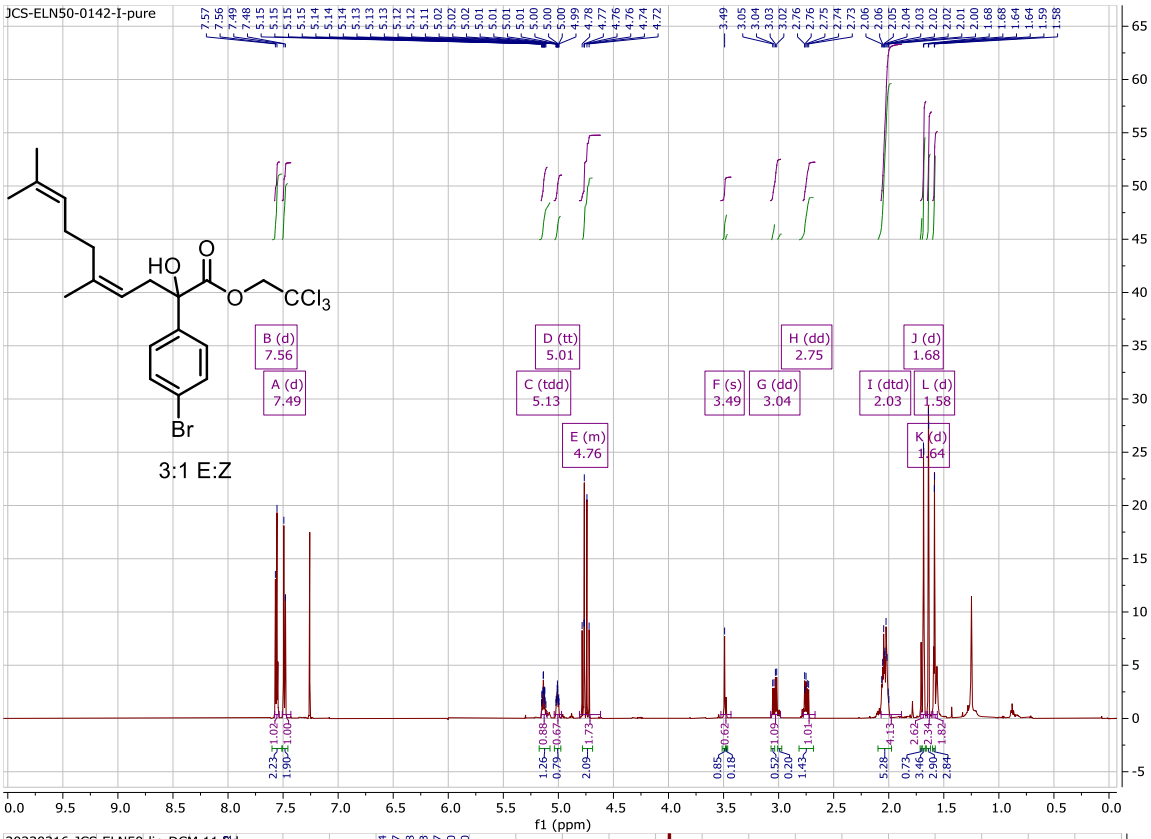
JCS-ELN50-0142-I-pure
HO
O
O
CCl3
Br
3:1 E:Z
B (d) 7.56
A (d) 7.49
D (tt) 5.01
C (tdd) 5.13
E (m) 4.76
F (s) 3.49
G (dd) 3.04
H (dd) 2.75
I (dtd) 2.03
J (d) 1.68
L (d) 1.58
K (d) 1.64
f1 (ppm)

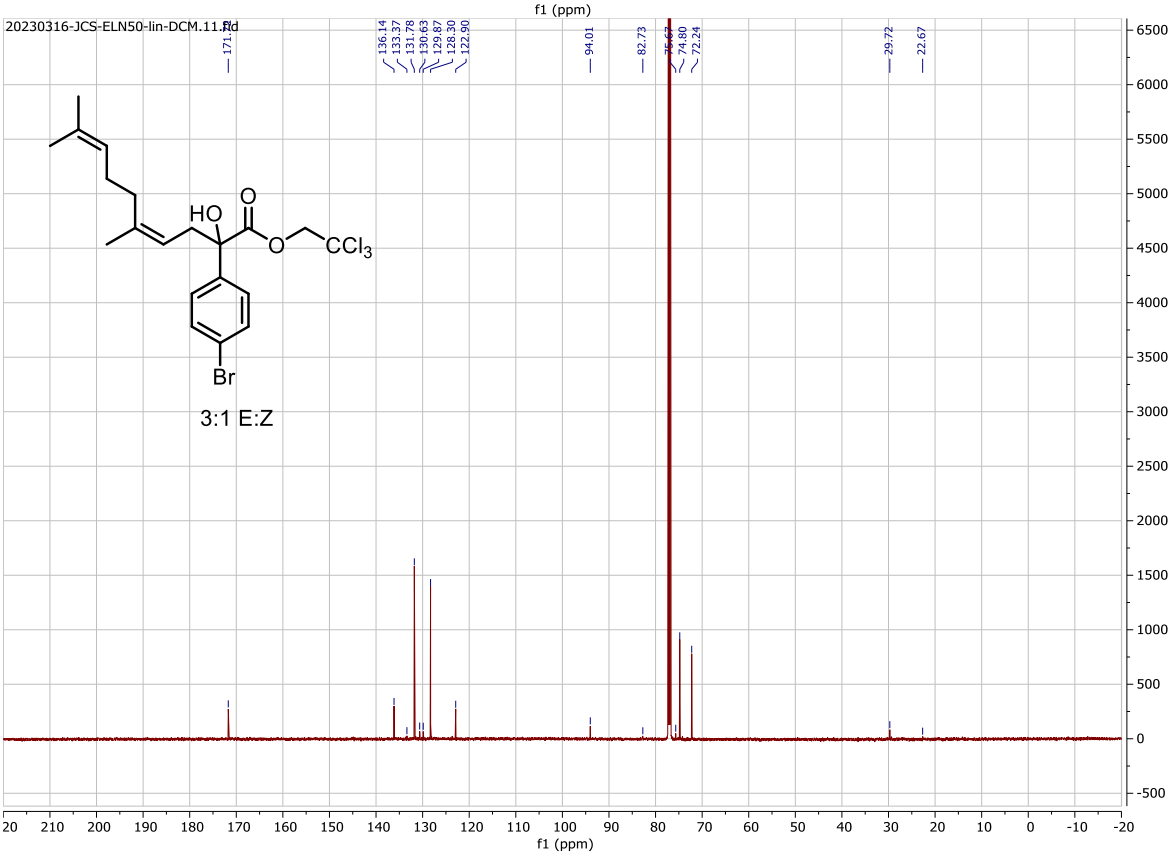
20230316-JCS-ELN50-lin-DCM.11.fid
HO
O
O
CCl3
Br
3:1 E:Z
171.
136.14
133.37
131.78
130.63
129.87
128.30
122.90
94.01
82.73
78.67
74.80
72.24
29.72
22.67
f1 (ppm)

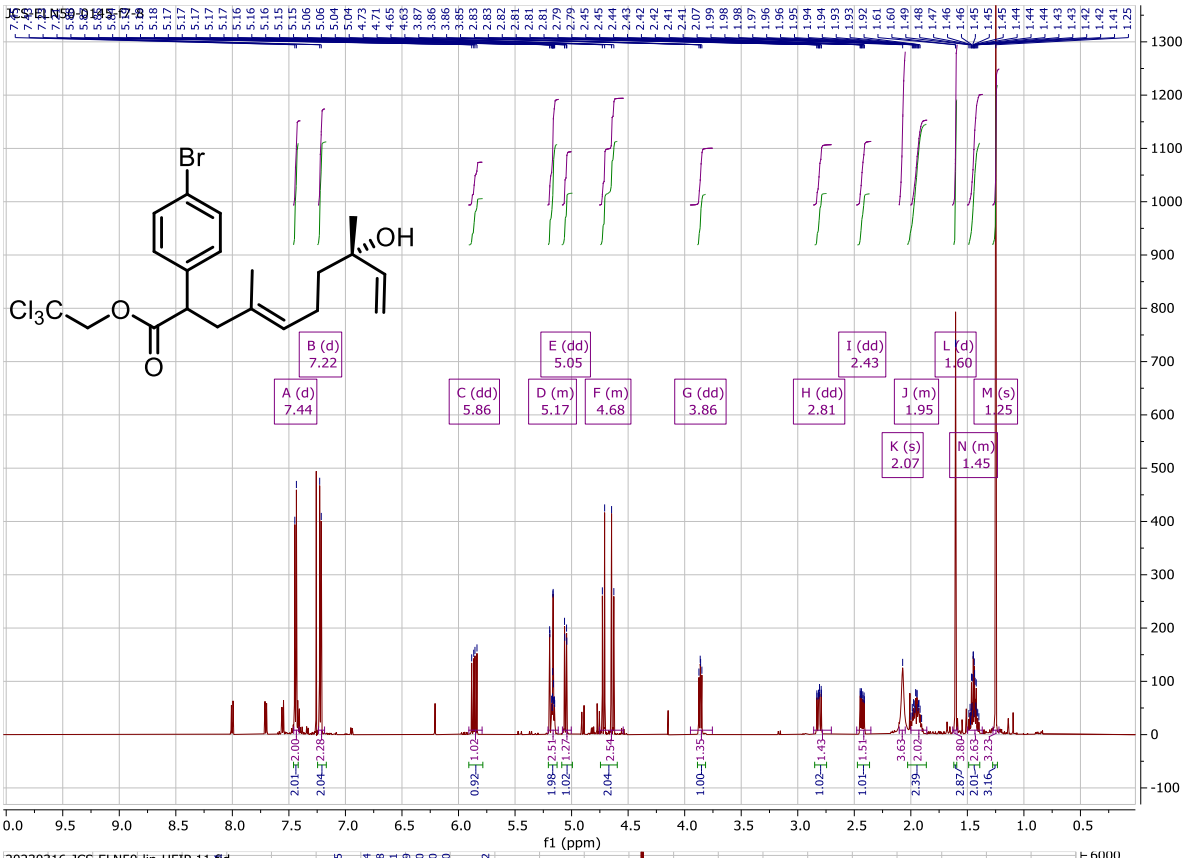
Br
OH
Cl3C
O
O
A (d) 7.44
B (d) 7.22
C (dd) 5.86
D (m) 5.17
E (dd) 5.05
F (m) 4.68
G (dd) 3.86
H (dd) 2.81
I (dd) 2.43
J (m) 1.95
K (s) 2.07
L (d) 1.60
M (s) 1.25
N (m) 1.45
f1 (ppm)

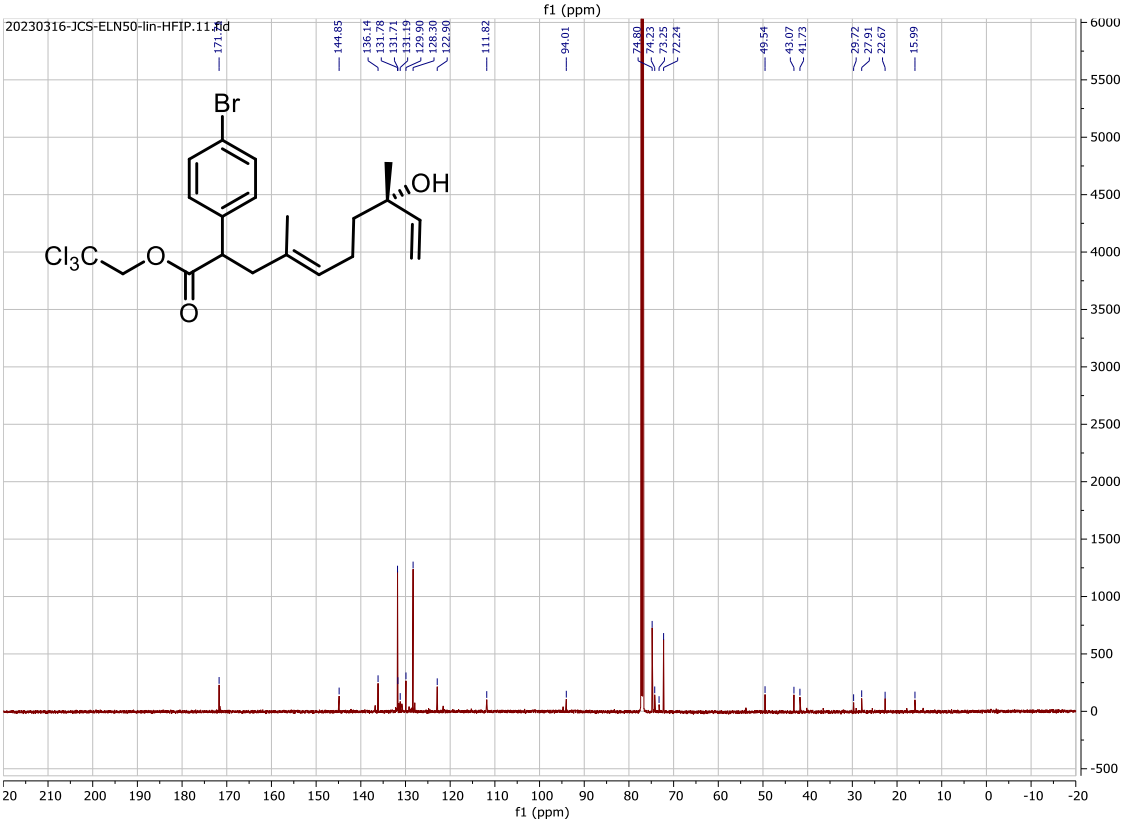
20230316-JCS-ELN50-lin-HFIP.11.fid
Br
OH
Cl3C
O
O
171.2
144.85
136.14
131.78
131.71
131.19
129.90
128.30
122.90
111.82
94.01
74.80
74.23
73.25
72.24
49.54
43.07
41.73
29.72
27.91
22.67
15.99
f1 (ppm)

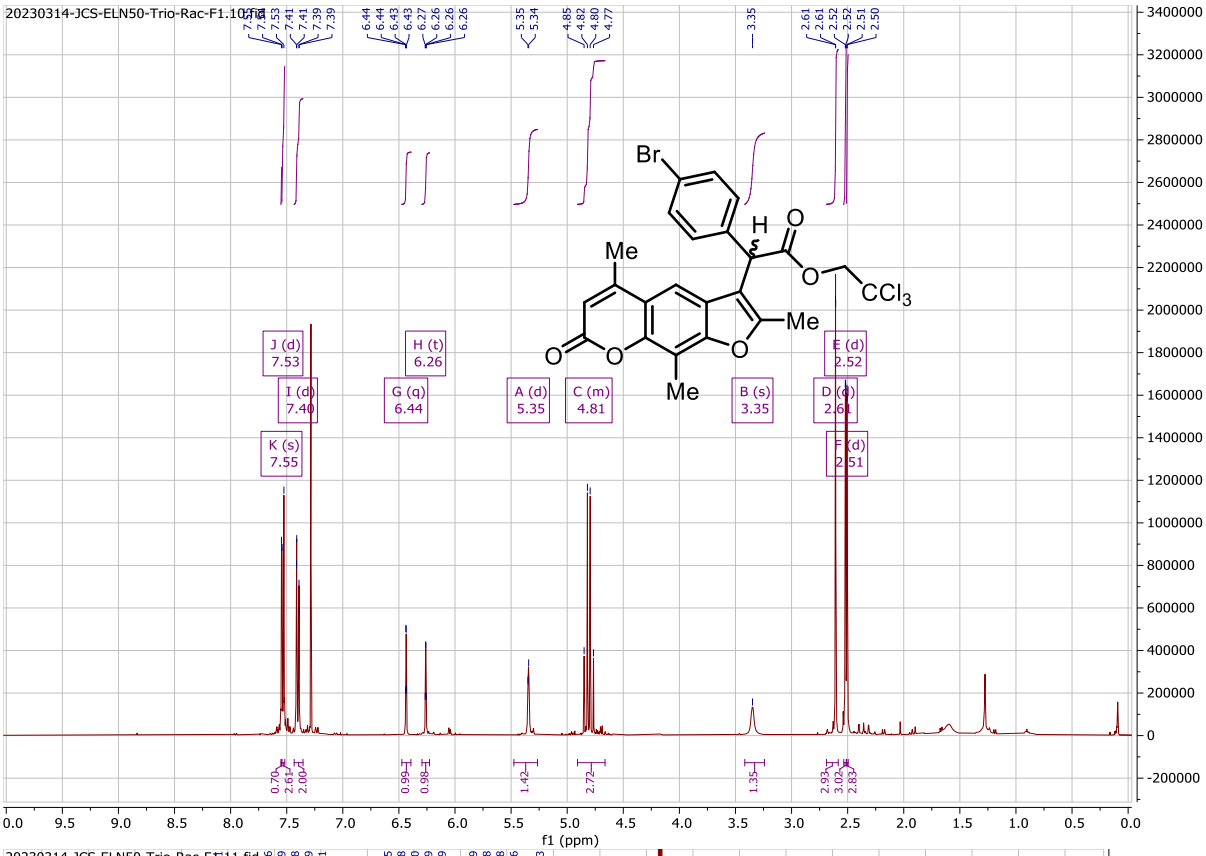
20230314-JCS-ELN50-Trio-Rac-F1.10.fid
J (d) 7.53
I (d) 7.40
K (s) 7.55
H (t) 6.26
G (q) 6.44
A (d) 5.35
C (m) 4.81
B (s) 3.35
E (d) 2.52
D (d) 2.61
F (d) 2.51
Br
H
O
Me
O
CCl3
Me
O
O
O
Me
f1 (ppm)

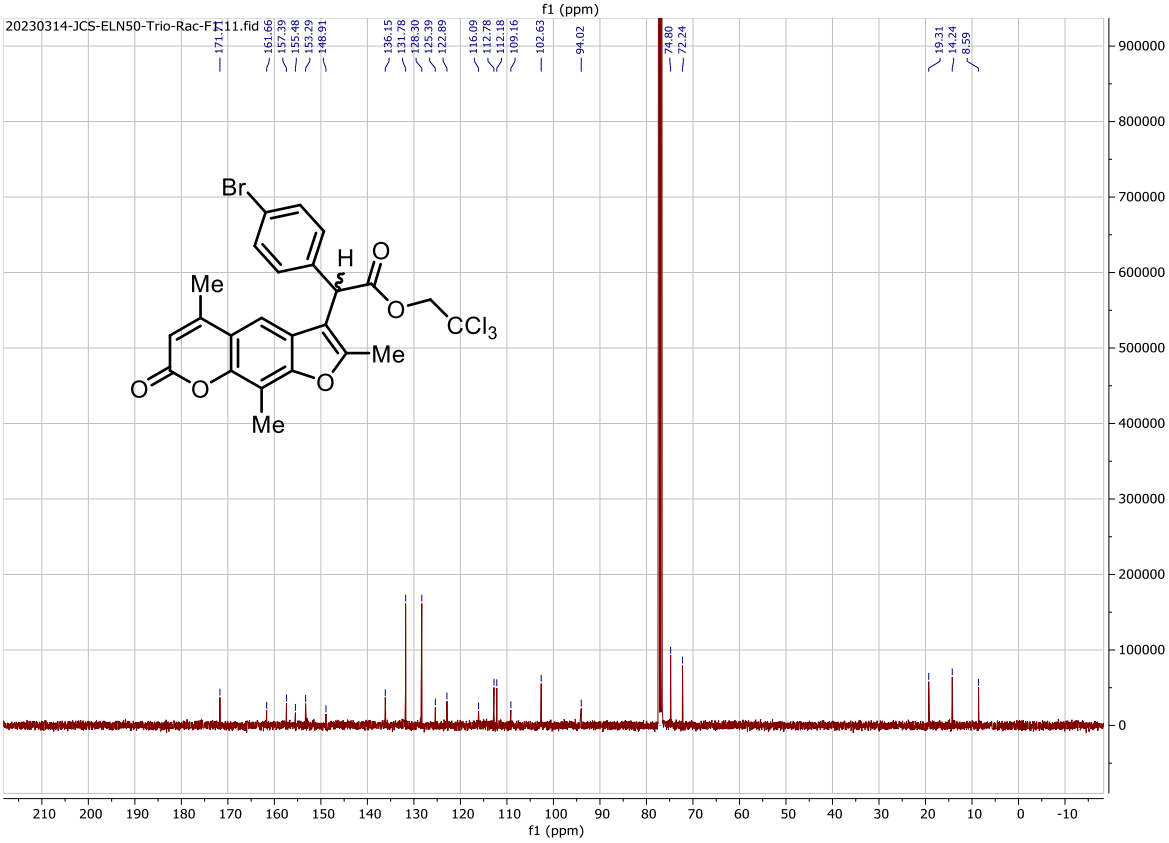
20230314-JCS-ELN50-Trio-Rac-F1.11.fid
171.1
161.66
157.39
155.48
153.29
148.91
136.15
131.78
128.30
125.39
122.89
116.09
112.78
112.18
109.16
102.63
94.02
74.80
72.24
19.31
14.24
8.59
Br
H
O
Me
O
CCl3
Me
O
O
O
Me
f1 (ppm)

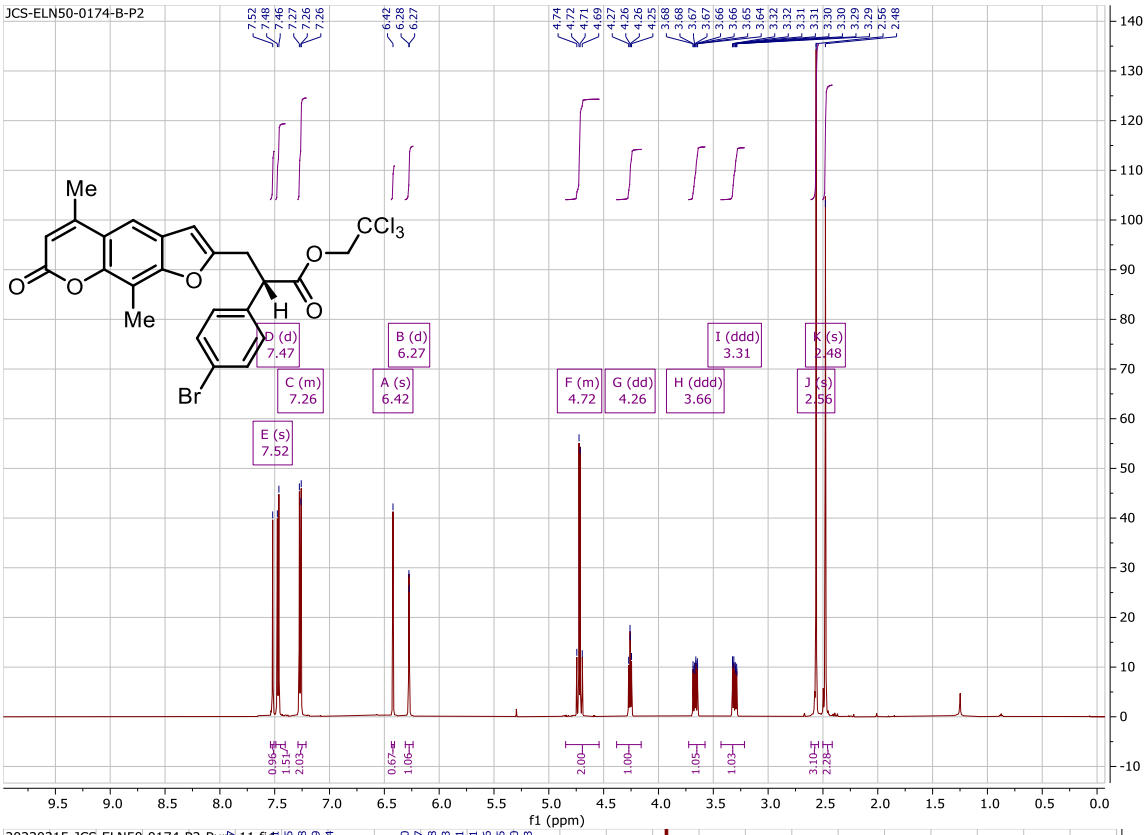
JCS-ELN50-0174-B-P2
Me
CCl3
O
O
O
O
H
O
Me
Br
D (d) 7.47
C (m) 7.26
E (s) 7.52
B (d) 6.27
A (s) 6.42
F (m) 4.72
G (dd) 4.26
H (ddd) 3.66
I (ddd) 3.31
K (s) 2.48
J (s) 2.56
f1 (ppm)

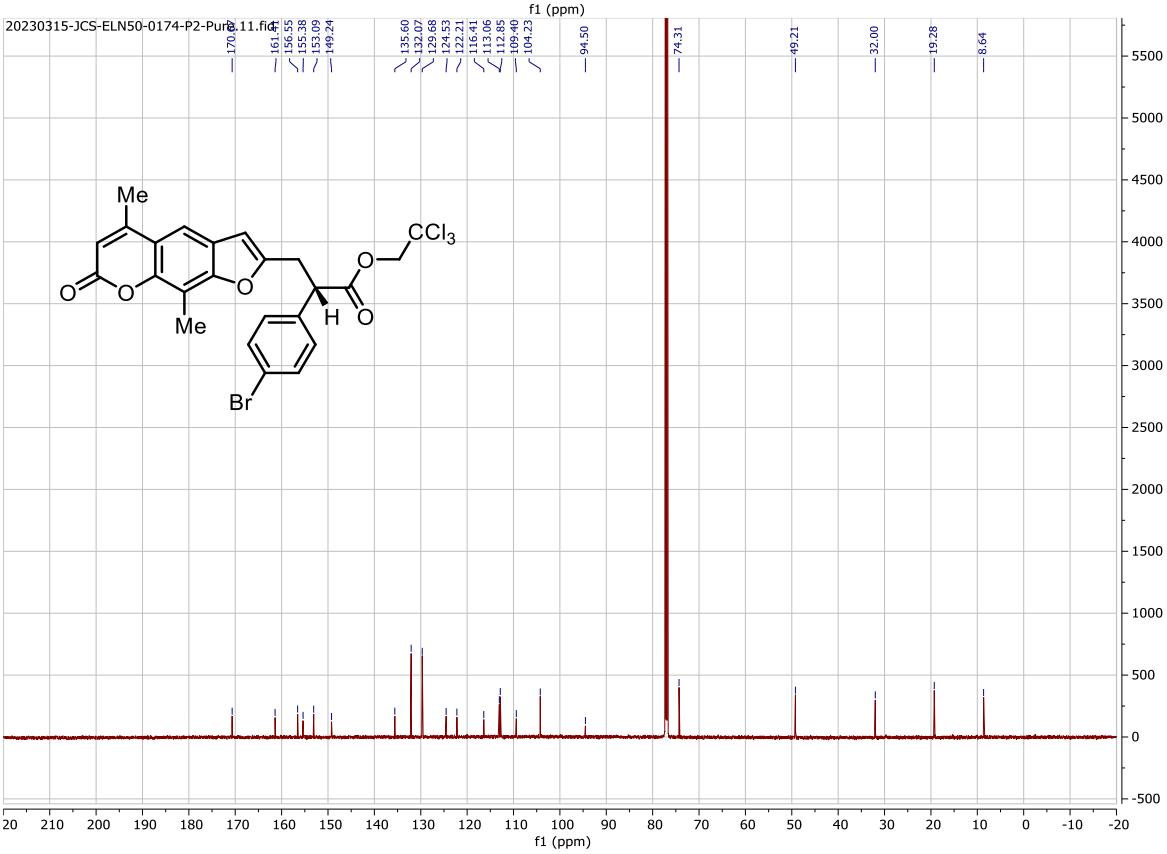
20230315-JCS-ELN50-0174-P2-Pure.11.fid
Me
CCl3
O
O
O
O
H
O
Me
Br
170.02
161.41
156.55
155.38
153.09
149.24
135.60
132.07
129.68
124.53
122.21
116.41
113.06
112.85
109.40
104.23
94.50
74.31
49.21
32.00
19.28
8.64
f1 (ppm)

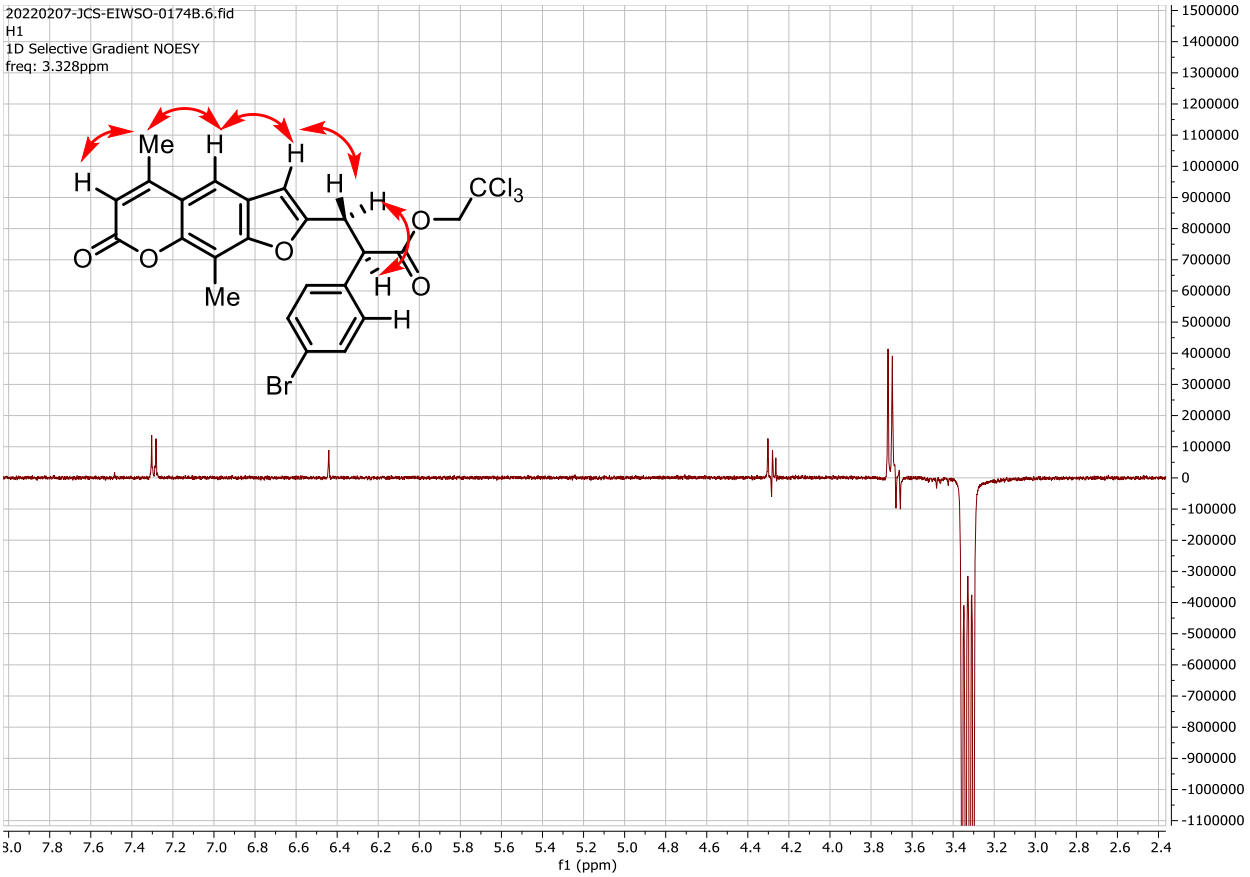
20220207-JCS-EIWSO-0174B.6.fid
H1
1D Selective Gradient NOESY
freq: 3.328ppm
Me
H
H
H
H
H
CCl3
O
O
O
O
Me
H
O
H
Br
f1 (ppm)

HPLC/SFC data:

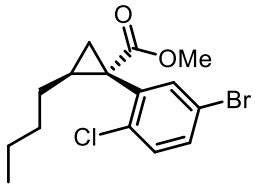

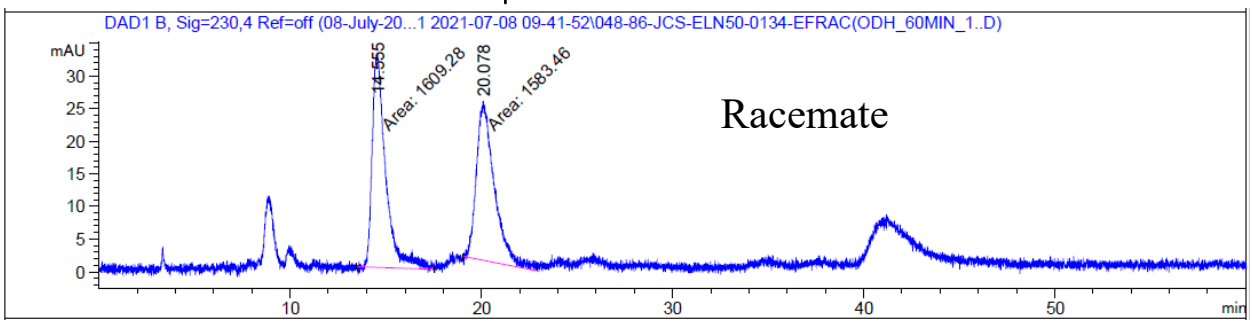

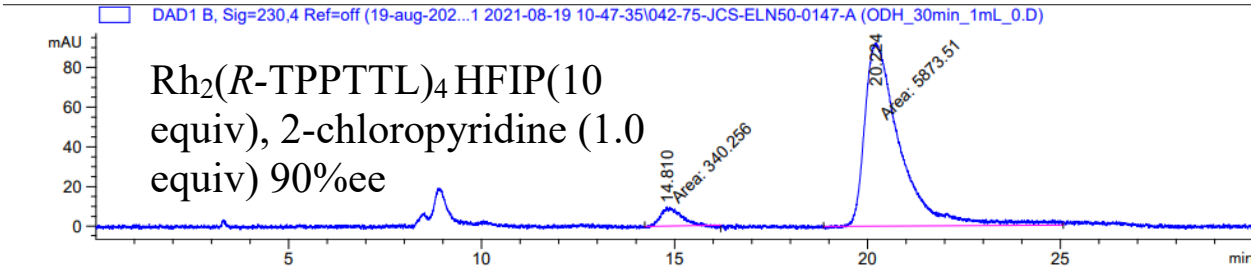

Signal 2: DAD1 B, Sig=230,4 Ref=off

Peak #	RetTime [min]	Type	Width [min]	Area [mAU*s]	Height [mAU]	Area %
1	14.810	MM	0.5894	340.25571	9.62150	5.4758
2	20.224	MM	1.0594	5873.51270	92.40273	94.5242
Totals :				6213.76840	102.02422	

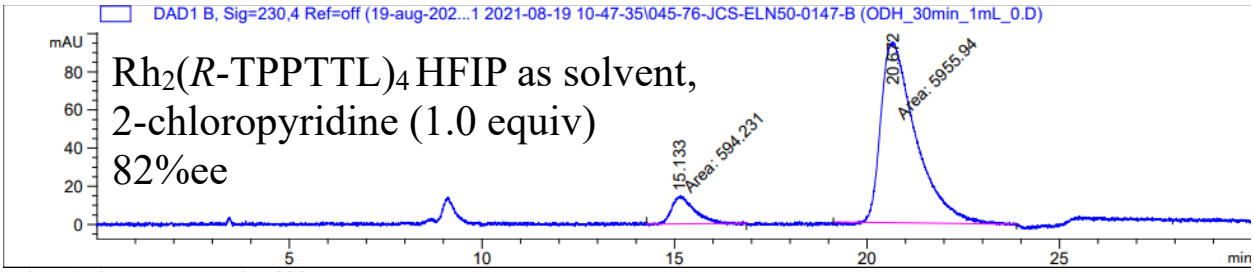

Signal 2: DAD1 B, Sig=230,4 Ref=off

Peak #	RetTime [min]	Type	Width [min]	Area [mAU*s]	Height [mAU]	Area %
1	15.133	MM	0.6742	594.23120	14.68917	9.0720
2	20.672	MM	1.0474	5955.94238	94.77296	90.9280
Totals :				6550.17358	109.46213	

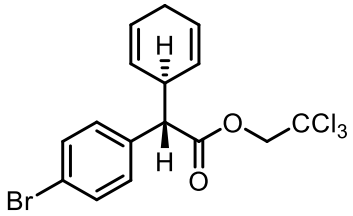

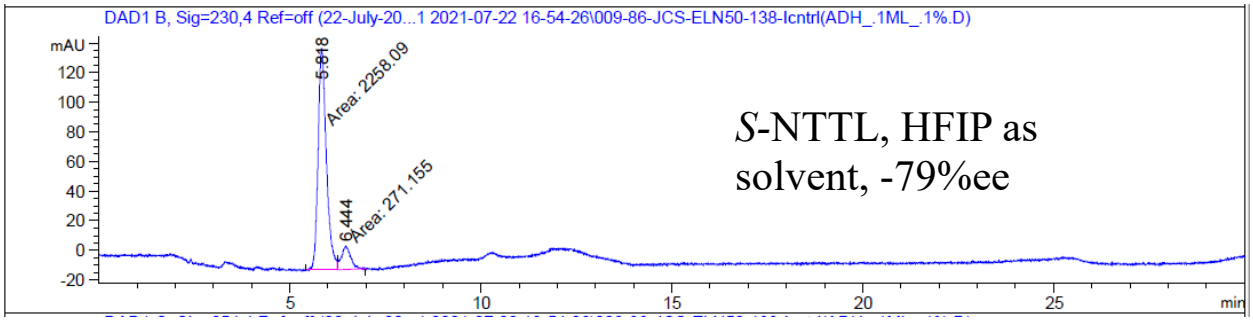

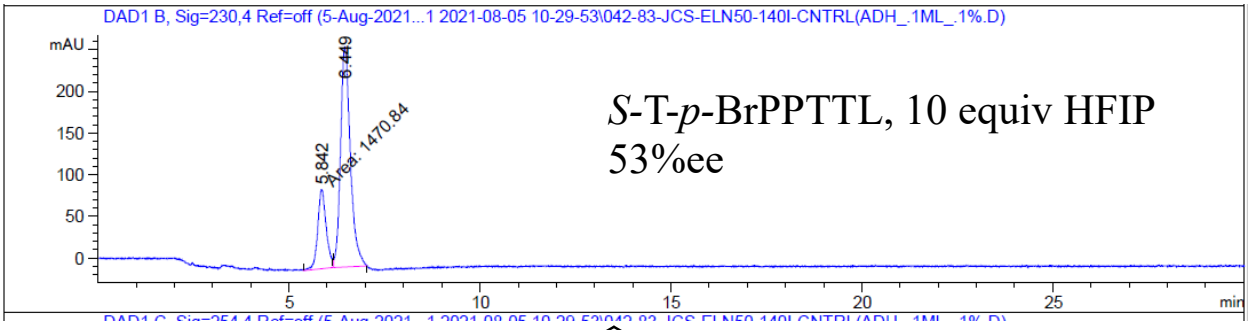

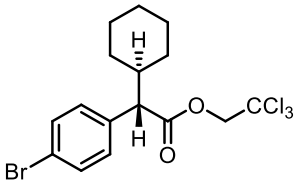

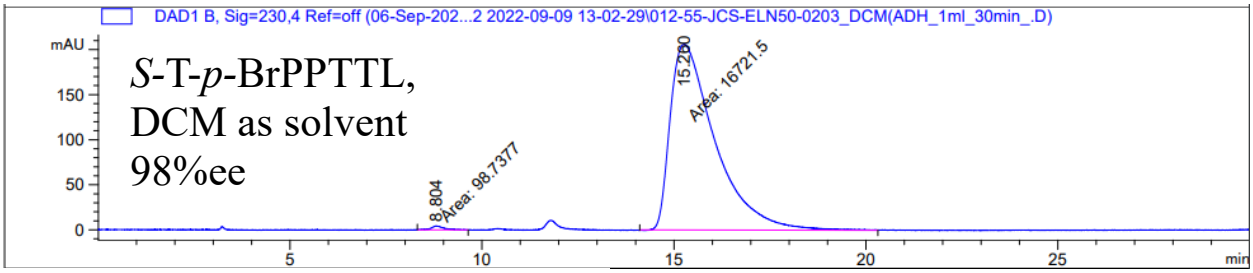


```
Signal 2: DAD1 B, Sig=230,4 Ref=off

Peak RetTime Type  Width     Area      Height     Area
  #   [min]        [min]   [mAU*s]     [mAU]       %
----|-------|----|-------|----------|----------|--------|
   1   8.804 MM    0.3675   98.73772    4.47801   0.5870
   2  15.260 MM    1.3531 1.67215e4   205.96581  99.4130

Totals :                  1.68202e4   210.44382
```

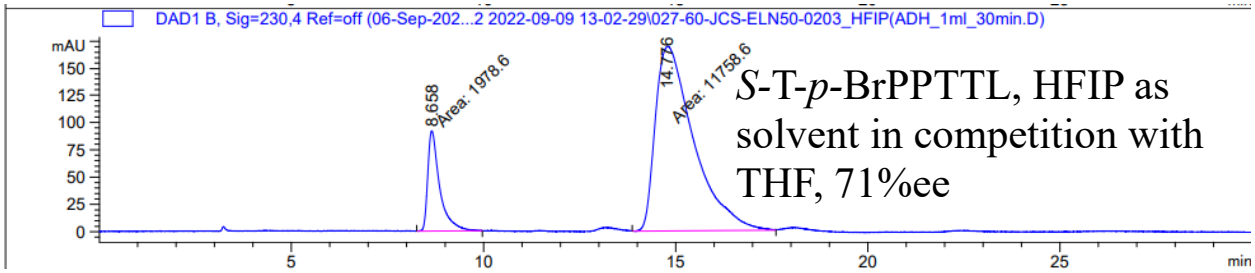

S-T-*p*-BrPPTTL, HFIP as solvent in competition with THF, 71%ee

Signal 2: DAD1 B, Sig=230,4 Ref=off

Peak #	RetTime [min]	Type	Width [min]	Area [mAU*s]	Height [mAU]	Area %
1	8.658	MM	0.3594	1978.59534	91.75107	14.4032
2	14.776	MM	1.1555	1.17586e4	169.60735	85.5968

Totals : 1.37372e4 261.35841

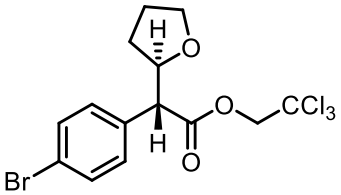

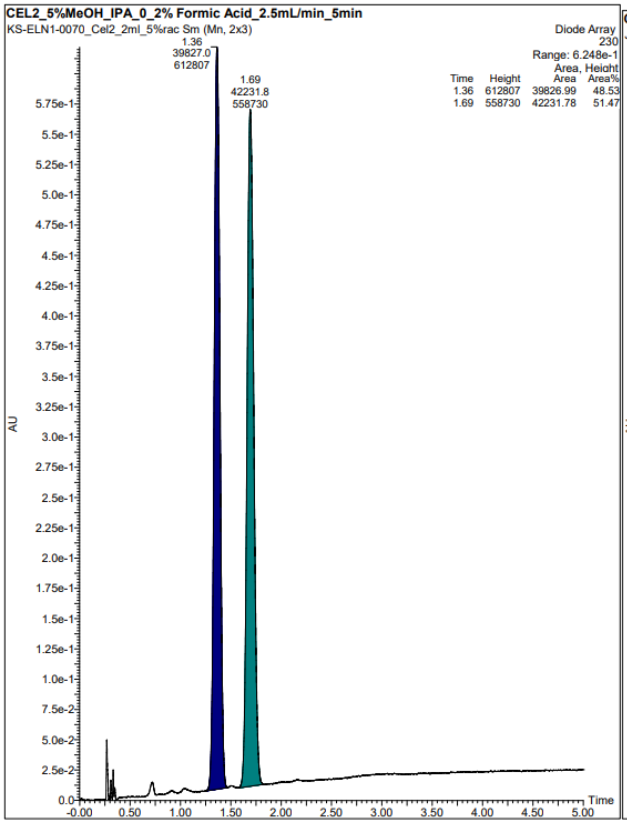

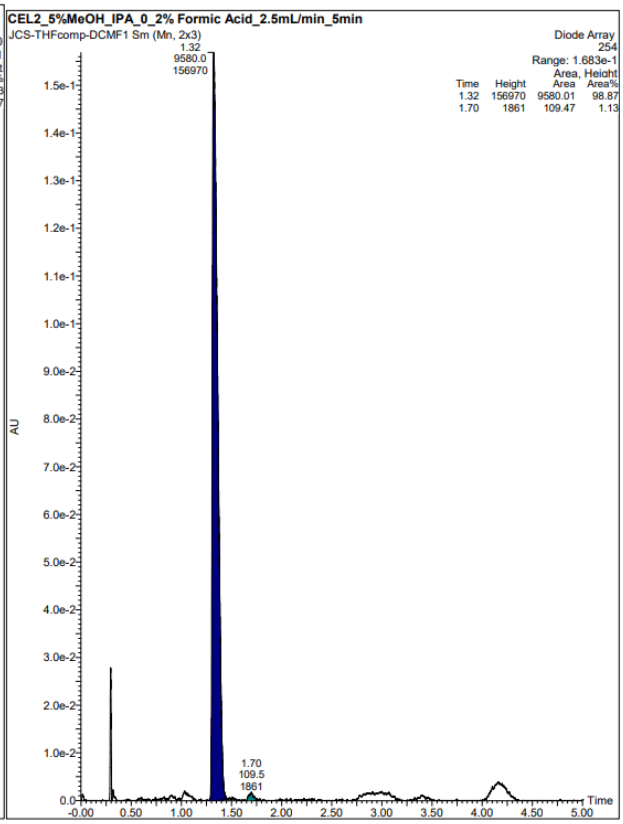

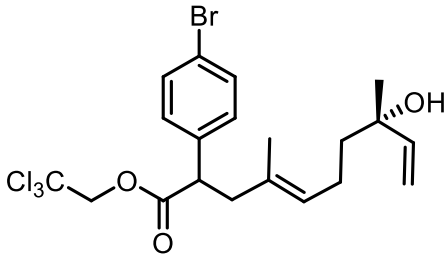
Br
OH
Cl3C
O
O

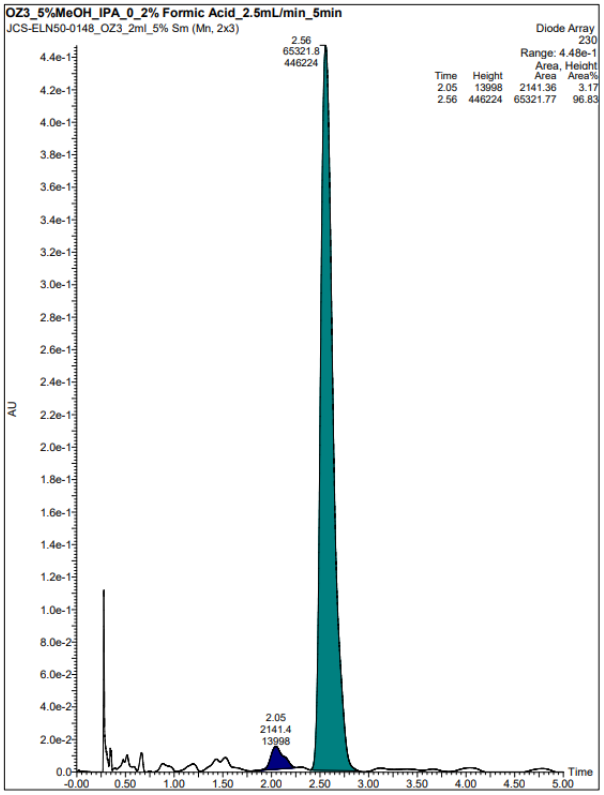
OZ3_5%MeOH_IPA_0_2% Formic Acid_2.5mL/min_5min
JCS-ELN50-0148_OZ3_2ml_5% Sm (Mn, 2x3)
Diode Array
230
Range: 4.48e-1
Area, Height
Time Height Area Area%
2.05 13998 2141.36 3.17
2.56 446224 65321.77 96.83
2.56
65321.8
446224
2.05
2141.4
13998
AU
Time

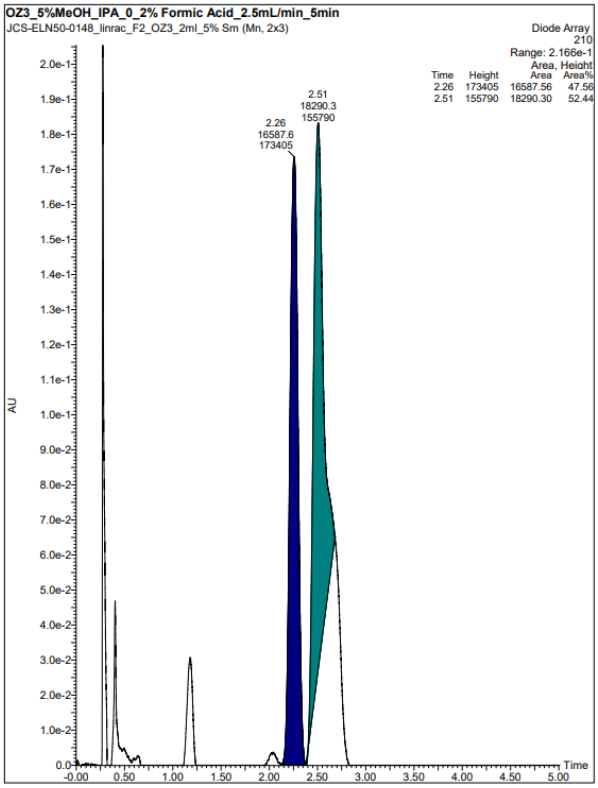
OZ3_5%MeOH_IPA_0_2% Formic Acid_2.5mL/min_5min
JCS-ELN50-0148_linrac_F2_OZ3_2ml_5% Sm (Mn, 2x3)
Diode Array
210
Range: 2.166e-1
Area, Height
Time Height Area Area%
2.26 173405 16587.56 47.56
2.51 155790 18290.30 52.44
2.26
16587.6
173405
2.51
18290.3
155790
AU
Time

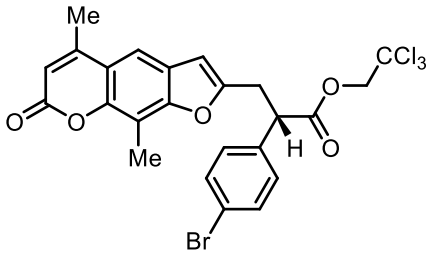
Me
CCl3
O
O
O
O
O
H
Me
Br

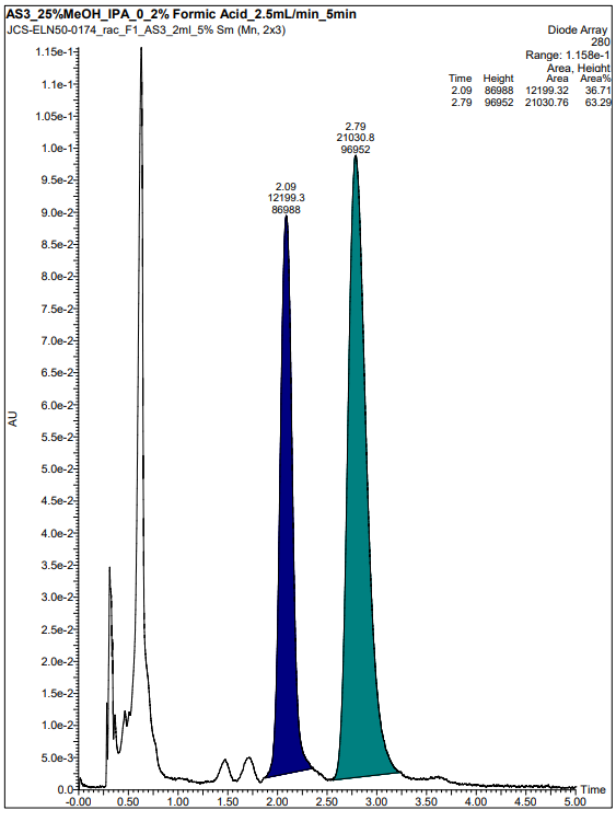
AS3_25%MeOH_IPA_0_2% Formic Acid_2.5mL/min_5min
JCS-ELN50-0174_rac_F1_AS3_2ml_5% Sm (Mn, 2x3)
Diode Array
280
Range: 1.158e-1
Area, Height
Time Height Area Area%
2.09 86988 12199.32 36.71
2.79 96952 21030.76 63.29
2.09
12199.3
86988
2.79
21030.8
96952
AU
Time

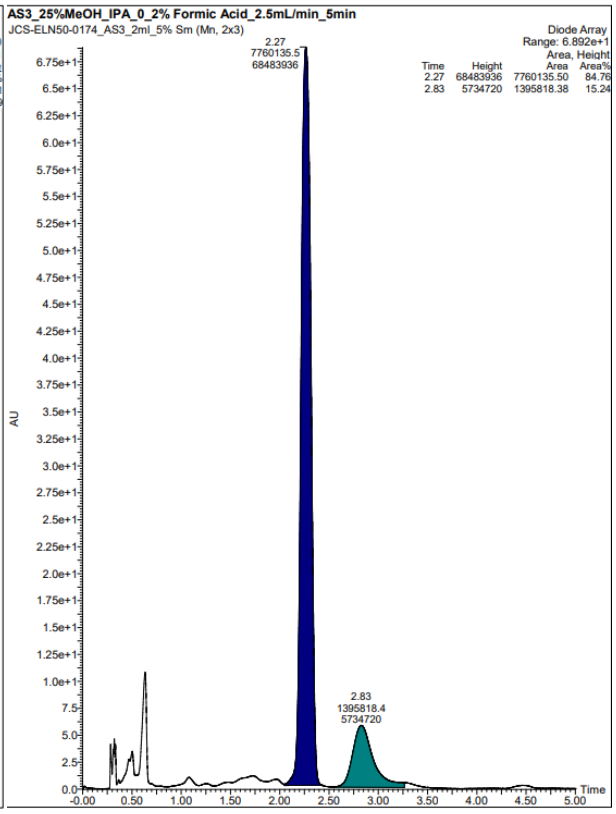
AS3_25%MeOH_IPA_0_2% Formic Acid_2.5mL/min_5min
JCS-ELN50-0174_AS3_2ml_5% Sm (Mn, 2x3)
Diode Array
Range: 6.892e+1
Area, Height
Time Height Area Area%
2.27 68483936 7760135.50 84.76
2.83 5734720 1395818.38 15.24
2.27
7760135.5
68483936
2.83
1395818.4
5734720
AU
Time

Figure 3-6: Asymmetric induction is a non-linear function of HFIP concentration

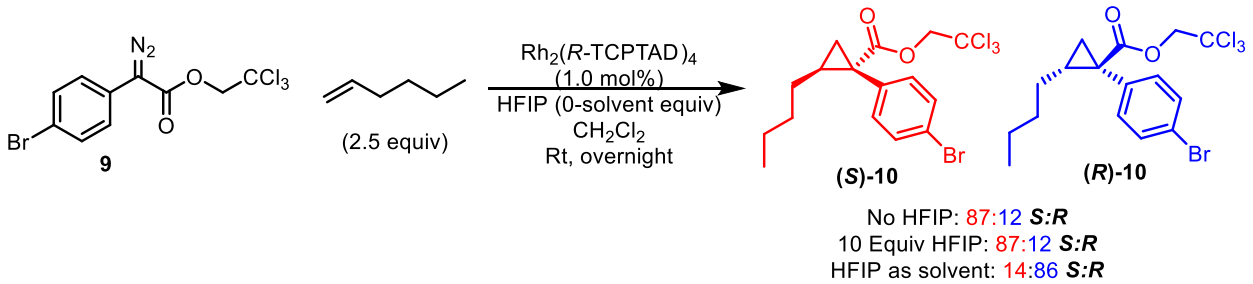

No HFIP: 87:12 ***S:R***
10 Equiv HFIP: 87:12 ***S:R***
HFIP as solvent: 14:86 ***S:R***

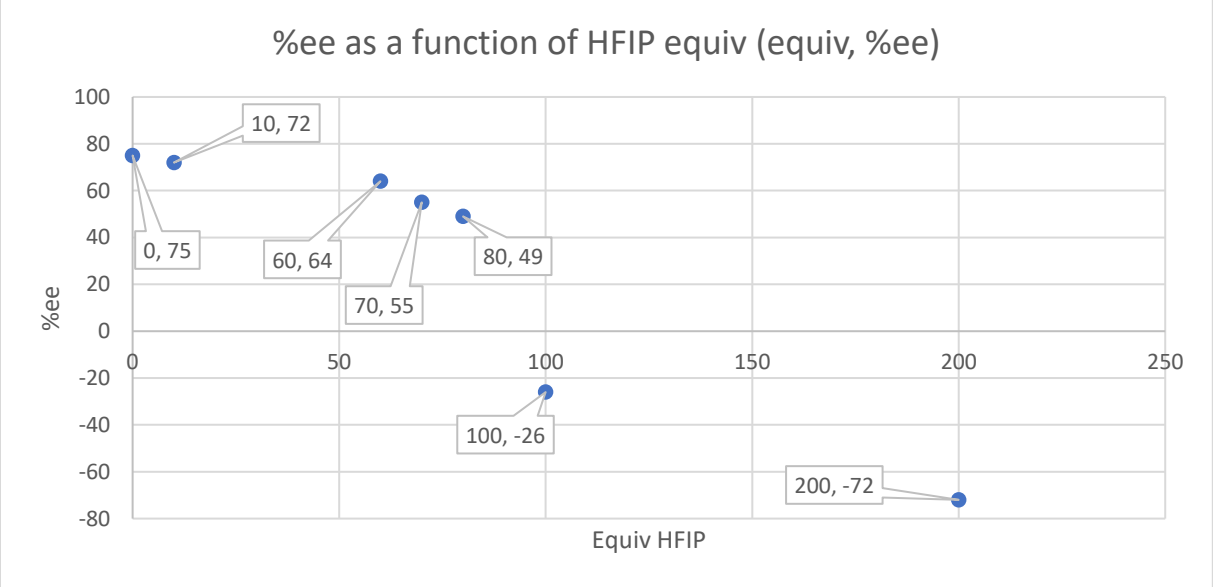

DCM as solvent: +71% ee

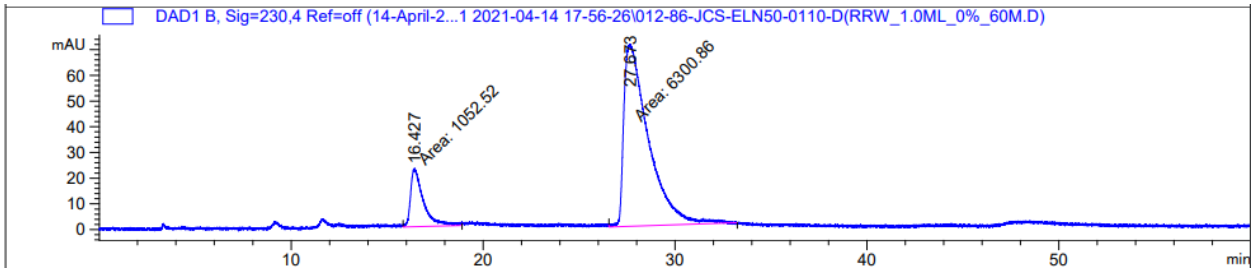

Signal 2: DAD1 B, Sig=230,4 Ref=off

Peak #	RetTime [min]	Type	Width [min]	Area [mAU*s]	Height [mAU]	Area %
1	16.427	MM	0.7759	1052.52429	22.60973	14.3135
2	27.673	MM	1.4834	6300.86182	70.79219	85.6865
Totals :				7353.38611		93.40192

60 equiv HFIP: 64% ee

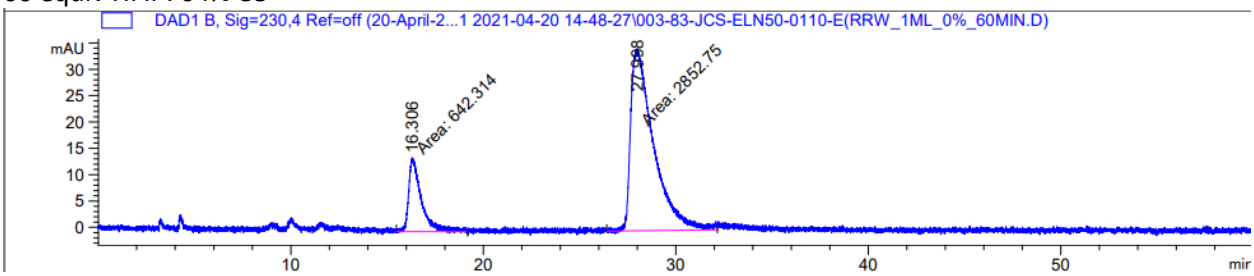

Signal 2: DAD1 B, Sig=230,4 Ref=off

Peak #	RetTime [min]	Type	Width [min]	Area [mAU*s]	Height [mAU]	Area %
1	16.306	MM	0.7617	642.31372	14.05462	18.3777
2	27.998	MM	1.3736	2852.75049	34.61340	81.6223
Totals :				3495.06421	48.66803	

70 equiv HFIP: 55% ee

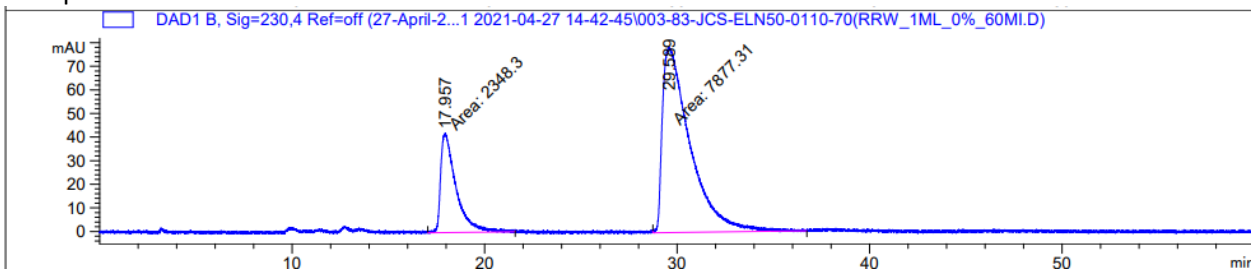

Signal 2: DAD1 B, Sig=230,4 Ref=off

Peak #	RetTime [min]	Type	Width [min]	Area [mAU*s]	Height [mAU]	Area %
1	17.957	MM	0.9295	2348.30200	42.10671	22.9649
2	29.589	MM	1.6736	7877.31201	78.44903	77.0351
Totals :				1.02256e4	120.55574	

80 equiv HFIP: 49% ee

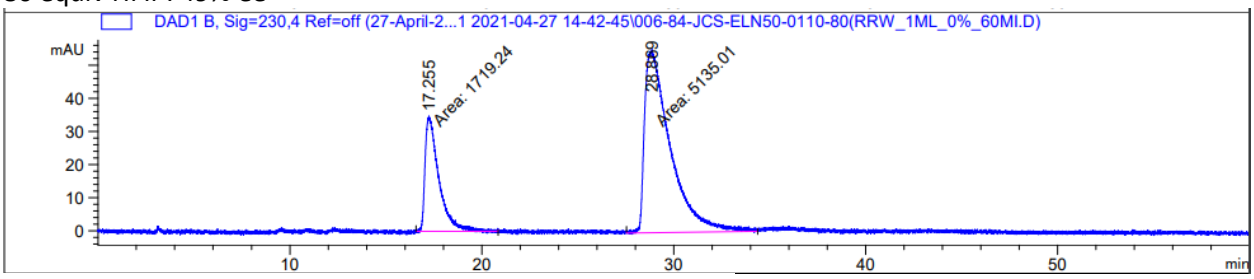

Signal 2: DAD1 B, Sig=230,4 Ref=off

Peak #	RetTime [min]	Type	Width [min]	Area [mAU*s]	Height [mAU]	Area %
1	17.255	MM	0.8247	1719.23743	34.74484	25.0828
2	28.869	MM	1.5452	5135.00879	55.38803	74.9172
Totals :				6854.24622	90.13287	

90 equiv HFIP: 39% ee

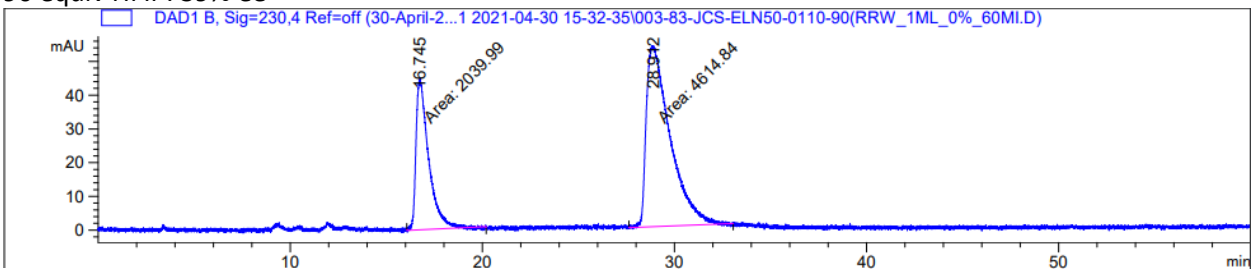

Signal 2: DAD1 B, Sig=230,4 Ref=off

Peak #	RetTime [min]	Type	Width [min]	Area [mAU*s]	Height [mAU]	Area %
1	16.745	MM	0.7620	2039.98511	44.61623	30.6542
2	28.912	MM	1.4356	4614.84326	53.57576	69.3458
Totals :				6654.82837	98.19199	

1:1 HFIP:DCM: -26% ee

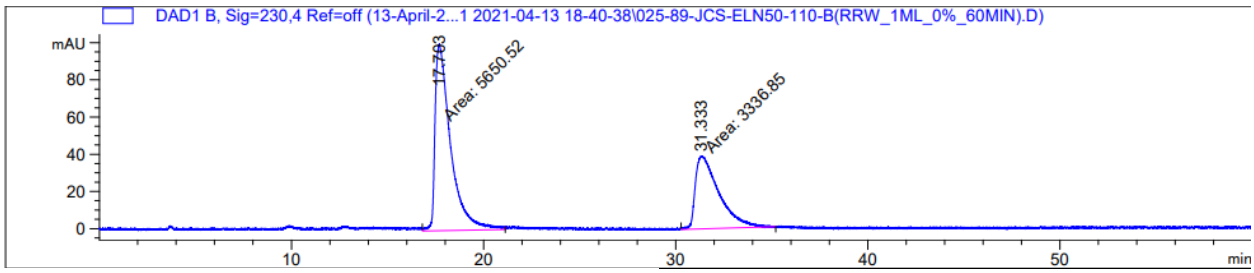

Signal 2: DAD1 B, Sig=230,4 Ref=off

Peak #	RetTime [min]	Type	Width [min]	Area [mAU*s]	Height [mAU]	Area %
1	17.703	MM	0.9361	5650.51709	100.60087	62.8718
2	31.333	MM	1.4198	3336.84668	39.17141	37.1282
Totals :				8987.36377	139.77228	

HFIP as solvent:-75% ee

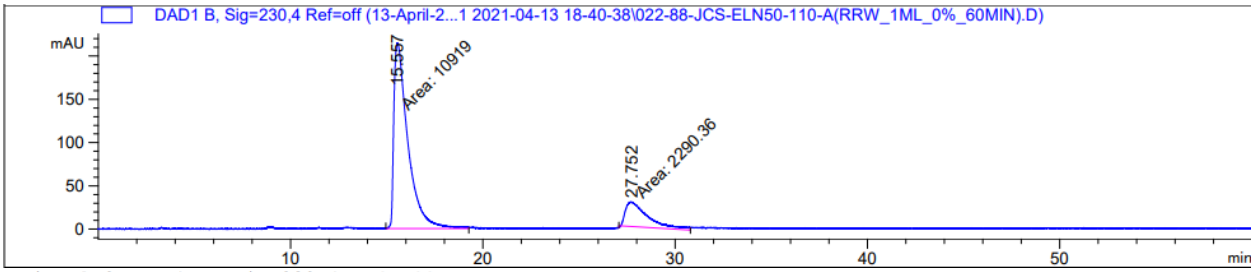

Signal 2: DAD1 B, Sig=230,4 Ref=off

Peak #	RetTime [min]	Type	Width [min]	Area [mAU*s]	Height [mAU]	Area %
1	15.557	MM	0.8483	1.09190e4	214.53247	82.6611
2	27.752	MM	1.3495	2290.35986	28.28736	17.3389
Totals :				1.32094e4	242.81983	

Figure 3-7: Inversion in the enantioselectivity of **132** is not a function of solvent polarity.

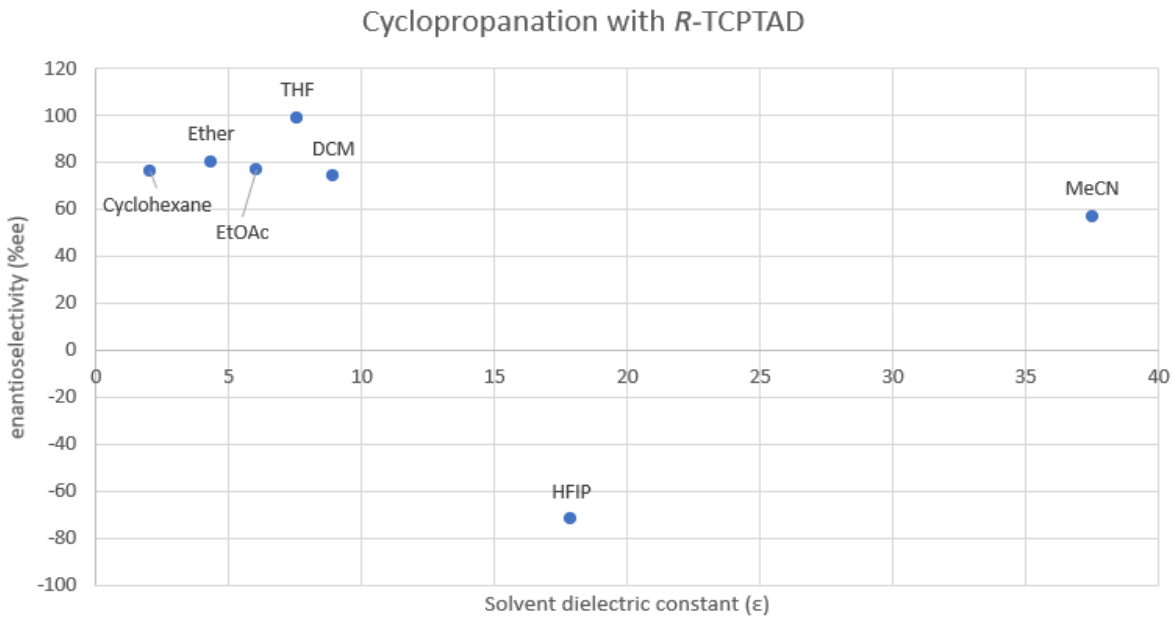

Supplemental solvent screen:

Cyclohexane: 75% ee

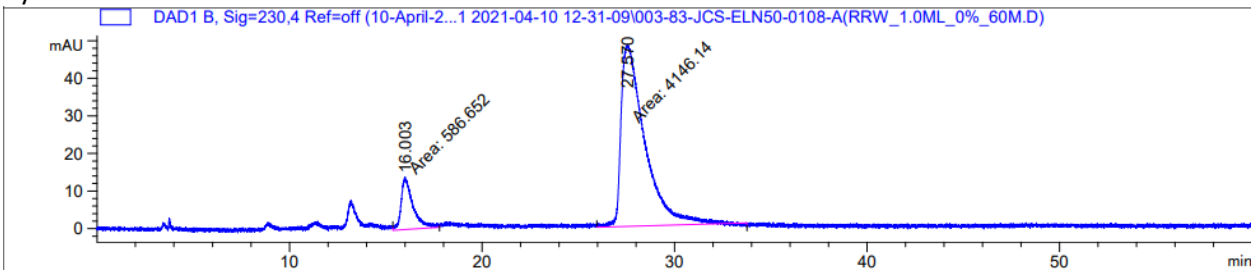


```
Signal 2: DAD1 B, Sig=230,4 Ref=off

Peak RetTime Type  Width     Area      Height     Area
  #   [min]        [min]   [mAU*s]     [mAU]       %
----|-------|----|-------|----------|----------|--------|
   1  16.003 MM    0.7042  586.65210   13.88408  12.3955
   2  27.570 MM    1.4336 4146.13623   48.20232  87.6045

Totals :                 4732.78833   62.08640
```

Diethyl ether: 85% ee

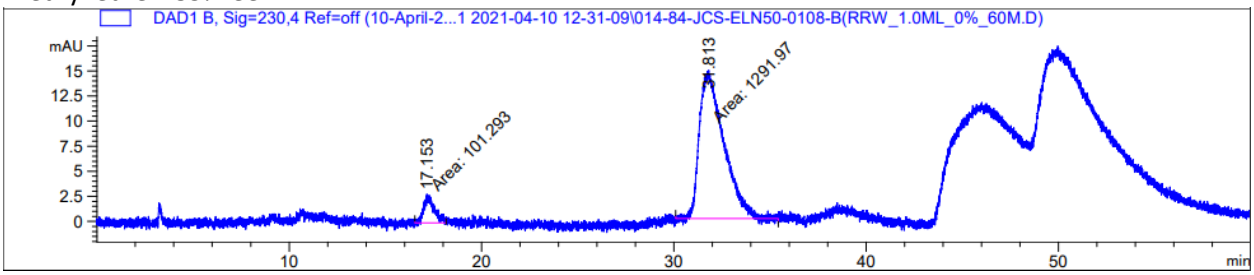

Signal 2: DAD1 B, Sig=230,4 Ref=off

Peak #	RetTime [min]	Type	Width [min]	Area [mAU*s]	Height [mAU]	Area %
1	17.153	MM	0.5907	101.29270	2.85820	7.2702
2	31.813	MM	1.4583	1291.96594	14.76533	92.7298
Totals :				1393.25864	17.62353	

Ethyl acetate: 77% ee

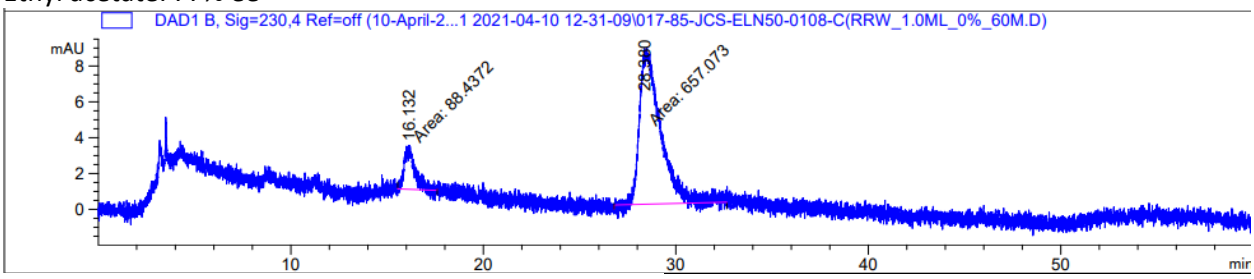

Signal 2: DAD1 B, Sig=230,4 Ref=off

Peak #	RetTime [min]	Type	Width [min]	Area [mAU*s]	Height [mAU]	Area %
1	16.132	MM	0.5996	88.43725	2.45838	11.8627
2	28.380	MM	1.2559	657.07275	8.71966	88.1373
Totals :				745.51000	11.17804	

THF: >99% ee

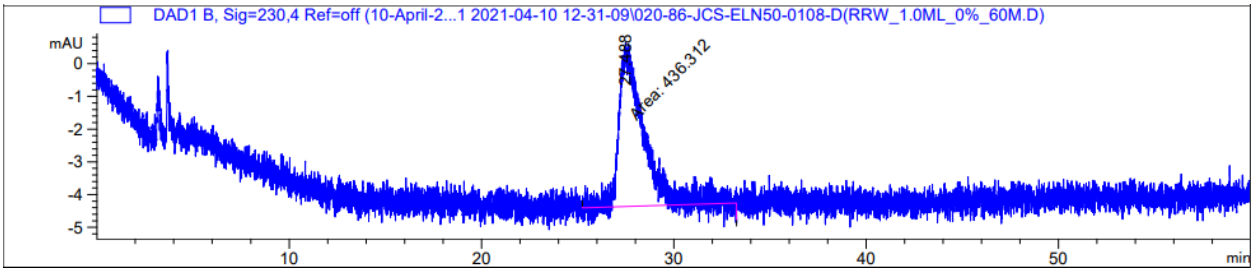

Signal 2: DAD1 B, Sig=230,4 Ref=off

Peak #	RetTime [min]	Type	Width [min]	Area [mAU*s]	Height [mAU]	Area %
1	27.488	MM	1.4544	436.31168	4.99996	100.0000
Totals :				436.31168	4.99996	

MeCN: 57% ee

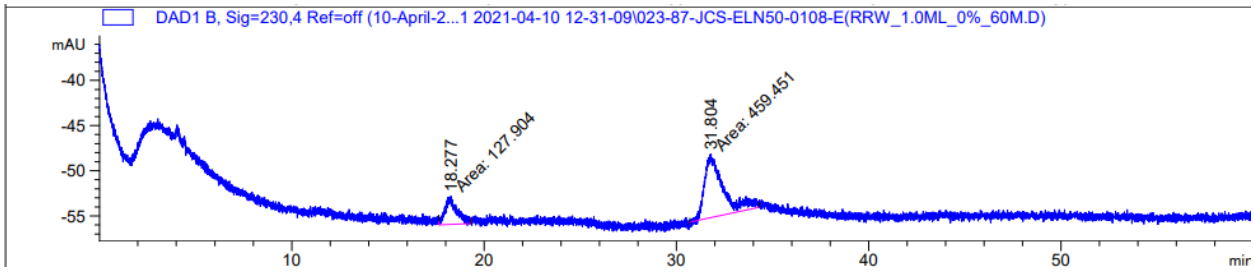

Signal 2: DAD1 B, Sig=230,4 Ref=off

Peak #	RetTime [min]	Type	Width [min]	Area [mAU*s]	Height [mAU]	Area %
1	18.277	MM	0.6752	127.90361	3.15704	21.7762
2	31.804	MM	1.0931	459.45056	7.00528	78.2238
Totals :				587.35417	10.16232	

11. References

1. Green, S. P.; Wheelhouse, K. M.; Payne, A. D.; Hallett, J. P.; Miller, P. W.; Bull, J. A., Thermal Stability and Explosive Hazard Assessment of Diazo Compounds and Diazo Transfer Reagents. *Org. Process. Res. Dev.* **2020,** *24* (1), 67-84.
2. Guptill, D. M.; Davies, H. M. L., 2,2,2-Trichloroethyl Aryldiazoacetates as Robust Reagents for the Enantioselective C–H Functionalization of Methyl Ethers. *J. Am. Chem. Soc.* **2014,** *136* (51), 17718-17721.
3. Ma, M.; Li, C.; Peng, L.; Xie, F.; Zhang, X.; Wang, J. J. T. I., An efficient synthesis of aryl α-keto esters. **2005,** *46* (22), 3927-3929.
4. Ueda, J.; Harada, S.; Nakayama, H.; Nemoto, T., Silver-catalyzed regioselective hydroamination of alkenyl diazoacetates to synthesize γ-amino acid equivalents. *Org. Biomol. Chem.* **2018,** *16* (25), 4675-4682.
5. Fu, J.; Ren, Z.; Bacsa, J.; Musaev, D. G.; Davies, H. M. L., Desymmetrization of cyclohexanes by site- and stereoselective C–H functionalization. *Nature* **2018,** *564* (7736), 395-399.
6. Qin, C.; Davies, H. M. L., Role of Sterically Demanding Chiral Dirhodium Catalysts in Site-Selective C–H Functionalization of Activated Primary C–H Bonds. *J. Am. Chem. Soc.* **2014,** *136* (27), 9792-9796.
7. Garlets, Z. J.; Boni, Y. T.; Sharland, J. C.; Kirby, R. P.; Fu, J.; Bacsa, J.; Davies, H. M., Design, Synthesis, and Evaluation of Extended C4–Symmetric Dirhodium Tetracarboxylate Catalysts. *ACS. Catal.* **2022,** *12*, 10841-10848.
8. Ghanem, A.; Gardiner, M. G.; Williamson, R. M.; Müller, P., First X-ray structure of a N-naphthaloyl-tethered chiral dirhodium (II) complex: structural basis for tether substitution improving asymmetric control in olefin cyclopropanation. *Chem. A Eur. J.* **2010,** *16* (11), 3291-3295.
9. Reddy, R. P.; Davies, H. M., Dirhodium tetracarboxylates derived from adamantylglycine as chiral catalysts for enantioselective C− H aminations. *Org. Lett.* **2006,** *8* (22), 5013-5016.
10. Wei, B.; Sharland, J. C.; Lin, P.; Wilkerson-Hill, S. M.; Fullilove, F. A.; McKinnon, S.; Blackmond, D. G.; Davies, H. M. L., In Situ Kinetic Studies of Rh(II)-Catalyzed Asymmetric Cyclopropanation with Low Catalyst Loadings. *ACS Catal.* **2020,** *10* (2), 1161-1170.
11. Wertz, B.; Ren, Z.; Bacsa, J.; Musaev, D. G.; Davies, H. M., Comparison of 1, 2, 2-Diarylcyclopropanecarboxylates as Chiral Ligands for Dirhodium-Catalyzed Cyclopropanation and C–H Functionalization. *J. Org. Chem.* **2020,** *85* (19), 12199-12211.
12. Qin, C.; Davies, H. M., Role of sterically demanding chiral dirhodium catalysts in site-selective C–H functionalization of activated primary C–H bonds. *J. Am. Chem. Soc.* **2014,** *136* (27), 9792-9796.
13. Fu, J.; Ren, Z.; Bacsa, J.; Musaev, D. G.; Davies, H. M., Desymmetrization of cyclohexanes by site-and stereoselective C–H functionalization. *Nature* **2018,** *564* (7736), 395-399.
14. Ren, Z.; Sunderland, T. L.; Tortoreto, C.; Yang, T.; Berry, J. F.; Musaev, D. G.; Davies, H. M., Comparison of reactivity and enantioselectivity between chiral bimetallic catalysts: bismuth–rhodium-and dirhodium-catalyzed carbene chemistry. *ACS. Catal.* **2018,** *8* (11), 10676-10682.
15. Liao, K.; Pickel, T. C.; Boyarskikh, V.; Bacsa, J.; Musaev, D. G.; Davies, H. M., Site-selective and stereoselective functionalization of non-activated tertiary C–H bonds. *Nature* **2017,** *551* (7682), 609-613.

Appendix D: Chapter 4 Supporting information.

1. General considerations

Geometry, frequency, and energy calculations for all reported structures were performed with the Gaussian-16 suite of programs[1] at the [B3LYP-D3(BJ)]/[6-31G(d,p) (for C, H, O, N, Cl, Br and F) + Lanl2dz (Rh)] level of theory with the corresponding Hay-Wadt effective core potential[2] for Rh (referred to as B3LYP-D3(BJ)/BS1). After validation studies at this level were performed with the DCC coordination system, all subsequent studies were performed at this level also. Thus, here we used the B3LYP[3] density functional with Grimme's empirical dispersion-correction (D3)[4] and Becke-Johnson (BJ)'s damping schemes.[5] Bulk solvent effects were incorporated in all calculations (including the geometry optimization and frequency calculations) at the self-consistent reaction field polarizable continuum model (IEF-PCM)[6] level. We chose dichloromethane as the solvent for all calculations.

To validate the [B3LYP-D3(BJ)]/BS1 calculated energetics, we performed single-point energy calculations with the B3LYP-D3(BJ), M06[7] and wB97xd[8] density functionals at the [B3LYP-D3(BJ)]/BS1 calculated geometries. In these calculations, we used two sets of basis sets, called as BS2 and BS3, both of them utilize the Stuttgart relativistic small-core effective core potential and associated basis sets for rhodium atoms, which were extended by the polarization 4f-function (ζ_f (Rh) = 1.350).[9] For the main group elements, BS2 and BS3 use the correlation-consistent cc-pvtz and split-valence 6-311+G(2d,p) basis sets, respectively.[10] The resulted approaches are labeled as [B3LYP-D3(BJ)]/BS2//[B3LYP-D3(BJ)]/BS1, [B3LYP-D3(BJ)]/BS3//[B3LYP-D3(BJ)]/BS1, M06/BS2//[B3LYP-D3(BJ)]/BS2, M06/BS3//[B3LYP-D3(BJ)]/BS1, wB97xd/BS2//[B3LYP-D3(BJ)]/BS2, and wB97xd/BS3//[B3LYP-D3(BJ)]/BS1. The presented Gibbs free energies at the DFT/BSn//[B3LYP-D3(BJ)]/BS1 level of theory (where DFT = B3LYP-D3(BJ), M06 and wB97xd, and BSn = BS1, BS2 and BS3} include the [B3LYP-D3(BJ)]/BS1 calculated enthalpy and entropy corrections. The calculated total and relative energies are presented in Tables D1-D4, respectively.

As seen in Table D2, in general, the DCC-catalyst interaction energies calculated by the [B3LYP-D3(BJ)] and wB97xd density functionals are consistent with each other, while those obtained by the M06 density functional are significantly different from their [B3LYP-D3(BJ)] and wB97xd calculated values. From Table D2, we also can conclude that the increase in the size of the used basis sets from BS1 to BS2 (or BS3) significantly decreases (i.e. destabilizes) the calculated DCC-catalyst interaction energies, while the calculated energies at the BS2 and BS3 are very close to each other.

In order to further elucidate the impact of quality of the used basis sets to the calculated geometries, as well as enthalpy and entropy corrections, we re-optimized geometries and re-calculated frequencies of all reported DCC-involving structures at the [B3LYP-D3(BJ)]/BS2 level of theory. Amazingly, both the [B3LYP-D3(BJ)]/BS2//[B3LYP-D3(BJ)]/BS1 and [B3LYP-D3(BJ)]/BS2 calculations have provided almost identical results. These extensive validations shown that, the calculated trends and made qualitative conclusions are independent from the use of [B3LYP-D3(BJ)] and wB97xd density functionals (except M06) and size of the basis sets. Therefore, in our discussion we use the most practical [B3LYP-D3(BJ)]/BS1 calculated results for all calculations herein presented.

2. Analysis of DCC coordination.

Table D1. The total energies (in hartree) of all structures involved in the reactions DCC + $Rh_2(AcO)_4$ and DCC + (Car)$Rh_2(AcO)_4$ calculated at different levels of theory (see text above).

Structure	$-E_{tot}$	$-E_{tot}$+ZPEC	-H	-G
	[B3LYP-D3(BJ)]/BS1			
DCC	618.227028	617.890234	617.874703	617.935059
$Rh_2(AcO)_4$	1133.220474	1133.009877	1132.987377	1133.062808
DCC-$Rh_2(AcO)_4$	1751.487838	1750.938543	1750.899811	1751.012682
(Car)-$Rh_2(AcO)_4$ (**8**)	2305.528370	2305.158162	2305.117516	2305.237818
DCC–$Rh_2(AcO)_4$–(Car) (**9b**)	2923.784206	2923.075702	2923.01869	2923.175929
$Rh_2(AcO)_4$–(Car)(DCC) (**10b**)	2923.788384	2923.078663	2923.022301	2923.174341
DCC–$Rh_2(AcO)_4$–(Car)(DCC)	3542.048162	3540.999883	3540.927237	3541.116083
	[B3LYP-D3(BJ)]/BS2			
DCC	618.425539	618.090418	618.074868	618.135579
$Rh_2(AcO)_4$	1135.724077	1135.514402	1135.492056	1135.567257
DCC-$Rh_2(AcO)_4$	1754.184086	1753.637331	1753.598697	1753.711501
(Car)-$Rh_2(AcO)_4$	2308.490261	2308.121960	2308.081430	2308.201623
DCC–$Rh_2(AcO)_4$–(Car)	2926.938362	2926.233521	2926.176459	2926.335323
$Rh_2(AcO)_4$–(Car)(DCC)	2926.940515	2926.234926	2926.178116	2926.334106
	[B3LYP-D3(BJ)]/BS2//[B3LYP-D3(BJ)]/BS1			
DCC	618.424810			
$Rh_2(AcO)_4$	1135.723090			
DCC-$Rh_2(AcO)_4$	1754.182075			
(Car)-$Rh_2(AcO)_4$	2308.487675			
DCC–$Rh_2(AcO)_4$–(Car)	2926.934942			
$Rh_2(AcO)_4$–(Car)(DCC)	2926.933919			
DCC–$Rh_2(AcO)_4$–(Car)(DCC)	3545.384147			
	[B3LYP-D3(BJ)]/BS3//[B3LYP-D3(BJ)]/BS1			
DCC	618.387126			
$Rh_2(AcO)_4$	1135.673283			
DCC-$Rh_2(AcO)_4$	1754.093909			
(Car)-$Rh_2(AcO)_4$	2308.374440			
DCC–$Rh_2(AcO)_4$–(Car)	2926.783669			
$Rh_2(AcO)_4$–(Car)(DCC)	2926.781831			
DCC–$Rh_2(AcO)_4$–(Car)(DCC)	3545.194392			
	M06/BS2//[B3LYP-D3(BJ)]/BS1			
DCC	617.869273			
$Rh_2(AcO)_4$	1135.019123			

DCC-$Rh_2(AcO)_4$	1752.919729
(Car)-$Rh_2(AcO)_4$	2307.125573
DCC–$Rh_2(AcO)_4$–(Car)	2925.012710
$Rh_2(AcO)_4$–(Car)(DCC)	2925.014093
DCC–$Rh_2(AcO)_4$–(Car)(DCC)	3542.905271

M06/BS3//[B3LYP-D3(BJ)]/BS1

DCC	617.837318
$Rh_2(AcO)_4$	1134.990369
DCC-$Rh_2(AcO)_4$	1752.858201
(Car)-$Rh_2(AcO)_4$	2307.062510
DCC–$Rh_2(AcO)_4$–(Car)	2924.917630
$Rh_2(AcO)_4$–(Car)(DCC)	2924.919702
DCC–$Rh_2(AcO)_4$–(Car)(DCC)	3542.779302

wB97xd/BS2//[B3LYP-D3(BJ)]/BS1

DCC	618.162099
$Rh_2(AcO)_4$	1135.322516
DCC-$Rh_2(AcO)_4$	1753.518776
(Car)-$Rh_2(AcO)_4$	2307.669999
DCC–$Rh_2(AcO)_4$–(Car)	2925.854727
$Rh_2(AcO)_4$–(Car)(DCC)	2925.855063
DCC–$Rh_2(AcO)_4$–(Car)(DCC)	3544.043786

wB97xd/BS3//[B3LYP-D3(BJ)]/BS1

DCC	618.127999
$Rh_2(AcO)_4$	1135.273939
DCC-$Rh_2(AcO)_4$	1753.435656
(Car)-$Rh_2(AcO)_4$	2307.556538
DCC–$Rh_2(AcO)_4$–(Car)	2925.707144
$Rh_2(AcO)_4$–(Car)(DCC)	2925.707561
DCC–$Rh_2(AcO)_4$–(Car)(DCC)	3543.862607

Table D2. The calculated DCC-catalyst interaction energies (in kcal/mol) at the different levels of theory (see text above, "minus" means that DCC-catalyst interaction is thermodynamically stable).

Structure	$-E_{tot}$	$-E_{tot}$+ZPEC	-H	-G
	[B3LYP-D3(BJ)]/BS1			
DCC + $Rh_2(AcO)_4$	0.0	0.0	0.0	0.0
DCC-$Rh_2(AcO)_4$	-25.3	-24.1	-23.7	-9.3
DCC + (Car)-$Rh_2(AcO)_4$	0.0	0.0	0.0	0.0
DCC–$Rh_2(AcO)_4$–(Car) (**9b**)	-18.1	-17.1	-16.6	-1.9
$Rh_2(AcO)_4$–(Car)(DCC) (**10b**)	-20.7	-19.0	-18.8	-0.9
	[B3LYP-D3(BJ)]/BS2			
DCC + $Rh_2(AcO)_4$	0.0	0.0	0.0	0.0
DCC-$Rh_2(AcO)_4$	-21.6	-20.4	-19.9	-5.4
DCC + (Car)-$Rh_2(AcO)_4$	0.0	0.0	0.0	0.0
DCC–$Rh_2(AcO)_4$–(Car)	-14.2	-13.3	-12.7	1.2
$Rh_2(AcO)_4$–(Car)(DCC)	-15.5	-14.2	-13.7	2.0
	[B3LYP-D3(BJ)]/BS2//[B3LYP-D3(BJ)]/BS1			
DCC + $Rh_2(AcO)_4$	0.0			0.0
DCC-$Rh_2(AcO)_4$	-21.5			-5.5
DCC + (Car)-$Rh_2(AcO)_4$	0.0	0.0	0.0	0.0
DCC–$Rh_2(AcO)_4$–(Car)	-14.1			2.1
$Rh_2(AcO)_4$–(Car)(DCC)	-13.5			6.3
	[B3LYP-D3(BJ)]/BS3//[B3LYP-D3(BJ)]/BS1			
DCC + $Rh_2(AcO)_4$	0.0	0.0	0.0	0.0
DCC-$Rh_2(AcO)_4$	-21.0			-5.0
DCC + (Car)-$Rh_2(AcO)_4$	0.0	0.0	0.0	0.0
DCC–$Rh_2(AcO)_4$–(Car)	-13.9			2.3
$Rh_2(AcO)_4$–(Car)(DCC)	-12.7			7.1
	M06/BS2//[B3LYP-D3(BJ)]/BS1			
DCC + $Rh_2(AcO)_4$	0.0	0.0	0.0	0.0
DCC-$Rh_2(AcO)_4$	-19.7			-3.7
DCC + (Car)-$Rh_2(AcO)_4$	0.0	0.0	0.0	0.0
DCC–$Rh_2(AcO)_4$–(Car)	-11.2			5.0
$Rh_2(AcO)_4$–(Car)(DCC)	-12.1			7.7
	M06/BS3//[B3LYP-D3(BJ)]/BS1			
DCC + $Rh_2(AcO)_4$	0.0	0.0	0.0	0.0
DCC-$Rh_2(AcO)_4$	-19.2			-3.1

DCC + (Car)-$Rh_2(AcO)_4$	0.0	0.0	0.0	0.0
DCC–$Rh_2(AcO)_4$–(Car)	-11.2			5.0
$Rh_2(AcO)_4$–(Car)(DCC)	-12.5			7.3
wB97xd/BS2//[B3LYP-D3(BJ)]/BS1				
DCC + $Rh_2(AcO)_4$	0.0	0.0	0.0	0.0
DCC-$Rh_2(AcO)_4$	-21.4			-5.4
DCC + (Car)-$Rh_2(AcO)_4$	0.0	0.0	0.0	0.0
DCC–$Rh_2(AcO)_4$–(Car)	-14.2			2.0
$Rh_2(AcO)_4$–(Car)(DCC)	-14.4			5.4
wB97xd/BS3//[B3LYP-D3(BJ)]/BS1				
DCC + $Rh_2(AcO)_4$	0.0	0.0	0.0	0.0
DCC-$Rh_2(AcO)_4$	-21.2			-5.1
DCC + (Car)-$Rh_2(AcO)_4$	0.0	0.0	0.0	0.0
DCC–$Rh_2(AcO)_4$–(Car)	-14.2			2.0
$Rh_2(AcO)_4$–(Car)(DCC)	-14.5			5.3

Table D3. The total energies (in hartree) of all structures involved in the reactions pyridine + $Rh_2(AcO)_4$ and pyridine+ (Car)$Rh_2(AcO)_4$ calculated at different levels of theory (see text above).

Structure	$-E_{tot}$	$-E_{tot}$+ZPEC	-H	-G
[B3LYP-D3(BJ)]/BS1				
Pyridine	248.3084357	248.219396	248.214184	248.246797
$Rh_2(AcO)_4$	1133.220474	1133.009877	1132.987377	1133.062808
Pyridine-$Rh_2(AcO)_4$	1381.569184	1381.269072	1381.240842	1381.329827
(Car)-$Rh_2(AcO)_4$ (**8**)	2305.528370	2305.158162	2305.117516	2305.237818
Pyridine–$Rh_2(AcO)_4$–(Car) (**9a**)	2553.859769	2553.399283	2553.352479	2553.487663
$Rh_2(AcO)_4$–(Car)(Pyridine) (**10a**)	2553.902282	2553.438293	2553.393082	2553.520175
[B3LYP-D3(BJ)]/BS2				
Pyridine	248.3945238	248.306267	248.301097	248.333642
$Rh_2(AcO)_4$	1135.724077	1135.514402	1135.492056	1135.567257
Pyridine-$Rh_2(AcO)_4$	1384.158457	1383.857689	1383.829749	1383.917470
(Car)-$Rh_2(AcO)_4$	2308.490261	2308.121960	2308.081430	2308.201623
Pyridine–$Rh_2(AcO)_4$–(Car)	2556.905871	2556.447436	2556.400815	2556.536296
$Rh_2(AcO)_4$–(Car)(Pyridine)	2556.947757	2556.485965	2556.440791	2556.568820
[B3LYP-D3(BJ)]/BS2//[B3LYP-D3(BJ)]/BS1				
Pyridine	248.3945238			
$Rh_2(AcO)_4$	1135.723090			
Pyridine-$Rh_2(AcO)_4$	1384.157033			
(Car)-$Rh_2(AcO)_4$	2308.487675			
Pyridine–$Rh_2(AcO)_4$–(Car)	2556.903004			

$Rh_2(AcO)_4$–(Car)(Pyridine) 2556.937094

Table D4. The calculated pyridine-catalyst interaction energies (in kcal/mol) at the different levels of theory (see text above, "minus" means that pyridine-catalyst interaction is thermodynamically stable).

Structure	$-E_{tot}$	$-E_{tot}$+ZPEC	-H	-G
[B3LYP-D3(BJ)]/BS1				
Pyridine + $Rh_2(AcO)_4$	0.0	0.0	0.0	0.0
Pyridine-$Rh_2(AcO)_4$	-25.3	-25.0	-24.6	-12.7
Pyridine + (Car)-$Rh_2(AcO)_4$	0.0	0.0	0.0	0.0
Pyridine –$Rh_2(AcO)_4$–(Car) (**9a**)	-14.4	-13.6	-13.0	-1.9
$Rh_2(AcO)_4$–(Car)(Pyridine)(**10a**)	-41.1	-38.1	-38.5	-22.3
[B3LYP-D3(BJ)]/BS2				
Pyridine + $Rh_2(AcO)_4$	0.0	0.0	0.0	0.0
Pyridine-$Rh_2(AcO)_4$	-25.0	-23.2	-22.4	-10.4
Pyridine + (Car)-$Rh_2(AcO)_4$	0.0	0.0	0.0	0.0
Pyridine –$Rh_2(AcO)_4$–(Car)	-13.2	-12.1	-11.5	-0.6
$Rh_2(AcO)_4$–(Car)(Pyridine)	-21.6	-20.4	-36.6	-21.1
[B3LYP-D3(BJ)]/BS2//[B3LYP-D3(BJ)]/BS1				
Pyridine + $Rh_2(AcO)_4$	0.0	0.0	0.0	0.0
Pyridine-$Rh_2(AcO)_4$	-24.7			-12.1
Pyridine + (Car)-$Rh_2(AcO)_4$	0.0	0.0	0.0	0.0
Pyridine –$Rh_2(AcO)_4$–(Car)	-13.1			-0.6
$Rh_2(AcO)_4$–(Car)(Pyridine)	-34.4			-15.6

Table D5. The total energies (in hartrees) of all structures involved in the reactions DCC+ (Carbene)$Rh_2(TPPTTL)_4$ calculated **BS1** level of theory.

Structure	$-E_{tot}$	$-E_{tot}$+ZPEC	-H	-G
$Rh_2(TPPTTL)_4$ (**5**)	7507.529159	7505.182880	7505.031339	7505.383157
$Rh_2(TPPTTL)_4$(DCC) (**11**)	8125.805677	8123.120082	8122.952478	8123.340331
(Carbene)-$Rh_2(TPPTTL)_4$ (**12**)	8679.883519	8677.377058	8677.207783	8677.597591
(DCC)-$Rh_2(TPPTTL)_4$-(Carbene) (**13**)	9298.151016	9295.304829	9295.119636	9295.543510

Table D6. The calculated DCC/Car1-Rh2(TPPTTL)4 interaction energies (in kcal/mol) at **BS1**. "Minus" means that interaction is thermodynamically stable).

Structure	ΔE_{tot}	$_{\Delta}E_{tot}$+ZPEC	ΔH	ΔG
DCC + $Rh_2(TPPTTL)_4$	0.0	0.0	0.0	0.0
(DCC)-$Rh_2(TPPTTL)_4$ (**11**)	-31.0	-29.5	-29.2	-14.4
DCC + $Rh_2(TPPTTL)_4$-(Car1)	0.0	0.0	0.0	0.0
(DCC)-$Rh_2(TPPTTL)_4$-(Car1) (**13**)	-25.4	-23.6	-23.4	-7.3

NBO Analyses:

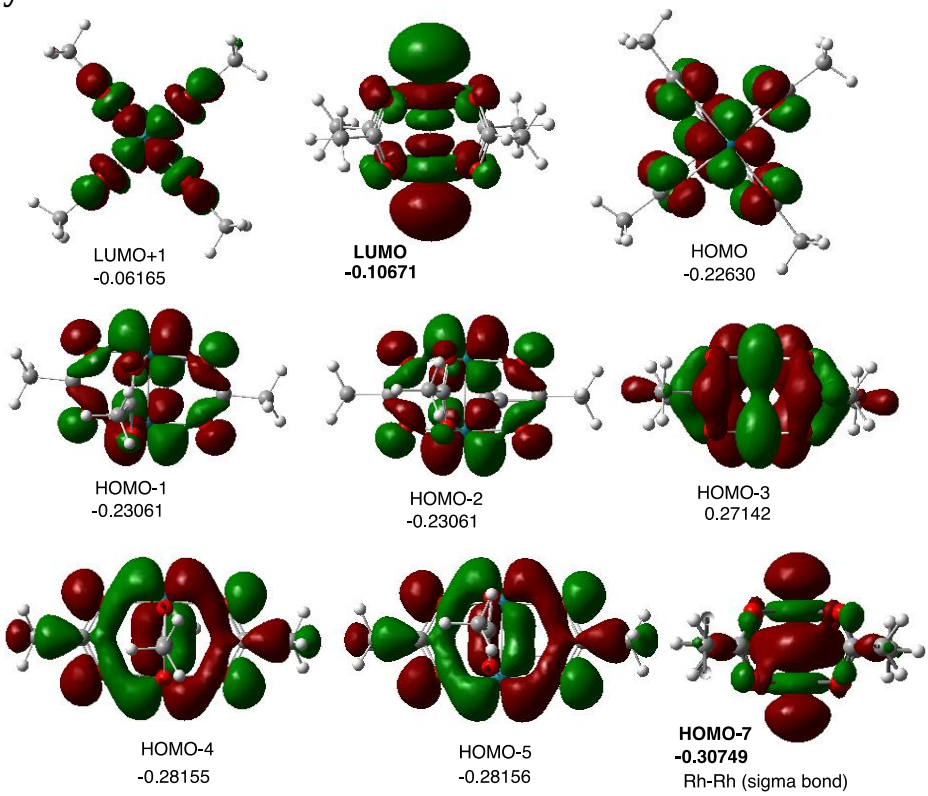

Figure D1. The calculated frontiers natural bonds for the $Rh_2(AcO)_4$. For the nature of the Rh-Rh bonding (HOMO-7), see Table D7.

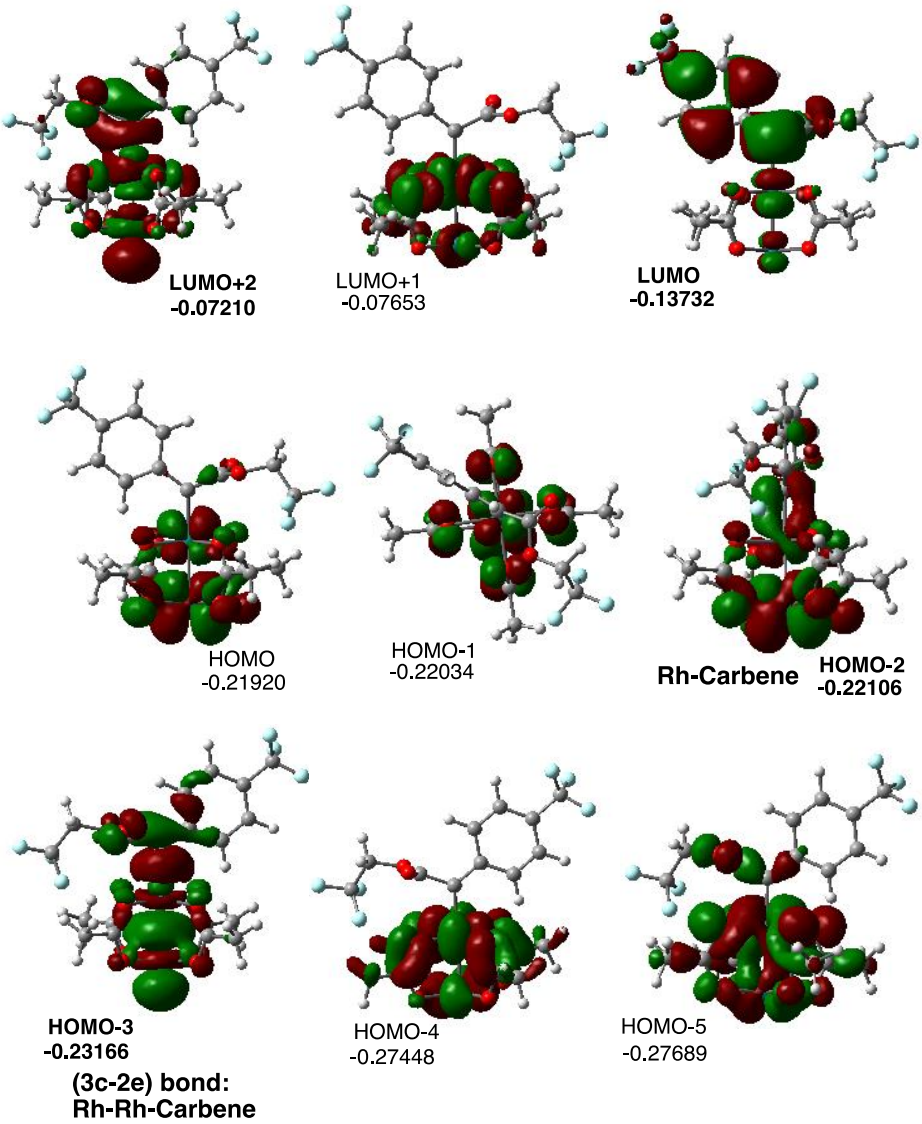

Figure D2. The calculated frontiers natural bonds for the (Carbene)-$Rh_2(AcO)_4$ (**8**). For the nature of the Rh-Rh and Rh-Carbene bonds, see Table D7.

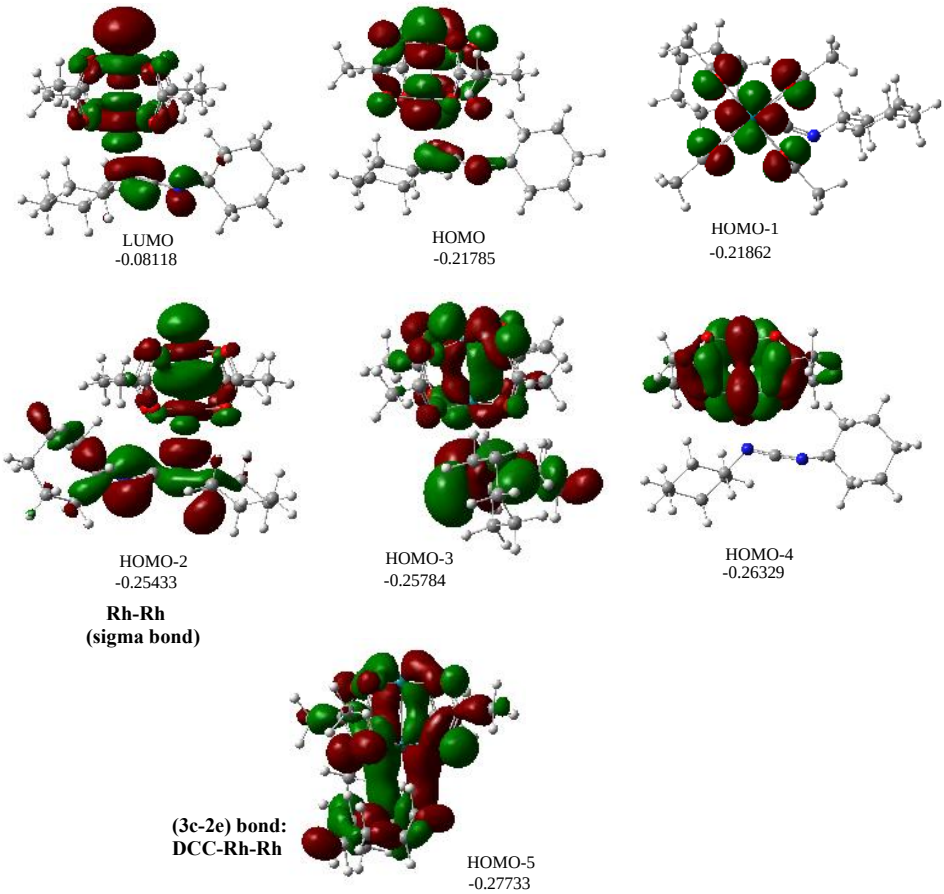

Figure D3. The calculated frontiers natural bonds for the (DCC)-$Rh_2(AcO)_4$ (**9b**). For the nature of the Rh-Rh and Rh-DCC bonds, see Table D7.

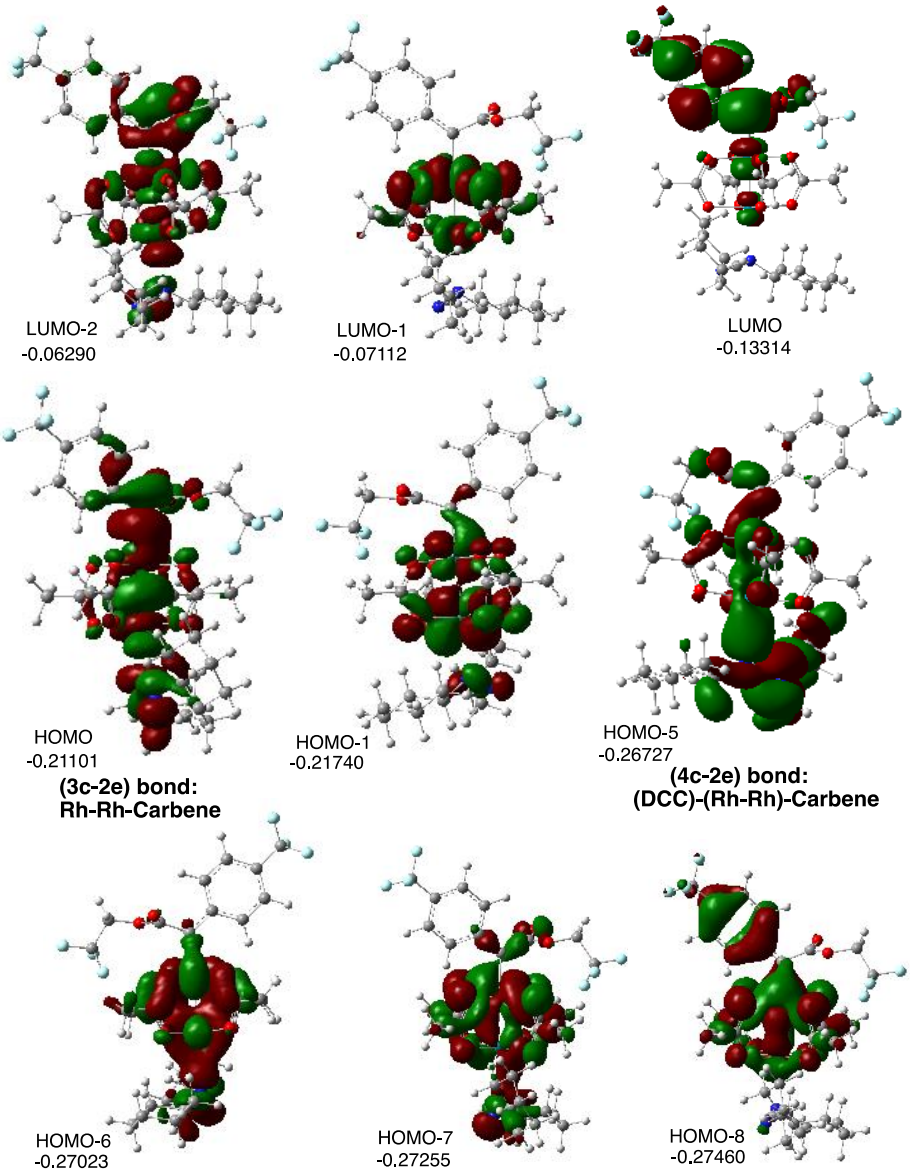

Figure D4. The calculated frontiers natural bonds for the (DCC)-$Rh_2(AcO)_4$ (**10b**). For the nature of the Rh-Rh and Rh-DCC bonds, see Table D7.

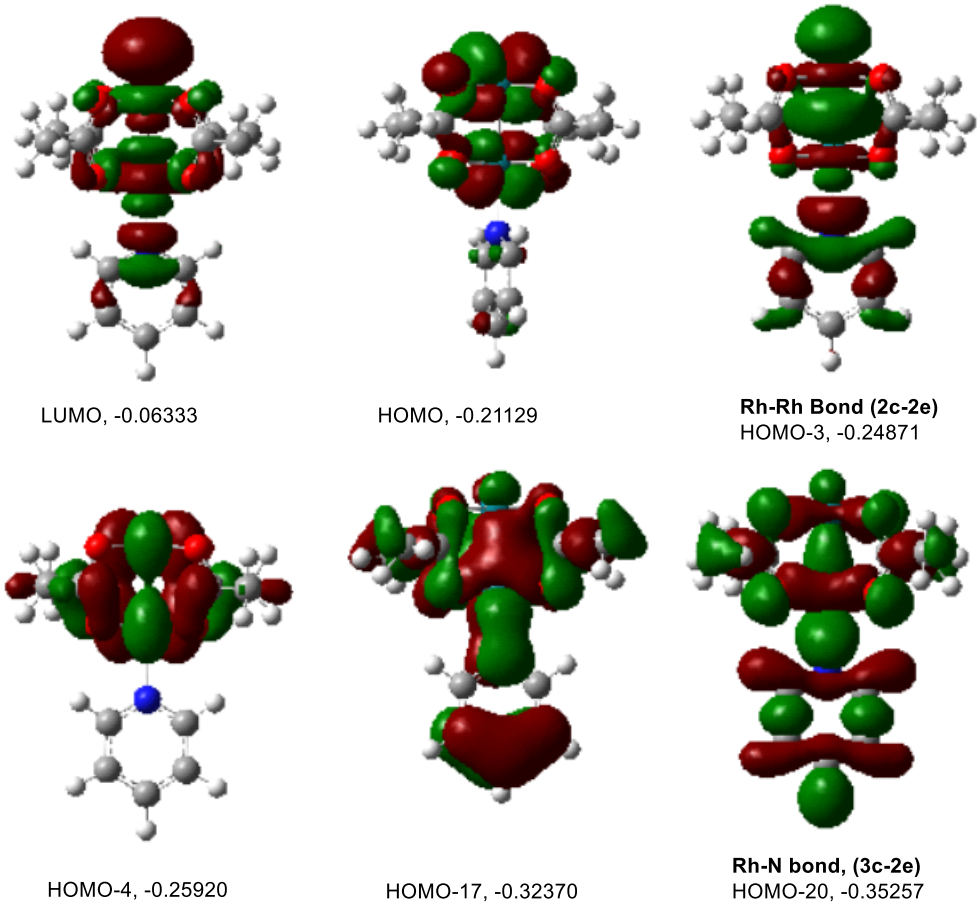

Figure D5. The calculated frontiers natural bonds for the (Pyridine)-$Rh_2(AcO)_4$. For the nature of the Rh-Rh and Rh-Pyridine bonds, see Table D8.

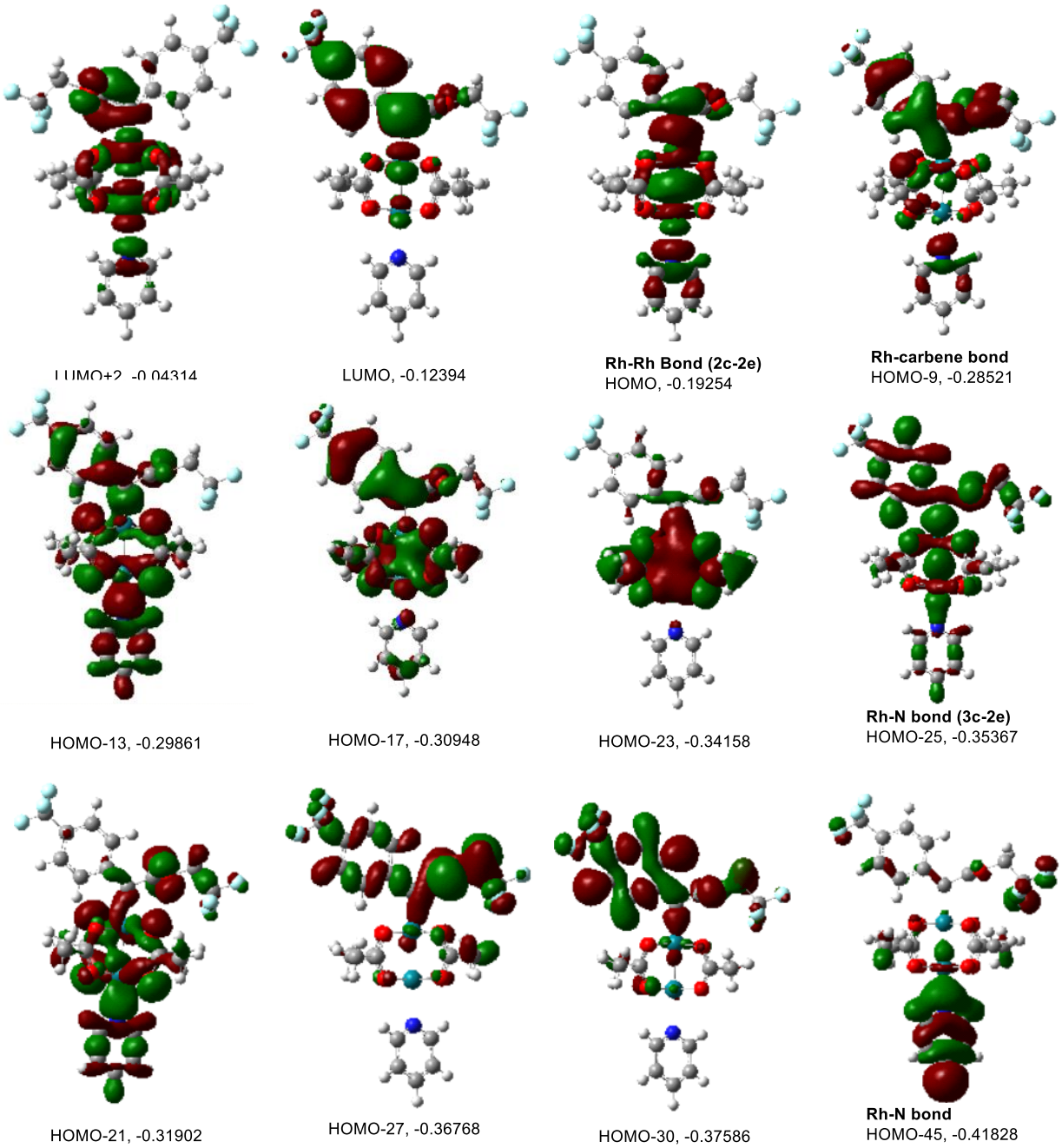

Figure D6. The calculated frontiers natural bonds for the (Pyridine)-$Rh_2(AcO)_4$–(Carbene) (**9a**). For the nature of the selective bonds, see Table D8.

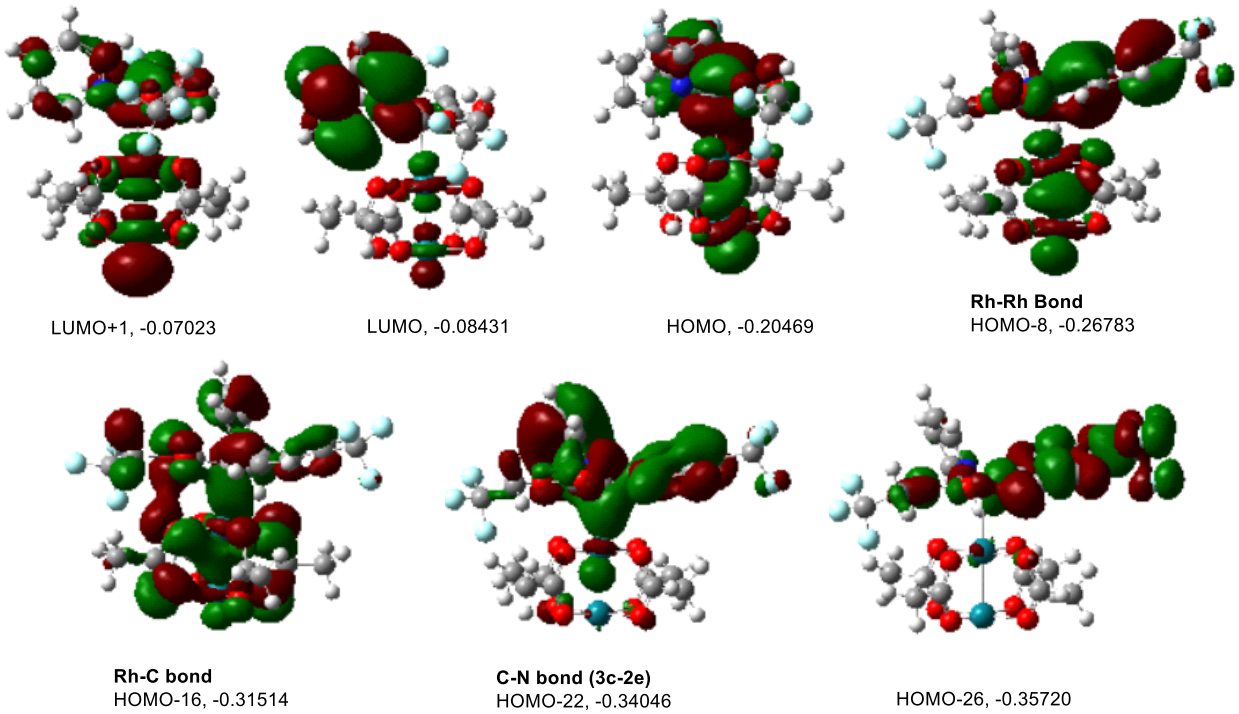

Figure D7. The calculated frontiers natural bonds for the ($Rh_2(AcO)_4$–(Carbene)(Pyridine) (**10a**). For the nature of the selective bonds, see Table D8.

Table D7. The important bonds for the calculated $Rh_2(AcO)_4$, (Carbene)–$Rh_2(AcO)_4$, (DCC)–$Rh_2(AcO)_4$, and (DCC)–$Rh_2(AcO)_4$–(Carbene) systems. Here, occ stands for the occupation number (in |e|) of the presented molecular orbital. Contributions (in %) from each participating atom are presented in the second column, which was divided to its s-, p- and d-AO contributions in the third, fourth and fifth columns. Here, we also have presented the calculated Natural Charges for critical atoms in |e|.

A. $Rh_2(AcO)_4$:

Natural Charges: Rh = +0.71

1.	(occ=1.87339)	Rh(1) - O(2)		
Rh(1):	(11.50%)	0.3391 s(13.52%)	p 3.69(49.88%)	d2.71(36.59%)
O(2):	(88.50%)	0.9408 s(16.49%)	p 5.06(83.47%)	d 0.00(0.04%)
2.	(occ=1.87337)	Rh(1) - O(3)		
Rh(1)	(11.51%)	0.3393 s(13.56%)	p 3.68(49.84%)	d 2.70(36.60%)
O(3)	(88.49%)	0.9407 s(16.47%)	p 5.07(83.49%)	d 0.00(0.04%)
3.	(occ=1.87322)	Rh(1) - O(4)		
Rh(1)	(11.51%)	0.3392 s(13.54%)	p 3.68(49.85%)	d 2.70(36.61%)

O(4)	(88.49%)	0.9407 s(16.46%)	p 5.07(83.49%)	d 0.00(0.04%)

4.	(occ=1.87324)	Rh(1) - O(5)		
Rh(1)	(11.50%)	0.3391 s(13.51%)	p 3.69(49.89%)	d 2.71(36.60%)
O(5)	(88.50%)	0.9408 s(16.48%)	p 5.07(83.48%)	d 0.00(0.04%)

5.	(occ=1.66099)	Rh(1) -Rh(6)		
Rh(1)	(50.00%)	0.7071 s(42.31%)	p 0.07(3.02%)	d 1.29(54.67%)
Rh(6)	(50.00%)	0.7071 s(42.31%)	p 0.07(3.02%)	d 1.29(54.67%)

Four Rh(2)-O bonds are not shown because they are identical to the Rh(1)-O bonding shown above.

B: Carbene-$Rh_2(AcO)_4$ (8):

Natural Charges:
Rh(1) = +0.55
Rh(2) = +0.45
C(Carbene) = +0.08

1.	(occ=1.60805)	Rh(1) -Rh(2)		
Rh(1)	(58.24%)	0.7631 s(48.60%)	p 0.03(1.36%)	d 1.03(50.04%)
Rh(2)	(41.76%)	0.6463 s(34.79%)	p 0.41(14.18%)	d 1.47(51.03%)

2.	(occ=1.88122)	Rh(1) - O(3)		
Rh(1)	(10.65%)	0.3263 s(12.36%)	p 4.06(50.12%)	d 3.04(37.52%)
O(3)	(89.35%)	0.9453 s(18.61%)	p 4.37(81.35%)	d 0.00(0.04%)

3.	(occ=1.87944)	Rh(1) - O(16)		
Rh(1)	(10.98%)	0.3314 s(12.45%)	p 3.98(49.49%)	d 3.06(38.06%)
O(16)	(89.02%)	0.9435 s(18.43%)	p 4.42(81.53%)	d 0.00(0.04%)

4.	(occ=1.88013)	Rh(1) - O(19)		
Rh(1)	(10.83%)	0.3291 s(12.43%)	p 4.00(49.76%)	d 3.04(37.80%)
O(19)	(89.17%)	0.9443 s(18.39%)	p 4.43(81.57%)	d 0.00(0.04%)

5.	(occ=1.88108)	Rh(1) - O(24)		
Rh(1)	(10.70%)	0.3272 s(12.43%)	p 4.01(49.90%)	d 3.03(37.67%)
O(24)	(89.30%)	0.9450 s(18.57%)	p 4.38(81.39%)	d 0.00(0.04%)

6.	(occ=1.87433)	Rh(2) - O(5)		
Rh(2)	(14.36%)	0.3790 s(11.27%)	p 4.58(51.60%)	d 3.30(37.14%)
O(5)	(85.64%)	0.9254 s(19.48%)	p 4.13(80.48%)	d 0.00(0.04%)

7.	(occ=1.87167)	Rh(2) - O(15)		
Rh(2)	(14.61%)	0.3823 s(11.52%)	p 4.44(51.14%)	d 3.24(37.34%)
O(15)	(85.39%)	0.9240 s(19.05%)	p 4.25(80.91%)	d 0.00(0.04%)

8. (occ=1.87240) Rh(2) - O(17)

Rh(2)	(14.67%)	0.3830	s(11.00%)	p 4.65(51.16%)	d 3.44(37.84%)
O(17)	(85.33%)	0.9237	s(19.27%)	p 4.19(80.69%)	d 0.00(0.04%)

9. (occ=1.87681) Rh(2) - O(26)

Rh(2)	(14.17%)	0.3764	s(11.64%)	p 4.41(51.37%)	d 3.18(36.99%)
O(26)	(85.83%)	0.9265	s(19.66%)	p 4.08(80.30%)	d 0.00(0.04%)

C. DCC- $Rh_2(AcO)_4$:

Natural Charges:
Rh(38) = +0.54
Rh(39) = + 0.64
N(Rh) = -0.54
N = -0.48

7. (occ=1.78578) N(3) -Rh(38)

N(3)	(89.72%)	0.9472	s(23.85%)	p 3.19(76.11%)	d 0.00(0.04%)
Rh(38)	(10.28%)	0.3206	s(23.87%)	p 2.09(49.97%)	d 1.10(26.16%)

42. (occ=1.50787) Rh(38) -Rh(39)

Rh(38)	(38.79%)	0.6228	s(14.91%)	p 3.26(48.58%)	d 2.45(36.51%)
Rh(39)	(61.21%)	0.7823	s(44.54%)	p 0.05(2.17%)	d 1.20(53.29%)

43. (occ=1.87748) Rh(38) - O(40)

Rh(38)	(12.42%)	0.3524	s(14.96%)	p 3.35(50.05%)	d 2.34(34.99%)
O(40)	(87.58%)	0.9358	s(19.25%)	p 4.19(80.71%)	d 0.00(0.04%)

44. (occ=1.87812) Rh(38) - O(53)

Rh(38)	(12.31%)	0.3509	s(15.44%)	p 3.23(49.84%)	d 2.25(34.73%)
O(53)	(87.69%)	0.9364	s(19.19%)	p 4.21(80.77%)	d 0.00(0.04%)

45. (occ=1.88001) Rh(38) - O(56)

Rh(38)	(12.32%)	0.3510	s(15.29%)	p 3.29(50.31%)	d 2.25(34.40%)
O(56)	(87.68%)	0.9364	s(19.28%)	p 4.19(80.68%)	d 0.00(0.04%)

46. (occ=1.87650) Rh(38) - O(61)

Rh(38)	(12.46%)	0.3530	s(15.50%)	p 3.20(49.62%)	d 2.25(34.88%)
O(61)	(87.54%)	0.9356	s(19.05%)	p 4.25(80.91%)	d 0.00(0.04%)

47. (occ=1.87593) Rh(39) - O(42)

Rh(39)	(11.17%)	0.3342	s(13.16%)	p 3.78(49.69%)	d 2.82(37.15%)
O(42)	(88.83%)	0.9425	s(17.87%)	p 4.59(82.09%)	d 0.00(0.04%)

48. (occ=1.87612) Rh(39) - O(52)

Rh(39)	(10.94%)	0.3307	s(13.17%)	p 3.80(50.06%)	d 2.79(36.76%)
O(52)	(89.06%)	0.9437	s(17.88%)	p 4.59(82.08%)	d 0.00(0.04%)

49. (occ=1.87608) Rh(39) - O(54)

Rh(39)	(11.09%)	0.3331 s(13.17%)	p 3.78(49.79%)	d 2.81(37.05%)
O(54)	(88.91%)	0.9429 s(17.79%)	p 4.62(82.17%)	d 0.00(0.04%)

50. (occ=1.87575) Rh(39) - O(63)

Rh(39)	(11.03%)	0.3321 s(13.10%)	p 3.81(49.90%)	d 2.83(37.00%)
O(63)	(88.97%)	0.9432 s(17.87%)	p 4.59(82.09%)	d 0.00(0.04%)

D. DCC- $Rh_2(AcO)_4$-Carbene (9b):

Natural Charges:
Rh(38) = +0.49
Rh(39) = + 0.43
N(Rh) = -0.55
N = -0.52
C(Carbene) = +0.06

41. (occ=1.59111) Rh(38) -Rh(39)

Rh(38)	(54.56%)	0.7387 s(44.82%)	p 0.09(4.22%)	d 1.14(50.96%)
Rh(39)	(45.44%)	0.6741 s(34.39%)	p 0.42(14.32%)	d 1.49(51.29%)

42. (occ=1.88127) Rh(38) - O(40)

Rh(38)	(10.91%)	0.3304 s(12.43%)	p 4.03(50.11%)	d 3.01(37.46%)
O(40)	(89.09%)	0.9439 s(20.11%)	p 3.97(79.85%)	d 0.00(0.04%)

43. (occ=1.88011) Rh(38) - O(53)

Rh(38)	(11.17%)	0.3343 s(12.44%)	p 4.01(49.83%)	d 3.03(37.73%)
O(53)	(88.83%)	0.9425 s(19.68%)	p 4.08(80.28%)	d 0.00(0.04%)

44. (occ=1.88188) Rh(38) - O(56)

Rh(38)	(11.03%)	0.3321 s(12.82%)	p 3.91(50.13%)	d 2.89(37.05%)
O(56)	(88.97%)	0.9432 s(19.83%)	p 4.04(80.13%)	d 0.00(0.04%)

45. (occ=1.88131) Rh(38) - O(61)

Rh(38)	(10.99%)	0.3315 s(12.43%)	p 4.01(49.91%)	d 3.03(37.65%)
O(61)	(89.01%)	0.9434 s(20.00%)	p 4.00(79.96%)	d 0.00(0.04%)

46. (occ=1.87532) Rh(39) - O(42)

Rh(39)	(14.19%)	0.3767 s(11.23%)	p 4.59(51.61%)	d 3.31(37.15%)
O(42)	(85.81%)	0.9263 s(20.14%)	p 3.96(79.82%)	d 0.00(0.04%)

47. (occ=1.87280) Rh(39) - O(52)

Rh(39)	(14.28%)	0.3779 s(11.54%)	p 4.45(51.37%)	d 3.22(37.10%)
O(52)	(85.72%)	0.9259 s(19.81%)	p 4.05(80.15%)	d 0.00(0.04%)

48. (occ=1.87392) Rh(39) - O(54)

Rh(39)	(14.42%)	0.3797 s(10.95%)	p 4.67(51.19%)	d 3.46(37.86%)

O(54)	(85.58%)	0.9251 s(19.94%)	p 4.01(80.02%)	d 0.00(0.04%)

49.	(occ=1.87789)	Rh(39) - O(63)		
Rh(39)	(13.94%)	0.3734 s(11.37%)	p 4.53(51.45%)	d 3.27(37.18%)
O(63)	(86.06%)	0.9277 s(20.26%)	p 3.94(79.71%)	d 0.00(0.04%)

Table D8. The important bonds for the calculated (Pyridine)–$Rh_2(AcO)_4$, (Pyridine)–$Rh_2(AcO)_4$–(Carbene), and $Rh_2(AcO)_4$–(Carbene)(Pyridine) systems. Here, occ stands for the occupation number (in |e|) of the presented molecular orbital. Contributions (in %) from each participating atom are presented in the second column, which was divided to its s-, p- and d-AO contributions in the third, fourth and fifth columns. Here, we also have presented the calculated Natural Charges for critical atoms in |e|.

A. Pyridine-$Rh_2(AcO)_4$:

Natural Charges:

Bottom Rh (29) = +0.53

Pyridine N (30) = -0.42

Top Rh (41) = + 0.59

37.	(occ=1.88393)	Rh(29) - N(30)		
Rh(29)	(11.69%)	0.3420 s(23.06%)	p 2.14(49.26%)	d 1.20(27.68%)
N(30)	(88.31%)	0.9397 s(26.63%)	p 2.75(73.36%)	d 0.00(0.01%)

38.	(occ=1.56302)	Rh(29) -Rh(41)		
Rh(29)	(34.97%)	0.5913 s(14.33%)	p 3.44(49.30%)	d 2.54(36.37%)
Rh(41)	(65.03%)	0.8064 s(38.25%)	p 0.09(3.40%)	d 1.53(58.35%)

B. Pyridine–$Rh_2(AcO)_4$–(Car) (9a):

Natural Charges:

Rh (1) = +0.46

Rh (2) = +0.42

C (31)(Carbene) = + 0.03

N (56) = -0.45

1.	(occ=1.60795)	Rh(1) -Rh(2)		
Rh(1)	(51.64%)	0.7186 s(40.31%)	p 0.17(6.76%)	d 1.31(52.93%)
Rh(2)	(48.36%)	0.6954 s(36.27%)	p 0.35(12.78%)	d 1.40(50.95%)

C. **$Rh_2(AcO)_4$–(Car)(Pyridine) (10a):**

Natural Charges:

Rh (1) = + 0.58

Rh (2) = + 0.49

C (31)(Carbene) = - 0.14

N (56) = -0.28

1.	(occ=1.62772)	Rh (1) - Rh (2)		
Rh(1)	(55.46%)	0.7447 s(45.93%)	p 0.04(1.87%)	d 1.14(52.21%)
Rh(2)	(44.54%)	0.6674 s(39.04%)	p 0.22(8.47%)	d 1.34(52.48%)

40.	(occ=1.97559)	C(31) - N(56)		
C(31)	(34.28%)	0.5855 s(22.93%)	p 3.36(76.92%)	d 0.01(0.15%)
N(56)	(65.72%)	0.8107 s(31.63%)	p 2.16(68.35%)	d 0.00(0.02%)

Table D9: Cartesian Coordinates (in Å) of all calculated structures for DCC coordination.

DCC: [B3LYP-D3(BJ)]/BS1
C -0.88801100 0.42240400 0.80691400
N -0.02317100 1.05174700 0.20573300
N -1.75188100 -0.08797100 1.51306000
C -2.98383200 -0.71456200 1.00139400
C -3.00575000 -2.19439200 1.40382200
C -4.20095600 0.02725900 1.56753400
H -3.01275000 -0.64915400 -0.09579700
C -4.31447800 -2.86831700 0.97096700
H -2.89656000 -2.25544300 2.49456000
H -2.14043500 -2.70391900 0.96568800
C -5.51061000 -0.64422800 1.13369100
H -4.12508900 0.02681400 2.66275100
H -4.17339000 1.07360100 1.24423900
C -5.53620700 -2.12656000 1.52940600
H -4.31818600 -3.91442800 1.29676100
H -4.37003500 -2.88143300 -0.12629500
H -6.36260500 -0.11439100 1.57392700
H -5.61758800 -0.55932100 0.04342200
H -6.46069900 -2.59806300 1.17727800
H -5.53656900 -2.20702400 2.62515700
C 1.19752000 0.45691400 -0.36639400
C 1.06610600 0.39033700 -1.89383200
C 2.40959400 1.30117000 0.04318700
H 1.33375600 -0.56449900 0.01720800
C 2.35346300 -0.14002900 -2.53899300
H 0.85049400 1.40065700 -2.26524500
H 0.20883800 -0.23887500 -2.15793700
C 3.69811900 0.77101300 -0.59987400
H 2.23080600 2.33615300 -0.27647700
H 2.49496900 1.31286300 1.13523900
C 3.57094600 0.69818300 -2.12720400
H 2.24474800 -0.15035600 -3.62922000
H 2.51104300 -1.18230000 -2.22911700
H 4.54368300 1.40658600 -0.31441600
H 3.91299400 -0.23233100 -0.20688700
H 4.48495700 0.28201800 -2.56582900
H 3.46099500 1.71509900 -2.52854600

$Rh_2(AcO)_4$: [B3LYP-D3(BJ)]/BS1
Rh 0.01306100 0.00304900 -1.18804600
O -1.43504900 1.47366900 -1.13355400
O 1.48272300 1.45014900 -1.10704000
O 1.45997600 -1.46730100 -1.11362900
O -1.45781300 -1.44517100 -1.14014300
Rh -0.01270400 -0.00349700 1.20621500
C -1.89076900 -1.85102700 -0.01302300
O -1.48189200 -1.45108000 1.12521400
C 1.85057800 -1.89165500 0.02225200
O 1.43588500 -1.47364700 1.15173000
C -1.85022100 1.89120600 -0.00407900
O -1.46009600 1.46638100 1.13179200
O 1.45770400 1.44519400 1.15830900
C 1.89117800 1.85052100 0.03119700
C 3.00456800 2.86635300 0.04822300
H 2.91531700 3.51094600 0.92367400
H 3.96044400 2.33530700 0.10941900
H 2.99532500 3.45824000 -0.86747800
C 2.86565200 -3.00583600 0.02973900
H 3.46137000 -2.97171800 0.94252300
H 2.33354500 -3.96260900 -0.00081500
H 3.50655100 -2.94156800 -0.85042000
C -2.86530200 3.00538000 -0.01152600
H -2.33321400 3.96214700 0.01955900
H -3.46070100 2.97158500 -0.92453100
H -3.50650600 2.94078900 0.86838600
C -3.00424700 -2.86676300 -0.03001400
H -3.96010800 -2.33563800 -0.09076500
H -2.91530600 -3.51110400 -0.90568300
H -2.99476400 -3.45892000 0.88550900

DCC–$Rh_2(AcO)_4$: [B3LYP-D3(BJ)]/BS1
C -2.23260300 -1.88191100 -0.27737700

N -2.17451100 -2.40911400 -1.36913000
N -2.35175400 -1.47227800 0.88828000
C -2.75495900 -0.07691300 1.20289600
C -3.47923600 -0.04736000 2.55057600
C -1.52400800 0.83986400 1.19652100
H -3.44939300 0.25646200 0.41999300
C -3.85485300 1.38986500 2.93517800
H -2.81586500 -0.47423400 3.30823100
H -4.36954200 -0.68320000 2.49955100
C -1.90590500 2.27296800 1.59038300
H -0.79616500 0.43845400 1.90783400
H -1.06380500 0.81906000 0.20161900
C -2.62187800 2.30284500 2.94708500
H -4.34403400 1.39153400 3.91551000
H -4.58824200 1.78345900 2.21756200
H -1.00748500 2.89969400 1.61467500
H -2.56725000 2.70032500 0.82385400
H -2.91001200 3.32892200 3.20235900
H -1.92860700 1.96221300 3.72841900
C -0.96541800 -2.50690100 -2.21174300
C -0.38631200 -3.92138100 -2.07669900
C -1.32438200 -2.18529400 -3.66406500
H -0.21655100 -1.78863800 -1.85415200
C 0.83236100 -4.09703900 -2.99166100
H -1.16651100 -4.64393400 -2.34849500
H -0.12733800 -4.09819000 -1.03055800
C -0.10497600 -2.36449000 -4.57861700
H -2.13075700 -2.86046100 -3.97824500
H -1.71388800 -1.16366800 -3.73034200
C 0.48873700 -3.77401000 -4.45167700
H 1.21505500 -5.11982700 -2.90216700
H 1.63703500 -3.42977000 -2.65443500
H -0.38869500 -2.15874300 -5.61641200
H 0.66100600 -1.62421200 -4.30966200
H 1.37997300 -3.86830600 -5.08213900
H -0.24075500 -4.50769900 -4.82117800
Rh -1.15902200 -2.83408000 2.27073800
Rh 0.21687400 -4.31411100 3.59919300
O -2.70911500 -3.22125000 3.58506400
C -2.51469000 -4.02880800 4.55144900
O -1.42565700 -4.63112800 4.81507600
C -3.69834000 -4.31247400 5.44372400
H -3.36985600 -4.72733900 6.39674200
H -4.27620000 -3.40018200 5.60258800
H -4.34753200 -5.04042800 4.94602800
H 2.55338500 -2.05605400 -0.27582800
C 2.69466600 -2.96395500 0.31090000
C 1.56223000 -3.14660800 1.29067300
H 3.64991200 -2.93612700 0.83767500
H 2.70739700 -3.82171900 -0.36969300
O 1.77167300 -3.90533900 2.28836400
O 0.46800300 -2.54837300 1.02507200
O 0.74740800 -2.68570000 4.75934500
C 0.26881600 -1.54497000 4.46786900
O -0.51718700 -1.29088100 3.49752800
C 0.63068700 -0.38404300 5.36101100
H 1.54722500 -0.59343600 5.91286600
H 0.73854700 0.52608200 4.76840300
H -0.18331900 -0.22645700 6.07649100
O -1.71080600 -4.47734900 1.14515300
C -1.19539400 -5.61278300 1.41072200
O -0.38528200 -5.85826300 2.35870600
C -1.55859300 -6.74940600 0.48821500
H -2.60227300 -6.66712900 0.18026600
H -0.93615500 -6.67969800 -0.41015800
H -1.37536600 -7.70990400 0.97005200

(Car)–$Rh_2(AcO)_4$ (8):
[B3LYP-D3(BJ)]/BS1

Rh -0.71785900 -2.23204800 2.03839400
Rh 0.24675400 -3.95425600 3.50021000
O -2.57140800 -2.71639200 2.83570200
C -2.65852600 -3.65777700 3.67665300
O -1.68370800 -4.34859300 4.13657700
C -4.02498900 -4.02458000 4.20047500
H -4.03358000 -3.93535400 5.29006000
H -4.78826400 -3.37871400 3.76775100
H -4.23719600 -5.06848600 3.95273500
H 3.49454700 -1.53727800 0.44931500
C 3.54655300 -2.18274800 1.32559600
C 2.16081100 -2.51209600 1.82115900
H 4.09419600 -1.67915500 2.12553100
H 4.08471600 -3.10333300 1.08942800
O 2.08523000 -3.42439900 2.71195600
O 1.18817600 -1.85919600 1.33503200
O 0.43535800 -2.48281400 4.93476500
C 0.13738600 -1.27362300 4.64801800
O -0.37513200 -0.86853700 3.56245600
C 0.44547100 -0.25700300 5.71891500
H 1.52334500 -0.26050500 5.90253500
H 0.12163100 0.73731200 5.41310600
H -0.04997200 -0.54357900 6.65015400
O -0.97215300 -3.71267600 0.60672600
C -0.56658600 -4.88688100 0.84940300
O -0.00069700 -5.28058300 1.92782900
C -0.74903200 -5.93967000 -0.21587900
H -1.29029800 -5.53348000 -1.06972600
H 0.23218700 -6.29999000 -0.53799100
H -1.29203800 -6.79085700 0.20326400
C 1.01702700 -5.34231800 4.73332800
C 0.64912300 -6.71480600 4.84945300
C 1.98855400 -4.79558100 5.69969100

C 1.38440600 -7.60177700 5.68569200
C -0.46228200 -7.22576300 4.12780600
O 1.64226100 -4.47775300 6.82094500
O 3.22701100 -4.63689500 5.18959300
C 1.03674300 -8.93672700 5.77897500
H 2.23030200 -7.23005100 6.25271100
C -0.81441200 -8.56280300 4.23605300
H -1.03680900 -6.55672700 3.50566400
C 4.15170400 -3.87401300 5.97046200
C -0.06398400 -9.41292800 5.05292100
H 1.60042200 -9.60843900 6.41557400
H -1.66930000 -8.94877000 3.69449400
H 5.06342900 -4.45913400 6.09314700
H 3.72534400 -3.62733500 6.94262600
C 4.47900800 -2.59594200 5.22168000
C -0.40438200 -10.88050000 5.12951700
F 5.07550600 -2.84691800 4.03889600
F 3.37891800 -1.85822900 4.97374000
F 5.32555400 -1.84904700 5.95945700
F -1.67580400 -11.12698300 4.75848100
F -0.24046200 -11.36139700 6.37950900
F 0.40044800 -11.60125700 4.31731600

DCC–$Rh_2(AcO)_4$–(Car) (9b)
[B3LYP-D3(BJ)]/BS1
C -2.33763900 -1.56256900 -0.44303800
N -2.13210100 -2.05993100 -1.53867700
N -2.64257800 -1.17828200 0.68940600
C -2.80818600 0.24733800 1.05083600
C -3.53901200 0.34351900 2.39219900
C -1.44203700 0.94711200 1.10711900
H -3.42138900 0.73158200 0.27756800
C -3.68038600 1.80401400 2.84035700
H -2.96374000 -0.21999600 3.13388900
H -4.52134400 -0.13465500 2.30660500
C -1.58631100 2.40660300 1.55758100
H -0.80937800 0.39931600 1.81263100
H -0.96572100 0.89020700 0.12091600
C -2.31526300 2.50193500 2.90432100
H -4.17828400 1.84478200 3.81559700
H -4.32780300 2.34370100 2.13493200
H -0.59680000 2.87316100 1.62209200
H -2.15096400 2.96974100 0.80142900
H -2.43697300 3.55092800 3.19777000
H -1.70233200 2.02350400 3.68055600
C -0.79518300 -2.35560000 -2.09148300
C -0.55007600 -3.86814600 -2.02598000
C -0.71342100 -1.83872000 -3.53036300
H -0.03190600 -1.85671500 -1.48189200
C 0.78914100 -4.24008500 -2.67513400
H -1.37206600 -4.37611500 -2.54744500
H -0.58250500 -4.18326200 -0.98125000
C 0.63187500 -2.20714500 -4.17002200
H -1.53512600 -2.28441900 -4.10618300
H -0.86521600 -0.75367300 -3.54030900
C 0.88038500 -3.72052800 -4.11565600
H 0.92298700 -5.32750200 -2.64788800
H 1.60873100 -3.80934900 -2.08545300
H 0.66106800 -1.84936700 -5.20516900
H 1.44057100 -1.68930900 -3.63578200
H 1.85930400 -3.96067200 -4.54601600
H 0.12840100 -4.23159600 -4.73261600
Rh -1.44980400 -2.79085300 2.27005100
Rh -0.14710900 -4.37154100 3.63180300
O -3.06113600 -3.17309200 3.52250200
C -2.93782000 -4.02748900 4.44806000
O -1.87846700 -4.68824600 4.72531700
C -4.13108700 -4.29203500 5.33341300
H -3.95706900 -3.82904000 6.30991100
H -5.03548200 -3.87251600 4.89324600
H -4.24698700 -5.36658500 5.49037000
H 2.31661900 -2.12636200 -0.20574000
C 2.53089400 -2.85787200 0.57270200
C 1.30653700 -3.10995400 1.41718700
H 3.34160100 -2.50603100 1.21271400
H 2.85548600 -3.79768600 0.11730800
O 1.45090700 -3.92601800 2.38632200
O 0.23701800 -2.50288000 1.10653900
O 0.34584400 -2.77511900 4.84612200
C -0.02339900 -1.59786300 4.52133600
O -0.77182400 -1.29492000 3.54491300
C 0.50005700 -0.48011100 5.38904300
H 1.59084900 -0.46315400 5.31551400
H 0.08980300 0.47849800 5.07238500
H 0.24098100 -0.67300800 6.43324800
O -2.01242200 -4.40659900 1.09433400
C -1.52384800 -5.55091000 1.33384200
O -0.72347500 -5.84118400 2.28574100
C -1.87961300 -6.67578900 0.39344600
H -2.81076100 -6.45592900 -0.12903200
H -1.07905900 -6.77514300 -0.34740600
H -1.95599200 -7.61766500 0.93905100
C 0.93586800 -5.66654100 4.77093900
C 0.67319100 -7.04614100 5.02353800
C 2.06404600 -5.03114200 5.46494000
C 1.64821300 -7.88355300 5.63225200
C -0.57654100 -7.61179300 4.65714800
O 1.94976400 -4.63693000 6.61110900
O 3.16128300 -4.86913500 4.69248000
C 1.39691900 -9.22888800 5.83690000
H 2.60523500 -7.46719400 5.92675800
C -0.83225700 -8.95529900 4.88606100

H -1.32957800 -6.97522500 4.21681800
C 4.18201100 -4.00595900 5.19921300
C 0.15494600 -9.75969200 5.46405100
H 2.14482700 -9.86572500 6.29387200
H -1.79206800 -9.38271500 4.62174300
H 5.12181500 -4.55818000 5.23441400
H 3.92154100 -3.64110400 6.19276800
C 4.33459500 -2.83141000 4.25200100
C -0.09915900 -11.23517200 5.64462100
F 4.71504100 -3.22785300 3.01929400
F 3.19001800 -2.13361200 4.11816900
F 5.28112400 -1.99445500 4.72401300
F -1.41024100 -11.50371400 5.80828400
F 0.55742400 -11.72907900 6.71440100
F 0.31999100 -11.93031000 4.56337000

$Rh_2(AcO)_4$–(Car)–DCC (10b)
[B3LYP-D3(BJ)]/BS1
Rh -1.16440300 -2.26969100 2.64745200
Rh 0.25110300 -3.82654300 3.91041800
O -2.70386200 -2.76934100 3.94605700
C -2.50928600 -3.64408700 4.84079900
O -1.41017700 -4.25991700 5.06557900
C -3.66617900 -4.01663800 5.73503600
H -3.38336300 -3.86658400 6.78027000
H -4.54399400 -3.41710900 5.49610800
H -3.89605700 -5.07785000 5.60339700
H 2.43080000 -1.56190000 -0.08230800
C 2.69050600 -2.29058500 0.68509600
C 1.53997300 -2.49886600 1.63602400
H 3.56470900 -1.95681400 1.24705200
H 2.93902900 -3.25326300 0.22748100
O 1.76239300 -3.30396100 2.60130500
O 0.45150700 -1.88643800 1.41249800
O 0.70837400 -2.23900400 5.16042400
C 0.24175400 -1.07690000 4.90397800
O -0.53958700 -0.78245400 3.95186100
C 0.69516400 0.03136400 5.82130200
H 1.72658300 0.28916200 5.56518700
H 0.06241300 0.91075500 5.70308400
H 0.68225400 -0.31228600 6.85758000
O -1.69341100 -3.84890000 1.42038600
C -1.17642900 -4.98632600 1.63002700
O -0.33703000 -5.26947000 2.55332500
C -1.56340400 -6.12863600 0.72886300
H -2.19866900 -5.78094300 -0.08532200
H -0.65120000 -6.59485700 0.34914300
H -2.09549500 -6.88321500 1.31627000
C 1.48965500 -5.02744100 4.95166400
C 1.50695700 -6.44632000 5.08487900
C 2.49287600 -4.23732000 5.69582900
C 2.60992800 -7.11261300 5.69160900
C 0.44021900 -7.22780100 4.57107500
O 2.38995300 -4.04404100 6.89203100
O 3.43533700 -3.69632100 4.90223000
C 2.66406100 -8.49290000 5.73377500
H 3.42603100 -6.53358000 6.10723500
C 0.49345400 -8.61354600 4.62691700
H -0.40359900 -6.72863200 4.11844500
C 4.21527100 -2.63239800 5.44747600
C 1.60756700 -9.23920100 5.19114000
H 3.51460900 -8.99570700 6.17932800
H -0.31848400 -9.20951600 4.22974900
H 5.21000500 -2.99667500 5.71137000
H 3.73015300 -2.20778200 6.32638000
C 4.35175800 -1.56880000 4.37591500
C 1.71980600 -10.74256500 5.20414800
F 4.91852500 -2.05540800 3.24907500
F 3.16811700 -1.03248000 4.02102400
F 5.13613900 -0.57469400 4.83490600
F 0.58668900 -11.34746800 4.79570400
F 2.01194800 -11.20444400 6.43657300
F 2.71555700 -11.15203700 4.38247300
N 1.63190900 -7.44803900 0.77165900
C 2.58281100 -6.67295400 0.79566000
C 1.68250200 -8.88128200 0.43877300
N 3.43592600 -5.79293400 0.75663400
C 2.68630000 -9.62411800 1.33281400
C 0.27624600 -9.47015300 0.58421700
H 2.00040200 -8.98647000 -0.60865500
C 4.37505500 -5.46672700 1.84854700
C 2.66996000 -11.13622000 1.07633100
H 2.42946000 -9.42372900 2.37908800
H 3.69046800 -9.21838900 1.16815500
C 0.26612500 -10.97867000 0.31064600
H -0.07133100 -9.27325700 1.60685100
H -0.41066100 -8.94909000 -0.09074200
C 4.58863400 -6.64845900 2.80138300
C 5.70577300 -5.01440300 1.23695700
H 3.93475700 -4.63065900 2.40476500
C 1.25730800 -11.71684000 1.21886900
H 3.35823600 -11.63124000 1.76948200
H 3.04246200 -11.33613800 0.06236700
H -0.74703800 -11.37308300 0.44619300
H 0.53449800 -11.15813300 -0.73978400
C 5.60872600 -6.31504900 3.89521800
H 4.95153800 -7.50350300 2.21552200
H 3.63156700 -6.94740000 3.23819400
C 6.74589000 -4.69663600 2.32091600
H 6.07827900 -5.82047600 0.59059500
H 5.53564300 -4.14299500 0.59514600
H 1.26358400 -12.78744800 0.98428700

H 0.93217500 -11.62358400 2.26213400
C 6.94449200 -5.87680800 3.28146900
H 5.74967300 -7.18316900 4.54943400
H 5.21415600 -5.50506700 4.52092500
H 7.69710700 -4.42398200 1.85000600
H 6.41448400 -3.82215900 2.89112900
H 7.65631900 -5.60749600 4.07022100
H 7.38276200 -6.72269000 2.73391500

DCC–$Rh_2(AcO)_4$–(Car)–DCC
[B3LYP-D3(BJ)]/BS1

C -2.22443000 -1.62200200 -0.37960000
N -1.95868100 -2.19821200 -1.42181600
N -2.59456300 -1.15714500 0.70301200
C -2.79345000 0.28856900 0.94450400
C -3.56941000 0.47580400 2.25043800
C -1.44047000 1.01460800 0.99307100
H -3.38718400 0.70172800 0.11661500
C -3.75031000 1.96366000 2.57778800
H -3.00714000 -0.01501800 3.05197800
H -4.53986600 -0.02753200 2.17331900
C -1.62172800 2.50183300 1.32316500
H -0.82451700 0.53291600 1.75923400
H -0.92815700 0.88945800 0.03161700
C -2.39943300 2.68960400 2.63244700
H -4.28240200 2.07102700 3.52962100
H -4.38136600 2.43419700 1.81074000
H -0.64197900 2.98900100 1.38487700
H -2.16704900 2.99476500 0.50623300
H -2.54790200 3.75604400 2.83736200
H -1.80681200 2.28526000 3.46456900
C -0.59828900 -2.49465800 -1.91403100
C -0.28730800 -3.97958400 -1.68777000
C -0.50475100 -2.12690600 -3.39749000
H 0.12748800 -1.90047200 -1.34640900
C 1.08129800 -4.35651400 -2.26906000
H -1.07433500 -4.57635500 -2.16780500
H -0.32804900 -4.18908100 -0.61836700
C 0.87042100 -2.49751600 -3.96918100
H -1.29202400 -2.66768900 -3.93901300
H -0.70371800 -1.05694900 -3.52469700
C 1.18364800 -3.98441200 -3.75322000
H 1.26054800 -5.42597700 -2.11740800
H 1.86774600 -3.83170800 -1.71175000
H 0.90899600 -2.24630900 -5.03500200
H 1.64257300 -1.89109400 -3.47549500
H 2.18208300 -4.22193900 -4.13811800
H 0.46970300 -4.58989700 -4.32884300
Rh -1.38277600 -2.58638900 2.44738500
Rh 0.01547600 -4.03499700 3.85582700
O -2.95970400 -3.02865100 3.72796200
C -2.77272500 -3.81685100 4.70059300
O -1.66776600 -4.38351900 5.00804800
C -3.94134600 -4.11076400 5.60935800
H -3.80222800 -3.57009000 6.55098000
H -4.87510300 -3.79073900 5.14737600
H -3.97637200 -5.17772400 5.83935500
H 2.30738700 -1.76417700 -0.08382800
C 2.58627300 -2.41466300 0.74459900
C 1.37729800 -2.75758000 1.57701800
H 3.32020300 -1.91493300 1.37987100
H 3.04582200 -3.33295900 0.37129700
O 1.56346100 -3.56816700 2.54325900
O 0.27275700 -2.21496500 1.26797700
O 0.45338600 -2.36067600 4.99214500
C -0.03323500 -1.22807100 4.65871100
O -0.80989400 -1.01113300 3.68229600
C 0.37770900 -0.05270200 5.51089000
H 1.44487000 0.13003300 5.36081800
H -0.18991300 0.83636100 5.23692300
H 0.22450700 -0.28888500 6.56660600
O -1.86738900 -4.26047700 1.33985100
C -1.37268900 -5.38429100 1.65672000
O -0.56702100 -5.60223500 2.62183800
C -1.73901100 -6.56336200 0.79306600
H -2.63990500 -6.34794200 0.21884600
H -0.90751000 -6.74231300 0.10584200
H -1.87673300 -7.45766300 1.40275900
C 1.26257700 -5.18588100 4.97504000
C 1.26042800 -6.60392300 5.13161600
C 2.27257300 -4.39057300 5.68663300
C 2.43555000 -7.30269600 5.52155600
C 0.08545000 -7.34537100 4.85324000
O 2.14305100 -4.15118500 6.87434400
O 3.24311200 -3.88139100 4.90098800
C 2.45347900 -8.68481600 5.55516200
H 3.33489100 -6.74825700 5.76237000
C 0.09448200 -8.73122500 4.93615200
H -0.81412000 -6.81381700 4.57802500
C 4.02781500 -2.82481000 5.45457400
C 1.28130000 -9.39436200 5.25538700
H 3.36230200 -9.21616200 5.81425400
H -0.80337600 -9.29875700 4.72648500
H 5.01666900 -3.19914900 5.72688900
H 3.53970200 -2.39981400 6.33149800
C 4.18517800 -1.75410000 4.39394000
C 1.34193000 -10.89963600 5.27943200
F 4.80381900 -2.22298000 3.28563900
F 3.00531500 -1.23884300 3.99762900
F 4.93435900 -0.74851200 4.88536900
F 1.67095000 -11.36078500 6.50385900
F 2.28446300 -11.35421400 4.42026600

F 0.17065000 -11.46861300 4.92920300
N 1.72963400 -6.76379000 0.40620400
C 2.81855400 -6.22830600 0.58084200
C 1.51178900 -8.21374100 0.28740000
N 3.86699400 -5.59351400 0.64334100
C 2.72246800 -8.98071000 -0.25621000
C 1.08114000 -8.77477100 1.64934300
H 0.67544100 -8.34037600 -0.41174200
C 4.63006100 -5.35341900 1.88478600
C 2.42539500 -10.48469500 -0.34617100
H 3.57324900 -8.81389500 0.41849500
H 3.00638200 -8.58106900 -1.23620900
C 0.75215800 -10.26732400 1.53959000
H 1.90691600 -8.62795100 2.35823300
H 0.23579600 -8.20014000 2.03177400
C 4.66275200 -6.60556600 2.77181900
C 6.04485000 -4.90733700 1.50308000
H 4.13091300 -4.54668200 2.43299900
C 1.95447300 -11.05236600 1.00026800
H 3.31611500 -11.01743900 -0.69728700
H 1.64331900 -10.65136200 -1.09953200
H 0.44299400 -10.66129200 2.51142100
H -0.10424300 -10.39887200 0.86378200
C 5.55060400 -6.40513700 4.00546800
H 5.04711600 -7.44347100 2.17458100
H 3.64134300 -6.86669200 3.06878200
C 6.93754100 -4.71746800 2.73651500
H 6.47903300 -5.67379700 0.84726500
H 5.98773900 -3.98249700 0.91835100
H 1.70247900 -12.11367800 0.89498400
H 2.77189700 -10.99221900 1.73111800
C 6.96924400 -5.98006900 3.60699200
H 5.57758300 -7.32718500 4.59770500
H 5.10893400 -5.62881500 4.64248700
H 7.95093800 -4.44571500 2.42049200
H 6.55777700 -3.87798100 3.32992600
H 7.57969600 -5.81060900 4.50130400
H 7.44607800 -6.79625500 3.04692400

DCC: [B3LYP-D3(BJ)]/BS2

C -0.92921600 0.52046700 0.76490600
N -0.05880800 1.10403600 0.14447200
N -1.80000400 0.05204200 1.47579500
C -3.02222800 -0.60555200 0.98660100
C -2.95054500 -2.10497000 1.27760900
C -4.24071100 0.02595600 1.65795200
H -3.10614100 -0.46439200 -0.09591000
C -4.24048000 -2.81307800 0.85977300
H -2.78209600 -2.23915500 2.34981600
H -2.08975000 -2.53332300 0.76142100
C -5.53190300 -0.67931200 1.23942700
H -4.11102400 -0.04648000 2.74147600
H -4.28271600 1.08777400 1.41031900
C -5.46531000 -2.18087900 1.52282300
H -4.17589500 -3.87344700 1.10950900
H -4.34915200 -2.75369400 -0.22763700
H -6.38118600 -0.23059000 1.75731100
H -5.69950000 -0.52197500 0.16934200
H -6.37703200 -2.67151200 1.17714000
H -5.41102000 -2.34034900 2.60425500
C 1.16731700 0.47858500 -0.37583900
C 1.06751000 0.33632600 -1.89518900
C 2.37471000 1.32783100 0.01723900
H 1.28290100 -0.51896800 0.06048000
C 2.35920100 -0.23257100 -2.48504000
H 0.86669000 1.32375000 -2.32026300
H 0.21612300 -0.29941300 -2.14404800
C 3.66770700 0.75920000 -0.56973000
H 2.21328200 2.34443000 -0.35233000
H 2.43809200 1.38851900 1.10482700
C 3.57319300 0.60936800 -2.08895100
H 2.27324400 -0.29110100 -3.57137300
H 2.49939300 -1.25708500 -2.12654300
H 4.50785000 1.40178800 -0.30125400
H 3.86774700 -0.21982100 -0.12315200
H 4.48764700 0.16147600 -2.48216200
H 3.48633800 1.60134000 -2.54319900

$Rh_2(AcO)_4$: [B3LYP-D3(BJ)]/BS2

Rh 0.01298900 0.00303900 -1.18347300
O -1.42402500 1.46325300 -1.12717600
O 1.47216200 1.43910700 -1.10079500
O 1.44894400 -1.45684100 -1.10733100
O -1.44751200 -1.43412000 -1.13371700
Rh -0.01265200 -0.00346900 1.20166000
C -1.88147500 -1.83888300 -0.01294000
O -1.47157800 -1.43979000 1.11898500
C 1.83853200 -1.88226000 0.02220000
O 1.42461700 -1.46343400 1.14536700
C -1.83819500 1.88182900 -0.00401100
O -1.44886100 1.45616200 1.12551400
O 1.44759900 1.43394500 1.15190300
C 1.88180700 1.83845800 0.03112900
C 2.98904800 2.85314800 0.04798700
H 2.90165700 3.49511500 0.92047200
H 3.94108600 2.32307700 0.10863300
H 2.98106200 3.44288100 -0.86423900
C 2.85253800 -2.99022500 0.02968200
H 3.44585600 -2.95771200 0.93920000
H 2.32147100 -3.94316300 -0.00092800
H 3.49103200 -2.92741800 -0.84726900
C -2.85220300 2.98979300 -0.01147700

H -2.32114300 3.94272800 0.01937900
H -3.44537400 2.95743000 -0.92109600
H -3.49083800 2.92683800 0.86536100
C -2.98868100 -2.85361200 -0.02978400
H -3.94074300 -2.32356700 -0.09026600
H -2.90136700 -3.49548000 -0.90235000
H -2.98056900 -3.44344500 0.88237600

DCC–$Rh_2(AcO)_4$: [B3LYP-D3(BJ)]/BS2
C -2.18197200 -1.91036300 -0.25038100
N -2.13949200 -2.43468300 -1.33329600
N -2.27739100 -1.48789200 0.90404800
C -2.72566400 -0.10174200 1.19531200
C -3.48045600 -0.07567500 2.51946800
C -1.52721800 0.84789900 1.20390900
H -3.40774500 0.19922200 0.39510200
C -3.90871100 1.34952000 2.87236800
H -2.82841400 -0.47134500 3.29766800
H -4.34587100 -0.73640800 2.45761300
C -1.95996100 2.26997600 1.56536100
H -0.80435800 0.48144300 1.93253900
H -1.04612200 0.82852600 0.22408900
C -2.71155300 2.30095600 2.89717900
H -4.41637600 1.34959700 3.83834300
H -4.63624900 1.70669500 2.13649500
H -1.08430400 2.92008900 1.60491100
H -2.60894500 2.66549500 0.77759900
H -3.04046700 3.31737100 3.12132200
H -2.03161100 2.00223600 3.70081900
C -0.96352100 -2.51444700 -2.21886600
C -0.36340500 -3.91675200 -2.11378800
C -1.37293900 -2.18928000 -3.65146400
H -0.21730600 -1.78980600 -1.88335700
C 0.82513600 -4.06833500 -3.06366000
H -1.13846200 -4.64533600 -2.36603400
H -0.06948700 -4.10121300 -1.08235200
C -0.18579900 -2.34446000 -4.60415900
H -2.17760300 -2.86958000 -3.94346600
H -1.77475500 -1.17596500 -3.69733400
C 0.43441800 -3.73951600 -4.50536900
H 1.22061700 -5.08310600 -2.99573900
H 1.62872800 -3.39718800 -2.74598600
H -0.50705300 -2.14112400 -5.62680800
H 0.57329500 -1.59498400 -4.35971700
H 1.30544300 -3.81153800 -5.15906700
H -0.28892100 -4.48057300 -4.85937200
Rh -1.11192200 -2.82997500 2.29471500
Rh 0.23479100 -4.30878700 3.63678000
O -2.66196700 -3.18892200 3.59429100
C -2.48405600 -3.98302000 4.56697600
O -1.40402500 -4.58546600 4.84207800
C -3.66989100 -4.24849600 5.45283900
H -3.34626600 -4.56716100 6.43967900
H -4.29627900 -3.36290100 5.52281200
H -4.26268400 -5.04907800 5.00706800
H 2.61918900 -2.09889800 -0.20204700
C 2.73034800 -3.01808500 0.36574600
C 1.59535000 -3.18335000 1.33746500
H 3.68305200 -3.03320400 0.88896700
H 2.71274600 -3.85871500 -0.32993600
O 1.78572800 -3.93963800 2.33425800
O 0.51580900 -2.57189100 1.07106000
O 0.78423600 -2.68589300 4.76778000
C 0.32201500 -1.54586900 4.46834800
O -0.45894500 -1.29604400 3.50097400
C 0.70388500 -0.38587600 5.34545900
H 1.64407800 -0.58164500 5.85312800
H 0.76764800 0.52689700 4.75856100
H -0.07534500 -0.25059400 6.09751600
O -1.67735200 -4.46940100 1.19838600
C -1.18661700 -5.60545300 1.47679900
O -0.38426400 -5.84790800 2.42553300
C -1.57338200 -6.74699800 0.57888600
H -2.60756100 -6.64323800 0.26011400
H -0.94290500 -6.71310800 -0.31125700
H -1.42040500 -7.69881500 1.07909800

(Car)–$Rh_2(AcO)_4$: [B3LYP-D3(BJ)]/BS2
Rh -0.76496700 -2.23605500 2.01755700
Rh 0.21971000 -3.92488700 3.48717500
O -2.60254400 -2.75201900 2.78029000
C -2.67932500 -3.67377700 3.63657900
O -1.69478200 -4.32542600 4.11536700
C -4.03783800 -4.06632100 4.14468600
H -4.03655100 -4.06924300 5.23332300
H -4.79760500 -3.38679600 3.77164400
H -4.26048600 -5.08050200 3.81199400
H 3.42711800 -1.56056100 0.40237400
C 3.48058700 -2.08613200 1.35112500
C 2.10310500 -2.45157700 1.82670900
H 3.94065100 -1.43443500 2.09438600
H 4.09862500 -2.97602700 1.26384900
O 2.03362600 -3.36673400 2.70677300
O 1.12346600 -1.82024300 1.33988600
O 0.38009600 -2.44479600 4.89436200
C 0.02427700 -1.25534300 4.61711000
O -0.49597900 -0.87518600 3.53189000
C 0.27216100 -0.22885000 5.68614400
H 1.34597700 -0.05047800 5.75413300
H -0.23322100 0.70215400 5.44886500
H -0.06159800 -0.60773200 6.64996800
O -0.96030900 -3.70273100 0.58939000

C -0.54702600 -4.86745100 0.83934900
O -0.00612900 -5.24608200 1.92892100
C -0.69082600 -5.92047800 -0.22317600
H -1.18445400 -5.51585400 -1.10101400
H 0.29597800 -6.29513400 -0.49375300
H -1.26309500 -6.75836000 0.17339700
C 1.00190100 -5.29211500 4.71459300
C 0.63668600 -6.66335600 4.85600700
C 2.01083000 -4.76871300 5.65221700
C 1.37971800 -7.53404200 5.69079500
C -0.47276700 -7.18989800 4.15848900
O 1.71528000 -4.40390700 6.76530200
O 3.24769300 -4.71256000 5.11934200
C 1.03949600 -8.86311500 5.80849400
H 2.22949500 -7.15859800 6.24106000
C -0.81836700 -8.52105500 4.28798900
H -1.05608600 -6.54000700 3.53248300
C 4.27313000 -4.10921800 5.90800100
C -0.06262800 -9.35350300 5.10693700
H 1.61468600 -9.51818900 6.44529100
H -1.67310800 -8.91226800 3.75847300
H 5.13117100 -4.77523500 5.90899400
H 3.92956300 -3.92800800 6.92216900
C 4.67818300 -2.79057900 5.28051200
C -0.40013300 -10.81772200 5.21822900
F 5.18111200 -2.94927400 4.04308700
F 3.64792300 -1.93256100 5.18916700
F 5.63257400 -2.20953400 6.03376800
F -1.65900000 -11.08661900 4.83169100
F -0.26269900 -11.26848800 6.48038700
F 0.41995800 -11.56376600 4.44510100

DCC–$Rh_2(AcO)_4$–(Car)
[B3LYP-D3(BJ)]/BS2
C -2.26621300 -1.59805700 -0.44964200
N -2.08427600 -2.10397500 -1.53474500
N -2.52586500 -1.20822600 0.68183100
C -2.83786000 0.19293900 1.02974700
C -3.65263000 0.21673900 2.31930400
C -1.54765600 1.00425200 1.16731100
H -3.43949200 0.62204500 0.22252000
C -3.94433500 1.65060100 2.76230600
H -3.08386500 -0.30315900 3.09132400
H -4.57942100 -0.34004600 2.17235800
C -1.84176700 2.43700600 1.61496300
H -0.91052700 0.50826800 1.90004800
H -1.01647900 0.99948400 0.21336700
C -2.65492200 2.45966900 2.91043900
H -4.49762600 1.63915200 3.70295500
H -4.59089400 2.13747600 2.02510000
H -0.90426200 2.98108000 1.74300600
H -2.40140500 2.95703600 0.83095200
H -2.88374200 3.48854400 3.19466400
H -2.05409300 2.03285500 3.71928400
C -0.77437800 -2.29285400 -2.18233700
C -0.38132600 -3.76771600 -2.09648000
C -0.84777900 -1.82051700 -3.63160100
H -0.02341400 -1.70343500 -1.65002600
C 0.93418600 -4.03021300 -2.83056100
H -1.18181000 -4.36526600 -2.54153800
H -0.30888800 -4.05353100 -1.04926200
C 0.47013400 -2.08188000 -4.36290400
H -1.66166800 -2.35661500 -4.12788100
H -1.09991300 -0.75911100 -3.65736900
C 0.87088800 -3.55606000 -4.28304100
H 1.17333300 -5.09415400 -2.78497500
H 1.74538200 -3.50624300 -2.31726400
H 0.38297800 -1.76556000 -5.40363300
H 1.25942300 -1.47006800 -3.91493900
H 1.83289300 -3.71274600 -4.77454000
H 0.13621000 -4.15816900 -4.82681000
Rh -1.36338100 -2.76656700 2.26581500
Rh -0.07765800 -4.34453800 3.63058700
O -2.98080600 -3.14716500 3.47836100
C -2.86316900 -3.97853000 4.41824800
O -1.80558000 -4.62395300 4.70996200
C -4.05782800 -4.23521700 5.29397600
H -3.87291100 -3.80209000 6.27758500
H -4.94966700 -3.78784100 4.86623600
H -4.19737400 -5.30653000 5.42562600
H 2.38386800 -2.13710800 -0.19747100
C 2.59875200 -2.85488700 0.58765000
C 1.38017300 -3.09146800 1.43483500
H 3.41020900 -2.49202600 1.21545500
H 2.92024400 -3.79808200 0.14721800
O 1.51172700 -3.90907100 2.39788000
O 0.32176200 -2.47264500 1.13435800
O 0.41123100 -2.75069700 4.82355200
C 0.01487900 -1.58217400 4.52161100
O -0.73252500 -1.28585800 3.54928900
C 0.50641700 -0.46539400 5.39964400
H 1.55293800 -0.27179900 5.16028400
H -0.07120300 0.43809700 5.22927600
H 0.45434900 -0.76016300 6.44538300
O -1.90257800 -4.35778900 1.08096400
C -1.43440400 -5.50255000 1.32556300
O -0.66195800 -5.79614600 2.29239800
C -1.78387900 -6.61915200 0.38220500
H -2.71266400 -6.40131100 -0.13698700
H -0.98615100 -6.70532500 -0.35762800
H -1.85346000 -7.56290300 0.91691100
C 0.97463700 -5.64922300 4.77129300

C 0.64896500 -7.00306300 5.08738200
C 2.16963500 -5.08923100 5.41302900
C 1.57326700 -7.84789900 5.74764400
C -0.61010500 -7.53634400 4.73384000
O 2.14152500 -4.63541200 6.53402900
O 3.25819100 -5.09937900 4.61141200
C 1.26229000 -9.16206600 6.02201600
H 2.54143000 -7.46556600 6.03535600
C -0.92626400 -8.84868400 5.02596000
H -1.32875600 -6.90192900 4.24756200
C 4.44651800 -4.49492900 5.11764100
C 0.00921100 -9.65841500 5.66334900
H 1.97677000 -9.79882500 6.52108000
H -1.89581600 -9.24357800 4.76375600
H 5.27301600 -5.17319100 4.92639800
H 4.35885200 -4.29069700 6.18077600
C 4.70843000 -3.19271400 4.38842700
C -0.31294100 -11.10502800 5.93197100
F 4.88961700 -3.37706900 3.06718100
F 3.70344000 -2.31309100 4.53651700
F 5.82887300 -2.62287200 4.87384600
F -1.63508100 -11.31923200 6.05772700
F 0.27448900 -11.55411700 7.05728000
F 0.11950800 -11.89422300 4.92265600

$Rh_2(AcO)_4$–(Car)–DCC
[B3LYP-D3(BJ)]/BS2
Rh -0.80238600 -1.87842100 2.61418600
Rh 0.63736000 -3.45815600 3.79834600
O -2.40323400 -2.72662800 3.58272900
C -2.20858400 -3.69404600 4.36778200
O -1.07571700 -4.20080000 4.65484400
C -3.40085900 -4.33102700 5.02409800
H -3.22296600 -4.43497200 6.09280000
H -4.29572900 -3.74306500 4.84592500
H -3.53663900 -5.33164500 4.61240600
H 3.05406900 -0.04899600 1.01319000
C 3.21133200 -1.08965500 1.28324700
C 2.00241700 -1.63119600 1.99198400
H 4.09608200 -1.19940800 1.90108600
H 3.35804800 -1.66404800 0.36716600
O 2.20400000 -2.58219300 2.81151100
O 0.87972000 -1.12574000 1.71192300
O 0.78440300 -2.03352800 5.26730600
C 0.20236200 -0.90979500 5.13829400
O -0.53715600 -0.56960400 4.17388200
C 0.44894300 0.09337700 6.22945300
H 1.39054400 0.60293800 6.02009200
H -0.34878000 0.83002900 6.25630300
H 0.54351800 -0.40624600 7.19005900
O -0.97954800 -3.27052500 1.12348100
C -0.37965400 -4.37609400 1.22600800
O 0.36312600 -4.72613500 2.20028800
C -0.52771000 -5.35667200 0.09938400
H 0.29967700 -5.20316700 -0.59490800
H -0.46138500 -6.37721400 0.46393700
H -1.46328500 -5.18599700 -0.42497800
C 1.79015600 -4.70712000 4.85075100
C 1.71479600 -6.12851500 4.95884800
C 2.73650400 -4.02828700 5.75787200
C 2.65675600 -6.85708000 5.72788300
C 0.69615100 -6.84546700 4.29667200
O 2.48846400 -3.85996800 6.92804200
O 3.84759800 -3.59834200 5.13057000
C 2.57896600 -8.22634100 5.82840500
H 3.44799400 -6.33845000 6.24656800
C 0.61247000 -8.22074000 4.41046400
H -0.02095700 -6.30971400 3.70197100
C 4.81439500 -2.89340100 5.90693500
C 1.54643300 -8.90567100 5.17763500
H 3.30256600 -8.77016100 6.41741200
H -0.17448400 -8.75605800 3.90492000
H 5.77884200 -3.37185300 5.75903500
H 4.54476300 -2.89275000 6.95879500
C 4.90170100 -1.46295100 5.41655800
C 1.47214900 -10.40084100 5.34318000
F 5.26399800 -1.39165300 4.12185100
F 3.73524000 -0.80778700 5.54365500
F 5.82749100 -0.79963500 6.13381600
F 0.38701700 -10.93787400 4.76123200
F 1.44052200 -10.74820200 6.64555200
F 2.55510000 -11.00875200 4.80664400
N 1.05185800 -8.48653800 0.89605800
C 1.89060300 -7.60363100 0.82350500
C 1.28910100 -9.91474600 0.64051800
N 2.60598200 -6.63879800 0.65314000
C 2.60762000 -10.40011300 1.24547100
C 0.10519400 -10.72209400 1.16406900
H 1.33822300 -10.04722100 -0.44595600
C 3.47118100 -5.95718100 1.61822600
C 2.80696500 -11.90033100 1.02358100
H 2.59960700 -10.18162900 2.31559800
H 3.43625200 -9.83741800 0.81200800
C 0.30575500 -12.21995200 0.93091000
H -0.00095800 -10.52967000 2.23326600
H -0.80901600 -10.37025400 0.68399600
C 4.35709100 -6.94773700 2.37638400
C 4.30587300 -4.90961800 0.88897300
H 2.82191400 -5.43984600 2.32718700
C 1.61808900 -12.70854800 1.54656600
H 3.73040800 -12.22382500 1.50709800
H 2.92993800 -12.09257500 -0.04675300

H	-0.53836800	-12.77475900	1.34379900
H	0.31600300	-12.42044600	-0.14515800
C	5.32348400	-6.23399000	3.32245800
H	4.92097600	-7.53335600	1.64464700
H	3.72875700	-7.64909800	2.92877200
C	5.24459700	-4.18688600	1.85315900
H	4.88092100	-5.40895800	0.10325500
H	3.63680000	-4.20203200	0.39757700
H	1.76238800	-13.76948600	1.33418000
H	1.56498500	-12.60753600	2.63395800
C	6.14972300	-5.17431700	2.59106200
H	5.97448800	-6.96678100	3.80275000
H	4.75736100	-5.74744600	4.11704500
H	5.84346700	-3.45422600	1.30930800
H	4.64500600	-3.63449000	2.57758300
H	6.78880300	-4.64296200	3.29940500
H	6.81507100	-5.66570300	1.87391000

Pyridine:
[B3LYP-D3(BJ)]/BS1

C	-4.32909200	-1.34628600	0.00002700
C	-2.93353500	-1.35010300	-0.00007000
C	-2.26547700	-0.12588900	-0.00028100
C	-3.02094200	1.04638700	-0.00040400
C	-4.41250800	0.94100100	-0.00031700
N	-5.07022600	-0.22814800	-0.00009000
H	-1.18057100	-0.08629300	-0.00035200
H	-4.87796200	-2.28605800	0.00018500
H	-2.38991100	-2.28883900	0.00004000
H	-2.54727300	2.02228800	-0.00054900
H	-5.02848100	1.83821300	-0.00037700

Pyridine-$Rh_2(AcO)_4$:
[B3LYP-D3(BJ)]/BS1

O	-0.68111300	-1.09080200	2.21745100
O	-2.86624700	-1.07104500	0.29699600
O	-0.94495700	-1.03394300	-1.88724700
O	1.23989100	-1.05432900	0.03737600
O	-2.85542600	-3.32609400	0.25463200
O	-0.94234300	-3.28968500	-1.91472300
O	1.24332500	-3.30958500	0.01118000
O	-0.67118600	-3.34658100	2.18266500
C	-0.62436800	-2.22461100	2.77582500
C	1.81823800	-2.17697600	-0.02274800
C	-0.99584900	-2.15186800	-2.47667200
C	-3.43738900	-2.19871000	0.32438100
C	3.31431400	-2.18376400	-0.17527900
H	3.55342500	-2.28637900	-1.23522300
H	3.74010700	-1.25261800	0.18732800
H	3.74545100	-3.03192400	0.35063300
C	-1.16185100	-2.14344000	-3.97150600
H	-0.81157100	-1.20420400	-4.38990000
H	-0.63268500	-2.98186800	-4.41732800
H	-2.22313600	-2.25224200	-4.20195600
C	-4.93300000	-2.22073600	0.47999300
H	-5.36467000	-1.27352200	0.17007700
H	-5.36097300	-3.04103600	-0.09103200
H	-5.16880500	-2.38434300	1.53296000
C	-0.46006600	-2.25749700	4.27056700
H	-1.00371000	-3.09886500	4.69315200
H	0.59870700	-2.39117300	4.49927400
H	-0.79584500	-1.32445300	4.71370900
Rh	-0.80568000	-3.39100800	0.13169800
N	-0.79768400	-5.54226800	0.08949600
C	0.24206400	-6.22593500	0.58073900
C	-1.82790100	-6.20976800	-0.44247600
C	0.28853500	-7.60986100	0.55676300
H	1.04810300	-5.63491700	0.98935200
C	-1.85416500	-7.59305200	-0.50332400
C	-0.77745900	-8.30748000	0.00468000
H	1.14687300	-8.12364100	0.96307100
H	-2.70483200	-8.09340900	-0.94130500
H	-0.76915500	-9.38758700	-0.02917500
H	-2.64209100	-5.60665600	-0.81572900
Rh	-0.81384000	-0.97380000	0.16786200

Pyridine–$Rh_2(AcO)_4$–(Car) (9a):
[B3LYP-D3(BJ)]/BS1

Rh	-0.76351600	-2.24855500	2.05525800
Rh	0.25316500	-3.94524500	3.51075200
O	-2.60157100	-2.83016200	2.77967400
C	-2.66353000	-3.77136700	3.61759200
O	-1.67038700	-4.40436100	4.09389000
C	-4.02027700	-4.20013200	4.10475000
H	-4.05802800	-4.11980000	5.19043100
H	-4.79997900	-3.58935600	3.66063500
H	-4.17918100	-5.24689700	3.84661500
H	3.43914500	-1.34598000	0.57187600
C	3.49516500	-1.95935300	1.46604800
C	2.12033500	-2.37780700	1.90884100
H	3.95898100	-1.38522500	2.26847900
H	4.11406100	-2.83622400	1.28976300
O	2.06150400	-3.31523100	2.76133700
O	1.13045900	-1.76340100	1.41983800
O	0.34252100	-2.47464300	4.94211400
C	-0.04571100	-1.29493100	4.68665900
O	-0.56273300	-0.90700900	3.60020200
C	0.15331200	-0.27611500	5.77449100
H	1.21086400	-0.01076200	5.81058500
H	-0.43106500	0.61737200	5.57664700

H	-0.11520200	-0.70155700	6.73885700
O	-0.89609400	-3.68872100	0.59269600
C	-0.46032500	-4.85085300	0.82590300
O	0.07826500	-5.23518400	1.90964000
C	-0.60059500	-5.88687000	-0.25493500
H	-0.86270400	-5.42342800	-1.20109100
H	0.32497500	-6.45053300	-0.35192100
H	-1.38688300	-6.58654300	0.03164900
C	1.06603000	-5.35570400	4.76792800
C	0.70743700	-6.73235300	4.90124500
C	2.05134200	-4.83464800	5.71477500
C	1.40652300	-7.60326700	5.77193600
C	-0.36186600	-7.26091300	4.14603800
O	1.74937400	-4.44888600	6.82229500
O	3.30345300	-4.78573900	5.19863000
C	1.06214200	-8.93345900	5.87143500
H	2.22358900	-7.22451400	6.36794300
C	-0.71240800	-8.59328000	4.25401300
H	-0.90577500	-6.60891400	3.48668100
C	4.32429200	-4.22077100	6.01656500
C	-0.00069000	-9.42500900	5.11221100
H	1.60275400	-9.58872900	6.53789300
H	-1.53571800	-8.98636700	3.67788200
H	5.19260500	-4.87102300	5.96013600
H	3.99062700	-4.11883800	7.04537100
C	4.71087400	-2.85308400	5.49079300
C	-0.34175300	-10.88889400	5.20489000
F	5.16859100	-2.90350400	4.22678000
F	3.68307300	-1.98682800	5.51119600
F	5.69426900	-2.33902200	6.25688700
F	-1.57569000	-11.16114900	4.74557400
F	-0.27841300	-11.33967100	6.47353900
F	0.52285900	-11.63661600	4.48239400
N	-1.68854300	-0.64521500	0.67230100
C	-1.76767100	0.62858400	1.06870300
C	-2.10583600	-0.96452600	-0.55645700
C	-2.26613500	1.63228500	0.25189800
H	-1.41700000	0.83396300	2.07072300
C	-2.61770600	-0.02293700	-1.43636200
H	-2.01747700	-2.00695800	-0.82966500
C	-2.69902700	1.30090700	-1.02518600
H	-2.31055600	2.64911400	0.61347200
H	-2.94251800	-0.32584300	-2.42098000
H	-3.09169400	2.05964000	-1.68746000

$Rh_2(AcO)_4$–(Car)(Pyridine) (10a): [B3LYP-D3(BJ)]/BS1

Rh	-1.47443100	-2.42108700	2.45856000
Rh	-0.10556500	-3.94797000	3.76477300
O	-3.11881000	-3.18418300	3.42234600
C	-2.95295800	-4.06876400	4.31357000
O	-1.84221800	-4.56540900	4.66860600
C	-4.17221700	-4.56589000	5.04120400
H	-4.26101300	-4.02001500	5.98204000
H	-5.06866000	-4.39233400	4.45289500
H	-4.06540600	-5.62247800	5.27468500
H	2.38128800	-0.98572400	0.51315900
C	2.61707400	-1.70489900	1.29131500
C	1.36358400	-2.24630700	1.92115800
H	3.21937800	-1.22650800	2.06358800
H	3.20248100	-2.52536100	0.87850900
O	1.52069000	-3.17483700	2.77161700
O	0.25648400	-1.74256100	1.57421500
O	0.05822800	-2.42966800	5.14497000
C	-0.51394500	-1.31744500	4.94233700
O	-1.23319800	-1.02676200	3.94234600
C	-0.29152400	-0.24693000	5.97525800
H	0.66893100	0.23077300	5.77627700
H	-1.07309200	0.50533600	5.92270900
H	-0.25093200	-0.68424000	6.97002200
O	-1.64654900	-3.89822600	1.03824600
C	-1.10877300	-5.02113900	1.24563100
O	-0.42519100	-5.33655400	2.27133900
C	-1.27567600	-6.09253000	0.20412500
H	-1.90161200	-5.74517100	-0.61175000
H	-0.29574500	-6.37727000	-0.17884900
H	-1.71811900	-6.97609700	0.66264100
C	1.26439100	-5.47320900	4.93446800
C	0.44161600	-6.67998200	5.17394400
C	1.56906300	-4.56241000	6.04396500
C	0.59542400	-7.83068600	4.38579900
C	-0.56052600	-6.70608700	6.15982300
O	0.98612400	-4.46305700	7.10262700
O	2.61714500	-3.73777700	5.72932700
C	-0.20505800	-8.94723200	4.56485100
H	1.34408800	-7.87413000	3.61135400
C	-1.35404600	-7.82142700	6.34406200
H	-0.71582000	-5.84064100	6.77531700
C	2.86705200	-2.68103000	6.63622200
C	-1.18497400	-8.95204900	5.54835500
H	-0.05739500	-9.81458700	3.93873900
H	-2.11311300	-7.81062700	7.11330100
H	3.44797000	-3.02158100	7.49310600
H	1.93878500	-2.23280000	6.97777400
C	3.67448100	-1.64206200	5.89308000
C	-2.09257100	-10.12472500	5.72150400
F	4.81793500	-2.14653800	5.38842000
F	2.99878200	-1.09339100	4.86663900
F	4.00917600	-0.64232700	6.73413100
F	-2.38167200	-10.36698000	7.02104900
F	-1.57706200	-11.26545700	5.21542800
F	-3.29048300	-9.94401000	5.10261000

N	2.49783000	-5.80370900	4.16947300
C	3.59256600	-6.19985900	4.85843100
C	2.52120200	-5.78328100	2.82536300
C	4.76042200	-6.53144700	4.21606400
H	3.49214400	-6.24043100	5.92935500
C	3.66601400	-6.11980600	2.13163400
H	1.60337300	-5.51622100	2.33851600
C	4.80696600	-6.48375700	2.82709000
H	5.61539800	-6.83104600	4.80125000
H	3.64604000	-6.09032400	1.05367200
H	5.71439400	-6.73997000	2.30037700

Pyridine:
[B3LYP-D3(BJ)]/BS2

C	-4.32909200	-1.34628600	0.00002700
C	-2.93353500	-1.35010300	-0.00007000
C	-2.26547700	-0.12588900	-0.00028100
C	-3.02094200	1.04638700	-0.00040400
C	-4.41250800	0.94100100	-0.00031700
N	-5.07022600	-0.22814800	-0.00009000
H	-1.18057100	-0.08629300	-0.00035200
H	-4.87796200	-2.28605800	0.00018500
H	-2.38991100	-2.28883900	0.00004000
H	-2.54727300	2.02228800	-0.00054900
H	-5.02848100	1.83821300	-0.00037700

Pyridine-$Rh_2(AcO)_4$:
[B3LYP-D3(BJ)]/BS2

O	-0.68111300	-1.09080200	2.21745100
O	-2.86624700	-1.07104500	0.29699600
O	-0.94495700	-1.03394300	-1.88724700
O	1.23989100	-1.05432900	0.03737600
O	-2.85542600	-3.32609400	0.25463200
O	-0.94234300	-3.28968500	-1.91472300
O	1.24332500	-3.30958500	0.01118000
O	-0.67118600	-3.34658100	2.18266500
C	-0.62436800	-2.22461100	2.77582500
C	1.81823800	-2.17697600	-0.02274800
C	-0.99584900	-2.15186800	-2.47667200
C	-3.43738900	-2.19871000	0.32438100
C	3.31431400	-2.18376400	-0.17527900
H	3.55342500	-2.28637900	-1.23522300
H	3.74010700	-1.25261800	0.18732800
H	3.74545100	-3.03192400	0.35063300
C	-1.16185100	-2.14344000	-3.97150600
H	-0.81157100	-1.20420400	-4.38990000
H	-0.63268500	-2.98186800	-4.41732800
H	-2.22313600	-2.25224200	-4.20195600
C	-4.93300000	-2.22073600	0.47999300
H	-5.36467000	-1.27352200	0.17007700
H	-5.36097300	-3.04103600	-0.09103200
H	-5.16880500	-2.38434300	1.53296000
C	-0.46006600	-2.25749700	4.27056700
H	-1.00371000	-3.09886500	4.69315200
H	0.59870700	-2.39117300	4.49927400
H	-0.79584500	-1.32445300	4.71370900
Rh	-0.80568000	-3.39100800	0.13169800
N	-0.79768400	-5.54226800	0.08949600
C	0.24206400	-6.22593500	0.58073900
C	-1.82790100	-6.20976800	-0.44247600
C	0.28853500	-7.60986100	0.55676300
H	1.04810300	-5.63491700	0.98935200
C	-1.85416500	-7.59305200	-0.50332400
C	-0.77745900	-8.30748000	0.00468000
H	1.14687300	-8.12364100	0.96307100
H	-2.70483200	-8.09340900	-0.94130500
H	-0.76915500	-9.38758700	-0.02917500
H	-2.64209100	-5.60665600	-0.81572900
Rh	-0.81384000	-0.97380000	0.16786200

Pyridine–$Rh_2(AcO)_4$–(Car):
[B3LYP-D3(BJ)]/BS2

Rh	-0.76351600	-2.24855500	2.05525800
Rh	0.25316500	-3.94524500	3.51075200
O	-2.60157100	-2.83016200	2.77967400
C	-2.66353000	-3.77136700	3.61759200
O	-1.67038700	-4.40436100	4.09389000
C	-4.02027700	-4.20013200	4.10475000
H	-4.05802800	-4.11980000	5.19043100
H	-4.79997900	-3.58935600	3.66063500
H	-4.17918100	-5.24689700	3.84661500
H	3.43914500	-1.34598000	0.57187600
C	3.49516500	-1.95935300	1.46604800
C	2.12033500	-2.37780700	1.90884100
H	3.95898100	-1.38522500	2.26847900
H	4.11406100	-2.83622400	1.28976300
O	2.06150400	-3.31523100	2.76133700
O	1.13045900	-1.76340100	1.41983800
O	0.34252100	-2.47464300	4.94211400
C	-0.04571100	-1.29493100	4.68665900
O	-0.56273300	-0.90700900	3.60020200
C	0.15331200	-0.27611500	5.77449100
H	1.21086400	-0.01076200	5.81058500
H	-0.43106500	0.61737200	5.57664700
H	-0.11520200	-0.70155700	6.73885700
O	-0.89609400	-3.68872100	0.59269600
C	-0.46032500	-4.85085300	0.82590300
O	0.07826500	-5.23518400	1.90964000
C	-0.60059500	-5.88687000	-0.25493500
H	-0.86270400	-5.42342800	-1.20109100

H	0.32497500	-6.45053300	-0.35192100
H	-1.38688300	-6.58654300	0.03164900
C	1.06603000	-5.35570400	4.76792800
C	0.70743700	-6.73235300	4.90124500
C	2.05134200	-4.83464800	5.71477500
C	1.40652300	-7.60326700	5.77193600
C	-0.36186600	-7.26091300	4.14603800
O	1.74937400	-4.44888600	6.82229500
O	3.30345300	-4.78573900	5.19863000
C	1.06214200	-8.93345900	5.87143500
H	2.22358900	-7.22451400	6.36794300
C	-0.71240800	-8.59328000	4.25401300
H	-0.90577500	-6.60891400	3.48668100
C	4.32429200	-4.22077100	6.01656500
C	-0.00069000	-9.42500900	5.11221100
H	1.60275400	-9.58872900	6.53789300
H	-1.53571800	-8.98636700	3.67788200
H	5.19260500	-4.87102300	5.96013600
H	3.99062700	-4.11883800	7.04537100
C	4.71087400	-2.85308400	5.49079300
C	-0.34175300	-10.88889400	5.20489000
F	5.16859100	-2.90350400	4.22678000
F	3.68307300	-1.98682800	5.51119600
F	5.69426900	-2.33902200	6.25688700
F	-1.57569000	-11.16114900	4.74557400
F	-0.27841300	-11.33967100	6.47353900
F	0.52285900	-11.63661600	4.48239400
N	-1.68854300	-0.64521500	0.67230100
C	-1.76767100	0.62858400	1.06870300
C	-2.10583600	-0.96452600	-0.55645700
C	-2.26613500	1.63228500	0.25189800
H	-1.41700000	0.83396300	2.07072300
C	-2.61770600	-0.02293700	-1.43636200
H	-2.01747700	-2.00695800	-0.82966500
C	-2.69902700	1.30090700	-1.02518600
H	-2.31055600	2.64911400	0.61347200
H	-2.94251800	-0.32584300	-2.42098000
H	-3.09169400	2.05964000	-1.68746000

$Rh_2(AcO)_4$–(Car)(Pyridine): [B3LYP-D3(BJ)]/BS2

Rh	-1.47443100	-2.42108700	2.45856000
Rh	-0.10556500	-3.94797000	3.76477300
O	-3.11881000	-3.18418300	3.42234600
C	-2.95295800	-4.06876400	4.31357000
O	-1.84221800	-4.56540900	4.66860600
C	-4.17221700	-4.56589000	5.04120400
H	-4.26101300	-4.02001500	5.98204000
H	-5.06866000	-4.39233400	4.45289500
H	-4.06540600	-5.62247800	5.27468500
H	2.38128800	-0.98572400	0.51315900
C	2.61707400	-1.70489900	1.29131500
C	1.36358400	-2.24630700	1.92115800
H	3.21937800	-1.22650800	2.06358800
H	3.20248100	-2.52536100	0.87850900
O	1.52069000	-3.17483700	2.77161700
O	0.25648400	-1.74256100	1.57421500
O	0.05822800	-2.42966800	5.14497000
C	-0.51394500	-1.31744500	4.94233700
O	-1.23319800	-1.02676200	3.94234600
C	-0.29152400	-0.24693000	5.97525800
H	0.66893100	0.23077300	5.77627700
H	-1.07309200	0.50533600	5.92270900
H	-0.25093200	-0.68424000	6.97002200
O	-1.64654900	-3.89822600	1.03824600
C	-1.10877300	-5.02113900	1.24563100
O	-0.42519100	-5.33655400	2.27133900
C	-1.27567600	-6.09253000	0.20412500
H	-1.90161200	-5.74517100	-0.61175000
H	-0.29574500	-6.37727000	-0.17884900
H	-1.71811900	-6.97609700	0.66264100
C	1.26439100	-5.47320900	4.93446800
C	0.44161600	-6.67998200	5.17394400
C	1.56906300	-4.56241000	6.04396500
C	0.59542400	-7.83068600	4.38579900
C	-0.56052600	-6.70608700	6.15982300
O	0.98612400	-4.46305700	7.10262700
O	2.61714500	-3.73777700	5.72932700
C	-0.20505800	-8.94723200	4.56485100
H	1.34408800	-7.87413000	3.61135400
C	-1.35404600	-7.82142700	6.34406200
H	-0.71582000	-5.84064100	6.77531700
C	2.86705200	-2.68103000	6.63622200
C	-1.18497400	-8.95204900	5.54835500
H	-0.05739500	-9.81458700	3.93873900
H	-2.11311300	-7.81062700	7.11330100
H	3.44797000	-3.02158100	7.49310600
H	1.93878500	-2.23280000	6.97777400
C	3.67448100	-1.64206200	5.89308000
C	-2.09257100	-10.12472500	5.72150400
F	4.81793500	-2.14653800	5.38842000
F	2.99878200	-1.09339100	4.86663900
F	4.00917600	-0.64232700	6.73413100
F	-2.38167200	-10.36698000	7.02104900
F	-1.57706200	-11.26545700	5.21542800
F	-3.29048300	-9.94401000	5.10261000
N	2.49783000	-5.80370900	4.16947300
C	3.59256600	-6.19985900	4.85843100
C	2.52120200	-5.78328100	2.82536300
C	4.76042200	-6.53144700	4.21606400
H	3.49214400	-6.24043100	5.92935500

C	3.66601400	-6.11980600	2.13163400
H	1.60337300	-5.51622100	2.33851600
C	4.80696600	-6.48375700	2.82709000
H	5.61539800	-6.83104600	4.80125000
H	3.64604000	-6.09032400	1.05367200
H	5.71439400	-6.73997000	2.30037700

Rh2(TPPTTL)4 (5) [B3LYP-D3(BJ)]/BS1

O	16.52499100	11.17319300	28.71252800
O	15.48732000	10.71308600	26.75633600
O	17.43025700	9.99241900	23.96298200
O	16.75518400	7.83392500	27.92687300
N	17.46357700	9.08758600	26.10409100
C	16.51138400	10.78227800	27.50873000
C	17.79620000	10.33074000	26.80351100
H	17.93068400	11.05623300	25.99414500
C	17.20482300	9.06669200	24.72083500
C	16.63131600	7.72096000	24.43048700
C	16.58662500	7.00125300	25.62957800
C	16.94034400	7.94351700	26.72823200
C	16.19277300	5.66632900	25.68169600
C	15.77789600	5.08123700	24.45470500
C	15.81074700	5.81073800	23.24321600
C	16.23733400	7.16490600	23.21969700
C	19.13267000	10.30867700	27.59940000
C	19.51281000	11.77557000	27.88335100
H	20.48665900	11.81176900	28.38232200
H	18.77519500	12.25248500	28.53179400
H	19.57946600	12.35693400	26.96093100
C	20.19805500	9.67351100	26.68715200
H	20.21710300	10.15014400	25.70490500
H	20.01372400	8.60473600	26.54461000
H	21.18811500	9.78966100	27.13889300
C	19.09333600	9.52816800	28.92483600
H	20.07326200	9.61171500	29.40776600
H	18.88044500	8.47006100	28.76805200
H	18.33980200	9.93099000	29.60239000
O	14.59411800	9.44903400	30.04409400
O	13.50343700	9.11512500	28.09162600
O	12.77304600	6.02839600	27.05679400
O	11.28422800	8.52892100	30.56462400
N	12.29040300	7.02957200	29.09980700
C	13.96589200	8.72986700	29.21330300
C	13.68580600	7.24759400	29.49076100
H	14.25492200	6.71579800	28.72035300
C	11.97485300	6.55447200	27.80848600
C	10.52343700	6.83282700	27.61041800
C	10.03329300	7.41640600	28.78268700
C	11.20702900	7.73986300	29.64032200
C	8.68071500	7.68548200	28.97260500
C	7.81556000	7.37711200	27.88924500
C	8.32363700	6.87377400	26.66938100

C	9.70377000	6.58448600	26.51399000
C	14.11565800	6.63012500	30.85280800
C	15.65609900	6.56187800	30.84665800
H	16.02715000	5.98953800	29.99301800
H	16.00515900	6.07557700	31.76336200
H	16.09328300	7.56142600	30.79888800
C	13.54688300	5.20112700	30.90795500
H	12.45644600	5.21040100	30.99220600
H	13.95049400	4.67712600	31.78011900
H	13.81697900	4.63069600	30.01666400
C	13.64831900	7.39486400	32.10343300
H	14.01711200	8.42128100	32.10402100
H	14.04233200	6.88606400	32.99012500
H	12.56125000	7.42365700	32.17920900
O	12.81997900	11.72683300	30.49351500
O	11.85932900	11.44132100	28.46611600
O	8.47373900	11.51687600	28.12863700
O	11.52136700	14.64830600	29.44231100
N	9.88313600	13.01537600	29.21578800
C	11.82696400	11.71529400	29.70884500
C	10.40904700	12.05503600	30.19086900
H	9.83118800	11.14556300	29.99448700
C	9.03981400	12.59324300	28.16718000
C	9.02907000	13.70663000	27.17450200
C	9.84951900	14.72942400	27.66071100
C	10.53388600	14.21419000	28.87773800
C	9.99633000	15.94807400	26.99975400
C	9.34512300	16.06591200	25.74435100
C	8.59684300	14.99573800	25.20800600
C	8.39547800	13.79940300	25.94001900
C	10.16867300	12.40940600	31.68392000
C	10.41186900	11.12186000	32.49628100
H	10.19531700	11.30810700	33.55309100
H	11.44946100	10.79211800	32.41103900
H	9.76923600	10.30677500	32.15341600
C	8.69186600	12.82143700	31.82263000
H	8.02791200	12.06371900	31.40033000
H	8.49465300	13.77097200	31.31673500
H	8.43928600	12.94132000	32.88081900
C	11.05195900	13.54024400	32.23741000
H	10.82854600	13.67017100	33.30208000
H	10.86144100	14.48722100	31.73070200
H	12.11165300	13.30547900	32.13186300
O	14.78014100	13.48881600	29.15887100
O	13.85486700	13.07213900	27.13757700
O	13.38591700	15.87729200	24.95624400
O	17.05568900	13.79843800	26.71057800
N	15.23379400	15.12480600	26.14776200
C	14.41916200	13.82628000	27.99379800
C	14.63835100	15.25549800	27.47860500
H	13.62999400	15.63304800	27.27785800

C	14.49171700	15.36751400	24.97826100
C	15.32778700	14.86201000	23.85018800
C	16.50592100	14.33176400	24.38577700
C	16.38361500	14.36679500	25.86899600
C	17.52232700	13.80691700	23.58664900
C	17.24807900	13.72368600	22.19604800
C	16.05243000	14.24617600	21.65553800
C	15.07155200	14.84940900	22.48441500
C	15.32370400	16.30044700	28.40315300
C	14.36130000	16.57664400	29.57475900
H	13.37899000	16.89570000	29.21808600
H	14.77034600	17.37177100	30.20639900
H	14.22563700	15.68439700	30.18855700
C	15.50442400	17.58847100	27.57818500
H	16.25218700	17.45509500	26.79099100
H	15.83993600	18.40095900	28.23007600
H	14.56733200	17.89639700	27.10930300
C	16.69479900	15.87205600	28.95309900
H	16.61822500	14.95767300	29.54230400
H	17.08002300	16.66988600	29.59754600
H	17.41749600	15.70289400	28.15338100
C	10.25772900	6.11011700	25.21783100
C	9.86692600	4.89004000	24.65341900
C	11.15088500	6.93309700	24.51887800
C	10.35762400	4.50248100	23.40637100
H	9.17048300	4.25235400	25.18744900
C	11.62897400	6.55211900	23.26745400
H	11.45277200	7.88071200	24.95405400
C	11.23391800	5.33525700	22.70605200
H	10.05032900	3.55346300	22.97787900
H	12.30438300	7.21175700	22.73296600
H	11.61800000	5.03267400	21.73766300
C	7.40068700	6.64483500	25.51910700
C	6.39910700	5.66778700	25.58132700
C	7.52915500	7.41716600	24.35799200
C	5.53860400	5.46955700	24.50240500
H	6.29158700	5.07087200	26.48086200
C	6.66551000	7.22250200	23.28080500
H	8.30128600	8.17679600	24.30620700
C	5.66765100	6.24803100	23.34975400
H	4.76678800	4.70829400	24.56224400
H	6.77146000	7.83157000	22.38809400
H	4.99556200	6.09555500	22.51089200
C	6.34534900	7.57251200	28.04740400
C	5.63519300	6.79068800	28.96766200
C	5.65845900	8.52391900	27.28437000
C	4.25823200	6.95042200	29.11650700
H	6.16674400	6.05867100	29.56733000
C	4.28236100	8.68568700	27.43716200
H	6.20162200	9.13800000	26.57546600
C	3.57730200	7.89902400	28.35061300

H	3.71847900	6.33509800	29.82987600
H	3.75872500	9.42564700	26.84070700
H	2.50513500	8.02529300	28.46566500
C	8.16265600	8.19667100	30.26877100
C	8.46055100	7.50432400	31.45123000
C	7.33487900	9.32660600	30.33134800
C	7.93015500	7.92174800	32.67077400
H	9.09533800	6.62495700	31.40847300
C	6.79670200	9.73550300	31.55050100
H	7.12265300	9.88473500	29.42856800
C	7.08924500	9.03523200	32.72265500
H	8.16540000	7.37200500	33.57689700
H	6.14640300	10.60390300	31.58450900
H	6.66667700	9.35632800	33.66970700
C	7.54404300	12.70668400	25.39491800
C	6.26619500	12.48008300	25.91814300
C	7.99570200	11.92566900	24.32365600
C	5.44578700	11.49628200	25.36766700
H	5.91341000	13.08548700	26.74699600
C	7.18248200	10.92657200	23.78939800
H	8.98216200	12.10783000	23.90940300
C	5.90327300	10.71113600	24.30690100
H	4.44889300	11.34457800	25.76835000
H	7.54479100	10.32311500	22.96325000
H	5.27317800	9.93128000	23.89192300
C	7.93398600	15.14834300	23.87937400
C	6.55498700	15.37846600	23.80221200
C	8.67796700	15.04684700	22.69778500
C	5.92983100	15.51101000	22.56242500
H	5.97558400	15.45224700	24.71690300
C	8.05186400	15.17619800	21.45829600
H	9.74566400	14.86325200	22.74886100
C	6.67702100	15.40960900	21.38695000
H	4.86043300	15.69259200	22.51483400
H	8.63705000	15.09447800	20.54778900
H	6.19069000	15.51100100	20.42159300
C	9.32387600	17.38550900	25.04352400
C	8.41659900	18.35722100	25.48489500
C	10.17352300	17.67773600	23.97114500
C	8.35881700	19.60557900	24.86606100
H	7.76008700	18.13018300	26.31931800
C	10.11528900	18.92769000	23.35465100
H	10.89201700	16.93954300	23.63254800
C	9.21004000	19.89364600	23.79785600
H	7.65137300	20.35027600	25.21805600
H	10.78073900	19.14714500	22.52761300
H	9.16949100	20.86487100	23.31422100
C	10.67200600	17.10570000	27.64146400
C	10.27384800	17.49330300	28.93017800
C	11.64202900	17.86681800	26.97395100
C	10.82078700	18.62366100	29.53403700

H	9.51623400	16.91531100	29.44970500
C	12.17701500	19.00595500	27.57473500
H	11.98547800	17.55797200	25.99580700
C	11.76911200	19.38998700	28.85312700
H	10.49763000	18.91186600	30.52959200
H	12.91892300	19.59298300	27.04283900
H	12.18808100	20.27801100	29.31620500
C	13.82541700	15.41475600	21.89956700
C	13.63089500	16.79962600	21.84751000
C	12.86311800	14.56501900	21.34039500
C	12.50128300	17.32724700	21.22409000
H	14.37753000	17.45990300	22.27701600
C	11.72154500	15.09369900	20.73829800
H	13.01835500	13.49130600	21.36979200
C	11.53912200	16.47697800	20.67451200
H	12.37858500	18.40336300	21.15888700
H	10.98196900	14.42403300	20.31030600
H	10.65370900	16.88979500	20.20179500
C	15.84574700	14.25084300	20.17722300
C	15.84388000	15.46466000	19.47696700
C	15.64144600	13.05979200	19.47224400
C	15.63922600	15.48485000	18.09776500
H	16.00144700	16.39252900	20.01670800
C	15.42942400	13.07934300	18.09420600
H	15.65195800	12.12025900	20.00818400
C	15.42780900	14.29215900	17.40233800
H	15.64394300	16.43197400	17.56691500
H	15.26447000	12.14791100	17.56082900
H	15.26427600	14.30834600	16.32916900
C	18.26274400	13.14117300	21.26702200
C	19.21016000	13.96573200	20.65109300
C	18.26644900	11.76677900	20.99659800
C	20.15446800	13.42322400	19.77869700
H	19.20527100	15.03136700	20.85848200
C	19.20865700	11.22650400	20.12183900
H	17.54205600	11.12019000	21.48047000
C	20.15511900	12.05244100	19.51177800
H	20.88737100	14.07095700	19.30719400
H	19.19744300	10.16046700	19.92036800
H	20.88918800	11.63079800	18.83182200
C	18.88320800	13.56235100	24.13712500
C	19.49595500	14.61165900	24.84298800
C	19.61494500	12.38924000	23.90622400
C	20.80983500	14.50046700	25.29207800
H	18.94254600	15.52913400	25.01622200
C	20.93644100	12.28762100	24.34141100
H	19.14740800	11.55536400	23.40389400
C	21.54008800	13.33903900	25.03209600
H	21.26587700	15.32497300	25.83131000
H	21.49482100	11.37844500	24.14221900
H	22.56888500	13.25308700	25.36777900

C	16.19761000	7.96342900	21.96452900
C	17.05409800	7.68412200	20.89372300
C	15.22133300	8.95795500	21.82221300
C	16.92972400	8.38363500	19.69338700
H	17.80343400	6.90628800	20.99785600
C	15.08187500	9.63941900	20.61442500
H	14.55504900	9.17278100	22.65217000
C	15.93757100	9.35535400	19.54735500
H	17.59773200	8.15988500	18.86748800
H	14.30089300	10.38538300	20.50562200
H	15.83372000	9.88732000	18.60715600
C	16.32259300	4.86457200	26.92806500
C	17.56953000	4.81964500	27.57003800
C	15.27017600	4.09067200	27.43649200
C	17.76649500	4.00938400	28.68688600
H	18.39244700	5.40792600	27.17662100
C	15.47254800	3.27274500	28.54692100
H	14.29844100	4.13372800	26.96446200
C	16.71878500	3.22605800	29.17459700
H	18.73935600	3.98276700	29.16790800
H	14.65265400	2.66805200	28.92163300
H	16.87151000	2.58583400	30.03793600
C	15.24930100	3.68597500	24.44689000
C	16.07492800	2.58470300	24.70043700
C	13.88659000	3.47989200	24.20019500
C	15.54597300	1.29436900	24.69389800
H	17.12901500	2.74204200	24.90591900
C	13.35642700	2.19099300	24.20210700
H	13.24297600	4.33227200	24.01735800
C	14.18559900	1.09373300	24.44591800
H	16.19525500	0.44559000	24.88601200
H	12.29629300	2.04935200	24.01466500
H	13.77521500	0.08852900	24.44566900
C	15.45076400	5.13214300	21.96234000
C	16.17759500	4.00947000	21.54058700
C	14.41511100	5.60698600	21.14729400
C	15.86465400	3.36765600	20.34334600
H	16.99024500	3.63923900	22.15571600
C	14.09693000	4.96325000	19.95226200
H	13.86420800	6.48935800	21.44460400
C	14.81865500	3.83872500	19.54721000
H	16.43943900	2.50067700	20.03236200
H	13.28779000	5.34461000	19.33679000
H	14.57239700	3.33779900	18.61607000
Rh	13.64554900	11.07883700	27.55492100
Rh	14.71159600	11.47978300	29.66780300

DCC-Rh2(TPPTTL)4 (11)[B3LYP-D3(BJ)]/BS1

Rh	14.83668700	11.19786900	29.70920900
Rh	13.86170300	10.77148700	27.52735000
O	16.68607300	10.75072900	28.85922800

O	15.72543000	10.25482400	26.87318200
O	17.89590800	10.33855200	24.16708000
O	16.90093500	7.36094800	27.48048700
N	17.76508300	8.94703000	26.01984900
C	16.72015600	10.35779900	27.65640800
C	18.05919200	9.99753500	26.99510500
H	18.28869800	10.87047400	26.37340800
C	17.55382800	9.28412300	24.66831300
C	16.84020600	8.12733700	24.05641900
C	16.65310300	7.16367200	25.05182500
C	17.10486800	7.75248600	26.34544200
C	16.03923100	5.94145400	24.79738200
C	15.58482600	5.71645000	23.47072800
C	15.75037000	6.70266400	22.46911800
C	16.38530300	7.94037200	22.75442100
C	19.31109200	9.76118300	27.89265000
C	19.80557600	11.14786200	28.35024500
H	20.66866500	11.03440200	29.01464800
H	19.02729400	11.68841900	28.88907900
H	20.11239700	11.75664600	27.49645500
C	20.40078700	9.11755900	27.01675700
H	20.56114600	9.68995500	26.09917500
H	20.13883500	8.09241800	26.74043800
H	21.34594700	9.09027700	27.56851000
C	19.06174700	8.86729000	29.11959800
H	19.99387000	8.77730100	29.68837500
H	18.73652000	7.86864500	28.82683500
H	18.30179900	9.29503300	29.77425400
O	14.54483900	9.18474400	30.13612400
O	13.50636300	8.84954900	28.15298300
O	12.06615200	5.40034900	27.77088800
O	11.45017300	8.70344400	30.88066400
N	12.07419800	6.93137200	29.50928900
C	13.90489900	8.47947400	29.30081300
C	13.53386300	7.02045300	29.61051000
H	13.88765500	6.46337300	28.73669700
C	11.46810900	6.17994800	28.48691300
C	10.02323900	6.54153500	28.50617700
C	9.81655500	7.43656100	29.56119800
C	11.15441000	7.80210600	30.11733400
C	8.54394500	7.88539600	29.90640800
C	7.47120700	7.45588300	29.07783400
C	7.68534400	6.57455900	27.99224900
C	8.98582100	6.08503000	27.70053800
C	14.14371300	6.32057300	30.85090200
C	15.67798500	6.36744200	30.71163300
H	16.00207900	5.93908500	29.75739600
H	16.13717800	5.78546300	31.51710400
H	16.05234500	7.39113900	30.77084400
C	13.69082800	4.84861800	30.81586900
H	12.60374400	4.76458100	30.90947000

H	14.14250900	4.30471100	31.65152100
H	13.99444700	4.36133300	29.88562500
C	13.70773700	6.94806500	32.18072300
H	13.97467800	8.00151600	32.23685900
H	14.19671800	6.42043800	33.00737400
H	12.62770500	6.86324600	32.32551200
O	12.92609200	11.65854000	30.36751700
O	12.05004500	11.34265800	28.30562900
O	8.37936100	11.33729200	28.32725600
O	11.66717300	14.50818100	28.50873300
N	10.01330500	12.90995600	28.82513500
C	11.98509600	11.70270600	29.52027600
C	10.59796900	12.19405100	29.95499300
H	9.99408800	11.28194400	30.02941000
C	8.97588800	12.36311200	28.05269000
C	8.79587000	13.28747600	26.89595300
C	9.71229900	14.33666900	27.03310800
C	10.60459100	14.00847800	28.18414200
C	9.74172200	15.41711700	26.15511100
C	8.82784800	15.37962400	25.06681200
C	7.92353100	14.30498800	24.91300500
C	7.89202800	13.23252100	25.84165200
C	10.46469200	12.92495600	31.32592000
C	10.66375700	11.86690600	32.42629100
H	10.54332200	12.33010000	33.41106700
H	11.66098200	11.43437900	32.36261400
H	9.93454000	11.05948200	32.34106500
C	9.03476300	13.48819900	31.41835700
H	8.28931200	12.72309300	31.18972200
H	8.88806800	14.32413400	30.72845900
H	8.84661400	13.85128500	32.43358900
C	11.46619800	14.07449500	31.53860800
H	11.32413200	14.48234900	32.54555400
H	11.31758000	14.88099800	30.81983900
H	12.49604000	13.72583200	31.45072400
O	15.07605100	13.17594700	29.09249500
O	14.26814000	12.71625200	27.02756800
O	14.18037500	15.77399600	24.78666900
O	17.50552700	13.36976500	26.79720400
N	15.78468500	14.77206800	26.11743400
C	14.79063300	13.48072700	27.89600400
C	15.03743500	14.90074700	27.36730200
H	14.04554400	15.24131800	27.05154700
C	15.24448500	15.19676800	24.89392400
C	16.23570200	14.81118200	23.84994100
C	17.31923800	14.19880700	24.48915800
C	16.96134800	14.03329500	25.93227800
C	18.47948000	13.85696200	23.79971300
C	18.48649600	14.10554700	22.39897700
C	17.37997400	14.70287000	21.74898000
C	16.22315900	15.07498100	22.48465800

C	15.60099300	15.98858700	28.31989500
C	14.62553300	16.15168600	29.50218400
H	13.61204100	16.36137200	29.14560800
H	14.94714200	16.99129500	30.12689100
H	14.58834700	15.25567400	30.12187100
C	15.63937500	17.31620000	27.53930500
H	16.32824300	17.26090400	26.69101800
H	15.98477600	18.11906000	28.19840500
H	14.64968700	17.58558100	27.16178100
C	17.01726900	15.66866900	28.82168200
H	17.07042800	14.67372200	29.25905800
H	17.31221000	16.40180500	29.57975600
H	17.74764400	15.71748500	28.00988400
C	8.29120900	8.66392600	31.14935100
C	7.57573300	9.86960700	31.14898800
C	8.68623900	8.10806700	32.37520800
C	7.23969900	10.48672400	32.35350300
H	7.28520900	10.31743500	30.20780300
C	8.35040200	8.72851600	33.57696000
H	9.23308800	7.17055500	32.38317900
C	7.61936300	9.91798400	33.57032900
H	6.67748000	11.41485500	32.34088700
H	8.64577900	8.27499400	34.51682000
H	7.34969400	10.39770400	34.50607700
C	6.09549000	7.96946500	29.34695800
C	5.38664100	7.57093600	30.48654100
C	5.51194200	8.88117400	28.45946200
C	4.10747000	8.06946300	30.72978000
H	5.84328600	6.87476300	31.18302900
C	4.23593200	9.38524300	28.70706900
H	6.06166100	9.20197500	27.58236400
C	3.52916200	8.97932100	29.84116400
H	3.56417600	7.75050500	31.61412300
H	3.80008500	10.09551300	28.01190100
H	2.53475100	9.37069400	30.03340100
C	6.53760300	6.14651300	27.14074700
C	5.42138700	5.50548400	27.69564400
C	6.56418000	6.37622200	25.75866300
C	4.34811300	5.12664700	26.89043000
H	5.39357400	5.30783500	28.76109900
C	5.48785200	6.00824100	24.95315400
H	7.43871300	6.83799600	25.31663600
C	4.37287700	5.38516200	25.51810400
H	3.49164000	4.63019700	27.33622000
H	5.52293100	6.20500300	23.88597100
H	3.53361400	5.09635600	24.89292600
C	9.24545500	5.13638800	26.58406500
C	8.67613600	3.85715200	26.58283800
C	10.06980100	5.51936700	25.51811400
C	8.93783500	2.97077300	25.53800300
H	8.02929500	3.55987500	27.40182300

C	10.32223900	4.63782700	24.46960100
H	10.51114300	6.51085900	25.51537900
C	9.76185800	3.35847400	24.47935200
H	8.49843300	1.97804700	25.55164700
H	10.96183700	4.94689600	23.65090600
H	9.96875400	2.66760900	23.66786100
C	15.88676800	4.92510300	25.87214200
C	17.02694000	4.40312200	26.49942500
C	14.62188000	4.47716900	26.26907500
C	16.90457200	3.43878400	27.49758000
H	18.00869000	4.75322300	26.19605700
C	14.49964600	3.51848800	27.27414700
H	13.73094900	4.88446400	25.80612700
C	15.63855200	2.99206300	27.88601600
H	17.79480800	3.03709800	27.97183800
H	13.51042900	3.20217100	27.58463500
H	15.54099600	2.24280000	28.66574600
C	14.90751500	4.42908800	23.13986800
C	15.57751600	3.20966600	23.30760400
C	13.59146900	4.41829600	22.65870900
C	14.94562400	2.00579700	22.99870000
H	16.59494500	3.20766200	23.68372100
C	12.95852400	3.21499400	22.35148600
H	13.06943500	5.35848000	22.51820400
C	13.63345900	2.00430500	22.52099400
H	15.47889200	1.06936900	23.13065800
H	11.94004400	3.22300100	21.97565700
H	13.14076900	1.06719300	22.28098400
C	15.25722700	6.44373000	21.08457000
C	15.81102300	5.41227700	20.31555400
C	14.23938400	7.23335700	20.53365800
C	15.35614600	5.17485000	19.01923000
H	16.59660300	4.79523000	20.73918500
C	13.77913600	6.99149700	19.24015800
H	13.81164300	8.03832100	21.12212000
C	14.33751600	5.96259600	18.47845500
H	15.79668300	4.37483200	18.43212100
H	12.98581100	7.60704100	18.82722200
H	13.98139300	5.77606100	17.46995100
C	16.50577300	9.00814600	21.72504200
C	17.20909900	8.79521300	20.53270200
C	15.86322300	10.23668000	21.92930900
C	17.25540200	9.78843100	19.55520000
H	17.70627900	7.84540300	20.36755100
C	15.90598000	11.22690400	20.95094700
H	15.32137500	10.40786200	22.85369000
C	16.59494400	11.00295300	19.75622600
H	17.80225400	9.61262100	18.63396800
H	15.39960300	12.17013800	21.12673400
H	16.62801600	11.77451500	18.99420600
C	19.70008600	13.37818100	24.50422700

C	20.26711600	14.18769800	25.49879900
C	20.34762100	12.18879700	24.14479100
C	21.46709200	13.82641900	26.11008100
H	19.77523000	15.11474300	25.77614600
C	21.54696500	11.82879100	24.75622900
H	19.90844900	11.55109600	23.38971000
C	22.11432800	12.64753600	25.73539300
H	21.89751300	14.46782300	26.87295500
H	22.04212200	10.90821100	24.46325800
H	23.05105600	12.36577700	26.20628500
C	19.69322100	13.72708300	21.60561500
C	20.91276000	14.39007200	21.79260200
C	19.61765100	12.68347600	20.67641800
C	22.03558900	14.02127100	21.05334500
H	20.97881100	15.19087100	22.52211800
C	20.74278900	12.30888800	19.94311800
H	18.67873300	12.16061700	20.53883000
C	21.95436700	12.97853100	20.12687100
H	22.97458800	14.54548600	21.20288600
H	20.67096600	11.49229200	19.23078300
H	22.83061400	12.68885300	19.55492300
C	17.43383800	14.99618700	20.28650800
C	18.45310300	15.79924900	19.75479100
C	16.44708000	14.50419100	19.42058300
C	18.49489500	16.08570600	18.39112900
H	19.21538300	16.19965100	20.41322900
C	16.49268500	14.78154000	18.05514200
H	15.63191100	13.91241100	19.81861900
C	17.51910100	15.57193300	17.53449800
H	19.29046600	16.71166000	17.99871600
H	15.72268700	14.38420500	17.40097500
H	17.55443500	15.79123700	16.47186200
C	15.05234300	15.75014600	21.86065900
C	15.18765500	17.01099900	21.26592300
C	13.78997000	15.14365900	21.89667000
C	14.07548400	17.66123300	20.73167500
H	16.16483500	17.48107700	21.22835700
C	12.68010500	15.78973000	21.35512600
H	13.68025100	14.16881200	22.36107900
C	12.81853900	17.05423500	20.77826000
H	14.19036000	18.64325400	20.28313700
H	11.70654500	15.31269700	21.39403600
H	11.95082900	17.56405100	20.37190400
C	10.63510300	16.58219200	26.38848400
C	10.54446800	17.28352600	27.60073700
C	11.53456100	17.02369500	25.41182300
C	11.33012900	18.41171200	27.82537600
H	9.84556400	16.94719200	28.36015900
C	12.32412100	18.14929100	25.63879300
H	11.63031700	16.48146400	24.47965500
C	12.21961800	18.85100900	26.84056000

H	11.24531900	18.94994100	28.76440700
H	13.03086600	18.46408800	24.87832500
H	12.83219100	19.73054800	27.01361500
C	8.83446000	16.47832900	24.05731800
C	8.51743900	17.79305700	24.42175800
C	9.16916200	16.20386700	22.72466200
C	8.53346600	18.81302300	23.47112300
H	8.26440900	18.01440600	25.45336500
C	9.18932600	17.22383400	21.77463800
H	9.40942500	15.18622000	22.43602900
C	8.87191300	18.53235700	22.14538100
H	8.28255100	19.82724000	23.76630700
H	9.44848800	16.99539300	20.74533900
H	8.88657600	19.32724100	21.40613300
C	6.96140300	14.30017700	23.77178700
C	5.95576700	15.27155000	23.68927200
C	7.04518900	13.31966900	22.77484400
C	5.04993700	15.26278900	22.62916500
H	5.88900000	16.03493000	24.45757800
C	6.14378200	13.31450400	21.71131400
H	7.81898400	12.56178700	22.83512700
C	5.14243800	14.28511900	21.63611300
H	4.27273800	16.01928500	22.57891800
H	6.22314200	12.55216400	20.94229500
H	4.43874000	14.27958500	20.80939300
C	6.96016000	12.08754200	25.64947400
C	5.57578700	12.25091000	25.77597500
C	7.47021300	10.84419600	25.25587500
C	4.71361000	11.18652300	25.50901400
H	5.17643700	13.21595900	26.07013600
C	6.60720400	9.78886000	24.96974700
H	8.54336500	10.71690900	25.15277900
C	5.22644300	9.95387100	25.09916400
H	3.64141100	11.32428700	25.61042400
H	7.01061000	8.83827700	24.64397800
H	4.56019400	9.12271800	24.89070900
C	14.95450200	10.83802900	32.72192300
N	15.58768300	11.47286200	31.86064200
N	14.41143800	10.11894700	33.53219200
C	13.34209900	10.45584500	34.48629100
C	12.31828900	9.31779500	34.53636400
C	13.97639000	10.70116900	35.86218200
H	12.84465300	11.37657000	34.16177700
C	11.24610200	9.59660700	35.59722000
H	12.85090400	8.38949300	34.77838300
H	11.86547900	9.18073900	33.55016600
C	12.89688500	10.99535900	36.91067800
H	14.54526000	9.80742000	36.14847300
H	14.68887800	11.53039700	35.79127600
C	11.86446800	9.86274000	36.97552000
H	10.55839800	8.74690000	35.64925100

H	10.64570500	10.46302900	35.28965900
H	13.36500700	11.14759000	37.88929800
H	12.38949900	11.93529700	36.65386100
H	11.08111800	10.10372600	37.70292400
H	12.35775500	8.94773900	37.33144000
C	16.76495400	12.27088500	32.32071100
C	18.02803000	11.75994100	31.63053900
C	16.51341800	13.75196200	32.03775300
H	16.86983300	12.12830700	33.40496700
C	19.24747800	12.60581000	32.01501800
H	17.86912600	11.80031000	30.55143400
H	18.18450400	10.70635200	31.88734000
C	17.73974800	14.60111200	32.39895200
H	16.27773200	13.85921900	30.97745200
H	15.63137500	14.08464600	32.59713900
C	19.00797000	14.08815700	31.70288500
H	20.12982100	12.23792700	31.48004900
H	19.45492800	12.48783000	33.08762900
H	17.55070800	15.64614700	32.12986100
H	17.89254100	14.57852600	33.48688400
H	19.87410400	14.68702800	32.00661600
H	18.90166800	14.21186200	30.61739700

Rh2(TPPTTL)4-Carbene (12) [B3LYP-D3(BJ)]/BS1

Rh	15.00850000	11.53300000	29.72640000
Rh	13.95460000	11.29000000	27.50840000
O	16.77700000	10.88220000	28.86240000
O	15.75430000	10.56670000	26.86660000
O	18.10500000	10.07250000	24.12090000
O	16.45830000	7.60870000	27.57370000
N	17.64760000	8.93100000	26.08230000
C	16.75560000	10.52800000	27.65420000
C	18.02350000	10.03830000	26.95490000
H	18.26790000	10.84670000	26.25480000
C	17.70120000	9.07530000	24.69100000
C	17.13880000	7.82460000	24.12770000
C	16.64800000	7.04500000	25.17850000
C	16.87060000	7.81610000	26.44650000
C	16.04550000	5.80670000	24.94410000
C	15.92290000	5.40590000	23.58230000
C	16.43030000	6.20400000	22.53040000
C	17.06640000	7.43680000	22.79910000
C	19.29850000	9.78460000	27.80570000
C	19.77520000	11.13800000	28.36980000
H	20.72140000	10.99930000	28.90280000
H	19.04690000	11.55940000	29.06410000
H	19.94460000	11.86060000	27.56430000
C	20.38660000	9.24370000	26.85900000
H	20.55230000	9.92270000	26.01710000
H	20.11880000	8.26110000	26.46010000
H	21.33010000	9.14100000	27.40400000

C	19.07320000	8.78230000	28.94900000
H	20.00330000	8.66420000	29.51510000
H	18.78140000	7.80040000	28.56990000
H	18.29480000	9.12800000	29.63130000
O	14.46120000	9.56670000	30.09970000
O	13.35170000	9.43490000	28.12880000
O	12.19440000	5.91980000	27.44360000
O	10.95510000	9.25170000	30.29460000
N	11.85400000	7.45970000	29.13010000
C	13.73510000	8.97760000	29.25600000
C	13.26510000	7.54400000	29.49270000
H	13.76720000	6.96960000	28.70490000
C	11.43700000	6.60820000	28.09750000
C	9.95910000	6.74010000	28.02970000
C	9.55930000	7.69530000	28.97200000
C	10.80650000	8.27310000	29.58230000
C	8.20810000	7.94340000	29.22000000
C	7.26690000	7.14980000	28.50060000
C	7.68510000	6.17760000	27.56140000
C	9.06090000	5.98670000	27.28470000
C	13.61840000	6.85270000	30.83900000
C	15.15210000	6.71800000	30.91940000
H	15.54310000	6.17370000	30.05320000
H	15.42340000	6.15880000	31.82050000
H	15.63810000	7.69370000	30.95950000
C	13.01070000	5.43630000	30.81000000
H	11.91700000	5.46740000	30.80210000
H	13.32280000	4.88620000	31.70300000
H	13.34510000	4.87650000	29.93110000
C	13.08340000	7.60960000	32.06510000
H	13.49180000	8.62010000	32.11560000
H	13.37030000	7.07290000	32.97560000
H	11.99330000	7.68210000	32.04840000
O	13.16450000	12.14950000	30.43290000
O	12.26060000	12.08580000	28.35650000
O	8.62310000	11.87520000	28.53040000
O	11.81400000	15.11270000	28.76970000
N	10.18720000	13.48850000	29.09090000
C	12.21670000	12.29250000	29.61640000
C	10.82890000	12.68130000	30.11960000
H	10.27180000	11.73600000	30.09490000
C	9.11460000	12.97390000	28.35010000
C	8.80270000	13.99630000	27.32060000
C	9.77590000	14.99910000	27.38590000
C	10.74100000	14.62040000	28.46960000
C	9.75510000	16.09500000	26.52230000
C	8.72660000	16.10790000	25.53660000
C	7.74840000	15.08810000	25.48130000
C	7.75860000	14.01760000	26.40600000
C	10.68670000	13.24440000	31.56390000
C	10.98970000	12.10460000	32.55740000

H	10.81320000	12.45480000	33.57970000
H	12.02630000	11.77340000	32.48010000
H	10.33760000	11.24420000	32.37670000
C	9.21820000	13.67090000	31.75060000
H	8.53260000	12.85130000	31.51570000
H	8.96350000	14.52440000	31.11590000
H	9.05100000	13.96310000	32.79200000
C	11.60490000	14.44530000	31.84330000
H	11.46760000	14.77110000	32.88000000
H	11.37500000	15.28780000	31.18830000
H	12.65500000	14.18250000	31.70170000
O	15.44290000	13.48390000	29.18570000
O	14.60660000	13.18830000	27.09870000
O	14.28810000	16.53200000	25.30910000
O	17.68460000	13.74900000	26.55930000
N	16.00250000	15.32210000	26.28040000
C	15.15890000	13.87430000	28.02140000
C	15.40570000	15.32710000	27.61240000
H	14.39740000	15.72420000	27.44270000
C	15.32320000	15.90500000	25.20230000
C	16.11970000	15.58270000	23.99180000
C	17.22450000	14.81440000	24.37970000
C	17.07510000	14.52770000	25.84800000
C	18.18380000	14.40170000	23.45130000
C	17.97740000	14.80050000	22.09820000
C	16.84170000	15.55330000	21.71680000
C	15.88110000	15.95460000	22.67570000
C	16.09200000	16.28660000	28.62190000
C	15.18400000	16.41510000	29.86140000
H	14.16890000	16.71170000	29.57540000
H	15.58410000	17.18330000	30.53070000
H	15.12240000	15.47560000	30.41210000
C	16.19020000	17.67110000	27.95160000
H	16.84850000	17.64920000	27.07820000
H	16.60100000	18.39390000	28.66310000
H	15.20720000	18.02940000	27.63000000
C	17.49730000	15.81950000	29.03100000
H	17.46530000	14.83970000	29.51040000
H	17.92900000	16.53750000	29.73630000
H	18.16340000	15.75590000	28.16680000
C	7.75470000	8.93980000	30.22650000
C	6.85020000	9.94970000	29.87360000
C	8.19520000	8.85220000	31.55440000
C	6.39510000	10.85420000	30.82950000
H	6.51140000	10.03690000	28.84870000
C	7.73480000	9.75400000	32.51260000
H	8.88950000	8.06830000	31.83760000
C	6.83070000	10.75670000	32.15260000
H	5.70580000	11.63850000	30.53380000
H	8.07810000	9.67110000	33.53910000
H	6.47220000	11.45930000	32.89860000

C	5.80650000	7.31430000	28.76310000
C	5.28460000	7.07860000	30.04250000
C	4.93340000	7.68190000	27.73110000
C	3.91790000	7.20410000	30.28450000
H	5.95500000	6.79780000	30.84790000
C	3.56630000	7.80960000	27.97390000
H	5.32690000	7.86570000	26.73900000
C	3.05360000	7.57130000	29.25040000
H	3.52790000	7.01390000	31.27970000
H	2.90090000	8.09090000	27.16310000
H	1.98870000	7.66910000	29.43800000
C	6.68980000	5.27820000	26.90760000
C	5.91610000	4.40980000	27.69080000
C	6.53880000	5.25380000	25.51570000
C	5.00470000	3.54010000	27.09480000
H	6.03050000	4.42100000	28.76960000
C	5.62070000	4.38920000	24.92030000
H	7.13600000	5.91330000	24.90050000
C	4.85120000	3.52960000	25.70640000
H	4.41540000	2.87080000	27.71420000
H	5.50850000	4.38710000	23.84030000
H	4.13890000	2.85500000	25.24130000
C	9.57230000	4.99710000	26.29630000
C	9.43600000	3.62160000	26.51980000
C	10.27120000	5.44220000	25.16700000
C	10.01700000	2.70580000	25.64200000
H	8.88880000	3.27330000	27.38970000
C	10.84280000	4.52670000	24.28530000
H	10.38090000	6.50710000	24.99270000
C	10.72850000	3.15580000	24.52730000
H	9.91930000	1.64140000	25.83270000
H	11.39310000	4.88100000	23.41980000
H	11.19790000	2.44630000	23.85380000
C	15.60920000	4.92140000	26.05660000
C	16.51840000	4.58680000	27.07270000
C	14.32180000	4.37180000	26.09230000
C	16.14750000	3.71900000	28.09730000
H	17.52080000	5.00130000	27.04970000
C	13.95090000	3.50180000	27.11550000
H	13.59900000	4.63380000	25.33010000
C	14.86150000	3.16960000	28.11870000
H	16.86270000	3.46580000	28.87390000
H	12.94210000	3.10270000	27.13070000
H	14.57350000	2.48990000	28.91500000
C	15.27320000	4.10720000	23.23820000
C	15.82150000	2.89190000	23.66790000
C	14.10130000	4.09020000	22.47030000
C	15.20790000	1.68400000	23.33980000
H	16.72600000	2.89840000	24.26720000
C	13.48480000	2.88280000	22.14450000
H	13.67560000	5.02780000	22.12900000

C	14.03560000	1.67540000	22.58020000
H	15.64450000	0.74930000	23.67810000
H	12.57590000	2.88570000	21.55050000
H	13.55670000	0.73470000	22.32670000
C	16.37710000	5.71410000	21.12220000
C	17.16920000	4.62840000	20.72690000
C	15.55150000	6.33470000	20.17680000
C	17.13370000	4.16990000	19.41060000
H	17.80890000	4.14290000	21.45690000
C	15.51150000	5.87300000	18.86110000
H	14.92920000	7.17060000	20.47840000
C	16.30330000	4.79010000	18.47420000
H	17.75360000	3.32830000	19.11660000
H	14.86150000	6.35890000	18.13980000
H	16.27340000	4.43130000	17.45000000
C	17.74340000	8.25660000	21.75400000
C	19.12740000	8.12170000	21.58870000
C	17.05030000	9.20160000	20.99070000
C	19.81240000	8.92800000	20.68010000
H	19.66530000	7.39220000	22.18630000
C	17.73620000	10.00790000	20.08120000
H	15.98100000	9.31710000	21.12560000
C	19.11790000	9.87700000	19.92750000
H	20.88640000	8.81860000	20.56370000
H	17.19090000	10.74200000	19.49950000
H	19.65010000	10.51650000	19.23190000
C	19.36690000	13.59100000	23.84240000
C	20.21240000	14.02610000	24.87350000
C	19.66820000	12.39700000	23.17360000
C	21.33960000	13.28490000	25.22270000
H	19.98890000	14.95130000	25.39390000
C	20.79190000	11.65330000	23.52610000
H	19.01680000	12.03720000	22.38700000
C	21.63370000	12.09670000	24.54740000
H	21.98970000	13.63570000	26.01810000
H	20.99530000	10.72200000	23.00750000
H	22.51210000	11.51960000	24.81990000
C	18.97870000	14.43820000	21.05320000
C	20.29430000	14.91210000	21.14010000
C	18.61070000	13.64480000	19.95940000
C	21.22230000	14.60540000	20.14620000
H	20.58660000	15.52080000	21.98950000
C	19.53840000	13.33850000	18.96550000
H	17.59660000	13.27080000	19.89350000
C	20.84700000	13.81810000	19.05500000
H	22.23750000	14.98250000	20.22270000
H	19.23750000	12.72820000	18.11940000
H	21.56900000	13.58070000	18.27990000
C	16.64130000	15.96310000	20.29670000
C	17.52480000	16.86060000	19.68400000
C	15.55320000	15.46720000	19.56660000

C	17.32600000	17.25380000	18.36140000
H	18.37030000	17.24380000	20.24580000
C	15.35980000	15.85520000	18.24130000
H	14.86790000	14.77040000	20.03520000
C	16.24420000	16.75020000	17.63550000
H	18.01600000	17.95220000	17.89790000
H	14.51810000	15.45790000	17.68230000
H	16.09160000	17.05340000	16.60430000
C	14.67180000	16.74770000	22.31740000
C	14.78140000	18.09600000	21.95870000
C	13.40620000	16.15220000	22.37380000
C	13.63620000	18.84510000	21.68310000
H	15.76230000	18.55760000	21.90640000
C	12.26540000	16.89660000	22.08140000
H	13.32280000	15.10710000	22.64840000
C	12.37490000	18.24870000	21.74880000
H	13.73030000	19.89400000	21.41910000
H	11.28840000	16.42800000	22.12800000
H	11.48060000	18.83010000	21.54760000
C	10.71810000	17.21970000	26.66090000
C	10.84090000	17.88020000	27.89340000
C	11.47560000	17.66800000	25.57280000
C	11.69780000	18.97020000	28.02830000
H	10.25380000	17.54300000	28.74130000
C	12.33140000	18.75880000	25.70640000
H	11.40800000	17.15910000	24.62010000
C	12.44380000	19.41530000	26.93210000
H	11.77950000	19.47570000	28.98570000
H	12.92080000	19.07610000	24.85270000
H	13.10880000	20.26740000	27.03680000
C	8.63450000	17.24000000	24.56850000
C	8.40940000	18.54770000	25.01840000
C	8.76840000	17.00950000	23.19310000
C	8.32550000	19.60340000	24.11210000
H	8.30910000	18.73460000	26.08240000
C	8.69020000	18.06580000	22.28560000
H	8.93460000	15.99890000	22.83610000
C	8.47020000	19.36690000	22.74300000
H	8.14880000	20.61120000	24.47520000
H	8.80160000	17.87150000	21.22330000
H	8.40840000	20.18970000	22.03750000
C	6.62660000	15.18220000	24.50050000
C	5.58390000	16.09140000	24.71600000
C	6.59600000	14.36540000	23.36390000
C	4.52840000	16.18310000	23.80880000
H	5.60660000	16.72860000	25.59440000
C	5.54250000	14.45890000	22.45440000
H	7.40810000	13.66770000	23.18620000
C	4.50560000	15.36750000	22.67530000
H	3.72500000	16.89130000	23.98690000
H	5.53310000	13.82360000	21.57410000

H	3.68520000	15.44040000	21.96810000
C	6.64460000	13.03350000	26.51940000
C	5.74610000	13.17190000	27.58650000
C	6.48110000	11.97240000	25.62330000
C	4.70070000	12.26510000	27.75440000
H	5.87490000	13.99190000	28.28620000
C	5.43500000	11.06400000	25.79260000
H	7.17650000	11.84740000	24.80210000
C	4.54450000	11.20610000	26.85790000
H	4.01040000	12.38440000	28.58380000
H	5.32150000	10.24410000	25.09350000
H	3.73900000	10.49300000	26.99340000
C	13.18170000	10.89330000	25.69950000
C	11.87590000	10.40690000	25.38450000
C	14.19070000	10.81940000	24.61690000
C	11.54690000	10.01920000	24.05320000
C	10.88530000	10.28020000	26.39460000
O	14.68580000	9.76400000	24.27660000
O	14.50670000	12.02880000	24.10940000
C	10.29910000	9.50720000	23.75880000
H	12.27950000	10.11360000	23.26140000
C	9.62750000	9.77620000	26.09130000
H	11.11940000	10.57960000	27.40500000
C	15.45040000	12.04560000	23.03000000
C	9.34920000	9.37740000	24.78220000
H	10.05900000	9.19560000	22.74880000
H	8.87620000	9.69130000	26.86530000
H	16.14880000	11.20970000	23.08930000
H	15.98640000	12.98790000	23.09980000
C	14.69400000	12.00900000	21.71710000
C	8.01350000	8.78810000	24.41920000
F	14.04260000	10.83720000	21.53220000
F	13.76930000	12.98860000	21.63700000
F	15.54720000	12.17010000	20.68320000
F	8.16860000	7.63440000	23.72730000
F	7.30210000	9.62140000	23.62470000
F	7.26040000	8.51600000	25.50240000

DCC-Rh2(TPPTTL)4-Carbene (13) [B3LYP-D3(BJ)]/BS1

Rh	14.97374600	11.44584700	29.68634600
Rh	13.99957100	11.22198800	27.42545400
O	16.81060400	10.99701500	28.82175600
O	15.86075700	10.62155800	26.80189700
O	17.95694200	10.06789700	24.10094600
O	16.95690400	7.74335700	27.88146100
N	17.85799900	9.03029900	26.16964300
C	16.84595100	10.65550200	27.61116100
C	18.16179000	10.23327700	26.94469500
H	18.33806000	10.99945300	26.18127400
C	17.67597200	9.09536700	24.77689200
C	17.06439100	7.79524900	24.37711700

C	16.84674700	7.05042200	25.53814600
C	17.21831000	7.89906000	26.70227600
C	16.27227500	5.78003600	25.51816300
C	15.80228300	5.32512700	24.26024900
C	15.97794900	6.09992300	23.08965400
C	16.65517200	7.34679900	23.12460900
C	19.45460700	10.15582300	27.80405700
C	19.81505000	11.59297100	28.23133400
H	20.75177200	11.58285900	28.79819600
H	19.03868000	12.02781200	28.86201200
H	19.95114200	12.24224000	27.36215800
C	20.57481500	9.61364000	26.89792000
H	20.66810800	10.20766000	25.98563300
H	20.38861700	8.57379200	26.61405900
H	21.53128800	9.65463400	27.42879100
C	19.34348800	9.25561200	29.04660000
H	20.28251200	9.31281900	29.60824000
H	19.17417800	8.21263900	28.77327500
H	18.53077100	9.57182000	29.69975900
O	14.56145700	9.40956100	29.94742000
O	13.51065800	9.30873000	27.94527200
O	12.36300300	5.89709100	26.97737800
O	11.17004900	8.99145500	30.11255300
N	12.04704800	7.28461400	28.80851500
C	13.88747500	8.82186100	29.06165000
C	13.45085500	7.35896000	29.20992900
H	13.98330500	6.83595600	28.40767500
C	11.62382700	6.55194900	27.69014900
C	10.14398600	6.73300400	27.62333700
C	9.75883400	7.57001700	28.67840400
C	11.00947300	8.07107300	29.32978900
C	8.41807000	7.81798400	28.96821000
C	7.45637400	7.12895500	28.17451800
C	7.84973500	6.28776100	27.10755500
C	9.22222200	6.12567000	26.77763700
C	13.77341000	6.59789900	30.52592600
C	15.30442700	6.44465500	30.61273400
H	15.70456600	5.93100700	29.73478600
H	15.56292300	5.85676900	31.49950000
H	15.79125000	7.41828300	30.69015800
C	13.12869400	5.20242000	30.42641300
H	12.03731700	5.26337900	30.47374500
H	13.46663000	4.58159600	31.26181800
H	13.40364300	4.69885300	29.49790600
C	13.24801000	7.29316200	31.78851400
H	13.68056400	8.28426800	31.91477200
H	13.51542000	6.69155200	32.66425900
H	12.16058000	7.39199900	31.77357900
O	13.07350000	11.93242200	30.35361600
O	12.24540300	11.91079800	28.24749900
O	8.55267900	11.86630100	28.34108800

O	11.86778900	14.97587000	28.63240000
N	10.19492700	13.39263600	28.91353000
C	12.16327300	12.11437700	29.50298400
C	10.77698800	12.56551400	29.95995400
H	10.17622500	11.64753500	29.93081900
C	9.08761600	12.94796000	28.18209100
C	8.79270800	14.02143400	27.19989900
C	9.80125100	14.98735800	27.28453800
C	10.77493200	14.53013800	28.33085800
C	9.79373800	16.12301800	26.47312500
C	8.74736700	16.20714100	25.50907700
C	7.73928400	15.21995300	25.42836000
C	7.72924100	14.11556300	26.31266700
C	10.62200200	13.15887000	31.39159900
C	10.85595300	12.02217800	32.40110000
H	10.69351100	12.39409600	33.41776700
H	11.87389700	11.64203900	32.32797500
H	10.16211500	11.19352700	32.23077700
C	9.16989000	13.65007600	31.54169900
H	8.45644200	12.85585400	31.30159400
H	8.96317900	14.50640700	30.89361200
H	8.99420600	13.96093200	32.57627600
C	11.58840800	14.31931900	31.68326600
H	11.44642700	14.65291400	32.71690200
H	11.40982900	15.17050200	31.02397700
H	12.62783300	14.00847700	31.56224200
O	15.28730600	13.45494300	29.21474700
O	14.54871000	13.16252600	27.09403800
O	14.15490700	16.39973100	25.26832000
O	17.62619900	13.79922500	26.68421700
N	15.89725100	15.30568700	26.31862900
C	15.04163000	13.85307700	28.04353300
C	15.26875100	15.31361200	27.63817400
H	14.25684200	15.68937300	27.44627900
C	15.21723800	15.81522800	25.20181200
C	16.05157600	15.47521900	24.01574000
C	17.16701000	14.76015800	24.46712800
C	17.00055300	14.53096500	25.93807500
C	18.18073400	14.35859000	23.60001600
C	18.00607000	14.67354000	22.22303000
C	16.87644000	15.39533900	21.77044100
C	15.87065600	15.81860900	22.67940600
C	15.92356300	16.29472000	28.64552700
C	15.01717400	16.39491600	29.88855900
H	13.99609600	16.67064900	29.60476000
H	15.40272500	17.16871800	30.56016800
H	14.97703900	15.45281300	30.43524700
C	15.97446300	17.68095900	27.97387900
H	16.62602800	17.67689500	27.09513500
H	16.36955000	18.41685800	28.68118200
H	14.97883500	18.00910200	27.65970700

C	17.34490400	15.87339800	29.04628600
H	17.35743500	14.86576000	29.46046400
H	17.73289900	16.56391900	29.80244100
H	18.02452800	15.89538700	28.19082400
C	8.00320600	8.70901100	30.08488800
C	7.12547000	9.77693800	29.85483900
C	8.46518100	8.47454100	31.38790600
C	6.72540200	10.59926800	30.90563100
H	6.76859400	9.97648300	28.85229000
C	8.05855600	9.29300600	32.44039700
H	9.13650500	7.64343600	31.57671900
C	7.18741900	10.35920500	32.20131000
H	6.05727300	11.43129100	30.70597500
H	8.42091900	9.09889100	33.44504000
H	6.87455500	11.00021000	33.01978100
C	6.00495400	7.27251100	28.49248300
C	5.51776300	6.88281600	29.74791200
C	5.10818900	7.78059900	27.54377100
C	4.16113300	6.99272700	30.04716900
H	6.20720900	6.49324300	30.48944500
C	3.75099300	7.88982700	27.84367200
H	5.47418000	8.08893900	26.57246500
C	3.27232600	7.49689500	29.09497200
H	3.79819500	6.68255700	31.02227200
H	3.06543200	8.27742600	27.09629100
H	2.21493900	7.58153000	29.32596500
C	6.82073800	5.48308200	26.38261800
C	6.08454400	4.52261200	27.09186800
C	6.59017200	5.63573600	25.01044100
C	5.13141400	3.73882800	26.44432800
H	6.26019000	4.39559300	28.15487300
C	5.63094000	4.85661700	24.36428100
H	7.16213200	6.35895800	24.44748400
C	4.89813000	3.90644500	25.07743200
H	4.57170600	2.99795800	27.00706300
H	5.45908500	4.99203400	23.30073200
H	4.15326200	3.29897700	24.57253300
C	9.66708400	5.40147800	25.55670200
C	9.39572100	4.04467800	25.34264000
C	10.33636500	6.13007600	24.56328100
C	9.78557100	3.43046700	24.15252500
H	8.87121300	3.47620000	26.10289700
C	10.70929700	5.52010700	23.36762500
H	10.54969600	7.17997600	24.72727400
C	10.43741900	4.16643200	23.15960600
H	9.57329100	2.37713400	23.99716500
H	11.20124800	6.10594100	22.59770000
H	10.73653500	3.68661200	22.23320200
C	16.33719300	4.89900300	26.71559100
C	17.59881000	4.67268200	27.29075900
C	15.22294400	4.24153700	27.25374600

C	17.74792000	3.79964000	28.36583200
H	18.46803300	5.17358200	26.87603400
C	15.37826300	3.35316400	28.31857200
H	14.23658500	4.43912500	26.85892700
C	16.63627400	3.12738600	28.87795400
H	18.73201300	3.63581600	28.79417700
H	14.50893500	2.83962700	28.71632100
H	16.74933000	2.43584000	29.70718000
C	15.21061700	3.95739900	24.14192100
C	16.02757300	2.88712500	23.75886500
C	13.85541000	3.72435100	24.40482300
C	15.50089200	1.59989700	23.64918800
H	17.07709200	3.06836000	23.54850200
C	13.32893600	2.43729800	24.29417600
H	13.21277300	4.54696500	24.70125400
C	14.14963400	1.37220800	23.91813900
H	16.14508000	0.77711500	23.35394300
H	12.27690700	2.27411600	24.50040100
H	13.73856400	0.37073200	23.83384500
C	15.48789100	5.56646800	21.78613600
C	16.39024700	5.23588700	20.76736500
C	14.11538400	5.40011100	21.56017500
C	15.92852100	4.74384200	19.54689400
H	17.45414600	5.36979200	20.93428600
C	13.65233500	4.91478500	20.33818400
H	13.41350700	5.65506900	22.34535000
C	14.55835000	4.58336000	19.32812400
H	16.63851700	4.48690100	18.76667100
H	12.58516900	4.79736000	20.17463300
H	14.19928600	4.20342400	18.37655600
C	16.89973800	8.15245000	21.89984400
C	18.20670800	8.51315700	21.54511200
C	15.83469700	8.56903300	21.08970900
C	18.44698700	9.27196600	20.40041700
H	19.03410400	8.19903800	22.17270100
C	16.07602800	9.32076500	19.94151600
H	14.81990900	8.31065800	21.36785100
C	17.38107300	9.67439800	19.59334900
H	19.46318400	9.55266800	20.14160000
H	15.24192300	9.64807900	19.33026400
H	17.56340000	10.26406000	18.70006900
C	19.41954400	13.69608500	24.08837200
C	20.22933900	14.36115700	25.01969300
C	19.83297100	12.45546800	23.58681600
C	21.44159900	13.80649500	25.42666200
H	19.91370900	15.32358100	25.40956800
C	21.04398700	11.90133500	23.99604200
H	19.20907500	11.92215500	22.88203200
C	21.85562000	12.57701800	24.90975700
H	22.06354200	14.33587700	26.14177000
H	21.35166600	10.93860600	23.59990700

H	22.80040000	12.14412900	25.22361300
C	19.03409800	14.21585100	21.24126800
C	20.33155900	14.74262400	21.26784200
C	18.71766300	13.22403300	20.30453900
C	21.29600900	14.28819100	20.36975900
H	20.58415600	15.50170700	22.00114300
C	19.68584700	12.76304800	19.41311200
H	17.71907300	12.80500300	20.28630900
C	20.97670100	13.29463600	19.44127700
H	22.29759600	14.70621800	20.39819100
H	19.43155200	11.98809400	18.69667400
H	21.72946300	12.93629600	18.74589000
C	16.75243100	15.75578300	20.32824900
C	17.72140300	16.56269900	19.71582700
C	15.65918800	15.31326100	19.57194800
C	17.60249700	16.91600500	18.37273700
H	18.56810900	16.91289700	20.29616100
C	15.54573500	15.65951400	18.22609700
H	14.90014200	14.69834600	20.03778800
C	16.51574400	16.46193100	17.62213000
H	18.35839200	17.54546300	17.91316800
H	14.69721100	15.30302900	17.65005000
H	16.42478000	16.73345700	16.57488200
C	14.70114900	16.63879500	22.25575300
C	14.89271100	17.92594700	21.73604800
C	13.39720500	16.15389800	22.41307900
C	13.79733600	18.72106100	21.39742000
H	15.90114700	18.30493600	21.60652900
C	12.30454000	16.94140900	22.05708500
H	13.24382800	15.16252100	22.82010300
C	12.49910500	18.23157300	21.55940200
H	13.95918100	19.72190200	21.00899100
H	11.29886200	16.55526500	22.18185000
H	11.64291000	18.84855200	21.30478100
C	10.77667300	17.22424100	26.65317500
C	10.93967900	17.80520700	27.92080900
C	11.50856100	17.73572000	25.57532100
C	11.81039500	18.87753300	28.10091400
H	10.37145600	17.42153400	28.76166200
C	12.37805300	18.80881100	25.75406500
H	11.41299800	17.28729500	24.59545000
C	12.52975200	19.38631700	27.01476300
H	11.92275900	19.32051900	29.08575600
H	12.94769300	19.17602200	24.90644500
H	13.20545600	20.22471200	27.15456300
C	8.66590000	17.38744400	24.59897900
C	8.45058400	18.67169100	25.11581900
C	8.80696700	17.22831500	23.21443300
C	8.38653200	19.77489600	24.26616000
H	8.34498700	18.80304700	26.18766700
C	8.75037200	18.33228400	22.36367300

H	8.96538400	16.23638300	22.80551700
C	8.54206400	19.60974400	22.88778900
H	8.21851000	20.76406200	24.68089100
H	8.86858000	18.19294900	21.29341000
H	8.49765000	20.46976900	22.22680700
C	6.60633000	15.38836900	24.46995800
C	5.55071900	16.25341700	24.78144000
C	6.57813200	14.68482300	23.26011500
C	4.48383700	16.41211600	23.89668700
H	5.57172300	16.80311800	25.71720100
C	5.51337300	14.84536800	22.37346200
H	7.39929400	14.02068700	23.00933800
C	4.46292400	15.70895400	22.69037800
H	3.67039800	17.08551300	24.14906800
H	5.50527800	14.29676100	21.43663200
H	3.63349500	15.83405300	22.00117100
C	6.59452000	13.15664800	26.41198800
C	5.79696200	13.18270100	27.56528300
C	6.32834600	12.20865200	25.42014200
C	4.75046200	12.27624100	27.72219100
H	6.00813200	13.91245000	28.34082300
C	5.28148300	11.29934400	25.57773400
H	6.95113700	12.16737300	24.53611000
C	4.49036100	11.33098200	26.72679000
H	4.13994400	12.30572600	28.61960800
H	5.09465700	10.56151000	24.80573000
H	3.68054300	10.62079800	26.85126500
C	15.05522400	10.85478100	32.95271800
N	15.71832400	11.52665700	32.15840700
N	14.42152400	10.07559400	33.64680600
C	13.29858200	10.39815500	34.54257600
C	12.16580600	9.38947000	34.32201500
C	13.78564700	10.36666300	35.99734600
H	12.92859600	11.40698800	34.32042400
C	11.00636100	9.63540700	35.29535600
H	12.57177200	8.38180700	34.47359600
H	11.81989300	9.44078000	33.28654200
C	12.62588800	10.62062000	36.96974600
H	14.23017600	9.38227500	36.19271600
H	14.57783300	11.11137000	36.13241000
C	11.48406100	9.61883900	36.75298200
H	10.22987700	8.87789300	35.13876300
H	10.54464400	10.60675400	35.07483200
H	12.99101000	10.57037500	38.00146500
H	12.24517500	11.64033900	36.82015600
H	10.65092800	9.84052200	37.42955200
H	11.83747400	8.60955500	37.00518600
C	16.95406200	12.23536100	32.57047100
C	18.14885100	11.61513400	31.84019200
C	16.80380900	13.72262100	32.23974500
H	17.09634700	12.11984000	33.65401100

C	19.44335800	12.38652300	32.12322400
H	17.93622900	11.62720600	30.76804600
H	18.24846500	10.56373900	32.13342500
C	18.10190800	14.49464300	32.50813500
H	16.52700600	13.80669000	31.18544600
H	15.97445400	14.14238400	32.82110000
C	19.28969000	13.86959600	31.76443200
H	20.26680800	11.93765800	31.55662600
H	19.70398200	12.29499600	33.18681300
H	17.97188600	15.54130500	32.21180900
H	18.31276000	14.49603800	33.58664700
H	20.21172100	14.41603000	31.99382500
H	19.12801500	13.96095200	30.68210200
C	13.22032200	10.87105400	25.58686500
C	11.88780000	10.48505600	25.23230500
C	14.22472100	10.75298600	24.51473200
C	11.51981200	10.34108200	23.86371800
C	10.91059200	10.22624200	26.22826000
O	14.64891700	9.66709700	24.17031900
O	14.62911400	11.94333700	24.02249600
C	10.24235300	9.95193700	23.51348000
H	12.24361600	10.53705400	23.08299100
C	9.62947900	9.82146400	25.87229800
H	11.17748200	10.33514700	27.26849700
C	15.52103500	11.90603300	22.90017000
C	9.30666700	9.67888900	24.52114500
H	9.97150600	9.83528000	22.47031900
H	8.89198200	9.61709700	26.63716400
H	16.08051600	10.97165300	22.86094200
H	16.19918500	12.74918200	23.00502100
C	14.69300200	12.08572600	21.64463900
C	7.95483700	9.18126700	24.09006100
F	13.84497600	11.05183900	21.43967700
F	13.93594600	13.20446600	21.70145700
F	15.48394700	12.19055300	20.55845600
F	8.07863400	8.07962600	23.31056700
F	7.29405200	10.09808100	23.34618700
F	7.16855000	8.85616700	25.13459400

2. Analysis of 2-chloropyridine coordination.

Table D10. The total energies (in hartree) of all structures involved in the reactions 2Clpyridine + $Rh_2(AcO)_4$, 2Clpyridine+ (Car1)$Rh_2(AcO)_4$, and 2Clpyridine+ styrene + (Car1)$Rh_2(AcO)_4$ calculated **BS1** level of theory (see text above).

Structure	$-E_{tot}$	$-E_{tot}$+ZPEC	-H	-G
2-Clpyridine	707.906103	707.826758	707.820447	707.85648
Styrene	309.684578	309.550918	309.543227	309.58227
$Rh_2(AcO)_4$	1133.220474	1133.009877	1132.987377	1133.062808

2Clpyridine-$Rh_2(AcO)_4$	1841.159267	1840.867685	1840.838108	1840.93031
2(2Clpyridine)-$Rh_2(AcO)_4$	2549.089427	2548.717632	2548.680500	2548.793268
(Car1)-$Rh_2(AcO)_4$ (**14**)	4202.251773	4201.901925	4201.867390	4201.970813
$Rh_2(AcO)_4$–(Car1)(2Clpyridine)-ester side (**21**)	4910.177688	4909.746846	4909.704484	4909.825252
$Rh_2(AcO)_4$–(Car1)(2Clpyridine)-carbonyl side (**20**)	4910.179834	4909.749191	4909.706720	4909.828134
$Rh_2(AcO)_4$–(Car1)(styrene)-ester side (**19**)	4511.961532	4511.476164	4511.432556	4511.556028
$Rh_2(AcO)_4$–(Car1)(styrene)-carbonyl side (**18**)	4511.957276	4511.472200	4511.428413	4511.552566
$Rh_2(AcO)_4$–(Car1)(styrene)-ester side-cyclopropanation transition state (**24**)	4511.960628	4511.474719	4511.432395	4511.551818
$Rh_2(AcO)_4$–(Car1)(2Clpyridine)-carbonyl side-(styrene)-ester side (**25**)	5219.884619	5219.318814	5219.267976	5219.408219
$Rh_2(AcO)_4$–(Car1)(2Clpyridine)-carbonyl side-(styrene)-ester side-cyclopropanation transition state (**23**)	5219.886106	5219.319648	5219.270972	5219.405408
Cyclopropane product **26**	3378.777147	3378.499846	3378.480950	3378.548664

Table D11. The total energies (in hartree) of all structures involved in the reactions styrene + (Car2)$Rh_2(AcO)_4$ calculated **BS1** level of theory for comparison with Car1.

Structure	$-E_{tot}$	$-E_{tot}$+ZPEC	-H	-G
Styrene	309.684578	309.550918	309.543227	309.58227
$Rh_2(AcO)_4$	1133.220474	1133.009877	1132.987377	1133.062808
(Car2)-$Rh_2(AcO)_4$ (**15**)	4202.251773	4201.901925	4201.867390	4201.970813
$Rh_2(AcO)_4$–(Car1)(styrene)-ester side (**17**)	Could not be computed due to barrierless TS for cyclopropanation			
$Rh_2(AcO)_4$–(Car1)(styrene)-carbonyl side (**16**)	4511.965292	4511.480241	4511.436354	4511.561769

Table D12. The total energies (in hartree) of all structures involved in the reactions styrene + (Car1)$Rh_2(TPPTTL)_4$ calculated **BS1** level of theory.

Structure	$-E_{tot}$	$-E_{tot}$+ZPEC	-H	-G
$Rh_2(TPPTTL)_4$ (**5**)	7507.529159	7505.182880	7505.031339	7505.383157
$Rh_2(TPPTTL)_4$(2Clpyridine)	8923.436005	8920.926931	8920.761511	8921.142967

(Car1)-Rh_2(TPPTTL)$_4$ (**27**)

10576.608885 10574.121261 10573.957877 10574.332315

(2Clpyridine)-Rh_2(TPPTTL)$_4$-(Car1) (**29**)

11284.541006 11281.972846 11281.802086 11282.194753

Table D13. The calculated 2Clpyridine/styrene/Car1-catalyst interaction energies (in kcal/mol) at **BS1** and comparison with catalyst-Car2. "Minus" means that interaction is thermodynamically stable).

Structure	ΔE_{tot}	$_{\Delta}E_{tot}$+ZPEC	ΔH	ΔG
[B3LYP-D3(BJ)]/BS1				
2Clpyridine + $Rh_2(AcO)_4$	0.0	0.0	0.0	0.0
2Clpyridine-$Rh_2(AcO)_4$	-20.5	-19.4	-19.0	-4.2
2(2Clpyridine) + $Rh_2(AcO)_4$	0.0	0.0	0.0	0.0
2(2Clpyridine)-$Rh_2(AcO)_4$	-35.5	-33.9	-32.7	-9.9
2Clpyridine + (Car1)-$Rh_2(AcO)_4$	0.0	0.0	0.0	0.0
$Rh_2(AcO)_4$–(Car1)(2Clpyridine)-carbonyl (**20**)	-13.8	-12.9	-11.8	-0.5
$Rh_2(AcO)_4$–(Car1)(2Clpyridine)-ester (**21**)	-12.4	-11.4	-10.4	+1.3
Styrene + (Car1)-$Rh_2(AcO)_4$	0.0	0.0	0.0	0.0
$Rh_2(AcO)_4$–(Car1)(styrene)-carbonyl (**18**)	-13.1	-12.1	-11.2	+0.3
$Rh_2(AcO)_4$–(Car1)(styrene)-ester (**19**)	-15.8	-14.6	-13.8	-1.8
Styrene + 2Clpyridine+(Car1)-$Rh_2(AcO)_4$	0.0	0.0	0.0	0.0
$Rh_2(AcO)_4$–(Car1)-(2Clpyridine)-carbonyl-(styrene)-ester (**25**)	-26.4	-24.6	-23.2	+0.8
$Rh_2(AcO)_4$–(Car1) (**14**)	0.0	0.0	0.0	0.0
$Rh_2(AcO)_4$–(Car2) (**15**)	-3.8	-3.7	-3.1	-5.7
$Rh_2(AcO)_4$–(Car1) -(styrene)-ester	0.0	0.0	0.0	0.0
$Rh_2(AcO)_4$–(Car2) -(styrene)-ester	-1.1	-1.6	-1.2	-3.4
2(2Clpyridine) + Rh_2(TPPTTL)$_4$	0.0	0.0	0.0	0.0
2(2Clpyridine)-Rh_2(TPPTTL)$_4$	-59.4	-56.8	-56.0	-29.3
(2Clpyridine) + Rh_2(TPPTTL)$_4$-(Car1)	0.0	0.0	0.0	0.0
(2Clpyridine)-Rh_2(TPPTTL)$_4$-(Car1) (**29**)	-16.3	-15.5	-14.9	-3.7

Table D14. The calculated car1-catalyst transition state barriers to cyclopropanation (in kcal/mol) at **BS1** both with and without 2Clpyridine.

Structure	ΔE_{tot}	$_{\Delta}E_{tot}$+ZPEC	ΔH	ΔG
$Rh_2(AcO)_4$–(Car1)(styrene)-ester (**24**)				
	0.0	0.0	0.0	0.0
Transition state barrier:	+0.6	+0.5	+0.1	+2.6
$Rh_2(AcO)_4$–(Car1)-(2Clpyridine)-carbonyl-(styrene)-ester (**23**)				
	0.0	0.0	0.0	0.0
Transition state barrier:	-0.9	-0.5	-1.87	+1.8
$Rh_2(AcO)_4$–(Car1)-(styrene)-ester (**24**)				
	0.0	0.0	0.0	0.0
$Rh_2(AcO)_4$ + Cyclopropane **26**	-22.7	-21.2	-22.5	-35.9
$Rh_2(AcO)_4$–(Car1) -(2Clpyridine)-carbonyl-(styrene)-ester (**23**)				
	0.0	0.0	0.0	0.0
$Rh_2(AcO)_4$ -(2Clpyridine)+ Cyclopropane **26**				
	-32.5	-30.6	-32.1	-44.4

Table D15: Cartesian Coordinates (in Å) of all 2-clpyridine related calculated structures.

2-Clpyridine [B3LYP-D3(BJ)]/BS1

C	1.46279300	-1.21212200	0.00030900
C	2.23926800	-0.05632900	0.00018100
C	1.58922700	1.17946900	-0.00002700
C	0.19682600	1.21541100	-0.00019500
C	-0.46493100	-0.01268600	-0.00021800
N	0.11873100	-1.19655700	0.00010400
H	2.15505900	2.10530500	-0.00007200
H	1.92694800	-2.19487900	0.00046100
H	3.32106500	-0.12430700	0.00028400
H	-0.35383200	2.14766300	-0.00030200
Cl	-2.23643900	-0.01413700	-0.00008300

Styrene [B3LYP-D3(BJ)]/BS1

C	0.83700200	0.88511400	0.19319900
C	2.23635000	0.99411100	0.08950900
C	2.84496500	2.23707900	-0.05708700
C	2.07261400	3.40268300	-0.10393200
C	0.68394600	3.31142500	-0.00222500
C	0.07533700	2.06512600	0.14470500
H	2.85261600	0.10145800	0.12396100
H	3.92634200	2.29958900	-0.13519500
H	2.55113800	4.37044400	-0.21851000
H	0.07391600	4.20908300	-0.03726200
H	-1.00657500	1.99887900	0.22318100
C	0.14145000	-0.40226200	0.34894800
C	0.69415700	-1.62034500	0.41132800
H	-0.94298300	-0.32452300	0.41809500

H	1.76604800	-1.78371600	0.34974900
H	0.07711700	-2.50511600	0.52808400

2Clpyridine-Rh2(AcO)4 [B3LYP-D3(BJ)]/BS1

O	-0.61325500	-1.17171200	2.23159100
O	-2.86108600	-0.93531400	0.36803100
O	-0.98200800	-0.88804000	-1.87719000
O	1.25333300	-1.12104000	-0.01358600
O	-2.95852900	-3.19872500	0.26606800
O	-1.06138200	-3.15070300	-2.01601500
O	1.15472200	-3.38159600	-0.14273100
O	-0.71601100	-3.43260800	2.09632100
C	-0.61382700	-2.33616500	2.73995800
C	1.78057200	-2.27042800	-0.13252700
C	-1.07149100	-1.98126900	-2.52072800
C	-3.48298500	-2.04431600	0.38448300
Rh	-0.79878700	-0.95603100	0.18276700
C	3.27783200	-2.33709500	-0.30776300
H	3.50230800	-2.45338400	-1.37325200
H	3.74706600	-1.42137700	0.05221200
H	3.67961700	-3.20530100	0.21760300
C	-1.23690400	-1.89302200	-4.01839800
H	-0.87145700	-0.93471600	-4.38825800
H	-0.71234400	-2.71684900	-4.50516900
H	-2.30166700	-1.97976300	-4.25948700
C	-4.97774800	-2.00121400	0.59020200
H	-5.36750600	-1.00797500	0.36695100
H	-5.46402600	-2.75255400	-0.03467300
H	-5.19609300	-2.24045800	1.63622100
C	-0.51765300	-2.44162200	4.24215900
H	-1.52804600	-2.54491000	4.65178200
H	0.05285100	-3.32863800	4.52243200
H	-0.06121600	-1.54440700	4.66076100
Rh	-0.91063500	-3.36949100	0.03459500
N	-0.86423000	-5.61339000	0.00717000
C	0.11484700	-6.12103100	0.78514400
C	-1.63748900	-6.46812900	-0.66339900
C	0.34462700	-7.48380900	0.90770200
H	0.71531900	-5.38959700	1.31090500
C	-1.48406500	-7.85339500	-0.60467600
C	-0.47072700	-8.36617000	0.19777600
H	1.14487900	-7.84013900	1.54518900
H	-2.14389300	-8.49526300	-1.17414200
H	-0.32295200	-9.43857100	0.26586900
Cl	-2.90834400	-5.81671000	-1.66534800

2(2Clpyridine)-Rh2(AcO)4 [B3LYP-D3(BJ)]/BS1

O	-0.98615900	-1.14577200	1.98360900
O	-2.77748600	-0.97634600	-0.30653400
O	-0.48934500	-1.04823700	-2.12987900
O	1.32727500	-1.22342800	0.20477700
O	-2.88886800	-3.24018500	-0.35513700
O	-0.56181700	-3.31439800	-2.18663700

O	1.22050400	-3.48625500	0.11190900
O	-1.07242700	-3.40936900	1.92533100
C	-1.10816300	-2.28919600	2.52682500
C	1.84548600	-2.38278700	0.22901900
C	-0.44712800	-2.16946000	-2.72813100
C	-3.40709000	-2.08099400	-0.38084800
C	3.34671100	-2.46147200	0.37514300
H	3.79624200	-2.46531400	-0.62364500
H	3.72315700	-1.59361200	0.91792000
H	3.63231800	-3.38426900	0.88206400
C	-0.20352900	-2.14098400	-4.21886600
H	0.87604100	-2.18469400	-4.39863900
H	-0.66563300	-3.00580700	-4.69683500
H	-0.58591000	-1.21497400	-4.65014600
C	-4.91239800	-2.00121300	-0.47621100
H	-5.21083600	-1.10826000	-1.02760000
H	-5.31335400	-2.89676200	-0.95198900
H	-5.32493700	-1.93099200	0.53597600
C	-1.35106700	-2.32106900	4.01697100
H	-2.43014000	-2.38014100	4.19505100
H	-0.88638000	-3.20478700	4.45715400
H	-0.97042400	-1.41410000	4.48758500
Rh	-0.83657200	-3.44459800	-0.13915400
N	-0.82569500	-5.78271800	-0.01605500
C	-0.04958400	-6.22972500	0.99157900
C	-1.45171600	-6.68557500	-0.76407900
C	0.11515700	-7.57993700	1.27144600
H	0.44206000	-5.45984900	1.57389000
C	-1.35390000	-8.06344000	-0.56795800
C	-0.55080000	-8.51321400	0.47522400
H	0.75017800	-7.88883100	2.09338700
H	-1.89048800	-8.74657200	-1.21394700
H	-0.44841200	-9.57709900	0.66102400
Cl	-2.45658400	-6.09784000	-2.07177200
Rh	-0.71801700	-1.01591600	-0.06909700
N	-0.77310800	1.31490700	0.16093000
C	0.02726700	2.24841700	-0.34337100
C	-1.78010100	1.71572700	0.96272200
C	-0.11127900	3.61352100	-0.09067200
C	-2.00549200	3.04957400	1.27673900
H	-2.40797100	0.92178800	1.34862400
C	-1.15293000	4.01547000	0.73933900
H	0.57621300	4.32334800	-0.53269000
H	-2.82913900	3.32107400	1.92648500
H	-1.29453300	5.06797400	0.96085500
Cl	1.32946700	1.72037400	-1.38752600

(Car1)-Rh2(AcO)4 (14) [B3LYP-D3(BJ)]/BS1

O	-0.20012000	-0.99960100	2.42984000
O	-2.13296700	-0.18682300	0.37958500
O	-0.04077600	-0.44675400	-1.66701700

O	1.87789500	-1.19951300	0.36601700
O	-2.68211400	-2.35389500	-0.00840700
O	-0.55273000	-2.63484000	-1.98649000
O	1.33393200	-3.38959500	0.12809000
O	-0.79663500	-3.16432200	2.11077100
C	-0.51606700	-2.17050600	2.84136900
C	2.16314600	-2.44112100	0.25791800
C	-0.26788100	-1.46950700	-2.39656300
C	-2.96573200	-1.13067900	0.15660400
C	3.63384100	-2.77999900	0.26960100
H	4.07827200	-2.46350100	-0.67930500
H	4.13386500	-2.23111000	1.07058400
H	3.77971000	-3.85272400	0.39420000
C	-4.41470800	-0.71916000	0.06273200
H	-4.57400600	-0.20987600	-0.89318200
H	-5.06590100	-1.59137900	0.11669700
H	-4.65477600	-0.01324500	0.86040500
C	-0.54639500	-2.35058000	4.33893800
H	-0.83517300	-3.36867300	4.59789400
H	0.44314300	-2.12892800	4.74848600
H	-1.25161700	-1.63918700	4.77700300
Rh	-0.69514600	-2.96431000	0.04758300
Rh	-0.10613400	-0.60289100	0.40099800
C	0.36401500	1.34632100	0.64029100
C	1.55686300	1.85320100	1.23402300
C	2.22551200	1.02403200	2.18131500
C	2.12934600	3.14096200	0.99116900
C	3.35225100	1.45522000	2.86266300
H	1.79649300	0.05605700	2.39359700
C	3.27708700	3.55604000	1.64817100
C	3.88167900	2.71791300	2.59086900
H	3.70164300	4.52794100	1.42904300
H	4.77197200	3.06187600	3.10723200
C	-0.74751500	2.24044700	0.25693900
O	-1.05916500	2.26719600	-1.03381500
C	-2.26594900	2.98542500	-1.36491800
H	-2.18234000	4.03061500	-1.05980600
H	-2.35993000	2.90829700	-2.44627800
H	-3.12023200	2.52158000	-0.86869200
O	-1.38495700	2.77275400	1.15385600
C	-0.19977200	-1.24245500	-3.88741400
H	-1.02446600	-0.58867000	-4.18687600
H	0.73413000	-0.73546600	-4.14125000
H	-0.27268600	-2.18867800	-4.42295000
Br	1.41396900	4.33536000	-0.30496000
H	3.82089500	0.81093600	3.59795600

Rh2(AcO)4–(Car1)(2Clpyridine)-ester side (21) [B3LYP-D3(BJ)]/BS1

O	-0.10782200	-0.98683200	2.34125500
O	-2.26987800	-0.31914500	0.50748600
O	-0.41662300	-0.30866700	-1.73036700

O	1.79877800	-0.91579300	0.08054800
O	-2.62310500	-2.54850000	0.25977200
O	-0.86107400	-2.50942100	-2.06186300
O	1.43818300	-3.11399500	-0.35649400
O	-0.33629600	-3.21294400	1.97894800
C	-0.16121000	-2.20668000	2.72511400
C	2.18145500	-2.09461200	-0.22659000
C	-0.71316800	-1.31279100	-2.45711700
C	-3.01350100	-1.35659300	0.44210100
C	3.65699200	-2.26591000	-0.49136200
H	3.84009800	-2.07281600	-1.55324300
H	4.23434800	-1.54453800	0.08720700
H	3.96820400	-3.28630900	-0.26481200
C	-4.49692300	-1.11163500	0.57859100
H	-4.85675500	-0.60814300	-0.32429700
H	-5.03146200	-2.05313400	0.70292700
H	-4.68861500	-0.45016300	1.42626200
C	0.00059500	-2.43466000	4.20784600
H	-0.04225200	-3.49821800	4.44051400
H	0.95683800	-2.01838100	4.53648800
H	-0.79157600	-1.90511200	4.74444700
Rh	-0.60548000	-2.92049000	-0.05432700
Rh	-0.21635200	-0.51886400	0.31987000
C	0.11846500	1.46297600	0.62083800
C	1.21757200	2.04404100	1.31939900
C	1.96494100	1.20509200	2.19354400
C	1.61589200	3.41749100	1.26175000
C	2.97935900	1.69801300	2.99889200
H	1.69023500	0.16376100	2.24744200
C	2.64832500	3.90312300	2.04722600
C	3.32050300	3.04789400	2.92699900
H	2.93649700	4.94445700	1.97283000
H	4.11888600	3.44728800	3.54414300
C	-1.04349200	2.28569700	0.22791300
O	-1.26920600	2.40237600	-1.07892700
C	-2.46019000	3.13069500	-1.43961700
H	-2.39507500	4.15901000	-1.07649100
H	-2.49179500	3.11040200	-2.52724600
H	-3.34203300	2.64578500	-1.01774200
O	-1.78821600	2.68952200	1.10892400
C	-0.87622000	-1.05017300	-3.93485300
H	-1.15581800	-0.01155600	-4.11189600
H	0.07952700	-1.24301900	-4.43198700
H	-1.62301100	-1.72619300	-4.35393400
N	2.25028300	1.92020100	-1.68742400
C	1.48444900	1.80168700	-2.78355700
C	3.42671300	1.32540100	-1.70359100
C	1.89073800	1.10238200	-3.91734700
H	0.51234400	2.27728800	-2.72654400
C	3.93713200	0.57967800	-2.76622500
Cl	4.43151800	1.52984500	-0.26371100

C	3.13680500	0.47445300	-3.90209000
H	1.24556400	1.04875500	-4.78606500
H	4.91543500	0.11962100	-2.70697400
H	3.48720800	-0.08696300	-4.76218400
H	3.50839800	1.03269700	3.67203200
Br	0.83396800	4.65725600	0.05236400

Rh2(AcO)4–(Car1)(2Clpyridine)-carbonyl side (20) [B3LYP-D3(BJ)]/BS1

O	0.02998800	-1.29799300	2.36578600
O	-2.37575900	-0.75520400	0.82718200
O	-0.78445300	-0.45193600	-1.60577700
O	1.65834600	-0.98105800	-0.06036300
O	-2.60663000	-2.96547100	0.37096500
O	-0.96921300	-2.67206300	-2.03312400
O	1.44760900	-3.20622300	-0.44858500
O	-0.20886900	-3.51391000	1.94895200
C	0.01453200	-2.52892400	2.71103600
C	2.11592800	-2.13398900	-0.37248600
C	-1.00815900	-1.45128700	-2.36897200
C	-3.05110100	-1.83437800	0.73063700
C	3.58798900	-2.19126200	-0.70005800
H	3.74354600	-1.77358000	-1.70005200
H	4.15284500	-1.58187000	0.00819000
H	3.94293000	-3.22163100	-0.68562800
C	-4.50653900	-1.73774900	1.11792500
H	-5.06974500	-2.57299400	0.70142900
H	-4.58021400	-1.77088700	2.21009100
H	-4.92402700	-0.78708800	0.78193000
C	0.26546300	-2.80335500	4.17366900
H	-0.60615200	-2.47650500	4.74969100
H	0.42908900	-3.86718900	4.34356500
H	1.12814600	-2.22759400	4.51667100
Rh	-0.59114400	-3.16401500	-0.05654800
Rh	-0.34965400	-0.75293500	0.39733400
C	-0.11257200	1.26192500	0.67518200
C	0.80703900	1.92472000	1.53258800
C	1.74651500	1.10705100	2.23403900
C	0.91942900	3.34148600	1.74931200
C	2.72632700	1.63634200	3.05356800
H	1.67940200	0.04047500	2.09629900
C	1.89318500	3.86496200	2.58942300
C	2.79729900	3.01904500	3.23484000
H	1.94432000	4.93500000	2.74402500
H	3.55288700	3.45091500	3.88304900
C	-0.97319000	1.98952800	-0.28610000
O	-0.26677300	2.34063000	-1.37008800
C	-1.03582300	2.86521000	-2.47045500
H	-1.50474100	3.80939400	-2.18457800
H	-0.32123200	3.02215400	-3.27628000
H	-1.79968500	2.14479500	-2.76763700
O	-2.17319400	2.13744600	-0.15072600

C	-1.37133700	-1.11898400	-3.79569900
H	-2.39701900	-0.73677700	-3.81721300
H	-0.71505800	-0.33300700	-4.17480500
H	-1.30687000	-2.00643200	-4.42499500
N	-2.12297800	3.28707400	3.51694600
C	-2.46366800	2.05348300	3.10048200
C	-1.12123100	3.37278800	4.37000600
C	-1.82211700	0.89857500	3.53741300
H	-3.26365000	2.00014600	2.37026000
C	-0.39624900	2.29448200	4.87926400
Cl	-0.66812700	5.00651100	4.88544700
C	-0.76987000	1.02653900	4.44479300
H	-2.11102500	-0.06433100	3.14082400
H	0.42478700	2.44883300	5.56750800
H	-0.22909500	0.15295900	4.78836200
Br	-0.23283200	4.62147900	0.95570900
H	3.42709000	0.97940200	3.55622100

Rh2(AcO)4–(Car1)(styrene)-ester side (19) [B3LYP-D3(BJ)]/BS1

O	-0.42412100	-0.96913600	2.79250300
O	-2.41925800	-0.10088800	0.84643900
O	-0.50483400	-0.37979400	-1.30161100
O	1.56653000	-1.19693800	0.61536200
O	-3.03019100	-2.26297000	0.51512000
O	-1.04255500	-2.56207900	-1.61398200
O	0.96692600	-3.36817100	0.34718800
O	-1.02724400	-3.13386600	2.48451000
C	-0.72436000	-2.14109500	3.20871800
C	1.82074600	-2.43950900	0.44631100
C	-0.77302100	-1.39358700	-2.02669500
C	-3.27981800	-1.03442600	0.69951500
C	3.28389700	-2.79831500	0.35210200
H	3.70976900	-2.33286800	-0.54184100
H	3.81550800	-2.39535800	1.21810200
H	3.41478000	-3.87869500	0.30007600
C	-4.72706500	-0.61218100	0.78024100
H	-4.97361500	-0.38930000	1.82320100
H	-4.88168900	0.29966600	0.19951500
H	-5.37888400	-1.40787800	0.42003500
C	-0.72711900	-2.32516500	4.70659500
H	-1.57389400	-1.77674800	5.13088000
H	-0.81480800	-3.38045400	4.96377200
H	0.18679500	-1.90503800	5.13281600
Rh	-1.05790400	-2.90669100	0.42384000
Rh	-0.40365700	-0.55267400	0.75868200
C	0.15863100	1.39728300	1.02841900
C	1.27549900	1.86430200	1.77782300
C	1.91379200	0.94392800	2.66248600
C	1.79885300	3.19903100	1.77600000
C	2.93453400	1.32538700	3.51433800
H	1.54543800	-0.06873200	2.68318100

C	2.84509800	3.56927300	2.60589400
C	3.40650200	2.63837200	3.48284900
H	3.23330300	4.57851600	2.56100700
H	4.22075300	2.94677500	4.12972200
C	-0.90093400	2.32228700	0.57909800
O	-1.05097700	2.45264200	-0.73663600
C	-2.18113600	3.24472400	-1.15207600
H	-2.09325100	4.26288500	-0.76606500
H	-2.14991400	3.24425900	-2.24000600
H	-3.10880900	2.79532200	-0.79257600
O	-1.64959600	2.79464700	1.42265600
C	-0.75242200	-1.15418500	-3.51727500
H	-1.04752400	-2.05332100	-4.05749400
H	-1.42619800	-0.32983400	-3.76468200
H	0.25671700	-0.85646800	-3.81666000
Br	1.15645800	4.54746300	0.60250200
H	3.37698900	0.60005600	4.18784200
C	1.93915500	1.32750600	-1.62268100
C	2.82593300	2.31200200	-1.41344200
H	1.99040200	0.37177500	-1.11544600
H	1.11190900	1.45659100	-2.30817400
C	3.95213200	2.28216500	-0.47665900
H	2.70712700	3.24728900	-1.95717600
C	4.74425100	3.43516300	-0.32407300
C	4.26341500	1.14990700	0.30019700
C	5.80562200	3.46324300	0.57647300
H	4.50766600	4.31768900	-0.91192500
C	5.33057300	1.17572800	1.19116700
H	3.64914600	0.26012700	0.22572500
C	6.10317500	2.33132500	1.34009700
H	6.39878500	4.36616900	0.68608800
H	5.55037300	0.29634700	1.78903100
H	6.92927300	2.34893200	2.04434900

Rh2(AcO)4–(Car1)(styrene)-carbonyl side (18) [B3LYP-D3(BJ)]/BS1

O	-0.47402500	-1.28838600	2.40963100
O	-2.23924300	0.01632100	0.47996900
O	-0.21253200	-0.38913600	-1.62004900
O	1.54475200	-1.64071900	0.28529300
O	-3.13716900	-1.99591300	-0.06372700
O	-1.10404500	-2.41256900	-2.13482800
O	0.65140100	-3.67841700	-0.16565300
O	-1.39056800	-3.29868400	1.89803700
C	-0.96461200	-2.43038900	2.71423700
C	1.62427800	-2.89202800	0.03482800
C	-0.62315400	-1.27896800	-2.43805300
C	-3.21808100	-0.76393800	0.22082100
C	3.02175100	-3.45665200	-0.04572700
H	3.48800800	-3.11498000	-0.97531500
H	3.62241700	-3.08075700	0.78531500
H	2.99731600	-4.54611800	-0.03630600

C	-4.59031400	-0.13826500	0.28227800
H	-4.81912400	0.11829100	1.32116700
H	-4.59954200	0.78800200	-0.29704400
H	-5.34453700	-0.82778800	-0.09593100
C	-1.05646200	-2.73736500	4.18861200
H	-1.91083000	-2.19694000	4.60905800
H	-1.20045100	-3.80597700	4.34764700
H	-0.15608600	-2.39107300	4.69922400
Rh	-1.27920200	-2.91591800	-0.13702000
Rh	-0.30841100	-0.72680200	0.42394500
C	0.49586000	1.08698300	0.84375600
C	1.75434300	1.31221900	1.46333500
C	2.26783100	0.27894300	2.30410700
C	2.54367700	2.50212200	1.35992000
C	3.44762600	0.43045700	3.00999200
H	1.67256200	-0.61340000	2.42111600
C	3.74471600	2.63436500	2.03559800
C	4.18643500	1.60719300	2.87412000
H	4.32362000	3.54258400	1.93351500
H	5.11383600	1.73805200	3.42135900
C	-0.43549700	2.19168000	0.54016300
O	-0.68019000	2.40678000	-0.74824900
C	-1.68996800	3.39779000	-1.03064600
H	-1.38864000	4.36733700	-0.62790600
H	-1.75879700	3.43823500	-2.11581200
H	-2.64314800	3.09543100	-0.59363900
O	-1.01891100	2.73696900	1.46783600
C	-0.54242300	-0.91616200	-3.90132700
H	-0.67094200	-1.80184800	-4.52336600
H	-1.33648500	-0.19831400	-4.13084100
H	0.41417400	-0.43527800	-4.11538200
Br	2.04777300	3.95033900	0.23222100
H	3.79032300	-0.35851100	3.66978500
C	0.12940000	0.81731900	5.46592700
C	0.25864700	1.81994100	4.58781400
H	0.78270600	0.70190000	6.32636700
H	-0.65139800	0.07448100	5.34632000
C	1.27006800	2.88786800	4.61846800
H	-0.44331000	1.88657800	3.75934100
C	1.09026100	4.01626800	3.80099500
C	2.42480200	2.82199900	5.41845400
C	2.02198700	5.05401600	3.79514300
H	0.22171500	4.06098400	3.15205600
C	3.35765000	3.85508500	5.40909500
H	2.60386500	1.94547500	6.03272700
C	3.16009200	4.97792700	4.59821900
H	1.86541000	5.91287800	3.14993800
H	4.24725300	3.78196300	6.02781300
H	3.89214600	5.77975400	4.58915600

Rh2(AcO)4–(Car1)(styrene)-ester side-cyclopropanation transition state (24) [B3LYP-D3(BJ)]/BS1

Imaginary λ=-164

O	-0.27964700	-0.75121700	2.62199700
O	-2.20202000	0.04641800	0.57354700
O	-0.31890800	-0.61882400	-1.51927400
O	1.67785100	-1.41802900	0.46371100
O	-2.99768700	-2.08016500	0.59524300
O	-1.15283100	-2.72681500	-1.57501200
O	0.87881700	-3.53869100	0.37983100
O	-0.98794700	-2.90575600	2.56109000
C	-0.63028400	-1.85033500	3.16641000
C	1.81538800	-2.68791200	0.39026700
C	-0.76375200	-1.65084300	-2.12187800
C	-3.13800800	-0.81833300	0.58507000
C	3.23704300	-3.18832800	0.30495100
H	3.69502100	-2.81565400	-0.61597000
H	3.81365300	-2.79028100	1.14417900
H	3.26583700	-4.27748200	0.31467800
C	-4.54620200	-0.27314000	0.55242500
H	-5.24805600	-1.00100500	0.96062400
H	-4.60089200	0.66576200	1.10549000
H	-4.81869500	-0.07080000	-0.48891500
C	-0.63322300	-1.86720300	4.67643900
H	-1.51439500	-1.32464900	5.03412600
H	-0.67062900	-2.89056300	5.04981600
H	0.25200900	-1.35287600	5.05605100
Rh	-1.09520300	-2.88399200	0.48990200
Rh	-0.22252500	-0.57956400	0.55515800
C	0.55900100	1.42401700	0.72155200
C	1.51435400	1.81894300	1.75263200
C	2.18154400	0.80933500	2.48953300
C	1.88152900	3.15664300	2.07749300
C	3.08102100	1.09565100	3.50840900
H	1.96713600	-0.21735600	2.24222200
C	2.78653100	3.45139800	3.09042200
C	3.38232600	2.42006000	3.81702700
H	3.03797700	4.48414500	3.29807600
H	4.08767900	2.66113100	4.60553000
C	-0.57171100	2.33835100	0.43734600
O	-0.81392200	2.59770800	-0.85699900
C	-2.03263100	3.31842200	-1.11339400
H	-2.01407000	4.28843000	-0.61138600
H	-2.07218300	3.44837200	-2.19385700
H	-2.89040300	2.74166000	-0.76230800
O	-1.30638500	2.69439400	1.34707000
C	-0.84857800	-1.55528000	-3.62675900
H	-1.00918800	-2.53935200	-4.06685900
H	-1.68554000	-0.90195400	-3.89342600
H	0.06416000	-1.10548000	-4.02334100
Br	1.22384900	4.67017600	1.10865800
H	3.55533400	0.28366200	4.04929800
C	1.77757600	1.31544300	-1.10691400

C	2.54305500	2.46119000	-1.10598800
H	2.19917800	0.37094700	-0.78775300
H	0.91242000	1.25168900	-1.74895800
C	3.78343700	2.62701400	-0.39287200
H	2.14843100	3.34644100	-1.59770600
C	4.37607600	3.90891200	-0.33291800
C	4.39026700	1.56586700	0.31687200
C	5.51180500	4.12972700	0.43181100
H	3.90957500	4.72818500	-0.87035400
C	5.52626500	1.79227300	1.08250300
H	3.96118400	0.57219100	0.27805200
C	6.08320500	3.07246200	1.15114400
H	5.94988700	5.12112200	0.48190500
H	5.97352700	0.97482500	1.63791600
H	6.96550700	3.24674400	1.75902300

Rh2(AcO)4–(Car1)(2Clpyridine)-carbonyl side-(styrene)-ester side (25) [B3LYP-D3(BJ)]/BS1

O	-0.12364300	-1.30229600	2.44992600
O	-2.48397100	-0.87404700	0.82249300
O	-0.82657000	-0.55851500	-1.56211100
O	1.58420600	-0.97794600	0.08455500
O	-2.61337100	-3.10191900	0.40901600
O	-0.91475100	-2.79124300	-1.95729600
O	1.46768000	-3.21016900	-0.30092900
O	-0.24326100	-3.53371200	2.06001600
C	-0.09745700	-2.52737000	2.81370000
C	2.09293300	-2.11276600	-0.20571600
C	-0.97199500	-1.57782700	-2.31712400
C	-3.11261700	-1.98090600	0.72676300
C	3.57593700	-2.11819400	-0.48757800
H	3.73777300	-1.79029900	-1.51969000
H	4.08811000	-1.41693500	0.17345600
H	3.98356500	-3.12249300	-0.37067400
C	-4.58629400	-1.92928100	1.05088900
H	-5.08063400	-2.84991300	0.74146100
H	-4.70589300	-1.80141900	2.13153100
H	-5.04549200	-1.06758200	0.56181900
C	0.10906500	-2.76933900	4.28940200
H	-0.77845300	-2.42997400	4.83264500
H	0.27016100	-3.82858000	4.48768100
H	0.96142200	-2.18510100	4.64457500
Rh	-0.58100600	-3.23316600	0.03898700
Rh	-0.44494400	-0.80359000	0.45855700
C	-0.29824100	1.22737500	0.72445000
C	0.60398000	1.91552900	1.57726400
C	1.55811400	1.12704800	2.29480000
C	0.67808600	3.33309700	1.79643400
C	2.49630300	1.68188000	3.14214600
H	1.53324100	0.06053900	2.14915800
C	1.61039400	3.88339400	2.66468000
C	2.52042800	3.06520500	3.33291600

H	1.63704800	4.95485300	2.80798100
H	3.24903800	3.51835300	3.99588400
C	-1.28575900	1.90886400	-0.14424200
O	-0.76031400	2.27379300	-1.31965700
C	-1.69504800	2.78111300	-2.28982800
H	-2.15922500	3.69934500	-1.92291200
H	-1.10478400	2.98109800	-3.18221100
H	-2.46506200	2.03566000	-2.49667100
O	-2.46407400	2.00834500	0.14887300
C	-1.22558900	-1.27914100	-3.77514500
H	-2.08885600	-0.61494700	-3.86721100
H	-0.35987500	-0.75446800	-4.18965600
H	-1.40046600	-2.19878500	-4.33277200
N	-2.37193200	3.32674400	3.68006800
C	-2.72365900	2.10639700	3.23601600
C	-1.33265300	3.38928500	4.48943700
C	-2.04866000	0.94227200	3.59083900
H	-3.56028600	2.07306000	2.54761200
C	-0.58250900	2.29935900	4.93054000
Cl	-0.86031900	5.00980900	5.03242100
C	-0.96090600	1.04597200	4.45838900
H	-2.33933300	-0.00816200	3.16351800
H	0.26518900	2.43412100	5.58968100
H	-0.39521800	0.16556400	4.73679400
Br	-0.46104700	4.58767500	0.94299000
H	3.20838200	1.04490400	3.65450000
C	3.32685000	3.32439900	-0.34556100
C	4.33424100	2.64699600	0.36361200
C	5.16513300	3.32973600	1.24699200
C	5.00753000	4.70512900	1.44588300
C	4.01114800	5.39204800	0.74932800
C	3.17851000	4.70647000	-0.13251300
H	4.44467500	1.57417800	0.24415700
H	5.92947300	2.78676600	1.79500700
H	5.65199900	5.23309100	2.14204900
H	3.87585300	6.45868900	0.90130700
H	2.39007300	5.23837200	-0.65700000
C	2.40732600	2.64056200	-1.26460900
C	2.56305700	1.41895400	-1.78818400
H	1.50726800	3.19652400	-1.51266700
H	3.43831100	0.80713700	-1.59440400
H	1.79462400	0.98443800	-2.41738700

Rh2(AcO)4–(Car1)(2Clpyridine)-carbonyl side-(styrene)-ester side-cyclopropanation transition state (23) [B3LYP-D3(BJ)]/BS, Imaginary λ=-155

O	-0.31655900	-1.09114200	2.08279700
O	-2.28213000	-0.77584000	-0.02997100
O	-0.19982600	-0.81884400	-2.05345700
O	1.85162000	-1.12836200	-0.00976300
O	-2.46408300	-3.03355700	-0.19175400
O	-0.34724300	-3.07811400	-2.19564200

O	1.66806800	-3.38595000	-0.09068400
O	-0.47276700	-3.34984400	1.93747500
C	-0.42125500	-2.26089400	2.58297700
C	2.33541700	-2.31175100	-0.05677900
C	-0.27622700	-1.91577300	-2.69943100
C	-2.94476800	-1.85927000	-0.12991000
C	3.84186100	-2.40252000	-0.07654000
H	4.21904700	-1.91274500	-0.97905900
H	4.25005200	-1.86588600	0.78409700
H	4.16800800	-3.44197600	-0.05875200
C	-4.44986900	-1.73282000	-0.16299800
H	-4.86565700	-2.17974500	0.74510600
H	-4.75028700	-0.68709800	-0.22261600
H	-4.84594500	-2.28811400	-1.01679100
C	-0.47219100	-2.32964200	4.09067600
H	-1.24365300	-1.65206900	4.46441900
H	-0.67405100	-3.34676300	4.42522300
H	0.48919100	-1.99750700	4.49449700
Rh	-0.41333300	-3.28765800	-0.13994400
Rh	-0.20677400	-0.83865500	0.02646500
C	0.01172800	1.29582200	0.29957400
C	0.79634300	1.86676800	1.38744000
C	1.69098300	1.02917100	2.09902000
C	0.77748900	3.22921100	1.80230400
C	2.44574800	1.47954700	3.17282500
H	1.77006000	0.00105200	1.78751300
C	1.53151300	3.68918800	2.87518900
C	2.36077100	2.81135700	3.57165900
H	1.47368200	4.73186700	3.16088300
H	2.93830600	3.17816700	4.41352600
C	-1.30475000	1.89684600	-0.01561200
O	-1.52783700	2.19628000	-1.30522400
C	-2.86739400	2.62795400	-1.60540700
H	-3.11263100	3.52749600	-1.03600400
H	-2.87247000	2.83876900	-2.67367500
H	-3.58205900	1.83860600	-1.36493600
O	-2.16775100	1.96561100	0.84824600
C	-0.31541400	-1.80232600	-4.20469700
H	-1.34212200	-1.57773600	-4.51274300
H	0.32397500	-0.98361100	-4.53909000
H	-0.00945100	-2.74090800	-4.66742000
N	-1.49264700	3.89372300	4.70297500
C	-1.73442900	2.88075300	3.85185200
C	-0.69829700	3.63595900	5.72468500
C	-1.19357200	1.60646500	4.00717500
H	-2.36146500	3.10531100	2.99627100
C	-0.10237700	2.40657200	5.99771000
Cl	-0.36617500	4.99360600	6.81998600
C	-0.36532500	1.37052900	5.10369400
H	-1.38236300	0.83938200	3.26737100
H	0.54301800	2.27597400	6.85718400

H	0.08905000	0.39796800	5.25545100
Br	-0.24744900	4.56520600	0.89725600
H	3.10303400	0.79107600	3.69321500
C	2.82928300	3.37404300	-0.59651600
C	3.68373400	2.48228700	0.09108000
C	4.67965100	2.96779000	0.92792800
C	4.84970100	4.34541800	1.09133900
C	4.03089300	5.24433900	0.39601200
C	3.03416700	4.76407100	-0.44014800
H	3.55646500	1.41285300	-0.02302900
H	5.31832000	2.27418700	1.46438200
H	5.62343000	4.72020200	1.75407100
H	4.16887000	6.31334300	0.52024700
H	2.37696600	5.45316300	-0.96052700
C	1.71465400	2.91387300	-1.38389100
C	1.29145800	1.60445900	-1.46310500
H	1.11269200	3.68232300	-1.86154700
H	1.93925600	0.79582800	-1.15023000
H	0.50705400	1.33676300	-2.15445300

Cyclopropane product 26 [B3LYP-D3(BJ)]/BS1

O	3.80431400	6.13232200	9.20364400
O	6.01350500	6.42238200	8.84055400
C	2.21669400	7.95678500	6.98871800
C	2.35663300	5.70066800	6.20610400
C	0.85149700	7.98768900	6.70935900
C	4.86364200	6.43677300	8.43613700
C	3.00556300	6.82815400	6.72971000
C	4.46879400	6.78666100	7.03488100
C	0.99295000	5.70849000	5.92402300
C	0.23984400	6.85780500	6.16748300
C	5.42627600	7.73622100	6.33981000
C	3.90927700	5.94005700	2.51819900
C	5.49111100	6.29396200	5.97096000
C	4.31358000	6.50345300	3.72768000
C	5.05714000	5.75619300	4.65197900
C	4.24254100	4.61971900	2.20798600
C	5.39093700	4.43297400	4.32733400
C	4.10326900	5.79661800	10.57135900
H	6.22735200	8.14033500	6.94781200
H	0.52122800	4.82156700	5.51378200
H	4.98102900	8.43245900	5.63877600
H	6.30690900	5.74070400	6.42580500
H	4.03596500	7.52753300	3.95219300
H	3.33200600	6.53474100	1.81662700
H	3.92651000	4.18297100	1.26565200
H	-0.82245300	6.87879000	5.94622700
H	4.58837600	6.63754400	11.07156600
H	3.14254800	5.57852000	11.03509100
H	4.75836800	4.92403800	10.61579800
C	4.98799600	3.86744000	3.11772800

H	5.96922500	3.84393400	5.03397300
H	5.25720800	2.84118500	2.88658700
H	2.94493700	4.81166400	6.01099800
H	0.27657100	8.88132900	6.92123700
Br	2.99014800	9.51195700	7.80218400

(Car2)-Rh2(AcO)4 (15) [B3LYP-D3(BJ)]/BS1

O	0.02930000	-1.04217600	2.39112600
O	-2.17140700	-0.30264600	0.63110300
O	-0.41912500	-0.47779700	-1.67923900
O	1.81668600	-1.23886000	0.07177200
O	-2.72465500	-2.49279500	0.40166100
O	-0.96736500	-2.66824300	-1.92465000
O	1.26710000	-3.42632100	-0.17564300
O	-0.48261500	-3.24004400	2.14997800
C	-0.16230700	-2.22595600	2.83746800
C	2.09725100	-2.47233800	-0.12377000
C	-0.77030800	-1.49697100	-2.36653800
C	-3.00486100	-1.27062700	0.58662200
C	3.56109200	-2.78853500	-0.30929500
H	3.93652900	-2.25964600	-1.18985900
H	4.12256700	-2.42747300	0.55660200
H	3.71090100	-3.86085100	-0.43063400
C	-4.45754900	-0.89594100	0.75238500
H	-4.79387900	-0.37421700	-0.14913200
H	-5.06778300	-1.78642700	0.90176000
H	-4.57164800	-0.21064800	1.59500300
C	-0.00856200	-2.39920000	4.32860800
H	0.06698600	-3.45561600	4.58562700
H	0.87217000	-1.85646300	4.67795300
H	-0.88455800	-1.97122200	4.82654900
Rh	-0.74820800	-3.03480000	0.10428900
Rh	-0.15417400	-0.66253000	0.36377900
C	0.35252400	1.27708200	0.58037400
C	1.31848300	1.82436500	1.46647400
C	2.19485600	0.97568700	2.19957500
C	1.44297100	3.23358100	1.64155500
C	3.14485000	1.50666800	3.05494800
H	2.12339500	-0.09305700	2.06522900
C	2.37535300	3.76680400	2.51079700
C	3.22183000	2.89485900	3.20918700
H	2.45779000	4.83742300	2.65103400
C	-0.43330700	2.20906200	-0.25635500
O	0.13339900	2.41551500	-1.44849800
C	-0.65097900	3.17380600	-2.39599300
H	-0.86208800	4.17078000	-2.00524800
H	-0.03963600	3.23466100	-3.29403700
H	-1.58761000	2.65266200	-2.60343400
O	-1.49312700	2.68498100	0.11299400
C	-0.97691800	-1.25160400	-3.84170900
H	-1.86006500	-0.61968100	-3.97701400

H	-0.11870800	-0.71302600	-4.25018900
H	-1.11968100	-2.19296900	-4.37165200
H	3.81868600	0.86019400	3.60334600
H	0.77985700	3.90192900	1.10365800
Br	4.50771400	3.61969700	4.39591400

Rh2(AcO)4–(Car2)(styrene)-carbonyl side (17) [B3LYP-D3(BJ)]/BS1

O	0.05984500	-1.45011500	2.59126700
O	-2.07740600	0.03070700	1.25826300
O	-0.65703400	-0.15351500	-1.26937600
O	1.51758600	-1.64594400	0.09282200
O	-3.15464400	-1.90866700	0.77619700
O	-1.67829700	-2.12596500	-1.73344100
O	0.45994300	-3.60784500	-0.33874400
O	-1.04957200	-3.38141600	2.16520800
C	-0.40624700	-2.59326200	2.91951300
C	1.48738300	-2.87053000	-0.27563900
C	-1.28639000	-0.95989500	-2.03511300
C	-3.11676400	-0.70711600	1.17928100
C	2.81200800	-3.46426900	-0.69002200
H	3.09879000	-3.04839600	-1.66113300
H	3.58461900	-3.18925900	0.03119100
H	2.73691000	-4.54837700	-0.77212700
C	-4.41597100	-0.05682600	1.58976900
H	-4.25848600	0.56899900	2.47030200
H	-4.75987000	0.58957500	0.77570900
H	-5.17673600	-0.81186200	1.78817800
C	-0.15059100	-3.01457400	4.34565700
H	-0.53129900	-2.24500600	5.02218300
H	-0.62615800	-3.97151700	4.55846600
H	0.92799500	-3.09312800	4.51021600
Rh	-1.39096200	-2.82955500	0.19668000
Rh	-0.23232300	-0.71019400	0.68300500
C	0.76044500	1.02434200	0.98077300
C	1.89770500	1.27590100	1.78602400
C	2.49029900	0.23734800	2.55792800
C	2.45539500	2.58472400	1.87747200
C	3.55744400	0.50029600	3.39675000
H	2.08092500	-0.75972600	2.49423800
C	3.52161700	2.85235500	2.71382700
C	4.05073800	1.80806200	3.47896000
H	3.92261300	3.85311700	2.80103900
C	0.21706000	2.13987600	0.17139800
O	0.88527000	2.27979000	-0.98050300
C	0.28591600	3.16634100	-1.95100900
H	0.18206500	4.17115500	-1.53847000
H	0.96573400	3.16764900	-2.80077900
H	-0.69245600	2.77997800	-2.24302400
O	-0.74836900	2.80651600	0.50332200
C	-1.60109100	-0.44220800	-3.41781400
H	-1.89664400	-1.25950000	-4.07550100

H	-2.42540600	0.27479700	-3.34526800
H	-0.73616900	0.08404100	-3.82655300
H	4.00077600	-0.28656300	3.99431200
C	-1.26273500	0.75323400	4.50518100
C	-0.83083500	1.80035100	3.79197900
H	-0.93867400	0.56414600	5.52516900
H	-1.95809200	0.04530100	4.06985100
C	0.14375500	2.80818300	4.23717100
H	-1.22353800	1.93750800	2.78759200
C	0.18976700	4.05387400	3.58557500
C	1.06059100	2.56650000	5.27537200
C	1.09702700	5.03680800	3.98009100
H	-0.48758600	4.23663500	2.75707100
C	1.97407800	3.54348400	5.66208200
H	1.07470700	1.59608300	5.76115100
C	1.99296500	4.78605700	5.02050600
H	1.11299700	5.99346800	3.46619300
H	2.68617400	3.33131700	6.45362800
H	2.71055700	5.54362500	5.32035000
H	2.02660800	3.39358100	1.29890300
Br	5.46728600	2.18196700	4.67877400

Rh2(TPPTTL)4 (5) [B3LYP-D3(BJ)]/BS1

O	16.52499100	11.17319300	28.71252800
O	15.48732000	10.71308600	26.75633600
O	17.43025700	9.99241900	23.96298200
O	16.75518400	7.83392500	27.92687300
N	17.46357700	9.08758600	26.10409100
C	16.51138400	10.78227800	27.50873000
C	17.79620000	10.33074000	26.80351100
H	17.93068400	11.05623300	25.99414500
C	17.20482300	9.06669200	24.72083500
C	16.63131600	7.72096000	24.43048700
C	16.58662500	7.00125300	25.62957800
C	16.94034400	7.94351700	26.72823200
C	16.19277300	5.66632900	25.68169600
C	15.77789600	5.08123700	24.45470500
C	15.81074700	5.81073800	23.24321600
C	16.23733400	7.16490600	23.21969700
C	19.13267000	10.30867700	27.59940000
C	19.51281000	11.77557000	27.88335100
H	20.48665900	11.81176900	28.38232200
H	18.77519500	12.25248500	28.53179400
H	19.57946600	12.35693400	26.96093100
C	20.19805500	9.67351100	26.68715200
H	20.21710300	10.15014400	25.70490500
H	20.01372400	8.60473600	26.54461000
H	21.18811500	9.78966100	27.13889300
C	19.09333600	9.52816800	28.92483600
H	20.07326200	9.61171500	29.40776600
H	18.88044500	8.47006100	28.76805200

H	18.33980200	9.93099000	29.60239000
O	14.59411800	9.44903400	30.04409400
O	13.50343700	9.11512500	28.09162600
O	12.77304600	6.02839600	27.05679400
O	11.28422800	8.52892100	30.56462400
N	12.29040300	7.02957200	29.09980700
C	13.96589200	8.72986700	29.21330300
C	13.68580600	7.24759400	29.49076100
H	14.25492200	6.71579800	28.72035300
C	11.97485300	6.55447200	27.80848600
C	10.52343700	6.83282700	27.61041800
C	10.03329300	7.41640600	28.78268700
C	11.20702900	7.73986300	29.64032200
C	8.68071500	7.68548200	28.97260500
C	7.81556000	7.37711200	27.88924500
C	8.32363700	6.87377400	26.66938100
C	9.70377000	6.58448600	26.51399000
C	14.11565800	6.63012500	30.85280800
C	15.65609900	6.56187800	30.84665800
H	16.02715000	5.98953800	29.99301800
H	16.00515900	6.07557700	31.76336200
H	16.09328300	7.56142600	30.79888800
C	13.54688300	5.20112700	30.90795500
H	12.45644600	5.21040100	30.99220600
H	13.95049400	4.67712600	31.78011900
H	13.81697900	4.63069600	30.01666400
C	13.64831900	7.39486400	32.10343300
H	14.01711200	8.42128100	32.10402100
H	14.04233200	6.88606400	32.99012500
H	12.56125000	7.42365700	32.17920900
O	12.81997900	11.72683300	30.49351500
O	11.85932900	11.44132100	28.46611600
O	8.47373900	11.51687600	28.12863700
O	11.52136700	14.64830600	29.44231100
N	9.88313600	13.01537600	29.21578800
C	11.82696400	11.71529400	29.70884500
C	10.40904700	12.05503600	30.19086900
H	9.83118800	11.14556300	29.99448700
C	9.03981400	12.59324300	28.16718000
C	9.02907000	13.70663000	27.17450200
C	9.84951900	14.72942400	27.66071100
C	10.53388600	14.21419000	28.87773800
C	9.99633000	15.94807400	26.99975400
C	9.34512300	16.06591200	25.74435100
C	8.59684300	14.99573800	25.20800600
C	8.39547800	13.79940300	25.94001900
C	10.16867300	12.40940600	31.68392000
C	10.41186900	11.12186000	32.49628100
H	10.19531700	11.30810700	33.55309100
H	11.44946100	10.79211800	32.41103900
H	9.76923600	10.30677500	32.15341600

C	8.69186600	12.82143700	31.82263000
H	8.02791200	12.06371900	31.40033000
H	8.49465300	13.77097200	31.31673500
H	8.43928600	12.94132000	32.88081900
C	11.05195900	13.54024400	32.23741000
H	10.82854600	13.67017100	33.30208000
H	10.86144100	14.48722100	31.73070200
H	12.11165300	13.30547900	32.13186300
O	14.78014100	13.48881600	29.15887100
O	13.85486700	13.07213900	27.13757700
O	13.38591700	15.87729200	24.95624400
O	17.05568900	13.79843800	26.71057800
N	15.23379400	15.12480600	26.14776200
C	14.41916200	13.82628000	27.99379800
C	14.63835100	15.25549800	27.47860500
H	13.62999400	15.63304800	27.27785800
C	14.49171700	15.36751400	24.97826100
C	15.32778700	14.86201000	23.85018800
C	16.50592100	14.33176400	24.38577700
C	16.38361500	14.36679500	25.86899600
C	17.52232700	13.80691700	23.58664900
C	17.24807900	13.72368600	22.19604800
C	16.05243000	14.24617600	21.65553800
C	15.07155200	14.84940900	22.48441500
C	15.32370400	16.30044700	28.40315300
C	14.36130000	16.57664400	29.57475900
H	13.37899000	16.89570000	29.21808600
H	14.77034600	17.37177100	30.20639900
H	14.22563700	15.68439700	30.18855700
C	15.50442400	17.58847100	27.57818500
H	16.25218700	17.45509500	26.79099100
H	15.83993600	18.40095900	28.23007600
H	14.56733200	17.89639700	27.10930300
C	16.69479900	15.87205600	28.95309900
H	16.61822500	14.95767300	29.54230400
H	17.08002300	16.66988600	29.59754600
H	17.41749600	15.70289400	28.15338100
C	10.25772900	6.11011700	25.21783100
C	9.86692600	4.89004000	24.65341900
C	11.15088500	6.93309700	24.51887800
C	10.35762400	4.50248100	23.40637100
H	9.17048300	4.25235400	25.18744900
C	11.62897400	6.55211900	23.26745400
H	11.45277200	7.88071200	24.95405400
C	11.23391800	5.33525700	22.70605200
H	10.05032900	3.55346300	22.97787900
H	12.30438300	7.21175700	22.73296600
H	11.61800000	5.03267400	21.73766300
C	7.40068700	6.64483500	25.51910700
C	6.39910700	5.66778700	25.58132700
C	7.52915500	7.41716600	24.35799200

C	5.53860400	5.46955700	24.50240500
H	6.29158700	5.07087200	26.48086200
C	6.66551000	7.22250200	23.28080500
H	8.30128600	8.17679600	24.30620700
C	5.66765100	6.24803100	23.34975400
H	4.76678800	4.70829400	24.56224400
H	6.77146000	7.83157000	22.38809400
H	4.99556200	6.09555500	22.51089200
C	6.34534900	7.57251200	28.04740400
C	5.63519300	6.79068800	28.96766200
C	5.65845900	8.52391900	27.28437000
C	4.25823200	6.95042200	29.11650700
H	6.16674400	6.05867100	29.56733000
C	4.28236100	8.68568700	27.43716200
H	6.20162200	9.13800000	26.57546600
C	3.57730200	7.89902400	28.35061300
H	3.71847900	6.33509800	29.82987600
H	3.75872500	9.42564700	26.84070700
H	2.50513500	8.02529300	28.46566500
C	8.16265600	8.19667100	30.26877100
C	8.46055100	7.50432400	31.45123000
C	7.33487900	9.32660600	30.33134800
C	7.93015500	7.92174800	32.67077400
H	9.09533800	6.62495700	31.40847300
C	6.79670200	9.73550300	31.55050100
H	7.12265300	9.88473500	29.42856800
C	7.08924500	9.03523200	32.72265500
H	8.16540000	7.37200500	33.57689700
H	6.14640300	10.60390300	31.58450900
H	6.66667700	9.35632800	33.66970700
C	7.54404300	12.70668400	25.39491800
C	6.26619500	12.48008300	25.91814300
C	7.99570200	11.92566900	24.32365600
C	5.44578700	11.49628200	25.36766700
H	5.91341000	13.08548700	26.74699600
C	7.18248200	10.92657200	23.78939800
H	8.98216200	12.10783000	23.90940300
C	5.90327300	10.71113600	24.30690100
H	4.44889300	11.34457800	25.76835000
H	7.54479100	10.32311500	22.96325000
H	5.27317800	9.93128000	23.89192300
C	7.93398600	15.14834300	23.87937400
C	6.55498700	15.37846600	23.80221200
C	8.67796700	15.04684700	22.69778500
C	5.92983100	15.51101000	22.56242500
H	5.97558400	15.45224700	24.71690300
C	8.05186400	15.17619800	21.45829600
H	9.74566400	14.86325200	22.74886100
C	6.67702100	15.40960900	21.38695000
H	4.86043300	15.69259200	22.51483400
H	8.63705000	15.09447800	20.54778900

H	6.19069000	15.51100100	20.42159300
C	9.32387600	17.38550900	25.04352400
C	8.41659900	18.35722100	25.48489500
C	10.17352300	17.67773600	23.97114500
C	8.35881700	19.60557900	24.86606100
H	7.76008700	18.13018300	26.31931800
C	10.11528900	18.92769000	23.35465100
H	10.89201700	16.93954300	23.63254800
C	9.21004000	19.89364600	23.79785600
H	7.65137300	20.35027600	25.21805600
H	10.78073900	19.14714500	22.52761300
H	9.16949100	20.86487100	23.31422100
C	10.67200600	17.10570000	27.64146400
C	10.27384800	17.49330300	28.93017800
C	11.64202900	17.86681800	26.97395100
C	10.82078700	18.62366100	29.53403700
H	9.51623400	16.91531100	29.44970500
C	12.17701500	19.00595500	27.57473500
H	11.98547800	17.55797200	25.99580700
C	11.76911200	19.38998700	28.85312700
H	10.49763000	18.91186600	30.52959200
H	12.91892300	19.59298300	27.04283900
H	12.18808100	20.27801100	29.31620500
C	13.82541700	15.41475600	21.89956700
C	13.63089500	16.79962600	21.84751000
C	12.86311800	14.56501900	21.34039500
C	12.50128300	17.32724700	21.22409000
H	14.37753000	17.45990300	22.27701600
C	11.72154500	15.09369900	20.73829800
H	13.01835500	13.49130600	21.36979200
C	11.53912200	16.47697800	20.67451200
H	12.37858500	18.40336300	21.15888700
H	10.98196900	14.42403300	20.31030600
H	10.65370900	16.88979500	20.20179500
C	15.84574700	14.25084300	20.17722300
C	15.84388000	15.46466000	19.47696700
C	15.64144600	13.05979200	19.47224400
C	15.63922600	15.48485000	18.09776500
H	16.00144700	16.39252900	20.01670800
C	15.42942400	13.07934300	18.09420600
H	15.65195800	12.12025900	20.00818400
C	15.42780900	14.29215900	17.40233800
H	15.64394300	16.43197400	17.56691500
H	15.26447000	12.14791100	17.56082900
H	15.26427600	14.30834600	16.32916900
C	18.26274400	13.14117300	21.26702200
C	19.21016000	13.96573200	20.65109300
C	18.26644900	11.76677900	20.99659800
C	20.15446800	13.42322400	19.77869700
H	19.20527100	15.03136700	20.85848200
C	19.20865700	11.22650400	20.12183900

H	17.54205600	11.12019000	21.48047000
C	20.15511900	12.05244100	19.51177800
H	20.88737100	14.07095700	19.30719400
H	19.19744300	10.16046700	19.92036800
H	20.88918800	11.63079800	18.83182200
C	18.88320800	13.56235100	24.13712500
C	19.49595500	14.61165900	24.84298800
C	19.61494500	12.38924000	23.90622400
C	20.80983500	14.50046700	25.29207800
H	18.94254600	15.52913400	25.01622200
C	20.93644100	12.28762100	24.34141100
H	19.14740800	11.55536400	23.40389400
C	21.54008800	13.33903900	25.03209600
H	21.26587700	15.32497300	25.83131000
H	21.49482100	11.37844500	24.14221900
H	22.56888500	13.25308700	25.36777900
C	16.19761000	7.96342900	21.96452900
C	17.05409800	7.68412200	20.89372300
C	15.22133300	8.95795500	21.82221300
C	16.92972400	8.38363500	19.69338700
H	17.80343400	6.90628800	20.99785600
C	15.08187500	9.63941900	20.61442500
H	14.55504900	9.17278100	22.65217000
C	15.93757100	9.35535400	19.54735500
H	17.59773200	8.15988500	18.86748800
H	14.30089300	10.38538300	20.50562200
H	15.83372000	9.88732000	18.60715600
C	16.32259300	4.86457200	26.92806500
C	17.56953000	4.81964500	27.57003800
C	15.27017600	4.09067200	27.43649200
C	17.76649500	4.00938400	28.68688600
H	18.39244700	5.40792600	27.17662100
C	15.47254800	3.27274500	28.54692100
H	14.29844100	4.13372800	26.96446200
C	16.71878500	3.22605800	29.17459700
H	18.73935600	3.98276700	29.16790800
H	14.65265400	2.66805200	28.92163300
H	16.87151000	2.58583400	30.03793600
C	15.24930100	3.68597500	24.44689000
C	16.07492800	2.58470300	24.70043700
C	13.88659000	3.47989200	24.20019500
C	15.54597300	1.29436900	24.69389800
H	17.12901500	2.74204200	24.90591900
C	13.35642700	2.19099300	24.20210700
H	13.24297600	4.33227200	24.01735800
C	14.18559900	1.09373300	24.44591800
H	16.19525500	0.44559000	24.88601200
H	12.29629300	2.04935200	24.01466500
H	13.77521500	0.08852900	24.44566900
C	15.45076400	5.13214300	21.96234000
C	16.17759500	4.00947000	21.54058700

C	14.41511100	5.60698600	21.14729400
C	15.86465400	3.36765600	20.34334600
H	16.99024500	3.63923900	22.15571600
C	14.09693000	4.96325000	19.95226200
H	13.86420800	6.48935800	21.44460400
C	14.81865500	3.83872500	19.54721000
H	16.43943900	2.50067700	20.03236200
H	13.28779000	5.34461000	19.33679000
H	14.57239700	3.33779900	18.61607000
Rh	13.64554900	11.07883700	27.55492100
Rh	14.71159600	11.47978300	29.66780300

Rh2(TPPTTL)4(2Clpyridine) [B3LYP-D3(BJ)]/BS1

Rh	14.85059100	11.49956400	29.60987600
Rh	13.78187100	11.17839800	27.44418200
O	16.66699400	11.20149600	28.64925400
O	15.64578200	10.76023500	26.68075900
O	17.56136200	10.14898900	23.90314000
O	16.93623000	7.86921400	27.80585500
N	17.63475200	9.16985000	26.01060700
C	16.65914900	10.82681100	27.44133700
C	17.95965100	10.39386200	26.74805000
H	18.11134800	11.13795100	25.95920900
C	17.33508500	9.20298300	24.63594300
C	16.70701400	7.88869800	24.31648300
C	16.67455600	7.13085400	25.49134100
C	17.09539700	8.01949800	26.60843500
C	16.21351200	5.81723500	25.52346500
C	15.68418500	5.30544900	24.30907700
C	15.66164200	6.09083200	23.13424200
C	16.20357900	7.40322300	23.11563400
C	19.28330200	10.34991700	27.56682900
C	19.68730500	11.81060700	27.84881000
H	20.64977000	11.83177400	28.37043700
H	18.94503900	12.30641200	28.47649100
H	19.78490700	12.38568900	26.92585100
C	20.35242300	9.68986900	26.67677200
H	20.39078100	10.15352800	25.68874400
H	20.15569500	8.62202100	26.54452800
H	21.33808300	9.79857800	27.14011500
C	19.21357400	9.58454400	28.90066400
H	20.19449400	9.64232800	29.38582100
H	18.96487200	8.53311400	28.75464000
H	18.47163700	10.02156900	29.56963400
O	14.66446700	9.44475400	29.89805100
O	13.51572900	9.21801200	27.95906900
O	12.57350200	5.97927000	26.94403400
O	11.32018100	8.70150300	30.39316800
N	12.23458200	7.14328800	28.93047700
C	13.98198200	8.78841900	29.05816700
C	13.64592600	7.30564900	29.28716200

H	14.17799400	6.78010400	28.48689900
C	11.83255700	6.56649300	27.71061700
C	10.36352000	6.81436100	27.60467700
C	9.95763400	7.49393200	28.75830200
C	11.18735600	7.87530000	29.50834300
C	8.61974800	7.75527300	29.03922100
C	7.67339400	7.33501300	28.06718200
C	8.08909300	6.72071100	26.86517100
C	9.45706200	6.43932300	26.61922900
C	14.07096000	6.62051400	30.61742000
C	15.60939000	6.52274400	30.60551600
H	15.97015700	5.98966200	29.72244900
H	15.94968500	5.98230900	31.49502700
H	16.06237400	7.51593300	30.60943500
C	13.47161300	5.20237500	30.61882900
H	12.38332700	5.23146200	30.72556200
H	13.87880100	4.62919200	31.45780100
H	13.70965600	4.66714100	29.69727400
C	13.61841500	7.34814500	31.89439600
H	14.00044500	8.36798300	31.92667000
H	14.00520600	6.80456100	32.76383800
H	12.53125200	7.38817800	31.97549900
O	12.93573800	11.77252000	30.39382900
O	12.00210200	11.60047100	28.33905300
O	8.65360000	11.41505300	28.04015400
O	11.55909700	14.72666300	29.21779500
N	9.97189500	13.03232200	29.07083000
C	11.96209000	11.81394300	29.59262600
C	10.54193400	12.13559100	30.08190900
H	9.98739200	11.20153700	29.94104200
C	9.17242900	12.51543600	28.02938400
C	9.14001500	13.56740400	26.96986000
C	9.92705400	14.63628600	27.40478000
C	10.59679800	14.22286200	28.66694000
C	10.04522000	15.82247300	26.68398200
C	9.40281700	15.85747900	25.42080300
C	8.68397300	14.73995200	24.93390100
C	8.50844600	13.57792800	25.73043100
C	10.32238100	12.55451900	31.56276500
C	10.54542000	11.29250600	32.41975800
H	10.36561700	11.52615800	33.47436300
H	11.56887000	10.92893900	32.31611900
H	9.86635600	10.48803200	32.12720500
C	8.85858800	13.00843300	31.70250700
H	8.17169000	12.25823400	31.30362100
H	8.68161200	13.95025400	31.17494600
H	8.61752400	13.16030500	32.75950800
C	11.24286700	13.67973800	32.06681100
H	11.02953600	13.85867100	33.12666800
H	11.07951500	14.61023700	31.52186900
H	12.29322600	13.40388000	31.96737900

O	14.96682700	13.54160700	29.15286000
O	14.11068200	13.16449000	27.09709000
O	13.57031100	15.78696800	24.93736700
O	17.31920700	13.92264900	26.74199500
N	15.47034400	15.19853200	26.14415300
C	14.64617000	13.89785700	27.98446500
C	14.86420000	15.33100400	27.47417800
H	13.85363900	15.69614000	27.26114800
C	14.70723600	15.35041200	24.97217200
C	15.56002500	14.85251500	23.85450900
C	16.74973200	14.36122100	24.40202000
C	16.63209400	14.44708300	25.88490200
C	17.77367700	13.83363600	23.61365000
C	17.51088800	13.73725100	22.22127200
C	16.32410100	14.26270400	21.66371600
C	15.31702400	14.83334100	22.48591300
C	15.52083800	16.38526900	28.40541600
C	14.52990500	16.65219800	29.55619300
H	13.56370600	16.99658900	29.17676500
H	14.93190300	17.42798200	30.21584600
H	14.36427800	15.74990800	30.14838200
C	15.70086600	17.67611400	27.58614000
H	16.45023400	17.54826800	26.79958900
H	16.03090500	18.48837000	28.24128000
H	14.76226900	17.98106500	27.11614400
C	16.88081000	15.96890800	28.98949900
H	16.78990500	15.06080100	29.58568200
H	17.24951300	16.77264600	29.63634200
H	17.62127900	15.79153600	28.20830600
Cl	13.32001300	8.68335800	24.85124700
N	12.72197200	11.20274000	25.35037400
C	12.66576700	10.24661300	24.42683200
C	12.12500800	10.42880900	23.15193000
H	12.10586600	9.61139900	22.44274600
C	11.63152700	11.69070200	22.83113200
H	11.21185000	11.87647000	21.84812600
C	11.68205200	12.70358700	23.78960400
H	11.32315900	13.70220900	23.58176900
C	12.22341800	12.41546500	25.03473000
H	12.29867300	13.17036300	25.80590200
Cl	14.36170800	10.94663500	33.22132300
N	16.09986900	12.00378000	31.54048000
C	15.83370500	11.80414100	32.82744000
C	16.65436500	12.23756900	33.86957500
H	16.37925300	12.04207000	34.89814500
C	17.81971700	12.92022400	33.53562200
H	18.48357700	13.27445900	34.31706100
C	18.11699600	13.13862900	32.18939400
H	19.01399500	13.66474900	31.88493400
C	17.23354200	12.66462700	31.22904400
H	17.41535700	12.79983100	30.17082100

C	9.88235400	5.81089300	25.33796400
C	9.60074700	4.46947800	25.05639100
C	10.50763200	6.59892700	24.36477400
C	9.94750000	3.92343000	23.81973900
H	9.10058200	3.85973900	25.80185300
C	10.84746000	6.05475200	23.12800000
H	10.71353400	7.64118100	24.57820500
C	10.57347400	4.71341400	22.85237500
H	9.72158200	2.88235400	23.60964300
H	11.32277900	6.67744200	22.37923400
H	10.85236200	4.28872800	21.89319800
C	7.08012500	6.33741100	25.83436300
C	6.14555200	5.32500200	26.08409400
C	7.06384100	6.98994900	24.59537100
C	5.20922600	4.97294900	25.11249900
H	6.15158900	4.81903600	27.04392600
C	6.12449700	6.64205600	23.62550200
H	7.78102300	7.77855900	24.39917800
C	5.19465100	5.63172500	23.88085100
H	4.49109600	4.18485700	25.31758000
H	6.11988200	7.16046900	22.67124100
H	4.46399300	5.35930000	23.12544900
C	6.21704200	7.53015100	28.32331800
C	5.58678500	6.84255400	29.36816900
C	5.46498300	8.39931000	27.52502300
C	4.22391000	7.01653200	29.60586100
H	6.16955100	6.17623900	29.99600900
C	4.10409200	8.57854300	27.76719900
H	5.95136400	8.93878800	26.72120100
C	3.47847100	7.88607600	28.80636400
H	3.74497000	6.47497700	30.41594000
H	3.53018700	9.25741400	27.14353600
H	2.41783200	8.02385000	28.99300300
C	8.18879900	8.36143800	30.32678900
C	8.55641400	7.75088500	31.53392900
C	7.35713200	9.48923200	30.35885900
C	8.08720500	8.24543800	32.75000400
H	9.19582700	6.87407800	31.51468400
C	6.88107800	9.97607100	31.57508600
H	7.09003600	9.98107700	29.43225800
C	7.24034200	9.35531000	32.77324200
H	8.37535900	7.75865900	33.67663200
H	6.22714900	10.84239200	31.58672800
H	6.86587000	9.73623500	33.71837300
C	7.67153900	12.43733400	25.26437200
C	6.42566300	12.19841200	25.85693600
C	8.09418000	11.62403200	24.20629200
C	5.60330300	11.17932200	25.37964600
H	6.09677200	12.82603400	26.67919300
C	7.28077500	10.58896500	23.74539400
H	9.05725500	11.80718000	23.74513200

C	6.02913100	10.36872400	24.32445800
H	4.62983600	11.01930400	25.83193800
H	7.62124200	9.96130500	22.92727400
H	5.39569600	9.56500700	23.96424400
C	8.04492800	14.81134200	23.58785200
C	6.65151000	14.74327000	23.45356200
C	8.83017200	14.94483800	22.43473200
C	6.05707600	14.79960300	22.19368800
H	6.03461800	14.64552100	24.33998600
C	8.23677700	14.99319800	21.17411500
H	9.90803500	15.01787900	22.51844900
C	6.84819000	14.91973300	21.04898800
H	4.97601000	14.74991300	22.10673100
H	8.85926100	15.09028300	20.29009600
H	6.38572300	14.95895700	20.06757000
C	9.32376000	17.15034800	24.67495000
C	8.18988300	17.95037100	24.86851200
C	10.33379400	17.59162600	23.81434400
C	8.06915300	19.17912200	24.22033900
H	7.40440100	17.60394200	25.53312300
C	10.21252600	18.82280700	23.16912600
H	11.21229800	16.97708800	23.65002100
C	9.08447500	19.61979100	23.36972800
H	7.18607700	19.79000100	24.38123500
H	11.00354700	19.16267500	22.51065400
H	8.99757300	20.57738700	22.86554900
C	10.65276700	17.02981900	27.30603900
C	10.12475500	17.48634500	28.52392400
C	11.69866500	17.74596700	26.70980500
C	10.62266800	18.63882800	29.12842900
H	9.31073800	16.93861300	28.98867400
C	12.18830400	18.90553300	27.31171800
H	12.14614100	17.38178300	25.79602700
C	11.65422000	19.35690400	28.51964400
H	10.20010100	18.97945600	30.06870000
H	12.99229500	19.45692700	26.83457600
H	12.03914400	20.25977500	28.98365200
C	14.06682500	15.36955800	21.88387700
C	13.81106400	16.74557200	21.87765500
C	13.16845200	14.50349900	21.24915400
C	12.68791400	17.24754300	21.22352400
H	14.50854800	17.42062000	22.36300100
C	12.02675800	15.00376900	20.62313300
H	13.37317500	13.43876000	21.24332800
C	11.78657200	16.37935800	20.60311700
H	12.52187200	18.31876900	21.18924500
H	11.33404900	14.32080400	20.14071200
H	10.90548100	16.77396200	20.10730700
C	16.17031500	14.34441900	20.17982500
C	16.13443100	15.60483500	19.56581000
C	16.06495300	13.20126100	19.38084800

C	15.98842500	15.71700400	18.18398800
H	16.22097400	16.49781500	20.17557700
C	15.91373600	13.31186500	17.99916400
H	16.10473400	12.22621400	19.84400900
C	15.87385400	14.56988200	17.39536300
H	15.96519600	16.70014800	17.72380500
H	15.82983900	12.41406300	17.39393900
H	15.75769500	14.65657700	16.31937600
C	18.52256800	13.12558100	21.30793500
C	19.50337300	13.91199900	20.69566300
C	18.47506600	11.75060200	21.04182300
C	20.42758000	13.33142100	19.82595900
H	19.53897000	14.97749000	20.90075900
C	19.39597000	11.17303000	20.16838300
H	17.72601300	11.13480300	21.52781700
C	20.37417300	11.96165100	19.55842200
H	21.18649000	13.94928000	19.35548300
H	19.34183600	10.10803300	19.96562100
H	21.09136700	11.51204100	18.87834200
C	19.13509200	13.59967200	24.16801400
C	19.74634300	14.65764600	24.86165000
C	19.86940600	12.42591600	23.94809100
C	21.06053900	14.55340200	25.31150700
H	19.19145800	15.57583500	25.02581100
C	21.19086400	12.33063500	24.38491700
H	19.40242400	11.58739800	23.45268600
C	21.79268000	13.39027300	25.06439500
H	21.51543300	15.38457900	25.84144700
H	21.75021800	11.41971800	24.19672000
H	22.82155000	13.30963700	25.40126200
C	16.15453200	8.21872800	21.87177000
C	16.85601900	7.82475500	20.72601300
C	15.30898300	9.33314600	21.80626700
C	16.69676300	8.52115300	19.52781800
H	17.50825700	6.95882600	20.77081100
C	15.12275900	10.00663800	20.60164500
H	14.77579900	9.64602200	22.69426900
C	15.81470900	9.60104900	19.45754700
H	17.24475900	8.20721400	18.64492500
H	14.43348800	10.84387200	20.55718200
H	15.66786800	10.12228300	18.51687800
C	16.37072100	4.96771200	26.73374100
C	17.64360700	4.84976000	27.31247800
C	15.31071300	4.22195700	27.26814800
C	17.85815600	3.99457900	28.39169600
H	18.47111700	5.41731400	26.89870600
C	15.53159800	3.35576500	28.33791900
H	14.31862500	4.32644400	26.85000100
C	16.80266000	3.23660200	28.90251900
H	18.85044900	3.91202600	28.82435600
H	14.70584900	2.77257100	28.73285200

H	16.96893500	2.55985900	29.73498700
C	15.13296500	3.91942700	24.27363300
C	15.98459500	2.81493400	24.39559500
C	13.75582800	3.71225400	24.12953700
C	15.46863900	1.52001900	24.36229200
H	17.05079600	2.97535100	24.52122400
C	13.24003700	2.41738000	24.10465200
H	13.08951100	4.56358600	24.04801600
C	14.09424600	1.31809300	24.21721500
H	16.13859400	0.67033100	24.45258600
H	12.17014400	2.27303800	23.99962800
H	13.69122500	0.31008700	24.19536100
C	15.04542200	5.53791900	21.89238500
C	15.57986700	4.40846900	21.25971200
C	13.90713800	6.14582200	21.34813300
C	14.98039400	3.89099600	20.11215300
H	16.46245500	3.93250000	21.67305100
C	13.30187700	5.62527500	20.20534000
H	13.50069900	7.02833400	21.82773900
C	13.83610100	4.49369300	19.58475900
H	15.40587700	3.01550600	19.63124500
H	12.41504900	6.10331300	19.80012300
H	13.36665700	4.08728300	18.69419500

(Car1)-Rh2(TPPTTL)4 (27) [B3LYP-D3(BJ)]/BS1

Rh	14.95238400	11.56582900	29.71485500
Rh	13.87820100	11.20263000	27.52398000
O	16.76561900	11.20355600	28.78087800
O	15.73935300	10.64597000	26.83916500
O	18.05775800	10.02662700	24.08013100
O	16.88497600	7.87111900	27.92753700
N	17.78431700	9.11712900	26.18681900
C	16.75767500	10.77094000	27.59777300
C	18.06649400	10.35698600	26.90934600
H	18.20686100	11.09734400	26.11334800
C	17.67124600	9.11402600	24.78923500
C	17.01623700	7.82815000	24.42310600
C	16.80700700	7.10482500	25.60095400
C	17.15442700	7.99340500	26.74613500
C	16.23318400	5.83218800	25.60753900
C	15.75945200	5.35243900	24.35846900
C	15.94235200	6.09824100	23.17173200
C	16.58637000	7.36236100	23.18486900
C	19.38123000	10.35058800	27.73737700
C	19.70618100	11.80837600	28.11954900
H	20.67580000	11.84597900	28.62674400
H	18.95032200	12.21929800	28.79066700
H	19.76354500	12.44789400	27.23362300
C	20.49805300	9.82235800	26.81800800
H	20.55687600	10.40368500	25.89424300
H	20.33586000	8.77320200	26.55459700

H	21.46282700	9.89811200	27.32929900
C	19.31968100	9.47939300	29.00278000
H	20.27894600	9.54576300	29.52748100
H	19.13642000	8.43064100	28.76115900
H	18.53164200	9.81566000	29.67813300
O	14.71248900	9.51743200	30.05299800
O	13.50605400	9.29492900	28.14943200
O	12.70745700	6.14289400	27.05209100
O	11.29605500	8.72856800	30.52154800
N	12.27804800	7.19390700	29.08034800
C	14.00632200	8.86256900	29.24249800
C	13.67728300	7.38085200	29.46969200
H	14.23618000	6.85888300	28.68447900
C	11.92362700	6.65234900	27.83056900
C	10.44915900	6.84292600	27.70298200
C	9.99430300	7.47773800	28.86355200
C	11.19865700	7.89222500	29.64185300
C	8.64406700	7.72759600	29.09354000
C	7.73698900	7.30353400	28.08351900
C	8.20239700	6.71237100	26.88565600
C	9.58928600	6.49050100	26.66925000
C	14.08714900	6.71587400	30.81639500
C	15.62464200	6.59900800	30.81400000
H	15.97921200	6.02273500	29.95535900
H	15.95448400	6.09157900	31.72639900
H	16.09295200	7.58426300	30.77757800
C	13.47728500	5.30271900	30.84067800
H	12.38757600	5.33828600	30.92810400
H	13.86793800	4.74820600	31.69963700
H	13.73056100	4.74510000	29.93610800
C	13.63434600	7.47323000	32.07689800
H	14.03830500	8.48622200	32.09898300
H	14.00066700	6.93653700	32.95884900
H	12.54770900	7.53746000	32.14431300
O	13.06180800	11.89498800	30.50687800
O	12.15188100	11.86254500	28.43441200
O	8.46026900	11.95162100	28.46705200
O	11.87297700	14.87609500	29.25335200
N	10.13811200	13.33505500	29.25088400
C	12.10486100	12.02636100	29.69983900
C	10.69588200	12.37386300	30.19996800
H	10.11090900	11.46231200	30.02952300
C	9.10779800	12.97747400	28.36670300
C	9.02436100	14.07679100	27.35576700
C	9.99630900	15.02792600	27.68800200
C	10.80433500	14.48869500	28.81614500
C	10.16805900	16.21463300	26.97680300
C	9.38435600	16.35713900	25.80341200
C	8.41587400	15.39123900	25.44907800
C	8.19952500	14.22872900	26.23978700
C	10.50246900	12.74994300	31.69602000

C	10.77992900	11.49092700	32.54084700
H	10.57210300	11.70501900	33.59427100
H	11.82091900	11.17629800	32.45178000
H	10.14309200	10.65722300	32.23168100
C	9.02708300	13.15144700	31.88024700
H	8.35644000	12.36981300	31.51487000
H	8.79549200	14.07952100	31.34950800
H	8.81807700	13.30857800	32.94303700
C	11.39878900	13.90624400	32.16873400
H	11.20609300	14.09499100	33.23040500
H	11.19400000	14.82622100	31.61781500
H	12.45580500	13.66492900	32.04701600
O	15.08875200	13.57639500	29.19203300
O	14.31912800	13.15607400	27.10117200
O	13.52004600	15.91617900	25.10479900
O	17.42444400	14.08832700	26.58816900
N	15.48852700	15.30234800	26.17364000
C	14.79592800	13.91087000	28.01220200
C	14.95976800	15.36043000	27.53595000
H	13.93172900	15.71486500	27.40090800
C	14.66794600	15.51454100	25.05298400
C	15.49338200	15.15115400	23.86512200
C	16.74936900	14.73751800	24.32164900
C	16.67822800	14.65462000	25.81044600
C	17.77914900	14.39129800	23.45160300
C	17.49073600	14.46415300	22.06233300
C	16.20065200	14.81649100	21.60359000
C	15.16812500	15.16501600	22.51323500
C	15.65938400	16.38942100	28.47264100
C	14.69136200	16.67422600	29.63817200
H	13.73692700	17.06355400	29.27500400
H	15.13271000	17.41934900	30.30821900
H	14.49158900	15.76778300	30.21240500
C	15.86626300	17.68385500	27.66476200
H	16.62759200	17.55633200	26.88971700
H	16.19471600	18.48612800	28.33296900
H	14.93937900	18.00409600	27.18348100
C	17.01741700	15.93386200	29.03437600
H	16.91492000	15.02568200	29.62977300
H	17.41490400	16.72630700	29.67804700
H	17.74141800	15.74236800	28.24144400
C	8.17944700	8.38712700	30.34224800
C	7.38125100	9.53847800	30.29627700
C	8.52233900	7.84366500	31.58792900
C	6.92684100	10.12549500	31.47562000
H	7.12337800	9.98001200	29.34234000
C	8.06948500	8.43421800	32.76659200
H	9.13628500	6.94957100	31.62910300
C	7.26736100	9.57609800	32.71344500
H	6.30571000	11.01431400	31.42586800
H	8.33914000	8.00043700	33.72449000

H	6.91132500	10.03557800	33.63029200
C	6.27338400	7.51040800	28.28792400
C	5.61563600	6.86212400	29.34147400
C	5.54015600	8.35566600	27.44523600
C	4.24869400	7.04727800	29.54330500
H	6.18141400	6.21481200	30.00361600
C	4.17491100	8.54612500	27.65120800
H	6.03623200	8.86935100	26.63001900
C	3.52397500	7.89086700	28.69870600
H	3.75078300	6.53437200	30.36038100
H	3.61802800	9.20355900	26.99099700
H	2.45992600	8.03748000	28.85613000
C	7.22028600	6.30299000	25.83763200
C	6.26748400	5.31392600	26.11548100
C	7.23421400	6.89297000	24.56681700
C	5.34298800	4.92849100	25.14579100
H	6.25081800	4.85131700	27.09659200
C	6.30373500	6.51555500	23.60025300
H	7.98352600	7.63876200	24.33092300
C	5.35455900	5.53215400	23.88646400
H	4.61301600	4.15822400	25.37491300
H	6.32379600	6.98751000	22.62271300
H	4.63152700	5.23589300	23.13279300
C	10.09069000	6.01690900	25.35151500
C	9.72076000	4.77593400	24.81983500
C	10.85443800	6.89684100	24.57222900
C	10.08392600	4.43425500	23.51768600
H	9.12485100	4.09347700	25.41633100
C	11.19853400	6.56467000	23.26362500
H	11.14735200	7.85436900	24.98460600
C	10.80586600	5.33418800	22.73098900
H	9.78778400	3.47259800	23.11071400
H	11.75998800	7.27270900	22.66152300
H	11.05875700	5.07646600	21.70779400
C	16.31764300	4.97218300	26.81936100
C	17.57726200	4.82705600	27.42613800
C	15.23486600	4.25213300	27.34288400
C	17.75371200	3.98091000	28.51836500
H	18.42644000	5.36857000	27.02147500
C	15.41698100	3.39351000	28.42704200
H	14.25067100	4.37805900	26.91881200
C	16.67253400	3.25307000	29.01943500
H	18.73644300	3.88188600	28.96903400
H	14.56962900	2.83445900	28.81160600
H	16.80737400	2.58403500	29.86373300
C	15.09802300	4.01569400	24.27068800
C	15.84198400	2.87670200	23.94535900
C	13.71981200	3.89662900	24.49269400
C	15.21819400	1.63216900	23.84704200
H	16.90894300	2.96956300	23.76742200
C	13.09692500	2.65303500	24.39106100

H	13.13893500	4.77506400	24.75406400
C	13.84410800	1.51805400	24.06867200
H	15.80481700	0.75373900	23.59541500
H	12.02805800	2.57805500	24.56119500
H	13.35867400	0.54997700	23.98987400
C	15.54197500	5.51439400	21.85807000
C	16.53020300	5.19880100	20.91550600
C	14.19963300	5.28410200	21.53706800
C	16.18201500	4.66035800	19.67729900
H	17.57286300	5.37839100	21.15727400
C	13.85016100	4.75213600	20.29676100
H	13.43253000	5.52613800	22.26033800
C	14.83963600	4.43684000	19.36323100
H	16.95834000	4.41640500	18.95846700
H	12.80449500	4.58273300	20.05736700
H	14.56707800	4.02056200	18.39825000
C	16.69443400	8.18799300	21.95192600
C	17.93721400	8.58276100	21.44387200
C	15.52613300	8.60011900	21.29523200
C	18.01254800	9.37276300	20.29729100
H	18.84418000	8.27410100	21.95237900
C	15.60064500	9.39650400	20.15351500
H	14.56164700	8.31541800	21.69981400
C	16.84482900	9.78391400	19.64950200
H	18.98282100	9.67367600	19.91562200
H	14.68822600	9.71918600	19.66101700
H	16.90194300	10.40406800	18.75987000
C	19.11091500	13.96148900	23.95243200
C	19.85464300	14.80425600	24.78941800
C	19.64336400	12.71849500	23.58555100
C	21.11434500	14.41632500	25.24355200
H	19.44575300	15.76807900	25.07578100
C	20.90247300	12.33220300	24.04101400
H	19.06998100	12.04894400	22.95786600
C	21.64311400	13.17930800	24.86800800
H	21.68281300	15.08009000	25.88762500
H	21.30312000	11.36649500	23.74916000
H	22.62392300	12.87589200	25.22090300
C	18.55662400	14.12322200	21.07633900
C	19.70227500	14.92223100	20.97598100
C	18.43143700	13.00083200	20.24812000
C	20.70132900	14.61096000	20.05408500
H	19.80823200	15.78662400	21.62368500
C	19.43260800	12.68685100	19.33092200
H	17.55275400	12.37169500	20.32786400
C	20.56909800	13.49256700	19.22845300
H	21.58262700	15.24090200	19.98185800
H	19.32470500	11.81479200	18.69327900
H	21.34720500	13.24918500	18.51156900
C	15.89997300	14.76362200	20.14272000
C	16.49289100	15.66724100	19.25360800

C	15.03266900	13.78225200	19.64371000
C	16.22398300	15.59147800	17.88714800
H	17.17124800	16.42329100	19.63550100
C	14.77124900	13.70077600	18.27696300
H	14.56747500	13.08042800	20.32778200
C	15.36555800	14.60621900	17.39469500
H	16.68771900	16.29969200	17.20734700
H	14.10418400	12.93054600	17.90191100
H	15.16081100	14.54427900	16.33034800
C	13.78118200	15.41343400	22.03666100
C	13.47570900	16.48660900	21.19133100
C	12.77897000	14.49257800	22.37017200
C	12.18635700	16.63155000	20.67952400
H	14.25221500	17.19531100	20.92322800
C	11.49605400	14.62788600	21.84239200
H	13.01815300	13.65526300	23.01642900
C	11.19683400	15.69803200	20.99567200
H	11.95746900	17.46578200	20.02377000
H	10.73853700	13.88913000	22.08549200
H	10.19973100	15.80465300	20.58050100
C	10.95851700	17.33823900	27.55086000
C	10.63780500	17.75393200	28.85443100
C	11.93917500	18.04550300	26.84245300
C	11.26926200	18.85317100	29.43141100
H	9.87120700	17.22109600	29.40816700
C	12.56013700	19.15472000	27.41698800
H	12.23120600	17.71843500	25.85627600
C	12.22967100	19.56446200	28.70919500
H	11.00293500	19.15963000	30.43828600
H	13.30927200	19.69855100	26.85014800
H	12.71712400	20.42838300	29.15037200
C	9.52808500	17.58135000	24.95914200
C	8.67091200	18.67130800	25.14430200
C	10.51601100	17.64319500	23.96842300
C	8.80128700	19.81182300	24.35127300
H	7.90185900	18.62105800	25.90885200
C	10.64328300	18.78228100	23.17401100
H	11.18719800	16.80293200	23.82520600
C	9.78739000	19.86924600	23.36384500
H	8.13231100	20.65343500	24.50349100
H	11.41057300	18.81350500	22.40760600
H	9.88732000	20.75619800	22.74553500
C	7.53399900	15.65376400	24.27326100
C	6.16717300	15.89185200	24.46678600
C	8.04904900	15.66211000	22.97156500
C	5.33088900	16.13423000	23.37763800
H	5.76239800	15.88107300	25.47378000
C	7.21205600	15.89590000	21.88161800
H	9.10534500	15.48165500	22.81799200
C	5.85040500	16.13375000	22.08116200
H	4.27408000	16.32178900	23.54135600

H	7.62202800	15.89221200	20.87598400
H	5.19872800	16.31823500	21.23267100
C	7.16506500	13.22354200	25.87408200
C	6.20204400	12.81701900	26.80765200
C	7.12958700	12.67267500	24.58439400
C	5.23090100	11.87828900	26.46350300
H	6.21553500	13.23813400	27.80615400
C	6.15411800	11.73937700	24.23655600
H	7.87170500	12.97313600	23.85441700
C	5.20315300	11.33517400	25.17645800
H	4.49750600	11.57050800	27.20158300
H	6.14481800	11.32059800	23.23484400
H	4.44557100	10.60580700	24.90603900
C	13.02150200	10.81160700	25.71599400
C	11.64850900	10.51744300	25.47165800
C	14.02124500	10.65851100	24.64307200
C	10.98297800	10.53262100	24.19740700
C	10.83650700	10.18407600	26.59636600
O	14.37792100	9.52773100	24.34845700
O	14.52010700	11.78835600	24.15461300
C	9.62010300	10.30423800	24.09644300
C	9.48221200	9.93385400	26.48649400
H	11.31736400	10.11624700	27.55706700
C	15.43883900	11.62767500	23.04535800
C	8.86828300	10.01685400	25.24019900
H	9.13752500	10.35172300	23.12836500
H	8.90658100	9.70258200	27.36907900
H	16.30681400	11.04691000	23.34738700
H	15.72119900	12.63430000	22.76681200
H	14.93006300	11.12820400	22.22083400
H	7.80139500	9.86218300	25.14188100
Br	11.86693000	10.89912000	22.55153900

(2Clpyridine)-Rh2(TPPTTL)4-(Car1) (28) [B3LYP-D3(BJ)]/BS1

Rh	14.90887200	11.58647400	29.72404800
Rh	13.84354800	11.22588300	27.52556000
O	16.73004500	11.23806800	28.80004400
O	15.71870000	10.67695600	26.85398800
O	18.05655400	10.04783500	24.11488600
O	16.88240400	7.90438700	27.96998600
N	17.78016600	9.14860300	26.22636200
C	16.73041500	10.80511400	27.61683700
C	18.04836900	10.39590500	26.94242300
H	18.18954700	11.13100900	26.14193100
C	17.67254900	9.13750000	24.82803200
C	17.02551100	7.84662700	24.46586600
C	16.81114700	7.12989800	25.64661800
C	17.15299800	8.02499000	26.78860200
C	16.24007000	5.85606900	25.65659600
C	15.77545200	5.36804300	24.40736200
C	15.96595600	6.10633200	23.21720600

C	16.60813300	7.37118400	23.22716900
C	19.35849300	10.40600500	27.77826900
C	19.66705700	11.86821400	28.15756100
H	20.63299300	11.91615700	28.67111000
H	18.90262000	12.27312400	28.82265700
H	19.72397500	12.50593100	27.27037300
C	20.48532000	9.88490300	26.86717200
H	20.54206800	10.46173200	25.94047900
H	20.33541100	8.83264300	26.60867700
H	21.44705100	9.97364800	27.38222600
C	19.30066800	9.54218000	29.04852700
H	20.26205500	9.61054500	29.56947600
H	19.11381700	8.49225300	28.81518400
H	18.51837500	9.88621900	29.72504700
O	14.68673100	9.53039100	30.04351200
O	13.47112300	9.31154300	28.14985100
O	12.69233700	6.15607500	27.05176000
O	11.25884400	8.72782100	30.52516100
N	12.25124200	7.20482600	29.07842800
C	13.97512500	8.87618200	29.23588500
C	13.64905300	7.39534900	29.47135600
H	14.20992400	6.86934700	28.69053000
C	11.90414200	6.66564300	27.82603900
C	10.43073900	6.85565100	27.68977600
C	9.96898700	7.49170200	28.84674500
C	11.16826100	7.90072700	29.63616900
C	8.61695600	7.73951500	29.06850400
C	7.71622200	7.30993900	28.05508800
C	8.18840500	6.71224900	26.86308700
C	9.57700900	6.49501100	26.65390700
C	14.05843700	6.73832600	30.82326900
C	15.59200700	6.58063200	30.80168000
H	15.91578100	5.95511700	29.96623800
H	15.92601900	6.10947100	31.73183100
H	16.08680900	7.54856100	30.70738900
C	13.41461700	5.34102300	30.87639700
H	12.32870400	5.40404300	30.99107000
H	13.81345300	4.78454100	31.73032200
H	13.63067200	4.76922300	29.97068300
C	13.64421700	7.52476300	32.07965800
H	14.09287000	8.51877000	32.09117900
H	13.99032700	6.97948000	32.96458000
H	12.56182600	7.63752100	32.14873300
O	13.01057200	11.89891200	30.50756700
O	12.10877300	11.87561600	28.43296700
O	8.42837500	11.95824600	28.44934100
O	11.82166200	14.89623100	29.27098900
N	10.09278300	13.34749500	29.25226500
C	12.05737300	12.03427300	29.69746300
C	10.64925200	12.38327300	30.19968400
H	10.06148400	11.47387000	30.02769600

C	9.07227400	12.98730800	28.35805000
C	8.99310100	14.08781000	27.34802500
C	9.96101000	15.04025500	27.68743300
C	10.75949300	14.50339900	28.82368900
C	10.13924100	16.22516300	26.97486700
C	9.36459100	16.36578400	25.79525000
C	8.39709000	15.40060000	25.43638300
C	8.17585200	14.23868900	26.22648100
C	10.45816300	12.75617200	31.69710100
C	10.73588400	11.49477600	32.53855600
H	10.52636900	11.70575300	33.59235500
H	11.77758200	11.18255700	32.44952400
H	10.10077200	10.66083500	32.22638800
C	8.98339500	13.15832400	31.88427600
H	8.31141500	12.37726300	31.51987500
H	8.75143600	14.08662400	31.35400800
H	8.77614200	13.31548100	32.94746800
C	11.35676200	13.90908100	32.17427800
H	11.16480900	14.09231500	33.23725300
H	11.15158800	14.83217800	31.62875100
H	12.41336600	13.66828600	32.05105200
O	15.04355800	13.59509300	29.19805100
O	14.28165800	13.17979200	27.10455800
O	13.49218900	15.91725500	25.11369800
O	17.40722300	14.12034400	26.60631600
N	15.46567200	15.32501000	26.18722800
C	14.75756100	13.93047300	28.01803700
C	14.93333900	15.38114900	27.54913000
H	13.90880100	15.74424800	27.41133000
C	14.64266500	15.52257900	25.06536000
C	15.46868600	15.15519800	23.87910200
C	16.72707600	14.75181100	24.33731400
C	16.65721400	14.67908100	25.82688500
C	17.75820600	14.40559300	23.46880600
C	17.46877300	14.46894900	22.07940000
C	16.17698300	14.81297200	21.61913400
C	15.14273200	15.15981200	22.52735300
C	15.63552100	16.39860300	28.49691800
C	14.65496400	16.69020100	29.65048400
H	13.71594500	17.10612600	29.27681900
H	15.10180300	17.41682200	30.33729200
H	14.42849400	15.78095100	30.20886300
C	15.86981800	17.69335000	27.69757600
H	16.63758200	17.55883300	26.92994200
H	16.20274100	18.48753700	28.37334000
H	14.95283900	18.02975400	27.20789200
C	16.97879100	15.92314800	29.07853100
H	16.85163800	15.01919800	29.67482700
H	17.37771500	16.71110100	29.72716300
H	17.71108100	15.72093800	28.29600400
C	8.14258100	8.39919000	30.31364200

C	7.34322600	9.54934100	30.26124500
C	8.47568600	7.85609100	31.56214500
C	6.87835600	10.13584600	31.43678800
H	7.09272800	9.99063800	29.30534000
C	8.01236000	8.44601200	32.73704700
H	9.09051100	6.96287300	31.60848300
C	7.20929800	9.58691600	32.67737100
H	6.25660200	11.02392700	31.38175700
H	8.27462500	8.01249700	33.69713200
H	6.84522100	10.04599000	33.59127200
C	6.25120400	7.51651300	28.24998600
C	5.58677700	6.87238300	29.30191200
C	5.52324800	8.35822900	27.39924600
C	4.21860100	7.05818800	29.49431300
H	6.14840700	6.22784300	29.97025300
C	4.15671600	8.54957300	27.59588200
H	6.02467900	8.86888900	26.58535900
C	3.49921000	7.89841100	28.64178600
H	3.71551900	6.54854400	30.31027300
H	3.60404400	9.20461000	26.92981700
H	2.43419300	8.04566500	28.79194700
C	7.21186100	6.28737400	25.81598200
C	6.26098000	5.29900800	26.10328400
C	7.22992500	6.85876600	24.53672700
C	5.34225700	4.89661400	25.13502900
H	6.24140300	4.85007600	27.09066400
C	6.30517200	6.46434700	23.57139000
H	7.97841300	7.60282300	24.29321500
C	5.35768000	5.48222500	23.86725200
H	4.61385800	4.12716000	25.37181000
H	6.32858000	6.92202000	22.58714900
H	4.63916900	5.17277200	23.11454600
C	10.08783400	6.01472300	25.34232300
C	9.72778300	4.76813600	24.81714700
C	10.85303900	6.89278500	24.56243400
C	10.10286000	4.41851000	23.52046100
H	9.13052700	4.08726300	25.41413900
C	11.20866400	6.55265800	23.25896100
H	11.13800900	7.85459600	24.97034500
C	10.82667500	5.31607000	22.73272400
H	9.81462800	3.45237600	23.11839600
H	11.77073700	7.25930900	22.65580700
H	11.08921300	5.05173800	21.71365200
C	16.31792700	4.99973400	26.87168800
C	17.57587700	4.84801000	27.47993100
C	15.23047400	4.28554100	27.39366000
C	17.74685300	3.99826400	28.57038500
H	18.42802200	5.38631400	27.07716200
C	15.40675900	3.42428600	28.47672900
H	14.24761400	4.41760000	26.96813500
C	16.66150800	3.27470400	29.06872400

H	18.72862100	3.89308200	29.02181000
H	14.55570800	2.87049500	28.86072200
H	16.79223300	2.60303900	29.91158800
C	15.11820500	4.02895600	24.32364200
C	15.86910900	2.88915500	24.01747200
C	13.73807100	3.90786700	24.53178000
C	15.25013600	1.64187000	23.92404900
H	16.93777000	2.98360800	23.85088000
C	13.12006100	2.66137400	24.43530600
H	13.15191700	4.78683400	24.77902900
C	13.87402800	1.52568600	24.13176600
H	15.84206900	0.76286600	23.68725500
H	12.04964400	2.58472600	24.59465800
H	13.39234800	0.55541200	24.05691500
C	15.57627400	5.51286700	21.90462300
C	16.57222100	5.18572800	20.97424900
C	14.23618900	5.28471900	21.57298900
C	16.23378700	4.63789400	19.73744800
H	17.61318100	5.36386700	21.22430500
C	13.89652500	4.74348400	20.33392700
H	13.46320000	5.53571300	22.28696000
C	14.89362200	4.41651000	19.41261000
H	17.01596200	4.38502600	19.02808900
H	12.85257400	4.57606300	20.08589000
H	14.62864700	3.99300800	18.44865600
C	16.73331000	8.18505400	21.98813500
C	17.98461200	8.56786500	21.49170800
C	15.57564100	8.59565700	21.31226500
C	18.07886900	9.34426600	20.33736900
H	18.88335800	8.26011500	22.01526900
C	15.66912200	9.37802700	20.16221000
H	14.60459200	8.32172000	21.70847100
C	16.92160000	9.75319700	19.66977500
H	19.05546400	9.63611500	19.96479400
H	14.76483600	9.69997800	19.65447200
H	16.99343400	10.36227900	18.77356900
C	19.09262200	13.98606400	23.97153700
C	19.83218800	14.83832100	24.80258400
C	19.63165700	12.74355600	23.61276000
C	21.09401800	14.46009800	25.25901600
H	19.41813800	15.80173000	25.08287800
C	20.89305900	12.36710600	24.07022500
H	19.06137000	12.06655000	22.99028800
C	21.62939400	13.22352100	24.89146100
H	21.65905600	15.13118500	25.89854100
H	21.29870900	11.40159900	23.78462400
H	22.61195900	12.92773400	25.24599400
C	18.53472800	14.12431200	21.09473300
C	19.67730900	14.92647600	20.98549300
C	18.41240900	12.99409400	20.27673000
C	20.67603300	14.61066100	20.06475100

H	19.78112300	15.79681900	21.62554000
C	19.41314400	12.67567100	19.36066000
H	17.53631300	12.36220000	20.36324200
C	20.54649000	13.48460400	19.24914200
H	21.55497100	15.24307300	19.98553700
H	19.30718900	11.79743500	18.73128300
H	21.32430900	13.23777400	18.53310800
C	15.87729700	14.75415300	20.15823800
C	16.46940800	15.65620600	19.26691400
C	15.01180800	13.77020000	19.66114500
C	16.20150700	15.57649800	17.90049100
H	17.14629900	16.41436500	19.64722500
C	14.75118900	13.68490900	18.29449300
H	14.54689900	13.06975800	20.34670700
C	15.34467200	14.58882200	17.41012200
H	16.66465700	16.28361100	17.21912800
H	14.08542700	12.91271900	17.92114600
H	15.14052600	14.52385100	16.34583000
C	13.75426500	15.39665000	22.04912600
C	13.44198300	16.46566500	21.20100400
C	12.75946300	14.46725800	22.38157800
C	12.15336700	16.59764100	20.68396400
H	14.21315600	17.18065200	20.93410100
C	11.47714400	14.59028800	21.84907400
H	13.00512700	13.63244700	23.02880000
C	11.17160500	15.65541800	20.99825700
H	11.91916300	17.42820500	20.02544400
H	10.72533600	13.84530500	22.09090000
H	10.17567900	15.75086500	20.57758900
C	10.92841700	17.34907700	27.55043500
C	10.59819400	17.77251600	28.84902800
C	11.91804300	18.04877700	26.84700400
C	11.22902700	18.87223800	29.42584500
H	9.82512600	17.24509800	29.39896500
C	12.53909600	19.15795800	27.42149700
H	12.21689800	17.71558200	25.86496600
C	12.19888600	19.57575600	28.70861700
H	10.95520900	19.18492200	30.42880500
H	13.29566300	19.69556100	26.85856800
H	12.68623500	20.43972900	29.14984400
C	9.51785400	17.58695400	24.94822100
C	8.66504900	18.68154500	25.12598000
C	10.51111100	17.64119000	23.96230600
C	8.80491700	19.81919400	24.33042300
H	7.89195800	18.63715200	25.88682000
C	10.64803100	18.77755800	23.16560000
H	11.17918500	16.79743800	23.82501400
C	9.79640500	19.86915100	23.34800600
H	8.13917700	20.66441500	24.47681400
H	11.41950100	18.80302100	22.40317700
H	9.90380500	20.75391000	22.72778700

C	7.52093600	15.66324900	24.25630500
C	6.15359100	15.90337300	24.44369000
C	8.04156000	15.67021600	22.95689500
C	5.32238400	16.14635700	23.35078700
H	5.74437800	15.89371500	25.44891400
C	7.20974800	15.90498800	21.86321400
H	9.09815500	15.48801700	22.80798100
C	5.84755500	16.14475500	22.05658000
H	4.26510400	16.33534800	23.50982500
H	7.62429100	15.90084600	20.85943800
H	5.19987200	16.32990500	21.20516900
C	7.14347700	13.23365700	25.85485900
C	6.17324100	12.82945200	26.78205100
C	7.11676600	12.68125000	24.56576400
C	5.20246900	11.89265400	26.43171600
H	6.18070200	13.25135100	27.78034300
C	6.14155200	11.75008800	24.21169000
H	7.86528700	12.97880800	23.84108100
C	5.18258400	11.34913000	25.14469500
H	4.46320600	11.58675200	27.16474400
H	6.13889200	11.33023200	23.21037200
H	4.42496200	10.62178700	24.86895400
C	12.98089000	10.81392200	25.68245400
C	11.60980500	10.51734400	25.42338300
C	13.98794500	10.65448600	24.62640900
C	10.95577500	10.50729000	24.14410200
C	10.78761600	10.20531200	26.54624300
O	14.36653500	9.52438600	24.34970300
O	14.48710700	11.78489800	24.13039600
C	9.59528700	10.26837000	24.03268600
C	9.43559900	9.94264700	26.42831200
H	11.25986300	10.16738300	27.51342600
C	15.42164800	11.61787900	23.03784200
C	8.83466600	9.99449600	25.17402100
H	9.12185100	10.29565300	23.05922500
H	8.85195900	9.72743500	27.31007900
H	16.27448600	11.01916300	23.34743100
H	15.72795800	12.62141300	22.77297700
H	14.91900300	11.13590400	22.19893300
H	7.77039400	9.82783600	25.06742800
Br	11.85729200	10.85180500	22.50171700
N	16.19916200	11.65482100	31.85744200
C	16.93099300	10.53180500	31.99015500
C	16.53816900	12.70230100	32.59597600
C	18.02051100	10.43950700	32.84792600
H	16.61477600	9.69733800	31.37565300
C	17.61551400	12.72402900	33.48294900
Cl	15.54395100	14.14118400	32.44093500
C	18.37164700	11.56120700	33.60162200
H	18.57978900	9.51384100	32.91673700
H	17.84189900	13.61624000	34.05289700

H	19.21958100	11.53320600	34.27788500

(2Clpyridine)-Rh2(TPPTTL)4-(Car1)-2Clpyridine (29) [B3LYP-D3(BJ)]/BS1

Rh	14.92580900	11.18513900	29.81485300
Rh	13.88214700	10.91953500	27.59118800
O	16.76910200	10.87671400	28.90699000
O	15.77380000	10.39458200	26.93636300
O	18.24062400	10.07749700	24.08374900
O	17.31528000	7.71980500	27.89607600
N	17.98655000	9.12937100	26.17638400
C	16.78598800	10.56105200	27.68639900
C	18.11675600	10.37284500	26.93647700
H	18.10530200	11.15585100	26.17039800
C	17.89820500	9.13538800	24.77252500
C	17.37748500	7.79238300	24.37976000
C	17.26002900	7.03325200	25.54706700
C	17.51884600	7.92411800	26.71211100
C	16.86744700	5.70149100	25.53470300
C	16.55610100	5.13525300	24.27563500
C	16.56489100	5.93020700	23.10292100
C	16.97045500	7.29280800	23.14363000
C	19.45729600	10.53916800	27.70178200
C	19.54829700	11.99408900	28.20199100
H	20.52697200	12.16010500	28.66414300
H	18.77682700	12.20836900	28.94348900
H	19.43369000	12.70405300	27.37786900
C	20.59210000	10.29965900	26.68753500
H	20.50267500	10.96795300	25.82581200
H	20.58991400	9.26844300	26.32212600
H	21.55883600	10.48681300	27.16540500
C	19.61959700	9.57103400	28.88327500
H	20.58986400	9.74660300	29.36083100
H	19.58436500	8.52873500	28.55978800
H	18.83767900	9.72488200	29.62739200
O	14.59268600	9.15750000	30.08778200
O	13.44179700	8.95622000	28.15288600
O	12.65748800	4.84962800	28.07276200
O	10.91553300	8.73210900	29.79602100
N	12.08127000	6.84398200	29.10953700
C	13.83836400	8.53883900	29.28626700
C	13.39866000	7.11832300	29.67500100
H	14.06974700	6.45123200	29.12235400
C	11.82415900	5.69303000	28.35184800
C	10.37943600	5.73544700	28.00966900
C	9.82288000	6.87326900	28.60722900
C	10.93268500	7.63990200	29.25877200
C	8.46124500	7.15449400	28.51331300
C	7.66680100	6.23781100	27.76810800
C	8.23840100	5.10071700	27.15443200
C	9.62835500	4.83551500	27.26412600
C	13.52355400	6.72625100	31.18739400

C	15.01888600	6.58540100	31.53725300
H	15.51676100	5.87784900	30.86537600
H	15.12035200	6.20554500	32.55889000
H	15.53351400	7.54326200	31.47479600
C	12.85650300	5.35213200	31.39186400
H	11.77502400	5.39655100	31.23494100
H	13.02768500	5.01839300	32.41941200
H	13.26821700	4.59632300	30.71803100
C	12.85545100	7.74031600	32.13254900
H	13.29227800	8.73375900	32.02560300
H	12.99417000	7.40996300	33.16754800
H	11.78271600	7.81831800	31.94550200
O	13.02735400	11.53319500	30.58630000
O	12.16104100	11.60226000	28.49987400
O	8.56974200	12.16816800	28.36744800
O	12.16527900	14.68545800	29.59708800
N	10.30948100	13.30862200	29.36999700
C	12.09799200	11.74418500	29.76470900
C	10.71052600	12.19845400	30.23434000
H	10.04493400	11.38153000	29.93493300
C	9.28222900	13.15288600	28.42803400
C	9.29576700	14.38330700	27.58515900
C	10.34467300	15.19465600	28.03473700
C	11.08182700	14.44687600	29.09470800
C	10.62962100	16.43296200	27.46066600
C	9.84572100	16.79883700	26.33506500
C	8.75844500	16.00542600	25.90704700
C	8.47344800	14.75581300	26.52426500
C	10.46371700	12.44014200	31.74760200
C	10.64680500	11.09501200	32.47748500
H	10.37295500	11.20882500	33.53139100
H	11.68181000	10.75421800	32.42490700
H	10.00865300	10.32023500	32.04119400
C	9.00003900	12.89309800	31.90692500
H	8.31035400	12.17584100	31.45349500
H	8.83144700	13.86962700	31.44301900
H	8.75414500	12.97882500	32.96999900
C	11.38944000	13.49958100	32.36511900
H	11.17103900	13.58640600	33.43524600
H	11.23856200	14.48060800	31.90964300
H	12.43739100	13.22553000	32.24574800
O	15.13601900	13.20213500	29.38042700
O	14.40055800	12.87465500	27.26396800
O	13.26512900	15.58089600	25.66222100
O	17.48230600	14.03752700	26.44725500
N	15.41594500	15.09802200	26.39878100
C	14.88022100	13.58409000	28.20764400
C	15.09037800	15.05308000	27.82337500
H	14.08296100	15.48216200	27.86917400
C	14.41731000	15.26888400	25.42250200
C	15.07594100	15.00567300	24.10868000

C	16.42498100	14.73475300	24.35325500
C	16.58380300	14.57800500	25.82815600
C	17.34233400	14.52884100	23.32823500
C	16.84012300	14.58532500	22.00184200
C	15.45640300	14.75413000	21.75800500
C	14.54258300	14.96923000	22.82433900
C	15.98417700	15.93611400	28.75596400
C	15.12645300	16.28524500	29.98947100
H	14.21273900	16.81120800	29.70407100
H	15.69829000	16.93178000	30.66353200
H	14.84638500	15.38050500	30.53145300
C	16.33206200	17.22841700	27.99598700
H	17.04212800	17.03941900	27.18545900
H	16.79199900	17.94461200	28.68423100
H	15.44196300	17.69477200	27.56907000
C	17.29281600	15.27931200	29.23548300
H	17.09491700	14.36375000	29.79368900
H	17.80945300	15.98099000	29.89993300
H	17.95343000	15.03820200	28.40398500
C	7.83349400	8.30698900	29.21128100
C	7.05742100	9.24104400	28.51316500
C	7.93851700	8.41242300	30.60544200
C	6.38257300	10.24903200	29.19681700
H	6.97106400	9.16634900	27.43496400
C	7.25667200	9.41713200	31.28948300
H	8.53650700	7.69096000	31.15221000
C	6.46949000	10.33294400	30.58657700
H	5.79885000	10.97231900	28.63987500
H	7.33559700	9.48181700	32.37015600
H	5.93335900	11.11160600	31.12029800
C	6.19812700	6.47283100	27.64254100
C	5.37364000	6.44004000	28.77453000
C	5.62786800	6.73190900	26.39008200
C	4.00247300	6.66049900	28.65564300
H	5.81209800	6.24781600	29.74827800
C	4.25773800	6.96167600	26.27239400
H	6.26413100	6.75620100	25.51271700
C	3.44074800	6.92500500	27.40440500
H	3.37341100	6.62813200	29.53995100
H	3.82880900	7.16871500	25.29665800
H	2.37343200	7.10137100	27.31254300
C	7.37326800	4.13262600	26.41860300
C	6.37389000	3.42325400	27.09832100
C	7.56593400	3.89549900	25.05164800
C	5.58053400	2.49698000	26.42313600
H	6.22059400	3.60038500	28.15754900
C	6.76667800	2.97564900	24.37459700
H	8.34149800	4.43392700	24.52115300
C	5.77258800	2.27239700	25.05808800
H	4.81319600	1.95073500	26.96320100
H	6.92293900	2.80727200	23.31344400

H	5.15283200	1.55309300	24.53151000
C	10.23666400	3.64683900	26.60301200
C	9.90449600	2.35351000	27.02423200
C	11.09847000	3.81163000	25.51124700
C	10.42207400	1.24152300	26.36082000
H	9.22993700	2.22199600	27.86388300
C	11.60104600	2.70005900	24.83749300
H	11.36352500	4.80782900	25.18279400
C	11.26437000	1.41175400	25.25996100
H	10.15921400	0.24333800	26.69719100
H	12.25677400	2.84039700	23.98451700
H	11.65289300	0.54628600	24.73179600
C	16.86333100	4.89623400	26.78819300
C	18.04983300	4.31292600	27.24677900
C	15.68306900	4.71526500	27.51389700
C	18.05284800	3.55397600	28.41839000
H	18.96698100	4.45333600	26.68290300
C	15.68404900	3.94903900	28.67844400
H	14.75903800	5.16387300	27.17066800
C	16.86936000	3.36865300	29.13613700
H	18.97822100	3.10540700	28.76691700
H	14.75207800	3.80340300	29.21254700
H	16.86975100	2.77269100	30.04372300
C	16.29821200	3.66797200	24.18727100
C	17.22259300	2.85278800	23.51939600
C	15.17184400	3.07733500	24.77392500
C	17.02853000	1.47436600	23.44322900
H	18.09364200	3.30686100	23.05772700
C	14.97799900	1.69800100	24.69804700
H	14.43882200	3.69521800	25.27941800
C	15.90540000	0.89242100	24.03505400
H	17.75466300	0.85613400	22.92417100
H	14.09974200	1.25757500	25.15762600
H	15.75311100	-0.18107000	23.97861900
C	16.15514900	5.32499900	21.80409600
C	17.00143300	5.38662700	20.68821400
C	14.91324700	4.68649200	21.67332500
C	16.61215000	4.83068200	19.47036400
H	17.96647900	5.87354100	20.77718900
C	14.51783000	4.14035200	20.45374600
H	14.25870600	4.61404200	22.53366600
C	15.36700200	4.21040200	19.34702300
H	17.28178900	4.88326400	18.61740200
H	13.54862700	3.65829700	20.37020000
H	15.06196300	3.78271800	18.39699300
C	16.83059900	8.18013500	21.95584700
C	17.92281000	8.85713400	21.40249200
C	15.55688200	8.37103600	21.39893300
C	17.74679100	9.70521300	20.30868500
H	18.90806100	8.72396200	21.83387400
C	15.38060700	9.21944400	20.30773400

H	14.70268000	7.87239200	21.84020400
C	16.47648500	9.88817300	19.75734000
H	18.60127300	10.22917400	19.89307500
H	14.38933600	9.35839500	19.88647400
H	16.33801800	10.54671400	18.90525700
C	18.76279700	14.20875200	23.63144900
C	19.53873300	15.09529000	24.38998200
C	19.33070500	13.00277700	23.19829900
C	20.85911300	14.78391600	24.70985400
H	19.10200500	16.02987300	24.72825900
C	20.64794700	12.68753700	23.52769500
H	18.74125100	12.30149100	22.62068100
C	21.41685900	13.57667000	24.28172700
H	21.45057900	15.48099400	25.29541400
H	21.06951000	11.74279300	23.19915300
H	22.44305100	13.32978900	24.53589100
C	17.78834500	14.39044400	20.86739200
C	18.82769800	15.30675200	20.66138000
C	17.67530600	13.28600900	20.01364100
C	19.73188800	15.12701500	19.61491200
H	18.92695400	16.15838800	21.32670200
C	18.58239200	13.10265900	18.97168700
H	16.88042100	12.56778800	20.17203400
C	19.61231800	14.02401000	18.76706600
H	20.53010200	15.84716600	19.46348900
H	18.48433400	12.24124100	18.31773900
H	20.31712900	13.88242200	17.95358300
C	14.93220100	14.61087100	20.36779500
C	15.26529900	15.52985200	19.36659700
C	14.11561900	13.51638400	20.04776300
C	14.79147400	15.35844600	18.06593100
H	15.90342500	16.37357400	19.60859100
C	13.65126700	13.33970800	18.74578700
H	13.84225400	12.80439300	20.81981000
C	13.98755000	14.26089200	17.75076900
H	15.05386700	16.07990300	17.29820300
H	13.02637300	12.48366000	18.51000300
H	13.62415400	14.12498100	16.73682400
C	13.07627900	15.00997900	22.58149100
C	12.49378200	15.96098500	21.73405400
C	12.27439700	14.00404800	23.14000400
C	11.13593500	15.88910500	21.42578200
H	13.11064100	16.73999000	21.29884300
C	10.91884900	13.93087300	22.82675100
H	12.73183600	13.25929800	23.78150200
C	10.35004800	14.86293800	21.95651000
H	10.69381700	16.62707700	20.76364200
H	10.31402400	13.13398800	23.24501700
H	9.29815400	14.79550300	21.69864900
C	11.53730200	17.40624700	28.12826400
C	11.27851800	17.71250000	29.47487600

C	12.55742000	18.10303100	27.46584500
C	12.00529300	18.69882700	30.13791800
H	10.48348400	17.18737100	29.99459100
C	13.27283600	19.10168900	28.12644600
H	12.79363700	17.85693300	26.44129500
C	13.00026500	19.40639700	29.46054700
H	11.78507300	18.92263700	31.17716800
H	14.05074900	19.64084400	27.59509500
H	13.56064600	20.18497100	29.96886600
C	10.15575000	18.05633200	25.59260200
C	9.52289000	19.26400400	25.89861100
C	11.08694400	18.00915800	24.54597100
C	9.81567000	20.41458400	25.16437200
H	8.79927300	19.29906300	26.70703600
C	11.37406300	19.15764300	23.81013800
H	11.58687700	17.07309500	24.31946600
C	10.73875700	20.36344200	24.11758700
H	9.32042800	21.34964000	25.40809300
H	12.09149800	19.10734100	22.99656700
H	10.96164000	21.25874100	23.54513400
C	7.80193400	16.54409000	24.89309600
C	6.46863400	16.75818800	25.27440200
C	8.18453900	16.85278100	23.58276600
C	5.54022100	17.26113400	24.36454900
H	6.16140200	16.52485200	26.28869100
C	7.25459500	17.34649900	22.66866000
H	9.20865500	16.69833600	23.27616800
C	5.92923000	17.55344000	23.05523800
H	4.51360900	17.42398600	24.67838800
H	7.56973300	17.57028500	21.65371900
H	5.20592900	17.94100200	22.34428500
C	7.38688500	13.87835600	26.01223900
C	6.35810100	13.42270800	26.84632200
C	7.37967500	13.50583000	24.66048900
C	5.34386700	12.61193400	26.33796800
H	6.35218100	13.70680900	27.89251300
C	6.36780400	12.69304700	24.15243600
H	8.17021100	13.86015000	24.00922100
C	5.34712200	12.24013200	24.99128900
H	4.54445200	12.27631900	26.99158400
H	6.37881900	12.41311900	23.10344100
H	4.55667700	11.60837800	24.59821400
C	13.09962600	10.67066400	25.63790000
C	11.76521100	10.60909900	25.14709900
C	14.23620700	10.49343100	24.72456700
C	11.33835400	10.46791700	23.77730300
C	10.71738000	10.68669800	26.11623000
O	14.72912700	9.39430400	24.53104400
O	14.68421400	11.65420800	24.23672700
C	9.99248500	10.42263200	23.44573300
C	9.37592300	10.65022500	25.77971800

H	11.00812000	10.78589000	27.15145500
C	15.74907800	11.56942500	23.26246500
C	9.01371200	10.51267100	24.43995100
H	9.70120200	10.30883400	22.40921200
H	8.62555800	10.74639800	26.55312600
H	16.69875400	11.73597600	23.76298200
H	15.54851400	12.35115900	22.53782400
H	15.75146500	10.59161400	22.78996200
H	7.96890700	10.47594000	24.15723100
Br	12.52232400	10.32105500	22.29376800
N	16.23159500	11.15604400	31.89228900
C	17.08422600	10.11377300	31.88783400
C	16.38282300	12.07394700	32.83674200
C	18.10335400	9.97039100	32.82106600
H	16.93175800	9.39080300	31.09537300
C	17.37255900	12.03316300	33.81997200
Cl	15.25017400	13.41398500	32.83213100
C	18.24988000	10.95257100	33.80277500
H	18.76501200	9.11349900	32.77417800
H	17.44374400	12.81834000	34.56191900
H	19.03529400	10.88059000	34.54771700
N	10.90843200	6.73427300	22.98916100
C	12.24091300	6.66901000	23.15814800
C	10.19535700	7.12061100	24.02995400
C	12.87720100	6.98889200	24.35554500
H	12.81119500	6.35251900	22.29018200
C	10.70852000	7.46331500	25.27931100
Cl	8.44436600	7.21110200	23.78269100
C	12.09262000	7.40599000	25.43316700
H	13.95558100	6.95084100	24.43334500
H	10.05400300	7.78294900	26.07698200
H	12.55060100	7.70338500	26.37158300

2. Analysis of HFIP interactions.

Table D16. The total energies (in hartree) of all structures involved in the reactions HFIP+(Car3)$Rh_2(AcO)_4$, calculated at **BS1** level of theory (see text above).

Structure	$-E_{tot}$	$-E_{tot}$+ZPEC	-H	-G
HFIP	789.803267	789.741478	789.731804	789.776252
H_2O	76.424984	76.403644	76.399864	76.421958
DMAP	382.302898	382.140544	382.130935	382.174646
Pyridine	248.308435	248.219396	248.214184	248.246797
DCM	959.701593	959.672125	959.667596	959.698961
$Rh_2(AcO)_4$	1133.220474	1133.009877	1132.987377	1133.062808
(Car3)-$Rh_2(AcO)_4$ (**22**)	5620.344475	5619.994458	5619.954672	5620.072664
$Rh_2(AcO)_4$–(Car1)(HFIP)-ester O	6410.173600	6409.760121	6409.709303	6409.852571
$Rh_2(AcO)_4$–(Car1)(HFIP)-carbonyl O (**33**)				

	6410.170147	6409.756302	6409.705563	6409.852363
$Rh_2(AcO)_4$–(Car1)(HFIP)$_2$	7200.009513	7199.531358	7199.470248	7199.634868
DMAP-HFIP	1172.134519	1171.908579	1171.888317	1171.960443
Pyridine-HFIP	1038.137394	1037.984488	1037.968680	1038.030091
$(H_2O)HFIP_2$	1656.068839	1655.917446	1655.893649	1655.974166
$(H_2O)_2HFIP_3$	2522.350548	2522.108280	2522.072043	2522.181309
(DCM)HFIP	1749.516292	1749.423019	1749.407574	1749.468658
$(DCM)HFIP_2$	2539.333664	2539.176914	2539.150437	2539.237908
$HFIP_2$	1579.627333	1579.500574	1579.479850	1579.552131
$HFIP_3$	2369.454736	2369.263518	2369.232375	2369.329690

Table D17. The total energies (in hartree) of all structures involved in the reactions Car 3+ HFIP+H_2O + $Rh_2(TCPTAD)_4$ calculated **BS1** level of theory.

Structure	$-E_{tot}$	$-E_{tot}$+ZPEC	-H	-G
$Rh_2(TCPTAD)_4$	12092.791560	12091.44903	12091.34614	12091.59905
$Rh_2(TCPTAD)_4$(Car3) (**35**)	16579.963422	16578.479862	16578.360773	16578.64248
$(HFIP)_4(H2O)_3$-$Rh_2(TCPTAD)_4$	15481.529730	15479.850139	15479.698686	15480.052963
$Rh_2(TCPTAD)_4(HFIP)_4$ (**34**)	15252.176965	15250.57699	15250.431668	15250.77502
$Rh_2(TCPTAD)_4$(Car3)$(HFIP)_3$	18949.472400	18947.79665	18947.64488	18948.00111
$Rh_2(TCPTAD)_4$(Car3)$(HFIP)_4$ (**36**)	19739.305358	19737.56401	19737.40206	19737.77964

Table D18. The calculated HFIP interaction energies (in kcal/mol) at **BS1** for achiral systems**.** "Minus" means that interaction is thermodynamically stable).

Structure	ΔE_{tot}	$_{\Delta}E_{tot}$+ZPEC	ΔH	ΔG
HFIP + (Car3)-$Rh_2(AcO)_4$	0.0	0.0	0.0	0.0
$Rh_2(AcO)_4$–(Car3)(HFIP)-carbonyl O (**33**)	-14.1	-12.8	-11.8	-2.2
$Rh_2(AcO)_4$–(Car3)(HFIP)-ester O	-16.2	-15.2	-14.3	-2.3
2(HFIP) + (Car3)-$Rh_2(AcO)_4$	0.0	0.0	0.0	0.0
$Rh_2(AcO)_4$–(Car3)$(HFIP)_2$	-36.7	-33.8	-32.6	-6.1
X(HFIP)	0.0	0.0	0.0	0.0
$(HFIP)_2$	-13.1	-11.1	-10.2	+0.2
$(HFIP)_3$	-28.2	-24.5	-23.2	-0.1

X(HFIP)+Y(H_2O)	0.0	0.0	0.0	0.0
$(HFIP)_2(H_2O)$	-23.4	-19.3	-18.9	+0.2
$(HFIP)_3(H_2O)_2$	-57.0	-48.0	-48.3	-5.4
X(HFIP)+DCM	0.0	0.0	0.0	0.0
(HFIP)(DCM)	-7.2	-5.9	-5.1	+4.1
$(HFIP)_2$(DCM)	-16.0	-13.7	-12.1	+8.5
HFIP+DMAP	0.0	0.0	0.0	0.0
HFIP-DMAP	-17.8	-16.7	-16.1	-6.0
HFIP+Pyridine	0.0	0.0	0.0	0.0
HFIP-Pyridine	-16.1	-14.8	-14.2	-4.4

Table D19. The calculated HFIP interaction energies (in kcal/mol) at **BS1** for $Rh_2(TCPTAD)_4$ system**.** "Minus" means that interaction is thermodynamically stable).

Structure	ΔE_{tot}	$_{\Delta}E_{tot}$+ZPEC	ΔH	ΔG
4(HFIP)+3(H_2O)+$Rh_2(TCPTAD)_4$	0.0	0.0	0.0	0.0
$(HFIP)_4(H_2O)_3$-$Rh_2(TCPTAD)_4$	-157.0	-140.7	-141.6	-52.1
4(HFIP)+ $Rh_2(TCPTAD)_4$	0.0	0.0	0.0	0.0
$(HFIP)_4$-$Rh_2(TCPTAD)_4$ (**34**)	-108.1	-101.7	-99.3	-44.5
4(HFIP)+$Rh_2(TCPTAD)_4$(Car3)	0.0	0.0	0.0	0.0
$(HFIP)_4$-$Rh_2(TCPTAD)_4$(Car3) (**36**)	-80.9	-74.2	-71.6	-20.2
3(HFIP)+$Rh_2(TCPTAD)_4$(Car3)	0.0	0.0	0.0	0.0
$(HFIP)_3$-$Rh_2(TCPTAD)_4$(Car3)	-62.2	-58.0	-55.7	-18.7
(HFIP)+ $(HFIP)_3$-$Rh_2(TCPTAD)_4$(Car3)	0.0	0.0	0.0	0.0
$(HFIP)_4$-$Rh_2(TCPTAD)_4$(Car3) (**36**)	-18.6	-16.2	-15.9	-1.4
Distortion+$Rh_2(TCPTAD)_4$(Car3)	0.0	0.0	0.0	0.0
$Rh_2(TCPTAD)_4$(Car3) Distorted ligand single point calculation	+29.2	N/A	N/A	N/A

NBO Analyses:

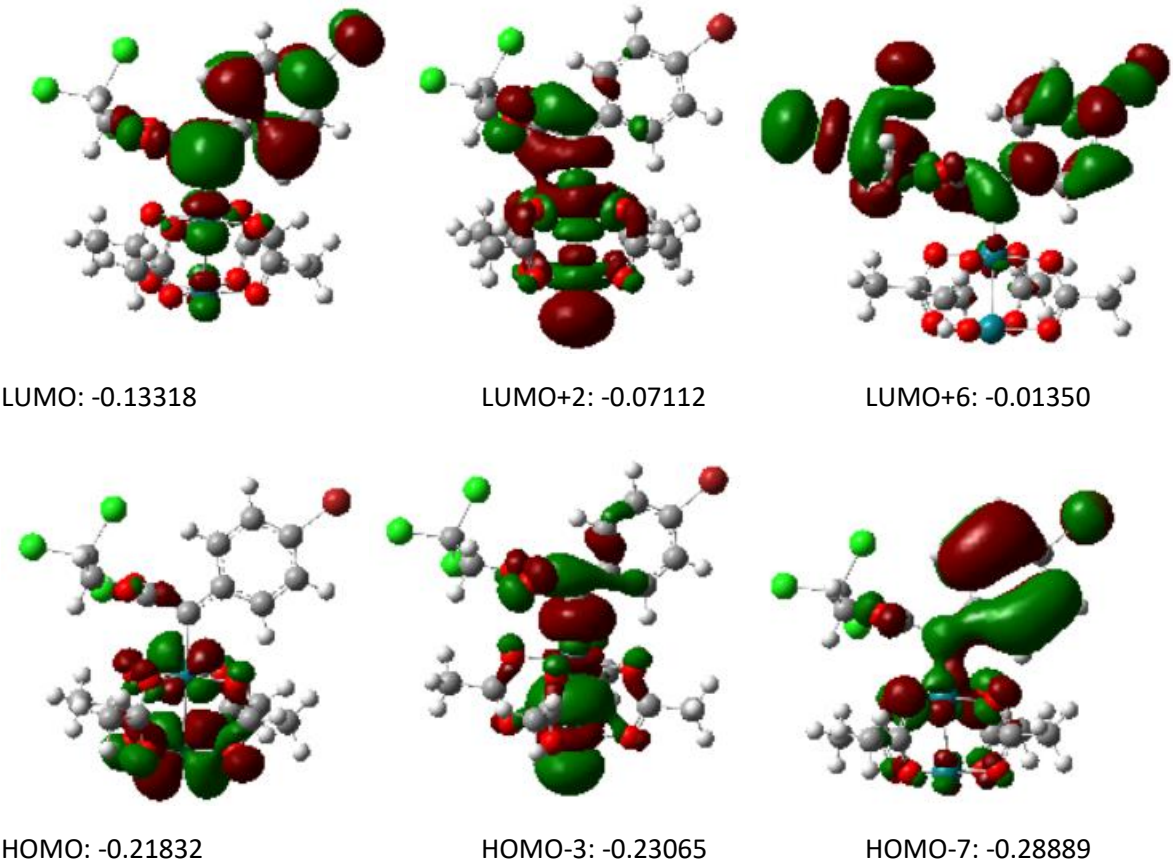

Figure D8. The calculated frontiers natural bonds for $Rh_2(AcO)_4$-(Car3) (**22**), energies reported in Hartreees. For the nature of the Rh-Rh and Rh-Carbene bonds, see Table S19.

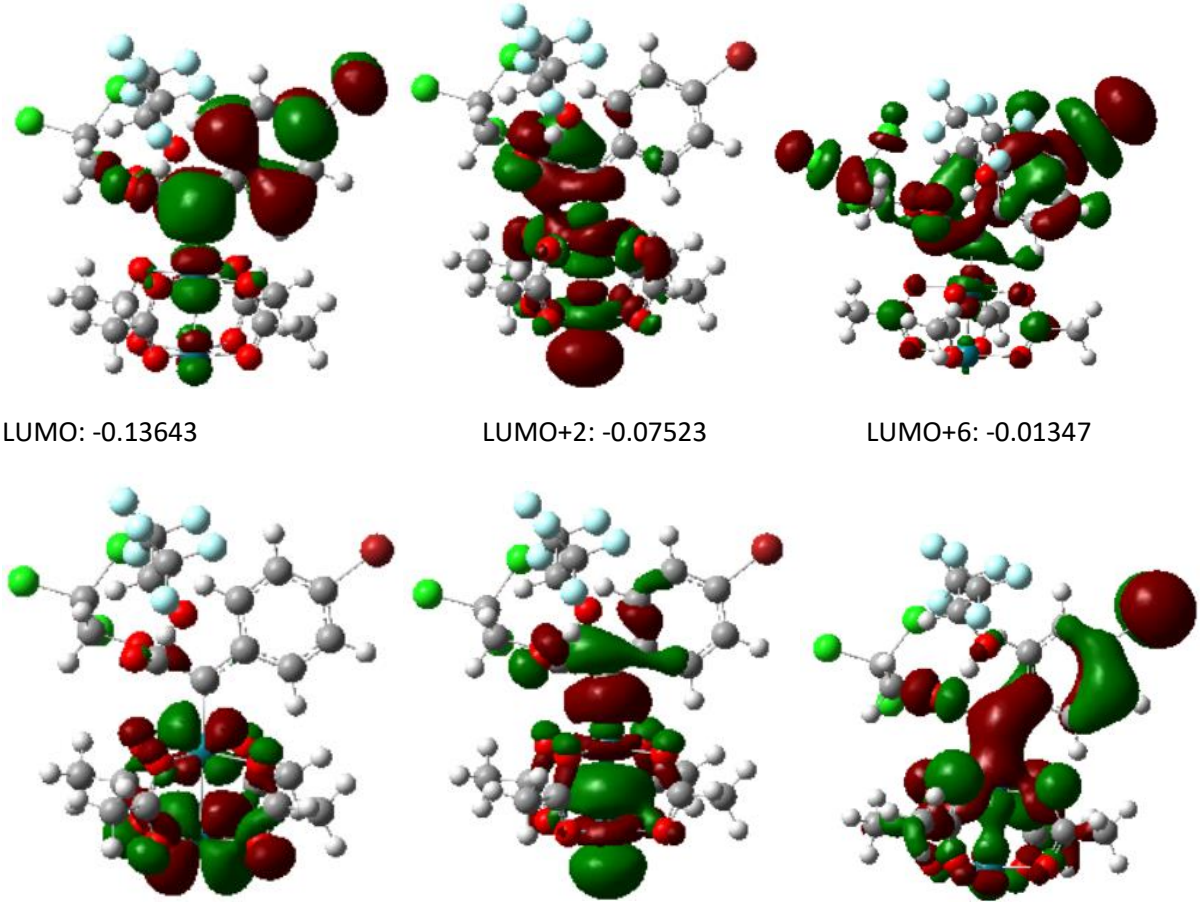

Figure D9. The calculated frontiers natural bonds for $Rh_2(AcO)_4$-(Car3)-HFIP carbonyl-O (**33**), energies reported in Hartreees. For the nature of the Rh-Rh and Rh-Carbene bonds, see Table S19.

Table D20: NBO's reported for HFIP coordinated carbene structure.

A: Carbene-$Rh_2(AcO)_4$ (22):

Natural Charges:
Rh(26) = +0.45
Rh(25) = +0.54
C27(Carbene) = +0.06

3. occ= (1.87804) BD (1) O 1 -Rh 26

O(1)	(85.84%)	0.9265	s(19.75%)	p 4.06(80.21%)	d 0.00(0.04%)
Rh(26)	(14.16%)	0.3763	s(11.69%)	p 4.38(51.22%)	d 3.17(37.09%)

6. occ= (1.87345) BD (1) O 2 -Rh 26

O(2)	(85.51%)	0.9247	s(19.36%)	p 4.16(80.60%)	d 0.00(0.04%)

Rh(26) (14.49%) 0.3807 s(11.44%) p 4.47(51.13%) d 3.27(37.42%)

9. occ= (1.87586) BD (1) O 3 -Rh 26

O(3) (85.63%) 0.9254 s(19.50%) p 4.13(80.46%) d 0.00(0.04%)

Rh(26) (14.37%) 0.3790 s(11.22%) p 4.57(51.29%) d 3.34(37.49%)

12. occ= (1.87533) BD (1) O 4 -Rh 26

O(4) (85.71%) 0.9258 s(19.60%) p 4.10(80.36%) d 0.00(0.04%)

Rh(26) (14.29%) 0.3780 s(11.42%) p 4.51(51.52%) d 3.24(37.06%)

14. occ= (1.88180) BD (1) O 5 -Rh 25

O(5) (89.04%) 0.9436 s(18.40%) p 4.43(81.56%) d 0.00(0.04%)

Rh(25) (10.96%) 0.3310 s(10.69%) p 4.69(50.07%) d 3.67(39.25%)

17. occ= (1.88277) BD (1) O 7 -Rh 25

O(7) (89.18%) 0.9443 s(18.61%) p 4.37(81.36%) d 0.00(0.04%)

Rh(25) (10.82%) 0.3290 s(10.86%) p 4.62(50.12%) d 3.59(39.02%)

19. occ= (1.92630) BD (1) O 8 -Rh 25

O(8) (86.04%) 0.9276 s(18.54%) p 4.39(81.42%) d 0.00(0.04%)

Rh(25) (13.96%) 0.3737 s(26.40%) p 0.43(11.45%) d 2.35(62.15%)

33. occ= (1.65183) BD (1)Rh 25 -Rh 26

Rh(25) (60.36%) 0.7769 s(39.85%) p 0.08(3.33%) d 1.43(56.82%)

Rh(26) (39.64%) 0.6296 s(34.86%) p 0.40(13.92%) d 1.47(51.22%)

B: Carbene3-$Rh_2(AcO)_4$-HFIP (33):

Natural Charges:
Rh(25) = +0.55
Rh(26) = +0.46
C27(Carbene) = +0.05

3. occ= (1.87734) BD (1) O 1 -Rh 26

O(1)	(85.78%)	0.9262	s(19.69%)	p 4.08(80.27%)	d 0.00(0.04%)
Rh(26)	(14.22%)	0.3771	s(11.74%)	p 4.36(51.15%)	d 3.16(37.10%)

6. (1.87338) BD (1) O 2 -Rh 26

O(2)	(85.49%)	0.9246	s(19.31%)	p 4.18(80.65%)	d 0.00(0.04%)
Rh(26)	(14.51%)	0.3809	s(11.42%)	p 4.48(51.16%)	d 3.28(37.42%)

9. occ= (1.87512) BD (1) O 3 -Rh 26

O(3)	(85.56%)	0.9250	s(19.39%)	p 4.16(80.57%)	d 0.00(0.04%)
Rh(26)	(14.44%)	0.3800	s(11.19%)	p 4.58(51.30%)	d 3.35(37.51%)

12. occ= (1.87520) BD (1) O 4 -Rh 26

O(4)	(85.68%)	0.9256	s(19.59%)	p 4.10(80.37%)	d 0.00(0.04%)
Rh(26)	(14.32%)	0.3784	s(11.53%)	p 4.46(51.44%)	d 3.21(37.03%)

14. occ= (1.88121) BD (1) O 5 -Rh 25

O(5)	(89.03%)	0.9435	s(18.32%)	p 4.45(81.63%)	d 0.00(0.04%)
Rh(25)	(10.97%)	0.3313	s(10.72%)	p 4.67(50.07%)	d 3.66(39.21%)

17. occ= (1.88220) BD (1) O 7 -Rh 25

O(7)	(89.14%)	0.9441	s(18.51%)	p 4.40(81.45%)	d 0.00(0.04%)
Rh(25)	(10.86%)	0.3296	s(10.90%)	p 4.60(50.12%)	d 3.58(38.98%)

19. occ= (1.92586) BD (1) O 8 -Rh 25

O(8)	(86.03%)	0.9275	s(18.46%)	p 4.41(81.50%)	d 0.00(0.04%)
Rh(25)	(13.97%)	0.3738	s(26.53%)	p 0.43(11.50%)	d 2.34(61.97%)

33. occ= (1.65189) BD (1)Rh 25 -Rh 26

Rh(25)	(59.92%)	0.7741	s(39.53%)	p 0.09(3.38%)	d 1.44(57.09%)

Rh(26) (40.08%) 0.6331 s(35.17%) p 0.39(13.55%) d 1.46(51.28%)

Table D21: Cartesian Coordinates (in Å) of all HFIP related calculated structures.

HFIP	**[B3LYP-D3(BJ)]/BS1**		
C	-0.07859000	1.02687800	0.01036200
H	0.26164600	1.50667900	-0.91194800
C	-1.61021200	1.07251000	0.00184700
C	0.47531400	-0.40168000	0.00503000
O	0.37389000	1.66891600	1.17490700
H	0.91647600	2.42619700	0.92454700
F	-2.02155400	2.35368800	-0.01070800
F	-2.13410200	0.48149600	1.08998600
F	-2.11611000	0.46325800	-1.08783100
F	0.05810000	-1.08927700	-1.07548100
F	0.10457700	-1.08509900	1.10182900
F	1.82023800	-0.36191800	-0.02182400

H2O	**[B3LYP-D3(BJ)]/BS1**		
O	0.10256400	-0.19280200	1.35261500
H	1.06687900	-0.14100600	1.35261500
H	-0.17051100	0.73349700	1.35261500

DMAP	**[B3LYP-D3(BJ)]/BS1**		
N	5.73483900	-3.38162800	-0.16201000
C	5.60955100	-2.94696900	-1.42763600
C	4.87359900	-4.34861100	0.19814100
C	4.68318100	-3.42035000	-2.34616700
H	6.29760300	-2.16007100	-1.73386700
C	3.90490900	-4.90252300	-0.62685600
H	4.95931100	-4.70880100	1.22249400
C	3.78395700	-4.44472100	-1.96161200
H	4.66312600	-2.99663100	-3.34171200
H	3.25676600	-5.67519900	-0.23448500
N	2.85793500	-4.96126900	-2.82607000
C	2.71335100	-4.39373400	-4.15835500
H	1.95030900	-4.94981200	-4.70176100
H	2.41297800	-3.33791700	-4.12629600
H	3.64970500	-4.46495400	-4.72333100
C	1.89319800	-5.94343300	-2.35421700
H	1.25939900	-6.24834700	-3.18611500
H	2.39419900	-6.83759900	-1.96610300
H	1.24986000	-5.54088100	-1.56043600

DCM	**[B3LYP-D3(BJ)]/BS1**		
C	4.99004300	-3.73437700	-0.84609100
H	4.79876000	-4.61265500	-0.23627600
H	4.09238700	-3.14392600	-1.00544200
Cl	5.58367200	-4.28641100	-2.44605400
Cl	6.18467000	-2.70959000	0.01397300

(Car3)-Rh2(AcO)4 (22) [B3LYP-D3(BJ)]/BS1

O	-0.00721600	-1.09679400	2.43641700
O	-2.23591000	-0.33238500	0.72759800
O	-0.51832300	-0.41438200	-1.61085500
O	1.75591100	-1.19481900	0.09919400
O	-2.76401300	-2.51902400	0.42041100
O	-1.01773500	-2.60607700	-1.92134800
O	1.23585500	-3.38231100	-0.20496100
O	-0.50504700	-3.28946600	2.13242000
C	-0.18619900	-2.29541300	2.84852300
C	2.05271300	-2.41763200	-0.13405700
C	-0.85627300	-1.41740000	-2.32828000
C	-3.05834200	-1.30807200	0.65260000
C	3.51833100	-2.70589300	-0.34715700
H	3.86158200	-2.18055400	-1.24312700
H	4.09187200	-2.32230400	0.50059000
H	3.68732100	-3.77615600	-0.46122800
C	-4.51446100	-0.95849500	0.83924800
H	-4.86960000	-0.43580800	-0.05460700
H	-5.10826600	-1.86034500	0.98692900
H	-4.63035100	-0.28218300	1.68863400
C	-0.01839600	-2.51370900	4.33184100
H	0.05999600	-3.57746600	4.55533300
H	0.86566900	-1.98174700	4.68930100
H	-0.88963700	-2.10141000	4.85083400
Rh	-0.78268200	-3.02645400	0.09627000
Rh	-0.21882800	-0.65874900	0.42359900
C	0.30119100	1.27996100	0.64375900
C	1.30006700	1.84129600	1.47590200
C	2.12654700	1.00640500	2.28099100
C	1.52213100	3.24981700	1.51279400
C	3.11978100	1.55009600	3.07584000
H	1.97343200	-0.06228100	2.25612400
C	2.50321800	3.79714800	2.31600500
C	3.29637700	2.93859900	3.09068400
H	2.66483600	4.86741500	2.34780300
C	-0.45618600	2.16749800	-0.25878000
O	0.21128600	2.33286700	-1.42237800
C	-0.53916100	2.88036800	-2.50317700
H	-1.14892000	3.72116400	-2.17031000
H	-1.17492000	2.10369400	-2.93386700
O	-1.55432200	2.62657200	-0.01767000
C	-1.10231400	-1.12665600	-3.78837000
H	-2.08260700	-0.64943900	-3.89071300
H	-0.34976300	-0.43041500	-4.16305500
H	-1.09500900	-2.04889000	-4.36924300
H	3.75333100	0.91516200	3.68264700
H	0.90648000	3.90729700	0.90883800
Br	4.64804000	3.68152200	4.18676700
C	0.45301600	3.36264400	-3.55659700

Cl	1.50714900	4.64788000	-2.87276500
Cl	-0.50048300	4.02574300	-4.92819700
Cl	1.47559600	2.00417700	-4.13933700

Rh2(AcO)4–(Car1)(HFIP)-ester O [B3LYP-D3(BJ)]/BS1

O	-0.04348400	-1.13582600	2.33606800
O	-2.46826000	-0.48103500	0.85577400
O	-0.96079100	-0.39480600	-1.63192400
O	1.49398300	-1.06465000	-0.15323800
O	-2.87032200	-2.69582600	0.56378400
O	-1.37879000	-2.60255800	-1.94641300
O	1.08618800	-3.26596700	-0.51575600
O	-0.39888300	-3.35271700	2.00815900
C	-0.08147700	-2.35636900	2.72111300
C	1.83914200	-2.24713700	-0.49565700
C	-1.32438600	-1.39859600	-2.33563400
C	-3.22267900	-1.51264000	0.85137500
C	3.27227300	-2.40985900	-0.93579000
H	3.39343700	-1.93898100	-1.91503300
H	3.93529200	-1.89092000	-0.24080600
H	3.53576400	-3.46513200	-1.00163500
C	-4.66860500	-1.27172900	1.21072300
H	-5.13945000	-0.68302700	0.41749400
H	-5.19835300	-2.21714700	1.32453400
H	-4.72783400	-0.69078000	2.13404400
C	0.28696200	-2.59971600	4.16382500
H	0.26373200	-3.66478000	4.39210800
H	1.28510800	-2.19712200	4.35624600
H	-0.41479600	-2.06661800	4.81145000
Rh	-0.90430100	-3.05636700	0.01871500
Rh	-0.46769500	-0.66625300	0.36507900
C	-0.06093500	1.30177300	0.59049700
C	1.01132600	1.91364600	1.27508700
C	1.97999700	1.11765600	1.95111900
C	1.23044900	3.32136500	1.19267400
C	3.12315600	1.69205700	2.47437600
H	1.82110100	0.05192600	2.02594200
C	2.36533800	3.89930600	1.72157200
C	3.31113700	3.07317800	2.34403900
H	2.54080900	4.96402800	1.63789500
C	-0.95943400	2.14648200	-0.21695500
O	-0.41858400	2.36945300	-1.44920800
C	-1.28774800	2.93445400	-2.42983100
H	-1.87741400	3.74498400	-2.00052300
H	-1.94558400	2.15864500	-2.82699000
O	-2.05536600	2.53921600	0.11942200
C	-1.74608500	-1.09192600	-3.75142300
H	-2.75076600	-0.65667300	-3.73139500
H	-1.07134300	-0.35620900	-4.19233800
H	-1.76580900	-2.00193100	-4.35087100
H	3.87292500	1.08622400	2.96782100

H	0.50611200	3.95035000	0.68744600
Br	4.89962900	3.84991000	3.01354300
C	-0.41228700	3.48317700	-3.55229800
Cl	0.71324600	4.72769000	-2.90270300
Cl	-1.48595000	4.20453900	-4.78687500
Cl	0.55712300	2.15320400	-4.29326100
H	1.56708500	1.99680900	-1.71743600
O	2.44134900	1.97182800	-1.30079400
C	3.43581200	2.34708600	-2.20490300
H	3.05451800	2.89008500	-3.07451700
C	4.13783800	1.08966200	-2.72865500
C	4.38046800	3.29698500	-1.46504300
F	3.22143400	0.27385000	-3.29475800
F	4.74164100	0.40051900	-1.74273400
F	5.06312900	1.38170000	-3.66004900
F	5.42100800	3.65688700	-2.23988400
F	4.87139000	2.74402500	-0.34116600
F	3.71466000	4.41475500	-1.11605400

Rh2(AcO)4–(Car3)(HFIP)-carbonyl O (33) [B3LYP-D3(BJ)]/BS1

O	-0.00167000	-1.04211600	2.34932600
O	-2.24032700	-0.52241500	0.56954100
O	-0.47744700	-0.64217800	-1.73663500
O	1.80604600	-1.17969100	0.05129300
O	-2.62774700	-2.75352200	0.41763600
O	-0.86855100	-2.86990800	-1.91296900
O	1.41885300	-3.40575900	-0.15292300
O	-0.34072800	-3.27870700	2.17409000
C	-0.10436200	-2.22332500	2.83246900
C	2.17755200	-2.39251300	-0.11873600
C	-0.75810400	-1.70257800	-2.39322300
C	-3.00003000	-1.55050500	0.56199200
C	3.66038000	-2.60447600	-0.29818600
H	3.98913900	-2.09640900	-1.20933600
H	4.19623700	-2.15538600	0.54209700
H	3.89171400	-3.66701600	-0.36526000
C	-4.47664000	-1.28109500	0.71548600
H	-4.86329400	-0.89106600	-0.23165200
H	-5.00831400	-2.19888400	0.96626100
H	-4.64157700	-0.52168200	1.48221100
C	0.05357000	-2.33815800	4.32815700
H	0.17495400	-3.38059900	4.62159000
H	0.91001100	-1.74629000	4.65809300
H	-0.84002100	-1.92986300	4.81085400
Rh	-0.61811700	-3.15387700	0.12405500
Rh	-0.20222300	-0.74570200	0.31186700
C	0.18343900	1.23601900	0.42792900
C	1.11769900	1.91269900	1.24246000
C	1.97850700	1.18723900	2.11751300
C	1.21627800	3.33594200	1.22229700
C	2.87606300	1.85137700	2.93248000

H	1.92134800	0.10885400	2.13261700
C	2.09895200	4.00262300	2.04714800
C	2.92287100	3.25157700	2.89713100
H	2.15335200	5.08372800	2.04133800
C	-0.66085400	2.00822600	-0.49627600
O	-0.07837300	2.16599900	-1.69025400
C	-0.87809200	2.74987700	-2.72117100
H	-1.52018700	3.53088700	-2.31378700
H	-1.48001900	1.97325600	-3.19713100
O	-1.79333800	2.39645700	-0.23370300
C	-1.00219700	-1.51502900	-3.87021400
H	-2.03225200	-1.17173600	-4.01361600
H	-0.33349600	-0.74950200	-4.26754400
H	-0.86912700	-2.45716600	-4.40231900
H	3.53366100	1.30282600	3.59539600
H	0.58579800	3.91028400	0.55818300
Br	4.13745900	4.15791700	4.02748200
C	0.07424200	3.35845100	-3.74611700
Cl	1.07723600	4.63280800	-2.97297200
Cl	-0.93351000	4.08188700	-5.04490700
Cl	1.14333300	2.09478100	-4.44485200
H	-1.97454200	3.19790100	1.30738600
O	-1.88949300	3.85450800	2.02990500
C	-2.49340300	5.04359000	1.61666700
H	-3.34477600	4.89010200	0.94308700
C	-1.48245700	5.91890400	0.86068200
C	-3.03384200	5.73420900	2.87139000
F	-1.06702200	5.26680500	-0.25610600
F	-0.38632600	6.17754700	1.59823500
F	-2.01049500	7.08924200	0.46911900
F	-3.62539700	6.90681600	2.57174400
F	-2.05653400	5.97853800	3.76310200
F	-3.94910200	4.94930700	3.46497500

Rh2(AcO)4–(Car3)(HFIP)2 [B3LYP-D3(BJ)]/BS1

O	-2.72538500	0.27762400	-0.27956500
O	-4.80406900	1.21038100	-2.09360000
O	-2.66133400	1.85187300	-4.10733800
O	-0.68136600	0.94339600	-2.22416500
O	-4.95665600	-0.87208700	-2.97870500
O	-2.91138200	-0.21084800	-4.99488500
O	-0.81956900	-1.10787600	-3.18337100
O	-2.84541600	-1.80775900	-1.16915100
C	-2.77459600	-1.00043100	-0.19744900
C	-0.17562300	-0.11248000	-2.73548100
C	-2.73274900	1.03455100	-5.09339300
C	-5.45676500	0.19379400	-2.51132700
C	1.32991200	-0.13784400	-2.82316200
H	1.64000000	0.56921200	-3.59726400
H	1.76192900	0.19461700	-1.87669000
H	1.68603700	-1.13650000	-3.07460000

C	-6.95987100	0.30154700	-2.43925300
H	-7.29300400	1.08521800	-3.12511400
H	-7.42599300	-0.64524600	-2.71047600
H	-7.25898600	0.59351500	-1.42956800
C	-2.76580800	-1.56749100	1.20012900
H	-2.61167300	-2.64587200	1.17307400
H	-1.98414600	-1.08599100	1.79182900
H	-3.72684500	-1.35085800	1.67698600
Rh	-2.89602500	-1.07857100	-3.11275800
Rh	-2.73199700	1.17031000	-2.13114700
C	-2.63574000	3.04578500	-1.40239600
C	-1.56636800	3.64881400	-0.69750500
C	-0.58441000	2.84405500	-0.05762700
C	-1.43195100	5.06387800	-0.64143600
C	0.47696600	3.42753200	0.61143300
H	-0.69015000	1.76924400	-0.08021100
C	-0.35590800	5.64911400	-0.00273000
C	0.58711500	4.82318600	0.62073400
H	-0.24517900	6.72521200	0.01606600
C	-3.88139900	3.81704700	-1.62147700
O	-4.22825700	3.95139200	-2.90382200
C	-5.51683100	4.50435900	-3.15936300
H	-5.53495700	5.55820900	-2.88133700
H	-6.28327300	3.95301100	-2.61195800
O	-4.57112800	4.17654600	-0.67767800
C	-2.54891100	1.63673700	-6.46155800
H	-2.90310200	0.95390400	-7.23318900
H	-3.07273700	2.59189500	-6.52552500
H	-1.47982500	1.82138900	-6.60930800
H	1.21741600	2.81927400	1.11590200
H	-2.15617300	5.68923900	-1.14608800
Br	2.05931700	5.62276100	1.50731800
C	-5.77976300	4.38662800	-4.65815700
Cl	-4.50628000	5.23719000	-5.59155700
Cl	-7.37435700	5.16755500	-4.96513200
Cl	-5.85162300	2.66797900	-5.17318500
H	-2.04258600	3.46472800	-4.12869400
O	-1.63111900	4.31683700	-3.85783400
C	-0.50257100	4.59293800	-4.61945300
H	-0.67579100	4.52744700	-5.70215300
C	0.63274400	3.61153100	-4.29604200
C	-0.12210900	6.04663700	-4.32633200
F	0.26248700	2.36785800	-4.69223800
F	0.90340300	3.55846800	-2.98357900
F	1.77150300	3.91633800	-4.94662700
F	0.92421500	6.43841900	-5.07959700
F	0.21097200	6.22995200	-3.03422300
F	-1.15763600	6.85525900	-4.60499500
H	-4.47640700	6.48185300	-0.79485000
O	-4.03772600	6.78008800	-1.60435500
C	-4.00594900	8.17988400	-1.68593400

H	-4.72096800	8.66675300	-1.01703600
C	-4.39320500	8.55665000	-3.11948700
C	-2.60379100	8.66688600	-1.29730400
F	-5.62240000	8.07469500	-3.39370800
F	-3.54033000	8.04307000	-4.01979300
F	-4.42345500	9.89102300	-3.27887500
F	-2.49377800	10.00148400	-1.39538200
F	-1.64909200	8.10555100	-2.06102900
F	-2.35305700	8.31459400	-0.01793200

DMAP-HFIP [B3LYP-D3(BJ)]/BS1

H	6.63619100	-2.47793900	0.88747200
O	7.35288500	-1.97072200	1.40770200
C	8.55163400	-2.65964200	1.37071900
H	9.33711100	-2.03772600	1.81509300
C	8.48292300	-3.93628500	2.22185500
C	9.02607600	-2.96641400	-0.06188300
F	8.29101100	-3.61468000	3.51501300
F	7.46138700	-4.73602000	1.85008900
F	9.61963900	-4.66109200	2.14254100
F	8.84287100	-1.88832700	-0.84906700
F	10.33875000	-3.27617100	-0.08716900
F	8.35860900	-3.99570600	-0.62626000
N	5.52903700	-3.16804300	-0.06916300
C	5.48979500	-2.79138900	-1.35923200
C	4.68017600	-4.14006700	0.30573500
C	4.62995100	-3.33178500	-2.29727900
H	6.19903400	-2.02090500	-1.64955200
C	3.77815000	-4.74973200	-0.54724100
H	4.73680000	-4.44686000	1.34649200
C	3.72102700	-4.34927100	-1.90731600
H	4.66903100	-2.97120600	-3.31608700
H	3.13239100	-5.52641400	-0.16063400
N	2.84712600	-4.91084600	-2.78837800
C	2.85085900	-4.49616000	-4.18511600
H	2.06814000	-5.03408900	-4.71777700
H	2.65241700	-3.42271100	-4.28242700
H	3.80996700	-4.71438500	-4.67108700
C	1.96280200	-5.98484000	-2.35567000
H	1.33731800	-6.28957600	-3.19331400
H	2.52659600	-6.86075400	-2.01156600
H	1.30589100	-5.65730800	-1.54161300

Pyridine-HFIP [B3LYP-D3(BJ)]/BS1

H	6.60951600	-2.52146500	0.82528000
O	7.26533500	-1.95461600	1.34330900
C	8.49805100	-2.58459500	1.39929300
H	9.22383400	-1.90330200	1.85631000
C	8.44220300	-3.82661600	2.30080400
C	9.06073000	-2.92325000	0.00698900
F	8.16909600	-3.46153000	3.56682700

F	7.47647600	-4.68587500	1.91135300
F	9.61138000	-4.50025600	2.30815700
F	8.87805700	-1.88249700	-0.82872400
F	10.38210200	-3.18202300	0.06233400
F	8.46104000	-3.99758900	-0.55065600
N	5.57334000	-3.33384700	-0.19549000
C	5.60475000	-2.98016900	-1.48854700
C	4.75572500	-4.32667700	0.18120300
C	4.81491200	-3.59635000	-2.45548300
H	6.29666700	-2.18393600	-1.74750200
C	3.92968400	-4.99936800	-0.71621800
H	4.77418500	-4.58863200	1.23492000
C	3.95939400	-4.62493100	-2.05974200
H	4.87265400	-3.27746200	-3.49012700
H	3.28285300	-5.79657100	-0.36752100
H	3.32941900	-5.12814100	-2.78614100

(H2O)HFIP2 [B3LYP-D3(BJ)]/BS1

O	1.77394700	0.52667700	4.77869800
H	1.51649400	0.38569500	5.70945200
H	2.15433800	1.41466400	4.76524400
F	1.68127000	-0.40069100	10.21678700
F	-0.21365400	0.62416300	9.91130700
F	1.48219300	1.69611500	10.76921300
F	3.60571000	0.04343600	8.36271100
F	3.31397900	1.71143300	7.00246300
F	3.60508300	2.08098900	9.13029800
O	1.01741200	0.27351500	7.51024900
H	0.04948100	0.29620300	7.54186600
C	1.52058600	1.19869300	8.44571100
H	1.13496300	2.21288900	8.29235900
C	1.12819400	0.76925400	9.86558300
C	3.03567000	1.25257200	8.24399100
F	2.64317700	-2.07106500	6.56901500
F	3.99948300	-3.54656200	5.72346600
F	6.34400400	-0.43237000	4.16689100
F	6.72251400	-1.54002600	6.00242500
F	6.07024800	-2.58848300	4.20931900
O	3.69118200	-1.20483600	4.17081300
H	2.93897500	-0.57846600	4.33112700
C	4.45982100	-1.23221800	5.33133200
H	4.43357300	-0.29140600	5.89296700
C	3.93717000	-2.32151700	6.27739900
C	5.91522400	-1.45947900	4.92439800
F	4.61883300	-2.36042200	7.44007300

(H2O)2HFIP3 [B3LYP-D3(BJ)]/BS1

O	4.06062400	0.53292900	2.06547300
H	5.01497100	0.67936800	2.02104000
H	3.95134900	-0.23417300	2.66807700
O	1.59902800	0.34990000	4.76629400

H	1.47296500	0.52242100	5.71673800
H	1.88716400	1.19799200	4.37355100
F	1.03958100	-0.22399400	10.13105500
F	-0.14679900	1.58083500	9.85656800
F	1.77226500	1.68317200	10.88616700
F	3.02854000	-0.62224800	8.26085700
F	3.75870600	1.16786600	7.27052000
F	3.92499400	0.98122200	9.43288400
O	0.96509400	0.88315000	7.48690500
H	0.16381000	1.42358000	7.42707700
C	1.77226200	1.38472200	8.52614500
H	1.93327600	2.46527200	8.45483700
C	1.11031600	1.09258500	9.87919500
C	3.13697600	0.70935400	8.38641900
F	4.71405500	4.62178100	3.05173800
F	5.79904100	2.73880300	3.00147400
F	5.99178200	4.05845700	4.72358200
F	2.79056200	4.88050800	4.93920900
F	2.12728800	3.07371000	5.94614000
F	3.99587200	4.01912800	6.53453100
O	3.02229800	2.43851900	3.51209800
H	3.44248900	1.75047300	2.90718200
C	3.95616500	2.84867000	4.46744200
H	4.40097200	2.01952300	5.02821600
C	5.12439900	3.59354400	3.80678400
C	3.21658800	3.72900000	5.47928000
F	2.89035400	-2.80665300	6.25473900
F	4.51344400	-3.71933700	5.12607800
F	5.95195800	0.14025900	4.24246900
F	6.71696700	-1.30741300	5.68006600
F	6.11917700	-1.95627300	3.68889700
O	3.51166000	-1.24510000	4.11223900
H	2.71024600	-0.70158500	4.40012400
C	4.38488200	-1.33419100	5.20162700
H	4.20531600	-0.56053400	5.95090300
C	4.18555500	-2.67752000	5.91117900
C	5.81472800	-1.13152000	4.70229400
F	4.92116900	-2.75510000	7.03693600

(DCM)HFIP [B3LYP-D3(BJ)]/BS1

H	7.51992700	-1.83883300	0.39396400
O	7.54596900	-1.87355300	1.36543100
C	8.67720400	-2.59953900	1.76193100
H	8.74743300	-2.54752900	2.85070300
C	9.94487200	-1.96273400	1.17945400
F	10.09402400	-0.71808900	1.66012800
F	11.05090100	-2.66359400	1.47713300
F	9.85106900	-1.87505100	-0.16613000
C	5.06491500	-3.55039000	-0.13624900
H	5.57842400	-3.38107000	0.80532900
H	4.01734700	-3.26785000	-0.09870500

Cl	5.16795900	-5.29068800	-0.53248500
Cl	5.86459300	-2.51538000	-1.37593200
C	8.52718100	-4.07899800	1.38390400
F	9.55619600	-4.82284500	1.81622500
F	7.39847700	-4.57017900	1.93396500
F	8.42655300	-4.23010600	0.04647600

(DCM)HFIP2 [B3LYP-D3(BJ)]/BS1

H	7.38375700	-1.95621200	0.60790500
O	8.30484300	-2.00356900	0.30056800
C	8.80589200	-3.28262500	0.56093200
H	9.85358400	-3.30300000	0.25188100
C	8.07002300	-4.34601600	-0.26679000
F	8.08190600	-3.99858500	-1.56702200
F	8.63202700	-5.55768700	-0.15310100
F	6.77596000	-4.44881700	0.11818200
C	4.62896700	-2.46818800	-1.11496500
H	4.84047500	-3.53181000	-1.10297300
H	3.60401700	-2.24843500	-1.39703700
Cl	5.71684800	-1.69743600	-2.31850100
Cl	4.89699900	-1.82812100	0.54057200
C	8.75943800	-3.57788500	2.06592400
F	9.15712900	-4.82932100	2.35270100
F	9.55768300	-2.72265300	2.72521700
F	7.50510700	-3.41707300	2.54166700
H	6.57264600	-3.71562200	-3.51927900
O	6.87655000	-4.28429300	-4.24561400
C	6.06130200	-5.41542500	-4.33055200
H	6.41943300	-6.02020100	-5.16730900
C	4.61147400	-5.02187800	-4.64464200
C	6.16880900	-6.29011500	-3.07288800
F	4.55586800	-4.37842700	-5.82043300
F	3.80028500	-6.09105600	-4.70973600
F	4.12000700	-4.18583700	-3.69951600
F	5.54333700	-7.46790200	-3.23259000
F	7.45580900	-6.53250300	-2.78548200
F	5.62006300	-5.67697000	-1.99519800

HFIP2 [B3LYP-D3(BJ)]/BS1

H	6.64939200	-2.54128400	0.61116500
O	7.20177700	-2.01679900	1.22662200
C	8.43994900	-2.62408100	1.41743000
H	8.96306500	-2.07986800	2.20893800
C	8.28599700	-4.07136300	1.90319900
C	9.33893900	-2.52892100	0.17244500
F	7.62892500	-4.09550300	3.07382100
F	7.57500900	-4.81395800	1.02367200
F	9.47757200	-4.67131600	2.07771800
F	9.31548600	-1.28331600	-0.32118700
F	10.61371000	-2.84188900	0.46662000
F	8.93773800	-3.36749300	-0.81618100

H	4.61470600	-3.02186600	-0.54194600
O	5.47271200	-3.45782600	-0.41560200
C	5.97106600	-3.87283100	-1.66607600
C	5.02826900	-4.91577100	-2.27538500
H	6.93524800	-4.34748100	-1.48840300
C	6.19803600	-2.65925000	-2.57622200
F	3.77270000	-4.42705600	-2.36117700
F	4.99114600	-6.00712300	-1.49558400
F	5.42111300	-5.28513300	-3.50425700
F	5.02797500	-2.04744800	-2.85759100
F	6.98393800	-1.76344200	-1.95339200
F	6.78393800	-3.00411800	-3.73144200

HFIP3 **[B3LYP-D3(BJ)]/BS1**

H	6.78546000	-3.37275500	0.75550900
O	6.95261100	-2.92933900	1.61763300
C	8.32491300	-2.72305000	1.81867600
H	8.47860600	-2.43789400	2.86187600
C	9.09005600	-4.02860300	1.57423300
C	8.83316000	-1.56068100	0.95567500
F	8.72066600	-4.95007800	2.47772800
F	8.80698600	-4.51921300	0.34790100
F	10.41843300	-3.85853100	1.66228700
F	8.07498900	-0.46669600	1.19977200
F	10.10624600	-1.24699800	1.23817700
F	8.74420500	-1.83668300	-0.35608700
H	5.22502900	-2.70363100	-0.59789400
O	5.56552000	-3.62331500	-0.57367100
C	5.58520900	-4.20558300	-1.84750800
C	4.18852400	-4.11408500	-2.47363200
H	5.83068300	-5.26347700	-1.73225500
C	6.67850100	-3.58078600	-2.72345000
F	3.76518800	-2.83194900	-2.49951300
F	3.31213800	-4.81871300	-1.73975600
F	4.16516300	-4.58974600	-3.72874200
F	6.43705300	-2.27725400	-2.95964500
F	7.86366100	-3.67659900	-2.09766100
F	6.78093500	-4.20891300	-3.90770500
H	5.78685600	-1.52755300	1.16459800
O	5.06861600	-1.24678100	0.56343400
C	5.12132200	0.13578400	0.32136500
H	5.83717500	0.64819300	0.96797900
C	5.56491100	0.36424400	-1.12767800
C	3.73444100	0.71251500	0.62019200
F	6.80509600	-0.12750500	-1.29956700
F	4.74914300	-0.26687800	-1.99295300
F	5.58567200	1.67041500	-1.44487200
F	3.42524700	0.49650600	1.91067800
F	3.69804100	2.03959700	0.39926100
F	2.78401400	0.13633000	-0.13615500

Rh2(TCPTAD)4 [B3LYP-D3(BJ)]/BS1

Rh	6.02048800	12.66299800	6.88839500
Rh	8.08750700	12.68919200	5.67400100
Cl	9.92437500	21.14308000	4.20306400
Cl	15.33289400	13.03613800	9.58652000
Cl	11.17481300	4.87799400	4.25017700
Cl	8.00310200	12.29376800	-2.70192700
Cl	8.20752500	19.21946000	6.01553600
Cl	12.32589700	12.11337800	9.81317600
Cl	8.61692700	6.64787900	4.74813300
Cl	6.56566800	13.28288800	-0.07059300
Cl	9.98771900	20.74240600	1.09641400
Cl	16.02072100	15.95096800	8.66349200
Cl	13.66936400	5.14898700	6.12668300
Cl	8.93548500	9.31287200	-2.96112500
Cl	8.33357700	18.41008400	-0.23715800
Cl	13.70792600	17.98152600	7.96711600
Cl	13.63402600	7.19750300	8.52602000
Cl	8.44507100	7.28538100	-0.59334000
O	7.15604000	13.86757800	4.26173800
O	8.58479200	14.38964000	6.71848100
O	8.90447500	11.52365400	7.17107600
O	7.45167000	10.98795400	4.68331100
O	5.17726900	13.72727200	5.34683500
O	6.62521300	14.38194200	7.84564100
O	6.97404400	11.57873100	8.34580800
O	5.53513600	10.94801700	5.87817600
O	6.42858800	16.68861900	5.44259500
O	9.56225500	13.55856600	9.42797000
O	7.79078500	8.72174200	6.97270200
O	5.59683300	11.85409700	2.54784500
O	6.46964200	16.13600100	0.88498900
O	10.56368300	17.77208100	7.90407200
O	11.52709700	9.27639300	9.58666500
O	7.13876400	7.53770300	2.26358200
N	6.16067900	16.20004300	3.18713600
N	9.72598900	15.75662900	8.69533200
N	9.47578700	9.20487200	8.49720400
N	6.22649600	9.62532800	2.71449200
C	6.66365400	16.92304900	4.27402700
C	10.23233100	14.52072400	9.10955100
C	8.91514300	8.54500100	7.39681900
C	6.13400200	10.86954200	2.08274500
C	7.53873500	17.98377600	3.68681500
C	11.72107800	14.65560200	9.06474600
C	9.97736800	7.62064200	6.89294500
C	6.81375500	10.70728800	0.76203100
C	8.25038500	19.00224200	4.30024400
C	12.71528600	13.73496400	9.35658000
C	9.97402700	6.75013500	5.81461100
C	7.03942600	11.62851500	-0.24850500

C	9.01506800	19.86106500	3.48002000
C	14.05865400	14.15176400	9.22963900
C	11.13562600	5.98016600	5.58373000
C	7.70437300	11.18071800	-1.41111600
C	9.04346000	19.68080500	2.08360100
C	14.36795900	15.46022200	8.81110200
C	12.25896900	6.10636300	6.42321400
C	8.12815500	9.84238900	-1.52514200
C	8.30577700	18.63926800	1.47871700
C	13.33873600	16.37585400	8.50054500
C	12.24915000	7.01709900	7.50255000
C	7.90752600	8.92689300	-0.47245200
C	7.56270900	17.80759300	2.30081800
C	12.02728200	15.94914800	8.63409700
C	11.09925300	7.76050900	7.71427200
C	7.25020400	9.38400400	0.65837400
C	6.69282900	16.63656900	1.96827700
C	10.74102400	16.65811800	8.35068700
C	10.79955000	8.81613800	8.73037200
C	6.90169100	8.68142300	1.93263100
C	5.31888600	15.00460600	3.29785800
H	5.50465500	14.44494700	2.37669500
C	8.31351700	16.02283800	8.40997600
H	8.32998000	16.85467400	7.69690100
C	8.83747700	10.31413700	9.21336000
H	9.66691200	10.91515300	9.59964100
C	5.80934100	9.36009200	4.09273300
H	6.41462900	8.50304800	4.40789400
C	5.92101200	14.12994500	4.40614100
C	7.78477500	14.82682200	7.60424300
C	8.16933600	11.20829200	8.15769100
C	6.29745300	10.53445300	4.95671200
C	3.80116400	15.30691300	3.35325900
C	7.50389700	16.49266700	9.64540500
C	7.98005700	9.87080100	10.42555400
C	4.31652300	8.95049800	4.22570400
C	3.35484800	16.04896900	4.63352300
H	3.88030500	17.00758400	4.70753400
H	3.62173400	15.46294000	5.51470700
C	7.29255200	15.38610800	10.70305800
H	8.26178800	15.01367000	11.04907600
H	6.76302900	14.54110500	10.25678600
C	6.71952800	9.06920000	10.02872000
H	7.01379900	8.16667300	9.48125300
H	6.09353200	9.66455300	9.36155700
C	3.33538100	10.11534000	3.95680400
H	3.53396100	10.93715300	4.64693600
H	3.48742700	10.50246600	2.94449800
C	1.83518100	16.29688900	4.59796200
H	1.53769600	16.81032800	5.52032000
C	6.49406800	15.94209300	11.89690900

H	6.34631600	15.13897300	12.62930200
C	5.92683600	8.67342400	11.28837700
H	5.03002400	8.12025500	10.98409300
C	1.88289000	9.63153900	4.11205200
H	1.20772800	10.47752300	3.93234600
C	1.48541800	17.17240600	3.38174700
H	0.40725400	17.37484400	3.35779300
H	1.99583900	18.14101600	3.45729700
C	7.27378900	17.09909600	12.54572900
H	6.72455300	17.48659900	13.41289100
H	8.24435300	16.73969600	12.91065300
C	6.80128000	7.78650600	12.19127200
H	6.23812700	7.47937800	13.08153100
H	7.08577800	6.87139100	11.65643600
C	1.59958700	8.51544000	3.09153300
H	0.55923500	8.17738700	3.17711500
H	1.73416000	8.89717700	2.07145000
C	1.91450900	16.44844000	2.09323700
H	1.68549300	17.07507100	1.22282500
C	7.48165300	18.21831200	11.50962700
H	8.05240700	19.03918200	11.96018400
C	8.05991200	8.56870300	12.60671100
H	8.69936700	7.93589000	13.23387600
C	2.55852600	7.33870200	3.34682800
H	2.37780500	6.54699400	2.60982800
C	3.43042800	16.18717500	2.13310000
H	3.75536900	15.69543400	1.20879000
H	3.96075300	17.14472500	2.19153500
C	8.27153300	17.66143900	10.31212400
H	9.25105400	17.31195900	10.65712900
H	8.45342600	18.45289400	9.57554400
C	8.84639300	8.97681500	11.34809300
H	9.15403100	8.07438600	10.80778800
H	9.76126600	9.51074500	11.62896400
C	4.01325300	7.82310200	3.20666700
H	4.70715200	6.98849300	3.35950000
H	4.17206300	8.19162300	2.18694300
C	3.02488100	13.97145800	3.22792900
H	3.27106800	13.31771200	4.06616800
H	3.33932700	13.45282300	2.31426100
C	6.12930300	17.03356400	9.17873300
H	6.28424300	17.82609800	8.43510300
H	5.56375500	16.23751200	8.69129100
C	7.57108900	11.12622500	11.23806300
H	6.97090500	11.79389200	10.61806100
H	8.47468800	11.67696000	11.52907000
C	4.07197100	8.37496300	5.64425100
H	4.75667000	7.53324600	5.81403300
H	4.29267200	9.13137300	6.39872200
C	1.51015800	14.23269900	3.19652600
H	0.98636600	13.27144600	3.12266200

C	5.33628200	17.58101500	10.37854200
H	4.36326400	17.94301900	10.02515400
C	6.77410700	10.71774500	12.48858700
H	6.48148300	11.62353000	13.03365400
C	2.61476700	7.90316200	5.78808200
H	2.46488700	7.52023600	6.80476900
C	1.16238200	15.11046500	1.98208200
H	0.08068900	15.28965200	1.93987800
H	1.44344300	14.59597900	1.05444400
C	6.11478600	18.73621100	11.02973500
H	5.54840300	19.14534500	11.87569000
H	6.25271800	19.55069200	10.30726500
C	7.64631700	9.82740900	13.38898000
H	8.53740900	10.37981200	13.71312100
H	7.09362200	9.54385800	14.29348100
C	2.32899800	6.79047200	4.76583800
H	1.29616900	6.43490600	4.86931600
H	2.98827700	5.93288700	4.95019100
C	1.09240200	14.95176000	4.49232900
H	0.00806600	15.11972600	4.49765100
H	1.32779000	14.32388100	5.36134900
C	5.12695400	16.45458800	11.40779900
H	4.55781000	15.63262700	10.95484700
H	4.53945600	16.82688100	12.25647300
C	5.51447400	9.94240100	12.05779300
H	4.88260800	10.57722000	11.42329200
H	4.92038600	9.67124100	12.93949300
C	1.66804600	9.09237100	5.53788400
H	1.86088800	9.88595500	6.27137800
H	0.62541700	8.77633700	5.66833000

Rh2(TCPTAD)4(Car3) (35) [B3LYP-D3(BJ)]/BS1

Rh	0.80194200	0.20623800	0.18876300
Rh	2.97812200	0.18139500	-0.97906100
Cl	7.63001100	5.25048600	-3.65086300
Cl	10.36492700	1.10360500	2.78062300
Cl	7.80006600	-4.05915000	-3.69399200
Cl	0.67978500	0.25433600	-9.50288900
Cl	5.17133400	5.22124200	-1.69067600
Cl	7.43453300	-0.02285100	3.08505500
Cl	4.73538200	-4.12734700	-2.94013200
Cl	-0.78553700	0.54332900	-6.72663400
Cl	7.45005500	3.77226700	-6.41807100
Cl	10.82192700	4.08990300	1.94268800
Cl	9.95185500	-3.50744200	-1.48684700
Cl	2.64389300	-2.13355200	-10.00236600
Cl	4.72980700	2.47500000	-7.34365100
Cl	8.35964700	5.91742700	1.20204600
Cl	9.06879900	-2.95056700	1.48704400
Cl	3.26897500	-4.18556000	-7.68287200
O	2.09562600	1.29535500	-2.42383600

O	3.48216400	1.89151700	0.06936100
O	3.64817900	-0.96452300	0.58509000
O	2.28842500	-1.47062500	-1.97927600
O	0.09399800	1.40373600	-1.38134800
O	1.49067100	1.90490700	1.14819000
O	1.65118800	-1.00979700	1.64412900
O	0.32405100	-1.52854700	-0.85242300
O	2.20846500	4.22673500	-1.92256000
O	4.56418800	1.21427800	2.73905300
O	3.14212500	-3.73455700	-0.27669200
O	-0.29021400	-0.76865500	-3.88959900
O	1.92541400	2.08090700	-5.95848100
O	5.24258800	5.49800000	1.22773700
O	6.26625600	-2.71769500	2.92834800
O	2.37865400	-4.41565100	-4.67869400
N	1.66205000	3.24529400	-3.96381400
N	4.56423900	3.40657300	1.96715300
N	4.44884100	-3.18190700	1.56960900
N	0.90451300	-2.75969600	-3.98321500
C	2.51837800	3.88067900	-3.04311700
C	5.16050000	2.21420300	2.39913500
C	4.22774000	-3.54191500	0.22865800
C	0.34062600	-1.59730400	-4.51628500
C	3.84768100	3.98318200	-3.71627800
C	6.63670000	2.46256300	2.34832500
C	5.57874100	-3.62155600	-0.40432000
C	0.73686400	-1.57498500	-5.95815300
C	5.03768500	4.53846300	-3.27252900
C	7.70015200	1.61637800	2.62632500
C	5.93367400	-3.84219800	-1.72686600
C	0.40065100	-0.68906600	-6.96992000
C	6.15101000	4.49647800	-4.13893000
C	9.00860900	2.13208700	2.47739100
C	7.30618700	-3.79975000	-2.05453700
C	1.02348300	-0.86017100	-8.22721300
C	6.06098800	3.85465900	-5.38934000
C	9.21504700	3.46541500	2.07233700
C	8.27276000	-3.54452400	-1.06284300
C	1.91277900	-1.93099300	-8.44979500
C	4.84626400	3.27101500	-5.81141800
C	8.11664600	4.29910000	1.76536700
C	7.88725800	-3.30728200	0.27399200
C	2.19986400	-2.85264200	-7.41766900
C	3.75388800	3.35728800	-4.96124900
C	6.84208100	3.77494000	1.91347900
C	6.53532900	-3.34803200	0.57559700
C	1.60510900	-2.64684200	-6.18302600
C	2.37102900	2.80831600	-5.09392000
C	5.50438300	4.38744900	1.64613000
C	5.81371600	-3.04454500	1.84937900
C	1.72265900	-3.42077700	-4.90847100

C	0.45478700	2.51889300	-3.53376100
H	0.29769700	1.77496500	-4.32320400
C	3.13495700	3.57834400	1.70256400
H	3.09091600	4.40056400	0.97753500
C	3.45214500	-2.47167900	2.38489100
H	4.05592100	-1.92285900	3.11798200
C	0.80494000	-3.17711200	-2.57946700
H	1.65864900	-3.84494500	-2.43187200
C	0.88225600	1.68221800	-2.31797000
C	2.65191500	2.34142500	0.92461000
C	2.84044500	-1.39190100	1.46826600
C	1.13701600	-1.95010500	-1.71657900
C	-0.83769800	3.35597500	-3.45711600
C	2.31342300	4.01903500	2.94533800
C	2.48949100	-3.37791400	3.18749800
C	-0.47291900	-3.98571300	-2.25844000
C	-0.87548500	4.36233700	-2.28695600
H	-0.03458700	5.05702800	-2.36471400
H	-0.76347800	3.82828800	-1.33817600
C	2.13033200	2.89821900	3.99342800
H	3.10948500	2.55144900	4.33863700
H	1.62539000	2.04275300	3.53866900
C	1.40703900	-4.05792900	2.32241700
H	1.87866600	-4.66559500	1.54599400
H	0.81298300	-3.29570700	1.81298100
C	-1.78640000	-3.18298100	-2.39265400
H	-1.75908700	-2.31534400	-1.73014500
H	-1.89178100	-2.80776300	-3.41631600
C	-2.20203300	5.14448900	-2.30776900
H	-2.21108400	5.84956700	-1.46778700
C	1.31292400	3.42191500	5.18988000
H	1.18463600	2.60882600	5.91456000
C	0.50140000	-4.93791900	3.20137600
H	-0.26179400	-5.40503800	2.56697400
C	-2.98966400	-4.08280700	-2.05062300
H	-3.90991400	-3.49332300	-2.14178900
C	-2.32045800	5.91900800	-3.63336500
H	-3.25120600	6.49983000	-3.64893500
H	-1.49141700	6.63182100	-3.72750300
C	2.05890800	4.59348300	5.85153900
H	1.49657800	4.95809200	6.72028600
H	3.03768900	4.25737000	6.21662500
C	1.34800800	-6.02849300	3.88158000
H	0.70920500	-6.67761700	4.49362500
H	1.82297800	-6.66265600	3.12225800
C	-3.03848400	-5.27187200	-3.02619500
H	-3.90598600	-5.90622200	-2.80526000
H	-3.15507600	-4.90908100	-4.05532600
C	-2.29911600	4.92586400	-4.81003300
H	-2.37092200	5.47299000	-5.75776200
C	2.23881300	5.72664400	4.82590200

H	2.78691800	6.55836400	5.28466200
C	2.42315300	-5.36505700	4.76219900
H	3.03893300	-6.13698800	5.23928700
C	-1.74069300	-6.09022000	-2.89868700
H	-1.76144700	-6.93066200	-3.60283600
C	-0.97834300	4.13820600	-4.78570000
H	-0.93709400	3.43970400	-5.63108600
H	-0.13276100	4.82600000	-4.89764000
C	3.04647400	5.20257400	3.62500300
H	4.03384000	4.87759700	3.97175600
H	3.20852500	6.00529500	2.89682200
C	3.32497700	-4.47890000	3.88454200
H	3.82309400	-5.09478600	3.12760300
H	4.11335600	-4.01699100	4.49211300
C	-0.53744900	-5.19041500	-3.22980200
H	0.39443300	-5.76498900	-3.16879200
H	-0.62679800	-4.83046100	-4.26137600
C	-2.04490300	2.39116400	-3.33341400
H	-1.96582400	1.82166100	-2.40491800
H	-2.02077800	1.66861500	-4.15820600
C	0.92574800	4.52889200	2.48137900
H	1.06363500	5.33640500	1.74970900
H	0.38245400	3.72434800	1.98281900
C	1.80300600	-2.52866600	4.28676800
H	1.21533500	-1.73203400	3.82504000
H	2.57165800	-2.05174100	4.90979000
C	-0.35411200	-4.53564000	-0.81643200
H	0.57989900	-5.10214600	-0.71612800
H	-0.30348800	-3.70576300	-0.10931800
C	-3.36541900	3.17909800	-3.35598500
H	-4.20113900	2.47519600	-3.26228100
C	0.11452000	5.04331800	3.68387700
H	-0.86698400	5.38165900	3.33062000
C	0.89618400	-3.41325100	5.15994300
H	0.41618600	-2.78759500	5.92202800
C	-1.55852700	-5.43191900	-0.48404800
H	-1.45350900	-5.80101800	0.54342000
C	-3.48315300	3.95145500	-4.68135400
H	-4.43047300	4.50401400	-4.71555700
H	-3.48579700	3.24978000	-5.52536400
C	0.85968200	6.21268200	4.34817300
H	0.28069100	6.59740300	5.19701000
H	0.97698500	7.03801900	3.63448100
C	1.74178000	-4.50384700	5.84030900
H	2.49795900	-4.04257700	6.48807900
H	1.10713800	-5.13206900	6.47789500
C	-1.60594200	-6.61968300	-1.46020500
H	-2.45329200	-7.27360400	-1.21912500
H	-0.69339200	-7.22149300	-1.36403700
C	-3.38510000	4.16942100	-2.17680300
H	-4.33155900	4.72452800	-2.16626600

H	-3.31855800	3.62334500	-1.22711700
C	-0.06634500	3.90150900	4.70138100
H	-0.61169800	3.06877600	4.23910600
H	-0.66587600	4.24953400	5.55190200
C	-0.17913700	-4.07010700	4.27481500
H	-0.79519900	-3.29777300	3.79647700
H	-0.84840700	-4.68486500	4.88974500
C	-2.85264100	-4.60731400	-0.60949000
H	-2.83294100	-3.76775500	0.09708300
H	-3.72046400	-5.22743500	-0.35210700
C	4.72948800	0.03928900	-1.95179900
C	4.92089700	-0.35868500	-3.29975700
C	5.94255200	0.36097900	-1.16577300
C	6.20548200	-0.73894800	-3.78720000
C	3.84699900	-0.27941600	-4.23090500
O	6.36979400	-0.24135000	-0.20785400
O	6.49443700	1.49784900	-1.68466200
C	6.41082700	-1.01281600	-5.12463400
H	7.03810700	-0.82913900	-3.10052100
C	4.06483100	-0.48438300	-5.58008500
H	2.87128400	0.01866000	-3.88098800
C	7.67087900	2.02074700	-1.08224300
C	5.33979900	-0.86148100	-6.01604600
H	7.38557600	-1.31561100	-5.48449500
H	3.26945100	-0.32538100	-6.29368600
H	7.58598000	3.10604300	-1.12503100
H	7.76655600	1.67710900	-0.05341000
C	8.93131000	1.60140000	-1.85788200
Br	5.62206400	-1.15698400	-7.85906900
Cl	9.30834900	-0.13916600	-1.60530100
Cl	8.72857700	1.89689000	-3.61468600
Cl	10.28360600	2.59488700	-1.21582200

(HFIP)4(H2O)3-Rh2(TCPTAD)4 [B3LYP-D3(BJ)]/BS1

Rh	-2.23210800	11.32977500	11.41348500
Rh	-0.27989900	11.33570600	12.82279900
Cl	4.85312500	12.43964500	10.39507300
Cl	7.25402100	13.93183200	11.80386100
Cl	3.98328800	18.14509900	12.93044800
Cl	6.81734500	16.76489500	13.07237100
Cl	6.55779000	8.72224300	10.69024400
Cl	6.89711300	6.70845500	13.09573800
Cl	1.50931800	6.00059800	13.29514000
Cl	4.38510600	5.33566300	14.36414700
Cl	-0.47175000	17.52268100	14.12247300
Cl	0.63852600	19.15256300	16.57913500
Cl	-1.49266400	15.47860800	19.99007300
Cl	0.11674600	18.14472100	19.50049000
Cl	-0.19270700	5.35698800	18.47209600
Cl	-1.37394600	6.69589700	21.07378600
Cl	-4.36553700	10.05840200	18.00585700

Cl	-3.51136800	8.97505800	20.83225100
O	0.05557600	13.30247900	12.22781200
O	1.79386100	11.16615400	13.70369200
O	-5.71206200	11.67834200	11.28988800
H	-5.05942000	11.88711500	11.97153400
H	-5.38877500	10.85570800	10.88911800
O	-1.78022300	13.25695400	10.91934200
O	1.20738100	17.31382100	11.69908400
O	1.84309600	13.13051700	9.91595300
O	-0.99702300	10.67757400	9.85600200
O	0.78942000	10.69904500	11.23040900
O	0.39951500	7.76401300	10.90655800
O	4.07739300	9.85686300	9.13172600
O	-3.31746800	11.98701800	13.04999800
O	-1.50169200	11.97792700	14.38873900
O	-2.79525300	13.34824900	18.09944000
O	-2.22712900	14.90934300	13.82900100
O	-0.73675900	9.40660900	13.33052800
O	-2.52166600	9.33942700	11.95107500
O	-3.42304700	9.44089800	15.04882900
O	-0.56687500	5.86930300	15.39129400
N	1.18376600	15.19394600	10.76069400
N	2.04283400	8.93863600	9.76061700
N	-2.76444700	13.90921400	15.85237200
N	-2.05775800	7.57724000	14.87745000
C	3.90372600	8.16324200	10.89057000
C	5.18073600	7.92583500	11.37341200
C	5.32352800	7.02679800	12.45259200
C	4.19466600	6.40736500	13.02083900
C	2.89950800	6.67642700	12.52539100
C	2.78155100	7.54327500	11.44961000
C	1.56950300	8.03671900	10.72403300
C	-0.70185700	13.77664300	11.31329300
C	2.10454500	14.18087500	10.46523800
C	1.20048200	9.91968500	9.06532700
H	1.87572500	10.76255600	8.87543400
C	0.22240900	10.46562900	10.11676300
C	3.42013200	14.67056500	10.97814600
C	4.64716500	14.03026900	11.04172500
C	5.70769100	14.70033300	11.68944200
C	5.51153200	15.97269400	12.25964500
C	-2.18517400	14.90333800	15.04060400
C	-1.54749200	15.86943900	15.98351000
C	-0.80841300	17.01343100	15.73401600
C	-0.29677600	17.72210300	16.84394900
C	-0.52710700	17.26763000	18.15627100
C	-1.26013700	16.08389000	18.38566000
C	-1.76271900	15.40940200	17.28492300
C	-2.49106200	14.11337900	17.19628200
C	4.25028300	16.60376700	12.18978700
C	3.22658700	15.93582700	11.53855500

C	-3.52085800	12.75731700	15.34714500
H	-3.41946100	11.98749100	16.11845000
C	-2.73611900	12.20171500	14.14889100
C	1.78701800	16.29665200	11.37786100
C	-0.26605800	15.08039300	10.63327000
H	-0.65706300	15.89138800	11.25977000
C	3.43370300	9.09092900	9.81985700
C	-1.32862000	6.74668300	15.74073600
C	-1.71457100	7.16197900	17.12255400
C	-1.31993000	6.66441000	18.35419000
C	-1.86515500	7.25857900	19.51290400
C	-2.81005200	8.29684000	19.40791600
C	-3.19628600	8.78644200	18.14263200
C	-2.62407300	8.21734000	17.01933900
C	-2.79510700	8.53962700	15.56965700
C	-2.02100000	7.44369300	13.41819000
H	-1.09667700	6.89705600	13.21025900
C	-1.76110300	8.84293000	12.84186000
H	2.29290700	10.87674600	12.92477800
H	1.80527300	10.42054700	14.36122200
O	-0.64174300	10.32630900	16.46984200
H	-0.77473800	10.64493100	17.38236500
H	-0.96079400	11.02101300	15.86321300
F	-1.44703600	10.99304900	22.07031800
F	-2.56517800	12.57218000	21.07517100
F	-0.64642000	13.01327200	22.01112500
F	0.19498300	9.62264400	20.37600300
F	1.29180700	10.88336300	18.98735200
F	1.37674900	11.29398900	21.12541000
O	-1.47971300	11.21490400	19.03703500
H	-2.11912000	11.89376900	18.73115800
C	-0.62258900	11.82137000	19.96555800
H	-0.24094500	12.78448800	19.61290400
C	-1.33009000	12.09152000	21.30441200
C	0.57197400	10.88574500	20.13208600
F	-5.80359600	8.03912400	8.06644700
F	-3.77613400	7.25751500	8.25753800
F	-4.33333500	8.43683800	6.51870600
F	-5.97674100	10.90137600	8.18617600
F	-4.13517700	11.91799800	8.75293500
F	-4.31732100	11.03714800	6.77973800
O	-4.48202300	9.40879300	9.96070300
H	-3.73575000	9.16417800	10.53975400
C	-4.05911500	9.55987900	8.62753600
H	-2.97312800	9.64082400	8.54019800
C	-4.50977400	8.31605800	7.84576700
C	-4.64002700	10.86693700	8.07567900
F	3.28656400	15.49520800	15.29637300
F	3.39592600	13.95601800	13.76292100
F	4.10831500	13.53347600	15.77233900
F	1.40066000	14.97157400	17.36205000

F	0.20609300	13.16536200	17.11264400
F	2.31427000	13.01304400	17.61361700
O	0.79635900	14.43451000	14.72138600
H	0.60464600	14.04535600	13.84695500
C	1.74828000	13.66285300	15.39744300
H	1.73780500	12.61575800	15.09672100
C	3.15460000	14.17637500	15.07433900
C	1.42769700	13.71511100	16.88566700
F	1.13633900	8.25100400	18.03449900
F	2.52412700	7.05714700	16.85395700
F	4.12942600	10.65239200	15.33533700
F	4.95251700	9.28066600	16.81259700
F	4.04975100	8.50982500	14.98612800
O	1.59830500	9.42185800	15.63708600
H	0.71909600	9.75438400	16.02182400
C	2.58847300	9.43188600	16.62832600
H	2.54850500	10.32036200	17.26367800
C	2.38969000	8.21015000	17.53094200
C	3.95109200	9.45717600	15.93630100
F	3.24726200	8.19769900	18.56462400
C	-0.81199500	15.31701000	9.18920900
C	-0.60881500	14.11207800	8.24006200
C	-2.32219100	15.65963400	9.26584500
C	-0.08074600	16.54115300	8.58558300
H	-1.10470500	13.22728900	8.64407500
H	0.45502000	13.87522600	8.16198600
C	-1.17144300	14.43474700	6.84416400
H	-2.46213400	16.52809000	9.92386400
H	-2.87282500	14.82540700	9.70296800
C	-2.87557500	15.97260200	7.86415800
H	0.99246600	16.33388100	8.51150200
H	-0.19749500	17.40702400	9.24860200
C	-0.63244300	16.86367600	7.18419700
H	-1.02196900	13.56254400	6.19572300
C	-2.67378400	14.74936100	6.95020600
C	-0.42742900	15.64859400	6.26122500
H	-3.94547700	16.19744800	7.94964600
C	-2.13393900	17.18572200	7.27843800
H	-0.09162300	17.72916000	6.78307300
H	-3.21078300	13.88273000	7.35291400
H	-3.08679300	14.95380700	5.95435500
H	0.64239100	15.42293400	6.16645500
H	-0.80128900	15.87544100	5.25485700
H	-2.52907200	17.42823000	6.28408000
H	-2.29133200	18.06571500	7.91483900
C	0.66454200	9.45702300	7.69581900
C	-0.42215800	8.36658900	7.78119200
C	0.10999300	10.69219900	6.94339700
C	1.85194600	8.88815100	6.87786100
H	-1.25473300	8.71803000	8.39313800
H	-0.02146000	7.48104500	8.28627500

C	-0.90089300	7.99098100	6.36565900
H	0.88704900	11.46608500	6.89348500
H	-0.73189100	11.11911100	7.49440400
C	-0.33803000	10.29907000	5.52639700
H	2.26459500	8.01271200	7.39140800
H	2.65226900	9.63456800	6.81961700
C	1.39271200	8.48767200	5.46631700
H	-1.69367600	7.23918100	6.44692800
C	-1.44181100	9.23544500	5.63458100
C	0.28667200	7.42089300	5.56888800
H	-0.73113100	11.18817500	5.01848300
C	0.85254200	9.73009500	4.73729600
H	2.24932900	8.07909700	4.91720400
H	-2.30100800	9.65616900	6.16118000
H	-1.79406400	8.95118500	4.63536900
H	0.67642000	6.52271000	6.06433800
H	-0.04113100	7.12174300	4.56573600
H	0.53726100	9.46481900	3.72059300
H	1.64286000	10.48582200	4.64604600
C	-3.19186000	6.59875600	12.85516300
C	-4.58305200	7.25097900	13.02400700
C	-2.92548300	6.29977700	11.35966400
C	-3.20866400	5.24057200	13.60584300
H	-4.61225800	8.22473900	12.53039200
H	-4.78173700	7.42852400	14.08583200
C	-5.67355400	6.32755000	12.44715000
H	-1.94592100	5.81605300	11.25681600
H	-2.87697000	7.22451400	10.78283700
C	-4.02848600	5.38901300	10.79040300
H	-3.40339700	5.40789600	14.67083300
H	-2.22532000	4.76295600	13.52842200
C	-4.29835200	4.31530200	13.03940700
H	-6.64721300	6.81824200	12.56418800
C	-5.39936500	6.07162500	10.95490900
C	-5.67145600	4.98905900	13.20590400
H	-3.82931000	5.21540500	9.72808200
C	-4.02747900	4.05131000	11.54882700
H	-4.27978900	3.36917300	13.59335300
H	-5.42381400	7.01507700	10.40355400
H	-6.18480700	5.43043600	10.53540300
H	-5.88165100	5.15684800	14.26991300
H	-6.46178100	4.33449000	12.81806200
H	-4.79584400	3.38420200	11.13885300
H	-3.06020100	3.54790300	11.42540400
C	-5.03867100	13.05157700	15.19256900
C	-5.36096400	14.12578300	14.12960500
C	-5.79251200	11.74011500	14.85761200
C	-5.56818700	13.56344800	16.55907400
H	-4.98491000	13.82007000	13.15042500
H	-4.85687800	15.06426400	14.38558600
C	-6.88292000	14.36622500	14.06697300

H	-5.56826300	10.98546100	15.61747400
H	-5.45062000	11.33438300	13.90589200
C	-7.30902300	11.99672700	14.79242000
H	-5.06912200	14.50202800	16.82338600
H	-5.32953900	12.84025100	17.34674600
C	-7.08482500	13.80895200	16.50516300
H	-7.08704600	15.11978800	13.29693500
C	-7.60752100	13.05430800	13.71332900
C	-7.38320100	14.87055700	15.43173500
H	-7.81119500	11.05631200	14.53521900
C	-7.80657500	12.49589200	16.15783700
H	-7.41763200	14.16898800	17.48601300
H	-7.28016200	12.68812700	12.73587900
H	-8.68887600	13.23326400	13.65663900
H	-6.88908300	15.81555700	15.69157000
H	-8.46107100	15.06957900	15.38718800
H	-8.89132400	12.65758000	16.13108900
H	-7.60858800	11.74289900	16.93160900

Rh2(TCPTAD)4(HFIP)4 (34) [B3LYP-D3(BJ)]/BS1

Rh	-2.11019900	11.12073300	11.59703100
Rh	-0.29770700	11.15233900	13.17264100
Cl	4.73857000	12.18167300	9.94969500
Cl	7.40297000	13.83663200	10.35208200
Cl	4.47692000	18.16054500	11.92167000
Cl	7.26712600	16.81362200	11.32679100
Cl	6.18980300	7.95664000	12.19511800
Cl	5.83964600	5.70417100	14.37662900
Cl	0.69361700	4.92441500	12.77003400
Cl	3.11345800	4.18297400	14.64650000
Cl	-0.71517700	17.64879200	14.19793900
Cl	0.56480500	19.08807100	16.69209900
Cl	-1.36851300	15.17622900	19.96037600
Cl	0.24326300	17.86261800	19.55636600
Cl	-0.30028900	5.51672900	18.89759500
Cl	-1.54248800	6.93432900	21.42769300
Cl	-4.51582700	10.14995100	18.18615800
Cl	-3.70248100	9.17102100	21.07565400
O	0.11830700	13.10070600	12.51654600
O	-1.62784200	13.02548900	11.09742800
O	1.49131100	17.14762700	11.80676300
O	1.69189100	12.89078300	10.09406300
O	-0.80161300	10.44902600	10.14031300
O	0.85146500	10.35848000	11.67958800
O	0.14253200	7.40330600	10.89320900
O	4.24447900	9.30327600	10.12572700
O	-3.30370400	11.81340800	13.11476300
O	-1.57329000	11.95376600	14.56619300
O	-2.96774700	13.28419800	18.03121900
O	-2.30452500	14.93001700	13.81573700
O	-0.89265300	9.29212200	13.74295100

O	-2.48555900	9.15320300	12.15771200
O	-3.57847000	9.37549700	15.27087800
O	-0.68611800	5.86077900	15.78469700
N	1.25034300	15.00345100	10.94839500
N	2.06371000	8.50830100	10.19817000
N	-2.92967300	13.92762100	15.81656100
N	-2.23354300	7.48882300	15.19823900
C	3.58717300	7.45580200	11.58606500
C	4.68264300	7.12428900	12.36759200
C	4.52008400	6.10837200	13.33428700
C	3.29290100	5.42767200	13.45902400
C	2.19733200	5.76814600	12.63801100
C	2.35977700	6.80716500	11.73611400
C	1.35011400	7.53815100	10.91175200
C	-0.60473300	13.57942800	11.57458900
C	2.07799200	13.96569200	10.50940600
C	1.43275400	9.65434600	9.52877700
H	2.20603100	10.42977700	9.53067000
C	0.38291400	10.19209200	10.51305000
C	3.47471300	14.47451600	10.65732700
C	4.68588200	13.84202100	10.42446800
C	5.86801700	14.58416500	10.63479200
C	5.80657800	15.91992500	11.07724900
C	-2.29884000	14.90762500	15.02857800
C	-1.63015000	15.83064100	15.99574700
C	-0.91333500	16.99674900	15.78229500
C	-0.34220200	17.63228800	16.90794100
C	-0.49447400	17.08780900	18.19814600
C	-1.22943900	15.89920700	18.39191500
C	-1.79722000	15.30204100	17.27890700
C	-2.61329200	14.06266200	17.15932600
C	4.56203400	16.53467200	11.33443400
C	3.41316200	15.79158200	11.11780500
C	-3.66217200	12.76482800	15.30460300
H	-3.64411000	12.04529100	16.12922600
C	-2.78672100	12.12832600	14.22335500
C	1.97684800	16.13168300	11.35803300
C	-0.20833400	14.94238100	10.99695000
H	-0.49831000	15.68225700	11.75363500
C	3.41695400	8.53430500	10.56663000
C	-1.47192100	6.72914300	16.09818200
C	-1.85529300	7.21850600	17.45836200
C	-1.46348800	6.78584700	18.71386800
C	-2.02924900	7.42156600	19.84091500
C	-2.97596900	8.45148000	19.68397600
C	-3.34597600	8.89182300	18.39419500
C	-2.76659100	8.26749500	17.30192400
C	-2.95725800	8.49697100	15.83726600
C	-2.14682300	7.31593300	13.74725100
H	-1.22296200	6.74843100	13.59518100
C	-1.84224000	8.69727000	13.15471800

F	-0.16419900	10.22485400	21.37619400
F	-0.23053700	12.38039800	21.66108500
F	1.52626400	11.45494800	20.76225300
F	0.00355700	9.34024700	18.79815000
F	-0.59397000	10.75052100	17.25179800
F	1.39416500	10.87193200	18.13338500
O	-1.82884000	11.40957500	19.60263300
H	-2.30080700	12.09483600	19.09066600
C	-0.45858400	11.59915200	19.45588400
H	-0.18965900	12.60323500	19.11554600
C	0.18194500	11.40495200	20.83223300
C	0.09656500	10.61984200	18.41614500
F	-5.25832300	7.67479100	8.05391200
F	-3.20782700	7.12863000	8.54006700
F	-3.62698800	8.33551300	6.77644700
F	-5.76826900	10.43328900	8.04667000
F	-4.36610600	11.65410100	9.17668500
F	-3.84558900	10.97976900	7.17807300
O	-4.42255900	9.13403700	10.17471100
H	-3.73979400	8.96003800	10.84823700
C	-3.82246900	9.36701200	8.92988400
H	-2.75088800	9.57714100	9.00720900
C	-3.99156800	8.11728200	8.05578800
C	-4.46528100	10.61641900	8.31877100
F	2.45225800	16.62185700	15.56527900
F	3.50669700	15.63807500	13.94088200
F	4.00282000	15.15407100	16.00443700
F	1.43056400	14.90220800	17.41346000
F	0.42495300	13.18482900	16.55064000
F	2.54337300	13.06807700	17.05493200
O	0.81751800	14.80440500	14.46999700
H	0.56726000	14.16942500	13.76472700
C	1.94563300	14.33377800	15.13111800
H	2.40496500	13.47496900	14.63751300
C	2.98769900	15.45502900	15.17070900
C	1.59189500	13.87945500	16.55575200
F	0.89543800	8.63731300	16.08566800
F	1.62301300	8.33791500	14.05363900
F	3.95574900	11.79834100	14.41361700
F	4.59877000	9.72043200	14.55788100
F	3.19194700	10.32668300	13.01403700
O	1.33664200	11.10001000	14.94374300
H	0.75591200	11.20032600	15.71605100
C	2.40982800	10.23990700	15.27121300
H	2.78700600	10.46375500	16.27132400
C	1.96598500	8.76923900	15.27544400
C	3.55244400	10.51802700	14.29052700
F	2.94262000	7.97244200	15.73803900
C	-0.89718600	15.33873800	9.65412000
C	-0.71481800	14.27825400	8.54135000
C	-2.40744500	15.58707900	9.90648900

C	-0.28568300	16.66913700	9.14881400
H	-1.11279300	13.31537600	8.86523000
H	0.35102100	14.13373300	8.34008100
C	-1.42378200	14.73307500	7.25375700
H	-2.51995300	16.36280300	10.67577700
H	-2.88217400	14.68124100	10.28417600
C	-3.10189800	16.03069900	8.60701300
H	0.78375200	16.53715300	8.95014000
H	-0.37881400	17.43904200	9.92273600
C	-0.97990800	17.12913300	7.85284200
H	-1.29479100	13.95737900	6.48863900
C	-2.92359600	14.93797500	7.53540100
C	-0.80291500	16.05338600	6.76637000
H	-4.16952500	16.17722900	8.81019100
C	-2.47961700	17.34767100	8.11556000
H	-0.52009600	18.06826800	7.52283000
H	-3.37381500	13.99667700	7.87549300
H	-3.44150500	15.23089800	6.61349000
H	0.26309000	15.90824700	6.54989200
H	-1.28263900	16.37819300	5.83474900
H	-2.97711500	17.68400600	7.19736000
H	-2.62107900	18.13337700	8.86837500
C	1.04404000	9.41513900	8.05803600
C	-0.06388000	8.36114400	7.86181400
C	0.59667500	10.76205800	7.43624000
C	2.30894000	8.93386900	7.30447800
H	-0.95733400	8.65540100	8.41385800
H	0.25859700	7.40077600	8.27758000
C	-0.37733100	8.19804300	6.36286200
H	1.38547500	11.51027700	7.58322700
H	-0.29406100	11.13062100	7.94963700
C	0.29883500	10.58487500	5.93816900
H	2.65115300	7.98326600	7.72959300
H	3.11959600	9.65923900	7.44477600
C	2.00899300	8.75392800	5.80653900
H	-1.18145500	7.46308400	6.24870900
C	-0.82445600	9.54706900	5.76899200
C	0.88689400	7.71390700	5.63062100
H	-0.02273500	11.54872500	5.52433200
C	1.56351300	10.10015200	5.20890200
H	2.91776100	8.40669700	5.30049700
H	-1.73460300	9.89697800	6.26449600
H	-1.06445200	9.42245900	4.70544200
H	1.20721600	6.74398300	6.03193600
H	0.67351600	7.56914700	4.56420500
H	1.36082800	9.98762800	4.13650100
H	2.36616300	10.84142300	5.31183300
C	-3.30416100	6.47381100	13.15625100
C	-4.68542400	7.16258700	13.23282600
C	-2.97110100	6.11928100	11.68656900
C	-3.39010900	5.14539500	13.95205200

H	-4.66615800	8.12174700	12.71093000
H	-4.93420900	7.37821600	14.27707300
C	-5.76620500	6.24674700	12.62667400
H	-1.99885900	5.61494400	11.64605000
H	-2.87340500	7.02120100	11.08324300
C	-4.06211400	5.21162200	11.09270100
H	-3.63067000	5.35667500	14.99984200
H	-2.41614100	4.64222400	13.93986100
C	-4.47249500	4.22551800	13.36105200
H	-6.73261100	6.76273300	12.67604500
C	-5.42321200	5.92933400	11.15971000
C	-5.83627000	4.93681400	13.42998300
H	-3.81065000	4.99904300	10.04777600
C	-4.13061900	3.90250300	11.89588000
H	-4.50704700	3.29947600	13.94724200
H	-5.39439300	6.84973300	10.57011300
H	-6.20208100	5.28837600	10.72724600
H	-6.09781300	5.14734900	14.47484100
H	-6.62052900	4.28638000	13.02337500
H	-4.89120900	3.23619200	11.47032800
H	-3.16928600	3.37577500	11.84179000
C	-5.14865300	13.05153800	14.97828300
C	-5.35640000	13.99959700	13.77518000
C	-5.87065700	11.70652700	14.70809800
C	-5.80195500	13.70020500	16.22481000
H	-4.88822200	13.57765200	12.88297200
H	-4.87333200	14.96226600	13.97143900
C	-6.86099700	14.22282100	13.53282500
H	-5.72525600	11.03671000	15.56284800
H	-5.42802800	11.21499300	13.83984500
C	-7.37032800	11.94455600	14.46651300
H	-5.31520600	14.65723200	16.44465300
H	-5.65442400	13.05561200	17.09997700
C	-7.30407800	13.93648700	15.98846000
H	-6.98517000	14.88708700	12.66913000
C	-7.54744200	12.87369100	13.25175100
C	-7.49115500	14.86990000	14.77883000
H	-7.85338300	10.98039200	14.26689600
C	-7.99901700	12.59212900	15.71189500
H	-7.73474900	14.39982000	16.88415800
H	-7.11067100	12.40898800	12.35822100
H	-8.61420600	13.02956300	13.04780800
H	-7.01987900	15.84111400	14.97638300
H	-8.55908000	15.05600300	14.60987800
H	-9.07371700	12.74931200	15.55685700
H	-7.88913600	11.92590900	16.57705000

Rh2(TCPTAD)4(Car3)(HFIP)4 (36) [B3LYP-D3(BJ)]/BS1

Rh	1.12542300	-0.04732800	-0.10223400
Rh	3.25758500	0.24335300	-1.28656100
Cl	3.19873000	9.64010600	-1.30756600

Cl	10.61569700	3.01840800	3.10475400
Cl	-0.31741300	-9.32519900	0.56427500
Cl	2.10681500	1.20953100	-9.96707700
Cl	1.87214400	7.15681300	0.11600900
Cl	8.04451300	1.21452400	3.41345400
Cl	-0.89416700	-6.28730400	1.18404600
Cl	0.78506400	1.61348500	-7.12949900
Cl	3.41727000	9.72813600	-4.43250200
Cl	10.41332600	5.82116500	1.72317200
Cl	2.63415600	-10.36221900	0.37916000
Cl	3.65482400	-1.43321600	-10.61825500
Cl	2.32730400	7.32846600	-6.16522500
Cl	7.61991500	6.92126800	0.75964100
Cl	5.04497800	-8.36947800	0.79698800
Cl	3.84122400	-3.73512000	-8.47038900
O	2.26450300	1.71725600	-2.41981900
O	3.71778600	1.74079700	0.06419900
O	3.93607800	-1.33373100	-0.04229400
O	2.61518100	-1.21425900	-2.59850800
O	0.28576000	1.21769000	-1.46118300
O	1.69512900	1.56503400	1.05809200
O	2.05569300	-1.32583000	1.19480500
O	0.72222600	-1.60221800	-1.41862700
O	1.05821600	4.27130200	-0.88649000
O	5.02255500	1.61262600	2.73065000
O	0.88563500	-3.79840000	1.56322500
O	0.64906900	-0.13145400	-4.53158000
O	1.10289000	4.50104200	-5.46580400
O	4.68081400	5.74603200	0.77190500
O	5.23984100	-5.28295000	1.40167300
O	2.70423500	-4.09808200	-5.53923700
N	0.88369300	4.10304200	-3.18820800
N	4.50143500	3.64936300	1.75390200
N	3.19112100	-4.18037200	1.50962800
N	1.47820900	-2.28142600	-4.77262000
C	1.17951900	4.76027200	-1.99299400
C	5.35517900	2.70111700	2.31406200
C	1.84463600	-4.53791600	1.44430400
C	1.16686000	-0.99778200	-5.20966200
C	1.69759400	6.10416000	-2.38318400
C	6.72162700	3.30541800	2.28137400
C	1.81231700	-6.00889600	1.19153700
C	1.64585200	-0.91642900	-6.62188700
C	2.09195500	7.17461600	-1.59819200
C	7.93451000	2.79614200	2.71829000
C	0.73054700	-6.86298900	1.04086200
C	1.55489300	0.11793400	-7.54019800
C	2.64135400	8.30038400	-2.24964100
C	9.08336300	3.60012200	2.55528300
C	0.99903100	-8.22449700	0.78145800
C	2.17698000	-0.05913200	-8.79612600

C	2.73543700	8.34084400	-3.65391900
C	8.98900700	4.86674900	1.94393900
C	2.32644300	-8.69053000	0.69972700
C	2.87729500	-1.24698500	-9.08674800
C	2.26733800	7.26306000	-4.43682400
C	7.74166600	5.36451100	1.50289300
C	3.41181100	-7.80539300	0.88043400
C	2.96115100	-2.28541900	-8.13202500
C	1.76594500	6.15222600	-3.77804100
C	6.62307500	4.56564300	1.68685500
C	3.12542300	-6.47122200	1.12139700
C	2.32830500	-2.10027400	-6.91314600
C	1.23314400	4.86142300	-4.31540000
C	5.18605500	4.79268500	1.32181000
C	4.03302900	-5.30836700	1.34714600
C	2.23956600	-2.99269500	-5.71208800
C	0.27457300	2.77750300	-3.27903400
H	0.54717600	2.40380900	-4.27052400
C	3.06241200	3.47070400	1.57144200
H	2.78668100	4.21582400	0.81551100
C	3.78590700	-2.86764100	1.81614500
H	4.82869300	-2.98399300	1.52970200
C	1.10886600	-2.82469700	-3.46533600
H	1.79594000	-3.66325300	-3.31160500
C	0.98466400	1.83790000	-2.29079700
C	2.80436400	2.13146700	0.86674000
C	3.19768400	-1.76404600	0.91839200
C	1.49095200	-1.78408300	-2.39905300
C	-1.28271100	2.81158700	-3.19877500
C	2.22085200	3.78577300	2.84487600
C	3.78164500	-2.51332900	3.33096000
C	-0.33764000	-3.39777200	-3.44230000
C	-1.82940600	3.26474100	-1.82359300
H	-1.47729300	4.27779500	-1.60081200
H	-1.45682600	2.61099400	-1.03466600
C	2.28378900	2.67956800	3.92242900
H	3.31905800	2.51439000	4.23393800
H	1.91788200	1.73868200	3.50571000
C	2.39288100	-2.58429000	3.99672300
H	1.99639000	-3.60283400	3.92626400
H	1.69695600	-1.92202000	3.48510400
C	-1.43360800	-2.31240800	-3.54066500
H	-1.35037800	-1.62529600	-2.69588600
H	-1.30196100	-1.72294900	-4.45253600
C	-3.36934900	3.25344000	-1.83386600
H	-3.72955800	3.55774800	-0.84365000
C	1.43544700	3.07987400	5.14480600
H	1.49162100	2.27616000	5.88916800
C	2.49705000	-2.19279300	5.48225300
H	1.49591500	-2.24314700	5.92726100
C	-2.82855300	-2.96439400	-3.55313500

H	-3.58506800	-2.17259800	-3.62076000
C	-3.88204700	4.23916900	-2.89768400
H	-4.97911700	4.25710700	-2.90297100
H	-3.54193700	5.25559200	-2.66218800
C	1.98417300	4.38542500	5.74714600
H	1.40296400	4.66637700	6.63446800
H	3.02341200	4.24422600	6.07087800
C	3.44171800	-3.16839500	6.20527400
H	3.50961100	-2.91122900	7.26983800
H	3.04615300	-4.19045600	6.14328300
C	-2.95390700	-3.90647500	-4.76173600
H	-3.95523600	-4.35408300	-4.78911700
H	-2.82394600	-3.34430900	-5.69547300
C	-3.35676500	3.81148100	-4.27912100
H	-3.69654900	4.52273200	-5.04157200
C	1.90928700	5.50398000	4.69154700
H	2.31458200	6.43389000	5.10874100
C	4.83594100	-3.10284400	5.55550200
H	5.51133000	-3.80683800	6.05679200
C	-1.88469600	-5.00958000	-4.65932900
H	-1.95635600	-5.67745500	-5.52620700
C	-1.81589400	3.80200600	-4.26588700
H	-1.43211500	3.52700900	-5.25493700
H	-1.45555800	4.81444900	-4.05052400
C	2.74930100	5.10324700	3.46738700
H	3.79274800	4.97688900	3.77739900
H	2.73043100	5.90221900	2.71741500
C	4.72875300	-3.49044600	4.06878800
H	4.34558900	-4.51481400	3.98758200
H	5.71606800	-3.47724000	3.59690600
C	-0.49113500	-4.35943400	-4.64905100
H	0.28817900	-5.12971400	-4.60857500
H	-0.35249400	-3.80783300	-5.58538900
C	-1.83714100	1.40850300	-3.55074500
H	-1.47079800	0.66936300	-2.83896700
H	-1.46508300	1.11239400	-4.53670500
C	0.73994200	4.01251900	2.44111800
H	0.68831300	4.79350300	1.67477100
H	0.33508600	3.10090200	2.00103900
C	4.34060500	-1.08422200	3.47748300
H	3.68827600	-0.37092100	2.97028000
H	5.32371600	-1.01956200	3.00042000
C	-0.55653700	-4.22210700	-2.14824300
H	0.21337400	-5.00307900	-2.07743100
H	-0.45502200	-3.58212800	-1.27141100
C	-3.37319100	1.41536900	-3.54734900
H	-3.72931900	0.40390700	-3.77978200
C	-0.09864700	4.41202400	3.66701000
H	-1.13902100	4.55579200	3.35006000
C	4.44522000	-0.69514900	4.96009300
H	4.83767700	0.32504300	5.02203900

C	-1.95666500	-4.86506100	-2.15958700
H	-2.09049700	-5.42593800	-1.22952500
C	-3.88377000	2.40399000	-4.60841500
H	-4.98084100	2.40967700	-4.62924700
H	-3.54126800	2.09473400	-5.60409300
C	0.44671500	5.71831500	4.26631400
H	-0.15655400	6.02211900	5.13114500
H	0.38567400	6.52652500	3.52608600
C	5.39219500	-1.67228900	5.67741900
H	6.39382700	-1.61854600	5.23151500
H	5.49189100	-1.39756600	6.73518300
C	-2.08571900	-5.81259200	-3.36281400
H	-3.07316400	-6.29094500	-3.36397000
H	-1.33717000	-6.61244600	-3.29503000
C	-3.87663600	1.83484500	-2.15528800
H	-4.97328400	1.81268600	-2.12659100
H	-3.51686200	1.12543700	-1.39859300
C	-0.02888900	3.29193800	4.72094300
H	-0.43823900	2.36317000	4.31148000
H	-0.63660500	3.55875300	5.59502400
C	3.04706900	-0.76059300	5.60063000
H	2.37097300	-0.05868600	5.09923500
H	3.10040400	-0.46392300	6.65596200
C	-3.03061400	-3.76580700	-2.25715700
H	-2.96735600	-3.09996700	-1.39311500
H	-4.02962100	-4.22018800	-2.24754700
C	5.03479400	0.44725600	-2.24821800
C	5.27064500	0.46465700	-3.64183900
C	6.21933700	0.52478400	-1.35945100
C	6.59195800	0.36328300	-4.17872700
C	4.18755200	0.61272800	-4.55360800
O	6.58879800	-0.35560200	-0.61953100
O	6.81662700	1.74534700	-1.47352700
C	6.82178900	0.39593400	-5.53732100
H	7.43353600	0.23149900	-3.51487400
C	4.42506900	0.70303400	-5.91016900
H	3.18298900	0.71385000	-4.16953000
C	7.96677600	2.00864600	-0.67110900
C	5.72879700	0.57374000	-6.39733400
H	7.82434800	0.29814000	-5.93389100
H	3.61886500	0.88886900	-6.59933800
H	7.82952400	2.99871400	-0.24390400
H	8.07817000	1.24960600	0.10240000
C	9.23618300	2.03697700	-1.53420500
Br	6.00661800	0.64352900	-8.26166400
Cl	9.61829200	0.40753200	-2.18154200
Cl	9.03839300	3.18478800	-2.89696600
Cl	10.57509900	2.57732200	-0.46602100
H	6.83104400	-2.56087500	0.66098200
O	7.13985200	-2.30014100	1.55443600
C	8.45950500	-2.71383400	1.71927600

H	8.79294000	-2.42242300	2.71878600
C	8.56577100	-4.24259200	1.63665800
C	9.37009200	-2.00098500	0.71041300
F	7.82381700	-4.80527400	2.60368900
F	8.11908000	-4.70116700	0.44637900
F	9.83341000	-4.67144000	1.78951400
F	9.30393200	-0.66803500	0.90598800
F	10.65986400	-2.36306700	0.83533400
F	8.98498100	-2.26010300	-0.55519700
C	4.83361400	4.19494400	-4.59900500
F	4.60388500	5.47876500	-4.93394700
F	3.75477800	3.47963900	-4.98122800
F	5.88970500	3.76269400	-5.31285900
C	5.07592100	3.99927500	-3.09269800
O	3.88562700	3.96190200	-2.36859800
H	5.67512700	3.09169500	-2.98753600
C	5.91573600	5.13912800	-2.51312400
H	3.43246600	3.10139200	-2.47690000
F	5.18898800	6.24100000	-2.28478600
F	6.46354600	4.74961400	-1.34120100
F	6.92501300	5.46716000	-3.34408500
H	5.09172600	-2.48303100	-0.75714400
O	5.78254700	-3.18029400	-0.70055700
C	5.87528400	-3.97362600	-1.83891600
C	4.57692800	-4.78727900	-2.05912400
H	6.68555100	-4.68692300	-1.67880100
C	6.23151900	-3.14902800	-3.08273500
F	3.50228500	-4.10283800	-1.59355000
F	4.62858100	-5.95165800	-1.38830500
F	4.34945400	-5.07348800	-3.34862700
F	5.16966700	-2.41685500	-3.49309800
F	7.23448800	-2.29919800	-2.80540800
F	6.61608600	-3.93098100	-4.10280700
H	-0.37703200	-3.31707500	2.86455000
O	-0.98207100	-2.64255500	3.21949200
C	-1.01999400	-1.62980800	2.25362000
C	-2.18893300	-1.86551800	1.29152500
H	-0.10823600	-1.61726200	1.65305200
C	-1.11253200	-0.29110400	2.98402800
F	-3.38749200	-1.71187600	1.88110000
F	-2.11979100	-3.12720400	0.81925000
F	-2.14370000	-1.02958000	0.22823500
F	-2.11325000	-0.26670500	3.87820900
F	0.03622100	-0.05276300	3.65137200
F	-1.30529200	0.73519300	2.12488200

Rh2(TCPTAD)4(Car3)(HFIP)3 [B3LYP-D3(BJ)]/BS1

Rh	1.04226200	0.32741900	0.05624500
Rh	3.15559600	0.33282200	-1.18581600
Cl	4.53054500	9.25705700	-1.92247300
Cl	10.31509500	0.57847000	3.38012400

Cl	4.92020100	-8.43324400	-1.96435400
Cl	1.33809100	0.38222700	-9.73427100
Cl	2.96234500	7.05596800	-0.29729300
Cl	7.32369200	-0.41446200	3.18107700
Cl	2.59485100	-6.39549200	-1.37912300
Cl	0.12566800	1.01146900	-6.89459600
Cl	4.62347000	9.13837900	-5.05309200
Cl	11.03768900	3.53638400	2.64091000
Cl	7.68943100	-8.12297600	-0.53468600
Cl	2.84915600	-2.31327500	-10.23965700
Cl	3.19374700	6.78413400	-6.59116200
Cl	8.76643600	5.56686400	1.81605300
Cl	8.17098200	-5.75598800	1.49299400
Cl	3.09452000	-4.44884300	-7.93979700
O	2.24248200	1.74627600	-2.43218900
O	3.72883700	1.92582900	0.00835300
O	3.86482000	-0.98295600	0.24104200
O	2.37305000	-1.25855500	-2.24437200
O	0.22363100	1.46341500	-1.45526900
O	1.69561700	2.00736700	0.99643700
O	1.98372700	-0.77840500	1.48496700
O	0.51281200	-1.40386300	-0.97834600
O	1.38433900	4.46164700	-1.10031700
O	4.60017800	1.00473400	2.60171200
O	2.38672800	-3.75295700	0.33388400
O	0.20329200	-0.45970400	-4.12211200
O	1.60076000	4.21856700	-5.67168400
O	5.61713200	5.37252900	1.62076800
O	6.41739900	-3.33612100	2.48199200
O	2.34688600	-4.44421600	-4.85068400
N	1.20828600	4.12361600	-3.38695500
N	4.77382800	3.26111200	2.08402300
N	4.24453800	-3.33497300	1.66184000
N	1.10400400	-2.59426200	-4.19578200
C	1.60720800	4.81735200	-2.24019400
C	5.26721200	2.00733600	2.44799800
C	3.49708500	-4.05386000	0.72506600
C	0.72058800	-1.37123800	-4.74022400
C	2.36417200	6.00692100	-2.73210100
C	6.74530600	2.17526200	2.58626100
C	4.36334700	-5.19939100	0.30818800
C	1.12314300	-1.41802400	-6.17805500
C	2.99910000	7.01378200	-2.02716400
C	7.72350900	1.24778000	2.90995500
C	4.12268000	-6.23227300	-0.58256800
C	0.94585400	-0.48616400	-7.18851000
C	3.70248700	7.99193100	-2.76288800
C	9.06406500	1.69093000	2.94992300
C	5.16948100	-7.14424300	-0.83899000
C	1.49299600	-0.77266300	-8.45818100
C	3.74755000	7.93575700	-4.16886500

C	9.38774200	3.02334700	2.62339700
C	6.41508000	-7.00184900	-0.19933600
C	2.17380400	-1.98489800	-8.68313000
C	3.10200200	6.89198300	-4.86617100
C	8.37552400	3.94397000	2.26748500
C	6.63857600	-5.94499800	0.71024000
C	2.31472600	-2.93626800	-7.64744000
C	2.42173000	5.93934000	-4.12661000
C	7.06233000	3.50064700	2.27510300
C	5.59932800	-5.06040800	0.94608200
C	1.79654300	-2.62218600	-6.40044200
C	1.71996900	4.69186000	-4.56108500
C	5.78741300	4.21728500	1.94417700
C	5.54403800	-3.83510200	1.80233900
C	1.82509400	-3.38207200	-5.10810100
C	0.39744800	2.90624000	-3.37995900
H	0.61751700	2.41400700	-4.33338700
C	3.37991200	3.53656300	1.73858500
H	3.42040600	4.41663500	1.08633900
C	3.79851000	-2.10970000	2.32673400
H	4.71977300	-1.58629100	2.59774900
C	0.87346100	-2.98520200	-2.80274000
H	1.64290800	-3.73596600	-2.59123100
C	0.97992600	1.97038300	-2.31524700
C	2.88664200	2.38764000	0.84751500
C	3.14159000	-1.21801300	1.26650100
C	1.25892400	-1.78014100	-1.92872300
C	-1.12977400	3.19563100	-3.34596200
C	2.48740600	3.89475700	2.96302700
C	3.00553500	-2.35865100	3.63824600
C	-0.51239000	-3.65456500	-2.58940200
C	-1.59627800	3.92011400	-2.06273200
H	-1.05998600	4.86786800	-1.95037200
H	-1.36484800	3.30938700	-1.18636400
C	2.18842400	2.68189700	3.87516700
H	3.12481200	2.25817300	4.25121400
H	1.68771300	1.89945900	3.30436100
C	1.63174800	-3.03912400	3.43254100
H	1.76743100	-4.01111200	2.94463700
H	1.00695300	-2.42833400	2.77949800
C	-1.70469400	-2.68810500	-2.77101300
H	-1.63548100	-1.85741500	-2.06787400
H	-1.68428400	-2.25590900	-3.77707100
C	-3.10981100	4.20129600	-2.13377900
H	-3.41754700	4.70719500	-1.21063500
C	1.30211900	3.10884400	5.05745100
H	1.09465800	2.22794700	5.67788700
C	0.93267200	-3.23596100	4.79218400
H	-0.04226400	-3.70875800	4.62172700
C	-3.03439000	-3.43933000	-2.56430400
H	-3.85922200	-2.72705800	-2.68212900

C	-3.41371700	5.10113200	-3.34415200
H	-4.48662600	5.32652300	-3.38625700
H	-2.88452400	6.05779600	-3.24718900
C	2.03694100	4.17212600	5.89205400
H	1.42521700	4.47096200	6.75255700
H	2.97283700	3.75705900	6.28746600
C	1.79488300	-4.13581800	5.69410200
H	1.29426300	-4.29818200	6.65703100
H	1.92776500	-5.12030800	5.22761000
C	-3.15674900	-4.56473600	-3.60663100
H	-4.11209100	-5.08999900	-3.48437100
H	-3.14449700	-4.14469900	-4.62059800
C	-2.97311600	4.38473500	-4.63302200
H	-3.17059900	5.02691600	-5.49974900
C	2.33405500	5.39625600	5.00714400
H	2.87585700	6.15105000	5.58984900
C	3.16364900	-3.46857600	5.91795600
H	3.79205800	-4.11339600	6.54426400
C	-1.98670200	-5.54892300	-3.43069200
H	-2.05592400	-6.34452100	-4.18221300
C	-1.46414500	4.10062300	-4.56043600
H	-1.12437900	3.62064700	-5.48580300
H	-0.92670200	5.05157300	-4.47674000
C	3.21002700	4.96969500	3.81495600
H	4.15864400	4.57066400	4.19172800
H	3.44999300	5.83892300	3.19164000
C	3.85974200	-3.26480900	4.56028600
H	4.01307600	-4.24101700	4.08533200
H	4.85000700	-2.81751700	4.70529000
C	-0.65972400	-4.79722200	-3.62864300
H	0.18535200	-5.49020400	-3.54225000
H	-0.63548100	-4.38426500	-4.64314000
C	-1.92552400	1.87530800	-3.50185800
H	-1.71869400	1.21375900	-2.65993000
H	-1.59807900	1.35307500	-4.40665200
C	1.15623700	4.51204100	2.46331800
H	1.37543700	5.38457600	1.83539600
H	0.62169600	3.79429800	1.84129500
C	2.80646500	-1.00258800	4.35966800
H	2.21755200	-0.33313400	3.73348600
H	3.78109300	-0.52540400	4.51118700
C	-0.56910700	-4.29889500	-1.18214700
H	0.26218700	-5.00142500	-1.07144800
H	-0.43224400	-3.54832700	-0.40461500
C	-3.43539800	2.16399300	-3.56925900
H	-3.96984800	1.21094600	-3.66366200
C	0.27685400	4.92691800	3.65504300
H	-0.66325000	5.34235200	3.27209800
C	2.10147900	-1.20732600	5.70948200
H	1.96200500	-0.22907600	6.18667400
C	-1.90683000	-5.03369900	-0.98057500

H	-1.92487100	-5.45767600	0.03058400
C	-3.73985700	3.05935800	-4.78149100
H	-4.81762100	3.25327400	-4.84983300
H	-3.44015800	2.55449000	-5.70875000
C	1.01082800	5.98768400	4.49245100
H	0.38689700	6.30559200	5.33732100
H	1.20765900	6.87816800	3.88178500
C	2.96442100	-2.10794300	6.60877800
H	3.93681800	-1.63338100	6.79276200
H	2.48177500	-2.24883000	7.58404700
C	-2.02802800	-6.16024400	-2.01988400
H	-2.96599800	-6.71059800	-1.87513300
H	-1.20723500	-6.87870600	-1.89740700
C	-3.87833200	2.87702200	-2.27942800
H	-4.95795000	3.07205200	-2.31001400
H	-3.69109300	2.23770000	-1.41316600
C	-0.02044200	3.69118800	4.52594100
H	-0.55528900	2.93571400	3.93738600
H	-0.67187700	3.97046800	5.36369300
C	0.73129900	-1.86856200	5.47252800
H	0.10751900	-1.22479600	4.84177000
H	0.20593400	-1.99917400	6.42718300
C	-3.07706400	-4.04793500	-1.15080700
H	-3.01871900	-3.25918100	-0.39644400
H	-4.02909700	-4.57351400	-1.00310500
C	4.85681500	0.22981500	-2.29170500
C	4.95163100	0.32327700	-3.69807800
C	6.08631400	-0.05523800	-1.52618100
C	6.21868800	0.33293700	-4.36322400
C	3.77846400	0.44471500	-4.50235200
O	6.40964100	-1.16349300	-1.14440600
O	6.78464700	1.07762500	-1.27389500
C	6.31001100	0.44082500	-5.73497900
H	7.13175700	0.26226100	-3.79002600
C	3.87081800	0.57079600	-5.87075100
H	2.81072700	0.44172100	-4.02879500
C	7.97430500	0.98641400	-0.48724300
C	5.12931500	0.54203000	-6.48205800
H	7.27361100	0.43610900	-6.22768900
H	2.98534300	0.69137900	-6.47398400
H	7.98602000	1.87391600	0.14038700
H	7.96840900	0.07657900	0.11283700
C	9.23320700	1.01179400	-1.36689700
Br	5.21591900	0.61775700	-8.36352900
Cl	9.35891200	-0.47181800	-2.37120900
Cl	9.20568900	2.44411800	-2.44203300
Cl	10.63587000	1.10673300	-0.25142700
C	5.59624600	4.04833400	-4.23315100
F	5.52596300	5.36781500	-4.49329100
F	4.56348700	3.45077100	-4.86429600
F	6.73698100	3.58057000	-4.77319200

C	5.53163900	3.73134600	-2.73152500
O	4.23112800	3.83252000	-2.23965400
H	5.96426000	2.73820600	-2.60253200
C	6.40390500	4.68969400	-1.91097500
H	3.73673800	3.00276200	-2.36329200
F	5.77111200	5.83656700	-1.63074700
F	6.74488700	4.10459900	-0.74125300
F	7.54527000	4.99531200	-2.55866600
H	7.00648800	-2.28074600	-2.64531100
O	7.02393300	-2.32613300	-3.61700300
C	6.47628000	-3.53145100	-4.06114800
C	5.46591500	-4.08450100	-3.05376200
H	7.23523900	-4.31501700	-4.19108200
C	5.86184300	-3.29036700	-5.44110500
F	4.42641000	-3.26221800	-2.83286000
F	6.11402700	-4.23600300	-1.87261100
F	4.98888000	-5.28045800	-3.42842100
F	4.76657700	-2.50022700	-5.39104900
F	6.75377900	-2.68998800	-6.24583300
F	5.50787200	-4.45998200	-5.99668500
H	-0.92984600	-1.64890100	0.08291700
O	-1.62543600	-1.59622500	0.76431500
C	-2.10098700	-0.28408000	0.84481900
C	-3.53692900	-0.24678400	0.30957900
H	-1.52453400	0.42155900	0.23535000
C	-1.99291500	0.19264100	2.29945000
F	-4.30167100	-1.20924800	0.84560500
F	-3.51672200	-0.43287600	-1.02973300
F	-4.12980100	0.94036300	0.55028700
F	-2.82725100	-0.47549700	3.11376500
F	-0.73725300	0.00439700	2.75399700
F	-2.26790300	1.50908600	2.40242600

Rh2(TCPTAD)4(Car3)-distorted ligand single point calculation [B3LYP-D3(BJ)]/BS1

Rh	1.12542300	-0.04732800	-0.10223400
Rh	3.25758500	0.24335300	-1.28656100
Cl	3.19873000	9.64010600	-1.30756600
Cl	10.61569700	3.01840800	3.10475400
Cl	-0.31741300	-9.32519900	0.56427500
Cl	2.10681500	1.20953100	-9.96707700
Cl	1.87214400	7.15681300	0.11600900
Cl	8.04451300	1.21452400	3.41345400
Cl	-0.89416700	-6.28730400	1.18404600
Cl	0.78506400	1.61348500	-7.12949900
Cl	3.41727000	9.72813600	-4.43250200
Cl	10.41332600	5.82116500	1.72317200
Cl	2.63415600	-10.36221900	0.37916000
Cl	3.65482400	-1.43321600	-10.61825500
Cl	2.32730400	7.32846600	-6.16522500
Cl	7.61991500	6.92126800	0.75964100
Cl	5.04497800	-8.36947800	0.79698800

Cl	3.84122400	-3.73512000	-8.47038900
O	2.26450300	1.71725600	-2.41981900
O	3.71778600	1.74079700	0.06419900
O	3.93607800	-1.33373100	-0.04229400
O	2.61518100	-1.21425900	-2.59850800
O	0.28576000	1.21769000	-1.46118300
O	1.69512900	1.56503400	1.05809200
O	2.05569300	-1.32583000	1.19480500
O	0.72222600	-1.60221800	-1.41862700
O	1.05821600	4.27130200	-0.88649000
O	5.02255500	1.61262600	2.73065000
O	0.88563500	-3.79840000	1.56322500
O	0.64906900	-0.13145400	-4.53158000
O	1.10289000	4.50104200	-5.46580400
O	4.68081400	5.74603200	0.77190500
O	5.23984100	-5.28295000	1.40167300
O	2.70423500	-4.09808200	-5.53923700
N	0.88369300	4.10304200	-3.18820800
N	4.50143500	3.64936300	1.75390200
N	3.19112100	-4.18037200	1.50962800
N	1.47820900	-2.28142600	-4.77262000
C	1.17951900	4.76027200	-1.99299400
C	5.35517900	2.70111700	2.31406200
C	1.84463600	-4.53791600	1.44430400
C	1.16686000	-0.99778200	-5.20966200
C	1.69759400	6.10416000	-2.38318400
C	6.72162700	3.30541800	2.28137400
C	1.81231700	-6.00889600	1.19153700
C	1.64585200	-0.91642900	-6.62188700
C	2.09195500	7.17461600	-1.59819200
C	7.93451000	2.79614200	2.71829000
C	0.73054700	-6.86298900	1.04086200
C	1.55489300	0.11793400	-7.54019800
C	2.64135400	8.30038400	-2.24964100
C	9.08336300	3.60012200	2.55528300
C	0.99903100	-8.22449700	0.78145800
C	2.17698000	-0.05913200	-8.79612600
C	2.73543700	8.34084400	-3.65391900
C	8.98900700	4.86674900	1.94393900
C	2.32644300	-8.69053000	0.69972700
C	2.87729500	-1.24698500	-9.08674800
C	2.26733800	7.26306000	-4.43682400
C	7.74166600	5.36451100	1.50289300
C	3.41181100	-7.80539300	0.88043400
C	2.96115100	-2.28541900	-8.13202500
C	1.76594500	6.15222600	-3.77804100
C	6.62307500	4.56564300	1.68685500
C	3.12542300	-6.47122200	1.12139700
C	2.32830500	-2.10027400	-6.91314600
C	1.23314400	4.86142300	-4.31540000
C	5.18605500	4.79268500	1.32181000

C	4.03302900	-5.30836700	1.34714600
C	2.23956600	-2.99269500	-5.71208800
C	0.27457300	2.77750300	-3.27903400
H	0.54717600	2.40380900	-4.27052400
C	3.06241200	3.47070400	1.57144200
H	2.78668100	4.21582400	0.81551100
C	3.78590700	-2.86764100	1.81614500
H	4.82869300	-2.98399300	1.52970200
C	1.10886600	-2.82469700	-3.46533600
H	1.79594000	-3.66325300	-3.31160500
C	0.98466400	1.83790000	-2.29079700
C	2.80436400	2.13146700	0.86674000
C	3.19768400	-1.76404600	0.91839200
C	1.49095200	-1.78408300	-2.39905300
C	-1.28271100	2.81158700	-3.19877500
C	2.22085200	3.78577300	2.84487600
C	3.78164500	-2.51332900	3.33096000
C	-0.33764000	-3.39777200	-3.44230000
C	-1.82940600	3.26474100	-1.82359300
H	-1.47729300	4.27779500	-1.60081200
H	-1.45682600	2.61099400	-1.03466600
C	2.28378900	2.67956800	3.92242900
H	3.31905800	2.51439000	4.23393800
H	1.91788200	1.73868200	3.50571000
C	2.39288100	-2.58429000	3.99672300
H	1.99639000	-3.60283400	3.92626400
H	1.69695600	-1.92202000	3.48510400
C	-1.43360800	-2.31240800	-3.54066500
H	-1.35037800	-1.62529600	-2.69588600
H	-1.30196100	-1.72294900	-4.45253600
C	-3.36934900	3.25344000	-1.83386600
H	-3.72955800	3.55774800	-0.84365000
C	1.43544700	3.07987400	5.14480600
H	1.49162100	2.27616000	5.88916800
C	2.49705000	-2.19279300	5.48225300
H	1.49591500	-2.24314700	5.92726100
C	-2.82855300	-2.96439400	-3.55313500
H	-3.58506800	-2.17259800	-3.62076000
C	-3.88204700	4.23916900	-2.89768400
H	-4.97911700	4.25710700	-2.90297100
H	-3.54193700	5.25559200	-2.66218800
C	1.98417300	4.38542500	5.74714600
H	1.40296400	4.66637700	6.63446800
H	3.02341200	4.24422600	6.07087800
C	3.44171800	-3.16839500	6.20527400
H	3.50961100	-2.91122900	7.26983800
H	3.04615300	-4.19045600	6.14328300
C	-2.95390700	-3.90647500	-4.76173600
H	-3.95523600	-4.35408300	-4.78911700
H	-2.82394600	-3.34430900	-5.69547300
C	-3.35676500	3.81148100	-4.27912100

H	-3.69654900	4.52273200	-5.04157200
C	1.90928700	5.50398000	4.69154700
H	2.31458200	6.43389000	5.10874100
C	4.83594100	-3.10284400	5.55550200
H	5.51133000	-3.80683800	6.05679200
C	-1.88469600	-5.00958000	-4.65932900
H	-1.95635600	-5.67745500	-5.52620700
C	-1.81589400	3.80200600	-4.26588700
H	-1.43211500	3.52700900	-5.25493700
H	-1.45555800	4.81444900	-4.05052400
C	2.74930100	5.10324700	3.46738700
H	3.79274800	4.97688900	3.77739900
H	2.73043100	5.90221900	2.71741500
C	4.72875300	-3.49044600	4.06878800
H	4.34558900	-4.51481400	3.98758200
H	5.71606800	-3.47724000	3.59690600
C	-0.49113500	-4.35943400	-4.64905100
H	0.28817900	-5.12971400	-4.60857500
H	-0.35249400	-3.80783300	-5.58538900
C	-1.83714100	1.40850300	-3.55074500
H	-1.47079800	0.66936300	-2.83896700
H	-1.46508300	1.11239400	-4.53670500
C	0.73994200	4.01251900	2.44111800
H	0.68831300	4.79350300	1.67477100
H	0.33508600	3.10090200	2.00103900
C	4.34060500	-1.08422200	3.47748300
H	3.68827600	-0.37092100	2.97028000
H	5.32371600	-1.01956200	3.00042000
C	-0.55653700	-4.22210700	-2.14824300
H	0.21337400	-5.00307900	-2.07743100
H	-0.45502200	-3.58212800	-1.27141100
C	-3.37319100	1.41536900	-3.54734900
H	-3.72931900	0.40390700	-3.77978200
C	-0.09864700	4.41202400	3.66701000
H	-1.13902100	4.55579200	3.35006000
C	4.44522000	-0.69514900	4.96009300
H	4.83767700	0.32504300	5.02203900
C	-1.95666500	-4.86506100	-2.15958700
H	-2.09049700	-5.42593800	-1.22952500
C	-3.88377000	2.40399000	-4.60841500
H	-4.98084100	2.40967700	-4.62924700
H	-3.54126800	2.09473400	-5.60409300
C	0.44671500	5.71831500	4.26631400
H	-0.15655400	6.02211900	5.13114500
H	0.38567400	6.52652500	3.52608600
C	5.39219500	-1.67228900	5.67741900
H	6.39382700	-1.61854600	5.23151500
H	5.49189100	-1.39756600	6.73518300
C	-2.08571900	-5.81259200	-3.36281400
H	-3.07316400	-6.29094500	-3.36397000
H	-1.33717000	-6.61244600	-3.29503000

C	-3.87663600	1.83484500	-2.15528800
H	-4.97328400	1.81268600	-2.12659100
H	-3.51686200	1.12543700	-1.39859300
C	-0.02888900	3.29193800	4.72094300
H	-0.43823900	2.36317000	4.31148000
H	-0.63660500	3.55875300	5.59502400
C	3.04706900	-0.76059300	5.60063000
H	2.37097300	-0.05868600	5.09923500
H	3.10040400	-0.46392300	6.65596200
C	-3.03061400	-3.76580700	-2.25715700
H	-2.96735600	-3.09996700	-1.39311500
H	-4.02962100	-4.22018800	-2.24754700
C	5.03479400	0.44725600	-2.24821800
C	5.27064500	0.46465700	-3.64183900
C	6.21933700	0.52478400	-1.35945100
C	6.59195800	0.36328300	-4.17872700
C	4.18755200	0.61272800	-4.55360800
O	6.58879800	-0.35560200	-0.61953100
O	6.81662700	1.74534700	-1.47352700
C	6.82178900	0.39593400	-5.53732100
H	7.43353600	0.23149900	-3.51487400
C	4.42506900	0.70303400	-5.91016900
H	3.18298900	0.71385000	-4.16953000
C	7.96677600	2.00864600	-0.67110900
C	5.72879700	0.57374000	-6.39733400
H	7.82434800	0.29814000	-5.93389100
H	3.61886500	0.88886900	-6.59933800
H	7.82952400	2.99871400	-0.24390400
H	8.07817000	1.24960600	0.10240000
C	9.23618300	2.03697700	-1.53420500
Br	6.00661800	0.64352900	-8.26166400
Cl	9.61829200	0.40753200	-2.18154200
Cl	9.03839300	3.18478800	-2.89696600
Cl	10.57509900	2.57732200	-0.46602100

References:

1. Frisch, M. J.; Trucks, G. W.; Schlegel, H. B.; Scuseria, G. E.; Robb, M. A.; Cheeseman, J. R.; Scalmani, G.; Barone, V.; Petersson, G. A.; Nakatsuji, H.; Li, X.; Caricato, M.; Marenich, A. V.; Bloino, J.; Janesko, B. G.; Gomperts, R.; Mennucci, B.; Hratchian, H. P.; Ortiz, J. V.; Izmaylov, A. F.; Sonnenberg, J. L.; Williams-Young, D.; Ding, F.; Lipparini, F.; Egidi, F.; Goings, J.; Peng, B.; Petrone, A.; Henderson, T.; Ranasinghe, D.; Zakrzewski, V. G.; Gao, J.; Rega, N.; Zheng, G.; Liang, W.; Hada, M.; Ehara, M.; Toyota, K.; Fukuda, R.; Hasegawa, J.; Ishida, M.; Nakajima, T.; Honda, Y.; Kitao, O.; Nakai, H.; Vreven, T.; Throssell, K.; Montgomery, J. A., Jr.; Peralta, J. E.; Ogliaro, F.; Bearpark, M. J.; Heyd, J. J.; Brothers, E. N.; Kudin, K. N.; Staroverov, V. N.; Keith, T. A.; Kobayashi, R.; Normand, J.; Raghavachari, K.; Rendell, A. P.; Burant, J. C.; Iyengar, S. S.; Tomasi, J.; Cossi, M.; Millam, J. M.; Klene, M.; Adamo, C.; Cammi, R.; Ochterski, J. W.; Martin, R. L.; Morokuma, K.; Farkas, O.; Foresman, J. B.; Fox, D. J., *Gaussian 16, Revision C.01*, **Gaussian**, Inc., Wallingford CT, 2019.

2. (a) Hay, P. J.; Wadt, W. R., Ab initio effective core potentials for molecular calculations. Potentials for K to Au including the outermost core orbitals. *J. Chem. Phys.* **1985,** *82*, 299-310; (b) Wadt, W. R.; Hay, P. J., Ab initio effective core potentials for molecular calculations. Potentials for main group elements Na to Bi. *J. Chem. Phys.* **1985,** *82*, 284-298.

3. (a) Becke, A. D., Density-functional exchange-energy approximation with correct asymptotic behavior. *Phys. Rev. A* **1988,** *38*, 3098-3100; (b) Lee, C.; Yang, W.; Parr, R. G., Development of the Colle-Salvetti correlation-energy formula into a functional of the electron density. *Phys. Rev. B* **1988,** *37*, 785-789; (c) Becke, A. D., A new mixing of Hartree–Fock and local density-functional theories. *J. Chem. Phys.* **1993,** *98*, 1372-1377.

4. (a) Grimme, S.; Antony, J.; Ehrlich, S.; Krieg, H., A consistent and accurate ab initio parametrization of density functional dispersion correction (DFT-D) for the 94 elements H-Pu. *J. Chem. Phys.* **2010,** *132*, 154104; (b) Grimme, S.; Hansen, A.; Brandenburg, J. G.; Bannwarth, C., Dispersion-corrected mean-field electronic structure methods. *Chem. Rev.* **2016**, *116*, 5105-5154

5. Becke, A. D; Johnson, E. R., Exchange-hole dipole moment and the dispersion interaction. *J. Chem. Phys.* **2005,** *122*, 154104.

6. Cancès, E.; Mennucci, B.; Tomasi, J., A new integral equation formalism for the polarizable continuum model: Theoretical background and applications to isotropic and anisotropic dielectrics. *J. Chem. Phys.* **1997,** *107*, 3032-3041.

7. Zhao, Y.; Truhlar, D. G. A new local density functional for main-group thermochemistry, transition metal bonding, thermochemical kinetics, and noncovalent interactions. *J. Chem. Phys.* **2006,** *125*, 194101.

8. Chai, J.-D.; Head-Gordon, M. Long-range Corrected Hybrid Density Functionals with Damped Atom-Atom Dispersion Corrections. *Phys. Chem. Chem. Phys.* **2008**, *10*, 6615-6620;

9. Küchle, W.; Dolg, M.; Stoll, H.; Preuss, H. Energy-adjusted pseudopotentials for the actinides. Parameter sets and test calculations for thorium and thorium monoxide. *J. Chem. Phys.* **1994**, *100*, 7535-7542.

10. Pritchard, B. P.; Altarawy, D.; Didier, B.; Gibson, T. D.; Windus, T. L. A New Basis Set Exchange: An Open, Up-to-date Resource for the Molecular Sciences Community. *J. Chem. Inf. Model.* **2019**, *59,* 4814-4820

Appendix E: Chapter 5 Supporting information.

CAUTION: Diazo compounds are high energy compounds and need to be treated with respect. Even though we experienced no energetic decomposition in this work, care should be taken in handling large quantities of diazo compounds. Large scale reactions should be conducted behind a blast shield. For a more complete analysis of the risks associated with diazo compounds see the recent review by Bull *et. al.*[1]

1. General Considerations

All experiments were carried out in oven-dried glassware under argon atmosphere unless otherwise stated. Flash column chromatography was performed on silica gel. Unless otherwise noted, all other reagents were obtained from commercial sources (Sigma Aldrich, Fisher, TCI Chemicals, AK Scientific, Combi Blocks, Oakwood Chemicals, Ambeed) and used as received without purification. ^{1}H, ^{13}C, and ^{19}F NMR spectra were recorded at either 400 MHz (^{13}C at 100 MHz) on Bruker 400 spectrometer or 600 MHz (^{13}C at 151 MHz) on INOVA 600 or Bruker 600 spectrometer. NMR spectra were run in solutions of deuterated chloroform ($CDCl_3$) with residual chloroform taken as an internal standard (7.26 ppm for ^{1}H, and 77.16 ppm for ^{13}C), and were reported in parts per million (ppm). The abbreviations for multiplicity are as follows: s = singlet, d = doublet, t = triplet, q = quartet, p = pentet, m = multiplet, dd = doublet of doublet, etc. Coupling constants (J values) are obtained from the spectra. Thin layer chromatography was performed on aluminum-back silica gel plates with UV light and cerium aluminum molybdate (CAM) or permanganate ($KMnO_4$) stain to visualize. Mass spectra were taken on a Thermo Finnigan LTQ-FTMS spectrometer with APCI, ESI or NSI. IR spectra were collected on a Nicolet iS10 FT-IR spectrometer from Thermo Scientific and reported in unit of cm^{-1}. Enantiomeric excess (% ee) data were obtained on a Varian Prostar chiral HPLC instrument, an Agilent 1100 HPLC, or a Waters SFC, eluting the purified products using a mixed solution of HPLC-grade 2-propanol (*i*-PrOH) and *n*-hexane for HPLC, and a mixed solution of supercritical CO2 and acetonitrile+0.2% formic acid (MeCN+0.2%FA).

2. Preparation of starting materials

General Method A: Synthesis of disubstituted α, β, and γ allyl diazoacetates:

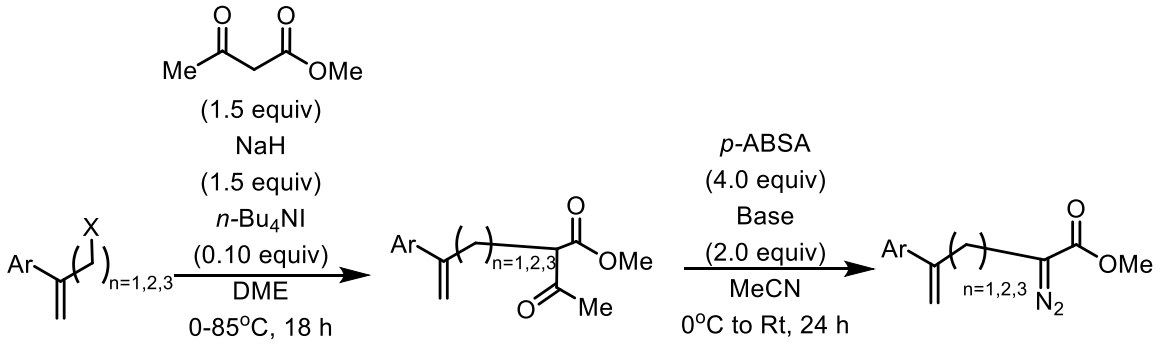

A-1: Synthesis of acetoacetate precursor compounds:

Under an argon atmosphere, a solution of methyl 3-oxobutanoate (1.5 equiv.) in anhydrous dimethoxyethane (DME) was added dropwise to a stirred suspension of NaH (60% suspension on mineral oil, 1.5 equiv.) in anhydrous DME at 0 °C in 1 hour. Then, *n*-Bu_4NI (0.1 equiv.) was added in one portion, followed by dropwise addition of (3-bromoprop-1-en-2-yl)arene, (3-bromobut-1-en-2-yl)arene, or (3-chloropent-1-en-2-yl)arene (1.0 equiv.) in anhydrous DME at 0 °C over 1 hour via addition funnel. The resulting mixture was then heated to 85 °C and stirred overnight. After reaction completion, the mixture was cooled to 0 °C, diluted slowly with 1 N HCl, and extracted with diethyl ether (Et_2O). The combined organic extracts were washed by brine, dried over anhydrous Na_2SO_4 and concentrated in vacuo. After a short flash chromatographic purification (0-10% Et_2O /hexanes), aggregation of product containing fractions and removal of solvent *in vacuo,* the resulting crude product was used directly without full characterization or further purification in the next step.

A-2: Synthesis of diazo compounds:

Under an argon atmosphere, in a flame-dried RBF, crude methyl 2-acetyl-4-arylpent-4-enoate, methyl 2-acetyl-5-arylhex-5-enoate, or methyl 2-acetyl-6-aryllhept-6-enoate (1.0 equiv.) and *p*-acetamidobenzenesulfonyl azide (*p*-ABSA) (2.0 equiv.) was dissolved in MeCN, and the reaction mixture was cooled to 0 °C. DBU (4.0 equiv.) was added dropwise at 0 °C. The reaction mixture was then warmed to room temperature and stirred overnight to afford a dark red solution. The crude reaction mixture was then extracted with Et_2O, washed by brine, dried over anhydrous Na_2SO_4, and concentrated in vacuo. Sample was chromatographed 0-3% Et_2O /hexanes and product containing fractions were aggregated. Solvent was removed *in vacuo* to afford the desired product as a highly colored oil. The products are stable if stored at -20°C for at least 4 months.

General Method B: General method for the synthesis of trisubstituted allyl-diazoacetates:

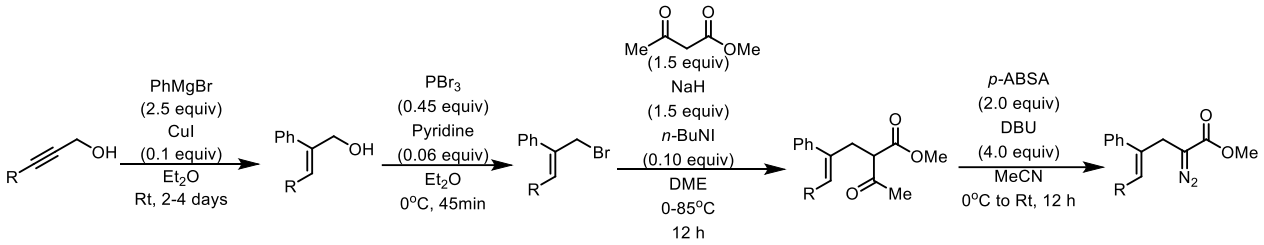

B-1: Copper-mediated addition of phenylmagnesium bromide to propargyl alcohols:

PhMgBr solution (3.0 M in Et_2O) was added dropwise to a suspension of Cu(I)I (10 mol%) and propargyl alcohol in dry Et_2O (125 ml) at 0°C in a flame dried RBF. The reaction mixture was then warmed to room temperature and stirred for 2-4 days. The resultant mixture was then cooled to 0°C, the reaction mixture was carefully quenched by dropwise addition of saturated aqueous NH_4Cl to yield a blueish-gray suspension. The reaction mixture was brought to room temperature and extracted with Et_2O, washed with brine, dried over Na_2SO_4 and concentrated *in vacuo.* The obtained compound was purified by column chromatography (0-30% Et_2O/hexanes) to give the desired product. Spectra of the purified products obtained via this method, (*E*)-2-phenylbut-2-en-1-ol (3.41g, 23 mmol, 65% yield), (*E*)-2-phenylhex-2-en-1-ol (2.46g, 27 mmol, 28% yield), and (*E*)-2,3-diphenylprop-2-en-1-ol (7.53g, 35.8 mmol, 95% yield), matched those reported in the literature.[2, 3]

B-2: Bromination of trisubstituted allyl-alcohols:

In a flame-dried RBF under an inert argon atmosphere, alkene (1 equiv.) was dissolved in dry Et_2O. To this solution was added pyridine (0.06 equiv.) and the reaction mixture was cooled to 0°C. Then PBr_3 (0.45 equiv.) was added dropwise. The reaction was warmed to room temperature with additional stirring for 45min or until disappearance of starting material by TLC. After completion of reaction, the mixture was quenched by addition of ice cubes to yield a cloudy suspension. The

aqueous and organic layers were separated, and the organic layer was dried over Na_2SO_4. Solvent was removed *in vacuo* and crude product was purified via silica plug (10% Et_2O /hexanes as eluent). After removal of solvent *in vacuo* the product was obtained, usually as a yellow oil. Spectra of the purified products obtained via this method, (*E*)-(1-bromobut-2-en-2-yl)benzene (4.1 g, 19 mmol, 84% yield), (*E*)-(1-bromohex-2-en-2-yl)benzene (920mg, 3.85 mmol, 68% yield), and (*E*)-(3-bromoprop-1-ene-1,2-diyl)dibenzene (3.52g, 12.9 mmol, 54% yield) matched those reported in the literature.[2, 3]

B-3: Synthesis of trisubstituted α-allyl-acetoacetates:

Under an argon atmosphere, a solution of methyl 3-oxobutanoate (1.5 equiv.) in anhydrous dimethoxyethane (DME) was added dropwise to a stirred suspension of NaH (60% suspension on mineral oil, 1.5 equiv.) in anhydrous DME at 0 °C in 1 hour. Then, *n*-Bu_4NI (0.1 equiv.) was added in one portion, followed by dropwise addition of trisubstituted allyl-bromide (1.0 equiv.) in anhydrous DME at 0 °C over 1 hour via addition funnel. The resulting mixture was then heated to 85 °C and stirred overnight. After reaction completion, the mixture was cooled to 0 °C, diluted slowly with 1 N HCl, and extracted with ethyl acetate (EtOAc). The combined organic extracts were washed by brine, dried over anhydrous Na_2SO_4 and concentrated in vacuo. After a short flash chromatographic purification (0-10% EtOAc /hexanes), aggregation of product containing fractions and removal of solvent *in vacuo,* the resulting crude (*Z)*-trisubstituted α-allyl-acetoacetate was used directly without full characterization or further purification in the next step. Nomenclature dictates the reassignment of the alkene geometry as "*Z*" after this synthetic step but the stereochemistry of the alkene is preserved throughout the synthesis.

Methyl (*Z*)-2-acetyl-4-phenylhex-4-enoate (86% yield, 4.1041 g, 16.66 mmol) 1H NMR: δ 7.41 – 7.31 (m, 2H), 7.29 – 7.19 (m, 2H), 7.15 – 7.06 (m, 2H), 5.62 (qt, *J* = 6.8, 1.2 Hz, 1H), 3.65 (d, *J* = 1.4 Hz, 3H), 3.42 (t, *J* = 7.5 Hz, 1H), 2.91 (d, *J* = 7.4 Hz, 2H), 2.12 (s, 2H), 1.53 (dd, *J* = 6.9, 1.2 Hz, 3H).

Methyl (*Z*)-2-acetyl-4-phenyloct-4-enoate (61% yield, 646mg, 2.35mmol) 1H NMR: δ 7.32 (t, *J* = 7.5 Hz, 2H), 7.24 (s, 1H), 7.11 (d, *J* = 7.5 Hz, 2H), 5.51 (t, *J* = 7.4 Hz, 1H), 3.82 – 3.57 (m, 3H), 3.43 (t, *J* = 7.5 Hz, 1H), 2.89 (dd, *J* = 7.7, 2.9 Hz, 3H), 2.12 (s, 3H), 1.99 – 1.77 (m, 3H), 1.30 (p, *J* = 7.3 Hz, 3H), 0.80 (t, *J* = 7.5 Hz, 3H).

Methyl (*Z*)-2-acetyl-4,5-diphenylpent-4-enoate (93% yield, 3.68g, 11.9mmol) 1H NMR: δ 7.59 – 7.37 (m, 3H), 7.38 – 7.22 (m, 4H), 7.21 – 7.14 (m, 2H), 7.10 (tt, *J* = 3.3, 1.3 Hz, 3H), 6.97 – 6.87 (m, 2H), 6.54 (d, *J* = 1.1 Hz, 1H), 3.73 (s, 3H), 3.37 (ddd, *J* = 5.5, 4.2, 2.2 Hz, 1H), 3.11 (dd, *J* = 7.5, 1.2 Hz, 2H), 2.20 (s, 3H).

B-4: Synthesis of diazo compounds:

Under an argon atmosphere, in a flame-dried RBF, *Z*-alkene (1.0 equiv.) and *p*-acetamidobenzenesulfonyl azide (*p*-ABSA) (2.0 equiv.) was dissolved in MeCN, and the reaction mixture was cooled to 0 °C. DBU (4.0 equiv.) was added dropwise at 0 °C. The reaction mixture was then warmed to room temperature and stirred overnight to afford a dark red solution. The crude reaction mixture was then extracted with EtOAc, washed by brine, dried over anhydrous Na_2SO_4, and concentrated in vacuo. Sample was chromatographed (0-3% or 10% diethyl ether /hexanes for alkyl or aryl products respectively) and product containing fractions were aggregated. Solvent was removed *in vacuo* to afford the diazo as a bright yellow-orange oil. The products are indefinitely stable if refrigerated except for methyl (Z)-2-diazo-4-phenyloct-4-enoate which decomposed after 4 months at 0°C.

3. One-pot synthesis of difluorinated carbocycles and other products

General Method C: One-pot synthesis of difluorobicylco[1.1.1]pentanes:

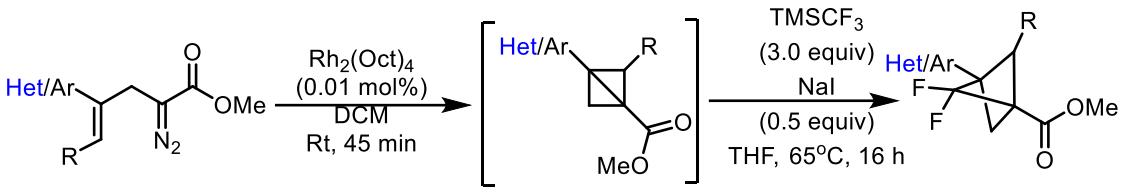

To a 16 mL flame-dried vial, kept under a dry atmosphere of argon, was added dry DCM (1.0 mL) and $Rh_2(Oct)_4$ (16 uL, c = 1.00 mg/ mL in DCM, 0.0001 equiv.). Diazo compound (0.2 mmol, 1.0 equiv.), dissolved in dry DCM (1 mL), was then added to the former solution drop-wise over 30 mins at room temperature via syringe pump. The mixture was allowed to stir for another 15 min after the addition; when the diazo compound was fully consumed by IR analysis (disappearance of diazo ($C=N_2$) stretch at ~2100 cm^{-1}), the reaction mixture was concentrated in vacuo and analyzed by ^1H NMR in $CDCl_3$ over K_2CO_3 to confirm the presence of bicyclo[1.1.0]butane product. Once bicyclo[1.1.0]butane presence was confirmed the solution was evaporated to dryness *in vacuo*. The mixture was then dissolved in THF (2 mL). $TMSCF_3$ (3 equiv) and NaI (0.5 equiv) were added to the solution. The resulting mixture was stirred at 65 °C overnight. After completion, the reaction mixture was concentrated under reduced pressure, then the residue was dissolved in EtOAc, washed with DI water and brine, and dried over anhydrous Na_2SO_4. The solvent was removed *in vacuo* and the crude product was purified by column chromatography (gradient, 0-10% Et_2O /hexanes) and product containing fractions were aggregated. The solvent was removed *in vacuo* to afford the desired product in up to 65% yield.

General Method D: One-pot synthesis of chiral methylene difluorocyclobutenes:

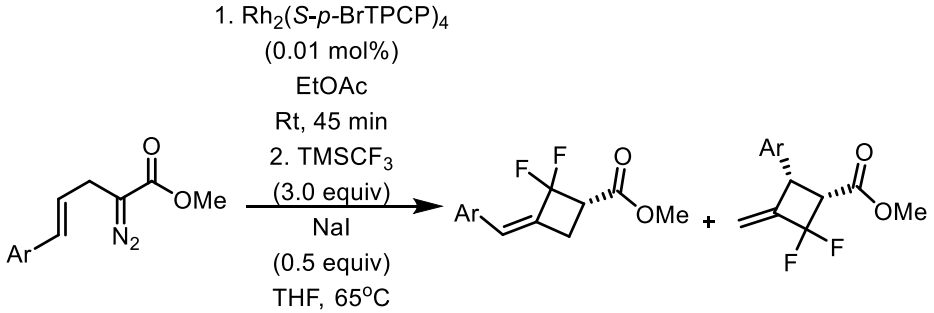

To a 16 mL flame-dried vial, kept under a dry atmosphere of argon, was added dry EtOAc (1.0 mL) and Rh_2(*S*-*p*-BrTPCP)$_4$ (16 uL, c = 1.00 mg/ mL in EtOAc, 0.0001 equiv.). Diazo compound (0.2 mmol, 1.0 equiv.), dissolved in dry EtOAc(1 mL), was then added to the former solution drop-wise over 30 mins at room temperature via syringe pump. The mixture was allowed to stir for another 15 min after the addition; when the diazo compound was fully consumed by IR analysis (disappearance of diazo ($C=N_2$) stretch at ~2100 cm^{-1}), the reaction mixture was concentrated in vacuo and analyzed by ^1H NMR in $CDCl_3$ over K_2CO_3 to confirm the presence of bicyclo[1.1.0]butane product. Once bicyclo[1.1.0]butane presence was confirmed as the spectra matched those reported in the literature, the solution was evaporated to dryness *in vacuo*. The mixture was then dissolved in THF (2 mL). $TMSCF_3$ (3 equiv) and NaI (0.5 equiv) were added to the solution. The resulting mixture was stirred at 65 °C overnight. After completion, the reaction mixture was concentrated under reduced pressure, then the residue was dissolved in diethyl ether, washed with DI water and brine, and dried over anhydrous Na_2SO_4. The solvent was removed *in vacuo* and the crude product was purified by column chromatography (gradient, 0-2% Et_2O /hexanes) and product containing fractions were aggregated. The solvent was removed *in vacuo* to afford the desired products in up to 74% yield as a mixture of methylene difluorocyclobutenes. The products appear as a single peak, to separate them one must collect low volume fractions (3-5ml) and NMR each vial individually. Additionally, the products are unstable upon isolation within a matter of hours and lose difluoromethane to generate a diene. As such, though confident characterization of a scope of these products was obtained by analysis of the material by NMR, the presence of this diene impurity prevents high confidence in the full data suite, especially the assigned enantiomeric excess and FTIR data obtained for products prepared according to this general method. As a result, these compounds should be regarded as unstable intermediates rather than isolable reaction products.

4. Known compounds:

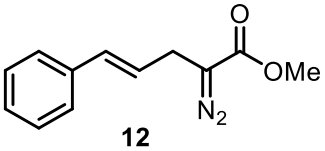

12

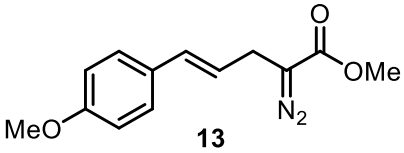

13

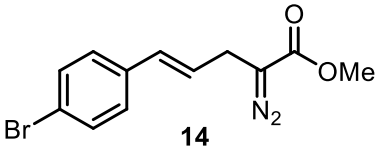

14

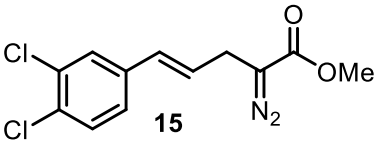

15

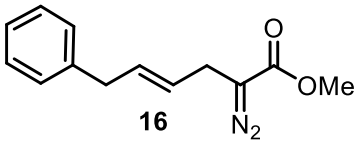

16

Compounds **12-16** were synthesized according to known methods and spectra matched the literature reported spectra.[4]

5. Characterization of novel precursor compounds:

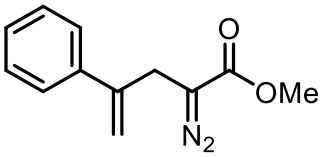

Methyl 2-diazo-4-phenylpent-4-enoate: Product is obtained from methyl 2-acetyl-4-phenylpent-4-enoate (5.23 g, 22.5 mmol) via method **A-2** and is obtained as a bright yellow liquid in 67% yield (3.28 g, 15.2 mmol).
1H NMR: (600 MHz, $CDCl_3$) δ 7.46 (d, *J* = 6.8 Hz, 2H), 7.39 – 7.35 (m, 2H), 7.34 – 7.30 (m, 1H), 5.51 (s, 1H), 5.21 (d, *J* = 1.1 Hz, 1H), 3.78 (s, 3H), 3.55 (d, *J* = 1.3 Hz, 2H).
^{13}C NMR (151 MHz, $CDCl_3$) δ 142.91, 139.12, 128.57, 128.54, 128.09, 126.06, 126.04, 114.85, 51.97, 29.14.
FTIR(neat): 3015, 2970, 2950, 2079, 1738, 1683, 1435, 1365, 1348, 1228, 1216, 1203, 1114, 904, 779, 732, 699, 579, 528cm^{-1}
HRMS: (+pAPCI, M+1H) Expected: 217.09715 Found: 217.09742

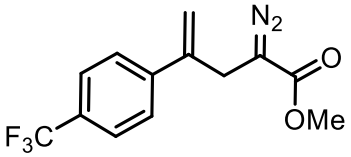

Methyl 2-diazo-4-(4-(trifluoromethyl)phenyl)pent-4-enoate: Product is obtained from methyl 2-acetyl-4-(4-trifluoromethylphenyl)pent-4-enoate (215mg, 716µmol) via method **A-2** and is obtained as a bright yellow liquid in 39% yield (80mg, 0.28mmol).
^{1}H NMR (600 MHz, CDCl3) δ 7.62 (d, J = 8.3 Hz, 2H), 7.56 (d, J = 8.1 Hz, 2H), 5.57 (s, 1H), 5.31 (s, 1H), 3.78 (s, 3H), 3.56 (s, 2H).
^{13}C NMR (151 MHz, CDCl3) δ 167.20, 142.61, 141.97, 130.39, 130.17, 129.96, 129.74, 126.79, 126.39, 126.11, 125.55, 125.52, 125.50, 125.47, 125.43, 124.98, 123.18, 121.38, 116.86, 52.09, 29.12.
^{19}F NMR (565 MHz, CDCl3) δ -62.62.
FTIR(neat): 2955, 2082, 1666, 1616, 1574, 1437, 1405, 1344, 1322, 1164, 1113, 1164, 1113, 1065, 1014, 976, 915, 847, 813, 751, 733, 721, 604, 536cm^{-1}
HRMS: (+pAPCI, M+1H) Expected: 285.08454 Found: 285.08496

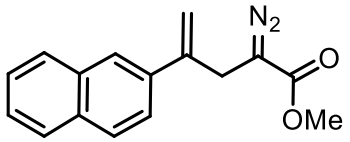

Methyl 2-diazo-4-(naphthalen-2-yl)pent-4-enoate: Product is obtained from methyl 2-acetyl-4-(naphthalen-2-yl)pent-4-enoate (631mg, 2.23mmol) via method **A-2** and is obtained as a bright yellow liquid in 62% yield (370mg, 1.39mmol).
^{1}H NMR (600 MHz, CDCl3) δ 7.90 (d, J = 1.9 Hz, 1H), 7.87 – 7.74 (m, 3H), 7.63 (dd, J = 8.6, 1.9 Hz, 1H), 7.54 – 7.36 (m, 2H), 5.66 (s, 1H), 5.31 (s, 1H), 3.79 (s, 3H), 3.68 (s, 2H).
^{13}C NMR (151 MHz, CDCl3) δ 167.44, 142.72, 136.23, 133.34, 133.07, 128.36, 128.14, 127.56, 126.32, 126.22, 125.02, 124.18, 115.40, 52.01, 29.21.
FTIR(neat): 3056, 2950, 2077, 1682, 1624, 1595, 1505, 1434, 1137, 1034, 1177, 1132, 1108, 1017, 975, 951, 893, 858, 818, 770, 747, 731, 669, 636, 572, 530, 473cm^{-1}
HRMS: (+pAPCI, M+1H) Expected: 267.1128 Found: 267.11163

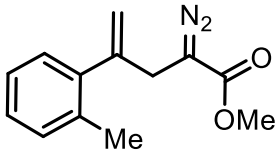

Methyl 2-diazo-4-(*o*-tolyl)pent-4-enoate: Product is obtained from methyl 2-acetyl-4-(*o*-tolyl)pent-4-enoate (303mg, 1.231 mmol) via method **A-2** and is obtained as a bright yellow liquid in 69% yield (195mg, 847µmol).
^{1}H NMR (600 MHz, CDCl3) δ 7.21 (dd, J = 4.0, 1.3 Hz, 2H), 7.19 – 7.14 (m, 1H), 7.12 (d, J = 7.6 Hz, 1H), 5.34 (d, J = 1.5 Hz, 1H), 5.07 (d, J = 1.2 Hz, 1H), 3.75 (s, 4H), 3.35 (s, 1H), 2.34 (s, 4H).
^{13}C NMR (151 MHz, CDCl3) δ 167.37, 144.71, 140.95, 135.05, 130.28, 128.30, 127.49, 125.68, 116.03, 51.97, 31.58, 19.69.
FTIR(neat): 2952, 2078, 1688, 1487, 1435, 1339, 1304, 1188, 1107, 1043, 976, 910, 813, 769, 748, 730, 683, 593, 531, 500, 456cm^{-1}
HRMS: (+pAPCI, M+1H) Expected: 231.1128 Found: 231.11308

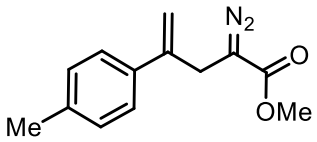

Methyl 2-diazo-4-(*p*-tolyl)pent-4-enoate: Product is obtained from methyl 2-acetyl-4-(*p*-tolyl)pent-4-enoate (5.00 g, 20.3 mmol) via method **A-2** and is obtained as a bright yellow liquid in 39% yield (1.83 g, 7.95 mmol).
^{1}H NMR (600 MHz, CDCl3) δ 7.36 (d, J = 7.9 Hz, 2H), 7.17 (d, J = 7.9 Hz, 2H), 5.47 (s, 1H), 5.16 (d, J = 1.0 Hz, 1H), 3.78 (s, 3H), 3.53 (s, 2H), 2.37 (s, 3H).
^{13}C NMR (151 MHz, CDCl3) δ 167.46, 142.60, 137.93, 136.13, 129.22, 125.89, 114.10, 51.97, 29.11, 21.14.
FTIR(neat): 2951, 2078, 1685, 1626, 1566, 1514, 1435, 1341, 1315, 1302, 1181, 1112, 1018, 975, 902, 825, 751, 734, 677, 641, 577, 535, 482 cm^{-1}
HRMS: (+pESI, M+1H) Expected: 231.1128 Found: 231.11274

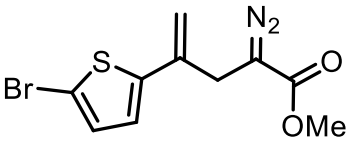

Methyl 4-(5-bromothiophen-2-yl)-2-diazopent-4-enoate: Product is obtained from methyl 2-acetyl-4-(5-bromothiophen-2-yl)pent-4-enoate (1.380g, 4.352mmol) via method **A-2** and is obtained as a bright yellow oil in 8% yield (106mg, 353µmol). The compound degrades rapidly and should therefore be used immediately after preparation.
1H NMR (400 MHz, CDCl3) δ 7.02 – 6.92 (m, 1H), 6.85 (d, *J* = 3.9 Hz, 1H), 5.43 (s, 1H), 5.06 (d, *J* = 1.3 Hz, 1H), 3.80 (s, 3H), 3.44 (d, *J* = 1.3 Hz, 2H).
13C NMR: (151 MHz, CDCl3) δ 167.19, 144.49, 136.02, 130.51, 124.70, 113.70, 111.92, 65.87, 52.12, 32.66, 29.72, 28.91.

FTIR(neat): 2951, 2923, 2851, 2081, 1684, 1617, 1525, 1435, 1341, 1303, 1178, 1109, 1036, 964, 891, 794, 735, 703, 672, 590, 533, 458cm^{-1}
HRMS: (+pESI, M+1H) Expected: 300.96409 Found: 300.964

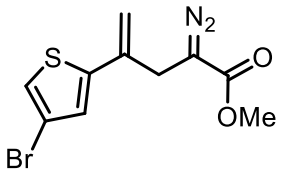

Methyl 4-(4-bromothiophen-2-yl)-2-diazopent-4-enoate: Product is obtained from methyl 2-acetyl-4-(4-bromothiophen-2-yl)pent-4-enoate (232 mg, 731 µmol) via method **A-2** and is obtained as a bright yellow oil in 24% yield (53 mg, 180 µmol).
^{1}H NMR (600 MHz, $CDCl_3$) δ 7.13 (d, *J* = 1.4 Hz, 1H), 7.02 (d, *J* = 1.4 Hz, 1H), 5.54 (s, 1H), 5.12 (s, 1H), 3.82 (s, 3H), 3.46 (s, 2H).
^{13}C NMR (151 MHz, $CDCl_3$) δ 167.15, 144.02, 135.80, 126.81, 122.17, 114.23, 110.09, 52.16, 29.21.
FTIR(neat): 3108, 2951, 2082, 1686, 1620, 1513, 1436, 1341, 1304, 1190, 1112, 1040, 975, 897, 864, 816, 734, 592, 535 cm^{-1}
HRMS: (+pESI, M+Na) Expected: 322.94603 Found: 322.94598

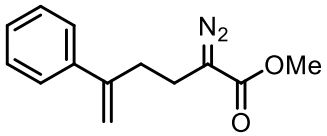

Methyl 5-phenyl-2-diazohex-5-enoate: Product is obtained from methyl 2-acetyl-5-phenylhex-5-enoate (1.69 g, 6.86 mmol) via method **A-2** and is obtained as a bright yellow liquid in 50% yield (786 mg, 3.41 mmol).
1H NMR: (600 MHz, CDCl3) δ 7.42 (d, J = 7.4 Hz, 2H), 7.37 (t, J = 7.3 Hz, 2H), 7.30 (t, J = 7.3 Hz, 1H), 5.37 (s, 1H), 5.16 (d, J = 1.3 Hz, 1H), 3.77 (s, 3H), 2.77 (t, J = 7.3 Hz, 2H), 2.48 (t, J = 7.3 Hz, 2H).
13C NMR (151 MHz, CDCl3) δ 167.83, 146.69, 140.30, 128.47, 127.68, 126.12, 114.11, 51.88, 33.58, 22.55.
FTIR(neat): 2951, 2075, 1684, 1626, 1599, 1574, 1496, 1435, 1349, 1310, 1169, 1118, 1028, 965, 898, 844, 814, 777, 739, 703, 616, 544 cm^{-1}
HRMS: (+p APCI, M+1H) Expected: 231.1128 Found: 231.11222

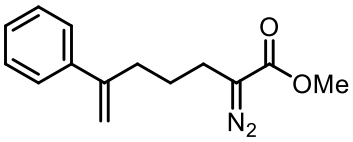

Methyl 2-diazo-6-phenylhept-6-enoate: Product is obtained from methyl 2-acetyl-6-phenylhept-6-enoate (1.168 g, 4.49mmol) via method **A-2** and is obtained as a bright yellow liquid in 31% yield (343 mg, 1.40mmol).
1H NMR (400 MHz, CDCl3) δ 7.44 – 7.39 (m, 2H), 7.36 (ddd, J = 8.1, 6.9, 1.0 Hz, 2H), 7.33 – 7.26 (m, 1H), 5.32 (d, J = 1.4 Hz, 1H), 5.11 (d, J = 1.4 Hz, 1H), 3.77 (s, 4H), 2.61 (td, J = 7.5, 1.3 Hz, 3H), 2.36 (t, J = 7.5 Hz, 3H), 1.71 (tt, J = 8.2, 6.9 Hz, 3H).
13C NMR (101 MHz, CDCl3) δ 169.83, 147.54, 140.86, 128.38, 128.35, 127.51, 126.24, 126.12, 113.00, 51.88, 34.34, 26.15, 22.75.
FTIR(neat): 2949, 2077, 1738, 1738, 1686, 1626, 1600, 1573, 1495, 1435, 1344, 1306, 1266, 1188, 1160, 1118, 1075, 1027, 896, 808, 778, 758, 738, 699, 539, 500 cm-1
HRMS: (+p ESI M+1H) Expected: 245.12845 Found: 245.12839

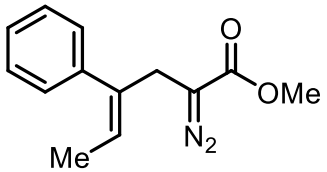

Methyl (Z)-2-diazo-4-phenylhex-4-enoate: Product is obtained from methyl (*Z*)-2-acetyl-4-phenylhex-4-enoate (4.00 g, 16.24 mmol) via method **B-4** and is obtained as a bright yellow liquid in 70% yield (2.62 g, 11.4 mmol).

1H NMR: (600 MHz, CDCl3) δ 7.45 – 7.32 (m, 2H), 7.30 – 7.23 (m, 1H), 7.21 – 7.08 (m, 1H), 5.70 (qt, J = 6.9, 1.2 Hz, 1H), 3.69 (s, 2H), 3.35 (d, J = 1.4 Hz, 2H), 1.62 (dd, J = 6.9, 1.2 Hz, 3H).
13C NMR (151 MHz, CDCl3) δ 171.05, 139.15, 136.28, 128.68, 128.53, 128.43, 128.38, 128.30, 127.93, 127.11, 124.50, 60.35, 51.81, 32.59, 20.99, 14.71, 14.19.
FTIR(neat): 2952, 2079, 1737, 1687, 1493, 1436, 1338, 1295, 1240, 1187, 1116, 1075, 1046, 911, 804, 781, 763, 732, 730, 699, 647, 611, 569, 531 cm^{-1}
HRMS: (+pAPCI, M+1H) Expected: 231.1128 Found: 231.11311

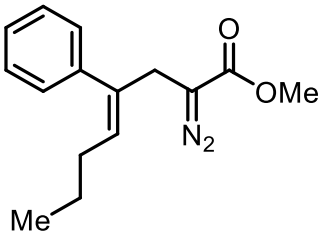

Methyl (Z)-2-diazo-4-phenyloct-4-enoate: Product is obtained from methyl (*Z*)-2-acetyl-4-phenyloct-4-enoate (2.432g, 8.862mmol) via method **B-4** and is obtained as a bright yellow liquid (1.709g, 75% yield, 6.614mmol) which slowly decomposed in the refrigerator (4 months).
^{1}H NMR (600 MHz, CDCl3) δ 7.39 – 7.32 (m, 2H), 7.31 – 7.25 (m, 1H), 7.21 – 7.16 (m, 2H), 5.63 – 5.57 (m, 1H), 3.72 (s, 3H), 3.36 (s, 2H), 1.99 (q, J = 7.6 Hz, 2H), 1.38 (h, J = 7.4 Hz, 2H), 0.86 (t, J = 7.4 Hz, 3H).
^{13}C NMR (151 MHz, CDCl3) δ 139.51, 130.68, 128.38, 128.27, 127.08, 51.85, 32.72, 30.93, 23.04, 13.72.
FTIR(neat): 2956, 2871, 2078, 1689, 1493, 1435, 1378, 1294, 1187, 1107, 1022, 909, 805, 781, 741, 698, 623, 610, 533 cm^{-1}
HRMS: (+pAPCI, M+1H) Expected: 259.1441 Found: 259.14432

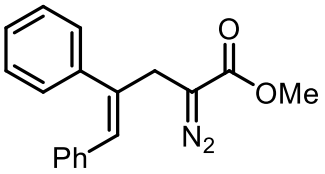

Methyl (Z)-2-diazo-4,5-diphenylpent-4-enoate: Product is obtained from methyl (*Z*)-2-acetyl-4,5-diphenylpent-4-enoate (3.683 g, 11.94 mmol) via method **B-4** and is obtained as a bright orange liquid in 72% yield (2.51g, 8.59 mmol).
^{1}H NMR (600 MHz, $CDCl_3$) δ 7.57 – 7.50 (m, 1H), 7.46 – 7.38 (m, 2H), 7.34 (d, *J* = 7.4 Hz, 2H), 7.26 – 7.21 (m, 1H), 7.16 – 7.11 (m, 2H), 7.01 (dd, *J* = 7.5, 2.2 Hz, 2H), 6.59 (s, 1H), 3.76 (s, 3H), 3.54 (d, *J* = 1.3 Hz, 2H).
^{13}C NMR (151 MHz, $CDCl_3$) δ 167.49, 141.03, 139.55, 137.41, 137.00, 136.50, 136.15, 131.73, 129.23, 128.83, 128.78, 128.72, 128.70, 128.65, 128.60, 128.56, 128.01, 127.98, 127.65, 127.36, 126.88, 126.41, 51.98, 34.16, 23.66.
FTIR(neat): 3015, 2970, 2950, 2077, 1738, 1688, 1493, 1435, 1338, 1295, 1188, 1106, 918, 806, 758, 741, 693, 574, 537, 508 cm^{-1}
HRMS: (+pAPCI, M+1H) Expected: 293.12845 Found: 293.1286

6. Characterization of known reaction intermediates and scope products

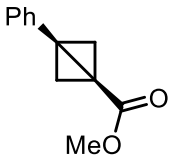

Methyl 3-phenylbicyclo[1.1.0]butane-1-carboxylate (11): Product is obtained as an intermediate during method **C** from the reaction between methyl 2-diazo-4-phenylpent-4-enoate (43mg, 0.20mmol) and $Rh_2(Oct)_4$ (15µg, 0.020µmol) as an

off-white amorphous solid in >99%yield (38mg, 0.20mmol). Spectra matched the previously reported compound in literature.[5]
1H NMR: (600 MHz, CDCl3) δ 7.34 – 7.30 (m, 4H), 7.28 – 7.24 (m, 1H), 3.51 (s, 3H), 2.95 (s, 1H), 1.63 (s, 1H).
13C NMR (151 MHz, CDCl3) δ 170.09, 133.61, 128.48, 126.99, 125.94, 51.81, 35.77, 32.96, 23.25.
FTIR(neat): 3016, 2970, 2949, 1738, 1602, 1526, 1443, 1402, 1365, 1343, 1228, 1216, 1204, 1154, 1112, 1068, 1025, 998, 890, 784, 745, 694, 548, 527, 515 cm^{-1}
HRMS: (+pAPCI, M+1H) Expected: 189.09101 Found: 189.0908

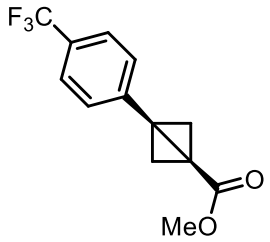

Methyl 3-(4-(trifluoromethyl)phenyl)bicyclo[1.1.0]butane-1-carboxylate(26): Product is obtained as an intermediate during method **C** from the reaction between methyl 2-diazo-4-(4-trifluoromethyl)phenylpent-4-enoate (20mg, 70µmol) and $Rh_2(Oct)_4$ (5.5µg, 0.0070µmol) as a white amorphous solid in >99% yield (18mg, 0.20mmol). Spectra matched the previously reported compound in literature.[5]
1H NMR (600 MHz, CDCl3) δ 7.57 (d, J = 8.1 Hz, 2H), 7.40 (d, J = 8.4 Hz, 2H), 3.52 (s, 3H), 2.98 (s, 2H), 1.69 (s, 2H).
13C NMR (151 MHz, CDCl3) δ 169.47, 138.26, 126.11, 125.48, 125.45, 125.43, 125.40, 52.03, 35.99, 31.68, 24.46.
19F NMR (565 MHz, CDCl3) δ -62.49 (s, 3F).
FTIR(neat): 3015, 2970, 2950, 1738, 1617, 1440, 1365, 1324, 1228, 1216, 1204, 1161, 1116, 1063, 1014, 891, 843, 754, 693, 538, 527, 515 cm^{-1}
HRMS: (+pAPCI, M+1H) Expected: 257.07839 Found: 257.07769

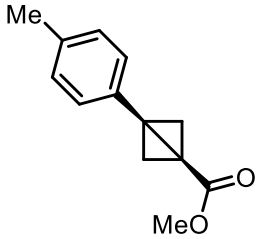

Methyl 3-(*p*-tolyl)bicyclo[1.1.0]butane-1-carboxylate(25): Product is obtained as an intermediate during method **C** from the reaction between methyl 2-diazo-4-(*p*-tolyl)pent-4-enoate (46mg, 0.20mmol) and $Rh_2(Oct)_4$ (15µg, 0.020µmol) as a white crystalline solid in 72% yield (29mg, 0.14mmol)). Spectra matched the previously reported compound in literature.[5].
^{1}H NMR (600 MHz, CDCl3) δ 7.21 (d, J = 8.1 Hz, 1H), 7.13 (d, J = 7.8 Hz, 1H), 3.51 (s, 1H), 2.92 (s, 1H), 2.34 (s, 2H), 1.60 (s, 1H).
13C NMR: (151 MHz, CDCl3) δ 170.23, 136.78, 130.38, 129.23, 125.86, 51.78, 35.78, 33.24, 22.90, 21.14.
FTIR(neat): 2951, 1707, 1607, 1532, 1499, 1440, 1404, 1344, 1194, 1157, 1112, 1097, 1067, 1018, 984, 891, 820, 770, 745, 539 cm^{-1}
HRMS: (+pAPCI, M+H_2O) Expected: 217.08592 Found: 217.08616

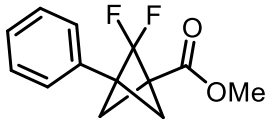

Methyl 2,2-difluoro-3-phenylbicyclo[1.1.1]pentane-1-carboxylate(40): This compound was prepared according to method **C** from methyl 2-diazo-4-phenylpent-4-enoate (43mg, 0.20mmol) and was isolated as a white amorphous solid in 65% yield (31mg, 0.13mmol). Spectra matched the previously reported compound in literature. [5]
1H NMR (600 MHz, CDCl3) δ 7.40 – 7.29 (m, 2H), 3.82 (s, 3H), 2.66 (t, J = 1.1 Hz, 2H), 2.21 – 2.03 (m, 2H).
13C NMR (151 MHz, CDCl3) δ 165.75, 128.60, 128.35, 127.07, 127.05, 52.23, 52.09, 43.22, 43.17, 43.13.

^{19}F NMR (565 MHz, CDCl3) δ -120.89 (t, J = 10.2 Hz).
FTIR(neat): 2956, 1793, 1514, 1496, 1439, 1392, 1323, 1238, 1202, 1142, 1110, 1090, 1022, 989, 954, 907, 857, 798, 765, 732, 697, 648, 601, 500 cm^{-1}
HRMS: (+pAPCI, M+1H) Expected: 239.08781 Found: 239.08823

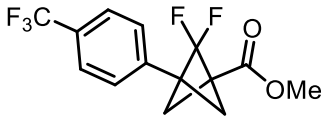

Methyl 2,2-difluoro-3-(4-(trifluoromethyl)phenyl)bicyclo[1.1.1]pentane-1-carboxylate(42): This compound was prepared according to method **C** from methyl 2-diazo-4-(4-trifluoromethyl)phenylpent-4-enoate (20mg, 70µmol) and was isolated as a clear colorless oil in 30% yield (6mg, 20µmol). Spectra matched the previously reported compound in literature. [5]
^{1}H NMR (600 MHz, CDCl3) δ 7.65 (d, J = 7.9 Hz, 1H), 7.42 (d, J = 7.9 Hz, 1H), 3.83 (d, J = 1.0 Hz, 1H), 2.69 (d, J = 1.1 Hz, 1H), 2.18 (ddd, J = 10.8, 9.6, 1.3 Hz, 1H).
^{13}C NMR (151 MHz, CDCl3) δ 165.37, 135.86, 130.74, 130.53, 127.54, 125.65, 125.62, 125.60, 125.57, 124.83, 123.02, 122.68, 54.33, 52.34, 50.32, 43.30, 43.26, 43.21.
^{19}F NMR (471 MHz, cdcl3) δ -62.75, -120.70 (t, J = 10.2 Hz).
FTIR(neat): 2958, 1738, 1622, 1503, 1440, 1411, 1395, 1321, 1243, 1108, 1066, 1028, 1017, 990, 954, 843, 790, 751, 711, 603, 507, 483cm^{-1}
HRMS: (+pAPCI, M+1H) Expected: 307.0752 Found: 307.07544

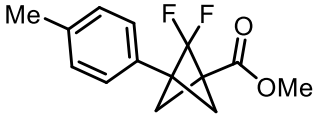

Methyl 2,2-difluoro-3-(*p*-tolyl)bicyclo[1.1.1]pentane-1-carboxylate(43): This compound was prepared according to method **C** from methyl 2-diazo-4-(*p*-tolyl)pent-4-enoate (46mg, 0.20mmol) and was isolated as a white crystalline solid in 42% yield (21mg, 83µmol). The structure was confirmed by X-Ray crystallography and spectra matched the previously reported compound in literature.[5]
1H NMR (600 MHz, CDCl3) δ 7.19 (s, 4H), 3.81 (s, 3H), 2.63 (s, 2H), 2.37 (s, 3H), 2.11 (t, J = 10.4 Hz, 2H).
13C NMR (151 MHz, CDCl3) δ 165.83, 138.21, 129.27, 129.01, 126.97, 122.88, 54.82, 54.69 (t, J = 19.3 Hz), 52.20, 50.15 (t, J = 19.5 Hz), 43.17 (t, J = 7.4 Hz), 21.24.
^{19}F NMR (565 MHz, CDCl3) δ -121.01 (t, J = 10.4 Hz).
FTIR(neat): 2955, 1738, 1525, 1500, 1438, 1392, 1323, 1240, 1200, 1141, 1108, 1032, 989, 954, 906, 858, 822, 796, 769, 730, 602, 587, 505, 480 cm^{-1}
HRMS: (+pAPCI, M+1H) Expected: 253.10346 Found: 253.10347

7. Characterization of novel compounds:

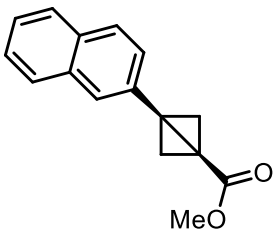

Methyl 3-(naphthalen-2-yl)bicyclo[1.1.0]butane-1-carboxylate(28): Product is obtained as an intermediate during method **C** from the reaction between methyl 2-diazo-naphthalen-2-ylpent-4-enoate (53mg, 0.20mmol) and $Rh_2(Oct)_4$ (15µg, 0.020µmol) as a yellow crystalline solid in 92% yield (44mg, 0.18mmol).

1H NMR (600 MHz, CDCl3) δ 7.85 – 7.81 (m, 3H), 7.80 (d, J = 8.6 Hz, 1H), 7.48 (dddd, J = 20.4, 8.0, 6.8, 1.4 Hz, 2H), 7.41 (dd, J = 8.5, 1.7 Hz, 1H), 3.48 (s, 3H), 3.08 (s, 2H), 1.71 (s, 2H).
13C NMR (151 MHz, CDCl3) δ 170.05, 133.39, 132.50, 131.27, 128.21, 127.70, 127.57, 126.36, 125.76, 125.65, 123.23, 51.87, 35.99, 33.44, 23.53.
FTIR(neat): 3016, 2970, 2949, 1738, 1628, 1600, 1501, 1439, 1365, 1334, 1228, 1216, 1203, 1155, 1134, 1090, 1065, 958, 950, 901, 856, 817, 772, 748, 653, 527, 516, 477 cm^{-1}
HRMS: (+pAPCI, M+1H) Expected: 239.10666 Found: 239.10661

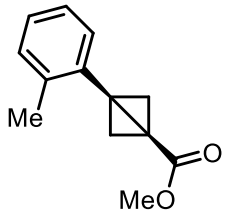

Mmethyl 3-(*o*-tolyl)bicyclo[1.1.0]butane-1-carboxylate(27): Product is obtained as an intermediate during method **C** from the reaction between methyl 2-diazo-4-(*o*-tolyl)pent-4-enoate (46mg, 0.20mmol) and $Rh_2(Oct)_4$ (15µg, 0.020µmol) as a clear colorless oil in 82% yield (33mg, 0.16mmol).
^{1}H NMR (600 MHz, $CDCl_3$) δ 7.25 – 7.15 (m, 3H), 7.12 (td, *J* = 7.5, 1.7 Hz, 1H), 7.06 (d, *J* = 7.5 Hz, 1H), 3.70 (s, 3H), 2.63 (s, 2H), 2.47 (s, 3H), 1.65 (s, 2H).
13C NMR (151 MHz, CDCl3) δ 171.25, 139.14, 132.47, 130.61, 127.29, 125.95, 125.08, 51.94, 38.86, 30.88, 20.66, 20.27.
FTIR(neat): 3016, 2970, 2948, 1738, 1484, 1439, 1365. 1228, 1216, 1204, 1156, 1131, 1091, 1070, 892, 753, 720, 538, 527, 515 cm^{-1}
HRMS: (+pAPCI, M+1H) Expected: 203.10666 Found: 203.10631

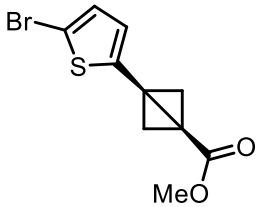

Methyl 3-(5-bromothiophen-2-yl)bicyclo[1.1.0]butane-1-carboxylate(31): Product is obtained as an intermediate during method **C** from the reaction between methyl 2-diazo-4-(5-bromothiophen-2-yl)pent-4-enoate and $Rh_2(Oct)_4$ (15µg, 0.020µmol).
^{1}H NMR (600 MHz, CDCl3) δ 6.92 (d, J = 3.8 Hz, 1H), 6.75 (d, J = 3.8 Hz, 1H), 3.62 (s, 3H), 2.85 (s, 2H), 1.75 (s, 2H).
^{13}C NMR (151 MHz, CDCl3) δ 169.24, 139.00, 130.44, 125.58, 109.92, 52.15, 38.05, 29.94, 23.75.
FTIR(neat): 3001, 2969, 2949, 1738, 1623, 1551, 1498, 1498, 1436, 1365, 1299, 1229, 1216, 1203, 1154, 1112, 1062, 1028, 997, 961, 880, 860, 794, 768, 735, 654, 577, 539, 527, 515 cm^{-1}
HRMS: (+pAPCI, M+1H) Expected: 272.95794 Found: 272.95814

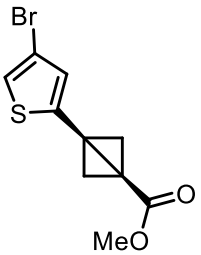

Methyl 3-(4-bromothiophen-2-yl)bicyclo[1.1.0]butane-1-carboxylate(30): Product is obtained as an intermediate during method **C** from the reaction between methyl 2-diazo-4-(4-bromothiophen-2-yl)pent-4-enoate (30mg, 0.10mmol) and $Rh_2(Oct)_4$ (7.8µg, 0.010µmol) as an off-white solid in 95% yield (26mg, 95µmol).
1H NMR (600 MHz, CDCl3) δ 7.05 (d, J = 1.5 Hz, 1H), 6.89 (d, J = 1.1 Hz, 1H), 3.60 (s, 4H), 2.88 (s, 2H), 1.76 (s, 2H).

13C NMR (151 MHz, CDCl3) δ 169.06, 139.01, 134.49, 131.54, 127.44, 121.37, 109.83, 52.15, 37.94, 29.38, 24.22.
FTIR(neat): 3016, 2970, 2949, 1738, 1440, 1365, 1306, 1228, 1216, 1157, 1091, 1032, 885, 818, 769, 740, 593, 538, 527, 515 cm^{-1}
HRMS: (+pAPCI, M+1H) Expected: 272.95794 Found: 272.95735

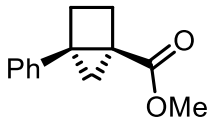

methyl (1S,4S)-4-phenylbicyclo[2.1.0]pentane-1-carboxylate(38): Product is obtained as a clear colorless oil in 7% ee from method **C** from the reaction between methyl 2-diazo-5-phenylhex-5-enoate (46mg, 0.20mmol) and Rh_2(*S-p*-BrTPCP)$_4$ (29µg, 0.020µmol) in >99% yield (40 mg, 0.20 mmol).
^{1}H NMR (600 MHz, $CDCl_3$)) δ 7.44 – 7.30 (m, 4H), 7.24 (t, J = 6.9 Hz, 1H), 3.61 (s, 2H), 2.63 (td, J = 10.9, 8.2 Hz, 2H), 2.36 (dt, J = 4.7, 1.7 Hz, 1H), 1.86 (t, J = 7.4 Hz, 1H), 1.74 (t, J = 7.2 Hz, 1H), 1.72 (d, J = 4.7 Hz, 1H).
^{13}C NMR (151 MHz, $CDCl_3$) δ 171.11, 138.23, 128.17, 127.02, 126.51, 51.46, 42.86, 35.66, 29.21, 25.05, 21.32.
FTIR(neat): 2946, 2864, 1708, 1601, 1500, 1435, 1375, 1329, 1288, 1239, 1191, 1147, 1103, 1075, 1028, 1000, 962, 924, 898, 811, 783, 733, 694, 664, 547, 516 cm^{-1}
HRMS: (+pAPCI, M+1H) Expected: 203.10666 Found: 203.10617
SFC: (OJ-3, 5%MeOH:IPA+2%FA/CO2, 2.5 ml/min, 5 min) Rt: 0.70 min, 0.85 min.

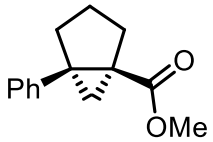

Methyl (1S,5S)-5-phenylbicyclo[3.1.0]hexane-1-carboxylate(39): Product is obtained as a light pink oil in 65% ee from method **C** from the reaction between methyl 2-diazo-6-phenylhept-6-enoate (53mg, 0.22mmol) and Rh_2(*S-p*-BrTPCP)$_4$ (39µg, 0.022µmol) in 96% yield (45mg, 0.21mmol).
^{1}H NMR (600 MHz, $CDCl_3$) δ 7.31 – 7.25 (m, 4H), 7.24 – 7.18 (m, 1H), 3.37 (s, 3H), 2.59 (td, *J* = 12.4, 8.2 Hz, 1H), 2.11 (ddd, *J* = 24.3, 12.5, 7.9 Hz, 2H), 2.02 (dd, *J* = 12.9, 7.9 Hz, 1H), 1.94 – 1.91 (m, 1H), 1.84 (dt, *J* = 13.3, 8.1 Hz, 1H), 1.41 – 1.27 (m, 1H).
^{13}C NMR (151 MHz, $CDCl_3$) δ 172.84, 140.94, 128.84, 128.12, 126.61, 51.25, 44.56, 37.51, 36.57, 29.00, 21.18, 17.75.
FTIR(neat): 2948, 2871, 1715, 1602, 1497, 1435, 1435, 1365, 1272, 1229, 1216, 1200, 1151, 1110, 1077, 1032, 945, 889, 777, 753, 699, 537cm^{-1}
HRMS: (+pAPCI, M+1H) Expected: 217.12231 Found: 217.12227
SFC: (SSW, 3%MeOH:IPA+2%FA/CO2, 2.5 ml/min, 5 min) Rt: 1.11 min, 1.46 min.

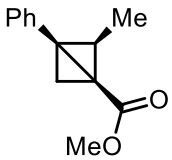

Methyl 2-methyl-3-phenylbicyclo[1.1.0]butane-1-carboxylate(34): Product is obtained as an intermediate in 50% ee during method **C** from the reaction between methyl (Z)-2-diazo-4-phenylhex-4-enoate (52mg, 0.20mmol) and Rh_2(Oct)$_4$ (15µg, 0.020µmol) as a yellow oil in 84% yield (39mg, 0.17mmol) and is observed via 1H NMR.
1H NMR (600 MHz, CDCl3) δ 7.34 – 7.31 (m, 3H), 7.29 – 7.23 (m, 1H), 3.69 (s, 3H), 2.67 (d, J = 1.5 Hz, 1H), 1.81 (q, J = 6.1 Hz, 1H), 1.46 (d, J = 6.1 Hz, 3H), 1.40 (d, J = 1.5 Hz, 1H).
13C NMR (151 MHz, CDCl3) δ 171.04, 133.29, 128.49, 128.33, 128.01, 127.76, 126.98, 51.53, 44.79, 36.60, 34.83, 24.03, 12.13.
FTIR(neat): 2948, 1708, 1602, 1522, 1483, 1439, 1371, 1331, 1192, 1155, 1120, 1097, 1042, 1025, 910, 843, 755, 701, 696, 596 cm^{-1}
HRMS: (+pAPCI, M+1H) Expected: 203.10666 Found: 203.10651
Chiral HPLC: (OD-H, 60 min, 1.0 ml/min, 0% IPA/Hexanes) RT: 20.3 min, 25.6 min.

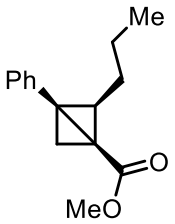

Methyl 3-phenyl-2-propylbicyclo[1.1.0]butane-1-carboxylate(35): Product is obtained as an intermediate during method **C** from the reaction between methyl (Z)-2-diazo-4-phenyloct-4-enoate (52mg, 0.20mmol) and $Rh_2(Oct)_4$ (15µg, 0.020µmol) as a yellow oil in 84% yield (39mg, 0.17mmol)and is observed via 1H NMR.
^{1}H NMR (600 MHz, CDCl3) δ 7.30 (d, J = 4.5 Hz, 4H), 7.26 – 7.21 (m, 1H), 3.66 (s, 3H), 2.58 (d, J = 1.4 Hz, 2H), 1.82 (ddd, J = 10.1, 8.2, 5.5 Hz, 1H), 1.78 – 1.71 (m, 1H), 1.68 (dd, J = 8.1, 5.2 Hz, 1H), 1.63 (dtt, J = 9.9, 7.5, 5.5 Hz, 1H), 1.54 – 1.43 (m, 1H), 1.33 (d, J = 1.4 Hz, 2H), 0.95 (t, J = 7.3 Hz, 3H).
^{13}C NMR (151 MHz, CDCl3) δ 170.93, 133.53, 128.46, 127.85, 127.00, 51.55, 50.93, 36.31, 34.16, 28.70, 22.90, 22.63, 14.17.
FTIR(neat): 2957, 2872, 1736, 1713, 1603, 1439, 1365, 1332, 1228, 1194, 1155, 1099, 1027, 912, 782, 753, 696, 527 cm^{-1}
HRMS: (+pAPCI, M+1H) Expected: 231.13796 Found: 231.13814
SFC: (SSW, 3%MeOH:IPA+2%FA/CO2, 2.5 ml/min, 5 min) Rt: 1.23 min, 1.31 min.

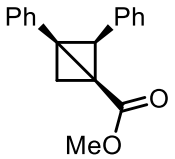

Methyl 2,3-diphenylbicyclo[1.1.0]butane-1-carboxylate(32): Product is obtained as an intermediate during method **C** from the reaction between methyl (Z)-2-diazo-4,5-diphenylpent-4-enoate (58mg, 0.20mmol) and $Rh_2(Oct)_4$ (15µg, 0.020µmol) as an off-white solid in 34% yield (18mg, 68µmol) and is observed via 1H NMR.
1H NMR (600 MHz, CDCl3) δ 7.28 – 7.23 (m, 2H), 7.22 – 7.14 (m, 5H), 6.98 (dd, J = 8.1, 1.6 Hz, 2H), 3.68 (s, 3H), 2.68 (d, J = 0.8 Hz, 1H), 2.66 (s, 1H), 1.52 (s, 1H).
13C NMR (151 MHz, CDCl3) δ 169.83, 133.08, 131.99, 129.24, 128.53, 128.36, 127.31, 127.09, 126.94, 51.66, 51.12, 36.39, 34.00, 25.26.
FTIR(neat): 3027, 2946, 1705, 1605, 1521, 1498, 1580, 1439, 1413, 1267, 1198, 1155, 1087, 1026, 970, 936, 910, 878, 781, 760, 698 cm^{-1}
HRMS: (+pAPCI, M+1H) Expected: 265.12231 Found: 265.12219

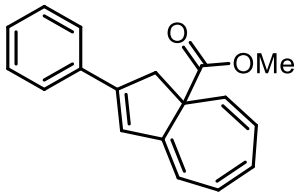

Methyl 2-phenylazulene-3a(3H)-carboxylate(33): Product is obtained during method **C** from the reaction between methyl (E)-2-diazo-4,5-diphenylpent-4-enoate (58mg, 0.20mmol) and $Rh_2(Oct)_4$ (15µg, 0.020µmol) and isolated as a bright yellow solid in 6% yield (3mg, 0.01mmol).
1H NMR (600 MHz, CDCl3) δ 7.56 – 7.48 (m, 2H), 7.44 – 7.36 (m, 2H), 7.32 (tt, J = 7.2, 1.2 Hz, 1H), 6.78 (t, J = 1.7 Hz, 1H), 6.54 (dd, J = 10.9, 6.7 Hz, 1H), 6.46 (d, J = 6.7 Hz, 1H), 6.36 (dtd, J = 27.9, 7.0, 4.3 Hz, 2H), 5.74 (d, J = 9.8 Hz, 1H), 3.67 (dd, J = 17.7, 1.7 Hz, 1H), 3.59 (s, 3H), 3.31 (d, J = 17.8 Hz, 1H).
13C NMR (151 MHz, CDCl3) δ 173.92, 147.31, 146.74, 134.85, 129.90, 128.63, 128.47, 127.70, 127.38, 127.33, 125.76, 124.67, 118.13, 54.87, 52.26, 49.21.
FTIR(neat): 3018, 2949, 1732, 1614, 1522, 1493, 1446, 1383, 1267, 1217, 1190, 1173, 1051, 1029, 897, 795, 756, 690cm^{-1}
HRMS: (+pAPCI, M+1H) Expected: 265.12231 Found: 265.12226

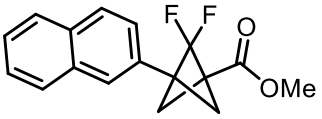

Methyl 2,2-difluoro-3-(naphthalen-2-yl)bicyclo[1.1.1]pentane-1-carboxylate(46): This compound was prepared according to method **C** from methyl 2-diazo-naphthalen-2-ylpent-4-enoate (53mg, 0.20mmol) and was isolated as a white amorphous solid in 40% yield (23mg, 80µmol).
^{1}H NMR (600 MHz, CDCl3) δ 7.86 (dd, J = 8.9, 3.6 Hz, 3H), 7.75 (s, 1H), 7.52 (tq, J = 7.3, 3.6 Hz, 2H), 7.42 (dd, J = 8.4, 1.7 Hz, 1H), 3.84 (s, 3H), 2.75 (s, 2H), 2.23 (t, J = 10.2 Hz, 2H).
^{13}C NMR (151 MHz, CDCl3) δ 165.78, 133.09, 133.07, 129.43, 128.46, 127.82, 127.80, 126.56, 126.40, 126.37, 124.92, 124.45, 122.96, 121.00, 55.06, 54.93, 52.28, 50.30, 43.38, 43.33, 43.28.
^{19}F NMR (376 MHz, $CDCl_3$) δ -120.70 (t, J = 10.3 Hz).
FTIR(neat): 3024, 2954, 1736, 1602, 1504, 1438, 1397, 1350, 1317, 1249, 1236, 1205, 1141, 1105, 1016, 989, 958, 897, 860, 818, 749, 720, 602, 514, 478 cm^{-1}
HRMS: (+pAPCI, M+1H) Expected: 289.10346 Found: 289.10364

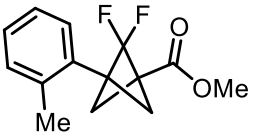

Methyl 2,2-difluoro-3-(*o*-tolyl)bicyclo[1.1.1]pentane-1-carboxylate(43): This compound was prepared according to method **C** from methyl 2-diazo-4-(*o*-tolyl)pent-4-enoate (46mg, 0.20mmol) and was isolated as a clear colorless oil in 42% yield (21mg, 83µmol).
^{1}H NMR (600 MHz, CDCl3) δ 7.26 – 6.98 (m, 4H), 3.82 (d, J = 0.6 Hz, 3H), 2.75 (d, J = 1.3 Hz, 2H), 2.43 (s, 3H), 2.24 (ddd, J = 10.8, 9.5, 1.3 Hz, 1H).
^{13}C NMR (151 MHz, CDCl3) δ 165.71, 165.70, 137.31, 131.02, 130.36, 128.68, 128.47, 125.97, 123.39, 55.72, 52.23, 50.47, 43.61, 43.56, 43.51, 20.40, 20.39, 20.38.
^{19}F NMR (376 MHz, $CDCl_3$) δ -117.61 (t, J = 10.2 Hz).
FTIR(neat): 2956, 1736, 1509, 1490, 1438, 1383, 1318, 1240, 1198, 1140, 1106, 988, 954, 862, 800, 762, 730, 603, 515, 478 cm^{-1}
HRMS: (+pAPCI, M+1H) Expected: 253.10346 Found: 253.1035

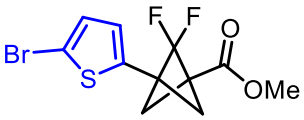

Methyl 3-(5-bromothiophen-2-yl)-2,2-difluorobicyclo[1.1.1]pentane-1-carboxylate(45): This compound was prepared according to method **C** from methyl 4-(5-bromothiophen-2-yl)-2-diazopent-4-enoate (60mg, 0.20mmol) and was isolated as a white amorphous solid in 36% yield (23mg, 71µmol).
^{1}H NMR (600 MHz, CDCl3) δ 6.97 (d, J = 3.7 Hz, 1H), 6.76 (d, J = 3.9 Hz, 1H), 3.81 (s, 3H), 2.62 (s, 2H), 2.16 (t, J = 9.5, 2H).
^{13}C NMR (151 MHz, CDCl3) δ 165.15, 135.22, 130.08, 126.96, 124.08, 122.11, 120.14, 112.47, 52.34, 50.97, 50.84, 50.55, 50.42, 44.48, 44.44, 44.39.
^{19}F NMR (471 MHz, cdcl3) δ -121.04 (t, J = 10.0 Hz).
FTIR(neat): 2954, 1739, 1501, 1449, 1438, 1374, 1327, 1289, 1242, 1201, 1181, 1150, 1103, 1054, 990, 959, 838, 795, 723, 600, 498 cm^{-1}
HRMS: (+pAPCI, M+1H) Expected: 322.95475 Found: 322.95498

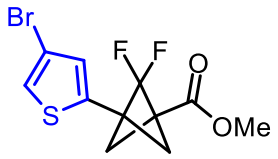

Methyl 3-(4-bromothiophen-2-yl)-2,2-difluorobicyclo[1.1.1]pentane-1-carboxylate(44): This compound was prepared according to method **C** from methyl 4-(4-bromothiophen-2-yl)-2-diazopent-4-enoate (26mg, 86µmol) and was isolated as a yellow oil with a peppery aroma in 43% yield (12mg, 37µmol).
^{1}H NMR (600 MHz, cdcl3) δ 7.16 (t, J = 1.6 Hz, 1H), 6.90 (t, J = 1.5 Hz, 1H), 3.77 (s, 3H), 2.60 (s, 2H), 2.14 (t, J = 10.4 Hz, 2H).
13C NMR (151 MHz, CDCl3) δ 165.08, 134.96, 129.18, 123.15, 122.14, 109.93, 65.87, 52.36, 44.46, 29.72, 15.29.
19F NMR (565 MHz, CDCl3) δ -120.98 (t, J = 10.1 Hz).
FTIR(neat): 3111, 2955, 1740, 1499, 1441, 1374, 1292, 1245, 1203, 1153, 1103, 990, 840, 811, 742, 585 cm^{-1}
HRMS: (+pAPCI, M+1H) Expected: 322.95475 Found: 322.95479

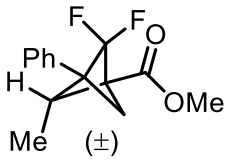

Methyl 2,2-difluoro-4-methyl-3-phenylbicyclo[1.1.1]pentane-1-carboxylate(48): Product is obtained as a minor product from general method **C** from the reaction between methyl (Z)-2-diazo-4-phenylhex-4-enoate (200mg, 0.869mmol) and Rh_2(*S*-NTTL)$_4$ and was obtained in 11% yield (24mg, 95µmol) as a mixture of enantiomers.
1H NMR: (600 MHz, CDCl3) δ 7.43 – 7.31 (m, 3H), 7.24 (dd, J = 8.0, 1.6 Hz, 2H), 3.80 (s, 3H), 3.28 (ttd, J = 6.4, 5.4, 3.0 Hz, 1H), 2.79 (ddd, J = 19.3, 3.9, 1.1 Hz, 1H), 2.66 (dtd, J = 7.2, 3.4, 1.6 Hz, 1H), 1.31 (dd, J = 6.4, 1.1 Hz, 3H).
13C NMR: (151 MHz, CDCl3) δ 165.63, 131.28, 128.62, 128.31, 128.21, 127.16, 52.07, 51.27, 47.97 (dd, J = 6.5, 1.8 Hz), 36.92 (dd, J = 7.1, 1.5 Hz), 6.04 (d, J = 5.7 Hz).
19F NMR: (565 MHz, CDCl3) δ -125.39 (d, J = 136.5 Hz), -126.35 (dd, J = 137.1, 19.3 Hz).
FTIR(neat): 2995, 2916, 2848, 1736, 1605, 1494, 1438, 1406, 1385, 1318, 1239, 1181, 1201, 1123, 1097, 1043, 959, 846, 765, 718, 697, 577 cm^{-1}
HRMS: (+pAPCI, M+1H) Expected: 253.10346 Found: 253.10329

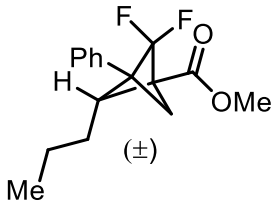

Methyl 2,2-difluoro-4-propyl-3-phenylbicyclo[1.1.1]pentane-1-carboxylate(49): Product is obtained as a minor product from general method **C** from the reaction between methyl (Z)-2-diazo-4-phenyloct-4-enoate (52mg, 0.20mmol) and Rh_2(*S*-NTTL)$_4$ and was obtained in 12% yield (8mg, 30µmol) as a mixture of enantiomers.
1H NMR: (600 MHz, CDCl3) δ 7.40 – 7.32 (m, 3H), 7.26 – 7.23 (m, 2H), 3.80 (s, 3H), 3.18 (qd, J = 6.9, 3.0 Hz, 1H), 2.80 (dq, J = 18.4, 2.2 Hz, 1H), 2.62 (p, J = 3.9 Hz, 1H), 1.77 (td, J = 14.2, 6.5 Hz, 1H), 1.68 – 1.59 (m, 1H), 1.43 – 1.23 (m, 2H), 0.89 (t, J = 7.4 Hz, 3H).
13CNMR: (151 MHz, CDCl3) δ 165.86, 128.56, 128.16, 127.22, 52.08, 36.61, 23.76, 21.80, 14.19.
19F NMR: (376 MHz, CDCl3) δ -125.93 (dt, J = 135.8, 3.3 Hz), -126.48 (ddd, J = 136.7, 17.3, 3.0 Hz).
FTIR(neat): 2969, 1738, 1437, 1365, 1318, 1229, 1216, 1204, 1109, 901, 697, 527 cm^{-1}
HRMS: (+pAPCI, M+1H) Expected: 281.1348 Found: 281.13512

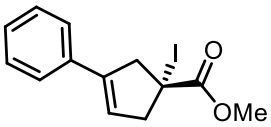

Methyl 1-iodo-3-phenylcyclopent-3-ene-1-carboxylate (53): Product is obtained as the major product from general method **C** from the reaction between methyl 5-phenyl-2-diazohex-5-enoate (46mg, 0.20mmol) and $Rh_2(Oct)_4$ and was obtained as a racemate in 47% yield (31mg, 94µmol) as a white crystalline solid. Product is highly unstable and decomposes releasing iodine within a day.

1H NMR (600 MHz, CDCl3) δ 7.44 (d, J = 7.3 Hz, 2H), 7.37 (t, J = 7.6 Hz, 2H), 7.28 (m, 1H), 6.17 (s, 1H), 3.85 (s, 3H), 3.45 (dd, J = 44.3, 17.6 Hz, 2H), 3.28 (ddd, J = 49.2, 19.2, 1.8 Hz, 2H).

13C NMR (151 MHz, CDCl3) δ 173.43, 140.93, 135.07, 128.55, 127.83, 125.57, 122.79, 53.28, 50.04, 49.98, 38.37, 37.11, 32.76, 31.95, 29.72, 27.10, 22.71, 19.74, 14.14

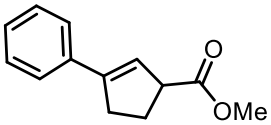

Methyl 3-phenylcyclopent-2-ene-1-carboxylate (54): Product is obtained as the major product from general method **C** from the reaction between methyl 5-phenyl-2-diazohex-5-enoate (200mg, 869µmol) and $Rh_2(Oct)_4$ and was obtained as a racemate in 70% yield (125mg, 618µmol) as a yellow oil.

1H NMR (600 MHz, CDCl3) δ 7.33 (dd, J = 8.2, 6.8 Hz, 2H), 7.25 (tt, J = 7.4, 1.8 Hz, 1H), 7.19 (dd, J = 6.7, 1.1 Hz, 2H), 6.81 (q, J = 2.2 Hz, 1H), 4.07 (ddq, J = 9.6, 7.5, 2.6 Hz, 1H), 3.80 (s, 3H), 2.84 – 2.74 (m, 1H), 2.67 (dddt, J = 16.2, 8.8, 7.3, 2.5 Hz, 1H), 2.54 (dtd, J = 13.0, 8.8, 4.1 Hz, 1H), 1.92 (ddt, J = 13.1, 9.4, 7.2 Hz, 1H).

13C NMR (151 MHz, CDCl3) δ 175.04, 165.80, 145.90, 145.18, 144.19, 137.13, 135.71, 128.64, 128.51, 128.36, 127.67, 127.26, 126.58, 126.43, 125.90, 123.04, 65.87, 51.92, 51.90, 51.55, 51.08, 33.76, 32.80, 31.46, 26.71.

FTIR(neat): 3026, 2970, 2949, 1737, 1629, 1601, 1494, 1435, 1365, 1261, 1229, 1216, 1202, 1090, 1009, 975, 942, 909, 836, 748, 697, 539 cm^{-1}

HRMS: (+pAPCI, [M+]) Expected: 203.10666 Found: 203.10587

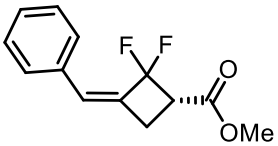

Methyl (R,Z)-3-benzylidene-2,2-difluorocyclobutane-1-carboxylate(9): Product is obtained as the major product from general method **D** from the reaction between **12** and Rh_2(*S*-BTPCP)$_4$ and was obtained in 47% yield in 75% ee as a clear colorless oil.

1H NMR (500 MHz, cdcl3) δ 7.37 – 7.18 (m, 5H), 6.74 (s, 1H), 4.34 (dtd, J = 24.6, 8.0, 2.1 Hz, 1H), 3.66 (s, 3H), 3.11 (dq, J = 8.0, 1.6 Hz, 2H).

13C NMR (151 MHz, CDCl3) δ 137.00, 135.72, 134.88, 128.42, 128.27, 128.24, 128.18, 128.06, 75.34 (dd, J = 22.1, 19.8 Hz), 51.90, 51.74, 31.60, 28.12, 28.09, 22.67.

19F NMR (565 MHz, CDCl3) δ -86.76 (d, J = 41.8 Hz, 1F), -89.86 (dd, J = 41.7, 24.6 (H-F coupling) Hz, 1F).

FTIR(neat): 3027, 2952, 2849, 1745, 1719, 1507, 1495, 1436, 13798, 1290, 1232, 1180, 1116, 1072, 959, 923, 820, 750, 696, 450 cm^{-1}

HRMS: (+pAPCI, M+1H) Expected: 239.08781 Found: 239.08759

Chiral SFC: (CEL-1, 2.5ml/min, 1%MeCN+0.2%FA, 5min) Rt: 0.60min, 2.42min

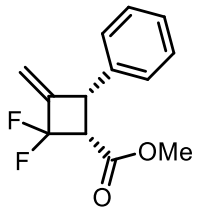

Methyl (1S,4R)-2,2-difluoro-3-methylene-4-phenylcyclobutane-1-carboxylate(10): Product is obtained as the minor product from general method **D** from the reaction between **12** and Rh_2(*S*-BTPCP)$_4$ and was obtained in 24% yield in 91% ee as a clear colorless oil.

1H NMR (600 MHz, CDCl3) δ 7.37 – 7.30 (m, 2H), 7.27 – 7.18 (m, 3H), 6.36 (s, 1H), 5.68 (dd, J = 1.4, 0.8 Hz, 1H), 4.76 (d, J = 10.4 Hz, 1H), 4.63 (ddd, J = 24.0, 10.4, 2.4 Hz, 1H), 3.71 (s, 3H).

13C NMR (151 MHz, CDCl3) δ 166.50, 128.76, 128.65, 128.44, 127.46, 127.00, 126.93, 125.86, 80.30 (dd, J = 23.6, 18.6 Hz, C-F coupling), 51.98, 41.20, 41.17.

19F NMR (565 MHz, CDCl3) δ -87.47 (d, J = 40.7 Hz, 1F), -88.44 (dd, J = 40.6, 23.8 (H-F coupling) Hz, 1F).

FTIR(neat): 3030, 2954, 1741, 1723, 1628, 1495, 1438, 1315, 1267, 1181, 1150, 1097, 1072, 1031, 990, 946, 926, 861, 847, 814, 758, 698, 561 cm^{-1}

HRMS: (+pAPCI, M+1H) Expected: 239.08781 Found: 239.08759

Chiral HPLC: (AD-H, 1ml, 0% 30min) Rt: 4.85min, 5.20min

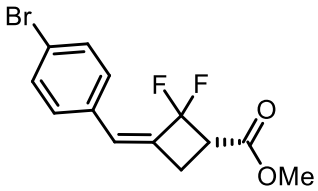

Methyl (R,Z)-3-(4-bromobenzylidene)-2,2-difluorocyclobutane-1-carboxylate(19): Product is obtained as the major product from general method **D** from the reaction between **14** and Rh_2(*S*-BTPCP)$_4$ and was obtained in 42% yield in 98% ee.

1H NMR (600 MHz, cdcl3) δ 7.42 (d, J = 8.5 Hz, 2H), 7.09 (d, J = 8.8 Hz, 1H), 6.64 (s, 1H), 4.31 (dtd, J = 24.6, 7.2, 2.1 Hz, 1H), 3.65 (s, 2H), 3.07 (dq, J = 8.0, 1.6 Hz, 2H).

13C NMR: (151 MHz, CDCl3) δ 168.72, 134.66, 133.89, 131.34, 129.83, 122.17, 75.16, 51.85, 29.72, 28.10, 28.07, 15.29, 14.13.

19F NMR: (565 MHz, CDCl3) δ -86.49 (d, J = 41.6 Hz), -89.64 (dd, J = 41.0, 24.5 Hz).

FTIR(neat): 3016, 2970, 2950, 1743, 1622, 1586, 1487, 1436, 1365, 1291, 1228, 1217, 1116, 1072, 1009, 960, 808, 711, 527 cm^{-1}

HRMS: (+pAPCI, M+1H) Expected: 316.99833 Found: 316.99801

Chiral SFC: (OZ-3-1, 2.5ml/min, 1%MeCN+0.2%FA, 5min) Rt: 0.80min, 0.91min

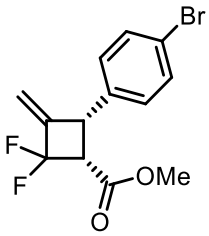

Methyl (1S,4R)-4-(4-bromophenyl)-2,2-difluoro-3-methylenecyclobutane-1-carboxylate(20): Product is obtained as the minor product from general method **D** as a clear colorless oil from the reaction between **14** and Rh_2(*S*-BTPCP)$_4$ and was obtained in 21% yield and 95% ee.

1H NMR (600 MHz, CDCl3) δ 7.45 (d, J = 8.4 Hz, 2H), 7.11 (d, J = 8.3 Hz, 2H), 6.37 (s, 1H), 5.70 (s, 1H), 4.70 (d, J = 10.3 Hz, 1H), 4.59 (ddd, J = 23.6, 10.3, 1.9 Hz, 1H), 3.71 (s, 3H).

13C NMR (151 MHz, CDCl3) δ 166.24, 141.51, 140.12, 131.83, 131.75, 129.17, 128.04, 126.19, 120.86, 79.85 (dd, J = 24.1, 18.4 Hz, C-F coupling), 67.44, 53.22, 52.07, 48.42, 40.83, 40.80.
19F NMR (565 MHz, CDCl3) δ -86.83 (d, J = 39.1 Hz), -87.83 (dd, J = 38.9, 23.6 Hz).
FTIR(neat): 2951, 1740, 1721, 1628, 1486, 1435, 1404, 1267, 1184, 1149, 1072, 1090, 1010, 949, 923, 815, 563 cm^{-1}
HRMS: (+pAPCI, M+1H) Expected: 316.99833 Found: 316.99801
Chiral HPLC: (OD-H, 1ml, 0% 60min) Rt: 11.53min, 13.35min

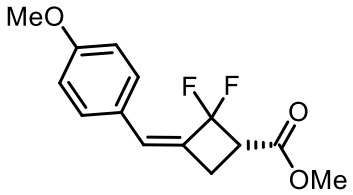

Methyl (R,Z)-2,2-difluoro-3-(4-methoxybenzylidene)cyclobutane-1-carboxylate(17): Product is obtained as the major product from general method **D** as a clear colorless oil from the reaction between **13** and Rh_2(*S*-BTPCP)$_4$ and was obtained in 37% yield and 86% ee.
1H NMR (600 MHz, CDCl3) δ 7.24 (d, J = 8.8 Hz, 2H), 6.87 (d, J = 8.7 Hz, 2H), 6.69 (s, 1H), 4.35 (dtd, J = 24.7, 7.7, 1.9 Hz, 1H), 3.83 (s, 3H), 3.71 (s, 3H), 3.10 (dd, J = 8.0, 1.7 Hz, 2H).
13C NMR (151 MHz, CDCl3) δ 169.33, 159.55, 134.94, 129.93, 129.24, 128.05, 113.60, δ 75.60 (dd, J = 23.9, 19.7 Hz, C-F coupling), 55.26, 51.70, 28.29, 28.26.
19F NMR (565 MHz, CDCl3) δ -87.04 (d, J = 42.1 Hz. 1F), -90.11 (dd, J = 42.3, 24.8 Hz, 1F).
FTIR(neat): 2952, 2839, 1745, 1717, 1606, 1575, 1510, 1463, 1438, 1378, 1342, 1288, 1253, 1217, 1176, 1121, 1104, 1072, 1032, 960, 820, 759, 526cm^{-1}
HRMS: (+pAPCI, M+1H) Expected: 269.09838 Found: 269.09856
Chiral HPLC: (OD-H, 1ml, 0% 60min) Rt: 27.78 min, 40.23min

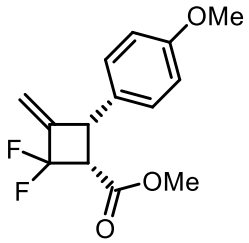

Methyl (1S,4R)-2,2-difluoro-4-(4-methoxyphenyl)-3-methylenecyclobutane-1-carboxylate(18): Product is obtained as the minor product from general method **D** as a clear colorless oil from the reaction between **13** and Rh_2(*S*-BTPCP)$_4$ and was obtained in 19% yield in 91% ee.
1H NMR: (600 MHz, cdcl3) δ 7.11 (d, J = 9.0 Hz, 2H), 6.82 (d, J = 8.5 Hz, 2H), 6.28 (d, J = 0.6 Hz, 1H), 5.62 (d, J = 0.9 Hz, 1H), 4.67 (d, J = 10.5 Hz, 1H), 4.56 (ddd, J = 23.8, 10.7, 2.6 Hz, 1H), 3.77 (s, 3H), 3.67 (s, 3H).
HSQC: 13C NMR was assigned by way of HSQC due to the small amount of product that could be isolated from the mixture of regioisomers, at 4096 scans 13C spectrum was still too weak to positively identify peaks corresponding to the carbons, instead the HSQC was able to identify the relevant correlations. (151 MHz, CDCl3) δ 128.44, 125.54, 125.54, 113.95, 55.36, 51.82, 40.55.
HMBC: Through long range coupling, quaternary carbons were also assigned: 13C NMR (151 MHz, CDCl3) δ 166.42, 166.42, 158.28, 133.43.
19F NMR: (565 MHz, CDCl3) δ -87.75 (d, J = 40.8 Hz, 1F), -88.61 (dd, J = 40.8, 24.2 Hz, 1F).
FTIR(neat): 2954, 2918, 2849, 1742, 1724, 1610, 1512, 1463, 1439, 1302, 1254, 1179, 1151, 1091, 1035, 921, 826, 778, 570cm^{-1}
HRMS: (+pAPCI, M+1H) Expected: 269.09838 Found: 269.09856
Chiral HPLC: (OD-H, 1ml, 0% 60min) Rt: 42.62min, 52.83min

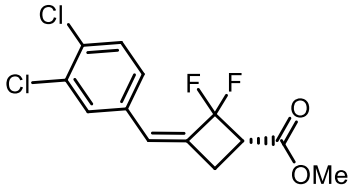

Methyl (R,Z)-3-(3,4-dichlorobenzylidene)-2,2-difluorocyclobutane-1-carboxylate(21): Product is obtained as the major product from general method **D** from the reaction between **15** and Rh_2(*S*-BTPCP)$_4$ and was obtained in 40% yield in 95% ee.

1H NMR: (600 MHz, CDCl3) δ 7.40 (d, J = 8.3 Hz, 1H), 7.36 (d, J = 2.1 Hz, 1H), 7.12 – 7.06 (m, 1H), 6.65 (s, 1H), 4.34 (dtd, J = 24.5, 8.0, 2.0 Hz, 1H), 3.70 (s, 3H), 3.12 (dd, J = 7.9, 1.6 Hz, 2H).

13C NMR: (151 MHz, CDCl3) δ 168.29, 135.75, 133.31, 132.60, 132.31, 132.04, 130.12, 130.10, 127.52, 74.97 (dd, J = 24.6, 19.7 Hz), 51.96, 28.02, 27.99.

19F NMR (565 MHz, CDCl3) δ -86.21 (d, J = 40.9 Hz), -89.39 (dd, J = 40.5, 24.4 Hz).

FTIR(neat): 2952, 1746, 1722, 1551, 1471, 1437, 1369, 1341, 1293, 1226, 1179, 1135, 1113, 1075, 1030, 967, 889, 815, 675, 526cm^{-1}

HRMS: (+pAPCI, M+1H) Expected: 307.00987 Found: 307.0099

Chiral SFC: (OX-3, 2.5ml, 1% 5min) Rt: 0.83min, 1.59min

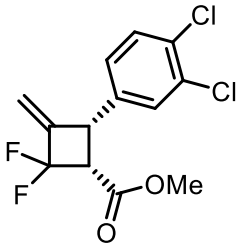

Methyl (1S,4R)-4-(3,4-dichlorophenyl)-2,2-difluoro-3-methylenecyclobutane-1-carboxylate(22): Product is obtained as the minor product from general method **D** from the reaction between **15** and Rh_2(*S*-BTPCP)$_4$ and was obtained in 20% yield in 91% ee.

1H NMR (600 MHz, CDCl3) δ 7.39 (d, J = 8.3 Hz, 1H), 7.31 (d, J = 2.2 Hz, 1H), 7.08 (dd, J = 8.3, 2.2 Hz, 1H), 6.40 (s, 1H), 5.74 (d, J = 1.3 Hz, 1H), 4.70 (d, J = 10.2 Hz, 1H), 4.59 (ddd, J = 23.6, 10.3, 2.1 Hz, 1H), 3.76 – 3.70 (s, 3H).

13C NMR (151 MHz, CDCl3) δ 166.00, 132.69, 130.57, 129.37, 126.87, 126.69, 79.51 (dd, J = 24.3, 18.5 Hz), 52.16, 40.65, 40.61.

19F NMR (565 MHz, CDCl3) δ -86.21 (d, J = 37.6 Hz), -87.28 (dd, J = 37.8, 23.6 Hz).

FTIR(neat): 2953, 1743, 1723, 1629, 1470, 1438, 1397, 1323, 1269, 1185, 1153, 1095, 1031, 955, 927, 878, 817, 749, 675, 513 cm^{-1}

HRMS: (+pAPCI, M+1H) Expected: 307.00987 Found: 307.0099

Chiral HPLC: (OD-H, 1ml, 0% 60min) Rt: 10.89min, 11.74min

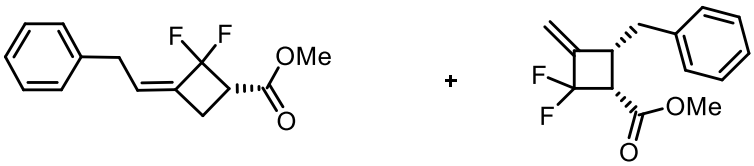

Methyl (R,Z)-2,2-difluoro-3-(2-phenylethylidene)cyclobutane-1-carboxylate(23), methyl (1S,4S)-4-benzyl-2,2-difluoro-3-methylenecyclobutane-1-carboxylate(24): Products are obtained from general method **D** as an irresolvable mixture which appears as a clear colorless oil from the reaction between **16** and Rh_2(*S*-BTPCP)$_4$ and was obtained in 73% combined yield in 90% ee.

1H NMR: (600 MHz, CDCl3) δ 6.20 (s, 1H), 6.15 (t, J = 7.5 Hz, 2H), 5.55 (s, 1H), 4.49 – 4.32 (m, 1H), 4.27 (ddd, J = 24.9, 8.9, 6.9 Hz, 1H), 3.86 (d, J = 7.5 Hz, 3H), 3.82 (s, 3H), 3.80 (s, 2H), 3.68 (q, J = 8.6 Hz, 1H), 3.02 (dd, J = 13.6, 6.2 Hz, 1H), 2.99 (d, J = 7.7 Hz, 3H), 2.76 (dd, J = 13.6, 8.7 Hz, 1H).

13C NMR: (151 MHz, CDCl3) δ 167.50, 166.70, 144.08, 141.82, 139.82, 138.92, 138.21, 134.63, 129.50, 129.24, 129.20, 129.14, 128.64, 128.57, 128.29, 126.37, 126.34, 125.97, 125.85, 125.53, 116.36, 51.95, 51.58, 40.73, 38.31, 38.28, 35.81, 34.38, 29.72, 27.41, 27.38, 21.19.
19F NMR (565 MHz, CDCl3) δ -87.69 (d, J = 34.1 Hz), -87.77 (d, J = 32.5 Hz), -88.51 (dd, J = 42.2, 24.9 Hz), -90.63 (dd, J = 43.5, 25.0 Hz).
FTIR(neat): 3028, 2922, 2850, 1744, 1716, 1602, 1515, 1495, 1436, 1378, 1290, 1208, 1178, 1140, 1117, 993, 940, 925, 823, 748, 699, 540, 488 cm^{-1}
HRMS: (+pAPCI, M+1H) Expected: 253.1035 Found: 253.1033
Chiral HPLC: (OD-H, 1ml, 0% 60min) Rt: 9.10min, 17.81min, 19.79min, 24.76min.

8. NMR spectra:

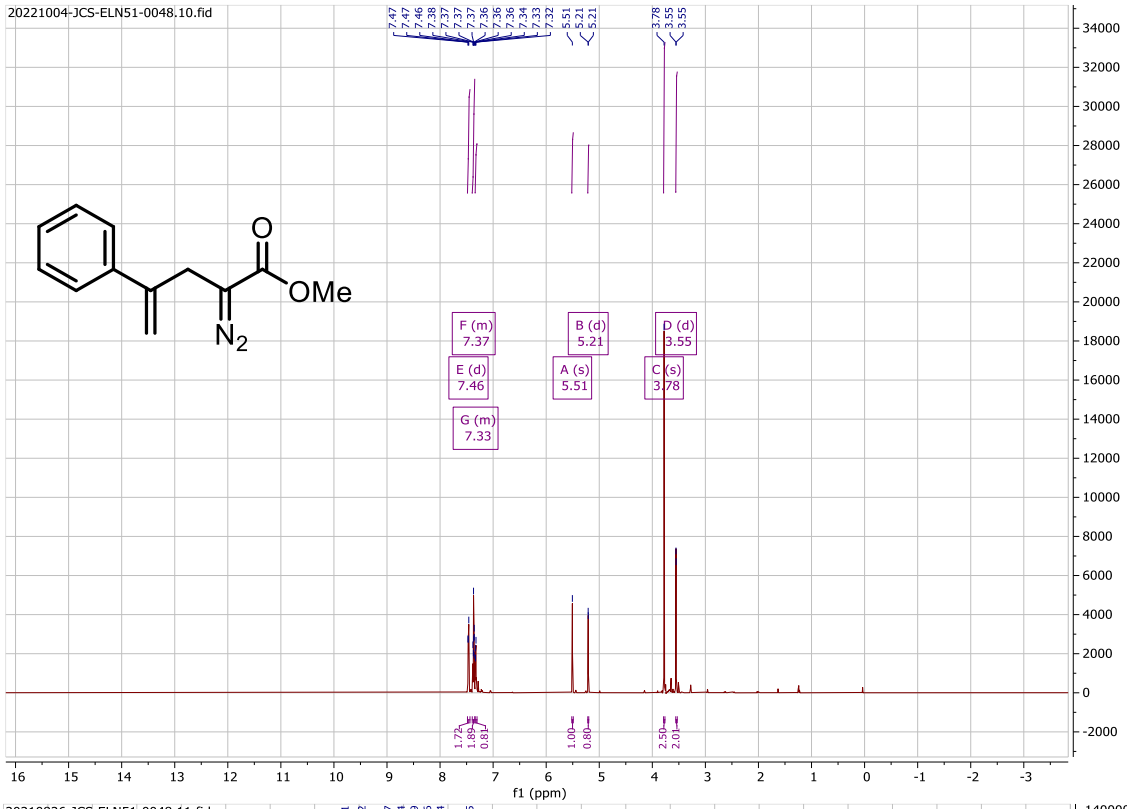

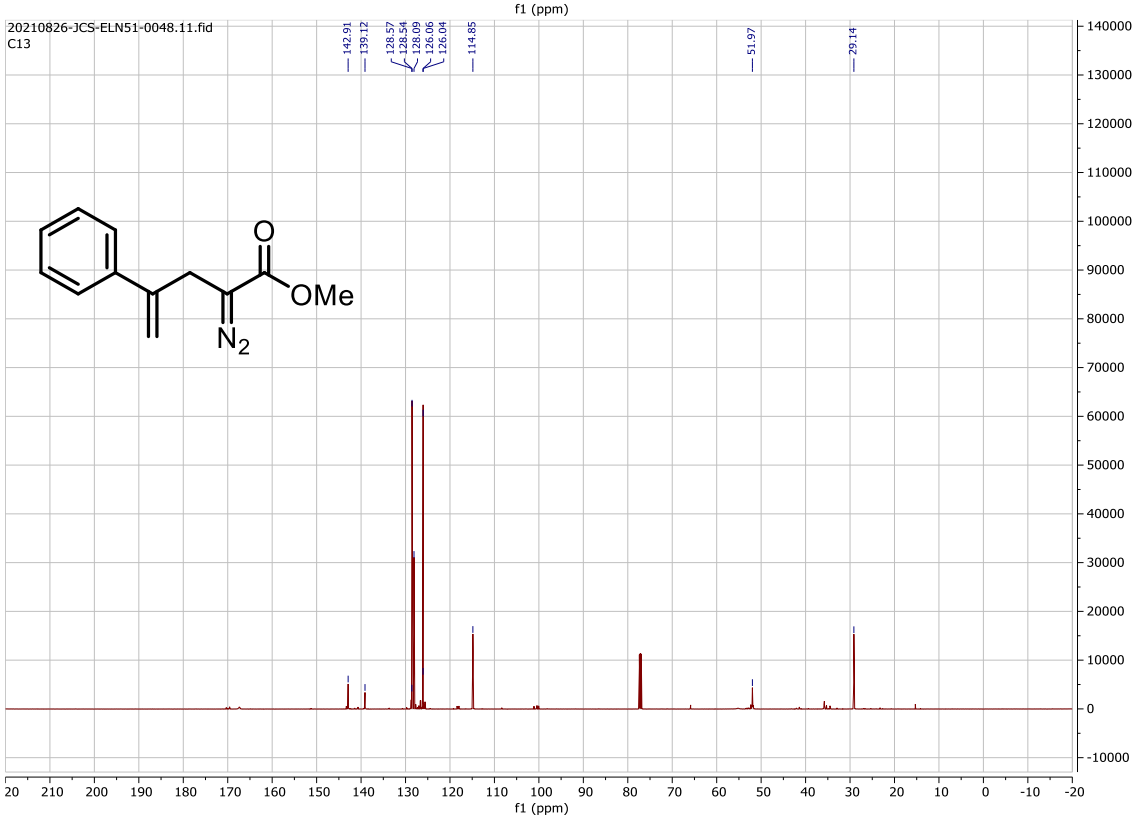

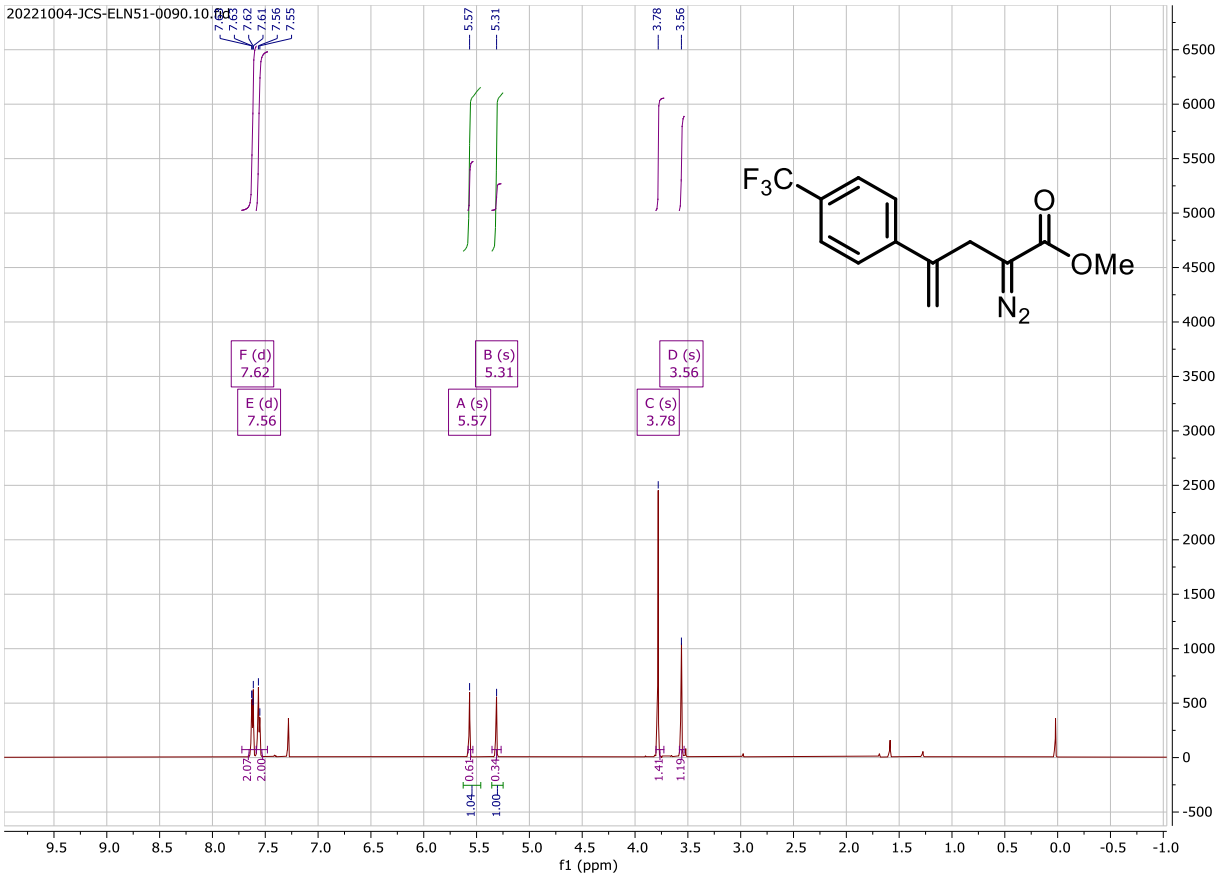
20221004-JCS-ELN51-0090.10.fid
F (d) 7.62
E (d) 7.56
B (s) 5.31
A (s) 5.57
D (s) 3.56
C (s) 3.78
F3C
O
OMe
N2
f1 (ppm)

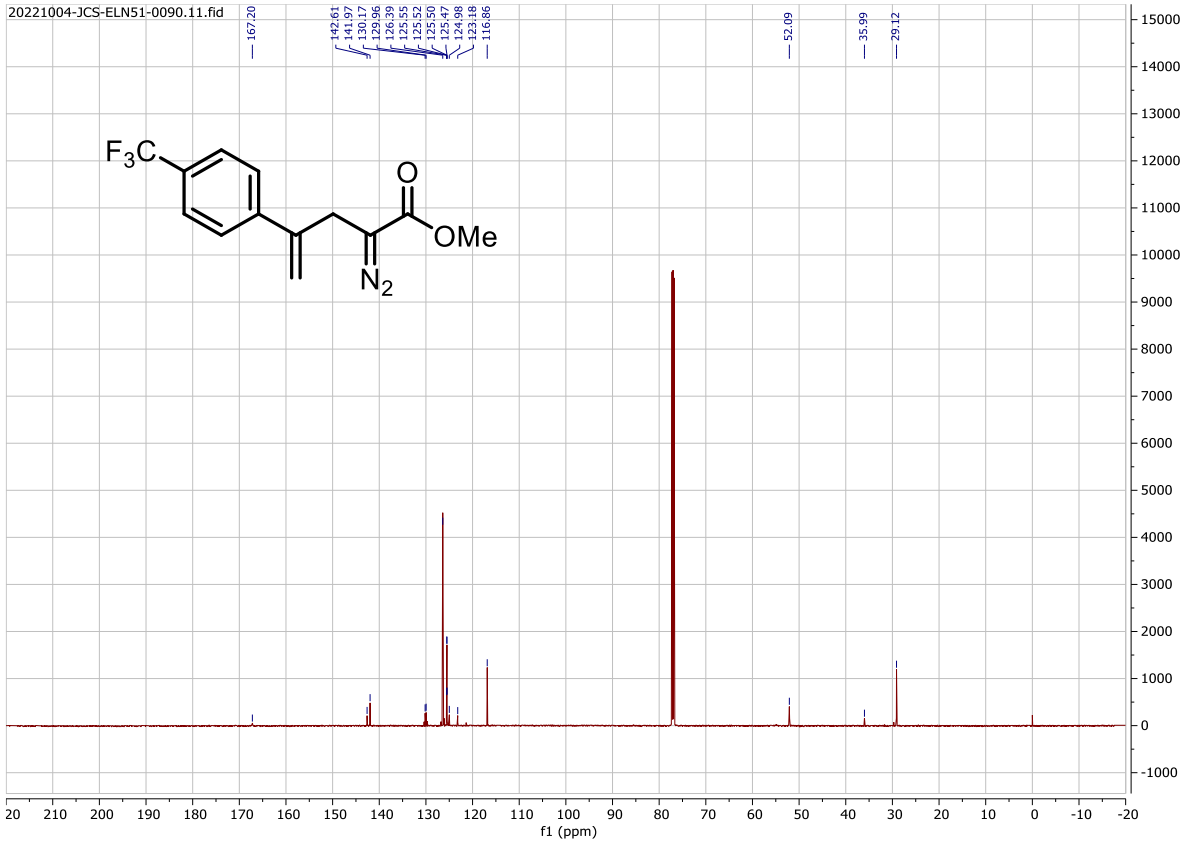
20221004-JCS-ELN51-0090.11.fid
167.20
142.61
141.97
130.17
129.96
126.39
125.55
125.52
125.50
125.47
124.98
123.18
116.86
52.09
35.99
29.12
F3C
O
OMe
N2
f1 (ppm)

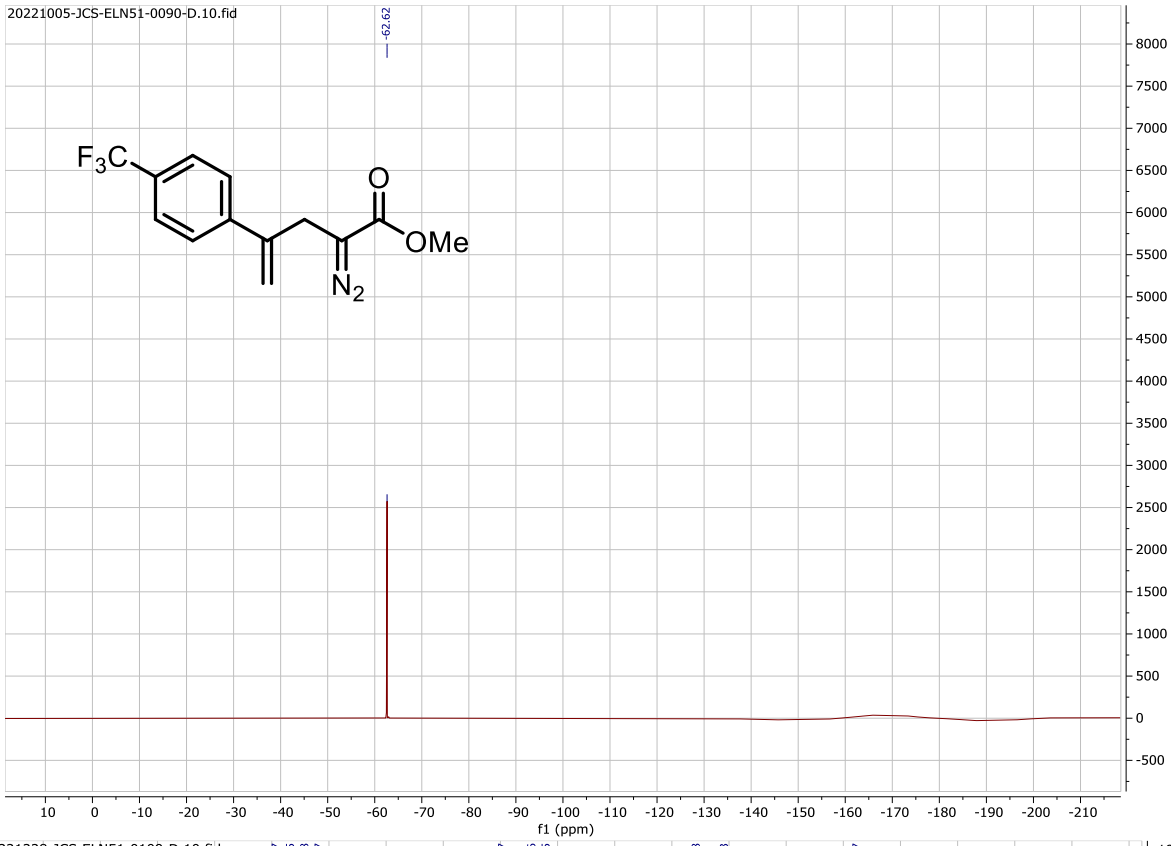
20221005-JCS-ELN51-0090-D.10.fid
-62.62
F3C
O
OMe
N2
f1 (ppm)

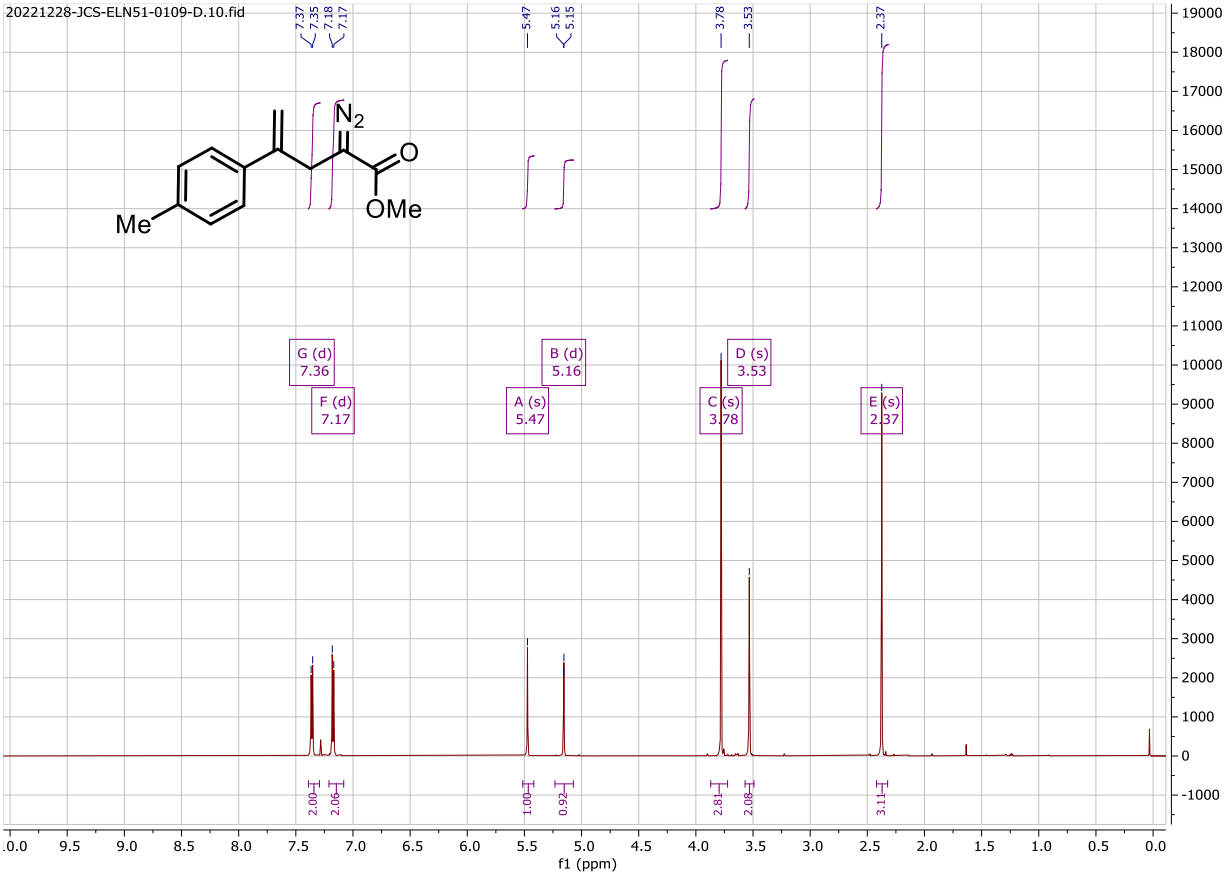
20221228-JCS-ELN51-0109-D.10.fid
7.37
7.35
7.18
7.17
5.47
5.16
5.15
3.78
3.53
2.37
N2
O
OMe
Me
G (d)
7.36
F (d)
7.17
B (d)
5.16
A (s)
5.47
D (s)
3.53
C (s)
3.78
E (s)
2.37
2.00
2.06
1.00
0.92
2.81
2.08
3.11
f1 (ppm)

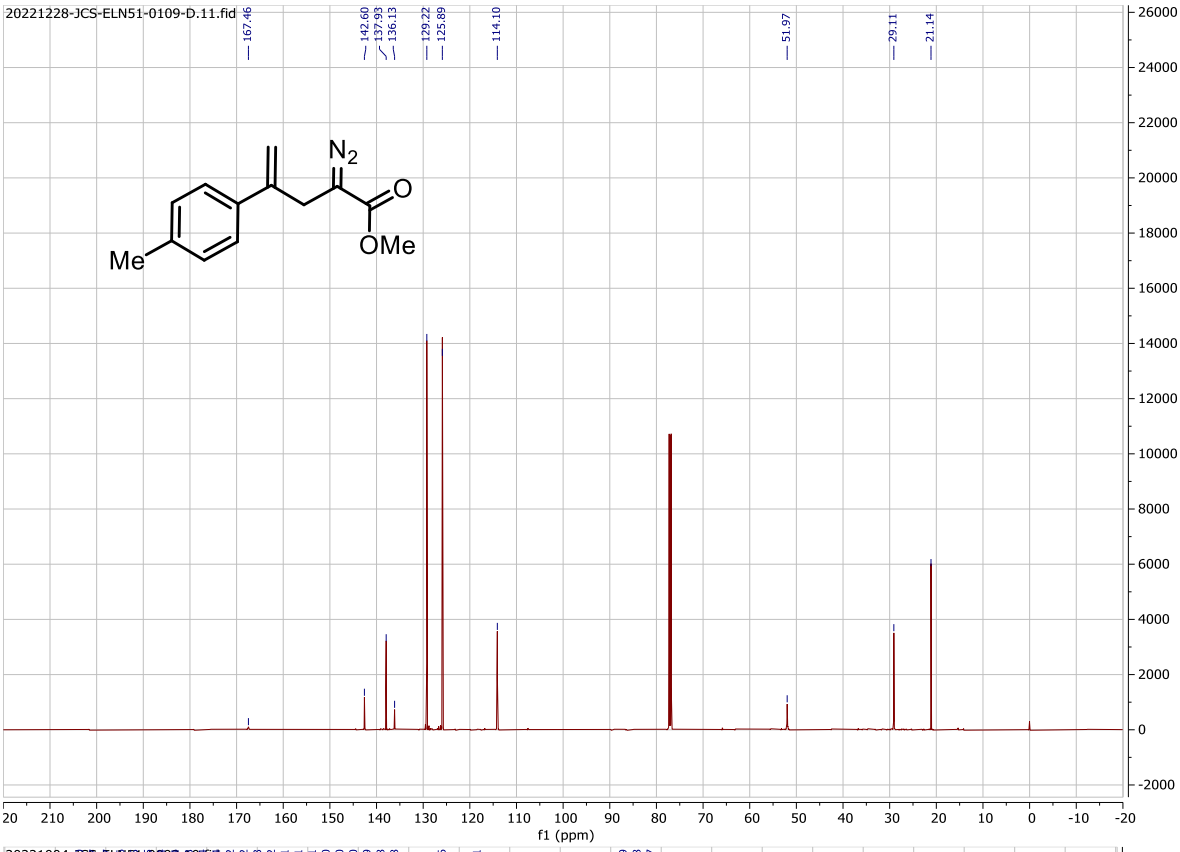
20221228-JCS-ELN51-0109-D.11.fid
167.46
142.60
137.93
136.13
129.22
125.89
114.10
51.97
29.11
21.14
N2
O
OMe
Me
f1 (ppm)

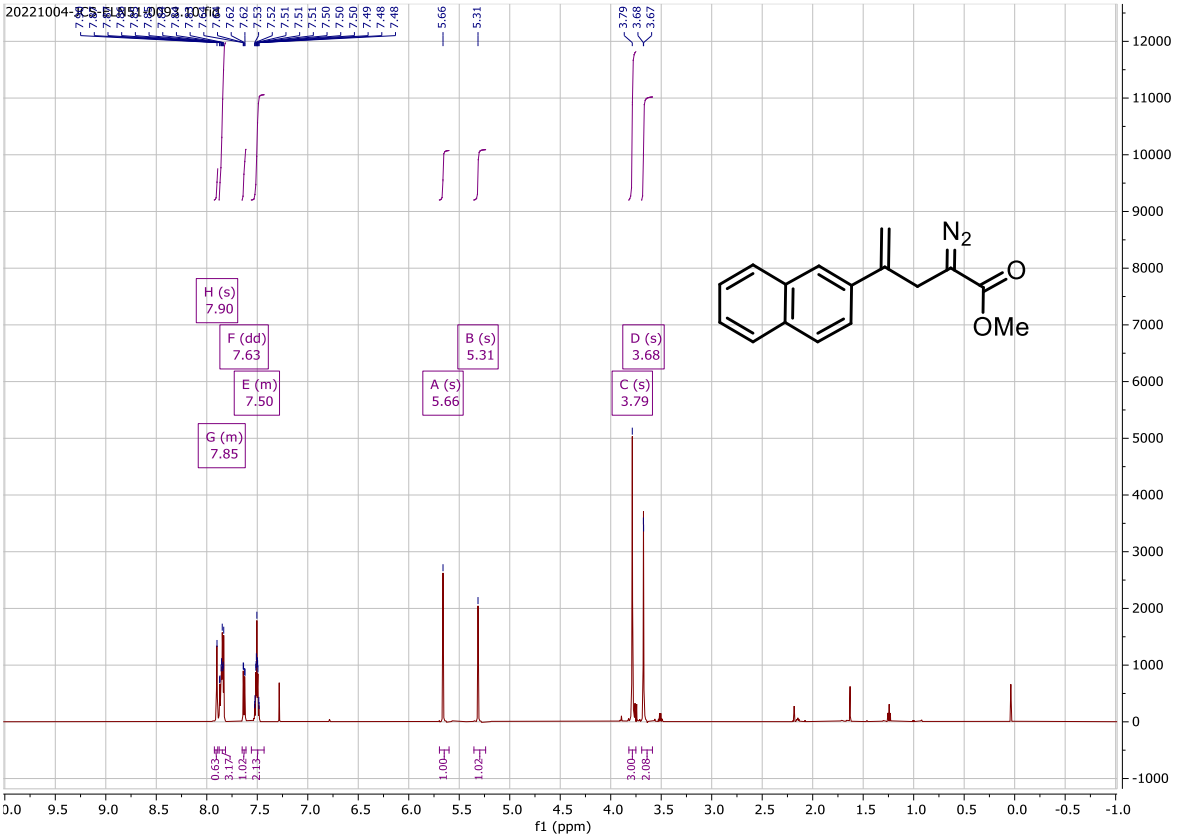
5.66
5.31
3.79
3.68
3.67
H (s)
7.90
F (dd)
7.63
E (m)
7.50
G (m)
7.85
B (s)
5.31
A (s)
5.66
D (s)
3.68
C (s)
3.79
N2
O
OMe
f1 (ppm)

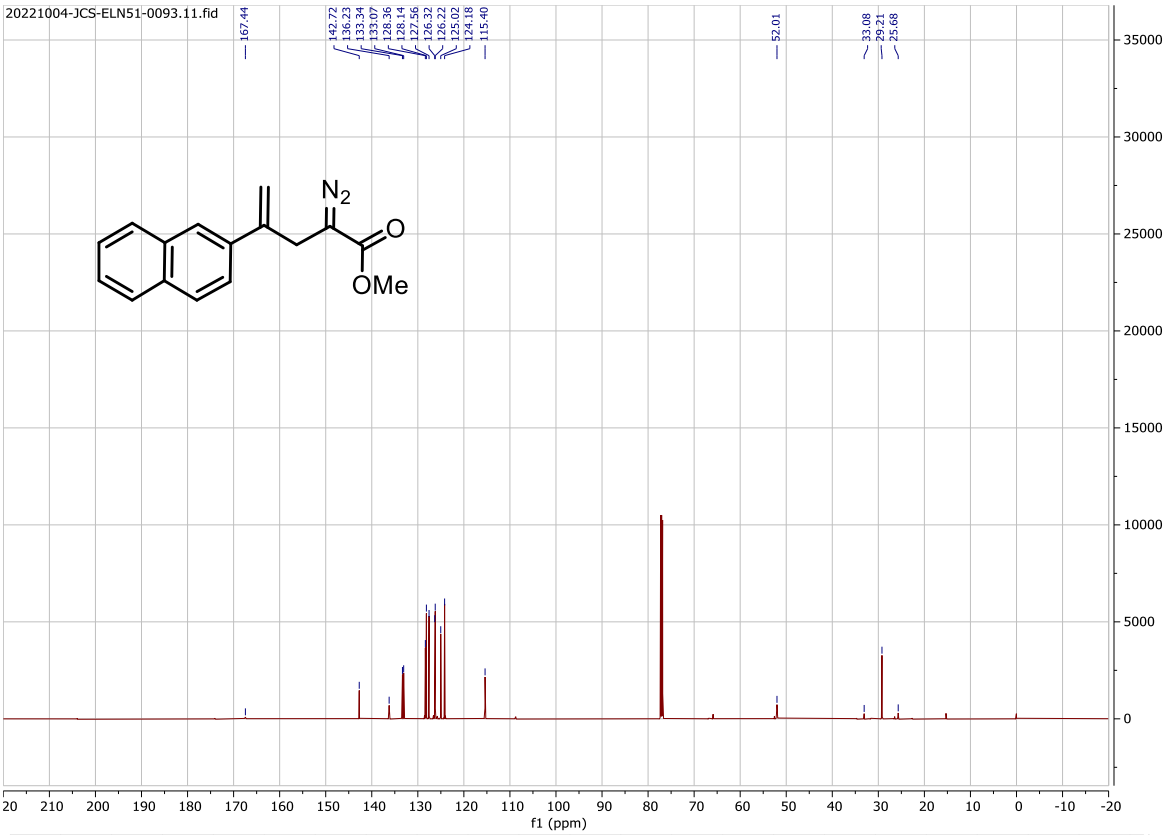
20221004-JCS-ELN51-0093.11.fid
167.44
142.72
136.23
133.34
133.07
128.36
128.14
127.56
126.32
126.22
125.02
124.18
115.40
52.01
33.08
29.21
25.68
N2
O
OMe
f1 (ppm)

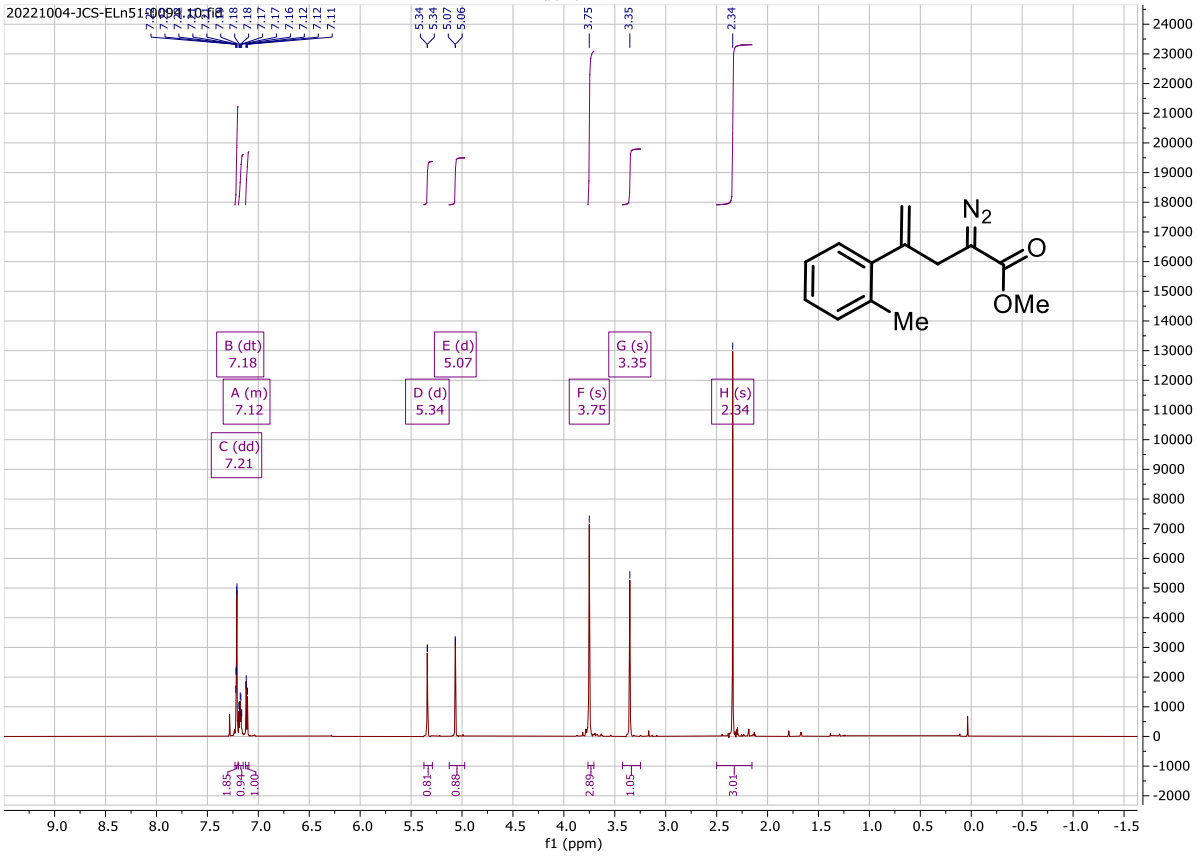
20221004-JCS-ELn51-0094.10.fid
7.18
7.17
7.16
7.12
7.11
5.34
5.34
5.07
5.06
3.75
3.35
2.34
N2
O
OMe
Me
B (dt)
7.18
A (m)
7.12
C (dd)
7.21
E (d)
5.07
D (d)
5.34
G (s)
3.35
F (s)
3.75
H (s)
2.34
1.85
0.94
1.00
0.81
0.88
2.89
1.05
3.01
f1 (ppm)

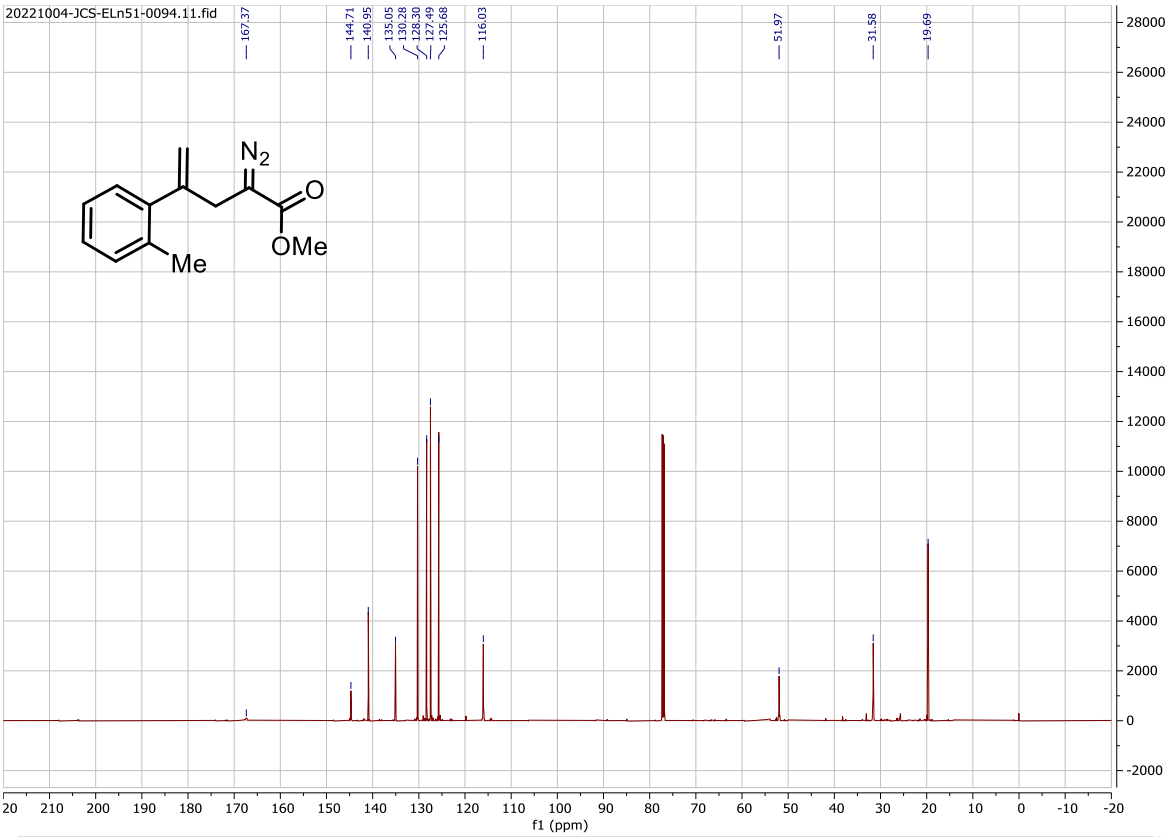
20221004-JCS-ELn51-0094.11.fid
167.37
144.71
140.95
135.05
130.28
128.30
127.49
125.68
116.03
51.97
31.58
19.69
N2
O
OMe
Me
f1 (ppm)

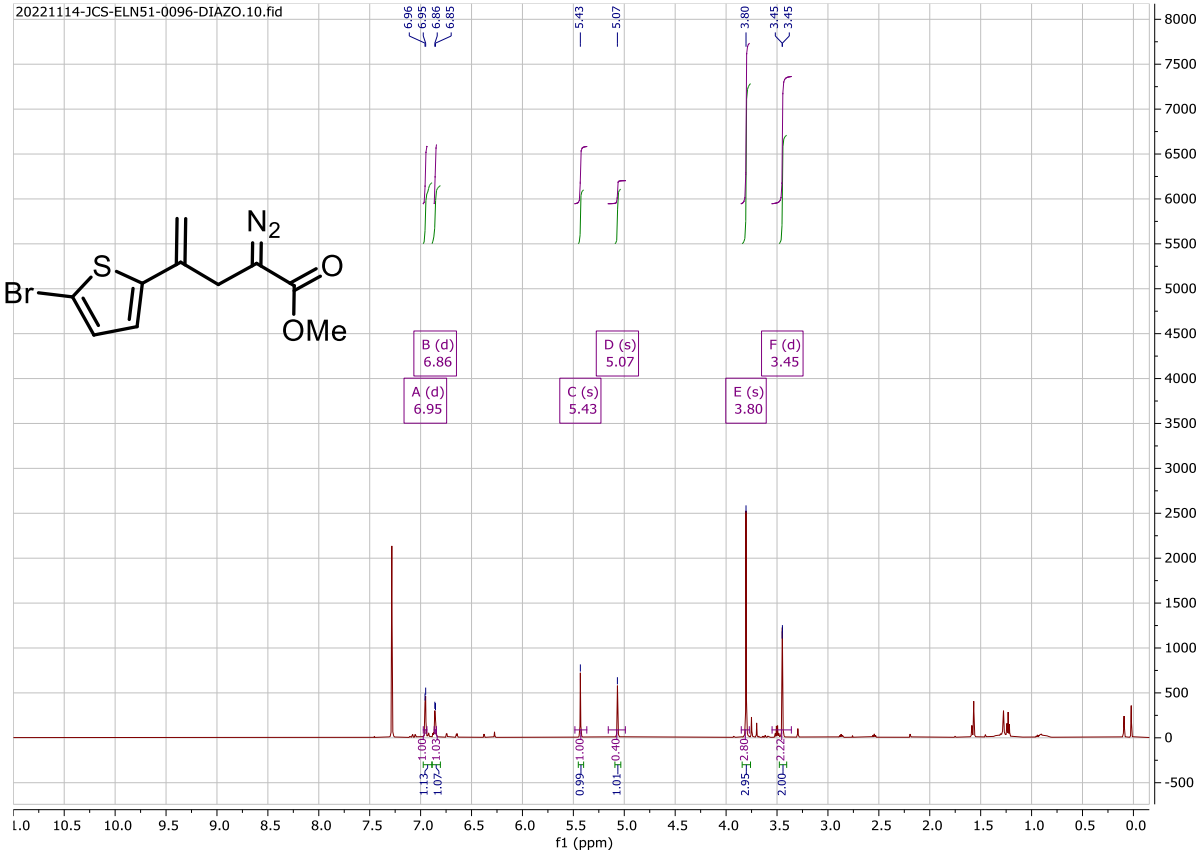
20221114-JCS-ELN51-0096-DIAZO.10.fid
6.96
6.95
6.86
6.85
5.43
5.07
3.80
3.45
3.45
N2
S
Br
O
OMe
B (d)
6.86
A (d)
6.95
D (s)
5.07
C (s)
5.43
F (d)
3.45
E (s)
3.80
1.13
1.00
1.07
1.03
0.99
1.00
1.01
0.40
2.95
2.80
2.00
2.22
f1 (ppm)

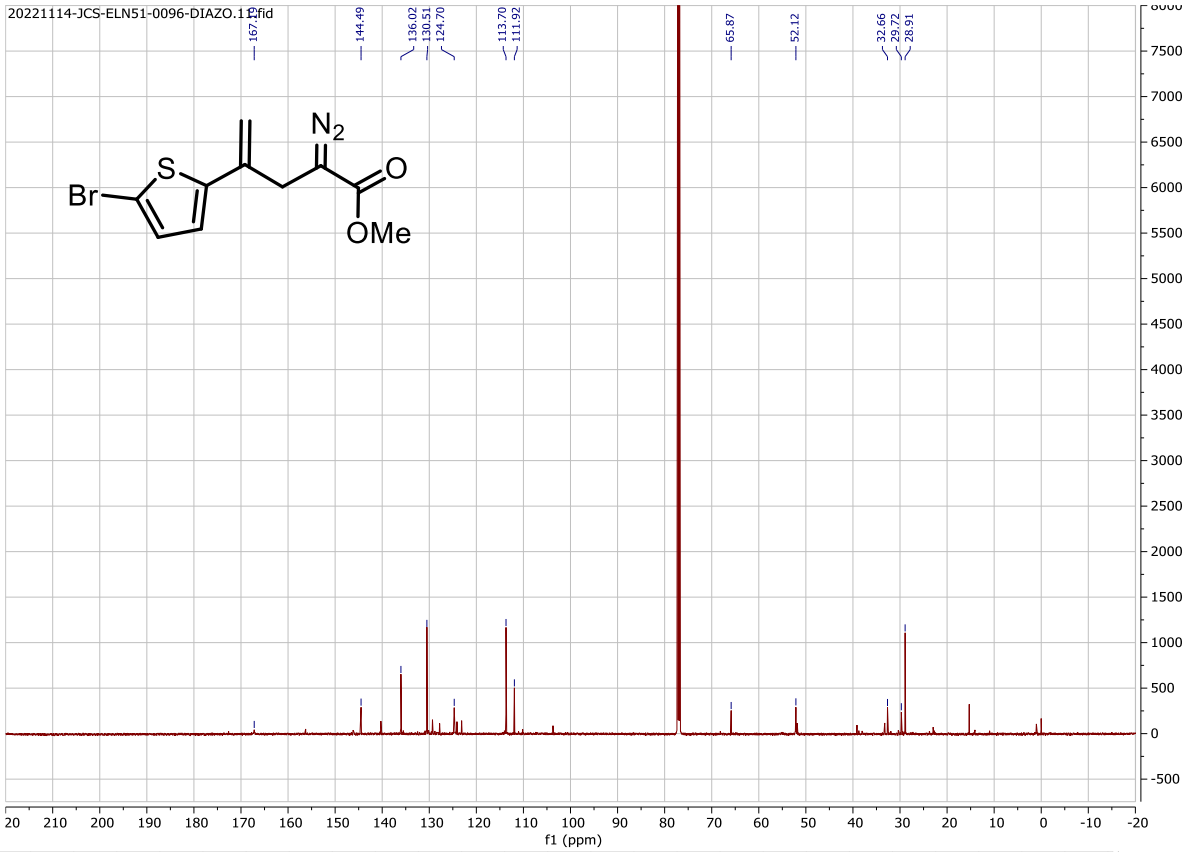
20221114-JCS-ELN51-0096-DIAZO.11.fid
167.11
144.49
136.02
130.51
124.70
113.70
111.92
65.87
52.12
32.66
29.72
28.91
N2
O
S
Br
OMe
f1 (ppm)

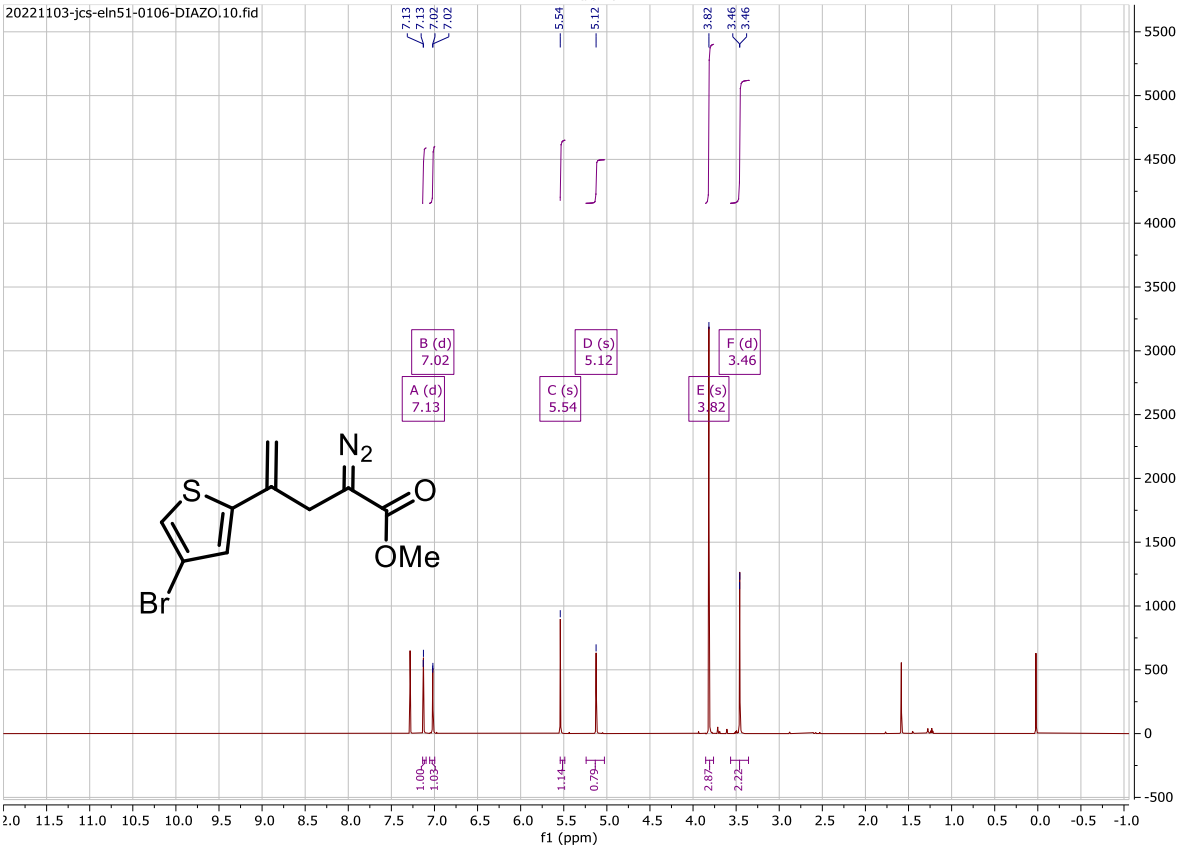
20221103-jcs-eln51-0106-DIAZO.10.fid
7.13
7.13
7.02
7.02
5.54
5.12
3.82
3.46
3.46
B (d)
7.02
A (d)
7.13
C (s)
5.54
D (s)
5.12
E (s)
3.82
F (d)
3.46
N2
O
S
OMe
Br
1.00
1.03
1.14
0.79
2.87
2.22
f1 (ppm)

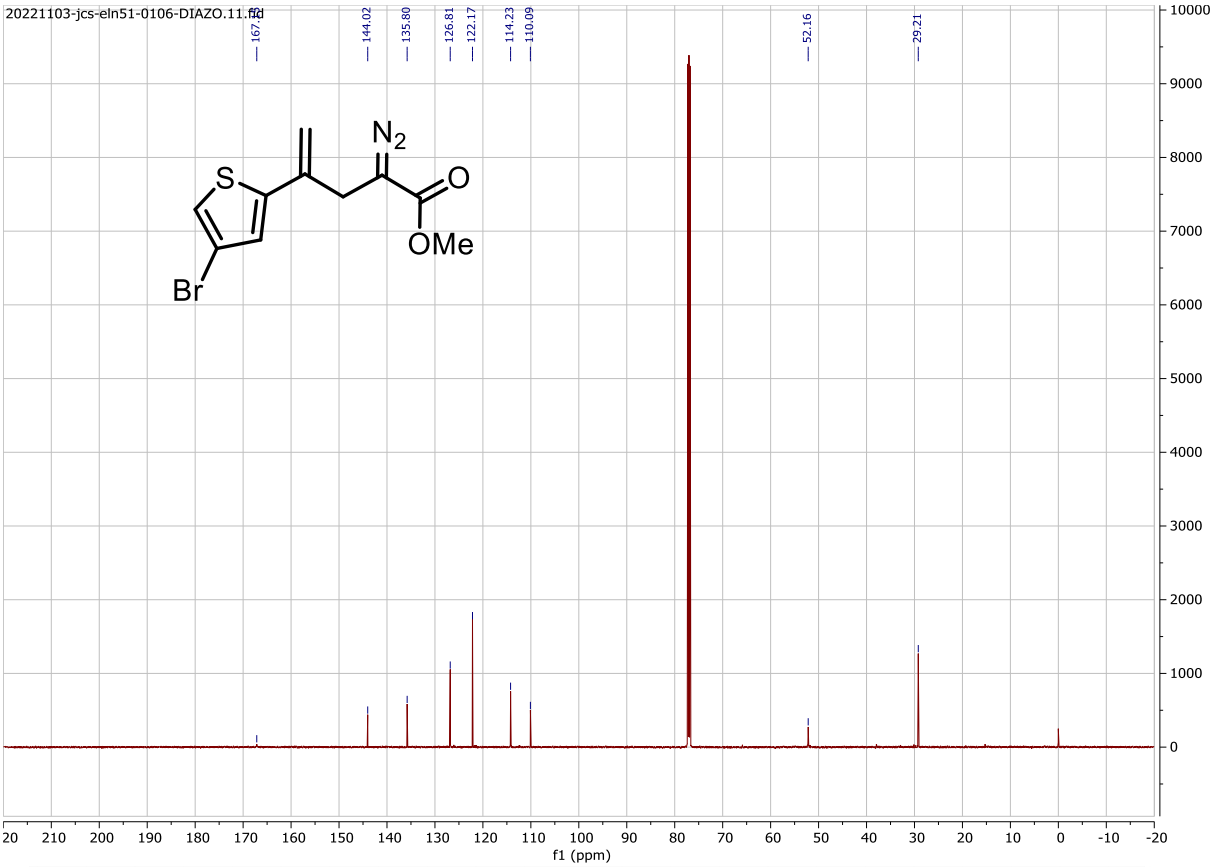
20221103-jcs-eln51-0106-DIAZO.11.fid
167.72
144.02
135.80
126.81
122.17
114.23
110.09
52.16
29.21
N2
O
OMe
S
Br
f1 (ppm)

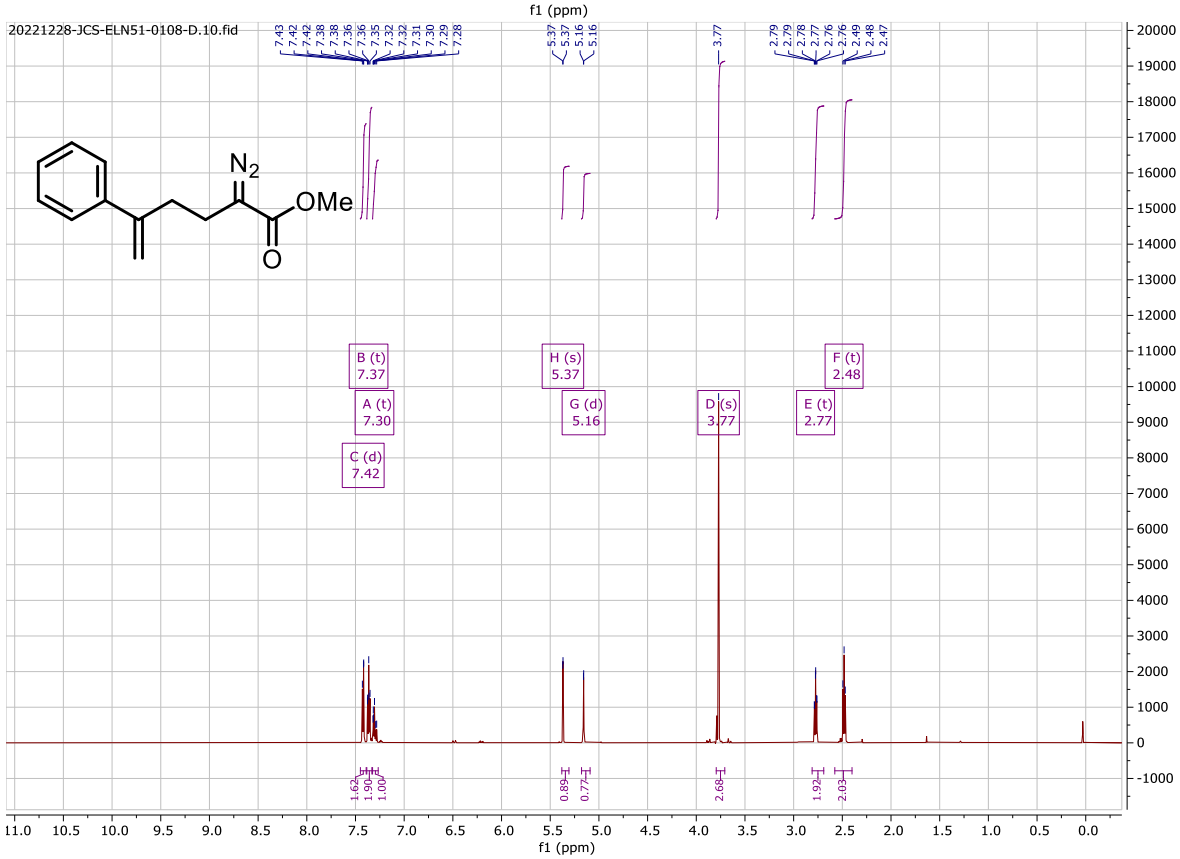
20221228-JCS-ELN51-0108-D.10.fid
7.43
7.42
7.42
7.42
7.38
7.38
7.36
7.36
7.35
7.32
7.32
7.31
7.30
7.29
7.28
5.37
5.37
5.16
5.16
3.77
2.79
2.79
2.78
2.77
2.76
2.76
2.49
2.48
2.47
N2
OMe
O
B (t)
7.37
A (t)
7.30
C (d)
7.42
H (s)
5.37
G (d)
5.16
D (s)
3.77
E (t)
2.77
F (t)
2.48
1.62
1.90
1.00
0.89
0.77
2.68
1.92
2.03
f1 (ppm)

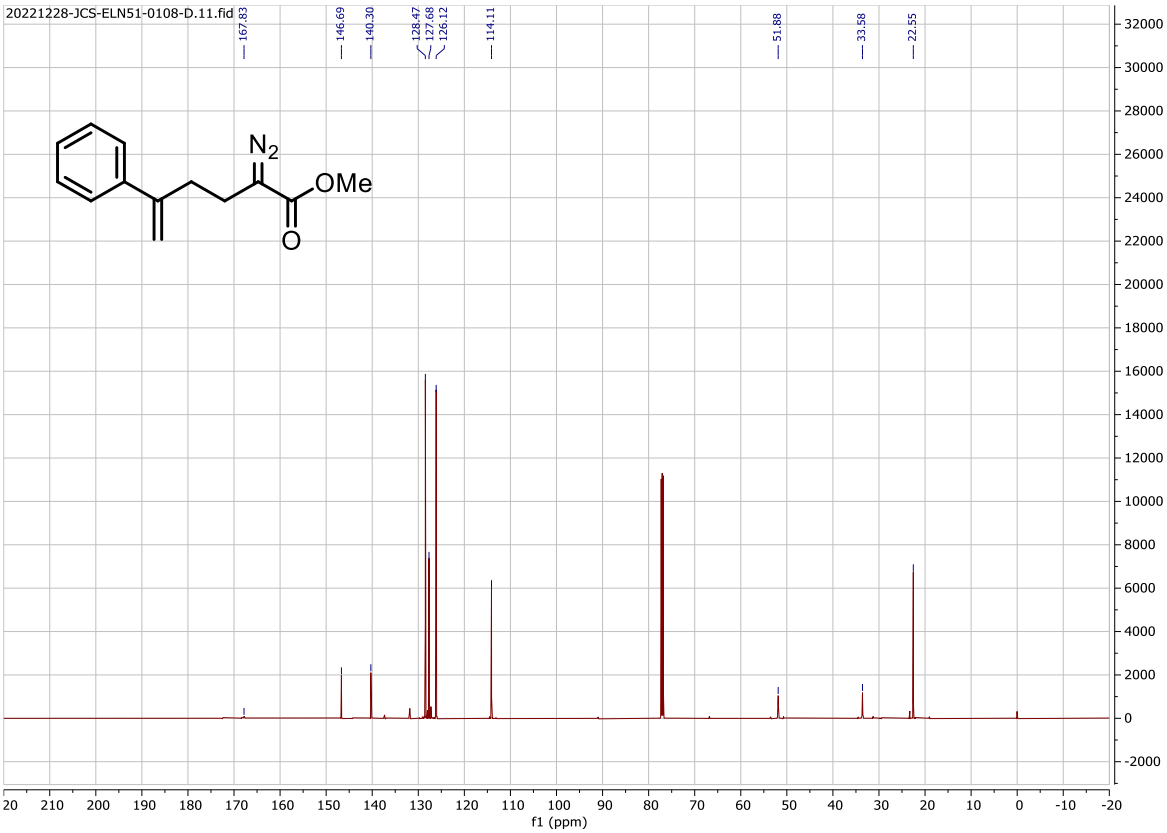
20221228-JCS-ELN51-0108-D.11.fid
167.83
146.69
140.30
128.47
127.68
126.12
114.11
51.88
33.58
22.55
N2
OMe
O
f1 (ppm)

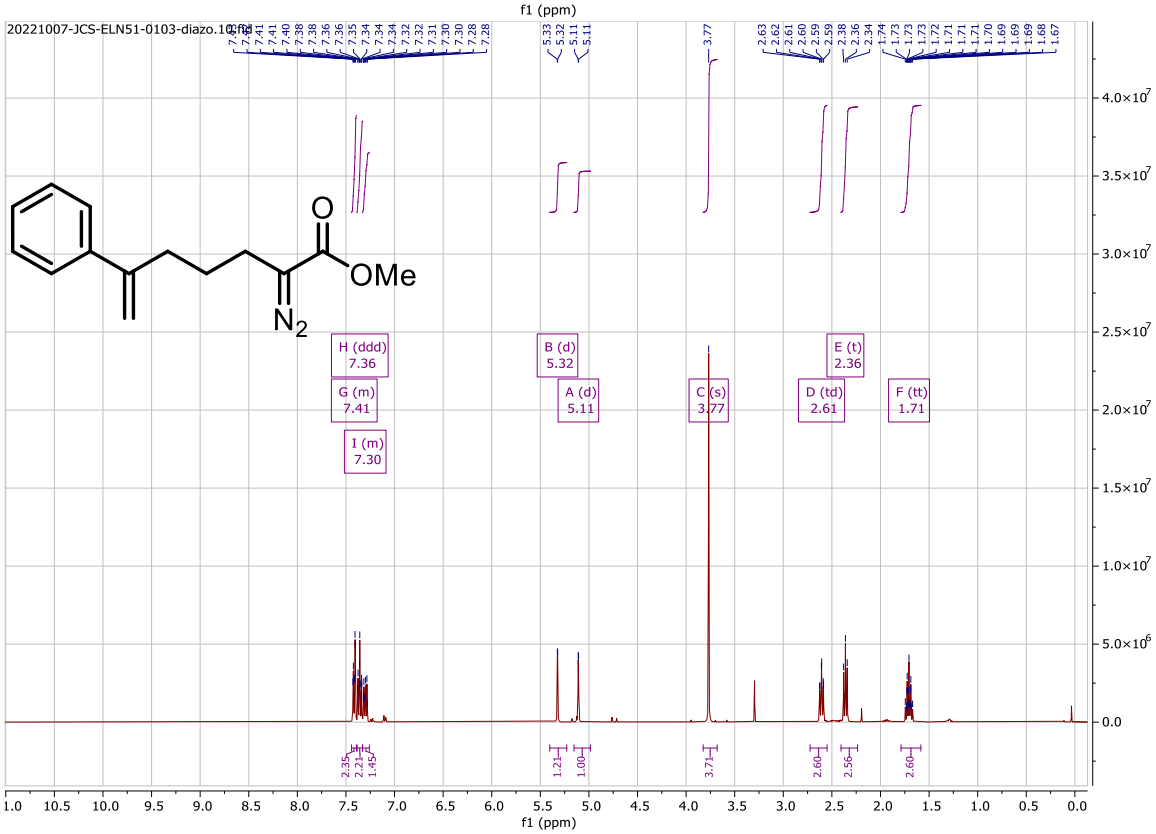
20221007-JCS-ELN51-0103-diazo.10.fid
O
OMe
N2
H (ddd) 7.36
G (m) 7.41
I (m) 7.30
B (d) 5.32
A (d) 5.11
C (s) 3.77
D (td) 2.61
E (t) 2.36
F (tt) 1.71
f1 (ppm)

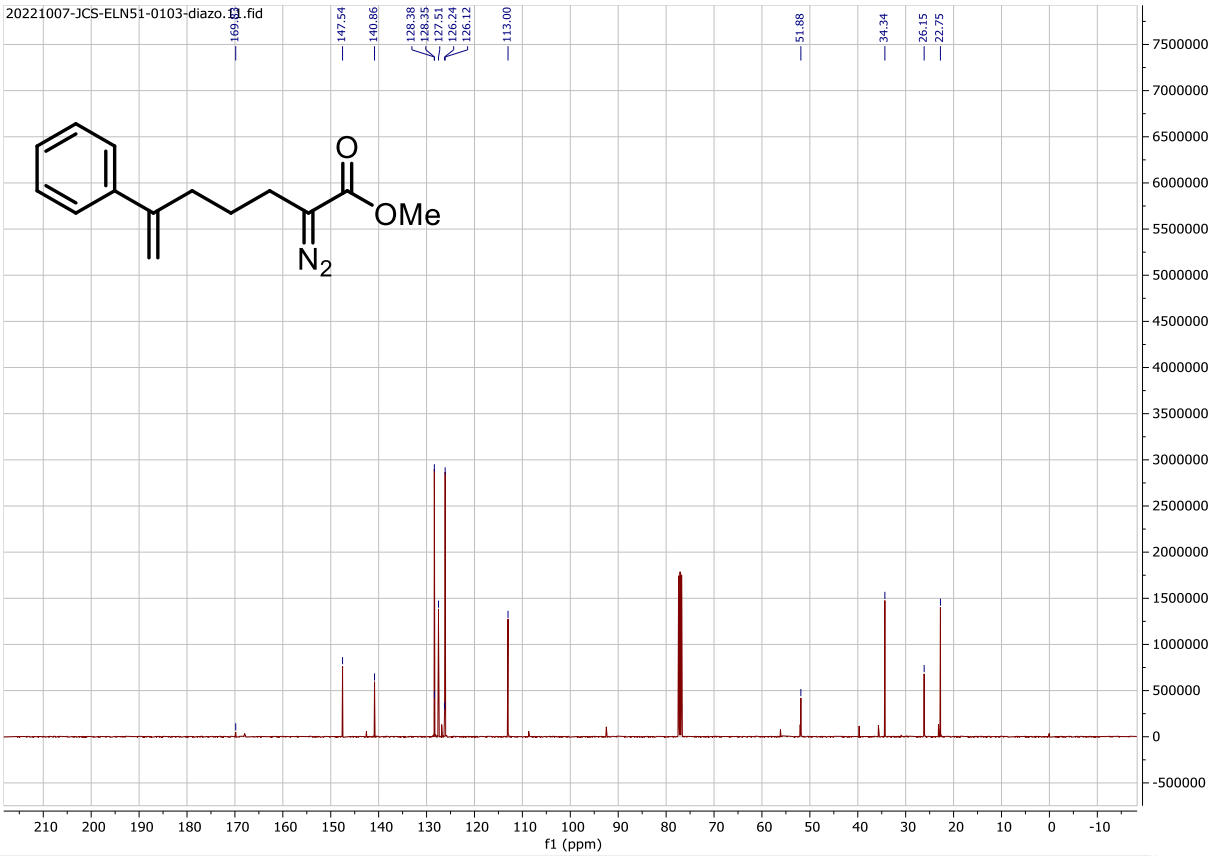
20221007-JCS-ELN51-0103-diazo.1.1.fid
169.12
147.54
140.86
128.38
128.35
127.51
126.24
126.12
113.00
51.88
34.34
26.15
22.75
O
OMe
N2
f1 (ppm)

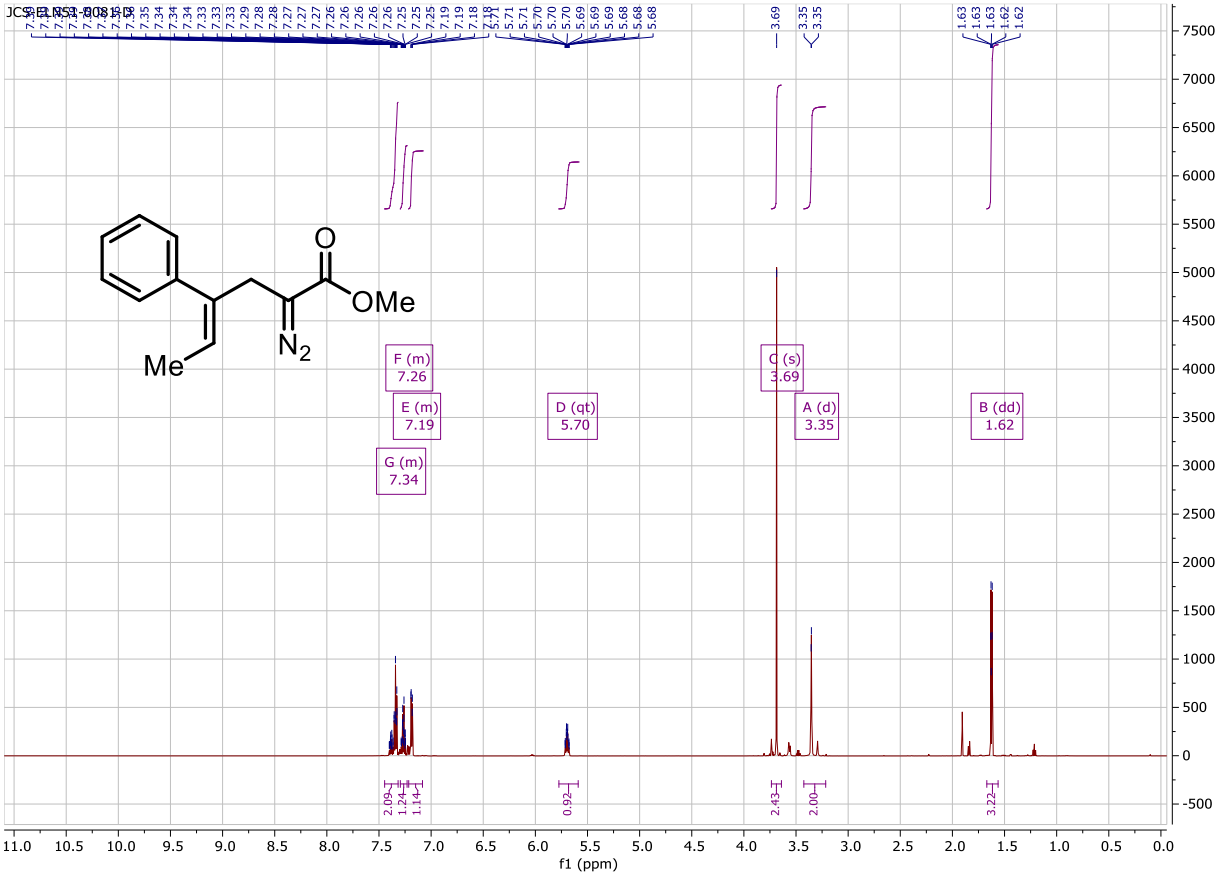
JCS-ELN51-0081-D
3.69
3.35
3.35
1.63
1.63
1.63
1.62
1.62
O
OMe
N2
Me
F (m)
7.26
E (m)
7.19
G (m)
7.34
D (qt)
5.70
C (s)
3.69
A (d)
3.35
B (dd)
1.62
2.09
1.24
1.14
0.92
2.43
2.00
3.22
f1 (ppm)

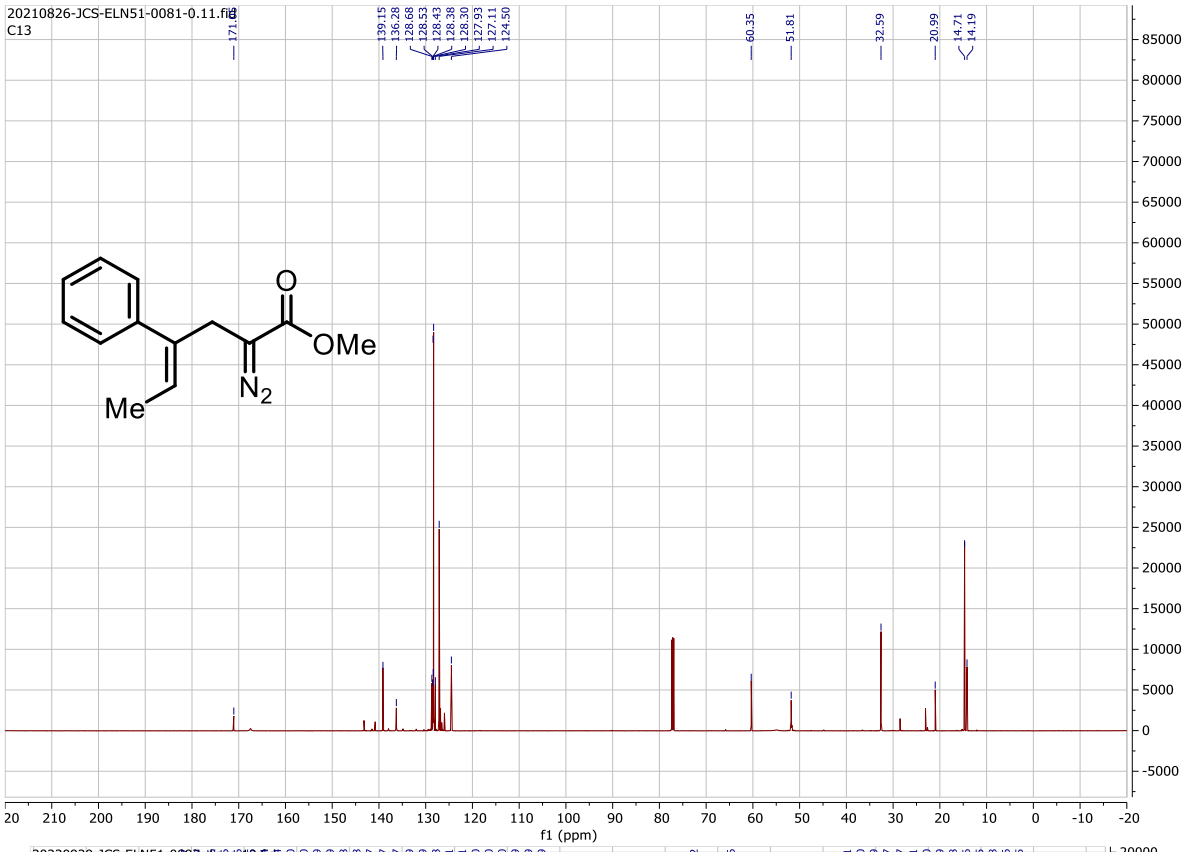
20210826-JCS-ELN51-0081-0.11.fid
C13
171.18
139.15
136.28
128.68
128.53
128.43
128.38
128.30
127.93
127.11
124.50
60.35
51.81
32.59
20.99
14.71
14.19
O
OMe
N2
Me
f1 (ppm)

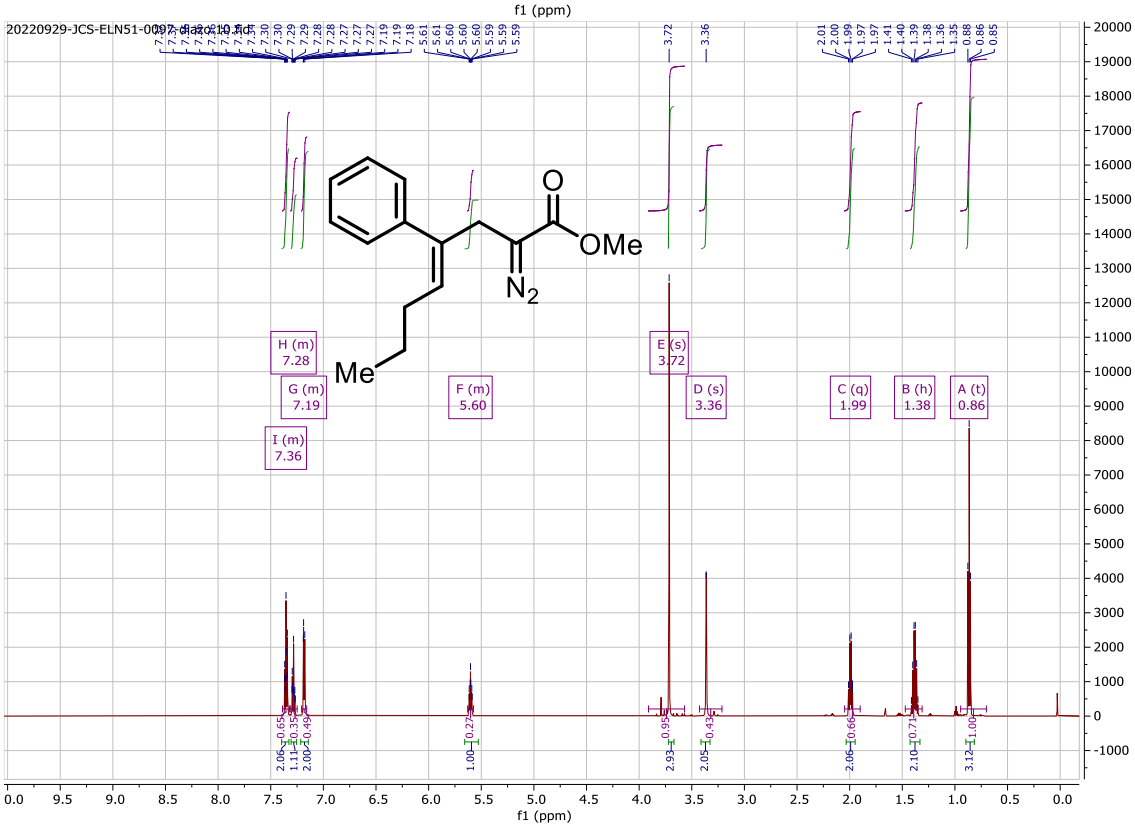
20220929-JCS-ELN51-0097-dia20210.fid
3.72
3.36
2.01
2.00
1.99
1.97
1.97
1.41
1.40
1.39
1.38
1.36
1.35
0.88
0.86
0.85
O
OMe
N2
Me
H (m)
7.28
G (m)
7.19
I (m)
7.36
F (m)
5.60
E (s)
3.72
D (s)
3.36
C (q)
1.99
B (h)
1.38
A (t)
0.86
f1 (ppm)

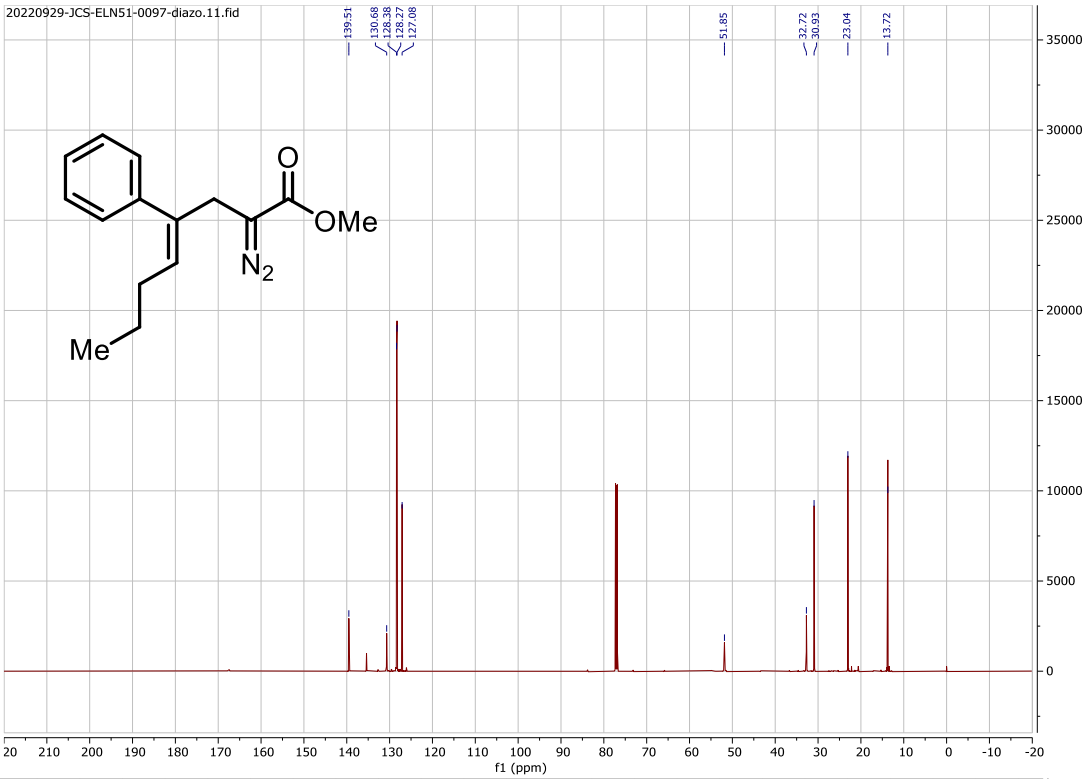
20220929-JCS-ELN51-0097-diazo.11.fid
139.51
130.68
128.38
128.27
127.08
51.85
32.72
30.93
23.04
13.72
O
OMe
N2
Me
f1 (ppm)

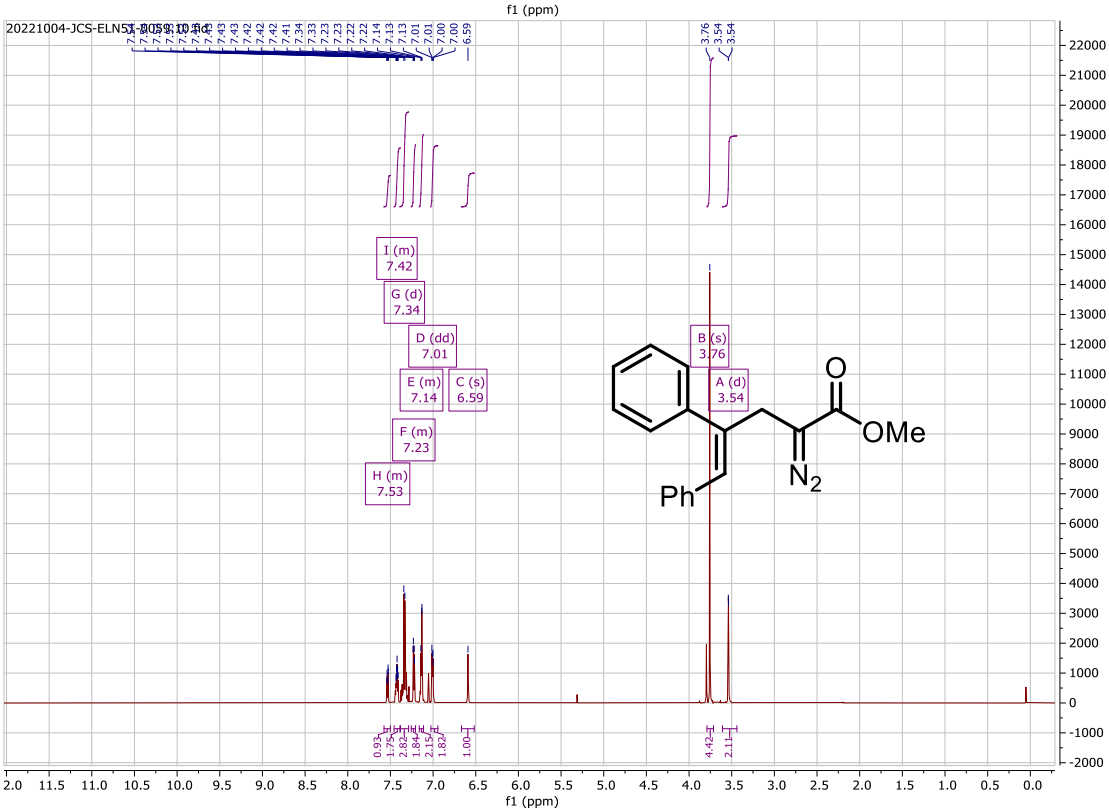
20221004-JCS-ELN51-0059.10.fid
3.76
3.54
3.54
I (m)
7.42
G (d)
7.34
D (dd)
7.01
E (m)
7.14
C (s)
6.59
F (m)
7.23
H (m)
7.53
B (s)
3.76
A (d)
3.54
O
OMe
N2
Ph
0.93
1.75
2.82
1.84
2.15
1.82
1.00
4.42
2.11
f1 (ppm)

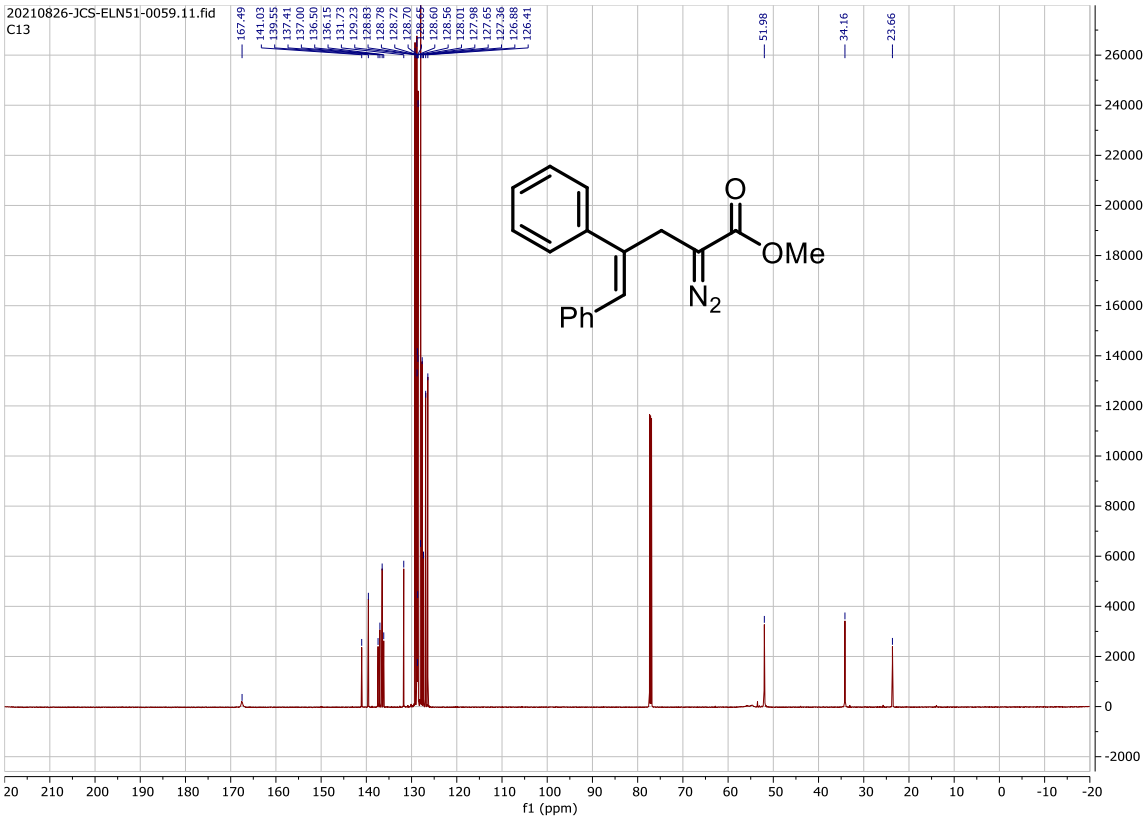
20210826-JCS-ELN51-0059.11.fid
C13
167.49
141.03
139.55
137.41
137.00
136.50
136.15
131.73
129.23
128.83
128.78
128.72
128.70
128.65
128.60
128.56
128.01
127.98
127.65
127.36
126.88
126.41
51.98
34.16
23.66
O
OMe
N2
Ph
f1 (ppm)

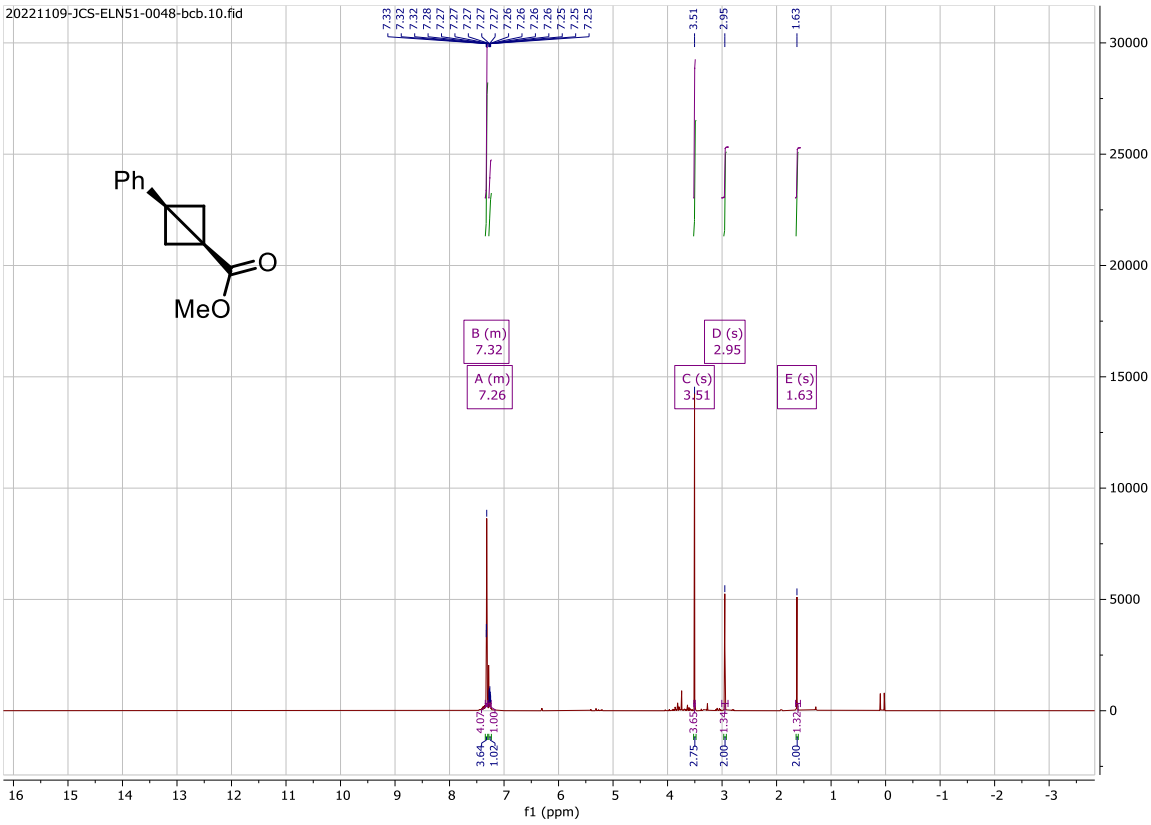
20221109-JCS-ELN51-0048-bcb.10.fid
7.33
7.32
7.32
7.28
7.27
7.27
7.27
7.27
7.27
7.26
7.26
7.26
7.26
7.25
7.25
7.25
3.51
2.95
1.63
Ph
O
MeO
B (m)
7.32
A (m)
7.26
D (s)
2.95
C (s)
3.51
E (s)
1.63
4.07
1.00
3.64
1.02
3.63
2.75
1.34
2.00
1.32
2.00
f1 (ppm)

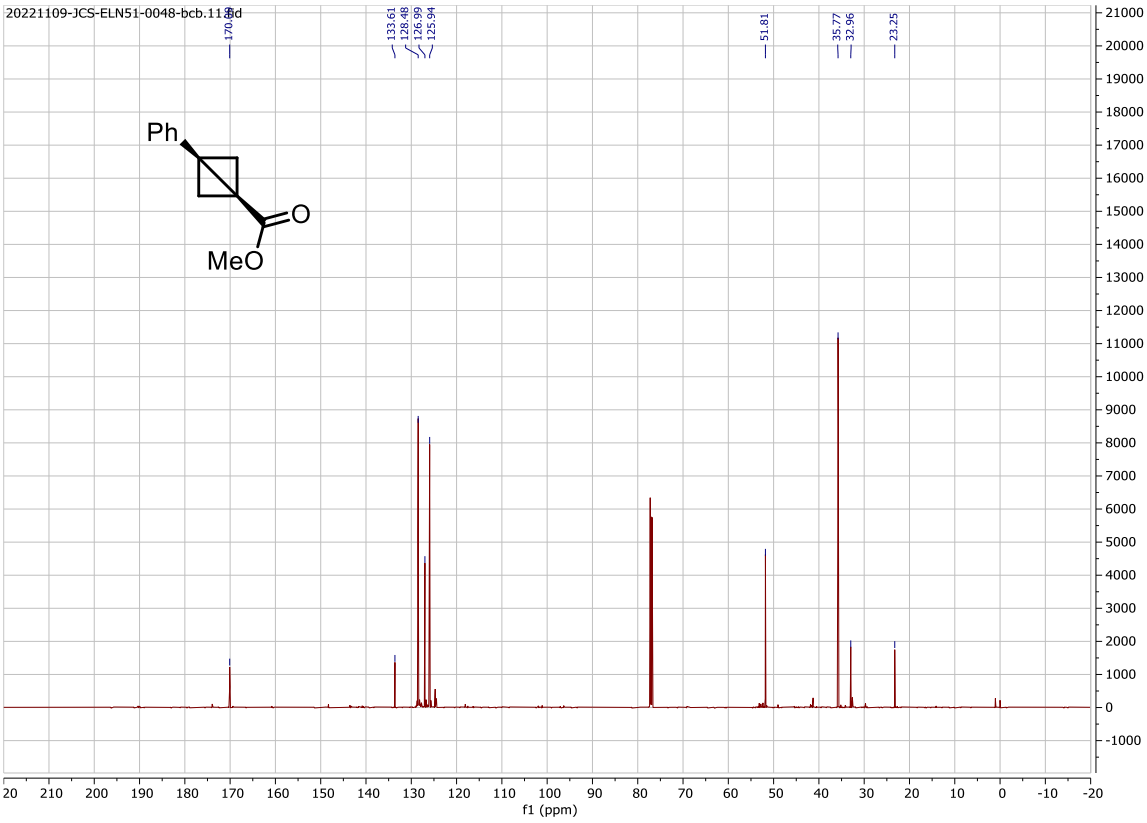
20221109-JCS-ELN51-0048-bcb.11.fid
170.88
133.61
128.48
126.99
125.94
51.81
35.77
32.96
23.25
Ph
O
MeO
f1 (ppm)

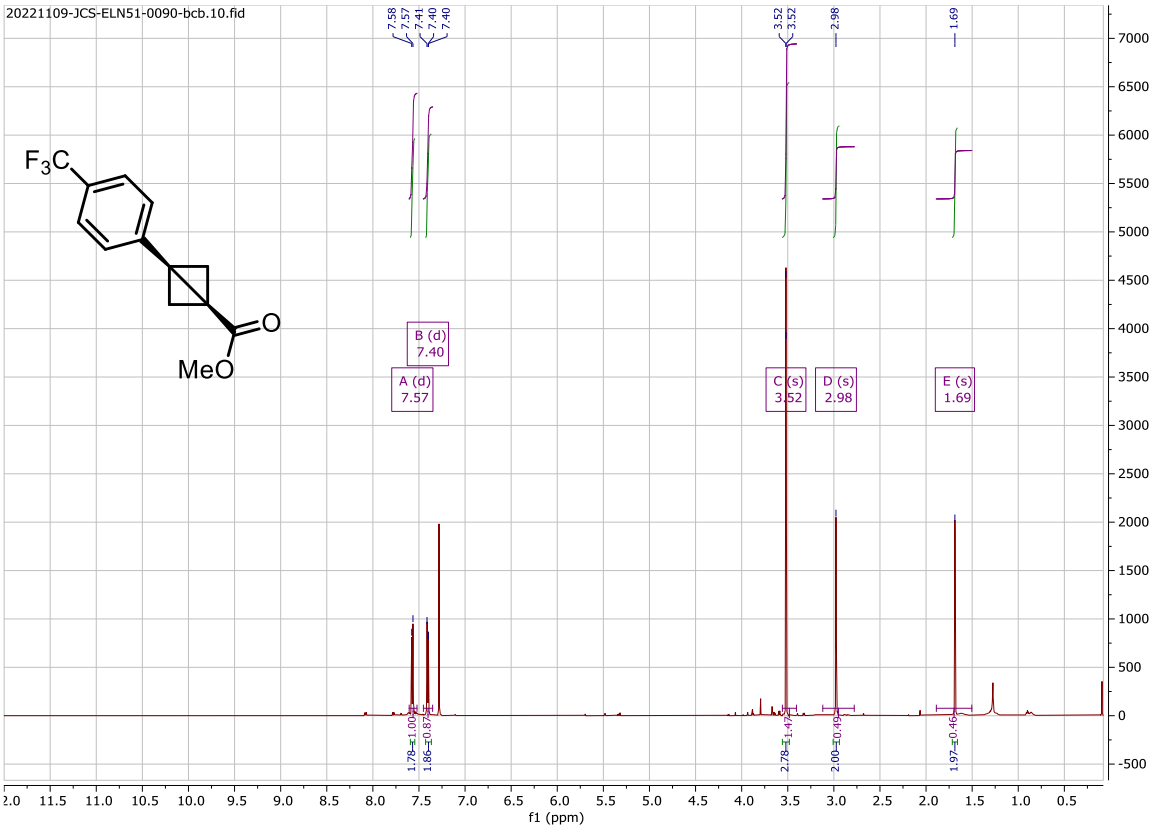
20221109-JCS-ELN51-0090-bcb.10.fid
7.58
7.57
7.41
7.40
7.40
3.52
3.52
2.98
1.69
F3C
O
MeO
B (d)
7.40
A (d)
7.57
C (s)
3.52
D (s)
2.98
E (s)
1.69
1.78 1.00
1.86 0.87
2.78 1.47
2.00 0.49
1.97 0.46
f1 (ppm)

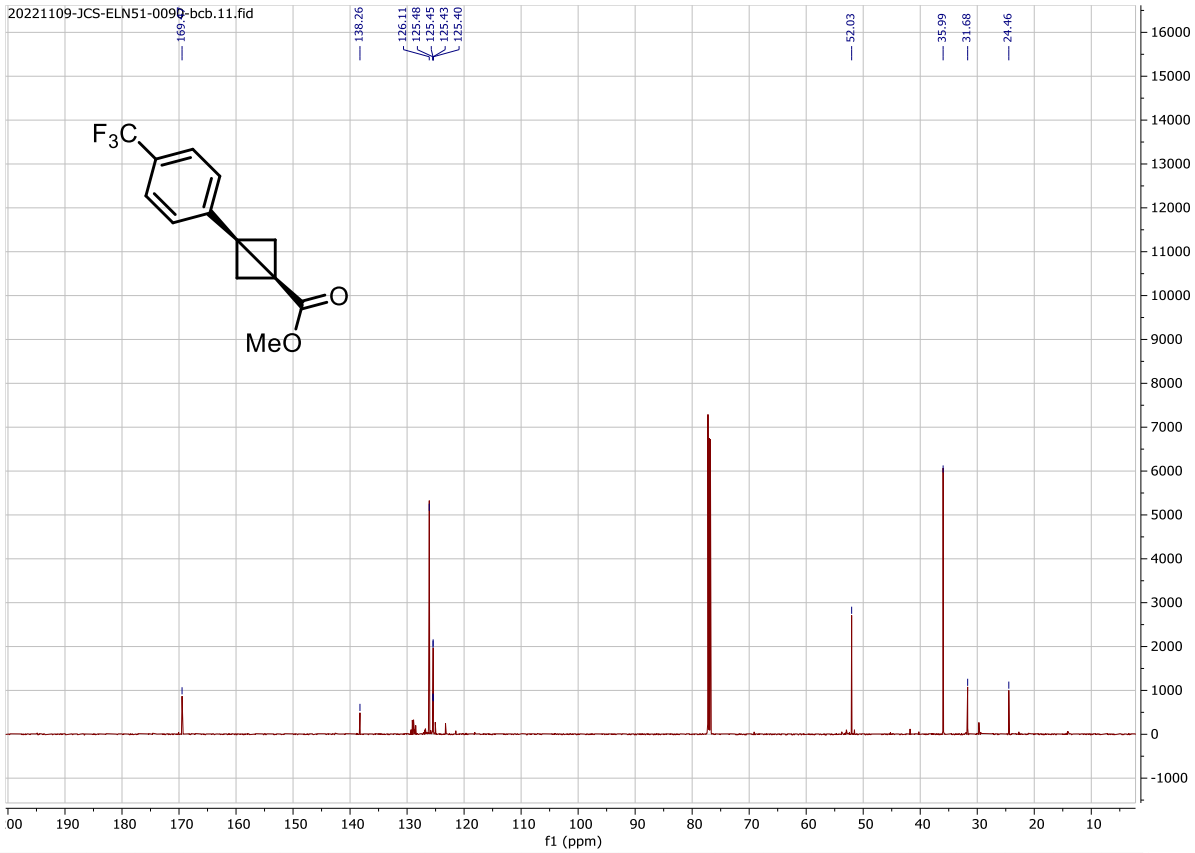
20221109-JCS-ELN51-0090-bcb.11.fid
169.9
138.26
126.11
125.48
125.45
125.43
125.40
52.03
35.99
31.68
24.46
F3C
O
MeO
f1 (ppm)

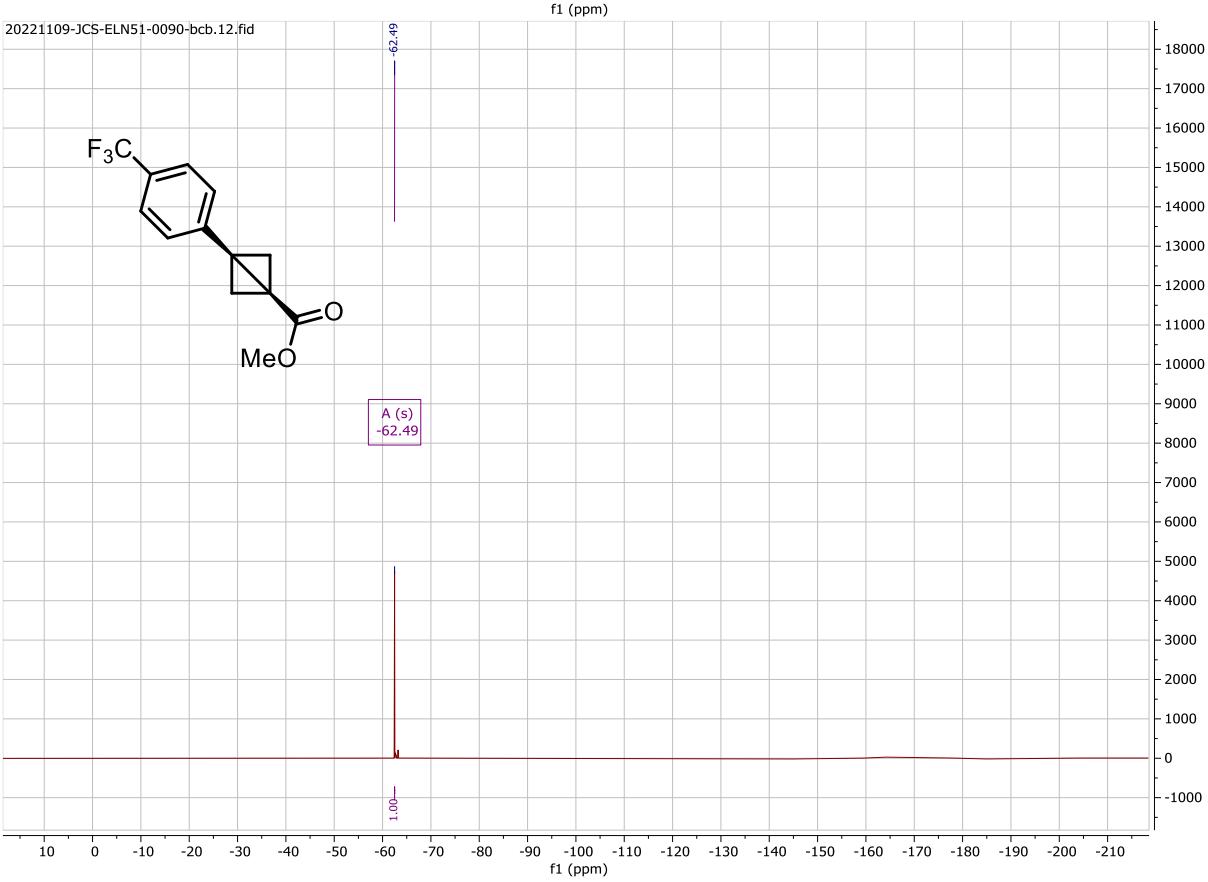
20221109-JCS-ELN51-0090-bcb.12.fid
-62.49
F3C
O
MeO
A (s)
-62.49
1.00
f1 (ppm)

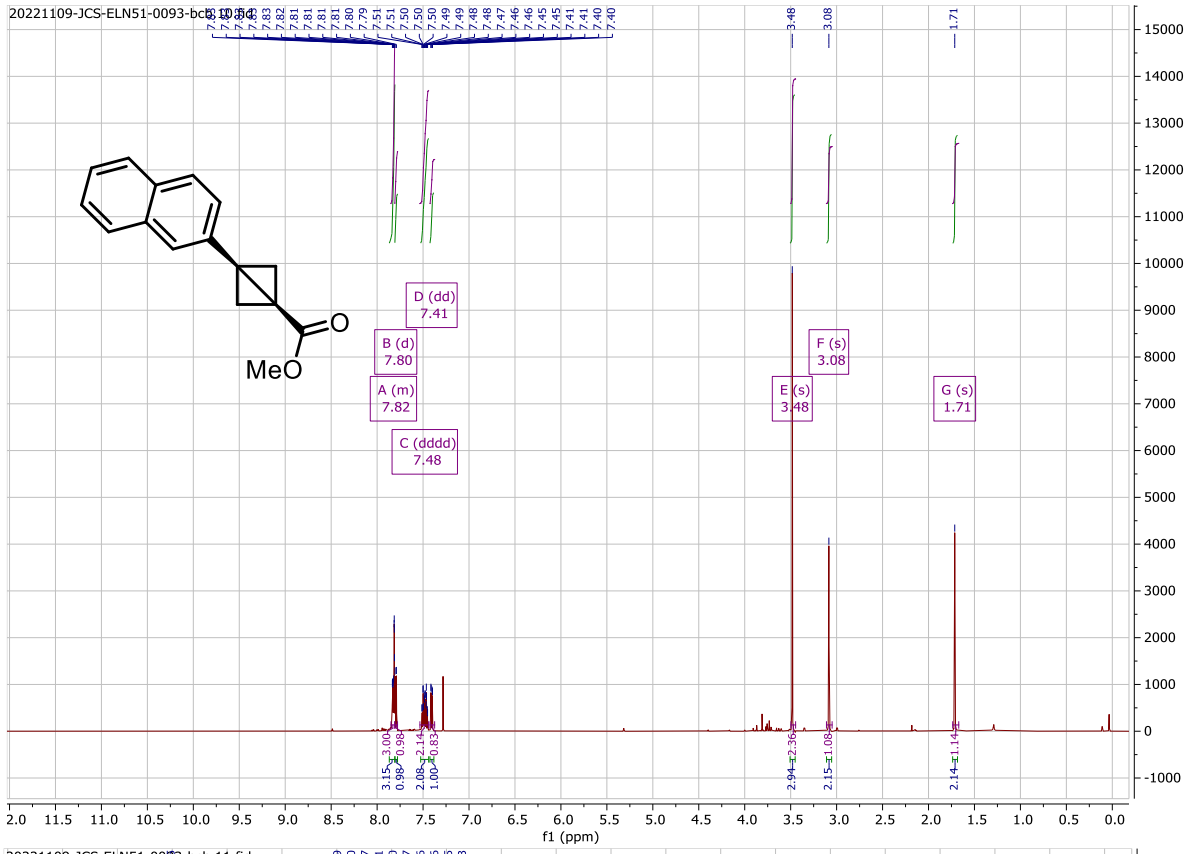
20221109-JCS-ELN51-0093-bcb.10.fid
MeO
O
D (dd)
7.41
B (d)
7.80
A (m)
7.82
C (dddd)
7.48
E (s)
3.48
F (s)
3.08
G (s)
1.71
f1 (ppm)

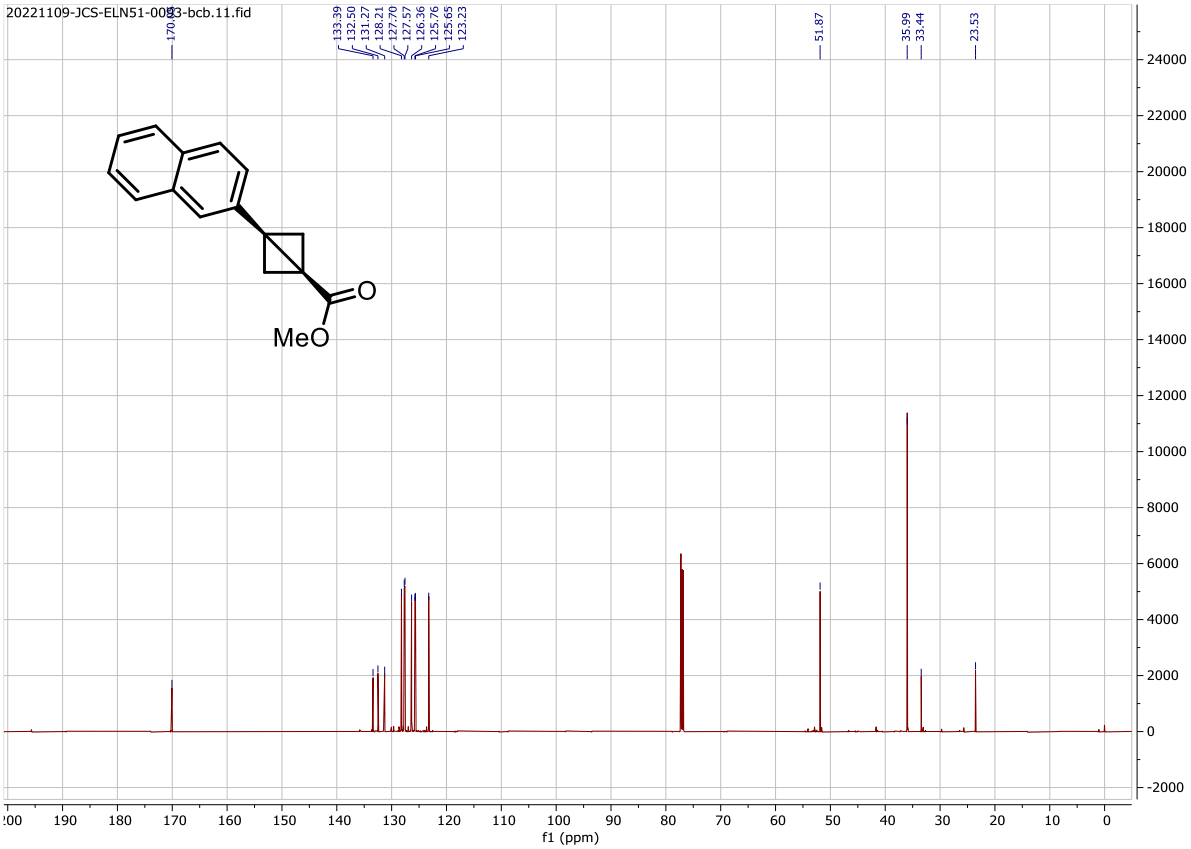
20221109-JCS-ELN51-0093-bcb.11.fid
MeO
O
170.03
133.39
132.50
131.27
128.21
127.70
127.57
126.36
125.76
125.65
123.23
51.87
35.99
33.44
23.53
f1 (ppm)

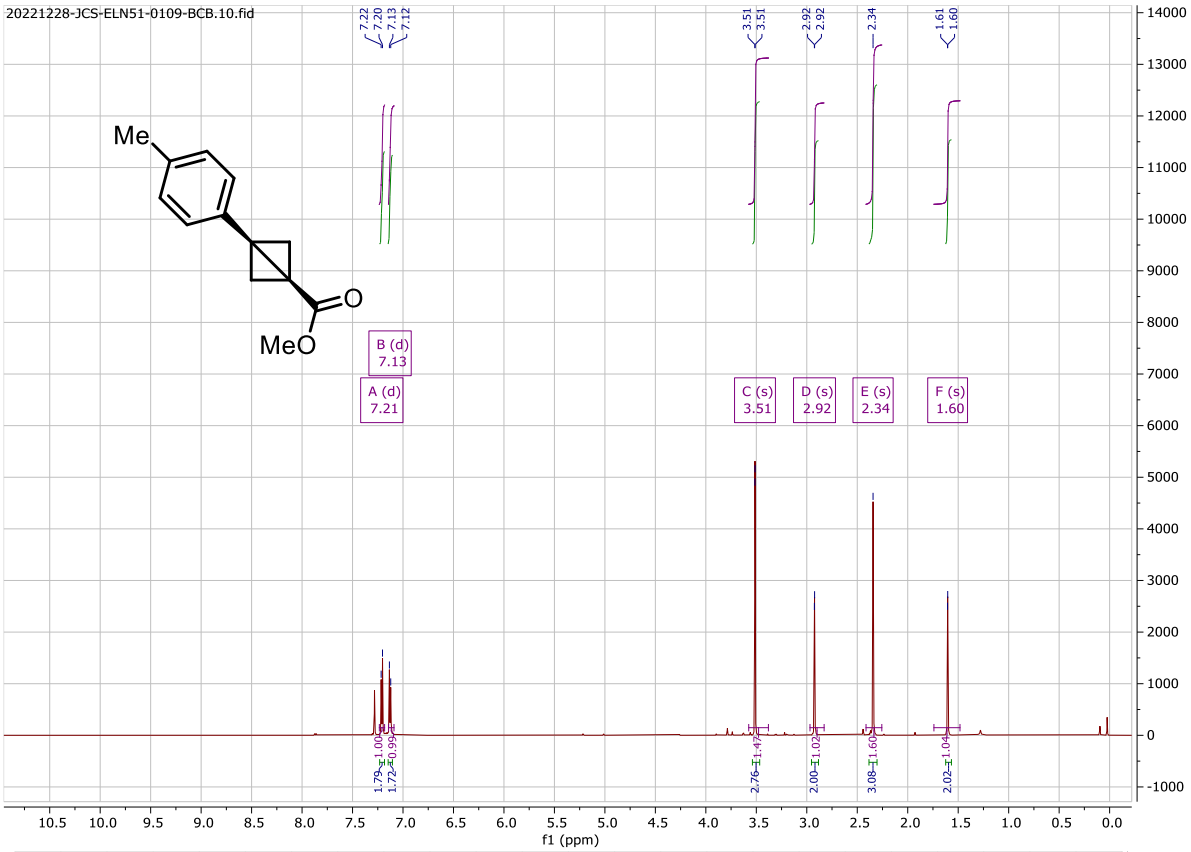
20221228-JCS-ELN51-0109-BCB.10.fid
Me
O
MeO
B (d)
7.13
A (d)
7.21
C (s)
3.51
D (s)
2.92
E (s)
2.34
F (s)
1.60
f1 (ppm)

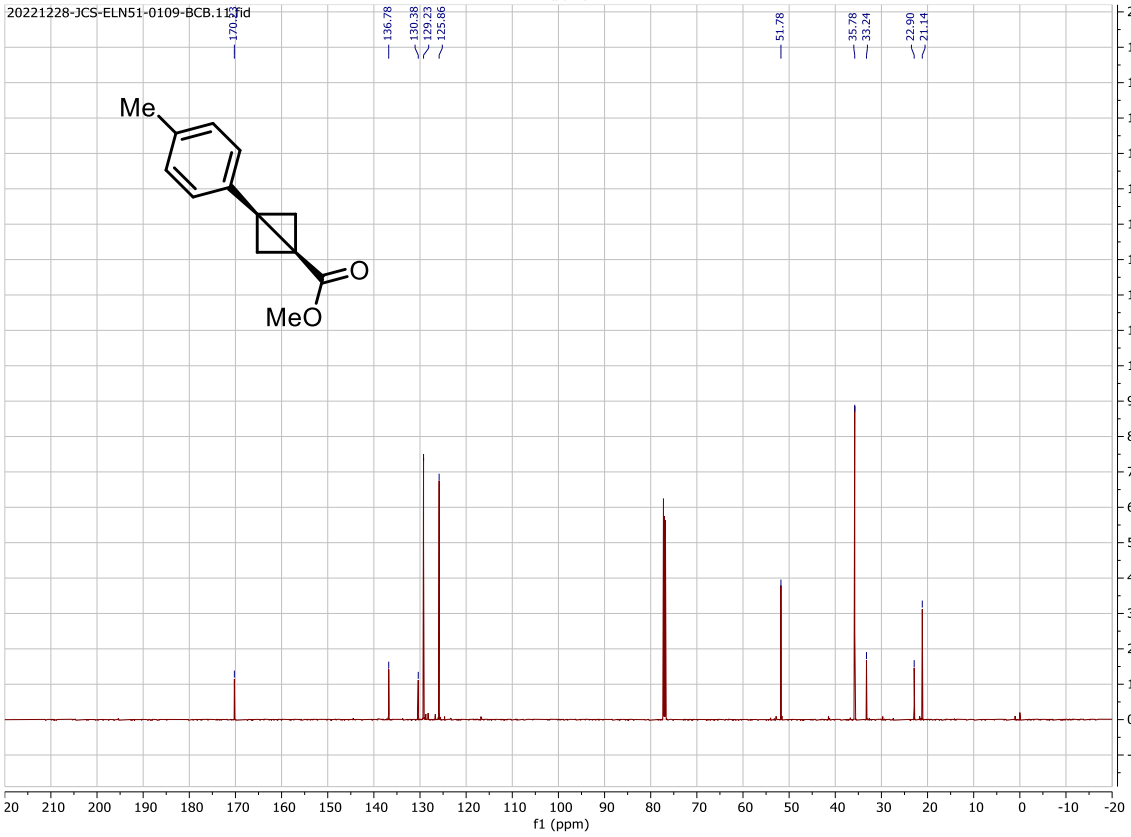
20221228-JCS-ELN51-0109-BCB.11.fid
Me
O
MeO
170.21
136.78
130.38
129.23
125.86
51.78
35.78
33.24
22.90
21.14
f1 (ppm)

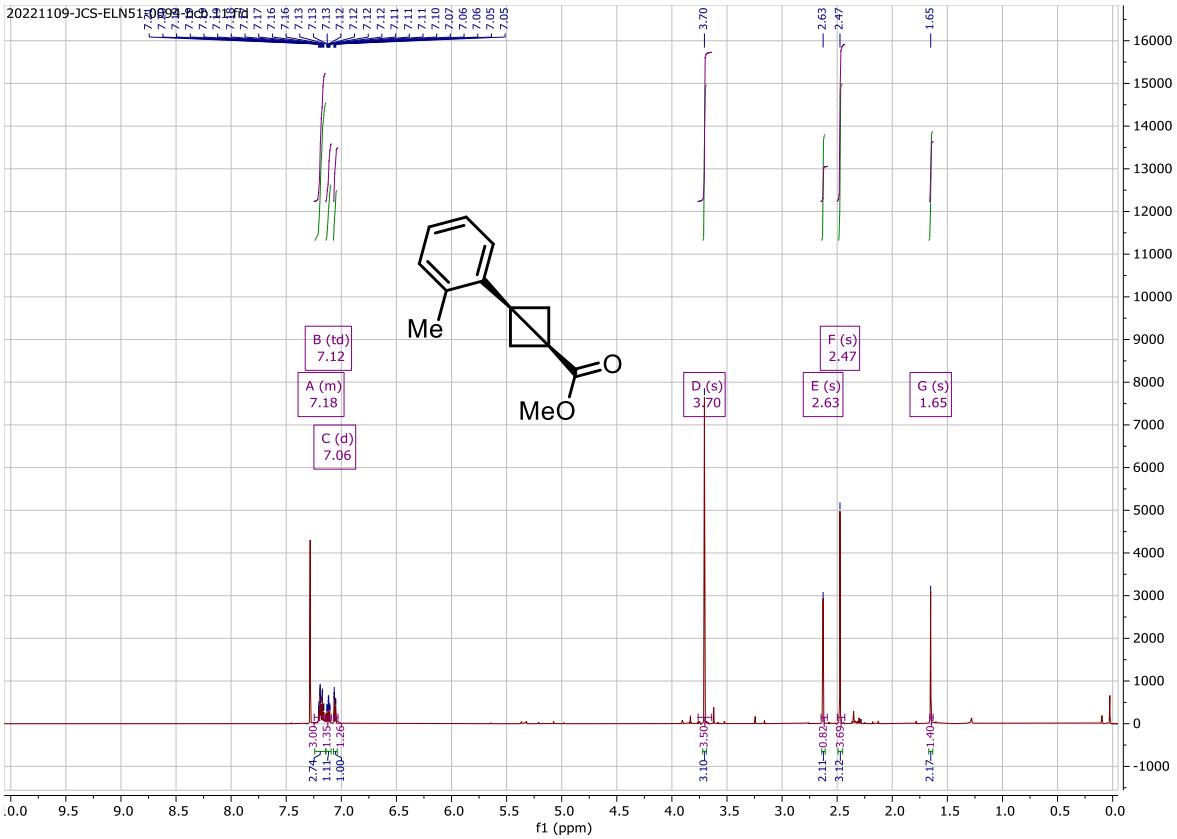
20221109-JCS-ELN51-0094-bcb.11.fid
Me
O
MeO
B (td)
7.12
A (m)
7.18
C (d)
7.06
D (s)
3.70
E (s)
2.63
F (s)
2.47
G (s)
1.65
f1 (ppm)

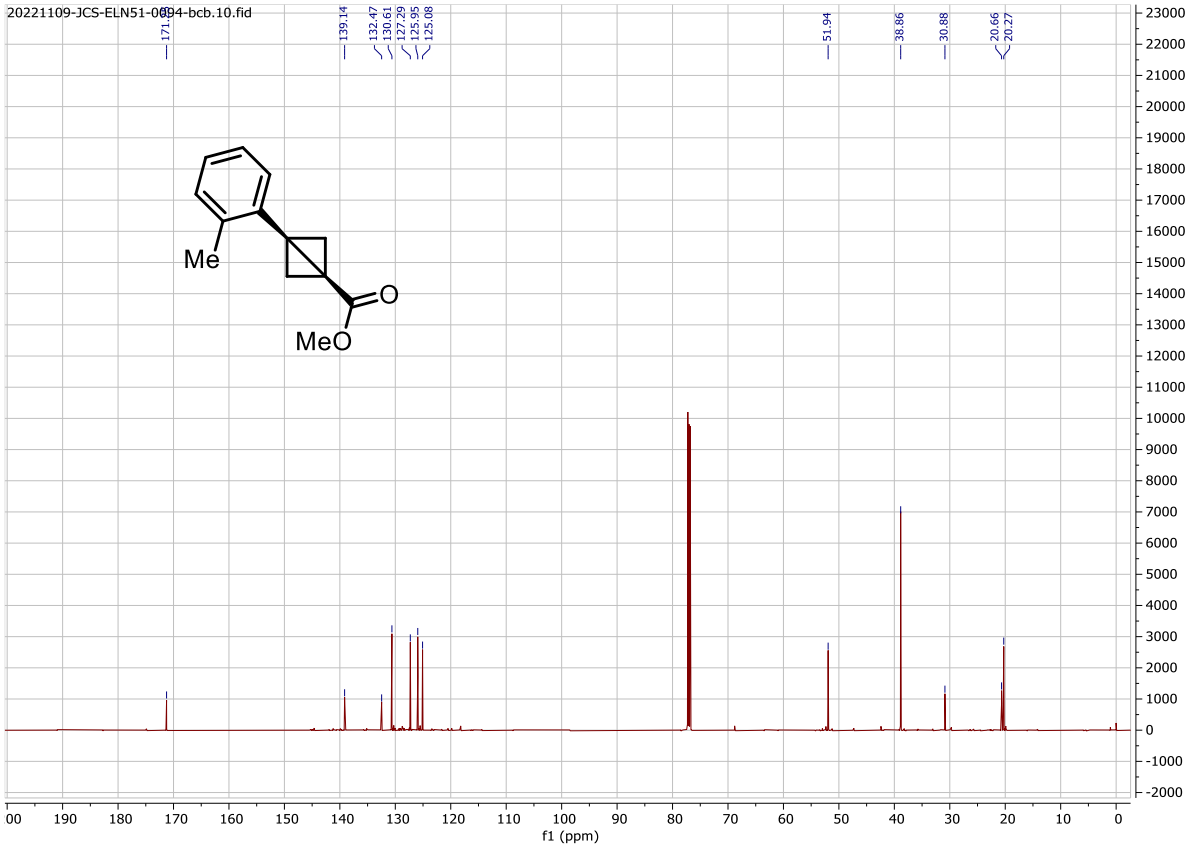
20221109-JCS-ELN51-0094-bcb.10.fid
171.61
139.14
132.47
130.61
127.29
125.95
125.08
51.94
38.86
30.88
20.66
20.27
Me
O
MeO
f1 (ppm)

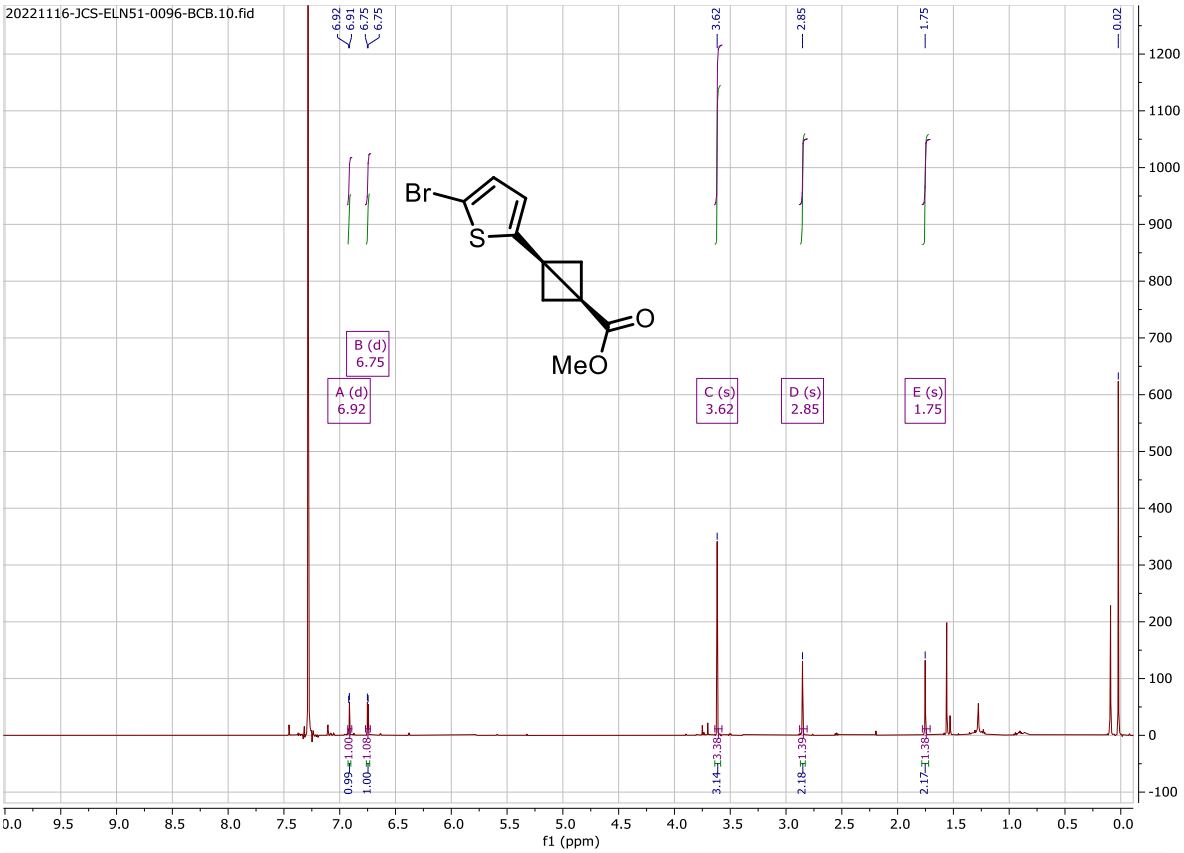
20221116-JCS-ELN51-0096-BCB.10.fid
6.92
6.91
6.75
6.75
3.62
2.85
1.75
0.02
Br
S
O
MeO
B (d)
6.75
A (d)
6.92
C (s)
3.62
D (s)
2.85
E (s)
1.75
0.99
1.00
1.08
3.14
3.38
2.18
1.39
2.17
1.38
f1 (ppm)

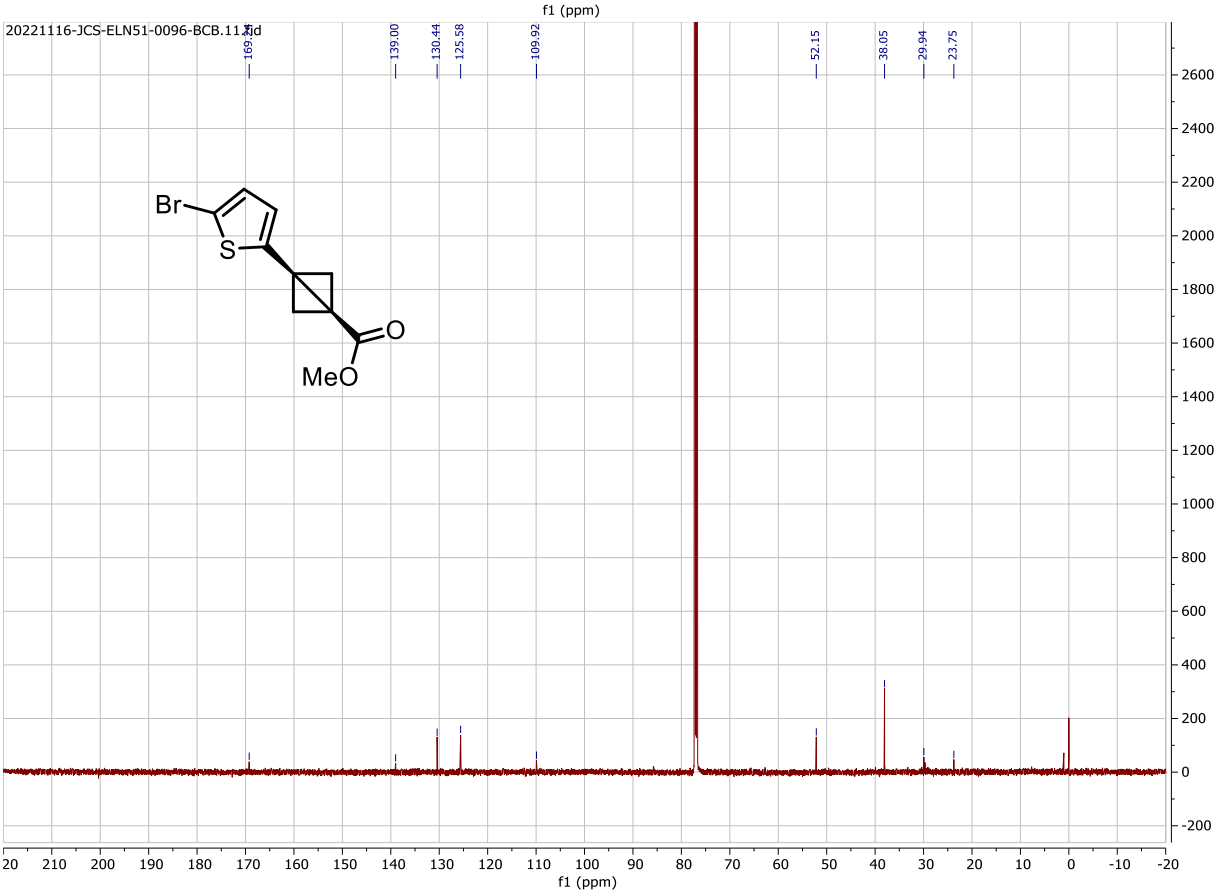
20221116-JCS-ELN51-0096-BCB.11.fid
169.21
139.00
130.44
125.58
109.92
52.15
38.05
29.94
23.75
Br
S
O
MeO
f1 (ppm)

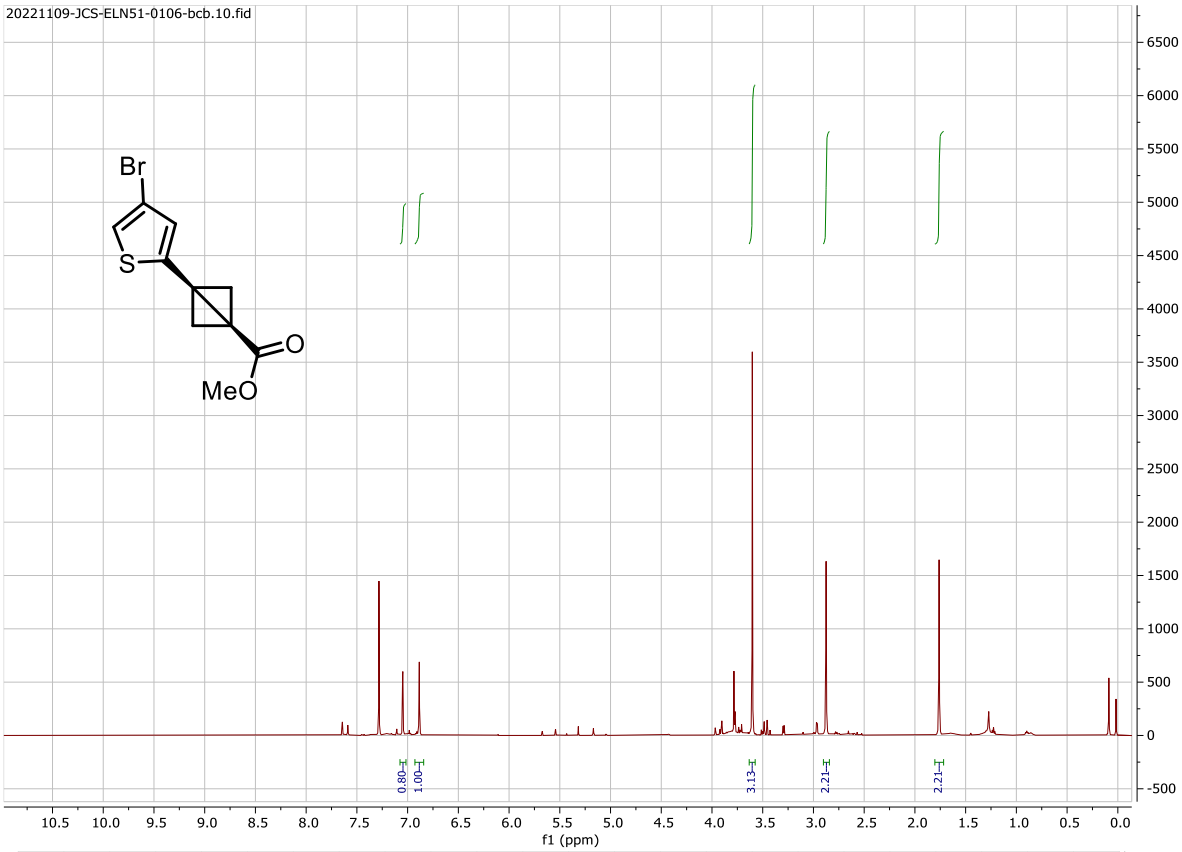
20221109-JCS-ELN51-0106-bcb.10.fid
Br
S
O
MeO
0.80
1.00
3.13
2.21
2.21
f1 (ppm)

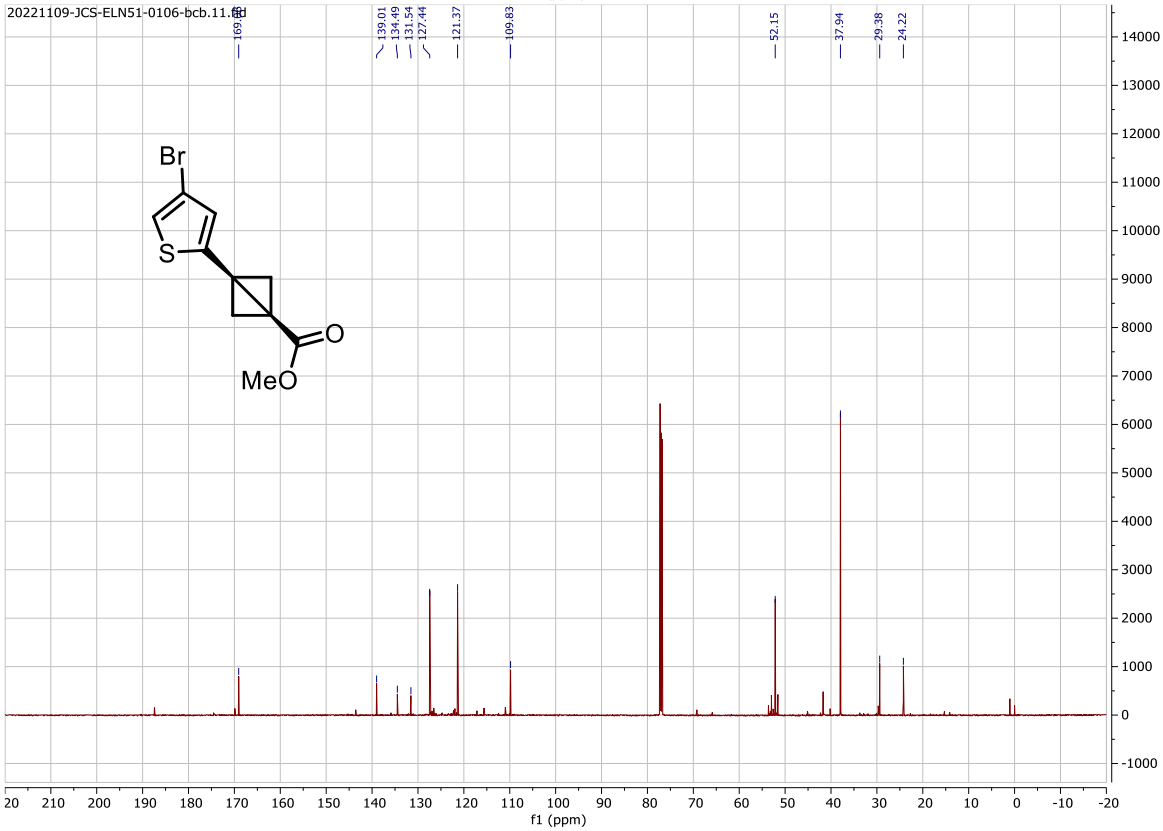
20221109-JCS-ELN51-0106-bcb.11.fid
169.81
139.01
134.49
131.54
127.44
121.37
109.83
52.15
37.94
29.38
24.22
Br
S
O
MeO
f1 (ppm)

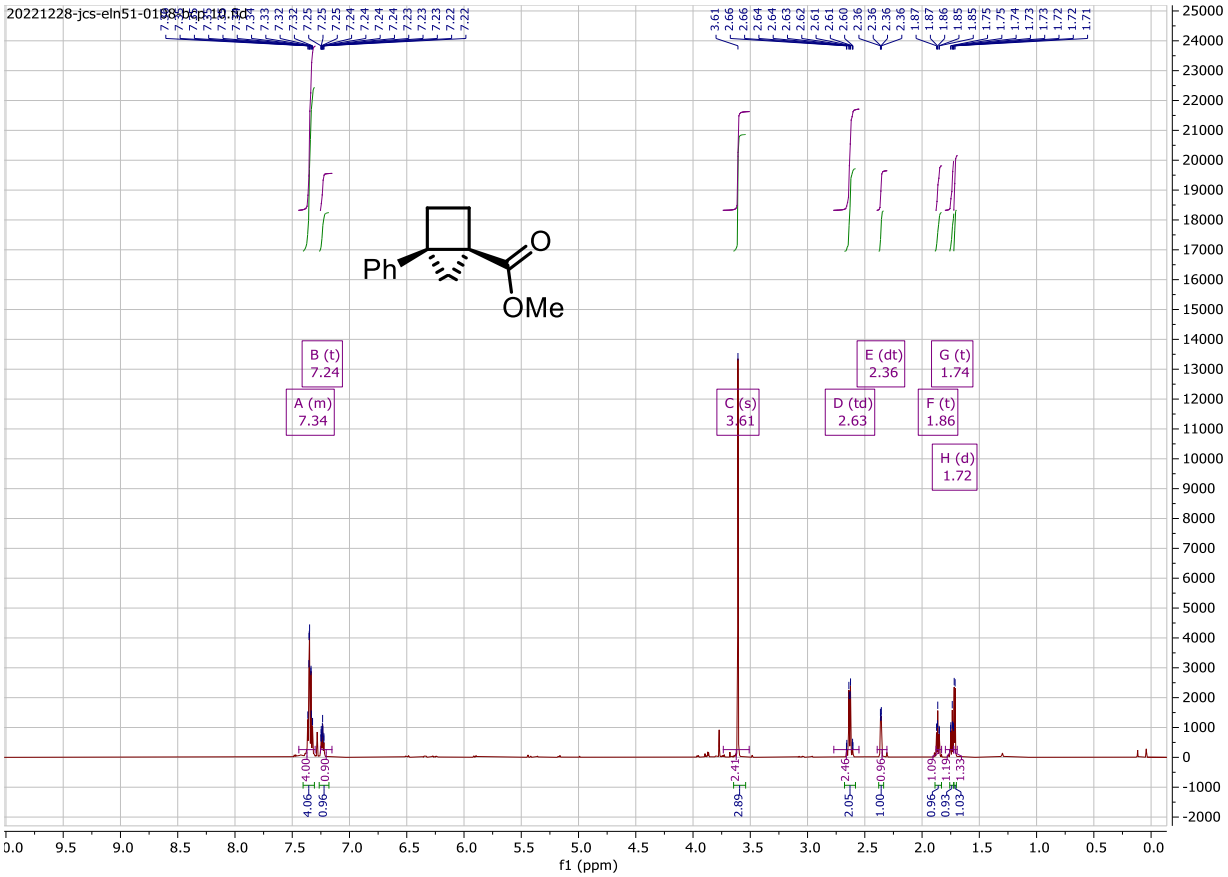
20221228-jcs-eln51-0108-bcp.10.fid
Ph
O
OMe
B (t)
7.24
A (m)
7.34
C (s)
3.61
D (td)
2.63
E (dt)
2.36
F (t)
1.86
G (t)
1.74
H (d)
1.72
f1 (ppm)

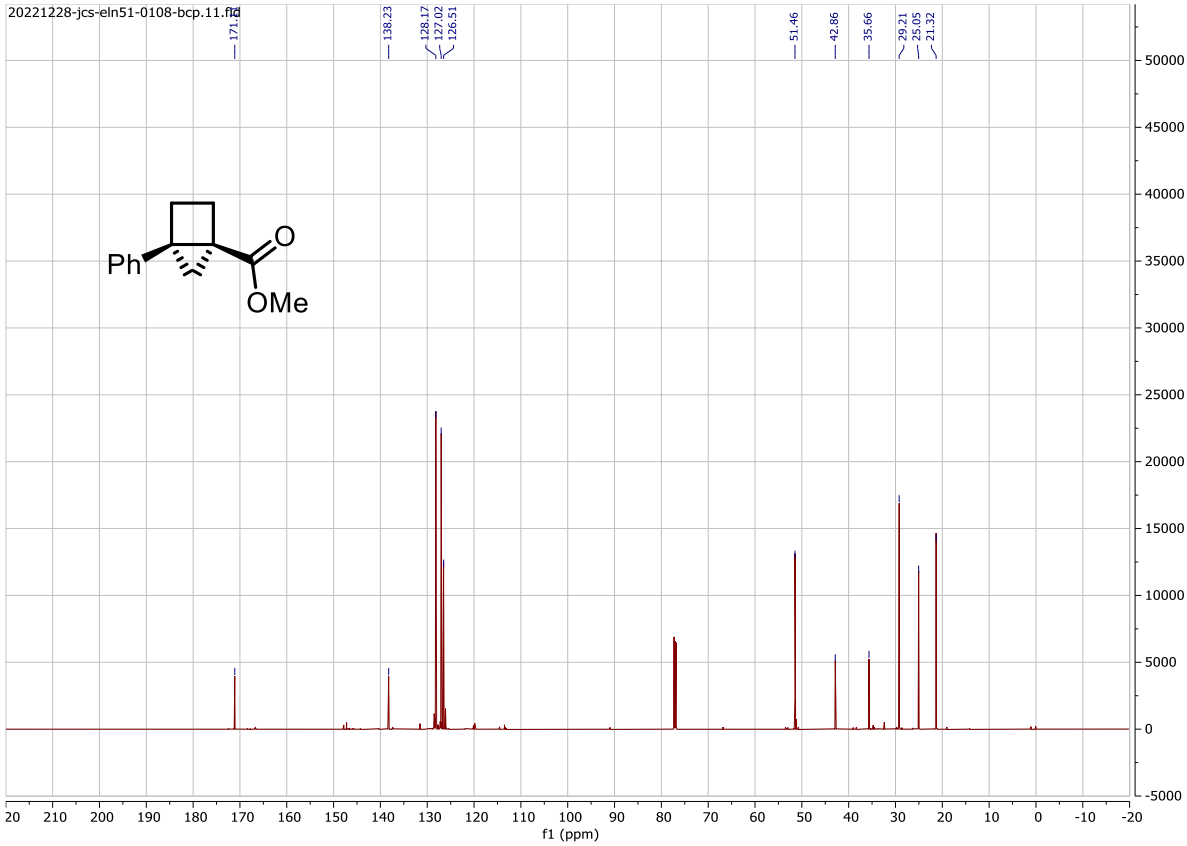
20221228-jcs-eln51-0108-bcp.11.fid
171.12
138.23
128.17
127.02
126.51
51.46
42.86
35.66
29.21
25.05
21.32
Ph
O
OMe
f1 (ppm)

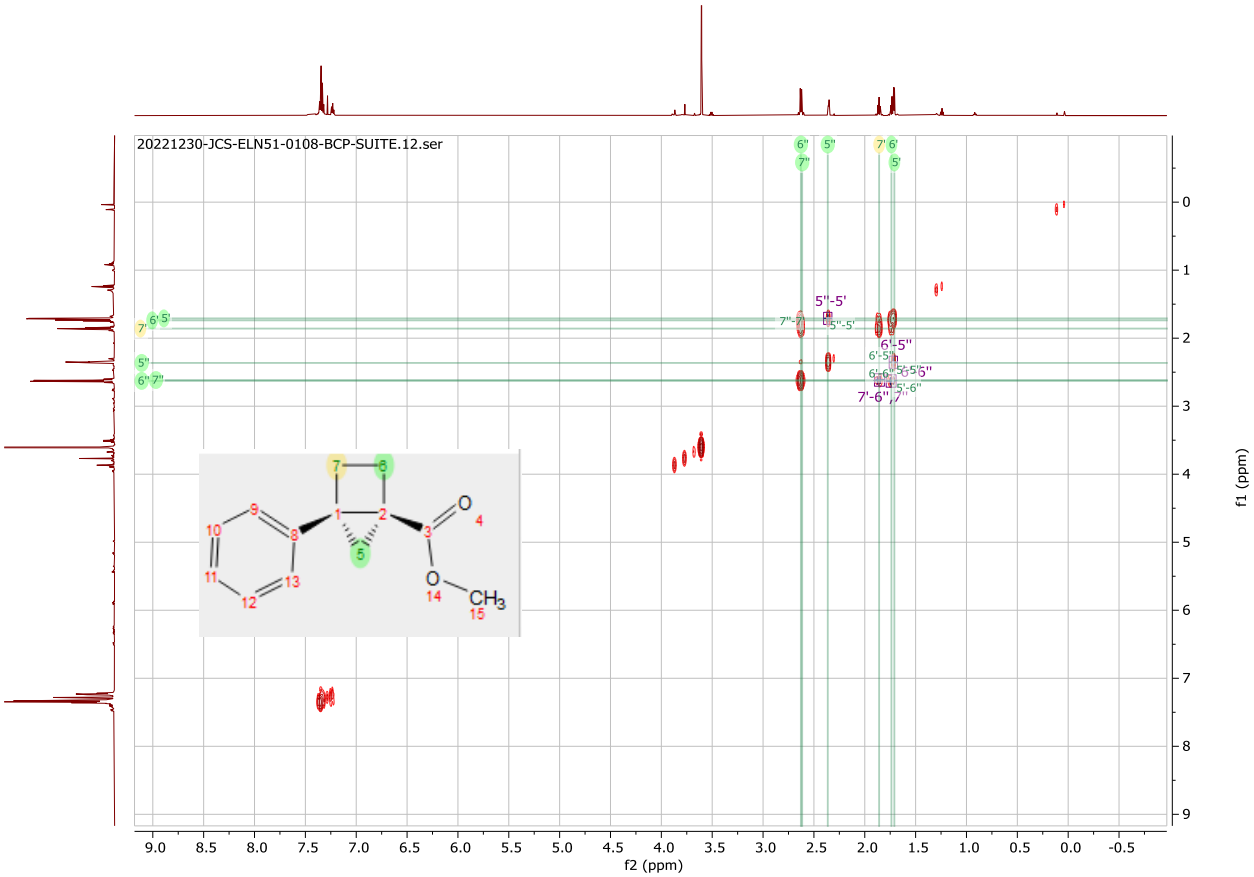
20221230-JCS-ELN51-0108-BCP-SUITE.12.ser
f2 (ppm)
f1 (ppm)


20221018-JCS-ELN51-0103-BCH.20.fid
Ph
OMe
I (m) 7.28
H (m) 7.22
G (s) 3.37
D (m) 1.93
B (ddd) 2.11
A (td) 2.59
F (m) 1.34
C (dd) 2.02
E (dt) 1.84
f1 (ppm)

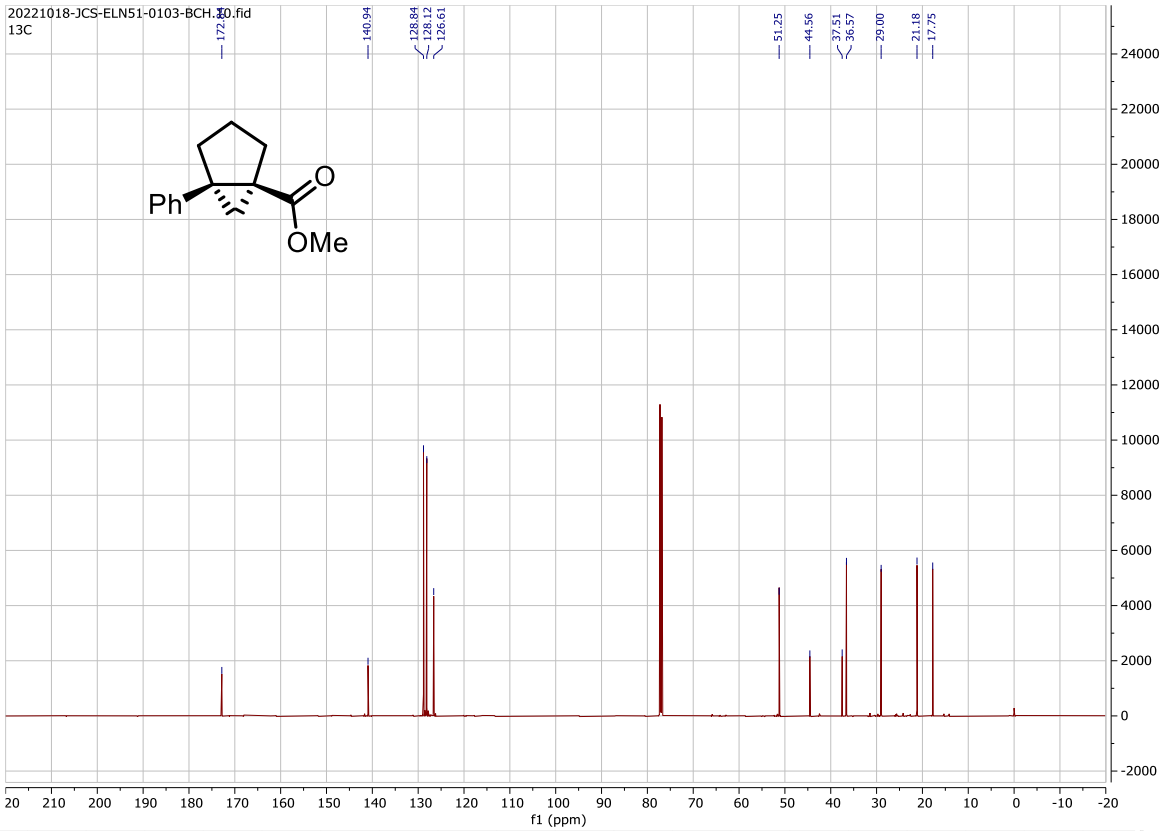
20221018-JCS-ELN51-0103-BCH.40.fid
13C
172.84
140.94
128.84
128.12
126.61
51.25
44.56
37.51
36.57
29.00
21.18
17.75
Ph
O
OMe
f1 (ppm)

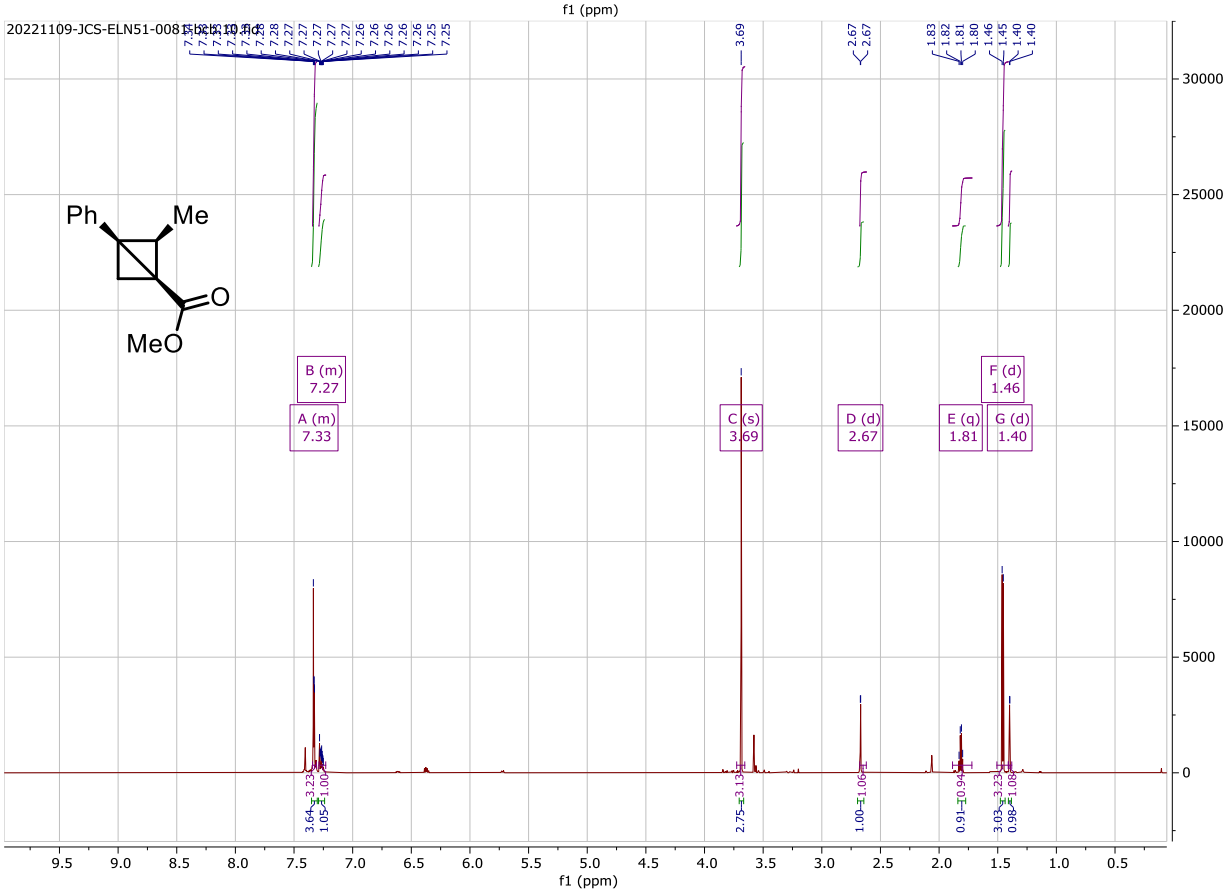
20221109-JCS-ELN51-008-1H.40.fid
Ph
Me
O
MeO
B (m)
7.27
A (m)
7.33
C (s)
3.69
D (d)
2.67
E (q)
1.81
F (d)
1.46
G (d)
1.40
f1 (ppm)

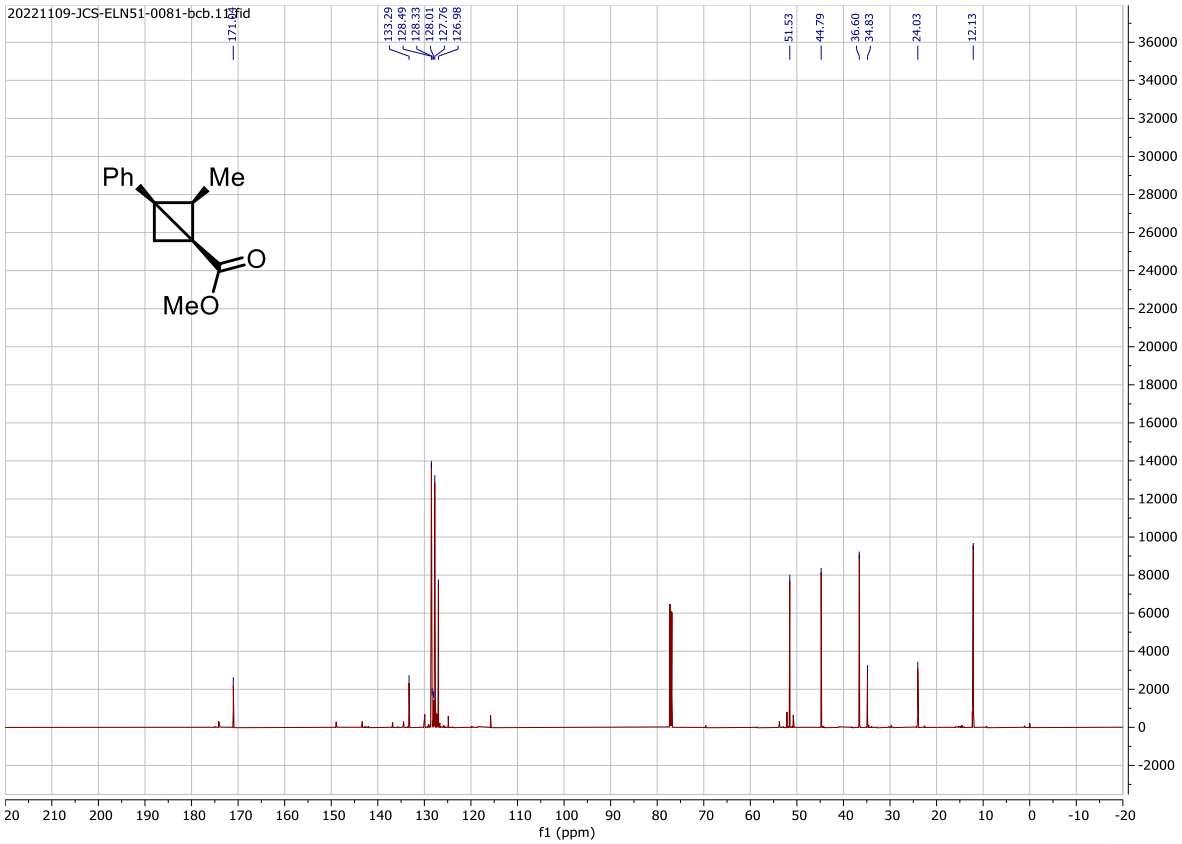
20221109-JCS-ELN51-0081-bcb.11.fid
171.15
133.29
128.49
128.33
128.01
127.76
126.98
51.53
44.79
36.60
34.83
24.03
12.13
Ph
Me
O
MeO
f1 (ppm)

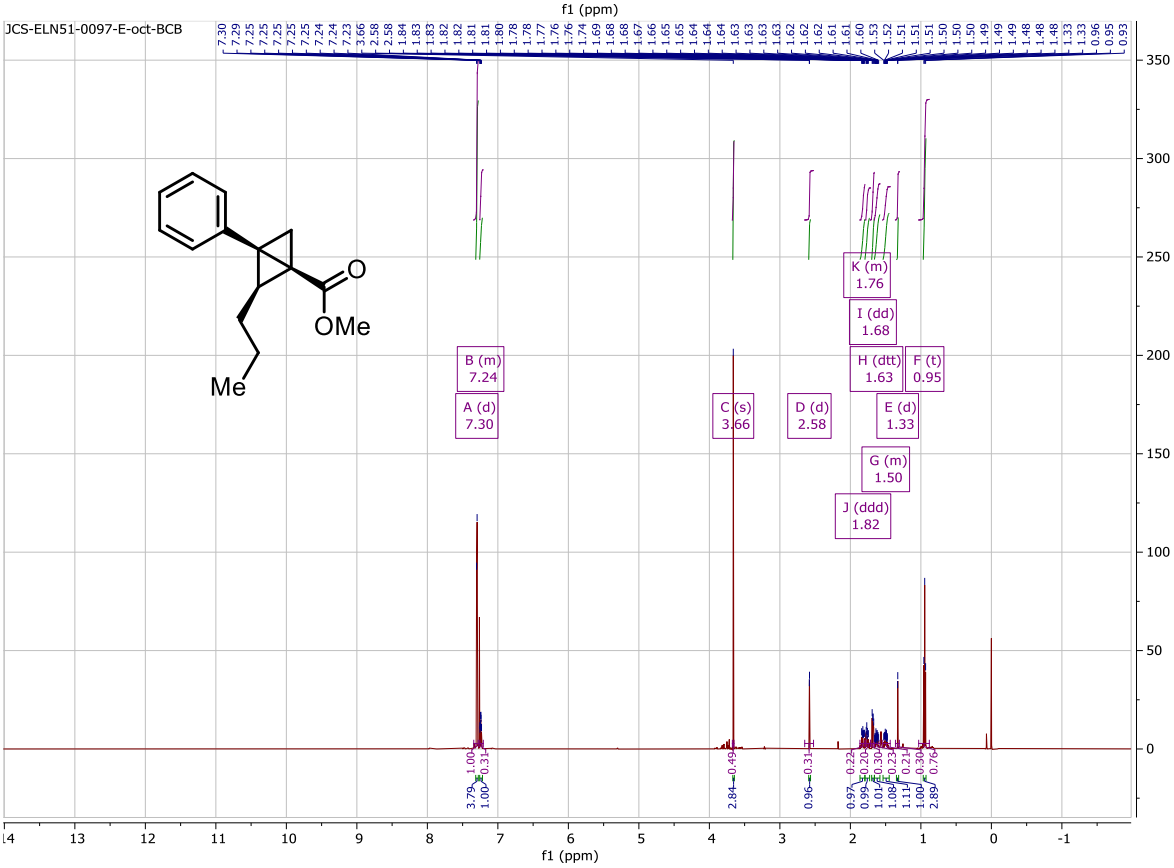
JCS-ELN51-0097-E-oct-BCB
O
OMe
Me
B (m)
7.24
A (d)
7.30
C (s)
3.66
D (d)
2.58
K (m)
1.76
I (dd)
1.68
H (dtt)
1.63
F (t)
0.95
E (d)
1.33
G (m)
1.50
J (ddd)
1.82
f1 (ppm)

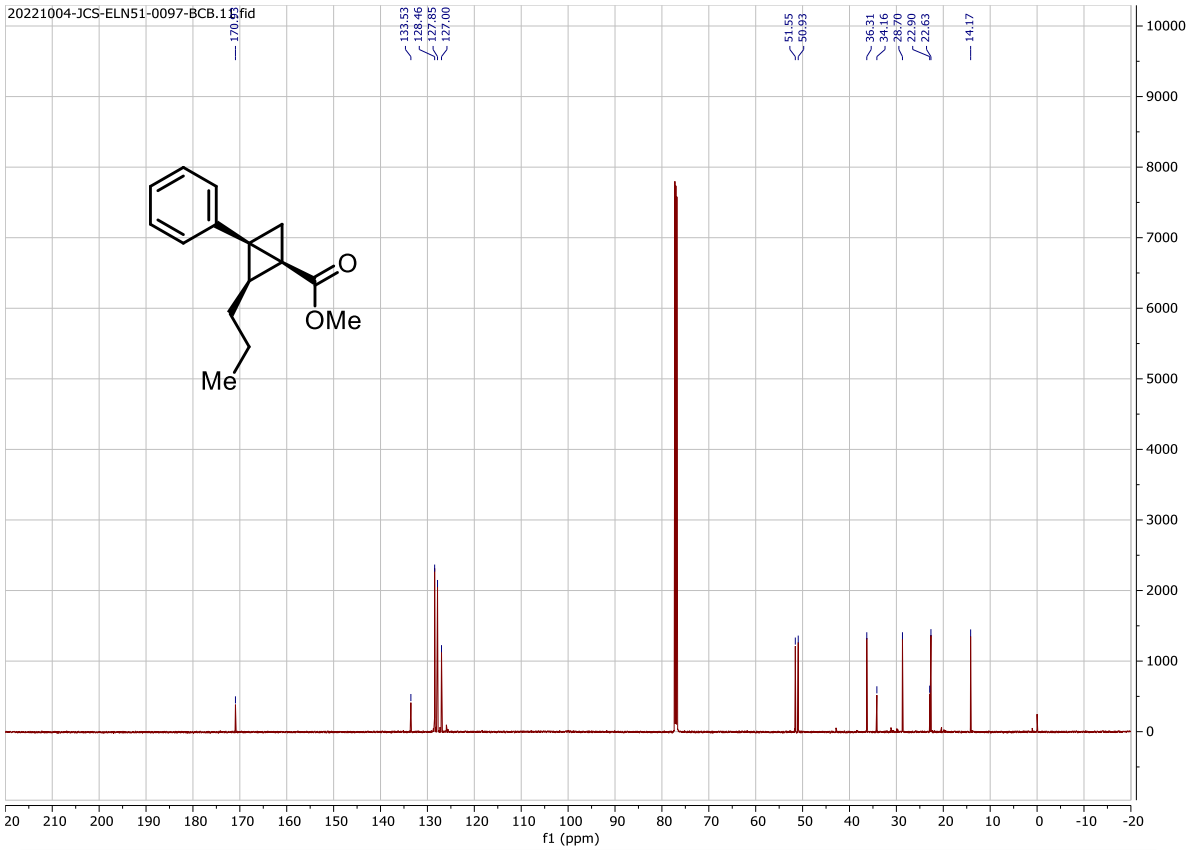
20221004-JCS-ELN51-0097-BCB.11.fid
170.51
133.53
128.46
127.85
127.00
51.55
50.93
36.31
34.16
28.70
22.90
22.63
14.17
O
OMe
Me
f1 (ppm)

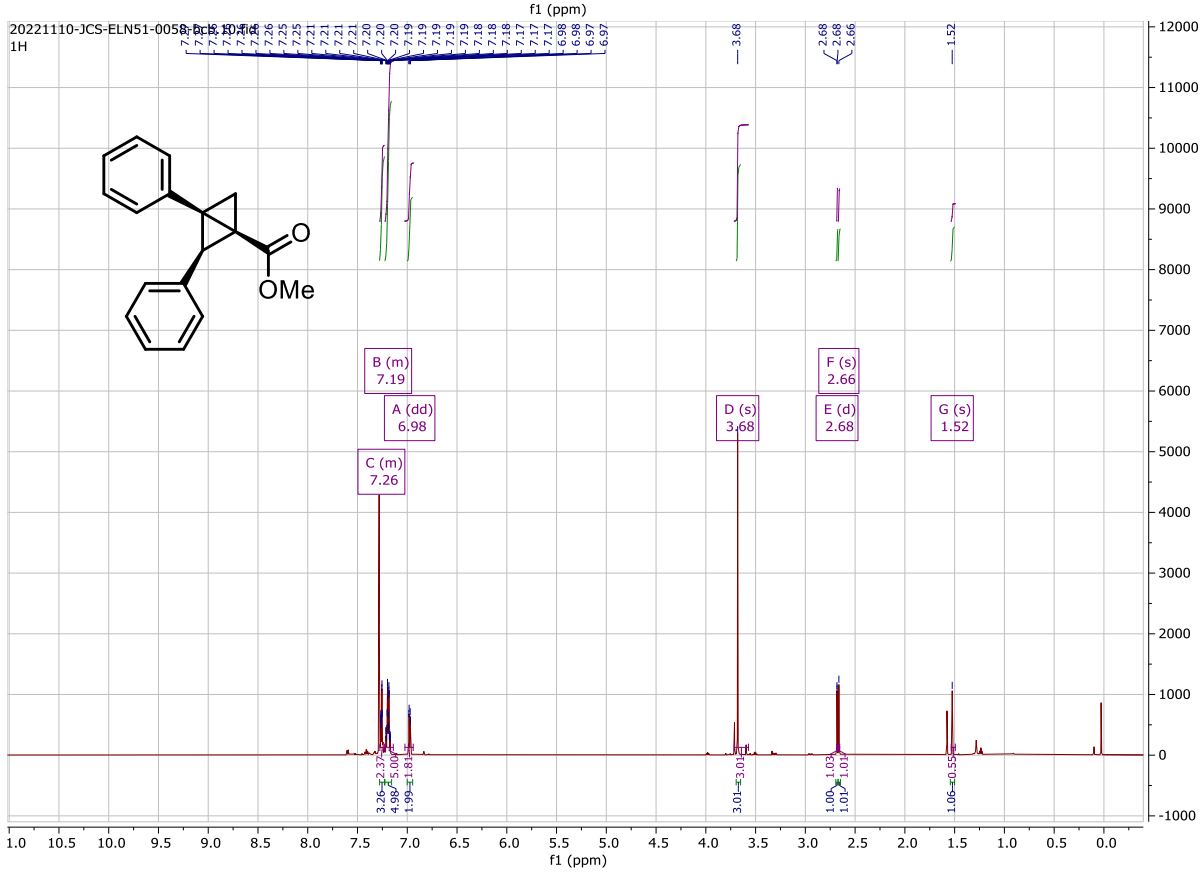
20221110-JCS-ELN51-0058-bcb.10.fid
1H
3.68
2.68
2.66
1.52
O
OMe
B (m)
7.19
A (dd)
6.98
C (m)
7.26
D (s)
3.68
F (s)
2.66
E (d)
2.68
G (s)
1.52
f1 (ppm)

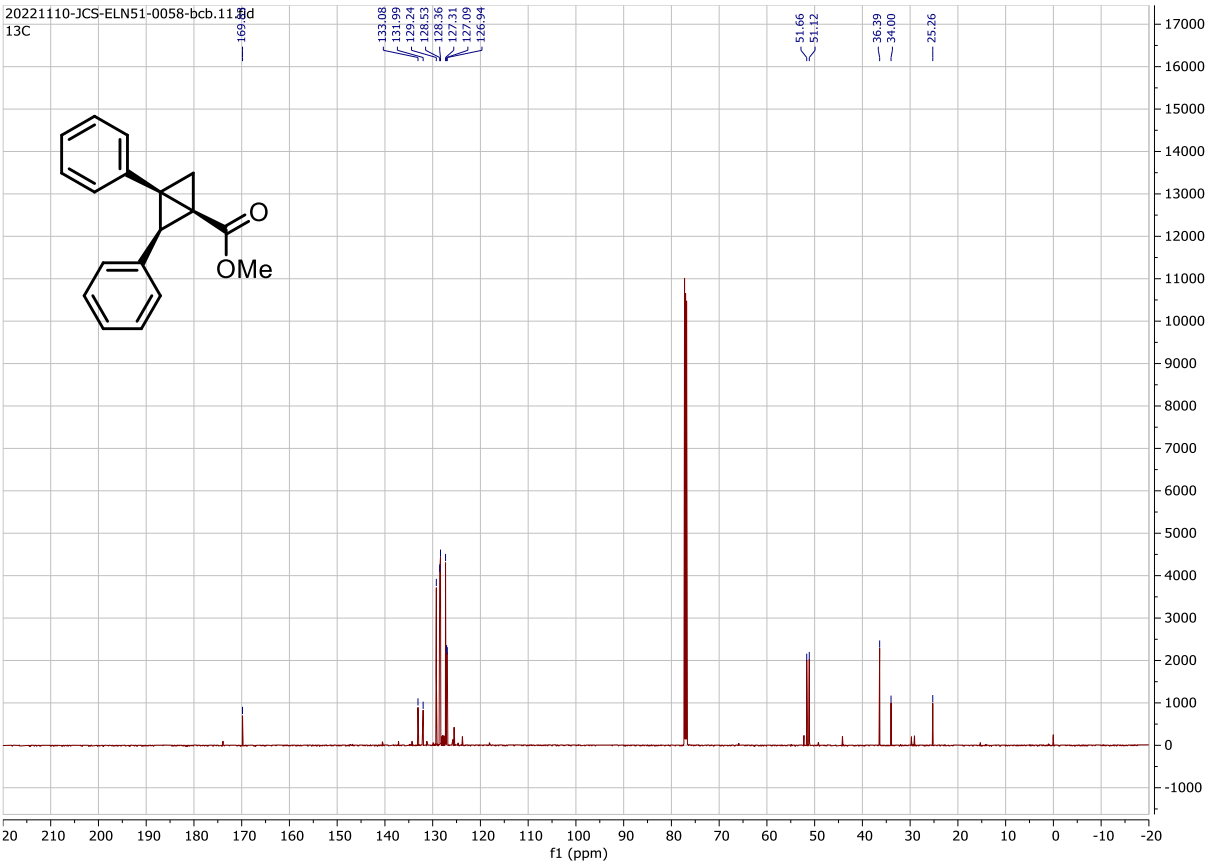
20221110-JCS-ELN51-0058-bcb.11.fid
13C
169.88
133.08
131.99
129.24
128.53
128.36
127.31
127.09
126.94
51.66
51.12
36.39
34.00
25.26
O
OMe
f1 (ppm)

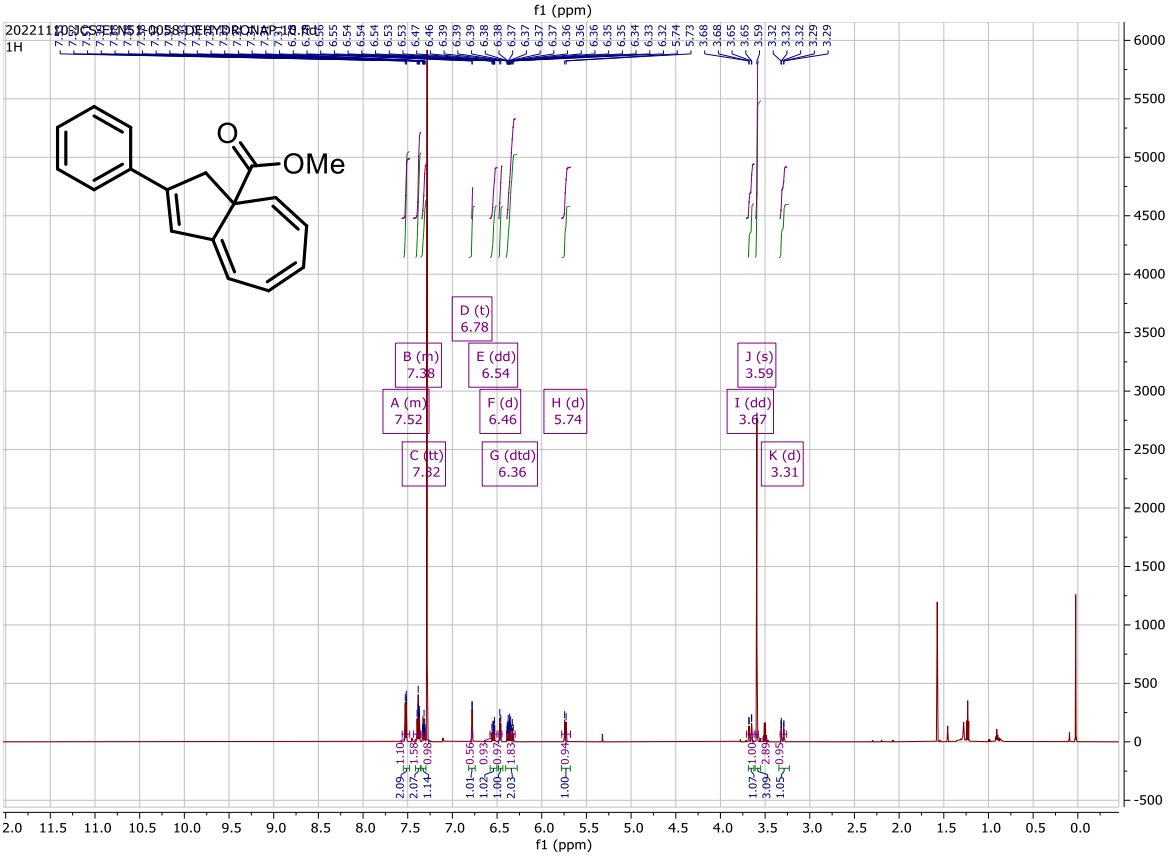
1H
O
OMe
D (t)
6.78
B (m)
7.38
E (dd)
6.54
J (s)
3.59
A (m)
7.52
F (d)
6.46
H (d)
5.74
I (dd)
3.67
C (tt)
7.32
G (dtd)
6.36
K (d)
3.31
f1 (ppm)

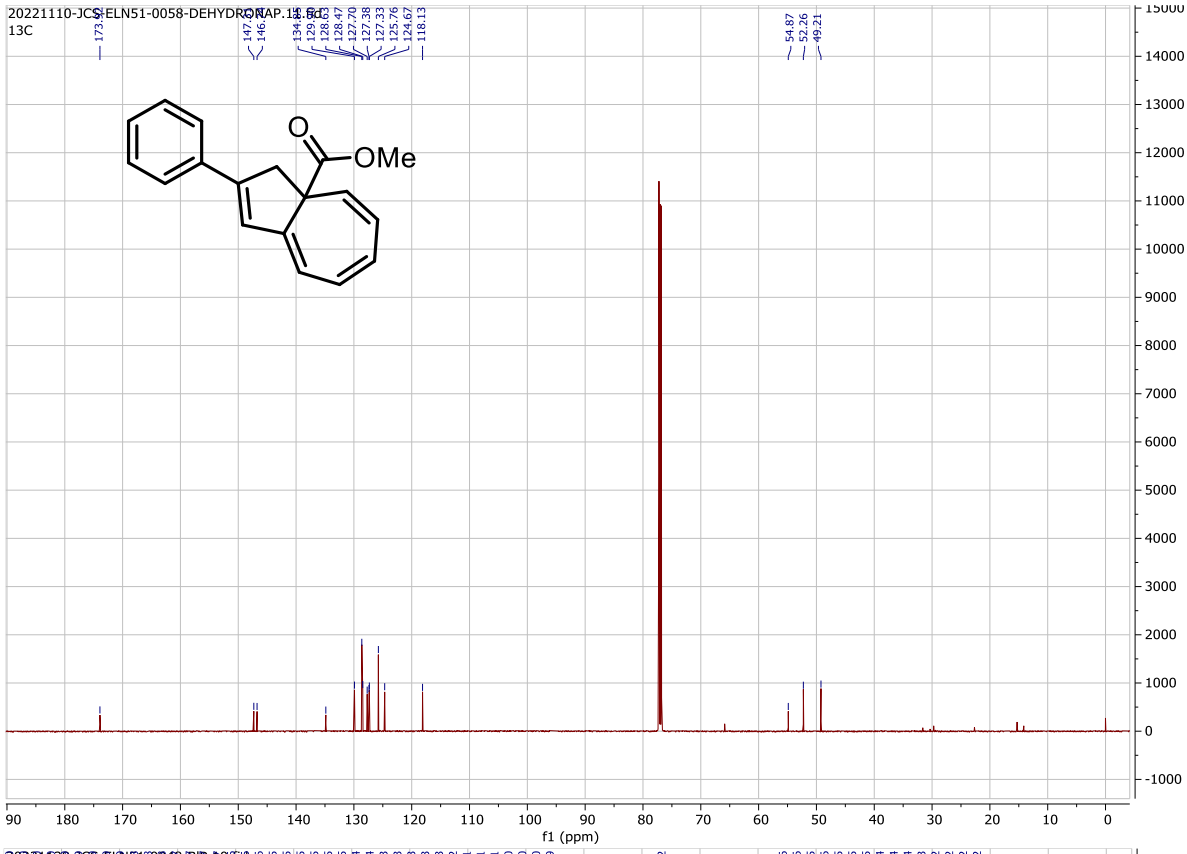
13C
173.7
147.08
146.7
134.8
129.51
128.65
128.47
127.70
127.38
127.33
125.76
124.67
118.13
54.87
52.26
49.21
O
OMe
f1 (ppm)

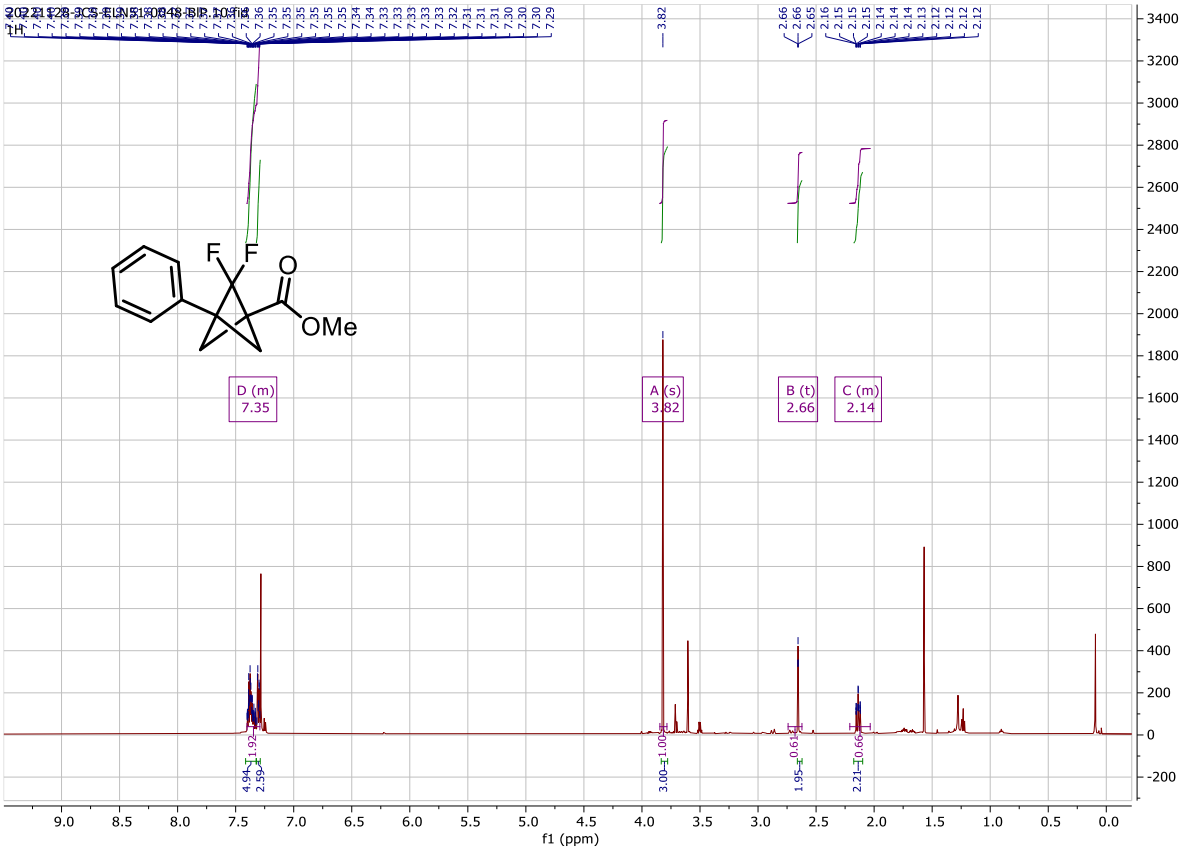
1H
3.82
2.66
2.15
F
F
O
OMe
D (m)
7.35
A (s)
3.82
B (t)
2.66
C (m)
2.14
4.94
1.92
2.59
3.00
1.00
1.95
0.61
2.21
0.66
f1 (ppm)

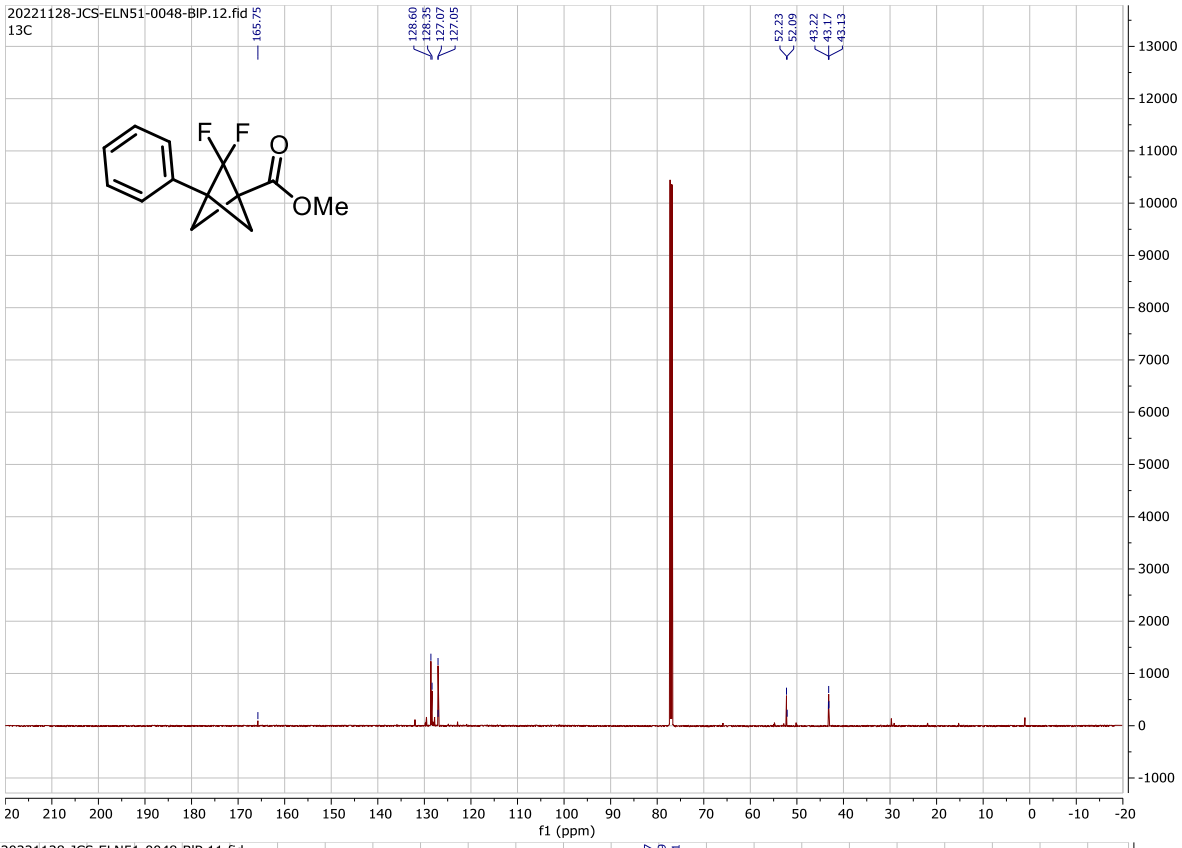
20221128-JCS-ELN51-0048-BIP.12.fid
13C
165.75
128.60
128.35
127.07
127.05
52.23
52.09
43.22
43.17
43.13
F F
O
OMe
f1 (ppm)

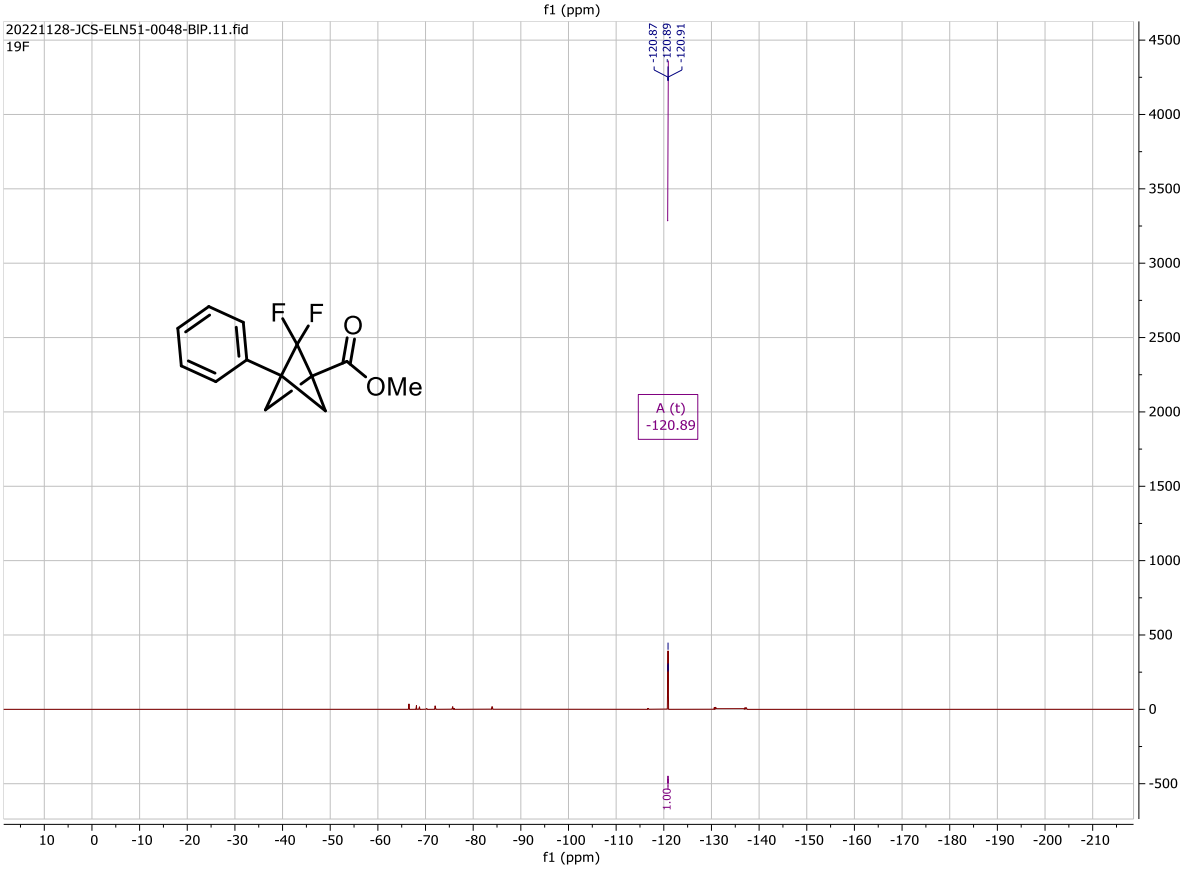
20221128-JCS-ELN51-0048-BIP.11.fid
19F
-120.87
-120.89
-120.91
F F
O
OMe
A (t)
-120.89
1.00
f1 (ppm)

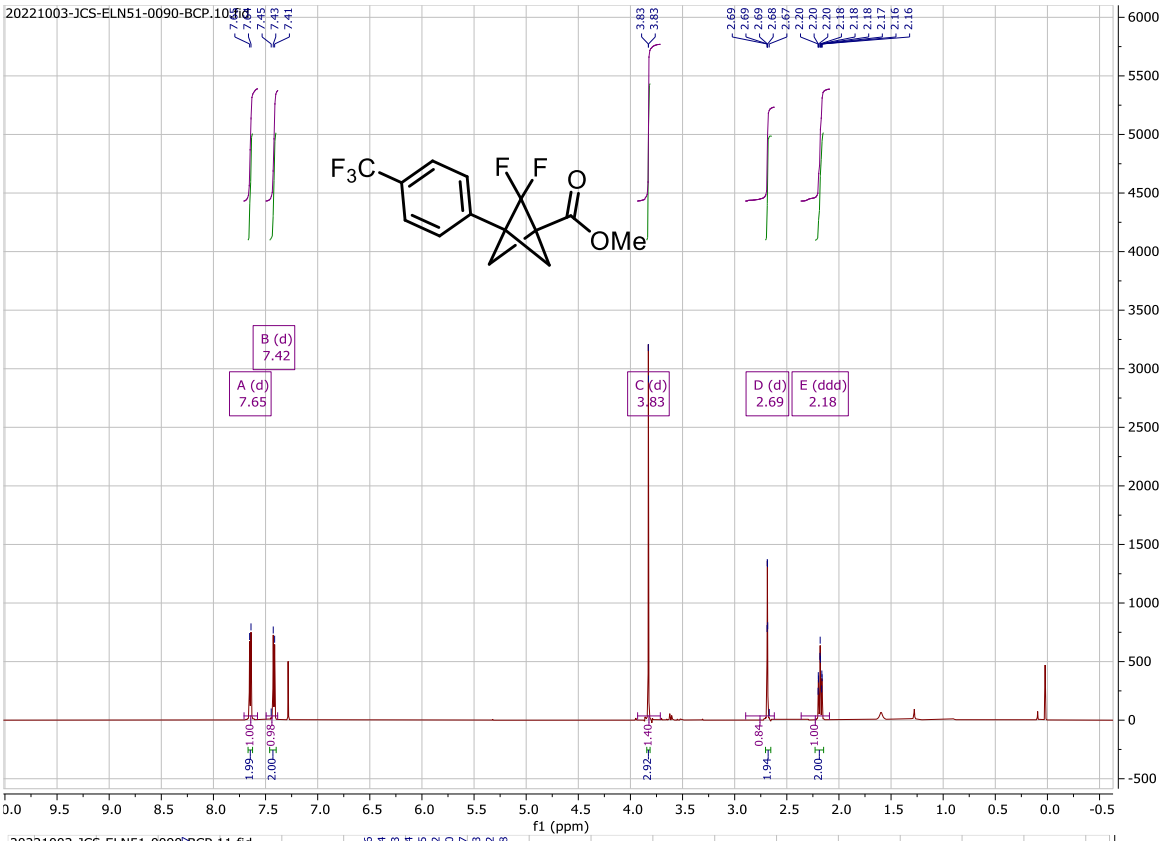
20221003-JCS-ELN51-0090-BCP.10.fid
F3C
F F
O
OMe
B (d)
7.42
A (d)
7.65
C (d)
3.83
D (d)
2.69
E (ddd)
2.18
f1 (ppm)

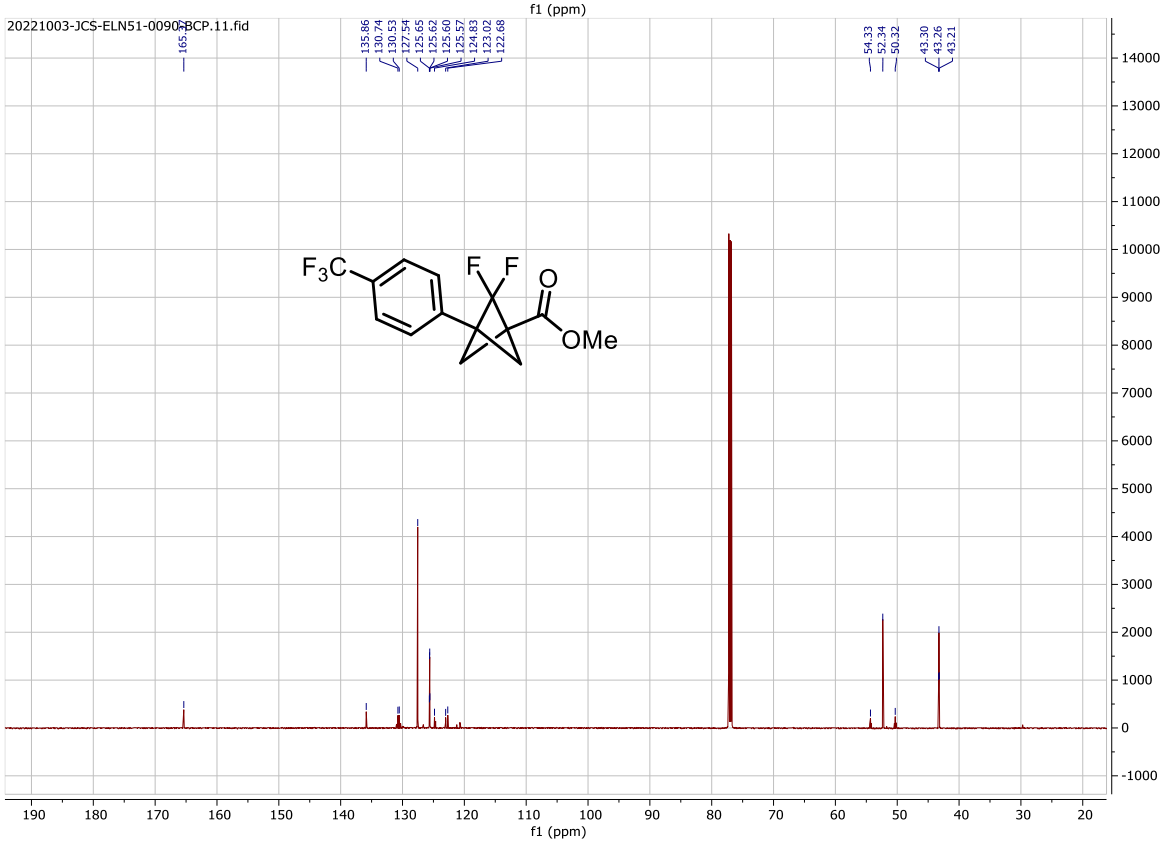
20221003-JCS-ELN51-0090-BCP.11.fid
F3C
F F
O
OMe
f1 (ppm)

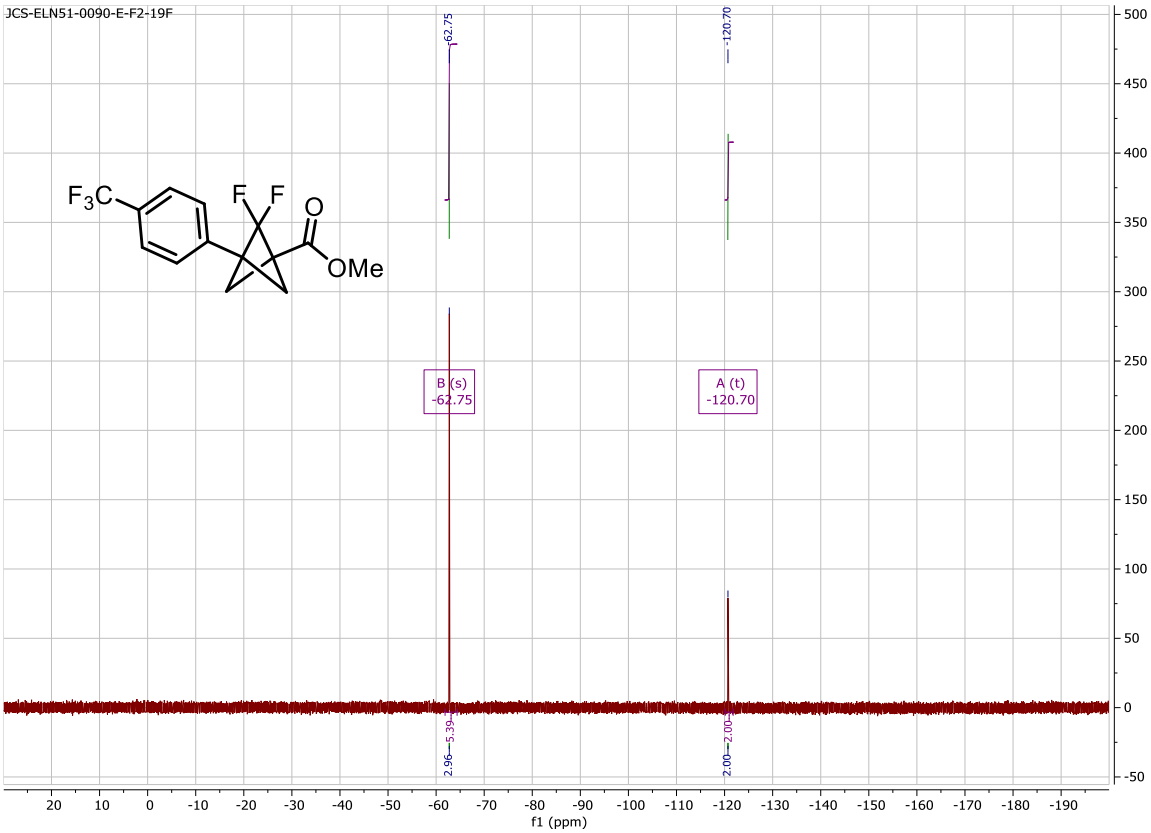
JCS-ELN51-0090-E-F2-19F
F3C
F F
O
OMe
B (s)
-62.75
A (t)
-120.70
f1 (ppm)

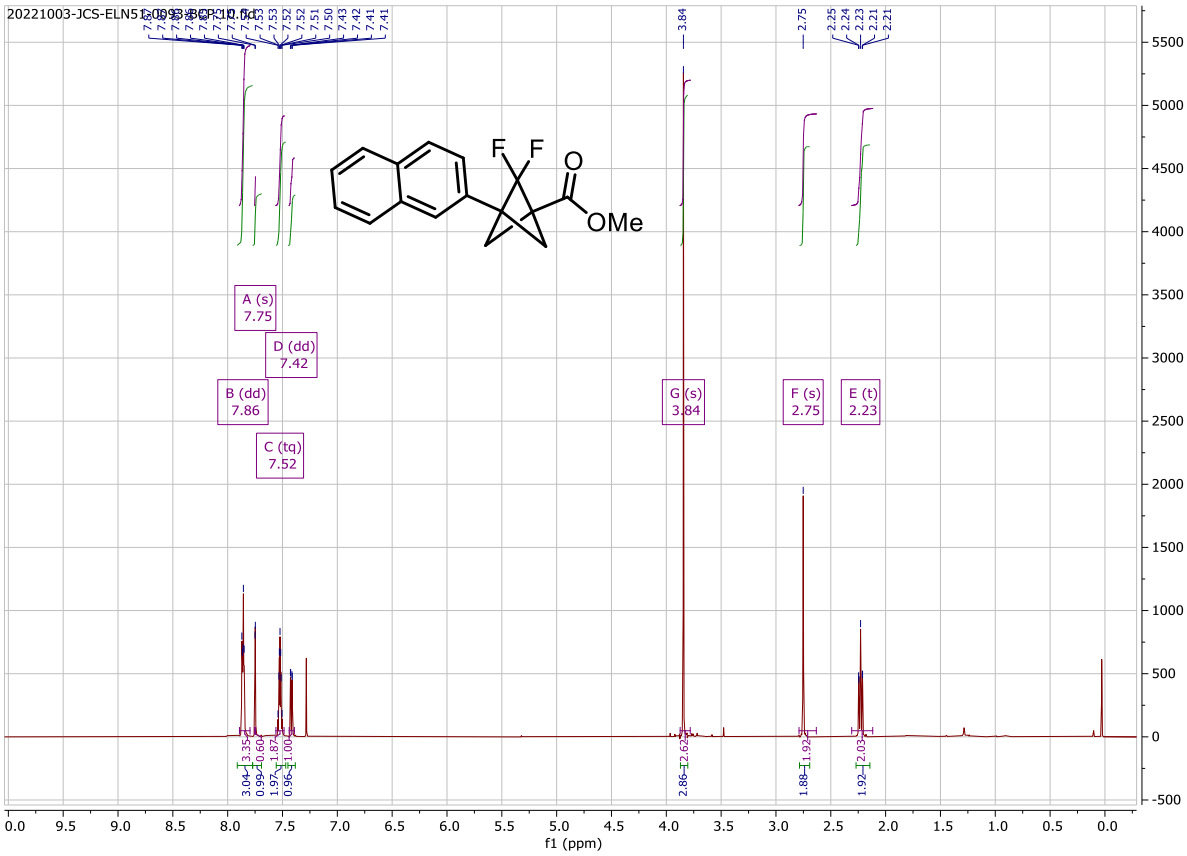
20221003-JCS-ELN51-0093-BCP-10.fid
F F
O
OMe
A (s)
7.75
D (dd)
7.42
B (dd)
7.86
C (tq)
7.52
G (s)
3.84
F (s)
2.75
E (t)
2.23
f1 (ppm)

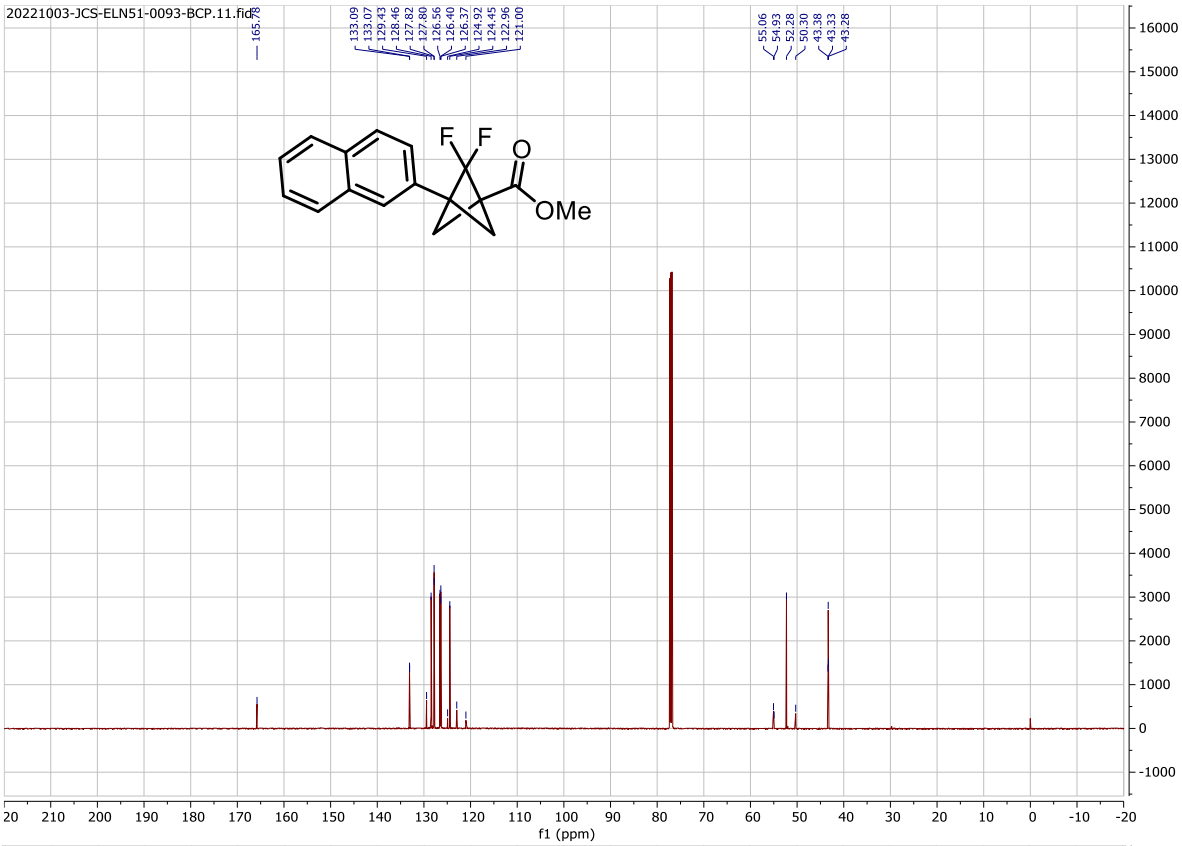
20221003-JCS-ELN51-0093-BCP.11.fid
165.78
133.09
133.07
129.43
128.46
127.82
127.80
126.56
126.40
126.37
124.92
124.45
122.96
121.00
55.06
54.93
52.28
50.30
43.38
43.33
43.28
F
F
O
OMe
f1 (ppm)

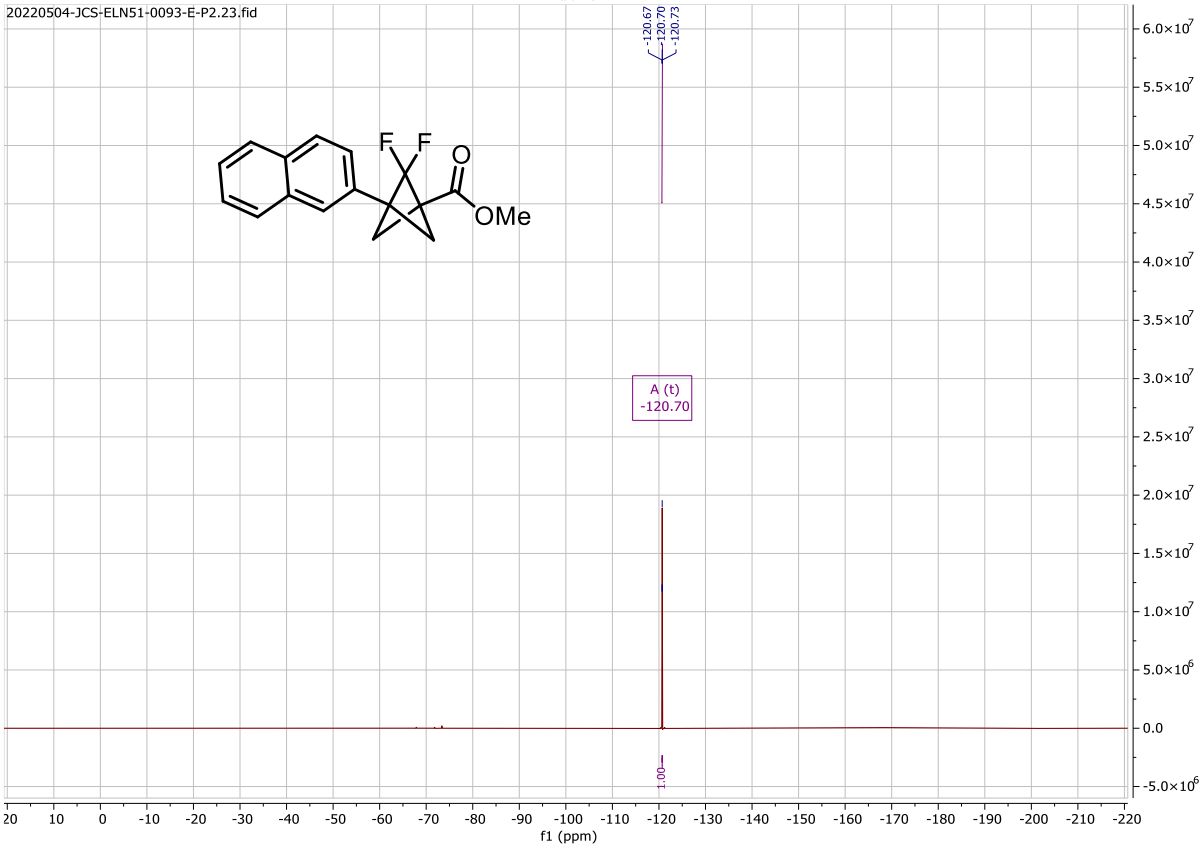
20220504-JCS-ELN51-0093-E-P2.23.fid
-120.67
-120.70
-120.73
F
F
O
OMe
A (t)
-120.70
1.00
f1 (ppm)

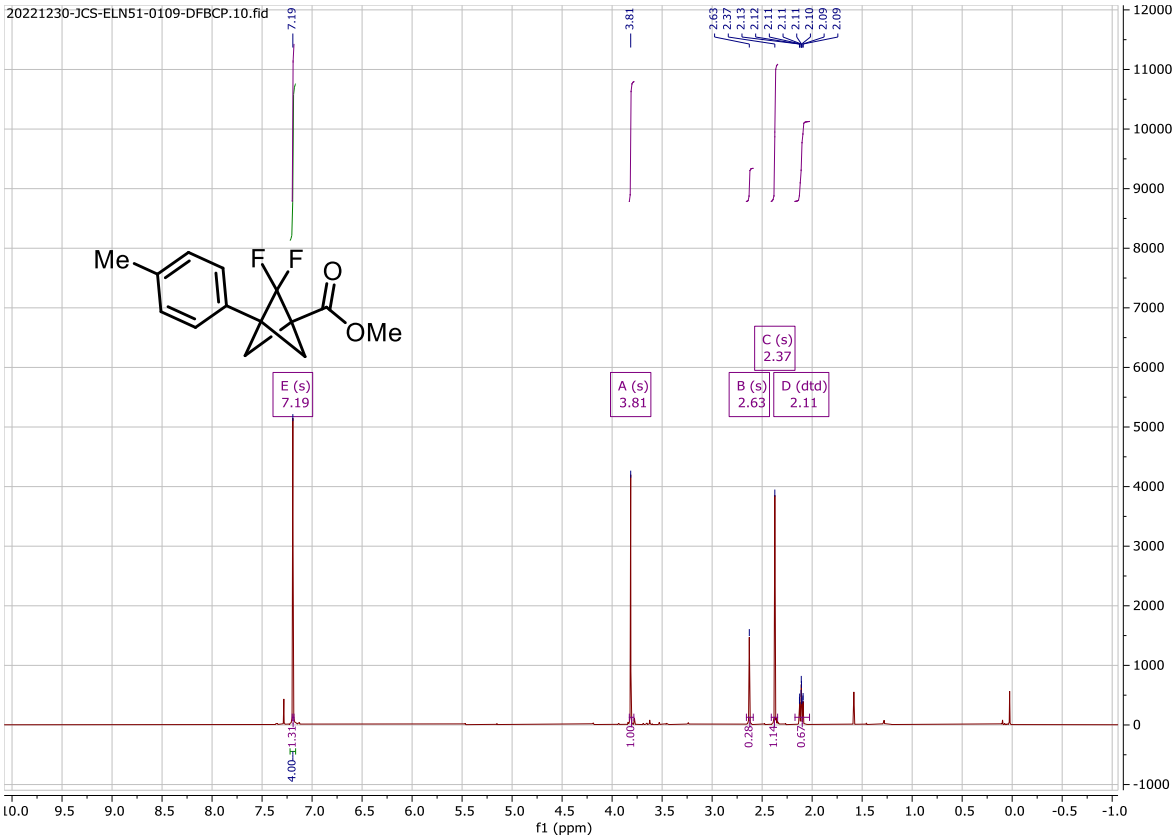
20221230-JCS-ELN51-0109-DFBCP.10.fid
Me
F
F
O
OMe
E (s)
7.19
A (s)
3.81
B (s)
2.63
C (s)
2.37
D (dtd)
2.11
f1 (ppm)

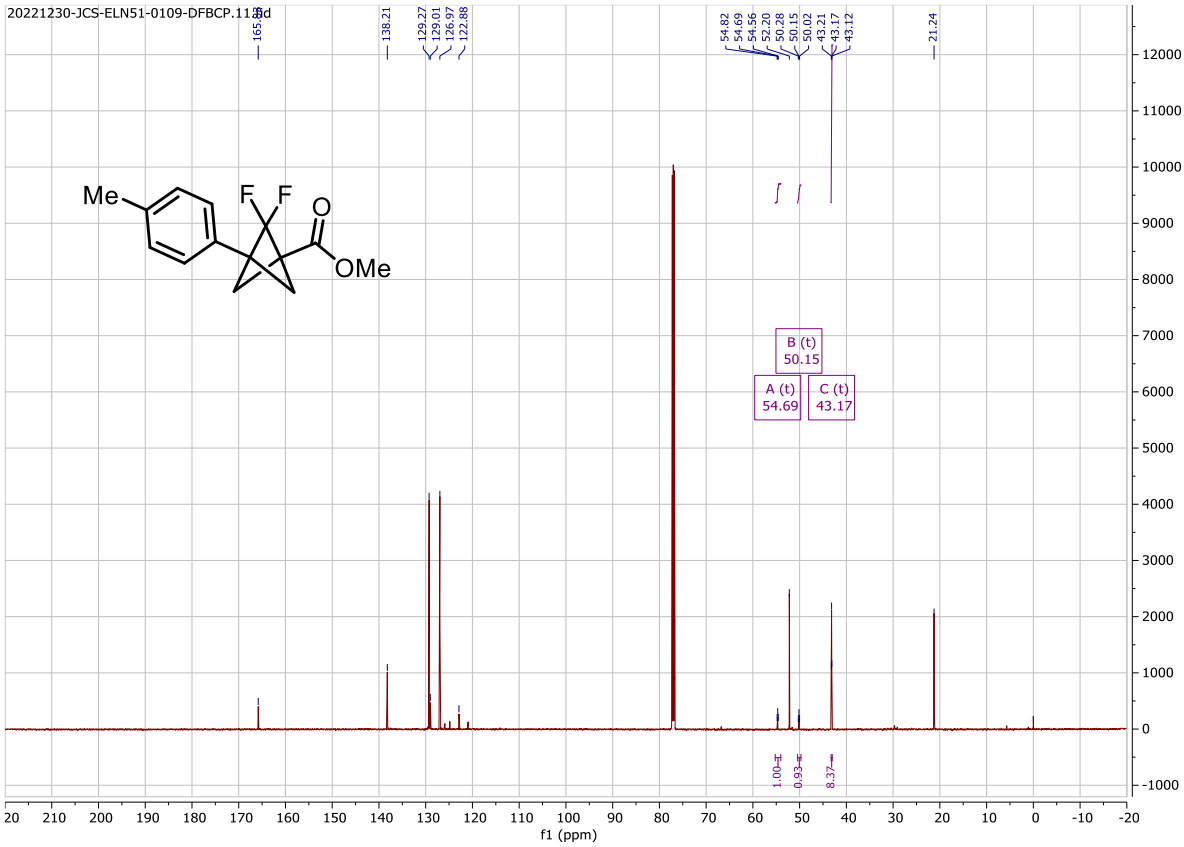
20221230-JCS-ELN51-0109-DFBCP.11.fid
Me
F
F
O
OMe
A (t)
54.69
B (t)
50.15
C (t)
43.17
f1 (ppm)

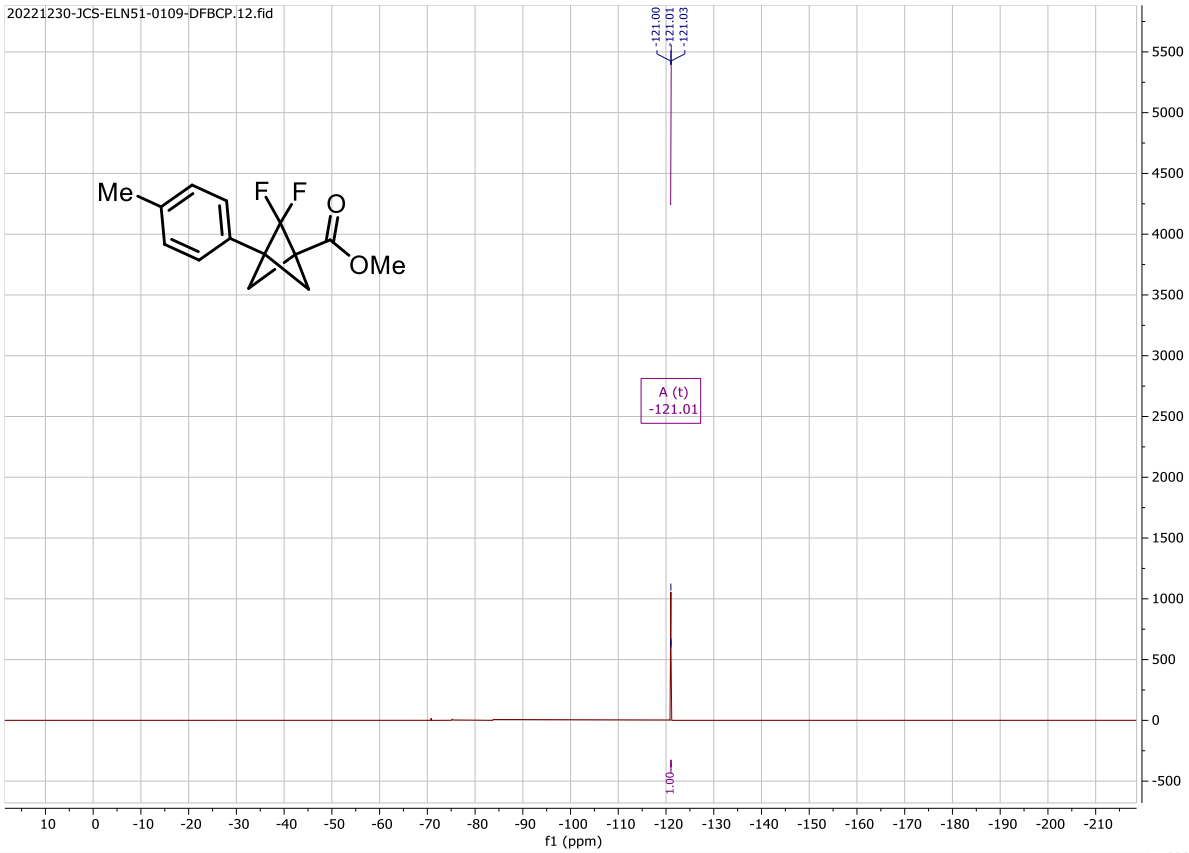
20221230-JCS-ELN51-0109-DFBCP.12.fid
Me
F F
O
OMe
A (t)
-121.01
f1 (ppm)

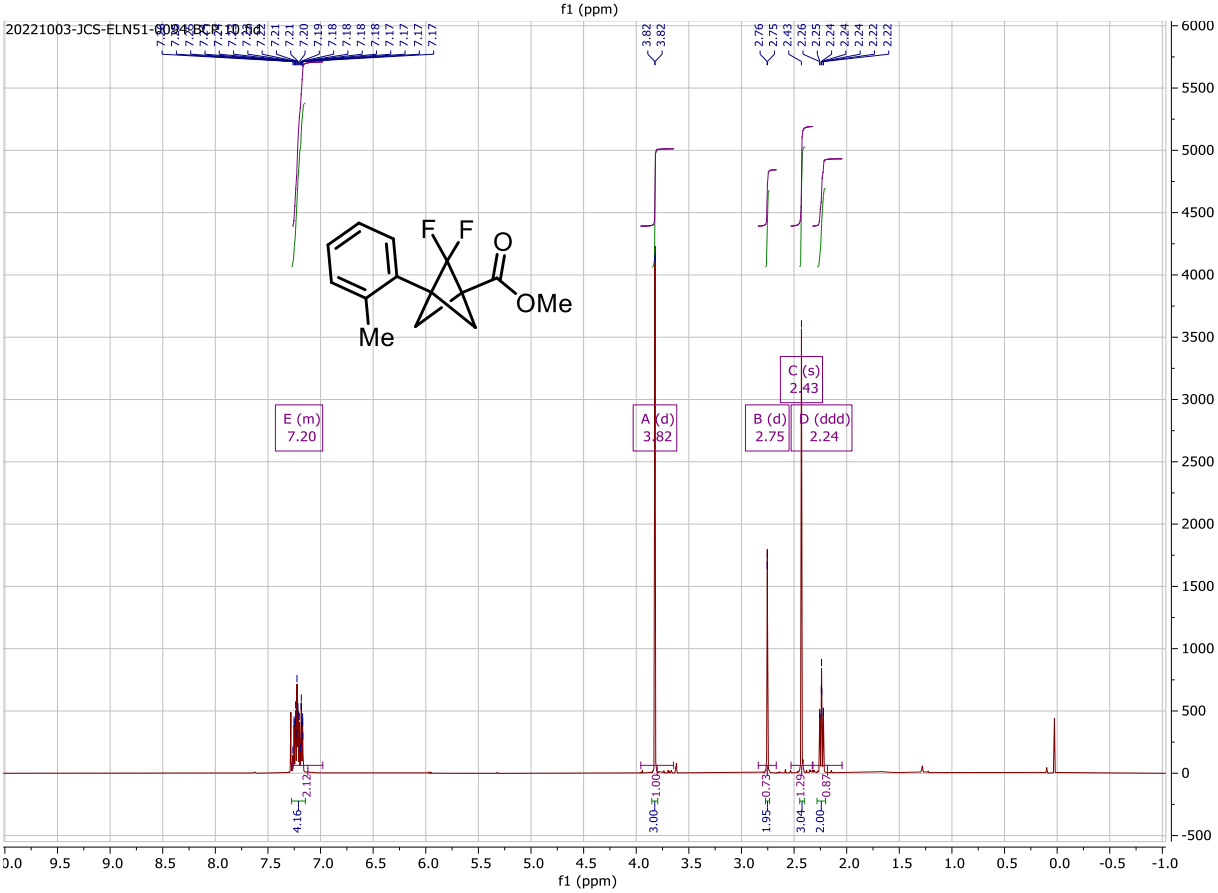
20221003-JCS-ELN51-0094-BCP.10.fid
F F
O
OMe
Me
E (m)
7.20
A (d)
3.82
B (d)
2.75
C (s)
2.43
D (ddd)
2.24
f1 (ppm)

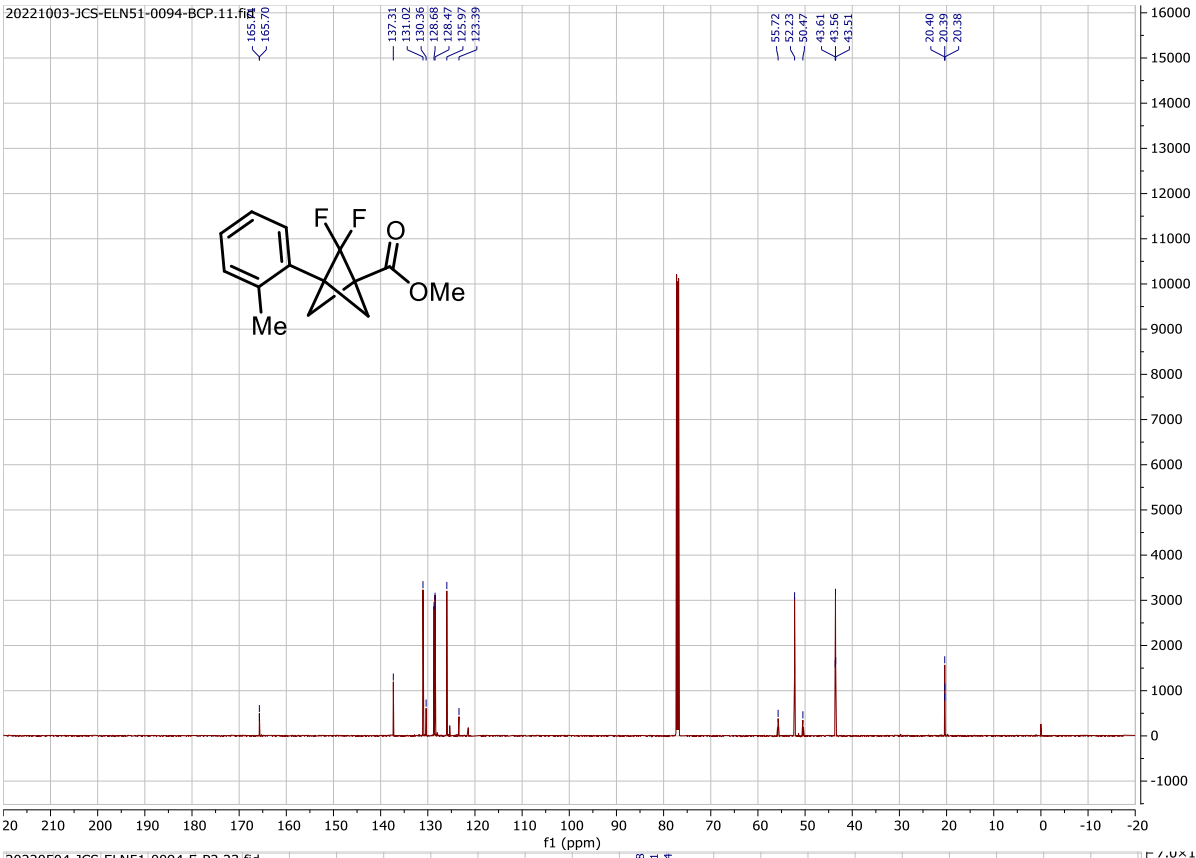
20221003-JCS-ELN51-0094-BCP.11.fid
165.74
165.70
137.31
131.02
130.36
128.68
128.47
125.97
123.39
55.72
52.23
50.47
43.61
43.56
43.51
20.40
20.39
20.38
F
F
O
OMe
Me
f1 (ppm)

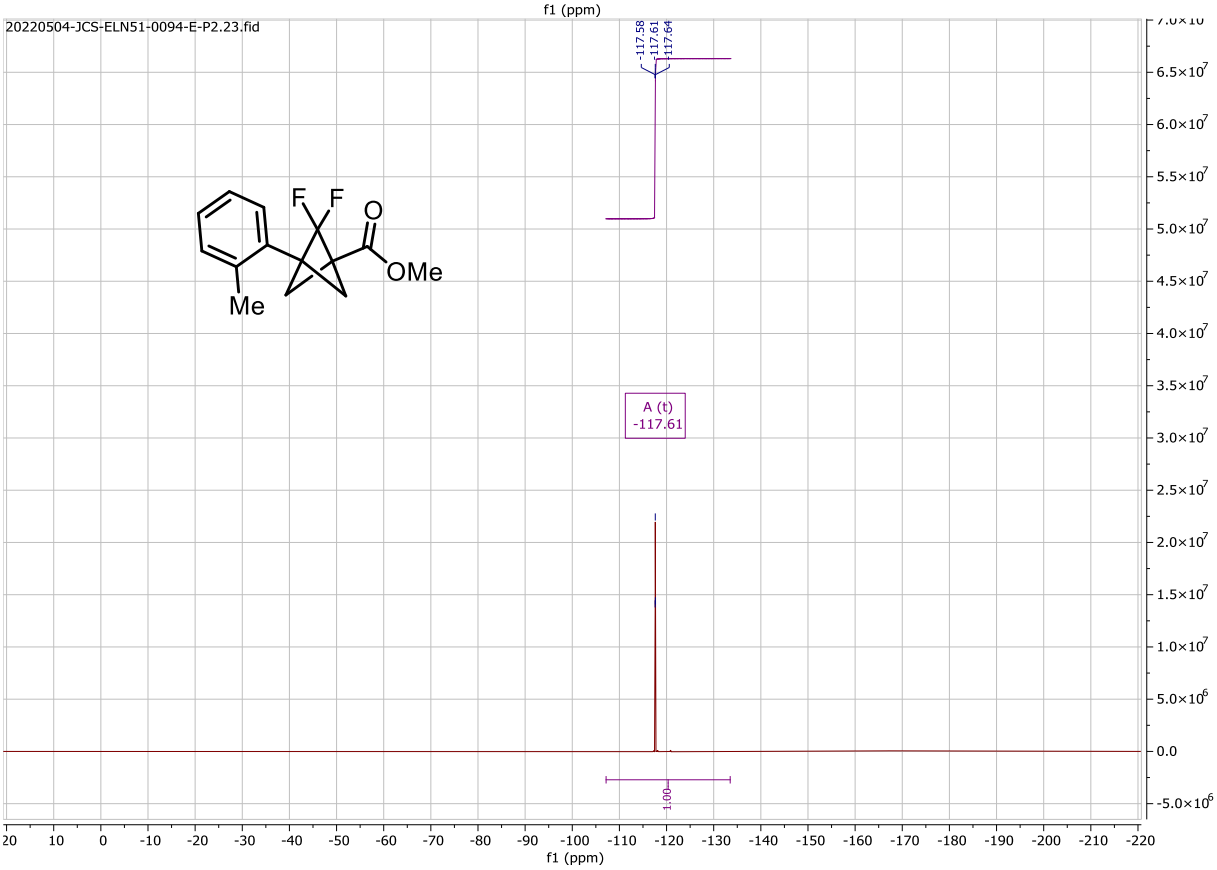
20220504-JCS-ELN51-0094-E-P2.23.fid
-117.58
-117.61
-117.64
F
F
O
OMe
Me
A (t)
-117.61
1.00
f1 (ppm)

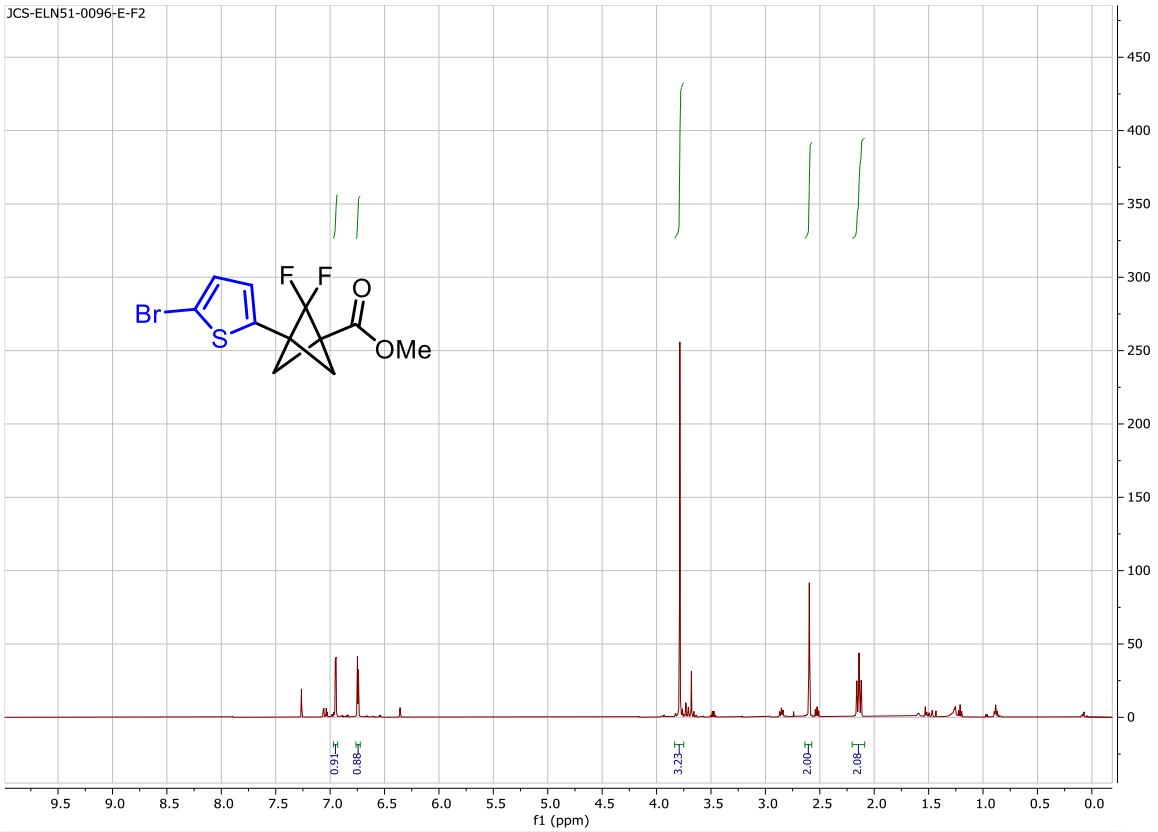
JCS-ELN51-0096-E-F2
Br
S
F
F
O
OMe
0.91
0.88
3.23
2.00
2.08
f1 (ppm)

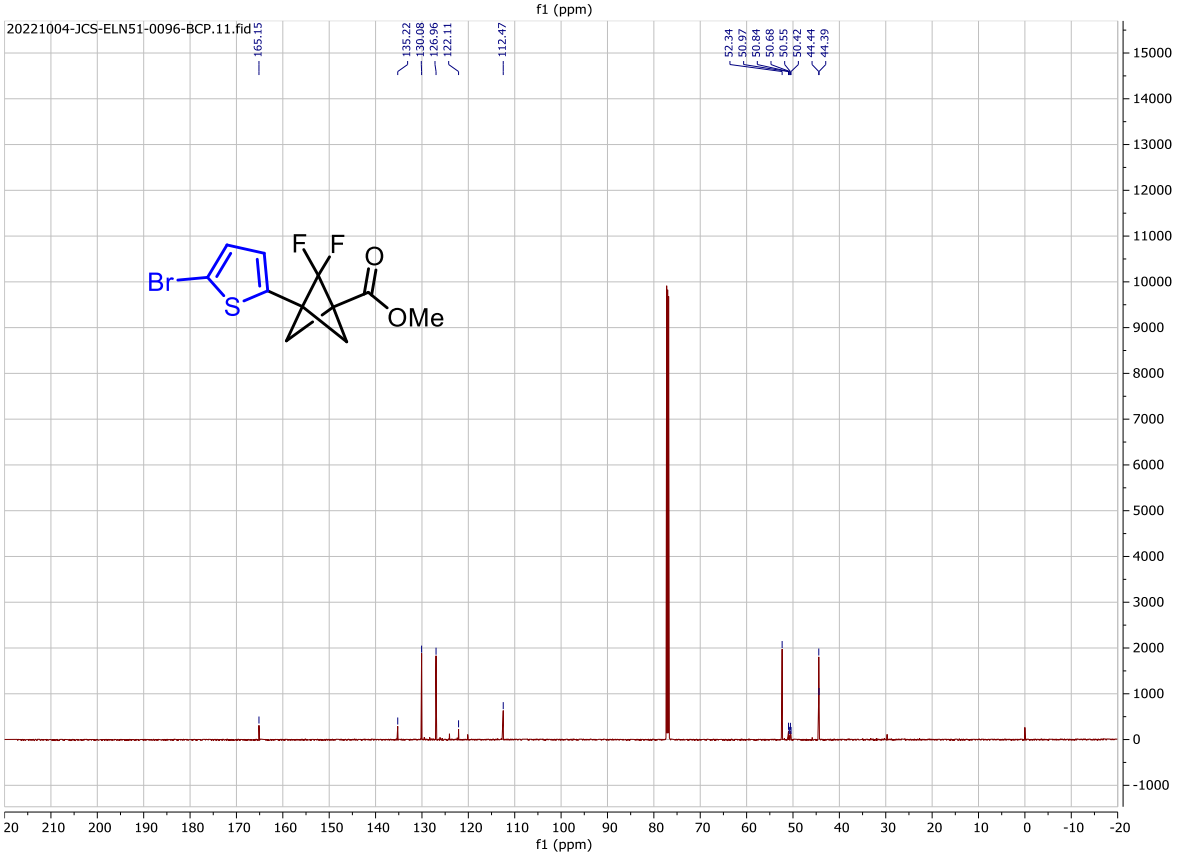
20221004-JCS-ELN51-0096-BCP.11.fid
165.15
135.22
130.08
126.96
122.11
112.47
52.34
50.97
50.84
50.68
50.55
50.42
44.44
44.39
Br
S
F
F
O
OMe
f1 (ppm)

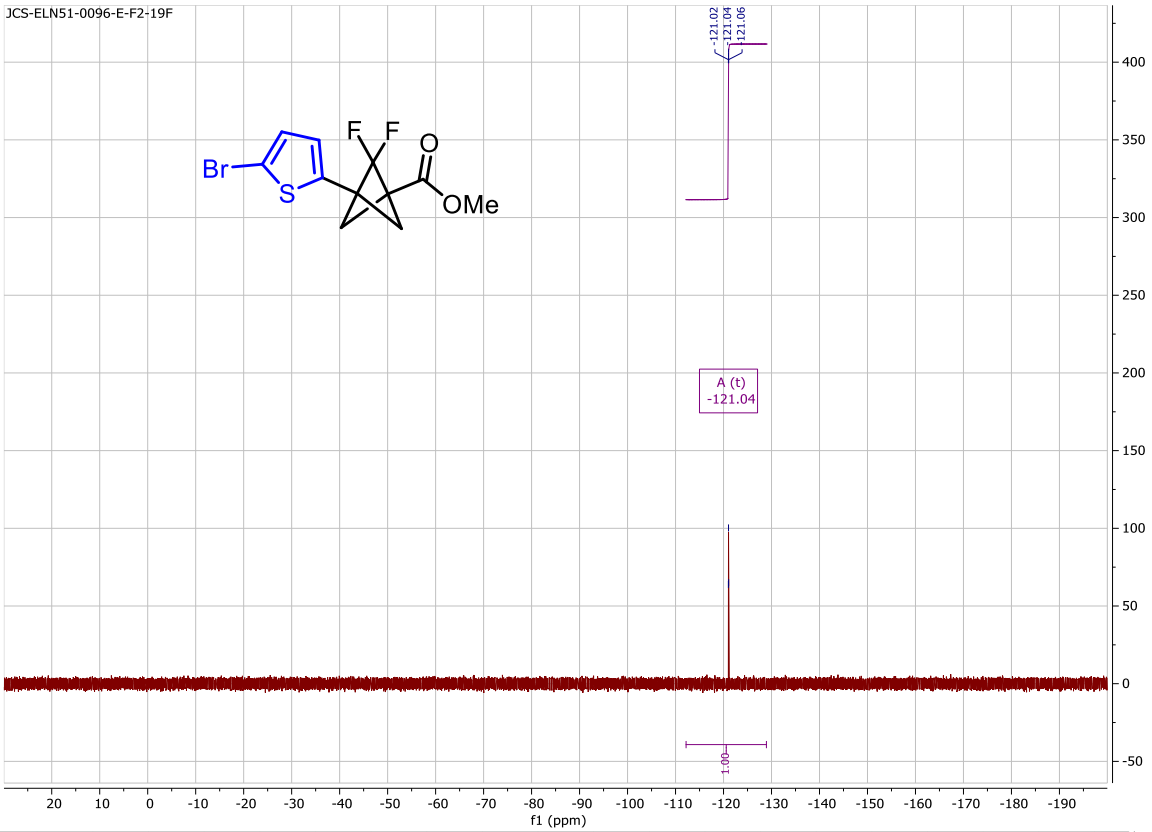
JCS-ELN51-0096-E-F2-19F
-121.02
-121.04
-121.06
Br
S
F
F
O
OMe
A (t)
-121.04
1.00
f1 (ppm)

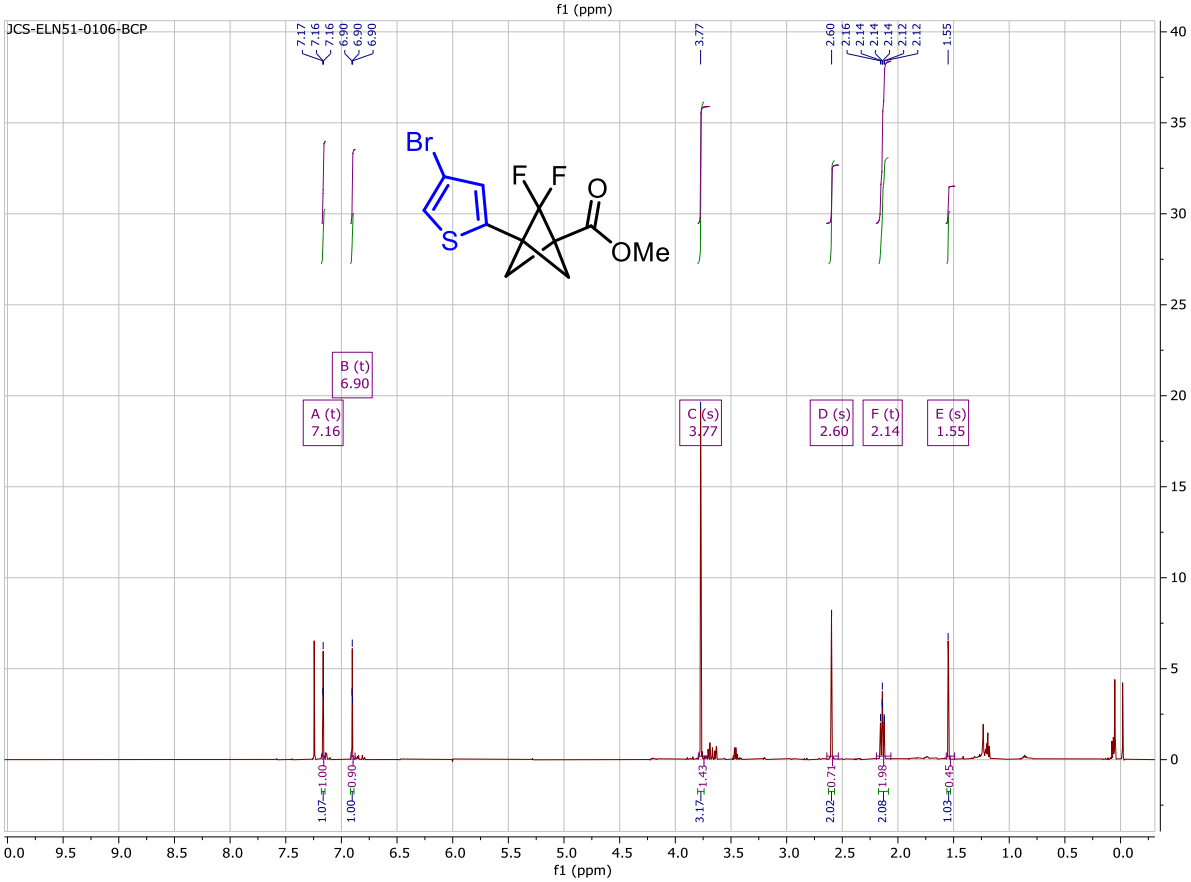
JCS-ELN51-0106-BCP
7.17
7.16
7.16
6.90
6.90
6.90
3.77
2.60
2.16
2.14
2.14
2.14
2.12
2.12
1.55
Br
S
F
F
O
OMe
B (t)
6.90
A (t)
7.16
C (s)
3.77
D (s)
2.60
F (t)
2.14
E (s)
1.55
1.07
1.00
1.00
0.90
3.17
1.43
2.02
0.71
2.08
1.98
1.03
0.45
f1 (ppm)

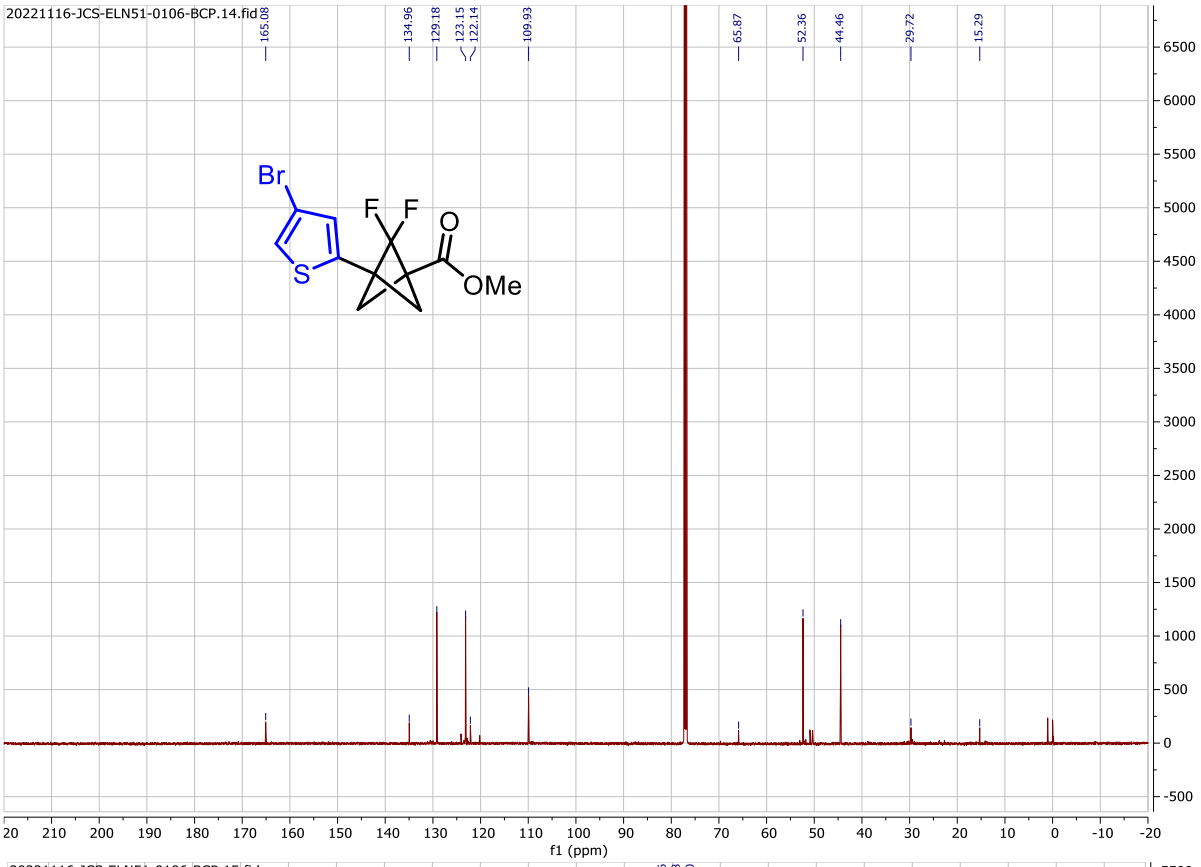
20221116-JCS-ELN51-0106-BCP.14.fid
165.08
134.96
129.18
123.15
122.14
109.93
65.87
52.36
44.46
29.72
15.29
Br
F
F
O
S
OMe
f1 (ppm)

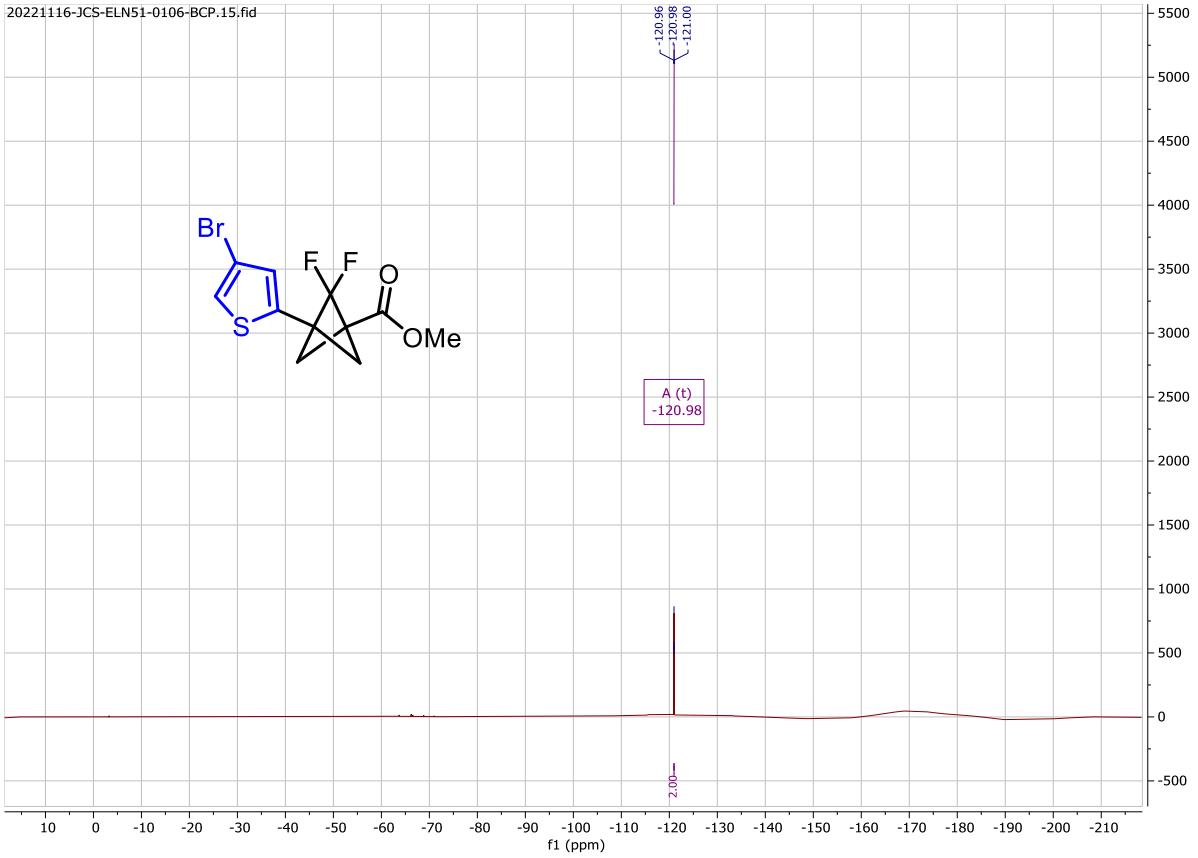
20221116-JCS-ELN51-0106-BCP.15.fid
-120.96
-120.98
-121.00
Br
F
F
O
S
OMe
A (t)
-120.98
2.00
f1 (ppm)

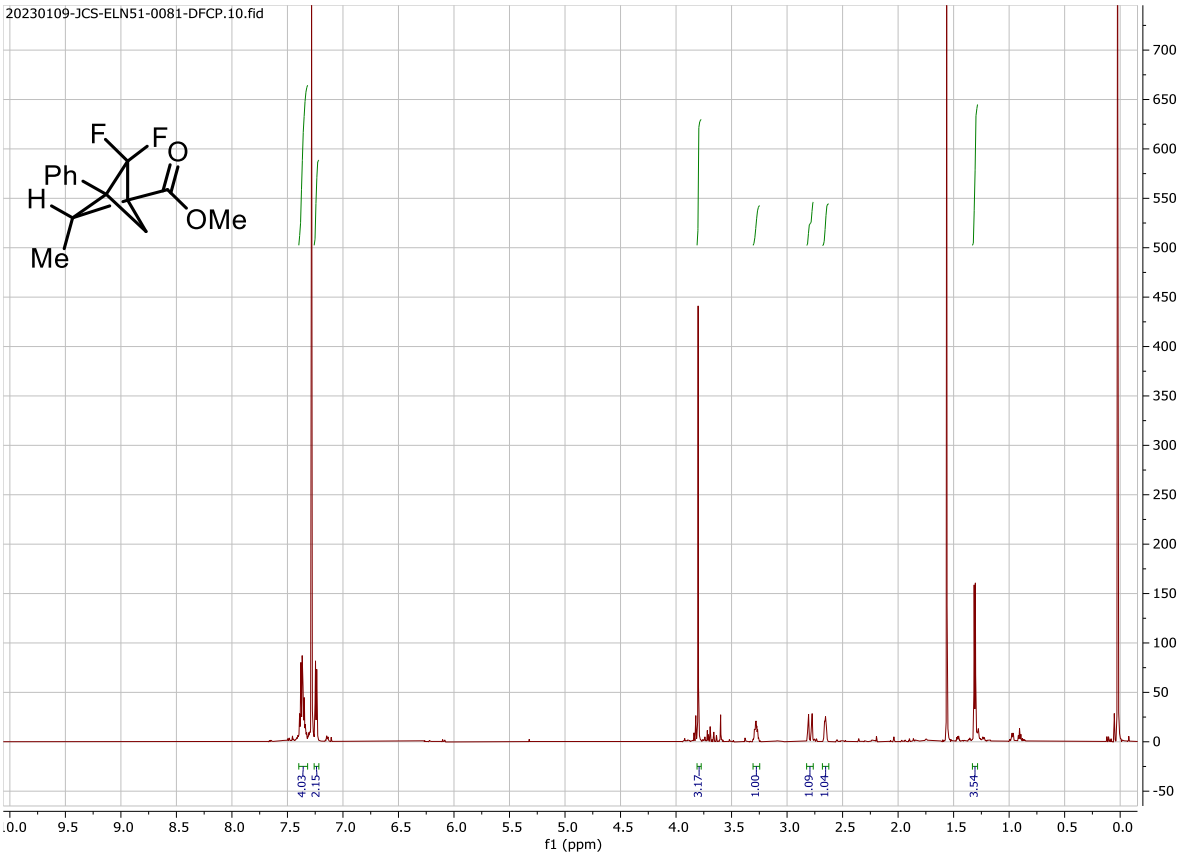
20230109-JCS-ELN51-0081-DFCP.10.fid
F
F
O
Ph
H
OMe
Me
4.03
2.15
3.17
1.00
1.09
1.04
3.54
f1 (ppm)

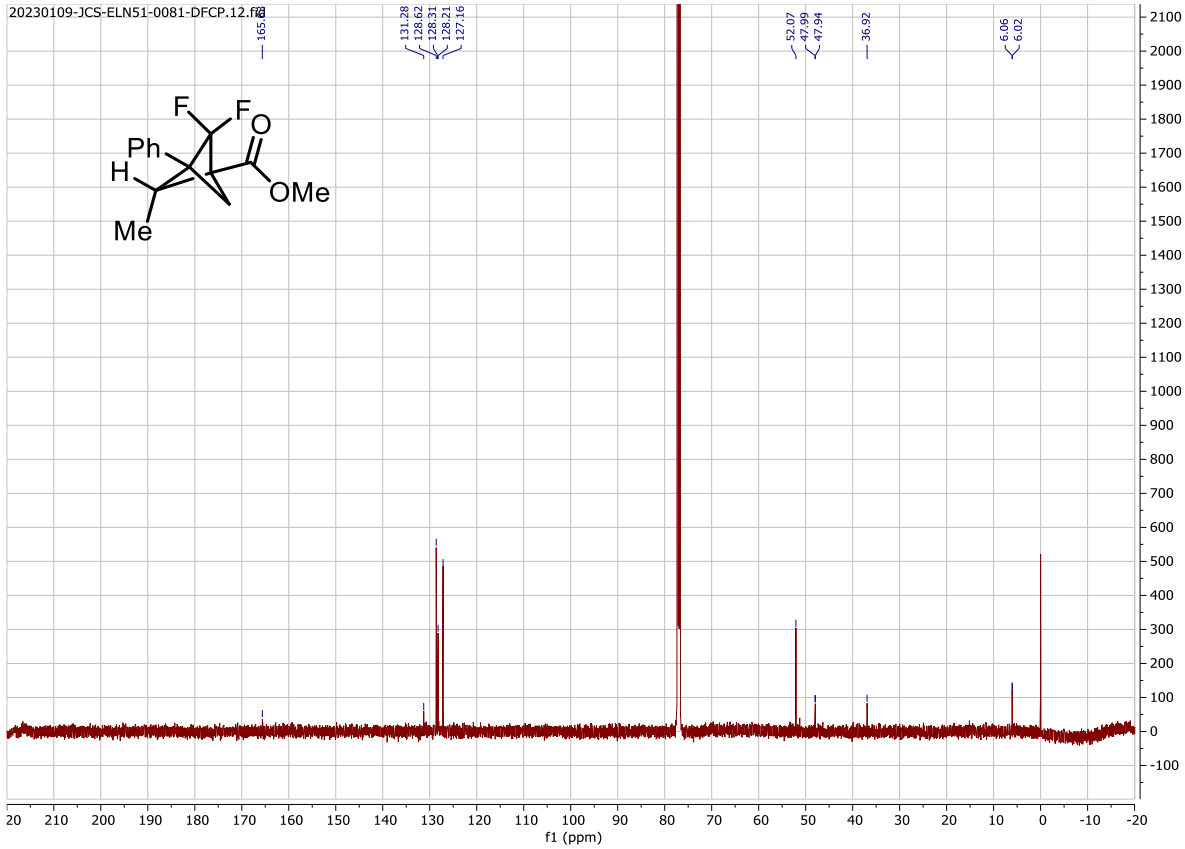
20230109-JCS-ELN51-0081-DFCP.12.fid
165.8
131.28
128.62
128.31
128.21
127.16
52.07
47.99
47.94
36.92
6.06
6.02
F
F
O
Ph
H
OMe
Me
f1 (ppm)

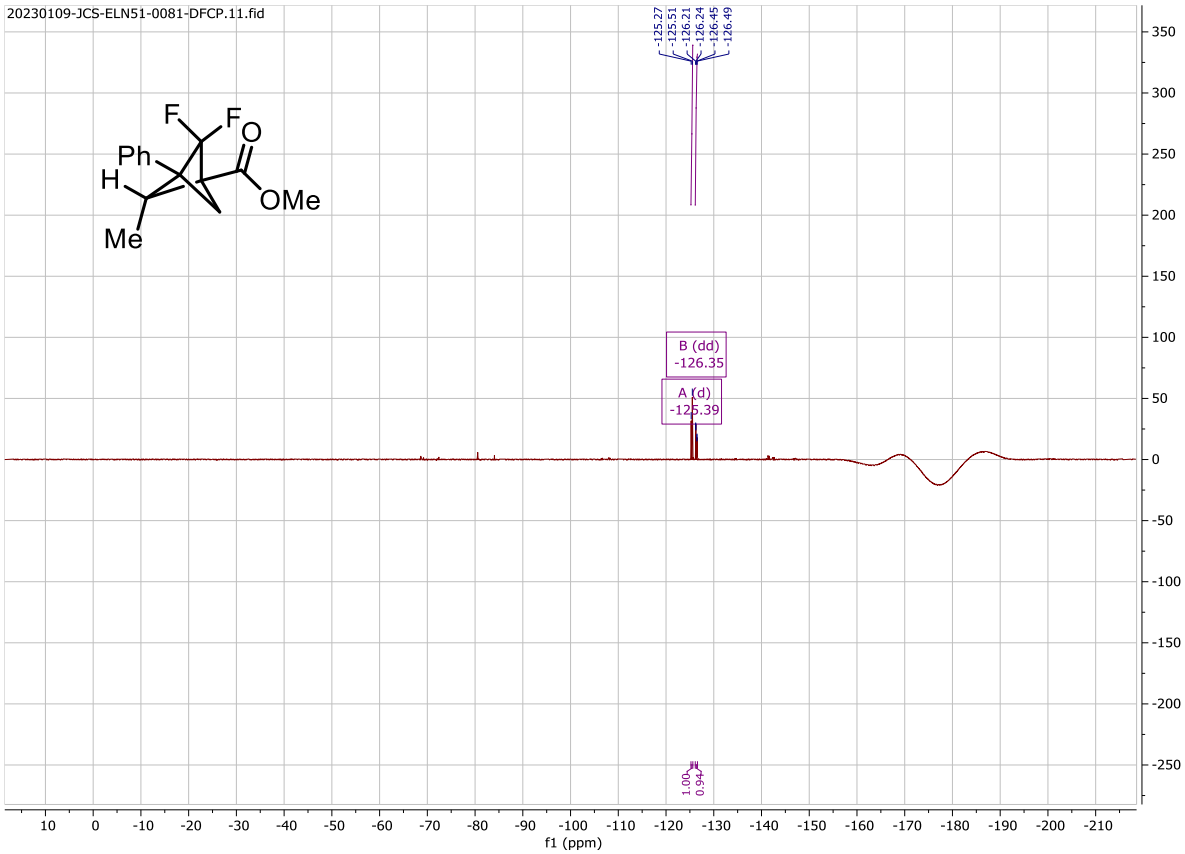
20230109-JCS-ELN51-0081-DFCP.11.fid
-125.27
-125.51
-126.21
-126.24
-126.45
-126.49
B (dd)
-126.35
A (d)
-126.39
1.00
0.94
f1 (ppm)

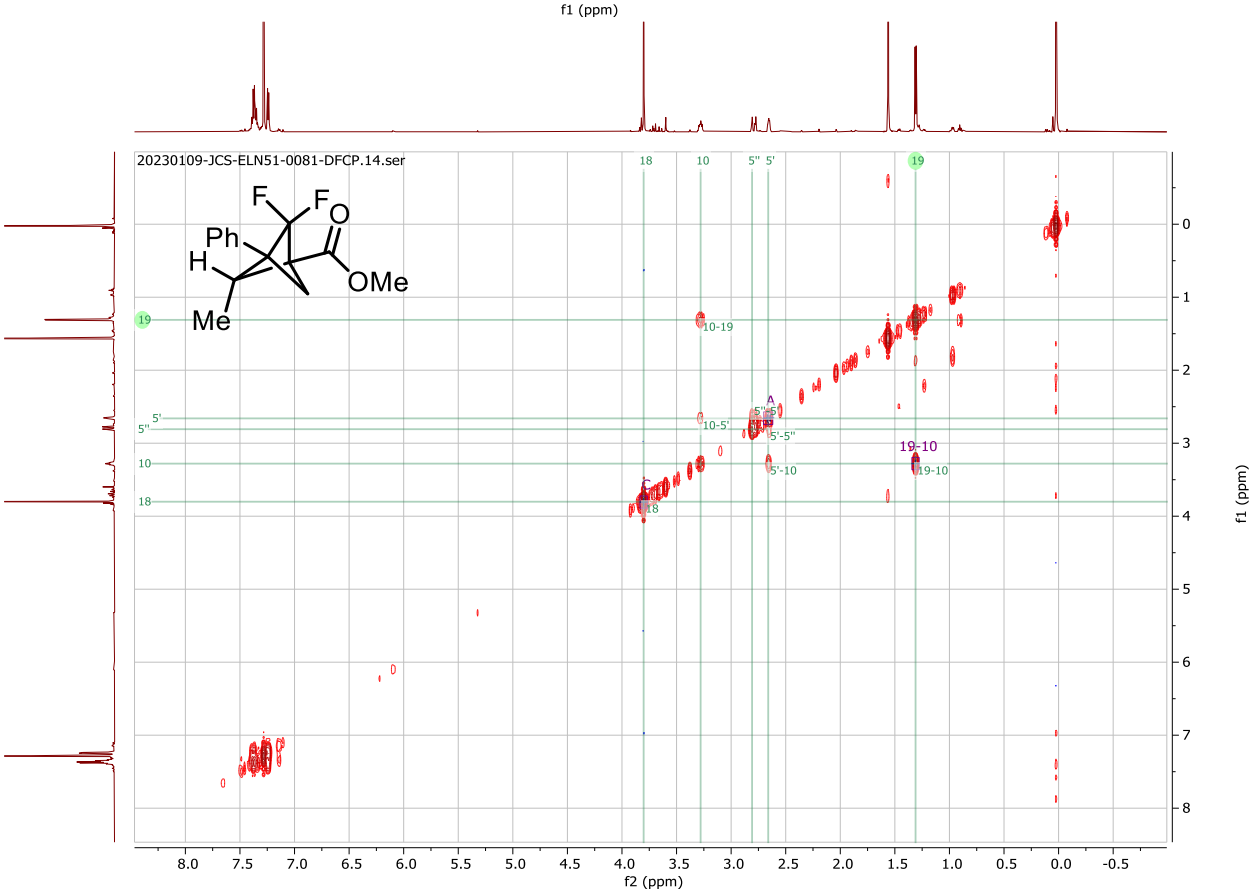
20230109-JCS-ELN51-0081-DFCP.14.ser
18
10
5'' 5'
19
10-19
10-5'
5'-5''
5'-10
19-10
f2 (ppm)
f1 (ppm)

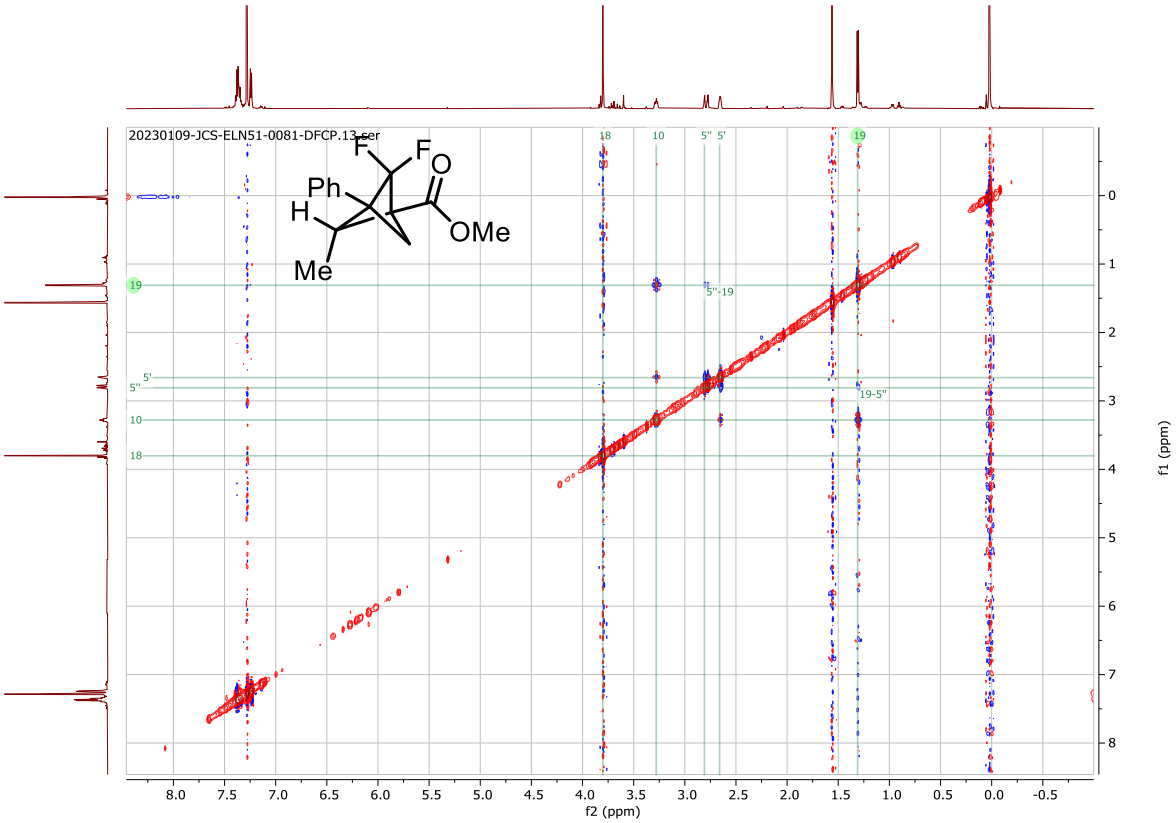
20230109-JCS-ELN51-0081-DFCP.13.ser
F
F
O
Ph
H
OMe
Me
18
10
5'' 5'
19
5''-19
19-5''
5'
5''
f2 (ppm)
f1 (ppm)

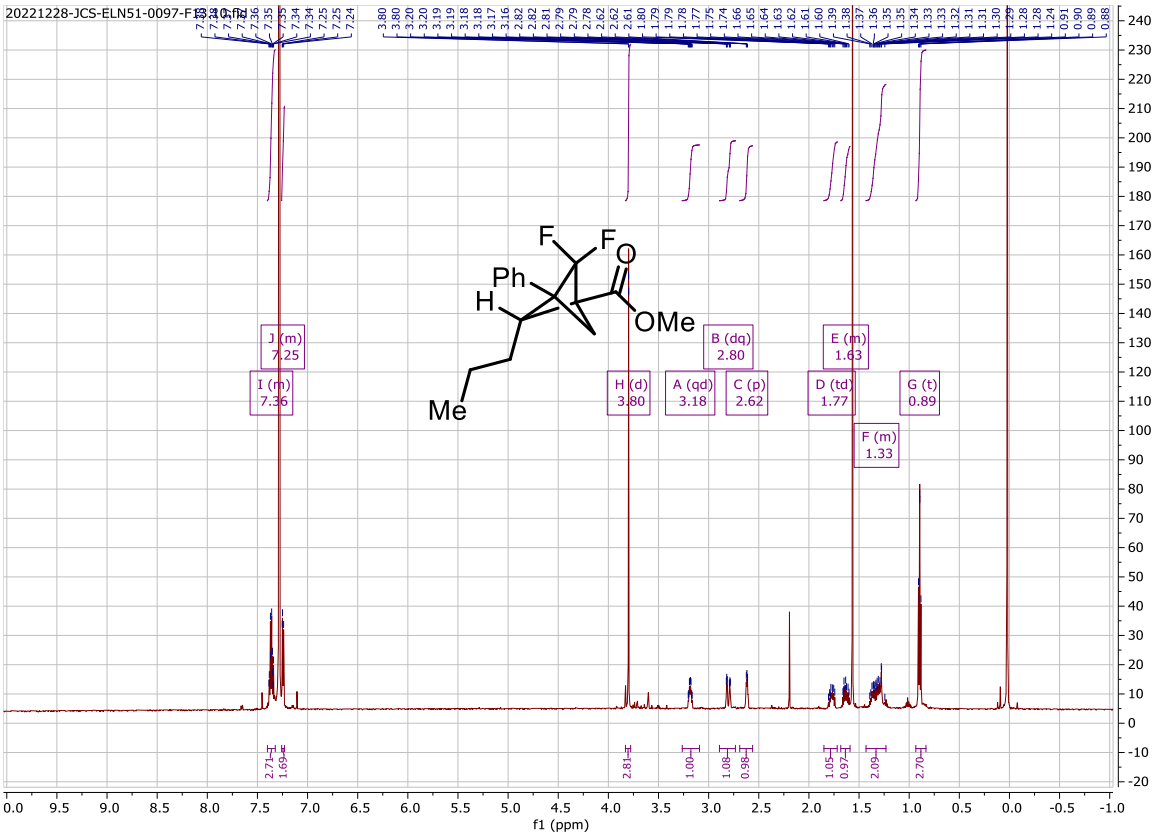
20221228-JCS-ELN51-0097-F1310.fid
F
F
O
Ph
H
OMe
Me
J (m) 7.25
I (m) 7.36
H (d) 3.80
A (qd) 3.18
B (dq) 2.80
C (p) 2.62
D (td) 1.77
E (m) 1.63
F (m) 1.33
G (t) 0.89
2.71
1.69
2.81
1.00
1.08
0.98
1.05
0.97
2.09
2.70
f1 (ppm)

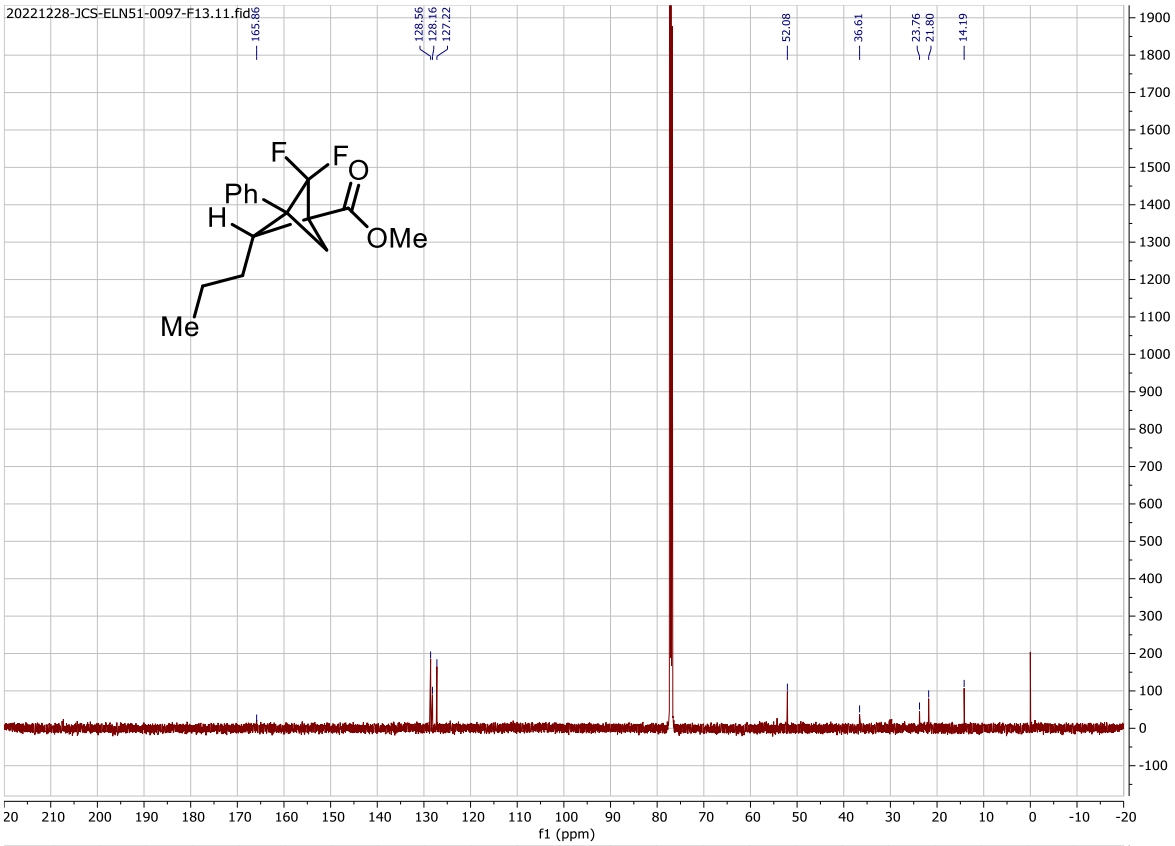
20221228-JCS-ELN51-0097-F13.11.fid
165.86
128.56
128.16
127.22
52.08
36.61
23.76
21.80
14.19
F
F
O
Ph
H
OMe
Me
f1 (ppm)

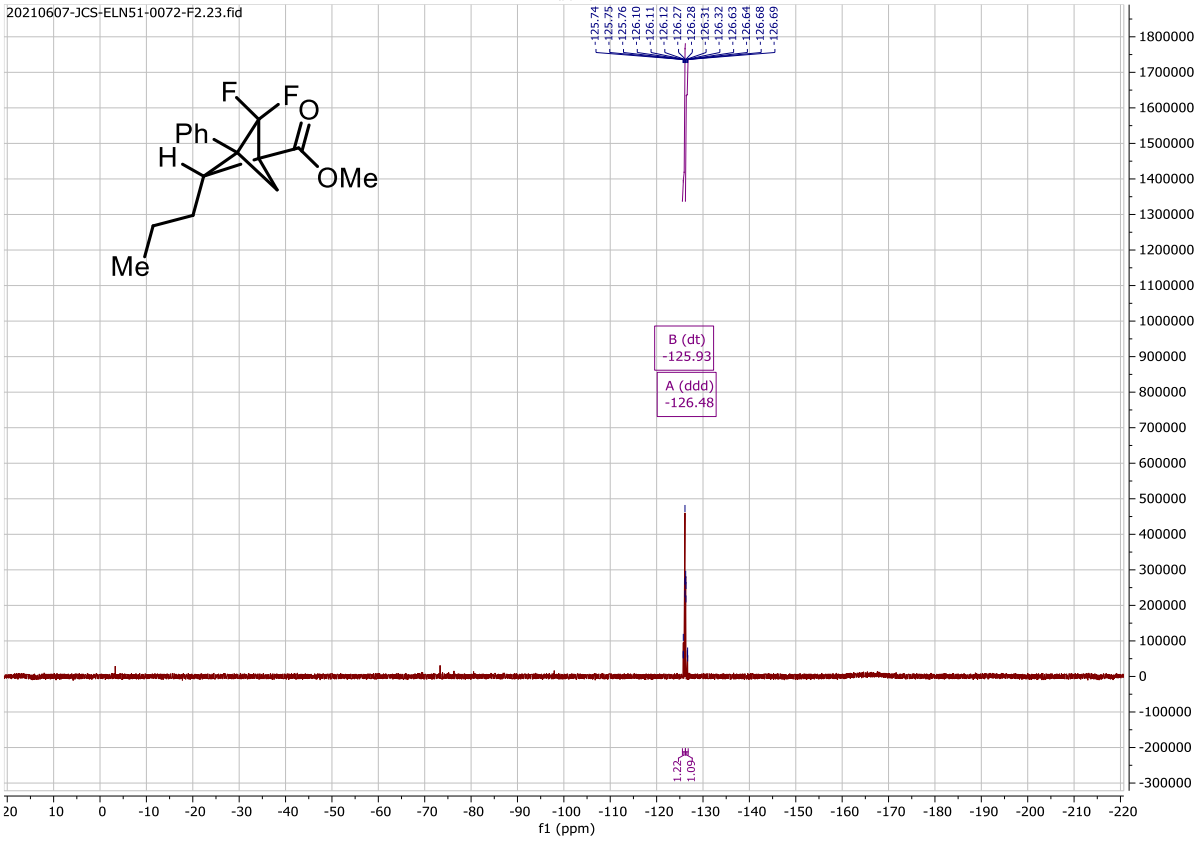
20210607-JCS-ELN51-0072-F2.23.fid
-125.74
-125.75
-125.76
-126.10
-126.11
-126.12
-126.27
-126.28
-126.31
-126.32
-126.63
-126.64
-126.68
-126.69
F
F
O
Ph
H
OMe
Me
B (dt)
-125.93
A (ddd)
-126.48
1.22
1.09
f1 (ppm)

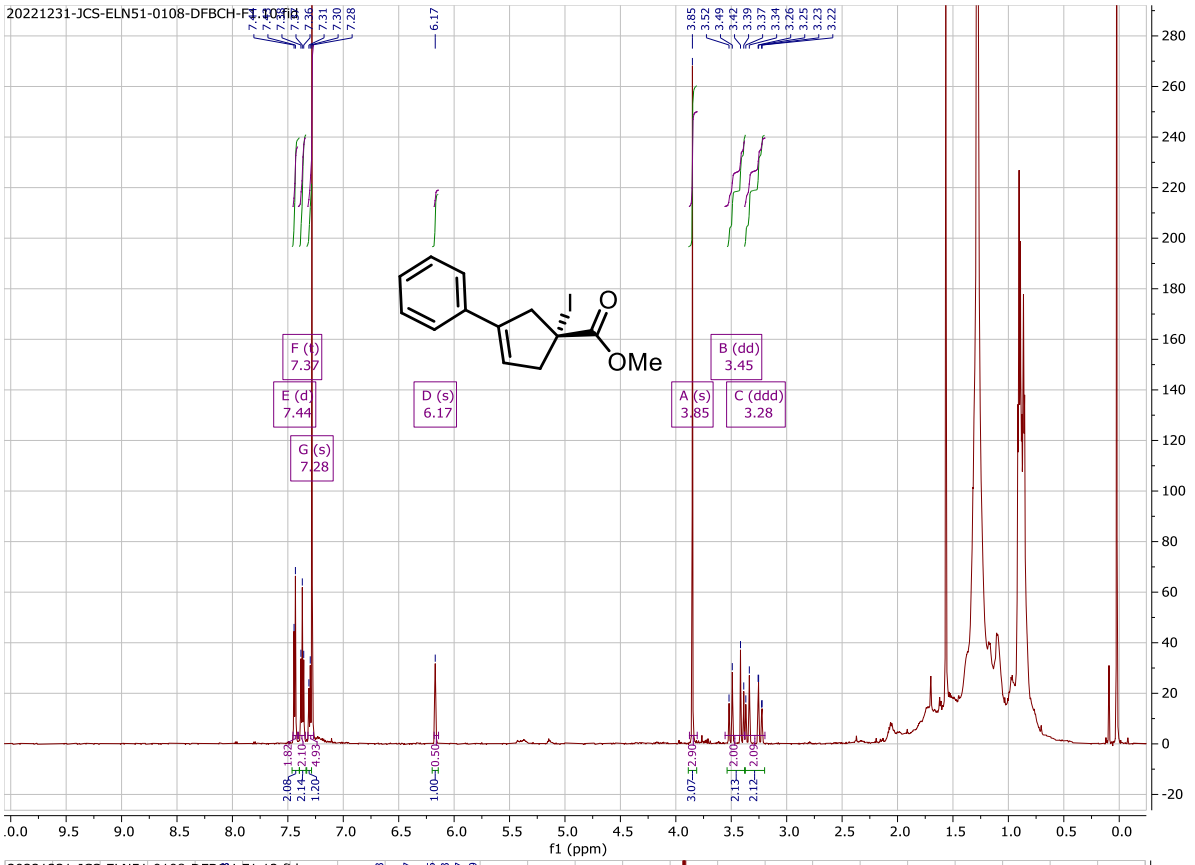
20221231-JCS-ELN51-0108-DFBCH-F1.10.fid
F (t) 7.37
E (d) 7.44
G (s) 7.28
D (s) 6.17
A (s) 3.85
B (dd) 3.45
C (ddd) 3.28
OMe
f1 (ppm)

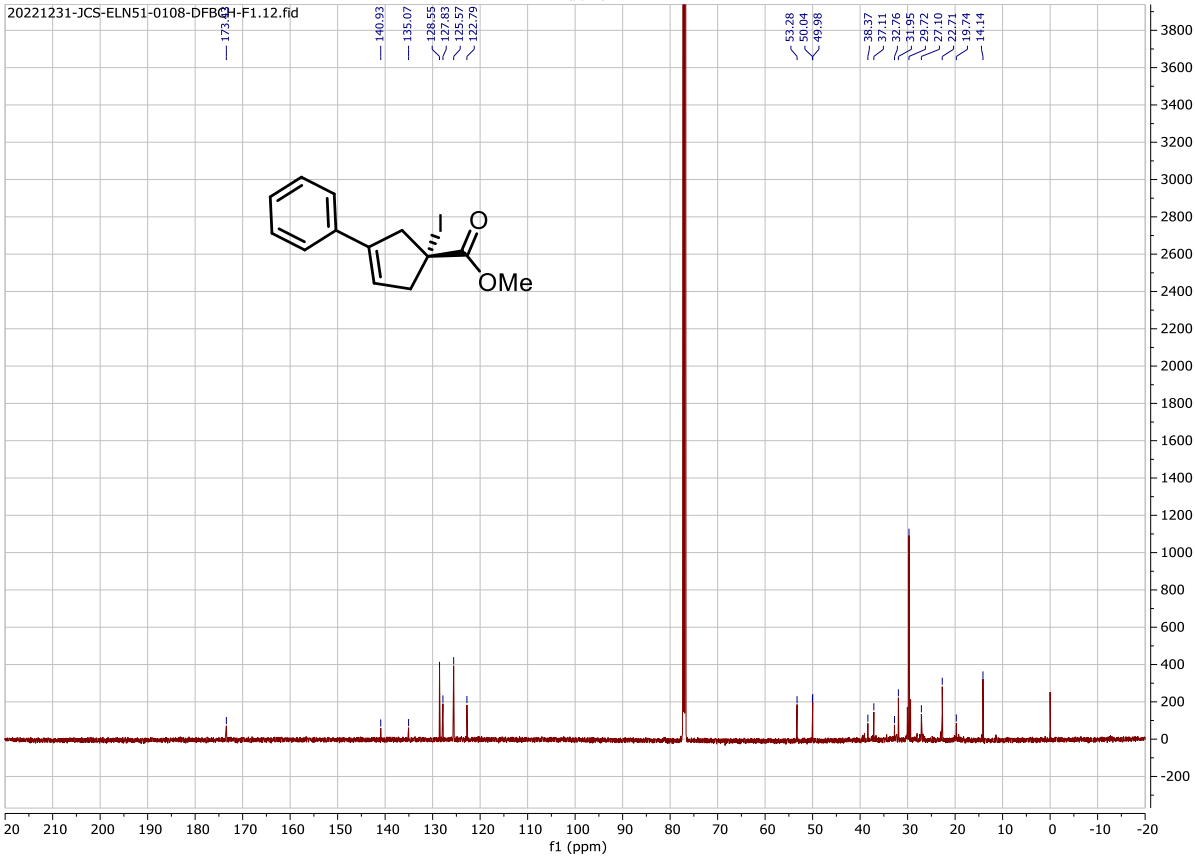
20221231-JCS-ELN51-0108-DFBCH-F1.12.fid
173.41
140.93
135.07
128.55
127.83
125.57
122.79
53.28
50.04
49.98
38.37
37.11
32.76
31.95
29.72
27.10
22.71
19.74
14.14
OMe
f1 (ppm)

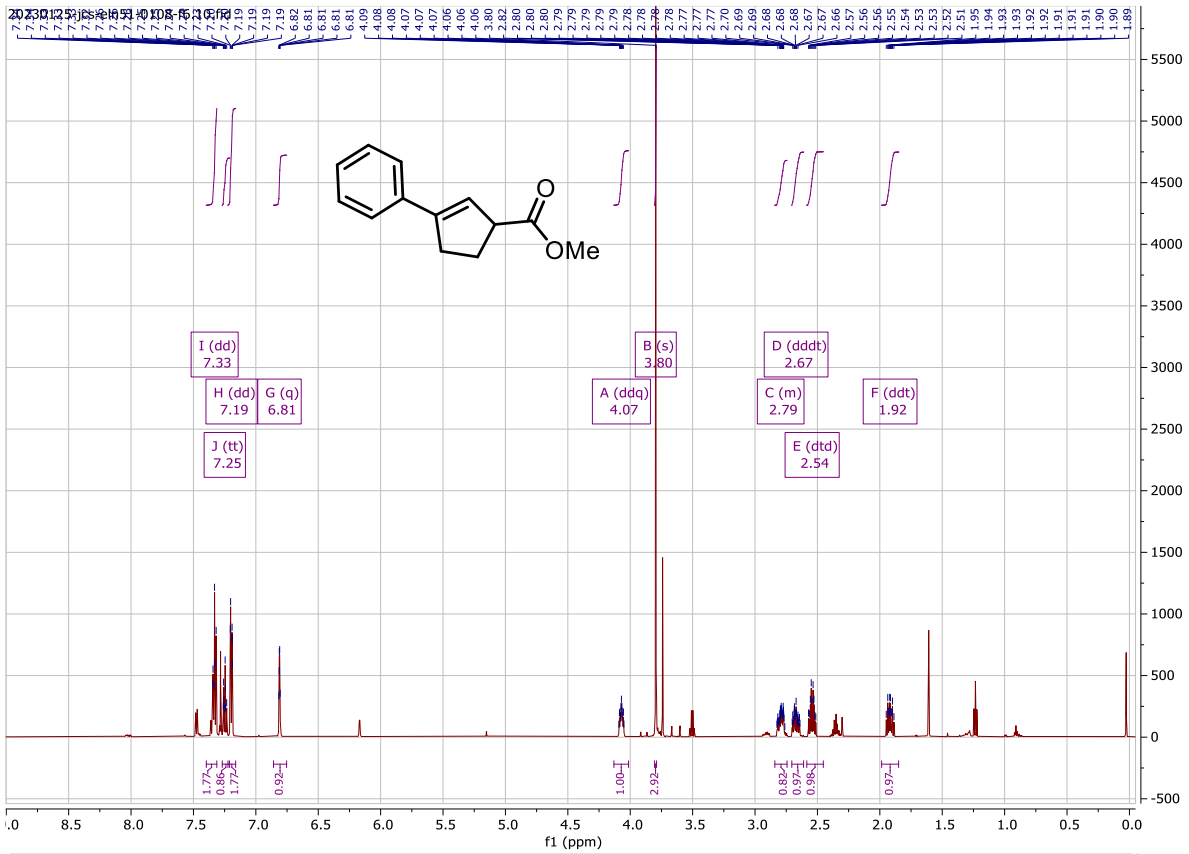
20230125-jcs-el651-0108-f6.10.fid
OMe
I (dd)
7.33
H (dd)
7.19
G (q)
6.81
J (tt)
7.25
B (s)
3.80
A (ddq)
4.07
D (dddt)
2.67
C (m)
2.79
F (ddt)
1.92
E (dtd)
2.54
f1 (ppm)

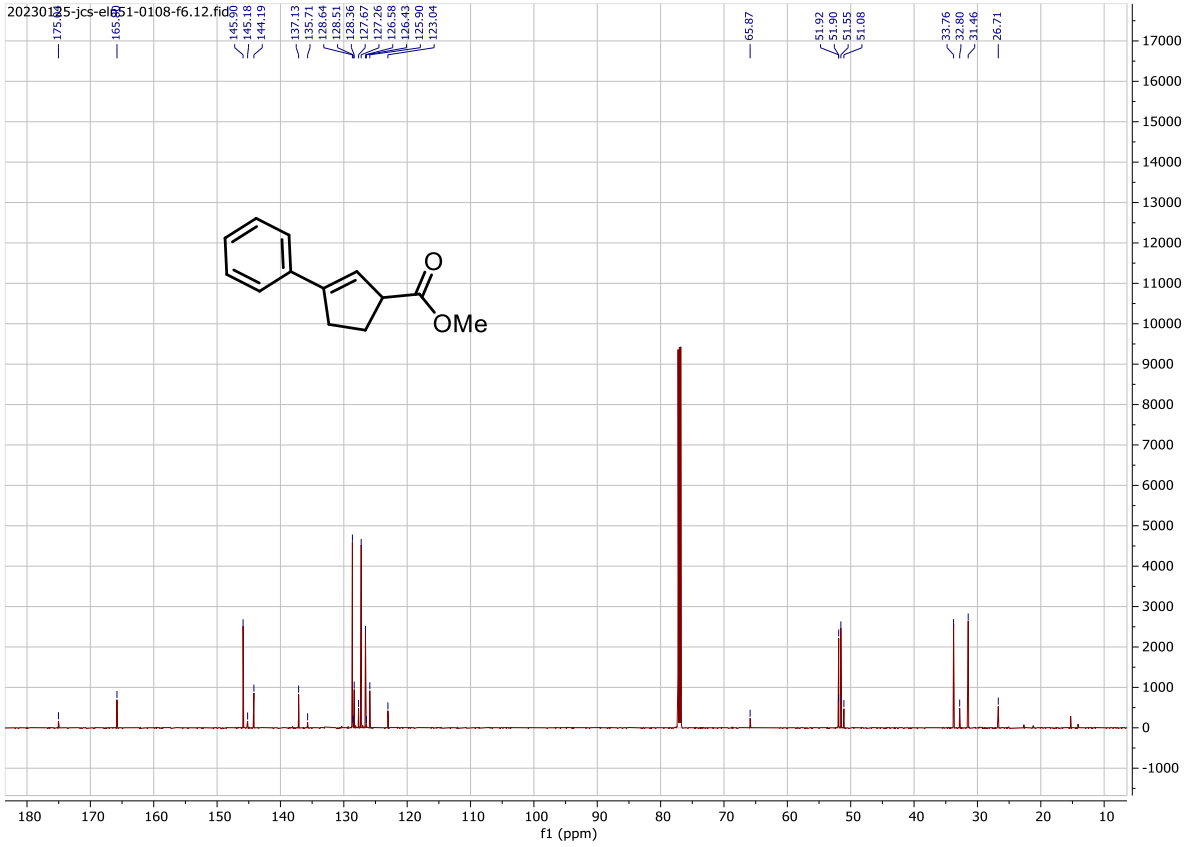
20230125-jcs-el651-0108-f6.12.fid
OMe
175.09
165.85
145.50
145.18
144.19
137.13
135.71
128.64
128.51
128.36
127.67
127.26
126.58
126.43
125.90
123.04
65.87
51.92
51.90
51.55
51.08
33.76
32.80
31.46
26.71
f1 (ppm)

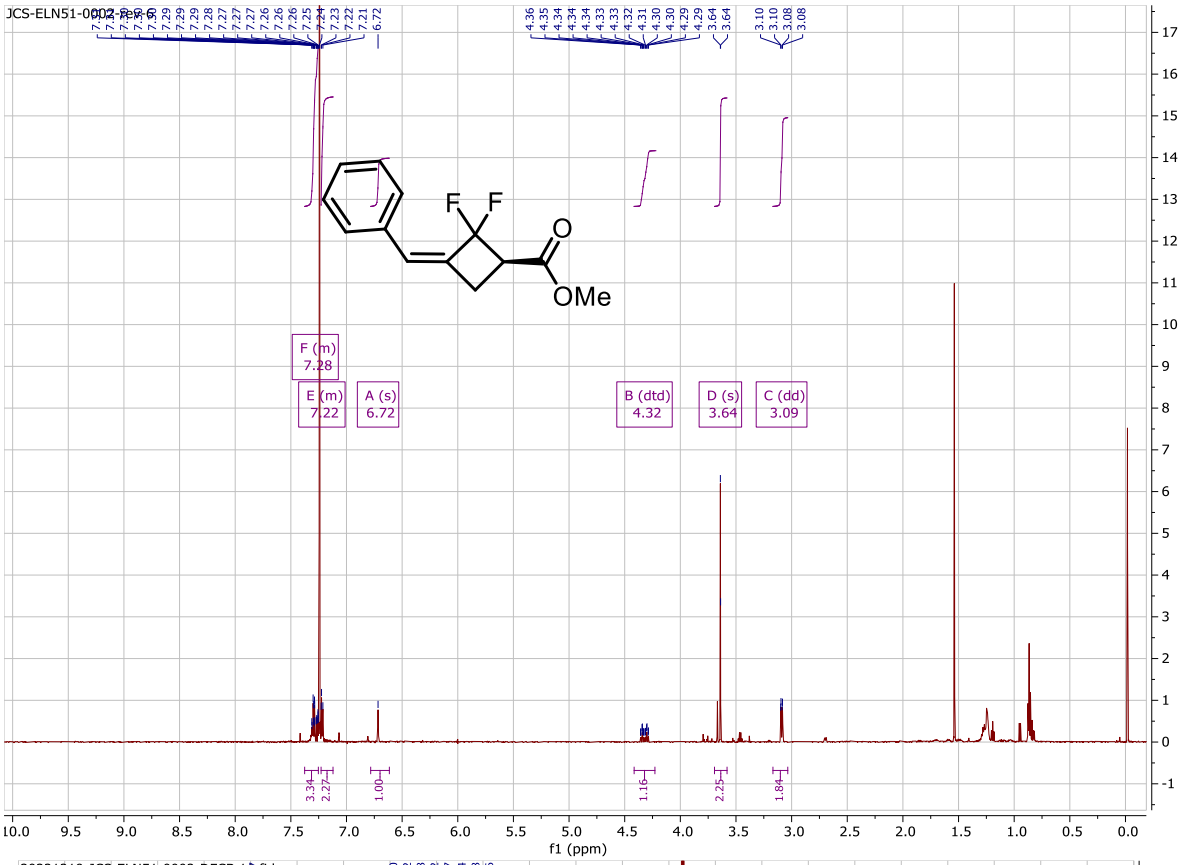
JCS-ELN51-0002-Rev.1
F (m)
7.28
E (m)
7.22
A (s)
6.72
B (dtd)
4.32
D (s)
3.64
C (dd)
3.09
3.34
2.27
1.00
1.16
2.25
1.84
f1 (ppm)

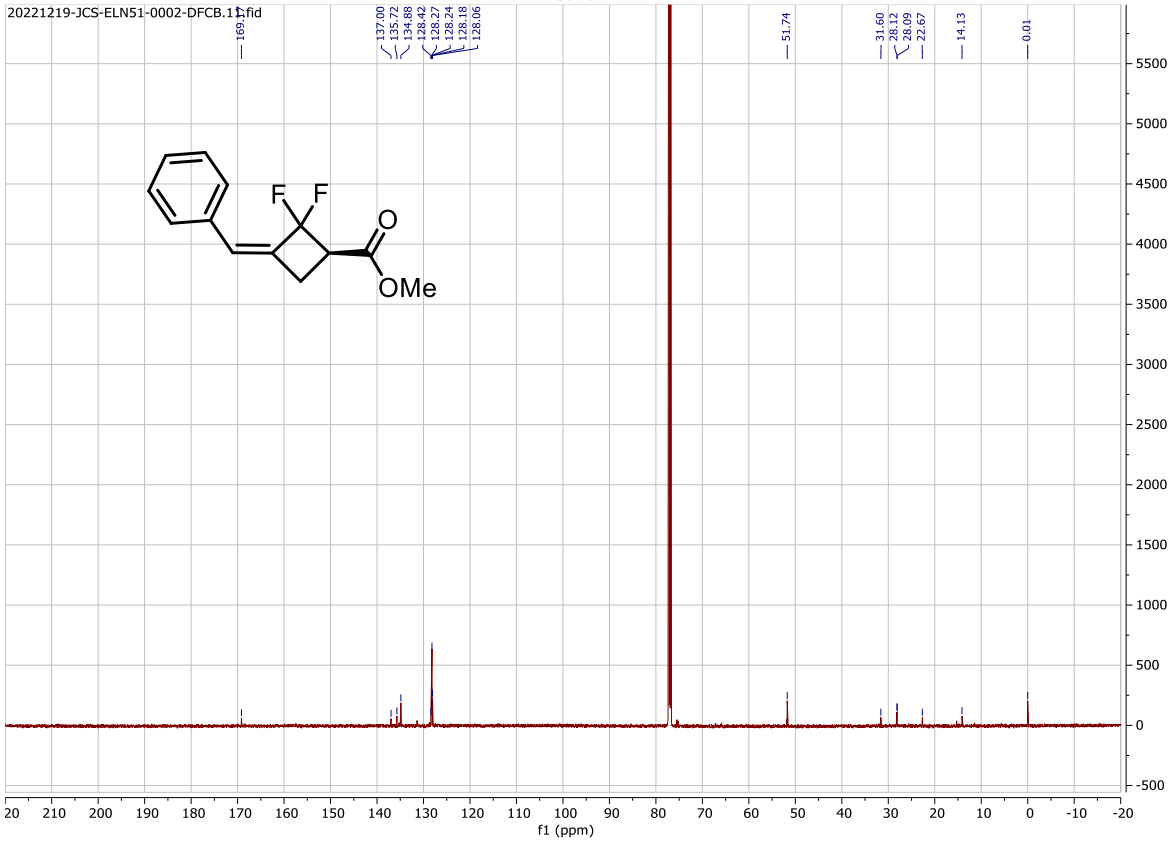
20221219-JCS-ELN51-0002-DFCB.11.fid
169.17
137.00
135.72
134.88
128.42
128.27
128.24
128.18
128.06
51.74
31.60
28.12
28.09
22.67
14.13
0.01
f1 (ppm)

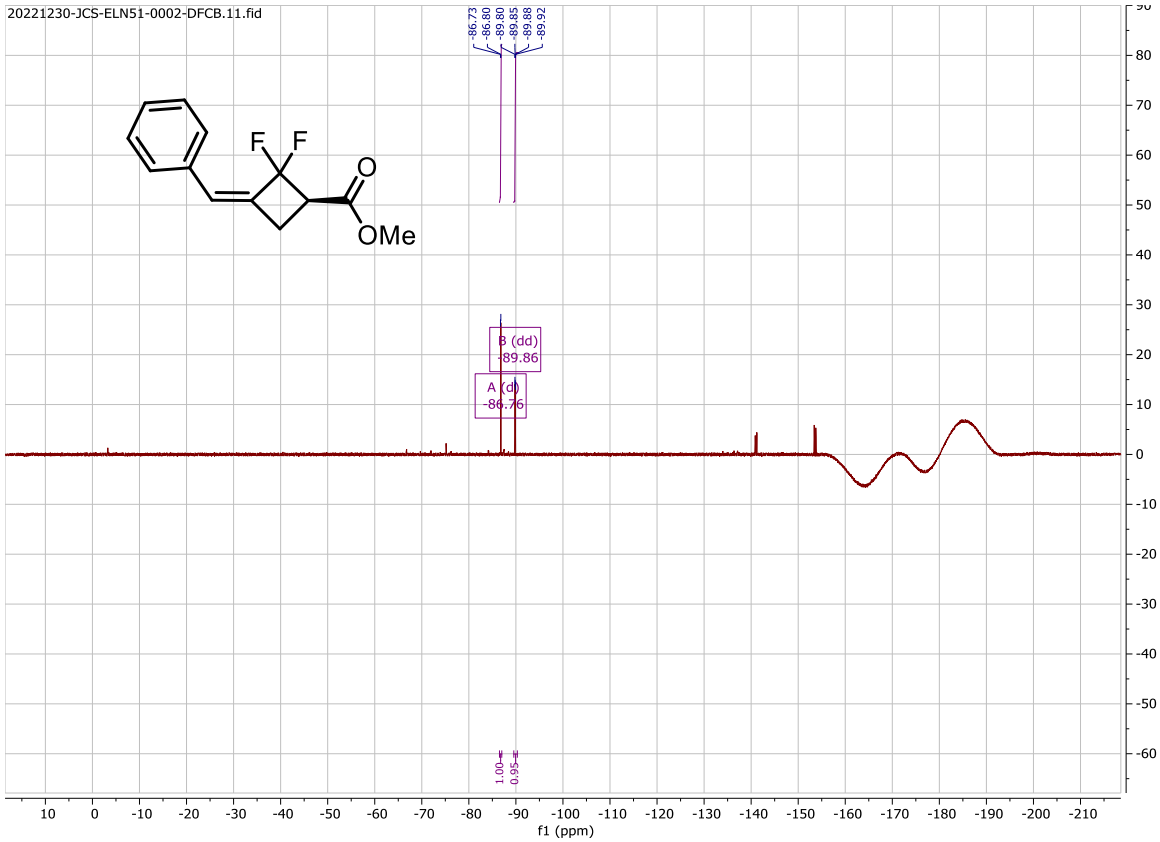
20221230-JCS-ELN51-0002-DFCB.11.fid
F
F
O
OMe
B (dd)
-89.86
A (dd)
-86.76
f1 (ppm)

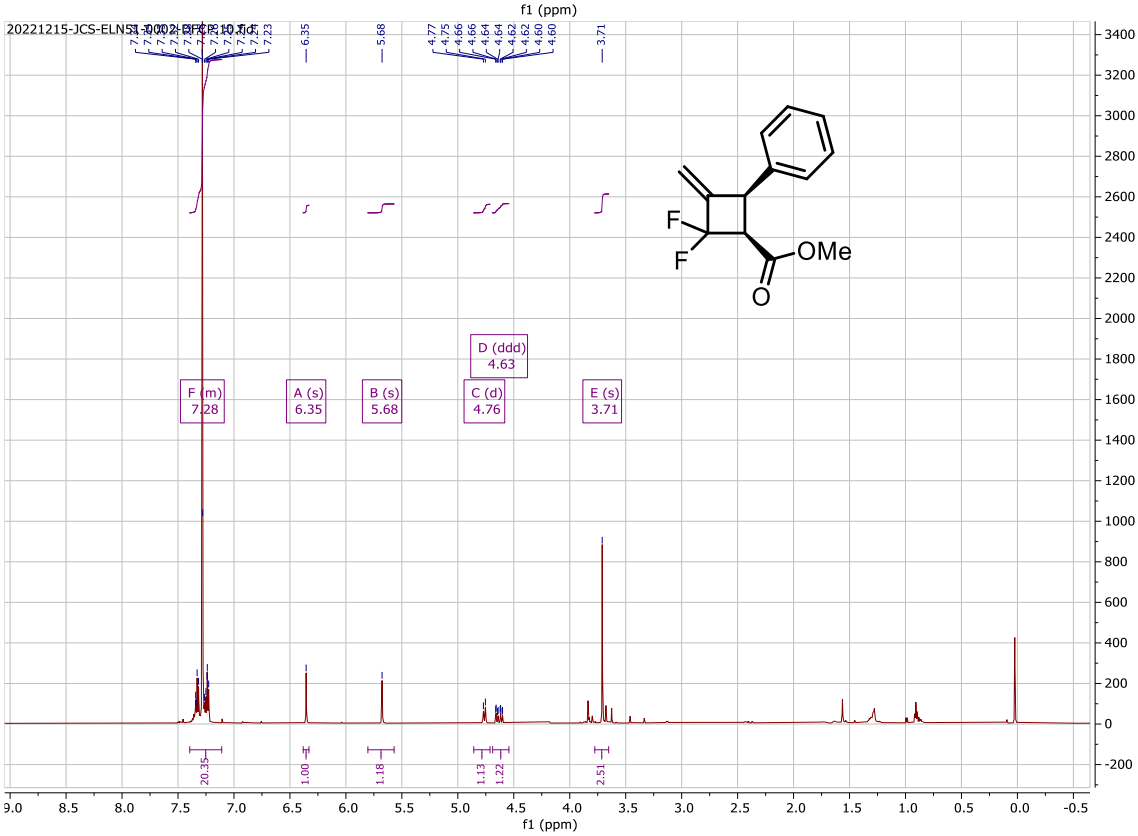
20221215-JCS-ELN51-0002-DFCB.10.fid
F
F
OMe
O
D (ddd)
4.63
F (m)
7.28
A (s)
6.35
B (s)
5.68
C (d)
4.76
E (s)
3.71
f1 (ppm)

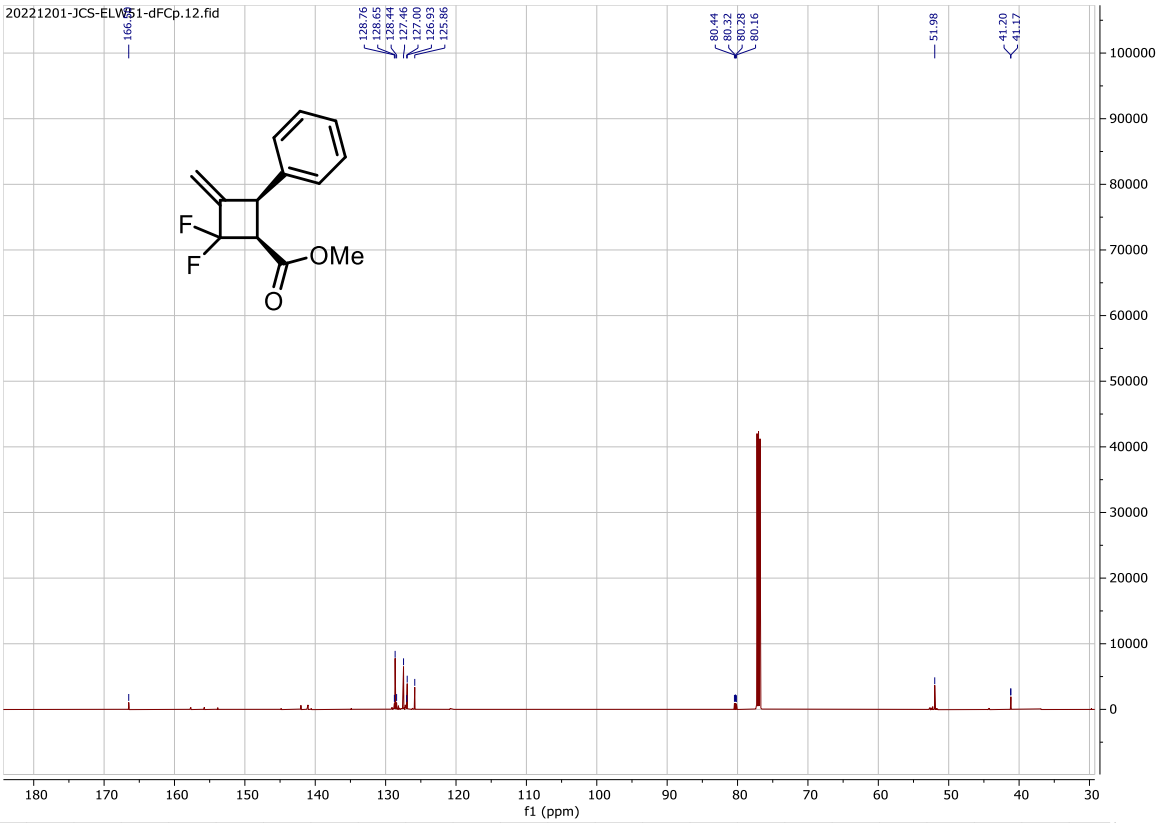
20221201-JCS-ELN51-dFCp.12.fid
166.75
128.76
128.65
128.44
127.46
127.00
126.93
125.86
80.44
80.32
80.28
80.16
51.98
41.20
41.17
F
F
OMe
O
f1 (ppm)

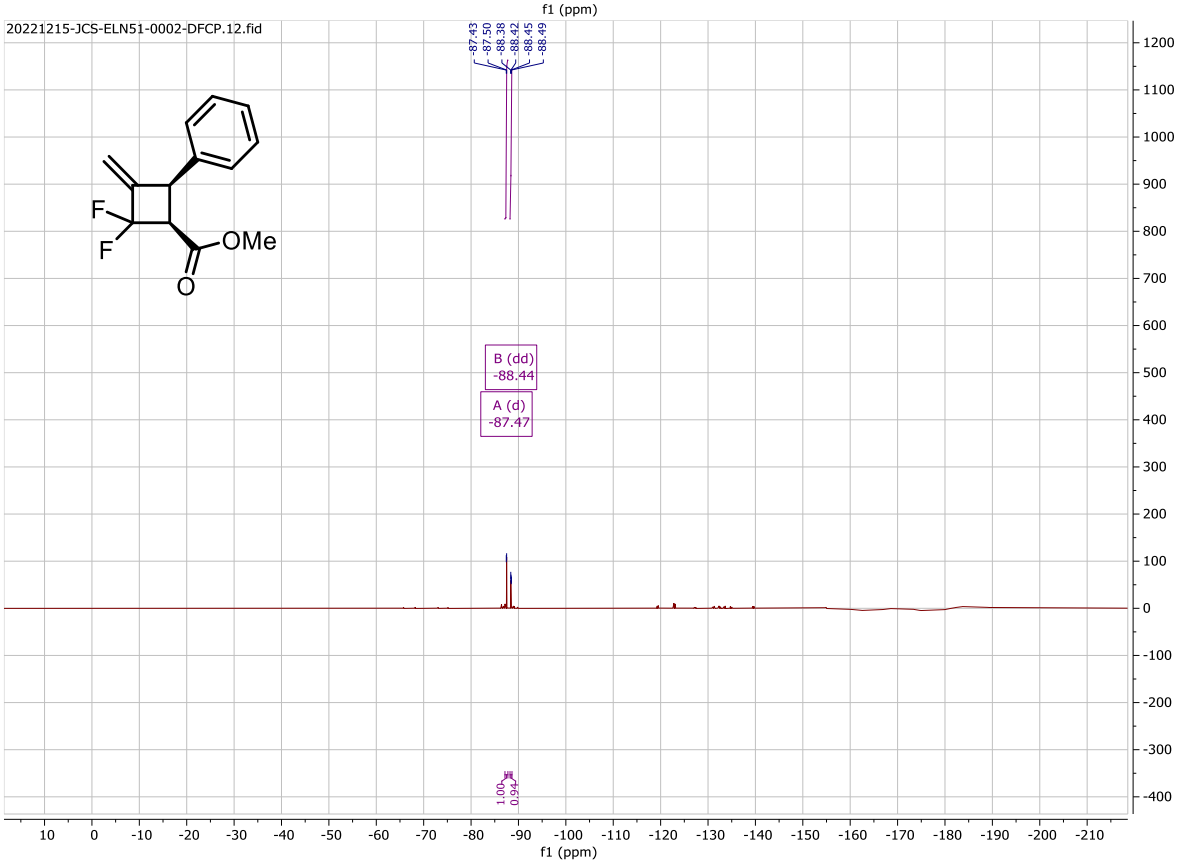
20221215-JCS-ELN51-0002-DFCP.12.fid
-87.43
-87.50
-88.38
-88.42
-88.45
-88.49
F
F
OMe
O
B (dd)
-88.44
A (d)
-87.47
1.00
0.94
f1 (ppm)

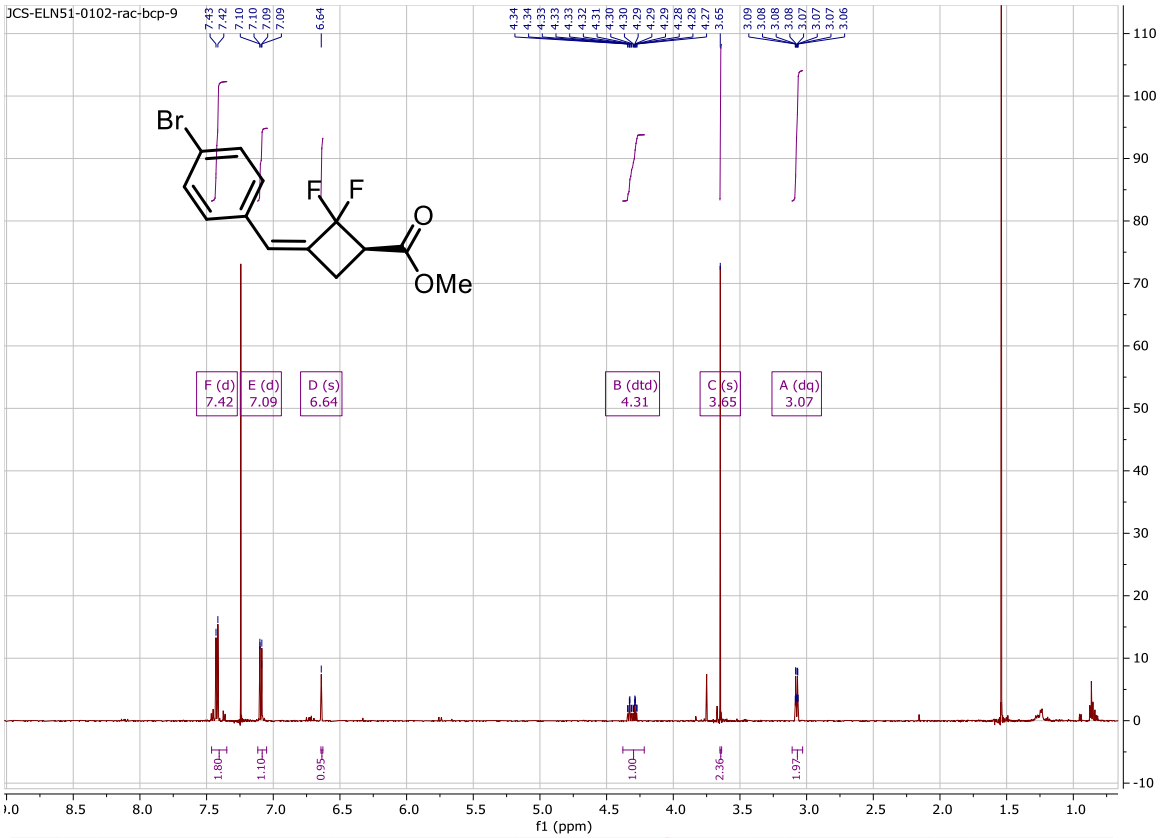
JCS-ELN51-0102-rac-bcp-9
Br
F
F
O
OMe
F (d) 7.42
E (d) 7.09
D (s) 6.64
B (dtd) 4.31
C (s) 3.65
A (dq) 3.07
f1 (ppm)

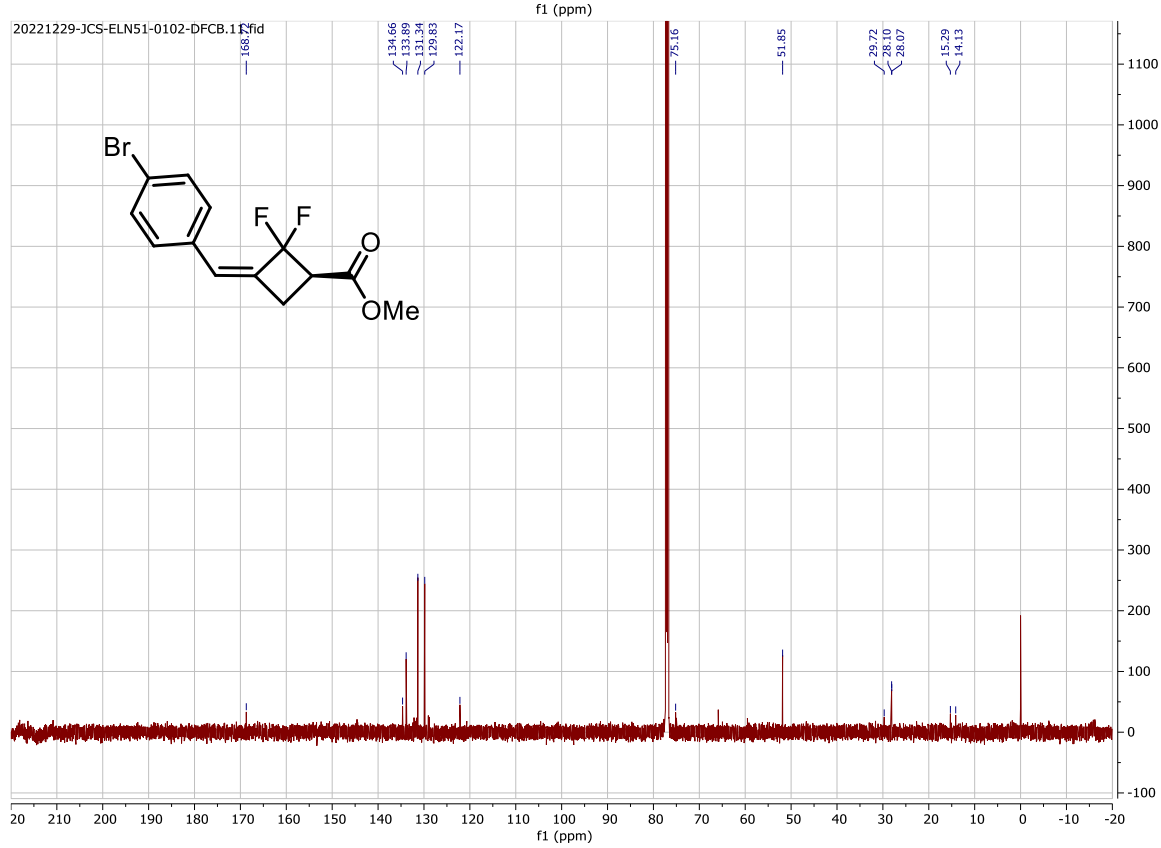
20221229-JCS-ELN51-0102-DFCB.11.fid
Br
F
F
O
OMe
168.71
134.66
133.89
131.34
129.83
122.17
75.16
51.85
29.72
28.10
28.07
15.29
14.13
f1 (ppm)

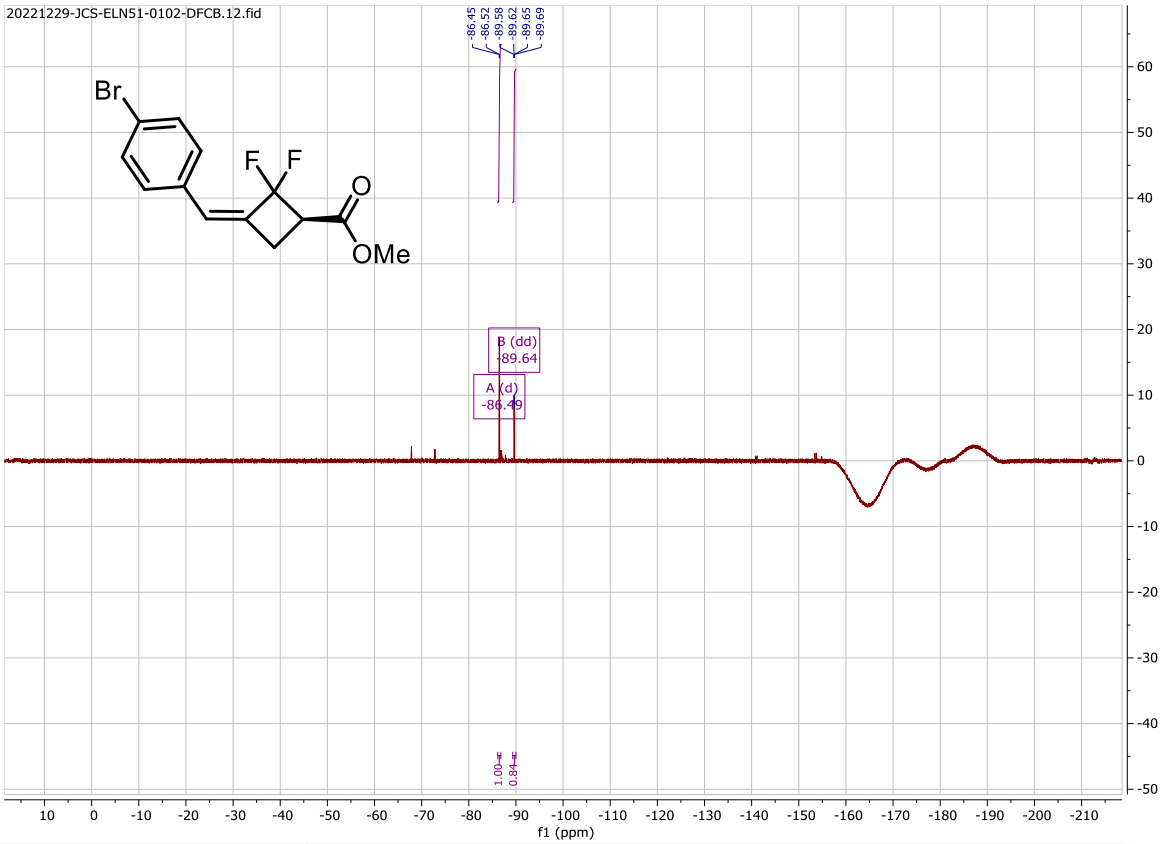
20221229-JCS-ELN51-0102-DFCB.12.fid
Br
F F
O
OMe
B (dd)
-89.64
A (d)
-86.49
f1 (ppm)

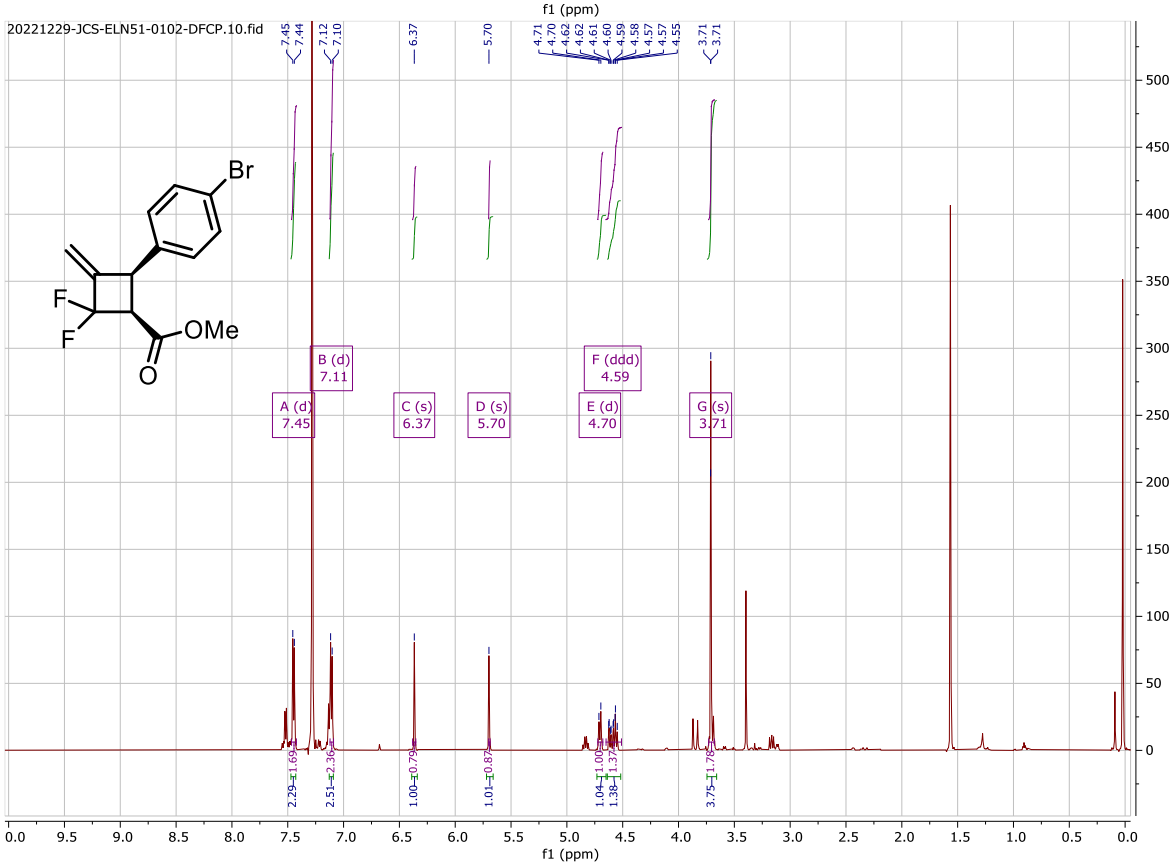
20221229-JCS-ELN51-0102-DFCP.10.fid
Br
F
F
OMe
O
B (d)
7.11
A (d)
7.45
C (s)
6.37
D (s)
5.70
F (ddd)
4.59
E (d)
4.70
G (s)
3.71
f1 (ppm)

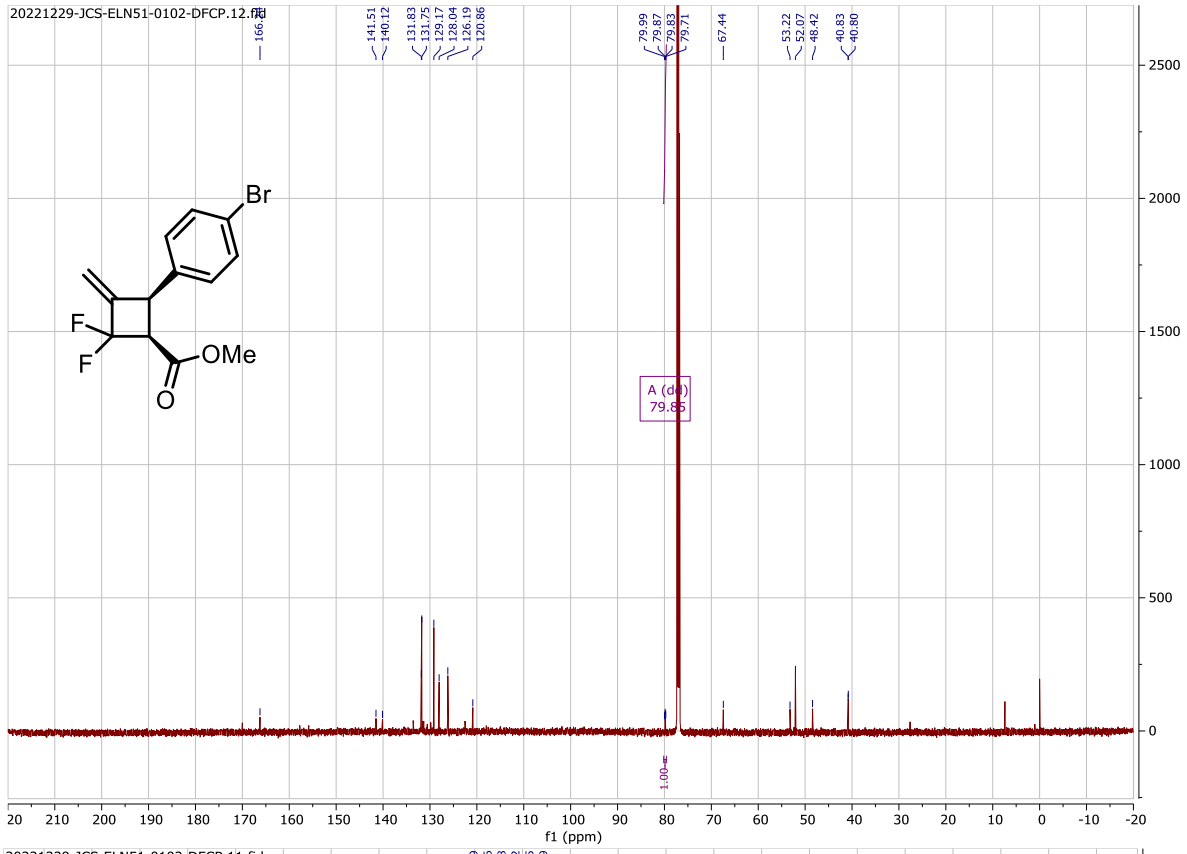
20221229-JCS-ELN51-0102-DFCP.12.fid
166.21
141.51
140.12
131.83
131.75
129.17
128.04
126.19
120.86
79.99
79.87
79.83
79.71
67.44
53.22
52.07
48.42
40.83
40.80
A (dd)
79.85
1.00
Br
F
F
OMe
O
f1 (ppm)

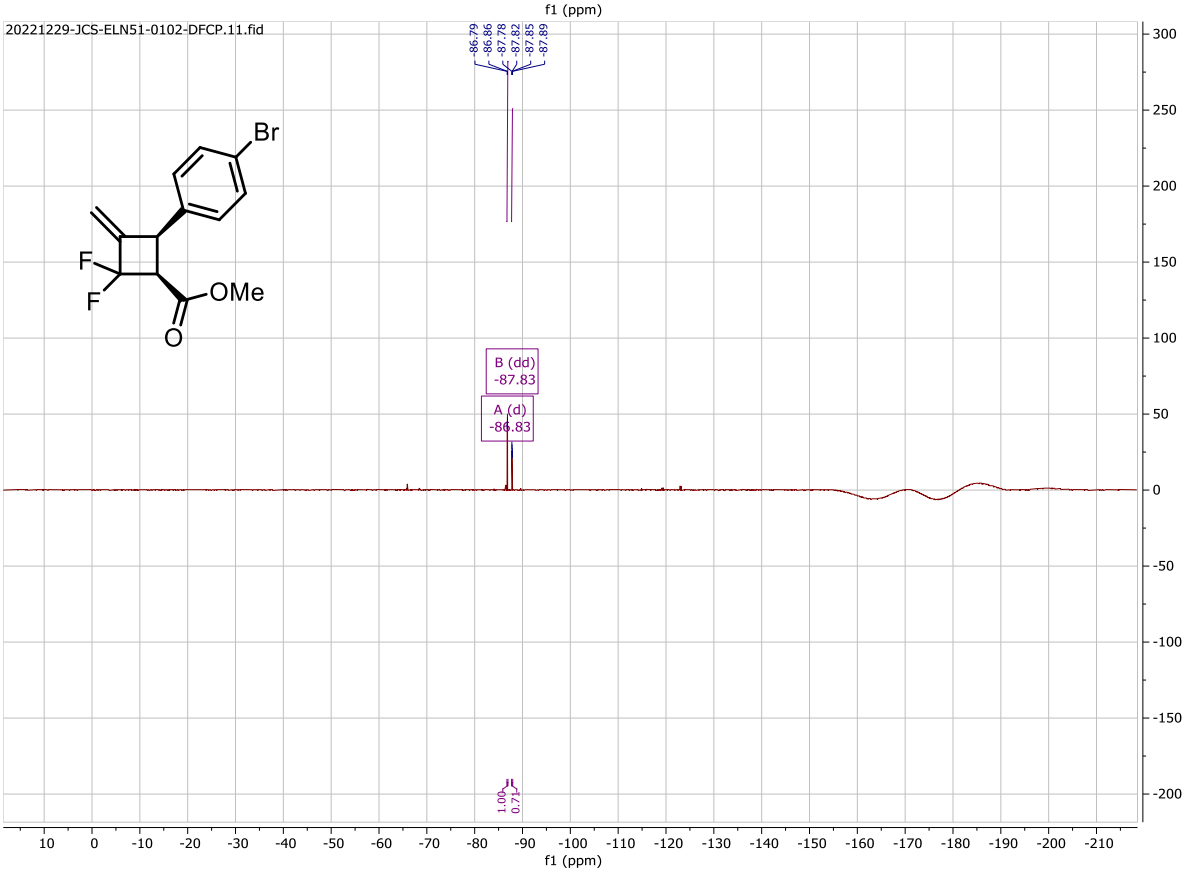
20221229-JCS-ELN51-0102-DFCP.11.fid
-86.79
-86.86
-87.78
-87.82
-87.85
-87.89
B (dd)
-87.83
A (d)
-86.83
1.00
0.71
Br
F
F
OMe
O
f1 (ppm)

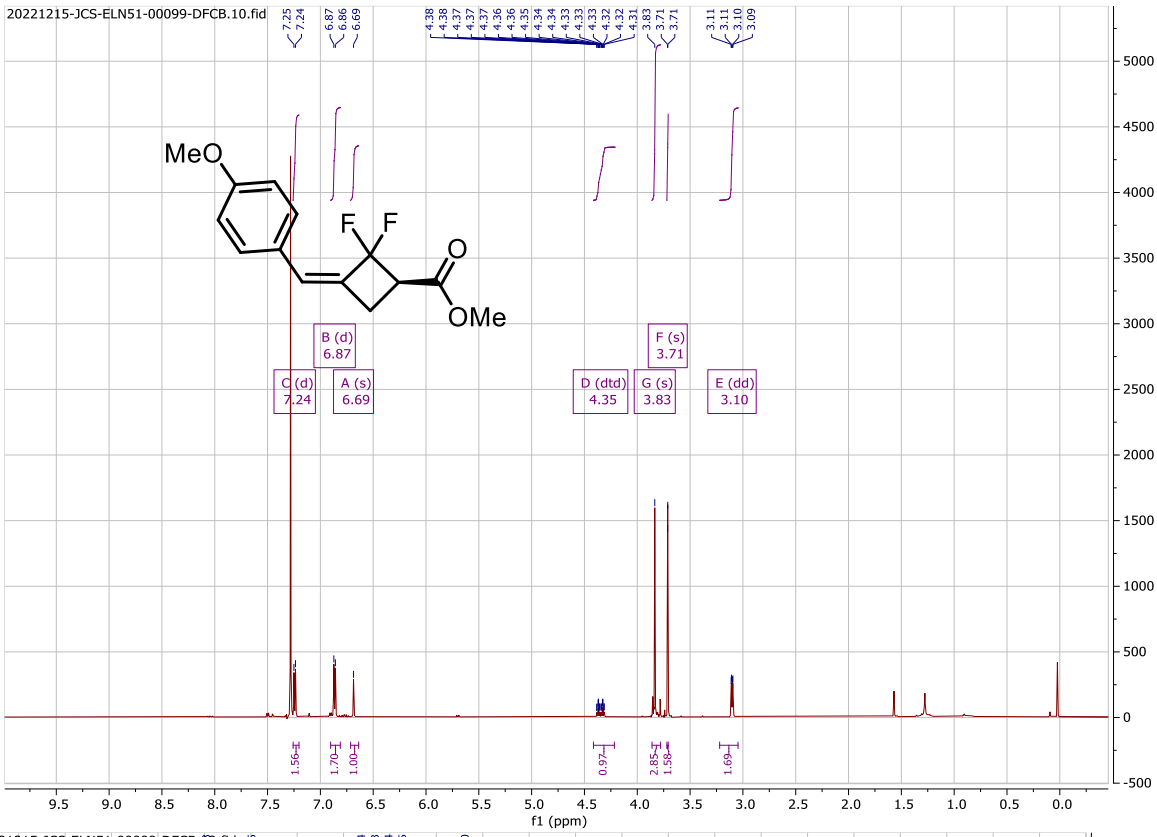
20221215-JCS-ELN51-00099-DFCB.10.fid
MeO
F
F
O
OMe
C (d) 7.24
B (d) 6.87
A (s) 6.69
D (dtd) 4.35
G (s) 3.83
F (s) 3.71
E (dd) 3.10
f1 (ppm)

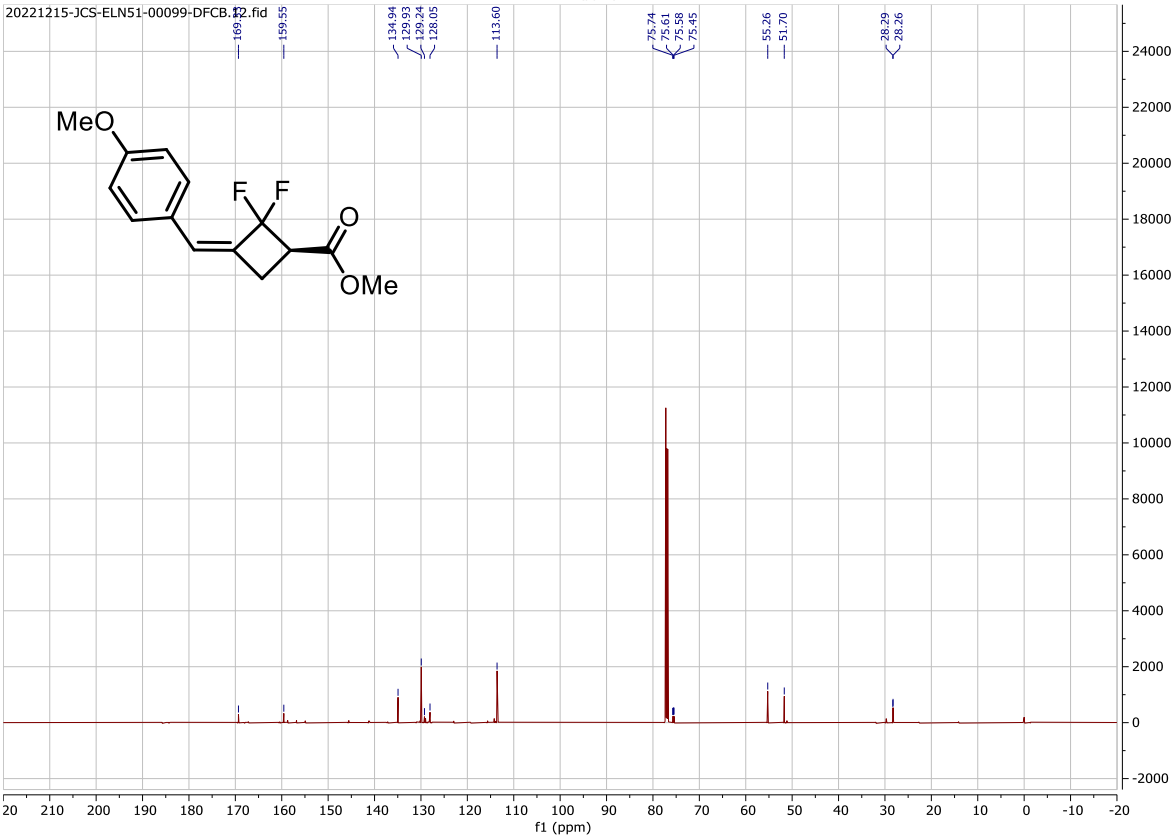
20221215-JCS-ELN51-00099-DFCB.12.fid
MeO
F
F
O
OMe
169.42
159.55
134.94
129.93
129.24
128.05
113.60
75.74
75.61
75.58
75.45
55.26
51.70
28.29
28.26
f1 (ppm)

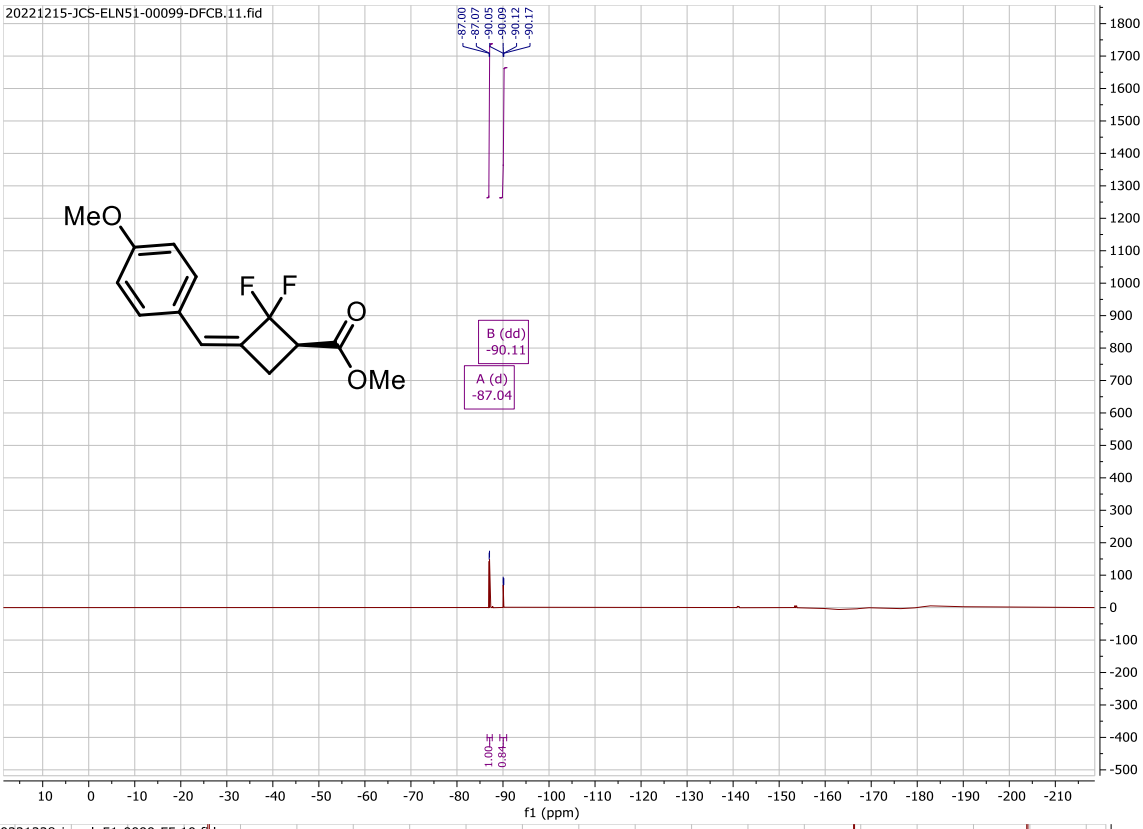
20221215-JCS-ELN51-00099-DFCB.11.fid
MeO
F
F
O
OMe
B (dd)
-90.11
A (d)
-87.04
f1 (ppm)

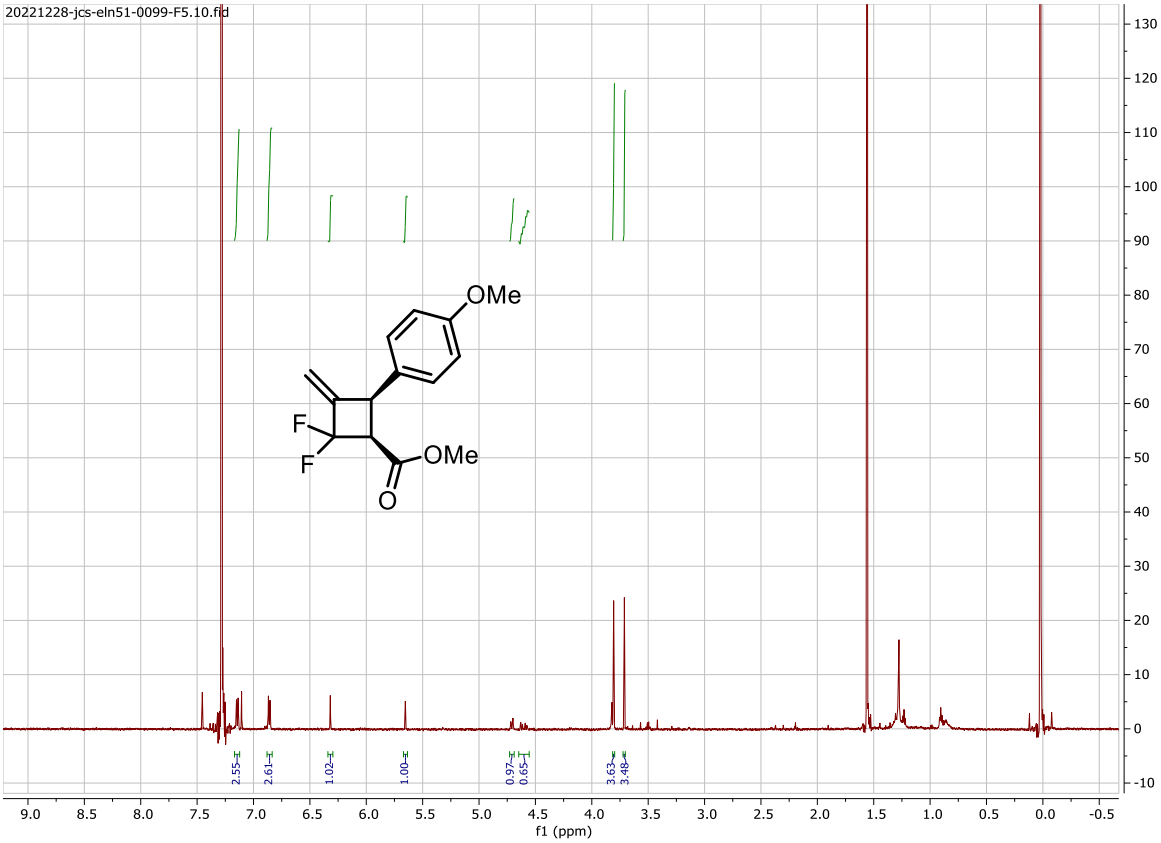
20221228-jcs-eln51-0099-F5.10.fid
OMe
F
F
OMe
O
f1 (ppm)

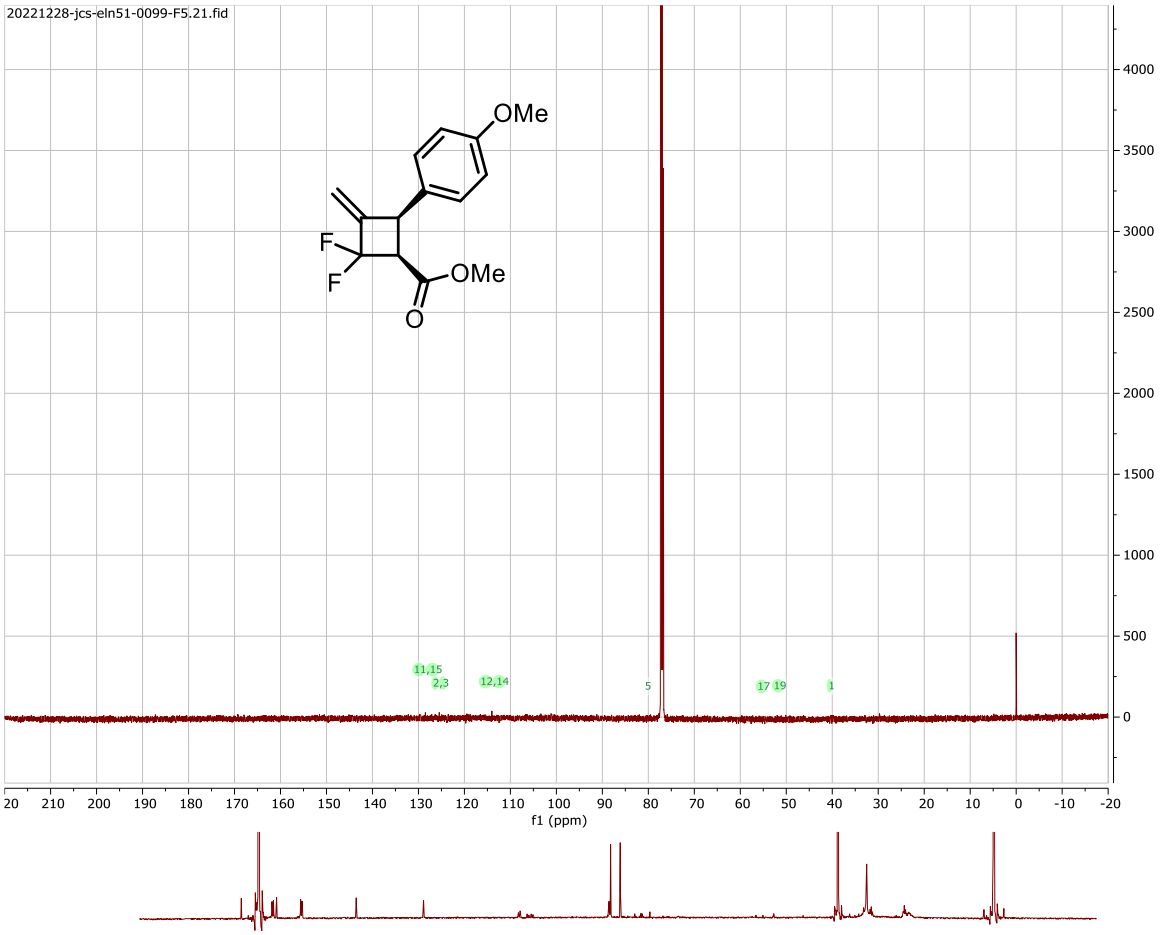
20221228-jcs-eln51-0099-F5.21.fid
OMe
F
F
OMe
O
f1 (ppm)

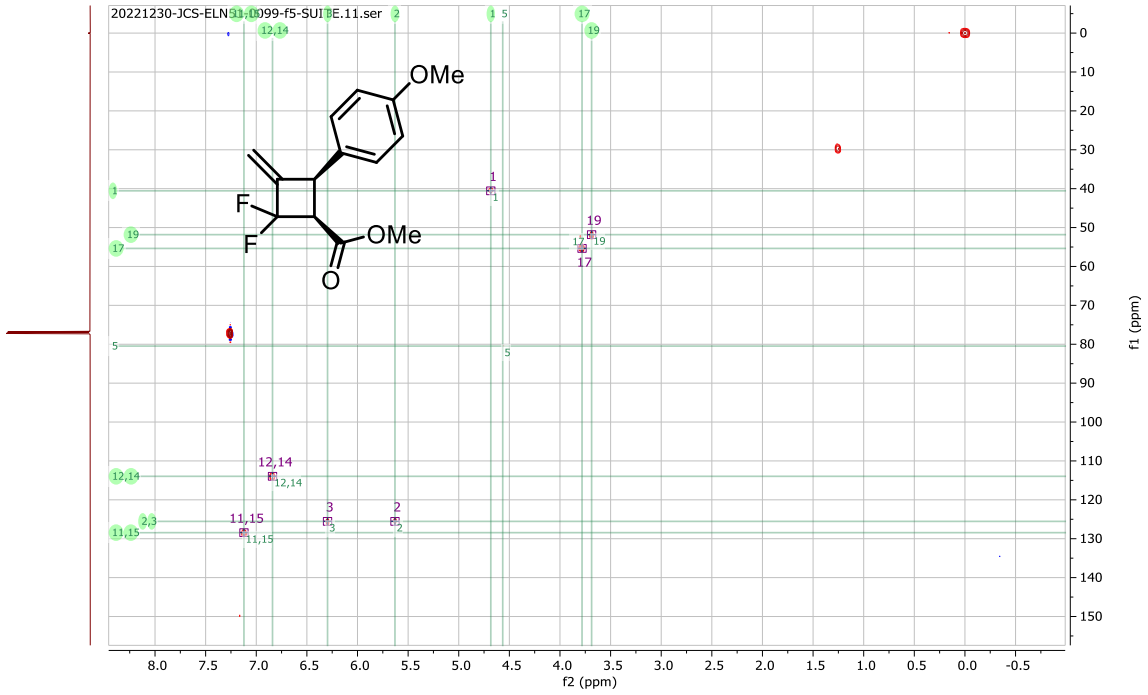
20221230-JCS-ELN51-0099-f5-SUITE.11.ser
OMe
F
F
OMe
O
f2 (ppm)
f1 (ppm)

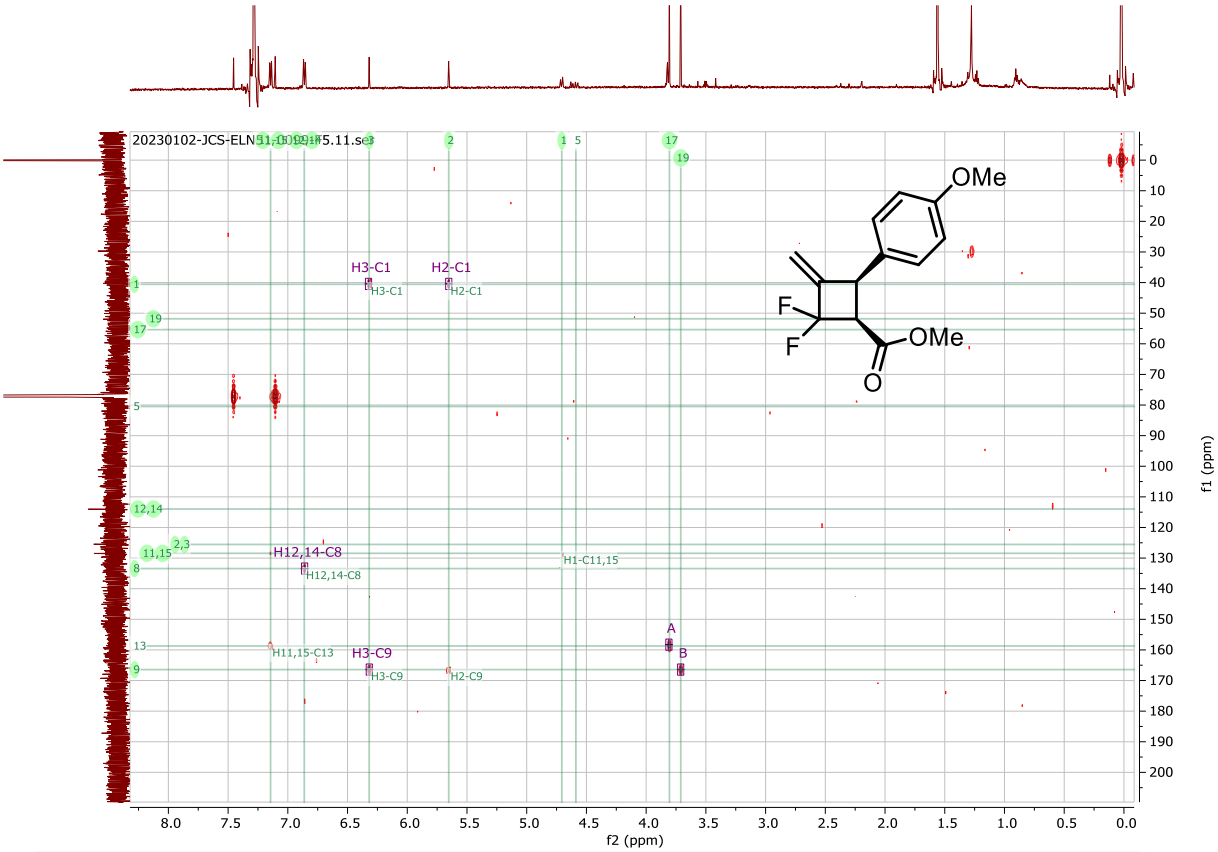
20230102-JCS-ELN51-0099-F5.11.se3
H3-C1
H2-C1
H12,14-C8
H1-C11,15
H11,15-C13
H3-C9
H2-C9
OMe
F
F
OMe
O
f1 (ppm)
f2 (ppm)

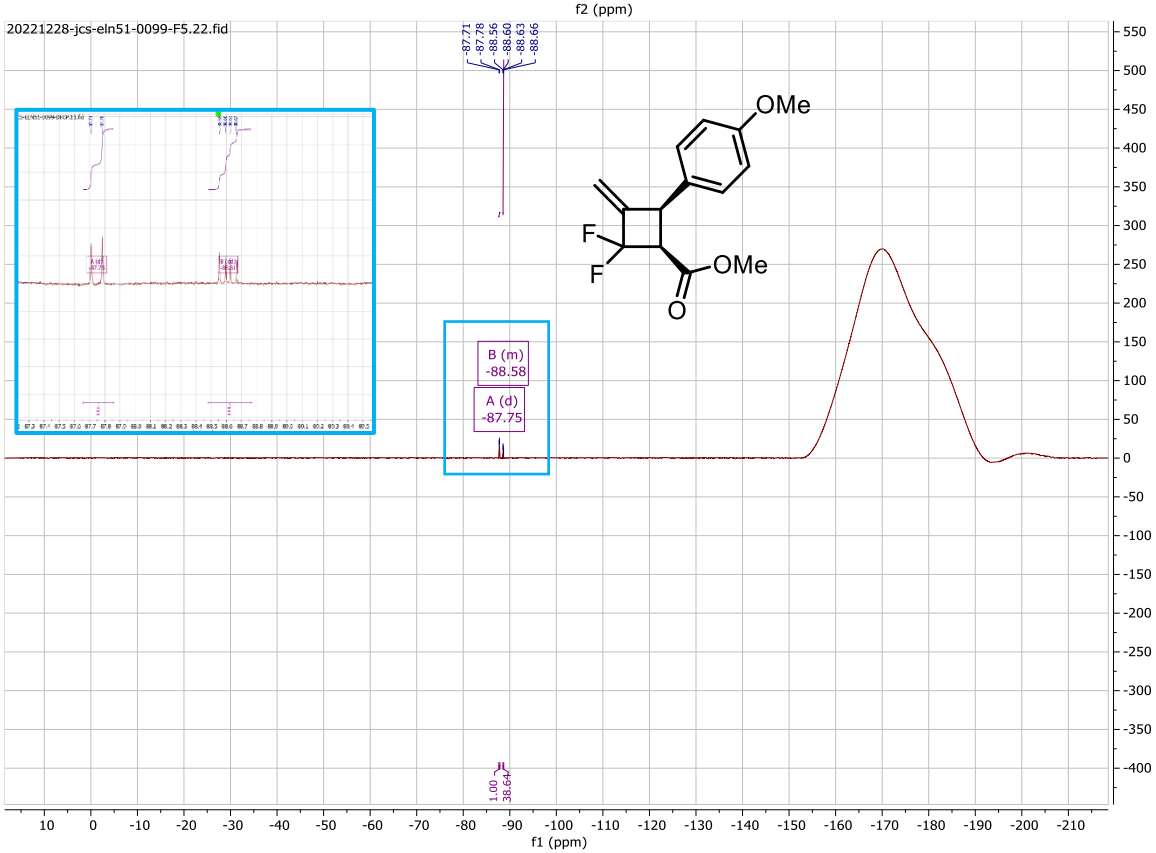
20221228-jcs-eln51-0099-F5.22.fid
-87.71
-87.73
-88.55
-88.60
-88.63
-88.66
OMe
F
F
OMe
O
B (m)
-88.58
A (d)
-87.75
1.00
38.64
f1 (ppm)

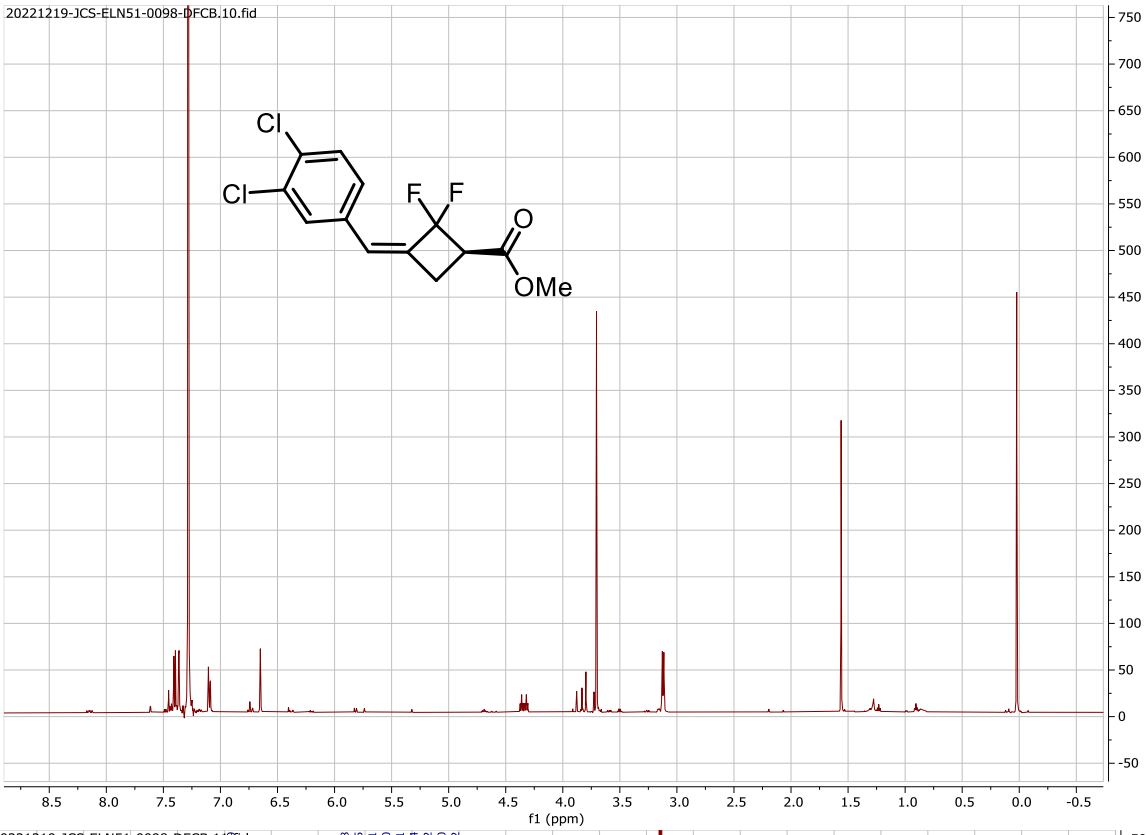
20221219-JCS-ELN51-0098-DFCB.10.fid
Cl
Cl
F
F
O
OMe
f1 (ppm)

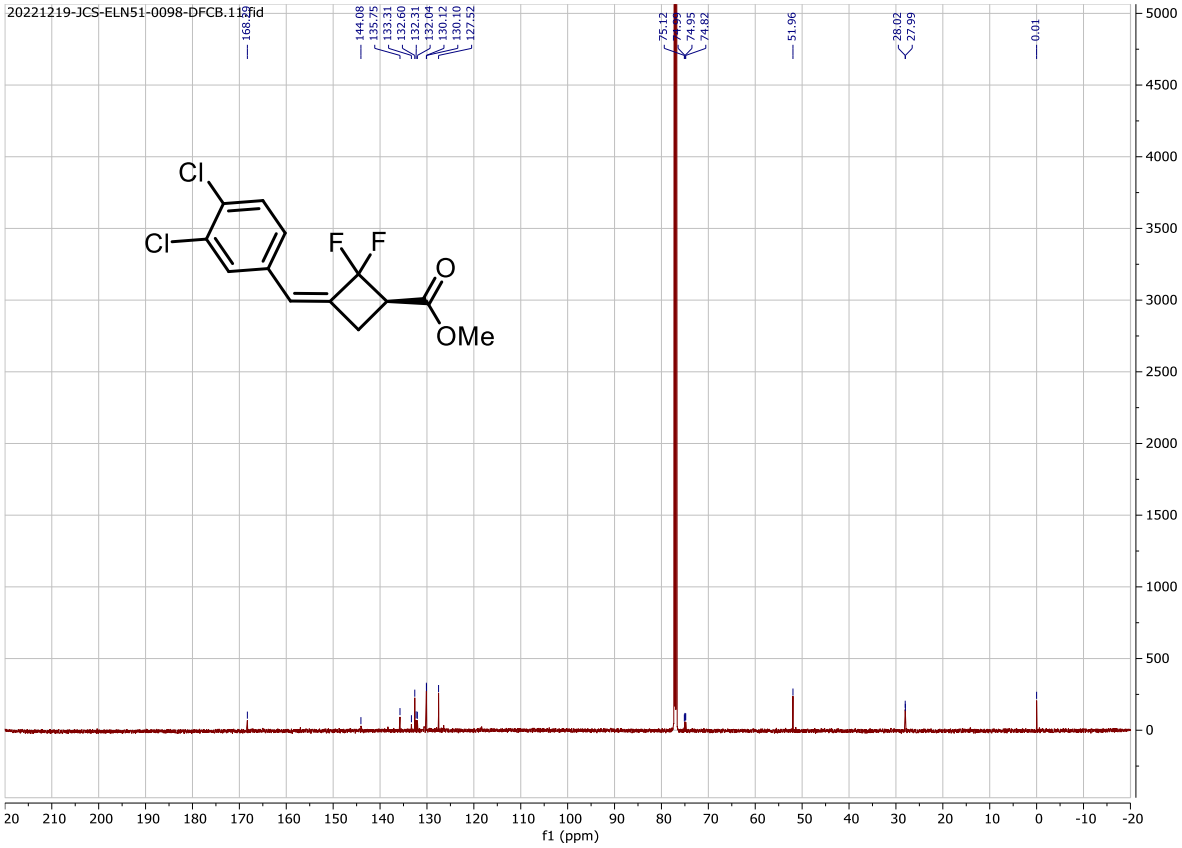
20221219-JCS-ELN51-0098-DFCB.11.fid
168.25
144.08
135.75
133.31
132.60
132.31
132.04
130.12
130.10
127.52
75.12
74.95
74.82
51.96
28.02
27.99
0.01
Cl
Cl
F
F
O
OMe
f1 (ppm)

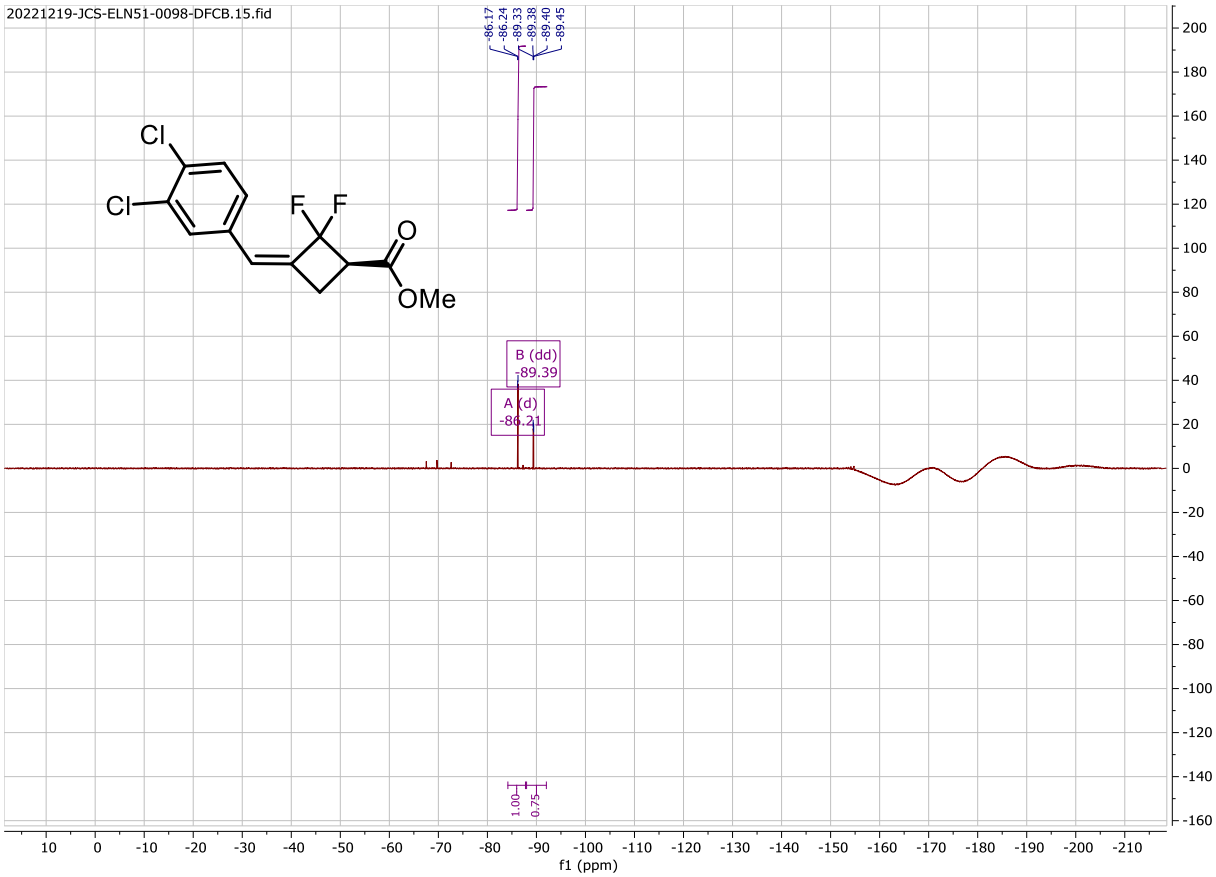
20221219-JCS-ELN51-0098-DFCB.15.fid
Cl
Cl
F
F
O
OMe
B (dd)
-89.39
A (d)
-86.21
f1 (ppm)

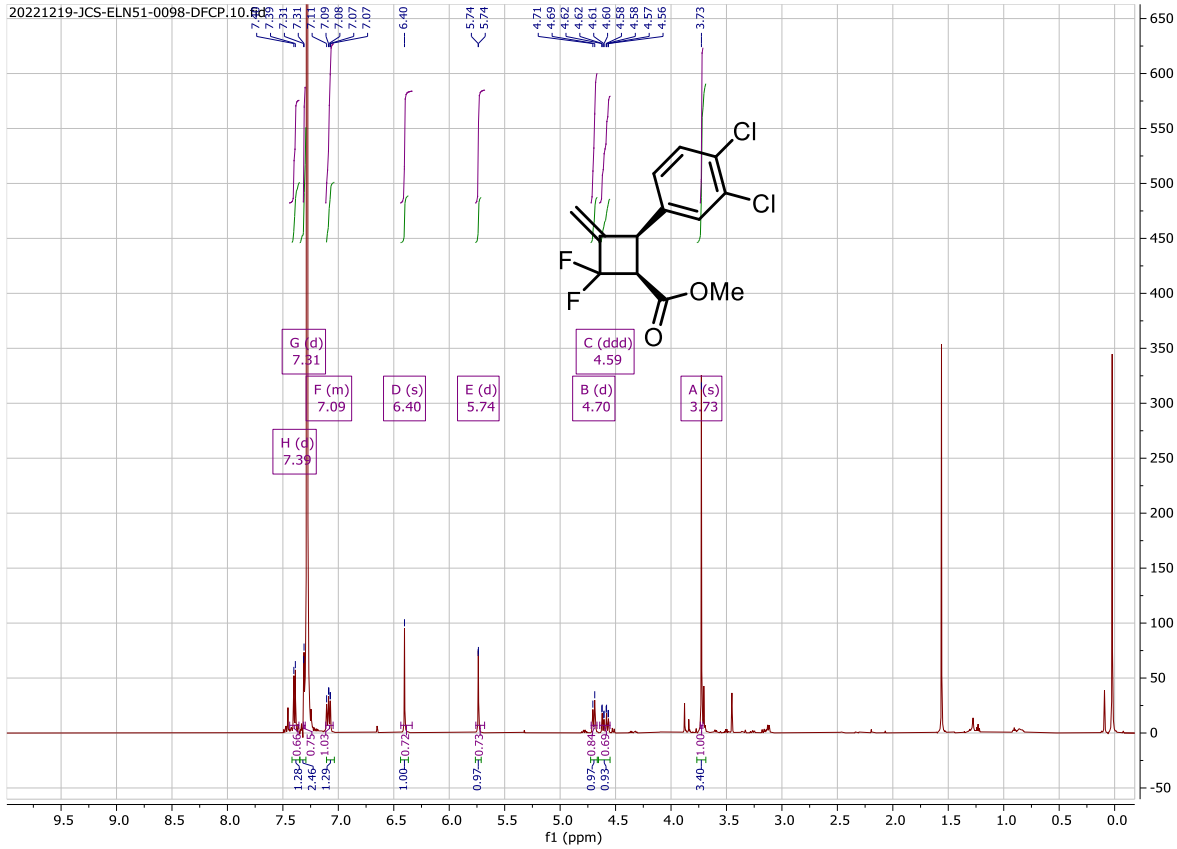
20221219-JCS-ELN51-0098-DFCP.10.fid
Cl
Cl
F
F
OMe
O
G (d)
7.31
F (m)
7.09
D (s)
6.40
E (d)
5.74
C (ddd)
4.59
B (d)
4.70
A (s)
3.73
H (d)
7.39
f1 (ppm)

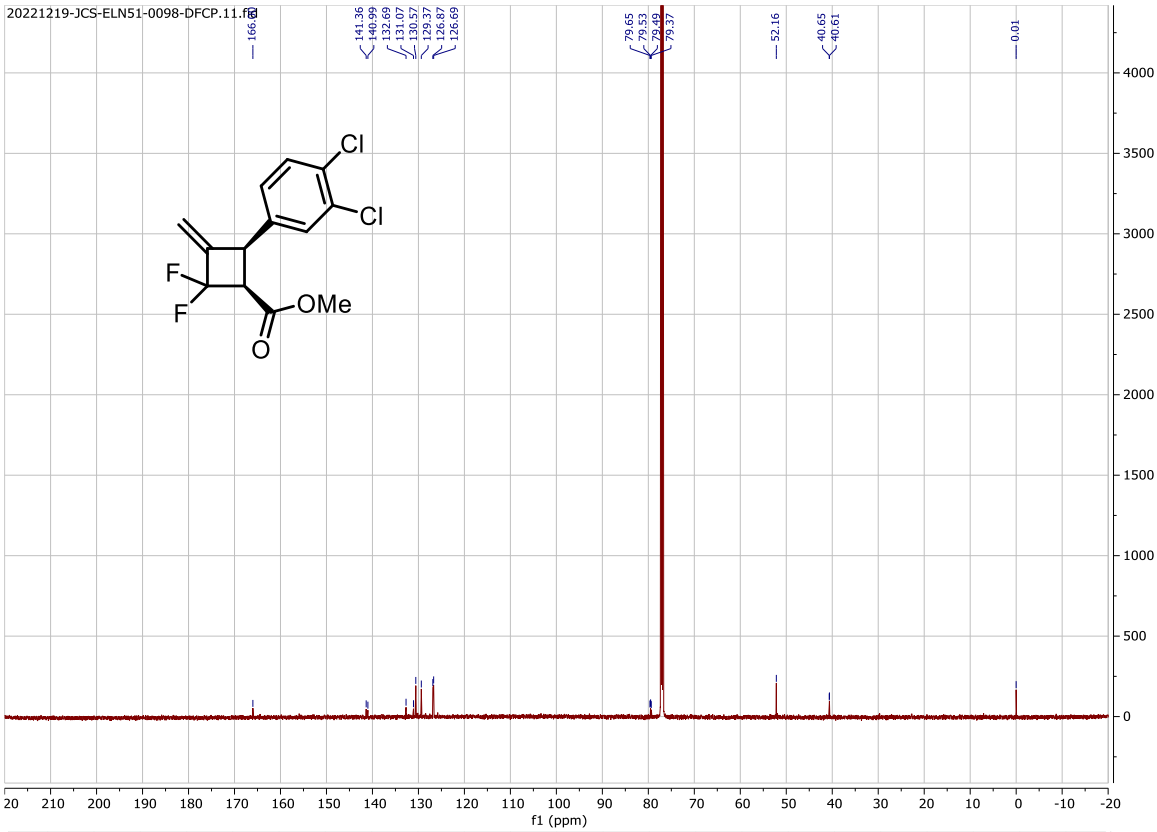
20221219-JCS-ELN51-0098-DFCP.11.fid
166.64
141.36
140.99
132.69
131.07
130.57
129.37
126.87
126.69
79.65
79.53
79.49
79.37
52.16
40.65
40.61
0.01
Cl
Cl
F
F
OMe
O
f1 (ppm)

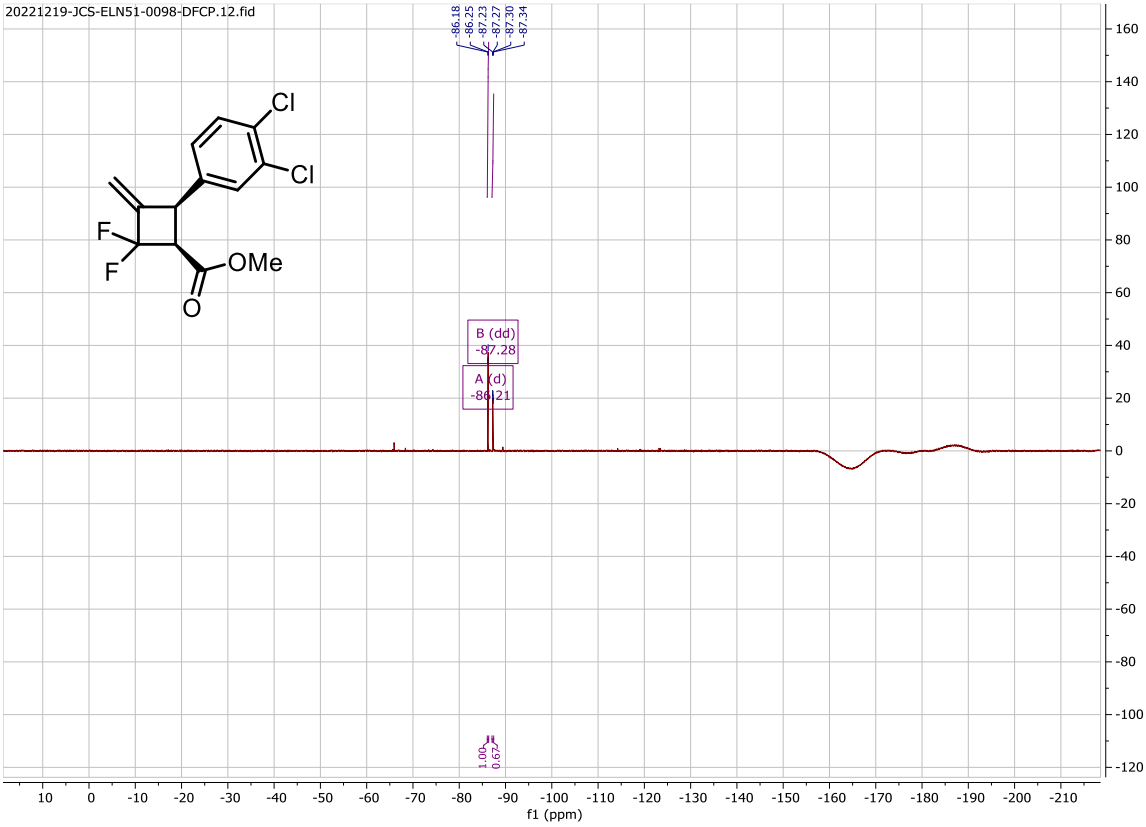
20221219-JCS-ELN51-0098-DFCP.12.fid
-86.18
-86.25
-87.23
-87.27
-87.30
-87.34
Cl
Cl
F
F
OMe
O
B (dd)
-87.28
A (d)
-86.21
1.00
0.67
f1 (ppm)

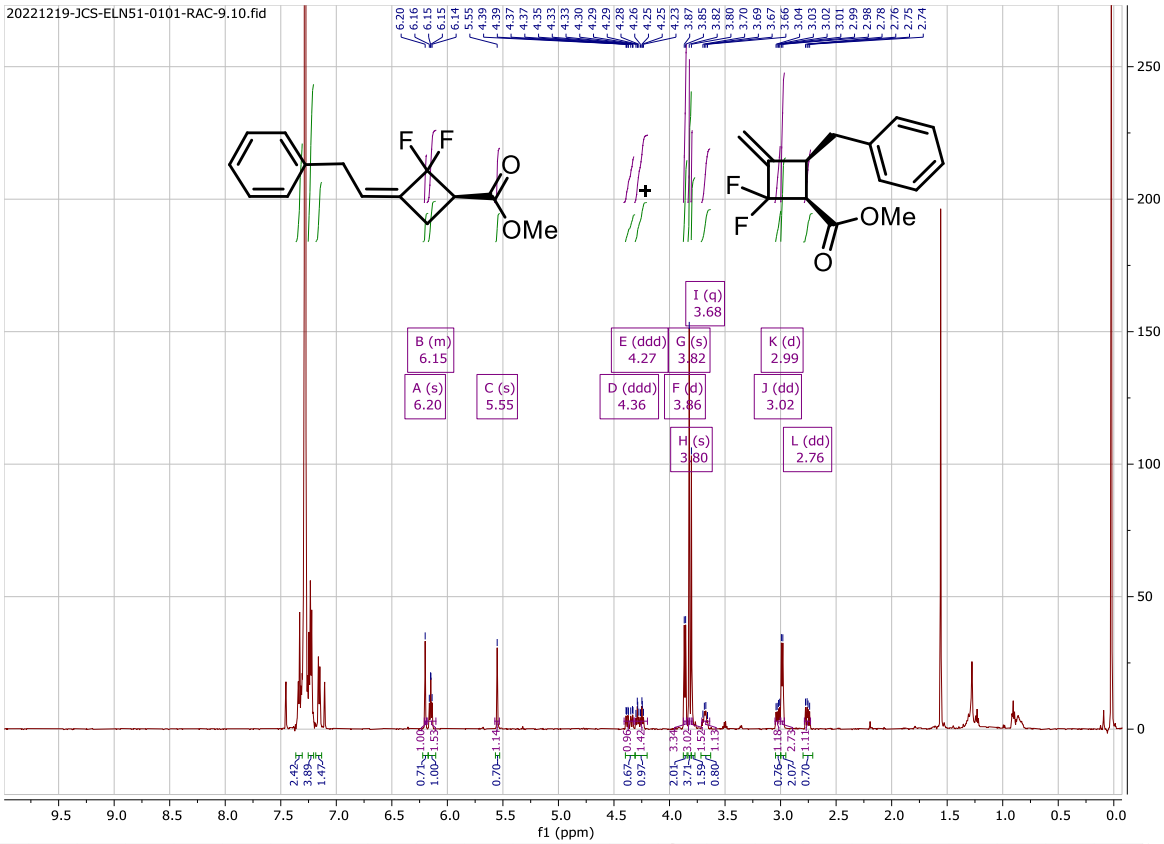
20221219-JCS-ELN51-0101-RAC-9.10.fid
A (s) 6.20
B (m) 6.15
C (s) 5.55
D (ddd) 4.36
E (ddd) 4.27
F (d) 3.86
G (s) 3.82
H (s) 3.80
I (q) 3.68
J (dd) 3.02
K (d) 2.99
L (dd) 2.76
f1 (ppm)

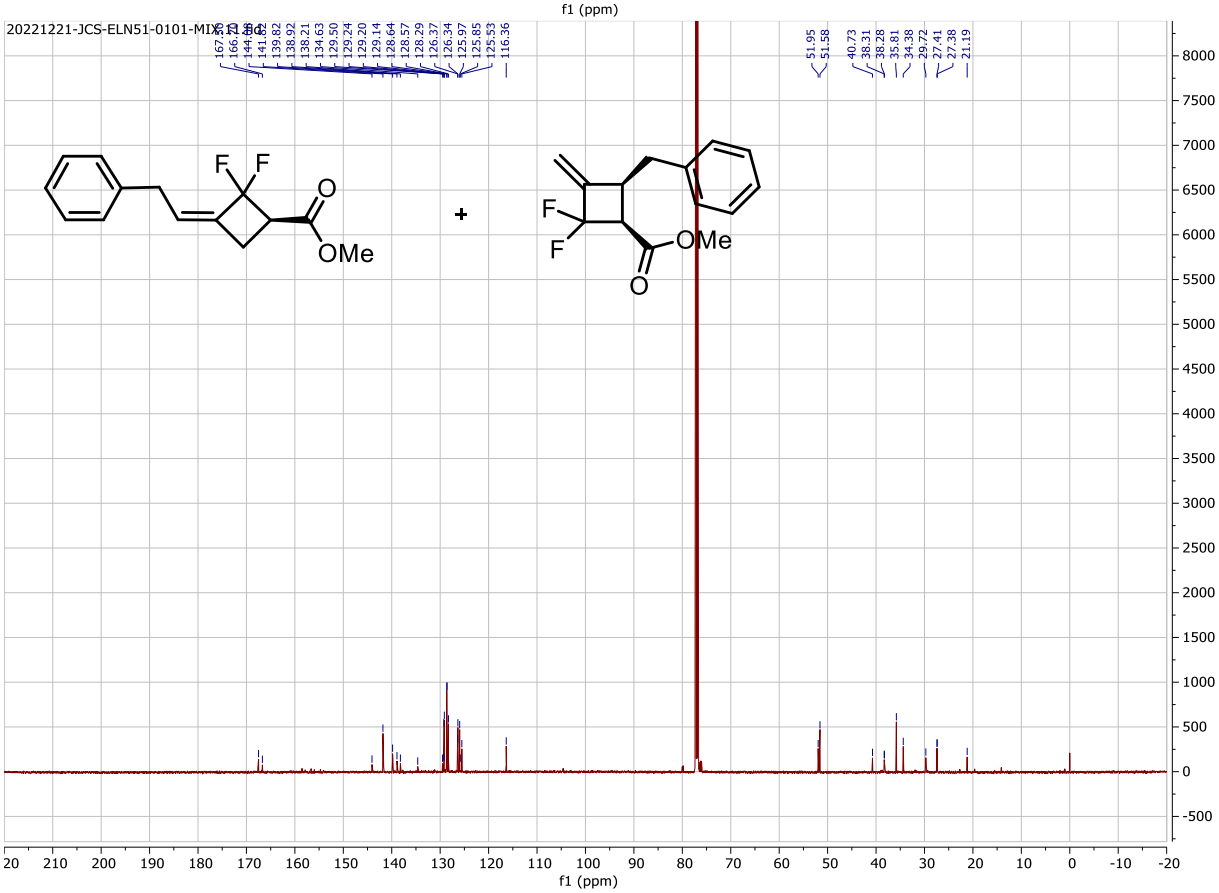
20221221-JCS-ELN51-0101-MIX-13.fid
f1 (ppm)

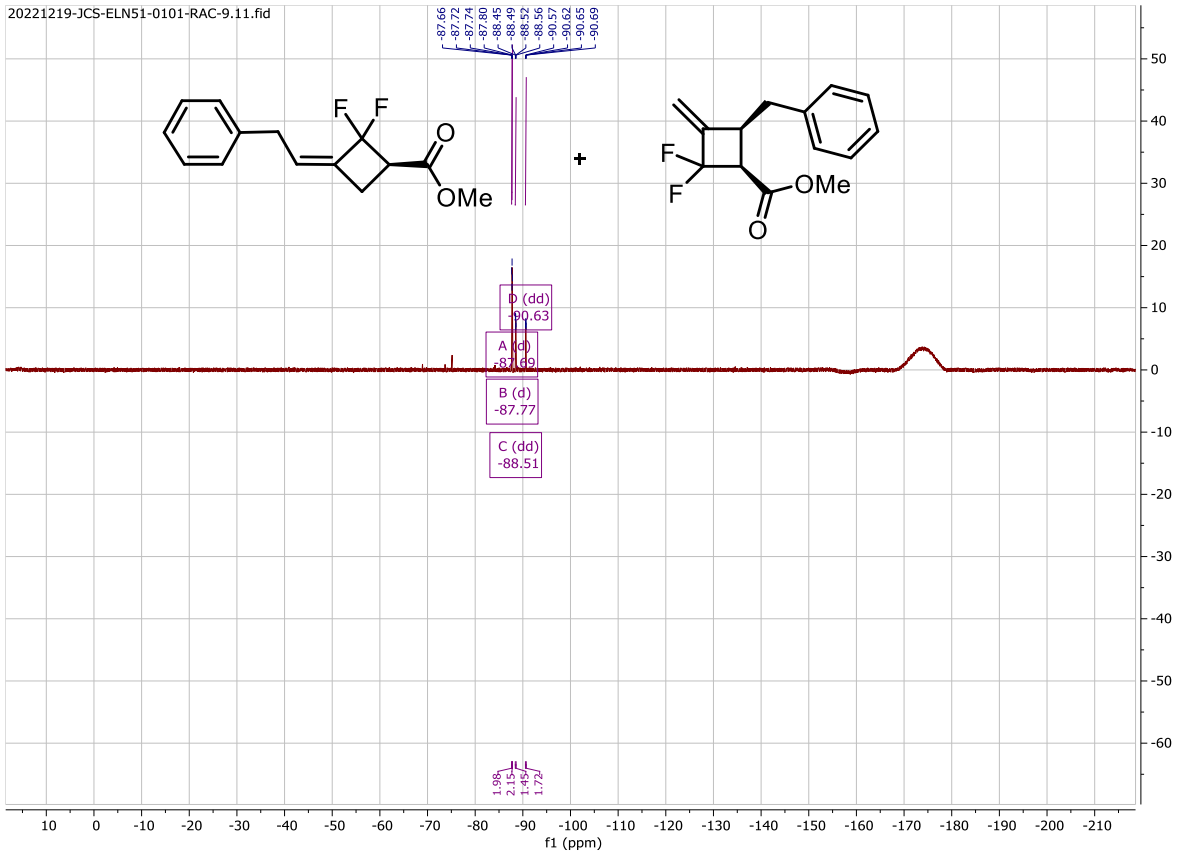
20221219-JCS-ELN51-0101-RAC-9.11.fid
-87.66
-87.72
-87.74
-87.80
-88.45
-88.49
-88.52
-88.56
-90.57
-90.62
-90.65
-90.69
F
F
O
OMe
+
F
F
OMe
O
D (dd)
-90.63
A (dd)
-87.69
B (d)
-87.77
C (dd)
-88.51
1.98
2.15
1.45
1.72
f1 (ppm)

9. HPLC/SFC Data:

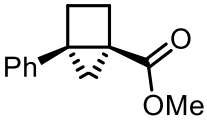

Racemate:

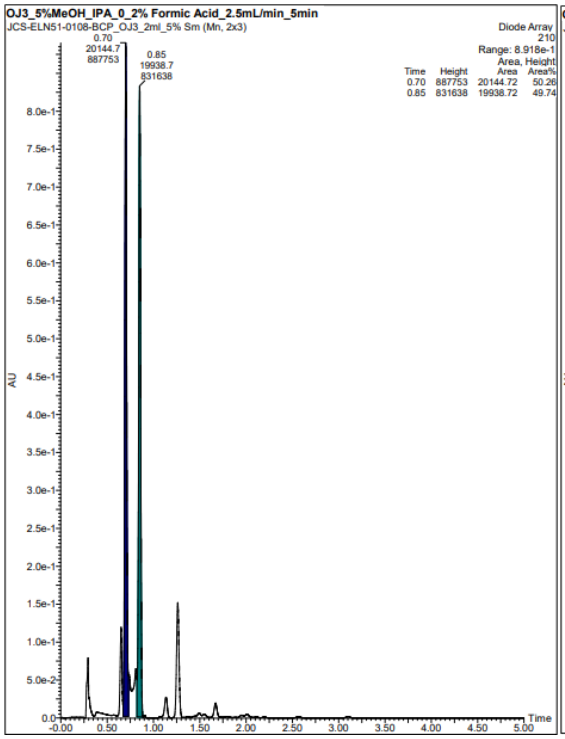

***S-p*-BrTPCP: 7% ee**

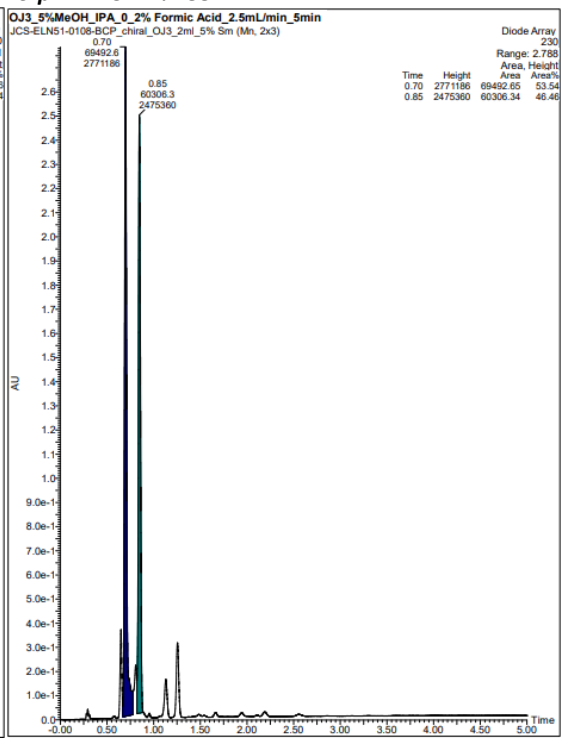

***R*-NTTL: 11% ee**

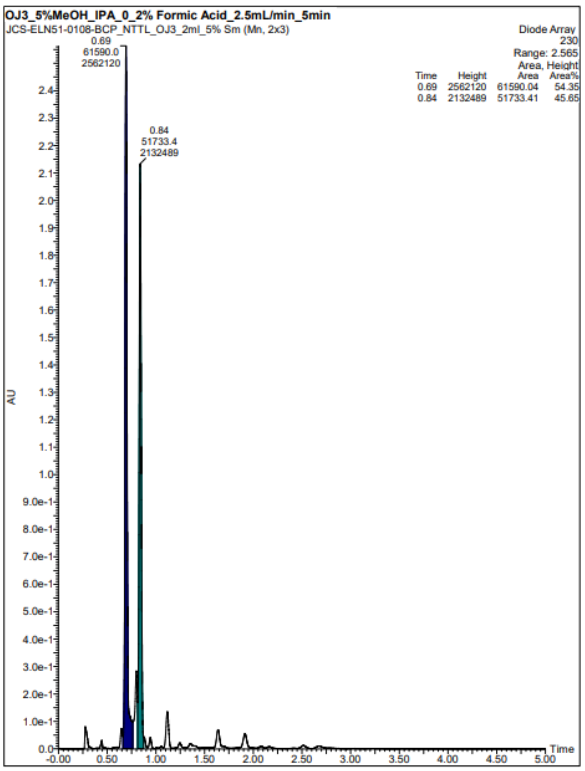

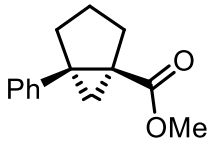

Racemate:

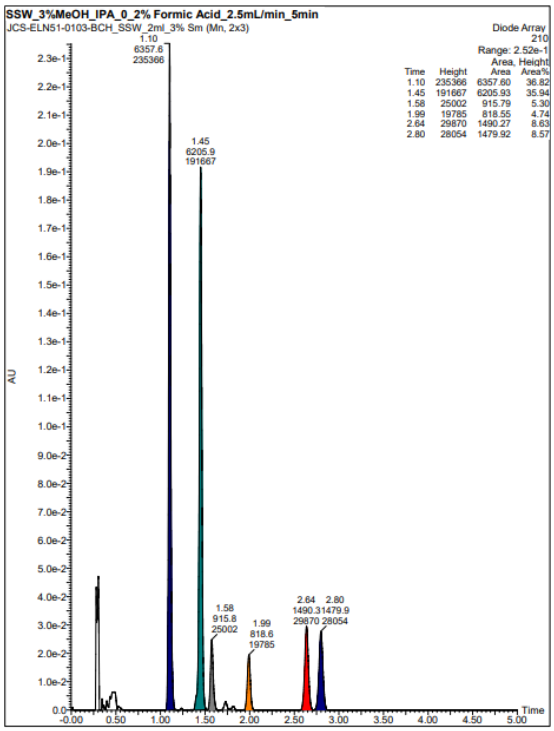

***S-p*-BrTPCP: 65% ee**

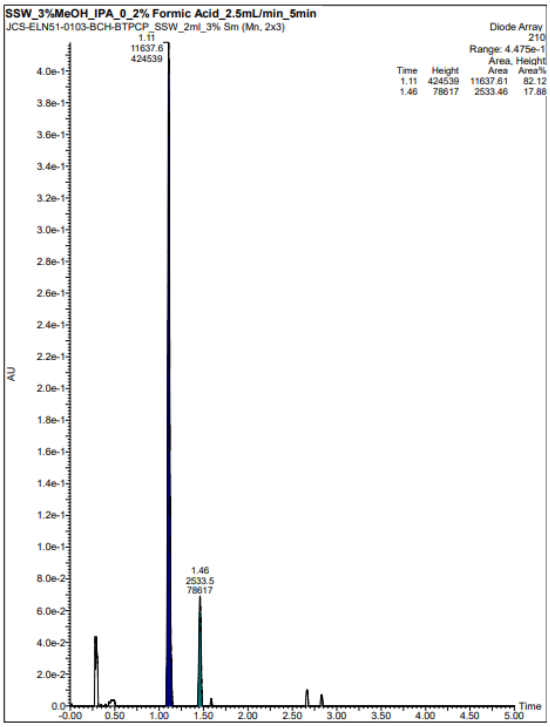

***R*-NTTL:**

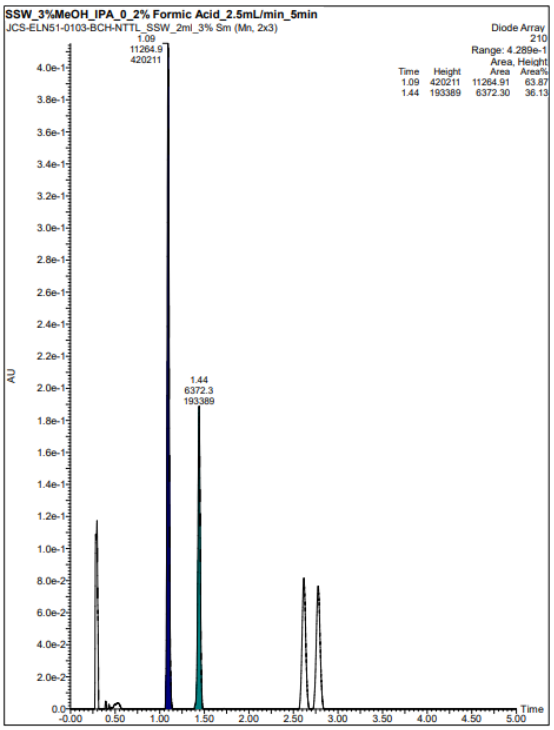

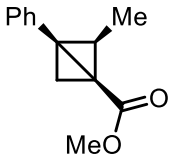
Ph
Me
O
MeO

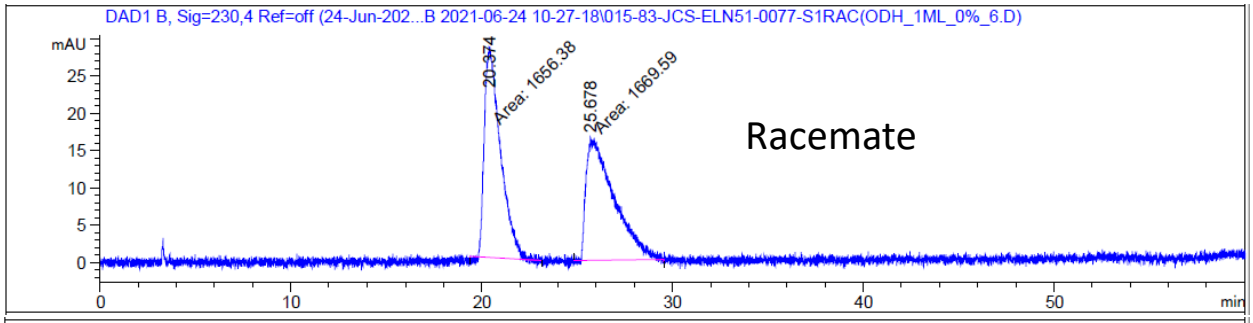
DAD1 B, Sig=230,4 Ref=off (24-Jun-202...B 2021-06-24 10-27-18\015-83-JCS-ELN51-0077-S1RAC(ODH_1ML_0%_6.D)
mAU
20.374
Area: 1656.38
25.678
Area: 1669.59
Racemate
min

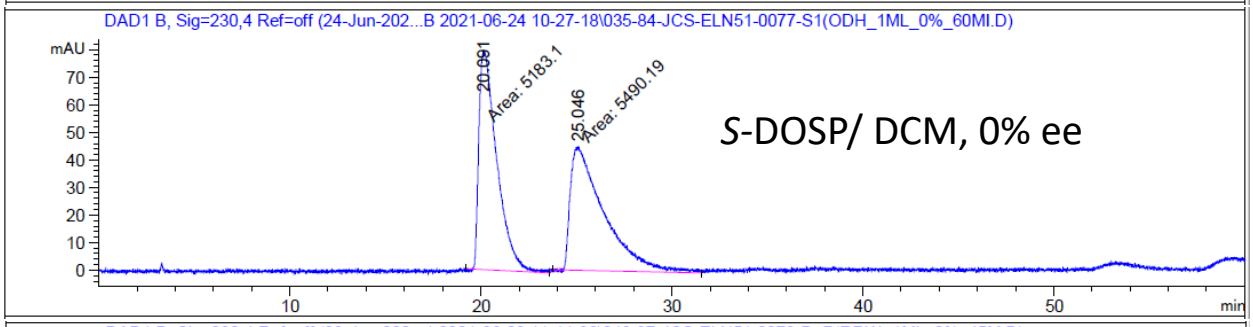
DAD1 B, Sig=230,4 Ref=off (24-Jun-202...B 2021-06-24 10-27-18\035-84-JCS-ELN51-0077-S1(ODH_1ML_0%_60MI.D)
mAU
20.091
Area: 5183.1
25.046
Area: 5490.19
S-DOSP/ DCM, 0% ee
min

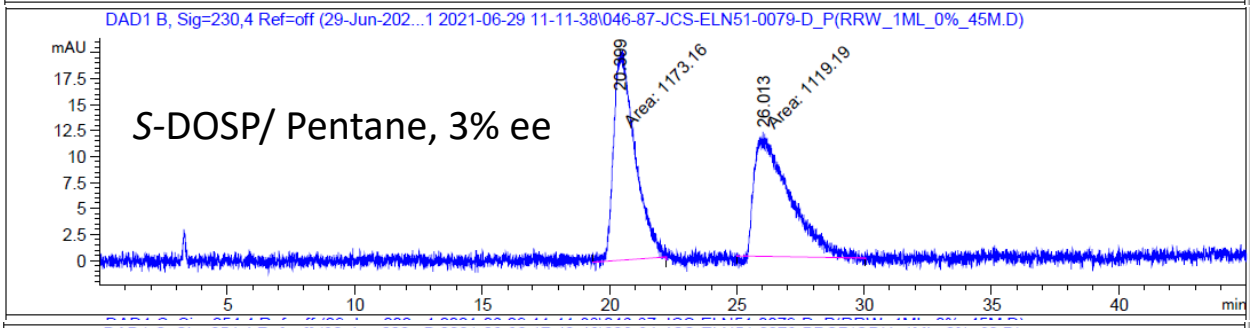
DAD1 B, Sig=230,4 Ref=off (29-Jun-202...1 2021-06-29 11-11-38\046-87-JCS-ELN51-0079-D_P(RRW_1ML_0%_45M.D)
mAU
S-DOSP/ Pentane, 3% ee
Area: 1173.16
26.013
Area: 1119.19
min

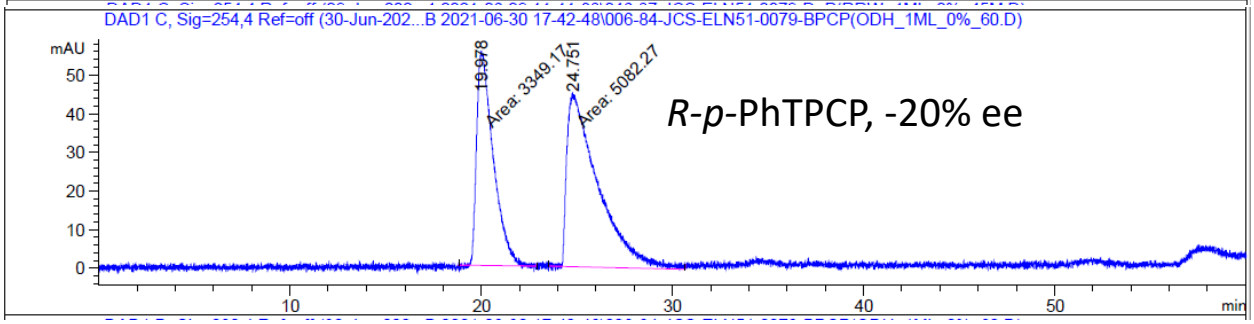
DAD1 C, Sig=254,4 Ref=off (30-Jun-202...B 2021-06-30 17-42-48\006-84-JCS-ELN51-0079-BPCP(ODH_1ML_0%_60.D)
mAU
19.978
Area: 3349.17
24.751
Area: 5082.27
R-p-PhTPCP, -20% ee
min

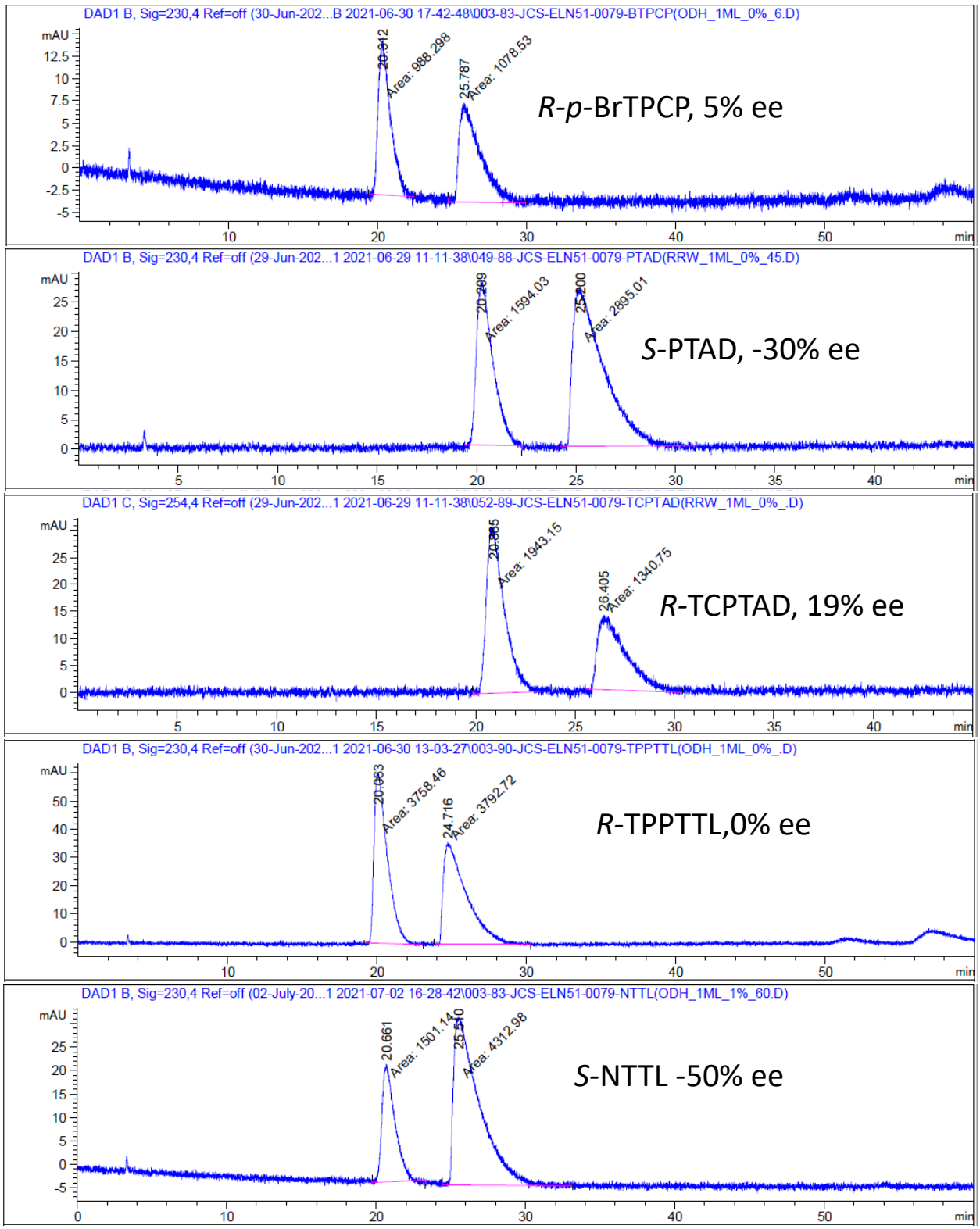
DAD1 B, Sig=230,4 Ref=off (30-Jun-202...B 2021-06-30 17-42-48\003-83-JCS-ELN51-0079-BTPCP(ODH_1ML_0%_6.D)
mAU
20.012
Area: 988.298
25.787
Area: 1078.53
R-p-BrTPCP, 5% ee
min
DAD1 B, Sig=230,4 Ref=off (29-Jun-202...1 2021-06-29 11-11-38\049-88-JCS-ELN51-0079-PTAD(RRW_1ML_0%_45.D)
mAU
20.269
Area: 1594.03
25.200
Area: 2895.01
S-PTAD, -30% ee
min
DAD1 C, Sig=254,4 Ref=off (29-Jun-202...1 2021-06-29 11-11-38\052-89-JCS-ELN51-0079-TCPTAD(RRW_1ML_0%_.D)
mAU
Area: 1943.15
26.405
Area: 1340.75
R-TCPTAD, 19% ee
min
DAD1 B, Sig=230,4 Ref=off (30-Jun-202...1 2021-06-30 13-03-27\003-90-JCS-ELN51-0079-TPPTTL(ODH_1ML_0%_.D)
mAU
20.063
Area: 3758.46
24.716
Area: 3792.72
R-TPPTTL,0% ee
min
DAD1 B, Sig=230,4 Ref=off (02-July-20...1 2021-07-02 16-28-42\003-83-JCS-ELN51-0079-NTTL(ODH_1ML_1%_60.D)
mAU
20.661
Area: 1501.14
Area: 4312.98
S-NTTL -50% ee
min

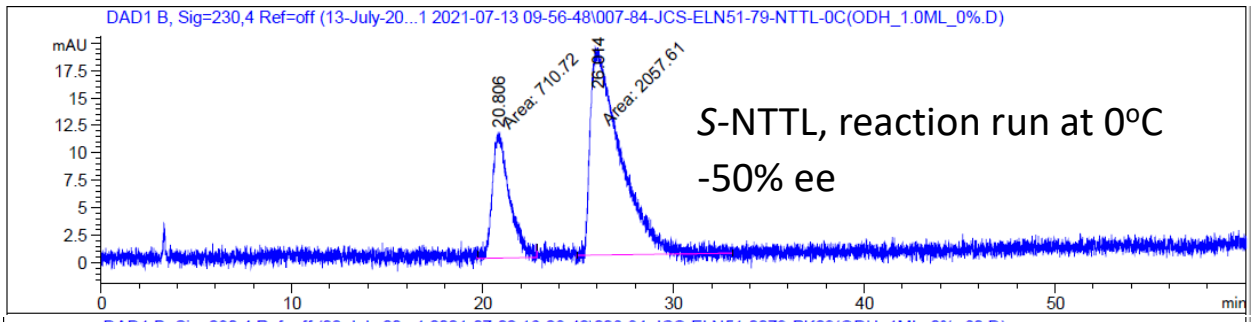
DAD1 B, Sig=230,4 Ref=off (13-July-20...1 2021-07-13 09-56-48\007-84-JCS-ELN51-79-NTTL-0C(ODH_1.0ML_0%.D)
mAU
20.806
Area: 710.72
Area: 2057.61
S-NTTL, reaction run at 0°C
-50% ee
min

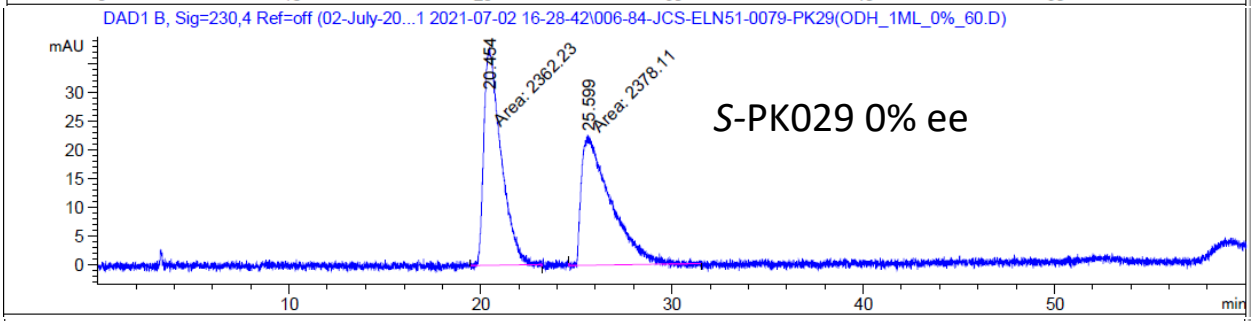
DAD1 B, Sig=230,4 Ref=off (02-July-20...1 2021-07-02 16-28-42\006-84-JCS-ELN51-0079-PK29(ODH_1ML_0%_60.D)
mAU
20.454
Area: 2362.23
25.599
Area: 2378.11
S-PK029 0% ee
min

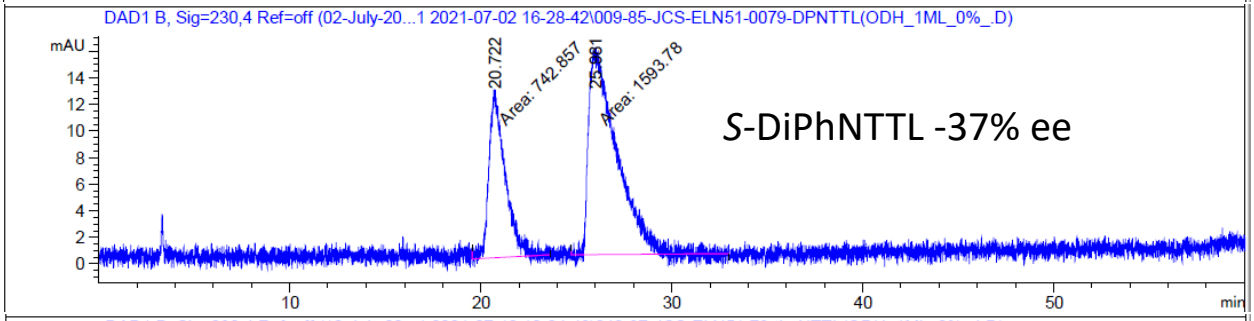
DAD1 B, Sig=230,4 Ref=off (02-July-20...1 2021-07-02 16-28-42\009-85-JCS-ELN51-0079-DPNTTL(ODH_1ML_0%_.D)
mAU
20.722
Area: 742.857
Area: 1593.78
S-DiPhNTTL -37% ee
min

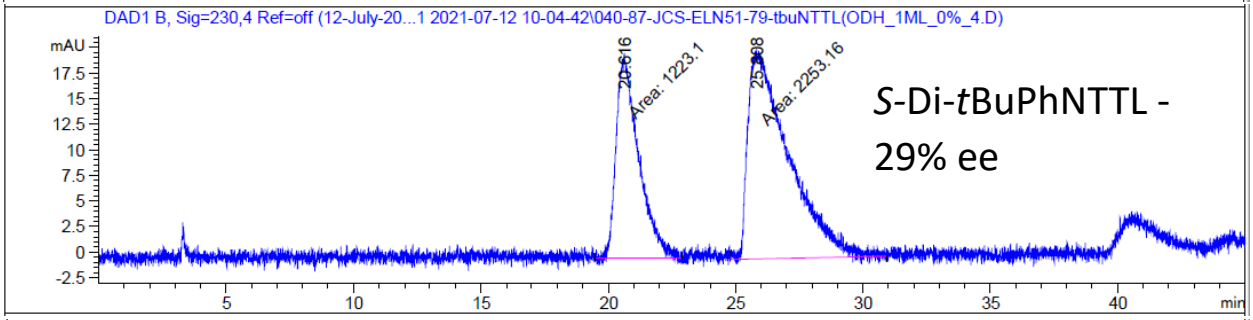
DAD1 B, Sig=230,4 Ref=off (12-July-20...1 2021-07-12 10-04-42\040-87-JCS-ELN51-79-tbuNTTL(ODH_1ML_0%_4.D)
mAU
20.616
Area: 1223.1
Area: 2253.16
S-Di-tBuPhNTTL -
29% ee
min

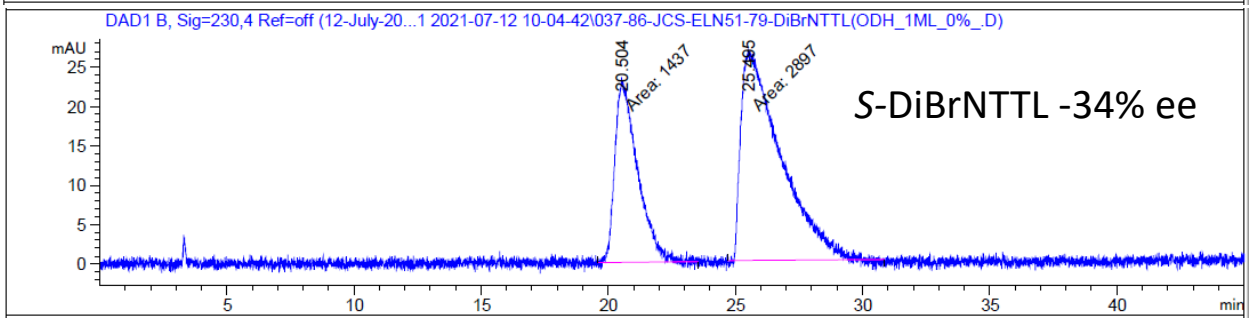
DAD1 B, Sig=230,4 Ref=off (12-July-20...1 2021-07-12 10-04-42\037-86-JCS-ELN51-79-DiBrNTTL(ODH_1ML_0%_.D)
mAU
20.504
Area: 1437
Area: 2897
S-DiBrNTTL -34% ee
min

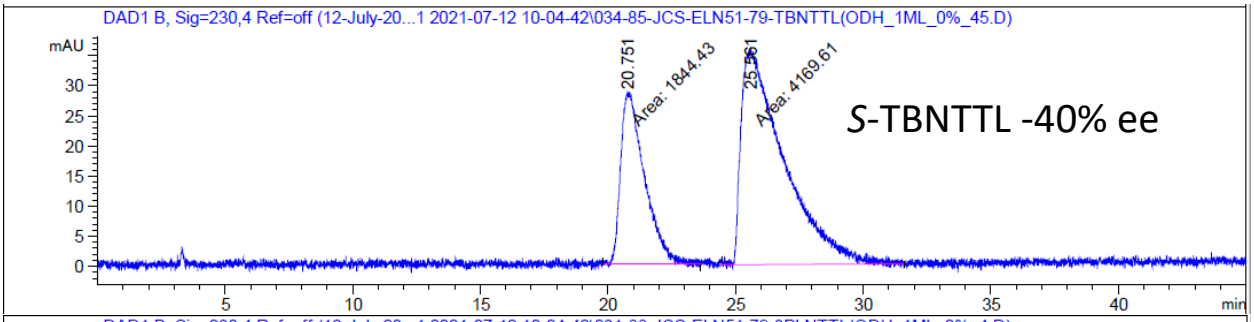

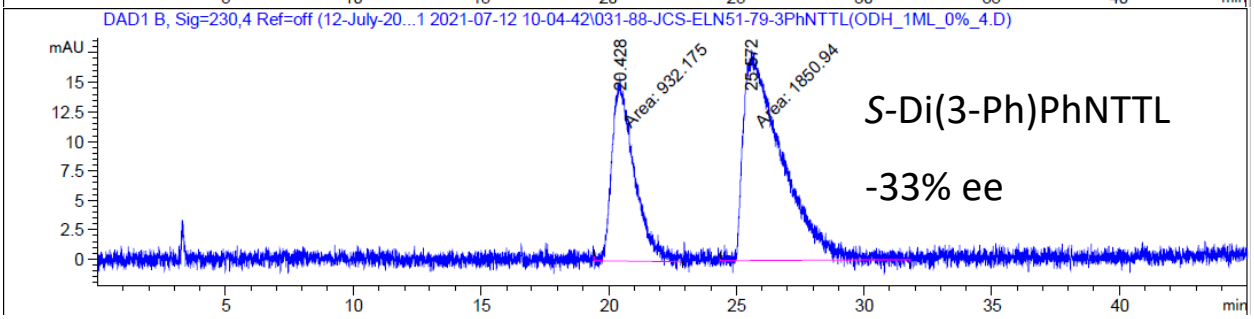

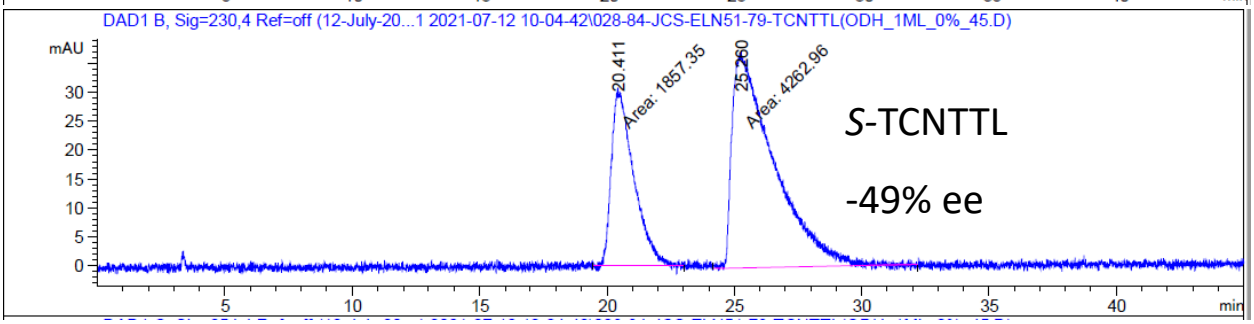

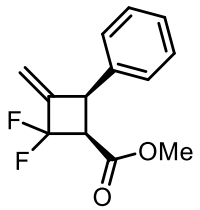

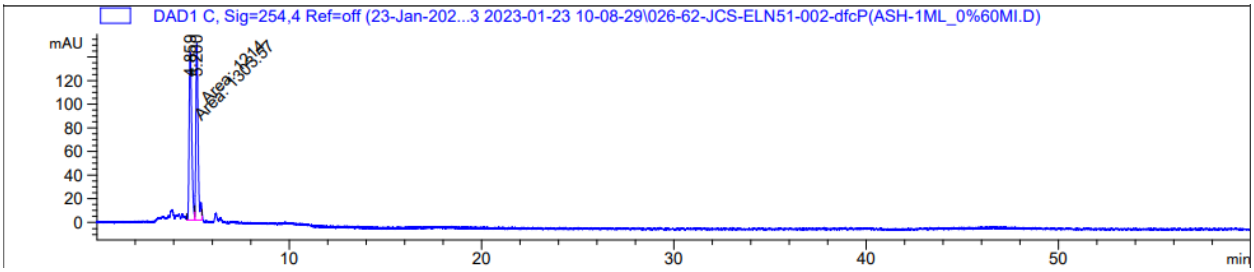

Signal 3: DAD1 C, Sig=254,4 Ref=off

Peak #	RetTime [min]	Type	Width [min]	Area [mAU*s]	Height [mAU]	Area %
1	4.859	MM	0.1528	1303.57104	142.19475	51.7789
2	5.200	MM	0.1353	1213.99963	149.57280	48.2211
Totals :				2517.57068	291.76755	

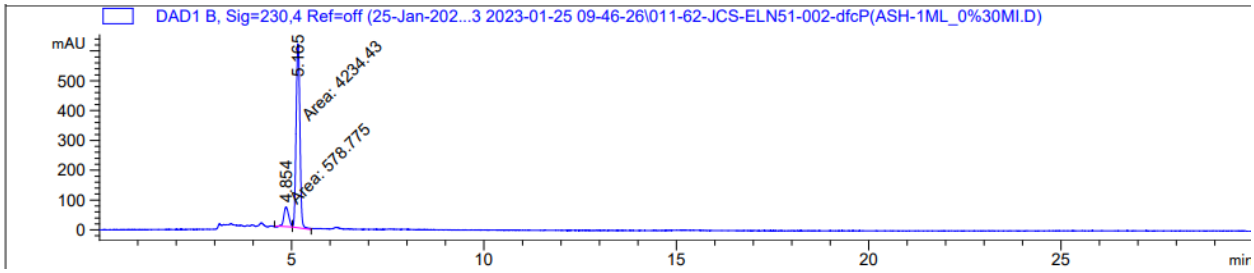

Signal 2: DAD1 B, Sig=230,4 Ref=off

Peak #	RetTime [min]	Type	Width [min]	Area [mAU*s]	Height [mAU]	Area %
1	4.854	MM	0.1462	578.77502	65.97089	12.0247
2	5.165	MM	0.1144	4234.42871	616.86493	87.9753

Totals : 4813.20374 682.83582

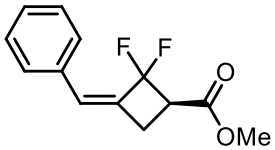

Racemate:

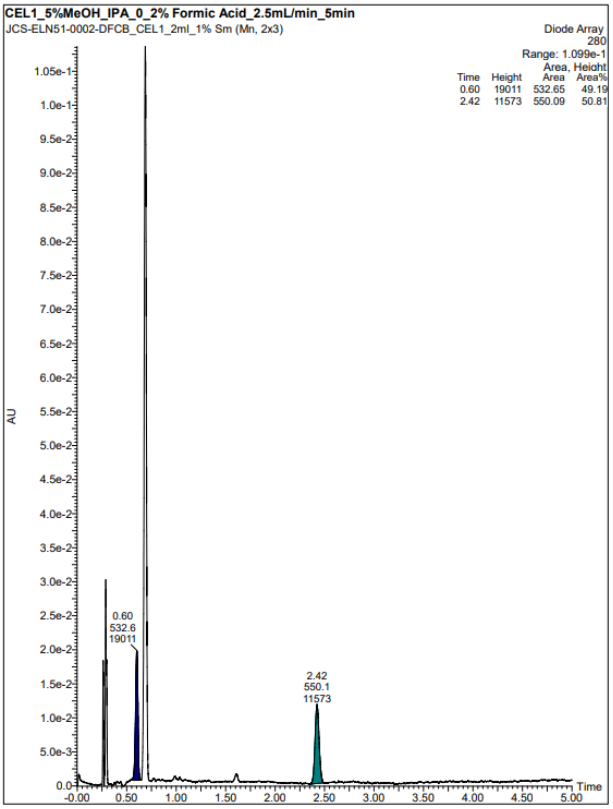

Chiral:

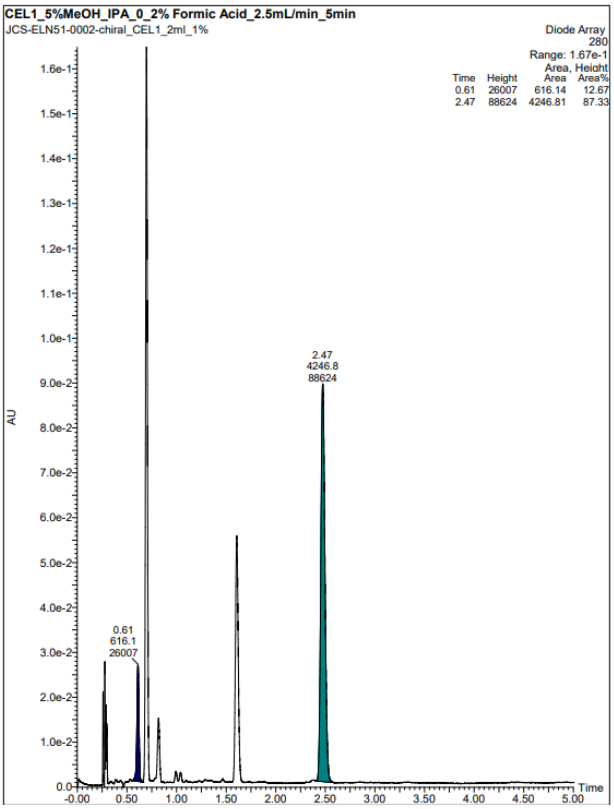

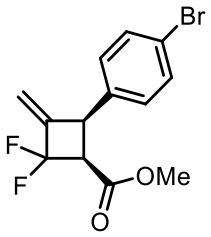

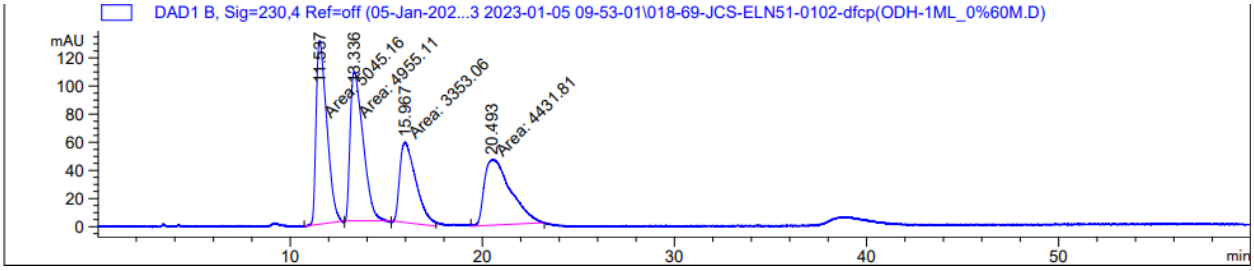

Signal 2: DAD1 B, Sig=230,4 Ref=off

Peak #	RetTime [min]	Type	Width [min]	Area [mAU*s]	Height [mAU]	Area %
1	11.537	MM	0.6437	5045.16016	130.62349	28.3673
2	13.336	MM	0.7758	4955.11230	106.44539	27.8610
3	15.967	MM	0.9761	3353.05664	57.25277	18.8531
4	20.493	MM	1.5800	4431.80664	46.75036	24.9186

Totals : 1.77851e4 341.07201

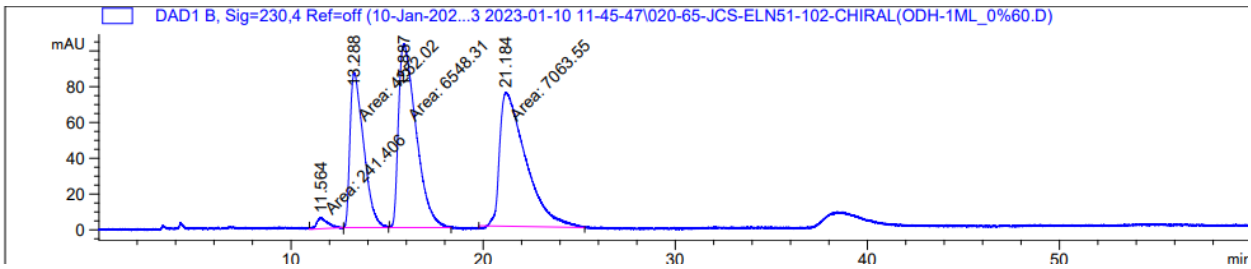

Signal 2: DAD1 B, Sig=230,4 Ref=off

Peak #	RetTime [min]	Type	Width [min]	Area [mAU*s]	Height [mAU]	Area %
1	11.564	MM	0.6497	241.40572	6.19271	1.3333
2	13.288	MM	0.8176	4252.02295	86.67820	23.4850
3	15.887	MM	1.0613	6548.30811	102.83199	36.1679
4	21.184	MM	1.5726	7063.54688	74.85870	39.0137

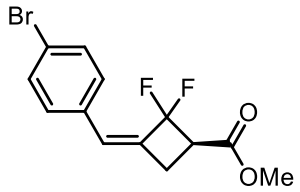

Racemate:

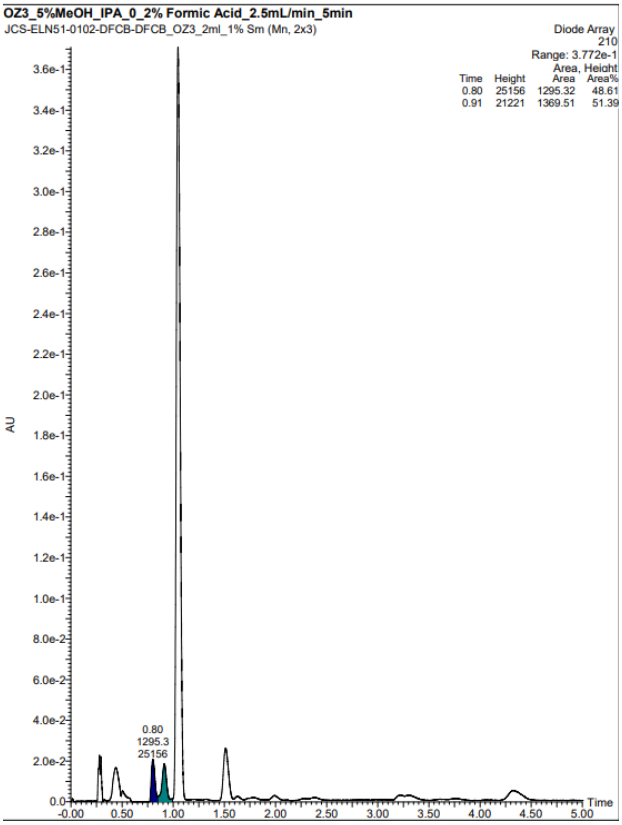

Chiral:

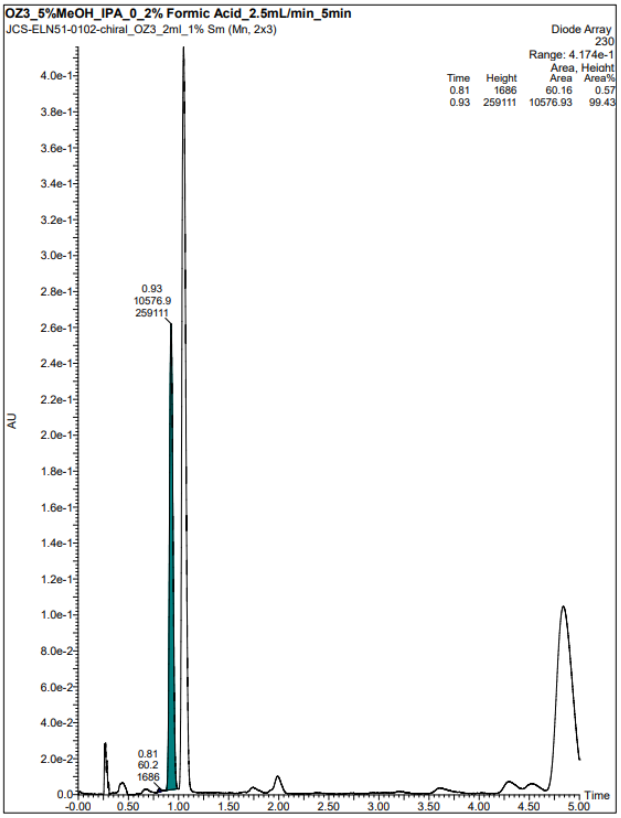

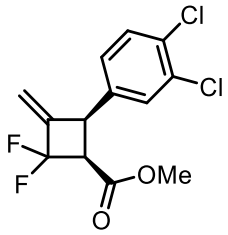

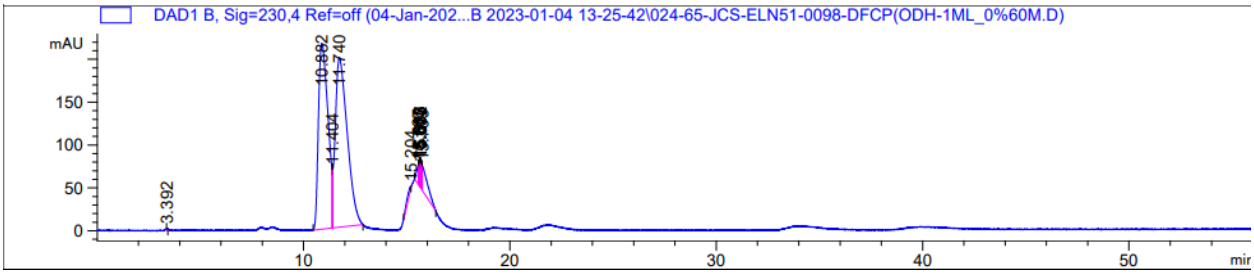

Signal 1: DAD1 A, Sig=210,4 Ref=off

Peak #	RetTime [min]	Type	Width [min]	Area [mAU*s]	Height [mAU]	Area %
1	10.891	MM	0.5172	2.08496e4	671.92285	45.4748
2	11.738	MM	0.7004	2.49991e4	594.86774	54.5252

Totals : 4.58487e4 1266.79059

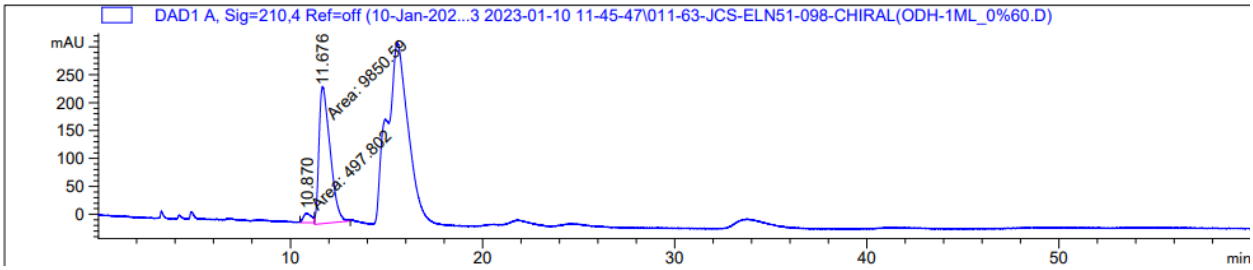

Signal 1: DAD1 A, Sig=210,4 Ref=off

Peak #	RetTime [min]	Type	Width [min]	Area [mAU*s]	Height [mAU]	Area %
1	10.870	MM	0.4854	497.80197	17.09164	4.8104
2	11.676	MM	0.6682	9850.58789	245.69438	95.1896

Totals : 1.03484e4 262.78602

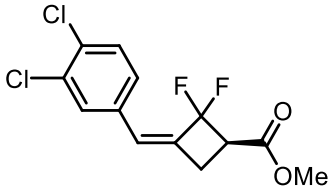

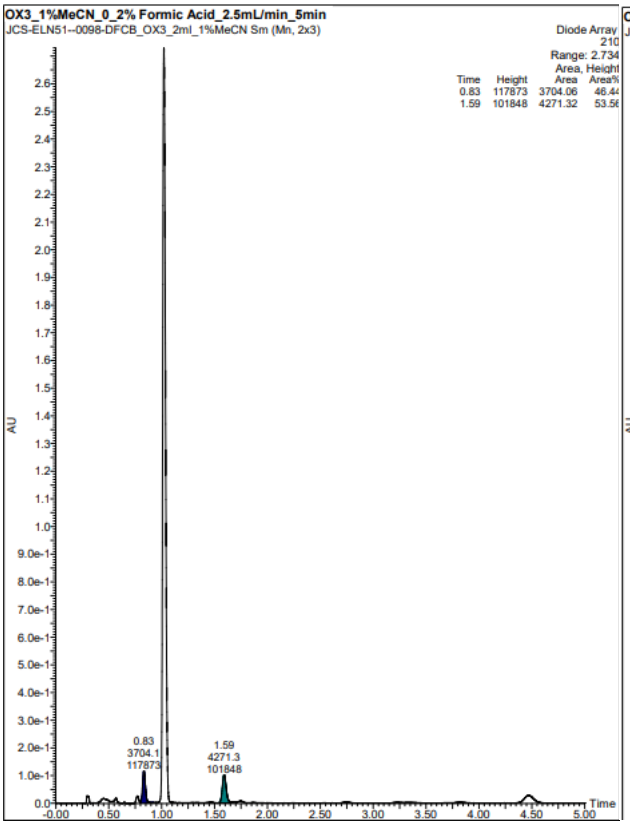

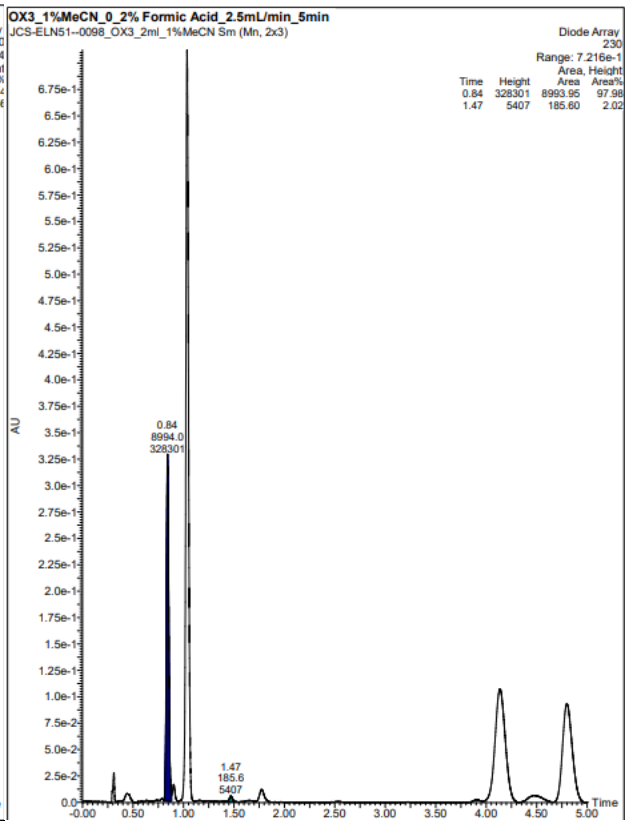

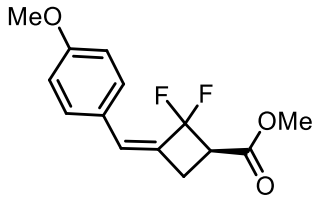

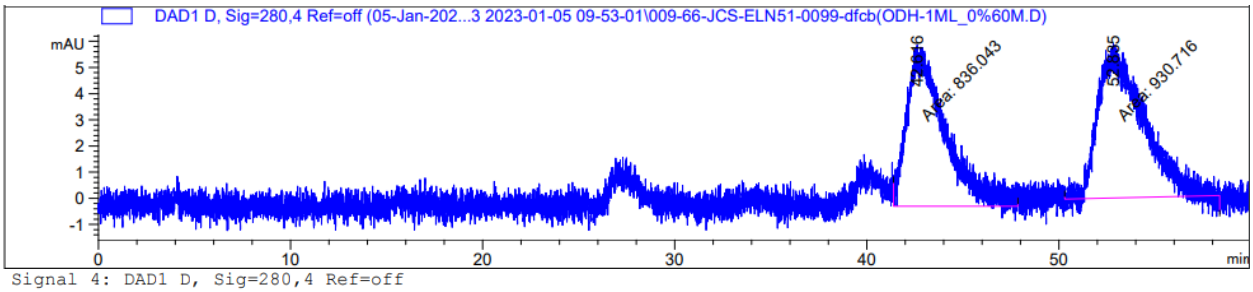

Signal 4: DAD1 D, Sig=280,4 Ref=off

Peak #	RetTime [min]	Type	Width [min]	Area [mAU*s]	Height [mAU]	Area %
1	42.616	MM	2.2583	836.04321	6.17007	47.3207
2	52.835	MM	2.6307	930.71600	5.89642	52.6793

Totals : 1766.75922 12.06648

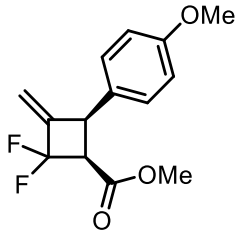

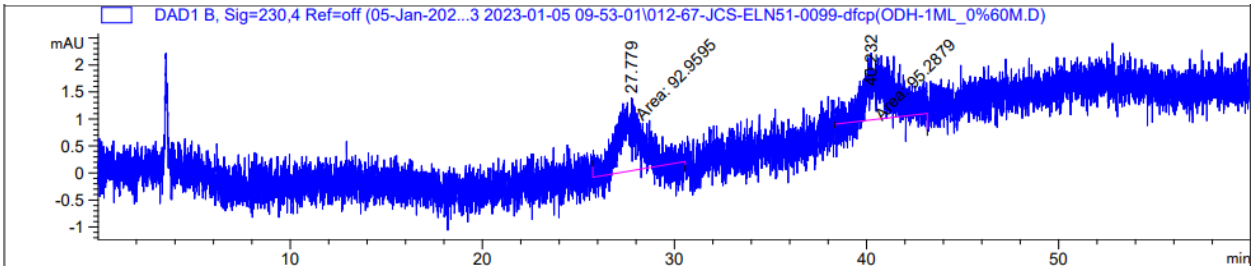

Signal 2: DAD1 B, Sig=230,4 Ref=off

Peak #	RetTime [min]	Type	Width [min]	Area [mAU*s]	Height [mAU]	Area %
1	27.779	MM	1.1467	92.95953	1.35112	49.3816
2	40.232	MM	1.2647	95.28786	1.25571	50.6184

Totals : 188.24738 2.60683

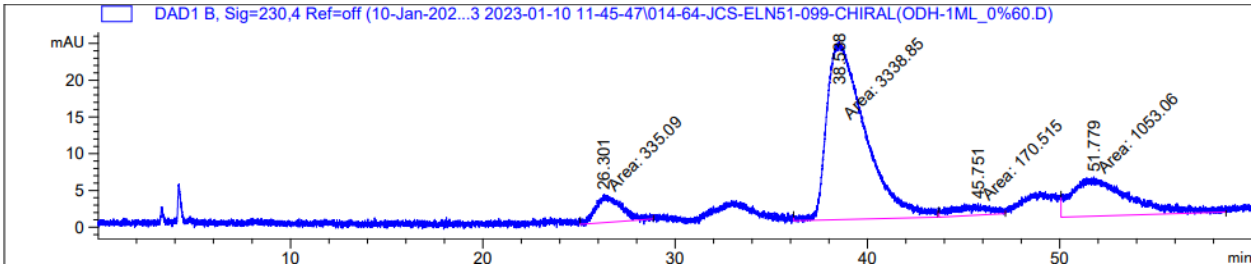

Signal 2: DAD1 B, Sig=230,4 Ref=off

Peak #	RetTime [min]	Type	Width [min]	Area [mAU*s]	Height [mAU]	Area %
1	26.301	MM	1.4445	335.08954	3.86632	6.8420
2	38.538	MM	2.2988	3338.85254	24.20752	68.1744
3	45.751	MM	1.8074	170.51495	1.57240	3.4817
4	51.779	MM	3.2620	1053.06152	5.38044	21.5019

Totals : 4897.51855 35.02668

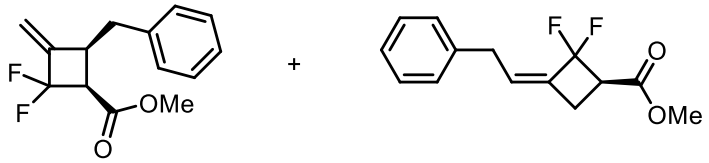

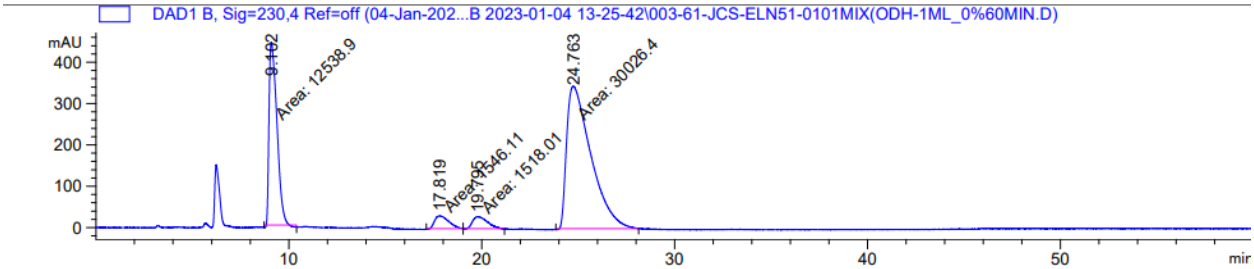

Signal 2: DAD1 B, Sig=230,4 Ref=off

Peak #	RetTime [min]	Type	Width [min]	Area [mAU*s]	Height [mAU]	Area %
1	9.102	MM	0.4726	1.25389e4	442.20712	27.4799
2	17.819	MM	0.8343	1546.10693	30.88548	3.3884
3	19.795	MM	0.8770	1518.00854	28.84764	3.3268
4	24.763	MM	1.4529	3.00264e4	344.43179	65.8049

Totals : 4.56294e4 846.37203

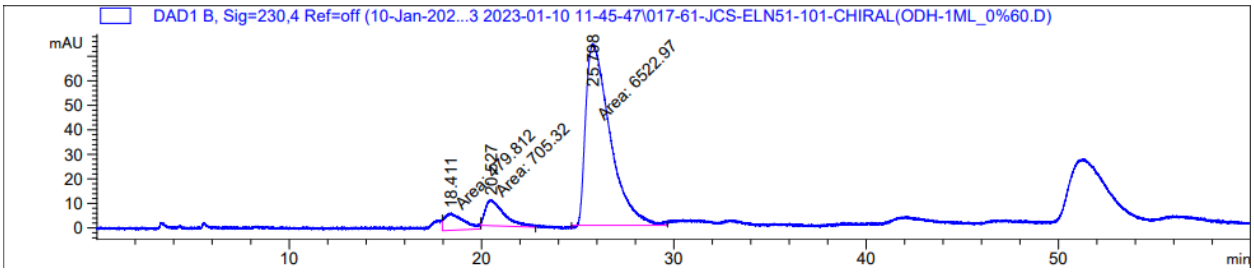

Signal 2: DAD1 B, Sig=230,4 Ref=off

Peak #	RetTime [min]	Type	Width [min]	Area [mAU*s]	Height [mAU]	Area %
1	18.411	MM	1.1306	479.81186	7.07342	6.2248
2	20.527	MM	1.1114	705.32050	10.57736	9.1504
3	25.798	MM	1.4662	6522.96973	74.14896	84.6248

Totals : 7708.10208 91.79974

10. References

1. Green, S. P.; Wheelhouse, K. M.; Payne, A. D.; Hallett, J. P.; Miller, P. W.; Bull, J. A., Thermal stability and explosive hazard assessment of diazo compounds and diazo transfer reagents. *Org. Proc. Res. Dev.* **2019,** *24* (1), 67-84.
2. Chauhan, D. P.; Varma, S. J.; Gudem, M.; Panigrahi, N.; Singh, K.; Hazra, A.; Talukdar, P., Intramolecular cascade rearrangements of enynamine derived ketenimines: access to acyclic and cyclic amidines. *Org. Biomol. Chem.* **2017,** *15* (22), 4822-4830.
3. Malkov, A. V.; Czemerys, L.; Malyshev, D. A., Vanadium-catalyzed asymmetric epoxidation of allylic alcohols in water. *J. Org. Chem.* **2009,** *74* (9), 3350-3355.
4. Qin, C.; Davies, H. M., Enantioselective synthesis of 2-arylbicyclo [1.1. 0] butane carboxylates. *Org. Lett.* **2013,** *15* (2), 310-313.
5. Bychek, R. M.; Hutskalova, V.; Bas, Y. P.; Zaporozhets, O. A.; Zozulya, S.; Levterov, V. V.; Mykhailiuk, P. K., Difluoro-substituted bicyclo [1.1. 1] pentanes for medicinal chemistry: Design, synthesis, and characterization. *J. Org. Chem.* **2019,** *84* (23), 15106-15117.